

# Lipids and Endothelium-Dependent Vasodilation—A Review

Lars Lind\*

Department of Medicine, Uppsala University Hospital and AstraZeneca R&D, Mölndal, Sweden

**ABSTRACT:** Studies using both *in vitro* and *in vivo* techniques have repeatedly shown that endothelium-dependent vasodilation (EDV) is impaired in different forms of experimental as well as human hypercholesterolemia. Clearly this impaired EDV can be reversed by lowering cholesterol levels by diet or medical therapy. Competitive blocking of L-arginine, changes in nitric oxide synthase activity, increased release of endothelin-1, and inactivation of nitric oxide due to superoxide ions all contribute to the impairment in EDV during dyslipidemia. The oxidation of low density lipoprotein, with its compound lysophosphatidylcholine, plays a critical role in these events. However, data on the role of triglycerides and fat-rich meals regarding EDV are not so consistent as data for cholesterol, although a view that the compositions of individual fatty acids and antioxidants are of major importance is emerging. Thus, this review shows that while impaired EDV is a general feature of hypercholesterolemia, the mechanisms involved and the therapeutic opportunities available still have to be investigated. Furthermore, discrepancies regarding the role of triglycerides and fat content in food may be explained by divergent effects of different fatty acids on the endothelium.

Paper no. L8726 in *Lipids* 37, 1–15 (January 2002).

Hypercholesterolemia has long been regarded as a major cardiovascular risk factor due to findings in epidemiological studies (1). Since the introduction of the statins, lipid lowering by these agents has had positive effects in recent years on cardiovascular morbidity and mortality (2–4).

Furchgott and Zawadzki (5) discovered in 1980 that the endothelium takes an active part in the regulation of blood flow. That the endothelium also participates in the pathogenesis of atherosclerosis was discovered later. Endothelial-derived factors contribute to maintaining a state favoring vessel patency, blood fluidity, nonadherence of circulating blood cells, and inhibition of smooth muscle cell proliferation (6–8).

In 1986, Ludmer and co-workers (9) showed that acetylcholine produced vasoconstriction in atherosclerotic coronary arteries, whereas a vasodilatory response was seen in normal arteries in humans. In fact, vasodilation was impaired in atherosclerotic-prone humans even before the development of atherosclerotic lesions could be detected with coronary angiograms (10). It was therefore suggested that an impairment

in endothelium-dependent vasodilation (EDV) could be taken as an early marker of atherosclerosis formation. Although dyslipidemia also could cause impairment in other functions of the endothelium (11), the present review will focus on the role of cholesterol, triglycerides, fatty acids, and fat intake on EDV.

## Endothelium-Derived Vasoactive Factors

*Nitric oxide (NO).* Palmer *et al.* (12) discovered that the endothelium-dependent relaxing factor, called EDRF, was identical to NO, being synthesized from the amino acid L-arginine by NO synthase (NOS) (13). NO diffuses to the smooth muscle cells in the vessels inducing formation of cGMP, which promotes vasodilation (14,15). NO is rapidly converted to metabolites, such as nitrite, nitrate, and radical forms of NO. Several analogs of L-arginine, such as N<sup>G</sup>-monomethyl-L-arginine, competitively inhibit NO production (14–16).

*Endothelin.* The main vasoconstrictive endothelin is endothelin-1 (ET-1), produced from the propeptide big ET-1 by endothelin-converting enzyme (17,18). The main vasoconstrictive endothelin receptor subtype is called ET<sub>A</sub> and is present on VSMC (19), whereas ET<sub>B</sub>-receptors, located on endothelial cells, induce vasodilation through release of NO (19–21).

*Other endothelium-derived vasoactive factors.* Apart from NO, hyperpolarizing factors (EDHF) can contribute to part of the acetylcholine-induced vasodilation (14,22,23) by opening K<sup>+</sup>-channels (24,25). Recent studies suggest that EDHF could be either a cytochrome p450-derived arachidonic acid metabolite (26,27) or the potassium ion (28). Acetylcholine could induce endothelial release of vasoconstricting factors (EDCF), such as thromboxane A<sub>2</sub> or prostaglandin H<sub>2</sub> (29–33). The endothelium could also produce other vasoactive compounds, such as the vasodilatory prostacyclin (PGI<sub>2</sub>).

## Models to Investigate EDV

*Experimental in vitro and in vivo studies.* The most widely used *in vitro* method to study EDV is to expose vessel rings mounted on a wire myograph to vasodilators, such as acetylcholine (34–70). *In vivo* studies in animals most often use acetylcholine in isolated organ preparations *in vivo* (71–78).

*Human studies of coronary circulation.* Registration of the change in vascular diameter in epicardial arteries during coronary angiography subjected to local infusion of acetylcholine is a common way to evaluate coronary EDV (79–82).

*Human forearm model.* Evaluation of the forearm blood flow response to intra-arterial infusion of vasodilator agents

\*Address correspondence at Department of Internal Medicine, University Hospital of Uppsala, S-751 85 Uppsala, Sweden.  
E-mail: lars.lind@medsci.uu.se

Abbreviations: ADMA, asymmetric dimethylarginine; EDCF, endothelium-derived vasoconstricting factor; EDHF, endothelium-derived hyperpolarizing factor; EDV, endothelium-dependent vasodilation; ET-1, endothelin-1; HDL, high density lipoprotein; LDL, low density lipoprotein; lp(a), lipoprotein(a); LPC, lysophosphatidylcholine; LPL, lipoprotein lipase; NO, nitric oxide; NOS, nitric oxide synthase; VSMC, vascular smooth muscle cells.

by venous occlusion plethysmography is the most widely used method to study EDV in resistance arteries in humans (83–89).

**Human brachial artery ultrasound method.** High-resolution ultrasound is used to measure changes in brachial artery diameter during reactive hyperemia, flow-mediated vasodilation (90–92). Apart from these methods, the *in vitro* method has also been used for human subcutaneous small arteries (93).

### Animal Models of Hypercholesterolemia and Atherosclerosis

The most widely used model of hypercholesterolemia and atherosclerosis is the cholesterol-fed New Zealand white rabbit (34–59). Other animals, such as the rat, monkey, pig, and

the Watanabe rabbit, have also been used (60–62). In recent years, the use of knock-out mice for the apolipoprotein E or the low density lipoprotein (LDL)-receptor gene have gained in popularity (69,70).

### Effects of Hypercholesterolemia on EDV in Animal Models

Table 1 summarizes the studies in which acetylcholine has been used to induce EDV in different animal models and different types of vessels in *in vitro* experimental studies. In the vast majority of the studies evaluating the aorta, a negative effect on EDV was seen in different animals (34–50, 60–64, 69). An impaired EDV was also seen in other vessels, includ-

**TABLE 1**  
Studies in Experimental Cholesterol-Fed (CF) Animals or Inheritable Forms of Atherosclerosis Using Acetylcholine to Evaluate Endothelium-Dependent Vasodilation (EDV)<sup>a</sup>

Model	Vessel type	Effect on EDV	Reference
<i>In vitro</i>			
CF rabbit	Aorta	Negative	34–50
CF rabbit	Coronary Pulmonary artery Corpus cavernosus Carotid artery Subclavian artery	Negative	41, 51–57
CF rabbit	Femoral artery Mesenteric artery Cerebral artery Basilar artery	No effect	41, 58
CF rabbit	Aorta	No effect	59
Watanabe rabbit	Aorta Coronary artery	Negative	60–62
Watanabe rabbit	Renal artery Basilar artery	No effect	61
CF rat	Aorta Skeletal muscle artery	Negative	63, 64
CF rat	Aorta	No effect	65
Yoshida rat	Aorta	Negative	66
Froxfeld rabbit	Subclavian artery	Negative	56
CF chicken	Pulmonary artery	Negative	67
CF monkey	Mesenteric artery	Negative	68
ApoE knock-out	Aorta	Negative	69
ApoE + LDL rec knock-out	Coronary	Negative	70
<i>In vivo</i>			
CF rabbit	Hindlimb and mesenteric	Negative	71–73
Watanabe	Hindlimb	No effect	74
CF rabbit	Kidney	No effect	75
CF pig	Kidney	Negative	76
CF monkey	Femoral artery	Negative	77
ApoE knock-out	Skin	Negative	78

<sup>a</sup>Effect on EDV denotes the influence of the animal model compared to control animals regarding EDV. LDL, low density lipoprotein; ApoE, apolipoprotein E.



ing the coronary arteries, during hypercholesterolemia (41,51–57,67,68,70). Also, *in vivo* studies using different perfused vascular beds have found that hypercholesterolemia impairs EDV (71–73,76–78). However, studies using small cerebral arteries or the renal vasculature generally have been unable to show a deleterious effect of hypercholesterolemia on EDV (41,58,61,75).

### Effects of Hypercholesterolemia on EDV in Humans

In humans, the effects of hypercholesterolemia on EDV have been even more consistent than in the experimental studies. In the 14 studies summarized in Table 2, all but one (92) showed that hypercholesterolemic subjects have an impaired EDV in different vascular beds (79–91,93). Additionally, several studies have demonstrated an inverse relationship between serum cholesterol levels and EDV in apparently healthy humans (94–98; see Fig. 1).

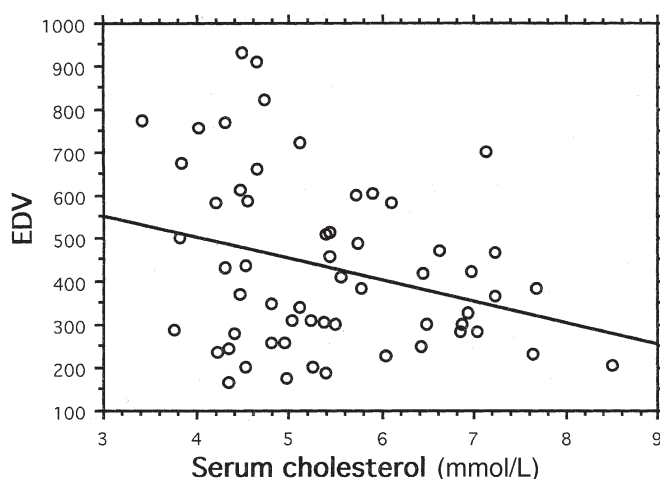
Thus, it can be concluded that hypercholesterolemia, both in animal models and in humans, has a deleterious effect on EDV in the majority of vascular beds studied.

### Effects of Different Types of Lipoproteins on EDV

Although native LDL reportedly induces an impairment in EDV when added to aortic preparations *in vitro* (99–101) and reduces NOS mRNA expression (102) and cGMP levels (103), oxidized LDL is more potent than the native form (104–106). A graded effect of the degree of oxidation of LDL on EDV was seen (107), confirming that oxidation of the LDL particle is essential for the endothelial effects (108–116). Also in humans, the lag phase of LDL oxidation was related to the degree of coronary EDV (117).

A major component in oxidized LDL is lysophosphatidylcholine (LPC). When aortic rings were exposed to pure LPC, a reduction in EDV similar to that with oxidized LDL was seen (109,118–123). The deleterious effect of LPC might be acting through a protein kinase-C pathway (124) and by elevated levels of phospholipase D (125). Plasma phospholipid transfer protein could abolish this impairment in EDV caused by LPC (126).

When aortic rings were exposed to high density lipoprotein (HDL) only, an impairment in EDV, similar to that of LDL, was found (100). However, when HDL was given together



**FIG. 1.** Relationship between serum cholesterol levels and endothelium-dependent vasodilation (EDV) in a sample of apparently healthy subjects (for details, see Ref. 97).

with oxidized LDL, HDL could inhibit the reduction in EDV induced by oxidized LDL (105,127) due to removal of LPC from oxidized LDL (122). Also, synthetic large “empty” phospholipid vesicles that accelerate reverse cholesterol transport improved EDV (128). In humans, a positive correlation between HDL levels and EDV has been reported (129,130).

Lipoprotein(a), especially in its oxidized form, has been reported to impair EDV (131). This effect can be reversed by adding HDL (132). In humans, lp(a) levels have been inversely related to coronary EDV and basal NO release (133–135).

### Effects of Triglycerides and Fatty Acids on EDV

Under experimental conditions, very low density lipoproteins and remnants of chylomicrons impair EDV (100,136,137). When Intralipid plus heparin was infused in humans to increase free fatty acids and triglycerides, a rapid reduction in EDV was seen (138–142). This effect was most pronounced in subjects with the BB-paraoxonase genotype (143). In the laboratory, oleic acid induced an impairment in EDV *in vitro* (144). However, later studies showed that the effect of fatty acids was not a simple one, as palmitic acid, but not stearic acid, reduced NO production in cultured cells (145). On the contrary, the two polyunsaturated fatty acids, eicosapentaenoic acid and docosahexaenoic acid, but not arachidonic acid, improved EDV (146) and NO production (147). The n-3 fatty acid supplementation in humans also improved EDV (148). We recently showed divergent effects of different fatty acids in a population study (129).

In humans with isolated hypertriglyceridemia, both an impaired (149–152) and a normal EDV have been reported (153,154). In our own population study, subjects with serum triglycerides >1.7 mmol/L showed an impaired EDV (Fig. 2) (97). As triglycerides are cleared from the circulation by lipoprotein lipase (LPL), an LPL activator improves EDV in rats (155).

**TABLE 2**  
Comparison of EDV in Human Subjects with Hypercholesterolemia (HC) and Controls Using Different Methods<sup>a</sup>

Methods	Effect of HC on EDV	Reference
Coronary	Negative	79–82
Forearm	Negative	83–89
FMD (femoral artery)	Negative	90,91
FMD (brachial artery)	No effect	92
<i>In vitro</i>	Negative	93

<sup>a</sup>FMD, flow-mediated vasodilation evaluated by ultrasound. See Table 1 for other abbreviation.

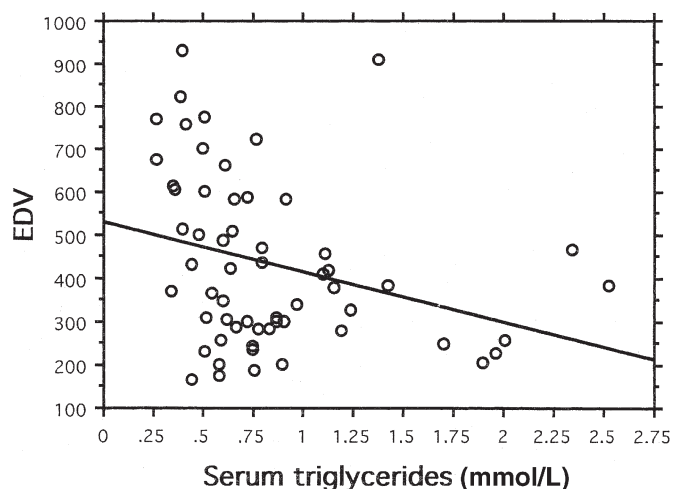


FIG. 2. Relationship between serum triglyceride levels and EDV in a sample of apparently healthy subjects (for details, see Ref. 97). See Figure 1 for abbreviation.

### Effects of a Fat-Rich Meal on EDV

Several studies (156–164), but not all (165–167), showed that meals rich in fat reduce EDV. This was not seen on low-fat diets. Antioxidant vitamins, folic acid, and red wine blunted the deleterious effects of a high-fat meal on EDV (156,157, 161). Also, food prepared in used cooking fat impaired EDV (168). A meal rich in olive oil impaired EDV only when antioxidant vitamins were not given (169), whereas an improvement was seen when hypercholesterolemic subjects were given a Mediterranean diet (170). Statin, but not fibrate, pretreatment blunted the negative effect of a high-fat meal on EDV (162).

Thus, compared to cholesterol, the effects of triglycerides and fatty acids on EDV are more complex, probably due to divergent effects of different fatty acids.

## PATHOLOGICAL CONSIDERATIONS

### Asymmetric Dimethylarginine (ADMA)

As a product of dimethylation of proteins, ADMA is formed and acts as a competitive inhibitor of NOS. ADMA levels are increased in subjects with both hypercholesterolemia (171) and isolated hypertriglyceridemia (151), and by cholesterol feeding in rabbits (172). This latter effect can be reversed by addition of L-arginine (171). The L-arginine-to-ADMA ratio is related to breakdown products of NO ( $\text{NO}_x$ ) (171), and cholesterol feeding reduces the breakdown of ADMA (173,174).

### Oxygen Free Radicals

The superoxide ion ( $\text{O}_2^-$ ) rapidly inactivates NO to form peroxynitrite ( $\text{ONOO}^-$ ) (175). Cholesterol feeding in animals increases the amount of  $\text{O}_2^-$  in vessels (176–178) and the metabolite of  $\text{ONOO}^-$ , nitrotyrosine (175). Supplementation with L-arginine, probucol, or a statin (177,179,180) reduces

this effect of cholesterol feeding on  $\text{O}_2^-$ -production. A number of antioxidants improve EDV during conditions of high cholesterol levels in humans and animal experiments (see Tables 3 and 4). However, all antioxidant interventions have not been effective in this respect. In humans, serum levels of vitamin E are directly related to EDV, whereas a marker of lipid peroxidation, plasma isoprostane 8-iso-PGF<sub>2 $\alpha$</sub> , is inversely related to EDV (181,182).

### Endothelin and Hypercholesterolemia

Elevated levels of ET-1 have been found in the circulation in hypercholesterolemic humans (183), whereas statin treatment has been shown to reduce ET-1 mRNA expression (184). Furthermore, endothelin-receptor blockade reverses the impaired EDV seen in experimental models (185,186).

### Effects of Hypercholesterolemia on NOS

Cholesterol feeding both increases caveolin binding to NOS (187) and externalizes NOS from within the caveolae (188). Dosing with tetrahydrobiopterin, a co-factor of NOS, of hypercholesterolemic subjects improved their impaired EDV within a short period of time (Table 4). Furthermore, statins may influence NOS activity directly (189,190) by an improved caveolin–NOS interaction (191).

### Endothelium-Derived Hyperpolarizing or Contracting Factors

Inhibition of cyclooxygenase improved EDV in cholesterol-fed rats, implying an importance of a prostanoid-derived EDCF during hypercholesterolemia (192). NO-dependent vasodilation was impaired in cholesterol-fed rabbits, but vasodilation mediated by EDHF was normal (193).

Thus, several factors, such as an endogenous inhibitor of NOS, effects on the enzyme itself, oxidative inactivation of NO, or an altered activity of other endothelium-derived vasoactive compounds, could be involved in the impaired EDV seen in dyslipidemia.

## EFFECTS OF INTERVENTIONS IN HYPERCHOLESTEROLEMIA

### Interventions in Animal Models

Treatment with statins in several models of hypercholesterolemia resulted in a positive effect on EDV in all (194–201) but two studies (202, 203); even then, cholesterol was not reduced (204) (Table 3). In addition, cholesterol lowering by dietary means or by cholestyramine improved EDV (205). However, the duration of hypercholesterolemia was of major importance for the effect of therapy. Once atherosclerosis had reached a certain degree, a reduction in cholesterol levels could not reverse the impairment in EDV in these models (206,207).

**TABLE 3**  
**Effects of Different Interventions on EDV in Different Animal Models<sup>a</sup>**

Intervention	Model	Type of vessel	Effect on EDV	Reference
Statins	CF rabbit, mice, monkey	Aorta	Positive	194–201
Statins	CF rabbit, Watanabe	Aorta	No effect	202,203
Statins	Watanabe	Langendorf heart	Positive	203
Cholestyramin	CF mice	Aorta	Positive	205
Dietary cholesterol-lowering	CF rabbit	Aorta	Positive	206,207
L-Arginine	CF rabbit	Aorta, hindlimb, basilar artery	Positive	202,208–214
Probucol	CF rabbit	Aorta	Positive	177,215,216
SOD	CF rabbit	Aorta	Positive and no effect	217,218
Vitamin E	CF rabbit	Aorta, carotid, Langendorf heart, perfused ear, pulse wave	Positive	208,219–226
Vitamin E	CF rabbit	Renal artery	No effect	224
Vitamin E	CF dog	Coronaries <i>in vivo</i>	Positive	227
β-Carotene	CF rabbit	Aorta	Positive	226
Tomatoes	CF rabbit	Aorta	Positive	228
NEP inhibition	CF rabbit	Aorta	Positive	229
α-Blockade	CF mice	Aorta	Positive	194
ACE-inhibition	CF rabbit	Aorta	Positive	230–232
Calcium blockers	CF rabbit	Aorta	Positive (and one no effect)	232–235
Endothelin antagonist	CF rabbit	Aorta	Positive	211
Endothelin antagonist	CF pig	Coronaries <i>in vivo</i>	Positive or no effect	236,237
Prostacyclin	CF rabbit	Langendorf heart	Positive	238
Heparin	Watanabe	Aorta	Positive	239
Cod liver oil	CF pigs	Coronaries	Positive	240
Estrogen	CF rabbit	Aorta	Positive and no effect	241,242
Estrogen	CF swine	Coronary	Positive	243

<sup>a</sup>SOD, superoxide dismutase; NEP, neuroendopeptidase; ACE, angiotensin-converting enzyme; see Table 1 for other abbreviations.

Treatment with L-arginine has been shown to improve EDV without any alterations in serum cholesterol levels (202,208–214). Also, different antioxidants or free-radical scavengers, such as probucol, superoxide dismutase, vitamin E, tomato carotenoids, and β-carotene, have positive effects on EDV in hypercholesterolemic animals (202,215–228).

**TABLE 4**  
**Effects of Different Interventions on EDV in Subjects with Hypercholesterolemia<sup>a</sup>**

Intervention	Model	Effect on EDV	Duration of treatment	Reference
Statins	Forearm	Positive	1–6 mon	246,247
Statins	FMD	Positive	6–12 wk	248–251
Statins	Coronary	Positive	5–6 mon	252,253
Statin + probucol	Coronary	Positive	12 mon	254
Statin + vitamin E	FMD	Positive	8 wk	255
Lipid-lowering drugs	Coronary, forearm, and FMD	Positive	12 mon and 12 wk	251,254,256
Cholestyramine	Coronary	Positive	6 mon	257
L-Arginine	Coronary and FMD	Positive	Acute	260,261
L-Arginine	Forearm	Positive and no effect	Acute	262,263
L-Arginine	FMD	Positive	4 wk	264
Vitamin E	FMD	Positive	4 wk	265
Vitamin E	Forearm	Positive and no effect	4 wk	266–268
Antioxidant vitamins	Forearm	No effect	4 wk	269
SOD	Forearm	No effect	Acute	270
Vitamin C	Forearm	Positive	Acute	271
Glutathione	Femoral artery	Positive	Acute	272
Folic acid	Forearm	Positive	Acute and 4 wk	273,274
Tetrahydrobiopterin	Forearm	Positive	Acute	275
ASA	Forearm	Positive	Acute	89
LDL-Apheresis	Forearm	Positive	Acute	276
Nifedipine	Forearm	Positive	6 wk	277
Estrogen	FMD	Positive	6 wk	248
Fish oil	FMD and <i>in vitro</i>	Positive	6 wk to 4 mon	93,278,279
Exercise training	Forearm	No effect	4 wk	280

<sup>a</sup>ASA, acetylic salicylic acid; LDL, low density lipoprotein; see Tables 1, 2, and 3 for other abbreviations.

Commonly used antihypertensive therapies, such as angiotensin-converting enzyme inhibition, calcium and  $\alpha$ -receptor blockade, endothelin receptor blockade, and neuroendopeptidase inhibition, all have positive effects on EDV (194,211, 229–237); a number of other drugs, such as heparin and estrogens (see Table 3) (238–245) have also exhibited this effect.

### Effects in Humans

Statins and other lipid-lowering drugs, such as cholestyramine, improve EDV in hypercholesterolemic patients after only 2 wk of treatment (246–258) in most studies (259) (Table 4). In the CARE study, EDV measured after 5 yr of treatment was related to reduction in serum cholesterol levels during that period (258).

An improvement of EDV was seen during both acute (260–263) and long-term treatment (4 wk) with L-arginine in hypercholesterolemic patients (264). Although a mixture of antioxidant vitamins or SOD produced no effects, vitamin C and E supplementation reportedly induced a positive effect on EDV (265–272) in most studies (259). A number of other interventions, including estrogen and calcium antagonists, have shown beneficial effects on EDV in hypercholesterolemic subjects (89,93,273–279). Exercise training for 4 wk, however, did not improve EDV (280).

### FUTURE ISSUES

Clearly, hypercholesterolemia impairs EDV, and lowering of cholesterol levels can reverse this condition. A publication bias may exist whereby negative studies are less likely to be published. However, several issues can be identified for future research in the field of cholesterol and EDV. Furthermore, the role of triglycerides and fatty acids deserves further investigation from the following starting points:

(i) To identify which mechanism that impairs EDV (which is associated with hypercholesterolemia and other lipids) is the major one, or whether several mechanisms act in concert.

(ii) To investigate whether supplementation with L-arginine, alone or in combination with other lipid-lowering regimens, also improves EDV during long-term treatment.

(iii) To further investigate the effect of the statins, as some statins induce vasodilation *in vitro* within minutes by a NO-dependent mechanism (189).

(iv) To identify the characteristics of the point of no return of atheroma-lesion formation, after which no major improvement in EDV can be obtained merely by lowering cholesterol levels in some animal models.

(v) To further characterize the production and metabolism of ADMA (281–283) and how these events are related to the impaired EDV seen in dyslipidemia.

(vi) To explore the future of gene therapy; for example, adenoviral gene transfer of NOS in cholesterol-fed animals improved EDV (284–286).

(vii) To consider the possibility of angiogenesis therapy in patients with coronary heart disease; the effects on EDV of

factors influencing angiogenesis should be explored. It was recently shown that basic fibroblast growth factor improved EDV in hypercholesterolemic rabbit aorta *in vitro* (287).

(viii) To investigate in more detail the action of different fatty acids on EDV in order to establish the optimal composition of lipids in food.

(ix) To establish the relevance of studying arteries in the upper limb not clinically affected by atherosclerosis as a means of revealing that impairments in EDV measured by the human forearm technique or by brachial artery ultrasound are related to atherosclerosis and an impaired EDV in the coronary circulation (288–290).

(x) Last, but not least, to investigate the use of impaired EDV as a predictor of cardiovascular events (291,292); it remains to be established that a reversal of endothelial dysfunction translates into an improved risk for cardiovascular events before EDV can be accepted as valid biomarker for atherosclerosis.

### REFERENCES

1. Kannel, W.B., and Larson, M. (1993) Long-Term Epidemiologic Prediction of Coronary Disease. The Framingham Experience, *Cardiology* 82, 137–152.
2. Randomised Trial of Cholesterol Lowering in 4444 Patients with Coronary Heart Disease: The Scandinavian Simvastatin Survival Study (4S), *Lancet* 344, 1383–1389.
3. Shepherd, J., Cobbe, S.M., Ford, I., *et al.* (1995) Prevention of Coronary Heart Disease with Pravastatin in Men with Hypercholesterolemia, West of Scotland Coronary Prevention Study Group, *N. Engl. J. Med.* 333, 1301–1307.
4. Sacks, F.M., Pfeffer, M.A., Moye, L.A., *et al.* (1996) The Effect of Pravastatin on Coronary Events After Myocardial Infarction in Patients with Average Cholesterol Levels. Cholesterol and Recurrent Events Trial Investigators, *N. Engl. J. Med.* 335, 1001–1009.
5. Furchgott, R.F., and Zawadzki, J.V. (1980) The Obligatory Role of Endothelial Cells in the Relaxation of Arterial Smooth Muscle by Acetylcholine, *Nature* 299, 373–376.
6. Jern, C., Selin, L., and Jern, S. (1994) *In vivo* Release of Tissue-Type Plasminogen Activator Across the Human Forearm During Mental Stress, *Thromb. Haemost.* 72, 285–291.
7. Groves, P.H., Banning, A.P., Penny, W.J., *et al.* (1995) The Effects of Exogenous Nitric Oxide on Smooth Muscle Cell Proliferation Following Porcine Carotid Angioplasty, *Cardiovasc. Res.* 30, 87–96.
8. Sarkar, R., Meinberg, E.G., Stanley, J.C., *et al.* (1996) Nitric Oxide Reversibility Inhibits the Migration of Cultured Vascular Smooth Muscle Cells, *Circ. Res.* 78, 225–230.
9. Ludmer, P.L., Selwyn, A.P., Shook, T.L., *et al.* (1986) Paradoxical Vasoconstriction Induced by Acetylcholine in Atherosclerotic Coronary Arteries, *N. Engl. J. Med.* 315, 1046–1051.
10. Werns, S.W., Walton, J.A., Hsia, H.H., *et al.* (1989) Evidence of Endothelial Dysfunction in Angiographically Normal Coronary Arteries of Patients with Coronary Artery Disease, *Circulation* 79, 287–291.
11. De Caterina, R., Spiecker, M., Solaini, G., Basta, G., Bosetti, F., Libby, P., and Liao, J. (1999) The Inhibition of Endothelial Activation by Unsaturated Fatty Acids, *Lipids* 34 (Suppl.), S191–S194.
12. Palmer, R.M.J., Ferrige, A.G., and Moncada, S. (1987) Nitric Oxide Release Accounts for the Biological Activity of Endothelium-Derived Relaxing Factor, *Nature* 327, 524–526.



13. Palmer, R.M.J., Ahston, D.S., and Moncada, S. (1988) Vascular Endothelial Cells Synthesize Nitric Oxide from L-Arginine, *Nature* 333, 664–666.
14. Moncada, S., Palmer, R.M.J., and Higgs, E.A. (1991) Nitric Oxide: Physiology, Pathophysiology, and Pharmacology, *Pharmacol. Rev.* 43, 109–142.
15. Moncada, S., and Higgs, E.A. (1993) L-Arginine–Nitric Oxide Pathway, *New Engl. J. Med.* 329, 2002–2012.
16. Rees, D.D., Palmer, R.M.J., Schulz, R., *et al.* (1990) Characterization of Three Inhibitors of Endothelial Nitric Oxide Synthase *in vitro* and *in vivo*, *Br. J. Pharmacol.* 101, 746–752.
17. Yangisawa, M., Kurihara, H., Kimura, S., *et al.* (1988) A Novel Potent Vasoconstrictor Peptide Produced by Vascular Endothelial Cells, *Nature* 332, 411–415.
18. Lüscher, T.F. (1992) Endothelin: Systemic Arterial and Pulmonary Effects of a New Peptide with Potent Biological Properties, *Am. Rev. Resp. Dis.* 146, S56–S60.
19. Webb, D.J., Haynes, W.G., and Ferro, C.J. (1995) Endothelin as a Regulator of Tone in Man: Studies in Upper Limb Resistance and Capacitance Vessels, in *The Endothelium in Cardiovascular Disease* (Lüscher, T.F., ed.), pp. 43–56, Springer Verlag, Berlin.
20. Schiffrin, E.L. (1995) Endothelin; Potential Role in Hypertension and Vascular Hypertrophy, *Hypertension* 25, 1135–1143.
21. Clozel, M., Gray, G.A., Breu, V., *et al.* (1992) The Endothelin ET<sub>B</sub> Receptor Mediates Both Vasodilation and Vasoconstriction *in vivo*, *Biochem. Biophys. Res. Com.* 186, 867–873.
22. Feletou, M., and Vanhoutte, P.M. (1988) Endothelin-Dependent Hyperpolarization of Canine Coronary Smooth Muscle, *Br. J. Pharmacol.* 93, 515–524.
23. Fujii, K., Tominaga, M., Ohmori, S., *et al.* (1992) Decreased Endothelin-Dependent Hyperpolarization to Acetylcholine in Smooth Muscle of the Mesenteric Artery of Spontaneously Hypertensive Rats, *Circ. Res.* 70, 660–669.
24. Chen, G., and Suzuki, H. (1989) Some Electrical Properties of the Endothelin-Dependent Hyperpolarization Recorded from Rat Arterial Smooth Muscle Cells, *J. Physiol.* 410, 91–106.
25. Fujii, K., Tominaga, M., Ohmori, S., *et al.* (1992) Decreased Endothelin-Dependent Hyperpolarization to Acetylcholine in Smooth Muscle of the Mesenteric Artery of Spontaneously Hypertensive Rats, *Circ. Res.* 70, 660–669.
26. Hecker, M., Bara, A.T., Bauersachs, J., and Busse, R. (1994) Characterization of Endothelin-Derived Hyperpolarizing Factor as a Cytochrome P450-Derived Arachidonic Acid Metabolite in Mammals, *J. Physiol.* 481, 407–414.
27. Campbell, W.B., Gebremedhin, D., Pratt, P.F., and Harder, D.R. (1996) Identification of Epoxyeicosatrienoic Acids as Endothelin-Derived Hyperpolarizing Factors, *Circ. Res.* 78, 415–423.
28. Edwards, G., Donk, K.A., Gardener, M.J., *et al.* (1998) K<sup>+</sup> Is an Endothelin-Derived Hyperpolarizing Factor in Rat Arteries, *Nature* 396, 269–272.
29. Ito, T., Kato, T., Iwama, Y., *et al.* (1991) Prostaglandin H<sub>2</sub> as an Endothelin-Derived Contracting Factor and Its Interaction with Endothelin-Derived Nitric Oxide, *J. Hypertens.* 9, 729–736.
30. Lüscher, T.F., and Vanhoutte, P.M. (1986) Endothelin-Dependent Contractions to Acetylcholine in the Aorta of the Spontaneously Hypertensive Rat, *Hypertension* 8, 344–348.
31. Kato, T., Iwama, Y., Okumura, K., *et al.* (1990) Prostaglandin H<sub>2</sub> May Be the Endothelin-Derived Contracting Factor Released by Acetylcholine in the Aorta of the Rat, *Hypertension* 15, 475–481.
32. Küng, S.F., and Lüscher, T.F. (1995) Different Mechanisms of Endothelial Dysfunction with Aging and Hypertension in Rat Aorta, *Hypertension* 25, 194–200.
33. Noll, G., Tschudi, M., Nava, E., and Lüscher, T.F. (1997) Endothelin and High Blood Pressure, *Int. J. Microcirc.* 17, 273–279.
34. Jayakody, R.L., Senaratne, M.P., Thomson, A.B., and Kappagoda, C.T. (1985) Cholesterol Feeding Impairs Endothelin-Dependent Relaxation of Rabbit Aorta, *Can. J. Physiol. Pharmacol.* 63, 1206–1209.
35. Verbeuren, T.J., Jordaens, F.J., Zonnekyen, L.L., *et al.* (1986) Effect of Hypercholesterolemia on Vascular Reactivity in the Rabbit. I. Endothelin-Dependent and Endothelin-Independent Contractions and Relaxations in Isolated Arteries of Control and Hypercholesterolemic Rabbits, *Circ. Res.* 58, 552–564.
36. Sreeharan, N., Jayakody, R.L., Senaratne, M.P., *et al.* (1986) Endothelin-Dependent Relaxation and Experimental Atherosclerosis in the Rabbit Aorta, *Can. J. Physiol. Pharmacol.* 64, 1451–1453.
37. Ibengwe, J.K., and Suzuki, H. (1986) Changes in Mechanical Responses of Vascular Smooth Muscles to Acetylcholine, Noradrenaline, and High-Potassium Solution in Hypercholesterolemic Rabbits, *Br. J. Pharmacol.* 87, 395–402.
38. Chappell, S.P., Lewis, M.J., and Henderson, A.H. (1987) Effect of Lipid Feeding on Endothelin Dependent Relaxation in Rabbit Aortic Preparations, *Cardiovasc. Res.* 21, 34–38.
39. Hof, R.P., and Hof, A. (1988) Vasoconstrictor and Vasodilator Effects in Normal and Atherosclerotic Conscious Rabbits, *Br. J. Pharmacol.* 95, 1075–1080.
40. Jayakody, L., Kappagoda, T., Senaratne, M.P., and Thomson, A.B. (1988) Impairment of Endothelin-Dependent Relaxation: An Early Marker of Atherosclerosis in the Rabbit, *Br. J. Pharmacol.* 94, 335–346.
41. Kanamaru, K., Waga, S., Tochio, H., and Nagatani, K. (1989) The Effects of Atherosclerosis on Endothelin-Dependent Relaxation in the Aorta and Intracranial Arteries of Rabbits, *J. Neurosurg.* 70, 793–798.
42. Ragazzi, E., Frolidi, G., Pandolfo, L., *et al.* (1989) Segmental Impairment of Endothelin-Mediated Relaxation in Thoracic Aortas from Atherosclerotic Rabbits. Comparison to Cholesterol Infiltration and Energy Metabolism, *Artery* 16, 327–345.
43. Minor, R.L., Jr., Myers, P.R., Guerra, R., Jr., *et al.* (1990) Diet-Induced Atherosclerosis Increases the Release of Nitrogen Oxides from Rabbit Aorta, *J. Clin. Invest.* 86, 2109–2116.
44. Merkel, L.A., Rivera, L.M., Bilder, G.E., and Perrone, M.H. (1990) Differential Alterations of Vascular Reactivity in Rabbit Aorta with Modest Elevation of Serum Cholesterol, *Circ. Res.* 67, 550–555.
45. Lang, D., Smith, J.A., and Lewis, M.J. (1993) Induction of a Calcium-Independent NO Synthase by Hypercholesterolemia in the Rabbit, *Br. J. Pharmacol.* 108, 290–292.
46. Hutchison, I.R., Smith, J.A., and Griffith, T.M. (1994) Abolition of Flow-Dependent EDRF Release Before That Evoked by Agonists in Hypercholesterolemic Rabbits, *Br. J. Pharmacol.* 113, 190–194.
47. Weisbrod, R.M., Griswold, M.C., Du, Y., *et al.* (1997) Reduced Responsiveness of Hypercholesterolemic Rabbit Aortic Smooth Muscle Cells to Nitric Oxide, *Arterioscler. Thromb. Vasc. Biol.* 17, 394–402.
48. Fontes Ribeiro, C.A., Almeida, L., Paiva, I., *et al.* (1998) Influence of 0.1 or 0.2% Cholesterol-Enriched Diet on the Induction of Atherosclerosis and Aorta Reactivity *in vitro*, *J. Cardiovasc. Pharmacol.* 31, 690–699.
49. Kojda, G., Husgen, B., Hacker, A., *et al.* (1998) Impairment of Endothelin-Dependent Vasorelaxation in Experimental Atherosclerosis Is Dependent on Gender, *Cardiovasc. Res.* 37, 738–747.
50. Sun, Y.P., Lu, N.C., Parmely, W.W., and Hollenbeck, C.B. (2000) Effects of Cholesterol Diets on Vascular Function and Atherogenesis in Rabbits, *Proc. Soc. Exp. Biol. Med.* 224, 166–171.



51. Takahashi, K., Ohyanagi, M., Ikeoka, K., and Iwasaki, T. (1999) Acetylcholine-Induced Response of Coronary Resistance Arterioles in Cholesterol-Fed Rabbits, *Jpn. J. Pharmacol.* 81, 156–162.
52. Simonsen, U., Prieto, D., Mulvany, M.J., *et al.* (1992) Effect of Induced Hypercholesterolemia in Rabbits on Functional Responses of Isolated Large Proximal and Small Distal Coronary Arteries, *Arterioscler. Thromb.* 12, 380–392.
53. Osborne, J.A., Siegman, M.J., Sedar, A.W., *et al.* (1989) Lack of Endothelium-Dependent Relaxation in Coronary Resistance Arteries of Cholesterol-Fed Rabbits, *Am. J. Physiol.* 256, C591–C597.
54. Ibengwe, J.K., and Suzuki, H. (1987) Protective Action of Elastase on Changes in Mechanical Properties of Vascular Smooth Muscles During Atherosclerogenesis in Hypercholesterolemic Rabbits, *Arch. Int. Pharmacodyn. Ther.* 287, 48–64.
55. Laight, D.W., Matz, J., Caesar, B., *et al.* (1996) Investigation of Endogenous Nitric Oxide Vascular Function in the Carotid Artery of Cholesterol-Fed Rabbits, *Br. J. Pharmacol.* 117, 1471–1474.
56. Greenlees, C., Wainwright, C.L., and Wadsworth, R.M. (1996) Vasorelaxant and Antiaggregatory Properties of the Endothelium: A Comparative Study in Normocholesterolaemic and Hereditary and Dietary Hypercholesterolaemic Rabbits, *Br. J. Pharmacol.* 119, 1470–1476.
57. Azadzi, K.M., and Saenz de Tajeda, I. (1991) Hypercholesterolemia Impairs Endothelium-Dependent Relaxation of Rabbit Corpus Cavernosum Smooth Muscle, *J. Urol.* 146, 238–240.
58. Simonsen, U., Ehrnroth, E., Gerdes, L.U., *et al.* (1991) Functional Properties *in vitro* of Systemic Small Arteries from Rabbits Fed a Cholesterol-Rich Diet for 12 Weeks, *Clin. Sci.* 80, 119–129.
59. Mudaliar, J.H., Freischlag, J.A., Johnson, D., *et al.* (1997) Combined Exposure to Cigarette Smoke and Hypercholesterolemia Decreases Vasorelaxation of the Aorta, *J. Vasc. Surg.* 25, 884–889.
60. Chinellato, A., Banchieri, N., Pandolfo, L., *et al.* (1991) Aortic Response to Relaxing Agents in Watanabe Heritable Hyperlipidemic (WHHL) Rabbits of Different Age, *Atherosclerosis* 89, 223–230.
61. Kitagawa, S., Yamaguchi, Y., Sameshima, E., and Kunimoto, M. (1994) Differences in Endothelium-Dependent Relaxation in Various Arteries from Watanabe Heritable Hyperlipidaemic Rabbits with Increasing Age, *Clin. Exp. Pharmacol. Physiol.* 21, 963–970.
62. Ragazzi, E., Chinatellato, A., De Biasi, M., *et al.* (1989) Endothelium-Dependent Relaxation, Cholesterol Content and High-Energy Metabolite Balance in Watanabe Hyperlipemic Rabbit Aorta, *Atherosclerosis* 80, 125–134.
63. Schuschke, D.A., Joshua, I.G., and Miller, F.N. (1991) Comparison of Early Microcirculatory and Aortic Changes in Hypercholesterolemic Rats, *Arterioscler. Thromb.* 11, 154–160.
64. O'Rourke, M., and Docherty, J.R. (1998) Effects of a High-Cholesterol Diet on Vascular and Endothelial Function in Rat Aorta, *Pharmacology* 56, 1–6.
65. Kitagawa, A., Yamaguchi, Y., Kunimoto, M., *et al.* (1992) Impairment of Endothelium-Dependent Relaxation in Aorta from Rats with Atherosclerosis Induced by Excess Vitamin D and a High-Cholesterol Diet, *Jpn. J. Pharmacol.* 59, 339–347.
66. Chinatello, A., Ragazzi, E., Petrelli, L., *et al.* (1994) Effects of Cholesterol-Supplemented Diet in Heritable Hyperlipidemic Yoshida Rats: Functional and Morphological Characterization of Thoracic Aorta, *Atherosclerosis* 106, 51–63.
67. Aksulu, H.E., Cellek, S., and Turker, R.K. (1986) Cholesterol Feeding Attenuates Endothelium-Dependent Relaxation Response to Acetylcholine in the Main Pulmonary Artery of Chickens, *Eur. J. Pharmacol.* 129, 397–400.
68. Toda, N., Miyazaki, M., and Hazama, F. (1988) Functional and Histological Changes in Mesenteric Arteries and Aortas from Monkeys Fed on High Cholesterol Diet, *Jpn. J. Pharmacol.* 48, 441–451.
69. Deckert, V., Lizard, G., Duverger, N., *et al.* (1999) Impairment of Endothelium-Dependent Arterial Relaxation by High-Fat Feeding in ApoE-Deficient Mice: Toward Normalization by Human ApoA-I Expression, *Circulation* 100, 1230–1235.
70. Lamping, K.G., Nuno, D.W., Chappell, D.A., and Faraci, F.M. (1999) Agonist-Specific Impairment of Coronary Vascular Function in Genetically Altered, Hyperlipidemic Mice, *Am. J. Physiol.* 276, R1023–R1029.
71. Wright, C.E., and Angus, J.A. (1986) Effects of Hypertension and Hypercholesterolemia on Vasodilatation in the Rabbit, *Hypertension* 8, 361–371.
72. Bossaller, C., Yamamoto, H., Lichtlen, P.R., and Henry, P.D. (1987) Impaired Cholinergic Vasodilation in the Cholesterol-Fed Rabbit *in vivo*, *Basic Res. Cardiol.* 82, 396–404.
73. Rozsa, Z., Pataricza, J., Nemeth, J., and Papp, J.G. (1998) Differential Efficacy of Vasodilators in Hypercholesterolaemic Rabbits, *J. Pharm. Pharmacol.* 50, 1035–1044.
74. Cirillo, R., Aliev, G., Italiano, G., and Prosdoci, M. (1992) Functional Responses of Hindlimb Circulation in Aged Normal and WHHL Rabbits, *Atherosclerosis* 93, 133–144.
75. Carroll, J.F., Mizelle, H.L., Cockrell, K., *et al.* (1997) Cholesterol Feeding Does Not Alter Renal Hemodynamic Response to Acetylcholine and Angiotensin II in Rabbits, *Am. J. Physiol.* 272, R940–R947.
76. Fedlstein, A., Krier, J.D., Sarafow, M.H., *et al.* (1999) *In vivo* Renal Vascular and Tubular Function in Experimental Hypercholesterolemia, *Hypertension* 34, 859–864.
77. McLenachan, J.M., Williams, J.K., Fish, R.D., *et al.* (1991) Loss of Flow-Mediated Endothelium-Dependent Dilatation Occurs Early in the Development of Atherosclerosis, *Circulation* 84, 1273–1278.
78. Yang, R., Powell-Braxton, L., Ogaoawara, A.K., *et al.* (1999) Hypertension and Endothelial Dysfunction in Apolipoprotein E Knockout Mice, *Arterioscler. Thromb. Vasc. Biol.* 19, 2762–2768.
79. Drexler, H., and Zeiher, A.M. (1991) Endothelial Function in Human Coronary Arteries *in vivo*. Focus on Hypercholesterolemia, *Hypertension* 18, II90–II99.
80. Zeiher, A.M., Drexler, H., Saurbier, B., and Just, H. (1993) Endothelium-Mediated Coronary Blood Flow Modulation in Humans. Effects of Age, Atherosclerosis, Hypercholesterolemia, and Hypertension, *J. Clin. Invest.* 92, 652–662.
81. Shiode, N., Kato, M., Hiraoka, A., *et al.* (1996) Impaired Endothelium-Dependent Vasodilation of Coronary Resistance Vessels in Hypercholesterolemic Patients, *Intern. Med.* 35, 89–93.
82. Shiode, N., Nakayama, K., Morishima, N., *et al.* (1996) Nitric Oxide Production by Coronary Conductance and Resistance Vessels in Hypercholesterolemia Patients, *Am. Heart. J.* 131, 1051–1057.
83. Chowienzyk, P.J., Watts, G.F., Cockcroft, J.R., and Ritter, J.M. (1992) Impaired Endothelium-Dependent Vasodilation of Forearm Resistance Vessels in Hypercholesterolaemia, *Lancet* 340, 1430–1432.
84. Creager, M.A., Cooke, J.P., Mendelsohn, M.E., *et al.* (1990) Impaired Vasodilation of Forearm Resistance Vessels in Hypercholesterolemic Humans, *J. Clin. Invest.* 86, 228–234.
85. Casino, P.R., Kilcoyne, C.M., Quyyumi, A.A., *et al.* (1993) The Role of Nitric Oxide in Endothelium-Dependent Vasodilation of Hypercholesterolemic Patients, *Circulation* 88, 2541–2547.
86. Gilligan, D.M., Guetta, C., and Panza, J.A. (1994) Selective Loss of Microvascular Endothelial Function in Human Hypercholesterolemia, *Circulation* 90, 35–41.

87. Lewis, T.V., Dart, A.M., and Chin-Dusting, J.P. (1999) Endothelium-Dependent Relaxation by Acetylcholine Is Impaired in Hypertriglyceridemic Humans with Normal Levels of Plasma LDL Cholesterol, *J. Am. Coll. Cardiol.* 33, 805–812.
88. Preik, M., Kelm, M., Schoebel, F., *et al.* (1996) Selective Impairment of Nitric Oxide Dependent Vasodilation in Young Adults with Hypercholesterolaemia, *J. Cardiovasc. Risk* 3, 465–471.
89. Noon, J.P., Walker, B.R., Hand, M.F., and Webb, D.J. (1998) Impairment of Forearm Vasodilation to Acetylcholine in Hypercholesterolemia Is Reversed by Aspirin, *Cardiovasc. Res.* 38, 480–484.
90. Arcaro, G., Zenere, B.M., Travia, D., *et al.* (1995) Non-invasive Detection of Early Endothelial Dysfunction in Hypercholesterolaemic Subjects, *Atherosclerosis* 114, 247–254.
91. Sorensen, K.E., Celermajer, D.S., Georgakopoulos, D., *et al.* (1994) Impairment of Endothelium-Dependent Dilation Is an Early Event in Children with Familial Hypercholesterolemia and Is Related to the Lipoprotein(a) Level, *J. Clin. Invest.* 93, 50–55.
92. Schnell, G.B., Robertson, A., Houston, D., *et al.* (1999) Impaired Brachial Artery Endothelial Function Is Not Predicted by Elevated Triglycerides, *J. Am. Coll. Cardiol.* 33, 2038–2043.
93. Goode, G.K., Garcia, S., and Heagerty, A.M. (1997) Dietary Supplementation with Marine Fish Oil Improves *in vitro* Small Artery Endothelial Function in Hypercholesterolemic Patients: A Double-Blind Placebo-Controlled Study, *Circulation* 96, 2802–2807.
94. Vita, J.A., Treasure, C.B., Nabel, E.G., *et al.* (1980) Coronary Vasomotor Response to Acetylcholine Relates to Risk Factors for Coronary Artery Disease, *Circulation* 81, 491–497.
95. Celermajer, D.S., Sorensen, K.E., Bull, C., *et al.* (1994) Endothelium-Dependent Dilation in the Systemic Arteries of Asymptomatic Subjects Relates to Coronary Risk Factors and Their Interaction, *J. Am. Coll. Cardiol.* 24, 1468–1474.
96. Gerhard, M., Roddy, M.A., Creager, S.J., and Creager, M.A. (1996) Aging Progressively Impairs Endothelium-Dependent Vasodilation in Forearm Resistance Vessels of Humans, *Hypertension* 27, 849–853.
97. Sarabi, M., Millgard, J., and Lind, L. (1999) Effects of Age, Gender and Metabolic Factors on Endothelium-Dependent Vasodilation: A Population-Based Study, *J. Intern. Med.* 246, 265–274.
98. Steinberg, H.O., Bayazeed, B., Hook, G., *et al.* (1997) Endothelial Dysfunction Is Associated with Cholesterol Levels in the High Normal Range in Humans, *Circulation* 96, 3287–3293.
99. Andrews, H.A., Bruckdorfer, K.R., Dunn, R.C., and Jacobs, M. (1987) Low-Density Lipoproteins Inhibit Endothelium-Dependent Relaxation in Rabbit Aorta, *Nature* 327, 237–239.
100. Takahashi, M., Yui, Y., Yasumoto, H., *et al.* (1990) Lipoproteins Are Inhibitors of Endothelium-Dependent Relaxation of Rabbit Aorta, *Am. J. Physiol.* 258, H1–H8.
101. Hein, T.W., and Kuo, L. (1998) LDLs Impair Vasomotor Function of the Coronary Microcirculation: Role of Superoxide Anions, *Circ. Res.* 83, 404–414.
102. Vidal, F., Colome, C., Martinez-Gonzalez, J., and Badimon, L. (1998) Atherogenic Concentrations of Native Low-Density Lipoproteins Down-Regulate Nitric-Oxide-Synthase mRNA and Protein Levels in Endothelial Cells, *Eur. J. Biochem.* 252, 378–384.
103. Pohl, U., Heydari, N., and Galle, J. (1995) Effects of LDL on Intracellular Free Calcium and Nitric Oxide-Dependent cGMP Formation in Porcine Endothelial Cells, *Atherosclerosis* 117, 169–178.
104. Galle, J., Mulisch, A., Busse, R., and Bassenge, E. (1991) Effects of Native and Oxidized Low Density Lipoproteins on Formation and Inactivation of Endothelium-Derived Relaxing Factor, *Arterioscler. Thromb.* 11, 198–203.
105. Galle, J., Ochslin, M., Schollmeyer, P., and Wanner, C. (1994) Oxidized Lipoproteins Inhibit Endothelium-Dependent Vasodilation. Effects of Pressure and High-Density Lipoprotein, *Hypertension* 23, 556–564.
106. Bruckdorfer, K.R. (1996) Antioxidants, Lipoprotein Oxidation, and Arterial Function, *Lipids* 31 (Suppl.), S83–S85.
107. Mougnot, N., Lesnik, P., Ramirez-Gil, J.F., *et al.* (1997) Effects of the Oxidation State of LDL on the Modulation of Arterial Vasomotor Response *in vitro*, *Atherosclerosis* 133, 183–192.
108. Kugiyama, K., Kerns, S.A., Morrisett, J.D., *et al.* (1990) Impairment of Endothelium-Dependent Arterial Relaxation by Lysolecithin in Modified Low-Density Lipoproteins, *Nature* 344, 160–162.
109. Yokoyama, M., Hirata, K., Miyake, R., *et al.* (1990) Lysophosphatidylcholine: Essential Role in the Inhibition of Endothelium-Dependent Vasorelaxation by Oxidized Low Density Lipoprotein, *Biochem. Biophys. Res. Commun.* 168, 301–308.
110. Berkenboom, G., Langer, J., Carpentier, Y., *et al.* (1997) Ramipril Prevents Endothelial Dysfunction Induced by Oxidized Low-Density Lipoproteins: A Bradykinin-Dependent Mechanism, *Hypertension* 30, 371–376.
111. Cox, D.A., and Cohen, M.L. (1997) Influence of Gender on Vasomotor Effects of Oxidized Low-Density Lipoprotein in Porcine Coronary Arteries, *Am. J. Physiol.* 272, H2577–H2583.
112. Buckley, C., Bund, S.J., McTaggart, F., *et al.* (1996) Oxidized Low-Density Lipoproteins Inhibit Endothelium-Dependent Relaxations in Isolated Large and Small Rabbit Coronary Arteries, *J. Auton. Pharmacol.* 16, 261–267.
113. Deckert, C., Pergesol, I., Viens, I., *et al.* (1997) Inhibitors of Arterial Relaxation Among Components of Human Oxidized Low-Density Lipoproteins. Cholesterol Derivatives Oxidized in Position 7 Are Potent Inhibitors of Endothelium-Dependent Relaxation, *Circulation* 95, 723–731.
114. Myers, P.R., Wright, T.F., Tanner, M.A., and Ostlund, R.E., Jr. (1994) The Effects of Native LDL and Oxidized LDL on EDRF Bioactivity and Nitric Oxide Production in Vascular Endothelium, *J. Lab. Clin. Med.* 124, 672–683.
115. Matthys, K.E., Van Hove, C.E., Kockx, M.M., *et al.* (1998) Exposure to Oxidized Low-Density Lipoprotein *in vivo* Enhances Intimal Thickening and Selectivity Impairs Endothelium-Dependent Dilation in the Rabbit, *Cardiovasc. Res.* 37, 239–246.
116. Napoli, C., Paterno, R., Faraci, F.M., *et al.* (1997) Mildly Oxidized Low-Density Lipoprotein Impairs Responses of Carotid but Not Basilar Artery in Rabbits, *Stroke* 28, 2266–2271.
117. Anderson, R.J., Meredith, I.T., Charbonneau, F., *et al.* (1996) Endothelium-Dependent Coronary Vasomotion Relates to the Susceptibility of LDL to Oxidation in Humans, *Circulation* 93, 1647–1650.
118. Doi, H., Kugiyama, K., Ohgushi, M., *et al.* (1999) Membrane Active Lipids in Remnant Lipoproteins Cause Impairment of Endothelium-Dependent Vasorelaxation, *Arterioscler. Thromb. Vasc. Biol.* 19, 1918–1924.
119. Tang, Y.H., Lu, R., and Li, Y.J. (1997) Effects of Calcitonin Gene-Related Peptide-Induced Preconditioning on Attenuated Endothelium-Dependent Vasorelaxation Induced by Lysophosphatidylcholine, *Chung Kuo Yao Li Hsueh Pao* 18, 405–407.
120. Freeman, J.E., Kuo, W.Y., Drenger, B., *et al.* (1996) Analysis of Lysophosphatidylcholine-Induced Endothelial Dysfunction, *J. Cardiovasc. Pharmacol.* 28, 345–352.
121. Cowan, C.L., and Steffen, R.P. (1995) Lysophosphatidylcholine Inhibits Relaxation of Rabbit Abdominal Aorta Medi-

- ated by Endothelium-Derived Nitric Oxide and Endothelium-Derived Hyperpolarizing Factor Independent of Protein Kinase C Activation, *Arterioscler. Thromb. Vasc. Biol.* 15, 2290–2297.
122. Matsuda, Y., Hirata, K., Inoue, N., *et al.* (1993) High Density Lipoprotein Reverses Inhibitory Effect of Oxidized Low Density Lipoprotein on Endothelium-Dependent Arterial Relaxation, *Circ. Res.* 72, 1103–1109.
  123. Murohara, T., Kugiyama, K., Ohgushi, M., *et al.* (1994) LPC in Oxidized LDL Elicits Vasoconstriction and Inhibits Endothelium-Dependent Relaxation, *Am. J. Physiol.* 267, H2441–H2449.
  124. Ohgushi, M., Kugiyama, K., and Fukunaga, K. (1993) Protein Kinase C Inhibitors Prevent Impairment of Endothelium-Dependent Relaxation by Oxidatively Modified LDL, *Arterioscler. Thromb.* 13, 1525–1532.
  125. Cox, D.A., and Cohen, M.L. (1997) Relationship Between Phospholipase D Activation and Endothelial Vasomotor Dysfunction in Rabbit Aorta, *J. Pharmacol. Exp. Ther.* 283, 305–311.
  126. Desrumaux, C., Deckert, C., Athias, A., *et al.* (1999) Plasma Phospholipid Transfer Protein Prevents Vascular Endothelium Dysfunction by Delivering Alpha-Tocopherol to Endothelial Cells, *FASEB J.* 13, 883–892.
  127. Plane, F., Bruckdorfer, K.R., Kerr, P., *et al.* (1992) Oxidative Modification of Low-Density Lipoproteins and the Inhibition of Relaxations Mediated by Endothelium-Derived Nitric Oxide in Rabbit Aorta, *Br. J. Pharmacol.* 105, 216–222.
  128. Williams, K.J., Scalia, R., Mazany, K.D., *et al.* (2000) Rapid Restoration of Normal Endothelial Functions in Genetically Hyperlipidemic Mice by a Synthetic Mediator of Reverse Lipid Transport, *Arterioscler. Thromb. Vasc. Biol.* 20, 1033–1039.
  129. Sarabi, M., Vessby, B., Millgard, J., and Lind, L. (2001) Endothelium-Dependent Vasodilation Is Related to the Fatty Acid Composition of Serum Lipids in Healthy Subjects, *Atherosclerosis* 156, 349–355.
  130. Kuhn, F.E., Mohler, E.R., Satler, L.F., *et al.* (1991) Effects of High-Density Lipoprotein on Acetylcholine-Induced Coronary Vasoreactivity, *Am. J. Cardiol.* 68, 1425–1430.
  131. Galle, J., Bengen, J., Schollmeyer, P., and Wanner, C. (1995) Impairment of Endothelium-Dependent Dilatation in Rabbit Renal Arteries by Oxidized Lipoprotein(a). Role of Oxygen-Derived Radicals, *Circulation* 92, 1582–1589.
  132. Galle, J., Bengen, J., Schollmeyer, P., and Wanner, C. (1994) Oxidized Lipoprotein(a) Inhibits Endothelium-Dependent Dilatation: Prevention by Higher Density Lipoprotein, *Eur. J. Pharmacol.* 265, 111–115.
  133. Tsurumi, Y., Nagashima, H., Ichikawa, K., *et al.* (1995) Influence of Plasma Lipoprotein(a) Levels of Coronary Vasomotor Response to Acetylcholine, *J. Am. Coll. Cardiol.* 26, 1242–1250.
  134. Schachinger, V., Halle, M., Minners, J., *et al.* (1997) Lipoprotein(a) Selectively Impairs Receptor-Mediated Endothelial Vasodilator Function of the Human Coronary Circulation, *J. Am. Coll. Cardiol.* 30, 927–934.
  135. Schlaich, M.P., John, S., Langenfeld, M.R., *et al.* (1998) Does Lipoprotein(a) Impair Endothelial Function? *J. Am. Coll. Cardiol.* 31, 359–365.
  136. Doi, H., Kugiyama, K., Ohgushi, M., *et al.* (1998) Remnants of Chylomicron and Very Low Density Lipoprotein Impair Endothelium-Dependent Vasorelaxation, *Atherosclerosis* 137, 341–349.
  137. Hayashi, T., Naito, M., Ishikawa, T., *et al.* (1989) Beta-Migrating Very Low Density Lipoprotein Attenuates Endothelium-Dependent Relaxation in Rabbit Atherosclerotic Aortas, *Blood Vessels* 26, 290–299.
  138. Steinberg, H.O., Tarshoby, M., Monestel, R., *et al.* (1997) Elevated Circulating Free Fatty Acid Levels Impairs Endothelium-Dependent Vasodilation, *J. Clin. Invest.* 100, 1230–1239.
  139. Lundman, P., Eriksson, M., Schenk-Gustafsson, K., *et al.* (1997) Transient Triglyceridemia Decreases Vascular Reactivity in Young, Healthy Men Without Risk Factors for Coronary Heart Disease, *Circulation* 96, 3266–3268.
  140. de Kreutzenberg, S.V., Crepaldi, C., Marchetto, S., *et al.* (2000) Plasma Free Fatty Acids and Endothelium-Dependent Vasodilation: Effect of Chain-Length and Cyclooxygenase Inhibition, *J. Clin. Endocrinol. Metab.* 85, 793–798.
  141. Lind, L., Fugmann, A., Vessby, B., Millgård, J., Berne, C., and Lithell, H. (2000) Impaired Endothelial Function Induced by Free Fatty Acids Is Reversed by Insulin, *Clin. Sci.* 99, 169–174.
  142. de Kreutzenberg, S.V., Crepaldi, C., Marchetto, S., Calo, L., Tiengo, A., Del Prato, S., and Avogaro, A. (2000) Plasma Free Fatty Acids and Endothelium-Dependent Vasodilation: Effect of Chainlength and Cyclooxygenase Inhibition, *J. Clin. Endocrinol. Metab.* 85, 793–798.
  143. Paolisso, G., Manzella, D., Tagliamonte, M.R., *et al.* (2001) The BB-Paraoxonase Genotype Is Associated with Impaired Brachial Reactivity After Acute Hypertriglyceridemia in Healthy Subjects, *J. Clin. Endocrinol. Metab.* 86, 1078–1082.
  144. Davda, R.K., Stepniakowski, K.T., Lu, G., *et al.* (1995) Oleic Acid Inhibits Endothelial Nitric Oxide Synthase by a Protein Kinase C-Independent Mechanism, *Hypertension* 26, 764–770.
  145. Moers, A., and Schrezenmeir, J. (1997) Palmitic Acid but Not Stearic Acid Inhibits NO-Production in Endothelial Cells, *Exp. Clin. Endocrinol. Diabetes* 105 (Suppl. 2), 78–80.
  146. Lawson, D.L., Mehta, J.L., Saldeen, K., *et al.* (1991) Omega-3 Polyunsaturated Fatty Acids Augment Endothelium-Dependent Vasorelaxation by Enhanced Release of EDRF and Vasodilator Prostaglandins, *Eicosanoids* 4, 217–223.
  147. Okuda, Y., Kawashima, K., Sawada, T., *et al.* (1997) Eicosapentaenoic Acid Enhances Nitric Oxide Production by Cultured Human Endothelial Cells, *Biochem. Biophys. Res. Commun.* 232, 487–491.
  148. Goodfellow, J., Bellamy, M.F., Ramsey, M.W., Jones, C.J., and Lewis, M.J. (2000) Dietary Supplementation with Marine Omega-3 Fatty Acids Improves Systemic Large Artery Endothelial Function in Subjects with Hypercholesterolemia, *J. Am. Coll. Cardiol.* 35, 265–270.
  149. Lewis, T.V., Dart, A.M., and Chin-Dusting, J.P. (1999) Endothelium-Dependent Relaxation by Acetylcholine Is Impaired in Hypertriglyceridemic Humans with Normal Levels of Plasma LDL Cholesterol, *J. Am. Coll. Cardiol.* 33, 805–812.
  150. de Man, F.H., Weverling-Rijnsburger, A.W., van der Laarse, A., *et al.* (2000) Not Acute but Chronic Hypertriglyceridemia Is Associated with Impaired Endothelium-Dependent Vasodilation: Reversal After Lipid-Lowering Therapy by Atorvastatin, *Arterioscler. Thromb. Vasc. Biol.* 20, 744–750.
  151. Lundman, P., Eriksson, M.J., Stuhlinger, M., Cooke, J.P., Hamsten, A., and Tornvall, P. (2001) Mild-to-Moderate Hypertriglyceridemia in Young Men Is Associated with Endothelial Dysfunction and Increased Plasma Concentrations of Asymmetric Dimethylarginine, *J. Am. Coll. Cardiol.* 38, 111–116.
  152. Lupattelli, G., Lombardini, R., Schillaci, G., Giuffetti, G., Marchesi, S., Siepi, D., and Mannarino, E. (2000) Flow-Mediated Vasoactivity and Circulating Adhesion Molecules in Hypertriglyceridemia: Association with Small, Dense LDL Cholesterol Particles, *Am. Heart J.* 140, 521–526.
  153. Chowienczyk, P.J., Watts, G.F., Wierzbicki, A.S., *et al.* (1997) Preserved Endothelial Function in Patients with Severe Hypertriglyceridemia and Low Functional Lipoprotein Lipase Activity, *J. Am. Coll. Cardiol.* 29, 964–968.
  154. Schnell, G.B., Robertson, A., Houston, D., *et al.* (1999)



- Impaired Brachial Artery Endothelial Function Is Not Predicted by Elevated Triglycerides, *J. Am. Coll. Cardiol.* 33, 2038–2043.
155. Hara, T., Kusunoki, M., Tsutsumi, K., *et al.* (1998) A Lipoprotein Lipase Activator, NO-1886, Improves Endothelium-Dependent Relaxation of Rat Aorta Associated with Aging, *Eur. J. Pharmacol.* 350, 75–79.
  156. Plotnick, G.D., Corretti, M.C., and Vogel, R.A. (1997) Effects of Antioxidant Vitamins on the Transient Impairment of Endothelium-Dependent Brachial Artery Vasoactivity Following a Single High-Fat Meal, *JAMA* 278, 1682–1686.
  157. Cuevas, A.M., Guasch, V., Castillo, O., *et al.* (2000) A High-Fat Diet Induces and Red Wine Counteracts Endothelial Dysfunction in Human Volunteers, *Lipids* 35, 143–148.
  158. Ong, P.J., Dean, T.S., Hayward, C.S., *et al.* (1999) Effects of Fat and Carbohydrate Consumption on Endothelial Function, *Lancet* 354, 2134.
  159. Marchesi, S., Lupattelli, G., Schillaci, G., Pirro, M., Siepi, D., Roscini, A.R., Pasqualini, L., and Mannarino, E. (2000) Impaired Flow-Mediated Vasoactivity During Post-prandial Phase in Young Healthy Men, *Atherosclerosis* 153, 397–402.
  160. Bae, J.H., Bassenge, E., Kim, K.B., Kim, Y.N., Kim, K.S., Lee, H.J., Moon, K.C., Lee, M.S., Park, K.Y., and Schwemmer, M. (2001) Postprandial Hypertriglyceridemia Impairs Endothelial Function by Enhanced Oxidant Stress, *Atherosclerosis* 155, 517–523.
  161. Wilmink, H.W., Stroes, E.S., Erkelens, W.D., Gerritsen, W.B., Wever, R., Banga, J.D., and Rabelink, T.J. (2000) Influence of Folic Acid on Postprandial Endothelial Dysfunction, *Arterioscler. Thromb. Vasc. Biol.* 20, 185–188.
  162. Wilmink, H.W., Twickler, M.B., Banga, J.D., Dallinga-Thie, G.M., Eetink, H., Erkelens, D.W., Rabelink, T.J., and Stroes, E.S. (2001) Effect of Statin Versus Fibrate on Postprandial Endothelial Dysfunction: Role of Remnant-like Particles, *Cardiovasc. Res.* 50, 577–582.
  163. Gokce, N., Duffy, S.J., Hunter, L.M., Keaney, J.E., and Vita, J.A. (2001) Acute Hypertriglyceridemia Is Associated with Peripheral Vasodilation and Increased Basal Flow in Healthy Young Adults, *Am. J. Cardiol.* 88, 153–159.
  164. Sarabi, M., Fugmann, A., Karlstrom, B., Berne, C., Lithell, H., and Lind, L. (2001) An Ordinary Mixed Meal Transiently Impairs Endothelium-Dependent Vasodilation in Healthy Subjects, *Acta Physiol. Scand.* 172, 107–113.
  165. Djousse, L., Ellison, R.C., McLennan, C.E., *et al.* (1999) Acute Effects of a High-Fat Meal With and Without Red Wine on Endothelial Function in Healthy Volunteers, *Am. J. Cardiol.* 84, 660–664.
  166. Munthwyler, J., Sutsch, G., Kim, J.H., Schmid, H., Follath, F., Kiowski, W., and Amann, F.W. (2001) Postprandial Lipaemia and Endothelial Function Among Healthy Men, *Swiss Med. Wkly.* 131, 214–218.
  167. Gudmundsson, G.S., Sinkey, C.A., Chenard, C.A., Stumbo, P.J., and Haynes, W.G. (2000) Resistance Vessel Endothelial Function in Healthy Humans During Transient Postprandial Hypertriglyceridemia, *Am. J. Cardiol.* 85, 381–385.
  168. Williams, M.J., Sutherland, W.H., McCormick, M.P., *et al.* (1999) Impaired Endothelial Function Following a Meal Rich in Used Cooking Fat, *J. Am. Coll. Cardiol.* 33, 1050–1055.
  169. Vogel, R.A., Corretti, M.C., and Plotnick, G.D. (2000) The Postprandial Effect of Components of the Mediterranean Diet on Endothelial Function, *J. Am. Coll. Cardiol.* 36, 1455–1460.
  170. Fuentes, F., Lopez-Miranda, J., Sanchez, E., Sanchez, F., Paez, J., Paz-Rojas, E., Marin, C., Gomez, P., Jimenez-Pererez, J., Ordovas, J.M., and Perez-Jimenez, F. (2001) Mediterranean and Low-Fat Diets Improve Endothelial Function in Hypercholesterolemic Men, *Ann. Intern. Med.* 134, 1115–1119.
  171. Boger, R.H., Bode-Boger, S.M., Szuba, A., *et al.* (1998) Asymmetric Dimethylarginine (ADMA): A Novel Risk Factor for Endothelial Dysfunction: Its Role in Hypercholesterolemia, *Circulation* 98, 1842–1847.
  172. Xiong, Y., Li, Y.J., Yu, X.J., *et al.* (1996) Endogenous Inhibitors of Nitric Oxide Synthesis and Lipid Peroxidation in Hyperlipidemic Rabbits, *Chung Kuo Yao Li Hsueh Pao* 17, 149–152.
  173. Boger, R.H., Sydow, K., Borlak, J., *et al.* (2000) LDL Cholesterol Upregulates Synthesis of Asymmetrical Dimethylarginine in Human Endothelial Cells: Involvement of S-Adenosylmethionine-Dependent Methyltransferases, *Circ. Res.* 87, 99–105.
  174. Ito, A., Tsao, P.S., Adimoolam, S., Kimoto, M., *et al.* (1999) Novel Mechanism for Endothelial Dysfunction: Dysregulation of Dimethylarginine Dimethylaminohydrolase, *Circulation* 99, 3092–3095.
  175. Hayashi, T., Yamada, K., Esaki, T., *et al.* (1999) Endothelium-Dependent Relaxation of Rabbit Atherosclerotic Aorta Was Not Restored by Control of Hyperlipidemia: The Possible Role of Peroxynitrate (ONN<sup>-</sup>), *Atherosclerosis* 147, 349–363.
  176. Ohara, Y., Peterson, T.E., Sayegh, H.S., *et al.* (1995) Dietary Correction of Hypercholesterolemia in the Rabbit Normalizes Endothelial Superoxide Anion Production, *Circulation* 92, 898–903.
  177. Inoue, N., Ohara, Y., Fukui, T., *et al.* (1998) Probucol Improves Endothelium-Dependent Relaxation and Decreases Vascular Superoxide Production in Cholesterol-Fed Rabbits, *Am. J. Med. Sci.* 315, 242–247.
  178. Kim, S.C., Kim, I.K., Seo, K.K., *et al.* (1997) Involvement of Superoxide Radical in the Impaired Endothelium-Dependent Relaxation of Cavertous Smooth Muscle in Hypercholesterolemic Rabbits, *Urol. Res.* 25, 341–346.
  179. Candipan, R.C., Wang, B.Y., Buitrago, R., *et al.* (1996) Regression or Progression. Dependency on Vascular Nitric Oxide, *Arterioscler. Thromb. Vasc. Biol.* 16, 44–50.
  180. Wagner, A.H., Kohler, T., Ruckschloss, U., *et al.* (2000) Improvement of Nitric Oxide-Dependent Vasodilation by HMG-CoA Reductase Inhibitors Through Attenuation of Endothelial Superoxide Anion Formation, *Arterioscler. Thromb. Vasc. Biol.* 20, 61–69.
  181. Kinlay, S., Fang, J.C., Hikita, H., *et al.* (1999) Plasma Alpha-Tocopherol and Coronary Endothelium-Dependent Vasodilator Function, *Circulation* 100, 219–221.
  182. Sarabi, M., Vessby, B., Basu, S., *et al.* (1999) Relationships Between Endothelium-Dependent Vasodilation, Serum Vitamin E and Plasma Isoprostane 8-iso-PGF<sub>2α</sub> Levels in Healthy Subjects, *J. Vasc. Res.* 36, 486–491.
  183. Mangiafico, R.A., Malatino, L.S., Santonocito, M., *et al.* (1996) Raised Plasma Endothelin-1 Concentrations in Patients with Primary Hypercholesterolemia Without Evidence of Atherosclerosis, *Int. Angiol.* 15, 240–244.
  184. Hernandez-Perera, O., Perez-Sala, D., Navarro-Antolin, J., *et al.* (1998) Effects of the 3-Hydroxy-3-Methylglutaryl-CoA Reductase Inhibitors, Atorvastin and Simvastatin, on the Expression of Endothelin-1 and Endothelial Nitric Oxide Synthase in Vascular Endothelial Cells, *J. Clin. Invest.* 101, 2711–2719.
  185. Best, P.J., Lerman, L.O., Romero, J.C., *et al.* (1999) Coronary Endothelial Function Is Preserved with Chronic Endothelin Receptor Antagonism in Experimental Hypercholesterolemia *in vitro*, *Arterioscler. Thromb. Vasc. Biol.* 19, 2769–2775.
  186. Barton, M., Haudenschild, C.C., d'Uscio, L.V., *et al.* (1998) Endothelin ETA Receptor Blockade Restores NO-Mediated Endothelial Function and Inhibits Atherosclerosis in Apolipoprotein E-Deficient Mice, *Proc. Natl. Acad. Sci. USA* 95, 14367–14372.
  187. Feron, O., Dessy, C., Moniotte, S., *et al.* (1999) Hypercholesterolemia Decreases Nitric Oxide Production by Promoting the

- Interaction of Caveolin and Endothelial Nitric Oxide Synthase, *J. Clin. Invest.* 103, 897–905.
188. Blair, A., Shaul, P.W., Yuhanna, I.S., *et al.* (1999) Oxidized Low Density Lipoprotein Displaces Endothelial Nitric-Oxide Synthase (eNOS) from Plasmalemmal Caveolae and Impairs eNOS Activation, *J. Biol. Chem.* 274, 32512–32519.
  189. Kaesemeyer, W.H., Caldwell, R.B., Huang, J., and Caldwell, R.W. (1999) Pravastatin Sodium Activates Endothelial Nitric Oxide Synthase Independent of Its Cholesterol-Lowering Actions, *J. Am. Coll. Cardiol.* 33, 234–241.
  190. Nakashima, Y., Toyokawa, Y., and Tanaka, S. (1996) Simvastatin Increases Plasma NO<sub>2</sub><sup>-</sup> and NO<sub>3</sub><sup>-</sup> Levels in Patients with Hypercholesterolemia, *Atherosclerosis* 127, 43–47.
  191. Feron, O., Dessy, C., Desager, J.P., and Balligand, J.L. (2001) Hydroxy-Methylglutaryl-Coenzyme A Reductase Inhibition Promotes Endothelial Nitric Oxide Synthase Activation Through a Decrease in Caveolin Abundance, *Circulation* 103, 113–118.
  192. Bank, N., and Aynedjian, H.S. (1992) Role of Thromboxane in Impaired Renal Vasodilation Response to Acetylcholine in Hypercholesterolemic Rats, *J. Clin. Invest.* 89, 1636–1642.
  193. Najibi, S., Cowan, C.L., Palacino, J.J., and Cohen, R.A. (1994) Enhanced Role of Potassium Channels in Relaxations to Acetylcholine in Hypercholesterolemic Rabbit Carotid Artery, *Am. J. Physiol.* 266, H2061–H2067.
  194. Kamata, K., Kojima, S., Sugiura, M., and Kasuya, Y. (1996) Preservation of Endothelium-Dependent Vascular Relaxation in Cholesterol-Fed Mice by the Chronic Administration of Prazosin or Pravastatin, *Jpn. J. Pharmacol.* 70, 149–156.
  195. Senaratne, M.P., Thomson, A.B., and Kappagoda, C.T. (1991) Lovastatin Prevents the Impairment of Endothelium-Dependent Relaxation and Inhibits Accumulation of Cholesterol in the Aorta in Experimental Atherosclerosis in Rabbits, *Cardiovasc. Res.* 25, 568–578.
  196. Dowell, F.J., Hamilton, C.A., Lindop, G.B., and Reid, J.L. (1995) Development and Progression of Atherosclerosis in Aorta from Heterozygous and Homozygous WHHL Rabbits. Effects of Simvastatin Treatment, *Arterioscler. Thromb. Vasc. Biol.* 15, 1152–1160.
  197. Jorge, P.A., Ozaki, M.R., and Metzke, K. (1994) Effects of Simvastatin and Pravastatin on Endothelium-Dependent Relaxation in Hypercholesterolemic Rabbits, *Exp. Toxicol. Pathol.* 46, 465–469.
  198. Jorge, P.A., Osaki, M.R., and de Almeida, E. (1997) Rapid Reversal of Endothelial Dysfunction in Hypercholesterolaemic Rabbits Treated with Simvastatin and Pravastatin, *Clin. Exp. Pharmacol. Physiol.* 24, 948–953.
  199. Galle, J., Busse, R., and Bassenge, E. (1991) Hypercholesterolemia and Atherosclerosis Change Vascular Reactivity in Rabbits by Different Mechanism, *Arterioscler. Thromb.* 11, 1712–1718.
  200. Brandes, R.P., Behra, A., Leberherz, C., *et al.* (1999) Lovastatin Maintains Nitric Oxide—But Not EDHF-Mediated Endothelium-Dependent Relaxation in the Hypercholesterolemic Rabbit Carotid Artery, *Atherosclerosis* 142, 97–104.
  201. Williams, J.K., Sukhova, G.K., Herrington, D.M., and Libby, P. (1998) Pravastatin Has Cholesterol-Lowering Independent Effects on the Artery Wall of Atherosclerotic Monkeys, *J. Am. Coll. Cardiol.* 31, 684–691.
  202. Boger, R.H., Bode-Boger, S.M., Brandes, R.P., *et al.* (1997) Dietary L-Arginine Reduces the Progression of Atherosclerosis in Cholesterol-Fed Rabbits: Comparison with Lovastatin, *Circulation* 96, 1282–1290.
  203. Kroon, A.A., Stalenhoef, A.F., Buikema, H., *et al.* (1993) The Effect of Cholesterol Reduction on the Endothelial Function and Progression of Atherosclerosis in WHHL Rabbits, *Atherosclerosis* 103, 221–230.
  204. Wilson, S.H., Simari, R.D., Best, P.J., Peterson, T.E., Lerman, L.O., Aviram, M., Nath, K.A., Holmes, D.R., Jr., and Lerman, A. (2001) Simvastatin Preserves Coronary Endothelial Function in Hypercholesterolemia in the Absence of Lipid Lowering, *Arterioscler. Thromb. Vasc. Biol.* 21, 122–128.
  205. Kamata, K., Sugiura, M., Kojima, S., and Kasuya, Y. (1996) Preservation of Endothelium-Dependent Relaxation in Cholesterol-Fed and Streptozotocin-Induced Diabetic Mice by the Chronic Administration of Cholestyramine, *Br. J. Pharmacol.* 118, 385–391.
  206. Kappagoda, C.T., Thomson, A.B., and Senaratne, M.P. (1990) A Model for Demonstration of Reversal of Impairment of Endothelium-Dependent Relaxation in the Cholesterol-Fed Rabbit, *Can. J. Physiol. Pharmacol.* 68, 845–850.
  207. Dowell, F.J., Hamilton, C.A., and Reid, J.L. (1996) Effects of Manipulation of Dietary Cholesterol on the Function of the Thoracic Aorta from New Zealand White Rabbits, *J. Cardiovasc. Pharmacol.* 27, 235–239.
  208. Boger, R.H., Bode-Boger, S.M., Phivthong-ngam, L., *et al.* (1998) Dietary L-Arginine and Alpha-Tocopherol Reduce Vascular Oxidative Stress and Preserve Endothelial Function in Hypercholesterolemic Rabbits via Different Mechanisms, *Atherosclerosis* 141, 31–43.
  209. Singer, A.H., Tsao, P.S., Wang, B.Y., *et al.* (1995) Discordant Effects of Dietary L-Arginine on Vascular Structure and Reactivity in Hypercholesterolemic Rabbits, *J. Cardiovasc. Pharmacol.* 25, 710–716.
  210. Cooke, J.P., Singer, A.H., Tsao, P., *et al.* (1992) Antiatherogenic Effects of L-Arginine in the Hypercholesterolemic Rabbit, *J. Clin. Invest.* 90, 1168–1172.
  211. Phivthong-ngam, L., Bode-Boger, S.M., Boger, R.H., *et al.* (1998) Dietary L-Arginine Normalizes Endothelin-Induced Vascular Contractions in Cholesterol-Fed Rabbits, *J. Cardiovasc. Pharmacol.* 32, 300–307.
  212. Girerd, X.J., Hirsch, A.T., Cooke, J.P., *et al.* (1990) L-Arginine Augments Endothelium-Dependent Vasodilation in Cholesterol-Fed Rabbits, *Circ. Res.* 67, 1301–1308.
  213. Jeremy, R.W., McCarron, H., and Sullivan, D. (1996) Effects of Dietary L-Arginine on Atherosclerosis and Endothelium-Dependent Vasodilation in the Hypercholesterolemic Rabbit. Response According to Treatment Duration, Anatomic Site, and Sex, *Circulation* 94, 498–506.
  214. Rossitch, E., Jr., Alexander, E., III, Black, P.M., and Cooke, J.P. (1991) L-Arginine Normalizes Endothelial Function in Cerebral Vessels from Hypercholesterolemic Rabbits, *J. Clin. Invest.* 87, 1295–1299.
  215. Keany, J.F., Xu, A., Cunningham, D., *et al.* (1995) Dietary Probucoyl Preserves Endothelial Function in Cholesterol-Fed Rabbits by Limiting Vascular Oxidative Stress and Superoxide Generation, *J. Clin. Invest.* 95, 2520–2529.
  216. Simon, B.C., Haudenschild, C.C., and Cohen, R.A. (1993) Preservation of Endothelium-Dependent Relaxation in Atherosclerotic Rabbit Aorta by Probucoyl, *J. Cardiovasc. Pharmacol.* 21, 893–901.
  217. Mugee, A., Elwell, J.H., Peterson, T.E., *et al.* (1991) Chronic Treatment with Polyethylene-Glycolated Superoxide Dismutase Partially Restores Endothelium-Dependent Vascular Relaxations in Cholesterol-Fed Rabbits, *Circ. Res.* 69, 1293–1300.
  218. Kamata, K., Nakajima, M., and Sugiura, M. (1999) Effects of Superoxide Dismutase on the Acetylcholine-Induced Relaxation Response in Cholesterol-Fed and Streptozotocin-Induced Diabetic Mice, *J. Smooth Muscle Res.* 35, 33–46.
  219. Andersson, T.L., Matz, J., Ferns, G.A., and Anggard, E.E. (1994) Vitamin E Reverses Cholesterol-Induced Endothelial Dysfunction in the Rabbit Coronary Circulation, *Atherosclerosis* 111, 39–45.



220. Matz, J., Andersson, T.L., Ferns, G.A., and Angaard, E.E. (1994) Dietary Vitamin E Increases the Resistance to Lipoprotein Oxidation and Attenuates Endothelial Dysfunction in the Cholesterol-Fed Rabbit, *Atherosclerosis* 110, 241–249.
221. Klemsdal, T.O., Andersson, T.L., Matz, J., *et al.* (1994) Vitamin E Restores Endothelium-Dependent Vasodilation in Cholesterol-Fed Rabbits: *In vivo* Measurements by Photoplethysmography, *Cardiovasc. Res.* 28, 1397–1402.
222. Keany, J.F., Jr., Gaziano, J.M., Xu, A., *et al.* (1994) Low-Dose Alpha-Tocopherol Improves and High-Dose Alpha-Tocopherol Worsens Endothelial Vasodilator Function in Cholesterol-Fed Rabbits, *J. Clin. Invest.* 93, 844–851.
223. Ribeiro, J.P.A., Neyra, L.C., Ozaki, R.M., and de Almeida, E. (1998) Improvement in the Endothelium-Dependent Relaxation in Hypercholesterolemic Rabbits Treated with Vitamin E, *Atherosclerosis* 140, 333–339.
224. Stewart-Lee, A.L., Ferns, G.A., and Anggard, E.E. (1995) Differences in Onset of Impaired Endothelial Responses and in Effects of Vitamin E in the Hypercholesterolemic Rabbit Carotid and Renal Arteries, *J. Cardiovasc. Pharmacol.* 25, 906–913.
225. Stewart-Lee, A.L., Forster, L.A., Nourooz-Zadeh, J., *et al.* (1994) Vitamin E Protects Against Impairment of Endothelium-Mediated Relaxations in Cholesterol-Fed Rabbits, *Arterioscler. Thromb.* 14, 494–499.
226. Keany, J.F., Jr., Gaziano, J.M., Xu, A., *et al.* (1993) Dietary Antioxidants Preserve Endothelium-Dependent Vessel Relaxation in Cholesterol-Fed Rabbits, *Proc. Natl. Acad. Sci.* 90, 11880–11884.
227. Jorge, P.A., Osaki, M.R., de Almeida, E., *et al.* (1996) Effects of Vitamin E on Endothelium-Dependent Coronary Flow in Hypercholesterolemic Dogs, *Atherosclerosis* 126, 43–51.
228. Saganuma, H., and Inakuma, T. (1999) Protective Effect of Dietary Tomato Against Endothelial Dysfunction in Hypercholesterolemic Mice, *Biosci. Biotechnol. Biochem.* 63, 78–82.
229. Kugiyama, K., Sugiyama, S., Matsumura, T., *et al.* (1996) Suppression of Atherosclerotic Changes in Cholesterol-Fed Rabbits Treated with an Oral Inhibitor of Neutral Endopeptidase 24.11 (EC 3.4.24.11), *Arterioscler. Thromb. Vasc. Biol.* 16, 1080–1087.
230. Finta, K.M., Fischer, M.J., Lee, L., *et al.* (1993) Ramipril Prevents Impaired Endothelium-Dependent Relaxation in Arteries from Rabbits Fed an Atherogenic Diet, *Atherosclerosis* 100, 149–156.
231. Hernandez, A., Barberi, L., Bellerio, R., *et al.* (1998) Delapril Slows the Progression of Atherosclerosis and Maintains Endothelial Function in Cholesterol-Fed Rabbits, *Atherosclerosis* 137, 71–76.
232. Riezebos, J., Vleeming, W., Beems, R.B., *et al.* (1994) Comparison of the Antiatherogenic Effects of Isradipine and Ramipril on Cholesterol-Fed Rabbits: I. Effect on Progression of Atherosclerosis and Endothelial Dysfunction, *J. Cardiovasc. Pharmacol.* 23, 415–423.
233. Kappagoda, C.T., Thomson, A.B., and Senaratne, M.P. (1991) Effects of Nisoldipine on Atherosclerosis in the Cholesterol Fed Rabbit: Endothelium Dependent Relaxation and Aortic Cholesterol Content, *Cardiovasc. Res.* 25, 270–282.
234. Habib, J.B., Bossaller, C., Wells, S., *et al.* (1986) Preservation of Endothelium-Dependent Vascular Relaxation in Cholesterol-Fed Rabbit by Treatment with the Calcium Blocker PN 200110, *Circ. Res.* 58, 305–309.
235. Becker, R.H., Linz, W., Wiemer, G., and Nordlander, M. (1991) Low-Dose Felodipine Treatment Attenuates Endothelial Dysfunction in Rabbits Fed an Atherogenic Diet, *J. Cardiovasc. Pharmacol.* 18, S36–S41.
236. Hasdai, D., Best, P.H., Cannan, C.R., *et al.* (1998) Acute Endothelin-Receptor Inhibition Does Not Attenuate Acetylcholine-Induced Coronary Vasoconstriction in Experimental Hypercholesterolemia, *Arterioscler. Thromb. Vasc. Biol.* 18, 108–113.
237. Best, P.J., McKenna, C.J., and Hasdai, D. (1999) Chronic Endothelin Antagonism Preserves Coronary Endothelial Function in Experimental Hypercholesterolemia, *Circulation* 99, 1747–1752.
238. Wooditsch, I., Hohnfeld, T., Stroback, H., and Schror, K. (1992) Oral Cicaprost Protects from Hypercholesterolaemia-Induced Impairment of Coronary Vasodilation, *Agents Action Suppl.*, 297–304.
239. Chinellato, A., Ragazzi, E., Pandolfo, L., *et al.* (1992) Protective Role of Heparin on *in vitro* Functional Aortic Response in Watanabe Heritable Hyperlipidemic Rabbits, *Atherosclerosis* 92, 17–24.
240. Shimokawa, H., and Vanhoutte, P.M. (1988) Dietary Cod-Liver Oil Improves Endothelium-Dependent Responses in Hypercholesterolemic and Atherosclerotic Porcine Coronary Arteries, *Circulation* 78, 1421–1430.
241. Hutchinson, S.J., Sudhir, K., Chou, T.M., *et al.* (1997) Testosterone Worsens Endothelial Dysfunction Associated with Hypercholesterolemia and Environmental Tobacco Smoke Exposure in Male Rabbit Aorta, *J. Am. Coll. Cardiol.* 29, 800–807.
242. Ghanam, K., Javellaud, J., Ea-Kim, L., and Oudart, N. (1998) The Protective Effect of 17-Beta-Estradiol on Vasomotor Responses of Aorta from Cholesterol-Fed Rabbit Is Reduced by Inhibitors of Superoxide Dismutase and Catalase, *Biochem. Biophys. Res. Commun.* 249, 858–864.
243. Keany, J.F., Jr., Shwaery, G.T., Xu, A., *et al.* (1994) 17-Beta-Estradiol Preserves Endothelial Vasodilator Function and Limits Low-Density Lipoprotein Oxidation in Hypercholesterolemic Swine, *Circulation* 89, 2251–2259.
244. Kang, S.Y., Kim, S.H., Schini, V.B., and Kim, N.D. (1995) Dietary Ginsenosides Improve Endothelium-Dependent Relaxation in the Thoracic Aorta of Hypercholesterolemic Rabbit, *Gen. Pharmacol.* 26, 483–487.
245. Rossoni, B., Berti, F., Trento, F., *et al.* (1999) Chronic Oral Defibrotide Counteracts Hypercholesterolemia Noxious Effects on Cardiovascular Function in the Rabbit, *Thromb. Res.* 94, 327–338.
246. John, S., Schlaich, M., Langenfeld, M., *et al.* (1998) Increased Bioavailability of Nitric Oxide After Lipid-Lowering Therapy in Hypercholesterolemic Patients: A Randomized Placebo-Controlled, Double-Blind Study, *Circulation* 98, 211–216.
247. O'Driscoll, G., Green, D., and Taylor, R.R. (1997) Simvastatin, an HMG-Coenzyme A Reductase Inhibitor, Improves Endothelial Function Within 1 Month, *Circulation* 95, 1126–1131.
248. Koh, K.K., Cardillo, C., Bui, M.N., *et al.* (1999) Vascular Effects of Estrogen and Cholesterol-Lowering Therapies in Hypercholesterolemic Postmenopausal Women, *Circulation* 99, 354–360.
249. Dupuis, J., Tardif, J.C., Cernacek, P., and Theroux, P. (1999) Cholesterol Reduction Rapidly Improves Endothelial Function After Acute Coronary Syndromes. The RECIFE (Reduction of Cholesterol in Ischemia and Function of the Endothelium) Trial, *Circulation* 99, 3227–3233.
250. Vogel, R.A., Corretti, M.C., and Plotnick, G.D. (1996) Changes in Flow-Mediated Brachial Artery Vasoactivity with Lowering of Desirable Cholesterol Levels in Healthy Middle-Aged Men, *Am. J. Cardiol.* 77, 37–40.
251. Simons, L.A., Sullivan, D., Simons, J., and Celermajer, D.S. (1998) Effects of Atorvastatin Monotherapy and Simvastatin Plus Cholestyramine on Arterial Endothelial Function in Patients with Severe Primary Hypercholesterolaemia, *Atherosclerosis* 137, 197–203.
252. Treasure, C.B., Klein, J.L., Weintraub, W.S., *et al.* (1995) Beneficial Effects of Cholesterol-Lowering Therapy on the Coro-

- nary Endothelium in Patients with Coronary Artery Disease, *N. Engl. J. Med.* 332, 481–487.
253. Egashira, K., Hirooka, Y., Kai, H., *et al.* (1994) Reduction in Serum Cholesterol with Pravastatin Improves Endothelium-Dependent Coronary Vasomotion in Patients with Hypercholesterolemia, *Circulation* 89, 2519–2524.
  254. Anderson, T.J., Meredith, I.T., Yeung, A.C., *et al.* (1995) The Effect of Cholesterol-Lowering and Antioxidant Therapy on Endothelium-Dependent Coronary Vasomotion, *N. Engl. J. Med.* 332, 488–493.
  255. Neunteufl, T., Kostner, K., Katzenschlager, R., *et al.* (1998) Additional Benefit of Vitamin E Supplementation to Simvastatin Therapy on Vasoreactivity of the Brachial Artery of Hypercholesterolemic Men, *J. Am. Coll. Cardiol.* 32, 711–716.
  256. Stroes, E.S., Koomans, H.A., de Bruin, T.W., and Rabelink, T.J. (1995) Vascular Function in the Forearm of Hypercholesterolaemic Patients Off and On Lipid-Lowering Medication, *Lancet* 346, 467–471.
  257. Leung, W.H., Lau, C.P., and Wong, C.K. (1993) Beneficial Effect of Cholesterol-Lowering Therapy on Coronary Endothelium-Dependent Relaxation in Hypercholesterolaemic Patients, *Lancet* 341, 1496–1500.
  258. Cohen, J.D., Drury, J.H., Ostdiek, J., *et al.* (2000) Benefits of Lipid Lowering on Vascular Reactivity in Patients with Coronary Artery Disease and Average Cholesterol Levels: A Mechanism for Reducing Clinical Events? *Am. Heart J.* 139, 734–738.
  259. Duffy, S.J., O'Brien, R.C., New, G., Harper, R.W., and Meredith, I.T. (2001) Effect of Antioxidant Treatment and Cholesterol Lowering on Resting Arterial Tone, Metabolic Vasodilation and Endothelial Function in the Human Forearm: A Randomized, Placebo-Controlled Study, *Clin. Exp. Pharmacol. Physiol.* 28, 409–418.
  260. Drexler, H., Eiber, A.M., Meinzer, K., and Just, H. (1991) Correction of Endothelial Dysfunction in Coronary Microcirculation of Hypercholesterolaemic Patients by L-Arginine, *Lancet* 338, 1546–1550.
  261. Boger, R.H., Bode-Boger, S.M., Szuba, A., *et al.* (1998) Asymmetric Dimethylarginine (ADMA): A Novel Risk Factor for Endothelial Dysfunction: Its Role in Hypercholesterolemia, *Circulation* 98, 1842–1847.
  262. Creager, M.A., Gallagher, S.J., Girerd, X.J., *et al.* (1992) L-Arginine Improves Endothelium-Dependent Vasodilation in Hypercholesterolemic Humans, *J. Clin. Invest.* 90, 1248–1253.
  263. Casino, P.R., Kilcoyne, C.M., Quyyumi, A.A., *et al.* (1994) Investigation of Decreased Availability of Nitric Oxide Precursor as the Mechanism Responsible for Impaired Endothelium-Dependent Vasodilation in Hypercholesterolemic Patients, *J. Am. Coll. Cardiol.* 23, 844–850.
  264. Clarkson, P., Adams, M.R., Powe, A.J., *et al.* (1996) Oral L-Arginine Improves Endothelium-Dependent Vasodilation in Hypercholesterolemic Young Adults, *J. Clin. Invest.* 97, 1989–1994.
  265. Kugiyama, K., Motoyama, T., Doi, H., *et al.* (1999) Improvement of Endothelial Vasomotor Dysfunction by Treatment with Alpha-Tocopherol in Patients with High Remnant Lipoproteins Levels, *J. Am. Coll. Cardiol.* 33, 1512–1518.
  266. Green, D., O'Driscoll, G., Rankin, J.M., *et al.* (1998) Beneficial Effects of Vitamin E Administration on Nitric Oxide Function in Subjects with Hypercholesterolaemia, *Clin. Sci.* 95, 361–367.
  267. Heitzer, T., Yla-Herttuala, S., Wild, E., *et al.* (1999) Effect of Vitamin E on Endothelial Vasodilator Function in Patients with Hypercholesterolemia, Chronic Smoking or Both, *J. Am. Coll. Cardiol.* 33, 499–505.
  268. Chowienzyk, P.J., Kneale, B.J., Brett, S.E., *et al.* (1998) Lack of Effect of Vitamin E on L-Arginine-Responsive Endothelial Dysfunction in Patients with Mild Hypercholesterolaemia and Coronary Artery Disease, *Clin. Sci.* 94, 129–134.
  269. Gilligan, D.M., Sack, M.N., Guetta, C., *et al.* (1994) Effect of Antioxidant Vitamins on Low Density Lipoprotein Oxidation and Impaired Endothelium-Dependent Vasodilation in Patients with Hypercholesterolemia, *J. Am. Coll. Cardiol.* 24, 1611–1617.
  270. Garcia, C.E., Kilcoyne, C.M., Cardillo, C., *et al.* (1995) Evidence That Endothelial Dysfunction in Patients with Hypercholesterolemia Is Not Due to Increased Extracellular Nitric Oxide Breakdown by Superoxide Anions, *Am. J. Cardiol.* 76, 1157–1161.
  271. Ting, H.H., Timimi, F.K., Haley, E.A., *et al.* (1997) Vitamin C Improves Endothelium-Dependent Vasodilation in Forearm Resistance Vessels of Humans with Hypercholesterolemia, *Circulation* 95, 2617–2622.
  272. Prasad, A., Andrews, N.P., Padder, F.A., *et al.* (1999) Glutathione Reverses Endothelial Dysfunction and Improves Nitric Oxide Bioavailability, *J. Am. Coll. Cardiol.* 34, 507–514.
  273. Verhaar, M.C., Wever, R.M., Kastelein, J.J., *et al.* (1998) 5-Methyltetrahydrofolate, the Active Form of Folic Acid, Restores Endothelial Function in Familial Hypercholesterolemia, *Circulation* 97, 237–241.
  274. Verhaar, M.C., Wever, R.M., Kastelein, J.J., *et al.* (1999) Effects of Oral Folic Acid Supplementation on Endothelial Function in Familial Hypercholesterolemia. A Randomized Placebo-Controlled Trial, *Circulation* 100, 335–338.
  275. Stroes, E., Kastelein, J., Cosentino, F., *et al.* (1997) Tetrahydrobiopterin Restores Endothelial Function in Hypercholesterolemia, *J. Clin. Invest.* 99, 41–46.
  276. Tamai, O., Matsuoka, H., Itabe, H., *et al.* (1997) Single LDL Apheresis Improves Endothelium-Dependent Vasodilation in Hypercholesterolemic Humans, *Circulation* 95, 76–82.
  277. Verhaar, M.C., Honing, M.L., van Dam, T., *et al.* (1999) Nifedipine Improves Endothelial Function in Hypercholesterolemia, Independently of an Effect on Blood Pressure or Plasma Lipids, *Cardiovasc. Res.* 42, 752–760.
  278. Chin, P., and Dart, A.M. (1994) HBPRCA Astra Award. Therapeutic Restoration of Endothelial Function in Hypercholesterolaemic Subjects: Effect of Fish Oils, *Clin. Exp. Pharmacol. Physiol.* 21, 749–755.
  279. Goodfellow, J., Bellamy, M.D., Ramsey, M.W., *et al.* (2000) Dietary Supplementation with Marine Omega-3 Fatty Acids Improves Systemic Large Artery Endothelial Function in Subjects with Hypercholesterolemia, *J. Am. Coll. Cardiol.* 35, 265–270.
  280. Lewis, T.V., Dart, A.M., Chin-Dusting, J.P., and Kingwell, B.A. (1999) Exercise Training Increases Basal Nitric Oxide Production from the Forearm in Hypercholesterolemic Patients, *Arterioscler. Thromb. Vasc. Biol.* 19, 2782–2787.
  281. McDermott, J.R. (1976) Studies on the Catabolism of N<sup>G</sup>-Methylarginine, N<sup>G</sup>, N<sup>G</sup>-Dimethylarginine and N<sup>G</sup>, N<sup>G</sup>-Dimethylarginine in the Rabbit, *Biochem. J.* 154, 179–184.
  282. Vallance, P., Leone, A., Calver, A., *et al.* (1992) Accumulation of an Endogenous Inhibitor of NO Synthesis in Chronic Renal Failure, *Lancet* 339, 572–575.
  283. MacAllister, R.J., Fickling, S.A., Whitley, G.S.J., and Vallance, P. (1994) Metabolism of Methylarginines by Human Vasculature: Implications for the Regulation of Nitric Oxide Synthesis, *Br. J. Pharmacol.* 112, 43–48.
  284. Ooboshi, H., Toyoda, K., Faraci, F.M., *et al.* (1998) Improvement of Relaxation in an Atherosclerotic Artery by Gene Transfer of Endothelial Nitric Oxide Synthase, *Arterioscler. Thromb. Vasc. Biol.* 18, 1752–1758.
  285. Mozes, G., Kullo, I.J., Mohacsi, T.G., *et al.* (1998) *Ex vivo* Gene Transfer of Endothelial Nitric Oxide Synthase to Atherosclerotic Rabbit Aortic Rings Improves Relaxations to Acetylcholine, *Atherosclerosis* 141, 265–271.
  286. Sato, J., Mohacsi, T., Noel, A., *et al.* (2000) *In vivo* Gene

- Transfer of Endothelial Nitric Oxide Synthase to Carotid Arteries from Hypercholesterolemic Rabbits Enhances Endothelium-Dependent Relaxations, *Stroke* 31, 968–975.
287. Meurice, T., Bauters, C., Vallet, B., *et al.* (1997) bFGF Resores Endothelium-Dependent Responses of Hypercholesterolemic Rabbit Thoracic Aorta, *Am. J. Physiol.* 272, H613–H617.
288. Hirooka, Y., Egashira, K., Imaizumi, T., Tagawa, T., Kai, H., Sugimachi, M., and Takeshita, A. (1994) Effect of L-Arginine on Acetylcholine-Induced Endothelium-Dependent Vasodilation Differs Between the Coronary and Forearm Vasculatures in Humans, *J. Am. Coll. Cardiol.* 24, 948–955.
289. Anderson, T.I., Uehata, A., Gerhard, M.D., Meredith, I.T., Knab, S., Delagrang, D., Lieberman, E.H., Ganz, P., Creager, M.A., Yeung, A.C., *et al.* (1995) Close Relation of Endothelial Function in the Human Coronary and Peripheral Circulations, *J. Am. Coll. Cardiol.* 26, 1235–1241.
290. Neunteufl, T., Katzenschlager, R., Hassan, A., Klaar, U., Schwarzacher, S., Glogar, D., Bauer, P., and Weidinger, F. (1997) Systemic Endothelial Dysfunction Is Related to the Extent and Severity of Coronary Artery Disease, *Atherosclerosis* 129, 111–118.
291. Schachinger, V., Britten, M.B., and Zeiher, A.M. (2000) Prognostic Impact of Coronary Vasodilatory Function on the Long-Term Outcome of Coronary Heart Disease, *Circulation* 101, 1899–1906.
292. Suwaidi, J.A., Hamasaki, S., Higano, S.T., Nishimura, R.A., Holmes, D.R., and Lerman, A. (2000) Long-Term Follow-Up of Patients with Mild Coronary Artery Disease and Endothelial Dysfunction, *Circulation* 101, 948–954.

[Received January 16, 2001, and in revised form November 13, 2001; revision accepted November 18, 2001]

# Abietoid Seed Fatty Acid Compositions—A Review of the Genera *Abies*, *Cedrus*, *Hesperopeuce*, *Keteleeria*, *Pseudolarix*, and *Tsuga* and Preliminary Inferences on the Taxonomy of Pinaceae

Robert L. Wolff<sup>a,\*</sup>, Olivier Lavalie<sup>b</sup>, Frédérique Pédrone<sup>a</sup>, Elodie Pasquier<sup>a</sup>,  
Frédéric Destailats<sup>a,d</sup>, Anne M. Marpeau<sup>c</sup>, Paul Angers<sup>d</sup>, and Kurt Aitzetmüller<sup>e</sup>

<sup>a</sup>Institut des Science et Techniques des Aliments de Bordeaux, <sup>b</sup>Institut National d'Ingénieurs des Techniques Agricoles, <sup>c</sup>Laboratoire de Chimie des Substances Végétales, Institut du Pin, Université Bordeaux 1, Talence, France, <sup>d</sup>Department of Food Science and Nutrition, and Dairy Research Center, Université Laval, Sainte Foy, Québec, Canada, and <sup>e</sup>Bundesanstalt für Getreide-, Kartoffel- und Fettforschung, Institute for Chemistry and Physics of Lipids, Münster, Germany

**ABSTRACT:** The seed fatty acid (FA) compositions of Abietoids (*Abies*, *Cedrus*, *Hesperopeuce*, *Keteleeria*, *Pseudolarix*, and *Tsuga*) are reviewed in the present study in conclusion to our survey of Pinaceae seed FA compositions. Many unpublished data are given. Abietoids and Pinoids (*Pinus*, *Larix*, *Picea*, and *Pseudotsuga*)—constituting the family Pinaceae—are united by the presence of several  $\Delta 5$ -olefinic acids, taxoleic (5,9-18:2), pinolenic (5,9,12-18:3), coniferonic (5,9,12,15-18:4), keteleeronic (5,11-20:2), and sciadonic (5,11,14-20:3) acids, and of 14-methyl hexadecanoic (anteiso-17:0) acid. These acids seldom occur in angiosperm seeds. The proportions of individual  $\Delta 5$ -olefinic acids, however, differ between Pinoids and Abietoids. In the first group, pinolenic acid is much greater than taxoleic acid, whereas in the second group, pinolenic acid is greater than or equal to taxoleic acid. Moreover, taxoleic acid in Abietoids is much greater than taxoleic acid in Pinoids, an apparent limit between the two subfamilies being about 4.5% of that acid relative to total FA. *Tsuga* spp. appear to be a major exception, as their seed FA compositions are much like those of species from the Pinoid group. In this respect, *Hesperopeuce mertensiana*, also known as *Tsuga mertensiana*, has little in common with Abietoids and fits the general FA pattern of Pinoids well. *Tsuga* spp. and *H. mertensiana*, from their seed FA compositions, should perhaps be separated from the Abietoid group and their taxonomic position revised. It is suggested that a “Tsugoid” subfamily be created, with seed FA in compliance with the Pinoid pattern and other botanical and immunological criteria of the Abietoid type. All Pinaceae genera, with the exception of *Pinus*, are quite homogeneous when considering their overall seed FA compositions, including  $\Delta 5$ -olefinic acids. In all cases but one (*Pinus*), variations from one species to another inside a given genus are of small amplitude. *Pinus* spp., on the other hand, have highly variable levels of  $\Delta 5$ -olefinic acids in their FA compositions, particularly when sections (e.g., *Cembroides* vs. *Pinus* sections) or subsections (e.g., *Flexiles* and *Cembrae* subsections from the section *Strobis*) are compared, although they show qualitatively the same FA patterns characteristic of

Pinoids. Multicomponent analysis of Abietoid seed FA allowed grouping of individual species into genera that coincide with the same genera otherwise characterized by more classical botanical criteria. Our studies exemplify how seed FA compositions, particularly owing to the presence of  $\Delta 5$ -olefinic acids, may be useful in sustaining and adding some precision to existing taxonomy of the major family of gymnosperms, Pinaceae.

Paper no. L8927 in *Lipids* 37, 17–26 (January 2002).

The family Pinaceae (Coniferophytina) contains a total of 12 genera: *Abies*, *Cathaya*, *Cedrus*, *Keteleeria*, *Larix*, *Nothotsuga*, *Picea*, *Pinus*, *Pseudolarix*, *Pseudotsuga*, *Tsuga*, and *Hesperopeuce* (1). Among these genera, *Pinus* is the largest and most heteromorphic genus, with *Abies* being ranked second and *Picea* third. Other genera contain considerably fewer species, some of them even being monospecific. The seed fatty acid (FA) compositions available for the most common pine species, totaling approximately one-half of extant species, were recently reviewed (2). A review on the genera *Picea*, *Larix*, and *Pseudotsuga* also appeared more recently (3). The usefulness of seed FA compositions in the taxonomy of conifers at the level of families as well as genera has been demonstrated (2–7).

The genera *Larix* and *Picea* are closely related to *Pinus*, although their relationships remain unclear. *Pinus*, *Larix*, and *Picea* are sometimes put together along with *Cathaya* and *Pseudotsuga* into a “Pinoid” group (equivalent to a subfamily), as opposed to an “Abietoid” group that embraces *Abies*, *Cedrus*, *Tsuga*, *Nothotsuga*, *Pseudolarix*, and *Keteleeria* (8). But other subfamily arrangements have been proposed, e.g., Pinoideae (*Pinus*), Laricoideae (*Larix*, *Pseudolarix*, *Cedrus*), and Abietoideae (*Abies*, *Cathaya*, *Keteleeria*, *Picea*, *Pseudotsuga*, *Tsuga*); Pinoideae (*Pinus*), Piceoideae (*Picea*), Laricoideae (*Larix*, *Cathaya*, *Pseudotsuga*), and Abietoideae (all other genera) (9); or more recently (10), Pinoideae, encompassing three tribes [Pineae (*Pinus*), Abietae (*Cathaya*, *Picea*, *Tsuga*, *Cedrus*, *Keteleeria*, and *Abies*), and Lariceae (*Larix*, *Pseudotsuga*)], and Pseudolariceae (*Pseudolarix*). Clearly, there is a lack of general agreement regarding the intergeneric relationships among Pinaceae. Here, we will review the Abietoid group as retained and immunologically de-

\*To whom correspondence should be addressed at INRA, Unité de Nutrition Lipidique, 17, rue Sully, BP 86510, 21065 Dijon Cedex, France.

E-mail: wolff@dijon.inra.fr

Abbreviations: anteiso-17:0, 14-methylhexadecanoic; FA, fatty acid; FAME, fatty acid methyl ester; GLC, gas-liquid chromatography; UPIFA, unsaturated polymethylene-interrupted fatty acid.



fined by Price *et al.* (8), thus including *Abies*, *Tsuga*, *Hesperopeuce*, *Cedrus*, *Keteleeria*, and *Pseudolarix*. *Nothotsuga* was not available from our usual tree-seed sources.

In this study, a compilation of data available for *Abies*, *Tsuga*, *Hesperopeuce*, *Cedrus*, *Keteleeria*, and *Pseudolarix* seed FA compositions is made, including numerous unpublished seed FA compositions, in particular, *Keteleeria*, for which no data were previously available. Species examined here represent approximately one-fourth of the species of the Abietoid group. Except for the seed FA compositions from *Abies* and *Cedrus* spp. that present some similarities, other genera are quite distinct one from another, with *Tsuga* in particular being quite close to Pinoids. Principal component analysis and discriminant analysis permit distinction among all Abietoid genera. This allows conclusions to be drawn on general features of the quantitative distribution of seed FA in *Abies*, *Tsuga*, *Hesperopeuce*, *Cedrus*, *Keteleeria*, and *Pseudolarix*, with emphasis on  $\Delta 5$ -unsaturated polymethylene-interrupted FA ( $\Delta 5$ -UPIFA, or  $\Delta 5$ -olefinic acids).

$\Delta 5$ -UPIFA with chain lengths  $C_{18}$  and  $C_{20}$  are characteristic of Pinaceae seed lipids but rarely occur in angiosperms. In this series of particular FA, the  $\Delta 5$ -double bond is separated from the next ethylenic bond by either two [5,9-18:2 (taxoleic), 5,9,12-18:3 (pinolenic), and 5,9,12,15-18:4 (coniferonic) acids] or four [5,11-20:2, 5,11,14-20:3 (sciadonic), and 5,11,14,17-20:4 (juniperonic) acids] methylene groups instead of only one, as in linoleic or  $\alpha$ -linolenic acids (of the methylene-interrupted type). All ethylenic bonds are in the *cis* configuration. A seventh  $\Delta 5$ -UPIFA, ephedrenic (5,11-18:2) acid, occurs in significant amounts only in *Ginkgo biloba* and *Ephedra* spp. seed lipids (11). Thus,  $\Delta 5$ -UPIFA are common constituents of seed oils from all Coniferophyte families and also some Cycadophyte families (12). In addition to seeds, these FA also occur in the leaf and wood lipids of Coniferophytes (13,14). A FA metabolically related to pinolenic acid, dihomopinolenic (7,11,14-20:3) acid, also is generally present in Pinaceae (15).

## MATERIAL AND METHODS

*Seeds, oil extraction, and fatty acid methyl ester (FAME) preparation.* The seeds analyzed here were purchased from Lawyer Nursery, Inc. (Plains, MT), F.W. Schuhmacher Co., Inc. (Sandwich, MA), Sandeman Seeds (Pulborough, Great Britain), Vilmorin S.A. (La Méniltré, France), Versepuy (Le Puy-en-Velay, France), and the National Office of Forests (ONF, Champagnole, France). Seeds were kept at 4°C until use. Lipid extraction, always performed starting with 10-g samples taken from 15  $\pm$  5 g of powdered seeds, and FAME preparation were performed as described in detail elsewhere for other gymnosperm seeds (4,6). All FAME preparations were made in duplicate and each solution was analyzed once by gas-liquid chromatography (GLC). Generally, FAME were prepared within 24 h after lipid extraction and immediately analyzed.

*Analytical GLC.* All FAME preparations were analyzed in a Carlo Erba 4130 chromatograph (Carlo Erba, Milano, Italy)

equipped with a DB-Wax column (30 m  $\times$  0.32 mm i.d., 0.5  $\mu$ m film; J&W Scientific, Folsom, CA). The oven temperature was 190°C and the inlet pressure of the carrier gas (helium) was 140 kPa. Occasionally, to confirm some identifications, a CP-Sil 88 column (50 m  $\times$  0.25 mm i.d., 0.2  $\mu$ m film; Chrompack, Middelburg, The Netherlands) was operated with temperature programming in a Carlo Erba HRGC chromatograph from 150 to 185°C at 4°C/min with H<sub>2</sub> at 100 kPa. The injector (split mode) and flame-ionization detector were maintained at 250°C for both columns. SP 4290 integrators (Spectra Physics, San Jose, CA) calculated quantitative data. In some instances, particularly to detect potential late-eluting components but also to confirm identifications, a Silar 5 CP column (50 m  $\times$  0.25 mm i.d., 0.2  $\mu$ m film; Chrompack), fitted in a Hewlett-Packard HP 5890 gas chromatograph (Avondale, PA), was used in the temperature program mode (isothermal for 1 min at 165°C; from 165 to 205°C at a rate of 1°C/min; isothermal at 205°C for 60 min). Nitrogen was the carrier gas, and the injector and detector temperatures were maintained at 230 and 260°C, respectively.

*Identification of FAME peaks.* The seed lipids from selected conifer species (15,16) or Ranunculaceae species (17) were used as sources of  $\Delta 5$ -olefinic acid methyl esters with known structures to identify FA from seed lipids by GLC, either by coinjection, comparison of the equivalent chain lengths (DB-Wax column), or retention times (CP-Sil 88 and Silar 5 CP).

*Data analysis.* Principal component analysis was performed with the program STATBOX (Grimmer, Paris, France). The classification of Abietoid spp. was performed with the program XLSTAT (copyright T. Fahmy, Paris, France). To compare the variability of interspecific seed FA compositions of Abietoid spp. and *Picea* and *Larix* spp., ascending hierarchical classifications were computed using the Ward method. This method consists of minimizing the loss of intraclass inertia at each step. The results are presented as a dendrogram (discussed below) in which the aggregation level can be interpreted as a dissimilarity index between the objects.

## RESULTS AND DISCUSSION

*Abies seed FA compositions.* Literature data on the seed FA compositions of species studied here, except for those from our Institutes (4,18), are particularly scarce. We are aware of only two papers partially describing the  $C_{18}$  unsaturated acids in fir (*A. alba*) seeds, indicating the presence of 5,9-18:2 and 5,9,12-18:3 acids characterized both by their GLC behavior (19) and their <sup>13</sup>C nuclear magnetic resonance spectra (20), but no mention of  $C_{20}$  acids was made. Although Takagi and Itabashi (21) did not analyze the seed FA of any of the genera reviewed here in their major study on gymnosperm seed lipids, Jamieson and Reid (14) reported on the leaf FA of several *Abies* and *Tsuga* species. Qualitatively, these acids were identical to those found in the leaves of other Pinaceae, i.e., *Pinus*, *Picea*, *Larix*, *Cedrus*, and *Pseudotsuga* (14).

*Abies* is the most important genus in the Abietoid group, with approximately 80 species and infraspecific taxa (Table 1). The



classification of the genus *Abies* was reviewed in 1989 by Farjon and Rushforth (22), who proposed a new classification scheme, mostly based on morphological characters. *Abies* was divided into 10 sections, some of which were further divided into subsections. Debazac (23) adopted a geographical classification. However, the differences in seed FA compositions between species were rather small, and we do not adopt either classification. Here we summarize data for 20 *Abies* spp. (Table 2). Some supplementary species were also checked, but owing to some overlap of resin components (terpenes?) in the C<sub>16</sub>–C<sub>17</sub> region, they are not reported here. However, they did not differ

appreciably in FA from other species reported here. In *Abies* spp. (Table 2), the level of total saturated acids is rather low, always less than 8–9% of total FA. These acids occur in the usual decreasing order 16:0 > 18:0 > 20:0 > 22:0, also encountered in *Tsuga*, *Cedrus*, and *Keteleeria*. In contrast to the genera reviewed earlier (*Pinus*, *Picea*, *Larix*, *Pseudotsuga*), anteiso-17:0 is higher than 0.6% in *Abies* spp., whereas the corresponding values in other genera are less than 0.4%, with the exception of *Pseudotsuga menziesii* (1.2%) (3).

The most prominent unsaturated FA in *Abies* spp. is linoleic acid, in the range of 37–46%, and values are usually

**TABLE 1**  
List of *Abies* spp. That Have (or Have Not Yet) Been Examined for Their Seed Fatty Acid Compositions

Species <sup>a</sup>	Trivial name <sup>b</sup>	Reference
1. <i>A. alba</i>	European silver fir	18
2. <i>A. amabilis</i>	Pacific silver fir, Cascade fir	—
3. <i>A. balsamea</i> var. <i>balsamea</i>	Balsam fir, Canada fir	4
4. <i>A. balsamea</i> var. <i>phanerolepis</i>	Caanan fir	—
5. <i>A. beshanzuensis</i>	Baishan fir	—
6. <i>A. borisii-regis</i>	Boris fir, Macedonian fir	This study
7. <i>A. bracteata</i>	Bristlecone fir, Santa Lucia fir	—
8. <i>A. cephalonica</i>	Greek fir	4
9. <i>A. chengii</i>	Cheng fir	—
10. <i>A. chensiensis</i> ssp. <i>chensiensis</i>	Shensi fir	—
11. <i>A. chensiensis</i> ssp. <i>salouenensis</i>	—	—
12. <i>A. chensiensis</i> ssp. <i>yulongxueshanensis</i>	—	—
13. <i>A. cilicica</i> ssp. <i>cilicica</i>	Cilician fir	—
14. <i>A. cilicica</i> ssp. <i>isaurica</i>	—	—
15. <i>A. concolor</i>	White fir	18
16. <i>A. concolor</i> ssp. <i>lowiana</i>	Sierra white fir, Pacific white fir	18
17. <i>A. delavayi</i> var. <i>delavayi</i>	Delavay's fir	This study
18. <i>A. delavayi</i> var. <i>motuoensis</i>	—	—
19. <i>A. delavayi</i> var. <i>nukiangensis</i>	—	—
20. <i>A. densa</i>	—	—
21. <i>A. durangensis</i> var. <i>coahuilensis</i>	—	—
22. <i>A. durangensis</i> var. <i>durangensis</i>	—	—
23. <i>A. fabri</i> ssp. <i>fabri</i>	Yunnan fir	—
24. <i>A. fabri</i> ssp. <i>minensis</i>	—	—
25. <i>A. fanjingshanensis</i>	Fanjingshan fir	—
26. <i>A. fansipanensis</i>	—	—
27. <i>A. fargesii</i> var. <i>fargesii</i>	Farges fir	—
28. <i>A. fargesii</i> var. <i>faxoniana</i>	—	—
29. <i>A. fargesii</i> var. <i>sutchuenensis</i>	—	—
30. <i>A. firma</i>	Japanese fir, Momi fir	—
31. <i>A. forrestii</i> var. <i>ferreana</i>	—	—
32. <i>A. forrestii</i> var. <i>forrestii</i>	Forrest fir	—
33. <i>A. forrestii</i> var. <i>georgei</i>	—	—
34. <i>A. forrestii</i> var. <i>smithii</i>	—	—
35. <i>A. fraseri</i>	Fraser fir	4
36. <i>A. grandis</i>	Grand fir	4
37. <i>A. guatemalensis</i> var. <i>guatemalensis</i>	Guatemalan fir	—
38. <i>A. guatemalensis</i> var. <i>jaliscana</i>	—	—
39. <i>A. hickelii</i> var. <i>hickelii</i>	Hickel fir	—
40. <i>A. hickelii</i> var. <i>oaxacana</i>	—	—
41. <i>A. hidalgensis</i>	—	—
42. <i>A. holophylla</i>	Needle fir, Manchurian fir	—
43. <i>A. homolepis</i> var. <i>homolepis</i>	Nikko fir	This study
44. <i>A. homolepis</i> var. <i>umbellata</i>	—	—
45. <i>A. kawakamii</i>	Taiwan fir	—
46. <i>A. koreana</i>	Korean fir	This study

Continued

**TABLE 1**  
**Continued**

Species <sup>a</sup>	Trivial name <sup>b</sup>	Reference
47. <i>A. lasiocarpa</i> var. <i>arizonica</i>	Corkbark fir	—
48. <i>A. lasiocarpa</i> var. <i>lasiocarpa</i>	Alpine fir	4
49. <i>A. magnifica</i> var. <i>magnifica</i>	California red fir, silvertip fir	—
50. <i>A. magnifica</i> var. <i>shastensis</i>	Shasta red fir	—
51. <i>A. mariesii</i>	Aomoritomatsu (Jap.)	—
52. <i>A. nebrodensis</i>	Silician fir	—
53. <i>A. nephrolepis</i>	Manchurian fir, Khingan fir	This study
54. <i>A. nordmanniana</i> ssp. <i>equi-trojani</i> ( <i>bornmuelleriana</i> )	—	4
55. <i>A. nordmanniana</i> ssp. <i>nordmanniana</i>	Nordmann fir	4
56. <i>A. numidica</i>	Algerian fir	This study
57. <i>A. pindrow</i> var. <i>brevifolia</i>	—	—
58. <i>A. pindrow</i> var. <i>pindrow</i>	West Himalayan fir	This study
59. <i>A. pinsapo</i> var. <i>marocana</i>	Moroccan fir	—
60. <i>A. pinsapo</i> var. <i>pinsapo</i>	Spanish fir	4
61. <i>A. pinsapo</i> var. <i>tazaotana</i>	—	—
62. <i>A. procera</i>	Noble fir	This study
63. <i>A. recurvata</i> var. <i>ernestii</i>	—	—
64. <i>A. recurvata</i> var. <i>recurvata</i>	Min fir	—
65. <i>A. religiosa</i>	Oyamel (Mex.), Sacred fir	—
66. <i>A. sachalinensis</i> var. <i>gracilis</i>	—	—
67. <i>A. sachalinensis</i> var. <i>mayriana</i>	—	—
68. <i>A. sachalinensis</i> var. <i>nemorensis</i>	—	—
69. <i>A. sachalinensis</i> var. <i>sachalinensis</i>	Sakhalin fir	—
70. <i>A. sibirica</i> ssp. <i>semenovii</i>	—	—
71. <i>A. sibirica</i> ssp. <i>sibirica</i>	Siberian fir	—
72. <i>A. spectabilis</i>	East Himalayan fir	—
73. <i>A. squamata</i>	Flaky fir	—
74. <i>A. veitchii</i> var. <i>sikokiana</i>	—	—
75. <i>A. veitchii</i> var. <i>veitchii</i>	Shirabe (Jap.), Veitch's silver fir	This study
76. <i>A. vejarii</i> ssp. <i>mexicana</i>	—	—
77. <i>A. vejarii</i> ssp. <i>vejarii</i>	Vejar fir	—
78. <i>A. yuanbaoshanensis</i>	—	—
79. <i>A. ziyuanensis</i>	Ziyuan fir	—

<sup>a</sup>List established according to Farjon's *World Checklist and Bibliography of Conifers* (25).

<sup>b</sup>List mostly based on tree-seed sellers' catalogs. The website <http://www.geocities.com/RainForest/Canopy> was also consulted. Abbreviations: Jap., Japanese; Mex., Mexican.

lower than those determined in *Pinus*, *Larix*, and *Picea*. Oleic acid is ranked second, varying between 20 and 35%. Here too, similar values are frequently encountered in the genus *Pinus*. The most discriminating feature is the amount of taxoleic acid, almost always higher than 4.5% (*A. procera* is an exception, with only 3.5%) and sometimes as much as 8%. A value of 4.5% is the highest encountered in *Pinus*, *Picea*, *Larix*, or *Pseudotsuga* (2,3), whereas a value of 8% is close to that presented by *Taxus baccata* seeds (24). The percentage of pinolenic acid lies within the limits of 9–17%, which on average is lower than in *Pinus*, *Picea*, *Larix*, and *Pseudotsuga* spp. This may be interpreted in terms of  $\Delta 5$ -desaturase activities, which are higher for oleic acid than for linoleic acid in *Abies* as compared to the preceding genera. With regard to the C<sub>20</sub>  $\Delta 5$ -UPIFA in *Abies* spp., 5,11-20:2 and sciadonic acid levels are not quantitatively very distinct from those occurring in *Pinus* spp. For the latter acid, the range is most often 1.7–2.7%, with only *A. procera* showing a lower value. The sums of  $\Delta 5$ -UPIFA are rather homogenous within the genus, between approximately 18 and 24% (except for *A. procera*, 16%).

*Tsuga seed FA compositions.* In addition to the species listed in Table 3, some authors [e.g., Farjon (25)] include *T. mertensiana* and its infraspecific taxa in the genus *Tsuga*, whereas other authors (1) consider it a distinct genus, *Hesperopeuce*. We have adopted the point of view that will be discussed next. Among the Abietoid genera studied here, the genus *Tsuga* is the closest to genera of the Pinoid group in its seed FA composition, with little in common with *Abies*, *Cedrus*, *Keteleeria*, or *Pseudolarix*. In a previous multicomponent analysis of conifer seed FA compositions (4), the two *Tsuga* species available at that time (as well as *P. menziesei*) were slightly set over in a bulky and stretched *Pinus* group, but were otherwise distinct from *Picea* and *Larix*. Since then, *Picea* and *Larix* spp. have been shown to constitute two clearly disjunct groups (3) with regard to their seed FA composition. *Tsuga* spp. have higher (ca. 50%) and lower (ca. 14%) average levels of linoleic and oleic acids, respectively, than most *Pinus*, *Larix*, and *Picea* species, but they are hardly distinguishable from *Pinus* spp. on the basis of their C<sub>18</sub>  $\Delta 5$ -UPIFA profiles. Within the genus, variations between species are of small amplitude, as is the case for *Picea* and *Larix* species.

**TABLE 2**  
**Fatty Acid Compositions (wt% of total fatty acids) of the Seed Lipids from *Abies* spp.**

Species <sup>a,b</sup>	16:0	16:1 <sup>c</sup>	aiso-17:0 <sup>d</sup>	18:0	9-18:1	11-18:1	9,12-18:2	9,12,15-18:3	X <sup>e</sup> (19:10)	20:0	11-20:1
1. <i>A. alba</i>	4.12	0.05	0.81	1.66	25.82	0.32	42.7	10.52	0.08	0.39	0.59
3. <i>A. balsamea</i> var. <i>balsamea</i>	3.15	0.05	0.57	1.53	20.93	0.41	45.83	0.43	0.14	0.49	0.78
6. <i>A. borisii-regis</i>	3.64	0.11	0.71	2.17	28.05	0.32	41.27	0.41	0.09	0.40	0.57
8. <i>A. cephalonica</i>	3.35	0.11	0.76	1.79	27.63	0.44	40.28	0.39	0.14	0.51	0.61
15. <i>A. concolor</i>	4.10	0.10	0.73	1.55	37.43	0.43	37.17	0.47	0.12	0.56	0.76
16. <i>A. concolor</i> ssp. <i>lowiana</i>	3.30	0.06	0.75	1.58	24.55	0.39	45.16	0.35	0.11	0.49	0.85
17. <i>A. delavayi</i> var. <i>delavayi</i>	4.47	0.16	0.90	2.33	28.23	0.57	42.02	0.57	0.13	0.67	0.73
35. <i>A. fraseri</i>	2.88	0.06	0.67	1.33	24.38	0.39	44.61	0.46	0.12	0.42	0.84
36. <i>A. grandis</i>	4.02	0.09	0.83	2.04	26.69	0.44	38.63	0.62	0.11	0.46	0.55
43. <i>A. homolepis</i> var. <i>homolepis</i>	3.24	0.06	0.76	1.86	25.07	0.35	44.68	0.34	0.08	0.72	0.98
46. <i>A. koreana</i>	3.54	0.08	0.75	1.91	24.88	0.45	44.54	0.48	0.14	0.44	0.53
48. <i>A. lasiocarpa</i> var. <i>lasiocarpa</i>	2.96	0.17	0.70	1.43	19.58	0.50	47.47	0.44	0.09	0.53	0.56
53. <i>A. nephrolepis</i>	3.14	0.06	0.60	1.55	24.13	0.33	44.78	0.35	0.10	0.57	0.84
54. <i>A. nordmanniana</i> ssp. <i>equi-trojani</i>	3.74	0.10	0.85	1.94	26.85	0.40	41.48	0.33	0.11	0.49	0.87
54. <i>A. bornmuelleriana</i>	3.60	0.08	0.71	1.91	29.07	0.40	39.95	0.34	0.10	0.40	0.57
55. <i>A. nordmanniana</i> ssp. <i>nordmanniana</i>	3.27	0.08	0.76	1.89	29.96	0.39	40.92	0.42	0.13	0.44	0.68
56. <i>A. numidica</i>	3.74	0.08	0.71	2.29	28.51	0.34	40.35	0.37	0.12	0.43	0.67
58. <i>A. pindrow</i> var. <i>pindrow</i>	3.27	0.10	0.69	1.54	30.12	0.44	40.74	0.42	0.13	0.55	0.93
60. <i>A. pinsapo</i> var. <i>pinsapo</i>	3.49	0.05	0.65	1.97	29.14	0.38	40.38	0.29	0.11	0.48	0.74
62. <i>A. procera</i>	3.51	0.09	0.87	1.99	35.14	0.55	39.63	0.56	0.08	0.60	0.51
75. <i>A. veitchii</i> var. <i>veitchii</i>	3.12	0.06	0.67	1.97	23.10	0.40	45.74	0.62	0.13	0.69	0.75

Species	11,14-20:2	22:0	5,9-18:2	5,9,12-18:3	5,9,12,15-18:4	5,11-20:2	5,11,14-20:3	7,11,14-20:3	ΣΔ5 <sup>f</sup>	Others <sup>g</sup>	Reference
1. <i>A. alba</i>	0.28	0.30	6.24	12.47	— <sup>h</sup>	0.24	0.24	0.10	21.09	1.22	18
3. <i>A. balsamea</i> var. <i>balsamea</i>	0.50	0.28	5.93	14.94	—	0.24	2.73	0.14	23.98	0.93	4
6. <i>A. borisii-regis</i>	0.26	0.37	6.65	12.25	—	0.28	1.94	0.06	21.18	0.45	This study
8. <i>A. cephalonica</i>	0.42	0.43	7.39	11.94	—	0.21	2.25	0.07	21.86	1.28	4
15. <i>A. concolor</i>	0.26	0.34	5.56	8.78	—	0.24	1.12	0.09	15.79	0.19	18
16. <i>A. concolor</i> ssp. <i>lowiana</i>	0.58	0.27	5.66	13.32	Trace <sup>i</sup>	0.20	1.87	0.07	21.12	0.44	18
17. <i>A. delavayi</i> var. <i>delavayi</i>	0.27	0.10	4.96	10.88	Trace	0.25	1.70	Trace	17.79	1.06	This study
35. <i>A. fraseri</i>	0.39	0.29	5.93	14.04	0.05	0.34	2.29	0.12	22.77	0.39	4
36. <i>A. grandis</i>	0.37	1.37	7.70	11.15	—	0.23	2.38	Trace	21.46	2.32	4
43. <i>A. homolepis</i> var. <i>homolepis</i>	0.61	0.13	5.39	12.20	—	0.18	2.38	0.11	20.26	0.86	This study
46. <i>A. koreana</i>	0.53	0.20	6.05	13.29	—	0.18	1.88	Trace	21.40	0.19	This study
48. <i>A. lasiocarpa</i> var. <i>lasiocarpa</i>	0.37	0.39	4.45	17.11	Trace	0.14	1.67	0.09	23.46	1.35	4
53. <i>A. nephrolepis</i>	0.50	0.23	6.55	14.21	Trace	0.24	1.75	Trace	22.75	0.07	This study
54. <i>A. nordmanniana</i> ssp. <i>equi-trojani</i>	0.45	0.40	7.02	12.01	Trace	0.25	2.23	0.09	21.63	0.39	4
54. <i>A. bornmuelleriana</i>	0.45	0.21	7.48	11.02	—	0.65	2.21	0.10	21.46	0.41	4
55. <i>A. nordmanniana</i> ssp. <i>nordmanniana</i>	0.40	0.28	6.60	11.27	0.03	0.24	1.95	0.09	20.18	0.20	4
56. <i>A. numidica</i>	0.49	0.26	6.98	11.48	0.05	0.27	2.58	0.10	21.39	0.18	This study
58. <i>A. pindrow</i> var. <i>pindrow</i>	0.60	0.60	5.68	10.97	Trace	0.28	2.52	0.04	19.49	0.38	This study
60. <i>A. pinsapo</i> var. <i>pinsapo</i>	0.37	0.32	8.20	10.39	—	0.40	2.29	0.08	21.36	0.27	4
62. <i>A. procera</i>	0.21	0.35	3.53	11.15	0.06	0.16	0.90	0.14	15.94	0.03	This study
75. <i>A. veitchii</i> var. <i>veitchii</i>	0.49	0.37	4.97	14.03	—	0.20	1.89	Trace	21.09	0.80	This study

<sup>a</sup>The numbers refer to species listed in Table 1.

<sup>b</sup>Some earlier chromatograms from our laboratory have been revised to take into account aiso-17:0, 11-18:1, 7,11,14-20:3 acids, and component X. Initial nomenclature (essentially that employed by tree-seed sellers) has been modified to fit recent recommendations by Farjon (25). *Abies bornmuelleriana* is retained here, although it is considered a synonym of *A. nordmanniana* ssp. *equi-trojani* by this author.

<sup>c</sup>Two isomers, 7- and 9-16:1 acids.

<sup>d</sup>14-Methylhexadecanoic acid, or anteiso-17:0.

<sup>e</sup>Unidentified component with an equivalent chain length of 19.10 on the DB-Wax column.

<sup>f</sup>Sum of Δ5-olefinic acids, including the 7,11,14-20:3 acid.

<sup>g</sup>Minor and/or unidentified fatty acids.

<sup>h</sup>Not detected or not reported.

<sup>i</sup>Trace amounts.

**Hesperopeuce seed FA composition.** The taxonomic ranking of *H. mertensiana* is rather controversial because it is sometimes considered a *Tsuga* species or even a hybrid (26). Some infrageneric taxa can be distinguished (not reported in

Table 4). A distinctive feature of *H. mertensiana* seed FA (Table 4) is the absence of α-linolenic acid, which otherwise represents 0.3–0.8% in *Tsuga* spp. Also, the proportions of linoleic and oleic acids are distinct: linoleic acid, 43.9 vs.

**TABLE 3**  
**List of *Tsuga*, *Hesperopeuce*, *Cedrus*, *Keteleeria*, and *Pseudolarix* spp. That Have (or Have Not Yet) Been Examined for Their Seed Fatty Acid Compositions**

Species <sup>a</sup>	Trivial name <sup>b</sup>	Reference
80. <i>T. canadensis</i>	Eastern hemlock, Hemlock spruce	18
81. <i>T. caroliniana</i>	Carolina hemlock	This study
82. <i>T. chinensis</i>	Taiwan hemlock	This study
83. <i>T. diversifolia</i>	Northern Japanese hemlock	—
84. <i>T. dumosa</i>	Himalayan hemlock	—
85. <i>T. heterophylla</i>	Western hemlock	12
86. <i>T. sieboldii</i>	Southern Japanese hemlock	—
87. <i>H. mertensiana</i>	Mountain hemlock	27
88. <i>C. atlantica</i>	Atlas cedar	18
89. <i>C. atlantica</i> var. <i>glauca</i>	Atlas cedar	12
90. <i>C. brevifolia</i>	<i>Cyprus cedar</i>	This study
91. <i>C. deodara</i>	Deodar, Himalayan cedar	12
92. <i>C. libani</i>	Lebanese cedar, Cedar of Lebanon	12
93. <i>K. davidiana</i>	—	This study
94. <i>K. evelyniana</i>	—	This study
95. <i>K. fortunei</i>	—	—
96. <i>P. amabilis</i>	Golden larch	27

<sup>a</sup>List established according to Farjon's *World Checklist and Bibliography of Conifers* (25).

<sup>b</sup>List mostly based on tree-seed sellers' catalogs. The website <http://www.geocities.com/RainForest/Canopy> was also consulted.

49.7–50.8%, and oleic acid, 23.3 vs. 13.0–14.8%, in *Hesperopeuce* and *Tsuga* spp., respectively (27).

**Cedrus seed FA compositions.** The genus *Cedrus* encompasses four species (all of which are presented in this study) that are closely allied (28) and a few varieties (Table 3). In contrast to *Abies* spp., the principal unsaturated FA in *Cedrus* spp. seeds is oleic acid (41–45%), with linoleic acid representing only 23–30% (Table 4). As in *Abies*, anteiso-17:0 acid is relatively high, between 0.4 and 1%. Despite the considerable differences in the amounts of their precursors, oleic and linoleic acids, taxoleic and pinolenic acids have a distribution profile similar to that in *Abies* spp. (4.6–7.7 and 9.6–10.9%, respectively). On the other hand, the C<sub>20</sub> Δ5-UIFA are less abundant in *Cedrus* than in *Abies* seeds. In this regard, it is worth noting the particular abundance of dihomopinolenic (7,11,14–20:3) acid, the elongation metabolite of pinolenic acid; there is about twice as much in *Cedrus* than in *Abies* spp. Incidentally, the same Δ5-UIFA were present in the pollen grain lipids collected from *C. atlantica* (Wolff, R.L., unpublished observations).

**Keteleeria seed FA composition.** The genus *Keteleeria* was revised recently (29) and was shown to contain three species only (Table 3). An interesting point is the pink color of the washing upper phase during the Folch *et al.* (30) purification of lipids. Among all other Pinaceae, this was observed only for *Abies* seeds. However, no further studies of the pigment(s) were made. The prominence of oleic acid over linoleic acid is exacerbated in *Keteleeria* (Table 4), where the former acid reaches 55% but the latter acid represents only 22% of total FA. This apparently results in a higher level of taxoleic acid as compared to pinolenic acid, although both acids, in particular the latter one, are comparatively low. Also, oleic acid seems to be particularly intensively elongated and further Δ5-desaturated if one considers the exceptionally high levels of 11-20:1

(3.1%) and 5,11-20:2 (1.8%) that are reached in no other Pinaceae species. As the latter acid has no trivial name, we suggest naming it “keteleeronic” acid. The overall content of Δ5-UIFA is the lowest (*ca.* 10%) inside the Abietoid group.

In brief, considering their seed FA compositions, *Abies*, *Cedrus*, and *Keteleeria*, are justifiably grouped in the Abietoid subfamily, whereas *Tsuga* would fit the overall seed FA pattern of the Pinoid group.

**Pseudolarix seed FA composition.** *Pseudolarix* is a monospecific genus with *P. amabilis* as a single species. The main feature of its seed FA is the presence of high contents of α-linolenic and coniferonic acids, 5.2 and 1.8%, respectively (Table 4). No Pinaceae seeds analyzed thus far showed such high quantities, although some Cupressaceae species might present higher levels of coniferonic acid (4). Also, taxoleic and pinolenic acids are present in approximately equal amounts, about 7.5%, which is encountered in Pinaceae only in *C. libani* (*ca.* 10% for both C<sub>18</sub> Δ5-UIFA).

**Multicomponent analysis.** A principal component analysis was processed for species listed in Tables 2 and 4. Minor components, such as 17:0 acid, were not included in that study. In addition, the mean compositions of seed FA from *Larix* and *Picea* spp. established in a previous study (3) were included in the statistical analysis. Figure 1 shows the first two component axes, which explain 32 and 19% of the total inertia. On this plot, the different genera are quite well separated. *Abies* spp. are scattered around the mean (gravity center) at the center of the plot.

On axis 1 (horizontal), 9,12-18:2 and 5,9,12-18:3 acids can be identified as representative of *Tsuga*, *Hesperopeuce*, *Picea*, and *Larix* spp. Axis 2 (vertical) allows differentiation between these genera: 11,14-20:2 and 5,11,14-20:3 acids can particularly be associated with *Tsuga* spp. In contrast, 11-18:1 is representative of *Picea* and *Larix* spp. *Pseudolarix* and

**TABLE 4**  
**Fatty Acid Compositions (wt% of total fatty acids) of the Seed Lipids from *Tsuga*, *Hesperopeuce*, *Cedrus*, *Keteleeria*, and *Pseudolarix* spp.**

Species <sup>a,b</sup>	16:0	16:1 <sup>c</sup>	aiso-17:0 <sup>d</sup>	18:0	9-18:1	11-18:1	9,12-18:2	9,12,15-18:3	20:0	11-20:1
80. <i>T. canadensis</i>	3.46	0.06	0.52	1.73	14.72	0.31	49.96	0.34	0.42	0.77
81. <i>T. caroliniana</i>	4.80	0.08	0.25	2.07	14.08	0.38	50.74	0.46	0.38	0.56
82. <i>T. chinensis</i>	4.75	0.11	0.25	2.27	14.76	0.50	50.53	0.51	0.42	0.49
85. <i>T. heterophylla</i>	3.10	0.05	0.57	1.99	13.00	0.28	50.83	0.82	0.32	0.53
87. <i>H. mertensiana</i>	3.63	0.11	0.51	1.53	23.27	0.57	43.92	— <sup>e</sup>	0.35	0.45
88. <i>C. atlantica</i>	5.20	0.16	0.98	2.86	41.47	0.43	28.90	0.42	1.06	0.67
89. <i>C. atlantica</i> var. <i>glauca</i>	4.85	0.15	0.76	3.51	41.43	0.40	26.84	0.14	1.08	0.70
90. <i>C. brevifolia</i>	4.74	0.37	0.71	2.64	43.32	0.98	25.49	0.10	0.73	0.62
91. <i>C. deodara</i>	3.99	0.15	0.42	1.70	44.02	0.92	30.01	0.18	0.54	1.11
92. <i>C. libani</i>	4.31	0.13	0.51	2.21	45.41	0.77	23.36	0.11	0.69	0.68
93. <i>K. davidiana</i>	4.15	0.19	0.07	2.71	55.16	0.17	22.23	0.19	0.78	3.06
94. <i>K. evelyniana</i>	4.70	0.04	Trace <sup>f</sup>	2.30	55.20	0.21	24.08	0.20	0.54	2.57
96. <i>P. amabilis</i>	4.00	0.29	0.37	2.42	26.50	0.24	35.55	5.18	0.51	1.61

Species	11,14-20:2	22:0	5,9-18:2	5,9,12-18:3	5,9,12,15-18:4	5,11-20:2	5,11,14-20:3	7,11,14-20:3	ΣΔ5 <sup>g</sup>	Others <sup>h</sup>
80. <i>T. canadensis</i>	0.94	0.25	2.62	19.53	— <sup>g</sup>	0.12	3.74	0.41	26.42	0.10
81. <i>T. caroliniana</i>	0.72	0.11	1.88	19.44	Trace <sup>h</sup>	0.69	2.65	0.27	24.93	0.44
82. <i>T. chinensis</i>	0.85	0.16	1.85	18.67	0.05	0.07	2.80	0.30	23.77	0.66
85. <i>T. heterophylla</i>	0.68	0.17	1.48	24.11	0.09	0.07	1.26	0.13	27.14	0.52
87. <i>H. mertensiana</i>	0.55	—	2.24	19.40	—	0.07	1.31	0.27	23.29	1.77
88. <i>C. atlantica</i>	0.36	0.38	5.57	10.49	—	0.14	0.69	0.24	17.13	—
89. <i>C. atlantica</i> var. <i>glauca</i>	0.33	0.31	7.32	9.94	—	0.13	0.48	0.20	18.07	1.43
90. <i>C. brevifolia</i>	0.31	Trace	7.73	10.93	—	Trace	0.55	0.35	19.56	0.43
91. <i>C. deodara</i>	0.49	Trace	4.60	9.61	—	0.11	0.93	0.16	15.41	1.06
92. <i>C. libani</i>	0.24	0.25	9.45	10.50	—	0.17	0.60	0.15	20.87	0.46
93. <i>K. davidiana</i>	0.36	0.51	3.45	1.43	—	1.83	3.23	0.05	9.99	0.43
94. <i>K. evelyniana</i>	0.32	Trace	3.55	1.59	—	1.61	2.53	Trace	9.28	0.56
96. <i>P. amabilis</i>	0.52	—	7.75	7.35	1.78	1.19	3.57	0.12	21.76	0.94

<sup>a</sup>The numbers refer to species listed in Table 3.

<sup>b</sup>Some earlier chromatograms from our laboratory have been revised to take into account aiso-17:0, 11-18:1, and 7,11,14-20:3 acids.

<sup>c</sup>Two isomers, 7- and 9-16:1 acids.

<sup>d</sup>14-Methylhexadecanoic acid, or anteiso-17:0.

<sup>e</sup>Not detected or not reported.

<sup>f</sup>Trace amounts.

<sup>g</sup>Sum of Δ5-olefinic acids, including the 7,11,14-20:3 acid.

<sup>h</sup>Minor and/or unidentified fatty acids.

*Keteleeria* spp. do not seem very different one from another. Three FA are more particularly representative of these genera: 5,11-20:2, 11-20:2, and 5,11,14-20:3 acids. *Pseudolarix* is also characterized by 16:1 and 9,12,15-18:3 acids and *Keteleeria* by 9-18:1 acid (in fact, this does not appear clearly on the first two axes). As for *Pseudolarix* and *Keteleeria* spp., *Cedrus* spp. is located on the positive direction of axis 1. Differences appear on axis 2: *Cedrus* spp. is associated with eight FA, namely 16:1, 16:0, anteiso-17:0, 18:0, 11-18:1, 9-18:1, 5,9-18:2, and 20:0 acids, which are essentially saturated and monoenoic FA.

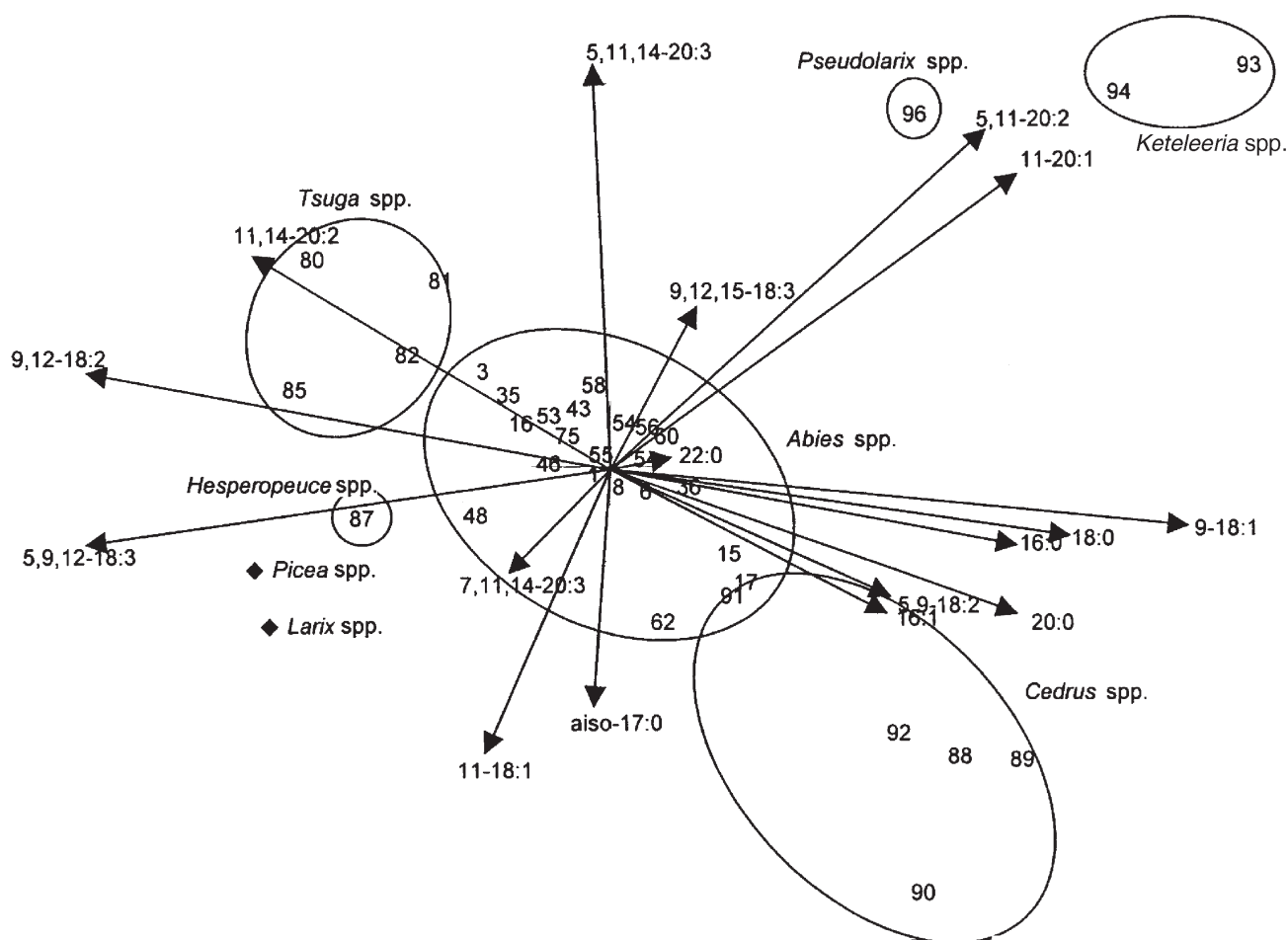
The dendrogram in Figure 2 confirms the principal component analysis results. In particular, the importance of interspecific variability is clearly demonstrated. It is worthwhile to note the closeness between some genera. On the one hand, *Larix*, *Picea*, and *Hesperopeuce* lie in close proximity, whereas *Tsuga* spp. are only slightly dissimilar. On the other hand, *Keteleeria* spp. and *Pseudolarix* lie close to one another. The latter two genera are thus grouped together with

*Cedrus*. The intraspecific dissimilarities among *Abies* spp. are of small amplitude, as observed above.

As a first observation, it can be inferred from our data that all genera of the Pinaceae family are united by the same qualitative seed FA chromatographic profiles, including Δ5-UPIFA. However, on a quantitative basis, many differences allow distinctions between the different genera.

*Pinus* is the Pinaceae genus that presents the greatest number of species, and is also generally recognized as the most heteromorphic genus when considering botanical criteria. This also holds for *Pinus* spp. seed FA compositions, particularly when considering Δ5-UPIFA. Their sum varies from less than 0.6% (*P. monophylla*, subsection *Cembroides*) to 30% (*P. sylvestris*, subsection *Sylvestres*). Taxoleic acid always represents less than 4.5% of total FA in *Pinus* spp. seeds. In *Abies* spp., as well as in *Cedrus* spp. and *P. amabilis*, the corresponding value is practically systematically higher than 4.5%. *Tsuga* spp. and *Keteleeria* spp., on the other hand, present values similar to those found in *Pinus* spp. The highest values of tax-





**FIG. 1.** First two components of the principal component analysis based on data for Abietoid seed fatty acids summarized in Tables 2 and 4. Also plotted are the gravity centers of *Picea* and *Larix* spp. from a previous study (Ref. 3).

oleic acid presented by *Picea* and *Larix* spp. seeds also are lower than 4.6%. Thus, with regard to the percentage of taxoleic acid, *Pinus*, *Larix*, *Picea* spp., and *Pseudotsuga menziesii* (Pinoids) are united by levels less than 4.6%, a situation shared by *Tsuga* spp. and *Keteleeria* spp. (Abietoids).

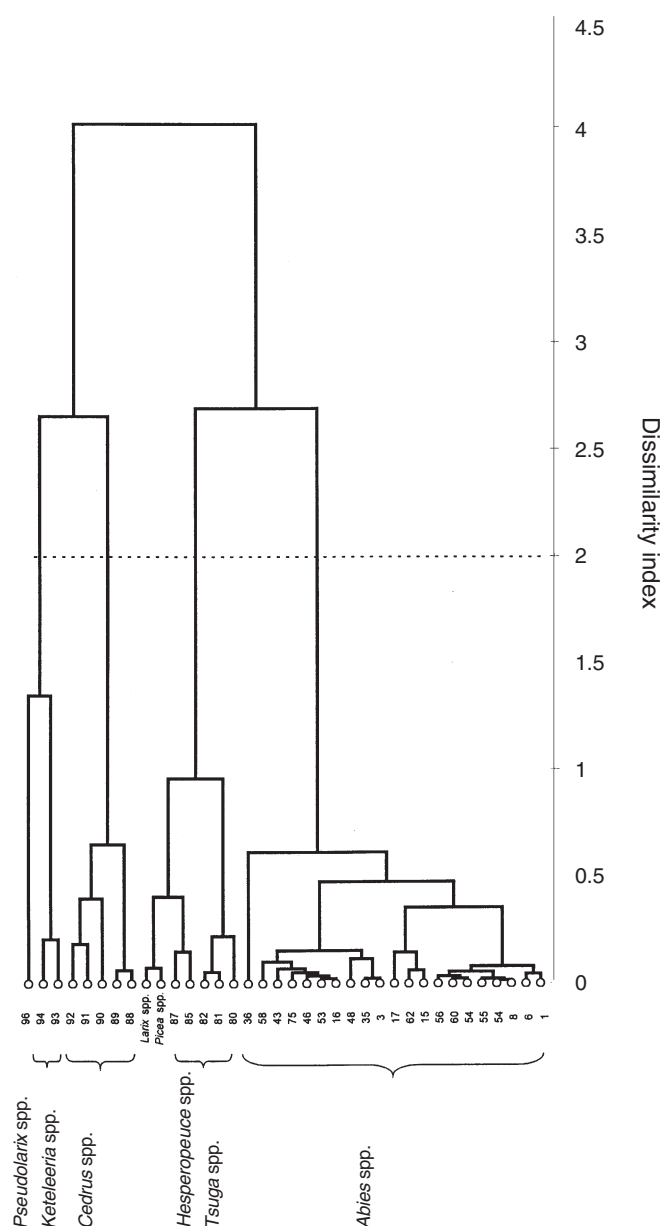
If one considers pinolenic acid, *Pinus* spp. are heterogeneous and present seed FA containing a maximum of 25.3% (*P. strobus*), with the bulk of species between 14 and 23%. This is most often less than values determined for *Larix* and *Picea* spp. but similar to those found in *Tsuga* spp.

As emphasized elsewhere (3), *Picea* and *Larix* spp. display seed FA compositions that vary little from one species to another in a given genus. This apparently also holds for *Tsuga* and *Keteleeria* spp. This adds to the general recognition that all of these genera are natural groups. A particular point is that the ratio of pinolenic/taxoleic acids in Pinoids (and in *Tsuga* spp.) is always higher than that in Abietoids (results not shown). This tendency culminates in *C. libani* and in *P. amabilis*, where the ratio approaches 1.

Among botanical criteria distinguishing Pinoids from Abietoids is the presence of resin vesicles in the coat of seeds from species of the latter group but not the former one. Resin

components are extracted by the solvents used in our studies and appear as a dense region of peaks preceding palmitic acid methyl ester during GLC. This occurs when analyzing seed FA methyl esters prepared from *Abies*, *Cedrus*, and *Keteleeria* spp. seeds but not from *Tsuga* spp. seeds. Indeed, resin vesicles in the seeds from the latter genus are reported to be very small and to contain little resin.

Price *et al.* (8), Prager *et al.* (31), and Frankis (9) have constructed possible phylogenetic sequences based either on immunological characteristics and distances (8,31) or on selected botanical features (9) that are rather similar in that they both distinguish two groups more or less corresponding to Pinoids and Abietoids. However, they differ in some details. Our studies (2,3, present study) agree with such a division, with some peculiarities of *Tsuga* spp. and *H. mertensiana* seed FA that resemble Pinoids and share little in common with other Abietoids. There are two possibilities: (i) the similarity of *Tsuga* spp. and *H. mertensiana* with Pinoids is due to evolutionary convergence or (ii) *H. mertensiana* is derived through the intergeneric hybridization of *Tsuga* × *Picea* (26). Regarding the second hypothesis, *Tsuga* would in some manner be a relative to *Picea*, which would indicate a relationship between *Tsuga*



**FIG. 2.** Intra- and intergeneric dissimilarities computed from Abietoid seed fatty acid compositions summarized in Tables 3 and 4. Also plotted are the gravity centers of *Picea* and *Larix* spp. from a previous study (Ref. 3).

and *Picea* with Pinoids. To take this possibility into account, we suggest a new group, Tsugoids, encompassing *Tsuga* spp. and *H. mertensiana*, which would be between Pinoids and Abietoids.

## REFERENCES

- Page, C.N. (1990) Gymnosperms: Coniferophytina (Conifers and Ginkgoids), in *The Families and Genera of Vascular Plants* (Kubitski, K., ed.), Vol. 1, *Pteridophytes and Gymnosperms* (Kramer, K.U., and Green, P.S., eds.), pp. 319–329, Springer-Verlag, Berlin.
- Wolff, R.L., Pédrone, F., Pasquier, E., and Marpeau, A.M. (2000) General Characteristics of *Pinus* spp. Seed Fatty Acid Compositions, and Importance of  $\Delta 5$ -Olefinic Acids in the Phylogeny and Taxonomy of the Genus, *Lipids* 35, 1–22.
- Wolff, R.L., Lavialle, O., Pédrone, F., Pasquier, E., Deluc, L.G., Marpeau, A.M., and Aitzetmüller, K. (2001) Fatty Acid Compositions of Pinaceae as Taxonomic Markers, *Lipids* 36, 439–451.
- Wolff, R.L., Deluc, L.G., Marpeau, A.M., and Comps, B. (1997) Chemotaxonomic Differentiation of Conifer Families and Genera Based on the Seed Oil Fatty Acids Compositions: Multivariate Analyses, *Trees* 12, 57–65.
- Wolff, R.L., Comps, B., Deluc, L.G., and Marpeau, A.M. (1997) Fatty Acids of the Seeds from Pine Species of the *Ponderosa-Banksiana* and *Halepensis* Sections. The Peculiar Taxonomic Position of *Pinus pinaster*, *J. Am. Oil Chem. Soc.* 74, 45–50.
- Wolff, R.L., Comps, B., Marpeau, A.M., and Deluc, L.G. (1997) Taxonomy of *Pinus* Species Based on the Seed Oil Fatty Acid Compositions, *Trees* 12, 113–118.
- Wolff, R.L. (1998) Clarification on the Taxonomic Position of *Sciadopitys verticillata* Among Coniferophytes Based on Seed Oil Fatty Acid Compositions, *J. Am. Oil Chem. Soc.* 75, 757–758.
- Price, R.A., Olsen-Stojkovich, J., and Lowenstein, J.M. (1987) Relationships Among the Genera of Pinaceae: An Immunological Comparison, *Syst. Bot.* 12, 91–97.
- Frankis, M.P. (1988) Generic Inter-relationships in Pinaceae, *Notes RBG Edinb.* 45, 527–548.
- Li, L.C. (1995) Studies on the Karyotype and Phylogeny of the Pinaceae, *Acta Phytotax. Sin. (Zhiwu Fenlei Xuebao)* 33, 417–432 (in Chinese; summary in English and descriptions in Latin).
- Wolff, R.L., Christie, W.W., Pédrone, F., Marpeau, A.M., Tsevegsüren, N., Aitzetmüller, K., and Gunstone, F.D. (1999)  $\Delta 5$ -Olefinic Acids in the Seed Lipids from Four *Ephedra* Species and Their Distribution Between the  $\alpha$  and  $\beta$  Positions of Triacylglycerols. Characteristics Common to Coniferophytes and Cycadophytes, *Lipids* 34, 855–864.
- Wolff, R.L. (1999) The Phylogenetic Significance of Sciadonic (all-*cis* 5,11,14-20:3) Acid in Gymnosperms and Its Quantitative Significance in Land Plants, *J. Am. Oil Chem. Soc.* 76, 1515–1516.
- Ekman, R. (1980) New Polyenoic Fatty Acids in Norway Spruce Wood, *Phytochemistry* 19, 147–148.
- Jamieson, G.R., and Reid, E.H. (1972) The Leaf Lipids of Some Conifer Species, *Phytochemistry* 11, 269–275.
- Berdeaux, O., and Wolff, R.L. (1996) Gas-Liquid Chromatography-Mass Spectrometry of the 4,4-Dimethylloxazoline Derivatives of  $\Delta 5$ -Unsaturated Polymethylene-Interrupted Fatty Acid from Conifer Seed Oils, *J. Am. Oil Chem. Soc.* 73, 1323–1326.
- Wolff, R.L. (1998) A Practical Source of  $\Delta 5$ -Olefinic Acids for Identification Purposes, *J. Am. Oil Chem. Soc.* 75, 891–892.
- Tsevegsüren, N., and Aitzetmüller, K. (1997) Unusual  $\Delta 5$ *cis*-FA in Seed Oils of *Cimicifuga* Species, *J. High Resolut. Chromatogr.* 20, 237–241.
- Wolff, R.L., Deluc, L.G., and Marpeau, A.M. (1996) Conifer Seeds: Oil Content and Fatty Acid Distribution, *J. Am. Oil Chem. Soc.* 73, 765–771.
- Kovac, M., and Vardjan, M. (1981) Metabolism of Lipids in Fir Seeds (*Abies alba* Mill.), *Acta Bot. Croat.* 40, 95–109.
- Rutar, V., Kovac, M., and Lahajna, V. (1989) Nondestructive Study of Liquids in Single Fir Seeds Using Nuclear Magnetic Resonance and Magic Angle Sample Spinning, *J. Am. Oil Chem. Soc.* 66, 961–965.
- Takagi, T., and Itabashi, Y. (1982) *cis*-5 Olefinic Unusual Fatty Acid in Seed Lipids of Gymnospermae and Their Distribution in Triacylglycerols, *Lipids* 17, 716–723.
- Farjon, A., and Rushforth, K.D. (1989) A Classification of *Abies* Miller (Pinaceae), *Notes RBG Edinb.* 46, 59–79.
- Debazac, E.B. (1964) *Manuel des Conifères*, Ecole Nationale des Eaux et Forêts, Nancy, pp. 49–78 (in French).

24. Wolff, R.L., Pédrone, F., Marpeau, A.M., Christie, W.W., and Gunstone, F.D. (1998) The Seed Fatty Acid Composition and the Distribution of  $\Delta 5$ -Olefinic Acids in the Triacylglycerols of Some Taxaceae (*Taxus* and *Torreya*), *J. Am. Oil Chem. Soc.* 75, 1637–1641.
25. Farjon, A. (1998) *World Checklist and Bibliography of Conifers*, pp.137–237, The Royal Botanic Gardens, Kew, United Kingdom.
26. Taylor, R.J. (1972) The Relationship and Origin of *Tsuga heterophylla* and *Tsuga mertensiana* Based on Phytochemical and Morphological Interpretations, *Am. J. Bot.* 59, 149–157.
27. Wolff, R.L., Destailats, F., and Angers, P. (2001)  $\alpha$ -Linolenic Acid and Its  $\Delta 5$ -Desaturation Product, Coniferonic Acid, in the Seeds of *Tsuga* and *Hesperopeuce* as a Taxonomic Means to Differentiate the Two Genera, *Lipids* 36, 211–212.
28. Farjon, A. (1990) Pinaceae: Drawings and Descriptions of the Genera *Abies*, *Cedrus*, *Pseudolarix*, *Keteleeria*, *Nothotsuga*, *Tsuga*, *Cathaya*, *Pseudotsuga*, *Larix* and *Picea*, *Regnum Veg.* 121, 111–121.
29. Farjon, A. (1989) A Second Revision of the *Keteleeria* Carrière (Taxonomic Notes on Pinaceae II), *Notes RBG Edinb.* 46, 81–99.
30. Folch, J., Lees, M., and Sloane-Stanley, G.H. (1957) A Simple Method for the Isolation and Purification of Total Lipides [sic] from Animal Tissues, *J. Biol. Chem.* 226, 497–509.
31. Prager, E.M., Fowler, D.P., and Wilson, A.C. (1976) Rates of Evolution in Conifers (Pinaceae), *Evolution* 30, 637–649.

[Received October 1, 2001; in revised form and accepted November 23, 2001]

# Assessment of Dietary and Genetic Factors Influencing Serum and Adipose Fatty Acid Composition in Obese Female Identical Twins

Marie Kunešová<sup>a,\*</sup>, Vojtěch Hainer<sup>a</sup>, Eva Tvrzická<sup>b</sup>, Stephen D. Phinney<sup>c</sup>,  
Vladimír Štich<sup>d</sup>, Jana Pařízková<sup>a</sup>, Aleš Žák<sup>b</sup>, and Albert J. Stunkard<sup>e</sup>

<sup>a</sup>Obesity Management Centre, Third Medical Department, First Medical School, Charles University, Prague, Czech Republic,

<sup>b</sup>Fourth Medical Department, Charles University, Prague, <sup>c</sup>Galileo Laboratories, Santa Clara, California 95054,

<sup>d</sup>Third Medical School, Charles University, Prague, Czech Republic, and <sup>e</sup>Department of Psychiatry, University of Pennsylvania, Philadelphia, Pennsylvania 19104

**ABSTRACT:** Fourteen pairs of obese female monozygotic twins were recruited for a study of genetic influences on serum and adipose fatty acid (FA) composition. Following 1 wk of inpatient stabilization, fasting serum and adipose tissue obtained by surgical excision were analyzed by thin-layer and gas chromatography. Intrapair resemblances (IPR) for individual FA were assessed by Spearman rank correlation and by analysis of variance and were found in serum cholesteryl esters (CE), triglycerides (TG), and adipose TG. With two exceptions (CE linoleate and adipose eicosapentaenoate), these IPR were limited to the nonessential FA. Palmitate had significant IPR in four lipid fractions; in serum CE and adipose TG palmitate was strongly correlated with multiple measures of adiposity. In contrast to other lipid fractions, serum phosphatidylcholine (PC) FA had 12 IPR, of which 6 were essential FA including arachidonate ( $r = 0.76$ ,  $P < 0.0005$ ), eicosapentaenoate ( $r = 0.78$ ,  $P < 0.0005$ ), and docosahexaenoate ( $r = 0.86$ ,  $P < 0.0001$ ). The PC IPR could not be explained by analysis of preadmission 7-d food records. After dividing the pairs into two groups differing and nondiffering according to fat intake of individuals in the pair, there was no evidence of a gene–environment interaction between fat intake and FA composition. The IPR for nonessential FA indicate that there is active genetic control of either food choices or postabsorptive metabolic processing. The high level of IPR in the PC fraction in contrast to the other lipid fractions suggests strong genetic influence over selection of specific FA for this membrane fraction independent of diet.

Paper no. L8727 in *Lipids* 37, 27–32 (January 2002).

Beyond their function as energy substrates in the nonesterified form and as energy reserves in triglycerides (TG), individual fatty acid (FA) species possess a range of metabolically important properties. Chain length and degree of unsaturation affect the physical properties of membrane phospholipids and TG, and some members of the essential n-6 and n-3 families provide substrates for eicosanoids. In addition, enzymes involved in FA metabolism have demonstrated selectivity for specific FA. An example of this is hormone-sensitive lipase in rat adipocytes. This enzyme has been shown *in vitro* (1) and *in vivo* (2) to be

\*To whom correspondence should be addressed at Obesity Management Centre, Third Medical Department, First Medical School, Charles University, U nemocnice 1, 128 08 Prague, Czech Republic.  
E-mail: marie.kunesova@lfl.cuni.cz

Abbreviations: AT, adipose tissue; CE, cholesteryl esters; FA, fatty acid(s); FAME, fatty acid methyl esters; GC, gas chromatography; IPR, intra-pair resemblance; PC, phosphatidylcholine; TG, triglycerides.

selective for release of specific FA based on their chain length, number of double bonds, and position of double bonds. This selectivity has been demonstrated in obese humans undergoing weight loss as indicated by a disproportionate decrease in  $\alpha$ -linolenate (18:3n-3) from adipose reserves (3–5). This selectivity allows specific tissue lipid fractions to maintain FA compositions that differ from those of the diet and from one another. In addition to selective release, these tissue differences could also result from selective uptake of individual fatty acids into adipose tissue (6). This effect could be achieved at any one of multiple steps in the digestion, absorption, hepatic processing, and endothelial release where interindividual variation in the processing of specific fatty acids could occur.

A number of important physiological functions are affected by the FA composition of tissue lipids, particularly the phospholipids in membranes. Odin *et al.* (7) reported variations in the rate of hepatocyte lipogenesis by varying the composition of the cell membranes in tissue culture, and Clarke and Jump (8) subsequently demonstrated that dietary fat composition directly affects FA synthase gene expression. Pelikánová *et al.* (9) and Borkman *et al.* (10) noted that variations in insulin sensitivity correlate with serum and muscle phospholipid arachidonate (20:4n-6). In addition, a relationship was found between the FA composition of child's muscle and maternal serum insulin concentration (11). These influences of phospholipid FA composition on metabolic pathways of fuel trafficking raise the potential for FA such as arachidonic acid to participate actively in the regulation of energy balance.

Genetically obese animals have been reported to have distortions in hepatic phospholipid arachidonate distribution relative to the lean genotype. The Zucker rat has reduced phospholipid arachidonate but increased cholesteryl ester compared to the lean genotype (12–14), and in the BSB mouse arachidonate is maldistributed into cholesteryl esters (15). While it is not clear if these alterations in 20:4n-6 distribution are a direct result of single or multiple genes causing their obesity, enhancing endogenous arachidonic acid production in the obese Zucker rat reduces food intake and weight gain (14,16). It remains to be determined specifically how increasing arachidonate production affects appetite in the Zucker rat or if altered arachidonate metabolism is either an important pathogenic factor or mediator in human obesity.



Studies of phenotypic variation within and between monozygotic human twins provide a powerful tool to assess genetically mediated traits (17–19). Previous human twin studies involving FA analysis have revealed intra-pair similarities in twins with schizophrenia (20) and in the branched-chain FA content of ear cerumen (21), but there have been no studies of twins selected for the phenotypic trait of obesity. To determine if genetic variation is associated with alterations in FA distribution in obese humans, we have undertaken a study of adult monozygotic twins, examining serum lipid fractions and adipose FA for variations due to diet, obesity, and genetic factors.

## MATERIALS AND METHODS

**Subjects.** Fourteen pairs of obese monozygotic premenopausal females aged  $39 \pm 1.7$  yr (mean  $\pm$  standard error, range 23–50), mean body mass index  $34.22 \pm 1.46$  kg/m<sup>2</sup> (range 24.84–59.47) were recruited for the study through the media and gave their written informed consent to participate in this study. The study was approved by the Charles University Medical Ethics Committee.

The monozygosity of the twins was established on the basis of their physical appearance, the loci of human leukocyte antigen system, and DNA of the apo B gene. The initial physician evaluation included medical history and physical examination. None of the subjects had a history of recent illness or severe cardiovascular or metabolic disease. Two pairs of twins were light smokers. None of the subjects had recently been on a diet or involved in a weight reduction regimen, and their body weight had been stable during the 6 mo prior to recruitment. Each pair had been reared together; however, with the exception of the youngest pair, they had been living apart for at least 10 yr at the time of recruitment. The initial 12 pairs were enrolled over a 15-wk period, and 2 pairs were enrolled in the following year. As part of a long-term study, four sets of twins at a time were admitted for a 1-wk inpatient baseline evaluation period in the Obesity Unit in the Fourth Department of Medicine, Charles University in Prague.

**Body composition and regional tissue distribution.** Body density was determined by the hydrostatic weighing technique, and percentage of body fat was estimated from body density by the method described by Pařízková (22) using the equation of Brozek (23). Pulmonary residual volume was determined using the helium dilution method (24). Fat mass was obtained by multiplying percentage of body fat by body weight. Anthropometric estimation of body fat was performed by measurement of 10 skinfolds according to Pařízková (22) and of 4 skinfolds according to Durnin (25). Waist and hip circumferences and sagittal abdominal diameter at the level L4/5 were measured following the standardized procedure recommended at the Airlie Conference (26).

**General test period.** After recruitment for the study but prior to the inpatient protocol, the subjects were instructed by the dietitian to record their food consumption for 7 d. These food records were evaluated by the Czech PC program

Výziva (KTS, Prague, Czech Republic), which includes more than 2000 items and evaluates 14 nutrients, minerals, and vitamins. During the 1-wk inpatient evaluation, the patients ate a diet prepared in the hospital kitchen providing daily energy intake calculated to achieve weight stability for each individual. Fat amount and compositions of the diet did not change in comparison with their previous diet. As a result, each subject's weight remained stable during this inpatient phase, and at the end of this week fasting blood was drawn for lipid fraction FA analysis. The same day AT was obtained by making a small surgical incision after lidocaine anesthesia on the abdomen about 20 mm to the left of the umbilicus, removing 300 mg of fat tissue.

**FA composition measurement.** Methanol, chloroform, dichloromethane, *n*-hexane, and *n*-heptane (analytical grade) were purchased from Lachema (Neratovice, Czech Republic), distilled before use, and checked by gas chromatography (GC). Acetic acid, sodium sulfate, sodium carbonate, and sulfuric acid were purchased from Lachema (Brno, Czech Republic). Standards of fatty acid methyl esters (FAME) were purchased from Sigma (St. Louis, MO). As a source for distilled water, Valvert drinking water (Etalle, Belgium) was used and checked as a blank sample by GC before use.

**Sample preparation.** Total lipid was extracted from 1 mL of serum and approximately 5 mg of AT by the method of Folch *et al.* (27) using dichloromethane instead of chloroform (28). Individual lipid classes—CE, TG, and phosphatidylcholine (PC)—were separated by thin-layer chromatography on silica gel with the mobile phase heptane/diethyl ether/acetic acid (80:20:3, by vol) being used for the separation of CE and TG and chloroform/methanol/water (60:30:5, by vol) for the separation of PC.

Separated CE (without isolation from the layer material) were saponified 20 h at 30°C with 2 M potassium hydroxide/methanol in darkness under nitrogen atmosphere. After cooling, samples were acidified with 2 M sulfuric acid, and lipid components (FA and sterols) were extracted twice with 2 mL of hexane and stepwise dried using a short column (20  $\times$  8 mm) of freshly activated sodium sulfate (45 min at 120°C). Combined hexane fractions were evaporated under nitrogen at 50°C. FA were separated by thin-layer chromatography on silica gel with the mobile phase heptane/diethyl ether/acetic acid (80:20:3, by vol).

**Preparation of FAME.** Isolated TG and PC were trans-methylated without previous separation from the layer material with 1 M sodium methoxide in methanol (60 min at laboratory temperature in darkness under nitrogen). Reaction mixture was neutralized by 0.5 N acetic acid. Methyl esters were extracted twice into hexane, dried by anhydrous sodium sulfate, and evaporated under nitrogen at 40°C. Samples were stored at –20°C before GC analysis. Separated FA from CE were esterified with methanol/5% sulfuric acid without previous isolation from the layer material (60 min at laboratory temperature in darkness under nitrogen). Reaction mixture was neutralized by 10% solution of sodium carbonate. Methyl esters were extracted twice into hexane, dried by anhydrous

**TABLE 1**  
**Characteristics of the Group**

	Mean	Standard error	Range
Age (yr)	39.0	1.7	23–50
Body weight (kg)	93.9	4.0	66.4–159.95
BMI (kg/m <sup>2</sup> ) <sup>a</sup>	34.22	1.46	24.84–59.47
Fat mass (kg)	44.28	3.07	21.8–96.41

<sup>a</sup>BMI, body mass index.**TABLE 2**  
**Food Composition in Free Living Conditions**

	Mean	r <sup>b</sup>
Energy (kJ)	8521 ± 590	0.64
Protein (g)	68.2 ± 5.0	0.47
Animal protein (g)	35.0 ± 2.6	-0.11
Plant protein (g)	33.2 ± 3.8	0.42
Fat (g)	80.9 ± 6.3	0.60*
Carbohydrates (g)	262.7 ± 18.7	0.60*
Linoleic acid (g)	7.29 ± 0.66	0.66*
Cholesterol (mg)	344 ± 20	0.07
Dietary fiber (g)	8.49 ± 1.30	0.24
C vitamin (mg)	43.33 ± 4.05	0.16

<sup>a</sup>Values are expressed as mean ± standard error.<sup>b</sup>r, intra-pair Spearman correlation coefficient. \*P < 0.05.

sodium sulfate, and evaporated under nitrogen at 40°C. Samples were stored at -20°C before GC analysis.

**GC of FAME.** GC was performed with a Model 9000 gas chromatograph (Chrompack, Middelburg, The Netherlands) equipped with a capillary split/splitless injector and flame-ionization detector. The chromatograph was interfaced with an IBMPS/2 Model 30 computer and Epson LQ 550 printer (Seico Epson Corp., Japan). Chrompack integration software was used for data acquisition and handling.

Determinations of FAME were performed on a fused-silica capillary column (25 m × 0.25 mm i.d.) coated with chemically bonded CP-WAX 52 CB stationary phase (Chrompack). The

oven temperature was programmed from 150 to 230°C at 2°C/min and then kept isothermal for 10 min. The injector and detector temperatures were 250°C. The carrier gas (hydrogen) was maintained at a head pressure of 80 kPa, with a splitting ratio of 1:20.

**Statistical methods.** The data were analyzed by Spearman rank correlation. For similarity within twin pairs analysis of variance (ANOVA) was used. The intraclass correlation coefficient was computed from the between-pairs and the within-pairs least squares. Twin pairs concordant and discordant for dietary fat content were compared for intrapair differences in FA composition in individual lipid classes using ANOVA. The analysis was performed with the Statgraphics package (Manugistic Inc., Rockville, MD) on a PC microcomputer.

## RESULTS

Table 1 presents the characteristics of the subjects. Preadmission-reported intakes of selected nutrients are shown in Table 2. Proteins represent 13.5%, fats 36.5% (linoleic acid 3.29%), and carbohydrates 50% of daily energy intake. Significant intrapair resemblances (IPR) expressed as Spearman correlations were found in energy content, carbohydrates, and linoleic acid (Table 2).

The composition of FA in serum PC, CE, and TG, and in AT TG are presented in Table 3. Because linoleate is the primary substrate for the other n-6 essential FA, its correlations between diet and these lipid fractions were calculated. No correlations for the linoleic acid content in food (expressed in g/d) with percentage of linoleic acid in serum lipids and AT TG were found. To assess the contribution of varying amounts of dietary fat to intrapair differences, the FA composition in individual lipid classes examined was compared in the twins concordant and discordant in fat intake according to the baseline food records. The groups did not differ with the exception of two FA in AT TG. These were oleate (higher per-

**TABLE 3**  
**Fatty Acid (FA) Composition in Serum and Adipose Tissue (AT) Lipids in Obese Female Monozygotic Twins<sup>a</sup>**

FA	Serum PC (n = 28)	Serum CE (n = 22)	Serum TG (n = 28)	AT (n = 24)
TG				
14:0	0.57 ± 0.04	1.15 ± 0.10	1.04 ± 0.09	2.03 ± 0.08
16:0	38.30 ± 1.31	20.33 ± 0.81	27.17 ± 0.38	21.9 ± 0.37
16:1n-7	1.34 ± 0.07	4.25 ± 0.19	4.93 ± 0.20	5.15 ± 0.18
18:0	18.96 ± 0.83	7.76 ± 0.92	3.35 ± 0.10	4.47 ± 0.17
18:1n-9	16.06 ± 0.77	23.81 ± 3.31	44.38 ± 0.57	49.6 ± 0.30
18:1n-7	3.24 ± 0.12	1.99 ± 0.06	4.15 ± 0.07	4.67 ± 0.09
18:2n-6	13.36 ± 0.94	34.80 ± 1.60	12.30 ± 0.59	10.4 ± 0.33
18:3n-6	0.13 ± 0.04	0.42 ± 0.04	0.20 ± 0.04	0.03 ± 0.008
18:3n-3	0.28 ± 0.08	0.48 ± 0.05	0.74 ± 0.10	0.86 ± 0.05
20:3n-6	1.51 ± 0.21	0.40 ± 0.03	0.15 ± 0.01	0.17 ± 0.01
20:4n-6	4.42 ± 0.72	3.78 ± 0.29	0.81 ± 0.07	0.38 ± 0.09
20:5n-3	0.42 ± 0.09	0.10 ± 0.04	0.12 ± 0.03	0.04 ± 0.01
22:5n-3	0.27 ± 0.05	0.08 ± 0.02	0.23 ± 0.02	0.15 ± 0.02
22:6n-3	1.05 ± 0.23	0.22 ± 0.03	0.43 ± 0.06	0.19 ± 0.04

<sup>a</sup>Values are expressed as mean ± standard error (in mol%). TG, triglycerides; PC, phosphatidylcholine; CE, cholesteryl esters.

centage in discordant than in concordant group,  $P < 0.05$ ) and docosahexaenoate (higher level in concordant group than in discordant group,  $P < 0.05$ ).

Table 4 shows IPR expressed as intra-class correlation coefficients for individual FA within the lipid fractions. In serum PC, 12 of 14 FA examined were significantly similar within pairs when compared to between pairs. In serum CE and TG, and also in AT TG, significant IPR in numerous saturated and monounsaturated FA were found. However, in the serum CE and TG fractions, only two significant IPR were found for polyunsaturates (CE, 18:2n-6, 18:3n-3,  $P < 0.05$ ).

Because of its consistent intra-pair correlations across lipid fractions, Spearman correlation coefficients were assessed for palmitoleic acid in serum CE and in AT TG vs. body weight, fat content, and some anthropometric measures of body fat content and distribution (Table 5). There were no significant correlations for palmitoleic acid in serum PC or TG against these variables, nor for palmitic acid in serum and adipose TG. Significant positive correlations also were found between myristic acid (14:0) in serum CE and adipose TG and some body composition measures (data not shown).

## DISCUSSION

The primary observation of this study was the high degree of IPR for FA in the serum PC fractions of monozygotic twins. These included nonessential FA, the essential precursor 18:3n-3 (but not 18:2n-6), and multiple anabolic products of both the n-3 and n-6 families of essential FA.

Despite the highly significant IPR in the serum PC fraction, these observations alone do not prove unequivocally that there is genetically mediated interindividual variation in membrane phospholipids in humans independent of diet. To do so would require a precisely controlled diet composition study lasting for 2 yr or longer—the duration necessary to achieve AT equilibration with dietary fat composition (29).

These cautions notwithstanding, careful evaluation of our data supports a role for genetic influence over PC FA composition. Although our analysis of the dietary intake antecedent to study enrollment lacks detailed FA intake information, and

recall methods have been shown to have limitations, our analysis of dietary variables revealed significant IPR for 18:2n-6 intake (Table 2). However, no significant correlations were found between individually reported 18:2n-6 intakes and the 18:2n-6 contents in serum and adipose FA (Table 4). Furthermore, no significant differences in FA composition of serum and AT lipids were found between pairs of twins discordant in and concordant in dietary fat intake. In this context, the fact that a very high frequency of statistically significant IPR for FA was observed in the PC fraction (Table 5), but not including 18:2n-6, argues in favor of the FA composition of this particular fraction being under genetic control. In AT TG, only oleate and docosahexaenoate were significantly different in the comparison of twin pairs concordant in and discordant in dietary fat intake, probably reflecting different dietary fat intakes of these specific FA.

Another strong point in favor of the metabolic regulation of PC FA composition being under genetic control is the fact that strong IPR were observed for PC 20:3n-6 and 22:5n-3. Both of these FA are metabolic intermediates in the pathways between dietary essential substrates (18:2n-6 and 18:3n-3) and their predominant respective pathway products (20:4n-6 and 22:6n-3; see Fig. 1). Although dietary intake of both the precursors and products can affect their proportions in serum and tissue (30,31), these intermediates are found in very low levels in common human foods. Thus, the observed IPR are attributable to metabolic similarities in FA anabolic activity and selective partitioning within twin pairs rather than to similarity in their dietary habits.

An unanticipated observation in this study was the surprisingly consistent high degree of correlation between the proportions of 16:1n-7 in serum CE and adipose TG on the one hand and multiple variables of body fatness on the other (Table 6). These strong and consistent correlations between palmitoleic acid in serum CE and adipose TG vs. body weight and anthropometric measures of body fat and AT distribution are striking, particularly for serum CE 16:1n-7 and waist circumference, which was previously validated as a measure of body fat distribution (32–34). This observation, coupled with the high degree of intra-pair resemblance in 16:1n-7 in multiple

**TABLE 4**  
The Intra-Pair Resemblance for the Relative Content of FA in Serum and AT Lipids<sup>a</sup>

FA	Serum PC		Serum CE		Serum TG		AT TG	
	<i>r</i>	<i>P</i>	<i>r</i>	<i>P</i>	<i>r</i>	<i>P</i>	<i>r</i>	<i>P</i>
14:0	0.63	<0.005	0.74	<0.005	0.66	<0.005	0.45	<0.06
16:0	0.70	<0.001	0.57	<0.05	0.39	<0.07	0.56	<0.05
16:1n-7	0.61	<0.01	0.59	<0.05	0.72	<0.001	0.48	<0.05
18:0	0.65	<0.005	0.68	<0.01	0.43	<0.05	0.52	<0.05
18:1n-9	0.89	<0.0001	0.00	NS	0.25	NS	0.00	NS
18:1n-7	0.66	<0.005	0.11	NS	0.54	<0.05	0.41	<0.08
18:2n-6	0.42	<0.06	0.48	<0.05	0.10	NS	0.36	NS
18:3n-6	0.7	NS	0.39	NS	0.28	NS	0.33	NS
18:3n-3	0.82	<0.0001	0.50	<0.05	0.21	NS	0.18	NS
20:3n-6	0.74	<0.001	0.24	NS	0.13	NS	0.08	NS
20:4n-6	0.76	<0.0005	0.24	NS	0.05	NS	0.23	NS
20:5n-3	0.78	<0.0005	0.01	NS	0.33	NS	0.66	<0.01
22:5n-3	0.91	<0.0001	0.00	NS	0.07	NS	0.17	NS
22:6n-3	0.86	<0.0001	0.00	NS	0.19	NS	0.31	NS

<sup>a</sup>*r*, intra-class correlation coefficient. For other abbreviations see Table 3.

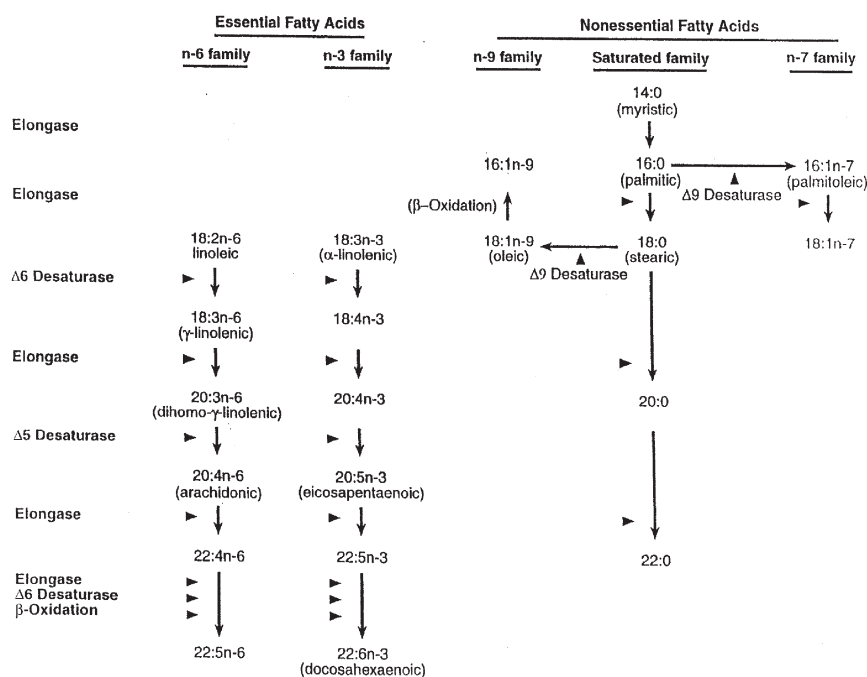


FIG. 1. Nomenclature and metabolic pathways of long-chain fatty acids.

serum and adipose TG fractions, presents a picture of 16:1n-7 as both a metabolic product under genetic control and one that is also closely linked to adiposity.

The mechanism leading to these associations is not immediately apparent. Selective release of 16:1n-7 by hormone-sensitive lipase has been observed in both rodents (1,2) and humans (3–5). However, this appears to be a relatively uniform process among individuals, and thus cannot readily explain the positive associations noted here.

A more likely process to explain the association of 16:1n-7 with adiposity is lipogenesis. Lands (35) noted that 16:1n-7 is an expected product of lipogenesis and that its content in serum CE will appropriately reflect the hepatic lipid pool. In this regard, it is noteworthy that the obese Zucker rat, a profoundly lipogenic animal, has dramatically increased proportions of 16:1n-7 in its liver TG and CE as well as in Serum CE fractions compared to lean controls fed the same diet (13). Although

Hellerstein *et al.* (36) find little evidence for hepatic lipogenesis in humans, their isotope technique is based on the quantitation of 16:0 as the primary product of lipogenesis. It is also worth noting that Aarsland *et al.* (37) published evidence for appreciable whole-body lipogenesis with carbohydrate overfeeding in humans, and they postulated that it occurs primarily in AT rather than liver. These pieces of evidence thus mesh nicely with our observed correlations between 16:1n-7 and adiposity, making 16:1n-7 in serum CE and adipose TG a candidate biomarker for processes leading to obesity.

The IPR in FA composition in obese adult identical twins clearly transcend dietary similarities, making a strong case for post-diet genetically mediated selectivity as a factor regulating tissue FA composition in humans. This pattern of IPR was most pronounced in the PC fraction, implying that the greatest effect of this selectivity, differentiating an individual from her diet, would be seen in membrane lipids. This in turn would magnify the effects of selectivity on cellular function, particularly because the PC selectivity was most pronounced among the highly unsaturated essential FA, which impart unique properties to membranes. Among the nonessential FA, there were consistent IPR for 16:1n-7 across all lipid fractions, and 16:1n-7 in serum CE and adipose TG correlated strongly with indices of adiposity. This pattern of correlations for palmitoleate suggests that it is an important product of endogenous lipogenesis, and that this shift of carbon into lipid storage pools participates directly or indirectly in the pathogenesis of obesity.

#### ACKNOWLEDGMENTS

We express our gratitude to Věra Lánská and Lubomír Poušek for statistical management and for graphical documentation of the study.

TABLE 5  
Correlation Coefficients Between Palmitoleic Acid (16:1) Content in Serum CE and AT TG and Some Anthropometric Measures

	CE		AT	
	$r^a$	$p^b$	$r^a$	$p^b$
Weight (kg)	0.60	<0.01	0.59	<0.005
BMI (kg/m <sup>2</sup> )	0.60	<0.01	0.56	<0.01
Fat (kg)	0.73	<0.001	0.70	<0.001
Sum of 10 skf (mm)	0.59	<0.01	0.59	<0.005
Sum of 4 skf (mm)	0.70	<0.005	0.51	<0.05
Waist (cm)	0.78	<0.0001	0.49	<0.05
SAD (cm)	0.67	<0.005	0.51	<0.05

<sup>a</sup> $r$ , Spearman correlation coefficient; skf, skinfold; SAD, sagittal abdominal diameter. For other abbreviations see Tables 1 and 3.



The project was supported by the Charles University (grant GA UK 203030/54 91/99).

## REFERENCES

- Raclot, T., and Groscolas, R. (1993) Differential Mobilization of White Adipose Tissue Fatty Acids According to Chain Length, Unsaturation, and Positional Isomerism, *J. Lipid Res.* 34, 1515–1526.
- Raclot, T., Mioskowski, E., Bach, A.C., and Groscolas, R. (1995) Selectivity of Fatty Acid Mobilization: A General Feature of Adipose Tissue, *Am. J. Physiol.* 296, R1060–R1067.
- Phinney, S.D., Tang, A.B., Johnson, S.B., and Holman, R.T. (1990) Reduced Adipose 18:3 $\omega$ 3 with Weight Loss by Very Low Calorie Dieting, *Lipids* 25, 798–806.
- Hudgins, L.C., and Hirsch, J. (1991) Changes in Abdominal and Gluteal Adipose Tissue Fatty Acid Compositions in Obese Subjects After Weight Gain and Weight Loss, *Am. J. Clin. Nutr.* 53, 1372–1377.
- Tang, A.B., Nishimura, K.Y., and Phinney, S.D. (1992) Preferential Reduction in Adipose Tissue  $\alpha$ -Linolenic Acid(18:3 $\omega$ 3) During Very Low Calorie Dieting Despite Supplementation with 18:3 $\omega$ 3, *Lipids* 28, 987–993.
- Summers, L.K.M., Barnes, C., Fielding, B.A., Beysen, C., Ilic, V., Humpreys, S.M., and Fray, K.N. (2000) Uptake of Individual Fatty Acids into Adipose Tissue in Relation to Their Presence in the Diet, *Am. J. Clin. Nutr.* 71, 1470–1477.
- Odin, R.S., Finke, B.A., Blake, W.L., Phinney, S.D., and Clarke, S.D. (1987) Modification of Fatty Acid Composition of Membrane Phospholipid in Hepatocyte Monolayer with n-3, n-6, and n-9 Fatty Acids and Its Relationship to Triacylglycerol Production, *Biochim. Biophys. Acta* 921, 378–391.
- Clarke, S.D., and Jump, D.B. (1994) Dietary Polyunsaturated Fatty Acid Regulation of Gene Transcription, *Annu. Rev. Nutr.* 14, 83–98.
- Pelikánová, T., Kouhout, M., Válek, J., Baše, J., and Kazdová, L. (1989) Insulin Secretion and Insulin Action Related to the Serum Phospholipid Fatty Acid Pattern in Healthy Men, *Metabolism* 38, 188–192.
- Borkman, M., Storlien, L.H., Pan, D.A., Jenkins, A.B., Chisholm, D.J., and Campbell, L.V. (1993) The Relation Between Insulin Sensitivity and the Fatty Acid Composition on Skeletal Muscle Phospholipids, *N. Engl. J. Med.* 328, 238–244.
- Baur, L.A., O'Connor, J., Pan, D.A., and Storlien, H. (1999) Relationship Between Maternal Risk of Insulin Resistance and the Child's Muscle Membrane Fatty Acid Composition, *Diabetes* 48, 112–116.
- Blond, J.P., Henchiri, C., and Bézard, J. (1989) Delta-6 and Delta-5 Desaturase Activities in Liver from Obese Zucker Rats at Different Ages, *Lipids* 24, 389–395.
- Guesnet, P., Bourre, J.-M., Guerre-Millo, M., Pascal, G., and Durand, G. (1990) Tissue Phospholipid Fatty Acid Composition in Genetically Lean or Obese Zucker Female Rats on the Same Diet, *Lipids* 25, 517–522.
- Phinney, S.D., Tang, A.B., Thurmond, D.C., Nakamura, M.T., and Stern, J.S. (1993) Abnormal Polyunsaturated Lipid Metabolism in the Obese Zucker Rat with Partial Metabolic Correction by  $\gamma$ -Linolenic Acid Administration, *Metabolism* 42, 1127–1140.
- Phinney, S.D., Fisler, J.S., Tang, A.B., and Warden, C.H. (1994) Liver Fatty Acid Composition Correlates with Body Fat and Sex in a Multigenic Mouse Model of Obesity, *Am. J. Clin. Nutr.* 60, 61–67.
- Thurmond, D.C., Tang, A.B., Nakamura, M.T., Stern, J.S., and Phinney, S.D. (1993) Time-Dependent Effects of Progressive Gamma-Linoleate Feeding on Hyperphagia, Weight Gain, and Erythrocyte Fatty Acid Composition During Growth of Zucker Obese Rats, *Obes. Res.* 1, 118–125.
- Bouchard, C., Tremblay, A., Despres, J.-P., Nadeau, A., Lupien, P.J., Thériault, G., Dussault, J., Moorjani, S., Pinault, S., and Fournier, G. (1990) The Response to Long-Term Overfeeding in Identical Twins, *N. Engl. J. Med.* 322, 1477–1482.
- Stunkard, A.J., Harris, J.R., Pedersen, N.L., and McClearn, G.E. (1990) The Body-Mass Index of Twins Who Have Been Reared Apart, *N. Engl. J. Med.* 322, 1483–1487.
- Hainer, V., Stunkard, A.J., Kunesová, M., Pařízková, J., Štich, V., and Allison, D.B. (2000) Intrapair Resemblance in Very Low Calorie Diet Induces Weight Loss in Female Obese Identical Twins, *Int. J. Obes. Relat. Metab. Disord.* 24, 1051–1057.
- Bates, C., Horrobin, D.F., and Ellis, K. (1992) Fatty Acids in Plasma Phospholipids and Cholesterol Esters from Identical Twins Concordant and Discordant for Schizophrenia, *Schizophr. Res.* 6, 1–7.
- Stewart, M.E., McDonnell, M.W., and Downing, D.T. (1986) Possible Genetic Control of the Proportions of Branched-Chain Fatty Acids in Human Sebaceous Wax Esters, *J. Invest. Dermatol.* 86, 706–708.
- Pařízková, J. (1977) *Body Fat and Physical Fitness*, 1st edn., pp. 32–51. M. Nijhoff, Hague.
- Brožek, J., Grande, F., Anderson, J.T., and Keys, A. (1967) Densitometric Analysis of Body Composition. Revision of Some Quantitative Assumptions, *Am. N.Y. Acad. Sci.* 110, 113–140.
- Meneely, G.R., and Kaltreider, N.L. (1949) The Volume of the Lung Determined by Helium Dilution: Description of the Method and Comparison with Other Procedures, *J. Clin. Invest.* 28, 129–139.
- Durnin, J.V., and Wommersley, A.G. (1974) Body Fat Assessed from Total Body Density and Its Estimation from Skinfold Thickness: Measurements on 481 Men and Women Aged from 16 to 72 Years, *Brit. J. Nutr.* 32, 77–97.
- Lohman, T., Roche, A., and Martorel, R., eds. (1989) *Standardization of Anthropometric Measurements*, pp. 39–80, Human Kinetics, Champaign.
- Folch, J., Lees, M., and Sloane-Stanley, G.H. (1957) A Simple Method for the Isolation and Purification of Total Lipides from Animal Tissues, *J. Biol. Chem.* 226, 497–509.
- Carlson, L.A. (1985) Extraction of Lipids from Human Whole Serum and Lipoproteins and From Rat Liver Tissue with Methylene Chloride-Methanol: A Comparison with Extraction with Chloroform-Methanol, *Clin. Chim. Acta* 149, 89–93.
- Hirsch, J. (1962) Composition of Adipose Tissue, in *Adipose Tissue as an Organ* (L.W. Kinsella, ed.), pp. 79–123, Thomas, Springfield, IL.
- Sinclair, H.M. (1982) The Relative Importance of Essential Fatty Acids of the Linoleic and Linolenic Families: Studies with an Eskimo Diet, *Prog. Lipid Res.* 20, 897–899.
- Phinney, S.D., Odin, R.S., Johnson, S.B., and Holman, R.T. (1990) Reduced Arachidonate in Serum Phospholipids and Cholesteryl Ester Associated with Vegetarian Diets in Humans, *Am. J. Clin. Nutr.* 51, 385–392.
- Björntorp, P. (1993) Visceral Obesity: A “Civilization Syndrome,” *Obesity Res.* 1, 206–222.
- Kissebah, A.H., and Krakower, G.R. (1994) Regional Adiposity and Morbidity, *Physiol. Rev.* 74, 761–811.
- Kunešová, M., Hainer, V., Hergetová, H., Žák, A., Pařízková, J., Hořejš, J. and Štich, V. (1995) Simple Anthropometric Measurements—Relation to Body Fat Mass, Visceral Adipose Tissue and Risk Factors of Atherogenesis, *Sborn. Léč.* 96, 257–268.
- Lands, W.E.M. (1995) Long-Term Fat Intake and Biomarkers, *Am. J. Clin. Nutr.* 61, 721S–725S.
- Hellerstein, M.K., Christiansen, M., Kaempfer, S., Kletke, C., Wu, K., Reid, J.S., Mulligan, K., Hellerstein, N.S., and Shackleton, C.H. (1991) Measurement of *de novo* Hepatic Lipogenesis in Humans Using Stable Isotopes, *J. Clin. Invest.* 87, 1841–1852.
- Aarsland, A., Chinkes, D., and Wolfe, R.R. (1997) Hepatic and Whole-Body Fat Synthesis in Humans During Carbohydrate Overfeeding, *Am. J. Clin. Nutr.* 65, 1774–1782.

[Received January 17, 2001 and in final revised form October 3, 2001; revision accepted October 4, 2001]

# Plant Sterol Esters Lower Plasma Lipids and Most Carotenoids in Mildly Hypercholesterolemic Adults

Joseph T. Judd<sup>a,\*</sup>, David J. Baer<sup>a</sup>, Shirley C. Chen<sup>b</sup>, Beverly A. Clevidence<sup>a</sup>,  
Richard A. Muesing<sup>c</sup>, Matthew Kramer<sup>d</sup>, and Gert W. Meijer<sup>b</sup>

<sup>a</sup>Beltsville Human Nutrition Research Center, ARS, USDA, Beltsville, Maryland 20705,

<sup>b</sup>Unilever Bestfoods NA, Englewood Cliffs, New Jersey 07632,

<sup>c</sup>The George Washington University Lipid Research Clinic, Washington, DC 20037,

and <sup>d</sup>Biometrical Consulting Service, Beltsville Area ARS, Beltsville, Maryland 20705

**ABSTRACT:** The ability of plant sterol esters (PSE) in salad dressing to modify plasma lipids and carotenoids was determined in 26 men and 27 women fed controlled, weight-maintaining, isocaloric diets. Diets contained typical American foods that provided 32% of energy from fat. Dressings contained 8 g (ranch) or 4 g (Italian) of fat per serving. PSE (3.6 g/d) were provided in two servings/d of one of the dressings. Diets with ranch or Italian dressing without and with PSE were fed for 3 wk/diet and crossed over randomly within dressings. Diets were adjusted to similar fat and fatty acid concentrations. Type of salad dressing did not affect plasma lipids, lipoproteins, carotenoids, or fat-soluble vitamins ( $P > 0.05$ ). Switching from a self-selected baseline diet to the control diet resulted in reduction in low density lipoprotein (LDL) cholesterol of 7.9%, a decrease in high density lipoprotein (HDL) cholesterol of 3.1%, and a decrease in triglycerides (TG) of 9.3%. Consumption of 3.6 g of PSE resulted in further decreases in LDL cholesterol (9.7%) and TG (7.3%) but no additional change in HDL cholesterol. Total plasma carotenoids decreased 9.6% with PSE. An automated stepwise procedure was developed to produce candidate mixed models relating plasma carotenoid response to PSE. These models adjusted for preintervention plasma carotenoid levels and effects of diets on blood lipids. There were significant decreases in  $\beta$ -carotene,  $\alpha$ -carotene, and  $\beta$ -cryptoxanthin (females only) not associated with changes in plasma lipids. Plasma carotenoids on all diets remained within normal ranges. We conclude that low-fat foods, such as salad dressings, are effective carriers for PSE.

Paper no. L8820 in *Lipids* 37, 33–42 (January 2002).

Although there is increased public health emphasis on maintenance of body weight and modification of lifestyle factors to reduce the risk of cardiovascular disease (CVD), elevated blood cholesterol remains of great concern and the target of both dietary recommendations (1) and drug treatments to re-

duce CVD risk. The blood cholesterol-reducing effect of plant sterols is well documented (2). However, plant sterols in natural food sources are low, ranging from 0.1 to 0.5 g/d, and therefore may not have substantial impact on cholesterol concentrations (3). Recent studies have demonstrated that plant sterol-enriched margarines lower total and low density lipoprotein (LDL) cholesterol in normocholesterolemic and mildly hypercholesterolemic subjects (4,5). Currently, such table spreads, prepared from vegetable oil and relatively high in fat (32–65%), are the major carriers for plant sterol esters (PSE) available to the public on the open market. PSE is dissolved in the fat phase of these products, termed in food technology as “fat continuous” products; that is, they are “water-in-oil” products in which water is emulsified into a continuous fat phase.

The efficacy of lower fat products as carriers of sterol esters has not been demonstrated in carefully controlled studies of blood lipids and lipoproteins. Examples of fat-based products lower in fat are salad dressings that are similar to those fed in the current study. These are “fat-in-water” products and employ the “water continuous” concept in which the fat is emulsified in a “water continuous” phase. The first objective of the present study was to determine effects of PSE in products in which fat is emulsified in a “water continuous” phase and in which the food carriers’ fat contents are reduced compared with those of margarines, the usual carriers of PSE. Indirectly, we planned to compare the efficacy of these reduced- and low-fat carriers of PSE with blood cholesterol and carotenoid effects reported for higher-fat, “fat continuous” products such as margarines.

Little is known about the effect of baseline blood lipid, fat-soluble vitamin, and carotenoid concentrations on the lipid- and carotenoid-modifying response to PSE consumption. Thus, a second objective of the current study was to examine the relationship of pretrial plasma concentrations of blood lipids and fat-soluble nutrients with the response to PSE consumption. This was achieved by including the appropriate individual pretrial variables as covariates and determining if the slopes of the control vs. PSE diets differed (i.e., if a covariate by treatment interaction was present).

## SUBJECTS AND METHODS

*Study design.* Two types of salad dressing were compared in a parallel arm design. Within each dressing (arm), there was a

\*To whom correspondence should be addressed at Beltsville Human Nutrition Research Center, Building 308, BARC-East, Beltsville, MD 20705.

E-mail: judd@bhnrc.arsusda.gov

Abbreviations: ANOVA, analysis of variance; Apo A1, apolipoprotein A1; Apo B, apolipoprotein B; BHNRC, Beltsville Human Nutrition Research Center; BIC, Schwartz’s Bayesian information criteria; BMI, body mass index; CVD, cardiovascular disease; HDL, high density lipoprotein; HPLC, high-performance liquid chromatography; LDL, low density lipoprotein; Lp(a), lipoprotein (a); NCEP, National Cholesterol Education Program; PSE, plant sterol esters; SEE, standard error of the estimated or corrected mean; SEM, standard error of the mean; SFA, saturated fatty acid; TC, total cholesterol; TG, triglycerides; USDA, U.S. Department of Agriculture.

randomized crossover between dressing with and without added PSE. The study cohort was divided into two groups balanced for gender, age, body mass index (BMI), and plasma total cholesterol (TC), and the groups were randomly assigned to the salad dressings. Participants consumed each diet for a period of 3 wk followed by blood sampling during the fourth week. Following the final blood sample in the first dietary period, volunteers were switched to the second diet with no washout between periods. There was no crossover between dressing types. The products were fed as part of a carefully controlled, moderately low fat, low saturated fat, weight maintenance diet. Within each dressing, a double-blind protocol was followed.

**Subjects.** The study protocol was approved by the Johns Hopkins University, School of Hygiene and Public Health, Committee on Human Research. Men and women with normal to slightly elevated blood cholesterol concentration were recruited by advertisement in the area of the Beltsville Agricultural Research Center, Beltsville, MD. Minimum eligibility criteria were based on general health, age (25–65 yr), and BMI within 85–120% of gender-specific ideal BMI specified by life insurance reference tables (6). Subjects selected for the study were required to have fasting plasma high density lipoprotein (HDL) cholesterol concentrations greater than 25 mg/dL for men and 35 mg/dL for women and fasting plasma triglyceride (TG) concentrations less than 300 mg/dL. Volunteers who reported taking lipid-lowering drugs, blood pressure medications, or dietary supplements or who had eating habits inconsistent with the study protocol (e.g., those on vegetarian or low-fat diets) were excluded. Volunteers were evaluated by a physician and determined to be in good health with no signs or symptoms of hypertension, hyperlipemia, diabetes, peripheral vascular disease, gout, liver or kidney disease, or endocrine disorders.

Women taking hormones for birth control ( $n = 2$ ) or postmenopausal hormone replacements ( $n = 3$ ) were included in the study with the requirement that they continue the same regimen (type of hormone, schedule, and dose) throughout the dietary intervention. Although smokers and nonsmokers were accepted for the study, only 5 of the 53 participants completing the study smoked. Exercise was not controlled, but subjects were encouraged to maintain their normal exercise patterns (type of exercise, duration, and frequency) throughout the study and were required to record exercise on their daily questionnaire.

**Basal diet and salad dressings.** Ranch and Italian salad dressings with PSE prepared from soybean oil were fed as part of a mixed diet (basal diet) composed of foods commonly eaten in the United States. Control ranch and Italian dressings having no added sterols but which matched the fat and fatty acid concentrations in the test dressings were fed for comparison. The fat level of both the control (–PSE) and the sterol-containing (+PSE) ranch dressing was 27%. The control and sterol-containing Italian dressings had 17 and 13% fat, respectively. The difference in fat content of the two Italian dressings as well as that between the ranch and Italian dress-

ings was balanced in the total diet by adding appropriate amounts of fat and fatty acids in other foods. Two servings, 30 g (2 tablespoons) per serving, of experimental salad dressing were fed each day. Group 1 was fed the basal diet with Italian dressing that provided 4 g of fat per serving while group 2 was fed ranch dressing that provided 8 g of fat per serving. PSE, prepared from soybean sterols, were added to each dressing so that two servings of +PSE dressing provided 3.6 g of PSE, equivalent to 2.2 g/d of free sterol. Salad dressings were prepared by Lipton (Englewood Cliffs, NJ).

**Dietary intervention.** Monday through Friday, all subjects consumed breakfast and dinner at the Beltsville Human Nutrition Research Center (BHNRC) human study facility under the supervision of a dietitian. At breakfast, each subject was provided with a carry-out lunch to be consumed that day. Snack items were included in the daily menu, and subjects were provided the option of consuming the snacks at dinner or later in the evening. One serving of the salad dressing was provided with lunch, and one serving with dinner. Meals for the weekend were packaged for home consumption and provided to the subjects, with written instructions, after dinner on Friday. Weekend menus contained the same type of foods and balance of nutrients as the weekday menus. Unlimited amounts of coffee, tea, and diet sodas were allowed, but all additives (sugar and milk) for coffee and tea were provided with the meals. Only foods provided by the Human Study Facility were allowed to be consumed during the study.

Each weekday morning, subjects were weighed before breakfast when they arrived at the facility. Energy intake was adjusted in 200-kcal increments for women and 400-kcal increments for men to maintain initial body weight. Subjects were fed the same items and the same proportions of each item relative to total dietary energy. Therefore, the relative amounts of nutrients, other than those provided by the salad dressing, were constant for all subjects. Each day, subjects completed a questionnaire detailing beverage intake, factors related to dietary compliance, exercise, medications, and illnesses. The questionnaires were routinely reviewed by a study investigator, and problems were discussed with the subject during the next meal.

**Analysis of diets.** Two composites of the 7-d menu cycle were made at two energy levels. Thus, four weekly diet composites were analyzed for dry matter, crude protein, crude fat, total dietary fiber, and ash (Corning Hazleton, Inc., Madison, WI). Fatty acid compositions of food composites were determined by gas chromatographic separation of fatty acid methyl esters. Carotenoid content of the controlled diets was estimated using data for carotenoids in foods which were compiled at BHNRC (7).

**Blood sample collection and analysis.** Baseline samples were collected on 2 d during the week immediately before initiation of the controlled feeding. Subsequently, samples were collected on two different days during the fourth week of the intervention. The subjects were randomly divided into two groups. One group had samples drawn on Monday and Wednesday and the other on Tuesday and Thursday.



Procedures for collection and processing of fasting blood samples were those described in the protocol for the Lipid Research Clinics Program (8). Plasma was harvested and stored in cryogenic vials at  $-80^{\circ}\text{C}$ . Before storage, the sample to be used for HDL cholesterol determination was precipitated by the sequential precipitation procedure of Gidez *et al.* (9). Supernatants from the HDL precipitation were stored at  $-80^{\circ}\text{C}$  for later analysis of cholesterol. Analyses for TC, TG, HDL, lipoprotein (a) [Lp(a)], and apolipoproteins were performed after the final blood collection. All samples from one subject were included in the same analytical run.

Lipid and lipoprotein analyses (TC, TG, HDL cholesterol, and apolipoproteins) were performed at the Lipid Research Clinic Laboratory, The George Washington University Medical Center, which maintains standardization with the Centers for Disease Control and Prevention, U.S. Department of Health and Human Services. Plasma TC, HDL cholesterol, and TG were determined enzymatically with commercial kits (Sigma Chemical Company, St. Louis, MO) on an Abbott VP analyzer (Abbott Laboratories, Chicago, IL). LDL cholesterol was calculated by the Friedewald equation (10). Plasma apolipoproteins A1 (Apo A1) and B (Apo B) concentrations were determined by rate nephelometry (Beckman ICS Immunochemical Analyzer; Beckman Instruments, Fullerton, CA).

Carotenoids from 0.4 mL of plasma were extracted into organic solvents containing an internal standard (11), concentrated, and analyzed by high-performance liquid chromatography (HPLC) with a Hewlett-Packard (Wilmington, DE) Series 1050 chromatograph with diode array detection. Carotenoids were separated on a reversed-phase  $\text{C}_{18}$  analytical column (Microsorb-MV; Varian Analytical Instruments, Walnut Creek, CA),  $250 \times 4.6$  mm, protected by a  $5\text{-}\mu\text{m}$  Brownlee  $\text{C}_{18}$  guard cartridge,  $30 \times 4.6$  mm, under isocratic conditions (12). The precision and accuracy of the HPLC system were verified using Standard Reference Material 968b (National Institute of Standards and Technology, Gaithersburg, MD).

*Statistical analysis.* There were a large number of independent variables, and potential interactions among them, that we wanted to consider as predictors of response to PSE consumption for each of the blood lipid, lipoprotein, and carotenoid variables. Therefore, we developed an automated stepwise model selection procedure (13), used for each of the dependent variables. Our procedure selected a mixed analysis of variance (ANOVA) model that minimized Schwartz's Bayesian information criteria (BIC) (14), where a smaller BIC corresponds to a better "fitting" model, given all the candidate independent variables. The basic within-individual covariance structure remained unchanged (that of a crossover design) while selecting the independent variables.

Models were tested in a standard stepwise approach (15). All models included an intercept term. Selection started by adding the single best independent variable or interaction term to the model. With that variable in the model, the next best variable was added. This process was repeated until no other variables could be added. After five or more independent variables were in the model, all variables currently in the

model were also tested to see if any could be removed. We used the resulting "final" model as a basis for further model development, usually by eliminating variables that changed BIC only marginally, because the resulting simpler models were easier to interpret and seemed to "fit" about as well, based on BIC.

For all dependent variables, one important predictor was the variable's pretrial value, which we refer to as baseline. This is because subjects with high posttreatment values were likely to come into the experiment with high pretreatment values, just as those with low posttreatment values came in with low pretreatment values. The baseline value of the dependent variable adjusts posttreatment scores by the variable's initial value, resulting in a more sensitive test of the treatment effects because much of the "noise" due to initial intersubject variation has been statistically removed. Since it was not initially evident to us that there would be a linear relationship between pre- and posttreatment values, we allowed for non-linearity by including a quadratic effect (the square of the baseline concentration of the dependent variable) as a candidate independent variable. In general, the quadratic effect was not included in the final model, that is, there was a linear relationship between pre- and posttreatment values.

Other candidate independent variables for both blood lipids and carotenoids included characteristics of the individual (age, sex, and BMI), pretrial plasma concentration of the dependent variable (baseline, baseline squared), design variables (period and sequence in which the diets were administered and carryover effect), and the variables of most interest, treatment and dressing. First-order interaction terms among these variables were also candidate independent variables. In addition, because carotenoids are carried by lipoproteins and concentrations may be dependent on changes in blood lipids (16), blood lipid variables were included as candidate covariates in models for carotenoids (i.e., TG, TC, LDL cholesterol, HDL cholesterol, and the sum of TG + TC).

For the carotenoids, there were 57 candidate independent variables (not including the intercept) for the routine to select from. There were fewer, 49, candidate variables for the blood lipids than for carotenoids, because blood lipid variables, other than the baseline level of the dependent variable, were not allowed into the model. For example, LDL cholesterol was not adjusted using HDL cholesterol, TC, or TG.

## RESULTS

*Subjects.* Twenty-eight men and 28 women completed the screening process and began the controlled feeding. One woman and two men withdrew for personal reasons not related to the study. Thus, 26 men and 27 women completed the feeding phase of the study. Data were analyzed statistically only for subjects who completed both feeding periods. Characteristics of these participants at baseline are presented in Table 1.

*Diets and salad dressings.* The background diets with salad dressing added were planned to be prudent, healthful diets having moderate levels of fat but lower levels of satu-



**TABLE 1**  
**Characteristics of the Participants at Baseline<sup>a</sup>**

	Men (n = 26)	Women (n = 27)	All (n = 53)
Age (yr)	45.8 ± 1.34	48.4 ± 1.68	47.1 ± 1.54
Body mass index (kg/m <sup>2</sup> )	26.7 ± 0.37	25.5 ± 0.73	26.3 ± 0.37
Plasma concentration (mg/dL)			
Total cholesterol	214 ± 5.0	220 ± 5.6	218 ± 3.8
Low density lipoprotein (LDL) cholesterol	141 ± 4.4	139 ± 4.0	140 ± 2.9
High density lipoprotein (HDL) cholesterol	46.3 ± 2.98	56.4 ± 2.65	51.4 ± 2.09
Ratio of total to HDL cholesterol	5.0 ± 0.23	4.2 ± 0.20	4.5 ± 0.16
Triglycerides	135 ± 12.4	123 ± 11.7	129 ± 8.5
Apolipoprotein A1	197 ± 5.9	213 ± 5.2	205 ± 4.1
Apolipoprotein B	92 ± 2.6	97 ± 2.9	95 ± 2.0
Lipoprotein (a)	22 ± 4.3	23 ± 3.6	23 ± 2.8

<sup>a</sup>Sample mean ± SEM.

rated fatty acids (SFA) and cholesterol, as well as higher levels of dietary fiber than reported for the average U.S. diet (17). Diets were calculated using data from the U.S. Department of Agriculture (USDA) nutrient database (18) so that total fat would be approximately 30% of energy and protein 16% of energy. Analyzed macronutrient and fatty acid compositions of the basal diet and diets with salad dressings are presented in Table 2. Analyzed compositions of diets as fed

in the study showed 32.2–32.7% of energy from fat and 15.7–16.2% from protein. The values for dietary fat are slightly lower than those reported for the U.S. diet (17). In order to avoid confounding the effect of dietary fatty acid intake on blood lipids with those of PSE, considerable effort was made to formulate diets that would vary little in the major SFA (myristic, palmitic, and stearic acids), as well as in major mono- and polyunsaturated fatty acids (oleic and linoleic

**TABLE 2**  
**Composition of Diets Containing Ranch or Italian Dressings With and Without Supplementation with Plant Sterol Esters (PSE) Prepared from Soybean Oil**

	Diets with:			
	Ranch dressing		Italian dressing	
	–PSE (n = 12 men + 14 women)	+PSE	–PSE (n = 14 men + 13 women)	+PSE
Added sterol esters (g/d)	0	3.6	0	3.6
Free sterol equivalents added (g/d)	0	2.2	0	2.2
Percent of energy <sup>a</sup> from:				
Protein <sup>b</sup>	16.2	15.7	16.5	15.8
Fat <sup>b,c</sup>	32.7	32.2	32.5	32.7
From 2 servings of dressing <sup>d</sup>	5.5	5.5	2.8	2.8
From basal diet <sup>d</sup>	27.2	26.7	29.7	29.9
Saturated fatty acids (SFA) <sup>b,c</sup>	7.9	7.6	7.6	7.4
Myristic acid (14:0)	0.5	0.4	0.4	0.4
Palmitic acid (16:0)	4.5	4.3	4.2	4.5
Stearic acid (18:0)	2.4	2.3	2.3	2.2
Other SFA	0.5	0.6	0.7	0.3
Monounsaturated fatty acids (MUFA) <sup>b,c</sup>	11.2	10.9	11	11
Oleic acid (all 18:1 isomers)	10.7	10.4	10.5	10.7
Other MUFA	0.5	0.5	0.5	0.3
Polyunsaturated fatty acids (PUFA) <sup>b,c</sup>	10.3	9.9	10	9.8
Linoleic acid (18:2)	9.1	8.7	8.8	8.6
Other PUFA	1.2	1.2	1.2	1.2
Dietary cholesterol (g/d/1000 kcal)	88	97	94	92
Dietary fiber (g/d/1000 kcal)	13	12	11	13

<sup>a</sup>Average energy intake for men was 2766 kcal/d; for women, 2163 kcal/d.<sup>b</sup>Diet composites with salad dressing included were analyzed at 2200 and 3200 kcal. Values are the average of the two composites.<sup>c</sup>Ratio of fatty acids, PUFA:MUFA:SFA = 1.3:1.4:1<sup>d</sup>Percentages of energy (en%) from salad dressing fat calculated at 2200 and 3200 kcal were, for ranch, 6.5 en% at 2200 kcal and 4.5 en% at 3200 kcal, and, for Italian, 3.3 en% at 2200 kcal and 2.2 en% at 3200 kcal.

acids). Ratios of polyunsaturated to monounsaturated to saturated fatty acids averaged 1.3:1.4:1 and were very consistent across diets. The diets averaged 12 g of dietary fiber per 1000 kcal. Mean total dietary fiber intake was 33 g/day for men and 26 g/day for women. These values are considerably higher than the average intake reported for the U.S. diet, 17.4 g/d for men and 13.7 g/d for women (17), but were constant across all diets.

**Blood lipids and lipoproteins.** As expected from documented inherent gender differences, women had higher concentrations of HDL cholesterol (+10 mg/dL) and apo A1 (+16 mg/dL) than did men but were not different from men in concentrations of LDL cholesterol and apo B. The ratio of total/HDL cholesterol was higher for men than for women,  $4.96 \pm 0.23$  vs.  $4.12 \pm 0.20$ .

The effects of type of salad dressing, gender, and gender  $\times$  dressing interaction were found to be nonsignificant ( $P > 0.05$ ) in the mixed ANOVA model; thus, data for the type of salad dressing and gender are combined. Blood lipid and lipoprotein changes due to the addition of 3.6 g PSE/d to the controlled diets are shown in Table 3. Inclusion of 3.6 g PSE/d in the controlled diet resulted in highly significant reductions ( $P < 0.005$ ) in TC [6.8% (13.8 mg/dL)], LDL cholesterol [9.8% (12.5 mg/dL)], apo B [3.3% (3.03 mg/dL)], and TG [7.3% (8.5 mg/dL)]. HDL cholesterol was unaffected by including PSE in the controlled diet ( $P = 0.33$ ). As with HDL cholesterol, apo A1 was unaffected by PSE ( $P = 0.56$ ).

The effect of PSE on the ratio of TC to HDL cholesterol depended on the ratio prior to dietary intervention, that is, there was a treatment by baseline interaction. Even so, PSE consumption always resulted in lower ratios. At a baseline ratio of 4.5, the average of the ratio at the start of the study (Table 1), the ratio decreased by 0.36 (7.5%,  $P = 0.0001$ ). At the minimum and maximum baseline ratio, the decrease was 6.9 and 7.7%, respectively. There were no significant interactions of gender or BMI with PSE effect on the ratio.

**Carotenoids.** There were no differences in the effect of PSE consumption on plasma carotenoid concentrations between Italian and ranch dressings. There were no significant interactions of gender with PSE consumption except for  $\beta$ -cryptoxanthin, where there was a significant treatment effect for females, but not for males (Table 4).

All plasma carotenoids decreased to some degree with consumption of PSE (Table 4). This general decrease in carotenoids was reflected by a 9.6% decrease ( $P < 0.0022$ ) in the sum of those carotenoids determined in our analytical procedure, i.e., total carotenoids. Among the major plasma carotenoids,  $\beta$ -carotene and  $\alpha$ -carotene decreased by 12.7 ( $P = 0.0009$ ) and 12.8% ( $P = 0.0226$ ), respectively. Lycopene decreased with consumption of PSE; however, the magnitude of the decrease varied directly with BMI (i.e., there was a significant treatment  $\times$  BMI interaction (Table 4). Estimation of the effect of BMI showed that the decrease in lycopene due to PSE became statistically significant ( $P = 0.05$ ) at BMI between 22 and 23 and ranged from 4.1  $\mu$ g/dL at BMI 22 ( $P = 0.0843$ ) to 10.9  $\mu$ g/dL at BMI 30 ( $P = 0.0001$ ). At the average BMI in this study (Table 1), the decrease in lycopene would approximate 20% of the mean lycopene concentration for the control (–PSE) treatment. Decreases in the lutein–zeaxanthin carotenoid fraction, anhydrolutein,  $\alpha$ -cryptoxanthin, and  $\beta$ -cryptoxanthin (for males only) due to PSE consumption were not statistically significant ( $P > 0.05$ ).

**Fat-soluble vitamins.** Modeling of  $\alpha$ - and  $\gamma$ -tocopherol and retinol by the same procedure and for the same covariates used for carotenoids showed no significant effects of dressing or treatment and no significant interactions of baseline concentration of the fat-soluble vitamin, gender, or BMI with dressing or treatment. The estimated means and standard errors of the estimated means (SEE) are shown in Table 4.

**Relationships of baseline subject characteristics with blood lipid and lipoprotein responses to PSE.** In Table 5 we present coefficients for independent variables entering into the model with probability values of  $\leq 0.05$  for the lipid and lipoprotein dependent variables. The coefficient for the intercept is included for completeness. There were no significant effects or interactions of type of dressing and treatment in the final model, indicating that the response to PSE consumption (treatment) was the same for both Italian and ranch dressings (Table 5). As expected, baseline concentration was a significant predictor of final concentration for all blood lipids and lipoproteins. However, there was no significant interaction of the baseline concentration with PSE (treatment effects), so the magnitude of change in the plasma lipid was the same over all baseline levels; that is, the effect of treatment on a

**TABLE 3**  
Plasma Lipid, Lipoprotein, and Apolipoprotein Concentrations of Men and Women Consuming 3.6 g PSE/d<sup>a</sup>

Plasma concentration (mg/dL) <sup>b</sup>	(LSMean $\pm$ SEE) <sup>c</sup>			<i>t</i> -test ( <i>P</i> -value)
	Without added PSE	With 3.6 g PSE/d	Difference	
Total cholesterol	202 $\pm$ 1.7	187 $\pm$ 1.7	–13.8 $\pm$ 1.6	<0.0001
LDL cholesterol	129 $\pm$ 1.5	116 $\pm$ 1.5	–12.5 $\pm$ 1.5	<0.0001
HDL cholesterol	50 $\pm$ 0.6	50 $\pm$ 0.6	0.4 $\pm$ 0.44	0.3353
Triglycerides	117 $\pm$ 3.7	109 $\pm$ 3.7	–8.5 $\pm$ 2.9	0.0047
Apolipoprotein A1	199 $\pm$ 2	198 $\pm$ 2	–0.9 $\pm$ 1.6	0.5996
Apolipoprotein B	93 $\pm$ 0.8	90 $\pm$ 0.8	–3.0 $\pm$ 0.7	<0.0001

<sup>a</sup>See Tables 1 and 2 for abbreviations.

<sup>b</sup>Estimated mean and standard error of the estimate from a mixed model analysis of variance that adjusted for baseline subject characteristics, type of dressing (ranch or Italian), period, and carryover;  $n = 53$  (26 men, 27 women).

**TABLE 4**  
**Plasma Carotenoid and Fat-Soluble Vitamin Concentrations of Men and Women Consuming 3.6 g PSE/d<sup>a</sup>**

Plasma concentration (µg/dL)	(LSMean ± SEE) <sup>b</sup>			t-test (P-value)
	Without added PSE	With 3.6 g PSE/d	Difference	
Total carotenoids <sup>b</sup>	116 ± 2.7	105 ± 2.7	-11.2 ± 3.5	0.0022
β-Carotene	21 ± 0.7	18 ± 0.7	-2.7 ± 0.75	0.0009
α-Carotene	11 ± 0.4	9 ± 0.4	-1.4 ± 0.57	0.0226
Lutein + zeaxanthin	15 ± 0.4	15 ± 0.4	0 ± 0.4	0.9980
Anhydrolutein	11 ± 0.3	11 ± 0.3	0 ± 0.4	0.9054
α-Cryptoxanthin	7 ± 0.2	6 ± 0.3	-0.5 ± 0.3	0.0691
β-Cryptoxanthin, males	10 ± 0.5	10 ± 0.5	-0.2 ± 0.48	0.6509
β-Cryptoxanthin, females	11 ± 0.6	10 ± 0.6	-1.5 ± 0.65	0.0312
Phytofluene	6 ± 0.2	5 ± 0.2	-0.5 ± 0.19	0.0110
α-Tocopherol	1360 ± 55	1276 ± 55	-85 ± 46	0.0669
γ-Tocopherol	205 ± 11	204 ± 11	-1.4 ± 11	0.8947
Retinol	41 ± 2	39 ± 2	-2 ± 1.8	0.3358

<sup>a</sup>Estimated mean and standard error of the estimate from a mixed model analysis of variance that adjusted for baseline subject characteristics, type of dressing (ranch or Italian), period, and carryover and covariance with blood lipids and lipoproteins; *n* = 53 (26 men, 27 women).

<sup>b</sup>There was a significant interaction of treatment (PSE) with body mass index (BMI) for lycopene; thus, LSMeans are uninformative. The decrease in lycopene due to PSE consumption was significant at BMI = 23 (-4.93 ± 2.01 µg/dL or -13.2%; *P* = 0.0181). At BMI = 30, lycopene decreased by 10.9 ± 2.10 µg/dL or 29% (*P* < 0.0001). For abbreviation see Table 2.

blood lipid or lipoprotein was independent of the baseline concentration. Because baseline was a significant indicator of the final concentration, it was included in all models. The importance of the relationship of baseline LDL cholesterol concentration to LDL cholesterol in both control and PSE diets is depicted graphically in Figure 1 for men and women.

There were no significant effects on blood lipids and lipoproteins due to gender, age, or BMI. In addition, there were no significant interactions of gender, age, or BMI with dressing or treatment, indicating that responses to dressing and PSE were also independent of these subject characteristics. Note that these relationships of blood lipids and PSE to

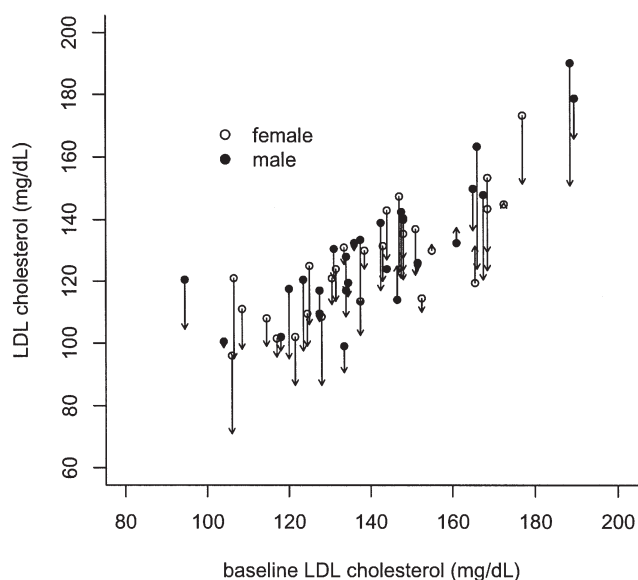
**TABLE 5**  
**Effect of Subject Characteristics Prior to Dietary Intervention on Plasma Lipid and Lipoprotein Changes due to Consumption of Plant Sterol Esters (PSE)**

Independent variables <sup>b</sup>	Dependent variable (Y) estimated by the model <sup>a</sup>					
	Total cholesterol (TC)	Triglycerides (TG)	LDL cholesterol	Apolipoprotein B	HDL cholesterol	Apolipoprotein A1
	Mean of the coefficient for independent variable ± SEE (P-value)					
Intercept	78 ± 12 (NS) <sup>c</sup>	20 ± 9 (0.0224)	11 ± 8 (NS)	42 ± 46 (NS)	6 ± 2 (0.0048)	366 ± 104 (0.0011)
Baseline concentration of Y	0.82 ± 0.05 (<0.0001)	0.61 ± 0.06 (<0.0001)	0.74 ± 0.06 (<0.0001)	8.9 ± 0.5 (<0.0001)	0.85 ± 0.04 (<0.0001)	7.8 ± 0.5 (<0.0001)
Dressing	(NS)	(NS)	(NS)	(NS)	(NS)	(NS)
Treatment	-13.8 ± 1.62 (<0.0001)	-8.50 ± 2.88 (0.0047)	-12.5 ± 1.48 (<0.0001)	-30.4 ± 7.1 (<0.0001)	-0.42 ± 0.44 (NS)	-9.49 ± 16.2 (NS)
Period	(NS)	(NS)	(NS)	(NS)	(NS)	68.7 ± 21.5 (0.0024)
Interaction among independent variables						
Dressing with period	5.36 ± 2.16 (0.0162)	(NS)	(NS)	30.6 ± 9.4 (0.0021)	1.57 ± 0.60 (0.0121)	(NS)
Gender (male) with age	(NS)	0.40 ± 0.14 (0.0064)	(NS)	(NS)	(NS)	(NS)
Gender with period	(NS)	(NS)	(NS)	(NS)	(NS)	-64.7 ± 28.8 (0.0292)

<sup>a</sup>Dependent variable (Y) estimated by:  $Y$  (mg/dL) = Intercept +  $b$  +  $b^2$  + Dressing + Treatment + Diet Sequence + Period + Age + BMI + TC + TG + (TC + TG) + LDL cholesterol + HDL cholesterol + interactions among independent variables, where  $b$  = baseline concentration of dependent variable Y; Dressing = ranch vs. Italian. BMI, body mass index; for other abbreviations, see Table 1.

<sup>b</sup>There were no significant main effects of sequence of the diet administration, gender, age, or BMI of the participants (data omitted from the table).

<sup>c</sup>NS, not significant.



**FIG. 1.** Preintervention (baseline) plasma low density lipoprotein (LDL) cholesterol concentration vs. change in LDL cholesterol in response to diets supplemented with 3.6 g/d of plant sterol esters (PSE) prepared from vegetable oil. For each participant, an arrow indicates the direction and magnitude of change from the control diet (-PSE) to the intervention diet (+PSE). Baseline concentrations for men and women were distributed similarly, as were responses to the intervention diet.

age and BMI cannot be extrapolated to a wider range than that in this study because age and BMI were selection criteria.

There was no effect of controlled diets with or without PSE on Lp(a) (data not shown).

*Relationships of baseline subject characteristics with plasma carotenoid responses to PSE, after adjusting for blood lipid changes.* In modeling responses of carotenoids to PSE, we were interested in determining if blood lipid concentrations were a determinant of carotenoid response. In addition to the independent and design variables considered for blood lipids and lipoproteins, TG, TC, LDL cholesterol, HDL cholesterol, and total plasma lipids (estimated as the sum of TG + TC) were included as candidate covariates in modeling carotenoid responses. Baseline carotenoid concentration was a significant predictor of final carotenoid concentration for all carotenoids (Table 6). As observed for blood lipids, carotenoid responses were independent of dressing at the  $P = 0.05$  level of significance. There were no significant interactions of baseline plasma carotenoid concentration with effects of dressing or treatment for any carotenoid.

After adjusting for the blood lipid covariates, baseline concentration of the dependent carotenoid variable, subject characteristics, and variables associated with study design (Table 6), there remained significant effects of PSE for total carotenoids,  $\beta$ -carotene, and  $\alpha$ -carotene. Thus, blood lipid responses to the diets do not completely determine the plasma carotenoid responses to PSE consumption.

## DISCUSSION

In this study, a large dietary trial showed that reduced-fat and low-fat salad dressings are effective carriers of PSE prepared from soybean oil. The dressings were compared within diets that were balanced for fat, fatty acids, and other nutrients. The reduction in CVD risk factors was not affected by the amount of fat in the dressing that carried the PSE. When two servings per day were fed as part of a mixed diet, the reduced-fat ranch salad dressing (8 g of fat per serving) and the low-fat Italian dressing (4 g of fat per serving), each supplemented with 1.1 g of free sterol equivalent per serving, resulted in approximately equal reductions in the major blood lipids. Each dressing was compared to a control dressing of similar fat and fatty acid composition but with no added PSE.

The effectiveness of reduced- and low-fat foods as carriers of PSE was demonstrated by highly significant reductions in blood lipid risk factors for CVD. TC and LDL cholesterol, indicators of increased risk, declined about 7% and 10%, respectively, with consumption of 3.6 g PSE/d, while HDL cholesterol, associated with reduced risk (19,20), remained unchanged. Lower ratios of TC to HDL cholesterol have been postulated to be strong, independent indicators of decreased risk for CVD (21,22). As would be expected considering the observation of major reductions in LDL cholesterol and sparing of HDL cholesterol by PSE consumption in the current study, the ratio of TC to HDL cholesterol was reduced by 6.9–7.7%, again indicating decreased risk for CVD with consumption of PSE. Increased blood TG concentrations have also been postulated as a risk factor for CVD (23). TG concentrations were reduced by 7% by PSE.

Changes in the major apolipoproteins of LDL (Apo B) and HDL (Apo A1) and changes in cholesterol associated with the corresponding lipoprotein were directionally similar. Similar changes in blood cholesterol and apolipoproteins have been shown in other studies of PSE (4,5). We did not directly determine lipoprotein particle composition. However, changes in LDL cholesterol and Apo B were directionally similar but not directly proportional. This may indicate a reduction in the cholesterol content of the lipoprotein particle as well as a reduction in the number of particles. Lp(a), similar to LDL in lipid composition and with Apo B as one major apolipoprotein but with a second major apolipoprotein referred to as Apo (a), may be a risk factor for the development of CVD (24,25). The particle has been reported to be more atherogenic than LDL (26,27). In our studies, and in those of others, Lp(a) has been altered by changes in dietary fatty acid intake. SFA tend to lower Lp(a) (28–30), whereas *trans* monounsaturated fatty acids raise Lp(a) (31,32). Although we did not expect that PSE would affect Lp(a) because the reputed action site of PSE lies ex-systemically at the level of the gastrointestinal tract (33), nonetheless it is important to know whether this highly atherogenic particle is affected by PSE in the diet before we can evaluate the overall reduction in CVD risk associated with PSE consumption. In the current study, Lp(a) was unaffected by inclusion of PSE in the diet.



**TABLE 6**  
**Effect of Subject Characteristics Prior to Dietary Intervention on Plasma Carotenoid Changes due to Consumption of Plant Sterol Esters (PSE)**

Independent variables <sup>b</sup>	Dependent variable (Y) estimated by the model <sup>a</sup>					
	Total carotenoids	β-Carotene	α-Carotene	Lycopene	Lutein + zeaxanthin	Anhydrolutein
	Mean of the coefficient for independent variable and SEE (P-value)					
Intercept	3.8 ± 13 (NS)	12 ± 2 (<0.0001)	5 ± 0.6 (<0.0001)	18 ± 3 (<0.0001)	-1.4 ± 2.4 (NS)	-4 ± 2 (0.0446)
Baseline concentration of Y	0.48 ± 0.06 (<0.0001)	0.33 ± 0.08 (<0.0001)	0.42 ± 0.04 (<0.0001)	0.28 ± 0.04 (<0.0001)	0.49 ± 0.05 (<0.0001)	0.48 ± 0.06 (<0.0001)
Dressing	(NS) <sup>c</sup>	(NS)	(NS)	(NS)	(NS)	(NS)
Treatment <sup>d</sup>	-11.2 ± 3.48 (0.0022)	-2.65 ± 0.75 (0.0009)	-1.35 ± 0.57 (0.0226)	-14.7 ± 10.9 (NS)	-0.0 ± 0.41 (NS)	-0.05 ± 0.38 (NS)
Sequence <sup>e</sup>	(NS)	-7.71 ± 2.38 (0.0022)	(NS)	(NS)	(NS)	(NS)
Period	(NS)	(NS)	(NS)	-4.45 ± 1.47 (0.0039)	(NS)	(NS)
Total cholesterol (TC) <sup>f</sup>	(NS)	(NS)	(NS)	(NS)	(NS)	(NS)
Triglycerides (TG) <sup>f</sup>	(NS)	(NS)	(NS)	0.07 ± 0.02 (0.0006)	(NS)	(NS)
TC + TG <sup>f</sup>	(NS)	(NS)	(NS)	(NS)	0.02 ± 0.01 (0.0009)	0.02 ± 0.01 (<0.0001)
LDL cholesterol <sup>f</sup>	0.32 ± 0.11 (0.0055)	(NS)	(NS)	(NS)	(NS)	(NS)
HDL cholesterol <sup>f</sup>	(NS)	(NS)	(NS)	(NS)	(NS)	(NS)
Interaction of treatment with other variables						
Treatment with BMI	(NS)	(NS)	(NS)	-0.85 ± 0.41 (0.0427)	(NS)	(NS)

<sup>a</sup>Dependent variable (Y) estimated by:  $Y$  (mg/dL) = Intercept +  $b$  +  $b^2$  + Dressing + Treatment + Diet Sequence + Period + Age + BMI + TC + TG + (TC + TG) + LDL cholesterol + HDL cholesterol + Interactions among independent variables, where  $b$  = baseline concentration of dependent variable Y; Dressing = ranch vs. Italian. BMI, body mass index; for other abbreviations see Table 1.

<sup>b</sup>There were no significant main effects of gender, age, or BMI of the participants (data omitted from the table).

<sup>c</sup>NS, not significant.

<sup>d</sup>Treatment = +PSE vs. -PSE.

<sup>e</sup>Diet sequences: Baseline to -PSE to +PSE vs. Baseline to +PSE to -PSE.

<sup>f</sup>Covariates: TC, TG, LDL cholesterol, HDL cholesterol, and sum of TC and TG.

In the 1994 report of strategies for blood cholesterol reduction from the National Cholesterol Education Program (NCEP) (34), it was estimated that for every 1% reduction in cholesterol concentration, the risk of CVD decreased by an average of 2%. Application of this prediction to TC reduction observed in the present study would indicate an average reduction in risk for CVD of 28%. This is based on changes from initial (baseline) plasma TC concentrations when a moderately low-fat, low-SFA diet with 3.6 g PSE/d was consumed. This may be partitioned as 14% reduction in risk due to consumption of the reduced-SFA diet without PSE, with a further reduction of 14% due to addition of PSE to the diet. Thus PSE consumption results in a reduction in risk beyond that resulting from reduced consumption of SFA. From this, we postulate that inclusion of PSE in the diet may have benefits unrelated to saturated fat intake and that even those people unwilling to commit to changes in type or amount of fat intake may benefit significantly from consumption of food products containing PSE.

When effects of PSE consumption (and type of dressing) were modeled, baseline (preintervention) concentration of a

plasma constituent was always an important predictor of final concentration. However, there was no interaction of baseline concentrations with response to PSE for any plasma lipid or lipoprotein. This indicates that people may benefit from a reduction in CVD risk with consumption of PSE regardless of their starting blood cholesterol level. For individuals having a normal cholesterol level, regular PSE consumption may help prevent the development of elevated cholesterol often associated with aging and changes in lifestyle as we age.

Unlike plasma lipids and lipoproteins, decreases in the TC/HDL cholesterol ratio with PSE consumption was related to the ratio at entrance of the subjects into the dietary intervention. Thus, if the ratio is an independent indicator of CVD risk (19,20), people with higher ratios, and thus at higher risk, may benefit from a greater reduction in risk when they consume PSE than do those who have lower ratios.

In this investigation, we found that plasma carotenoid concentrations decreased with addition of PSE to the diet. For example, β- and α-carotene both decreased by about 13%, while lycopene decreased by about 20%. Plasma concentrations of fat-soluble nutrients such as carotenoids may be lowered by

PSE either directly by reduced absorption or indirectly through undefined mechanisms. Plasma concentrations of some, if not all, carotenoids may be related to the concentration of the plasma lipoproteins on which they are carried (16) and may decrease or increase as plasma lipoproteins change. Thus, in experimental studies, fat-soluble carotenoids and vitamins are commonly normalized to plasma lipid concentrations. This may not be appropriate, however, when both the carotenoid and the plasma lipid are dependent variables and both are subject to change with treatment.

We saw no evidence that PSE consumption affected fat-soluble vitamin absorption. However, this investigation was conducted over a relatively short time period, and results cannot be extrapolated to what might occur over longer periods. Concentrations of plasma carotenoids in this study remained well within what may be considered normal levels. Again, as for the fat-soluble vitamins, caution must be exercised in extrapolating our results to long-term effects on carotenoids. However, plasma carotenoids are strongly related to dietary intake. On diets sufficiently rich in carotenoids, we expect that plasma concentrations of carotenoids will reach a lower plateau due to PSE consumption but will remain within normal ranges. The effects of PSE on plasma carotenoid concentrations when the diet is marginal or low in carotenoids may be of more concern.

This study did not directly compare salad dressings with vegetable oil spreads, which are the common form of commercially available food carriers of PSE. However, the extent of LDL cholesterol lowering by PSE delivered by dressings in this study, averaging 17% compared with the subjects' cholesterol level at entry, and 9.7% compared with the control diet, matched what can be extrapolated from clinical studies in which PSE were delivered by spreads having a higher fat content (4,5). In theory, there should not be any difference in the *in vivo* digestion of the fat in a spread product and the fat in a dressing product despite the differences in how they are structured. Each type of product should deliver PSE to the digestive milieu. Our data clearly support this supposition.

Reduction in SFA intake remains the primary dietary goal for individuals and for the population at large to lower LDL cholesterol and reduce the risk of CVD. In the 2001 report from the NCEP on the treatment of high blood cholesterol in adults, Adult Treatment Panel III (ATP-III) (35), the recommended intake of saturated fat is less than 7% of energy with total fat intake of 25–35% of energy. Food carriers of PSE including both vegetable oil-based spreads and reduced-fat salad dressings, each having high levels of polyunsaturated fatty acids, can be incorporated in NCEP ATP-III type diets. However, dressings with lower total fat/serving may be more readily used to deliver PSE while replacing SFA. For example, two servings per day of low-fat salad dressing, such as the Italian dressing fed in this study, carrying 3.6 g of PSE, would provide about 8 g of fat and 1 g of SFA per day but would deliver PSE in amounts that significantly reduce blood cholesterol risk of CVD. For women consuming 2163 kcal per day, the average intake in this study, two servings per day of the Italian dressing added to a

diet having 30% of calories from fat would provide only 11% of the daily fat intake and 5% of the SFA recommended as the maximum SFA intake in an NCEP ATP-III type diet. Corresponding amounts for men consuming 2766 kcal per day (the average energy intake in this study) would be 9% of daily fat intake and 4% of the SFA intake. These amounts of fat are readily balanced by removal of dietary fat from other sources and would be especially beneficial if the fat replaced is animal fat or vegetable oil-containing products high in either SFA or *trans* unsaturated fatty acids.

We conclude that low-fat foods, such as reduced- and low-fat salad dressings, are effective carriers for PSE. Such reduced-fat foods can be readily included in diets low in SFA as well as diets moderately low in total fat, i.e., prudent diets, to lower blood cholesterol and reduce the risk of CVD. Furthermore, the reductions in LDL cholesterol and in the ratio of TC to HDL cholesterol are not conditioned by the plasma lipid level of the person when consumption begins. Thus, PSE addition to the diet, coupled with the primary goal of reducing saturated fat intake, may help to both prevent development of high LDL cholesterol and reduce CVD risk.

#### ACKNOWLEDGMENT

Partial financial support was provided by Unilever Bestfoods NA (formerly Lipton) through a Research Support Agreement with the Agricultural Research Service, USDA.

#### REFERENCES

1. Dietary Guidelines Advisory Committee (2000) Report of the Dietary Guidelines Advisory Committee on the Dietary Guidelines for Americans, 2000, U.S. Department of Agriculture, Agricultural Research Service, Beltsville, MD.
2. Pollak, O.J., and Kritchevsky, D. (1981) *Sitosterol (Monographs on Atherosclerosis, Vol. 10)*, Karger, Basel.
3. de Vries, J.H.M., Kromhout, J.A., van de Bovenkamp, P., van Straveren, W.A., Mensink, R.P., and Katan, M.B. (1997) The Fatty Acid and Sterol Content of Food Composites of Middle-Aged Men in Seven Countries, *J. Food Comp. Anal.* 10, 115–141.
4. Weststrate, J.A., and Meijer, G.W. (1998) Plant Sterol-Enriched Margarines and Reduction of Plasma Total- and LDL-Cholesterol Concentrations in Normocholesterolaemic and Mildly Hypercholesterolaemic Subjects, *Eur. J. Clin. Nutr.* 52, 334–343.
5. Hendriks, H.F.J., Weststrate, J.A., van Vliet, T., and Meijer, G.W. (1999) Spreads Enriched with Three Different Levels of Vegetable Oil Sterols and the Degree of Cholesterol Lowering in Normocholesterolaemic and Mildly Hypercholesterolaemic Subjects, *Eur. J. Clin. Nutr.* 53, 319–327.
6. Society of Actuaries and Association of Life Insurance Medical Directors of America 1979 (1980) *Weight of Insured Persons in the United States Associated with Lowest Mortality*, Association of Life Insurance Medical Directors of America, Philadelphia.
7. U.S. Department of Agriculture, Agricultural Research Service (1998) USDA-NCC Carotenoid Database for U.S. Foods—1998, Nutrient Data Laboratory Home Page, <http://www.nal.usda.gov/fnic/foodcomp>.
8. National Heart Lung and Blood Institute (1982) Lipid and Lipoprotein Analysis, in *Manual of Laboratory Operations, Lipid Research Clinics Program* (Hainline, A., Karon, J., and Lippel, K., eds.), 2nd edn., Department of Health and Human Services, Bethesda, MD.

9. Gidez, L.I., Miller, G.J., Burstein, M., Slagle, S., and Eder, H.A. (1982) Separation and Quantitation of Subclasses of Human Plasma High-Density Lipoproteins by a Simple Precipitation Procedure, *J. Lipid Res.* 23, 1206–1223.
10. Friedewald, W.T., Levy, R.I., and Fredrickson, D.S. (1972) Estimation of the Concentration of Low-Density Lipoprotein Cholesterol Without Use of the Preparative Ultracentrifuge, *Clin. Chem.* 18, 499–502.
11. Khachik, F., Beecher, G.R., Goli, M.B., Lusby, W.R., and Smith, J.C. (1992) Separation and Identification of Carotenoids and Their Oxidation Products in the Extracts of Human Plasma, *Anal. Chem.* 64, 2111–2122.
12. Bieri, J.G., Brown, E.D., and Smith, J.C. (1985) Determination of Individual Carotenoids in Human Plasma by High Performance Liquid Chromatography, *J. Liq. Chromatogr.* 8, 473–484.
13. Burnham, K.P., and Anderson, D.R. (1998) *Model Selection and Inference; A Practical Information-Theoretic Approach*, Springer-Verlag, New York.
14. Littell, R.C., Milliken, G.A., Stroup, W.W., and Wolfinger, R.D. (1996) *SAS System for Mixed Models*, SAS Institute, Inc., Cary, NC.
15. Schwartz, G. (1978) Estimating the Dimension of a Model, *Ann. Statistics* 6, 461–464.
16. Clevidence, B.A., and Bieri, J.G. (1993) Association of Carotenoids with Human Plasma Lipoproteins, *Methods Enzymol.* 214.
17. U.S. Department of Agriculture, Agricultural Research Service, (1996) Data Tables: Results for USDA's 1995 Continuing Survey of Food Intakes by Individuals and 1995 Diet and Health Knowledge Survey, Beltsville Human Nutrition Research Center, Food Surveys Research Group, Beltsville, MD.
18. U.S. Department of Agriculture, Human Nutrition Information Service (1976–1990) Composition of Foods, *Agriculture Handbook No. 8*, Sections 1–22, U.S. Government Printing Office, Washington, DC.
19. Miller, G.J., and Miller, N.E. (1975) Plasma High-Density Lipoprotein Concentration and Development of Ischemic Heart Disease, *Lancet* i, 16–20.
20. Gordon, D.J., Probstfield, J.L., Garrison, R.J., Neaton, J.D., Castelli, W.P., Knoke, J.D., Jacobs, D.R., Jr., Bangdiwala, S., and Tyroler, H.A. (1989) High-Density Lipoprotein Cholesterol and Cardiovascular Disease: Four Prospective American Studies, *Circulation* 79, 8–15.
21. Lichtenstein, A.H., Ausman, L.M., McNamara, J.R., and Schaefer, E.J. (1996) *Trans* and Saturated Fatty Acid Content of Dietary Fat Effects Plasma Lipid and Lipoprotein Concentrations, *Circulation* 94, 1–97.
22. Chisholm, A., Mann, J., Sutherland, W., Duncan, A., Skeaff, M., and Frampton, C. (1996) Effect on Lipoprotein Profile of Replacing Butter with Margarine in a Low Fat Diet: Randomized Crossover Study with Hypercholesterolaemic Subjects, *Br. Med. J.* 312, 931–934.
23. Hokanson, J.E., and Austin, M.A. (1996) Plasma Triglyceride Level Is a Risk Factor for Cardiovascular Disease Independent of High-Density Lipoprotein Cholesterol Level: A Meta-analysis of Population-Based Prospective Studies, *J. Cardiovasc. Risk* 3, 213–229.
24. Bostom, A.G., Gagnon, D.R., Cupples, L.A., Wilson, P.W.F., Jenner, J.L., Ordovas, J.M., Schaefer, E.J., and Castelli, W.P. (1994) A Prospective Investigation of Elevated Lipoprotein(a) Detected by Electrophoresis and Cardiovascular Disease in Women: The Framingham Heart Study, *Circulation* 90, 1688–1695.
25. Schaefer, E.J., Lamon-Fava, S., Jenner, J.L., McNamara, J.R., Ordovas, J.M., Davis, E., Abolafia, J.M., Lippel, K., and Levy, R.I. (1994) Lipoprotein (a) Levels and Risk of Coronary Heart Disease in Men: The Lipid Research Clinics Coronary Primary Prevention Trial, *J. Am. Med. Assoc.* 271, 999–1003.
26. Hoefler, G., Harnoncourt, F., Paschke, E., Mirtl, W., Pfeiffer, K.H., and Kostner, G.M. (1988) Lipoprotein Lp(a): A Risk Factor for Myocardial Infarction, *Arteriosclerosis* 8, 398–401.
27. Rosengren, A., Wilhelmsen, L., Eriksson, E., Risberg, B., and Wedel, H. (1990) Lipoprotein (a) and Coronary Heart Disease: A Prospective Case-Control Study in a General Population Sample of Middle Aged Men, *Br. Med. J.* 301, 1248–1251.
28. Clevidence, B.A., Judd, J.T., Schaefer, E.J., Jenner, J.L., Lichtenstein, A.H., Muesing, R.A., Wittes, J.A., and Sunkin, M.E. (1997) Plasma Lipoprotein(a) Levels in Men and Women Consuming Diets Enriched in Saturated, *cis* or *trans* Monounsaturated Fatty Acids, *Arterioscler. Thromb. Vasc. Biol.* 17, 1–5.
29. Almendingen, K., Jordal, O., Kierulf, P., Sandstad, B., and Pedersen, J.I. (1995) Effects of Partially Hydrogenated Fish Oil, Partially Hydrogenated Soybean Oil, and Butter on Serum Lipoproteins and Lp(a) in Men, *J. Lipid Res.* 36, 1370–1384.
30. Judd, J.T., Baer, D.J., Clevidence, B.A., Muesing, R.A., Chen, S.C., Weststrate, J.A., Meijer, G.W., Wittes, J., Lichtenstein, A.H., Vilella-Bach, M., and Schaefer, E.J. (1998) Effects of Margarine Compared with Those of Butter on Blood Lipid Profiles Related to Cardiovascular Disease Risk Factors in Normolipemic Adults Fed Controlled Diets, *Am. J. Clin. Nutr.* 68, 768–777.
31. Mensink, R.P., Zock, P.L., Katan, M.B., and Hornstra, G. (1992) Effect of Dietary *cis* and *trans* Fatty Acids on Serum Lipoprotein(a) Levels in Humans, *J. Lipid Res.* 33, 1493–1501.
32. Nestel, P., Noakes, M., Belling, B., McArthur, R., Clifton, P., Janus, E., and Abbey, M. (1992) Plasma Lipoprotein Lipid and Lp(a) Changes with Substitution of Elaidic Acid for Oleic Acid in the Diet, *J. Lipid Res.* 33, 1029–1036.
33. Normen, L., Dutta, P., Lia, A., and Andersson, H. (2000) Soy Sterol Esters and  $\beta$ -Sitosterol Ester as Inhibitors of Cholesterol Absorption in Human Small Bowel, *Am. J. Clin. Nutr.* 71, 908–913.
34. National Cholesterol Education Program (1994) Second Report of the Expert Panel on Detection, Evaluation, and Treatment of High Blood Cholesterol in Adults (Adult Treatment Panel II), *Circulation* 89, 1329–1445.
35. National Cholesterol Education Program (2001) Executive Summary: Third Report of the Expert Panel on Detection, Evaluation, and Treatment of High Blood Cholesterol in Adults (Adult Treatment Panel III), *J. Am. Med. Assoc.* 285, 2486–2497.

[Received April 27, 2001, and in revised form July 27, 2001; revision accepted October 2, 2001]

# Exercise Training-Induced Changes in Sensitivity to Endothelin-1 and Aortic and Cerebellum Lipid Profile in Rats

Eduardo Latorre<sup>c</sup>, María Morán<sup>b</sup>, M. Dolores Aragonés<sup>a</sup>, Ana Saborido<sup>a</sup>, Inmaculada Fernández<sup>a</sup>, Jerónimo Delgado<sup>b</sup>, R. Edgardo Catalán<sup>c</sup>, and Alicia Megías<sup>b,\*</sup>

<sup>a,b</sup>Departamento de Bioquímica y Biología Molecular I, <sup>a</sup>Facultad de Química y <sup>b</sup>Facultad de Biología, Universidad Complutense, E-28040 Madrid, Spain, and <sup>c</sup>Departamento de Biología Molecular, Centro de Biología Molecular "Severo Ochoa," Universidad Autónoma de Madrid, E-28049 Madrid, Spain

**ABSTRACT:** The purpose of this work was to study whether exercise training induces changes in the lipid profile of rat aorta and nervous system and in the *in vitro* intrinsic responsiveness of these tissues to endothelin-1 (ET-1) treatment. The exercise program performed successfully produced the characteristic metabolic alterations of the trained state. Exercise training induced a large and significant increase in the levels of both aortic ethanolamine plasmalogens (PlasEtn) and glucosylceramides. In contrast, a decrease of aortic ceramide and cholesterol levels was evoked by exercise training. ET-1 increased PlasEtn content only in sedentary animals. An exercise-induced increase in cerebellum levels of ceramides and ceramide monohexosides was found. The cerebellum ceramide content was increased by ET-1 more noticeably in sedentary rats than in trained animals. In contrast, cerebral cortex was observed to be largely insensitive to both exercise training and ET-1 treatment. It was concluded that exercise training (i) induces changes in both vascular and cerebellar lipid profiles, the former being much more pronounced than the latter, and (ii) diminishes the aortic and cerebellar sensitivity to ET-1 action.

Paper no. L8768 in *Lipids* 37, 43–52 (January 2002).

Sphingolipids and their breakdown products, ceramides, have emerged as important components of signal transduction systems (1). Ceramides play a role as secondary messengers mediating agonist action in postmitotic neuronal (2) and vascular cells (3) and are also involved in cellular proliferation, differentiation, and apoptosis phenomena (1). In addition, there is increasing experimental evidence showing that a highly complex network of interactions exists between glycerolipid and sphingolipid metabolism. We recently reported that an increase in the endogenous ceramide level elicited by sphingomyelinase (SPHase) treatment can affect choline and ethanolamine phosphoglycerides in the brain (4).

In previous studies focused on signal transduction systems, we described that sphingolipids as well as glycerolipids have a central role in the molecular mechanism of endothelin-1 (ET-1) action (5–9). ET-1 is a potent regulatory peptide gen-

erated by endothelial cells that was first isolated from cultured porcine aorta endothelial cells (10). It is now clear that ET-1 has a wide range of biological actions in both vascular and nonvascular tissues, including the nervous system (11,12). Thus, the ET-1 behavior as vasoactive peptide and neuropeptide is widely known. Therefore, the distribution and characteristics of ET-1 receptors and the signal transduction systems involved in the ET-1 molecular mechanism are being extensively studied. In this context, we reported that ET-1 is able to modulate phosphoinositide turnover and protein kinase C activity in the nervous system and in the blood-brain barrier (6–9), as well as the brain sphingolipid signal transduction system evoking ceramide production (5).

It is well known that endurance exercise training has beneficial effects on physiopathological states of the cardiovascular and nervous systems, but the molecular mechanisms involved are not completely understood. Endurance exercise causes a redistribution of tissue blood flow (13,14) and alterations in the levels of some neuropeptides (15), including those of plasma ET-1, that are augmented by exercise (13). Since aortic blood flow increases during treadmill training in the rat (16), it is conceivable that chronic exercise induces adaptive changes in the aorta, thereby contributing somehow to the modification of aortic function, as has been widely reported (17–19). In addition, there is evidence of exercise-induced changes in the nervous system (20–23), and it has been suggested that in the brain these changes might be mediated, at least in part, through neuroregulatory feedback from arterial baroreceptors to the brain (24). On the other hand, cardiovascular and neurodegenerative diseases are known to be associated with cellular apoptosis (2,3) and with oxidative stress or the vulnerability to it (25).

With this background and our interest in the molecular mechanisms involved in ET-1 actions, we have hypothesized that vascular and brain responses to ET-1 may be modified by long-term endurance exercise training. The aim of the present study was to investigate whether a long-term period of treadmill running induces alterations in the ET-1 regulatory actions on: (i) lipid second messengers, such as ceramide and diacylglycerols (DAG), considered, respectively, as being apoptotic and survival signal transducers (2), (ii) their potential lipid precursors, and (iii) ceramide monohexosides and cholesterol (CH). The study of all these lipid molecules was carried out

\*To whom correspondence should be addressed.  
E-mail: amegias@bbm1.ucm.es

Abbreviations: BSS, balanced salt solution; CH, cholesterol; DAG, diacylglycerol; ET-1, endothelin-1; PlasEtn, ethanolamine plasmalogens; PtdEtn, phosphatidylethanolamine; PL, phospholipids; SPH, sphingomyelin; SPHase, sphingomyelinase; TL, total lipids; TLC, thin-layer chromatography.



because they have a causal involvement in the physiological actions of ET-1 (5) and may be involved in some beneficial effects of exercise, i.e., prevention of diseases and delay of aging, as suggested by previous evidence (25–28). In addition, differences found in the trained animals in the profile of these lipids involved in the ET-1 signal transduction systems are discussed in terms of adaptation to long-term training.

## MATERIALS AND METHODS

**Materials.** Ceramides type III from bovine brain sphingomyelin (SPH), containing primarily stearic and nervonic acids; ceramides type IV from bovine brain galactocerebrosides, containing  $\alpha$ -hydroxy fatty acids; ceramide monohexoside standards (bovine brain galactocerebrosides and human spleen glucocerebrosides); ET-1, and other standard lipids were purchased from Sigma Chemical Co. (St. Louis, MO). [ $\gamma$ - $^{32}$ P]ATP (specific activity: 3000 Ci/mmol) was obtained from Nuclear Ibérica, S.A., (Madrid, Spain) and *Escherichia coli* DAG kinase was from Calbiochem (San Diego, CA). High-performance thin-layer chromatography (TLC) plates were obtained from Merck (Darmstadt, Germany). All other reagents were of the highest analytical grade available.

**Animals and exercise training program.** Male Wistar rats (initial body weight  $150 \pm 9$  g) were obtained from Charles River (Barcelona, Spain). They were housed in an animal room at 22–24°C and given free access to commercial rat chow and tap water. The animals were adapted to an inverse 12:12 h light-dark cycle (dark period 0800 to 2000) before the beginning of the exercise regimen. Rat care and handling and all the experimental procedures employed were in accordance with internationally accepted principles concerning the care and use of laboratory animals.

Sixteen rats were randomly allotted to sedentary ( $n = 8$ ) and exercise-trained ( $n = 8$ ) groups. The rats of the trained group were exercised on a motor-driven rodent treadmill (Columbus Instruments, Columbus, OH) and performed five exercise sessions per week for 24 wk. Mild electrical stimulation was used to encourage the rats to run (grid shock  $<1$  mA). During the first 4 wk, the speed and duration of the daily exercise sessions were progressively increased until the rats were capable of running continuously for 45 min at  $25 \text{ m}\cdot\text{min}^{-1}$ . After 12 wk, the duration of the exercise sessions was increased to 60 min, and these conditions were maintained until completion of the exercise program. The selected treadmill speed corresponds to 60–70% of  $\text{VO}_{2\text{max}}$  according to the data of Brooks and White (29). During the 24-wk training period, sedentary control rats performed a single weekly exercise session for 5 min at  $15 \text{ m}\cdot\text{min}^{-1}$  to familiarize them with treadmill exercise and handling.

**Treadmill endurance test.** Two weeks before the end of the training period, a treadmill endurance exercise test was administered to all sedentary and trained rats the day before the weekly animal rest. The exercise test started with a 5 min warm-up at  $20 \text{ m}\cdot\text{min}^{-1}$  with a 5% slope after which animals ran at  $25 \text{ m}\cdot\text{min}^{-1}$  with a 5% slope until exhaustion. Rats were

judged to be exhausted when they could no longer continue at the required pace or maintain upright posture on the treadmill; at this point, they were usually unable to rapidly upright themselves when placed on their backs. Total exercise duration was recorded.

**Tissue preparation.** At the conclusion of the training program, 48 h after the final exercise training session, the rats were anesthetized with diethyl ether and killed as previously described (4), and the tissues were quickly dissected. The soleus muscles were removed, trimmed of connective tissue, weighed, fast-frozen in liquid nitrogen, and stored at  $-80^\circ\text{C}$  until further use. Aortas were removed and placed under a dissecting microscope in cold balanced salt solution (BSS) with the following composition (in mM): 135 NaCl, 4.5 KCl, 1.5  $\text{CaCl}_2$ , 0.5  $\text{MgCl}_2$ , 5.6 glucose, 10 HEPES, pH 7.4. The vessels were then cleaned of adherent fat and connective tissue with a cotton swab moistened in BSS, and the cleaned aortas were then cut into rings (4 mm long). Aortic strips were incubated as described later. Brains were removed, pial vessels and white matter were carefully discarded, and cerebral cortex and cerebellum were obtained. Slices (dimensions:  $350 \times 350 \mu\text{m}$ ) of both regions were prepared with a MacIlwain tissue chopper. They were equilibrated in BSS with 95%  $\text{O}_2/5\%$   $\text{CO}_2$  for 1 h.

To study the ET-1 effect, aorta strips and cerebral cortex and cerebellum slices from each animal were randomly divided into two portions, transferred into glass tubes containing BSS, and incubated for 30 min without or with ET-1 (final concentration  $10^{-7}$  M). These conditions have been designed to evoke physiological and biochemical alterations in aortic (30) and brain (5) intact tissue preparations. The incubation mixtures were continuously gassed with 95%  $\text{O}_2/5\%$   $\text{CO}_2$ . Reactions were stopped by removing the medium and replacing it with 0.38 mL of BSS containing 10 mM EDTA and 1 mL of chloroform/methanol/13 M HCl (100:100:1, by vol).

**Determination of citrate synthase activity in muscle homogenate.** Soleus muscle was homogenized twice for 30 s with a Polytron PT-10 at the maximum speed setting in 6.5 vol of 20 mM 3-(*N*-morpholino)propane sulfonic acid (MOPS), pH 7.0 containing 0.25 M sucrose,  $5 \text{ mg}\cdot\text{mL}^{-1}$  defatted BSA, and protease inhibitors at the following concentrations: 0.23 mM phenylmethylsulfonyl fluoride,  $100 \mu\text{g}\cdot\text{mL}^{-1}$  benzamidine, and  $0.5 \mu\text{g}\cdot\text{mL}^{-1}$  each of aprotinin, leupeptin, and pepstatin A. The resulting homogenate was diluted with 5 vol of the same buffer, filtered through two layers of cheesecloth, and used for analysis. The protein concentration of the homogenates was determined by the method of Lowry *et al.* (31).

Citrate synthase (EC 4.1.3.7) was measured in the muscle homogenates at  $37^\circ\text{C}$  as described previously (32). The assay mixture contained in a total volume of 1 mL (in mM) was as follows: 100 Tris-HCl, pH 8.1; 1 5,5'-dithiobis-(2-nitrobenzoate); 0.3 acetyl-CoA; 0.5 oxalacetate; 0.2% (wt/vol) Triton X-100, and a suitable amount of protein (60  $\mu\text{g}$ ). The reaction was started by addition of oxalacetate, and the increase in absorbance was recorded at 412 nm ( $\epsilon = 13.6 \text{ mM}^{-1}\cdot\text{cm}^{-1}$ ) in a thermostatically controlled UVIKON 930 spectrophotometer

(Kontron Instruments, Milan, Italy). The enzymatic activity was expressed in units per g of tissue wet weight ( $\mu\text{mol}\cdot\text{min}^{-1}\cdot\text{g}$  tissue wet weight $^{-1}$ ).

**Extraction of total lipids, separation of glycerolipids and sphingolipids.** Lipids were extracted by the method of Bligh and Dyer (33). The organic phases were dried under an  $\text{N}_2$  atmosphere and the total lipids were weighed and dissolved in chloroform/methanol (2:1, vol/vol). Lipids were separated by TLC.

For the sphingolipid studies, one aliquot of total lipids was subjected to alkaline hydrolysis in 0.1 M methanolic KOH at 37°C for 1 h to remove glycerolipids, as previously described (5). SPH, ceramides, and ceramide monohexosides were resolved using chloroform/methanol/water (65:25:4, by vol). Lipid standards were co-chromatographed with samples. Lipids were visualized by iodine vapors, and the bands corresponding to ceramide monohexosides and ceramides were scraped from the plates and extracted with chloroform/methanol (60:40, vol/vol) for their subsequent quantitation. SPH bands were quantitated without extraction, as described next.

**Radioenzymatic determination of ceramide and ceramide monohexoside levels.** Extracted ceramides and ceramide monohexosides were phosphorylated in the presence of DAG kinase, as described previously (34) with some modification (4). Aliquots of the dried lipids were solubilized and emulsified in 40  $\mu\text{L}$  of octyl- $\beta$ -D-glucoside/cardiolipin solution and sonicated in a bath sonicator (50–60 Hz) for 1 min. The reaction mixture containing 5  $\mu\text{g}$  of enzyme and the emulsified lipid substrate was preincubated at room temperature for 10 min, and the reaction was started by adding 10  $\mu\text{L}$  of 10 mM [ $\gamma$ - $^{32}\text{P}$ ]ATP in 20 mM imidazole buffer, pH 6.6. After incubation for 30 min at 25°C, phosphorylated derivatives of ceramides and ceramide monohexosides were extracted, fractionated by TLC, and quantitated by liquid scintillation counting (4). Calibration curves were derived using known amounts of ceramide and ceramide monohexoside.

**Radioenzymatic determination of DAG mass.** Aliquots of total lipids were phosphorylated in the presence of DAG kinase according to Preiss *et al.* (35). After DAG kinase assay, samples were fractionated by TLC (6). Spots corresponding to phosphatidic acid were visualized by autoradiography and quantitated by liquid scintillation counting. Calibration curves were derived using known quantities of 1-stearoyl,2-arachidonoyl glycerol.

**Quantitative determination of glycerophospholipids and CH. Analysis of the subclasses of ethanolamine phospholipids.** Aliquots of total lipids were dissolved in chloroform/methanol (2:1, vol/vol). For glycerophospholipid and CH studies, one aliquot of total lipid was separated using sequential one-dimensional TLC. The first system employed was chloroform/methanol/acetic acid/water (25:15:4:1.5, by vol) and the second was chloroform/methanol/acetic acid (65:2.5:4, by vol). The first system reached 4 cm from the top plate, whereas the second was developed through the plate. After development, spots were visualized by iodine vapors.

In the experiments where 1-alkenyl-2-acyl-*sn*-glycero-3-phosphoethanolamine (ethanolamine plasmalogens; PlasEtn)

were quantitated, total lipids were quantitatively split into two portions and dried under  $\text{N}_2$ . One portion was exposed to fumes from 12 M HCl in a Pyrex tray for 13 min to cleave the ether bond of the plasmalogen fraction while the 1-alkyl-2-acyl- and 1,2-diacyl-*sn*-glycero-3-phosphoethanolamine (phosphatidylethanolamine, PtdEtn) fractions remained intact. The small alkylacyl fraction was not quantitated separately. After separation by sequential one-dimensional TLC, as described previously, spots corresponding to ethanolamine phosphoglycerides, choline phosphoglycerides, and CH were scraped. Phosphorus content of glycerophospholipids and SPH was quantitated as described previously (36). In the case of ethanolamine phosphoglycerides, the untreated sample gave the total ethanolamine phosphoglyceride content, whereas the acid-resistant one gave the PtdEtn fraction level. The PlasEtn content was obtained by subtracting the latter from the former value. Identification was carried out by using respective standards. CH mass was quantitated as described previously (36).

**Statistical analysis.** All samples were individually processed and assayed in duplicate. Means  $\pm$  SD of eight independent preparations are presented. To evaluate differences between the sedentary and the exercised group, a Student's *t*-test for unpaired values was used. Measurements of lipid levels were analyzed using two-way analysis of variance to test for the two main effects (exercise training and ET-1 treatment) and for the interaction between them; a Scheffé *post hoc* analysis was performed to establish specific differences. When appropriate, effects of ET-1 in a single group were evaluated by paired *t*-testing. For all statistical analysis, significance was established at  $P < 0.05$ .

## RESULTS

**Exercise training effectiveness.** As a prerequisite of our study, we confirmed that the exercise program employed produced the characteristic effects of the endurance training. The exercise program induced several changes indicative of a trained state in male rats, as shown in Table 1. First, animal body weight was lower in the trained group compared with the sedentary group (19%,  $P < 0.05$ ), a common finding for trained male rats (37,38). Second, the results of the treadmill endurance test showed that running time until fatigue was significantly longer in trained than in control animals. Finally, the citrate synthase activity measured in the homogenates of soleus muscles of exercised rats was 60% over that of the

**TABLE 1**  
Effect of Exercise Training Program on Rat Body Weight, Exercise Endurance Capacity, and Skeletal Muscle Citrate Synthase Activity (CS)<sup>a</sup>

Group	Body weight (g)	Endurance time <sup>b</sup> (min)	CS activity ( $\mu\text{mol}\cdot\text{min}^{-1}\cdot\text{g}^{-1}$ )
Sedentary	625 $\pm$ 36	13 $\pm$ 6	30 $\pm$ 6
Trained	508 $\pm$ 50 <sup>c</sup>	162 $\pm$ 19 <sup>c</sup>	48 $\pm$ 5 <sup>c</sup>

<sup>a</sup>Values are means  $\pm$  SD ( $n = 8$ ).

<sup>b</sup>Endurance time is defined as the time during which the rat shows the ability to keep pace with the treadmill at 25  $\text{m}\cdot\text{min}^{-1}$  and 5% slope.

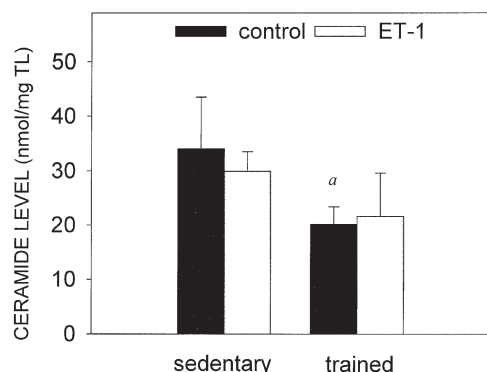
<sup>c</sup>Significant difference between sedentary and trained groups ( $P < 0.05$ ).

sedentary group, indicating that the exercise program induced the well-characterized enhancement of skeletal muscle oxidative capacity (37,38).

**Aortic responses to ET-1 treatment and exercise training.** In the ceramide radioenzymatic assay, two different molecular species of phosphorylated ceramide that showed different migration values ( $R_f$  values) in the TLC were found. The major band had an  $R_f$  value of 0.14, whereas a value of 0.32 was observed for the minor band. These bands run in parallel with the band corresponding to the phosphorylated ceramide type IV standard, which is rich in hydroxy fatty acids. The phosphorylated derivative of the ceramide type III standard (without hydroxy acids) was found to overlap to some degree with that of ceramide type IV. Therefore, it may only be concluded that aorta ceramides exist both with or without hydroxy acids. In addition, differences in the length of the fatty acid chain cannot be discarded, as it has been previously discussed (34). Figure 1 shows that ET-1 treatment did not change the level of the major ceramide species. However, the training induced a significant decrease (40%,  $P < 0.05$ ). With respect to the minor ceramide species [basal value:  $0.78 \pm 0.2$  nmol/mg total lipids (TL)], we could only observe a training-evoked slight, but not significant, decrease (30%) in their levels (data not shown).

DAG levels (basal value:  $9.1 \pm 2.5$  nmol/mg TL) remained unchanged after both ET-1 treatment and exercise-training (data not shown).

The variations exhibited by the potential phospholipid (PL) precursors of these second messengers are shown in Table 2. Neither ET-1 treatment nor exercise training produced any significant change in the levels of SPH and choline phosphoglycerides. Exercise training, but not ET-1, significantly decreased the ethanolamine phosphoglyceride level. Further separation of these PL into diacyl and alkenylacyl molecular forms gave the results shown in Figure 2. In sedentary, but not in trained animals, the basal levels of both diacyl (Fig. 2A) and plasmalogen forms (Fig. 2B) were significantly ( $P < 0.05$ ) modified by ET-1 treatment in a specific manner, since the peptide evoked a significant decrease (37%) in the level of diacyl forms and a large increase (145%) in the plasmalogen content.



**FIG. 1.** Effects of exercise training and *in vitro* endothelin-1 (ET-1) treatment on aortic ceramide levels. Data are represented as means  $\pm$  SD ( $n = 8$ ). <sup>a</sup>Significantly different from the sedentary control group at the level of  $P < 0.05$ . TL, total lipids.

**TABLE 2**  
Distribution of Aortic Phospholipid Subclasses (nmol/mg total lipids) in Sedentary and Trained Rats, Effect of *in Vitro* Endothelin-1 (ET-1) Treatment<sup>a</sup>

Group	Treatment	Choline phosphoglycerides	Ethanolamine phosphoglycerides	SPH
Sedentary	Control	11.5 $\pm$ 2.7	8.8 $\pm$ 1.1	1.7 $\pm$ 0.2
	ET-1	9.5 $\pm$ 2.9	7.0 $\pm$ 2.1	1.7 $\pm$ 0.3
Trained	Control	12.1 $\pm$ 1.0	4.1 $\pm$ 1.0 <sup>b</sup>	1.8 $\pm$ 0.4
	ET-1	10.2 $\pm$ 2.5	3.6 $\pm$ 1.1 <sup>c</sup>	1.2 $\pm$ 0.3

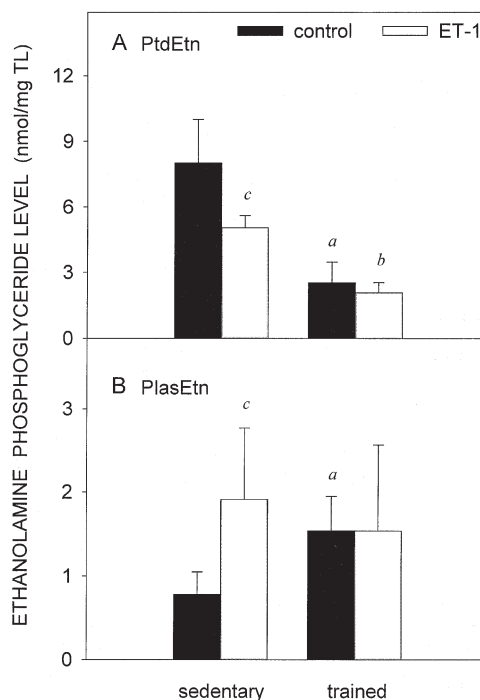
<sup>a</sup>Data are presented as means  $\pm$  SD ( $n = 8$ ).

<sup>b</sup>Significantly different from the sedentary control group at the level of  $P < 0.05$ .

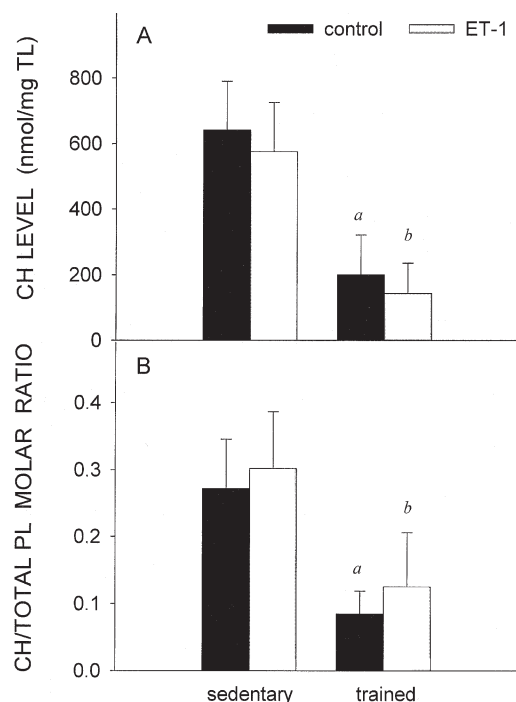
<sup>c</sup>Significantly different from the ET-1-treated aortic strips from the sedentary group ( $P < 0.05$ ). SPH, sphingomyelin.

In the sedentary control group the plasmalogen fraction (mean value, 0.78 nmol/mg TL, Fig. 2B) made up 9% of the total ethanolamine phosphoglycerides, whereas in the trained control group this percentage was 38% (mean value of plasmalogens, 1.54 nmol/mg TL, Fig. 2B), which represents a fourfold increase. Obviously, an exercise-elicited decrease was found in the content of diacyl molecular forms, the difference being much less noticeable (91% in the control of sedentary group vs. 62% in the control of the trained group).

Figure 3 shows that ET-1 never altered the CH level and the CH/total PL molar ratio. However, aortas from trained rats



**FIG. 2.** Alterations induced by exercise training and *in vitro* ET-1 treatment on aorta ethanolamine phosphoglycerides. (A) Levels of phosphatidylethanolamine (PtdEtn); (B) levels of ethanolamine plasmalogen (PlasEtn). Data are expressed as means  $\pm$  SD ( $n = 8$ ). <sup>a</sup>Significantly different from the sedentary control group ( $P < 0.05$ ). <sup>b</sup>Significantly different from the ET-1-treated aorta from sedentary group ( $P < 0.05$ ). <sup>c</sup>Significant difference between control and ET-1-treated aorta of the sedentary group ( $P < 0.05$ ). For other abbreviations see Figure 1.

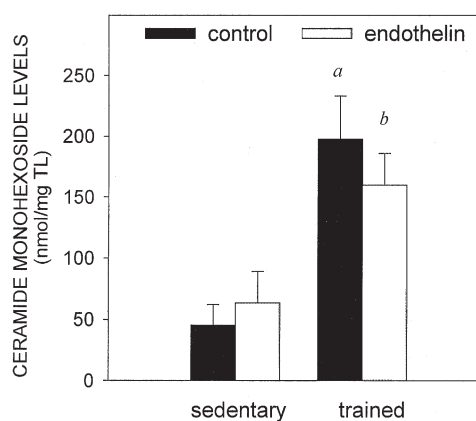


**FIG. 3.** Alterations induced by exercise training on aorta cholesterol (CH) levels (A) and CH/total phospholipids (PL) molar ratio (B). Effect of *in vitro* ET-1 treatment. Data are represented as means  $\pm$  SD ( $n = 8$ ). <sup>a</sup>Significantly different from the sedentary control group ( $P < 0.05$ ). <sup>b</sup>Significantly different from the ET-1 treated aorta from sedentary group ( $P < 0.05$ ). For other abbreviations see Figure 1.

showed a significant decrease (70% under the value observed in their sedentary counterparts) in both the CH level and the CH/total PL ratio.

Previous evidence of a potential role for ceramide monohexosides in the ET-1 molecular mechanism of action (5) and in the vascular physiology (27) prompted us to evaluate potential alterations in their levels. The aortic ceramide monohexoside fraction was found to co-migrate with the glucocerebroside standard, as previously described for aortic glycosphingolipids (39). In sedentary animals, but not in trained ones, ET-1 treatment induced a slight, but not significant, increase in the ceramide monohexoside levels (Fig. 4). However, there were significantly higher ceramide monohexoside levels in aortas from trained rats compared with those of their sedentary counterparts.

**Cerebral cortex and cerebellum response to ET-1 treatment and exercise training.** Two different molecular species of ceramide were found in cerebral cortex and cerebellum as we detected in aorta. Neither ET-1 treatment nor exercise training modified ceramide levels in cerebral cortex (Table 3). In contrast, in the cerebellum, ET-1 treatment increased ( $P < 0.05$ ) the level of the ceramide species that runs more slowly in the chromatography (Fig. 5A), which was more noticeable in sedentary rats than in trained ones, i.e., 300 and 78% over their respective control value. The other ceramide species were not significantly altered by ET-1 treatment (Fig. 5B). Exercise training was found to enhance the levels of both ceramide species, 400 and 87% over their sedentary counterparts (Figs. 5 A and B, respectively).



**FIG. 4.** Exercise training-induced alterations in aorta ceramide monohexoside levels. Effect of *in vitro* ET-1 treatment. Data are represented as means  $\pm$  SD ( $n = 8$ ). <sup>a</sup>Significantly different from the sedentary control group ( $P < 0.05$ ). <sup>b</sup>Significantly different from the ET-1 treated aortas from the sedentary group ( $P < 0.05$ ). For abbreviations see Figure 1.

DAG levels in cerebral cortex (Table 3) and cerebellum (basal value:  $90.5 \pm 38$  nmol/mg TL, data not shown) were not significantly altered by ET-1 treatment or exercise training.

Tables 4 and 5 show that no significant changes were observed in the levels of cerebral cortex and cerebellum PL in response to either ET-1 treatment or exercise training except for a decrease in the cerebral cortex SPH content of sedentary animals following ET-1 treatment (53% under control value).

Table 6 shows that ET-1 evoked a decrease in the CH content (30% under control value) in cerebral cortex from trained rats, whereas in sedentary animals the peptide produced no effects. In cerebellum, the sensitivity to the ET-1 lowering effect of the CH levels was reversed, i.e., it was observed in sedentary rats, but not in trained animals. Exercise training did not give rise to any difference.

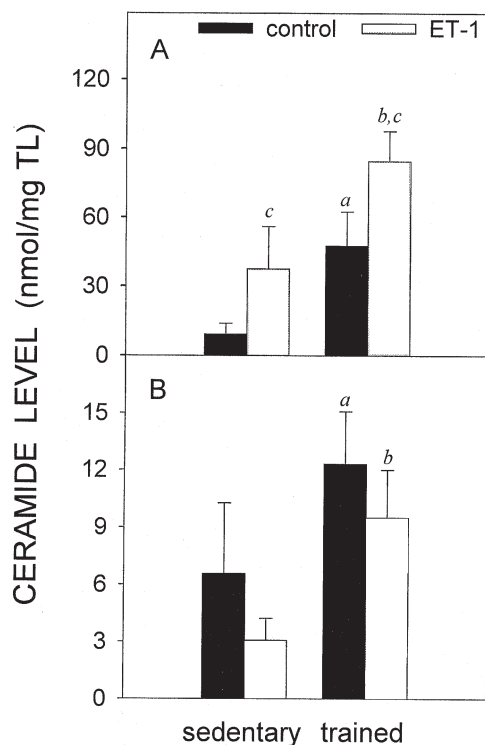
The ceramide monohexoside fraction from cerebral cortex migrated as a doublet and co-migrated with glucocerebroside standard, whereas that from cerebellum migrated slightly more slowly and showed some degree of overlapping with the galactocerebroside standard. Since cerebral cortex is not a myelinated region and shows a poor synthesis of galactocerebroside, it is likely that this lipid fraction is mainly glucosylceramide. In contrast, in the fraction from cerebellum both glucosyl and galactosylceramide are present. Figure 6 shows that levels of ceramide monohexosides in cerebral cortex (6A) and cerebellum (6B) were not modified by ET-1 treat-

**TABLE 3**  
Lipid Fraction Levels (nmol/mg total lipids) in Cerebral Cortex of Sedentary and Trained Rats, Effect of *in Vitro* ET-1 Treatment<sup>a</sup>

Group	Treatment	Ceramides			DAG
Sedentary	Control	103 $\pm$ 22	0.29 $\pm$ 0.13	31 $\pm$ 6	
	ET-1	68 $\pm$ 26	0.18 $\pm$ 0.09	35 $\pm$ 6	
Trained	Control	87 $\pm$ 12	0.21 $\pm$ 0.10	23 $\pm$ 11	
	ET-1	93 $\pm$ 23	0.21 $\pm$ 0.09	25 $\pm$ 5	

<sup>a</sup>Data are presented as means  $\pm$  SD ( $n = 8$ ). DAG, diacylglycerol; see Table 2 for other abbreviation.



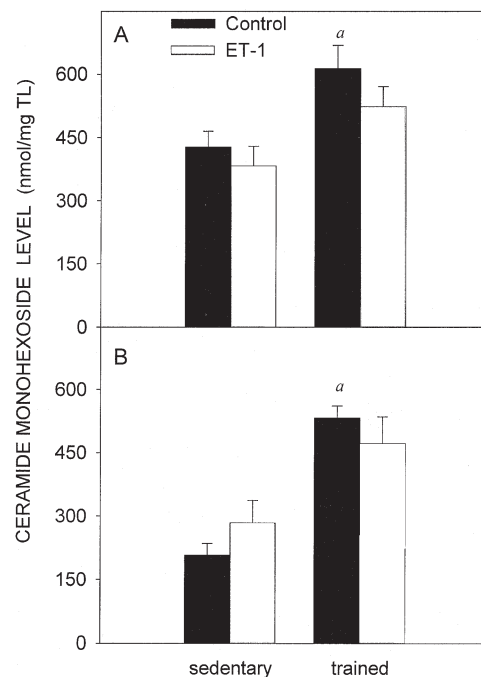


**FIG. 5.** Exercise training-induced alterations in ceramide levels of cerebellum. Effect of *in vitro* ET-1 treatment. (A) and (B): Levels of the major and minor ceramide molecular species, respectively. Data are represented as means  $\pm$  SD ( $n = 8$ ). <sup>a</sup>Significantly different from the sedentary control group ( $P < 0.05$ ). <sup>b</sup>Significantly different from the ET-1-treated slices from the sedentary group ( $P < 0.05$ ). <sup>c</sup>Significant difference between control and ET-1-treated slices of the same group ( $P < 0.05$ ).

ment but were significantly enhanced by exercise training. The extent of the increase was greater in cerebellum (Fig. 6B, 156% over the value found in the sedentary counterpart) than in cerebral cortex (Fig. 6A, 43% over the value found in the sedentary counterpart).

## DISCUSSION

We studied the ET-1-induced variations in aortic and nervous system sphingolipid and glycerolipid profile and the potential alteration of the sensitivity of these systems to the peptide in-



**FIG. 6.** Alterations induced by exercise training on ceramide monohexoside levels in cerebral cortex (A) and cerebellum (B). Effect of *in vitro* ET-1 treatment. Data are represented as means  $\pm$  SD ( $n = 8$ ). <sup>a</sup>Significantly different from the sedentary control group ( $P < 0.05$ ).

duced by exercise training. This physiological condition has been described as producing beneficial adaptive changes in the cardiovascular (17–19) and nervous systems (20–23) and altering the endogenous level of ET-1 (13). In experiments where vascular tissue was studied, intact aortic strips were chosen, and when nervous system was analyzed, slices of cerebral cortex (the brain area influenced by afferent systems from working muscle and emotional processes) and cerebellum (the brain area involved in the motor processes) were used.

The training program employed in this study can be regarded as a moderate stimulus for normal rodent standards. The 6-mon training period caused a reduction in the body weight of the rats and produced an increase in exercise tolerance associated with an enhanced oxidative capacity of skeletal muscle. We selected the present conditions of treadmill

**TABLE 4**  
Distribution of Cerebral Cortex Phospholipid Subclasses (nmol/mg total lipids) in Sedentary and Trained Rats, Effect of *in Vitro* ET-1 Treatment<sup>a</sup>

Group	Treatment	Choline phosphoglycerides	Ethanolamine phosphoglycerides <sup>c</sup>		
			PtdEtn	PlasEtn	SPH
Sedentary	Control	244 $\pm$ 41	188 $\pm$ 20	90 $\pm$ 17	18.5 $\pm$ 6.5
	ET-1	234 $\pm$ 61	180 $\pm$ 18	92 $\pm$ 27	9.9 $\pm$ 0.2 <sup>b</sup>
Trained	Control	250 $\pm$ 34	180 $\pm$ 13	75 $\pm$ 9	9.2 $\pm$ 1.8
	ET-1	275 $\pm$ 41	191 $\pm$ 44	59 $\pm$ 27	9.6 $\pm$ 1.8

<sup>a</sup>Data are presented as means  $\pm$  SD ( $n = 8$ ).

<sup>b</sup>Significant difference between control and ET-1 treated slices from the sedentary group ( $P < 0.05$ ).

<sup>c</sup>PtdEtn, phosphatidylethanolamine; PlasEtn, ethanolamine plasmalogens; for other abbreviations see Table 2.

**TABLE 5**  
**Distribution of Cerebellum Phospholipid Subclasses (nmol/mg total lipids)**  
**in Sedentary and Trained Rats, Effect of *in Vitro* ET-1 Treatment<sup>a</sup>**

Group	Treatment	Choline phosphoglycerides	Ethanolamine phosphoglycerides		
			PtdEtn	PlasEtn	SPH
Sedentary	Control	214 ± 30	471 ± 36	196 ± 57	20 ± 6
	ET-1	186 ± 23	417 ± 99	133 ± 51	24 ± 7
Trained	Control	294 ± 35	405 ± 79	218 ± 94	19 ± 5
	ET-1	293 ± 15	386 ± 88	355 ± 148	22 ± 4

<sup>a</sup>Data are presented as means ± SD (*n* = 8). See Tables 2 and 4 for abbreviations.

training for the following reasons. First, we previously showed that a steady-state or constant-speed protocol of the same intensity as that used in this work is more effective in enhancing exercise endurance capacity and skeletal muscle citrate synthase activity than other programs consisting of either a constant higher speed (30 m·min<sup>-1</sup>) or high-speed interval running (38). Second, it has been reported that a treadmill for rats running at 21.4 m·min<sup>-1</sup> results in a significant redistribution of tissue blood flow whereby it is greatly increased in the working muscles (40). Moreover, active muscle showed gradual increases in blood flow that were linearly related to time from 5 to 54 min of low-intensity treadmill exercise. Furthermore, ET-1 levels have been shown to increase in plasma of rats immediately after 45 min of treadmill exercise at 25 m·min<sup>-1</sup> (13). Therefore, we reasoned that chronic exposure to sessions of treadmill exercise under the conditions selected for this study (i.e., 25 m·min<sup>-1</sup> exercise intensity and 45 or 60 min duration of the sessions), would be expected not only to induce adaptations that enhance muscle perfusion, flow capacity, and oxidative metabolism but also to modify tissue responsiveness to ET-1 because the exercise sessions should have produced transient and repetitive increases in endogenous levels of the peptide in our rats. Finally, we chose a prolonged training period of 6 mon to allow for the possibility that some adaptive events require longer periods than those necessary to induce skeletal muscle adaptations (38,41).

To our knowledge, this is the first time that the aorta ceramide pattern has been described. ET-1 treatment did not elicit any significant changes in the levels of both ceramide fractions. However, we did detect a decrease in the overall ceramide level due to exercise training without significant alteration in the SPH content. Since there are conflicting results regarding the exact role of the cellular pools of SPH in

ceramide-mediated signaling (42), the possibility of the involvement of a minor pool of SPH remains open. In addition, the possibility of an accelerated glycosphingolipid biosynthesis from ceramides (as discussed below) induced by training cannot be discarded.

Evidence about the physiopathological role of vascular ceramide is controversial. Ceramide has been described to exert a vasodilatory action in *in vitro* systems (3,43). In contrast, several studies indicate that SPHase activity and ceramide-mediated cell signaling are somehow involved in the atherogenic process (3,27,28). If an increase of vascular ceramide production is a risk factor for the induction of apoptosis, the exercise-induced decrease in aortic ceramide levels reported here is consistent with the idea that exercise may protect against cardiovascular diseases. In fact, the apparent protective effect of adequate Mg<sup>2+</sup> intake on vascular function may be related to a decrease of ceramide levels in aorta smooth muscle cells (44).

The role of diacyl molecular forms of choline and ethanolamine phosphoglycerides as second messenger sources is well established. In this regard the involvement of different phospholipases in the transduction mechanism of ET-1 in aorta is well known (45). In the present experimental conditions, only ethanolamine phosphoglycerides were found to exhibit variations as a consequence of training. The alterations observed might be the result of an enhancement of their hydrolysis by a phospholipase A<sub>2</sub>, since DAG levels were unmodified.

In recent years the alkenyl-acyl molecular forms (plasmalogens) have been described to have a potential role in signal transduction systems (46,47). Thus, several plasmalogen-hydrolyzing phospholipases A<sub>2</sub> from different sources have been described to be regulated by several agonists (48,49). However, our data do not allow elucidation of the molecular mech-

**TABLE 6**  
**Effects of Exercise Training on Cholesterol Level (nmol/mg total lipids) and Cholesterol/Total Phospholipid Molar Ratio of Cerebral Cortex and Cerebellum, Effect of *in Vitro* ET-1 Treatment<sup>a</sup>**

Group	Treatment	Cholesterol		Cholesterol/total phospholipid	
		Cerebral cortex	Cerebellum	Cerebral cortex	Cerebellum
Sedentary	Control	522 ± 70	378 ± 90	0.27 ± 0.05	0.21 ± 0.04
	ET-1	524 ± 60	252 ± 50 <sup>b</sup>	0.29 ± 0.03	0.23 ± 0.03
Trained	Control	515 ± 10	400 ± 90	0.23 ± 0.05	0.24 ± 0.04
	ET-1	362 ± 60 <sup>b</sup>	392 ± 40	0.18 ± 0.03	0.26 ± 0.02

<sup>a</sup>Data are represented as means ± SD (*n* = 8).

<sup>b</sup>Significant difference between control and ET-1 treated slices from the same group (*P* < 0.05). For abbreviation see Table 2.

anism(s) responsible for the increase of aortic PlasEtn levels induced by both ET-1 treatment and exercise training. It is interesting to point out that plasmalogens are uniquely susceptible to oxidation and have a protective role against oxidative damage within cellular membranes (25). In this respect, it has been suggested that an increase in the overall vinyl ether linkage per acyl chain in lipid extracts from cerebrovascular smooth muscle may represent a possible compensatory mechanism against lipid oxidation (50). On the contrary, aging is associated with a decline in the PlasEtn content of aortas that is more pronounced in atherogenic than in normal vessels (25). Thus, the increasing effect of exercise training on aorta PlasEtn levels observed in this work may account, at least in part, for the well-known beneficial effects of exercise on the cardiovascular system. In support of this idea, exercise has been shown to attenuate the increase in blood pressure and to reduce the lipid peroxidation in aorta of fructose-fed rats (51).

CH on its own can alter arterial smooth muscle, as indicated by observations demonstrating a correlation between CH enrichment and augmented membrane calcium permeability as well as with vasoconstrictory activity (52). Furthermore, arterial smooth muscle had increased CH levels and a high CH/total PL ratio during atherogenesis (26). In addition, antioxidant treatment has been reported to reduce the aorta CH concentration in hypercholesterolemic rabbits (53). In the present study, we did not observe any differences in the aorta CH content due to ET-1 treatment. However, a noticeable and expected reduction of CH levels induced by exercise training was found. This is another finding consistent with the hypothesis that exercise training reduces the risk of cardiovascular diseases.

The biosynthesis of complex glycosphingolipid, one of the metabolic fates of ceramides, begins with the sequential transfer of a glucose residue forming glucosylceramide followed by the addition of galactose, resulting in the synthesis of lactosylceramide. This latter step is particularly relevant in vascular metabolism. Thus, lactosylceramide has been reported to be more prevalent in atherosclerotic aorta and to induce proliferation of aortic smooth muscle cells through superoxide generation (27). Furthermore, oxidized LDL stimulate endogenous synthesis of lactosylceramide from glucosylceramide (27). In addition, a coordinated regulation of lactosylceramide and CH synthesis by LDL has been postulated (27). In this study we found that exercise evokes a notable increase in glucosylceramide levels, suggesting a deviation of ceramides toward glucosylceramide formation (see previous discussion) and/or a reduced lactosylceramide formation. This and the CH lowering effect of exercise demonstrated here constitute further evidence of the protective effect of exercise against vascular disease. The fact that ET-1 seems to evoke a slight increase in glucosylceramide levels in the sedentary group, but not in the exercised animals, supports the notion that exercise training reduces sensitivity to ET-1 action. This observation is probably related to the down-regulation and/or altered expression of ET-1 receptors secondary to the increased endogenous generation of ET-1 as it occurs during exercise (13). Accordingly, the contractile re-

sponse of coronary arteries to ET-1 is attenuated in trained animals (54,55), a fact that has been hypothesized to be the result of an altered coupling between ET-1 receptors and second messenger (phosphatidic acid) production (54).

It is interesting to note that in sedentary animals, *in vitro* ET-1 treatment elicited a small increase of aortic basal levels of glucosylceramide and a marked enhancement of those of PlasEtn, suggesting that the peptide may function as a vasoprotective agent. This potential beneficial action of ET-1 might be consistent with previous observations of vasodilatory responses to the peptide (11) and reinforces the view of the complex regulation of the vascular function by ET-1. Nevertheless, cautions must be taken when data obtained *in vitro* are extrapolated to physiopathological states. First, since the aorta ring is not in its normal biochemical environment, the response to ET-1 observed *in vitro* might somehow differ from that occurring in physiological conditions. In fact, changes in the vascular sensitivity to ET-1 are known to occur when experimental conditions are altered (56). Second, the concentration of ET-1 used ( $10^{-7}$  M) is higher than the physiological one (13); nevertheless, it is difficult to know the exact amount of the peptide that reaches discrete aorta regions since it is released in an autocrine/paracrine fashion.

Comparative analysis of the present and previous results (5) shows that the response to ET-1 within the nervous system is tissue-specifically altered with age. Thus, in sedentary adult rats, ET-1 scarcely modified the levels of sphingolipids in the cerebral cortex. In contrast, in cerebral cortex from young animals, ET-1 increased both SPHase activity and ceramide monohexoside synthesis (5). In cerebellum, ET-1 evoked an increase in the level of ceramide in adult as well as in young rats. In addition, the cerebellum response to ET-1 observed in trained animals was less noticeable than that observed in the cerebellum of their sedentary counterparts. The biochemical significance of this finding in the context of cerebellum physiology is not yet known.

As observed in aorta, exercise training induces an increase in the net levels of ceramide monohexosides in the nervous system. It has been reported that glucosylceramide synthesis is a means through which neuroepithelioma cells attempt to escape from apoptosis (57). Therefore, it is likely that the increased content of these sphingolipids (probably glucosylceramide) in the nervous system has a beneficial significance, as it occurs in the vascular tissue (27). It is clear that ceramide monohexoside levels are somehow involved in the response to exercise training.

Information exists concerning the endurance exercise-induced actions on the brain. Exercise training increases brain resistance to the damage and neurodegeneration that occurs with age (23), reduces lipid peroxidation by increasing brain antioxidant capacity (20), and enhances the velocity of the fast axonal transport of proteins and the quantity transported (58). As stated above, there is good evidence that PlasEtn are effective as ubiquitous endogenous antioxidants (25). In addition, PlasEtn are known to decline in neuronal tissues of patients with Alzheimer's disease and with age (25). In fact,

when the basal levels of PlasEtn in young animals (4) are compared with those presently observed in adult animals, a decrease of about 30% in the net content of cerebral PlasEtn with age is noted. On the other hand, the enhanced vulnerability to oxidative stress associated with aging is, at least in part, the result of higher levels of CH in brain tissue (59). However, our results demonstrate that neither PlasEtn nor CH levels from the nervous system underwent changes in response to exercise training, which is in contrast with that observed in aorta. Thus, the tissue specificity of the putative antioxidant role of the PlasEtn and CH systems appears to emerge from the present study.

Two major conclusions emerge from the present work: (i) exercise training induces tissue-specific changes in the lipid profile, the vascular tissue being much more sensitive than the nervous system is, and (ii) the sensitivity to ET-1 treatment is lower in tissues from trained animals in comparison with their sedentary counterparts. These responses likely result in a greater resistance to oxidative stress, and they may be related to adaptive mechanisms to the previously reported increase in the endogenous level of ET-1 induced by exercise (13). It must be remembered that these changes represent a response induced by an endurance exercise training that is very prolonged for the mean life span of rats, and it is not known whether the same effects would be produced by shorter training programs. In any case, our data may help to elucidate the molecular basis of the beneficial effects elicited by physical exercise in both vascular and nervous systems.

## ACKNOWLEDGMENTS

This work was supported by grants from Dirección General de Investigación Científica y Técnica (DGICYT) and PB-98-0822 from Dirección General de Enseñanza Superior e Investigación Científica (DGESIC).

## REFERENCES

- Huwiler, A., Kolter, T., Pfeilschifter, J., and Sandhoff, K. (2000) Physiology and Pathophysiology of Sphingolipid Metabolism and Signalling, *Biochim. Biophys. Acta* 1485, 63–69.
- Ariga, T., Jarvis, W.D., and Yu, R.K. (1998) Role of Sphingolipid-Mediated Cell Death in Neurodegenerative Diseases, *J. Lipid Res.* 39, 1–16.
- Johns, D.G., Charpie, J.R., and Webb, C. (1998) Is Ceramide Signaling a Target for Vascular Therapeutic Intervention? *Curr. Pharm. Des.* 4, 481–488.
- Latorre, E., Aragonés, M.D., Fernández, I., and Catalán, R.E. (1999) Platelet-Activating Factor Modulates Brain Sphingomyelin Metabolism, *Eur. J. Biochem.* 261, 1–9.
- Catalán, R.E., Aragonés, M.D., Martínez, A.M., and Fernández, I. (1996) Involvement of Sphingolipids in the Endothelin-1 Signal Transduction Mechanism in Rat Brain, *Neurosci. Lett.* 220, 121–124.
- Catalán, R.E., Martínez, A.M., Aragonés, M.D., Fernández, I., Miguel, B.G., Pérez, M.J., and Calcerrada, M.C. (1995) Endothelin-Stimulated Phosphoinositide Turnover and Protein Kinase C Translocation in Rat Synaptosomes, *Biochem. Mol. Biol. Int.* 38, 7–14.
- Catalán, R.E., Martínez, A.M., Aragonés, M.D., and Hernández, F. (1995) Endothelin-1 Stimulates Myristoylated Alanine-Rich C-Kinase Substrate (MARCKS) Phosphorylation in Rat Cerebellar Slices, *Neurosci. Lett.* 194, 53–56.
- Catalán, R.E., Martínez, A.M., Aragonés, M.D., Martínez, A., and Díaz, G. (1996) Endothelin Stimulates Phosphoinositide Hydrolysis and PAF Synthesis in Brain Microvessels, *J. Cer. Blood Flow Metab.* 16, 1325–1334.
- Catalán, R.E., Martínez, A.M., Aragonés, M.D., Hernández, F., and G. Díaz, G. (1996) Endothelin Stimulates Protein Phosphorylation in Blood-Brain Barrier, *Biochem. Biophys. Res. Commun.* 219, 366–369.
- Yanagisawa, M., Kurihara, M., Kimura, S., Tomobe, Y., Kobayashi, M., Mitsui Y., Yazaki, Y., Goto, K., and Masaki, T. (1988) A Novel Potent Vasoconstrictor Peptide Produced by Vascular Endothelial Cells, *Nature (London)* 332, 411–415.
- Haynes, W.G., and Webb, D.J. (1998) Endothelin as a Regulator of Cardiovascular Function in Health and Disease, *J. Hypertens.* 16, 1081–1098.
- Gulati, A., and Srimal, R.C. (1992) Endothelin Mechanisms in the Central Nervous System: A Target for Drug Development, *Drug Dev. Res.* 26, 361–387.
- Maeda, S., Miyauchi, T., Kobayashi, T., Goto, K., and Matsuda, M. (1998) Exercise Causes Tissue-Specific Enhancement of Endothelin-1 mRNA Expression in Internal Organs, *J. Appl. Physiol.* 85, 425–431.
- Norton, K.I., Jones, M.T., and Armstrong, R.B. (1990) Oxygen Consumption and Distribution of Blood Flow in Rats Climbing a Laddermill, *J. Appl. Physiol.* 68, 241–247.
- Onuoha, G.N., Nicholls, D.P., Patterson, A., and Beringer, T. (1998) Neuropeptide Secretion in Exercise, *Neuropeptides* 32, 319–325.
- Lash, J.M. (1998) Exercise Training Enhances Adrenergic Constriction and Dilatation in the Rat Spinotrapezius Muscle, *J. Appl. Physiol.* 85, 168–174.
- Raven, P.B., Welch-O'Connor, R.M., and Shi, X. (1998) Cardiovascular Function Following Reduced Aerobic Activity, *Med. Sci. Sports Exerc.* 30, 1041–1052.
- Best, P.J., Tajik, A.J., Gibbons, R.J., and Pellikka, P.A. (1998) The Safety of Treadmill Exercise Stress Testing in Patients with Abdominal Aortic Aneurysms, *Ann. Intern. Med.* 129, 628–631.
- McMurray, R.G., Ainsworth, B.E., Harrel, J.S., Griggs, T.R., and Williams, O.D. (1998) Is Physical Activity or Aerobic Power More Influential on Reducing Cardiovascular Disease Risk Factors? *Med. Sci. Sports Exerc.* 30, 1521–1529.
- Itoh, H., Ohkuwa, T., Yamamoto, T., Sato, Y., Miyamura, M., and Naoi, M. (1998) Effects of Endurance Physical Training on Hydroxyl Radical Generation in Rat Tissues, *Life Sci.* 63, 1921–1929.
- Kanda, K., and Hashizume, K. (1998) Effects of Long-Term Physical Exercise on Age-Related Changes of Spinal Motoneurons and Peripheral Nerves in Rats, *Neurosci. Res.* 31, 69–75.
- Mechau, D., Mücke, S., Weib, M., and Liesen, H. (1998) Effect of Increasing Running Velocity on Electroencephalogram in a Field Test, *Eur. J. Appl. Physiol.* 78, 340–345.
- Oliff, H.S., Berchtold, N.C., Isackson, P., and Cotman, C.W. (1998) Exercise-Induced Regulation of Brain-Derived Neurotrophic Factor (BDNF) Transcripts in the Rat Hippocampus, *Mol. Brain Res.* 61, 147–153.
- Lacey, B.C., and Lacey, J.L. (1978) Two-Way Communication Between the Heart and the Brain, *Am. Psychol.* 33, 99–113.
- Brosche, T., and Platt, D. (1998) The Biological Significance of Plasmalogens in Defense Against Oxidative Damage, *Exp. Gerontol.* 33, 363–369.
- Chen, M., Mason, R.P., and Tulenko, T.N. (1995) Atherosclerosis Alters the Composition, Structure and Function of Arterial Smooth Muscle Cell Plasma Membranes, *Biochim. Biophys. Acta* 1272, 101–112.
- Chatterjee, S. (1998) Sphingolipids in Atherosclerosis and



- Vascular Biology, *Arterioscler. Thromb. Vasc. Biol.* 18, 1523–1533.
28. Augé, N., Nègre-Salvayre, A., Salvayre, R., and Levade, T. (2000) Sphingomyelin Metabolites in Vascular Cell Signalling and Atherogenesis, *Prog. Lipid Res.* 39, 207–229.
  29. Brooks, G.A., and White T.P. (1978) Determination of Metabolic and Heart Rate Responses of Rat to Treadmill Exercise, *J. Appl. Physiol.* 45, 1009–1015.
  30. Aoki, H., Kobayashi, S., Nishimura, J., and Kanaide, H. (1994) Sensitivity of G-Protein Involved in Endothelin-1-Induced  $Ca^{2+}$  Influx to Pertussis Toxin in Porcine Endothelial Cell *in situ*, *Br. J. Pharmacol.* 111, 989–996.
  31. Lowry, O.H., Rosebrough, N.J., Farr, A.L., and Randall, R.J. (1951) Protein Measurement with the Folin Phenol Reagent, *J. Biol. Chem.* 193, 265–275.
  32. Molano, F., Saborido, A., Delgado, J., Morán, M., and Megías, A. (1999) Rat Liver Lysosomal and Mitochondrial Activities Are Modified by Anabolic-Androgenic Steroids, *Med. Sci. Sports Exerc.* 31, 243–250.
  33. Bligh, E.G., and Dyer, W.J. (1959) A Rapid Method of Total Lipid Extraction and Purification, *Can. J. Biochem. Physiol.* 39, 911–917.
  34. Van Veldhoven, P.P., Bishop, W.R., Yurivich, D.A., and Bell, R.M. (1995) Ceramide Quantitation: Evaluation of a Mixed Micellar Assay Using *E. coli* Diacylglycerol Kinase, *Biochem. Mol. Biol. Int.* 36, 21–30.
  35. Preiss, J., Loomis, C.R., Bishop, W.R., Stein, R., Nidel, J.E., and Bell, R.M. (1986) Quantitative Measurement of *sn*-1,2-Diacylglycerols Present in Platelets, Hepatocytes, and *ras*- and *sis*-Transformed Normal Rat Kidney Cells, *J. Biol. Chem.* 261, 8597–8600.
  36. Catalán, R.E., Martínez, A.M., and Aragonés, M.D. (1984) Evidence for a Role of Somatostatin in Lipid Metabolism of Liver and Adipose Tissue, *Regul. Peptides* 8, 147–159.
  37. Booth, F.W., and Thomason, D.B. (1991) Molecular and Cellular Adaptation of Muscle in Response to Exercise: Perspectives of Various Models, *Physiol. Rev.* 71, 541–585.
  38. Delgado, J., Saborido, A., Morán, M., and Megías, A. (1999) Chronic and Acute Exercise Do Not Alter  $Ca^{2+}$  Regulatory Systems and Ectonucleotidase Activities in Rat Heart, *J. Appl. Physiol.* 87, 152–160.
  39. Mukhin, D.N., Chao, F.F., and Kruth, H.S. (1995) Glycosphingolipid Accumulation in the Aortic Wall Is Another Feature of Human Atherosclerosis, *Arterioscler. Thromb. Vasc. Biol.* 15, 1607–1615.
  40. Laughlin, M.H., Armstrong, R.B., White, J., and Rouk, K. (1982) A Method for Using Microspheres to Measure Muscle Blood Flow in Exercising Rat, *J. Appl. Physiol.* 52, 1629–1635.
  41. Saborido, A., Molano, F., Moro, G., and Megías, A. (1995) Regulation of Dihydropyridine Receptor Levels in Skeletal and Cardiac Muscle by Exercise Training, *Pflügers Arch.-Eur. J. Physiol.* 429, 364–369.
  42. Andrieu-Abadie, N., Carpentier, S., Salvayre, R., and Levade, T. (1988) The Tumor Necrosis Factor-Sensitive Pool of Sphingomyelin Is Resynthesized in a Distinct Compartment of the Plasma Membrane, *Biochem. J.* 333, 91–97.
  43. Johns, D.G., and Webb, R.C. (1998) TNF- $\alpha$ -induced Endothelium-Independent Vasodilatation: A Role for Phospholipase  $A_2$ -Dependent Ceramide Signalling, *Am. J. Physiol.* 275, H1592–H1598.
  44. Morril, G.A., Gupta, R.K., Kostellow, A.B., Ma, G-Y., Zhang, A., Altura, B.T., and Altura, B.M. (1998)  $Mg^{2+}$  Modulates Membrane Sphingolipid and Lipid Second Messenger Levels in Vascular Smooth Muscle Cells, *FEBS Lett.* 440, 167–171.
  45. Jones, A.W., Magliola, L., Waters, C.B., and Rubin, L.J. (1998) Endothelin-1 Activates Phospholipases and Channels at Similar Concentrations in Porcine Coronary Arteries, *Am. J. Physiol.* 274, C1583–C1591.
  46. Farooqui, A.A., Yang, H-CH., and Horrocks, L.A. (1995) Plasmalogens, Phospholipase  $A_2$  and Signal Transduction, *Brain Res. Rev.* 21, 152–161.
  47. Farooqui, A.A., Yang, H.C., Rosenberger, T.A., and Horrocks, L.A. (1997) Phospholipase  $A_2$  and Its Role in Brain Tissue, *J. Neurochem.* 69, 889–901.
  48. McHowat, J., Liu, S., and Creer, M.H. (1998) Selective Hydrolysis of Plasmalogen Phospholipids by  $Ca^{2+}$ -Independent  $PLA_2$  in Hypoxic Ventricular Myocytes, *Am. J. Physiol.* 274, C1727–C1737.
  49. McHowat, J., and Creer, M.H. (2000) Selective Plasmalogen Substrate Utilization by Thrombin-Stimulated  $Ca^{2+}$ -Independent  $PLA_2$  in Cardiomyocytes, *Am. J. Physiol.* 278, H1933–H1940.
  50. Morril, G.A., Gupta, R.K., Kostellow, A.B., Ma, G-Y., Zhang, A., Altura, B.T., and Altura, B.M. (1997)  $Mg^{2+}$  Modulates Membrane Lipids in Vascular Smooth Muscle: A Link to Atherogenesis, *FEBS Lett.* 408, 191–194.
  51. Anuradha, C.V., and Balakrishnan, S.D. (1998) Effect of Exercise-Training on Lipid Peroxidation and Antioxidant Enzymes in the Aorta of Fructose-Fed Rats, *Med. Sci. Res.* 26, 439–443.
  52. Bialecki, R.A., and Tulenko, T.N. (1989) Excess Membrane Cholesterol Alters Calcium Channels in Arterial Smooth Muscle, *Am. J. Physiol.* 257, C306–C314.
  53. Schwenke, D.C., and Behr, S.R. (1998) Vitamin E Combined with Selenium Inhibits Atherosclerosis in Hypercholesterolemic Rabbits Independently of Effects on Plasma Cholesterol Concentrations, *Circ. Res.* 83, 366–377.
  54. Jones, A.W., Rubin, L.J., and Magliola, L. (1999) Endothelin-1 Sensitivity of Porcine Coronary Arteries Is Reduced by Exercise Training and Is Gender Dependent, *J. Appl. Physiol.* 87, 1172–1177.
  55. Bowles, D.K., Laughlin, M.H., and Sturek, M. (1995) Exercise Training Alters the  $Ca^{2+}$  and Contractile Responses of Coronary Arteries to Endothelin-1, *J. Appl. Physiol.* 78, 1079–1087.
  56. White, L.R., Leseth, K.H., Juul, R., Adner, M., Cappelen, J., Aasly, J., and Edvinsson, L. (1998) Increased Endothelin  $ET_B$  Contractile Activity in Cultured Segments of Human Temporal Artery, *Acta Physiol. Scand.* 164, 21–27.
  57. Spinedi, A., Di Bartolomeo, S., and Piacentini, M. (1998) Apoptosis Induced by *N*-Hexanoylsphingosine in CHP-100 Cells Associates with Accumulation of Endogenous Ceramide and Is Potentiated by Inhibition of Glucocerebroside Synthesis, *Cell Death Differ.* 5, 785–791.
  58. Jasmin, B.J., Lavoie, P.A., and Gardiner, P.F. (1988) Fast Axonal Transport of Labeled Proteins in Motoneurons of Exercise-Trained Rats, *Am. J. Physiol.* 255, C731–C736.
  59. Urano, S., Sato, Y., Otonari, T., Makabe, S., Suzuki, S., Ogata, M., and Endo, T. (1998) Aging and Antioxidative Stress in Neurodegeneration, *Biofactors* 7, 103–112.

[Received March 7, 2001, and in final revised form October 29, 2001; revision accepted November 26, 2001]

# Selective Effect of Cholesterylphosphoserine on Intracellular Cholesterol Transport

F. Cusinato and A. Bruni\*

Department of Pharmacology and Anesthesiology, University of Padova, 35131 Padova, Italy

**ABSTRACT:** Cholesteryl-3 $\beta$ -phosphoserine (CPHS) is a synthetic steroid affecting intracellular cholesterol transport. To compare CPHS with the well-known inhibitors progesterone and U18666A, we examined cholesterol transport in three human cell lines: the monocytic U-937, the endothelial ECV-304, and the lymphoid Jurkat. Under low density lipoprotein (LDL) loading, CPHS inhibited cholesterol esterification in U-937 and ECV-304 cells but not in Jurkat cells. In contrast, CPHS inhibited the mobilization of plasma membrane cholesterol induced by 25-hydroxycholesterol, brefeldin A, or sphingomyelinase in all cell lines. In cells pulse-labeled with [<sup>3</sup>H]cholesterol, CPHS decreased incorporation of cholesterol and inhibited its esterification. In prelabeled cells, CPHS promoted cholesterol efflux and enhanced the cyclodextrin-mediated removal of plasma membrane cholesterol. CPHS did not affect endogenous cholesterol synthesis nor acyl-coenzyme A:cholesterol acyltransferase activity. These data suggest that, unlike progesterone and U18666A, CPHS inhibits intracellular cholesterol transport by specifically affecting the movements of cholesterol in the plasma membrane. Owing to this restricted site of action, CPHS may help to clarify the role of the plasma membrane in cholesterol trafficking. For example, the lack of an effect of CPHS on the esterification of LDL-derived cholesterol in Jurkat cells suggests that most of the LDL-derived cholesterol in these cells is directly delivered to the endoplasmic reticulum without cycling through the plasma membrane.

Paper no. L8829 in *Lipids* 37, 53–59 (January 2002).

In eukaryotic cells, cholesterol is required for the proper functioning of plasma membranes. Together with the barrier function, cholesterol regulates the activity of membrane-bound transporters, ion channels, signaling molecules, and transport vesicles (1–3). To fulfill this function, a continuous flow of cholesterol to the plasma membrane is provided by endogenous synthesis and lipoprotein uptake. Back transport to the endoplasmic reticulum followed by esterification and an efficient system of efflux maintain cholesterol homeostasis. Certain steroids are known to influence intracellular cholesterol trafficking. For example, the role of progesterone and 3 $\beta$ -[2-(diethylamino)ethoxy]androst-5-en-17-one (U18666A) in the accumulation of low density lipoprotein (LDL)-derived cho-

lesterol in late endosomes and lysosomes, thus reproducing the phenotype of Niemann–Pick disease (4–6), has been well characterized. In addition, these steroids inhibit endogenous cholesterol synthesis (7,8). We have recently shown that a synthetic cholesteryl ester, cholesteryl-3 $\beta$ -phosphoserine (CPHS), inhibits the transport of plasma membrane cholesterol to the endoplasmic reticulum in the Jurkat lymphoid cell line (9). This observation prompted the present study aimed at establishing whether the mechanism of action of CPHS is different from that of progesterone and U18666A. Unlike the neutral progesterone and the basic U18666A, which may cross the plasma membrane, CPHS is acidic owing to the presence of a phosphoserine polar group, negatively charged at physiological pH. As has been known for many years (10), negatively charged amphiphiles may become arrested in the plasma membrane as they are repelled by the negatively charged lipids of the cytoplasmic leaflet. In agreement with this, by following the binding of fluorescent annexin V to the phosphoserine group of CPHS, we have shown that this steroid accumulates in the plasma membrane without penetrating inside the cells (9). This might indicate that the site of action of CPHS is different from that of progesterone and U18666A. Such a result would be interesting because the availability of inhibitors acting in different ways is of help in clarifying complex biological sequences such as intracellular cholesterol transport. A controversial aspect of cholesterol trafficking is the proportion of LDL-derived cholesterol that can be transported from lysosomes to the endoplasmic reticulum without cycling through the plasma membrane. This proportion might differ in the various populations of mammalian cells. To test the applicability of CPHS in the investigation of this question, we followed the intracellular cholesterol transport in three cell lines—the lymphoid Jurkat, the monocytic U-937, and the endothelial ECV-304. We selected these cells because they were previously shown to be CPHS-sensitive (9). In addition, they might be of interest as models of the cell populations involved in the formation of atherosclerotic plaque (11). Cholesterol transport was tested by the addition of LDL to cells previously incubated in the absence of lipoproteins to increase the expression of LDL receptor. The plasma membrane  $\rightarrow$  endoplasmic reticulum segment of this transport was examined in the absence of lipoproteins by the addition of cholesterol in the incubation medium (12) or by the use of agents known to mobilize plasma membrane cholesterol. In agreement with our hypothesis, the data show that CPHS affects intracellular cholesterol trafficking only when the trans-

\*To whom correspondence should be addressed at Department of Pharmacology and Anesthesiology, University of Padova, Largo E. Meneghetti 2, 35131 Padova, Italy. E-mail: alessandro.bruni@unipd.it

Abbreviations: 25-OH, 25-hydroxycholesterol; ACAT, acyl-coenzyme A:cholesterol acyltransferase; BSA, bovine serum albumin; CPHS, cholesterylphosphoserine; cyclodextrin, hydroxypropyl- $\beta$ -cyclodextrin; LDL, low density lipoprotein; U18666A, 3 $\beta$ -[2-(diethylamino)ethoxy]androst-5-en-17-one.

port pathway involves the plasma membrane. In contrast, the role of progesterone and U18666A extends to inhibition of the intracellular steps of cholesterol synthesis and transport.

## MATERIALS AND METHODS

**Reagents.** The sodium salt of cholesteryl-3 $\beta$ -phospho-L-serine (a generous gift of Dr. G. Kirschner, Fidia Research Laboratories, Abano Terme, Padova, Italy) was dispersed at 1 mg/mL in 50% ethanol containing 5 mM Tris-HCl, pH 7.8, and briefly warmed at 50°C to obtain a clear solution which could be stored at 4°C for a week. The final CPHS concentration was verified by phosphorus determination. Progesterone and 25-hydroxycholesterol were obtained from Sigma (St. Louis, MO), and U18666A was obtained from Biomol (Plymouth Meeting, PA). These steroids were dissolved in ethanol. The influence of equivalent concentrations of ethanol in our tests was routinely checked. Low-density lipoproteins were prepared from human plasma, supplemented with 1 mM EDTA, by preparative ultracentrifugation ( $d$  1.019–1.063 g/mL). 25-Hydroxycholesteryl linoleate and squalene epoxides were prepared as described in References 13 and 14, respectively. Hydroxypropyl- $\beta$ -cyclodextrin (cyclodextrin) and other chemicals of reagent grade were from Sigma.

**Cell cultures.** The human cell lines used in this study were obtained from the Istituto Zooprofilattico Sperimentale della Lombardia e dell'Emilia, Brescia, Italy. The T cell line Jurkat and a strain of the monocytic cell line U-937 with a normal cholesterol metabolism (15) were used as cell suspensions maintained in RPMI 1640 medium. Adherent cultures of ECV-304 endothelial cells were maintained in M199 medium and applied as a monolayer in six-well plates. At confluence, each well contained  $400 \pm 55$   $\mu$ g of cell proteins, corresponding to  $7 \times 10^5$  cells. All media were supplemented with 10% (vol/vol) fetal calf serum (Poesys; PAA Laboratories GmbH, Linz, Austria), 2 mM L-glutamine, and antibiotics. To exclude the possibility of CPHS-induced cytotoxicity, the release of accumulated [ $^3$ H]adenine was measured (16). The spontaneous release was not changed by 10  $\mu$ M CPHS, whereas it was increased up to 7% by 20  $\mu$ M CPHS. As a cautionary limit, 10  $\mu$ M was selected as the maximal concentration to be used.

**Esterification of LDL-derived cholesterol.** To enhance LDL internalization, the cells were previously incubated in serum-free media supplemented with 5 mg/mL of bovine serum albumin (BSA) and 10  $\mu$ g/mL of transferrin. The preincubation was 48 h with the Jurkat cells and 24 h with the other cells. Jurkat and U-937 cells ( $5 \times 10^6$ ) were suspended in 1 mL of RPMI 1640 medium. Confluent monolayers of ECV-304 were incubated in 3 mL of M199. All cell cultures, supplemented with 5 mg/mL of BSA, were incubated for 4 h at 37°C in the presence of 25–50  $\mu$ g of LDL proteins. The inhibitory steroids and 5  $\mu$ Ci of [ $^3$ H]oleate (prepared at pH 7.4 in Tris buffer free of divalent cations but containing 1 mg/mL of BSA) were then added, and the incubation was continued for an additional 2–3 h. 25-Hydroxycholesterol (2.5  $\mu$ M) was

added together with the [ $^3$ H]oleate to the cultures of U-937 and ECV-304 cells. After the incubation, the cells were washed, and the lipids extracted as detailed below.

**Esterification of plasma membrane cholesterol.** Jurkat and U-937 cells ( $5 \times 10^6$ ) suspended in 1 mL of RPMI 1640 medium or confluent monolayers of ECV-304 cells in 3 mL of M199 were incubated for 2–3 h at 37°C with 5 mg/mL of BSA and 5  $\mu$ Ci of [ $^3$ H]oleate. To mobilize the plasma membrane cholesterol, cells were preincubated for 30 min with 5  $\mu$ M brefeldin A or 0.12 U of sphingomyelinase from *Bacillus cereus*. Alternatively, 2.5  $\mu$ M of 25-hydroxycholesterol was added together with the [ $^3$ H]oleate. The transport of plasma membrane cholesterol to the endoplasmic reticulum was specifically tested by measuring the incorporation and the esterification of [ $^3$ H]cholesterol in Jurkat and U-937 cells (12). Cells ( $5 \times 10^6$ ) resuspended in 1 mL of RPMI 1640 medium containing 1 mg/mL of BSA were incubated for 45 min at 37°C in the presence of 2  $\mu$ Ci of [ $^3$ H]cholesterol added in 5  $\mu$ L of ethanol. Lipids were extracted from washed cells and resolved by thin-layer chromatography.

**Extraction of plasma membrane cholesterol with cyclodextrin (17).** Suspensions of Jurkat cells ( $5 \times 10^6$ /mL of RPMI 1640 medium containing 1 mg/mL of BSA) were incubated for 15 min at room temperature with 2  $\mu$ Ci/mL of [ $^3$ H]cholesterol added in ethanol (5  $\mu$ L/mL). After centrifugation, the cells were washed twice in RPMI/BSA and resuspended in the same medium in aliquots of  $5 \times 10^6$  cells/mL. One aliquot was supplemented with cyclodextrin (2% wt/vol) and incubated for 10 min at 37°C with continuous shaking. After centrifugation, the radioactivity was measured in the supernatant and in the sediment. The other aliquots were incubated at 37°C with or without 10  $\mu$ M CPHS for the times indicated in Figure 4. After centrifugation, the supernatants were saved for the determination of CPHS-induced cholesterol efflux, and the sediments were extracted with cyclodextrin as described above. The cholesterol remaining in the final sediment after the action of cyclodextrin was extracted with chloroform/methanol to quantify the esterified fraction.

**Lipid extraction.** At the end of the above incubations, Jurkat and U-937 cells were washed, resuspended in 0.1 mL of 0.15 M NaCl, and extracted with 20 vol of chloroform/methanol (2:1, vol/vol). The lipid extract, washed twice with 0.2 vol of 0.1 M HCl, was taken to dryness and resolved with the appropriate standards in a monodimensional thin-layer chromatography system using petroleum ether/diethylether/acetic acid (90:10:1, by vol). In cases in which 25-hydroxycholesterol had been added to the cell cultures, the thin-layer plates were developed in hexane/ethyl acetate (85:15, vol/vol) to resolve the cholesteryl esters and the esters of 25-hydroxycholesterol (18). Lipid spots were visualized with iodine, scraped, and quantified by scintillation counting. The adherent ECV-304 cells were washed and detached with isopropyl alcohol (19). After transfer to glass tubes, an equal volume of petroleum ether was added to the cell suspension. The lipid extract was filtered, taken to dryness, and applied to the thin-layer chromatographic plates.



**Synthesis of cholesterol.** Cells were depleted of lipoproteins by incubation for 24 h in serum-free medium containing 5 mg/mL of BSA and 10  $\mu$ g/mL of transferrin. The cells were then incubated for 3 h at 37°C in serum-free medium containing 5 mg/mL of BSA and 10  $\mu$ Ci of [<sup>3</sup>H]acetate. After washing, the cells were collected in 0.5 mL of 0.1 M NaOH and incubated for 30 min at 37°C. A 0.5-mL volume of 1 M KOH in methanol was then added, and the samples were saponified for 1 h at 55°C. The nonsaponifiable lipids were extracted with petroleum ether and resolved by thin-layer chromatography in hexane/ethyl acetate (85:15, vol/vol). Standards of cholesterol, lanosterol, squalene, and squalene epoxides demonstrated a clear separation of these components. Desmosterol, a major final product of sterol metabolism in nonhepatic cells (20), comigrated with cholesterol.

**Subcellular acyl-coenzyme A:cholesterol acyltransferase (ACAT) activity.** Jurkat cells ( $5 \times 10^7$ ) were lysed by freezing and thawing, homogenized, and centrifuged for 10 min at 800  $\times g$  in the cold. Aliquots of the supernatant (100  $\mu$ g of protein) were mixed with 1  $\mu$ Ci of [<sup>3</sup>H]cholesterol dissolved in ethanol (1% final concentration). After 20 min at 37°C, 24  $\mu$ M of oleoyl-coenzyme A was added, and the incubation was continued for an additional 45 min at 37°C (18).

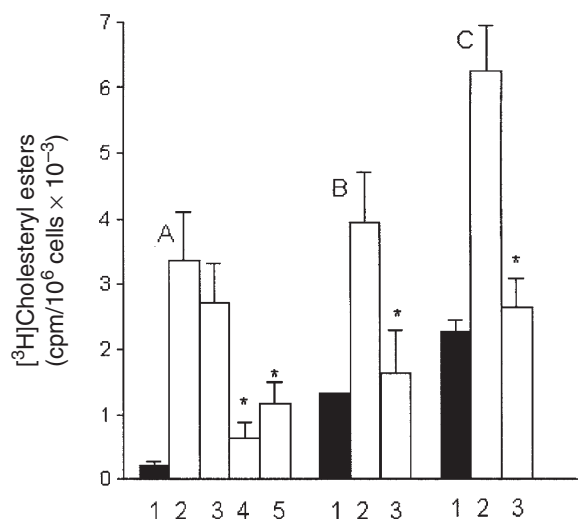
## RESULTS

After a preincubation in a lipoprotein-free medium, Jurkat cells became very active in the uptake of LDL-cholesterol, as revealed by its esterification (Fig. 1A). The LDL-induced stimulation of cholesterol esterification was detected in all experiments, although to a variable extent (mean value of  $21 \pm 14$

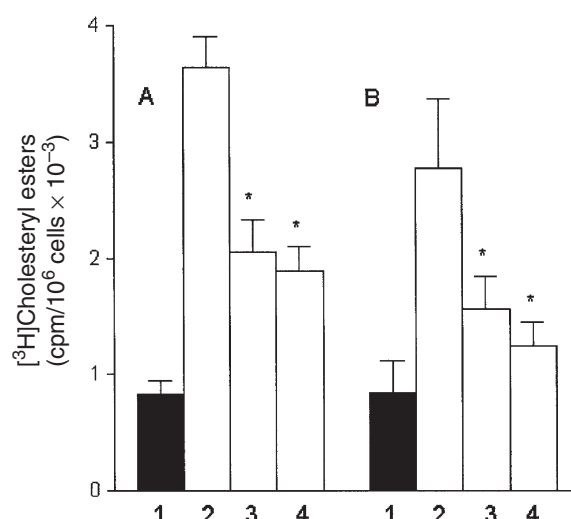
times the unstimulated value in 20 experiments). The inhibitory effect of CPHS was marginal and not significant ( $20.7 \pm 16\%$  in 11 experiments). In contrast, the inhibition by U18666A and progesterone was reproducible and significant (mean values of  $76.8 \pm 8.8\%$  and  $65.4 \pm 7.2\%$ , respectively).

Unlike the Jurkat cells, U-937 and ECV-304 cells showed LDL-stimulated cholesterol esterification only upon the addition of 25-hydroxycholesterol, a sterol inducing the mobilization of plasma membrane cholesterol (Fig. 1, B and C). As suggested for macrophages (21), this may reflect the large proportion of LDL-cholesterol transported to the plasma membrane in these cells and the high capacity of their plasma membranes to accommodate the newly transported cholesterol. Under this condition, LDL caused a similar stimulation of cholesterol esterification in U-937 and ECV-304 cells (a mean of  $2.9 \pm 0.9$  times the value obtained with 25-hydroxycholesterol alone in eight experiments). The LDL-induced stimulation was abolished by CPHS. Separate experiments showed that progesterone and U18666A were similarly active (data not shown).

The transport of cholesterol from the plasma membrane to the endoplasmic reticulum in the absence of LDL was studied by the addition of reagents inducing the mobilization of plasma membrane cholesterol. To this end, cells were preincubated with brefeldin A, sphingomyelinase, or 25-hydroxycholesterol. As shown in Figure 2 for U-937 cells, brefeldin A and sphingomyelinase stimulated the esterification of plasma membrane cholesterol severalfold, and their effect was inhibited by both CPHS and progesterone. U18666A was not tested in these experiments. The best results with 25-hydroxycholesterol were obtained in Jurkat cells, in which



**FIG. 1.** Esterification of low density lipoprotein (LDL)-derived cholesterol. Suspensions of Jurkat (A) and of U-937 cells (B) or monolayers of ECV-304 cells (C) were incubated for 4 h at 37°C with 25–50  $\mu$ g of LDL proteins. Inhibitory steroids and 5  $\mu$ Ci of [<sup>3</sup>H]oleate were then added, and the incubation was continued for an additional 2–3 h. 25-Hydroxycholesterol (2.5  $\mu$ M) was added together with the [<sup>3</sup>H]oleate in U-937 and ECV-304 cells. 1, Without LDL; 2, LDL; 3, LDL, 10  $\mu$ M cholesteryl-3 $\beta$ -phosphoserine (CPHS); 4, LDL, 2.5  $\mu$ M U18666A; 5, LDL, 10  $\mu$ M progesterone. Data are means  $\pm$  SEM from 11 (A) and six experiments (B,C). \* $P < 0.01$ .



**FIG. 2.** Esterification of plasma membrane cholesterol, mobilized by brefeldin A or sphingomyelinase. U-937 cells were incubated for 30 min at 37°C with 5  $\mu$ M brefeldin A (A) or 0.12 U/mL of bacterial sphingomyelinase (B). Inhibitory steroids and 5  $\mu$ Ci of [<sup>3</sup>H]oleate were then added, and the incubation was continued for an additional 2 h. 1, Cells not treated with brefeldin A or sphingomyelinase; 2, treated cells; 3, treated cells, 10  $\mu$ M CPHS; 4, treated cells, 10  $\mu$ M progesterone. Data are means  $\pm$  SEM from four or five experiments. \* $P < 0.05$ . See Figure 1 for abbreviation.

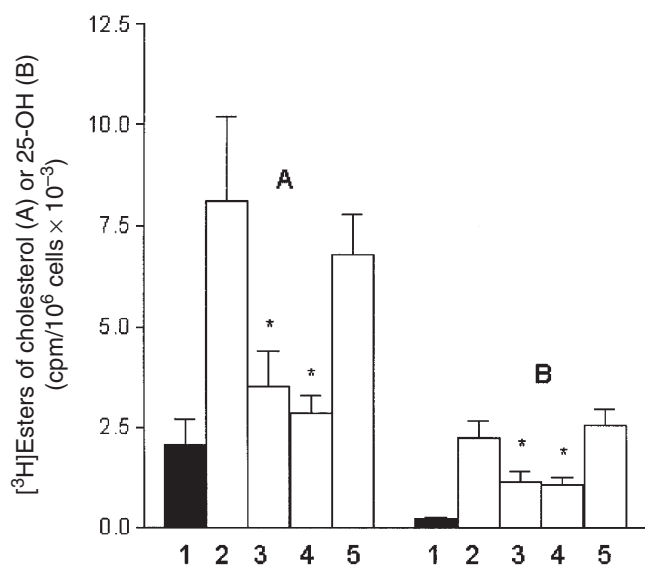


the stimulation of cholesterol esterification and the esterification of 25-hydroxycholesterol could be simultaneously tested, in accord with previous observations on hepatoma cells (18). CPHS and progesterone produced a significant inhibition of cholesterol esterification (Fig. 3A) and 25-hydroxycholesterol esterification (Fig. 3B), whereas U18666A was essentially without effect under these conditions. To confirm the action of CPHS on the esterification of plasma membrane cholesterol, we examined the esterification of [ $^3\text{H}$ ]cholesterol, added as an ethanolic solution to the incubation medium in Jurkat and U-937 cells. In these experiments, the concentration of ethanol (5  $\mu\text{L}/\text{mL}$  of RPMI 1640 medium) was critical to obtain reproducible results. After the incorporation, the added cholesterol mixed with the plasma membrane pool of cholesterol, and then it was delivered to the endoplasmic reticulum for esterification (12). In Jurkat cells, CPHS caused a dose-dependent inhibition of both cholesterol incorporation and esterification (Table 1). CPHS also decreased the percentage of incorporated cholesterol delivered for esterification, indicating a wide influence on the movements of plasma membrane cholesterol. The action of CPHS was dose-dependent with an  $\text{IC}_{50}$  (concentration at which 50% inhibition occurs) at 3  $\mu\text{M}$ . Progesterone and U18666A inhibited the esterification of cholesterol but did not affect its incorporation. Similar results were obtained in U-937 cells. The inhibition of cholesterol incorporation by CPHS suggested that this steroid might also affect its efflux. To investigate this possibility, we tested the passive cholesterol desorption from the cells, a component of cholesterol efflux (22). Jurkat cells were incubated overnight with [ $^3\text{H}$ ]cholesterol (0.2  $\mu\text{Ci}/10^6$

cells) in RPMI 1640 medium containing 5 mg/mL of BSA and 10  $\mu\text{g}/\text{mL}$  of transferrin. After this treatment, the cells showed  $33,900 \pm 7,600$  cpm/ $10^6$  cells in six experiments. Labeled cells ( $5 \times 10^6/\text{mL}$ ) were then incubated for 15 min at  $37^\circ\text{C}$  in RPMI 1640 medium containing 1 mg/mL of BSA. During this time, the passive desorption of cholesterol was  $2.5 \pm 0.6\%$  of total cpm (mean  $\pm$  SD,  $n = 6$ ). The addition of 10  $\mu\text{M}$  CPHS during the 15 min of incubation increased this value to  $4.4 \pm 1\%$  ( $P < 0.01$ ), whereas 10  $\mu\text{M}$  progesterone or 2.5  $\mu\text{M}$  U18666A was without effect.

To confirm the action of CPHS on the movements of plasma membrane cholesterol, we examined the combined effect of CPHS and cyclodextrin, a reagent that extracts cholesterol from the plasma membrane but not from intracellular sites (23,24). Owing to this property, cyclodextrin has become the agent of choice when it is necessary to monitor the arrival of intracellular cholesterol to the plasma membrane (17,25). Since cyclodextrin is more effective in cells grown in suspension and incubated with continuous shaking (23), our experiments were performed in Jurkat cells, which also yielded the most reproducible results when labeled cholesterol was added to the incubation medium. In Jurkat cells prelabeled with [ $^3\text{H}$ ]cholesterol, cyclodextrin (2% wt/vol) extracted  $67.8 \pm 3.1\%$  ( $n = 5$ ) of the incorporated cholesterol in 10 min (Fig. 4A). CPHS did not alter the effect of cyclodextrin. When 30 min of incubation preceded the addition of cyclodextrin, the fraction of extracted cholesterol decreased, indicating cholesterol migration to sites not accessible to cyclodextrin. This decrease in cyclodextrin efficiency was highly reproducible ( $P < 0.001$ ) and completely prevented by CPHS. CPHS did not change the labeled cholesterol pool remaining in the cell pellet when the preincubation was not performed but inhibited the significant increase ( $P < 0.001$ ) occurring after 30 min of preincubation. The same results were obtained when cells were preincubated for 60 and 120 min before the addition of cyclodextrin (not shown in Fig. 4A). We obtained evidence of cholesterol transfer to sites inaccessible to cyclodextrin by measuring cholesterol esterification inside the cells. In these tests, we found that esterified cholesterol became detectable after 30 min of preincubation, increasing thereafter (Fig. 4B). As expected, CPHS inhibited cholesterol esterification. During cell incubation at  $37^\circ\text{C}$  in the absence of cyclodextrin, the activating effect of CPHS on cholesterol efflux was confirmed (Fig. 4C). The action of CPHS was more manifest in the first 30 min, suggesting an induced desorption of cholesterol located in the external layer of the plasma membrane.

Next, we studied the action of inhibitory steroids on endogenous cholesterol synthesis and on ACAT activity. As reported in Figure 5 for U-937 cells, 3 h of incubation with [ $^3\text{H}$ ]acetate resulted in the labeling of cholesterol plus desmosterol ( $22.3 \pm 6.2\%$  of total cpm,  $n = 9$ ). CPHS and progesterone did not cause significant effects, whereas U18666A inhibited endogenous cholesterol synthesis by  $81.1 \pm 7.6\%$  (Fig. 5C). Progesterone caused the accumulation of lanosterol (Fig. 5B), reducing the cholesterol/lanosterol ratio from  $7.4 \pm 4.2$  to  $2.5 \pm 1.2$  (inhibition of  $64.6 \pm 10.2\%$ ,  $P < 0.05$ ). U18666A caused the accumulation of squalene epoxides (Fig. 5A) and inhibited the label-



**FIG. 3.** Esterification of plasma membrane cholesterol activated by 25-hydroxycholesterol (25-OH). Jurkat cells were incubated for 2 h at  $37^\circ\text{C}$  in RPMI 1640 medium with 5 mg/mL of bovine serum albumin (BSA), 2.5  $\mu\text{M}$  25-OH, and 5  $\mu\text{Ci}$  of [ $^3\text{H}$ ]oleate. Esters of cholesterol (A) or of 25-OH (B) were extracted and resolved by thin-layer chromatography. 1, Without 25-OH; 2, 25-OH; 3, 25-OH, 10  $\mu\text{M}$  CPHS; 4, 25-OH, 10  $\mu\text{M}$  progesterone; 5, 25-OH, 2.5  $\mu\text{M}$  U18666A. Data are means  $\pm$  SEM from five experiments. \* $P < 0.01$ . See Figure 1 for abbreviation.

**TABLE 1**  
**Cholesterol Incorporation and Esterification in Jurkat Cells<sup>a</sup>**

Added steroid	cpm/10 <sup>6</sup> cells × 10 <sup>-3</sup>		CE × 100 CE + FC
	CE	FC	
None	1.08 ± 0.10	56.1 ± 5.8	1.89 ± 0.05
2.5 μM CPHS <sup>b</sup>	0.63 ± 0.11 (40 ± 9%) <sup>c</sup>	44.9 ± 2.0 (15 ± 8%)	1.37 ± 0.21 (28 ± 6%) <sup>c</sup>
5 μM CPHS	0.41 ± 0.05 (59 ± 7%) <sup>d</sup>	37.8 ± 3.2 (27 ± 10%) <sup>c</sup>	1.05 ± 0.10 (45 ± 4%) <sup>d</sup>
10 μM CPHS	0.31 ± 0.04 (69 ± 6%) <sup>d</sup>	32.2 ± 3.2 (39 ± 10%) <sup>d</sup>	0.94 ± 0.06 (50 ± 2%) <sup>d</sup>
10 μM Progesterone	0.48 ± 0.06 (52 ± 9%) <sup>d</sup>	48.4 ± 2.8 (18 ± 10%)	0.96 ± 0.07 (49 ± 3%) <sup>d</sup>
2.5 μM U18666A	0.55 ± 0.09 (46 ± 10%) <sup>d</sup>	52.0 ± 3.9 (14 ± 8%)	1.03 ± 0.12 (46 ± 5%) <sup>d</sup>

<sup>a</sup>Jurkat cells (5 × 10<sup>6</sup>) were incubated for 45 min at 37°C in 1 mL of RPM 1640 medium containing 1 mg of bovine serum albumin, 2 μCi of [<sup>3</sup>H]cholesterol (added in 5 μL of ethanol), and the added steroid indicated. After lipid extraction, cholesteryl esters (CE) and free cholesterol (FC) were separated by thin-layer chromatography. Data are means ± SEM from 4–5 experiments (percent inhibition in parenthesis).

<sup>b</sup>CPHS, cholesteryl-3β-phosphoserine.

<sup>c</sup>P < 0.05.

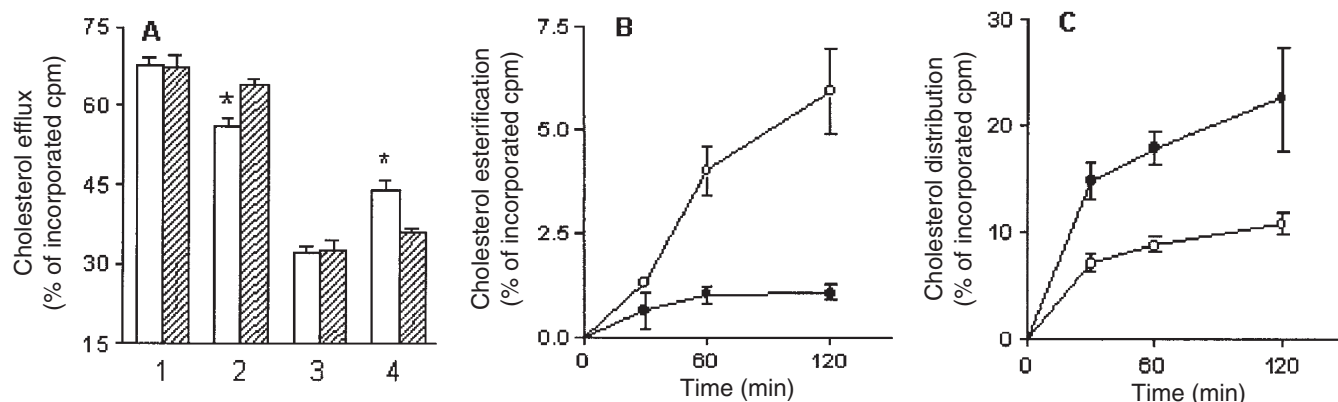
<sup>d</sup>P < 0.01.

ing of lanosterol by 74 ± 19% (Fig. 5B). CPHS did not alter the labeling of cholesterol precursors. Similar results were obtained with ECV-304 cells. In Jurkat cells, after 3 h of incubation with [<sup>3</sup>H]acetate, the label was mainly distributed in lanosterol (65.6 ± 8.1%, *n* = 3). Cholesterol/desmosterol took up 4.2 ± 2% of the label. Slow conversion of lanosterol to cholesterol was also observed in human lymphocytes (26). A clear precursor–product relationship between lanosterol and cholesterol in these cells was reached after 6 h of incubation. The high extent of labeling of lanosterol in Jurkat cells was inhibited by U18666A (inhibition of 91.2 ± 1% in three experiments, *P* < 0.01). CPHS and progesterone were without effect.

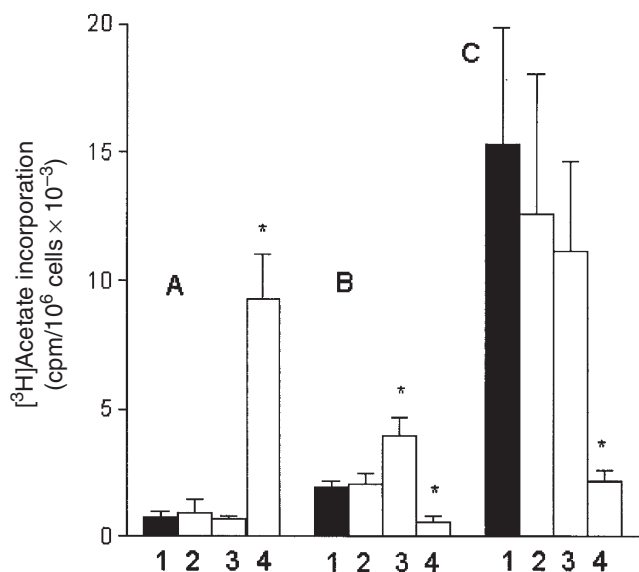
ACAT activity was tested in homogenates of Jurkat cells labeled with [<sup>3</sup>H]cholesterol. After 30 min of incubation of 1 μCi of [<sup>3</sup>H]cholesterol and 100 μg of protein with 25 μM oleoyl-coenzyme A, 1.15 ± 0.23% of cpm was recovered in cholesteryl esters (*n* = 5). The presence of 10 μM of CPHS, 10 μM progesterone, or 2.5 μM U18666A did not cause a significant change in this value.

## DISCUSSION

The results of this study show a clear difference between the newly introduced CPHS and the well-known progesterone and U18666A in the inhibition of intracellular cholesterol transport. As demonstrated by several previous studies in other cells, we confirmed with the lymphoid Jurkat, the monocytic U-937, and the endothelial ECV-304 that progesterone and U18666A inhibit the two main routes of the intracellular transport of LDL-derived cholesterol, namely, the direct route from lysosomes to the endoplasmic reticulum and the indirect route in which cholesterol is first transported from lysosomes to the plasma membrane and then from this site to the endoplasmic reticulum (4,5,19,27). Other effects of progesterone and U18666A confirmed in the present study include their inhibition of endogenous cholesterol synthesis. Progesterone influences the terminal steps of cholesterol synthesis, causing accumulation of lanosterol (7), whereas U18666A inhibits 2,3-oxidosqualene cyclase with subsequent accumulation of oxidized products of squalene and inhibition of lanos-



**FIG. 4.** Synergism between CPHS and cyclodextrin (CD). Aliquots of 5 × 10<sup>6</sup> Jurkat cells prelabeled with [<sup>3</sup>H]cholesterol (580 ± 110 cpm × 10<sup>-3</sup>) were either extracted with 2% CD in the presence or absence of 10 μM CPHS or preincubated at 37°C with or without CPHS before the extraction with CD. (A) Distribution of label in supernatants (1,2) and pellets (3,4) after the extraction with CD. 1 and 3, Without preincubation; 2 and 4, after 30 min of preincubation. The shaded bars indicate the addition of CPHS. (B) Percentage of label found in the cholesteryl ester fraction of lipid extract in cells preincubated and treated with CD. (○), Preincubation without CPHS; (●), preincubation with CPHS. (C) Percent of the incorporated cholesterol released by the cells during the preincubation in the absence (○) or in the presence of CPHS (●). Data are means ± SEM from five experiments. \**P* < 0.01. See Figure 1 for abbreviation.



**FIG. 5.** Inhibition of the endogenous synthesis of cholesterol. Lipoprotein-depleted U-937 cells ( $5 \times 10^6$ ) were incubated for 3 h at 37°C in 1 mL of RPMI 1640 medium containing 5 mg of BSA, 10  $\mu$ Ci of [ $^3$ H]acetate, and the inhibitory steroids. Nonsaponifiable lipids were extracted and resolved by thin-layer chromatography. A, Squalene epoxides; B, lanosterol; C, cholesterol plus desmosterol. 1, Untreated sample; 2, 10  $\mu$ M CPHS; 3, 10  $\mu$ M progesterone; 4, 2.5  $\mu$ M of U18666A. Data are means  $\pm$  SEM from six experiments. \* $P < 0.01$ . See Figures 1 and 3 for abbreviations.

terol and cholesterol synthesis (8). In addition, we found that U18666A does not influence the mobilization of plasma membrane cholesterol promoted by 25-hydroxycholesterol nor does it inhibit the esterification of this oxysterol. The best model to detect the U18666A-induced inhibition of the plasma membrane  $\rightarrow$  endoplasmic reticulum segment of cholesterol transport has been the esterification of [ $^3$ H]cholesterol added to the incubation medium. These results are consistent with a minor influence of this steroid on the transport of cholesterol from the plasma membrane to the endoplasmic reticulum (19,28).

In comparison to progesterone and U18666A, CPHS shows a restricted area of influence. This steroid does not affect endogenous cholesterol synthesis nor ACAT activity. In addition, it shows little activity on the transport of LDL-derived cholesterol to the intracellular sites of esterification in Jurkat cells. The inhibitory activity of CPHS became apparent when we tested the esterification of LDL-derived cholesterol in U-937 and ECV-304 cells or when we specifically monitored the plasma membrane  $\rightarrow$  endoplasmic reticulum segment of cholesterol transport. The inhibition of this route has been observed in all cell lines, using several models of cholesterol transport, including the esterification of labeled cholesterol added to the incubation medium, the stimulation of cholesterol esterification by brefeldin A or sphingomyelinase in cells depleted of lipoproteins, and the 25-hydroxycholesterol-induced mobilization of plasma membrane cholesterol. Taken together, these data suggest that the plasma membrane  $\rightarrow$  endoplasmic reticulum segment of cholesterol transport is the main site of CPHS action and that this pathway is not obliga-

tory during the esterification of LDL cholesterol in Jurkat cells. In an attempt to clarify whether the CPHS-sensitive site is in the plasma membrane itself or in the postmembrane steps, we examined the action of CPHS on the movements of plasma membrane cholesterol. A first effect of CPHS observed in cells pulse-labeled with [ $^3$ H]cholesterol is the inhibition of cholesterol incorporation into the plasma membrane. In addition, CPHS activates cholesterol efflux in prelabeled cells. This action of CPHS is rapid and more manifest in the first minutes of cell incubation with the steroid. The simplest explanation of these effects is that CPHS, inserting into the plasma membrane, displaces the cholesterol contained in the exofacial leaflet of the membrane bilayer, favoring its desorption. In the external leaflet of the plasma membrane, cholesterol preferentially associates with the sphingolipids, forming the microdomains known as lipid rafts (29). In accord with a CPHS-lipid rafts interaction, our previous data demonstrate that this steroid associates with sphingomyelin and cholesterol, forming a detergent-insoluble complex (9). Alternatively or in addition, the phosphoserine group of CPHS activates the ABCA1 permease (30), thus promoting cholesterol efflux. This possibility is supported by confocal microscopy images obtained with fluorescent annexin V in Jurkat cells showing that CPHS distributes in the external cell surface, exposing its phosphoserine group to the extracellular medium (9). Additional support for the hypothesis that CPHS acts on the plasma membrane has been obtained by examining its combined effect with cyclodextrin, a cholesterol-depleting agent also acting in the plasma membrane (23,24). Confirming previous data on suspensions of mouse fibroblasts (23), we found that in Jurkat cells the addition of 2% cyclodextrin depletes  $67.8 \pm 3.1\%$  of cell cholesterol in 10 min. This high efficiency decreases after a brief preincubation of labeled cells at 37°C, indicating a rapid migration of cholesterol to sites inaccessible to cyclodextrin, and cholesterol esterification begins to be detected. The addition of CPHS inhibits cholesterol migration, thus improving the extraction by cyclodextrin and decreasing the amount of cholesterol remaining in the cells.

Owing to its selective effect on plasma membranes, CPHS may become a useful reagent for the study of the involvement of the plasma membrane in cholesterol transport in different mammalian cells. For example, we interpret the ineffectiveness of CPHS in inhibiting the esterification of LDL-derived cholesterol in Jurkat cells as indicating that in these cells most of the LDL-derived cholesterol is directly delivered to the endoplasmic reticulum, without cycling through the plasma membrane. In contrast, in U-937 and ECV-304 cells, a large proportion of LDL-derived cholesterol follows the CPHS-sensitive pathway. In accord with this, the high capacity of these cells to store LDL-derived cholesterol in the plasma membrane is indicated by the observation that the addition of 25-hydroxycholesterol is required to initiate the transfer of cholesterol to the sites of esterification in the endoplasmic reticulum. In contrast, the oxysterol is not required in Jurkat cells. Variations in cholesterol synthesis, transport, and efflux



in mammalian cells are known (2). The application of inhibitors with a defined mechanism of action may prove to be invaluable in clarifying these differences.

## ACKNOWLEDGMENTS

This work received financial support from the Italian MURST (Co-finanziamento No. 9906104773007). We are grateful to Dr. Irene Cortella (Department of Medical and Surgical Sciences, University of Padova) for her assistance in preparing the LDL.

## REFERENCES

- Liscum, L., and Munn, N.J. (1999) Intracellular Cholesterol Transport, *Biochim. Biophys. Acta* 1438, 19–37.
- Fielding, C.J., and Fielding, P.E. (1997) Intracellular Cholesterol Transport, *J. Lipid Res.* 38, 1503–1521.
- Incardona, J.P., and Eaton, S. (2000) Cholesterol in Signal Transduction, *Curr. Opin. Cell Biol.* 12, 193–203.
- Liscum, L., and Faust, J.R. (1989) The Intracellular Transport of Low Density Lipoprotein-Derived Cholesterol Is Inhibited in Chinese Hamster Ovary Cells Cultured with 3 $\beta$ -[2-(Diethylamino)ethoxy]androst-5-en-17-one, *J. Biol. Chem.* 264, 11796–11806.
- Butler, J.D., Blanchette-Mackie, J., Goldin, E., O'Neill, R.R., Carstea, G., Roff, C.F., Patterson, M.C., Patel, S., Comly, M.E., Cooney, A., et al. (1992) Progesterone Blocks Cholesterol Translocation from Lysosomes, *J. Biol. Chem.* 267, 23797–23805.
- Neufeld, E.B., Wastney, M., Patel, S., Suresh, S., Cooney, A.M., Dwyer, N.K., Roff, C.F., Ohno, K., Morris, J.A., Carstea, E.D., et al. (1999) The Niemann–Pick C1 Protein Resides in a Vesicular Compartment Linked to Retrograde Transport of Multiple Lysosomal Cargo, *J. Biol. Chem.* 274, 9627–9635.
- Metherall, J.E., Waugh, K., and Li, H. (1996) Progesterone Inhibits Cholesterol Biosynthesis in Cultured Cells. Accumulation of Cholesterol Precursors, *J. Biol. Chem.* 271, 2627–2633.
- Sexton, R.C., Panini, S.R., Azran, F., and Rudney, H. (1983) Effects of 3 $\beta$ -[2-(Diethylamino)ethoxy]androst-5-en-17-one on the Synthesis of Cholesterol and Ubiquinone in Rat Intestinal Epithelial Cell Cultures, *Biochemistry* 22, 5687–5692.
- Cusinato, F., Habeler, W., Calderazzo, F., Nardi, F., and Bruni, A. (1998) Loss of Phosphoserine Polar Group Asymmetry and Inhibition of Cholesterol Transport in Jurkat Cells Treated with Cholesterylphosphoserine, *J. Lipid Res.* 39, 1844–1851.
- Scheetz, M.P., and Singer, S.J. (1974) Biological Membranes as Bilayer Couples. A Molecular Mechanism of Drug–Erythrocyte Interaction, *Proc. Natl. Acad. Sci. USA* 71, 4457–4461.
- Lusis, A.J. (2000) Atherosclerosis, *Nature* 407, 233–241.
- Lange, Y. (1994) Cholesterol Movement from Plasma Membrane to Rough Endoplasmic Reticulum. Inhibition by Progesterone, *J. Biol. Chem.* 269, 3411–3414.
- Billheimer, J.T., Avart, S., and Milani, B. (1983) Separation of Steryl Esters by Reversed-Phase Liquid Chromatography, *J. Lipid Res.* 24, 1646–1650.
- Nadeau, R.G., and Hanzlik, R.P. (1969) Synthesis of Labeled Squalene and Squalene 2,3-Oxide, *Methods Enzymol.* 15, 346–351.
- Billheimer, J.T., Chamoun, D., and Esfahani, M. (1987) Defective 3-Ketosteroid Reductase Activity in a Human Monocyte-like Cell Line, *J. Lipid Res.* 28, 704–709.
- Warner, G.J., Stoudt, G., Bamberger, M., Johnson, W.J., and Rothblat, G.H. (1995) Cell Toxicity Induced by Inhibition of Acyl Coenzyme A:Cholesterol Acyltransferase and Accumulation of Unesterified Cholesterol, *J. Biol. Chem.* 270, 5772–5778.
- Lange, Y., Ye, J., Rigney, M., and Steck, T. (2000) Cholesterol Movement in Niemann–Pick Type C Cells and in Cells Treated with Amphiphiles, *J. Biol. Chem.* 275, 17468–17475.
- Lange, Y., Ye, J., and Strebel, F. (1995) Movement of 25-Hydroxycholesterol from the Plasma Membrane to the Rough Endoplasmic Reticulum in Cultured Hepatoma Cells, *J. Lipid Res.* 36, 1092–1097.
- Underwood, K.W., Jacobs, N.L., Howley, A., and Liscum, L. (1998) Evidence for a Cholesterol Transport Pathway from Lysosomes to Endoplasmic Reticulum That Is Independent of the Plasma Membrane, *J. Biol. Chem.* 273, 4266–4274.
- Johnson, W.J., Fischer, R.T., Phillips, M.C., and Rothblat, G.H. (1995) Efflux of Newly Synthesized Cholesterol and Biosynthetic Sterol Intermediates from Cells. Dependence on Acceptor Type and on Enrichment of Cells with Cholesterol, *J. Biol. Chem.* 270, 25037–25046.
- Xu, X.X., and Tabas, I. (1991) Lipoproteins Activate Acyl-Coenzyme A:Cholesterol Acyltransferase in Macrophages Only After Cellular Cholesterol Pools Are Expanded to a Critical Threshold Level, *J. Biol. Chem.* 266, 17040–17048.
- Fielding, C.J., and Fielding, P.E. (1995) Molecular Physiology of Reverse Cholesterol Transport, *J. Lipid Res.* 36, 211–228.
- Yancey, P.G., Rodriguez, W.V., Kilsdonk, E.P., Stoudt, G.W., Johnson, W.J., Phillips, M.C., and Rothblat, G.H. (1996) Cellular Cholesterol Efflux Mediated by Cyclodextrins. Demonstration of Kinetic Pools and Mechanism of Efflux, *J. Biol. Chem.* 271, 16026–16034.
- Neufeld, E.B., Cooney, A.M., Pitha, J., Dawidowicz, E.A., Dwyer, N.K., Pentchev, P.G., and Blanchette-Mackie, E.J. (1996) Intracellular Trafficking of Cholesterol Monitored with Cyclodextrin, *J. Biol. Chem.* 271, 21604–21613.
- Heino, S., Lusa, S., Somerharju, P., Ehnholm, C., Olkkonen, V.M., and Ikonen, E. (2000) Dissecting the Role of the Golgi Complex and Lipid Rafts in Biosynthetic Transport of Cholesterol to the Cell Surface, *Proc. Natl. Acad. Sci. USA* 97, 8375–8380.
- Ho, Y.K., Faust, J.R., Bilheimer, D.W., Brown, M.S., and Goldstein, J.L. (1977) Regulation of Cholesterol Synthesis by Low Density Lipoprotein in Isolated Human Lymphocytes, *J. Exp. Med.* 145, 1531–1549.
- Harmala, A.S., Porn, M.I., Mattjus, P., and Slotte, J.P. (1994) Cholesterol Transport from Plasma Membranes to Intracellular Membranes Is Inhibited by 3 $\beta$ -[2-(Diethylamino)ethoxy]androst-5-en-17-one, *Biochim. Biophys. Acta* 1211, 317–325.
- Underwood, K.W., Andemariam, B., McWilliams, G.L., and Liscum, L. (1996) Quantitative Analysis of Hydrophobic Amine Inhibition of Intracellular Cholesterol Transport, *J. Lipid Res.* 37, 1556–1568.
- Simons, K., and Ikonen, E. (1997) Functional Rafts in Cell Membranes, *Nature* 387, 569–572.
- Chambenoit, O., Hamon, Y., Marguet, D., Rigneault, H., Rosseneu, M., and Chimini, G. (2001) Specific Docking of Apolipoprotein A-I at the Cell Surface Requires a Functional ABCA1 Transporter, *J. Biol. Chem.* 276, 9955–9960.

[Received May 10, 2002, and in revised form November 26, 2001; revision accepted December 5, 2001]



# Reduced Secretion of Triacylglycerol in CaCo-2 Cells Transfected with Intestinal Fatty Acid-Binding Protein

Ane Gedde-Dahl<sup>a,\*</sup>, Mari Ann Kulseth<sup>b</sup>, Trine Ranheim<sup>b</sup>, Christian A. Drevon<sup>b</sup>,  
and Arild C. Rustan<sup>a</sup>

<sup>a</sup>Department of Pharmacology, School of Pharmacy, and <sup>b</sup>Institute for Nutrition Research, University of Oslo, N-0316 Oslo, Norway

**ABSTRACT:** The fatty acid-binding proteins are hypothesized to be involved in cellular fatty acid transport and trafficking. We established CaCo-2 cells stably transfected with intestinal fatty acid-binding protein (I-FABP) and examined how the expression of this protein may influence fatty acid metabolism. I-FABP expression was detectable in I-FABP-transfected cells, whereas parent CaCo-2 cells as well as mock-transfected cells failed to express detectable levels of I-FABP mRNA or protein at any stage of differentiation. For studies of lipid metabolism, cells were incubated with [<sup>14</sup>C]oleic acid in taurocholate micelles containing monoolein, and distribution of labeled fatty acid in cellular and secreted lipids was examined. In one transfected cell clone, expressing the highest level of I-FABP, labeled cellular triacylglycerol increased approximately twofold as compared to control cells. The level of intracellular triacylglycerol in two other I-FABP-transfected clones resembled that of control cells. However, secretion of triacylglycerol was markedly reduced in all the I-FABP-expressing cell lines. Our data suggest that increased expression of I-FABP leads to reduced triacylglycerol secretion in intestinal cells.

Paper no. L8852 in *Lipids* 37, 61–68 (January 2002).

Fatty acid-binding proteins (FABP) are small (14–15 kDa) cytosolic proteins especially abundant in tissues with active fatty acid metabolism (1–3). A role for intracellular FABP in fatty acid transport has been hypothesized for several decades, and several studies have supported this proposed function (4). The small intestine contains two different types of FABP: intestinal fatty acid-binding protein (I-FABP) (5), exclusively expressed in intestinal epithelium (6,7), and liver fatty acid-binding protein (L-FABP) (5), which is present in the liver and the intestine (8,9). It has been postulated that I-FABP, which is highly expressed in the tips of small intestine villi (2), targets the delivery of fatty acids from the brush-border membrane to specific sites of lipid metabolism, whereas L-FABP is important for the basic cellular economy of fatty

acids (10,11). The hypothesis that the two FABP in the intestine have different roles in fatty acid uptake and metabolism is supported by recent studies on lipid metabolism in mouse L-cell fibroblasts. Transfected L-cells expressing L-FABP increased fatty acid uptake and incorporated more fatty acids into phospholipids, whereas fibroblasts transfected to express I-FABP did not affect fatty acid uptake, but preferentially stimulated fatty acid incorporation into triacylglycerol as compared to control cells (11–13).

The human cell line CaCo-2 is generally considered a suitable model for enterocyte differentiation and growth regulation (14) and has been extensively used as an *in vitro* model for the investigation of intestinal lipoprotein metabolism [reviewed in (15–17)]. These cells have previously been reported to express only L-FABP (7,18–21), but the presence of endogenous I-FABP has recently been described (22–24). Furthermore, different patterns of expression and regulation have been reported for I-FABP and L-FABP in these cells (24).

Previously, cell lines transfected with I-FABP cDNA and cells that endogenously express I-FABP have provided insight on intracellular functions of I-FABP (11,13,21,25–30). With only a few exceptions (21,29), these studies have not examined the effect of I-FABP on secretion of lipids from an intact cell system. The aim of the present study was to examine synthesis and secretion of triacylglycerol in CaCo-2 cells stably transfected to express I-FABP.

## MATERIALS AND METHODS

**Materials.** [<sup>14</sup>C]oleic acid (58 Ci/mol) and [<sup>32</sup>P]dCTP were obtained from Du Pont, NEN<sup>®</sup> Research Products (Boston, MA). Bovine serum albumin (BSA) (essentially fatty acid free), oleic acid, 2-monooleoylglycerol, and sodium taurocholate were purchased from Sigma (St. Louis, MO). Silica gel F 1500 thin-layer chromatography (TLC) plates were purchased from Schleicher and Schuell (Dassel, Germany). The recombinant plasmids pJG19 and pJG418 containing cDNA encoding rat I-FABP (6) and rat L-FABP (8), respectively, were generously provided by Dr. J.I. Gordon, Washington University (St. Louis, MO).

**Cell culture.** CaCo-2 cells obtained from American Type Culture Collection (Manassas, VA) (passage 18) were grown in Dulbecco's modified Eagle's (DME) medium (4.5 g/L glucose

\*To whom correspondence should be addressed at Laboratory of Clinical Biochemistry, Haukeland Hospital, P.O. Box 1, N-5021 Bergen, Norway.

E-mail: ane.gedde-dahl@haukeland.no

Abbreviations: ANOVA, analysis of variance; apoB, apolipoprotein B; BSA, bovine serum albumin; dCTP, deoxy CTP; DME, Delbecco's modified Eagle's; FABP, fatty acid-binding protein; I-FABP, intestinal fatty acid-binding protein; L-FABP, liver fatty acid-binding protein; dNTP, deoxynucleoside triphosphate; PBS, phosphate-buffered saline; PCR, polymerase chain reaction; SDS, sodium dodecyl sulfate; TLC, thin-layer chromatography.

and 3.7 g/L sodium bicarbonate) (Bio-Whittaker, Walkersville, MD) supplemented with 20% fetal calf serum (GIBCO BRL, Paisley, United Kingdom), insulin (10 µg/mL) (Sigma), L-glutamine (2 mM), penicillin (50 IU/mL), streptomycin (50 µg/mL), and 1% nonessential amino acids (Bio-Whittaker) and maintained as previously described (31).

For experiments, cells were plated at  $2 \times 10^5$  cells/cm<sup>2</sup> on the apical side of 24.5-mm diameter collagen-treated cell culture filter inserts with 3.0 µm pore size (Transwell™-COL, Costar, Cambridge, MA) and grown to 14 d postconfluence (31).

**Plasmid construction.** The recombinant plasmid pJG19 containing a 564 bp cDNA encoding rat I-FABP (6) was digested with *Dra*I and used as template in a polymerase chain reaction (PCR) amplification. The PCR was performed in a 50-µL reaction solution containing PCR buffer (50 mM KCl, 10 mM Tris-HCl pH 8.4, 1.5 mM MgCl<sub>2</sub>, and 0.001% gelatin), 25 pmol of the upstream primer 5'-CCG AAT TCA CAG CTG ACA TCA TGG CAT-3', 25 pmol of the downstream primer 5'-CCT CTA GAT CTG ACA AGG CTT GGA AGC A-3', 200 µM deoxynucleoside triphosphate (dNTP) and 1 U Taq polymerase (AmpliTaq; PerkinElmer Cetus, Norwalk, CT). The DNA was denatured at 94°C for 3 min, and the PCR mixture was subjected to 35 cycles of PCR; each cycle consisted of 1 min at 94, 55, and 72°C. The PCR product was subcloned into the plasmid vector pCR™II by means of the Original TA Cloning® Kit (Invitrogen, San Diego, CA) allowing direct insertion of a PCR product. The cDNA encoding the rat I-FABP was thereafter excised using *Eco*RI (RE site in the upper primer) and *Xba*I (RE site in the lower primer) and subcloned into the mammalian expression vector pcDNA3 (Invitrogen). Restriction enzyme analysis and DNA sequencing were used to confirm a proper insertion of the cDNA insert.

**Transfection and clone selection.** The DNA-calcium phosphate co-precipitation method (32) was used for production of stably transfected cell lines. CaCo-2 cells were plated at  $3.8 \times 10^5$  cells/100-mm dishes 24 h prior to transfection with 20 µg DNA. Cells and DNA were coincubated for 14 h at 37°C in 5% CO<sub>2</sub>. After a 10% dimethylsulfoxide shock, cultures were incubated in fresh medium for 72 h before the cells were split 1:2 and 1:4 into G418 (Geneticin®) supplemented media (0.8 mg/mL active drug) (GIBCO BRL). Medium was changed two to three times/week. From 31 d postplating, independent G418-resistant cell colonies were isolated with cloning cylinders, detached with trypsin-EDTA, and transferred to 96-well tissue culture plates. The cloned cell lines were expanded and maintained in media containing G418 (0.4 mg/mL active drug).

Several independent stably transfected cell lines expressing I-FABP were established. Mock-transfected cells, designated CaCo-2 neo, were cloned following transfection with pcDNA3 without a cDNA insert. This cell line was used as a control for the I-FABP-transfected cells to control for possible effects of G418 sulfate on the cells. The wild-type parental cell line, CaCo-2, was also included for comparison.

**mRNA isolation and Northern blot analysis.** For mRNA analysis in undifferentiated cells, the cells were grown in plastic

tissue culture flasks and harvested at confluence. For mature monolayers, cells were plated on polycarbonate filter membranes (Transwell™; Costar) and grown to 14 d postconfluence. Poly(A)<sup>+</sup> mRNA was isolated from cells using the Dynabeads mRNA Direct kit (Dyna®; Oslo, Norway). Approximately 2 µg mRNA was separated on 1% agarose gel containing 6.7% formaldehyde and transferred to nylon membrane (Hybond-N; Amersham, Buckinghamshire, United Kingdom). I-FABP and L-FABP cDNA probes were recovered from digestion of pJG19 (6) and pJG418 (8), respectively. The probes for I-FABP, L-FABP, and human β-actin (Clontech, Palo Alto, CA, USA) were labeled with [<sup>32</sup>P]dCTP by random priming according to Sambrook *et al.* (33). Membranes were prehybridized, hybridized, and washed at 65°C as described by Church and Gilbert (34). Finally, the signals were analyzed by imaging using a Phosphorimager II (Molecular Dynamics, Sunnyvale, CA) and calibrated against β-actin as an internal standard using the software ImageQuaNT (Molecular Dynamics). Before rehybridization, the membranes were stripped in 0.1% sodium dodecyl sulfate (SDS) at 95°C. The size of the mRNA was determined with reference to an RNA molecular weight marker (GIBCO BRL) that was cut off the nylon membrane before hybridization and stained with methylene blue.

**Western blot analysis.** Cells grown to 14 d postconfluence on polycarbonate filter membranes (Transwell™, Costar) were harvested by scraping into phosphate-buffered saline (PBS), and the pelleted cells were resuspended in lysis buffer [NaCl (0.1 M), Tris-HCl (20 mM, pH 7.4), ethylenediamine tetracetic acid (10 mM), Triton X-100 (1%), aprotinin (10 µg/mL), and phenylmethylsulfonyl fluoride (1 mM)] for 30 min at 4°C. Lysed cells were centrifuged (12,000 × g, 10 min) and the supernatants were collected. Total protein was measured using BSA as standard (35). Protein lysates (100 µg) were separated on 14% precast gels (Novex, San Diego, CA) by SDS-polyacrylamide gel electrophoresis (36) and transferred to PVDF membranes (NEN® Research Products) by electroblotting. Blots were probed with rabbit anti-rat I-FABP antisera and rabbit anti-rat L-FABP antisera (generously provided by Dr. J.I. Gordon), which cross-react with human I-FABP and human L-FABP, respectively (19). Antigen-antibody complexes were detected by the use of the VECTASTAIN® ABC system according to the manufacturer's instructions (Vector Laboratories, Burlingame, CA). Blots were developed by tetramethylbenzidine substrate for horseradish peroxidase. To determine the amounts of I-FABP in the various cell lysates, the filters were scanned with a laser densitometer (Molecular Dynamics). Purified recombinant rat I-FABP (Molecular Probes Europe BV, Leiden, The Netherlands) was used as a standard to estimate I-FABP protein concentrations.

**Measurement of cell-associated and secreted lipids.** Apical and basolateral media were removed and the cells were rinsed once with serum-free DME medium; unattached and damaged cells were thereby washed off. Cell monolayers were incubated in serum-free DME medium containing [1-<sup>14</sup>C]oleic acid (1 µCi/mL, 0.6 mM) and 2-monooleoylglycerol (0.3 mM) in taurocholate micelles (12 mM sodium tau-

rocholate) prepared as previously described (37). The micelles were added to the upper chamber of the cell culture system, whereas the lower chamber contained serum-free DME medium only. After incubation, the media were collected from the apical and basolateral compartments of the tissue culture inserts, and the cells were scraped off the filter membranes into PBS. Samples were taken for protein determination, using BSA as a reference protein (35).

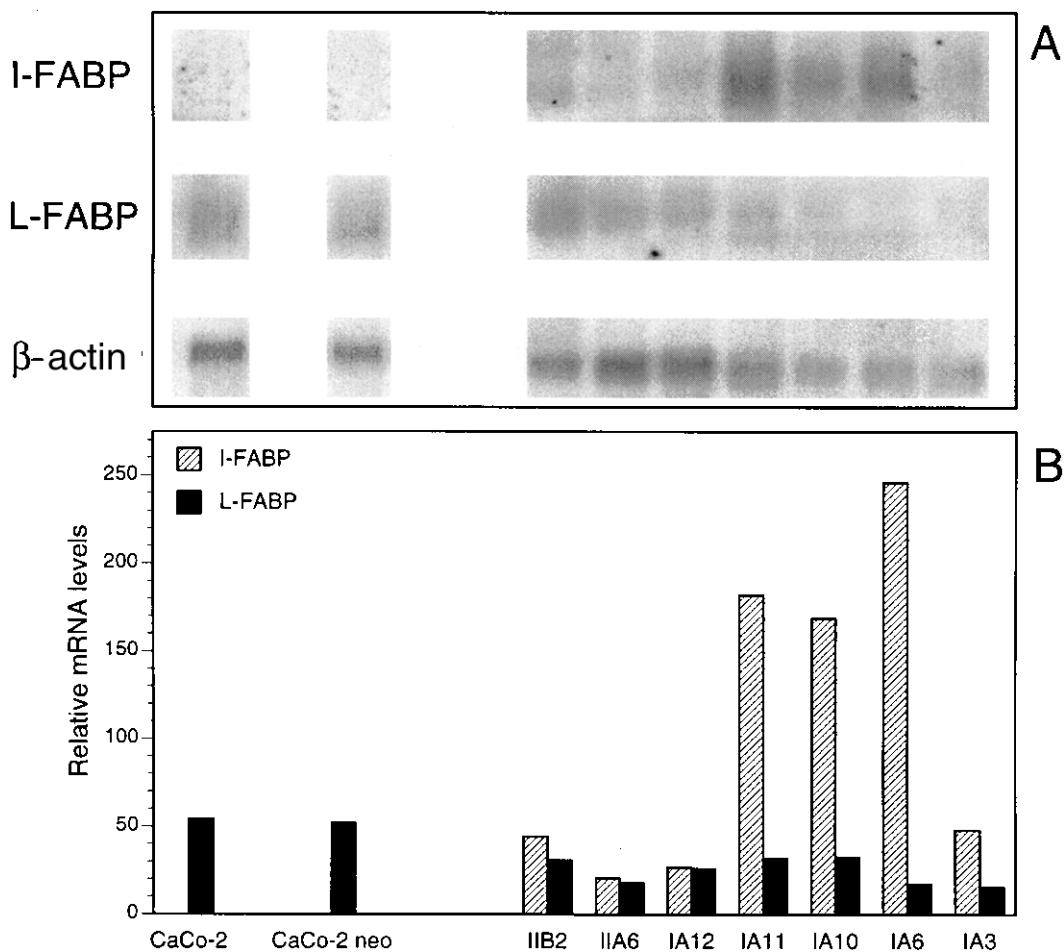
The homogenized cell fraction was mixed with 20 vol of chloroform/methanol (2:1, vol/vol) (38). Four volumes of a 0.9% sodium chloride solution of pH 2 were added, and the mixture was allowed to separate into two phases. The organic phase was dried under a stream of nitrogen at 40°C. The residual lipid extract was redissolved in 200  $\mu$ L hexane and separated by TLC, using hexane/diethyl ether/acetic acid (80:20:1, by vol) as developing solvent. The various lipid bands were visualized by iodine vapor and cut into 8 mL liquid scintillation fluid (InstaGel II Plus, Packard Instrument, Downers Grove, IL); and the radioactivity was then quantified using a liquid scintillation counter (TRI-CARB 1900 TR, Packard Instrument).

Samples of basolateral media, devoid of cellular debris, were added to 4 vol of chloroform/methanol (2:1, vol/vol) and 2% serum as unlabeled carrier for the lipids. The water phase was reextracted once with 4 vol of chloroform/methanol (2:1, vol/vol), and the combined organic phases were further treated in the same way as for the cells.

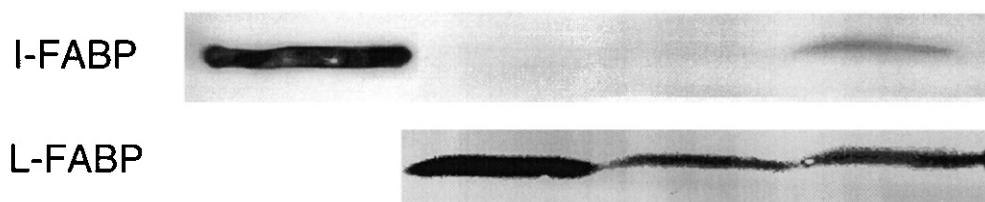
**Statistical analysis.** All values are reported as mean  $\pm$  standard error of the mean. Comparison of different treatments was evaluated by analysis of variance (ANOVA) (StatView<sup>®</sup> 5.0, SAS Institute, Cary, NC). The analysis of variance results were *post-hoc* tested by Fisher's protected least significant difference. Statistical significance was defined as  $P < 0.05$ .

## RESULTS

**I-FABP and L-FABP expression.** Transfection of CaCo-2 cells resulted in several stably transfected cell lines expressing I-FABP (Fig. 1). Northern and Western blot analyses of differentiated cells did not show detectable levels of I-FABP mRNA or protein in parent CaCo-2 cells or mock-transfected cells (CaCo-



**FIG. 1.** Expression of intestinal fatty acid-binding protein (I-FABP) and liver fatty acid-binding protein (L-FABP) mRNA in differentiated CaCo-2 cells. Poly(A)<sup>+</sup> mRNA was isolated from transfected and nontransfected cells, and Northern blot analyses were performed with cDNA probes for I-FABP and L-FABP. (A) Lane 1, CaCo-2; lane 2, CaCo-2 neo; lanes 3–9, different clones of I-FABP transfected cells (IIB2, IIA6, IA12, IA11, IA10, IA6, IA3). The expression levels were related to  $\beta$ -actin in each sample and the relative mRNA levels are shown in (B).



**FIG. 2.** Detection of I-FABP and L-FABP protein in differentiated CaCo-2 cells. Western blot analyses of protein lysates (100  $\mu$ g) from transfected and nontransfected cells were performed using antiserum raised against rat I-FABP and rat L-FABP. Lane 1, 0.3  $\mu$ g purified rat I-FABP; lane 2, CaCo-2; lane 3, CaCo-2 neo; lane 4, clone IA6. Quantification of the I-FABP band revealed that the band from clone IA6 corresponded to approximately 0.5  $\mu$ g/mg protein. For abbreviations see Figure 1.

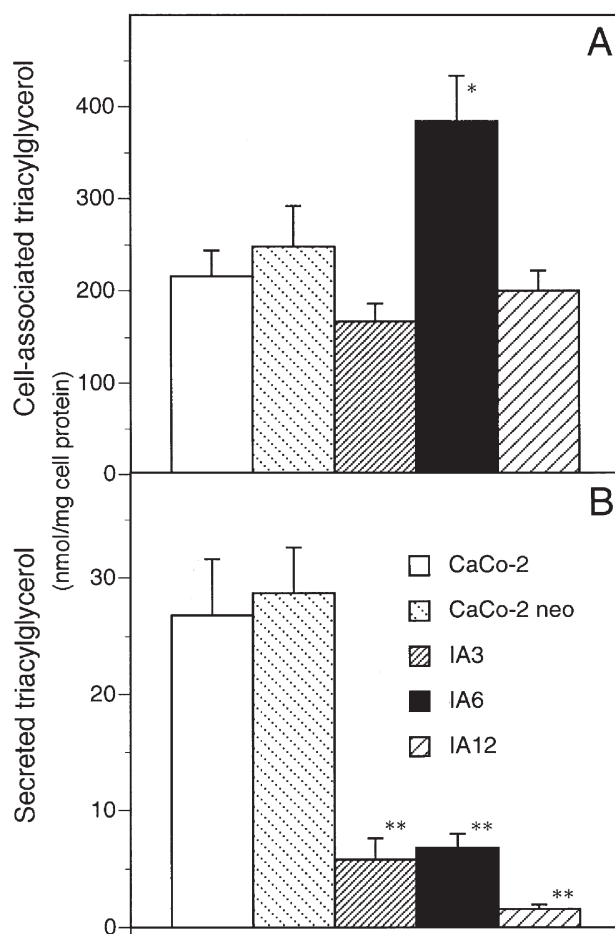
2 neo) (Figs. 1 and 2). The expression of L-FABP was already present in undifferentiated cells (data not shown), and the expression increased with differentiation, as reported earlier by several investigators (18–21,24). For the wild-type parental cell line, the relative amounts of L-FABP mRNA in 14 d postconfluent monolayers were 10 times those in undifferentiated cultures (data not shown). However, I-FABP-expressing cells showed lower levels of L-FABP mRNA than control cells (Fig. 1).

**[<sup>14</sup>C]Oleic acid esterification and distribution.** As shown in Figure 1, the different transfected clones expressed various levels of I-FABP mRNA. The effect of I-FABP on oleic acid metabolism was examined in three clones expressing different levels of I-FABP, namely, IA3, IA6, and IA12 (Fig. 3).

To study fatty acid incorporation, esterification, and secretion, cell lines were incubated up to 24 h with taurocholate micelles containing [<sup>14</sup>C]oleic acid (0.6 mM) and 2-monoacylglycerol (0.3 mM). Incorporation of labeled oleic acid into cellular triacylglycerol was significantly increased in clone IA6 as compared to the other cell lines examined (Fig. 3A). After 5 h incubation, this clone incorporated  $57 \pm 3\%$  of [<sup>14</sup>C]oleic acid into triacylglycerol, whereas nontransfected cells and mock-transfected cells incorporated  $44 \pm 4$  and  $39 \pm 4\%$ , respectively ( $P < 0.05$ ). However, the other I-FABP-expressing cell lines did not show increased incorporation into triacylglycerol (Fig. 3A). On the other hand, secretion of labeled triacylglycerol was markedly reduced in all I-FABP transfectants when compared to control cells (Fig. 3B).

The clone expressing the highest level of I-FABP, clone IA6, was studied in more detail (Table 1). Incorporation of labeled fatty acid into cellular triacylglycerol as well as total incorporation into cellular lipids was increased in this clone when compared to parent CaCo-2 cells (Table 1). However, total incorporation was not significantly different between clone IA6 and mock-transfected cells. The increased incorporation into triacylglycerol, without affecting cellular phospholipids, resulted in a twofold higher triacylglycerol/phospholipid ratio for I-FABP-expressing cells (Table 1). The levels of free [<sup>14</sup>C]oleic acid as well as the incorporation into diacylglycerol were similar in all cell lines, whereas the incorporation into cholesteryl esters was reduced both in I-FABP-expressing and mock-transfected cells (Table 1). However, the proportion of [<sup>14</sup>C]oleic acid in cholesteryl esters was less than 1% of the total incorporation into cellular lipids.

Time course experiments showed that the observed differences in cell-associated and secreted triacylglycerol between the clone IA6 and control cells were evident also after 24 h of incubation (Fig. 4).



**FIG. 3.** Incorporation of [<sup>14</sup>C]oleic acid into cell-associated (A) and secreted (B) triacylglycerol. Cell monolayers were incubated with [<sup>14</sup>C]oleic acid (0.6 mM) and 2-monoolein (0.3 mM) for 5 h. Incorporation of [<sup>14</sup>C]oleic acid into cell-associated and secreted triacylglycerol was measured as described in the Materials and Methods section. Data, given as nmol/mg cell protein, represent mean  $\pm$  standard error of the mean of 6–14 filters from 2–5 independent experiments. \*Significantly different from all other cell lines. \*\*Significantly different from controls ( $P < 0.0001$ ).



**TABLE 1**  
**Metabolism of [<sup>14</sup>C]Oleic Acid in Nontransfected and Transfected CaCo-2 Cells<sup>a</sup>**

	Incorporation of [ <sup>14</sup> C]oleic acid (nmol/mg cell protein)		
	CaCo-2	CaCo-2 neo	Clone IA6
Triacylglycerol			
Cell-associated	216 ± 28	248 ± 44	384 ± 49 <sup>b,c</sup>
Secreted	27 ± 5	29 ± 4	7 ± 1 <sup>b,c</sup>
Phospholipids			
Cell-associated	111 ± 6	124 ± 5	110 ± 8
Secreted	1.4 ± 0.3	2.8 ± 1.0	1.0 ± 0.2 <sup>c</sup>
Diacylglycerol			
Cell-associated	34 ± 4	53 ± 6	51 ± 7
Free fatty acids			
Cell-associated	129 ± 19	169 ± 11	121 ± 19
Cholesteryl esters			
Cell-associated	3.9 ± 0.3	2.5 ± 0.3	3.4 ± 0.5
Total cellular incorporation	494 ± 43	597 ± 61	669 ± 69 <sup>b</sup>
TG/PL ratio, cellular lipids	2.1 ± 0.3	2.0 ± 0.3	3.6 ± 0.4 <sup>b,c</sup>
TG/PL ratio, secreted lipids	19 ± 1	16 ± 3	10 ± 3 <sup>b</sup>
TG secretion (% of synthesized)	11 ± 2	13 ± 3	2 ± 1 <sup>b,c</sup>

<sup>a</sup>Cell monolayers were incubated with [<sup>14</sup>C]oleic acid (0.6 mM) and 2-monoolein (0.3 mM) for 5 h. Cells were harvested and lipids were extracted and separated by thin-layer chromatography as described in the Materials and Methods section. Incorporation of [<sup>14</sup>C]oleic acid into cellular and secreted lipids was measured. Data represent mean ± standard error of the mean of 7–14 filters from 3–5 independent experiments. Abbreviations: TG, triacylglycerols; PL, phospholipids.

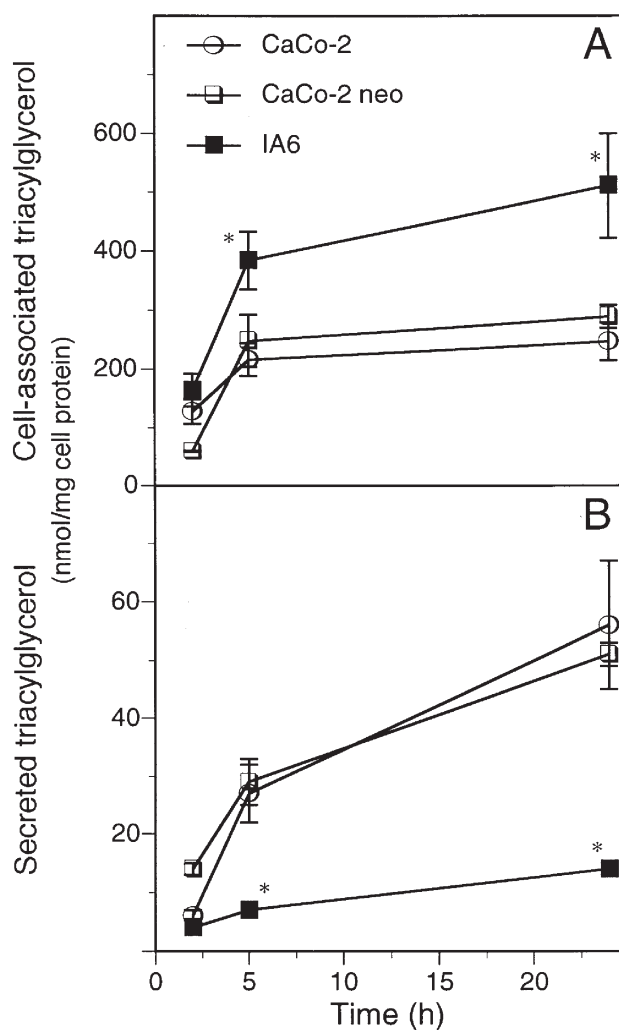
<sup>b</sup>Significantly different from CaCo-2.

<sup>c</sup>Significantly different from CaCo-2 neo.

## DISCUSSION

In the present study, we established CaCo-2 cells stably transfected with I-FABP, and examined how the expression of this protein may influence fatty acid metabolism in intestinal cells. Our main finding was that triacylglycerol secretion was inhibited in I-FABP-transfected cells independent of the level of I-FABP expression.

Differentiated as well as undifferentiated CaCo-2 cells fail to express I-FABP when grown on plastic supports (7,20,23). However, differentiated cells grown on filter inserts have recently been shown to express I-FABP endogenously (22–24), suggesting that I-FABP expression in CaCo-2 cells may depend on culture conditions as well as maturation. Darimont *et al.* (24) reported that when collagen was present during cell differentiation on filter inserts, the expression of endogenous I-FABP, but not L-FABP, was strongly reduced. In the present study, cells for Northern and Western blot hybridization studies were differentiated on uncoated polycarbonate filters, which are not known to inhibit I-FABP expression (24). Nevertheless, parent CaCo-2 cells as well as mock-transfected cells did not show detectable levels of I-FABP mRNA or protein (Figs. 1 and 2). Also in previous studies, I-FABP protein expression was not detectable in pre- or postconfluent cells grown on filter inserts (18,19,21). The use of different antibodies as well as various culture conditions may account for



**FIG. 4.** Time course for incorporation of [<sup>14</sup>C]oleic acid into cell-associated (A) and secreted (B) triacylglycerol. Cell monolayers were incubated with [<sup>14</sup>C]oleic acid (0.6 mM) and 2-monoolein (0.3 mM) for 2, 5, and 24 h. Incorporation of [<sup>14</sup>C]oleic acid into cell-associated and secreted triacylglycerol was measured as described in the Materials and Methods section. Data represent mean ± standard error of the mean from several independent experiments. \*Significant difference as compared to the other two cell lines.

the discrepancies observed between these studies and the recent demonstrations of endogenous I-FABP expression in these cells (22–24).

Previously, cell lines transfected with I-FABP cDNA and cells that endogenously express I-FABP have provided insight on intracellular functions of I-FABP (11,13,21,25–30). Only a few of these studies were performed with cells of intestinal origin (21,28,29). In our present study, fatty acid metabolism was examined using CaCo-2 human intestinal cells stably transfected with I-FABP. We found that incorporation of [<sup>14</sup>C]oleic acid into cellular triacylglycerol was significantly increased in clone IA6, expressing the highest level of I-FABP (Table 1, Figs. 3A, 4A). However, other I-FABP transfected cell lines with lower levels of I-FABP did not show increased incorporation into cellular triacylglycerol

(Fig. 3A). The reason for the lack of dose dependence between I-FABP level and cellular triacylglycerol is not known. Because several proteins are involved in cytosolic binding of fatty acids, binding to I-FABP will account for only a minority of fatty acid transport. It appears that other factors than the level of I-FABP expression may be rate-limiting in the regulation of triacylglycerol synthesis under the conditions of cell culture.

The data from clone IA6 support the hypothesis that I-FABP may be involved in targeting long-chain fatty acids to triacylglycerol synthesis. This is in accordance with Darimont *et al.* (39), who showed that reduced incorporation of [ $^{14}\text{C}$ ]palmitic acid into triacylglycerol was accompanied by a reduced level of I-FABP in CaCo-2 cells. Our observations are also similar to results from I-FABP transfected L-cell fibroblasts (11,13) and rat intestinal epithelial cells (hBRIE 380i) (28) showing that [ $^3\text{H}$ ]oleic acid incorporation into triacylglycerol was increased in I-FABP-expressing cells. In hBRIE 380i cells, however, the increase in fatty acid incorporation into triacylglycerol was correlated to cellular differentiation in addition to I-FABP expression, leading the authors to suggest that differentiation-dependent factors other than I-FABP may play a role in long-chain fatty acid targeting (28). This is supported by studies in non-I-FABP/non-L-FABP-expressing mouse embryonic stem cells demonstrating that differentiation increased the quantity of cellular lipids, primarily triacylglycerol, whereas expression of I-FABP further enhanced triacylglycerol production (27). In our present study, experiments examining oleic acid metabolism were conducted in differentiated cells, grown to 14 d postconfluence on filter membranes. We previously showed that this stage of differentiation exhibits the most metabolically active cells, as evaluated by the degree of triacylglycerol secretion (31).

In accordance with the studies in L-cell fibroblasts (13) and hBRIE 380i cells (28), no differences were detected between cell lines in the incorporation of [ $^{14}\text{C}$ ]oleic acid into total phospholipids (Table 1). Furthermore, compared to mock-transfectants, expression of I-FABP did not increase total incorporation of labeled oleic acid into the cells (Table 1). This also confirms observations in other I-FABP-expressing cells (11,28). The suggestion that I-FABP has a passive role with respect to fatty acid uptake has been demonstrated in L-cells (11,13), in which transfection with I-FABP stimulated fatty acid esterification into triacylglycerol without increasing fatty acid uptake.

With two exceptions (21,29) previous studies on the role of I-FABP expression on fatty acid esterification have not examined secretion of lipids from an intact cell system. We show here that secretion of labeled triacylglycerol was reduced in all I-FABP-expressing cell lines as compared to control cells (Fig. 3). A recent study showed that plasma concentration of triacylglycerol was higher in Fabp $^{-/-}$  mice, indicating that the rate of dietary fat transfer into the plasma compartment was actually increased in the absence of I-FABP (40). Furthermore, a nonsignificant reduction in lipid secretion was shown in I-FABP-transfected CaCo-2 cells as com-

pared to mock-transfected cells (29). The expression of I-FABP in mock-transfected cells was similar to that previously reported by the same authors for wild type CaCo-2 cells (24). However, no data for parent CaCo-2 cells were given in this study (29). Given the clonal variability evident for these cells, it remains to be confirmed whether the metabolic activity of these mock transfected cells resembled that of wild-type cells.

In CaCo-2 cells stably transfected with two naturally occurring isoforms of I-FABP, the Thr $^{54}$ -isoforms (mutated type) increased triacylglycerol secretion relative to the Ala $^{54}$ -form (21). However, nontransfected cells secreted more triacylglycerol than either of the I-FABP-transfected cell lines (Baier, L.J., personal communication). In accordance with our study (Fig. 1), the nontransfected cells contained higher levels of L-FABP than the I-FABP expressing cells, leading the authors to suggest a coregulation between the intestinal and liver forms of this protein. However, the issue of clonal variability rather than a specific effect of I-FABP expression must also be considered. Another study in CaCo-2 cells showed different levels of L-FABP in two different cell clones transfected with I-FABP (29).

The physiological significance of the two forms of FABP in intestinal cells is unknown. Different patterns of regulation have been reported for I-FABP and L-FABP in CaCo-2 cells (24,41). Furthermore, it was shown that the total amount of FABP in these cells was not proportional to the amount of lipid transport (21). Together, these observations support the hypothesis that L-FABP and I-FABP may not affect fatty acid transport in a simple combined fashion but that the proteins may play separate roles in intracellular lipid metabolism. The contribution of L-FABP to lipid transport in I-FABP-transfected cells remains unclear. Nevertheless, the decrease in L-FABP observed in the I-FABP transfected cells may provide a mechanism for the decrease in triacylglycerol secretion observed in our study.

Consideration has been given to the possibility that newly synthesized triacylglycerol is channeled to a cytosolic storage pool and not transferred directly to lipoprotein assembly. It can be speculated that these triacylglycerol molecules might be used for secretion at a later time. It has been demonstrated that the expression of L-FABP in transfected rat (McA-RH7777) hepatoma cells inhibits the assembly and secretion of apoB100VLDL without decreasing the biosynthesis of apolipoprotein B100 (apoB100) or triacylglycerol (42). This is explained by a diversion of fatty acids from the second step in the very low density lipoprotein assembly process, thereby promoting a "late" intracellular degradation of apoB100 (42). In I-FABP-transfected CaCo-2 cells, however, preliminary data indicate that the reduced triacylglycerol secretion observed was not accompanied by decreased apoB secretion (data not shown). It seems therefore that rather than an increased degradation of apoB, dense lipid-poor particles are secreted from the cells. Interestingly, it was recently suggested that there is no coordinated regulation of FABP and apoB-containing lipoproteins (41).

Fatty acid incorporation in secreted triacylglycerol was reduced in differentiated CaCo-2 cells stably transfected with I-FABP, independent of the intracellular level of triacylglycerol. These findings need further examinations to investigate the role of I-FABP-expression on intestinal triacylglycerol secretion.

## ACKNOWLEDGEMENTS

The authors are grateful to Dr. J.I. Gordon for providing I-FABP and L-FABP cDNA and anti-rat I-FABP and L-FABP antisera. We wish to thank Mari-Ann Baltzersen and Manigeh M. Beigi for technical assistance.

## REFERENCES

- Veerkamp, J.H., and Maatman, R.G. (1995) Cytoplasmic Fatty Acid-Binding Proteins: Their Structure and Genes, *Prog. Lipid Res.* 34, 17–52.
- Glatz, J.F.C., and Van der Vusse, G.J. (1996) Cellular Fatty Acid-Binding Proteins: Their Function and Physiological Significance, *Prog. Lipid Res.* 35, 243–282.
- Coe, N.R., and Bernlohr, D.A. (1998) Physiological Properties and Functions of Intracellular Fatty Acid-Binding Proteins, *Biochim. Biophys. Acta* 1391, 287–306.
- Storch, J., and Thumser, A.E.A. (2000) The Fatty Acid Transport Function of Fatty Acid-Binding Proteins, *Biochim. Biophys. Acta* 1486, 28–44.
- Ockner, R.K., Manning, J.A., Poppenhansen, R.B., and Ho, W.K. (1972) A Binding Protein for Fatty Acids in Cytosol of Intestinal Mucosa, Liver, Myocardium, and Other Tissues, *Science* 177, 56–58.
- Alpers, D.H., Strauss, A.W., Ockner, R.K., Bass, N.M., and Gordon, J.I. (1984) Cloning of a cDNA Encoding Rat Intestinal Fatty Acid Binding Protein, *Proc. Natl. Acad. Sci. USA* 81, 313–317.
- Sweetser, D.A., Birkenmeier, E.H., Klisak, I.J., Zollman, S., Sparkes, R.S., Mohandas, T., Lusic, A.J., and Gordon, J.I. (1987) The Human and Rodent Intestinal Fatty Acid Binding Protein Genes. A Comparative Analysis of Their Structure, Expression, and Linkage Relationships, *J. Biol. Chem.* 262, 16060–16071.
- Gordon, J.I., Alpers, D.H., Ockner, R.K., and Strauss, A.W. (1983) The Nucleotide Sequence of Rat Liver Fatty Acid Binding Protein mRNA, *J. Biol. Chem.* 258, 3356–3363.
- Bass, N.M., Manning, J.A., Ockner, R.K., Gordon, J.I., Seetharam, S., and Alpers, D.H. (1985) Regulation of the Biosynthesis of Two Distinct Fatty Acid-Binding Proteins in Rat Liver and Intestine. Influences of Sex Difference and of Clofibrate, *J. Biol. Chem.* 260, 1432–1436.
- Bass, N.M. (1988) The Cellular Fatty Acid Binding Proteins: Aspects of Structure, Regulation, and Function, *Int. Rev. Cytol.* 111, 143–184.
- Prows, D.R., Murphy, E.J., and Schroeder, F. (1995) Intestinal and Liver Fatty Acid Binding Proteins Differentially Affect Fatty Acid Uptake and Esterification in L-Cells, *Lipids* 30, 907–910.
- Murphy, E.J., Prows, D.R., Jefferson, J.R., and Schroeder, F. (1996) Liver Fatty Acid-Binding Protein Expression in Transfected Fibroblasts Stimulates Fatty Acid Uptake and Metabolism, *Biochim. Biophys. Acta* 1301, 191–198.
- Prows, D.R., Murphy, E.J., Moncecchi, D., and Schroeder, F. (1996) Intestinal Fatty Acid-Binding Protein Expression Stimulates Fibroblast Fatty Acid Esterification, *Chem. Phys. Lipids* 84, 47–56.
- Pinto, M., Robine-Leon, S., Appay, M.-D., Kedinger, M., Triadou, N., Dussaulx, E., Lacroix, B., Simon-Assmann, P., Haffen, K., Fogh, J., and Zweibaum, A. (1983) Enterocyte-Like Differentiation and Polarization of the Human Colon Carcinoma Cell Line Caco-2 in Culture, *Biol. Cell* 47, 323–330.
- Dashti, N. (1991) Synthesis and Secretion of Nascent Lipoprotein Particles, *Prog. Lipid Res.* 30, 219–230.
- Field, F.J., and Mathur, S.N. (1995) Intestinal Lipoprotein Synthesis and Secretion, *Prog. Lipid Res.* 34, 185–198.
- Levy, E., Mehran, M., and Seidman, E. (1995) Caco-2 Cells as a Model for Intestinal Lipoprotein Synthesis and Secretion, *FASEB J.* 9, 626–635.
- Trotter, P.J., and Storch, J. (1991) Fatty Acid Uptake and Metabolism in a Human Intestinal Cell Line (Caco-2): Comparison of Apical and Basolateral Incubation, *J. Lipid Res.* 32, 293–304.
- Levin, M.S., Talkad, V.D., Gordon, J.I., and Stenson, W.F. (1992) Trafficking of Exogenous Fatty Acids Within Caco-2 Cells, *J. Lipid Res.* 33, 9–19.
- Mallordy, A., Besnard, P., and Carlier, H. (1993) Research of an *in vitro* Model to Study the Expression of Fatty Acid-Binding Proteins in the Small Intestine, *Mol. Cell. Biochem.* 123, 85–92.
- Baier, L.J., Bogardus, C., and Sacchettini, J.C. (1996) A Polymorphism in the Human Intestinal Fatty Acid Binding Protein Alters Fatty Acid Transport Across Caco-2 Cells, *J. Biol. Chem.* 271, 10892–10896.
- Schmiedlin-Ren, P., Thummel, K.E., Fisher, J.M., Paine, M.F., Lown, K.S., and Watkins, P.B. (1997) Expression of Enzymatically Active CYP3A4 by Caco-2 Cells Grown on Extracellular Matrix-Coated Permeable Supports in the Presence of  $1\alpha,25$ -Dihydroxyvitamin D<sub>3</sub>, *Mol. Pharmacol.* 51, 741–754.
- Le Beyec, J., Delers, F., Jourdan, F., Schreider, C., Chambaz, J., Cardot, P., and Pinçon-Raymond, M. (1997) A Complete Epithelial Organization of Caco-2 Cells Induces I-FABP and Potentializes Apolipoprotein Gene Expression, *Exp. Cell Res.* 236, 311–320.
- Darimont, C., Gradoux, N., Cumin, F., Baum, H.P., and De Pover, A. (1998) Differential Regulation of Intestinal and Liver Fatty Acid-Binding Proteins in Human Intestinal Cell Line (Caco-2): Role of Collagen, *Exp. Cell Res.* 244, 441–447.
- Prows, D.R., and Schroeder, F. (1997) Metallothionein-IIA Promoter Induction Alters Rat Intestinal Fatty Acid Binding Protein Expression, Fatty Acid Uptake, and Lipid Metabolism in Transfected L-Cells, *Arch. Biochem. Biophys.* 340, 135–143.
- Murphy, E.J. (1998) L-FABP and I-FABP Expression Increase NBD-Stearate Uptake and Cytoplasmic Diffusion in L Cells, *Am. J. Physiol.* 275, G244–249.
- Atshaves, B.P., Foxworth, W.B., Frolov, A., Roths, J.B., Kier, A.B., Oetama, B.K., Piedrahita, J.A., and Schroeder, F. (1998) Cellular Differentiation and I-FABP Protein Expression Modulate Fatty Acid Uptake and Diffusion, *Am. J. Physiol.* 274, C633–644.
- Holehouse, E.L., Liu, M.-L., and Aponte, G.W. (1998) Oleic Acid Distribution in Small Intestinal Epithelial Cells Expressing Intestinal-Fatty Acid Binding Protein, *Biochim. Biophys. Acta* 1390, 52–64.
- Darimont, C., Gradoux, N., Persohn, E., Cumin, F., and De Pover, A. (2000) Effects of Intestinal Fatty Acid-Binding Protein Overexpression on Fatty Acid Metabolism in Caco-2 Cells, *J. Lipid Res.* 41, 84–92.
- Murphy, E.J., Prows, D.R., Stiles, T., and Schroeder, F. (2000) Liver and Intestinal Fatty Acid-Binding Protein Expression Increases Phospholipid Content and Alters Phospholipid Fatty Acid Composition in L-Cell Fibroblasts, *Lipids* 35, 729–738.
- Ranheim, T., Gedde-Dahl, A., Rustan, A.C., and Drevon, C.A. (1992) Influence of Eicosapentaenoic acid (20:5, n-3) on Secretion of Lipoproteins in CaCo-2 Cells, *J. Lipid Res.* 33, 1281–1293.
- Wigler, M., Pellicer, A., Silverstein, S., Axel, R., Urlaub, G., and Chasin, L. (1979) DNA-Mediated Transfer of the Adenine

- Phosphoribosyltransferase Locus into Mammalian Cells, *Proc. Natl. Acad. Sci. USA* 76, 1373–1376.
33. Sambrook, J., Fritsch, E.F., and Maniatis, T. (1989) *Molecular Cloning: A Laboratory Manual*, 2nd edn., Cold Spring Harbor Laboratory Press, Cold Spring Harbor, New York.
  34. Church, G.M., and Gilbert, W. (1984) Genomic Sequencing, *Proc. Natl. Acad. Sci. USA* 81, 1991–1995.
  35. Bradford, M.M. (1976) A Rapid and Sensitive Method for the Quantitation of Microgram Quantities of Protein Utilizing the Principle of Protein-Dye Binding, *Anal. Biochem.* 72, 248–254.
  36. Laemmli, U.K. (1970) Cleavage of Structural Proteins During the Assembly of the Head of Bacteriophage T4, *Nature* 227, 680–685.
  37. Ranheim, T., Gedde-Dahl, A., Rustan, A.C., and Drevon, C.A. (1994) Fatty Acid Uptake and Metabolism in Caco-2 Cells: Eicosapentaenoic Acid (20:5(n-3)) and Oleic Acid (18:1(n-9)) Presented in Association with Micelles or Albumin, *Biochim. Biophys. Acta* 1212, 295–304.
  38. Folch, J., Lees, M., and Sloane Stanley, G.H. (1957) A Simple Method for the Isolation and Purification of Total Lipides [*sic*] from Animal Tissues, *J. Biol. Chem.* 226, 497–509.
  39. Darimont, C., Gradoux, N., and De Pover, A. (1999) Epidermal Growth Factor Regulates Fatty Acid Uptake and Metabolism in Caco-2 Cells, *Am. J. Physiol.* 39, G606–G612.
  40. Vassileva, G., Huwyler, L., Poirier, K., Agellon, L.B., and Toth, M.J. (2000) The Intestinal Fatty Acid Binding Protein Is Not Essential for Dietary Fat Absorption in Mice, *FASEB J.* 14, 2040–2046.
  41. Dubé, N., Delvin, E., Yotov, W., Garofalo, C., Bendayan, M., Veerkamp, J.H., and Levy, E. (2001) Modulation of Intestinal and Liver Fatty Acid-Binding Proteins in Caco-2 Cells by Lipids, Hormones and Cytokines, *J. Cell. Biochem.* 81, 613–620.
  42. Lindberg, K., Oskarsson, J., Claesson, C., Carlsson, L., Lindholm, M., Asp, L., Borén, J., and Olofsson, S.-O. (1998) Liver Fatty Acid Binding Protein Inhibits Assembly and Secretion of ApoB100-Containing VLDL in a Rat Hepatoma Cell Line (McA-RH7777 Cells), *Circulation* 98, A916.

[Received June 6, 2001, and in revised form and accepted November 6, 2001]



# Regulation of Phosphatidic Acid Phosphohydrolase 1 by Fatty Acids

Noureddine Elabbadi<sup>a,1</sup>, Christopher P. Day<sup>b</sup>, Richard Virden<sup>a</sup>,  
and Stephen J. Yeaman<sup>a,b,\*</sup>

<sup>a</sup>School of Biochemistry and Genetics and <sup>b</sup>Centre for Liver Research, Medical School, University of Newcastle upon Tyne, Newcastle upon Tyne NE2 4HH United Kingdom

**ABSTRACT:** In the starved state and during metabolic stress, free fatty acids (FFA) are the principal hepatic energy supply, undergoing  $\beta$ -oxidation. Accordingly, it appears paradoxical that FFA have been reported to increase the liver's esterification capacity by translocating the rate-limiting enzyme phosphatidic acid phosphohydrolase (PAP-1) from the cytosol to the endoplasmic reticulum. We have therefore investigated the regulation of rat liver PAP-1. Oleic acid inhibited PAP activity in all subcellular fractions, with PAP-1 activity in cytosol being the most sensitive. Inhibition was also observed with oleoyl-CoA, linoleate, and palmitate. Fatty acids and their derivatives show detergent effects at high concentrations, and such effects can lead to enzyme inhibition. Inhibition by oleate, however, was reversed by phosphatidic acid and albumin and exhibited sigmoidal kinetics. These results demonstrate that PAP-1 is reversibly inhibited by FFA and their CoA esters, which may play a role in directing hepatic FFA to  $\beta$ -oxidation during times of increased energy demand.

Paper no. L8631 in *Lipids* 37, 69–73 (January 2002).

Phosphatidic acid phosphohydrolase (PAP) catalyzes the hydrolysis of phosphatidic acid (PA) to generate *sn*-1,2-diacylglycerol (DAG), a substrate for the synthesis of a number of phospholipids, as well as a direct precursor of triacylglycerol (TAG) (1,2). Regulation of PAP activity therefore plays a crucial role in determining the rate and direction of glycerolipid synthesis with, for example, elevated levels of PAP activity being associated with alcoholic fatty liver (3). In mammalian cells, two major forms of PAP activity have been identified (4,5). PAP-1, stimulated by  $Mg^{2+}$  and inhibited by *N*-ethylmaleimide (NEM) *in vitro*, is distributed between the cytosol and endoplasmic reticulum (ER) and is regarded as the metabolic form involved in the regulation of glycerolipid synthesis. PAP-2 [for which at least three isoforms exist (2,6)] is  $Mg^{2+}$ -independent and NEM-insensitive, is found mainly in the plasma membrane and, in view of its location, is thought to be

involved principally in cell-signaling and is a member of the lipid phosphate phosphohydrolase family (6–8).

The level of PAP-1 activity expressed *in vivo* has long been considered to be regulated by the ability of the cytosolic form to translocate to the ER, where its substrate, PA, is generated *via* the acylation of glycerol-3-phosphate (reviewed in Ref. 9). Largely indirect evidence suggests that, *in vivo*, this translocation is induced by the accumulation of fatty acids, acyl-CoA esters, and PA on the ER membranes and results in the enhanced synthesis of glycerolipid (10). Such evidence has come principally from experiments that have incubated cell-free tissue homogenates with lipids prior to the preparation of cyto-solic and microsomal fractions by ultracentrifugation (5,11–15).

In addition to their putative effect on the subcellular distribution of PAP-1, some studies have reported an effect of free fatty acids (FFA) on total enzyme activity. PAP-1 activity in rat hepatocytes is apparently increased by extracellular FFA concentrations of  $\geq 2$  mM above (10,16), whereas in rat adipocytes, stimulation of lipolysis by noradrenaline leads to a rapid decrease in PAP-1 activity. This effect, which is antagonized by insulin and a  $\beta$ -adrenergic antagonist, suggests either inhibition of PAP by fatty acids or a direct hormonal effect on the enzyme, possibly *via* reversible phosphorylation, although there is no direct evidence for this covalent modification (17,18). In view of these conflicting and somewhat paradoxical data, we have further investigated the effect of fatty acids on PAP-1 activity from rat liver. We show *in vitro* that PAP-1 is directly and reversibly inhibited by both FFA and their acyl CoA esters. This regulation of PAP-1 may be important in determining the balance between  $\beta$ -oxidation and esterification in situations such as starvation and metabolic stress in which there is an increased supply of fatty acids to the liver.

## MATERIALS AND METHODS

**Materials.** Male Wistar rats (150–200 g) were obtained from Newcastle University Comparative Biology Centre (United Kingdom). They were allowed free access to food and water prior to sacrifice by cervical dislocation, after which livers were immediately removed and stored at  $-20^{\circ}\text{C}$  until use. Phosphatidic acid, 1,2-dioleoyl-*sn*-glycerol, oleic acid, linoleic acid, palmitic acid, oleoyl-CoA, bovine serum albumin (BSA) (fatty acid-free), Triton X-100, and polyethylene glycol (MW 8,000) were from Sigma Chemical (Poole, Dorset, United Kingdom).

\*To whom correspondence should be addressed.

E-mail: s.j.yeaman@ncl.ac.uk.

<sup>1</sup>Current address: Faculte des Sciences et Techniques, University Cadi Ayyad, Beni-Mellal, Morocco.

Abbreviations: BSA, bovine serum albumin; DAG, diacylglycerol; DDT, dithiothreitol; ER, endoplasmic reticulum; FFA, free fatty acid; NEM, *N*-ethylmaleimide; PA, phosphatidic acid; PAP, phosphatidic acid phosphohydrolase; TAG, triacylglycerol.

*Preparation of subcellular fractions from rat liver.* Livers were suspended at 4°C in 4–5 vol of 50 mM Tris-HCl (pH 7.4) containing 0.25 M sucrose and 0.2 M DTT (buffer A) and minced with scissors before homogenization with a Teflon–glass homogenizer. The crude homogenate was then centrifuged at 4°C for 20 min at  $10,000 \times g$  and the supernatant (homogenate) collected. The pellet was resuspended in buffer A and stored at –20°C (low spin, “membrane” fraction). The homogenate was then centrifuged at  $150,000 \times g$  for 90 min at 4°C, the resulting supernatant being recentrifuged for a further 60 min at  $150,000 \times g$  to produce a cytosolic fraction. The pellets from both spins were collected and washed twice by resuspension and further centrifugation at  $150,000 \times g$  and finally resuspended in buffer A (microsomal fraction). Fractions were stored at –20°C or used immediately. A mitochondrial fraction was prepared by centrifuging crude homogenate at  $2,000 \times g$  for 15 min at 4°C. The resulting supernatant was centrifuged again at  $10,000 \times g$  for 10 min at 4°C, and the resulting pellet was resuspended in buffer A and used as crude mitochondrial fraction. Previous work in this laboratory using this methodology, coupled with marker enzymes, has shown that the low-spin “membrane” fraction contains essentially only PAP-2 and that over 80% of the PAP activity in the cytosol is due to PAP-1 (5).

For partial purification of PAP-1, cytosol was diluted in buffer A to give a final protein concentration of 6–7 mg/mL, and then solid polyethylene glycol (MW 8,000) was added (6 g per 100 mL of cytosol). The mixture was stirred for 1 h at 4°C and then centrifuged at  $5,000 \times g$  for 15 min. The precipitate (in which PAP-1 is enriched approximately 5- to 10-fold) was resuspended in buffer A. Contamination of this fraction with PAP-2 was negligible, as judged by the complete sensitivity of the activity to NEM.

*Determination of PAP activity.* Total PAP activity (*i.e.* measured in the absence of NEM) was measured at 30°C by the production of [ $^{32}$ P]P<sub>i</sub> from [ $^{32}$ P]PA, essentially as in References 5 and 19, except that Triton X-100 was omitted and the PA substrate was prepared by sonication. The standard incubation mixture (0.1 mL) contained 50 mM Tris HCl pH 7.5, 1.5 mM MgCl<sub>2</sub>, 0.1 mg/mL fatty acid-free BSA, 0.5 mM EDTA, 0.5 mM EGTA, 0.5 mM DTT, 125 mM sucrose, and 0.5 mM PA (10,000 dpm/nmol). One unit of PAP activity is defined as the release of 1 nmol of P<sub>i</sub>/min.

*Inhibition of PAP activity by fatty acids and their acyl-CoA esters.* The PAP activity of aliquots of subcellular fractions and partially purified PAP was assayed as described above except that fatty acids or their acyl-CoA esters were present in the basic assay system, and the concentration of [ $^{32}$ P]PA was reduced from 0.5 to 0.25 mM. In parallel, aliquots of the same subcellular fractions or partially purified PAP were first preincubated for 10 min at 37°C with fatty acids prior to assaying PAP activity. Palmitate and linoleate were suspended separately in buffer A containing 0.1% Triton X-100 and used as a stock solution, whereas oleate or oleoyl-CoA were directly suspended in buffer A. In all cases, the final concentration of Triton X-100 in the reaction mixture was less than 0.01%

(0.15 mM), at which levels Triton does not affect the observed activity (5). In some experiments, after the 10 min preincubation with oleate, various concentrations of BSA or PA were added to the incubations 5 min prior to the initiation of PAP assays. Kinetic data were fitted using nonlinear regression with bi-square weighting (20).

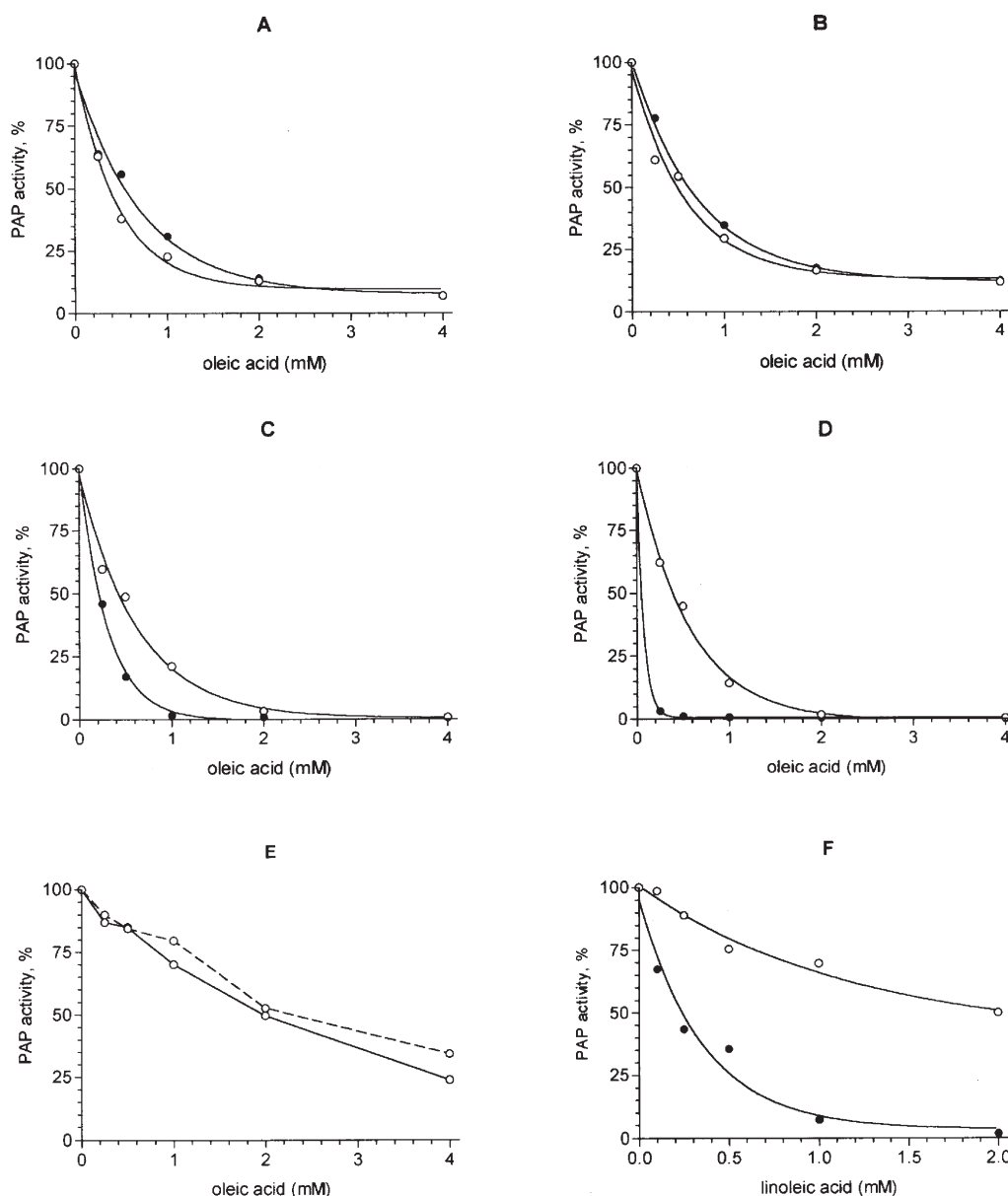
## RESULTS

Increasing concentrations of oleic acid progressively inhibited PAP activity in both the homogenate (Fig. 1A) and microsomal fractions of rat liver (Fig. 1B), which contain both PAP-1 and PAP-2, with 50% inhibition observed at approximately 0.6 mM of added fatty acid and more than 80% inhibition occurring at concentrations higher than 1.2 mM. In these fractions there was no significant increase in the inhibitory effect of oleic acid when it was present 10 min prior to initiating the assay reaction (Figs. 1A and B). PAP-1 activity in the cytosolic fraction (Fig. 1C) [which is essentially all PAP-1 (5)], or partially purified PAP-1 activity (Fig. 1D), was more sensitive to the presence of oleic acid in the reaction mixture, with 50% inhibition observed at approximately 0.4 mM and essentially 100% inhibition occurring at 2 mM oleic acid or above. Preincubation with oleic acid accentuated the inhibitory effect of oleic acid on PAP-1 activity in cytosol or partially purified PAP-1 preparations, with essentially complete inhibition observed at 1.0 and 0.5 mM, respectively. These results indicate that oleic acid is a potent inhibitor of PAP-1.

Mitochondrial and membrane-bound PAP activity [which is predominantly PAP-2 (5)] is less sensitive to the presence of oleic acid. At 1 mM oleate, PAP activity was only slightly inhibited (25% inhibition) and even at concentrations of 2–3 mM, the degree of inhibition was only 50–60% (Fig. 1E). These results suggest that PAP-1 and PAP-2 are affected to different extents by the presence of fatty acids. This is consistent with the results from the homogenate and microsomal fractions (Fig. 1A and B) in which a low level of PAP activity was maintained even at a high concentration of oleate, corresponding to the contribution of the PAP-2 isoform present in these fractions. The effect of other fatty acids and oleoyl CoA on partially purified PAP-1 was also examined. Linoleic acid inhibited this activity in a dose-dependent fashion, with increased inhibition observed following preincubation in the absence of PA (Fig. 1F).

Palmitic acid also inhibited PAP-1 activity, with 30% inhibition at 1 mM, increasing to 90% if the enzyme was preincubated in the absence of PA. The inhibitory effect of oleoyl CoA was similar to that observed with oleic acid (results not shown). The reversibility of oleate-induced inhibition of PAP-1 was investigated by addition of 3 mg/mL BSA, following preincubation of partially purified PAP-1 with 1 mM oleate but prior to assaying PAP activity. The presence of 1 mM oleate in the preincubation period reduced PAP-1 activity by about 70%. BSA completely reversed this inhibitory effect of oleate (results not shown).

To further elucidate the possible mechanism(s) of fatty acid-induced PAP-1 inhibition, we investigated the kinetics



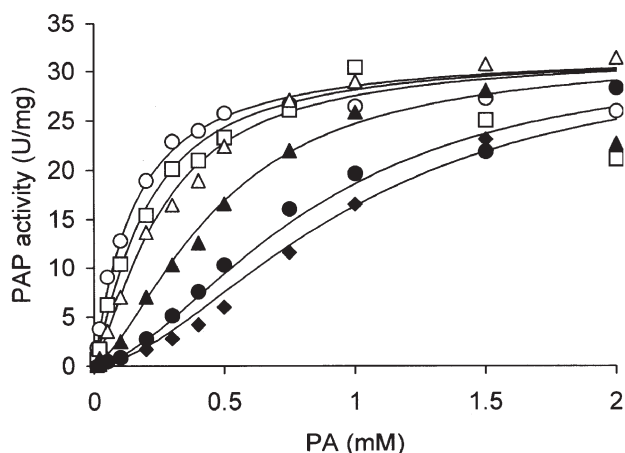
**FIG. 1.** Effects of oleate and linoleate on the subcellular phosphatidic acid phosphohydrolase (PAP) activity in rat liver. PAP activity was measured in aliquots of homogenate (A), microsomes (B), cytosol (C), partially purified PAP (D and F), mitochondria (E, solid line), or in membrane (low spin) fraction (E, broken line) in the presence of various concentrations of oleate (A–E) or linoleate (F) as indicated. The graphs show the inhibitory effect of these fatty acids on PAP activity with (●) or without (○) preincubation for 10 min at 37°C in the absence of substrate phosphatidic acid. Similar results were obtained in five further experiments. Results are expressed as % of control (without fatty acids).

of partially purified PAP-1 activity in the absence or presence of oleic acid. The results (Fig. 2) were suggestive of  $K$ -system inhibition (21), in which the effective value of the allosteric constant  $L$  increases and saturation curves become increasingly sigmoidal as a function of the concentration of an allosteric inhibitor. The combined data fitted an allosteric model better than the alternative of simple competitive inhibition by a factor of 4.4 in residual variance. Because the deduced value of  $L$  was small ( $0.4 \pm 0.2$ ), the saturation function in the absence of oleic acid was indistinguishable from the hyperbolic function of Michaelis–Menten kinetics. The

value of  $S_{0.5}$  ( $0.13 \pm 0.02$  mM) deduced using the allosteric model did not differ significantly from the value of  $K_m$  ( $0.17 \pm 0.02$  mM) deduced for competitive inhibition, and corresponding values of maximal velocity were  $32 \pm 1$  and  $35 \pm 1$  U/mg, respectively. Both models yielded similar values of  $K_i$  ( $0.05 \pm 0.01$  and  $0.10 \pm 0.01$  mM, respectively).

## DISCUSSION

The results reported here show that fatty acids and their acyl-CoA esters are inhibitors of hepatic PAP activity, in particu-



**FIG. 2.** Effect of phosphatidic acid (PA) concentration on the initial velocity of phosphatidic phosphohydrolase-1 (PAP-1) activity in the presence of oleate. Activity of partially purified PAP (specific activity 20 U/mg) was measured as a function of PA concentrations in the absence (○) or the presence of 0.05 (□), 0.1 (△), 0.25 (▲), 0.5 (●), or 0.6 mM (◆) oleate. The data represent a typical example of five different experiments. The lines show the best fit of the combined data to a two-state allosteric model, assuming two binding sites for PA, with binding favoring the *R* state by a factor of 100, and two allosteric binding sites for oleic acid.

lar PAP-1, the form of the enzyme principally involved in glycerolipid biosynthesis. The inhibition of PAP-1 by oleate appears to involve a negative allosteric interaction, resulting in a decreased affinity for its substrate, PA, suggesting that PAP-1 could be regulated *in vivo* by the intracellular ratio of PA/fatty acids. The levels of added fatty acids and acyl CoA used in this study are consistent with those used previously in similar work (e.g., Ref. 13) but are somewhat higher than values that are normally considered to be physiological, although it should be remembered that the liver will receive high levels of fatty acids from the portal vein. Fatty acids and their derivatives show detergent effects at high concentrations and such effects can lead to enzyme inhibition. It is important to point out, however, that the inhibitory effects of fatty acids are greater at lower levels of PA (Fig. 2) and that the PA concentrations used are also higher than might be considered physiological; this is necessary in order for the enzyme activity to be detectable. The concentrations of FFA actually present in the incubations will be lower than the added amounts owing to the presence of low levels of fatty acid-free BSA, and similarly, the situation in the cell is complicated by the presence of a number of binding proteins for fatty acids and acyl CoA esters. Thus, the concentration may vary within the cytosol and in the region of different membranes. The inhibition of PAP-1 by fatty acids also offers a possible explanation for the inhibitory effect of catecholamines on PAP-1 activity reported in adipocytes, with increased levels of fatty acids and their CoA esters being responsible (17,18).

A number of studies have shown that the rate of TAG synthesis is dependent on the concentration of FFA. However, since fatty acid supply also determines the rate of  $\beta$ -oxidation, factors regulating this pathway will also affect TAG syn-

thesis. This is illustrated by the stimulation of fatty acid esterification and TAG synthesis that occurs when hepatocytes are incubated with inhibitors of  $\beta$ -oxidation (22,23). However, when cells or tissues require an increased supply of energy (e.g., during metabolic stress), fatty acids need to be preferentially directed toward  $\beta$ -oxidation rather than esterification. In the liver during conditions of stress, the increased ratio of glucagon to insulin directs incoming fatty acids (derived from adipose tissue lipolysis) toward  $\beta$ -oxidation by inhibiting acetyl-CoA carboxylase activity, leading to a reduction in malonyl CoA levels and stimulation of carnitine palmitoyl transferase, thus promoting the entry of fatty acids into mitochondria. The inhibition of PAP-1 by fatty acids and their acyl-CoA esters will further favor  $\beta$ -oxidation over esterification. Only if the liver receives an influx of fatty acids sufficient to exceed the capacity for  $\beta$ -oxidation will they then be esterified to lysophosphatidic acid and PA on the ER. The translocation induced by fatty acids in intact cells (e.g., Ref. 10) could also be an indirect effect resulting from their incorporation into newly synthesized PA, which has been shown to promote the binding of PAP-1 to microsomal and mitochondrial membranes *in vitro* (24,25). This regulation of PAP-1 metabolic expression by membrane-bound PA is similar to the regulation of the intracellular distribution of DAG kinase by DAG (26), with the substrate in each case localizing the enzyme to the membrane. In the case of PAP-1, PA would act as the signal to promote the intracellular movement of the enzyme to the membranes, contributing to increased TAG synthesis, although clearly other enzymes in the pathway such as DAG acyltransferase may play a regulatory role (reviewed in Ref. 27). In the fed state, the high ratio of insulin to glucagon will block the entry of fatty acids into the mitochondria *via* elevation of malonyl CoA levels, and they will be preferentially esterified. The subsequent increase in PA on the ER membranes will then translocate PAP-1 and overcome any fatty acid-induced inhibition of PAP-1 activity.

## ACKNOWLEDGMENTS

This work was supported by a project grant from the Biotechnology and Biological Sciences Research Council, Swindon, United Kingdom.

## REFERENCES

1. Tijburg, L.B.M., Geelen, M.J.H., and van Golde, L.M.G. (1989) Regulation of the Biosynthesis of Triacylglycerol Phosphatidylcholine and Phosphatidylethanolamine in the Liver, *Biochim. Biophys. Acta* 1004, 1–19.
2. Brindley, D.N., and Waggoner, D.W. (1998) Mammalian Lipid Phosphate Phosphohydrolases, *J. Biol. Chem.* 273, 24281–24284.
3. Day, C.P., James, O.F.W., Brown, A.J.M., Bennett, M.K., Fleming, I.N., and Yeaman, S.J. (1993) The Activity of the Metabolic Form of Hepatic Phosphatidate Phosphohydrolase Correlates with the Severity of Alcoholic Fatty Liver in Human Beings, *Hepatology* 18, 832–838.
4. Jamal, Z., Martin, A., Gomez-Munoz, A., and Brindley, D.N. (1991) Plasma Membrane Fractions from Rat Liver Contain a Phosphatidate Phosphohydrolase Distinct from That in the



- Endoplasmic Reticulum and Cytosol, *J. Biol. Chem.* 266, 2988–2996.
5. Day, C.P., and Yeaman, S.J. (1992) Physical Evidence for the Presence of Two Forms of Phosphatidate Phosphohydrolase in Rat Liver, *Biochim. Biophys. Acta* 1127, 87–94.
  6. Fleming, I.N., and Yeaman, S.J. (1995) Purification and Characterization of *N*-Ethylmaleimide-Sensitive Phosphatidic Acid Phosphohydrolase (PAP2) from Rat Liver, *Biochem. J.* 308, 983–989.
  7. Waggoner, D.W., Gomez-Munoz, A., Dewald, J., and Brindley, D.N. (1996) Phosphatidate Phosphohydrolase Catalyzes the Hydrolysis of Ceramide 1-Phosphate, Lysophosphatidate, and Sphingosine 1-Phosphate, *J. Biol. Chem.* 271, 16506–16509.
  8. Kai, M., Wada, I., Imai, S., Sakane, F., and Kanoh, H., (1997) Cloning and Characterization of Two Human Isozymes of Mg<sup>2+</sup>-Independent Phosphatidic Acid Phosphatase, *J. Biol. Chem.* 272, 24572–24578.
  9. Brindley, D.N. (1985) Intracellular Translocation of Phosphatidate Phosphohydrolase and Its Possible Role in the Control of Glycerolipid Synthesis, *Prog. Lipids Res.* 23, 115–133.
  10. Cascales, C., Mangiapane, E.H., and Brindley, D.N. (1984) Oleic Acid Promotes the Activation and Translocation of Phosphatidate Phosphohydrolase from the Cytosol to Particulate Fractions of Isolated Rat Hepatocytes, *Biochem. J.* 219, 911–916.
  11. Martin-Sanz, P., Hopewell, R., and Brindley, D.N. (1984) Long-Chain Fatty Acids and Their Acyl-CoA Esters Cause the Translocation of Phosphatidate Phosphohydrolase from the Cytosolic to the Microsomal Fraction of Rat Liver, *FEBS Lett.* 175, 284–288.
  12. Martin-Sanz, P., Hopewell, R., and Brindley, D.N. (1985) Spermine Promotes the Translocation of Phosphatidate Phosphohydrolase from the Cytosol to the Microsomal Fraction of Rat Liver and It Enhances the Effects of Oleate in This Respect, *FEBS Lett.* 179, 262–266.
  13. Hopewell, R., Martin-Sanz, P., Martin, A., Saxton, J., and Brindley, D.N. (1985) Regulation of the Translocation of Phosphatidate Phosphohydrolase Between the Cytosol and the Endoplasmic Reticulum of Rat Liver, *Biochem. J.* 232, 485–491.
  14. Gomez-Munoz, A., Hamza, E.H., and Brindley, D.N. (1992) Effects of Sphingosine, Albumin and Unsaturated Fatty Acids on the Activation and Translocation of Phosphatidate Phosphohydrolases in Rat Hepatocytes, *Biochim. Biophys. Acta* 1127, 49–56.
  15. Asiedu, D., Skorve, J., Demoz, A., Willumsen, N., and Berge, R.K. (1992) Relationship Between Translocation of Long-Chain Acyl-CoA Hydrolase, Phosphatidate Phosphohydrolase and CTP:Phosphocholine Cytidylyltransferase and the Synthesis of Triglycerides and Phosphatidylcholine in Rat Liver, *Lipids* 27, 241–247.
  16. Gomez-Munoz, A., Hatch, G.M., Martin, A., Jamal, Z., Vance, D.E., and Brindley, D.N. (1992) Effects of Okadaic Acid on the Activities of Two Distinct Phosphatidate Phosphohydrolases in Rat Hepatocytes, *FEBS Lett.* 301, 103–106.
  17. Cheng, C.H.K., and Saggerson, E.D. (1978) Rapid Effects of Noradrenaline on Mg<sup>2+</sup>-Dependent Phosphatidate Phosphohydrolase Activity in Rat Adipocytes, *FEBS Lett.* 87, 65–68.
  18. Cheng, C.H.K., and Saggerson, E.D. (1978) Rapid Antagonistic Actions of Noradrenaline and Insulin on Rat Adipocyte Phosphatidate Phosphohydrolase Activity, *FEBS Lett.* 93, 120–124.
  19. Fleming, I.N., and Yeaman, S.J. (1995) Subcellular Distribution of *N*-Ethylmaleimide-Sensitive and Insensitive Phosphatidic Acid Phosphohydrolase in Rat Brain, *Biochim. Biophys. Acta* 1254, 161–168.
  20. Duggleby, R.G. (1981) A Nonlinear Regression Program for Small Computers, *Anal. Biochem.* 110, 9–18.
  21. Monod, J., Wyman, J., and Changeux, J.-P. (1965) On the Nature of Allosteric Transitions: A Plausible Model, *J. Mol. Biol.* 12, 88–117.
  22. Ide, T., and Ontko, J.A. (1981) Increased Secretion of Very Low Density Lipoprotein Triglyceride Following Inhibition of Long Chain Fatty Acid Oxidation in Isolated Rat Liver, *J. Biol. Chem.* 256, 10247–10255.
  23. Ontko, J.A. (1972) Metabolism of Free Fatty Acids in Isolated Liver Cells. Factors Affecting the Partition Between Esterification and Oxidation, *J. Biol. Chem.* 247, 1788–1800.
  24. Martin, A., Hopewell, R., Martin-Sanz, P., Morgan, J.E., and Brindley, D.N. (1986) Relationship Between the Displacement of Phosphatidate Phosphohydrolase from the Membrane-Associated Compartment by Chlorpromazine and the Inhibition of the Synthesis of Triacylglycerol and Phosphatidylcholine in Rat Hepatocytes, *Biochim. Biophys. Acta* 876, 581–591.
  25. Freeman, M., and Mangiapane, E.H. (1989) Translocation to Rat Liver Mitochondria of Phosphatidate Phosphohydrolase, *Biochem. J.* 263, 589–595.
  26. Besterman, J.M., Pollenz, R.S., Booker, E.L., and Cuatrecasas, P. (1986) Diacylglycerol-Induced Translocation of Diacylglycerol Kinase: Use of Affinity-Purified Enzyme in a Reconstitution System, *Proc. Natl. Acad. Sci. USA* 83, 9378–9382.
  27. Day, C.P., and Yeaman, S.J. (1994) The Biochemistry of Alcohol-Induced Fatty Liver, *Biochim. Biophys. Acta* 1215, 33–48.

[Received September 19, 2000, and in revised form July 23, 2001; revision accepted November 8, 2001]

# A New Cytotoxic Fatty Acid (5Z,9Z)-22-Methyl-5,9-tetracosadienoic Acid and the Sterols from the Far Eastern Sponge *Geodinella robusta*

Tatyana N. Makarieva<sup>a</sup>, Elena A. Santalova<sup>b</sup>, Irina A. Gorshkova<sup>a</sup>,  
Andrei S. Dmitrenok<sup>a</sup>, Alla G. Guzii<sup>b</sup>, Vladimir I. Gorbach<sup>a</sup>,  
Vassilii I. Svetashev<sup>c</sup>, and Valentin A. Stonik<sup>a,\*</sup>

<sup>a</sup>Laboratory of the Marine Natural Products, Pacific Institute of Bioorganic Chemistry of the Russian Academy of Sciences, 690022, Vladivostok, Russian Federation, <sup>b</sup>Bioorganic Chemistry and Biotechnology Department, Institute of Chemistry and Applied Ecology, Far-Eastern State University, 690600, Vladivostok, Russian Federation, and <sup>c</sup>Institute of Marine Biology of the Russian Academy of Sciences, 690022, Vladivostok, Russian Federation

**ABSTRACT:** A new fatty acid, (5Z,9Z)-22-methyl-5,9-tetracosadienoic acid (**1a**), and a rare fatty acid, (5Z,9Z)-23-methyl-5,9-tetracosadienoic acid (**2a**), the predominant constituents of the free fatty acid fraction from the lipids of the sponge *Geodinella robusta*, were isolated and partly separated by reversed phase high-performance liquid chromatography, followed by multi-fold crystallization from MeOH to give **1a** and **2a** in 70% and 60% purity, respectively. These fatty acids were identified as (5Z,9Z)-22- and (5Z,9Z)-23-methyl-5,9-tetracosadienoic acids by nuclear magnetic resonance techniques, including distortionless enhancement by polarization transfer, heteronuclear multiple quantum connectivity, and correlation spectroscopy experiments, as well as from mass-spectrometric data for their methyl esters, the methyl esters of their perhydro derivatives, and their pyrrolidides. Mixtures of **1a** and **2a** showed cytotoxic activity against mouse Ehrlich carcinoma cells and a hemolytic effect on mouse erythrocytes. The sterol fraction from the same sponge was analyzed by gas-liquid chromatography-mass spectrometry, and 24-methylenecholesterol was identified as a main constituent of this fraction. The implications of the co-occurrence of membranolytic long-chain fatty acids and 24-methylenecholesterol as a main membrane sterol are discussed in terms of the phenomenon of biochemical coordination.

Paper no. L8822 in *Lipids* 37, 75–80 (January 2002).

Sponges are characterized by the wide diversity in their fatty acid composition and, in contrast with higher animals, by the presence of very long chain constituents (so-called demospongiac acids) with novel branching and unsaturation patterns. The content of demospongiac acids may approach 85% of total

fatty acids in sponge phospholipids (1–5). As a rule, C<sub>26</sub> acids, accompanied by C<sub>28</sub> and sometimes C<sub>24</sub> acids, including those of *iso* and *anteiso* structures (4,6–9), dominate in the demospongiac acids of sponges (3). Demospongiac acids with 25 carbon atoms as predominant constituents have been found only in a few cases. For example, Bergquist *et al.* (3) found a preponderance of C<sub>25</sub> acids in lipids of *Leiosella* sp. and *Ircinia novaeseelandiae*, in contradistinction to the higher concentrations of C<sub>26</sub>–C<sub>28</sub> acids in other sponges.

Usually, the demospongiac acids are found mainly as structural components of membrane phospholipids (1–9). Recently, Nemoto *et al.* (10) isolated free demospongiac acids as human DNA topoisomerase-I inhibitors from the sponge *Amphimedon* sp. and characterized them by spectral methods, including nuclear magnetic resonance (NMR) spectroscopy. The majority of unusual fatty acids with very long chains have not been isolated from the corresponding sponges but have been identified solely using gas-liquid chromatography (GLC) and GLC-mass spectrometry (MS) methods. Therefore, NMR data for many demospongiac acids have not been reported.

In the course of our continuing studies on marine natural products (11), we found that the alcoholic extract from the Far Eastern sponge *Geodinella robusta* (class Demospongiae, subclass Tetractinomorpha, order Astrophorida, family Geodiidae) showed cytotoxic activity against mouse Ehrlich carcinoma cells. Thin-layer chromatography (TLC) revealed the presence of an extraordinarily high content of free fatty acids in this extract. Bioassay-guided isolation gave a fatty acid fraction that was analyzed by GLC-MS, and C<sub>25</sub>-demospongiac acids (**1a**, **2a**) were subsequently identified as the bioactive compounds. One of these fatty acids (**1a**) has not been described previously, whereas **2a** was found by Carballeira *et al.* in several *Ircinia* species and in *Spongia tubulifera* (12). In this paper, we report the compositions of free fatty acid and free sterol fractions from the sponge *Geodinella robusta* and the isolation and structure elucidation of the demospongiac acids **1a** and **2a**, including NMR data for these compounds.

\*To whom correspondence should be addressed at Laboratory of the Marine Natural Products, Pacific Institute of Bioorganic Chemistry of the Russian Academy of Sciences, Vladivostok, Pr. 100-letya Vladivostoka 159, 690022, Russian Federation. E-mail: piboc@stl.ru

Abbreviations: COSY, correlation spectroscopy; ECL, equivalent chain length; EI-MS, electron impact mass spectrometry; GLC, gas-liquid chromatography; GLC-MS, gas-liquid chromatography coupled with mass spectrometry; HPLC, high-performance liquid chromatography; NMR, nuclear magnetic resonance; TLC, thin-layer chromatography.

## EXPERIMENTAL PROCEDURES

**Extraction and isolation of demospongiac acids.** Specimens of *Geodinella robusta* were collected near Iturup Island (the Konservnaya Bay), Sea of Okhotsk, using scuba equipment at the depth of 5 m in August 1999. The sponges (0.25 kg dry weight) were carefully cleaned of all nonsponge debris, cut into small pieces, and immediately extracted at room temperature with ethanol for two consecutive 24-h periods. The combined extracts were concentrated *in vacuo*. The ethanol-soluble materials were dissolved in 90% ethanol (200 mL) and extracted with hexane (5 × 100 mL) to give 2.1 g of an oily residue after evaporation of the hexane extract. The material obtained was then chromatographed on a column of Sephadex LH-20 (Sigma Chemical Co., St. Louis, MO) using chloroform/ethanol (1:1, vol/vol) and rechromatographed on the same column using chloroform/ethanol (3:1, vol/vol) as the eluting solvent systems, to obtain 1.12 g of a mixture of nonpolar compounds. This mixture was separated by column chromatography on silica gel L (40–100 μm; Chemapol, Prague, Czech Republic) using petroleum ether gradually replaced with chloroform as the eluting solvent to obtain a crude fatty acid fraction (760 mg) after the removal of solvents *in vacuo*. This substance was subjected to high-performance liquid chromatography (HPLC) on an Altex (Berkeley, CA) Ultrasphere Si column (25 cm × 10 mm), eluted with hexane/ethyl acetate (5:1, vol/vol) at 2 mL/min, using a DuPont Series 8800 instrument (Boston, MA) equipped with a differential refractometer (RIDK-102). The fatty acid fraction obtained (394 mg) was subjected to HPLC on a Serva (Heidelberg, Germany) Octadecyl-Si 100 column (5 μm, 25 cm × 4.6 mm), using 96% methanol as the eluting solvent at 1 mL/min, to obtain 80.5 mg (0.03% on dry weight) of a mixture of acids **1a** and **2a** (1.5:1). Multifold crystallization of part of this mixture from methanol yielded 8.2 mg of the subfraction **I** (containing 70% acid **1a** and 30% acid **2b**) and 7.6 mg of the subfraction **II** (containing 60% acid **2a** and 40% acid **1a**).

The acids were converted to methyl esters by treatment with diazomethane. *N*-Acyl pyrrolidide derivatives were prepared by direct treatment of the methyl esters with pyrrolidine/acetic acid (10:1, vol/vol) in a capped vial (1 h, 100°C) followed by ethereal extraction from the acidified solution and purification by preparative TLC on silica gel L plates developed in CHCl<sub>3</sub>. The hydrogenations of methyl esters and *N*-acyl pyrrolidides with addition of 2H<sub>2</sub> were carried out in methanol solution using PtO<sub>2</sub> as catalyst. The β-*N*-acylglucosamides **1f** and **2f** were obtained from acids **1a** and **2a** and glucosamine by the method described elsewhere (13).

**Analysis of fatty acids.** Proton and carbon nuclear magnetic resonance (<sup>1</sup>H and <sup>13</sup>C NMR) 1D and 2D spectra of the acids were recorded using a Bruker WM-250 spectrometer (Karlsruhe, Germany) at 250 and 62.9 MHz and a Bruker DPX-300 spectrometer at 300 and 75 MHz, respectively, with tetramethylsilane as an internal standard. Proton NMR spectra of **1a** and **2a** were also obtained on a Bruker DPX-500 instrument at 500 MHz. The infrared (IR) spectrum was recorded on a Bruker "Vector 22" spectrophotometer.

**Capillary GLC.** GLC analyses of methyl esters of fatty acids were performed on a Sigma 2000 PerkinElmer chromatograph (Norwalk, CT) using an SPB-5 column [bonded; poly (5% diphenyl/95% dimethylsiloxane; 50 m × 0.32 mm)] at 260°C and on a Shimadzu Chromatograph 9A (Kyoto, Japan) with a Supelcowax 10 (Supelco, Bellefonte, PA) column (30 m × 0.32 mm) at 210°C, with helium as the carrier gas at 1 mL/min.

**GLC-MS.** GLC-MS analyses were carried out on a Hewlett-Packard 6890 GC System instrument (Palo Alto, CA) with a 5973 Mass Selective Detector, with an HP-5MS (cross-linked 5% phenyl methylsiloxane) capillary column (30 m × 250 μm × 0.25 μm) at 270°C. Helium was used as the carrier gas (1 mL/min), and the ionizing energy was 70 eV. Mass spectral and some other data of key fatty acids for this discussion are presented below.

**Methyl (5Z,9Z)-22-methyl-5,9-tetracosadienoate (1b).** MS *m/z* (relative intensity, %): 392 (M<sup>+</sup>, 5), 363 (1), 360 (3), 343 (3), 318 (2), 277 (2), 264 (2), 250 (3), 181 (7), 164 (6), 167 (3), 154 (7), 141 (35), 136 (16), 109 (52), 95 (30), 81 (100), 74 (20), 67 (63), 55 (61).

**Methyl 22-methyltetracosanoate (1c).** MS *m/z* (relative intensity, %): 396 (M<sup>+</sup>, 46), 367 (2), 353 (15), 339 (1), 311 (4), 297 (5), 199 (5), 143 (27), 129 (11), 111 (6), 87 (90), 74 (100), 57 (63).

**N-[(5Z,9Z)-22-Methyl-5,9-tetracosadienoyl]pyrrolidine (1d).** MS *m/z* (relative intensity, %): 431 (M<sup>+</sup>, 5), 416 (1), 402 (1.5), 378 (0.5), 206 (1), 194 (1.5), 180 (52), 152 (1.5), 140 (2), 126 (30), 113 (100), 98 (10), 85 (8), 70 (12), 55 (12).

**N-(22-Methyltetracosanoyl)pyrrolidine (1e).** MS *m/z* (relative intensity, %): 435 (M<sup>+</sup>, 5), 420 (2.5), 406 (5.5), 378 (4), 126 (30), 113 (100), 98 (10), 85 (7), 70 (12), 55 (10).

**Methyl (5Z,9Z)-23-Methyl-5,9-tetracosadienoate (2b).** MS *m/z* (relative intensity, %): 392 (M<sup>+</sup>, 7), 360 (1), 343 (4), 318 (1), 277 (4), 264 (1), 250 (4), 181 (6), 164 (6), 154 (4), 141 (40), 121 (15), 109 (54), 96 (35), 81 (100), 67 (82), 55 (62).

**Methyl 23-Methyltetracosanoate (2c).** MS *m/z* (relative intensity, %): 396 (M<sup>+</sup>, 40), 367 (2), 353 (15), 339 (1), 311 (4), 297 (5), 199 (5), 143 (27), 129 (11), 111 (6), 87 (90), 74 (100), 57 (45).

**N-[(5Z,9Z)-23-Methyl-5,9-tetracosadienoyl]pyrrolidine (2d).** MS *m/z* (relative intensity, %): 431 (M<sup>+</sup>, 5), 420 (1.5), 388 (1), 206 (1), 194 (1), 180 (50), 152 (1.5), 140 (2), 126 (15), 113 (100), 98 (12), 85 (6), 70 (12), 55 (14).

**N-(23-Methyltetracosanoyl)pyrrolidine (2e).** MS *m/z* (relative intensity, %): 435 (M<sup>+</sup>, 5), 420 (3.5), 392 (3), 126 (20), 113 (100), 98 (10), 85 (7), 70 (12), 55 (14).

**N-[(5Z,9Z)-22-Methyl-5,9-tetracosadienoyl]/(5Z,9Z)-23-methyl-5,9-tetracosadienoyl, 1.5:1]-2-amino-α-D-glucopyranose (1f and 2f).** <sup>13</sup>C NMR (C<sub>5</sub>D<sub>5</sub>N): 11.35, 19.14, 22.5, 26.23, 27.17, 27.43, 29.36, 29.49, 29.64, 29.77, 30.09, 34.38, 36.01, 36.65, 39.00, 55.79, 63.05, 72.86, 72.29, 73.67, 92.57 (C-1), 129.34, 129.79, 129.89, 130.40 ppm.

**Isolation and analysis of free sterol fraction.** The free sterols were isolated from the fraction of nonpolar compounds (1.12 g) by preparative TLC on silica gel L (5/40 μm;



Chemapol) with the use of chloroform/ethanol (20:1, vol/vol) as the developing solvent. Treatment of the sterol mixture obtained with pyridine/acetic anhydride (1:1, vol/vol; room temperature, 24 h) yielded the sterol acetates. The sterol acetates were separated by preparative TLC on silica gel L-AgNO<sub>3</sub> plates developed with hexane/benzene (5:3, vol/vol). The isolated subfractions were then analyzed by GLC and GLC-MS as previously described (14).

**Hemolysis.** Studies involving laboratory animals were approved by an Institutional Review Board and conformed to accepted Standards. Mouse erythrocytes were washed three times by centrifugation (600 × g, 5 min) in cold Tris buffer containing 150 mM NaCl, 1 mM KCl, and 1 mM HEPES (pH 7.4). The pellet was resuspended in the same solution to a final concentration of 1%. Erythrocytes were incubated with the compounds tested for 30 min at room temperature and then centrifuged (600 × g, 5 min). Optical density of the supernatant was measured spectrophotometrically at 540 nm.

**Cytotoxicity.** Ehrlich ascites carcinoma cells were grown intraperitoneally in albino mice. Cells were harvested on the seventh day after inoculation, washed twice with cold phosphate-buffered saline using centrifugation (600 × g, 5 min), and resuspended in 199 medium (0.7 × 10<sup>6</sup> cells/mL). The cell suspension was incubated with the test compounds in a 96-well microplate at 37°C for 24 h. Then total and viable cell numbers were determined microscopically using 0.17% Trypan Blue stain (15).

## RESULTS AND DISCUSSION

The major fatty acids of the free fatty acid fraction (0.03% of dry weight of the sponge) were identified in standard fashion from GLC equivalent chain length (ECL) values and electron impact mass spectrometry (EI-MS) of methyl esters. As shown in Table 1, the fatty acid fraction contained a variety of *isolanteiso* fatty acids (87.25%) ranging from 25 to 27 carbons in length. The most abundant fatty acids of *G. robusta* were generally *ai25:2* and *i25:2* together with *ai27:2* and *ai26:2*. It is noteworthy that the fatty acids with terminal *anteiso* branching were the predominant acids and their total content was as high as 57.6%. Another peculiarity of this sponge is that the percentage of C<sub>25</sub> constituents was more than 50%. Usually, the content of C<sub>25</sub> acids is in the range of 1–10% (3); for instance, C<sub>25</sub> acids represented only 10% of phospholipid fatty acid fraction from the sponges of genus *Ircinia* (12). The fatty acids with 26 carbon atoms (about 28% of the free fatty acid fraction in *G. robusta*) are typical acids from marine sponges belonging to the class Demospongiae and usually account for 50% of total demospongiic acid mixtures (2). In contrast, C<sub>27</sub> fatty acids (18% of the free fatty acid fraction in *G. robusta*) are not as widely distributed in sponges, although *ai-5,9-27:2* acid has been found as the major fatty acid constituent (18.4%) in phospholipids from the sponge *Petrosia ficiformis* (6). Cytotoxic properties were not reported for free fatty acids. Thus, we considered the *ai25:2* and *i25:2* constituents to be interesting for structural

**TABLE 1**  
Principal Free Fatty Acids from *Geodinella robusta*<sup>a</sup>

Fatty acid	ECL <sup>b</sup>	Abundance (%)
1 5,9-Tetracosadienoic (24:2)	24.31	0.95
2 Pentacosanoic ( <i>i25:0</i> )	24.55	0.85
3 Pentacosanoic ( <i>ai25:0</i> )	24.73	0.97
4 (5 <i>Z</i> ,9 <i>Z</i> )-23-Methyl-5,9-tetracosadienoic ( <i>i25:2</i> ) ( <b>1a</b> )	24.82	19.5
5 (5 <i>Z</i> ,9 <i>Z</i> )-22-Methyl-5,9-tetracosadienoic ( <i>ai25:2</i> ) ( <b>2a</b> )	25.01	30.0
6 9-Pentacosanoic (25:1)	25.16	0.86
7 Pentacosadienoic (25:2)	25.28	0.89
8 Hexacosanoic ( <i>i26:0</i> )	25.51	0.99
9 Hexacosanoic ( <i>ai26:0</i> )	25.68	0.94
10 5,9-Hexacosadienoic ( <i>i26:2</i> )	25.76	3.24
11 5,9-Hexacosadienoic ( <i>ai26:2</i> )	25.95	11.76
12 5,9-Hexacosadienoic (26:2)	26.25	3.76
13 5,9,17-Hexacosatrienoic (26:3)	26.45	0.89
14 5,9,19-Hexacosatrienoic (26:3)	26.56	6.40
15 5,9-Heptacosadienoic ( <i>i27:2</i> )	26.72	3.94
16 5,9-Heptacosadienoic ( <i>ai27:2</i> )	26.91	14.00

<sup>a</sup>Some minor acids (≤0.8%) are not included in this table.

<sup>b</sup>Equivalent chain length; Supelcowax 10 column, 210°C.

studies and probably bioactive compounds in the sponge *G. robusta*. In fact, separation of the free fatty acid fraction by HPLC allowed us to isolate a mixture of these two acids, and it was shown that they have a potent cytotoxic action against mouse Ehrlich carcinoma cells.

The separation of *iso* and *anteiso* demospongiic acids has not yet been reported in the literature (4,6–9,12). Efforts to separate the mixture of **1a** and **2a** as free acids by HPLC procedures on a Serva Octadecyl-Si 100 column with a solvent system of 95% EtOH with 0.01 M AcONH<sub>4</sub>, 85% acetone, or MeOH with 0.1% trifluoroacetic acid or on Zorbax ODS (Kyoto, Japan), with EtOH as the eluting solvent, were unsuccessful. Similarly, separation of methyl esters of **1a** and **2a** by HPLC on an Ultrasphere-Si column in hexane/ethyl acetate (200:1, vol/vol) was not obtained. Taking into consideration the fact that reversed phase HPLC is a more available method for separation of amphiphilic compounds, we carried out the modification of isolated 5,9-25:2 demospongiic acids by the method developed in 1982 (13) to obtain β-*N*-acylglucosamides **1f** and **2f** from acids **1a** and **2a** and glucosamine. However, separation of these derivatives on an ODS column, using MeOH and acetonitrile as eluting solvents, was also unsuccessful. Nevertheless, we achieved a partial separation of compounds **1a** and **2a** by HPLC on Serva Octadecyl-Si 100, using 96% MeOH as a developing solvent, followed by multifold crystallization from MeOH. By employing this procedure, we obtained subfraction I (containing 70% **1a** and 30% of **2a**) and subfraction II (containing 60% **2a** and 40% of **1a**).

The absorption band at 1710 cm<sup>-1</sup> (CHCl<sub>3</sub>) in the infrared spectrum of **1a** and a <sup>13</sup>C NMR signal at δ 178.7 ppm (Table 2) indicated the presence of a carboxyl group (Scheme 1). A chemical shift at δ 33.2 ppm was expected and observed for the C-2 signal of the neighboring methylene group (16). The methyl ester (**1b**) had an ECL value of 25.01 on GLC and gave



**TABLE 2**  
Nuclear Magnetic Resonance (NMR) Data for **1a** and **2a**<sup>a</sup>

Position	<b>1a</b> ( <i>anteiso</i> )		<b>2a</b> ( <i>iso</i> )	
	<sup>1</sup> H NMR (ppm)	<sup>13</sup> C NMR (ppm)	<sup>1</sup> H NMR (ppm)	<sup>13</sup> C NMR (ppm)
1		178.7 <i>s</i>		178.7 <i>s</i>
2	2.36 <i>t</i> (7.5)	33.2 <i>t</i>	2.36 <i>t</i> (7.5)	33.2 <i>t</i>
3	1.70 sept. (7.4)	24.6 <i>t</i>	1.70 sept. (7.5)	24.6 <i>t</i>
4	2.08 <i>m</i>	26.5 <i>t</i>	2.08 <i>m</i>	26.5 <i>t</i>
5	5.30–5.40 <i>m</i>	128.5 <i>d</i>	5.30–5.40 <i>m</i>	128.5 <i>d</i>
6	5.30–5.40 <i>m</i>	130.6 <sup>b</sup> <i>d</i>	5.30–5.40 <i>m</i>	130.6 <sup>b</sup> <i>d</i>
7	2.08 <i>m</i>	27.3 <i>t</i>	2.08 <i>m</i>	27.3 <i>t</i>
8	2.08 <i>m</i>	27.3 <i>t</i>	2.08 <i>m</i>	27.3 <i>t</i>
9	5.30–5.40 <i>m</i>	128.9 <i>d</i>	5.30–5.40 <i>m</i>	128.9 <i>d</i>
10	5.30–5.40 <i>m</i>	130.5 <sup>b</sup> <i>d</i>	5.30–5.40 <i>m</i>	130.5* <i>d</i>
11	2.02 <i>br. q</i> (6.8)	27.4 <i>t</i>	2.02 <i>br. q</i> (6.8)	27.4 <i>t</i>
12–21	1.2–1.4 <i>m</i>	29.4–30.1 <i>t</i>	1.2–1.4 <i>m</i>	29.4–30.1 <i>t</i>
22	1.51 sept. (6.5)	34.4 <i>d</i>	1.15 <i>m</i>	39.1 <i>t</i>
23	1.15 <i>m</i>	36.7 <i>t</i>	1.30 <i>m</i>	28.0 <i>d</i>
24	0.85 <i>t</i> (6.4)	11.4 <i>q</i>	0.86 <i>d</i> (6.6)	22.6 <i>q</i>
25	0.84 <i>d</i> (6.4)	19.2 <i>q</i>	0.86 <i>d</i> (6.6)	22.6 <i>q</i>

<sup>a</sup>In CDCl<sub>3</sub> with tetramethylsilane as internal standard.

<sup>b</sup>Signal assignments equivocal.

a molecular ion peak ( $M^+$ ) at  $m/z$  392. These data supported the 25:2 structure proposed for this compound. Compound **1b** was transformed into the perhydro derivative (**1c**) by catalytic hydrogenation. EI-MS of the latter compound gave a molecular ion peak at  $m/z$  396 ( $M^+$ ), confirming the presence of two double bonds in the original fatty acid. The presence of two unsaturated bonds in compound **1a** was also indicated by the <sup>1</sup>H NMR resonances at  $\delta$  5.30–5.40 (m, 4H) and by distortionless enhancement by polarization transfer <sup>13</sup>C NMR spectra, showing four CH signals at  $\delta$  128.5, 128.9, 130.5, and 130.6.

The  $\Delta^{5,9}$  unsaturation pattern was readily recognized in **1a** from the characteristic prominent peaks at  $m/z$  81 in the EI mass spectrum of the methyl ester (**1b**) and at  $m/z$  180 (C-7–C-8 cleavage) in the EI mass spectrum of the corresponding pyrrolidide (**1d**) (17). The mass spectrum of the pyrrolidide (**1d**) displayed an  $M^+$  peak at  $m/z$  431 and differences of 12 amu between homologous ions at  $m/z$  140 (C<sub>4</sub>) and  $m/z$  152

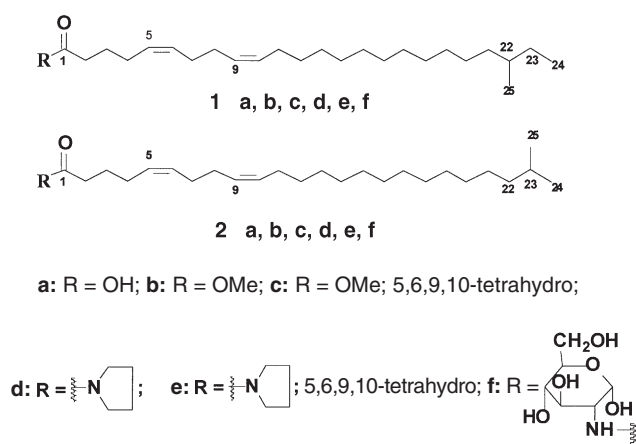
(C<sub>5</sub>), indicating a  $\Delta^5$  double bond, and between homologous ions at  $m/z$  194 (C<sub>8</sub>) and  $m/z$  206 (C<sub>9</sub>), indicating a  $\Delta^9$  double bond (6,17). Further confirmation of the double-bond positions was obtained from NMR correlation spectroscopy (COSY) experiments with consecutive COSY correlations from C-1 to C-11 clearly showing that the double bonds were located at C-5 and C-9 (Table 2). The geometry of the double bonds was established by analysis of the <sup>13</sup>C NMR chemical shifts of the neighboring carbons of the double bonds (18). It is known that carbons adjacent to *trans* double bonds have chemical shifts in the range of  $\delta$  29.5–38.0, whereas those adjacent to *cis* double bonds have values of  $\delta$  26.0–28.5. The <sup>13</sup>C NMR signals of compound **1a** were at  $\delta$  26.5 (C-4), 27.3 (C-7), 27.3 (C-8), and  $\delta$  27.4 (C-11) (Table 2), confirming the percentage of *cis* double bonds between C-5 and C-6 as well as between C-9 and C-10.

The methyl branching in **1a** was established because catalytic hydrogenation (PtO<sub>2</sub>) of methyl ester **1b** did not give a C<sub>25</sub> acid methyl ester with a normal saturated chain. Furthermore, the presence of two methyl groups in **1a** was revealed by <sup>13</sup>C NMR and <sup>1</sup>H NMR spectra. The chemical shift at 11.4 (CH<sub>3</sub>-24) shielded into a high field by the branching at the  $\beta$ -position indicated *anteiso* structure (<sup>1</sup>H NMR:  $\beta$  = 0.85, *t*,  $J$  = 6.4 Hz) while the signal at  $\delta$  19.2 (CH<sub>3</sub>-25) indicated a methyl group at C-22 (18,19). The doublet at  $\delta$  0.85 in the <sup>1</sup>H NMR spectrum and the signal at  $\delta$  34.4 (C-22) in the <sup>13</sup>C NMR spectrum (18) as well as COSY and heteronuclear multiple quantum connectivity experiments and gas–liquid chromatographic behavior of **1a** confirmed this conclusion. Moreover, EI-MS of the hydrogenated derivative of the pyrrolidide (**1e**,  $M^+$  435; Fig. 1) showed diagnostic fragments for the *ai*25:0 fatty acid (406,  $M^+$  – 29; 378,  $M^+$  – 29 – 28).

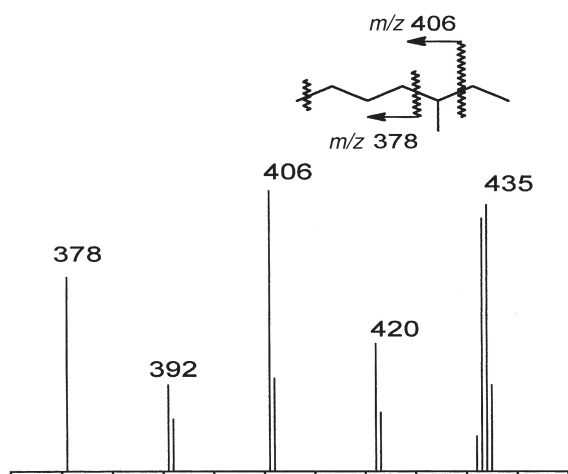
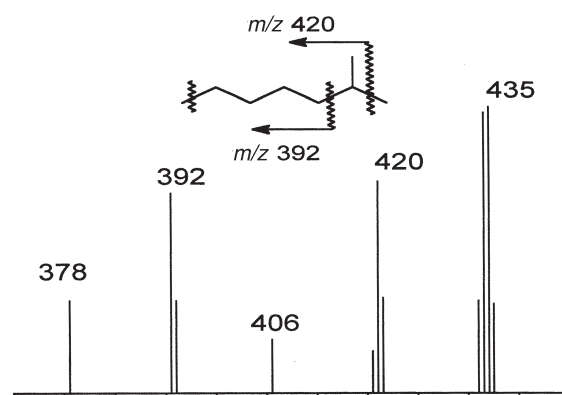
On the basis of the data discussed above, the structure of **1a** was determined as (5*Z*,9*Z*)-22-methyl-5,9-tetracosadienoic acid.

The fatty acid **2a** was easily presumed to be an isomer of **1a** by comparison of the spectral data of **1a** and **2a** (Table 2). The methyl ester (**2b**) had an ECL value of 24.82 on GLC, and EI-MS gave a molecular ion peak ( $M^+$ ) at  $m/z$  392. These data supported the C<sub>25:2</sub> structure. The positions and geometry of the double bonds as were determined for **2a** as 5*Z*,9*Z* by NMR data in the same manner as for **1a** (Table 2). The methyl branching was established based on the fact that catalytic hydrogenation (PtO<sub>2</sub>) of **2b** also did not give a methyl ester with a normal chain. The presence of two methyl groups was revealed by the signals at  $\delta$  22.6 in the <sup>13</sup>C NMR spectrum (C-24, C-25) and at  $\delta$  0.86 in the <sup>1</sup>H NMR spectrum (*d*,  $J$  = 6.6 Hz, an isopropyl group). The signal at  $\delta$  39.1 (C-22) in the <sup>13</sup>C NMR spectrum confirmed the position of methyl branching at C-23 (20,21). Mass spectrum of the tetrahydropyrrolidide (**2e**) obtained from **2a** exhibited a molecular ion peak at  $m/z$  435 (Fig. 2) and diagnostic fragmentation ions for the *iso* fatty acids at  $m/z$  420 ( $M^+$  – 15) and  $m/z$  392 ( $M^+$  – 15 – 28).

On the basis of data discussed above, the structure of **2a** was determined as (5*Z*,9*Z*)-23-methyl-5,9-tetracosadienoic acid.



**SCHEME 1**

FIG. 1. Partial mass spectrum of **1e**.FIG. 2. Partial mass spectrum of **2e**.

The GLC-MS and  $^1\text{H}$  NMR analyses of the fraction of free sterols and the corresponding subfractions, obtained by silica gel- $\text{AgNO}_3$  preparative TLC, revealed 18 known sterols. Table 3 lists the identified sterols as well as their content (%) in the free sterol fraction and GLC relative retention times. This sterol mixture contained  $\text{C}_{26}$  (5.9%),  $\text{C}_{27}$  (21%),  $\text{C}_{28}$  (49%), and  $\text{C}_{29}$  (19%)  $\Delta^5$  sterols and stanols. The major sterol was identified as 24-methylenecholesterol (38.25%).

The demospongiac acids from the Far Eastern marine sponge *G. robusta* demonstrated potent cytotoxic activities. In fact, toxic and hemolytic effects of the mixture of the acids **1a** and **2a** (1.5:1) against mouse Ehrlich carcinoma cells and erythrocytes were observed at  $\text{ED}_{50} = 1.8$  and  $1.5 \mu\text{g/mL}$ , respectively. The sponge *G. robusta* contained 24-methylenecholesterol as the principal constituent of the free sterol fraction instead of cholesterol, a main membrane sterol of the ma-

jority of animals. Earlier, Djerassi's group (22) distinguished some sponges containing unusual additionally alkylated side chains in sterols as also having the branched demospongiac fatty acids in their membrane phospholipids. It was suggested (22) that "such an unusual feature of the membrane . . . may represent a response to stress from the sponge's biotic environment, or it may reflect a specialized requirement of certain membrane-bound enzymes for internal fluidity" (p. 645). In the course of our continued investigations on membranolytic toxins from marine organisms, we have discovered that many toxin-producing marine animals (sponges, holothurians, etc.) contain unusual sterols instead of cholesterol in their membrane free sterol fractions (23). Moreover, we confirmed by experiments that inclusion of unusual sterols instead of cholesterol into cellular membranes protects cells against membranolytic action of different marine toxins (24). We call the phenomenon, which involves the mutually conditioned presence of two different series of secondary metabolites in living organisms, "biochemical coordination" (23,24). The find-

**TABLE 3**  
Sterols from the Sponge *Geodinella robusta* (gas-liquid chromatographic analysis of RRT<sup>a</sup> are given for acetates)

Sterol	Short designation	RRT <sup>a</sup>	% Content
1 24-Norcholesta-5,22-dien-3 $\beta$ -ol	$26\Delta^{5,22}$	0.695	5.22
2 24-Nor-5 $\alpha$ -cholest-22-en-3 $\beta$ -ol	$26\Delta^{22}$	0.713	0.67
3 27-Nor-24 $\xi$ -methylcholesta-5,22-dien-3 $\beta$ -ol	$27\Delta^{5,22}$	0.895	3.38
4 Cholesta-5,22-dien-3 $\beta$ -ol	$27\Delta^{5,22}$	0.920	3.88
5 5 $\alpha$ -Cholest-22-en-3 $\beta$ -ol	$27\Delta^{22}$	0.95	0.44
6 Cholest-5-en-3 $\beta$ -ol (cholesterol)	$27\Delta^5$	1.001	1.19
7 5 $\alpha$ -Cholestan-3 $\beta$ -ol	$27\Delta^0$	1.02	2.14
8 24 $\xi$ -Methylcholesta-5,22-dien-3 $\beta$ -ol	$28\Delta^{5,22}$	1.098	10.38
9 24 $\xi$ -Methyl-5 $\alpha$ -cholest-22-en-3 $\beta$ -ol	$28\Delta^{22}$	1.126	1.47
10 24-Methylcholesta-5,24(28)-dien-3 $\beta$ -ol	$28\Delta^{5,24(28)}$	1.238	38.25
11 24 $\xi$ -Methylcholest-5-en-3 $\beta$ -ol	$28\Delta^5$	1,249	Trace
12 24-Methylcholest-24(28)-en-3 $\beta$ -ol	$28\Delta^{24(28)}$	1.268	0.76
13 24 $\xi$ -Ethylcholesta-5,22-dien-3 $\beta$ -ol	$29\Delta^{5,22}$	1.333	1.33
14 24 $\xi$ -Ethylcholest-5-en-3 $\beta$ -ol	$29\Delta^5$	1.495	Trace
15 24-Ethylcholesta-5,24(28)-dien-3 $\beta$ -ol	$29\Delta^{5,22(28)}$	1.498	Trace
16 24-Ethylcholesta-5,24(28)Z-dien-3 $\beta$ -ol	$29\Delta^{5,22(28)}$	1.507	12.49
17 24 $\xi$ -Ethyl-5 $\alpha$ -cholest-24(28)E-en-3 $\beta$ -ol	$29\Delta^{22(28)}$	1.541	Trace
18 24 $\xi$ -Ethyl-5 $\alpha$ -cholestan-3 $\beta$ -ol	$29\Delta^0$	1.554	6.44

<sup>a</sup>Relative retention time (RRT) for the sterol acetate (RRT for cholesterol acetate = 1.00); HP-5MS column, 270°C.

ing of a new case where membranolytic toxins (fatty acids **1a** and **2a**) and the major sterol distinguished from cholesterol (24-methylenecholesterol) were found in the same animal (the sponge *G. robusta*) is of interest from the point of view of further studies on "biochemical coordination." Probably, 24-methylenecholesterol complements the unusual fatty acid toxicity in some unknown fashion.

## ACKNOWLEDGMENTS

We are very grateful to Drs. Ekaterina G. Lyakhova, Olga P. Moiseenko, and Mikhail V. Vysotskii for GLC analysis and MS measurements, We thank Dr. Vladimir B. Krasokhin for identification of the sponge, Dr. Nina G. Prokof'eva for performing bioassays, and Dr. Pavel A. Lukiyanov for collection of the Far Eastern sponge *G. robusta*. The research described in this publication was supported by grant no. REC-003 of the U.S. Civilian Research & Development Foundation for the Independent States of the Former Soviet Union (CRDF) and Russian Foundation of Basic Research (RFBR) grant no. 00-15-97806. The expedition on the R/V *Akademik Oparin*, during which the sponge was collected, was supported by grants DEB-9400821 and DEB-9505031 of the International Programs Divisions and Biological Science Foundation (principal investigator Theodore W. Pietscher) and of the Japan Society for the Promotion of Science (principal investigator Kunio Amaoka).

## REFERENCES

1. Jefferts, E., Morales, R.W., and Litchfield, C. (1974) Occurrence of *cis*-5, *cis*-9-Hexacosadienoic and *cis*-5, *cis*-9, *cis*-19-Hexacosatrienoic Acids in the Marine Sponge *Microcionia prolifera*, *Lipids* 9, 244–247.
2. Morales, R.W., and Litchfield, C. (1976) Unusual C24, C25 and C27 Polyunsaturated Fatty Acids of the Marine Sponge *Microcionia prolifera*, *Biochim. Biophys. Acta* 431, 206–216.
3. Bergquist, P.R., Lavis, A., Lawson, M.P., and Cambie, R.C. (1984) Fatty Acid Composition and the Classification of the Porifera, *Biochem. Syst. Ecol.* 12, 63–84.
4. Dasgupta, A., Ayanoglu, E., and Djerassi, C. (1984) Phospholipid Studies of Marine Organisms: New Branched Fatty Acids from *Strongylophora durissima*, *Lipids* 19, 768–776.
5. Ayanoglu, E., Popov, S., Kornprobst, J.M., Abound-Bichara, A., and Djerassi, C. (1983) Phospholipid Studies of Marine Organisms: New  $\alpha$ -Methoxy Acids from *Higginsia tethyoides*, *Lipids* 18, 830–836.
6. Ayanoglu, E., Walkup, R.D., Sica, D., and Djerassi, C. (1982) Phospholipid Studies of Marine Organisms. III. New Phospholipid Fatty Acids from *Petrosia ficiformis*, *Lipids* 17, 617–625.
7. Carballeira, N.M., Thompson, J.E., Ayanoglu, E., and Djerassi, C. (1986) Biosynthetic Studies of Marine Lipids. 5. The Biosynthesis of Long-Chain Branched Fatty Acids in Marine Sponges, *J. Org. Chem.* 51, 2751–2756.
8. Carballeira, N.M., and Shalabi F. (1990) Identification of Naturally Occurring *trans*, *trans* ( $\Delta$ 5,9 Fatty Acids from the Sponge *Plakortis halichondroides*, *Lipids* 25, 835–840.
9. Carballeira, N.M., Reyes, E.D., and Shalabi F. (1993) Identification of Novel *iso/anteiso*-Nonacosadienoic Acids from the Phospholipids of the Sponges *Chondrosia remiformis* and *Myrmekioderma styx*, *J. Nat. Prod.* 56, 1850–1855.
10. Nemoto, T., Yoshino, G., Ojika, M., and Sakagami, Y. (1997) Amphimic Acids and Related Long-Chain Fatty Acids as DNA Topoisomerase-I Inhibitors from an Australian Sponge, *Amphimedon* sp., *Tetrahedron* 53, 16699–16710.
11. Makarieva, T.N., Ilyin, S.G., Stonik, V.A., Lyssenko, K.A., and Denisenko, V.A. (1999) Pibocin, the First Ergoline Marine Alkaloid from the Far-Eastern Ascidian *Eudistoma* sp., *Tetrahedron Lett.* 40, 1591–1594.
12. Carballeira, N.M., Shalabi, F., Cruz, C., Rodriguez, J., and Rodriguez, E. (1991) Comparative Study of Fatty Acid Composition of Genus *Ircinia*. Identification of the New 23-Methyl-5,9-tetracosadienoic Acid, *Comp. Biochem. Physiol.* 100B, 489–492.
13. Gorbach, V.I., Ivanchina, E.V., Isakov, V.V., Luk'yanov, P.A., Solov'eva, T.A., and Ovodov, Yu, S. (1982) Synthesis of Lipid A Analogs. Preparation of ( $\beta$ -1,6)-Disaccharide 6'-Phosphates of 2-Acylamino-2-deoxy-D-glucose, *Bioorg. Chem.* 8, 1670–1676.
14. Stonik, V.A., Ponomarenko, L.P., Makarieva, T.N., Boguslavsky, V.M., Dmitrenok, A.S., Fedorov, S.N., and Strobikin, S.A. (1998) Free Sterol Compositions from the Sea Cucumbers *Pseudostichopus trachus*, *Holothuria (Mycrotele) nobilis*, *Holothuria scabra*, *Trochostoma orientale* and *Bathyploetes natans*, *Comp. Biochem. Physiol.* 120B, 337–347.
15. Sasaki, T., Ishida, H., Takasuka, N., Kamiya, H., Endo, Y., Tanaka, M., Hayashi, T., and Shimizu, Y. (1985) Antitumor Activity of Aqueous Extracts of Marine Animals, *J. Pharmacobio-Dyn.* 8, 969–974.
16. Stothers, J.B. (1972) *Carbon-13 NMR Spectroscopy*, Academic Press, New York, p. 74.
17. Andersson, B.A. (1978) Mass Spectrometry of Fatty Acid Pyrrolidides, *Prog. Chem. Fats Other Lipids* 16, 279–308.
18. Choudhury, S.R., Traquair, J.P., and Jarvis, W.R. (1995) New Extracellular Fatty Acids in Culture Filtrates of *Sporothrix flocculosa* and *S. rugulosa*, *Can. J. Chem.* 73, 84–87.
19. Niepel, T., Meyer, H., Wray, V., and Abraham, W.R. (1997) New Type of Glycolipid, 1- $[\alpha$ -Mannopyranosyl-(1 $\alpha$ -3)-(6-O-acetyl- $\alpha$ -mannopyranosyl)]-3-O-acylglycerol, from *Arthrobacter atrocyaneus*, *Tetrahedron* 53, 3593–3602.
20. Carballeira, N.M., Reyes, E.D., Sostre, A., Rodriguez, A.D., Rodriguez, J.L., and Gonzalez, F.A. (1997) Identification of the Novel Antimicrobial Fatty Acid (5Z,9Z)-14-Methyl-5,9-pentadecadienoic Acid in *Eunicea succinea*, *J. Nat. Prod.* 60, 502–504.
21. Reyes, E.D., and Carballeira N.M. (1997) Total Synthesis of the Antimicrobial Fatty Acid (5Z,9Z)-14-Methylpentadeca-5,9-dienoic Acid and Its Longer Chain Analog (5Z,9Z)-24-Methylpentacos-5,9-dienoic Acid, *Synthesis* 10, 1195–1198.
22. Walkup, R.D., Janieson G.C., Ratcliff, M.R., and Djerassi, C. (1981) Phospholipid Studies of Marine Organisms: 2. Phospholipid-Bound Fatty Acids and Free Sterols of the Sponge *Aplysia fistularis* (Pallas) forma *fulva* (Pallas) (= *Verongia Thiona*). Isolation and Structure Elucidation of Unprecedented Branched Fatty Acids, *Lipids* 16, 631–646.
23. Makarieva, T.N., Stonik, V.A., Ponomarenko, L.P., and Kalinovskiy, A.I. (1996) Isolation of (24R)-24,25-Methylene-5 $\alpha$ -cholestan-3 $\beta$ -ol, a New Cyclopropane-Containing Sponge Sterol, *J. Chem. Res. (S)* 10, 468–469.
24. Makarieva, T.N., Stonik, V.A., Ponomarenko, L.P., and Aminin, D.L. (1998) Unusual Marine Sterols May Protect Cellular Membranes Against Action of Some Marine Toxins, in *New Developments in Marine Biotechnology* (Le Gal, Y., and Halvorson, H.O., eds.), pp. 37–40, Plenum Press, New York.

[Received April 27, 2001, and in final revised form, November 28, 2001; revision accepted December 5, 2001]



# Formation of Triacylglycerol Core Aldehydes During Rapid Oxidation of Corn and Sunflower Oils with *tert*-Butyl Hydroperoxide/Fe<sup>2+</sup>

Olli Sjövall<sup>a,b</sup>, Arnis Kuksis<sup>a,\*</sup>, and Heikki Kallio<sup>b</sup>

<sup>a</sup>Banting and Best Department of Medical Research, University of Toronto, Toronto, Ontario, Canada M5G 1L6, and <sup>b</sup>Department of Biochemistry and Food Chemistry, FIN-20014 University of Turku, Finland

**ABSTRACT:** The lipid ester core aldehydes formed during a rapid oxidation (7.8 M *tert*-butyl hydroperoxide, 90 min at 37°C) of the triacylglycerols of purified corn and sunflower oils were isolated as dinitrophenylhydrazones by preparative thin-layer chromatography and identified by reversed-phase high-performance liquid chromatography with on-line electrospray ionization mass spectrometry and by reference to standards. A total of 113 species of triacylglycerol core aldehydes were specifically identified, accounting for 32–53% of the 2,4-dinitrophenylhydrazine (DNPH)-reactive material of high molecular weight representing 25–33% of the total oxidation products. The major core aldehyde species (50–60% of total triacylglycerol core aldehydes) were the mono(9-oxo)nonanoyl- and mono(12-oxo)-9,10-epoxy dodecenoyl- or (12-oxo)-9-hydroxy-10,11-dodecenoyl-diacylglycerols. A significant proportion of the total (9-oxo)nonanoyl and epoxidized (12-oxo)-9,10-dodecenoyl core aldehydes was found in complex combinations with hydroperoxy or hydroxy fatty acyl groups (6–10% of total triacylglycerol core aldehydes). Identified were also di(9-oxo)nonanoylmonoacylglycerols (0.5% of total) and tri(9-oxo)nonanoylglycerols (trace). The identification of the oxoacylglycerols was consistent with the products anticipated from *tert*-butyl hydroperoxide oxidation of the major species of corn and sunflower oil triacylglycerols (mainly linoleoyl esters). However, the anticipated (13-oxo)-9,11-trideca-dienoyl aldehyde-containing acylglycerols were absent because of further oxidation of the dienoic core aldehyde. A significant proportion of the unsaturated triacylglycerol core aldehydes contained *tert*-butyl groups linked to the unsaturated fatty chains *via* peroxide bridges (2–9%). The study demonstrates that rapid peroxidation with *tert*-butyl hydroperoxide constitutes an effective method for enriching natural oils and fats in triacylglycerol core aldehydes for biochemical and metabolic testing.

Paper no. L8703 in *Lipids* 37, 81–94 (January 2002).

Autoxidation of unsaturated triacylglycerols yields hydroperoxides as primary oxidation products. In the presence of divalent cations, the hydroperoxides readily undergo chain

\*To whom correspondence should be addressed at Banting and Best Department of Medical Research, University of Toronto, Charles H. Best Institute, 112 College Street, Toronto, Ontario, Canada M5G 1L6. E-mail: amis.kuksis@utoronto.ca

Abbreviations: ALD, aldehyde; CI, chemical ionization; CID, collision-induced dissociation; DLI, direct liquid inlet; DNPH, 2,4-dinitrophenylhydrazine; EI, electron impact; ESI, electrospray ionization; HPLC, high-performance liquid chromatography; LC, liquid chromatography; M, molecular ion; MS, mass spectrometry; Rt, retention time; TBHP, *tert*-butyl hydroperoxide; TCN, theoretical carbon number; TLC, thin-layer chromatography.

cleavage, yielding both volatile and nonvolatile carbonyl compounds of a large variety of structural types (1,2). Whereas the volatile carbonyl compounds have been extensively studied owing to their contribution to off-flavors, color, and aroma of stored food products (3,4), the nonvolatile acylglycerol aldehyde molecules have largely been ignored (5,6). Extensive research has shown that volatile carbonyls form adducts with proteins (7–9) and some of them precipitate adverse physiological effects (9–11). The chain cleavage products remaining associated with the acylglycerol molecules, although not directly contributing to off-flavors, color, and aroma, can serve as reservoirs of potentially toxic oxidation materials as well as complexing agents. Furthermore, polar glycerolipids containing an aldehyde group are likely to remain associated with cell membranes (12) and affect their structure and function, including receptor activity. Because the nonvolatile aldehydes have been shown (13,14) to react with amino compounds as readily as the volatile aldehydes and because hydroperoxides of dietary linoleic acid esters are converted to aldehydes in the stomach before being absorbed into the body (15,16), it is essential that acylglycerol core aldehydes be available for studies on the gastrointestinal fate and metabolic consequences of ingestion of the secondary products of triacylglycerol oxidation.

As synthetic lipid ester core aldehydes are not commercially available, previous biochemical and nutritional studies have been performed with the small amounts of products generated by autoxidation of unsaturated fats and oils (17,18). Because of low yields of oxoacylglycerols, direct identification of the potential dietary precursors and the absorbed materials has been difficult, and analysts have relied on indirect tests based on various color reactions (17,18). We have previously isolated the C<sub>5</sub> and C<sub>9</sub> core aldehydes of cholesteryl esters (19,20), glycerophospholipids (19), and standard triacylglycerols (21,22) following treatment with *tert*-butyl hydroperoxide (TBHP) and have identified them by reversed-phase high-performance liquid chromatography (HPLC) with on-line electrospray ionization mass spectrometry (LC/ESI/MS) after preparation of the 2,4-dinitrophenylhydrazones (13,22). In the present study, we have used this analytical method to identify over 113 core aldehydes and their derivatives generated from corn and sunflower oil triacylglycerols by a rapid oxidation with TBHP and ferrous ions.



## MATERIALS AND METHODS

**Materials.** Corn oil (Mazola; Best Foods Canada Inc., Etobicoke, Ontario, Canada) was purchased from a local grocery store, and sunflower seed oil (Kultasula) was obtained from a Finnish manufacturer (Raision Margariini Oy, Toijala, Finland). The triacylglycerols were purified by thin-layer chromatography (TLC) as previously described (22). Reference triacylglycerols, hydroperoxytriacylglycerols, and core aldehydes were available from a previous study (22), including the oxidation products of 16:0/18:1/18:2 (21).

**Oxidation.** The oxidation was accelerated by adding 1 mL of 70% TBHP in water (7.8 M) to 10 mg of purified triacylglycerols in the presence of 10  $\mu$ M FeSO<sub>4</sub> and 100  $\mu$ L of 0.2% taurocholic acid (16). The mixture was incubated on a mechanical agitator in the dark for 1.5 h at 37°C. The reaction was stopped by diluting with 5 mL of chloroform/methanol (2:1, vol/vol) and by washing three times with water (3  $\times$  1 mL). The solvent was evaporated under nitrogen at 38°C, and the lipid residue was subjected to preparation of derivatives of 2,4-dinitrophenylhydrazine (DNPH).

**Preparation of DNPH derivatives.** The DNPH derivatives of triacylglycerol core aldehydes were obtained by adding 2 mL of freshly prepared DNPH in 1 N HCl (3.6 mg/mL) to a 6–9-mg dry sample (6). The mixture was shaken vigorously and kept in the dark at room temperature for 4 h and then overnight at 4°C. The lipids were extracted with 5 mL of chloroform/methanol (2:1, vol/vol), the chloroform phase was blown down under nitrogen, and the residue was taken up in an appropriate solvent for chromatography and MS as described below.

**TLC.** Normal-phase TLC was used to purify triacylglycerols and their oxidized derivatives. Silica gel H (E. Merck & Co., Darmstadt, Germany) plates were prepared in the laboratory, and heptane/isopropyl ether/acetic acid (60:40:4, by vol) solution was used as the mobile phase (22). The DNPH derivatives of the core aldehydes were seen as yellow bands on the chromatoplates (in daylight). The compounds were recovered from the silica gel scrapings by extraction with chloroform/methanol (2:1, vol/vol). Extracts were washed with distilled water, dried with anhydrous Na<sub>2</sub>SO<sub>4</sub>, and saved in 2-propanol.

**HPLC, LC/ESI/MS, and LC/ESI/CID/MS.** Procedures for HPLC, LC/ESI/MS, and LC with on-line ESI/collision-induced dissociation/MS (LC/ESI/CID/MS) of triacylglycerols were as described previously (21,22). The reversed-phase HPLC profiles of native corn and sunflower oil triacylglycerols were recorded with the use of a direct liquid inlet (DLI) chemical ionization (CI) mass spectrometer (Hewlett-Packard, Palo Alto, CA) as a detector, as previously described (23). For ESI/CID/MS, the capillary exit voltage was raised to 300 V to obtain fragment ions from any clearly resolved components (pseudo MS/MS) (24,25). The triacylglycerol samples were dissolved in isopropanol by heating for 2–3 min at 80°C prior to injection. Addition of chloroform to assist the dissolution of triacylglycerols was avoided as it caused distortion of peak shape and variation in retention time.

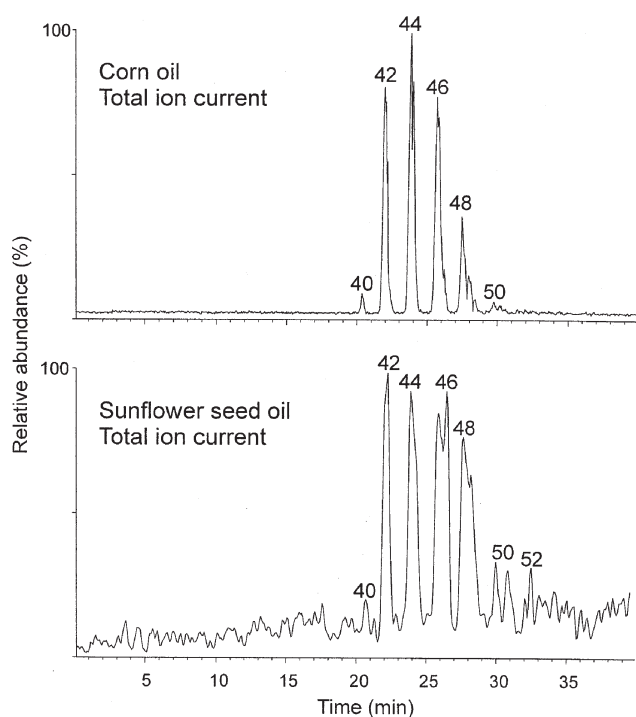
**GC/MS.** GC/MS analyses were performed using an HP5890A gas chromatograph (Hewlett-Packard, San Diego, CA) coupled to the single-quadrupole mass spectrometer described above. A fused-silica capillary column (15 m  $\times$  0.32 mm, i.d.) of the DB-1 bonded phase type (J&W Scientific, Rancho Cordova, CA) was used for the analysis with temperature programming from 200 to 300°C at 5°C/min. Spectra were recorded under electron impact (EI) (70 eV) ionization conditions.

**Peak identification and quantification.** The structures of the resolved oxoacylglycerols were established on the basis of their behavior on normal-phase TLC, reversed-phase HPLC, and LC/ESI/MS as follows. The tentative identities obtained by chromatography in relation to standards were confirmed by LC/ESI/MS, which provided high-intensity [M + 1]<sup>+</sup> and low-intensity [M – RCOOH]<sup>+</sup> ions for the underivatized oxoacylglycerols. The DNPH derivatives of the TBHP oxidation products of the oils gave [M – 1]<sup>–</sup> as the major ions on LC/ESI/MS in the negative mode. The DNPH derivatives of oxidized 16:0/18:1/18:2 were characterized by LC/ESI/CID/MS, which permitted the detection of greatly increased yields of the [M – RCOOH] ions. The data obtained with the TBHP oxidation products of 16:0/18:1/18:2 were used to assign the structures of the TBHP oxidation products of corn and sunflower oil triacylglycerols. The abundances of the major molecular ions of the core aldehydes in the TLC bands provided an estimate of the relative quantities of each component of each homologous series, which could be summed to match the estimates for the major oxoacylglycerol core aldehydes in the total negative ion profile.

## RESULTS

**Analysis of seed oils.** The molecular species composition of native corn and sunflower oil triacylglycerols was determined by reversed-phase HPLC and was found to be similar to that reported previously for commercial corn (23) and sunflower (26) seed oils. Figure 1 shows the triacylglycerol profiles of the two oils before oxidation as obtained by LC/DLI/CI/MS. Table 1 compares molecular species of triacylglycerols of corn and sunflower seed oils before oxidation. The major molecular species of triacylglycerols in both oils were 18:2/18:2/18:2 (20–22%), 18:1/18:2/18:2 (17–18%), 18:1/18:1/18:2 (12–21%), 16:0/18:2/18:2 (7–10%), 16:0/18:1/18:2 (4–9%), 18:1/18:1/18:1 (9–14%), and 18:0/18:1/18:1 (3–7%). The sunflower oil also contained minor amounts (1–5%) of 18:0/18:1/18:1, 22:1/18:1/18:2, and 22:0/18:1/18:2. The overall fatty acid composition of the original sunflower and corn oil triacylglycerols was similar to that reported previously (23,26), with linoleic (18:2), oleic (18:1), and palmitic (16:0) acids accounting for over 90% of the total, as shown in Table 2.

**Analysis of total oxidation mixtures.** Figure 2 compares the total reversed-phase HPLC elution profiles, as detected by light scattering, of corn and sunflower seed oil triacylglycerols following the TBHP treatment. The peaks corresponding to unoxidized triacylglycerols are eluted toward the end of the chromatograms and are identified by their theoretical



**FIG. 1.** Total positive ion current profiles of triacylglycerols of corn and sunflower seed oils before oxidation. Peak numbering refers to the partition number. Triacylglycerols were detected as the ammonium adducts  $[M + NH_4]^+$  in the positive ion mode. Conditions and instrumentation of reversed-phase high-performance liquid chromatography (HPLC) and mass spectrometry (MS) with direct liquid inlet (DLI) chemical ionization (CI) are described in the Materials and Methods section. Solvent gradient: 20–80% 2-propanol in methanol (0.85 mL/min) in 30 min.

**TABLE 1**  
Major Molecular Species of Triacylglycerols of Native Corn (Mazola, Canada) and Sunflower (Kultasula, Finland) Oils<sup>a</sup>

ACN/DB <sup>b</sup>	$[MH]^+$	Molecular species	Corn oil (mol%)	Sunflower oil (mol%)
54:7	894	18:2/18:2/18:3	4.2 ± 0.1	0.05 ± 0.1
54:6	896	18:2/18:2/18:2	22.3 ± 2.0	20.3 ± 2.1
52:5	870	16:0/18:2/18:3	0.9 ± 0.1	0.0 ± 0.0
54:5	898	18:1/18:2/18:2	18.0 ± 2.0	17.3 ± 2
52:4	872	16:0/18:2/18:2	9.9 ± 1.0	6.8 ± 1
54:4	900	18:1/18:1/18:2	12.0 ± 1.0	21.5 ± 1.0
52:3	873	16:0/18:1/18:2	8.6 ± 1.0	4.0 ± 1.0
50:2	848	16:0/16:0/18:2	3.2 ± 0.5	0.05 ± 0.1
54:3	902	18:1/18:1/18:1	9.0 ± 0.5	13.7 ± 1.1
52:2	876	16:0/18:1/18:1	6.0 ± 0.5	0.7 ± 0.1
50:1	850	16:0/16:0/18:1	2.3 ± 0.2	0.2 ± 0.1
48:0	824	16:0/16:0/16:0	0.4 ± 0.2	0.1 ± 0.5
54:2	904	18:0/18:1/18:1	2.8 ± 0.2	7.4 ± 0.2
52:1	878	16:0/18:0/18:1	0.9 ± 0.2	1.1 ± 0.2
58:4	956	18:1/18:2/22:1	—	4.8 ± 0.5
54:1	906	18:0/18:0/18:1	—	0.9 ± 0.5
58:3	958	18:1/18:2/22:0	—	1.2 ± 0.5

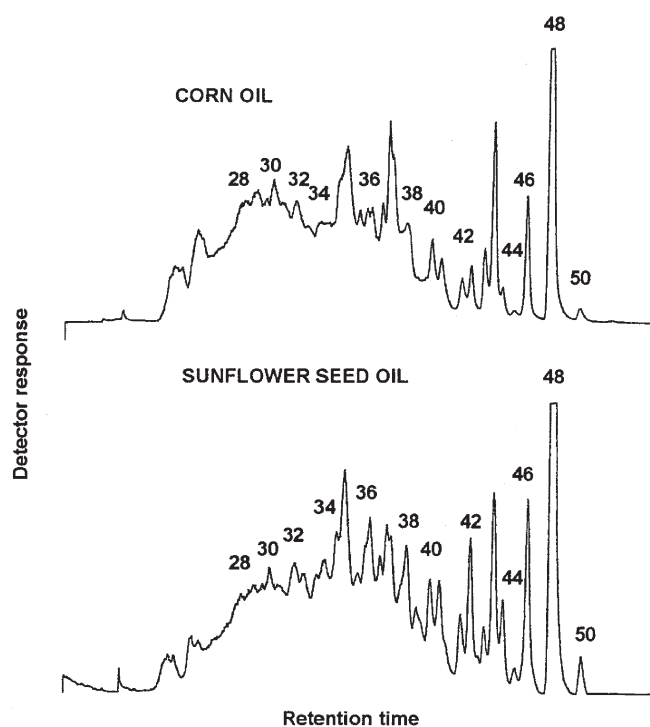
<sup>a</sup>Analysis by liquid chromatography with the use of a direct liquid inlet mass spectrometer as detector (LC/DLI/CI/MS) and using a linear gradient of 30–90% propionitrile in acetonitrile. Values are means ± range/2.

<sup>b</sup>ACN, acyl carbon number; DB, double bond.

**TABLE 2**  
Fatty Acid Composition of Corn (Mazola, Canada) and Sunflower (Kultasula, Finland) Oils<sup>a</sup>

Fatty acid	Corn oil (mol%)	Sunflower oil (mol%)
16:0	10.96 ± 0.8	6.4 ± 1.0
16:1n-7	0.09 ± 0.1	0.2 ± 0.2
18:0	1.85 ± 0.2	3.9 ± 0.8
18:1n-9	28.83 ± 1.7	34.0 ± 3.2
18:2n-6	56.59 ± 2.5	49.4 ± 4.0
18:3n-3	0.70 ± 0.3	0.3 ± 0.2
20:0	0.46 ± 0.1	1.2 ± 0.8
20:1n-9	0.40 ± 0.1	1.0 ± 0.1
22:0	0.11 ± 0.1	0.5 ± 0.2
22:1n-11	Trace	1.5 ± 0.5

<sup>a</sup>Gas-liquid chromatographic analysis (in duplicate) on a polar capillary column (21,22). Values are means ± range/2.



**FIG. 2.** Comparison of reversed-phase HPLC elution profiles of the corn and sunflower seed oils following oxidation with *tert*-butyl hydroperoxide (TBHP) and ferrous iron. Peak numbering for residual triacylglycerols is based on partition number. Conditions of HPLC separation and light-scattering detection as in the Materials and Methods section. Solvent gradient as in Figure 1. See Figure 1 for abbreviation.

carbon number (TCN). The oxidized triacylglycerols are eluted earlier with retention times corresponding to those recorded for synthetic triacylglycerols containing epoxy, hydroperoxy, and hydroxy fatty acids in combination with unmodified fatty acids or the core aldehydes as reported previously (22). On the basis of total peak area, up to 75–80% of the original oil has been oxidized. An examination of the total oxidation mixtures by reversed-phase LC/ESI/MS in the positive ion mode gave elution profiles similar to those obtained

by HPLC with light-scattering detection (chromatograms not shown). Although the residual triacylglycerol species were readily recognized, the parts of the chromatograms containing the oxygenated triacylglycerols were too complex for identification of the molecular species of the core aldehydes. Further reversed-phase HPLC analyses of the oxidized oils were performed following conversion of the aldehyde-containing triacylglycerols into DNPH derivatives.

Figure 3 (upper panel) shows the elution profile of the DNPH derivatives of oxidized sunflower oil triacylglycerols as recorded by reversed-phase LC/ESI/MS in the negative ion mode, along with the full mass spectrum averaged over the core aldehyde elution range (4–25 min). In the negative mode, only the DNPH derivatives and the presumed DNPH polymers (0–5 min) were ionized and detected. The negative ions recorded in the early part of the chromatogram (1.5–4.6 min) were of much lower molecular mass ( $m/z$  403–513) and were attributed to the DNPH derivatives of the short-chain aldehydes and presumed DNPH derivatives produced during the oxidation of the sunflower oil triacylglycerols and were not further investigated. Similar results were obtained for the negative ion mass chromatograms of oxidized corn oil.

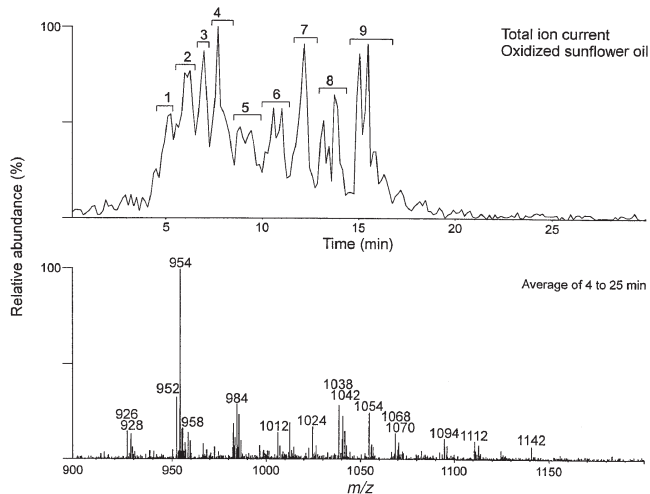
The major ions in the core aldehyde elution range (Fig. 3, lower panel) extend from  $m/z$  926 to  $m/z$  1142, the higher masses clearly exceeding those anticipated for the DNPH derivatives of the simple  $C_9$ – $C_{12:1}$  core aldehydes of sunflower

oil triacylglycerols. The major peaks or peak clusters are numbered 1–9 for reference. The major ions are tentatively identified and assigned to specific peak clusters by determining the full mass spectra associated with each peak cluster as given in Table 3. The peak clusters correspond to the polyoxygenated (clusters 1–3), dioxygenated (clusters 4 and 5), monooxygenated (cluster 6), and simple core aldehydes (clusters 7, 8, and 9) in the oxidized sunflower oil sample. The peaks were identified and quantified by ion extraction from the total negative ion current profile by the computer. All ions represent the DNPH derivatives of triacylglycerols containing at least one core aldehyde group per molecule. The peaks possess symmetrical shapes but are resolved into two or more components based on the relative proportions of the regio- and geometric isomers in the sample. The peaks belong to homologous series and may be aligned according to their TCN. Many more ions could be similarly extracted and identified on the basis of the relative retention times observed for standards or extrapolated from them.

**TABLE 3**  
The Major Ions [as 2,4-dinitrophenylhydrazine (DNPH) derivatives] in Peak Clusters of Total Ion Current Profile of *tert*-Butyl Hydroperoxide (TBHP)-Oxidized Sunflower Seed Oil<sup>a</sup>

Peak cluster	Time range (min)	$m/z$	Molecular structure <sup>a</sup>
1	4.66–5.52	996	6:0ALD/8:0ALD/8:0ALD
		1012	18:2/18:3/9:0ALD, diOOH
		1052	18:2/18:3/9:0ALD, OH, TBHP
		1128	9:0ALD/9:0ALD/9:0ALD
		1140	18:1/18:2/9:0ALD, OH, diTBHP
		1142	18:1/18:1/9:0ALD, OH, diTBHP
		1054	18:2/18:2/9:0, OH, TBHP
		1070	18:2/18:2/9:0ALD, OOH, TBHP
		982	18:2/18:2/9:0ALD, OOH
2	5.66–6.53	1012	16:0/18:3/12:1ALD, OOH, epoxy
		1038	18:2/18:2/12:1ALD, OOH, epoxy
		1056	18:1/18:2/9:0ALD, OH, TBHP
		958	16:0/18:2/9:0ALD, OOH
		984	18:1/18:2/9:0ALD, OOH
3	6.63–7.25	940	16:0/9:0ALD/18:3, OH
		966	18:2/9:0ALD/18:2, OH
		984	18:1/18:2/9:0ALD, OOH
		1032	16:0/18:1/9:0 ALD, OH, TBHP
4	7.25–8.54	1092	18:2/12:1ALD/18:3, TBHP, epoxy
		1112	18:2/18:2/8:0ALD, diTBHP
		996	16:1/18:3/8:0ALD, TBHP
		1022	18:2/18:3/8:0, TBHP
		1038	18:2/18:2/9:0ALD, TBHP
		1068	16:0/18:3/12:1ALD, epoxy, TBHP
		1070	16:0/12:1ALD/18:2, epoxy, TBHP
5	8.54–9.84	1094	18:2/18:2/12:1ALD, epoxy, TBHP
		1006	18:2/12:1ALD/18:2, epoxy
		1024	18:2/18:2/8:0ALD, TBHP
		1042	18:2/9:0ALD/22:0, OOH
		926	16:0/18:2/9:0ALD
6	9.98–11.27	952	18:1/18:2/9:0ALD
		982	16:0/18:2/12:1ALD, epoxy
		954	18:1/18:1/9:0ALD
7	11.56–12.57	1024	18:2/18:2/8:0ALD, TBHP
		1042	18:2/9:0ALD/22:0, OOH
8	12.71–14.58	926	16:0/18:2/9:0ALD
		952	18:1/18:2/9:0ALD
		982	16:0/18:2/12:1ALD, epoxy
9	14.72–16.01	954	18:1/18:1/9:0ALD
		928	16:0/18:1/9:0ALD

<sup>a</sup>Ions were derivatized by DNPH. ALD, aldehyde.



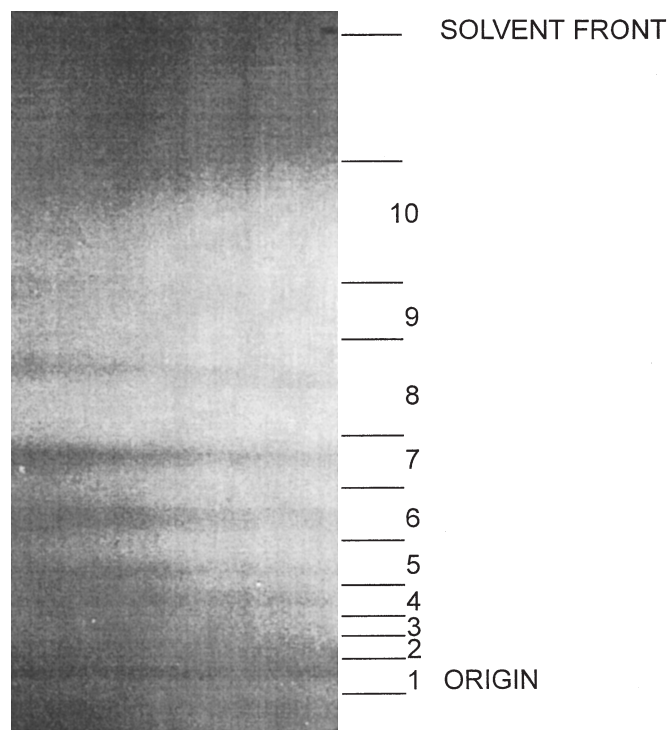
**FIG. 3.** Total negative ion elution profile of the 2,4-dinitrophenylhydrazine (DNPH) derivatives of oxidized sunflower oil triacylglycerols and full mass spectrum averaged over the acylglycerol elution range. Peaks are numbered as clusters in the elution profile and identified on the basis of subsequent analyses as follows: cluster 1, trialdehydes; cluster 2, core aldehyde trihydroxides or epoxydihydroxides; cluster 3, core aldehyde dihydroxides or epoxyhydroxides; cluster 4, core aldehyde hydroperoxides or epoxyhydroxides; cluster 5, core aldehyde hydroperoxides; cluster 6, TBHP adducts of core aldehyde epoxides; cluster 7, TBHP adducts of core aldehydes; cluster 8, core aldehydes; cluster 9, core aldehydes. For identification of ions, see Tables 4–6. Conditions for liquid chromatography with on-line electrospray ionization mass spectrometry (LC/ESI/MS) as in the Materials and Methods section. See Figure 2 for abbreviations.

**TLC of DNPH derivatives.** To confirm the identification of the triacylglycerol core aldehydes, the 2,4-DNPH-treated reaction mixture was subjected to TLC prefractionation. Figure 4 shows the TLC separation of the DNPH derivatives of oxidized sunflower seed oil. The complex mixture was resolved into a total of nine yellow bands and a residual triacylglycerol band (TLC band 10), which did not absorb in daylight but possessed a weak ultraviolet absorption. The oxotriacylglycerols were resolved on the basis of overall polarity and regio- and geometric configuration of the DNPH derivatives as subsequently established by reversed-phase LC/ESI/MS of the individual TLC bands in comparison to standards.

**TLC/LC/ESI/MS of DNPH derivatives.** The structures of the triacylglycerol core aldehydes were further confirmed and the core aldehyde content quantified by examining each TLC band by reversed-phase LC/ESI/MS.

**TLC band 10.** LC/ESI/MS with positive ionization showed that TLC band 10 was made up of residual triacylglycerols along with their TBHP adducts (27).

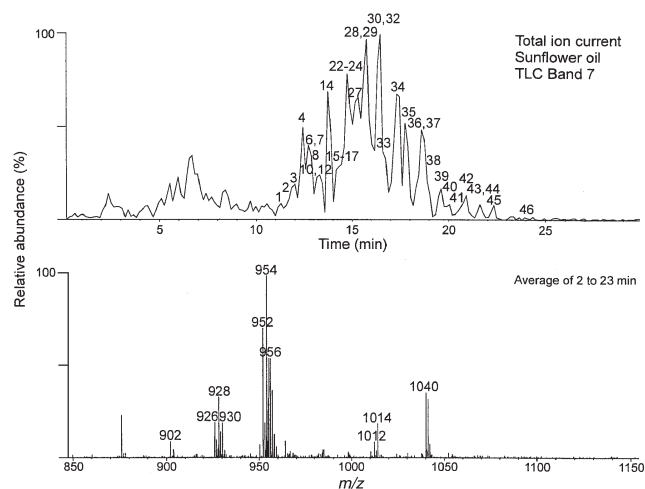
**TLC bands 9 and 8.** The DNPH derivatives recovered from TLC bands 9 and 8 showed mainly ions with masses below



**FIG. 4.** Normal-phase thin-layer chromatography (TLC) separation of the total mixture of oxidized sunflower oil triacylglycerols following derivatization with 2,4-dinitrophenylhydrazine. TLC band 10, residual triacylglycerols; yellow TLC bands (in daylight) represent, in descending order, the following major components: 9 and 8, short-chain aldehydes; 7 and 6, simple triacylglycerol core aldehydes; 5 and 4, dioxygenated core aldehydes; 3 and 2, polyoxygenated core aldehydes; 1, trioxxygenated core aldehydes. Heptane/isopropyl ether/acetic acid (60:40:4, by vol) solution was used as a mobile phase. The compounds were recovered by extraction with chloroform/methanol 2:1 (by vol) from silica gel 60 H plates. Procedures and conditions are given in the Materials and Methods section.

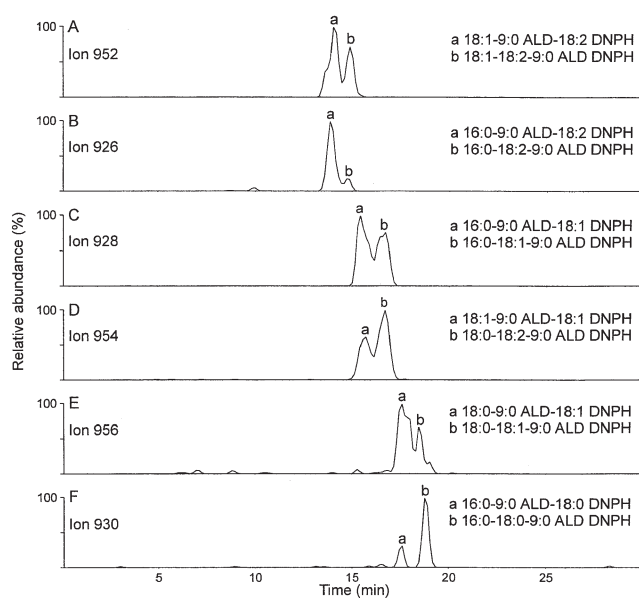
600, which suggested that the major components of those bands were DNPH derivatives of the volatile short-chain aldehydes also produced by peroxidation of the sunflower oil triacylglycerols, although artifacts arising from polymerization of DNPH also were present. A typical low-molecular-weight aldehyde, hexanal, as the DNPH derivative ( $m/z$  273), was found to migrate between residual triacylglycerols and the simple core aldehyde acylglycerols in our TLC system.

**TLC bands 7 and 6.** Figure 5 shows the total ion current profile (upper panel) of TLC band 7 from oxidized sunflower seed oil, along with the full mass spectrum ( $m/z$  850–1150; lower panel) averaged over the oxotriacylglycerol elution range (2–23 min.). The complex profile of the chromatogram (upper panel of Fig. 5) is deceptive in view of the relative simplicity of the total mass spectrum (lower panel of Fig. 5), which shows major ions at  $m/z$  928, 952, 954, and 956, with minor ions at  $m/z$  876, 1014, and 1040. The peak complexity is due to the chromatographic resolution of the regio- and geometric isomers of the DNPH derivatives of the core aldehydes, which possess identical molecular masses, as shown by the mass chromatograms recorded in Figure 6 for simple core aldehyde peaks eluted over the period of 14.2–18.8 min. These peaks represent combinations of 9:0ALD (where ALD is aldehyde) with the common sunflower oil fatty acids. The major species are: 18:1/9:0ALD/18:2 ( $m/z$  952), 18:1/18:1/9:0ALD ( $m/z$  954), 16:0/18:2/9:0ALD ( $m/z$  926), 18:0/9:0ALD/18:1 ( $m/z$  956), and 16:0/18:0/9:0ALD ( $m/z$  930), and there are many minor ones. These peaks clearly represent derivatives of homologous series of sunflower oil triacylglycerols. However, some fatty acids of the core aldehydes are more saturated than the fatty acids of the typical native



**FIG. 5.** Total negative ion current profile of TLC band 7 of the DNPH derivatives of oxidized sunflower seed oil (upper panel) and the full mass spectrum (lower panel) averaged over the core aldehyde elution range (2–23 min). Peak identification and ion assignment are given in Table 4. Earlier eluted ions are attributed to hydrazones of short-chain aldehydes and artifacts from polymerization of DNPH. LC/ESI/MS conditions are as given in the Materials and Methods section. See Figures 3 and 4 for abbreviations.





**FIG. 6.** Mass chromatograms of major ions of (9-oxo)nonanoyl acylglycerols as DNPH derivatives from TLC band 7 of oxidized sunflower oil. Ion identification is given in Table 4. LC/ESI/MS conditions are as described in the Materials and Methods section. ALD, aldehyde; see Figures 3 and 4 for other abbreviations.

sunflower oil. In addition to 9:0 core aldehydes, a series of compounds was found to correspond to 8:0 core aldehydes. However, there were no masses corresponding to the 13:2 and 12:1 core aldehydes in TLC band 7 nor in TLC bands 8 and 9, which were examined in case these core aldehydes had migrated ahead of the other 9:0 core aldehydes. The peaks eluted over the range of 11–13.5 min, and clearly ahead of the simple core aldehydes, represented the TBHP adducts of the unsaturated core aldehydes. The major adduct species were: 18:1/18:2/9:0ALD, TBHP ( $m/z$  1042), 18:1/18:1/9:0ALD, TBHP ( $m/z$  1040), and 16:0/18:2/9:0ALD, TBHP ( $m/z$  1014). No adducts were seen for the saturated triacylglycerol core aldehyde species. TLC band 7 contained the bulk of the triacylglycerol core aldehydes (mainly mono-9:0) with minor amounts found also in TLC band 6 ( $m/z$  928,  $m/z$  952, and  $m/z$  956) as listed in Table 4. A total of 32 9:0 and 14 8:0 core aldehyde-containing triacylglycerols, including the TBHP adducts, were identified in both corn and sunflower oils. The identifications were consistent with the ion masses, the reversed-phase HPLC retention times of standards, as well as the TCN, and the relative proportions of the parent triacylglycerols in the original oils. The abundance of the molecular ions in the major TLC bands provided an uncalibrated quantification of the various members of each homologous series. The major TBHP adduct species also corresponded to the major species of the triacylglycerol core aldehydes: 18:1/18:2TBHP/9:0ALD DNPH ( $m/z$  1040), 18:2/18:2TBHP/9:0ALD DNPH ( $m/z$  1038), 16:0/18:2TBHP/9:0ALD DNPH ( $m/z$  1014), and others. The masses of the TBHP adducts were consistent with the presence of peroxide bridging at the sites expected to be occupied by hydroperoxyl groups, the retention times on the reversed-phase

column, and TCN, as well as with the structures of the major molecular species of residual triacylglycerols in both corn and sunflower oils. There were no significant ions corresponding to the TBHP adducts of the 12:1 core aldehydes in these bands. A similar approach was used in examining other TLC bands.

**TLC bands 5 and 4.** TLC band 5 contained the bulk of the DNPH-derivatized material. The major ions were found at  $m/z$  956, 966, 982, and 984, with minor ions at  $m/z$  1006, 1008, 1068, 1012, 1024, and 1094, indicating the presence of core aldehydes in combination with two full-length normal or oxidized-chain fatty acids in the same triacylglycerol molecule. There were indications of the presence of several homologous series of the core aldehydes. The minor peaks eluted over the time period 7.5–11.7 min represented mostly the hydroperoxides of the 9:0 core aldehydes with  $m/z$  values of 982, 958, 984, 986, 988, and 1042. In the hydroperoxides of 9:0 core aldehydes, the hydroperoxyl group was located on one of two unsaturated fatty acids bound to the triacylglycerol molecule containing the aldehyde group. The peaks eluted over the time period 11.8–13.9 min included ions with  $m/z$  values of 1000 and 1026, which could be attributed to TBHP adducts of 12:1 core aldehydes. The peaks eluted over the time period 9.3–12.7 min represent the TBHP adducts of the 12:1 core aldehyde monoepoxides with  $m/z$  values of 1092, 1094, 1068, 1070, 1096, and 1098. The peaks emerging over the time period 12.3–20.3 min represent an orderly elution sequence of the monoepoxides of 12:1 core aldehydes with  $m/z$  values of 1006, 980, 956, 1008, 982, and 1010. The sudden appearance of the 12:1 aldehydes in the epoxy triacylglycerols suggests that the epoxy group is located on the 12:1 aldehyde chain. The monoepoxides of 12:1 core aldehydes have two fatty acids and the epoxidized 12:1 aldehyde chain esterified to a parent triacylglycerol. However, the structures of epoxy compounds are shown in this paper without the loss of double bonds to indicate the original composition of core aldehydes. TLC band 4 contained the regioisomers of the epoxy core aldehydes in TLC band 5 along with the corresponding TBHP adducts (mass chromatograms not shown). The chromatographic properties and the relative quantities of the epoxides of the 12:1 core aldehydes and the corresponding TBHP adducts in TLC bands 5 and 4 are given in Table 5 in order of the reversed-phase HPLC retention times. In all instances, the relative proportions of the aldehyde derivatives corresponded to the relative proportions of the major triacylglycerols in the original oils. In the case of corn oil, some of the core aldehyde hydroperoxides were found, in part, in TLC bands 6 and 4 and in TLC bands 4 and 3. The identification of all major aldehyde hydroperoxides was consistent with ion masses and relative retention times of standards, as well as the TCN and the total acyl carbon and double-bond numbers. The molecular-ion abundances in the major TLC bands provide uncorrected estimates of the relative quantities of the various members of each homologous series.

**TLC bands 3, 2, and 1.** These minor TLC fractions represent the core aldehydes of the more highly oxygenated tri-

TABLE 4

Composition and Structure of Triacylglycerol Core Aldehydes and Peroxide Adducts in TBHP-Oxidized Corn and Sunflower Seed Oils as Determined by Reversed-Phase Liquid Chromatography with On-line Electrospray Ionization Mass Spectrometry (LC/ESI/MS) (TLC bands 6 and 7)<sup>a</sup>

No	Avg Rt	TCN	ACN/DB	Mass <sup>b</sup>	Abundance <sup>c</sup>		Molecular structure <sup>d</sup>
					Corn	Sunflower	
1	11.23	31.33	45:4	1038	500	11400	18:2/9:0ALD/18:2, TBHP
2	11.43	30.99	42:2	1000	400	500	16:1/8:0ALD/18:1, TBHP
3	12.03	31.67	45:4	1038	6500		18:2/18:2/9:0ALD, TBHP
4	12.45	33.17	43:2	1014	2900	4900	16:0/9:0ALD/18:2, TBHP
5	12.59	32.51	42:2	1000	400		16:0/18:2/8:0ALD, TBHP
6	12.63	32.66	45:3	1040	8400	14500	18:1/9:0ALD/18:2, TBHP
7	12.79	33.51	43:2	1014	5400	3300	16:0/18:2/9:0ALD, TBHP
8	12.97	33.27	45:4	950	400	1900	18:2/9:0ALD/18:2
9	13.32	33.60	44:3	938	400		18:1/8:0ALD/18:2
10	13.37	33.00	45:3	1040	3500	5500	18:1/18:2/9:0ALD, TBHP
11	13.58	34.05	44:3	938	200		18:1/18:2/8:0ALD
12	13.63	33.72	45:4	950	300	2000	18:2/18:2/9:0ALD
13	13.94	33.06	44:3	1026	500		18:0/18:3/8:0ALD, TBHP
14	14.20	34.60	45:3	952	8100	18100	18:1/9:0ALD/18:2
15	14.20	35.11	43:2	926	6100	5900	16:0/9:0ALD/18:2
16	14.30	34.66	44:3	938	100		18:0/8:0ALD/18:3
17	14.58	34.21	45:2	1042	4100		18:1/9:0ALD/18:1, TBHP
18	14.70	35.15	44:2	940	500	1500	18:1/8:0ALD/18:1
19	14.70	35.89	40:0	888	200	500	16:0/8:0ALD/16:0
20	14.73	35.11	44:3	938	400		18:0/18:3/8:0ALD
21	14.79	35.38	42:1	914	500	1300	16:0/8:0ALD/18:1
22	14.80	35.56	43:2	926	1200	9100	16:0/18:2/9:0ALD
23	15.03	35.83	42:1	914	900	300	16:0/18:1/8:0ALD
24	15.03	36.11	45:3	952	4300	15500	18:1/18:2/9:0ALD
25	15.11	35.60	44:2	940	1600	2400	18:1/18:1/8:0ALD
26	15.36	36.34	40:0	888	100	200	16:0/16:0/8:0ALD
27	15.48	36.89	41:0	902	5900	2300	16:0/9:0ALD/16:0
28	15.52	34.44	45:2	1042	3200		18:1/18:1/9:0ALD, TBHP
29	15.76	36.38	43:1	928	16700	10600	16:0/9:0ALD/18:1
30	15.83	36.15	45:2	954	9500	14300	18:1/9:0ALD/18:1
31	16.41	37.38	44:1	942	400		18:0/8:0ALD/18:1
32	16.56	37.34	41:0	902	3500	1800	16:0/16:0/9:0ALD
33	16.61	36.83	43:1	928	13000	10200	16:0/18:1/9:0ALD
34	16.65	37.56	45:2	954	15300	12300	18:0/18:2/9:0ALD
35	17.60	38.89	43:0	930	2000	5300	16:0/9:0ALD/18:0
36	17.75	38.38	45:1	956	5500	10900	18:0/9:0ALD/18:1
37	18.75	38.83	45:1	956	5400	8100	18:0/18:1/9:0ALD
38	18.77	39.34	43:0	930	5800	11200	16:0/18:0/9:0ALD
39	19.71	40.89	45:0	958	5300	4100	18:0/9:0ALD/18:0
40	20.11	40.38	47:1	984	4100	1800	20:0/9:0ALD/18:1
41	20.58	41.11	49:2	1010	700		18:2/9:0ALD/22:0
42	21.13	41.34	45:0	958	1000	3600	18:0/18:0/9:0ALD
43	21.65	41.56	49:2	1010	700		22:0/18:2/9:0ALD
44	21.82	42.38	49:1	1012	400	700	18:1/9:0ALD/22:0
45	22.73	42.83	49:1	1012	100	2600	22:0/18:1/9:0ALD
46	24.19	44.89	49:0	1014	100	400	18:0/9:0ALD/22:0

<sup>a</sup>Abbreviations: Avg Rt, average retention time; TCN, theoretical carbon number; ACN, acyl carbon number; DB, double bond; TLC, thin-layer chromatography. See Table 3 for other abbreviations.

<sup>b</sup>[M + DNPH].

<sup>c</sup>Abundance of ion in the major TLC band.

<sup>d</sup>Core aldehyde regioisomers consistent with chromatographic and MS properties.

acylglycerols possessing complex elution profiles (total ion currents not shown). The tentative peak identifications again were based on the TLC/HPLC behavior of synthetic standards, the specificity of the negative ion response to the DNPH derivatives, and knowledge of the general nature of the products of TBHP oxidation of standard triacylglycerols. As an example, Figure 7 shows the single ion mass chro-

matograms of major hydroxy (9-oxo)nonanoyl acylglycerols extracted from TLC band 2. Table 6 summarizes the chromatographic properties of the identified peaks along with the ion abundance recorded for each molecular species in TLC bands 3 and 2 and in the most polar minor TLC band 1. There remained significant ion abundance at  $m/z$  1040, 1056, 958, 980, 960, 982, 986, 1008, and 1012 in TLC band 3 and at  $m/z$

Table 5

Composition and Structure of Triacylglycerol Core Aldehydes and Peroxide Adducts in TBHP-Oxidized Corn and Sunflower Seed Oils as Determined by Reversed-Phase LC/ESI/MS (TLC bands 4 and 5)<sup>a</sup>

No	Avg Rt	TCN	ACN/DB <sup>b</sup>	Mass <sup>c</sup>	Abundance <sup>d</sup>		Molecular structure <sup>b,e</sup>
					Corn	Sunflower	
1	7.52	24.87	45 : 4	982		3300	18:2/9:0ALD/18:2, OOH
2	8.20	26.71	43 : 2	958	9600	2900	16:0/9:0ALD/18:2, OOH
3	8.44	26.20	45 : 3	984	9500	8400	18:1/9:0ALD/18:2, OOH
4	9.23	27.28	45 : 2	986	7000	3100	18:1/9:0ALD/18:1, OOH
5	9.25	27.51	43 : 1	960		600	16:0/9:0ALD/18:1, OOH
6	9.32	25.81	48 : 6	1092		9500	18:2/12:1ALD/18:3, epoxy, TBHP
7	9.91	26.22	48 : 6	1092	1700	9200	18:2/18:3/12:1ALD, epoxy, TBHP
8	10.08	29.51	45 : 1	988		800	18:0/9:0ALD/18:1, OOH
9	10.77	27.20	48 : 5	1094		17500	18:2/12:1ALD/18:2, epoxy, TBHP
10	10.86	27.59	46 : 4	1068	4100	12200	16:0/2:1ALD/18:3, epoxy, TBHP
11	11.06	29.04	46 : 3	1070		1100	16:0/12:1ALD/18:2, epoxy, TBHP
12	11.24	27.72	48 : 5	1094	6400	5200	18:2/18:2/12:1ALD, epoxy, TBHP
13	11.31	28.81	48 : 4	1096	700	4000	18:1/12:1ALD/18:2, epoxy, TBHP
14	11.43	28.00	46 : 4	1068	7000	3200	16:0/18:3/12:1ALD, epoxy, TBHP
15	11.63	32.71	49 : 2	1042	1600	600	18:2/9:0ALD/22:0, OOH
16	11.68	33.51	49 : 1	1044	400	300	22:0/9:0ALD/18:1, OOH
17	11.81	31.44	44 : 3	1026		800	18:1/8:0ALD/18:2, TBHP
18	12.27	29.53	46 : 4	980	5100	8400	16:0/12:1ALD/18:3, epoxy
19	12.27	31.66	44 : 3	1026	3500	1800	18:1/8:0ALD/18:2, TBHP
20	12.32	29.14	48 : 5	1006	6300	13700	18:2/12:1ALD/18:2, epoxy
21	12.32	32.17	42 : 2	1000	900		16:0/8:0ALD/18:2, TBHP
22	12.44	29.22	48 : 4	1096		800	18:1/18:2/12:1ALD, epoxy, TBHP
23	12.55	29.66	48 : 5	1006	2700	8700	18:2/18:2/12:1ALD, epoxy
24	12.59	32.51	42 : 2	1000	500		16:0/18:2/8:0ALD, TBHP
25	12.65	30.05	46 : 4	980	3600	8700	16:0/18:3/12:1ALD, epoxy
26	12.66	32.00	44 : 3	1026	4100	2000	18:1/18:2/8:0ALD, TBHP
27	12.71	31.08	48 : 3	1098		6800	18:1/18:1/12:1ALD, epoxy, TBHP
28	13.45	30.53	44 : 2	956	8000	4100	16:0/12:1ALD/16:1, epoxy
29	13.54	30.75	48 : 4	1008	6400	11300	18:1/12:1ALD/18:2, epoxy
30	13.59	30.98	46 : 3	982	29700	17100	16:0/12:1ALD-18:2, epoxy
31	13.75	31.05	44 : 2	956	11000	5800	16:0-16:1/12:1ALD, epoxy
32	13.92	31.27	48 : 4	1008	19400	25800	18:1/18:2/12:1ALD, epoxy
33	13.94	33.06	44 : 3	1026	900		18:0/18:3/8:0ALD, TBHP
34	13.98	32.72	48 : 3	1010	3300	3500	18:1/12:1ALD/18:1, epoxy
35	14.04	31.50	46 : 3	982	16000	12200	16:0/18:2/12:1ALD, epoxy
36	15.57	32.53	46 : 2	984	1700	7300	16:0/12:1ALD/18:1, epoxy
37	15.63	33.24	48 : 3	1010	3800	8600	18:1/18:1/12:1ALD, epoxy
38	17.67	34.53	48 : 2	1012		1800	18:0/12:1ALD/18:1, epoxy
39	19.61	36.98	52 : 3	1066		1300	22:0/12:1ALD/18:2, epoxy
40	20.25	37.50	52 : 3	1066		800	22:0/18:2/12:1ALD, epoxy

<sup>a</sup>See Tables 3 and 4 for abbreviations.

<sup>b</sup>ACN/DB values of molecular structure are presented without loss of double bonds due to epoxidation.

<sup>c</sup>[M + DNPH].

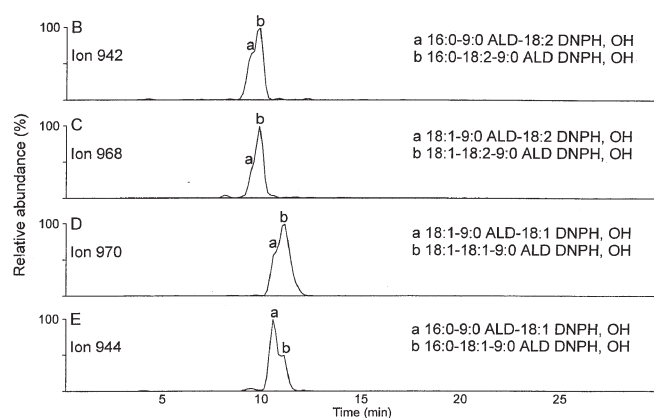
<sup>d</sup>Abundance of ion in the major TLC band.

<sup>e</sup>Core aldehyde regioisomers consistent with chromatographic and MS properties.

902, 984 1054, 1142, 1026, 944, 970, 1194, 986, 982, and 1012 in TLC band 2, for which identities consistent with the retention time, TCN, acyl carbon and double-bond numbers, and *m/z* values could not be immediately suggested.

Table 7 gives the estimated yields of the identified oxidation products for both seed oils. Depending on the mass range over which the total ion current is integrated, the overall yields of the identified aldehyde-containing triacylglycerols range from 32 to 43% of DNPH derivatives in the total oxidation mixture. The major product was the mixed acid acylglycerol containing the 9:0 monoaldehyde (44–60% of identified core aldehydes) followed by hydroperoxy (13–16% of the identified species) and mono-

epoxy aldehydes (11–12% of the identified species) and hydroperoxyepoxy aldehydes (up to 10% of the identified species). More of the TBHP adduct was obtained during the oxidation of the sunflower oil. The major ion masses correspond to the monoaldehyde esters of the 16:0/18:1/18:2 (16:0/18:1/9:0ALD DNPH, *m/z* 928), 16:0/18:2/18:0 (16:0/9:0ALD/18:0DNPH, *m/z* 930), 18:1/18:1/18:2 (18:1/18:1/9:0ALD DNPH, *m/z* 954), 18:1/18:2/18:2 (18:1/18:2/9:0ALD DNPH, *m/z* 952), and 18:0/18:1/18:2 (18:0/18:1/9:0ALD DNPH, *m/z* 956) species, which are the major triacylglycerols in corn and sunflower oils. Apparently, the linoleic acid residue in each instance was converted to the (9-oxo)nonanoate and, to a lesser extent, the



**FIG. 7.** Mass chromatograms of major ions of hydroxy (9-oxo)nonanoyl acylglycerols as DNP derivatives from TLC band 2 of oxidized sunflower oil. Ion identification is given in Table 6. LC/ESI/MS conditions are as described in the Materials and Methods section. See Figures 3, 4, and 6 for abbreviations.

(12-oxo)-9,10-dodecenoate, whereas most of the anticipated (13-oxo)-9,11-tridecadienoyl core aldehydes were oxidized further to the (9-oxo)nonanoyl core aldehydes.

**TABLE 7**  
**Proportion of Identified Core Aldehydes in Total TBHP Oxidation Mixture<sup>a</sup>**

Type of aldehyde	Corn oil <sup>b</sup> (mol%)	Sunflower oil <sup>b</sup> (mol%)
Mixed acid mono aldehydes (8:0)	0.3 ± 0.1	0.2 ± 0.1
Mixed acid mono aldehydes (9:0)	19.2 ± 3.2	18.9 ± 3.8
Hydroperoxy aldehydes (9:0)	5.0 ± 1.0	5.4 ± 1.1
Hydroxy aldehydes (9:0)	0.4 ± 0.2	0.5 ± 0.1
Epoxy aldehydes (12:1)	3.5 ± 0.7	4.9 ± 1.0
Hydroperoxyepoxy aldehydes (12:1)	0.1 ± 0.1	4.1 ± 0.8
Diepoxy aldehydes (12:1)	0.8 ± 0.3	0.3 ± 0.1
Dialdehydes (9:0)	0.5 ± 0.1	0.4 ± 0.2
TBHP adduct aldehydes (8:0)	0.3 ± 0.1	0.3 ± 0.2
TBHP adduct aldehydes (9:0)	0.6 ± 0.2	4.2 ± 1.0
TBHP adduct epoxy aldehydes (12:1)	1.5 ± 0.4	4.1 ± 0.9
Total	32.2 ± 6.4	43.1 ± 9.3

<sup>a</sup>See Table 3 for abbreviation.

<sup>b</sup>Proportion of integrated areas of ion current (mass range 750–1250) of total oxidation mixture.

The most polar oxotriacylglycerols were these with two or more functional groups, e.g., epoxy aldehyde esters and hydroperoxy aldehyde esters (mainly TLC bands 2 and 3). Oxo-

**TABLE 6**  
**Composition and Structure of Triacylglycerol Core Aldehydes and Peroxide Adducts in TBHP-Oxidized Corn and Sunflower Seed Oils as Determined by Reversed-Phase LC/ESI/MS (TLC bands 1, 2, and 3)<sup>a</sup>**

No	Avg Rt	TCN	ACN/DB <sup>b</sup>	Mass <sup>c</sup>	Abundance <sup>d</sup>		Molecular structure <sup>b,e</sup>
					Corn oil	Sunflower	
1	5.99	19.35	48:6	1036	700		18:2/12:1ALD/18:3, OOH, epoxy
2	6.41	24.33	36:3	1020	900	1700	18:3/9:0ALD/9:0ALD
3	6.67	20.74	48:5	1038	8200	6500	18:2/12:1ALD/18:2, OOH, epoxy
4	6.67	21.13	46:4	1012	4900	4000	16:0/12:1ALD/18:3, OOH, epoxy
5	6.85	25.42	46:4	996		2800	16:0/12:1ALD/18:3, diepoxy
6	7.13	22.58	46:3	1014	2700		16:0/12:1ALD/18:2, OOH, epoxy
7	7.24	25.78	36:2	1022	1600	4400	18:2/9:0ALD/9:0ALD
8	7.29	25.87	46:3	996		2400	16:0/18:3/12:1ALD, diepoxy
9	7.55	22.35	48:4	1040	1400	4000	18:1/12:1ALD/18:2, OOH, epoxy
10	7.95	27.56	34:0	998	1300	5300	16:0/9:0ALD/9:0ALD
11	8.05	27.05	36:1	1024	3300	3500	18:1/9:0ALD/9:0ALD
12	8.37	25.10	45:4	966		300	18:2/9:0ALD/18:2, OH
13	8.40	27.09	48:4	1024	2200		18:1/18:2/12:1ALD, diepoxy
14	8.65	29.56	36:0	1026		2000	18:0/9:0ALD/9:0ALD
15	8.78	25.55	45:4	966		7700	18:2/18:2/9:0ALD, OH
16	9.57	26.94	43:2	942	3500	8800	16:0/9:0ALD/18:2, OH
17	9.59	26.43	45:3	968	4900	12400	18:1/9:0ALD/18:2, OH
18	9.99	26.88	45:3	968	5600	35700	18:1/18:2/9:0ALD, OH
19	10.01	27.20	43:2	942	8700	13400	16:0/18:2/9:0ALD, OH
20	10.79	27.69	45:2	970	11000	32100	18:1/9:0ALD/18:1, OH
21	10.83	27.92	43:1	944	23900	36600	16:0/9:0ALD/18:1, OH
22	11.30	28.14	45:2	970	32500	45400	18:1/18:1/9:0ALD, OH
23	11.34	28.12	43:1	944	18300	18200	16:0/18:1/9:0ALD, OH
24	11.99	28.61	48:3	1026		5200	18:1/12:1ALD/18:1, diepoxy
25	12.50	29.92	45:1	972	500	17000	18:0/9:0ALD/18:1, OH
26	13.11	30.12	45:1	972	1400	14600	18:0/18:1/9:0ALD, OH
27	16.41	33.92	49:1	1028		6000	22:0/9:0ALD/18:1, OH
28	17.03	34.12	49:1	1028		1100	22:0/18:1/9:0ALD, OH

<sup>a</sup>See Tables 3 and 4 for abbreviations.

<sup>b</sup>ACN/DB values of molecular structure are presented without loss of double bonds due to epoxidation.

<sup>c</sup>[M + DNP].

<sup>d</sup>Abundance of ion in the major TLC band.

<sup>e</sup>Core aldehyde regioisomers consistent with chromatographic and MS properties.



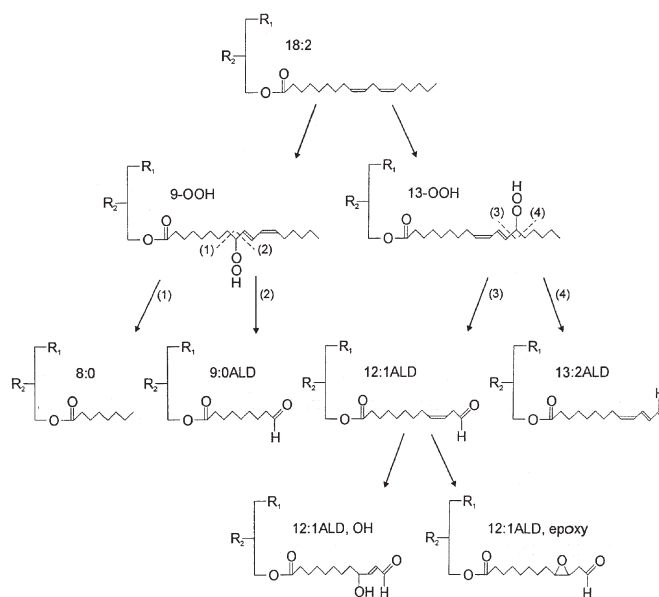
triacylglycerols of intermediate polarity were represented by triacylglycerols containing two core aldehyde groups (mainly TLC bands 4 and 5), whereas the least polar were the oxotriacylglycerols with a single core aldehyde group (TLC bands 6 and 7). There was partial resolution of triacylglycerols containing a single 9:0 or 12:1 core aldehyde in the primary and the secondary position. Further complications arose from a conversion of some of the aldehyde groups into acids by further oxidation. These oxidation products were seen as DNPH derivatives only when combined with another aldehyde or keto group in the same molecule (data not shown).

## DISCUSSION

TBHP is a synthetic organic hydroperoxide that is commonly employed to accelerate lipid peroxidation *in vitro*. The decomposition of the hydroperoxide to alkoxy or peroxy radicals stimulates the chain reaction of lipid peroxidation. The decomposition is aided by metal ions such as  $\text{Fe}^{2+}$  and their complexes (28). In order to increase the yield of the secondary oxidation products (e.g., core aldehydes) in the present study, the triacylglycerol peroxidation and hydroperoxide decomposition were further stimulated by elevated temperature (37°C) and the inclusion of bile salts as emulsifiers. As a result of oxidation, it was possible to obtain within 1–2 h a controlled oxidative destruction of corn and sunflower oil triacylglycerols equivalent to many months of autoxidation by thin-film exposure to air. About 90% destruction of 18:2 had occurred with relatively little loss of 18:1 as judged from the ratio of the unsaturated fatty acids to palmitic acid in the oxidized oil. The proportion of the saturated fatty acids (16:0, 18:0, 20:0, and 22:0) had proportionally increased in the oxidized corn and sunflower oil triacylglycerols along with the appearance of hydroperoxy and epoxy fatty acids (data not shown). It was, therefore, anticipated that the major triacylglycerol core aldehydes would have arisen largely from the oxidation of 18:2 and would be found in combination with palmitic and oleic acids as the DNPH derivatives of the oxotriacylglycerols.

The main mechanism for the formation of aldehydes from lipid hydroperoxides is homolytic scission ( $\beta$ -cleavage) of the two C–C bonds on either side of the hydroperoxy group (6,29) as shown in Figure 8. This reaction proceeds *via* the lipid alkoxy radical. Applying this mechanism to triacylglycerols, it would be anticipated that the cleavage of the carbon–carbon bond would result in aldehydes derived from the methyl termini of the fatty acid chains and of aldehydes still bound to the parent lipid molecule. Hydroperoxides also undergo heterolytic reactions yielding the same products as homolytic reactions. Another possible mechanism for the formation of aldehydes is the Hock–Criegee rearrangement (29,30). This acid-catalyzed carbon-to-oxygen rearrangement of hydroperoxides would be expected to yield products from linoleic acid hydroperoxide cleavage similar to those arising from homolytic scission (29).

Oxidation of methyl oleate (1–3,6), has shown that the 9-



**FIG. 8.** Postulated formation of triacylglycerol core aldehydes from linoleic acid-containing triacylglycerol. R<sub>1</sub> and R<sub>2</sub> are fatty acids esterified to a parent triacylglycerol. Positions of cleavage of the fatty acid chain of hydroperoxides are numbered 1 to 3. In oxidation by TBHP, the 9,10-epoxy derivative of the (12-oxo)dodecenoyl core aldehyde is assumed to be formed in preference to 9-hydroxy-10,11-dodecenoyl core aldehydes. Formation of the core aldehyde can take place on any *sn*-position of acylglycerol. See Figures 2 and 6 for abbreviations.

and 10-hydroperoxides are formed in amounts approximately similar to those of the 8- and 11-hydroperoxides. Therefore, the oleic acid-containing triacylglycerols would be expected to yield (8-oxo)octanoyl and (11-oxo)-9,10-undecenoyl acylglycerols, as well as (9-oxo)nonanoyl and (10-oxo)-8,9-decenoyl acylglycerols. Indeed, small amounts of (8-oxo)octanoyl-containing acylglycerols were observed. Specific masses corresponding to (10-oxo)- $\Delta^8$ -decenoyl and (11-oxo)-9,10-undecenoyl acylglycerols were not found, however. It is possible that the ions arising from the minor (11-oxo)-9,10-undecenoyl acylglycerols overlapped with those arising from the major (9-oxo)nonanoyl acylglycerols.

The major hydroperoxides arising from the oxidation of methyl linoleate are the 9-hydroperoxy and 13-hydroperoxy isomers in equal amounts (2,31). Recently, the 11-hydroperoxide of linoleic acid has been recognized as one of the primary oxidation products (32). It made up 5–10% of the abundance of 9- and 13-hydroperoxide in vitamin E-controlled autoxidation. However, in the absence of vitamin E, 11-peroxyl radicals are not stable and 9- and 13-hydroperoxides predominate (32). The core aldehydes derived from 9- and 13-hydroperoxides of linoleic acid-containing acylglycerols are expected to be 8-nonanoic acid and 9-oxononanoyl-, (12-oxo)-9,10-dodecenoyl, and (13-oxo)-9,11-tridecadienoyl acylglycerols (6,29,33,34). Figure 8 shows the proposed formation of the major core aldehydes from linoleic acid attributable to autoxidation and oxidation by TBHP. According to Frankel (33), the homolytic cleavage of the oxygen–oxygen

bond is the first step in the decomposition of unsaturated hydroperoxides (33). Decomposition proceeds with cleavage of the fatty acid chain on either side of the hydroperoxide group or by cleavage of the oxygen-carbon bond, leading to positional isomerization of the unsaturated hydroperoxides. Simple  $\beta$ -cleavage to 9- and 13-hydroperoxide would produce 9-oxo- and 12-oxo-derivatives as major core aldehydes. The formation of the (12-oxo)-9,10-dodecenoyl acylglycerols would involve another mechanism linked closely with the  $\beta$ -cleavage reaction and would depend upon an alkenyl radical formation. This 1-olefin radical could combine with a hydroxy radical to form an enol which would rearrange to an aldehyde (6,33). Esterbauer *et al.* (6) have pointed out still another possibility provided by the reaction with oxygen to form a hydroperoxide that can decompose again to the enol and then form the aldehyde. If this radical abstracted a hydrogen, it would become a core alkene, which would not be detected as the DNPH derivative unless another aldehyde group was present in the acylglycerol molecule. In the present study, there was no evidence for the presence of core aldehydes carrying short alkene chains in the acylglycerol molecules.

Acid-catalyzed cleavage of the fatty acid chain between the hydroperoxide group and the  $\alpha$ -olefinic carbon leads also to formation of the (12-oxo)-9,10-dodecenoyl acylglycerol from the 13-hydroperoxide of oxidized linoleic acid (29,30). Whereas the 9-oxononanoyl and (12-oxo)-9,10-dodecenoyl acylglycerols were readily detected, those corresponding to the (13-oxo)-9,11-tridecadienoyl acylglycerols were not found. Apparently, this unsaturated core aldehyde did not survive the oxidation and/or workup conditions. In plants, enzymatic processes resembling radical cleavage reactions take place. Gardner (34) has categorized two types of hydroperoxide lyases as heterolytic and homolytic types, found in higher plants and mushrooms, respectively. The heterolytic type of lyase catalyzes the cleavage of the fatty acid chain between the hydroperoxide group and the  $\alpha$ -olefinic carbon, resembling acid-catalyzed cleavage of the hydroperoxide. As a result of decomposition of the 13-hydroperoxide, (13-oxo)-9,11-tridecadienoyl is formed when homolytic lyase activity is present, mimicking  $\beta$ -scission.

The absence of the 12:1 aldehydes from the simple core aldehyde fractions and their appearance in the epoxy triacylglycerol fractions suggest that the epoxy group is associated with the 12:1 aldehyde chain. According to Frankel *et al.* (35) and Frankel (1,3), epoxy esters of 18:1 can arise from its reaction with hydroperoxides or from the hydroperoxides themselves. Gardner *et al.* (36) have discussed the enzymatic and nonenzymatic decomposition mechanisms for linoleic acid hydroperoxides leading to epoxide formation. The major pathways postulated for decomposition in the presence of  $\text{Fe}^{3+}$ /cysteine catalyst involved formation of an alkoxy radical by loss of OH, cyclization of the alkoxy radical to the  $\alpha$ -unsaturation, and reaction of the epoxy allylic radical either with  $\text{O}_2$  to form an epoxyhydroperoxy monoene or with OH to form the epoxyhydroxy monoene, as well as other reactions. Noordermeer *et al.* (37) have identified 9-hydroxy-(12-

oxo)-(10E)- and 11-hydroxy-(12-oxo)-(9Z)-dodecenoic acids in incubations of (12-oxo)-(9Z)-dodecenoic acid formed by a nonenzymatic process. Our results are in accordance with the findings of Noordermeer *et al.* (37), which showed that (12-oxo)dodecenoyl acylglycerols are readily further oxidized to the corresponding hydroxy, hydroperoxy, or epoxy compounds. It is possible that epoxy compounds may be formed more readily than hydroperoxy or hydroxy derivatives during TBHP oxidation. Indeed, TBHP has been employed as the oxidant for epoxidation of oleic, linoleic, linolenic, and arachidonic acids in aqueous buffers containing surfactant or in organic solvents (38). In the present study, tentative identifications were made of the diepoxides based on their migration on TLC.

The identity of the hydroperoxy linoleic and oleic acid components of the oxoacylglycerols was determined by GC-MS analysis following collection of individual HPLC peaks, hydrogenation (platinum oxide catalyst), and transmethylation with sodium methoxide. Samples were analyzed as their trimethylsilyl ether derivatives as described by Hughes *et al.* (39). In each case, the position of hydroxylation was determined from the major fragment ions formed on either side of the oxygen trimethylsilyl group. The *cis/trans* configuration of bonds was assigned on the basis of previous work. Porter *et al.* (40) had shown that the *cis/trans* isomers eluted earlier than the corresponding *trans/trans* isomers when normal-phase HPLC systems were used. According to Park *et al.* (41), the *cis/trans* isomer of the 9-hydroperoxy derivative of trilinoleoylglycerol eluted ahead of the 9-hydroperoxy *trans/trans* isomer from a reversed-phase column. However, the *trans/trans* isomer of the 13-hydroperoxy trilinoleoylglycerol eluted ahead of the corresponding *cis/trans* isomer.

In addition to core aldehydes, ketones were expected to be found among DNPH derivatives of TBHP-oxidized seed oil triacylglycerols. Because a homologous series of appropriate ions was not found, it was not possible to conclude that any isolated masses corresponding to hypothetical DNPH derivatives of ketotriacylglycerols were actually present. Individual keto compounds may have been present in our preparations, but specific identifications were not made owing to a lack of appropriate reference compounds. Possible ketotriacylglycerols could be represented by such ions as  $m/z$  1092,  $m/z$  1094, and  $m/z$  1096, which were tentatively assigned to the TBHP adducts of epoxy 12:1 aldehydes on the basis of their chromatographic behavior.

Many of the triacylglycerol core aldehydes appeared as double peaks, which were attributed to regioisomers. On the basis of previous work with standard oxotriacylglycerols (22,42), the earlier eluted peak was attributed to an aldehyde in the secondary position and the later eluted peak to an aldehyde in the primary position of the oxidized triacylglycerol molecule. A functional group in the *sn*-2 position is known to exert higher polarity than a similar group in the *sn*-1 or *sn*-3 position of the triacylglycerol molecule (22,43,44). Furthermore, each regioisomer possessed a double peak, which was

attributed to a partial resolution of the *syn/anti* isomers of the DNPH derivatives. Previous studies with DNPH derivatives of core aldehydes of known triacylglycerol structure (22) also had given two peaks, the main peak, representing 75–85% of the total, emerging ahead of the minor one, accounting for 15–25%, as estimated by reversed-phase HPLC with ultraviolet detection at 358 nm. However, a clear separation of the geometric isomers was not always obtained for the mixed triacylglycerols of the oxidized seed oils. Identification of regioisomers was complicated due to *syn/anti* isomerism of dinitrophenylhydrazones. Double peaks of DNPH derivatives have been reported to occur also in other analyses of DNPH derivatized carbonyl compounds. Kuklev *et al.* (45) have shown that the 12,13-epoxide runs ahead of the 9,10-epoxide of linoleate on adsorption TLC; this order would be reversed on reversed-phase HPLC. Likewise, 13-keto linoleate migrated ahead of 9-keto linoleate on TLC; again, the order would be reversed on reversed-phase HPLC. The nature of the solvent is known to affect the order of HPLC elution as well as the isomer ratios of these compounds (46).

The only unusual structures, although not unexpected (47), were the TBHP adducts of the unsaturated triacylglycerol core aldehydes. These compounds could have been formed in a termination reaction between a *tert*-butylhydroperoxy radical and an alkenyl radical or between a lipid hydroperoxy radical and the *tert*-butyl radical. The formation of the *tert*-butyl derivatives of the lipid hydroperoxides has a precedent in the existence of di-*tert*-butyl peroxide (40), as well as in the formation of cyclic peroxides during decomposition of linoleate hydroperoxides (31,48) and tocopherol adducts (42). Furthermore, Miyashita *et al.* (31) have demonstrated that oxygenation of methyl linoleate hydroperoxides yields dimers composed of octadecadienoate and octadecenoate moieties cross-linked through either ether or peroxy linkages across the 9- or 13-positions. Yamauchi *et al.* (49) have shown the formation of  $\alpha$ -tocopherol adducts with phosphatidylcholine peroxy radicals.

Finally, the absence of the (13-oxo)tridecadienoyl core aldehydes as oxidation products seems to be consistent with the absence of this core aldehyde also among the autoxidation products of cholesteryl linoleate (20,50) and of linoleate-containing glycerophospholipids (51). Very little work has been done on the triacylglycerol core aldehydes (21,22,42), and their structures have been assigned on the basis of the known routes of degradation of the hydroperoxides of methyl oleate and linoleate (1–3).

In conclusion, the present study demonstrates the formation of a large variety of triacylglycerol core aldehydes during a brief treatment of corn and sunflower oils, with TBHP. The identification of the high-molecular-weight aldehydes was simplified by derivatization with DNPH, normal-phase TLC isolation, and reversed-phase HPLC separation with on-line negative ion MS, which specifically detects the DNPH derivatives. By the combined application of the criteria of chemical derivatization, chromatographic, and MS behavior, it was possible to eliminate many of the uncertainties posed

by coincidental peaks and ions. The chromatographic and MS methods developed here for the characterization of the triacylglycerol core aldehydes arising from *tert*-butyl hydroperoxidation should be suitable for the identification of the core aldehydes among the autoxidation and enzymatic oxidation products of tissue triacylglycerols. This technology may also have applications in atherosclerosis research by permitting identification of aldehydic products formed during the autoxidation of low density lipoprotein (LDL), in which cholesteryl esters predominate. The study shows that rapid peroxidation with TBHP provides an effective method for enriching unsaturated vegetable oils in triacylglycerol core aldehydes for dietary and metabolic testing.

## ACKNOWLEDGMENTS

This work was supported by the Heart and Stroke Foundation of Ontario, Toronto, Ontario; the Medical Research Council of Canada, Ottawa, Ontario; and the Finnish Food Research Foundation, Helsinki, Finland.

## REFERENCES

1. Frankel, E.N. (1984) Lipid Oxidation: Mechanism, Products, and Biological Significance, *J. Am. Oil Chem. Soc.* 61, 1908–1917.
2. Porter, N.A., Caldwell, S.E., and Mills, K.A. (1995) Mechanisms of Free Radical Oxidation of Unsaturated Lipids, *Lipids* 30, 277–290.
3. Frankel, E.N. (1985) Chemistry of Autoxidation: Mechanism, Products, and Flavor Significance, in *Flavor Chemistry of Fats and Oils* (Min, D. and Smouse, T.H., eds.), pp. 1–37, American Oil Chemists' Society, Champaign.
4. Lee, I., Fatemi, S.H., Hammond, E.G., and White, P.J. (1995) Quantitation of Flavour Volatiles in Oxidized Soybean Oil by Dynamic Headspace Analysis, *J. Am. Oil Chem. Soc.* 72, 539–546.
5. Kuksis, A. (1990) Core Aldehydes—Neglected Products of Lipid Peroxidation, *inform 1*, 1055–1058.
6. Esterbauer, H., Zollner, H., and Schauer, R.S. (1989) Aldehydes Formed by Lipid Peroxidation: Mechanism of Formation, Occurrence, and Determination, in *Membrane Lipid Oxidation* (Vigo-Pelfrey, C., ed.), Vol. 1, pp. 239–268, CRC Press, Boca Raton.
7. Brunner, B.A., Jones, A.D., and German, J.B. (1995) Direct Characterization of Protein Adducts of the Lipid Peroxidation Product 4-Hydroxynonenal Using Electroaspray Mass Spectrometry, *Chem. Res. Toxicol.* 8, 552–559.
8. Bolgar, M.S., Yang, C., and Gaskell, S.J. (1996) First Direct Evidence for Lipid/Protein Conjugation in Oxidized Human Low Density Lipoprotein, *J. Biol. Chem.* 271, 27999–28001.
9. Fogelman, A.M., Schechter, I., Saeger, J., Hokum, M., Child, J.S., and Edwards, P.A. (1980) Malonaldehyde Alteration of Low Density Lipoproteins Leads to Cholesteryl Ester Accumulation in Human Monocyte-Macrophages, *Proc. Natl. Acad. Sci. USA* 77, 2214–2218.
10. Kaneko, T., Kaji, K., and Matsuo, M. (1988) Cytotoxicities of a Linoleic Acid Hydroperoxide and Its Related Aliphatic Aldehydes Toward Cultured Human Umbilical Vein Endothelial Cells, *Chem.-Biol. Interact.* 67(3–4), 295–304.
11. Szveda, L.I., Uchida, K., Tsai, L., and Stadtman, E.R. (1993) Inactivation of Glucose-6-Phosphate Dehydrogenase by 4-Hydroxy 2-Nonenal. Selective Modification of an Active Site Lysine, *J. Biol. Chem.* 268, 3342–3347.



12. Grzelinska, E., Bartosz, G., Gwozdziński, K., and Leyko, W. (1979) A Spin-Label Study of the Effect of  $\gamma$ -Radiation on Erythrocyte Membrane. Influence of Lipid Peroxidation on Membrane Structure, *Int. J. Radiat. Biol.* **36**, 325–334.
13. Ravandi, A., Kuksis, A., Shaikh, N., and Jackowski, G. (1997) Preparation of Schiff Base Adducts of Phosphatidylcholine Core Aldehydes and Aminophospholipids, Amino Acids, and Myoglobin, *Lipids* **32**, 989–1001.
14. Kurvinen, J.-P., Kuksis, A., Ravandi, A., Sjövall, O., and Kallio, H. (1999) Rapid Complexing of Oxoacylglycerols with Amino Acids, Peptides, and Aminophospholipids, *Lipids* **34**, 299–305.
15. Kanazawa, K., and Ashida, H. (1998) Dietary Hydroperoxides of Linoleic Acid Decompose to Aldehydes in Stomach Before Being Absorbed into the Body, *Biochim. Biophys. Acta* **1393**, 349–361.
16. Kanazawa, K., and Ashida, H. (1998) Catabolic Fate of Dietary Trilinoleoylglycerol Hydroperoxides in Rat Gastrointestines, *Biochim. Biophys. Acta* **1393**, 336–348.
17. Naruszewicz, M., Wozny, E., Mirkiewicz, G., Nowicka, G., and Szostak, W.B. (1987) The Effect of Thermally Oxidized Soya Bean Oil on Metabolism of Chylomicrons: Increased Uptake and Degradation of Oxidized Chylomicrons in Cultured Mouse Macrophages, *Atherosclerosis* **66**, 45–53.
18. Staprāns, I., Rapp, J.H., Pan, X.-M., Kim, K.Y., and Feingold, K.R. (1994) Oxidized Lipids in the Diet Are a Source of Oxidized Lipid in Chylomicrons of Human Serum, *Arterioscler. Thromb.* **14**, 1900–1905.
19. Kamido, H., Kuksis, A., Marai, L., Myher, J.J., and Pang, H. (1992) Preparation, Chromatography, and Mass Spectrometry of Cholesteryl Ester and Glycerolipid-Bound Aldehydes, *Lipids* **27**, 645–650.
20. Kamido, H., Kuksis, A., Marai, L., and Myher, J.J. (1993) Identification of Core Aldehydes Among *in vitro* Peroxidation Products of Cholesteryl Esters, *Lipids* **28**, 331–336.
21. Kuksis, A., Myher, J.J., Marai, L., and Geher, K. (1993) Analyses of Hydroperoxides and Core Aldehydes of Triacylglycerols, in 17th Nordic Lipid Symposium, *Lipidforum* (Mälikki, Y., ed.), pp. 230–238, Bergen, Norway.
22. Sjövall, O., Kuksis, A., Marai, L., and Myher, J. (1997) Elution Factors of Synthetic Oxotriacylglycerols as an Aid in Identification of Peroxidized Natural Triacylglycerols by Reversed-Phase High-Performance Liquid Chromatography with Electrospray Mass Spectrometry, *Lipids* **32**, 1211–1218.
23. Duffin, K.L., Henion, J.D., and Shieh, J.J. (1991) Electrospray and Tandem Mass Spectrometric Characterization of Acylglycerol Mixtures That Dissolved in Nonpolar Solvents, *Anal. Chem.* **63**, 1781–1788.
24. Myher, J.J., and Kuksis, A. (1995) Electrospray-MS for Lipid Identification, *inform* **6**, 1068–1072.
25. Marai, L., Myher, J.J., and Kuksis, A. (1983) Analysis of Triacylglycerols by Reversed-Phase High Pressure Liquid Chromatography with Direct Liquid Inlet Mass Spectrometry, *Can. J. Biochem. Cell Biol.* **61**, 840–849.
26. Reske, J., Siebrecht, J., and Hazebroek, J. (1997) Triacylglycerol Composition and Structure in Genetically Modified Sunflower and Soybean Oils, *J. Am. Oil Chem. Soc.* **74**, 989–998.
27. Sjövall, O., Kuksis, A., and Kallio, H. (2001) Regioisomers of Octanoic Acid-Containing Structured Triacylglycerols Analyzed by Tandem Mass Spectrometry Using Ammonia Negative Chemical Ionization, *Lipids* **36**, 1377–1382.
28. Halliwell, B., and Gutteridge, J.M.C. (1989) *Free Radicals in Biology and Medicine*, pp. 210–214, Clarendon Press, Oxford.
29. Gardner, H.W. (1989) Oxygen Radical Chemistry of Polyunsaturated Fatty Acids, *Free Radic. Biol. Med.* **7**, 65–86.
30. Porter, N.A. (1992) Alkyl Hydroperoxides in *Organic Peroxides* (Ando, W., ed.), pp. 101–156, John Wiley & Sons, Chichester.
31. Miyashita, K., Hara, N., Fujimoto, K., and Kaneda, T. (1985) Dimers Formed in Oxygenated Methyl Linoleate Hydroperoxides, *Lipids* **20**, 578–587.
32. Brash, A.R. (2000) Autoxidation of Methyl Linoleate: Identification of the Bis-allylic 11-Hydroperoxide, *Lipids* **35**, 947–952.
33. Frankel, E.N. (1980) Lipid Oxidation, *Prog. Lipid Res.* **19**, 1–22.
34. Gardner, H.W. (1991) Recent Investigations into the Lipoygenase Pathway of Plants, *Biochim. Biophys. Acta* **1084**, 221–239.
35. Frankel, E.N., Neff, W.E., Rohwedder, W.K., Khambay, B.P.S., Garwood, R.F., and Weedon, B.C.L. (1977). Analysis of Autoxidized Fats by Gas Chromatography–Mass Spectrometry: I. Methyl Oleate, *Lipids* **12**, 901–907.
36. Gardner, H., Weisleder, D., and Kleiman, R. (1978) Formation of *trans*-12,13-Epoxy-9-Hydroperoxy-*trans*-10-Octadecenoic Acid from 13-L-Hydroperoxy-*cis*-8,*trans*-11-octadecadienoic Acid Catalyzed by Either a Soybean Extract or Cysteine-FeCl<sub>3</sub>, *Lipids* **13**, 246–252.
37. Noordermeer, M.A., Feussner, I., Kolbe, A., Veldink, G.A., and Vliegenthart, J.F.G. (2000) Oxygenation of (3Z)-Alkenals to 4-Hydroxy-(2E)-Alkenals in Plant Extracts: A Nonenzymatic Process, *Biochem. Biophys. Res. Commun.* **277**, 112–116.
38. Piazza, G., Foglia, T., and Nuñez, A. (2001) Epoxidation of Carbon-Carbon Double Bonds in Fatty Acids and Other Compounds with Membrane-Supported Peroxygenase, in 92nd AOCS Annual Meeting & Expo Abstracts, Minneapolis, Minnesota (Abstract S80).
39. Hughes, H., Smith, C.V., Horning, E.C., and Mitchell, J.R. (1983) High-Performance Liquid Chromatography and Gas Chromatography–Mass Spectrometry Determination of Specific Lipid Peroxidation Products *in vivo*, *Anal. Biochem.* **130**, 431–436.
40. Porter, N.A., Wolf, R.A., and Weenen, H. (1979) The Free Radical Oxidation of Polyunsaturated Lecithins, *Lipids* **15**, 164–167.
41. Park, D.K., Terao, J., and Matsushita, S. (1981) High-Performance Liquid Chromatography of Hydroperoxides Formed by Autoxidation of Vegetable Oils, *Agric. Biol. Chem.* **45**, 2443–2448.
42. Steenhorst-Slikkerveer, L., Louter, A., Janssen, H.-G., and Bauer-Plank, C. (2000) Analysis of Nonvolatile Lipid Oxidation Products in Vegetable Oils by Normal-Phase High-Performance Liquid Chromatography with Mass Spectrometric Detection, *J. Am. Oil Chem. Soc.* **77**, 837–845.
43. Kusaka, T., Ishihara, S., Sakaida, M., Mifune, A., Nakano, Y., Tsuda, K., Ikeda, M., and Nakano, H. (1996) Composition Analysis of Normal Plant Triacylglycerols and Hydroperoxidized *rac*-1-Stearoyl-2-oleoyl-3-linoleoyl-*sn*-glycerols by Liquid Chromatography–Atmospheric Pressure Chemical Ionization Mass Spectrometry, *J. Chromatogr. A* **730**, 1–7.
44. Lin, J.-T., Snyder, L.R., and McKeon, T.A. (1998) Prediction of Relative Retention Times of Triacylglycerols in Non-aqueous Reversed-Phase High-Performance Liquid Chromatography, *J. Chromatogr. A* **808**, 43–49.
45. Kuklev, D.V., Christie, W.W., Durand, T., Rossi, J.C., Vidal, J.P., Kasyanov, S.P., Akulin, V.N., and Bezuglov, V.V. (1997) Synthesis of Keto- and Hydroxydienoic Compounds from Linoleic Acid, *Chem. Phys. Lipids* **85**, 125–134.
46. Viinänen, E., and Hopia, A. (1994) Reversed-Phase High-Performance Liquid Chromatographic Analysis of Triacylglycerol Autoxidation Products with Ultraviolet and Evaporative Light-Scattering Detectors, *J. Am. Oil Chem. Soc.* **71**, 537–539.
47. Sjövall, O., Kuksis, A., and Kallio, H. (2001) Reversed-Phase High-Performance Liquid Chromatographic Separation of *tert*-Butyl Hydroperoxide Oxidation Products of Unsaturated Triacylglycerols, *J. Chromatogr. A* **905**, 119–132.
48. Courtneidge, J.L. (1992) Polyfunctional Peroxides from *tert*-



- Butyl Hydroperoxide-Loaded Autoxidations of Polyunsaturated Substrates and an Assessment of the Rate Constants for Allylic Peroxyl Radical Ring Closures, *J. Chem. Soc., Chem. Commun.* 1270–1272.
49. Yamauchi, R., Hara, Y., Murase, H. and Kato, K. (2000) Analysis of the Addition Products of  $\alpha$ -Tocopherol with Phosphatidylcholine-Peroxyl Radicals by High-Performance Liquid Chromatography with Chemiluminescent Detection, *Lipids* 35, 1405–1410.
50. Kamal-Eldin, A., Marquez-Ruiz, G., Dobarganes, C., Appelqvist, L.-A. (1997) Characterization of Aldehydic Acids in Used and Unused Frying Oils, *J. Chromatogr. A* 776, 245–254.
51. Kamido, H., Kuksis, A., Marai, L., and Myher, J.J. (1995) Lipid Ester-Bound Aldehydes Among Copper-Catalyzed Peroxidation Products of Human Plasma Lipoproteins, *J. Lipid Res.* 36, 1876–1886.

[Received December 11, 2000, and in final revised form and accepted September 5, 2001]

# Fast and Reproducible Method for the Direct Quantitation of Adipose Tissue in Newborn Infants

T.A.M. Harrington<sup>a,b,c</sup>, E.L. Thomas<sup>a</sup>, N. Modi<sup>b</sup>, G. Frost<sup>c</sup>,  
G.A. Coutts<sup>a</sup>, and J.D. Bell<sup>a,\*</sup>

<sup>a</sup>The Robert Steiner MRI Unit, MRC Clinical Sciences Centre, and Departments of <sup>b</sup>Paediatrics and Neonatal Medicine and <sup>c</sup>Nutrition and Dietetics, Imperial College School of Medicine, Hammersmith Hospital, London, United Kingdom

**ABSTRACT:** The role of body fat content and distribution in infants is becoming an area of increasing interest, especially as perception of its function appears to be rapidly evolving. Although a number of methods are available to estimate body fat content in adults, many are of limited use in infants, especially in the context of regional distribution and internal depots. In this study we developed and implemented a whole-body magnetic resonance imaging (MRI)-based protocol that allows fast and reproducible measurements of adipose tissue content in newborn infants, with an intra-observer variability of <2.4% and an inter-observer variability of <7%. The percentage total body fat for this cohort of infants ranged from 13.3–22.6% (mean and standard deviation: 16.6 ± 2.9%), which agrees closely with published data. Subcutaneous fat accounted for just over 89% of the total body fat, whereas internal fat corresponded to almost 11%, most of which was nonabdominal fat. There were no gender differences in total or regional body fat content. These results show that whole-body MRI can be readily applied to the study of adipose tissue content and distribution in newborn infants. Furthermore, its noninvasive nature makes it an ideal method for longitudinal and interventional studies in newborn infants.

Paper no. L8876 in *Lipids* 37, 95–100 (January 2002).

Recent advances in molecular biology are helping to redefine the role of adipose tissue (AT). This organ was originally perceived as a passive storage site for excess fat, but it is now considered a highly active, finely tuned metabolic tissue, exerting control on numerous biochemical and physiological processes in both health and disease.

Body fat content and distribution in adults influence the risk of coronary heart disease, hypertension, and type II diabetes (1). Barker *et al.* (2–4) hypothesized that infants who are small and thin at birth are at increased risk of developing cardiovascular disease and type II diabetes in adulthood. However, the relationship between body weight, fat content,

and distribution in neonates and their contribution to chronic disease in adults is unclear. This is partly due to a lack of safe and accurate methods to determine AT content and distribution in newborn infants and track changes through time.

Existing techniques for measuring body fat include underwater weighing, body water dilution, anthropometry, impedance, dual-energy x-ray absorptiometry (DXA), and total body electrical conductivity (5). Some of these techniques are clearly unsuitable for neonatal studies, for both technical and practical reasons. Several postmortem studies of fetal and infant body composition have greatly enhanced our understanding of fat deposition during *in utero* development and postnatal growth. However, the very nature of this work makes serial studies impossible (6–9). Recent developments in DXA have enabled the serial measurement of total body fat in adults and infants (10–13). An important limitation of DXA is the inability to differentiate between different fat compartments so as to quantify visceral AT, perhaps the most important AT depot in human physiology, independently of total fat mass (1,14).

Magnetic resonance imaging (MRI) scanning is a technique that is of minimal risk to the neonate and is noninvasive, capable of quantifying total and discrete AT depots, and therefore ideal for examining changes over time. MRI assessment of AT has been validated in animals (15,16), human cadavers (17), and human adults (18). MRI accurately measures AT *in vivo*, showing good agreement with the values produced by dissection and chemical analysis (15–17). Furthermore, whole-body MRI gives an unbiased measurement of the fat content, both internal and subcutaneous, for a large range of body shapes and sizes (19). To date there has been limited application of MRI to the study of AT content in neonates (20,21). Deans *et al.* (20) measured body fat content of human fetuses *in utero* at 40 wk gestation and showed significant differences in fat content between infants from healthy women and those with gestational diabetes. Olhager *et al.* (21) measured total body fat in infants aged between 19 and 107 d old and made a detailed study of the reproducibility of the image analysis. However, a drawback of both the previous MRI studies is that they did not differentiate between different AT compartments. The aim of the present study was to develop an MRI protocol that would allow for routine and noninvasive quantification of total and regional AT in newborn infants.

\*To whom correspondence should be addressed at Hammersmith Hospital, Du Cane Road, London, W12 0HS, United Kingdom.

E-mail: jimmy.bell@csc.mrc.ac.uk

Abbreviations: AT, adipose tissue; CoV, coefficient of variation; DXA, dual-energy x-ray absorptiometry; MRI, magnetic resonance imaging; S/N, signal-to-noise ratio.

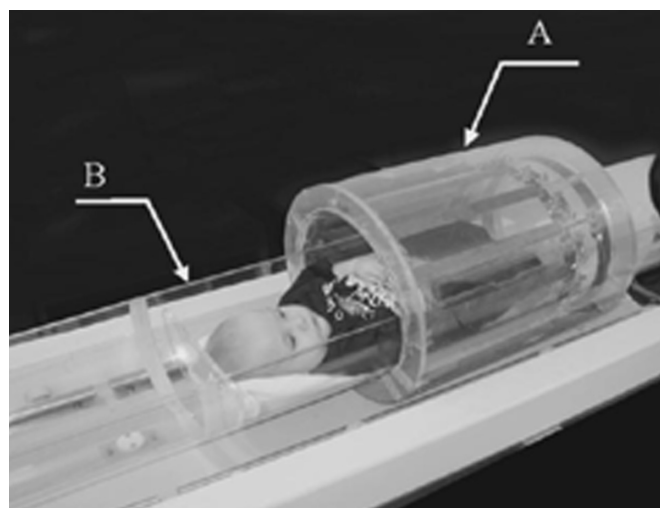
## SUBJECTS AND METHODS

**Subjects.** This study was approved by the Ethics Committee of the Imperial College School of Medicine and Hammer-smith Hospitals Trust, London. Parents of healthy newborn babies were approached for permission to recruit their babies. Informed parental consent was obtained.

Eight term Caucasian infants (4 males, 4 females) participated in the first phase of the study. Infants were scanned within 36 h of delivery. Anthropometric measurements were obtained at the same time.

**MRI. (i) Protocol.** All newborn infants underwent whole-body (head-to-toe) MRI using an Eclipse 1.5T Marconi Medical System scanner. The MRI sequence used in this study was adapted from a previously developed whole-body adult scanning protocol (19,22). Modification to the adult protocol took into account several factors pertinent to neonatal scanning, including signal-to-noise ratio (S/N), tissue contrast, and acoustic noise levels. A compromise between these factors and the need for good quality images led to the use of a  $T_1$ -weighted spin-echo sequence because it gives good tissue contrast, has relatively low acoustic noise, and is reasonably fast. Further reduction in scanning time was achieved by using 5-mm thick transverse images, with 5-mm gaps between slices. This method was shown to have little effect on the overall quantitation of body fat if the gaps between slices do not exceed one slice thickness (19).

S/N was maximized by using a small transmitter receiver birdcage coil (head coil, internal diameter 27 cm) instead of the conventional body coil (Fig. 1). Potential image distortions, which could compromise subsequent fat quantitation, were minimized by mapping the coil homogeneity. Phantom studies showed that the useful imaging length along the coil axis, before radiofrequency inhomogeneity results in signal



**FIG. 1.** Photograph showing the arrangement of the mobile platform (B) within the birdcage coil (A). The mobile platform allows the infant to be moved through the coil in a fast and accurate manner, without the need to remove the subject from the magnet. (See the Subjects and Methods section for more details.)

loss and imaging distortion, was limited to 20 cm. Given that the length of most infants was larger than the homogeneous area of the coil, a graduated (1 cm steps) mobile bed/platform was designed that allowed the infant to be repositioned within the coil with minimal disturbance. A photograph showing the bird-cage coil and mobile platform is shown in Figure 1.

**(ii) MRI scanning.** Infants were positioned supine during natural sleep on the platform and were swaddled to keep them as stationary as possible during the scan. We used a  $T_1$ -weighted spin-echo imaging sequence, repetition time (TR) = 600 ms, echo time (TE) = 16 ms, field of view = 24 cm, number of signals averaged = 2, and a  $256 \times 256$  matrix after phase conjugate symmetry giving a scanning time of 2.52 minutes per set of images. Twenty 5-mm thick transverse images with 5 mm gaps between slices gave 20 cm coverage. The platform was then moved 20 cms and imaging repeated. The overall scanning time was approximately 6 min. Infants were monitored using a pulse oximeter. Both a neonatal nurse and a pediatrician were present during the procedure.

**(iii) Data analysis.** Images were analyzed as previously described (19) using an image segmentation software program developed in-house that employs a threshold range and a contour-following algorithm with an interactive image editing facility. The threshold range, which isolates the AT, was computed automatically, calculated from the greyscale histogram within a contour that defined the outer boundary of subcutaneous AT and noise.

The volumes ( $\text{cm}^3$ ) of each AT compartment were determined by summing the relevant voxel counts and multiplying by the voxel dimensions in  $\text{cm}^3$ . Total body AT content was calculated by multiplying the AT volumes of each slice by the sum of the slice thickness (5 mm) and inter-slice distance (5 mm). Therefore, this analysis provides a direct measure of the volume of AT rather than the quantity of triglyceride contained within the AT. Each slice was reviewed using the interactive program that enables detection of unwanted pixels (such as milk in the stomach and bowels), which, because they contain fat, have intensity levels similar to AT. The AT depots were separated to measure pixel count in total AT, subcutaneous AT, and total internal AT. Total internal AT was subdivided into visceral and nonvisceral adipose tissue. Visceral AT content was obtained by quantifying AT in the slices from the sacrum to the slice containing the top of the liver or base of the lungs (19). Subcutaneous AT in this region of the body was termed abdominal subcutaneous AT. All other internal adipose tissue was considered nonvisceral AT.

The MRI data in liters is converted to percentage AT using the following equations:

$$\text{AT in kg} = \text{AT in liters} \times 0.9 \quad [1]$$

$$\text{Percentage AT} = (\text{AT in kg/body weight in kg}) \times 100 \quad [2]$$

The factor 0.9 in Equation 1 is the widely accepted value for the density of AT in  $\text{kg/L}$  and is required to convert the volume of adipose tissue in liters to the mass of AT in kg.

Total AT fat was calculated assuming 1 cm<sup>3</sup> of AT contains 0.66 g of fat (23; measured in infants):

$$\text{fat mass in kg} = \text{AT in liters} \times 0.66 \quad [3]$$

$$\text{total AT fat} = (\text{fat mass in kg/body weight in kg}) \times 100 \quad [4]$$

(iv) *Reproducibility measurements.* MRI studies have shown that the largest variability in the technique appears to be introduced during the data analysis stage (24). To assess the coefficient of variation (CoV) of the technique (intra-observer and inter-observer variability), whole-body images from a newborn, a 6-wk-old, and a 6-mon-old infant were analyzed by three independent observers.

*Anthropometry.* Infants' weights, lengths, and head circumferences were recorded by a single trained observer (TH). Scales used were accurate to 0.2 g (Marsden Professional Baby Scale), length was measured by using a Rollametre (Raven Equipment Ltd.), and head circumference using a measuring tape from the Child Growth Foundation.

*Statistical analysis.* All data are expressed as mean  $\pm$  standard deviation (SD). Data were tested for normality using the Shapiro–Wilk normality test. Differences between male and female infants were tested using the Student's unpaired *t*-test. Statistical analyses were performed using Unistat version 4.53. The level of significance was set at  $P < 0.05$ .

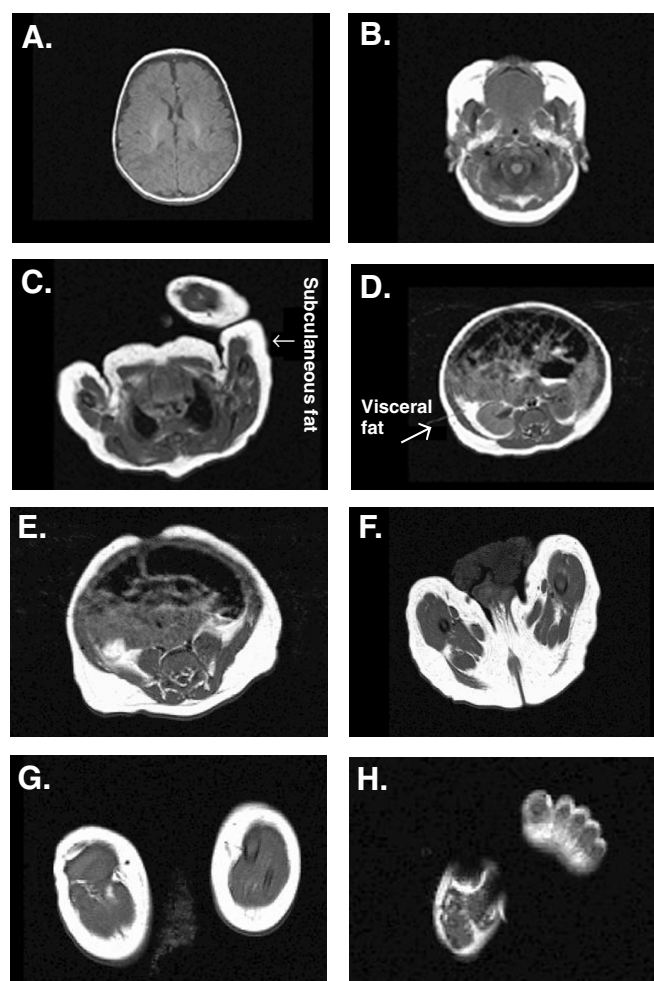
## RESULTS

Data were obtained from eight term Caucasian infants (4 males, 4 females) with a mean gestational age of  $39.1 \pm 1.6$  wk (range 36–41 wk) and a mean birth weight of  $3.5 \pm 0.5$  kg (range 2.6–4.3 kg).

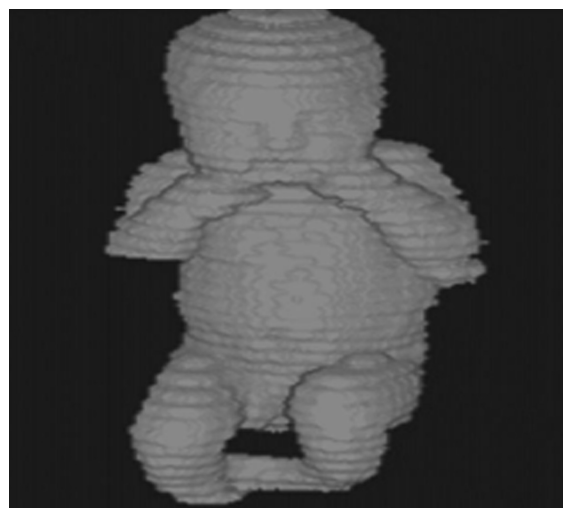
The protocol for whole-body AT imaging of newborn infants developed and implemented in this study resulted in an average of 40–50 images per infant. The overall scanning time was approximately 6 min. A selection of typical images from one of these infants is shown in Figure 2. The T<sub>1</sub>-weighted imaging protocol resulted in images with high contrast between AT and other tissues, with the former appearing as high signal intensity. A three-dimensional reconstruction of the total data set is shown in Figure 3.

The reproducibility of the MRI analysis method was assessed by measuring AT content in infants with different quantities of AT. The intra-observer CoV for subcutaneous AT appears to be directly related to the relative AT content of the infant (ranging from 1–7%), with thinner babies showing the largest CoV. For internal body AT the CoV appeared to be independent of body size (*ca.* 7%). The inter-observer CoV in this study was 2.4% for subcutaneous AT and 17.6% for internal AT. To minimize inter-observer variability, all images in this study were analyzed by the same observer (ELT).

The data obtained from the MRI may be expressed as absolute values in liters, percentage AT mass, or total AT fat (i.e., correcting for the lipid content of AT). All of these values are shown in Table 1. The data in the remainder of the



**FIG. 2.** Typical magnetic resonance images obtained from a full-term newborn male infant (6 h after birth). A total of 40–50 images was normally acquired for each infant; some representative slices are shown here: (A) the brain at the low ventricular level, (B) upper cervical spine, (C) apices of lung, (D) abdomen at level of kidneys, (E) lower abdomen, (F) upper femur, (G) calf, and (H) feet. The magnetic resonance imaging protocol used in this study leads to adipose tissue appearing as high intensity compared to other tissues.



**FIG. 3.** Three-dimensional reconstruction of a whole magnetic resonance imaging data set from a newborn infant.



**TABLE 1**  
**Adipose Tissue and Fat Content in Newborn Infants by Magnetic Resonance Imaging<sup>a</sup>**

	Total	Subcutaneous	Internal	Subcutaneous abdominal	Visceral	Nonvisceral internal
Adipose tissue (liters)	0.9 ± 0.3 (0.5–1.5)	0.8 ± 0.3 (0.5–1.3)	0.09 ± 0.2 (0.06 ± 0.14)	0.11 ± 0.06 (0.06 ± 0.25)	0.03 ± 0.01 (0.01–0.04)	0.06 ± 0.02 (0.05–0.01)
Adipose tissue (%)	22.7 ± 4.0 (18.5–30.8)	20.3 ± 3.9 (15.9–27.8)	2.4 ± 0.6 (1.5–3.0)	3.2 ± 1.2 (1.8–5.8)	0.9 ± 0.3 (0.3–1.3)	1.5 ± 0.4 (1.1–2.1)
Total adipose tissue fat (%)	16.6 ± 2.9 (13.5–22.6)	14.9 ± 2.9 (11.7–20.4)	1.8 ± 0.4 (1.1–2.2)	2.3 ± 0.9 (1.3–4.2)	0.7 ± 0.2 (0.2–1.0)	1.1 ± 0.3 (0.8–1.6)

<sup>a</sup>Results presented as mean ± standard deviation and range.

results and discussion are expressed as total AT fat to allow ready comparison with literature values.

Total AT fat as a percentage of body weight for all eight infants studied by MRI ranged from 13.5–22.6%, with a mean value of 16.6 ± 2.9%. The percentage subcutaneous fat was 14.9 ± 2.9% (range 11.7–20.4%) and internal 1.8 ± 0.4% (range 1.1–2.2%). The ratio of internal to subcutaneous AT fat was 0.12 ± 0.03 (range 0.07–0.16). Investigating the abdomen in more detail, we found there was 2.3 ± 1.0% (range 1.3–4.2%) abdominal subcutaneous AT fat as a percentage of body weight and 0.7 ± 0.2% (range 0.2–1.0%) visceral AT fat. Most of the internal fat in infants appears to be nonabdominal and generally is found in the pelvis and limbs, as the visceral AT fat measured in this study was approximately 33% of the total internal AT fat measured. There were no significant gender differences in total body or regional AT fat content.

## DISCUSSION

The increasing interest in the potential role of AT on physiological and biochemical processes in health and disease has led to the need for accurate methodologies to assess AT content and distribution in neonates and infants. In this study we have shown that MRI allows direct and reproducible quantitation of both subcutaneous and visceral AT depots in newborn infants.

The MRI protocol developed and implemented in this study shows high reproducibility, is relatively fast, with significantly reduced acoustic noise. The images obtained with this sequence gave good contrast between AT and other tissues including muscle and internal organs. It did not, however, allow differentiation between white and brown AT depots, and all AT appeared with the same relative intensity in the MRI. The lack of contrast between brown and AT in the MR images is not surprising given that this has only been achieved in rodents using very specialized sequences and at very high field strengths (25).

At present there is no established “gold standard” technique for measuring body composition in infants with which to make a direct comparison of the MRI results obtained in the present study. Most available methods for determining AT and fat content are indirect. They utilize the measurement of different body compartments with subsequent extrapolation

in order to derive a value for AT and fat mass. MRI protocols, similar to that described in the present study, have previously been validated in both adults and animals by chemical analysis of cadaver and animal carcasses, suggesting that this non-invasive method gives an accurate measurement of body AT fat content (15–17). Moreover, these studies have demonstrated that MRI can be used to determine different AT depots, something that cannot be readily achieved with other noninvasive methods (15–17).

The relative levels of total body AT fat in newborn infants obtained in the present study (*ca.* 16.6%) compare well with those previously reported using other techniques. Widdowson (6) and Hager *et al.* (26) both reported a percentage body fat of 16% in infants using chemical analysis and whole body potassium counting, respectively. Similarly White *et al.* (7) reported an AT content of 14% by chemical dissection. Fomon *et al.* (27,28) in different studies have reported a reference infant body composition of between 11% (chemical analysis) and 14% [using a combination of anthropometry and data by Southgate and Hey (9)]. Forsum *et al.* (29), using anthropometric and skinfold measurements, showed the percentage body fat in 22 ten-day-old female infants to be 15.9% (29). Similarly, Dauncey *et al.* (30) reported a body fat content of 12% in newborn infants using anthropometry. Ziegler *et al.* (8) published body composition for the reference fetus in which the lipid content for an infant between 37–40 wk gestation was approximately 10%. This is somewhat lower than the results of both the current study and other studies using chemical analysis, but as the authors point out, the fetuses included in the study were of a relatively small size. The MRI results obtained in the present study were also similar to those reported using DXA for a similar cohort of newborn infants (15.3%, Picaud *et al.*, 10; 15.7%, Rigo *et al.*, 11; 12.8%, Butte *et al.*, 13).

In contrast to total AT fat, regional distribution of subcutaneous and internal AT fat measurements in the current study cannot be readily compared with other published data. Previous MRI studies by Deans *et al.* (20) of fetal fat content at 40 wk gestation *in utero* have found similar body fat content to that in the present study (17.2%, *cf.* 16.6%) (20). However, the authors did not appear to differentiate between internal and subcutaneous AT. Similarly, Olhager *et al.* (21) have obtained comparable measures of fat content in infants (21). Olhager *et al.* produced a percentage body fat ranging from 17.4 to 22.4%. However, their

cohort of infants covered a broad age range, 19–107 d, compared to the present study where all infants scanned were less than 36 h old. Furthermore, the authors do not provide figures for regional fat depots although they do state that 90% of the total AT volume was subcutaneous. This value is similar to that observed in the present study (89%), and as we have shown in this study, most of the internal AT is principally nonabdominal AT.

No significant gender differences in total or regional AT fat content were observed in this study. Although female infants tended to have slightly less visceral fat compared with male infants, this did not reach the level of significance. Gender differences have previously been reported, mainly in studies with a large cohort of infants (11–13,30,31). This suggests that the gender differences are relatively small. Indeed Rigo *et al.* (11) reported that on average female infants have 50 g more fat than male infants at birth, which corresponds to a difference of approximately 1.5% between male and female infants. This is well within the CoV of most techniques, including MRI, and therefore unlikely to be detected in a small cohort of infants.

Interestingly, Kabir and Forsum (23) found a gender difference in nonsubcutaneous fat, assessed by a combination of body water dilution, skinfold thickness, and ultrasonography. This should correspond to our measure of internal fat in the current study, which was not significantly different between the male and female infants studied. This may be related to the methodology used by Kabir and Forsum for their measurement of nonsubcutaneous AT. It is possible that we did not observe a difference in total AT fat content by MRI due to the small size of this study.

Another important consideration when comparing the fat measurements obtained in the present study with previously published data is the makeup of the cohort of babies. Factors such as gestational age at birth, whether the infant was an appropriate size for its gestational age, the postnatal age at which the measurement was obtained, gender, and ethnicity are all factors that are known to influence body fat content and distribution. For instance, in the present study all measurements of body composition were made within 36 h of birth, whereas many papers in the literature do not give exact ages for the infants studied but say less than 1 mon. However, we know that there is a rapid accretion of body fat within the first few weeks of postnatal life (6).

In conclusion, our preliminary studies have demonstrated MRI to be a reliable, safe method for assessing total body AT, with the advantage of visualization of different AT depots. This opens up the possibility of assessing the effects of the intrauterine environment, dietary regimes, hormonal treatments, and genetic factors on the developing infant in a fast and reproducible way.

## ACKNOWLEDGMENTS

Financial support from the Medical Research Council, Marconi Medical Systems, and Serono UK are gratefully acknowledged. The authors would also like to thank Professor Graeme Bydder, Dr. Mary Rutherford, and Dr. Gavin Hamilton for their help with this project and the babies and their parents for participating in this study.

## REFERENCES

1. Bouchard, C., Bray, G.A., and Hubbard, V.S. (1990) Basic and Clinical Aspects of Regional Fat Distribution, *Am. Clin. Nutr.* 52, 946–950.
2. Barker, D.J.P., Winter, P.D., Osmond, C., Margetts, B., and Simmonds, S.J. (1989) Weight in Infancy and Death from Ischaemic Heart Disease, *Lancet* *ii*, 577–580.
3. Barker, D.J.P. (1990) The Fetal and Infant Origins of Adult Disease [editorial], *Br. Med. J.* 301, 111.
4. Barker, D.J.P., Hales, C.N., Fall, C., Osmond, C., Phipps, K., and Clark, P.M. (1993) Type 2 (non-insulin dependent) Diabetes Mellitus, Hypertension and Hyperlipidaemia (Syndrome X): Relation to Reduced Foetal Growth, *Diabetologia* 36, 62–67.
5. Brodie, D.A., and Stewart, A.D. (1999) Body Composition Measurement: A Hierarchy of Methods, *J. Pediatr. Endocrinol. Metab.* 12, 801–816.
6. Widdowson, E.M. (1981) Changes in Body Composition During Growth, in *Scientific Foundations of Paediatrics*, 2nd edn., (Davis, J.A., and Dobbing, J., eds.) Vol. 17, pp. 330–342, Heinemann Medical, London.
7. White, D.R., Widdowson, E.M., Woodard, H.Q., and Dickerson, J.W. (1991) The Composition of Body Tissues (II). Fetus to Young Adult, *Br. J. Radiol.* 64, 149–159.
8. Ziegler, E.E., O'Donnell, A.M., Nelson, S.E., and Fomon, S.J. (1976) Body Composition of the Reference Fetus, *Growth* 40, 329–341.
9. Southgate, D.A.T., and Hey, E.N. (1976) Chemical and Biochemical Development of the Human Fetus, in *The Biology of Human Fetal Growth*, (Roberts, D.F., and Thompson, A.M., eds.) Vol. 15, pp. 195–209, Taylor and Francis, London.
10. Picaud, J.C., Rigo, J., Nyamugabo, K., Milet, J., and Senterre, J. (1996) Evaluation of Dual-Energy X-Ray Absorptiometry for Body-Composition Assessment in Piglets and Term Human Neonates, *Am. J. Clin. Nutr.* 63, 157–163.
11. Rigo, J., Nyamugabo, K., Picaud, J.C., Gerard, P., Pieltain, C., and De Curtis, M. (1998) Reference Values of Body Composition Obtained by Dual Energy X-Ray Absorptiometry in Preterm and Term Neonates, *J. Pediatr. Gastroenterol. Nutr.* 27, 184–190.
12. Koo, W.W., Walters, J.C., and Hockman, E.M. (2000) Body Composition in Human Infants at Birth and Postnatally, *J. Nutr.* 130, 2188–2194.
13. Butte, N.F., Hopkinson, J.M., Wong, W.W., Smith, E.O., and Ellis, K.J. (2000) Body Composition During the First 2 Years of Life: An Updated Reference, *Pediatr. Res.* 47, 578–585.
14. Montague, C.T., and O'Rahilly, S. (2000) The Perils of Portliness: Causes and Consequences of Visceral Adiposity, *Diabetes* 49, 883–888.
15. Fowler, P.A., Fuller, M.F., Glasbey, C.A., Cameron, G.G., and Foster, M.A. (1992) Validation of the *in vivo* Measurement of Adipose Tissue by Magnetic Resonance Imaging of Lean and Obese Pigs, *Am. J. Clin. Nutr.* 56, 7–13.
16. Ross, R., Léger, L., Guardo, R., De Guise, J., and Pike, B.G. (1991) Adipose Tissue Volume Measured by Magnetic Resonance Imaging and Computerized Tomography in Rats, *J. Appl. Physiol.* 70, 2164–2172.
17. Abate, N., Burns, D., Peshock, R.M., Garg, A., and Grundy, S.M. (1994) Estimation of Adipose Tissue Mass by Magnetic Resonance Imaging: Validation Against Dissection in Human Cadavers, *J. Lipid Res.* 35, 1490–1496.
18. Fowler, P.A., Fuller, M.F., Glasbey, C.A., Foster, M.A., Cameron, G.G., McNeill, G., and Maughan, R.J. (1991) Total and Subcutaneous Adipose Tissue in Women: The Measurement of Distribution and Accurate Prediction of Quantity by Using Magnetic Resonance Imaging, *Am. J. Clin. Nutr.* 54, 18–25.
19. Thomas, E.L., Saeed, N., Hajnal, J.V., Brynes, A.E., Goldstone, A.P., Frost, G., and Bell, J.D. (1998) Magnetic Resonance Imaging of Total Body Fat, *J. Appl. Physiol.* 85, 1778–1785.

20. Deans, H.E., Smith, F.W., Lloyd, D.J., Law, A.N., and Sutherland, H.W. (1989) Fetal Fat Measurement by Magnetic Resonance Imaging, *Br. J. Radiol.* 62, 603–607.
21. Olhager, E., Thuomas, K.A., Wigstrom, L., and Forsum, E. (1998) Description and Evaluation of a Method Based on Magnetic Resonance Imaging to Estimate Adipose Tissue Volume and Total Body Fat in Infants, *Pediatr. Res.* 44, 572–577.
22. Barnard, M.L., Schwieso, J.E., Thomas, E.L., Bell, J.D., Saeed, N., Frost, G., Bloom, S.R., and Hajnal, J.V. (1996) Development of a Rapid and Efficient Magnetic Resonance Imaging Technique for Analysis of Body Fat Distribution, *NMR Biomed.* 9, 156–164.
23. Kabir, N., and Forsum, E. (1993) Estimation of Total Body Fat and Subcutaneous Adipose Tissue in Full-Term Infants Less Than 3 Months Old, *Pediatr. Res.* 34, 448–454.
24. Gronemeyer, S.A., Steen, R.G., Kauffman, W.M., Reddick, W.E., and Glass, J.O. (2000) Fast Adipose Tissue (FAT) Assessment by MRI, *Magn. Reson. Imaging* 18, 815–818.
25. Sbarbati, A., Guerrini, U., Marzola, P., Asperio, R., and Osculati, F. (1997) Chemical Shift Imaging at 4.7T of Brown Adipose Tissue, *J. Lipid Res.* 38, 343–347.
26. Hager, A., Sjostrom, L., Arvidsson, B., Bjorntorp, P., and Smith, U. (1977) Body Fat and Adipose Tissue Cellularity in Infants: A Longitudinal Study, *Metabolism* 26, 607–614.
27. Fomon, S.J. (1967) Body Composition of the Male Reference Infant During the First Year of Life, *Pediatrics* 40, 863–870.
28. Fomon, S.J., Haschke, F., Ziegler, E.E., and Nelson, S.E. (1982) Body Composition of Reference Children from Birth to Age 10 Years, *Am. J. Clin. Nutr.* 35, 1169–1175.
29. Forsum, E., and Sadurskis, A. (1986) Growth, Body Composition and Breast Milk Intake of Swedish Infants During Early Life, *Early Hum. Dev.* 14, 121–129.
30. Dauncey, M.J., Gandy, G., and Gairdner, D. (1977) Assessment of Total Body Fat in Infancy from Skinfold Thickness Measurements, *Arch. Dis. Child.* 52, 223–227.
31. Oakley, J.R., Parsons, R.J., and Whitelaw, A.G. (1977) Standards for Skinfold Thickness in British Newborn Infants, *Arch. Dis. Child.* 52, 287–290.

[Received July 23, 2001, and in revised form November 13, 2001; revision accepted November 15, 2001]

# Potential Bile Acid Metabolites. 24. An Efficient Synthesis of Carboxyl-Linked Glucosides and Their Chemical Properties

Takashi Iida<sup>a,\*</sup>, Ryusei Nakamori<sup>a</sup>, Rie Yabuta<sup>a</sup>, Satoru Yada<sup>a</sup>, Yuzuru Takagi<sup>a</sup>,  
Nariyasu Mano<sup>b</sup>, Shigeo Ikegawa<sup>b</sup>, Junichi Goto<sup>b</sup>, and Toshio Nambara<sup>c</sup>

<sup>a</sup>Department of Chemistry, College of Humanities & Sciences, Nihon University, Sakurajousui, Setagaya, Tokyo 156-8550, Japan; <sup>b</sup>Graduate School of Pharmaceutical Sciences, Tohoku University, Aobayama, Sendai 981-8578, Japan; and <sup>c</sup>Hoshi University, Shinagawa, Ebara, Tokyo 147-8501, Japan

**ABSTRACT:** A facile and efficient synthesis of the carboxyl-linked glucosides of bile acids is described. Direct esterification of unprotected bile acids with 2,3,4,6-tetra-*O*-benzyl- $\beta$ -D-glucopyranose in pyridine in the presence of 2-chloro-1,3,5-trinitrobenzene as a coupling agent afforded a mixture of the  $\alpha$ - and  $\beta$ -anomers (*ca.* 1:3) of the 1-*O*-acyl- $\beta$ -D-glucoside benzyl ethers of bile acids, which was separated effectively on a  $C_{18}$  reversed-phase chromatography column (isolated yields of  $\alpha$ - and  $\beta$ -anomers are 4–9% and 12–19%, respectively). Subsequent hydrogenolysis of the  $\alpha$ - and  $\beta$ -acyl glucoside benzyl ethers on a 10% Pd-C catalyst in acetic acid/methanol/EtOAc (1:2:2, by vol) at 35°C under atmospheric pressure gave the corresponding free esters in good yields (79–89%). Chemical specificities such as facile hydrolysis and transesterification of the acyl glucosides in various solvents were also discussed.

Paper no. L8894 in *Lipids* 37, 101–110 (January 2002).

A variety of the glycosidic conjugates of bile acids, which include  $\beta$ -D-glucuronides (1–4),  $\beta$ -D-glucosides (5–8), and  $\beta$ -D-*N*-acetylglucosaminides (9–11), have been identified in biological materials. Such glycosidation reactions are considered to be mechanisms for detoxification and elimination of such toxic and hydrophobic bile acids of lithocholic acid in patients with cholestasis. Since variations in the concentration and relative proportion of glycosidic conjugated bile acids are closely related to liver diseases, the identification, quantification, metabolism, physiological significance, and excretory route of the glycosidic conjugates are of special importance from a clinical point of view.

In conventional bile acid glycosides, a hydroxyl group in the 5 $\beta$ -steroid nucleus is attached by an ether linkage to an anomeric 1'- $\beta$ -hydroxyl group in the sugar moieties to form so-called hydroxyl-linked or ether glycosides. Meanwhile, Radomska-Pyrek *et al.* (12–15) have recently reported the simultaneous formation of a new type of glucuronide conju-

gate of short-chain ( $C_{20}$ – $C_{23}$ ) bile acid analogs,  $C_{24}$  lithocholic acid (LCA) (16), and hyodeoxycholic acid (HDCA) (17) in significant amounts by rat liver microsomal glucuronosyltransferase, together with the expected hydroxyl-linked metabolites. The novel glucuronide-conjugated bile acids, termed acyl, ester, or carboxyl-linked glucuronides, have an ester linkage between the terminal carboxyl group at C-24 in the side chain of bile acids and the 1'- $\beta$ -hydroxyl group in  $\beta$ -D-glucuronic acid. In more recent works, the occurrence of the carboxyl-linked 24-glucuronides of five common bile acids, i.e., LCA, chenodeoxycholic acid (CDCA), ursodeoxycholic acid (UDCA), deoxycholic acid (DCA), and cholic acid (CA), in incubation mixtures of rat liver microsomes and in human urine has been confirmed by Goto *et al.* (18,19). They have also revealed that LCA 24-glucuronide is easily bonded covalently with protein during incubation to give LCA-protein adduct, suggesting the presence of tissue-bound bile acids in the liver (20).

Although the carboxyl-linked 24-glycosides of bile acids in biological materials so far isolated or identified have been exclusively glucuronide conjugates, analogous glucosides and *N*-acetylglucosaminides may be also possible candidates as potential metabolites, because of the widespread occurrence of various hydroxyl-linked analogs in human biological materials. As part of our ongoing program of synthesizing new and scarce potential bile acid metabolites for use as reference standards, we have previously reported the preparation of a series of the ether glucosides of bile acids (21). In this paper, we extended our program to synthesize the  $\alpha$ - and  $\beta$ -anomers of acyl glucosides (15–28; Fig. 1) of five prominent bile acids (LCA, CDCA, UDCA, DCA, and CA) and 6-hydroxylated bile acids (HDCA and its 6 $\beta$ -epimer, murideoxycholic acid, MDCA).

## EXPERIMENTAL PROCEDURES

**Materials and methods.** LCA, DCA, and CA were purchased from Wako Pure Industries, Ltd. (Osaka, Japan). CDCA and UDCA were kindly donated by Tokyo Tanabe Co. (Tokyo, Japan). HDCA and 2-chloro-1,3,5-trinitrobenzene (CTNB) were available from Tokyo Kasei Kogyo Co., Ltd. (Tokyo, Japan). MDCA was prepared from HDCA (22). 2,3,4,6-Tetra-*O*-benzyl- $\beta$ -D-glucopyranose (TBGP) was purchased from

\*To whom correspondence should be addressed.  
E-mail: takaiida@chs.nihon-u.ac.jp

Abbreviations: CA, cholic acid; CDCA, chenodeoxycholic acid; CTNB, 2-chloro-1,3,5-trinitrobenzene; DCA, deoxycholic acid; ESI, electrospray ionization; FT, Fourier transform; HDCA, hyodeoxycholic acid; HR-MS, high-resolution mass spectra; IR, infrared; LCA, lithocholic acid; MDCA, murideoxycholic acid; NIM, negative ion mode; NMR, nuclear magnetic resonance; mp, melting points; PIM, positive ion mode; TBGP, 2,3,4,6-tetra-*O*-benzyl- $\beta$ -D-glucopyranose; UDCA, ursodeoxycholic acid.



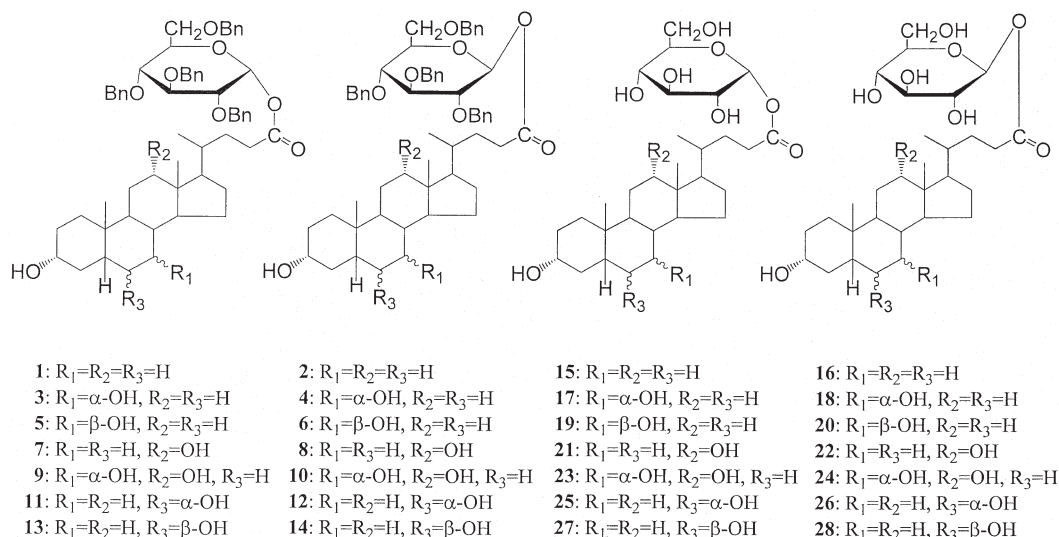


FIG. 1. Structures of bile acid C-24 acyl glucosides and their related compounds. Bn =  $-\text{CH}_2\text{C}_6\text{H}_5$ .

Sigma Chemical Co., (St. Louis, MO). All other reagents and solvents were of analytical reagent grade and used without further purification.

Normal-phase thin-layer chromatography (TLC) of the free 1-*O*-acyl-β-D-glucosides of bile acids (**15–28**) was performed on a precoated silica gel plate (E. Merck, Darmstadt, Germany) using chloroform/methanol/acetic acid (24:6:3, by vol; solvent system A) or EtOAc/acetic acid (9:1, vol/vol; solvent system B) mixtures as the developing solvents. Reversed-phase TLC was carried out on precoated C<sub>18</sub> silica gel plates (E. Merck) using a developing mixture of methanol/water (19:1, vol/vol; solvent system C). Liquid chromatography was performed using silica gel 60 (70–230 mesh; Wako Pure Chemical Industries, Tokyo, Japan) or Cosmosil 140C<sub>18</sub>-OPN (particle size, 140 μm; Nacalai Tesque, Inc., Kyoto, Japan) as an adsorbent.

Melting points (mp) were determined on an electric hot stage and are uncorrected. Infrared (IR) spectra were obtained on a Bio-Rad FTS-7 Fourier transform IR (FTIR) spectrometer (Philadelphia, PA) using KBr tablets. <sup>1</sup>H nuclear magnetic resonance (NMR) spectra were obtained on a JEOL JNM-EX 270 FT NMR instrument (Tokyo, Japan) at 270 MHz, with CDCl<sub>3</sub>, CDCl<sub>3</sub> containing 20% dimethylsulfoxide (DMSO)-*d*<sub>6</sub> or CD<sub>3</sub>OD containing 0.1% Me<sub>4</sub>Si as the solvent; chemical shifts are expressed as δ ppm relative to Me<sub>4</sub>Si. High-resolution mass spectra (HR-MS) were obtained on a JEOL JMS-LCmate double focusing magnetic mass spectrometer equipped with an electrospray ionization (ESI) probe under the positive ion mode (PIM) [M + Na]<sup>+</sup> for benzyl ester derivatives (**1–14**) or negative ion mode (NIM) [M – H]<sup>–</sup> for free esters (**15–28**). For reference compounds, polypropylene glycol (50 ppm) in methanol for **1** and **2**, or polyethyleneglycol (50 ppm) in methanol for **3–14** was used in PIM; and sodium trifluoroacetate (200 ppm) and sodium acetate (40 ppm) in methanol for **15** and **16**, or polyethyleneglycol sulfate (50 ppm) in methanol for **17–28** was used in NIM. The apparatus

used for medium-pressure liquid chromatography consisted of a YRD-880 RI-detector (Shimamura Instruments Works, Co., Tokyo, Japan) and a chromatographic pump uf-3040S.

*General procedure for the esterification of bile acids by CTNB.* To a stirred solution of bile acid (5 mmol) and TBGP (6 mmol) in dry pyridine (12 mL) was added CTNB (5 mmol) in one portion, and the mixture was stirred at room temperature for 3 h under a stream of N<sub>2</sub> (the reaction was monitored by TLC). To the mixture was added 8% sodium hydrogencarbonate solution (70 mL), Et<sub>2</sub>O (70 mL) and then water (35 mL), and the whole mixture was stirred until a clear solution was obtained. The organic layer was washed with 5% HCl and water, dried over Drierite, and evaporated under reduced pressure. Crystallization of the residue from benzene recovered excess amounts of the starting sugar derivative. Evaporation of the combined mother liquor gave an oily residue, which was treated on a column of silica gel (70 g, 70–250 mesh) by eluting with benzene or benzene/EtOAc (7:3 to 4:1, vol/vol) mixtures containing 1% acetic acid to give the crude esterified product. Separation of the α- and β-anomeric mixtures from the resulting product was then achieved by medium-pressure liquid chromatography on a C<sub>18</sub> reversed-phase column (100 g), eluting with methanol/water mixtures (19:1 to 9:1, vol/vol) containing 1% acetic acid as a mobile phase.

(i) *Benzyl 1-O-(24-lithocholyl)-2,3,4-tri-O-benzyl-D-glucopyranose (1 and 2).* The more polar component, which eluted first, was identified as the α-anomer (**1**): this compound was found to be homogeneous according to TLC and <sup>1</sup>H NMR analyses, but failed to crystallize: The yield of this oil was 8%. The less polar component was identified as the β-anomer (**2**). Although this compound was homogeneous according to TLC and <sup>1</sup>H NMR analyses, it could not be crystallized: The yield of this oil was 19%. Spectral and HR-MS data are shown in Table 1.

(ii) *Benzyl 1-O-(24-chenodeoxycholyl)-2,3,4-tri-O-benzyl-D-glucopyranose (3 and 4).* The more polar component,

which eluted first, was identified as the  $\alpha$ -anomer (**3**): The yield of this oil was 4%. The less polar component was identified as the  $\beta$ -anomer (**4**): The yield of the oil was 12%.

(iii) *Benzyl 1-O-(24-ursodeoxycholy)-2,3,4-tri-O-benzyl-D-glucopyranose (5 and 6)*. The more polar component, which eluted first, was identified as the  $\alpha$ -anomer (**5**): The yield of this oil was 9%. The less polar component was identified as the  $\beta$ -anomer (**6**): The yield of this oil was 14%.

(iv) *Benzyl 1-O-(24-deoxycholy)-2,3,4-tri-O-benzyl-D-glucopyranose (7 and 8)*. The more polar component was identified as the  $\alpha$ -anomer (**7**): The yield of this oil was 8%. The less polar component was identified as the  $\beta$ -anomer (**8**): The yield of this oil was 16%.

(v) *Benzyl 1-O-(24-choly)-2,3,4-tri-O-benzyl-D-glucopyranose (9 and 10)*. The more polar component was identified as the  $\alpha$ -anomer (**9**): The yield of this oil was 8%. The less polar component was identified as the  $\beta$ -anomer (**10**): The yield of this oil was 16%.

(vi) *Benzyl 1-O-(24-hyodeoxycholy)-2,3,4-tri-O-benzyl-D-glucopyranose (11 and 12)*. The more polar component was identified as the  $\alpha$ -anomer (**11**): The yield of this oil was 4%. The less polar component was identified as the  $\beta$ -anomer (**12**): The yield of this oil was 16%.

(vii) *Benzyl 1-O-(24-murideoxycholy)-2,3,4-tri-O-benzyl-D-glucopyranose (13 and 14)*. The more polar component was identified as the  $\alpha$ -anomer (**13**): The yield of this oil was 4%. The less polar component was identified as the  $\beta$ -anomer (**14**): The yield of this oil was 15%.

*General procedure for the deprotection of bile acid acyl glucoside benzyl ethers.* To a magnetically stirred solution of prereduced 10% Pd-C catalyst (120 mg) with hydrogen in acetic acid/methanol/EtOAc (5 mL; 1:2:2, by vol) was added a solution of acyl glucoside benzyl ether (0.27 mmol) in the same solvent (5 mL), and the mixture was hydrogenated at 35°C for 6 h under atmospheric pressure (1 atm). After the hydrogenolysis, the catalyst was filtered off on Celite and washed four times with methanol (each 4 mL). The combined mother liquor was evaporated *in vacuo* to give an oily residue, which was crystallized directly from EtOAc.

(i) *1-O-(24-Lithocholy)- $\alpha$ -D-glucopyranose (15)*. This was recrystallized from EtOAc as a colorless amorphous solid; yield, 79%; mp, 116–119°C. TLC,  $R_f$ : 0.52 (solvent A) and 0.58 (solvent C). Spectral and HR-MS data are shown in Table 2.

(ii) *1-O-(24-Lithocholy)- $\beta$ -D-glucopyranose (16)*. This was recrystallized from EtOAc as a colorless amorphous solid; yield, 86%; mp, 123–125°C. TLC,  $R_f$ : 0.53 (solvent A) and 0.57 (solvent C).

(iii) *1-O-(24-Chenodeoxycholy)- $\alpha$ -D-glucopyranose (17)*. This was recrystallized from EtOAc as a colorless amorphous solid; yield, 86%; mp, 126–129°C. TLC,  $R_f$ : 0.34 (solvent A) and 0.66 (solvent C).

(iv) *1-O-(24-Chenodeoxycholy)- $\beta$ -D-glucopyranose (18)*. This was recrystallized from EtOAc as colorless needles; yield, 88%; mp, 120–123°C. TLC,  $R_f$ : 0.35 (solvent A) and 0.65 (solvent C).

(v) *1-O-(24-Ursodeoxycholy)- $\alpha$ -D-glucopyranose (19)*. This was recrystallized from EtOAc as a colorless amorphous solid; yield, 87%; mp, 137–140°C. TLC,  $R_f$ : 0.37 (solvent A) and 0.73 (solvent C).

(vi) *1-O-(24-Ursodeoxycholy)- $\beta$ -D-glucopyranose (20)*. This was recrystallized from EtOAc as a colorless amorphous solid; yield, 80%; mp, 141–144°C. TLC,  $R_f$ : 0.39 (solvent A) and 0.72 (solvent C).

(vii) *1-O-(24-Deoxycholy)- $\alpha$ -D-glucopyranose (21)*. This was recrystallized from EtOAc as a colorless amorphous solid; yield, 82%; mp, 134–137°C. TLC,  $R_f$ : 0.38 (solvent A) and 0.64 (solvent C).

(viii) *1-O-(24-Deoxycholy)- $\beta$ -D-glucopyranose (22)*. This was recrystallized from EtOAc as a colorless amorphous solid; yield, 89%; mp, 131–134°C. TLC,  $R_f$ : 0.39 (solvent A) and 0.63 (solvent C).

(ix) *1-O-(24-Choly)- $\alpha$ -D-glucopyranose (23)*. This was recrystallized from EtOAc as a colorless amorphous solid; yield, 80%; mp, 141–143°C. TLC,  $R_f$ : 0.19 (solvent A) and 0.71 (solvent C).

(x) *1-O-(24-Choly)- $\beta$ -D-glucopyranose (24)*. This was recrystallized from EtOAc as a colorless amorphous solid; yield, 85%; mp, 164–166°C. TLC,  $R_f$ : 0.20 (solvent A) and 0.69 (solvent C).

(xi) *1-O-(24-Hyodeoxycholy)- $\alpha$ -D-glucopyranose (25)*. This was recrystallized from EtOAc as a colorless amorphous solid; yield, 85%; mp, 133–136°C. TLC,  $R_f$ : 0.32 (solvent A) and 0.73 (solvent C).

(xii) *1-O-(24-Hyodeoxycholy)- $\beta$ -D-glucopyranose (26)*. This was recrystallized from EtOAc as a colorless amorphous solid; yield, 89%; mp, 164–166°C. TLC,  $R_f$ : 0.33 (solvent A) and 0.72 (solvent C).

(xiii) *1-O-(24-Murideoxycholy)- $\alpha$ -D-glucopyranose (27)*. This was recrystallized from EtOAc as a colorless amorphous solid; yield, 79%; mp, 108–110°C. TLC,  $R_f$ : 0.38 (solvent A) and 0.74 (solvent C).

(xiv) *1-O-(24-Murideoxycholy)- $\beta$ -D-glucopyranose (28)*. This was recrystallized from EtOAc as a colorless amorphous solid; yield, 83%; mp, 146–148°C. TLC,  $R_f$ : 0.39 (solvent A) and 0.73 (solvent C).

## RESULTS AND DISCUSSION

The instability of acyl glucosides, which are susceptible to hydrolysis and transesterification under mild conditions (see below) (17), may hamper their identification and quantitation in biological materials as well as the chemical synthesis of authentic reference compounds. Previous syntheses of acyl glucuronides have required multiple steps with several protections and deprotections, resulting in low overall yields (23–26). A feasible, shorter method, however, has recently been reported for the preparation of acyl glucuronides, all of which are produced in a condensation reaction between carboxylic acids and a protected glucuronic acid derivative in the presence of diisopropyl- (or diethyl)-azodicarboxylate and triphenylphosphine as coupling agents (27,28). By utilizing

**TABLE 1**  
**Spectral Data<sup>a</sup> of Acyl Glucoside Benzyl Esters 1–14**

Product	IR (cm <sup>-1</sup> )	<sup>1</sup> H NMR (270 MHz) δ, J (Hz)	HR-MS		
			Molecular formula [M + Na] <sup>+</sup>	Calcd. (PIM)	Found
<b>1</b>	698, 738 (C <sub>6</sub> H <sub>5</sub> CH <sub>2</sub> -), 1072 (C–O), 1747 (C=O), 2851, 2916 (CH), 3283 (OH)	CDCl <sub>3</sub> : 0.61 (3H, <i>s</i> , 18-CH <sub>3</sub> ), 0.89 (3H, <i>d</i> , <i>J</i> = 4.3 Hz, 21-CH <sub>3</sub> ), 0.91 (3H, <i>s</i> , 19-CH <sub>3</sub> ), 3.61 (1H, <i>brm</i> , 3β-H), 3.65–3.94 (6H, <i>m</i> , 2'-, 3'-, 4'-, 5'-, and 6'-H), 4.45–4.98 (8H, <i>m</i> , 4 × CH <sub>2</sub> C <sub>6</sub> H <sub>5</sub> ), 6.38 (1H, <i>d</i> , <i>J</i> = 3.5 Hz, 1'β-H), 7.14–7.33 (20H, <i>m</i> , 4 × CH <sub>2</sub> C <sub>6</sub> H <sub>5</sub> )	C <sub>58</sub> H <sub>74</sub> O <sub>8</sub> Na	921.5281	921.5247
<b>2</b>	698, 738 (C <sub>6</sub> H <sub>5</sub> CH <sub>2</sub> -), 1073 (C–O), 1755 (C=O), 2852, 2916 (CH), 3332 (OH)	CDCl <sub>3</sub> : 0.62 (3H, <i>s</i> , 18-CH <sub>3</sub> ), 0.89 (3H, <i>d</i> , <i>J</i> = 5.6 Hz, 21-CH <sub>3</sub> ), 0.92 (2H, <i>s</i> , 19-CH <sub>3</sub> ), 3.56 (1H, <i>brm</i> , 3β-H), 3.59–3.76 (7H, <i>m</i> , 2'-, 3'-, 4'-, 5'-, 6'-, and 3β-H), 4.46–4.87 (8H, <i>m</i> , 4 × CH <sub>2</sub> C <sub>6</sub> H <sub>5</sub> ), 5.61 (1H, <i>d</i> , <i>J</i> = 7.0 Hz, 1'α-H), 7.15–7.30 (20H, <i>m</i> , 4 × CH <sub>2</sub> C <sub>6</sub> H <sub>5</sub> )	C <sub>58</sub> H <sub>74</sub> O <sub>8</sub> Na	921.5281	921.5325
<b>3</b>	698, 736 (C <sub>6</sub> H <sub>5</sub> CH <sub>2</sub> -), 1078 (C–O), 1744 (C=O), 2864, 2931 (CH), 3326 (OH)	CDCl <sub>3</sub> : 0.63 (3H, <i>s</i> , 18-CH <sub>3</sub> ), 0.90 (3H, <i>s</i> , 19-CH <sub>3</sub> ), 0.92 (3H, <i>d</i> , <i>J</i> = 6.3 Hz, 21-CH <sub>3</sub> ), 3.47 (1H, <i>brm</i> , 3β-H), 3.62–3.94 (6H, <i>m</i> , 2'-, 3'-, 4'-, 5'-, and 6'-H), 3.84 (1H, <i>m</i> , 7β-H), 4.46–4.98 (8H, <i>m</i> , 4 × CH <sub>2</sub> C <sub>6</sub> H <sub>5</sub> ), 6.38 (1H, <i>d</i> , <i>J</i> = 3.3 Hz, 1'β-H), 7.13–7.35 (20H, <i>m</i> , 4 × CH <sub>2</sub> C <sub>6</sub> H <sub>5</sub> )	C <sub>58</sub> H <sub>74</sub> O <sub>9</sub> Na	937.5230	937.5247
<b>4</b>	698, 736 (C <sub>6</sub> H <sub>5</sub> CH <sub>2</sub> -), 1077 (C–O), 1755 (C=O), 2852, 2917 (CH), 3341 (OH)	CDCl <sub>3</sub> : 0.64 (3H, <i>s</i> , 18-CH <sub>3</sub> ), 0.89 (3H, <i>s</i> , 19-CH <sub>3</sub> ), 0.91 (3H, <i>d</i> , <i>J</i> = 6.2 Hz, 21-CH <sub>3</sub> ), 3.46 (1H, <i>brm</i> , 3β-H), 3.58–3.73 (6H, <i>m</i> , 2'-, 3'-, 4'-, 5'-, and 6'-H), 3.84 (1H, <i>m</i> , 7β-H), 4.45–4.90 (8H, <i>m</i> , 4 × CH <sub>2</sub> C <sub>6</sub> H <sub>5</sub> ), 5.61 (1H, <i>d</i> , <i>J</i> = 8.4 Hz, 1'-H), 7.14–7.33 (20H, <i>m</i> , 4 × CH <sub>2</sub> C <sub>6</sub> H <sub>5</sub> )	C <sub>58</sub> H <sub>74</sub> O <sub>9</sub> Na	937.5230	937.5217
<b>5</b>	698, 737 (C <sub>6</sub> H <sub>5</sub> CH <sub>2</sub> -), 1075 (C–O), 1748 (C=O), 2862, 2926 (CH), 3302 (OH)	CDCl <sub>3</sub> : 0.65 (3H, <i>s</i> , 18-CH <sub>3</sub> ), 0.92 (3H, <i>d</i> , <i>J</i> = 6.6 Hz, 21-CH <sub>3</sub> ), 0.94 (3H, <i>s</i> , 19-CH <sub>3</sub> ), 3.59–3.97 (8H, <i>m</i> and <i>brm</i> , 3β- and 7α-H and 2'-, 3'-, 4'-, 5'-, and 6'-H), 4.46–4.98 (8H, <i>m</i> , 4 × CH <sub>2</sub> C <sub>6</sub> H <sub>5</sub> ), 6.38 (1H, <i>d</i> , <i>J</i> = 3.5 Hz, 1'β-H), 7.12–7.35 (20H, <i>m</i> , 4 × CH <sub>2</sub> C <sub>6</sub> H <sub>5</sub> )	C <sub>58</sub> H <sub>74</sub> O <sub>9</sub> Na	937.5230	937.5216
<b>6</b>	698, 736 (C <sub>6</sub> H <sub>5</sub> CH <sub>2</sub> -), 1081 (C–O), 1758 (C=O), 2866, 2930 (CH), 3302 (OH)	CDCl <sub>3</sub> : 0.65 (3H, <i>s</i> , 18-CH <sub>3</sub> ), 0.89 (3H, <i>d</i> , <i>J</i> = 6.3 Hz, 21-CH <sub>3</sub> ), 0.93 (3H, <i>s</i> , 19-CH <sub>3</sub> ), 3.56 (2H, <i>brm</i> , 3β- and 7α-H), 3.59–3.75 (6H, <i>m</i> , 2'-, 3'-, 4'-, 5'-, and 6'-H), 4.45–4.98 (8H, <i>m</i> , 4 × CH <sub>2</sub> C <sub>6</sub> H <sub>5</sub> ), 5.61 (1H, <i>d</i> , <i>J</i> = 8.0 Hz, 1'α-H), 7.11–7.32 (20H, <i>m</i> , 4 × CH <sub>2</sub> C <sub>6</sub> H <sub>5</sub> )	C <sub>58</sub> H <sub>74</sub> O <sub>9</sub> Na	937.5230	937.5243
<b>7</b>	698, 736 (C <sub>6</sub> H <sub>5</sub> CH <sub>2</sub> -), 1072 (C–O), 1743 (C=O), 2860, 2918 (CH), 3329 (OH)	CDCl <sub>3</sub> : 0.64 (3H, <i>s</i> , 18-CH <sub>3</sub> ), 0.90 (3H, <i>s</i> , 19-CH <sub>3</sub> ), 0.96 (3H, <i>d</i> , <i>J</i> = 6.1 Hz, 21-CH <sub>3</sub> ), 3.59 (1H, <i>brm</i> , 3β-H), 3.56–3.76 (6H, <i>m</i> , 2'-, 3'-, 4'-, 5'-, and 6'-H), 3.94 (1H, <i>m</i> , 12β-H), 4.46–4.98 (8H, <i>m</i> , 4 × CH <sub>2</sub> C <sub>6</sub> H <sub>5</sub> ), 6.38 (1H, <i>d</i> , <i>J</i> = 3.6 Hz, 1'β-H), 7.12–7.37 (20H, <i>m</i> , 4 × CH <sub>2</sub> C <sub>6</sub> H <sub>5</sub> )	C <sub>58</sub> H <sub>74</sub> O <sub>9</sub> Na	937.5230	937.5211

(continued on next page)

TABLE 1 (continued)

Product	IR (cm <sup>-1</sup> )	<sup>1</sup> H NMR (270 MHz) δ, J (Hz)	HR-MS		
			Molecular formula [M + Na] <sup>+</sup>	Calcd. (PIM)	Found
<b>8</b>	698, 737 (C <sub>6</sub> H <sub>5</sub> CH <sub>2</sub> -), 1077 (C-O), 1757 (C=O), 2859, 2932 (CH), 3317 (OH)	CDCl <sub>3</sub> : 0.65 (3H, s, 18-CH <sub>3</sub> ), 0.91 (3H, s, 19-CH <sub>3</sub> ), 0.94 (3H, d, J = 6.0 Hz, 21-CH <sub>3</sub> ), 3.52–3.88 (6H, m, 2'-, 3'-, 4'-, 5'-, and 6'-H), 3.61 (1H, brm, 3β-H), 3.96 (1H, m, 12β-H), 4.46–4.91 (8H, m, 4 × CH <sub>2</sub> C <sub>6</sub> H <sub>5</sub> ), 5.62 (1H, d, J = 8.0 Hz, 1'-H), 7.12–7.33 (20H, m, 4 × CH <sub>2</sub> C <sub>6</sub> H <sub>5</sub> )	C <sub>58</sub> H <sub>74</sub> O <sub>9</sub> Na	937.5230	937.5240
<b>9</b>	698, 736 (C <sub>6</sub> H <sub>5</sub> CH <sub>2</sub> -), 1076 (C-O), 1744 (C=O), 2868, 2933 (CH), 3327 (OH)	CDCl <sub>3</sub> : 0.65 (3H, s, 18-CH <sub>3</sub> ), 0.89 (3H, s, 19-CH <sub>3</sub> ), 0.97 (3H, d, J = 6.3 Hz, 21-CH <sub>3</sub> ), 3.46 (1H, brm, 3β-H), 3.61–3.77 (6H, m, 2'-, 3'-, 4'-, 5'-, and 6'-H), 3.84 (1H, m, 7β-H), 3.94 (1H, m, 12β-H), 4.46–4.98 (8H, m, 4 × CH <sub>2</sub> C <sub>6</sub> H <sub>5</sub> ), 6.38 (1H, d, J = 3.3 Hz, 1'β-H), 7.13–7.35 (20H, m, 4 × CH <sub>2</sub> C <sub>6</sub> H <sub>5</sub> )	C <sub>58</sub> H <sub>74</sub> O <sub>10</sub> Na	953.5179	953.5190
<b>10</b>	698, 745 (C <sub>6</sub> H <sub>5</sub> CH <sub>2</sub> -), 1076 (C-O), 1747 (C=O), 2869, 2931 (CH), 3351 (OH)	CDCl <sub>3</sub> : 0.66 (3H, s, 18-CH <sub>3</sub> ), 0.89 (3H, s, 19-CH <sub>3</sub> ), 0.96 (3H, d, J = 6.1 Hz, 21-CH <sub>3</sub> ), 3.45 (1H, brm, 3β-H), 3.56–3.78 (6H, m, 2'-, 3'-, 4'-, 5'-, and 6'-H), 3.84 (1H, m, 7β-H), 3.96 (1H, m, 12β-H), 4.46–4.91 (8H, m, 4 × CH <sub>2</sub> C <sub>6</sub> H <sub>5</sub> ), 5.62 (1H, d, J = 8.0 Hz, 1'α-H), 7.12–7.37 (20H, m, 4 × CH <sub>2</sub> C <sub>6</sub> H <sub>5</sub> )	C <sub>58</sub> H <sub>74</sub> O <sub>10</sub> Na	953.5179	953.5173
<b>11</b>	698, 737 (C <sub>6</sub> H <sub>5</sub> CH <sub>2</sub> -), 1071 (C-O), 1746 (C=O), 2850, 2916 (CH), 3302 (OH)	CDCl <sub>3</sub> : 0.61 (3H, s, 18-H), 0.90 (3H, s, 19-H), 0.91 (3H, d, J = 5.9 Hz, 21-H), 3.59–3.94 (8H, m, 2'-, 3'-, 4'-, 5'-, 6'-, 3β-, and 6β-H), 4.46–4.94 (8H, m, 4 × CH <sub>2</sub> C <sub>6</sub> H <sub>5</sub> ), 6.38 (1H, d, J = 3.5 Hz, 1'β-H), 7.14–7.36 (20H, m, 4 × CH <sub>2</sub> C <sub>6</sub> H <sub>5</sub> )	C <sub>58</sub> H <sub>74</sub> O <sub>9</sub> Na	937.5230	937.5219
<b>12</b>	698, 736 (C <sub>6</sub> H <sub>5</sub> CH <sub>2</sub> -), 1073 (C-O), 1758 (C=O), 2873, 2929 (CH), 3294 (OH)	CDCl <sub>3</sub> : 0.62 (3H, s, 18-H), 0.89 (3H, d, J = 7.0 Hz, 21-H), 0.90 (3H, s, 19-H), 3.56 (1H, brm, 3β-H), 3.59–3.73 (7H, m, 2'-, 3'-, 4'-, 5'-, 6'-, and 6β-H), 4.46–4.87 (8H, m, 4 × CH <sub>2</sub> C <sub>6</sub> H <sub>5</sub> ), 5.61 (1H, d, J = 8.1 Hz, 1'α-H), 7.12–7.36 (20H, m, 4 × CH <sub>2</sub> C <sub>6</sub> H <sub>5</sub> )	C <sub>58</sub> H <sub>74</sub> O <sub>9</sub> Na	937.5230	937.5206
<b>13</b>	698, 738 (C <sub>6</sub> H <sub>5</sub> CH <sub>2</sub> -), 1072 (C-O), 1747 (C=O), 2870, 2931 (CH), 3348 (OH)	CDCl <sub>3</sub> : 0.65 (3H, s, 18-H), 0.92 (3H, d, J = 6.2 Hz, 21-H), 1.10 (3H, s, 19-H), 3.59 (1H, m, 3β-H), 3.50–3.77 (7H, m, 2'-, 3'-, 4'-, 5'-, 6'-, and 6α-H), 4.45–4.98 (8H, m, 4 × CH <sub>2</sub> C <sub>6</sub> H <sub>5</sub> ), 6.38 (1H, d, J = 3.5 Hz, 1'β-H), 7.12–7.36 (20H, m, 4 × CH <sub>2</sub> C <sub>6</sub> H <sub>5</sub> )	C <sub>58</sub> H <sub>74</sub> O <sub>9</sub> Na	937.5230	937.5218
<b>14</b>	698, 738 (C <sub>6</sub> H <sub>5</sub> CH <sub>2</sub> -), 1083 (C-O), 1756 (C=O), 2866, 2940 (CH), 3317 (OH)	CDCl <sub>3</sub> : 0.66 (3H, s, 18-H), 0.90 (3H, d, J = 6.2 Hz, 21-H), 1.10 (3H, s, 19-H), 3.50–3.74 (7H, m, 2'-, 3'-, 4'-, 5'-, 6'-, and 6α-H), 3.61 (1H, m, 3β-H), 4.45–4.87 (8H, m, 4 × CH <sub>2</sub> C <sub>6</sub> H <sub>5</sub> ), 5.61 (1H, d, J = 7.8 Hz, 1'α-H), 7.12–7.36 (20H, m, 4 × CH <sub>2</sub> C <sub>6</sub> H <sub>5</sub> )	C <sub>58</sub> H <sub>74</sub> O <sub>9</sub> Na	937.5230	937.5248

<sup>a</sup>Abbreviations: IR, infrared; NMR, nuclear magnetic resonance; HR-MS, high-resolution mass spectra; PIM, positive ion mode.



**TABLE 2**  
Spectral Data<sup>a</sup> of Free Acyl Glucocides 15–28

Product	IR (cm <sup>-1</sup> )	<sup>1</sup> H NMR (270 MHz) δ, J (Hz)	HR-MS		
			Molecular formula [M - H] <sup>-</sup>	Calcd. (NIM)	Found
<b>15</b>	1088 (C–O), 1736 (C=O), 2866, 2932 (CH), 3248 (OH)	CDCl <sub>3</sub> + 20% DMSO- <i>d</i> <sub>6</sub> : 0.64 (3H, <i>s</i> , 18-H), 0.91 (3H, <i>s</i> , 19-H), 0.92 (3H, <i>d</i> , <i>J</i> = 5.7 Hz, 21-H), 3.12–3.80 (7H, <i>m</i> and <i>brm</i> , 2′-, 3′-, 4′-, 5′-, 6′-, and 3β-H), 6.16 (1H, <i>brs</i> , 1′β-H)	C <sub>30</sub> H <sub>49</sub> O <sub>8</sub>	537.3427	537.3408
<b>16</b>	1073 (C–O), 1739 (C=O), 2863, 2930 (CH), 3321 (OH)	CDCl <sub>3</sub> + 20% DMSO- <i>d</i> <sub>6</sub> : 0.64 (3H, <i>s</i> , 18-CH <sub>3</sub> ), 0.90 (3H, <i>s</i> , 19-CH <sub>3</sub> ), 3.45–3.81 (7H, <i>m</i> and <i>brm</i> , 2′-, 3′-, 4′-, 5′-, 6′-, and 3β-H), 5.55 (1H, <i>d</i> , <i>J</i> = 7.8 Hz, 1′α-H)	C <sub>30</sub> H <sub>49</sub> O <sub>8</sub>	537.3427	537.3389
<b>17</b>	1083 (C–O), 1737 (C=O), 2865, 2927 (CH), 3300 (OH)	CDCl <sub>3</sub> + 20% DMSO- <i>d</i> <sub>6</sub> : 0.65 (3H, <i>s</i> , 18-H), 0.89 (3H, <i>s</i> , 19-H), 0.93 (3H, <i>d</i> , <i>J</i> = 7.8 Hz, 21-H), 3.40–3.78 (8H, <i>m</i> and <i>brm</i> , 2′-, 3′-, 4′-, 5′-, 6′-, 3β-, and 7β-H), 6.15 (1H, <i>brs</i> , 1′β-H)	C <sub>30</sub> H <sub>49</sub> O <sub>9</sub>	553.3376	553.3346
<b>18</b>	1077 (C–O), 1750 (C=O), 2872, 2934 (CH), 3323 (OH)	CDCl <sub>3</sub> + 20% DMSO- <i>d</i> <sub>6</sub> : 0.65 (3H, <i>s</i> , 18-CH <sub>3</sub> ), 0.90 (3H, <i>s</i> , 19-CH <sub>3</sub> ), 0.92 (3H, <i>d</i> , <i>J</i> = 5.4 Hz, 21-H), 3.30–3.83 (8H, <i>m</i> and <i>brm</i> , 2′-, 3′-, 4′-, 5′-, 6′-, 3β-, and 7β-H), 5.55 (1H, <i>d</i> , <i>J</i> = 7.7 Hz, 1′α-H)	C <sub>30</sub> H <sub>49</sub> O <sub>9</sub>	553.3376	553.3419
<b>19</b>	1118 (C–O), 1736 (C=O), 2866, 2923 (CH), 3252 (OH)	CDCl <sub>3</sub> + 20% DMSO- <i>d</i> <sub>6</sub> : 0.67 (3H, <i>s</i> , 18-CH <sub>3</sub> ), 0.93 (3H, <i>s</i> , 19-CH <sub>3</sub> ), 0.93 (3H, <i>d</i> , <i>J</i> = 5.4 Hz, 21-H), 3.39–3.78 (8H, <i>m</i> and <i>brm</i> , 2′-, 3′-, 4′-, 5′-, 6′-, 3β-, and 7α-H), 6.17 (1H, <i>d</i> , <i>J</i> = 3.5 Hz, 1′β-H)	C <sub>30</sub> H <sub>49</sub> O <sub>9</sub>	553.3376	553.3342
<b>20</b>	1076 (C–O), 1745 (C=O), 2862, 2936 (CH), 3429 (OH)	CD <sub>3</sub> OD: 0.70 (3H, <i>s</i> , 18-CH <sub>3</sub> ), 0.95 (3H, <i>d</i> , <i>J</i> = 6.3 Hz, 21-CH <sub>3</sub> ), 0.96 (3H, <i>s</i> , 19-CH <sub>3</sub> ), 3.35–3.88 (8H, <i>m</i> and <i>brm</i> , 2′-, 3′-, 4′-, 5′-, 6′-, 3β-, and 7α-H), 5.50 (1H, <i>d</i> , <i>J</i> = 8.0 Hz, 1′α-H)	C <sub>30</sub> H <sub>49</sub> O <sub>9</sub>	553.3376	553.3406
<b>21</b>	1086 (C–O), 1734 (C=O), 2866, 2943 (CH), 3270 (OH)	CD <sub>3</sub> OD: 0.70 (3H, <i>s</i> , 18-CH <sub>3</sub> ), 0.92 (3H, <i>s</i> , 19-CH <sub>3</sub> ), 1.01 (3H, <i>d</i> , <i>J</i> = 6.3 Hz, 21-CH <sub>3</sub> ), 3.35–3.78 (7H, <i>m</i> and <i>brm</i> , 2′-, 3′-, 4′-, 5′-, 6′-, and 3β-H), 3.96 (1H, <i>m</i> , 12β-H), 6.12 (1H, <i>d</i> , <i>J</i> = 2.8 Hz, 1′β-H)	C <sub>30</sub> H <sub>49</sub> O <sub>9</sub>	553.3376	553.3440
<b>22</b>	1078 (C–O), 1742 (C=O), 2862, 2939 (CH), 3302 (OH)	CD <sub>3</sub> OD: 0.67 (3H, <i>s</i> , 18-CH <sub>3</sub> ), 0.92 (3H, <i>s</i> , 19-CH <sub>3</sub> ), 1.00 (3H, <i>d</i> , <i>J</i> = 6.3 Hz, 21-CH <sub>3</sub> ), 3.35–3.88 (6H, <i>m</i> , 2′-, 3′-, 4′-, 5′-, and 6′-H), 3.62 (1H, <i>brm</i> , 3β-H), 3.96 (1H, <i>m</i> , 12β-H), 5.50 (1H, <i>d</i> , <i>J</i> = 7.7 Hz, 1′α-H)	C <sub>30</sub> H <sub>49</sub> O <sub>9</sub>	553.3376	553.3405
<b>23</b>	1088 (C–O), 1732 (C=O), 2866, 2924 (CH), 3267 (OH)	CD <sub>3</sub> OD: 0.71 (3H, <i>s</i> , 18-CH <sub>3</sub> ), 0.91 (3H, <i>s</i> , 19-CH <sub>3</sub> ), 1.02 (3H, <i>d</i> , <i>J</i> = 5.8 Hz, 21-CH <sub>3</sub> ), 3.35–3.83 (8H, <i>m</i> and <i>brm</i> , 2′-, 3′-, 4′-, 5′-, 6′-, 3β-, and 7β-H), 3.96 (1H, <i>m</i> , 12β-H), 6.12 (1H, <i>d</i> , <i>J</i> = 2.7 Hz, 1′β-H)	C <sub>30</sub> H <sub>49</sub> O <sub>10</sub>	569.3325	569.3327

(continued on next page)

TABLE 2 (continued)

Product	IR (cm <sup>-1</sup> )	<sup>1</sup> H NMR (270 MHz) δ, J (Hz)	HR-MS		
			Molecular formula [M - H] <sup>-</sup>	Calcd. (NIM)	Found
24	1078 (C=O), 1743 (C=O), 2872, 2935 (CH), 3342 (OH)	CD <sub>3</sub> OD: 0.71 (3H, s, 18-CH <sub>3</sub> ), 0.91 (3H, s, 19-CH <sub>3</sub> ), 1.01 (3H, d, J = 6.0 Hz, 21-CH <sub>3</sub> ), 3.34–3.88 (8H, m and brm, 2'-, 3'-, 4'-, 5'-, 6'-, 3β-, and 7β-H), 3.96 (1H, m, 12β-H), 5.50 (1H, d, J = 7.7 Hz, 1'α-H)	C <sub>30</sub> H <sub>49</sub> O <sub>10</sub>	569.3325	569.3314
25	1731 (C=O), 2870, 2929 (CH), 3284 (OH)	CDCl <sub>3</sub> + 20% DMSO- <i>d</i> <sub>6</sub> : 0.64 (3H, s, 18-H), 0.89 (3H, s, 19-H), 0.92 (3H, d, J = 6.2 Hz, 21-H), 3.50–3.75 (8H, m and brm, 2'-, 3'-, 4'-, 5'-, 6'-, 3β-, and 6β-H), 6.15 (1H, brs, 1'β-H)	C <sub>30</sub> H <sub>49</sub> O <sub>9</sub>	553.3376	553.3385
26	1072 (C=O), 1759 (C=O), 2870, 2944 (CH), 3340 (OH)	CDCl <sub>3</sub> + 20% DMSO- <i>d</i> <sub>6</sub> : 0.64 (3H, s, 18-H), 0.89 (3H, s, 19-H), 0.91 (3H, d, J = 7.8 Hz, 21-H), 3.31–3.79 (8H, m and brm, 2'-, 3'-, 4'-, 5'-, 6'-, 3β-, and 6β-H), 5.52 (1H, d, J = 7.8 Hz, 1'α-H)	C <sub>30</sub> H <sub>49</sub> O <sub>9</sub>	553.3376	553.3404
27	1731 (C=O), 2873, 2944 (CH), 3256 (OH)	CDCl <sub>3</sub> + 20% DMSO- <i>d</i> <sub>6</sub> : 0.67 (3H, s, 18-H), 0.92 (3H, s, 19-H), 1.10 (3H, d, J = 4.3 Hz, 21-H), 3.34–3.80 (8H, m and brm, 2'-, 3'-, 4'-, 5'-, 6'-, 3β-, and 6α-H), 6.18 (1H, brs, 1'β-H)	C <sub>30</sub> H <sub>49</sub> O <sub>9</sub>	553.3376	553.3374
28	1076 (C=O), 1764 (C=O), 2874, 2939 (CH), 3279 (OH)	CDCl <sub>3</sub> + 20% DMSO- <i>d</i> <sub>6</sub> : 0.67 (3H, s, 18-CH <sub>3</sub> ), 0.92 (3H, d, J = 5.9 Hz, 21-H), 1.10 (3H, s, 19-CH <sub>3</sub> ), 3.45–3.81 (8H, m and brm, 2'-, 3'-, 4'-, 5'-, 6'-, 3β-, and 6α-H), 5.54 (1H, d, J = 7.8 Hz, 1'α-H)	C <sub>30</sub> H <sub>49</sub> O <sub>9</sub>	553.3376	553.3397

<sup>a</sup>DMSO, dimethylsulfoxide; for other abbreviations see Table 1.

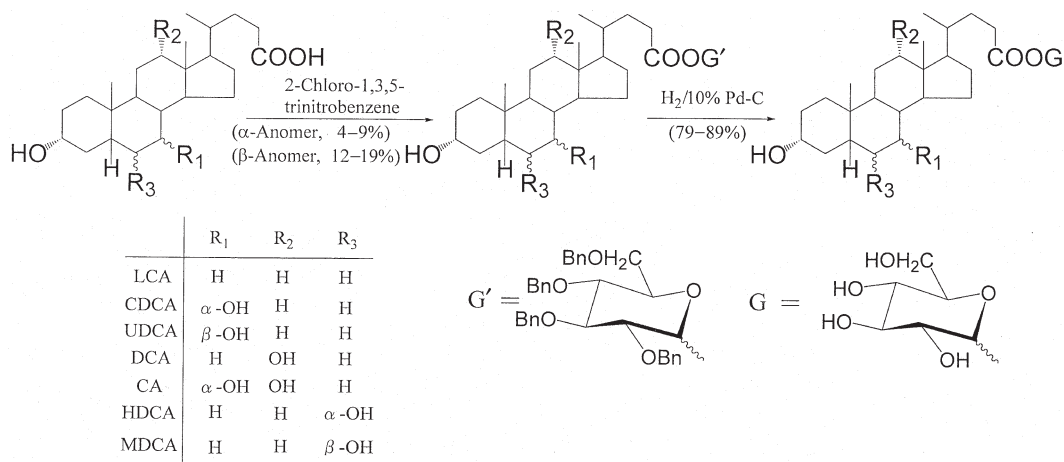
the Mitsunobu reaction, the 1-*O*-acyl-β-D-glucuronide derivatives of five common bile acids have been prepared by condensing bile acid acetates with methyl 2,3,4-tri-*O*-acetyl-D-glucopyranuronate (18). However, subsequent transformation of the resulting methyl ester-acetate derivatives of acyl glucuronides into the corresponding free ester forms was unsuccessful because of the instability of the C-24 ester linkages under alkaline hydrolysis conditions.

On the other hand, synthesis of the free 1-*O*-acyl-β-glucuronide of LCA, 1-*O*-(24-lithocholyl)-β-D-glucopyranuronic acid, has been successfully achieved in two steps by the Mitsunobu reaction of unprotected LCA with a fully benzylated derivative of glucuronic acid having a free C-1' hydroxyl group (benzyl 2,3,4-tri-*O*-benzyl-D-glucopyranuronate), followed by the hydrogenolysis of the resulting benzyl 1-*O*-(24-lithocholyl)-2,3,4-tri-*O*-benzyl-β-D-glucopyranuronate with Pd on charcoal as a catalyst (17). Subsequently, the 1-*O*-acyl-β-D-glucuronides of CDCA, UDCA, DCA, and CA have also been prepared by using a similar procedure (29).

In our synthesis of the analogous acyl glucosides of five common bile acids as well as HDCA and MDCA, we used TBGP as an alcoholic substrate. A preliminary experiment of the condensation of unprotected CDCA with TBGP by the

Mitsunobu reaction was discouraging; numerous by-products were formed, from which a mixture of the desired α- and β-anomers of the acyl glucosides benzyl ether derivative of CDCA was isolated in very low yield (6%) after tedious and repeated chromatographic purification. Similarly, the use of *N,N*-dicyclohexylcarbodiimide as a coupling agent (30) was also unsatisfactory.

However, when the mixtures of unprotected bile acids and TBGP were treated with CTNB as a condensing agent in pyridine (31), the nucleophilic acyl substitution reaction proceeded cleanly at room temperature for 3 h, *via* the activated ester intermediate of bile acid 1,3,5-trinitrobenzyl esters, to give the desired 1-*O*-acyl-D-glucoside benzyl ethers (1–14) (Fig. 2). After esterification, the reaction product was easily recovered by passage through a column of silica gel and elution with EtOAc/benzene mixtures; 1% acetic acid was added to all solvents used in the workup processes to prevent the decomposition of the resulting acyl glucosides (see below). Since each of the esterified products was a mixture of the α- and β-anomers of acyl glucoside benzyl ethers, as shown by <sup>1</sup>H NMR, they were then subjected to medium-pressure liquid chromatography on a C<sub>18</sub> reversed-phase column with elution by methanol/water mixtures. The reversed-phase



**FIG. 2.** Synthetic route to bile acid C-24 acyl glucosides. LCA, lithocholic acid; CDCA, chenodeoxycholic acid; UDCA, ursodeoxycholic acid; DCA, deoxycholic acid; CA, cholic acid; HDCA, hyodeoxycholic acid; MDCA, murideoxycholic acid.

chromatography resolved the two epimers effectively, and an  $\alpha$ -anomer (**1**, **3**, **5**, **7**, **9**, **11**, or **13**) was eluted first as a minor component (4–9% isolated yields), followed by the corresponding  $\beta$ -anomer (**2**, **4**, **6**, **8**, **10**, **12**, or **14**) as a major component (12–19% isolated yields), in an approximate  $\beta/\alpha$  ratio of 3:1, suggesting that the  $\alpha$ -anomers are more sterically unstable than the corresponding  $\beta$ -ones.

Subsequent treatment of **1–14** by hydrogenolysis in the presence of 10% Pd on charcoal as a catalyst (17,28) resulted in the complete elimination of the benzylic ether groups of a sugar moiety to form the  $\alpha$ - (**15**, **17**, **19**, **21**, **23**, **25**, or **27**) and  $\beta$ -anomers (**16**, **18**, **20**, **22**, **24**, **26**, or **28**) of free 1-*O*-acyl-D-glucosides. In our exploratory experiments, yield of the hydrogenolysis was influenced significantly by the reaction conditions. When the acyl glucoside benzyl ethers were subjected to hydrogenolysis in methanol/EtOAc mixtures (1:1, vol/vol) containing 20% acetic acid at 35°C under 1 atm, the time required for complete deprotection was only 6 h, and the yields of the resulting free acyl glucosides were 79–89%. However, when hydrogenolysis was carried out in methanol/EtOAc mixtures (1:1, vol/vol) under a positive pressure of 80 kg/cm<sup>2</sup>, the reaction took more than 24 h and yields of the desired free esters decreased steeply, probably due to the decomposition of ester linkage (see below) during the hydrogenolysis. The former procedure therefore seems to be the method of choice.

In TLC, the  $R_f$ -values observed for compounds **15–28**, which differ from one another in the number, position, and stereochemistry of hydroxyl groups in the aglycone moieties, increased in the following order in each series of the  $\alpha$ - and  $\beta$ -anomers: The acyl glucosides of CA (0.20) < HDCA (0.33) < CDCA (0.36), DCA (0.38), UDCA (0.39), MDCA (0.39) < LCA (0.53) on normal-phase TLC (solvent system A); those of LCA (0.57) < DCA (0.64), CDCA (0.65) < CA (0.70) < UDCA (0.73), HDCA (0.73), MDCA (0.74) on reversed-phase TLC (solvent system C). The TLC behaviors in each series of acyl glucosides on both the normal- and reversed-

phase TLC plates was similar to those observed for the corresponding ether glucosides (**32**). Although each pair of the corresponding  $\alpha$ - and  $\beta$ -anomers of the acyl glucosides had essentially identical mobility on TLC, they were nicely separated by medium-pressure liquid chromatography on a C<sub>18</sub> reversed-phase column, indicating that the  $\alpha$ -anomers are slightly more polar than the  $\beta$ -anomers.

Since previous workers pointed out the chemical specificity of acyl glucuronides (17), we examined the lability of the 1-*O*-acyl- $\beta$ -D-glucoside of DCA (**22**) as a representative substrate. Thus, **22** was stored at room temperature in various neutral, acidic, and alkaline solvents, and changes in the  $R_f$  values of the resulting solutions were monitored by normal-phase TLC (solvent system B). As a result, **22** ( $R_f$ , 0.22) was completely stable in acetone, acetic acid, and pyridine. However, when **22** was stored in methanol (or ethanol) containing 1% NaOH (or KOH), it was rapidly converted into the corresponding unconjugated DCA ( $R_f$ , 0.71). Interestingly, **22** was also decomposed readily within several hours on exposure in methanol (or ethanol) containing 1% HCl (or H<sub>2</sub>SO<sub>4</sub>) and gradually in a few days in the same solvent in the absence of acid. The  $R_f$  value (0.77) of the decomposed product differed from that (0.71) of the free acid of DCA, but it was in accord with that of the methyl ester derivative of DCA, clearly demonstrating the occurrence of acyl migration by transesterification. However, no intramolecular rearrangement was detected by acyl group migration of **22** to give positional isomers in which the aglycone is attached at the position of C-2', C-3', and C-4' of the  $\beta$ -D-glucoside moiety, in analogy with similar glucuronides (17). Since the carboxyl-linked glucosides of bile acids are susceptible to both hydrolysis and transesterification in alcoholic solvents, particular caution should therefore be paid in the isolation and purification processes.

<sup>1</sup>H NMR spectra provided confirmatory evidence for the structures of individual acyl glucosides (**15–28**). The resonance positions of 18-, 19-, and 21-methyl protons, as well as

methine protons at C-3, C-6, C-7, or C-12, are essentially unchanged compared to those observed for the corresponding unconjugated bile acids. An equatorial 1' $\beta$ -H signal in the  $\alpha$ -anomers (15, 17, 19, 21, 23, 25, and 27), which has a *cis* axial-equatorial relationship with adjacent axial 2' $\beta$ -H, occurs at a lower field of 6.12–6.17 ppm as a doublet with a coupling constant of 2.7–3.5 Hz (33). On the other hand, the corresponding axial 1' $\alpha$ -H signal in the  $\beta$ -anomers (16, 18, 20, 22, 24, 26, and 28) is shifted to a higher field and resonates at 5.50–5.55 ppm as a doublet with a coupling constant of 7.7–8.0 Hz owing to a *trans* diaxial relationship with 2' $\beta$ -H.

## ACKNOWLEDGMENTS

The authors are indebted to Messrs. K. Fujigaya and Y. Yamashita for their skillful technical assistance. This work was supported in part by a Grant-in-Aid for Scientific Research from the Ministry of Education, Science, Sports and Culture of Japan.

## REFERENCES

- Back, P., Spaczynski, K., and Gerok, W. (1974) Bile Salt Glucuronides in Urine, *Hoppe-Seyler's Z. Physiol. Chem.* 355, 749–752.
- Back, P. (1976) Bile Acid Glucuronides. II. Isolation and Identification of Chenodeoxycholic Acid Glucuronide from Human Plasma in Intrahepatic Cholestasis, *Hoppe-Seyler's Z. Physiol. Chem.* 357, 213–217.
- Almé, B., and Sjövall, J. (1980) Analysis of Bile Acid Glucuronides in Urine. Identification of 3 $\alpha$ ,6 $\alpha$ ,12 $\alpha$ -Trihydroxy-5 $\beta$ -cholanoic Acid, *J. Steroid Biochem.* 13, 907–916.
- Radomska-Pyrek, A., Zimniak, P., Irshaid, Y.M., Lester, R., Tephly, T.R., and St. Pyrek, J. (1987) Glucuronidation of 6 $\alpha$ -Hydroxy Bile Acids by Human Liver Microsomes, *J. Clin. Invest.* 80, 234–241.
- Matern, H., Matern, S., and Gerok, W. (1984) Formation of Bile Acid Glucosides by a Sugar Nucleotide-Independent Glucosyltransferase Isolated from Human Liver Microsomes, *Proc. Natl. Acad. Sci. USA* 81, 7036–7040.
- Marschall, H.-U., Egestad, B., Matern, H., Matern, S., and Sjövall, J. (1987) Evidence for Bile Acid Glucosides as Normal Constituents in Human Urine, *FEBS Lett.* 213, 411–414.
- Wietholtz, H., Marschall, H.-U., Reuschenbach, R., Matern, H., and Matern, S. (1991) Urinary Excretion of Bile Acid Glucosides and Glucuronides in Extrahepatic Cholestasis, *Hepatology* 13, 656–662.
- Radomska-Pyrek, A., Little, J., Pyrek, J.S., Drake, R.R., Igari, Y., Fournel-Gigleux, S., Magdalou, J., Burchell, B., Elbein, A.D., Siest, G., and Lester, R. (1993) A Novel UDP-Glc-Specific Glucosyltransferase Catalyzing the Biosynthesis of 6-*O*-Glucosides of Bile Acids in Human Liver Microsomes, *J. Biol. Chem.* 268, 15127–15135.
- Marschall, H.-U., Egestad, B., Matern, H., Matern, S., and Sjövall, J. (1989) *N*-Acetylglucosaminides. A New Type of Bile Acid Conjugate in Man, *J. Biol. Chem.* 264, 12989–12993.
- Marschall, H.-U., Matern, H., Wietholtz, H., Egestad, B., Matern, S., and Sjövall, J. (1992) Bile Acid *N*-Acetylglucosaminidation. *In vitro* and *in vivo* Evidence for a Selective Conjugation Reaction of 7 $\beta$ -Hydroxylated Bile Acids in Humans, *J. Clin. Invest.* 89, 1981–1987.
- Marschall, H.-U., Griffiths, W.J., Zhang, J., Wietholtz, H., Matern, H., Matern, S., and Sjövall, J. (1994) Positions of Conjugation of Bile Acids with Glucose and *N*-Acetylglucosamine *in vitro*, *J. Lipid Res.* 35, 1599–1610.
- Radomska-Pyrek, A., Zimniak, P., Chari, M., Golunski, E., Lester, R., and St. Pyrek, J. (1986) Glucuronides of Monohydroxylated Bile Acids: Specificity of Microsomal Glucuronyltransferase for the Glucuronidation Site, C-3 Configuration, and Side Chain Length, *J. Lipid Res.* 27, 89–101.
- Shattuck, K.E., Radomska-Pyrek, A., Zimniak, P., Adcock, E.W., Lester, R., and St. Pyrek, J. (1986) Metabolism of 24-Norlithocholic Acid in the Rat: Formation of Hydroxyl- and Carboxyl-Linked Glucuronides and the Effect on Bile Flow, *Hepatology* 6, 869–873.
- Radomska, A., Green, M.D., Zimniak, P., Lester, R., and Tephly, T.R. (1988) Biosynthesis of Hydroxyl-Linked Glucuronides of Short-Chain Bile Acids by Rat Liver 3-Hydroxysteroid UDP-Glucuronosyltransferase, *J. Lipid Res.* 29, 501–508.
- Radomska, A., Little, J.M., Lester, R., and St. Pyrek, J. (1992) Hepatic Metabolism of 3-Oxoandroster-4-ene-17 $\beta$ -carboxylic Acid in the Adult Rat: Formation of Carboxyl-Linked Glucuronides Both *in vivo* and *in vitro*, *Steroids* 57, 328–334.
- Zimniak, P., Radomska, A., Zimniak, M., and Lester, R. (1988) Formation of Three Types of Glucuronides of 6-Hydroxy Bile Acids by Rat Liver Microsomes, *J. Lipid Res.* 29, 183–190.
- Panfil, I., Lehman, P.A., Zimniak, P., Ernest, B., Franz, T., Lester, R., and Radomska, A. (1992) Biosynthesis and Chemical Synthesis of Carboxyl-Linked Glucuronides of Lithocholic Acid, *Biochim. Biophys. Acta* 1126, 221–228.
- Goto, G., Murano, N., Nakada, C., Motoyama, T., Oohashi, J., Yanagihara, T., Niwa, T., and Ikegawa, S. (1998) Separation and Characterization of Carboxyl-Linked Glucuronides of Bile Acids in Incubation Mixture of Rat Liver Microsomes, *Steroids* 63, 186–192.
- Ikegawa, S., Okuyama, H., Oohashi, J., Murano, N., and Goto, J. (1999) Separation and Detection of Bile Acid 24-Glucuronides in Human Urine by Liquid Chromatography Combined with Electrospray Ionization Mass Spectrometry, *Anal. Sci.* 15, 625–631.
- Ikegawa, S., Murano, N., Nagata, M., Ohba, S., and Goto, J. (1999) Covalent Binding of Bile Acid Acyl Glucuronide with Protein, *Anal. Sci.* 15, 213–215.
- Iida, T., Nishida, S., Yamaguchi, Y., Kodake, M., Chang, F.C., Niwa, T., Goto, J., and Nambara, T. (1995) Potential Bile Acid Metabolites. 23. Syntheses of 3-Glucosides of Nonamidated and Glycine- and Taurine-Amidated Bile Acids, *J. Lipid Res.* 36, 628–638.
- Iida, T., Momose, T., Tamura, T., Matsumoto, T., Chang, F.C., Goto, J., and Nambara, T. (1988) Potential Bile Acid Metabolites. 13. Improved Routes to 3 $\beta$ ,6 $\beta$ - and 3 $\beta$ ,6 $\alpha$ -Dihydroxy-5 $\beta$ -cholanoic Acids, *J. Lipid Res.* 29, 165–171.
- Bugianesi, R., and Shen, T.Y. (1971) A Chemical Synthesis of 1-*O*-Indomethacin- $\beta$ -D-glucosyluronic Acid, *Carbohydr. Res.* 19, 179–187.
- Compernelle, F. (1980) Synthesis of Biliverdin and Bilirubin 1-*O*-Acyl- $\beta$ -D-glucopyranuronic Acids, *Biochem. J.* 187, 857–863.
- DeMesmaeker, A., Hoffmann, P., and Ernst, B. (1989) A New Protected Form of Glucuronic Acid for the Synthesis of Labile 1-*O*-Acyl- $\beta$ -glucuronides, *Tetrahedron Lett.* 30, 3773–3776.
- Kirschning, A., Ries, M., Domann, S., Martin, W., Albrecht, W., Arnold, P., and Laufer, S. (1997) Synthesis and Biological Identification of the Acyl Glucuronides of the Anti-inflammatory Drug ML-300, *Bioorg. Med. Chem. Lett.* 7, 903–906.
- Smith, A.B., III, Hale, K.J., and Rivero, R.A. (1986) An Efficient Synthesis of Glycosyl Esters Exploiting the Mitsunobu Reaction, *Tetrahedron Lett.* 27, 5813–5816.
- Juteau, H., Gareau, Y., and Labelle, M. (1997) A Convenient Synthesis of  $\beta$ -Acyl Glucuronides, *Tetrahedron Lett.* 38, 1481–1484.



29. Goto, J., Murano, N., Oohashi, J., and Ikegawa, S. (1998) Synthesis of Bile Acid 24-Acyl Glucuronides, *Steroids* 63, 180–185.
30. Neises, B., and Steglich, W. (1985) Esterification of Carboxylic Acids with Dicyclohexylcarbodiimide/4-Dimethylaminopyridine, *Org. Synth.* 63, 183–187.
31. Takimoto, S., Inanaga, J., Katsuki, T., and Yamaguchi, M. (1981) Esterification of Carboxylic Acids by Alcohols with 2-Chloro-1,3,5-trinitrobenzene as Condensing Agent, *Bull. Chem. Soc. Jpn.* 54, 1470–1473.
32. Sasaki, T., Wakabayashi, M., Yamaguchi, T., Kasuga, Y., Nagatsuma, M., Iida, T., and Nambara, T. (1999) Separation of Double Conjugates of Bile Acids by Two-Dimensional High-Performance Thin-Layer Chromatography with Tetra-*n*-butylammonium Phosphate and Methyl  $\beta$ -Cyclodextrin, *Chromatographia* 49, 681–685.
33. Barnes, S., and Kirk, D.N. (1988) Nuclear Magnetic Resonance Spectroscopy of Bile Acids, in *The Bile Acids* (Setchell, K.D.R., Kritchevsky, D., and Nair, P.P., eds.), Vol. 4, pp. 65–136, Plenum Press, New York.

[Received August 13, 2001, and in revised form November 16, 2001; revision accepted November 23, 2001]

# Dibutyrate Derivatization of Monoacylglycerols for the Resolution of Regioisomers of Oleic, Petroselinic, and *cis*-Vaccenic Acids

Frédéric Destailats<sup>a</sup>, Joseph Arul<sup>a</sup>, James E. Simon<sup>b</sup>, Robert L. Wolff<sup>c</sup>,  
and Paul Angers<sup>a,\*</sup>

<sup>a</sup>Department of Food Science and Nutrition, and Dairy Research Center (STELA), Université Laval, Sainte-Foy, Québec, Canada G1K 7P4, <sup>b</sup>Department of Plant Science, Rutgers University, New Brunswick, New Jersey 08901, and <sup>c</sup>INRA-UNL, 21065 Dijon Cedex, France

**ABSTRACT:** Dibutyrate derivatives of monoacylglycerols of oleic, petroselinic, and *cis*-vaccenic acids were prepared by diesterification of monoacylglycerols with *n*-butyryl chloride. The resulting triacylglycerols were analyzed by gas chromatography (GC) with a 65% phenyl methyl silicone capillary column and separated on the basis of both fatty acid composition and regiospecific position. The petroselinic acid derivatives eluted first, followed sequentially by the oleic and *cis*-vaccenic acid derivatives, with the *sn*-2 positional isomer eluting before the *sn*-1(3) isomer in each case. Separation of the peaks was almost baseline between petroselinic and oleic acids as well as between oleic and *cis*-vaccenic acids. To assess the accuracy of the method, mixtures of triolein, tripetroselinin, and tri-*cis*-vaccenin in various known proportions were partially deacylated with the use of ethyl magnesium bromide and derivatized and analyzed as above. The results showed that this method compares favorably to the existing methods for analysis of oleic, petroselinic, and *cis*-vaccenic fatty acids by GC with respect to peak separation and accuracy, and it also provides information on the regiospecific distribution of the fatty acids. The method was applied to basil (*Ocimum basilicum*) and coriander (*Coriandrum sativum*) seed oils. *cis*-Vaccenic, oleic, and linoleic acids were mainly distributed at the *sn*-2 position in basil seed oil, and higher proportions of linolenic, palmitic, and stearic acids were distributed at the *sn*-1(3) position than at the *sn*-2 position. In coriander seed oil, petroselinic acid was mainly distributed at the *sn*-1(3) position, and both oleic and linoleic acids were mostly located at the *sn*-2 position, whereas palmitic, stearic, and *cis*-vaccenic acids were located only at the *sn*-1(3) position.

Paper no. L8786 in *Lipids* 37, 111–116 (January 2002).

Petroselinic (*cis*-6 18:1) and *cis*-vaccenic (*cis*-11 18:1) acids are two fatty acid isomers of oleic acid (*cis*-9 18:1), differing in the position of the double bond. These isomers are major fatty acid constituents in the lipids of plants of the *Araliaceae* (1) and *Apiaceae* (formerly *Umbelliferae*) (2–9) families and are also minor constituents of seed lipids of basil (unpub-

lished results) and of other plants (10–15). Regio- and stereospecific distribution of fatty acids in oils containing petroselinic and *cis*-vaccenic acids is not well documented (16,17), attributable to the difficulties involved in the analysis of mixtures of these isomers, which tend to coelute in gas chromatography (GC) (18–21). Until recently, their analysis has been laborious and required isolation of the 18:1 isomeric fatty acids, followed by oxidative cleavage of the double bond to produce, for example, azelaic and nonanoic acids from oleic acid and adipic and lauric acids from petroselinic acid. Analytical methods allowing direct and accurate quantitative analysis by GC of mixtures of derivatized oleic, petroselinic, and *cis*-vaccenic acids were developed by Wolff and Vandamme (20,21) with isopropyl derivatives, by Thies (22) with *n*-butyl derivatives, and by Liu and Hammond (23) with 2-phenylethyl derivatives. The latter can also be analyzed by high-performance liquid chromatography (HPLC). These methods use larger ester alcohol moieties than methanol, and this results in reduced relative polarity of the esterified acid, with the double bond in the hydrocarbon moiety making the primary contribution to the polarity of the esters. Thus, the position of the polar center, i.e., the double bond, plays a significant role in the adsorption of the ester to the hydrophobic polymer coating on the chromatographic column, where the ester with the double bond at position 6 is least strongly adsorbed and should elute faster than the esters with the double bond at position 9 or 11, given that there is no difference in their vapor pressure or boiling point. This reasoning led us to hypothesize that the use of dibutyrate derivatives of monoacylglycerols (24) would permit not only the separation of the fatty acid isomers oleic, petroselinic, and vaccenic acids, but also the determination of their regiospecific distribution.

The objectives of the present work were first to evaluate the separation of dibutyrate derivatives of monoacylglycerols of oleic, petroselinic, and *cis*-vaccenic acids by GC on the basis of both fatty acid composition and regiospecific distribution; second, to determine the accuracy of this method by analyzing dibutyrate derivatives of monoacylglycerols obtained by partial deacylation of mixtures of triolein, tripetroselinin, and tri-*cis*-vaccenin in known proportions; and third, to validate the method by analyzing natural samples of basil and coriander seed oils.

\*To whom correspondence should be addressed at Department of Food Science and Nutrition, Université Laval, Sainte-Foy, Québec, Canada G1K 7P4. E-mail: paul.angers@aln.ulaval.ca

Abbreviations: GC, gas chromatography; HPLC, high-performance liquid chromatography; TAG, triacylglycerol; TLC, thin-layer chromatography.

## MATERIALS AND METHODS

**Materials.** Monooleoylglycerol, monopetroselinoylglycerol, monostearoylglycerol, mono-*cis*-vaccenoylglycerol, triolein, tripetroselinin, and tri-*cis*-vaccenin were purchased from Nu-Chek-Prep (Elysian, MN). Ethylmagnesium bromide (3.0 M in diethyl ether), *n*-butyryl chloride, and triethylamine were obtained from Aldrich (Milwaukee, WI).

**Oil extraction.** Mature dry seeds (10 g) of basil (*Ocimum basilicum*) (25) and of coriander (*Coriandrum sativum*), purchased from a local seed retailer, were washed and finely ground in a mortar. Oil was extracted with hexane in a Soxhlet apparatus and recovered by filtering and drying the extract over anhydrous sodium sulfate and evaporating the solvent under vacuum at 30°C on a rotary evaporator (21% yield for basil oil and 23% for coriander oil). The oils were stored under nitrogen at -35°C until further use.

**Derivatization of monoacylglycerols.** Standard monoacylglycerols (10 mg) of oleic, petroselinic, *cis*-vaccenic, and stearic acids were solubilized in dry chloroform (0.5 mL). Triethylamine (100 µL) and *n*-butyryl chloride (50 µL) were sequentially added, and the reaction mixture was held at 60°C for 20 min in a closed vial with constant stirring. After cooling to room temperature, the reaction mixture was diluted with *n*-octane (1 mL), washed sequentially with 1-mL volumes each of cold diluted hydrochloric acid (0.1 N), water, and brine (saturated aqueous solution of sodium chloride), and dried over anhydrous sodium sulfate. Aliquots (50 µL) were diluted with *n*-octane (200 µL) and analyzed by GC.

**Partial deacylation of triacylglycerols (TAG).** Mixtures of standard TAG triolein, tripetroselinin, and tri-*cis*-vaccenin in different proportions (Table 1) and basil and coriander seed oils were partially deacylated with ethylmagnesium bromide according to a literature procedure (24). After workup, the residue was solubilized in dry chloroform, derivatized with *n*-butyryl chloride as described above for standard monoacylglycerols, and analyzed by GC.

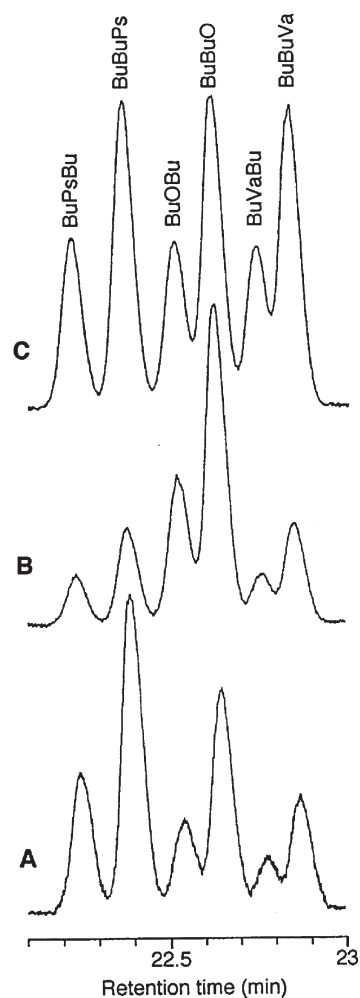
**GC of triacylglycerols.** Analysis was performed using a gas chromatograph (Hewlett-Packard Model 6890, Series II; Palo Alto, CA), equipped with a flame-ionization detector and connected to a ChemStation (Hewlett-Packard). Sample volumes (1.0 µL) in *n*-octane were injected onto a 65% phenyl methyl silicone capillary column (Restek, Bellefonte, PA; 30 m × 0.25 mm i.d., 0.10 µm film thickness) with a split ratio of 1:50. Injector and detector temperatures were set at 400°C, while the oven temperature was programmed from 190 to 300°C at 2.5°C min<sup>-1</sup> and to 360°C at 15°C min<sup>-1</sup> and held for 5 min at this temperature, for a total duration of 70 min. The linear velocity of the carrier gas (hydrogen) was 47 cm s<sup>-1</sup> at 190°C. Other chromatographic conditions used were isothermal oven temperatures from 190 to 260°C, in 5°C increments, other parameters being left unchanged. Peak areas and corrected response factors based on standards were used for quantitation. Resolution values were determined using peak base width.

**Experimental considerations.** The oil samples were crude and possibly contained components other than TAG, such as

phospholipids. These, however, do not interfere with the regiospecific analysis of TAG by the present method, which can be performed directly on the crude lipid extracts without further purification of TAG by thin-layer chromatography (TLC) or other methods (26).

## RESULTS AND DISCUSSION

**GC of TAG.** Dibutyrate derivatives of monoacylglycerols of oleic, petroselinic, and *cis*-vaccenic acids were separated by GC by both fatty acid composition and regiospecific position. The order of elution was similar to that reported for other GC methods employed in the analysis of these fatty acid isomers (20–22), with petroselinic acid derivatives eluting first, oleic acid derivatives second, and *cis*-vaccenic acid derivatives third. For each fatty acid derivative, the *sn*-2 positional isomer eluted before the *sn*-1(3) isomer (Fig. 1). The separation was nearly baseline ( $R_S = 1.28$ ) between the petroselinic and oleic acid de-



**FIG. 1.** Gas chromatograms of dibutyrate derivatives of monoacylglycerols obtained after partial deacylation of mixtures of tripetroselinin, triolein, and tri-*cis*-vaccenin by ethyl magnesium bromide, followed by derivatization with *n*-butyryl chloride. Bu, 4:0; Ps, *cis*-6 18:1; O, *cis*-9 18:1; Va, *cis*-11 18:1. Proportions of tripetroselinin/triolein/tri-*cis*-vaccenin in the initial mixtures were (A) 3:2:1, (B) 1:3:1, and (C) 1:1:1.

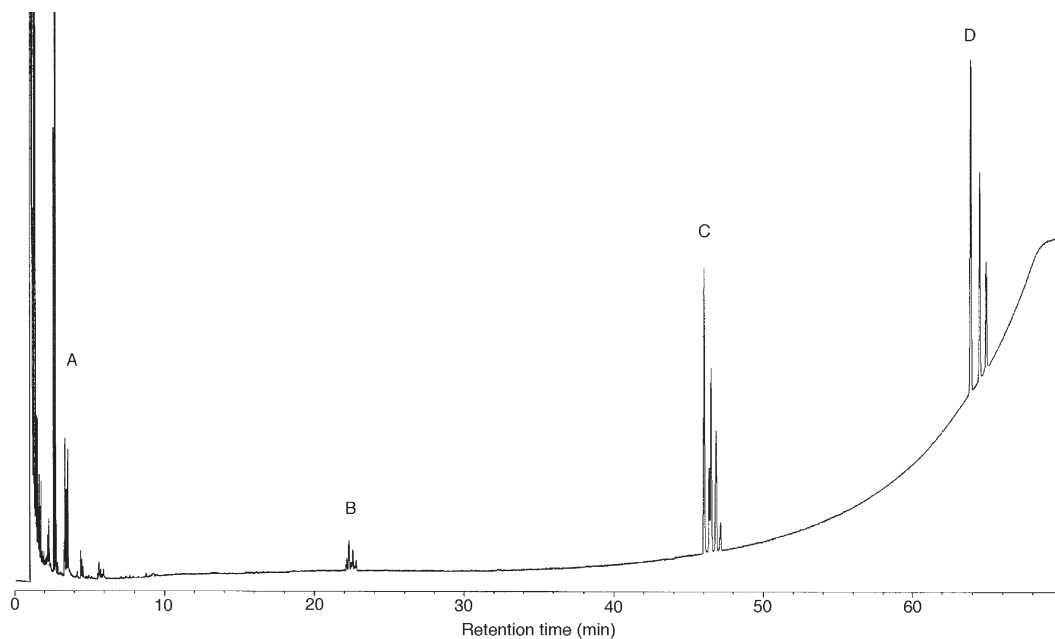
derivatives, and also close to baseline between the oleic and *cis*-vaccenic acid derivatives ( $R_S = 1.10$ ). The resolution of positional isomers was highest for petroselinic acid derivatives and lowest for *cis*-vaccenic acid derivatives, with  $R_S$  values of 1.37, 0.95, and 0.88 between the *sn*-2 and the *sn*-1(3) positional isomers of the petroselinic, oleic, and *cis*-vaccenic acid derivatives, respectively. However, separation between *sn*-2 and *sn*-1(3) isomers of the derivatives of the 18:1 isomers (as well as other fatty acids) depends on the quality of the column; columns with the same stationary phase can exhibit some variability in their resolution owing to variations in the polymer coating.

Analysis of dibutyrate derivatives of monoacylglycerols by this method does not require separation of glyceride species prior to derivatization because well-defined chromatographic resolution, free of overlap, of all species present in the samples is obtained with the use of proper chromatographic conditions (Fig. 2). The species included dibutyrate derivatives of monoacylglycerols, monobutyrate derivatives of diacylglycerols, TAG, and tertiary alcohols, some of which may have been partly derivatized or dehydrated during the derivatization procedure. However, we have encountered some overlapping of the elution regions for derivatives of mono- and diacylglycerols in samples containing  $C_8$  to  $C_{20}$  fatty acids, but not for individual species (data not shown).

The primary chromatographic conditions reported in the Materials and Methods section indeed allowed separation of dibutyrate derivatives of petroselinic, oleic, and *cis*-vaccenic acids. However, these conditions resulted in overlapping of petroselinic and stearic acid derivatives (Fig. 3, A1). Isothermal elution at 205°C resulted in separation of petroselinic and stearic acid derivatives, but the latter overlapped with oleic

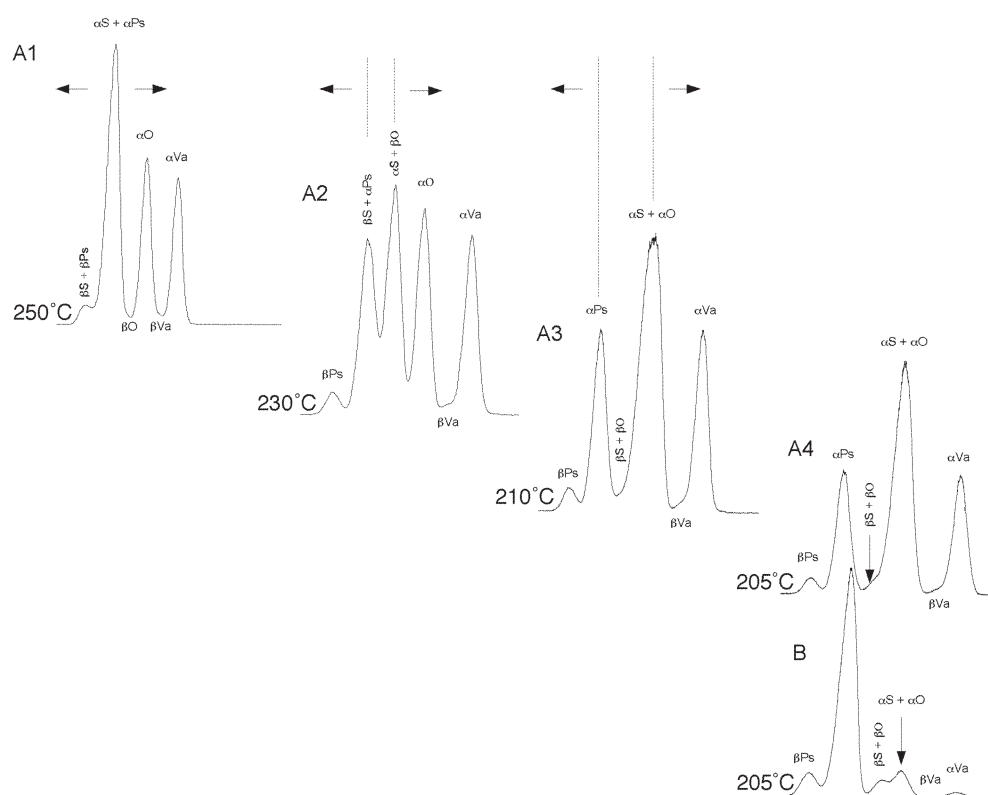
acid derivatives (Fig. 3, A4). Although we did not succeed in obtaining acceptable separation of stearic, petroselinic, and oleic acid derivatives under a single set of chromatographic conditions, the combined chromatograms obtained under two sets of chromatographic conditions (Fig. 3, A2 and A3) made possible the quantitation of acid derivatives in a given sample. A first set of conditions resulting in overlap of petroselinic and stearic acid derivatives but resolving oleic acid derivatives, and a second set of conditions resulting in overlap of oleic and stearic acid derivatives while resolving petroselinic acid derivatives permitted accurate determination of the values of these acid derivatives in coriander seed oil (Fig. 3, B).

**Fatty acid composition of TAG mixtures.** The accuracy of the present method for the analysis of petroselinic, oleic, and *cis*-vaccenic acids in samples, and for the determination of the regiospecific distribution of these acids, was evaluated by analyzing dibutyrate derivatives of monoacylglycerols from partial deacylation of three mixtures of triolein, tripetroselinin, and tri-*cis*-vaccenin in defined proportions. The experiments were carried out in triplicate, and the results are presented in Table 1. The expected and experimental values are in good agreement for all three mixtures, although minor deviations were noted. The values for the *sn*-1(3) isomer were slightly underestimated by roughly 1% for petroselinic acid, whereas they were slightly overestimated for oleic acid. Experimental values for the *sn*-2 isomers of petroselinic and oleic acids and the *sn*-1(3) isomer of *cis*-vaccenic acid were on target. Total fatty acid compositions of the mixtures calculated from the values for the *sn*-1(3) and *sn*-2 positions were also in agreement with the expected values.



**FIG. 2.** Gas chromatogram of products resulting from partial deacylation with ethyl magnesium bromide of a 3:2:1 mixture of tripetroselinin, triolein and tri-*cis*-vaccenin, followed by derivatization with *n*-butyryl chloride. (A) Tertiary alcohols and similar compounds; (B) dibutyrate derivatives of monoacylglycerols; (C) monobutyrate derivatives of diacylglycerols; (D) triacylglycerols.





**FIG. 3.** Partial gas chromatogram of a mixture of dibutyrate derivatives of monoacylglycerols of stearic, petroselinic, oleic and *cis*-vaccenic acids under selected isothermal conditions at 250°C (A1), 230°C (A2), 210°C (A3) and 205°C (A4); and of dibutyrate derivatives of monoacylglycerols obtained after partial deacylation of coriander (*Coriandrum sativum*) seed oil under isothermal conditions at 205°C (B).  $\alpha$  and  $\beta$  refer to *sn*-1(3) and *sn*-2 positional isomers, respectively. (Derivatives of other fatty acids not shown.)

*Regiospecific analysis of basil and coriander seed oils.* The analytical method was further validated by the analysis of basil (*Ocimum basilicum*) and coriander (*Coriandrum sativum*) seed oils. The results (Table 2) showed that in basil seed oil, linolenic acid was the most abundant fatty acid in both the *sn*-1(3) and *sn*-2 positions, amounting to 55.8 and 51.3%, respectively. The results also showed that  $C_{18:1}$  isomers were mostly distributed at the *sn*-2 position, whereas the saturated fatty acids, palmitic and stearic acids, were predominantly located at the *sn*-1(3) position. In coriander seed oil, petroselinic acid was the major acid both at the *sn*-1(3) position (80.1%) and at the *sn*-2 position (40.9%). Oleic and linoleic acids were mainly distributed at the *sn*-2 position,

whereas palmitic, stearic, and *cis*-vaccenic acids were distributed only at the *sn*-1(3) position. The calculated fatty acid compositions of both seed oil TAG obtained from the results of the regiospecific analysis were in good agreement with the experimental values obtained by GC analysis of fatty acid methyl ester derivatives (25) of basil seed oil and of fatty acid isopropyl ester derivatives (20) of coriander seed oil.

We have developed a simple, fast, and accurate method for the regiospecific analysis of petroselinic, oleic, and *cis*-vaccenic acids in triacylglycerols and validated it with natural oils of basil and coriander seeds. The simplicity of the protocol more than compensates for the possibility of small errors, indicated by the analysis of known mixtures of TAG

**TABLE 1**  
Experimental Values for Fatty Acid Distribution Between *sn*-1(3) and *sn*-2 Positions of Known Mixtures of Triolein, Tripetroselinin, and Tri-*cis*-vaccenin

Tripetroselinin/ triolein/ tri- <i>cis</i> -vaccenin	Fatty acid composition (mol%) <sup>a</sup>								
	Petroselinic			Oleic			<i>cis</i> -Vaccenic		
	<i>sn</i> -1(3)	<i>sn</i> -2	TAG <sup>b</sup>	<i>sn</i> -1(3)	<i>sn</i> -2	TAG	<i>sn</i> -1(3)	<i>sn</i> -2	TAG
33.3:33.3:33.3	32.5 ± 0.2	34.1 ± 0.5	33.0 ± 0.3	34.8 ± 0.3	34.3 ± 1.0	34.6 ± 0.5	32.7 ± 0.3	31.6 ± 0.6	32.3 ± 0.4
20.0:60.0:20.0	18.7 ± 0.5	20.5 ± 0.9	19.3 ± 0.7	61.4 ± 0.8	59.5 ± 0.7	60.7 ± 0.7	19.9 ± 0.3	20.0 ± 0.7	19.9 ± 0.1
50.0:33.3:16.7	48.4 ± 0.4	49.9 ± 0.4	48.9 ± 0.2	33.9 ± 0.1	32.8 ± 0.2	33.5 ± 0.1	17.7 ± 0.2	17.3 ± 0.5	17.6 ± 0.3

<sup>a</sup>Values are means of three replicate analyses ± standard deviations.

<sup>b</sup>Triacylglycerol, calculated from values for *sn*-1(3) and *sn*-2:  $[2 \times sn-1(3) + sn-2]/3$ .

**TABLE 2**  
**Experimental Values (mol%) for Fatty Acid Distribution Between *sn*-1(3) and *sn*-2 Positions and Fatty Acid Composition in Basil (*Ocimum basilicum*) and in Coriander (*Coriandrum sativum*) Seed Oils**

Fatty acid	Basil				Coriander			
	<i>sn</i> -1(3) <sup>a</sup>	<i>sn</i> -2 <sup>a</sup>	Calculated <sup>b</sup>	Experimental <sup>c</sup>	<i>sn</i> -1(3) <sup>a</sup>	<i>sn</i> -2 <sup>a</sup>	Calculated <sup>b</sup>	Experimental <sup>c</sup>
Palmitic	10.5 ± 0.2	2.6 ± 0.1	7.9	8.1	5.4 ± 0.1	— <sup>d</sup>	3.6	4.3
Stearic	5.7 ± 0.1	—	3.8	2.8	2.5 ± 0.2	—	1.7	1.0
Petroselinic	—	—	—	—	80.1 ± 0.4	40.9 ± 0.2	67.0	69.7
Oleic	8.6 ± 0.3	13.2 ± 0.4	10.1	13.0	5.5 ± 0.3	28.3 ± 0.4	13.1	11.1
<i>cis</i> -Vaccenic	1.0 ± 0.2	2.4 ± 0.2	1.5	0.8	1.6 ± 0.1	—	1.0	0.7
Linoleic	18.4 ± 0.3	30.6 ± 0.3	22.5	22.8	4.9 ± 0.1	30.8 ± 0.4	13.5	13.2
Linolenic	55.8 ± 0.6	51.3 ± 0.5	54.3	52.7	—	—	—	—

<sup>a</sup>Values are means of three replicate analyses ± standard deviations.

<sup>b</sup>Calculated from values for *sn*-1(3) and *sn*-2:  $[2 \times sn-1(3) + sn-2]/3$ .

<sup>c</sup>Experimental values obtained by gas chromatographic analysis of fatty acid methyl (basil) and isopropyl (coriander) esters (means of duplicate analyses).

<sup>d</sup>Concentrations lower than 0.1% are not reported.

of petroselinic, oleic, and *cis*-vaccenic acids. The existing methods for regiospecific analysis of triglycerides also have limitations with respect to accuracy, owing to additional steps in the protocols (TLC, back-calculations, etc.) (27–32). Thus, this method constitutes an improvement over the existing methods for the analysis of these acids in fats and oils: it provides a better separation of the isomers by GC and also provides information on triacylglycerol structure.

## ACKNOWLEDGMENTS

We acknowledge financial support of the Natural Sciences and Engineering Research Council of Canada and of Conseil de Recherche en Pêche et en Agroalimentaire du Québec (CORPAQ).

## REFERENCES

- Lognay, G., Marlier, M., Séverin, M., and Wathelet, J.-P. (1987) Étude des Lipides du Lierre (*Hedera helix* L.). Identification d'Acides Gras Monoéniques Isomères, *Rev. Fr. Corps Gras* 34, 407–411 (1987).
- Fore, S.P., Holmes, R.L., and Bickford, W.G. (1960) Preparation of Petroselinic Acid, *J. Am. Oil Chem. Soc.* 37, 490–491.
- Privett, O.S., Nadenicek, J.D., Weber, R.P., and Pusch, F.J. (1963) Petroselinic Acid and Nonsaponifiable Constituents of Parsley Seed Oil, *J. Am. Oil Chem. Soc.* 40, 28–30.
- Moreau, J.P., Holmes, R.L., and Ward, T.L. (1966) Evaluation of Yield and Chemical Composition of Fennel Seed from Different Planting Dates and Row-Spacings, *J. Am. Oil Chem. Soc.* 43, 352–354.
- Salveson, A., and Svendsen, A.B. (1976) Gas-Liquid Chromatographic Separation and Identification of the Constituents of Caraway Seed Oil, *Planta Med.* 30, 93–96.
- Mallet, J.F., Gaydou, E.M., and Archavlis, A. (1990) Determination of Petroselinic Acid in *Umbelliflorae* Seed Oils by Combined GC and <sup>13</sup>C NMR Spectroscopy Analysis, *J. Am. Oil Chem. Soc.* 67, 607–610.
- Charvet, A.-S., Comeau, L.C., and Gaydou, E.M. (1991) New Preparation of Pure Petroselinic Acid from Fennel Oil (*Foeniculum vulgare*), *J. Am. Oil Chem. Soc.* 68, 604–607.
- Liu, L.S., Hammond, E.G., and Wurtele, E.S. (1994) Accumulation of Petroselinic Acid in Developing Somatic Carrot Embryos, *Phytochemistry* 37, 749–753.
- Reiter, B., Lechner, M., and Lorbeer, E. (1998) The Fatty Acid Profiles—Including Petroselinic and *cis*-Vaccenic Acid—of Different *Umbelliferae* Seed Oils, *Fett-Lipid* 100, 498–502.
- Placek, L.L. (1963) A Review on Petroselinic Acid and Its Derivatives, *J. Am. Oil Chem. Soc.* 40, 319–329.
- Shibahara, A., Yamamoto, K., Nakayama, T., and Kajimoto, G. (1987) *cis*-Vaccenic Acid in Pulp Lipids of Commonly Available Fruits, *J. Am. Oil Chem. Soc.* 64, 397–401.
- Mallet, G., Dimitriades, C., and Ucciani, E. (1988) Quelques Exemples de Répartition Entre Pulpes et Graines des Acides Palmitoléique et *cis*-Vaccénique, *Rev. Fr. Corps Gras* 35, 479–483.
- Ratnayake, S., and McLaughlin, J.L. (1993) Petroselinic Acid from the Ripe Berries of *Aralia spinosa*, *Int. J. Pharm.* 31, 35–37.
- Spitzer, V. (1996) Fatty Acid Composition of Some Seed Oils of the *Sapindaceae*, *Phytochemistry* 42, 1357–1360.
- Wolff, R.L., Christie, W.W., Pédrone, F., Marpeau, A.M., Tsevegüren, N., Aitzetmüller, K., and Gunstone, F.D. (1999)  $\Delta^5$ -Olefinic Acids in the Seed Lipids from Four *Ephedra* Species and Their Distribution Between the  $\alpha$  and  $\beta$  Positions of Triacylglycerols. Characteristics Common to Coniferophytes and Cycadophytes, *Lipids* 34, 855–864.
- Asilbekova, D.T., Gusakova, S.D., and Glushenkova, A.I. (1983) Position Distribution of Petroselinic Acid in the Triacylglycerols of *Acanthopanax sessiflorus* [Isolated from the Seed Lipids], *Chem. Nat. Compd.* 19, 606–607.
- Scano, P., Casu, M., Lai, A., Saba, G., Dessi, M.A., Deiana, M., Corungiu, F.P., and Bandino, G. (1999) Recognition and Quantitation of *cis*-Vaccenic and Eicosenoic Fatty Acids in Olive Oils by <sup>13</sup>C Nuclear Magnetic Resonance Spectroscopy, *Lipids* 34, 757–759.
- Ucciani, E., Chevolleau, S., Mallet, G., and Morin, O. (1989) Application des Adduits Triméthylsilyloxy à l'Analyse des Acides Pétrosélinique et Oléique, *Rev. Fr. Corps Gras* 36, 433–436.
- Ratnayake, W.M.N., and Beare-Rogers, J.L. (1990) Problems of Analyzing C<sub>18</sub> *cis*- and *trans*-Fatty Acids of Margarine on the SP-2340 Capillary Column, *J. Chromatogr. Sci.* 28, 633–639.
- Wolff, R.L., and Vandamme, F.F. (1992) Separation of Petroselinic (*cis*-6 18:1) and Oleic (*cis*-9 18:1) Acids by Gas-Liquid Chromatography of Their Isopropyl Esters, *J. Am. Oil Chem. Soc.* 69, 1228–1231.
- Wolff, R.L. (1998) Comments on the Methodology for the Separation and Quantification of *cis*-6 (petroselinic) and *cis*-9 (oleic) 18:1 acids, *J. Am. Oil Chem. Soc.* 75, 893–894.
- Thies, W. (1995) Determination of the Petroselinic Acid in Seeds of *Coriandrum sativum* by Gas-Liquid Chromatography as *n*-Butyl Esters, *Fat Sci. Technol.* 97, 411–413.
- Liu, L., and Hammond, E.G. (1995) Phenylethyl Esters of Fatty Acids for the Analytical Resolution of Petroselinate and Oleate, *J. Am. Oil Chem. Soc.* 72, 749–751.

24. Angers, P., and Arul, J. (1999) A Simple Method for Regiospecific Analysis of Triacylglycerols by Gas Chromatography, *J. Am. Oil Chem. Soc.* 76, 481–484.
25. Angers, P., Morales, M.R., and Simon, J.E. (1996) Fatty Acid Variation in Seed Oil Among *Ocimum* Species, *J. Am. Oil Chem. Soc.* 73, 393–395.
26. Destailats, F., Angers, P., Wolff, R.L., and Arul, J. (2001) Regiospecific Analysis of Conifer Seed Triacylglycerols by Gas-Liquid Chromatography with Particular Emphasis on  $\Delta^5$ -Olefinic Acids, *Lipids* 36, 1247–1254.
27. Brockerhoff, H., (1971) Stereospecific Analysis of Triglycerides, *Lipids* 6, 942–956.
28. Tagaki, T., and Ando, Y. (1991) Stereospecific Analysis of Triacyl-*sn*-glycerols by Chiral High-Performance Liquid Chromatography, *Lipids* 26, 542–547.
29. Ando, Y., and Takagi, T. (1993) Micro Method for Stereospecific Analysis of Triacyl-*sn*-glycerols by Chiral-Phase High-Performance Liquid Chromatography, *J. Am. Oil Chem. Soc.* 70, 1047–1049.
30. Becker, C.C., Rosenquist, A., and H elmer, G. (1993) Regiospecific Analysis of Triacylglycerols Using Allyl Magnesium Bromide, *Lipids* 28, 147–149.
31. Angers, P., Tousignant,  .., Boudreau, A., and Arul, J. (1998) Regiospecific Analysis of Fractions of Bovine Milk Fat Triacylglycerols with the Same Partition Number, *Lipids* 33, 1195–1201.
32. Damiani, P., Santinelli, F., Simonetti, M.S., Castellini, M., and Rosi, M. (1994) Comparison Between Two Procedures for Stereospecific Analysis of Triacylglycerols from Vegetable Oils—I: Olive Oil, *J. Am. Oil Chem. Soc.* 71, 1157–1162.

[Received April 9, 2001, and in revised form November 26, 2001; revision accepted November 30, 2001]

## Cardiac and Vascular Structure and Function Are Related to Lipid Peroxidation and Metabolism

Peter Steer<sup>a</sup>, Jonas Millgård<sup>a</sup>, Dennis M. Sarabi<sup>a</sup>, Samar Basu<sup>b</sup>, Bengt Vessby<sup>b</sup>,  
Thomas Kahan<sup>c</sup>, Magnus Edner<sup>c</sup>, and Lars Lind<sup>a,\*</sup>

Departments of <sup>a</sup>Medical Sciences/Internal Medicine and <sup>b</sup>Public Health and Caring Sciences/Geriatrics, University Hospital, SE-751 85 Uppsala, Sweden, and <sup>c</sup>Division of Internal Medicine, Karolinska Institutet Danderyd Hospital, SE-182 88 Danderyd, Sweden

**ABSTRACT:** The present study investigated possible relationships between left ventricular mass, intima-media thickness of the carotid artery (IMT), total arterial compliance, and lipid status in a population sample of 58 apparently healthy subjects aged 20 to 69. By stepwise multiple regression analysis, including age, blood pressure, and smoking, left ventricular mass index, measured by M-mode echocardiography, increased by 13.0 g/m<sup>2</sup> for each 1 standard deviation (SD = 0.11 μM,  $r = 0.60$ ,  $P < 0.01$ ) increase in plasma malondialdehyde and 9.50 g/m<sup>2</sup> per SD increase in plasma 8-iso-prostaglandin F<sub>2α</sub> in women only (SD = 8.88 ng/L,  $r = 0.44$ ,  $P = 0.01$ ). Each 1-SD (SD = 0.27 g/L) increase in apolipoprotein B was associated with a 63 μm increase in IMT ( $r = 0.47$ ,  $P = 0.01$ ) and a 0.27 mL/min/m<sup>2</sup>/mm Hg ( $r = -0.60$ ,  $P < 0.01$ ) decrease in stroke index/pulse pressure ratio, reflecting total arterial compliance in women. In men, each 1-SD increase in the proportion of stearic acid (18:0) in serum cholesterol esters (SD = 0.12 percent units) reduced the transmitral E/A ratio, measured by Doppler echocardiography, reflecting left ventricular diastolic function, by 0.10 units ( $r = -0.29$ ,  $P < 0.05$ ). Thus, important cardiovascular characteristics, such as left ventricular mass, left ventricular diastolic function, carotid IMT, and total arterial compliance, were independently predicted by indices of lipid metabolism and peroxidation in apparently healthy subjects.

Paper no. L8762 in *Lipids* 37, 231–236 (March 2002).

Several characteristics of cardiovascular structure and function, e.g., left ventricular hypertrophy, increased intima-media thickness (IMT) of the carotid artery, and total arterial compliance, are associated with cardiovascular morbidity and mortality (1–3). IMT is regarded as an early marker of atherosclerosis and is related to coronary artery calcification (4). Left ventricular diastolic dysfunction is an early finding in hypertensive heart disease (5), but whether left ventricular

diastolic dysfunction is an independent cardiovascular risk factor has not been thoroughly investigated.

A number of epidemiologic studies have shown a strong relationship between serum cholesterol levels and coronary heart disease (CHD) (6). Moreover, high levels of LDL and nonesterified FA are associated with an increased risk of CHD (7,8). Also, saturated FA in serum, particularly palmitic acid (16:0), have been associated with an increased risk of CHD, whereas some PUFA, such as linoleic acid (18:2n-6), may be protective against CHD (9,10). Furthermore, serum levels of nonesterified FA and TG are related to relative wall thickness of the left ventricle in elderly men (11).

Lipid peroxidation has been implicated in the pathogenesis of atherosclerosis (12), CHD (13), and congestive heart failure (14–18). Indeed, oxidized LDL is found in atherosclerotic lesions (19). Oxidized LDL exerts several negative effects on the arterial wall, such as binding to scavenger receptors on macrophages, followed by internalization and formation of foam cells (20). Two biomarkers of lipid peroxidation are malondialdehyde (MDA) and 8-iso-prostaglandin F<sub>2α</sub> (8-iso-PGF<sub>2α</sub>) (21). MDA is produced as an end product by the peroxidation of FA, whereas 8-iso-PGF<sub>2α</sub> is synthesized through nonenzymatic free radical-catalyzed peroxidation of arachidonic acid (20:4n-6). Epidemiologic studies have demonstrated an inverse relationship between dietary intake of the antioxidant vitamin E and CHD, but intervention studies using vitamin E supplementation have produced a divergent picture regarding the use of this vitamin in the prevention of CHD (22–24). The antiatherosclerotic effect of vitamin E is thought to be mediated through protection of LDL from oxidation (25).

There is a significant gender difference in the incidence of cardiovascular disease, with premenopausal women at lower risk (26,27). Estrogen is considered to account for this effect, as the CHD risk in postmenopausal women approaches that of men, while estrogen replacement therapy reduces the risk of CHD.

As left ventricular hypertrophy, increased IMT of the carotid artery, and impaired arterial compliance all seem to be cardiovascular alterations commonly preceding a CHD event, we investigated whether these indices of cardiovascular structure and function are related to lipoprotein levels, plasma FA composition, biomarkers of lipid peroxidation,

\*To whom correspondence should be addressed.  
E-mail: lars.lind@medsci.uu.se

Abbreviations: AVPD, atrio-ventricular valve plane displacement; CHD, coronary heart disease; EF, ejection fraction; IMT, intima-media thickness; 8-iso-PGF<sub>2α</sub>, 8-iso-prostaglandin F<sub>2α</sub>; LVEDD, left ventricular diameter in end-diastole; LVESD, left ventricular diameter in end-systole; LVMI, left ventricular mass index; MDA, malondialdehyde; PL, phospholipid; PP, pulse pressure = systolic blood pressure – diastolic blood pressure; SI, stroke index.



and antioxidants, using data from a sample of apparently healthy subjects. Owing to gender differences in risk, we also investigated whether these relationships are influenced by gender.

## MATERIALS AND METHODS

Subjects were randomly chosen from the population registry of Uppsala, Sweden. The study sample (Table 1) consisted of 58 healthy subjects, aged 20 to 69 yr. None of the subjects was on regular medication or had a history of any disease known to affect the cardiovascular system or a history of any metabolic or other chronic disease. None of the women was on contraceptive or estrogen replacement therapy. Subjects with blood pressures higher than 160/95 mm Hg, fasting hyperglycemia (>6.0 mmol/L), or pronounced hypercholesterolemia (>7.0 mmol/L) at the initiation of the investigation were not included. Blood samples for determination of lipid metabolism were collected in the morning after an overnight fast. Ultrasonographic examinations were generally performed before noon on a subsequent day. The study was approved by the Ethics Committee of Uppsala University, and informed consent was obtained from each participant.

**Echocardiography.** A comprehensive 2-D echocardiographic examination was performed with an Acuson 128 XP/10 device (Mountain View, CA) equipped with a 3.5 MHz transducer, as described previously (28). In brief, all examinations were performed with the subjects in the standard left lateral position and in expiratory apnea or quiet breathing. All recordings were stored on videotape. Two experienced persons analyzed each recording, and the mean values of the two observations were used. Five representative cardiac beats were chosen and the average of these was calculated. Left ventricular dimensions were measured with M-mode using the leading-edge to leading-edge convention. The measurements included interventricular septal thickness, posterior wall thickness, and left ventricular diameter in end-diastole (LVEDD) and end-systole (LVESD). The left ventricular ejection fraction (EF) was calculated as  $(LVEDD^3 - LVESD^3)/LVEDD^3$ . Left ventricular systolic function was also assessed by the atrio-ventricular valve plane displacement method (AVPD) (29). Left ventricular mass was calculated using the M-mode formula of Troy, according to the recommendations by the American Society of

Echocardiography (30), and indexed for body surface area (left ventricular mass index, LVMI) to adjust for body size. Intra-observer and inter-observer coefficients of variation for LVMI were 1% and 12–15%, respectively (28). Stroke index (SI) was calculated by the use of the Teichholz formula (30). The inflow over the mitral valve was measured by pulsed Doppler with the sampling volume placed between the tips of the open mitral leaflets. The maximal velocity of the early filling period (E-wave) and the filling due to atrial contraction (A-wave) were used to calculate the E/A ratio, which was used as an index of left ventricular diastolic function.

**Carotid artery intima-media thickness.** The carotid artery IMT was assessed by high-resolution B-mode ultrasonography (Acuson 128 XP/10 and a 7.5 MHz transducer) of both the right and left common carotid artery, 1–2 cm proximal to the carotid bulb. Images were focused on the far wall of the right and left common carotid artery and recorded on videotape for later analysis. All ultrasonographic images were analyzed with a computerized system (28) by one person. The mean of the far-wall IMT of the right and left common carotid artery was used. The intra-observer coefficient of variation in our laboratory was <10%.

**Arterial compliance and blood pressure.** Blood pressure was recorded with a mercury sphygmomanometer after 15 min rest in the supine position. Pulse pressure (PP) was defined as systolic blood pressure minus diastolic blood pressure. SI was calculated by the use of the Teichholz formula (30). Total arterial compliance was assessed by the SI/PP ratio. This ratio has been shown to be closely related to arterial compliance calculated by the diastolic-decay time constant using a Windkessel model (31).

**Biochemical studies.** LDL and HDL were isolated by a combination of preparative ultracentrifugation and precipitation with a sodium phosphotungstate and magnesium chloride solution. TG and cholesterol concentrations were determined enzymatically in serum and in lipoprotein fractions (Instrumentation Laboratories Company, Lexington, MA), using a Monarch apparatus. The concentrations of serum apolipoprotein A-I and apolipoprotein B were determined by immunoturbidimetry in a Monarch apparatus. FA composition of serum cholesterol esters were analyzed with GLC as described previously (32). Three tocopherols,  $\alpha$ -,  $\beta$ -, and  $\gamma$ -tocopherol, were analyzed with HPLC (33). The serum tocopherol concentration was divided by the sum of the plasma cholesterol and TG concentrations (34). MDA was determined with the thiobarbituric acid test after HPLC separation with fluorescence detection (35). Plasma 8-iso-PGF<sub>2 $\alpha$</sub>  was analyzed by a newly developed radioimmunoassay (21).

**Statistical analysis.** Data are expressed as means  $\pm$  SD unless otherwise specified. Relationships of lipid peroxidation and metabolism variables to cardiac and vascular structure and function were evaluated by linear regression analysis. Subsequently, all lipid variables with a univariate *P*-value <0.05 were entered into forward stepwise multiple regression models to search for independent determinants of cardiovascular structure and function. Age, systolic and diastolic blood

**TABLE 1**  
**Basic Characteristics of Study Participants<sup>a</sup>**

	Men	Women
<i>n</i>	31	27
Age (yr)	52 $\pm$ 12	47 $\pm$ 14
Height (cm)	180 $\pm$ 5	168 $\pm$ 7
Weight (kg)	82.7 $\pm$ 10	67.6 $\pm$ 11.7
BMI (kg/m <sup>2</sup> )	25.4 $\pm$ 2.8	24.0 $\pm$ 3.5
Systolic blood pressure (mm Hg)	125 $\pm$ 14	117 $\pm$ 14
Diastolic blood pressure (mm Hg)	82 $\pm$ 8	75 $\pm$ 8
Smokers	5	3

<sup>a</sup>Means  $\pm$  SD or *n* are given. BMI, body mass index.

pressure, and smoking are related to most of the evaluated cardiovascular variables (36), and were included as confounders in all multiple regressions. Due to the protective effect of female gender against cardiovascular disease, gender was included as a confounder in all multiple regressions, and genders were also analyzed separately (26,27). As smoking contributes to oxidative stress, analysis was also performed after exclusion of smokers (37).  $P < 0.05$  was regarded as significant.

## RESULTS

Basic characteristics and cardiovascular and biochemical variables are given in Tables 1–4.

**Left ventricular geometry.** By multiple stepwise regression analysis, a 1-SD increase in plasma MDA level (SD = 0.13  $\mu\text{M}$ ) was associated with an increase in LVMI of 9.6  $\text{g}/\text{m}^2$  ( $r = 0.40$ ,  $P < 0.01$ ) in the total sample, independent of other confounders (age, gender, blood pressure, and smoking). When genders were analyzed separately, both MDA (13.0  $\text{g}/\text{m}^2$  per SD MDA,  $r = 0.60$ ,  $P < 0.01$ ) and the plasma 8-iso-PGF<sub>2 $\alpha$</sub>  level (9.50  $\text{g}/\text{m}^2$  per SD 8-iso-PGF<sub>2 $\alpha$</sub> ,  $r = 0.44$ ,  $P = 0.01$ ) were significant and independent predictors of LVMI in women only (Fig. 1).

**Left ventricular systolic function.** EF increased by 2.9 percent units for each 1-SD increase in the plasma 8-iso-PGF<sub>2 $\alpha$</sub>  level (SD = 8.31  $\text{ng}/\text{L}$ ,  $r = 0.38$ ,  $P < 0.01$ ), and decreased by 2.6 percent units for each 1-SD increase in the serum  $\gamma$ -tocopherol level (SD = 0.06  $\text{g}/\text{mol}$ ,  $r = -0.34$ ,  $P < 0.05$ ), independently of confounders. These relationships were only present in women when genders were analyzed separately (3.7 percent units per SD 8-iso-PGF<sub>2 $\alpha$</sub> ,  $r = 0.59$ ,  $P < 0.001$ ; and -3.5 percent units per SD  $\gamma$ -tocopherol,  $r = -0.57$ ,  $P < 0.001$  in women). There were no relationships between AVPD and markers of lipid peroxidation and metabolism in the total sample. However, when genders were analyzed separately, each 1-SD increase in the LDL/HDL ratio was associated with a 1.3-mm reduction of the AVPD ( $r = -0.48$ ,  $P < 0.05$ ) in men alone, independent of other confounders.

**TABLE 2**  
Indices of Cardiovascular Structure and Function in Men and in Women<sup>a</sup>

	Men	Women
<i>n</i>	31	27
Intraventricular septum thickness (cm)	1.08 ± 0.24	0.88 ± 0.18
Left ventricular end-diastolic diameter (cm)	5.2 ± 0.3	4.9 ± 0.4
Posterior wall thickness (cm)	0.85 ± 0.15	0.71 ± 0.16
Left ventricular mass index ( $\text{g}/\text{m}^2$ )	118 ± 25	91 ± 21
Atrio-ventricular valve plane displacement (cm)	1.51 ± 0.24	1.47 ± 0.24
Ejection fraction (%)	74 ± 8	74 ± 6
E/A ratio	1.14 ± 0.36	1.43 ± 0.51
Carotid intima-media thickness (mm)	0.80 ± 0.19	0.71 ± 0.14
Stroke index/pulse pressure ratio ( $\text{mL}/\text{min}/\text{m}^2/\text{mm Hg}$ )	1.14 ± 0.39	1.05 ± 0.36

<sup>a</sup>Means ± SD are given.

**TABLE 3**  
Fasting Levels<sup>a</sup> of Lipids, Lipoproteins, Apolipoproteins, Lipid-Adjusted Tocopherols, 8-Iso-prostaglandin F<sub>2 $\alpha$</sub>  and Malondialdehyde

	Men	Women
<i>n</i>	31	27
S-Cholesterol (mM)	5.27 ± 0.86	5.59 ± 1.4
S-Triglycerides (mM)	0.92 ± 0.50	0.74 ± 0.50
S-HDL cholesterol (mM)	1.29 ± 0.33	1.53 ± 0.36
S-LDL cholesterol (mM)	3.57 ± 0.78	3.73 ± 1.26
LDL/HDL ratio	2.97 ± 1.08	2.59 ± 1.12
S-Apolipoprotein A-I (g/L)	1.24 ± 0.15	1.41 ± 0.20
S-Apolipoprotein B (g/L)	0.87 ± 0.19	0.86 ± 0.27
S- $\alpha$ -Tocopherol (g/mol)	1.76 ± 0.21	1.86 ± 0.29
S- $\beta$ -Tocopherol (g/mol)	0.023 ± 0.006	0.031 ± 0.041
S- $\gamma$ -Tocopherol (g/mol)	0.130 ± 0.047	0.126 ± 0.072
P-8-Iso-prostaglandin F <sub>2<math>\alpha</math></sub> (ng/L)	16.38 ± 7.45	20.14 ± 8.88
P-Malondialdehyde ( $\mu\text{M}$ )	0.65 ± 0.13	0.56 ± 0.11

<sup>a</sup>Means ± SD are given. S, serum; P, plasma.

**Left ventricular diastolic function.** No relationships were found between the E/A ratio and markers of lipid peroxidation and metabolism in the total sample. However, when genders were analyzed separately, each increase in the proportion of stearic acid (18:0) in the cholesterol ester fraction of 1 SD was associated with a decrease in the E/A ratio of 0.10 units ( $r = -0.29$ ,  $P < 0.05$ , Fig. 2) independent of confounders in men alone.

**Carotid artery IMT.** No associations were found with carotid IMT in the total sample. However, when genders were analyzed separately, each increase in the serum apolipoprotein B level of 1 SD was associated with an increase in IMT of 63  $\mu\text{m}$  ( $r = 0.47$ ,  $P = 0.01$ ), independent of confounders in women.

**Arterial compliance.** No relationships were found between the SI/PP ratio and markers of lipid peroxidation and metabolism in the total sample. However, when genders were analyzed separately, each increase in the serum apolipoprotein B level of

**TABLE 4**  
FA Composition<sup>a</sup> of Serum Cholesterol Esters

FA	FA proportion (%)	
	Men	Women
<i>n</i>	31	27
Myristic acid, 14:0	0.9 ± 0.2	0.9 ± 0.2
Pentadecanoic acid, 15:0	0.2 ± 0.04	0.2 ± 0.03
Palmitic acid, 16:0	11.4 ± 0.6	11.2 ± 0.6
Palmitoleic acid, 16:1	3.7 ± 1.5	3.6 ± 0.9
Stearic acid, 18:0	0.9 ± 0.1	0.9 ± 0.1
Oleic acid, 18:1	21.9 ± 2.3	21.6 ± 1.7
Linoleic acid, 18:2n-6	49.2 ± 3.9	50.1 ± 3.5
$\alpha$ -Linolenic acid, 18:3n-3	0.9 ± 0.1	0.9 ± 0.2
$\gamma$ -Linolenic acid, 18:3n-6	0.8 ± 0.3	0.7 ± 0.3
Dihomo- $\gamma$ -linolenic acid, 20:3n-6	0.7 ± 0.2	0.7 ± 0.1
Arachidonic acid, 20:4n-6	6.7 ± 1.1	6.3 ± 1.3
Eicosapentaenoic acid, 20:5n-3	2.0 ± 1.0	2.0 ± 0.6
Docosapentaenoic acid, 22:5n-3	<0.05	<0.05
Docosahexaenoic acid, 22:6n-3	0.9 ± 0.3	1.0 ± 0.2

<sup>a</sup>Data are *n* or means ± SD.

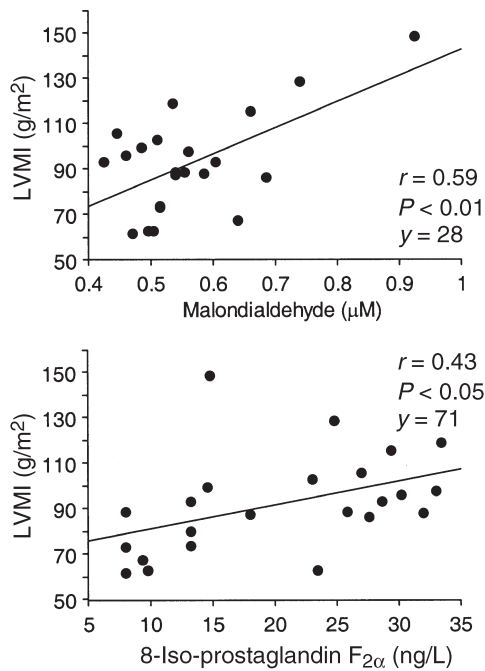


FIG. 1. Univariate regression of left ventricular mass index (LVMI) on plasma malondialdehyde and 8-iso-prostaglandin  $F_{2\alpha}$  in women.

1 SD was associated with a decrease in the SI/PP ratio of 0.27 mL/min/m<sup>2</sup>/mm Hg ( $r = -0.60$ ,  $P < 0.01$ ), independent of confounders in women alone.

**Smoking.** The regressions of LVMI and EF on markers of lipid peroxidation and metabolism were also studied with the eight smokers excluded, as smoking contributes to lipid peroxidation. However, exclusion of smokers did not alter the relationships between LVMI and EF and circulating levels of 8-iso-PGF<sub>2α</sub>, MDA, and serum  $\gamma$ -tocopherol.

## DISCUSSION

The major findings of the present study are that in apparently healthy subjects LVMI is predicted by biomarkers of lipid peroxidation in women, whereas left ventricular diastolic function is inversely related to the proportion of stearic acid

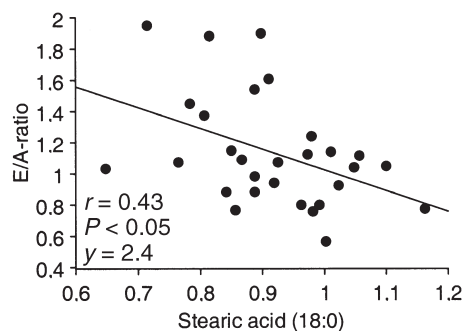


FIG. 2. Univariate regression of the E/A ratio on the proportion of stearic acid (18:0) in the serum cholesterol ester fraction in men.

(18:0) in men. Furthermore, apolipoprotein B is a main predictor of total arterial compliance and IMT in women.

Few studies have been devoted to the relation between lipid peroxidation and left ventricular mass. Experimental models to induce left ventricular hypertrophy by pressure overload in rodents have shown increased superoxide dismutase and glutathione peroxidase activity, and lower MDA content in the myocardium (17,38). The associations between lipid peroxidation and LVMI in the present study suggest that lipid peroxidation in plasma may be of importance for growth of the left ventricle in healthy subjects.

The E/A ratio, a sensitive way to evaluate left ventricular diastolic filling, was inversely related to the saturated FA stearic acid (18:0) in serum cholesterol esters in men. This is in accordance with previous findings that supplementation with saturated FA in humans results in impaired left ventricular diastolic filling, while addition of n-3 FA has the opposite effect (39). Taken together, these data suggest that FA composition influences left ventricular diastolic performance. The underlying mechanisms may involve alterations in myocyte relaxation, as recently proposed (39), or alterations in afterload.

In the present study, left ventricular systolic performance, as evaluated by EF, was related to 8-iso-PGF<sub>2α</sub> and inversely related to the antioxidant  $\gamma$ -tocopherol. Increased levels of biomarkers of lipid peroxidation have been found in myocardial tissue in experimental heart failure (17,18), and in the circulation and pericardial fluid in humans with heart failure (14–16,40). The unexpected relations between EF, 8-iso-PGF<sub>2α</sub>, and  $\gamma$ -tocopherol in the present study may reflect the fact that all subjects were healthy and had normal left ventricular systolic function. Furthermore, left ventricular systolic function, as assessed by the AVPD method, was inversely related to the LDL/HDL ratio in men. Cardiac afterload is mainly determined by arterial compliance and blood pressure and is related to both growth and an increased contractile function of the left ventricle (41). An increased myocardial fibrosis and an increase in relative wall thickness of the left ventricle, as seen in hypertensive left ventricular hypertrophy, will result in a reduced compliance of the left ventricle, as assessed by, e.g., the E/A ratio, and subsequently in a reduced systolic performance (5). Thus, the relations of LVMI, E/A ratio, and AVPD to markers of lipid metabolism and peroxidation may in part be explained by an increase in afterload due to structural vascular changes.

Structural vascular changes, as assessed by, e.g., carotid IMT measurements, influence total arterial compliance (42). Indeed, both carotid IMT and total arterial compliance were independently related to apolipoprotein B in women in this study. Apolipoprotein B has been shown previously to be related to IMT in subjects with CHD and non-insulin-dependent diabetes mellitus (43,44). IMT is also predicted by traditional cardiovascular risk factors, such as LDL cholesterol and saturated FA (45–47). Thus, our findings further support an impact of lipoprotein metabolism on arterial distensibility and atherosclerosis also in subjects without clinical signs of atherosclerosis.



**Limitations.** The aim of the present study was to generate new hypotheses in an area of research that has previously received little attention. A number of correlations were performed and, with the chosen significance level of 5%, one correlation in 20 may be significant merely by chance. This risk is even greater when genders are analyzed separately. Therefore, these results must be interpreted with caution until reproduced by other investigators. We observed a greater impact of lipid peroxidation on left ventricular mass and of apolipoprotein B on carotid IMT and arterial compliance in women, whereas stearic acid (18:0) appears to be more predictive of left ventricular diastolic function in men. The different patterns of relations of cardiac and vascular structure and function to markers of lipid peroxidation and metabolism in men and women appear to be gender specific, although the number of male and female subjects was limited and type I errors were likely to occur. Thus, larger studies are needed to confirm the findings and gender-specific differences of this study.

In conclusion, important structural and functional changes in the heart and blood vessels are related to indices of lipid metabolism and peroxidation in apparently healthy subjects.

## REFERENCES

- Levy, D., Garrison, R.J., Savage, D.D., Kannel, W.B., and Castelli, W.P. (1990) Prognostic Implications of Echocardiographically Determined Left Ventricular Mass in the Framingham Heart Study, *N. Engl. J. Med.* 322, 1561–1566.
- O'Leary, D.H., Polak, J.F., Kronmal, R.A., Manolio, T.A., Burke, G.L., and Wolfson, S.K., Jr. (1999) Carotid-Artery Intima and Media Thickness as a Risk Factor for Myocardial Infarction and Stroke in Older Adults. Cardiovascular Health Study Collaborative Research Group, *N. Engl. J. Med.* 340, 14–22.
- Dart, A.M., Lacombe, F., Yeoh, J.K., Cameron, J.D., Jennings, G.L., Laufer, E., and Esmore, D.S. (1991) Aortic Distensibility in Patients with Isolated Hypercholesterolaemia, Coronary Artery Disease, or Cardiac Transplant, *Lancet* 338, 270–273.
- Davis, P.H., Dawson, J.D., Mahoney, L.T., and Lauer, R.M. (1999) Increased Carotid Intimal-Medial Thickness and Coronary Calcification Are Related in Young and Middle-Aged Adults. The Muscatine Study, *Circulation* 100, 838–842.
- Schwartzkopf, B., Motz, W., Vogt, M., and Strauer, B.E. (1993) Heart Failure on the Basis of Hypertension, *Circulation* 87 (Suppl.), IV66–72.
- Jousilahti, P., Vartiainen, E., Pekkanen, J., Tuomilehto, J., Sundvall, J., and Puska, P. (1998) Serum Cholesterol Distribution and Coronary Heart Disease Risk: Observations and Predictions Among Middle-Aged Population in Eastern Finland, *Circulation* 97, 1087–1094.
- Frayn, K.N., Williams, C.M., and Arner, P. (1996) Are Increased Plasma Non-esterified Fatty Acid Concentrations a Risk Marker for Coronary Heart Disease and Other Chronic Diseases? *Clin. Sci.* 90, 243–253.
- Castelli, W.P., Doyle, J.T., Gordon, T., Hames, C.G., Hjortland, M.C., Hulley, S.B., Kagan, A., and Zukel, W.J. (1977) HDL Cholesterol and Other Lipids in Coronary Heart Disease. The Cooperative Lipoprotein Phenotyping Study, *Circulation* 55, 767–772.
- Simon, J.A., Hodgkins, M.L., Browner, W.S., Neuhaus, J.M., Bernert, J.T., Jr., and Hulley, S.B. (1995) Serum Fatty Acids and the Risk of Coronary Heart Disease, *Am. J. Epidemiol.* 142, 469–476.
- Miettinen, T.A., Naukkarinen, V., Huttunen, J.K., Mattila, S., and Kumlin, T. (1982) Fatty-Acid Composition of Serum Lipids Predicts Myocardial Infarction, *Br. Med. J.* 285, 993–996.
- Sundström, J., Lind, L., Nyström, N., Zethelius, B., Andrén, B., Hales, C.N., and Lithell, H.O. (2000) Left Ventricular Concentric Remodeling Rather Than Left Ventricular Hypertrophy Is Related to the Insulin Resistance Syndrome in Elderly Men, *Circulation* 101, 2595–2600.
- Jayakumari, N., Ambikakumari, V., Balakrishnan, K.G., and Iyer, K.S. (1992) Antioxidant Status in Relation to Free Radical Production During Stable and Unstable Anginal Syndromes, *Atherosclerosis* 94, 183–190.
- Chandra, M., Chandra, N., Agrawal, R., Kumar, A., Ghatak, A., and Pandey, V.C. (1994) The Free Radical System in Ischemic Heart Disease, *Int. J. Cardiol.* 43, 121–125.
- Diaz-Velez, C.R., Garcia-Castineiras, S., Mendoza-Ramos, E., and Hernandez-Lopez, E. (1996) Increased Malondialdehyde in Peripheral Blood of Patients with Congestive Heart Failure, *Am. Heart J.* 131, 146–152.
- Mallat, Z., Philip, I., Lebret, M., Chatel, D., Maclouf, J., and Tedgui, A. (1998) Elevated Levels of 8-Iso-prostaglandin  $F_{2\alpha}$  in Pericardial Fluid of Patients with Heart Failure: A Potential Role for *in vivo* Oxidant Stress in Ventricular Dilatation and Progression to Heart Failure, *Circulation* 97, 1536–1539.
- Keith, M., Geranmayegan, A., Sole, M.J., Kurian, R., Robinson, A., Omran, A.S., and Jeejeebhoy, K.N. (1998) Increased Oxidative Stress in Patients with Congestive Heart Failure, *J. Am. Coll. Cardiol.* 31, 1352–1356.
- Dhalla, A.K., Hill, M.F., and Singal, P.K. (1996) Role of Oxidative Stress in Transition of Hypertrophy to Heart Failure, *J. Am. Coll. Cardiol.* 28, 506–514.
- Kaul, N., Siveski-Iliskovic, N., Thomas, T.P., Hill, M., Khaper, N., and Singal, P.K. (1995) Probucol Improves Antioxidant Activity and Modulates Development of Diabetic Cardiomyopathy, *Nutrition* 11, 551–554.
- Ylä-Herttuala, S., Palinski, W., Rosenfeld, M.E., Parthasarathy, S., Carew, T.E., Butler, S., Witztum, J.L., and Steinberg, D. (1989) Evidence for the Presence of Oxidatively Modified Low Density Lipoprotein in Atherosclerotic Lesions of Rabbit and Man, *J. Clin. Invest.* 84, 1086–1095.
- Navab, M., Berliner, J.A., Watson, A.D., Hama, S.Y., Territo, M.C., Lusis, A.J., Shih, D.M., Van Lenten, B.J., Frank, J.S., Demer, L.L., *et al.* (1996) The Yin and Yang of Oxidation in the Development of the Fatty Streak. A Review Based on the 1994 George Lyman Duff Memorial Lecture, *Arterioscler. Thromb. Vasc. Biol.* 16, 831–842.
- Basu, S. (1998) Radioimmunoassay of 8-Iso-prostaglandin  $F_{2\alpha}$ : An Index for Oxidative Injury via Free Radical Catalysed Lipid Peroxidation, *Prostaglandins Leukot. Essent. Fatty Acids* 58, 319–325.
- Manson, J.E., Gaziano, J.M., Jonas, M.A., and Hennekens, C.H. (1993) Antioxidants and Cardiovascular Disease: A Review, *J. Am. Coll. Nutr.* 12, 426–432.
- Stephens, N.G., Parsons, A., Schofield, P.M., Kelly, F., Cheeseman, K., and Mitchinson, M.J. (1996) Randomised Controlled Trial of Vitamin E in Patients with Coronary Disease: Cambridge Heart Antioxidant Study (CHAOS), *Lancet* 347, 781–786.
- Yusuf, S., Dagenais, G., Pogue, J., Bosch, J., and Sleight, P. (2000) Vitamin E Supplementation and Cardiovascular Events in High-Risk Patients. The Heart Outcomes Prevention Evaluation Study Investigators, *N. Engl. J. Med.* 342, 154–160.
- Esterbauer, H., Puhl, H., Dieber-Rotheneder, M., Waeg, G., and Rabl, H. (1991) Effect of Antioxidants on Oxidative Modification of LDL, *Ann. Med.* 23, 573–581.



26. Lerner, D.J., and Kannel, W.B. (1986) Patterns of Coronary Heart Disease Morbidity and Mortality in the Sexes: A 26-Year Follow-up of the Framingham Population, *Am. Heart J.* 111, 383–390.
27. Kannel, W.B., Hjortland, M.C., McNamara, P.M., and Gordon, T. (1976) Menopause and Risk of Cardiovascular Disease: The Framingham Study, *Ann. Intern. Med.* 85, 447–452.
28. Malmqvist, K., Kahan, T., Edner, M., Held, C., Hägg, A., Lind, L., Müller-Brunotte, R., Nyström, F., Öhman, K.P., Osbakken, M.D., and Ostergern, J. (2001) Regression of Left Ventricular Hypertrophy in Human Hypertension with Irbesartan, *J. Hypertens.* 19, 1167–1176.
29. Höglund, C., Alam, M., and Thorstrand, C. (1988) Atrioventricular Valve Plane Displacement in Healthy Persons. An Echocardiographic Study, *Acta Med. Scand.* 224, 557–562.
30. Teichholz, L.E., Kreulen, T., Herman, M.V., and Gorlin, R. (1976) Problems in Echocardiographic Volume Determinations: Echocardiographic–Angiographic Correlations in the Presence of Absence of Asynergy, *Am. J. Cardiol.* 37, 7–11.
31. Randall, O.S., Westerhof, N., van den Bos, G.C., and Alexander, B. (1986) Reliability of Stroke Volume to Pulse Pressure Ratio for Estimating and Detecting Changes in Arterial Compliance, *J. Hypertens. (Suppl.)* 4, S293–S296.
32. Boberg, M., Croon, L.B., Gustafsson, I.B., and Vessby, B. (1985) Platelet Fatty Acid Composition in Relation to Fatty Acid Composition in Plasma and to Serum Lipoprotein Lipids in Healthy Subjects with Special Reference to the Linoleic Acid Pathway, *Clin. Sci.* 68, 581–587.
33. Öhrvall, M., Tengblad, S., and Vessby, B. (1993) Lower Tocopherol Serum Levels in Subjects with Abdominal Adiposity, *J. Intern. Med.* 234, 53–60.
34. Thurnham, D.I., Davies, J.A., Crump, B.J., Situnayake, R.D., and Davis, M. (1986) The Use of Different Lipids to Express Serum Tocopherol: Lipid Ratios for the Measurement of Vitamin E Status, *Ann. Clin. Biochem.* 23, 514–520.
35. Öhrvall, M., Tengblad, S., Ekstrand, B., Siegbahn, A., and Vessby, B. (1994) Malondialdehyde Concentration in Plasma Is Inversely Correlated to the Proportion of Linoleic Acid in Serum Lipoprotein Lipids, *Atherosclerosis* 108, 103–110.
36. Lind, L., Andersson, P.E., Andrén, B., Hänni, A., and Lithell, H.O. (1995) Left Ventricular Hypertrophy in Hypertension Is Associated with the Insulin Resistance Metabolic Syndrome, *J. Hypertens.* 13, 433–438.
37. Morrow, J.D., Frei, B., Longmire, A.W., Gaziano, J.M., Lynch, S.M., Shyr, Y., Strauss, W.E., Oates, J.A., and Roberts, L.J., 2nd (1995) Increase in Circulating Products of Lipid Peroxidation (F<sub>2</sub>-isoprostanes) in Smokers. Smoking as a Cause of Oxidative Damage, *N. Engl. J. Med.* 332, 1198–1203.
38. Gupta, M., and Singal, P.K. (1989) Higher Antioxidative Capacity During a Chronic Stable Heart Hypertrophy, *Circ. Res.* 64, 398–406.
39. Grimsgaard, S., Bonna, K.H., Hansen, J.B., and Myhre, E.S. (1998) Effects of Highly Purified Eicosapentaenoic Acid and Docosahexaenoic Acid on Hemodynamics in Humans, *Am. J. Clin. Nutr.* 68, 52–59.
40. Ghatak, A., Brar, M.J., Agarwal, A., Goel, N., Rastogi, A.K., Vaish, A.K., Sircar, A.R., and Chandra, M. (1996) Oxy Free Radical System in Heart Failure and Therapeutic Role of Oral Vitamin E, *Int. J. Cardiol.* 57, 119–127.
41. Ganau, A., Devereux, R.B., Roman, M.J., de Simone, G., Pickering, T.G., Saba, P.S., Vargiu, P., Simongini, I., and Laragh, J.H. (1992) Patterns of Left Ventricular Hypertrophy and Geometric Remodeling in Essential Hypertension, *J. Am. Coll. Cardiol.* 19, 1550–1558.
42. Lin, W.W., Chen, Y.T., Hwang, D.S., Ting, C.T., Wang, K.Y., and Lin, C.J. (1999) Evaluation of Arterial Compliance in Patients with Carotid Arterial Atherosclerosis, *Chung Hua I Hsueh Tsa Chih (Taipei)* 62, 598–604.
43. Sharrett, A.R., Patsch, W., Sorlie, P.D., Heiss, G., Bond, M.G., and Davis, C.E. (1994) Associations of Lipoprotein Cholesterol, Apolipoproteins A-I and B, and Triglycerides with Carotid Atherosclerosis and Coronary Heart Disease. The Atherosclerosis Risk in Communities (ARIC) Study, *Arterioscler. Thromb.* 14, 1098–1104.
44. Niskanen, L., Rauramaa, R., Miettinen, H., Haffner, S.M., Mercuri, M., and Uusitupa, M. (1996) Carotid Artery Intima–Media Thickness in Elderly Patients with NIDDM and in Nondiabetic Subjects, *Stroke* 27, 1986–1992.
45. Crouse, J.R., Goldbourt, U., Evans, G., Pinsky, J., Sharrett, A.R., Sorlie, P., Riley, W., and Heiss, G. (1996) Risk Factors and Segment-Specific Carotid Arterial Enlargement in the Atherosclerosis Risk in Communities (ARIC) Cohort, *Stroke* 27, 69–75.
46. Ferrieres, J., Elias, A., Ruidavets, J.B., Cantet, C., Bongard, V., Fauvel, J., and Boccalon, H. (1999) Carotid Intima–Media Thickness and Coronary Heart Disease Risk Factors in a Low-Risk Population, *J. Hypertens.* 17, 743–748.
47. Ma, J., Folsom, A.R., Lewis, L., and Eckfeldt, J.H. (1997) Relation of Plasma Phospholipid and Cholesterol Ester Fatty Acid Composition to Carotid Artery Intima–Media Thickness: The Atherosclerosis Risk in Communities (ARIC) Study, *Am. J. Clin. Nutr.* 65, 551–559.

[Received March 2, 2001, and in revised form December 6, 2001; revision accepted January 16, 2002]

# Fluctuations in Human Milk Long-Chain PUFA Levels in Relation to Dietary Fish Intake

Lotte Lauritzen<sup>a,\*</sup>, Marianne H. Jørgensen<sup>b</sup>, Harald S. Hansen<sup>c</sup>, and Kim F. Michaelsen<sup>a</sup>

<sup>a</sup>Center for Advanced Food Studies, Research Department of Human Nutrition, Royal Veterinary and Agricultural University, <sup>b</sup>Department of Pediatrics, University Hospital of Copenhagen, and <sup>c</sup>Department of Pharmacology, Royal Danish School of Pharmacy, Denmark

**ABSTRACT:** Within the Danish population, milk DHA (22:6n-3) levels vary by more than a factor of 10. This paper deals with fluctuations in the milk content of 22:6n-3 and other long-chain PUFA (LCPUFA) and the acute effects of fish meals and fish oil supplements on milk levels of LCPUFA. Twelve fish-eating mothers with 4-mon-old infants provided one blood and one adipose tissue sample, and seven consecutive morning hind-milk samples with dietary records from the previous days. Another 12 lactating women were given fish oil (2–8 g) for breakfast and delivered 6–12 milk samples during the following 24 h. The mean milk 22:6n-3 content of the fish-eating mothers was  $0.57 \pm 0.28$  FA% (= percentage of total area of FAME peaks in GLC) and the day-to-day variation (SD/mean) within the individual was  $35 \pm 17\%$ . Mean milk 22:6n-3 content on mornings with no fish the day before was  $0.42 \pm 0.15$  FA%; this was increased by  $82 \pm 17\%$  ( $n = 9$ ,  $P = 0.05$ ) if the mother had eaten fatty fish. Fish oil resulted in a twofold increase in milk 22:6n-3 levels, which peaked after 10 h and lasted for 24 h. The EPA content of milk was also increased by fish meals and fish oil supplements, but these had no effect on the level of arachidonic acid. The study showed that diurnal and day-to-day fluctuations in levels of milk n-3 LCPUFA are large, which makes it difficult to assess the 22:6n-3 intake of breast-fed infants from a single milk sample. In studies of the functional outcome of dietary 22:6n-3 in breast-fed infants it is suggested also to use a measure of maternal 22:6n-3 status.

Paper no. L8890 in *Lipids* 37, 237–244 (March 2002).

Studies on formula-fed infants have indicated the beneficial effects of dietary DHA (22:6n-3) on visual acuity and cognitive development (1–5). It is therefore likely that 22:6n-3 levels in maternal milk could affect the visual and mental development of breast-fed infants. A few cross-sectional studies (6–8) and one maternal intervention trial (9) indicate that this may be the case.

In most Western populations mean 22:6n-3 levels are around 0.1–0.4% of milk FA (FA%: percentage of the total area of FAME peaks in the gas–liquid chromatogram) (10),

\*To whom correspondence should be addressed at Research Department of Human Nutrition, The Royal Veterinary and Agricultural University, Rolighedsvej 30, DK-1958 Frederiksberg C, Denmark. E-mail: ll@kvl.dk

Abbreviations: 22:6n-3 response, area under the curve of milk 22:6n-3 vs. time (AUC, calculated by the trapezium rule), or the difference between peak and baseline levels of 22:6n-3 in milk; AUC, area under the curve of milk FA level vs. time after test meal; BMI, body mass index ( $\text{kg}/\text{m}^2$ ); FA%, percentage of the total area of FAME peaks in the chromatogram; LCPUFA, long-chain PUFA; RBC, erythrocytes.

but milk 22:6n-3 levels in populations with a high fish consumption have been found to be up to 10 times higher (11–13). Within the Danish population, milk 22:6n-3 levels vary by more than a factor of 10, and in a cross-sectional study 55% of this variation could be explained by differences in maternal fish intake (6). Many studies have shown that supplementation of lactating women with various 22:6n-3 rich oils give rise to an increase in milk 22:6n-3 levels (14–21), but few studies have looked at the day-to-day variation and the time course after 22:6n-3 supplementation.

The arachidonic acid (20:4n-6) content of human milk varies much less than the content of n-3 long-chain PUFA (LCPUFA) (22). A high maternal intake of fish and fish oil might also affect the milk content of EPA (20:5n-3) and other n-3 LCPUFA. The acids 20:5n-3 and 20:4n-6 compete with one another in many metabolic processes, and therefore 20:5n-3 might theoretically inhibit the synthesis and mammary secretion of 20:4n-6. This may be of concern since studies have indicated that the addition of n-3 LCPUFA to formula milk has a negative effect on 20:4n-6 levels in infant erythrocytes (RBC) (23–27), which could be prevented by simultaneous addition of 20:4n-6 (27).

There is a need to know in more detail how the dietary intake of fish and fish oil by the mother affects the LCPUFA supply of the breast-fed infant. We investigated day-to-day variations in LCPUFA levels of breast milk from individual women and related these to fish intake. Furthermore, maternal RBC and adipose tissue levels of 22:6n-3 were correlated with the levels of 22:6n-3 in breast milk in order to compare milk levels with biomarkers of maternal habitual fish intake. Finally, we compared the immediate effect of different doses and two kinds of fish oil supplements on milk LCPUFA levels. Our results indicate that there are considerable difficulties in assessing the dietary intake of LCPUFA in breast-fed infants.

## EXPERIMENTAL PROCEDURES

**Subjects.** Twenty-four lactating women were recruited. The only inclusion criteria were that their infants were term, normal weight for gestation, and around 4 mon of age (mean  $3.9 \pm 0.5$  mon old, range 3.1–5.3). Apart from breast milk, some infants were given tea and water, and the oldest of the infants (22.6 wk old) was given some porridge. The Scientific-Ethical Committees for Copenhagen and Frederiksberg (KF 01-299/97) approved the study protocols and all subjects gave written consent

to participate. After inclusion they were interviewed about their pregnancy, delivery, the frequency of their fish intake, and height and weight of both mothers and infants. All mothers were of normal weight [body mass index (BMI) <27 kg/m<sup>2</sup>], had an average of 1.5 (range 1–5) children, and a fish intake frequency of 3.8 ± 2.0 meals/wk.

**Design.** The mothers were divided into two groups (for a “7-d-study” and a “test-meal-study”) mainly according to their fish intake. In the 7-d-study, 12 mothers with a high fish intake (4.6 ± 1.5 meals/wk) provided one blood sample and one adipose tissue biopsy from the buttock. Every day for a week they delivered a milk sample along with a dietary record of the previous day (only food items, not quantities). The mothers were asked to collect the milk sample immediately after nursing their baby for the first time in the morning. Fish meals were classified as fatty or lean according to fat content [given in national food composition tables (28)] with a cutoff at 5 g fat/100 g fresh weight. We categorized the milk samples (fatty, lean, or no fish) according to the dietary intake of the mother the day before the sample was taken. On several days the mothers had more than one meal of fish, and in these cases the meal with the highest marine fat content was used for the categorization. For each mother, the mean FA composition was calculated for all days in each of the three categories (fatty, lean, or no fish). This way we could compare the effect of fish intake on the FA composition of the milk by a paired statistical analysis.

In the test-meal-study, the other 12 women with a lower fish intake (2.9 ± 2.5 meals/wk) were given a morning test meal containing two different doses of microencapsulated fish oil on two nonconsecutive days (see Table 1). We used two different kinds of fish oil, a standard fish oil (Dry n-3<sup>TM</sup> 18:12 from BASF Health and Nutrition A/S, Ballerup, Denmark), and a tuna oil with a low 20:5n-3 content (Dry n-3<sup>TM</sup> 5:25 from BASF Health and Nutrition A/S). All fish oil doses were supplied with 2½ dL of yogurt. Following the test meal, a hind-milk sample was expressed after each episode of nursing during the next 24 h. A single woman was given only one test meal and was asked to collect milk for a day without any intake of fish or fish oil.

**Sampling.** Milk samples (2–5 mL) were stored in the home at 5°C until they were collected no later than 30 h after expression. Aliquots (2 mL) of the milk samples were stored at –80°C with BHT (Sigma), final concentration 0.001%. All milk samples were analyzed within one year of collection. Ten to 50 mg adipose tissue biopsies were stored at –80°C

in physiological saline with 0.005% BHT. Blood samples (10 mL) were taken by venipuncture in ice-cold EDTA-conditioned tubes. RBC were separated from plasma and leukocytes immediately after sampling and washed three times in physiological saline. The isolated packed RBC were reconstituted 1:1 in physiological saline with 1 mM EDTA and 0.005% BHT and kept at –80°C until they were analyzed (maximum storage time 6½ mon).

**FA analysis.** Lipids from 1-mL aliquots of the milk samples were extracted with the Bligh and Dyer procedure (29) using 3 mL of a 1:2 mixture of chloroform/methanol followed by addition of 1 mL chloroform. Phases were separated by addition of 1 mL 0.28 N HCl and centrifugation. Lipids from 1.2 mL of reconstituted RBC were extracted using the Rose and Oklander procedure (30). Ice-cold isopropanol (6.6 mL) with 0.005% BHT was added, followed by 10 min ultrasonication and steady shaking for 50 min. Then 4.2 mL of chloroform was added and, after one more round of ultrasonication and shaking, the phases were separated by centrifugation. Lipids from 10–50 mg of adipose tissue were extracted with 4 mL of chloroform containing 0.005% BHT and phase-separated by addition of 0.8 mL of H<sub>2</sub>O and centrifugation.

The extracted lipids were reesterified with BF<sub>3</sub> in methanolic NaOH. The resulting FAME were extracted with heptane and separated by GLC on an HP-6890 (Hewlett-Packard) equipped with a 30-m SP2380 capillary column (0.32 mm i.d., 0.2 µm film thickness; Supelco, Bellefonte, PA) and an FID. The injector temperature was set at 250°C. Samples of 1 µL (1 mg FAME/40 µL) were automatically injected with a split ratio of 1:49. For the initial 3 min the oven temperature was 80°C, which was then increased to 110°C at 30°C/min, then to 208°C at 3°C/min, and finally to 240°C at 50°C/min, which was held for 10 min before cool-down and injection of a new sample (total run time 46 min). Helium was used as the carrier gas at a constant flow of 2 mL/min (pressure 10.7 psi, velocity 35 cm/s). All peaks from 12:0 to 22:6n-3, except for that of BHT, were integrated.

The FAME peaks were tentatively identified by comparison of retention times with those of known FAME mixtures (Nu-Chek-Prep Inc., Elysian, MN), a fish-oil mixture (Fish Qual; Laurodan Fine Chemicals AB, Malmö, Sweden), and the 22:5n-6 peak in a rat testis preparation. Furthermore, we verified our identification by TLC separation of FAME from one milk sample and a fish-oil sample on silver nitrate-impregnated silica gel plates in hexane/ether (85:15, vol/vol). Bands repre-

**TABLE 1**  
**Content of Test Meals<sup>a</sup>**

Test meal	Fish oil type	Fish oil (g)	No. of meals	n-3 LCPUFA (g)	20:5n-3 (g)	22:6n-3 (g)	20:4n-6 (g)
a	Standard type	2.1	4	0.7	0.37	0.25	0.03
b	Standard type	4.2	8	1.5	0.75	0.50	0.06
c	Standard type	8.3	6	2.9	1.50	1.00	0.12
e	Tuna oil	3.7	5	1.3	0.18	0.92	0.08

<sup>a</sup>Twelve women were each given two test meals (except one woman) with different doses of fish oil. The fish oil was provided microencapsulated with 2½ dL of yogurt at breakfast.

senting the different degrees of unsaturation were visualized, scraped from the TLC plates, extracted with heptane, and separated by GLC. Typically, more than 95% of the total chromatogram area was identified. Under the present GLC conditions, some FAME coelute, e.g., 20:4n-6 and 20:3n-3, but as the latter is a minor component even in fish oil (31), we assumed that this FA contributed less than 10% to the peak.

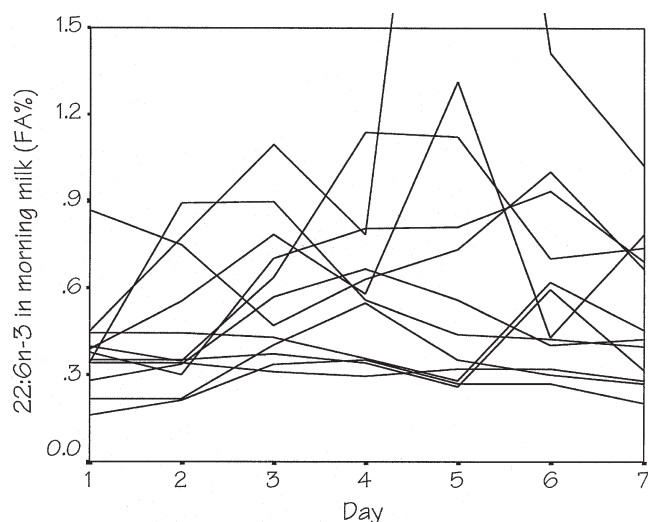
The FA composition of all samples was determined in duplicate and in a series of 8–18, each containing a blank and a reference sample. The series was rejected if major FA in the reference sample deviated by more than 2 SD from the previously established mean values. The individual sample was re-analyzed if the relative difference (difference/mean) of major FA in the duplicates was appreciably increased relative to the typical deviation for that particular FA. The interassay variation of 22:6n-3 in milk and RBC was 10 and 1.9%, respectively, and the mean interassay variation of all identified peaks with area% >0.5 was  $2.1 \pm 1.9\%$  ( $n = 14$ ) and  $5.3 \pm 3.4\%$  ( $n = 14$ ), respectively. All adipose tissue samples were analyzed in one run, and the intraassay variation of the identified FA was generally below 5%. The relative amounts of identified FA (FA%) are given as area%.

**Statistical analysis.** All results are given as mean  $\pm$  SD. The FA percentage for 22:6n-3 and other n-3 LCPUFA in milk did not agree with a Gaussian distribution, and neither did all of the 22:6n-3 responses [measured as area under the curve of milk 22:6n-3 vs. time (AUC, calculated by the trapezium rule) or as the difference between peak and baseline levels of 22:6n-3] to the test meals. Therefore, all statistical group comparisons of FA composition or 22:6n-3 levels were performed by Wilcoxon signed rank tests. Analysis of the test meal responses was performed with linear regression models on logarithmically transformed values. Mean milk 22:6n-3 levels and the 22:6n-3 levels in RBC and gluteal adipose tissue did not deviate from a Gaussian distribution; thus, correlation analyses between these parameters were done by linear regression analysis. All the statistical analyses were performed by SPSS (version 10.0, SPSS Inc., Chicago, IL).

## RESULTS

**Variations in milk 22:6n-3 levels according to fish meals.** The mean 22:6n-3 content of the breast milk of the mothers in the 7-d-study was  $0.57 \pm 0.28$  FA% ( $n = 12$  women), giving a between-person variation of 49%. The relative 22:6n-3 content of the milk from the individual women varied considerably from day to day (Fig. 1) and the mean day-to-day variation within milk from the individual woman [(CV% = (SD/mean) · 100)] was  $35 \pm 17\%$  ( $n = 12$ ).

During the experimental week the women had, altogether, 62 meals of fish [on average  $5.2 \pm 1.3$  per woman ( $n = 12$ )]. The most frequent fish meal type was lunch (35 meals), which typically included open-faced sandwiches with fatty fish. Lean fish was eaten more frequently for dinner. The milk samples were classified as described in the Experimental Procedures section. All subjects had at least one milk sample in



**FIG. 1.** Day-to-day variations in 22:6n-3 levels [peak area percentage (FA%)] in morning hind-milk samples from 12 lactating mothers of 4-month-old infants. One of the women had a milk 22:6n-3 content of 3.4 FA% after a lunch meal of herring and cod liver (outlier in the plot).

the category “lean fish” and 11 of the mothers also had at least one sample in the “fatty fish” category. During the experimental week, the mothers had on average  $2.6 \pm 1.2$  d ( $n = 12$ ) where they had no intake of fish on the previous day.

The milk 22:6n-3 level was significantly increased by maternal fish consumption (fatty or lean) on the previous day [ $0.63 \pm 0.31$  FA% compared with  $0.41 \pm 0.15$  FA% on days with no fish intake,  $n = 12$ ,  $P = 0.018$  (Wilcoxon signed rank tests)]. Thus, consumption of fish resulted in a 1.5-fold higher level of 22:6n-3 in the milk on the following morning. This increase was mainly due to intake of fatty fish, as the relative increase in milk 22:6n-3 after a day with fatty fish consumption was on average  $1.7 \pm 0.8$  times compared with no-fish levels ( $n = 11$ ). Meals of lean fish did not give rise to a significant increase in milk 22:6n-3 (Table 2). An extremely high

**TABLE 2**  
FA Composition [peak area percentage (FA%)] of Morning Milk According to Fish Intake the Previous Day<sup>a</sup>

	7-d mean	No fish	Fatty fish	Lean fish
n (women)	12	12	11	12
Days (n)	7	$2.6 \pm 1.2$	$2.4 \pm 1.5$	$1.9 \pm 1.1$
SFA	$42.9 \pm 2.9$	$44.1 \pm 3.6$	$48.9 \pm 11.6$	$43.2 \pm 4.6$
MUFA	$39.5 \pm 2.1$	$39.0 \pm 2.1$	$36.6 \pm 11.3$	$39.5 \pm 2.6$
18:2n-6	$10.6 \pm 1.5$	$10.2 \pm 1.6$	$10.0 \pm 3.4$	$11.0 \pm 2.3$
20:4n-6	$0.42 \pm 0.06$	$0.42 \pm 0.06$	$0.40 \pm 0.13$	$0.41 \pm 0.07$
18:3n-3	$1.5 \pm 0.3$	$1.4 \pm 0.2$	$1.4 \pm 0.5$	$1.5 \pm 0.5$
20:5n-3	$0.21 \pm 0.08$	$0.16 \pm 0.06$	$0.24 \pm 0.12^{**}$	$0.15 \pm 0.04$
22:5n-3	$0.30 \pm 0.10$	$0.25 \pm 0.06$	$0.31 \pm 0.10^{*}$	$0.24 \pm 0.06$
22:6n-3	$0.57 \pm 0.28$	$0.41 \pm 0.15$	$0.73 \pm 0.36^{**}$	$0.49 \pm 0.14$
Total n-6	$11.7 \pm 1.6$	$11.3 \pm 1.7$	$11.0 \pm 3.7$	$12.1 \pm 2.4$
Total n-3	$2.8 \pm 0.5$	$2.5 \pm 0.4$	$2.9 \pm 1.1^{*}$	$2.7 \pm 0.6$
n-6/n-3	$4.4 \pm 1.0$	$4.7 \pm 0.8$	$3.8 \pm 1.8$	$4.6 \pm 1.1$

<sup>a</sup>Daily milk samples from 12 women were categorized according to fish intake the day before. The individual mean FA compositions in each category were calculated, and the table provides the means of all women. *P*-value for statistical comparisons with No fish (Wilcoxon): \* $P < 0.05$ , and \*\* $P < 0.01$ . SFA, saturated FA; MUFA, monounsaturated FA.

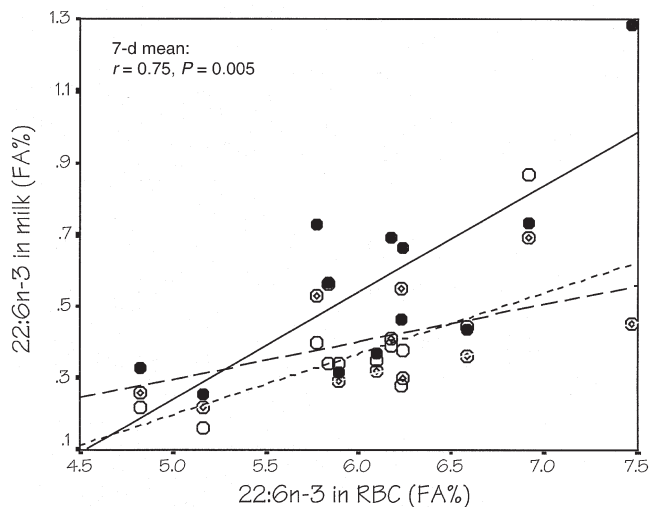


milk 22:6n-3 content (3.4 FA%) was found in one of the milk samples, which was collected the day after the mother had both herring and cod liver for lunch.

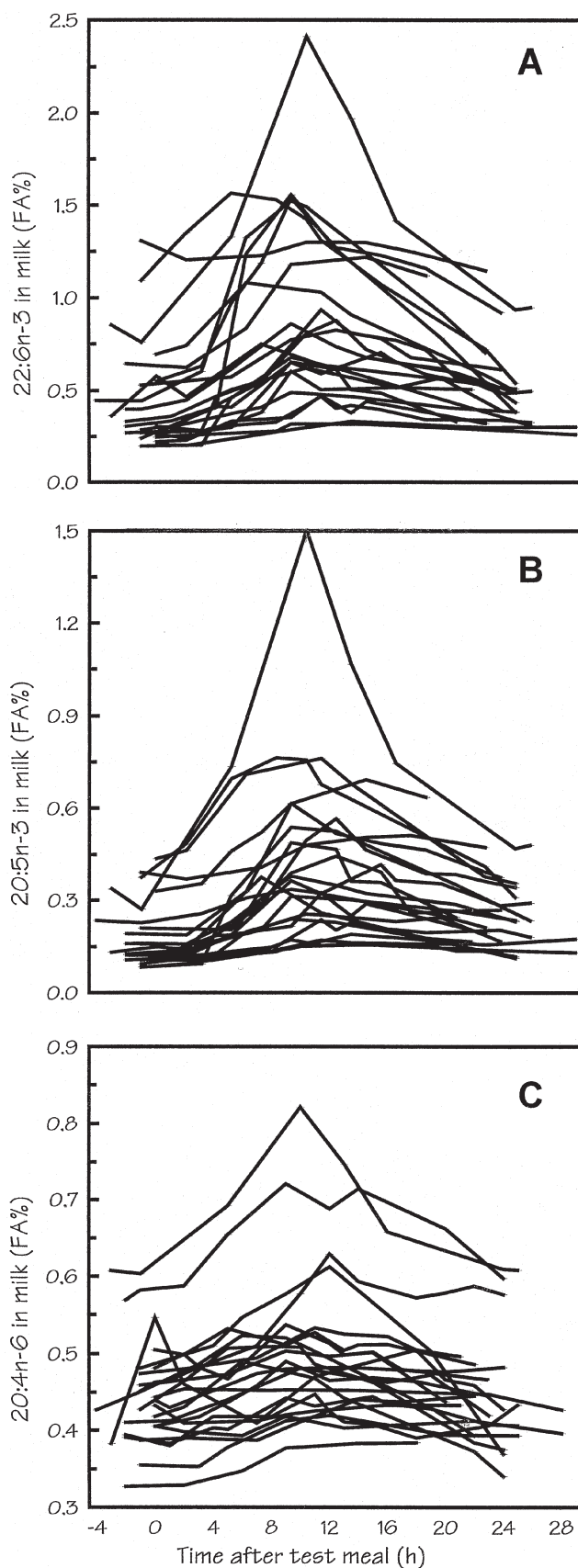
**Tissue markers of milk 22:6n-3.** The mean 22:6n-3 content of gluteal adipose tissues and RBC, two commonly used biomarkers of 22:6n-3 status, were  $0.20 \pm 0.05$  and  $6.10 \pm 0.71$  FA%, respectively. The average levels of 22:6n-3 in all seven milk samples from the same mother were significantly associated with that of RBC (Fig. 2), and also tended to be so with that of adipose tissues ( $r = 0.50$ ,  $P = 0.096$ ). The two indicators of 22:6n-3 status, RBC and adipose tissue, correlated with each other ( $r = 0.79$ ,  $P = 0.002$ ).

We also calculated correlation coefficients between the 22:6n-3 content of RBC and that of the milk for each of the 7 d. The 22:6n-3 content of the individual milk samples correlated significantly with the 22:6n-3 levels of RBC on 5 out of 7 d ( $P = 0.030$ – $0.001$ ), but on other days this association was less clear (day 3:  $P = 0.09$  and day 4:  $P = 0.52$ ). We also calculated the correlation between the 22:6n-3 status measures and the mean 22:6n-3 content of the milk on days after no fish in order to see whether maternal 22:6n-3 status was better reflected in the 22:6n-3 level of milk that was not influenced by a recent fish intake. The 22:6n-3 content of the no-fish milk samples was not significantly associated with that of RBC (Fig. 2), but correlated with that of adipose tissues ( $r = 0.69$ ,  $P = 0.012$ ).

**Effect of fish oil test meals on milk 22:6n-3.** In the test-meal study a fish oil-containing meal resulted in an acute increase in the relative 22:6n-3 content of the milk, which started after a few hours and peaked after  $10 \pm 2$  h ( $n = 23$ ) (Fig. 3A). At peak, milk 22:6n-3 reached levels  $2.3 \pm 1.1$  times higher than baseline levels (Table 3). The effect of fish oil was transient;  $23 \pm 2$  h after ingestion of the test meal the milk 22:6n-3 level



**FIG. 2.** Correlation between the levels [peak area percentage (FA%)] of 22:6n-3 in maternal erythrocytes (RBC) and milk on one individual day [here day 1 of the study ( $-\circ-$ ), on days with no prior fish consumption ( $-\circ\cdot-$ ), or as a mean of all seven days ( $-\bullet-$ ), the regression parameters of which are given in the figure]. The correlation coefficient for day 1 was  $r = 0.69$ ,  $P = 0.013$ , and for no-fish  $r = 0.51$ ,  $P = 0.09$ .



**FIG. 3.** The levels [peak area percentage (FA%)] of 22:6n-3 (A), 20:5n-3 (B), and 20:4n-6 (C) in human milk as a function of time (h) after ingestion of test meals with fish oil ( $n = 23$  test meals).

**TABLE 3**  
**FA Composition [peak area percentage (FA%)] of Breast Milk at Baseline, Peak, and One Day After a Test Meal with Fish Oil<sup>a</sup>**

	Baseline	Peak	End of period
<i>n</i> (test meals)	23	23	23
Time (h)	-1.1 ± 0.9	9.6 ± 2.1	23.4 ± 2.4
SFA	43.1 ± 3.9	42.5 ± 7.8	43.9 ± 4.0
MUFA	39.7 ± 2.9	39.2 ± 7.0	39.8 ± 2.6
18:2n-6	10.3 ± 1.5	10.3 ± 2.1	9.4 ± 1.7
20:4n-6	0.44 ± 0.06	0.50 ± 0.13***	0.44 ± 0.07
18:3n-3	1.3 ± 0.4	1.2 ± 0.3*	1.2 ± 0.4
20:5n-3	0.11 ± 0.03	0.44 ± 0.29***	0.26 ± 0.13**
22:5n-3	0.27 ± 0.11	0.40 ± 0.16***	0.30 ± 0.07**
22:6n-3	0.45 ± 0.29	0.94 ± 0.51***	0.54 ± 0.26*
Total n-6	11.5 ± 1.6	11.6 ± 2.3	10.5 ± 1.8
Total n-3	2.50 ± 0.67	3.39 ± 1.05***	2.61 ± 0.59
n-6/n-3	4.9 ± 0.9	3.7 ± 0.8***	4.2 ± 0.7***

<sup>a</sup>From 12 women, hind-milk samples were collected from every lactation in 24 h following ingestion of test meals (see Table 1). The data represent mean of all fish oil responses regardless of given dose and test subject. *P*-value for comparisons with baseline (Wilcoxon): \**P* < 0.05, \*\**P* < 0.01, and \*\*\**P* < 0.001.

was almost back at starting level, being only marginally increased by 1.3 ± 0.4 times morning levels (Table 3).

The magnitude of the 22:6n-3 responses in the milk (peak relative to start concentration) after the different test meals was significantly different [Table 4, part A, *P* = 0.007 (ANOVA with logarithmically transformed values)], but a dose response was not immediately evident. There were, however, differences in the BMI of the women given the various test meals, and the starting points for milk 22:6n-3 also deviated between test meals, although not significantly. A multiple linear regression analysis (taking account of test subject, BMI, habitual fish intake frequency, and the type and

dose of fish oil) showed a highly significant dose-response relationship between the amount of 22:6n-3 given in the test meal and the resultant response (AUC) in milk 22:6n-3 (Table 5). However, the size of the 22:6n-3 response was also inversely related to the BMI of the mother (Table 5). A simple linear model of the 22:6n-3 response vs. dose of 22:6n-3/BMI explains 56% (*P* < 0.001) of the variation in the 22:6n-3 responses (data not shown).

Type of fish oil [tuna oil (e) or ordinary fish oil (a-c)] also significantly affected the milk 22:6n-3 response in the multiple regression model that controlled for the 22:6n-3 dose given (Table 5), indicating that the response to a certain dose of 22:6n-3 was larger after tuna oil than after ordinary fish oil. This was not apparent in the direct group comparison (c vs. e, Table 4, part A), but the tuna oil 22:6n-3 response was significantly larger than the fish oil response if one compares test meals with similar amounts of n-3 LCPUFA (b vs. e, *P* = 0.004).

*Milk content of 20:5n-3 and 20:4n-6.* In the 7-d-study the levels of other n-3 LCPUFA in the milk were also significantly increased if the lactating woman had fatty fish the day before the milk sample was taken as compared with the levels if she had not had fish the previous day (Table 2). The 20:5n-3 response after a fish oil test meal appears very similar to that of 22:6n-3 (Fig. 3B), with approximately the same relative increase and the same time course. All the levels of n-3 LCPUFA, as well as the ratio between n-6 and n-3 PUFA, were significantly affected at the peak of the fish oil response (Table 3).

In the test-meal-study we used two different types of fish oil: the low-20:5n-3 tuna oil and an ordinary high-20:5n-3 fish oil. As expected, the 20:5n-3 increase after tuna oil (e) was significantly lower than following the dose of fish oil that gave a

**TABLE 4**  
**The Acute Response in Breast Milk Content of 22:6n-3 (A), 20:5n-3 (B), and 20:4n-6 (C) After Test Meals with Four Different Doses of Fish Oil (a-c,e)<sup>a</sup>**

Meals <sup>b</sup>	<i>n</i>	Baseline (FA%)	Peak (FA%)	Total AUC (FA%·time <sup>-1</sup> )	Corrected AUC (FA%·time <sup>-1</sup> ) <sup>c</sup>	BMI (kg/m <sup>2</sup> )
<b>A</b>						
a	4	0.33 ± 0.07	0.64 ± 0.23	11.9 ± 2.9	4.1 ± 2.0 <sup>a,b</sup>	22.3 ± 1.6
b	8	0.58 ± 0.42	0.82 ± 0.45	14.5 ± 7.1	2.4 ± 1.7 <sup>a</sup>	25.0 ± 1.7
c	6	0.43 ± 0.26	1.08 ± 0.69	16.7 ± 9.3	7.5 ± 4.2 <sup>b,c</sup>	24.0 ± 2.7
e	5	0.36 ± 0.13	1.23 ± 0.44	18.9 ± 6.7	10.8 ± 5.0 <sup>c</sup>	23.7 ± 1.8
<b>B</b>						
a		0.13 ± 0.03	0.28 ± 0.11	5.1 ± 1.2	2.1 ± 0.8 <sup>a</sup>	
b		0.21 ± 0.14	0.41 ± 0.22	8.0 ± 4.0	2.5 ± 1.1 <sup>a</sup>	
c		0.13 ± 0.05	0.51 ± 0.09	9.7 ± 4.5	6.2 ± 3.1 <sup>b</sup>	
e		0.18 ± 0.10	0.31 ± 0.18	5.5 ± 3.1	1.4 ± 1.1 <sup>a</sup>	
<b>C</b>						
a		0.45 ± 0.09	0.51 ± 0.14	12.2 ± 2.7	1.3 ± 0.9 <sup>a</sup>	
b		0.44 ± 0.04	0.48 ± 0.04	10.7 ± 0.8	0.4 ± 0.3 <sup>a</sup>	
c		0.44 ± 0.07	0.53 ± 0.10	11.2 ± 3.6	1.2 ± 0.8 <sup>a</sup>	
e		0.45 ± 0.03	0.44 ± 0.03	10.8 ± 1.5	0.6 ± 0.6 <sup>a</sup>	

<sup>a</sup>The responses in milk LCPUFA content after fish oil test meals are expressed as relative content at peak [area% (FA%)] and area under the curve (AUC) of relative FA content vs. time (approximately 24 h). Responses were compared by ANOVA and subsequent *post hoc* tests on logarithmically transformed responses. In each column, values with different superscript letters are significantly different (*P* < 0.05). BMI, body mass index.

<sup>b</sup>Fish oil-containing test meals as specified in Table 1.

<sup>c</sup>The total AUC response corrected for the area below baseline.

**TABLE 5**  
**Influence of Individual Parameters in a Multiple Linear Regression Model for the Breast Milk 22:6n-3 Increase After Fish Oil-Containing Test Meals<sup>a</sup>**

	Unstandardized coefficients	P
22:6n-3 in test meal (g)	0.572 ± 0.155	0.002
BMI (kg/m <sup>2</sup> )	-0.059 ± 0.019	0.007
Fish oil type (a,b,c = 1; e = 2) <sup>b</sup>	0.229 ± 0.107	0.049
Frequency of fish intake (wk <sup>-1</sup> )	0.004 ± 0.003	0.147
Subject	-0.012 ± 0.010	0.247

<sup>a</sup>The 22:6n-3 increase in the milk was expressed as the logarithm of the corrected AUC response (FA%·time<sup>-1</sup>). All included variables are given in the table. The model has an overall  $r = 0.85$  (adjusted  $r^2 = 0.63 \pm 0.18$ ) and  $P = 0.001$ .

<sup>b</sup>a, b, and c represent three different test meals with standard fish oil, and e represents meals with tuna oil as specified in Table 1.

similar amount of 22:6n-3 (c). However, there was no difference between the two types of fish oil if we compared test doses of oils that supplied similar amounts of total n-3 LCPUFA (b) (Table 4, part B). A proxy for the secreted amounts (measured as AUC of FA% vs. time) showed that the increase in 20:5n-3 was  $3.7 \pm 2.6$  FA%·time<sup>-1</sup> (here in average 23 h) and that 22:6n-3 increased with  $4.5 \pm 3.5$  FA%·time<sup>-1</sup>. Since the test meals on average contained  $0.9 \pm 0.5$  g 20:5n-3 and  $0.6 \pm 0.3$  g 22:6n-3, the increase in milk 20:5n-3 per g ingested 20:5n-3 was approximately half of that for 22:6n-3, being  $5.0 \pm 3.5$  and  $9.0 \pm 6.3$  AUC/g ( $n = 23$ ), respectively.

In the 7-d-study, the fish meals did not have any negative effect on milk 20:4n-6 levels (Table 2). In the test-meal-study, milk 20:4n-6 showed a tendency toward an increase after fish oil test meals (Fig. 3C). When the results obtained from the fish oil doses were pooled, the milk 20:4n-6 levels at the peak of the responses were significantly higher than at baseline (Table 3), but no statistical differences were apparent when we compared the peak and AUC responses of 20:4n-6 after the different test meal types (Table 4, part C).

## DISCUSSION

*The time course of changes in milk n-3 LCPUFA.* In the present study we found that 22:6n-3, 22:5n-3, 20:5n-3, and total n-3 PUFA were all maximally increased 10 h after a test meal containing 2–8 g of fish oil (Fig. 3). This is in agreement with previously published time courses for n-3 LCPUFA after consumption of 1 g of fish oil (15) or 0.5 g algal oil (21), and for 16:0, 18:1n-9, and 18:2n-6 after doses of <sup>1</sup>H- or <sup>13</sup>C-labeled FA (32,33). It is also consistent with the proposed route for mammary gland fat uptake from the circulation being through the modality of chylomicrons (33). Francois *et al.* (34) found similar time courses for 18:2n-6, 22:1n-11, 18:0, and 12:0 after consumption of vegetable oil, herring oil, or cocoa butter, but after consuming 20 g menhaden oil the levels of 22:6n-3 and 20:5n-3 increased much more slowly with a peak around 24 h postingestion. In considering the large fish oil dose given in that study (34), the peak 22:6n-3 and 20:5n-3 levels in the milk were low compared to the responses with test meals with fish oil seen in the present study. The delayed

peak could theoretically be explained by the high dose of fish oil given by Francois *et al.* However, consumption of 20 g of herring oil resulted in a faster 22:1n-11 response than did 7 g (34), and we found no delay of the peak after increasing the dose of fish oil from 2 to 8 g (data not shown).

We found that the acute milk response to dietary fish oil had almost disappeared after 24 h. In many studies on the effect of daily LCPUFA supplementation, milk samples are taken 24 h after the supplement (15,19,35). Therefore, these studies may underestimate the effect of supplements on the FA composition of the milk. In this study we found that there was a significant effect of fish intake the day before milk sampling on n-3 LCPUFA levels in morning milk. The milk samples were typically taken approximately 17 h after the fish meal, which, as judged from the curves in Figure 3, seems to be a representative time with respect to the day-mean of milk 22:6n-3. This effect was primarily due to meals of fatty fish as opposed to lean fish (Table 2).

*Factors affecting 22:6n-3 milk levels.* Milk 22:6n-3 levels were significantly and dose-dependently increased after test meals with fish oil (Tables 3 and 5), which in their content of n-3 LCPUFA were comparable to that of moderate-sized fish meals [an open-faced sandwich with fatty fish or a dinner serving of codfish (28)]. We found that milk 22:6n-3 levels were negatively influenced by the BMI of the mother (Table 5), as previously reported (18,19). As milk 22:6n-3 levels are expressed relative to that of other FA (FA%) the BMI effect probably reflects increasing dilution of dietary lipids in the plasma by the endogenous lipid pool. The LCPUFA content of human milk has been shown to reflect the FA composition of maternal plasma phospholipids (17,19), which in turn is determined by dietary FA and slightly modified by hepatic metabolism and FA from internal stores. Variations in the total amount of fat ingested in the test meal and in previous and following meals probably account for many of the individual differences.

*Factors affecting 20:5n-3 milk levels.* In the present study we compared marine oils with a low and a high 20:5n-3 content in order to see whether the first oil would increase milk 22:6n-3 levels without affecting levels of 20:4n-6 and 20:5n-3. We found no difference between the 20:5n-3 responses for doses of the two fish oil types that supplied similar amounts of n-3 LCPUFA. Ordinary fish oil has a high 20:5n-3 content compared with most fish consumed in Denmark [20:5n-3/22:6n-3 = 1.5 and 0.4 (28), respectively]. Thus, at a certain 22:6n-3 response one would expect that the 20:5n-3 response to fish oil would be 3–4 times higher than that of a meal of fish. However, the 20:5n-3 and 22:6n-3 responses in the milk after fish oil and meals of fatty fish were not so different (see Tables 2 and 3). The 20:5n-3 response after fish oil test meals also appears to be lower than that of 22:6n-3, based on our estimates of the secreted amounts of these two n-3 LCPUFA. This blunting of the 20:5n-3 response does not necessarily indicate a selective mechanism for mammary secretion of 22:6n-3, but may reflect a high hepatic conversion of plasma 20:5n-3 to 22:6n-3. However, the 22:6n-3 response to tuna oil was, if anything, larger than the response



to a similar dose of 22:6n-3 from fish oil. Furthermore, it was shown in another study that dietary flaxseed oil (11 g 18:3n-3 daily for 4 wk) significantly increased maternal plasma and breast milk 18:3n-3 and 20:5n-3 but had no effect on 22:6n-3 (36). Thus, the apparent lower 20:5n-3 secretion does not appear to be due to rapid elongation and desaturation.

**Factors affecting 20:4n-6 milk levels.** The content of 20:4n-6 in human milk varies much less than the content of n-3 FA, both within the individual and among different populations (1,10,37). In the current study the day-to-day variation in milk 20:4n-6 content of 12 women was only about 8% (data not shown). Four grams of fish oil with 1 FA% of 20:4n-6 (31) would increase the maternal 20:4n-6 intake 7–40% (38,39). In agreement with other studies (14,15,17–21), our results indicate that fish meals do not have a decreasing effect on milk 20:4n-6 and that milk 20:4n-6 was significantly increased by fish oil-containing test meals.

We expected that fish oil with a high 20:5n-3 content might have a negative effect on the 20:4n-6 level of the milk. However, the 20:4n-6 level of the milk was significantly increased at the peak of the n-3 LCPUFA response after test meals with fish oil (Table 3). Although tuna oil had a lower 20:5n-3 content and a higher 20:4n-6 content than the ordinary fish oil [2.2 and 1.4 FA%, respectively (see Table 1)], it did not seem to have the same positive effect on milk 20:4n-6 levels as ordinary fish oil. The 20:4n-6 level at the peak of the tuna oil response was not higher than at time 0 (Table 4, part C). The overall significant effect that fish oil had on milk 20:4n-6 levels occurred in spite of this. Thus, we found no indication that fish oil with a low 20:5n-3 content had a protective effect on milk 20:4n-6 content compared to a standard high-20:5n-3 fish oil.

**Biomarker of infant 22:6n-3 intake.** The present results indicate that variations in milk 22:6n-3 levels within the individual woman are of the same order of magnitude as the total variation between the individuals. The average milk 22:6n-3 content in this study was in agreement with previous observations in the Danish population (6,26,40), as was the observed variation between subjects (i.e., 64%). We found a within-subject day-to-day variation of 35% and a peak effect of fish oil on milk 22:6n-3 content on the order of a factor of 2.

To assess infant 22:6n-3 intake, one would want to determine the milk 22:6n-3 content that reflects the maternal habitual fish intake. Such typical milk 22:6n-3 content will be difficult to assess accurately in a population with a variable fish intake, because of the variability in milk n-3 LCPUFA. On several days within the 7-d study there was no correlation between the 22:6n-3 content of milk and that of RBC and gluteal adipose tissues (data not shown), both of which are commonly used biomarkers of the habitual intake of n-3 LCPUFA (41–45). Thus, there is a large risk that the 22:6n-3 level in a single milk sample does not reflect the habitual intake of the breast-fed infant. We hypothesized that milk levels of 22:6n-3 on mornings with no fish consumption the previous day would represent a resting level that would reflect the overall 22:6n-3 status of the mother. However, we found that this putative resting level of milk 22:6n-3 was poorly associated with 22:6n-3 levels in maternal RBC and adipose tissues.

In this study we found that 22:6n-3 levels in milk from individual fish-eating women can vary almost as much as 22:6n-3 levels in human milk in general. Furthermore, the present study indicates that n-3 LCPUFA from the maternal diet appears faster and to a larger extent in the milk than previously realized. The acute effect of fish meals on milk n-3 LCPUFA levels is more pronounced than the effect of the overall fish intake frequency. Thus, the present study has clearly demonstrated the drawbacks of using 22:6n-3 levels in single milk samples as a measure of the dietary intake of 22:6n-3 in breast-fed infants.

## ACKNOWLEDGMENTS

We gratefully acknowledge Pediatric Nurse Lise Lotte Ingholt for assisting in collecting the data and Technician Bettina Sørensen for performing the FA analysis. This study was financed in part by FØTEK—The Danish Research and Development Program for Food and Technology and BASF Health and Nutrition A/S.

## REFERENCES

1. Hamosh, M., and Salem, N. (1998) Long-Chain Polyunsaturated Fatty Acids, *Biol. Neonate* 74, 106–120.
2. Anderson, J.W., Johnstone, B.M., and Remley, D.T. (1999) Breast-Feeding and Cognitive Development: A Meta-Analysis, *Am. J. Clin. Nutr.* 70, 525–535.
3. Gibson, R.A., and Makrides, M. (1998) The Role of Long-Chain Polyunsaturated Fatty Acids (LCPUFA) in Neonatal Nutrition, *Acta Paediatr.* 87, 1017–1022.
4. SanGiovanni, J.P., Berkey, C.S., Dwyer, J.T., and Colditz, G.A. (2000) Dietary Essential Fatty Acids, Long-Chain Polyunsaturated Fatty Acids, and Visual Resolution Acuity in Healthy Fullterm Infants: A Systematic Review, *Early Hum. Dev.* 57, 165–188.
5. Lauritzen, L., Hansen, H.S., Jørgensen, M.H., and Michaelsen, K.F. (2001) The Essentiality of Long-Chain n-3 Fatty Acids in Relation to Development and Function of the Brain and Retina, *Prog. Lipid Res.* 40, 1–94.
6. Jørgensen, M.H., Hernell, O., Hughes, E., and Michaelsen, K.F. (2001) Is There a Relation Between Docosahexaenoic Acid Concentration in Mother's Milk and Visual Development in Term Infants? *J. Pediatr. Gastroenterol. Nutr.* 32, 293–296.
7. Innis, S.M., Gilley, J., Werker, J., MacKinnon, M., and Auestad, N. (2000) Long-Chain Polyunsaturated Fatty Acids, Growth and Neurodevelopment Among Breast-Fed Infants Followed Prospectively to 1 Year of Age, *FASEB J.* 14, A725 (Abstract).
8. Scott, D.T., Janowsky, J.S., Carroll, R.E., Taylor, J.A., Auestad, N., and Montalto, M.B. (1998) Formula Supplementation with Long-Chain Polyunsaturated Fatty Acids: Are There Developmental Benefits? *Pediatrics* 102, E591–E593.
9. Gibson, R.A., Neumann, M.A., and Makrides, M. (1997) Effect of Increasing Breast-Milk Docosahexaenoic Acid on Plasma and Erythrocyte Phospholipid Fatty Acids and Neural Indices of Exclusively Breast-Fed Infants, *Eur. J. Clin. Nutr.* 51, 578–584.
10. Koletzko, B., Thiel, I., and Abiodun, P.O. (1992) The Fatty Acid Composition of Human Milk in Europe and Africa, *J. Pediatr.* 120, S62–S70.
11. Jensen, R.G. (1999) Lipids in Human Milk, *Lipids* 34, 1243–1271.
12. Innis, S.M., and Kuhnlein, H.V. (1988) Long-Chain n-3 Fatty Acids in Breast-Milk of Inuit Women Consuming Traditional Foods, *Early Hum. Dev.* 18, 185–189.
13. Chulei, R., Xiaofang, L., Hongsheng, M., Xiulan, M., Guizheng, L., Gianhong, D., DeFrancesco, C.A., and Connor, W.E. (1995)



- Milk Composition in Women from Five Different Regions of China: The Great Diversity of Milk Fatty Acids, *J. Nutr.* 125, 2993–2998.
14. Harris, W.S., Connor, W.E., and Lindsey, S. (1984) Will Dietary Omega-3 Fatty Acids Change the Composition of Human Milk? *Am. J. Clin. Nutr.* 40, 780–785.
  15. Henderson, R.A., Jensen, R.G., Lammi-Keefe, C.J., Ferris, A.M., and Dardick, K.R. (1992) Effect of Fish Oil on the Fatty Acid Composition of Human Milk and Maternal and Infant Erythrocytes, *Lipids* 27, 863–869.
  16. Jensen, C.L., Prager, T.C., Zou, Y.L., Fraley, J.K., Maude, M., Anderson, R.E., and Heird, W.C. (1999) Effects of Maternal Docosahexaenoic Acid Supplementation on Visual Function and Growth of Breast-Fed Term Infants, *Lipids* 34, S225.
  17. Jensen, C.L., Maude, M., Anderson, R.E., and Heird, W.C. (2000) Effect of Docosahexaenoic Acid Supplementation of Lactating Women on the Fatty Acid Composition of Breast-Milk Lipids and Maternal and Infant Plasma Phospholipids, *Am. J. Clin. Nutr.* 71, 292S–299S.
  18. Makrides, M., Neumann, M.A., and Gibson, R.A. (1996) Effect of Maternal Docosahexaenoic Acid (DHA) Supplementation on Breast-Milk Composition, *Eur. J. Clin. Nutr.* 50, 352–357.
  19. Helland, I.B., Saarem, K., Saugstad, O.D., and Drevon, C.A. (1998) Fatty Acid Composition in Maternal Milk and Plasma During Supplementation with Cod Liver Oil, *Eur. J. Clin. Nutr.* 52, 839–845.
  20. Cherian, G., and Sim, J.S. (1996) Changes in the Breast-Milk Fatty Acids and Plasma Lipids of Nursing Mothers Following Consumption of n-3 Polyunsaturated Fatty Acid Enriched Eggs, *Nutrition* 12, 8–12.
  21. Fidler, N., Sauerwald, T., Pohl, A., Demmelmair, H., and Koletzko, B. (2000) Docosahexaenoic Acid Transfer into Human Milk After Dietary Supplementation: A Randomized Clinical Trial, *J. Lipid Res.* 41, 1376–1383.
  22. Sanders, T.A.B. (1990) Essential Fatty Acid Requirements of Vegetarians in Pregnancy, Lactation, and Infancy, *Am. J. Clin. Nutr.* 70, 555S–559S.
  23. Guesnet, P., Pugo-Gunsam, P., Maurage, C., Pinault, M., Girardeau, B., Alessandri, J.M., Durand, G., Antoine, J.M., and Couet, C. (1999) Blood Lipid Concentrations of Docosahexaenoic and Arachidonic Acids at Birth Determine Their Relative Postnatal Changes in Term Infants Fed Breast-Milk or Formula, *Am. J. Clin. Nutr.* 70, 292–298.
  24. Maurage, C., Guesnet, P., Pinault, M., de Lempdes, J.B.R., Durand, G., Antoine, J.M., and Couet, C. (1998) Effect of Two Types of Fish Oil Supplementation on Plasma and Erythrocyte Phospholipids in Formula-Fed Term Infants, *Biol. Neonate* 74, 416–429.
  25. Makrides, M., Neumann, M., Simmer, K., Pater, J., and Gibson, R. (1995) Are Long-Chain Polyunsaturated Fatty Acids Essential Nutrients in Infancy? *Lancet* 345, 1463–1468.
  26. Jørgensen, M.H., Højlmer, G., Lund, P., Hernell, O., and Michaelsen, K.F. (1998) Effect of Formula Supplemented with Docosahexaenoic Acid and Gamma-Linolenic Acid on Fatty Acid Status and Visual Acuity in Term Infants, *J. Pediatr. Gastroenterol. Nutr.* 26, 412–421.
  27. Carlson, S.E. (1996) Arachidonic Acid Status of Human Infants: Influence of Gestational Age at Birth and Diets with Very Long-Chain n-3 and n-6 Fatty Acids, *J. Nutr.* 126, 1092S–1098S.
  28. Møller, A., and Saxholt, E. (1996) *Levnedsmiddeltabeller (The Composition of Foods)*, 4th edn., Levnedsmiddelstyrelsen, Søborg, Denmark.
  29. Bligh, E.G., and Dyer, W.J. (1959) A Rapid Method of Total Lipid Extraction and Purification, *Can. J. Biochem. Physiol.* 37, 911–917.
  30. Rose, H.G., and Oklander, M. (1965) Improved Procedure for the Extraction of Lipids from Human Erythrocytes, *J. Lipid Res.* 6, 428–431.
  31. Sagredos, A.N. (1991) Fatty Acid Composition of Fish Oil Capsules, *Fett Wiss. Technol.–Fat Sci. Technol.* 93, 184–191.
  32. Emken, E.A., Adlof, R.O., Hachey, D.L., Garza, C., Thomas, M.R., and Brown-Booth, L. (1989) Incorporation of Deuterium-Labeled Fatty Acids into Human Milk, Plasma, and Lipoprotein Phospholipids and Cholesteryl Esters, *J. Lipid Res.* 30, 395–402.
  33. Demmelmair, H., Baumheuer, M., Koletzko, B., Dokoupil, K., and Kratl, G. (1998) Metabolism of U<sup>13</sup>C-Labeled Linoleic Acid in Lactating Women, *J. Lipid Res.* 39, 1389–1396.
  34. Francois, C.A., Connor, S.L., Wander, R.C., and Connor, W.E. (1998) Acute Effects of Dietary Fatty Acids on the Fatty Acids of Human Milk, *Am. J. Clin. Nutr.* 67, 301–308.
  35. Smit, E.N., Koopmann, M., Boersma, E.R., and Muskiet, F.A.J. (2000) Effect of Supplementation of Arachidonic Acid (AA) or a Combination of AA Plus Docosahexaenoic Acid on Breast-Milk Fatty Acid Composition, *Prostaglandins Leukotrienes Essent. Fatty Acids* 62, 335–340.
  36. Francois, C.A., Connor, S.L., Bolewicz, L., and Connor, W.E. (2000) Changes in Breast-Milk and Plasma n-3 Fatty Acids After Supplementation with Flaxseed Oil, *FASEB J.* 14, A724 (Abstract).
  37. Koletzko, B., Mrotzek, M., and Bremer, H.J. (1988) Fatty Acid Composition of Mature Human Milk in Germany, *Am. J. Clin. Nutr.* 47, 954–959.
  38. Phinney, S.D., Odin, R.S., Johnson, S.B., and Holman, R.T. (1990) Reduced Arachidonate in Serum Phospholipids and Cholesteryl Esters Associated with Vegetarian Diets in Humans, *Am. J. Clin. Nutr.* 51, 385–392.
  39. Mann, N.J., Johnson, L.G., Warrick, G.E., and Sinclair, A.J. (1995) The Arachidonic Acid Content of the Australian Diet Is Lower Than Previously Estimated, *J. Nutr.* 125, 2528–2535.
  40. Jørgensen, M.H., Hernell, O., Lund, P., Højlmer, G., and Michaelsen, K.F. (1996) Visual Acuity and Erythrocyte Docosahexaenoic Acid Status in Breast-Fed and Formula-Fed Term Infants During the First Four Months of Life, *Lipids* 31, 99–105.
  41. Olsen, S.F., Hansen, H.S., Sandström, B., and Jensen, B. (1995) Erythrocyte Levels Compared with Reported Dietary Intake of Marine n-3 Fatty Acids in Pregnant Women, *Br. J. Nutr.* 73, 387–395.
  42. Prisco, D., Filippini, M., Francalanci, I., Paniccina, R., Gensini, G.F., Abbate, K., and Neri Serneri, G.G. (1996) Effect of n-3 Polyunsaturated Fatty Acid Intake on Phospholipid Fatty Acid Composition in Plasma and Erythrocytes, *Am. J. Clin. Nutr.* 63, 925–932.
  43. Leaf, D.A., Connor, W.E., Barstad, L., and Sexton, G. (1995) Incorporation of Dietary n-3 Fatty Acids into the Fatty Acids of Human Adipose Tissue and Plasma Lipid Classes, *Am. J. Clin. Nutr.* 62, 68–73.
  44. Tjønneland, A., Overvad, K., Thorling, E., and Ewertz, M. (1993) Adipose Tissue Fatty Acids as Biomarkers of Dietary Exposure in Danish Men and Women, *Am. J. Clin. Nutr.* 57, 629–633.
  45. Marckmann, P., Lassen, A., Haraldsdottir, J., and Sandström, B. (1995) Biomarkers of Habitual Fish Intake in Adipose Tissue, *Am. J. Clin. Nutr.* 62, 956–959.

[Received August 9, 2001, and in revised form January 14, 2002; revision accepted February 6, 2002]

# Postprandial and Short-Term Effects of Dietary Virgin Olive Oil on Oxidant/Antioxidant Status

Montserrat Fitó<sup>a</sup>, Eva Gimeno<sup>b</sup>, María-Isabel Covas<sup>a,c,\*</sup>, Elisabet Miró<sup>d</sup>, María del Carmen López-Sabater<sup>b</sup>, Magí Farré<sup>d</sup>, Rafael de la Torre<sup>d</sup>, and Jaume Marrugat<sup>a</sup>

<sup>a</sup>Unitat de Lípids i Epidemiologia Cardiovascular and <sup>d</sup>Unitat de Farmacologia, Institut Municipal d'Investigació Mèdica (IMIM), 08003 Barcelona, Spain, <sup>b</sup>Departament de Bromatologia i Nutrició, Facultat de Farmàcia, Universitat de Barcelona, 08029 Barcelona, Spain, and <sup>c</sup>Laboratori de Referència de Catalunya, 08907 L'Hospitalet, Barcelona, Spain

**ABSTRACT:** It is generally believed that virgin olive oil consumption has beneficial effects, but little is known about its effects postprandially on oxidant/antioxidant status. The aim of this study was to determine changes in oxidative stress biomarkers and lipid profile after a single dose of virgin olive oil and after 1 wk of daily consumption. Sixteen subjects (9 men, 7 women) ingested 50 mL of virgin olive oil in a single dose. Blood samples were collected from 0 to 24 h. Thereafter, 14 participants (8 men, 6 women) followed a 1-wk 25 mg/d virgin olive oil dietary intervention. Blood samples were collected at the end of this period. Serum TAG ( $P = 0.016$ ), plasma FA ( $P < 0.001$ ), and lipid peroxidation products in plasma ( $P < 0.001$ ) and VLDL ( $P = 0.007$ ) increased, reaching a peak at 4–6 h, and returning to baseline values at 24 h after oil ingestion. The opposite changes were observed in plasma glutathione peroxidase ( $P = 0.001$ ) and glutathione reductase (GR) ( $P = 0.042$ ). No changes in LDL lipid peroxidation or resistance to oxidation were observed postprandially. At 24 h, plasma oleic acid remained increased ( $P < 0.05$ ) and resistance of LDL to oxidation improved ( $P < 0.05$ ). After 1 wk of virgin olive oil consumption, plasma oleic acid ( $P = 0.031$ ), resistance of LDL to oxidation ( $P < 0.05$ ), and plasma GR activity ( $P = 0.005$ ) increased. These results indicate that changes in oxidant/antioxidant status occur after oral virgin olive oil. Virgin olive oil consumption could provide short-term benefits for LDL resistance to oxidation and in glutathione-related enzyme activities.

Paper no. L8901 in *Lipids* 37, 245–251 (March 2002).

Coronary heart disease (CHD) is the main cause of mortality in industrialized countries; although mortality rates vary, the Mediterranean area has among the lowest (1). The Mediterranean diet has been shown to be associated with a benefit in secondary prevention of CHD (2). The lower incidence of CHD in Mediterranean countries has been attributed to a diet rich in fruits, vegetables, legumes, and grains, in which the major fat component is olive oil. These foods contain natural antioxidants that can prevent LDL oxidation (3).

\*To whom correspondence should be addressed at Unitat de Lípids i Epidemiologia Cardiovascular Institut Municipal d'Investigació Mèdica (IMIM), Carrer Doctor Aiguader, 80. 08003 Barcelona, Spain. E-mail: mcovas@imim.es

Abbreviations: Apo, apolipoprotein; CHD, coronary heart disease; GR, glutathione reductase; GSH-Px, glutathione peroxidase; MUFA, monounsaturated FA; OR, oxidation rate; SFA, saturated FA.

Evidence is increasing that dietary fat composition may influence oxidative modification of LDL (4). LDL oxidation is now widely regarded as playing an important role in the development of atherosclerosis (5). Postprandial lipemia has been recognized as a risk factor for atherosclerosis development, as it is associated with oxidative changes, including an increase in TAG-rich proteins and their remnants (6). This increase may directly damage the vascular endothelium *via* oxidative mechanisms (7). Meals rich in oxidized fats increase the oxidized lipid content of lipoproteins, and a reduction of serum paraoxonase activity after a cooked fat-rich meal has been reported (8,9).

Previous dietary intervention studies have shown that, compared to carbohydrate- or PUFA-enriched diets, monounsaturated FA (MUFA)-enriched diets reduced the LDL susceptibility to oxidation (10–13). In general, these studies utilized carefully prepared liquid-formula or solid diets highly enriched in MUFA. Whether a more realistic level of MUFA ingestion will lead to similar results is unknown.

The mechanisms underlying the apparent benefits of olive oil consumption are not completely understood. After an oral olive oil load, the magnitude of postprandial lipemia and remnant lipoprotein is reported to be lower than after ingesting butter (14), similar to that after eating a saturated fat-rich meal (15), or higher than after consuming a dose of safflower oil (16). The aim of the current study was to determine whether a bolus ingestion of virgin olive oil affected postprandial lipid peroxidation, serum antioxidant glutathione-related enzymes, and LDL oxidation resistance. The study also examined the effect on these oxidative stress markers after 1 wk of replacement of butter, margarine, or vegetable oils by crude virgin olive oil.

## MATERIALS AND METHODS

**Subjects.** Sixteen (9 men and 7 women) healthy volunteers (aged 25 to 65 yr) were recruited. The ethical committee (CEIC-IMAS) approved the protocol, and participants signed an informed consent. All volunteers were considered healthy on the basis of a physical examination and standard biochemical and hematological tests. Subjects had an average weight of  $75 \pm 13.47$  kg (men:  $83.2 \pm 4.4$ , women:  $59.7 \pm 6.11$ ) and a body mass index of  $25.6 \pm 3.1$  kg/m<sup>2</sup> (men:  $26.9 \pm 3.29$ , women:  $22.4 \pm 2.4$ ).

**Olive oil analyses.** The characteristics of the virgin olive oil used in the experiments are as follows: peroxide value (meq/kg), 9.8;  $K_{270}$  (extinction coefficient for light absorption at 270 nm), 0.10; FA (%): 16:0, 12.7; 16:1, 1.0; 18:0, 1.79; 18:1, 73.3; 18:2, 9.49; 18:3, 0.40; monounsaturated, 74.87; polyunsaturated, 9.89; saturated, 15.24; vitamin E (mg/kg), 156.20;  $\beta$ -carotene (mg/kg), 3.07; phenolic compounds (mg/kg), 253.36.

FA composition was determined by GC (17), and  $\alpha$ -tocopherol and  $\beta$ -carotene contents in olive oils were determined by RP-HPLC (18). Total phenolic content of olive oils was measured by the Folin–Ciocalteu method (19). Peroxide index and UV light absorption ( $K_{270}$ ), a measure of secondary oxidation compounds such as carbonyls (aldehydes and ketones), were determined following the analytical methods described in CEE/2568/91 of the European Union Commission (20).

**Study design.** Volunteers followed an antioxidant and olive oil-free diet for 5 d. A nutritionist instructed them on excluding several foods from their diet (coffee, tea, fruit, vegetables, wine, and olive oil). At 8 A.M. on day 5, in the fasting state, they were provided with 50 mL (44 g) of extra virgin olive oil administered in a single dose either ingested directly or with some bread. During the first postprandial 6 h, subjects abstained from food and drink with the exception of caffeine-free, low-energy drinks and water. Blood was collected at baseline (0 h) and at 2, 4, 6, 8, and 24 h after virgin olive oil administration. Thereafter, 14 participants (8 men, 6 women) followed their habitual diet for 1 wk, using the same virgin olive oil as source of crude dietary lipid. The participants' daily consumption of virgin olive oil ranged from 19 to 22 mL (17–19 g) per day (each individual was provided 25 mL/d). Blood samples were collected on day 12 of the study after a week of virgin olive oil consumption. Plasma was separated by centrifugation at  $1000 \times g$  at 4°C for 15 min.

**Dietary assessment.** Nutrient intakes were calculated from seven daily dietary records with the software *Diet Analysis Nutritionist IV* (N-Squared Computing, San Bruno, CA). The daily caloric intake of the subjects during the week of sustained olive oil ingestion ranged from 1465 to 2284 kcal (mean  $\pm$  SD,  $1748 \pm 331$  kcal) and consisted of lipids  $37.5 \pm 3\%$  (PUFA  $4.8 \pm 1.2$ , MUFA  $17.9 \pm 2.1$ , and saturated FA  $14.7 \pm 1.58\%$ ), carbohydrates  $44.2 \pm 5.1\%$ , and proteins  $18.3 \pm 2.7\%$ .

**Antioxidant enzyme activity measurements.** Glutathione peroxidase (GSH-Px) activity in plasma was measured by a modification of the Paglia and Valentine method (21) (Ransel RS 505; Randox Laboratory, Crumlin, Northern Ireland). Glutathione reductase (GR) activity in plasma was measured by glutathione reduction following the oxidation of NADPH to NADP<sup>+</sup> during the reduction of oxidized glutathione (Ransel GR 2368, Randox Laboratory) (22). Enzyme activities were measured in a Cobas Mira Plus analyzer (Hoffman-La Roche, Basel, Switzerland) at 37°C. Intra-assay CV were 3.6 and 3.5% for GSH-Px and GR, respectively. Interassay CV were 5.4 and 4.4% for GSH-Px and GR, respectively.

**Glucose, lipid, lipoprotein, and apolipoprotein (Apo) measurements.** Serum glucose, total cholesterol, HDL cholesterol,

and TAG levels were measured by standard enzymatic methods. Serum ApoA1 and ApoB were measured by immunoturbidimetric methods (Roche Diagnostics, Basel, Switzerland). LDL-cholesterol (LDL-C) was calculated by means of the Friedewald equation.

**FA measurements.** Plasma FA were directly transesterified without previous lipid extraction and measured by capillary GC (23). Intra- and interassay CV were 3.4 and 5.15%, respectively.

**Lipoprotein isolation.** Very low density lipoproteins (VLDL) and LDL isolation were performed by sequential flotation ultracentrifugation (24). Protein content was determined by the red pyrogallol method (Sigma, St. Louis, MO).

**LDL resistance to oxidation.** Conjugated diene formation after copper-mediated LDL oxidation was assessed as previously described (25). Briefly, dialyzed LDL (0.05 g protein/L) was incubated with cupric sulfate (5  $\mu$ M) in PBS at a final volume of 1 mL. Absorbance at 234 nm was continuously monitored at 2-min intervals for 5 h at 35°C. All samples from one individual were performed in the same run. For data presentation, the x-axis value corresponding to the intercept of the propagation phase tangent with the extrapolated line for the slow propagation reaction was calculated (lag time), oxidation rate (OR) was derived from the slope of the propagation phase tangent, and diene formation was calculated by the maximum increase of the absorbance at 234 nm. OR and diene formation were calculated using the molar absorbance  $\epsilon_{234\text{nm}}$  for conjugated dienes (29,500 L $\cdot$ mol<sup>-1</sup> $\cdot$ cm<sup>-1</sup>). Intra-assay CV were 3.29, 5.27, and 1.46% for lag time, OR, and diene formation, respectively.

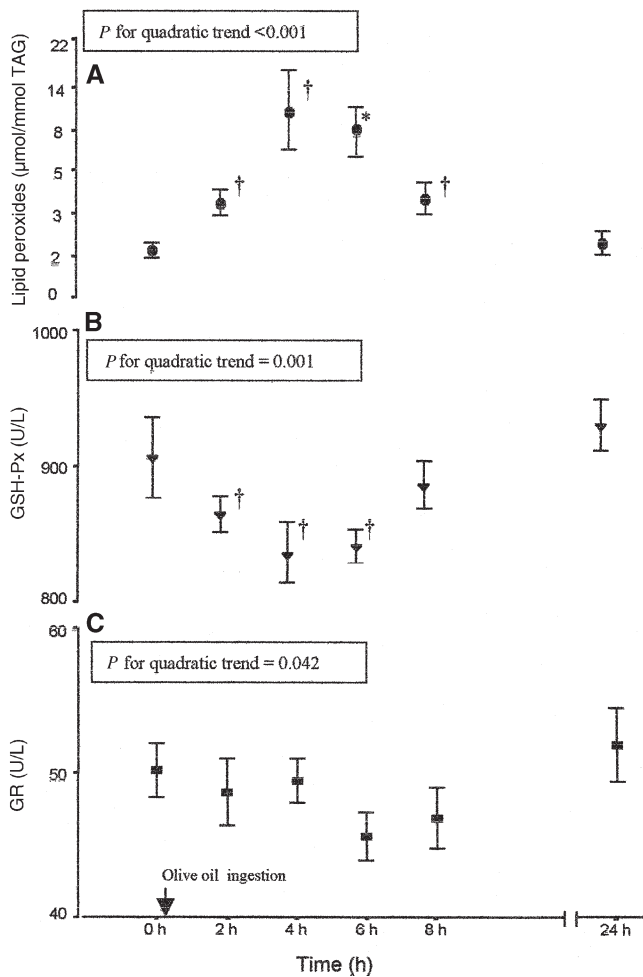
**Lipid peroxidation measurements.** Lipid peroxidation in plasma, VLDL, and LDL was measured by the TBARS test (26) adjusted by TAG or protein content. Solutions of 1,1,3,3-tetraethoxypropane in ethanol were used as standards for the assay. Intra- and interassay CV were 4.22–4.87% and 5.89–6.87%, respectively.

**Statistical analyses.** A general linear model was used to test the best fit of the repeated measurements: linear, quadratic, or cubic. Once statistical differences among the means were observed, a *post-hoc* multiple comparison test was done for each variable separately by Tukey's test. A Bonferroni's correction was applied, so for these multiple comparisons a *P* value <0.01 was considered statistically significant. Spearman's correlation coefficients were used to assess the relationship between two continuous variables. Paired Student's *t*-test for parametric variables and Wilcoxon's test for non-parametric variables (TAG and lipid peroxides) were used to assess differences between baseline values and those obtained after 1 wk of virgin olive oil consumption. A *P* value <0.05 was considered statistically significant. These statistical analyses were performed using the SPSS statistical package (SPSS Incorporated Co., Chicago, IL).

## RESULTS

**Effects of ingesting a single dose of virgin olive oil.** Figure 1 shows the time course of plasma lipid peroxides, GSH-Px, and GR activities for 24 h after ingesting 50 mL of olive oil.





**FIG. 1.** Time course of (A) plasma lipid peroxides, (B) glutathione peroxidase (GSH-Px), and (C) glutathione reductase (GR) after ingestion of 50 mL virgin olive oil ( $n = 16$ ). \* $P < 0.005$ ; † $P < 0.01$  vs. baseline (0 h).

Plasma lipid peroxidation increased to a peak at 4–6 h, and returned to baseline at 24 h. The opposite changes were observed in plasma GSH-Px and GR activities

The time course of lipid peroxide formation in VLDL and LDL, and LDL oxidation resistance-related variables, is shown in Table 1. Lipid peroxidation in VLDL increased, reaching a peak at 6 h and returning close to baseline at 24 h, whereas no significant changes in lipid peroxidation were observed in LDL. The lag time of conjugated diene formation

in LDL increased and the OR decreased at 24 h after virgin olive oil ingestion. No statistical differences were observed in diene formation with time in LDL oxidation.

Serum TAG and plasma FA increased after ingesting 50 mL of virgin olive oil, reaching a peak at 4–6 h postprandially (Table 2). Despite the increase of oleate and the decrease of linoleate percentages in plasma ( $P < 0.001$ ) (data not shown), linoleate concentration (g/L) in plasma increased after olive oil ingestion (Table 2). At 4 h postprandial time, the concentration (g/L) of linoleic acid in plasma was directly related to plasma lipid peroxides ( $P = 0.027$ ) and inversely to plasma GSH-Px ( $P = 0.008$ ) and GR activities ( $P = 0.068$ ) (Fig. 2). No relationship was obtained among plasma oleic, or other plasma FA levels, and lipid peroxides or glutathione-related enzymes at 4–6 h of virgin olive oil ingestion. Levels of serum glucose in plasma increased from baseline ( $3.9 \pm 0.6$  mmol/L, mean  $\pm$  SD) to 2 h ( $4.4 \pm 0.8$  mmol/L, mean  $\pm$  SD) after virgin olive oil ingestion ( $P = 0.021$ ) (data not shown).

At 24 h after olive oil ingestion, plasma MUFA/PUFA ratio and oleic acid concentrations remain increased (Table 2). At this time period plasma lipid peroxides were inversely related to plasma oleic acid ( $r = -0.565$ ,  $P = 0.028$ ) and directly to linoleic acid concentrations ( $r = 0.532$ ,  $P = 0.041$ ) (data not shown).

*Effects of ingesting virgin olive oil for 1 wk.* Table 3 shows the changes in lipids, lipoproteins, FA, and oxidative stress markers after 1 wk of olive oil consumption. Consumption of virgin olive oil (19–20 mL/d) during a week led to a significant decrease in LDL-cholesterol concentration. No significant changes were observed in the total plasma FA content. An increase was observed in the oleic acid percentage and MUFA/PUFA ratio from baseline time to the end of the study. No significant changes were observed in the linoleate percentage in the evaluated times. Changes in the concentration (g/L) of the individual plasma FA were similar to those observed in their percentages. An increase in plasma GR and GSH-Px and a decrease both in the lag time and in the OR of conjugated diene formation were observed.

After 1 wk of virgin olive oil consumption, plasma linoleate/oleate ratio was directly related to plasma lipid peroxides and inversely related to plasma GR activity (Fig. 3). In comparison with data from 24 h after 50 mL olive oil ingestion, only the lag time of conjugated diene formation was slightly increased ( $P = 0.047$ ).

**TABLE 1**  
**Time Course of Lipid Peroxides in Lipoproteins and LDL Oxidation-Related Variables<sup>a</sup>**

	Time after virgin olive oil ingestion						<i>P</i> trend
	Baseline (0 h)	2 h	4 h	6 h	8 h	24 h	
Lipid peroxides (nmol/mg of protein)							
VLDL	12.2 (6.9)	22.5 (14.7)	28.0 (8.9)	34.1 (9.0) <sup>b</sup>	24.3 (11.9)	16.8 (10.4)	0.007 (quadratic)
LDL	7.6 (2.5)	6.9 (3.8)	8.2 (2.8)	7.8 (3.5)	6.9 (2.2)	7.5 (2.6)	NS
LDL oxidation related variables							
Lag time (min)	142 (13)	148 (14)	151 (11)	146 (16)	152 (15)	149 (11) <sup>b</sup>	0.027 (linear)
Oxidation rate (mol diene/min/mol LDL)	6.41 (1.16)	5.68 (1.11)	5.65 (1.95)	5.34 (1.78)	5.08 (1.52)	4.84 (1.31) <sup>b</sup>	0.017 (linear)
Dienes (mol diene/mol LDL)	612 (130)	730 (102)	759 (215)	701 (215)	710 (181)	610 (128)	NS

<sup>a</sup>Values expressed as mean (SD),  $n = 16$ . NS, not significant ( $P > 0.01$ ).

<sup>b</sup>Significantly different from baseline values,  $P < 0.01$ .



**TABLE 2**  
**Time Course of Plasma FA and Serum TAG After Virgin Olive Oil Ingestion (50 mL)<sup>a</sup>**

	Time after virgin olive oil ingestion						<i>P</i> trend (quadratic)
	Baseline (0 h)	2 h	4 h	6 h	8 h	24 h	
FA (g/L)							
Palmitic (16:0)	0.66 (0.13)	0.68 (0.17)	0.68 (0.12) <sup>b</sup>	0.70 (0.10) <sup>c</sup>	0.69 (0.16)	0.69 (0.21)	0.001
Stearic (18:0)	0.23 (0.04)	0.24 (0.05)	0.24 (0.03) <sup>b</sup>	0.25 (0.03) <sup>b</sup>	0.25 (0.05)	0.24 (0.06)	<0.001
Oleic (18:1)	0.63 (0.15)	0.77 (0.28) <sup>b</sup>	0.83 (0.19) <sup>c</sup>	0.91 (0.21) <sup>c</sup>	0.82 (0.35) <sup>c</sup>	0.73 (0.25) <sup>b</sup>	<0.001
Linoleic (18:2)	0.96 (0.15)	0.99 (0.15)	1.01 (0.10) <sup>b</sup>	1.04 (0.13) <sup>b</sup>	1.02 (0.22)	0.94 (0.15)	<0.001
Arachidonic (20:4)	0.22 (0.05)	0.22 (0.04)	0.23 (0.04)	0.23 (0.04)	0.23 (0.05)	0.22 (0.04)	0.010
MUFA/PUFA <sup>d</sup> ratio	0.50 (0.09)	0.58 (0.15) <sup>b</sup>	0.65 (0.11) <sup>c</sup>	0.70 (0.15) <sup>c</sup>	0.60 (0.16) <sup>b</sup>	0.58 (0.15) <sup>b</sup>	<0.001
Total FA (g/L)	2.71 (0.44)	2.92 (0.61)	2.98 (0.47) <sup>b</sup>	3.13 (0.41) <sup>c</sup>	3.02 (0.71) <sup>b</sup>	2.83 (0.61)	<0.001
TAG (mmol/L)	1.29 (0.44)	1.49 (0.73)	1.52 (0.58)	1.60 (0.52) <sup>b</sup>	1.35 (0.74)	1.44 (0.73)	0.016
TAG (mg/dL)	114.2	131.9	134.5	141.6	119.5	127.4	

<sup>a</sup>Values expressed as mean (SD), *n* = 16.

<sup>b</sup>*P* < 0.01 vs. baseline values.

<sup>c</sup>*P* < 0.001 vs. baseline values.

<sup>d</sup>MUFA/PUFA ratio, monounsaturated FA/PUFA ratio.

## DISCUSSION

This study reports the effects of both single and sustained doses of virgin olive oil on the oxidant/antioxidant balance, and on plasma TAG and FA. Plasma lipid peroxides increased, and glutathione-related enzymes decreased postprandially after 50 mL of virgin olive oil. These opposite time courses are explainable by the fact that GSH-Px, a selenium-containing enzyme requiring glutathione, besides removing reactive oxygen species (H<sub>2</sub>O<sub>2</sub>), also detoxifies lipid peroxides to nontoxic alcohols, thus acting as a chain-breaking antioxidant (27). At the same time, GR regenerates oxidized glutathione to the reduced form required by GSH-Px activity (28). A decrease in the antioxidant defenses, with an increase of lipid oxidation, is a common feature in an increased oxidative status situation (29,30).

Lipid peroxides can be generated during digestion-absorption (29,30) by alkaline pH and by the catalysts of peroxidation (i.e., transition metals with catalytic action on lipid peroxidation). Dietary ingestion of oxidized lipids is one of the sources of postprandial lipid peroxidation products (8,9). The limiting quality value indices specified by the European Union Commission for virgin olive oil are 20 meq/kg for peroxide and 0.2 for secondary carbonyl products (*K*<sub>270</sub>). Although these indices are far lower than the established limits in the virgin olive oil used in the study, the contribution of oxidized lipids from the ingested virgin olive oil to the observed postprandial oxidative stress cannot be ignored. Hyperglycemia is also a widely known cause of enhanced free radical concentration (31). Although we have not measured glucose at the earlier postprandial phase, when its peak occurs, a

**TABLE 3**  
**Serum Lipids and Lipoproteins, Plasma FA, Lipid Peroxides, and Glutathione-Related Enzymes and LDL Oxidation-Related Variables After 1 wk of Virgin Olive Oil Consumption<sup>a</sup>**

	1 wk	Change from baseline	<i>p</i> <sup>b</sup>
Total cholesterol (mmol/L)	4.96 (1.03)	-0.38 (1.25)	0.783
TAG (mmol/L)	1.35 (0.39)	0.02 (0.34)	0.756
TAG (mg/dL)	119.5		
HDL-cholesterol (mmol/L)	1.16 (0.34)	0.07 (0.34)	0.536
LDL-cholesterol (mmol/L)	3.28 (0.79)	-0.09 (0.38)	0.029
Total FA (g/L)	2.81 (0.64)	0.08 (0.42)	0.481
FA (% of total)			
Palmitic (16:0)	22.73 (1.44)	-1.55 (1.72)	0.007
Stearic (18:0)	10.07 (16.24)	2.28 (6.73)	0.147
Oleic (18:1)	25.94 (4.46)	3.99 (5.97)	0.031
Linoleic (18:2)	35.71 (3.85)	-0.11 (2.4)	0.861
Arachidonic (20:4)	7.41 (3.82)	-0.52 (0.67)	0.013
MUFA/PUFA ratio	0.61 (0.16)	0.06 (0.10)	0.041
Lipid peroxides (μmol/mmol TAG)	1.65 (0.57)	-0.29 (0.72)	0.599
Glutathione peroxidase (U/L)	974 (97)	89 (108)	0.098
Glutathione reductase (U/L)	56.8 (11.3)	4.57 (4.82)	0.018
LDL oxidation-related variables			
Lag time (min)	163 (12)	17.8 (10.2)	0.005
Oxidation rate (mol diene/min/mol LDL)	5.3 (1.8)	-0.63 (1.5)	0.039
Dienes (mol diene/mol LDL)	573 (143)	-26.4 (121)	0.793

<sup>a</sup>Values expressed as mean (SD), *n* = 14. For abbreviation see Table 2.

<sup>b</sup>As found by paired Student's *t*-test, except for TAG and lipid peroxides, for which Wilcoxon's test was used.

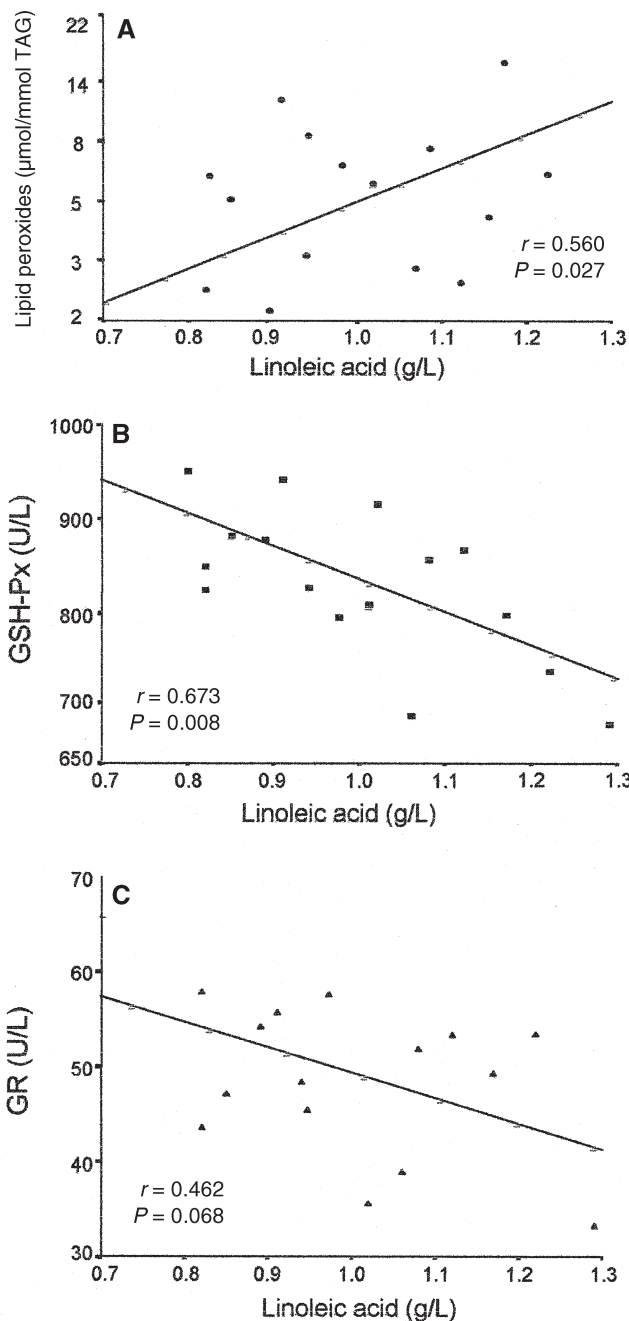


FIG. 2. Scatterplot showing the relationship between plasma linoleic acid concentration and plasma lipid peroxides, GSH-Px, and GR 4 h after ingestion of 50 mL virgin olive oil ( $n = 16$ ). For abbreviations see Figure 1.

moderate increase in glucose levels at 2 h postprandial state was observed. A postprandial increase in glucose and insulin has been related to oxidative stress in diabetic patients (32), but the relevance of glucose and insulin as free-radical generators in healthy individuals is unknown at present.

According to our results, postprandial VLDL are prone to oxidation after ingesting 50 mL of virgin olive oil. Postprandial TAG enrichment of VLDL is reportedly related to oxidative stress in type 2 diabetic patients (33), and postprandial remnantlike protein particles have been shown to increase intracellular oxidant content and impair endothelial function

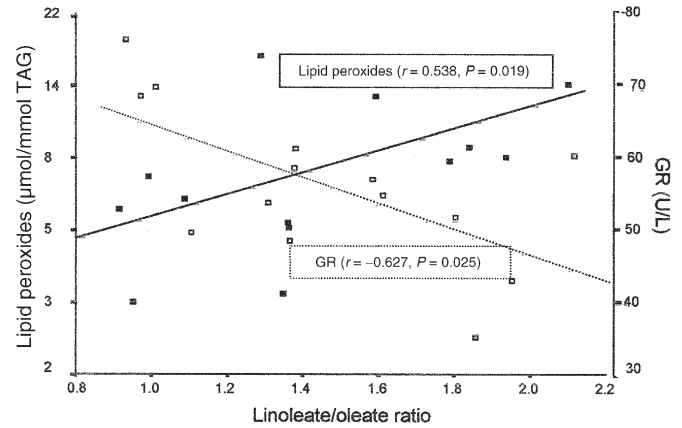


FIG. 3. Scatterplot showing the relationship between plasma linoleate/oleate ratio, plasma lipid peroxides, and glutathione reductase (GR) after 1 wk of olive oil consumption ( $n = 14$ ). TAG, triacylglycerols.

(34). After a meal rich in olive oil, the TAG in postprandial TAG-rich proteins generally reflect the composition of olive oil, although the proportion of the individual molecular species is altered by the processes leading to their formation, with an increase of linoleoyl-oleyl- and palmitoyl-oleyl-TAG (35). These results (35) are in agreement with the observed increase of oleic and linoleic acid in plasma in the postprandial state in this study. MUFA-TAG rich particles are reportedly relatively resistant to oxidation (36). However, linoleic acid is one of the most abundant and oxidizable FA (10), and its increase in plasma was related to an oxidant/antioxidant imbalance at 4 h postprandially in this study. Thus, despite the concomitant increase in the oleic acid content, the increase in linoleate content could be related to the observed oxidative stress situation postprandially.

Increased susceptibility of postprandial LDL to oxidation after a meal rich in dairy fat has been reported (37). In other studies, however, susceptibility of isolated LDL to oxidation and lipid peroxidation in LDL did not change in normal individuals after meals rich in dairy fat (38), thermally stressed cooking fat, or unheated fat (9). In the current study, the increase in lipid peroxidation in plasma and VLDL was not reflected in the resistance of isolated LDL to copper-catalyzed oxidation, nor in the lipid peroxidation products in LDL postprandially. We must point out, however, that the method of assaying lipid peroxides by TBARS assay may be insufficiently sensitive or specific (39) to detect modest differences in lipid oxidation products in LDL samples. Our results are in agreement with those of Nicolaiew *et al.* (40), who found no effect on the lag time of LDL oxidation at 6 h after virgin olive oil ingestion.

Virgin olive oil has phenolic compounds with *in vitro* antioxidant properties (24,41). We recently reported the bioavailability in humans of two characteristic olive oil phenolic compounds, tyrosol and hydroxytyrosol, from virgin olive oil in its natural form (42). The lack of changes in LDL oxidation observed in this study postprandially could be related to an increase in their antioxidant phenolic compound content. In a recent study, Bonanome *et al.* (43) reported the recovery

of tyrosol and hydroxytyrosol in all postprandial lipoprotein fractions, except in VLDL, after the ingestion of 100 g of virgin olive oil. Their findings (43) suggest that olive oil phenolic compounds are absorbed from the intestine through a pathway independent of chylomicron formation. The TAG enrichment of VLDL (6), together with a lack of phenolic compound incorporation (43), could be an explanation for the increase in VLDL lipid peroxidation observed in this study after the acute virgin olive oil ingestion.

At 24 h after olive oil ingestion, an improvement of LDL resistance to oxidation was observed, whereas plasma oleic acid and the MUFA/PUFA ratio remained elevated. At this time point, virgin olive oil was the sole source of antioxidants and oleic acid. Thus, the improvement of LDL resistance to oxidation could be related to virgin olive oil ingestion.

Concerning the 1-wk effects of sustained doses (around 20 mL/d) of virgin olive oil consumption, the increase in plasma oleic acid levels, without changes in the total FA content, confirms good compliance by the subjects and their responsiveness to the dietary intervention. Despite the short-term dietary intervention, the effects on plasma LDL-cholesterol and on susceptibility of LDL to oxidation were in line with those reported in previous dietary studies with MUFA-enriched diets (10–13) and with a lengthier (3–4 wk) dietary intervention time. One explanation for this fact could be that participants followed a washout period (4 d) with an antioxidant- and olive oil-free diet before the beginning of the study. Thus, besides virgin olive oil, other dietary antioxidant compounds could account for the increase in resistance to LDL oxidation and antioxidant enzymes. The effect of the short-term olive oil dietary intervention was reflected in a decrease of plasma linoleate/oleate ratio, this decrease being related to an apparently better plasma oxidant/antioxidant status. The protective mechanism of oleic acid-enriched diets on LDL susceptibility to oxidation has been attributed to a decrease in LDL linoleic acid content. However, recent studies on oleic acid-enriched liposomes suggest an independent protective mechanism of oleic acid on lipoprotein susceptibility to oxidation (44). The increase in glutathione-related enzymes could be attributed to a preservation of their enzymatic activities. Although little is known of the *in vivo* response of antioxidant enzymes to dietary fats or antioxidants, increased activity of GSH-Px and transferase has been reported in rabbits after olive oil supplementation (45).

To our knowledge, this is the first time that oxidative stress has been described after virgin olive oil ingestion. One limitation of this study, however, is the lack of a control group. It remains to be elucidated whether virgin olive oil ingestion affords more protection than other fat-rich meals for the postprandial oxidative stress situation. Further studies are also required to examine whether differences in the phenolic content of virgin oils could influence the postprandial oxidative stress after their ingestion.

An oxidative stress, reflected in an increase of plasma and VLDL lipid peroxidation, and a decrease in plasma GSH-Px and GR activity levels occur after an oral load of virgin olive oil. At this postprandial time, LDL seems to be protected from

oxidation. On the other hand, our results suggest that real-life moderate, sustained doses of virgin olive oil could provide benefits for the LDL resistance to oxidation and plasma glutathione-related enzyme activities.

## ACKNOWLEDGMENTS

This work was supported by grants ALI97-1607-CO2-01 from Comisión Interministerial de Ciencia y Tecnología (CICYT) and 98/9562 FPI from Fondo de Investigación Sanitaria (FIS) and by Federació de Cooperatives Agràries de Catalunya. We also appreciate the English revision made by Stephanie Lonsdale.

## REFERENCES

1. Pérez, G., Pena, A., Sala, J., Roset, P., Masiá, R., and Marrugat, J. (1998) Acute Myocardial Infarction Case Fatality, Incidence and Mortality Rates in a Population Registry in Gerona, Spain, 1990–1992, *Int. J. Epidemiol.* 27, 599–604.
2. De Lorgeril, M., Salen, P., Martin, J.L., Monjaud, I., Delaye, J., and Mamelle, N. (1999) Mediterranean Diet, Traditional Risk Factors, and the Rate of Cardiovascular Complications After Myocardial Infarction. Final Report of the Lyon Diet Heart Study, *Circulation* 99, 779–785.
3. Visioli, F. (2000) Antioxidants in Mediterranean Diets, in *Mediterranean Diets* (Simopoulos, A.P., and Visioli, F., eds.), Vol. 87, pp. 43–45, World Review of Nutrition and Dietetics Series, S. Karger, Basel, Switzerland.
4. Reaven, P.D., and Witztum, J.L. (1996) Oxidized Low Density Lipoproteins in Atherogenesis: Role of Dietary Modification, *Ann. Rev. Nutr.* 16, 51–71.
5. Witztum, J.L. (1994) The Oxidation Hypothesis of Atherosclerosis, *Lancet* 344, 793–795.
6. Cohn, S. (1998) Postprandial Lipemia: Emerging Evidence for Atherogenicity of Remnant Lipoproteins, *Can. J. Cardiol.* 14 (Suppl. B), 18B–27B.
7. Sattar, N., Petrie, J.R., and Jaap, A.J. (1998) The Atherogenic Lipoprotein Phenotype and Vascular Endothelial Dysfunction, *Atherosclerosis* 138, 229–235.
8. Staprans, I., Rapp, J.H., Pan, X.M., Kim, K.Y., and Feingold, K.R. (1994) Oxidized Lipids in the Diet Are a Source of Oxidized Lipid in Chylomicrons of Human Serum, *Arterioscler. Thromb.* 14, 1900–1905.
9. Sutherland, W.H., Walker, R.J., de Jong, S.A., van Rij, A.M., Phillips, V., and Walker, H.L. (1999) Reduced Postprandial Serum Paraoxonase Activity After a Meal Rich in Used Cooking Fat, *Arterioscler. Thromb. Vasc. Biol.* 19, 1340–1347.
10. Reaven, P., Parthasarathy, S., Grasse, B.J., Miller, E., Almazan, F., Mattson, F.H., Khoo, J.C., Steinberg, D., and Witztum, J.L. (1991) Feasibility of Using an Oleate-Rich Diet to Reduce the Susceptibility of Low-Density Lipoprotein to Oxidative Modification in Humans, *Am. J. Clin. Nutr.* 54, 701–706.
11. Berry, E.M., Eisenberg, S., Friedlander, Y., Harats, D., Kaufmann, N.A., Norman, Y., and Stein, Y. (1992) Effects of Diets Rich in Monounsaturated Fatty Acids on Plasma Lipoproteins: The Jerusalem Nutrition Study: Monounsaturated Fatty Acids vs. Carbohydrates, *Am. J. Clin. Nutr.* 56, 394–403.
12. Mata, P., Varela, O., Alonso, R., Lahoz, C., de Oya, M., and Badimon, L. (1997) Monounsaturated and Polyunsaturated n-6 Fatty Acid-Enriched Diets Modify LDL Oxidation and Decrease Human Coronary Smooth Muscle Cell DNA Synthesis, *Arterioscler. Thromb. Vasc. Biol.* 17, 2088–2095.
13. Reaven, P.D., Grasse, B.J., and Tribble, D.L. (1994) Effect of Linoleate-Enriched and Oleate-Enriched Diets in Combination with Alpha-Tocopherol on the Susceptibility of LDL and LDL Subfractions to Oxidative Modifications in Humans, *Arterioscler. Thromb.* 14, 557–566.

14. Thomsen, C., Rasmussen, O., Lousen, T., Holst, J.J., Fenselau, S., Schrezenmeir, J., and Hermansen, K. (1999) Differential Effects of Saturated and Monounsaturated Fatty Acids on Postprandial Lipemia and Incretin Responses in Healthy Subjects, *Am. J. Clin. Nutr.* 69, 1135–1143.
15. Roche, H.M., Zampelas, A., Jackson, K.G., Williams, C.M., and Gibney, M.J. (1998) The Effect of Test Meal Monounsaturated Fatty Acid: Saturated Fatty Acid Ratio on Postprandial Lipid Metabolism, *Brit. J. Nutr.* 79, 419–424.
16. Higashi, K., Ishikawa, T., Shige, H., Tomiyasu, K., Yoshida, H., Ito, T., Nakajima, K., Yonemura, A., Sawada, S., and Nakamura, H. (1997) Olive Oil Increases the Magnitude of Postprandial Chylomicron Remnants Compared to Milk Fat and Safflower Oil, *J. Am. Coll. Nutr.* 16, 429–434.
17. López, M.C., Satué, T., González, M., and Agramount, A. (1994) Fatty Acid Composition of Trout Oil, *Food Chem.* 50, 363–365.
18. Gimeno, E., Calero, E., Castellote, A.I., Lamuela, R., de la Torre, M.C., and López-Sabater, M.C. (2000) Simultaneous Determination of Alpha-Tocopherol and Beta-Carotene in Olive Oil by Reversed-Phase High-Performance Liquid Chromatography, *J. Chromatogr. A* 881, 251–254.
19. Singleton, V.L., and Ross, J.A. (1965) Colorimetry of Total Phenolics with Phosphomolybdic-Phosphotungstic Acid Reagent, *Am. J. Enol. Vitic.* 16, 144–158.
20. European Union Commission (1999) Commission Regulation (ECC) no. 2568/91 of 11 July 1991 on the Characteristics of Olive Oil and Olive-Residue Oil and on the Relevant Methods of Analysis, *Official Journal of the European Community* L248, 05/09/91, 0001–0082.
21. Paglia, D.E., and Valentine, W.N. (1967) Studies on the Quantitative and Qualitative Characterization of Erythrocyte Glutathione Peroxidase, *J. Lab. Clin. Med.* 70, 158–169.
22. Goldberg, D.M., and Spooner, R.J. (1983) Glutathione Reductase, in *Methods of Enzymology* (Bergmeyer, H.U., ed.), Vol. 3, pp. 258–265, Verlag Chemie, Basel, Switzerland.
23. Rodríguez-Palmero, M., López-Sabater, M.C., Castellote-Bargallo, A.I., de la Torre-Boronat, M.C., and Rivero-Urgell, M. (1998) Comparison of Two Methods for the Determination of Fatty Acid Profiles in Plasma and Erythrocytes, *J. Chromatogr. A* 793, 419–426.
24. Havel, R.J., Eder, H.A., and Bragdon, J.H. (1955) The Distribution and Chemical Composition of Ultracentrifugally Separated Lipoproteins in Human Serum, *J. Clin. Invest.* 34, 1345–1349.
25. Fitó, M., Covas, M.I., Lamuela-Raventós, R.M., Vila, J.S., Torrents, J., de la Torre, C., and Marrugat, J. (2000) Protective Effect of Olive Oil and Its Phenolic Compounds Against Low Density Lipoprotein Oxidation, *Lipids* 35, 633–638.
26. Hoving, E.B., Laing, C., Rutgers, H.M., Teggele, M., van Doornmal, J.J., and Muskiet, F.A. (1992) Optimized Determination of Malondialdehyde in Plasma Lipid Extracts Using 1,3-Diethyl-2-thiobarbituric Acid: Influence of Detection Method and Relations with Lipids and Fatty Acids in Plasma from Healthy Adults, *Clin. Chim. Acta* 208, 63–76.
27. Gutteridge, J.M.C. (1995) Lipid Peroxidation and Antioxidants as Biomarkers of Tissue Damage, *Clin. Chem.* 41, 1819–1828.
28. Ursini, F., Malorino, M., Brigellus-Flohe, R., Aumann, K.D., Roveri, A., Schomburg, D., and Flohe, L. (1995) The Diversity of Glutathione Peroxidases, *Methods Enzymol.* 252, 38–53.
29. Ruíz, C., Alegría, A., Barbera, R., Farre, R., and Lagarda, M.J. (1999) Lipid Peroxidation and Antioxidant Enzyme Activities in Patients with Type 1 Diabetes Mellitus, *Scand. J. Clin. Lab. Invest.* 59, 99–105.
30. Efe, H., Deger, O., Kirci, D., Karahan, S.C., Orem, A., and Calapoglu, M. (1999) Decreased Neutrophil Antioxidative Enzyme Activities and Increased Lipid Peroxidation in Hyperlipoproteinemic Human Subjects, *Clin. Chim. Acta.* 279, 155–165.
31. Ceriello, A. (2000) Oxidative Stress and Glycemic Regulation, *Metabolism* 49, 27–29.
32. Ceriello, A., Bortolotti, N., Motz, E., Pieri, C., Marra, M., Tonutti, L., Lizzio, S., Felett, F., Catone, B., and Taboga, C. (1999) Meal-Induced Oxidative Stress and Low-Density Lipoprotein Oxidation in Diabetes: The Possible Role of Hyperglycemia, *Metabolism* 48, 1503–1508.
33. Evans, M., Anderson, R.A., Graham, J.B., Ellis, G.R., Morris, K., Davies, S., Jackson, S.K., Lewis, M.J., Frenneaux, M.P., and Rees, A. (2000) Ciprofibrate Therapy Improves Endothelial Function and Reduces Postprandial Lipemia and Oxidative Stress in Type 2 Diabetes Mellitus, *Circulation* 101, 1773–1779.
34. Doi, H., Kugiyama, K., Oka, H., Sugiyama, S., Ogata, N., Koide, S.I., Nakamura, S.I., and Yasue, H. (2000) Remnant Lipoproteins Induce Proatherothrombotic Molecules in Endothelial Cells Through a Redox-Sensitive Mechanism, *Circulation* 102, 670–676.
35. Abia, R., Perona, J.S., Pacheco, Y.M., Montero, E., Muriana, F.J., and Ruiz-Gutierrez, V. (1999) Postprandial Triacylglycerols from Dietary Virgin Olive Oil Are Selectively Cleared in Humans, *J. Nutr.* 129, 2184–2191.
36. Mabile, L., Salvayre, R., Bonnafe, M.J., and Negre-Salvayre, A. (1995) Oxidizability and Subsequent Cytotoxicity of Chylomicrons to Monocytic V937 and Endothelial Cells Are Dependent on Dietary Fat Composition, *Free Radic. Biol. Med.* 19, 599–607.
37. Lechleitner, M., Hoppichler, F., Foger, B., and Patsch, J.R. (1994) Low-Density Lipoproteins of the Postprandial State Induce Cellular Cholesteryl Ester Accumulation in Macrophages, *Arterioscler. Thromb.* 14, 1799–1807.
38. Diwadkar, V.A., Anderson, J.W., Bridges, S.R., Gowri, M.S., and Oelgten, P.R. (1999) Postprandial Low-Density Lipoproteins in Type 2 Diabetes Are Oxidized More Extensively Than Fasting Diabetes and Control Samples, *Proc. Soc. Exp. Biol. Med.* 222, 178–184.
39. Moore, K., and Roberts, L.J. (1998) Measurement of Lipid Peroxidation, *Free Rad. Res.* 28, 659–671.
40. Nicolaiew, N., Lemort, N., Adorni, L., Berra, B., Montorfano, G., Rapelli, S., Cortesi, N., and Jacotot, B. (1998) Comparison Between Extra Virgin Olive Oil and Oleic Acid Rich Sunflower Oil: Effects on Postprandial Lipemia and LDL Susceptibility to Oxidation, *Ann. Nutr. Metab.* 42, 251–260.
41. Caruso, D., Berra, B., Giavarini, F., Cortesi, N., Fedeli, E., and Galli, G. (1999) Effect of Virgin Olive Oil Phenolic Compounds on *in vitro* Oxidation of Human Low Density Lipoproteins, *Nutr. Metab. Cardiovasc. Dis.* 9, 102–107.
42. Miró-Casas, E., Farré Alvadalejo, M., Covas, M.I., Ortuño Rodríguez, J., Menoyo Colomer, E., Lamuela Raventós, R.M., and de la Torre, R. (2001) Capillary Gas Chromatography–Mass Spectrometry Quantitative Determination of Hydroxytyrosol and Tyrosol in Human Urine, *Anal. Biochem.* 294, 63–72.
43. Bonanome, A., Pagnan, A., Caruso, D., Toia, A., Xamin, A., Fedeli, E., Berra, B., Zamburlini, A., Ursini, F., and Galli, G. (2000) Evidence of Postprandial Absorption of Olive Oil Phenols in Humans, *Nutr. Metab. Cardiovasc. Dis.* 10, 111–120.
44. Lee, C., Barnett, J., and Reaven, P.D. (1998) Liposomes Enriched in Oleic Acid Are Less Susceptible to Oxidation and Have Less Proinflammatory Activity When Exposed to Oxidizing Conditions, *J. Lipid Res.* 39, 1239–1247.
45. De la Cruz, J.P., Quintero, L., Villalobos, M.A., and Sanchez de la Cuesta, F. (2000) Lipid Peroxidation and Glutathione System in Hyperlipemic Rabbits: Influence of Olive Oil Administration, *Biochim. Biophys. Acta* 1485, 36–44.

[Received August 23, 2001, and in revised form January 3, 2002; revision accepted January 9, 2002]



# Dietary n-3 FA Modulate Long and Very Long Chain FA Content, Rhodopsin Content, and Rhodopsin Phosphorylation in Rat Rod Outer Segment After Light Exposure

Miyoung Suh<sup>a</sup>, Antony A. Wierzbicki<sup>a</sup>, and M. Thomas Clandinin<sup>a,b,\*</sup>

Nutrition and Metabolism Research Group, <sup>a</sup>Department of Agricultural, Food and Nutritional Science, and <sup>b</sup>Department of Medicine, University of Alberta, Edmonton, Alberta, Canada T6G 2P5

**ABSTRACT:** A previous study has shown that the long and very long chain FA (VLCFA) content of the rat retina responds to changes in dietary n-6/n-3 ratio of the fat fed (1). The present study tested whether similar changes in these FA are associated with alterations in rhodopsin content and rhodopsin phosphorylation after light treatment. Weanling rats were fed diets containing 20% (w/w, 40% energy) fat with either high (4.8%, w/w) or low (1.2%, w/w) n-3 FA. After 6 wk of feeding, half of the animals in each group were exposed to light for 48 h at 350 lx or were kept in complete darkness. In the rod outer segment, the high n-3 diet treatment increased the level of 20:5n-3 and 22:6n-3 and reduced the levels of 20:4n-6 and 24:4n-6 in PC, PE, and PS. After the feeding of a high n-3 FA diet, total n-3 pentaenoic VLCFA from C<sub>24</sub> to C<sub>34</sub> increased in PC, whereas the n-6 tetra- and pentaenoic VLCFA decreased. No changes occurred in n-3 hexaenoic VLCFA regardless of the level of 22:6n-3 in the diet. After light exposure, animals fed a high n-3 FA diet showed reduction in 22:6n-3 as well as in n-6 and n-3 VLCFA in PC. FFA and TG fractions contained increased levels of both 20:4n-6 and 22:6n-3 after light exposure. Dark-adapted rhodopsin content and rhodopsin phosphorylation in the rod outer segment of rats fed the low n-3 FA diet were higher than in animals fed a high n-3 FA diet. After light exposure, animals fed the low n-3 FA diet lost more rhodopsin compared to animals fed the high n-3 FA diet, resulting in less phosphorylation of rhodopsin. Results indicate that the FA composition, rhodopsin content, and phosphorylation in visual cells is influenced by the dietary n-3 FA fed as well as by light exposure. The results also imply that 22:6n-3 may not be the precursor for synthesis of hexaenoic VLCFA.

Paper no. L8551 in *Lipids* 37, 253–260 (March 2002).

The role of dietary fat in determining the content of very long chain fatty acids (VLCFA, of C<sub>24</sub>–C<sub>34</sub>) has not been studied extensively in visual cells. In previous studies we demonstrated that a diet high in n-3 FA containing 22:6n-3 increased the level of 22:6n-3 and decreased 20:4n-6 and n-6 tetraenoic

VLCFA in phospholipids of the rod outer segment (ROS) (1,2). VLCFA, comprising carbon chain lengths of up to C<sub>36</sub>, are highly concentrated in PC of photoreceptors (1–4). The functional role of VLCFA in the retina has not been identified. Thus, the objective of the present study was to assess whether these diet-induced changes in photoreceptor essential FA constituents are associated with alterations in rhodopsin content or phosphorylation after light exposure.

Studies have indicated dietary modulation of n-3 FA in membrane phospholipid components of nervous tissue in the brain and retina of the chick (5), monkey (6–8), and rat (9–11). Diet-induced modulation of docosahexaenoic acid (DHA, 22:6n-3) content in the membrane appears to be associated with a change in retinal function when measured by electroretinogram or visual acuity (6,12–14). In most of these studies (6,13,14), the level of saturated and monounsaturated FA was also varied because a fat source from a single oil was used. Also, experiments were performed on n-3 FA-deficient animals made deficient by feeding an imbalanced n-6/n-3 FA diet. This extreme diet regime is not reflective of the physiological intake for neonatal animals or of infant fat intakes. Studies investigating the effect of dietary fat on individual phospholipids in visual cells in normally growing animals by feeding diets that produce a range of nutritionally balanced FA intakes are limited.

Rhodopsin is firmly embedded in the lipid bilayer in the disk of the ROS, and rhodopsin function is sensitive to specific alterations in membrane phospholipids (15,16). The function of DHA or VLCFA in phospholipids of the ROS in relation to rhodopsin function is not clear. Bush *et al.* (15) reported that rats fed safflower oil devoid of n-3 FA exhibit a slower rate of rhodopsin regeneration than animals fed soybean oil containing n-3 FA. These results suggest that the n-3 FA is important for regeneration of rhodopsin. To regenerate rhodopsin, photoactivated rhodopsin has to be phosphorylated and then dephosphorylated to rebind an 11-*cis* retinal. It is not known whether these steps are also affected by dietary n-3 FA.

Rhodopsin and its membrane environment are responsive to light (17–20). For example, animals exposed to light have a lower level of rhodopsin together with a shortened ROS

\* To whom correspondence should be addressed at Nutrition and Metabolism Research Group, Agricultural, Food and Nutritional Science, 4-10 Agricultural Forestry, University of Alberta, Edmonton, Alberta, Canada T6G 2P5. E-mail: tom.clandinin@ualberta.ca

Abbreviations: LCFA, long chain fatty acids; ROS, rod outer segment; VLCFA, very long chain fatty acids.

length, a reduced number of photoreceptors, and a thinner outer nuclear layer, and they exhibit reduced rhodopsin synthesis (17–20). These changes may be partly associated with DHA, since this FA is reduced by constant illumination and bright cyclic illumination (21–23). However, the effect of light treatment on VLCFA content has not been explored. Collectively, these findings imply that altering membrane FA composition may modulate membrane functional components of photoreceptor cells after light exposure.

The present study was designed to determine whether dietary fat and light induce change in long-chain FA (LCFA) and whether VLCFA content of the ROS alters visual function in the photoreceptor cells of growing animals. The levels of polyenoic LCFA and VLCFA in individual phospholipids of the ROS after 48 h of light exposure were determined after a high or low dietary n-3 FA intake. To associate changes occurring in membrane composition with visual function, rhodopsin level and rhodopsin phosphorylation were also measured in the ROS.

## EXPERIMENTAL PROCEDURES

**Animals and diets.** This study was approved by the University of Alberta Animal Ethics Committee. Two hundred sixteen male weanling Sprague-Dawley rats were housed under cyclic light with 12-h dark and 12-h light periods. The intensity of illumination at the front of the cage was 110 lx and at the center of the cage 27 lx of cool, white fluorescent light. Animals were randomly assigned to two diet groups and fed semipurified diets (24) containing 20% (w/w) fat (40% energy as fat) of either a high (4.8% w/w of total FA) n-3 FA content providing 22:6n-3 (3.4% w/w of total FA) or a low n-3 FA content without 22:6n-3 (1.2% w/w of total FA). Shark oil was used to supply 22:6n-3 in the high n-3 diet, since it is high in content of 22:6n-3 (22%, w/w) and relatively low in 20:5n-3 (5.5%, w/w) compared to fish oils used previously (1). The fat mixture and FA composition of the diets fed are presented in Table 1 and reflect a range of dietary fat intakes typical in North America. Diets were prepared weekly, kept in the freezer, and fed to animals every other day.

After 6 wk of feeding, half of the rats in each diet group were transferred to polypropylene cages, housed in pairs, and exposed to 48 h of continuous light at the intensity of approximately 300–350 lx. This level of light intensity is equivalent to the light intensity experienced while standing in a well-lit office under the light source and is much less than 1% of the light intensity experienced when facing the sun on a clear day. The other half of the animals in each diet group were kept in complete darkness as a control. Body weight was measured weekly; the weight gain from weaning ( $54.1 \pm 4.5$  g) to 6 wk postweaning ( $374.6 \pm 30$  g) was 7.2 g per day. No effect of dietary treatment was observed on body weight or weight gain.

**Isolation of retina and ROS.** Animals were sacrificed by decapitation. All isolations were performed at 4°C. For lipid analysis, retinas were isolated either in dim red light for dark-

**TABLE 1**  
**Fat Mixture and FA Composition of Experimental Diets<sup>a</sup>**

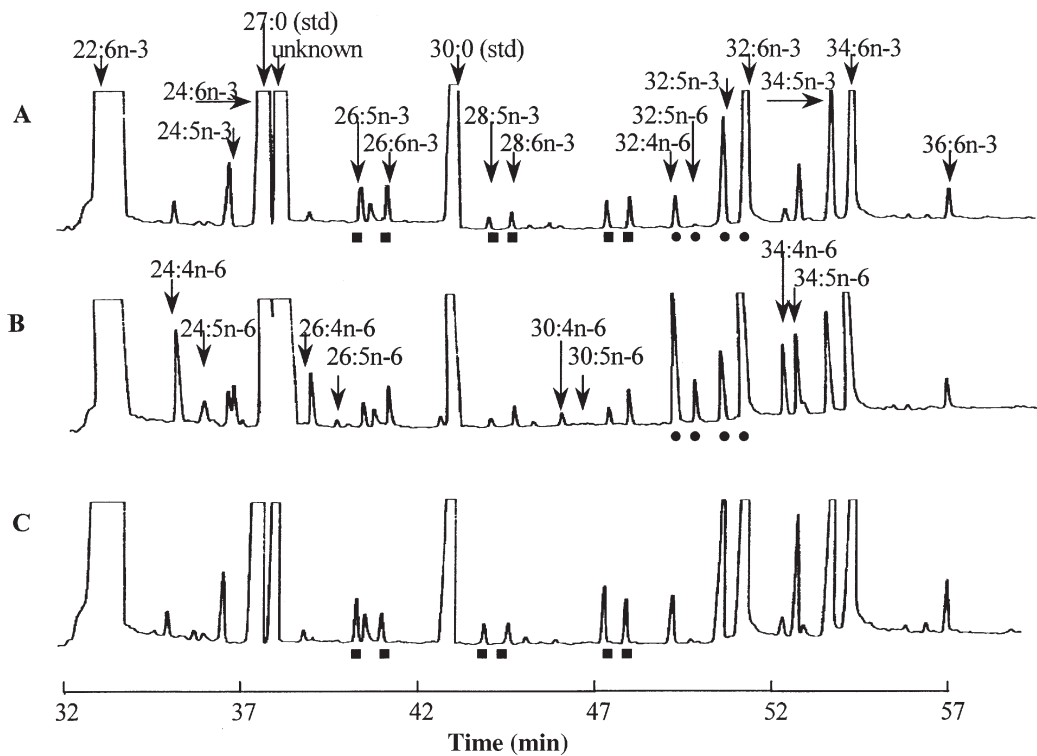
Diet	High n-3	Low n-3
Fat source (g/kg)		
Beef tallow	134.0	152.0
Safflower	33.0	44.0
Linseed oil	—	4.0
Shark oil	36.0	—
FA (% w/w)		
14:0	2.8	2.4
16:0	23.9	22.9
18:0	46.2	47.9
18:1n-9 + 18:1n-7	5.7	6.3
18:2n-6	11.3	16.3
18:3n-3	0.1	1.2
20:4n-6	0.3	—
20:5n-3	0.9	—
22:6n-3	3.4	—
ΣSAT	76.1	76.0
ΣMono	7.3	6.5
Σn-6	11.8	16.3
Σn-3	4.8	1.2
P/S ratio	0.22	0.23

<sup>a</sup>FA with chain lengths greater than C<sub>24</sub> were less than 0.02% (w/w) in both diets. ΣSAT, sum of saturated FA; Σmono, sum of monounsaturated FA; Σn-6, sum of n-6 FA; Σn-3, sum of n-3 FA; P/S ratio, polyunsaturated to saturated FA ratio.

adapted animals or in ambient laboratory light for light-exposed groups. For analysis of rhodopsin, light-exposed animals were dark-adapted for 1 h before sacrifice in dim red light. For each sample ( $n = 1$ ), 8 retinas were pooled for the separation of the ROS for lipid analysis, and 10 retinas were pooled for measurement of ROS rhodopsin content and rhodopsin phosphorylation. The ROS was isolated by discontinuous sucrose gradient centrifugation (25). The ROS for rhodopsin analysis was resuspended with 0.5 mL of washing buffer, 50 mM Tris-acetate (pH 7.4) containing 5 mL MgCl<sub>2</sub> and 0.1 mM EDTA and then stored at -70°C.

**Lipid analysis.** Lipids were extracted from the ROS (26). Individual phospholipids were separated using silica-gel TLC H-plates as described previously (1). After recovery of the phospholipids, the silica gel containing neutral lipids was scraped into 25-mL culture tubes and eluted three times with 10 mL of chloroform/methanol (1:1, vol/vol) containing 1 ppm ethoxyquin. The eluted lipids were applied to TLC G-plates to separate neutral lipids (1). Each phospholipid and neutral lipid was recovered, and FAME were prepared with a 14% (w/w) boron trifluoride-methanol reagent (27).

**Analysis of FAME.** FAME were separated on a polar BPX70 column (25 m × 0.22 mm i.d.) using a Hewlett-Packard 5890 GLC equipped with a Vista DS 654 data system (Varian, Palo Alto, CA), as described earlier (1). With this column, the resolution of n-6 tetraenoic and pentaenoic and n-3 pentaenoic and hexaenoic VLCFA was more distinct compared to the nonpolar BP1 column used earlier (1) (Fig. 1). Degree of unsaturation and n-series of VLCFA were confirmed by GC-MS (1). The content of VLCFA obtained was not corrected for detector response factors, since pure standards for these FA are not available.



**FIG. 1.** Typical chromatograms of very long chain FA (VLCFA) of PC in the rod outer segment following diet and light treatment. FAME were separated by GLC using a polar BPX 70 column (SGE, Rose Scientific, Edmonton, Canada). Although the amount of standard is different in (A) and (B), the proportion of the FA indicated by the circle (●) in  $C_{32}$  indicates an example of the influence of diet treatment. Those indicated by the square (■) in (A) and (C) reflect light treatment: The ratio of n-3 pentaene to hexaene of  $C_{26}$ ,  $C_{28}$ , and  $C_{30}$  FA increased after light exposure. (A), High n-3 diet/dark; (B), low n-3 diet/dark; (C), high n-3 diet/light. Std, standard.

**Rhodopsin measurement.** Rhodopsin content of the ROS was determined from animals of both dietary groups that were either dark adapted or light exposed. Rhodopsin was extracted by the method of Fulton *et al.* (28), using 1% (wt/vol) octylglucoside as a detergent (29). Each extract was scanned from 270 to 700 nm using a diode-array spectrophotometer (Hewlett-Packard 8452A), and rhodopsin was quantified by difference spectroscopy at an absorption of 498 nm before and after bleaching for 480 s with a cool, white fluorescent light with the intensity of 1,000 lx at a distance of 30 cm from the cuvette. A molar extinction coefficient of 40,000 (30) was used for the calculations of rhodopsin concentration.

**Rhodopsin phosphorylation in Vitro.** Rhodopsin phosphorylation was measured by the method used by Kuhn and Wilden (31) using [ $\gamma$ - $^{32}P$ ]ATP (SA 3000 Ci/mmol; New England Nuclear-DuPont, Boston, MA) as a monitor for phosphorylation. The reaction was initiated by the onset of illumination, which was cool, white fluorescence light at 700–800 lx at a distance of 50 cm from the water bath. The resulting radiolabeled solubilized ROS membrane containing 30  $\mu$ g of protein was loaded and run on a 10-cm linear gradient (7.5% acrylamide) polyacrylamide gel (32) for 2 h at a constant current at 40 mA at  $\approx$ 150 V. The gel was dried using gel drying film (Promega, Madison, WI). Incorporation of  $^{32}P_i$  was monitored by exposing x-ray film (Kodak X-OMAT AR film) to the gel at  $-70^\circ\text{C}$

for 1.5 h. The film was developed by Kodak M35A X-Omat Processors (Rochester, NY). The resulting autoradiograms were analyzed using a scanning densitometer (Ultrosan XL, Bromma, Sweden). The area under the peak was used to quantitate labeling with  $^{32}P_i$  and was divided by the rhodopsin content loaded on the gel to express the rhodopsin phosphorylation state.

**Statistical methods.** The effect of light and diet on the FA composition of phospholipids in the ROS and on the rhodopsin content and rhodopsin phosphorylation was analyzed by a two-way ANOVA with light and diet as the main factors. The *n* number of replicates is indicated in each table and figure caption. Duncan's multiple range test (33) was used for comparison of the main factors after a significant ANOVA. All data are expressed as mean  $\pm$  SEM.

## RESULTS

**Effect of dietary fat and light on LCFA and VLCFA composition of ROS phospholipids.** Both diet and light significantly altered the FA composition of major phospholipids of the ROS in rat retina. Feeding a high 22:6n-3 diet increased the level of 22:6n-3 in PE and PS in both dark- and light-exposed animals compared to feeding a low n-3 FA diet (Table 2). This diet also increased the level of 22:6n-3 in PI of light-adapted

**TABLE 2**  
**Effect of Dietary Fat and Light on the Level of 20:4n-6 and 22:6n-3 Phospholipids in the Rod Outer Segment<sup>a</sup>**

FA (% w/w)	High n-3		Low n-3		Significant effects	
	Dark	Light	Dark	Light	Light	Diet
PC						
20:4n-6	3.9 ± 0.2 <sup>b</sup>	4.2 ± 0.1 <sup>b</sup>	5.0 ± 0.2 <sup>a</sup>	5.1 ± 0.2 <sup>a</sup>		***
22:6n-3	32.5 ± 2.1 <sup>a</sup>	25.9 ± 1.1 <sup>b</sup>	27.2 ± 1.9 <sup>a,b</sup>	24.8 ± 2.4 <sup>b</sup>	*	
PE						
20:4n-6	5.9 ± 0.3 <sup>c</sup>	5.8 ± 0.2 <sup>c</sup>	7.6 ± 0.4 <sup>a</sup>	6.7 ± 0.1 <sup>b</sup>		***
22:6n-3	57.1 ± 1.3 <sup>a</sup>	58.1 ± 0.5 <sup>a</sup>	47.5 ± 0.9 <sup>c</sup>	53.1 ± 0.4 <sup>b</sup>	**	***
PS						
20:4n-6	2.5 ± 0.2 <sup>b</sup>	2.5 ± 0.1 <sup>b</sup>	3.1 ± 0.1 <sup>a</sup>	2.9 ± 0.1 <sup>a</sup>		***
22:6n-3	63.1 ± 0.9 <sup>a</sup>	59.9 ± 0.4 <sup>b</sup>	55.7 ± 0.6 <sup>c</sup>	52.4 ± 0.5 <sup>d</sup>	***	***
PI						
20:4n-6	37.3 ± 0.9 <sup>b</sup>	38.7 ± 0.8 <sup>b</sup>	39.5 ± 1.1 <sup>b</sup>	44.6 ± 0.7 <sup>a</sup>	**	**
22:6n-3	12.5 ± 1.0 <sup>b</sup>	15.8 ± 0.5 <sup>a</sup>	11.7 ± 1.0 <sup>b</sup>	12.2 ± 0.5 <sup>b</sup>	*	*

<sup>a</sup>Values given are means ( $n = 6$ ) ± SEM. For each  $n$ , eight retinas were pooled, except for PI ( $n = 3$ ), wherein 16 retinas were pooled. Significant effects of light and diet were analyzed by a two-way ANOVA. Values without a common roman superscript are significantly different: \* $P < 0.05$ ; \*\* $P < 0.01$ ; \*\*\* $P < 0.001$ . Significant interactions were identified only for 22:6n-3 in PE.

animals. Concomitantly, the level of 20:4n-6 decreased in all major phospholipids except PI of dark-adapted animals after feeding a high n-3 FA diet containing 22:6n-3 in comparison to feeding a low n-3 FA diet. The loss of rhodopsin from the low n-3 FA group was slightly higher than that observed for animals fed a high n-3 FA diet (59 and 51%, respectively) (Table 2). Animals fed a low n-3 FA diet containing no 22:6n-3 exhibited a significant decrease in 20:4n-6 in PE and 22:6n-3 in PS after light exposure. The level of 20:4n-6 in PI and 22:6n-3 in PE increased after light exposure.

VLCFA containing carbon chain lengths of up to C<sub>36</sub> in PC and C<sub>26</sub> in PS were also influenced by diet and light treatment (Table 3; Figs. 1 and 2). For example, in PC of dark-adapted animals, feeding a high n-3 FA diet containing 22:6n-3 increased the level of n-3 pentaenoic VLCFA of C<sub>24</sub>, C<sub>26</sub>, C<sub>30</sub>, C<sub>32</sub>, and C<sub>34</sub> carbons in chain length. This diet also decreased most of the n-6 tetraenoic VLCFA except for C<sub>30</sub> and decreased n-6 pentaenoic VLCFA of C<sub>24</sub>, C<sub>26</sub>, and C<sub>32</sub> carbons in chain length (Table 3). Hexaenoic n-3 VLCFA were not influenced by feeding a high n-3 FA diet. The high n-3 FA diet increased total n-3 pentaenoic VLCFA in PC while decreasing the n-6 tetra- and pentaenoic VLCFA (Fig. 2). In PS, the content of n-3 pentaenoic VLCFA of C<sub>24</sub> and C<sub>26</sub> and hexaenoic C<sub>26</sub> FA increased after feeding a high n-3 FA diet, whereas this diet decreased the level of n-6 tetraenes of C<sub>24</sub> and pentaenes of C<sub>24</sub> and C<sub>26</sub> carbons in chain length (Table 3).

In light-exposed animals, total n-6 tetraenoic and pentaenoic VLCFA decreased in animals fed a diet either high (46.0 and 32.5%, respectively) or low (18.4 and 47.2%, respectively) in n-3 FA (Fig. 2). Total n-3 pentaenoic and hexaenoic VLCFA also decreased in both groups fed either the high (16.9 and 14.3%) or the low (7.8 and 17.0%) n-3 FA diet. The loss of n-6 tetraenoic and pentaenoic VLCFA after light treatment was slightly greater than that of n-3 VLCFA (Fig. 2).

*Effect of dietary fat and light on FA composition of FFA and TAG fractions.* FFA and TAG fractions were also analyzed (Fig. 3) to identify the fate of 20:4n-6 and 22:6n-3 lost

from phospholipids after light treatment. In both FFA and TAG fractions, diet and light treatments influenced the level of 20:4n-6 and 22:6n-3. After consumption of the high n-3 FA diet, animals kept in the dark displayed a significant increase in 22:6n-3 content in both FFA and TAG compared to animals fed the low n-3 FA diet. In the TAG fraction, the increase in 22:6n-3 occurred concomitantly with increased levels of 20:4n-6. Exposure to light significantly increased the content of 20:4n-6 and 22:6n-3 above dark values in both dietary groups (Fig. 3).

*Effect of dietary fat and light on rhodopsin content.* Rhodopsin content of the ROS was determined in order to identify the relationship between dietary fat and retinal function. Animals fed a low n-3 FA diet exhibited a higher rhodopsin content in ROS maintained in the dark compared to ROS of animals fed the high n-3 FA (7.5 ± 0.5 nmol/mg protein and 6.1 ± 0.2 nmol/mg protein, respectively). Significant loss of rhodopsin was found after light exposure in both animal groups fed either a low or a high n-3 FA (3.1 ± 0.1 and 3.0 ± 0.3 nmol/mg protein, respectively). The loss from the low n-3 FA group was slightly higher than that observed for animals fed a high n-3 FA diet (59 and 51%, respectively).

*Effect of dietary fat and light on rhodopsin phosphorylation.* Rhodopsin phosphorylation in the ROS was analyzed *in vitro* to identify the effect of dietary fat on retinal function. Rhodopsin phosphorylation rate measured by the ratio of densitometer unit (O.D.·mm<sup>2</sup>) to rhodopsin present on the gel was altered by 1 h of incubation in continuous white light for both the dietary groups and also by the light treatment. Rhodopsin in the ROS of animals fed a low n-3 FA diet exhibited a higher phosphorylation state than that observed for animals fed the high n-3 FA diet in both dark- (59.8 ± 9.1 and 49.7 ± 8.8, respectively) and light (61.3 ± 10.1 and 53.5 ± 7.7, respectively) -exposed animals. This result, while not statistically significant, indicates that more phosphorylation of rhodopsin may have occurred following consumption of the low n-3 FA diet. After light exposure, rhodopsin from animals fed the low n-3 FA diet was phos-



**TABLE 3**  
**Effect of Dietary Fat on the Level of Very Long Chain Fatty Acid (VLCFA) Composition of PC (C<sub>24</sub>–C<sub>36</sub>) and PS (C<sub>24</sub>–C<sub>26</sub>) in the Rod Outer Segment of Dark-Adapted Rats<sup>a</sup>**

FA (% w/w)	PC		PS	
	High n-3	Low n-3	High n-3	Low n-3
<b>n-6 Tetraenoic VLCFA<sup>b</sup></b>				
24:4	0.06 ± 0.01***	0.15 ± 0.01	0.43 ± 0.01***	1.73 ± 0.18
26:4	0.02 ± 0.00***	0.06 ± 0.01	0.05 ± 0.02	0.03 ± 0.02
28:4	0.00 ± 0.00***	0.02 ± 0.00		
30:4	0.02 ± 0.01	0.03 ± 0.00		
32:4	0.11 ± 0.03***	0.29 ± 0.04		
34:4	0.04 ± 0.01***	0.21 ± 0.05		
<b>n-6 Pentaenoic VLCFA</b>				
24:5	0.02 ± 0.00***	0.05 ± 0.01	0.09 ± 0.02***	0.29 ± 0.03
26:5	0.00 ± 0.00**	0.02 ± 0.00	0.00 ± 0.00*	0.03 ± 0.02
28:5	0.00 ± 0.00	0.00 ± 0.00		
30:5	0.01 ± 0.00	0.01 ± 0.01		
32:5	0.02 ± 0.01***	0.14 ± 0.05		
34:5	0.03 ± 0.00	0.10 ± 0.04		
<b>n-3 Pentaenoic VLCFA</b>				
24:5	0.15 ± 0.02 **	0.08 ± 0.01	1.59 ± 0.08***	0.86 ± 0.08
26:5	0.08 ± 0.01**	0.04 ± 0.00	0.06 ± 0.01**	0.03 ± 0.01
28:5	0.03 ± 0.00	0.02 ± 0.00		
30:5	0.07 ± 0.01**	0.04 ± 0.01		
32:5	0.31 ± 0.05**	0.17 ± 0.03		
34:5	0.49 ± 0.06**	0.32 ± 0.08		
<b>n-3 Hexaenoic VLCFA</b>				
24:6	—	—	2.01 ± 0.44	1.80 ± 0.21
26:6	0.08 ± 0.01	0.08 ± 0.01	0.17 ± 0.01*	0.12 ± 0.03
28:6	0.06 ± 0.01	0.04 ± 0.01		
30:6	0.07 ± 0.01	0.07 ± 0.01		
32:6	1.32 ± 0.21	1.10 ± 0.17		
34:6	1.10 ± 0.14	1.00 ± 0.18		
36:6	0.09 ± 0.01	0.08 ± 0.01		

<sup>a</sup>Values given are means ( $n = 6$ ) ± SEM. For each  $n$ , eight retinas were pooled. Asterisks \* indicate the significant differences between diets within each phospholipid: \* $P < 0.05$ ; \*\* $P < 0.01$ ; \*\*\* $P < 0.001$ .

<sup>b</sup>24:6n-3 in PC was also detected but not represented because its resolution time was almost the same as the standard 27:0 in the analysis.

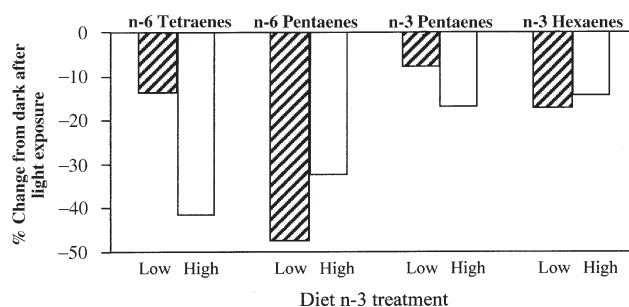
phorylated only 2.6% more than that of dark-adapted rhodopsin, compared to 7.8% for animals fed the high n-3 FA diet.

## DISCUSSION

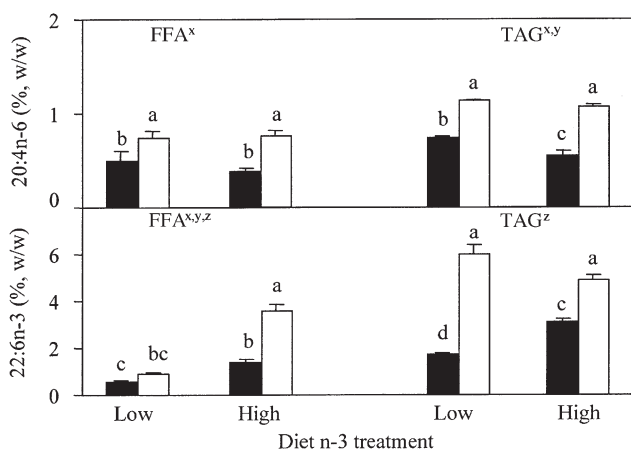
**Dietary fat and LCFA.** In normal growing rats, consumption of nutritionally adequate diets with a physiological change in the n-3 FA content produced considerable modification of the FA composition in photoreceptor cell membrane phospholipids. Higher n-3 FA level with addition of 22:6n-3 in the diet significantly increased membrane content of DHA in PE, PS, and PI and reduced 20:4n-6 content. This finding is in agreement with previous studies (1,10,11) and suggests that the neuronal cell is capable of replacing n-6 with n-3 FA. The replacement of n-6 with n-3 FA was more obvious in animals deficient in n-3 FA (8,34,35), perhaps owing to a significant difference in the ratio of n-6/n-3 FA diet in the control (n-6/n-3 = 7) vs. deficient diets (n-6/n-3 = 255). Changes in *de novo* synthesis and/or direct molecular replacement by deacylation–reacylation may be responsible.

PE and PS are located in the outer disk membrane monolayer (36). DHA is the major FA in these phospholipids in the

retina and ROS. In the present study, the level of DHA in the ROS was increased to 20 and 13% in PE and PS, respectively, after consumption of a diet containing a high n-3 FA content



**FIG. 2.** Effect of light on the change in level of total n-6 tetraenoic and pentaenoic and total n-3 pentaenoic and hexaenoic VLCFA (C<sub>24</sub>–C<sub>36</sub>) present in PC of the rod outer segment. The value for the percent change from dark as a result of light treatment was taken from the total mean ( $n = 6$ ) for each group from dark-adapted rats (Table 2). In both low and high n-3 FA diet groups, n-6 and n-3 VLCFA were reduced after light exposure ( $P < 0.05$ ). Diagonally lined box, low n-3 diet; open box, high n-3 diet. For abbreviation see Figure 1.



**FIG. 3.** Effect of dietary fat and light on the level of 20:4n-6 and 22:6n-3 in FFA and TAG components of the rod outer segment. The values are the mean ( $n = 3$ )  $\pm$  SEM. Sixteen retinas were pooled for each  $n$ . Values without a common letter within a lipid class were significantly different by diet and light treatment,  $P < 0.05$ . Superscripts indicate the following: x, significant effect of light ( $P < 0.003$ ); y, significant effect of diet ( $P < 0.02$ ); z, significant interaction effect ( $P < 0.003$ ). Unlike phospholipids, the levels of both 20:4n-6 and 22:6n-3 increased in the FFA and TAG after light exposure. (■), dark; (□), light.

as compared to those animals fed the low n-3 diet. DHA is the principal component of dipolyunsaturated phospholipids found in bovine and frog ROS (37–39). The relationship between FA composition in the phospholipid and an asymmetrical distribution of phospholipids in excitable membranes is not clearly established. However, this asymmetrical distribution of membrane phospholipids (36) highly enriched in 22:6n-3 may enable the optimal environment for rhodopsin conformational change induced by light exposure.

**Dietary fat and VLCFA.** The general compositional features of VLCFA in the ROS were similar to those reported earlier (1,40). The present experimental conditions identified one more series of n-6 pentaenoic VLCFA in addition to n-6 tetraenoic VLCFA. It is now clear that VLCFA are present in the ROS as either n-6 tetraenes and pentaenes or n-3 pentaenes and hexaenes.

A higher n-3 FA content in the diet significantly increased n-3 pentaenoic VLCFA in PC but not n-3 hexaenoic VLCFA. An increase in 22:6n-3 occurred in major phospholipids with no changes occurring in hexaenoic VLCFA in PC regardless of the level of 22:6n-3 in the diet. This unexpected result may imply that 22:6n-3 is not a precursor for further elongation and synthesis of hexaenoic VLCFA. Therefore, the identification of the precursors and their further metabolism to VLCFA remain to be elucidated.

The implications of altering levels of VLCFA by dietary treatment are still not known. Together with a high concentration of DHA, it is conceivable that these FA provide a suitable environment for rhodopsin since these VLCFA have a high affinity for rhodopsin (4). VLCFA may also be involved in membrane signal transduction, as recent evidence indicates the involvement of tetraenoic VLCFA in activation

of protein kinase C in rat brain (41) and  $Ca^{2+}$  modulation in human neutrophils (42).

**Light exposure on LCFA and VLCFA.** Light exposure reduced 20% of the 22:6n-3 content in PC and 5% in PS from the dark-adapted level after consumption of the high n-3 FA diet. Light-induced reduction in LCFA is mediated by phospholipase  $A_2$  (43–45). Rats raised in cyclic light at a light intensity of 800 lx from birth to 12 wk also exhibited reduced 22:6n-3 content in ROS phospholipid by 70% and reduced ROS length and rhodopsin content compared to rats raised at a light intensity of 5 lx (46). These changes on exposure to cyclic light are a form of retinal adaptation to light (46–48).

Light treatment also reduced n-3 pentaenoic and hexaenoic VLCFA in PC. This level of n-6 VLCFA was not associated with 20:4n-6 since this FA in PC was not affected by light exposure. Thus, these data suggest that VLCFA undergo a different metabolic process compared to LCFA following light exposure. VLCFA is esterified mainly in the *sn*-1 position of glycerol, whereas LCFA is esterified in the *sn*-2 position (3,49). This observation suggests that light may activate phospholipase  $A_1$ .

The present experiment demonstrated that FFA and TAG are involved in the uptake of 20:4n-6 and 22:6n-3 developed from phospholipids after light exposure for 48 h. FFA and TAG fractions contained increased levels of both 20:4n-6 and 22:6n-3 after light exposure, implying that FFA and TAG serve as sources for 20:4n-6 and 22:6n-3 to enable recycling of these essential FA after light exposure.

**Dietary fat and light on rhodopsin content and rhodopsin phosphorylation.** The present experiment demonstrated that rhodopsin content and rhodopsin phosphorylation in the ROS were higher in dark-adapted animals after consumption of a low n-3 FA diet compared to animals fed a high n-3 FA diet. The ratio of rhodopsin content (nmol/mg protein), when expressed as densitometer units, showed 20.4 and 14.6% higher phosphorylation in animals fed a low n-3 FA diet in both the dark- and light-exposed group, respectively. This implies that the enzymes involved in rhodopsin phosphorylation, rhodopsin kinase and protein kinase C, may be affected by dietary n-3 FA treatment. Light-exposed animals fed a low n-3 FA lost more rhodopsin content and had less rhodopsin phosphorylation compared to animals fed a high n-3 FA diet. It would be of interest to determine whether a low n-3 FA diet also leads to higher rhodopsin regeneration. Rhodopsin phosphorylation functioning as a turn-off mechanism to inactivate the bleached rhodopsin is a necessary step for rhodopsin restoration to the dark state. Together with the FA data, light-evoked reduction of LCFA and VLCFA seems to be associated with a reduced level of rhodopsin after light exposure.

In conclusion, it is clear that the ROS content of both LCFA and VLCFA responds to dietary fat and light exposure. It is also apparent that 22:6n-3 may not be a direct precursor for the synthesis of hexaenoic VLCFA. Light exposure induces loss of VLCFA. These compositional changes seem to be associated with rhodopsin content and rhodopsin phosphorylation since both parameters are also altered in concert by a change in exposure to light and diet n-3 FA.

## ACKNOWLEDGMENTS

This research was supported by grants from Natural Sciences and Engineering Research Council of Canada.

## REFERENCES

- Suh, M., Wierzbicki, A.A., and Clandinin, M.T. (1994) Dietary Fat Alters Membrane Composition in Rod Outer Segments in Normal and Diabetic Rats: Impact on Content of Very-Long-Chain ( $C \geq 24$ ) Polyenoic Fatty Acids, *Biochim. Biophys. Acta* 1214, 54–62.
- Suh, M., Wierzbicki, A.A., Lien, E., and Clandinin, M.T. (2000) Dietary 20:4n-6 and 22:6n-3 Modulates the Profile of Long- and Very-Long-Chain Fatty Acids ( $C_{24}$ – $C_{36}$ ), Rhodopsin Content and Kinetics in Developing Photoreceptor Cells, *Pediatr. Res.* 48, 524–530.
- Aveldano, M.I. (1987) A Novel Group of Very Long Chain Polyenoic Fatty Acids in Dipolyunsaturated Phosphatidylcholines from Vertebrate Retina, *J. Biol. Chem.* 262, 1172–1179.
- Aveldano, M.I. (1988) Phospholipid Species Containing Long and Very Long Polyenoic Fatty Acids Remain with Rhodopsin After Hexane Extraction of Photoreceptor Membranes, *Biochemistry* 27, 1229–1239.
- Anderson, G.J., Connor, W.E., and Corliss, J.D. (1990) Docosahexaenoic Acid Is the Preferred Dietary Omega-3 Fatty Acid for the Development of the Brain and Retina, *Pediatr. Res.* 27, 81–87.
- Neuringer, M., Connor, W.E., Lin, P.S., Barstad, L., and Luck, S. (1986) n-3 Fatty Acids in the Brain and Retina: Evidence for Their Essentiality, *Proc. Natl. Acad. Sci. USA* 3, 4021–4025.
- Lin, D.S., Anderson, G.J., Connor, W.E., and Neuringer, M. (1994) Effect of Dietary n-3 Fatty Acids upon the Phospholipid Molecular Species of the Monkey Retina, *Invest. Ophthalmol. Vis. Sci.* 35, 794–803.
- Connor, W.E., Neuringer, M., and Lin, D.S. (1990) Dietary Effects on Brain Fatty Acid Composition: The Reversibility of n-3 Fatty Acid Deficiency Turnover of Docosahexaenoic Acid in the Brain Erythrocytes and Plasma of Rhesus Monkeys, *J. Lipid Res.* 31, 237–247.
- Philbrick, D.J., Mahadevappa, V.G., Ackman, R.G., and Holub, B.J. (1987) Ingestion of Fish Oil or a Derived n-3 Fatty Acid Concentrate Containing Eicosapentaenoic Acid (EPA) Affects Fatty Acid Compositions of Individual Phospholipids of Rat Brain, Sciatic Nerve, and Retina, *J. Nutr.* 117, 1663–1670.
- Hargreaves, K.M., and Clandinin, M.T. (1987) Dietary Control of Diacylphosphatidylethanolamine Species in Brain, *Biochim. Biophys. Acta* 962, 98–104.
- Hargreaves, K.M., and Clandinin, M.T. (1987) Phosphocholine-transferase Activity in Plasma Membrane: Effect of Diet, *Biochem. Biophys. Res. Commun.* 145, 309–315.
- Pawlosky, R.J., Denkins, Y., Ward, G., and Salem, N., Jr. (1997) Retinal and Brain Accretion of Long-Chain Polyunsaturated Fatty Acids in Developing Felines: The Effect of Corn Oil Based Maternal Diets, *Am. J. Clin. Nutr.* 65, 465–472.
- Weisinger, H.S., Vingrys, A.J., and Sinclair, A.J. (1996) The Effect of Docosahexaenoic Acid on the Electroretinogram of the Guinea Pig, *Lipids* 31, 65–70.
- Weisinger, H.S., Vingrys, A.J., and Sinclair, A.J. (1996) Effect of Dietary n-3 Deficiency on the Electroretinogram of the Guinea Pig, *Ann. Nutr. Metab.* 40, 91–98.
- Bush, R.A., Malnoe, A., Reme, C.E., and Williams, T.P. (1994) Dietary Deficiency of n-3 Fatty Acids Alters Rhodopsin Content and Function in the Rat Retina, *Invest. Ophthalmol. Vis. Sci.* 35, 91–100.
- Zorn, M., and Futterman, S. (1971) Properties of Rhodopsin Dependent on Associated Phospholipid, *J. Biol. Chem.* 246, 881–886.
- Schremser, J.L., and Williams, T. (1995) Rod Outer Segment (ROS) Renewal as a Mechanism for Adaptation to a New Intensity Environment. I. Rhodopsin Levels and ROS Length, *Exp. Eye Res.* 61, 17–24.
- Schremser, J.L., and Williams, T. (1995) Rod Outer Segment (ROS) Renewal as a Mechanism for Adaptation to a New Intensity Environment. II. Rhodopsin Synthesis and Packing Density, *Exp. Eye Res.* 61, 25–32.
- Organisciak, D.T., Darrow, R.M., Jiang, Y.L., and Blanks, J.C. (1996) Retinal Light Damage in Rats with Altered Levels of Rod Outer Segment Docosahexaenoate, *Invest. Ophthalmol. Vis. Sci.* 37, 2243–2257.
- Penn, J.S., and Williams T.P. (1986) Photostasis: Regulation of Daily Photon-Catch by Rat Retinas in Response to Various Cyclic Illuminances, *Exp. Eye Res.* 43, 915–928.
- Wiegand, R.D., Joel, C.D., Rapp, L.M., Nielson, J.C., Maude, M.B., and Anderson, R.E. (1986) Polyunsaturated Fatty Acids and Vitamin E in Rat Rod Outer Segments During Light Damage, *Invest. Ophthalmol. Vis. Sci.* 27, 727–733.
- Penn, J.S., and Anderson, R.E. (1987) Effect of Light History on Outer-Segment Membrane Composition in the Rat, *Exp. Eye Res.* 44, 767–778.
- Wiegand, R.D., Koutz, C.A., Chen, H., and Anderson, R.E. (1995) Effect of Dietary Fat and Environmental Lighting on the Phospholipid Molecular Species of Rat Photoreceptor Membranes, *Exp. Eye Res.* 60, 291–306.
- Clandinin, M.T., and Yamashiro, S. (1980) Dietary Factors Affecting the Incidence of Dietary Fat Induced Myocardial Lesions, *J. Nutr.* 110, 1197–1203.
- Stinson, A.M., Wiegand, R.D., and Anderson, R.E. (1991) Metabolism of Lipid Molecular Species in Rat Rod Outer Segments, *Exp. Eye Res.* 52, 213–218.
- Folch, J., Lees, M., and Sloane Stanley, G.H. (1957) A Simple Method for Isolation and Purification of Total Lipides from Animal Tissues, *J. Biol. Chem.* 226, 497–509.
- Morrison, W.R., and Smith, L.M. (1964) Preparation of Fatty Acid Methyl Esters and Dimethylacetals from Lipids with Boron Fluoride-Methanol, *J. Lipid Res.* 5, 600–608.
- Fulton, A.B., Manning, K.A., Baker, B.N, Schukar, S.E., and Bailey, C.J. (1982) Dark-Adapted Sensitivity, Rhodopsin Content, and Background Adaptation in Pcd/Pcd Mice, *Invest. Ophthalmol. Vis. Sci.* 22, 386–393.
- Stubbs, G.W., Smith, H.G., and Litman, B.J. (1976) Alkyl Glucosides as Effective Solubilizing Agents for Bovine Rhodopsin—A Comparison with Several Commonly Used Detergents, *Biochim. Biophys. Acta* 425, 46–56.
- Hubbard, R., Brown, P.K., and Bownds, D. (1971) Methodology of Vitamins A and Retinal Pigments, *Methods Enzymol.* 18, 615–653.
- Kuhn, H., and Wilden, U. (1982) Light Regulated Binding of Rhodopsin Kinase and Other Proteins to Cattle Photoreceptor Membranes, *Methods Enzymol.* 81, 489–496.
- Laemmli, U.K. (1970) Cleavage of Structural Proteins During the Assembly of the Head of Bacteriophage T4, *Nature* 227, 680–685.
- Steel, R.G.D., and Torrie, J.H. (1990) *Principles and Procedures of Statistics*, 2nd edn., Chapters 8–9, McGraw-Hill, New York.
- Connor, W.E., Neuringer, M., and Reisbick, S. (1991) Essentiality of Omega-3 Fatty Acids: Evidence from the Primate Model and Implications for Human Nutrition, in *Health Effects of  $\omega$ 3 Polyunsaturated Fatty Acids in Seafoods* (Simopoulos, A.P., Kifer, R.R., Martin, R.E., and Barlow, S.M., eds.), Vol. 66, pp. 118–132, Karger Press, Basel.
- Neuringer, M., and Connor, W.E. (1986) n-3 Fatty Acids in the Brain and Retina: Evidence of Their Essentiality, *Nutr. Rev.* 44, 285–294.

36. Miljanich, G.P., Nemes, P.P., White, D.L., and Dratz, E.A. (1981) The Asymmetric Transmembrane Distribution of Phosphatidylethanolamine, Phosphatidylserine and Fatty Acids of the Bovine Retinal Rod Outer Segment Disk Membrane, *J. Membr. Biol.* 60, 249–255.
37. Aveldano, M.I. (1989) Dipolyunsaturated Species of Retina Phospholipids and Their Fatty Acids, in *Biomembranes and Nutrition: Nutrients Affecting Lipid Composition Properties of Cell Membranes* (Leger, C.L., and Bereziat, G., eds.), Vol. 195, pp. 87–96, INSERM, Paris.
38. Aveldano, M.I., and Bazan, N.G. (1983) Molecular Species of Phosphatidylcholine, -ethanolamine, -serine, and -inositol in Microsomal and Photoreceptor Membranes of Bovine Retina, *J. Lipid Res.* 24, 620–627.
39. Wiegand, R.D., and Anderson, R.E. (1983) Phospholipid Molecular Species of Frog Rod Outer Segment Membranes, *Exp. Eye Res.* 37, 159–173.
40. Aveldano, M.I., and Sprecher, H. (1987) Very Long Chain (C<sub>24</sub> to C<sub>36</sub>) Polyenoic Fatty Acids of the n-3 and n-6 Series in Dipolyunsaturated Phosphatidylcholines from Bovine Retina, *J. Biol. Chem.* 262, 1180–1186.
41. Hardy, S.J., Ferrante, A., Poulos, A., Robinson, B.S., Johnson, D.W., and Murray, A.W. (1994) Effect of Exogenous Fatty Acids with Greater Than 22 Carbon Atoms (Very Long Chain Fatty Acids) on Superoxide Production by Human Neutrophils, *J. Immunol.* 153, 1754–1761.
42. Hardy, S.J., Robinson, B.S., Ferrante, A., Hii, C.S.T., Johnson, D.W., Poulos, A., and Murray, A.W. (1995) Polyenoic Very-Long-Chain Fatty Acids Mobilize Intracellular Calcium from a Thapsigargin-Insensitive Pool in Human Neutrophils: The Relationship Between Ca<sup>2+</sup> Mobilization and Superoxide Production Induced by Long- and Very-Long-Chain Fatty Acids, *Biochem. J.* 311, 689–697.
43. Jung, H., and Reme, C. (1994) Light-Evoked Arachidonic Acid Release in the Retina: Illuminance/Duration Dependence and the Effects of Quinacrine, Mellitin and Lithium, *Graefes Arch. Clin. Exp. Ophthalmol.* 232, 167–175.
44. Reinboth, J.J., Gautschi, K., Clausen, M., and Reme, C.E. (1996) Light Elicits the Release of Docosahexaenoic Acid from Membrane Phospholipids in the Rat Retina *in vitro*, *Exp. Eye Res.* 63, 277–284.
45. Birkle, D.L., and Bazan, N.G. (1989) Light Exposure Stimulates Arachidonic Acid Metabolism in Intact Rat Retina and Isolated Rod Outer Segments, *Neurochem. Res.* 14, 185–190.
46. Penn, J.S., and Anderson, R.E. (1987) Effect of Light History on Retinal Antioxidants and Light Damage Susceptibility in the Rat, *Exp. Eye Res.* 44, 767–778.
47. Penn, J.S., and Thum, L. (1987) A Comparison of the Retinal Effects of Light Damage and High Illuminance Light History, in *Degenerative Retinal Disorders: Clinical and Laboratory Investigations* (Hollyfield, J.G., Anderson, R.E., and LaVail, M.M., eds.), Progress in Clinical and Biological Research Series, Vol. 247, pp. 425–438, Alan R. Liss, New York.
48. Penn, J.S., Thum, L., and Naash, M.I. (1989) Photoreceptor Physiology in the Rat Is Governed by the Light Environment, *Exp. Eye Res.* 49, 205–215.
49. Poulos, A., Sharp, P., Johnson, D., and Easton, C. (1988) The Occurrence of Polyenoic Very Long Chain Fatty Acids with Greater Than 32 Carbon Atoms in Molecular Species of Phosphatidylcholine in Normal and Peroxisome Deficient (Zellweger's syndrome) Brain, *Biochem. J.* 253, 645–650.

[Received June 7, 2000 and in revised form February 1, 2001; revision accepted February 4, 2002]



# Hypolipidemic Action of the Soybean Isoflavones Genistein and Genistin in Glomerulonephritic Rats

Takashi Kojima<sup>a</sup>, Takehiko Uesugi<sup>b</sup>, Toshiya Toda<sup>b</sup>,  
Yutaka Miura<sup>a</sup>, and Kazumi Yagasaki<sup>a,\*</sup>

<sup>a</sup>Department of Applied Biological Science, Tokyo Noko University, Fuchu, Tokyo 183-8509, Japan,  
and <sup>b</sup>Research & Development Laboratory, Fujicco Co., Ltd., Kobe 650-8558, Japan

**ABSTRACT:** Effects of genistein and its glycoside genistin were studied in nephritic rats with endogenous hyperlipidemia. Male Wistar rats with glomerulonephritis caused by a single intravenous injection of nephrotoxic serum were orally given 5 mg of genistein or 8 mg of genistin/d/100 g body weight for 12 d. These isoflavones suppressed nephritis-induced severe hypercholesterolemia and hypertriglyceridemia, and their hypolipidemic action was almost identical. Fecal steroid excretion was unchanged by administration of the two isoflavones. Genistein inhibited the incorporation of [1-<sup>14</sup>C]acetate into cholesterol and FA in liver slices from nephritic rats when added to an incubation buffer, whereas genistin did not. These results suggest that genistin may be hydrolyzed to genistein and that genistein itself and/or its metabolite(s) may be intracorporal entities suppressing hepatic lipid syntheses. They also suggest that the suppression of hepatic lipid synthesis may be one mechanism of the hypolipidemic action of genistein.

Paper no. L8929 in *Lipids* 37, 261–265 (March 2002).

Glomerulonephritis caused by immunological insult is often associated with apparent pathological changes of glomeruli such as glomerular cell proliferation, crescent formation, and extracellular matrix accumulation (1–4). Massive protein excretion into urine results in hypoalbuminemia (5), and secondary hyperlipidemia occurs by increased lipid and lipoprotein synthesis in the liver (6). These types of hyperlipidemia should be remedied since hyperlipidemia is believed to further the kidney dysfunction (7,8). Thus, trials to reduce hyperlipidemia have been conducted using the drug probucol (9), nutrients such as fish oil (10), and a low-protein diet (11); and all three treatments succeeded in reducing the endogenous hyperlipidemia. Besides hypolipidemic action, probucol reduced proteinuria (9), and an amino acid-fortified low soy protein diet, for instance, reduced both proteinuria and hypoalbuminemia (11).

Soybean isoflavones are known to have cancer chemopreventive (12,13) and antioxidative (13) activities, and reportedly improve cardiovascular risk factors by reducing serum

cholesterol concentrations in monkeys (14) and exogenously hypercholesterolemic rats (15). In the present study, we attempted to examine whether genistein and its glycoside genistin reduce endogenous hyperlipidemia and other symptoms in rats with glomerulonephritis.

## MATERIALS AND METHODS

**Animals and diets.** This experiment was conducted in accordance with guidelines established by the Animal Care and Use Committee at Tokyo Noko University. Male Wistar rats (3 wk of age) were obtained from Charles River Japan (Kanagawa, Japan). In an air-conditioned room with a temperature of 22 ± 2°C, a relative humidity of 60 ± 5%, and a light cycle from 8:00 A.M. to 8:00 P.M., animals were kept on a stock pellet diet (CE-2; CLEA Japan, Tokyo, Japan) for 6 d and then fed a basal 20% casein diet for another 5 d. All animals were moved on day 8 of the preliminary feeding from individual cages with wire bottoms into metabolism cages to acclimate them to these new surroundings, and to collect urine and feces. The composition of the 20% casein diet was as follows (16): 20% casein (Oriental Yeast Co., Tokyo, Japan), 5% corn oil (Hayashi Chemicals Co., Tokyo, Japan), 68.3%  $\alpha$ -cornstarch (Nihon Nosan Kogyo Co., Yokohama, Japan), 3.5% mineral mixture and 1% vitamin mixture (both AIN-76A composition; Nihon Nosan Kogyo Co.), 0.2% choline bitartrate (Wako Pure Chemical Industries, Osaka, Japan), and 2% cellulose powder (Oriental Yeast Co.). On the last day of the preliminary feedings (day 0), rats were divided into two groups of the same average body weight. One group, which received no antiserum injection, was regarded as the normal group, whereas rats of the other group were given a single intravenous injection into the tail vein of anti-rat kidney glomerular basement membrane (GBM) rabbit antiserum (0.4 mL/rat), which was produced by immunizing rabbits with the supernatant of trypsin-digested rat GBM (17,18), to induce nephritis. The following day (day 1), the animals were subcutaneously immunized with rabbit  $\gamma$ -globulin (8 mg/rat; Sigma Chemical Co., St. Louis, MO) in 0.2 mL of Freund's complete adjuvant (Wako Pure Chemical Industries) into the hind foot pads as described previously (19). On the third day after antiserum injection, nephritic rats were divided into three

\*To whom correspondence should be addressed at Department of Applied Biological Science, Tokyo Noko University, Saiwai-cho 3-5-8, Fuchu, Tokyo 183-8509, Japan. E-mail: yagasaki@cc.tuat.ac.jp

Abbreviations: BA, bile acid; Ch, cholesterol; GBM, glomerular basement membrane; LPO, lipid peroxide; NS, neutral sterol; PL, phospholipid.

groups of similar average body weights and urinary protein excretion rates, and the effects of genistein and genistin (Research & Development Laboratory, Fujicco Co., Kobe, Japan) were examined. Rats of two of the nephritis groups orally received 5 mg of genistein or 8 mg of genistin/d/100 g body weight for 12 d, whereas those of the other nephritis group, designated as the control group, were similarly given vehicle alone (0.5 mL of 0.5% carboxymethylcellulose aqueous solution/d/100 g body weight). Rats of the normal group were also given vehicle alone. Oral intubation of isoflavones or vehicle was carried out once a day at 9:00–10:00 A.M. The dose of 8 mg of genistin/d/100 g body weight was chosen to examine its antinephritic action, since genistin showed a pharmacological activity in the range of the dose; the glycoside significantly suppressed bone loss in ovariectomized rats (20). The dose of 8 mg of genistin is equimolar to that of 5 mg of genistin (18.5  $\mu\text{mol}$ ). Water and diets were available *ad libitum*. Urine excreted during the preceding 24 h by the rats individually housed in metabolism cages was collected at 9:00 A.M. each day. The animals were deprived of their diets at 9:00 A.M. on day 14 and given a final administration of isoflavones or vehicle. They were allowed free access to water until they were killed, which was done 4 h later by decapitation. Blood was collected and left to clot at room temperature to obtain serum. The liver and kidney were quickly removed, washed with cold 0.9% NaCl, blotted on filter paper, and weighed.

**Lipid analyses.** Total lipids from the liver were extracted according to the procedure of Folch *et al.* (21). After aliquots of the chloroform phase had been dried, cholesterol (Ch) (22), TG (23), and phospholipid (PL) (24) were determined as previously described (10,11). The serum TG and PL levels were also determined as mentioned above. The serum total Ch and lipid peroxide (LPO, as TBARS) levels were determined using commercial kits (Wako Pure Chemical Industries).

**Measurements of serum albumin, serum urea nitrogen, and urinary protein.** Serum albumin and urea nitrogen concentrations were also measured with commercial kits (Wako Pure Chemical Industries). Urinary protein was measured by the Bradford method (Bio-Rad Protein Assay; Bio-Rad Laboratories, Richmond, CA) (25).

**Fecal steroid excretion.** Feces were collected individually for 2 d before rats were killed. Neutral sterol (NS) and bile acid (BA) were extracted according to the method of Yama-

naka *et al.* (26). NS and BA were enzymatically determined with commercial kits (Wako Pure Chemical Industries) as described (27).

**Cholesterol and FA syntheses from [ $^{14}\text{C}$ ]acetate in liver slices.** Nephritis was induced by injecting anti-GBM rabbit antiserum and immunizing rabbit  $\gamma$ -globulin to rats fed the basal 20% casein diet as described above. On the 14th day after antiserum injection, rats were killed and livers were removed from nephritic rats and sliced with a razor. From one animal, three sets of liver slices were prepared. Liver slices weighing 100–120 mg (wet weight basis) were incubated for 2 h at 37°C in 1 mL of Krebs–Ringer phosphate buffer (pH 7.4) containing 37 kBq of [ $^{14}\text{C}$ ]acetate (37 kBq/ $\mu\text{mol}$ ; NEN Research Products, Boston, MA) in the absence or presence of 1 mM genistein or genistin. These isoflavones were suspended in DMSO (Sigma Chemical Co.). Syntheses of total FA and Ch in liver slices were estimated as described previously (28,29).

**Statistical analyses.** Results were expressed as mean  $\pm$  SEM. Statistical analyses were conducted either by ANOVA followed by Tukey's Q test or by Friedman test followed by Dunn's multiple comparison test (30). A *P* value below 0.05 was considered significant.

## RESULTS

As shown in Table 1, food intake and body weight gain were decreased by nephritis induction. The oral administration of either genistein or genistin exerted no further influence on this reduction. Conversely, relative liver and kidney weights were increased by nephritis, and neither genistein nor genistin showed any further effects on this rise.

Figure 1 shows time-dependent changes in protein excretion rate into urine. The urinary protein excretion was minimal in the normal state, but the excretion rate of nephritic control animals increased approximately linearly up to day 3 and thereafter remained high up to day 14. Genistin tended to suppress the increase in protein excretion in the early stage (day 5), whereas genistein did so in the middle stage (day 10). These suppressive effects of isoflavones, however, diminished in the late stage (day 14).

As expected from severe proteinuria, serum albumin concentration significantly decreased in the nephritic control group, indicating induction of hypoalbuminemia by the

**TABLE 1**  
Effects of Genistein and Genistin on Food Intake, Body Weight Gain, Liver Weight, and Kidney Weight in Nephritic Rats<sup>a</sup>

Measurement	Normal	Nephritis		
		Control	Genistein	Genistin
Food intake (g/11 d)	222.1 $\pm$ 7.8 <sup>a</sup>	165.3 $\pm$ 11.2 <sup>b</sup>	169.4 $\pm$ 10.9 <sup>b</sup>	183.8 $\pm$ 6.8 <sup>a,b</sup>
Body weight gain (g/11 d)	84.0 $\pm$ 5.1 <sup>a</sup>	47.6 $\pm$ 6.6 <sup>b</sup>	44.3 $\pm$ 5.8 <sup>b</sup>	48.6 $\pm$ 4.6 <sup>b</sup>
Liver weight (g/100 g body weight)	4.13 $\pm$ 0.17 <sup>a</sup>	5.85 $\pm$ 0.14 <sup>b</sup>	6.16 $\pm$ 0.27 <sup>b</sup>	6.12 $\pm$ 0.22 <sup>b</sup>
Kidney weight (g/100 g body weight)	0.87 $\pm$ 0.02 <sup>a</sup>	1.43 $\pm$ 0.08 <sup>b</sup>	1.39 $\pm$ 0.08 <sup>b</sup>	1.28 $\pm$ 0.05 <sup>b</sup>

<sup>a</sup>Each value represents the mean  $\pm$  SEM for five (genistein) or six (others) rats. Values not sharing a common superscript roman letter are significantly different at *P* < 0.05 by Tukey's Q test.

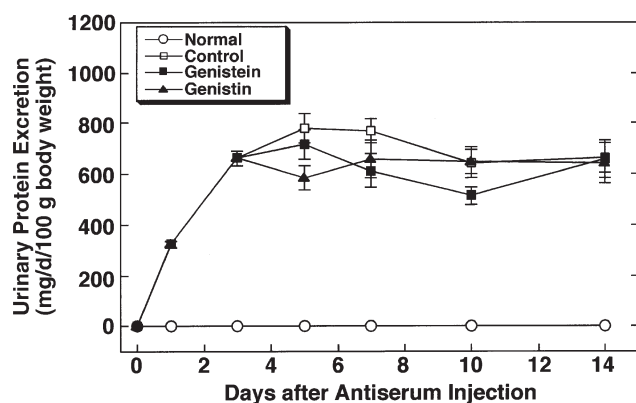


FIG. 1. Effects of genistein and genistin on urinary protein excretion in nephritic rats. Each value represents the mean  $\pm$  SEM for five (genistein) or six (others) rats.

nephritis (Table 2). Genistein tended to improve, and genistin significantly improved the nephritis-induced hypoalbuminemia. Serum urea nitrogen concentration was slightly elevated by nephritis induction and decreased to normal with the administration of isoflavones, although none of the changes was significant (Table 2).

As shown in Figure 2, the serum total Ch (Fig. 2A) and TG (Fig. 2B) levels were significantly and strikingly increased by nephritis induction, indicating the occurrence of severe hypercholesterolemia and hypertriglyceridemia. The serum Ch and TG levels of nephritic rats were 5- and 21-fold, respectively, higher than those of normal rats. Genistein and genistin suppressed both the severe hypercholesterolemia and hypertriglyceridemia, although the hypotriglyceridemic activity of genistein was not significant. Likewise, the serum PL and LPO levels of the nephritic control group were significantly higher than those of the normal group (Table 2). Genistein and genistin slightly suppressed these rises, although the suppression was not significant. Liver Ch content was significantly increased by nephritis induction, but this increase was not significantly changed by treatment with the isoflavones. In contrast, neither nephritis nor isoflavones affected liver TG and PL contents (Table 2).

Changes in fecal sterol excretion are indicated in Table 3. Excretion of feces (dry weight basis) in the nephritic control group was slightly but significantly increased when compared with that in the normal group. The same tendency was observed in the excretion of NS and total steroids. Genistein and genistin exerted little influence on these four parameters.

Figure 3 depicts *in vitro* effects of genistein and genistin on lipid syntheses in the liver slices from nephritic rats. Genistein proved to significantly suppress hepatic Ch synthesis (Fig. 3A) and FA synthesis (Fig. 3B), while its glycoside genistin showed no (Fig. 3A) or weak (Fig. 3B) inhibitory effects on Ch and FA syntheses, respectively.

DISCUSSION

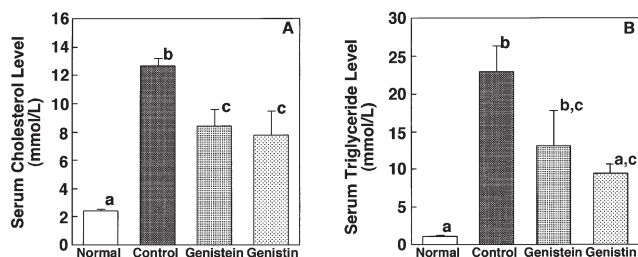
Rats with glomerulonephritis show hyperlipidemia as well as proteinuria, hypoalbuminemia, and pathological changes of glomeruli (1–4, 31). Glomerular scarring in this animal model developed and progressed as in human glomerulonephritis (17). In the present study, the effects of genistein, a potent and specific protein kinase inhibitor (32) that occurs naturally in soy foods, and its glycoside genistin were studied in nephritic rats with hyperlipidemia. These isoflavones suppressed severe hypercholesterolemia and hypertriglyceridemia in nephritic rats (Fig. 2).

Following ingestion, genistin is hydrolyzed in the large intestine by the action of bacteria to release genistein (33). Genistein is rapidly absorbed from the intestine, taken up by the liver, and excreted into bile as its glucuronide conjugate (34). These events are consistent with the fact that the hypolipidemic action of equimolar genistein and genistin was almost identical (Fig. 2). The hypocholesterolemic action of the isoflavones was not due to increased steroid excretion from the body, since excretion of neither NS nor BA into feces was enhanced by their administration (Table 3). Lipid syntheses by liver slices from nephritic rats are significantly enhanced over those from normal rats (35). Genistein inhibited the increased Ch and FA syntheses by liver slices from nephritic rats when added to the incubation buffer, whereas genistin did not (Fig. 3). Genistein reportedly inhibits the hepatocyte

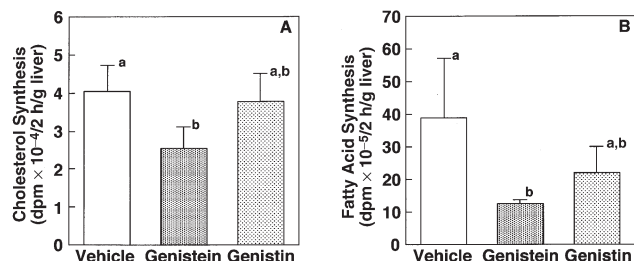
TABLE 2 Effects of Genistein and Genistin on Serum Albumin Level, Serum Urea Nitrogen Level, Serum Lipid Levels, and Liver Lipid Levels in Nephritic Rats<sup>a</sup>

Measurement	Normal	Nephritis		
		Control	Genistein	Genistin
Serum albumin (g/dL)	4.10 $\pm$ 0.08 <sup>a</sup>	2.59 $\pm$ 0.19 <sup>b</sup>	3.07 $\pm$ 0.15 <sup>b,c</sup>	3.42 $\pm$ 0.15 <sup>c</sup>
Serum urea nitrogen (mg/dL)	15.72 $\pm$ 1.13	18.81 $\pm$ 0.95	16.69 $\pm$ 3.15	13.11 $\pm$ 1.17
Serum lipids				
PL (mmol/L)	2.93 $\pm$ 0.10 <sup>a</sup>	10.77 $\pm$ 0.97 <sup>b</sup>	9.34 $\pm$ 1.62 <sup>b</sup>	8.50 $\pm$ 0.88 <sup>b</sup>
LPO (nmol/mL)	3.64 $\pm$ 0.09 <sup>a</sup>	10.57 $\pm$ 1.55 <sup>b</sup>	7.45 $\pm$ 0.60 <sup>b</sup>	8.05 $\pm$ 0.90 <sup>b</sup>
Liver lipids ( $\mu$ mol/g liver)				
Ch	5.18 $\pm$ 0.16 <sup>a</sup>	6.75 $\pm$ 0.50 <sup>b</sup>	6.59 $\pm$ 0.45 <sup>a,b</sup>	7.21 $\pm$ 0.39 <sup>b</sup>
TG	12.32 $\pm$ 0.96	17.18 $\pm$ 4.01	13.24 $\pm$ 2.64	21.35 $\pm$ 5.41
PL	35.88 $\pm$ 1.85	40.64 $\pm$ 1.07	39.21 $\pm$ 0.52	38.30 $\pm$ 1.00

<sup>a</sup>Each value represents the mean  $\pm$  SEM for five (genistein) or six (others) rats. Values not sharing a common superscript roman letter are significantly different at  $P < 0.05$  by Tukey's Q test. PL, phospholipid; LPO, lipid peroxide; Ch, cholesterol.



**FIG. 2.** Effects of genistein and genistin on serum total cholesterol (A) and TG (B) levels in nephritic rats. Each value represents the mean  $\pm$  SEM for five (genistein) or six (others) rats. Values not sharing a common letter are significantly different at  $P < 0.05$  by Tukey's Q test.



**FIG. 3.** Effects of genistein and genistin on *in vitro* cholesterol (A) and total FA (B) syntheses in liver slices from nephritic rats. Each value represents the mean  $\pm$  SEM for five incubations. Values not sharing a common letter are significantly different at  $P < 0.05$  by Dunn's multiple comparison test.

**TABLE 3**  
**Effects of Genistein and Genistin on Fecal Steroid Excretion and Feces Excretion in Nephritic Rats<sup>a</sup>**

Measurement	Nephritis			
	Normal	Control	Genistein	Genistin
Fecal steroid excretion ( $\mu\text{mol}/2 \text{ d}/100 \text{ g}$ body weight)				
Bile acid	2.43 $\pm$ 0.41	1.92 $\pm$ 0.47	1.02 $\pm$ 0.25	1.65 $\pm$ 0.13
Neutral sterol	8.28 $\pm$ 0.40	11.19 $\pm$ 1.33	8.84 $\pm$ 1.72	9.37 $\pm$ 0.82
Total	10.71 $\pm$ 0.52	13.12 $\pm$ 1.75	9.86 $\pm$ 1.93	11.02 $\pm$ 0.83
Feces excretion (g/2 d/100 g body weight)	0.55 $\pm$ 0.03 <sup>a</sup>	0.80 $\pm$ 0.05 <sup>b</sup>	0.65 $\pm$ 0.06 <sup>a,b</sup>	0.74 $\pm$ 0.04 <sup>b</sup>

<sup>a</sup>Each value represents the mean  $\pm$  SEM for five (genistein) or six (others) rats. Values not sharing a common superscript roman letter are significantly different at  $P < 0.05$  by Tukey's Q test.

growth factor-stimulated syntheses of lipids and secretion of lipoproteins in cultured rat hepatocytes (36). These previous and current *in vitro* findings suggest that genistein itself and/or its metabolite(s) may be intracorporal entities that suppress hepatic lipid syntheses and also suggest that the suppression of hepatic lipid synthesis may be one mode of the hypolipidemic action of genistein. In contrast to the present results, genistin reportedly did not reduce endogenous hypercholesterolemia and hypertriglyceridemia in ovariectomized rats at doses of 5 and 10 mg/d/100 g body weight (37). This discrepancy in genistin effect on endogenous hyperlipidemias between previous and present studies may be attributable to differences in disease models and hence to differences in mechanisms by which hyperlipidemias arise.

In addition to hypolipidemic action, genistein and genistin improved hypoalbuminemia that was induced in rats with glomerulonephritis (Table 2). However, urinary albumin excretion and hepatic albumin mRNA level were not altered by their administration (data not shown). These findings suggest that the isoflavones may increase the translational step of albumin synthesis and hence remedy hypoalbuminemia. Further studies are required to clarify the mechanisms for the remedial effect of isoflavones on hypoalbuminemia.

We demonstrated that amino acid-fortified low (8.5%) soy protein (11) and low casein (38) diets succeeded in simultaneously reducing the three major symptoms in nephritic rats, i.e., proteinuria, hypoalbuminemia, and hyperlipidemia, without causing severe protein malnutrition. Feeding fish oil, as compared with corn oil, to nephritic rats fed a 20% casein diet reduced hyperlipidemia but failed to improve proteinuria and

hypoalbuminemia (10), suggesting difficulties in the simultaneous control of proteinuria, hypoalbuminemia, and hyperlipidemia by nutrients without restricting protein intake. In the present study, genistein and genistin were demonstrated to improve two of the three symptoms simultaneously without any restriction of protein intake. Thus, isoflavone administration has the potential to mitigate protein restriction in nephritis treatment.

The doses of genistein and genistin employed in the present study seem too high to be obtained from eating soy foods in everyday life. Provided that other major isoflavones in soy foods at lower doses are also effective against nephritis, the ingestion of effective doses of isoflavones may be attainable from soy foods. Studies on dose-dependent effects of genistein, and genistin as well as on effects of other major isoflavones in soybean, daidzein and daidzin will clarify this aspect.

## REFERENCES

- Robbins, S.L., Cotran, R.C., and Kumar, V. (1984) Glomerular Diseases, in *Pathological Basis of Disease*, 3rd edn. (Robbins, S.L., Cotran, R.C., and Kumar, V., eds.), pp. 1002–1026, W.B. Saunders, Philadelphia.
- Morel-Maroger, S.L., Killen, P.D., Chi, E., and Striker, G.E. (1984) The Composition of Glomerulosclerosis. I. Studies in Focal Sclerosis, Crescentic Glomerulonephritis, and Membranoproliferative Glomerulonephritis, *Lab. Invest.* 51, 181–192.
- Floege, J., Alpers, C.E., Burns, M.W., Pritzl, P., Gordon, K., Couser, W.G., and Johnson, R.J. (1992) Glomerular Cells, Extracellular Matrix Accumulation, and the Development of Glomerulosclerosis in the Remnant Kidney Model, *Lab. Invest.* 66, 485–497.



4. Schnaper, H.W., Kopp, J.B., Poncelet, A.C., Hubchak, S.C., Stetler-Stevenson, W.G., Klotman, P.E., and Kleinman, H.K. (1996) Increased Expression of Extracellular Matrix Proteins and Decreased Expression of Matrix Proteases After Serial Passage of Glomerular Mesangial Cells, *J. Cell. Sci.* 109, 2521–2528.
5. Cameron, J.S. (1990) Proteinuria and Progression in Human Glomerular Diseases, *Am. J. Nephrol.* 10 (Suppl. 1), 81–87.
6. Appel, G.B., and Appel, A.S. (1990) Lipid-Lowering Agents in Proteinuric Diseases, *Am. J. Nephrol.* 10 (Suppl. 1), 110–115.
7. Moorhead, J.F., El-Nahas, M., Chan, M.K., and Varghese, Z. (1982) Lipid Nephrotoxicity in Chronic Progressive Glomerular and Tubulo-interstitial Disease, *Lancet* 2, 1309–1312.
8. Kasiske, B.L., O'Donnell, M.P., Cleary, M.P., and Keane, W.F. (1988) Treatment of Hyperlipidemia Reduces Glomerular Injury in Obese Zucker Rats, *Kidney Int.* 33, 667–672.
9. Hirano, T., Mamo, J.C.L., Nagano, S., and Sugisaki, T. (1991) The Lowering Effect of Probucol on Plasma Lipoprotein and Proteinuria in Puromycin Aminonucleoside-Induced Nephrotic Rats, *Nephron* 58, 95–100.
10. Fujisawa, K., Yagasaki, K., and Funabiki, R. (1994) Effects of Low Casein and Fish Oil on Hyperlipidemia and Proteinuria in Nephritic Rats, *Lipids* 29, 779–783.
11. Fujisawa, K., Yagasaki, K., and Funabiki, R. (1995) Reduction of Hyperlipidemia and Proteinuria Without Growth Retardation in Nephritic Rats by a Methionine-Supplemented, Low-Soy-Protein Diet, *Am. J. Clin. Nutr.* 61, 603–606.
12. Lamartiniere, C.A., Moore, J., Holland, M., and Barnes, S. (1995) Neonatal Genistein Chemoprevents Mammary Cancer, *Proc. Soc. Exp. Biol. Med.* 208, 120–123.
13. Wei, H., Bowen, R., Cai, Q., Barnes, S., and Wang, Y. (1995) Antioxidant and Antipromotional Effects of the Soybean Isoflavone Genistein, *Proc. Soc. Exp. Biol. Med.* 208, 124–130.
14. Anthony, M.S., Clarkson, T.B., Hughes, C.L., Jr., Morgan, T.M., and Burke, G.L. (1996) Soybean Isoflavones Improve Cardiovascular Risk Factors Without Affecting the Reproductive System of Peripubertal Rhesus Monkeys, *J. Nutr.* 126, 43–50.
15. Ni, W., Yoshida, S., Tsuda, Y., Nagao, K., Sato, M., and Imaizumi, K. (1999) Ethanol-Extracted Soy Protein Isolate Results in Elevation of Serum Cholesterol in Exogenously Hypercholesterolemic Rats, *Lipids* 34, 713–716.
16. Fujisawa, K., Yagasaki, K., Funabiki, R., Masuda, S., and Sasaki, R. (2000) Restoration of Low Casein Feed-Induced Decrease in Serum Erythropoietin Concentration by Fortifying Diet with Methionine and Threonine in Normal and Nephritic Rats, *Nutr. Res.* 20, 685–693.
17. Shibata, S., Miyakawa, Y., Naruse, T., Nagasawa, T., and Takuma, T. (1969) A Glycoprotein That Induces Nephrotoxic Antibody: Its Isolation and Purification from Rat Glomerular Basement Membrane, *J. Immunol.* 102, 593–601.
18. Suzuki, Y., Nagamatsu, T., Kito, T., Kohmura, T., and Ito, M. (1981) Pharmacological Studies on Experimental Nephritic Rats (11). Changes in Pathohistological and Biochemical Parameters in Anti-rat GBM Rabbit Serum-Induced Nephritis, *Folia Pharmacol. Jpn.* 77, 407–417.
19. Suzuki, Y., Tsukushi, Y., Ito, M., and Nagamatsu, T. (1987) Antinephritic Effect of Y-19018, a Thromboxane A Synthetase Inhibitor, on Crescentic-type Anti-GBM Nephritis in Rats, *Jpn. J. Pharmacol.* 45, 177–185.
20. Ishida, H., Uesugi, T., Hirai, K., Toda, T., Nukaya, H., Yokotsuka, K., and Tsuji, K. (1998) Preventive Effects of the Plant Isoflavones, Daidzin and Genistin, on Bone Loss in Ovariectomized Rats Fed a Calcium-Deficient Diet, *Biol. Pharm. Bull.* 21, 62–66.
21. Folch, J., Lees, M., and Sloane Stanley, G.H. (1957) A Simple Method for the Isolation and Purification of Total Lipides from Animal Tissues, *J. Biol. Chem.* 226, 497–509.
22. Zak, B. (1957) Simple Rapid Microtechnic for Serum Total Cholesterol, *Am. J. Clin. Pathol.* 27, 583–588.
23. Van Handel, E. (1961) Suggested Modifications of the Micro Determination of Triglycerides, *Clin. Chem.* 7, 249–251.
24. Chen, P.S., Toribara, T.Y., and Warner, H. (1956) Microdetermination of Phosphorus, *Anal. Chem.* 28, 1756–1758.
25. Bradford, M.M. (1976) A Rapid and Sensitive Method for the Quantitation of Microgram Quantities of Protein Utilizing the Principle of Protein–Dye Binding, *Anal. Biochem.* 72, 248–254.
26. Yamanaka, Y., Tsuji, K., and Ichikawa, T. (1986) Stimulation of Chenodeoxycholic Acid Excretion in Hypercholesterolemic Mice by Dietary Taurine, *J. Nutr. Sci. Vitaminol.* 32, 287–296.
27. Kawasaki, M., Yagasaki, K., Miura, Y., and Funabiki, R. (1995) Reduction of Hyperlipidemia in Hepatoma-Bearing Rats by Dietary Fish Oil, *Lipids* 30, 431–436.
28. Yagasaki, K., Okada, K., Mochizuki, T., Takagi, K., and Irikura, T. (1984) Effect of 4-(4'-Chlorobenzoyloxy)benzyl Nicotinate (KCD-232) on Triglyceride and Fatty Acid Metabolism in Rats, *Biochem. Pharmacol.* 33, 3151–3163.
29. Okada, K., Yagasaki, K., Mochizuki, T., Takagi, K., and Irikura, T. (1985) Effect of 4-(4'-Chlorobenzoyloxy)benzyl Nicotinate (KCD-232) on Cholesterol Metabolism in Rats, *Biochem. Pharmacol.* 34, 3361–3367.
30. Zar, J.H. (1999) *Biostatistical Analysis*, 4th edn., pp. 208–230, Prentice Hall International, Upper Saddle River, NJ.
31. Nihei, T., Miura, Y., and Yagasaki, K. (2001) Arginine as an Exacerbating Factor for Glomerulonephritis in Rats Fed a Methionine-Threonine-Supplemented Low Casein Diet, *Biosci. Biotechnol. Biochem.* 65, 1155–1162.
32. Akiyama, T., Ishida, J., Nakagawa, S., Ogawa, H., Watanabe, S., Itoh, N., Shibuya, M., and Fukami, Y. (1987) Genistein, a Specific Inhibitor of Tyrosine-Specific Protein Kinases, *J. Biol. Chem.* 262, 5592–5595.
33. Wiseman, H. (1999) The Bioavailability of Non-nutrient Plant Factors: Dietary Flavonoids and Phyto-oestrogens, *Proc. Nutr. Soc.* 58, 139–146.
34. Sfakianos, J., Coward, L., Kirk, M., and Barnes, S. (1997) Intestinal Uptake and Biliary Excretion of the Isoflavone Genistein in Rats, *J. Nutr.* 127, 1260–1268.
35. Fujisawa, K., Yagasaki, K., and Funabiki, R. (1994) Reduction of Hyperlipidemia and Proteinuria Without Growth Retardation in Nephritic Rats by Amino Acids-Fortified Low Casein Diets, *J. Nutr. Biochem.* 5, 21–27.
36. Kaibori, M., Kwon, A.H., Oda, M., Kamiyama, Y., Kitamura, N., and Okumura, T. (1998) Hepatocyte Growth Factor Stimulates Synthesis of Lipids and Secretion of Lipoproteins in Rat Hepatocytes, *Hepatology* 27, 1354–1361.
37. Uesugi, T., Toda, T., Tsuji, K., and Ishida, H. (2001) Comparative Study on Reduction of Bone Loss and Lipid Metabolism Abnormality in Ovariectomized Rats by Soy Isoflavones, Daidzin, Genistin, and Glycitin, *Biol. Pharm. Bull.* 24, 368–372.
38. Fujisawa, K., Yagasaki, K., Miura, Y., and Funabiki, R. (1995) Improvement of Hyperlipidemia and Proteinuria Without Noticeable Growth Retardation by Feeding a Methionine and Threonine Supplemented Low-Casein Diet to Nephritic Rats, *Biosci. Biotechnol. Biochem.* 59, 1896–1900.

[Received October 3, 2001, and in revised form December 18, 2001; revision accepted January 4, 2002]

# Egg Ovomucin Attenuates Hypercholesterolemia in Rats and Inhibits Cholesterol Absorption in Caco-2 Cells

Satoshi Nagaoka<sup>a,\*</sup>, Motoki Masaoka<sup>a</sup>, Qing Zhang<sup>a</sup>, Mineo Hasegawa<sup>b</sup>, and Kenji Watanabe<sup>a</sup>

<sup>a</sup>Department of Food Science, Faculty of Agriculture, Gifu University, Gifu 501-1193, Japan, and <sup>b</sup>Research Laboratory, Q.P. Corporation, Fuchu 183-0034, Japan

**ABSTRACT:** This experiment was designed to evaluate the effect of casein or ovomucin (OV) on the micellar solubility of cholesterol and the taurocholate binding capacity *in vitro*. We also evaluated the effects of casein or OV on cholesterol metabolism in rats and Caco-2 cells. OV had a significantly greater bile acid-binding capacity than that of casein *in vitro*. Micellar cholesterol solubility *in vitro* was significantly lower in the presence of OV compared to casein. The cholesterol micelles containing OV significantly suppressed cholesterol uptake by Caco-2 cells compared to the cholesterol micelles containing casein. Consistent with these *in vitro* findings, OV-feeding significantly increased the fecal excretion of bile acids or cholesterol compared with casein-feeding. Serum total cholesterol was significantly lower in rats fed OV than in those fed casein. The concentrations of total lipids in liver were significantly lower in the OV-fed group compared with the casein group. These results suggest that the suppression of cholesterol absorption by direct interaction between cholesterol mixed micelles and OV in the jejunal epithelia is part of the mechanism underlying the hypocholesterolemic action of OV. OV may also inhibit the reabsorption of bile acids in the ileum, thus lowering the serum cholesterol level.

Paper no. L8926 in *Lipids* 37, 267–272 (March 2002).

Egg protein consists of well-balanced amino acids with high biological value. However, egg is a cholesterol-rich food whose use is always strictly or carefully advocated for the prevention of hypercholesterolemia and its related diseases. As the cholesterol exists exclusively in the egg yolk, egg white is cholesterol-free. Egg intake is thought to increase serum cholesterol concentrations in experimental animals (1) and humans (2).

Egg white contains a wide variety of proteins such as ovalbumin, ovomucin (OV), ovotransferrin, and lysozyme (3,4). Several reports have indicated that the quality and quantity of dietary protein affect the serum cholesterol level (1,5–9). Only a few reports have dealt with the effect of egg white protein (EWP) on the serum cholesterol level in rats (10) and humans (11). Moreover, the mechanism by which the hypocholesterolemic effect of EWP is exerted in rats is not well understood. Although OV is one of the EWP, there is no information about the hypocholesterolemic action of OV. In earlier papers (12,13) we used cultured Caco-2 cells and found that soy protein peptic hydrolysate (SPH) directly inhibited the absorption of micellar

cholesterol. Our experimental system to evaluate cholesterol with Caco-2 cells is useful for clarifying the molecular mechanism underlying the mechanism for and effects of OV on cholesterol absorption from the small intestine. We postulate that OV-induced hypocholesterolemic action may have resulted in the inhibition of both cholesterol absorption in the intestinal epithelial cells and ileal reabsorption of bile acids. Thus, we used Caco-2 cells, rats, or *in vitro* assays to investigate the effects of the serum cholesterol-lowering action of OV.

## EXPERIMENTAL PROCEDURES

**Preparation of OV.** Fresh egg white was prepared from eggs (White Leghorn hens) according to the method of Xu *et al.* (14). OV from fresh egg white was prepared by the method of Kato *et al.* (15). Briefly, thick egg white separated from total egg white using a sieve was homogenized in a Waring blender for about 5 min and diluted with 3 vol of deionized water. The mixture was stirred for 1 h and then adjusted to pH 6.0 with 1 mol/L HCl. After the mixture stood overnight at 4°C, OV precipitated in this system and was then lyophilized.

**Chemical analyses.** Protein content was determined by the Kjeldahl method (16), with an N-to-protein conversion factor of 6.25. Lipids were extracted by using chloroform/methanol (2:1, vol/vol) and weighed. Sugar content was determined by the phenol-sulfonic acid method (17). Moisture was determined as the loss in weight after drying at 105°C for 24 h. Ash content was determined by the direct ignition method (550°C overnight). As shown in Table 1, amino acid composition was determined by the methods described previously (18). Tryptophan content was determined by the *p*-dimethyl-aminobenzaldehyde method (19,20). Casein was generously supplied by the Central Research Institute of Meiji Milk Products Co., Ltd. (Tokyo, Japan). The chemical composition of casein was as follows (g/kg): protein, 860; sugar 15; moisture, 110; lipid, 0; and ash, 15. The chemical composition of OV was as follows (g/kg): protein, 693; sugar 148; moisture, 120; lipid, 0; and ash, 39.

**Taurocholate-binding capacities.** The binding capacity of cholestyramine, casein, or OV with taurocholate was measured by the method described previously (13). The mixtures containing 1.85 kBq of tauro [carbonyl-<sup>14</sup>C]cholic acid (sodium salt) (1.89 Gbq/mmol; Amersham International, Buckinghamshire, United Kingdom), 0.1 mol/L sodium taurocholate in 5 mL of 0.1 mol/L Tris-HCl buffer (pH 7.4), and 1–500 mg binding substances [cholestyramine, casein: casein sodium (Wako Pure

\*To whom correspondence should be addressed.

E-mail: nagaoka@cc.gifu-u.ac.jp

Abbreviations: EWP, egg white protein; LTH,  $\beta$ -lactoglobulin tryptic hydrolysate; OV, ovomucin; SPH, soy protein peptic hydrolysate.

**TABLE 1**  
**Amino Acid Compositions of Casein and Ovomucin (OV) (g/kg)**

Amino acid	Casein	OV
Asp	89.5	102.8
Thr	56.2	83.9
Ser	53.8	92.8
Glu	201.6	97.7
Pro	75.6	90.8
Gly	19.8	67.1
Ala	38.8	51.3
Cys	2.4	39.5
Val	61.6	62.2
Met	32.4	21.7
Ile	53.1	45.4
Leu	94.3	64.2
Tyr	26.1	29.6
Phe	38.3	36.5
His	24.8	21.7
Lys	84.8	58.2
Arg	27.9	21.7
Trp	19.0	12.9

Chemical, Osaka, Japan), OV] were incubated at 37°C for 2 h, and the radioactivity in the supernatant (15,000 × g for 15 min) was measured by liquid scintillation counting.

**Micellar solubility of cholesterol and taurocholate.** Micellar solubility of cholesterol and taurocholate with proteins *in vitro* was measured by the method of Ikeda *et al.* (21) with some modifications. Micellar solutions (1 mL) containing 6.6 mmol/L sodium taurocholate, 0.5 mmol/L cholesterol, 1 mmol/L oleic acid, 0.5 mol/L monoolein, 0.6 mmol/L PC, 132 mmol/L NaCl; and 15 mmol/L sodium phosphate (pH 7.4), casein sodium or OV (5 mg/mL, respectively) were prepared by sonication. Then the mixture was incubated at 37°C for 24 h and ultracentrifuged at 100,000 × g for 60 min at 37°C. The supernatant was collected for the determination of cholesterol and taurocholate as described previously (13).

**Cholesterol absorption in Caco-2 cells.** Caco-2 cells were acquired from the American Type Culture Collection (Rockville, MD). The cells were maintained DMEM supplemented with 10% FBS, 4 mmol/L L-glutamine, 50 IU/mL of penicillin, and 50 mg/L streptomycin. The cells were incubated at 37°C in a humidified atmosphere of 5% CO<sub>2</sub> in air. The monolayers became confluent 3 to 4 d after seeding at between 7 × 10<sup>5</sup> and 1.2 × 10<sup>6</sup> cells per 100-mm diameter dish, and the cells were passed at a split ratio of 4 to 8 by trypsinizing with 0.25% trypsin and 0.8 mmol/L EDTA in PBS. Monolayers were grown in 24-well plastic dishes containing 1 mL of DMEM supplemented with FBS as described previously (13), fresh medium being added every 2 d. The experiments described usually used cultures 12–15 d after plating and were performed in medium-199/Earle's (GIBCO, Grand Island, NY) containing 1 mmol/L HEPES. Cell viability, as ascertained by trypan-blue exclusion, was unaffected by any of the experimental procedures. The number of passages of the cell line ranged from 70–85.

[<sup>14</sup>C]-Labeled micellar cholesterol uptake in Caco-2 cells was measured by the method described previously (13). The

final concentration of each [<sup>14</sup>C]-labeled micellar solution (0.5 mL) was as follows: 3.7 kBq [4-<sup>14</sup>C]cholesterol (2.1 Gbq/m mol; NEN, Boston, MA), 0.1 mmol/L cholesterol, 1 mmol/L oleic acid, 0.5 mmol/L monoolein, 6.6 mmol/L sodium taurocholate, 0.6 mmol/L PC, casein sodium, and OV (2.5 mg/0.5 mL, respectively). The micellar solution was mixed by ultrasonication.

After 14 d, the cells were rinsed two times with 1 mL of PBS. A [<sup>14</sup>C]-labeled micellar solution (0.5 mL) containing casein sodium or OV was then added to the dishes, which were incubated at 37°C for 20 min in a CO<sub>2</sub> incubator. After this incubation, the cells were rinsed two times with 1 mL of PBS. The cells were finally lysed in 0.1% SDS solution, after which 7.5 mL of Aquasol-2 (NEN) was added, and the radioactivity in the cellular debris was counted to determine the amount of cholesterol absorbed into the cells. The cellular protein was determined by a commercially available kit (Bio-Rad Protein Assay; Bio-Rad, Tokyo, Japan). The amount of cholesterol absorbed into the cells was expressed as pmol/mg protein.

**Effects of OV or casein on lipid metabolism in rats (animals and diets).** Male rats of the Wistar strain (Japan SLC, Hamamatsu, Japan) were used in the present animal studies. Room temperature was maintained at 22 ± 2°C with a 12-h cycle of light (0800–2000) and dark. The approval of the Gifu University Animal Care and Use Committee was given for our animal experiments. All the rats were housed individually in metal cages and were allowed free access to food and water. After acclimation to a commercial stock diet (CE-2; Japan CLEA, Tokyo, Japan) for 3 d, 5-wk-old rats weighing 115–130 g were divided into two groups of six rats each on the basis of body weight. The composition of the basal diet recommended by the American Institute of Nutrition (22) is shown in Table 2. OV was added to the diet at a nitrogen level equivalent to that of a casein diet at the expense of carbohydrates. Each group had free access to one of the respective test diets (Table 2) containing casein or OV as the protein source for 10 d. After 24 h without food, the rats were anesthetized with

**TABLE 2**  
**Composition of Experimental Diets (g/kg)**

Ingredient	Diet group	
	Casein	OV <sup>a</sup>
Casein	232.56	232.56
OV	—	72.15
Lard	50	50
Corn oil	10	10
Mineral mixture <sup>b</sup>	35	35
Vitamin mixture <sup>c</sup>	10	10
Choline chloride	2	2
Sucrose	200.98	176.93
Starch	401.96	353.86
Cellulose	50	50
Cholesterol	5	5
Sodium cholate	2.5	2.5

<sup>a</sup>See Table 1 for abbreviation.

<sup>b</sup>AIN-76 mineral mixture (21).

<sup>c</sup>AIN-76 vitamin mixture (21).



diethyl ether and killed. Blood was collected by cardiac puncture, and the liver was removed. Fecal collections (d 7–9) were completed prior to the 24-h food restriction and blood sampling. Feces were used for determining fecal steroids.

**Rat lipid analyses.** Various lipid concentrations were determined using commercially available kits as follows: serum and liver cholesterol with Monotest cholesterol (Boehringer Mannheim Yamanouchi, Tokyo, Japan); HDL-cholesterol with HDL-cholesterolase (Nissui, Tokyo, Japan); serum and liver TG with Triglycolor III (Boehringer Mannheim Yamanouchi); and serum phospholipid with Phospholipid C-Test Wako (Wako Pure Chemical, Osaka, Japan). Liver lipids were extracted by the method of Folch *et al.* (23), and total lipids were determined gravimetrically as described previously (24). Fecal acidic steroids were measured according to the method of Bruusgaard *et al.* (25) and Malchow-Moller *et al.* (26), whereas fecal neutral steroids were assayed with trimethylsilyl ether by using 1.5% OV-17 with a GC-14A instrument (Shimadzu, Kyoto, Japan) and 5  $\alpha$ -cholestane as the internal standard (27).

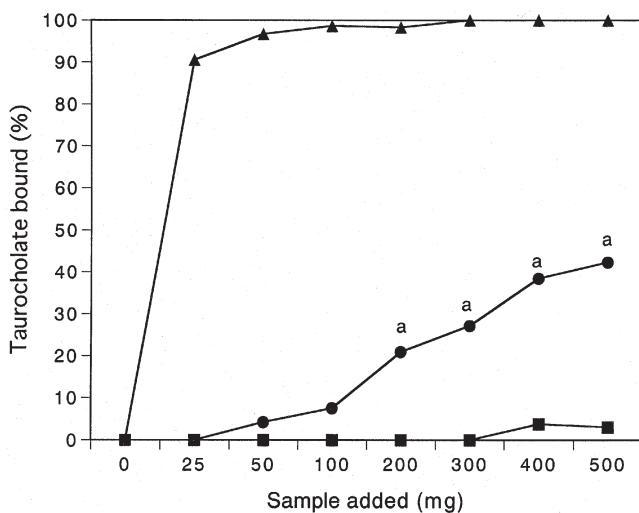
**Statistical analysis.** Results are expressed as mean  $\pm$  SEM. The statistical significance of differences was evaluated by Student's *t*-test (28).

## RESULTS

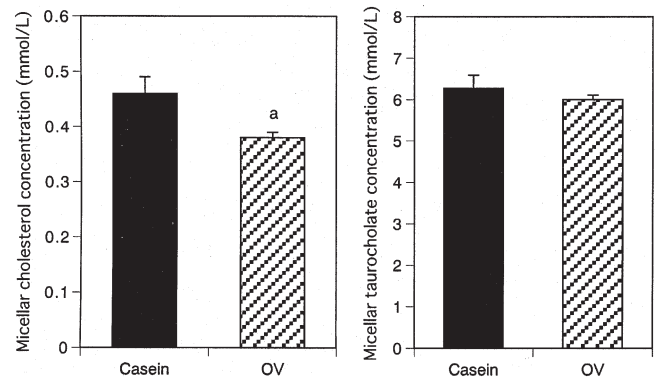
**Taurocholate binding capacities.** From 200 to 500 mg, the bile acid-binding capacity of OV was significantly greater than that of casein (Fig. 1).

**Micellar solubility of cholesterol and taurocholate.** The micellar solubility of cholesterol in the presence of OV was significantly lower than with casein. Micellar solubility of taurocholate was unchanged (Fig. 2).

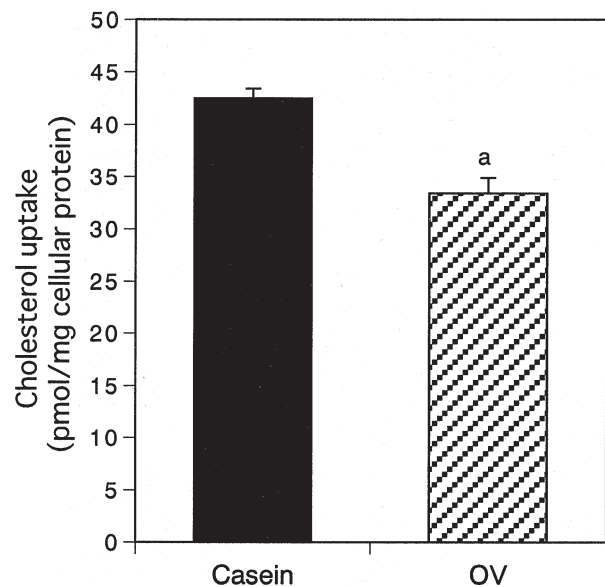
**Cholesterol absorption in Caco-2 cells.** The cholesterol micelles containing OV induced a significant suppression of cholesterol absorption in Caco-2 cells compared to the cholesterol micelles containing casein (Fig. 3).



**FIG. 1.** Binding of cholestyramine (▲), casein (■), or ovomucin (●) with taurocholate. Individual values represent means of assays performed in duplicate. Error bars (SEM) are too small to show. Statistical significance compared to casein by Student's *t*-test (a,  $P < 0.05$ ).



**FIG. 2.** Effect of casein or ovomucin (OV) on micellar solubility of cholesterol and taurocholate. Each value is expressed as mean  $\pm$  SEM of three determinations. Statistical significance compared to casein by Student's *t*-test (a,  $P < 0.05$ ).



**FIG. 3.** Effect of casein or ovomucin (OV) on cholesterol absorption in Caco-2 cells. Each value is expressed as mean  $\pm$  SEM of five determinations. Statistical significance compared to casein by Student's *t*-test (a,  $P < 0.001$ ).

**Effects of OV or casein on lipid metabolism in rats.** Food intake, growth rates, and the relative liver weight were unaffected by dietary OV (Table 3). Serum total cholesterol levels in the OV groups were significantly lower than in the casein group. The HDL-cholesterol in the OV group tended to increase compared with the casein group. The proportion in the OV group of HDL-cholesterol to serum total cholesterol [(b)/(a)], which is known as the atherogenic index, was significantly higher than in the casein group. The liver total lipids level was significantly lower in the OV group than in the casein group. Fecal dry weight was unchanged by OV feeding. The fecal excretion of bile acids and cholesterol was significantly increased by OV feeding compared with casein feeding.

## DISCUSSION

In this study we found, for the first time, that hen egg OV is a hypocholesterolemic protein. OV clearly demonstrated serum



**TABLE 3**  
**Effects of Dietary Casein and OV on Body and Liver Weights, Food Intake, Serum and Liver Lipids, and Fecal Steroid Excretion in Rats<sup>a</sup>**

	Diet group	
	Casein	OV
Body weight gain (g/10 d)	25.9 ± 1.1	22.4 ± 2.5
Liver weight (g/100 g body wt)	3.81 ± 0.06	3.61 ± 0.07
Food intake, d 6 (g/d)	14.2 ± 0.7	13.6 ± 0.6
Serum (mmol/L)		
Total cholesterol (a)	2.83 ± 0.21	1.96 ± 0.07 <sup>b</sup>
HDL cholesterol (b)	0.53 ± 0.04	0.66 ± 0.06
LDL + VLDL cholesterol	2.30 ± 0.22	1.30 ± 0.08 <sup>b</sup>
Atherogenic index: (b)/(a) (mol/mol)	0.19 ± 0.02	0.34 ± 0.03 <sup>b</sup>
TG	0.38 ± 0.04	0.37 ± 0.03
Phospholipids	1.13 ± 0.08	1.04 ± 0.05
Liver		
Total lipids (mg/g liver)	142.8 ± 4.41	124.0 ± 2.47 <sup>b</sup>
Cholesterol (μmol/g liver)	70.8 ± 2.4	66.9 ± 3.2
TG (μmol/g liver)	26.8 ± 2.9	24.8 ± 2.1
Phospholipid (μmol/g liver)	118.8 ± 3.2	98.7 ± 1.6
Feces		
Dry weight (g/3 d)	2.42 ± 0.06	2.58 ± 0.10
Cholesterol (μmol/3 d)	252.5 ± 6.7	281.3 ± 9.5 <sup>c</sup>
Bile acids (μmol/3 d)	126.5 ± 5.8	151.9 ± 7.2 <sup>c</sup>

<sup>a</sup>Mean ± SEM of six rats. For abbreviation see Table 1.

<sup>b</sup>Significantly different from casein group at  $P < 0.01$ .

<sup>c</sup>Significantly different from casein group at  $P < 0.05$ .

cholesterol-lowering effects compared with casein. The major differences in amino acid compositions between casein and OV are in the level of glycine and cystine (Table 1). The relationship between the serum cholesterol-lowering activity of dietary protein and the amino acid contents of protein has been reported previously (29–31). Sugiyama *et al.* (31) reported a significant negative correlation between blood cholesterol levels and the level of cystine in intact dietary proteins. Thus, as OV contains higher levels of cystine than casein, the differences in amino acids content may relate to the differences in serum cholesterol level in the present study.

The amount of OV in egg white is 3.5% (w/w) of the total EWP. Reportedly, OV, which is macromolecular and a highly glycosylated glycoprotein, has two subunits, one a protein-rich  $\alpha$ -subunit (M.W. 220 kDa) and one a carbohydrate-rich  $\beta$ -subunit (M.W. 400 kDa) (15,32). Recent studies suggest that OV exhibits both antiviral (18,33) and antitumor activities (4). All the sialic acid present in OV was described as *N*-acetylneuraminic acid (34). Previous studies (4,18,33) discussed the relationships between the *N*-acetylneuraminic acid of OV and its physiological activity. Our preliminary observations suggested that cholesterol absorption in Caco-2 cells or micellar solubility of cholesterol is unaffected by the *N*-acetylneuraminic acid *in vitro*. Whether the hypocholesterolemic action induced by OV *in vivo* is related to *N*-acetylneuraminic acid is currently being studied.

Taking dietary utilization of OV into account, OV is appropriate to use as a supplement in the diet containing an adequate protein rather than a main protein source in the diet. It is not easy to prepare a large amount of OV, which contains

only 3.5% (w/w) of the EWP. Thus, we simply added OV to the casein diet (20% casein), increasing the protein content of the diet (Table 2). We also found that the serum cholesterol level was significantly decreased in rats fed the diet containing 15% casein supplemented with 5% OV compared to that of 20% casein diet (Nagaoka, S., and Watanabe, K., unpublished results).

It has been postulated that the degree of serum cholesterol-lowering activity depends on the degree of fecal steroid excretion (acidic steroids + neutral steroids) (35). The present study demonstrated a higher fecal excretion of cholesterol (11.4% change) and acidic steroids by OV feeding (Table 3), indicating that the effect is due at least in part to an enhancement of fecal steroid excretion. Smith (36) reported that human gallbladder mucin binds to cholesterol in model bile. Thus, we speculate that an increased fecal excretion of cholesterol may be induced by the binding of cholesterol to OV in the intestine. There have been many studies on the hypocholesterolemic effects of proteins except for OV, most of which emphasized the hypothesis that a peptide with binding capacity to bile acid could inhibit the reabsorption of bile acid in the ileum and decrease the blood cholesterol level (37). These possibilities may be applicable to the case of OV on the basis of the evidence of fecal bile acid excretion (Table 3) and taurocholate-binding capacity (Fig. 1) in the present study.

Cholesterol is rendered soluble in bile salt-mixed micelles and then absorbed (38). The present study indicated that the micellar solubility of cholesterol in the presence of OV was significantly lower than with casein. Very interestingly, we found for the first time that the presence of SPH (13) or

$\beta$ -lactoglobulin tryptic hydrolysate (LTH) (39) significantly suppressed micellar solubility of cholesterol *in vitro*. Sitos-terol (21), sesamine (40), or catechin (41) also lowered the micellar solubility of cholesterol in conjunction with the serum cholesterol-lowering effects in rats. These findings, including those with OV, suggest that the suppression of micellar solubility of cholesterol induces the inhibition of cholesterol absorption in the jejunum, and this may be closely related to the lowering action of serum cholesterol. As shown in the cases of OV, LTH (39), or SPH (13), other dietary proteins or peptides may also affect such solubility.

In recent studies, monolayers of Caco-2 cell cultures were used as a model system to examine the process of lipid metabolism (42–44). For example, Field *et al.* (42) reported that Caco-2 cells, like the small intestine, had the ability to absorb micellar cholesterol and to express marker enzymes such as alkaline phosphatase as small intestinal epithelial cells. The experiments described usually used cultures 12–15 d after plating. This is optimal to determine the cholesterol uptake of the Caco-2 cell culture concomitant with the optimal expression of marker enzymes as small intestinal epithelial cells. In our previous paper (12), we found by using the Caco-2 cultured cell strain that the cholesterol micelles containing SPH (12) or LTH (39) significantly suppressed cholesterol absorption by Caco-2 cells *in vitro*. There is no information about the effects of OV on cholesterol absorption. We therefore used Caco-2 cells or rats to investigate the mechanisms of the serum cholesterol-lowering action of OV. Our experimental system to evaluate cholesterol absorption with Caco-2 cells is very useful for clarifying the molecular mechanism underlying the inhibitory effect of OV on cholesterol absorption from the small intestine, which was previously unknown. There have so far been a few experimental studies to evaluate some effects of proteins or peptides on cholesterol absorption by using cultured intestinal cells (12,13,39).

In this study, we found that OV lowers serum cholesterol levels in rats and inhibits cholesterol absorption in Caco-2 cells. The present results suggest that the suppression of cholesterol absorption by direct interaction between cholesterol-mixed micelles and OV in the jejunal epithelia is part of the mechanism of hypocholesterolemic action induced by OV. Whether OV micelles act directly to lower cholesterol absorption in rat jejunum epithelium *in vivo* is currently being studied.

There have been many studies on the hypocholesterolemic effects of proteins, most of which emphasized the hypothesis that a peptide with high bile acid-binding capacity could inhibit the reabsorption of bile acid in the ileum and decrease the blood cholesterol level (ileal effects). These possibilities may be applicable to the case of OV on the basis of the evidence of fecal bile acid excretion and bile acid-binding capacity in this study. Fecal excretion of bile acids was significantly increased by OV feeding compared with casein feeding, and the bile acid-binding capacity of OV was significantly greater than that of casein. However, our earlier studies (13,39), together with this study, suggest that the reduction of micellar solubility of cholesterol, which may cause the suppression of cholesterol absorption by

direct interaction between cholesterol-mixed micelles and OV in the jejunal epithelia, is part of the mechanism of hypocholesterolemic action induced by OV (jejunal effects). Thus, the hypocholesterolemic action of OV may involve both jejunal and ileal effects.

This study clearly indicates the hypocholesterolemic action of OV compared to casein in the animal model. Present findings concerning the hypocholesterolemic action of OV may enhance both industrial utilization of egg or egg proteins and their value for health enhancement.

## ACKNOWLEDGMENTS

This research is supported in part by Agriculture & Livestock Industries Corporation and the Kiei-kai Research Foundation.

## REFERENCES

1. Carrol, K.K., and Hamilton, R.M.G. (1975) Effects of Dietary Protein and Carbohydrate on Plasma Cholesterol Levels in Relation to Atherosclerosis, *J. Food Sci.* 40, 18–23.
2. Roberts, S.L., McMurry, M.P., and Conner, W.E. (1981) Does Egg Feeding (i.e., dietary cholesterol) Affect Plasma Cholesterol Levels in Humans? Results of Double-Blind Study, *Am. J. Clin. Nutr.* 34, 2092–2099.
3. Nakamura, R., Takayama, M., Nakamura, K., and Umemura, O. (1980) Constituent Proteins of Globulin Fraction Obtained from Egg White, *Agric. Biol. Chem.* 44, 2357–2362.
4. Watanabe, K., Tsuge, Y., Shimoyamada, M., Ogama, N., and Ebina, T. (1998) Antitumor Effects of Pronase-Treated Fragments, Glycopeptides, from Ovomucin in Hen Egg White in a Double Grafted Tumor System, *J. Agric. Food Chem.* 46, 3033–3038.
5. Nagaoka, S., Kanamaru, Y., and Kuzuya, Y. (1991) Effects of Whey Protein and Casein on the Plasma and Liver Lipids in Rats, *Agric. Biol. Chem.* 55, 813–818.
6. Nagaoka, S., Kanamaru, Y., Kuzuya, Y., Kojima, T., and Kuwata, T. (1992) Comparative Studies on the Serum Cholesterol Lowering Action of Whey Protein and Soybean Protein in Rats, *Biosci. Biotechnol. Biochem.* 56, 1484–1485.
7. Potter, S.M. (1995) Overview of Proposed Mechanisms for the Hypocholesterolemic Effect of Soy, *J. Nutr.* 125, 606S–611S.
8. Zhang, X., and Beynen, A.C. (1993) Influence of Dietary Fish Proteins on Plasma and Liver Cholesterol Concentrations in Rats, *Br. J. Nutr.* 69, 767–777.
9. Sirtori, C.R., Even, R., and Lovati, M.S. (1993) Soybean Protein Diet and Plasma Cholesterol: From Therapy to Molecular Mechanisms, *Ann. NY Acad. Sci.* 676, 188–201.
10. Yamamoto, S., Kina, T., Yamagata, N., Kokubu, T., Shinjo, S., and Asato, L. (1993) Favorable Effects of Egg White Protein on Lipid Metabolism in Rats and Mice, *Nutr. Res.* 13, 1453–1457.
11. Asato, L., Wang, M.F., Chan, Y.C., Yeh, S.H., Chung, H.M., Chung, S.Y., Chida, S., Uezato, T., Suzuki, I., Yamagata, N., *et al.* (1996) Effect of Egg White on Serum Cholesterol Concentration in Young Women, *J. Nutr. Sci. Vitaminol.* 42, 87–96.
12. Nagaoka, S., Awano, T., Nagata, N., Masaoka, M., Hori, G., and Hashimoto, K. (1997) Serum Cholesterol Reduction and Cholesterol Absorption Inhibition in CaCo-2 Cells by a Soyprotein Peptic Hydrolyzate, *Biosci. Biotech. Biochem.* 61, 354–356.
13. Nagaoka, S., Miwa, K., Eto, M., Kuzuya, Y., Hori, G., and Yamamoto, K. (1999) Soy Protein Peptic Hydrolysate with Bound Phospholipids Decreases Micellar Solubility and Cholesterol Absorption in Rats and Caco-2 Cells, *J. Nutr.* 129, 1725–1730.
14. Xu, J.Q., Shimoyamada, M., and Watanabe, K. (1998) Heat Aggregation of Dry-Heated Egg White and Its Inhibiting Effect on

- Heat Coagulation of Fresh Egg White, *J. Agric. Food Chem.* **46**, 3027–3032.
15. Kato, A., Nakamura, R., and Sato, Y. (1970) Studies on Changes in Stored Shell Eggs. Part IV. Changes in the Chemical Composition of Ovomucin During Storage, *Agric. Biol. Chem.* **34**, 1009–1013.
  16. AOAC (1984) *Official Methods of Analysis of the Association of Official Analytical Chemists*, 14th edn., Association of Official Analytical Chemists, Arlington.
  17. Dubois, M., Gilles, K.A., Hamilton, J.K., Rebers, P.A., and Smith, F. (1956) Colorimetric Method for Determination of Sugars and Related Substances, *Anal. Chem.* **28**, 350–356.
  18. Tsuge, Y., Shimoyamada, M., and Watanabe, K. (1997) Structural Features of Newcastle Disease Virus- and Anti-Ovomucin Antibody-Binding Glycopeptides from Pronase-Treated Ovomucin, *J. Agric. Food Chem.* **45**, 2393–2398.
  19. Spies, J.R., and Chambers, D.C. (1948) Chemical Determination of Tryptophan, *Anal. Chem.* **20**, 30–39.
  20. Spies, J.R., and Chambers, D.C. (1949) Chemical Determination of Tryptophan in Proteins, *Anal. Chem.* **20**, 1249–1266.
  21. Ikeda, I., Tanaka, K., Sugano, M., Vahouny, G.V., and Gallo, L.L. (1988) Inhibition of Cholesterol Absorption in Rats by Plant Sterols, *J. Lipid Res.* **29**, 1573–1582.
  22. American Institute of Nutrition (1977) Report of the American Institute of Nutrition *ad hoc* Committee on Standards for Nutritional Studies, *J. Nutr.* **107**, 1340–1348.
  23. Folch, J., Lees, M., and Sloane-Stanley, G.H. (1957) A Simple Method for the Isolation and Purification of Total Lipids from Animal Tissues, *J. Biol. Chem.* **226**, 497–509.
  24. Nagaoka, S., Miyazaki, H., Oda, H., Aoyama, Y., and Yoshida, A. (1990) Effects of Excess Dietary Tyrosine on Cholesterol, Bile Acid Metabolism and Mixed-Function Oxidase System in Rats, *J. Nutr.* **120**, 1134–1139.
  25. Bruusgaard, A., Sørensen, H., Gilhuus-Moe, C.C., and Skalhogg, B.A. (1977) Bile Acid Determination with Different Preparations of 3  $\alpha$ -Hydroxysteroid Dehydrogenase, *Clin. Chim. Acta* **77**, 387–395.
  26. Malchow-Møller, A., Arffmann, S., Larusso, N.F., and Krag, E. (1982) Enzymatic Determination of Total 3  $\alpha$ -Hydroxy Bile Acids in Faeces. Validation in Healthy Subjects of a Rapid Method Suitable for Clinical Routine Purpose, *Scand. J. Gastroenterol.* **17**, 331–333.
  27. Miettinen, T.A., Ahrens, E.H., and Grundy, S.M. (1965) Quantitative Isolation and Gas-Liquid Chromatographic Analysis of Total Dietary and Fecal Neutral Steroids, *J. Lipid Res.* **6**, 411–424.
  28. Snedecor, C.W., and Cochran, W.G. (1967) *Statistical Methods*, 6th edn., The Iowa State University Press, Ames (Japanese Edition: Iwanami Publishing, Tokyo).
  29. Huff, M.W., and Carroll, K.K. (1980) Effects of Dietary Proteins and Amino Acid Mixtures on Plasma Cholesterol Levels in Rabbits, *J. Nutr.* **110**, 1676–1685.
  30. Jacques, H., Deshaies, Y., and Savoie, L. (1986) Relationship Between Dietary Proteins, Their *in vitro* Digestion Products, and Serum Cholesterol in Rats, *Atherosclerosis* **61**, 89–98.
  31. Sugiyama, K., Ohkawa, S., and Muramatsu, K. (1986) Relationship Between Amino Acid Composition of Diet and Plasma Cholesterol Level in Growing Rats Fed a High Cholesterol Diet, *J. Nutr. Sci. Vitaminol.* **32**, 413–423.
  32. Itoh, T., Miyazaki, J., Sugawara, H., and Adachi, S. (1987) Studies on the Characterization of Ovomucin and Chalaza of the Hen's Egg, *J. Food Sci.* **52**, 1518–1521.
  33. Tsuge, Y., Shimoyamada, M., and Watanabe, K. (1997) Binding of Ovomucin to Newcastle Disease Virus and Anti-Ovomucin Antibodies and Its Heat Stability Based on Binding Abilities, *J. Agric. Food Chem.* **45**, 4629–4634.
  34. Robinson, D.S., and Monsey, J.B. (1971) Studies on the Composition of Egg-White Ovomucin, *Biochem. J.* **121**, 537–547.
  35. Nagata, Y., Ishiwaki, N., and Sugano, M. (1982) Studies on the Mechanisms of Antihypercholesterolemic Action of Soy Protein and Soy Protein-Type Amino Mixtures in Relation to the Casein Counterparts in Rats, *J. Nutr.* **112**, 1614–1625.
  36. Smith, B.F. (1987) Human Gallbladder Mucin Binds Biliary Lipids and Promotes Cholesterol Crystal Nucleation in Model Bile, *J. Lipid Res.* **28**, 1088–1097.
  37. Iwami, K., Sakakibara, K., and Ibuki, F. (1986) Involvement of Post-Digestion "Hydrophobic" Peptides in Plasma Cholesterol-Lowering Effect of Dietary Plant Proteins, *Agric. Biol. Chem.* **50**, 1217–1222.
  38. Wilson, M.D., and Rudel, L.L. (1994) Review of Cholesterol Absorption with Emphasis on Dietary and Biliary Cholesterol, *J. Lipid Res.* **28**, 1057–1066.
  39. Nagaoka, S., Futamura, Y., Miwa, K., Awano, T., Yamauchi, K., Kanamaru, Y., Kojima, T., and Kuwata, T. (2001) Identification of Novel Hypocholesterolemic Peptides Derived from Bovine Milk  $\beta$ -Lactoglobulin, *Biochem. Biophys. Res. Commun.* **281**, 11–17.
  40. Hirose, N., Inoue, T., Nishihara, K., Sugano, M., Akimoto, K., Shimizu, S., and Yamada, H. (1991) Inhibition of Cholesterol Absorption and Synthesis in Rats by Sesamin, *J. Lipid Res.* **32**, 629–638.
  41. Ikeda, I., Imasato, Y., Sasaki, E., Nakayama, M., Nagao, H., Takeo, T., Yayabe, F., and Sugano, M. (1992) Tea Catechins Decrease Micellar Solubility and Intestinal Absorption of Cholesterol in Rats, *Biochim. Biophys. Acta* **1127**, 141–146.
  42. Field, F.J., Albright, E., and Mathur, S. (1987) Regulation of Cholesterol Esterification by Micellar Cholesterol in CaCo-2 Cells, *J. Lipid Res.* **28**, 1057–1066.
  43. Hughes, T.E., Sasak, W.V., Ordovas, J.M., Forte, T.M., Lamon-Fava, S., and Schaefer, E.J. (1987) A Novel Cell Line (Caco-2) for the Study of Intestinal Lipoprotein Synthesis, *J. Biol. Chem.* **262**, 3762–3767.
  44. Ranheim, T., Gedde-Dahl, A., Rustan, A.C., and Drevon, C.A. (1992) Influence of Eicosapentaenoic Acid (20:5, n-3) on Secretion of Lipoproteins in CaCo-2 Cells, *J. Lipid Res.* **33**, 1281–1293.

[Received October 1, 2001, and in revised form December 14, 2001; revision accepted January 8, 2002]

# Evidence in Favor of a Facilitated Transport System for FA Uptake in Cultured L6 Cells

Carlos A. Marra<sup>a,\*</sup>, María Dolores Girón<sup>b</sup>,  
and María Dolores Suárez<sup>b</sup>

<sup>a</sup>INIBIOLP (Instituto de Investigaciones Bioquímicas de La Plata), CONICET-UNLP, Facultad de Ciencias Médicas, Universidad Nacional de La Plata, La Plata, Argentina, and <sup>b</sup>Departamento de Bioquímica y Biología Molecular, Facultad de Farmacia, Universidad de Granada, Campus Cartuja, Granada, España

**ABSTRACT:** In this manuscript we report a study of the transport of FA in L6 muscle cells. Cultured L6 cells took up labeled FA (C<sub>10</sub> to C<sub>20</sub>) as a linear function of time up to 15 min. Thereafter, the rate of uptake gradually declined although it persisted for at least 12 h after the addition of the substrate. Kinetic parameters ( $K_m$ ,  $V_m$ , and  $k_d$ ) were determined from a fitted Michaelis-Menten-type equation modified by a term for a saturable (linear) component of the measured total uptake.  $V_m$  values were different for some of the FA studied, and  $K_m$  data showed significant differences between saturated and unsaturated FA. The maximal rate of uptake was observed at pH 7.40 for decanoate, palmitate, and eicosatrienoate. Uptake was significantly influenced when the pH of the incubation medium was changed. Experiments designed to study the influence of FA/albumin molar ratio indicated that  $V_m$  was dependent on the total (bound and free) concentration of the FA. A concentrative uptake was demonstrated in short-term experiments with an apparent plateau of 20 and 40  $\mu$ M for palmitate and eicosatrienoate, respectively. A competitive inhibition was also observed between palmitate as substrate and the other FA. From our results we can postulate that the uptake of FA in L6 cells is the sum of passive diffusion plus a saturable component and that the rate of uptake is dependent on one (or more) protein structures, although their precise characteristics and functions remain to be elucidated.

Paper no. L8740 in *Lipids* 37, 273–283 (March 2002).

FA bound to albumin and serum lipoproteins represent the most suitable form in which to transport fat for its utilization. Different types of cultured cells are able to carry out the uptake and metabolism of FA. It was previously demonstrated that in cardiac myocytes the oxidation of long-chain FA is the predominant source of energy necessary for proper electrochemical function (1). As the capacity of this kind of cells to store FA in lipid pools is very limited, myocytes are dependent on a continuous supply of these substrates from the blood stream (2). The L6 rat skeletal muscle cell line would share similar metabolic characteristics with cardiac myocytes;

\*To whom correspondence should be addressed at Facultad de Medicina, Universidad Nacional de La Plata, 60 y 120 (1900) La Plata, Argentina. E-mail: camarra@atlas.med.unlp.edu.ar

Abbreviations: FABP, fatty acid-binding protein; IMEM-Zo, improved minimal essential medium-zinc optional; MEM, minimal essential medium; UFA, uncomplexed FA.

as a consequence, it may be a useful experimental model to investigate FA uptake.

Prior to their cellular uptake, FA must be dissociated from albumin, then they go through the plasma membrane. The driving force for this process is considered to be the concentration gradient existing across the biomembrane (1–4). Previous papers support the conclusion that transmembrane transport is governed by simple, nonfacilitated diffusion (2–6). However, it was also suggested that the plasma membrane fatty acid-binding protein (FABP), an FA transport protein, and a membrane translocase found in myocytes (2,7–11) would be involved in the FA uptake. However, the role of FABP remains a matter of discussion since transfection of L6 muscle cells with FABP-cDNA does not modify FA uptake (12). In addition, it was reported that high-affinity albumin-binding sites would participate in this process (13,14). Luiken *et al.* (2) recently discussed the idea that FA uptake in isolated cardiac myocytes would be the result of both passive and protein-mediated processes. At present no general agreement exists on this matter, and the exact mechanism of transmembrane transport of FA is still a topic of controversy. Contrary to previous results, which supported the idea of passive diffusion of FA into transformed cells (15), our findings favor a facilitated transport system operating in these skeletal muscle cells.

## MATERIALS AND METHODS

**Chemicals.** [1-<sup>14</sup>C]FA (98–99% pure, 50–60 mCi/mmol) were obtained from American Radiolabeled Chemicals, Inc. (St. Louis, MO). Unlabeled FA were provided by Nu-Chek-Prep (Elysian, MN). All acids were stored in benzene under an atmosphere of nitrogen at –20°C. Concentrations and purities were routinely checked by both gas-liquid radiochromatography and liquid-scintillation counting. Mass determinations were performed by GLC of FAME prepared in the presence of internal standards. FAME mixtures, HEPES delipidated serum albumin (BSA; fraction V from bovine), minimum essential medium Eagle (MEM) with Earle's salts, nonessential amino acids, L-glutamine, choline chloride, fetal bovine serum (FBS), Earle's balanced salts, and improved



minimal essential medium-zinc-optional (IMEM-Zo) were obtained from Sigma Chemical Co. (St. Louis, MO). All solvents were RPE grade and provided by Carlo Erba, Milano, Italy. Silicagel G-60 plates for TLC were provided by Fluka-Riedel-de Häen, Darmstadt, Germany. Other chemicals used were reagent grade and obtained from commercial sources.

**Cell culture and experimental procedure.** L6 muscle cells were grown in surface cultures in approximately 30 cm<sup>2</sup> flasks at 37°C with 5 mL MEM supplemented with 10% (vol/vol) FBS, 0.30 g/L glutamine, and 25 mM HEPES. When the cells were at the logarithmic phase of growth (approximately 72 h after seeding), the culture medium was replaced by IMEM-Zo minus linoleic acid and containing HEPES (25 mM final concentration). The cells were maintained in this medium for 24 h. Then the medium was aspirated and replaced by fresh medium at 37°C supplemented with different FA at various final concentrations. The FA were added as sodium salts bound to delipidated albumin according to Spector *et al.* (15). The uptake process was stopped following the method of Samuel *et al.* (16). After aspiration of the medium, the cells were washed twice with 5 mL of cold Earle's balanced salt solution containing 0.5% BSA. All operations were performed within 20 to 25 s. Control flasks were supplemented with defatted BSA at the same concentration used in the experimental ones. Radioactivity recovered in the last wash routinely represented 4 to 7% of the total radioactivity remaining bound to the cells. Cells were washed and then treated with 2 mL of 0.1 N NaOH and immediately shaken to produce cellular lysis. The resulting lysates were transferred to ice-cold tubes, and the culture flasks were washed twice with 1 mL each of 0.1 N NaOH. After stirring of the pooled solutions, an appropriate aliquot was directly transferred into scintillation vials containing 10 mL of ACS II Scintillation Cocktail for aqueous samples from Amersham Pharmacia Biotech (Buckinghamshire, England). A Beckman LS-5801 Liquid Scintillation Counter with 95% efficiency for <sup>14</sup>C was used. Counting of cellular-associated radioactivity by this method gives results similar to those obtained by extraction of total cellular lipids following the procedure of Folch *et al.* (17). Another aliquot of the cellular lysates was taken for protein measurement following the method of Lowry *et al.* (18). Differences in the uptake values of flasks from the same experimental group did not exceed 5%. Lipid analyses were performed on cellular pellets obtained from surface cultures of L6 cells during the logarithmic phase of growth. The attached cells were mechanically scraped off from the growing surface through the use of a rubber-tipped spatula. After centrifugation at 500 × *g* for 10 min in the cold, the pellet was washed again with 10 mL of Earle's balanced saline solution and centrifuged as described before. The final pellet was extracted according to the method of Folch *et al.* (17). Neutral and polar lipids were further isolated from the total lipid extract by silicic acid microchromatography (Bio-Rad Laboratories, Richmond, CA) according to the method of Hanahan *et al.* (19). The total amount of lipids in each fraction was determined gravimetrically (20). Samples for GLC were transesterified

and analyzed as previously described (21). Lipid analyses performed on culture medium were carried out after filtering through a 0.22 μ SM-11307 Sartorius Membranefilter (Göttingen, Germany) to remove cell debris. The filtrates were lyophilized, and the residual components extracted by the method of Folch *et al.* (17). The procedures employed for TLC analysis were described previously (22). In some experiments the initial rate of FA uptake was determined in modified incubation media. To study the effect of sodium concentration on uptake, we followed the procedure of Stremmel, Strohmeyer and Berk (23). A buffer containing 0.4 mM KH<sub>2</sub>PO<sub>4</sub>, 0.3 mM K<sub>2</sub>HPO<sub>4</sub>, and 15 mM HEPES at pH 7.40 was employed instead of IMEM-Zo medium. The desired concentration of NaCl or substitutes, such as choline chloride, KCl, CaCl<sub>2</sub>, or MgCl<sub>2</sub>, was added and, in order to perform the incubations at the same osmolarity (285 ± 5 mOsm/kg H<sub>2</sub>O), all media were checked by a Semi Micro Osmometer A-800 from Knauer GmbH (Berlin, Germany). Cell viability was assessed by the exclusion test of trypan blue (>96%) (24).

**Software and calculations.** Data are reported as the mean ± SE calculated from three or four independent analyses. The software used for statistical studies (correlation coefficient for nonlinear curve fitting, linear regressions, Student *t*-test, and ANOVA) and other calculations was Systat (version 8.0 for Windows) from SPSS Science (Chicago, IL). Data were also plotted and analyzed using Sigma Scientific Graphing Software (version 8.0) from Sigma Chemical Co. Graphics were constructed considering the amount of uncomplexed FA (UFA) in the presence of BSA. The UFA concentrations were calculated on the association constants determined by Spector *et al.* (25–27) for 12:0, 16:0, 18:0, and 18:2n-6 FA using a personal computer. In the case of the UFA, 18:3n-3 and 20:3n-6, the UFA concentrations were measured in separate experiments (in the absence of cells) by the two-phase partitioning method using heptane as the organic phase as described by Spector *et al.* (27–29). These measurements were performed with a fractional standard error among independent determinations of 2.5% or less. Uptake data were fitted to a modified hyperbolic function of the calculated UFA concentrations using the software mentioned before. During the data fitting, care was taken to find both global minima in the sum of squares and the best nonlinear regression coefficient. We found that, for all the FA studied, our results were best fitted by the following modified hyperbolic equation:

$$UT = V_m[UFA]/(K_m + [UFA]) + k_o [UFA] \quad [1]$$

where UT is the global uptake expressed in nmol FA/min/mg cellular protein, [UFA] is the UFA concentration in the presence of a specific BSA concentration (nM), *K*<sub>m</sub> is the UFA concentration at a half-maximal uptake rate (nM), *V*<sub>m</sub> is the maximal uptake rate of the saturable uptake component (nmol/min/mg cellular protein), and *k*<sub>o</sub> is the rate constant for the linear (nonsaturable) component (μL/min/mg cellular protein). The same equation can be expressed as the sum of two components, one of them with a saturable behavior

(rectangular hyperbola) and the other as an unsaturable component (a linear function of UFA concentration):

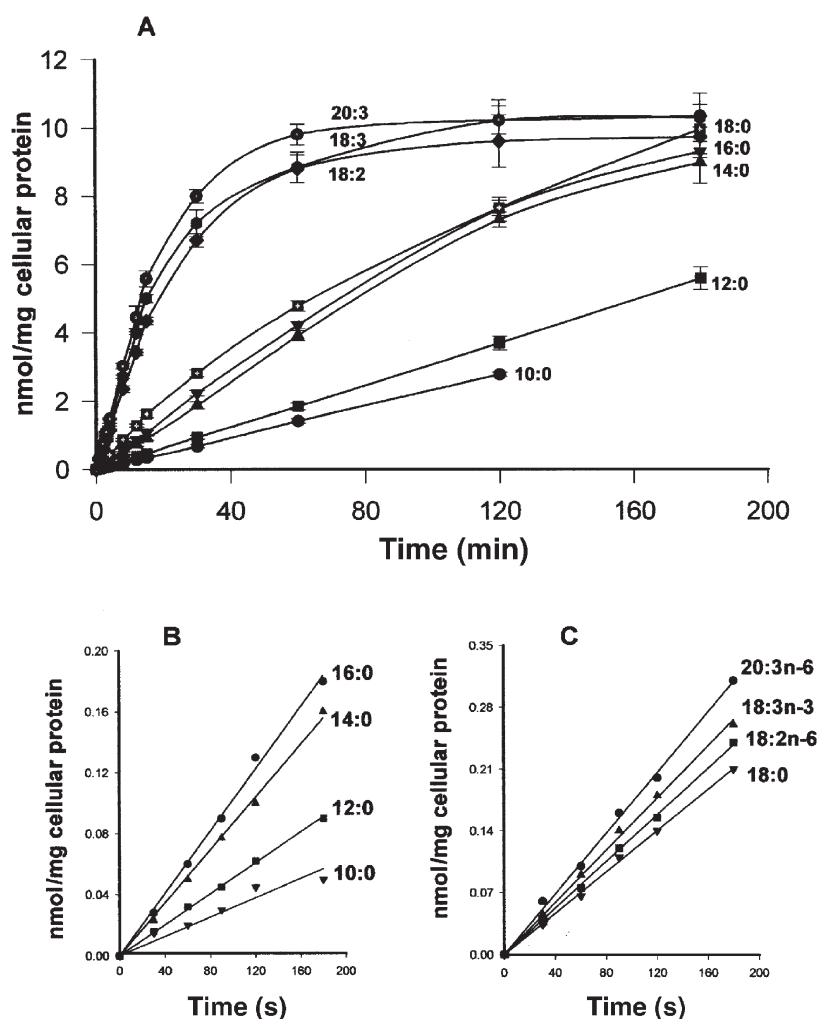
$$UT = (V_m [UFA]/(K_m + [UFA])) + k_o' [UFA] \quad [2]$$

Both equations were essentially identical to those employed by Trigatti and Gerber (14) and Stump, Fan, and Berk (30), and both of them gave statistically identical results for calculation of the kinetic parameters. Nonlinear correlation coefficients ( $R^2$ ) were within the range 0.980 to 0.997 depending on the FA studied.

## RESULTS

Owing to the significant modifications of the FA composition evoked by the culture time in complete medium (data not

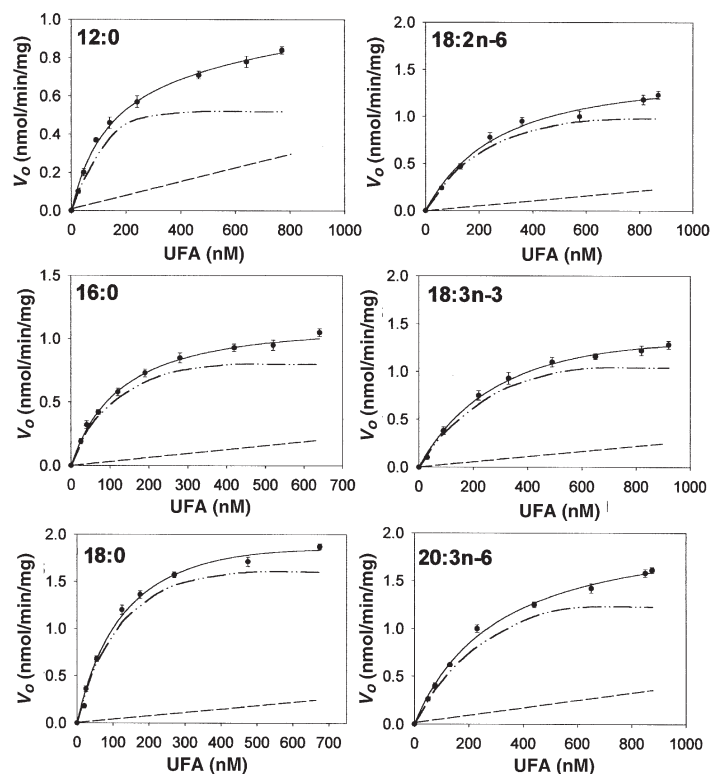
shown), the experiments described in this work were carried out using cultured monolayers of L6 muscle cells during the early logarithmic phase of growth (approximately 72 h after seeding). We chose for our experiments various FA of different chain length and degree of unsaturation. Experimental parameters such as the FA concentration, specific activities, and incubation times were determined by testing the initial rate of uptake under different assay conditions. When the time course of FA uptake was studied under physiological conditions, i.e., at exogenous concentrations of FA and albumin of 20 and 5  $\mu\text{M}$  (FA/BSA equal to 4:1), a rapid initial phase was observed for all substrates studied (Fig. 1A). This uptake was measurable within 30 s after FA addition (Figs. 1B and 1C) and linear with time for at least 15 min (Fig. 1A). Thereafter, the rate of uptake gradually declined for those FA from  $C_{14}$  to  $C_{20}$ . In contrast, the period of linear uptake was longer for



**FIG. 1.** The time course of FA uptake was determined in L6 cells using confluent monolayers of myocytes at an early logarithmic phase of growth. They were incubated in improved minimal essential medium-zinc optional (IMEM-Zo) medium with different FA (fixed initial concentration 20  $\mu\text{M}$ ) bound to delipidated albumin (FA/BSA molar ratio 4:1) and analyzed on cellular uptake at the times indicated. Samples were taken from 0 to 180 min (A) or registered during the initial 180 s at 30-s intervals (B and C). For details see Materials and Methods section. Data are the mean  $\pm$  SEM of three experiments.

shorter-chain FA ( $C_{10}$  and  $C_{12}$ ). For all the substrates studied, uptake was observed for at least 8–12 h (data not shown). It may be suggested that the fall-off in the rate of uptake could be the result of a toxic effect of the FA on the cells (3). After taking into account this possibility, the kinetic data were determined in the 0–3 min period after the FA addition. Exclusion of trypan blue was routinely performed for each determination, leading to the observation that more than 96% of cells were viable in all assays. Figure 2 shows the initial uptake rates for various FA as a function of the UFA concentration in the incubation medium calculated as mentioned in the Materials and Methods section. We chose the initial concentration of FA and BSA to obtain similar sets of UFA concentrations within the range 0 to 900 nM for each FA studied. Calculations for initial uptake rates were made from the slopes of the cumulative linear regressions curves over the first 3-min incubation period. As explained before, the uptake rates were fitted best ( $R^2$  within the range 0.980 to 0.997) by

the sum of the saturable (hyperbolic) plus nonsaturable (linear) components for all the FA studied. Computed values for the kinetic parameters obtained from these plots are presented in Table 1.  $V_m$  values varied from  $0.55 \pm 0.03$  to  $1.80 \pm 0.11$   $\text{nmol}\cdot\text{min}^{-1}\cdot\text{mg}$  cellular protein $^{-1}$ , and they were different from each other for the saturated FA studied. Results indicate that, in the case of the saturated FA,  $V_m$  values increased with the length of the carbon chain.  $V_m$  data for the UFA were very similar to each other, and these values were between those of palmitic and stearic acids. In the case of the  $K_m$  data, we also found significant differences between unsaturated FA ( $133 \pm 7$ ,  $130 \pm 8$ , and  $128 \pm 6$  nM for linoleate,  $\gamma$ -linolenate, and dihomo- $\gamma$ -linolenate, respectively) and saturated FA ( $75 \pm 4$ ,  $71 \pm 3$ , and  $68 \pm 3$  nM for  $C_{12}$ ,  $C_{16}$ , and  $C_{18}$ , respectively) (Table 1). From these kinetic parameters, it is possible to calculate the  $k_o$  constant and the percentage contribution of the uptake that is ascribed to the saturable component of the global kinetic behavior (Table 1). When the FA/BSA molar ratios



**FIG. 2.** Initial uptake rates of various [ $1\text{-}^{14}\text{C}$ ]FA as a function of the uncomplexed FA (substrate) concentration in the incubation medium. Monolayers of cultured L6 cells in IMEM-Zo medium were incubated at  $37^\circ\text{C}$  for 3 min with various concentrations of the indicated FA (fixed initial concentrations from 0 to  $500\ \mu\text{M}$ ) bound to delipidated BSA. The resultant FA/BSA molar ratios varied from 0.2:1 to 4:1. The resultant uncomplexed FA (UFA) concentrations were within the range 0 to 1000 nM; they were calculated, or experimentally determined, as indicated in the Materials and Methods section. The initial uptake rates were obtained from the linear regression slopes of the cumulative uptake curves over the initial 3-min incubation period and were fitted by a computer program to a nonlinear hyperbolic curve containing a term for nonsaturable uptake. (●), Experimentally measured total FA uptake; (—), computer-fitting of experimental data; (---), saturated uptake component; and (----), nonsaturable uptake component. Values are the means  $\pm$  SEM of three independent measurements. For abbreviation see Figure 1.

**TABLE 1**  
Kinetic Parameters Obtained from the Uptake of FA in L6 Cells<sup>a</sup>

FA	$V_m^b$	$K_m^b$	$k_o^c$	%NSC <sup>d</sup>
12:0	0.55 ± 0.03	75 ± 4	0.38 ± 0.02	34 ± 2
16:0	0.91 ± 0.05	71 ± 3	0.35 ± 0.03	20 ± 1
18:0	1.80 ± 0.11	68 ± 3	0.37 ± 0.03	14 ± 1
18:2n-6	1.11 ± 0.10	133 ± 7	0.25 ± 0.02	17 ± 2
18:3n-3	1.22 ± 0.13	130 ± 8	0.26 ± 0.03	17 ± 3
20:3n-6	1.40 ± 0.08	128 ± 6	0.37 ± 0.04	20 ± 2

<sup>a</sup>The kinetic parameters ( $V_m$ ,  $K_m$ , and  $k_o$ ) for each curve from Figure 2 were generated from a weighted least-squares calculation fitted from the individual data points for each FA by means of a Michaelis-Menten-type equation containing the term  $k_o \cdot [UFA]$  for nonsaturable (linear) uptake.

<sup>b</sup>nmol·min<sup>-1</sup>·mg cellular protein<sup>-1</sup>.

<sup>c</sup>nM.

<sup>d</sup>μL·min<sup>-1</sup>·mg cellular protein<sup>-1</sup>.

<sup>e</sup>Percentage contribution of the nonsaturable uptake component. UFA, uncomplexed FA; NSC, non-saturable component.

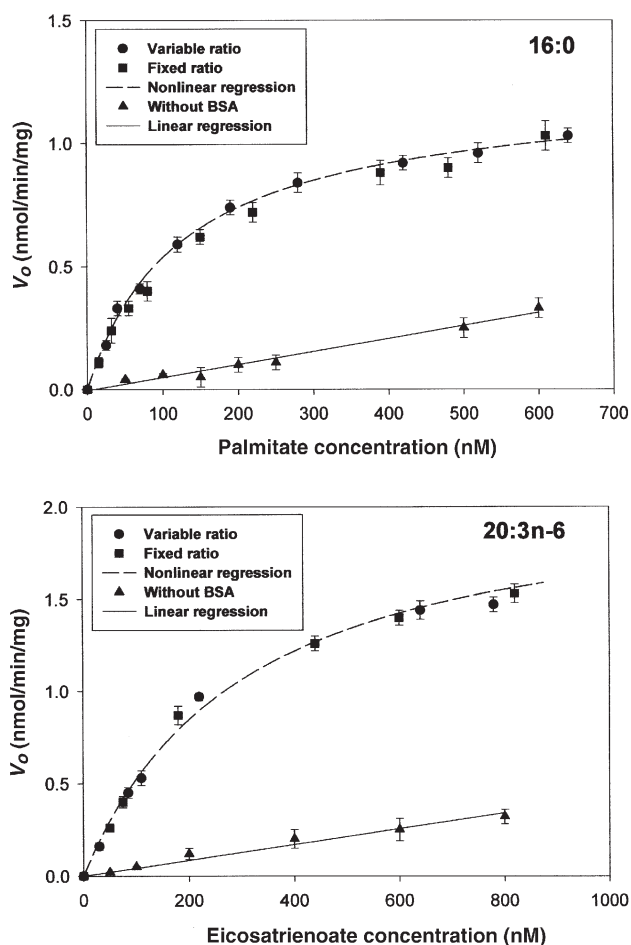
were maintained below 4:1, the linear component contributed 14 to 34% of the observed (total) uptake. The contribution observed for C<sub>18</sub> FA was of lesser extent than those from the other ones (Table 1). Within the saturated FA, the contribution of the nonsaturable uptake correlates inversely with the chain length, whereas in the case of the unsaturable FA this parameter remains almost constant (Table 1).

A series of experiments was designed to study the influence of FA/BSA molar ratio on the rate of uptake. To understand the role of BSA in the uptake of a saturated (palmitate) and an unsaturated (eicosatrienoate) FA, we performed some experiments at various concentrations of UFA in the incubation medium. The FFA concentration was selected to avoid exceeding its solubility (31,32). The incubations were performed at variable or fixed BSA concentrations (Fig. 3). In this setting, [<sup>14</sup>C]palmitate or [<sup>14</sup>C]eicosatrienoate at a fixed concentration was complexed to BSA at various concentrations or a BSA at a fixed concentration was complexed to FA at increasing concentrations producing a FA/BSA molar ratio that varied between 0.25:1 and 6:1 (Fig. 3, circles). Alternatively, the FA/BSA molar ratio was maintained constant at 6:1 as the FA concentration was increased (Fig. 3, squares). This provided various calculated UFA concentrations within the range 0 to 900 nM. Another uptake curve was obtained in the absence of BSA (Fig. 3, triangles). Results indicate a clear dependence of the uptake on the presence of BSA in the incubation medium. However, no significant differences were observed at the initial rate of uptake when the FA/BSA molar ratio was varied from 0.25:1 to 6:1. The uptake in the absence of BSA was clearly decreased with respect to that observed in the presence of the protein, and in this case, results were best fitted to a linear regression (Fig. 3, triangles).

The optimal pH for initial rates of uptake was found to be around 7.40 for decanoate, palmitate, and eicosatrienoate (Fig. 4). It is important to remark that we found maximal uptake at physiological pH for the three FA studied. Changing the pH of the incubation medium had the largest influence on the uptake of palmitate.

No differences were observed for the initial rates of uptake when using a medium supplemented with glucose (10 mM). We also found that the omission in the medium of K<sup>+</sup> (re-

placed by Na<sup>+</sup>) or Ca<sup>2+</sup> (replaced by Mg<sup>2+</sup>) had no significant influence on the rate of any of the FA studied (data not shown). However, when we examined the uptake of palmi-

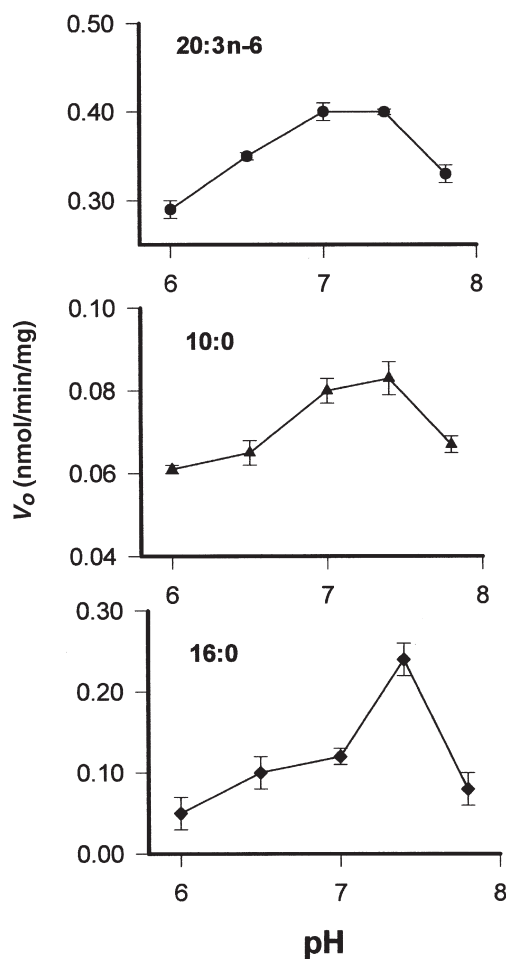


**FIG. 3.** L6 cells (approximately  $3 \cdot 10^6$  cells in 4 mL final incubation volume) were incubated at 37°C with labeled palmitic (A) or eicosatrienoic (B) acid. Incubations were conducted at variable FA/BSA molar ratios (0.75:1 to 6:1) (●) or at a fixed ratio of 6:1 (■). Other curves were obtained in the absence of albumin (▲). Uptake was measured as described in the Materials and Methods section and in the legend to Figure 1. Data are the mean ± SEM of three determinations.



tate and eicosatrienoate under the effect of isosmotic  $\text{Na}^+$  substitution with different proportions of choline chloride to achieve  $285 \pm 5$  mOsm/kg  $\text{H}_2\text{O}$  in all incubation flasks, the influx of FA was significantly depressed in a nonproportional fashion (Fig. 5). A major effect was observed with complete substitution of  $\text{Na}^+$  for choline chloride added at a final concentration of approximately 135 mM. The resultant uptake values were significantly depressed within the range 0 to 50 mM  $\text{Na}^+$  compared to the values measured at 140 mM.

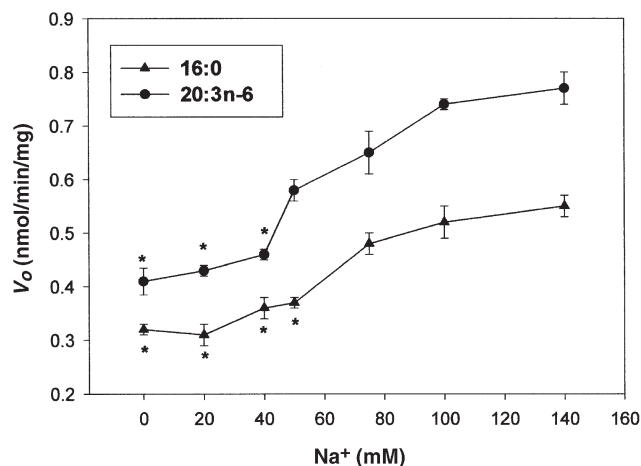
Table 2 shows the specific activities of labeled palmitic and eicosatrienoic acids in the medium after the incubation of the L6 cells from 1 to 5 min. The medium of each experiment was saved, and the unesterified FA were separated by TLC, methylated, and analyzed by quantitative GLC as described in the Materials and Methods section. We found no significant changes in the specific radioactivity of the FA assayed, although up to 23% of the exogenous acid was taken up by the cells. These results are in favor of a net uptake of FA rather than an exchange with FA previously present in the cells.



**FIG. 4.** Initial rates of FA uptake were determined in L6 cells incubated in IMEM-Zo medium buffered at different pH values.  $V_o$  values (nmol/min/mg of cellular protein) were determined at an FA/BSA molar ratio of 4:1 after a 3-min incubation period at 37°C. Data are the mean  $\pm$  SEM of three determinations.

We carried out another type of experiment by analyzing the composition and the concentrations of the different UFA in both the culture medium and the L6 cells. Results obtained clearly demonstrated that these cells do take up FA very efficiently from the culture medium. Moreover, a concentrative uptake could be demonstrated in short-term experiments conducted at different FA concentrations of FA under conditions where the substrates were mainly present as their unesterified form (Fig. 6). As expected, this concentrative uptake declined as the concentration of the acid increased. Apparent plateaus were reached at 20 and 40  $\mu\text{M}$  of external FA concentration for palmitate and eicosatrienoate, respectively (Fig. 6).

During FA uptake of L6 cells, a competitive inhibition takes place between palmitate as substrate and the other FA. In these experiments the initial rates of uptake for [ $1\text{-}^{14}\text{C}$ ]palmitate were determined at total concentrations of 16:0 varying from 0 to 200  $\mu\text{M}$  (UFA concentrations within the range 0 to 500 nM) with an FA/BSA molar ratio equal to 4:1, and in the simultaneous presence of different unlabeled FA as competitors added to the incubation medium at uncomplexed concentrations of 100 to 300 nM (approximately one to four times the  $K_m$  for the uptake of palmitate). Data were processed to obtain Dixon plots (21,33), and the kinetic parameters that characterized each incubation ( $V_m$  and  $K_i$ ) were calculated with the aid of the graphic software mentioned before. Dixon plots were constructed as the inverse of the initial velocities vs. inhibitor concentrations (Fig. 7). These types of kinetic analysis are frequently used to identify kinetic inhibition and to determine " $\alpha K_i$ " and " $K_i$ " values (33). The velocity equation for pure or mixed-type competitive inhibition may



**FIG. 5.** The influence of sodium ion concentration on initial uptake velocity ( $V_o$ ) of [ $1\text{-}^{14}\text{C}$ ]palmitate ( $\blacktriangle$ ) or [ $1\text{-}^{14}\text{C}$ ]eicosatrienoate ( $\bullet$ ) was studied in a buffered IMEM-Zo medium (pH 7.40) containing the indicated  $\text{Na}^+$  concentrations (as NaCl) plus sufficient choline chloride salt to achieve a total osmolarity of  $285 \pm 5$  mOsm/kg  $\text{H}_2\text{O}$  in all flasks.  $V_o$  values (nmol/min/mg of cellular protein) were determined at an FA/BSA molar ratio of 4:1 after a 3-min incubation period at 37°C. Values are the mean  $\pm$  SEM of three determinations. (\*)  $P < 0.01$  with respect to the  $V_o$  values measured at 140 mM sodium. For abbreviation see Figure 1.

**TABLE 2**  
**Specific Activity of the Incubation Medium After FA Uptake by L6 Cells<sup>a</sup>**

Time (min)	FA (10 $\mu$ M)	Uptake (nmol/mg)	Uptake (%)	Specific activity (dpm/nmol)
1	16:0	0.66 $\pm$ 0.05	4.0	3106 $\pm$ 195
5	16:0	1.75 $\pm$ 0.22	10.5	2967 $\pm$ 114
1	20:3n-6	1.50 $\pm$ 0.31	9.0	3110 $\pm$ 142
5	20:3n-6	3.80 $\pm$ 0.44	23.0	2807 $\pm$ 232

<sup>a</sup>FA were incubated at 10  $\mu$ M initial concentration as albumin complexes (FA/BSA molar ratio equal to 4:1) with  $3 \cdot 10^6$  cells (approximately 3 mg of cellular protein) at the times indicated. The incubation media were saved and analyzed as described in the Materials and Methods section. Each value is the mean  $\pm$  SEM of four determinations.

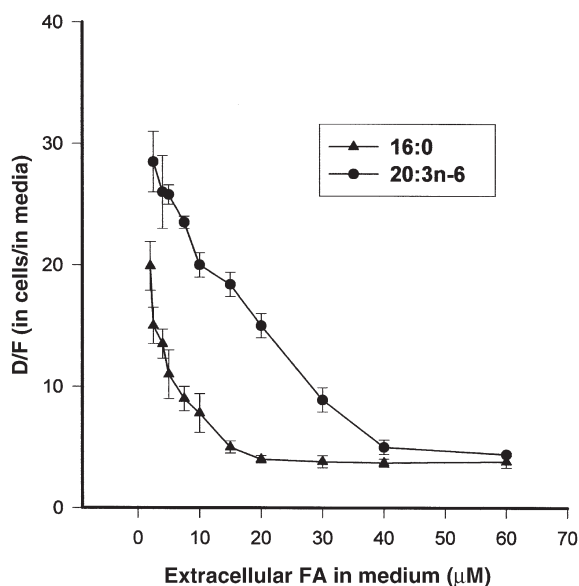
be converted into a linear form in which the varied ligand is the concentration of the FA added as competitor. The regression lines obtained at different substrate (palmitate) concentrations have positive slopes that are given by  $K_m/[S] \cdot V_m \cdot K_i$ . Since  $K_m$ ,  $[S]$ , and  $V_m$  are constants, the slopes are inversely proportional to  $K_i$ . By drawing a horizontal line at a height of  $1/V_m$ , these lines can be intercepted at the  $-[FA]$  (FA added as competitor), representing the kinetic parameter  $K_i$ . Results from Table 3 and Figure 7 indicate a competition between the FA for entry into the cells, since the presence of another FA in the incubation medium is accompanied by a decrease in palmitate uptake. The analysis of Dixon plots (Fig. 7) suggests that this inhibitory effect belongs to the type called "pure competitive" (33) with  $K_i$  values within the range 141 to 218 nM depending on the FA tested as competitor (Table 3). The values found when these FA were present either as substrates or as competitors strongly

suggest that they can interact with the same molecular system as palmitate, thus displaying a similar affinity.

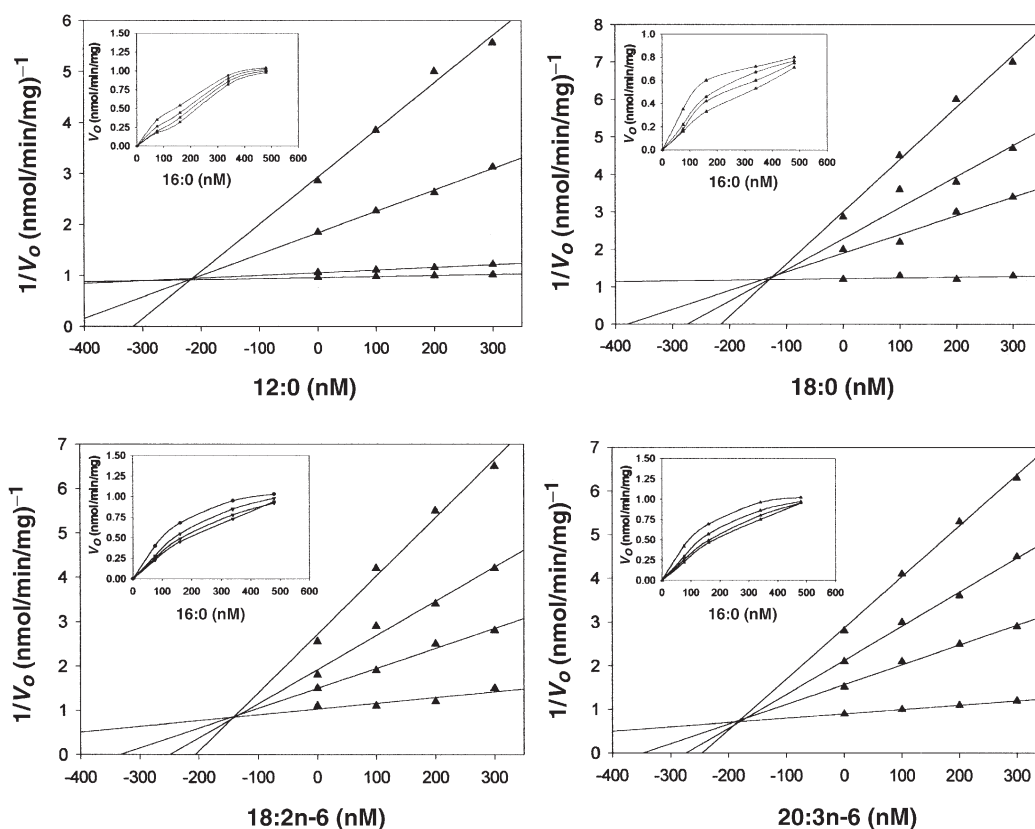
## DISCUSSION

It is generally assumed that the uptake of FA by mammalian cells occurs by passive diffusion (3,4,21). Active transport of FA has been described in bacteria and yeast (34). Active transport of FA in cardiac cells from chick embryo (16) or adult rats (2) has also been suggested. In addition, other authors reported a direct involvement of BSA (13,14,35), membrane proteins (23,35,36) and various cytosolic proteins (2,35,37–45) in the uptake of FA. However, up to now, the mechanism of cellular uptake of FA has been a controversial question that probably involves both a passive and a carrier-mediated transmembrane translocation (35,46,47). In the present paper, the experimental evidence indicates that in cultured myoblastoma cells a net uptake of FA occurs through a saturable transport system. Results from Figure 2 and Table 1 clearly show that the saturable component of the FA uptake exhibits a rather high affinity for  $C_{12}$  to  $C_{20}$  FA, with different initial velocities depending on the length of the carbon chain and/or unsaturation degree. After comparing results from other laboratories—recalculated using the same units—we observed that  $V_m$  values for some of the FA studied approached previously reported rates (3,7,23), and  $K_m$  for net uptake seems to be above the physiological concentrations on non-BSA-bound FA in plasma (25,35,48,49). Stearic acid has a  $V_m$  that is almost three times greater than that of 12:0; taking into account that one million L6 cells equals *ca.* 0.8 mg of cellular protein, this value is very similar to that reported by Stremmel (7) for oleic acid in cardiomyocytes. Moreover, we found that  $K_m$  data increased significantly with chain length from  $C_{12}$  to  $C_{18}$  (Table 1) in a way similar to that suggested by DeGrella and Light (3).  $K_m$  values showed clear differences between saturated FA and UFA (Table 1). Interpretation of these results may be carried out from different points of view, but we think they, may indicate the existence of a membrane-associated transport system with appropriate capacity to meet the needs of L6 cells for FA as metabolic precursors or as a source of energy.

Transmembrane FA transport could be linked to some ATP-consuming process such as conformational changes of membrane-associated proteins, or co-transport with—for



**FIG. 6.** FA uptake was determined in L6 cells incubated in IMEM-Zo medium supplemented with various concentrations of palmitate ( $\blacktriangle$ ) or eicosa-8,11,14-trienoate ( $\bullet$ ) bound to delipidated albumin (FA/BSA molar ratio 4:1). After 4 min of incubation, radioactivity was quantified in both cells (D) and media (F) as described in the Materials and Methods section. Data are the mean  $\pm$  SEM of three analyses. For abbreviation see Figure 1.



**FIG. 7.** Competition experiments were performed in the presence of labeled palmitate (0 to 200  $\mu\text{M}$  total concentration; FA/BSA molar ratio equal to 4:1) and different unlabeled FA (12:0, 18:0, 18:2, and 20:3) as competitors at three final concentrations. Uncomplexed palmitate concentration varied from 0 to 500 nM, and the concentrations of the FA added as competitors were within the range of 100 to 300 nM (one to four times higher than the basal  $K_m$  value for palmitate). Data were processed to obtain Dixon plots, and the kinetic parameters ( $V_m$  and  $K_i$ ) were calculated through a computer software program as detailed in the Materials and Methods section. The initial velocities were calculated from the slopes of the minimal-squares linear regression plots computer-generated from the 3-min initial uptake data according to the procedure described in the text. Each value represents the mean of duplicate experiments. Inset graphics show the Michaelis–Menten-type behavior for the different sets of experimental points.

instance— $\text{Na}^+$  (23,35,50–52). Although the available data from liver and cardiac muscle cells indicate that  $\text{Na}^+$ -dependent transport of FA represents a minor portion of total uptake, previous reports from other laboratories (23,35,50,51) and the present paper (Fig. 5) indicate a direct relationship

**TABLE 3**  
Kinetic Parameters for the Uptake of Palmitate in the Presence of Various FA as Competitors<sup>a</sup>

FA added as competitor	$V_m^a$ (nmol/min/mg cellular protein)	$K_i$ (nM)
None	0.91	—
16:0	0.88	218
18:0	0.78	129
18:2n-6	0.77	141
20:3n-6	0.89	178

<sup>a</sup>The kinetic parameters  $V_m$  and  $K_i$  were obtained from linear regression analysis of Dixon plots shown in Figure 7. For further details see the text. Data are expressed as the mean of duplicate experiments.

between FA uptake and sodium availability. The fact that FA uptake is facilitated specifically in the presence of  $\text{Na}^+$  suggests that L6 cells have a sodium-linked system for FA influx that may be dependent on  $\text{Na}^+/\text{K}^+$ -ATPase, similar to what had been found for the hepatocellular uptake of oleate previously reported by Stremmel *et al.* (23).

It is well-known that changing pH is a simple but potent strategy for altering the amount of FA partitioning into the biomembrane. The UFA is composed of anions and undissociated acid, but in practice, the total UFA concentration is considered to be the free anion concentration (27). This approach would be entirely valid if the pH of the medium is 7 or higher because the  $\text{p}K_a$  of FA is thought to be about 4.8 to 5.0 (27). For this reason, within the range of physiological pH values a considerable portion of total FA may be un-ionized. As reviewed by Spector (27), binding of FA to BSA is increased significantly when the pH of the medium is raised from 6.5 to 8.2. This would be reflected in the relative proportion between free and complexed FA. As discussed by

Hamilton (53), basic physical chemistry indicates that we expect an enhanced uptake of FA into cells when the pH of the medium is decreased. However, we found that decanoate, palmitate, and eicosatrienoate exhibited a maximal uptake at physiological pH (7.40) that was preceded by diminished uptake values in the pH range of 6.0 to 7.4 (Fig. 4). This fact suggests that a structure sensible to pH modification—other than the FA itself—may be involved in the uptake of the substrates. This is not the case when we assume that the uptake proceeds by passive diffusion, in which the driving force that determines the net uptake is the partition coefficient of FFA between medium and biomembrane (35,53). In the simple diffusion model, a very rapid rate of flip-flop of FA across the membrane is proposed (53). It has also been reported that the  $\text{Na}^+/\text{K}^+$  antiporter may act in response to the movement of  $\text{H}^+$  by FA flip-flop, and it may influence diffusion by local pH changes that modify the interfacial ionization of the substrate (53). Several experimental observations have described the structural changes of BSA within the pH interval we examined, including significant modifications around the physiological pH (27). Thus, BSA and/or a membrane protein could influence FA uptake by binding the substrate directly, enhancing partitioning into the membrane, or playing a role in its subsequent metabolism, for example, sequestering FA to a membrane-bound transporter. If a membrane-associated protein binds FA with high affinity in a pH-dependent manner, the rate of release from the protein will affect the rate of uptake, possibly slowing it down.

Experimental evidence from other authors indicates that only UFA enter the cells and that the rate of uptake is dependent upon the FA/BSA molar ratio, that is, upon the concentration of FFA (15,16,35,47,54). Figure 3 demonstrates that no significant differences are observed for the uptake of palmitate and eicosatrienoate at constant and variable ratios. Thus, under our experimental conditions, only the total FA concentration (bound and free) seems to be crucial for the rate of uptake. As the exogenous palmitate—or eicosatrienoate—concentrations were varied at a fixed FA/BSA ratio (Fig. 3), the uncomplexed substrate concentration, which is solely a function of the ratio (2,49,54), remained constant. Hence, the concentration of BSA in the medium was the only variable in this setting. Under these conditions, the FA uptake appeared to be saturable at increasing BSA concentration, indicating, as previously proposed by Trigatti and Gerber (14) and Glatz *et al.* (35), the possible involvement of an albumin receptor structure in the uptake mechanism. On the other hand, taking into account the high affinity of BSA for FFA, it might be assumed that these substrates cannot leave binding sites on albumin without catalysis performed by another protein. In this regard, it was reported that the rate of desorption of stearic acid from albumin may be accomplished in 70 s as determined by  $^{13}\text{C}$  NMR studies (53). This time seems to be too long compared to the time required for observing a significant uptake of FA in our experimental system (30 s) (Figs. 1B and 1C). It is evident that the presence of living cells influences the mechanism of FA desorption. We think, in conse-

quence, that the rate of spontaneous desorption is too slow to explain the uptake process without the intervention of another protein(s). The FA are maintained in a nonaggregated form by means of FA–albumin complexes as a source of substrate in transport studies (31,32). Under physiological conditions albumin is present in large quantities with respect to FA, strongly suggesting the existence of another structure that is involved in the uptake process. For this reason, we agree with other authors who postulate the presence of an albumin receptor in plasma membranes (13,14,35,53). This fact could explain the different results obtained for the FA uptake in experiments with artificial systems or cultured cells. Further support for the concept of a facilitated uptake for long-chain FA influx in L6 cells is found in Figure 6 and Table 2. We found a concentrative uptake of FA arising from the net incorporation of substrates rather than from an exchange with external FA. Moreover, the radioactivity was recovered exclusively in the methyl ester peak, indicating that the FA were not significantly metabolized and then released into the medium. The fact that L6 cells are able to take up FA in a concentrative fashion at all concentrations tested (Fig. 6) and that this uptake is dependent on sodium concentrations (Fig. 5) favors an active transport. We can assume therefore the existence of such a transport system in L6 cells for the uptake of FA. Notwithstanding, we should also keep in mind that FA-activating enzymes are present at the cytoplasmic level and in organelles. For this reason, a passive diffusion component cannot be ruled out. However, the fact that some FA do not compete with palmitate for activation but do compete for entry into cells (16) (Table 3) is a crucial argument against this possibility. Our results from competition studies are also in agreement with the hypothesis of a specific transport system operating in FA uptake. Similar values were found when FA were present either as substrates or as competitors, suggesting that they are recognized by the same protein structure (Table 3).

In conclusion, our results agree with previous reports (7,14,16,23,30,35) that postulate that the rate of entry of FA into L6 cells is determined by the sum of a diffusion-like (linear) component and a saturable (hyperbolic) component. As previously reported by Samuel *et al.* (16) for cultured cardiac cells, the contribution of passive diffusion in the total uptake of FA would account for no more than 30% of the total rate of uptake. In our experiments we found a contribution of 66 to 86% as saturable uptake (Table 1), which implies that 14 to 34% of the total uptake was evoked by passive diffusion. Thus, the importance of the saturable transport becomes evident. It is widely known that the cellular uptake of FA is a multistep process that involves a variety of membrane-associated events (3–5,7,8,14,23,30,35,37,52,53). Our results suggest the necessity of one or more protein structures to achieve these steps, although their precise function remains unknown. The physiological significance of this question is evident, since different tissues express a distinct set of proteins putatively involved in cellular uptake (2,5,8,10,11,13,14,23,35–45, 52,53). This phenomenon would explain the adaptation for



specific needs of each tissue and the central role related to FA availability and metabolism. These adaptive responses are complicated and not easily interpretable. For these reasons, we think they may not be the result of only passive (flip-flop) diffusion of FA through the plasma membranes.

## ACKNOWLEDGMENTS

The authors are grateful to Prof. Dra. María J.T. de Alaniz for stimulating discussion during the preparation of this manuscript. The helpful advice of Prof. Enrique Gustavo Bozarello regarding mathematical calculations is gratefully acknowledged. This study was supported in part by grants from CONICET, ANPCyT, Argentina.

## REFERENCES

1. Van der Vusse, G.J., Glatz, J.F.C., Stam, H.C.G., and Reneman, R.S. (1992) Fatty Acid Homeostasis in the Normoxic and Ischemic Heart, *Physiol. Rev.* 72, 881–940.
2. Luiken, J.J.F.P., Van Nieuwenhoven, F.A., America, G., Van der Vusse, G.J., and Glatz, J.F.C. (1997) Uptake and Metabolism of Palmitate by Isolated Cardiac Myocytes from Adult Rats: Involvement of Sarcolemmal Proteins, *J. Lipid. Res.* 38, 745–758.
3. DeGrella, R.F., and Light, R.J. (1980) Uptake and Metabolism of Fatty Acids by Dispersed Adult Rat Heart Myocytes. I. Kinetics of Homologous Fatty Acids, *J. Biol. Chem.* 255, 9731–9738.
4. DeGrella, R.F., and Light, R.J. (1980) Uptake and Metabolism of Fatty Acids by Dispersed Adult Rat Heart Myocytes. II. Inhibition by Albumin and Fatty Acid Homologues, and the Effect of Temperature and Metabolic Reagents, *J. Biol. Chem.* 255, 9739–9745.
5. Rose, H., Hennecke, T., and Kammermeier, H. (1990) Sarcolemmal Fatty Acid Transfer in Isolated Cardiomyocytes Governed by Albumin/Membrane-Lipid Partition, *J. Mol. Cell. Cardiol.* 22, 883–892.
6. Hamilton, J.A., Civelek, V.N., Kamp, F., Tonhein, K., and Corkey, B.E. (1994) Changes in Internal pH Caused by Movement of Fatty Acids into and out of Clonal Pancreatic  $\beta$ -Cells (HIT), *J. Biol. Chem.* 269, 20852–20856.
7. Stremmel, W. (1988) Fatty Acid Uptake by Isolated Heart Myocytes Represents a Carrier-Mediated Transport Process, *J. Clin. Invest.* 81, 844–852.
8. Sorrentino, D., Stump, D., Potter, B.J., Robinson, R.B., White, R., Kiang, C.L., and Berk, P.D. (1988) Oleate Uptake by Cardiac Myocytes Is Carrier Mediated and Involves a 40 kD Plasma Membrane Fatty Acid Binding Protein Similar to That in Liver, Adipose Tissue, and Gut, *J. Clin. Invest.* 82, 928–935.
9. Harmon, C.M., Luce, P., Beth, A.H., and Abumrad, N.A. (1991) Labeling of Adipocyte Membranes by Sulfo-*N*-succinimidyl Derivatives of Long-Chain Fatty Acids: Inhibition of Fatty Acid Transport, *J. Membrane Biol.* 121, 261–268.
10. Tanaka, T., and Kawamura, K. (1995) Isolation of Myocardial Membrane Long-Chain Fatty Acid-Binding Protein: Homology with a Rat Membrane Protein Implicated in the Binding or Transport of Long-Chain Fatty Acids, *J. Mol. Cell. Cardiol.* 27, 1613–1622.
11. Schaffer, J.E., and Lodish, H.F. (1994) Expression Cloning and Characterization of a Novel Adipocyte Long Chain Fatty Acid Transport Protein, *Cell* 79, 427–436.
12. Prinsen, C.F., and Veerkamp, J.H. (1998) Transfection of L6 Myoblasts with Adipocyte Fatty Acid-Binding Protein cDNA Does Not Affect Fatty Acid Uptake but Disturbs Lipid Metabolism and Fusion, *Biochem. J.* 329, 265–273.
13. Popov, D., Hasu, M., Ghinea, N., Simionescu, N., and Simionescu, M. (1992) Cardiomyocytes Express Albumin Binding Proteins, *J. Mol. Cell. Cardiol.* 24, 989–1002.
14. Trigatti, B.L., and Gerber, G.E. (1995) A Direct Role of Serum Albumin in the Cellular Uptake of Long-Chain Fatty Acids, *Biochem. J.* 308, 155–159.
15. Spector, A.A., Steinberg, D., and Tanaka, A. (1965) Uptake of Free Fatty Acids by Erlich Ascites Tumor Cells, *J. Biol. Chem.* 240, 1032–1041.
16. Samuel, D., Paris, S., and Ailhaud, G. (1976) Uptake and Metabolism of Fatty Acids and Analogues by Cultured Cardiac Cells from Chick Embryo, *Eur. J. Biochem.* 64, 583–595.
17. Folch, J., Lees, M., and Sloane Stanley, G.H. (1957) A Simple Method for the Isolation and Purification of Total Lipids from Animal Tissues, *J. Biol. Chem.* 226, 497–509.
18. Lowry, O.H., Rosebrough, N.J., Farr, A.L., and Randall, R.J. (1951) Protein Measurement with the Folin Phenol Reagent, *J. Biol. Chem.* 193, 265–275.
19. Hanahan, D.J., Dittner, J.C., and Warashima, E. (1957) A Column Chromatographic Separation of Classes of Phospholipids, *J. Biol. Chem.* 228, 685–690.
20. Marra, C.A., and de Alaniz, M.J.T. (1990) Mineralocorticoids Modify Rat Liver  $\Delta 6$  Desaturase Activity and Other Parameters of Lipid Metabolism, *Biochem. Int.* 22, 483–493.
21. Marra, C.A., and de Alaniz, M.J.T. (1999) Acyl-CoA Synthetase Activity in Liver Microsomes from Calcium-Deficient Rats, *Lipids* 34, 343–354.
22. Marra, C.A., and de Alaniz, M.J.T. (1992) Incorporation and Metabolic Conversion of Saturated and Unsaturated Fatty Acids in SK-Hep1 Human Hepatoma Cells in Culture, *Mol. Cell. Biochem.* 117, 107–118.
23. Stremmel, W., Strohmeyer, G., and Berk, P.D. (1986) Hepatocellular Uptake of Oleate Is Energy Dependent, Sodium Linked, and Inhibited by Antibody to a Hepatocyte Plasma Membrane Fatty Acid Binding Protein, *Proc. Natl. Acad. Sci. USA* 83, 3584–3588.
24. Jauregui, H.O., Hayner, N.T., Driscoll, J.L., Williams-Holland, R., Lipsky, M.H., and Galletti, P.M. (1981) Trypan Blue Dye Uptake and Lactate Dehydrogenase in Adult Rat Hepatocytes—Freshly Isolated Cells, Cell Suspensions, and Primary Monolayer Cultures, *In Vitro* 17, 1100–1110.
25. Spector, A.A., Fletcher, J.E., and Ashbrook, J.D. (1971) Analysis of Long-Chain Free Fatty Acid Binding to Bovine Serum Albumin by Determination of Stepwise Equilibrium Constants, *Biochemistry* 10, 3229–3232.
26. Ashbrook, J.D., Spector, A.A., Santos, E.C., and Fletcher, J.E. (1975) Long Chain Fatty Acid Binding to Human Plasma Albumin, *J. Biol. Chem.* 250, 2333–2338.
27. Spector, A.A. (1975) Fatty Acid Binding to Plasma Albumin, *J. Lipid Res.* 16, 165–179.
28. Spector, A.A., John, K., and Fletcher, J.E. (1969) Binding of Long-Chain Fatty Acids to Bovine Serum Albumin, *J. Lipid Res.* 10, 56–67.
29. Ashbrook, J.D., Spector, A.A., and Fletcher, J.E. (1972) Medium Chain Fatty Acid Binding to Human Plasma Albumin, *J. Biol. Chem.* 247, 7038–7042.
30. Stump, D.D., Fan, X., and Berk, P.D. (2001) Oleic Acid Uptake and Binding by Rat Adipocytes Define Dual Pathways for Cellular Fatty Acid Uptake, *J. Lipid Res.* 42, 509–520.
31. Corrin, H.L., Klevens, H.B., and Harkins, W.D. (1946) The Determination of Critical Concentrations for the Formation of Soap Micelles by the Spectral Behavior of Pinacyanol Chloride, *J. Chem. Phys.* 14, 480–486.
32. Klevens, H.B. (1953) Structure and Aggregation in Dilute Solutions of Surface Active Agents, *J. Am. Oil Chem. Soc.* 30, 74–80.
33. Segel, I.H. (1975) *Enzyme Kinetics and Analysis of Rapid Equilibrium and Steady-State Enzyme Systems*, pp. 105–175, Wiley Interscience Publication, John Wiley & Sons, New York.

34. Barber, E.D., and Lands, W.E.M. (1973) Quantitative Measurement of the Effectiveness of Unsaturated Fatty Acids Required for the Growth of *Saccharomyces cerevisiae*, *J. Bacteriol.* **115**, 543–551.
35. Glatz, J.F.C., Luiken, J.J.F.P., Van Nieuwenhoven, F.A., and Van der Vusse, G.J. (1997) Molecular Mechanism of Cellular Uptake and Intracellular Translocation of Fatty Acids, *Prostaglandins, Leukot. Essent. Fatty Acids* **57**, 3–9.
36. Reed, R.G., and Burrington, C.M. (1989) The Albumin Receptor Effect May Be Due to a Surface-Induced Conformational Change in Albumin, *J. Biol. Chem.* **17**, 9867–9872.
37. Luiken, J.J.F.P., Schaap, F.G., Van Nieuwenhoven, F.A., Van der Vusse, G.J., Bonen, A., and Glatz, J.F.C. (1999) Cellular Fatty Acid Transport in Heart and Skeletal Muscle as Facilitated by Proteins, *Lipids* **34** (Suppl.), S169–S175.
38. Jefferson, J.R., Powell, D.M., Rymaszewski, Z., Kukowska-Latallo, J., Lowe, J.B., and Schroeder, F. (1990) Altered Membrane Structure in Transfected Mouse L-Cell Fibroblasts Expressing Rat Liver Fatty Acid-Binding Protein, *J. Biol. Chem.* **265**, 11062–11068.
39. Prows, D.R., Murphy, E.J., and Schroeder, F. (1995) Intestinal and Liver Fatty Acid Binding Proteins Differentially Affect Fatty Acid Uptake and Esterification in L-Cells, *Lipids* **30**, 907–910.
40. Murphy, E.J., Prows, D.R., Jefferson, J.R., and Schroeder, F. (1996) Liver Fatty Acid Binding Protein Expression in Transfected Fibroblasts Stimulates Fatty Acid Uptake and Metabolism, *Biochim. Biophys. Acta* **1301**, 191–196.
41. Prows, D.R., Murphy, E.J., Moncecchi, D., and Schroeder, F. (1996) Intestinal Fatty Acid-Binding Protein Expression Stimulates Fibroblast Fatty Acid Esterification, *Chem. Phys. Lipids* **84**, 47–56.
42. Murphy, E.J. (1998) Sterol Carrier Protein-2 Expression Increases NBD-Stearate Uptake and Cytoplasmic Diffusion in L Cells, *Am. J. Physiol.* **275**, G244–G249.
43. Atshaves, B.P., Foxworth, W.B., Frolov, A., Roths, J.B., Kier, A.B., Oetama, B.K., Piedrahita, J.A., and Schroeder, F. (1998) Cellular Differentiation and I-FABP Protein Expression Modulate Fatty Acid Uptake and Diffusion, *Am. J. Physiol.* **274**, C633–C644.
44. Hotamisligil, G.S., Johnson, R.S., Distel, R.J., Ellis, R., Pappaioannou, V.E., and Spiegelman, B.M. (1996) Uncoupling of Obesity from Insulin Resistance Through a Targeted Mutation in aP2, the Adipocyte Fatty Acid Binding Protein, *Science* **274**, 1377–1379.
45. Murphy, E.J., Prows, D.R., Stiles, T., and Schroeder, F. (2000) Liver and Intestinal Fatty Acid-Binding Protein Expression Increases Phospholipid Content and Alters Phospholipid Fatty Acid Composition in L-Cell Fibroblasts, *Lipids* **35**, 729–738.
46. Rose, H., Hennecke, T., and Kammermeier, H. (1989) Is Fatty Acid Uptake in Cardiomyocytes Determined by Physicochemical Fatty Acid Partition Between Albumin and Membranes? *Mol. Cell. Biochem.* **88**, 31–36.
47. Bassingthwaite, J.B., Noodleman, L., Van der Vusse, G., and Glatz, J.F.C. (1989) Modeling of Palmitate Transport in the Heart, *Mol. Cell. Biochem.* **88**, 51–58.
48. Ricieri, G.V., and Kleinfeld, A.M. (1995) Unbound Free Fatty Acid Levels in Human Serum, *J. Lipid Res.* **36**, 229–240.
49. Richieri, G.V., Anel, A., and Kleinfeld, A.M. (1993) Interactions of Long-Chain Fatty Acids and Albumin: Determination of Free Fatty Acid Levels Using the Fluorescent Probe ADI-FAB, *Biochemistry* **32**, 7574–7580.
50. Sorrentino, D., Van Ness, K., Moukabary, K., and Berk, P.D. (1991) Hepatocellular  $^{22}\text{Na}^+$  Uptake: Effect of Oleate, *Am. J. Physiol.* **261**, G1024–G1029.
51. Vyska, K., Stremmel, W., Meyer, W., Notohamiprodjo, G., Minami, K., Meyer, H., and Körfer, R. (1994) Effects of Temperature and Sodium on Myocardial and Hepatocellular Fatty Acid Uptake, *Circ. Res.* **74**, 1–13.
52. Potter, B.J., Sorrentino, D., and Berk, P.D. (1988) Mechanisms of Cellular Uptake of Free Fatty Acids, *Annu. Rev. Nutr.* **9**, 253–270.
53. Hamilton, J.A. (1998) Fatty Acid Transport: Difficult or Easy? *J. Lipid Res.* **39**, 467–481.
54. Spector, R.A. (1993) The Role of Albumin Binding in Hepatic Organic Anion Transport, in *Hepatic Transport and Bile Secretion: Physiology and Pathophysiology* (Tavoloni, N., and Berk, P.D., eds.), pp. 171–196, Raven Press, New York.

[Received January 29, 2001, and in final revised form and accepted December 12, 2001]

# Platelet Phospholipids Are Differentially Protected Against Oxidative Degradation by Plasmalogens

Claude Leray, Jean-Pierre Cazenave, and Christian Gachet\*

Inserm U.311, Etablissement Français du Sang-Alsace, 67065 Strasbourg, France

**ABSTRACT:** The oxidative degradation of phospholipids in the presence and absence of plasmalogens (plasmalogen phosphatidylethanolamine: PPE) was followed by chemical analysis. Human platelet phospholipids, either intact or after removal of PPE by acid treatment, were oxidized with 28 mM 2,2'-azobis(2-amidinopropane di-HCl in Triton X-100 micelles (detergent/phospholipid 5:1, mol/mol). PPE (12% of all phospholipids, mol/mol) disappeared about three times more rapidly than glycerophospholipids, whereas sphingomyelin remained unaltered and the lysophosphatidylethanolamine (lysoPE) generated became progressively more unsaturated. After 60 min oxidation, the FA compositions of PS, PC, and PI were similar in extracts with or without plasmalogens. In contrast, diacyl phosphatidylethanolamine (DPE) became more saturated in the absence of PPE. The rate of phospholipid destruction was always unique to each class, but for all phospholipids slowed down in the presence of PPE. This protective effect increased in the order DPE < PS < PC < PI and did not seem to be simply related to the class unsaturation.  $\alpha$ -Tocopherol had no influence on the time courses of the quantities and compositions of the phospholipids, even at a molar ratio of  $\alpha$ -tocopherol to phospholipids four times higher than in platelet membranes. Thus, PPE protected phospholipids efficiently but differentially against peroxidative attack, whereas the contribution of  $\alpha$ -tocopherol appeared to be negligible even at a concentration four times greater than in platelet membranes.

Paper no. L8933 in *Lipids* 37, 285–290 (March 2002).

Several findings suggest that oxygen free radicals behave as stimulators of platelet aggregation, acting at different levels of the signal activation pathways (1,2). There is also a growing body of evidence to support the role of these active radicals in a number of pathological situations involving platelet activation, such as atherosclerosis (3) or reperfusion injury (4). Since the early demonstration of a preferential attack of "active" oxygen on the vinyl-ether linkage of plasmalogen phospholipids (5), further reports have indicated that these membrane components can play an important role in antioxidant defense (3,6,7). The most convincing systems are those employing cultured cells (8,9), LDL particles (10–12), liposomes (13–15), or micelles (12,16). The plasmalogen content of platelets is relatively high, as these compounds constitute more than half the PE pool, thus accounting for about 12% of

\*To whom correspondence should be addressed at Inserm U.311, 10 rue Spielmann, 67065 Strasbourg Cedex, France.  
E-mail: christian.gachet@efs-alsace.fr

Abbreviations: AAPH, 2,2'-azobis(2-amidinopropane) di-HCl; DPE, diacyl phosphatidylethanolamine; lysoPE, lysophosphatidylethanolamine; PPE, plasmalogen phosphatidylethanolamine (plasmalogens); SM, sphingomyelin.

all membrane phospholipids. The contribution of choline plasmalogens nevertheless remains marginal and amounts to no more than 0.8% of the PC pool (17). Although many reports have described the susceptibility of plasmalogens to various oxidative reactions (5,9,13,14), there are no studies concerning their specific protection of phospholipids. The aim of the present work was to evaluate the protection of individual platelet phospholipids by plasmalogens during peroxidative attack by estimating their concentrations and compositions in an *in vitro* system.

## MATERIALS AND METHODS

Washed human platelets were prepared from the blood of four pools of healthy donors (18), and platelet lipids were extracted immediately (19). Tocopherols were stripped from the samples down to undetectable levels by filtering chloroform solutions onto silica gel; after eluting neutral lipids with chloroform, phospholipids were eluted with methanol. Aliquots of total phospholipids (about 9  $\mu$ g P, final concentration 600  $\mu$ M) were mixed with 3 mM Triton X-100 (12) in PBS (0.5 mL), and peroxidation was induced by addition of 2,2'-azobis(2-amidinopropane) di-HCl (AAPH) at a final concentration of 28 mM (Polysciences Inc., Eppelheim, Germany). Two micellar systems were used; in one, the phospholipids were left intact, whereas in the other plasmalogens were destroyed by vortexing chloroform solutions in the presence of 0.4 M HCl for 15 min (20). Free aldehydes were removed by filtration on a silica gel column, and phospholipids were eluted as described above. To compare the protective efficiency of plasmalogens and  $\alpha$ -tocopherol, the oxidative degradation of phospholipids was also studied after addition of  $\alpha$ -tocopherol (final concentration 2.8 or 11.2  $\mu$ M; Sigma Chemical Co., Lyon, France) before AAPH to a phospholipid suspension without plasmalogens. In these experiments, the molar ratios of phospholipids to  $\alpha$ -tocopherol were similar to those in platelet membranes (about 214:1) for 2.8  $\mu$ M or up to fourfold lower (about 54:1) for 11.2  $\mu$ M  $\alpha$ -tocopherol. After incubation at 37°C for 0, 15, 30, 45, or 60 min, phospholipids were extracted with a Folch mixture. PE, PC, PS, PI, and sphingomyelin (SM) were separated by TLC (21), and their FA compositions were analyzed by GLC after direct transmethylation with BF<sub>3</sub>/methanol reagent (21). Addition of a known amount of heptadecanoic acid as an internal standard enabled estimation of the mass of each phospholipid. DPE and PPE were quantified after elution of the PE spots

and cleavage of the vinyl bond by acid treatment (21), the lysoPE representative of PPE and the remaining DPE being separated by a second TLC run.  $\alpha$ -Tocopherol was estimated by HPLC with fluorescence detection (19).

The Mann–Whitney test was used to compare the means between experimental groups.

## RESULTS

In the present study, the phospholipid composition of the platelet samples was similar to that previously reported (21) using the same analytical procedure. The average composition of the phospholipid mixture was (mol %): PPE (14.2  $\pm$  1.1), DPE (12.3  $\pm$  0.6), PC (46.3  $\pm$  2.6), PS (12.3  $\pm$  0.5), PI (4.7  $\pm$  0.2), and SM (10.2  $\pm$  0.6).

Exposure of intact platelet phospholipids to 28 mM AAPH led to a progressive loss of diacylphospholipids, which were at 25% of their initial level after 60 min oxidation. The AAPH concentration was selected to obtain a degradation rate similar to that previously observed in brain phospholipid mixtures (16). The destruction of PPE was more rapid than that of other phospholipids, occurring mainly within the first 15 min and reaching a loss of about 75% after 60 min. Moreover, the FA

composition of the remaining PPE was significantly altered (Table 1). The new FA profile after 60 min oxidation was characterized by important increases in saturated and n-9 FA, compensated by important decreases in n-6 and n-3 PUFA of, respectively, 24 and 45%. The lysoPE generated amounted to about 7% of total diacylphospholipids, and its FA composition differed significantly from that of the small amount present at time 0 (less than 1%). The concentration of arachidonic acid was four times its value at time 0, while an increase of n-6 and n-3 PUFA compensated for a decrease of n-9 FA. The FA compositions of DPE, PS, PC, and PI at time 0 and after 60 min of oxidation in the presence or absence of plasmalogens are given in Tables 2 and 3. AAPH induced important losses of PUFA (14% for DPE and about 27% for PS, PC, and PI) in intact phospholipid extracts (with plasmalogens), compensated by increases in the concentrations of saturated and monounsaturated FA. The FA compositions of PS (Table 2), PC, and PI (Table 3) in intact extracts were similar to those in extracts without plasmalogens after 60 min oxidation. In contrast, the composition of DPE was less affected by AAPH in the presence of plasmalogens (Table 2). Thus, plasmalogens significantly reduced the losses of n-6 PUFA (13 vs. 32%,  $P < 0.01$ ) and MUFA (13 vs. 35%,  $P < 0.001$ ), whereas saturated FA

**TABLE 1**  
Effects of AAPH on the FA Composition of Plasmenylethanolamine and Lysophosphatidylethanolamine in Intact Platelet Extracts<sup>a</sup>

	PPE		LysoPE	
	0	60 min	0	60 min
14:0	0.2 $\pm$ 0.0	2.2 $\pm$ 0.1***	6.0 $\pm$ 0.3	0.8 $\pm$ 0.0***
16:0	1.6 $\pm$ 0.1	10.0 $\pm$ 0.4***	22.3 $\pm$ 1.3	8.7 $\pm$ 0.5***
18:0	1.4 $\pm$ 0.1	9.9 $\pm$ 0.4***	24.5 $\pm$ 1.2	28.8 $\pm$ 1.5
Sum Sat	3.2 $\pm$ 0.2	22.0 $\pm$ 1.2***	52.8 $\pm$ 3.3	39.0 $\pm$ 2.1*
16:1n-9	0.5 $\pm$ 0.0	3.5 $\pm$ 0.2***	7.0 $\pm$ 0.3	2.8 $\pm$ 0.2***
18:1n-9	1.7 $\pm$ 0.1	5.1 $\pm$ 0.3***	11.1 $\pm$ 0.6	6.7 $\pm$ 0.4***
20:2n-9	0.7 $\pm$ 0.0	0.0 $\pm$ 0.0	6.5 $\pm$ 0.3	1.3 $\pm$ 0.0***
Sum n-9	2.9 $\pm$ 0.2	8.6 $\pm$ 0.4***	24.6 $\pm$ 1.8	11.0 $\pm$ 0.5***
18:1n-7	0.0 $\pm$ 0.0	0.1 $\pm$ 0.0	0.3 $\pm$ 0.0	0.5 $\pm$ 0.0
Sum n-7	0.1 $\pm$ 0.0	0.1 $\pm$ 0.0	0.3 $\pm$ 0.0	0.7 $\pm$ 0.0
18:2n-6	1.1 $\pm$ 0.0	1.7 $\pm$ 0.0	1.0 $\pm$ 0.0	1.9 $\pm$ 0.1
18:3n-6	0.6 $\pm$ 0.0	2.0 $\pm$ 0.1***	9.6 $\pm$ 0.5	1.5 $\pm$ 0.0
20:2n-6	0.1 $\pm$ 0.0	1.5 $\pm$ 0.0	0.0 $\pm$ 0.0	0.0 $\pm$ 0.0
20:3n-6	0.5 $\pm$ 0.0	0.5 $\pm$ 0.0	0.6 $\pm$ 0.0	0.4 $\pm$ 0.0
20:4n-6	63.2 $\pm$ 3.4	44.9 $\pm$ 2.0**	9.2 $\pm$ 0.4	34.0 $\pm$ 1.9***
22:4n-6	16.8 $\pm$ 0.8	12.3 $\pm$ 0.7**	1.4 $\pm$ 0.0	8.8 $\pm$ 0.6***
22:5n-6	0.9 $\pm$ 0.0	0.5 $\pm$ 0.0	0.0 $\pm$ 0.0	0.4 $\pm$ 0.0
Sum n-6	83.3 $\pm$ 4.3	63.4 $\pm$ 3.9**	21.8 $\pm$ 1.5	47.1 $\pm$ 2.6***
20:5n-3	0.5 $\pm$ 0.0	0.3 $\pm$ 0.0	0.0 $\pm$ 0.0	0.2 $\pm$ 0.0
22:5n-3	5.5 $\pm$ 0.3	3.3 $\pm$ 0.2**	0.5 $\pm$ 0.0	1.2 $\pm$ 0.0
22:6n-3	4.6 $\pm$ 0.3	2.3 $\pm$ 0.1***	0.0 $\pm$ 0.0	0.7 $\pm$ 0.0
Sum n-3	10.6 $\pm$ 0.5	5.8 $\pm$ 0.4***	0.5 $\pm$ 0.0	2.1 $\pm$ 0.1**
MUFA	2.3 $\pm$ 0.1	8.7 $\pm$ 0.6***	18.4 $\pm$ 1.2	10.5 $\pm$ 0.7***
PUFA	94.5 $\pm$ 5.9	69.2 $\pm$ 4.6*	28.7 $\pm$ 1.9	50.5 $\pm$ 3.5**

<sup>a</sup>Results are mean  $\pm$  SEM ( $n = 4$ ). AAPH, 2,2'-azobis(2-amidinopropane) di-HCl; lysoPE, lysophosphatidylethanolamine; MUFA, monounsaturated FA; PPE, plasmenylethanolamine (plasmalogens); Sum Sat, sum of the saturated FA; Sum n-9, sum of n-9 FA; Sum n-7, sum of n-7 FA; Sum n-6, sum of n-6 FA; Sum n-3, sum of n-3 FA. PPE amounted to 12.5% (mol/mol) of the total phospholipids at time 0 and 3.9% after 60 min; lysoPE amounted to 1% at time 0 and 6.9% after 60 min. The Mann–Whitney test was used to compare the means at 0 and 60 min for each compound: \* $P < 0.05$ , \*\* $P < 0.01$ , \*\*\* $P < 0.001$ .



**TABLE 2**  
**Effects of AAPH on the FA Composition of Diacyl PE and PS in Platelet Extracts With and Without PPE<sup>a</sup>**

	DPE			PS		
	0	C	AT	0	C	AT
16:0	8.5 ± 0.5	10.6 ± 0.5	6.6 ± 0.3***	2.6 ± 0.1	4.6 ± 0.2	3.0 ± 0.1***
18:0	34.7 ± 1.8	35.7 ± 1.6	54.5 ± 2.9**	44.2 ± 2.1	46.4 ± 2.2	52.7 ± 2.7
20:0	1.3 ± 0.1	1.4 ± 0.1	0.0 ± 0.0	1.6 ± 0.0	1.8 ± 0.0	2.1 ± 0.1
Sum Sat	44.9 ± 2.3	48.5 ± 2.5	61.5 ± 3.1*	49.4 ± 2.3	54.2 ± 3.0	58.0 ± 3.2
16:1n-9	0.4 ± 0.0	0.9 ± 0.0	0.3 ± 0.0	0.5 ± 0.0	1.4 ± 0.0	0.5 ± 0.0
18:1n-9	6.4 ± 0.3	8.8 ± 0.4	5.4 ± 0.3***	16.1 ± 0.8	19.0 ± 0.8	16.6 ± 0.6
20:1n-9	0.4 ± 0.0	0.4 ± 0.0	0.4 ± 0.0	0.2 ± 0.0	0.3 ± 0.0	0.3 ± 0.0
20:2n-9	0.3 ± 0.0	0.6 ± 0.0	0.0 ± 0.0	0.7 ± 0.0	0.6 ± 0.0	0.5 ± 0.0
Sum n-9	7.6 ± 0.3	10.8 ± 0.4	6.1 ± 0.3***	17.5 ± 0.9	21.4 ± 1.0	17.9 ± 0.8
16:1n-7	0.1 ± 0.0	0.1 ± 0.0	0.0 ± 0.0	0.0 ± 0.0	0.1 ± 0.0	0.0 ± 0.0
18:1n-7	1.0 ± 0.0	0.9 ± 0.0	0.6 ± 0.0	0.8 ± 0.0	0.8 ± 0.0	0.6 ± 0.0
Sum n-7	1.0 ± 0.0	1.0 ± 0.0	1.1 ± 0.0	0.8 ± 0.0	0.9 ± 0.0	0.6 ± 0.0
18:2n-6	4.2 ± 0.2	5.2 ± 0.3	3.0 ± 0.1***	0.6 ± 0.0	0.9 ± 0.0	0.7 ± 0.0
18:3n-6	0.5 ± 0.0	1.0 ± 0.0	0.8 ± 0.0	0.9 ± 0.0	0.9 ± 0.0	0.7 ± 0.0
20:2n-6	0.2 ± 0.0	0.0 ± 0.0	0.1 ± 0.0	0.2 ± 0.0	0.1 ± 0.0	0.0 ± 0.0
20:3n-6	0.6 ± 0.0	0.5 ± 0.0	0.5 ± 0.0	1.2 ± 0.0	1.0 ± 0.0	1.0 ± 0.0
20:4n-6	34.6 ± 1.6	27.9 ± 1.5	22.5 ± 1.0*	26.2 ± 1.2	17.7 ± 0.9	18.4 ± 0.8
22:4n-6	3.2 ± 0.1	3.0 ± 0.1	2.9 ± 0.2	1.5 ± 0.0	1.6 ± 0.0	1.6 ± 0.0
22:5n-6	0.4 ± 0.0	0.3 ± 0.0	0.0 ± 0.0	0.3 ± 0.0	0.2 ± 0.0	0.2 ± 0.0
Sum n-6	43.8 ± 2.0	38.0 ± 1.8	29.7 ± 1.6**	30.9 ± 1.5	22.2 ± 1.1	22.6 ± 1.0
22:5n-3	1.1 ± 0.0	0.9 ± 0.0	0.8 ± 0.0	0.5 ± 0.0	0.5 ± 0.0	0.5 ± 0.0
22:6n-3	1.5 ± 0.0	0.8 ± 0.0	0.7 ± 0.0	0.9 ± 0.0	0.7 ± 0.0	0.4 ± 0.0
Sum n-3	2.7 ± 0.1	1.7 ± 0.1	1.5 ± 0.1	1.4 ± 0.0	1.2 ± 0.0	0.9 ± 0.0
MUFA	8.3 ± 0.4	11.2 ± 0.5	7.2 ± 0.3***	17.6 ± 0.8	21.7 ± 1.0	18.0 ± 0.7*
PUFA	46.8 ± 2.6	40.2 ± 2.1	31.3 ± 1.4*	33.0 ± 1.7	24.1 ± 1.1	23.9 ± 1.0
DBI	189.5 ± 10.0	161.7 ± 8.3	127.0 ± 6.9*	147.0 ± 8.1	115.1 ± 5.4	111.2 ± 5.0

<sup>a</sup>Results are mean ± SEM ( $n = 4$ ). DPE, diacyl PE; 0, extracts at time 0 before addition of AAPH; C, control extracts with plasmalogens after 60 min oxidation; AT, acid-treated extracts (without plasmalogens) after 60 min oxidation; DBI, double bond index (number of double bonds for 100 mol FA). Other abbreviations as in legend of Table 1. The Mann-Whitney test was used to compare the means of C and AT extracts: \* $P < 0.05$ , \*\* $P < 0.01$ , \*\*\* $P < 0.001$ .

were correspondingly more abundant in extracts without plasmalogens (37%) than in intact extracts (8%) ( $P < 0.05$ ).

The time courses of the relative quantities of the phospholipids and their PUFA contents during AAPH oxidation are shown in Figure 1. In intact extracts, the rate of phospholipid destruction was constant over 1 h but differed according to the class, with only 40% of the initial DPE remaining after 60 min as compared to about 75% of PS and PI and 87% of PC. In the absence of plasmalogens, all phospholipids disappeared rapidly over the first half hour but more slowly thereafter, the destruction of DPE and PI being strongest (26–29% remaining) and that of PS and PC weakest (48–50% remaining). The time courses of the relative PUFA contents of all phospholipids were similar to those of their quantities in extracts with or without plasmalogens. In the absence of plasmalogens, the addition of  $\alpha$ -tocopherol (2.8 or 11.2  $\mu\text{M}$ ) before AAPH did not alter the time courses of the quantities and compositions of the phospholipids in the incubation mixture (data not shown). At both concentrations,  $\alpha$ -tocopherol was no longer detectable after 15 min oxidation in the presence of AAPH.

## DISCUSSION

Although the oxidative degradation of plasmalogens has been accurately described (11,14,22), their role in the protection of

diacyl phospholipids remains poorly understood. The effects of plasmalogens on the oxidative decay of total tissue phospholipids (15) or of certain specific molecular species (12,16) have been reported, but comparative effects on the degradation of individual phospholipids have not yet been described. As previously observed in various systems (14–16), there was a pronounced loss of PPE following exposure of intact platelet phospholipids to AAPH, as compared to the loss of total diacyl phospholipids. Furthermore, we observed an accumulation of lysoPE-bearing PUFA groups (50.5 ± 5.2% after 60 min). This specific destruction of PPE species having a polyunsaturated fatty acyl group esterified at the *sn*-2 position is in accordance with earlier reports (22). In contrast, an accumulation of lysoPE molecular species containing only monounsaturated fatty acyl groups was observed after oxidation of bovine brain PE (14). This discrepancy could be related to different experimental conditions and/or to the use of only PE (14) instead of a phospholipid mixture (present work). On a mass basis, the results show that plasmalogens strongly protect all diacyl phospholipids (Fig. 1). In the presence of plasmalogens (nontreated extracts), all phospholipids and their PUFA disappeared at a constant rate over a period of 1 h, whereas without plasmalogens (acid-treated extracts) the degradation proceeded more rapidly. Similar kinetics have been described by others in liposomal (15) and micellar

**TABLE 3**  
**Effects of AAPH on the FA Composition of PC and PI in Platelet Extracts With and Without PPE<sup>a</sup>**

	PC			PI		
	0	C	AT	0	C	AT
16:0	31.9 ± 1.5	33.4 ± 1.4	32.7 ± 1.3	3.0 ± 0.2	9.4 ± 0.5	5.6 ± 0.3**
18:0	15.4 ± 0.7	18.4 ± 0.8	18.1 ± 0.9	43.1 ± 2.0	44.5 ± 2.1	48.8 ± 2.4
20:0	1.2 ± 0.0	1.4 ± 0.0	1.4 ± 0.0	0.5 ± 0.0	0.7 ± 0.0	1.0 ± 0.0
Sum Sat	49.0 ± 2.5	53.6 ± 2.8	52.4 ± 3.2	47.0 ± 2.1	55.9 ± 2.6	56.0 ± 2.6
16:1n-9	0.3 ± 0.0	0.4 ± 0.0	0.4 ± 0.0	0.3 ± 0.0	2.5 ± 0.1	1.0 ± 0.0
18:1n-9	17.8 ± 0.8	20.4 ± 1.1	20.6 ± 1.2	2.0 ± 0.1	4.4 ± 0.2	4.1 ± 0.2
20:1n-9	0.7 ± 0.0	0.8 ± 0.0	0.8 ± 0.0	0.2 ± 0.0	0.3 ± 0.0	0.3 ± 0.0
20:2n-9	0.1 ± 0.0	0.1 ± 0.0	0.2 ± 0.0	0.8 ± 0.0	0.6 ± 0.0	0.9 ± 0.0
Sum n-9	18.9 ± 0.9	21.7 ± 1.0	22.0 ± 1.1	3.3 ± 0.2	7.8 ± 0.5	6.2 ± 0.4
16:1n-7	0.5 ± 0.0	0.6 ± 0.0	0.5 ± 0.0	0.0 ± 0.0	0.1 ± 0.0	0.1 ± 0.0
18:1n-7	2.0 ± 0.1	2.3 ± 0.1	2.2 ± 0.1	0.5 ± 0.0	0.6 ± 0.0	0.8 ± 0.0
Sum n-7	2.6 ± 0.1	3.0 ± 0.1	2.8 ± 0.1	0.5 ± 0.0	0.8 ± 0.0	0.9 ± 0.0
18:2n-6	9.1 ± 0.4	8.6 ± 0.4	8.7 ± 0.4	0.5 ± 0.0	1.1 ± 0.0	1.2 ± 0.0
18:3n-6	0.2 ± 0.0	0.2 ± 0.0	0.2 ± 0.0	1.3 ± 0.0	1.3 ± 0.0	1.3 ± 0.0
20:2n-6	0.6 ± 0.0	0.5 ± 0.0	0.5 ± 0.0	0.0 ± 0.0	0.0 ± 0.0	0.0 ± 0.0
20:3n-6	1.4 ± 0.1	1.1 ± 0.0	1.2 ± 0.0	0.3 ± 0.0	0.3 ± 0.0	0.4 ± 0.0
20:4n-6	15.8 ± 0.6	9.6 ± 0.5	10.4 ± 0.5	46.5 ± 2.3	31.6 ± 1.7	32.6 ± 1.9
22:4n-6	1.2 ± 0.0	0.9 ± 0.0	0.9 ± 0.0	0.4 ± 0.0	1.0 ± 0.0	1.1 ± 0.0
22:5n-6	0.2 ± 0.0	0.1 ± 0.0	0.1 ± 0.0	0.0 ± 0.0	0.0 ± 0.0	0.0 ± 0.0
Sum n-6	28.3 ± 1.4	21.1 ± 1.0	22.1 ± 1.3	49.0 ± 2.4	35.4 ± 1.9	36.5 ± 2.6
22:5n-3	0.4 ± 0.0	0.3 ± 0.0	0.3 ± 0.0	0.2 ± 0.0	0.2 ± 0.0	0.3 ± 0.0
22:6n-3	0.6 ± 0.0	0.2 ± 0.0	0.4 ± 0.0	0.1 ± 0.0	0.0 ± 0.0	0.1 ± 0.0
Sum n-3	1.2 ± 0.1	0.6 ± 0.0	0.8 ± 0.0	0.2 ± 0.0	0.2 ± 0.0	0.4 ± 0.0
MUFA	21.4 ± 1.0	24.6 ± 1.2	24.6 ± 1.3	3.0 ± 0.1	7.9 ± 0.4	6.2 ± 0.4
PUFA	29.6 ± 1.2	21.8 ± 0.9	23.0 ± 1.1	50.0 ± 2.8	36.2 ± 2.2	37.8 ± 2.4
DBI	120.8 ± 6.2	92.7 ± 4.8	97.4 ± 5.3	199.2 ± 8.6	147.9 ± 9.2	152.2 ± 10.1

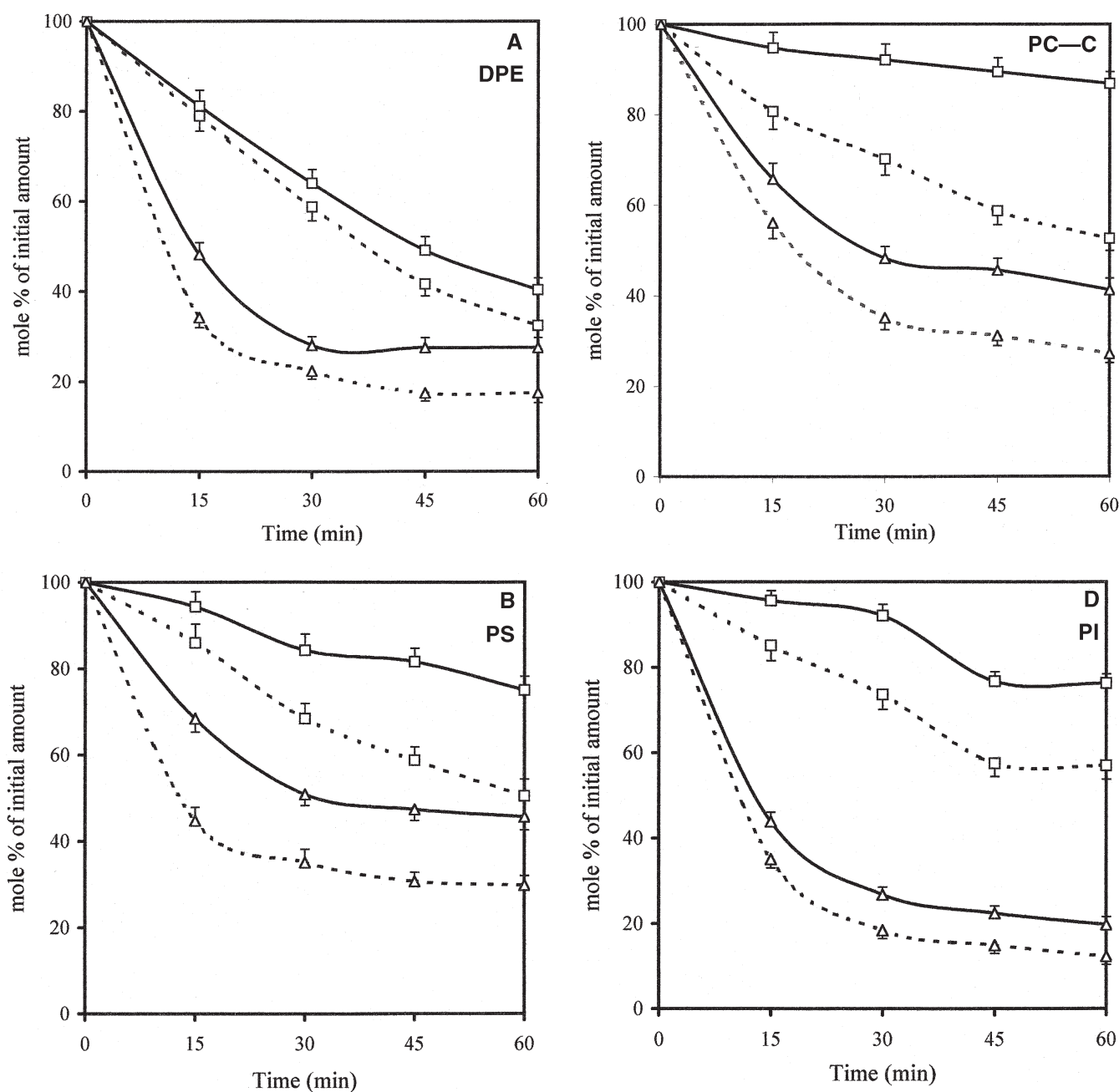
<sup>a</sup>Results are mean ± SEM ( $n = 4$ ). For abbreviations see Tables 1 and 2. The Mann-Whitney test was used to compare the means of C and AT extracts: \*\* $P < 0.01$ .

systems (16). Comparing the degradation rates of the different diacyl phospholipids and their PUFA over the first 30 min, we found that the protective effect of plasmalogens increased in the order DPE < PS < PC < PI. Thus, the degradation after 30 min oxidation decreased in the presence of plasmalogens by  $48 \pm 3$ ,  $66 \pm 4$ ,  $85 \pm 4$ , and  $88 \pm 5\%$  for DPE, PS, PC, and PI, respectively. Among DPE, PS, and PC, the efficiency of protection was inversely related to the double bond index (respectively,  $189 \pm 10$ ,  $147 \pm 8$ , and  $121 \pm 6$ ) or PUFA content (respectively,  $46.8 \pm 2.6$ ,  $33.0 \pm 1.7$ , and  $29.6 \pm 1.2\%$ ), the most unsaturated phospholipid (DPE) being least efficiently protected by plasmalogens. Unexpectedly, although PI is still more unsaturated than DPE, it appeared to be the most strongly protected of the diacyl phospholipids (Fig. 1).

These results demonstrate that plasmalogens participate actively in the inhibition of PUFA peroxidation and concomitantly in phospholipid degradation, the protection afforded depending on both the acyl chain unsaturation and the nature of the polar head. Interestingly, in the absence of plasmalogens the degradation rates of the four glycerophospholipids increased in the order PS < PC < DPE < PI, which is not the order of their increasing unsaturation (PC < PS < DPE < PI). Hence, if unsaturation is important for peroxidative susceptibility (23), there is also an obvious influence of the polar head group among the diacyl glycerophospholipids. Moreover, the least unsaturated phospholipid (SM) was unaffected by free

radical oxidation in our experimental system, even in the absence of plasmalogens (data not shown).

In natural membranes,  $\alpha$ -tocopherol is currently considered to be the major lipid-soluble antioxidant despite its low concentration, which approximates 1 mole for 220 moles of phospholipids, as for instance in platelets (19). The relative potency of  $\alpha$ -tocopherol as compared to plasmalogens as a protective agent against phospholipid degradation induced by peroxy radicals was evaluated by adding  $\alpha$ -tocopherol before AAPH to membrane extracts without plasmalogens. We observed that the rates of phospholipid degradation remained unchanged when using molar ratios of phospholipids to  $\alpha$ -tocopherol similar to that found in platelet membranes (214:1) or up to about fourfold lower (54:1). These unexpected results are probably at least partly due to total consumption of the added  $\alpha$ -tocopherol after 15 min oxidation. Although a significant decrease in degradation rate was previously reported (16), these authors used a higher  $\alpha$ -tocopherol amount (4:1 ratio of phospholipid to  $\alpha$ -tocopherol) and a lower AAPH concentration (2 mM) than in our experiments. Thus, in our conditions, plasmalogens appear to contribute more effectively than  $\alpha$ -tocopherol to the resistance of the unsaturated acyl chains of phospholipids to peroxidation. In spite of a scavenging activity estimated to be similar to (10) or fourfold higher (12) than that of plasmalogens, in platelet membranes only 1 mole of  $\alpha$ -tocopherol is able to compete with about 30 moles of plasmalogens



**FIG. 1.** 2,2'-Azobis(2-amidinopropane) di-HCl-mediated degradation of platelet phospholipids in the presence or absence of plasmalogens. Mean values ( $\pm$  SEM) in four independent experiments where the mass values obtained at time 0 were set to 100%. (A) diacyl phosphatidylethanolamine, (DPE) (B), PS; (C), PC; (D), PI. Relative mass of a given phospholipid in control extracts (with plasmalogens) ( $\square$ ), and in acid-treated extracts (without plasmalogens) ( $\triangle$ ); relative PUFA content of a given phospholipid in control extracts: ( $\square$ ), and in acid-treated extracts (without plasmalogens) ( $\triangle$ ).

for interaction with peroxy radicals. Any extrapolation of the present findings to biological membranes will nevertheless require further work to clarify the mechanisms responsible for the differential protection of phospholipids by plasmalogens.

## REFERENCES

- Iuliano, L., Colavita, A.R., Leo, R., Pratico, D., and Violi, F. (1997) Oxygen Free Radicals and Platelet Activation, *Free Rad. Biol. Med.* 22, 999–1006.
- Joseph, M. (1995) The Generation of Free Radicals by Blood Platelets, in *Handbook of Immunopharmacology* (Joseph, M., ed.), pp. 209–225, Academic Press, London.
- Brosche, T., and Platt, D. (1998) The Biological Significance of Plasmalogens in Defense Against Oxidative Damage, *Exp. Gerontol.* 33, 363–369.
- Bolli, R., Patel, B.S., Jeroudi, M.O., Lai, E.K., and McCay, P.B. (1988) Demonstration of Free Radical Generation in "Stunned" Myocardium of Intact Dogs with the Use of the Spin Trap  $\alpha$ -Phenyl *N-tert*-Butyl Nitron, *J. Clin. Invest.* 82, 476–485.
- Yavin, E., and Gatt, S. (1972) Oxygen-Dependent Cleavage of the Vinyl-Ether Linkage of Plasmalogens 1. Cleavage by Rat-Brain Supernatant, *Eur. J. Biochem.* 25, 431–436.

6. Garg, M.L., and Haerdi, J.C. (1993) The Biosynthesis and Functions of Plasmalogens, *J. Clin. Biochem. Nutr.* 14, 71–82.
7. Lee, T.C. (1998) Biosynthesis and Possible Biological Functions of Plasmalogens, *Biochim. Biophys. Acta* 1394, 129–145.
8. Morand, O.H., Zoeller, R.A., and Raetz, C.R.H. (1988) Disappearance of Plasmalogens from Membranes of Animal Cells Subjected to Photosensitized Oxidation, *J. Biol. Chem.* 263, 11597–11606.
9. Zoeller, R.A., Lake, A.C., Nagan, N., Gaposchkin, D.P., Legner, M.A., and Lieberthal, W. (1999) Plasmalogens as Endogenous Antioxidants: Somatic Cell Mutants Reveal the Importance of the Vinyl Ether, *Biochem. J.* 338, 769–776.
10. Engelmann, B., Brautigam, C., and Thiery, J. (1994) Plasmalogen Phospholipids as Potential Protectors Against Lipid Peroxidation of Low Density Lipoproteins, *Biochem. Biophys. Res. Comm.* 204, 1235–1242.
11. Felde, R., and Spiteller, G. (1995) Plasmalogen Oxidation in Human Serum Lipoproteins, *Chem. Phys. Lipids* 76, 259–267.
12. Hahnel, D., Beyer, K., and Engelmann, B. (1999) Inhibition of Peroxyl Radical-Mediated Lipid Oxidation by Plasmalogen Phospholipids and  $\alpha$ -Tocopherol, *Free Rad. Biol. Med.* 27, 1087–1094.
13. Zommarà, M., Tachibana, N., Mitsui, K., Nakatani, N., Sakono, M., Ikeda, I., and Imaizumi, K. (1995) Inhibitory Effect of Ethanolamine Plasmalogen on Iron- and Copper-Dependent Lipid Peroxidation, *Free Rad. Biol. Med.* 18, 599–602.
14. Khaselev, N., and Murphy, R.C. (1999) Susceptibility of Plasmalogen Glycerophosphoethanolamine Lipids Containing Arachidonate to Oxidative Degradation, *Free Rad. Biol. Med.* 26, 275–284.
15. Sindelar, P.J., Guan, Z., Dallner, G., and Ernster, L. (1999) The Protective Role of Plasmalogens in Iron-Induced Lipid Peroxidation, *Free Rad. Biol. Med.* 26, 318–324.
16. Reiss, D., Beyer, K., and Engelmann, B. (1997) Delayed Oxidative Degradation of Polyunsaturated Diacyl Phospholipids in the Presence of Plasmalogen Phospholipids *in vitro*, *Biochem. J.* 323, 807–814.
17. Takamura, H., Tanaka, K.I., Matsuura, T., and Kito, M. (1989) Ether Phospholipid Molecular Species in Human Platelets, *J. Biochem.* 105, 168–172.
18. Cazenave, J.P., Hemmendinger, S., Beretz, A., Sutter-Bay, A., and Launay, J. (1983) L'agrégation plaquettaire: Outil d'investigation clinique et étude pharmacologique. Méthodologie, *Ann. Biol. Clin.* 41, 167–179.
19. Leray, C., Andriamampandry, M., Gutbier, G., Cavadenti, J., Klein-Soyer, C., Gachet, C., and Cazenave, J.P. (1997) Quantitative Analysis of Vitamin E, Cholesterol and Phospholipid Fatty Acids in a Single Aliquot of Human Platelets and Cultured Endothelial Cells, *J. Chromatogr.* 696, 33–42.
20. Pugh, E.L., Kates, M., and Hanahan, D.J. (1977) Characterization of the Alkyl Ether Species of Phosphatidylcholine in Bovine Heart, *J. Lipid Res.* 18, 710–716.
21. Leray, C., Pelletier, X., Hemmendinger, S., and Cazenave, J.P. (1987) Thin-Layer Chromatography of Human Platelet Phospholipids with Fatty Acid Analysis, *J. Chromatogr.* 420, 411–416.
22. Khaselev, N., and Murphy, R.C. (2000) Structural Characterization of Oxidized Phospholipid Products Derived from Arachidonate-Containing Plasmalogen Glycerophosphocholine, *J. Lipid Res.* 41, 564–572.
23. Wang, J.Y., Shibata, T., Ueki, T., and Miyazawa, T. (1995) Susceptibility for Hydroperoxide Formation of Phosphatidylcholine and Phosphatidylethanolamine in Liposomes, *J. Nutr. Sci. Vitaminol. (Tokyo)* 41, 273–280.

[Received October 11, 2001, and in revised form January 24, 2002; revision accepted January 29, 2002]



# Lung Lipid Composition in Zinc-Deficient Rats

N.N. Gomez<sup>a</sup>, M.S. Ojeda<sup>a</sup>, and M.S. Gimenez<sup>b,\*</sup>

<sup>a</sup>Department of Biochemistry and Biological Sciences, Faculty of Chemistry, Biochemistry and Pharmacy, National University of San Luis, Argentina, and <sup>b</sup>Member of the Career of Scientific Investigations, Consejo Nacional de Investigaciones Científicas y Técnicas (CONICET), Argentina

**ABSTRACT:** There have been a limited number of studies investigating surfactant lipid changes in lung with trace elements. The present investigation was designed to examine the effect of moderate zinc deficiency on the lipid metabolism in rat lung. We also evaluated whether zinc deficiency, which is a widespread problem, could play a role in adult respiratory distress syndrome (ARDS). For that purpose, adult male Wistar rats were fed two diets differing in zinc concentration. The rats were divided into two groups. One group was fed a zinc-deficient diet containing 3 mg Zn/kg, and the other group received a zinc-adequate control diet with 30 mg Zn/kg according to AIN 93-M. After 2 mon of treatment, we observed that in the zinc-deficient group (i) total lipids, phospholipids, and cholesterol increased whereas TG decreased in whole lung; (ii) phospholipid (PC) concentration increased in lamellar bodies and alveolar macrophages and decreased in extracellular surfactant but did not change in microsomes; (iii) protein concentration decreased in whole lung, extracellular surfactant, lamellar bodies, and macrophages; (iv) the incorporation of [Me-<sup>14</sup>C]choline into PC (phospholipids) of lung slices increased; and (v) the activity of CTP/phosphocholine cytidyltransferase bound to the microsomes increased in the lung. These results suggest that the lipid concentration in the lung (especially the phospholipids) is modified directly or indirectly by a zinc-deficient diet. In a zinc-deficient diet, the lung changes the pattern of PC for an adaptive or recovery stage. Therefore, zinc deficiency implications are important for the design of therapies and public health interventions involving targeted zinc supplementation for high-risk groups or groups with certain diseases, such as ARDS.

Paper no. L8745 in *Lipids* 37, 291–296 (March 2002).

Serious surfactant deficiency may compromise the structural and functional integrity of the alveoli and become life threatening. An abnormal surfactant also appears to be an important characteristic of adult respiratory distress syndrome (ARDS) (1). A major early hallmark of ARDS is damage to the alveoli-capillary membrane with a concomitant increase in permeability to high-molecular-weight solutes. Surfactant changes are thought to play an important role in the pathogenesis of this condition (1,2).

Zinc deficiency (ZD) produces profound alterations in the metabolism of lipids (3,4). The effects of ZD not only depend on the type of dietary fat but also show organ-specific variations and influence the lipid metabolism in a variety of ways (3,5). Zinc-deficient rats exhibit elevated activities of lipogenic

enzymes in liver as well as elevated serum lipid concentrations (4). The effects of ZD on the FA composition of phospholipids are more pronounced in liver and plasma than in heart, testes, erythrocyte membranes, and mesentery of the small intestine (3). This might be due to the fact that the turnover rates of phospholipids in liver are higher than in other tissues (3). In ZD both pathways of PC biosynthesis in liver microsomes were significantly increased (5)

The alveolar surfaces of the lungs are lined with a lipid-protein complex called pulmonary surfactant. This material consists of approximately 90% lipids and 5–10% proteins. The surfactant lipids spread as a monolayer on the air-liquid interface.

PC is quantitatively the major component of surfactant and is undoubtedly its major surface-active component (3). *De novo* PC synthesis by type II epithelial cells from adult rats proceeds mainly *via* the CDP choline pathway (6). Dipalmitoylphosphatidylcholine may be synthesized directly *via* this pathway or by the remodeling of unsaturated PC species (7). Accumulating evidence is available from studies on a number of different cell types (6), where the enzyme cholinephosphate cytidyltransferase (CYT) catalyzes the rate-limiting step in the conversion of choline into PC. CYT (EC 2.7.7.15) is a regulatory enzyme in the synthesis of pulmonary surfactant PC *via* the Kennedy pathway (8). When CYT activity is assayed in different subcellular fractions, its greatest increase, as a function of development, is found in microsomes (9). Zimmermann *et al.* (10) speculate about the possibility that either a subcellular translocation of CYT from cytosol to microsomes or an increase in CYT gene expression is responsible for the developmental increase of *de novo* PC synthesis (10).

The lecithin/sphingomyelin ratio in amniotic fluid is used clinically as a marker of pulmonary maturation of the fetal lung and its production of surfactant (11). Zinc-deficient rats did not show an increase even at day 21 of gestation, suggesting that ZD interferes with surfactant biosynthesis in the fetal lung (11). Zinc may therefore have important implications for asthma and other inflammatory diseases, where the physical barrier is vulnerable and compromised (12).

The aim of the present study was to determine if ZD alters the metabolism of lipids in lung, in particular the synthesis of PC, the main component of the pulmonary surfactant. We also investigated whether ZD plays a role in ARDS.

## MATERIALS AND METHODS

**Chemicals and radioisotopes.** All reagents were of analytical grade. Lipid standards and protein were acquired from Sigma Chemical Co. (St. Louis, MO). Serum total lipids, cholesterol, and TG were determined by enzymatic methods using kits

\*To whom correspondence should be addressed at Area Química Biológica, Universidad Nacional de San Luis, Chacabuco y Pedernera, 5700 San Luis, Argentina. E-mail: mgimenez@unsl.edu.ar

Abbreviations: ARDS, adult respiratory distress syndrome; Co, control; CYT, cytidyltransferase; LPC, lysophosphatidylcholine; SPH, sphingomyelin; ZD, zinc deficiency.

from Boehringer Mannheim Diagnostics (Indianapolis, IN). [Methyl- $^{14}\text{C}$ ]phosphorylcholine (specific activity, 50 mCi/mmol) and [methyl- $^{14}\text{C}$ ]choline chloride (specific activity, 60 mCi/mol) were purchased from Dupont, New England Nuclear (Boston, MA).

**Animals and diets.** Adult male Wistar rats with an average body weight of  $200 \pm 10$  g were divided into two groups; one of them was fed a zinc-deficient diet containing 3 mg Zn/kg and the other a zinc-adequate control diet supplemented with 30 mg Zn/kg, added as  $\text{ZnCl}_2$ . All the other components of the diet remained constant. The diets were fortified with recommended amounts of vitamins and minerals according to AIN 93-M (13). The composition of the basal maintenance (semisynthetic) diet was as follows (g/kg diet): cornstarch, 465.692; casein ( $\geq 85\%$  protein), 140.000; dextrinized cornstarch, 155.000; sucrose, 100.000; fiber/cellulose, 50.000; soybean oil (containing liposoluble vitamins), 40.000; mineral mix (AIN-93M-MX), 35.000; vitamin mix (AIN-93-VX), 10.000; L-cystine, 1.800; ascorbic acid, 0.008; choline bitartrate (41% choline), 2.500. This diet had 1 mg Zn/kg dry matter. In the ZD diet, zinc was not incorporated into the mineral mix. All dietary ingredients were obtained in the purest form known with regard to zinc contamination, and newly obtained ingredients were monitored for zinc concentration.

Rats were housed individually in a controlled environment with a light-dark cycle of 14/10 h (lights on from 0600–2000) and at a temperature of 22 to 24°C. Fresh diets were given and leftover food discarded on a daily basis (20 g diet was adequate to ensure *ad libitum* feeding). Care and treatment of rats followed recommended guidelines (14). Body weights were recorded weekly.

At the end of the experimental period of 2 mon, 12 h after the last feeding all animals were sacrificed. Rats were anesthetized intraperitoneally with sodium pentobarbital (50 mg/kg, ip). The respiration of the rats was normal at all times prior to sacrifice. Blood for hematological measurements was collected into EDTA-coated vials. Blood for determination of serum zinc was collected into washed tubes, and the concentration of serum zinc was measured directly by aspirating a dilute solution (1:5, vol/vol) into the atomic absorption spectrophotometer (see below). The lungs were quickly removed, lavaged with ice-cold 0.9% saline solution, and weighed. Serum and tissue samples were stored at  $-80^\circ\text{C}$  until they were analyzed.

**Zinc analyses.** Aliquots of the diet, liver, and lung were collected without allowing any contact with metal. Each sample was wet-ashed with 16 N nitric acid as described by Clegg *et al.* (15). The zinc concentrations of the pretreated samples and the serum were quantified with a pyrolytically coated graphite tube from an atomic absorption spectrophotometer (model 5100, HGA-600 Graphite Furnace; PerkinElmer) fitted with an electrothermal atomizer and a hollow cathode lamp (PerkinElmer). A linear calibration curve was created using certified standard NIST solutions. All specimens were diluted with twice-distilled and deionized water and analyzed in duplicate. Prior to digesting the sample, different amounts of standard solution of each element were added. The recovery rate was between 98 and 99.2% for different elements.

**Isolation of extracellular pulmonary surfactant and macrophages.** In another experiment, the tracheas of anesthetized rats were cannulated and the lungs were filled with 2.5 mL ice-cold 0.15 M NaCl. Lavages containing the extracellular surfactant were then collected. This procedure was repeated nine times. The combined lavages were centrifuged at  $4^\circ\text{C}$  and  $580 \times g$  for 10 min to sediment macrophages. The resulting supernatant was centrifuged at  $198,000 \times g$  for 30 min in a Beckman ultracentrifuge LS 65 B, 65 Ty rotor to obtain the surfactant pellet (16).

**Isolation of lamellar bodies and microsomes.** After extraction of the extracellular pulmonary surfactant fraction, the lavaged lungs were used to isolate lamellar bodies and microsomes (16).

**Lipid analyses.** Lipids were extracted from total lung tissue, microsomes, lamellar bodies, extracellular surfactant, and macrophages. Total lipids were determined by dry weight. The lipids were resuspended in a hexane/isopropanol mixture (3:2, vol/vol) containing BHT as antioxidant (17). Aliquots were taken for determining phospholipids and measuring phosphorus (18) and total cholesterol (19). Other parts of the extracts were used for the separation of the different lipids on TLC plates coated with silica gel G (Merck, Darmstadt, Germany) using hexane/diethyl ether/acetic acid (80:20:1, by vol) as solvent. The lipids were detected by exposing the plates to iodine vapors. They were scraped off and used directly for determination of phospholipids (18), TG (20), and free and esterified cholesterol (19).

**Analysis of phospholipid composition.** Phospholipids were separated into component classes by TLC, using silica gel H plates and chloroform/methanol/water (65:25:4, by vol) as solvent (21). The individual phospholipids were identified and recovered as described previously and were quantified (18). The position of the phospholipids was determined using the respective standards. The results were expressed as the percentage of total phospholipid phosphorus.

**Incorporation of [Me- $^{14}\text{C}$ ]choline in lung slices.** The rate of PC synthesis in lung slices was determined by the rate of incorporation of [Me- $^{14}\text{C}$ ]choline. The lung slices (100 mg) were rapidly cut and placed into individual metabolic flasks containing DMEM (pH 7.4; GIBCO BRL). The flasks were continuously flushed with 95%  $\text{O}_2$ /5%  $\text{CO}_2$ . After the slices were preincubated for 10 min at  $37^\circ\text{C}$ , 1  $\mu\text{Ci}$ /assay [Me- $^{14}\text{C}$ ]choline was added to each flask. The incubation was stopped after 1 h by dilution with medium. After the incubation period, tissue slices were removed from the medium and the tissues were washed with ice-cold 0.9% NaCl. The tissues were homogenized, and the lipids were extracted and analyzed as described above.

**CTP:cholinephosphate CYT assay.** Lungs of control and zinc-deficient rats were used for the separation of cytosol and microsomes for enzymatic determination (22). Assay mixtures contained 20 mM Tris/succinate pH 7.8, 6 mM  $\text{MgCl}_2$ , 8 mM CTP, and 4 mM [Me- $^{14}\text{C}$ ]phosphorylcholine (specific radioactivity 1  $\mu\text{Ci}$ /assay). The reaction was started by addition of enzyme (100  $\mu\text{g}$  protein), and the assay mixture was incubated for 30 min at  $37^\circ\text{C}$ . The reaction was stopped with TCA (0.5%), and protein was removed by centrifugation ( $1000 \times g$  for 10 min). A 50  $\mu\text{L}$  sample was taken from the supernatant,

mixed with 2 nmol of unlabeled phosphorylcholine used as a carrier, and subjected to TLC on precoated silica gel H (Merck) with NaCl 0.5%/methanol/concentrated ammonia (50:50:5, by vol) used as developing solvent.

**Protein.** Protein content was determined by the method of Lowry *et al.* (23) with BSA as a standard.

**Enzyme markers.** To determine if the lamellar bodies were contaminated with microsomal, mitochondrial, or cell membranes, the activities of NADPH cytochrome c reductase (24), succinate dehydrogenase (25), and 5'-nucleotidase (26), respectively, were measured.

**Statistical analysis.** Values are expressed as mean  $\pm$  SD. Significant differences were considered at  $P < 0.05$ , as determined by Student's *t*-test.

## RESULTS

**Weight gain and zinc status of the rats.** After 8 wk of treatment, body weight gain was lower in zinc-deficient rats in comparison to controls, as previously reported by (3,4,27). The lung weight of zinc-deficient rats was also significantly lower ( $P < 0.001$ ) compared to the control (Co) (Table 1). Serum, liver, and lung zinc concentrations were significantly lower in rats fed the zinc-deficient diet compared with those of Co group (Table 2). Likewise, we found that glucose was influenced by ZD, and there was an increased level of it in plasma ( $P < 0.01$ ) (28). Other parameters, such as albumin, did not change, but globulin content fell with the zinc-deficient diet (Table 1). This was coincident with a previous report (29).

**Total lipids, cholesterol, and TG in serum and whole lung.** Total lipids and cholesterol increased and TG were not modified in the serum from the zinc-deficient rats after 2 mon of treatment. Total lipids and total free and esterified cholesterol increased, but TG decreased in whole lung of the zinc-deficient rats (Table 2).

**Phospholipid concentration in whole lung, intracellular, and extracellular compartments.** The phospholipid concentration increased in whole lung and lamellar bodies, whereas in extracellular surfactant and macrophages it decreased, but in microsomes it was not modified in the zinc-deficient group compared to the control group (Table 3).

On a percentage basis, the phospholipid composition in whole lung and other particles studied was modified after 2 mon of the zinc-deficient diet, compared to the control. In whole lung, PC and PS + PI increased; and lysophosphatidylcholine (LPC) and sphingomyelin (SPH) decreased. PE and phosphatidylglycerol (PG) did not change (Table 4). In microsomes, PS + PI increased; LPC and PE decreased; and SPH, PC, and PG did not change. In the lamellar bodies PC and PS + PI increased and LPC, SPH, PE, and PG decreased. In extracellular surfactant PS + PI increased and LPC, PC, and PE decreased, whereas SPH and PG did not change. In alveolar macrophages LPC, SPH, and PC did not change, but PS + PI, PE, and PG decreased (Table 4).

**Incorporation of [ $Me$ - $^{14}C$ ]choline into phospholipids of lung slices.** *De novo* synthesis of PC in the adult type II cell

**TABLE 1**  
**Body and Lung Weights and Serum Parameters of Male Rats<sup>a</sup>**

	Control	Zinc-deficient
Gain of body weight (g)	140 $\pm$ 24	87 $\pm$ 25 <sup>d</sup>
Lung weight (g)	1.9 $\pm$ 0.2	1.4 $\pm$ 0.1 <sup>d</sup>
Serum		
Glucose (mg/dL)	85.3 $\pm$ 5	111 $\pm$ 2 <sup>c</sup>
Total lipids (mg/dL)	350 $\pm$ 70	430 $\pm$ 160
Cholesterol (mg/dL)	49.4 $\pm$ 1.4	61.2 $\pm$ 2.6 <sup>c</sup>
TG (mg/dL)	91.1 $\pm$ 3	100 $\pm$ 9.8
Albumin (g/dL)	2.7 $\pm$ 0.02	2.9 $\pm$ 0.05
Globulin (g/dL)	4.9 $\pm$ 0.2	4.0 $\pm$ 0.5 <sup>a</sup>

<sup>a</sup>Results given as mean  $\pm$  SD;  $n = 12$  for each case. Across a row, values with different roman superscript letters indicate significant differences by analysis of Student's test: <sup>b</sup> $P < 0.05$ , <sup>c</sup> $P < 0.01$ , <sup>d</sup> $P < 0.001$ .

proceeds mainly *via* the CDP:choline pathway. The incorporation of choline in PC and SPH was modified by the zinc-deficient diet in relation to what was observed with the control diet. The incorporation of [ $Me$ - $^{14}C$ ]choline increased in PC in the zinc-deficient group compared to the control group. As well, the incorporation was significantly lower in SPH of the zinc-deficient group (Fig. 1).

**Activity of CTP:phosphocholine CYT.** The enzyme activity that takes place in the endoplasmic reticulum membranes increased in the lung of rats fed the zinc-deficient diet compared with those fed the control diet (Table 3).

**Protein concentration in whole lung, intracellular and extracellular compartments.** Proteins in whole lung, lamellar bodies, extracellular surfactant, and macrophages decreased in the zinc-deficient group, but in microsomes the proteins were similar in both cases (Table 3).

## DISCUSSION

The present study was undertaken to investigate the effect of moderate ZD in the adult rat lung. We also evaluated whether

**TABLE 2**  
**Lipids from Whole Lung and Macrophages and Zinc Concentrations in Serum, Lung, and Liver of Male Rat<sup>a</sup>**

	Control	Zinc-deficient
Whole lung ( $\mu$ g/g)		
Total lipids	6210 $\pm$ 560	7550 $\pm$ 107 <sup>a</sup>
Total cholesterol	2337 $\pm$ 349	3550 $\pm$ 74 <sup>a</sup>
Free cholesterol	1853 $\pm$ 462	2595 $\pm$ 505 <sup>a</sup>
Esterified cholesterol	444 $\pm$ 27.9	949 $\pm$ 23.8 <sup>b</sup>
TG	201 $\pm$ 8.7	96 $\pm$ 10 <sup>b</sup>
Macrophages ( $\mu$ g/g)		
Total cholesterol	65.2 $\pm$ 8.8	91.1 $\pm$ 9.4 <sup>b</sup>
Free cholesterol	23.1 $\pm$ 4	23.7 $\pm$ 3.6
Esterified cholesterol	41.1 $\pm$ 4.3	64.7 $\pm$ 7.8 <sup>b</sup>
Zinc		
Serum ( $\mu$ mol/L)	21 $\pm$ 1.9	16 $\pm$ 1.4 <sup>b</sup>
Lung ( $\mu$ g/g)	25.4 $\pm$ 2.8	16.4 $\pm$ 2.4 <sup>b</sup>
Liver ( $\mu$ g/g)	36.0 $\pm$ 3.6	24.0 $\pm$ 3.2 <sup>b</sup>

<sup>a</sup>Results given as mean  $\pm$  SD;  $n = 12$  for each case. Lung and liver zinc are expressed as  $\mu$ g/g wet tissue. Across a row, values with different roman superscript letters indicate significant differences by analysis of Student's test: <sup>a</sup> $P < 0.01$ , <sup>b</sup> $P < 0.001$ .



**TABLE 3**  
**Phospholipids, Proteins, and Activity of CTP-Phosphocholine Cytidylyltransferase of Lung<sup>a</sup>**

	Control	Zinc-deficient
Phospholipids (mg/g lung)		
Whole lung	25.4 ± 0.16	37.4 ± 1.2 <sup>b</sup>
Microsomes	3.6 ± 0.2	3.8 ± 0.5
Lamellar bodies	13 ± 2	22.9 ± 1.9 <sup>c</sup>
Surfactant	7.3 ± 0.9	4.8 ± 0.7 <sup>c</sup>
Macrophages	3.2 ± 0.7	2.1 ± 0.5 <sup>a</sup>
Proteins (mg/g lung)		
Whole lung	88.8 ± 10.2	59.7 ± 15 <sup>c</sup>
Microsomes	5.2 ± 1.3	5.0 ± 0.2
Lamellar bodies	7.9 ± 1	4.5 ± 0.3 <sup>a</sup>
Surfactant	4.8 ± 1	1.3 ± 0.6 <sup>b</sup>
Macrophages	1.5 ± 0.1	1.1 ± 0.01 <sup>b</sup>
CYT (dpm/min/mg prot.)		
Microsomal fraction	1572 ± 72	3999 ± 584 <sup>c</sup>

<sup>a</sup>Results given as mean ± SD; *n* = 10 for each case. Values with different roman superscript letters indicate significant difference of <sup>a</sup>*P* < 0.05, <sup>b</sup>*P* < 0.01, <sup>c</sup>*P* < 0.001. CYT, cytidylyltransferase.

ZD plays a role in ARDS. For this purpose, a rat model that permits the induction of moderate ZD was used. This model has the advantage that it permits long-term studies and is physiologically more relevant (3,4,30).

Suboptimal intake of dietary zinc is one of the most common nutritional problems worldwide and has been shown to exist in low-income groups, institutionalized patients, pregnant women and teenagers, and in elderly Americans (31). In our experiment, the low gain of body weight observed in the zinc-deficient group compared to the control group confirms previous results (3,4,27,29). The lower lung weight of the zinc-deficient group compared to the control group is similar to that observed in other organs, such as testes (27). The amount of food consumed by rats was similar in both diets (Table 1). This model typically consumes adequate quantities of food (1,30). In our experimental design, clinical signs such as dermatitis and alopecia were not observed.

Besides some studies of liver zinc uptake (32), very little is known about the utilization of zinc by peripheral tissues (31).

Some tissues lose zinc in order to support other tissues. For example, the zinc concentration in muscle is conserved in zinc-deficient animals, whereas zinc concentrations in bone, liver, and plasma drop (33). Our results show that in plasma, liver, and lung, the contents of zinc decreased in the zinc-deficient rats (Table 2). A reduction in plasma zinc reflects a loss of zinc from bone and liver and an increased risk for development of metabolic and clinical signs of ZD (33).

The amount of globulin (a blood plasma protein) decreased in the zinc-deficient group (Table 1). B-Lymphocyte development and antibody production, particularly immunoglobulin G, is compromised by the zinc-deficient diet (34).

Blood glucose levels increased in the zinc-deficient rats (*P* < 0.01). In ZD, the level of insulin mRNA did not change, suggesting either that translation was impaired or, more likely, that the degradation of insulin was enhanced. Another possible explanation could be an inhibition of insulin release (35).

Alveolar type II cells synthesize lipids and proteins of surfactant that are stored prior to secretion in intracellular organelles called lamellar bodies (36). The results obtained in different fractions of lungs show that ZD after 2 mon of treatment could cause changes in the synthesis, secretion, and clearance of phospholipids in surfactant.

Cholesterol is the major neutral lipid component of extracellular surfactant, and it is accepted that most cholesterol in the lung is taken up from circulating LDL or HDL (37). The increment of cholesterol in serum could be a cause of the increased cholesterol concentration observed in whole lung and macrophages in the zinc-deficient group compared to the control group. Studies utilizing isolated perfused rat lung demonstrated the uptake of lipoproteins from the perfusion medium (38).

The decreased TG concentrations observed in whole lung of the zinc-deficient group could be a consequence of a higher utilization of these as a precursor for the synthesis of phospholipids. In our laboratory we have found that the synthesis of TG decreased in lung and liver of castrated rat while the synthesis of phospholipids increased (39,40). Zinc is also known to play a major role in gene expression and protein

**TABLE 4**  
**Phospholipid Composition of Whole Lung and Subcellular Particles of Male Rat<sup>a</sup>**

	LPC	SPH	PC	PS + PI	PE	PG
Whole lung						
Control	7.2 ± 2	14.1 ± 0.7	64.5 ± 1.7	6.5 ± 0.3	2.7 ± 0.4	4.7 ± 1.0
Zinc-deficient	3.6 ± 0.2 <sup>b</sup>	10.5 ± 1.4 <sup>b</sup>	70.1 ± 2 <sup>c</sup>	10 ± 0.9 <sup>c</sup>	2.2 ± 0.9	3.6 ± 0.5
Microsomes						
Control	9.6 ± 1.3	16.9 ± 4.2	38 ± 3.7	7.5 ± 1	10 ± 1.2	13.1 ± 3
Zinc-deficient	5.6 ± 0.5 <sup>b</sup>	24.1 ± 4	36 ± 2.8	12.2 ± 1.8 <sup>b</sup>	6.4 ± 1.6 <sup>b</sup>	11.8 ± 0.8
Lamellar body						
Control	7.4 ± 0.7	12.3 ± 0.7	35.6 ± 5	13.5 ± 1.5	12.3 ± 2.6	17.8 ± 3
Zinc-deficient	5.1 ± 0.4 <sup>c</sup>	7.0 ± 0.8 <sup>b</sup>	50 ± 4 <sup>a</sup>	18.1 ± 1.0 <sup>a</sup>	7.6 ± 1.4 <sup>a</sup>	8.5 ± 1.1 <sup>a</sup>
Extracellular surfactant						
Control	6.0 ± 2	5.1 ± 0.4	64.2 ± 3	7.3 ± 0.7	6.5 ± 0.6	10.6 ± 1.4
Zinc-deficient	3.0 ± 0.6 <sup>a</sup>	5.0 ± 1	55.5 ± 2.2 <sup>b</sup>	13.2 ± 2.4 <sup>a</sup>	3.2 ± 0.3 <sup>b</sup>	10.7 ± 0.5
Alveolar macrophages						
Control	7.0 ± 0.4	11.4 ± 1.3	51 ± 2	11.6 ± 1.2	8.0 ± 0.7	10.6 ± 1
Zinc-deficient	6.9 ± 0.9	9.4 ± 2	55.8 ± 3	9.1 ± 0.3 <sup>a</sup>	5.3 ± 1.2 <sup>a</sup>	5.4 ± 0.9 <sup>c</sup>

<sup>a</sup>LPC, lysophosphatidylcholine; SPH, sphingomyelin; PG, phosphatidylglycerol. Results given as means ± SD for eight rats in each group expressed as percentage of total phospholipids. Across a row, values with different roman superscript letters indicate a significant difference: <sup>a</sup>*P* < 0.05, <sup>b</sup>*P* < 0.01, <sup>c</sup>*P* < 0.001.



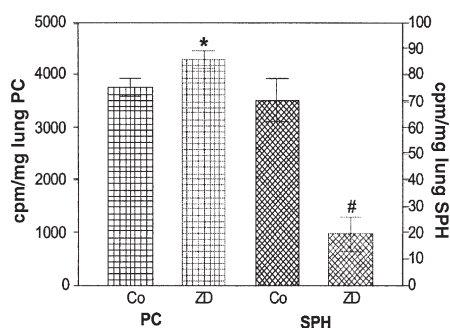


FIG. 1. Incorporation of  $^{14}\text{C}$ -choline into PC and SPH in lung of zinc-deficient (ZD) or control (Co) rat. Significant difference \* $P < 0.05$ ; # $P < 0.001$ . SPH, sphingomyelin.

synthesis. The protein concentration decreased in whole lung, lamellar bodies, surfactant, and macrophages with ZD. Dietary constituents such as zinc can alter gene expression directly by interacting with regulatory components in the genome and activating or inhibiting transcription (41).

Although we observed that the protein concentration in microsomes did not change, the data were similar to those previously reported in the liver microsomes from the zinc-deficient animals (5). The enzymatic activities of PE methyltransferase, phosphatidyl-dimethylethanolamine methyltransferase, and choline phosphotransferase had a linear relationship between time and concentration of microsomal protein (5).

The lower protein concentration in the extracellular surfactant could be a consequence of its decreased secretion from lamellar bodies or decreased synthesis of specific proteins by extracellular surfactant. Specific surfactant protein-A is the major surfactant protein in regard to relative abundance as well as size, and its main known functions are support of alveolar macrophage activities and regulation of surfactant secretion (1).

The lower content of phospholipid in extracellular surfactant may be a consequence of increased recycling by alveolar type II cells or type II pneumocytes for synthesis of new surfactant (42) or decreased secretion from lamellar bodies. This change could be associated with a posttranslational change in plasma membrane proteins (43).

The macrophage, a pivotal cell in many immunologic functions, is adversely affected by ZD, which can modify intracellular killing, cytokine production, and phagocytosis (31,35). It has been reported that the amount of macrophages decrease in ZD (31,34); this is coincident with our case because the low content of phospholipids in macrophages could be a consequence of a smaller amount of these cells in extracellular surfactant in the zinc-deficient rats (Table 3).

Adult type II cells may be different from other cells because of their exceptionally high rate of uptake and choline phosphorylation and their high rate of PC synthesis, even at low substrate concentration (22). In our experiments, the rate of PC synthesis from  $[\text{Me-}^{14}\text{C}]$ choline appeared to be sensitive to ZD because the radioactivity increased 12% in PC, but in SPH it decreased 73% in relation to the control group (Fig. 1).

The amount of cholesterol would change the synthesis of PC through stimulation of CYT (44). We do not know if the increased activity of CYT observed in the lung of the zinc-deficient rats is due to a pre- or posttranslational regulation. It may be that the cholesterol concentration is an indirect cause of the increased activity of this enzyme observed in microsomes of rat lung after 2 mon of zinc-deficient diet.

In the present study, the zinc-deficient diet increases the capacity to produce surfactant phospholipids. The amount of phospholipids may be higher due to the increase in type II cells and/or an increase in specific activity of phospholipid-synthesizing enzymes (45). The alveolar epithelial damage is followed *in vivo* by an adaptive or recovery stage in which type II cells proliferate, and in this stage the capacity to produce surfactant phospholipids may be higher (45). Clejan *et al.* (46) indicated that in the liver, small intestine, and testes the synthesis of phospholipids increased in ZD. These changes may be due to the increased availability of substrates as well as to increased activities of the enzymes involved in these processes. Perhaps this situation occurs in the initial period of deficiency, which corresponds with our experimental model.

This is the first demonstration that phospholipid synthesis can be enhanced in the adult rat lung by a physiological stimulus produced by a zinc-deficient diet (*in vivo*) after 2 mon of treatment.

In moderate ZD, the lung changes the pattern of PC. In addition, we know the role of zinc in immunity and its participation in the antioxidant defense system (10). Considering all these facts, ZD implications are important to consider when designing therapies and public health interventions involving targeted zinc supplementation for high-risk groups or groups with certain diseases, such as ARDS.

## ACKNOWLEDGMENTS

The authors are grateful to Dr. Adolfo Acosta, Dr. Fanny Zirulnik, Lic. Silvina M. Alvarez, Lic. María R. Fernandez, Isabel Sosa, and Rosario Dominguez for their technical assistance. This work was supported by a grant from CONICET-4931 and National University of San Luis, Project No. 8104.

## REFERENCES

1. Hamm, H., Fabel, H., and Bartsch, W. (1992) The Surfactant System of the Adult Lung: Physiology and Clinical Perspectives, *Clin. Invest.* 70, 637–657.
2. Notter, M.D. (1989) Physical Chemistry and Physiological Activity of Pulmonary Surfactants, in *Surfactant Replacement Therapy* (Shapiro, D.L., and Notter, R.H., eds.), A.R. Liss, New York, pp. 19–70.
3. Eder, K., and Kirchgessner, M. (1994) Levels of Polyunsaturated Fatty Acids in Tissues from Zinc-Deficient Rats Fed a Linseed Oil Diet, *Lipids* 29, 839–844.
4. Eder, K., and Kirchgessner, M. (1995) Zinc Deficiency and Activities of Lipogenic and Glycolytic Enzymes in Liver of Rats Fed Coconut Oil or Linseed Oil, *Lipids* 30, 63–69.
5. Cornatzer, W.E., Haning, J.A., Wallwork, J.C., and Sandstead, H.H. (1984) Effect of Zinc Deficiency on the Biosynthesis of Phosphatidylcholine in Rat Microsomes, *Biol. Trace Elem. Res.* 6, 393–401.

6. Rooney, S.A. (1985) The Surfactant System and Lung Phospholipid Biochemistry, *Am. Rev. Respir. Dis.* 131, 439–460.
7. Mason, R.J., and Nellenbogen, J. (1984) Synthesis of Saturated Phosphatidylcholine and Phosphatidylglycerol by Freshly Isolated Rat Alveolar Type II Cells, *Biochim. Biophys. Acta* 794, 392–402.
8. Sharma, A., Gonzalez, L.W., and Ballard, P.L. (1993) Hormonal Regulation of Cholinephosphate Cytidylyltransferase in Human Fetal Lung, *Biochim. Biophys. Acta* 1170, 237–244.
9. Barr, H.A., Nicholas, T.E., and Power, J.H.T. (1989) Effect of Hypernea on Enzymes of the CDP-Choline Path for Phosphatidylcholine Synthesis in Rat Lung, *Lipids* 24, 709–714.
10. Zimmermann, L.J., Hogan, M., Carlson, K.S., Smith, B.T., and Post, M. (1993) Regulation of Phosphatidylcholine Synthesis in Fetal Type II Cells by CTP:Phosphocholine Cytidylyltransferase, *Am. J. Physiol.* 264 (6Pt), L575–L580.
11. Vojnik, C., and Hurley, L.S. (1977) Abnormal Prenatal Lung Development Resulting from Maternal Zinc Deficiency in Rats, *J. Nutr.* 107, 862–872.
12. Truong-Tran, A.Q., Carter, J., Ruffin, R., and Zalewski, P.D. (2001) New Insights into the Role of Zinc in the Respiratory Epithelium, *Immunol. Cell. Biol.* 79, 170–177.
13. Reeves, P.G., Nielsen, F.H., and Fahey, G.C., Jr. (1993) AIN-93 Purified Diets for Laboratory Rodents: Final Report of the American Institute of Nutrition *ad hoc* Writing Committee on the Reformulation of the AIN-76A Rodent Diet, *J. Nutr.* 123, 1939–1951.
14. National Research Council (1985) *Guide for the Care and Use of Laboratory Animals*, Publication 85-23 (rev.), National Institutes of Health, Bethesda.
15. Clegg, M.S., Keen, C.L., Lonnerdal, B., and Hurley, L.S. (1981) Influence of Ashing Techniques on the Analysis of Trace Elements in Animal Tissue. I. Wet Ashing, *Biol. Trace Elem. Res.* 3, 107–115.
16. Adachi, H., Hayashi, H., Sato, H., Dempo, K., and Akino, T. (1989) Characterization of Phospholipids Accumulated in Pulmonary Surfactant Compartments of Rats' Intratracheally Exposed to Silica, *Biochem. J.* 262, 781–786.
17. Hara, A., and Radin, N.S. (1978) Lipid Extraction of Tissues with a Low-Toxicity Solvent, *Anal. Biochem.* 90, 420–426.
18. Rouser, G., Fluster, S., and Yamamoto, A. (1970) Two-Dimensional Thin-Layer Chromatographic Separation of Polar Lipid and Determination of Phospholipids Analysis of Spots, *Lipids* 5, 494–496.
19. Abell, L.L., Levy, B.B., Brodie, B.B., and Kendall, F.E. (1952) A Simplified Method for the Estimation of Total Cholesterol in Serum and Demonstration of Its Specificity, *J. Biol. Chem.* 195, 357–366.
20. Sardesai, V.M., and Manning, J.A. (1968) Determination of Triglycerides in Plasma and Tissues, *Clin. Chem.* 14, 156–161.
21. Kuroki, Y., and Akino, T. (1991) Pulmonary Surfactant Protein A (Sp-A) Specifically Binds Dipalmitoylphosphatidylcholine, *J. Biol. Chem.* 266, 3068–3073.
22. Haagsman, H.P., Schuurmans, E.A.J.M., Batenburg, J.J., and van Golde, L.M.G. (1988) Synthesis of Phosphatidylcholines in Ozone-Exposed Alveolar Type II Cells Isolated from Adult Rat Lung: Is Glycerolphosphate Acyltransferase a Rate-Limiting Enzyme? *Exp. Lung Res.* 14, 1–17.
23. Lowry, O.H., Rosebrough, N.J., Farr, A.L., and Randall, R.J. (1951) Protein Measurement with the Folin Phenol Reagent, *J. Biol. Chem.* 193, 265–275.
24. Omura, T., and Takesue, S. (1970) A New Method for Simultaneous Purification of Cytochrome b<sub>5</sub> and NADPH-Cytochrome C Reductase from Rat Liver Microsomes, *J. Biochem.* 67, 249–257.
25. Hansen, T.L., and Andersen, H. (1983) Succinate Dehydrogenase Activity in Cultured Human Skin Fibroblasts and Amniotic Fluid Cells, A Methodological Study, *Histochemistry* 78, 211–225.
26. Avruch, J., and Wallach, D.F.H. (1971) Preparation and Properties of Plasma Membrane and Endoplasmic Reticulum Fragments from Isolated Rat Fat Cells, *Biochim. Biophys. Acta* 233, 334–347.
27. Oteiza, P.L., Olin, K.L., Fraga, C.G., and Keen, C.L. (1996) Oxidant Defense Systems in Testes from Zinc-Deficient Rats, *Proc. Soc. Exptl. Biol. Med.* 213, 85–91.
28. Chen, M.D., Song, Y.M., and Lin, P.Y. (2000) Zinc Effects on Hyperglycemia and Hypoleptinemia in Streptozotocin-Induced Diabetic Mice, *Horm. Metab. Res.* 32, 107–109.
29. Ivandija, V.R.L., Luterotti, S., Dominis-Kramaric, M., and Bozac, R. (1998) Plasma Proteins and Hematological Parameters in Fattening Pigs Fed Different Sources of Dietary Zinc, *Acta Vet. Hung.* 46, 111–126.
30. Cunnane, S.C., and Yang, J. (1995) Zinc Deficiency Impairs Whole-Body Accumulation of Polyunsaturates and Increases the Utilization of 1-<sup>14</sup>C Linoleate for *de novo* Lipid Synthesis in Pregnant Rats, *Can. J. Physiol. Pharmacol.* 73, 1246–1252.
31. Walsh, C.T., Sandstead, H.H., Prasad, A.S., Newberne, P.M., and Fraker, P.J. (1994) Zinc: Health Effects and Research Priorities for the 1990s, *Environ. Health Perspect.* 102 (Suppl. 2), 5–46.
32. Pattison, S.E., and Cousins, R.J. (1986) Zinc Uptake and Metabolism by Hepatocytes, *Fed. Proc.* 45, 2805–2809.
33. King, J.C. (1990) Assessment of Zinc Status, *J. Nutr.* 120, 1474–1479.
34. Shankar, A.H., and Prasad, A.S. (1998) Zinc and Immune Function: The Biological Basis of Altered Resistance to Infection, *Am. J. Clin. Nutr.* 68 (Suppl.), 447S–463S.
35. Jhala, U.S., and Baly, D.L. (1991) Zinc Deficiency Results in a Post-Transcriptional Impairment in Insulin Synthesis, *FASEB J.* 5, A941.
36. Scott, J.E. (1992) Phosphatidylcholine Synthesis, Secretion and Reutilization During Differentiation of the Surfactant-Producing Type II Alveolar Cell from Fetal Rabbit Lung, *Exp. Lung Res.* 18, 563–580.
37. Hass, M.A., and Longmore, W.J. (1980) Regulation of Lung Surfactant Cholesterol Metabolism by Serum Lipoproteins, *Lipids* 15, 401–406.
38. Hass, M.A., and Longmore, W.J. (1974) Surfactant Cholesterol Metabolism of the Isolated Perfused Rat Lung, *Biochim. Biophys. Acta* 573, 166–174.
39. Michaut, M., Carrasco, M., and Gimenez, M.S. (1992) Effects of Castration on the Incorporation of [<sup>3</sup>H<sub>2</sub>O] in Lipids of Male Rat Liver, *Horm. Metab. Res.* 24, 593–594.
40. Ojeda, M.S., Gomez, N.N., and Gimenez, M.S. (1997) Androgen Regulation of Lung Lipids in the Male Rat, *Lipids* 32, 57–62.
41. Cousins, R.J. (1999) Nutritional Regulation of Gene Expression, *Am. J. Med.* 106 (1A), 20S–23S.
42. Fisher, A.B., and Dodia, C. (1994) Regulation of Surfactant Metabolism Degradation of Internalized Alveolar Phosphatidylcholine, *Prog. Respir. Res.* 27, 74–83.
43. O'Dell, B.L. (2000) Role of Zinc in Plasma Membrane Function, *J. Nutr.* 130 (5S Suppl.), 1432S–1436S.
44. Shiratori, Y., Houweling, M., Zha, X., and Tabas, Y. (1995) Stimulation of CTP-Phosphocholine Cytidylyltransferase by Free Cholesterol Loading of Macrophages Involves Signaling Through Protein Dephosphorylation, *J. Biol. Chem.* 270, 29894–29903.
45. Muller, B., and von Wichert, P. (1993) Effect of Nitrogen Dioxide Inhalation on Surfactant Phosphatidylcholine Synthesis in Rat Alveolar Type II Cells, *Biochim. Biophys. Acta* 1170, 38–43.
46. Clejan, S., Maddaiah, V.T., Castro-Magana, M., and Collipp, P.J. (1981) Zinc Deficiency-Induced Changes in the Composition of Microsomal Membranes and in the Enzymatic Regulation of Glycerolipid Synthesis, *Lipids* 16, 454–460.

[Received February 2, 2001; and in final revised form November 12, 2001; revision accepted November 17, 2001]

# Lipid Metabolism and FA Composition in Tissues of Eurasian Perch *Perca fluviatilis* as Influenced by Dietary Fats

Xueliang Xu\* and Patrick Kestemont

Facultés Universitaires N. D. de la Paix, Unité de Recherches en Biologie des Organismes, 5000 Namur, Belgium.

**ABSTRACT:** Eurasian perch, *Perca fluviatilis*, were fed a semipurified fat-free diet for 4 wk, followed by a 16% feeding supplementation of either olive oil (OO), safflower oil (SO), linseed oil (LO), or cod liver oil (CLO) as the only lipid source in each diet for 10 wk. Significant reductions in total lipid of tissues were observed (31.4% in viscera, 66.7% in muscle, and 74.1% in liver) after feeding the fat-free diet. The SO-, LO-, and CLO-fed fish significantly increased lipid deposition in liver and viscera compared to fish fed the OO diet; however, muscle lipid levels were not significantly affected. Large amounts of dietary 18:1n-9 were incorporated directly into tissue lipids when fish were fed the OO diet. The LO diet significantly elevated 18:4n-3, 20:5n-3, 22:5n-3, and 22:6n-3 in the liver compared to fish fed OO or SO diets, and the n-3/n-6 ratio was 16 times that of the SO group, with significantly high desaturation and elongation products of 18:3n-3. These results suggest that  $\Delta 6$  and  $\Delta 5$  desaturases are highly active in Eurasian perch, and that the enzymes at this dietary n-3/n-6 ratio favor 18:3n-3 over 18:2n-6 as substrate. The SO diet significantly increased 18:3n-6, 20:3n-6, and 22:5n-6 in the liver and significantly decreased EPA and DHA. This indicates that desaturation enzymes were not specifically favoring n-3 over n-6 acids in perch lipid metabolism, and that these elongation and desaturation enzymes were influenced by n-3 and n-6 FA content in the diet. The present study indicates that high tissue content of DHA in the muscle of Eurasian perch was attributable to the greater ability for n-3 acid bioconversion.

Paper no. L8853 in *Lipids* 37, 297–304 (March 2002).

Lipid nutrition research has demonstrated that DHA, EPA, and arachidonic acid (AA) are FA essential for maintaining cell integrity and supporting life in all animals, and are now being recognized as desirable in the human diet (1–8). As n-3 and n-6 18-carbon FA are precursors of these FA, the requirements in fish are, to a large extent, associated with the ability of animals to convert the 18-carbon FA to the longer-chain highly unsaturated FA (HUFA) (9–16). The nutritive value of dietary lipid sources therefore is also closely related to the animal's ability to produce chain elongation and desaturation (17–18), and the type and amount of dietary fat have been shown to be important factors (19–21). It is generally ac-

cepted that marine fish lack one or more of the desaturation enzymes necessary to complete the chain elongation and desaturation of n-3 and n-6 acids such as linoleic acid and linolenic acid to AA, EPA, and DHA (9,11,22–25). In contrast, freshwater fish are capable of performing this conversion by chain elongation and desaturation (24,26–30). Recent interest in fish oil for animal and human nutrition has increased the demand for the world's fish oil supply. At this date, aquaculture already consumes nearly 50% of the world supply of fish oil, and with the continuous rapid growth of world aquaculture, the demand for fish oil will exceed the supply in the near future (25). It is important therefore to develop alternatives to fish oil in fish feed formulations (25). During the past three decades, although many studies on n-3 and n-6 FA nutrition and metabolism have been conducted in both marine and freshwater fish (9,11,22,23,26,28,29,31–33), limited information has been published on lipids, FA composition, and metabolism of percid fish (34–37). In fact, no study has yet addressed the influence of dietary fat source on lipid metabolism and FA composition of Eurasian perch *Perca fluviatilis*.

The purposes of the present study were to investigate the influence of different lipid sources on FA composition and metabolism in the Eurasian perch, and to evaluate the potential alternatives to fish oil in fish feed formulations.

## MATERIALS AND METHODS

**Animals and diets.** Three hundred Eurasian perch (initial mean weight 25 g) were obtained from the Tihange Fish Culture Station (University of Liège, Belgium) and were fed on a semipurified fat-free basal diet in a 1.5 × 1.5 × 1 m fiberglass tank for 4 wk. The basal diet was composed of (by wt%): casein, 47; arginine HCl, 2; blood meal, 7; cornstarch, 18.4; vitamin mix, 2; mineral mix, 2; choline chloride, 0.5; ascorbic acid, 0.2; attractants (alanine, glycine, proline, and betaine), 1; cellulose, 2; carboxymethylcellulose, 2; testing lipid source, 16. (Vitamin and mineral mixes were purchased from INVE Aquaculture NV, Dendermonde, Belgium.) After that, 240 fish were divided randomly into eight 120-L rectangular tanks (30 fish per tank) to provide duplicates of the four dietary treatments. The diets were formulated to meet the protein and lipid requirements of Eurasian perch (36–38) and contained 45% protein and 16% lipid (a cod liver oil diet served

\*To whom correspondence should be addressed at Facultés Universitaires N. D. de la Paix, Unité de Recherches en Biologie des Organismes, rue de Bruxelles, 61, 5000 Namur, Belgium. E-mail: Xu.xueliang@fundp.ac.be.

Abbreviations: AA, arachidonic acid; CLO, cod liver oil; HUFA, highly unsaturated FA; LO, linseed oil; OO, olive oil; SO, safflower oil.



**TABLE 1**  
**FA Compositions (wt% of total FA) of the Diets<sup>a</sup>**

FA	Diet			
	OO	SO	LO	CLO
14:0	0.8	0.2	0.1	6.3
16:0	10.8	7.1	5.2	14.4
16:1	0.8	0.1	0.1	8.1
18:0	2.6	2.4	3.2	2.5
18:1	77.2	14.1	21.8	21.4
18:2n-6	5.9	75.0	15.5	4.4
18:3n-3	0.7	0.3	52.5	1.5
18:4n-3	—	—	0.4	2.0
20:1n-9	—	—	—	6.8
20:4n-6	—	—	—	0.3
20:4n-3	—	—	—	1.1
20:5n-3	—	—	—	10.1
21:5n-3	—	—	—	1.1
22:1n-11	—	—	—	6.4
22:5n-3	—	—	—	1.1
22:6n-3	—	—	—	10.3

<sup>a</sup>Total lipids were extracted from the diets as described in the Materials and Methods section. FA composition was determined by GC Trace 2000 (Thermo Quest, Carlo Erba, Italy) with on-column injection. Values were expressed as percentages of each FA over total FA identifiable. OO, olive oil; SO, sunflower oil; LO, linseed oil; CLO, cod liver oil. (—), not detected.

as the control treatment) with all ingredients identical except for the different lipid sources (Table 1). Fish were subjected to a natural photoperiod, and the water temperature during the experimental period was kept constant at 23°C. Fish were fed twice a day by hand to satiation for 10 wk. Fish were weighed in biomass at the start and finish of the experiment and at intervals of every 2 wk. Vitamin-free casein, olive oil (OO), sunflower oil (SO), linseed oil (LO), and cod liver oil (CLO) were purchased from Sigma-Aldrich (St. Louis, MO). Vitamin and mineral mixtures were purchased from INVE. An antioxidant (ethoxyquin 0.2%) was added to the oil before adding it to the basal mixture. The FA composition of each diet is presented in Table 1.

**Lipid extraction and FA analysis.** Three fish per tank were killed by a blow to the head, and liver, viscera, and muscle were dissected. Samples were stored at -80°C prior to lipid extraction. Total lipids of liver (0.5–0.8 g) and viscera (1 g) were extracted with chloroform/methanol (2:1, vol/vol) by the method of Folch *et al.* (39), and the total lipids of muscle tissues (50–100 g) were extracted with chloroform/methanol/water (2:2:1.8, by vol) by the method of Bligh and Dyer (40). BHA (0.02%) was added to chloroform/methanol as an antioxidant. The FA of total lipids were converted to methyl esters with BF<sub>3</sub>-MeOH (41), and FA were separated and quantified by GC (GC Trace, 2000; ThermoQuest, Carlo Erba, Italy) using a 30 m × 0.32 mm capillary column (FAME-Wax<sup>TM</sup>; Restek Corporation, Bellefonte, PA). Helium was used as carrier gas, and temperature programming was from 66 to 190°C at 40°C/min and then to 230°C at 2°C/min. Individual methyl esters were identified by comparison with standard fish oil (42) and quantified by the computing integrator Chrom-Card for Trace (ThermoQuest).

**Statistical analysis.** Results of replicate tanks with two different pooled samples from six fish were used for statistical analysis. Values shown in Tables 3–7 are the means ± SD, with *n* values indicating the numbers of different pooled samples per treatment. Statistical analysis was based on a one-way ANOVA processed by Duncan's multiple range test (43). The significant differences between treatments were evaluated at the 0.05 level.

## RESULTS AND DISCUSSION

Feeding fish with a fat-free diet had a pronounced effect on reducing the lipid deposition in liver, viscera, and muscle in Eurasian perch (Table 2). Total lipid content of these tissues dropped significantly, with a 31% fat reduction in the viscera, 66.7% in the muscle, and 74.1% in the liver, indicating that dietary fat is essential for building body lipids in fish. The fat-free diet also affected the FA composition of fish tissues

**TABLE 2**  
**Total Fat Content of Different Tissues and Growth Parameters After the 10 wk Feeding Trial**

Parameter	Before <sup>b</sup>	After <sup>c</sup>	OO Diet	SO Diet	LO Diet	CLO Diet
total lipid (%) <sup>a</sup>						
Liver	34.7 ± 2.9 <sup>a</sup>	9.0 ± 0.4 <sup>b</sup>	7.1 ± 0.5 <sup>c</sup>	8.3 ± 0.4 <sup>b,c</sup>	12.6 ± 0.1 <sup>d</sup>	9.4 ± 0.2 <sup>b</sup>
Viscera	72.9 ± 1.0 <sup>a</sup>	41.5 ± 2.6 <sup>b</sup>	43.8 ± 1.4 <sup>b</sup>	53.9 ± 0.8 <sup>c</sup>	64.5 ± 2.9 <sup>a</sup>	76.7 ± 3.4 <sup>a</sup>
Muscle	3.0 ± 0.1 <sup>a</sup>	1.0 ± 0.0 <sup>b</sup>	0.8 ± 0.0 <sup>b</sup>	1.0 ± 0.1 <sup>b</sup>	1.1 ± 0.2 <sup>b</sup>	1.1 ± 0.2 <sup>b</sup>
Initial weight (g) <sup>d</sup>			25.5 ± 2.3	26.0 ± 1.8	25.5 ± 3.2	24.5 ± 1.4
Final weight (g)			33.1 ± 3.4 <sup>a</sup>	35.9 ± 1.8 <sup>b</sup>	44.2 ± 2.8 <sup>c</sup>	59.2 ± 4.3 <sup>d</sup>
Weight gain (%) <sup>e</sup>			30.0 ± 5.6 <sup>a</sup>	41.0 ± 1.5 <sup>b</sup>	71.2 ± 1.5 <sup>c</sup>	141.7 ± 6.8 <sup>d</sup>
Feed efficiency ratio <sup>f</sup>			0.86 ± 0.03 <sup>a</sup>	1.10 ± 0.02 <sup>b</sup>	1.23 ± 0.01 <sup>b</sup>	1.28 ± 0.08 <sup>b</sup>

<sup>a</sup>Total lipids of liver, viscera and muscle are percentage by weight ± SD from three different pooled samples of six fish from duplicate tanks per treatment.

<sup>b</sup>Before feeding fat-free diet.

<sup>c</sup>After feeding fat-free diet.

<sup>d</sup>Values for initial weight and final weight are mean ± SD obtained from two biomass (25–30 fish) of duplicate tanks. Values in the same row with different superscript letters are significantly different (*P* < 0.05).

<sup>e</sup>Weight gain percent = (final weight – initial weight)/initial weight × 100%.

<sup>f</sup>Feed efficiency ratio = (g final biomass – g initial biomass + g dead fish) × (g feed supply)<sup>-1</sup>.



**TABLE 3**  
**FA Compositions (wt% total FA) of Liver and Viscera Before and After Feeding the Fat-Free Diet<sup>a</sup>**

	Dietary treatments					
	Liver		Viscera		Muscle	
	Before <sup>b</sup>	After <sup>c</sup>	Before <sup>b</sup>	After <sup>c</sup>	Before <sup>b</sup>	After <sup>c</sup>
Total lipid (%, wet wt)	34.7 ± 2.9 <sup>a</sup>	9.0 ± 0.4 <sup>c</sup>	72.9 ± 1.0 <sup>a</sup>	41.5 ± 2.6 <sup>c</sup>	3.0 ± 0.1 <sup>a</sup>	1.4 ± 0.1 <sup>b</sup>
FA						
14:0	4.3 ± 0.1 <sup>a</sup>	2.9 ± 0.3 <sup>b</sup>	6.3 ± 0.0	6.2 ± 0.1	19.4 ± 0.4	20.9 ± 0.6
16:0	17.0 ± 1.1	16.0 ± 1.1	13.9 ± 0.7 <sup>b</sup>	11.6 ± 0.1 <sup>a</sup>	2.9 ± 0.1	3.3 ± 0.0
18:0	1.3 ± 0.1	1.0 ± 0.4	0.9 ± 0.1	1.0 ± 0.1	—	—
20:0	—	—	0.2 ± 0.0	—	—	—
Total SFA	22.6 ± 1.4	19.9 ± 0.5	21.3 ± 0.4 <sup>b</sup>	18.7 ± 0.1 <sup>a</sup>	24.5 ± 0.6	25.6 ± 0.3
16:1	11.0 ± 1.2	7.9 ± 0.2	9.8 ± 1.1	8.4 ± 1.4	4.7 ± 0.7	3.9 ± 0.0
18:1	22.2 ± 1.6	17.8 ± 0.7	23.6 ± 0.1	24.8 ± 0.7	12.9 ± 0.6	11.4 ± 0.3
20:1	3.9 ± 0.7	2.7 ± 0.6	6.8 ± 0.6 <sup>a</sup>	9.0 ± 0.1 <sup>b</sup>	3.7 ± 0.0 <sup>a</sup>	2.0 ± 0.4 <sup>b</sup>
22:1	1.5 ± 0.4 <sup>a</sup>	— <sup>b</sup>	4.0 ± 0.3 <sup>a</sup>	5.3 ± 0.1 <sup>b</sup>	— <sup>a</sup>	0.8 ± 0.2 <sup>b</sup>
Total MUFA	38.5 ± 0.2 <sup>a</sup>	28.3 ± 2.8 <sup>b</sup>	44.3 ± 0.4 <sup>a</sup>	47.4 ± 0.8 <sup>b</sup>	21.3 ± 1.8 <sup>a</sup>	18.1 ± 0.4 <sup>b</sup>
18:2	5.1 ± 0.4	4.7 ± 0.2	5.1 ± 0.1	4.7 ± 0.1	2.4 ± 0.1	2.5 ± 0.1
18:3	—	0.1 ± 0.0	0.1 ± 0.0	0.1 ± 0.0	—	—
20:2	— <sup>a</sup>	0.2 ± 0.1 <sup>b</sup>	0.5 ± 0.0	0.5 ± 0.1	—	—
20:3	—	—	0.1 ± 0.0	—	—	—
20:4	0.7 ± 0.1	1.0 ± 0.0	0.4 ± 0.0	0.4 ± 0.0	1.2 ± 0.1	2.0 ± 0.0
22:4	— <sup>a</sup>	0.3 ± 0.1 <sup>b</sup>	0.2 ± 0.0	0.2 ± 0.1	0.2 ± 0.0	0.4 ± 0.1
22:5	—	—	—	—	0.3 ± 0.0	0.3 ± 0.1
Total n-6 FA	5.8 ± 0.6	6.2 ± 0.4	6.2 ± 0.0	5.8 ± 0.1	4.1 ± 0.1	5.2 ± 0.3
18:3	1.4 ± 0.1 <sup>a</sup>	0.8 ± 0.0 <sup>b</sup>	1.8 ± 0.1	1.3 ± 0.1	0.7 ± 0.0 <sup>a</sup>	0.4 ± 0.1 <sup>b</sup>
18:4	1.3 ± 0.1 <sup>a</sup>	0.8 ± 0.1 <sup>b</sup>	2.2 ± 0.1	1.3 ± 0.0	0.8 ± 0.1 <sup>a</sup>	0.4 ± 0.1 <sup>b</sup>
20:3	—	0.1 ± 0.0	0.2 ± 0.0	—	—	—
20:4	0.7 ± 0.0 <sup>a</sup>	0.4 ± 0.0 <sup>b</sup>	0.7 ± 0.0	0.6 ± 0.0	0.3 ± 0.1	0.3 ± 0.0
20:5	4.8 ± 1.3	5.6 ± 0.1	6.0 ± 0.4 <sup>b</sup>	3.8 ± 0.1 <sup>a</sup>	6.8 ± 0.8 <sup>a</sup>	9.2 ± 0.3 <sup>b</sup>
22:5	1.3 ± 0.0	1.6 ± 0.0	1.3 ± 0.0	1.5 ± 0.1	1.0 ± 0.1	0.9 ± 0.2
22:6	21.1 ± 1.2 <sup>a</sup>	33.0 ± 1.1 <sup>b</sup>	13.3 ± 0.3 <sup>a</sup>	16.2 ± 0.0 <sup>b</sup>	34.4 ± 0.2	34.5 ± 0.6
Total n-3 FA	30.5 ± 0.2 <sup>a</sup>	42.1 ± 0.7 <sup>b</sup>	25.4 ± 0.6	24.7 ± 0.1	44.0 ± 0.7	45.7 ± 0.8
n-3/n-6 Ratio	5.3 ± 0.6	6.8 ± 0.7	4.0 ± 0.4	4.3 ± 0.1	10.7 ± 0.3	8.8 ± 0.2

<sup>a</sup>Values are means ± SD obtained from two different pooled samples of six fish from duplicate tanks. Values in the same row (same tissue category) with different superscript letters are significantly different ( $P < 0.05$ ). (—), trace value ( $<0.05$ ) or not detected. SFA, saturated FA; MUFA, monounsaturated FA.

<sup>b</sup>Before feeding fat-free diet.

<sup>c</sup>After feeding fat-free diet.

(Table 3). Proportions of 18:3n-3, 18:4n-3, 20:4n-3, and total monounsaturated FA in the liver were significantly decreased, whereas DHA and total n-3 FA were significantly increased after a 4-wk fat-free diet. At the same time, 18:3n-6, 20:2n-6, 20:4n-6, and 22:4n-6 in the liver were also increased. By contrast, the FA composition of viscera and muscle remained almost unchanged after feeding the fat-free diet. The relatively high levels of HUFA (20:4n-6, 20:5n-3, and 22:6n-3) in the tissue lipids of perch fed the fat-free diet were probably the result of preferential utilization of short- and medium-chain FA as an energy source for basal maintenance, rather than an increase in the absolute content of the HUFA. AA, EPA, and especially DHA were preferentially retained in the larval lipids at the expense of other FA during the periods of starvation (44). The growth responses and feed efficiency of fish

fed four different dietary fat sources are presented in Table 2. The lowest growth rate (30%) and feed efficiency (0.86) were observed in fish fed the OO diet. LO- and SO-fed fish increased significantly in growth response (41 and 71.2%, respectively) and in improved feed efficiency (1.10 to 1.23, respectively) compared to OO fish. These results indicate that n-6 and n-3 FA may be essential for the growth of Eurasian perch. However, the highest growth rate (141.7%) and feed efficiency (1.28) were found in control fish fed the CLO diet. The differences in weight gain between the LO and the CLO fish may be attributed to the better palatability of the CLO diet.

The total lipid content of viscera, muscle, and liver of fish fed OO, SO, LO, or CLO diets is shown in Table 2. Significant differences in total lipid content of liver and viscera were

observed. The SO, LO, and CLO diets significantly increased lipid deposition in viscera as compared to the OO diet-fed fish, and the lipid content of the viscera in LO and CLO fish was significantly higher than that of the SO fish, which was comparable to or even higher than that of fish before feeding the fat-free diet, suggesting that lipid restoration in viscera was efficient compared to that of liver. The liver lipid content in LO fish was the highest among the four dietary fat treatment groups, and the lipid content of liver in CLO fish was significantly higher than that of OO diet-fed fish; however, there was no significant difference in liver lipid content between OO and SO diet-fed fish, and total lipid contents of livers from all dietary treatments were low compared to those of fish before feeding the fat-free diet, which might imply a slow restoration of liver lipids in Eurasian perch. The lipid content in muscle was not significantly affected by dietary fats and remained similar among the four treatments.

FA compositions in liver, viscera, and muscle from fish fed four different lipid sources clearly showed that significant changes were made by their responses to dietary FA (Tables 4–6). Considerable amounts of dietary FA were incorporated

into fish tissues, and extensive chain elongation and desaturation n-6 and n-3 FA were observed among the four dietary treatments. Predominant FA were 16:0, 16:1, 18:1, and 22:6n-3 in OO-fed fish, and among these FA, 18:1 was significantly increased in OO fish livers compared to those of SO, LO, and CLO fish. DHA and total n-3 FA in the livers of OO fish were significantly higher than those in SO fish, but they were significantly lower than those in LO and CLO fish, suggesting that n-3 desaturations were inhibited by the SO diet and enhanced by the LO diet.

The highest single FA was 18:2n-6 in SO-fed fish, accounting for 23.7% of total FA in the liver, 19.7% in the viscera, and 12.3% in the muscle, which was 8.5-, 4.3-, and 4.6-fold that of OO fish, 6.1-, 4.0-, and 4.0-fold that of LO fish, and 5.8-, 4.4-, and 5.9-fold that of CLO fish, respectively. These results suggest that linoleic acid is the type of FA that can be incorporated easily into all tissue lipids in Eurasian perch and stored in the lipid pool without modification. The considerable accumulations of 18:2n-6 have also been reported in liver phospholipids of gilthead bream (*Sparus aurata*) fed a diet containing soybean oil (21). The product of

**TABLE 4**  
**FA Compositions (wt% total FA) of Livers<sup>a</sup>**

	Dietary treatments			
	OO	SO	LO	CLO
Total lipid (%, wet wt)	7.1 ± 0.5 <sup>a</sup>	8.3 ± 0.4 <sup>a,b</sup>	12.6 ± 0.1 <sup>c</sup>	9.4 ± 0.2 <sup>b</sup>
FA				
14:0	1.6 ± 0.2	2.1 ± 0.0	2.3 ± 0.2	2.1 ± 0.3
16:0	16.8 ± 2.9	17.8 ± 1.3	14.5 ± 0.4	16.1 ± 1.8
18:0	2.6 ± 0.6	2.9 ± 0.4	2.4 ± 0.1	2.9 ± 0.3
20:0	—	0.1 ± 0.0	0.1 ± 0.0	—
Total SFA	21.0 ± 3.6	22.9 ± 1.4	19.3 ± 1.2	21.1 ± 2.4
16:1	11.2 ± 4.3	10.2 ± 1.5	8.9 ± 0.7	8.6 ± 0.6
18:1	26.9 ± 2.9 <sup>a</sup>	16.9 ± 0.7 <sup>b</sup>	16.3 ± 0.1 <sup>b</sup>	14.8 ± 0.5 <sup>c</sup>
20:1	2.1 ± 0.0	1.5 ± 0.6	3.0 ± 0.2	2.2 ± 0.1
22:1	—	—	2.0 ± 0.0	1.3 ± 0.3
Total monoenes	40.3 ± 4.9 <sup>a</sup>	28.5 ± 2.8 <sup>b</sup>	30.1 ± 0.1 <sup>b</sup>	26.8 ± 1.4 <sup>c</sup>
18:2n-6	2.8 ± 0.2 <sup>a</sup>	23.7 ± 2.1 <sup>c</sup>	3.9 ± 0.0 <sup>b</sup>	4.1 ± 0.6 <sup>b</sup>
18:3n-6	0.1 ± 0.0 <sup>a</sup>	1.0 ± 0.3 <sup>b</sup>	0.2 ± 0.0 <sup>a</sup>	0.1 ± 0.0 <sup>a</sup>
20:2n-6	0.4 ± 0.0 <sup>a</sup>	0.9 ± 0.1 <sup>b</sup>	0.2 ± 0.0 <sup>c</sup>	0.9 ± 0.2 <sup>b</sup>
20:3n-6	0.4 ± 0.1 <sup>a</sup>	3.4 ± 0.4 <sup>b</sup>	0.2 ± 0.0 <sup>c</sup>	0.2 ± 0.0 <sup>c</sup>
20:4n-6	2.0 ± 0.3	0.8 ± 0.1	1.1 ± 0.2	1.6 ± 0.6
22:4n-6	0.4 ± 0.2	0.6 ± 0.1	0.9 ± 0.1	—
22:5n-6	0.5 ± 0.1 <sup>a</sup>	2.9 ± 0.7 <sup>b</sup>	0.3 ± 0.0 <sup>a</sup>	0.5 ± 0.1 <sup>a</sup>
Total n-6 FA	6.5 ± 0.6 <sup>a</sup>	33.1 ± 4.2 <sup>b</sup>	6.4 ± 0.2 <sup>a</sup>	7.2 ± 1.5 <sup>a</sup>
18:3n-3	0.3 ± 0.0 <sup>a</sup>	0.2 ± 0.1 <sup>a</sup>	3.0 ± 0.1 <sup>b</sup>	3.1 ± 0.3 <sup>a</sup>
18:4n-3	0.2 ± 0.0 <sup>a</sup>	0.1 ± 0.0 <sup>a</sup>	0.7 ± 0.1 <sup>b</sup>	0.6 ± 0.1 <sup>b</sup>
20:3n-3	— <sup>a</sup>	— <sup>a</sup>	0.2 ± 0.0 <sup>b</sup>	0.2 ± 0.0 <sup>b</sup>
20:4n-3	0.1 ± 0.0 <sup>a</sup>	0.2 ± 0.0 <sup>a</sup>	0.6 ± 0.0 <sup>b</sup>	0.6 ± 0.1 <sup>b</sup>
20:5n-3	2.2 ± 0.1 <sup>a</sup>	1.2 ± 0.7 <sup>b</sup>	2.8 ± 0.0 <sup>c</sup>	2.9 ± 0.1 <sup>c</sup>
22:5n-3	0.7 ± 0.0 <sup>a</sup>	0.3 ± 0.1 <sup>b</sup>	1.2 ± 0.0 <sup>c</sup>	0.9 ± 0.1 <sup>a</sup>
22:6n-3	27.1 ± 0.8 <sup>a</sup>	12.6 ± 1.8 <sup>b</sup>	31.6 ± 0.4 <sup>c</sup>	32.2 ± 1.2 <sup>c</sup>
Total n-3 FA	30.4 ± 0.4 <sup>a</sup>	14.6 ± 2.4 <sup>b</sup>	40.0 ± 1.1 <sup>c</sup>	40.4 ± 1.4 <sup>c</sup>
n-3/n-6 Ratio	4.7 ± 0.3 <sup>b</sup>	0.4 ± 0.1 <sup>a</sup>	6.5 ± 0.4 <sup>d</sup>	5.6 ± 0.8 <sup>c</sup>

<sup>a</sup>Values are means ± SD obtained from two different pooled samples of six fish from duplicate tanks per treatment. Values in the same row with different superscript are significantly different ( $P < 0.05$ ). (—), trace value ( $< 0.05$ ) or not detected. For abbreviations see Tables 2 and 3.

**TABLE 5**  
**FA Compositions (wt% total FA) of Viscera<sup>a</sup>**

	Dietary treatments			
	OO	SO	LO	CLO
Total lipid (%, wet wt)	43.8 ± 1.4 <sup>a</sup>	53.9 ± 0.8 <sup>b</sup>	64.5 ± 2.9 <sup>c</sup>	76.7 ± 3.4 <sup>c</sup>
FA				
14:0	5.2 ± 0.7 <sup>a</sup>	4.6 ± 0.2 <sup>a</sup>	6.2 ± 0.1 <sup>b</sup>	5.6 ± 0.2 <sup>b</sup>
16:0	11.5 ± 0.0 <sup>a</sup>	11.5 ± 0.4 <sup>a</sup>	10.8 ± 0.6 <sup>a</sup>	14.1 ± 0.8 <sup>b</sup>
18:0	0.9 ± 0.1	0.9 ± 0.0	0.9 ± 0.1	0.6 ± 0.1
20:0	— <sup>a</sup>	1.1 ± 0.0 <sup>b</sup>	— <sup>a</sup>	0.2 ± 0.0 <sup>a</sup>
Total SFA	17.5 ± 0.6	18.1 ± 0.1	17.8 ± 0.6	20.4 ± 1.4
16:1	10.3 ± 0.5 <sup>a</sup>	7.6 ± 0.6 <sup>b</sup>	9.0 ± 0.4 <sup>b</sup>	13.4 ± 0.1 <sup>c</sup>
18:1	34.5 ± 4.2 <sup>a</sup>	22.9 ± 0.1 <sup>b</sup>	24.2 ± 1.1 <sup>b</sup>	24.3 ± 1.8 <sup>b</sup>
20:1	7.2 ± 0.9	7.3 ± 0.5	9.3 ± 2.3	7.3 ± 0.1
22:1	4.1 ± 0.6	1.5 ± 0.4	4.1 ± 0.7	3.2 ± 0.4
Total monoenes	56.0 ± 2.4	39.2 ± 0.2	46.5 ± 4.4	48.1 ± 0.6
18:2n-6	4.6 ± 0.2 <sup>a</sup>	19.7 ± 0.2 <sup>b</sup>	4.9 ± 0.1 <sup>a</sup>	4.5 ± 0.1 <sup>a</sup>
18:3n-6	0.1 ± 0.0	0.3 ± 0.0	0.1 ± 0.0	0.2 ± 0.0
20:2n-6	0.4 ± 0.1	0.5 ± 0.1	0.3 ± 0.1	0.3 ± 0.0
20:3n-6	— <sup>a</sup>	0.3 ± 0.0 <sup>b</sup>	0.1 ± 0.0 <sup>a</sup>	0.1 ± 0.0 <sup>a</sup>
20:4n-6	0.3 ± 0.0	0.4 ± 0.1	0.4 ± 0.0	0.4 ± 0.1
22:4n-6	—	—	0.1 ± 0.0	—
22:5n-6	0.3 ± 0.0	0.3 ± 0.1	0.2 ± 0.1	0.3 ± 0.1
Total n-6 FA	5.6 ± 0.1 <sup>a</sup>	21.4 ± 0.1 <sup>b</sup>	6.0 ± 0.2 <sup>a</sup>	5.7 ± 0.5 <sup>a</sup>
18:3n-3	0.9 ± 0.0 <sup>a</sup>	1.0 ± 0.0 <sup>a</sup>	1.4 ± 0.1 <sup>b</sup>	1.4 ± 0.1 <sup>b</sup>
18:4n-3	0.9 ± 0.1	1.0 ± 0.0	1.2 ± 0.0	1.5 ± 0.0
20:3n-3	0.1 ± 0.0	—	—	0.1 ± 0.0
20:4n-3	0.4 ± 0.0 <sup>a</sup>	0.4 ± 0.1 <sup>a</sup>	0.6 ± 0.0 <sup>a,b</sup>	0.8 ± 0.0 <sup>b</sup>
20:5n-3	2.5 ± 0.1 <sup>a</sup>	2.8 ± 0.1 <sup>a</sup>	3.2 ± 0.1 <sup>b</sup>	5.1 ± 0.1 <sup>c</sup>
22:5n-3	1.3 ± 0.1 <sup>a</sup>	1.2 ± 0.1 <sup>a</sup>	1.7 ± 0.1 <sup>b</sup>	1.8 ± 0.1 <sup>b</sup>
22:6n-3	12.7 ± 1.4 <sup>a</sup>	13.1 ± 0.0 <sup>a</sup>	16.0 ± 0.4 <sup>b</sup>	12.4 ± 0.1 <sup>a</sup>
Total n-3 FA	18.7 ± 1.7 <sup>a</sup>	19.3 ± 0.0 <sup>a</sup>	24.0 ± 0.2 <sup>b</sup>	22.9 ± 0.0 <sup>b</sup>
n-3/n-6	3.3 ± 0.4 <sup>a</sup>	0.9 ± 0.0 <sup>b</sup>	4.0 ± 0.1 <sup>c</sup>	4.0 ± 0.3 <sup>c</sup>
Ratio				

<sup>a</sup>Viscera may include mostly depot TAG. Values are means ± SD obtained from two different pooled samples of six fish from duplicate tanks per treatment. Values in the same row with different superscripts are significantly different ( $P < 0.05$ ). (—), trace value ( $< 0.05$ ) or not detected. For abbreviations see Tables 2 and 3.

$\Delta 6$  desaturation and elongation of 18:2n-6, 20:3n-6, was 17-fold that of the corresponding n-3 desaturation product, 20:4n-3, indicating that the  $\Delta 6$  desaturation enzyme was also favoring 18:2n-6 as a substrate when dietary 18:3n-3 content was low. A substantially high level of 22:5n-6 (9.7-fold that of LO fish) with a low level of 20:4n-6 was found in the livers of SO fish in the present study. This indicates that the conversion of 20:3n-6 to 20:4n-6 might be reduced during SO diet feeding or that the utilization of 20:4n-6 for 22:5n-6 increased and was more rapid during the same period, leading to the accumulation of 22:5n-6 as one of the predominant metabolic products of 18:2n-6. The n-3/n-6 ratios in the tissues of fish fed the SO diet were significantly decreased compared to those of OO, LO, and CLO fish, especially in the liver. The n-3/n-6 ratio was 0.4, almost 11.3 times lower than that of OO fish, 13 times lower than that of CLO, and 15.3 times lower than that of LO fish. Significant increases in  $\Delta 6$  and  $\Delta 5$  desaturation and elongation products of 18:2n-6 were found in SO-fed fish, and a significant decrease in 22:6n-3 and total n-3 FA was observed in SO-fed fish. These signifi-

cant changes in n-3/n-6 ratio and FA composition of fish fed different dietary fats indicate that the competition and inhibition between 18:2n-6 and 18:3n-3 for further desaturation and elongation were greatly influenced by the type of dietary fat and the content of n-3 and n-6 FA in the diet. Similar changes in FA composition and n-3/n-6 ratio have also been reported for salmon, rainbow trout, and tilapia (33,45–47).

Substantial amounts of chain elongation and desaturation products of 18:3n-3, such as 18:4n-3, 20:3n-3, 20:4n-3, 20:5n-3, 22:5n-3, and 22:6n-3, were found in the liver and the viscera of fish fed the LO diet combined with few or no corresponding products of 18:2n-6. This implies that chain elongation and desaturation of 18:3n-3 were actively occurring and that desaturation enzymes at this dietary n-3/n-6 ratio probably favored 18:3n-3 over 18:2n-6 as a substrate in Eurasian perch lipid metabolism. This is in agreement with previous studies in rats (48), rainbow trout (33), and Atlantic salmon (49). FA composition of the muscle from fish fed four diets remained similar, regardless of different dietary fats. DHA content and total n-3 FA in all tissues of LO fish were

**TABLE 6**  
**FA Compositions (wt% total FA) of Muscle<sup>a</sup>**

	Dietary treatments			
	OO	SO	LO	CLO
Total lipid (%, wet wt)	0.8 ± 0.0 <sup>a</sup>	1.0 ± 0.1 <sup>a</sup>	1.1 ± 0.2 <sup>a</sup>	1.1 ± 0.2 <sup>a</sup>
FA				
14:0	0.8 ± 0.1 <sup>a</sup>	0.7 ± 0.0 <sup>a</sup>	1.0 ± 0.1 <sup>b,c</sup>	1.4 ± 0.1 <sup>c</sup>
16:0	20.2 ± 0.1	19.8 ± 0.7	20.2 ± 0.1	21.6 ± 0.4
18:0	3.6 ± 0.1 <sup>a</sup>	0.3 ± 0.1 <sup>b</sup>	0.4 ± 0.1 <sup>b</sup>	3.6 ± 0.1 <sup>a</sup>
20:0	0.1 ± 0.0	0.3 ± 0.0	—	—
Total SFA	24.6 ± 0.1 <sup>a</sup>	21.1 ± 0.7 <sup>b</sup>	21.5 ± 0.1 <sup>b</sup>	26.6 ± 0.4 <sup>c</sup>
16:1	3.5 ± 0.0	3.0 ± 0.1	3.7 ± 0.1	4.8 ± 0.3
18:1	12.6 ± 1.7 <sup>a</sup>	14.2 ± 0.9 <sup>a,b</sup>	15.0 ± 2.6 <sup>b</sup>	12.4 ± 2.8 <sup>a</sup>
20:1	2.1 ± 0.2	1.6 ± 0.3	2.0 ± 0.2	2.3 ± 0.3
22:1	0.5 ± 0.1	0.3 ± 0.1	0.5 ± 0.1	0.7 ± 0.0
Total monoenes	18.6 ± 1.1	19.0 ± 0.8	21.1 ± 0.8	20.2 ± 0.9
18:2n-6	2.7 ± 0.8 <sup>a</sup>	12.3 ± 4.9 <sup>b</sup>	3.1 ± 0.6 <sup>a</sup>	2.1 ± 0.0 <sup>a</sup>
18:3n-6	0.2 ± 0.0	0.3 ± 0.0	0.2 ± 0.1	0.2 ± 0.0
20:2n-6	0.2 ± 0.0	0.5 ± 0.1	0.3 ± 0.1	0.2 ± 0.0
20:3n-6	0.2 ± 0.0 <sup>a</sup>	1.3 ± 0.6 <sup>b</sup>	0.2 ± 0.0 <sup>a</sup>	— <sup>a</sup>
20:4n-6	2.3 ± 0.1	1.8 ± 0.2	1.8 ± 0.0	1.6 ± 0.1
22:4n-6	0.4 ± 0.0	0.4 ± 0.0	0.5 ± 0.0	0.5 ± 0.1
22:5n-6	0.6 ± 0.0 <sup>a</sup>	1.3 ± 0.6 <sup>b</sup>	0.6 ± 0.1 <sup>a</sup>	0.6 ± 0.4 <sup>a</sup>
Total n-6 FA	6.5 ± 0.2 <sup>a</sup>	17.7 ± 0.7 <sup>b</sup>	6.6 ± 0.7 <sup>a</sup>	5.1 ± 0.0 <sup>a</sup>
18:3n-3	0.3 ± 0.0 <sup>a</sup>	0.2 ± 0.0 <sup>a</sup>	1.6 ± 0.1 <sup>b</sup>	0.5 ± 0.1 <sup>a</sup>
18:4n-3	0.1 ± 0.0 <sup>a</sup>	0.1 ± 0.0 <sup>a</sup>	0.3 ± 0.0 <sup>b</sup>	0.4 ± 0.1 <sup>b</sup>
20:3n-3	—	—	0.1 ± 0.0	0.1 ± 0.0
20:4n-3	0.3 ± 0.1 <sup>a</sup>	0.2 ± 0.0 <sup>a</sup>	0.4 ± 0.0 <sup>a,b</sup>	0.5 ± 0.1 <sup>b</sup>
20:5n-3	8.1 ± 0.4	5.4 ± 1.4	6.7 ± 0.4	7.7 ± 0.1
22:5n-3	0.9 ± 0.1 <sup>a</sup>	0.7 ± 0.1 <sup>a</sup>	1.0 ± 0.0 <sup>a</sup>	1.5 ± 1.1 <sup>b</sup>
22:6n-3	36.3 ± 1.3	31.5 ± 5.6	36.9 ± 0.9	31.5 ± 1.4
Total n-3 FA	45.9 ± 2.5	38.1 ± 5.8	46.9 ± 0.7	45.2 ± 1.5
n-3/n-6	7.1 ± 1.1 <sup>a</sup>	2.2 ± 0.4 <sup>b</sup>	7.1 ± 0.7 <sup>a</sup>	8.9 ± 0.8 <sup>a</sup>
Ratio				

<sup>a</sup>Values are means ± SD obtained from two different pooled samples of six fish from duplicate tanks per treatment. Values in the same row with different superscripts are significantly different ( $P < 0.05$ ). (—), trace value ( $< 0.05$ ) or not detected. For abbreviations see Tables 2 and 3.

comparable to or even higher than those of control fish fed the CLO diet, indicating a high capability of converting 18-carbon n-3 acids to the longest-chain HUFA possible in Eurasian perch. Unlike in carp and other fish, linoleic acid may be incorporated to a large extent in fish tissues; a relatively low percentage of linolenic acid was found in tissues of LO-fed perch, along with high percentages of 20:5n-3 and a high level of 22:6n-3. A high dietary 18:3n-3 content with low levels of 18:3n-3 in fish tissues is clear evidence that Eurasian perch may readily catabolize 18:3n-3 in excess of their biological needs; 18:3n-3 not only serves as a precursor for chain elongation and desaturation, but also Eurasian perch metabolize it as an energy source. Consistent with our finding, Bell *et al.* (50) also reported that relatively limited amounts of 18:3n-3 were found in the phospholipids of Atlantic salmon fed an LO diet as compared to a large amount of 18:2n-6 deposition in fish fed a sunflower oil diet. The present study shows that the different characteristics of deposition and utilization between 18:3n-3 and 18:2n-6 may be the key difference in these two important FA in fish lipid metabolism. However, the essentiality of 18:3n-3 for perch and its specific

biological and physiological functions remain unclear. Evidence of a specific metabolic function for 18:3n-3 other than as a precursor of n-3 HUFA has not been published (51).

The existence and function of  $\Delta 4$  have been disputed during the past decade. Low  $\Delta 4$  desaturase activities and a possibly related product have been reported by some investigators (52–55). However, recent evidence in rainbow trout with original findings in rats has reinforced the argument of DHA synthesis in that desaturations of both PUFA of the n-3 and n-6 series through the  $\Delta 6$  and  $\Delta 5$  enzymes are used to produce 24:6n-3 and 24:5n-6, which are then chain-shortened to 22:6n-3 and 22:5n-6, respectively, by  $\beta$ -oxidation (56–57). Since only low  $\Delta 4$  desaturase activity has been reported in fish, the large amounts of DHA synthesis found in the present study most likely resulted from this peroxisomal process. However, the exact DHA synthesis process in perch awaits further investigation.

Compared to marine fish, most freshwater fish contain high levels of 18-carbon n-6 and n-3 FA, but also substantial concentrations of EPA and DHA (10,24,58). The presence of substantial amounts of DHA with relatively low EPA was also



observed in our previous studies on Eurasian perch (36). Here high concentrations of DHA and less EPA were found in all tissue lipids of LO and CLO fish, which suggests that these FA patterns are the distinguishing feature and physiological nature of Eurasian perch lipids and are probably related to the high  $\Delta 6$  and  $\Delta 5$  desaturation enzyme activities that lead to the accumulation of DHA. Therefore, active metabolic bioconversion of n-3 and n-6 FA, and n-3 and n-6 FA competition and inhibition observed in the present study are the most appropriate explanations for the similarity of DHA concentration in LO and CLO fish and for the differences in n-3 and n-6 FA composition in LO and SO fish, all of which are closely linked to the influences of their dietary fats (30).

In summary, the results of the present study with Eurasian perch confirm that the competition for the same desaturation enzyme between n-3 and n-6 FA is greatly influenced by dietary fat, and perhaps is regulated by the content of n-3 and n-6 FA in the diet. Although it contains relatively low fat in the muscle, the Eurasian perch is a potential nutritional food fish for human consumption with a high DHA content. In view of the great ability for bioconversion of n-3 and n-6 FA observed in the present study of Eurasian perch, LO is a promising alternative to fish oil in perch feed formulations in terms of DHA synthesis. However, before drawing final conclusions, more work is needed to determine to what extent LO may replace the fish oil in the diet, as well as to better understand the effects of the dietary n-3/n-6 ratio on the lipid metabolism of fish in general.

## ACKNOWLEDGMENTS

The authors are grateful to Thierry Mayenne for his technical support. This study was jointly supported by the Walloon Region (General Directorate of Technology, Research, and Energy) and by the European Commission Agriculture and Fisheries (FAIR) specific RTD programme, CT 98-9241.

## REFERENCES

- Carlson, S.E. (1989) Polyunsaturated Fatty Acids and Infant Nutrition, in *Dietary  $\omega 3$  and  $\omega 6$  Fatty Acids: Biological Effects and Nutritional Essentiality* (Galli C., and Simopoulos, A.P., eds.), Series A: Life Sciences, Vol. 171, pp. 147–157, Plenum Press, New York.
- Horrobin, D.F., and Manku, M.S. (1990) Clinical Biochemistry of Essential Fatty Acids, in *Omega-6 Essential Fatty Acids: Pathophysiology and Roles in Clinical Medicine* (Horrobin, D.F., ed.), pp. 21–53, Wiley-Liss, New York.
- Simopoulos, A.P., Kifer, R.R., and Wykes, A.A. (1991)  $\omega 3$  Fatty Acids: Research Advances and Support in the Field Since June 1985 (Worldwide), in *Health Effects of  $\omega 3$  Polyunsaturated Fatty Acids in Seafoods* (Simopoulos, A.P., Kifer, R.R., Martin, R.E., and Barlow, S.M., eds.), World Review of Nutrition and Dietetics Series, Vol. 66, pp. 51–71, Karger, Basel.
- Lauritzen, L., Hansen, H.S., Jorgensen, M.H., and Michaelsen, K.F. (2001) The Essentiality of Long-Chain n-3 Fatty Acids in Relation to Development and Function of Brain and Retina, *Prog. Lip. Res.* 40, 1–94.
- Conquer, J.A., Tierney, M.C., Zecerich, J., Bettger, W.J., and Fisher, R.H. (2000). Fatty Acid Analyses of Blood Plasma of Patients with Alzheimer's Disease, Other Types of Dementia, and Cognitive Impairment, *Lipids* 35, 1305–1312.
- Ackman, R.G. (1999) Docosahexaenoic Acid in the Infant and Its Mother, *Lipids* 34, 125–128.
- Rapoport, S.I., Chang, M.C.J., and Spector, A.A. (2001) Delivery and Turnover of Plasma-Derived Essential PUFAs in Mammalian Brain, *J. Lipid Res.* 42, 678–685.
- Parrish, C.C., Myher, J.J., Kuksis, A., and Angel, A. (1997) Lipid Structure of Rat Adipocyte Plasma Membranes Following Dietary Lard and Fish Oil, *Biochim. Biophys. Acta* 1323, 235–262.
- Cowey, C.B., and Sargent, J.R. (1977) Lipid Nutrition in Fish, *Comp. Biochem. Physiol.* 57B, 269–273.
- Castell, J.D. (1979) Review of Lipid Requirement of Finfish, in *Finfish Nutrition and Fishfeed Technology* (Halver, J.E., and Tiews, K., eds.), Vol. 1, pp. 59–84, Heinemann, Berlin.
- Kanazawa, A., Teshima, S.I., and Ono, K. (1979) Relationship Between Essential Fatty Acid Requirements of Aquatic Animals and the Capacity for Bioconversion of Linolenic Acid to Highly Unsaturated Fatty Acids, *Comp. Biochem. Physiol.* 63B, 295–298.
- Xu, X.L., Ji, W.J., Castell, J.D., and O'Dor, R.K. (1993) The Nutritional Value of Dietary n-3 and n-6 Fatty Acids for Chinese Prawn *Penaeus chinensis*, *Aquaculture* 118:277–285.
- Sargent, J.R., McEvoy, L.A., and Bell, J.G. (1997) Requirements, Presentation, and Sources of Polyunsaturated Fatty Acids in Marine Fish Larval Feeds, *Aquaculture* 155, 117–127.
- Rainuzzo, J.R., Reitan, K.I., and Olsen, Y. (1997) The Significance of Lipids at Early Stages of Marine Fish: A Review, *Aquaculture* 155, 103–115.
- Takeuchi, T. (1997) Essential Fatty Acid Requirements of Aquatic Animals with Emphasis on Fish Larvae and Fingerlings, *Rev. Fish. Sci* 5, 1–25.
- Sargent, J., McEvoy, L., Estevez, A., Bell, G., Bell, M., Henderson, J., and Tocher, D. (1999) Lipid Nutrition of Marine Fish During Early Development: Current Status and Future Directions, *Aquaculture* 179:217–229.
- Brenner, R.R. (1981) Nutritional and Hormonal Factors Influencing Desaturation of Essential Fatty Acids, *Prog. Lipid Res.* 20, 41–47.
- Cinti, D.L., Cook, L., Nagi, M.N., and Suneja, S.K. (1992) The Fatty Acid Chain Elongation System of Mammalian Endoplasmic Reticulum, *Prog. Lipid Res.* 31, 1–51.
- Garg, M.L., Sebokova, E., Thomson, A.B.R., and Clandinin, M.T. (1988)  $\Delta 6$  Desaturase Activity in Liver Microsomes of Rats Fed Diets Enriched with Cholesterol and/or n-3 Fatty Acids, *Biochem. J.* 249, 351–356.
- Thomassen, M., and Rosjo, C. (1989) Different Fats in Feed for Salmon: Influence on Sensory Parameters, Growth Rate, and Fatty Acids in Muscle and Heart, *Aquaculture* 79, 129–135.
- Kalogeropoulos, N., Alexis, M.N., and Henderson, R.J. (1992) Effects of Dietary Soybean and Cod-Liver Oil Levels on Growth and Body Composition of Gilthead Bream (*Sparus aurata*), *Aquaculture* 104, 293–308.
- Owen, J.M., Adron, J.W., Sargent, J.R.S., and Cowey, C.B. (1972) Studies on the Nutrition of Marine Flatfish. The Effect of Dietary Fatty Acids on the Tissue Fatty Acids of the Plaice, *Pleuronectes platessa*, *Mar. Biol.* 13, 160–166.
- Léger, C., Gatesoupe, E.J., Metailler, R., Luquet, P., and Fremont, L. (1979) Effect of Dietary Fatty Acids Differing by Chain Lengths and  $\omega$  Series on the Growth and Lipid Composition of Turbot *Scophthalmus maximus* L., *Comp. Biochem. Physiol.* 64B, 345–350.
- Sargent, J.R., Henderson, R.J., and Tocher, D.R. (1989) The Lipids, in *Fish Nutrition*, 2nd edn. (Halver, J.E., ed.), pp. 153–218 Academic Press, San Diego.
- Sargent, J.R. (1999) Development in Lipid Nutrition Within the Aquagene Initiative, *Aquacult. News* 25 (Institute of Aquaculture, University of Stirling, Stirling, Scotland), 8–12.
- Kayama, M., Tsuchiya, Y., and Mead, J.F. (1963) A Model Experiment of Aquatic Food Chain with Special Significance in Fatty Acid Conversion, *Bull. Jpn. Soc. Sci. Fish.* 29, 452–458.

27. Owen, J.M., Adron, J.W., Middleton, C., and Cowey, C.B. (1975) Elongation and Desaturation of Dietary Fatty Acids in Turbot *Scophthalmus maximus* L. and Rainbow Trout *Salmo gairdneri* Rich, *Lipids* 10, 528–531.
28. Takeuchi, T., Watanabe, T., and Nose, T. (1979) Requirement for Essential Fatty Acids of Chum Salmon (*Oncorhynchus keta*) in Freshwater Environment, *Bull. Jpn. Soc. Sci. Fish.* 45, 1319–1323.
29. Yamada, K., Kobayashi, K., and Yone, Y. (1980) Conversion of Linolenic Acid to  $\omega$ -3 Highly Unsaturated Fatty Acids in Marine Fishes and Rainbow Trout, *Bull. Jpn. Soc. Sci. Fish* 46, 1231–1233.
30. Henderson, R.J., and Tocher, D.R. (1987) The Lipid Composition and Biochemistry of Freshwater Fish, *Prog. Lipid Res.* 26, 281–347.
31. Castell, J.D., Lee, D.J., and Sinnhuber, R.O. (1972) Essential Fatty Acid in the Diet of Rainbow Trout (*Salmo gairdneri*), Lipid Metabolism and Fatty Acid Composition, *J. Nutr.* 102, 93–100.
32. Yu, T.C., and Sinnhuber, R.O. (1975) Effect of Dietary Linolenic and Linoleic Acids on Growth and Lipid Metabolism of Rainbow Trout (*Salmo gairdneri*), *Lipids*, 10, 63–66.
33. Yu, T.C., and Sinnhuber, R.O. (1979) Effect of Dietary n-3 and n-6 Fatty Acids on Growth and Feed Conversion Efficiency of Coho Salmon (*Oncorhynchus kisutch*), *Aquaculture* 16, 31–38.
34. Dabrowski, K., Culver, D.A., Brooks, C.L., and Voss, A.C. (1993) Biochemical Aspects of the Early Life History of Yellow Perch *Perca flavescens*, in *Fish Nutrition in Practice* (Kaushik, S.J., and Luquet, P., eds.), pp. 531–540, Institut National de la Recherche Agronomique, Paris, France.
35. Thongard, S., Dabrowski, K., and Ebeling, J. (1995) Lipid and Fatty Acid Composition in Gonad and Liver of Wild and Captive Broodstock of Yellow Perch *Perca flavescens* and Consequently in Their Eggs and Larvae, World Aquaculture Society Annual Meeting, San Diego (abstract, p. 93).
36. Xu, X.L., Fontaine, P., M elard, C., and Kestemont, P. (2000) Effects of Different Dietary Fat Levels on Growth, Feed Efficiency, Lipid Composition, and Histological Changes of Eurasian Perch *Perca fluviatilis*, *Aqua 2000*, European Aquaculture Special Publication No. 28, Oostende, Belgium.
37. Kestemont, P., Vandeloise, E., M elard, C., Fontaine, P., and Brown, P., Growth and Nutritional Status of Eurasian Perch *Perca fluviatilis* L. Fed Graded Levels of Dietary Lipids With or Without Added Ethoxyquin, *Aquaculture*, in press.
38. Fiogb e, E.D., Kestemont, P., M elard, C., and Micha, J.C. (1996) The Effects of Dietary Crude Protein on Growth of Eurasian Perch *Perca fluviatilis*, *Aquaculture* 144, 239–249.
39. Folch, J., Lees, M., and Sloane Stanley, G.H. (1957) A Simple Method for the Isolation and Purification of Total Lipides from Animal Tissues, *J. Biol. Chem.* 226, 497–509.
40. Bligh, E.G., and Dyer, W.J. (1959) A Rapid Method of Total Lipid Extraction and Purification, *Can. J. Biochem. Physiol.* 37, 911–917.
41. Ackman, R.G. (1998) Remarks on Official Methods Employing Boron Trifluoride in the Preparation of Methyl Esters of the Fatty Acids of Fish Oils, *J. Am. Oil Chem. Soc.* 75, 541–545.
42. Ackman, R.G. (1980) Fish Lipids, Part I, in *Advances in Fish Science and Technology* (Connell, J.J., ed.), pp. 86–103, Fishing News Books, Farnham, United Kingdom.
43. Steel, R.G.D., and Torrie, J.H. (1960) *Principles and Procedures of Statistics*, p. 418, McGraw-Hill, New York.
44. Tandler, A., Watanabe, T., Satoh, S., and Fukusho, K. (1989). The Effect of Food Deprivation on the Fatty Acid and Lipid Profile of Red Seabream Larvae (*Pagrus major*), *Br. J. Nutr.* 62, 349–361.
45. Bell, J.G., Dick, J.R., and Sargent, J.R. (1993) Effect of Diets Rich in Linoleic or  $\alpha$ -Linolenic Acid on Phospholipid Fatty Acid Composition and Eicosanoid Production in Atlantic Salmon (*Salmo salar*), *Lipids* 28, 819–826.
46. Olsen, K.E., Henderson, R.J., and McAndrew, B.J. (1990) The Conversion of Linoleic Acid and Linolenic Acid to Longer Chain Polyunsaturated Fatty Acids by Tilapia (*Oreochromis nilotica*) in vivo, *Fish Physiol. Biochem.* 8, 261–270.
47. Olsen, R.E., and Ringo, E. (1992) Lipids of Arctic Charr, *Salvelinus alpinus* (L.) II. Influence of Dietary Fatty Acids on the Elongation and Desaturation of Linoleic and Linolenic Acid, *Fish Physiol. Biochem.* 9, 393–399.
48. Sprecher, H. (1989) (n-3) and (n-6) Fatty Acid Metabolism, in *Dietary Omega 3 and Omega 6 Fatty Acids: Biological Effects and Nutritional Essentiality* (Galli, C., and Simopoulos, A.P., eds.), Series A: Life Sciences, Vol. 171, pp. 69–79, Plenum Press, New York.
49. Bell, J.G., Tocher, D.R., Farndale, B.M., Cox, D.I., McKinney, R.W., and Sargent, J.R. (1997) The Effect of Dietary Lipid on Polyunsaturated Fatty Acid Metabolism in Atlantic Salmon (*Salmo salar*) Undergoing Parr–Smolt Transformation, *Lipids* 32, 515–525.
50. Bell, J.G., Dick, J.R., McVivar, A.H., Sargent, J.R., and Thompson, K.D. (1993) Dietary Sunflower, Linseed, and Fish Oil Affect Phospholipid Fatty Acid Composition, Development of Cardiac Lesions, Phospholipase Activity, and Eicosanoid Production in Atlantic Salmon (*Salmo salar*), *Prostaglandins, Leukotrienes Essent. Fatty Acids* 49, 665–673.
51. Innis, S.M. (1991) Essential Fatty Acids in Growth and Development, *Prog. Lipid Res.* 30, 39–103.
52. Mourente, G., and Odriozola, J.M. (1990) Effect of Broodstock Diets on Total Lipids and Fatty Acid Composition of Larvae of Gilthead Sea Bream (*Sparus aurata* L.) During Yolk Sac Stage, *Fish Physiol. Biochem.* 8, 103–110.
53. Tocher, D.R., and Dick, J.R. (1990) Incorporation and Metabolism of n-3 and n-6 Polyunsaturated Fatty Acids in Phospholipid Classes in Cultured Atlantic Salmon (*Salmo salar*) Cells, *Comp. Biochem. Physiol.* 96B, 73–79.
54. Olsen, R.E., Henderson, R.J., and Ringo, E. (1991) Lipid of Arctic Charr, *Salvelinus alpinus* (L.) I. Dietary Induced Changes in Lipid Class and Fatty Acid Composition, *Fish Physiol. Biochem.* 9, 151–164.
55. Christiansen, E.N., Lund, J.S., Rortveit, T., and Rustan, A.C. (1991) Effect of Dietary n-3 and n-6 Fatty Acids on Fatty Acid Desaturation in Rat Liver, *Biochim. Biophys. Acta* 1082, 57–62.
56. Voss, A., Rienhart, M., Sankarappa, S., and Sprecher, H. (1991) The Metabolism of 7,10,13,16,19-Docosapentaenoic Acid to 4,7,10,13,16,19-Docosahexaenoic Acid in Rat Liver Is Independent of a 4-Desaturase, *J. Biol. Chem.* 266, 19995–20000.
57. Buzzi, M., Henderson, R.J., and Sargent, J.R. (1996) The Desaturation and Elongation of Linolenic Acid and Eicosapentaenoic Acid by Hepatocytes and Liver Microsomes from Rainbow Trout (*Oncorhynchus mykiss*) Fed Diets Containing Fish Oil and Olive Oil, *Biochim. Biophys. Acta* 1299, 235–244.
58. Ackman, R.G. (1967) Characteristics of the Fatty Acid Composition and Biochemistry of Some Freshwater Fish Oils and Lipids in Comparison with Marine Oils and Lipids, *Comp. Biochem. Physiol.* 22:907–922.

[Received June 6, 2001 and in revised form October 3, 2001; revision accepted January 31, 2002]

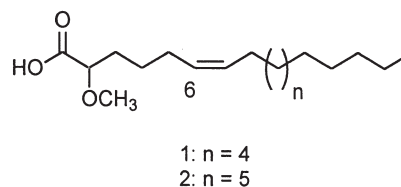
# Novel Methoxylated FA from the Caribbean Sponge *Sphaciospongia cuspidifera*

Néstor M. Carballeira\* and Johanna Alicea

Department of Chemistry, University of Puerto Rico, San Juan, Puerto Rico 00931-3346

**ABSTRACT:** The  $\Delta^6$  monoenoic methoxylated FA (6Z)-2-methoxy-6-heptadecenoic acid and (6Z)-2-methoxy-6-octadecenoic acid were identified for the first time in nature in the phospholipids from the uncommon Caribbean sponge *Sphaciospongia cuspidifera*. These findings expand the occurrence of  $\Delta^6$  2-methoxylated FA to  $C_{17}$ – $C_{18}$  chain lengths and establish a new FA biosynthetic possibility for these marine organisms. The novel methoxylated FA also could have originated from the phospholipids of a bacterium in symbiosis with the sponge.

Paper no. L8925 in *Lipids* 37, 305–308 (March 2002).



SCHEME 1

Methoxylated lipids have attracted much attention for their intriguing biological activities. Earlier work by Hallgren and collaborators with methoxy-substituted glycerol ethers from Greenland shark liver oil established their antibiotic effect against several bacterial strains, including *Streptococcus* and *Staphylococcus* (1,2). Some of these methoxy-substituted glycerol ethers also display antitumor activity against a variety of human tumors (2). Most recently, several phosphocholines possessing 2'-methoxy acyl chains, such as 1-*O*-(2'-methoxyhexadecyl)-*sn*-glycero-3-phosphocholine and 1-*O*-(2'-methoxy-4'*Z*-hexadecenyl)-*sn*-glycero-3-phosphocholine, were isolated from the sponge *Spirastrella abata* (3). These methoxylated lysophospholipids were also significantly cytotoxic against specific lines of lung, ovarian, and skin cancer cells with  $ED_{50}$  values of 4–6  $\mu\text{g/mL}$  (3).

Whereas the previous examples relate to ether lipids, some work has also been published regarding methoxylated phospholipid FA from marine sponges (4,5). For example, our group reported a whole series of  $\Delta^6$  2-methoxylated FA with  $C_{14}$ – $C_{16}$  chain lengths from the Caribbean sponge *Callyspongia fallax* (4). In addition, we showed that short-chain methoxylated FA such as (6Z)-2-methoxy-6-hexadecenoic acid display moderate antibacterial activity against Gram-positive bacteria (5). Despite these efforts, other  $\Delta^6$  2-methoxylated FA, in particular those with  $C_{17}$ – $C_{18}$  chain lengths, remain unknown. It is quite probable that these

$C_{17}$ – $C_{18}$   $\Delta^6$  2-methoxylated FA also display antimicrobial and/or antitumor activity as either FFA or bound to phospholipids. Therefore, as part of our continuing program in the isolation and characterization of novel FA from marine organisms we report the identification of the 2-methoxylated FA (6Z)-2-methoxy-6-heptadecenoic acid (1) and (6Z)-2-methoxy-6-octadecenoic acid (2) (Scheme 1) from the uncommon Caribbean sponge *Sphaciospongia cuspidifera* Lamarck (class Demospongiae, order Hadromerida, family Clionidae) (6). This finding expands the occurrence of  $\Delta^6$  2-methoxylated normal-chain FA in sponges to  $C_{14}$ – $C_{18}$  chain lengths.

## MATERIALS AND METHODS

**Instrumentation.** FAME were analyzed by direct ionization using GC–MS (Hewlett-Packard 5972A MS ChemStation) at 70 eV equipped with a 30 m  $\times$  0.25 mm special performance capillary column (HP-5MS) of polymethylsiloxane cross-linked with 5% phenyl methylpolysiloxane. The temperature program was as follows: 130°C for 1 min, increased at a rate of 3°C/min to 270°C, and maintained for 30 min at 270°C.

**Sponge collection.** *Sphaciospongia cuspidifera* Lamarck was collected from Cayo Enrique reef near La Parguera, Puerto Rico, in March 1991 at 20 m depth by scuba. A voucher specimen is stored at the Chemistry Department of the University of Puerto Rico, Río Piedras campus (6).

**Extraction and isolation of phospholipids.** The sponge (50 g) was carefully cleaned and cut into small pieces. Immediate extraction after collection with 3  $\times$  300 mL of  $\text{CHCl}_3/\text{MeOH}$  (1:1) yielded the total lipids (4 g). The neutral lipids (0.11 g), glycolipids (1.0 g), and phospholipids (1.1 g) were separated by column chromatography on Si gel (60–200 mesh) from 3 g of total lipids using the procedure of Privett *et al.* (7).

\*To whom correspondence should be addressed at Department of Chemistry, University of Puerto Rico, P.O. Box 23346, San Juan, Puerto Rico 00931-3346. E-mail: ncarballeira@upr.edu

Abbreviations: DMDS, dimethyl disulfide; ECL, equivalent chain-length; FCL, fractional chain-length.



**Derivatives.** The fatty acyl components of the phospholipids were obtained as their methyl esters (0.011 g) by reaction of the phospholipids (1.07 g) with methanolic HCl followed by column chromatography. They were stored at  $-20^{\circ}\text{C}$  in hexane with BHT as antioxidant until analyzed. The methyl esters were hydrogenated in 10 mL absolute methanol with catalytic amounts of platinum oxide ( $\text{PtO}_2$ ). The double-bond positions in these compounds were determined by dimethyl disulfide (DMDS) derivatization following a procedure that was previously described (8,9).

## RESULTS AND DISCUSSION

The Caribbean sponge *S. cuspidifera* presented a typical sponge phospholipid profile with PE and PS as the two most abundant phospholipids. Acid methanolysis provided a rather complex phospholipid FA composition of around 68 identifiable FA, as shown in Table 1. FA chain lengths ranged between  $\text{C}_{10}$  and  $\text{C}_{27}$ , mainly consisting of monoenoic and dienoic FA. The monoenoic FA were particularly abundant in

this sponge; they made up around 22% of the total FA composition. However, a most interesting finding was the identification of a whole series of n-7 and n-9 monounsaturated FA with chain lengths between  $\text{C}_{18}$  and  $\text{C}_{26}$ . As expected, the most characteristic FA from *S. cuspidifera* was the (5Z,9Z)-5,9-hexacosadienoic acid, which was identified in this sponge together with other  $\Delta^{5,9}$  diunsaturated very long chain acids such as the (5Z,9Z)-5,9-tetracosadienoic acid and the (5Z,9Z)-5,9-heptacosadienoic acid (6). All of these FA were characterized as methyl esters by GC-MS, and the double bond positions in the monoenoic esters were elucidated by DMDS derivatization as well as by GC comparisons with authentic standards.

The most interesting series of FA from *S. cuspidifera* were the monounsaturated FA (6Z)-2-methoxy-5-hexadecenoic acid, (5Z)-2-methoxy-6-hexadecenoic acid, (6Z)-2-methoxy-6-heptadecenoic acid (**1**), and (6Z)-2-methoxy-6-octadecenoic acid (**2**). The methoxylated acids **1** and **2** are unprecedented in nature. The relative GC retention times of their methyl esters, the mass spectra of both the methyl esters and

**TABLE 1**  
Identified Phospholipid FA from *Sphēciospongia cuspidifera*

FA	Relative abundance (wt %)	FA	Relative abundance (wt %)
Decanoic (10:0)	0.4	11,14,17-Eicosatrienoic (20:3n-3)	0.8
Dodecanoic (12:0)	0.2	8,11,14-Eicosatrienoic (20:3n-6)	0.3
(Z)-9-Tetradecenoic (14:1n-5)	0.1	Eicosadienoic (20:2)	1.5
Tetradecanoic (14:0)	1.8	18-Methylnonadecanoic ( <i>i</i> -20:0)	0.8
4,8,12-Trimethyltridecanoic (16:0)	8.2	17-Methylnonadecanoic ( <i>ai</i> -20:0)	1.7
13-Methyltetradecanoic ( <i>i</i> -15:0)	0.8	(Z)-11-Eicosenoic (20:1n-9)	0.2
12-Methyltetradecanoic ( <i>ai</i> -15:0)	0.6	(Z)-13-Eicosenoic (20:1n-7)	0.1
Pentadecanoic (15:0)	0.6	Eicosanoic (20:0)	2.3
(5Z,9Z)-5,9-Hexadecadienoic (16:2n-7)	0.2	Methyleicosanoic (21:0)	1.3
14-Methylpentadecanoic ( <i>i</i> -16:0)	0.2	19-Methyleicosanoic ( <i>i</i> -21:0)	0.5
(Z)-9-Hexadecenoic (16:1n-7)	0.3	18-Methyleicosanoic ( <i>ai</i> -21:0)	0.7
Hexadecanoic (16:0)	11.7	(Z)-14-Heneicosenoic (21:1n-7)	0.2
7-Methyl-6(Z)-hexadecenoic (17:1n-11)	0.5	Heneicosanoic (21:0)	0.6
15-Methylhexadecanoic ( <i>i</i> -17:0)	0.5	20-Methylheneicosanoic ( <i>i</i> -22:0)	0.1
14-Methylhexadecanoic ( <i>ai</i> -17:0)	2.5	19-Methylheneicosanoic ( <i>ai</i> -22:0)	0.2
(5Z)-2-Methoxy-5-hexadecenoic (2-OMe-16:1n-11)	0.5	(Z)-13-Docosenoic (22:1n-9)	0.4
(6Z)-2-Methoxy-6-hexadecenoic (2-OMe-16:1n-10)	2.5	(Z)-15-Docosenoic (22:1n-7)	0.3
(Z)-9-Heptadecenoic (17:1n-8)	0.2	Docosanoic (22:0)	0.8
Heptadecanoic (17:0)	0.7	(Z)-14-Tricosenoic (23:1n-9)	0.1
2-Methoxyhexadecanoic (2-OMe-16:0)	0.1	(Z)-16-Tricosenoic (23:1n-7)	0.1
(5Z,9Z)-5,9-Octadecadienoic (18:2n-9)	0.5	Tricosanoic (23:0)	0.5
(9Z,12Z)-9,12-Octadecadienoic (18:2n-6)	2.9	(5Z,9Z)-5,9-Tetracosadienoic (24:2n-15)	0.2
(Z)-9-Octadecenoic (18:1n-9)	5.2	(Z)-15-Tetracosenoic (24:1n-9)	2.4
(Z)-11-Octadecenoic (18:1n-7)	3.7	(Z)-17-Tetracosenoic (24:1n-7)	1.8
(6Z)-2-Methoxy-6-heptadecenoic (2-OMe-17:1n-11) <sup>a</sup>	0.3	Tetracosanoic (24:0)	0.3
Octadecanoic (18:0)	4.9	(5Z,9Z)-5,9-Pentacosadienoic (25:2n-16)	3.2
( <i>E</i> )-11-Methyl-12-octadecenoic (19:1n-7)	0.5	(Z)-9-Pentacosenoic (25:1n-16)	0.1
Methylnonadecanoic (19:0)	0.2	(Z)-16-Pentacosenoic (25:1n-9)	0.1
17-Methyloctadecanoic ( <i>i</i> -19:0)	0.4	(Z)-18-Pentacosenoic (25:1n-7)	0.1
16-Methyloctadecanoic ( <i>ai</i> -19:0)	0.3	(5Z,9Z)-5,9-Hexacosadienoic (26:2n-17)	17.7
Nonadecenoic (19:1)	0.2	(Z)-17-Hexacosenoic (26:1n-9)	4.6
(6Z)-2-Methoxy-6-octadecenoic (2-OMe-18:1n-12) <sup>a</sup>	0.1	(Z)-19-Hexacosenoic (26:1n-7)	1.1
Nonadecanoic (19:0)	0.6	Hexacosanoic (26:0)	0.1
5,8,11,14-Eicosatetraenoic (20:4n-6)	1.8	(5Z,9Z)-5,9-Heptacosadienoic (27:2n-18)	0.5

<sup>a</sup>Unprecedented in nature.



the corresponding DMDS derivatives, and corroboration of these mass spectra with synthetic analogs provided the basis for their characterization (5). For example, methyl (6Z)-2-methoxy-6-heptadecenoate exhibited unusual chromatographic properties, namely, an equivalent chain length (ECL) value of 17.91, for which the fractional value is well in agreement with those reported in the literature for other  $\Delta^6$  mono-unsaturated linear chain  $\alpha$ -methoxylated methyl esters (10). The mass spectrum of methyl (6Z)-2-methoxy-6-heptadecenoate contained a molecular ion peak at  $m/z$  312 and an intense peak at  $m/z$  104, arising from a favorable McLafferty rearrangement (Table 2). The additional 30 amu, when compared with the typical base peak of saturated FAME at  $m/z$  74, could only be accounted for by a methoxy group at the 2-position. Important for the structural characterization were also the prominent fragmentation ions at  $m/z$  280 ( $M^+ - \text{MeOH}$ ),  $m/z$  253 ( $M^+ - \text{CO}_2\text{CH}_3$ ), and  $m/z$  221 ( $M^+ - \text{CO}_2\text{CH}_3 - \text{MeOH}$ ), which confirmed the  $\alpha$ -methoxylation (11). The double bond at C-6 was determined by preparing the corresponding DMDS adduct, a convenient method for the location of double bonds by mass spectrometry (8,9). For example, the mass spectrum of methyl 2-methoxy-6,7-bis(methylthio)heptadecanoate afforded a molecular ion peak at  $m/z$  406 and an  $M^+ - 59$  peak at  $m/z$  347. The double bond was readily determined to be at carbon 6 by the prominent fragmentations at  $m/z$  205 [ $\text{C}_9\text{H}_{17}\text{SO}_3$ ] $^+$  and 201 [ $\text{C}_{12}\text{H}_{25}\text{S}$ ] $^+$ , since this constitutes cleavage between carbons 6 and 7. There was also an abundant ion at  $m/z$  173 [ $\text{C}_8\text{H}_{13}\text{SO}_2$ ] $^+$  resulting from the loss

of methanol from the  $m/z$  205 fragment. Upon catalytic hydrogenation ( $\text{PtO}_2$ ), methyl (6Z)-2-methoxy-6-heptadecenoate yielded the normal-chain methyl 2-methoxyheptadecanoate as evidenced by a strong fragmentation at  $m/z$  255 ( $M^+ - 59$ ) in the mass spectrum of the latter. The experimental data thus support methyl (6Z)-2-methoxy-6-heptadecenoate as the most probable structure for this methyl ester. In a similar fashion methyl (6Z)-2-methoxy-6-octadecenoate was characterized (Table 2). A GC co-elution of methyl (6Z)-2-methoxy-6-hexadecenoate from *S. cuspidifera* with a synthetic sample confirmed a Z double bond for the natural methyl ester (5). In addition, a straight line was obtained when the retention times of the  $\alpha$ -methoxylated  $\Delta^6$ -16:1,  $\Delta^6$ -17:1, and  $\Delta^6$ -18:1 methyl esters were plotted against chain length, thus also supporting the Z double bond stereochemistry for the  $\Delta^6$ -17:1 and  $\Delta^6$ -18:1 methoxylated methyl esters.

The novel FA identified in this sponge expand the present scheme ( $2\text{-OCH}_3\text{-}n:0 \rightarrow \Delta^6$  desaturase  $\rightarrow 2\text{-OCH}_3\text{-}n:1$ ,  $n = 14\text{--}18$ ) of possible biosynthetic pathways for  $\text{C}_{14}\text{--}\text{C}_{18}$   $\alpha$ -methoxylated FA in nature. *Sphaciospongia cuspidifera* is interesting because, despite the fact that it contains a series of 2-OME- $n:1$   $\Delta^6$  FA with chain lengths between 16 and 18 carbons, it also contains a 2-OME-16:1  $\Delta^5$  FA, in addition to what was originally reported (8). With the exception of the 2-methoxyheptadecanoic acid, which has not been encountered in nature, the saturated  $\text{C}_{16}$  and  $\text{C}_{18}$  2-methoxylated FA have been reported from the phospholipids of several sponges (12). Therefore, it is logical to assume that these saturated

**TABLE 2**  
Mass Spectral Data (70 eV) for the Novel Methoxylated Compounds and Their DMDS Derivatives<sup>a</sup>

Compound	ECL	$m/z$ (relative intensity)
Methyl (6Z)-2-methoxy-6-heptadecenoate	17.91	$M^+$ 312 (1), 280 (2), 253 (7), 221 (3), 195 (2), 180 (3), 167 (2), 166 (3), 153 (4), 150 (4), 143 (3), 141 (4), 138 (5), 135 (5), 127 (4), 125 (7), 123 (8), 121 (6), 111 (16), 104 (31), 98 (16), 97 (34), 87 (35), 85 (14), 84 (23), 83 (42), 81 (36), 75 (12), 71 (35), 69 (56), 67 (43), 57 (38), 55 (100)
Methyl 2-methoxy-6,7-bis(methylthio)heptadecanoate		$M^+$ 406 (7), 357 (1), 347 (3), 281 (2), 256 (3), 219 (4), 205 (78), 201 (26), 187 (3), 185 (3), 173 (26), 159 (5), 157 (8), 145 (19), 141 (11), 139 (6), 133 (7), 131 (5), 125 (17), 123 (15), 119 (12), 117 (7), 111 (24), 104 (7), 97 (48), 95 (40), 93 (18), 87 (43), 85 (25), 83 (47), 81 (45), 79 (22), 71 (65), 69 (71), 67 (45), 61 (30), 57 (83), 55 (100)
Methyl (6Z)-2-methoxy-6-octadecenoate	18.91	$M^+$ 326 (1), 294 (4), 267 (17), 234 (7), 227 (8), 208 (6), 167 (3), 166 (4), 153 (6), 150 (9), 141 (7), 135 (8), 127 (9), 125 (11), 123 (13), 121 (12), 111 (26), 104 (83), 97 (44), 95 (70), 91 (14), 87 (31), 85 (21), 83 (46), 81 (63), 75 (14), 71 (74), 69 (56), 68 (30), 67 (86), 57 (57), 55 (100)
Methyl 2-methoxy-6,7-bis(methylthio)octadecanoate		$M^+$ 420 (2), 372 (2), 361 (3), 313 (3), 265 (7), 245 (5), 231 (5), 217 (5), 215 (9), 205 (16), 201 (2), 187 (2), 185 (5), 173 (8), 159 (7), 157 (7), 145 (10), 141 (8), 137 (11), 133 (15), 131 (11), 125 (14), 123 (18), 119 (19), 117 (12), 111 (21), 104 (6), 97 (39), 95 (32), 93 (13), 87 (23), 85 (34), 83 (41), 81 (36), 79 (24), 71 (72), 69 (67), 67 (38), 61 (15), 55 (91)

<sup>a</sup>DMDS, dimethyldisulfide; ECL, equivalent chain-length.

2-methoxylated FA are the biogenetic precursors of the  $\Delta^6$  monounsaturated 2-methoxylated FA. However, *S. cuspidifera* is unusual because both  $\Delta^5$  and  $\Delta^6$  desaturases operate with the methoxylated FA from this sponge, but the  $\Delta^5$  desaturation seems to be limited to  $C_{16}$  chain lengths. In any instance, the identification of small amounts (3.5%) of  $\alpha$ -methoxylated  $C_{16}$ – $C_{18}$  FA in *S. cuspidifera* suggests that these acids are probably of bacterial or endosymbiotic origin.

As to the structure of the possible phospholipids containing the methoxylated FA, we can only speculate at this point. One possibility is novel PE with  $\Delta^5$  or  $\Delta^6$   $\alpha$ -methoxylated FA at the 2-position, and a saturated nonmethoxylated FA at the 1-position, similar to the structures of the hydroxylated PE from myxobacteria (13). However, these 2-methoxylated FA could also occupy the 1-position of PC with the nonmethoxylated FA at the 2-position, analogous to the lysoPC isolated from the sponge *S. abata* (3).

## ACKNOWLEDGMENTS

This work was supported by a grant from the SCORE program of the National Institutes of Health (grant no. S06GM08102). Johanna Alicia thanks Pfizer Inc. for an undergraduate fellowship. We appreciate the help of Dr. Vance P. Vicente in the collection and classification of the sponge.

## REFERENCES

- Hallgren, B., Niklasson, A., Stallberg, G., and Thorin, H. (1974) On the Occurrence of 1-*O*-(2-Methoxyalkyl)glycerols and 1-*O*-Phytanylglycerol in Marine Animals, *Acta Chem. Scand. B* 28, 1035–1040.
- Boeryd, B., Hallgren, B., and Stallberg, G. (1971) Studies on the Effect of Methoxy-Substituted Glycerol Ethers on Tumour Growth and Metastasis Formation, *Br. J. Exp. Pathol.* 52, 221–230.
- Alam, N., Bae, B.H., Hong, J., Lee, C.-O., Shin, B.A., Im, K.S., and Jung, J.H. (2001) Additional Bioactive Lyso-PAF Con-  
geners from the Sponge *Spirastrella abata*, *J. Nat. Prod.* 64, 533–535.
- Carballeira, N.M., and Pagán, M. (2001) New Methoxylated Fatty Acids from the Caribbean Sponge *Callyspongia fallax*, *J. Nat. Prod.* 64, 620–623.
- Carballeira, N.M., Emiliano, A., Hernández-Alonso, N., and González, F.A. (1998) Facile Total Synthesis and Antimicrobial Activity of the Marine Fatty Acids (*Z*)-2-Methoxy-5-hexadecenoic Acid and (*Z*)-2-Methoxy-6-hexadecenoic Acid, *J. Nat. Prod.* 61, 1543–1546.
- Vicente, V.P., Rützler, K., and Carballeira, N.M. (1991) Comparative Morphology, Ecology, and Fatty Acid Composition of West Indian *Sphēciospongia* (Demospongiae), *Mar. Ecol.* 12, 211–226.
- Privett, O.S., Dougherty, K.A., Erdahl, W.L., and Stolyhwo, A. (1973) Lipid Composition of Developing Soybeans, *J. Am. Oil Chem. Soc.* 50, 516–520.
- Carballeira, N.M., and Sepúlveda, J.A. (1992) Two Novel Naturally Occurring  $\alpha$ -Methoxy Acids from the Phospholipids of Two Caribbean Sponges, *Lipids* 27, 72–74.
- Dunkelblum, E., Tan, S.H., and Silk, R.J. (1985) Double-Bond Location in Monounsaturated Fatty Acids by Dimethyl Disulfide Derivatization and Mass Spectrometry, *J. Chem. Ecol.* 11, 265–277.
- Ayanoglu, E., Popov, S., Kornprobst, J.M., Aboud-Bichara, A., and Djerassi, C. (1983) Phospholipid Studies of Marine Organisms: V. New  $\alpha$ -Methoxy Acids from *Higginsia tethyoides*, *Lipids* 18, 830–836.
- Ayanoglu, E., Kornprobst, J.M., Aboud-Bichara, A., and Djerassi, C. (1983) Phospholipid Studies of Marine Organisms 4. (2*R*,21*Z*)-2-Methoxy-21-octacosenoic Acid, the First Naturally Occurring  $\alpha$ -Methoxy Acid from a Phospholipid, *Tetrahedron Lett.* 24, 1111–1114.
- Carballeira, N.M., Colón, R., and Emiliano, A. (1998) Identification of 2-Methoxyhexadecanoic Acid in *Amphimedon compressa*, *J. Nat. Prod.* 61, 675–676.
- Yamanaka, S., Fudo, R., Kawaguchi, A., and Komagata, K. (1988) Taxonomic Significance of Hydroxy Fatty Acids in Myxobacteria with Special Reference to 2-Hydroxy Fatty Acids in Phospholipids, *J. Gen. Appl. Microbiol.* 34, 57–66.

[Received September 11, 2001, and in revised form and accepted January 7, 2002]

# Changes in Lipid Molecular Species and Sterols of Microsomal Membranes During Aging of Potato (*Solanum tuberosum* L.) Seed-Tubers

Vladimir Zabrouskov and N. Richard Knowles\*

Department of Horticulture and Landscape Architecture, Washington State University, Pullman, Washington 99164-6414

**ABSTRACT:** Changes in sterols and the molecular species composition of polar lipids from microsomal membranes were characterized as a prerequisite to determining how lipid chemistry affects membrane susceptibility to peroxidation during aging of potato tubers. Polar lipid content of the microsomal fraction fell 17% (protein basis) as tubers aged from 2 to 38 mon at 4°C. In younger seed-tubers, PC concentration (protein basis) was the highest, followed by digalactosyldiacylglycerol (DGDG), PE, monogalactosyldiacylglycerol (MGDG), and PI. PC and PE increased 14 and 27%, respectively, whereas glycolipids fell 64 and PI 43% with advancing age. These changes resulted in PC and PE dominating the microsomal membrane lipids of 38-mon-old tubers. Nonpositional analysis of lipid molecular species across lipid pools showed an increase in 16:0/18:3, 18:3/18:3, and 18:2/18:3 (PC and PE only), and a decline in 18:2/18:2 and 16:0/18:2 (except for MGDG) with advancing tuber age. The increase in 18:3-bearing species effected a linear increase in double-bond index (DBI) of PC and PE during aging. The DBI of DGDG did not change with age; however, it fell 65% for MGDG, resulting in an overall decrease in average microsomal DBI. In addition,  $\Delta$ 5-avenasterol and stigmastanol concentrations increased 1.6- and 3.3-fold, respectively, effecting a significant increase in the sterol/phospholipid ratio with advancing tuber age. The increase in sterol/phospholipid ratio and the possibility that the increased unsaturation of microsomal membranes reflects a compensatory response to maintain optimal membrane function in light of the age-induced loss of galactolipid and PI are discussed.

Paper no. L8948 in *Lipids* 37, 309–315 (March 2002).

A decline in membrane integrity, leading to increased leakage and loss of selective permeability, is a central feature of the deterioration accompanying senescence in plants. Studies on senescing plant tissues using electron spin resonance (1), fluorescence depolarization (2), and freeze-fracture electron microscopy (3) have shown decreases in membrane fluidity, development of gel-phase domains, and increases in membrane permeability (4). Extensive phospholipid catabolism and lipid peroxidation during senescence (5) effect membrane

compositional changes (6) that include increases in sterols and sterol/phospholipid ratio (2,7), both of which are intrinsically involved in rigidification and the loss of membrane function. Furthermore, senescence-induced changes in phospholipid molecular species have been shown to increase the susceptibility of membrane lipids to enzymatic degradation (8–10).

While the relationships between lipid peroxidation and membrane deterioration during senescence have been investigated extensively, no detailed information is available on lipid catabolism in plant tissues during natural aging, as distinct from senescence, due primarily to the lack of an appropriate model system. Potato tubers are nonsenescing vegetative propagules that can maintain viability in storage for as long as 3 yr (4°C, 95% RH) and are thus well suited for studying the process of aging in plants, particularly as it relates to loss of membrane integrity and lipid catabolism. In addition to changes in plant growth potential (11), aging of seed-tubers is accompanied by increased respiration (12), decreased protein synthesis (13), increased protein catabolism (14), and oxidative stress (15).

As tuber age advances through 24 mon at 4°C, lipid peroxidation (16) contributes to a decrease in double-bond index (DBI) of total polar lipids that correlates with increased membrane permeability (17) and oxidative catabolism (15). Indeed, lipid peroxidation appears to play a pivotal role in the collective deterioration of metabolic systems during aging of seed-tubers. Using tubers transformed with sense constructs of FA desaturases, we demonstrated that high levels of linolenate in cell membranes enhanced oxidative stress and overall metabolic rate, which, in turn, accelerated aging and loss of growth potential (Zabrouskov, V., Kumar, G.N.M., Spychalla, J.P., and Knowles, N.R., unpublished data). Hence, compositional changes in lipid molecular species can render membranes more conducive to peroxidative damage. To date, detailed studies of lipid metabolism during tuber aging have been based mainly on relatively short-term durations (less than 12 mon) (18,19). Changes in lipid molecular species (vs. total esterified FA) and sterols during long-term aging of tubers, in relation to the susceptibility of membrane lipids to peroxidation and oxidative stress, are unknown.

This study characterizes the effects of age on lipid compositional changes (including sterols) in microsomal membranes of potato tubers. Molecular species analysis revealed that age-induced alterations in acyl chain composition and constituent pairing depended on lipid class. Age-induced changes to a

\*To whom correspondence should be addressed at Department of Horticulture and Landscape Architecture, P.O. Box 646414, Washington State University, Pullman, WA 99164. E-mail: rknowles@wsu.edu

Abbreviations: DBI, double-bond index; DGDG, digalactosyldiacylglycerol; DHB, 2,5-dihydroxybenzoic acid; MALDI TOF MS, matrix-assisted laser desorption/ionization time-of-flight mass spectrometry; MGDG, monogalactosyldiacylglycerol; PVP, polyvinylpyrrolidone.

given molecular species with a defined pair of acyl chains can thus be quite different from those of other species with the same pair of chains. A detailed account of these modifications is essential to gain a better understanding of the various metabolic processes that influence membrane susceptibility to deterioration during aging.

## MATERIALS AND METHODS

*Chemicals, membrane isolation, and lipid extraction.* All solvents (HPLC grade) and buffer salts were from J.T. Baker (Phillipsburg, NJ) and were used without further purification. 2,5-Dihydroxybenzoic acid (DHB) was from Aldrich Chemical Co. (Milwaukee, WI). The lipid and sterol standards were purchased from Avanti Polar Lipids (Alabaster, AL) and Supelco (Supelco Inc., Bellefonte, PA), respectively. Certified potato seed-tubers (Elite III, cv. Russet Burbank) were obtained at harvest and stored at 4°C (95% RH) for up to 38 mon.

Microsomal membranes were isolated as described by Kumar and Knowles (15), with modifications. After the appropriate storage interval, approximately 50 g of the apical third of each of three or four tubers (200 g total) was collectively homogenized with a Braun (Type 4-172, Braun Canada, Ltd., Mississauga, Ontario) hand homogenizer in 200 mL of ice-cold extraction medium. The medium (pH 7.5) contained 75 mM MOPS, 250 mM sucrose, 1 mM EDTA, 1 mM EGTA, 2.5 mM sodium bisulfite, 1.5% (wt/vol) polyvinylpyrrolidone, 1 mM *n*-propylgallate, 10 µg/mL BHT, and 1 mM DTT. The homogenate was filtered through two layers of Miracloth (Calbiochem, San Diego, CA) and the filtrate was centrifuged at 5000 × *g* for 5 min to sediment starch. The resulting supernatant was centrifuged at 10,000 × *g* for 30 min and the pellet discarded. The supernatant was then centrifuged at 105,000 × *g* for 45 min to pellet microsomal membranes. Microsomes were washed and pelleted twice (105,000 × *g*, 45 min) with washing buffer (pH 7.5), containing 5 mM MOPS, 250 mM sucrose, 1 mM EGTA, 1 mM DTT, 10 µg/mL BHT, and 10 mM KCl. The microsomal pellet was suspended in 1 mL of washing buffer and stored at -80°C until further analysis.

Lipids were extracted from microsomal membranes according to Folch *et al.* (20), and phospholipids and galactolipids were quantified with an Iatroscan (model MK-5; Iatron Labs, Tokyo, Japan). The Iatroscan couples TLC separation of analytes with FID. To separate lipid classes, approximately 1.5 µg of total lipid was spotted on a silica gel rod that was developed in chloroform/methanol/ammonium hydroxide/water (45:28:0.5:1, by vol). The rods were then processed in an Iatroscan. Hydrogen and air flow rates for the Iatroscan FID were 160 mL/min and 2 L/min, respectively. The rack speed for the silica gel rods was 30 cm/min. For analysis of FAME, lipid classes were separated by TLC (silica gel G) using chloroform/methanol/ammonium hydroxide/water (45:28:0.5:1, by vol) as the mobile phase. Lipid classes [PC, PE, PI, monogalactosyldiacylglycerol (MGDG), digalactosyldiacylglycerol (DGDG)] were eluted from the silica gel (twice)

with chloroform/methanol (1:1, vol/vol) at 55°C. Eluates were dried in a rotary evaporator and dissolved in chloroform. FAME were prepared by dissolving approximately 200 µg of lipid in 200 µL of hexane and transesterifying with 2 mL of methanol/BF<sub>3</sub> reagent (Sigma Chemical, St. Louis, MO) for 1.5 h at 90°C. After adding 1 mL of 0.088% (wt/vol) NaCl, FAME were extracted with 1 mL of hexane. FAME were separated on a 30 m × 0.25 mm × 0.25 µm INNOWax capillary column (Agilent Technologies, Wilmington, DE) and quantified using an HP 6890 GC (Agilent Technologies). The oven temperature was initially 160°C for 1 min and then increased (8°C/min) to 233°C. Injection volume was 1 µL, and the injector and detector temperatures were 240 and 250°C, respectively. Helium was the carrier gas at 1.7 mL/min.

*Nonpositional analysis of lipid molecular species.* PC and PE were digested to their corresponding DAG with phospholipase C in preparation for molecular species analysis by matrix-assisted laser desorption/ionization time-of-flight mass spectrometry (MALDI-TOF MS) (21). MGDG and DGDG were left intact for this analysis. DHB in acetone (0.5 M) was used as the matrix. The lipids in chloroform were mixed (1:5 vol/vol) with the matrix solution; and 1 µL, containing 30 to 100 ng of lipid, was applied to the sample plate. MALDI spectra were obtained using a PerSpective Biosystems (Framingham, MA) Voyager DE-RP time-of-flight mass spectrometer equipped with a nitrogen laser (337 nm). All spectra were the average of 256 laser shots. The laser was adjusted to one-third of maximum power, depositing approximately 100 µJ per laser pulse. The applied potential was 25,000 V, and a focusing guide wire was held at a potential of 0.1% of the accelerating voltage. A delay time of 100 ns was used between the time of the laser pulse and application of the accelerating voltage. The instrument was set in the reflector mode and spectra were acquired from 0 to 5000 *m/z*. A spectrum for each sample was acquired from two wells, and the results were averaged. Spectra of standard PC were used to calibrate the instrument. FAME data were used to determine certain isomeric abundances within the isobaric mix of particular molecular species (such as 18:1/18:2 and 18:0/18:3). Where FAME data were insufficient to deduce isomeric abundances (as in the case of DGDG and MGDG), the molecular species are presented as an isomeric mix.

*Sterol analysis.* Sterols were analyzed as described by Toivo *et al.* (22) with an acid hydrolysis step to account for glycosylated moieties. Microsomal lipids (0.25 to 1 mg in chloroform) were spiked with 20 µg of 5- $\alpha$ -cholestane as an internal standard, dried under N<sub>2</sub>, and dissolved in 10 mL of 1 M HCl in denatured ethanol (90%, Baker). The lipids were incubated for 1 h at 65°C in a dry bath. Samples were then cooled to room temperature prior to the sequential addition of 0.9 mL of 60% (wt/vol) aqueous KOH and 5 mL of 2.84% (wt/vol) KOH in denatured alcohol. After being shaken for 1 min, the mixture was incubated for 1 h at 65°C in a dry bath, cooled, and transferred to 50-mL plastic tubes with 8 mL of water (HPLC grade). Sterols were extracted with 10 mL of hexane (three times). The extracts were combined and dried in



a rotary evaporator (40°C). The underivatized free sterols were solubilized in 200  $\mu$ L of chloroform and 1  $\mu$ L was injected into a GC (HP 6890) equipped with a 15 m  $\times$  0.25 mm  $\times$  1  $\mu$ m DB-5MS column (J&W Scientific, Folsom, CA). Separation and quantification of sterols was accomplished in isothermal mode (285°C), and injector and detector temperatures were 300°C. The identity of sterols was confirmed based on retention times of authentic standards and GC-MS. Microsomal protein was quantified according to Bradford (23), following solubilization of the membranes in 0.05% (w/w) Triton X-100.

Concentrations of microsomal lipids and sterols were expressed on a protein basis to reflect the dynamics outside the particular lipid pool. Microsomal protein declined with age (~25% from 2 to 38 mon), thus contributing to the trends characterized in this study. However, the majority of age-induced changes in lipid molecular species were far greater than what could be attributed to changes in protein. Hence, in most cases, the trends shown on a protein basis were also evident on a mole percent basis.

**Experimental design.** The study was conducted as a randomized complete block design with four seed-tuber ages (2, 14, 26, and 38 mon of storage at 4°C) replicated three times. Variation attributable to age was partitioned in ANOVA. Treatment means are reported  $\pm$  SE.

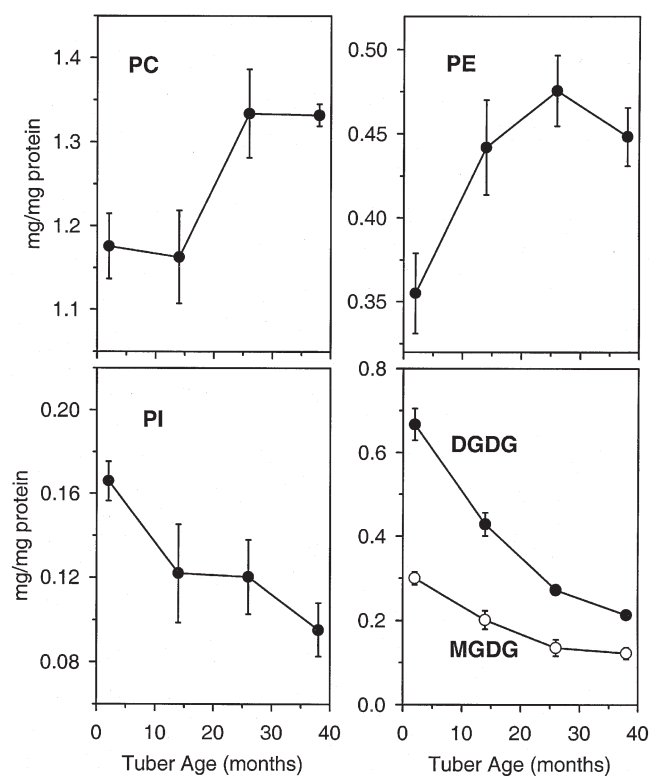
## RESULTS

The concentration of total polar lipids in microsomal membranes fell 17% (protein basis) as tuber age advanced from 2 to 38 mon (Fig. 1). In 2-mon-old tubers, PC accounted for 45%, DGDG 25%, PE 13%, MGDG 11%, and PI 6% of total polar lipid. The concentrations of PC and PE increased 14 and 27%, respectively, whereas glycolipids (DGDG and MGDG) fell 65% and PI 43% with advancing age (Fig. 1). These age-induced changes resulted in PC and PE dominating the microsomal lipids of 38-mon-old tubers, where they accounted for 60.3 and 20.4% of polar lipid, respectively.

Four major (16:0/18:2, 18:2/18:2, 18:2/18:3, and 16:0/18:3) and three relatively minor molecular species (18:0/18:2, 18:1/18:2, and 18:3/18:3) were identified within the PC pool (Fig. 2). Near-linear increases in PC 16:0/18:3, 18:2/18:3, 18:3/18:3, and 18:1/18:2 ranged from 1.7- to 8.5-fold through 38 mon of storage, reflecting a major effect of age on increased unsaturation. On the other hand, PC 16:0/18:2, 18:2/18:2, and 18:0/18:2 declined with advancing age, the greatest decline occurring over the initial 13 mon of storage.

PE had the same molecular species profile as PC; however, aging induced changes that differed from those of PC (Fig. 3). The greatest increases in PE 16:0/18:3, 18:2/18:3, 18:3/18:3, and 18:1/18:2 occurred during the initial 13 mon of storage. Furthermore, PE 16:0/18:2 and 18:2/18:2 remained relatively constant through the entire 38-mon storage period. These changes effected an overall increase in the level of PE, elevating it from third- to second-most abundant polar lipid in microsomal membranes as tubers aged through 38 mon.

DGDG had three major (16:0/18:2, 18:2/18:3, isobaric mix



**FIG. 1.** Age-induced changes in the concentrations of phospho- and galactolipids in microsomal membranes from potato tubers. DGDG, digalactosyldiacylglycerol; MGDG, monogalactosyldiacylglycerol. Error bars indicate SE.

of 18:2/18:2 + 18:1/18:3) and four minor (16:0/18:3, 18:3/18:3, isobaric mix of 18:0/18:2 + 18:1/18:1, 18:1/18:2 + 18:0/18:3) molecular species (Fig. 4). Except for 16:0/18:3, which remained constant with age, all molecular species declined proportionally during aging, resulting in a 65% drop in DGDG concentration of microsomal membranes and no change in the DBI of this pool.

Three major (18:2/18:3, 18:3/18:3, isobaric mix of 18:2/18:2 + 18:1/18:3) and four minor (16:0/18:2, 16:0/18:3, isobaric mix of 18:1/18:2 + 18:0/18:3, and 18:0/18:2 + 18:1/18:1) molecular species made up the initial MGDG pool at 2 mon (Fig. 5). Similar to DGDG, the concentrations of several MGDG molecular species (16:0/18:2, 18:2/18:3, 18:3/18:3, 18:2/18:2 + 18:1/18:3) fell with advancing age, while 16:0/18:3 increased from undetectable levels in 2-mon-old tubers to 5.4  $\mu$ g/mg protein in 38-mon-old tubers. Unlike DGDG, these changes defined a 65% drop in DBI, reflecting a significant loss of relative unsaturation in the MGDG fraction of membranes during aging. Moreover, this age-induced drop in unsaturation of MGDG offset increases in the DBI of PC and PE, resulting in an overall decline in DBI of polar lipids in the microsomal membrane fraction.

The total sterol fraction of microsomal membranes from potato tubers contained  $\Delta$ 5-avenasterol,  $\beta$ -sitosterol, stigmasterol, and cholesterol, in order of decreasing concentration (Fig. 6A). Concentrations of  $\Delta$ 5-avenasterol and stigmasterol increased 1.6- and 3.3-fold, respectively, as tuber age advanced

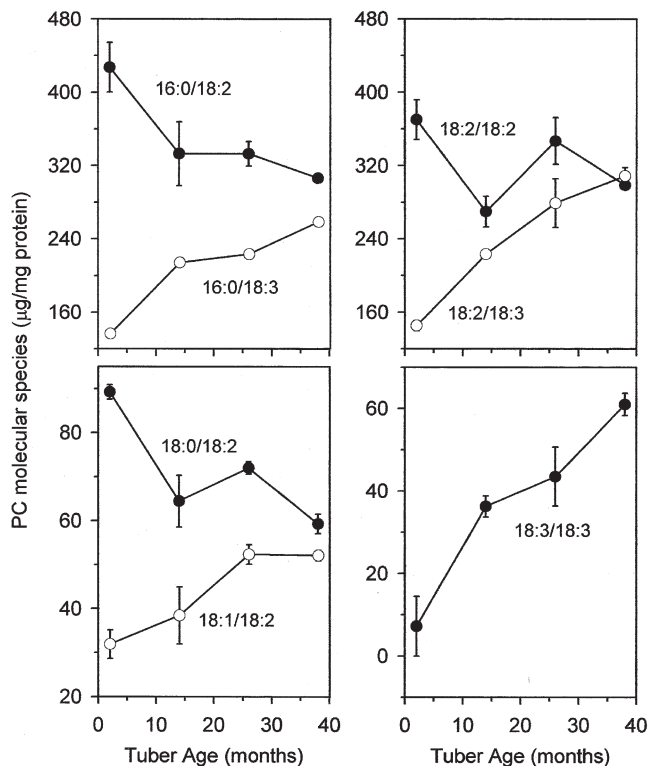


FIG. 2. Age-induced changes in the molecular species of PC in microsomal membranes from potato tubers. Error bars indicate SE.

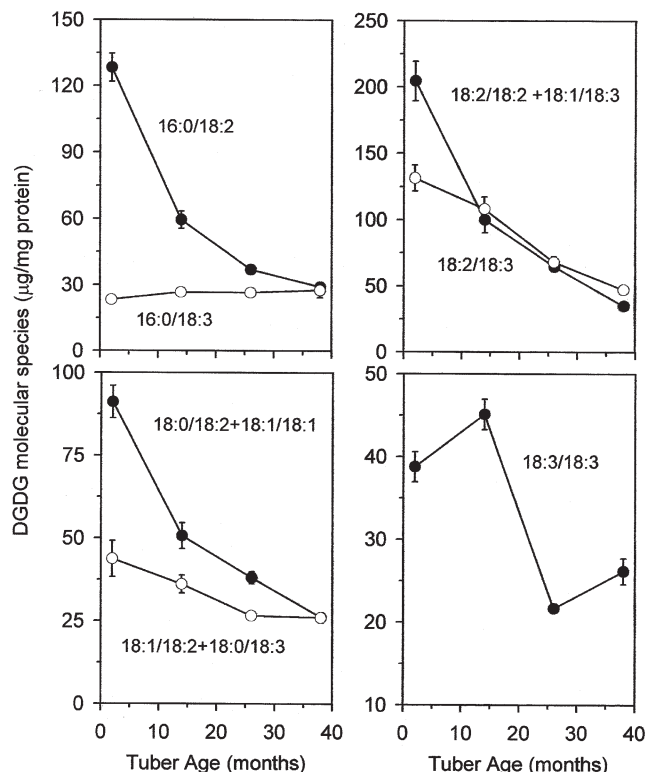


FIG. 4. Age-induced changes in the molecular species of DGDG in microsomal membranes from potato tubers. For abbreviation see Figure 1. Error bars indicate SE.

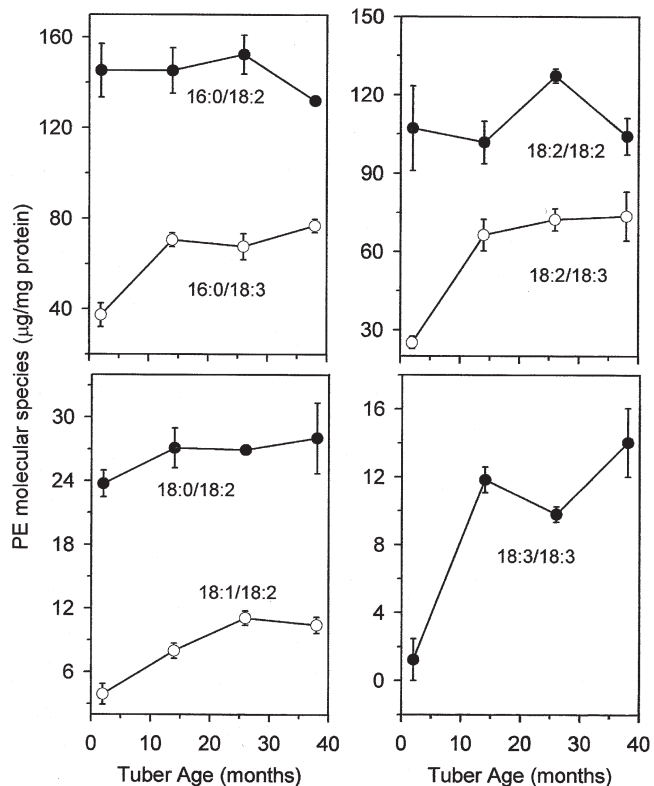


FIG. 3. Age-induced changes in the molecular species of PE in microsomal membranes from potato tubers. Error bars indicate SE.

to 38 mon, while  $\beta$ -sitosterol and cholesterol remained relatively constant. These changes resulted in a 57% increase in total sterol concentration over the aging interval (Fig. 6B). The sterol/phospholipid ratio also increased (41%) as tuber age advanced from 2 to 26 mon, stabilizing thereafter (Fig. 6B, inset).

## DISCUSSION

This study provides the first comprehensive characterization of changes in lipid composition of microsomal membranes during natural aging of potato tubers over their entire storage life. Results indicate that head group and FA composition of polar lipids are important determinants of the susceptibility of individual lipid species to age-induced metabolism. Specific mono- and digalactolipid molecular species (16:0/18:2, 18:2/18:2 + 18:1/18:3, 18:2/18:3, 18:3/18:3) were catabolized to a much greater extent than other species (16:0/18:3, 18:1/18:2 + 18:0/18:3) during aging, resulting in a decline of the entire galactolipid fraction. This likely reflects the deterioration of amyloplasts and could explain the progressive sweetening that occurs during aging (16). Differential susceptibility of microsomal membrane lipids to breakdown has also been reported during floral senescence (10), the process of which culminates in death of the flower. In this regard, it is worth reiterating that potato tubers do not undergo senescence. As natural vegetative propagules, potato tubers are suitably adapted for maximal longevity and thus are ideal for

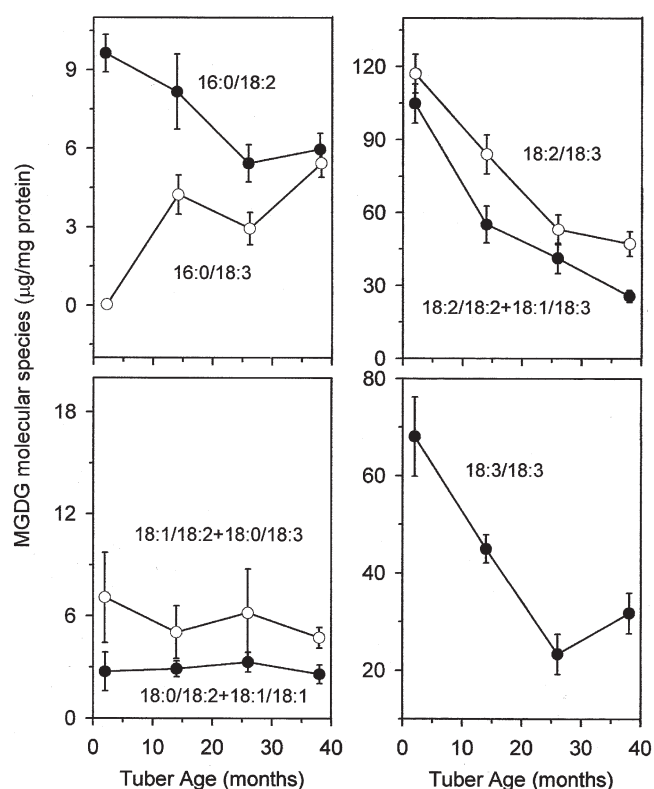


FIG. 5. Age-induced changes in the molecular species of MGDG in microsomal membranes from potato tubers. For abbreviation see Figure 1. Error bars indicate SE.

assessing the effects of age, as distinct from senescence, on membrane structure and function in herbaceous plants.

In contrast to galactolipids, unsaturated molecular species of PC and PE increased in microsomal membranes from tubers with advancing age, likely reflecting increases in the activities of 18:1 and 18:2 FA desaturases. Increases in  $\Delta 9$ -desaturase mRNA levels have been demonstrated during floral senescence (24). These changes, however, appear contradictory to the general increase in saturation of microsomal

membranes that accompanies senescence of flowers (24). Like senescing tissues, the mechanisms by which the molecular species composition of various lipid pools within potato tubers changed during aging are no doubt complex, involving the concerted actions of FA desaturases and membrane re-tailoring enzymes (lipases, acyltransferase, acyl CoA synthetase, etc.).

Although the fluidity of microsomal membranes often decreases during senescence (26), associations between fluidity, unsaturation, and desaturase activity remain speculative. Thompson and Martin (27) proposed that desaturases are activated when membrane fluidity drops below a threshold level. By using synthetic lipid bilayers, it was demonstrated that the physical properties of membranes cannot be predicted based solely on their overall FA profiles. Intramolecular positioning of acyl chains is an important factor determining the fluidity of membranes (28,29). A number of other factors have also been shown to affect membrane fluidity, including sterol content, sterol-to-phospholipid ratio, and lipid-to-protein ratio (30). Increase in sterol/phospholipid ratio leads to membrane rigidification (25) and is diagnostic of microsomal and plasma membrane deterioration during senescence (7). Stigmasterol has a disordering effect on artificial membranes (31) and has been shown to increase in the plasma membranes of mung bean hypocotyls during senescence (32). Moreover, an increase in the stigmasterol/sitosterol ratio has been proposed as a marker of physiologically older tissue (33). Thus, consistent with senescence, tuber aging resulted in an increase in sterol/phospholipid and stigmasterol/sitosterol ratios. In contrast to senescence (10), however, substantial increases in the major phospholipids of microsomal membranes were observed during tuber aging.

In addition to being developmentally linked (8–10,25), changes to membrane lipids are a common adaptive response of plants to various environmental stresses (27), such as temperature. Indeed, the early increases in 18:3-bearing species of potato tuber may simply reflect an adaptive response to maintain membrane fluidity at low temperature. Similar initial increases in phospholipid unsaturation in tubers during short-term storage have been reported (19). Moreover, increased unsaturation during acclimation of tubers to cold over the first weeks of storage is consistent with cold acclimation responses in other plants (27,34). Continued increases in 18:3 content of various PC and PE molecular species (18:3/18:3, 18:2/18:3, 16:0/18:3) beyond 13 mon, however, were unexpected. These latter increases may reflect a compensatory response to the age-induced loss of PI and increase in sterol content of membranes, thus characterizing age-specific effects on glycerolipid metabolism.

An increase in unsaturation alone does not necessarily translate into an increase in overall membrane fluidity. Previous studies on heart mitochondrial lipids of aging rats demonstrated that, despite age-related increases in unsaturation, there was an apparent decrease in membrane fluidity (35). The decrease was attributed to age-induced accumulation of peroxidized lipids in the lipid bilayer that greatly affected

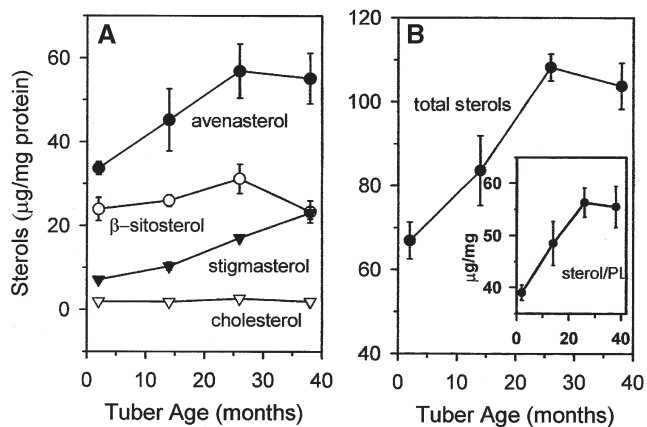


FIG. 6. Changes in the concentrations of individual (A) and total (B) sterols in microsomal membranes from potato tubers. Inset shows sterol/phospholipid (PL) ratio (µg/mg). Error bars indicate SE.

membrane architecture and thus membrane biophysical properties, including fluidity. These results were confirmed in a later study using artificial liposomes, where decreases in microfluidity, lateral diffusion, and liposome size were associated with peroxidation of PUFA in the lipid bilayer (36). Because unsaturated FA are more susceptible to free radical attack, their increase with age would only serve to magnify lipid oxidative damage. Indeed, products of lipid peroxidation accumulate in tubers during aging, despite a decrease in lipolytic activity (16). Additionally, older tubers have leakier membranes (17; Zabrouskov, V., Kumar, G.N.M., Spsychalla, P., and Knowles, N.R., unpublished data), reflecting age-induced increases in membrane permeability. Hence, maintaining membrane fluidity through increased unsaturation appears to be a response to maintain membrane function during aging of potatoes. However, increases in PUFA content are also likely to be detrimental by rendering membranes more susceptible to nonenzymatic and possibly enzymatic degradation, thus compromising membrane functional properties, including fluidity. While older tubers have lower lipoxigenase and lipolytic acylhydrolase activities (16; Zabrouskov, V., Kumar, G.N.M., Spsychalla, J.P., and Knowles, N.R., unpublished data), the role of lipolytic enzymes in the age-induced catabolism of tuber lipids remains unresolved, owing to the fact that lipases exhibit preferences for various phospholipid molecular species (8–10), resulting in their differential susceptibility to enzymatically mediated degradation. The genuine lipolytic potential within different ages of tubers therefore will depend on the phospholipid molecular species that are characteristic for a particular tuber age.

Thus, changes in molecular species of microsomal membranes during tuber aging are consistent with previous work demonstrating age-induced declines in membrane integrity and increases in lipid peroxidation, all of which contribute to oxidative stress and loss of growth potential. Our results provide a base for further studies to establish the impact of age-related changes in molecular species on (i) susceptibility of membrane lipids to enzymatic degradation and (ii) the physical parameters of membranes in relation to their architecture and function.

In summary, aging effected differential changes in the molecular species of lipids in microsomal membranes from potato that were dependent on the particular lipid class (or pool). The modifications were characterized by increases in 18:3/18:3 and 18:2/18:3 species of PC and PE, lower galactolipid content and unsaturation owing to decreases in 16:0/18:2, 18:2/18:2 + 18:1/18:3, 18:2/18:3, and 18:3/18:3 and an increase in 16:0/18:3 species, and higher sterols content and sterol/phospholipid ratio. These alterations in membrane lipid chemistry are consistent with previous studies showing a decline in membrane integrity, increased susceptibility of membranes to lipid peroxidation, and the development of oxidative stress during aging of potato tubers.

#### ACKNOWLEDGMENTS

We thank Dr. William F. Siems, Department of Chemistry, Washington State University, for help with the MS analysis of sterols.

This work was funded by grants from the United States Department of Agriculture—Cooperative State Research, Education, and Extension Service and Washington State Potato Commission to NRK.

#### REFERENCES

- McKerzie, B.D., Lepock, J.R., Kruuv, J., and Thompson, J.E. (1978) The Effect of the Cotyledon Senescence on the Composition and Physical Properties of Membrane Lipid, *Biochim. Biophys. Acta* 508, 197–212.
- Fobel, M., Lynch, D.V., and Thompson, J.E. (1987) Membrane Deterioration in Senescing Carnation Flowers, *Plant Physiol.* 85, 204–211.
- Platt-Aloia, K.A., and Thomson, W.W. (1985) Freeze-Fracture Evidence of Gel Phase Lipid in Membranes of Senescing Cotyledons, *Planta* 163, 360–369.
- Paliyath, G., and Thompson, J.E. (1987) Evidence for Early Changes in Membrane Structure During Post-Harvest Development of Cut Carnation Flowers, *New Phytol.* 114, 555–562.
- Yao, K., Paliyath, G., and Thompson, J.E. (1993) Localization of Peroxidized Lipids in Non-sedimentable Microvesicles of Senescing Bean Cotyledons, *J. Exp. Bot.* 44, 1267–1274.
- Suttle, J.C., and Kende, H. (1980) Ethylene Action and Loss of Membrane Integrity During Petal Senescence in *Tradescantia*, *Plant Physiol.* 65, 1067–1072.
- Thompson, J.E., Froese, C.D., Madey, E., Smith, M., and Hong, Y. (1998) Lipid Metabolism During Plant Senescence, *Prog. Lipid Res.* 37, 119–141.
- Brown, J.H., Lynch, D.V., and Thompson, J.E. (1987) Molecular Species Specificity of Phospholipid Breakdown in Microsomal Membranes of Senescing Carnation Petals, *Plant Physiol.* 85, 679–683.
- Brown, J.H., Paliyath, G., and Thompson, J.E. (1990) Influence of Acyl Chain Composition on the Degradation of Phosphatidylcholine by Phospholipase D in Carnation Microsomal Membranes, *J. Exp. Bot.* 41, 979–986.
- Brown, J.H., Chambers, J.A., and Thompson, J.E. (1991) Acyl Chain and Head Group Regulation of Phospholipid Catabolism in Senescing Carnation Flowers, *Plant Physiol.* 95, 909–916.
- Kumar, G.N.M. and Knowles, N.R. (1993) Involvement of Auxin in the Loss of Apical Dominance and Plant Growth Potential in Aging Potato Seed-Tubers, *Can. J. Bot.* 71, 541–550.
- Kumar, G.N.M., and Knowles, N.R. (1996) Nature of Enhanced Respiration During Sprouting of Aged Potato Seed-Tubers, *Physiol. Plant.* 97, 228–236.
- Kumar, G.N.M., and Knowles, N.R. (1993) Age of Potato Seed-Tubers Influences Protein Synthesis During Sprouting, *Physiol. Plant.* 89, 262–270.
- Kumar, G.N.M., Houtz, R.L., and Knowles, N.R. (1999) Age-Induced Protein Modifications and Increased Proteolysis in Potato Seed-Tubers, *Plant Physiol.* 119, 89–99.
- Kumar, G.N.M., and Knowles, N.R. (1996) Oxidative Stress Results in Increased Sinks for Metabolic Energy During Aging and Sprouting of Potato Seed-Tubers, *Plant Physiol.* 112, 1301–1313.
- Kumar, G.N.M., and Knowles, N.R. (1993) Changes in Lipid Peroxidation and Lipolytic and Free-Radical Scavenging Enzymes Activities During Aging and Sprouting of Potato (*Solanum tuberosum*) Seed-Tubers, *Plant Physiol.* 102, 115–124.
- Knowles, N.R., and Knowles, L.O. (1989) Correlations Between Electrolyte Leakage and Degree of Saturation of Polar Lipids from Aged Potato (*Solanum tuberosum* L.) Tuber Tissue, *Ann. Bot.* 63, 331–338.
- Spsychalla, J. (1998) Post-Harvest Potato Tuber Glycerolipid Metabolism, in *The Molecular and Cellular Biology of the Potato*, pp. 108–123, CAB International, Oxon, United Kingdom.



19. Spychalla, J.P., and Desborough, S.L. (1990) Fatty Acids, Membrane Permeability, and Sugars of Stored Potato Tubers, *Plant Physiol.* **94**, 1214–1218.
20. Folch, J., Lees, M., and Sloane-Stanley, G.H. (1957) A Simple Method for the Isolation and Purification of Total Lipids from Animal Tissue, *J. Biol. Chem.* **226**, 497–509.
21. Zabrouskov, V., Al-Saad, K.A., Siems, W.F., Hill, H.H., and Knowles, N.R. (2001) Analysis of Plant Phosphatidylcholines by Matrix-Assisted Laser Desorption/Ionization Time-of-Flight Mass Spectrometry, *Rapid Commun. Mass Spectrom.* **15**, 935–940.
22. Toivo, J., Lampi, A.M., Aalto, S., and Piironen, V. (2000) Factors Affecting Sample Preparation in the Gas Chromatographic Determination of Plant Sterols in Whole Wheat Flour, *Food Chem.* **68**, 239–245.
23. Bradford, M. (1976) A Rapid and Sensitive Method for Quantitation of Microgram Quantities of Proteins Utilizing the Principles of Protein-Dye Binding, *Anal. Biochem.* **72**, 247–254.
24. Fikuchi-Mizutani, M., Savin, K., Cornish, E., Tanaka, Y., Ashikari, T., Kusumi, T., and Murata, N. (1995) Senescence-Induced Expression of a Homologue of  $\Delta 9$  Desaturase in Rose Petals, *Plant Mol. Biol.* **29**, 627–635.
25. Itzhaki, H., Borochoy, A., and Mayak, S. (1990) Age-Related Changes in Petal Membranes from Attached and Detached Rose Flowers, *Plant Physiol.* **94**, 1233–1236.
26. Thompson, J.E., Mayak S., Shinitzky, M., and Hlevy, A.H. (1982) Acceleration of Membrane Senescence in Cut Carnation Flowers by Treatment with Ethylene, *Plant Physiol.* **69**, 859–863.
27. Thompson, G.A., Jr., and Martin, C.E. (1984) Regulation of Phospholipid Fatty Acid Composition, in *Physiology of Membrane Fluidity*, Vol. 1, pp. 99–129, CRC Press, Boca Raton.
28. Philips, M.C., Hauser, H., and Paltauf, F. (1972) The Inter- and Intra-molecular Mixing of Hydrocarbon Chains in Lecithin/Water Systems, *Chem. Phys. Lipids* **8**, 127–133.
29. Philips, M.C., Ladbroke, B.D., and Chapman, D. (1970) Molecular Interactions in Mixed Lecithin Systems, *Biochim. Biophys. Acta* **196**, 35–44.
30. Williams, J.P., Mobashsher, U.K., Mitchell, K., and Johnson, G. (1988) The Effect of Temperature on the Level and Biosynthesis of Unsaturated Fatty Acids in Diacylglycerols of *Brassica napus* Leaves, *Plant Physiol.* **87**, 904–910.
31. Marsan, M.P., Muller I., and Milon A. (1996) Ability of Clionasterol and Poriferasterol to Regulate Membrane Lipid Dynamics, *Chem. Phys. Lipids* **84**, 117–121.
32. Stalleart, V.M., and Geuns, J.M. (1994) Phospholipid and Free Sterol Composition of Hypocotyl Plasma Membranes of Aging Mung Bean Seedlings, *Phytochemistry* **36**, 1170–1180.
33. Geuns, J.M.C (1975) Regulation of Sterol Biosynthesis in Etiolated Mung Bean Hypocotyl Sections, *Phytochemistry* **14**, 975–978.
34. Uemura, M., Joseph, R., and Steponkus, P. (1995) Cold Acclimation of *Arabidopsis thaliana*, *Plant Physiol.* **109**, 15–30.
35. Lee, J., Yu, B., and Herlihy, J. (1999) Modulation of Cardiac Mitochondrial Membrane Fluidity by Age and Calorie Intake, *Free Radic. Biol. Med.* **26**, 260–265.
36. Borst, J.W., Visser, N.V., Kouptsova, O., and Visser, A. (2000) Oxidation of Unsaturated Phospholipids in Membrane Bilayer Mixtures Is Accompanied by Membrane Fluidity Changes, *Biochim. Biophys. Acta* **1487**, 61–73.

[Received November 7, 2001, and in final revised form and accepted January 30, 2002]

# Selective (*R*)-3-Hydroxylation of FA by *Stenotrophomonas maltophilia*

Kerstin Weil<sup>a</sup>, Patrick Gruber<sup>a</sup>, Frank Heckel<sup>a</sup>, Dag Harmsen<sup>b</sup>, and Peter Schreier<sup>a,\*</sup>

<sup>a</sup>Lehrstuhl für Lebensmittelchemie and <sup>b</sup>Institut für Hygiene und Mikrobiologie, Universität Würzburg, D-97074 Würzburg, Germany

**ABSTRACT:** Soil samples were screened for microorganisms selectively transforming FA. One of the isolated strains was identified as the bacterium *Stenotrophomonas maltophilia* by its phenotypic features and genotypic characterization by sequencing the ribosomal RNA gene. Using linoleic acid as substrate resulted in the formation of two major compounds. After liquid chromatographic isolation and separation, their structures were elucidated by HPLC–tandem MS, GC–MS, and NMR techniques to be 3-hydroxy-Z6-dodecenoic acid and 3-hydroxy-Z5,Z8-tetradecadienoic acid. In additional experiments, other FA, such as  $\alpha$ -linolenic, oleic, palmitoleic, myristoleic, and *cis*-vaccenic acids, were converted to 3-hydroxylated metabolites of shorter chain lengths as well. Determination of the enantiomeric composition revealed highly enriched (*R*)-hydroxylation (88–98% enantiomeric excess).

Paper no. L8827 in *Lipids* 37, 317–323 (March 2002).

Long-chain hydroxy FA and other oxygenated FA derivatives (oxylipins) are widely distributed in both the animal and plant kingdoms and exert different biological actions (1,2). During the last decade, knowledge has accumulated regarding the biosynthesis of oxylipins by fungi and related organisms (3). A large number of unsaturated hydroxy FA, which are formed by lipoxygenase, dioxygenase, or cytochrome P450-mediated pathways, have been found in various fungal species (4–6). Bacterial conversions of unsaturated FA have been exploited, too. For instance, oleic acid and linoleic acid were transformed to the corresponding 10-hydroxy and 10-keto FA by hydratases from *Flavobacterium* sp. DS5 (7) and *Nocardia cholesterolicum* (8). In addition, oleic acid was converted to 7,10-dihydroxy-E8-octadecenoic acid via a 10-hydroxy-Z8-octadecenoic acid as intermediate by *Pseudomonas aeruginosa* PR3 (9). 12,13,17-Trihydroxy-Z9-octadecenoic acid was produced from linoleic acid by a Gram-positive strain identified as *Clavibacter* sp. ALA2 (10). Other trihydroxy acids, such as 9,12,13-trihydroxy-10-octadecenoic acid and 9,12,13-trihydroxy-10,15-octadecadienoic acid, as well as epoxy unsaturated FA have been found in some rice cultivars (11). Finally, several cytochrome P450 enzymes have been isolated from different strains of *Bacillus megaterium* and characterized.

\*To whom correspondence should be addressed at Lehrstuhl für Lebensmittelchemie, Universität Würzburg, Am Hubland, D-97074 Würzburg, Germany. E-mail: schreier@pzl.uni-wuerzburg.de.

Abbreviations: CD, circular dichroism; EMBL, European Molecular Laboratory Biology Database; ESI, electrospray ionization; HPLC–MS/MS, HPLC–tandem mass spectrometry; HRGC, high-resolution gas chromatography; MDGC, multidimensional GC; TE buffer (Tris + EDTA, pH 7.6).

They are capable of catalyzing the  $\omega$ -1,  $\omega$ -2, and  $\omega$ -3 hydroxylation of long-chain FA, amides, and alcohols (12,13).

In this report, we describe the biotransformation of linoleic acid and other unsaturated FA into (*R*)-3-hydroxylated metabolites of shorter chain length by a *Stenotrophomonas maltophilia* strain isolated from topsoil.

## MATERIALS AND METHODS

**Isolation procedure and bacterial growth.** Microorganisms were isolated from a soil sample taken in the Würzburg University area. The bacterial cultures were maintained on plate count agar (Creatogen Biosciences GmbH, Augsburg, Germany).

**Phenotypic characterization of the microorganism.** Phenotypic characterization of the isolated strain was carried out by investigations concerning appearance (microscopic study including Gram stain) and behavior (optimal growth temperature) of the bacteria. Sensitivity against antibiotics (ampicillin, piperacillin, imipenem, meropenem, cefotaxime, cefotiam, gentamicin, amikacin, cotrimoxazol, ofloxacin) was tested by means of an agar diffusion test. In addition, classification using the commercially available test-stripe APIZYM 20 NE (bioMérieux Deutschland GmbH, Nürtingen, Germany) was done. Enzyme assays were performed according to Smibert and Krieg (14).

**Preparation, amplification, and sequencing of bacterial ribosomal RNA gene.** The preparation of intact bacterial cells for the PCR was performed as described (15). Briefly, cells were cultivated in Luria Bertani broth, centrifuged, washed with 1 M NaCl, resuspended in TE buffer (10 mM Tris, 1 mM EDTA, pH 7.6), and diluted in TE buffer to an optical density of 1.0 at 600 nm. A 1- $\mu$ L aliquot of each cell suspension was used for the PCR.

Partial-length small subunit ribosomal RNA gene (16S) was amplified using PCR with primers 27f and 342r (16), one of which was biotinylated in each of two reciprocal reactions. Single-stranded DNA were sequenced with internal primers by using the Taq-cycle DyeDeoxy™ Terminator method combined with a 373A automatic sequencer (ABI Division of PerkinElmer, Weiterstadt, Germany). For all newly determined nucleotide sequences (variable region V1–V3 of the 16S-rRNA), data were obtained for both DNA strands; sequences from primer regions were not included in the analysis. Finally, a homology search with the sequence data against the European Molecular Biology Laboratory (EMBL) database was performed (17).

**Materials and chemicals.** Linoleic,  $\alpha$ -linolenic, oleic, and Z5-dodecenoic acids were obtained from Aldrich (Sigma-Aldrich Chemie GmbH, Deisenhofen, Germany). Palmitoleic and myristoleic acids were acquired from Sigma (Sigma-Aldrich Chemie GmbH, Deisenhofen, Germany). *cis*-Vaccenic acid was purchased from ICN (ICN Pharmaceuticals, Inc., Cosa Mesa, CA). Reagents and solvents were of analytical or HPLC grade. As rotary shaker, a GFL 3031 (Gesellschaft für Labortechnik mbH, Burgwedel, Germany) was used. A Wolf SanoClav-MCN autoclave (Wolf, Geisslingen, Germany) was employed for sterilization, and a laminar AirFlow bench was used for sterile work (NuAire Inc., Plymouth, MN). A Beckman J2-21 centrifuge was applied for cell separations (Beckman, Fullerton, CA).

**Biotransformation and product isolation.** Liquid minimal medium (100 mL), prepared according to Dworkin and Foster (18), with an additional trace-element solution (5 mL/L) (19) was autoclaved, and glucose (5 g/L) was added under sterile conditions. The culture used to inoculate the liquid medium was taken from freshly grown plates with an inoculating loop. The liquid culture was allowed to grow for about 23 h at 30°C in a rotary shaker at 120 rpm until 100 mg of the FA was added under sterile conditions. After further incubation for 18 h under the same conditions, the culture was worked up by sonication of the bacterial broth for 15 min and centrifugation at 15,000  $\times$  g for 20 min. The supernatant (approximately 100 mL), adjusted to pH 3 by adding 2 mL of HCl (10%), was extracted three times each with 50 mL diethyl ether. The combined extract was dried over Na<sub>2</sub>SO<sub>4</sub> and, after filtration, the solvent was removed under reduced pressure (rotary evaporator). For subsequent HPLC analysis, the residue was dissolved in 5 mL of methanol/water mixture (1:1, vol/vol).

For the isolation and purification of the transformation products, the combined extract obtained from eight conversions was applied onto a glass column (10  $\times$  2 cm) filled with RP18 (octadecyl reversed phase) material (40–63  $\mu$ m particle size; Merck KGaA, Darmstadt, Germany). Separation was carried out by employing a gradient composed of mobile phase A (water/0.05% formic acid) and B (acetonitrile). The share of solvent B increased from 40 to 100% in 5% steps using 100-mL fractions. Fractions (12 mL) were collected and analyzed by analytical HPLC. Fractions containing the target compounds were combined and lyophilized. Yields of transformation products ranged from 10 to 15%.

**Derivatization of products.** Methylation with diazomethane was performed by a standard procedure (20).

**HPLC.** Analytical separation was carried out on a Eurospher 100 C-18 column (250  $\times$  4 mm, 5  $\mu$ m particle size; Knauer, Berlin, Germany) using a flow rate of 1 mL/min, employing a Knauer HPLC pump MaxiStar coupled to (i) a Knauer multi-wavelength UV/visible detector (234 nm) and (ii) an ELSD (Sedere, Alfortville Cedex, France) kept at 40°C and 2.2 bar compressed air. Data acquisition was achieved using Eurochrom 2000 software (Knauer). The following gradient was applied: solvent A (water/0.05% formic acid), solvent B (acetonitrile): 0–30 min, 5–80% B, 30–40 min, 80–100% B, 40–45 min, 100% B.

**HPLC–tandem mass spectrometry (HPLC–MS/MS).** Analysis of the isolated products was performed using a triple-stage quadrupole TSQ 7000 HPLC–MS/MS system (Finnigan MAT, Bremen, Germany) using electrospray ionization (ESI) in either the positive or the negative mode. ESI capillary voltage was set to 4 kV (positive mode) and 3 kV (negative mode), respectively. The temperature of the heated capillary was 250°C. Nitrogen served both as sheath (60 psi) and auxiliary gas (10 L/min). Positive and negative ions were detected by scanning from 150 to 400 u with a total scan duration of 1.0 s for a single full spectrum. MS/MS experiments were performed at a collision gas pressure of 1.8 mTorr argon and a collision-induced dissociation offset voltage of –12 eV scanning a mass range of 20 to 280 u within 2.0 s. Data acquisition and evaluation were carried out on a Personal DECstation 5000/33 (Digital Equipment, Unterföhring, Germany) and ICIS 8.1 software (Finnigan MAT).

**High-resolution GC–MS (HRGC–MS).** After methylation of the isolated compounds with diazomethane, HRGC–MS analysis was performed using a Fisons MD 800 mass spectrometer coupled to a Fisons GC 8000 with split injector (1:20). The system was equipped with the Mass Lab software (version 1.3) (Fisons, Mainz-Kastel, Germany). A J&W DB Wax fused-silica capillary column (30 m  $\times$  0.25 mm i.d., 0.25  $\mu$ m film thickness; J&W Scientific, Folsom, CA) was employed. The temperature program was 3 min isothermal at 50°C and then increased at 4°C/min to 240°C using a flow rate of 1.5 mL/min helium. The MS operating parameters were as follows: ionization voltage 70 eV (electron impact ionization), ion source and interface temperatures 210 and 250°C, respectively.

**Multidimensional GC (MDGC).** A double-oven MDGC system consisting of two Fisons GC 8000 apparatus was used (Fisons, Mainz-Kastel, Germany). Split injection (1:10) and FID detection in ovens 1 and 2 were employed. Preseparation was achieved in oven 1 on a J&W DB Wax fused-silica capillary column (30 m  $\times$  0.25 mm i.d., 0.25  $\mu$ m film thickness; J&W Scientific). In oven 2, a chiral fused-silica capillary column was connected to the precolumn by a moving column–stream switching system. As chiral phase, a 2,3-*O*-diethyl-6-*O*-*tert*-butyldimethyl-silyl- $\beta$ -cyclodextrin column (MEGA, Milano, Italy) was employed for the separation of the 3-hydroxy acid methyl esters. Helium was used as the carrier gas (1.9 mL/min).

**NMR.** <sup>1</sup>H and <sup>13</sup>C NMR spectra were recorded on a Bruker WM 400 spectrometer (Bruker, Ettlingen, Germany) with CDCl<sub>3</sub> (Merck KGaA) as solvent and are reported in ppm ( $\delta$ ) relative to CDCl<sub>3</sub> as internal reference; coupling constants (*J*) are given in Hertz (Hz).

(i) *3-Hydroxy-Z6-dodecenoic acid 1* (21). <sup>13</sup>C NMR (100 MHz, CDCl<sub>3</sub>):  $\delta$  177.6 (C-1), 131.2 (C-7), 128.4 (C-6), 67.7 (C-3), 41.2 (C-2), 36.4 (C-4), 31.5 (C-10), 29.3 (C-9), 27.2 (C-8), 23.3 (C-5), 22.6 (C-11), 14.0 (C-12).

ESI–MS (full scan, positive mode): *m/z* 237 [M + Na]<sup>+</sup>, 232 [M + NH<sub>4</sub>]<sup>+</sup>. ESI–MS (full scan, negative mode): *m/z* 427 [2M – H]<sup>–</sup>, 213 [M – H]<sup>–</sup>. ESI–MS/MS (*m/z* 232, –12 eV): *m/z* (%) 232 [M + NH<sub>4</sub>]<sup>+</sup> (4), 215 [M + H]<sup>+</sup> (28), 197

$[M - H_2O + H]^+$  (26), 179  $[M - 2H_2O + H]^+$  (6), 155  $[C_{10}H_{19}O]^+$  (100), 137  $[C_{10}H_{19}O - H_2O]^+$  (11).

HRGC-EI-MS (70 eV) (methyl ester):  $m/z$  (%) 228 (1), 210 (3), 136 (18), 110 (11), 103 (16), 100 (22), 93 (16), 84 (32), 81 (37), 80 (30), 79 (36), 69 (40), 67 (44), 55 (70), 54 (44), 43 (75), 41 (100).

(ii) *3-Hydroxy-Z5,Z8-tetradecadienoic acid 2* (21).  $^{13}C$  NMR (100 MHz,  $CDCl_3$ ):  $\delta$  177.5 (C-1), 131.8 (C-5), 130.8 (C-9), 127.1 (C-8), 124.2 (C-6), 67.9 (C-3), 40.6 (C-2), 34.3 (C-4), 31.5 (C-12), 29.2 (C-11), 27.2 (C-10), 25.8 (C-7), 22.5 (C-13), 14.0 (C-14).

ESI-MS (full scan, positive mode):  $m/z$  263  $[M + Na]^+$ , 258  $[M + NH_4]^+$ . ESI-MS (full scan, negative mode):  $m/z$  479  $[2M - H]^-$ , 239  $[M - H]^-$ . ESI-MS/MS ( $m/z$  258, -12 eV):  $m/z$  (%) 258  $[M + NH_4]^+$  (10), 241  $[M + H]^+$  (95), 223  $[M - H_2O + H]^+$  (100), 205  $[M - 2H_2O + H]^+$  (28), 181  $[C_{12}H_{21}O]^+$  (88), 163  $[C_{12}H_{21}O - H_2O]^+$  (61).

HRGC-EI-MS (70 eV) (methyl ester):  $m/z$  (%) 254 (1), 236 (1), 152 (7), 133 (7), 119 (11), 105 (27), 103 (53), 95 (18), 91 (20), 81 (38), 79 (45), 71 (54), 67 (65), 61 (29), 55 (61), 43 (100), 41 (82).

(iii) *3-Hydroxy-Z6,Z9-dodecadienoic acid 3*.  $^{13}C$  NMR (100 MHz,  $CDCl_3$ ):  $\delta$  176.7 (C-1), 132.1 (C-6), 129.2 (C-10), 128.8 (C-9), 127.1 (C-7), 67.7 (C-3), 41.1 (C-2), 36.4 (C-4), 25.6 (C-8), 23.3 (C-5), 20.6 (C-11), 14.2 (C-12).

ESI-MS (full scan, positive mode):  $m/z$  235  $[M + Na]^+$ , 230  $[M + NH_4]^+$ . ESI-MS (full scan, negative mode):  $m/z$  423  $[2M - H]^-$ , 211  $[M - H]^-$ . ESI-MS/MS ( $m/z$  230, -12 eV):  $m/z$  (%) 230  $[M + NH_4]^+$  (7), 213  $[M + H]^+$  (70), 195  $[M - H_2O + H]^+$  (100), 177  $[M - 2H_2O + H]^+$  (11), 153  $[C_{10}H_{17}O]^+$  (70), 135  $[C_{10}H_{17}O - H_2O]^+$  (36).

HRGC-EI-MS (70 eV) (methyl ester):  $m/z$  (%) 226 (1), 208 (1), 152 (21), 134 (23), 119 (43), 108 (60), 105 (88), 103 (16), 95 (36), 93 (89), 91 (77), 81 (66), 80 (66), 79 (100), 71 (63), 67 (89), 55 (80), 43 (49), 41 (65).

(iv) *3-Hydroxy-Z5,Z8,Z11-tetradecatrienoic acid 4* (22).  $^{13}C$  NMR (100 MHz,  $CDCl_3$ ):  $\delta$  176.9 (C-1), 132.2 (C-5), 131.6 (C-12), 128.9 (C-9), 127.5 (C-8), 126.9 (C-11), 124.5 (C-6), 67.9 (C-3), 40.6 (C-2), 34.5 (C-4), 25.8 (C-7), 25.6 (C-19), 20.6 (C-13), 14.2 (C-14).

ESI-MS (full scan, positive mode):  $m/z$  261  $[M + Na]^+$ , 256  $[M + NH_4]^+$ . ESI-MS (full scan, negative mode):  $m/z$  475  $[2M - H]^-$ , 237  $[M - H]^-$ . ESI-MS/MS ( $m/z$  256, -12 eV):  $m/z$  (%) 256  $[M + NH_4]^+$  (20), 239  $[M + H]^+$  (46), 221  $[M - H_2O + H]^+$  (100), 203  $[M - 2H_2O + H]^+$  (42), 179  $[C_{12}H_{19}O]^+$  (71), 161  $[C_{12}H_{19}O - H_2O]^+$  (97).

HRGC-EI-MS (70 eV) (methyl ester):  $m/z$  (%) 234 (1), 178 (5), 160 (9), 145 (9), 133 (11), 131 (25), 117 (26), 105 (52), 103 (54), 95 (48), 91 (71), 81 (28), 79 (100), 71 (72), 67 (71), 61 (32), 55 (47), 43 (52), 41 (53).

(v) *3-Hydroxy-Z5-tetradecenoic acid 5* (21).  $^{13}C$  NMR (100 MHz,  $CDCl_3$ ):  $\delta$  177.0 (C-1), 133.9 (C-6), 123.9 (C-5), 68.1 (C-3), 40.7 (C-2), 34.5 (C-4), 31.9 (C-12), 29.6 (C-10), 29.5 (C-9), 29.3 (C-8), 29.3 (C-11), 27.5 (C-7), 22.6 (C-13), 14.0 (C-14).

ESI-MS (full scan, positive mode):  $m/z$  265  $[M + Na]^+$ ,

260  $[M + NH_4]^+$ . ESI-MS (full scan, negative mode):  $m/z$  483  $[2M - H]^-$ , 241  $[M - H]^-$ . ESI-MS/MS ( $m/z$  260, -12 eV):  $m/z$  (%) 260  $[M + NH_4]^+$  (10), 243  $[M + H]^+$  (43), 225  $[M - H_2O + H]^+$  (23), 207  $[M - 2H_2O + H]^+$  (11), 183  $[C_{12}H_{23}O]^+$  (100), 165  $[C_{12}H_{23}O - H_2O]^+$  (9).

HRGC-EI-MS (70 eV) (methyl ester):  $m/z$  (%) 256 (1), 238 (3), 164 (13), 140 (8), 126 (8), 104 (18), 103 (100), 84 (40), 83 (20), 71 (86), 69 (35), 61 (49), 55 (71), 43 (73), 41 (69).

(vi) *3-Hydroxy-Z5-dodecenoic acid 6* (23).  $^{13}C$  NMR (100 MHz,  $CDCl_3$ ):  $\delta$  177.0 (C-1), 133.9 (C-6), 123.9 (C-5), 68.0 (C-3), 40.5 (C-2), 34.4 (C-4), 31.7 (C-10), 29.5 (C-8), 28.9 (C-9), 27.5 (C-7), 22.6 (C-11), 14.0 (C-12).

ESI-MS (full scan, positive mode):  $m/z$  237  $[M + Na]^+$ , 232  $[M + NH_4]^+$ . ESI-MS (full scan, negative mode):  $m/z$  427  $[2M - H]^-$ , 213  $[M - H]^-$ . ESI-MS/MS ( $m/z$  232, -12 eV):  $m/z$  (%) 232  $[M + NH_4]^+$  (6), 215  $[M + H]^+$  (25), 197  $[M - H_2O + H]^+$  (16), 179  $[M - 2H_2O + H]^+$  (12), 155  $[C_{10}H_{19}O]^+$  (100), 137  $[C_{10}H_{19}O - H_2O]^+$  (11).

HRGC-EI-MS (70 eV) (methyl ester):  $m/z$  (%) 210 (5), 178 (4), 161 (3), 150 (7), 136 (10), 126 (18), 104 (14), 103 (100), 84 (30), 71 (70), 69 (45), 61 (30), 55 (55), 43 (90), 41 (32).

(vii) *3-Hydroxy-Z5-decenoic acid 8* (24).  $^{13}C$  NMR (100 MHz,  $CDCl_3$ ):  $\delta$  176.8 (C-1), 133.7 (C-6), 123.9 (C-5), 68.0 (C-3), 40.6 (C-2), 34.4 (C-4), 31.7 (C-8), 27.1 (C-7), 22.3 (C-9), 13.8 (C-10).

ESI-MS (full scan, positive mode):  $m/z$  209  $[M + Na]^+$ , 204  $[M + NH_4]^+$ . ESI-MS (full scan, negative mode):  $m/z$  427  $[2M - H]^-$ , 213  $[M - H]^-$ . ESI-MS/MS ( $m/z$  204, -12 eV):  $m/z$  (%) 204  $[M + NH_4]^+$  (9), 187  $[M + H]^+$  (28), 169  $[M - H_2O + H]^+$  (41), 151  $[M - 2H_2O + H]^+$  (18), 127  $[C_8H_{15}O]^+$  (100), 109  $[C_8H_{15}O - H_2O]^+$  (22).

HRGC-EI-MS (70 eV) (methyl ester):  $m/z$  (%) 182 (3), 150 (6), 133 (3), 122 (8), 108 (17), 103 (100), 84 (14), 71 (77), 69 (21), 61 (43), 55 (53), 43 (79), 41 (33).

## RESULTS

*Phenotypic characterization of the microorganism.* With linoleic acid as substrate, different soil samples were investigated in order to detect microorganisms selectively degrading FA. Of the bacteria screened, one culture, isolated from a humid soil sample, converted the exogenous substrate to more polar compounds at greater than a trace amount. This strain was a Gram-negative, nonfermentative rod ( $0.5 \times 2 \mu\text{m}$ ) that exhibited optimal growth at  $30^\circ\text{C}$ . The following reactions of the commercially available test-stripe APIZYM 20 NE showed positive results: existence of urease,  $\beta$ -glucosidase, protease, and  $\beta$ -galactosidase as well as assimilation of glucose, arabinose, mannose, mannitol, *N*-acetylglucosamine, maltose, capric acid, malic acid, and citric acid. Checks concerning aminopeptidase, catalase, and DNase were positive, whereas no oxidase activity could be detected. The isolated strain was very resistant to antibiotics. Only two antibiotic substances, i.e., cotrimoxazol and oflocacin, inhibited the bacterial growth. Comparison of these data with those of known strains revealed that the strain belongs to the genus



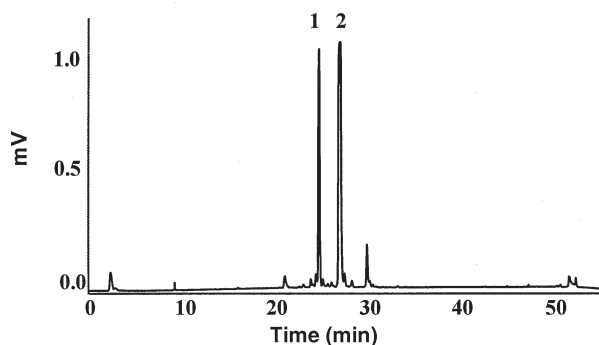
*Stenotrophomonas* and has 99% similarity to the species *S. maltophilia*.

**Genotypic identification of the bacterial strain.** To confirm the phenotypic characterization, the isolated strain was subjected to sequencing of the first 300 base pairs of its small subunit ribosomal RNA gene (16S) by means of the Taq-cycle-DyeDeoxy™-terminator technique. The resulting nucleotide sequences were compared with the sequence data of the EMBL database, which disclosed that a *Pseudomonas* sp. had been isolated. Prior to its second reclassification in 1993, *S. maltophilia* had been named *Pseudomonas maltophilia* and before that *Xanthomonas maltophilia* (25,26).

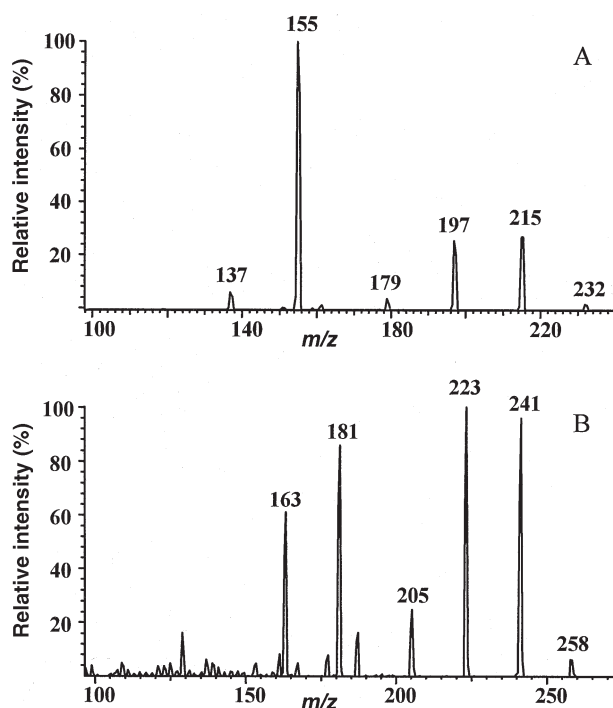
**Structure determination of the biotransformation products of linoleic acid.** HPLC analysis of the extract obtained by incubation of linoleic acid with the *S. maltophilia* strain showed two major products **1** and **2** (Fig. 1). Their isolation was performed by liquid chromatography. Fractions containing the target compounds (HPLC control) were combined. Lyophilization revealed two colorless, oily liquids.

The identification of **1** and **2** was carried out by HPLC–MS/MS analysis. In the full scan mode, the spectrum of compound **1** displayed pseudomolecular ions at  $m/z$  232 [ $M + NH_4$ ]<sup>+</sup> and  $m/z$  237 [ $M + Na$ ]<sup>+</sup>. Fragmentation of the ammonium adduct ion (Fig. 2A) revealed characteristic ions at  $m/z$  215, 197, and 179, which are caused by subsequent elimination of the ammonium as well as one and two water molecules. The other prominent signals at  $m/z$  155 and 137 are due to a cleavage of the molecule and following splitting-off of water. Analogously, the spectrum of compound **2** revealed pseudomolecular ions at  $m/z$  258 [ $M + NH_4$ ]<sup>+</sup> and  $m/z$  263 [ $M + Na$ ]<sup>+</sup>. The product ion spectrum (Fig. 2B) showed fragments at  $m/z$  241, 223, 205, 181, and 163 due to dissociation processes similar to that of product **1**.

In addition, HRGC–MS analysis was carried out after methylation of **1** and **2** with diazomethane. Both compounds exhibited a characteristic signal at  $m/z$  103 [ $C_4H_7O_3$ ], which is indicative of a hydroxylation at the C-3 position as induced by an  $\alpha$ -cleavage of the molecule. Further fragments were caused by decomposition of the carbon chain, mainly next to the double bonds. The molecular ion of the methyl esters of **1** and **2** at



**FIG. 1.** RP-HPLC separation (ELSD detection) of the extract obtained after incubation of linoleic acid with *Stenotrophomonas maltophilia* strain isolated from topsoil: **1**: 3-hydroxy-Z6-dodecenoic acid; **2**: 3-hydroxy-Z5,Z8-tetradecadienoic acid.



**FIG. 2.** HPLC–electrospray-tandem mass spectrometry product ion spectra of compounds **1** (A) and **2** (B); precursor ions  $m/z$  232 and 258 [ $M + NH_4$ ]<sup>+</sup>, respectively (positive mode, collision-induced dissociation offset voltage –12 eV, 1.8 mTorr argon as collision gas).

$m/z$  254 and 228, respectively, as well as fragments of  $m/z$  236 and 210 corresponding to [ $M - H_2O$ ] were also observed.

Structural elucidation of **1** and **2** was completed by recording different 1D and 2D NMR spectra (*cf.* Materials and Methods section). On the basis of the received results, products **1** and **2** were identified as 3-hydroxy-Z6-dodecenoic acid and 3-hydroxy-Z5,Z8-tetradecadienoic acid, respectively.

**Substrate specificity.** To elucidate the scope of substrate acceptability, various other FA were fed to *S. maltophilia* (*cf.* Materials and Methods section). Product separation and structure elucidation was performed as mentioned above for linoleic acid. Figure 3 summarizes the substrates used (including linoleic acid) and their biotransformation products observed (for spectroscopic data, see the Materials and Methods section).

**Stereochemistry of biotransformation products.** Analysis of the enantiomeric distribution of the methylated 3-hydroxylated products **1** to **7** by MDGC revealed ratios ranging from 99:1 to 94:6% (*cf.* Fig. 3). Stereochemical evaluation was carried out by MDGC after transformation of the 3-hydroxylated microbial products into the corresponding saturated 1,3-diols by hydrogenation and subsequent reduction of the carboxylic function with  $LiAlH_4$  (27) and comparison with reference data. A racemic reference substance was synthesized by aldol addition with methyl acetate and subsequent hydrogenation, followed by reduction of the methyl ester with  $LiAlH_4$  (27). Enantioselective synthesis of (*S*)-dodecane-1,3-diol was carried out by asymmetric epoxidation under Sharpless conditions (28) and treatment of the epoxide formed with sodium bis(2-methoxy-ethoxy)aluminum (Red-Al) (29).



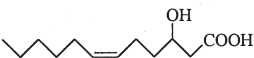
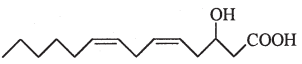
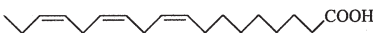


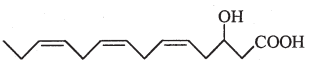


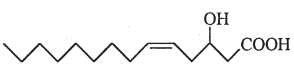






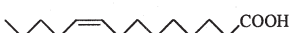

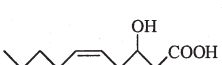
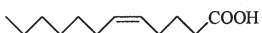

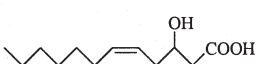
			(R)	(S)	
 <b>linoleic acid</b> <b>(Z9,Z12-octadecadienoic acid)</b>		 <b>3-hydroxy-Z6-dodecenoic acid 1</b>	31%	94	6
		 <b>3-hydroxy-Z5,Z8-tetradecadienoic acid 2</b>	57%	97	3
 <b>α-linolenic acid</b> <b>(Z9,Z12,Z15-octadecatrienoic acid)</b>		 <b>3-hydroxy-Z6,Z9-dodecadienoic acid 3</b>	24%	95	5
		 <b>3-hydroxy-Z5,Z8,Z11-tetradecatrienoic acid 4</b>	62%	95	5
 <b>oleic acid</b> <b>(Z9-octadecenoic acid)</b>		 <b>3-hydroxy-Z5-tetradecenoic acid 5</b>	91%	93	7
 <b>cis-vaccenic acid</b> <b>(Z11-octadecenoic acid)</b>		 <b>3-hydroxy-Z5-dodecenoic acid 6</b>	89%	98	2
 <b>palmitoleic acid</b> <b>(Z9-hexadecenoic acid)</b>		 <b>3-hydroxy-Z5-dodecenoic acid 6</b>	81%	98	2
 <b>myristoleic acid</b> <b>(Z9-tetradecenoic acid)</b>		 <b>3-hydroxy-Z5-decenoic acid 7</b>	87%	99	1
 <b>Z5-dodecenoic acid</b>		 <b>3-hydroxy-Z5-dodecenoic acid 6</b>	86%	96	4

FIG. 3. Substrates fed to *Stenotrophomonas maltophilia* and main products formed after an incubation time of 18 h (percentage of total transformation and enantiomeric composition given).

In addition, circular dichroism (CD) spectroscopy (30) was employed. The details of the configurational assignment including synthesis of the reference compounds as well as MDGC analysis and CD spectroscopy are reported elsewhere (31). Both methods revealed highly enriched (*R*)-configured 3-hydroxy derivatives for all substrates under study.

## DISCUSSION

The capability of producing (*R*)-3-hydroxylated FA metabolites is not restricted to *S. maltophilia* alone. In 1967, the occurrence of (*R*)-3-hydroxy palmitic acid and related saturated compounds was reported in yeasts such as *Rhodotorula graminis* (32) and *Saccharomyces malanga* (33). Medium-chain 3-hydroxy FA are present in the glycolipids of the smut fungi *Ustilago zaeae* and *U. nuda* (34). Similar data have been found for the yeast *Dipodascopsis uninucleata* (22) and the soil fungus *Mucor genevensis* (35). In these organisms, 3-hydroxylated FA appear to be implicated in the regulation of vegetative growth and sexual reproduction within the life cycle. A recent immunofluorescence microscopic study using an antibody that exhibited group-specificity toward (*R*)-3-hydroxy-oxylipins revealed that in *D. uninucleata* (*R*)-hydroxylated compounds occur selectively in the gametangia, in asci as well as between the released ascospores (36).

The biosynthetic pathway to the (*R*)-3-hydroxy enoic FA remains to be elucidated. From the structural identification of the FA derivatives formed after incubation with *S. maltophilia*, it is evident that during transformation of the admitted substrate the carbon chain remained unchanged from the  $\omega$ -end. Only even-numbered products were detected. Owing to these observations, FA degradation by  $\beta$ -oxidation is assumed. While during "normal"  $\beta$ -oxidation an intermediary (*S*)-3-hydroxyacyl-CoA is formed as the major metabolite of the enoyl-CoA hydratase-catalyzed reaction, we have clearly demonstrated that *S. maltophilia* converts different FA into (*R*)-3-hydroxylated products of shorter chain length. Thus, as a metabolic route to (*R*)-3-hydroxy FA a reaction sequence analogous to  $\beta$ -oxidation is conceivable; however, the sequence would imply the occurrence of a 2-enoyl CoA hydratase with opposite stereochemistry. The occurrence of such enzymes has already been demonstrated in microorganisms. Recently, an (*R*)-specific *trans*-2,3-enoylacyl-CoA hydratase has been isolated and characterized from *Rhodospirillum rubrum* (37).

## ACKNOWLEDGMENTS

This work was supported by the Deutsche Forschungsgemeinschaft, Bonn (SFB 347 "Selective Reactions of Metal-Activated Molecules") and Fond der Chemischen Industrie. Dr. Matthias Grüne and Elfriede Ruckdeschl are thanked for the measurement of NMR spectra.

## REFERENCES

- Gardner, H.W. (1991) Recent Investigations into the Lipoygenase Pathway of Plants, *Biochim. Biophys. Acta* 1024, 221–239.
- Nomura, T., and Ogata, O. (1976) Distribution of Prostaglandins in the Animal Kingdom, *Biochim. Biophys. Acta* 43, 127–131.
- Van Dyk, M.S., Kock, J.L.F., and Botha, A. (1994) Hydroxy Long Chain Fatty Acids in Fungi, *World J. Microbiol. Biotechnol.* 10, 495–504.
- Hamberg, M., Herman, R.P., and Jacobsen, U. (1987) Stereochemistry of Two Epoxy Alcohols from *Saprolegnia parasitica*, *Biochim. Biophys. Acta* 879, 410–418.
- Brodowsky, I.B., Hamberg, M., and Oliw, E.H. (1992) A Linoleic Acid 8(*R*) Dioxygenase and Hydroperoxide Isomerase of Fungus *Gaeomannomyces graminis*, *J. Biol. Chem.* 267, 14738–14745.
- Su, C., Brodowsky, I.B., and Oliw, E.H. (1995) Studies on Linoleic Acid 8*R*-Dioxygenase and Hydroperoxide Isomerase of Fungus *Gaeomannomyces graminis*, *Lipids* 30, 43–50.
- Hou, C.T. (1995) Production of Hydroxy Fatty Acids from Unsaturated Fatty Acids by *Flavobacterium* sp. DS5 Hydratase, a C-10 Positional- and *cis* Unsaturation-Specific Enzyme, *J. Am. Oil Chem. Soc.* 72, 1265–1270.
- Koritala, S., and Bagby, M.O. (1992) Microbial Conversion of Linoleic and Linolenic Acids to Unsaturated Hydroxy Fatty Acids, *J. Am. Oil Chem. Soc.* 69, 575–578.
- Kuo, T.M., Manthey, L.K., and Hou, C.T. (1998) Fatty Acid Bioconversion by *Pseudomonas aeruginosa* PR3, *J. Am. Oil Chem. Soc.* 75, 875–879.
- Hou, C.T. (1996) A Novel Compound, 12,13,17-Trihydroxy-9(*Z*)-octadecenoic Acid, from Linoleic Acid by a New Microbial Isolate *Clavibacter* sp. ALA2, *J. Am. Oil Chem. Soc.* 73, 1359–1362.
- Kato, T., Yamaguchi, Y., Abe, N., Ueyehara, T., Namai, T., Yamana, S., and Harada, N. (1984) Unsaturated Hydroxy Fatty Acids, the Self-Defensive Substances in Rice Plant Suffering from Rice Blast Disease, *Chem. Lett.* 25, 409–412.
- Miura, Y., and Fulco, A.J. (1975)  $\omega$ -1,  $\omega$ -2 and  $\omega$ -3 Hydroxylation of Long-Chain Fatty Acids, Amides and Alcohols by a Soluble Enzyme System from *Bacillus megaterium*, *Biochim. Biophys. Acta* 388, 305–317.
- Truan, G., Komandla, M.R., Falck, J.R., and Peterson, J.A. (1999) P450BM-3: Absolute Configuration of the Primary Metabolites of Palmitic Acid, *Arch. Biochem. Biophys.* 366, 192–198.
- Smibert, R.M., and Krieg, N.L. (1994) Phenotypic Characterization, in *Methods for General and Molecular Bacteriology* (Gerhardt, P., ed.), pp. 607–654, American Society for Microbiology, Washington, DC.
- Woods, C.R., Versalovic, J., Koeuth, T., and Lupski, J.R. (1993) Whole-Cell Repetitive Element Sequence-Based Polymerase Chain Reaction Allows Rapid Assessment of Clonal Relationships of Bacterial Isolates, *J. Clin. Microbiol.* 31, 1927–1931.
- Lane, D.J. (1991) Rapid Determination of 16S Ribosomal RNA Sequences for Phylogenetic Analyses, in *Nucleic Acid Techniques in Bacterial Systematics* (Stackebrandt, E., and Goodfellow, M., eds.), pp. 115–175, Wiley, Chichester.
- Harmsen, D., Rothgänger, J., Singer, C., Albert, J., and Frosch, M. (1999) Intuitive Hypertext-Based Molecular Identification of Microorganisms, *Lancet* 353, 291.
- Dworkin, M., and Foster, J.W. (1958) Experiments with Some Microorganisms Which Utilize Ethane and Hydrogen, *J. Bacteriol.* 75, 592–603.
- Atlas, R.M., and Parks, L.C. (eds.) (1993) *Handbook of Microbiological Media*, CRC Press, Boca Raton.
- Black, T.H. (1983) The Preparation and Reactions of Diazomethane, *Aldrichimica Acta* 16, 3–10.
- de Waard, P., van der Wal, H., Huijberts, G.N.M., and Eggink, G. (1993) Heteronuclear NMR Analysis of Unsaturated Fatty Acids in Poly(3-hydroxyalkanoates). Study of  $\beta$ -Oxidation in *Pseudomonas putida*, *J. Biol. Chem.* 268, 315–319.

22. Venter, P., Kock, J.L.F., Sravan Kumar, G., Botha, A., Coetzee, D.J., Botes, P.J., Bhatt, R.K., Falck, J.R., Schewe, T., and Nigam, S. (1997) Production of 3R-Hydroxy-polyenoic Fatty Acids by the Yeast *Dipodascopsis uninucleata*, *Lipids* 32, 1277–1283.
23. Huijberts, G.N.M., de Rijk, T., de Waard, P., and Eggink, G. (1994) <sup>13</sup>C Nuclear Magnetic Resonance Studies of *Pseudomonas putida* Fatty Acid Metabolic Routes Involved in Poly(3-hydroxyalkanoate) Synthesis, *J. Bacteriol.* 176, 1661–1666.
24. Abe, H., Doi, Y., Fukushima, T., and Eya, H. (1994) Biosynthesis from Gluconate of a Random Copolyester Consisting of 3-Hydroxybutyrate and Medium-Chain-Length 3-Hydroxyalkanoates by *Pseudomonas* sp. 61-3, *Int. J. Biol. Macromol.* 16, 115–119.
25. Palleroni, N.J., and Bradbury, J.F. (1993) *Stenotrophomonas*, a New Genus for *Xanthomonas maltophilia*, *Int. J. Syst. Bacteriol.* 43, 606–609.
26. Swings, J., De Vos, P., Van den Mooter, M., and De Ley, J. (1983) Transfer of *Pseudomonas maltophilia* Hugh 1981 to the Genus *Xanthomonas* as *Xanthomonas maltophilia* (Hugh 1981) comb. nov., *Int. J. Syst. Bacteriol.* 33, 409–413.
27. Beuerle, T., Engelhard, S., Bicchi, C., and Schwab, W. (1999) Isolation, Identification and Enantioselective Synthesis of Octane-1,3,7-triol: Determination of the Absolute Configuration, *J. Nat. Prod.* 62, 35–40.
28. Katsuki, T., and Sharpless, K.B. (1980) The First Practical Method for Asymmetric Epoxidation, *J. Am. Chem. Soc.* 102, 5974–5976.
29. Viti, S.M. (1982) Regioselective Reduction of 2,3-Epoxy Alcohols, *Tetrahedron Lett.* 23, 4541–4544.
30. Nakanishi, K., and Berova, N. (1994) The Exciton Chirality Method, in *Circular Dichroism Principles and Applications* (Nakanishi, K., Berova, N., and Woody, R., eds.), pp. 361–398, VCH Publishers, New York.
31. Weil, K., Humpf, H.U., Schwab, W., and Schreier, P. (2001) Absolute Configuration of 3-Hydroxy Acids Formed by *Stenotrophomonas maltophilia*: Application of Multidimensional Gas Chromatography and Circular Dichroism Spectroscopy, *Chirality* 14, 51–58 (2002).
32. Stodala, F.H., Deinema, M.H., and Spencer, J.F.T. (1967) Extracellular Lipids of Yeasts, *Bacteriol. Rev.* 31, 194–213.
33. Vesonder, R.F., Wickerham, L.J., and Rohwedder, W.K. (1968) 3-D-Hydroxypalmitic Acid: A Metabolic Product of the Yeast NRRL Y-6954, *Can. J. Chem.* 46, 2628–2629.
34. Lösel, D.M. (1988) Fungal Lipids, in *Microbial Lipids* (Rathledge, C., and Wilkinson S.G., eds.), pp. 699–806, Academic Press, San Diego.
35. Pohl, C.H., Botha, A., Kock, J.L.F., Coetzee, D.J., Botes, P.J., Schewe, T., and Nigam, S. (1998) Oxylipin Formation in Fungi: Biotransformation of Arachidonic Acid to 3-Hydroxy-5,8-tetradecadienoic Acid by *Mucor genevensis*, *Biochem. Biophys. Res. Commun.* 253, 703–706.
36. Kock, J.L.F., Venter, P., Linke, D., Schewe, T., and Nigam, S. (1998) Biological Dynamics and Distribution of 3-Hydroxy Fatty Acids in the Yeast *Dipodascopsis uninucleata* as Investigated by Immunofluorescence Microscopy: Evidence for a Putative Regulatory Role in the Sexual Reproductive Cycle, *FEBS Lett.* 427, 345–348.
37. Reiser, S.E., Mitsky, T.A., and Gruys, K.J. (2000) Characterization and Cloning of an (R)-Specific *trans*-2,3-Enoylacyl-CoA Hydratase from *Rhodospirillum rubrum* and Use of This Enzyme for PHA Production in *Escherichia coli*, *Appl. Microbiol. Biotechnol.* 53, 209–218.

[Received May 3, 2001, and in revised form December 3, 2001; revision accepted January 2, 2002]



# Saturated and Unsaturated Anteiso-C<sub>19</sub> Acids in the Seed Lipids from *Hesperopeuce mertensiana* (Pinaceae)

Frédéric Destailats<sup>a</sup>, Robert L. Wolff<sup>b,\*</sup>, and Paul Angers<sup>a</sup>

<sup>a</sup>Department of Food Science and Nutrition, and Dairy Research Center (STELA), Université Laval, Sainte Foy, Québec, Canada, G1K 7P4, and <sup>b</sup>Institut des Science et Techniques des Aliments de Bordeaux, Université Bordeaux 1, Talence, France

**ABSTRACT:** Minor uncommon FA from *Hesperopeuce mertensiana* (a gymnosperm species of the Pinaceae family) seed oil were characterized through a combination of silver ion TLC of their FAME, and GLC coupled with MS of their picolinyl derivatives. These uncommon components have the structures 16-methyloctadecanoic (anteiso-19:0), 16-methyl-*cis*-9-octadecenoic (anteiso-19:1), and 16-methyl-*cis*-9,*cis*-12-octadecadienoic (anteiso-19:2) acids. These branched C<sub>19</sub> acids were identified earlier in the wood of *Picea abies*, which would indicate that such acids could be widespread, though minor, components of Pinaceae lipids.

Paper no. L8953 in *Lipids* 37, 325–328 (March 2002).

It is generally admitted that branched (br) FA, mostly with iso- and anteiso- structures, are characteristic of animal fats, particularly ruminant fats. On the other hand, it is also widely recognized that these acids do not, or very rarely, occur in the plant kingdom. In fact, this is a simplistic point of view. Gymnosperms, which are one of the most prominent elements of the extant flora, do indeed contain br-FA, i.e., br-15:0 and br-17:0 acids, in their leaves (1), anteiso-17:0 acid in their seeds (2), and several saturated and unsaturated anteiso-C<sub>19</sub> acids in their wood (3).

We had some indications that sustained the possibility of the presence of anteiso-C<sub>19</sub> acids in the seed lipids from Pinaceae. First of all, Plattner *et al.* (4) characterized such uncommon FA in the seed lipids from *Larix leptolepis* (= *L. kaempferi*) by MS coupled with GLC. Second, analyses by GLC of fractions isolated by silver ion TLC (Ag-TLC) from FAME prepared from *L. decidua* indicated the presence of some unidentified peaks in the C<sub>19</sub> acid region (5). In one particular case, that of *Hesperopeuce mertensiana*, 1.7% of seed FA had not been identified in a previous study (6).

We report here on the GLC–MS characterization of these uncommon FA prepared from *H. mertensiana* seeds in the form of their picolinyl esters (7). Globally, they are similar to the br-C<sub>19</sub> acids characterized by Ekman in the wood of *Picea abies* (3), although present in minute amounts, which would indicate that they are more widespread in conifers than considered thus far.

## MATERIALS AND METHODS

**Sample.** The seed oil prepared from *H. mertensiana* was available from an earlier investigation, and details of its source, extraction, and FA composition are given elsewhere (6).

**GLC of FAME.** Methylation of O-acetylated FA (ca. 10 mg in 2 mL hexane) was carried out in a sealed tube with 0.4 N sodium methoxide in methanol (0.5 mL). Analyses of the FAME were performed with a Hewlett-Packard gas chromatograph, model 5890 Series II, equipped with an FID and connected to a computer with a Hewlett-Packard ChemStation (Hewlett-Packard, Palo Alto, CA). Samples in hexane (1.0 µL) were injected onto an open tubular DB-225 capillary column (30 m × 0.25 mm i.d., 0.25 µm film thickness; J&W, Folsom, CA). The injector and detector temperatures were maintained at 250°C, while the oven temperature was 190°C isothermal. Hydrogen was the carrier gas, with a head pressure of 140 kPa.

**Fractionation of FAME by Ag-TLC.** FAME were fractionated by TLC on silica gel plates impregnated with AgNO<sub>3</sub>. The plates were immersed in a 5% AgNO<sub>3</sub> solution in acetonitrile for 15 min in the dark and activated at 100°C for 1 h. Fractionation was performed according to number and configuration of double bonds, using a mixture of hexane and diethyl ether (80:20, vol/vol) as developing solvent. At the end of the chromatographic runs, the plates were sprayed with a solution of 2',7'-dichlorofluorescein and viewed under UV light. The bands corresponding to saturated, monounsaturated, diunsaturated, and triunsaturated FA were separately scraped off and transferred into test tubes, and methanol (1.5 mL), hexane (2 mL), and an aqueous solution of NaCl (5% wt/vol, 1.5 mL) were successively added with thorough mixing after each addition. After standing for ca. 1 min, the hexane phase was withdrawn, the solvent was evaporated under a stream of nitrogen, and the residue was redissolved in dry methylene chloride (1 mL) prior to further derivatization.

**Picolinyl ester preparation.** Picolinyl esters were prepared from fractionated FAME according to Destailats and Angers (8). A solution of potassium *tert*-butoxide in THF (100 µL, 1.0 M; Aldrich Chemicals, Milwaukee, WI) was added to 3-pyridylcarbinol (200 µL; Aldrich Chemicals). After homogenization, the FAME solutions (1 mL) were added to the reagent, and the mixtures were held at 40°C for 15 min in a closed vial. After cooling to room temperature, the reaction mixture was washed with distilled water (1 mL) and the organic phase was withdrawn, dried over anhydrous sodium sulfate, and filtered before analysis.

\*To whom correspondence should be addressed at INRA-UNL, 17 rue Sully, BP 86510, 21065 Dijon cedex, France. E-mail: wolff@dijon.inra.fr  
Abbreviations: Ag-TLC, silver ion TLC; amu, atomic mass unit; br, branched.

**GLC-MS analysis.** FA picolinyl esters were analyzed by GLC-MS (Hewlett-Packard model 6890 Series II gas chromatograph attached to an Agilent model 5973N selective quadrupole mass detector; Palo Alto, CA) under an ionization voltage of 70 eV at 250°C, and connected to a computer with a Hewlett-Packard ChemStation. The injector, in split mode (25:1), and the interface temperatures were maintained at 230°C, and He was used as carrier gas under constant flow (1 mL min<sup>-1</sup>). GLC separation was performed on a BPX-70 capillary column (SGE, Melbourne, Australia; 60 m × 0.25 mm i.d., 0.25 μm film thickness) with an oven temperature of 200°C isothermal for 10 min, increased to 240°C at 5°C min<sup>-1</sup>, isothermal at this temperature for 20 min, and then increased to 260°C at 5°C min<sup>-1</sup>, for a total run time of 47 min.

## RESULTS

Picolinyl ester derivatives, prepared from FAME separated by Ag-TLC and under mild reaction conditions (8), were used to achieve structural determination of presumably C<sub>19</sub> FA. The mass spectra of three uncommon FA found in *H. mertensiana* seed oil are given in Figure 1.

A first spectrum (Fig. 1A) shows a molecular ion at  $m/z = 389$ , characteristic of a saturated C<sub>19</sub> structure. Loss of carbon-16 and its associated methyl group resulted in two distinctive ion fragments at  $m/z = 360$  and 332. Further fragmentation produced ions of  $m/z$  ranging from 164 to 332, with successive increments of 14 atomic mass units (amu), thus confirming the saturated structure of anteiso-19:0 (16-methyl stearic) acid (7). A second mass spectrum (Fig. 1B) indicates a monounsaturated C<sub>19</sub> structure, with a molecular ion at  $m/z = 387$ . A fragmentation pattern similar to that observed for anteiso-19:0 acid (ion fragments at  $m/z = 358$  and 330) attributable to loss of carbon-16 and its associated methyl group, confirms the anteiso-structure of this FA (16-methyl 18:1). A Δ9 location for the double bond on the hydrocarbon chain was deduced from a 26 amu gap (-C<sub>2</sub>H<sub>2</sub>) between ion fragments at  $m/z = 234$  and 260, characteristic of vinylic fragmentations between carbon atoms C<sub>8</sub>-C<sub>9</sub> and C<sub>10</sub>-C<sub>11</sub>, respectively (7). Moreover, ion fragments at  $m/z = 220$  and 274, resulting from allylic fragmentation, confirmed this position. This FA (as FAME) co-eluted with oleic (*cis*-9 18:1) acid in Ag-TLC fractionation, indicating a similar double bond configuration, and thus completing determination of the 16-methyl-*cis*-9 18:1 (anteiso-19:1) acid structure.

Finally, the spectrum given in Figure 1C resembles that of anteiso-19:1 acid, but the molecular ion at  $m/z = 385$  rather indicates a dienoic acid. Indeed, the spectrum gave diagnostic ions of a monomethylene-interrupted double bond system at  $m/z = 234$ , 260, 274, and 300, indicating ethylenic bonds at positions 9 and 12. Moreover, this compound co-eluted with linoleic (*cis*-9,*cis*-12 18:2) acid in Ag-TLC, indicative of an all-*cis* double bond system. Typical anteiso- fragmentation resulted in ions at  $m/z = 328$  and 356, and completed structure elucidation of this 16-methyl-*cis*-9,*cis*-12 18:2 (anteiso-19:2) acid.

## DISCUSSION

We have shown that *H. mertensiana* seed lipids contain several anteiso-C<sub>19</sub> acids, all of which were earlier characterized in the wood of *P. abies* (3). However, we could not positively identify the anteiso-5,9,12 19:3 present in *P. abies* wood (3). To which extent these findings apply to other Pinaceae seed oils needs further investigation, as no intensive research of these FA was made during our systematic studies of gymnosperm seed lipids. However, *H. mertensiana* and *Picea* spp. are generally not recognized as close relatives. The first species belongs to the Abietoid group, whereas *Picea* spp. belongs to the Pinoid group [this classification is based on botanical as well as immunological observations (9)]. We recently suggested that a Tsugoid group be created (9), considering the closeness of the seed FA compositions of *Tsuga* spp. and *H. mertensiana* on the one hand, and of *Larix*, *Picea*, and most *Pinus* spp. on the other hand, which consistently differed from other Abietoid seed FA.

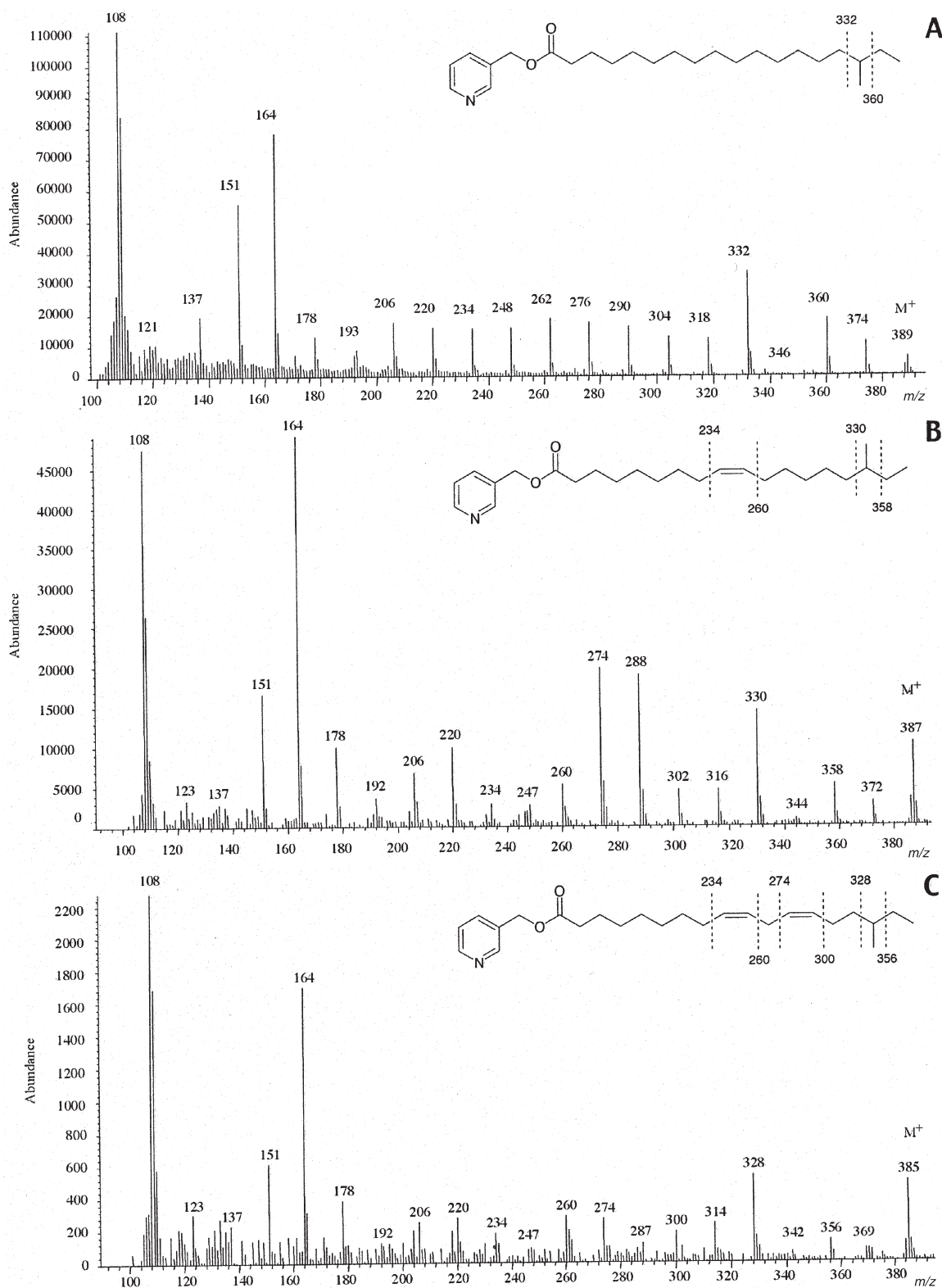
From a quantitative point of view, the anteiso-C<sub>19</sub> acids remain of minor significance (anteiso-19:0, 0.14% of total FA, anteiso-19:1, 0.14%, and anteiso-19:2, 0.05%), and some of them are hindered in chromatograms by other FA of considerably higher levels, but this may vary with the GLC column used. As such, structures of minor FA still remain to be determined. Whatever the distribution of these FA in the seeds of Pinaceae, they do not alter our conclusions reported in three recent reviews for that family (5,9,10). The metabolic origin of br-FA in Pinaceae, however, remains unknown, except that they occur in their leaf, wood, and seed lipids.

## ACKNOWLEDGMENTS

We acknowledge financial support from the Natural Sciences and Engineering Council of Canada, and the Conseil de Recherches en Pêche et en Agroalimentaire du Québec (CORPAQ). The authors are also grateful to the Fondation de l'Université Laval for a Ph.D. award to Frédéric Destailats.

## REFERENCES

1. Jamieson, G.R., and Reid, E.H. (1972) The Leaf Lipids of Some Conifer Species, *Phytochemistry* 11, 269-275.
2. Wolff, R.L., Christie, W.W., and Coakley, D. (1997) Unusual Occurrence of 14-Methylhexadecanoic Acid in Pinaceae Seed Oils Among Plants, *Lipids* 32, 971-973.
3. Ekman, R. (1980) New Polyenoic Acids in Norway Spruce Wood, *Phytochemistry* 19, 147-148.
4. Plattner, R.D., Spencer, G.F., and Kleiman, R. (1975) *cis*-5 Polyenoic Acids in *Larix leptolepis* Seed Oil, *Lipids* 10, 413-416.
5. Wolff, R.L., Lavielle, O., Pédrone, F., Pasquier, E., Deluc, L.G., Marpeau, A.M., and Aitzetmüller, K. (2001) Fatty Acid Compositions of Pinaceae as Taxonomic Markers, *Lipids* 36, 439-451.
6. Wolff, R.L., Destailats, F., and Angers, P. (2001) α-Linolenic Acid and Its Δ5-Desaturation Product, Coniferonic Acid, in the Seeds of *Tsuga* and *Hesperopeuce* as a Taxonomic Means to Differentiate the Two Genera, *Lipids* 36, 211-212.
7. Harvey, D.J. (1982) Picolinyl Esters as Derivatives for the



**FIG. 1.** Mass spectra of picolinyl ester derivatives of 16-methyl 18:0 (anteiso-19:0) acid (A), 16-methyl-*cis*-9 18:1 (anteiso-19:1) acid (B), and 16-methyl-*cis*-9,*cis*-12 18:2 (anteiso-19:2) acid (C) prepared from *Hesperopeuce mertensiana* (Pinaceae) seed lipids.

- Structural Determination of Long Chain Branched and Unsaturated Fatty Acids, *Biomed. Mass Spectrom.* 9, 33–38.
8. Destailats, F., and Angers, P. (2002) One-Step Methodology for the Synthesis of FA Picolinyl Esters from Intact Lipids, *J. Am. Oil Chem. Soc.* 79, 253–256.
  9. Wolff, R.L., Lavialle, O., Pédrone, F., Pasquier, E., Destailats, F., Marpeau, A.M., Angers, P., and Aitzetmüller, K. (2002) Abietoid Seed Fatty Acid Compositions—A Review of the Genera *Abies*, *Cedrus*, *Hesperopeuce*, *Keteleeria*, *Pseudolarix*, and *Tsuga* and Preliminary Inferences on the Taxonomy of Pinaceae, *Lipids* 37:17–26.
  10. Wolff, R.L., Pédrone, F., Pasquier, E., and Marpeau, A.M. (2000) General Characteristics of *Pinus* spp. Seed Fatty Acid Compositions, and Importance of  $\Delta^5$ -Olefinic Acids in the Taxonomy and Phylogeny of the Genus, *Lipids* 35, 1–22.

[Received November 26, 2001; in revised form January 25, 2002; accepted January 31, 2002]



# Distribution of Medium-Chain FA in Different Lipid Classes After Administration of Specific Structured TAG in Rats

Huiling Mu\* and Carl-Erik Høy

BioCentrum-DTU and Center for Advanced Food Studies, Technical University of Denmark, DK-2800 Lyngby, Denmark

**ABSTRACT:** Structured TAG (STAG) containing medium-chain FA (MCFA) in the *sn*-1,3 positions and essential FA in the *sn*-2 position were synthesized by lipase-catalyzed acidolysis. In our previous studies we found that part of the MCFA from STAG could be absorbed in the small intestine; however, it was unclear how they were absorbed. In order to get a better understanding of the metabolism of STAG to improve future design and application of STAG, in the present study lymph lipids collected after feeding STAG were fractionated into different classes and the FA composition of each lipid class was studied by GC after methylation to FAME. Caprylic acid was detected in the fraction of TAG only after administration of 1,3-dioctanoyl-2-linoleyl-*sn*-glycerol (8:0/18:2/8:0), whereas lauric acid was detected in TAG, DAG, and FFA as well as phospholipids after administration of 1,3-didodecanoyl-2-linoleyl-*sn*-glycerol (12:0/18:2/12:0). We conclude that the enterocyte has the ability to reacylate the MCFA into TAG and that the intestinal absorption of MCFA from STAG mainly occurs by resynthesis of TAG. Caprylic acid from STAG is not incorporated into phospholipids, whereas lauric acid from STAG can be incorporated into phospholipids.

Paper no. L8934 in *Lipids* 37, 329–331 (March 2002).

Medium-chain TAG (MCT) provide the advantage of being rapidly digested and thus rapidly providing energy. Therefore, they have been used in clinical nutrition for patients suffering from malabsorption. However, these patients also suffer from a lack of essential FA, a problem that is not solved by using MCT. New lipase-catalyzed acidolysis makes it possible to synthesize structured TAG (STAG) containing medium-chain FA (MCFA) in the *sn*-1,3 positions and essential FA in the *sn*-2 position (1). The absorption of essential FA from these STAG was better in comparison with that from conventional long-chain TAG (2).

To study the effect of chain length of MCFA on the absorption of long-chain FA (LCFA) and the distribution of MCFA between the portal vein and lymphatics in rats with normal fat absorption, we studied the lymphatic transport of FA from specific STAG containing different MCFA varying from caprylic acid (8:0) to lauric acid (12:0) in *sn*-1,3 positions and linoleic acid in the *sn*-2 position. Earlier we found that the chain length of the MCFA in the primary positions of

STAG did not affect the maximal intestinal absorption of LCFA in the *sn*-2 position, whereas the distribution of FA between the lymphatics and the portal vein reflected the chain length of the FA (3). Even though several studies on the absorption of STAG have been reported (4–7), the absorption pathway is still unclear and the intestinal absorption of MCFA from MLM (medium-long-medium)-type STAG is not well understood. A better understanding of the metabolism of STAG may help in the future design and application of STAG. Therefore, lymph lipids collected after feeding STAG were fractionated into different classes, and the FA composition of each lipid class was studied by GC after methylation to FA methyl esters (FAME). The primary target of this study was to find out in which lipid fraction the MCFA exist and whether the distribution of MCFA in different lipid classes changes with the variation in chain length of the MCFA. Therefore, one baseline fraction of lymph and the lymph fractions with maximal absorption of MCFA after administration of different STAG were studied.

## EXPERIMENTAL PROCEDURES

**STAG.** The STAG were synthesized by lipase-catalyzed inter-esterification of safflower oil (Róco, Copenhagen, Denmark) and MCFA (Sigma Chemical Co., St. Louis, MO) in a packed-bed reactor (1). The individual STAG were purified by preparative HPLC (3). The composition of the purified STAG was determined by GC after methylation with 2 M KOH in methanol and Grignard degradation (8). The purity of 8:0/18:2/8:0 and 12:0/18:2/12:0 was 94 and 87%, respectively.

**Animal experiments.** Animal experiments were approved by the Danish Animal Experiments Inspectorate. Male albino Wistar rats were used in the study. More details about surgery and lymph collection have been described previously (3). The lymph FA composition was studied and reported previously (3). The lymph used in this study was collected during the maximal absorption of MCFA after administration of STAG 8:0/18:2/8:0, 12:0/18:2/12:0, or maximal absorption of linoleic acid after administration of safflower oil.

**Analytical procedure.** The lymph from all six rats was pooled together for each group and 200  $\mu$ L lymph, together with internal standards of PC 15:0, DAG 15:0, FFA 15:0, and TAG 15:0, were extracted with chloroform and methanol. After washing with water, drying with anhydrous sodium sulfate, and evaporating under nitrogen, the residues were redissolved in 150  $\mu$ L chloroform/methanol (95:5, vol/vol). The

\*To whom correspondence should be addressed at BioCentrum-DTU, Section for Biochemistry and Nutrition, Building 224, Technical University of Denmark, DK-2800 Lyngby, Denmark.

E-mail: huiling.mu@biocentrum.dtu.dk

Abbreviations: LCFA, long-chain FA; MCFA, medium-chain FA; MCT, medium-chain TAG; STAG, structured triacylglycerol.

total lipids from the lymph samples were separated into different lipid classes on a silica TLC plate (art. 5721; Merck, Darmstadt, Germany), which was developed in a closed chamber with hexane/diethyl ether/acetic acid (80:20:1, by vol). Following visualization by spraying with 2,7-dichlorofluorescein (0.2% in ethanol), TAG, FFA, DAG, and phospholipids were scraped off and methylated to FAME catalyzed with  $\text{BF}_3$ . The FAME of each lipid fraction were analyzed on an HP 6890 gas chromatograph (Hewlett-Packard, Waldbronn, Germany) equipped with a capillary column (SP-2380, 60 m  $\times$  0.25 mm i.d.; Supelco Inc., Bellefonte, PA). Oven temperature was programmed from 70°C (2 min) to 200°C at a rate of 15°C/min and then to 230°C at a rate of 1.5°C/min and held for 20 min. An FID was used at 300°C, and the injector temperature was 260°C. The injector was used in split mode with a ratio 1:20. The carrier gas was helium with a column flow of 2 mL/min. The FA were identified by comparing the retention time with standards of known FA composition.

**Statistical methods.** The statistical program InStat (GraphPad Software Inc., San Diego, CA) was used in the statistical evaluation. A one-way ANOVA was applied to analyze differences among different lymph groups. The Tukey–Kramer multiple comparisons test was used to evaluate statistical significance.

## RESULTS AND DISCUSSION

Caprylic acid was detected only in lymph TAG after administration of the STAG 8:0/18:2/8:0, whereas lauric acid was also detected in other lipid fractions, i.e., phospholipids, FFA, and DAG, after administration of 12:0/18:2/12:0 (Table 1). A significantly higher level of lauric acid than caprylic acid ( $P < 0.001$ ) was

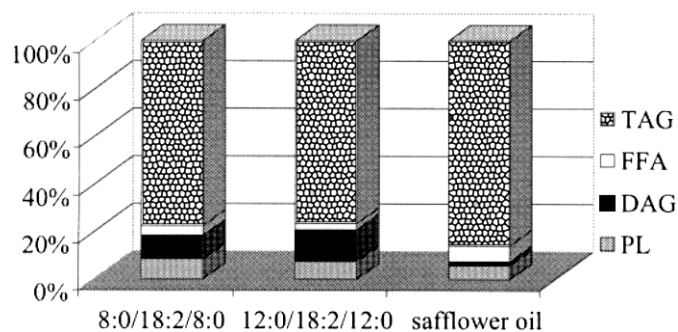
detected in lymph TAG, partly because the caprylic acid was preferably transported *via* the portal vein and partly because of the low activity of acyl-transferase toward caprylic acid. The relatively high level of oleic acid in lymph lipids after administration of the STAG 8:0/18:2/8:0 may have been due to a greater endogenous contribution when most of the caprylic acid was transported *via* the portal vein.

The distribution of linoleic acid in different lymph lipids was similar after administration of the two STAG and safflower oil (Fig. 1), except that more linoleic acid was detected in DAG after administration of the STAG ( $P < 0.01$ ). When the total FA distributions of different lipid classes were compared, the level of phospholipids was higher ( $P < 0.05$ ) after administration of 8:0/18:2/8:0 than the others (Fig. 2), which may reflect the formation of smaller chylomicrons. It has been reported previously that the number of chylomicrons and the production of apolipoprotein are not changed after a diet containing lipids, but the chylomicron size is increased (9). Since most of the absorbed caprylic acid was transported *via* the portal vein, the chylomicron size decreased, which may have required more phospholipid molecules to form the surface and consequently resulted in more secretion of phospholipids from bile. Comparing the FA profile of lymph phospholipids after administration of the STAG and safflower oil, the levels of palmitic acid ( $P < 0.05$ ) and arachidonic acid ( $P < 0.01$ ) were higher after administration of 8:0/18:2/8:0 than 12:0/18:2/12:0 and safflower oil. Since the major FA of bile phospholipids are palmitic acid (35.7%), stearic acid (6.2%), oleic acid (6.1%), linoleic acid (31.0%), and arachidonic acid (8.3%) (Fruekilde, M.-B., and Høy, C.E., unpublished results), the relatively high levels of palmitic and arachidonic acids in lymph phospholipids after administration of 8:0/18:2/8:0 may have resulted from the contribution of bile phospholipids.

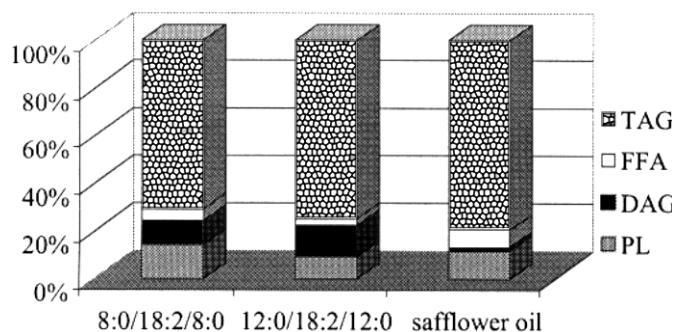
**TABLE 1**  
FA Composition (mol%) of Different Lymph Lipids After Administration of Structured TAG and Safflower Oil<sup>a</sup>

FA	8:0/18:2/8:0				12:0/18:2/12:0				Safflower oil			
	PL	DAG	FFA	TAG	PL	DAG	FFA	TAG	PL	DAG	FFA	TAG
8:0	—	—	—	7.3	—	—	—	—	—	—	—	—
10:0	—	—	—	—	—	—	—	0.1	—	—	—	—
12:0	—	—	—	—	3.0	38.1	24.9	48.2	—	—	—	—
14:0	0.8	7.6	4.6	0.6	0.9	3.3	3.4	0.6	—	0.7	0.4	0.2
16:0	24.7	16.0	15.2	10.8	21.5	5.9	8.7	3.2	22.0	14.0	8.2	10.6
16:1	0.6	—	1.4	0.5	0.7	—	1.5	0.4	—	0.6	0.8	0.3
18:0	20.8	8.0	7.1	3.7	17.7	2.9	3.8	0.9	13.4	4.9	2.8	2.7
18:1n-9	4.3	15.4	17.1	17.7	3.1	1.7	5.0	1.5	13.7	12.8	13.1	12.7
18:1n-7	2.3	—	2.7	2.3	2.3	—	1.3	0.7	—	1.0	1.3	1.1
18:2n-6	29.1	51.7	46.4	52.7	37.0	45.8	45.7	42.5	45.8	57.6	66.2	69.8
18:3n-3	0.3	—	1.1	0.6	0.3	—	0.9	0.4	—	0.6	0.9	0.6
20:0	—	—	—	0.2	0.2	—	—	0.1	—	—	—	0.3
20:1n-9	—	—	—	—	—	—	—	—	—	1.0	0.7	0.7
20:2	—	—	—	0.2	0.3	—	—	0.1	—	—	—	0.1
20:3n-6	0.5	—	—	0.2	0.4	—	—	0.1	—	—	0.3	0.0
20:4n-6	15.5	1.3	3.9	2.6	11.0	2.4	3.6	0.9	5.2	6.6	5.3	0.8
22:0	0.1	—	—	—	0.2	—	—	0.1	—	—	—	0.2
22:4	0.2	—	—	—	0.2	—	—	—	—	—	—	—
22:6	1.0	—	—	0.6	1.0	—	1.0	0.2	—	—	—	—

<sup>a</sup>PL, phospholipids; below 0.1% or not detected.



**FIG. 1.** The distribution of linoleic acid (wt%) in different lipid fractions of lymph after intragastric administration of specific structured TAG (STAG) 8:0/18:2/8:0 and 12:0/18:2/12:0. PL, phospholipids.



**FIG. 2.** The distribution of total FA (wt%) in different lipid fractions of lymph after intragastric administration of specific STAG 8:0/18:2/8:0, 12:0/18:2/12:0, and safflower oil. For abbreviations see Figure 1.

In summary, this study provides evidence that caprylic acid is not incorporated into phospholipids and that the intestinal absorption of caprylic acid from STAG mainly occurs by resynthesis of TAG. Lauric acid from the STAG can be incorporated into phospholipids.

#### ACKNOWLEDGMENTS

We thank Jannie Agersten for her technical assistance, Maj-Britt Fruekilde for providing the FA composition of bile phospholipids, and the Center for Advanced Food Studies (LMC) for financial support.

#### REFERENCES

- Mu, H., Xu, X., and Høy, C.E. (1998) Production of Specific Structured Triacylglycerols by Lipase-Catalyzed Interesterification in a Laboratory Scale Continuous Reactor, *J. Am. Oil Chem. Soc.* 75, 1187–1193.
- Ikeda, I., Tomari, Y., Sugano, M., Watanabe, S., and Nagata, J. (1991) Lymphatic Absorption of Structured Glycerolipids Containing Medium-Chain Fatty Acids and Linoleic Acid, and Their Effect on Cholesterol Absorption in Rats, *Lipids* 26, 369–373.
- Mu, H., and Høy, C.-E. (2000) Effect of Medium-Chain Fatty Acids on Lymphatic Absorption of Essential Fatty Acids in Specific Structured Lipids, *Lipids* 35, 83–89.
- Jandacek, R.J., Whiteside, J.A., Holcombe, B.N., Volpenhein, R.A., and Taulbee, J.D. (1987) The Rapid Hydrolysis and Efficient Absorption of Triglycerides with Octanoic Acid in the 1 and 3 Positions and Long-Chain Fatty Acid in the 2 Position, *Am. J. Clin. Nutr.* 45, 940–945.
- Christensen, M.S., Müllertz, A., and Høy, C.E. (1995) Absorption of Triglycerides with Defined or Random Structure by Rats with Biliary and Pancreatic Diversion, *Lipids* 30, 521–526.
- Christensen, M.S., Høy, C.E., Becker, C.C., and Redgrave, T.G. (1995) Intestinal Absorption and Lymphatic Transport of Eicosapentaenoic (EPA), Docosahexaenoic (DHA), and Decanoic Acids: Dependence on Intramolecular Triacylglycerol Structure, *Am. J. Clin. Nutr.* 61, 56–61.
- Tso, P., Lee, T., and DeMichele, S.J. (1999) Lymphatic Absorption of Structured Triglycerides vs. Physical Mix in a Rat Model of Fat Malabsorption, *Am. J. Physiol.* 277, G333–G400.
- Becker, C.C., Rosenquist, A., and Højlmer, G. (1993) Regiospecific Analysis of Triacylglycerols Using Allyl Magnesium Bromide, *Lipids* 28, 147–149.
- Hayashi, H., Fujimoto, K., Cardelli, J.A., Nutting, D.F., Bergstedt, S., and Tso, P. (1990) Fat Feeding Increases Size, but Not Number, of Chylomicrons Produced by Small Intestine, *Am. J. Physiol.* 259, G709–G719.

[Received October 11, 2001; in revised form January 24, 2002; accepted February 7, 2002]

## Habitual Fish Intake Is Associated with Decreased LDL Susceptibility to *ex vivo* Oxidation

Juan Carlos Ruiz de Gordo<sup>a,\*</sup>, Mertxe de Renobales<sup>a</sup>, Ana del Cerro<sup>a</sup>,  
Eva Fernández de Labastida<sup>a</sup>, Pilar Amiano<sup>b</sup>, Miren Dorronsoro<sup>b</sup>,  
and the EPIC Group of Spain<sup>1</sup>

<sup>a</sup>Bioquímica y Biología Molecular, Facultad de Farmacia, Universidad del País Vasco/Euskal Herriko Unibertsitatea, Vitoria-Gasteiz, Spain, and <sup>b</sup>Delegación de Sanidad de Guipuzkoa, Donostia-San Sebastián, Spain

**ABSTRACT:** A sample of 101 free-living individuals eating their habitual diets had fish consumptions ranging from less than one serving per week to over five servings per week. Statistically significant positive correlations were found between the amounts of EPA (20:5), DHA (22:6), and total n-3 PUFA ingested with the diet and their amounts in serum and in the phospholipid and cholesterol ester fractions of isolated LDL. No statistically significant correlations were observed between the intake and the serum or LDL amounts of any other FA [total n-6 PUFA, linoleic acid (18:2), arachidonic acid (20:4), monounsaturated FA, or saturated FA]. The increase in serum n-3 PUFA did not affect the Trolox-equivalent antioxidant capacity of serum (1.18 ± 0.17 mmol/L). When isolated LDL were subjected to Cu<sup>2+</sup>-induced *ex vivo* oxidation, a statistically significant but negative correlation was found between intake of n-3 PUFA and the rate of appearance of conjugated dienes as well as with the total amount of conjugated dienes. In contrast, intake of n-6 PUFA showed a significant and positive correlation with these two oxidation parameters. The observed results suggest that 22:6 but not 20:5 could have a possible protective effect, whereas perhaps 20:4 and 18:2 could have a prooxidant effect.

Paper no. L8798 in *Lipids* 37, 333–341 (April 2002).

In their classic study with Greenland Eskimos, Dyerberg *et al.* (1,2) showed that there was a direct relationship between

\*To whom correspondence should be addressed at Dpto. de Bioquímica y Biología Molecular, Facultad de Farmacia, Universidad del País Vasco/Euskal Herriko Unibertsitatea, Aptdo. 450, E-01080 Vitoria-Gasteiz, Spain. E-mail: gbpruarj@vc.ehu.es

<sup>1</sup>E EPIC Group of Spain: A. Agudo, Instituto Catalán de Oncología, Barcelona; P. Amiano, Dpto. de Sanidad del Gobierno Vasco, San Sebastián; A. Barcos, Dpto. de Salud de Navarra, Pamplona; A. Barricarte, Dpto. de Salud de Navarra, Pamplona; J.M. Begiristain, Dpto. de Sanidad del Gobierno Vasco, San Sebastián; M.D. Chirlaque, Consejería de Sanidad y Política Social, Murcia; M. Dorronsoro, Dpto. de Sanidad del Gobierno Vasco, San Sebastián; C. Lasheras, Consejería de Sanidad y Servicios Sociales, Asturias; C. Martínez, Escuela Andaluza de Salud Pública, Granada; C. Navarro, Consejería de Sanidad y Política Social, Murcia; G. Pera, Institut de Recerca Epidemiològica i Clínica, Mataró; J.R. Quirós, Consejería de Sanidad y Servicios Sociales, Asturias; M. Rodríguez, Escuela Andaluza de Salud Pública, Granada; M.J. Tormo, Consejería de Sanidad y Política Social, Murcia; and C.A. González, Instituto Catalán de Oncología, Barcelona. Abbreviations: MUFA, monounsaturated FA; DHA, 22:6, or 4,7,10,13,16,19-docosahexaenoic acid; EPA, 20:5, or 5,8,11,14,17-eicosapentaenoic acid; 18:2: linoleic acid; TEAC, Trolox equivalent antioxidant capacity, TNBS, trinitrobenzene sulfonic acid.

a high dietary intake of fish and high plasma levels of n-3 PUFA. Parkinson *et al.* (3) compared the habitual diets of Alaskan Eskimos with those of a nonnative population used as control and related the amount of n-3 PUFA ingested to plasma n-3 PUFA levels. Similar conclusions have been reached in other studies carried out in Finland (4) and the Madeira Islands (5) by comparing the serum amounts of n-3 PUFA among populations with different dietary habits and lifestyles. Likewise, a number of other workers administering very high levels of dietary supplements (mostly in the form of oil capsules) to volunteer individuals on low-fish diets have obtained similar results with n-3 PUFA in total plasma (6–14), particularly in plasma phospholipids and cholesteryl esters (6,14–23). However, few studies have been done comparing individuals with similar lifestyles consuming their habitual diets ranging from less than one serving of fish per week to up to five or more servings per week (23–28). Likewise, the relation between the increase in lipoprotein n-3 PUFA and fish intake has been documented in cases where fish oil supplements were given (8,10,15,29–34) or in groups of people with extreme dietary habits (35). But the relationship of habitual diets with different amounts of fish on the levels of n-3 PUFA in plasma and in lipoprotein lipids in free-living individuals has not been well documented.

Dietary FA potentially can modify LDL oxidation by changing its FA composition. PUFA are the most susceptible to oxidation (36), and diets enriched with n-6 PUFA result in increased LDL oxidation in humans (19,37–42). The peroxidation of PUFA in LDL has been linked to atherosclerosis (43–45). Fish is high in n-3 PUFA, primarily EPA (20:5) and DHA (22:6), both of which are highly susceptible to oxidation (36,46). Several studies have shown that diet supplementation with n-3 PUFA increased LDL oxidation in healthy subjects (19,31,47) and hypertriglyceridemic patients (10,29). This result was also reported in a small group of people who habitually consume very large amounts of fish (35). By contrast, in other diet intervention studies with high doses of n-3 PUFA, the susceptibility of LDL to oxidation did not change (30,32) or decreased (34). However, we are not aware of any study with free-living individuals who consumed a variety of diets with no supplements in which oxidation of LDL was studied.



The purpose of this work was to study the correlation between a wide range of dietary fish intake (mostly white, lean fish) in a large number of healthy, free-living individuals, their serum and LDL levels of n-3 and n-6 PUFA, and the susceptibility of these PUFA to *ex vivo* oxidation. To assess the antioxidant capacity of LDL, the following indices of oxidizability were used: conjugated dienes (total amount, rate at which they increased, and length of the lag phase), TBARS, and the reaction with trinitrobenzene sulfonic acid (TNBS) after oxidation with  $\text{CuSO}_4$ . Total antioxidant capacity of serum was also determined because literature data are contradictory: Some studies show that fish oil supplements do not affect serum oxidation (4,13,16,22,29), whereas others show an increase in serum oxidation (7,21).

## EXPERIMENTAL PROCEDURES

**Subjects.** The study was carried out with a sample of the cohort of participants from the province of Gipuzkoa (Basque country, Spain) participating in the EPIC (European Prospective Investigation in Cancer and Nutrition) project among nine European countries (48,49). Each participant agreed in writing to the study. The sample consisted of 120 randomly selected healthy individuals of both sexes aged 35–65 with fish intakes ranging from less than one serving per week to five or more servings per week. Subjects were divided into the following four categories of fish intake according to their dietary habits: occasional consumers,  $\leq 31.0$  g/d; low consumers, 31.1–64.0 g/d; moderate consumers, 64.1–115.0 g/d; and high consumers,  $>115.0$  g/d.

**Dietary habits.** Information on daily dietary intake over the previous year was obtained by a personal interview with

each individual (conducted by trained interviewers) using the method of dietetic history with a computerized questionnaire, especially designed and validated by the EPIC Group of Spain (50–52), as described in a previous study (53). Energy and nutrient intake were estimated from Food Composition Tables (54) using a computerized database designed for the EPIC project. The intake of the major FA was calculated from specific Spanish food-composition tables (55–57).

Fish consumption ranged from 0 to 250.70 g/d among the final sample of 101 free-living individuals (46 men and 55 women). Fish, FA, and antioxidant vitamin intakes of grouped individuals according to habitual fish consumption are shown in Table 1. The group of high consumers had an intake of n-3 PUFA 2.2-fold higher than the occasional consumers. The average amount of 20:5 and 22:6 consumed was 6.0- and 4.5-fold higher, respectively, in the high consumer group than for occasional consumers. Saturated FA, monounsaturated FA (MUFA), n-6 PUFA, antioxidant vitamins, and total calorie intake were not significantly different among groups of consumers. Statistically significant differences were found only for the intake of n-3 PUFA ( $P > 0.001$ ) but not for that of n-6 PUFA, MUFA, and saturated FA. The total amount of dietary 20:5 and 22:6 intake in the high-consumer individuals (0.30 and 0.90 g/d, respectively) was comparable to that of other fish diets (4–6,23,24)

**Reagents.** All reagents were purchased from Sigma-Aldrich (Madrid, Spain) and were analytical reagent grade or better. Solvents (highest grade available) were purchased from Teknochroma (Barcelona, Spain) and were not redistilled before use.

**Blood samples.** A fasting blood sample from each individual was collected during a second personal interview. Plasma, serum, and other fractions were separated immediately and

**TABLE 1**  
Fish, FA, and Antioxidant Vitamin Intake of the Subjects According to Habitual Fish Consumption (mean  $\pm$  SD)

Data	Fish consumption groups <sup>b</sup>				P
	$\leq 31.0$ g/d (n = 26)	31.1–64.0 g/d (n = 24)	64.1–115.0 g/d (n = 27)	$>115.0$ g/d (n = 24)	
Age (yr)	50.42 $\pm$ 9.87	50.60 $\pm$ 8.10	47.22 $\pm$ 6.79	52.00 $\pm$ 5.64	NS <sup>c</sup>
Fish consumption (g/d)	19.20 $\pm$ 11.90	51.10 $\pm$ 14.30	83.63 $\pm$ 16.89	151.20 $\pm$ 38.31	<0.001
Lean fish	11.58 $\pm$ 10.36	27.81 $\pm$ 14.93	52.34 $\pm$ 23.09	113.80 $\pm$ 46.57	<0.001
Fatty fish	5.18 $\pm$ 6.48	16.44 $\pm$ 12.99	20.67 $\pm$ 23.50	27.60 $\pm$ 26.94	<0.001
FA intake (g/d) <sup>a</sup>					
Saturated FA	29.16 $\pm$ 8.72	29.26 $\pm$ 6.70	28.26 $\pm$ 10.23	29.80 $\pm$ 10.57	NS
Monounsaturated FA	35.29 $\pm$ 8.06	39.44 $\pm$ 8.49	38.28 $\pm$ 10.71	44.50 $\pm$ 13.03	NS
Total n-6 PUFA	15.08 $\pm$ 9.23	14.23 $\pm$ 6.53	13.55 $\pm$ 5.93	17.60 $\pm$ 17.00	NS
Total n-3 PUFA	1.00 $\pm$ 0.25	1.49 $\pm$ 0.48	1.56 $\pm$ 0.50	2.20 $\pm$ 0.92	<0.001
EPA (20:5)	0.05 $\pm$ 0.05	0.13 $\pm$ 0.07	0.21 $\pm$ 0.13	0.30 $\pm$ 0.18	<0.001
DHA (22:6)	0.19 $\pm$ 0.15	0.44 $\pm$ 0.22	0.58 $\pm$ 0.41	0.90 $\pm$ 0.50	<0.001
Antioxidant intake (mg/d)					
Ascorbic acid	144.10 $\pm$ 91.54	153.90 $\pm$ 81.10	150.90 $\pm$ 85.50	150.20 $\pm$ 88.90	NS
Vitamin E	12.40 $\pm$ 8.50	11.58 $\pm$ 8.30	11.90 $\pm$ 6.60	13.70 $\pm$ 10.10	NS
$\beta$ -Carotene	2.69 $\pm$ 1.54	2.59 $\pm$ 1.18	2.50 $\pm$ 1.44	2.70 $\pm$ 1.84	NS
Retinol	0.57 $\pm$ 0.80	0.71 $\pm$ 0.71	0.67 $\pm$ 0.64	0.55 $\pm$ 0.80	NS
Total calorie intake (kcal)	2329.30 $\pm$ 546.34	2377.20 $\pm$ 621.21	2451.80 $\pm$ 801.29	2641.90 $\pm$ 818.26	NS

<sup>a</sup>Adjusted for energy intake.

<sup>b</sup>Reproduced in part from Reference 53 with permission.

<sup>c</sup>NS, not significantly different values among fish consumption groups, where significant differences are taken as  $P < 0.05$ .

kept at  $-180^{\circ}\text{C}$  in liquid nitrogen until analyzed. Serum was used for all analyses reported herein. Samples were analyzed without knowing their identity. A 0.1-mL serum aliquot for the Trolox (a water-soluble vitamin E analog) equivalent antioxidant capacity (TEAC), as oxidizability measurement in total serum, was sealed under nitrogen and kept at  $-80^{\circ}\text{C}$  for up to 2 d.

Lipoproteins were separated by ultracentrifugation on a NaBr density gradient as described by Kelly and Kruski (58). The NaBr (containing 0.05% EDTA) gradient was prepared in a Buchler Auto DensiFlow (Buchler Instruments, Fort Lee, NJ), and the ultracentrifugation was carried out in a Beckman L8-M ultracentrifuge with a SW 40 Ti rotor (Beckman Instruments, Palo Alto, CA) for 24 h at  $110,000 \times g$  and  $14^{\circ}\text{C}$ . The yellow-orange band corresponding to the LDL was collected. A 100- $\mu\text{L}$  aliquot was used to determine the total protein concentration (59). BHT (1%) was added to a 0.5-mL aliquot, and this sample was stored at  $-80^{\circ}\text{C}$  until the lipid analysis was done. The remainder was used immediately for lipoprotein oxidizability measurements.

**Lipid analysis.** Total serum FA were quantitated as FAME following the method of Lepage and Roy (60) as modified by Matorras *et al.* (61). Briefly, 2.0 mL toluene/methanol (1:4 vol/vol) containing 10  $\mu\text{g}$  *n*-heptadecanoic acid as internal standard was added to 100  $\mu\text{L}$  serum in a stoppered glass tube. After mixing, 200  $\mu\text{L}$  acetyl chloride was added, and the tube was incubated overnight (16–18 h) at  $60^{\circ}\text{C}$ . Then 500  $\mu\text{L}$  *n*-heptane containing 250  $\mu\text{g}$  BHT and 3.0 mL 10% potassium carbonate was added. The tube was centrifuged to separate the phases, and the upper phase was transferred to a glass vial. The solvent was evaporated under a stream of nitrogen on a sand bath at  $35^{\circ}\text{C}$ , and the residue was dissolved in 50  $\mu\text{L}$  *n*-heptane.

FAME were separated by capillary GC on a 30-m capillary SP-2330 column (0.32 mm internal diameter, 0.20 mm film thickness). The chromatograph was from Hewlett-Packard (model 5890 series II, Palo Alto, CA), equipped with an FID, split-splitless injector, automatic sampler, and work station. The carrier gas (He) flow through the column was 0.95 mL/min. Oven temperature was programmed from 80 (1 min) to  $140^{\circ}\text{C}$  at  $50^{\circ}\text{C}/\text{min}$  and to  $190^{\circ}\text{C}$  at  $5^{\circ}\text{C}/\text{min}$ . After 5 min at  $190^{\circ}\text{C}$ , the temperature was increased to  $215^{\circ}\text{C}$  at  $5^{\circ}\text{C}/\text{min}$  and held at  $215^{\circ}\text{C}$  for 8 min. Injector and detector temperatures were  $250^{\circ}\text{C}$ , and the split-splitless valve was set at 1:10. Serum samples were extracted in duplicate, and each sample was injected twice into the gas chromatograph.

LDL lipids were extracted and lipid classes were separated by TLC on silica gel plates as described (62,63). Phospholipids and cholesterol esters were recovered and derivatized, and the resulting FAME were quantitated as described above.

**Oxidizability measurements.** The TEAC value of serum was determined using a commercially available kit (catalog no. NX2332; Randox, Crumlin, United Kingdom), based on the method of Miller *et al.* (64).

**Oxidizability measurements in LDL.** The antioxidant capacity of LDL was evaluated by three different methods: con-

jugated dienes after oxidation with  $\text{CuSO}_4$ , TBARS, and the reaction with TNBS. Total amount of conjugated dienes, the rate of diene appearance, and the length of the lag phase for the oxidation of these dienes were determined by the modified method of Puhl *et al.* (65) as follows: an aliquot of LDL containing 50  $\mu\text{g}$  protein/mL, PBS (0.15 M NaCl, 0.01 M phosphate buffer, pH 7.4), and 5  $\mu\text{M}$   $\text{CuSO}_4$  was incubated at  $30^{\circ}\text{C}$  in a spectrophotometric cuvette, and the increase in absorbance at 234 nm was recorded during 4 h. To determine TBARS the method described by Kleinveld *et al.* (66) was used. After oxidizing LDL aliquots as described above at  $30^{\circ}\text{C}$  for 3 h, 0.1 mL EDTA (6.7 mg/mL) and 0.1 mL TCA (100%) were added. The mixture was centrifuged at  $7,500 \times g$  for 15 min. To 0.5 mL of the supernatant was added 1.0 mL thiobarbituric acid (TBA: 0.67%), and the mixture was incubated in a double boiler for 15 min. Absorbance at 532 nm was read after the samples had cooled. Results are expressed as equivalents of malondialdehyde generated by the acid hydrolysis of 1,1,3,3-tetramethoxypropane. The oxidation of the protein fraction of LDL was determined according to the method of Steinbrecher (67) for the  $\epsilon$ -amino group of lysine residues. Aliquots of LDL were oxidized as described above for 6 h. The reaction was stopped by the introduction of 0.1 mL EDTA (6.7 mg/mL), and 1.0 mL  $\text{NaHCO}_3$  (4%) and 50  $\mu\text{L}$  TNBS were added. The mixture was incubated at  $37^{\circ}\text{C}$  for 1 h. Then 0.1 mL 1 M HCl and 0.1 mL SDS (10%) were added, and the absorbance was read at 340 nm. The value obtained was compared to that of the nonoxidized (but otherwise identically treated) LDL aliquot.

**Statistical analysis.** Statistical treatment of the data (SPSS Statistical Software, Chicago, IL) was done for a final sample of 101 individuals due to the loss of some samples during analytical manipulations. Results are presented as mean  $\pm$  SD. One-way ANOVA were done to compare the intake and FA composition of serum and LDL among the groups of occasional ( $\leq 31.0$  g/d), low (31.1–64.0 g/d), moderate (64.1–115.0 g/d), and high ( $> 115.0$  g/d) fish consumers. The influence of fish intake on the FA composition of serum and LDL was studied by simple linear regression analysis. Multiple linear regression analysis was used to study the influence of PUFA intake and LDL FA composition (independent variables) on the oxidation parameters of serum and LDL (dependent variables). In this analysis  $r$  represents the value of the multiple correlation coefficient for all variables and  $\beta$  represents the direction and value of the regression coefficient of each independent variable. Statistical significance was considered to be  $P < 0.05$  for all results.

## RESULTS AND DISCUSSION

**FA in serum and LDL.** The amounts of unsaturated FA present in serum and in LDL phospholipid and cholesterol esters are listed in Tables 2 and 3, respectively. Statistically significant differences among consumer groups were observed only for the percentage of *n*-3 PUFA in serum ( $P < 0.001$ ) and in LDL phospholipids ( $P < 0.01$ ) and cholesterol esters ( $P < 0.001$ ).

**TABLE 2**  
**FA (Percentage of total FA expressed as nmol/mL) in Serum According to Habitual Fish Consumption (mean ± SD)**

FA	Fish consumption groups <sup>a</sup>				P
	≤31.0 g/d (n = 26)	31.1–64.0 g/d (n = 24)	64.1–115.0 g/d (n = 27)	>115.0 g/d (n = 24)	
Saturated FA	32.12 ± 2.27	31.26 ± 2.23	31.46 ± 2.36	31.25 ± 1.92	NS <sup>b</sup>
Monounsaturated FA	20.82 ± 4.28	20.13 ± 4.38	19.62 ± 4.30	20.72 ± 3.38	NS
Total n-6 PUFA	42.86 ± 5.11	43.63 ± 5.58	43.94 ± 5.17	42.34 ± 5.09	NS
Linoleic acid (18:2)	33.60 ± 4.92	35.04 ± 5.12	35.49 ± 4.82	33.87 ± 5.53	NS
Arachidonic acid (20:4)	7.31 ± 1.53	6.94 ± 1.30	6.85 ± 1.51	6.66 ± 1.41	NS
Total n-3 PUFA	4.20 ± 0.89	4.83 ± 1.07	4.99 ± 1.19	5.68 ± 1.18	<0.001
EPA (20:5)	0.39 ± 0.17	0.58 ± 0.29	0.52 ± 0.16	0.75 ± 0.32	<0.001
DHA (22:6)	3.47 ± 0.76	3.91 ± 0.83	4.14 ± 1.04	4.58 ± 0.90	<0.001

<sup>a</sup>Reproduced in part from Reference 53 with permission.

<sup>b</sup>NS, not significantly different values among fish consumption groups, where significant differences are taken as  $P < 0.05$ .

Fish intake was positively correlated with the values of n-3 PUFA in serum ( $P < 0.001$ ), 20:5, 22:6, and total n-3 PUFA (Table 4). The same was true for phospholipids and cholesterol esters of isolated LDL (Table 5). No statistically significant differences were observed in the correlations between fish intake and the amounts of the other FA, n-6 PUFA (total, linoleic, or arachidonic acids), MUFA, or saturated FA, either in total serum lipids or in those of isolated LDL. This result is consistent with the fact that the dietary intake of these FA was essentially identical ( $P > 0.05$ ) for all subjects. In diet intervention studies in which subjects have been given large amounts of n-3 PUFA, other authors have shown that n-3 PUFA in total serum (9,17,23) or LDL (33) can be used as serum markers of fish intake. Our results are in agreement with this observation even though in our study only a small fraction of the subjects (10%) would have ingested amounts of n-3 PUFA ( $\geq 2.5$  g/d) similar to the lower value of the

dietary supplements given in those studies (2.5–7.7 g/d). The correlation between intake of n-3 PUFA and their serum concentrations agrees with published studies of fish intake (23–28).

*Serum and LDL oxidizability.* Total antioxidant capacity of serum samples was measured with the Randox commercial reagent kit developed after the method of Miller *et al.* (64). Average values obtained for the TEAC measurements of all serum samples were  $1.18 \pm 0.17$  mmol/L (range: 0.65–1.74). The observed increase in total serum n-3 PUFA levels with fish intake did not affect the total antioxidant capacity of serum. These observations are similar to those of other investigators who showed that dietary supplements of either fish oil or n-3 PUFA have no effect on oxidation of serum lipids, both in humans (4,13,16,29) and in rats (68). This could be explained by the relatively high vegetable and fruit intake (the average was 616 g, or 7.7 servings per day) in all individuals (69), which would

**TABLE 3**  
**Percent FA Composition of LDL (expressed as nmol/mg protein) According to Habitual Fish Consumption (mean ± SD).**

FA	Fish consumption groups <sup>a</sup>				P
	≤31.0 g/d (n = 26)	31.1–64.0 g/d (n = 24)	64.1–115.0 g/d (n = 27)	>115.0 g/d (n = 24)	
Phospholipids					
Saturated FA	53.13 ± 4.38	53.55 ± 4.16	53.52 ± 5.29	52.37 ± 4.32	NS
Monounsaturated FA	11.80 ± 5.99	10.42 ± 2.07	11.12 ± 4.78	11.55 ± 4.74	NS
Total n-6 PUFA	29.75 ± 5.32	30.18 ± 3.86	29.20 ± 4.87	29.12 ± 5.71	NS
Linoleic acid (18:2)	18.51 ± 4.17	20.20 ± 3.26	18.91 ± 3.76	19.31 ± 4.67	NS
Arachidonic acid (20:4)	7.62 ± 2.42	7.32 ± 1.31	7.19 ± 2.10	7.18 ± 1.81	NS
Total n-3 PUFA	5.31 ± 1.28	5.85 ± 1.37	6.16 ± 1.55	6.95 ± 1.69	<0.01
EPA (20:5)	0.51 ± 0.20	0.61 ± 0.21	0.69 ± 0.21	0.73 ± 0.30	<0.01
DHA (22:6)	4.74 ± 1.24	5.17 ± 1.28	5.44 ± 1.52	6.14 ± 1.47	<0.01
Cholesterol esters					
Saturated FA	18.88 ± 5.36	18.04 ± 5.06	19.19 ± 4.97	16.46 ± 3.36	NS
Monounsaturated FA	17.48 ± 4.21	17.01 ± 4.27	16.16 ± 3.37	18.07 ± 4.29	NS
Total n-6 PUFA	61.64 ± 6.73	62.62 ± 6.45	62.31 ± 5.59	62.66 ± 6.25	NS
Linoleic acid (18:2)	53.48 ± 7.08	55.09 ± 6.68	54.52 ± 5.43	54.73 ± 7.37	NS
Arachidonic acid (20:4)	6.70 ± 2.16	6.51 ± 1.13	6.80 ± 1.80	6.82 ± 1.50	NS
Total n-3 PUFA	2.00 ± 0.44	2.32 ± 0.52	2.35 ± 0.44	2.81 ± 0.83	<0.001
EPA (20:5)	0.49 ± 0.16	0.64 ± 0.24	0.70 ± 0.30	0.90 ± 0.41	<0.001
DHA (22:6)	1.23 ± 0.31	1.34 ± 0.27	1.39 ± 0.32	1.54 ± 0.46	<0.05

<sup>a</sup>Reproduced in part from Reference 53 with permission.

<sup>b</sup>NS, not significantly different values among fish consumption groups, where significant differences are taken as  $P < 0.05$ .

**TABLE 4**  
**Linear Correlation Between Fish Intake (g/d) and Serum FA Composition<sup>a</sup> (percentages of the total FA expressed as nmol/mL)**

FA	<i>r</i>	<i>P</i>
Saturated FA	0.035	NS
Monounsaturated FA	0.059	NS
Total n-6 PUFA	0.089	NS
Linoleic acid (18:2)	0.120	NS
Arachidonic acid (20:4)	-0.080	NS
Total n-3 PUFA	0.415	<0.001
EPA (20:5)	0.412	<0.001
DHA (22:6)	0.390	<0.001

<sup>a</sup>*r*, correlation coefficient; NS, no statistically significant correlation, where statistical significance is *P* < 0.05.

provide a number of low M.W. antioxidants. It is known that the presence of antioxidant compounds in serum such as albumin, urate, ascorbate, bilirubin, or  $\alpha$ -tocopherol can stop the appearance and propagation of free radicals (64). Thus, even though the level of serum n-3 PUFA increased significantly with fish intake, no differences were observed in the susceptibility to oxidation of serum samples from individuals with widely different fish intakes.

Isolated LDL fractions were subjected to Cu<sup>2+</sup>-induced oxidation *ex vivo*, and the following lipid oxidation parameters were measured: duration of the lag phase, rate of conjugated diene production, total diene concentration, and TBARS. In addition, the percentage of nonoxidized protein (TNBS) was also measured. Intake of n-3 and n-6 PUFA was significantly correlated with the rate of conjugated diene appearance (*P* < 0.05) and the total diene concentration (*P* < 0.05) (Table 6). The average rate of conjugated diene production (propagation rate) was 17.63  $\pm$  5.33 nmol·min<sup>-1</sup>·mg protein<sup>-1</sup> (range: 7.73–37.90 nmol·min<sup>-1</sup>·mg protein<sup>-1</sup>), and the average amount of conjugated dienes was 518.19  $\pm$  111.34 nmol·mg

**TABLE 5**  
**Linear Correlation Between Fish Intake (g/d) and Percent FA Composition of LDL Phospholipid and Cholesterol Ester Fractions**

FA	<i>r</i>	<i>P</i>
Phospholipid		
Saturated FA	0.005	NS
Monounsaturated FA	0.002	NS
n-6 PUFA	-0.117	NS
Linoleic acid (18:2)	-0.013	NS
Arachidonic acid (20:4)	-0.105	NS
n-3 PUFA	0.346	<0.001
EPA (20:5)	0.320	<0.001
DHA (22:6)	0.316	<0.001
Cholesterol esters		
Saturated FA	-0.090	NS
Monounsaturated FA	0.045	NS
n-6 PUFA	0.000	NS
Linoleic acid (18:2)	-0.007	NS
Arachidonic acid (20:4)	0.002	NS
n-3 PUFA	0.397	<0.001
EPA (20:5)	0.445	<0.001
DHA (22:6)	0.230	<0.05

<sup>a</sup>*r*, correlation coefficient; NS, no statistically significant correlation, where statistical significance is *P* < 0.05.

**TABLE 6**  
**Multiple Linear Regression Analysis Between the Intake of Total n-3 and n-6 PUFA (as independent variables) and Individual Lipid Oxidation Parameters for LDL (as dependent variables)**

Parameter <sup>a</sup>	Multiple regression	Total n-6	Total n-3
Lag phase			
<i>r</i>	0.079		
$\beta$		0.001	-0.079
<i>P</i>	NS	NS	NS
Rate of conjugated diene appearance			
<i>r</i>	0.306		
$\beta$		0.263	-0.271
<i>P</i>	<0.01	<0.05	<0.05
Conjugated diene concentration			
<i>r</i>	0.274		
$\beta$		0.247	-0.230
<i>P</i>	<0.05	<0.05	<0.05
TBARS			
<i>r</i>	0.062		
$\beta$		-0.049	-0.025
<i>P</i>	NS	NS	NS

<sup>a</sup>*r*, multiple correlation coefficient for all variables;  $\beta$ , regression coefficient for each independent variable; NS, no statistically significant correlation, where significance is taken as *P* < 0.05.

protein<sup>-1</sup> (range: 229.91–849.91 nmol·mg protein<sup>-1</sup>). These two parameters negatively correlated with n-3 PUFA intake, indicating that higher amounts of these highly unsaturated FA gave lower propagation rates and, therefore, lower conjugated diene concentrations. Thus, the increased levels of n-3 PUFA present in LDL as a result of higher dietary fish intakes did not result in higher LDL *ex vivo* oxidizability. In contrast, intake of n-6 PUFA presented a positive correlation with these two lipid oxidation parameters (*P* < 0.05). As expected, the intake of saturated FA and MUFA showed no statistically significant correlation with any of the LDL oxidation parameters measured. The average duration of the lag phase was 70  $\pm$  12 min (range: 38–102 min), and the TBARS measurements gave an average value of 86.08  $\pm$  16.96 nmol·mg protein<sup>-1</sup> (range: 45.38–136.32 nmol·mg protein<sup>-1</sup>). The observed differences in LDL lipid composition as a result of the different fish intakes did not significantly affect these parameters of lipid oxidation. Other investigators, directing diet intervention studies in which subjects were given higher amounts of n-3 PUFA than the majority of subjects herein ingested, have shown that a decrease in the lag phase and an increase in the TBARS value was related to the prooxidant effect of fish oil and n-3 PUFA (10,19,29,31,35,47). In contrast, other investigators have not found any effect of dietary supplements containing fish oil or n-3 PUFA on these LDL lipid peroxidation parameters (30,32,34).

The percentage of nonoxidized protein (TNBS measurements) was 54.29  $\pm$  12.14 (range: 22.40–87.42). The lack of significant differences in these values indicated that the observed differences in lipid composition did not affect the oxidizability of the protein composition of LDL as a result of the oxidation of the lipid components.



**TABLE 7**  
**Multiple Linear Regression Analysis Between the Percent Total n-3 and n-6 PUFA in LDL Phospholipids and Cholesterol Esters, (as independent variables) and Lipid Oxidation Parameters (as dependent variables)**

Parameter <sup>a</sup>	Phospholipids			Cholesterol esters		
	Multiple regression	Total n-6	Total n-3	Multiple regression	Total n-6	Total n-3
Lag phase						
<i>r</i>	0.143			0.169		
$\beta$		-0.146	0.043		-0.164	-0.038
<i>P</i>	NS	NS	NS	NS	NS	NS
Rate of conjugated diene appearance						
<i>r</i>	0.324			0.471		
$\beta$		0.211	-0.311		0.354	-0.323
<i>P</i>	<0.01	<0.05	<0.01	<0.001	<0.001	<0.001
Conjugated diene concentration						
<i>r</i>	0.132			0.375		
$\beta$		0.114	-0.105		0.347	-0.153
<i>P</i>	NS	NS	NS	<0.01	<0.001	NS
TBARS						
<i>r</i>	0.204			0.225		
$\beta$		0.090	0.159		0.138	0.173
<i>P</i>	NS	NS	NS	NS	NS	NS

<sup>a</sup>For footnotes see Table 5.

The increase in total n-3 PUFA in LDL phospholipids and cholesterol esters was negatively correlated ( $P < 0.01$  and  $P < 0.001$ , respectively) with the propagation rate of  $\text{Cu}^{2+}$ -induced oxidation, whereas total n-6 PUFA showed a statistically significant positive correlation ( $P < 0.05$  and  $P < 0.001$ , respectively) (Table 7). Of the two major n-3 PUFA, only the amount of 22:6 showed a statistically significant but negative correlation with the rate of appearance of conjugated dienes, both in the cholesterol ester ( $P < 0.05$ ) and phospholipid ( $P < 0.001$ ) fractions of the LDL (Table 8), indicating that as the percentage of this FA in the corresponding fraction in the

LDL increased, the formation of conjugated dienes decreased (Table 8). This unexpected protective effect of total n-3 PUFA, and of 22:6 in particular, has also been observed by some authors in LDL isolated from humans (31), nonhuman primates (70), and Yucatan minipigs (71). In these studies, propagation rates decreased in the presence of higher amounts of n-3 PUFA. In contrast, in cholesterol esters it was the percentage of linoleic acid and not that of arachidonic acid that correlated positively with the rate of propagation ( $P < 0.01$ ) as well as with the total conjugated diene concentration ( $P < 0.05$ ), in agreement with results from other studies

**TABLE 8**  
**Multiple Linear Regression Analysis Between the LDL Percent PUFA (as independent variables) and Lipid Oxidation Parameters (as dependent variables)**

Parameter <sup>a</sup>	Phospholipids					Cholesterol esters				
	Multiple regression	18:2	20:4	20:5	22:6	Multiple regression	18:2	20:4	20:5	22:6
Lag phase										
<i>r</i>	0.401					0.451				
$\beta$		0.004	-0.423	-0.090	0.152		-0.159	-0.469	-0.142	0.191
<i>P</i>	<0.01	NS	<0.001	NS	NS	<0.001	NS	<0.001	NS	NS
Rate of conjugated diene appearance										
<i>r</i>	0.407					0.457				
$\beta$		0.347	0.034	0.142	-0.427		0.385	0.041	-0.120	-0.241
<i>P</i>	<0.001	<0.01	NS	NS	<0.001	<0.001	<0.001	NS	NS	<0.05
Conjugated diene concentration										
<i>r</i>	0.275					0.372				
$\beta$		0.292	-0.068	0.147	-0.204		0.372	-0.065	-0.056	-0.067
<i>P</i>	NS	<0.05	NS	NS	NS	<0.01	<0.01	NS	NS	NS
TBARS										
<i>r</i>	0.457					0.360				
$\beta$		-0.096	0.433	0.190	0.018		0.097	0.315	0.100	0.052
<i>P</i>	<0.001	NS	<0.001	NS	NS	<0.01	NS	<0.01	NS	NS

<sup>a</sup>For footnotes see Table 6.

(41,42). We have also observed that the amount of arachidonic acid is positively correlated with an increase in the value of TBARS, for phospholipids ( $P < 0.001$ ) and cholesterol esters ( $P < 0.01$ ), and a decrease in the duration of the lag phase for phospholipids and cholesterol esters ( $P < 0.001$ ) (Table 8), both of which would be consistent with the prooxidant effect of n-6 PUFA.

Thomas *et al.* (72) showed that the rate of conjugated diene appearance during peroxidation of LDL was similar when LDL were enriched with n-3 PUFA or MUFA, but it was considerably higher when LDL were enriched with n-6 PUFA. Furthermore, Frankel *et al.* (30) showed that, after intake of fish oil supplements, the PUFA composition of LDL as well as the oxidation products is modified, although these changes taken together do not affect the susceptibility to *ex vivo* peroxidation of LDL. *In vitro* studies with PUFA in aqueous micelles indicate that n-3 PUFA have greater resistance to oxidation than n-6 PUFA (46,73,74).

As a consequence of an habitually higher fish intake the percentage of n-3 PUFA increased significantly in serum and in LDL, but this increase did not result in a loss of serum antioxidant capacity or in an increase in susceptibility toward  $\text{Cu}^{2+}$ -induced oxidation in LDL. Furthermore, these FA, particularly 22:6, appear to confer some antioxidative character because of a decrease in the propagation velocity of the lipid peroxidation.

## REFERENCES

- Dyerberg, J., Bang, H.O., and Hjörne, N. (1975) Fatty Acid Composition of the Plasma Lipids in Greenland Eskimos, *Am. J. Clin. Nutr.* 28, 958–966.
- Bang, H.O., Dyerberg, J., and Hjörne, N. (1976) The Composition of Food Consumed by Greenland Eskimos, *Acta Med. Scand.* 200, 69–73.
- Parkinson, A.J., Cruz, A.L., Heyward, W.L., Bulkow, L.R., Hall, D., Barstæd, L., and Connor, W.E. (1994) Elevated Concentrations of Plasma  $\omega$ -3 Polyunsaturated Fatty Acids Among Alaskan Eskimos, *Am. J. Clin. Nutr.* 59, 384–388.
- Anttolainen, M., Valsta, L.M., Alftan, G., Kleemola, P., Salminen, I., and Tamminen, M. (1996) Effect of Extreme Fish Consumption on Dietary and Plasma Antioxidant Levels and Fatty Acid Composition, *Eur. J. Clin. Nutr.* 50, 741–746.
- Torres, I.C., Mira, L., Ornelas, C.P., and Melim, A. (2000) Study of the Effects of Dietary Fish Intake on Serum Lipids and Lipoproteins in Two Populations with Different Dietary Habits, *Br. J. Nutr.* 83, 371–379.
- Vidgren, H.M., Ågren, J.J., Schwab, U., Rissanen, T., Hänninen, O., and Uusitupa, M.I.J. (1997) Incorporation of n-3 Fatty Acids into Plasma Lipid Fractions, and Erythrocyte Membranes and Platelets During Dietary Supplementation with Fish, Fish Oil, and Docosahexaenoic Acid-Rich Oil Among Healthy Young Men, *Lipids* 32, 697–705.
- Meydani, M., Natiello, F., Goldin, B., Free, N., Woods, M., Schaefer, E., Blumberg, J.B., and Gorbach S.L. (1991) Effect of Long-Term Fish Oil Supplementation on Vitamin E Status and Lipid Peroxidation in Women, *J. Nutr.* 121, 484–491.
- Sadou, H., Léger, C.L., Descomps, B., Barjon, J.N., Monnier, L., and Crastes de Paulet, A. (1995) Differential Incorporation of Fish-Oil Eicosapentaenoate and Docosahexaenoate into Lipids of Lipoprotein Fractions as Related to Their Glyceryl Esterification: A Short-Term (postprandial) and Long-Term Study in Healthy Humans, *Am. J. Clin. Nutr.* 62, 1193–1200.
- Palozza, P., Sgarlata, E., Luberto, C., Piccioni, E., Anti, M., Marra G., Armelao, F., Franceschelli, P., and Bartoli, G.M. (1996) n-3 Fatty Acids Induce Oxidative Modifications in Human Erythrocytes Depending on Dose and Duration of Dietary Supplementation, *Am. J. Clin. Nutr.* 64, 297–304.
- Hau, M.F., Smelt, A.H.M., Bindels, A.J.G.H., Sijbrands, E.J.G., Van der Laarse, A., Onkenhout, W., van Duyvenvoorde, W., and Princen, H.M.G. (1996) Effects of Fish Oil on Oxidation Resistance of VLDL in Hypertriglyceridemic Patients, *Arterioscler. Thromb. Vasc. Biol.* 16, 1197–1202.
- Rodríguez-Palmero, M., López-Sabater, M.C., Castellote-Bargallo, A.I., de la Torre-Boronat, M.C., and Rivero-Urgell, M. (1997) Administration of Low Doses of Fish Oil-Derived n-3 Fatty Acids to Elderly Subjects, *Eur. J. Clin. Nutr.* 51, 554–560.
- Nelson, G.J., Schmidt, P.C., Bartolini, G.L., Kelley, D.S., and Kyle, D. (1997) The Effect of Dietary Docosahexaenoic Acid on Plasma Lipoproteins and Tissue Fatty Acid Composition in Humans, *Lipids* 32, 1137–1146.
- Turley, E., Wallace, J.M.W., Gilmore, W.S., and Strain, J.J. (1998) Fish Oil Supplementation With and Without Added Vitamin E Differentially Modulates Plasma Antioxidant Concentrations in Healthy Women, *Lipids* 33, 1163–1167.
- Vognild, E., Elvevoll, E.O., Brox, J., Olsen, R.L., Barstad, H., Aursand, M., and Østerud, B. (1998) Effects of Dietary Marine Oils and Olive Oil on Fatty Acid Composition, Platelet Membrane Fluidity, Platelet Responses, and Serum Lipids in Healthy Humans, *Lipids* 33, 427–436.
- Nenseter, M.S., Rustan, A.C., Lund-Katz, S., Søyland, E., Mælandsmo, G., Phillips, M.C., and Drevon, C.A. (1992) Effect of Dietary Supplementation with n-3 Polyunsaturated Fatty Acids on Physical Properties and Metabolism of Low Density Lipoprotein in Humans, *Arterioscler. Thromb.* 12, 369–379.
- Eritsland, J., Arnesen, H., Seljeflot, I., and Høstmark, A.T. (1995) Long-Term Metabolic Effects of n-3 Polyunsaturated Fatty Acids in Patients with Coronary Artery Disease, *Am. J. Clin. Nutr.* 61, 831–836.
- Andersen, L.F., Solvoll, K., and Drevon, C.A. (1996) Very-Long-Chain n-3 Fatty Acids as Biomarkers for Intake of Fish and n-3 Fatty Acid Concentrates, *Am. J. Clin. Nutr.* 64, 305–311.
- Adler, A.J., and Holub, B.J. (1997) Effect of Garlic and Fish-Oil Supplementation on Serum Lipid and Lipoprotein Concentrations in Hypercholesterolemic Men, *Am. J. Clin. Nutr.* 65, 445–450.
- Mata, P., Varela, O., Alonso, R., Lahoz, C., de Oya, M., and Badimon, L. (1997) Monounsaturated and Polyunsaturated n-6 Fatty Acid-Enriched Diets Modify LDL Oxidation and Decrease Human Coronary Smooth Muscle Cell DNA Synthesis, *Arterioscler. Thromb. Vasc. Biol.* 17, 2088–2095.
- Conquer, J.A., and Holub, B.J. (1997) Dietary Docosahexaenoic Acid as a Source of Eicosapentaenoic Acid in Vegetarians and Omnivores, *Lipids* 32, 341–345.
- Allard, J.P., Kurian, R., Aghdassi, E., Muggli, R., and Royall, D. (1997) Lipid Peroxidation During n-3 Fatty Acid and Vitamin E Supplementation in Humans, *Lipids* 32, 535–541.
- Saldeen, T., Wallin, R., and Marklinder, I. (1998) Effects of a Small Dose of Stable Fish Substituted for Margarine in Bread on Plasma Phospholipid Fatty Acids and Serum Triglycerides, *Nutr. Res.* 18, 1483–1492.
- Hjartåker, A., Lund, E., and Bjerve, K.S. (1997) Serum Phospholipid Fatty Acid Composition and Habitual Intake of Marine Foods Registered by a Semi-quantitative Food Frequency Questionnaire, *Eur. J. Clin. Nutr.* 51, 736–742.

24. Børnaa, K.H., Bjerve, K.S., and Nordøy, A. (1992) Habitual Fish Consumption, Plasma Phospholipid Fatty Acids, and Serum Lipids: The Tromsø Study, *Am. J. Clin. Nutr.* 55, 1126–1134.
25. Bjerve, K.S., Brubakk, A.M., Fougner, K.J., Johnsen, H., Midtjell, K., and Vik, T. (1993) Omega-3 Fatty Acids: Essential Fatty Acids with Important Biological Effects, and Serum Phospholipid Fatty Acids as Markers of Dietary  $\omega$ -3-Fatty Acid Intake, *Am. J. Clin. Nutr.* 57, 801S–806S.
26. Svensson, B.G., Åkesson, B., Nilsson, A., and Skerfving, S. (1993) Fatty Acid Composition of Serum Phosphatidylcholine in Healthy Subjects Consuming Varying Amounts of Fish, *Eur. J. Clin. Nutr.* 47, 132–140.
27. Nakamura, T., Takebe, K., Tando, Y., Arai, Y., Yamada, N., Ishii, M., Kikuchi, H., Machida, K., Imamura, K., and Terada, A. (1995) Serum Fatty Acid Composition in Normal Japanese and Its Relationship with Dietary Fish and Vegetable Oil Contents and Blood Lipid Levels, *Ann. Nutr. Metab.* 39, 261–270.
28. Ma, J., Folsom, A.R., Shahar, E., and Eckfeldt, J.H. (1995) Plasma Fatty Acid Composition as an Indicator of Habitual Dietary Fat Intake in Middle-Aged Adults, *Am. J. Clin. Nutr.* 62, 564–571.
29. Lussier-Cacan, S., Dubreuil-Quidoz, S., Roederer, G., Leboeuf, N., Boulet, L., de Langavant, G.C., Davignon, J., and Naruszewicz, M. (1993) Influence of Probuocol on Enhanced LDL Oxidation After Fish Oil Treatment of Hypertriglyceridemic Patients, *Arterioscler. Thromb.* 13, 1790–1797.
30. Frankel, E.N., Parks, E.J., Xu, R., Schneeman, B.O., Davis, P.A., and German, J.B. (1994) Effect of n-3 Fatty Acid-Rich Fish Oil Supplementation on the Oxidation of Low Density Lipoproteins, *Lipids* 29, 233–236.
31. Suzukawa, M., Abbey, M., Howe, P.R.C., and Nestel, P.J. (1995) Effects of Fish Oil Fatty Acids on Low Density Lipoprotein Size, Oxidizability, and Uptake by Macrophages, *J. Lipid Res.* 36, 473–484.
32. Bonanome, A., Biasia, F., De Luca, M., Munaretto, G., Biffanti, S., Pradella, M., and Pagnan, A. (1996) n-3 Fatty Acids Do Not Enhance LDL Susceptibility to Oxidation in Hypertriglyceridemic Hemodialyzed Subjects, *Am. J. Clin. Nutr.* 63, 261–266.
33. Clandinin, M.T., Foxwell, A., Goh, Y.K., Layne, K., and Jumpsen, J.A. (1997) Omega-3 Fatty Acid Intake Results in a Relationship Between the Fatty Acid Composition of LDL Cholesterol Ester and LDL Cholesterol Content in Humans, *Biochim. Biophys. Acta* 1346, 247–252.
34. Ramírez-Tortosa, C., López-Pedrosa, J.M., Suárez, A., Ros, E., Mataix, J., and Gil, A. (1999) Olive Oil- and Fish Oil-Enriched Diets Modify Plasma Lipids and Susceptibility of LDL to Oxidative Modification in Free-Living Male Patients with Peripheral Vascular Disease: The Spanish Nutrition Study, *Br. J. Nutr.* 82, 31–39.
35. Korpela, R., Seppo, L., Laakso, J., Lilja, J., Karjala, K., Lähdenmäki, T., Solatunturi, E., Vapaatalo, H., and Tikkanen, M.J. (1999) Dietary Habits Affect the Susceptibility of Low-Density Lipoprotein to Oxidation, *Eur. J. Clin. Nutr.* 52, 802–807.
36. Esterbauer, H. (1995) The Chemistry of Oxidation of Lipoproteins, in *Oxidative Stress, Lipoproteins and Cardiovascular Dysfunction* (Rice-Evans, C., and Bruckdorfer, K.R., eds.), pp. 55–79, Portland Press, London.
37. Berry, E.M., Eisenberg, S., Haratz, D., Friedlander, Y., Norman, Y., Kaufmann N.A., and Stein, Y. (1991) Effects of Diets Rich in Monounsaturated Fatty Acids on Plasma Lipoproteins—The Jerusalem Nutrition Study: High MUFAs vs. High PUFAs, *Am. J. Clin. Nutr.* 53, 899–907.
38. Reaven, P., Parthasarathy, S., Grasse, B.J., Miller, E., Almazan, F., Mattson, F.H., Khoo, J.C., Steinberg, D., and Witztum, J.L. (1991) Feasibility of Using an Oleate-Rich Diet to Reduce the Susceptibility of Low-Density Lipoprotein to Oxidative Modification in Humans, *Am. J. Clin. Nutr.* 54, 701–706.
39. Bonanome, A., Pagnan, A., Biffanti, S., Opportuno, A., Sorgato, F., Dorella, M., Maiorino, M., and Ursini, F. (1992) Effect of Dietary Monounsaturated and Polyunsaturated Fatty Acids on the Susceptibility of Plasma Low Density Lipoproteins to Oxidative Modification, *Arterioscler. Thromb.* 12, 529–533.
40. Reaven, P., Parthasarathy, S., Grasse, B.J., Miller, E., Steinberg, D., and Witztum, J.L. (1993) Effects of Oleate-Rich and Linoleate-Rich Diets on the Susceptibility of Low Density Lipoprotein to Oxidative Modification in Mildly Hypercholesterolemic Subjects, *J. Clin. Invest.* 91, 668–676.
41. Abbey, M., Belling, G.B., Noakes, M., Hirata F., and Nestel, P.J. (1993) Oxidation of Low-Density Lipoproteins: Intraindividual Variability and the Effect of Dietary Linoleate Supplementation, *Am. J. Clin. Nutr.* 57, 391–398.
42. Louheranta, A.M., Porkkala-Sarataho, E.K., Nyssönen, M.K., Salonen, R.M., and Salonen, J.T. (1996) Linoleic Acid Intake and Susceptibility of Very-Low-Density and Low-Density Lipoproteins to Oxidation in Men, *Am. J. Clin. Nutr.* 63, 698–703.
43. Gutteridge, J.M.C., and Halliwell, B. (1994) *Antioxidants in Nutrition, Health, and Disease*, pp. 124–135, Oxford University Press, Oxford.
44. Rice-Evans, C. (1995) Free Radicals and Antioxidants in Atherosclerosis, in *Immunopharmacology of Free Radical Species* (Blake, D., and Winyard, P.G., eds.), pp. 39–52, Academic Press, London.
45. Parthasarathy, S., Santanam, N., Ramachandran, S., and Meilhack, O. (1999) Oxidants and Antioxidants in Atherogenesis: An Appraisal, *J. Lipid Res.* 40, 2143–2157.
46. Bruna, E., Petit, E., Bejjean-Leymarie, M., Huynh, S., and Nouvelot, A. (1989) Specific Susceptibility of Docosahexaenoic Acid and Eicosapentaenoic Acid to Peroxidation in Aqueous Solution, *Lipids* 24, 970–975.
47. Oostenburg, G.S., Mensink, R.P., and Hornstra, G. (1994) Effects of Fish Oil and Vitamin E Supplementation on Copper-Catalysed Oxidation of Human Low Density Lipoprotein *in vitro*, *Eur. J. Clin. Nutr.* 48, 895–898.
48. Riboli, E. (1992) Nutrition and Cancer: Background and Rationale of the European Prospective Investigation into Cancer and Nutrition (EPIC), *Ann. Oncol.* 3, 783–791.
49. Grupo EPIC de España (1994) El Estudio Prospectivo Europeo Sobre Dieta, Cáncer y Salud (EPIC) en España, *Med. Clin. (Barc.)* 102, 781–785.
50. EPIC Group of Spain (1997) Relative Validity and Reproducibility of a Diet History Questionnaire in Spain. I. Foods, *Int. J. Epidemiol.* 26, S91–S99.
51. EPIC Group of Spain (1997) Relative Validity and Reproducibility of a Diet History Questionnaire in Spain. II. Nutrients, *Int. J. Epidemiol.* 26, S100–S109.
52. EPIC Group of Spain (1997) Relative Validity and Reproducibility of a Diet History Questionnaire in Spain. III. Biochemical Markers, *Int. J. Epidemiol.* 26, S110–S117.
53. Amiano, P., Dorronsoro, M., de Renobales, M., Ruiz de Gordoa, J.C., Irigoien, I., and the EPIC Group of Spain (2001) Very-Long-Chain  $\omega$ -3 Fatty Acids as Markers for Habitual Fish Intake in a Population Consuming Mainly Lean Fish: The EPIC Cohort of Gipuzkoa, *Eur. J. Clin. Nutr.* 55, 827–832.
54. Slimani, N., Torrent, M., Farriol, N., Moreno, I., Hémon, B., González, C.A., and Riboli, E. (1991) *European Prospective Investigation into Cancer and Nutrition (EPIC). Food Composition Tables—Spain*, International Agency for Research on Cancer, Lyon.
55. Vilardell, F., Portero, M., Aragón, M., Bellmunt, M.J., Pamplona, R., and Prat, J. (1995) Composición en Ácidos Grasos de los Pescados Más Comunes en la Dieta Española. Dieta y Lípidos Marinos, *Clin. Invest. Arterioscler.* 7, 45–51.

56. Portero, M., Aragón, M., Vilardell, F., Pamplona, R., Bellmunt, M.J., and Prat, J. (1996) Composición en Ácidos Grasos de los Pescados en Conserva Más Comunes en la Dieta Española. Dieta y Lípidos Marinos (II), *Clin. Invest. Arterioscler.* 8, 9–14.
57. MSC (Ministerio de Sanidad y Consumo) (1995) *Tablas de Composición de Alimentos Españoles*, Secretaría General Técnica, Centro de Publicaciones, Madrid.
58. Kelley, J.L., and Kruski, A.W. (1986) Density Gradient Ultracentrifugation of Serum Lipoproteins in a Swinging Bucket Rotor, in *Methods in Enzymology* (Segrest, J.P., and Albers, J.J., eds.), Vol. 128, pp. 170–181, Academic Press, Orlando.
59. Lowry, O.H., Rosebrough, N.J., Farr, A.L., and Randall, R.J. (1951) Protein Measurement with the Folin Phenol Reagent, *J. Biol. Chem.* 193, 265–275.
60. Lepage, G., and Roy, C.C. (1986) Direct Transesterification of All Classes of Lipids in a One-Step Reaction, *J. Lipid Res.* 27, 114–120.
61. Matorras, R., Perteagudo, L., Sanjurjo, P., Sasieta, M., and Ruiz, J.I. (1998) Long Chain  $\omega$ -3 Polyunsaturated Fatty Acids and Lipid Pattern in the Mother and the Newborn Infant, *J. Perinat. Med.* 26:313–319.
62. Hamilton, R.J., Hamilton, S., and Sewell, P.A. (1992) Extraction of Lipids and Derivative Formation, in *Lipid Analysis: A Practical Approach* (Hamilton, R.J., and Hamilton, S., eds.), pp. 13–64, Oxford University Press, Oxford.
63. Henderson, R.J., and Tocher, D.R. (1992) Thin-Layer Chromatography, in *Lipid Analysis: A Practical Approach* (Hamilton, R.J., and Hamilton, S., eds.), pp. 65–111, Oxford University Press, Oxford.
64. Miller, N.J., Rice-Evans, C., Davies, M.J., Gopinathan, V., and Milner, A. (1993) A Novel Method for Measuring Antioxidant Capacity and Its Application to Monitoring the Antioxidant Status in Premature Neonates, *Clin. Sci.* 84:407–412.
65. Puhl, H., Waeg, G., and Esterbauer, H. (1994) Methods to Determine Oxidation of Low-Density Lipoproteins, in *Methods in Enzymology* (Packer, L., ed.), Vol. 233, pp. 425–441, Academic Press, San Diego.
66. Kleinveld, H.A., Hak-Lemmers, H.L.M., Stalenhoef, A.F.H., and Demacker, P.N.M. (1992) Improved Measurement of Low-Density-Lipoprotein Susceptibility to Copper-Induced Oxidation: Application of a Short Procedure for Isolating Low-Density Lipoprotein, *Clin. Chem.* 38, 2066–2072.
67. Steinbrecher, U.P. (1987) Oxidation of Human Low Density Lipoprotein Results in Derivatization of Lysine Residues of Apolipoprotein B by Lipid Peroxide Decomposition Products, *J. Biol. Chem.* 262, 3603–3608.
68. Vaagenes, H., Muna, Z.A., Madsen, L., and Berge, R.K. (1998) Low Doses of Eicosapentaenoic Acid, Docosahexaenoic Acid, and Hypolipidemic Eicosapentaenoic Acid Derivatives Have No Effect on Lipid Peroxidation in Plasma, *Lipids* 33, 1131–1137.
69. EPIC Group of Spain (1999) Dietary Intake of Vegetables and Fruits Among Adults in Five Regions of Spain, *Eur. J. Clin. Nutr.* 53, 174–180.
70. Thomas, M.J., and Rudel, L.L. (1996) Dietary Fatty Acids, Low Density Lipoprotein Composition and Oxidation and Primate Atherosclerosis, *J. Nutr.* 126, 1058S–1062S.
71. Whitman, S.C., Fish, J.R., Rand, M.L., and Rogers, K.A. (1994) n-3 Fatty Acid Incorporation into LDL Particles Renders Them More Susceptible to Oxidation *in vitro* but Not Necessarily More Atherogenic *in vivo*, *Arterioscler. Thromb.* 14, 1170–1176.
72. Thomas, M.J., Thornburg, T., Manning, J., Hooper, K., and Rudel, L.L. (1994) Fatty Acid Composition of Low-Density Lipoprotein Influences Its Susceptibility to Autoxidation, *Biochemistry* 33, 1828–1834.
73. Miyashita, K., Nara, E., and Ota, T. (1993) Oxidative Stability of Polyunsaturated Fatty Acids in an Aqueous Solution, *Biosci. Biotechnol. Biochem.* 57, 1638–1640.
74. Yazu, K., Yamamoto, Y., Ukegawa, K., and Niki, E. (1996) Mechanism of Lower Oxidizability of Eicosapentaenoate Than Linoleate in Aqueous Micelles, *Lipids* 31, 337–340.

[Received April 25, 2001, and in revised form December 27, 2001; revision accepted February 14, 2002]



# Dietary Conjugated Linolenic Acid in Relation to CLA Differently Modifies Body Fat Mass and Serum and Liver Lipid Levels in Rats

Kazunori Koba<sup>a,\*</sup>, Asuka Akahoshi<sup>b</sup>, Masao Yamasaki<sup>c</sup>, Kazunari Tanaka<sup>a</sup>,  
Koji Yamada<sup>c</sup>, Toshio Iwata<sup>d</sup>, Takeshi Kamegai<sup>d</sup>,  
Kentaro Tsutsumi<sup>d</sup>, and Michihiro Sugano<sup>b</sup>

<sup>a</sup>Faculty of Nursing and Nutrition, Siebold University of Nagasaki, Nagasaki 851-2195, Japan, <sup>b</sup>Faculty of Environmental and Symbiotic Sciences, Prefectural University of Kumamoto, Kumamoto 862-8502, Japan,

<sup>c</sup>Laboratory of Food Chemistry, Department of Bioscience and Biotechnology, Graduate School Kyushu University, Fukuoka 812-8581, Japan, and <sup>d</sup>Rinoru Oil Mills Co., Ltd., Tokyo 103-0027, Japan

**ABSTRACT:** The present study compared the effect of dietary conjugated linolenic acid (CLNA) on body fat and serum and liver lipid levels with that of CLA in rats. FFA rich in linoleic acid,  $\alpha$ -linolenic acid, CLA, or CLNA were used as experimental fats. Male Sprague–Dawley rats (4 wk old) were fed purified diets containing 1% of one of these experimental fats. After 4 wk of feeding, adipose tissue weights, serum and liver lipid concentrations, serum tumor necrosis factor (TNF)- $\alpha$  and leptin levels, and hepatic  $\beta$ -oxidation activities were measured. Compared with linoleic acid, CLA and, more potently, CLNA were found to reduce perirenal adipose tissue weight. The same trend was observed in the weight of epididymal adipose tissue. CLNA, but not CLA, was found to significantly increase serum and liver TG concentrations. Serum FFA concentration was also increased in the CLNA group more than in the other groups. The activity of  $\beta$ -oxidation in liver mitochondria and peroxisomes was significantly higher in the CLNA group than in the other groups. Thus, the amount of liver TG exceeded the ability of hepatic  $\beta$ -oxidation. Significant positive correlation was found between the adipose tissue weights and serum leptin levels in all animals (vs. perirenal:  $r = 0.557$ ,  $P < 0.001$ ; vs. epididymal:  $r = 0.405$ ,  $P < 0.05$ ). A less significant correlation was found between adipose tissue weights and serum TNF- $\alpha$  level (vs. perirenal:  $r = 0.069$ ,  $P > 0.1$ ; vs. epididymal:  $r = 0.382$ ,  $P < 0.05$ ). Although the mechanism for the specific effect of CLNA is not clear at present, these findings indicate that in rats CLNA modulated the body fat and TG metabolism differently from CLA.

Paper no. L8937 in *Lipids* 37, 343–350 (April 2002).

CLA is a FA that has 18 carbons and one conjugated double bond, including multiple positional and geometric isomers (9*c*, 11*t*; 10*t*, 12*c*; etc.), and is exclusively found in a trace amount

\*To whom correspondence should be addressed at Department of Nutrition, Faculty of Nursing and Nutrition, Siebold University of Nagasaki, 1-1-1 Manabino, Nagayo, Nagasaki 851-2195, Japan.  
E-mail: koba@sun.ac.jp

Abbreviations: CLNA, conjugated linolenic acid; CPT, carnitine palmitoyl-transferase; DTNB, 5,5-dithiobis-(2-nitrobenzoic acid); LA, linoleic acid; LNA,  $\alpha$ -linolenic acid; PPAR, peroxisome proliferator-activated receptor; TNF, tumor necrosis factor; UCP, uncoupling protein.

in ruminant meats and dairy products (1,2). CLA has been shown to reduce body fat in rodents (3,4) and humans, although results were not always unequivocal (5–9). The exact mechanism of the anti-obese effect of CLA is not clear. Animal studies showed that it could be attributed in part to a decrease in the activity of lipoprotein lipase (10–12), an increase in lipolysis in adipocytes (10), or a moderate increase in FA oxidation in adipose tissue (10), muscle (10), and liver (13). Compared with linoleic acid (LA), CLA has been shown to lower plasma concentrations of cholesterol and TG and regress established atheroma in rabbits (14,15), whereas it increases liver TG concentrations in mice (16,17) but not in rats (13,18). It has been demonstrated that more highly unsaturated FA, such as LA metabolites, are more hypocholesterolemic than LA (19). Similar to LA, CLA is thought to be metabolized to conjugated eicosatrienoic or eicosatetraenoic acids through desaturation and elongation in rats (20,21). From these backgrounds, it is of interest to know how a more highly unsaturated conjugated FA affects lipid metabolism.

CLNA is one of the more highly unsaturated forms of conjugated FA and possibly includes multiple positional (8, 10, 12; 9, 11, 13; etc.) and geometric (*cis* and *trans*) isomers. CLNA occurs abundantly in some specific seed oils, such as karela oil (22), tung oil (23,24), and pomegranate oil (24). There is evidence showing that karela oil, as compared with linseed oil [rich in  $\alpha$ -linolenic acid (ALA)], increased the serum cholesterol and TG concentrations in rats fed a high-fat diet (20% fat containing 10% CLNA) (22). Igarashi and Miyazawa showed that CLNA, but not CLA, exhibited cytotoxic effects on some lines of human tumor cells (23). They also reported that conjugated eicosapentaenoic and docosahexaenoic acids with conjugated trienoic structures exhibited the strongest cytotoxic effect on human tumor cells, possibly due to the induction of apoptosis of the cells through lipid peroxidation (25). From these observations, feeding of CLNA with conjugated trienoic structure was expected to affect lipid metabolism more than was CLA. To date, no additional

evidence is available to show the biological effects of CLNA. The objective of the present study using a rat model was to examine how CLNA affects body fat mass, and serum and liver lipids.

## MATERIALS AND METHODS

**Experimental fats.** Experimental fats used in the present study were FFA that were rich in LA, LNA, CLA, and CLNA, all supplied by Rinoru Oil Mills Co., Ltd. (Tokyo, Japan). LA- and LNA-rich FA were derived from safflower oil and perilla oil, respectively, and from them CLA- and CLNA-rich FA were prepared by alkaline isomerization. The FA profile was measured as described previously (26). Briefly, approximately 25 mg of the FFA sample was methylated with 2 mL of BF<sub>3</sub>-methanol at 40°C for 10 min. FAME were analyzed by GLC with a J&W DB-23 capillary column (30 m × 0.25 mm i.d.; Agilent Technologies, Palo Alto, CA). The FA profile of the experimental fats is shown in Table 1. For the confirmation of CLNA analysis, we observed two peaks for conjugated diene and six peaks for conjugated triene by HPLC (27) monitoring at 234 and 268 nm, respectively (23). It was confirmed by GC/MS that the former peaks contained 18:3 and 18:2 and the latter peaks contained 18:3. Although CLNA contained 18:3 conjugated diene and triene, the identification of individual components awaits further study.

**Animals and diets.** Thirty-two male weanling Sprague-Dawley rats (4 wk old) purchased from SEAC Yoshitomi Co. (Fukuoka, Japan) were acclimatized for 3 d in a room maintained at 21–23°C with a 12-h light–dark cycle. Animals were randomly assigned to four groups of eight animals each according to the experimental fats: LA, ALN, CLA, and CLNA. Diets were prepared according to the AIN-93G formula (28) and contained (by wt %) casein 20; soybean oil 6; experimental fat 1; cornstarch 39.7; dextrinized cornstarch 13.2; sucrose 10; cellulose 5; mineral mixture (AIN-93G-MX) 3.5; vitamin mixture (AIN-93-VX) 1; L-cystine 0.3; choline bitartrate 0.25; and *t*-butylhydroquinone 0.0014. Animals were maintained on their respective diets *ad libitum* for 4 wk. During the feeding period, body weight and food consumption were recorded every other day. After 16 h of food deprivation, animals were anesthetized with diethyl ether, and blood was collected from the abdominal aorta. Serum was separated by centrifugation. The liver and other tissues, including perirenal and epididymal white adipose tissues and interscapular brown adipose tissue, were excised and weighed.

**Serum and liver lipid analysis.** Serum total and HDL cholesterol were measured using commercial assay kits (Cholesterol CII-test Wako; Wako Pure Chemical Industries, Osaka, Japan; and HDL-C2; Daiichi Pure Chemicals, Tokyo, Japan). Serum phospholipid, TG, FFA, and TBARS were also measured using commercial assay kits (Phospholipid B-, Triglyceride G-, NEFA-, and Lipid Peroxide-Test Wako; Wako Pure Chemical Industries).

Total liver lipids were extracted by the method of Folch *et al.* (29). The concentrations of liver cholesterol, phospholipid, and TG were measured by the methods of Ide *et al.* (30), Rouser *et al.* (31), and Fletcher (32), respectively.

**Preparation of liver mitochondria/peroxisomes.** An aliquot of liver was homogenized in 7 vol of a 0.25-M sucrose solution. The homogenate was centrifuged at 1,000 × *g* for 10 min at 4°C. The supernatant was centrifuged at 16,000 × *g* for 20 min to sediment mitochondria/peroxisomes. The pellet was suspended in a solution containing 0.3 M mannitol, 10 mM HEPES, and 0.1 mM EGTA. The suspension was stored at –80°C until used for the measurement of carnitine palmitoyltransferase (CPT) and peroxisomal β-oxidation activities. The protein content of the suspension was measured by the method of Lowry *et al.* (33).

**Measurement of CPT activity.** The activity of CPT was measured spectrophotometrically by monitoring the release of CoA-SH from palmitoyl-CoA using 5,5-dithiobis-(2-nitrobenzoic acid) (DTNB) (34). The carnitine-dependent reaction was initiated by addition of enzyme (sample suspension) to the reaction cuvette containing 58 mM Tris HCl (pH 8.0), 1.25 mM EDTA, 0.1% Triton X-100, 0.25 mM DTNB, 37.5 mM palmitoyl-CoA, and 1.25 mM L-carnitine. The reaction compartment was thermostated at 27°C. The reaction was followed at 412 nm. The carnitine-independent reaction was conducted by an identical procedure without L-carnitine. The difference between L-carnitine-dependent and -independent reaction rates was regarded as CPT activity. Data were expressed as nmol CoA/min/mg protein.

**Measurement of peroxisomal β-oxidation.** The peroxisomal β-oxidation was measured spectrophotometrically by monitoring the reduction of NAD to NADH in the presence of palmitoyl-CoA (35). The reaction was initiated by the addition of enzyme (sample suspension) to the reaction cuvette containing 50 mM Tris HCl (pH 8.0), 20 mM NAD, 0.33 M DTT, 1.5% BSA, 2% Triton X-100, 10 mM CoA, 1 mM FAD, 100 mM KCN, and 5 mM palmitoyl-CoA. The reaction compartment

**TABLE 1**  
**FA Composition of Experimental Fats (FFA Form)**

FA	Experimental fat (% wt) <sup>a</sup>			
	LA	LNA	CLA	CLNA
16:0	7.4	5.8	7.4	5.9
18:0	2.6	1.6	2.7	1.6
18:1n-9	17.7	13.6	17.8	14.2
18:2n-6	70.9	21.9	1.5	0.5
18:3n-3	0.3	55.5	—	—
Conjugated 18:2	—	—	68.9	24.7
(9c,11t)	—	—	(31.8)	(8.0)
(10t,12c)	—	—	(32.7)	(15.1)
(9c,11c/10c,12c)	—	—	(2.1)	(1.4)
(9t,11t/10t,12t)	—	—	(2.3)	(0.2)
Conjugated 18:3	—	—	—	49.1
(Conjugated diene)	—	—	—	(31.9)
(Conjugated triene)	—	—	—	(17.2)

<sup>a</sup>LA, linoleic acid; LNA, α-linolenic acid; CLNA, conjugated linolenic acid.

was thermostated at 37°C. The reaction rate was followed at 340 nm. Data were expressed as nmol NAD reduced/min/mg protein.

**Serum concentration of tumor necrosis factor (TNF)- $\alpha$  and leptin.** The concentration of serum TNF- $\alpha$  and leptin was measured by ELISA using a commercial kit (Rat TNF- $\alpha$  ELISA YK 040 and Rat Leptin ELISA YK 050; Yanaihara Institute Inc., Shizuoka, Japan).

**Measurement of uncoupling protein (UCP) 1 of brown adipose tissue by western blotting.** An aliquot of brown adipose tissue was homogenized in PBS containing 0.5% sodium deoxycholate, 0.1% SDS, 2 mM EDTA, 1% NP-40 (Sigma, St. Louis, MO), 5 mg/mL phenylmethylsulfonyl fluoride, and 2 mg/mL aprotinin. The homogenate was centrifuged at 10,000  $\times$  g for 10 min at 4°C. The supernatant was used for the following measurements. The protein concentration was determined using a commercial kit (BCA Protein Assay Reagent; Pierce Chemical Co., Rockford, IL). The sample (50 mg protein/lane) was electrophoresed using SDS polyacrylamide gel (12%) transferred to nitrocellulose membrane. UCP 1 was probed with rabbit anti-rat UCP 1 antibody at 4°C for 16 h (2000 times diluted solution), which was kindly provided by Dr. Teruo Kawada (Kyoto University, Kyoto, Japan). Then the membrane was reacted with goat anti-rabbit IgG POD (peroxidase) conjugated (secondary antibody; ICN Pharmaceuticals, Aurora, OH) at 37°C for 1 h. Detected protein was visualized using equivalent chain length western blotting detection reagents (Amersham Pharmacia Biotech, Buckinghamshire, England), and the bands were quantitated using NIH (National Institutes of Health) Image. The amount of  $\beta$ -actin was also measured by western blotting and anti-rat  $\beta$ -actin clone AC-15 (3000  $\times$  dilution; Sigma) and anti-mouse IgG HRP conjugated (3000  $\times$  dilution; ICN) were used as primary and secondary antibodies. Values of UCP 1 were divided by those of  $\beta$ -actin to be normalized.

**Statistical analysis.** Results were expressed as means and pooled SE unless otherwise indicated. All data were analyzed by a one-way ANOVA followed by the Tukey–Kramer test to determine the dietary fat-dependent difference. All analyses were performed with SuperANOVA software (Abacus Concepts, Berkeley, CA).

## RESULTS

**Body weight gain, food intake, and tissue weights.** During 4 wk of feeding, food intake tended to be higher in rats fed LNA and CLA than in those fed LA and CLNA (Table 2). The relative weight of perirenal adipose tissue was significantly lower in rats fed CLA and CLNA than in those fed LA, and it tended to be lower in the CLNA group than in the CLA group. This trend also was observed in the weight of epididymal adipose tissue. The relative liver weight was significantly heavier in rats fed CLNA than in those fed other fats. This trend also was observed in the relative heart weight.

**Serum and liver lipid concentrations.** The concentration of serum cholesterol was significantly lower in the CLNA group than in the LA group (Table 3). Although CLA exhibited the same trend as CLNA, the cholesterol-lowering effect against LA was not statistically significant. The concentration of HDL-cholesterol was significantly lower in rats fed CLNA than in those fed other fats. As a result, the ratio of HDL/total cholesterol was significantly lower in the CLNA group than in the LNA group (data not shown). The serum TG concentration of the CLNA group was more than twice that of the LA, LNA, and CLA groups. The serum FFA concentration of the CLNA group was significantly higher than that of the other groups. The serum TBARS value, an index of the potential for lipid peroxidation, was significantly higher in rats fed CLNA than in those fed CLA. However, there was no significant difference in this value between the other groups.

**TABLE 2**  
Effect of Conjugated Linolenic Acid on the Body Weight, Food Intake, and Tissue Weights

	Groups <sup>a</sup>				Pooled SE <sup>b</sup>
	LA	LNA	CLA	CLNA	
Body weight (g)					
Initial	77	77	77	77	2
Gain	198	212	216	197	8
Food intake (g/d)	18.4 <sup>a</sup>	20.0 <sup>b</sup>	19.3 <sup>a,b</sup>	18.2 <sup>a</sup>	0.5
Tissue weights (g/100 g body weight)					
White adipose tissue					
Perirenal	1.95 <sup>a</sup>	1.90 <sup>a,b</sup>	1.40 <sup>b,c</sup>	1.29 <sup>c</sup>	0.20
Epididymal	1.22	1.20	1.09	1.00	0.09
Brown adipose tissue	0.17	0.15	0.15	0.18	0.03
Liver	3.10 <sup>a</sup>	3.26 <sup>a</sup>	3.31 <sup>a</sup>	3.80 <sup>b</sup>	0.11
Kidney	0.86 <sup>a,b</sup>	0.81 <sup>a</sup>	0.87 <sup>a,b</sup>	0.93 <sup>b</sup>	0.03
Spleen	0.23	0.24	0.25	0.25	0.02
Heart	0.41 <sup>a</sup>	0.45 <sup>a,b</sup>	0.46 <sup>b</sup>	0.49 <sup>b</sup>	0.02
Lung	0.61	0.61	0.59	0.55	0.04
Brain	0.63	0.59	0.59	0.66	0.04

<sup>a</sup>Values not sharing a common roman superscript letter (a,b,c) are significantly different at  $P < 0.05$ .

<sup>b</sup>All data are expressed as means and pooled SE of 7 or 8 rats. For abbreviations see Table 1.

**TABLE 3**  
**Effect of Conjugated Linolenic Acid on Serum and Liver Lipid Concentrations**

	Groups <sup>a</sup>				Pooled SE <sup>b</sup>
	LA	LNA	CLA	CLNA	
Serum lipids (mmol/L)					
Cholesterol					
Total cholesterol	1.87 <sup>a</sup>	1.80 <sup>a,b</sup>	1.72 <sup>a,b</sup>	1.48 <sup>b</sup>	0.13
HDL cholesterol	0.92 <sup>a</sup>	0.95 <sup>a</sup>	0.84 <sup>a</sup>	0.65 <sup>b</sup>	0.06
Phospholipid	1.55	1.45	1.48	1.64	0.13
TG	1.23 <sup>a</sup>	1.02 <sup>a</sup>	1.10 <sup>a</sup>	2.91 <sup>b</sup>	0.47
FFA	0.85 <sup>a</sup>	0.79 <sup>a</sup>	0.78 <sup>a</sup>	1.21 <sup>b</sup>	0.10
TBARS (× 10 <sup>3</sup> )	3.74 <sup>a,b</sup>	3.92 <sup>a,b</sup>	3.57 <sup>a</sup>	4.92 <sup>b</sup>	0.45
Liver lipids (μmol/g)					
Cholesterol	10.0 <sup>a</sup>	11.9 <sup>b</sup>	9.72 <sup>a</sup>	9.23 <sup>a</sup>	0.68
Phospholipid	42.3	42.2	43.1	42.5	1.0
TG	5.95 <sup>a</sup>	6.22 <sup>a</sup>	4.75 <sup>a</sup>	11.5 <sup>b</sup>	1.32

<sup>a</sup>All data are expressed as mean and pooled SE of 8 rats. For abbreviations see Table 1.

<sup>b</sup>Values not sharing a common roman superscript letter (a,b) are significantly different at  $P < 0.05$ .

Effects of different dietary fats on the liver lipid concentrations are shown in Table 3. The concentration of liver cholesterol was significantly higher in rats fed the LNA diet than in those fed other fats. The TG concentration of the CLNA group was approximately twice that of the other three groups.

***β-Oxidation activity in liver mitochondria and peroxisomes.*** The β-oxidation activity was examined in liver mitochondria and peroxisomes. The activity of CPT, a key enzyme in the FA oxidation pathway, was measured as an index of liver mitochondrial β-oxidation. Since freezing–thawing mitochondria inactivates CPT I but not CPT II (36), the CPT activity measured in the present study most likely represented CPT II activity (37). As shown in Figure 1A, CPT II activity was 7 μmol/mg protein in rats fed LA. The activity was increased 20% by either LNA or CLA and 57% by CLNA. The activity in rats fed CLNA was significantly higher than that in animals fed other fats. On the other hand, relative to LA, peroxisomal β-oxidation, measured using palmitoyl-CoA as a substrate, was increased threefold by CLNA but was unaffected by the other dietary treatments (Fig. 1B).

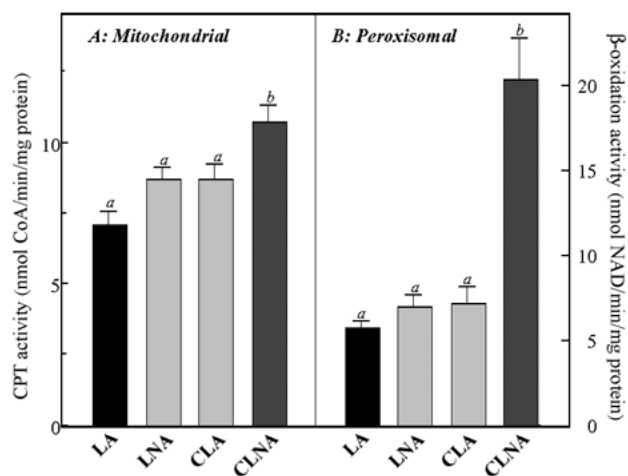
***Serum concentration of TNF-α and leptin.*** As shown in Figure 2A, the serum concentration of TNF-α was significantly higher in rats fed LNA, CLA, and CLNA than in those fed LA. The concentration of serum leptin tended to be higher in rats fed LNA than in those fed LA (Fig. 2B). The leptin concentration of CLA-fed rats tended to be lower, whereas the leptin concentration of CLNA-fed rats was significantly lower than that of LNA-fed rats.

The correlations between serum TNF-α or leptin concentrations and adipose tissue weight are shown in Figure 3. A positive correlation was observed between the serum TNF-α concentration and epididymal but not perirenal adipose tissue (Fig. 3A). On the other hand, serum leptin exhibited a significant positive correlation with weights of both perirenal and epididymal adipose tissues (Fig. 3B).

***UCP 1 level of brown adipose tissue.*** NIH-imaged UCP 1 levels normalized by β-actin were  $1.36 \pm 0.12$ ,  $1.40 \pm 0.10$ ,  $1.33 \pm 0.13$ , and  $1.35 \pm 0.12$  for the LA, LNA, CLA, and CLNA groups (mean ± SE), respectively. No statistically significant difference was observed.

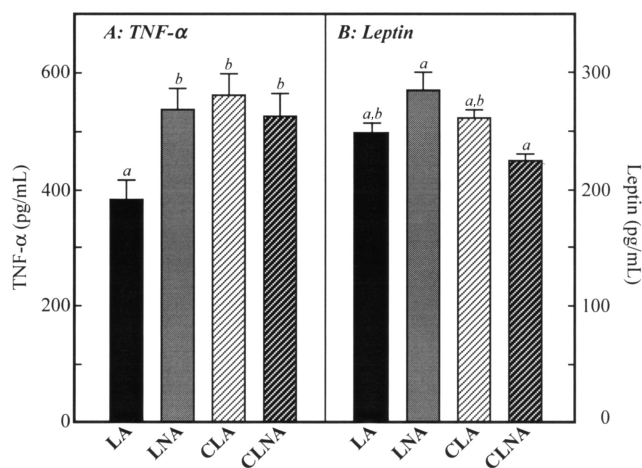
## DISCUSSION

The present study examined how dietary CLNA affects body fat mass and serum and liver lipid levels in rats. The effect of dietary CLNA was compared with that of CLA, LNA, and LA. In agreement with the earlier findings using mice as an experi-



**FIG. 1.** Effect of conjugated linolenic acid (CLNA) on liver mitochondrial (A) and peroxisomal (B) β-oxidation activity. LA, linoleic acid; LNA, α-linolenic acid; CPT, carnitine palmitoyltransferase. All data are expressed as mean ± SE of eight rats. Values not sharing a common letter (a,b) are significantly different at  $P < 0.05$ .



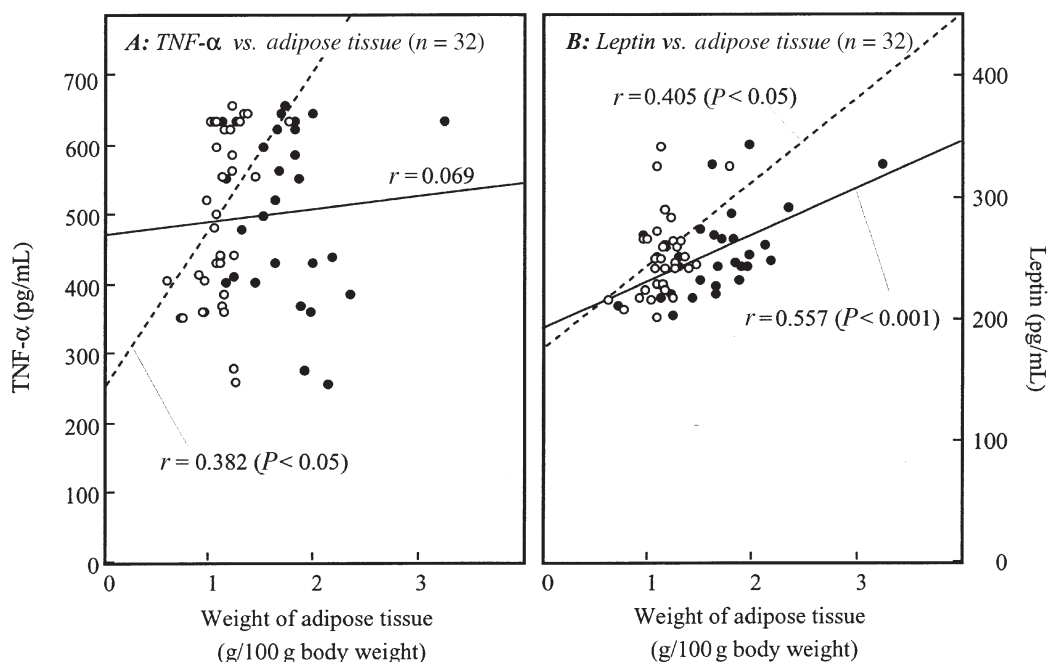


**FIG. 2.** Effect of CLNA on tumor necrosis factor (TNF)- $\alpha$  (A) and leptin (B) concentrations in serum. For other abbreviations see Figure 1. All data are expressed as mean  $\pm$  SE of 8 rats. Values not sharing a common letter (a,b) are significantly different at  $P < 0.05$ .

mental animal (3,4), feeding of CLA reduced the perirenal adipose tissue weight more than LA did. However, the difference between LNA and CLA was not statistically significant. On the other hand, feeding of CLNA reduced the weight of perirenal adipose tissue significantly more than LA and LNA did. This suggests that the body fat-reducing effect of CLNA is at least comparable to or even stronger than that of CLA under the experimental conditions described in the present study.

Serum lipid concentration was modified by dietary CLNA.

The concentration of serum TG increased 2.5-fold in rats fed CLNA as compared with the animals fed LA, LNA, or CLA. Since serum TG was normally associated with lipoproteins (38), one may expect that the increase in serum TG concentration might cause an increase in serum cholesterol concentration. However, serum cholesterol concentration was significantly lower in rats fed CLNA than in those fed LA. Serum phospholipid concentration was comparable among the groups. Since the rats were fasted for 16 h prior to collection of blood, this elevated level of TG in rats fed CLNA in the present study might be indicative of an inability to clear VLDL, possibly due to an inhibition of lipoprotein lipase activity (10–12). It is plausible that the increase in the serum concentration of TBARS (Table 3) and the whitish color of the serum may be responsible for the hypertriglyceridemia caused by CLNA. Dhar *et al.* (22) reported that karela oil containing CLNA increased the serum concentration of cholesterol and TG, whereas it tended to decrease the liver TG. The difference in the dietary level of experimental fat and the type of FA molecule may be the cause of the discrepancy. The dietary level of the experimental fat was 20% (as karela oil) in their report, whereas it was only 1% (as CLNA) in the present study. Also, karela oil contains mainly 9*c*, 11*t*, 13*t*-18:3 (39), whereas the CLNA used in the present study was a mixture of conjugated diene and triene, which possibly contains multiple positional and geometric isomers. In the present study, adipose tissue did not grow as rapidly in rats fed CLNA or CLA. In an early report, Park *et al.* (10) suggested that CLA reduced the body fat through a reduction of fat deposition and an increase of lipolysis in adipocytes. It was demonstrated that 10*t*, 12*c*-18:2 but



**FIG. 3.** Correlation between TNF- $\alpha$  concentration and adipose tissue weight (A) and leptin concentration and adipose tissue weight (B). ●, Perirenal adipose tissue; ○, epididymal adipose tissue. —, vs. perirenal adipose tissue; ----, vs. epididymal adipose tissue. For abbreviation see Figure 2.

not 9*c*,11*t*- and 9*t*,11*c*-isomers inhibited lipoprotein lipase activity (12) and depressed the concentration of intracellular TG in 3T3-L1 preadipocytes (11,12). As shown in Table 1, CLA contained 33% of 10*t*,12*c*-18:2, whereas CLNA contained 15% of this isomer, and 32 and 17% of conjugated 18:3 with diene and triene structures (Table 1). Therefore, conjugated diene and/or triene isomers of 18:3 may reduce the fat deposition more efficiently than CLA. Moreover, feeding of CLNA, but not CLA, increased the serum concentration of FFA significantly more than that of LA and LNA, suggesting that CLNA may increase FA mobilization from the adipose tissues.

Previous studies have established that adipocytokines, such as leptin and TNF- $\alpha$  secreted from adipocytes, can modulate the amount of adipose tissue (40). Therefore, the correlation between these adipocytokine levels and adipose tissue weights was investigated to clarify which adipocytokine was more closely related to the adipose tissue weights (Fig. 3). As a result, serum leptin level was found to exhibit a significant positive correlation with the weight of perirenal and epididymal adipose tissues. Adipose tissue weight was related to serum leptin concentration more than to TNF- $\alpha$  concentration (40). Relative to the group fed LA, TNF- $\alpha$  levels were elevated by LNA, CLA, and CLNA to a similar extent (Fig. 2). An early report in animals showed that TNF- $\alpha$  decreased the synthesis of lipoprotein lipase in adipose tissue but increased the activity of lipoprotein lipase in liver (41). TNF- $\alpha$  was reported to decrease peroxisome proliferator-activated receptor (PPAR)- $\gamma$  mRNA level in 3T3-L1 preadipocytes (42). PPAR- $\gamma$  is known to play an important role for the differentiation of adipocytes (43,44). Recently, studies in obese women showed that PPAR- $\gamma$  mRNA levels in adipose tissue were positively associated with the serum concentrations of HDL-cholesterol (45,46). Serum HDL-cholesterol concentrations were also shown to exhibit a positive correlation with leptin mRNA levels in adipose tissue (45). In the present study, serum leptin concentration exhibited a significant positive correlation with serum HDL-cholesterol ( $r = 0.596$ ,  $n = 32$ ,  $P < 0.001$ , data not shown). Also, serum leptin and HDL-cholesterol levels were the lowest in the CLNA group. This could be one explanation why CLA and, more potently, CLNA decreased the weight of white adipose tissues as compared with the corresponding nonconjugated FA, even under the equally high concentration of serum TNF- $\alpha$ . In the present study, the level of UCP 1 was also measured, which is a thermogenic uncoupling protein and expresses exclusively in brown adipose tissue (47). Although TNF- $\alpha$  was reported to increase UCP 1 level of brown adipose tissue (48), the effect of dietary fat on the UCP1 level was not clear in the present study.

CLA and CLNA also affected differently the concentration of liver TG. CLA tended to suppress the liver TG concentration as compared with LA or LNA (Table 3) without affecting the liver weight (Table 2). The liver mitochondrial CPT II activity and peroxisomal  $\beta$ -oxidation activity tended to be higher in rats fed CLA than in those fed LA (Fig. 1). The

increase in  $\beta$ -oxidation activity may cause a decreased concentration of TG in the liver. In contrast to CLA, CLNA increased liver TG concentration twofold as compared with LA or LNA. This may be one reason why the liver weight was significantly increased only by CLNA (Table 2). Also, CLNA, as compared with other FA significantly enhanced the activities of both liver mitochondrial and peroxisomal  $\beta$ -oxidation (Fig. 1). Peroxisomal  $\beta$ -oxidation in particular increased 3–3.5-fold in CLNA-fed rats as compared with other groups of animals. It was reported that an enhancement of hepatic  $\beta$ -oxidation was regulated through activation of PPAR- $\alpha$  in the liver (49). Moya-Camarena *et al.* (50) demonstrated, using a rat hepatoma cell line, that CLA is an activator of PPAR- $\alpha$ . Also, feeding of the prototypical peroxisome proliferator Wy-14,643 (0.01 wt% in the diet) increased hepatic total lipid content and mRNA level of acyl CoA oxidase, the first step enzyme of peroxisomal  $\beta$ -oxidation in rats (51), consistent with the phenomena observed in rats fed the CLNA diet in the present study. Therefore, it was suggested that CLNA feeding affected hepatic lipid metabolism much more potently than did CLA. It seems likely that the accumulation of liver TG in the CLNA group may have resulted from a situation in which the amount of FA influx exceeded the ability of FA to oxidize in liver, even though the  $\beta$ -oxidation activity was considerably enhanced in these animals.

CLNA feeding resulted in a net reduction in adipose tissue weight. This effect was more potent than with CLA. Also, serum and liver TG concentrations were increased more than twofold by CLNA in contrast to CLA. The adipose tissue weight-reducing effect of CLNA may be related to a decrease either in TG deposition from circulation and/or in lipolysis in adipose tissues. Although the underlying mechanism is not clear at the moment, these findings indicate that CLNA modulates the body fat and TG metabolism differently from CLA in rats. Studies with a more purified form of CLNA are necessary before definite conclusions are drawn. Also, studies on the individual isomers of CLNA are important for future research. Some specific seed oils containing CLNA will be useful for this purpose.

## ACKNOWLEDGMENTS

We thank Eri Nishida, Ayako Shibuta, and Yukari Okawa for their technical support. A part of this study was supported by The Kieikai Research Foundation.

## REFERENCES

1. Ha, Y.L., Grimm, N.K., and Pariza, M.W. (1989) Newly Recognized Anticarcinogenic Fatty Acids: Identification and Quantitation in Natural and Processed Cheese, *J. Agric. Food Chem.* 37, 75–81.
2. Chin, S.F., Liu, W., Storkson, J.M., and Pariza, M.W. (1992) Dietary Source of Conjugated Diene Isomers of Linoleic Acid, a Novelty Recognized Class of Anticarcinogens, *J. Food Comp. Anal.* 5, 185–207.
3. West, D.B., De Lany, J.P., Camet, P.M., Blohm, F., Truett, A.A.,

- and Scimeca, J.A. (1998) Effects of Conjugated Linoleic Acid on Body Fat and Energy Metabolism in the Mouse, *Am. J. Physiol.* 275, R667–R672.
4. De Lany, J.P., Blohm, F., Truett, A.A., Scimeca, J.A., and West, D.B. (1999) Conjugated Linoleic Acid Rapidly Reduces Body Fat Content in Mice Without Affecting Energy Intake, *Am. J. Physiol.* 276, R1172–R1179.
  5. Berven, G., Bye, A., Hais, O., Blankson, H., Fagertun, H., Thom, E., Wadestein, J., and Gudmundsen, O. (2000) Safety of Conjugated Linoleic Acid (CLA) in Overweight or Obese Human Volunteers, *Eur. J. Lipid Sci.* 102, 455–462.
  6. Zambell, K.L., Keim N.L., Van Loan, M.D., Gale, B., Benito, P., Kelley, D.S., Nelson, G.J. (2000) Conjugated Linoleic Acid Supplementation in Humans: Effects on Body Composition and Energy Expenditure, *Lipids* 35, 777–782.
  7. Medina, E.A., Horn, W.F., Keim, N.L., Havel, P.J., Benito, P., Kelley, D.S., Nelson, G.J., and Erickson K.L. (2000) Conjugated Linoleic Acid Supplementation in Humans: Effects on Circulating Leptin Concentrations and Appetite, *Lipids* 35, 783–788.
  8. Blankson, H., Stakkestad, J.A., Fagertun, H., Thom, E., Wadestein, J., and Gudmundsen, O. (2000) Conjugated Linoleic Acid Reduces Body Fat Mass in Overweight and Obese Humans, *J. Nutr.* 130, 2943–2948.
  9. Smedman, A., and Vessby, B. (2001) Conjugated Linoleic Acid Supplementation in Humans—Metabolic Effects, *Lipids* 36, 773–781.
  10. Park, Y., Albright, K.J., Liu, W., Storkson, J.M., Cook, M.E., and Pariza, M.W. (1997) Effect of Conjugated Linoleic Acid on Body Composition in Mice, *Lipids* 32, 853–858.
  11. Park, Y., Storkson, J.M., Albright, K.J., Liu, W., and Pariza, M.W. (1999) Evidence that *trans*-10,*cis*-12 Isomer of Conjugated Linoleic Acid Induces Body Composition Changes in Mice, *Lipids* 34, 235–241.
  12. Lin, Y., Kreeft, A., Schuurbiens, J.A., and Draijer, R. (2001) Different Effects of Conjugated Linoleic Acid Isomers on Lipoprotein Lipase Activity in 3T3-L1 Adipocytes, *J. Nutr. Biochem.* 12, 183–189.
  13. Sakono, M., Miyanaga, F., Kawahara, S., Yamaguchi, K., Fukuda, N., Watanabe, K., Iwata, T., and Sugano, M. (1999) Dietary Conjugated Linoleic Acid Reciprocally Modifies Ketogenesis and Lipid Secretion by the Rat Liver, *Lipids* 34, 997–1000.
  14. Lee, K.N., Kritchevsky, D., and Pariza, M.W. (1994) Conjugated Linoleic Acid and Atherosclerosis in Rabbits, *Atherosclerosis* 108, 19–25.
  15. Krichevsky, D., Tepper, S.A., Wright, S., Tso, P., Czarnecki, S.K. (2000) Influence of Conjugated Linoleic Acid (CLA) on Establishment and Progression of Atherosclerosis in Rabbits, *J. Am. Coll. Nutr.* 19, 472S–477S.
  16. Belury, M.A., and Kempa-Steczko, A. (1997) Conjugated Linoleic Acid Modulates Hepatic Lipid Composition in Mice, *Lipids* 32, 199–204.
  17. Belury, M.A., Moya-Camarena, S.Y., Liu, K.L., and Heuvel, J.P.V. (1997) Dietary Conjugated Linoleic Acid Induces Peroxisome-Specific Enzyme Accumulation and Ornithine Decarboxylase Activity in Mouse Liver, *J. Nutr. Biochem.* 8, 579–584.
  18. Yamasaki, M., Mansho, K., Mishima, H., Kasai, M., Sugano, M., Tachibana, H., and Yamada, K. (1999) Dietary Effect of Conjugated Linoleic Acid on Lipid Levels in White Adipose Tissue of Sprague–Dawley Rats, *Biosci. Biotechnol. Biochem.* 63, 1104–1106.
  19. Horrobin, D.F., and Manku, M.S. (1983) How Do Polyunsaturated Fatty Acids Lower Plasma Cholesterol Levels? *Lipids* 18, 558–562.
  20. Sébédio, J.-L., Juaneda, P., Dobson, G., Ramilison, I., Martin, J.C., Chardigny, J.M., and Christie, W.W. (1997) Metabolites of Conjugated Isomers of Linoleic Acid (CLA) in the Rat, *Biochim. Biophys. Acta* 1345, 5–10.
  21. Banni, S., and Martin, J.C. (1998) Conjugated Linoleic Acid and Metabolites, in *Trans Fatty Acids in Human Nutrition* (Sébédio, J.-L., and Christie, W.W., eds.), pp. 261–302, Oily Press, Aberdeen, United Kingdom.
  22. Dhar, P., and Bhattacharyya, D.K. (1998) Nutritional Characteristics of Oil Containing Conjugated Octadecatrienoic Fatty Acid, *Ann. Nutr. Metab.* 42, 290–296.
  23. Igarashi, M., and Miyazawa, T. (2000) Newly Recognized Cytotoxic Effect of Conjugated Trienoic Fatty Acids on Cultures Human Tumor Cells, *Cancer Lett.* 148, 173–179.
  24. Suzuki, R., Noguchi, R., Ota, T., Abe, M., Miyashita, K., and Kawada, T. (2001) Cytotoxic Effect of Conjugated Trienoic Fatty Acids on Mouse Tumor and Human Monocytic Leukemia Cells, *Lipids* 36, 477–482.
  25. Igarashi, M., and Miyazawa, T. (2000) Do Conjugated Eicosapentaenoic Acid and Conjugated Docosahexaenoic Acid Induce Apoptosis via Lipid Peroxidation in Cultured Human Tumor Cells? *Biochem. Biophys. Res. Comm.* 270, 649–656.
  26. Kamegai, T., Kasai, M., and Ikeda, I. (2001) Improved Method for Preparation of the Methyl Ester of Conjugated Linoleic Acid, *J. Oleo Sci.* 50, 237–241.
  27. Banni, S., Carta, G., Contini, M.S., Angioni, E., Deiana, M., Dessi, M.A., Melis, M.P., and Corongiu, F.P. (1996) Characterization of Conjugated Diene Fatty Acids in Milk, Dairy Products, and Lamb Tissues, *J. Nutr. Biochem.* 7, 150–155.
  28. Reeves, P.G., Nielsen, F.H., and Fahey, G.C. (1993) AIN-93 Purified Diets for Laboratory Rodents: Final Report of the American Institute of Nutrition *Ad Hoc* Writing Committee on the Reformulation of the AIN-76A Rodent Diet, *J. Nutr.* 123, 1939–1951.
  29. Folch, J., Lees, M., and Slone-Stanley, G.H. (1957) A Simple Method for the Isolation and Purification of Total Lipids from Animal Tissues, *J. Biol. Chem.* 226, 497–509.
  30. Ide, T., Oku, H., and Sugano, M. (1982) Reciprocal Responses to Clofibrate in Ketogenesis and Triglyceride and Cholesterol Secretion in Isolated Rat Liver, *Metabolism* 31, 1065–1072.
  31. Rouser, G., Siakotos, A.N., and Fleischer, S. (1966) Quantitative Analysis of Phospholipids by Thin-Layer Chromatography and Phosphorus Analysis of Spots, *Lipids* 1, 85–86.
  32. Fletcher, M.J. (1968) A Calorimetric Method for Estimating Serum Triglycerides, *Clin. Chim. Acta* 22, 393–397.
  33. Lowry, O.H., Rosebrough, N.J., Farr, A.L., and Randall, R.J. (1951) Protein Measurement with Folin Phenol Reagent, *J. Biol. Chem.* 193, 265–275.
  34. Lieber, L.L., Abraham, T., and Helmrath, T. (1972) A Rapid Spectrophotometric Assay for Carnitine Palmitoyltransferase, *Anal. Biochem.* 50, 509–518.
  35. Lazarow, P.B. (1981) Assay of Peroxisomal  $\beta$ -Oxidation of Fatty Acids, *Methods Enzymol.* 72, 315–319.
  36. MacGarry J.D., and Brown, N.F. (1997) The Mitochondrial Carnitine Palmitoyltransferase System. From Concept to Molecular Analysis, *Eur. J. Biochem.* 244, 1–14.
  37. Ashakumary, L., Rouyer, I., Takahashi, Y., Ide, T., Fukuda, N., Aoyama, T., Hashimoto, T., Mizugaki, M., and Sugano, M. (1999) Sesamin, A Sesame Lignan, Is a Potent Inducer of Hepatic Fatty Acid Oxidation in the Rat, *Metabolism* 48, 1303–1313.
  38. Havel, R.J., and Kane, J.P. (1995) Structure and Metabolism of Plasma Lipoproteins, in *The Metabolic Basis of Inherited Disease*, 7th edn. (Scriver, C.R., Beaudet, A.L., Sly, W.S., and Valle, D., eds.), pp. 1841–1851, McGraw-Hill, New York.
  39. Dhar, P., Ghosh, S., and Bhattacharyya, D.K. (1999) Dietary Effects of Conjugated Octadecatrienoic Fatty Acid (9 *cis*, 11 *trans*, 13 *trans*) Levels on Blood Lipids and Nonenzymatic *in Vitro* Lipid Peroxidation in Rats, *Lipids* 34, 109–114.
  40. Halle, M., Berg, A., Northoff, H., and Keul, J. (1998) Importance of TNF- $\alpha$  and Leptin in Obesity and Insulin Resistance: A

- Hypothesis on the Impact of Physical Exercise, *Exerc. Immunol. Rev.* 4, 77–94.
41. Semb, H., Peterson, J., Tavernier, J., and Olivecrona, T. (1987) Multiple Effects of Tumor Necrosis Factor on Lipoprotein Lipase *in vivo*, *J. Biol. Chem.* 262, 8390–8394.
  42. Zhang, B., Berger, J., Hu, E., Szalkowski, D., White-Carrington, S., Spiegelman, B.M., and Moller, D.E. (1996) Negative Regulation of Peroxisome Proliferator-Activated Receptor- $\gamma$  Gene Expression Contributes to the Antiadipogenic Effects of Tumor Necrosis Factor- $\alpha$ , *Mol. Endocrinol.* 10, 1457–1466.
  43. Spiegelman, B.M. (1998) PPAR- $\gamma$ : Adipogenic Regulator and Thiazolidinedione Receptor, *Diabetes* 47, 507–514.
  44. Grimaldi, P.A. (2001) The Role of PPARs in Adipocyte Differentiation, *Prog. Lipid Res.* 40, 269–281.
  45. Bastard, J.P., Hainque, B., Dusserre, E., Bruckert, E., Robin, D., Vallier, P., Perche, S., Robin, P., Turpin, G., Jardel, C., et al. (1999) Peroxisome Proliferator Activated Receptor- $\gamma$ , Leptin and Tumor Necrosis Factor- $\alpha$  mRNA Expression During Very Low Calorie Diet in Subcutaneous Adipose Tissue in Obese Women, *Diabetes Metab. Res. Rev.* 15, 92–98.
  46. Zeghari, N., Vidal, H., Younsi, M., Ziegler, O., Drouin, P., and Donner, M. (2000) Adipocyte Membrane Phospholipids and PPAR- $\gamma$  Expression in Obese Women: Relationship to Hyperinsulinemia, *Am. J. Physiol. Endocrinol. Metab.* 279, E736–E743.
  47. Ricquier, D. (1998) Neonatal Brown Adipose Tissue. UCP1 and the Novel Uncoupling Proteins, *Biochem. Soc. Trans.* 26, 120–123.
  48. Masaki, T., Yoshimatsu, H., Chiba, S., Hidaka, S., Tajima, D., Kakuma, T., Kurokawa, M., and Sakata, T. (1999) Tumor Necrosis Factor- $\alpha$  Regulates *in vivo* Expression of the Rat UCP Family Differentially, *Biochim. Biophys. Acta* 1436, 585–592.
  49. Cook, W.S., Yeldandi, A.V., Rao, M.S., Hashimoto, T., and Reddy, J.K. (2000) Less Extrahepatic Induction of Fatty Acid  $\beta$ -Oxidation Enzymes by PPAR- $\alpha$ , *Biochem. Biophys. Res. Commun.* 278, 250–257.
  50. Moya-Camarena, S.Y., Van den Heuvel, J.P., Blanchard, S.G., Leesnitzer, L.A., and Belury, M.A. (1999) Conjugated Linoleic Acid Is a Potent Naturally Occurring Ligand and Activator of PPAR- $\alpha$ , *J. Lipid Res.* 40, 1426–1433.
  51. Moya-Camarena, S.Y., Van den Heuvel J.P., and Belury, M.A. (1999) Conjugated Linoleic Acid Activates Peroxisome Proliferator-Activated Receptor  $\alpha$  and  $\beta$  Subtypes but Does Not Induce Hepatic Peroxisome Proliferation in Sprague–Dawley Rats, *Biochim. Biophys. Acta* 1436, 331–342.

[Received October 15, 2001; accepted February 17, 2002]



# Effect of Sesaminol on Plasma and Tissue $\alpha$ -Tocopherol and $\alpha$ -Tocotrienol Concentrations in Rats Fed a Vitamin E Concentrate Rich in Tocotrienols

Kanae Yamashita<sup>a,\*</sup>, Saiko Ikeda<sup>a</sup>, Yoshie Iizuka<sup>a</sup>, and Ikuo Ikeda<sup>b</sup>

<sup>a</sup>Department of Food and Nutrition, Sugiyama Jogakuen University, Nagoya 464-8662, Japan, and <sup>b</sup>Laboratory of Nutrition Chemistry, Department of Bioscience and Biotechnology, Faculty of Agriculture, Graduate School Kyushu University, Fukuoka 812-8581, Japan

**ABSTRACT:** We have shown that sesame lignans added to rat diet resulted in significantly greater plasma and tissue concentrations of  $\alpha$ - and  $\gamma$ -tocopherol concentrations in supplemented rats than in rats without supplementation. In the present studies we examined whether sesaminol, a sesame lignan, enhances tocotrienol concentrations in plasma and tissues of rats fed diets containing a tocotrienol-rich fraction of palm oil (T-mix). In Experiment 1, effects of sesaminol on tocotrienol concentrations in plasma, liver, and kidney were evaluated in rats fed diets containing 20 mg/kg of T-mix (20T) and 50 mg/kg of T-mix (50T) with or without 0.1% sesaminol. Although the T-mix contained 23%  $\alpha$ -tocopherol, 22%  $\alpha$ -tocotrienol, and 34%  $\gamma$ -tocotrienol,  $\alpha$ -tocopherol constituted most or all of the vitamin E in plasma and tissue (from 97% in kidney to 100% in plasma), with no or very little  $\alpha$ -tocotrienol and no  $\gamma$ -tocotrienol at all. Addition of sesaminol to the T-mix resulted in significantly higher plasma, liver, and kidney  $\alpha$ -tocopherol concentrations compared to values for T-mix alone. Further, T-mix with sesaminol resulted in significantly higher  $\alpha$ -tocotrienol concentrations in kidney, although the concentration was very low. In Experiment 2, we examined whether sesaminol caused enhanced absorption of  $\alpha$ -tocopherol and  $\alpha$ -tocotrienol in a dosage regimen supplying T-mix and sesaminol on alternating days and observed significantly higher levels of  $\alpha$ -tocopherol and  $\alpha$ -tocotrienol in rats fed sesaminol, even without simultaneous intake, compared to those in rats without sesaminol. In Experiment 3,  $\alpha$ -tocopherol was supplied to the stomach with and without sesaminol, and  $\alpha$ -tocopherol concentrations in the lymph fluid were measured.  $\alpha$ -Tocopherol concentrations were not different between groups. These results indicated that sesaminol produced markedly higher  $\alpha$ -tocopherol concentrations in plasma and tissue and significantly greater  $\alpha$ -tocotrienol concentrations in kidney and various other tissues, but the concentrations of  $\alpha$ -tocotrienol were extremely low compared to those of  $\alpha$ -tocopherol (Exps. 1 and 2). However, the sesaminol-induced increases of  $\alpha$ -tocopherol and  $\alpha$ -tocotrienol concentrations in plasma and tissue were not caused by their enhanced absorption since sesaminol did not enhance their absorption.

Paper no. L8752 in *Lipids* 37, 351–358 (April 2002).

\*To whom correspondence should be addressed at Dept. of Food and Nutrition, School of Life Studies, Sugiyama Jogakuen University, 17-3 Hoshigaoka-Motomachi, Chikusa-ku, Nagoya, 464-8662, Japan.  
E-mail: kanaey@food.sugiyama-u.ac.jp

Abbreviations: AIN, American Institute of Nutrition;  $\alpha$ -CEHC, 2,5,7,8-tetramethyl-2 (2'-carboxyethyl)-6-hydroxychroman;  $\gamma$ -CEHC, 2,7,8-trimethyl-2 (2'-carboxyethyl)-6-hydroxychroman; T-mix, tocotrienol-rich fraction from palm oil containing  $\alpha$ -tocopherol; Toc, tocopherol; Toc3, tocotrienol;  $\alpha$ -TTP,  $\alpha$ -tocopherol transfer protein.

Sesame seed has long been used as a health food for its purported anti-aging effects, but it contains only  $\gamma$ -tocopherol and negligible amounts of  $\alpha$ -tocopherol, which suggests low physiological vitamin E activity. However, sesame seed contains substantial amounts of the characteristic lignans sesamin and sesaminol. In earlier experiments we found that sesame seed and its lignans produced elevated levels of  $\alpha$ - and  $\gamma$ -tocopherol concentrations in plasma and tissue (1–3). Subsequently, we investigated the mechanisms by which sesame lignans caused higher tocopherol concentration in rats. In a previous paper (4), we examined whether the secretion of tocopherols into bile was suppressed by sesame seed feeding. However, we found that concentrations of  $\alpha$ - or  $\gamma$ -tocopherol in bile showed a good correlation with concentrations of  $\alpha$ - or  $\gamma$ -tocopherol in liver. We concluded that suppression of tocopherol secretion into bile did not cause higher tocopherol levels in the rat body. Thus, as a further possibility, we decided to examine whether sesame lignans enhance absorption of tocopherols. In the present experiments we used a tocotrienol-rich palm oil fraction as a dietary source of vitamin E, since some papers have shown that tocotrienols concentrated in palm oil exhibit stronger functions than  $\alpha$ -tocopherol as antioxidants and antitumor agents (5–7). If sesame lignans produce higher tocotrienol concentrations in *in vivo* tests, tocotrienols with sesame lignans might show stronger effects than tocotrienol alone. Therefore, in the first experiment of the present series we attempted to determine whether sesame lignans produced higher tocotrienol concentrations following the use of sesaminol and a tocotrienol-rich fraction of palm oil containing some  $\alpha$ -tocopherol (T-mix). In these experiments we sought to determine whether sesaminol acted at the site of absorption and whether enhanced absorption of vitamin E was dependent on sesaminol being supplemented simultaneously with T-mix. In Experiment 2, we examined the effect of sesaminol on vitamin E concentrations in plasma and tissues of rats when given in a regimen that provided T-mix and sesaminol on alternating days. In Experiment 3, we measured the direct effects of sesaminol on  $\alpha$ -tocopherol concentrations in lymph fluid after  $\alpha$ -tocopherol had been supplied into the rat stomach with and without sesaminol.

## MATERIALS AND METHODS

**Materials.**  $\alpha$ -Tocopherol,  $\gamma$ -tocopherol, and vitamin E homologs used for biochemical analysis were gifts of Eisai Co.

(Tokyo, Japan). Pure  $\alpha$ -tocotrienol,  $\gamma$ -tocotrienol, and tocotrienol-rich palm oil fraction (T-mix) were gifts of Lion Corporation (Tokyo, Japan). Sesaminol (30% ethanol solution; 74.5% purity as solid) was donated by Takemoto Oil & Fat Co. (Aichi, Japan). Vitamin E-stripped corn oil was purchased from Funahashi Nogyo Co. (Chiba, Japan). A vitamin E-free vitamin mixture and a mineral mixture were both made according to AIN-76 formulation (8) by Nihon Nosan Kogyo (Yokohama, Japan). Solvents used for chromatography were HPLC grade from Katayama Chemicals Co., Ltd. (Osaka, Japan). Thiobarbituric acid was purchased from Merck (Darmstadt, Germany). All reagents for the measurement of pyruvate kinase (EC 2.7.1.40) activity were purchased from Boehringer-Mannheim Yamanouchi (Tokyo, Japan). All other chemicals were of analytical grade.

**Animals and diets.** Three-week-old male Wistar strain rats (Japan SLC Inc., Shizuoka, Japan) were housed individually in stainless-steel wire-mesh cages at 24.5°C and 55% RH, with a 12-h light/dark cycle in Experiments 1 and 2. Rats were maintained in accordance with the Guidelines for Animal Experimentation of Nagoya University. Rats were allowed free access to a nonpurified diet for 3–5 d and given an experimental diet for 8 wk. The experimental diets in Experiments 1 and 2 were in accordance with AIN-76 formulation (8) and consisted of 20% protein, 10% fat, vitamins excluding vitamin E, and minerals, as shown in Table 1. In Experiment 3, 8-wk-old male Sprague-Dawley rats (Seiwa Experimental Animals, Fukuoka, Japan) weighing 280–320 g were given *ad libitum* a commercial nonpurified diet (type NMF; Oriental Yeast Co., Tokyo, Japan) and drinking water. Rats were maintained in accordance with the

Guidelines for Animal Experimentation of Kyushu University.

In Experiment 1, effects of sesaminol on tocotrienol concentrations in plasma, liver, and kidney were evaluated in rats fed diets containing 20 mg/kg T-mix (20T) and 50 mg/kg T-mix (50T) with or without 0.1% sesaminol. We set up the vitamin E-free diet as a vitamin E-deficient control, 50 mg  $\alpha$ -tocopherol diet as a vitamin E-sufficient control, and 20T and 50T diets with or without sesaminol. Although the 20T diet was a vitamin E-insufficient diet, we anticipated more pronounced effects of sesaminol in this diet because sesaminol caused greater changes in a low  $\alpha$ -tocopherol diet than a normal vitamin E diet in our previous study (3). To examine the extent to which tocotrienols affected vitamin E activity in the 50T diet, this diet was compared to a 50 mg  $\alpha$ -tocopherol diet. 20T and 50T diets contained, respectively, 4.6 and 11.5 mg  $\alpha$ -tocopherol, 4.4 and 11.0 mg  $\alpha$ -tocotrienol (Toc3), 1 and 2.5 mg  $\beta$ -Toc3, 6.8 and 17.0 mg  $\gamma$ -Toc3, and 2 and 5 mg  $\delta$ -Toc3. Thirty-six rats were randomly divided into six groups and fed the diets shown in Table 1 for 8 wk.

Addition of sesaminol to 20T produced higher concentrations of  $\alpha$ -tocopherol in plasma and tissue than were found with 20T alone (Experiment 1). In Experiment 2, to clarify the mechanism by which sesaminol induced higher  $\alpha$ -tocopherol concentrations, we investigated whether sesaminol would cause enhanced absorption of  $\alpha$ -tocopherol. We thought that enhanced absorption would take place when  $\alpha$ -tocopherol and sesaminol were present at the absorption site at the same time. Group 1 was fed a diet containing 20T throughout; group 2 was fed a diet containing 40T and a vitamin E-free diet on alternating days, with a diet containing 40T on the final day

**TABLE 1**  
**Composition of Diets (Experiments 1 and 2)**

Experiment 1	Control (-E)	20 mg T-mix	20 mg T-mix + 0.1% sesaminol	50 mg T-mix	50 mg T-mix + 0.1% sesaminol	50 mg $\alpha$ -tocopherol
	g/kg diet					
Casein (-E)	200	200	200	200	200	200
Mineral mixture (AIN-76)	35	35	35	35	35	35
Vitamin mixture [AIN-76 (-E)]	10	10	10	10	10	10
Corn starch (-E)	655	655	651	655	654	655
Stripped corn oil	100	96	96	90	90	90
0.5% T-mix <sup>a</sup> in stripped corn oil		4	4	10	10	
0.5% $\alpha$ -Toc <sup>b</sup> in stripped corn oil						10
Sesaminol <sup>c</sup>			1		1	
Experiment 2	Control (-E)	20 mg T-mix	40 mg T-mix	0.2% Sesaminol		
g/kg diet						
Casein (-E)	200	200	200	200		
Mineral mixture (AIN-76)	35	35	35	35		
Vitamin mixture [AIN-76 (-E)]	10	10	10	10		
Cornstarch (-E)	655	655	655	647		
Stripped corn oil	100	96	92	100		
0.5% T-mix <sup>a</sup> in stripped corn oil		4	8			
Sesaminol <sup>c</sup>				2		

<sup>a</sup>Tocotrienol-rich fraction from palm oil that contained  $\alpha$ -Toc, 23%;  $\gamma$ -Toc, 0.4%;  $\alpha$ -Toc3, 22%;  $\beta$ -Toc3, 5%;  $\gamma$ -Toc3, 34%;  $\delta$ -Toc3, 10%. Abbreviations: Toc, tocopherol; Toc3, tocotrienol.

<sup>b</sup>Pure *RRR*- $\alpha$ -tocopherol.

<sup>c</sup>30% Ethanol solution, 78% purity as solid. The sesaminol-dissolving ethanol was canceled by reducing cornstarch.

(40T/-E/40T); group 3 was fed the same diet as group 2 except for a vitamin E-free diet on the final day (-E/40T/-E); group 4 was fed a diet containing 40T and a vitamin E-free with sesaminol diet on alternating days, with a diet containing 40T on the final day (40T/S/40T); and group 5 was fed the same diet as group 4 except for a vitamin E-free with sesaminol diet on the final day (S/40T/S). The rationale for the dietary groups was as follows: To ensure that all rats consumed nearly the same amount of T-mix as the animals in group 1, rats were fed a diet containing twice the amount T-mix on one day and a vitamin E-free diet or a vitamin E-free with sesaminol diet on the other day. Since we thought there might be a difference in  $\alpha$ -tocopherol concentration in rats fed 40T and rats fed vitamin E-free diet on the final day, we omitted T-mix for the two groups (groups 3 and 5) on the last day. After being on experiment for 8 wk, the animals were sacrificed.

In Experiment 1, we determined tocopherol and tocotrienol concentrations in plasma, liver, and kidney as well as TBARS in liver, red blood cell hemolysis, and plasma pyruvate kinase activity as indices of vitamin E status. In Experiment 2, only tocopherol and tocotrienol concentrations in plasma and tissues were determined. After 8 wk of feeding and 24 h of fasting, rats were anesthetized with Nembutal, and blood samples were drawn from the heart using heparinized needles and syringes. The tissues were excised after the liver had been perfused with physiological saline. A hemolysis test of red blood cells was conducted immediately after collection of blood samples. Plasma was prepared, and measurements of pyruvate kinase activity were made within 7 h after the rats were killed. The remaining plasma and tissues were kept at  $-80^{\circ}\text{C}$  until analysis. Tocopherol and tocotrienol concentrations in plasma and tissue as well as TBARS in liver were determined.

In Experiment 3, to obtain more direct evidence of  $\alpha$ -tocopherol absorption, we examined  $\alpha$ -tocopherol concentrations in the lymph fluid of rats supplied  $\alpha$ -tocopherol with and without sesaminol into the stomach. Sixteen rats were anesthetized with Nembutal; then an indwelling catheter was placed in the stomach and a cannula in the left thoracic lymphatic channel. Lymph fluid collections were performed according to the method described by Ikeda *et al.* (9). After administration of 3 mL of a test emulsion contained 200 mg sodium taurocholate, 50 mg FA-free albumin, 200 mg triolein, and 10 mg  $\alpha$ -tocopherol with or without 100 mg sesaminol, lymph fluid was collected for 24 h in four tubes containing EDTA, three tubes collected at 3-h intervals during the first 0–9 h, and one tube collected for 15 h during the latter 9–24 h.

*Analysis of samples.* Analytical procedures were essentially the same as described by Yamashita *et al.* (4). Tocopherol and tocotrienol concentrations in plasma and tissue were analyzed by HPLC according to the method of Ueda and Igarashi (10). Lymph fluid was treated in the same manner as plasma. Instrumentation used for HPLC was a Shimadzu Model LC-9A (Shimadzu, Kyoto, Japan) with a Shimadzu RF-535 fluorescence detector (excitation, 298 nm; emission, 325 nm). The analytical column used was a Develosil 60-5 (4.6 mm i.d.  $\times$  250 mm; Nomura Chemical, Aichi, Japan).

The mobile phase was hexane containing 1% (vol/vol) dioxan and 0.2% (vol/vol) isopropyl alcohol (99:1, vol/vol), and the flow rate was 1 mL/min. Lipid peroxides in liver were determined as TBARS by the thiobarbituric acid colorimetric method of Ohkawa *et al.* (11). Oxidative hemolysis of red blood cells was measured using dialuric acid (12). Plasma pyruvate kinase activity was determined according to the method described by Gutmann and Bernt (13).

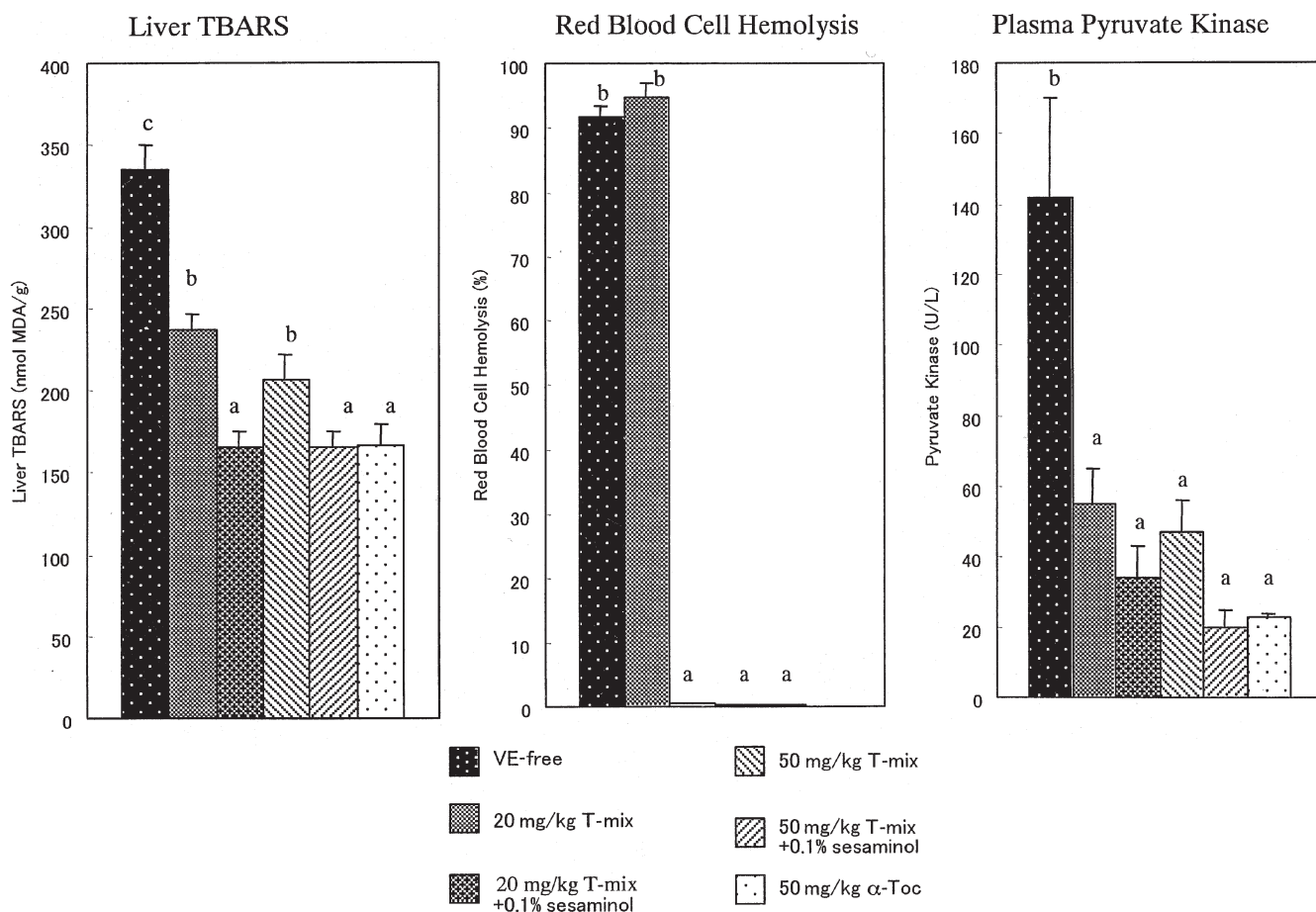
*Statistical analysis.* Data are expressed as mean  $\pm$  SEM. Experiments 1 and 2 were analyzed by using one-way ANOVA in SPSS Base 9.0 (Chicago, IL). When one-way ANOVA revealed  $P < 0.05$ , the data were further analyzed using Duncan's multiple comparisons test (14). Experiment 3 was performed by using Student's *t*-test to compare the effect with and without sesaminol. Differences were considered statistically significant at  $P < 0.05$ .

## RESULTS

In Experiment 1, the diets exhibited no significant effect on food intake or animal growth except for liver weight. As in our previous studies (1–3), we observed significantly greater liver weights (107–110%) in rats fed sesaminol-containing diets. We determined liver TBARS concentrations, red blood cell hemolysis, and plasma pyruvate kinase activity as vitamin E status indices. As shown in Figure 1, liver TBARS were significantly lower in the 20T and 50T groups than in the vitamin E-free group. The addition of sesaminol to the 20T and 50T diets significantly suppressed liver TBARS, and these values were nearly the same as those in the 50 mg  $\alpha$ -tocopherol control diet. Red blood cell hemolysis in the 20T group showed the same high value as in the vitamin E-free group, but the other groups showed almost no hemolysis. Plasma pyruvate kinase activity showed significantly higher activity in the vitamin E-free group than the other groups. Although the activities in the other groups were not statistically different, all groups showed similar patterns with respect to liver TBARS.

$\alpha$ -Tocopherol concentrations in plasma, liver, and kidney are shown in Figure 2. In spite of the greater intake of tocotrienol, vitamin E analogs detected were nearly all  $\alpha$ -tocopherol, with a very small amount of  $\alpha$ -tocotrienol. We could not detect  $\gamma$ -tocotrienol in the plasma, liver, or kidney. The groups receiving sesaminol had significantly higher  $\alpha$ -tocopherol concentrations than those receiving T-mix alone. In the kidney, supplementation of sesaminol to T-mix resulted in significantly higher concentrations of  $\alpha$ -tocotrienol compared to groups receiving T-mix alone, although the concentrations were extremely low compared to  $\alpha$ -tocopherol. Plasma  $\alpha$ -tocopherol, kidney  $\alpha$ -tocopherol, and kidney tocotrienol concentrations were not significantly different between the groups receiving 20T with sesaminol and 50T alone.

In Experiment 2, we investigated whether sesaminol enhanced the absorption of  $\alpha$ -tocopherol and  $\alpha$ -tocotrienol in rats fed a T-mix-containing diet. We examined whether sesaminol induced higher  $\alpha$ -tocopherol and  $\alpha$ -tocotrienol concentrations in plasma and tissue if rats were not fed sesaminol concurrently with T-mix. Plasma and tissue con-



**FIG. 1.** Effect of sesaminol on TBARS in liver, red blood cell hemolysis, and plasma pyruvate kinase activity. Thirty-six rats were divided into six groups and fed experimental diets for 8 wk. The experimental diets consisted of vitamin E-free (VE-free) as vitamin E-deficient control; 20 mg/kg of tocotrienol-rich palm oil (T-mix); 20 mg T-mix + 0.1% sesaminol; 50 mg T-mix; 50 mg T-mix + 0.1% sesaminol; and 50 mg  $\alpha$ -tocopherol ( $\alpha$ -Toc) as a vitamin E-sufficient control. The 20 and 50 mg/kg T-mix diets contained, respectively, 4.6 and 11.5 mg  $\alpha$ -Toc, 4.4 and 11.0 mg  $\alpha$ -tocotrienol ( $\alpha$ -Toc3), 1 and 2.5 mg  $\beta$ -Toc3, 6.8 and 17.0 mg  $\gamma$ -Toc3, and 2 and 5 mg  $\delta$ -Toc3. Values are means  $\pm$  SE of six rats. Values not sharing the same superscript letter are significantly different at  $P < 0.05$ . Abbreviation: MDA, malondialdehyde.

centrations of  $\alpha$ -tocopherol and  $\alpha$ -tocotrienol are shown in Table 2. All rats consumed nearly the same amounts of  $\alpha$ -tocopherol and  $\alpha$ -tocotrienol, and much larger amounts of  $\gamma$ -tocotrienol. In spite of these facts, almost all vitamin E detected in the plasma and tissue was  $\alpha$ -tocopherol. Small amounts of  $\alpha$ -tocotrienol were detected, but  $\gamma$ -tocotrienol was not detected in the plasma and tissue. Plasma and tissue concentrations of  $\alpha$ -tocopherol were below normal since rats were fed low vitamin E diets for 8 wk. In groups that received sesaminol on alternate days with 40T, significantly higher plasma and tissue concentrations of  $\alpha$ -tocopherol and  $\alpha$ -tocotrienol were observed. We detected very low concentrations of  $\alpha$ -tocotrienol in plasma and tissue, but there were differences in the ratios of  $\alpha$ -tocotrienol to  $\alpha$ -tocopherol in plasma and tissue. The ratios in plasma and tissue were high in sesaminol-fed groups, and those in liver and plasma were extremely low compared to those in kidney, adrenal, and testes. There were no significant differences in  $\alpha$ -tocopherol or  $\alpha$ -tocotrienol concentrations between groups 2 and 3, or groups 4 and 5, that is, between groups that were fed 40T and vitamin E-free diets on the final day except for concentrations of

$\alpha$ -tocopherol in liver and plasma and  $\alpha$ -tocotrienol in liver, testes, and lung.

In Experiment 3, we determined the  $\alpha$ -tocopherol recovered in the lymph fluid of rats intragastrically administered a test emulsion containing 10 mg  $\alpha$ -tocopherol with or without sesaminol. Lymph flow rate was linear during the experiments, and it was  $160.6 \pm 17.4$  and  $162.2 \pm 8.0$  mL for 24 h in rats given  $\alpha$ -tocopherol and  $\alpha$ -tocopherol with sesaminol, respectively. There was no significant difference between the groups. The results are shown as the percentage of  $\alpha$ -tocopherol in lymph fluid recovered over the experimental period from the 10 mg administered intragastrically, and as  $\alpha$ -tocopherol concentrations in lymph fluid collected at each interval. As shown in Figure 3, lymphatic recovery of  $\alpha$ -tocopherol was not enhanced by sesaminol.

## DISCUSSION

As shown in Figure 2, despite feeding with a mixture of  $\alpha$ -tocopherol,  $\alpha$ -tocotrienol and  $\gamma$ -tocotrienol, most of the vitamin E detected in plasma, liver, and kidney was  $\alpha$ -tocopherol;



a very slight concentration of  $\alpha$ -tocotrienol was found, but  $\gamma$ -tocotrienol was not found. These results agree with the tissue concentrations of tocopherols and tocotrienol in humans and hamsters found by Hayes *et al.* (15) and in humans by Mensink *et al.* (16). It is generally thought that discrimination between the structural forms of vitamin E in hepatic  $\alpha$ -tocopherol transfer protein ( $\alpha$ -TTP) caused these results (17–19). The addition of sesaminol to diets containing T-mix caused significantly higher concentrations of  $\alpha$ -tocopherol and  $\alpha$ -tocotrienol in plasma and tissue, but most vitamin E detected was still  $\alpha$ -tocopherol (90–99%). Liver  $\alpha$ -tocopherol concentration in the 20T with sesaminol group was lower than in the 50T group. However, liver TBARS concentration in the 20T with sesaminol group was lower than in the 50T (Fig. 1). This result could not be explained by the  $\alpha$ -tocopherol concentration, because the  $\alpha$ -tocopherol concentration in 50T was higher than in 20T with sesaminol. There are reports that sesaminol itself exhibits strong antioxidative activity *in vitro* and *in vivo* (20–22). Sesaminol might have contributed to the lower TBARS concentration in the 20T or 50T with sesaminol groups. Since the 20T diet contained insufficient vitamin E, hemolysis in this diet group had the same high level as in the vitamin E-free group. It is well known that hemolysis does not occur in proportion to the concentration of vitamin E in red blood cells but occurs below a certain critical concentration (12,23). We observed substantial hemolysis in animals consuming 20T, but not in 50T diets. Addition of sesaminol to 20T completely suppressed hemolysis. Plasma pyruvate kinase activity did not exhibit significant differences among groups except for vitamin E-free animals, but all groups showed similar patterns with respect to liver TBARS. These results indicated that sesaminol improved vitamin E indices in rats receiving 20T or 50T diets by promoting significantly higher  $\alpha$ -tocopherol concentrations and by possibly acting as antioxidant.

A further concern is how sesaminol produced higher  $\alpha$ -tocopherol and  $\alpha$ -tocotrienol concentrations *in vivo*. In a previous paper (4), we examined whether the secretion of tocopherol into the bile was suppressed with sesame seed feeding. However, we could not observe suppressed secretion of tocopherol into the bile in rats fed sesame seed. According to past studies, no discrimination exists among vitamin E analogs during absorption (24–26), but Hayes *et al.* (15) reported lower absorption of tocotrienols and Ikeda *et al.* (9) enhanced absorption of  $\alpha$ -tocotrienol. Further, Hirose *et al.* (27) reported sesamin, the main sesame lignan, suppressed cholesterol absorption. Therefore, we hypothesized that vitamin E absorption might be enhanced by sesaminol, and in Experiments 2 and 3, we examined the effect of sesaminol on absorption of vitamin E. Using a total of five groups in Experiment 2, we examined whether there were higher concentrations of vitamin E in plasma and tissue of rats fed sesaminol and T-mix on alternate days, not concurrently. As shown in Table 2, we observed significantly higher concentrations of  $\alpha$ -tocopherol and  $\alpha$ -tocotrienol in groups 4 and 5, fed sesaminol, than in groups 1, 2, and 3, not fed sesaminol. Even if rats were fed sesaminol 24 h after T-mix, sesaminol showed an effect similar to that

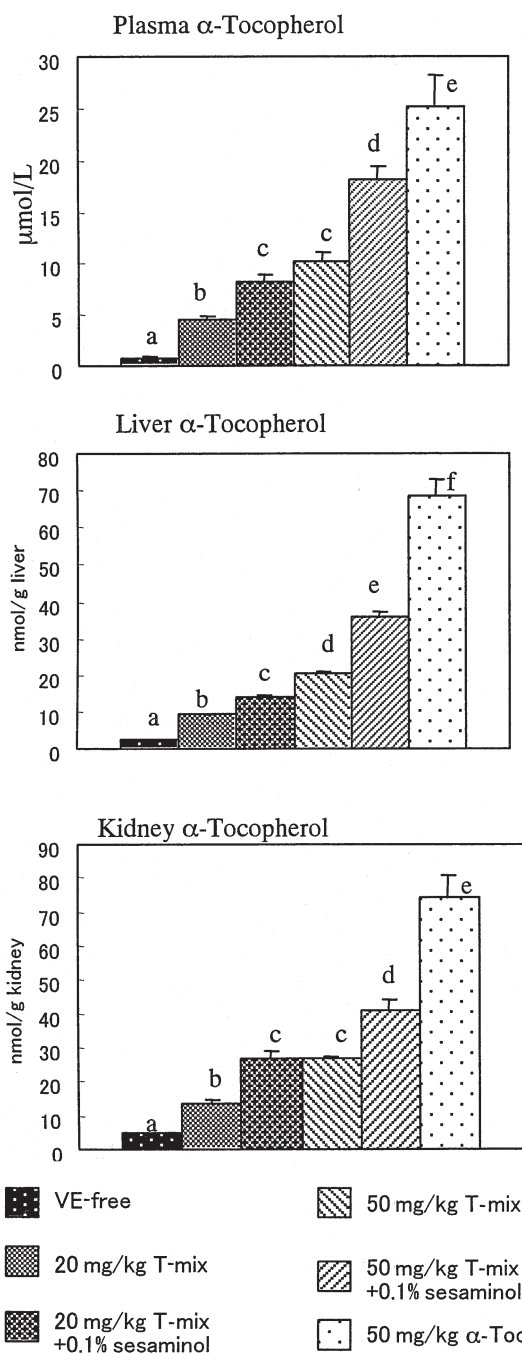


FIG. 2. Effect of sesaminol on  $\alpha$ -tocopherol concentrations in the plasma, liver, and kidney of rats fed diets containing 20 and 50 mg/kg T-mix. Values are means  $\pm$  SE of six rats. Values not sharing the same superscript letter are significantly different at  $P < 0.05$ . For abbreviations see Figure 1.

found with rats that were fed sesaminol and T-mix simultaneously in Experiment 1. These results indicated that the higher vitamin E concentrations with sesaminol were not caused by enhanced vitamin E absorption. Further, we knew that vitamin E concentrations *in vivo* did not significantly change 24 or 48 h after T-mix had been supplied because there were almost no significant differences in groups 2 and 3 or groups 4 and 5. In addition to Experiment 2, we found more direct evidence that

**TABLE 2**  
 **$\alpha$ -Tocopherol and  $\alpha$ -Tocotrienol Concentrations in the Plasma and Tissue of Rats in Experiment 2**

	20T <sup>a</sup> (Group 1)	40T/-E/40T <sup>b</sup> (Group 2)	-E/40T/-E <sup>c</sup> (Group 3)	40T/S/40T <sup>d</sup> (Group 4)	S/40T/S <sup>e</sup> (Group 5)
Liver <sup>f,g</sup>					
$\alpha$ -Tocopherol	7.27 $\pm$ 0.48 <sup>a</sup>	8.62 $\pm$ 0.24 <sup>b</sup>	7.04 $\pm$ 0.05 <sup>a</sup>	12.21 $\pm$ 0.40 <sup>c</sup>	13.13 $\pm$ 0.44 <sup>c</sup>
$\alpha$ -Tocotrienol	ND	0.04 $\pm$ 0.02 <sup>a</sup>	ND	0.13 $\pm$ 0.02 <sup>b</sup>	0.13 $\pm$ 0.02 <sup>b</sup>
$\alpha$ -Toc3/ $\alpha$ -Toc	—	1:216	—	1:94	1:101
Kidney <sup>f,g</sup>					
$\alpha$ -Tocopherol	6.84 $\pm$ 0.21 <sup>a</sup>	7.07 $\pm$ 0.32 <sup>a</sup>	7.05 $\pm$ 0.16 <sup>a</sup>	12.07 $\pm$ 0.44 <sup>b</sup>	13.32 $\pm$ 1.00 <sup>b</sup>
$\alpha$ -Tocotrienol	0.28 $\pm$ 0.03 <sup>a</sup>	0.39 $\pm$ 0.03 <sup>a</sup>	0.34 $\pm$ 0.03 <sup>a</sup>	1.13 $\pm$ 0.06 <sup>b</sup>	1.28 $\pm$ 0.10 <sup>b</sup>
$\alpha$ -Toc3/ $\alpha$ -Toc	1:24	1:18	1:20	1:11	1:10
Adrenal <sup>f,g</sup>					
$\alpha$ -Tocopherol	53.02 $\pm$ 3.37 <sup>a</sup>	61.33 $\pm$ 3.16 <sup>a</sup>	62.21 $\pm$ 3.35 <sup>a</sup>	97.60 $\pm$ 5.85 <sup>b</sup>	94.07 $\pm$ 4.54 <sup>b</sup>
$\alpha$ -Tocotrienol	2.23 $\pm$ 0.21 <sup>a</sup>	3.20 $\pm$ 0.29 <sup>a</sup>	2.41 $\pm$ 0.14 <sup>a</sup>	6.76 $\pm$ 0.71 <sup>b</sup>	6.30 $\pm$ 0.19 <sup>b</sup>
$\alpha$ -Toc3/ $\alpha$ -Toc	1:24	1:19	1:26	1:14	1:15
Testes <sup>f,g</sup>					
$\alpha$ -Tocopherol	13.28 $\pm$ 0.35 <sup>a</sup>	13.05 $\pm$ 0.60 <sup>a</sup>	13.12 $\pm$ 0.53 <sup>a</sup>	17.91 $\pm$ 0.53 <sup>b</sup>	18.28 $\pm$ 0.79 <sup>b</sup>
$\alpha$ -Tocotrienol	0.59 $\pm$ 0.01 <sup>a</sup>	0.67 $\pm$ 0.07 <sup>a</sup>	0.57 $\pm$ 0.05 <sup>a</sup>	1.31 $\pm$ 0.05 <sup>b</sup>	1.57 $\pm$ 0.12 <sup>c</sup>
$\alpha$ -Toc3/ $\alpha$ -Toc	1:23	1:19	1:23	1:13	1:12
Lung <sup>f,g</sup>					
$\alpha$ -Tocopherol	12.67 $\pm$ 0.26 <sup>a</sup>	13.93 $\pm$ 0.56 <sup>a</sup>	12.88 $\pm$ 0.46 <sup>a</sup>	20.14 $\pm$ 0.53 <sup>b</sup>	19.77 $\pm$ 0.35 <sup>b</sup>
$\alpha$ -Tocotrienol	0.40 $\pm$ 0.03 <sup>a</sup>	0.57 $\pm$ 0.03 <sup>b</sup>	0.36 $\pm$ 0.04 <sup>a</sup>	1.14 $\pm$ 0.06 <sup>c</sup>	1.00 $\pm$ 0.05 <sup>c</sup>
$\alpha$ -Toc3/ $\alpha$ -Toc	1:32	1:24	1:36	1:18	1:20
Plasma <sup>f,h</sup>					
$\alpha$ -Tocopherol	3.58 $\pm$ 0.21 <sup>a</sup>	4.23 $\pm$ 0.30 <sup>a</sup>	3.95 $\pm$ 0.18 <sup>a</sup>	7.74 $\pm$ 0.51 <sup>c</sup>	5.98 $\pm$ 0.41 <sup>b</sup>
$\alpha$ -Tocotrienol	0.04 $\pm$ 0.02 <sup>a</sup>	0.05 $\pm$ 0.02 <sup>a</sup>	0.03 $\pm$ 0.01 <sup>a</sup>	0.20 $\pm$ 0.06 <sup>b</sup>	0.13 $\pm$ 0.04 <sup>a,b</sup>
$\alpha$ -Toc3/ $\alpha$ -Toc	1:90	1:85	1:135	1:39	1:46

<sup>a</sup>Group 1 was fed throughout a diet containing 20 mg/kg T-mix (20T).

<sup>b</sup>Group 2 was fed on alternating days a diet containing 40 mg T-mix and a vitamin E-free diet, with a diet containing 40 mg/kg T-mix on the final day (40T/-E/40T).

<sup>c</sup>Group 3 was fed the same diet as group 2 but fed a vitamin E-free diet on the final day (-E/40T/-E).

<sup>d</sup>Group 4 was fed on alternating days a diet containing 40 mg/kg T-mix and a vitamin E-free with 2 g/kg sesaminol diet, with a diet containing 40 mg/kg T-mix on the final day (40T/S/40T).

<sup>e</sup>Group 5 was fed the same diet as Group 4 but fed a vitamin E-free with 2 g/kg sesaminol diet on the final day (S/40T/S).

<sup>f</sup>Values are means  $\pm$  SEM,  $n = 6$ , ND = not detected. Values with different superscript roman letters (a-c) in the same line are significantly different,  $P < 0.05$ .

<sup>g</sup>Units: nmol/g wt tissue.

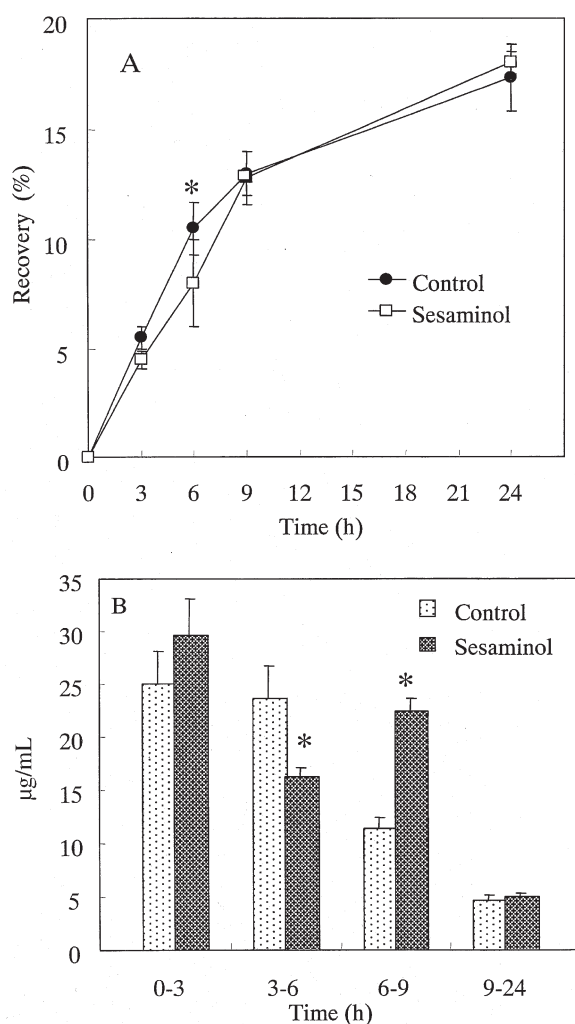
<sup>h</sup>Units:  $\mu$ mol/L.

sesaminol did not enhance the absorption of  $\alpha$ -tocopherol in Experiment 3, in which  $\alpha$ -tocopherol was supplied to the stomach with and without sesaminol, and  $\alpha$ -tocopherol concentration was determined in the lymph fluid (Fig. 3). Because enhanced absorption was not observed in rats fed sesaminol, we must consider other potential mechanisms by which sesaminol may enhance  $\alpha$ -tocopherol and  $\alpha$ -tocotrienol concentrations. As mentioned previously, sesaminol has strong antioxidative properties. Therefore, the antioxidative activity of sesaminol may act to produce a sparing effect on vitamin E, or to promote the recycling of vitamin E, as it does with vitamin C. To clarify such mechanisms, it might be fruitful to investigate the contributions of antioxidative activity in sesaminol to vitamin E concentrations.

There was organ specificity in the accumulation of tocotrienol (Table 2), since ratios of tocotrienol to tocopherol were low in liver and plasma compared to kidney, adrenal, testes, and lung. Addition of sesaminol to T-mix resulted in significantly higher ratios in all tissues and plasma. We could not determine why sesaminol produced the higher ratio of tocotrienol to tocopherol. Although the concentrations of tocotrienols were extremely low in plasma and tissue examined

in the present experiments, Podda *et al.* (28) reported significant presence of tocotrienols in skin of hairless mice, and Hayes *et al.* (15) reported substantial amounts of tocotrienols in adipose tissue of hamsters. We have also observed considerable quantities of  $\alpha$ - and  $\gamma$ -tocotrienols in the skin of rats and mice (29) and in adipose tissues of rats (30) fed diets containing the same T-mix as in the present experiment. At the present time, we are inclined to think that the skin and adipose tissue are unique tissues in which substantial amounts of tocotrienols exist in spite of the simultaneous presence of  $\alpha$ -tocopherol. These facts suggest that tocotrienols exhibit tissue specificity in acting as vitamin E.

Recently, Parker *et al.* (31) reported that the metabolism of  $\gamma$ -tocopherol to  $\gamma$ -carboxyethylhydroxy chroman ( $\gamma$ -CEHC) was inhibited by sesamin in rat primary hepatocytes. Possibly, the catabolism of  $\alpha$ -tocopherol and  $\alpha$ -tocotrienol to  $\alpha$ -CEHC is inhibited by sesaminol in the present experiments. Inhibition of tocopherol and tocotrienol catabolism by sesame lignans is the most likely cause of higher concentrations of tocopherols and tocotrienols in plasma and tissue. However, the concentrations of  $\alpha$ -tocotrienol were extremely small compared to those of  $\alpha$ -tocopherol. We need to consider the



**FIG. 3.** (A) Lymphatic recovery of  $\alpha$ -tocopherol in rats intragastrically administered a test emulsion containing  $\alpha$ -tocopherol with and without sesaminol, and (B)  $\alpha$ -tocopherol concentration in lymph fluid after administration of  $\alpha$ -tocopherol collected over 24 h at each time interval. The test emulsion contained 200 mg sodium taurocholate, 50 mg FA-free albumin, 200 mg triolein, and 10 mg  $\alpha$ -tocopherol with or without 100 mg sesaminol. An asterisk (\*) indicates significant difference between control and sesaminol groups,  $P < 0.01$  by Student's *t*-test.

contribution of  $\alpha$ -TTP and the modulated affinity of vitamin E to  $\alpha$ -TTP by sesame lignans, and will pursue this possibility in future research.

In the present studies we observed that sesaminol induced significantly higher concentrations of  $\alpha$ -tocopherol and  $\alpha$ -tocotrienol in rats fed diets containing palm oil extracts rich in  $\alpha$ -tocopherol,  $\alpha$ -tocotrienol, and  $\gamma$ -tocotrienol than in controls, and further, that sesaminol may have acted as an antioxidant *in vivo*. The results of Experiments 2 and 3 indicated that the higher concentrations of  $\alpha$ -tocopherol and  $\alpha$ -tocotrienol induced by sesaminol were not caused by their enhanced absorption.

#### ACKNOWLEDGMENTS

This study was supported by a grant-in-aid for scientific research (C) from the Ministry of Education, Science and Culture Japan and the

Science Research Promotion Fund from the Japan Private School Promotion Foundation.

#### REFERENCES

1. Yamashita, K., Nohara, Y., Katayama, K., and Namiki, M. (1992) Sesame Seed Lignans and  $\gamma$ -Tocopherol Act Synergistically to Produce Vitamin E Activity in Rats, *J. Nutr.* **122**, 2440–2446.
2. Imai, T., Iizuka, Y., Namiki, M., and Yamashita, K. (1995) Marked Increase of  $\alpha$ -Tocopherol Concentration in Rats Fed Sesame Seed, *J. Home Econ. Jpn.* **46**, 627–633.
3. Yamashita, K., Iizuka, Y., Imai, T., and Namiki, M. (1995) Sesame Seed and Its Lignans Produce Marked Enhancement of Vitamin E Activity in Rats Fed a Low  $\alpha$ -Tocopherol Diet, *Lipids* **30**, 1019–1028.
4. Yamashita, K., Takeda, N., and Ikeda, S. (2000) Effects of Various Tocopherol-Containing Diets on Tocopherol Secretion into Bile, *Lipids* **35**, 163–170.
5. Theriault, A., Chao, J., Wang, Q., Gapor, A., and Adeli, K. (1999) Tocotrienol: A Review of Its Therapeutic Potential, *Clin. Biochem.* **32**, 309–319.
6. Kamat, J.P., Sarma, H.D., Devasagayam, T.P.A., Nesaretnam, K., and Basiron, Y. (1997) Tocotrienols from Palm Oil as Effective Inhibitors of Protein Oxidation and Lipid Peroxidation in Rat Liver Microsomes, *Mol. Cell. Biochem.* **170**, 131–138.
7. McIntyre, B.S., Briski, K.P., Tirmenstein, M.A., Fariss, M.W., Gapor, A., and Sylvester, P.W. (2000) Antiproliferative and Apoptotic Effects of Tocopherols and Tocotrienols on Normal Mouse Mammary Epithelial Cells, *Lipids* **35**, 171–180.
8. American Institute of Nutrition (1977) Report of the American Institute of Nutrition *ad hoc* Committee on Standards for Nutritional Studies, *J. Nutr.* **107**, 1340–1348.
9. Ikeda, I., Imasato, Y., Sasaki, E., and Sugano, M. (1996) Lymphatic Transport of  $\alpha$ -,  $\gamma$  and  $\delta$ -Tocotrienols and  $\alpha$ -Tocopherol in Rats, *Int. J. Vitam. Nutr. Res.* **66**, 217–221.
10. Ueda, T., and Igarashi, O. (1987) New Solvent System for Extraction of Tocopherols from Biological Specimens for HPLC Determination and the Evaluation of 2,2,5,7,8-Pentamethyl-6-chromanol as an Internal Standard, *J. Micronutr. Anal.* **3**, 185–198.
11. Ohkawa, H., Ohishi, N., and Yagi, K. (1979) Assay for Lipid Peroxides in Animal Tissues by Thiobarbituric Acid Reaction, *Anal. Biochem.* **95**, 351–358.
12. Mino, M., Kitagawa, M., and Nakagawa, S. (1981) Changes of  $\alpha$ -Tocopherol Levels in Red Blood Cells and Plasma with Respect to Hemolysis Induced by Dialuric Acid in Vitamin E-Deficient Rats, *J. Nutr. Sci. Vitaminol.* **27**, 199–207.
13. Gutmann, I., and Bernt, E. (1974) Pyruvate Kinase Assay in Serum and Erythrocytes, in *Methods of Enzymatic Analysis* (Bergmeyer, H.U., ed.), Vol. 2, pp. 774–778.
14. Duncan, D.B. (1957) Multiple Range Tests for Correlated and Heteroscedastic Means, *Biometrics* **13**, 164–176.
15. Hayes, K.C., Pronczuk, A., and Liang, J.S. (1993) Differences in the Plasma Transport and Tissue Concentrations of Tocopherols and Tocotrienols: Observations in Humans and Hamsters, *Proc. Soc. Exp. Biol. Med.* **202**, 353–359.
16. Mensink, R.P., Houwelingen, A.C., and Hornstra, G. (1999) A Vitamin E Concentrate Rich in Tocotrienols Had No Effect on Serum Lipids, Lipoproteins, or Platelet Function in Men with Mildly Elevated Serum Lipid Concentrations, *Am. J. Clin. Nutr.* **69**, 213–219.
17. Catignani, G.L., and Bieri, J.G. (1977) Rat Liver  $\alpha$ -Tocopherol Binding Protein, *Biochim. Biophys. Acta* **497**, 349–357.
18. Traber, M.G., and Kaden, H.J. (1989) Preferential Incorporation of  $\alpha$ -Tocopherol vs.  $\gamma$ -Tocopherol in Human Lipoproteins, *Am. J. Clin. Nutr.* **49**, 518–526.

19. Sato, Y., Hagiwara, K., Arai, H., and Inoue, K. (1991) Purification and Characterization of the  $\alpha$ -Tocopherol Transfer Protein from Rat Liver, *FEBS Lett.* 288, 41–45.
20. Kang, M.-H., Katsuzaki, H., and Osawa, T. (1998) Inhibition of 2,2'-Azobis(2,4-dimethylvaleronitrile)-Induced Lipid Peroxidation by Sesaminol, *Lipids* 33, 1031–1036.
21. Kang, M.-H., Kawai, Y., Naito, M., and Osawa, T. (1999) Dietary Defatted Sesame Flour Decreases Susceptibility to Oxidative Stress in Hypercholesterolemic Rabbits, *J. Nutr.* 129, 1885–1890.
22. Kang, M.-H., Naito, M., Sakai, K., Uchida, K., and Osawa, T. (2000) Mode of Action of Sesame Lignans in Protecting Low-Density Lipoprotein Against Oxidative Damage *in vitro*, *Life Sci.* 66, 161–171.
23. Mino, M., Nishida, Y., Murata, K., Kakegawa, M., Katsui, G., and Yuguchi, Y. (1978) Studies on the Factors Influencing the Hydrogen Peroxide Hemolysis Test, *J. Nutr. Sci. Vitaminol. (Tokyo)* 24, 383–395.
24. Peake, I.R., Windmueller, H.G., and Bieri, J.G. (1972) A Comparison of the Intestinal Absorption, Lymph and Plasma and Tissue Uptake of Alpha and Gamma Tocopherols in the Rat, *Biochim. Biophys. Acta* 260, 679–688.
25. Traber, M.G., Kayden, H.J., Green, J.B., and Green, M.H. (1986) Absorption of Water-Miscible Forms of Vitamin E in a Patient with Cholestasis and in Thoracic Duct-Cannulated Rats, *Am. J. Clin. Nutr.* 44, 914–923.
26. Traber, M.G., Burton, G.W., Hughes, L., Ingold, K.U., Hidaka, H., Malloy, M., Kane, J., Hyams, J., and Kayden, H. (1992) Discrimination Between Forms of Vitamin E by Humans With and Without Genetic Abnormalities of Lipoprotein Metabolism, *J. Lipid Res.* 33, 1171–1182.
27. Hirose, N., Inoue, T., Sugano, M., Akimoto, K., Shimizu, S., and Yamada, H. (1991) Inhibition of Cholesterol Absorption and Synthesis in Rats by Sesamin, *J. Lipid Res.* 32, 629–638.
28. Podda, M., Weber, C., Traber, M.G., and Packer, L. (1996) Simultaneous Determination of Tissue Tocopherols, Tocotrienols, Ubiquinol, and Ubiquinones, *J. Lipid Res.* 37, 893–901.
29. Ikeda, S., Niwa, T., and Yamashita, K. (2000) Selective Uptake of Dietary Tocotrienols into Rat Skin, *J. Nutr. Sci. Vitaminol. (Tokyo)* 46, 141–143.
30. Ikeda, S., Toyoshima, K., and Yamashita, K. (2001) Dietary Sesame Seeds Elevate  $\alpha$ - and  $\gamma$ -Tocotrienol Concentrations in Skin and Adipose Tissue of Rats Fed Tocotrienol-Rich Fraction Extracted from Palm Oil, *J. Nutr.* 131, 2892–2897.
31. Parker, R.S., Sontag, T.J., and Swanson, J.E. (2000) Cytochrome P4503A-Dependent Metabolism of Tocopherols and Inhibition by Sesamin, *Biochem. Biophys. Res. Commun.* 277, 531–534.

[Received February 16, 2002, and in final revised form and accepted February 25, 2002]



# Effects of Dietary Lipids on Daunomycin-Induced Nephropathy in Mice: Comparison Between Cod Liver Oil and Soybean Oil

Takayasu Ohtake<sup>a,1</sup>, Masato Kimura<sup>b,\*</sup>, Hitomi Takemura<sup>b</sup>, and Akira Hishida<sup>c</sup>

<sup>a</sup>Department of Medicine, Fujinomiya City General Hospital, Fujinomiya, Japan, <sup>b</sup>Shizuoka University School of Nursing, Shizuoka, Japan, and <sup>c</sup>First Department of Medicine, Hamamatsu University School of Medicine, Hamamatsu, Japan

**ABSTRACT:** Although it is well known that dietary lipids affect the course of glomerulonephritis in rats and humans, the precise mechanisms involved have not been fully elucidated. The aim of this study was to investigate the effects of different types of dietary lipids (fish oil and vegetable oil) on daunomycin (DM)-induced nephropathy in mice fed on soybean oil (SO) or cod liver oil (CLO). Urinary protein excretion, serum albumin, creatinine, total cholesterol, and TG were measured, and glomerular histological changes were evaluated. Antioxidant enzymes were also measured, along with the levels of lipid peroxide, GSH, thromboxane (Tx) B<sub>2</sub>, and 6-keto prostaglandin F<sub>1α</sub> in renal cortical tissue. Dietary CLO significantly reduced urinary albumin excretion and ameliorated the histological changes induced by DM. The increase of tissue lipid peroxide levels seen in SO-fed mice was suppressed in CLO-fed mice, whereas CLO-fed mice showed higher GSH levels than SO-fed mice throughout the experiment. In addition, renal tissue GSH peroxidase activity was significantly higher at 72 h after DM injection in CLO-DM mice than in SO-DM mice. Both renal cortical TxB<sub>2</sub> and 6-keto PGF<sub>1α</sub> levels were significantly lower in CLO-DM mice than in SO-DM mice. These results suggest that inhibition of oxidative damage by dietary CLO played an important role in the prevention of DM nephropathy in this mouse model. The effect of CLO was closely associated with the inhibition of Tx synthesis.

Paper no. L8896 in *Lipids* 37, 359–366 (April 2002).

Daunomycin (DM), an anthracycline compound, induces nephropathy and massive proteinuria in rats and mice after a single injection (1,2). Although two well-known biological mediators, eicosanoids and reactive oxygen species (ROS), have been suggested to cause the nephrotoxicity of anthracyclines (3–6), the exact mechanisms underlying anthracycline nephropathy have not been fully established.

<sup>1</sup>Current address: Department of Medicine, Shonan Kamakura General Hospital, 1201-1, Yamazaki, Kamakura 247-8533, Japan.

\*To whom correspondence should be addressed at Shizuoka University School of Nursing, 52-1 Yada, Shizuoka 422-8526, Japan.  
E-mail: kimura@u-shizuoka-ken.ac.jp

Abbreviations: AA, arachidonic acid; ADR, adriamycin; AOE, antioxidant enzyme; CLO, cod liver oil; CyA, cyclosporin A; DM, daunomycin; DMTU, dimethylthiourea; FO, fish oil; GSH-Px, glutathione peroxidase; PG, prostaglandin; PL, phospholipase; ROS, reactive oxygen species; SO, soybean oil; SOD, superoxide dismutase; Tx, thromboxane.

Remuzzi *et al.* (3) demonstrated that glomerular thromboxane (Tx)A<sub>2</sub> production was increased at 14 and 30 d after a single injection of adriamycin (ADR) in rats, whereas administration of selective Tx synthetase inhibitors for 14 to 18 d after ADR injection caused a significant reduction of proteinuria. Accordingly, increased Tx production was thought to be responsible for proteinuria by altering glomerular basement membrane permeability to protein, but why the generation of TxA<sub>2</sub> increased in ADR nephropathy was not clarified. Milner *et al.* (4) found that dimethylthiourea (DMTU), a hydroxyl radical scavenger, prevented glomerular injury in rats with ADR nephropathy, and Okasora *et al.* (5) demonstrated that administration of superoxide dismutase (SOD) together with ADR suppressed the development of proteinuria in rats.

We previously reported the existence of differences in the nephrotoxicity of DM among several strains of inbred mice (2). We found that A/J and BALB/c mice were sensitive to DM, whereas C57BL/6J, DAB-2, and B10D2/o mice were resistant. Using DM-sensitive A/J mice and DM-resistant C57BL/6J mice, we also found that DM nephropathy seemed to be mediated by ROS and that intrinsic antioxidant enzymes (AOE), including SOD and glutathione peroxidase (GSH-Px), apparently play an important role in modulating the sensitivity to DM (6).

Recently, fish oil (FO) supplementation has been reported to improve renal damage when compared to vegetable oil supplementation in rats with ADR nephropathy (7,8). Ito *et al.* (7) reported that the beneficial effect of FO was related to reduced glomerular production of TxA<sub>2</sub> and a decrease of circulating lipids, and Barcelli *et al.* (8) found that FO decreased the production of TxB<sub>2</sub>, prostaglandin (PG)E<sub>2</sub>, and 6-keto-PGF<sub>1α</sub> in isolated glomeruli. However, there has been no investigation of the effect of FO on oxidative renal damage mediated by ROS, even though this is thought to be one of the major factors in anthracycline nephropathy (4–6).

Soybean oil (SO) is the usual dietary lipid source in standard laboratory chow, and injection of DM causes severe nephropathy in standard chow-fed A/J mice (2,6). In the present study, we used SO for the control and cod liver oil (CLO) for the experimental dietary lipid. Although we did not compare a typical control diet with the FO diet, it was thought to be meaningful to clarify the effects of these lipids on DM

nephropathy. Accordingly, we investigated (i) the effects of two different dietary lipids (SO and CLO) on DM nephropathy in mice and (ii) how dietary lipids modified oxidative damage, AOE activity, and eicosanoid production in renal tissue during the course of DM nephropathy.

## MATERIALS AND METHODS

**Animals and diets.** Inbred male A/J mice were bred in our laboratory. They had free access to standard laboratory chow and water. After weaning at 4 wk of age, they were allocated to two indicated isocaloric diets containing 7% SO or 6% CLO plus 1% SO. The reason for the 1% SO supplement to the latter diet was to supply EFA. The composition of diets after the addition of fat was: cornstarch 40.5% w/w, casein 25% w/w,  $\alpha$ -starch 10% w/w, cellulose powder 8% w/w, fat 7% w/w (two different types as mentioned above), minerals 3.5% w/w, granulated sugar 5% w/w, and vitamins 1% w/w (Oriental Yeast Co. Ltd., Tokyo, Japan). FA composition varied between SO and CLO as described in Table 1. The contents of antioxidants in the SO and CLO diets were analyzed at the Japan Food Research Laboratories and were found to be almost identical between the two diets, i.e., vitamin E of 74 and 70 mg/kg, and vitamin C of 56 and 58 mg/kg in the SO and CLO diets, respectively. And the content of selenium, which is a substrate of GSH-Px, was also identical, i.e., 0.16 and 0.15 mg/kg in SO and CLO diets, respectively. Diets were kept at 4°C in airtight bags and provided daily to minimize autoxidation of dietary lipids. Paired feeding was applied, with the amount of daily diet adjusted to the lower food consumptions of the two groups throughout the experiment. Since the SO-fed mice ate their food more quickly than the CLO-fed mice, the food receptacle in the SO-fed group was not refilled until the CLO-fed group had finished their ration. Food consumption was 7 g/mouse/d and yielded a calorie intake of almost 28 kcal/mouse/d in both groups at the time of saline or DM injection.

**Study design.** Mice were pair-fed for 10 wk, i.e., 8 wk before and 2 wk after DM injection, and body weights were recorded weekly. Eight weeks after the diets had started, mice

were injected with DM, 20 mg/kg body weight, or a vehicle (saline) through the tail vein, and they were divided into four groups, i.e., SO-DM: DM-injected mice with SO diet; SO-C: saline-injected mice with SO diet; CLO-DM: DM-injected mice with CLO diet; CLO-C: saline-injected mice with CLO diet. Before and 7 and 14 d after injection, 24-h urine samples were collected in the metabolic cages. Fifteen days after injection, mice were anesthetized with diethyl ether and blood was obtained *via* a cardiac puncture. Blood samples were assayed for albumin, creatinine, total cholesterol, and TG concentrations. After blood sampling, the kidneys were removed and fixed in 10% neutral buffered formalin solution for histological study. This study was approved by the research committees in the Shizuoka University School of Nursing and the Hamamatsu University School of Medicine.

**Analytical methods.** (i) *Serum and urine.* The urinary concentration of albumin was measured with a radial immunodiffusion method using rabbit anti-mouse albumin serum (9). Twenty-four-hour urine samples were collected in a small plastic tube. Urine volumes were less than 2 mL both in the basal state and after the onset of nephritis. All samples were diluted to 2 mL with saline solution and applied to immunodiffusion. The protein concentration in the tissue homogenate was determined by the method of Lowry *et al.* (10) with crystalline bovine albumin used as the standard. Serum concentrations of albumin and creatinine were measured with the bromocresol green method and Jaffe's reaction, respectively, using a Hitachi 736 autoanalyzer (Hitachi, Ltd., Tokyo, Japan). TG and cholesterol were measured by enzymatic methods on a Hitachi autoanalyzer.

(ii) *Morphological studies.* Formalin-fixed renal tissue was stained with periodic acid-Schiff. Mesangial matrix expansion, ballooning of the glomerular epithelial cells, and intracapillary thrombi are the characteristics of DM-induced glomerulopathy. These glomerular morphological changes were evaluated in all four groups 15 d after DM or saline injection. (i) Mesangial matrix expansion was graded from 0 to 4: Grade 1 represented minimal expansion involved in less than 25% of tufts, and grade 4, severe expansion in almost all tuft areas, while intermediate scores were assigned arbitrarily according to the severity and extent. The mean scores of 20 glomeruli per mouse, were calculated and five mice in each group were evaluated. (ii) One hundred glomeruli per mouse were used to estimate the ballooning change. If at least one epithelial ballooning was seen in a glomerulus, it was estimated as positive. The total positive glomerular numbers of 100 glomeruli were counted in five mice from each group. (iii) Intracapillary thrombus formation was evaluated in the same way as the epithelial ballooning. A positive grading means that the glomerulus had at least one thrombus in its tufts. The positive glomerular numbers of 100 glomeruli were counted in five mice from each group.

(iii) *Tissue preparation.* For the measurements of lipid peroxide and AOE (SOD, catalase, and GSH-Px) and reduced GSH content in the renal cortex, 8 to 11 mice from each group (mentioned before) were sacrificed before and 24 and 72 h

**TABLE 1**  
**FA Composition of Lipids**

FA	Oil (%)	
	Soybean	Cod liver
14:1	—	4.7
16:0	10.3	12.4
16:1	0.1	7.2
18:0	3.8	2.2
18:1 (oleic)	24.3	18.5
18:2 (linoleic)	52.7	1.0
18:3 ( $\alpha$ -linoleic)	7.9	0.6
20:0	0.3	6.5
20:4 (arachidonic)	—	0.6
20:5 (EPA)	—	11.6
22:0	0.4	10.6
22:6 (DHA)	—	10.2

after injection with DM or saline. The kidneys were perfused with cold saline. The renal cortical tissues were collected and frozen in liquid nitrogen. Tissue samples were stored at  $-85^{\circ}\text{C}$  until the analyses.

Renal cortical  $\text{TxB}_2$  (a stable metabolite of  $\text{TxA}_2$ ) and 6-keto  $\text{PGF}_{1\alpha}$  (a stable metabolite of  $\text{PGL}_2$ ) contents were measured 24 and 72 h after DM injection. Five mice from each group were sacrificed at the indicated times. Kidneys were perfused with 5 mL of ice-cold saline containing EDTA (10 mM) and indomethacin (0.1 mM), as used in the previous paper (11). The renal cortical tissue was immediately excised and stored at  $-85^{\circ}\text{C}$  until the analyses.

**Lipid peroxide measurement.** Tissue lipid peroxide content was determined as described previously (6). Cortical tissue (15–20 mg) in each tissue sample was used for the assay, and the fluorescence intensity of the *n*-butanol layer was measured using a spectrofluorometer FP-777 (Japan Spectroscopic Co., Ltd., Tokyo, Japan). The set wavelengths were excitation at 515 nm and emission at 535 nm, and 0.1–1.0 nmol of 1,1,3,3-tetramethoxypropane solution was used as the standard. Data are expressed as nmol/mg protein.

**Measurement of AOE activities and GSH content.** SOD, catalase, and GSH-Px activities and GSH content in the cortical tissue were measured as described before (6). SOD activity was expressed as units of nitrite per mg of protein. Catalase activity was calculated as *K*, the rate constant of a first-order reaction,  $\text{s}^{-1}/\text{mg}$  protein, and GSH-Px activity was expressed as nanomoles of NADPH oxidized to NADP per minute per milligram of protein, using the extinction coefficient of NADPH at 340 nm,  $6.22 \times 10^3 \text{ mol}^{-1} \text{ cm}^{-1}$ . The content of GSH was expressed as nanomoles per milligram of protein.

**Measurement of  $\text{TxB}_2$  and 6-keto  $\text{PGF}_{1\alpha}$ .** About 30 mg of renal cortical tissue was homogenized in 3 mL of 95% ethanol at  $4^{\circ}\text{C}$  and then centrifuged at  $600 \times g$  for 10 min. Then the supernatant was used for measurements of arachidonic acid (AA) metabolites by radioimmunoassay methods ( $^{125}\text{I}$ - $\text{TxB}_2$  and  $^{125}\text{I}$ -6-keto  $\text{PGF}_{1\alpha}$  kit; Daiichi RI, Tokyo, Japan) as used in the previous paper (11). Data are expressed as pg/mg protein.

**Statistics.** Results are presented as mean  $\pm$  SEM. Differences between groups were determined by ANOVA and two-tailed Student's *t*-test. A level of  $P < 0.05$  was accepted as significant.

## RESULTS

**Effect of dietary lipids on body weight.** The body weights in the two diet groups (10 mice in each group) are shown in Table 2. No significant difference was observed at various intervals under paired feeding.

**Effect of dietary lipids on urinary albumin excretion and serum parameters.** Urinary albumin excretion is shown in Figure 1. The basal urinary albumin excretion was less than 0.1 mg/d in both dietary groups. A significant increase in urinary albumin was observed in the SO-DM mice 1 wk after DM injection. Two weeks after injection, a further elevation

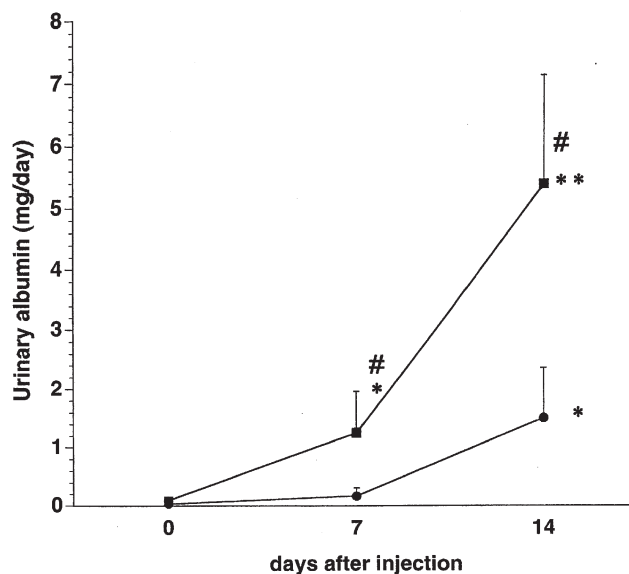
**TABLE 2**  
Effect of Dietary FA Substitution on Body Weight<sup>a</sup>

Age (wk)	Body weights (g)	
	Soybean oil diet	Cod liver oil diet
4	15.1 $\pm$ 0.48	15.6 $\pm$ 0.52
6	19.4 $\pm$ 0.51	21.0 $\pm$ 0.94
8	21.9 $\pm$ 0.41	23.0 $\pm$ 0.68
10	24.7 $\pm$ 0.75	25.2 $\pm$ 1.02
12	26.0 $\pm$ 0.73	25.6 $\pm$ 1.02

<sup>a</sup>The temporal change in body weight of soybean oil-fed and cod liver oil-fed mice from day of weaning to the day of injection. Data are expressed as mean  $\pm$  SEM ( $n = 10$  for each diet group).

of albumin excretion was observed in this group. The CLO-DM mice did not show a significant increase in albuminuria on day 7. Thereafter, the albuminuria on day 14 in CLO-DM mice significantly increased when compared to control mice (CLO-C), but it was significantly lower than that in SO-DM mice ( $1.51 \pm 0.86$  vs.  $5.41 \pm 1.76$  mg/d,  $P < 0.05$ ).

Serum parameters on day 15 are presented in Table 3. The serum creatinine and TG levels were not different among the four groups. Serum albumin levels significantly decreased in SO-DM mice compared to the other three groups. In contrast, they were not significantly decreased by DM injection in CLO-DM mice. The total cholesterol level was significantly higher in SO-DM mice. The cholesterol levels were low in CLO-fed mice compared to SO-fed mice. Although the total cholesterol levels increased in CLO-DM mice after DM injection, they were still lower than the SO control mice (SO-C).



**FIG. 1.** Urinary albumin excretion in SO-DM (■) and CLO-DM (●) mice after DM injection. Data are expressed as mean  $\pm$  SEM ( $n = 10$ ). Urinary albumin excretions in SO-fed mice and CLO-fed mice with saline injection (SO-C and CLO-C) are under 0.1 mg/d through the experimental period. \* $P < 0.05$  and \*\* $P < 0.01$  vs. pretreatment value in the same group; <sup>#</sup> $P < 0.05$  vs. CLO-DM at the same time point. SO-DM, soybean oil diet–daunomycin-treated animals; CLO, cod liver oil diet–DM-treated animals; SO-C and CLO-C, soybean oil- and cod liver oil-fed control animals.



**TABLE 3**  
**Effect of Dietary Oils and Daunomycin (DM) Injection on Serum Parameters<sup>a</sup>**

Parameter	Group			
	SO-C	SO-DM	CLO-C	CLO-DM
Albumin (g/dL)	3.53 ± 0.09	2.58 ± 0.41 <sup>a</sup>	3.50 ± 0.06	3.26 ± 0.25 <sup>c</sup>
Creatinine (mg/dL)	0.33 ± 0.02	0.35 ± 0.03	0.36 ± 0.02	0.33 ± 0.02
Total cholesterol (mg/dL)	112.2 ± 5.36	152.5 ± 16.65 <sup>b</sup>	67.8 ± 2.24 <sup>b</sup>	107.8 ± 10.91 <sup>c,d</sup>
TG (mg/dL)	76.8 ± 11.5	87.6 ± 11.8	60.2 ± 6.2	52.3 ± 6.0 <sup>d</sup>

<sup>a</sup>SO-C, saline-injected mice fed soybean oil (SO) diet; SO-DM, DM-injected mice fed SO diet; CLO-C, saline-injected mice fed cod liver oil (CLO) diet; CLO-DM, DM-injected mice fed CLO diet. Five to eight mice from each group were killed on day 15. Values are expressed as mean ± SEM. <sup>a</sup>*P* < 0.01 vs. SO-C; <sup>b</sup>*P* < 0.05 vs. SO-C; <sup>c</sup>*P* < 0.05 vs. SO-DM; <sup>d</sup>*P* < 0.05 vs. CLO-C.

**Morphological studies.** DM-induced histological changes in SO-fed and CLO-fed mice are shown in Figure 2. The degrees of expansion of the mesangial matrix, glomerular epithelial cell ballooning, and glomerular intracapillary thrombus were almost completely suppressed by CLO supplementation (Fig. 3).

**Lipid peroxide content in the renal tissue.** The basal lipid peroxide levels in renal cortical tissues were not different in either diet group (Fig. 4A). In SO-DM, a significant increase in peroxide levels was observed 72 h after DM injection. No significant increase in lipid peroxide level was evident in CLO-DM over 72 h after DM injection.

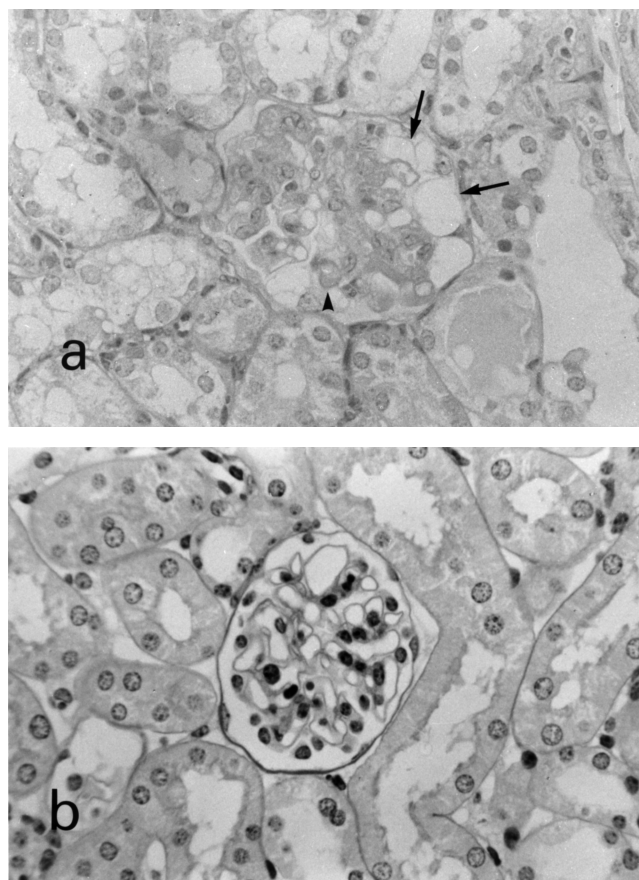
**GSH content in the renal tissue.** The basal GSH content was 1.4-fold higher in CLO-fed mice (CLO-C and CLO-DM) than in SO-fed mice (SO-C and SO-DM) (Fig. 4B). After DM injection, a significant decrease in GSH content was observed in both DM-treated groups (SO-DM and CLO-DM). However, the levels of GSH were consistently higher in CLO-DM than in SO-DM over 72 h after DM injection.

**Antioxidant enzyme activity in the renal tissue.** The basal levels of tissue antioxidant enzymes (SOD, catalase, and GSH-Px) activities were not different between the two diet groups (Table 4). After DM treatment, SOD activity increased transiently, but not significantly, in both diet groups (SO-DM and CLO-DM) after 24 h and returned to the basal levels after 72 h. Catalase activity at the basal level was almost the same in both diet groups. The activity decreased significantly in SO-DM at 72 h after DM injection. No marked change in catalase activity was found in the CLO-fed groups. Tissue GSH-Px activity in CLO-fed mice was higher than that in SO-fed mice in the basal state, although not significantly. The activity in CLO-DM mice increased after DM injection. The GSH-Px activity transiently increased after 24 h in SO-DM mice, but not significantly, and decreased below the basal level after 72 h. Consequently, the activities in SO-DM and CLO-DM after 72 h were significantly different.

**TxB<sub>2</sub> and 6-keto PGF<sub>1α</sub> in the renal cortical tissue.** Tissue eicosanoids 24 and 72 h after DM or saline injection are shown in Table 5. The tissue TxB<sub>2</sub> levels in the saline control groups (SO-C and CLO-C) were not significantly different

between the two diets. Acceleration of the production of tissue TxB<sub>2</sub> was found 72 h after DM injection in SO-DM mice. On the contrary, in CLO-DM mice, significant elevation of tissue Tx synthesis was not found over 72 h after DM injection.

Tissue 6-keto PGF<sub>1α</sub> increased 72 h after DM injection in SO-DM mice, although the increase was not statistically



**FIG. 2.** Morphological changes in DM-induced nephropathy (periodic acid-Schiff stain). (a) Mesangial matrix expansion, glomerular epithelial ballooning (arrow), and intracapillary thrombus (arrowhead) are seen in SO-DM at 2 wk after DM injection. (b) Histological changes in CLO-DM at 2 wk after DM injection. For abbreviations see Figure 1.



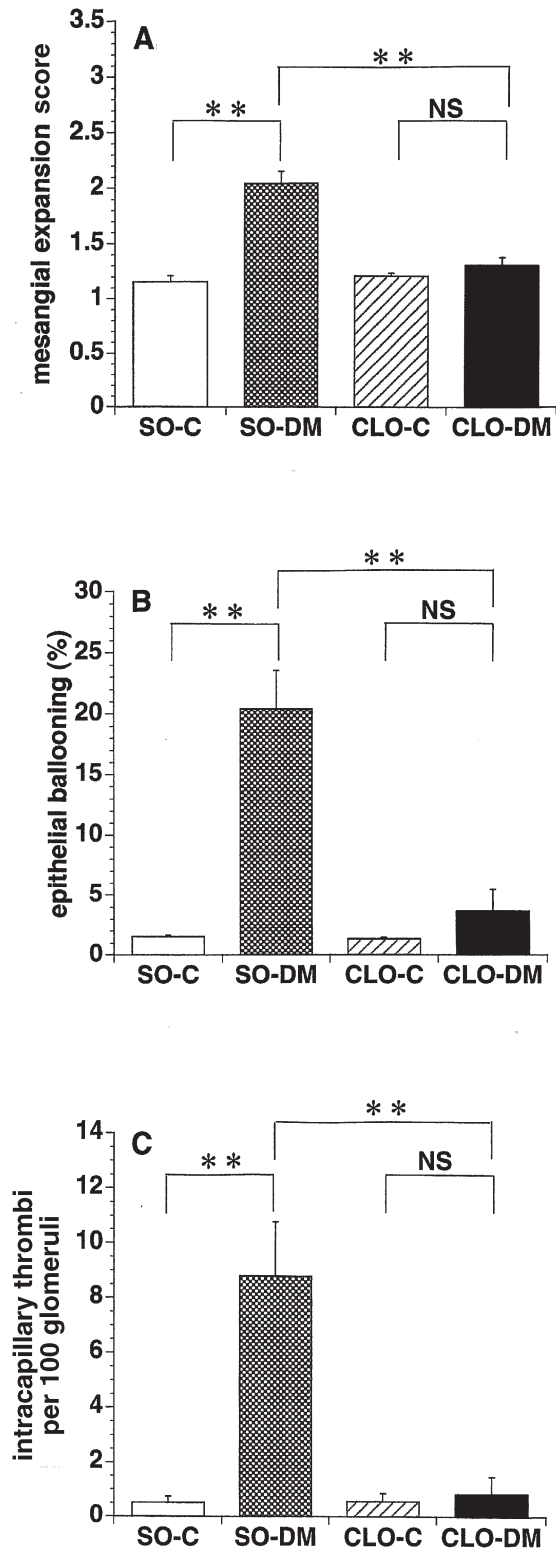


FIG. 3. Morphological study. (A) The mesangial matrix expansion score; (B) the number of glomeruli with epithelial ballooning per 100 glomeruli; (C) the number of glomeruli with intracapillary thrombi per 100 glomeruli. \*\* $P < 0.01$ ; NS, statistically not significant. For abbreviations see Figure 1.

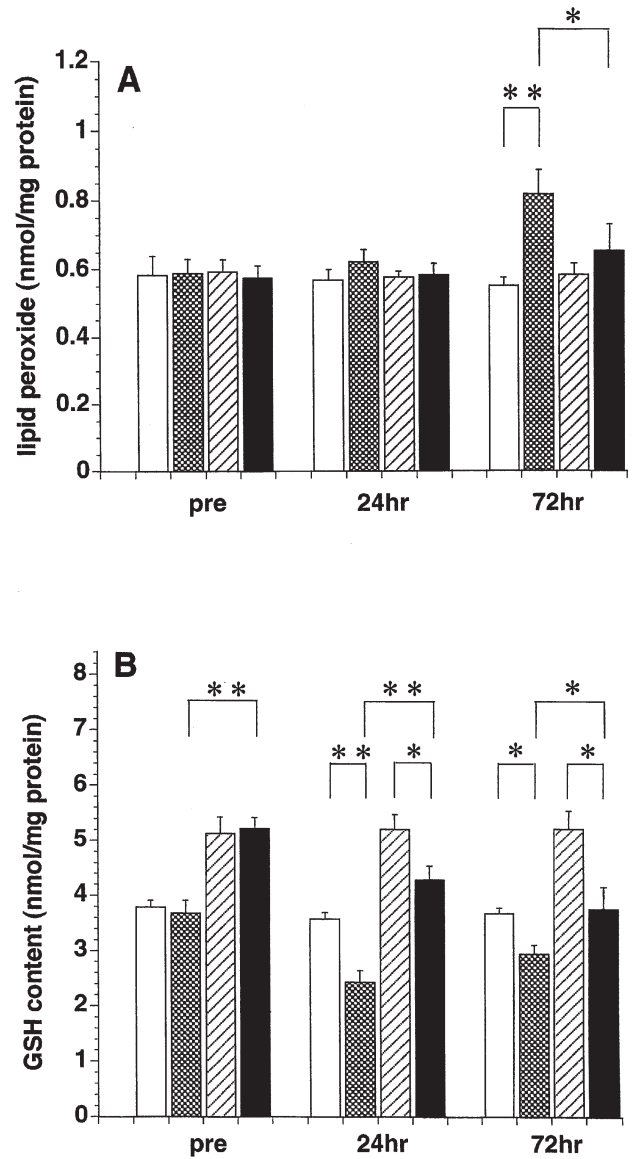


FIG. 4. (A) Lipid peroxide levels in the renal cortical tissue; (B) GSH content in the renal cortical tissue. Eight to 11 mice were sacrificed at specified intervals, and data are expressed as mean  $\pm$  SEM. Open bars: The values of SO-C; cross-hatched bars: SO-DM; diagonally lined bars: CLO-C; and solid bars: CLO-DM. \* $P < 0.05$ , \*\* $P < 0.01$ . For abbreviations see Figure 1.

significant compared to the saline control group (SO-C). No increase in 6-keto  $\text{PGF}_{1\alpha}$  levels was found in CLO-DM mice after DM injection. When compared 72 h after DM injection, a significant difference in tissue 6-keto  $\text{PGF}_{1\alpha}$  was found between SO-DM and CLO-DM mice.

## DISCUSSION

In the present study, dietary lipids dramatically modified the course of DM nephropathy in mice. Replacement of SO with CLO in the diet effectively ameliorated renal injury induced by the injection of DM. The characteristic histological changes of DM nephropathy, i.e., mesangial expansion,

**TABLE 4**  
Effect of Dietary Oils and DM Injection on Antioxidant Enzyme Activities on Renal Tissue<sup>a</sup>

Enzyme	Group			
	SO-C	SO-DM	CLO-C	CLO-DM
SOD				
Pre	116.6 ± 3.2	120.2 ± 4.6	124.2 ± 6.8	130.6 ± 8.7
24 h	118.5 ± 6.8	136.7 ± 16.4	118.9 ± 6.2	149.0 ± 9.2
72 h	115.2 ± 6.9	112.2 ± 4.2 <sup>a</sup>	125.2 ± 7.1	130.5 ± 8.0
Catalase				
Pre	8.2 ± 0.3	8.5 ± 0.4	7.8 ± 0.4	7.6 ± 0.7
24 h	7.9 ± 0.2	7.5 ± 0.3	7.5 ± 0.4	7.6 ± 0.6
72 h	8.3 ± 0.2	6.5 ± 0.5 <sup>b</sup>	7.9 ± 0.6	7.3 ± 0.8
GSH-Px				
Pre	2.72 ± 0.19	2.84 ± 0.16	3.08 ± 0.21	3.17 ± 0.17
24 h	2.91 ± 0.13	3.36 ± 0.15	2.98 ± 0.25	3.31 ± 0.29
72 h	2.81 ± 0.18	2.77 ± 0.20 <sup>c</sup>	3.05 ± 0.23	3.50 ± 0.22 <sup>c</sup>

<sup>a</sup>Eight to 11 mice from each group were sacrificed at specified intervals, and values are expressed as mean ± SEM. Units are: SOD, nitrite units/mg protein; catalase,  $k \times 10^{-2}$ /s/mg protein; GSH-Px,  $10^4$  nmol/min/mg protein. Statistics: <sup>a</sup> $P < 0.05$  vs. 24-h value in SO-DM; <sup>b</sup> $P < 0.01$  vs. pre value in SO-DM; <sup>c</sup> $P < 0.01$  vs. 72-h value in SO-DM. SOD, superoxide dismutase; GSH-Px, glutathione peroxidase; for other abbreviations see Table 3.

epithelial ballooning, and intracapillary thrombus formation, were decreased by dietary CLO to levels similar to those seen in saline control mice. Albuminuria was increased slightly at 14 d in CLO-DM mice, but the increase was significantly suppressed, by 30%, in SO-DM mice. These effects of CLO were associated with the suppression of lipid peroxide, a high tissue GSH content, and an increase of GSH-Px activity, as well as with suppression of renal cortical  $\text{TxB}_2$  and 6-keto  $\text{PGF}_{1\alpha}$  production in the early period after DM injection.

The main differences between SO and CLO are in the ratio and type of PUFA. SO contains about 60% PUFA, whereas CLO contains about 35% PUFA. In SO, PUFA are mainly n-6 FA (linoleic acid), whereas PUFA in CLO are n-3 FA, i.e., EPA and DHA. There are two possible explanations for why these differences of dietary FA composition modified the course of DM nephropathy. One is the inhibition of Tx and PG production, and the other is that oxidative damage to renal tissue was reduced by CLO supplementation.

There are two possible explanations for the prevention of Tx production by CLO. One is that EPA and DHA can compete with AA as a substrate for cyclooxygenase, resulting in the formation of trienoic eicosanoids ( $\text{TxA}_3$  and  $\text{PGI}_3$ ) that

are less biologically active than dienoic prostanoids ( $\text{TxA}_2$  and  $\text{PGI}_2$ ), as suggested in previous reports (7,8). The other possibility is that factors promoting Tx biosynthesis may be inhibited by dietary CLO supplementation. Angiotensin II, arginine-vasopressin, platelet-activating factor, interleukin-1, and ROS (13) are known to stimulate Tx synthesis. In the present study, we did not investigate whether any of these factors were modified by dietary CLO supplementation, apart from ROS, so it is difficult to speculate about this issue. As a result of the inhibition of Tx production, basement membrane permeability to protein might be decreased, and consequently albuminuria would decrease. In addition, Tx and PG are important factors that influence renal vascular resistance and/or arterial blood pressure (13). Therefore, a possibility exists that the effects of CLO might occur through eicosanoid-mediated alterations of glomerular hemodynamics, but we did not investigate these parameters in the present study.

Regarding lipid peroxidation in the kidneys, the high content of PUFA in SO appears to enhance the susceptibility of the mice ingesting SO to lipid peroxidation, and the high GSH content of renal tissue from mice on a CLO diet may also have been an important factor in preventing oxidative tissue

**TABLE 5**  
 $\text{TxB}_2$  and 6-Keto  $\text{PGF}_{1\alpha}$  Content 24 and 72 h After Treatment in the Renal Cortical Tissue<sup>a</sup>

	Group			
	SO-C	SO-DM	CLO-C	CLO-DM
$\text{TxB}_2$ (pg/mg protein)				
24 h	2.23 ± 0.09	2.20 ± 0.18	2.36 ± 0.67	2.14 ± 0.02
72 h	2.30 ± 0.11	3.32 ± 0.32 <sup>a,b,c</sup>	2.09 ± 0.67	2.22 ± 0.12
6-keto $\text{PGF}_{1\alpha}$ (pg/mg protein)				
24 h	2.04 ± 0.79	2.03 ± 0.44	1.56 ± 0.50	1.76 ± 0.29
72 h	2.26 ± 0.23	3.52 ± 0.81 <sup>b</sup>	1.76 ± 0.17	1.40 ± 0.24

<sup>a</sup>Five mice from each group were sacrificed at specified intervals. Values are expressed as mean ± SEM. Statistics: <sup>a</sup> $P < 0.01$  vs. 72 h value in SO-C; <sup>b</sup> $P < 0.01$  vs. 72 h value in CLO-DM; <sup>c</sup> $P < 0.05$  vs. 24 h value in SO-DM.  $\text{TxB}_2$ , thromboxane  $\text{B}_2$ ;  $\text{PGF}_{1\alpha}$ , prostaglandin  $\text{F}_{1\alpha}$ ; for other abbreviations see Table 3.

damage. GSH acts directly as a hydroxyl radical scavenger, and it is also a substrate for GSH-Px, an enzyme that metabolizes hydrogen peroxide. The GSH and GSH-Px system maintains a favorable redox status in cells and confers resistance to oxidative damage. The high renal tissue GSH content might have enhanced the tissue redox potential, thus leading to less lipid peroxidation in CLO-fed mice. This is the second study, to our knowledge, to indicate that FO supplementation increases the GSH content of renal tissue. Milner *et al.* (14) showed that FO supplementation increased the renal GSH content in a rat model of ADR nephropathy, but they did not clarify the mechanism involved. Outside the kidney, Ibrahim *et al.* (15) have reported elevation of the GSH content in the mouse liver by dietary FO. Because unsaturated and unstable long-chain n-3 FA are more susceptible to oxidation than n-6 FA, the increased GSH content of renal cortical tissue may have been a response to increased oxidative stress. The precise mechanism by which CLO supplementation caused GSH to increase still needs to be clarified.

With respect to enhanced GSH-Px activity, the findings of Chandrasekar and Fernandes (16) may be pertinent. They reported that FO increased the renal expression of mRNA for SOD, catalase, and GSH-Px when compared with the levels found in corn oil-fed control mice, and that treatment with FO delayed the onset and progression of renal disease in lupus-prone NZB/NZW F1 female mice. In the present study, although GSH-Px activity was only significantly elevated at 72 h after DM injection in CLO-DM mice, the pretreatment values found in both CLO-DM and CLO-C mice were higher than those seen in SO-fed mice. The higher GSH-Px activity in CLO-fed mice may have reflected upregulation of its mRNA in renal tissue.

We also need to take into account the direct relationship between ROS and eicosanoid production. An *in vitro* experiment by Baud *et al.* (17) provided clear evidence that the production of TxB<sub>2</sub> and 6-keto PGF<sub>1α</sub> in isolated rat glomeruli was increased twofold by stimulation with ROS, which caused activation of membrane phospholipase (PL) A<sub>2</sub> and led glomerular Tx production to increase as a consequence of the enhanced availability of AA. An increase of lipid peroxidation as a result of stimulation by ROS has also been suggested to increase the susceptibility of membrane lipids to PLA<sub>2</sub>. But few studies have evaluated the relationship between ROS and eicosanoid production in an *in vivo* model of renal injury. Shibouta *et al.* (18) reported the simultaneous enhancement of the production of renal cortical TxA<sub>2</sub>, leukotrienes, and malondialdehyde in rats with puromycin nephrosis, and Parra *et al.* (19) found that glomerular TxB<sub>2</sub> and ROS syntheses were simultaneously increased in rats with cyclosporin A (CyA) nephrotoxicity. Interestingly, the administration of vitamin E (a free radical scavenger) prevented an increase in glomerular TxB<sub>2</sub> production in these rats, suggesting that the increase of TxB<sub>2</sub> synthesis depended on the overproduction of ROS.

In the case of DM nephropathy, the initial stimulus that induces nephropathy is the injection of DM. After being

injected, DM is converted to a semiquinone radical and promotes the free radical cascade (20). DM nephropathy can be prevented by administration of SOD or DMTU (6), and it was ameliorated along with the inhibition of enhanced lipid peroxidation by dietary CLO supplementation in the present study. Thus, scavenging of ROS may be the primary effect of CLO supplementation. ROS produced after injection of DM may act on cell membrane PUFA, and lipid peroxide that is produced as a result may be rapidly metabolized by the enhanced GSH-GSHPx system in mice receiving dietary CLO. The inhibitory effect of CLO supplementation on TxB<sub>2</sub> production in DM nephropathy may occur *via* a mechanism similar to that shown in rat CyA nephropathy, i.e., the increase of TxB<sub>2</sub> synthesis was inhibited by blocking the overproduction of ROS through CLO supplementation.

We studied the effects of dietary CLO compared with SO, not necessarily the beneficial effects of FO in general. This study could not distinguish between the beneficial effect of CLO, the adverse effect of SO, or a combination of the two. A further study is needed to clarify the relative beneficial or unfavorable effects of FO and vegetable oil. By using several diets that differ in only one FA, we could further extend our understanding of the interaction between PUFA and renal injury.

Dietary CLO supplementation could significantly reduce DM-induced glomerular injury when compared to that in SO-fed mice. The mechanisms linking ROS and eicosanoids during the progression of DM nephropathy have not been fully clarified, but the effect of CLO supplementation was probably due to modification of oxidative damage as well as alteration of eicosanoid production. The effect of CLO may be possibly related to an enhanced redox potential (a high GSH level and increased GSH-Px activity), together with the suppression of TxB<sub>2</sub> production in renal tissue.

## ACKNOWLEDGMENTS

We thank Mitsuko Asano (Shizuoka University School of Nursing) for technical assistance, and Yoshiyuki Ito (Fujinomiya City General Hospital) for editorial assistance. We also thank Japan Food Research Laboratories (Tokyo, Japan) for the analyses of the content of antioxidants in the diets.

## REFERENCES

1. Sternberg, S.S., and Philips, F.S. (1967) Biphasic Intoxication and Nephrotic Syndrome in Rats Given Daunomycin, *Proc. Am. Assoc. Cancer Res.* 8, 64.
2. Kimura, M., Takahashi, H., Ohtake, T., Satou, T., Hishida, A., Nishimura, M., and Honda, N. (1993) The Interstrain Differences in Murine Daunomycin (DM)-Induced Nephrosis, *Nephron* 63, 193–198.
3. Remuzzi, G., Imberti, L., Rossini, M., Morelli, C., Carminati, C., Cattaneo, G.M., and Bertani, T. (1985) Increased Glomerular Thromboxane Synthesis as a Possible Cause of Proteinuria in Experimental Nephrosis, *J. Clin. Invest.* 75, 94–101.
4. Milner, L.S., Weis, H., and Houser, M.T. (1991) Amelioration of Glomerular Injury in Doxorubicin Hydrochloride Nephrosis by Dimethylthiourea, *J. Lab. Clin. Med.* 118, 427–434.

5. Okasora, T., Takikawa, T., Utsunomiya, Y., Senoh, I., Hayashibara, H., Shiraki, K., Kasagi, T., and Shimizu, F. (1992) Suppressive Effect of Superoxide Dismutase on Adriamycin Nephropathy, *Nephron* 60, 199–203.
6. Ohtake, T., Kimura, M., Nishimura, M., and Hishida, A. (1997) Roles of Reactive Oxygen Species and Antioxidant Enzymes in Murine Daunomycin-Induced Nephropathy, *J. Lab. Clin. Med.* 129, 81–88.
7. Ito, Y., Barcelli, U., Yamashita, W., Weiss, M., Glas-Greenwalt, P., and Pollak, V.E. (1988) Fish Oil Has Beneficial Effects on Lipids and Renal Disease of Nephrotic Rats, *Metabolism* 37, 352–357.
8. Barcelli, U.O., Beach, D.C., Thompson, B., Weiss, M., and Pollak, V.E. (1988) A Diet Containing n-3 and n-6 Fatty Acids Favorably Alters the Renal Phospholipids, Eicosanoid Synthesis and Plasma Lipids in Nephrotic Rats, *Lipids* 23, 1059–1063.
9. Mancini, G., Carbonara, A.O., and Heremans, J.F. (1965) Immunochemical Quantitation of Antigens by Single Radial Immunodiffusion, *Immunochemistry* 2, 235–254.
10. Lowry, O.M., Rosebrough, N.J., Farr, A.L., and Randall, R.J. (1951) Protein Measurement with the Folin Phenol Reagent, *J. Biol. Chem.* 193, 265–275.
11. Kato, A., Hishida, A., and Nakajima, T. (1995) Role of Thromboxane A<sub>2</sub> and Prostacyclin in Uninephrectomy-Induced Attenuation of Ischemic Renal Injury, *Kidney Int.* 48, 1577–1583.
12. Remuzzi, G., FitzGerald, G.A., and Patrono, C. (1992) Thromboxane Synthesis and Action Within the Kidney, *Kidney Int.* 41, 1483–1493.
13. Kasiske, B.L., O'Donnell, M.P., and Keane, W.F. (1989) Fish Oil Diet Decreases Prostacyclin and Increases Resistance in Isolated Rat Kidneys, *Am. J. Physiol* 256, F843–F851.
14. Milner, L.S., Weis, S., Kazakoff, P., Watkins, L., and Houser, M.T. (1994) Synergistic Effects of Fish Oil Diet and Dimethylthiourea in Acute Adriamycin Nephrosis, *Am. J. Med. Sci.* 308, 266–270.
15. Ibrahim, W., Lee, U.S., Yeh, C.C., Szabo, J., Bruckner, G., and Chow, C.K. (1997) Oxidative Stress and Antioxidant Status in Mouse Liver: Effects of Dietary Lipid, Vitamin E and Iron, *J. Nutr.* 127, 1401–1406.
16. Chandrasekar, B., and Fernandes, G. (1994) Decreased Pro-inflammatory Cytokines and Increased Antioxidant Enzyme Gene Expression by  $\omega$ -3 Lipids in Murine Lupus Nephritis, *Biochem. Biophys. Res. Comm.* 200, 893–898.
17. Baud, L., Nivez, M.P., Chansel, D., and Ardaillou, R. (1981) Stimulation by Oxygen Radicals of Prostaglandin Production by Rat Renal Glomeruli, *Kidney Int.* 20, 332–339.
18. Shibouta, Y., Terashita, Z., Imura, Y., Shino, A., Kawamura, M., Ohtsuki, K., Ohkawa, S., Nishikawa, K., and Fujiwara, Y. (1991) Involvement of Thromboxane A<sub>2</sub>, Leukotrienes and Free Radicals in Puromycin Nephrosis in Rats, *Kidney Int.* 39, 920–929.
19. Parra, T., de Arriba, G., Arribas, I., Perez de Lima, G., Rodriguez-Puyol, D., and Rodriguez-Puyol, M. (1998) Cyclosporine A Nephrotoxicity: Role of Thromboxane and Reactive Oxygen Species, *J. Lab. Clin. Med.* 131, 63–70.
20. Doroshov, J.H., and Davies, K.J.A. (1986) Redox Cycling of Anthracycline by Cardiac Mitochondria. 2. Formation of Superoxide Anion, Hydrogen Peroxide, and Hydroxyl Radical, *J. Biol. Chem.* 261, 3068–3074.

[Received August 17, 2001, and in revised form February 15, 2002; revision accepted March 19, 2002]



# Long-Term n-3 FA Deficiency Modifies Peroxisome Proliferator-Activated Receptor $\beta$ mRNA Abundance in Rat Ocular Tissues

Cecilia V. Rojas<sup>a,\*</sup>, Rebecca S. Greiner<sup>b</sup>, Lidia C. Fuenzalida<sup>a</sup>, Jessica I. Martínez<sup>a</sup>, Norman Salem, Jr.<sup>b</sup>, and Ricardo Uauy<sup>a</sup>

<sup>a</sup>INTA, Universidad de Chile, Santiago, Chile, and <sup>b</sup>Division of Intramural Clinical and Biological Research, Laboratory of Membrane Biochemistry and Biophysics, National Institute on Alcohol Abuse and Alcoholism, National Institutes of Health, Rockville, Maryland 20852

**ABSTRACT:** Peroxisomal proliferator-activated receptors (PPAR) are a FA-response system involved in diverse cellular responses. FA regulate PPAR activity and modulate PPAR mRNA abundance. Increasing evidence indicates that PUFA are required for optimal neuronal development and function. To gain insight into the mechanism for nutrition-induced impairment of neuronal development and function we investigated the effect of chronic n-3 FA deficiency on PPAR mRNA levels in rat brain and ocular tissues. Rats were fed for three generations a diet designed to reduce DHA levels in tissues, and the abundance of PPAR $\alpha$  and PPAR $\beta$  transcripts was measured by hybridization with specific probes. Chronic consumption of the  $\alpha$ -linolenic acid (LNA)-insufficient diet caused a remarkable modification in DHA content in membrane phospholipids. The results reported here indicate that PPAR $\alpha$  mRNA levels did not exhibit significant variation in ocular, hepatic, or nervous tissues from rats fed the experimental diet. In contrast, PPAR $\beta$  mRNA normalized to  $\beta$ -actin mRNA was 21% higher in ocular tissue from F3 generation rats consuming the LNA-deficient diet but was independent of diet in hepatic and nervous tissues. The absolute abundance of PPAR $\beta$  transcripts showed a 17% increase in ocular tissue from rats consuming the LNA-deficient diet (F3 generation). The biological significance of the reported changes in PPAR $\beta$  mRNA in ocular tissue remains to be determined.

Paper no. L8931 in *Lipids* 37, 367–374 (April 2002).

FA are one of the main energy substrates for most mammalian species. In addition, FA serve as components of membrane phospholipids, precursors for the synthesis of molecules involved in cellular signaling, and modulators of gene expression (1–3). An inadequate FA balance, particularly a deficit of long-chain PUFA, is associated with reduced fetal growth and impaired neurodevelopment and nerve transmission in animal models (4–6). Furthermore, dietary studies in humans indicate that PUFA status affects sensory and cognitive development in premature and term infants (7–10).

Investigations over the past decades support the involvement of peroxisome proliferator activated-receptors (PPAR)

in many of the physiological responses to FA. PPAR are ligand-dependent transcription factors, initially recognized as mediators of FA effects on lipid metabolism, controlling gene expression for  $\beta$ -oxidation and lipid biosynthesis. Lately, it became apparent that PPAR not only participate in the regulation of FA oxidation and lipogenesis but also play a role in a wide array of cellular responses, including inflammation, thermogenesis, and cell differentiation (3,11,12).

Three PPAR isoforms encoded by individual genes, namely,  $\alpha$ ,  $\beta$  and  $\gamma$ , have been described. These isoforms display a tissue-selective pattern of expression (13). PPAR $\alpha$  is expressed in liver, brown adipose tissue, skeletal muscle, kidney, and adrenal glands. PPAR $\gamma$  is mainly expressed in white adipose tissue and, to a lesser extent, in spleen, gut, and the immune system. PPAR $\beta$  displays a broad pattern of expression with relatively higher levels in skeletal muscle, testis, placenta, and neuronal tissues (i.e., cerebellum, oligodendrocytes) (14–17). The presence of both PPAR $\alpha$  and PPAR $\beta$  transcripts has been reported both in outer and inner layers of rat retina (13). Regarding PPAR function, the  $\alpha$  isoform appears primarily to regulate the transcription of several FA-metabolizing enzymes in hepatic mitochondria and peroxisomes. PPAR $\gamma$  is implicated in the control of lipogenesis, regulating the maturation of preadipocytes and the accumulation of lipid droplets in the cytoplasm of fat cells (18,19). The physiological role of PPAR $\beta$  remains unclear, although it reportedly regulates acylCoA synthetase 2 in rat brain cultures (20), but it also seems to participate in early differentiation of adipocyte precursor cells (21). Furthermore, PPAR $\beta$ -null mice display alterations in development, epidermal cell proliferation, myelination of the corpus callosum, and lipid metabolism (22). Recently, PPAR $\beta$  has also been implicated in colorectal cancer (23), in bone resorption (24), and in the stimulation of reverse cholesterol transport (25).

PPAR activity is mainly controlled by ligand binding (26). Different FA and their derivatives (such as conjugated FA, eicosanoids, and prostaglandins) are able to activate PPAR isoforms (2,26). Among FA, DHA has been reported as a potent PPAR activator (27). FA activation of PPAR $\alpha$  seems to account for many of the short-term effects of dietary fat on gene expression in liver, at least in rodents. However, there is increasing evidence that under different nutritional states, not

\*To whom correspondence should be addressed at INTA, Universidad de Chile, Casilla 138-11, Santiago, Chile. E-mail crojas@uec.inta.uchile.cl  
Abbreviations: DPAn-6, docosapentaenoate; GAPDH, glyceraldehyde-3-phosphate dehydrogenase; LA, linoleic acid; LNA,  $\alpha$ -linolenic acid; PPAR, peroxisome proliferator-activated receptor; RXR, retinoic acid receptor.

only PPAR activity but also its mRNA abundance are modified. After feeding, PPAR $\gamma$  increases in adipose tissue in response to sterol regulatory element binding protein 1 (28,29), thus stimulating uptake of FA and their conversion to TG, whereas, PPAR $\gamma$  diminishes in murine liver during fasting periods (28). Starvation causes a decrease in PPAR $\alpha$  mRNA levels in liver (30). In contrast, fasting results in high expression of PPAR $\alpha$  (30,31), increasing the ketonemia and thus providing fuel for different tissues. The recently identified fasting-induced adipose factor gene (FIAF) seems to be a target for the PPAR $\alpha$ -mediated response to fasting (32).

This work addresses the effect of long-term n-3 FA deficiency on the abundance of PPAR mRNA in rat tissues. Rats were chronically fed diets sufficient in linoleic acid (LA: 18:2n-6) but low or adequate in  $\alpha$ -linolenic acid (LNA: 18:3n-3). Consumption of diets containing oils low in LNA significantly reduced DHA (22:6n-3) content in F2 generation rat brain and liver FA. PPAR $\alpha$  and PPAR $\beta$  mRNA levels were analyzed in nervous, ocular, and hepatic tissues from F2 and F3 generation rats. Our results show a moderate increase in PPAR $\beta$  mRNA in ocular tissues from rats with an inadequate dietary supply of n-3 FA. In contrast, levels of neither PPAR $\alpha$  mRNA in all three tissues nor PPAR $\beta$  mRNA in hepatic or nervous tissues were significantly modified.

## MATERIALS AND METHODS

**Diets.** Diets based on the AIN93 diet (33) were designed to contain 10% total lipids and either deficient or adequate amounts of LNA (34). The experimental diets were composed of (in g/100 g diet): 20 vitamin-free casein, 60 carbohydrates (15 cornstarch, 10 sucrose, 20 dextrose, and 15 maltose-dextrin), 10 cellulose vitamins/minerals, and 10 lipids. Safflower oil was used to provide an adequate amount of LA (18:2n-6), and flaxseed oil was the source of LNA (18:3n-3) in the LNA-sufficient diet. The LNA-deficient diet contained 8.1 g/100 g of hydrogenated coconut oil (abundant in lauric and myristic acids) and 1.9 g/100 g of safflower oil. The LNA-adequate diet contained 7.75 g/100 g of hydrogenated coconut oil, 1.77 g/100 g of safflower oil, and 0.48 g/100 g of flaxseed. Fatty acyl composition analysis of the diets showed that 18:3n-3 was 3.1 and 0.04% of total FA in the LNA-sufficient and the LNA-deficient diet, respectively (34).

**Experimental design.** Female Long-Evans rats (Charles River, Portage, MI) were randomly divided into two groups of 12 rats each and reared on n-3 adequate or deficient diets beginning at 21 d of life. These females (F1 generation) were mated with chow-fed males and similarly, F2 generation females were mated with chow-fed males. Their male offspring (F2 and F3 generations) were weaned to the diet of the dam and maintained on this diet until sacrifice at 12 wk of age. No obvious differences in reproduction efficiency or pup size were observed in this study between dietary groups. Animals were killed by decapitation and the tissues rapidly excised and stored at  $-80^{\circ}\text{C}$  until analysis. Cerebellum, liver, and whole eyeballs were collected from the F2 and F3 generation

rats. All animal procedures were approved by the NIAAA Animal Care and Use Committee, NIH.

**FA analysis.** FA composition was determined in rat brain and liver. Lipids were extracted in the presence of tricosanoic acid (23:0) as internal standard (35). FA were transmethylated and analyzed by GC (36). The identification of individual FA was based on the retention time, and their content was expressed as a weight percentage of total FA (37).

**Slot blot analysis.** Frozen tissue samples (approximately 100 mg) were ground in a prechilled mortar. Total RNA was extracted with guanidine isothiocyanate/phenol (TRIZOL reagent; GIBCO BRL, Bethesda, MD) according to the manufacturer's instructions, precipitated in ethanol, and stored at  $-80^{\circ}\text{C}$ . Before use, samples were resuspended in diethyl pyrocarbonate-treated doubly distilled water and incubated for 45 min at  $37^{\circ}\text{C}$  with 0.03 units of RNase-free RQ1 DNase (Promega Corp., Madison, WI) per microgram of RNA.

Total RNA (0.5 to 1  $\mu\text{g}$ ) was denatured at  $68^{\circ}\text{C}$  in 0.21 M sodium citrate, 0.021 M sodium chloride, pH 7.0, 69% deionized formamide, 9% formaldehyde, and transferred to nitrocellulose membranes (Schleicher & Schuell GmbH, Dassel, Germany) by filtration under negative pressure. RNA was fixed to membranes using a UV cross linker (Stratagene, La Jolla, CA) and hybridized with  $^{32}\text{P}$ -labeled cDNA probes for PPAR $\alpha$ , PPAR $\beta$ , glyceraldehyde-3-phosphate dehydrogenase (GAPDH), or  $\beta$ -actin. Probes for PPAR $\alpha$ , PPAR $\beta$ , GAPDH, and  $\beta$ -actin transcripts were obtained by reverse transcription-PCR using primers specific for the corresponding cDNA sequences available on databases (PPAR $\alpha$ , Genebank accession # M88592; PPAR $\beta$ , Genebank accession # U40064;  $\beta$ -actin, Genebank accession # V01217; GAPDH Genebank accession # X02231 X00972). PCR-amplified fragments, cloned into pCR II (Invitrogen, Carlsbad, CA) or pBluescript (Stratagene) vectors, constituted nucleotides 1030 to 1775 of PPAR $\alpha$  cDNA, nucleotides 86 to 392 of PPAR $\beta$  cDNA, nucleotides 1253 to 2381 of  $\beta$ -actin gene, and nucleotides 87 to 626 of GAPDH cDNA. The identity of cloned fragments was confirmed by direct cDNA sequencing. The specificity of all probes used in slot blot hybridizations was verified by Northern analysis. Unique bands of the predicted size were observed in autoradiograms. Hybridization with nonlimiting amounts of radioactive probes was carried out for 24 h at  $42^{\circ}\text{C}$  in 0.02 M sodium phosphate buffer, pH 6.5, containing  $6\times$  SSC (0.9 M sodium chloride, 0.09 M sodium citrate pH 7.0),  $5\times$  Denhardt's solution (0.1% wt/vol polyvinylpyrrolidone, 0.1% wt/vol Ficoll type 400, 0.1% wt/vol BSA), 5% wt/vol dextran sulfate in formamide, 0.1 mg/mL denatured salmon sperm DNA, and  $^{32}\text{P}$ -labeled probes. Labeling of the probes was carried out by the PCR Radioactive Labeling System (GIBCO BRL) and  $\alpha$ - $^{32}\text{P}$ -dCTP (111 TBq/mmol, 370 MBq/mL; NEN Life Science Products, Inc., Boston, MA). Membranes were washed with a solution containing  $0.2\times$  SSC (0.015 M sodium chloride, 0.0015 M sodium citrate, pH 7.0), and 0.1% SDS at 60, 63, or  $68^{\circ}\text{C}$  for PPAR $\beta$ , PPAR $\alpha$ , or  $\beta$ -actin and GAPDH, respectively. Membranes were exposed to X-ray films using intensifying screens, and densitometric analysis of autoradio-

grams was carried out with a Bio-Rad GS-670 image densitometer. PPAR signal intensities for each tissue in individual animals were standardized with those of the reference mRNA measured in parallel. The mean  $\pm$  SD of two experiments was determined for each dietary group. Hybridizations to mRNA from different tissues were carried out independently. To compare PPAR mRNA abundance among samples and experiments,  $\beta$ -actin and GAPDH mRNA were used as an internal reference. Thus, results for PPAR $\alpha$  and PPAR $\beta$  mRNA were expressed relative to  $\beta$ -actin and GAPDH mRNA.

*Statistical analysis.* Statistical differences between the mean values of dietary groups were assessed by the two-tailed unpaired *t*-test and were considered significantly different at  $P < 0.05$ .

## RESULTS

*Effect of diet on FA composition.* Analysis of liver and brain lipids from rats fed LNA-deficient or LNA-adequate diets shows significant differences in FA composition (Table 1), particularly in DHA, which accounts for over 99 and 85% of total n-3 FA in brain and liver, respectively. A fivefold lower level of DHA was found in brain and an 11-fold DHA decrease in liver from rats fed the LNA-deficient diet. A concomitant compensatory increase in 22-carbon n-6 FA, particularly in docosapentaenoate (DPA $n$ -6, 22:5n-6) and, to a lesser extent, in 22:4n-6 was detected in the lipids of hepatic and nervous tissue. Thus, the total n-6 to n-3 ratio increased almost 10-fold in brain lipids and 14-fold in liver lipids.

**TABLE 1**  
**FA Composition<sup>a</sup> of Total Lipid Extracts from Rat Liver and Brain**

FA	Liver		Brain	
	LNA-deficient	LNA-adequate	LA-deficient	LNA-adequate
	(% total FA)			
Saturated				
14:0	1.60 $\pm$ 0.17*	1.20 $\pm$ 0.21	0.30 $\pm$ 0.20	0.60 $\pm$ 0.40
16:0	17.1 $\pm$ 1.00*	19.8 $\pm$ 1.90	16.30 $\pm$ 0.20	17.0 $\pm$ 0.90
18:0	18.9 $\pm$ 0.80	17.9 $\pm$ 1.90	18.50 $\pm$ 0.20	18.6 $\pm$ 0.50
20:0	0.09 $\pm$ 0.01*	0.08 $\pm$ 0.00	0.70 $\pm$ 0.09	0.60 $\pm$ 0.07
22:0	0.30 $\pm$ 0.20*	0.20 $\pm$ 0.10	0.90 $\pm$ 0.06*	0.80 $\pm$ 0.05
24:0	0.65 $\pm$ 0.06*	0.44 $\pm$ 0.03	1.70 $\pm$ 0.20	1.60 $\pm$ 0.20
Total	38.60 $\pm$ 1.10	39.60 $\pm$ 1.00	38.50 $\pm$ 0.60	39.20 $\pm$ 1.20
Monounsaturated				
14:1	0.02 $\pm$ 0.01	0.02 $\pm$ 0.02	ND <sup>b</sup>	ND
16:1	1.80 $\pm$ 0.40	2.40 $\pm$ 0.70	0.30 $\pm$ 0.03	0.40 $\pm$ 0.06
18:1n-9	7.80 $\pm$ 1.30	9.90 $\pm$ 1.40	15.3 $\pm$ 0.50*	16.2 $\pm$ 0.40
18:1n-7	4.70 $\pm$ 0.60	5.10 $\pm$ 0.80	3.70 $\pm$ 0.10*	3.60 $\pm$ 0.10
20:1	0.19 $\pm$ 0.02	0.16 $\pm$ 0.04	2.00 $\pm$ 0.20	1.90 $\pm$ 0.30
22:1	0.004 $\pm$ 0.01	ND	0.20 $\pm$ 0.02	0.20 $\pm$ 0.03
24:1	0.30 $\pm$ 0.07*	0.21 $\pm$ 0.20	3.30 $\pm$ 0.30	3.30 $\pm$ 0.30
Total	14.80 $\pm$ 1.90	17.90 $\pm$ 2.60	24.90 $\pm$ 0.70	25.50 $\pm$ 0.90
n-6 series				
18:2n-6	10.5 $\pm$ 1.20	11.0 $\pm$ 1.20	4.60 $\pm$ 0.30*	5.10 $\pm$ 0.40
18:3n-6	0.04 $\pm$ 0.01*	0.07 $\pm$ 0.01	ND	ND
20:3n-6	0.60 $\pm$ 0.10*	0.90 $\pm$ 0.10	0.30 $\pm$ 0.03*	0.30 $\pm$ 0.02
20:4n-6	22.3 $\pm$ 0.80*	19.2 $\pm$ 1.60	8.80 $\pm$ 0.30	8.40 $\pm$ 0.40
22:4n-6	0.80 $\pm$ 0.10*	0.27 $\pm$ 0.20	3.60 $\pm$ 0.08*	2.70 $\pm$ 0.09
22:5n-6	5.30 $\pm$ 0.70*	0.20 $\pm$ 0.05	9.00 $\pm$ 0.50*	0.40 $\pm$ 0.05
Total	39.90 $\pm$ 2.10*	31.90 $\pm$ 2.40	22.30 $\pm$ 0.70*	12.40 $\pm$ 0.50
n-3 series				
18:3n-3	0.006 $\pm$ 0.005*	0.28 $\pm$ 0.05	ND	ND
20:5n-3	ND	0.47 $\pm$ 0.10	ND	ND
22:5n-3	0.07 $\pm$ 0.03*	0.50 $\pm$ 0.09	0.008 $\pm$ 0.02*	0.13 $\pm$ 0.01
22:6n-3	0.60 $\pm$ 0.02*	6.60 $\pm$ 0.50	2.30 $\pm$ 0.10*	11.8 $\pm$ 0.70
Total	0.70 $\pm$ 0.05*	7.80 $\pm$ 0.60	2.30 $\pm$ 0.10*	11.90 $\pm$ 0.70
20:3n-9	0.17 $\pm$ 0.02	0.14 $\pm$ 0.03	0.08 $\pm$ 0.003	0.06 $\pm$ 0.01
18:2n-6/18:3n-3	1062 $\pm$ 83*	39.9 $\pm$ 5.3	NA <sup>b</sup>	NA
22:5n-6/22:6n-3	8.8 $\pm$ 1.1*	0.03 $\pm$ 0.006	3.9 $\pm$ 0.2*	0.03 $\pm$ 0.004
22:5 + 22:6	5.9 $\pm$ 0.7*	6.8 $\pm$ 0.48	11.3 $\pm$ 0.6	12.2 $\pm$ 0.7
Total n-6/total n-3	58.7 $\pm$ 5.0*	4.1 $\pm$ 0.3	9.6 $\pm$ 0.5*	1.0 $\pm$ 0.04
Total n-6 + total n-3	40.6 $\pm$ 2.1	39.8 $\pm$ 2.8	24.6 $\pm$ 0.7	24.4 $\pm$ 1.1

<sup>a</sup>Data are mean  $\pm$  SD for F2 generation rats. \*Statistically significant differences  $P < 0.05$ .

<sup>b</sup>NA, not available; ND, not detectable; LNA,  $\alpha$ -linolenic acid; LA, linoleic acid. Values may not equal 100% due to unidentified peaks.

Changes in lipid composition were not evaluated in ocular tissue because the whole sample was used for mRNA quantification, and other studies show that retinal responses are similar to those of brain with respect to DHA loss and replacement with DPAn-6 (4,38,39).

**Effect of diets on PPAR mRNA abundance.** GAPDH and  $\beta$ -actin transcripts are widely accepted as reference genes for expression analysis. Because changes in either GAPDH or  $\beta$ -actin mRNA levels have been reported under some experimental conditions (40–42), the abundance of both transcripts was evaluated in the tissues analyzed here (Table 2). Data are expressed as the mean value of  $\beta$ -actin and GAPDH mRNAs in tissues from rats fed the LNA-deficient diet and as a percentage of the value obtained from the LNA-adequate group. GAPDH mRNA levels in different tissues were independent of the dietary supply of LNA, except for a 10% decrease in nervous tissue in F3 generation rats fed the LNA-deficient diet. In addition, significantly lower levels of  $\beta$ -actin mRNA were detected in ocular (10%), nervous (20%), and hepatic (42%) tissues from F2 generation rats fed the LNA-deficient diet as compared to those that consumed the LNA-adequate diet. Therefore, data normalized to  $\beta$ -actin mRNA in all tissues from F2 generation rats and to GAPDH mRNA in nervous tissue (F3 generation) were not included for analysis. In addition, a lower level (37%) of  $\beta$ -actin transcripts was also found in liver from F3 generation rats. However, this difference was not statistically significant, probably owing to variability within the group.

The abundance of PPAR mRNA in nervous and ocular tissues was evaluated and expressed relative to both  $\beta$ -actin and GAPDH mRNA levels in the same tissue, as pointed out in the Materials and Methods section (Tables 3 and 4). Analysis of mRNA in hepatic tissue was included as a control, because of reported high levels of PPAR $\alpha$  mRNA expression. As shown in Table 3, most of the differences detected in the relative abundance of PPAR $\alpha$  mRNA in ocular, nervous, and hepatic tissue from F2 and F3 generation rats fed LNA-deficient or LNA-adequate diets were not statistically significant. PPAR $\alpha$  mRNA abundance normalized to  $\beta$ -actin mRNA was 61% higher in hepatic tissue from F3 generation rats consuming the LNA-deficient diet than that measured in rats fed the LNA-adequate diet. However, the latter could be explained,

at least in part, by the lower  $\beta$ -actin mRNA measured in hepatic tissue from these rats (Table 2). This is confirmed when results are examined relative to GAPDH mRNA. In this case, PPAR $\alpha$  levels do not significantly differ in the liver samples. As illustrated in Table 4, PPAR $\beta$  mRNA abundance also displayed significantly higher levels when expressed relative to  $\beta$ -actin mRNA but not to GAPDH mRNA.

The results of the PPAR $\beta$  mRNA abundance determination in nervous and hepatic tissues shown in Table 4 indicate no significant changes, except a 51% increment in PPAR $\beta$  mRNA normalized to  $\beta$ -actin mRNA in the F3 generation (possibly influenced by the decrease observed in  $\beta$ -actin transcripts in liver). In ocular tissue, significantly higher PPAR $\beta$  mRNA abundance relative to  $\beta$ -actin transcripts (21%) was found in F3 generation rats from the LNA-deficient group (Table 4). It is likely that the increase in the normalized PPAR $\beta$  level in ocular tissue arises mainly from a moderately higher absolute abundance of PPAR $\beta$  mRNA (17%) in the rats consuming the n-3-deficient diet (Table 4).

## DISCUSSION

Effects of dietary FA at the level of gene expression are part of an adaptive metabolic response to the amount and type of fat. These are mediated, at least in part, by the PPAR system. Although the activity of PPAR isoforms is mainly regulated by ligand binding and phosphorylation status, control at the transcriptional level is also apparent. Changes in the abundance of PPAR $\alpha$ , which influences the expression of enzymes for FA oxidation, have been detected in liver during fasting periods, with a concomitant increase in the level of PPAR $\alpha$  mRNA (31). Moreover, food intake increases PPAR $\gamma$  mRNA levels, whereas PPAR $\gamma$  abundance decreases during fasting periods (28). Changes in PPAR $\alpha$  mRNA levels in response to total dietary fat intake and to FA composition have also been documented. Feeding rats a diet rich in LNA for 12 wk after weaning caused a decrease in PPAR $\alpha$  mRNA abundance in the epididymal fat pads (43). In contrast, an increased expression of PPAR $\alpha$  mRNA in rat liver was observed in 5-wk-old rats fed a high-fat diet (250 g/kg of either coconut oil or olive oil or safflower oil) over a 4-wk period (44).

**TABLE 2**  
 **$\beta$ -Actin and GAPDH mRNA Abundance in LNA-Deficient Rats**

Tissue	Rat generation	$\beta$ -Actin <sup>a</sup>	% <sup>b</sup>	GAPDH <sup>a</sup>	% <sup>b</sup>
Ocular	F2	23.3 $\pm$ 1.1 (6)	90.1 $\pm$ 4.8 <sup>*,c</sup>	11.5 $\pm$ 0.2 (6)	99.1 $\pm$ 1.7
	F3	28.0 $\pm$ 1.8 (6)	97.6 $\pm$ 6.4	13.3 $\pm$ 1.1 (6)	92.7 $\pm$ 8.3
Nervous	F2	16.1 $\pm$ 2.5 (5)	80.1 $\pm$ 15.4 <sup>*,d</sup>	10.5 $\pm$ 0.6 (6)	98.5 $\pm$ 5.8
	F3	18.5 $\pm$ 2.3 (5)	110.4 $\pm$ 12.2	10.5 $\pm$ 0.4 (6)	90.4 $\pm$ 3.6 <sup>*,e</sup>
Hepatic	F2	1.4 $\pm$ 0.4 (5)	57.5 $\pm$ 30.4 <sup>*,f</sup>	4.4 $\pm$ 0.6 (6)	84.3 $\pm$ 14.0
	F3	1.3 $\pm$ 0.6 (6)	62.9 $\pm$ 46.5	5.3 $\pm$ 0.3 (6)	97.8 $\pm$ 5.9

<sup>a</sup>Data are mean  $\pm$  SD. In parentheses are the number of samples. <sup>\*</sup>Statistically significant differences: <sup>c</sup> $P = 0.03$ , <sup>d</sup> $P = 0.04$ , <sup>e</sup> $P = 0.0008$ , <sup>f</sup> $P = 0.02$ .

<sup>b</sup>The mean value of  $\beta$ -actin mRNA and GAPDH mRNA for the LNA-deficient diet was expressed as a percentage of the value for the group fed the LNA-adequate diet. GAPDH, glyceraldehyde-3-phosphate dehydrogenase; for other abbreviation see Table 1.



**TABLE 3**  
**PPAR $\alpha$  mRNA Relative Abundance<sup>a</sup> in Tissues from LNA-Deficient Rats**

Tissue	Generation	PPAR $\alpha$ <sup>b</sup>	% <sup>c</sup>	PPAR $\alpha$ / $\beta$ -actin <sup>b</sup>	% <sup>c</sup>	PPAR $\alpha$ /GAPDH <sup>b</sup>	% <sup>c</sup>
Ocular	F2	0.78 $\pm$ 0.19	109 $\pm$ 24	0.02 $\pm$ 0.01 (6)	118 $\pm$ 25	0.04 $\pm$ 0.01 (6)	111 $\pm$ 22
	F3	0.98 $\pm$ 0.09	113 $\pm$ 9	0.02 $\pm$ 0.002 (6)	123 $\pm$ 10	0.04 $\pm$ 0.003 (6)	122 $\pm$ 7
Nervous	F2	1.69 $\pm$ 0.10	106 $\pm$ 6	0.06 $\pm$ 0.01 (5)	133 $\pm$ 18 <sup>*d</sup>	0.16 $\pm$ 0.02 (5)	108 $\pm$ 9
	F3	1.69 $\pm$ 0.10	105 $\pm$ 6	0.05 $\pm$ 0.01 (4)	98 $\pm$ 15	0.16 $\pm$ 0.01 (5)	121 $\pm$ 7 <sup>*e</sup>
Hepatic	F2	0.38 $\pm$ 0.15	98 $\pm$ 4	0.28 $\pm$ 0.07 (5)	171 $\pm$ 26 <sup>*f</sup>	0.06 $\pm$ 0.02 (6)	116 $\pm$ 33
	F3	0.34 $\pm$ 0.05	95 $\pm$ 15	0.31 $\pm$ 0.14 (5)	161 $\pm$ 45 <sup>*g</sup>	0.04 $\pm$ 0.01 (6)	105 $\pm$ 15

<sup>a</sup>Because hybridization assays to mRNA from different tissues were carried out independently (see Materials and Methods section), the comparison of absolute PPAR $\alpha$  mRNA values should be restricted to the same tissue.

<sup>b</sup>Data are mean  $\pm$  SD. In parentheses are the number of samples. <sup>c</sup>Statistically significant differences: <sup>d</sup> $P = 0.007$ , <sup>e</sup> $P = 0.0027$ , <sup>f</sup> $P = 0.0009$ , and <sup>g</sup> $P = 0.02$ .

<sup>c</sup>The mean value of PPAR $\alpha$  mRNA relative to  $\beta$ -actin or to GAPDH mRNA for the LNA-deficient diet was expressed as percentage of the value for the group fed the LNA-adequate diet. PPAR $\alpha$ , peroxisome proliferator-activated receptor  $\alpha$ ; for other abbreviations see Tables 1 and 2.

The effect of high- and low-fat diets on PPAR $\alpha$  mRNA abundance in kidney of 3-wk-old rats also has been investigated previously (45). In this study, pups were kept on a low-fat diet (less than 1% fat) from day 16 to 21; then a group was placed on a high-fat diet (supplemented with 25% coconut oil) for 24 h. Despite marked changes in the mRNA levels for enzymes involved in  $\beta$ -oxidation in the kidney cortex, the authors reported no significant modification of PPAR $\alpha$  mRNA abundance, suggesting that modulation of the expression of the PPAR $\alpha$  gene is not involved in this physiological response to a high-fat diet. A diet high in fat causes a small increase in PPAR $\gamma$  in rat adipose tissue (28). However, the infusion of lipids (Intralipid) in humans results in a marked increase in subcutaneous adipose tissue PPAR $\gamma$  mRNA (46). Considering the PPAR $\beta$  ligand-binding profile (26), it is likely that FA are physiological regulators of its activity as a transcription factor. However, information regarding the regulation of PPAR $\beta$  gene expression is not yet available.

Many investigations support the role of n-3 FA, particularly DHA, on the development and function of the nervous system in humans (4,38,47,48), particularly in the visual system (7,10,47). High DHA levels are found in the inner membranes of photoreceptor outer segments, in certain brain areas,

and in specific neuronal cell types. Dietary n-3 FA deficiency alters rat retinal function (49). Moreover, DHA promotes differentiation of developing photoreceptors in culture (50). Interestingly, PPAR $\beta$  mRNA is more prominent than other PPAR isoforms in many areas of the rat adult brain (15) and its level is particularly high during embryonic development (51). Expression of PPAR $\beta$  is also abundant in differentiating oligodendrocytes, cells involved in myelin sheath formation (16). Consistently, PPAR $\beta$  null mice show alterations in myelination of the corpus callosum and in lipid metabolism (22). As in other cell types, it likely that PPAR transcriptional activity is modulated by FA in neuronal cells although their PPAR-responsive genes have not been identified.

The purpose of this study was to explore whether long-term modification of FA intake, specifically n-3 FA deficiency, affects the abundance of PPAR $\alpha$  and  $\beta$  mRNA in neural tissues. It is well known that the content and composition of dietary lipids can alter FA composition in biological membranes (38,39,52–54). These studies demonstrate that when two or more generations of animals are maintained on an n-3-deficient diet, a marked modification of the FA composition in the nervous system occurs. Therefore, in the present study, rats were fed the experimental diet for three gener-

**TABLE 4**  
**PPAR $\beta$  mRNA Relative Abundance<sup>a</sup> in Tissues from LNA-Deficient Rats**

Tissue	Generation	PPAR $\beta$ <sup>b</sup>	% <sup>c</sup>	PPAR $\beta$ / $\beta$ -actin <sup>b</sup>	% <sup>c</sup>	PPAR $\beta$ /GAPDH <sup>b</sup>	% <sup>c</sup>
Ocular	F2	1.63 $\pm$ 0.33	122 $\pm$ 20	0.04 $\pm$ 0.01 (6)	136 $\pm$ 14 <sup>*d</sup>	0.09 $\pm$ 0.02 (6)	123 $\pm$ 20
	F3	1.59 $\pm$ 0.10	117 $\pm$ 6 <sup>*e</sup>	0.03 $\pm$ 0.004 (6)	121 $\pm$ 12 <sup>*f</sup>	0.07 $\pm$ 0.01 (6)	126 $\pm$ 14
Nervous	F2	2.14 $\pm$ 0.26	96 $\pm$ 12	0.07 $\pm$ 0.01 (5)	122 $\pm$ 14	0.20 $\pm$ 0.02 (5)	97 $\pm$ 9
	F3	1.65 $\pm$ 0.10	100 $\pm$ 6	0.06 $\pm$ 0.01 (5)	104 $\pm$ 9	0.16 $\pm$ 0.01 (5)	112 $\pm$ 4 <sup>*g</sup>
Hepatic	F2	0.18 $\pm$ 0.06	75 $\pm$ 33	0.12 $\pm$ 0.02 (5)	130 $\pm$ 14 <sup>*h</sup>	0.04 $\pm$ 0.01 (6)	87 $\pm$ 31
	F3	0.35 $\pm$ 0.09	117 $\pm$ 12	0.27 $\pm$ 0.10 (5)	151 $\pm$ 36 <sup>*i</sup>	0.04 $\pm$ 0.01 (6)	112 $\pm$ 2

<sup>a</sup>Because hybridization assays to mRNA from different tissues were carried out independently (see Materials and Methods section), the comparison of absolute PPAR $\beta$  mRNA values should be restricted to the same tissue.

<sup>b</sup>Data are mean  $\pm$  SD. In parentheses are the number of samples. <sup>c</sup>Statistically significant differences: <sup>d</sup> $P = 0.001$ , <sup>e</sup> $P = 0.005$ , <sup>f</sup> $P = 0.004$ , <sup>g</sup> $P = 0.03$ , <sup>h</sup> $P = 0.02$ , and <sup>i</sup> $P = 0.02$ .

<sup>c</sup>The mean value of PPAR $\beta$  mRNA relative to  $\beta$ -actin or to GAPDH mRNA for the LNA-deficient diet was expressed as a percentage of the value for the group fed the LNA-adequate diet. For abbreviations see Tables 1–3.

ations. The effects of the diet deficient in LNA were compared to those of a diet providing adequate levels of this FA. One would expect that n-3 FA deficiency would resemble genetic diseases associated with impaired DHA synthesis, which preferentially affect the function of excitable tissues such as brain, retina, and muscle (55,56). Despite no apparent differences in body or brain weight, siblings of these rats that consumed the n-3-deficient diet showed poorer performance in spatial and olfactory-cued learning tests than those that received the control diet (33,57,58). As shown here, long-term inadequate dietary provision of n-3 fat sources results in a remarkable decrease in DHA in rat brain phospholipids (five-fold) and in liver (11-fold), and a concomitant increase in DPAn-6 FA (>20-fold).

In the present study, quantitation of PPAR mRNA in hepatic, ocular, and nervous tissues from rats fed the LNA-deficient or -adequate diet was referred to both  $\beta$ -actin and GAPDH mRNA abundance. Results shown here indicate that reference transcripts did not differ significantly in most tissues from rats consuming the LNA-deficient diet. However,  $\beta$ -actin mRNA levels in the F2 but not in the F3 generation were consistently lower in the LNA-deficient rats for all three tissue types analyzed here. In addition, GAPDH mRNA was also significantly lower in nervous tissue of F3 generation rats fed the LNA-deficient diet. We do not have a clear explanation for the apparent selective decrease in  $\beta$ -actin mRNA. As a matter of speculation, we propose that the expression of  $\beta$ -actin and GAPDH genes is sensitive, to a different extent, to an undefined factor that is dissimilarly present in F2 vs. F3 generation rats fed the LNA-deficient diet. Therefore, taking into account the results discussed above, PPAR data normalized to  $\beta$ -actin mRNA (F2 generation) and GAPDH mRNA (F3 generation, nervous tissue) were excluded from the analysis.

Our findings indicate that the marked decrease in DHA levels in tissues did not correlate with substantial changes in the level of PPAR $\alpha$  or PPAR $\beta$  transcripts in rat liver or brain. We found a modest increase in the abundance of PPAR $\beta$  mRNA in ocular tissues from rats consuming the LNA-deficient diet compared to those fed the LNA-adequate diet. In F3 generation rats, the PPAR $\beta$  mRNA level was 17% higher, and PPAR $\beta$  mRNA normalized to  $\beta$ -actin showed a 21% increase in ocular tissues from the n-3 FA deficient group.

Given that the biological activity of PPAR transcription factors is primarily controlled by ligand binding, the functional relevance of an increment in the abundance of the corresponding transcripts remains a matter of speculation. Considering that the precise function of PPAR $\beta$  has not been determined, the theoretical outcome of an eventual increase in PPAR $\beta$  protein (as a consequence of higher mRNA levels) could be inferred from emerging information that supports the role of PPAR $\beta$  as a dietary lipid sensor and modulator of lipid homeostasis. Reportedly, PPAR $\beta$ -null mice have reduced adipose tissue depots. Moreover, the advent of a selective PPAR $\beta$  ligand has provided evidence for its role as a regulator of the expression of the gene encoding the ABCA1 reverse cholesterol transporter (25). Therefore, changes in PPAR $\beta$

mRNA absolute abundance in ocular tissue could hypothetically stimulate the efflux of cholesterol from cells. However, modulation of other cellular pathways cannot be excluded.

Our results indicate that PPAR gene expression is moderately sensitive to long-term n-3 FA deficiency in the whole-body experimental model tested here. The dietary intervention in this study is highly specific to the n-3 FA series, preserving the total amount of fat as well as the amount of n-6 FA. The response to this dietary intervention conceivably includes mechanisms other than the transcriptional control of PPAR genes. It is possible that the consequences of dietary intake of n-3 FA primarily involve modulation of the activity rather than amount of PPAR. In addition, other transcription factors may be involved in the response to n-3 deficiency. Recent experiments using cell lines show that DHA is a potent activator of the transcriptional activity of 9-*cis* retinoic acid receptor (RXR) isoforms. Moreover, the reported effect was highly specific to DHA in comparison to other C<sub>22</sub>, C<sub>20</sub>, and C<sub>18</sub> unsaturated FA (59). Given the fact that RXR responsiveness to DHA is affected by heterodimerization and that PPAR and RXR are common partners, it is possible that DHA deficiency alters cellular pathways under the transcriptional control of both RXR and PPAR or other heterodimerization partners.

## ACKNOWLEDGMENT

Supported by Cátedra Presidencial 1996 to R.U.

## REFERENCES

- Clarke, S.D., and Jump, D.B. (1994) Dietary Polyunsaturated Fatty Acid Regulation of Gene Transcription, *Annu. Rev. Nutr.* 14, 83–98.
- Kliwer, S.A., Sundseth, S.S., Jones, S.A., Brown, P.S., Wisely, G.B., Koble, C.S., Devchand, P., Wahli, W., Willson, T.M., Lenhard, J.M., and Lehmann, J.M. (1997) Fatty Acids and Eicosanoids Regulate Gene Expression Through Direct Interactions with Peroxisome Proliferator-Activated Receptor  $\alpha$  and  $\gamma$ , *Proc. Nat. Acad. Sci. USA* 94, 4318–4323.
- Jump, D.B., and Clarke, S.D. (1999) Regulation of Gene Expression by Dietary Fat, *Annu. Rev. Nutr.* 19, 63–90.
- Neuringer, M., Anderson, G.J., and Connor, W.E. (1988) The Essentiality of n-3 Fatty Acids for the Development and Function of the Retina and Brain, *Annu. Rev. Nutr.* 8, 517–541.
- Bourre, J.M., Francois, M., Youyou, A., Dumont, O., Piciotti, M., Pascal, G., and Durand, G. (1989) The Effects of Dietary  $\alpha$ -Linoleic Acid on the Composition of Nerve Membranes, Enzymatic Activity, Amplitude of Electrophysiological Parameters, Resistance to Poison and Performance of Learning Tasks in Rats, *J. Nutr.* 119, 1880–1892.
- Carlson, S.E. (2000) Behavioral Methods Used in the Study of Long-Chain Polyunsaturated Fatty Acid Nutrition in Primate Infants, *Am. J. Clin. Nutr.* 71, 268S–274S.
- Uauy, R., Birch, E.E., Birch, D.G., and Peirano, P. (1992) Visual and Brain Function Measurements in Studies of n-3 Fatty Acid Requirements of Infants, *J. Pediatr.* 120, S168–S180.
- Carlson, S.E., Werkman, S.H., Rhodes, P.G., and Tolley, E.A. (1993) Visual-Acuity Development in Healthy Preterm Infants: Effect of Marine-Oil Supplementation, *Am. J. Clin. Nutr.* 58, 35–42.
- Neuringer, M., Connor, W.E., Van Petten, C., and Barstad, L. (1984) Dietary Omega-3 Fatty Acid Deficiency and Visual Loss in Infant Rhesus Monkeys, *J. Clin. Invest.* 73, 272–276.

10. Birch, E.E., Hoffman, D.R., Uauy, R., Birch, D.G., and Prestidge, C. (1998) Visual Acuity and the Essentiality of Docosahexaenoic Acid and Arachidonic Acid in the Diet of Term Infants, *Pediatr. Res.* 44, 201–209.
11. Devchand, P.R., Keller, H., Peters, J.M., Vázquez, M., González, F.J., and Wahli, W. (1996) The PPAR $\alpha$ -Leukotriene B<sub>4</sub> Pathway to Inflammation Control, *Nature* 384, 39–43.
12. Kersten, S., Desvergne, B., and Wahli, W. (2000) Roles of PPARs in Health and Disease, *Nature* 405, 421–424.
13. Braissant, O., Foufelle, F., Scotto, C., Dauça, M., and Wahli, W. (1996) Differential Expression of Peroxisome Proliferator Activated Receptor (PPARs): Tissue Distribution of PPAR- $\alpha$ , - $\beta$  and - $\gamma$  in the Adult Rat, *Endocrinology* 137, 354–366.
14. Mukherjee, R., Jow, L., Croston, G.E., and Paterniti, J.R., Jr. (1997) Identification, Characterization, and Tissue Distribution of Human Peroxisome Proliferator-Activated Receptor (PPAR) Isoforms PPAR $\gamma$ 2 versus PPAR $\gamma$ 1 and Activation with Retinoid Receptor Agonists and Antagonists, *J. Biol. Chem.* 272, 8071–8076.
15. Cullingford, T.E., Bhakoo, K., Peuchen, S., Dolphin, C.T., Patel, R., and Clark, J.B. (1998) Distribution of mRNAs Encoding the Peroxisome Proliferator-Activated Receptor  $\alpha$ ,  $\beta$ , and  $\gamma$  and the Retinoid X Receptor  $\alpha$ ,  $\beta$ , and  $\gamma$  in Rat Central Nervous System, *J. Neurochem.* 70, 1366–1375.
16. Granneman, J., Skoff, R., and Yang, X. (1998) Member of the Peroxisome Proliferator-Activated Receptor Family of Transcription Factors Is Differentially Expressed by Oligodendrocytes, *J. Neurosci. Res.* 51, 563–573.
17. Kremarik-Bouillaud, P., Schohn, H., and Dauça, M. (2000) Regional Distribution of PPAR Beta in the Cerebellum of the Rat, *J. Chem. Neuroanat.* 19, 225–232.
18. Gregoire, F.M., Smas, C.M., and Sul, H.S. (1998) Understanding Adipocyte Differentiation, *Physiol. Rev.* 78, 783–809.
19. Rosen, E.D., Sarraf, P., Troy, A.E., Bradwin, G., Moore, K., Milstone, D.S., Spiegelman, B.M., and Mortensen, R.M. (1999) PPAR Is Required for the Differentiation of Adipose Tissue *in vivo* and *in vitro*, *Mol. Cell* 4, 611–617.
20. Bassu-Modak, S., Braissant, O., Escher, P., Desvergne, B., Honegger, P., and Wahli, W. (1999) Peroxisome Proliferator-Activated Receptor Beta Regulates Acyl-CoA Synthetase 2 in Reaggregated Rat Brain Cell Cultures, *J. Biol. Chem.* 274, 35881–35888.
21. Bastie, C., Luquet, S., Holst, D., Jehl-Petri, C., and Grimaldi, P.A. (2000) Alterations of Peroxisome Proliferator-Activated Receptor ( $\delta$ ) Activity Affect Fatty Acid-Controlled Adipose Differentiation, *J. Biol. Chem.* 275, 38768–38773.
22. Peters, J.M., Lee, S.S., Li, W., Ward, J.M., Gavrillova, O., Everett, C., Reitman, M.L., Hudson, L.D., and González, F.J. (2000) Growth, Adipose, Brain, and Skin Alterations Resulting from Targeted Disruption of the Mouse Peroxisome Proliferator-Activated Receptor Beta (Delta), *Mol. Cell. Biol.* 20, 5119–5128.
23. He, T.C., Chan, T.A., Vogelstein, B., and Kinzler, K.W. (1999) PPAR Delta Is an APC-Regulated Target of Nonsteroidal Anti-inflammatory Drugs, *Cell* 29, 335–345.
24. Mano, H., Kimura, C., Fujisawa, Y., Kameda, T., Watanabe-Mano, M., Kaneko, H., Kaneda, T., Hakeda, Y., and Kumegawa, M. (2000) Cloning and Function of Rabbit Peroxisome Proliferator-Activated Receptor  $\delta/\beta$  in Mature Osteoclasts, *J. Biol. Chem.* 275, 8126–8132.
25. Oliver, W.R., Shenk, J.L., Snaith, M.R., Russell, C.S., Plunket, K.D., Bodkin, N.L., Lewis, M.C., Winegar, D.A., Sznajdman, M.L., Lambert, M.H., et al. (2001) A Selective Peroxisome Proliferator-Activated Receptor  $\delta$  Agonist Promotes Reverse Cholesterol Transport, *Proc. Natl. Acad. Sci. USA* 98, 5306–5311.
26. Forman, B.H., Chen, J., and Evans, R.M. (1997) Hypolipidemic Drugs, Polyunsaturated Fatty Acids, and Eicosanoids Are Ligands for Peroxisome Proliferator Activated Receptor  $\alpha$  and  $\gamma$ , *Proc. Natl. Acad. Sci. USA* 94, 4312–4317.
27. Yu, K., Bayona, W., Kallen, C.B., Harding, H.P., Ravera, C.P., McMahon, G., Brown, M., and Lazar, M.A. (1995) Differential Activation of Peroxisome Proliferator-Activated Receptors by Eicosanoids, *J. Biol. Chem.* 270, 23975–23983.
28. Vidal-Puig, A., Jiménez-Liñán, M., Lowell, B.B., Hamann, A., Hu, E., Spiegelman, B., Flier, J.S., and Moller, D.E. (1996) Regulation of PPAR $\gamma$  Gene Expression by Nutrition and Obesity in Rodents, *J. Clin. Invest.* 97, 2553–2561.
29. Fajas, L., Schoonjans, K., Gelman, L., Kim, J.B., Najib, J., Martin, G., Fruchart, J.C., Briggs, M., Spiegelman, B.M., and Auwerx, J. (1999) Regulation of Peroxisome Proliferator-Activated Receptor Gamma Expression by Adipocyte Differentiation and Determination Factor 1/Sterol Regulatory Element Binding Protein 1: Implications for Adipocyte Differentiation and Metabolism, *Mol. Cell. Biol.* 19, 5495–5503.
30. Hashimoto, T., Cook, W.S., Qi, C., Yeldandi, A.V., Reddy, J.K., and Rao, M.S. (2000) Defect in Peroxisome Proliferator-Activated Receptor  $\alpha$ -Inducible Fatty Acid Oxidation Determine the Severity of Hepatic Steatosis in Response to Fasting, *J. Biol. Chem.* 275, 28918–28928.
31. Kersten, S., Seydoux, J., Peters, J.M., González, F.J., Desvergne, B., and Wahli, W. (1999) Peroxisome Proliferator Activated Receptor  $\alpha$  Mediates the Adaptive Response to Fasting, *J. Clin. Invest.* 103, 1489–1498.
32. Kersten, S., Mandard, S., Tan, N.S., Escher, P., Metzger, D., Chambon, P., González, F.J., Desvergne, B., and Wahli, W. (2000) Characterization of the Fasting-Induced Adipose Factor FIAF, a Novel Peroxisome Proliferator-Activated Receptor Target Gene, *J. Biol. Chem.* 275, 28488–28493.
33. Reeves, P.G., Neilsen, F.H., and Fahey, G.C. (1993) Committee Report on the AIN-93 Purified Rodent Diet, *J. Nutr.* 123, 1939–1951.
34. Greiner, R.S., Moriguchi, T., Hutton, A., Slotnick, B.M., and Salem, N., Jr. (1999) Rats with Low Levels of Brain Docosahexaenoic Acid Show Impaired Performance in Olfactory-Based and Spatial Learning Tasks, *Lipids* 34 (Suppl.), S239–S243.
35. Bligh, E.G., and Dyer, W.J. (1959) A Rapid Method of Total Lipid Extraction and Purification, *Can. J. Biochem. Physiol.* 37, 911–917.
36. Morrison, W.R., and Smith, L.M. (1961) Preparation of Fatty Acid Methyl Esters and Dimethylacetals from Lipids with Boron Fluoride-Methanol, *J. Lipid Res.* 35, 600–608.
37. Salem, N., Jr., Reyzer, M., and Karanian, J. (1996) Losses of Arachidonic Acid in Rat Liver After Alcohol Inhalation, *Lipids* 31, S153–S156.
38. Salem, N., Jr. (1989) Omega-3 Fatty Acids: Molecular and Biochemical Aspects, in *New Protective Roles of Selected Nutrients in Human Nutrition* (Spiller, G., and Scala, J., eds.), pp. 109–228, Alan R. Liss, New York.
39. Hamilton, J., Greiner, R., Salem, N., and Kim, H. (2000) n-3 Fatty Acid Deficiency Decreases Phosphatidylserine Accumulation Selectively in Neuronal Tissues, *Lipids* 35, 863–869.
40. Rolland, V., Dugail, I., Le Liepvre, X., and Lavau, M. (1995) Evidence of Increased Glyceraldehyde-3-phosphate Dehydrogenase and Fatty Acid Synthetase Promoter Activities in Transiently Transfected Adipocytes from Genetically Obese Rats, *J. Biol. Chem.* 270, 1102–1106.
41. Weisinger, G., Gavish, M., Mazurika, C., and Zinder, O. (1999) Transcription of Actin, Cyclophilin and Glyceraldehyde Phosphate Dehydrogenase Genes: Tissue- and Treatment-Specificity, *Biochim. Biophys. Acta* 1446, 225–232.
42. Zhong, H., and Simons, J.W. (1999) Direct Comparison of GAPDH,  $\beta$ -Actin, Cyclophilin, and 28S rRNA as Internal Standards for Quantifying RNA Levels Under Hypoxia, *Biochem. Biophys. Res. Commun.* 259, 523–526.

43. Okuno, M., Kajiwara, K., Imai, S., Kobayashi, T.Y., Honma, N., Maki, T., Suruga, K., Goda, T., Takase, S., Muto, Y., and Moriwaki, H. (1997) Perilla Oil Prevents the Excessive Growth of Visceral Adipose Tissue in Rats by Down-Regulating Adipocyte Differentiation, *J. Nutr.* 127, 1752–1757.
44. Bonilla, S., Redonnet, A., Noel-Suberville, C., Pallet, V., Garcin, H., and Higuieret, P. (2000) High-Fat Diets Affect the Expression of Nuclear Retinoic Acid Receptor in Rat Liver, *Br. J. Nutr.* 83, 665–671.
45. Ouali, F., Djouadi, F., Merlet-Bénichou, C., and Bastin J. (1998) Dietary Lipids Regulate  $\beta$ -Oxidation Enzyme Gene Expression in the Developing Rat Kidney, *Am. J. Physiol.* 275 (Renal Physiol. 44), F777–F784.
46. Nisoli, E., Carruba, M.O., Tonello, C., Macor, C., Federspil, G., and Vettor, R. (2000) Induction of Fatty Acid Translocase/CD36, Peroxisome Proliferation-Activated Receptor-Gamma2, Leptin, Uncoupling Proteins 2 and 3, and Tumor Necrosis Factor-Alpha Gene Expression in Human Subcutaneous Fat by Lipid Infusion, *Diabetes* 49, 319–324.
47. Makrides, M., Neumann, M., Simmer, K., Pater, J., and Gibson, R. (1995) Are Long-Chain Polyunsaturated Fatty Acids Essential Nutrients in Infancy? *Lancet* 345, 1463.
48. Fernstrom, J.D. (1999) Effects of Dietary Polyunsaturated Fatty Acids on Neuronal Function, *Lipids* 34, 161–169.
49. Bush, R.A., Armand, M., Remé, C.E., and Williams, T.P. (1994) Dietary Deficiency of n-3 Fatty Acid Alters Rhodopsin Content and Function in the Rat Retina, *Invest. Ophthalmol. Vis. Sci.* 35, 91–100.
50. Rotstein, N., Politi, L.E., and Avelaño, M.I. (1998) Docosahexaenoic Acid Promotes Differentiation of Developing Photoreceptors in Culture, *Invest. Ophthalmol. Vis. Sci.* 39, 2750–2758.
51. Braissant, O., and Wahli, W. (1998) Differential Expression of Peroxisome Proliferator Activated Receptor- $\alpha$ , - $\beta$  and - $\gamma$  During Rat Embryonic Development, *Endocrinology* 139, 2748–2754.
52. Foot, M., Cruz, T.F., and Clandinin, M.T. (1982) Influence of Dietary Fat on the Lipid Composition of Rat Brain Synaptosomal and Microsomal Membranes, *Biochem. J.* 208, 631–640.
53. Bourre, J.M., Pascal, D., Durand, G., Masson, M., Dumont, O., and Piciotti, M. (1984) Alterations in the Fatty Acid Composition of Rat Brain Cells (neurons, astrocytes and oligodendrocytes) and of Subcellular Fractions (myelin synaptosomes) Induced by a Diet Devoid of n-3 Fatty Acids, *J. Neurochem.* 43, 342–348.
54. Yamamoto, N., Saitoh, M., Moriuchi, A., Nomura, M., and Okuyama, H. (1987) Effect of Dietary  $\alpha$ -Linolenate/Linoleate Balance on Brain Lipid Composition and Learning Ability of Rats, *J. Lipid Res.* 28, 144–151.
55. Martínez, M. (1992) Abnormal Profiles of Polyunsaturated Fatty Acids in the Brain, Liver, Kidney and Retina of Patients with Peroxisomal Disorders, *Brain Res.* 583, 171–182.
56. Infante, J.P., and Huszagh, V.A. (2000) Secondary Carnitine Deficiency and Impaired Docosahexaenoic (22:6n-3) Acid Synthesis: A Common Denominator in the Pathophysiology of Disease of Oxidative Phosphorylation and  $\beta$ -Oxidation, *FEBS Lett.* 468, 1–5.
57. Moriguchi, T., Greiner, R.S., and Salem N., Jr. (2000) Behavioral Deficits Associated with Dietary Induction of Decreased Brain Docosahexaenoic Acid Concentration, *J. Neurochem.* 75, 2563–2573.
58. Greiner, R.S., Moriguchi, T., Hutton, A., Slotnick, B.M., and Salem, N., Jr. (2001) Olfactory Discrimination Deficits in n-3 Fatty Acid Deficient Rats, *Physiol. Behav.* 72, 379–385.
59. Mata de Urquiza, M., Liu, S., Sjöberg, M., Zetterström, R.H., Griffiths, W., Sjövall, J., and Perlmann, T. (2000) Docosahexaenoic Acid, a Ligand for the Retinoid X Receptor in Mouse Brain, *Science* 290, 2140–2144.

[Received October 3, 2001, and in revised form February 11, 2002; revision accepted February 22, 2002]



# Dietary Cholesterol Modulates $\Delta 6$ and $\Delta 9$ Desaturase mRNAs and Enzymatic Activity in Rats Fed a Low-EFA Diet

Rodolfo R. Brenner\*, Ana M. Bernasconi, María S. González, and Omar J. Rimoldi

Instituto de Investigaciones Bioquímicas de La Plata (INIBIOLP), CONICET-UNLP,  
Facultad de Ciencias Médicas, 1900-La Plata, Argentina

**ABSTRACT:** The effects of a 1% addition of cholesterol to a diet low in EFA on FA desaturases were examined. The administration of cholesterol markedly increased the esterified cholesterol content in microsomes and total liver lipids from the first day, whereas the proportion of free cholesterol remained unaltered throughout the treatment. An excellent homeostasis in the free cholesterol content was apparently evoked by the acyl-CoA cholesterol acyltransferase. The cholesterol esters were mainly oleate, palmitate, and stearate, and the addition of cholesterol increased the relative proportions of cholesterol palmitoleate and oleate. The addition of cholesterol to a low-EFA diet induced, as in animals fed a high-EFA diet, a marked increase in liver stearoyl-CoA desaturase-1 mRNA and enzyme activity. This increased activity apparently evoked a similar enhancement of palmitoleic and oleic acids in total and microsomal liver lipids. The cholesterol-rich diet depressed the liver  $\Delta 6$  and  $\Delta 5$  desaturase activity. However, the abundance of  $\Delta 6$  desaturase mRNA was not modified throughout the treatment. This indicates that the depressive effect is evoked at a step beyond that controlled by the mRNA level. The depression of both enzymatic activities was consistent with the decrease in the percentages of arachidonic acid and DHA in total and microsomal liver lipids. Taken together, these results indicate that through its modulating effect on the desaturases, dietary cholesterol may lead an animal or human fed low-EFA diet to a true deficiency by the decreased synthesis of the highly polyunsaturated acids derived from linoleic and  $\alpha$ -linolenic acids.

Paper no. L8938 in *Lipids* 37, 375–383 (April 2002).

Very early research in the 1960s (1,2) showed, by the measurement of parameters used then, that feeding cholesterol to animals with a suboptimal EFA intake led to an exacerbation of the signs of EFA deficiency. The real biological effects of EFA deficiency are mainly due to a decrease in the highly polyunsaturated acids of the n-6 and n-3 families and not to linoleic or  $\alpha$ -linolenic acids. It has repeatedly been shown in later publications that administration of dietary cholesterol to

\*To whom correspondence should be addressed at INIBIOLP, Facultad de Ciencias Médicas, 60 y 120, 1900-La Plata, Argentina.  
E-mail: rbrenner@atlas.med.unlp.edu.ar

Abbreviations: HPTLC, high-performance thin-layer chromatography; Ptd-Cho, phosphatidylcholine; SCD, stearoyl-CoA desaturase; SREBP, sterol regulatory element binding protein.

rats evokes not only its incorporation into the cell but also an increase in liver  $\Delta 9$  desaturase activity and a decrease in  $\Delta 6$  and  $\Delta 5$  desaturase activities, followed by important changes in the FA composition of cell phospholipids (3–8).

These effects of cholesterol were shown in rats fed diets rich in linoleic acid, and they provoked a decrease in the polyunsaturated acids as arachidonic acid was synthesized in the animal from dietary linoleic acid. Therefore, enhancing the effects of EFA deficiency evoked by cholesterol might be the consequence of the depression of  $\Delta 5$  and  $\Delta 6$  desaturases.

However, a linoleic acid-rich diet causes a depressive effect on the  $\Delta 9$  desaturase gene expression (9). In addition, Clarke's group (10) showed not only that the addition of linoleic acid to a fat-free diet depressed the hepatic  $\Delta 6$  desaturase activity, but also that this depression was paralleled by a reduction in the corresponding  $\Delta 6$  desaturase mRNA. The same authors (11) also found that a diet containing 10% safflower seed oil depressed the hepatic mRNA of  $\Delta 5$  desaturase compared to that of rats fed a fat-free diet or a diet containing triolein. In addition to these results, we have repeatedly shown in our laboratory, as well as in a recent review (12), that, in general, hormones (except insulin) evoke effects on the  $\Delta 9$  desaturase that are antagonistic to those found for both  $\Delta 6$  and  $\Delta 5$  desaturation activities, indicating different mechanisms of regulation. Therefore, we consider it necessary to prove definitively if—in a diet low in EFA that already enhances  $\Delta 9$ ,  $\Delta 6$ , and  $\Delta 5$  desaturation of FA—the addition of 1% cholesterol is still able to modify activities and even push animals to a true EFA deficiency. Moreover, in spite of the enhancing effect of a high-cholesterol, EFA-rich diet on the abundance of stearoyl-CoA desaturase-1 (SCD-1) mRNA in rat liver shown by Landau *et al.* (7), the effect of a high-cholesterol diet on the  $\Delta 6$  desaturase mRNA level has not yet been investigated.

All these results prompted us to investigate at different times the simultaneous effect of a diet low in EFA and one containing 1% cholesterol on the incorporation of cholesterol into total liver cells and microsomes; the  $\Delta 9$ ,  $\Delta 6$ , and  $\Delta 5$  desaturation activities; and the abundance of  $\Delta 9$  and  $\Delta 6$  desaturase mRNA. The total FA composition of liver cells and microsomes, as well as the distribution of cholesterol and cholesterol esters and their FA composition, was also checked.

We found that dietary cholesterol was incorporated into liver microsomes and total liver cells, increasing the cholesterol ester fraction but not the relative ratio of free cholesterol. Dietary cholesterol evoked an increase in  $\Delta 9$  desaturase mRNA that correlated with the enzymatic activity. However, it did not modify the abundance of  $\Delta 6$  desaturase mRNA but decreased the enzymatic activities of both  $\Delta 6$  and  $\Delta 5$  desaturases. The FA composition of microsomes, total liver lipids, and cholesterol esters followed the enzymatic activity changes rather well and showed a drastic decrease in highly polyunsaturated acids.

## MATERIALS AND METHODS

**Materials.** [1- $^{14}$ C]Stearic acid (56 mCi/mmol, 98% radiochemically pure) and [1- $^{14}$ C]linoleic acid (55 mCi/mmol, 99% radiochemically pure) were purchased from Amersham Life Science (Amersham, England). [1- $^{14}$ C]Eicosa-8,11,14-trienoic acid (52 mCi/mmol, 98% radiochemically pure) was provided by New England Nuclear (Boston, MA). Unlabeled FA were provided by Nu-Chek-Prep (Elysian, MN). Cofactors used for enzymatic reactions were obtained from Sigma Chemical Co. (St. Louis, MO). Solvents for HPLC were purchased from Carlo Erba (Milan, Italy).

Rat SCD-1 ( $\Delta 9$  desaturase) cDNA was a kind gift from Dr. Juris Tsunehiro Ozols (Department of Biochemistry, University of Connecticut, Central Health, Farmington, CT), and rat  $\Delta 6$  desaturase cDNA was a kind gift from Dr. T. Aki (Department of Molecular Biotechnology, Hiroshima University, Higashi-Hiroshima, Japan). Restriction enzymes and other DNA nuclei-modifying enzymes were obtained from Promega (Madison, WI). All plasmid DNA were isolated by SDS-NaOH methods (13).

**Animals and diets.** Animal care and handling were in accordance with internationally accepted principles concerning the care and use of laboratory animals. Forty male Wistar rats were fed for 10 d after weaning with a control diet low in EFA composed of 62 wt% starch, 22.6 wt% delipidated casein, 9.4 wt% cacao butter, 2 wt% vitamins (14), and 4 wt% minerals (14). The FA composition of the food was 32.2 wt% 16:0, 0.6 wt% 16:1, 28.7 wt% 18:0, 34.0 wt% 18:1, and 4.5 wt% 18:2; cholesterol was not detected. After this time, 20 animals were kept on the control low-EFA diet, whereas the other 20 animals were fed the same diet as the control with the addition of 1 wt% cholesterol. Lots of five animals from each group were sacrificed by decapitation without anesthesia and exsanguinated on days 1, 3, 7, and 21. The liver from each animal was rapidly excised and placed in an ice-cold homogenizing solution (1:3 wt/vol) composed of 0.25 M sucrose, 0.15 M KCl, 0.1 mM EDTA, 1.41 mM *N*-acetyl cysteine, 5 mM  $\text{MgCl}_2$ , and 62 mM phosphate buffer (pH 7.4). Microsomes were obtained by differential ultracentrifugation at  $100,000 \times g$  (Beckman Ultracentrifuge) as described elsewhere (15). They were stored at  $-80^\circ\text{C}$ .

Protein concentration was measured according to the procedure of Lowry *et al.* (16).

**Lipid analysis.** Lipids were extracted from total liver and microsomes according to the procedure of Folch *et al.* (17). Total lipid content was measured by aliquot evaporation to constant weight. Total phosphorus was determined by the method of Chen *et al.* (18).

Free and esterified cholesterol were measured in total homogenate and microsomal liver lipids. They were separated by TLC on Whatman high-performance thin-layer chromatography (HPTLC) plates of  $20 \times 10$  cm (Linear-K preadsorbent strip), using hexane/ethyl ether/acetic acid (80:20:1, by vol). Cholesterol and esterified cholesterol spots were visualized by the ferric chloride method of Lowry (19). They were quantified by comparison to curves constructed using commercial standards (1–5  $\mu\text{g}$ ). After staining, the plates were scanned and the densitometric quantitation was performed using 1D Image Analysis Software (Kodak, Rochester, NY) from multiple exposures. The cholesterol esters separated by TLC were saponified with alcoholic KOH, and the FA were separated and methylated with  $\text{BF}_3$  at  $64^\circ\text{C}$  for 1 h.

FA composition of the cholesterol esters, microsomal liver lipids, and total lipids of liver, adrenals, and testicles were analyzed by GLC of their methyl esters in a Hewlett-Packard HP 6890 apparatus. They were injected into an Omega Wax 250 (Supelco, Bellefonte, PA) capillary column of 30 m, 0.25 mm i.d., and 0.25  $\mu\text{m}$  film. The temperature was programmed to obtain a linear increase of  $3^\circ\text{C}/\text{min}$  from 175 to  $230^\circ\text{C}$ . The chromatographic peaks were identified by comparison of their retention times with those of standards.

**FA desaturation assays.**  $\Delta 9$ ,  $\Delta 6$ , and  $\Delta 5$  desaturations were estimated in hepatic microsomes using as substrates 50  $\mu\text{M}$  [1- $^{14}$ C]stearic acid, 33  $\mu\text{M}$  [1- $^{14}$ C]linoleic acid, and 50  $\mu\text{M}$  [1- $^{14}$ C]eicosa-8,11,14-trienoic acid, respectively. The acids were incubated with 2.5, 2.0, and 1.95 mg of microsomal protein, respectively, in a final volume of 1.5 mL at  $36^\circ\text{C}$  (3). The reaction mixture consisted of 0.25 M sucrose, 0.15 M KCl, 1.41 mM *N*-acetyl-L-cysteine, 40 mM NaF, 60  $\mu\text{M}$  CoA (sodium salt), 1.3 mM ATP, 0.87 mM NADH, 5 mM  $\text{MgCl}_2$ , and 40 mM potassium phosphate buffer (pH 7.4). After 1 min preincubation at  $36^\circ\text{C}$ , the reaction was started by addition of microsomal protein, and the mixture was incubated in open tubes for 15 min in a thermoregulated shaking water bath. The desaturation reaction was stopped with 10% (wt/vol) KOH in ethanol followed by saponification. The extracted FFA were dissolved in methanol/water/acetic acid (85:15:0.2, by vol) and fractionated by RP-HPLC (20). Separations were performed on an Econosil  $\text{C}_{18}$  10- $\mu\text{m}$  particle size reversed-phase column ( $250 \times 4.6$  mm) (Alltech Associates, Inc., Deerfield, IL) coupled to a guard column (10  $\times$  4 mm), and filled with pellicular  $\text{C}_{18}$ , using a mobile phase (methanol/water/acetic acid, 90:10:0.2, by vol) at a flow rate of 1 mL/min and a Merck-Hitachi L-6200 solvent delivery system (Darmstadt, Germany). The column eluate was monitored by a UV spectrometer at 205 nm for FA identification on the basis of retention times. Radioactivity associated with FA was measured by a Radiomatic Instrument (Tampa, FL) Flo-One Beta flow-through liquid scintillation counter fitted with a

0.5-mL cell. Ultima Flo-M scintillation cocktail (Packard Instruments, Downers Grove, IL) was used at a rate of 3 mL/min.

**Northern blots of Δ9 and Δ6 desaturase mRNA.** Total liver RNA of the different animals tested was isolated with a Wizard RNA Isolation System (Promega) according to the manufacturer's instructions. Twenty micrograms of total RNA was size-fractionated on a 1% formaldehyde gel and then transferred to a Zeta-Probe nylon membrane (Bio-Rad, Richmond, CA). The Δ9 and Δ6 desaturase and β-actin probes were prepared by incorporating [<sup>32</sup>P]dCTP by random prime labeling. Northern blot hybridization analyses were performed as described by Sambrook *et al.* (13). The autoradiographic signal for Δ9 and Δ6 desaturase mRNA was quantified from multiple exposures using 1D Image Analysis Software (Kodak). They were normalized to mRNA for β-actin, with all mRNA probed on the same gel.

**Statistical analysis.** Data in the tables are expressed as mean ± SD. They were analyzed using ANOVA (Instat v.2.0 Graph Pad Software, San Diego, CA) to identify time and diet effects and their interactions. When effects were identified as significant (*P* < 0.05), Tukey's *post-hoc* tests were utilized to identify significant effects of diet at particular time points or significant effects of time on a particular diet.

**RESULTS**

**Effect of dietary cholesterol on free cholesterol and cholesterol ester content in liver homogenate and microsomes.** Dietary cholesterol has repeatedly been shown to be incorporated into liver (3–5,7). In the present experiment, the same is shown in total liver and liver microsomes (Table 1). However, the incorporation of cholesterol apparently did not increase the lipid content of the liver microsomes since the lipid/protein ratio of these organelles was steadily maintained at 0.52 mg/mg throughout the 21 d of the experiment. Nevertheless, the total lipid content of total liver increased due to cholesterol incorporation. In the control rats the lipid/protein ratio

(by wt) was maintained at 0.22 throughout the 21 d, whereas it increased in the cholesterol-treated animals from 0.22 to 0.37 on day 7 and to 0.50 on day 21.

When we compared the extent to which the relative cholesterol increase in the lipid fraction was due to the free or esterified form, we found that in cytosol and microsomes the increase was due to cholesterol esters but not to free cholesterol.

In total liver homogenate (Table 1) the percentage of free cholesterol in the lipids compared to the control animals was not increased and remained unmodified on days 1, 7, and 21 after cholesterol administration. However, the percentage of cholesterol ester in the same lipids was very significantly increased as early as 24 h after cholesterol administration and was progressively enhanced on days 7 and 21. In spite of that, the amounts of both cholesterol forms increased in the cell because the total lipids increased.

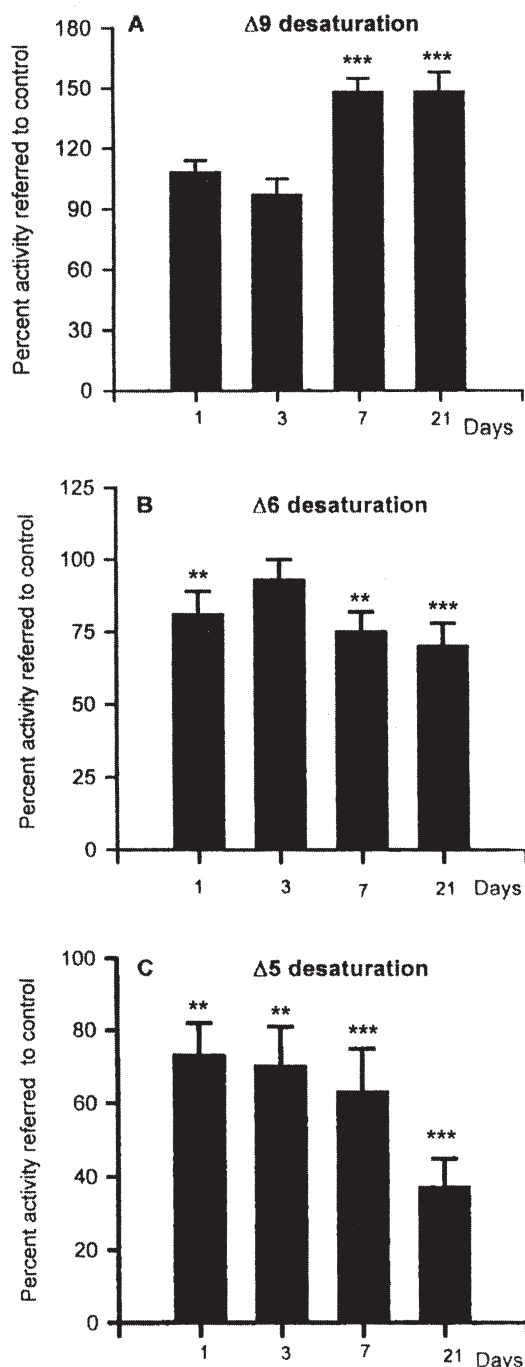
Similarly, in rat liver microsomal lipids (Table 1), although no modification of the free cholesterol was shown compared to the control animals on days 1, 7, and 21, a very significant increase in cholesterol esters was also found after 24 h of treatment. In microsomes the higher level of esters was maintained on the following days, at least up to the end of the experiment (21 d). Since the lipid/protein ratio was maintained in the microsomes, only the cholesterol ester fraction was quantitatively increased.

**Effect of dietary cholesterol on liver Δ9 desaturation activity and the abundance of mRNA.** The liver Δ9 desaturation activity for the conversion of stearic acid to oleic acid is shown in Figure 1. After 24 h of cholesterol feeding, no significant change in Δ9 desaturation activity was shown. After 7 d, it reached significance compared to the activity of control animals. These results are similar to results from experiments (3–5,7) in which a different diet rich in EFA was administered. An EFA-rich diet is known to depress Δ9 desaturation activity (21). Therefore, in spite of these differential effects of low-EFA and EFA-sufficient diets on the liver Δ9 desaturation activity, the addition of cholesterol evoked a relative activation of the reaction.

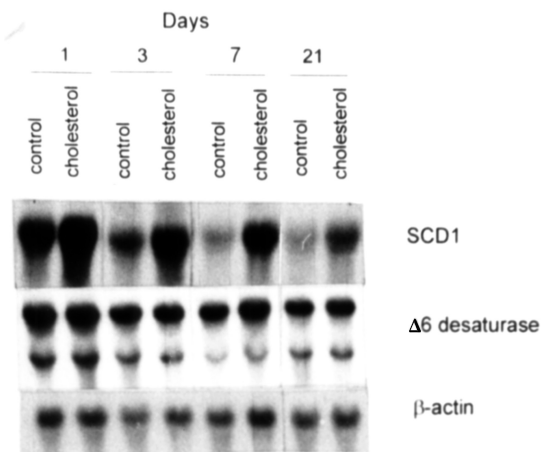
**TABLE 1**  
**Free and Esterified Cholesterol (wt%) of Total Lipids<sup>a</sup>**

Treatment	Time						
	1 d		7 d		21 d		
	Control (a)	Cholesterol (b)	Control (c)	Cholesterol (d)	Control (e)	Cholesterol (f)	
Total liver	Free cholesterol	6.23 ± 1.69	5.82 ± 1.57	5.69 ± 1.71	5.10 ± 1.25	2.84 ± 0.86 <sup>a**,c*</sup>	2.27 ± 0.03 <sup>b**,d*</sup>
	Esterified cholesterol	3.32 ± 1.91	10.50 ± 2.91 <sup>a*</sup>	5.78 ± 2.21	16.32 ± 3.52 <sup>c**</sup>	2.82 ± 0.85	30.00 ± 8.49 <sup>b***,d***,e***</sup>
Liver microsomes	Free cholesterol	4.91 ± 1.70	4.35 ± 0.89	4.07 ± 1.18	4.19 ± 1.50	3.28 ± 0.47	4.26 ± 0.55
	Esterified cholesterol	3.02 ± 0.99	13.27 ± 3.45 <sup>a***</sup>	3.03 ± 0.80	8.32 ± 1.25 <sup>c***</sup>	4.19 ± 0.87	10.70 ± 0.98 <sup>e***</sup>

<sup>a</sup>Results are the mean ± SD (*n* = 5 animals) expressed as weight percentage of total lipids. Different roman superscript letters indicate significant differences between this value and that in the group headed by the same letter. \*\*\**P* < 0.001, \*\**P* < 0.01, \**P* < 0.05.



**FIG. 1.** Relative FA desaturation activities in cholesterol-treated rats.  $\Delta 9$ ,  $\Delta 6$ , and  $\Delta 5$  desaturation in EFA-deficient rats during cholesterol supplementation (at 1, 3, 7, and 21 d) using liver microsomes. Microsomal protein was incubated with (A) [ $1\text{-}^{14}\text{C}$ ]stearic acid; (B) [ $1\text{-}^{14}\text{C}$ ]linoleic acid, or (C) [ $1\text{-}^{14}\text{C}$ ]eicosatrienoic acid. The assay mixture contained 60  $\mu\text{M}$  CoA, 1.3 mM ATP, 0.45 mM NADH, 5 mM  $\text{MgCl}_2$  in 40 mM potassium phosphate buffer, 0.25 M sucrose, 0.15 M KCl, 1.41 mM *N*-acetyl-L-cysteine, and 40 mM NaF; final pH: 7.0. Data are expressed as a percentage of the control group at each time point and represent means  $\pm$  SD ( $n = 4$ ). Control enzymatic activities (nmol product/min-mg protein) on day 1 were (A)  $0.407 \pm 0.048$ ; (B)  $0.668 \pm 0.031$ ; and (C)  $1.165 \pm 0.201$ . Symbols above columns indicate statistically significant differences from values of control groups: \*\*\* $P < 0.001$ ; \*\* $P < 0.01$  using the Student's *t*-test (Excel Microsoft).



**FIG. 2.** Effect of a cholesterol-rich diet on the levels of liver, stearoyl-CoA desaturase-1 (SCD-1), and  $\Delta 6$  desaturase mRNA. Total liver mRNA from control and cholesterol-fed animals at the periods indicated were electrophoresed on a 1% agarose-formaldehyde gel, blotted to nylon membrane, and probed with  $^{32}\text{P}$ -random primed cDNA. mRNA levels of SCD-1 and  $\Delta 6$  desaturases were compared to  $\beta$ -actin signals.

The relative abundance of SCD-1 mRNA in the livers of rats fed the cholesterol diet was significantly higher than in the livers of animals fed the low-EFA diet alone (Fig. 2). A 1.5-fold increase compared to the controls was evident 24 h after feeding the cholesterol diet, and it apparently reached a steady state on the following days at approximately twofold. It is important to note that this enhancement is evoked by the cholesterol diet independent of any apparent EFA deficiency effect known to induce the SCD-1 mRNA (22).

However, we have to remark that the relatively significant increase in the  $\Delta 9$  desaturation activity evoked by cholesterol in this experiment was shown only after 7 d of treatment (Fig. 1), whereas the relative increase in liver SCD-1 mRNA was already shown in the first 24 h (Fig. 2).

*Effect of dietary cholesterol on liver  $\Delta 6$  and  $\Delta 5$  desaturation activities and level of  $\Delta 6$  desaturase mRNA.* The activities of microsomal liver  $\Delta 6$  and  $\Delta 5$  desaturations of linoleic and eicosatrienoic n-6 acids, respectively, in rats fed a low-EFA control diet and the same diet plus 1% cholesterol are shown in Figure 1. As expected, the relative activities of both reactions are depressed to some extent by the addition of dietary cholesterol.

On this occasion we also measured the abundance of  $\Delta 6$  desaturase mRNA in liver cells by Northern blot analysis (Fig. 2). Two transcripts of mRNA  $\Delta 6$  desaturase were found. It is important to remark that Cho *et al.* (11) also found two transcripts of this enzyme, a major one of 3.8 kb and a minor one of 1.9 kb in rat liver and similar ones in mouse. Both mRNA transcripts, the major one and the minor one (see Fig. 2), are not significantly altered when compared to control animals by the effect of cholesterol addition to the diet as measured after 1, 3, 7, and 21 d of treatment. From these data, the depressive effect of cholesterol-rich diets on the  $\Delta 6$  desaturation



**TABLE 2**  
**FA Composition (wt%) of Total Liver Lipids<sup>a</sup>**

FA	1 d		7 d		21 d	
	Control (a)	Cholesterol (b)	Control (c)	Cholesterol (d)	Control (e)	Cholesterol (f)
16:0	20.24 ± 1.00	19.68 ± 1.57	20.34 ± 1.07	19.57 ± 1.92	21.53 ± 0.82	16.84 ± 0.20 <sup>e****</sup>
16:1	2.05 ± 0.06	2.82 ± 0.31 <sup>a*</sup>	1.47 ± 0.31	5.12 ± 1.93 <sup>b**,c***</sup>	2.18 ± 0.27	6.54 ± 0.82 <sup>b***,e***</sup>
18:0	20.77 ± 0.43	18.58 ± 1.20	23.41 ± 2.15	14.29 ± 0.65 <sup>b**,c***</sup>	22.77 ± 2.07	14.36 ± 1.25 <sup>b**,e***</sup>
18:1n-9	25.54 ± 0.42	30.06 ± 2.71 <sup>a***</sup>	24.18 ± 0.66	38.73 ± 0.92 <sup>b***,c***</sup>	25.00 ± 0.66	45.66 ± 2.03 <sup>b***,d***,e***</sup>
18:2n-6	5.60 ± 0.34	5.78 ± 0.40	5.92 ± 0.45	5.29 ± 0.23	6.24 ± 0.10	4.67 ± 0.30 <sup>b***,e***</sup>
20:3n-9	8.43 ± 1.03	7.63 ± 0.69	5.72 ± 0.85 <sup>a**</sup>	5.86 ± 1.32	3.82 ± 1.19 <sup>a***</sup>	4.12 ± 1.07 <sup>b***</sup>
20:3n-6	1.14 ± 0.11	1.14 ± 0.17	1.08 ± 0.07	0.95 ± 0.11	0.90 ± 0.25	0.65 ± 0.08 <sup>b***</sup>
20:4n-6	12.63 ± 0.83	11.00 ± 0.73	13.58 ± 1.42	7.65 ± 1.35 <sup>b***,c***</sup>	14.06 ± 1.35	5.65 ± 0.28 <sup>b***,e***</sup>
22:5n-6	1.03 ± 0.10	0.95 ± 0.04	1.29 ± 0.30	0.72 ± 0.29 <sup>c***</sup>	0.88 ± 0.03	0.44 ± 0.08 <sup>b**,e**</sup>
22:5n-3	0.13 ± 0.04	0.12 ± 0.03	0.12 ± 0.04	0.06 ± 0.06	0.33 ± 0.08 <sup>a***,c***</sup>	0.12 ± 0.01 <sup>e***</sup>
22:6n-3	2.45 ± 0.33	2.25 ± 0.37	2.88 ± 0.45	1.76 ± 0.37 <sup>c***</sup>	2.29 ± 0.40	0.95 ± 0.01 <sup>b***,d*,e***</sup>

<sup>a</sup>Only principal FA were considered. Values are given as mean ± SD (n = 5 animals). Different roman superscript letters indicate significant differences between this value and that in the group headed by the same letter. \*\*\*P < 0.001, \*\*P < 0.01, \*P < 0.05.

activity cannot be attributed to a decrease in the enzyme mRNA level.

*Effect of dietary cholesterol on the FA composition of liver lipids, microsomes, and cholesterol esters.* (i) The effect of the cholesterol-rich and low-EFA diets on the FA composition of total liver lipids is shown in Table 2. In control animals, the effect of the low-EFA and high-oleic content of the diet is shown by the high proportions of oleic acid that were maintained up to 21 d and by the presence of a significant level of eicosa-5-8,11-trienoic acid of the n-9 series. Unexpectedly, the proportion of the latter decreased from 8.43 to 3.82% during the experiment from day 1 to 21 of control diet feeding. The already low proportions of linoleic acid, arachidonic acid, and DHA evoked by the low-EFA diet were not further decreased for the additional 21 d of the experiment.

The addition of 1% cholesterol to the control diet evoked the expected effects, increasing progressively and significantly the proportions of palmitoleic and, especially, oleic acids. It did not modify the level of 20:3n-9 found in control rats, nor did it modify the percentage of linoleic acid for 21 d. Rather, it decreased significantly and progressively the proportions of arachidonic acid and DHA.

(ii) The effect of the control diet, low in EFA, on the microsomal FA (Table 3) also showed, as in total liver lipids, a high level of oleic acid, approximately threefold higher than in the Leikin and Brenner (3) experiment, in which corn oil was administered. It also evoked a high level of 20:3n-9 acid, typical of EFA deficiency, but as in total liver lipids, a progressive decrease in this acid was shown during the 21-d experiment. No significant changes were observed during this time on the already low levels of linoleic acid, arachidonic acid, and DHA, which were half the amounts found with a high-EFA diet (3).

An analysis of the effect of the cholesterol-rich diet over time on the comparative FA composition of rat liver microsomes (Table 3) followed the same general pattern as that of the total liver lipids. An increase in palmitoleic and oleic acids (the main components) was shown, and this increase became very significant on day 7. As in total liver lipids, no relatively significant decrease occurred in the percentage of 20:3n-9.

Linoleic acid, a minor component, was modified very little; arachidonic acid, a major component, decreased significantly and progressively; and DHA, a minor component, was not significantly altered.

**TABLE 3**  
**FA Composition (wt%) of Liver Microsomal Lipids<sup>a</sup>**

FA	1 d		7 d		21 d	
	Control (a)	Cholesterol (b)	Control (c)	Cholesterol (d)	Control (e)	Cholesterol (f)
16:0	19.58 ± 0.25	20.16 ± 1.13	19.76 ± 0.96	21.27 ± 0.85	22.13 ± 1.94 <sup>a*,c*</sup>	20.39 ± 0.39
16:1	1.95 ± 0.07	2.41 ± 0.31	1.18 ± 0.30	3.57 ± 0.60 <sup>b***,c***</sup>	2.13 ± 0.21 <sup>c**</sup>	4.14 ± 0.38 <sup>b***,e***</sup>
18:0	21.25 ± 0.93	20.05 ± 1.76	24.55 ± 2.16	19.25 ± 1.78 <sup>c**</sup>	23.92 ± 2.87	20.09 ± 0.26 <sup>e*</sup>
18:1n-9	24.31 ± 0.31	26.57 ± 1.51	22.28 ± 1.87	27.54 ± 2.13 <sup>c***</sup>	24.45 ± 1.87	29.05 ± 1.58 <sup>e**</sup>
18:2n-6	4.53 ± 0.06	5.19 ± 0.20	5.39 ± 0.56	5.96 ± 0.90	5.29 ± 0.32	6.22 ± 0.33 <sup>b*</sup>
20:3n-9	10.60 ± 0.95	9.50 ± 0.65	7.24 ± 0.86 <sup>a***</sup>	8.48 ± 0.47	5.79 ± 0.41 <sup>a***</sup>	6.91 ± 1.18 <sup>b***,d*</sup>
20:3n-6	1.17 ± 0.08	1.16 ± 0.03	1.21 ± 0.06	1.23 ± 0.18	1.10 ± 0.16	1.11 ± 0.09
20:4n-6	12.76 ± 0.11	11.63 ± 1.15	13.91 ± 1.79	9.88 ± 0.71 <sup>c**</sup>	12.60 ± 2.33	9.65 ± 1.27 <sup>e*</sup>
22:5n-6	1.06 ± 0.18	1.06 ± 0.07	1.36 ± 0.25 <sup>a*</sup>	0.91 ± 0.12 <sup>c**</sup>	0.79 ± 0.14 <sup>c***</sup>	0.66 ± 0.07 <sup>b**</sup>
22:5n-3	0.17 ± 0.01	0.10 ± 0.09	0.13 ± 0.09	0.05 ± 0.07	0.13 ± 0.16	0.13 ± 0.09
22:6n-3	2.62 ± 0.06	2.17 ± 0.26	2.99 ± 0.73	1.87 ± 0.32 <sup>c**</sup>	1.68 ± 0.22 <sup>a**,c***</sup>	1.63 ± 0.37

<sup>a</sup>Only principal FA were considered. Data are the mean ± SD (n = 5 animals). Different roman superscript letters indicate significant differences between this value and that in the group headed by the same letter. \*\*\*P < 0.001, \*\*P < 0.01, \*P < 0.05.

**TABLE 4**  
**FA Composition (wt%) of Liver Cholesterol Esters<sup>a</sup>**

	FA	1 d		7 d		21 d	
		Control (a)	Cholesterol (b)	Control (c)	Cholesterol (d)	Control (e)	Cholesterol (f)
Total liver	16:0	28.19 ± 0.98	23.37 ± 2.81 <sup>a*</sup>	30.58 ± 0.59	16.90 ± 3.16 <sup>b**,c***</sup>	43.00 ± 2.88 <sup>a***,c***</sup>	20.68 ± 2.39 <sup>e***</sup>
	16:1	5.26 ± 0.96	9.65 ± 0.01 <sup>a***</sup>	8.91 ± 0.50 <sup>a***</sup>	8.50 ± 0.24	6.25 ± 2.48 <sup>c*</sup>	10.53 ± 0.57 <sup>e***</sup>
	18:0	26.35 ± 1.31	11.84 ± 1.31 <sup>a***</sup>	20.06 ± 4.24 <sup>a*</sup>	9.16 ± 4.77 <sup>c***</sup>	19.63 ± 0.71 <sup>a**</sup>	6.16 ± 0.36 <sup>b*,e***</sup>
	18:1n-9	31.81 ± 0.85	47.95 ± 5.20 <sup>a***</sup>	28.74 ± 5.07	61.51 ± 8.07 <sup>b**,c***</sup>	28.71 ± 2.94	61.04 ± 2.39 <sup>b**,e***</sup>
	18:2n-6	5.99 ± 0.72	3.92 ± 0.91	5.17 ± 2.60	1.76 ± 0.94 <sup>c**</sup>	2.41 ± 0.25 <sup>a**,c*</sup>	1.59 ± 0.67
	20:3n-9	1.09 ± 1.54	2.58 ± 0.10	4.62 ± 1.10 <sup>a***</sup>	0.92 ± 0.46 <sup>c***</sup>	Trace	Trace
	20:4n-6	1.30 ± 1.84	0.69 ± 0.06	1.93 ± 0.59	0.35 ± 0.13 <sup>c*</sup>	Trace	Trace
Liver microsomes	16:0	33.36 ± 0.47	28.29 ± 0.84	38.29 ± 1.61	36.88 ± 6.47 <sup>b**</sup>	42.30 ± 1.31 <sup>a***</sup>	39.55 ± 2.10 <sup>b***</sup>
	16:1	7.15 ± 0.14	7.92 ± 1.02	5.62 ± 2.04	6.43 ± 1.93	3.95 ± 0.68 <sup>a**</sup>	4.83 ± 0.96
	18:0	18.35 ± 0.19	16.88 ± 1.93	22.23 ± 1.05 <sup>a**</sup>	19.13 ± 0.84 <sup>c*</sup>	21.64 ± 0.34 <sup>a**</sup>	21.47 ± 2.10 <sup>b***</sup>
	18:1n-9	27.48 ± 3.50	37.61 ± 2.55 <sup>a***</sup>	28.40 ± 4.42	33.68 ± 3.06	29.13 ± 1.41	31.18 ± 1.72 <sup>b*</sup>
	18:2n-6	13.67 ± 2.70	9.31 ± 1.44 <sup>a**</sup>	3.01 ± 0.39 <sup>a***</sup>	3.89 ± 1.75 <sup>b***</sup>	2.98 ± 0.15 <sup>a***</sup>	2.98 ± 1.01 <sup>b***</sup>

<sup>a</sup>Only principal FA were considered. Data are presented as mean ± SD ( $n = 5$  animals). Different roman superscript letters indicate significant differences between this value and that in the group headed by the same letter. \*\*\* $P < 0.001$ , \*\* $P < 0.01$ , \* $P < 0.05$ .

(iii) The FA composition of cholesterol esters of total liver lipids is shown in Table 4. In these lipids, the predominant FA were 16:0, 18:1n-9, and 18:0. They had very little arachidonic and eicosatrienoic n-9 acids, and DHA was not detected.

The addition of cholesterol to the diet provoked an increase in cholesteryl palmitoleate from the first 24 h. Cholesteryl oleate also increased rapidly and doubled after 7 d, reaching a value of  $\cong 61\%$ , which was maintained for 21 d. Cholesteryl stearate, linoleate, and arachidonate were also reduced after 24 h.

(iv) In liver control microsomes (Table 4) the predominant cholesterol esters were 16:0 > 18:1n-9 > 18:0. However, the percentage of cholesteryl palmitate increased somewhat with time, whereas the oleate ester remained unaltered. The percentage of cholesteryl linoleate was higher than that in total liver cholesterol esters, but it decreased rapidly up to the experimental time of 21 d. No arachidonate was detected.

The addition of cholesterol to the diet did not significantly modify the relative microsomal percentage of cholesteryl palmitate, palmitoleate, and stearate; it increased cholesteryl oleate after the first 24 h of cholesterol administration and somewhat decreased linoleate esters.

The relative proportion of cholesterol esters, in both total liver and liver microsomes followed the pattern of saturated and monounsaturated amounts found in total liver and microsomal lipids rather well, but the percentage of polyunsaturated acid cholesterol esters was either markedly diminished or undetected, as shown for arachidonate in total liver.

To compare the effect of the diets on the FA composition of liver lipids with other organs, the FA of testes and adrenals were analyzed for the same time periods. The relative compositions of neither testes nor adrenal FA were significantly altered by the cholesterol diet throughout the 21-d experiment. The low-EFA diet evoked only a reduced increase of 20:3n-9 acid in both tissues (data not shown).

## DISCUSSION

*Incorporation of cholesterol into liver lipids.* Ingested cholesterol has repeatedly been shown to be incorporated into ani-

mal tissues, especially in liver (3–8). Table 1 confirms these results in our rats and shows a significant incorporation into liver microsomes and total cellular homogenate as early as 24 h after ingestion. However, these tables also show that the true relative increase of cholesterol in microsomal and total liver lipids was evoked in the cholesterol ester fraction and not in the free cholesterol. The relative increase of microsomal cholesterol esters was found after 24 h, and similar figures were maintained throughout time, showing that the esterification of any incorporated cholesterol is immediate and that the homeostasis of microsomal free cholesterol is very efficient. The same efficient homeostasis of free cholesterol is also shown in total liver homogenate, which does not modify the steady and similar relative values in the lipids of control and cholesterol-treated rats from 24 h up to at least 21 d (Table 1). The cholesterol provided by the cholesterol-rich diet is also especially derived in total cells to the cholesterol ester fraction, which in this case increased 10-fold after 21 d of treatment. It offered excellent protection in the cell cytosol against the deleterious effect of the high free cholesterol contents.

This homeostasis is undoubtedly evoked by the ACAT enzymes. In rodents (mice) two ACAT with approximately 40% identity have been cloned, ACAT-1, whose liver activity in these animals is doubtful, and ACAT-2, recently recognized, which is apparently active in the lives of mice (23,24). These enzymes are mainly located in the cell endoplasmic reticulum, and the mechanism of action in cholesterol homeostasis (24) is interpreted in the following way. In cholesterol-loaded cells and when cholesterol is added to the microsomes, cholesterol esterification is activated and increased (24). Therefore, the endoplasmic reticulum ACAT esterifies the added cholesterol (24) and only some controlled amount of it; in accordance with our results in Table 1, it accumulates in this organelle. The excess is removed from the endoplasmic reticulum, increasing the amount of cholesterol esters in other parts of the cell such as cytosol, storing it harmlessly in cytosolic droplets (25), or exporting it as lipoproteins (24,26). This mechanism is in accordance with the results in Table 1, which also show

an increased accumulation with time of cholesterol esters in extramicrosomal places.

The FA compositions of cholesterol esters in liver cellular homogenate and microsomes of control rats (Table 4) showed typical and similar patterns evoked mainly by the specificity of ACAT fatty acyl-CoA in choosing FA provided by the diet, provided by the cellular lipids, and specifically synthesized in accordance with the corresponding activities of  $\Delta 9$ ,  $\Delta 6$ , and  $\Delta 5$  desaturases. The most abundant esters found were the oleate, palmitate, and stearate (Table 4), which were also the predominant FA in the food. Linoleic acid, a lesser component in the food and liver lipids, appeared as a minor component of total liver cholesterol esters and a little higher in the microsomal esters. However, in either control or treated animals, the percentage of cholesteryl linoleate significantly decreased with time for the 21 d of the experiment. These results may be easily explained as an effect of EFA deficiency in the diet. Arachidonic acid cholesterol ester was a very minor component in total liver and was below detection limits in microsomes.

The typical composition of the cholesterol esters found (Table 4) is in accordance with the known fatty acyl-CoA specificity of rodent ACAT-2, which does not practically accept arachidonyl-CoA (23), whereas ACAT-1 has a broader spectrum that also includes arachidonyl-CoA (24). Moreover, it has been shown (24) that in ACAT-1 knockout mice (ACAT-1  $-/-$ ) livers, no problem exists in the synthesis of large amounts of cholesterol esters.

The addition of cholesterol to the diet evoked significant increases in total liver (Table 4) of cholesterol esters of palmitoleic and oleic acids and decreases in palmitate and stearate. These results are in accordance with the evoked increases in SCD-1 mRNA (Fig. 2) and  $\Delta 9$  desaturation activity (Fig. 1). Moreover, Miyazaki *et al.* (27) already proved that the activation of SCD-1 is specifically responsible for the increase in the relative proportion of cholesterol oleate. In an earlier work, Miyazaki *et al.* (28) showed that oleate and palmitoleate, which arise in rodents from SCD-activity, are the preferred substrates for ACAT synthesis of cholesterol esters. In addition, they concluded that the regulation of liver SCD-1 activity plays an important role in the mechanisms of cellular cholesterol homeostasis. In the present experiment, the increases in cholesterol esters of oleic and palmitoleic acids in liver are shown to be produced together with relative increases in SCD-1 mRNA (Fig. 2).

*Effect of cholesterol on the  $\Delta 9$  desaturase activity and corresponding levels of mRNA.* It has repeatedly been shown that the addition of 1% cholesterol to an EFA-rich diet evokes a relatively higher activity of the liver  $\Delta 9$  desaturation (3–5,7) of both palmitic and stearic acids and SCD-1 mRNA (7). In the present research, the addition of cholesterol shows a similar effect but in animals fed a low-EFA diet. However, the increase in liver SCD-1 mRNA was immediate (24 h), whereas the enzymatic activity was only significantly enhanced on day 7 (Fig. 1A).

At present, we know that from the three genes of  $\Delta 9$  desaturase characterized in rodents, SCD-1, SCD-2 (22), and SCD-3 (29,30), only SCD-1 is regularly expressed in liver, and it is the one we measured. SCD-2 apparently can only be expressed in liver by a very strong stimulus (31), which is not the present case.

Our results confirm those of Landau *et al.* (7) for animals fed a high-EFA diet and show that the effect of dietary cholesterol on the activation of the SCD-1 is evoked first by an increase in its mRNA and afterward, with some retardation and less pronounced, by the enzymatic activity independent of the EFA content of the diet. Therefore, these effects supplement possible activating effects evoked by low-EFA diets. However, we do not yet envisage a clear mechanism that would explain the way this activation is produced.

The possible role of the sterol regulatory element-binding proteins (SREBP) in this dietary cholesterol-enhancing effect of the enzyme activity is not yet understood (8) when compared to the findings of Shimomura *et al.* (31) and the Goldstein group, which showed an SREBP-dependent depression in cell cultures (32). This problem was thoroughly discussed by Ntambi (22) without reaching a definitive conclusion.

*Effect of cholesterol on the  $\Delta 6$  and  $\Delta 5$  desaturation activities and the level of  $\Delta 6$  desaturase mRNA.* Results displayed in Figure 1 show that cholesterol-treated rats fed a low-EFA diet have lower liver  $\Delta 6$  and  $\Delta 5$  FA desaturation activities than control rats. They confirm similar experiments (3–5) done with rats receiving a high-EFA diet and explain the depression found in some of the n-6 and n-3 PUFA (mainly the 20:4n-6) of those animals (Tables 2 and 3).

One of the possible mechanisms by which dietary cholesterol might modulate the  $\Delta 6$  desaturation activity is through the depression of  $\Delta 6$  desaturase mRNA. The present experimental data displayed in Figure 2 discard this possibility and reject the suggestion that it could be evoked either through a mechanism depressing the enzyme mRNA transcription or any other mechanism that could alter its abundance of mRNA. Therefore, cholesterol downregulation of rat liver  $\Delta 6$  desaturation activity must be ascribed to an effect produced at a later step than that of mRNA.

In spite of the fact that our studies on the effect of cholesterol on the abundance of  $\Delta 5$  desaturase mRNA in rats are still in progress, we expect that a result similar to that found for the  $\Delta 6$  desaturase will be found due to the extreme similarity in the activity regulation in animals (33). Besides, Clarke's group (11) showed that, in addition to the great similarity of the cDNA of both enzymes, it is very possible that the transcription of  $\Delta 5$  and  $\Delta 6$  desaturase genes may be coordinately governed by regulatory sequences within the 11,000-bp region that is common for both genes.

Another possible mechanism suggested to explain the way in which cholesterol could depress  $\Delta 6$  and  $\Delta 5$  desaturation is by a modification of the biophysical properties of microsomal lipid environment in which the desaturation systems are embedded (3,4). This suggestion has not been proved, in spite

of the fact that Leikin and Shinitzky (34,35) isolated from microsomes by hydrostatic pressure a lipid fraction constituted by PtdCho and cholesterol that included a  $\Delta 6$  desaturation system constituted by the NADH-cytochrome  $b_5$  reductase, cytochrome  $b_5$ , and the  $\Delta 6$  desaturase. Moreover, *in vitro* incorporation of free cholesterol into isolated rat liver microsomes provokes just the opposite effect, enhancing both  $\Delta 6$  and  $\Delta 5$  desaturation (36). Therefore, another mechanism, different from these genetic and biophysical ones, must be sought. Cholesterol would appear to modulate  $\Delta 6$  and  $\Delta 5$  desaturase activities by a mechanism different from that of  $\Delta 9$  desaturase.

**FA composition of liver lipids.** The FA composition found in total liver and microsomal lipids (Tables 2 and 3) of control rats fed a low-EFA diet agrees with the well-known effect of this type of diet, i.e., depression of mainly the linoleic and arachidonic acid proportions and an increase in oleic acid, and specifically 20:3n-9, in animal tissues. These changes are evoked by the decreased exogenous supply of linoleic and  $\alpha$ -linolenic acids. On one hand, they activate oleic acid biosynthesis (9) and, on the other hand, as shown previously (37), they decrease the very active competition of linoleic and  $\alpha$ -linolenic acids with oleic acid for the  $\Delta 6$  desaturase that catalyzes and regulates the conversion of oleic acid to 20:3n-9. However, we cannot explain why the level of 20:3n-9 is not increased, or at least maintained, in control animals (Tables 2 and 3) for the additional 21 d of the experiment in which they were fed the same low-EFA diet.

It is apparent that administration of cholesterol provokes, in both total liver and microsomal lipids, and independent of the FA composition of the diet, an increase in palmitoleic and oleic acids that, as has been shown in similar experiments (3–8), must be attributed to the increase in  $\Delta 9$  desaturation activity. It is also apparently preceded by an increase in liver SCD-1 mRNA (Fig. 2).

The depression of  $\Delta 6$  and  $\Delta 5$  desaturation activity produced by the cholesterol-rich diet (Fig. 1) would explain, as in other experiments (3–6,8), the decrease in arachidonic acid in both total liver and microsomal lipids and DHA only in total liver lipids (Tables 2 and 3). Moreover Bernasconi *et al.* (8) showed that the administration of cholesterol to rats fed an EFA-rich diet specifically depressed the 18:0/20:4 and 16:0/20:4 PC molecular species and increased the 18:1-containing species.

Another important conclusion that may be deduced from these results is that a cholesterol-rich diet evokes an additional EFA deficiency effect on an already EFA-deficient or, even more important from a nutritional point of view, on an EFA-limited diet. This effect is mainly due not to a decrease in linoleic acid, but to an important decrease in the synthesis and amount of the highly polyunsaturated acids, arachidonic acid and DHA. These two acids, as is well known, are the main effectors among the EFA that control very important physiological functions in animal tissues.

Therefore, another important new finding shown here is that in animals or humans receiving diets near the limit of EFA necessity, the addition of cholesterol to these diets may push them into a true EFA deficiency.

## ACKNOWLEDGMENTS

This study was supported by a grant from CONICET, Argentina. The authors are very grateful to Dr. Tsunehiro Aki from Japan and to Dr. Juri Ozols from the United States for providing the cDNA of rat  $\Delta 6$  and  $\Delta 9$  desaturases, respectively, and to Mrs. L. Hernández for her technical assistance.

## REFERENCES

- Holman, R.T., and Peiffer, J.J. (1960) Acceleration of Essential Fatty Deficiency by Dietary Cholesterol, *J. Nutr.* 70, 411–417.
- Gambal, D., and Quackenbush, F.W. (1960) Effect of Cholesterol and Other Substances on Essential Fatty Acid Deficiencies, *J. Nutr.* 70, 497–501.
- Leikin, A.I., and Brenner, R.R. (1987) Cholesterol-Induced Microsomal Changes Modulate Desaturase Activities, *Biochim. Biophys. Acta* 922, 294–303.
- Leikin, A.I., and Brenner, R.R. (1988) *In vivo* Cholesterol Removal from Liver Microsomes Induces Changes in Fatty Acid Desaturase Activities, *Biochim. Biophys. Acta* 963, 311–319.
- Garg, M.L., Snowswell, A.M., and Sabine, J.R. (1986) Influence of Dietary Cholesterol on Desaturase Enzymes of Rat Liver Microsomes, *Prog. Lipid Res.* 25, 639–644.
- Igal, R.A., and Gómez Dumm, I.N.T. de (1994) Changes in Adrenal Gland and Liver Polyunsaturated Fatty Acids Biosynthesis in Hypercholesterolemic Rats, *Nutr. Res.* 14, 241–254.
- Landau, J.M., Sekowski, A., and Hamm, M.W. (1997) Dietary Cholesterol and the Activity of Stearoyl-CoA Desaturase in Rats: Evidence for an Indirect Effect, *Biochim. Biophys. Acta* 1345, 349–357.
- Bernasconi, A.M., Garda, H.A., and Brenner, R.R. (2000) Dietary Cholesterol Induces Changes in Molecular Species of Hepatic Microsomal Phosphatidyl Choline, *Lipids* 35, 1335–1344.
- Ntambi, J.M. (1992) Dietary Regulation of Stearoyl-CoA Desaturase 1 Gene Expression in Mouse Liver, *J. Biol. Chem.* 267, 10925–10930.
- Nakamura, M.T., Cho, H.P., and Clarke, S.D. (2000) Regulation of Hepatic  $\Delta 6$  Desaturase Expression and Its Role in the Polyunsaturated Fatty Acid Inhibition of Fatty Acid Synthase Gene Expression in Mice, *J. Nutr.* 130, 1561–1565.
- Cho, H.P., Nakamura, M.T., and Clarke, S.D. (1999) Cloning Expression and Fatty Acid Regulation of the Human  $\Delta 5$  Desaturase, *J. Biol. Chem.* 274, 37335–37339.
- Brenner, R.R. (2000) Hormonal Interplay in Fatty Acid Desaturases Activities, presented at 51st Harden Conference, Fatty Acid Desaturases: Form, Function and Future, 30 July–2 August 2000, Wye College, United Kingdom. Abstracts published by the Biochemical Society, London.
- Sambrook, J., Fritsch, E.F., and Maniatis, T. (1989) *Molecular Cloning, a Laboratory Manual*, Cold Spring Harbor Laboratory Press, New York.
- Reeves, P.G., Nielsen, F.H., and Fakey, G.C., Jr. (1993) AIN93 Purified Diets Laboratory Rodents: Final Report of the American Institute of Nutrition *Ad Hoc* Writing Committee on the Reformulation of the AIN-76 A Rodent Diet, *J. Nutr.* 123, 1939–1951.
- Catalá, A., Nervi, A.M., and Brenner, R.R. (1975) Separation of a Protein-Factor Necessary for the Oxidative Desaturation of Fatty Acids in the Rat, *J. Biol. Chem.* 250, 7481–7484.
- Lowry, O.H., Rosebrough, N.J., Farr, A.L., and Randall, R.J. (1951) Protein Measurement with Folin Phenol Reagent, *J. Biol. Chem.* 193, 265–275.
- Folch, J., Lees, M., and Sloane-Stanley, G.H. (1957) A Simple Method for the Isolation and Purification of Total Lipides from Animal Tissues, *J. Biol. Chem.* 226, 497–509.
- Chen, P.S., Toribara, T., and Warner, H. (1956) Microdetermination of Phosphorus, *Anal. Chem.* 28, 1756–1758.
- Lowry, R.R. (1968) Ferric Chloride Spray Detector for Choles-



- terol and Cholesterol Esters on Thin-Layer Chromatograms, *J. Lipid Res.* 9, 397.
20. Garda, H.A., Leikin, A.I., and Brenner, R.R. (1992) Determination of Fatty Acid Desaturases Activities by RP-HPLC, *An. Asoc. Quím. Arg.* 80, 365–371.
  21. Jeffcoat, R., and James, A.T. (1978) The Control of Stearoyl-CoA Desaturase by Dietary Linoleic Acid, *FEBS Lett.* 85, 114–118.
  22. Ntambi, J.M. (1999) Regulation of Stearoyl-CoA Desaturase by Polyunsaturated Fatty Acids and Cholesterol, *J. Lipid Res.* 40, 1549–1558.
  23. Cases, S., Novak, S., Zheng, Y., Myers, H.M., Lear, S.R., Sandet, E., Welch, C.B., Luses, A.J., Spencer, T.A., Krause, B.R., *et al.* (1998) ACAT-2, Second Mammalian Acyl-CoA:Cholesterolacyltransferase, *J. Biol. Chem.* 273, 26755–26764.
  24. Buhman, K.F., Accad, M., and Farese, R.V., Jr. (2000) Mammalian Acyl-CoA:Cholesterol Acyltransferases, *Biochim. Biophys. Acta* 1529, 142–154.
  25. Kellner-Weibel, G., McHendry-Rinde, B., Haynes, M.P., and Adelman, S. (2001) Evidence That Newly Synthesized Esterified Cholesterol Is Deposited in Existing Cytoplasmic Lipid Inclusions, *J. Lipid Res.* 42, 768–777.
  26. Davis, R.A. (1999) Cell and Molecular Biology of the Assembly and Secretion of Apolipoprotein B-Containing Lipoproteins by the Liver, *Biochim. Biophys. Acta* 1440, 1–31.
  27. Miyazaki, M., Kim, Y.C., and Ntambi, J.M. (2001) A Lipogenic Diet in Mice with a Disruption of Stearoyl-CoA Desaturase 1 Gene Reveals a Stringent Requirement of Endogenous Monounsaturated Fatty Acids for Triglyceride Synthesis, *J. Lipid Res.* 42, 1018–1024.
  28. Miyazaki, M., Kim, Y.C., Gray-Keller, M.P., Attie, A.D., and Ntambi, J.M. (2000) The Biosynthesis of Hepatic Cholesterol Esters and Triglycerides Is Impaired in Mice with a Disruption of the Gene for Stearoyl-CoA Desaturase 1, *J. Biol. Chem.* 275, 30132–30138.
  29. Zheng, Y., Prouty, S.M., Harmon, A., Sundberg, J.P., Stenn, K.S., and Parimoo, S. (2001) SCD-3 a Novel Gene of the Stearoyl-CoA Desaturase Family with Restricted Expression in Skin, *Genomics* 71, 182–191.
  30. Miyazaki, M., Kim, H.J., Man, W.C., and Ntambi, J.M. (2001) Oleoyl-CoA Is the Major *de novo* Product of Stearoyl-CoA Desaturase 1 Gene Isoform and Substrate for the Biosynthesis of the Harderian Gland 1-Alkyl-2,3-diacylglycerol, *J. Biol. Chem.* (in press).
  31. Shimomura, I., Shimano, H., Korn, B.S., Bashmakov, Y., and Horton, J.D. (1998) Nuclear Sterol Regulatory Element-Binding Proteins Activate Genes Responsible for Entire Program of Unsaturated Fatty Acid Biosynthesis in Transgenic Mouse Liver, *J. Biol. Chem.* 273, 35299–35306.
  32. Pai, J., Guryev, O., Brown, M.S., and Goldstein, J.L. (1998) Differential Stimulation of Cholesterol and Unsaturated Fatty Acid Biosynthesis in Cells Expressing Individual Nuclear Sterol Regulatory Element-Binding Proteins, *J. Biol. Chem.* 273, 26138–26148.
  33. Brenner, R.R. (1990) Endocrine Control of Fatty Acid Desaturation, *Biochem. Soc. Trans.* 18, 773–775.
  34. Leikin, A.I., and Shinitzky, M. (1994) Shedding and Isolation of the  $\Delta 6$  Desaturase System from Rat Liver Microsomes by Application of High Hydrostatic Pressure, *Biochim. Biophys. Acta* 1211, 150–155.
  35. Leikin, A.I., and Shinitzky, M. (1995) Characterization of the Lipid Surrounding the  $\Delta 6$  Desaturase of Rat Liver Microsomes, *Biochim. Biophys. Acta* 1256, 13–17.
  36. Garda, H.A., and Brenner, R.R. (1985) *In vitro* Modification of Cholesterol Content of Rat Liver Microsomes. Effects upon Membrane “Fluidity” and Activities of Glucose-6-Phosphatase and Fatty Acid Desaturation Systems, *Biochim. Biophys. Acta* 819, 45–54.
  37. Brenner, R.R., and Peluffo, R.O. (1966) Effect of Saturated and Unsaturated Fatty Acids on the Desaturation *in Vitro* of Palmitic, Stearic, Oleic, Linoleic and Linolenic Acids, *J. Biol. Chem.* 241, 5213–5219.

[Received October 22, 2001, and in final revised form January 16, 2002; revision accepted February 7, 2002]

# Increased Cardiomyocyte Apoptosis Following Ischemia and Reperfusion in Diet-Induced Hypercholesterolemia: Relation to Bcl-2 and Bax Proteins and Caspase-3 Activity

Tzung-Dau Wang<sup>a</sup>, Wen-Jone Chen<sup>b</sup>, Sophia Seh-Yi Su<sup>a</sup>, Shyh-Chyi Lo<sup>c</sup>,  
Wan-Wan Lin<sup>d</sup>, and Yuan-Teh Lee<sup>a,\*</sup>

Departments of <sup>a</sup>Internal Medicine (Cardiology), <sup>b</sup>Emergency Medicine, and <sup>c</sup>Laboratory Medicine, National Taiwan University Hospital, Taipei, 100, Taiwan, Republic of China, and <sup>d</sup>Department of Pharmacology, College of Medicine, National Taiwan University, Taipei (100), Taiwan, Republic of China

**ABSTRACT:** It has been reported that apoptosis is a significant contributor to myocardial cell death as a result of reperfusion injury. However, whether the extent of cardiomyocyte apoptosis following ischemia and reperfusion varies in different pathophysiological backgrounds is still uncertain. In this study, we examined whether hypercholesterolemia increases the extent of myocardial reperfusion injury by aggravating cardiomyocyte apoptosis and the effects of hypercholesterolemia on the expression of Bcl-2 and Bax proteins and the activation of caspase-3. Twenty-eight male New Zealand white rabbits were fed standard chow (control,  $n = 14$ ) or chow supplemented with 1% cholesterol (hypercholesterolemic,  $n = 14$ ) for 8 wk. Anesthetized rabbits were then subjected to 30 min of left circumflex artery occlusion followed by 4 h of reperfusion. Apoptosis was identified as "DNA ladders" by gel electrophoresis and confirmed histologically using the terminal deoxynucleotidyl transferase-mediated dUTP-biotin nick end labeling (TUNEL) assay. The infarct size (% of risk region) was significantly greater in hypercholesterolemic rabbits than in controls ( $39 \pm 6$  vs.  $23 \pm 2\%$ ,  $P = 0.02$ ). Very few TUNEL-positive cardiomyocytes could be identified in the nonischemic regions in both groups, consistent with an absence of DNA laddering. In contrast, TUNEL-positive cardiomyocytes were significantly displayed in the ischemic, nonnecrotic myocardium, and DNA ladder occurred in all animals. The percentage of TUNEL-positive cardiomyocytes in the ischemic nonnecrotic myocardium was significantly higher in hypercholesterolemic rabbits compared with controls ( $40 \pm 5$  vs.  $17 \pm 1\%$ ,  $P < 0.001$ ). Western blot analysis showed that, in the nonischemic myocardium, hypercholesterolemic rabbits exhibited an approximately 50% increase in the expression of Bcl-2 ( $P < 0.05$ ), but not Bax, than control rabbits. However, compared with controls, hypercholesterolemic rabbits exhibited a more pronounced decrease in the expression of Bcl-2 ( $42 \pm 4$  vs.  $26 \pm 2\%$ ,  $P < 0.01$ ) and a similar extent of increase in the expression of Bax in the ischemic myocardium. Furthermore, hypercholesterolemic rabbits were associated with a markedly increased activation of caspase-3 within the ischemic myocardium compared to con-

trol rabbits. This study demonstrates that although hypercholesterolemia is associated with an increased myocardial Bcl-2/Bax ratio at baseline, it still significantly exacerbates cardiac reperfusion injury, not only by increasing the infarct size but also by increasing the extent of cardiomyocyte apoptosis.

Paper no. L8833 in *Lipids* 37, 385–394 (April 2002).

Timely reperfusion of jeopardized myocardium by thrombolytic therapy or angioplasty is now the standard of care in patients with acute myocardial infarction (1). However, the process of reperfusion, although beneficial in terms of myocardial salvage, has been shown to be injurious to the ischemic myocardium as well (2). Although reperfusion-related cardiomyocyte deaths are traditionally assumed to be necrotic, recent studies have demonstrated that a substantial proportion of cardiomyocyte deaths are actually apoptotic following ischemia and reperfusion (3–6). Under experimental conditions, 10–15% of cardiomyocytes rendered ischemic and reperfused were recognized as apoptotic by using the *in situ* terminal deoxynucleotidyl transferase-mediated dUTP-biotin nick end labeling (TUNEL) assay (7). Moreover, in acute myocardial infarction in humans, 12% of cardiomyocytes were TUNEL-positive in the border zone of infarction (8). Nevertheless, whether the extent of cardiomyocyte apoptosis following ischemia and reperfusion varies in different pathophysiological background (e.g., hypercholesterolemia and hypertension) remains to be elucidated.

Hypercholesterolemia and ensuing atherosclerosis have been implicated in the pathophysiology of coronary artery disease (9–11). It is noteworthy that, in the Scandinavian Simvastatin Survival Study, the mortality rate of definite myocardial infarction in the placebo group was 28% higher than that in the simvastatin group (10). This finding indicates that hypercholesterolemia may have an adverse effect on the evolution of myocardial infarction, possibly by aggravating the severity of reperfusion injury. Moreover, we previously demonstrated that the detrimental effect of hypercholesterolemia on postinfarct left ventricular ejection fraction is independent of the patency rate of infarct-related artery and the infarct size estimated by serum cardiac enzyme changes (12). Because cardiomyocyte apoptosis, which could not be evaluated by conventional serum

\*To whom correspondence should be addressed at Department of Internal Medicine (Cardiology), National Taiwan University Hospital, 7, Chung-Shan South Road, Taipei, 100, Taiwan, Republic of China.  
E-mail: ytleee@ha.mc.ntu.edu.tw

Abbreviations: AMC, 7-amino-4-methyl coumarin; GAPDH, glyceraldehyde-3-phosphate dehydrogenase; TTC, 2,3,5-triphenyltetrazolium chloride; TUNEL, terminal deoxynucleotidyl transferase-mediated dUTP-biotin nick end labeling.

cardiac enzyme changes (13), affects myocardial mechanics by reducing the force-generating capacity of the muscle, we speculated that hypercholesterolemia may increase the magnitude of cardiomyocyte apoptosis following ischemia and reperfusion and thereby aggravate the extent of postinfarct left ventricular systolic dysfunction.

Despite previous experiments that have uniformly shown that hypercholesterolemia results in larger infarct size in hearts exposed to ischemia and reperfusion (14–16), two recent studies demonstrated that prolonged exposure to hypercholesterolemia (over 5 wk) protects the heart from reperfusion injury (17,18). Hence, the effects of prolonged hypercholesterolemia on reperfusion injury after myocardial ischemia still deserve further investigation.

In the present study, we examined whether prolonged hypercholesterolemia (8 wk) increases the extent of experimental myocardial reperfusion injury by aggravating cardiomyocyte apoptosis. Although a large number of genes have been reported to be involved in the regulation of apoptotic cell death, the antiapoptotic Bcl-2 and proapoptotic Bax play major roles in regulating myocardial apoptosis following ischemia and reperfusion (19). Furthermore, apoptotic cell death is mediated by a family of aspartate-specific cysteine proteases known as caspases. Of the 14 caspases characterized, caspase-3 plays a critical role in cardiomyocyte apoptosis and represents the final common pathway of the caspase cascade (7). We thus determined the effects of hypercholesterolemia on the expression of Bcl-2 and Bax and the activation of caspase-3 in both ischemic and nonischemic myocardium to identify the underlying molecular mechanisms induced by hypercholesterolemia.

## MATERIALS AND METHODS

**Animals and diet.** Adult male New Zealand white rabbits (2.4–2.8 kg) were housed in individual cages in environmentally controlled rooms (12 h light-dark cycle, relative humidity  $50 \pm 5\%$ , and  $20 \pm 1^\circ\text{C}$ ). Twenty-eight rabbits were randomly assigned to two different dietary groups: Animals in the control group ( $n = 14$ ) were fed standard rabbit pellets (Purina 5321, St. Louis, MO), whereas those in the cholesterol-fed group ( $n = 14$ ) received a diet enriched with 1% cholesterol and 10% coconut oil added to the standard Purina rabbit pellets for a total of 8 wk. At the end of the 8-wk feeding period, the rabbits were studied. The animals had free access to water. Blood samples were taken to determine plasma levels of cholesterol and TG just before the administration of the diet and at the end of the 8-wk feeding period. All experiments were performed in accordance with the *Guide for the Care and Use of Laboratory Animals* (NIH Publication No. 85-23, revised 1996). The experimental protocol was approved by the Institutional Animal Care and Use Committee.

**Surgical procedures.** After 12 h of fasting, the rabbits were anesthetized with pentobarbital (25 mg/kg i.v.), and anesthesia was maintained during the experiment by intravenous injection of small amounts of pentobarbital (5 mg/kg), sufficient to abolish the corneal reflex. An intratracheal tube was

inserted through a midline incision, and all rabbits were given intermittent positive-pressure ventilation *via* a Harvard small animal respirator (Harvard Apparatus). The respirator was adjusted to maintain arterial blood gases within the physiological range. The standard limb leads of the electrocardiogram were monitored during the experiment. A polyethylene catheter was inserted through the right femoral artery and positioned in the abdominal aorta for blood gas and arterial pressure monitoring (Gould Instruments, Essex, United Kingdom). A midline sternotomy was performed, and the heart was exposed after the pericardium was incised. A 5-0 silk suture on a small curved needle was passed through the myocardium beneath the major marginal branch of the left circumflex coronary artery located on the dorsal surface of the heart, 10 to 12 mm from its origin. A reversible tie was subsequently made and loosely placed on the myocardial surface. After a 20-min stabilization period after thoracotomy, myocardial ischemia was initiated by complete ligation of the marginal coronary artery. Myocardial ischemia was confirmed by ST-segment elevation on the electrocardiogram and regional cyanosis of the myocardial surface. The ligature was released after 30 min of ischemia, and the ischemic myocardium was reperfused for 4 h. Reperfusion was confirmed by myocardial blush over the risk area after the ligature was released. We eliminated from analysis the rabbits that did not complete the experiment.

**Determination of area at risk and infarct size.** At the end of the reperfusion period, the marginal coronary artery was again occluded through ligation of the tie that remained at the site of previous occlusion. Immediately after ligation, 5 mL of 1% Evans blue dye (Sigma, St. Louis, MO) was injected directly into the left atrial cavity to delineate the area of the left ventricular myocardium perfused by patent coronary arteries. The area-at-risk was thus determined by negative staining. The heart was then rapidly removed and placed in ice-cold 0.9% saline, and the atria, right ventricle, and great vessels were removed. The left ventricle was sliced into sections 2 mm thick parallel to the atrioventricular groove. The unstained portion of the myocardium (i.e., the area-at-risk) was separated from the stained portion (i.e., the nonischemic area). The unstained portion was subsequently sliced into 1-mm thick sections and counterstained with 10 mL of 1% solution of the 2,3,5-triphenyltetrazolium chloride (TTC) (Sigma) in 20 mM PBS, pH 7.4 at  $37^\circ\text{C}$  for 15 min to detect the presence of coenzyme and dehydrogenase. The necrotic portion of the myocardium, which did not stain, was separated from the stained portion (i.e., ischemic but nonnecrotic area). The nonischemic portion was also counterstained with TTC as done for the ischemic portion to avoid the possible confounding effect of TTC staining on apoptosis and Western blotting analyses. All three portions of the left ventricular myocardium (i.e., nonischemic, ischemic nonnecrotic, and ischemic necrotic) were weighed individually. The results were expressed as the percentage of the infarct (ischemic necrotic) area to the area-at-risk or the total left ventricular mass. The individual portions of the myocardium were further sectioned into  $1 \times 1$  mm transmural

myocardial columns and either fixed in 10% buffered formalin for *in situ* nick end labeling or rapidly frozen in liquid nitrogen and stored at  $-70^{\circ}\text{C}$  for DNA and protein isolation. The entire procedure took approximately 25 min to complete. Because differences in this additional time may affect comparability of the results of apoptosis and Western blotting analyses, we carefully monitored the entire procedure to ensure that the time taken for processing both ischemic and nonischemic myocardia was the same.

**DNA laddering.** Frozen tissue samples (20–30 mg each) were minced in 600  $\mu\text{L}$  of lysis buffer (Puregene DNA Isolation Kit, Minneapolis, MN) and quickly homogenized on ice. The tissue was digested with 150  $\mu\text{g}/\text{mL}$  of proteinase K at  $55^{\circ}\text{C}$  for 16 h and incubated with RNase A at  $37^{\circ}\text{C}$  for 2 h. After incubation, tissues were precipitated and centrifuged at 14,000 rpm for 10 min. The DNA in supernatants was extracted with phenol/chloroform and precipitated with isopropanol. After centrifugation at 14,000 rpm for 30 min, the resulting DNA pellets were washed with 70% ethanol and dissolved in TE buffer (10 mM Tris and 1 mM EDTA). The concentration and purity of DNA were determined by measurement of the optical density at 260 nm and the ratio of optical density at 260 nm to that at 280 nm.

To augment the detection of DNA laddering, we employed a terminal deoxynucleotidyl transferase labeling reaction prior to electrophoretic analysis. Briefly, 2  $\mu\text{g}$  of isolated DNA was added into a reaction mixture containing 60 EU/mL terminal deoxynucleotidyl transferase (Boehringer Mannheim, Mannheim, Germany) and 6 nmol/mL biotinylated dUTP (Boehringer Mannheim). After 15 min incubation at  $37^{\circ}\text{C}$ , the biotin-labeled DNA was precipitated with ethanol, resuspended in TE buffer, and separated by electrophoresis on a 1.8% agarose gel. The electrophoretically separated DNA was subsequently transferred onto a nylon membrane (Millipore, Bedford, MA) and detected by the Biotin Detection Kit (KPL Laboratory, Gaithersburg, MD) using a chemiluminescent substrate and exposure on an X-ray film.

**In situ nick end labeling.** The TUNEL protocol was performed with the use of a FragEL DNA fragment detection kit (Oncogene, Cambridge, MA) according to the manufacturer's instructions with minor modifications. Briefly, the fixed transmural ventricular slices were embedded in paraffin, and 4- $\mu\text{m}$  thick sections were deparaffinized by washing in xylene and a descending ethanol series. Subsequently, the tissue sections were stripped of proteins through incubation with 20  $\mu\text{g}/\text{mL}$  proteinase K for 15 min at room temperature. The slides were incubated with 3% hydrogen peroxide for 5 min to allow inactivation of endogenous peroxidase and then incubated for 90 min at  $37^{\circ}\text{C}$  with terminal deoxynucleotidyl transferase and biotinylated dUTP to label the 3'-OH ends of DNA. After the end labeling, the slides were coated with streptavidin-conjugated peroxidase for 30 min at room temperature and visualized with the use of chromogen 3,3'-diaminobenzidine and hydrogen peroxide. Counterstaining was performed with methyl green. Using this method, each cardiomyocyte could be defined, and TUNEL-positive or -negative nuclei were stained dark brown or light green, respectively, under light microscopy. When the

TUNEL method was performed, positive controls were always included. As a positive control, sections of heart tissue were exposed to DNase I for 20 min before nick end labeling.

Cardiomyocytes from six separate sections that were picked randomly from three of the transmural slices of both nonischemic and ischemic nonnecrotic portions of the left ventricular myocardium were analyzed per animal. In each section, cardiomyocytes with counterstained nuclei were counted in 20 random high-power fields ( $\times 400$ ) from the endocardial to epicardial portion and the index of apoptosis was determined (i.e., number of apoptotic myocytes/total number of myocytes  $\times 100$ ). TUNEL-positive cardiomyocytes were carefully distinguished from TUNEL-positive noncardiomyocytes, such as macrophages. This evaluation was carried out independently by two persons who were unaware of the experimental protocol.

**Western blots.** For immunoblot assays of Bcl-2 and Bax proteins, tissue samples (80–100 mg) were homogenized in a lysis buffer (2%  $\beta$ -mercaptoethanol, 10 mM Tris, pH 7.4, 140 mM NaCl, 1 mM phenylmethylsulfonyl fluoride, 10  $\mu\text{g}/\text{mL}$  leupeptin, 10  $\mu\text{g}/\text{mL}$  pepstatin, 10  $\mu\text{g}/\text{mL}$  aprotinin, 1% NP-40, and 0.5% deoxycholic acid). After centrifugation at 14,000 rpm for 20 min, protein concentration was determined by the method of Lowry *et al.* (20), using BSA as the standard. Aliquots containing 50  $\mu\text{g}$  protein were resuspended in the same volume of 2 $\times$  sample buffer (20%  $\beta$ -mercaptoethanol, 4% SDS, 20% glycerol, 0.0125% bromophenol blue, and 0.125 mM Tris, pH 6.4), and they were boiled for 5 min. Proteins were then size-fractionated on 12% polyacrylamide gels by electrophoresis using a Mini-Protean II Dual Stab Cell (Bio-Rad, Hercules, CA), and they were electrotransferred to PVDF membranes (Millipore) by a semidry blotting system (3 mA/cm<sup>2</sup> for 45 min in a buffer consisting of 48 mM Tris, 39 mM glycine, 0.037% SDS, and 20% methanol). Nonspecific binding was blocked with 5% nonfat dry milk in PBS for 3 h. Then membranes were incubated with specific antibodies overnight at  $4^{\circ}\text{C}$ . For Bcl-2 detection, a mouse monoclonal anti-rat Bcl-2 antibody (PharMingen, San Diego, CA) was used at 1:500 in the blocking solution; for Bax immunodetection, a mouse monoclonal anti-rat Bax antibody (PharMingen) was used at 1:500 in the blocking solution. After washing, Bcl-2 and Bax-bound antibodies were detected by alkaline phosphatase-conjugated anti-mouse IgG (Promega, Madison, WI) at 1:5000 in PBS. The immunoreactivity on the membranes was detected by treatment with nitro blue tetrazolium/5-bromo-4-chloro-3-indolyl-phosphate (Promega). For negative controls, membranes were incubated with normal goat serum without specific antibodies. The specificity of the bands was checked by preabsorbing anti-Bcl-2 and anti-Bax with the corresponding synthetic peptides. The density of each protein band was quantified by the National Institutes of Health (NIH) Image software and then calculated as the ratio of Bcl-2 or Bax to glyceraldehyde-3-phosphate dehydrogenase (GAPDH). The values for each sample were presented in percentage of control (nonischemic tissue of rabbits fed with standard diets) on the same gel.



**Caspase activity assay.** In a separate series of experiments, both normally fed and cholesterol-fed rabbits were subjected to 30-min ischemia followed by 4-h reperfusion. After rabbits were euthanized by pentobarbital overdose, the hearts were excised and the ischemic and nonischemic portions of the left ventricular myocardium were separately dissected. Tissues were homogenized by a Polytron homogenizer in ice-cold lysis buffer and centrifuged at 14,000 rpm for 30 min. Homogenates (100  $\mu$ g of protein) were applied for the measurement of caspase activity by CasPACE assay system (Promega) according to the instructions. Briefly, the fluorogenic substrates for caspase-3 are labeled with fluorochrome 7-amino-4-methyl coumarin (AMC). The substrates produce a blue fluorescence that can be detected by exposure to UV light at 360 nm. AMC is released from the substrates upon cleavage by caspase-3. Free AMC produces a yellow-green fluorescence that is measured by a fluorometer at 460 nm. Fluorescent units were converted to pmol AMC using a standard curve generated with free AMC. The values for each sample were then normalized by the value of the control (non-ischemic myocardium of control rabbits).

**Statistics.** Results are presented as mean  $\pm$  SEM computed from the average measurements obtained from each group of rabbits. Student's *t*-test or two-way ANOVA followed by Scheffé's *post hoc* test was used to assess the statistical significance of variations observed between groups where appropriate. A value of  $P < 0.05$  was accepted as statistically significant.

## RESULTS

**Characteristics and mortality.** Table 1 summarizes plasma cholesterol and TG levels and body weight in rabbits before and after 8 wk of normal diet or cholesterol-enriched diet feeding. Rabbits in both groups began the dietary regimen with equivalent plasma total cholesterol and TG concentrations. Plasma total cholesterol and TG levels were markedly increased in cholesterol-fed rabbits by the end of the 8-wk feeding period. All rabbits exhibited a similar weight gain

**TABLE 1**  
Characteristics of Experimental Groups

	Control (n = 14)	Cholesterol-fed <sup>a</sup> (n = 14)
Baseline		
Total cholesterol (mmol/L)	1.5 $\pm$ 0.1	1.5 $\pm$ 0.1
HDL cholesterol (mmol/L)	0.6 $\pm$ 0.1	0.6 $\pm$ 0.1
LDL cholesterol (mmol/L)	0.5 $\pm$ 0.1	0.5 $\pm$ 0.1
TG (mmol/L)	0.5 $\pm$ 0.1	0.5 $\pm$ 0.1
Body weight (kg)	2.6 $\pm$ 0.1	2.6 $\pm$ 0.1
After 8-wk feeding period		
Total cholesterol (mmol/L)	1.6 $\pm$ 0.1	35.6 $\pm$ 0.9*
HDL cholesterol (mmol/L)	0.6 $\pm$ 0.1	4.9 $\pm$ 0.1*
LDL cholesterol (mmol/L)	0.6 $\pm$ 0.1	30.4 $\pm$ 1.5*
TG (mmol/L)	0.5 $\pm$ 0.1	2.1 $\pm$ 0.1*
Body weight (kg)	3.0 $\pm$ 0.1	3.1 $\pm$ 0.1

<sup>a</sup>Laboratory chow was supplemented with 1% cholesterol and 10% coconut oil. \* $P < 0.001$  for cholesterol-fed vs. control.

**TABLE 2**  
Hemodynamic Data for Normally Fed and Cholesterol-Fed Rabbits<sup>a</sup>

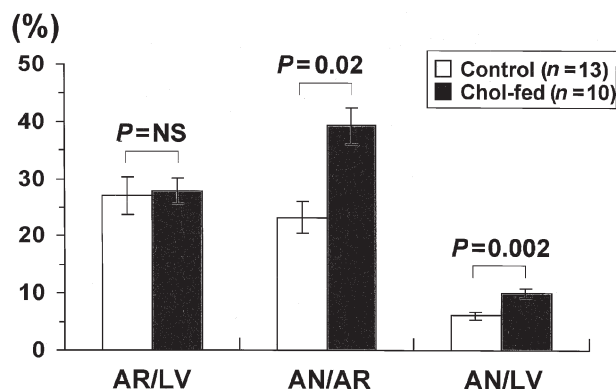
	Control (n = 13)		Cholesterol-fed (n = 10)	
	HR (bpm)	MABP (mm Hg)	HR (bpm)	MABP (mm Hg)
Baseline	266 $\pm$ 9	90 $\pm$ 5	271 $\pm$ 7	78 $\pm$ 5
30 min Ischemia	281 $\pm$ 10	62 $\pm$ 6	264 $\pm$ 8	54 $\pm$ 3
120 min Reperfusion	284 $\pm$ 9	65 $\pm$ 6	272 $\pm$ 7	55 $\pm$ 4
240 min Reperfusion	286 $\pm$ 10	66 $\pm$ 6	273 $\pm$ 8	56 $\pm$ 3

<sup>a</sup>HR, heart rate; MABP, mean arterial blood pressure.

throughout the 8-wk feeding period. Four cholesterol-fed rabbits died of ventricular fibrillation (two during reperfusion and two during coronary occlusion), whereas only one rabbit in the control group died during reperfusion. However, the difference in mortality rate between both groups (29% in the cholesterol-fed group vs. 7% in the control group) did not reach statistical significance ( $P = 0.15$ ), which might be limited by the small sample size.

**Hemodynamic data.** There was no significant difference in heart rate between control and cholesterol-fed groups either before or after ischemia and reperfusion. In contrast, mean arterial blood pressure was decreased in cholesterol-fed rabbits compared to control, though not statistically significantly, both before and after ischemia and reperfusion (Table 2). During the 30-min period of ischemia, both control and cholesterol-fed rabbits showed a comparable degree of decrease in blood pressure, which then slightly elevated during the reperfusion period.

**Myocardial infarct size after ischemia and reperfusion.** In order to determine the effect of hypercholesterolemia on myocardial vulnerability following ischemia and reperfusion, we measured the amount of infarct (necrotic) tissue either as a percentage of area-at-risk or as a percentage of total left ventricle (Fig. 1). There was no significant difference in area-at-risk as a percentage of total left ventricular mass, indicating a comparable

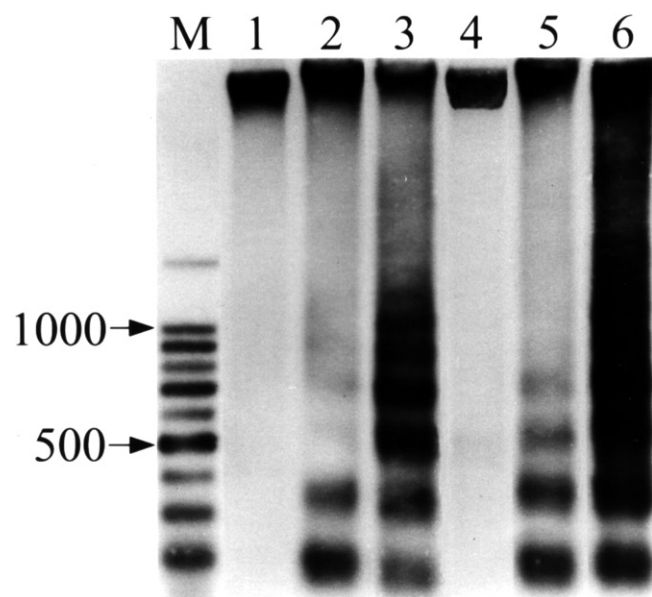


**FIG. 1.** Tissue wet weights of area-at-risk (AR) as a percentage of the total left ventricular wet weight (LV) (left), infarct tissue (area of necrosis, AN) as a percent of the AR (middle), and AN as a percent of the total LV (right) for both groups of rabbits that underwent myocardial ischemia and reperfusion. The infarct size (% of risk region) was significantly greater in cholesterol-fed rabbits than in controls (39  $\pm$  6 vs. 23  $\pm$  2%,  $P = 0.02$ ). Error bars indicate  $\pm$ SEM.

degree of jeopardy had occurred in both groups. However, the infarct size, whether expressed as a percentage of area-at-risk or as a percentage of total left ventricle, was greater by approximately 70% in cholesterol-fed rabbits than in normally fed rabbits ( $P = 0.002$ ). Thus, hypercholesterolemia did have a detrimental effect on myocardial vulnerability following ischemia and reperfusion.

**DNA fragmentation (DNA ladder) in hearts subjected to ischemia and reperfusion.** Myocardial DNA fragmentation in the nonischemic, ischemic but nonnecrotic, and necrotic (TTC unstained) areas in both groups is shown in Figure 2. DNA ladders were not detected in the nonischemic left ventricles of either normally fed or cholesterol-fed rabbits (lanes 1 and 4, respectively). Typical nucleosomal DNA ladders indicative of apoptosis were clearly demonstrated in myocardial specimens sampled from the ischemic, nonnecrotic left ventricles of both normally fed and cholesterol-fed rabbits (lanes 2 and 5, respectively). The intensity of the ladders was more pronounced in cholesterol-fed rabbits. In specimens sampled from the necrotic (TTC unstained) myocardium, patterns of background smear, a hallmark of necrosis, were evident in both normally fed and cholesterol-fed rabbits (lanes 3 and 6). DNA laddering was also present in specimens from the necrotic myocardium. Likewise, the intensity of the ladders and background smear in the necrotic samples was also more prominent in cholesterol-fed rabbits.

**In situ determination of apoptosis in ischemic-reperfused myocardium.** Heart tissue from the nonischemic area exhibited very low levels of staining for TUNEL in both normally



**FIG. 2.** DNA laddering. Laddering represents multiples of 180-bp internucleosomal DNA fragments and corroborates histological evidence of apoptosis. DNA was extracted from the myocardium of normally fed rabbits (lanes 1–3) and of cholesterol-fed rabbits (lanes 4–6). Lanes 1 and 4 are from the nonischemic zones. Lanes 2 and 5 are from the ischemic, nonnecrotic zones. Lanes 3 and 6 are from the necrotic (infarcted) zones. Lane M is 100-bp ladder marker. The figure is representative of at least six separate experiments.

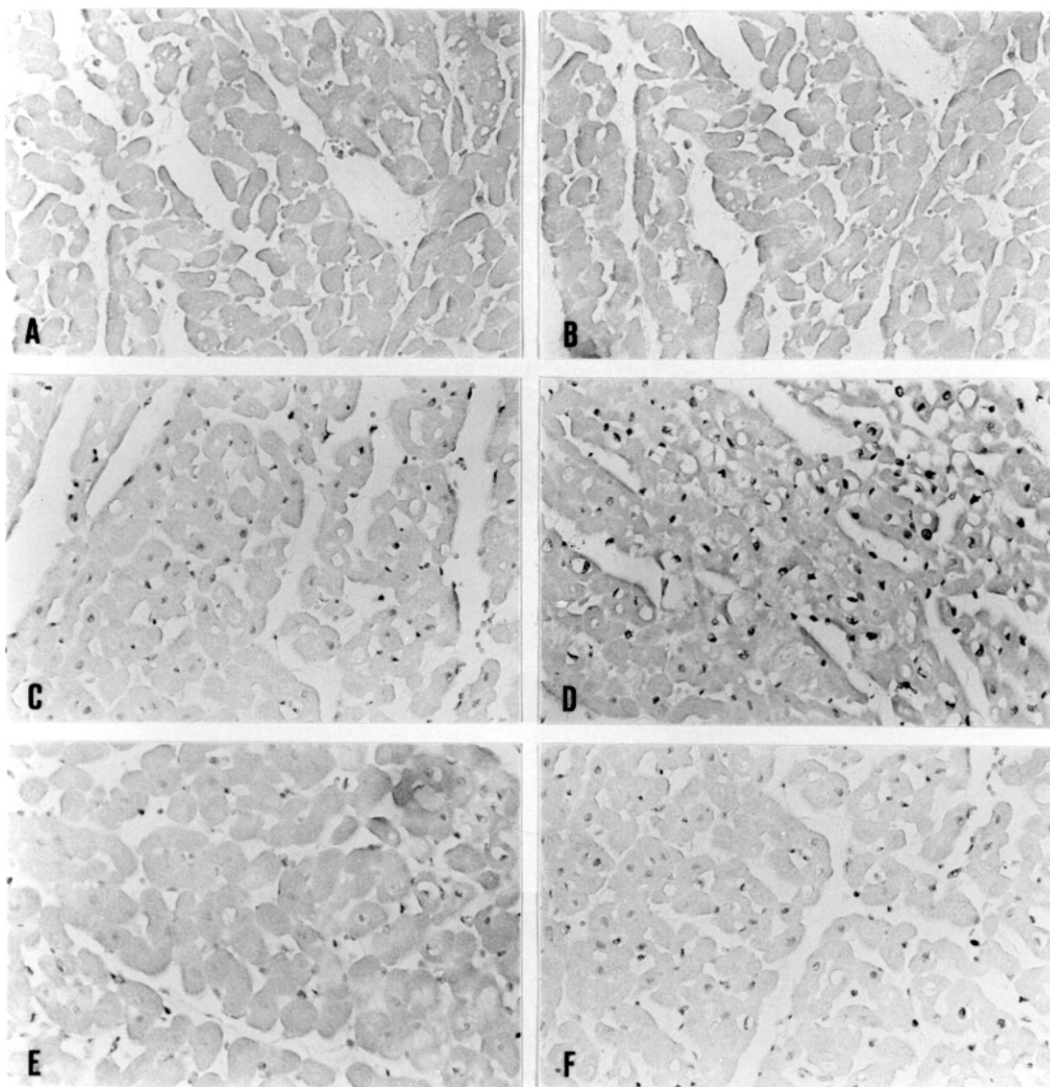
fed ( $0.3 \pm 0.1\%$ ) and cholesterol-fed ( $0.4 \pm 0.1\%$ ) rabbits (Figs. 3A and 3B, respectively), consistent with an absence of DNA laddering. In contrast, significant numbers of cardiomyocyte nuclei from the ischemic nonnecrotic myocardium were stained positively for TUNEL in both groups (Figs. 3C–F). The positive TUNEL staining was primarily confined to the cardiomyocytes, which could be easily distinguished from other nonmyocytes by their morphology. Furthermore, apoptotic myocytes were localized to a greater degree in the subendocardial area and were individually dispersed among otherwise normal cardiomyocytes (Figs. 3C and 3D). The percentage of TUNEL-positive cardiomyocytes in the ischemic nonnecrotic myocardium in cholesterol-fed rabbits was significantly higher than that in normally fed rabbits ( $40.3 \pm 4.7$  vs.  $17.1 \pm 1.4\%$ ;  $P < 0.001$ ) (Fig. 4). This finding is consistent with a more pronounced DNA laddering in the ischemic myocardium of cholesterol-fed rabbits than control. Because DNA degradation occurred nonspecifically in necrotic myocardium, and this might also be stained by TUNEL, the extent of cardiomyocyte apoptosis in the necrotic areas was thus not assessed.

The percentage of TUNEL-positive cardiomyocytes in myocardium from sham-operated control rabbits ( $0.3 \pm 0.1\%$ ) was similar to that in the nonischemic myocardium of both control and cholesterol-fed rabbits. This finding demonstrates that both TTC staining and the additional time for processing the myocardium did not affect the analyses of apoptosis.

**Expression of Bcl-2 and Bax proteins after ischemia and reperfusion.** The expression of Bcl-2 and Bax proteins was analyzed by Western blot analysis, as illustrated in Figure 5. Densitometrically, the amount of Bcl-2 expressed in the nonischemic area was approximately 50% higher ( $P < 0.05$ ) in cholesterol-fed rabbits than in normally fed rabbits. However, there was no significant difference in the expression of Bax between both groups in the nonischemic area. Furthermore, for rabbits in both groups, the expression of Bcl-2 and Bax in the nonischemic myocardium was similar to that in sham-operated rabbits (data not shown). This finding suggests that myocardial ischemia and reperfusion did not affect the expression of Bcl-2 and Bax in the nonischemic myocardium. Therefore, the expression of both Bcl-2 and Bax in the nonischemic myocardium could be viewed as a reflection of baseline myocardial status.

Compared with that in the nonischemic myocardium, the expression of Bcl-2 in the ischemic myocardium increased by  $34 \pm 3\%$ , whereas the expression of Bax decreased by  $22 \pm 2\%$ . Changes of the amount of Bax expressed following ischemia and reperfusion were similar between both groups. However, compared with normally fed rabbits, cholesterol-fed rabbits were associated with more pronounced decrease in the expression of Bcl-2 in the ischemic myocardium ( $42 \pm 4$  vs.  $26 \pm 2\%$ ;  $P < 0.01$ ). Furthermore, changes of the expression of both Bcl-2 and Bax proteins became significant 2 h after reperfusion, which was earlier than the development of cardiomyocyte apoptosis as assessed by DNA ladder formation (data not shown).

**Caspase-3 activity after ischemia and reperfusion.** For normally fed rabbits, there was a 1.8-fold increase in cas-



**FIG. 3.** Paraffin sections stained with terminal deoxynucleotidyl transferase-mediated dUTP-biotin nick end labeling (TUNEL) and methyl green in the nonischemic zones (A, normally fed rabbits; B, cholesterol-fed rabbits), subendocardium of the ischemic zones (C, normally fed rabbits; D, cholesterol-fed rabbits), and subepicardium of the ischemic zones (E, normally fed rabbits; F, cholesterol-fed rabbits) are presented (200 $\times$  magnification). The apoptotic cardiomyocyte is detected by the brown nuclear staining in contrast to the methyl green-stained normal cardiomyocyte nucleus. Figures are representative of at least six separate experiments.

pase-3 activity in the ischemic myocardium compared with that in the nonischemic myocardium (Fig. 6). However, for cholesterol-fed rabbits, there was a much greater increase (2.5-fold) in caspase-3 activity in the ischemic myocardium compared with that in the nonischemic myocardium. Caspase-3 activity in the nonischemic myocardium was similar between normally fed and cholesterol-fed rabbits. Like Bcl-2 and Bax, caspase-3 activity was markedly increased 2 h after reperfusion (data not shown).

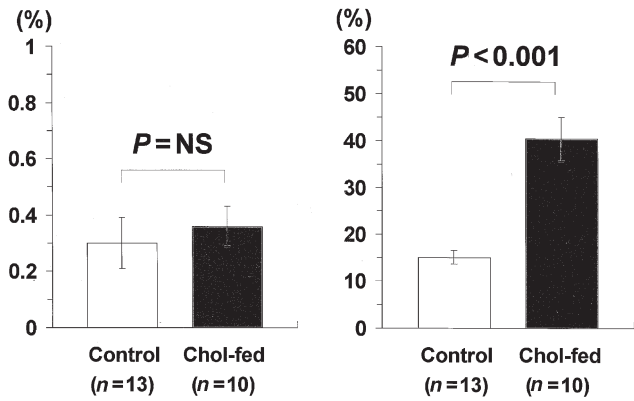
## DISCUSSION

This study shows, for the first time, that long-term (8 wk) hypercholesterolemia significantly increases the extent of cardiomyocyte apoptosis as well as infarct size following exper-

imental myocardial ischemia and reperfusion. In the nonischemic myocardium, hypercholesterolemia increases the expression of anti-apoptotic Bcl-2 protein but not pro-apoptotic Bax protein. However, in the ischemic-reperfused myocardium, hypercholesterolemic rabbits exhibited a more pronounced decrease in the expression of Bcl-2, a similar extent of increase in the expression of Bax, and a significantly increased activation of caspase-3. These findings may partly explain why hypercholesterolemia is associated with greater cardiomyocyte apoptosis after ischemia and reperfusion.

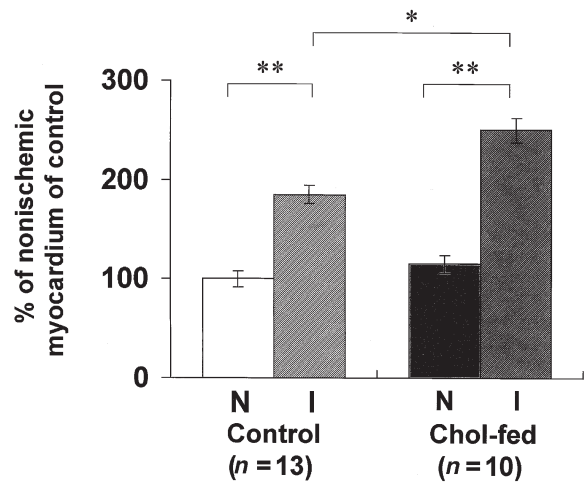
Although there are several studies showing that cardiomyocyte apoptosis is a significant contributor to myocardial cell death following ischemia and reperfusion (3–8), it is still not known whether the severity of reperfusion-related cardiomyocyte apoptosis varies in patients with different





**FIG. 4.** Percentage of cardiomyocyte nuclei stained positive for TUNEL in the nonischemic (left) and ischemic nonnecrotic (right) areas from both normally fed and cholesterol-fed rabbits. The percentage of TUNEL-positive cardiomyocytes in the ischemic nonnecrotic myocardium in cholesterol-fed rabbits was significantly higher than that in normally fed rabbits ( $40.3 \pm 4.7\%$  vs.  $17.1 \pm 1.4\%$ ;  $P < 0.001$ ). Error bars indicate  $\pm$ SEM. For abbreviation see Figure 3.

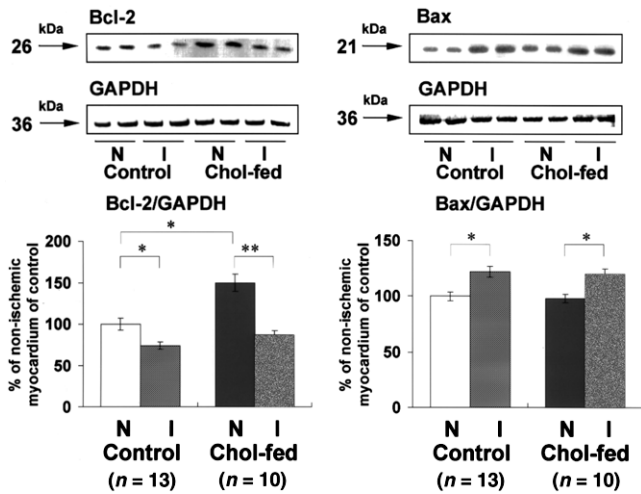
co-morbid conditions. The present study is the first to demonstrate that hypercholesterolemia is associated with a more than twofold increase in the number of cardiomyocytes undergoing apoptosis following experimental ischemia and reperfusion in the ischemic nonnecrotic myocardium. In this study, we defined apoptosis by two conventional methods, DNA laddering by agarose gel electrophoresis and histochemical visualization of nuclear DNA fragments by the



**FIG. 6.** Caspase-3 activity in the nonischemic (N) and ischemic (I) myocardium. Caspase-3 activity was measured by the ability of tissue homogenates to cleave DEVD-fluorochrome 7-amino-4-methyl coumarin (AMC). The values for each sample are presented in percentage of control (nonischemic myocardium of control rabbits). For control rabbits, there was a 1.8-fold increase in caspase-3 activity in the ischemic myocardium compared with that in the nonischemic myocardium. However, for cholesterol-fed rabbits, there was a much greater 2.5-fold increase in caspase-3 activity in the ischemic myocardium compared with that in the nonischemic myocardium. Caspase-3 activity in the nonischemic myocardium was similar between control and cholesterol-fed rabbits. \* $P < 0.05$ , \*\* $P < 0.001$ . Error bars indicate  $\pm$ SEM.

TUNEL staining. While TUNEL staining has been criticized for lack of specificity when used in tissue where necrosis occurs along with apoptotic cell death (21), recent studies have demonstrated that in areas where necrotic cells are not present to any significant amount, good correlation is found between the TUNEL test and other more sophisticated methods (22,23). We herein assessed the magnitude of cardiomyocyte apoptosis only in ischemic areas without evidence of necrosis, confirmed by the absence of background smear on agarose gel electrophoresis. Previous studies examining the effects of ischemia-reperfusion on cardiomyocyte apoptosis by TUNEL staining often included both necrotic and non-necrotic areas (3,6,24). However, the extent of cardiomyocyte apoptosis following ischemia and reperfusion in normocholesterolemic rabbits reported here agrees with most previous studies with this methodological flaw (7). Although DNA laddering may be due to noncardiomyocyte apoptosis, we demonstrated that most TUNEL-positive cells had typical morphological features of cardiomyocytes. This observation is consistent with recent reports that showed that DNA fragmentation on gel electrophoresis was essentially associated with cardiomyocyte apoptosis (3,6).

Adult cardiomyocytes are terminally differentiated cells and thought to have, at best, a very limited capacity for self-renewal (25). Viewed from this perspective, death of a significant number of cardiomyocytes, by either necrosis or apoptosis, can have lasting adverse consequences on overall cardiac performance. Because postinfarct left ventricular systolic function is the most important determinant of long-term



**FIG. 5.** Expression of Bcl-2 and Bax proteins was visualized in the nonischemic (N) and ischemic nonnecrotic (I) myocardium by Western blot analysis. The ratio of Bcl-2 or Bax band density to glyceraldehyde-3-phosphate dehydrogenase (GAPDH) band density was calculated and then normalized by the value of control (nonischemic myocardium of control rabbits). In the nonischemic myocardium, cholesterol-fed rabbits exhibited an approximately 50% increase in the expression of Bcl-2 ( $P < 0.05$ ), but not Bax, than control rabbits. However, compared with control, cholesterol-fed rabbits exhibited a more pronounced decrease in the expression of Bcl-2 ( $42 \pm 4$  vs.  $26 \pm 2\%$ ,  $P < 0.01$ ) and a similar extent of increase in the expression of Bax in the ischemic myocardium. Figures are representative of at least six separate experiments. \* $P < 0.05$ , \*\* $P < 0.001$ . Error bars indicate  $\pm$  SEM.



survival in patients with myocardial infarction, our observation that hypercholesterolemia increases the extent of cardiomyocyte apoptosis as well as infarct size following ischemia and reperfusion is consistent with the clinical phenomenon that hypercholesterolemic patients treated with lipid-lowering drugs had a better prognosis after sustaining a myocardial infarction than those treated with placebo, even in the current reperfusion era (10,12). Moreover, because cardiac enzymes are released only when cardiomyocytes break down and cardiomyocytes typically rupture during necrosis but not apoptosis (13), evaluation of infarct size by cardiac enzyme values may underestimate the severity of myocardial infarction, especially in patients with predisposing conditions that may aggravate the magnitude of apoptosis. This explains our previous observation that the deleterious effect of dyslipidemia on postinfarct left ventricular systolic function was independent of the size of myocardial infarction estimated by cardiac enzyme changes (12).

In view of the markedly increased activation of caspase-3 and the significant contribution of cardiomyocyte apoptosis as a result of reperfusion injury, it is speculated that anti-apoptotic interventions, such as caspase inhibitors, may reduce myocardial reperfusion injury by attenuating cardiomyocyte apoptosis within the ischemic myocardium. Despite several studies that have demonstrated that *in vivo* administration of various caspase inhibitors is effective in reducing the extent of apoptosis, their effect on infarct size reduction was still controversial (24,26). One possible reason is that because the apoptotic cardiomyocytes are mostly scattered, not grouped together, in the ischemic myocardium as shown in the present and other studies (3,5,6,24,26), evaluation of infarct size by the traditional TTC staining at the gross examination may underestimate the impact of apoptosis inhibition, which was evident at the histological examination. Since the magnitude of cardiomyocyte apoptosis doubled in hypercholesterolemic rabbits, we speculated that caspase inhibitors might have a greater protective effect on myocardial ischemia-reperfusion injury in animals with underlying hypercholesterolemia. Further investigations are needed to test this hypothesis.

Compared with normally fed rabbits, rabbits in the cholesterol-fed group had a higher mortality rate following myocardial ischemia and reperfusion. Because rabbits dying in the procedure might have had a greater extent of cardiomyocyte apoptosis as well as larger infarct size, our observation may underestimate the impact of hypercholesterolemia on reperfusion-related cardiac injuries. This may also explain why mice fed a cholesterol-enriched diet for 12 wk had a significantly decreased infarct size following ischemia and reperfusion than normocholesterolemic mice in one recent study (17).

The multigene family of Bcl-2-like proteins, some of which, such as Bcl-2 itself, inhibit apoptosis and others, such as Bax, that promote apoptosis, is one of the best-known regulators of the apoptotic process (19). The ratio of Bcl-2 to Bax, the so-called death-switch, is often used as an indicator of

apoptosis. An increase in this ratio is used to signify attenuation of the apoptotic process, whereas a decrease in this ratio is used to signify exacerbation of the apoptotic process. In this study, compared with normally fed rabbits, the expression of Bcl-2 was significantly upregulated in the nonischemic myocardium of hypercholesterolemic rabbits, whereas the expression of Bax was similar between both groups. This intriguing finding indicates that hypercholesterolemia may render the myocardium more resistant to pro-apoptotic stimuli by increasing the Bcl-2/Bax ratio. Although we did not perform immunohistochemical staining to ensure the exact origin of both Bcl-2 and Bax proteins, several studies demonstrated that the expression of both Bcl-2 and Bax primarily originates from cardiomyocytes (6,27). It is still not known whether hypercholesterolemia has a direct effect on the expression of Bcl-2 and Bax in cardiomyocytes. However, prolonged hypercholesterolemia may confer to the heart a relatively oxygen-deprived milieu by leading to coronary atherosclerosis and subsequent depressed pump function, as manifested by decreased mean arterial blood pressure at baseline in cholesterol-fed rabbits in the present and other studies (17,18). Hence, we speculated that hypercholesterolemia may cause the heart to develop a preconditioning-like response and thereby upregulate the expression of Bcl-2. In keeping with our observation, one study reported that ischemic preconditioning was associated with upregulation of Bcl-2 in rats (28). Furthermore, in explanted failed human hearts, Olivetti *et al.* (29) reported a near doubling of the expression of Bcl-2 without changes in the expression of Bax. This preconditioning-like effect of hypercholesterolemia also explains why isolated perfused heart of the cholesterol-fed rabbits, in the absence of invading activated inflammatory cells, was more resistant to ischemia-reperfusion injury in one recent study (18).

Although cholesterol-fed rabbits were associated with an increased Bcl-2/Bax ratio in the nonischemic myocardium, these rabbits also exhibited a more pronounced decrease in the expression of Bcl-2 and a similar extent of increase in the expression of Bax in the ischemic myocardium compared with normally fed rabbits. This finding is in accordance with our observation that hypercholesterolemia increased cardiomyocyte apoptosis following ischemia and reperfusion. Several studies demonstrated that hypercholesterolemia is associated with massive generation of oxygen-derived free radicals (30), increased interactions between circulating leukocytes and the endothelium (31,32), impaired anticoagulant mechanisms (15), and underdevelopment of collateral circulation following ischemia and reperfusion (33). These adverse effects may offset the cardioprotective action conferred by an increased Bcl-2/Bax ratio and thus render the heart more susceptible to the ischemia-reperfusion insult.

*Limitations.* First, some other members of the Bcl-2 family, such as Bcl-x and Bax, may also be involved in regulation of apoptosis (19). However, these proteins were not measured in the present study. Second, it has been reported that infiltrated inflammatory cells express high levels of Bax (34). Because immunohistochemical staining was not done in the

present study, we cannot exclude the possibility that the increased Bax expression following ischemia and reperfusion may be partly due to invading activated inflammatory cells, such as neutrophils. Nevertheless, although several previous studies demonstrated that the number of neutrophils accumulated in the ischemic myocardium was significantly higher in cholesterol-fed rabbits than in normally fed ones (32), the increase in Bax expression in the ischemic myocardium was similar between both groups in this study. Hence, the contribution of inflammatory cells to the increase in Bax expression may be small. Third, because the positive TUNEL has been observed in necrotic cells as well as apoptotic cells, we cannot accurately assess the extent of cardiomyocyte apoptosis in the necrotic myocardium. Further studies using the more specific Taq polymerase-based *in situ* ligation assay may resolve this problem (7).

**Clinical implications.** In this study, we demonstrated that although hypercholesterolemia is associated with an increased myocardial Bcl-2/Bax ratio at baseline, diet-induced hypercholesterolemia significantly exacerbates cardiac reperfusion injury, not only by increasing the infarct size but also by increasing the extent of cardiomyocyte apoptosis. The increased extent of cardiomyocyte apoptosis may adversely influence the left ventricular remodeling process and subsequently lead to poor prognosis. Because the magnitude of reperfusion-related cardiomyocyte apoptosis is significantly greater in hypercholesterolemic rabbits, we speculated that the administration of anti-apoptotic agents following the establishment of successful revascularization might provide additional benefits in salvaging the ischemic myocardium.

## ACKNOWLEDGMENTS

The authors are indebted to Ms. Rong-Jane Chen for her excellent technical work. This study was funded in part by a grant from the National Taiwan University Hospital (NTUH89-M013).

## REFERENCES

- Ryan, T.J., Antman, E.M., Brooks, N.H., Califf, R.M., Hillis, L.D., Hiratzka, L.F., Rapaport, E., Riegel, B., Russell, R.O., Smith, E.E., *et al.* (1999) 1999 Update: ACC/AHA Guidelines for the Management of Patients with Acute Myocardial Infarction: Executive Summary and Recommendations: A Report of the American College of Cardiology/American Heart Association Task Force on Practice Guidelines (Committee on Management of Acute Myocardial Infarction), *Circulation* 100, 1016–1030.
- Braunwald, E., and Kloner, R.A. (1985) Myocardial Reperfusion: A Double-Edged Sword? *J. Clin. Invest.* 76, 1713–1719.
- Gottlieb, R.A., Bursleson, K.O., Kloner, R.A., Babior, B.M., and Engler, R.L. (1994) Reperfusion Injury Induces Apoptosis in Rabbit Cardiomyocytes, *J. Clin. Invest.* 94, 1621–1628.
- Saraste, A., Pulkki, K., Kallajoki, M., Henriksen, K., Parvinen, M., and Voipio-Pulkki, L.M. (1997) Apoptosis in Human Acute Myocardial Infarction, *Circulation* 95, 320–323.
- Fliiss, H., and Gattinger, D. (1996) Apoptosis in Ischemic and Reperfused Rat Myocardium, *Circ. Res.* 79, 949–956.
- Zhao, Z.Q., Nakamura, M., Wang, N.P., Wilcox, J.N., Shearer, S., Ronson, R.S., Guyton, R.A., and Vinten-Johansen, J. (2000) Reperfusion Induces Myocardial Apoptotic Cell Death, *Cardiovasc. Res.* 45, 651–660.
- Yaoita, H., Ogawa, K., Maehara, K., and Maruyama, Y. (2000) Apoptosis in Relevant Clinical Situations: Contribution of Apoptosis in Myocardial Infarction, *Cardiovasc. Res.* 45, 630–641.
- Olivetti, G., Quaini, F., Sala, R., Lagrasta, C., Corradi, D., Bonacina, E., Gambert, S.R., Cigola, E., and Anversa, P. (1996) Acute Myocardial Infarction in Humans Is Associated with Activation of Programmed Myocyte Cell Death in the Surviving Portion of the Heart, *J. Mol. Cell. Cardiol.* 28, 2005–2016.
- Keys, A. (1970) Coronary Heart Disease in Seven Countries, *Circulation* 41 (Suppl. I), I1–I8.
- Scandinavian Simvastatin Survival Study Group (1994) Randomized Trial of Cholesterol Lowering Therapy in 4444 Patients with Coronary Heart Disease: The Scandinavian Simvastatin Survival Study (4S), *Lancet* 344, 1383–1389.
- Shepherd, J., Cobbe, S.M., Ford, I., Isles, C.G., Lorimer, A.R., MacFarlane, P.W., McKillop, J.H., and Packard, C.J. (1995) Prevention of Coronary Heart Disease with Pravastatin in Men with Hypercholesterolemia. The West of Scotland Coronary Prevention Study Group, *N. Engl. J. Med.* 333, 1301–1307.
- Wang, T.D., Wu, C.C., Chen, W.J., Lee, C.M., Chen, M.F., Liao, C.S., Sung, F.C., and Lee, Y.T. (1998) Dyslipidemias Have a Detrimental Effect on Left Ventricular Systolic Function in Patients with a First Myocardial Infarction, *Am. J. Cardiol.* 81, 531–537.
- James, T.N. (2000) Homage to James B. Herrick: A Contemporary Look at Myocardial Infarction and at Sickle-Cell Heart Disease, *Circulation* 101, 1874–1887.
- Osborne, J.A., Lento, M.R., Siegfried, M.R., Stahl, G.L., Fushman, B., and Lefer, A.M. (1989) Cardiovascular Effects of Acute Hypercholesterolemia in Rabbits: Reversal with Lovastatin Treatment, *J. Clin. Invest.* 83, 465–473.
- Golino, P., Maroko, P.R., and Carew, T.E. (1987) Efficacy of Platelet Depletion in Counteracting the Detrimental Effect of Acute Hypercholesterolemia on Infarct Size and the No-Reflow Phenomenon in Rabbits Undergoing Coronary Artery Occlusion–Reperfusion, *Circulation* 76, 173–180.
- Tilton, R.G., Cole, P.A., Zions, J.D., Daugherty, A., Larson, K.B., Suter, S.P., Kilo, C., and Williamson, J.R. (1987) Increased Ischemia–Reperfusion Injury to the Heart Associated with Short-Term, Diet-Induced Hypercholesterolemia in Rabbits, *Circ. Res.* 60, 551–559.
- Girod, W.G., Jones, S.P., Sieber, N., Aw, T.Y., and Lefer, D.J. (1999) Effects of Hypercholesterolemia on Myocardial Ischemia–Reperfusion Injury in LDL Receptor-Deficient Mice, *Arterioscler. Thromb. Vasc. Biol.* 19, 2776–2781.
- Le Grand, B., Vie, B., Faure, P., Degryse, A.-D., Mouillard, P., and John, G.W. (1995) Increased Resistance to Ischemic Injury in the Isolated Perfused Atherosclerotic Heart of the Cholesterol-Fed Rabbit, *Cardiovasc. Res.* 30, 689–696.
- Kirshenbaum, L.A., and de Moissac, D. (1997) The Bcl-2 Gene Product Prevents Programmed Cell Death of Ventricular Myocytes, *Circulation* 96, 1580–1585.
- Lowry, O.H., Rosebrough, N.J., Farr, A.L., and Randall, R.J. (1951) Protein Measurement with the Folin-Phenol Reagent, *J. Biol. Chem.* 193, 265–275.
- Ohno, M., Takemura, G., Ohno, A., Misao, J., Hayakawa, Y., Minatoguchi, S., Fujiwara, T., and Fujiwara, H. (1998) ‘Apoptotic’ Myocytes in Infarct Area in Rabbit Hearts May Be Oncotic Myocytes with DNA Fragmentation. Analysis by Immunogold Electron Microscopy Combined with *in situ* Nick End-Labeling, *Circulation* 98, 1422–1430.
- Leri, A., Liu, Y., Malhotra, A., Li, Q., Stiegler, P., Claudio, P.P., Giordano, A., Kajstura, J., Hintze, T.H., and Anversa, P. (1998) Pacing-Induced Heart Failure in Dogs Enhances the Expression

- of p53 and p53-Dependent Genes in Ventricular Myocytes, *Circulation* 97, 194–203.
23. Oskarsson, H.J., Coppey, L., Weiss, R.M., and Li, W.G. (2000) Antioxidants Attenuate Myocyte Apoptosis in the Remote Non-infarcted Myocardium Following Large Myocardial Infarction, *Cardiovasc. Res.* 45, 679–687.
  24. Okamura, T., Miura, T., Takemura, G., Fujiwara, H., Iwamoto, H., Kawamura, S., Kimura, M., Ikeda, Y., Iwatate, M., and Matsuzaki, M. (2000) Effect of Caspase Inhibitors on Myocardial Infarct Size and Myocyte DNA Fragmentation in the Ischemia-Reperfused Rat Heart, *Cardiovasc. Res.* 45, 642–650.
  25. Anversa, P., Palackal, T., Sonnenblick, E.H., Olivetti, G., Meggs, L.G., and Capasso, J.M. (1990) Myocyte Cell Loss and Myocyte Cellular Hyperplasia in the Hypertrophied Aging Rat Heart, *Circ. Res.* 67, 871–885.
  26. Yaoita, H., Ogawa, K., Maehara, K., and Maruyama, Y. (1998) Attenuation of Ischemia/Reperfusion Injury in Rats by a Caspase Inhibitor, *Circulation* 97, 276–281.
  27. Condorelli, G., Morisco, C., Stassi, G., Notte, A., Farina, F., Sgaramella, G., de Rienzo, A., Roncarati, R., Trimarco, B., and Lembo, G. (1999) Increased Cardiomyocyte Apoptosis and Changes in Proapoptotic and Antiapoptotic Genes Bax and Bcl-2 During Left Ventricular Adaptations to Chronic Pressure Overload in the Rat, *Circulation* 99, 3071–3078.
  28. Maulik, N., Engelman, R.M., Rouson, J.A., Flack, J.E., Deaton, D., and Das, D.K. (1999) Ischemic Preconditioning Reduces Apoptosis by Upregulating Anti-death Gene Bcl-2, *Circulation* 100 (Suppl. 19), II369–II375.
  29. Olivetti, G., Abbi, R., Quaini, F., Kajstura, J., Cheng, W., Nitahara, J.A., Quaini, E., Di Loreto, C., Beltrami, C.A., Krajewski, S., et al. (1996) Apoptosis in the Failing Human Heart, *N. Engl. J. Med.* 336, 1131–1141.
  30. Ohara, U., Peterson, T.E., and Harrison, D.G. (1993) Hypercholesterolemia Increases Endothelial Superoxide Anion Production, *J. Clin. Invest.* 91, 2546–2551.
  31. Tsao, P.S., McEvoy, L.M., Drexler, H., Butcher, E.C., and Cooke, J.P. (1994) Enhanced Endothelial Adhesiveness in Hypercholesterolemia Is Attenuated by L-Arginine, *Circulation* 89, 2176–2182.
  32. Hoshida, S., Yamashita, N., Kawahara, K., Kuzuya, T., and Hori, M. (1999) Amelioration by Quinapril of Myocardial Infarction Induced by Coronary Occlusion/Reperfusion in a Rabbit Model of Atherosclerosis, *Circulation* 99, 434–440.
  33. Chilian, W.M. (1997) Coronary Microcirculation in Health and Disease, *Circulation* 95, 522–528.
  34. Kockx, M.M., De Meyer, G.R., Muhring, J., Jacob, W., Bult, H., and Herman, A.G. (1998) Apoptosis and Related Proteins in Different Stages of Human Atherosclerotic Plaques, *Circulation* 97, 2307–2315.

[Received May 18, 2001, and in revised form October 22, 2001; revision accepted February 13, 2002]

# Effect of SMP-500, a Novel ACAT Inhibitor, on Hepatic Cholesterol Disposition in Rats

Katsuhisa Ioriya\*, Takeshi Nishimura, and Naohito Ohashi

Research Division, Sumitomo Pharmaceuticals Co., Ltd., Osaka, Japan

**ABSTRACT:** The effects of SMP-500, a novel ACAT inhibitor, on serum lipid levels, hepatic lipid secretion rate, and hepatic lipid disposition in rats were studied to clarify its lipid-lowering action. SMP-500 reduced the serum cholesterol level in a dose-dependent manner in rats fed a hypercholesterolemic diet. SMP-500 also reduced hepatic free cholesterol content in addition to hepatic total and esterified cholesterol contents. Biliary concentrations of cholesterol and bile acid were increased by SMP-500; however, the bile flow and lithogenic index were not affected. SMP-500 increased cholesterol 7 $\alpha$ -hydroxylase mRNA level. Therefore, it is suggested that the increase in concentrations of cholesterol and bile acid in bile is due to both the increase of bile acid production through the increase of cholesterol 7 $\alpha$ -hydroxylase and the decrease of hepatic free cholesterol content. An inhibitory effect of SMP-500 both on the cholesterol secretion and on the TG secretion from liver was observed. SMP-500 reduced the serum TG level in sucrose-fed rats. From these results, one may hypothesize that the suppression of hepatic VLDL secretion probably plays an important role on both cholesterol- and TG-lowering effects of SMP-500.

Paper no. L8923 in *Lipids* 37, 395–400 (April 2002).

Hypercholesterolemia and cardiovascular disease are major health problems in many industrialized countries. One therapeutic approach for reducing hypercholesterolemia is to inhibit enzymes essential for cholesterol metabolism. ACAT is a primary enzyme responsible for the intracellular esterification of cholesterol (1). ACAT plays important roles in physiological processes. In the small intestine, ACAT facilitates the absorption of exogenous cholesterol, which is incorporated into chylomicrons (2,3). In liver, ACAT also plays an important role in the assembly of VLDL, which is secreted into blood (4–6). Under pathological states, ACAT is presumed to play a crucial role in foam cell formation of macrophages in the arterial wall, a characteristic feature of atherosclerotic lesions (7–9).

\*To whom correspondence should be addressed at 1-98, Kasugade Naka 3-chome, Konohana-ku, Osaka, 554-0022, Japan  
E-mail: ioriya@sumitomopharm.co.jp

Abbreviations: ACAT, acyl-CoA:cholesterol acyltransferase; HC, high-cholesterol; LI, lithogenic index; MC, methyl cellulose; RT-PCR, reverse transcription-PCR; SMP-500, *N*-(2,6-bis(1-methylethyl)phenyl)-*N'*-(1-butyl-1,2-dihydro-2-oxo-4-(3-(3-pyridylmethoxy)phenyl)-1,8-naphthyridin-3-yl)-urea nitrate.

Therefore, an ACAT inhibitor is expected to lower serum cholesterol through suppression of intestinal cholesterol absorption and hepatic VLDL secretion and to prevent atherosclerosis through the inhibition of foam cell formation of macrophages (10,11). Several ACAT inhibitors have been synthesized, and their pharmacological activities have been evaluated in animals and humans (12–19).

Recently, we reported a novel ACAT inhibitor, SMP-500, that can potently inhibit ACAT and cause cholesterol lowering in hyperlipidemic and normolipidemic animals (20). Interestingly, SMP-500 reduced hepatic free cholesterol contents. That data suggested that SMP-500 directly facilitates the mobilization of cholesterol from liver.

Rats can be made hypercholesterolemic when cholesterol is fed in combination with lipophilic bile salts (21). Rats also have a high activity of cholesterol 7 $\alpha$ -hydroxylase, the major rate-limiting enzyme in bile acid biosynthesis from free cholesterol (22–24). Therefore, the rat is a good animal model for the study of cholesterol disposition from liver. In this study, to clarify the role of SMP-500 in liver, we investigated the effect of SMP-500 on both disposition and secretion of hepatic cholesterol in rats, and the lowering effect of SMP-500 on serum TG and serum cholesterol.

## EXPERIMENTAL PROCEDURES

**Materials.** SMP-500, *N*-(2,6-bis(1-methylethyl)phenyl)-*N'*-(1-butyl-1,2-dihydro-2-oxo-4-(3-(3-pyridylmethoxy)phenyl)-1,8-naphthyridin-3-yl)-urea nitrate, was synthesized at the Research Division, Sumitomo Pharmaceuticals Co. Ltd., Osaka, Japan.

**Animals.** SD rats (SLC Japan, Hamamatu, Japan) were individually housed in metal cages in a room with controlled temperature (23  $\pm$  3°C), relative humidity (50  $\pm$  20%), and light (12/12 h light/dark cycle). They had free access to water and a stock diet, CE-2 (Clea Japan Inc., Tokyo). All procedures related to the use of animals in these studies were reviewed and approved by the Institutional Animal Care and Use Committee at Sumitomo Pharmaceuticals Research Division.

**Cholesterol-lowering effect.** SD rats were fed either CE-2 diet containing 1.5% cholesterol, 0.5% cholic acid, 5.5% peanut oil [high-cholesterol (HC) diet] (25) or CE-2 (normal group), and started on the HC diet at the same time as SMP-500. SMP-500 was suspended in 0.5% methylcellulose (MC) and administered by gavage to the HC diet-fed rats once a day



for 6 d. In control and normal groups, 0.5% MC solution was administered. On the day after the final administration, rats were anesthetized with diethylether. Blood samples were collected from the orbital sinus using a capillary tube. Serum concentrations of total and HDL cholesterol were measured by enzymatic methods using commercial kits (Wako Pure Chemical Industries, Ltd., Osaka, Japan). The non-HDL cholesterol level was calculated as the difference between the HDL cholesterol level and the total cholesterol level. After collecting the blood samples from the rats, laparotomy was performed to remove the liver, which was immediately frozen in liquid nitrogen. Lipids of these samples were extracted with chloroform/methanol mixture according to the method of Folch *et al.* (26). The amounts of total and free cholesterol were measured by the method of Kunitomo *et al.* (27). The esterified cholesterol was calculated as the difference between the free and the total cholesterol.

**Bile flow and biliary cholesterol secretion.** SMP-500 was suspended in 0.5% MC and administered by gavage to HC diet-fed rats once a day for 6 d. On the day after the final administration, rats were fitted with a cannula on the bile duct, and bile was collected for 1 h under anesthesia (50 mg/kg; Nembutal®, Abbot Laboratories, IL). The serum total cholesterol level and biliary total bile acid, cholesterol and phospholipid were measured with enzymatic methods using commercial kits, as described above. The lithogenic index (LI), expressed as the cholesterol saturation of bile, was calculated by the method of Admirand and Small (28).

**Lipid secretion rate.** The effect of SMP-500 on the rate of lipid secretion from liver was determined by measuring the plasma cholesterol and TG levels after intravenous administration of Triton WR-1339 to rats (29). SMP-500 was suspended in 0.5% MC and administered by gavage to normal diet-fed rats once a day for 3 d. After the second administration, rats were fasted. On the next day, 1 h after the final administration, 400 mg/kg Triton WR-1339, as a 10% solution in 0.9% NaCl, was administered intravenously *via* the tail vein under diethylether anesthesia. Two hours later, rats were anesthetized with diethylether, and blood samples were collected from the orbital sinus and supplemented with 1 mg/mL of EDTA. The plasma VLDL fraction was then isolated by ultracentrifugation (30), and VLDL-cholesterol and VLDL-TG levels were measured by enzymatic methods using commercial kits, as described above.

**TG-lowering effect in sucrose-fed rats.** Rats were fed a high-sucrose diet (High Sucrose AIN-76A; Purina, St. Louis, MO) (25) for 2 wk, and orally administered SMP-500 suspended in 0.5% MC, once a day for 6 d utilizing the same diet. On the day after the final administration, rats were anesthetized with diethylether. Blood samples were collected from the orbital sinus of nonfasted rats, and the serum TG levels were measured by enzymatic methods using commercial kits, as described above.

**Cholesterol 7 $\alpha$ -hydroxylase mRNA level in HepG2 cells.**  $\beta$ -VLDL was isolated from rabbit plasma by ultracentrifugation (30). HepG2 cells were purchased from the American Type

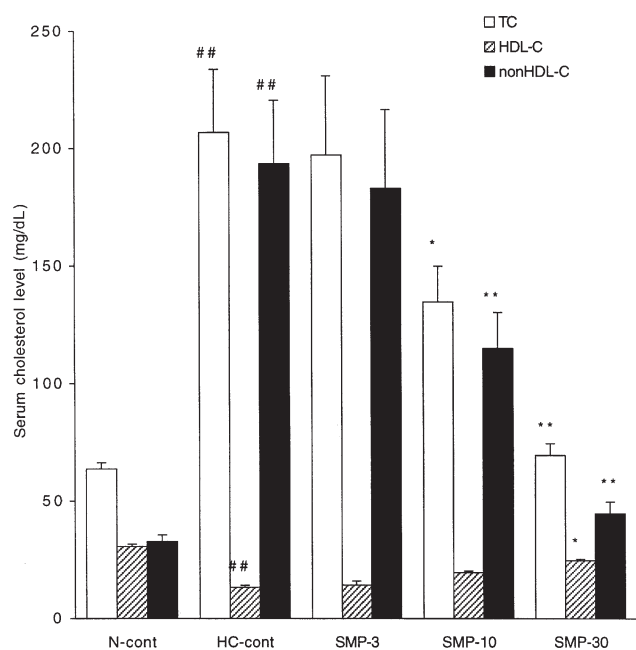
Culture Collection (Manassas, VA), and cultured in DMEM/F-12 (GIBCO, Grand Island, NY) containing 10% FCS (GIBCO), 100 units/mL penicillin, and 100  $\mu$ g/mL streptomycin in a humidified incubator (5% CO<sub>2</sub>) at 37°C. Cells were grown to confluence and then the medium was changed to a fresh medium containing 10% lipoprotein-deficient serum and  $\beta$ -VLDL (200  $\mu$ g/mL) with or without SMP-500, followed by incubation for 24 h. SMP-500 was dissolved in DMSO, and the final concentration of DMSO in the medium was 0.1% (vol/vol). Isolation of total RNA and real-time quantitative reverse transcription (RT)-PCR were performed as described previously (31). Total RNA was isolated from HepG2 cells using TRIzol reagent (Life Technologies, Inc., Rockville, MD). The mRNA for cholesterol 7 $\alpha$ -hydroxylase was measured by real-time quantitative RT-PCR using a PE Applied Biosystems prism model 7700 sequence detection instrument (Applied Biosystems, Foster, CA). The sequences of forward and reverse primers as designed by Primer Express (PE ABI) were 5'-GCGCATGTTTCTCAATGACACT-3' and 5'-CGCTGAATGTGTTTGCTT-3', respectively. The TaqMan<sup>TM</sup> fluorogenic probe used was 5'-6FAM-ATGATCTGGAGAAGGCCAA-GACACACCTC-TAMRA-3'. Cholesterol 7 $\alpha$ -hydroxylase mRNA levels were corrected for  $\beta$ -actin RNA, which was measured using a kit (PE ABI, P/N 401846) from PerkinElmer as per the manufacturer's protocol.

**Statistical analysis.** Data were expressed as mean  $\pm$  SEM. Differences among the groups were determined by Dunnett's multiple comparisons test. Student's *t*-test was also used to compare data between two groups. Differences were considered statistically significant when the *P*-value was less than 0.05.

## RESULTS

SMP-500 was administered by gavage once a day to rats fed a HC diet for 6 d. The serum total cholesterol level markedly increased during feeding with the HC diet in the control groups to approximately 3.2-fold in comparison to the value of the normal diet group (HC diet group: 207  $\pm$  26 mg/dL, normal diet group: 64  $\pm$  4 mg/dL) (Fig. 1). The increased amount of total cholesterol level was due to an increase in the non-HDL cholesterol level. SMP-500 significantly reduced the serum total and non-HDL cholesterol levels in a dose-dependent manner at doses of 10 mg/kg/d or higher (Fig. 1). Compared with HC-fed controls, serum total cholesterol level was reduced by 35 and 66% and non-HDL cholesterol level was reduced 41 and 77% in animals administered SMP-500 at 10 and 30 mg/kg/d, respectively. The total cholesterol content in liver from the HC diet group was approximately nine times higher than that of the normal group (HC diet group: 23.1  $\pm$  0.7 mg/g tissue, normal diet group: 2.5  $\pm$  0.1 mg/g tissue) (Fig. 2A). The increase in the hepatic total cholesterol content was mainly due to an increase in the hepatic cholesteryl ester content. SMP-500 markedly reduced the hepatic total and esterified cholesterol content (Figs. 2A, 2B) and significantly reduced the hepatic free cholesterol content (Fig. 2C).

SMP-500 was administered by gavage once a day to rats fed

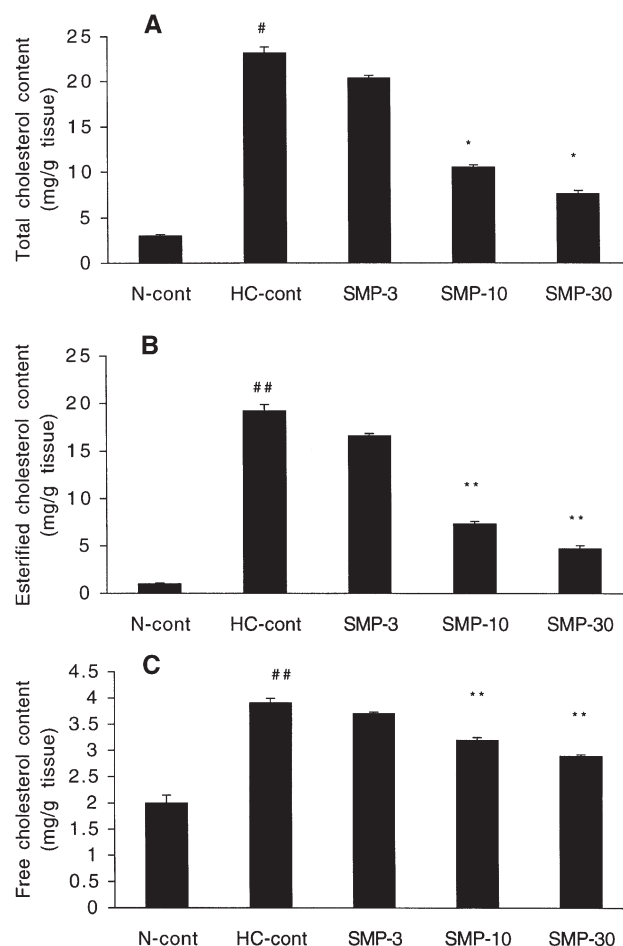


**FIG. 1.** Effect of SMP-500 on serum cholesterol levels in hypercholesterolemic rats. SMP-500 was administered by gavage to the high-cholesterol (HC) diet-fed rats once a day at doses of 3, 10, and 30 mg/kg/d for 6 d. Each point represents the mean  $\pm$  SEM ( $n = 6$ ). SMP-500, *N*-(2,6-bis(1-methylethyl)-phenyl)-*N'*-(1-butyl-1,2-dihydro-2-oxo-4(3-(3-pyridylmethoxy)phenyl)-1,8-naphthyridin-3-yl)-urea nitrate; N-cont, normal diet control; HC-cont, HC diet-fed control; SMP-3, 10, and 30, SMP-500 at doses of 3, 10 and 30 mg/kg/d, respectively; \* $P < 0.05$ ; \*\* $P < 0.01$ , significantly different from HC-cont using Dunnett's multiple comparisons test. ## $P < 0.01$ , significantly different from N-cont using Student's *t*-test.

the HC diet for 6 d. On the day after the final administration, rats were anesthetized with sodium pentobarbital, the bile duct was cannulated, and the bile was collected for 1 h. The concentrations of both biliary cholesterol and bile acid in collected bile were increased, whereas the concentration of biliary phospholipid was not affected by SMP-500 (Table 1). However, the total bile efflux and the LI were not affected by SMP-500 (Table 1).

SMP-500 was administered by gavage to normal diet-fed rats once a day for 3 d. One hour after the final administration of SMP-500, Triton WR-1339 (400 mg/kg) was intravenously injected to determine its effect on lipid secretion from the liver into blood. Two hours later, the cholesterol and TG levels in the plasma VLDL fraction had increased. In the plasma VLDL fraction, the increased cholesterol level was  $72 \pm 4$  mg/dL/2 h and that of TG was  $729 \pm 28$  mg/dL/2 h. SMP-500 decreased the cholesterol influx into the plasma at doses of 10 mg/kg or more and the TG influx into the plasma at a dose of 30 mg/kg (Fig. 3). The reduction in cholesterol influx into the plasma was 18 and 29% and in TG influx into the plasma 8 and 18% at doses of 10 and 30 mg/kg/d, respectively.

Rats were fed a high-sucrose diet for 2 wk, and further fed the same diet while being administered SMP-500 suspended in 0.5% MC once a day for 6 d. The serum TG level in this



**FIG. 2.** Effect of SMP-500 on the hepatic total (A), esterified (B), and free cholesterol (C) content in rats. SMP-500 was administered by gavage to the HC diet-fed rats once a day for 6 d. Each column represents the mean  $\pm$  SEM ( $n = 6$ ). For abbreviations see Figure 1. \*\* $P < 0.01$ , significantly different from HC-cont using Dunnett's multiple comparisons test; ## $P < 0.01$ , significantly different from N-cont using Student's *t*-test.

model increased from approximately 190 to 350 mg/dL after feeding rats the high-sucrose diet in the first 2 wk and that in the control group increased from  $350 \pm 28$  mg/dL to  $403 \pm 38$  mg/dL throughout the period of administration of SMP-500 or vehicle. SMP-500 significantly reduced the serum TG level in a dose-dependent manner (Fig. 4). The reduction in the serum TG levels were 8, 18, and 29% at doses of 10, 30, and 100 mg/kg/d, respectively.

To investigate the mechanism for the increase of bile acid concentration in bile induced by SMP-500, the mRNA for cholesterol 7 $\alpha$ -hydroxylase was measured by real-time quantitative RT-PCR in HepG2 cells. Treatment with SMP-500 for 24 h increased cholesterol 7 $\alpha$ -hydroxylase mRNA level approximately 1.3-fold compared with control cells (Fig. 5).

## DISCUSSION

Recently, we reported a novel ACAT inhibitor, SMP-500, that can potentially inhibit ACAT and cause cholesterol lowering in

**TABLE 1**  
**Effect of SMP-500 on Biliary Secretion of Bile Acid, Cholesterol, and Phospholipid in HC Diet-Fed Rats<sup>a,b</sup>**

	STC (mg/dL)	Biliary concentration (mmol/L)			Flow ( $\mu$ L/h)	LI
		Cholesterol	TBA	PL		
Control	174 $\pm$ 17	0.57 $\pm$ 0.01	48.6 $\pm$ 1.2	9.3 $\pm$ 0.4	1752 $\pm$ 101	0.27 $\pm$ 0.07
SMP-10	118 $\pm$ 10 **	0.66 $\pm$ 0.02*	57.1 $\pm$ 1.3*	9.3 $\pm$ 0.2	1628 $\pm$ 198	0.25 $\pm$ 0.02
SMP-30	72 $\pm$ 6**	0.76 $\pm$ 0.01*	60.3 $\pm$ 1.8*	10.0 $\pm$ 0.3	1679 $\pm$ 131	0.27 $\pm$ 0.04

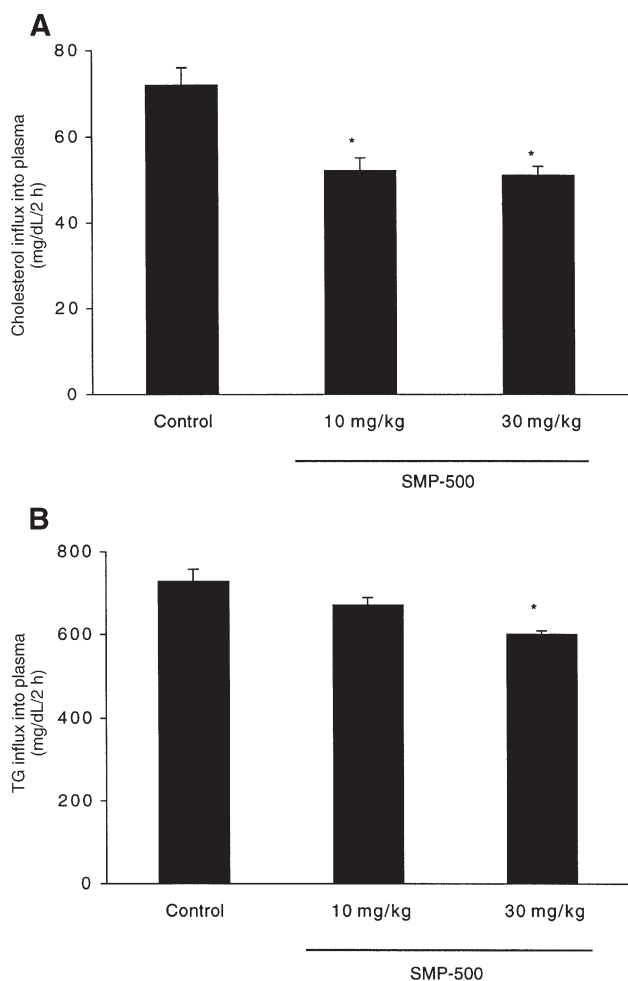
<sup>a</sup>Each value represents the mean  $\pm$  SEM ( $n = 12$ ). SMP-500 was orally administered to high-cholesterol (HC) diet-fed rats once a day for 6 d. On the day after final administration, bile was collected from the bile duct for an hour under anesthesia. The lithogenic index (LI) was calculated by the method of Admirand and Small (28). \* $P < 0.05$ , \*\* $P < 0.01$ , significant difference from HC control by Dunnett's multiple comparison test.

<sup>b</sup>SMP-10 and 30, SMP-500 at doses of 10 and 30 mg/kg/d, respectively; STC, serum total cholesterol; TBA, total bile acid; PL, phospholipid; SMP-500, *N*-(2,6-bis(1-methylethyl)phenyl)-*N'*-(1-butyl-1,2-dihydro-2-oxo-4-(3-(3-pyridylmethoxy)phenyl)-1,8-naphthyridin-3-yl)-urea nitrate.

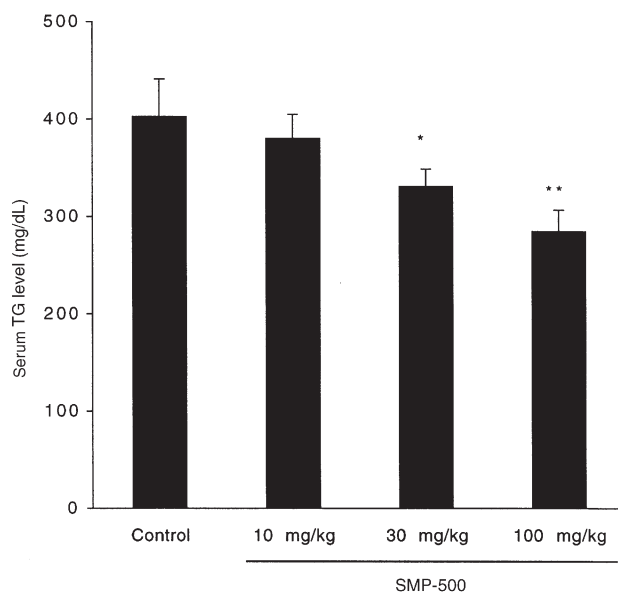
mice, rabbits, and hamsters (20). Interestingly, SMP-500 reduced hepatic free cholesterol contents. These data suggested that SMP-500 directly facilitates the mobilization of chole-

sterol from liver. In this article, we investigated the effect of SMP-500 on both the component in bile and VLDL secretion in rats to clarify its role in liver. In rats fed a HC diet, SMP-500 strongly reduced the serum total cholesterol levels. The hypocholesterolemic effect of SMP-500 was due to a reduction in non-HDL cholesterol level. SMP-500 reduced the hepatic free cholesterol content as well as the hepatic total and esterified cholesterol contents. These data were consistent with the results obtained by using other animals in our previous studies (20).

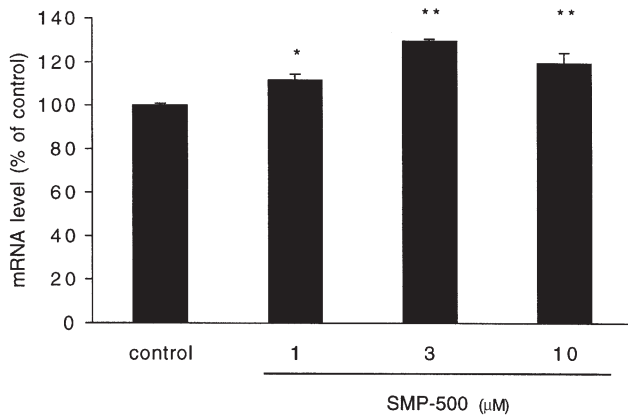
First, the bile efflux and the biliary secretions of bile acid and cholesterol were measured. The biliary concentrations of cholesterol and bile acid were increased by SMP-500, although the bile efflux and the LI were not affected. These data suggested that SMP-500 facilitated hepatic cholesterol removal through increases in bile acid production and chole-



**FIG. 3.** Effect of SMP-500 on cholesterol influx (A) and TG influx (B) into plasma in rats. Rats fed a normal diet were administered SMP-500 by gavage once a day for 3 d. One hour after the final administration, they were intravenously injected with Triton-WR1339, and the plasma lipid levels were measured before and 2 h after injection. The difference in the plasma lipid levels is expressed as the lipid secretion from liver. All data represent the mean  $\pm$  SEM ( $n = 6$ ). \* $P < 0.05$ , significant difference from control using Dunnett's multiple comparisons test. For abbreviation see Figure 1.



**FIG. 4.** Effect of SMP-500 on serum TG levels in sucrose-fed rats. Rats were fed a sucrose diet for 2 wk, and further fed sucrose and administered SMP-500 by gavage once a day for 7 d. All data represent the mean  $\pm$  SEM ( $n = 6$ ). \* $P < 0.05$ ; \*\* $P < 0.01$ , significant difference from control using Dunnett's multiple comparisons test. For abbreviation see Figure 1.



**FIG. 5.** Effect of SMP-500 on cholesterol 7 $\alpha$ -hydroxylase mRNA level in HepG2 cells. Cells were incubated for 24 h in medium containing 10% lipoprotein-deficient serum and  $\beta$ -VLDL (200  $\mu$ g/mL) with or without SMP-500. Cholesterol 7 $\alpha$ -hydroxylase mRNA level was measured by real-time quantitative reverse transcription-PCR. Cholesterol 7 $\alpha$ -hydroxylase mRNA levels were corrected for  $\beta$ -actin RNA. All values are expressed as a percentage of mRNA level in control cells and represent the mean  $\pm$  SEM ( $n = 6$ ). \* $P < 0.05$ ; \*\* $P < 0.01$ , significant difference from control using Dunnett's multiple comparisons test. For abbreviation see Figure 1.

terol influx into the bile. The treatment of SMP-500 in HepG2 cells for 24 h increased cholesterol 7 $\alpha$ -hydroxylase mRNA level compared with the control. It has been reported that CI-1011 (32) and HL-004 (33) facilitate bile acid production through an increase of cholesterol 7 $\alpha$ -hydroxylase activity and mRNA level. The inhibition of hepatic ACAT activity causes a change in the metabolic pathway of cholesterol by increasing the supply of free cholesterol as a substrate. Free cholesterol is also reported to be an inducer of cholesterol 7  $\alpha$ -hydroxylase (24,34,35), resulting in an enhanced production of bile acids (21,22,36). These processes are common in several species, such as rats or humans (37,38). SMP-500 is thought to have a similar effect on cholesterol 7  $\alpha$ -hydroxylase. As a result, SMP-500 reduced the hepatic free cholesterol content. CI-1011 and HL-004 (two other ACAT inhibitors), however, did not change the hepatic free cholesterol content, although they were thought to facilitate bile acid production through a temporary increase in free cholesterol (32,33). SMP-500 increased the concentration of cholesterol in bile and, on the other hand, CI-1011 and HL-004 had no effect. The decrease of hepatic free cholesterol by SMP-500 may be due to this effect.

ACAT also plays an important role in the assembly of VLDL (4–6). VLDL-cholesterol and TG influx into plasma was measured using the Triton model to investigate the effect of SMP-500 on VLDL secretion. As expected, an inhibitory effect of SMP-500 on cholesterol influx into plasma was observed. This effect by SMP-500 is also involved in its cholesterol-lowering effect. In addition, the inhibitory effect of SMP-500 on TG influx into plasma was shown. It has been reported that some ACAT inhibitors reduce serum TG level (25,39–41). These reports indicate that a reduction of serum TG depends on the suppression of VLDL secretion by hepatic

ACAT inhibition and that a reduction of serum cholesterol depends on both the inhibition of cholesterol absorption and the suppression of VLDL secretion. These mechanisms may also be involved in the observed effects of SMP-500, although further studies will be necessary for clarifying this mechanism.

In this study, we demonstrated that SMP-500 dose-dependently reduces serum cholesterol level in rats. We clarified that SMP-500 facilitated hepatic cholesterol clearance through increases in bile acid that were due to the increase in cholesterol 7 $\alpha$ -hydroxylase mRNA level and cholesterol concentration in the bile and to suppressed VLDL-cholesterol secretion that was involved in the hypocholesterolemic effect of this compound. In addition, SMP-500 reduced serum TG level. These results suggest that SMP-500 may have therapeutic potential for both hypercholesterolemia and hypertriglyceridemia.

#### ACKNOWLEDGMENTS

The authors are grateful to Dr. Noriaki Imanishi for valuable discussions and encouragement throughout this work, and also thank Rika Yamaguchi for her excellent technical assistance.

#### REFERENCES

1. Suckling, K.E., and Stange, E.F. (1985) Role of Acyl-CoA: Cholesterol Acyltransferase in Cellular Cholesterol Metabolism, *J. Lipid Res.* 26, 647–671.
2. Field, F.J., and Salome, R.G. (1982) Effect of Dietary Fat Saturation, Cholesterol and Cholestyramine on Acyl-CoA Cholesterol Acyltransferase Activity in Rabbit Intestinal Microsomes, *Biochim. Biophys. Acta* 712, 557–570.
3. Heider, J.G., Pickens, C.E., and Kelly, L.A. (1983) Role of Acyl-CoA:Cholesterol Acyltransferase in Cholesterol Absorption and Its Inhibition by 57-118 in the Rabbit, *J. Lipid Res.* 24, 1127–1134.
4. Drevon, C.A., Engelhorn, S.C., and Steinberg, D. (1980) Secretion of Very Low Density Lipoproteins Enriched in Cholesteryl Esters by Cultured Rat Hepatocytes During Simulation of Intracellular Cholesterol Esterification, *J. Lipid Res.* 21, 1065–1071.
5. Khan, B., Wilcox, H.G., and Heimberg, M. (1989) Cholesterol Is Required for Secretion of Very Low Density Lipoprotein by Rat Liver, *Biochem. J.* 258, 807–816.
6. Cianflone, K.M., Yasrael, Z., Rodriguez, M.A., and Sniderman, A.D. (1990) Regulation of ApoB Secretion from HepG2 Cells: Evidence for a Critical Role for Cholesteryl Ester Synthesis in the Response to a Fatty Acid Challenge, *J. Lipid Res.* 31, 2045–2055.
7. Brecher, P.I., and Chobanian, A.V. (1974) Cholesterol Ester Synthesis in Normal and Atherosclerotic Aortas of Rabbit and Rhesus Monkeys, *Circ. Res.* 35, 692–701.
8. Day, A.J., and Proudlock, J.W. (1974) Changes in Aortic Cholesterol-Esterifying Activity in Rabbits Fed Cholesterol for Three Days, *Atherosclerosis* 19, 253–258.
9. Hashimoto, S., and Dayton, S. (1977) Studies of the Mechanism of Augmented Synthesis of Cholesteryl Ester in Atherosclerotic Rabbit Aortic Microsomes, *Atherosclerosis* 28, 447–452.
10. Sliskovic, D.R., and Trivedi, B.K. (1994) ACAT Inhibitors: Potential Antiatherosclerotic Agents, *Curr. Med. Chem.* 1, 204–225.
11. Sliskovic, D.R., and White, A.D. (1991) Therapeutic Potential of ACAT Inhibitors as Lipid Lowering and Anti-atherosclerotic Agents, *Trends Pharmacol. Sci.* 12, 194–199.
12. Nicolosi, R.J., Wilson, T.A., and Krause, B.R. (1998) The ACAT Inhibitor, CI-1011 Is Effective in the Prevention and Regression of Aortic Fatty Streak Area in Hamsters, *Atherosclerosis* 137, 77–85.



13. Burnett, J.R., Wilcox, L.J., Telford, D.E., Kleinstiver, S.J., Barrett, P.H.R., Newton, R.S., and Huff, M.W. (1999) Inhibition of ACAT by Avasimibe Decreases Both VLDL and LDL Apolipoprotein B Production in Miniature Pigs, *J. Lipid Res.* 40, 1317–1327.
14. Kusunoki, J., Aragane, K., Kitamine, T., Kozono, H., Kano, K., Fujinami, K., Kojima, K., Chiwata, T., and Sekine, Y. (2000) Postprandial Hyperlipidemia in Streptozotocin-Induced Diabetic Rats Is Due to Abnormal Increase in Intestinal Acyl Coenzyme A:Cholesterol Acyltransferase Activity, *Arterioscler. Thromb. Vasc. Biol.* 20, 171–178.
15. Junquero, D., Oms, P., Carilla-Durand, E., Autin, J.M., Tarayre, J.P., Degryse, A.D., Patoiseau, J.F., Colpaert, F.C., and Delhon, A. (2001) Pharmacological Profile of F 12511, (S)-2',3',5'-trimethyl-4'-hydroxy- $\alpha$ -dodecylthioacetanilide a Powerful and Systemic Acylcoenzyme A:Cholesterol Acyltransferase Inhibitor, *Biochem. Pharmacol.* 61, 97–108.
16. Junquero, D., Bruniquel, F., N'Guyen, X., Autin, J.M., Patoiseau, J.F., Degryse, A.D., Colpaert, F.C., and Delhon, A. (2001) F 12511, a Novel ACAT Inhibitor, and Atorvastatin Regulate Endogenous Hypercholesterolemia in a Synergistic Manner in New Zealand Rabbits Fed a Casein-Enriched Diet, *Atherosclerosis* 155, 131–142.
17. Koren, M., Insull, W., Schrott, H., Davila, M., Heinonen, T., McLain, R.W., and Black, D. (1998) ACAT Inhibitor Avasimibe Lowers VLDL-C and Triglycerides in Patients with Hypertriglyceridemia, *Circulation* 98, I-240.
18. Harris, W.S., Dujovne, C.A., von Bergmann, K., Neal, J., Akester, J., Windsor, S.L., Greene, D., and Look, Z. (1990) Effect of the ACAT Inhibitor CL 277,082 on Cholesterol Metabolism in Humans, *Clin. Pharmacol. Ther.* 48, 189–194.
19. Hainer, J.W., Terry, J.G., Cornell, J.M., Zyruk, H., Jenkins, R.M., Shand, D.L., Gillies, P.J., Livak, K.J., Hunt T.L., and Crouse, J.R. III (1994) Effect of the ACAT Inhibitor Dup128 on Cholesterol Absorption and Serum Cholesterol in Humans, *Clin. Pharmacol. Ther.* 56, 65–74.
20. Ioriya, K., Noguchi, T., Muraoka, M., Fujita, K., Shimizu, H., and Ohashi, N. (2002) Effect of SMP-500, a Novel Acyl-CoA:Cholesterol Acyltransferase Inhibitor, on the Cholesterol Esterification and Its Hypocholesterolemic Properties, *Pharmacology* 65, 18–25.
21. Cohen, B.I., Raicht, R.F., and Mosbach, E.H. (1977) Sterol Metabolism Studies in the Rat. Effect of Primary Bile Acids (sodium taurochenodeoxycholate and sodium taurocholate) on Sterol Metabolism, *J. Lipid Res.* 18, 223–231.
22. Bostrom, H., and Wikvall, K. (1982) Hydroxylations in Biosynthesis of Bile Acids: Isolation of Subfractions with Different Substrate Specificity from Cytochrome P-450LM4, *J. Biol. Chem.* 257, 11755–11759.
23. Chiang, J.Y.L., Malmer, M., and Hutterer F. (1983) A Form of Rabbit Liver Cytochrome P-450 That Catalyzes the 7 $\alpha$ -Hydroxylation of Cholesterol, *Biochim. Biophys. Acta* 750, 291–299.
24. Horton, J.D., Cuthbert, J.A., and Spady, D.K. (1995) Regulation of Hepatic 7 $\alpha$ -Hydroxylase Expression and Response to Dietary Cholesterol in the Rat and Hamster, *J. Biol. Chem.* 270, 5381–5387.
25. Krause, B.R., Anderson, M., Bisgaier, C.L., Bocan, T., Bousley, R., DeHart, P., Essenburg, A., Hamelehle, K., Homan, R., Kieft, K., et al. (1993) *In vivo* Evidence That the Lipid-Regulating Activity of the ACAT Inhibitor CI-976 in Rats Is Due to Inhibition of Both Intestinal and Liver ACAT, *J. Lipid Res.* 34, 279–294.
26. Folch, J., Lees, M., and Sloane Stanley, G.H. (1957) A Simple Method for the Isolation and Purification of Total Lipids from Animal Tissues, *J. Biol. Chem.* 226, 497–509.
27. Kunitomo, K., Yamaguchi, Y., Matsushima, K., and Bando, Y. (1983) Microanalysis of Tissue Cholesterol Using a Fluorometric Enzymatic Method, *Jpn. J. Clin. Chem.* 12, 117–124.
28. Admirand, W.H., and Small, D.M. (1968) The Physicochemical Basis of Cholesterol Gallstone Formation in Man, *J. Clin. Invest.* 47, 1043–1052.
29. Sugiyama, Y., Odaka, H., Itokawa, S., Ishikawa, E., Tomari, Y., and Ikeda, H. (1995) TMP-153, a Novel ACAT Inhibitor, Lowers Serum Cholesterol Through Its Hepatic Action in Golden Hamsters, *Atherosclerosis* 118, 145–153.
30. Havel, R.J., Eder, H.A., and Bradgon, J.H. (1955) The Distribution and Chemical Composition of Ultracentrifugally Separated Lipoproteins in Human Serum, *J. Clin. Invest.* 34, 1345–1353.
31. Pugazhenthii, S., Nesterova, A., Sable, C., Heidenreich, K.A., Boxer, L.M., Heasley, L.E., and Reusch, J.E.B. (2000) Akt/Protein Kinase B Up-regulates Bcl-2 Expression Through cAMP-Response Element-Binding Protein, *J. Biol. Chem.* 275, 10761–10766.
32. Post, S.M., Zoetewij, J.P., Bos, M.H.A., de Wit, E.C.M., Havinga, R., Kuipers, F., and Princen, H.M.G. (1999) Acyl-Coenzyme A:Cholesterol Acyltransferase Inhibitor, Avasimibe, Stimulates Bile Acid Synthesis and Cholesterol 7 $\alpha$ -Hydroxylase in Cultured Rat Hepatocytes and *in vivo* in the Rat, *Hepatology* 30, 491–500.
33. Murakami, S., Yamagishi, I., Sato, M., Tomisawa, K., Nara, Y., and Yamori, Y. (1997) ACAT Inhibitor HL-004 Accelerates the Regression of Hypercholesterolemia in Stroke-Prone Spontaneously Hypertensive Rats (SHRSP): Stimulation of Bile Acid Production by HL-004, *Atherosclerosis* 133, 97–104.
34. Pandak, W.M., Li, Y.C., Chiang, J.Y.L., Studer, E.J., Gurley, E.C., Heuman, D.M., Vlahcevic, Z.R., and Hylemon, P.B. (1991) Regulation of Cholesterol 7  $\alpha$ -Hydroxylase mRNA and Transcriptional Activity by Taurocholate and Cholesterol in the Chronic Biliary Diverted Rat, *J. Biol. Chem.* 266, 3416–3421.
35. Shefer, S., Nguyen, L.B., Salen, G., Ness, G.C., Chowdhary, I.R., Lerner, S., Batta, A.K., and Tint, G.S. (1992) Differing Effects of Cholesterol and Taurocholate on Steady State Hepatic HMG-CoA Reductase and Cholesterol 7  $\alpha$ -Hydroxylase Activities and mRNA Levels in the Rat, *J. Lipid Res.* 33, 1193–1200.
36. Twisk, J., Lehmann, E.M., and Princen, M.G. (1993) Differential Feedback Regulation of Cholesterol 7  $\alpha$ -Hydroxylase mRNA and Transcriptional Activity by Rat Bile Acids in Primary Monolayer Cultures of Rat Hepatocytes, *Biochem. J.* 290, 685–691.
37. Spady, D.K., and Cuthbert, J.A. (1992) Regulation of Hepatic Sterol Metabolism in the Rat. Parallel Regulation of Activity and mRNA for 7  $\alpha$ -Hydroxylase but Not 3-Hydroxy-3-methylglutaryl-Coenzyme A Reductase or Low Density Lipoprotein Receptor, *J. Biol. Chem.* 267, 5584–5591.
38. Erickson, S.K., and Fielding, P.E. (1986) Parameters of Cholesterol Metabolism in Human Hepatoma Cell Line, HepG2, *J. Lipid Res.* 27, 875–883.
39. Krause, B.R., Black, A., Bousley, R., Essenburg, A., Cornicelli, J., Holmes, A., Homan, R., Kieft, K., Sekerke, C., Shaw-Hes, M.K., et al. (1993) Divergent Pharmacologic Activities of PD-132301-2 and CL-277082, Urea Inhibitors of Acyl-CoA:Cholesterol Acyltransferase, *J. Pharm. Exper. Therap.* 267, 734–743.
40. Riddell, D., Bright, C.P., Burton, B.J., Bush, R.C., Harris, N.V., Hele, D., Moore, U.M., Naik, K., Parrott, D.P., Smith, C., et al. (1996) Hypolipidaemic Properties of a Potent and Bioavailable Alkylsulphinyl-Diphenylimidazole ACAT Inhibitor (RP 73163) in Animals Fed Diets Low in Cholesterol, *Biochem. Pharmacol.* 52, 1177–1186.
41. Lee, H.T., Sliskovic, D.R., Picard, J.A., Roth, B.D., Wierenga, W., Hicks, J.L., Bousley, R.F., Hamelehle, K.L., Homan, R., Speyer, C., et al. (1996) Inhibitors of Acyl-CoA:Cholesterol O-Acyl Transferase (ACAT) as Hypocholesterolemic Agents. CI-1011: An Acyl Sulfamate with Unique Cholesterol-Lowering Activity in Animals Fed Noncholesterol-Supplemented Diets, *J. Med. Chem.* 39, 5031–5034.

[Received September 26, 2001, and in final revised form January 21, 2002; revision accepted January 22, 2002]

# Synthesis and Phospholipase C Inhibitory Activity of D609 Diastereomers

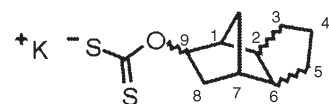
Albert González-Roura, Josefina Casas, and Amadeu Llebaria\*

Research Unit on BioActive Molecules (RUBAM), Department of Biological Organic Chemistry, IIQAB-CSIC, 08034-Barcelona, Spain

**ABSTRACT:** The potassium xanthate D609 is widely accepted as a selective inhibitor of PC-specific phospholipase C (PC-PLC). The tricyclo[5.2.1.0<sup>2,6</sup>]decane skeleton present in D609 can lead to four diastereomeric pairs, but the diastereoselectivity of PC-PLC inhibition has never been reported. In this article, the synthesis of racemic D609 diastereomers and that of other xanthates, as well as their inhibitory effect on PC-PLC is reported. All xanthates obtained were competitive inhibitors of PC-PLC from *Bacillus cereus* (PLC*Bc*). No significant differences were found in the activity of D609 diastereomers ( $K_i$  13–17  $\mu\text{M}$ ), suggesting the absence of a diastereochemical control of the enzyme by xanthate inhibitors. This result was confirmed after obtaining other potassium xanthates differing from D609 in the aliphatic chain. Among them, the potassium *O*-*n*-decenylxanthate was the most active inhibitor of PLC*Bc* ( $K_i$  10  $\mu\text{M}$ ). These data indicate that the essential structural requirements for PLC*Bc* *in vitro* inhibition by xanthates are the presence of a Zn-chelating dithiocarbonate head and a sufficiently hydrophobic aliphatic moiety.

Paper no. L8955 in *Lipids* 37, 401–406 (April 2002).

PC-specific phospholipase C (PC-PLC) is a crucial enzyme in lipid metabolism that hydrolyzes PC into phosphorylcholine and DAG and has been implicated in the cellular signal transduction cascade (1). Among different biological effects, the tricyclic potassium xanthate D609 (Fig. 1) is a potent inhibitor of PC-PLC (2). The inhibitory effect is selective for PC-PLC as compared to other phospholipases (3), which has made D609 a universally accepted pharmacological tool to assess the involvement of a PC-PLC enzyme in a given cellular process. However, a few reports show that D609 can also inhibit the enzymes of the sphingomyelin cycle, namely, sphingomyelinases and sphingomyelin synthase (4,5). The effect on sphingomyelin synthase is especially critical, since this enzyme catalyzes the transfer of phosphorylcholine from PC to ceramide to give sphingomyelin and DAG. At this point, it is worth mentioning that the possible differential ef-



D609

FIG. 1. Chemical structure of D609.

fects of D609 diastereomers and other xanthates on PC-PLC have not been reported; in addition, the exact diastereomeric composition of the commercially available D609 inhibitor is not specified. Therefore, we were interested in determining the effect of the different D609 diastereomers and other xanthates on lipid-metabolizing enzymes, since some discrepancies existing in the literature might arise from different D609 diastereomers or its mixtures used in the experimentation. The use of structurally simpler xanthates, without stereogenic centers, avoids misleading and controversial results arising from the use of stereochemically different tools.

In this article we describe the synthesis of a series of xanthates and the preparation of D609 diastereomers in racemic form, as well as their evaluation as inhibitors of the PC-PLC of *Bacillus cereus* (PLC*Bc*). This commercially available enzyme is currently accepted as a surrogate of the elusive mammalian PC-PLC, both enzymes having antigenic similarities (6). The structure and mechanism of PLC*Bc* are well known (7–12), and several inhibitors other than D609 have been disclosed for this enzyme (13,14).

## EXPERIMENTAL PROCEDURES

**Materials and methods.** FTIR spectra are reported in  $\text{cm}^{-1}$ .  $^1\text{H}$  and  $^{13}\text{C}$  NMR spectra were obtained in  $\text{CDCl}_3$ ,  $\text{CD}_3\text{OD}$ , DMSO, or  $\text{D}_2\text{O}$  solutions at 200 or 300 MHz for  $^1\text{H}$  and 50 or 75 MHz for  $^{13}\text{C}$ . Chemical shifts are reported in  $\delta$  units, parts per million (ppm) relative to the singlet at 7.24 ppm of  $\text{CDCl}_3$  for  $^1\text{H}$  and ppm relative to the center line of a triplet at 77.0 ppm of  $\text{CDCl}_3$  for  $^{13}\text{C}$ . Electrospray (ESP) mass spectra in negative mode were obtained by HPLC–MS using acetonitrile/water (1:1) at 0.5 mL/min as mobile phase. Solvents were distilled prior to use and dried by standard methods. Ketone **9** and the mixture of alcohols **10** are commercial products

\*To whom correspondence should be addressed at Research Unit on BioActive Molecules (RUBAM), Department of Biological Organic Chemistry, IIQAB-CSIC, Jordi Girona, 18-26, 08034-Barcelona, Spain. E-mail: alsqob@iiqab.csic.es

Abbreviations: DAG, diacylglycerol; ESP, electrospray; PC-PLC, phosphatidylcholine-specific phospholipase C; PLC*Bc*, PC-PLC from *Bacillus cereus*.

(TCD-keton A and TCD-alcohol E, respectively) and were obtained from Celanese Chemicals Europe GmbH (Oberhausen, Germany). Racemic diastereomeric alcohols **5–8** were obtained following described procedures: *O*-*exo*,*C*-*exo* **5** (15); *O*-*endo*,*C*-*exo* alcohol **6** (16,17); *O*-*exo*,*C*-*endo* **7** (18); and *O*-*endo*,*C*-*endo* **8** (15,17,18) and characterized by comparison with reported spectroscopic data (17).

**Determination of CMC.** The CMC of xanthates and PC were determined in 96-well microtiter plates by dye-binding with Coomassie brilliant Blue G-250 (19). Using this method, CMC of 1,2-dihexanoyl-*sn*-glycero-3-phosphocholine was determined to be 6.23 mM.

**General procedure for the synthesis of potassium xanthates (1–4, 14–17).** The alcohol (1.1 eq) was slowly added to a solution of *t*-BuOK (1 eq.) in anhyd. THF (3 mL/mmol) at 0°C under nitrogen. Carbon disulfide (1.1 eq) was added dropwise, and the solution was stirred for 4 h at this temperature. The reaction mixture was diluted with ether (15 mL/mmol) and concentrated to give the crude product. The residue was washed with ether and dried to give the corresponding potassium xanthate as a white powder.

**Potassium O-*exo*-tricyclo[5.2.1.0<sup>2,6</sup>]-*exo*-dec-9-ylthiocarbonate 1.** (63% yield) IR (cm<sup>-1</sup>): 2943, 2862, 1118, 1098, 1079. <sup>1</sup>H NMR (200 MHz, CD<sub>3</sub>OD): δ 0.84–1.10 (*m*, 2H), 1.14–1.54 (*m*, 4H), 1.56–2.06 (*m*, 7H), 2.20–2.26 (*m*, 1H), 5.05–5.15 (*m*, 1H). <sup>13</sup>C NMR (75 MHz, DMSO): δ 27.7, 29.6, 31.5, 31.8, 39.3, 39.6, 42.8, 46.0, 47.1, 82.1, 229.5. Mass spectrum (ESP<sup>-</sup>): *m/z* 227 (M – K, base peak), 151 (alcohol fragment). CMC: 3.16 mM.

**Potassium O-*endo*-tricyclo[5.2.1.0<sup>2,6</sup>]-*exo*-dec-9-ylthiocarbonate 2.** (52% yield) IR (cm<sup>-1</sup>): 2945, 2860, 1107, 1087, 1070. <sup>1</sup>H NMR (200 MHz, CD<sub>3</sub>OD): δ 0.85–1.50 (*m*, 6H), 1.60–1.74 (*m*, 1H), 1.80–2.18 (*m*, 5H), 2.36–2.44 (*m*, 1H), 2.50–2.65 (*m*, 1H), 5.40–5.55 (*m*, 1H). <sup>13</sup>C NMR (75 MHz, DMSO): δ 26.9, 30.7, 31.4, 32.2, 36.6, 38.7, 40.6, 44.5, 47.5, 79.6, 230.0. Mass spectrum (ESP<sup>-</sup>): *m/z* 227 (M – K, base peak), 151 (alcohol fragment). CMC: 3.63 mM.

**Potassium O-*exo*-tricyclo[5.2.1.0<sup>2,6</sup>]-*endo*-dec-8-ylthiocarbonate 3.** (65% yield) IR (cm<sup>-1</sup>): 2950, 2860, 1147, 1122, 1103, 1089, 962. <sup>1</sup>H NMR (200 MHz, CD<sub>3</sub>OD): δ 1.36–1.90 (*m*, 9H), 2.08–2.24 (*m*, 2H), 2.30–2.59 (*m*, 3H), 5.38–5.48 (*m*, 1H). <sup>13</sup>C NMR (75 MHz, DMSO): δ 26.0, 26.9, 28.0, 34.0, 40.1, 40.3, 43.8, 43.9, 46.6, 78.6, 229.6. Mass spectrum (ESP<sup>-</sup>): *m/z* 227 (M – K, base peak), 151 (alcohol fragment). CMC: 2.57 mM.

**Potassium O-*endo*-tricyclo[5.2.1.0<sup>2,6</sup>]-*endo*-decan-9-ylthiocarbonate 4.** (62% yield) IR (cm<sup>-1</sup>): 2948, 2875, 1154, 1126, 1101, 1069, 1008. <sup>1</sup>H NMR (300 MHz, CD<sub>3</sub>OD): 1.40–1.68 (*m*, 7H), 1.92–2.32 (*m*, 4H), 2.45–2.64 (*m*, 3H), 5.44–5.52 (*m*, 1H). <sup>13</sup>C NMR (75 MHz, DMSO): δ 26.2, 27.0, 28.5, 28.6, 40.9, 41.1, 43.4, 44.6, 45.8, 81.4, 229.6. Mass spectrum (ESP<sup>-</sup>): *m/z* 227 (M – K, base peak), 151 (alcohol fragment). CMC: 2.63 mM.

**Potassium O-*n*-decylthiocarbonate 14.** (91% yield) IR (cm<sup>-1</sup>): 3370, 2953, 2915, 2851, 1471, 1138, 1118, 1104, 1064. <sup>1</sup>H NMR (200 MHz, CD<sub>3</sub>OD): δ 0.90 (*t*, 3H, *J* = 6.3 Hz),

1.20–1.50 (*m*, 16H), 1.64–1.82 (*m*, 2H), 4.38 (*t*, 2H, *J* = 6.7 Hz). <sup>13</sup>C NMR (75 MHz, DMSO): δ 13.9, 22.1, 25.8, 28.65, 28.7, 28.9, 29.0, 29.05, 31.3, 70.6, 230.3. Mass spectrum (ESP<sup>-</sup>): *m/z* 233 (M – K, base peak), 157 (alcohol fragment). CMC: 3.81 mM.

**Potassium O-*n*-butylthiocarbonate 15.** (52% yield) IR (cm<sup>-1</sup>): 2959, 2943, 2870, 1461, 1173, 1151, 1136, 1106, 1074. <sup>1</sup>H NMR (200 MHz, CD<sub>3</sub>OD): δ 0.95 (*t*, 3H, *J* = 7.3 Hz), 1.36–1.54 (*m*, 2H), 1.65–1.79 (*m*, 2H), 4.39 (*t*, 2H, *J* = 6.6 Hz). <sup>13</sup>C NMR (75 MHz, DMSO): δ 13.7, 19.0, 30.8, 70.3, 230.3. Mass spectrum (ESP<sup>-</sup>): *m/z* 149 (M – K). CMC: > 10 mM.

**Potassium O-2-phenylethylthiocarbonate 16.** (81% yield) IR (cm<sup>-1</sup>): 1121, 1103, 1084, 1069, 1045, 1021, 756, 698, 507. <sup>1</sup>H NMR (200 MHz, CD<sub>3</sub>OD): δ 3.04 (*t*, 2H, *J* = 7.3 Hz), 4.60 (*t*, 2H, *J* = 7.3 Hz), 7.15–7.28 (*m*, 5H). <sup>13</sup>C NMR (75 MHz, DMSO): δ 34.9, 71.3, 126.3, 128.4, 129.0, 139.1, 229.8. Mass spectrum (ESP<sup>-</sup>): *m/z* 197 (M – K, base peak), 121 (alcohol fragment). CMC: >10 mM.

**Potassium O-7-tridecylthiocarbonate 17.** (77% yield) IR (cm<sup>-1</sup>): 2955, 1466, 1457, 1379, 1130, 1090, 672. <sup>1</sup>H NMR (200 MHz, CD<sub>3</sub>OD): δ 0.89 (*t*, 6H, *J* = 6.7 Hz), 1.20–1.80 (*m*, 20H), 5.48–5.60 (*m*, 1H). <sup>13</sup>C-NMR (75 MHz, D<sub>2</sub>O): δ 16.3, 24.9, 27.5, 31.4, 34.1, 35.7, 86.7, 234.2. Mass spectrum (ESP<sup>-</sup>): *m/z* 275 (M – K, base peak), 199 (alcohol fragment). CMC: 4.16 mM.

**Enzymatic assays.** Inhibition studies were performed *in vitro* using commercially available PLCβc. Quantification of the enzymatic activity was performed following an indirect method described by Hergenrother and Martin (20). Briefly, 1,2-dihexanoyl-*sn*-glycero-3-phosphocholine (2 mM final concentration) was incubated with PC-PLC in the absence or presence of inhibitors (0–2 mM, final concentration) at 37°C in 96-well plates, and after 1.5 min the reaction was quenched with Tris-HCl 2M, pH 8. A molybdenum blue complex with the phosphate produced after alkaline phosphatase hydrolysis of phosphorylcholine was formed and read with a microplate reader. All assays were performed at least in triplicate. The IC<sub>50</sub> values were determined by plotting percent activity vs. log[I], using at least five different inhibitor concentrations (0.0003–1 mM). As indicated previously, CMC values of tested xanthates ranged from 2.6 to >10 mM; therefore, all assays were performed below the CMC of substrate and inhibitors.

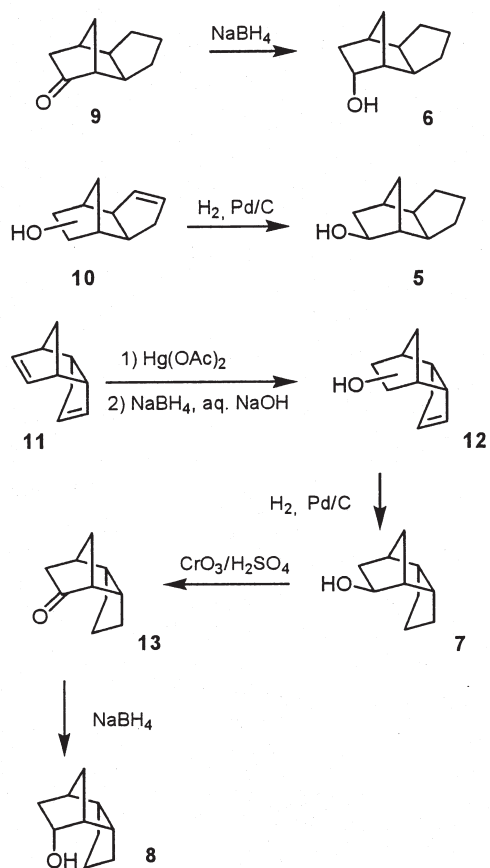
Kinetic parameters for more active inhibitors were determined by Lineweaver–Burke plots of assays performed with the corresponding xanthate derivative (10 μM) and five different substrate concentrations (0.6–5 mM). *K<sub>i</sub>* values were calculated with the following equation:

$$K_i = K_m[I]/(K_{m,app} - K_m) \quad [1]$$

## RESULTS AND DISCUSSION

**Synthesis.** The classical approach to the synthesis of xanthates is based on the reaction of the corresponding sodium or potassium alcoholate with carbon disulfide. Therefore, the prepara-





SCHEME 1

tion of racemic tricyclic xanthates **1–4** required the synthesis of diastereomeric alcohols **5–8** (Fig. 2). This was accomplished as detailed in Scheme 1. The alcohols **5** and **6**, displaying an *exo* cyclopentane group, were obtained from commercially available ketone **9** and a mixture of regioisomeric alcohols **10**, respectively. After reduction of ketone **9**, pure *O-endo,C-exo* alcohol **6** was obtained in 31% isolated yield after chromatography to separate it from the *O-exo,C-exo* epimeric alcohol **5**, which was a minor product of this reaction. Complete chromatographic separation of **5** from **6** proved unfeasible, but catalytic hydrogenation of double bonds in **10** directly gave high-purity *O-exo,C-exo* alcohol **5** in almost quantitative yield.

The alcohols **7** and **8** having an *endo* cyclopentane attached to the norbornene skeleton were obtained from *endo*-dicyclopentadiene **11** following reported procedures. Thus, olefin regioselective acetoxymercuration-demercuration sequence on *endo*-dicyclopentadiene with *in situ* hydrolysis of the resulting acetate afforded a mixture of regioisomeric racemic alcohols **12**. After catalytic hydrogenation the desired *O-exo,C-endo* isomer **7** was obtained in 74% yield over two steps. The racemic epimeric alcohol **8** was obtained by oxidation of **7** to the corresponding tricyclic ketone **13** followed by NaBH<sub>4</sub> reduction to give the *O-endo,C-endo* alcohol **8** in 62% yield after two steps.

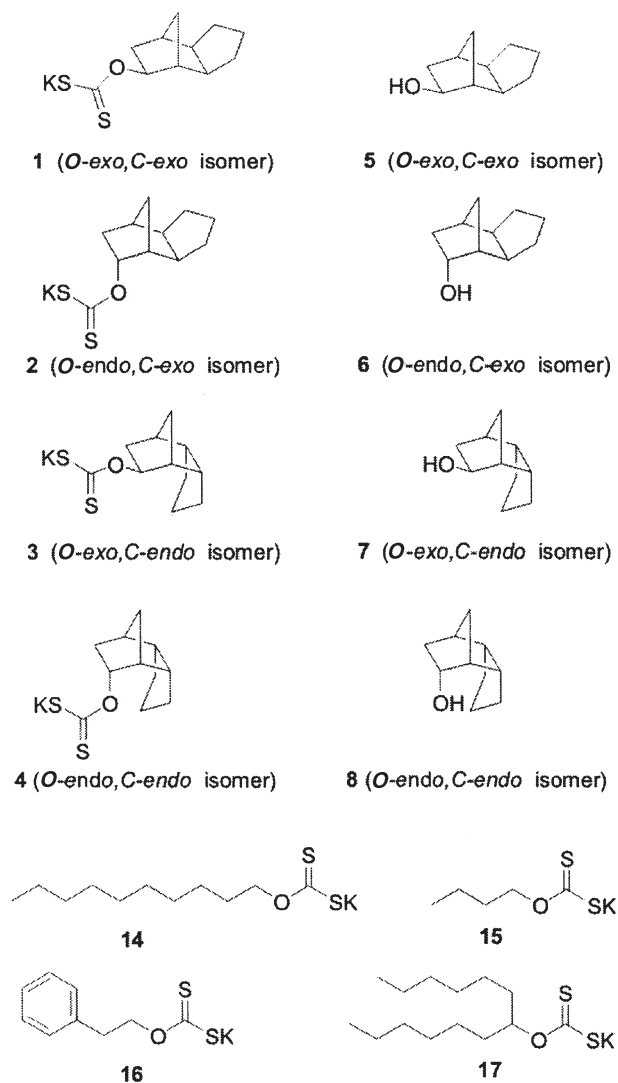


FIG. 2. Tested xanthates and D609 alcohol precursors.

With racemic diastereomeric alcohols **4–8** in hand, the corresponding xanthates were synthesized by reaction with carbon disulfide in the presence of an equivalent of potassium *t*-butoxide in THF. This method was also employed to synthesize the xanthates **14** (from *n*-decanol), **15** (from *n*-butanol), **16** (from 2-phenylethanol), and **17** (from 7-tridecanol) also required for this study (Fig. 2).

**Inhibition studies.** Enzymatic assays were performed on commercial PLCBc using the method described by Hergenrother and Martin (20). This is based on a colorimetric determination of phosphate after alkaline phosphatase hydrolysis of the phosphorylcholine produced by PLCBc-catalyzed hydrolysis of PC.

To check the reliability of the colorimetric method for testing xanthate derivatives as inhibitors of PC-PLC, we performed experiments aimed to exclude a possible effect of xanthates on alkaline phosphatase. We found that all xanthates at 1 or 2 mM concentration did not affect the enzymatic activity of



alkaline phosphatase in the assay conditions (45–450  $\mu\text{M}$  phosphorylcholine and 6 U/mL of enzyme, 2 h at 37°C).

Kinetic parameters calculated for PLCBc with 1,2-dihexanoyl-*sn*-glycero-3-phosphocholine ( $V_{\text{max}}$ : 2600  $\pm$  670  $\mu\text{M}/\text{min}\cdot\text{mg}$  and  $K_m$ : 2.6  $\pm$  0.14 mM,  $n = 5$ ) were close to those described in the literature using this substrate (20). Therefore, a substrate concentration of 2 mM was chosen to test the activity of alcohol **5** and the different synthesized xanthates. Among these compounds only alcohol **5** was inactive, this indicating that the presence of the oxygen-bonded dithiocarbonate group is essential for inhibitory activity.

All tested xanthates exhibited a dose-dependent inhibition (Fig. 3 and Table 1) of PLCBc with different degrees of activity. Among the four D609 diastereomers analyzed, compounds with a *C-exo* configuration (**1–2**) showed slightly lower  $\text{IC}_{50}$  values than the corresponding *C-endo* isomers (**3–4**). In addition to xanthates bearing a tricyclo[5.2.1.0<sup>2,6</sup>]decane skeleton, the xanthate **14**, derived from *n*-decanol, also showed a remarkable inhibitory activity on PLCBc. Therefore, the presence of a tricyclic system as hydrophobic moiety in xanthates does not seem to be an essential structural requirement for *in vitro* PLCBc inhibition. Other xanthates resulted in less active inhibitors. Thus, potassium *O-n*-butylxanthate **15**, potassium *O-2*-phenylethylxanthate **16**, or potassium *O-7*-tridecylxanthate **17** differ in the length of the hydrophobic chains attached to the dithiocarbonate group, which must be the reason for their different PC-PLC inhibitory activities. The  $\text{IC}_{50}$  values obtained decrease in parallel to the increase on the hydrophobicity of xanthate aliphatic chain. This effect is especially noteworthy in the case of *n*-butanol-derived xanthate, which was found to be the least active xanthate used in this study. These results are in agreement with the low inhibitory activity reported for potassium *O*-ethylxanthate (46% inhibition at 0.63 mM) (3). The use of xanthate **17** derived from a secondary alcohol containing a double hydrophobic chain or the presence of a phenylethyl

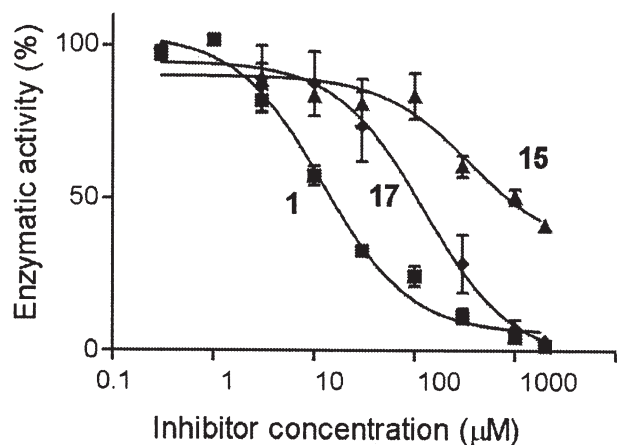


FIG. 3. Dose-dependent inhibition of phosphatidylcholine/specific phospholipase C of *Bacillus cereus* by different xanthate derivatives. Compounds (**1**: *O-exo,C-exo* isomer D609, **15**: potassium *n*-butylxanthate, **17**: *O-7*-tridecylxanthate) were incubated with 2 mM of PC for 1.5 min at 37°C.

TABLE 1  
Inhibition of PLCBc<sup>a</sup> by Different Xanthate Derivatives

Compound	$\text{IC}_{50}$ ( $\mu\text{M}$ )	$K_i$ ( $\mu\text{M}$ )	Type of inhibition
<b>1</b>	10	13	Competitive
<b>2</b>	7	17	Competitive
<b>3</b>	45	15	Competitive
<b>4</b>	32	13	Competitive
<b>14</b>	30	10	Competitive
<b>15</b>	1000	—	—
<b>16</b>	190	—	—
<b>17</b>	170	—	—

<sup>a</sup>PLCBc, PC-specific phospholipase from *Bacillus cereus*.

group on compound **16** did not result in a significant improvement as compared to the compounds with a single chain and did not reach the inhibitory effect of D609.

Inhibition parameters for the most active xanthates were also calculated. Lineweaver–Burke plots obtained for xanthate **14** (Fig. 4) were very similar to those achieved with xanthates **1–4**. The curves obtained in the absence and in the presence of inhibitor cross in the ordinate axis, indicating a competitive type of inhibition of PC-PLC by all compounds. Calculated inhibition constants were comparable (10–17  $\mu\text{M}$ , Table 1), and similar to that reported for D609 using dipalmitoyl PC or *p*-nitrophenylphosphatidylcholine as substrate (3).

The results described show the absence of substantial differences in the activity of D609 diastereomers, suggesting the lack of a diastereochemical control of the enzyme by this family of inhibitors. In addition, simple straight-chain xanthates with sufficient lipophilic chains inhibit PLCBc even more potently than D609. This result confirms the lack of selectivity of this enzyme for the hydrocarbon chain present in xanthates. In this context, it has been described that PLCBc presents a shallow cleft for docking the phospholipid substrate, with a minimum acyl chain length being required for good enzymatic activity (12,21).

Although different types of enzymes are reported to be inhibited by xanthates, the mechanisms of inhibition are differ-

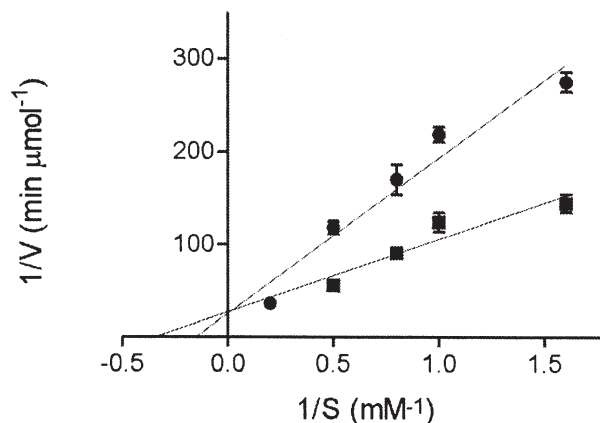


FIG. 4. Lineweaver–Burke plot for the phosphatidylcholine specific phospholipase C of *Bacillus cereus* inhibition by potassium *O-n*-decylxanthate (**14**). [I] = 0 (■) and 10  $\mu\text{M}$  (●).

ent. Thus, the xanthate derivative of cholesterol exhibited a good inhibitory activity of Cdc25A phosphatase, an enzyme involved in the regulation of the G1/S transition of the cell cycle, and the xanthate group would surrogate the phosphate moiety in a cysteinyl-phosphate enzyme intermediate formed during the reaction course (22). On the other hand, different xanthates, including D609, were found to be specific mechanism-based inactivators of cytochrome P450 2B1 and 2B6, and the inactivation is caused by covalent binding of a reactive xanthate intermediate to the apoprotein (23). Contrary to the results reported in the present paper for the inhibition of PC-PLC, reported  $K_i$  values for the inactivation of P-450 2B1 were not strongly dependent on the length of the aliphatic chain substituent. Concerning the effects of D609 on sphingomyelin synthase, the almost complete absence of structural, mechanistic, and biochemical data for this enzyme (24) precluded any hypothesis on the mechanism of inhibition by D609. In regard to PC-PLC inhibition by xanthates, our results and previously published data indicate that active xanthates are competitive inhibitors, suggesting that they have affinity for the PC binding site. Different experimental evidences indicate that the three zinc ions are present in the active center of PC-PLC, which are essential for full activity, and are involved in substrate binding and activation of the phosphate moiety toward nucleophilic attack through charge neutralization. An active site base-activated water molecule acts as the nucleophilic species (10). Xanthate derivatives that have the appropriate lipophilic chain would fit in the active center of PC-PLC, and the dithiocarbonate group could act as a surrogate of the phosphate group and presumably would bond to active-site Zn ions in view of the charge and metal coordinating ability of the sulfur atoms present in this group.

The *in vitro* inhibitory activity of a series xanthates on PLC $\beta$ c indicated that the essential structural requirements are the presence of a sufficiently hydrophobic aliphatic chain and a dithiocarbonate head group.

## ACKNOWLEDGMENTS

This work was supported by the Dirección General de Enseñanza Superior e Investigación Científica (grant PB97-1171, grant PB97-1253, and a Predoctoral fellowship to Albert González-Roura) and DURSI, Generalitat de Catalunya (grant 1999-SGR 00187). We thank Dr. Gemma Fabriàs for helpful comments on the manuscript and Dr. Antonio Delgado and Dr. Jesús Joglar for their assistance in different aspects of this work. We thank Celanese Chemicals Europe GmbH for a generous gift of chemicals.

## REFERENCES

- Exton, J.H. (1994) Phosphatidylcholine Breakdown and Signal Transduction, *Biochim. Biophys. Acta* 1212, 26–42.
- Muller-Decker, K. (1989) Interruption of TPA-Induced Signals by an Antiviral and Antitumoral Xanthate Compound: Inhibition of a Phospholipase C-Type Reaction, *Biochem. Biophys. Res. Commun.* 162, 198–205.
- Amtmann, E. (1996) The Antiviral, Antitumoral Xanthate D609 Is a Competitive Inhibitor of Phosphatidylcholine-Specific Phospholipase C, *Drugs Exp. Clin. Res.* 22, 287–294.
- Luberto, C., and Hannun, Y.A. (1998) Sphingomyelin Synthase, a Potential Regulator of Intracellular Levels of Ceramide and Diacylglycerol During SV40 Transformation. Does Sphingomyelin Synthase Account for the Putative Phosphatidylcholine-Specific Phospholipase C? *J. Biol. Chem.* 273, 14550–14559.
- Luberto, C., Yoo, D.S., Suidan, H.S., Bartoli, G.M., and Hannun, Y.A. (2000) Differential Effects of Sphingomyelin Hydrolysis and Resynthesis on the Activation of NF-Kappa B in Normal and SV40-Transformed Human Fibroblasts, *J. Biol. Chem.* 275, 14760–14766.
- Clark, M.A., Shorr, R.G., and Bomalaski, J.S. (1986) Antibodies Prepared to *Bacillus cereus* Phospholipase C Crossreact with a Phosphatidylcholine Preferring Phospholipase C in Mammalian Cells, *Biochem. Biophys. Res. Commun.* 140, 114–119.
- Hough, E., Hansen, L.K., Birknes, B., Jynge, K., Hansen, S., Hordvik, A., Little, C., Dodson, E., and Derewenda, Z. (1989) High-Resolution (1.5 Å) Crystal Structure of Phospholipase C from *Bacillus cereus*, *Nature* 338, 357–360.
- Hansen, S., Hough, E., Svensson, L.A., Wong, Y.L., and Martin, S.F. (1993) Crystal Structure of Phospholipase C from *Bacillus cereus* Complexed with a Substrate Analog, *J. Mol. Biol.* 234, 179–187.
- Martin, S.F., Spaller, M.R., and Hergenrother, P.J. (1996) Expression and Site-Directed Mutagenesis of the Phosphatidylcholine-Preferring Phospholipase C of *Bacillus cereus*: Probing the Role of the Active Site Glu146, *Biochemistry* 35, 12970–12977.
- Martin, S.F., and Hergenrother, P.J. (1998) General Base Catalysis by the Phosphatidylcholine-Preferring Phospholipase C from *Bacillus cereus*: The Role of Glu4 and Asp55, *Biochemistry* 37, 5755–5760.
- Martin, S.F., and Hergenrother, P.J. (1999) Catalytic Cycle of the Phosphatidylcholine-Preferring Phospholipase C from *Bacillus cereus*. Solvent Viscosity, Deuterium Isotope Effects, and Proton Inventory Studies, *Biochemistry* 38, 4403–4408.
- Martin, S.F., Follows, B.C., Hergenrother, J.P., and Trotter, B.K. (2000) The Choline Binding Site of Phospholipase C (*Bacillus cereus*): Insights into Substrate Specificity, *Biochemistry* 39, 3410–3415.
- Martin, S.F., Wong, Y.-L., and Wagman, A.S. (1994) Design, Synthesis, and Evaluation of Phospholipid Analogues as Inhibitors of the Bacterial Phospholipase C from *Bacillus cereus*, *J. Org. Chem.* 59, 4821–4831.
- Martin, S.F., Follows, B.C., Hergenrother, P.J., and Franklin, C.L. (2000) A Novel Class of Zinc-Binding Inhibitors for the Phosphatidylcholine-Preferring Phospholipase C from *Bacillus cereus*, *J. Org. Chem.* 65, 4509–4514.
- Cristol, S.J., Seifert, W.K., and Colloway, S.B. (1960) Bridged Polycyclic Compounds. X. The Synthesis of *endo* and *exo*-1,2-Dihydrodicyclopentadienes and Related Compounds, *J. Am. Chem. Soc.* 82, 2351–2356.
- Wilder, P.J., Portis, A.R., Jr., Wright, G.W., and Sheperd, J.M. (1974) Oxymercuration–Demercuration and Hydroboration–Oxidation of *endo*-Dicyclopentadiene (*endo* Tricyclo[5.2.1.0<sup>2,6</sup>]deca-3,8-diene), *J. Org. Chem.* 39, 1636–1641.
- Dawson, B.A., and Stothers, J.B. (1983) Carbon-13 NMR Spectra of Several Dicyclopentadiene Derivatives, *Org. Magn. Reson.* 21, 217–220.
- Brown, H.C., Rothberg, I., and Van der Jagt, D.J. (1972) Convenient Synthetic Routes to the 5,6-Trimethylenenorbornanones, *J. Org. Chem.* 37, 4098–4103.
- Shiotsuki, T., Huang, T.L., Uematsu, T., Bonning, B.C., Ward, V.K., and Hammock, B.D. (1994) Juvenile Hormone Esterase Purified by Affinity Chromatography with 8-Mercapto-1,1,1-trifluoro-2-octanone as a Rationally Designed Ligand, *Protein Expr. Purif.* 5, 296–306.
- Hergenrother, P.J., and Martin, S.F. (1997) Determination of the

- Kinetic Parameters for Phospholipase C (*Bacillus cereus*) on Different Phospholipid Substrates Using a Chromogenic Assay Based on the Quantitation of Inorganic Phosphate, *Anal. Biochem.* 251, 45–49.
21. Martin, S.F., and Pitzer, G.E. (2000) Solution Conformations of Short-Chain Phosphatidylcholine. Substrates of the Phosphatidylcholine-Preferring PLC of *Bacillus cereus*, *Biochim. Biophys. Acta* 1464, 104–112.
22. Peng, H., Xie, W., Otterness, D.M., Cogswell, J.P., McConnell, R.T., Carter, H.L., Powis, G., Abraham, R.T., and Zalkow, L.H. (2001) Syntheses and Biological Activities of a Novel Group of Steroidal Derived Inhibitors for Human Cdc25A Protein Phosphatase, *J. Med. Chem.* 44, 834–848.
23. Yanev, S.G., Kent, U.M., Roberts, E.S., Ballou, D.P., Hollenberg, P.F. (2000) Mechanistic Studies of Cytochrome P450 2B1 Inactivation by Xanthates, *Arch. Biochem. Biophys.* 378, 157–166.
24. Nikolova-Karakashian, M. (2000) Assays for the Biosynthesis of Sphingomyelin and Ceramide Phosphoethanolamine, *Methods Enzymol.* 311, 31–42.

[Received November 27, 2001 and in revised form January 31, 2002; revision accepted February 14, 2002]

# FA Composition of Heart and Skeletal Muscle During Embryonic Development of the King Penguin

Frederic Decrock<sup>a</sup>, René Groscolas<sup>a</sup>, and Brian K. Speake<sup>b,\*</sup>

<sup>a</sup>Centre d'Ecologie et Physiologie Energétiques, Centre National de la Recherche Scientifique, Associé à l'Université Louis Pasteur, 67087 Strasbourg, France, and <sup>b</sup>Lipid Laboratory, Avian Science Research Centre, Scottish Agricultural College, Ayr KA6 5HW, United Kingdom

**ABSTRACT:** Since the yolk lipids of the king penguin (*Aptenodytes patagonicus*) naturally contain the highest concentrations of DHA and EPA yet reported for the eggs of any avian species, the effects of this (n-3)-rich yolk on the FA profiles of the embryonic heart and skeletal muscle were investigated. The concentrations (mg/g wet tissue) of phospholipid (PL) in the developing heart and leg muscle of the penguin doubled between days 27 and 55 from the beginning of egg incubation (i.e., from the halfway stage of embryonic development to 2 d posthatch), whereas no net increase occurred in pectoral muscle. During this period, the concentration of TAG in heart decreased by half but increased two- and sixfold in leg and pectoral muscle, respectively. The most notable change in cholesteryl ester concentration occurred in pectoral muscle, increasing ninefold between days 27 and 55. Arachidonic acid (ARA) was the major polyunsaturate in PL of the penguin's heart, where it formed about 20% (w/w) of FA at day 55. At the equivalent developmental stage, the heart PL of the chicken contained a 1.3-fold greater proportion of ARA, contained a fifth less DHA, and was almost devoid of EPA, whereas the latter FA was a significant component (7% of FA) of penguin heart PL. Similarly, in PL of leg and pectoral muscle, the chicken displayed about 1.4-fold more ARA, up to 50% less DHA, and far less EPA in comparison with the penguin. Thus, although ARA-rich PL profiles are achieved in the heart and muscle of the penguin embryo, these profiles are significantly affected by the high n-3 content of the yolk.

Paper no. L8884 in *Lipids* 37, 407–415 (April 2002).

During development of the avian embryo, FA derived from yolk lipids are distributed to the growing tissues where they are used for energy metabolism, membrane biogenesis, and the formation of fat stores (1). As a result of the selective uptake and incorporation of certain PUFA, the phospholipids (PL) of the various embryonic tissues display highly distinctive FA profiles (1). Particular attention has been focused on the high proportions of DHA (22:6n-3) in the PL of the embryonic brain and retina, largely because this n-3 polyunsatu-

rate is believed to perform essential roles during neuronal differentiation (2–4). However, the development and subsequent functioning of the embryonic heart and skeletal muscles are also dependent on lipid-related events. For example, the early stages of skeletal myogenesis, characterized by the proliferation of myoblasts and their subsequent fusion to form multinucleate myotubes, are dependent on high rates of PL metabolism associated with membrane rearrangements (5–7). Also, studies in mammals have demonstrated that the proportion of C<sub>20-22</sub> polyunsaturates and the n-3/n-6 ratio in muscle PL are positively correlated with the tissue's sensitivity to insulin and that inadequacies in the provision of certain PUFA during development could contribute to insulin resistance (8,9). Most notably, investigations using mammalian cardiomyocytes have revealed a central role for PL-derived arachidonic acid (ARA, 20:4n-6) in the signal transduction mechanisms that regulate the heart beat (10,11). Moreover, DHA and EPA (20:5n-3) have been shown to exert powerful antiarrhythmic effects on heart cells by modulating membrane ion channels (12,13). In addition, the intramyocellular TAG of both heart and skeletal muscle could function as an important energy reserve during development (14,15).

Given the regulatory roles of C<sub>20-22</sub> polyunsaturates of both the n-6 and n-3 series in cardiac and skeletal muscle (8–13), the avian embryo may require the provision of these FA from the yolk in adequate amounts and in the appropriate n-3/n-6 ratio to support the functional differentiation of these tissues. For a particular avian species, major distortions of the yolk's polyunsaturate profile away from that which is normally encountered by the embryo, as achieved by altering the diet of the hen, could conceivably result in impairments of myocellular function. If so, this is analogous to the well-studied consequences of n-3 or n-6 deprivation during development on the subsequent performance of the brain and retina (16,17). However, different avian species utilize a variety of dietary modes resulting in a great diversity of species-specific yolk FA compositions (18,19). For those species whose eggs naturally contain a great excess of n-3 over n-6 FA, or vice versa, the embryo could possibly express adaptations to ensure that a more balanced spectrum of polyunsaturates is delivered/incorporated into the muscle cells. Alternatively, the lipid-dependent regulatory mechanisms in the developing heart and skeletal muscle of such species may possess sufficient

\*To whom correspondence should be addressed at Avian Science Research Centre, Scottish Agricultural College, Auchincruive, Ayr, KA6 5HW, United Kingdom. E-mail: b.speake@au.sac.ac.uk

Abbreviations: ARA, arachidonic acid; CE, cholesteryl ester; PL, phospholipid.



flexibility to accommodate the excess of one or the other type of polyunsaturate.

The eggs of some piscivorous birds provide an extreme case since their yolks are exceptionally enriched with DHA and EPA due to the large amounts of these FA in the fish they eat (20–22). For example, the n-3/n-6 ratio of the yolk lipids of the king penguin (*Aptenodytes patagonicus*) is 3.0 compared with only 0.1 in eggs of the chicken (20,21). We recently described the rearrangements in FA composition that occur as lipids are transferred from the yolk of the king penguin to the embryonic plasma and liver (21). In the present work, and based on comparison with the chicken, we show how the (n-3)-rich yolk of the king penguin affects the FA profiles of lipids of the developing heart and skeletal muscle in this species.

## MATERIALS AND METHODS

### *The penguin colony, egg incubation, and tissue collection.*

The breeding colony of king penguins (Crozet Archipelago, South Indian Ocean), the natural incubation of eggs in the wild, and the sampling of eggs for the collection of embryonic tissues (during the austral summer of 1998/1999) were described in detail previously (21). In brief, eggs in the range of 280–320 g were removed from the incubating parent after 27, 33, 40, and 47 d of development. Hatching occurs after  $53 \pm 1$  d in this species but began about 3 d earlier (23,24). Additionally, some eggs in which hatching had commenced were transferred from the parent to a laboratory incubator maintained at 37.5°C and 100% relative humidity until the chicks were completely hatched. These were either sampled immediately on hatching or were maintained for 2 d and provided with drinking water but no food. The reason for not obtaining newly hatched and 2-d posthatch chicks directly from the colony is that parents commence feeding their chicks before they have fully emerged from the shell. The FA composition of this food (myctophid fishes) differs from that of the yolk (21) and would therefore interfere with any assessment of yolk-to-muscle lipid transfer. Unfed newly hatched chicks rely on the residual contents of the internalized yolk sac for their source of nutrients (1). Embryos and chicks were sacrificed by decapitation and hearts and muscles were dissected and immediately stored frozen at –20°C. Samples were maintained at –20°C during air transport to Britain, where they were stored at –80°C for up to 6 mon prior to analysis. The use of fewer than 60 eggs to generate samples for the present work and for a related study (21) had negligible impact on the local population of 30,000 breeding pairs given that natural mortality is several thousand eggs and chicks per year.

*Incubation of chicken eggs.* Fertile eggs of the domestic chicken (Ross 1 broiler-breeder strain) were obtained from a commercial hatchery. The laying hens were provided with a standard commercial diet in which 18:2n-6 and 18:3n-3, formed about 44 and 6% (w/w) respectively, of total FA but ARA and DHA were present only in trace amounts (less than 0.5%), and EPA was not detected. The proportions (wt% of total FA) of

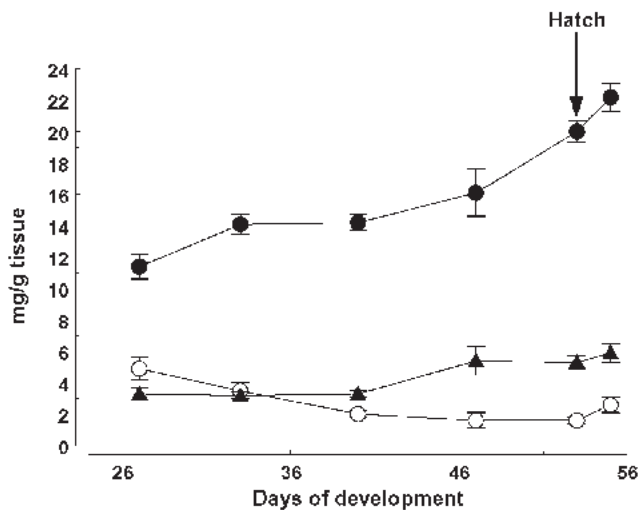
18:2n-6, 18:3n-3, ARA, EPA, and DHA in the total lipids of the unincubated eggs were 15.3, 0.6, 1.5, 0.1, and 1.4%, respectively, consistent with the well-established FA composition of chicken eggs (1,2,25). This contrasts markedly with eggs of the king penguin, where the proportions of 18:2n-6, 18:3n-3, ARA, EPA, and DHA in total lipids were 1.9, 0.1, 1.6, 3.0, and 5.9%, respectively (21). Eggs were incubated at 37.8°C and 60% relative humidity in a benchtop incubator (Brinsea Products, Banwell, United Kingdom). Hatching occurred after 21 d and the chicks were maintained for 2 d with drinking water but no food provided. After sacrifice by decapitation, heart and muscle samples were dissected and stored at –80°C for up to 1 mon prior to analysis.

*Lipid analysis.* The methodology for lipid and FA analysis was previously described in detail (21,26). In brief, total lipids were extracted from samples of heart and skeletal muscle using the modified Folch method (27), lipid classes were separated by TLC on silica gel G using a solvent system of hexane/diethyl ether/formic acid (80:20:1, by vol), and, following exhaustive elution of the identified bands from the silica (26), the isolated PL, TAG, and cholesteryl ester (CE) were subjected to transmethylation. The resultant FAME were analyzed by GLC using a Carbowax capillary column (30 m  $\times$  0.25 mm, film thickness 0.25  $\mu$ m; Alltech, Carnforth, United Kingdom) in a CP9001 Instrument (Chrompack, Middleburg, The Netherlands) with peak integration and data analysis performed by an EZ Chrom Data Analysis System (Scientific Software, San Ramon, CA). Peaks were quantified with reference to a 19:0 standard and identified by comparison with standard FAME (Sigma, Poole, United Kingdom). FA compositions are expressed as wt%. Since minor FA (<0.2%) were not included in the tables, the sum of the presented values is less than 100%. The amounts of the lipid classes were calculated from the FA mass derived from each class together with the acyl group contribution to the M.W. of these compounds. Free cholesterol was determined using an enzymatic/colorimetric assay kit (Boehringer, Lewes, United Kingdom).

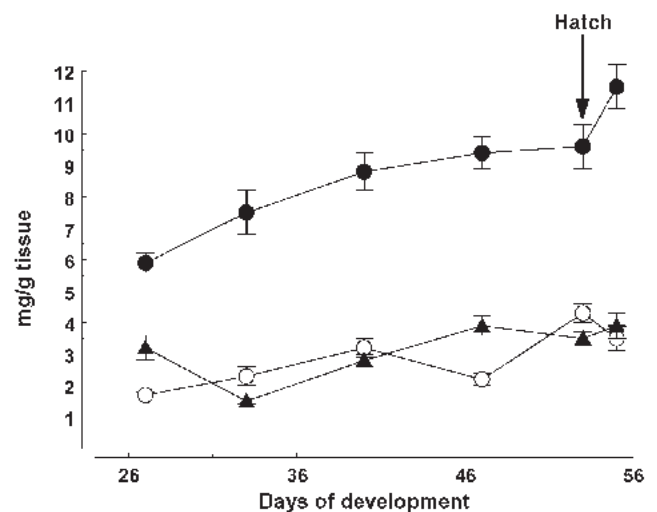
*Data analysis.* Results are expressed as mean  $\pm$  SE of values from  $n = 4$ –8 embryos or chicks. Comparison of FA compositions between two developmental stages or between penguin and chicken utilized the unpaired two-tailed Student's *t*-test after arcsine transformation of percentage values. Tissue lipid class concentrations throughout development were compared by one-way ANOVA and *post-hoc* Bonferroni tests.

## RESULTS

*Concentrations of lipid classes in heart and skeletal muscle during development of the king penguin.* Developmental changes in the tissue concentrations of PL, TAG, and CE (expressed as mg/g wet tissue) are shown in Figures 1–3. The concentration of PL in the heart of the king penguin increased by almost twofold ( $P < 0.001$ ) between day 27 of embryonic development (i.e., the halfway stage of the embryonic period) and 2 d posthatch (Fig. 1). It should be noted that the



**FIG. 1.** Concentrations (mg/g wet tissue) of phospholipid (●), TAG (○), and cholesteryl ester (▲) in the heart of the king penguin during development. Values are means of  $n = 8$  (days 27 and 33), 6 (day 40), and 4 (days 47, 53, and 55) with SE indicated by error bars.



**FIG. 2.** Concentrations (mg/g wet tissue) of phospholipid (●), TAG (○), and cholesteryl ester (▲) in leg muscle of the king penguin during development. Values are means ( $n = 4$ ) with SE indicated by error bars.

concentration of PL in the heart at the time of hatching was approximately twice as high as in the two skeletal muscle sites (Fig. 1 vs. Figs. 2 and 3). The concentration of TAG in the heart of the day 27 embryo was less than half of the value for PL at that stage and decreased by 67% ( $P < 0.01$ ) throughout the latter half of the embryonic period. Thus, by the time of hatching, the concentration of PL in the heart was 12.5 times greater than that of TAG. At day 27, CE was a relatively minor component of the heart lipids (less than a third of the PL content), but its concentration had increased by 1.8-fold ( $P < 0.02$ ) at 2 d posthatch.

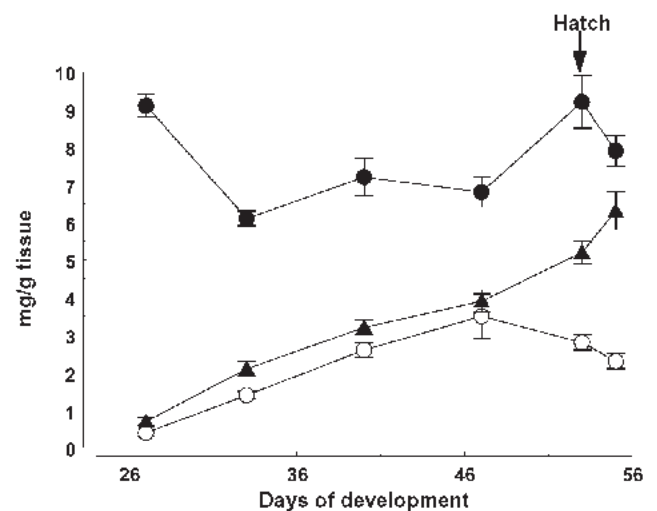
PL was the major lipid class of leg muscle throughout development and its concentration increased twofold ( $P < 0.001$ ) between day 27 of embryonic life and day 2 after hatching; the apparent abrupt rise between hatching and 2 d posthatch did not reach statistical significance (Fig. 2). The concentration of TAG in this tissue also doubled ( $P < 0.001$ ) during this same period. After a decrease of 50% ( $P < 0.01$ ) between days 27 and 33, the concentration of CE was restored to its initial value by the time of hatching.

In contrast with heart and leg muscle, the concentration of PL in pectoral muscle did not undergo a net increase during this period; instead it decreased by 30% ( $P < 0.001$ ) between days 27 and 33 with the original concentration being restored by the time of hatching (Fig. 3). On the other hand, the concentrations of TAG and CE in pectoral muscle increased during development, the latter continuously so that its concentration at 2 d posthatch was 9.0 times greater ( $P < 0.001$ ) than at day 27, and the former peaked at day 47 when its concentration was 8.8 times higher ( $P < 0.01$ ) than at day 27.

*FA profiles of heart lipids during development of the king penguin.* To illustrate developmental change, the FA profiles of heart lipids at 27 and 55 days of incubation were compared, the latter time point representing day 2 after hatching. These

times represent the earliest and latest developmental stages that were sampled. ARA was the main polyunsaturate of the heart PL (Table 1), and substantial proportions of EPA and DHA were also present; however, 18:2n-6 was a very minor FA and no 18:3n-3 was detected. Between days 27 and 55, the proportions of 16:0 and 22:5n-3 in PL decreased, whereas those of 18:0, 18:1n-9, and 18:2n-6 increased; however, the most striking change was a reduction in the proportion of DHA to less than half its day 27 value.

At day 27, the most notable feature of the heart's TAG was the very high proportion of DHA. By day 55, however, the proportion of DHA had decreased by two-thirds, accompanied by a major increase in the contribution of 18:1n-9 and lesser



**FIG. 3.** Concentrations (mg/g wet tissue) of phospholipid (●), TAG (○), and cholesterol ester (▲) in pectoral muscle of the king penguin during development. Values are means ( $n = 4$ ) with SE indicated by error bars.

**TABLE 1**  
**FA Profiles<sup>a</sup> of Heart Lipids<sup>b</sup> During Development of the King Penguin**

	Phospholipid		TAG		Cholesteryl ester	
	Day 27 <sup>c</sup>	Day 55	Day 27	Day 55	Day 27	Day 55
16:0	20.5 ± 1.1	17.9 ± 0.7 <sup>d</sup>	15.0 ± 1.7	19.8 ± 1.0 <sup>d</sup>	7.9 ± 0.8	8.7 ± 0.8
16:1n-7	0.7 ± 0.1	0.8 ± 0.1	0.6 ± 0.1	2.4 ± 0.2 <sup>e</sup>	1.0 ± 0.1	1.8 ± 0.2 <sup>d</sup>
18:0	18.8 ± 0.3	21.2 ± 0.4 <sup>e</sup>	13.3 ± 0.3	10.8 ± 0.6 <sup>d</sup>	8.3 ± 0.3	5.2 ± 0.2 <sup>e</sup>
18:1n-9	16.3 ± 0.3	19.1 ± 0.5 <sup>e</sup>	22.4 ± 0.5	40.0 ± 0.5 <sup>e</sup>	44.3 ± 1.4	59.5 ± 2.9 <sup>e</sup>
18:1n-7	3.0 ± 0.1	2.7 ± 0.2	3.1 ± 0.1	3.7 ± 0.1 <sup>d</sup>	2.9 ± 0.1	3.8 ± 0.1 <sup>e</sup>
18:2n-6	1.2 ± 0.1	2.2 ± 0.2 <sup>d</sup>	2.1 ± 0.1	2.6 ± 0.2 <sup>d</sup>	3.7 ± 0.3	2.2 ± 0.1 <sup>d</sup>
18:3n-3	0.0	0.0	0.5 ± 0.1	0.4 ± 0.1	1.9 ± 0.2	0.3 ± 0.1 <sup>e</sup>
20:1n-9	0.4 ± 0.0	0.3 ± 0.1	1.4 ± 0.1	2.3 ± 0.2 <sup>d</sup>	2.2 ± 0.1	3.3 ± 0.4 <sup>d</sup>
20:4n-6	16.1 ± 0.5	19.7 ± 1.8	4.4 ± 0.1	3.2 ± 0.3 <sup>d</sup>	2.5 ± 0.1	2.3 ± 0.1
22:4n-6	0.6 ± 0.1	0.7 ± 0.1	0.7 ± 0.1	0.3 ± 0.1	0.0	0.0
20:5n-3	8.2 ± 0.2	7.1 ± 0.7	3.1 ± 0.1	2.9 ± 0.3	3.7 ± 0.3	3.7 ± 0.2
22:5n-3	1.5 ± 0.1	1.1 ± 0.1 <sup>d</sup>	3.2 ± 0.2	2.0 ± 0.3 <sup>d</sup>	1.0 ± 0.1	0.6 ± 0.1 <sup>d</sup>
22:6n-3	10.5 ± 0.5	4.7 ± 0.2 <sup>e</sup>	26.7 ± 1.9	7.9 ± 0.8 <sup>e</sup>	13.0 ± 1.2	5.3 ± 0.5 <sup>e</sup>

<sup>a</sup>Wt% of FA in that lipid class; values are mean ± SE of *n* = 8 and 4 hearts at days 27 and 55, respectively.

<sup>b</sup>Total lipid formed 2.4 and 3.6 wt% of wet tissue at days 27 and 55, respectively; phospholipid, TAG, cholesteryl ester, and free cholesterol, respectively, formed 47.5, 20.5, 13.8, and 8.6 wt% of total lipid at day 27, and 61.8, 7.2, 16.3, and 7.1% at day 55.

<sup>c</sup>Days from the beginning of egg incubation; day 55 is 2 d posthatch.

<sup>d</sup>*P* < 0.05; comparison with day 27.

<sup>e</sup>*P* < 0.001; comparison with day 27.

increases in the proportions of 16:0 and 16:1n-7. DHA was the major polyunsaturate of heart CE at day 27; it was still the major polyunsaturate at day 55 although its proportion was much lower than at day 27. The other main difference during development was the 1.3-fold increase in the proportion of 18:1n-9 in CE.

*FA profiles of leg muscle lipids during development of the king penguin.* DHA was the main polyunsaturate of the PL fraction of leg muscle (Table 2) at both time points although its proportion had decreased by a quarter at the latter stage, commensurate with increased contributions from ARA and EPA. Also, the proportion of 18:0 in PL increased 1.3-fold

over this period. DHA was also the main polyunsaturate of the TAG fraction at both stages, even though its proportion had decreased by more than a third at day 55. Reductions in the contributions from ARA and EPA were also evident at the latter stage. A major increase in the proportion of 16:0, an increase in that of 18:1n-9, and a reduced contribution from 18:0 also occurred during development. Again, DHA was the predominant polyunsaturate of CE at both stages although its proportion decreased by more than half during development. The proportion of ARA was also lower at the later stage, and there was an increased contribution from 18:1n-9.

**TABLE 2**  
**FA Profiles<sup>a</sup> of Leg Muscle Lipids<sup>b</sup> During Development of the King Penguin**

	Phospholipid		TAG		Cholesteryl ester	
	Day 27 <sup>c</sup>	Day 55	Day 27	Day 55	Day 27	Day 55
16:0	22.2 ± 1.4	19.1 ± 0.4	14.2 ± 0.3	23.6 ± 0.8 <sup>d</sup>	8.0 ± 0.7	8.5 ± 0.3
16:1n-7	0.8 ± 0.1	0.6 ± 0.1	1.3 ± 0.2	2.0 ± 0.3	1.3 ± 0.2	1.6 ± 0.1
18:0	14.9 ± 0.4	19.6 ± 0.2 <sup>e</sup>	15.4 ± 1.9	9.3 ± 0.4 <sup>e</sup>	7.3 ± 0.3	5.5 ± 0.1 <sup>e</sup>
18:1n-9	23.0 ± 0.2	21.0 ± 0.9	34.8 ± 0.3	40.2 ± 1.1 <sup>e</sup>	48.7 ± 0.7	59.6 ± 1.5 <sup>f</sup>
18:1n-7	3.0 ± 0.1	2.5 ± 0.1 <sup>e</sup>	3.7 ± 0.1	3.7 ± 0.2	3.3 ± 0.1	3.1 ± 0.1
18:2n-6	1.1 ± 0.1	1.7 ± 0.1 <sup>e</sup>	2.7 ± 0.3	2.1 ± 0.1	2.7 ± 0.2	2.3 ± 0.1
18:3n-3	0.0	0.0	0.3 ± 0.1	0.2 ± 0.0	0.5 ± 0.1	0.3 ± 0.1
20:1n-9	0.6 ± 0.1	0.6 ± 0.1	2.6 ± 0.1	3.6 ± 0.3 <sup>e</sup>	2.0 ± 0.2	3.6 ± 0.4 <sup>e</sup>
22:1n-9 <sup>f</sup>	0.0	0.0	1.4 ± 0.2	0.5 ± 0.1 <sup>e</sup>	0.4 ± 0.1	0.3 ± 0.1
20:4n-6	8.9 ± 0.3	10.7 ± 0.3 <sup>e</sup>	2.2 ± 0.2	1.2 ± 0.1 <sup>e</sup>	3.7 ± 0.1	2.6 ± 0.3 <sup>e</sup>
20:5n-3	4.6 ± 0.2	6.1 ± 0.5 <sup>e</sup>	2.9 ± 0.3	1.1 ± 0.1 <sup>e</sup>	5.3 ± 0.5	4.4 ± 0.3
22:5n-3	2.3 ± 0.1	2.8 ± 0.2	2.1 ± 0.4	2.7 ± 0.1	0.9 ± 0.1	0.6 ± 0.1
22:6n-3	15.2 ± 0.5	11.4 ± 0.4 <sup>e</sup>	12.0 ± 1.8	7.4 ± 0.5 <sup>e</sup>	12.0 ± 0.6	5.2 ± 0.5 <sup>f</sup>

<sup>a</sup>Wt% of FA in that lipid class; values are mean ± SE (*n* = 4).

<sup>b</sup>Total lipid formed 1.3 and 2.3 wt% of wet tissue at days 27 and 55, respectively; phospholipid, TAG, cholesteryl ester, and free cholesterol, respectively, formed 45.7, 12.9, 24.3, and 4.2 wt% of total lipid at day 27, and 49.8, 15.3, 16.8, and 7.6% at day 55.

<sup>c</sup>Days from the beginning of egg incubation; day 55 is 2 d posthatch.

<sup>d</sup>*P* < 0.001; comparison with day 27.

<sup>e</sup>*P* < 0.05; comparison with day 27. <sup>f</sup>Also contains 22:1n-11.

**TABLE 3**  
**FA Profiles<sup>a</sup> of Pectoral Muscle Lipids<sup>b</sup> During Development of the King Penguin**

	Phospholipid		TAG		Cholesteryl ester	
	Day 27 <sup>c</sup>	Day 55	Day 27	Day 55	Day 27	Day 55
16:0	25.5 ± 0.9	20.4 ± 0.4 <sup>d</sup>	18.7 ± 1.7	20.2 ± 1.1	10.0 ± 0.3	8.4 ± 0.2 <sup>d</sup>
16:1n-7	1.1 ± 0.1	0.6 ± 0.1 <sup>d</sup>	1.8 ± 0.2	1.5 ± 0.2	1.6 ± 0.2	1.5 ± 0.1
18:0	13.6 ± 0.3	18.0 ± 0.2 <sup>e</sup>	14.3 ± 1.1	11.3 ± 0.3 <sup>d</sup>	6.8 ± 0.6	5.7 ± 0.1
18:1n-9	22.9 ± 0.4	23.4 ± 0.5	32.3 ± 1.4	37.2 ± 0.6 <sup>d</sup>	47.9 ± 1.5	62.3 ± 0.5 <sup>e</sup>
18:1n-7	3.0 ± 0.1	1.9 ± 0.1 <sup>e</sup>	3.6 ± 0.1	3.3 ± 0.2	3.2 ± 0.1	3.3 ± 0.1
18:2n-6	1.1 ± 0.1	1.6 ± 0.1 <sup>d</sup>	2.2 ± 0.2	2.1 ± 0.1	2.5 ± 0.3	2.3 ± 0.1
18:3n-3	0.0	0.0	0.8 ± 0.1	0.3 ± 0.1 <sup>d</sup>	0.8 ± 0.2	0.2 ± 0.0
20:1n-9	0.4 ± 0.1	0.7 ± 0.1	1.6 ± 0.2	2.9 ± 0.2 <sup>d</sup>	1.8 ± 0.1	2.4 ± 0.2 <sup>d</sup>
20:4n-6	8.7 ± 0.3	11.8 ± 0.3 <sup>e</sup>	3.2 ± 0.4	2.7 ± 0.3	3.8 ± 0.1	2.5 ± 0.2 <sup>d</sup>
22:4n-6	0.8 ± 0.1	1.3 ± 0.1 <sup>d</sup>	0.0	0.0	0.0	0.0
20:5n-3	4.1 ± 0.3	3.6 ± 0.4	3.0 ± 0.4	1.6 ± 0.1 <sup>d</sup>	5.3 ± 0.3	4.2 ± 0.2 <sup>d</sup>
22:5n-3	2.0 ± 0.1	2.2 ± 0.1	2.1 ± 0.3	3.0 ± 0.3	0.6 ± 0.1	0.5 ± 0.1
22:6n-3	14.1 ± 0.5	11.8 ± 0.5 <sup>d</sup>	12.3 ± 1.3	10.1 ± 0.6	10.7 ± 0.9	4.5 ± 0.2 <sup>e</sup>

<sup>a</sup>Wt% of FA in that lipid class; values are mean ± SE ( $n = 4$ ).

<sup>b</sup>Total lipid formed 1.1 and 2.0 wt% of wet tissue at days 27 and 55, respectively; phospholipid, TAG, cholesteryl ester, and free cholesterol, respectively, formed 82.5, 3.7, 6.0, and 6.1 wt% of total lipid at day 27; and 39.6, 11.6, 31.4, and 8.6% at day 55.

<sup>c</sup>Days from beginning of egg incubation; day 55 is 2 d posthatch.

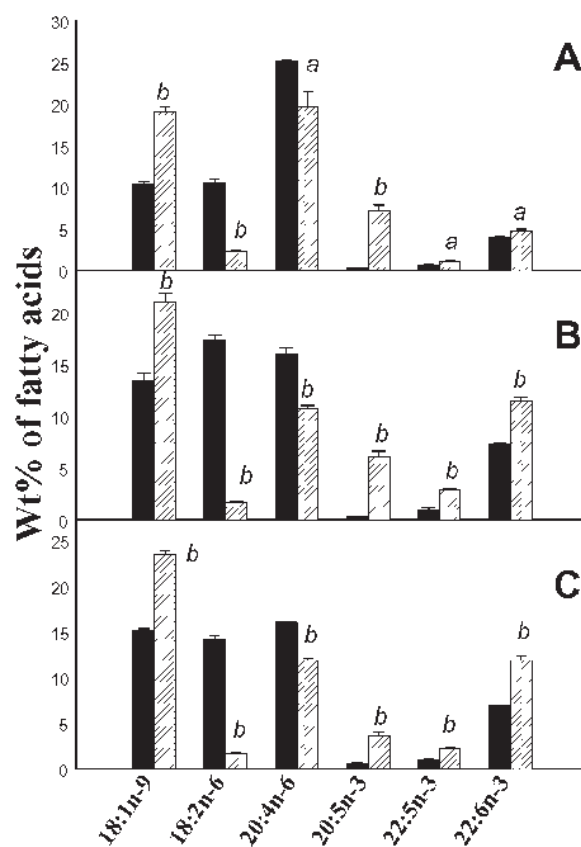
<sup>d</sup> $P < 0.05$ ; comparison with day 27.

<sup>e</sup> $P < 0.001$ ; comparison with day 27.

*FA profiles of pectoral muscle lipids during development of the king penguin.* DHA, the major polyunsaturate of pectoral muscle PL (Table 3), decreased by a fifth between the two stages, commensurate with an increased proportion of ARA. A decrease in the proportion of 16:0 in PL during development was balanced by an increased contribution from 18:0. DHA was again the major PUFA of the TAG fraction, with no significant decrease during development; the proportions of 18:0 and EPA were lower at day 55, whereas the proportion of 18:1n-9 was higher. In CE, DHA was also the main polyunsaturate, although its proportion decreased by half during development; the contributions of ARA and EPA were also less at the later stage, whereas the proportion of 18:1n-9 increased 1.3-fold during development, and that of 16:0 decreased slightly.

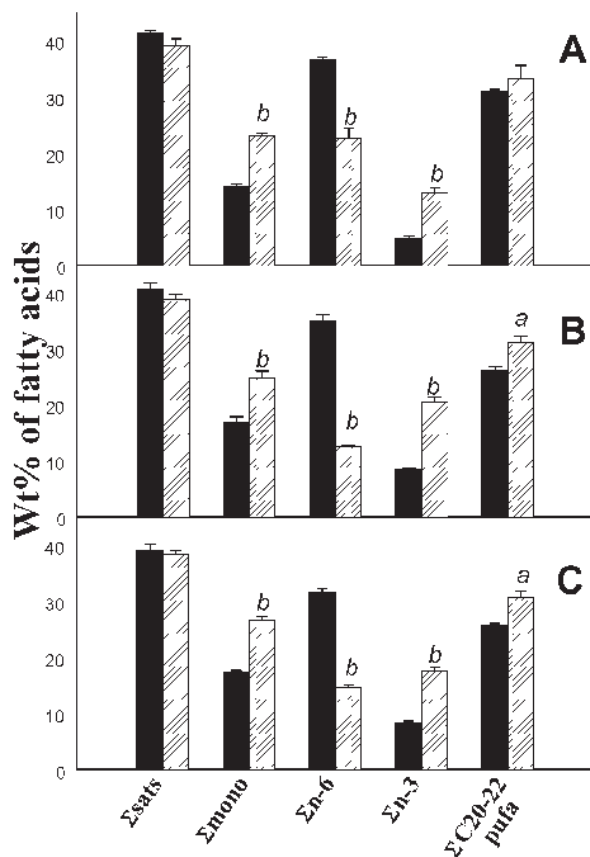
Data (not shown) from intermediate stages indicate that, for heart, leg, and pectoral muscle, the differences in FA composition between days 27 and 55 reflect continuous trends during this period.

*Comparison with the chicken.* The FA profiles of the PL fraction of the heart, leg, and pectoral muscle of the newly hatched chicken were compared (Figs. 4 and 5) with the equivalent values for the penguin at the same developmental stage (i.e., 2 d posthatch). The PL fraction was chosen since it is the main structural and functional lipid of the cell membranes. For all three tissues, the proportions of total saturates (16:0 plus 18:0) in PL did not differ between the two avian species (Fig. 5). The heart PL of the chicken displayed only half the proportion of 18:1n-9 but nearly five times as much 18:2n-6 compared with the values for the penguin; also, a 1.3-fold greater contribution from ARA in the chicken was counterbalanced by a near-absence of EPA and a lower (by a fifth) proportion of DHA (Fig. 4A). The heart PL of the chicken



**FIG. 4.** Proportions (wt% of total FA) of unsaturated FA in phospholipid of heart (A), leg muscle (B), and pectoral muscle (C) in the chicken (filled bars) and king penguin (diagonally lined bars), both at 2 d posthatch. Values are mean ( $n = 8$  and 4 for chicken and penguin, respectively) with SE indicated by error bars. <sup>a</sup> $P < 0.05$ ; <sup>b</sup> $P < 0.001$ ; comparison with chicken.





**FIG. 5.** Composite parameters (wt% of total FA) for phospholipid FA of heart (A), leg muscle (B), and pectoral muscle (C) of the chicken (filled bars) and king penguin (diagonally lined bars), both at 2 d posthatch. Abbreviations: sats, saturated FA; mono, monounsaturated FA; pufa, polyunsaturated FA. Values are means ( $n = 8$  and  $4$  for chicken and penguin, respectively) with SE indicated by error bars. <sup>a</sup> $P < 0.05$ ; <sup>b</sup> $P < 0.001$ ; comparison with chicken.

contained lower proportions of total monounsaturates and n-3 polyunsaturates but more n-6 polyunsaturates than that of the penguin, whereas the contributions of total  $C_{20-22}$  polyunsaturates did not differ between the two species (Fig. 5A). The n-6/n-3 ratio in heart PL was 7.6 for the chicken compared with only 1.8 for the penguin.

Compared with the penguin, the leg muscle PL of the chicken contained a much greater (10.2-fold) proportion of 18:2n-6 and commensurately less 18:1n-9; the contribution from ARA was 1.5 times greater in the chicken tissue, but again, EPA was almost absent and the proportion of DHA was about a third lower than in the PL of the penguin leg muscle (Fig. 4B). Thus, the leg muscle PL of the chicken was characterized by lower proportions of total monounsaturates and n-3 polyunsaturates but a higher proportion of n-6 polyunsaturates than were present in the corresponding penguin samples; the total contribution of  $C_{20-22}$  polyunsaturates was also slightly less in the case of the chicken (Fig. 5B). The n-6/n-3 ratio in leg muscle PL was 4.2 for the chicken compared with only 0.6 for the penguin.

The pectoral muscle PL of the chicken contained almost

nine times the proportion of 18:2n-6 but a lower (by a third) proportion of 18:1n-9, than that of the penguin; the contribution from ARA was 1.4 times greater in the chicken tissue, but EPA was a very minor FA and the proportion of DHA was little more than half the value for the penguin (Fig. 4C). Consequently, the contributions of total monounsaturates, n-3 polyunsaturates, and total  $C_{20-22}$  polyunsaturates were lower and that of total n-6 polyunsaturates was higher in the case of the chicken tissue (Fig. 5C). The n-6/n-3 ratio in pectoral muscle PL was 3.8 for the chicken but only 0.8 for the penguin.

## DISCUSSION

*Concentrations of lipid classes in heart and skeletal muscle during development of the king penguin.* The increased concentrations of PL in heart and leg muscle that were observed during the second half of the penguin's embryonic period may reflect the proliferation of myoblasts and subsequently, during myogenic differentiation, the formation of membranous structures, such as the sarcoplasmic reticulum and transverse tubules. In the chicken, the phase of skeletal myoblast proliferation is largely confined to the first half of embryonic development; cell fusion to form multinucleate myotubes occurs around the middle period, and myotube maturation proceeds throughout the final trimester (7). If skeletal myogenesis in the leg of the king penguin employs a similar ontogeny, then the second half of embryonic development, as studied here, is largely characterized by the stages of myoblast fusion and myotube maturation, with any cell division limited to the beginning of this period.

In contrast to the results for heart and leg muscle, the concentration of PL in the pectoral muscle of the penguin did not display a net increase over the same developmental period. This may relate to differences in the rates of maturation between the different muscle sites, such as leg muscle developing in advance of pectoral muscle. We have no quantitative data on this point, but on dissection, the pectoral muscle of the newly hatched penguin chick was markedly underdeveloped compared to leg muscle and to the situation in the adult (Decrock, F., and Groscolas, R., unpublished observations). Such observations are consistent with the fact that, at the beginning of posthatch life, the king penguin's main form of locomotion is walking; it is only later (at 1 yr of age) that it needs a powerful pectoral muscle for swimming (24).

Studies on mammalian skeletal muscle have demonstrated that intramyocellular TAG represents a dynamic energy store that accumulates particularly during periods of high fat intake and is utilized during or just after exercise (28–30). Mobilization of this TAG is catalyzed by intramuscular hormone-sensitive lipase, which is activated by adrenergic stimulation and muscle contraction (14,31). The changing concentration of TAG in the pectoral muscle of the developing king penguin may be consistent with such a role, increasing continuously and substantially (8.8-fold) between days 27 and 47 of egg incubation [a time of rapid provision of yolk-derived lipid to

the embryo (21)] followed by a 35% decrease, which, although not reaching statistical significance, could indicate mobilization of TAG to provide energy for this muscle during the hatching period. In leg muscle, the concentration of TAG increased 2.5-fold between day 27 and hatching, although the pattern of change was not continuous and the 20% decrease within 2 d posthatch did not reach significance. These findings provisionally suggest that TAG is deposited in the skeletal muscle of the developing penguin at a time when the embryo is replete with lipid and that it functions as a reserve of energy, possibly to assist with the demands of the hatching and early posthatch periods. Mobilization of the embryo's TAG stores for energy during hatching is suggested by observations that between days 49 and 54 the total lipid content of the king penguin embryo/chick decreased by 22%, and subcutaneous adipose tissue decreased by 35% (Groscolas, R., and Decrock, F., unpublished data).

By contrast, TAG did not accumulate in the heart of the embryonic king penguin; in fact, the concentration of this lipid in the heart decreased as development progressed. In mammals, myocardial TAG exists in a dynamic state, capable of providing as much as 40% of the energy needs of the beating heart while being rapidly resynthesized to minimize depletion (15). The net decrease in the heart's TAG content throughout the second half of the penguin's embryonic period, despite the intensive transfer of lipid from yolk to embryo, may reflect the substantial use of myocardial TAG as an energy source for the working heart during development.

A consequence of the transfer of lipids from yolk to the avian embryo is the formation in the plasma of CE-rich lipoprotein remnants, which are mainly taken up by the liver (1). However, in the chicken embryo, skeletal muscle is also a significant site for the disposal of plasma CE (32). This would also appear to be the case during the development of the king penguin, particularly in the pectoral muscle where the concentration of CE increased continuously from day 27 of egg incubation to day 2 after hatching.

*Effect of the (n-3)-rich yolk of the king penguin on the FA profiles of embryonic muscle.* The FA composition of the initial yolk of the king penguin (21) forms a dramatic contrast with that of the domestic chicken. Since the chicken's diet was almost devoid of ARA and DHA, the presence of these long-chain polyunsaturates in the chicken's egg is most likely due to desaturation/elongation of dietary 18:2n-6 and 18:3n-3 in the liver of the hen (1,25). In the total yolk lipid, the penguin eggs contained 4.2 times the proportion of DHA and 6.4 times the proportion of C<sub>20-22</sub> n-3 FA in the chicken eggs used in this study. The proportion of ARA was similar for the two species, whereas the chicken yolks displayed an eightfold greater proportion of 18:2n-6. Consequently, the n-3/n-6 ratio of the yolk was 3.0 for the penguin but only 0.1 for the chicken.

An aim of the present work was to evaluate the impact of such disparities on the FA profiles of the developing heart and muscle. Despite the preponderance of C<sub>20-22</sub> n-3 FA in the yolk of the king penguin, the PL of the developing heart of

this species contained ARA as the main polyunsaturate, consistent with an essential role for this n-6 FA in the regulation of cardiomyocyte contraction (10,11). The characteristic fatty acyl profile of the penguin eggs was not, however, without effect on the heart's PL composition since the proportion of ARA was less than in the chicken's heart at the same developmental stage, whereas in the heart of the penguin the contribution from DHA was slightly higher and that of EPA was far more pronounced. It is notable that the total proportion of C<sub>20</sub> polyunsaturates (i.e., ARA plus EPA) in the posthatch heart PL, at  $26.8 \pm 2.7\%$  and  $25.4 \pm 0.2\%$  for the penguin and chicken, respectively, did not differ significantly between the two species. Thus, it is feasible that in the penguin's cardiomyocytes EPA makes a contribution to the signaling functions that in other species are performed entirely by ARA.

Similarly, the skeletal muscle PL of the posthatch king penguin displayed less ARA, more DHA, and far more EPA than the equivalent chicken samples. Nevertheless, the proportions of total C<sub>20</sub> polyunsaturates were again very similar for the two species. Thus, in leg muscle PL, ARA plus EPA formed  $16.8 \pm 0.6$  and  $16.3 \pm 0.6\%$  for the penguin and chicken, respectively, the equivalent values for pectoral muscle being  $15.4 \pm 0.5$  and  $16.5 \pm 0.1\%$ . In neither case were these summed proportions significantly different between the two species. Again, this may imply that some of the regulatory functions normally attributable to ARA have, in the penguin's skeletal muscle, been partly delegated to EPA.

These findings suggest that the PL FA profiles of the developing heart and skeletal muscle of the king penguin represent a compromise between the tissue-specific requirements for particular polyunsaturates (i.e., those that have a defined role in the function and regulation of myocytes) and the pattern of FA that are supplied from the yolk. Thus, the typical "high-ARA" profile of heart PL is upheld in the penguin embryo but in a modified form in which the contribution from n-3 FA is greater than in other avian species (1,33). However, the variation in functional maturity between tissues of the precocial chicken and the semialtricial penguin at the time of hatching (34) should also be considered as a possible contributory factor to the differences in tissue FA profiles.

A consistent finding was that the proportion of DHA in penguin muscle PL was high at day 27 of incubation but then decreased significantly during the second half of the embryonic period; in the case of the two skeletal muscle sites, this was accompanied by a significant increase in the proportion of ARA. The biological relevance of these changes in polyunsaturate composition is not clear but could relate to maturation-dependent modifications in membrane fluidity or lipid-mediated regulatory mechanisms. It is also unclear whether the decreases in the proportion of DHA in myocellular TAG and CE that occurred during the second half of embryonic life are related in some way to the functions of these lipids in the maturing muscle.

The FA composition of the food (myctophid fishes) that is supplied to the newly hatched king penguin by its parents differs from that of the yolk in several respects (21,22). As a

result, the hatchling will consume higher proportions of EPA, DHA, and long-chain (C<sub>20-22</sub>) monounsaturates and a lower proportion of ARA than the embryo (21). The consequences of this nutritional transition on the FA profiles and physiology of the cardiac and skeletal muscles during the posthatch period remain to be investigated.

The king penguin, whose eggs exhibit the highest proportion of C<sub>20-22</sub> n-3 FA yet reported for any bird (21), provides an extreme example to assess the relationship between the FA composition of the yolk and that of embryonic tissues such as the heart, which in most species is dominated by ARA (1,33). The data suggest that the esterification reactions involved in the synthesis of heart PL display a high degree of selectivity in the penguin embryo to sustain a "high-ARA" profile despite the predominance of n-3 FA in the lipids supplied from the yolk. This profile is, however, modified by the presence of higher proportions of EPA and DHA than are found in the heart PL of other species (1,33). In the penguin embryo, the FA-dependent signal transduction cascades that regulate cardiac function (10,11) are presumably adapted to accommodate this modified composition, possibly by employing EPA as well as ARA in these roles. A similar argument may apply to any regulatory roles of n-6 and n-3 polyunsaturates in the developing skeletal muscle.

## ACKNOWLEDGMENTS

We are grateful to Institut Français pour la Recherche et la Technologie Polaires (Program 119) and to the Scottish Executive Rural Affairs Department for financial support. Logistical support was provided by Terres Australes et Antarctiques Françaises. The project was approved by the ethical committee of the Institut Français pour la Recherche et la Technologie Polaires and conformed to the Agreed Measures for the Conservation of Antarctic and Subantarctic Fauna.

## REFERENCES

- Speake, B.K., Murray, A.M.B., and Noble, R.C. (1998) Transport and Transformations of Yolk Lipids During Development of the Avian Embryo, *Prog. Lipid Res.* 37, 1–32.
- Maldjian, A., Cristofori, C., Noble, R.C., and Speake, B.K. (1996) The Fatty Acid Composition of Brain Phospholipids from Chicken and Duck Embryos, *Comp. Biochem. Physiol.* 115B, 153–158.
- Anderson, G.J., Connor, W.E., Corliss, J.D., and Lin, D.S. (1989) Rapid Modulation of the n-3 Docosahexaenoic Acid Levels in the Brain and Retina of the Newly Hatched Chick, *J. Lipid Res.* 30, 433–441.
- Cherian, G., and Sim, J. (1992) Preferential Accumulation of n-3 Fatty Acids in the Brain of Chicks from Eggs Enriched with n-3 Fatty Acids, *Poult. Sci.* 71, 1658–1668.
- Kent, C., Schimmel, S.D., and Vagelos, P.R. (1974) Lipid Composition of Plasma Membranes from Developing Chick Muscle Cells in Culture, *Biochim. Biophys. Acta* 360, 312–321.
- Sauro, V.S., Brown, G.A., Hamilton, M.R., Strickland, C.K., and Strickland, K.P. (1988) Changes in Phospholipid Metabolism Dependent on Calcium-Regulated Myoblast Fusion, *Biochem. Cell. Biol.* 66, 1110–1118.
- Granata, F., Iorio, E., Carpinelli, G., Giannini, M., and Poda, F. (2000) Phosphocholine and Phosphoethanolamine During Chick Embryo Myogenesis: A <sup>31</sup>P-NMR Study, *Biochim. Biophys. Acta* 1483, 334–342.
- Storlien, L.H., Pan, D.A., Kriketos, A.D., O'Connor, J., Catterson, I.D., Cooney, G.J., Jenkins, A.B., and Baur, L.A. (1996) Skeletal Muscle Membrane Lipids and Insulin Resistance, *Lipids* 31, S261–S265.
- Baur, L.A., O'Connor, J., Pan, D.A., Kriketos, A.D., and Storlien, L.H. (1998) The Fatty Acid Composition of Skeletal Muscle Membrane Phospholipid: Its Relationship with the Type of Feeding and Plasma Glucose Levels in Young Children, *Metabolism* 47, 106–112.
- Hohl, C.M., and Rosen, P. (1987) The Role of Arachidonic Acid in Rat Heart Cell Metabolism, *Biochim. Biophys. Acta* 921, 356–363.
- Pavoine, C., Magne, S., Sauvadet, A., and Pecker, F. (1999) Evidence for a β<sub>2</sub>-Adrenergic/Arachidonic Acid Pathway in Ventricular Cardiomyocytes. Regulation by the (β<sub>1</sub>-Adrenergic/cAMP Pathway, *J. Biol. Chem.* 274, 628–637.
- Kang, J.X., and Leaf, A. (1996) The Cardiac Antiarrhythmic Effects of Polyunsaturated Fatty Acids, *Lipids* 31, S41–S44.
- Leaf, A., Kang, J.X., Xiao, Y.F., Billman, G.E., and Voskuyl, R.A. (1999) The Antiarrhythmic and Anticonvulsant Effects of Dietary n-3 Fatty Acids, *J. Membr. Biol.* 172, 1–11.
- Langfort, J., Ploug, T., Ihlemann, J., Saldo, M., Holm, C., and Galbo, H. (1999) Expression of Hormone-Sensitive Lipase and Its Regulation by Adrenaline in Skeletal Muscle, *Biochem. J.* 340, 459–465.
- Swanton, E.M.S., and Saggerson, E.D. (1997) Effects of Adrenaline on Triacylglycerol Synthesis and Turnover in Ventricular Myocytes from Adult Rats, *Biochem. J.* 328, 913–922.
- Neuringer, M., Anderson, G.J., and Connor, W.E. (1988) The Essentiality of n-3 Fatty Acids for the Development and Function of the Retina and Brain, *Annu. Rev. Nutr.* 8, 517–541.
- Innis, S.M. (2000) The Role of Dietary n-6 and n-3 Fatty Acids in the Developing Brain, *Dev. Neurosci.* 22, 474–480.
- Speake, B.K., Surai, P.F., Noble, R.C., Beer, J.V., and Wood, N.A.R. (1999) Differences in Egg Lipid and Antioxidant Composition Between Wild and Captive Pheasants and Geese, *Comp. Biochem. Physiol. B* 124, 101–107.
- Surai, P.F., Speake, B.K., Bortolotti, G.R., and Negro, J.J. (2001) Captivity Diets Alter Egg Yolk Lipids of a Bird of Prey (the American kestrel) and of a Galliforme (the red-legged partridge), *Physiol. Biochem. Zool.* 74, 153–160.
- Speake, B.K., Decrock, F., Surai, P.F., and Groscolas, R. (1999) Fatty Acid Composition of the Adipose Tissue and Yolk Lipids of a Bird with a Marine-Based Diet, the Emperor Penguin (*Aptenodytes forsteri*), *Lipids* 34, 283–290.
- Decrock, F., Groscolas, R., McCartney, R.J., and Speake, B.K. (2001) Transfer of n-3 and n-6 Polyunsaturated Fatty Acids from Yolk to Embryo During Development of the King Penguin, *Am. J. Physiol. Regul. Integr. Comp. Physiol.* 280, R843–R853.
- Raclot, T., Groscolas, R., and Cherel, Y. (1998) Fatty Acid Evidence for the Importance of Myctophid Fishes in the Diet of King Penguins, *Aptenodytes patagonicus*, *Mar. Biol. (Berl.)* 132, 523–533.
- Groscolas, R. (1990) Metabolic Adaptations to Fasting in Emperor and King Penguins, in *Penguin Biology* (Davis, L.S., and Darby, J.T., eds.), Academic, San Diego, pp. 269–296.
- Stonehouse, B. (1960) The King Penguin *Aptenodytes patagonica* of South Georgia. 1. Breeding Behavior and Development, *Falk. Isl. Dep. Survey Scient. Rep.* 23, 1–81.
- Speake, B.K., and Thompson, M.B. (1999) Comparative Aspects of Yolk Lipid Utilisation in Birds and Reptiles, *Poult. Avian Biol. Revs.* 10, 181–211.

26. Royle, N.J., Surai, P.F., McCartney, R.J., and Speake, B.K. (1999) Parental Investment and Egg Yolk Lipid Composition in Gulls, *Funct. Ecol.* *13*, 298–306.
27. Hamilton, S., Hamilton, R.J., and Sewell, P.A. (1992) Extraction of Lipids and Derivative Formation, in *Lipid Analysis: A Practical Approach* (Hamilton, R.J., and Hamilton, S., eds.), IRL, Oxford, pp. 13–64.
28. Decombaz, J., Fleith, M., Hoppler, H., Kries, R., and Boesch, C. (2000) Effect of Diet on the Replenishment of Intramyocellular Lipids After Exercise, *Eur. J. Nutr.* *39*, 244–247.
29. Brechtel, K., Niess, A.M., Machann, J., Rett, K., Schick, F., Claussen, C.D., Dickhuth, H.H., Haering, H.U., and Jacob, S. (2001) Utilization of Intramyocellular Lipids (IMCLs) During Exercise as Assessed by Proton Magnetic Resonance Spectroscopy (<sup>1</sup>H-MRS), *Horm. Metab. Res.* *33*, 63–66.
30. Kiens, B., and Richter, E.A. (1998) Utilization of Skeletal Muscle Triacylglycerol During Postexercise Recovery in Humans, *Am. J. Physiol. Endocrinol. Metab.* *275*, E332–E337.
31. Langfort, J., Ploug, T., Ihlemann, J., Holm, C., and Galbo, H. (2000) Stimulation of Hormone-Sensitive Lipase Activity by Contractions in Rat Skeletal Muscle, *Biochem. J.* *351*, 207–214.
32. Tarugi, P., Reggiani, D., Ottaviani, E., Ferrari, S., Tiozzo, R., and Calandra, S. (1989) Plasma Lipoproteins, Tissue Cholesterol Overload, and Skeletal Muscle Apolipoprotein A-I Synthesis in the Developing Chick, *J. Lipid Res.* *30*, 9–22.
33. Speake, B.K., McCartney, R.J., Feast, M., Maldjian, A., and Noble, R.J. (1996) The Relationship Between the Fatty Acid Profiles of the Yolk and the Embryonic Tissue Lipids: A Comparison Between the Lesser Black Backed Gull (*Larus fuscus*) and the Pheasant (*Phasianus colchicus*), *Comp. Biochem. Physiol.* *115B*, 493–499.
34. Choi, I.H., Ricklefs, R.E., and Shea, R.E. (1993) Skeletal Muscle Growth, Enzyme Activities, and the Development of Thermogenesis: A Comparison Between Altricial and Precocial Birds, *Physiol. Zool.* *66*, 455–473.

[Received August 3, 2001, and in revised form February 15, 2002; revision accepted February 22, 2002]



# Cloning and Molecular Characterization of the $\Delta 6$ -Desaturase from Two *Echium* Plant Species: Production of GLA by Heterologous Expression in Yeast and Tobacco

Federico García-Maroto<sup>a</sup>, José A. Garrido-Cárdenas<sup>a</sup>, Juan Rodríguez-Ruiz<sup>b</sup>, Miguel Vilches-Ferrón<sup>b</sup>, Ana C. Adam<sup>c</sup>, Julio Polaina<sup>c</sup>, and Diego López Alonso<sup>b,\*</sup>

Departamentos de <sup>a</sup>Bioquímica and <sup>b</sup>Biología Aplicada, Facultad de Ciencias Experimentales, Universidad de Almería, E-04120 Almería, Spain, and <sup>c</sup>Instituto de Agroquímica y Tecnología de Alimentos, Consejo Superior de Investigaciones Científicas, E-46100 Burjassot, Valencia, Spain

**ABSTRACT:** The synthesis of GLA ( $\Delta 6,9,12$ -18:3) is carried out in a number of plant taxa by introducing a double bond at the  $\Delta 6$  position of its precursor, linoleic acid ( $\Delta 9,12$ -18:2), through a reaction catalyzed by a  $\Delta 6$ -desaturase enzyme. We have cloned genes encoding the  $\Delta 6$ -desaturase (D6DES) from two different Macaronesian *Echium* species, *E. pitardii* and *E. gentianoides* (Boraginaceae), which are characterized by the accumulation of high amounts of GLA in their seeds. The *Echium* D6DES genes encode proteins of 438 amino acids bearing the prototypical cytochrome b<sub>5</sub> domain at the N-terminus. Cladistic analysis of desaturases from higher plants groups the *Echium* D6DES proteins together with other  $\Delta 6$ -desaturases in a different cluster from that of the highly related  $\Delta 8$ -desaturases. Expression analysis carried out in *E. pitardii* shows a positive correlation between the D6DES transcript level and GLA accumulation in different tissues of the plant. Although a ubiquitous expression in all organs is observed, the transcript is particularly abundant in developing fruits, whereas a much lower level is present in mature leaves. Functional characterization of the D6DES gene from *E. gentianoides* has been achieved by heterologous expression in tobacco plants and in the yeast *Saccharomyces cerevisiae*. In both cases, overexpression of the gene led to the synthesis of GLA. Biotechnological application of these results can be envisaged as an initial step toward the generation of transgenic oleaginous plants producing GLA.

Paper no. L8951 in *Lipids* 37, 417–426 (April 2002).

GLA ( $\Delta 6,9,12$ -18:3) is recognized as an EFA in human nutrition. Its deficiency causes several health disorders, and it has also been claimed that its administration prevents some diseases (1–3). In particular, GLA has been shown to improve skin function in elderly people (4), attenuate body fat accumulation (5), and have a selective tumoricidal action over human gliomas (6,7).

GLA is synthesized from linoleic acid ( $\Delta 9,12$ -18:2, LA) by the activity of the enzyme  $\Delta 6$ -desaturase (D6DES) that introduces a new double bond into the  $\Delta 6$  carbon (8). The same

enzyme is able to introduce a  $\Delta 6$  desaturation into  $\alpha$ -linolenic acid ( $\Delta 9,12,15$ -18:3, ALA), producing octadecatetraenoic acid ( $\Delta 6,9,12,15$ -18:4, OTA) (9). Although present in humans, D6DES activity is apparently too low to provide enough GLA to satisfy body needs. Therefore, GLA has interest as an essential nutrient and as a component of some pharmaceutical products and functional foods.

GLA is currently marketed from seeds of a few plant species, e.g., evening primrose (*Oenothera biennis*), common borage (*Borago officinalis*), and black currant (*Ribes nigrum*). However, current sources have been recognized as inadequate for the continuous demand of an expanding market (10–12), since they are not oil-rich plants, and their agronomic practices are not as well developed as for other crops. Therefore, attempts have been made to find alternative sources (13). In this sense, GLA production from genetically modified organisms, including oilseed plants, has been suggested as a possible alternative (13–16). Initial attempts at overexpression of D6DES genes in heterologous systems have emphasized the importance of the gene origin and host organism. For instance, functional expression of the D6DES gene from a cyanobacterium was very inefficient when performed in a higher plant, tobacco (15), whereas performance of the *Borago* D6DES was much better in the same host plant (17). Therefore, D6DES genes from higher plants seem to be a better choice (instead of those from fungi or cyanobacteria) when used as transgenes in oilseed crops.

A group of endemic Macaronesian plants from the genus *Echium* (Boraginaceae) were recently identified as among the richest sources of GLA found in nature (18). Among them, *E. gentianoides* showed an exceptional GLA content in the seed, 28% of total FA (19), which makes this species an interesting source of the D6DES gene. However, *E. gentianoides* is a perennial shrub whose flowering takes about 2–3 yr in its natural habitat, a major problem when a study of gene expression in floral tissues and developing fruits is intended. To overcome this problem, a closely related species, *E. pitardii*, was also used in our studies to perform a molecular characterization of the D6DES gene. Although somewhat less efficient in GLA seed accumulation (22%), *E. pitardii* has the advantage of an annual life cycle that is completed in about 4 mon in the laboratory.

\*To whom correspondence should be addressed at Universidad de Almería, Departamento de Biología Aplicada, 04120 Almería, Spain. E-mail: dlopez@ual.es

Abbreviations: ALA,  $\alpha$ -linolenic acid; CaMV, cauliflower mosaic virus; DIG, digoxigenin; GAPDH, glyceraldehyde-3-phosphate dehydrogenase; IPCR, inverse polymerase chain reaction; LA, linoleic acid; MS, mass spectrometry; OTA, octadecatetraenoic acid; PCR, polymerase chain reaction.

In this work, we obtained the genomic sequences for the  $\Delta 6$ -desaturase genes of *E. gentianoides* (*EGD6DES*) and *E. pitardii* (*EPD6DES*). A molecular characterization of these genes, including the expression pattern analysis, was performed. Functionality of the putative *D6DES* product was proved by heterologous expression of *EGD6DES* in tobacco *calli* and in the yeast *Saccharomyces cerevisiae*. In transgenic tobacco *calli* the synthesis of GLA and OTA was achieved from the endogenous substrates LA and ALA, respectively, whereas GLA production in the yeast took place from exogenously incorporated LA. These results pave the way for the generation of oilseed plants overexpressing the *EGD6DES* gene.

## MATERIALS AND METHODS

**Plant material.** Seeds from *E. gentianoides* Webb ex Coincy and *E. pitardii* A. Chev. were collected in their natural habitats at the Macaronesian island of La Palma (Canary Islands) during the summers of 1999 and 2000. Tobacco plants, *Nicotiana tabacum* var. Wisconsin 38, were used for transformation experiments. All plants were grown at 25°C under controlled conditions in growth cabinets with a 16 h light/8 h dark photoperiod.

**Microbial strains.** *Agrobacterium tumefaciens* LBA4404 (20) was used as a vector for plant transformation. The *S. cerevisiae* strain used in this work was Sc340: *MATa ade1 leu2 ura3 his3::P<sub>GAL10</sub>-GAL4-URA3* (21,22). Cloning procedures in *Escherichia coli* were carried out with strain DH5 $\alpha$  as the host.

**Cloning and sequence analysis of the *D6DES* genes.** Cloning of the *D6DES* gene from *EGD6DES* was achieved by polymerase chain reaction (PCR) amplification of a partial sequence, followed by bi-directional genomic walking through inverse PCR (IPCR). Initially, a 550 bp PCR fragment corresponding to amino acid positions 187 to 369 (Fig. 1) was obtained by using the degenerate oligonucleotides BO-1 [5'-AT(A/C)AG(T/C)AT(T/C)GGTTGGTG-GAA(A/G)TGG-3'] and BO-2 [5'-AATCCACC(A/G)TG-(A/G)AACCA(A/G)TCCAT-3'] as primers and genomic DNA from *E. gentianoides* as a template, following standard PCR protocols. The product was cloned into the pGEM-T-Easy® vector (Promega, Madison, WI) and the sequences for several clones were obtained from both strands by the dideoxy method using a PerkinElmer (Foster City, CA) ABI-377 DNA automated sequencer. Two sequences were obtained that were identified as corresponding to the putative  $\Delta 6$ -desaturase and the highly related  $\Delta 8$ -desaturase, based on the comparison to the orthologous genes from *B. officinalis*. From the *D6DES* partial sequence, two nested upstream primers, GE-1 (5'-GAGGTGAGCGAGCTAAACA ACTTG-3') and GE-2 (5'-AACATATTGACCCTAGCGGAACA-3'), and two nested downstream primers, GE-3 (5'-CTCGGTGACTGGAATGCAACAAG-3') and GE-4 (5'-CGGCGAGT-GTTTATGTTGGTCAG-3'), were designed to perform the IPCR essentially as described (23). The DNA was digested with one of the enzymes *Hind*III or *Ssp*I and subjected to circularization followed by two nested rounds of PCR amplification. Suitable fragments were analyzed and sequenced as de-

scribed before. With this approach, we obtained about 2.5 kbp of genomic sequence, comprising 120 bp upstream of the initiation ATG and some 1.1 kbp downstream of the stop codon.

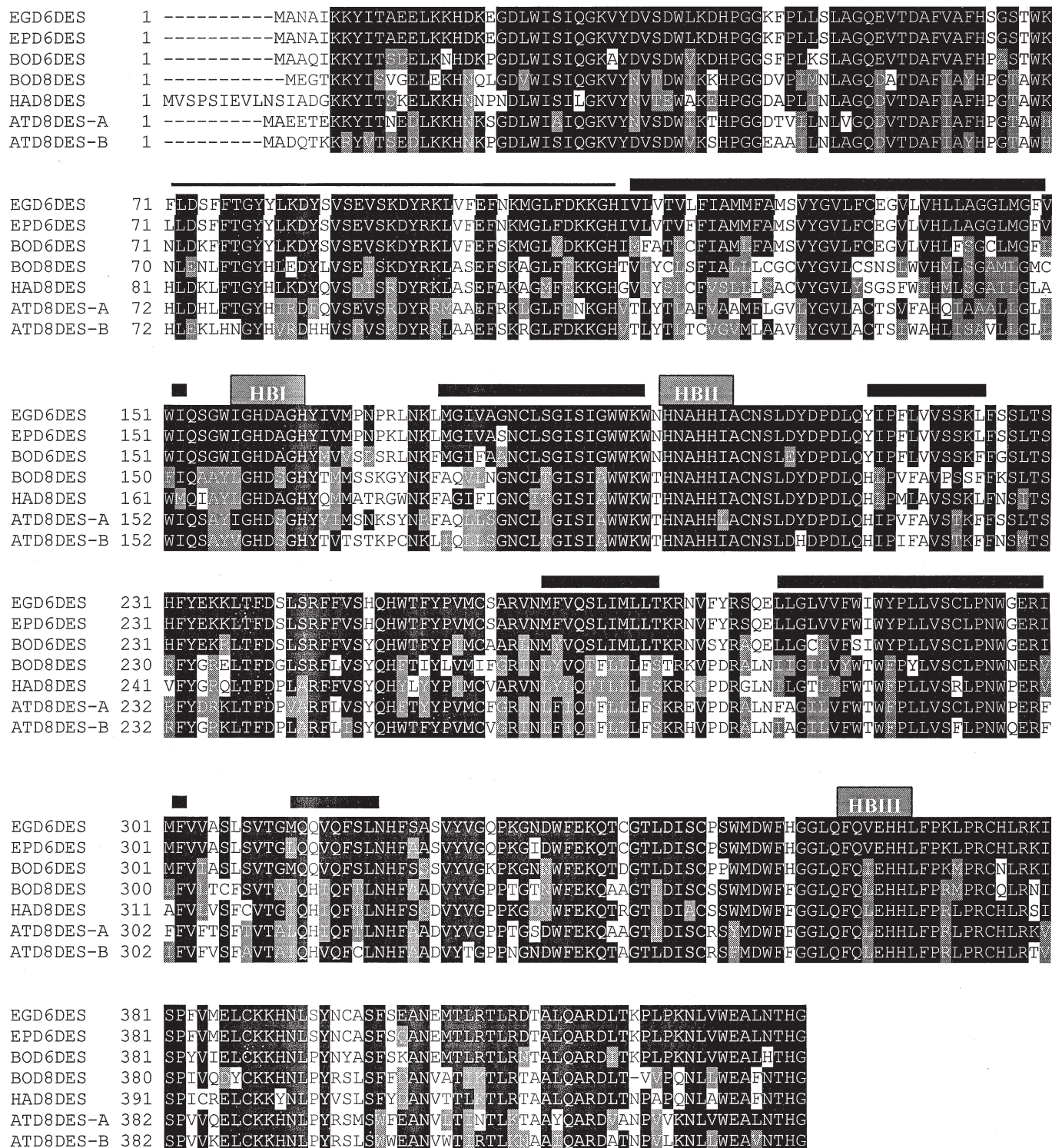
A genomic DNA fragment containing the whole coding sequence (besides 36 and 97 bp of the 5'- and 3'-untranslated regions, respectively) for *EGD6DES* was obtained by PCR amplification using suitable upstream GE-5 (5'-TGGATCACCAAA-CACAGTAGTAAG-3') and downstream GE-6 (5'-TCCAACA-AGTAGAACCAATGCAAG-3') primers and a reading-proof polymerase (AccuTaq®, Sigma). The fragment was cloned and sequenced as indicated. Similarly, a whole genomic clone for the *D6DES* gene from *EPD6DES* was obtained by PCR on genomic DNA, using the same GE-5 and GE-6 flanking primers.

**Cladistic analysis.** Alignment of amino acid sequences for desaturase proteins was done using the program Clustal X v.1.7 (24) (European Molecular Biology Laboratory, Heidelberg, Germany) with the default settings. For the selected sequences in Figure 1, the alignment was visualized using the Boxshade v. 3.21 program (European Molecular Biology Laboratory). The whole alignment output was used to generate a phylogenetic tree (Fig. 2) based on the neighbor-joining algorithm of Saitou and Nei (25) with the following parameters: The whole amino acid sequence of the protein was considered, positions with gaps were not excluded, and distances were not corrected for multiple substitutions. Bootstrap values over 1,000 replicates were also calculated using the same program. The resulting phenogram was drawn using the program TreeView (University of Glasgow, Glasgow, United Kingdom) (26).

**Southern and Northern blot analysis.** Genomic DNA was isolated from *Echium* seedlings by a cetyltrimethylammonium bromide-based extraction procedure (27). DNA (about 3  $\mu$ g) was restricted with the appropriate restriction enzymes, separated on a 0.8% agarose gel, and transferred by capillarity onto Hybond® N+ nylon membranes (Amersham, Buckinghamshire, United Kingdom). Filters were fixed by baking, prehybridized at 42°C for 5 h in the 50% formamide/High SDS buffer recommended by the digoxigenin (DIG) manufacturer (Boehringer-Mannheim, Mannheim, Germany), and hybridized at the same temperature and same buffer solution (stringent conditions), containing the DIG-labeled *EGD6DES* specific probe at 25 ng/mL. High stringency washes were performed twice at 65°C during 15 min in buffer containing 0.5  $\times$  SSC (1  $\times$  SSC = 150 mM NaCl, 15 mM sodium citrate, pH 7.0) and 0.1% SDS, and the luminogenic substrate CSPD® (Boehringer-Mannheim) was used for detection following the instructions provided with the DIG detection kit. Images were obtained by exposure of Biomax ML® films (Kodak, Rochester, NY) for 10–25 min and final developing by standard procedures. The *EGD6DES* probe was obtained by random primed labeling from a PCR fragment (Fig. 3) generated with primers GE-4 and GE-6, corresponding to the last 115 amino acids of the protein and about 100 bp of the 3'-untranslated region. Probe specificity was previously confirmed by the absence of cross-hybridization under the same conditions with a highly homologous  $\Delta 8$ -desaturase fragment from *Echium* (not shown).



Cytochrome b<sub>5</sub>



**FIG. 1.** Sequence comparison between *Echium* D6DES and related D6DES and D8DES proteins from higher plants. The amino acid sequences of  $\Delta 6$ -desaturases of *E. gentianoides* (EGD6DES, acc. no. AY055117), *E. pitardii* (EPD6DES, AY055118), *Borago officinalis* (BOD6DES, U79010), and  $\Delta 8$ -desaturases from *B. officinalis* (BOD8DES, AF133728), *Helianthus annuus* (HAD8DES, S68358), and *Arabidopsis thaliana* (ATD8DES-A, AAC62885.1; and ATD8DES-B, CAB71088.1) are aligned by using the Clustal X (v1.7) software (European Molecular Biology Laboratory, Heidelberg, Germany). The Boxshade program (European Molecular Biology Laboratory) is used to highlight the homology between protein sequences. Shading is applied when there is agreement for a fraction of sequences above 0.5. Amino acids identical to EGD6DES are enclosed in black boxes and similar residues are in grey boxes. The N-terminal cytochrome-b<sub>5</sub> domain, as well as the position of the three characteristic histidine boxes (HBI to HBIII), are also indicated. Putative transmembrane regions of EPD6DES predicted by the TMPRED software (48) are marked with thick black bars.

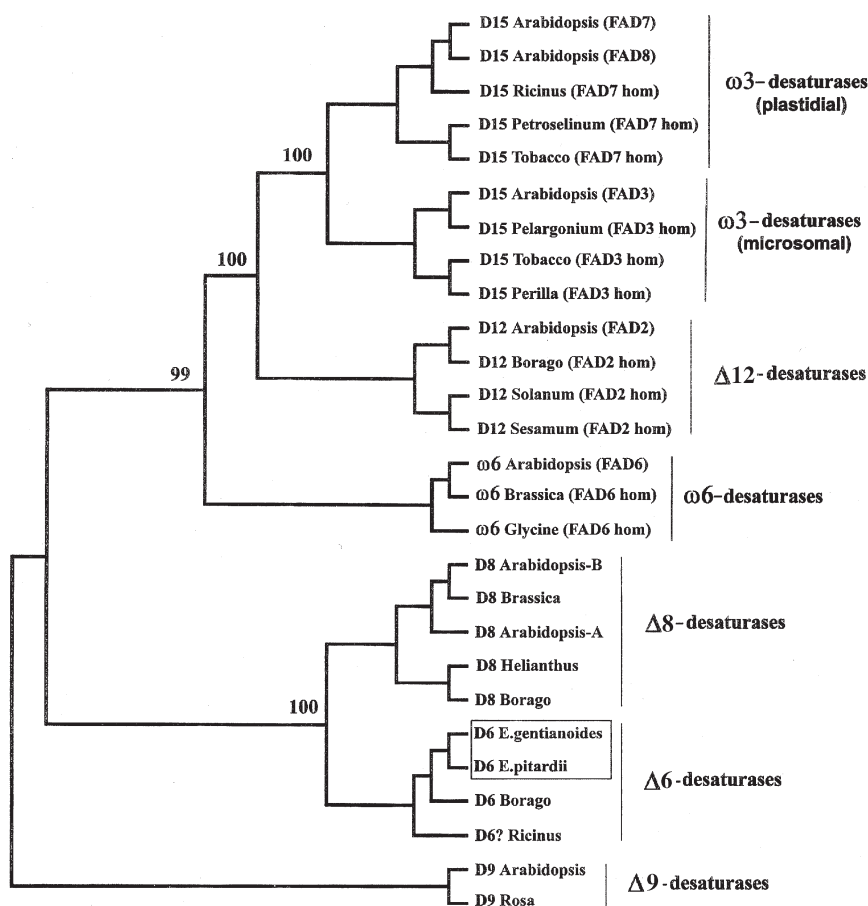


FIG. 2. Neighbor-joining tree illustrating relationships among *Echium* D6DES proteins and other desaturases from dicot species. Amino acid sequences were analyzed as described in the Materials and Methods section. EGD6DES and EPD6DES proteins reported in this paper are indicated enclosed by a square. The tree was rooted using  $\Delta 9$ -desaturases as the outgroup. Bootstrap values are expressed as percentages (over 1000 replicates) at relevant nodes.

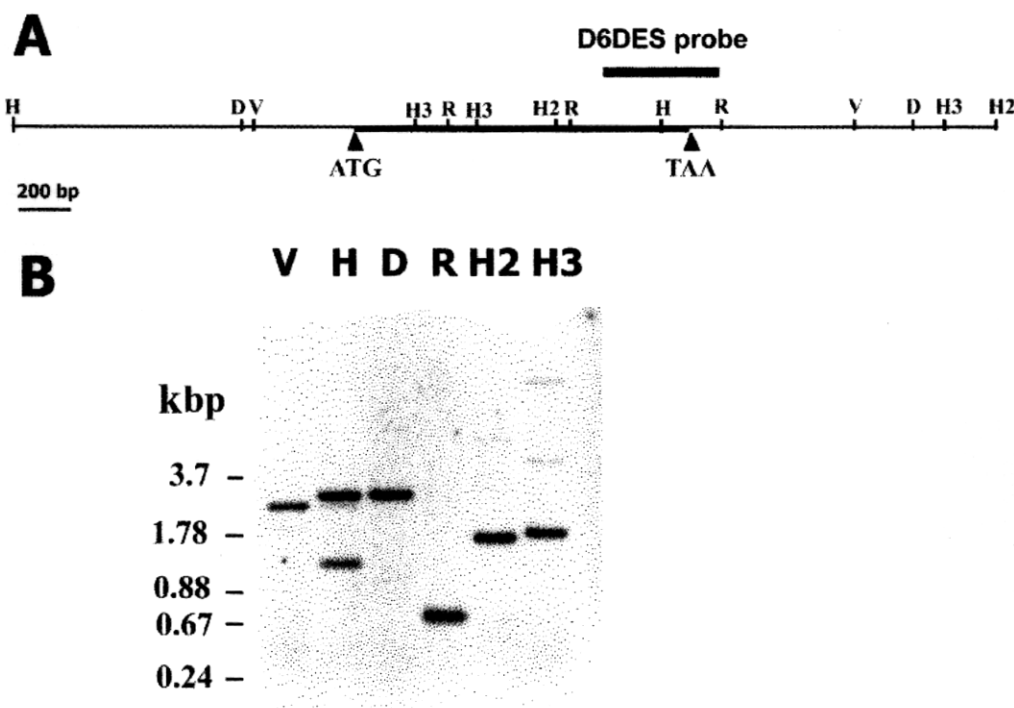
Total RNA was extracted from different tissues of *E. pitardii* plants grown to maturity following the method of Chang *et al.* (28). About 5  $\mu$ g per lane of total RNA was loaded onto an agarose/formaldehyde gel, electrophoretically separated, and transferred to Hybond-N+ membranes. Filters were hybridized at 50°C (stringent conditions) as described for Southern analysis using the same *EGD6DES* specific probe. Stringent washes, accomplished at 68°C, and detection of the DIG labeled probe were as indicated before. As a control, the filters were rehybridized with a 900 bp cDNA probe from tobacco, which encodes part of the cytosolic glyceraldehyde-3-phosphate dehydrogenase gene (29). In this case, hybridization was done in the same conditions, but the final washes were performed at 65°C.

**Tobacco transformation and generation of calli.** A full DNA genomic fragment encoding the whole EGD6DES protein and part of the 5' and 3'-untranslated regions was obtained by PCR as indicated before. The fragment was sequenced to check for the absence of PCR mutations and cloned in the sense orientation at the polylinker of the transcriptional fusion vector pJIT60 (30) between a 35S CaMV promoter containing a duplicate enhancer sequence and

appropriate termination-polyadenylation signals. The *KpnI-XhoI* "cassette" containing the transcriptional fusion was liberated and cloned into the pBIN19 binary vector (31), and the resulting construct was used to transform the *A. tumefaciens* LBA4404 strain. Tobacco leaf disc transformation was achieved essentially as described by Horsch *et al.* (32). The *calli* were obtained by incubation of tobacco leaf disks in Murashige-Skoog medium containing 30 g/L glucose, 0.1 mg/L 6-benzylamino-purine, 1 mg/L  $\alpha$ -naphthalene acetic acid, 100 mg/L kanamycin, 500 mg/L cefotaxime, and 1 mL/L vitamins (stock solution from Sigma). Incubation was performed in petri dishes kept in growth chambers at 25°C under a 12L/12D photoperiod regime.

**Yeast transformation.** *Saccharomyces cerevisiae* Sc340 strain was transformed by the procedure of Ito *et al.* (33) with plasmid pYexD6D. This plasmid was constructed by cloning the *E. gentianoides* D6DES gene under control of the *CYC-GAL* hybrid promoter of expression vector pEMBLyex4 (34). Transformant colonies were selected by complementation of the *leu2d* marker. Yeast-transformed clones were grown for about 48 h at 30°C in standard minimal medium supplemented with the auxotrophic requirement of the strain. The





**FIG. 3.** Genomic structure of the *D6DES* gene of *Echium gentianoides*. (A) Restriction map of the *EGD6DES* genomic sequence reconstructed by inverse polymerase chain reaction. Enzyme symbols are stated below. Position of the *EGD6DES*-specific probe is indicated by a bar. (B) Southern blot analysis of *EGD6DES* in *E. gentianoides*. DNA was digested with *Hind*III (H3), *Hind*II (H2), *Rsa*I (R), *Dra*I (D), *Hae*III (H), or *Vsp*I (V) restriction endonucleases, and hybridization was performed under stringent conditions, as described in the Materials and Methods section, using the *EGD6DES*-specific probe (Fig. 3B). Size markers (kbp) positions are indicated.

cells were collected by centrifugation and transferred to a medium suited for the induction of the *GAL* promoter, which contained 1% yeast extract, 2% peptone, 0.5% glucose, and 1% galactose. The induction medium also contained 25  $\mu$ M of the GLA precursor LA (final concentration) prepared in Tergitol (1% final concentration). The transformant cells were incubated in the induction medium at 20°C and samples were taken for analysis after 24 and 48 h.

**FA analysis.** The biomass (tobacco *calli* or yeast) was previously lyophilized. Simultaneous lipid extraction and generation of FAME were performed as described elsewhere (35). For some experiments, fresh tobacco *calli* were directly analyzed following the same method. FA composition was determined by GLC as in (35). GC-MS analysis was carried out using a Varian (Palo Alto, CA) 3400 gas chromatograph-Saturn 3 ion trap mass spectrometer operating at an ionization voltage of 70 eV with a scan range of 60–650 Da. The mass spectra of the relevant peaks were compared to those of standards processed by the same equipment.

## RESULTS

**Cloning of genes encoding the  $\Delta$ 6-desaturase from *Echium* plants.** The complete genomic sequence for the *D6DES* gene of *E. gentianoides* was obtained by PCR amplification of a partial sequence fragment, followed by walking in both directions by IPCR (see the Materials and Methods section).

Degenerated primers corresponding to highly conserved motifs (ISIGWWKW, and MDWFHGG) of  $\Delta$ 6- and  $\Delta$ 8-desaturases (Fig. 1) were used to amplify from the genomic DNA of *E. gentianoides* a 550 bp PCR fragment that was subsequently cloned in a T-vector. Several clones were sequenced, allowing the identification of putative  $\Delta$ 6- and  $\Delta$ 8-desaturase sequences based on the comparison to the *Borago* orthologues. From the partial *D6DES* sequence, gene-specific primers were designed that allowed the obtaining of several IPCR clones and the assemblage of a 2.5 kbp genomic sequence containing the whole coding region. Finally, genomic fragments comprising the coding sequence of genes from *EGD6DES* and *EPD6DES* were obtained by PCR amplification on genomic DNA using flanking primers derived from the *E. gentianoides* sequence. None of these genes contained intervening sequences showing 98% of identity at the DNA level. The two genes presented very similar open reading frames encoding proteins of the same length, 438 amino acids (Fig. 1). The *Echium* proteins shared a high similarity, with only seven amino acid changes (three of them conservative). Both proteins are highly homologous to  $\Delta$ 6- and  $\Delta$ 8-plant desaturases (Fig. 1). They exhibit the prototypical cytochrome  $b_5$  domain at the N-terminus, as reported for other  $\Delta$ 6- and  $\Delta$ 8-desaturases (36). In addition, three Histidine boxes, the third one conforming to the characteristic consensus QXXHH of these desaturases, are found at the corresponding positions. Putative trans-membrane regions are predicted to occur

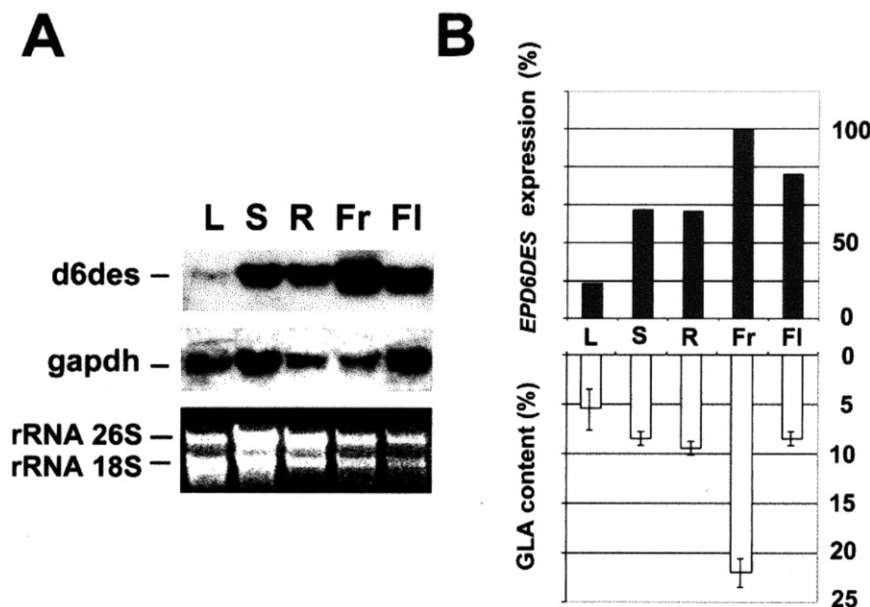
(Fig. 1) according to their location as membrane-bound proteins. Protein BLAST search revealed the highest homology to D6DES of *B. officinalis*, sharing 85% of identical residues with EGD6DES. Clustering analysis including representative members of the different desaturase classes shows a clear grouping of the two *Echium* proteins with the D6DES of *Borago* and a still uncharacterized protein from *Ricinus* (acc. no. AF005096). These proteins make up a separate clade (supported by a 100% bootstrap value) to that of the highly related  $\Delta 8$ -desaturases. This provides evidence for the identification of the *Echium* gene products as  $\Delta 6$ -desaturases.

**Genomic organization and expression analysis of the *Echium*  $\Delta 6$ -desaturase.** Genomic structure and organization of the *D6DES* gene in *Echium* was investigated by Southern blot analysis. Genomic DNA from *E. gentianoides* was digested with six different restriction enzymes followed by hybridization with a *EGD6DES* specific probe (see the Materials and Methods section) under stringent conditions. Single hybridization bands were obtained with five enzymes that do not cut within the probe (Fig. 3B), thus indicating that the *EGD6DES* gene is represented in the haploid genome by a single copy. Moreover, sizes for the hybridization fragments comprising the coding region are in agreement with the genomic sequence assembled by IPCR walking (Fig. 3A), thus confirming that the *D6DES* genes do not possess introns.

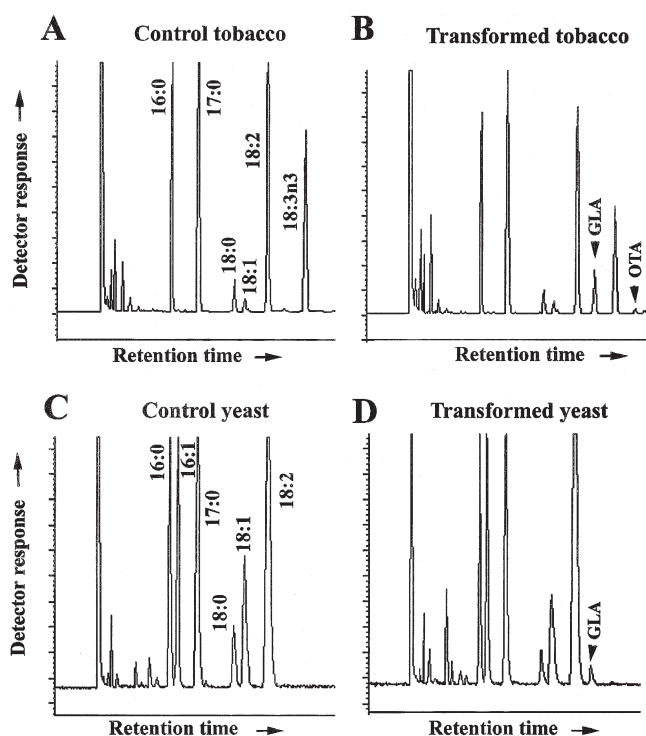
Similar results were obtained from Southern analysis in *E. pitardii* (results not shown).

The expression pattern of the *D6DES* was analyzed by Northern blot on total RNA from different tissues of *E. pitardii*. Hybridization with the *EGD6DES* specific probe under stringent conditions resulted in relatively strong hybridization signals for samples corresponding to stems, roots, flowers, and developing fruits, this latter tissue giving the highest intensity. Conversely, the *EPD6DES* RNA was found at a comparative low level in the leaves (Fig. 4A). In the same experiment expression of the housekeeping gene *GAPDH* served as a positive hybridization control. The relative transcript levels (normalized in base to RNA loading) of *EPD6DES* showed a good correlation with the GLA content determined for the different tissues (Fig. 4B). This might be an indication that in *Echium* plants the GLA content in a given tissue might be primarily governed by the steady-state level of the *D6DES* mRNA.

**Functional analysis of the *Echium*  $\Delta 6$ -desaturase by heterologous expression in tobacco calli.** In order to demonstrate that the *Echium* genes actually encode enzymes with a  $\Delta 6$ -desaturase activity, we have introduced *via Agrobacterium* the complete *EGD6DES* gene under the control of a constitutive 35S CaMV double promoter in tobacco, a plant that does not accumulate GLA. The phospholipid-bound LA, which is



**FIG. 4.** Expression analysis of the *EPD6DES* gene. (A) Northern experiment of the *D6DES* of *Echium pitardii*. Equivalent amounts of total RNA from leaves (L), stems (S), roots (R), developing fruits (Fr), and developing flowers (F) were hybridized with the *EGD6DES*-specific probe (Fig. 3A) under high-stringency conditions, as indicated in the Materials and Methods section. The expression pattern of the cytosolic glyceraldehyde-3-phosphate dehydrogenase (*GAPDH*), a constitutive gene used as a control, is shown below beside the ethidium bromide staining of the gel. The *GAPDH* probe was obtained from tobacco. (B) Comparison of the GLA content and *D6DES* expression in different tissues of *E. pitardii*. Relative *D6DES* expression (above), normalized in base to RNA loading, is expressed as a percentage over the maximum level attained in developing fruits. GLA content is shown (below) as a percentage of total FA. These data were determined in triplicate as described in the Materials and Methods section, and the mean values beside their SE intervals are indicated in the figure.



**FIG. 5.** Identification by GC of GLA in tobacco and yeast transformed with the *Echium D6DES* gene. FAME of total lipids of tobacco *calli* (A,B) and *Saccharomyces cerevisiae* (sc340) grown under inductive conditions in the presence of the linolenic acid substrate (C,D). (A) Control tobacco *calli* transformed with the pBIN19 vector alone. (B) Tobacco *calli* transformed with the *EGD6DES* gene under control of the CaMV constitutive promoter. (C) Control yeast transformed with the pEMBLyex4 vector alone. (D) Yeast transformed with the *EGD6DES* gene under control of the  $P_{CYC-GAL}$  inducible promoter. Positions of the additional peaks (GLA and OTA) are indicated by arrows. Heptadecanoic acid (17:0) is included in the analysis as an internal standard. OTA, octadecatetraenoic acid.

the main substrate for D6DES, is present at a high level in tobacco tissues. Therefore, synthesis of GLA was expected in the transformed plants. To speed-up the assay, *calli* derived from leaf discs were analyzed for FA composition. As a negative control tobacco *calli* transformed with the pBIN19 vector alone was used. A total of 22 *calli* samples representing individual transformation events were screened for both the control and 35S::*EGD6DES* constructs. In all transgenic samples harboring *EGD6DES*, the presence of an additional peak with a retention time corresponding to GLA was apparent (Fig. 5B), as compared to the control (Fig. 5A). Further identification of this compound as GLA was achieved by GC-MS using the pure GLA-methyl ester as a standard (data not shown). The mass spectra of the unknown and GLA standard were identical. In this experiment, GLA was found in variable amounts ranging in the different samples from 1.9 to 11.8% on total FA (Table 1). This variation should be attributed to positional effects of the T-DNA insertion in each individual *callus*. The presence of a second additional peak corresponding to the OTA was also observed in a number of transgenic samples (Figs. 5A and 5B). Identification by GC-MS of the new peak was

**TABLE 1**  
FA Composition of Total Lipids from Tobacco *Calli* Transformed with the *EGD6DES* gene

FA <sup>b</sup>	Control <sup>a</sup>		35S:: <i>EGD6DES</i>	
	Range <sup>c</sup>	Mean <sup>c</sup> ± SEM	Range <sup>c</sup>	Mean <sup>c</sup> ± SEM
16:0	18.0–19.8	19.2 ± 0.06	18.3–20.6	19.2 ± 0.08
18:0	3.2–3.7	3.4 ± 0.02	3.0–4.0	3.3 ± 0.03
Δ9-18:1	0.8–2.0	1.3 ± 0.03	1.3–2.4	1.8 ± 0.03
LA	35.3–40.6	37.9 ± 0.16	31.6–41.6	35.3 ± 0.31
GLA	—	—	1.9–11.8	6.5 ± 0.27
ALA	17.8–25.6	22.4 ± 0.24	16.4–23.4	18.6 ± 0.21
OTA	—	—	0.0–1.6	0.5 ± 0.06
Total FA	1.3–1.5	1.4 ± 0.01	1.2–1.8	1.5 ± 0.02

<sup>a</sup>Control experiment correspond to *calli* transformed with the empty vector pBIN19.

<sup>b</sup>Contributions of individual FA are expressed as percentage of total FA. Total FA are calculated as percentage of the dry callus weight.

<sup>c</sup>The results are from the analysis of 10 individual *calli*. LA, linoleic acid; ALA,  $\alpha$ -linolenic acid; OTA, octadecatetraenoic acid.

achieved by comparison with the OTA standard (data not shown). Again this compound was expected to be produced by the D6DES activity using the endogenous ALA as a substrate. It is noteworthy that, when detected, the amount of OTA was consistently lower than GLA (Table 1).

*Functional expression of the Δ6-desaturase from Echium in the yeast S. cerevisiae.* The complete coding region of *EGD6DES* (see the Materials and Methods section) was cloned in the yeast expression vector pEMBLyex4 under control of the  $P_{CYC-GAL}$  promoter inducible by galactose. The resulting plasmid (pYexD6D) was used to transform *S. cerevisiae* strain Sc340. This strain carries a construction in which the *GAL4* gene under control of the  $P_{GAL10}$  promoter is located at the site that interrupts the *HIS3* gene. *GAL4* encoded an enhancer protein that triggers the expression of genes activated by galactose. The *GAL4* protein is present in the cell in very low amounts. Therefore, the Sc340 construction amplifies the expression of genes placed under control of *GAL* promoters (21,22). The transformed yeast strains were cultured under inductive conditions in the presence of LA provided as exogenous substrate. This FA is not synthesized by the yeast, but it is efficiently incorporated, reaching about 70% of the total FA in the cell under our experimental conditions. Extracts of yeast cells transformed with the *EGD6DES* gene showed a peak not present in the extracts of control cultures transformed with the vector alone (Figs. 5C and 5D). The retention time in GC experiments coincides with that of GLA, and the identity of the compound was confirmed by GC-MS analysis (not shown). In this case, GLA accumulation reached a maximum of 1.5% of total FA.

## DISCUSSION

*Functional characterization of the Echium D6DES gene.* Here we provide evidence for the identification of the gene products *EGD6DES* and *EPD6DES* as functional  $\Delta 6$ -desaturases. First, a high similarity of their protein sequences was found with other previously characterized D6DES, mainly *B.*



*officinalis*, a species belonging to the same family of plants. However, as it has been pointed out (11), sequence similarity among desaturases should be considered cautiously before assigning a particular function to an unknown protein. For example, a sunflower desaturase, showing a high homology to the *Borago* D6DES (BOD6DES), was identified as a  $\Delta 8$ -desaturase active on sphingolipids rather than on glycerolipids (37). This is further supported by directed mutagenesis experiments in which few amino acid changes in a desaturase resulted in drastic alterations in the substrate specificity regarding acyl chain length and desaturation position (38). Nevertheless, clustering analysis of desaturases from higher plants separates with a high reliability the group integrated by BOD6DES and the *Echium* desaturases from that of the  $\Delta 8$ -desaturases, thus indicating that the *Echium* products are likely to be  $\Delta 6$ -desaturases.

To obtain a direct proof for the activity of the putative *Echium* desaturases we overexpressed the *EGD6DES* gene in tobacco *calli*. FA composition of these undifferentiated cells is similar to that of nonphotosynthetic tissues, such as the root, where a higher amount of LA (45%) relative to ALA (26%) is found (39). These compounds were previously shown to act as substrates of D6DES enzymes, giving rise to GLA and OTA, respectively (9,40). Both products were detected in transformed *calli*, thus demonstrating the ability of the *Echium* enzyme to desaturate the  $\Delta 6$  position of FA containing previous double bonds at  $\Delta 9$  and  $\Delta 12$  carbons. These results also indicate that the activity of a single D6DES enzyme is enough to synthesize both GLA and OTA.

The activity of EGD6DES has been further analyzed by heterologous expression in a yeast system. As expected, desaturation of exogenously provided LA was observed in transformed cells. A similar experiment has been carried out with the D6DES from the fungus *Mortierella alpina* (13). In this case  $\Delta 6$ -desaturation of the endogenous 16:1n-7 and 18:1n-9 was observed in transformed yeast that were not supplemented with LA. Accumulation of 16:2n-7 has also been reported by yeast expression of the *Borago* D6DES (41). However, in our experiments we did not detect the accumulation of such compounds. This discrepancy could be attributed to differences in the experimental conditions, or it might reflect a different behavior of the D6DES from those organisms.

*Gene structure and expression analysis of the Echium D6DES gene.* We have shown that the *D6DES* of *Echium* do not contain introns. The same seems to be true for the *Borago D6DES* and the *D8DES* from *Echium* and *Borago*, since partial sequences obtained by genomic PCR also present continuous open reading frames (results not shown). Moreover, the whole coding sequences of the two *D8DES* genes (F2A19.180; At2g46210) present in the *Arabidopsis* genome are also contained within single exons. This is in contrast to the gene structure of D6DES from other organisms such as the moss *Physcomitrella* (42), the worm *Caenorhabditis* (43), and *Homo* (44), where a number of introns interrupt both the desaturase and cytochrome  $b_5$  domains. Although we cannot exclude the existence in *Echium* of an additional version of

the *D6DES* gene containing introns, this is not supported by Southern analyses since they do not reveal the presence of further loci. It seems likely therefore that loss of introns of the *D6DES* gene may have occurred during evolution of higher plants, followed, at least in Boraginaceae species, by high divergence or loss of the interrupted gene. Loss of introns has been well documented in a number of instances, with retroposition as the most direct mechanism (revised in 45). The fact that *D8DES* genes are also continuous suggests that the retroposition event took place before the duplication and further divergence of the *D6DES/D8DES* lineages.

We have also studied the expression of the *D6DES* gene in different tissues of *E. pitardii*. High relative levels of D6DES transcript is found in all tissues of the plant except in leaves of mature plants, where it is barely detectable. This correlates with the accumulation of GLA in those tissues, as the synthesis of this compound in the mature leaves is about five times below that of the developing fruits. The lower GLA level in the leaves has also been reported in other plants (46,47), and competition between the D6DES and the  $\omega 3$ -desaturase for the same substrate (LA) to give either GLA or ALA, respectively, was suggested as the cause (9). It is likely that this competition has its origin at the transcriptional level. This correlation suggests that, at least in *Echium*, the steady-state level of the D6DES transcript might be the limiting factor in the accumulation of GLA in the different tissues.

## ACKNOWLEDGMENTS

We are indebted to Dr. Edgar B. Cahoon for helpful suggestions about this work. We are also grateful to Drs. Antonio Valverde and Amadeo Rodriguez for their help in the GC-MS analyses and to Jerónimo Pérez and Juan Carlos Gázquez for providing facilities and technical assistance in greenhouse plant culture. This work was supported by an UAL-CAJAMAR research project and by the Plan Andaluz de Investigación (PAI-III, CVI-279).

## REFERENCES

1. Gunstone, F.D. (1992)  $\gamma$ -Linolenic Acid—Occurrence and Physical and Chemical Properties, *Prog. Lipid Res.* 31, 145–161.
2. Gunstone, F.D. (1998) Movements Towards Tailor-Made Fats, *Prog. Lipid Res.* 37, 277–305.
3. Horrobin, D.F. (1992) Nutritional and Medical Importance of  $\gamma$ -Linolenic Acid, *Prog. Lipid Res.* 31, 163–194.
4. Brosche, T., and Platt, D. (2000) Effect of Borage Oil Consumption on Fatty Acid Metabolism, Transepidermal Water Loss and Skin Parameters in Elderly People, *Arch. Gerontol. Geriatr.* 30, 139–150.
5. Takahashi, Y., Ide, T., and Fujita, H. (2000) Dietary  $\gamma$ -Linolenic Acid in the Form of Borage Oil Causes Less Body Fat Accumulation Accompanying an Increase in Uncoupling Protein 1 mRNA Level in Brown Adipose Tissue, *Comp. Biochem. Physiol.* 127, 213–222.
6. Das, U.N., Prasad, V.V.S.K., and Reddy, D.R. (1995) Local Application of  $\gamma$ -Linolenic Acid in the Treatment of Human Gliomas, *Cancer Lett.* 94, 147–155.
7. Preuss, M., Girnun, G.D., Darby, C.J., Khoo, N., Spector, A.A., and Robbins, M.E. (2000) Role of Antioxidant Enzyme Expression in the Selective Cytotoxic Response of Glioma Cell to  $\gamma$ -Linolenic Acid Supplementation, *Free Radic. Biol. Med.* 28, 1143–1156.



8. Harwood, J.L. (1996) Recent Advances in the Biosynthesis of Plant Fatty Acids, *Biochim. Biophys. Acta* 1301, 7–56.
9. Griffiths, G., Brechany, E.Y., Jackson, F.M., Christie, W.W., Stymne, S., and Stobart, K. (1996) Distribution and Biosynthesis of Stearidonic Acid in Leaves of *Borago officinalis*, *Phytochemistry* 43, 381–386.
10. Gill, I., and Valivety, R. (1997) Polyunsaturated Fatty Acids, Part 1: Occurrence, Biological Activities and Applications, *Trends Biotechnol.* 15, 401–409.
11. Napier, J.A., Michaelson, L.V., and Stobart, A.K. (1999) Plant Desaturases: Harvesting the Fat of the Land, *Curr. Opin. Plant Biol.* 2, 123–127.
12. Sakuradani, E., Kobayashi, M., and Shimizu, S. (1999)  $\Delta^6$ -Fatty Acid Desaturase From an Arachidonic Acid-Producing *Mortierella* Fungus. Gene Cloning and Its Heterologous Expression in a Fungus, *Aspergillus*, *Gene* 238, 445–453.
13. Huang, Y.-S., Chaudhary, S., Thurmond, J.M., Bobik, E.G., Yuan, L., Chan, G.M., Kirchner, S.J., Mukerji, P., and Knutzon, D.S. (1999) Cloning of  $\Delta^{12}$ - and  $\Delta^6$ -Desaturases from *Mortierella alpina* and Recombinant Production of  $\gamma$ -Linolenic Acid in *Saccharomyces cerevisiae*, *Lipids* 34, 649–659.
14. Murphy, D.J. (1995) The Use of Conventional and Molecular Genetics to Produce New Diversity in Seed Oil Composition for the Use of Plant Breeders—Progress, Problems and Future Prospects, *Euphytica* 85, 433–440.
15. Reddy, A.S., and Thomas, T.L. (1996) Expression of a Cyanobacterial  $\Delta^6$ -Desaturase Gene Results in  $\gamma$ -Linolenic Acid Production in Transgenic Plants, *Nat. Biotechnol.* 14, 639–642.
16. López Alonso, D., and García Maroto, F. (2000) Plants as ‘Chemical Factories’ for the Production of Polyunsaturated Fatty Acids, *Biotechnol. Adv.* 18, 481–497.
17. Sayanova, O., Smith, M.A., Lapinskas, P., Stobart, A.K., Dobson, G., Christie, W.W., Shewry, P.R., and Napier, J.A. (1997) Expression of a Borage Desaturase cDNA Containing an N-Terminal Cytochrome  $b_5$  Domain Results in the Accumulation of High Levels of  $\Delta^6$ -Desaturated Fatty Acids in Transgenic Tobacco, *Proc. Nat. Acad. Sci. USA* 94, 4211–4216.
18. Guil-Guerrero, J.L., Gómez-Mercado, F., García-Maroto, F., and Campra-Madrid, P. (2000) Occurrence and Characterization of Oils Rich in  $\gamma$ -Linolenic Acid Part I: *Echium* Seeds from Macaronesia, *Phytochemistry* 53, 451–456.
19. Guil-Guerrero, J.L., Gómez-Mercado, F., Rodríguez-García, I., Campra-Madrid, P., and García-Maroto, F. (2001) Occurrence and Characterization of Oils Rich in  $\gamma$ -Linolenic Acid (III): The Taxonomical Value of the Fatty Acids in *Echium* (Boraginaceae), *Phytochemistry* 58, 117–120.
20. Hoekema, A., Hirsch, P.R., Hooykaas, P.J.J., and Schilperoot, R.A. (1983) A Binary Plant Vector Strategy Based on Separation of Vir- and T-Region of the *Agrobacterium tumefaciens* Ti-Plasmid, *Nature* 303, 179–180.
21. Schultz, L.D., Hofmann, K.J., Mylin, L.M., Montgomery, D.L., Ellis, R.W., and Hopper, J.E. (1987) Regulated Overproduction of the GAL4 Gene Product Greatly Increases Expression from Galactose-Inducible Promoters on Multi-Copy Expression Vectors in Yeast, *Gene* 61, 123–133.
22. Mylin, L.M., Hofmann, K.J., Schultz, L.D., and Hopper, J.E. (1990) Regulated *GAL4* Expression Cassette Providing Controllable and High-Level Output from High-Copy Galactose Promoter in Yeast, *Meth. Enzymol.* 185, 297–309.
23. Ochman, H., Medhora, M., Garza, D., and Hartl, D.L. (1990) Amplification of Flanking Sequences by Inverse PCR, in *PCR Protocols: A Guide to Methods and Applications* (Innis, M.A., Gelfand, D.H., Sninsky, J.J., and White, T.J., eds.), pp. 219–227, Academic Press, London.
24. Thompson, J.D., Higgins, D.G., and Gibson, T.C. (1994) CLUSTALW: Improving the Sensitivity of Progressive Multiple Sequence Alignment Through Sequence Weighting, Position-Specific Gap Penalties and Weight Matrix Choice, *Nucl. Acids Res.* 22, 4673–4680.
25. Saitou, N., and Nei, M. (1987) The Neighbor-Joining Method: A New Method for Reconstructing Phylogenetic Trees, *Mol. Biol. Evol.* 4, 406–425.
26. Page, R.D.M. (1996) TREEVIEW: An Application to Display Phylogenetic Trees on Personal Computers, *Comput. Appl. Biosci.* 12, 357–358.
27. Taylor, B., and Povel, A. (1982) Isolation of Plant DNA and RNA, *Focus* 4, 4–6.
28. Chang, S., Puryear, J., and Cairney, J. (1993) A Simple and Efficient Method for Isolating RNA from Pine Trees, *Plant Mol. Biol. Rep.* 11, 113–116.
29. Shih, M.C., Lazan, G., and Goodman, H.M. (1986) Evidence in Favor of the Symbiotic Origin of Chloroplasts: Primary Structure and Evolution of Tobacco Glyceraldehyde-3-phosphate Dehydrogenases, *Cell* 47, 73–80.
30. Guerineau, F. (1995) Tools for Expressing Foreign Genes in Plants, *Methods Mol. Biol.* 49, 1–32.
31. Bevan, M. (1984) Binary *Agrobacterium* Vectors for Plant Transformation, *Nucl. Acids Res.* 12, 8711–8721.
32. Horsch, R.B., Fry, J.E., Hoffmann, N.L., Wallroth, M., Eichholtz, D., Rogers, S.G., and Fraley, R.T. (1985) A Simple and General Method for Transferring Genes into Plants, *Science* 227, 1229–1231.
33. Ito, H., Fukuda, K., Murata, K., and Kimura, A. (1983) Transformation of Intact Yeast Cells Treated with Alkali Cations, *J. Bacteriol.* 153, 163–168.
34. Cesareni, G., and Murray, A.H. (1987) Plasmid Vectors Carrying the Replication Origin of Filamentous Single-Stranded Phages, in *Genetic Engineering* (Setlow, J.K., ed.), Vol. 9, pp. 135–154, Plenum Press, New York.
35. Rodríguez-Ruiz, J., Belarbi, E.-H., García Sánchez, J.L., and López Alonso, D. (1998) Rapid Simultaneous Lipid Extraction and Transesterification for Fatty Acid Analyses, *Biotechnol. Tech.* 12, 689–691.
36. Napier, J.A., Sayanova, O., Sperling, P., and Heinz, E. (1999) A Growing Family of Cytochrome  $b_5$ -Domain Fusion Proteins, *Trends Plant Sci.* 4, 2–4.
37. Sperling, P., Zähringer, U., and Heinz, E. (1998) A Sphingolipid Desaturase from Higher Plants. Identification of a New Cytochrome  $b_5$  Fusion Protein, *J. Biol. Chem.* 273, 28590–28596.
38. Cahoon, E.B., Lindqvist, Y., Schneider, G., and Shanklin, J. (1997) Redesign of Soluble Fatty Acid Desaturases from Plants for Altered Substrate Specificity and Double Bond Position, *Proc. Natl. Acad. Sci. USA* 94, 4871–4877.
39. Sayanova, O., Davies, G.M., Smith, M.A., Griffith, G., Stobart, A.K., Shewry, P.R., and Napier, J.A. (1999) Accumulation of  $\Delta^6$ -Unsaturated Fatty Acids in Transgenic Tobacco Plants Expressing a  $\Delta^6$ -Desaturase from *Borago officinalis*, *J. Exp. Bot.* 50, 1647–1652.
40. Stymne, S., and Stobart, A.K. (1986) Biosynthesis of  $\gamma$ -Linolenic Acid in Cotyledons and Microsomal Preparations of the Developing Seeds of Common Borage (*Borago officinalis*), *Biochem. J.* 240, 385–393.
41. Sayanova, O., Beaudoin, F., Libisch, B., Shewry, P., and Napier, J. (2000) Mutagenesis of the Borage  $\Delta^6$  Fatty Acid Desaturase, *Biochem. Soc. Trans.* 28, 636–638.
42. Girke, T., Schmidt, H., Zähringer, U., Reski, R., and Heinz, E. (1998) Identification of a Novel  $\Delta^6$ -Acyl-Group Desaturase by Targeted Gene Disruption in *Physcomitrella patens*, *Plant J.* 15, 39–48.
43. Napier, J.A., Hey, S.J., Lacey, D.J., and Shewry, P.R. (1998) Identification of a *Caenorhabditis elegans*  $\Delta^6$ -Fatty-Acid-Desaturase by Heterologous Expression in *Saccharomyces cerevisiae*, *Biochem. J.* 330, 611–614.
44. Cho, H.P., Nakamura, M.T., and Clarke, S.D. (1999) Cloning,

- Expression, and Nutritional Regulation of the Mammalian  $\Delta$ -6 Desaturase, *J. Biol. Chem.* 274, 471–477.
45. Brosius, J. (1999) RNAs from All Categories Generate Retrosequences That May Be Exapted as Novel Genes or Regulatory Elements, *Gene* 238, 115–134.
46. Sayanova, O., Napier, J., and Shewry, P.R. (1999)  $\Delta^6$ -Unsaturated Fatty Acids in Species and Tissues of the Primulaceae, *Phytochemistry* 52, 419–422.
47. Guil-Guerrero, J.L., García-Maroto, F., Campra-Madrid, P., and Gómez-Mercado, F. (2000) Occurrence and Characterization of Oils Rich in  $\gamma$ -Linolenic Acid Part II: Fatty Acids and Squalene from Macaronesian *Echium* Leaves, *Phytochemistry* 54, 525–529.
48. Hofmann, K., and Stoffel, W. (1993) TMbase—A Database of Membrane Spanning Proteins Segments, *Biol. Chem. Hoppe Seyler* 374, 166.

[Received November 16, 2001; accepted February 13, 2002]

# Biosynthesis of New Divinyl Ether Oxylinins in *Ranunculus* Plants

Mats Hamberg\*

Department of Medical Biochemistry and Biophysics, Division of Physiological Chemistry II,  
Karolinska Institutet, S-171 77 Stockholm, Sweden

**ABSTRACT:** [1-<sup>14</sup>C]Linolenic acid was incubated with homogenates of leaves from the aquatic plants *Ranunculus lingua* (greater spearwort) or *R. peltatus* (pond water-crowfoot). Analysis by reversed-phase high-performance liquid radiochromatography demonstrated the formation of a new divinyl ether FA, i.e., 12-[1'(E),3'(Z)-hexadienyloxy]-9(Z),11(Z)-dodecadienoic acid [11(Z)-etherolenic acid] as well as a smaller proportion of ω5(Z)-etherolenic acid previously identified in terrestrial *Ranunculus* plants. The same divinyl ethers were formed upon incubation of 13(S)-hydroperoxy-9(Z),11(E),15(Z)-octadecatrienoic acid, a lipoxygenase metabolite of linolenic acid, whereas the isomeric hydroperoxide, 9(S)-hydroperoxy-10(E),12(Z),15(Z)-octadecatrienoic acid, was not converted into divinyl ethers in *R. lingua* or *R. peltatus*. Incubation of [1-<sup>14</sup>C]linoleic acid or 13(S)-hydroperoxy-9(Z),11(E)-octadecadienoic acid produced the divinyl ether 12-[1'(E)-hexenyloxy]-9(Z),11(Z)-dodecadienoic acid [11(Z)-etheroleic acid] and a smaller amount of ω5(Z)-etheroleic acid. The experiments demonstrated the existence in *R. lingua* and *R. peltatus* of a divinyl ether synthase distinct from those previously encountered in higher plants and algae.

Paper no. L8992 in *Lipids* 37, 427–433 (April 2002).

The divinyl ether synthase pathway of FA hydroperoxide metabolism was discovered by Galliard and Phillips, who in 1972 described the structures and biosynthesis of colneleic and colnelenic acids (1). These two divinyl ether FA were formed from the 9(S)-hydroperoxide derivatives of linoleic and linolenic acids, respectively, in homogenates of potato tubers (1), and were later identified also in preparations of tomato roots (2) and potato leaves (3). The enzyme responsible, i.e., divinyl ether synthase, is a membrane-bound P-450 protein, and the gene encoding it was recently cloned (4). Studies using other plant tissues have shown that hydroperoxides generated by 13-lipoxygenase activity can also serve as precursors of divinyl ethers. Evidence for this was first provided by Proteau and Gerwick (5), who isolated 12-[1'(Z),3'(Z)-hexadienyloxy]-6(Z),9(Z),11(E)-dodecatrienoic acid and 12-[1'(Z),3'(Z)-hexadienyloxy]-9(Z),11(E)-dodecadienoic acid [ω5(Z)-etherolenic acid] from the brown alga

\*E-mail: Mats.Hamberg@mbb.ki.se

Abbreviations and trivial names: Colneleic acid, 9-[1'(E),3'(Z)-nonadienyloxy]-8(E)-nonenoic acid; colnelenic acid, 9-[1'(E),3'(Z),6'(Z)-nonatrienyloxy]-8(E)-nonenoic acid; etheroleic acid, 12-[1'(E)-hexenyloxy]-9(Z),11(E)-dodecadienoic acid; etherolenic acid, 12-[1'(E),3'(Z)-hexadienyloxy]-9(Z),11(E)-dodecadienoic acid; 9-H(P)OD, 9-hydro(pero)xy-10(E),12(Z)-octadecadienoic acid; 13 H(P)OD, 13-hydro(pero)xy-9(Z),11(E)-octadecadienoic acid; 9-H(P)OT, 9 hydro(pero)xy-10(E),12(Z),15(Z)-octadecatrienoic acid; 13-H(P)OT, 13-hydro(pero)xy-9(Z),11(E),15(Z)-octadecatrienoic acid.

*Laminaria sinclairii*, compounds presumably derived from the 13-hydroperoxides of stearidonic and linolenic acids, respectively. Subsequently, Grechkin *et al.* (6) obtained 12-[1'(E),3'(Z)-hexadienyloxy]-9(Z),11(E)-dodecadienoic acid (etherolenic acid) and 12-[1'(E)-hexenyloxy]-9(Z),11(E)-dodecadienoic acid (etheroleic acid) following incubation of the 13(S)-hydroperoxides of linolenic and linoleic acids, respectively, with an extract of garlic bulbs. Hamberg (7) isolated the 1'(Z) isomers of these divinyl ethers, i.e., ω5(Z)-etherolenic acid and ω5(Z)-etheroleic acid, following incubation of the 13-hydroperoxides with leaves from *Ranunculus* plants.

The present study reports the structures of additional divinyl ethers, i.e., the 11(Z) isomers of etheroleic and etherolenic acids, and their biosynthesis in leaves from two aquatic *Ranunculus* plants.

## EXPERIMENTAL PROCEDURES

**Plant materials.** Specimens of greater spearwort (*R. lingua* L.) and pond water-crowfoot (*R. peltatus* L.) were collected in freshwater lakes in the Stockholm area in 1999. Leaves were either used directly or shock-frozen in liquid nitrogen and stored at -80°C.

**FA, FA hydroperoxides, and divinyl ethers.** Linoleic and linolenic acids were purchased from Nu-Chek-Prep (Elysian, MN). [1-<sup>14</sup>C]Linolenic acid (DuPont NEN, Boston, MA) was mixed with unlabeled material and purified by SiO<sub>2</sub> chromatography to afford a specimen having a specific radioactivity of 5.5 kBq/μmol. The FA hydroperoxides used in the present work, i.e., 9(S)-hydroperoxy-10(E),12(Z),15(Z)-octadecatrienoic acid [9(S)-HPOT], 13(S)-hydroperoxy-9(Z),11(E),15(Z)-octadecatrienoic acid [13(S)-HPOT], 9(S)-hydroperoxy-10(E),12(Z)-octadecadienoic acid [9(S)-HPOD], and 13(S)-hydroperoxy-9(Z),11(E)-octadecadienoic acid [13(S)-HPOD] were purchased from Larodan Fine Chemicals (Malmö, Sweden). From the same source were also obtained [17,17,18,18,18-<sup>2</sup>H<sub>5</sub>]linolenic acid, 12-oxo-10,15(Z)-phytodienoic acid as well as the divinyl ether FA used, i.e., colneleic, colnelenic, etheroleic, etherolenic, ω5(Z)-etheroleic, and ω5(Z)-etherolenic acids.

**Enzyme preparations.** Leaves of *R. lingua* or *R. peltatus* were minced and homogenized at 0°C in 0.1 M potassium phosphate buffer pH 6.7 (5:1, vol/wt) using an Ultra-Turrax homogenizer. The homogenate was filtered through gauze, and the filtrate was used in incubations carried out on a small scale. Centrifugation of the whole homogenate at 1100 × g for 15 min provided a low-speed particulate fraction, and further centrifu-

gation of the supernatant at  $105,000 \times g$  for 60 min provided a high-speed particulate fraction. The two particulate fractions, which both contained divinyl ether synthase activity, were re-suspended in volumes of phosphate buffer equal to those of the corresponding supernatants and used in large-scale incubations.

**Incubations on a small scale and treatments.** [ $1\text{-}^{14}\text{C}$ ]-Linolenic acid, [ $1\text{-}^{14}\text{C}$ ]linoleic acid, or hydroperoxides (300  $\mu\text{M}$ ) were stirred with the whole homogenate preparations from *R. lingua* or *R. peltatus* (2–15 mL) at 23°C for 20 min. The mixtures were acidified to pH 4 and rapidly extracted with 2 vol of diethyl ether. Material obtained after evaporation of the solvent was dissolved in 3 mL of 2-propanol/chloroform (1:2, vol/vol) and subjected to solid-phase extraction using an aminopropyl column (0.5 g; Supelco, Bellefonte, PA). After rinsing with 5 mL of the same solvent mixture, acidic components were eluted with 10 mL of diethyl ether/acetic acid (98:2, vol/vol). The material obtained was subjected to RP-HPLC radiochromatography using a column of Nucleosil 100-5  $\text{C}_{18}$  (250  $\times$  4.6 mm) (Macherey-Nagel, Düren, Germany) and a solvent system composed of acetonitrile/water/acetic acid (60:40:0.02, by vol). The flow rate was 1.5 mL/min, and the detector was set at 210 nm.

**Preparation of compound 4.** Crystalline compound 4, which was needed for structural and chromatographic studies, was prepared in the following way. Suspensions of the low-speed and high-speed particulate fractions obtained from 26 g of leaves of *R. lingua* were separately stirred at 23°C for 20 min with 300  $\mu\text{M}$  13(*S*)-HPOT. The mixtures were pooled, acidified to pH 4, and extracted with two portions of diethyl ether. The residue remaining after evaporation of the solvent was dissolved in 12 mL of 2-propanol/chloroform (1:2, vol/vol) and subjected to solid-phase extraction (four columns). Material obtained from five such batches was subjected to RP-HPLC using a column of Nucleosil  $\text{C}_{18}$  100-7 (250  $\times$  10 mm) and a solvent system of acetonitrile/water/acetic acid (60:40:0.02, by vol) to afford 4.5 mg of pure compound 4 (168–177 mL effluent; yield, 4%). The low yield was caused mainly by the strong hydroperoxide lyase activity in the tissue used, which diverted the main part of the incubated hydroperoxide into 12-oxo-9(*Z*)-dodecenoic acid and 3(*Z*)-hexenal. Crystallization of compound 4 from hexane at  $-25^\circ\text{C}$  afforded white crystals, m.p. 66–67°C. When carrying out the m.p. determinations, it was noted that further heating of melted samples led to the development of a faint odor of 3(*Z*)-hexenal, suggesting the presence of a 1,3-hexadienyloxy partial structure in compound 4.

**Preparation of methyl [17,17,18,18,18- $^2\text{H}_5$ ] $\omega$ 5(*Z*)-etherolenate.** [17,17,18,18,18- $^2\text{H}_5$ ]13(*S*)-HPOT (18 mg) was prepared by incubation of [17,17,18,18,18- $^2\text{H}_5$ ]linolenic acid with soybean lipoxygenase followed by purification by open-column  $\text{SiO}_2$  chromatography. The hydroperoxide (300  $\mu\text{M}$ ) was incubated with a suspension of the  $105,000 \times g$  particulate fraction from a homogenate of 40 g of leaves of *R. acris* as described earlier (7). Purification by RP-HPLC and  $\text{SiO}_2$  chromatography and methyl esterification by treatment with diazomethane afforded 6 mg of the title compound. Analysis

by GC-MS showed a single peak and a mass spectrum displaying a molecular ion at  $m/z$  311. The isotopic purity was 95%.

**Chemical, chromatographic, and instrumental methods.** Detailed descriptions of the methodology used for isolation and structural analysis are given or referred to in a previous study on hydroperoxide metabolism in terrestrial *Ranunculus* plants (7).

## RESULTS

**Isolation of oxidation products of linolenic acid.** [ $1\text{-}^{14}\text{C}$ ]-Linolenic acid (300  $\mu\text{M}$ ) was stirred at 23°C for 20 min with a whole homogenate preparation (10 mL) of *R. lingua*. Material obtained following extraction with diethyl ether and solid-phase extraction was subjected to RP-HPLC radiochromatography. Four major products were observed, i.e., compounds 1 (6% of the recovered radioactivity), 2 (5%), 3 (1%; 34.0 mL effluent), and 4 (10%; 35.8 mL effluent). Compound 1 was identified as 12-oxo-10,15(*Z*)-phytodienoic acid by UV spectroscopy and GC-MS using the authentic compound as reference (*cf.* Ref. 7). In a similar way, compound 2 was found to be identical to 13(*S*)-HOT. Compound 3 was spectroscopically and chromatographically indistinguishable from 12-[1'(*Z*),3'(*Z*)-hexadienyloxy]-9(*Z*),11(*E*)-dodecadienoic acid [ $\omega$ 5(*Z*)-etherolenic acid] recently isolated following incubation of linolenic acid with preparations of *R. acris* or other terrestrial *Ranunculus* plants (7). Compound 4 was a new divinyl ether oxylipin, and its structure was determined as described below. Incubation of [ $1\text{-}^{14}\text{C}$ ]linolenic acid with a whole homogenate preparation from *R. peltatus*, another aquatic *Ranunculus* plant, produced compounds 1 (16% of the recovered radioactivity), 3 (15%), and 4 (52%) as the main products.

**Structure of compound 4.** Compound 4 showed strong UV absorption with  $\lambda_{\text{max}}$  (EtOH) = 267 nm,  $\epsilon$  = 41,600 [reference:  $\omega$ 5(*Z*)-etherolenic acid,  $\lambda_{\text{max}}$  (EtOH) = 267 nm,  $\epsilon$  = 41,200], suggesting a dibutadienyl ether structure (Table 1). The FTIR spectrum (film) of the methyl ester of compound 4 showed bands at 1740 (ester C=O), 1646 (C=C), 1595 (C=C), 1165 (C–O–C), and 910  $\text{cm}^{-1}$  (*trans*-substituted vinyl ether). The mass spectrum of the methyl ester of compound 4 showed prominent ions at  $m/z$  306 (23%;  $\text{M}^+$ ), 277 (2;  $\text{M}^+ - 29$ ; loss of  $\cdot\text{C}_2\text{H}_5$ ), 275 (3;  $\text{M}^+ - 31$ ; loss of  $\cdot\text{OCH}_3$ ), 245 [4%;  $\text{M}^+ - (29 + 32)$ ], 217 (2), 199 (3), 163 [9%;  $\text{M}^+ - 143$ ; loss of  $\cdot(\text{CH}_2)_6\text{-COOCH}_3$ ], 149 (21), 131 (27), 107 (31), 81 (100), and 55 (98). Catalytic hydrogenation of the methyl ester of compound 4 provided an octahydro derivative, the mass spectrum of which showed ions at  $m/z$  314 (0.1%;  $\text{M}^+$ ), 283 (2%;  $\text{M}^+ - 31$ ; loss of  $\cdot\text{OCH}_3$ ), 229 [18%;  $\text{M}^+ - 85$ ; loss of  $\cdot(\text{CH}_2)_5\text{-CH}_3$ ], 214 [15%;  $\text{M}^+ - 100$ ; loss of  $\text{-OHC-(CH}_2)_4\text{-CH}_3$ ], 197 [49%;  $\text{M}^+ - (85 + 32)$ ], 143 {27%; [( $\text{CH}_2)_6\text{-COOCH}_3$ ] $^+$ }, 129 {11%; [( $\text{CH}_2)_5\text{-COOCH}_3$ ] $^+$ }, 97 {31%; [( $\text{CH}_2)_4\text{-CH=C=O}$ ] $^+$ }, 87 {59%; [( $\text{CH}_2)_2\text{-COOCH}_3$ ] $^+$ }, 74 {69%; [ $\text{CH}_2\text{=C(OH)-OCH}_3$ ] $^+$ }, and 55 (100). Oxidative ozonolysis performed on the methyl ester of compound 4 produced monomethyl azelate as the major nonvolatile fragment. Collectively, these data indicated that compound 4 possessed a



**TABLE 1**  
**UV Data and Chromatographic Properties of Divinyl Ethers**

Compound <sup>a</sup>	$\lambda_{\max}^b$ (nm)	Retention vol <sup>c</sup> (mL)	Retention time <sup>d</sup> (min)	C-value <sup>e</sup>
Compound <b>4</b>	267	30.9	34.7	19.96
Etherolenic acid	268	25.8	31.3	19.74 <sup>f</sup>
$\omega$ 5(Z)-Etherolenic acid	267	27.2	32.1	19.74
Colnelenic acid	253	30.2	28.9	19.45 <sup>f</sup>
Compound <b>6</b>	253	23.0	43.7	19.60
Etheroleic acid	250	21.4	38.3	19.33
$\omega$ 5(Z)-Etheroleic acid	250	20.8	41.9	18.83
Colneleic acid	250	25.5	46.4	19.41

<sup>a</sup>Abbreviations: Compound **4**, 12-[1'(E),3'(Z)-hexadienyloxy]-9(Z),11(Z)-dodecadienoic acid; etherolenic acid, 12-[1'(E),3'(Z)-hexadienyloxy]-9(Z),11(E)-dodecadienoic acid;  $\omega$ 5(Z)-etherolenic acid, 12-[1'(Z),3'(Z)-hexadienyloxy]-9(Z),11(E)-dodecadienoic acid; colnelenic acid, 9-[1'(E),3'(Z),6'(Z)-nonatrienyloxy]-8(E)-nonenoic acid; compound **6**, 12-[1'(E)-hexenyloxy]-9(Z),11(Z)-dodecadienoic acid; etheroleic acid, 12-[1'(E)-hexenyloxy]-9(Z),11(E)-dodecadienoic acid;  $\omega$ 5(Z)-etheroleic acid, 12-[1'(Z)-hexenyloxy]-9(Z),11(E)-dodecadienoic acid; colneleic acid, 9-[1'(E),3'(Z)-nonadienyloxy]-8(E)-nonenoic acid.

<sup>b</sup>UV spectra were recorded on the free acids dissolved in 99.5% ethanol.

<sup>c</sup>Straight-phase HPLC was performed on the methyl esters using a column of Nucleosil 50-5 and a solvent system of ethyl acetate/hexane (8:992, vol/vol) at a flow rate of 1.0 mL/min. The detector was set at 250 nm.

<sup>d</sup>Capillary electrophoresis. Data from Reference 8.

<sup>e</sup>GLC was performed on the methyl esters using a methyl silicone capillary column (25 m) at 230°C. The C-values indicate the retention times relative to those of standards of saturated FAME.

<sup>f</sup>Partial degradation on the capillary column.

9,11-dodecadienoate moiety linked to a 1,3-hexadienyl group by an ether oxygen, i.e., a skeletal structure identical to that of etherolenic acid (**6**) and  $\omega$ 5(Z)-etherolenic acid (**7**). The distinguishing feature of compound **4**, i.e., the geometrical configuration of the double bond system, was established by NMR analysis of the methyl ester.

Eight of the deshielded signals due to the eight olefinic

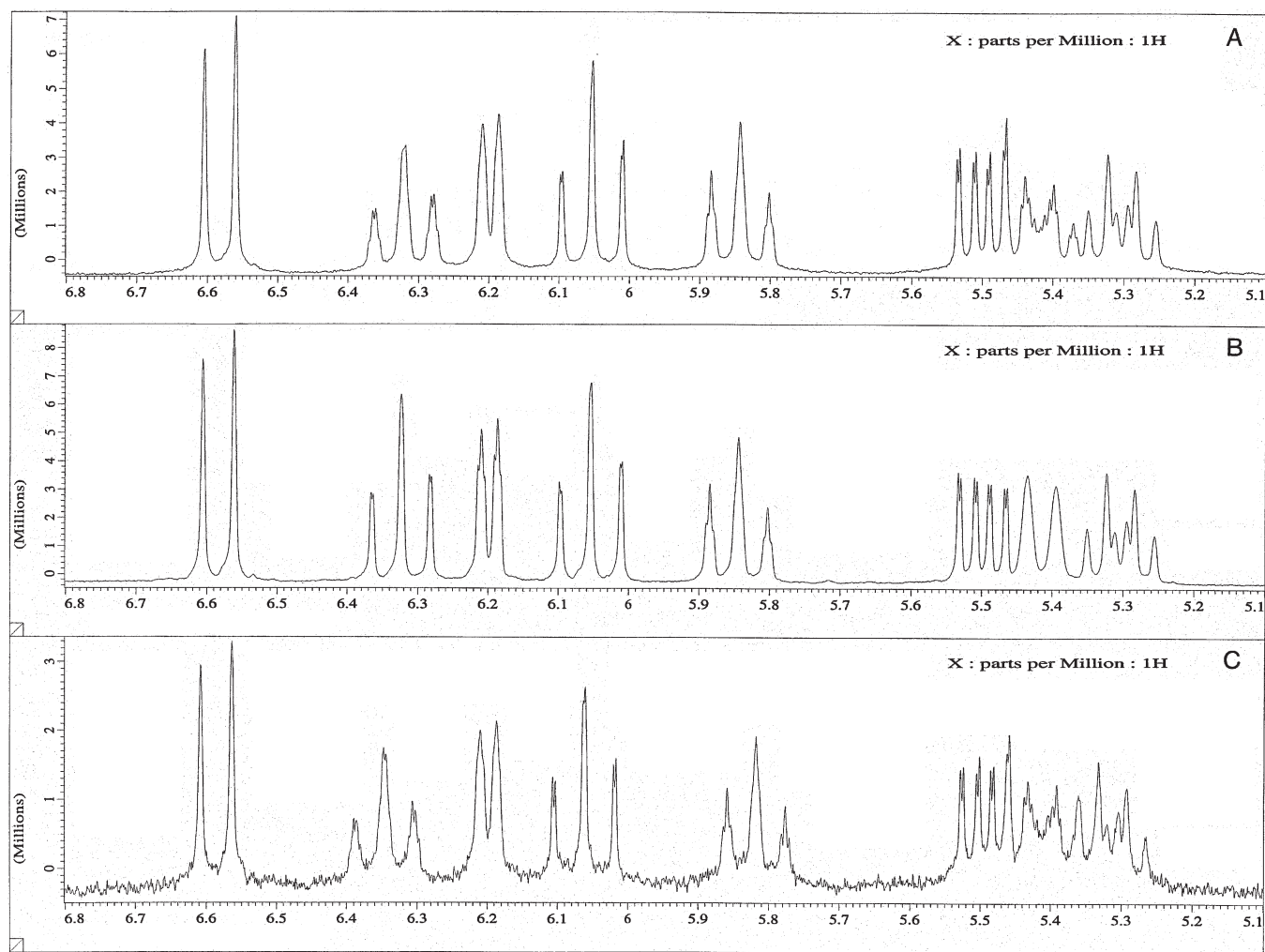
protons of compound **4** were observed (Table 2, Fig. 1C). Correlation of the signals with the different protons was achieved by spin-spin decoupling experiments and by using the NMR spectra of methyl etherolenate (**6**) and methyl  $\omega$ 5(Z)-etherolenate (**7**) as references. The signals centered at 5.41 and 6.33 ppm were due to the protons at C-9 and C-10, respectively, whereas the signals at 5.82 and 5.31 ppm were due to the protons at C-3' and C-4', respectively. As shown by the values of  $J_{9,10}$  and  $J_{3',4'}$  (11.1 and 10.6 Hz, respectively), both the  $\Delta^9$  and  $\Delta^{3'}$  double bonds had the *Z* geometrical configuration. Earlier work on divinyl ether FA and on other vinyl ether compounds, such as ethyl propenyl ether (5-7,9,10), showed that the coupling constants of protons across *Z* and *E* vinyl ether double bonds have values of 6-7 and 11-12 Hz, respectively. As seen in Table 2, the  $J_{11,12}$  determined for the signals of the vinylic protons at C-11 (5.49 ppm) and C-12 (6.20 ppm) was 6.2 Hz, thus demonstrating that the  $\Delta^{11}$  double bond had the *Z* configuration. In the same way, the coupling constant of the vinylic protons of the  $\Delta^{1'}$  double bond (signals centered at 6.59 and 6.06 ppm) was 11.9 Hz. This showed that the  $\Delta^{1'}$  double bond had the *E* geometrical configuration. On the basis of the data presented, compound **4** was identified as 12-[1'(E),3'(Z)-hexadienyloxy]-9(Z),11(Z)-dodecadienoic acid [11(Z)-etherolenic acid] (Scheme 1).

Compound **4** and  $\omega$ 5(Z)-etherolenic acid differed only with respect to their alternative placements of their *E,Z*-butadienyl ether and *Z,Z*-butadienyl ether partial structures (Scheme 1), and accordingly, their NMR spectra were virtually identical (Figs. 1A and 1C). Therefore, the NMR signal assignments made for compound **4** were in part based on those previously made for  $\omega$ 5(Z)-etherolenic acid (**7**). It was deemed important to confirm the correctness of the latter

**TABLE 2**  
**Proton NMR Data for the Methyl Esters of Compounds 4 and 6<sup>a</sup>**

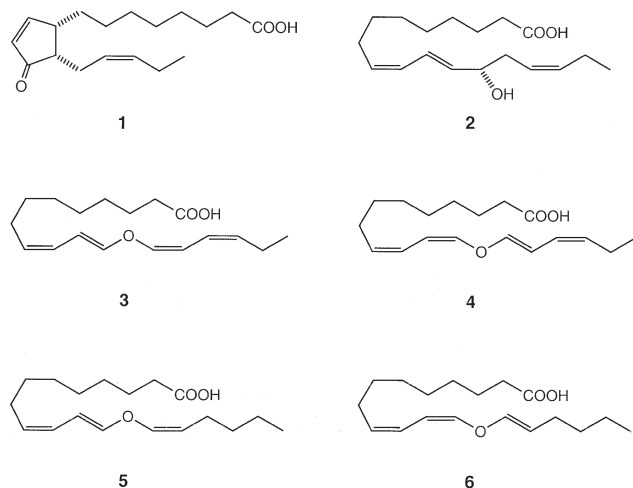
Methyl ester of compound <b>4</b>				Methyl ester of compound <b>6</b>			
Carbon #	$\delta$ (ppm)	Multiplicity	<i>J</i> (Hz)	Carbon #	$\delta$ (ppm)	Multiplicity	<i>J</i> (Hz)
2	2.30	<i>t</i>	7.5	2	2.30	<i>t</i>	7.4
3	1.62	<i>m</i>		3	1.62	<i>m</i>	
4	1.31	<i>m</i>		4	1.31	<i>m</i>	
5	1.31	<i>m</i>		5	1.31	<i>m</i>	
6	1.31	<i>m</i>		6	1.31	<i>m</i>	
7	1.31	<i>m</i>		7	1.31	<i>m</i>	
8	2.13	<i>m</i>		8	2.11	<i>m</i>	
9	5.41	<i>m</i>		9	5.35	<i>m</i>	
10	6.33	<i>ddd</i>	1.0, 11.1, 11.4	10	6.34	<i>dd</i>	11.1, 11.5
11	5.49	<i>ddd</i>	1.0, 6.2, 11.4	11	5.42	<i>dd</i>	11.5, 6.2
12	6.20	<i>d</i>	6.2	12	6.14	<i>d</i>	6.2
1'	6.59	<i>d</i>	11.9	1'	6.30	<i>dt</i>	12.1, 1.2
2'	6.06	<i>ddd</i>	1.0, 11.4, 11.9	2'	5.13	<i>dt</i>	12.1, 7.7
3'	5.82	<i>m</i>	10.6, 11.4	3'	1.94	<i>m</i>	
4'	5.31	<i>dt</i>	10.6, 7.7	4'	1.31	<i>m</i>	
5'	2.13	<i>m</i>		5'	1.31	<i>m</i>	
6'	0.99	<i>t</i>	7.5	6'	0.89	<i>t</i>	7.0
OCH <sub>3</sub>	3.66	<i>s</i>		OCH <sub>3</sub>	3.66	<i>s</i>	

<sup>a</sup>Proton NMR spectra were recorded at 270 MHz in CDCl<sub>3</sub> with tetramethylsilane as internal chemical shift reference. For names of compounds **4** and **6** see Table 1.



**FIG. 1.** Partial proton NMR spectra of divinyl ethers. (A) Methyl ester of  $\omega 5(Z)$ -etherolenic acid [= 12-[1'(Z),3'(Z)-hexadienyloxy]-9(Z),11(E)dodecadienoic acid, methyl ester); (B) methyl ester of [17,17,18,18,18- $^2\text{H}_5$ ] $\omega 5(Z)$ -etherolenic acid; (C) methyl ester of compound **4** [= - $\omega 5(Z)$ etherolenic acid]. The region  $\delta$  5.1–6.8 ppm containing signals due to the olefinic protons are shown. Solvent, deuteriochloroform.

assignments in an independent way. To this end, an NMR analysis of [17,17,18,18,18- $^2\text{H}_5$ ] $\omega 5(Z)$ -etherolenic acid prepared by incubation of [17,17,18,18,18- $^2\text{H}_5$ ]**13(S)**-HPOT



**SCHEME 1**

with *R. acris* (cf. Ref. 7) was performed. As expected, the NMR spectrum of the methyl ester of this compound lacked signals due to the methyl protons and the 5' protons. Importantly, the multiplet at 5.41 ppm ascribed to the 4' protons of unlabeled  $\omega 5(Z)$ -etherolenic acid (**7**) simplified to a doublet (5.41 ppm;  $J_{3',4'} = 10.9$  Hz) (Fig. 1B), thus confirming that the spin system 1'–4' corresponded to the Z,Z-butadienyl moiety as previously concluded (**7**). By means of exclusion, this experiment gave independent proof for the location at C-9 to C-12 of the corresponding moiety of compound **4**.

**Incubation of 13(S)-HPOT.** [1- $^{14}\text{C}$ ]**13(S)**-HPOT (300  $\mu\text{M}$ ) was stirred at 23°C for 20 min with a whole homogenate preparation (10 mL) of *R. lingua* or *R. peltatus*, and the materials obtained following extraction with diethyl ether and solid-phase extraction were subjected to RP-HPLC radiochromatography. The pattern of radioactive products was similar to that observed following incubation of [1- $^{14}\text{C}$ ]linolenic acid; however, the amount of compound **3** [ $\omega 5(Z)$ -etherolenic acid] relative to that of compound **4** was higher and more variable. Thus, the ratio of compound **3**/compound **4** observed with linolenic acid

incubated with *R. lingua* was 1:10, whereas 13(*S*)-HPOT incubated with the same plant gave ratios of up to 50:50.

**Incubation of linoleic acid and 13(*S*)-HPOD.** Incubation of [ $1\text{-}^{14}\text{C}$ ]linoleic acid (300  $\mu\text{M}$ ) as described above led to the formation of two divinyl ethers, i.e., compound **5** and compound **6** in proportions 20:80. Compound **5** was found to be identical to 12-[1'(*Z*)-hexenyloxy]-9(*Z*),11(*E*)-dodecadienoic acid [ $\omega 5$ (*Z*)-etheroleic acid], a compound previously obtained from linoleic acid incubated with an enzyme preparation from *R. acris* and other terrestrial *Ranunculus* plants (7). The structure of compound **6**, the major divinyl ether formed from linoleic acid, was determined as described below. Incubation of 13(*S*)-HPOD with whole homogenate preparations of *R. lingua* or *R. peltatus* provided the same divinyl ethers as those formed from linoleic acid although in proportions 40:60 (compound **5**/compound **6**).

**Structure of compound 6.** The UV spectrum of **6** showed  $\lambda_{\text{max}}$  (EtOH) = 253 nm (Table 1), and the FTIR spectrum (film) of the methyl ester showed absorption bands at 1741 (ester carbonyl), 1647 (C=C), 1601 (C=C), 1158 (C-O-C), and 933 and 916  $\text{cm}^{-1}$  (*trans*-substituted vinyl ether). The mass spectrum showed prominent ions at  $m/z$  308 (31%;  $\text{M}^+$ ), 277 (2%;  $\text{M}^+ - 31$ ; loss of  $\cdot\text{OCH}_3$ ), 251 [3%;  $\text{M}^+ - 57$ ; loss of  $\cdot(\text{CH}_2)_3\text{-CH}_3$ ], 219 [2%;  $\text{M}^+ - (57 + 32)$ ], 177 (13), 165 [20%;  $\text{M}^+ - 143$ ; loss of  $\cdot(\text{CH}_2)_6\text{-COOCH}_3$ ], 159 (14), 135 (25), 81 (60), 67 (70), and 55 (100). Catalytic hydrogenation of **6** produced a derivative identical to that formed from **4** upon the same treatment (see above). Oxidative ozonolysis performed on the methyl ester of **6** yielded monomethyl azelate as the main product. The data mentioned indicated the presence in **6** of a tri-unsaturated ether partial structure spanning from C-9 to C-14. NMR spectroscopy showed six groups of signals due to olefinic protons (Table 2). The protons at the  $\Delta^9$  double bonds gave rise to signals at 5.35 and 6.34 ppm. The value of  $J_{9,10}$  (11.1 Hz) demonstrated that this double bond had the *Z* geometrical configuration. The signals at 5.42 and 6.14 ppm were due to the protons at the  $\Delta^{11}$  double bond. The observed  $J_{11,12}$  (6.2 Hz) was in agreement with a vinyl ether double bond having the *Z* configuration. In the same way, the  $\Delta^{1'}$  double bond was assigned the *E* configuration based on the  $J_{1',2'}$  (12.1 Hz) measured from the signals at 6.30 and 5.13 ppm (protons at C-1' and C-2', respectively). On the basis of these results, compound **6** was assigned the structure 12-[1'(*E*)-hexenyloxy]-9(*Z*),11(*Z*)-dodecadienoic acid [11(*Z*)-etheroleic acid]. This compound was obtained earlier as a minor by-product in the biosynthesis of etheroleic acid from 13(*S*)-HPOD using a crude enzyme preparation from garlic bulbs (10).

**Incubations of 9(*S*)-HPOT, 9(*S*)-HPOD, and  $\omega 5$ (*Z*)-etherolenic acid.** Incubation of 9(*S*)-HPOT (300  $\mu\text{M}$ ) with the whole homogenate preparations of *R. lingua* or *R. peltatus* did not result in the formation of divinyl ethers. The compounds observed were identified as unconverted hydroperoxide accompanied by smaller amounts of 9(*S*)-HOT and 9-oxo-10(*E*),12(*Z*),15(*Z*)-octadecatrienoic acid. Incubation of 9(*S*)-HPOD likewise produced small amounts of 9-HOD and

9-oxo-10(*E*),12(*Z*)-octadecadienoic acid but no divinyl ethers. Incubation of  $\omega 5$ (*Z*)-etherolenic acid did not lead to conversion into other compounds, thus excluding the presence of isomerase(s) catalyzing interconversion of divinyl ether isomers in the preparations used.

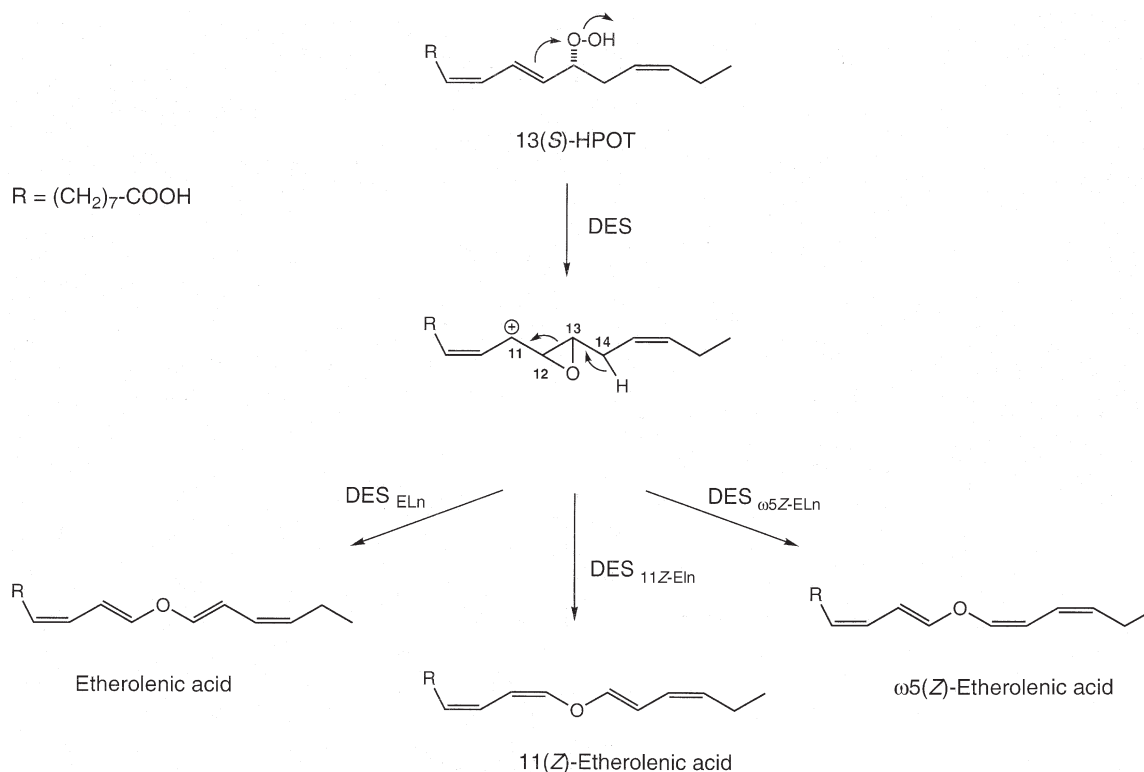
**Chromatographic separation of divinyl ether FA.** As seen in Table 1, straight-phase HPLC allowed separation of the methyl esters of etherolenic and etheroleic acids from their corresponding  $\omega 5$ (*Z*) and 11(*Z*) isomers. Furthermore, complete resolution of the divinyl ether isomers could be effected by capillary electrophoresis (8). Also GLC was useful for identification and separation of divinyl ethers, although the methyl ester of etherolenic acid was inseparable from its  $\omega 5$ (*Z*) isomer.

## DISCUSSION

In a previous study, leaves of terrestrial *Ranunculus* plants were shown to metabolize linolenic acid and 13(*S*)-HPOT extensively into a single crystalline divinyl ether FA identified as  $\omega 5$ (*Z*)-etherolenic acid (7). The present study describes the formation of a higher-melting form of this divinyl ether in leaves from two aquatic *Ranunculus* plants, i.e., greater spearwort (*R. lingua*) and pond water-crowfoot (*R. peltatus*). The new divinyl ether, compound **4**, was separable from previously recognized divinyl ether FA by chromatographic methods (Table 1) but gave results similar to those of  $\omega 5$ (*Z*)-etherolenic acid when analyzed by UV and FTIR spectroscopy as well as MS. NMR spectrometry performed on the methyl ester of compound **4** and using the methyl esters of  $\omega 5$ (*Z*)-etherolenic acid and [ $17,17,18,18,18\text{-}^2\text{H}_5$ ] $\omega 5$ (*Z*)-etherolenic acid as references (Fig. 1) demonstrated the presence in compound **4** of a *Z,Z*-butadienyl structure located in the 9–12 position and an *E,Z*-butadienyl structure located in the 13–16 position. Accordingly, compound **4** was identified as the 11(*Z*) isomer of etherolenic acid (Scheme 1). Linoleic acid and 13(*S*)-HPOD were metabolized in an analogous way to produce compound **6** [11(*Z*)-etheroleic acid] as the main divinyl ether product.

The finding that biosynthesis of divinyl ethers from linolenic and linoleic acids in *R. lingua* and *R. peltatus* was accompanied by the formation of smaller amounts of 12-oxo-10,15(*Z*)-phytodienoic acid, 13-HOT, and 13-HOD demonstrated the presence of 13-lipoxygenase activity in the preparations used. This fact, coupled with the result that 13(*S*)-HPOT and 13(*S*)-HPOD served as efficient precursors of divinyl ethers, indicated that a two-step pathway involving 13-lipoxygenase and divinyl ether synthase was responsible for biosynthesis of divinyl ethers in the plants studied (Fig. 2). Divinyl ether synthases emerge as a group of isoenzymes catalyzing the conversion of FA hydroperoxides into regioisomeric and stereoisomeric divinyl ethers. One such enzyme, i.e., the one catalyzing the conversion of 9(*S*)-HPOD into colnelic acid, has been found to be a cytochrome P-450, protein and the gene encoding it has been cloned (4).

Conversion of 13-hydroperoxides into 11(*Z*)-etheroleic and 11(*Z*)-etherolenic acids by divinyl ether synthase in *R. lingua* and *R. peltatus* is remarkable in the sense that it



**FIG. 2.** Biosynthesis of isomeric divinyl ethers from 13(*S*)-hydroperoxy-9(*Z*),11(*E*),15(*Z*)-octadecatrienoic acid [13(*S*)-HPOT]. DES, divinyl ether synthase; ELn, etherolenic acid; see Figure 1 for other abbreviations.

involves a thermodynamically unfavorable  $E \rightarrow Z$  isomerization of the  $\Delta^{11}$  double bond (Fig. 2). An epoxide carbocation has been proposed to serve as an enzyme-bound intermediate in the biosynthesis of divinyl ethers (10–12), and a basic amino acid residue in the active site of divinyl ether synthases has been proposed to effect the stereoselective removal of a proton from the noncharged carbon  $\alpha$  to the epoxide (11,12). It can be speculated that the active sites of the divinyl ether synthase isoenzymes catalyzing the biosynthesis of etherolenic, 11(*Z*)-etherolenic, and  $\omega 5$ (*Z*)-etherolenic acids show subtle differences with respect to the positioning of amino acid residues needed for binding and further conversion of the epoxide carbocation intermediate. This may force the intermediate to adopt different conformations by rotation of the 11,12 and 13,14 single bonds to provide conformers that serve as precursors of the different geometrical isomers of etherolenic acid (Fig. 2).

The function of divinyl ether FA in plants is not well-established. A role in plant–pathogen interactions is suggested by the antifungal properties of colnelic and colnelenic acids (3) and by the pathogen-induced formation of these compounds in potato leaves (3) or in cell cultures from potato (13).

#### ACKNOWLEDGMENTS

Gunvor Hamberg is thanked for expert technical assistance and for collection and identification of the plant materials used. The author is greatly indebted to Professor Per-Erik Jansson and Reine Eserstam (Clinical Research Center, Huddinge University Hospital,

Stockholm) for their help with the NMR analyses. This work was supported by Vesical Co., Stockholm, Sweden, and by the Swedish Council for Forestry and Agricultural Research (project 980.0897/00).

#### REFERENCES

- Galliard, T., and Phillips, D.R. (1972) The Enzymic Conversion of Linoleic Acid into 9-(Nona-1',3'-dienoxy)non-8-enoic Acid, a Novel Unsaturated Ether Derivative Isolated from Homogenates of *Solanum tuberosum* Tubers, *Biochem. J.* 129, 743–753.
- Caldelari, D., and Farmer, E.E. (1998) A Rapid Assay for the Coupled Cell Free Generation of Oxylipins, *Phytochemistry* 47, 599–604.
- Weber, H., Chételat, A., Caldeleri, D., and Farmer, E.E. (1999) Divinyl Ether Fatty Acid Synthesis in Late Blight-Diseased Potato Leaves, *Plant Cell* 11, 485–493.
- Itoh, A., and Howe, G.A. (2001) Molecular Cloning of a Divinyl Ether Synthase, *J. Biol. Chem.* 276, 3620–3627.
- Proteau, P.J., and Gerwick, W.H. (1993) Divinyl Ethers and Hydroxy Fatty Acids from Three Species of *Laminaria* (Brown Algae), *Lipids* 28, 783–787.
- Grechkin, A.N., Fazliev, F.N., and Mukhtarova, L.S. (1995) The Lipoxigenase Pathway in Garlic (*Allium sativum* L.) Bulbs: Detection of the Novel Divinyl Ether Oxylipins, *FEBS Lett.* 371, 159–162.
- Hamberg, M. (1998) A Pathway for Biosynthesis of Divinyl Ether Fatty Acids in Green Leaves, *Lipids* 33, 1061–1071.
- Öhman, M., Wang, H., Hamberg, M., and Blomberg, L.G. (2001) Separation of Divinyl Ether Fatty Acid Isomers by Micellar Electrokinetic Chromatography, *Electrophoresis* 22, 1163–1169.



9. *The Sadtler Standard Spectra*, Vol. 12, Sadtler Research Laboratories, Philadelphia, 1969, Spectrum #7748.
10. Grechkin, A.N., Ilyasov, A.V., and Hamberg, M. (1997) On the Mechanism of Biosynthesis of Divinyl Ether Oxylipins by Enzyme from Garlic Bulbs, *Eur. J. Biochem.* 245, 137–142.
11. Crombie, L., Morgan, D.O., and Smith, E.H. (1991) An Isotopic Study ( $^2\text{H}$  and  $^{18}\text{O}$ ) of the Enzymic Conversion of Linoleic Acid into Colneleic Acid with Carbon Chain Fracture: The Origin of Shorter Chain Aldehydes, *J. Chem. Soc., Perkin Trans. 1*, 567–757.
12. Fahlstadius, P., and Hamberg, M. (1990) Stereospecific Removal of the *pro-R* Hydrogen at C-8 of (9*S*)-Hydroperoxyoctadecadienoic Acid in the Biosynthesis of Colneleic Acid, *J. Chem. Soc., Perkin Trans. 1*, 2027–2030.
13. Göbel, C., Feussner, I., Schmidt, A., Scheel, D., Sanchez-Serrano, J., Hamberg, M., and Rosahl, S. (2001) Oxylipin Profiling Reveals the Preferential Stimulation of the 9-Lipoxygenase Pathway in Elicitor-Treated Potato Cells, *J. Biol. Chem.* 276, 6267–6273.

[Received January 28, 2002, and in revised form and accepted March 14, 2002]

# Evidence for [1,5] Sigmatropic Rearrangements of CLA in Heated Oils

Frédéric Destailats and Paul Angers\*

Department of Food Science and Nutrition, and Dairy Research Center (STELA),  
Université Laval, Sainte-Foy, Québec, Canada, G1K 7P4

**ABSTRACT:** Linoleic acid was heated at 200°C under helium. Analysis of degradation products by GC on a long polar open tubular capillary column showed the presence of CLA isomers. The identified mono *trans* CLA isomers were *cis*-9,*trans*-11, *trans*-9,*cis*-11, *trans*-10,*cis*-12, *cis*-10,*trans*-12, *trans*-8,*cis*-10, and *cis*-11,*trans*-13 18:2 acids. Oils containing different levels of linoleic acid (peanut, sesame seed, and safflower seed oils) were also heat treated, resulting in similar CLA distributions. Elution order was confirmed using *cis*-9,*trans*-11 and *trans*-10,*cis*-12 acid methyl esters standards and their respective configuration isomers (*trans*-9,*cis*-11, *cis*-10,*trans*-12), obtained after mild selenium-catalyzed isomerization. These results indicated that two conjugated mono *trans* isomers of 18:2 acid, *cis*-8,*trans*-10 and *trans*-11,*cis*-13 18:2 were absent from the series, thus strongly suggesting that some constraints were preventing their formation. By heating pure methyl rumenate (*cis*-9,*trans*-11 18:2) under similar conditions, isomerization resulted principally in a nearly equimolar mixture of methyl rumenate and *trans*-8,*cis*-10 18:2. Similarly, the methyl ester of *trans*-10,*cis*-12 18:2 acid was partially transformed into *cis*-11,*trans*-13 18:2 acid. Respective geometrical isomers were also formed in trace amounts. A concerted pericyclic isomerization mechanism, a [1,5] sigmatropic rearrangement, is proposed that limits the conjugated system to isomerization from a *cis*-*trans* acid to a *trans*-*cis* acid, and vice versa. This mechanism is consistent with undetected *cis*-8,*trans*-10 and *trans*-11,*cis*-13 18:2 isomers in heated oils containing linoleic acid.

Paper no. L8962 in *Lipids* 37, 435–438 (April 2002).

During the last decade, more than 600 scientific articles have been published on analysis, physiology, nutrition, and technological implications of CLA. These conjugated FA are naturally present in milk fat and in the meat of ruminants and may result in beneficial health effects, which have recently been reviewed (1). CLA, especially all-*trans*-9,11-18:2 and -10,12-18:2 acid isomers, are also found in trace amounts in processed materials such as partially hydrogenated oils (2). Juanéda *et al.* (3) showed that CLA had been formed in frying oils collected from restaurants. Their structures have been determined by a combination of GC and silver ion HPLC. The formed CLA consisted mainly of *trans*-9,*trans*-11, *trans*-10,*trans*-12, *cis*-9,*trans*-11, *trans*-10,*cis*-12, *trans*-8,*cis*-10, *cis*-11,*trans*-13 18:2 acids, and minor amounts of *cis*-9,*cis*-11, *cis*-10,*cis*-12, and *cis*-11,*cis*-13 18:2 acids. Indeed, occurrence of CLA in heat-treated sunflower

seed oil, high in linoleic (*cis*-9,*cis*-12 18:2) acid, has been demonstrated by Sébédio *et al.* (4), who observed the presence of similar isomers. Obviously, some constraints prevented the formation of two conjugated mono *trans* isomers of 18:2 acid in heated oils, *cis*-8,*trans*-10 and *trans*-11,*cis*-13 18:2, which were absent from the series.

In this study, successive experiments were performed to identify reaction mechanisms causing the formation of *trans*-8,*cis*-10 and *cis*-11,*trans*-13 18:2 acids in heated oil, while preventing the formation of their respective *cis*-8,*trans*-10 and *trans*-11,*cis*-13 18:2 configuration isomers. Comprehensive chemical observations are a prerequisite step to further interpretations of chemical behavior of CLA.

## MATERIALS AND METHODS

**Samples and reagents.** Linoleic (*cis*-9,*cis*-12 18:2), *cis*-9,*trans*-11 (rumenic), and *trans*-10,*cis*-12 18:2 acid methyl esters were purchased from Nu-Chek-Prep (Elysian, MN). *n*-Hexadecane, *n*-hexane, selenium metal (-100 mesh, 99.999%), and silver nitrate were obtained from Aldrich Chemicals (Milwaukee, WI). Peanut, sesame seed, and safflower seed oils were purchased from a local store.

**Heat treatment.** Methyl linoleate (50  $\mu$ L) was heated under helium in a sealed glass vial for 120 h at 200°C in the oven of a 5890A gas chromatograph (Hewlett-Packard, Palo Alto, CA). Methyl rumenate (25  $\mu$ L) and methyl *trans*-10,*cis*-12 18:2 (25  $\mu$ L) acids were diluted in hexadecane (500  $\mu$ L) and separately heated under helium at 200°C for 13 h in the same apparatus. After cooling to room temperature, samples were diluted with *n*-hexane (*ca.* 1 mL) prior to GLC analysis. Oils of peanuts, sesame seeds, and safflower seeds (25 mL each) were heated at 200°C in open 50-mL flasks. Samples were collected after 18 h of heat treatment and transesterified (5) prior to analysis. All experiments were performed in duplicate.

**Fractionation of FAME by Ag-TLC.** Methylation of FA from heated oil samples was carried out in sealed tubes with 0.4 N sodium methoxide in methanol. FAME from heated oils were fractionated according to number and configuration of double bonds by TLC on silica gel plates (20  $\times$  20 cm) impregnated with AgNO<sub>3</sub>. The plates were immersed in a 5% AgNO<sub>3</sub> solution in acetonitrile for 15 min in the dark, and activated at 100°C for 1 h. The developing solvent was a mixture of hexane and diethyl ether (80:20, vol/vol). At the end of the chromatographic runs, the plates were sprayed with a solution of 2',7'-dichlorofluorescein and then viewed under UV light. The bands

\*To whom correspondence should be addressed at Department of Food Science and Nutrition, Université Laval, Sainte-Foy (Québec) Canada G1K 7P4. E-mail: paul.angers@aln.ulaval.ca

corresponding to monounsaturated FA, which also contained the CLA isomers, were scraped off and transferred into test tubes. Methanol (1.5 mL), hexane (2 mL), and a 5% (wt/vol) aqueous solution of NaCl (1.5 mL) were successively added to the silica gels. Thorough mixing followed each addition. After standing for *ca.* 1 min, the hexane phase was withdrawn and concentrated under a stream of dry nitrogen before analysis.

**Synthesis of CLA isomers.** Configurational isomers of methyl-9,11-linoleate were synthesized using a modified literature procedure (6): to a stirred solution of methyl rumenate (100  $\mu$ L) in anhydrous hexadecane (0.5 mL), contained in a flame-dried flask under inert atmosphere (He), selenium (7 mg) was added. After 20 h at 120°C, under constant stirring, the solution was cooled to room temperature, filtered, diluted in hexane (*ca.* 2 mL), and analyzed by GC. The reaction products consisted of a mixture of methyl *trans*-9,*trans*-11 (**12**), *trans*-9,*cis*-11 (**5**), *cis*-9,*trans*-11 (**2**), and *cis*-9,*cis*-11 (**9**) linoleate. A similar experiment on methyl *trans*-10,*cis*-12 (**7**) linoleate yielded the corresponding configurational isomers methyl *trans*-10,*trans*-12 (**11**), *trans*-10,*cis*-12 (**7**), *cis*-10,*trans*-12 (**4**), and *cis*-10,*cis*-12 (**10**) linoleate.

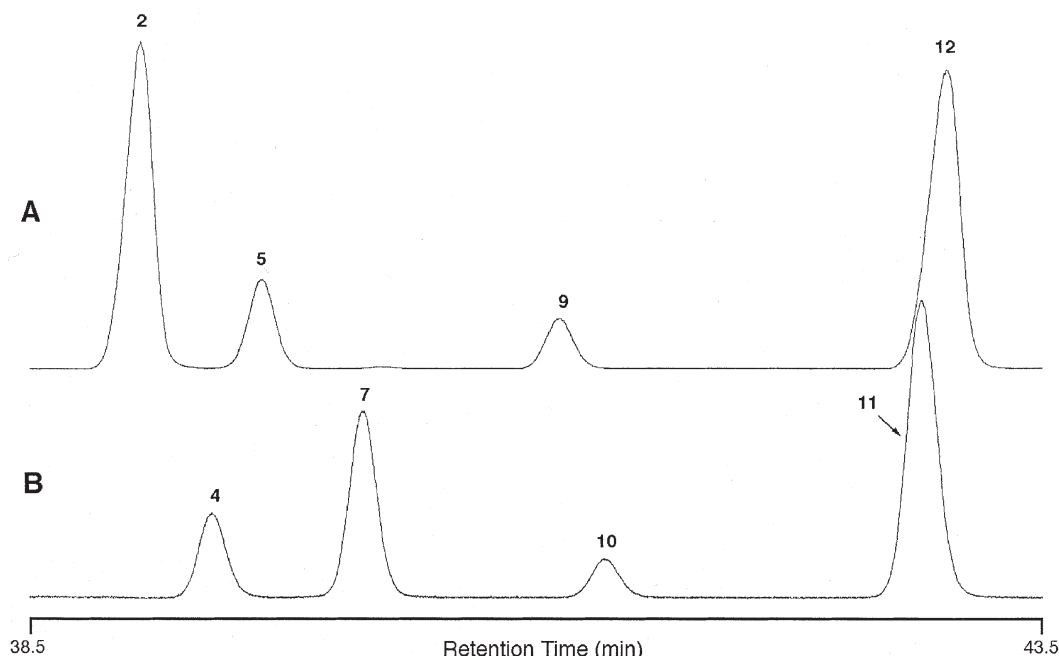
**FAME analysis.** Analysis of conjugated methyl linoleate isomers was performed on a 6890 Series II gas chromatograph (Hewlett-Packard), equipped with a fused-silica BPX-70 capillary column (equivalent to 70% cyanopropyl; 120 m  $\times$  0.25 mm i.d., 0.25  $\mu$ m film thickness; SGE, Melbourne, Australia), and connected to a ChemStation (Hewlett-Packard). Injection (split mode) and detection (flame-ionization) were performed at 250°C. Oven temperature programming was 60°C isothermal for 1 min, increased to 170°C at

20°C min<sup>-1</sup>, and held isothermal for 40 min at 170°C (3). The inlet pressure of the carrier gas (H<sub>2</sub>) was 300 kPa at 170°C. Identification of individual *cis-trans* CLA isomers was achieved based on literature data (3,5,7,8), and confirmed with both commercially available and synthesized standards.

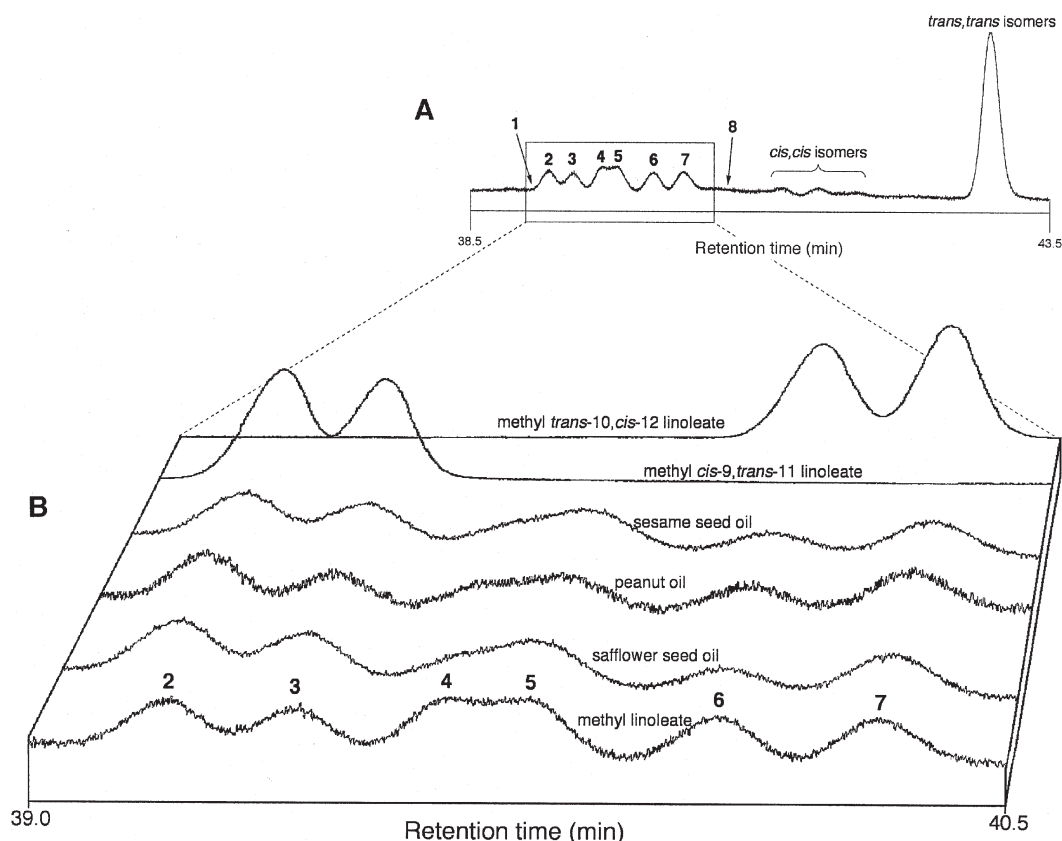
## RESULTS AND DISCUSSION

**Identification of individual *cis-trans* CLA isomers.** Structural determination of configurational CLA isomers presents some difficulties and may be confusing for closely related structural pairs. Analysis of individual CLA isomers has been achieved both by silver-ion HPLC (2,3,5,8,9), and by GC under appropriate eluting conditions using long polar open tubular capillary columns (3,5,7,8). We analyzed 18:2 conjugated isomers by GC on a 120-m highly polar BPX-70 column coated with 70% cyanoalkylpolysiloxane equivalent polymer. Separations were performed under temperature programming mode according to literature (3) and required high pressure (300 kPa at 170°C) to prevent excessive diffusion and to optimize run time. Elution order for mono *trans* 9,11 and 10,12 CLA was confirmed by using commercial rumenic (**2**) and *trans*-10,*cis*-12 (**7**) acid methyl esters standards, and their respective configuration isomers, *trans*-9,*cis*-11 (**5**) and *cis*-10,*trans*-12 (**4**), were obtained by isomerization of **2** and **7**, respectively, under mild conditions, using selenium metal as catalyst (6). Corresponding gas chromatograms are presented in Figure 1.

**CLA isomers from heated methyl linoleate and vegetable oils.** Methyl linoleate was heat treated at 200°C for 120 h under helium to ensure the formation of isomeric CLA. Similarly,



**FIG. 1.** Gas chromatogram of all configurational isomers of (A) methyl 9,11-linoleate and (B) methyl 10,12-linoleate, for confirmation of elution order of methyl *trans*-9,*cis*-11 (**5**) and *cis*-10,*trans*-12 (**4**) linoleate isomers. Isomers **5**, **9** (methyl *cis*-9,*cis*-11 linoleate), and **12** (methyl *trans*-9,*trans*-11 linoleate) were synthesized from **2** (methyl rumenate) by selenium-catalyzed isomerization. Similarly, isomers **4**, **10** (methyl *cis*-10,*cis*-12 linoleate), and **11** (methyl *trans*-10,*trans*-12 linoleate) were prepared from **7** (methyl *trans*-10,*cis*-12 linoleate). Analysis was performed on a 120-m BPX-70 capillary column (see Materials and Methods section for details).



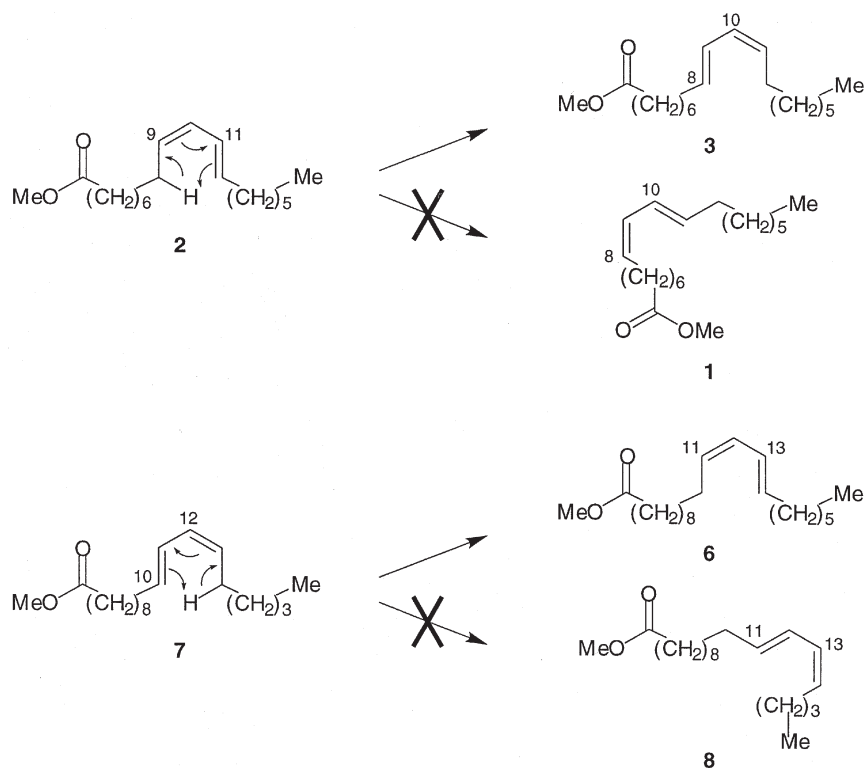
**FIG. 2.** Gas chromatogram region of (A) methyl CLA isomers from heated methyl linoleate, and (B) details of mono *trans* methyl CLA isomers from heated samples of methyl linoleate, safflower seed oil, peanut oil, sesame seed oil, methyl rumenate **2** (*cis*-9,*trans*-11 18:2), and methyl ester of *trans*-10,*cis*-12 18:2 acid **7**. Analysis was performed on a 120 m BPX-70 capillary column (see Materials and Methods section for details). Identification of CLA isomers is **2** (*cis*-9,*trans*-11), **3** (*trans*-8,*cis*-10), **4** (*cis*-10,*trans*-12), **5** (*trans*-9,*cis*-11), **6** (*cis*-11,*trans*-13), and **7** (*trans*-10,*cis*-12). Arrows in panel A indicate respective location for peaks of undetected **1** (*cis*-8,*trans*-10) and **8** (*trans*-11,*cis*-13) 18:2 isomers.

refined vegetable oils containing different levels of linoleic acid—peanut (28%), sesame seed (44%), and safflower seed (70%) oils—were heated at 200°C for 18 h in open flasks, in order to partly simulate oxygen uptake during the frying process. Respective CLA levels of 0.10, 0.25, and 1.1% were obtained. After methylation of heated oils, FAME were fractionated by Ag-TLC to achieve concentration of CLA isomers while removing saturated FA that elute within the CLA pattern on GC. A chromatogram exhibiting the *cis,trans* and *trans,cis* CLA elution zone (Fig. 2) shows distribution of mono *trans* CLA isomers from heated methyl linoleate and vegetable oils. They consisted of **2** *cis*-9,*trans*-11, **3** *trans*-8,*cis*-10, **4** *cis*-10,*trans*-12, **5** *trans*-9,*cis*-11, **6** *cis*-11,*trans*-13, and **7** *trans*-10,*cis*-12 18:2 acids. Relative CLA isomer distribution was identical for methyl linoleate and for peanut, sesame seed, and safflower seed oils. It was also similar to those from frying oils (3). As expected, two CLA isomers, **1** *cis*-8,*trans*-10 and **8** *trans*-11,*cis*-13 18:2 acids, were not detected in products from heat-treated methyl linoleate and vegetable oils.

**Evidence of [1,5] sigmatropic rearrangement.** The question that arises from the absence of **1** and **8** in the products from heated linoleic acid derivatives is, why? Obviously, a concerted mechanism, sensitive to steric or configurational factors, such as an internal pericyclic rearrangement of conjugated double bonds, must prevail. Indeed, sigmatropic

rearrangements are sensitive to such factors and thus have been extensively used in organic synthesis (10,11). To verify this hypothesis, methyl rumenate **2** was heated at 200°C under helium for 13 h. Owing to configuration constraints that would prevent the formation of mono *trans* isomer **1** in a [1,5] sigmatropic rearrangement, only mono *trans* isomer **3** should be formed (Fig. 3). Indeed, the resulting products of heat treatment of **2** were composed in quasi equal proportions of **2** and **3** (Fig. 2). Geometrical all-*cis* and all-*trans* isomers were also formed in small amounts. Sigmatropic rearrangement resulting in shift of the double bonds leading to 10,12 CLA isomers was not observed again as a result of unfavorable steric factors and configurations. Similarly, heat treatment of **7** resulted mainly in the formation of **6** (Figs. 2,3). These results suggested the establishment of an equilibrium between *cis,trans* and *trans,cis* systems in CLA that is in agreement with a [1,5] sigmatropic rearrangement (10). In the present case, the intramolecular process involved sigmatropic migration of an allylic hydrogen. This resulted in a shift of one carbon position for the conjugated system and imposed geometrical configurations for the two double bonds. In particular, the *cis* configurations in **3** and **6** were imposed by the cyclic geometry of the pericyclic mechanism, and the *trans* configurations, by steric factors. In addition, the process also prevented the formation of **1** and **8** CLA isomers, which were not detected in heated





**FIG. 3.** [1,5] Sigmatropic rearrangement of **2** (*cis*-9,*trans*-11 18:2) into **3** (*trans*-8,*cis*-10 18:2) and **7** (*trans*-10,*cis*-12 18:2) into **6** (*cis*-11,*trans*-13 18:2) acid isomers. Geometrical constraints prevent isomerization of **2** into **1** (*cis*-8,*trans*-10 18:2) and **7** into **8** (*trans*-11,*cis*-13 18:2) acid isomers.

linoleic acid derivatives (Fig. 2). Very likely, a [1,5] sigmatropic rearrangement may also occur between **4** and **5** acids, whose presence gives some clues on the formation of CLA from linoleic acid. Indeed, the formation of CLA very likely proceeds also through a concerted mechanism that results in abstraction of active hydrogen at C-11 by C-9 or C-13 (12). Moreover, the presence of **4** and **5** suggests that geometrical isomerization may also occur during this process, resulting in a mixture of all configuration isomers of 9,11 and 10,12 CLA. Further heat treatment then causes mono *trans* CLA to rearrange through a [1,5] sigmatropic mechanism, thus completing logical links between the three *cis,trans* and the three *trans,cis* CLA isomers found in heated vegetable oils.

## ACKNOWLEDGMENTS

We acknowledge financial support of Natural Sciences and Engineering Council of Canada, of Fonds FCAR, and of CORPAQ (Gouvernement du Québec). The authors are also grateful to Fondation de l'Université Laval for a Ph.D. scholarship to F. Destailats, and to Claire Japiot for technical assistance.

## REFERENCES

- Turini, M.E., and Martin, J.C. (2001) Sources, Functions, and Analysis of Conjugated Linoleic Acid and Its Metabolites, in *Structured and Modified Lipids* (Gunstone, F.D., ed.), Marcel Dekker, New York, pp. 251–284.
- Jung, M.Y., and Ha, Y.L. (1999) Conjugated Linoleic Acid Isomers in Partially Hydrogenated Soybean Oil Obtained During Nonselective and Selective Hydrogenation Process, *J. Agric. Food Chem.* **47**, 704–708.
- Juanéda, P., Cordier, O., Gregoire, S., and Sébédio, J.L. (2001) Conjugated Linoleic Acid (CLA) Isomers in Heat-Treated Vegetable Oils, *Oleagineux Corps Gras Lipides* **8**, 94–97.
- Sébédio, J.L., Grandgirard, A., and Prevost, J. (1988) Linoleic Acid Isomers in Heat-Treated Sunflower Oils, *J. Am. Oil Chem. Soc.* **65**, 362–366.
- Christie, W.W., Sébédio, J.L., and Juanéda, P. (2001) A Practical Guide to the Analysis of Conjugated Linoleic Acid (CLA), *inform* **12**, 147–152.
- Kass, J.P., and Burr, G.O. (1939) The Elaidinization of Linoleic Acid, *J. Am. Chem. Soc.* **61**, 1062–1066.
- Kramer, J.K.G., Cruz-Hernandez, C., and Zhou, J. (2001) Conjugated Linoleic Acids and Octadecenoic Acids: Analysis by GC, *Eur. J. Lipid Sci. Technol.* **103**, 600–609.
- Eulitz, K., Yurawecz, M.P., Sehat, N., Fritsche, J., Roach, J.A.G., Mossoba, M.M., Kramer, J.K.G., Adlof, R.O., and Ku, Y. (1999) Preparation, Separation, and Confirmation of the Eight Geometrical *cis/trans* Conjugated Linoleic Acid Isomers 8,10- Through 11,13-18:2, *Lipids* **34**, 873–877.
- Yurawecz, M.P., and Morehouse, K.M. (2001) Silver-Ion HPLC of Conjugated Linoleic Acid Isomers, *Eur. J. Lipid Sci. Technol.* **103**, 609–613.
- Spangler, C.W. (1976) Thermal [1,*j*] Sigmatropic Rearrangements, *Chem. Rev.* **76**, 187–217.
- Quinn, J.F., Bos, M.E., and Wulff, W.D. (1999) Novel [1,5] Sigmatropic Rearrangements of Cyclohexadienones Generated from Fischer Carbene Complexes. A New Strategy for Installing the C-20 Angular Ethyl Group in Aspidospermidine Alkaloids, *Organic Lett.* **1**, 161–164.
- Mounts, T.L., and Dutton, H.J. (1970) Conjugation of Polyunsaturated Acids, *Lipids* **5**, 997–1005.

[Received December 7, 2001, and in revised form March 6, 2002; revision accepted March 10, 2002]

# Issues Concerning the Monitoring of Statin Therapy in Hypercholesterolemic Subjects with High Plasma Lipoprotein(a) Levels

Angelo M. Scanu<sup>a,b,\*</sup> and Janet Hinman<sup>a</sup>

Departments of <sup>a</sup>Medicine and <sup>b</sup>Biochemistry and Molecular Biology, University of Chicago, Chicago, Illinois 60637

**ABSTRACT:** Most studies on the topic have shown that statin therapy decreases plasma LDL levels but not those of lipoprotein(a) [Lp(a)]. This specificity of action, although previously noted, has not been systematically investigated. In the current study we approached this problem by monitoring LDL- and Lp(a) cholesterol in 80 hypercholesterolemic subjects with high Lp(a) levels, at entry and 8 mon after initiation of statin therapy. We found that commonly used direct and indirect LDL cholesterol assays gave an LDL cholesterol value that comprised both true LDL- and Lp(a) cholesterol. We estimated these two analytes from the values of Lp(a) protein determined by ELISA and from knowledge of the Lp(a) chemical composition, complemented by data from immunochemical and ultracentrifugal analyses. Statin therapy, while not affecting plasma Lp(a) protein levels ( $21.7 \pm 10.4$ , before, and  $22.0 \pm 10.1$  mg/dL, after), caused a decrease in the estimated or true LDL cholesterol ( $P < 0.0001$ ) to values in some cases as low as 10 mg/dL. This drop in true LDL was validated by the decrease in the LDL band in the ultracentrifugation profiles, and its magnitude was proportional to the degree of total cholesterol lowering and to the pretreatment true LDL/Lp(a) cholesterol weight ratio. We conclude that true LDL but not Lp(a) cholesterol is affected by statin therapy and that this specific response cannot be monitored by current LDL cholesterol assays and must, rather, rely on estimates of these two analytes.

Paper no. L8996 in *Lipids* 37, 439–444 (May 2002).

Lipoprotein(a) [Lp(a)] is an LDL variant in which apolipoprotein B-100 (apoB-100) is linked by a single disulfide bond to apolipoprotein(a), [apo(a)], the characteristic glycoprotein of Lp(a) (1). As a consequence of this linkage, Lp(a) acquires metabolic properties that differ from those of LDL; among them is the inability to be taken up and degraded *via* the LDL receptor pathway (2,3). This impaired mechanism has been attributed to the failure of statins to lower the plasma levels of Lp(a) significantly, in contrast to LDL (4). The difference in metabolic behavior and pharmacological response of these two lipoproteins is not routinely recognized when statins or other hypolipidemic agents are used to treat subjects with high plasma Lp(a) levels (5). A main reason for this lack of recognition is the reliance placed on LDL cholesterol assays

that measure both LDL and Lp(a) cholesterol (6). The metabolic consequences and clinical magnitude of the different responses of LDL and Lp(a) to statins have not been clearly established. In the present study we investigated 80 hypercholesterolemic subjects on statin therapy who had both high plasma LDL and Lp(a) levels, and we also determined the LDL, Lp(a), and HDL distribution by physical, chemical, and immunochemical methods both at entry and after 8 mon at completion of the study. Furthermore, we examined the performance of direct and indirect assays for total LDL cholesterol and estimated this value by subtracting the amount contributed by Lp(a) from the total cholesterol. We report here that statin treatment can cause a significant depletion of plasma LDL but not of Lp(a), thus causing an unusually high Lp(a)/LDL profile that, if unrecognized, introduces a confounder in monitoring hypercholesterolemic subjects with high Lp(a).

## MATERIALS AND METHODS

**Human subjects.** The 80 subjects were chosen from the patient population seen in the Lipid Clinic of the University of Chicago, presenting with either a personal or a family history of plasma lipid abnormalities with or without an established atherosclerotic cardiovascular disease assessed by the occurrence of one or more episodes of myocardial infarction, positive thallium stress test, and/or coronary angiography. The characteristics of the subjects studied are summarized in Table 1. All of them at entry had a significant elevation of plasma total cholesterol (above 200 mg/dL), LDL cholesterol (above 100 mg/dL), apoB-100 (above 100 mg/dL), and Lp(a) protein (above 10 mg/dL). The plasma TG did not exceed the 300 mg/dL level, thus permitting the application of the Friedewald *et al.* formula (7).

**Study plan.** At entry each subject was examined for plasma levels of total and LDL cholesterol, apoB-100, Lp(a) protein, and Lp(a) cholesterol, HDL cholesterol, and apolipoproteins A-1 (apoA-1) along with a lipoprotein profile obtained by isopycnic density gradient ultracentrifugation. In addition, genotyping and phenotyping of apo(a) and genotyping of apolipoprotein E (apoE) were also conducted. The same analyses, except for genotyping, were carried out after 8 mon during which time the patients were under statin treatment. The statins used were: atorvastatin (Pfizer, New York, NY), cerivastatin (Bayer, New Haven, CT), pravastatin (Bristol-Meyers Squibb, Princeton, NJ) and simvastatin (Merck, West

\*To whom correspondence should be addressed at Department of Medicine, MC5041, University of Chicago, 5841 S. Maryland Ave., Chicago, IL 60637. E-mail: ascanu@medicine.bsd.uchicago.edu

Abbreviations: apo(a), apolipoprotein(a); apoB, apolipoprotein B; apoA-I, apolipoprotein A-I; CK, creatine kinase; est-LDL, estimated LDL cholesterol as determined by subtracting Lp(a) cholesterol from total LDL cholesterol; Lp(a), lipoprotein(a).

**TABLE 1**  
**Characteristics of Subjects at Entry**

Number	80	Lp(a) protein (mg/dL)	21.7 ± 10.4
Age (yr)	58.1 ± 14.0 <sup>a</sup>	Apo(a) genotype (kb)	60–140
Body mass index (kg/m <sup>2</sup> )	27.5 ± 4.6	Lp(a) cholesterol (mg/dL)	36.9 ± 17.7
Race (Caucasian/African-American/Oriental)	61/16/2	HDL cholesterol (mg/dL)	48.3 ± 26.6
Gender (male/female)	50/30	ApoA-1	130.9 ± 21.6
Smoker, +/ex/-	5/11/64	TG (mg/dL)	174.3 ± 72.4
Diabetes, +/-	12/68	Apo E genotype	
Systolic BP >140 mm Hg, +/-	8/72	3/3	49
ASCVD, +/-	30/50	3/4	21
Total cholesterol (mg/dL)	252.0 ± 36.3	2/2	2
Total LDL cholesterol (mg/dL) <sup>b</sup>	167.7 ± 38.9	2/3	7
ApoB-100 (mg/dL)	132.8 ± 30.9	2/4	1

<sup>a</sup>Mean ± SD.

<sup>b</sup>Calculated using the Friedewald formula. Abbreviations: BP, blood pressure; ASCVD, atherosclerotic cardiovascular disease; Apo, apolipoprotein.

Point, PA) (Table 2). Their choice and dosage were individualized according to clinical presentation, degree of hypercholesterolemia, and drug response. At the beginning of the study and during the course of the therapy each subject received nutritional and exercise counseling.

**Blood collection.** All subjects gave informed consent according to a protocol approved by the Institutional Review Advisory Board of the University of Chicago. The subjects fasted overnight before blood was withdrawn from the antecubital vein. The blood was collected into EDTA-containing tubes that were centrifuged within 30 min of collection. Following addition of an antiproteolytic cocktail (8), the plasma was either examined immediately or stored at 4°C in airtight containers until use within no more than 2 d.

**Laboratory analyses.** Total plasma cholesterol, TG, and HDL cholesterol were determined in a Vitros DT60 II System (Ortho Clinical Diagnostics, Rochester, NY) following the instructions by the manufacturer. Validation of the results was obtained from the College of American Pathologists (Northfield, IL). In all cases, the total LDL cholesterol was calculated according to the formula of Friedewald *et al.* (7). For comparative purposes, in 10 randomly selected subjects we also determined the total LDL cholesterol by direct assays, using each of the two following procedures: (i) Sigma Diagnostic procedure #353 (Sigma, St. Louis, MO), which utilizes latex beads coated with affinity-purified goat polyclonal antisera to specific human apolipoproteins to remove HDL and VLDL from the plasma sample; (ii) Sigma Diagnostic EZ LDL<sup>TM</sup> Homogeneous Method, in which, as a first step, an enzyme is used to bind to LDL cholesterol, rendering it unreactive and, as a second step, the enzyme is removed, thus permitting the colorimetric measurement of LDL cholesterol. The techniques

were carried out according to the manufacturer's instructions. In all cases, Lp(a), in terms of protein, was determined by ELISA as described by Fless *et al.* (9). Lp(a) cholesterol was estimated by multiplying the Lp(a) protein value by 1.7, a factor obtained from the average protein/total cholesterol weight ratio of six Lp(a) preparations differing in density (10). We estimated LDL cholesterol (est-LDL) by subtracting Lp(a) cholesterol from total LDL cholesterol. ApoB was determined by ELISA as previously described (11) and apoA-I by an ELISA developed in our laboratory using monospecific polyclonal antibodies raised in the rabbit utilizing reference materials kindly provided by Dr. Santica Marcovina of the Northwest Lipid Research Laboratories (Seattle, WA). Genotyping of apo(a) was carried out according to Lackner *et al.* (12) and that of apoE according to Hixson and Vernier (13). Phenotyping of apo(a) was conducted as previously described (14). All subjects had two alleles that ranged between 60 and 140 kb. Two apo(a)-size isoforms were present in the plasma; however, except for those cases in whom the two isoforms differed by 2–3 kringsles, the smaller sizes (12–15 kringsles) were the dominant ones. Creatine kinase (CK) and liver function tests were carried out at 4-mon intervals in the General Clinical Chemistry Laboratory of the University of Chicago.

**Isopycnic density gradient ultracentrifugation.** This was carried out according to an updated version (14) of a previously described technique (15). In brief, a nonlinear salt gradient was constructed to maximize the separation of LDL, Lp(a), and HDL classes. VLDL remained at the top of the tube. This discontinuous gradient was centrifuged in a swinging bucket rotor, SW40 (Beckman, Palo Alto, CA) at 284,000 × *g* for 50 h. At the end of the run, the effluent emerging from the top of the tube was monitored at 280 nm in a UA-5 ISCO absorbance monitor (Isco, Lincoln, NE) and recorded on a chart with a chart speed of 60 cm/h and a pump flow rate of 1 mL/cm. Density calibration was carried out as reported previously (14) by measuring the densities of each collected gradient fraction (0.9 mL) using a Mettler/Paar Precision Density Meter Model DMA 02C, and the distribution of Lp(a) was determined throughout the profile by ELISA. The subjects selected for the study had plasma levels of Lp(a) protein above

**TABLE 2**  
**Statin Regimen for the 8-mon Study**

Statin	Number of subjects	Dose (mg/d)
Atorvastatin	48	10–80
Simvastatin	17	20–40
Cerivastatin	8	0.2–0.4
Pravastatin	7	20–40

10 mg/dL, which permitted detection of a peak in the density gradient profile. In preliminary studies, we also established that in the hypertriglyceridemic subjects less than 1% of the total plasma apo(a) was present in the low-density portion of the gradient containing the TG-rich particles.

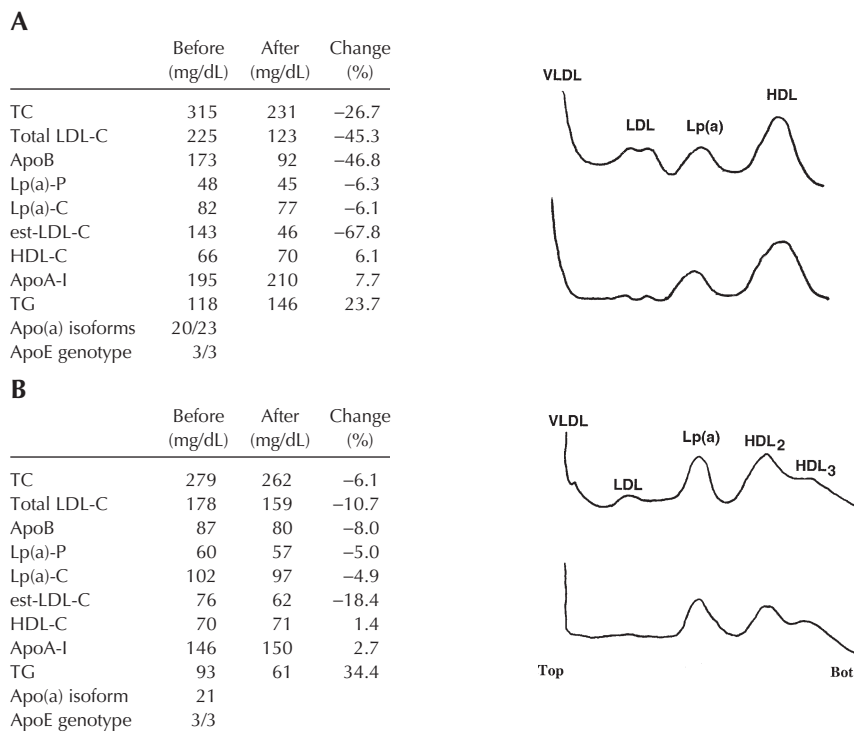
**Electrophoresis and immunoblotting.** For apo(a) phenotyping, the electrophoretic analyses were carried out on SDS-PAGE (4% polyacrylamide) on a Novex system (Novex, San Diego, CA) as previously described (16). Following electroblotting, the Immobilon blots were blocked in PBS containing 5% dry powdered milk and 0.3% Tween 20, followed by incubation with a specific anti-Lp(a) antibody prepared in the laboratory as previously described (16). M.W. markers representing apo(a) recombinants of a defined number of kringles were obtained from Dr. Eduardo Angles Cano (INSERM U 143, Paris, France).

**Statistical analyses.** The changes of the various parameters following statin treatment were determined by the paired two-tailed *t*-test. Because of the potential skewed distribution of

some of the parameters, particularly Lp(a) protein and Lp(a) cholesterol, all data were also examined by the Wilcoxon rank-sum test. We considered values of  $P < 0.05$  as significant.

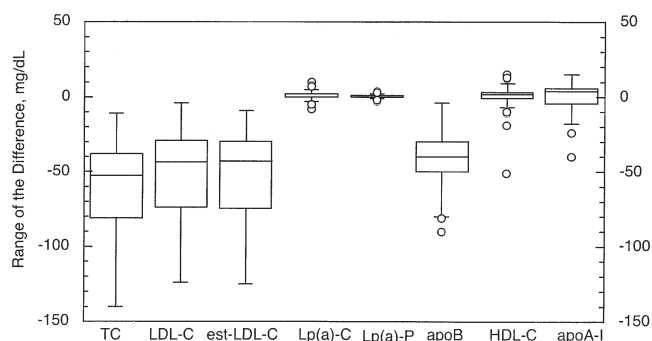
## RESULTS

In the 10 subjects used in the comparative studies, the mean total LDL cholesterol value  $\pm$  SD ( $126.7 \pm 67.2$  mg/dL) obtained by the formula of Friedewald *et al.* was in close agreement with the mean values  $\pm$  SD obtained by the Sigma 353 and EZ direct assays,  $132.2 \pm 63.2$  and  $133.2 \pm 66.5$  mg/dL, respectively. Since the formula of Friedewald *et al.* previously has been shown to provide the combined values of LDL cholesterol and Lp(a) cholesterol (6), it is apparent from our results that commonly used LDL cholesterol assays jointly measure both parameters. Figure 1 shows the lipoprotein and apolipoprotein values obtained in two representative subjects before and 8 mon after continual statin therapy. The subject in panel A exhibited a marked change in total cholesterol,



**FIG. 1.** Single spin profiles in two subjects before and after statin therapy. (A) This subject experienced a marked change in plasma total and est-LDL cholesterol and a modest change in Lp(a) protein while on atorvastatin, 20 mg daily. The marked drop in "true" LDL and apoB is reflected by the single spin profile (lower pattern) in which the double LDL peak is markedly reduced while the bands corresponding to Lp(a) and HDL remained essentially unchanged in keeping with the chemical and immunochemical data. (B) This subject had, at entry, a very high plasma level of Lp(a) protein indicating that a high percentage of the plasma cholesterol was carried by Lp(a). The hypocholesterolemic response elicited by cerivastatin 0.4 mg daily involved only est-LDL, as reflected by the chemical and ultracentrifugal data. Also in this case, chemical, immunochemical, and ultracentrifugal results showed little change in Lp(a) and HDL. In all cases the ultracentrifugal profiles were continuously recorded at 280 nm. The vertical axis represents optical density readings and the horizontal axis the gradient from top to bottom. TC, total cholesterol; LDL-C, total LDL cholesterol; est-LDL-C, estimated LDL cholesterol; Lp(a)-C, Lp(a) cholesterol; Lp(a)-P, Lp(a) protein; HDL-C, HDL cholesterol; apoB and apoA-I, apolipoproteins B and A-I; Lp(a), lipoprotein(a).





**FIG. 2.** Box plot of the range of difference of each parameter before and after statin treatment. Each box encloses 50% of the data with the median value of the parameter displayed as a line. The top and bottom of each box marks the  $\pm 25\%$  limit of the parameter studied. The lines extending from the top and bottom of each box mark the minimal and maximal values within the data set that fall within the acceptable range. Any outlier outside of this range is displayed as an individual point. For abbreviations see Figure 1.

LDL cholesterol, apoB, and est-LDL cholesterol, whereas there was comparatively little change in Lp(a) protein and Lp(a) cholesterol. In keeping with the chemical and immunochemical findings, the ultracentrifugal lipoprotein profiles showed that, after statin therapy (lower profiles), there was a marked reduction of the two LDL bands with little change in the Lp(a) and HDL bands. For the subject in panel B (Fig. 1), about 58% of the total LDL cholesterol (178 mg/dL) at entry, was in Lp(a) (102 mg/dL). Again, statin therapy had little effect on Lp(a) protein and Lp(a) cholesterol, as also reflected by the ultracentrifugation profiles. Both subjects in Figure 1, who differed in their apo(a), had the same apoE genotype, E3/3. In the 80 subjects, the effects on the various parameters of statin therapy are summarized in Figure 2. Major changes are evident for total cholesterol, LDL cholesterol, est-LDL cholesterol and apoB. The statistical analyses of the data (Table 3) using the paired *t*-test indicated that all these changes were highly significant. On the other hand, for Lp(a) protein and Lp(a) cholesterol, the mean change and the 95% confidence interval values after statin therapy were in each case very small, indicating that despite the *P* values, the changes were of either little or no biological relevance. The

Wilcoxon treatment of the data gave results comparable to those obtained with the paired *t*-test. Taken together, our results indicate that, whenever present, the drop in total plasma cholesterol occurred at the expense of the est-LDL cholesterol or true LDL cholesterol.

The statins were well tolerated with no evidence of side effects. The liver function tests and CK values remained within normal limits.

## DISCUSSION

The results of the current studies show that in hypercholesterolemic subjects with high plasma Lp(a) levels, statin treatment causes a decrease of total plasma LDL at the expense of the LDL component without a significant effect on Lp(a). This specificity in response could not be identified by either the indirect Friedewald *et al.* method or by the two direct "LDL cholesterol" assays, since all of them measured the total LDL cholesterol, i.e., the sum of LDL- and Lp(a) cholesterol. These results are in agreement with the ultracentrifugation-based  $\beta$  quantification data also shown to measure total LDL cholesterol (6). We believe that this is also likely to apply to any method that makes use of reagents reacting with apoB-100. Based on experimental findings in the current study, which was aimed at developing an understanding of the magnitude of the statin effect on true LDL- and Lp(a) cholesterol, we estimated those parameters based on the Lp(a) protein values and the data on the chemical composition of Lp(a) (see the Materials and Methods section for details) In our work, we used the factor 1.7 to estimate Lp(a) cholesterol from the Lp(a) protein ELISA data. However, this factor may not be universally applicable owing to the wide interindividual variation in Lp(a) in terms of apo(a) size, lipid content, and composition. From our own data and those in the literature, the protein-to-total cholesterol weight ratio may vary from 1.3 to 2 and in extreme cases 2.5 (5). Our conclusion that the statin effect is at the expense of true LDL was corroborated by both the density gradient ultracentrifugal profiles and the apoB-100 data. We attempted to compare the estimated Lp(a) cholesterol values with those obtained by the direct Lp(a) cholesterol assay of Seman *et al.* (17) utilizing a

**TABLE 3**  
Statistical Evaluation of the Parameters Studied in the 80 Subjects<sup>a</sup>

	Mean change	SD	Range	95% CI	<i>P</i> -value
	mg/dL				
Total cholesterol	-60.4	30.6	-140 to -11	-67.2 < -60.4 < -53.6	<0.0001
Total LDL cholesterol	-51.3	29.2	-124 to -4	-57.8 < -51.3 < -44.8	<0.0001
est-LDL cholesterol	-51.9	28.9	-125 to -7	-58.3 < -51.9 < -45.4	<0.0001
ApoB	-42.3	20.5	-90 to -4	-46.2 < -42.3 < -38.4	<0.0001
ApoA-I	0.83	9.11	-40 to 15	-2.17 < 0.83 < 3.83	0.41
HDL cholesterol	0.39	7.71	-51 to 15	-1.33 < 0.39 < 2.11	0.65
Lp(a) protein	0.34	1.23	-3 to 4	0.07 < 0.34 < 0.61	0.016
Lp(a) cholesterol	0.57	2.09	-5 to 7	0.11 < 0.57 < 1.04	0.017

<sup>a</sup>CI, confidence interval; est-LDL, estimated LDL cholesterol determined by subtracting Lp(a) cholesterol from total LDL cholesterol; ApoB and ApoA-I, apolipoproteins B and A-I; Lp(a), lipoprotein(a).

commercial kit developed by Genzyme. Unfortunately, we were unable to arrive at a credible comparison because the number of available observations is limited by the fact that the kit has been removed from the market. An ultracentrifugation method, VAP (Atherotec, Birmingham, AL), has been proposed for simultaneously determining the cholesterol distribution among the main plasma lipoproteins. However, this approach suffers from the fact that both LDL and Lp(a) are highly heterogeneous in density (14), causing overlaps among these species and thus difficulties in making unequivocal lipoprotein assignments in the absence of appropriate apolipoprotein markers.

From our studies it is apparent that statin therapy, by specifically lowering the plasma LDL levels, leaves a residual statin-resistant hypercholesterolemia mainly sustained by Lp(a), the magnitude of which depends on pretreatment plasma LDL cholesterol and the LDL/Lp(a) cholesterol ratio. This specificity in response supports the notion that LDL and Lp(a) have distinct metabolic pathways (3,4). Moreover, the fact that the drop in plasma LDL involved the whole lipoprotein particle, as was shown by the chemical, immunochemical, and ultracentrifugal data, provides evidence that the LDL particles were removed *in toto* via the LDL receptor pathway.

The treatment with statins of hypercholesterolemic subjects with high plasma Lp(a) levels was prompted by the notion that decreasing the plasma LDL levels reduces the cardiovascular pathogenic potential of Lp(a) (18). Of note, the safety limit for the hypocholesterolemic effect of hypolipidemic agents has not been established. This situation cannot be compared with hypo- $\beta$ - and  $\alpha$ - $\beta$ -lipoproteinemia since these disorders are genetically determined and characterized by very low to absent plasma levels of LDL and apoB-100 (19), however, with little or no Lp(a)/apo(a) (3), and thus they are not directly comparable to the statin-induced LDL-deficient/high Lp(a) phenotype. Concerns about plasma cholesterol lowering have been raised because of reports associating plasma cholesterol levels with mood changes (20,21), depression and suicide attempts (22–25), and violent crime (26). However, the threshold of plasma cholesterol associated with these pathologies has not been uniformly established nor has the type of lipoprotein accounting for the cholesterol lowering been determined. In this study, statins caused an important drop in true LDL but did not significantly affect the levels of Lp(a) and HDL. Thus, in this unique scenario, we may speculate that the potentially harmful lowering of LDL may be functionally compensated by the cholesterol contained in either Lp(a) or HDL, or both. This would be in keeping with the lack of psychological problems reported in extensive statin trials, which likely included subjects of the type examined in the current study.

Atorvastatin, cerivastatin, simvastatin, and pravastatin, the four statins represented in this study, all exhibited similar behavior at the doses used by significantly lowering the plasma levels of true LDL while not affecting those of Lp(a). Thus, this appears to represent a class effect. A main message from our studies is that when hypercholesterolemic subjects with

elevated plasma levels of Lp(a) are treated with statins, the currently available assays that measure total LDL-cholesterol cannot be used to monitor compliance with the National Cholesterol Education Program III (NCEP III) guidelines (27) and therapeutic response. Recently, the two-step non-HDL cholesterol assay has been suggested as a better tool for cardiovascular risk and treatment assessment (28) and a better predictor (29) than the three-step LDL cholesterol assays. Although this approach clearly deserves further evaluation, the fact that the non-HDL cholesterol includes Lp(a) among the atherogenic lipoproteins requires attention.

## ACKNOWLEDGMENTS

Celina Edelstein provided invaluable assistance during the preparation of the manuscript and Ditta Pfaffinger, critical technical help. We are grateful to Drs. Theodore Karrison and Dezheng Huo of our Department of Health Studies for advice in the statistical analyses. Supported by the National Heart, Lung, and Blood Institute grants HL 63115 and 63209.

## REFERENCES

1. Scanu, A.M., Nakajima, K., and Edelstein, C. (2001) Apolipoprotein(a): Structure and Biology, *Front. Biosci.* 6, 546–554.
2. Scanu, A.M., and Fless, G.M. (1990) Lipoprotein (a): Heterogeneity and Biological Relevance, *J. Clin. Invest.* 85, 1709–1715.
3. Utermann, G. (1995) Lipoprotein(a), in *The Metabolic and Molecular Basis of Inherited Disease* (Scriver, C.R., Beaudet, A.L., Sly, W.S., and Valle, D., eds.), pp. 1887–1912, McGraw-Hill, New York.
4. Lawn, M.R., and Scanu, A.M. (1996) Lipoprotein(a), in *Atherosclerosis and Coronary Artery Disease* (Fuster, V., Ross, R., and Topol, E.J., eds.), pp. 151–161, Lippincott-Raven, Philadelphia.
5. Scanu, A.M. (2001) Lipoprotein(a), Friedewald Formula and NCEP Guidelines, National Cholesterol Education Program, *Am. J. Cardiol.* 87, 608–609.
6. Bachorik, P.S. (1997) Measurement of Low-Density-Lipoprotein Cholesterol, in *Handbook of Lipoprotein Testing* (Rifai, N., Warnick, E.R., and Dominiczak, M.H., eds.), pp. 235–243, AAC Press, Washington, DC.
7. Friedewald, W.T., Levy, R.I., and Fredrickson, D.S. (1972) Estimation of the Distribution of Low Density Lipoprotein Cholesterol in Plasma Without the Use of the Preparative Centrifuge, *Clin. Chem.* 18, 499–502.
8. Edelstein, C., and Scanu, A.M. (1986) Precautionary Measures for Collecting Blood Destined for Lipoprotein Isolation, *Methods Enzymol.* 128, 151–155.
9. Fless, G.M., Snyder, M.L., and Scanu, A.M. (1989) Enzyme-Linked Immunoassay for Lp(a), *J. Lipid Res.* 30, 651–662.
10. Fless, G.M., Zummallen, M.E., and Scanu, A.M. (1987) Heterogeneity of Human Plasma Lp(a), in *Proceedings of the Workshop on Lipoprotein Heterogeneity* (Lippel, K., ed.), pp. 141–153, NIH Publication No. 87-2646, NIH, Bethesda.
11. Fless, G.M., Rolih, C.A., and Scanu, A.M. (1984) Heterogeneity of Human Plasma Lp(a): Isolation and Characterization of the Lipoprotein Subspecies and Their Apoproteins, *J. Biol. Chem.* 259, 11470–11478.
12. Lackner, C., Boerwinkle, E., Leffert, C.C., Rahmig, T., and Hobbs, H.H. (1991) Molecular Basis of Apolipoprotein(a) Isoform Size Heterogeneity as Revealed by Pulsed-Field Gel Electrophoresis, *J. Clin. Invest.* 87, 2153–2161.

13. Hixson, J.E., and Vernier, D.T. (1990) Restriction Isotyping of Human Apolipoprotein E by Gene Amplification and Cleavage with *HhaI*, *J. Lipid Res.* 31, 545–548.
14. Nakajima, K., Hinman, J., Pfaffinger, D., Edelstein, C., and Scanu, A.M. (2001) Changes in Plasma Triglyceride Levels Shift Lipoprotein(a) Density in Parallel with That of Low-Density Lipoprotein Independently of Apolipoprotein(a) Size, *Arterioscler. Thromb. Vasc. Biol.* 21, 1238–1243.
15. Nilsson, J., Mannickarottu, V., Edelstein, C., and Scanu, A.M. (1981) An Improved Detection System Applied to the Study of Serum Lipoproteins After Single-Step Density Gradient Ultracentrifugation, *Anal. Biochem.* 110, 342–348.
16. Edelstein, C., Italia, J.A., Klezovitch, O., and Scanu, A.M. (1996) Functional and Metabolic Differences Between Elastase-Generated Fragments of Human Lipoprotein(a) and Apolipoprotein(a), *J. Lipid Res.* 37, 1786–1801.
17. Seman, L.J., Jenner, J.L., McNamara, J.R., and Schaefer, E.J. (1994) Quantification of Lipoprotein(a) in Plasma by Assaying Cholesterol in Lectin-Bound Plasma Fraction, *Clin. Chem.* 40, 400–403.
18. Maher, V.M.G., and Brown, B.G. (1995) Lipoprotein(a) and Coronary Heart Disease, *Curr. Opin. Lipid.* 6, 229–235.
19. Kane, J.P., and Havel, R.J. (1995) Disorders of the Biogenesis and Secretion of Lipoproteins Containing the B Apolipoproteins, in *Metabolic and Molecular Basis of Inherited Disease* (Scriver, C.R., Beaudet, A.L., Sly, W.S., and Valle, D., eds.), pp. 1853–1885, McGraw-Hill, New York.
20. Brown, S.L. (1996) Lowered Serum Cholesterol and Low Mood, *Br. Med. J.* 313, 637–638.
21. Lindberg, G., Larsson, G., Setterlind, S., and Rastam, L. (1994) Serum Lipid and Mood in Working Men and Women in Sweden, *J. Epidemiol. Commun. Health* 48, 360–363.
22. Partonen, T., Haukka, J., Virtamo, J., Taylor, P.R., and Lonngvist, J. (1999) Association of Low Serum Total Cholesterol with Major Depression and Suicide, *Br. J. Psychiatry* 175, 259–262.
23. Manfredini, R., Caracciolo, S., Salmi, R., Boari, B., Tomelli, A., and Gallerani, M. (2000) The Association of Low Serum Cholesterol with Suicidal Behaviours: New Hypotheses for the Missing Link, *J. Int. Med. Res.* 28, 247–257.
24. Ellison, L.F., and Morrison, H.I. (2001) Low Serum Cholesterol and Risk of Suicide, *Epidemiology* 12, 169–172.
25. Alvarez, J.-C., Cremniter, D., Gluck, N., Quintin, P., Leboyer, N., Berlin, I., Therond, P., and Spreux-Varoquax, O. (2000) Low Serum Cholesterol in Violent but Not in Non-violent Suicide Attempters, *Psychiatry Res.* 95, 103–108.
26. Golomb, B.A., Stattin, H., and Mednick, S. (2000) Low Cholesterol and Violent Crime, *J. Psychoatr. Res.* 34, 301–309.
27. Executive Summary of the Third Report of the National Cholesterol Education Program (NECP) (2001) Expert Panel on Detection, Evaluation and Treatment of High Blood Cholesterol in Adults (Adult Treatment Panel III), *JAMA* 285, 2486–2497.
28. Frost, P.H., and Havel, R.J. (1998) Rationale for Use of Non-High-Density Lipoprotein Cholesterol Rather Than Low-Density Lipoprotein Cholesterol as a Tool for Lipoprotein Cholesterol Screening and Assessment of Risk and Therapy, *Am. J. Cardiol.* 81, 26B–31B.
29. Cui, Y., Blumenthal, R.S., Flaws, J.A., Whiteman, M.K., Langenberg, P., Bachorik, P.S., and Bush, T.L. (2001) Non-high-Density Lipoprotein Cholesterol Level as a Predictor of Cardiovascular Disease Mortality, *Arch. Intern. Med.* 161, 1413–1419.

[Received February 1, 2002, and in revised form March 27, 2002; revision accepted April 15, 2002]

# High Doses of Atorvastatin and Simvastatin Induce Key Enzymes Involved in VLDL Production

Núria Roglans<sup>a</sup>, Joan C. Verd<sup>a</sup>, Cristina Peris<sup>a</sup>, Marta Alegret<sup>a</sup>,  
Manuel Vázquez<sup>a</sup>, Tomás Adzet<sup>a</sup>, Cristina Díaz<sup>b</sup>, Gonzalo Hernández<sup>b</sup>,  
Juan C. Laguna<sup>b</sup>, and Rosa M. Sánchez<sup>a,\*</sup>

<sup>a</sup>Unidad de Farmacología y Farmacognosia, Departamento Farmacología y Química Terapéutica, Facultad de Farmacia, 08028-Barcelona, Spain, and <sup>b</sup>Departamento I+D, División Médica, Pfizer S.A. 28108-Madrid, Spain

**ABSTRACT:** Treatments with high doses of 3-hydroxy-3-methylglutaryl-coenzyme A (HMG-CoA) reductase inhibitors may induce the expression of sterol regulatory element binding protein (SREBP)-target genes, causing different effects from those attributed to the reduction of hepatic cholesterol content. The aim of this study was to investigate the effects of high doses of statins on the key enzymes involved in VLDL production in normolipidemic rats. To examine whether the effects caused by statin treatment are a consequence of HMG-CoA reductase inhibition, we tested the effect of atorvastatin on these enzymes in mevalonate-fed rats. Atorvastatin and simvastatin enhanced not only HMG-CoA reductase but also the expression of the SREBP-2 gene itself. As a result of the overexpression of SREBP-2 caused by the statin treatment, genes regulated basically by SREBP-1, as FA synthase and acetyl-coenzyme A carboxylase, were also induced and their mRNA levels increased. DAG acyltransferase and microsomal TG transfer protein mRNA levels as well as phosphatidate phosphohydrolase activity were increased by both statins. Simvastatin raised liver cholesterol content, ACAT mRNA levels, and CTP:phosphocholine cytidyltransferase activity, whereas it reduced liver DAG and phospholipid content. Mevalonate feeding reversed all changes induced by the atorvastatin treatment. These results show that treatment with high doses of statins induces key enzymes controlling rat liver lipid synthesis and VLDL assembly, probably as a result of SREBP-2 overexpression. Despite the induction of the key enzymes involved in VLDL production, both statins markedly reduced plasma TG levels, suggesting that different mechanisms may be involved in the hypotriglyceridemic effect of statins at high or low doses.

Paper no. L8856 in *Lipids* 37, 445–454 (May 2002).

Inhibitors of the rate-limiting step in cholesterol biosynthesis, 3-hydroxy-3-methylglutaryl coenzyme A (HMG-CoA) reductase, are efficient drugs used to lower plasma cholesterol levels (1). However, their ability to reduce TG concentrations depends on the baseline TG levels and on the potency and efficacy of the statin used (2–4). Daily doses of HMG-CoA reduc-

tase inhibitors used for the treatment of hyperlipidemias are progressively increasing in order to achieve optimal control of plasma lipid levels. However, it is still unknown whether the mechanisms involved in the hypolipidemic action are the same at high doses of statins or whether different effects may be responsible for the lipid-lowering activity of these drugs.

HMG-CoA reductase inhibitors have been shown to lower apolipoprotein B (apoB) concentrations in several animal models by decreasing hepatic VLDL apoB secretion into plasma, but not all studies have been consistent with this concept (5,6). Although the HMG-CoA reductase inhibitors have similar pharmacodynamic properties, they differ in their pharmacokinetic behavior. Therefore, the differences in apoB secretion observed *in vivo* among reported studies may, in part, pertain to the type and especially the dose of HMG-CoA reductase inhibitor administered (7). It has been proposed that inhibition of HMG-CoA reductase could limit the availability of cholesterol for VLDL production and decrease hepatic VLDL secretion, with the subsequent lowering of plasma TG (6,8). Nevertheless, the decrease in the cellular cholesterol content elicited by drug treatment not only limits cholesterol availability but also leads to the activation of the sterol regulatory element binding proteins (SREBP), membrane-bound transcription factors that transcriptionally regulate multiple genes involved in cholesterol metabolism and TG synthesis (9).

The role of SREBP in lipoprotein production has not yet been elucidated. However, it has been reported that SREBP-1 and SREBP-2 bind to the microsomal TG transfer protein (MTP) promoter (10). Furthermore, data obtained from transfected cells suggest that lipogenesis and the assembly and secretion of apoB-containing lipoproteins might be coordinately regulated by SREBP (11). We hypothesized that the effects of statins on VLDL production and secretion may differ depending on the dose used. Thus, treatments with high doses of HMG-CoA reductase inhibitors may induce an intense stimulus in the expression of SREBP-target genes, causing different effects from those attributed to the reduction of hepatic cholesterol content.

Both adequate supply of lipids and functional MTP are required for efficient formation of apoB-containing lipoproteins (12). Here we investigate the effect of high doses of atorvastatin and simvastatin on MTP and key enzymes involved in hepatic lipid synthesis in normolipidemic rats, an animal model widely used to study the hypotriglyceridemic effect of

\*To whom correspondence should be addressed at Unidad de Farmacología y Farmacognosia, Departamento Farmacología y Química Terapéutica, Facultad de Farmacia, Núcleo Universitario de Pedralbes, Barcelona E-08028, Spain. E-mail: sanchez@farmacia.far.ub.es

Abbreviations: ACC, acetyl-CoA carboxylase; apo, apolipoprotein; APRT, adenosyl phosphoribosyl transferase; CT, CTP:phosphocholine cytidyltransferase; DGAT, diacylglycerol acyltransferase; FAS, fatty acid synthase; HMG-CoA, 3-hydroxy-3-methylglutaryl-coenzyme A; MTP, microsomal triglyceride transfer protein; PAP, phosphatidate phosphohydrolase; RT-PCR, reverse transcription polymerase chain reaction; SREBP, sterol regulatory element binding protein.



statins. In addition, we have studied whether the effects caused by statin treatment are a consequence of HMG-CoA reductase inhibition by determining the effect of atorvastatin on these enzymes in mevalonate-fed rats.

## METHODS

**Animals and treatments.** Male Sprague–Dawley rats (Harlan, France) were maintained with water and food *ad libitum* at constant humidity and temperature with a light/dark cycle of 12 h. The animals (average weight  $207 \pm 11$  g) were randomized into three groups and fed a standard diet (Panlab, Barcelona, Spain) or the same diet supplemented with atorvastatin or simvastatin (0.1% w/w) for 3 d.

A subgroup of 12 animals was randomized into three groups of treatment: control, mevalonate, and atorvastatin-mevalonate groups. The control group was fed a standard diet (Panlab); mevalonate and atorvastatin-mevalonate groups were fed the same diet supplemented with mevalonate (0.1% w/w) or atorvastatin (0.1% w/w) plus mevalonate (0.1% w/w), respectively. Animals were treated for 3 d and killed by decapitation between 9 and 10 A.M. at the beginning of the light period. Treatment diets were prepared as described in Alegret *et al.* (13). Mevalonate was supplied by Sigma-Aldrich (St. Louis, MO), atorvastatin calcium was supplied by Pfizer S.A. (Madrid, Spain), and the simvastatin lactone form was a generous gift from Merck (Barcelona, Spain).

Golden Syrian hamsters (Harlan, France) weighing 35–40 g were maintained in the same conditions described above. All procedures were conducted in accordance with the principles and guidelines established by the University of Barcelona Bioethics Committee as stated in Law 5/1995, 21st July, from the Generalitat de Catalunya.

**Sample preparation.** Rat liver homogenate and subcellular fractions were obtained as described previously (14) and stored at  $-80^{\circ}\text{C}$  until needed. The protein concentration of each fraction was determined by the method of Bradford (15). Between 10 and 100 mg of liver tissue of each rat was immediately frozen in liquid  $\text{N}_2$  and used for the extraction of total RNA with the Ultraspec™ (Biotechx, Houston, TX) reagent, following the instructions provided by the manufacturer. Blood samples were collected at the time of death in heparinized tubes; plasma was obtained by centrifugation and stored at  $-80^{\circ}\text{C}$  until needed.

**Lipid analysis.** Plasma total cholesterol, TG, and phospholipid concentrations were measured with the Boehringer-Mannheim GmbH (Mannheim, Germany) colorimetric tests (Monotest Cholesterol-CHODPAP No. 290319, Peridochrom-Triglyceride-GPO-PAP No. 701882, and MPR2 No. 691844 phospholipid, respectively). VLDL and LDL from plasma samples were precipitated by using reagent No. 543004, also from Boehringer-Mannheim GmbH, and HDL-cholesterol concentration was determined in the supernatant.

Liver lipid was extracted and measured as described previously (14). DAG concentration was measured with the Amersham-Pharmacia-Biotech-Europe GmbH (Freiburg, Germany) radioactive test (DAG reagents system RPN 200).

**Enzyme assays.** HMG-CoA reductase, phosphatidate phosphohydrolase (PAP), and CTP:phosphocholine cytidyltransferase (CT) activities were determined as described previously (14). DAG acyltransferase (DGAT) activity was measured as described previously (13). MTP activity was assayed by the commercial kit WAK-MTP-100 (Wak-Chemie Medical GmbH, Bad Homburg, Germany), following the instructions provided by the manufacturer.

**Immunoblot analysis.** Crude nuclear extract from livers was prepared, and immunoblot analysis for endogenous SREBP-2 was performed as described previously (16,17).

**mRNA analysis.** (i) *Reverse transcription PCR (RT-PCR).* Relative levels of specific mRNA were assessed by RT-PCR, as described previously (18). To check the absence of contamination, negative controls were included in each experiment. Preliminary experiments were carried out to establish conditions for exponential amplification of all the genes studied, calculating the range of cycle numbers at which a linear relationship was detected between input RNA and final product. For each primer set, an increasing number of PCR cycles with otherwise fixed conditions were performed to determine the optimal number of cycles to be used. The same procedure was followed for RNA concentration (19). Adenosyl phosphoribosyl transferase (APRT) was used as an internal control and was coamplified with target sequences in the same tube, except for SREBP-2 and FA synthase (FAS). These sequences were amplified in parallel with APRT in separate tubes and in duplicate. The number of cycles was 26 for ACAT-1, 24 for DGAT, 22 for HMG-CoA reductase, 21 for CT, 30 for SREBP-2, 23 for acetyl-CoA reductase (ACC), and 18 for FAS. Twenty-three cycles were used for APRT when it was amplified separately. Primer sequences and resulting PCR products are listed in Table 1. Five microliters of each PCR reaction mixture was subjected to electrophoresis in 5% polyacrylamide gel in  $1 \times$  TBE (Tris-borate-EDTA). Gels were dried, autoradiographed on RX-OMAT S Kodak film (Rochester, NY), and quantified by image analysis (Vilbert Lourmat Imaging, Scientific and Technical Services, University of Barcelona). The mRNA levels were always expressed as a ratio relative to APRT mRNA levels.

(ii) *Northern blot analysis.* Rat MTP cDNA was cloned by RT-PCR amplification. First-strand cDNA was reverse transcribed from hamster liver total RNA (1  $\mu\text{g}$ ) by using SuperScript™ II from GIBCO BRL Life Technologies (Paisley, United Kingdom). The cDNA was amplified by PCR using sense (forward) and antisense (reverse) primers designed from the hamster MTP cDNA sequence (GenBank accession number: X59657). Sense and antisense primers were designed at 29 to 49 bp (5'-GGG AAG GCT GGT CTT CAC GGT-3') and at 456 to 476 bp (5'-TGG TTT CCA GGC CAG CTT TCA-3'), respectively, relative to the translation start site. The PCR was conducted for 34 cycles, and PCR products were fractionated on 1% agarose gels, and DNA fragments of the appropriate size (448 bp) were excised and purified by Jetsorb, Gel Extraction Kit (GenoMed, Bad Oeynthausen, Germany). These cDNA probes were  $^{32}\text{P}$ -labeled

**TABLE 1**  
**Primers Used for the PCR Reaction<sup>a</sup>**

Primers	Sense and antisense	PCR product (bp)	GenBank accession number
ACAT-1	5'-GGTGTGCGCTCACGACCTTCT-3' 5'-TCAGAATGAACCGGGAGGCTG-3'	498	BAA25372
DGAT	5'-TGTCAGTGGGTGCCCTGACAG-3' 5'-CCAACTGCAGGAGCTCTGCC-3'	613	AF296131
HMG-CoA Rd	5'-CCGACAAGAAACCTGCTGCCA-3' 5'-CAGTGCCACACACAATTCCGGG-3'	470	X55286
SREBP-2	5'-CATGGACACCCTCACGGAGCTGGGCGACGA-3' 5'-TGCATCATCCAATAGAGGGCTTCTGGCTC-3'	920	U12330
CT	5'-GGTTTACGGCAGCCAGCTCCT-3' 5'-ACGGACAATGCGGGTGATGAT-3'	516	M36071
ACC	5'-CGAGGCCGCTCAGCAACAGTA-3' 5'-TGGGTTCTCCGAGGCTTCG-3'	211	AB004329
FAS	5'-GTCTGCAGCTACCCACCCGTG-3' 5'-CTTCTCCAGGGTGGGGACCAG-3'	214	M76767
APRT	5'-AGCTTCCCAGACTTCCCCATC-3' 5'-GACCACTTTCTGCCCCGGTTC-3'	329	L04970

<sup>a</sup>DGAT, diacylglycerol acyltransferase; HMG-CoA Rd, 3-hydroxy-3-methylglutaryl-coenzyme A reductase; SREBP, sterol regulatory element binding protein; CT, CTP:phosphocholine cytidyltransferase; ACC, acetyl-CoA carboxylase; FAS, FA synthase; APRT, adenosyl phosphoribosyl transferase.

by a Random Priming Mix™ procedure from Promega-Boehringer Ingelheim (Heidelberg, Germany).

Twenty micrograms of total rat liver RNA was denatured and electrophoresed in 1% agarose gel and transferred to nylon membrane filter (Zeta-Probe; Bio-Rad, Barcelona, Spain). The filter was hybridized using ExpressHyb™ solution (Clontech Laboratories Inc., Palo Alto, CA) according to the instructions of the manufacturer and exposed to Kodak X-OMAT X-ray film at -80°C (20). mRNA levels were evaluated by densitometric scanning of the autoradiograph as described above and corrected for the amount of APRT using a cDNA probe.

**Statistics.** The results are the mean ± SEM of *n* experiments assayed in duplicate. Significant differences were established by an ANOVA test, using the computer program GraphPad InStat™ (GraphPad Software v2.03, San Diego, CA). When the number of animals was too small or the variance was not homogeneous, a nonparametric test was performed (Kruskal-Wallis test). When significant variations were found, the Student-Newman-Keuls multiple comparisons test was performed. Linear correlation between variables was calculated by using the above-mentioned program. Level of statistical analysis was set at *P* < 0.05.

## RESULTS

**Plasma and liver lipid.** Statin administration reduced plasma TG without affecting cholesterol and phospholipid levels (Table 2). Mevalonate feeding did not affect plasma lipid values, but reversed all the modifications induced by the atorvastatin treatment (Table 3).

In contrast to atorvastatin, the simvastatin treatment increased liver free cholesterol and decreased phospholipid and DAG concentration (20, 41, and 35% vs. control, respectively).

TG content was not significantly modified by statin administration (Table 2). Mevalonate feeding raised liver free cholesterol, TG, and phospholipid content (2.6-, 3.4-, and 2.3-fold vs.

**TABLE 2**  
**Effect of Atorvastatin (ATV) and Simvastatin (SVT) Treatment on Plasma and Liver Lipid Levels<sup>a</sup>**

	Control	ATV	SVT
Plasma			
Total cholesterol	111 ± 3	116 ± 10	111 ± 8
TG	103 ± 6	66 ± 13*	65 ± 8*
Phospholipid	199 ± 7	187 ± 18	192 ± 17
Liver			
Free cholesterol	8.3 ± 0.4	8.7 ± 0.4	9.9 ± 0.5*
TG	18.8 ± 2.2	20.6 ± 2.4	25.1 ± 3.3
Phospholipid	76 ± 4.2	66 ± 7.5	45 ± 2.2*
DAG	8.6 ± 0.6	8.2 ± 0.6	5.6 ± 0.3**

<sup>a</sup>Data are the mean ± SEM (*n* = 6). Plasma lipid levels are expressed as mg/dL. Liver free cholesterol, TG, and phospholipid are expressed as 10<sup>-3</sup> mg/mg of liver postnuclear supernatant protein and DAG content as pmol/mg of liver postnuclear supernatant protein. \**P* < 0.05; \*\**P* < 0.01.

**TABLE 3**  
**Effect of ATV Treatment on Plasma and Liver Lipid Levels in MVL-Fed Rats<sup>a</sup>**

	Control	MVL	ATVMVL
Plasma			
Total cholesterol	116 ± 6	105 ± 6	110 ± 7
TG	122 ± 9	119 ± 9	90 ± 11
Phospholipid	194 ± 9	175 ± 9	171 ± 8
Liver			
Free cholesterol	6.1 ± 1.0	16.2 ± 3.1*	11.3 ± 0.7
TG	14.9 ± 2.8	51.2 ± 12.3*	38.6 ± 3.8
Phospholipid	66 ± 10.8	151 ± 28.1*	84 ± 24.6

<sup>a</sup>Data are the mean ± SEM (*n* = 4) and are expressed as mg/dL of plasma or 10<sup>-3</sup> mg/mg of liver postnuclear supernatant protein. \**P* < 0.05. MVL, mevalonate; ATVMVL, atorvastatin-mevalonate.

control, respectively). These changes were blunted when animals were fed with both atorvastatin and mevalonate (Table 3).

**SREBP-2 and enzyme involved in cholesterol synthesis and esterification.** Atorvastatin and simvastatin treatments raised the mRNA levels of SREBP-2 (Fig. 1A). The increase in SREBP-2 mRNA levels is a consequence of SREBP-2 activation, as the SREBP-2 gene is a target gene of itself (21). Therefore, the nuclear form of SREBP-2 (active form) should increase after statin treatment. We checked this issue in a small subgroup of animals and, as expected, the nuclear form of SREBP-2 was increased by statin treatment ( $0.83 \pm 0.12$  and  $2.07 \pm 0.50$  (arbitrary units), respectively, for control and simvastatin groups ( $n = 4$ ;  $P < 0.05$ ). Statin treatment also increased mRNA levels of HMG-CoA reductase (Fig. 1B), whereas ACAT mRNA levels were only increased by simvastatin (1.54-fold induction vs. control group; Fig. 2). Despite statins being competitive inhibitors of HMG-CoA reductase, when microsomal HMG-CoA reductase activity from livers of statin-treated animals was measured, an increase in enzyme activity was detected because the inhibitors had been removed from the microsomes when samples were obtained (22). Accordingly, both statins enhanced microsomal HMG-CoA reductase activity ( $0.192 \pm 0.0512$ ,  $1.31 \pm 0.074$ , and  $2.65 \pm 0.083$  nmol/min/mg, for the control, atorvastatin, and simvastatin groups ( $n = 6$ ), respectively;  $P < 0.001$ ). Although atorvastatin was more potent than simvastatin in increasing mRNA levels (16- and 8-fold, respectively, relative to control), HMG-CoA reductase activity was lower in atorvastatin than in simvastatin-treated animals, given that this drug is more difficult to remove from microsomes than other HMG-CoA reductase inhibitors (23).

Mevalonate feeding downregulated SREBP-2 and HMG-CoA reductase. mRNA levels were reduced 50 and 56% vs. the control group, respectively, whereas HMG-CoA reductase activity decreased 88% vs. the control (Table 4). Even in the presence of mevalonate, atorvastatin increased mRNA levels of both genes and HMG-CoA reductase activity relative to the mevalonate group, achieving values similar to control group (Figs. 1C,D, Table 4).

**Enzyme involved in FA synthesis.** Atorvastatin and simvastatin treatment increased the mRNA levels of FAS and ACC (2.5- and 1.4-fold induction vs. control group, respectively; Figs. 3A,B). Mevalonate feeding did not affect mRNA levels of FA biosynthetic enzymes but reversed the changes induced by atorvastatin treatment in the mRNA levels of these genes (Table 4).

**Enzyme involved in TG synthesis.** As shown in Figure 4A, PAP activity was markedly increased by simvastatin and atorvastatin administration (3.7- and 3.4-fold induction vs. the control value, respectively). mRNA levels of DGAT were enhanced by statin treatment (Fig. 4B). As a result DGAT activity was also increased ( $17.9 \pm 1.48$ ,  $25.1 \pm 0.84$ , and  $20.8 \pm 0.35$  nmol/min/mg for the control, atorvastatin, and simvastatin groups ( $n = 4$ ), respectively;  $P < 0.05$ ). Mevalonate feeding did not modify significantly the PAP activity (Table 4) or the DGAT mRNA levels (data not shown) but blocked the increase in enzyme activity caused by atorvastatin.

**TABLE 4**  
Effect of ATV Treatment on Enzymes Involved in Hepatic Lipid Synthesis and VLDL Assembly in MVL-Fed Rats<sup>a</sup>

	Control	MVL	ATVMVL
HMG-CoA Rd (activity)	$0.185 \pm 0.029$	$0.0225 \pm 0.005^a$	$0.23 \pm 0.067^c$
FAS (mRNA)	$0.434 \pm 0.037$	$0.461 \pm 0.077$	$0.369 \pm 0.029$
ACC (mRNA)	$1.155 \pm 0.052$	$1.345 \pm 0.085$	$1.332 \pm 0.141$
PAP (activity)	$0.662 \pm 0.047$	$0.680 \pm 0.071$	$0.607 \pm 0.026$
CT (mRNA)	$0.545 \pm 0.172$	$0.762 \pm 0.092^a$	$0.718 \pm 0.025$
CT (activity)	$624.5 \pm 32.7$	$912.8 \pm 63.5^a$	$826.8 \pm 25.1$
MTP (mRNA)	$0.327 \pm 0.029$	$0.405 \pm 0.006$	$0.382 \pm 0.017$
MTP (activity)	$208 \pm 13$	$249 \pm 50$	$263 \pm 33$

<sup>a</sup>Data are the mean  $\pm$  SEM ( $n = 4$ ) and are expressed as pmol/min/mg (HMG-CoA Rd); nmol/min/mg (PAP activity); fluorescence arbitrary units/h/mg (MTP activity) and arbitrary units (mRNA). PAP, phosphatidate phosphohydrolase; MTP, microsomal TG transfer protein. For other abbreviations see Tables 1 and 3. <sup>a</sup>Values significantly different from control ( $P < 0.05$ ). <sup>c</sup>Values significantly different from MVL ( $P < 0.05$ ).

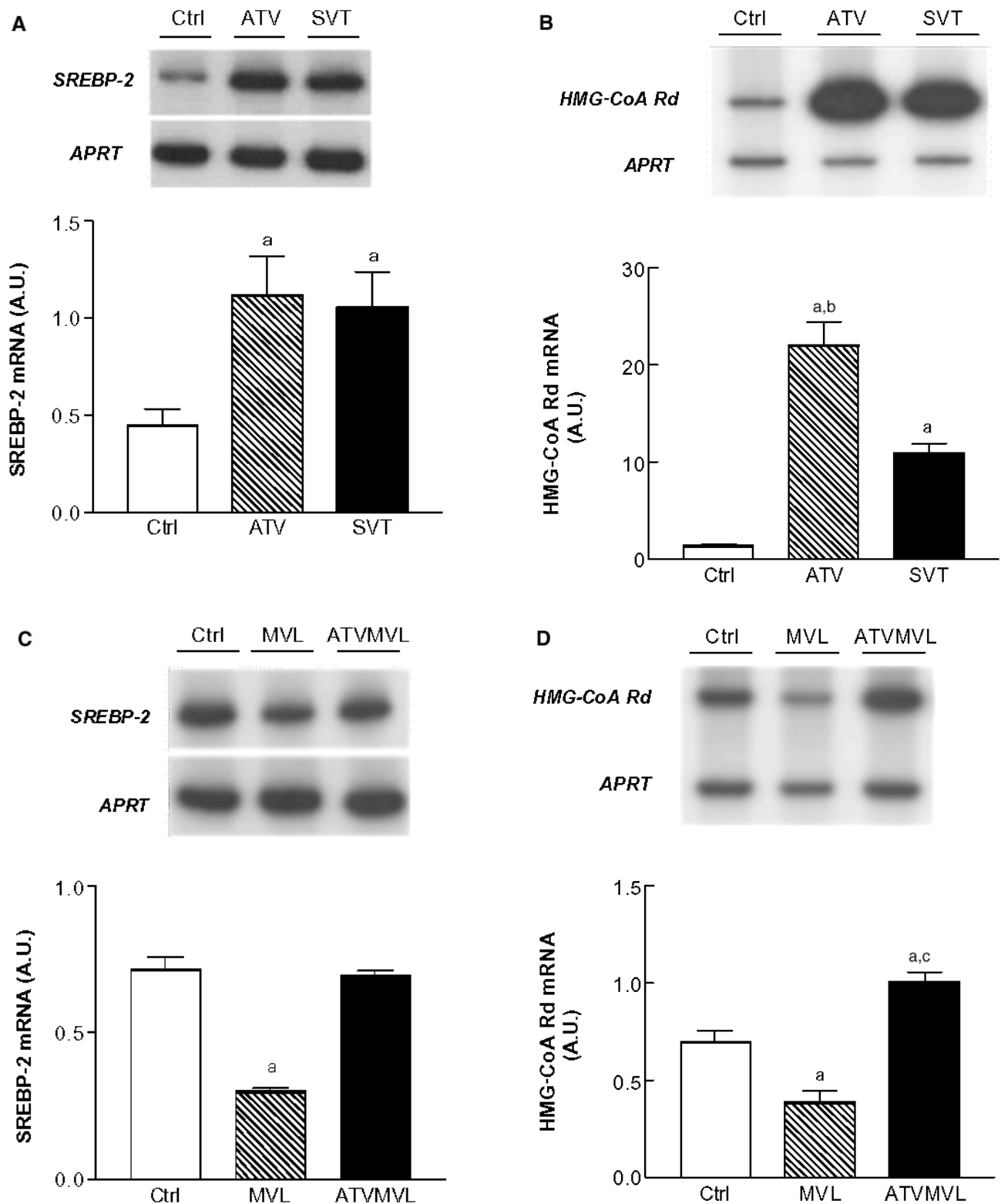
**Enzyme involved in phospholipid synthesis.** Figure 5 shows the effect of statin administration on CT. After atorvastatin treatment no significant changes were observed. In contrast, simvastatin increased the enzyme activity (1.4-fold vs. control value) without significantly affecting mRNA levels ( $0.78 \pm 0.014$ ,  $0.85 \pm 0.15$ , and  $0.96 \pm 0.11$  for the control, atorvastatin, and simvastatin groups ( $n = 6$ ), respectively). When animals were fed with a diet supplemented with mevalonate, mRNA levels and CT activity rose relative to the control group (1.4- and 1.5-fold, respectively) (Table 4).

**Enzyme involved in lipoprotein assembly.** Statin administration increased mRNA levels of MTP, the enzyme that catalyzes the transference of hepatic lipid to apoB, although this increase was statistically significant only for atorvastatin (Fig. 6). Neither atorvastatin nor simvastatin affected MTP activity [ $306 \pm 9.9$ ,  $381 \pm 23$ , and  $346 \pm 40$  for the control, simvastatin, and atorvastatin group ( $n = 6$ ), respectively]. Further, mevalonate feeding did not affect MTP mRNA levels or enzyme activity but blocked the increase in the mRNA levels caused by atorvastatin (Table 4).

## DISCUSSION

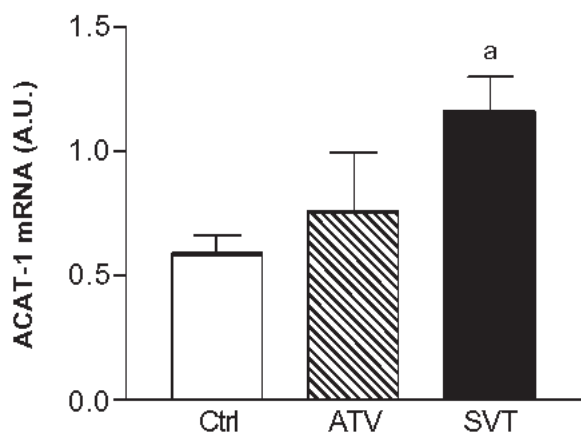
HMG-CoA reductase inhibitors deplete cellular cholesterol causing SREBP activation and enhancing the expression of SREBP-2 target genes, as HMG-CoA reductase or LDL receptors. However, SREBP have been shown to regulate many other enzymes involved in hepatic lipid synthesis and VLDL assembly (9). In the present study, we have focused on the effects of high doses of atorvastatin and simvastatin on key enzymes involved in VLDL production in normolipidemic rats.

Atorvastatin and simvastatin not only induce HMG-CoA reductase but also raise mRNA levels of SREBP-2 (Fig. 1). Generally, despite the induction of HMG-CoA reductase, HMG-CoA reductase activity and cholesterol synthesis remain inhibited, while statins present inside the hepatocyte and plasma cholesterol levels decrease. However, it is well established that HMG-CoA reductase inhibitors do not lower



**FIG. 1.** Effect of statin treatment on mRNA levels of sterol regulatory element binding protein-2 (SREBP-2) and 3-hydroxy-3-methylglutaryl-CoA reductase (HMG-CoA Rd) in normolipidemic rats (A,B) and mevalonate-fed rats (C,D). Total liver RNA was subjected to reverse transcription PCR (RT-PCR), and adenosyl phosphoribosyl transferase (APRT) was used as a reference gene to normalize mRNA levels of SREBP-2 (A,C) and HMG-CoA Rd (B,D). Bars represent the mean  $\pm$  SEM of the values obtained from six (A,B) or four (C,D) animals in each treatment group. A representative autoradiography of a RT-PCR assay for one animal of each treatment group is shown in the upper part of the figures. Ctrl, control; ATV, atorvastatin; SVT, simvastatin; MVL, mevalonate; ATVMVL, atorvastatin-mevalonate. <sup>a</sup>Values significantly different from control ( $P < 0.05$ ); <sup>b</sup>significant differences between values from ATV and SVT groups ( $P < 0.05$ ); <sup>c</sup>values significantly different from MVL ( $P < 0.05$ ).

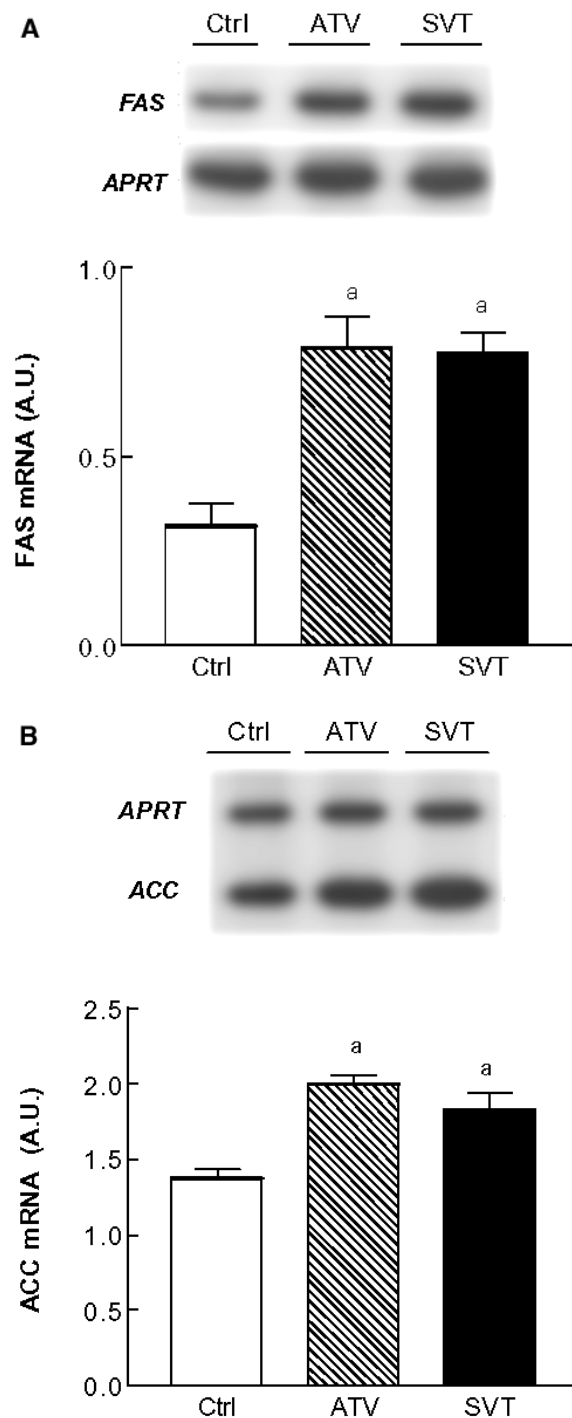




**FIG. 2.** Effect of statin treatment on mRNA levels of ACAT in normolipidemic rats. APRT-normalized mRNA levels of ACAT as measured by RT-PCR. Bars represent the mean  $\pm$  SEM of the values obtained from six animals in each treatment group: Ctrl, ATV, and SVT. For abbreviations see Figure 1. <sup>a</sup>Values significantly different from control ( $P < 0.05$ ).

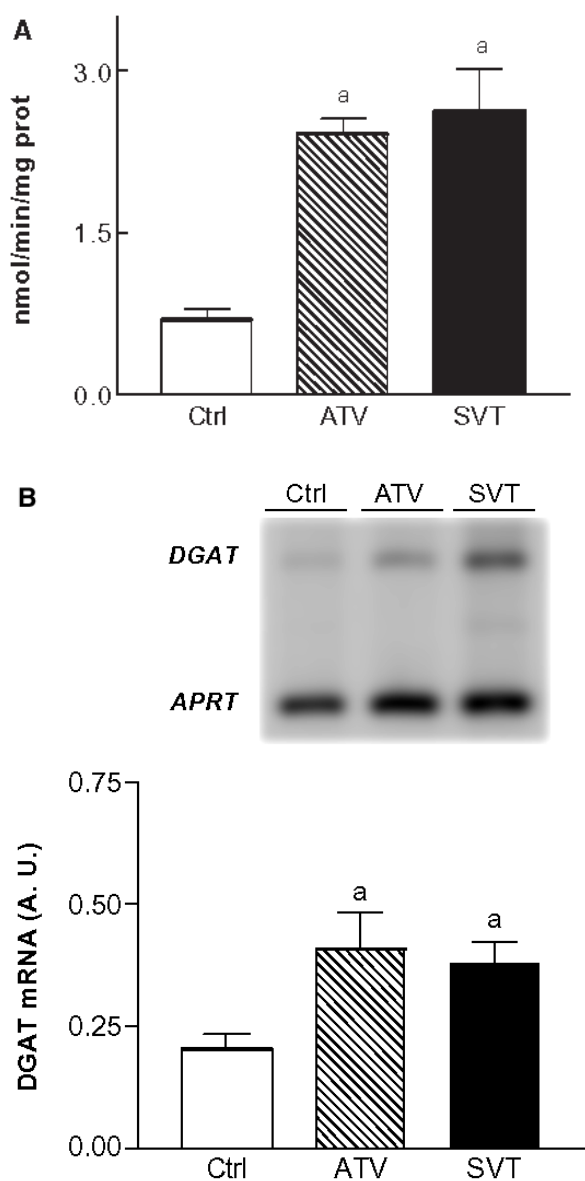
plasma cholesterol in rats, as HDL is the main transporter of rat plasma cholesterol (8). In fact, the great activation of SREBP elicited by treatment with high doses of statins may cause a superinduction of HMG-CoA reductase, which can compensate for the inhibitory effect of the drug and increase hepatic cholesterol (24). This effect depends on the dose, the potency, and the duration of action of the compound used. Thus, in the present study, simvastatin, but not atorvastatin, increased liver cholesterol content (Table 2). This difference may be attributable to the longer duration of action of atorvastatin, which maintains its inhibitory effect on HMG-CoA reductase for more than 24 h (2). This increase in hepatic cholesterol content was associated with higher ACAT mRNA levels. We cannot ensure that both effects are related, as little is known about the regulation of ACAT expression. However, it has been described that a high-fat, high-cholesterol diet causes an increase in ACAT mRNA levels in rabbit liver (25). Therefore, the increase in mRNA levels could be addressed to eliminate the excess of cholesterol produced by the simvastatin treatment (26).

Treatment with atorvastatin and simvastatin markedly reduced plasma TG levels. Although the mechanism underlying their TG-lowering effect is still unclear, low doses of statins may reduce apoB secretion in normolipidemic rats and other animal models (6,8). TG availability has been shown to be one of the major factors in the posttranslational regulation of apoB secretion (27,28). The effect of statins on TG synthesis has been tested in cell culture and animal models. These results show that low doses of statins affect neither the rate of TG synthesis nor the activity of key enzymes involved in the biosynthetic pathway (13,14,29,30). However, in the present study, the main enzymes involved in FA and TG synthesis were induced by treatment with high doses of atorvastatin and simvastatin. It is interesting to point out that the genes involved in FA synthesis are selectively activated by SREBP-1, but at high levels of expression, SREBP-2 also activates the enzyme cascade required for FA synthesis (31,32). Therefore,



**FIG. 3.** Effect of statin treatment on mRNA levels of FA synthase (FAS) and acetyl-CoA carboxylase (ACC) in normolipidemic rats. APRT-normalized mRNA levels of FAS (A) and ACC (B) as measured by RT-PCR. Bars represent the mean  $\pm$  SEM of the values obtained from six animals in each treatment group. A representative autoradiograph is shown in the upper part of each figure, with signals corresponding to FAS or ACC and the reference gene, APRT, for one Ctrl, one ATV-, and one SVT-treated rat. For abbreviations see Figure 1. <sup>a</sup>Values significantly different from control ( $P < 0.001$ ).

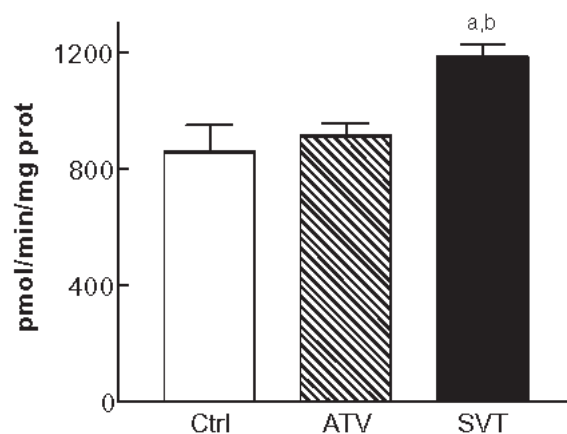
the increase in the mRNA levels of FAS and ACC may be attributed to the overexpression of SREBP-2 induced by the administration of high doses of statins. Thus, while low doses



**FIG. 4.** Effect of statin treatment on mRNA levels of diacylglycerol acyltransferase (DGAT) and phosphatidate phosphohydrolase (PAP) activity in normolipidemic rats. (A) PAP activity. The results are the mean  $\pm$  SEM of the values obtained from six animals in each treatment group. (B) APRT-normalized mRNA levels of DGAT as measured by RT-PCR. Bars represent the mean  $\pm$  SEM of the values obtained from six animals in each treatment group. A representative autoradiograph is shown in the upper part of each figure, with signals corresponding to DGAT and the reference gene, APRT, for one Ctrl, one ATV- and one SVT-treated rat. For abbreviations see Figure 1. <sup>a</sup>Values significantly different from control ( $P < 0.05$ ).

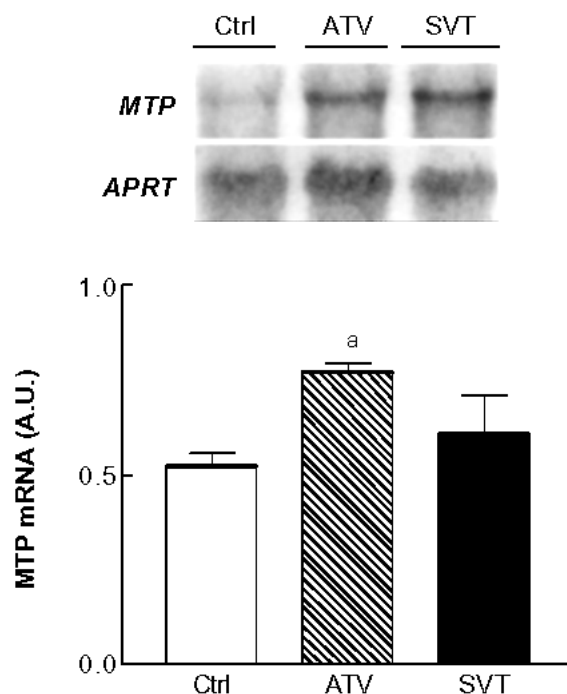
of statins induce only SREBP-2 target-genes, such as HMG-CoA reductase, high doses of statins cause such great activation of SREBP-2 that SREBP-1 target genes, such as FAS and ACC, are also induced by drug treatment.

DGAT and PAP may also be transcriptionally regulated by SREBP, as other enzymes involved in glycerolipid synthesis (33). Nevertheless, we cannot discard the notion that the induction of these enzymes was due to FA activation (34–36). Thus,



**FIG. 5.** Effect of ATV and SVT treatment on CTP:phosphocholine cytidyltransferase (CT) activity in normolipidemic rats. The results are the mean  $\pm$  SEM of the values obtained from six animals in each treatment group. For abbreviations see Figure 1. <sup>a</sup>Values significantly different from Ctrl ( $P < 0.01$ ). <sup>b</sup>Significant differences between values from ATV and SVT groups ( $P < 0.01$ ).

in the present study we have shown a concomitant increase in FAS mRNA levels, DGAT activities, and PAP activities. Given that others have shown that the increase in FAS mRNA parallels the relative increase in FA synthesis measured *in vivo*



**FIG. 6.** Effect of statin treatment on mRNA levels of microsomal TG transfer protein (MTP) in normolipidemic rats. Total liver RNA was subjected to electrophoresis and blot hybridization with the MTP <sup>32</sup>P-labeled probe and with a control <sup>32</sup>P probe directed against APRT. The mRNA levels were calculated after correction for loading differences with APRT. Bars represent the mean  $\pm$  SEM of the values obtained from six animals in each treatment group. A representative autoradiograph is shown in the upper part of the figure, with signals corresponding to MTP and the reference gene, APRT, for one Ctrl, one ATV-, and one SVT-treated rat. For abbreviations see Figure 1. <sup>a</sup>Values significantly different from control ( $P < 0.05$ ).

(9,32), the changes in DGAT and PAP found in the present study might be secondary to the induction of FA synthesis. In this sense, it is interesting to point out that we have found an almost 50% direct correlation between mRNA levels of FAS and PAP activity ( $n = 18$ ;  $r^2 = 0.470$ ;  $P = 0.0017$ ).

PAP is the branch point between TG and phospholipid synthesis and catalyzes the production of DAG. Despite the induction of FA and TG biosynthetic enzymes, hepatic TG content was unaffected by atorvastatin and simvastatin. Instead, DAG and phospholipid contents were decreased by the simvastatin treatment. It has been reported that statins increase biliary cholesterol and phospholipid secretion in rats owing to the induction of hepatic synthesis of cholesterol (24,37). From our results we can deduce that the DAG produced by PAP is shunted to the synthesis of phospholipids in order to supply enough phospholipid to eliminate the excess of cholesterol synthesized. The balance between cholesterol, TG, and phospholipid synthesis was maintained after atorvastatin treatment without changes in liver content of cholesterol, TG, DAG, or phospholipid. However, simvastatin caused a greater increase in cholesterol synthesis, probably because of its shorter duration of action. As a consequence, the DAG supply was not sufficient to sustain phospholipid synthesis for biliary cholesterol secretion, and the liver cholesterol content rose while the DAG and phospholipid contents decreased (Table 2).

Phospholipid synthesis is mainly regulated by CT activity, the rate-limiting enzyme of PC synthesis (38). The effects of statins on CT activity are not clear, and they seem to depend on the type of compound and experimental model used (13,14). In the present study, no change in CT activity was observed after the atorvastatin treatment. However, the simvastatin treatment caused an increase in this enzyme activity and a decrease in liver phospholipid content. The decrease of liver phospholipid caused by simvastatin (Table 2) may activate the translocation of CT (39,40), explaining the increase in the enzyme activity shown in the present study (Fig. 5). Although CT translocation is also activated by FA and DAG in cultured cells (40), we can discard the view that the increase in CT activity caused by simvastatin was a consequence of FA or DAG activation, since atorvastatin also enhanced FA synthesis and PAP activity without modifying CT activity.

MTP plays a pivotal role in VLDL assembly by mediating the transfer of hepatic lipid to nascent apoB (12). The effect of statins on MTP has not been tested in animal models. In the present study, treatment with high doses of atorvastatin and simvastatin caused an increase in MTP mRNA levels (Fig. 6), as a result of HMG-CoA reductase inhibition, although the enzyme activity was unaffected by drug treatment. This divergence is not surprising because of the long half-life of MTP (4.4 d) (41), which it makes difficult to observe a rise in MTP activity subsequent to a 1.4-fold increase in the mRNA levels. Transcriptional regulation of MTP has not been fully elucidated, but both SREBP and FA seem to control MTP expression (10,42,43). Horton *et al.* (31) showed a fourfold increase in MTP mRNA levels in SREBP-2

transgenic mice. Therefore, the increase in MTP mRNA levels observed in the present study might be a consequence of SREBP-2 overexpression, although we cannot discern whether MTP induction is a result of direct SREBP or FA activation.

Despite the induction of the key enzymes involved in lipid synthesis and lipoprotein assembly, plasma cholesterol was unchanged and TG levels were reduced by statin treatment. These results suggest the following: (i) apoB secretion is not enhanced in the present study. Nevertheless, given that treatment with high doses of lovastatin for 7 d raised plasma cholesterol levels (24), we cannot discard the view that longer treatment periods with high doses of statins may increase apoB secretion in normolipidemic rats. (ii) The blockage of apoB secretion does not seem to be one of the mechanisms involved in the TG-lowering effect of statins at high doses in normolipidemic rats. It has been reported that statins reduce cholesterol availability for apoB secretion, and this effect depends on the extent of HMG-CoA reductase inhibition (7). However, the reduction of plasma TG levels observed in the present study is difficult to explain by this mechanism, especially for simvastatin, because the induction of HMG-CoA reductase caused by high doses of this drug can overcome its inhibitory effect and increase hepatic cholesterol content (Table 2). Although the aim of this study was not to investigate the mechanisms involved in the hypotriglyceridemic effect of statins, we can speculate that the decrease in plasma TG levels observed in this study might be due to an induction of lipoprotein lipase by SREBP (44,45).

In summary, we have shown that treatment with high doses of statins induces key enzymes controlling rat liver lipid synthesis and VLDL assembly. High doses of atorvastatin and simvastatin induce not only SREBP-2 target genes involved in cholesterol synthesis as SREBP-2 or HMG-CoA reductase, but also SREBP-1 target genes, as FAS or ACC. PAP, DGAT, and MTP were also induced by the statin treatment as a result of SREBP or FA activation. After the atorvastatin treatment, the balance between hepatic cholesterol, TG, and phospholipid synthesis was maintained without changes in liver lipid content. In contrast, simvastatin increased liver cholesterol and reduced DAG and phospholipid content. Despite the induction of the key enzymes involved in VLDL production, both statins markedly reduced plasma TG levels, suggesting that different mechanisms may be involved in the hypotriglyceridemic effect of statins at high or low doses in normolipidemic rats.

## ACKNOWLEDGMENTS

Financial support was partly provided by Fundació Privada Catalana de Nutrició i Lípids (FPCNL), Parke-Davis (981-SPA-07), Comisión Interministerial de Ciencia y Tecnología (CICYT) (SAF98-0105), Fondo de Investigación sanitaria de la Seguridad Social (FIS<sub>ss</sub>) (00/1124; 00/0201), and grant SGR 99-33 from Generalitat de Catalunya. Núria Roglans is the recipient of a Research and Teaching grant from the University of Barcelona. We thank Dr. Robin Rycroft (Language Advice Service of the University of

Barcelona) and Dr. Albert Tauler (Unidad de Bioquímica y Biología Molecular, Facultad de Farmacia, Universidad de Barcelona) for their helpful assistance.

## REFERENCES

- Davignon, J., Montigny, M., and Dufour, R. (1992) HMG-CoA Reductase Inhibitors: A Look Back and a Look Ahead, *Can. J. Pharmacol.* 8, 843–864.
- Lea, A.P., and McTavish D. (1997) Atorvastatin. A Review of Its Pharmacology and Therapeutic Potential in the Management of Hyperlipidemias, *Drugs* 53, 828–847.
- Jones, P., Kafonek, S., Laurora, I., and Hunninghake, D. (1998) Comparative Dose Efficacy Study of Atorvastatin Versus Simvastatin, Pravastatin, Lovastatin and Fluvastatin in Patients with Hypercholesterolemia (The Curves Study), *Am. J. Cardiol.* 81, 582–587.
- Stein, E.A., Lane, M.L., and Laskarzewski, P. (1998) Comparison of Statins in Hypertriglyceridemia, *Am. J. Cardiol.* 81, 66B–69B.
- Thompson, G.R., Naumova, R.P., and Watts, G.F. (1996) Role of Cholesterol in Regulating Apolipoprotein B Secretion by the Liver, *J. Lipid. Res.* 37, 439–447.
- Huff, M.W., and Burnett, J.R. (1997) 3-Hydroxy-3-methylglutaryl Coenzyme A Reductase Inhibitors and Hepatic Apolipoprotein B Secretion, *Curr. Opin. Lipidol.* 8, 138–145.
- Burnett, J.R., Wilcox, L.J., Telford, D.E., Kleinstiver, S.J., Barrett, P.H.R., Newton, R., and Huff, M.W. (1999) The Magnitude of Decrease in Hepatic Very Low Density Lipoprotein Apolipoprotein B Secretion Is Determined by the Extent of 3-Hydroxy-3-methylglutaryl Coenzyme A Reductase Inhibition in Miniature Pigs, *Endocrinology* 140, 5293–5302.
- Krause, B.R., and Newton, R.S. (1995) Lipid-Lowering Activity of Atorvastatin and Lovastatin in Rodent Species: Triglyceride-Lowering in Rats Correlates with Efficacy in LDL Models, *Atherosclerosis* 117, 237–244.
- Horton, J.D., and Shimomura, I. (1999) Sterol Regulatory Element-Binding Proteins: Activators of Cholesterol and Fatty Acid Biosynthesis, *Curr. Opin. Lipidol.* 10, 143–150.
- Sato, R., Miyamoto, W., Inoue, J., Terada, T., Imanaka, T., and Maeda, M. (1999) Sterol Regulatory Element-Binding Protein Negatively Regulates Microsomal Triglyceride Transfer Protein Gene Transcription, *J. Biol. Chem.* 274, 24714–24720.
- Wang, S.-L., Du, E.Z., Martin, D., and Davis, R.A. (1997) Coordinate Regulation of Lipogenesis, the Assembly and Secretion of Apolipoprotein B-Containing Lipoproteins by Sterol Response Element Binding Protein-1, *J. Biol. Chem.* 272, 19351–19358.
- Olofsson, S.-O., Asp, L., and Bören, J. (1999) The Assembly and Secretion of Apolipoprotein B-Containing Lipoproteins, *Curr. Opin. Lipidol.* 10, 341–346.
- Alegret, M., Verd, J.C., Díaz, C., Hernández, G., Adzet, T., Sánchez, R.M., and Laguna, J.C. (1998) Effect of Hypolipidemic Drugs on Key Enzyme Activities Related to Lipid Metabolism in Normolipidemic Rabbits, *Eur. J. Pharmacol.* 37, 283–291.
- Verd, J.C., Peris, C., Alegret, M., Díaz, C., Hernández, G., Vázquez, M., Adzet, T., Laguna, J.C., and Sánchez, R.M. (1999) Different Effect of Simvastatin and Atorvastatin on Key Enzymes Involved in VLDL Synthesis and Catabolism in High Fat/Cholesterol Fed Rabbits, *Br. J. Pharmacol.* 27, 1479–1485.
- Bradford, M. (1976) A Rapid Sensitive Method for the Quantitation of Microgram Quantities of Protein Utilizing the Principles of Protein-Dye Binding, *Anal. Biochem.* 72, 248–254.
- Helenius, M., Hänninen, M., Lehtinen, S.K., and Salminen, A. (1996) Aging-Induced Upregulation of Nuclear Binding Activities of Oxidative Stress Responsive NF- $\kappa$ B Transcription Factor in Mouse Cardiac Muscle, *J. Mol. Cell. Cardiol.* 28, 487–498.
- Roglans, N., Peris, C., Verd, J.C., Alegret, M., Vázquez, M., Sánchez, R.M. and Laguna, J.C. (2001) Increase in Hepatic Expression of SREBP-2 by Gemfibrozil Administration to Rats, *Biochem. Pharmacol.* 62, 803–809.
- Cabrero, A., Llaverías, G., Roglans, N., Alegret, M., Sánchez, R.M., Adzet, T., Laguna, J.C., and Vázquez, M. (1999) Uncoupling Protein-3 mRNA Levels Are Increased in White Adipose Tissue and Skeletal Muscle of Bezafibrate-Treated Rats, *Biochem. Biophys. Res. Commun.* 260, 547–556.
- Gause, W.C., and Adamovicz, J. (1995) Use of PCR to Quantitate Relative Differences in Gene Expression, in *PCR Primer. A Laboratory Manual* (Dieffenbach, C.W., and Dveksler, G.S., eds.), pp. 293–311, Cold Spring Harbor Laboratory Press, Cold Spring Harbor, New York.
- Fernández de Mattos, S., de los Pinos, E., and Tauler, A. (2000) Activation of Phosphatidylinositol 3-Kinase Is Required for Transcriptional Activity of F-Type 6-Phosphofructo-2-kinase/Fructose-2,6-biphosphatase: Assessment of the Role of Protein Kinase B and p70 S6 Kinase, *Biochem. J.* 349, 59–65.
- Sato, R., Inoue, J., Kawabe, Y., Kodama, T., Takano, T., and Maeda, M. (1996) Sterol-Dependent Transcriptional Regulation of Sterol Regulatory Element-Binding Protein-2, *J. Biol. Chem.* 271, 26461–26464.
- Goldstein, J.L., and Brown, M.S. (1990) Regulation of the Mevalonate Pathway, *Nature* 343, 425–430.
- Ness, G.C., Chambers, C.M., and López, D. (1998) Atorvastatin Action Involves Diminished Recovery of Hepatic HMG-CoA Reductase Activity, *J. Lipid. Res.* 39, 75–84.
- Linscheer, W.G., Atreyee, B., Uma, K.M., John, W., Sandor, N., and Jyotirmoy, N. (1995) Lovastatin Induces Synthesis of Cholesterol, Which Acts as a Secretagogue of Biliary Phospholipids in Rats, *Am. J. Physiol.* 268, G242–G250.
- Uelmen, P.J., Oka, K., Sullivan, M., Chang, C.C.Y., Chang T.Y., and Chan, L. (1995) Tissue-Specific Expression and Cholesterol Regulation of Acylcoenzyme A:Cholesterolacyltransferase (ACAT) in Mice. Molecular Cloning of Mouse ACAT cDNA, Chromosomal Localization, and Regulation of ACAT *in vivo* and *in vitro*, *J. Biol. Chem.* 270, 26192–26201.
- Chang, T.-Y., Chang, C.C.Y., Lin, S., Yu, C., Li, B.L., and Miyazaki, A. (2001) Roles of Acyl-Coenzyme A:Cholesterol Acyltransferase-1 and -2, *Curr. Opin. Lipidol.* 12, 289–296.
- Lewis, G.F. (1997) Fatty Acid Regulation of Very Low Density Lipoprotein Production, *Curr. Opin. Lipidol.* 8, 146–153.
- Ginsberg, H.N. (1995) Synthesis and Secretion of Apolipoprotein B from Cultured Liver Cells, *Curr. Opin. Lipidol.* 6, 275–280.
- Mohammadi, A., Macri, J., Newton, R., Romain, T., Dulay, D., and Adeli, K. (1998) Effects of Atorvastatin on the Intracellular Stability and Secretion of Apolipoprotein B in HepG2 cells, *Arterioscler. Thromb. Vasc. Biol.* 18, 783–793.
- Wilcox, L.J., Barrett, P.H.R., and Huff, M.W. (1999) Differential Regulation of Apolipoprotein B Secretion from HepG2 Cells by Two HMG-CoA Reductase Inhibitors, Atorvastatin and Simvastatin, *J. Lipid. Res.* 40, 1078–1089.
- Horton, J.D., Shimomura, I., Brown, M.S., Hammer, R.E., Goldstein, J.L., and Shimano, H. (1998) Activation of Cholesterol Synthesis in Preference to Fatty Acid Synthesis in Liver and Adipose Tissue of Transgenic Mice Overproducing Sterol Regulatory Element-Binding Protein-2, *J. Clin. Invest.* 101, 2331–2339.
- Boizard, M., Liepvre, X.L., Lemarchand, P., Fougelle, F., Ferre, P., and Dugail, I. (1998) Obesity-Related Overexpression of Fatty-Acid Synthase Gene in Adipose Tissue Involves Sterol Regulatory Element-Binding Protein Transcription Factors, *J. Biol. Chem.* 273, 29164–29171.
- Ericsson, J., Jackson, S.M., Kim, J.B., Spiegelman, B.M., and



- Edwards, P.A. (1997) Identification of Glycerol-3-phosphate Acyltransferase as an Adipocyte Determination and Differentiation Factor-1 and Sterol Regulatory Element-Binding Protein-Responsive Gene, *J. Biol. Chem.* **272**, 7298–7305.
34. Lamb, R.G., and McCue, S.B. (1983) The Effect of Fatty Acid Exposure on the Biosynthesis of Glycerolipids by Cultured Hepatocytes, *Biochim. Biophys. Acta* **753**, 356–363.
35. Tijburg, L.B.M., Geelen, M.J.H., and Van Golde, L.M.G. (1989) Regulation of the Biosynthesis of Triacylglycerol, Phosphatidylcholine and Phosphatidylethanolamine in the Liver, *Biochim. Biophys. Acta* **1004**, 1–19.
36. Faresee, R.V., Cases, S., and Smith, S.J. (2000) Triglyceride Synthesis: Insights from the Cloning of Diacylglycerol Acyltransferase, *Curr. Opin. Lipidol.* **11**, 229–234.
37. Hooiveld, G.J.E.J., Vos, T.A., Scheffer, G.L., Van Goor, H., Koning, H., Bloks, V., Loot, A.E., Meijer, D.K., Jansen, P.L., Kuipers, F., et al. (1999) 3-Hydroxy-3-methylglutaryl-Coenzyme A Reductase Inhibitors (statins) Induce Hepatic Expression of the Phospholipid Translocase *mdr2* in Rats, *Gastroenterology* **117**, 678–687.
38. Boggs, K.P., Rock, C.O., and Jackowski, S. (1995) Lysophosphatidylcholine and 1-*O*-Octadecyl-2-*O*-methyl-*rac*-glycero-3-phosphocholine Inhibit the CDP-Choline Pathway of Phosphatidylcholine Synthesis at the CTP:Phosphocholine Cytidylyl Transferase Step, *J. Biol. Chem.* **270**, 7757–7764.
39. Vance, D. (1990) Phosphatidylcholine Metabolism: Masochistic Enzymology, Metabolic Regulation and Lipoprotein Assembly, *Biochem. Cell. Biol.* **68**, 1151–1165.
40. Tronchère, H., Record, M., Tercé, F., and Chap, H. (1994) Phosphatidylcholine Cycle and Regulation of Phosphatidylcholine Biosynthesis by Enzyme Translocation, *Biochim. Biophys. Acta* **1212**, 137–151.
41. Lin, M.C.M., Gordon, D., and Wetterau, J.R. (1995) Microsomal Triglyceride Transfer Protein (MTP) Regulation in HepG2 Cells: Insulin Negatively Regulates MTP Gene Expression, *J. Lipid Res.* **36**, 1073–1081.
42. Hagan, D.L., Kienzle, B., Jamil, H., and Hariharan, N. (1994) Transcriptional Regulation of Human and Hamster Microsomal Triglyceride Transfer Protein Genes. Cell Type-Specific Expression and Response to Metabolic Regulators, *J. Biol. Chem.* **269**, 28737–28744.
43. Kuriyama, H., Yamashita, S., Shimomura, I., Funahashi, T., Ishigami, M., Aragane, K., Miyaoka, K., Nakamura, T., Takemura, K., Man, Z., et al. (1998) Enhanced Expression of Hepatic Acyl-Coenzyme A Synthetase and Microsomal Triglyceride Transfer Protein Messenger RNAs in the Obese and Hypertriglyceridemic Rat with Visceral Fat Accumulation, *Hepatology* **27**, 557–562.
44. Schoonjans, K., Peinado-Onsurbe, J., Fruchart, J.C., Tailleux, A., Fiévet, C., and Auwerx, J. (1999) 3-Hydroxy-3-methylglutaryl CoA Reductase Inhibitors Reduce Serum Triglyceride Levels Through Modulation of Apolipoprotein C-III and Triglyceride Levels Through Modulation of Apolipoprotein C-III and Lipoprotein Lipase, *FEBS Lett.* **452**, 160–164.
45. Schoonjans, K., Gelman, L., Haby, C., Briggs, M., and Auwerx, J. (2000) Induction of LPL Gene Expression by Sterols Is Mediated by a Sterol Regulatory Element and Is Independent of the Presence of Multiple E Boxes, *J. Mol. Biol.* **304**, 323–334.

[Received June 8, 2001; in revised form March 13, 2002; accepted March 26, 2002]

# Effect of Dietary Cholesterol Oxidation Products on the Plasma Clearance of Chylomicrons in the Rat

D.F. Vine<sup>b</sup>, K.D. Croft<sup>a</sup>, L.J. Beilin<sup>a</sup>, and J.C.L. Mamo<sup>b,\*</sup>

<sup>a</sup>University of Western Australia, Department of Medicine, Royal Perth Hospital, Perth, Western Australia, Australia, and <sup>b</sup>Curtin University of Technology, Department of Nutrition, Dietetics and Food Science, School of Public Health, Perth, Western Australia

**ABSTRACT:** Oxidized cholesterol in the diet have been shown to exacerbate arterial cholesterol deposition and the development of atherosclerosis in animal models. Dietary oxidized cholesterol are absorbed through the intestine and incorporated into lymph chylomicrons. The aim of this study was to investigate the effect of oxidized cholesterol on the metabolism of nascent chylomicrons *in vivo*. It was shown that oxidized cholesterol markedly delay the clearance of chylomicrons from plasma compared to rats given TG alone. However, there was no difference in the clearance of chylomicrons containing oxidized cholesterol vs. purified cholesterol, although the presence of oxysterols did appear to exacerbate the removal of these particles from circulation. The impaired clearance of chylomicrons containing oxidized cholesterol was not due to impaired lipolysis and slower conversion to the remnant form. Moreover, the incorporation of oxidized cholesterol did not alter the hepatic or splenic uptake of chylomicrons compared to chylomicrons isolated from rats given purified cholesterol or TG alone. Collectively, the results of this study suggest that the exacerbated delay in clearance of chylomicron remnants enriched with oxysterols may be due to impaired uptake by tissues other than the liver and spleen. Apolipoprotein (apo) analysis showed that oxysterol incorporation reduced the apoE content and altered the apoC phenotype of chylomicrons, which may have an impact on the removal of chylomicron remnants from plasma. In conclusion, dietary oxysterols appear to have the potential to adversely affect chylomicron metabolism. Therefore, further investigations in humans are required to determine whether dietary oxidized cholesterol found in cholesterol-rich processed foods delay the clearance of postprandial remnants, which may contribute to and exacerbate the development of atherosclerosis.

Paper no. L8972 in *Lipids* 37, 455–462 (May 2002).

The onset of atherosclerosis is marked by the accumulation of cholesterol and oxidized cholesterol in the arterial wall (1,2). The oxidized cholesterol content of early foam cells and fatty streaks closely resembles the oxidized cholesterol found in cholesterol-rich processed foods (3–8). We and others have shown that dietary oxidized cholesterol are absorbed from the intestine and incorporated into lymph chylomicrons (9,10). In humans, absorption of oxidized cholesterol from cholesterol-rich processed foods results in increased circulating levels of

cholesterol oxidation products in plasma lipoproteins (11,12). Early studies showed that feeding oxidized cholesterol resulted in focal arterial damage and fibrous lesions in rat and rabbit models (13–15). More recently we have shown that short-term feeding of oxidized cholesterol to rabbits result in a marked increase in aortic cholesterol concentration compared to rabbits fed purified cholesterol (16). Longer-term feeding of oxidized cholesterol to rabbits has shown that these sterols accelerate and exacerbate the development of atherosclerotic lesions (17,18). Epidemiological evidence also suggests oxysterols are proatherogenic, because the consumption of ghee, which is rich in oxysterols, has been associated with an increased incidence of coronary heart disease (19). Given postprandial lipoproteins transport dietary oxidized cholesterol to the circulation, and chylomicron remnants penetrate and are retained by the arterial wall (20), it has been proposed that dietary lipids may be a potential source of early lesion oxidized cholesterol (9,16).

The consumption of dietary cholesterol has been associated with delayed clearance and accumulation of chylomicron remnants in plasma (21,22). The consumption of cholesterol may often include cholesterol-rich processed foods that contain oxidized cholesterol products (3). The absorption and incorporation of oxidized cholesterol into lymph chylomicrons may modulate the metabolism and tissue uptake of these particles. We have previously shown that chylomicrons enriched with oxysterols have an increased size due to a greater content of cholesterol and TG in these particles compared to rats given purified cholesterol (9). The size of chylomicrons can influence their kinetics, with larger chylomicrons having delayed clearance from plasma compared to smaller chylomicrons (23). Furthermore, increasing the cholesterol content can further delay the clearance of chylomicrons (21,24).

Like cholesterol, oxidized cholesterol products appear to affect chylomicron metabolism. Mortimer and co-workers (25) reported that the inclusion of the oxidized cholesterol 7 $\alpha$ -hydroxycholesterol, 7 $\beta$ -hydroxycholesterol, 25-hydroxycholesterol, and 3-ketocholesterol into chylomicron-like lipid emulsions retarded plasma clearance. However, the effects of dietary oxidized cholesterol products on chylomicron composition and metabolism remain unclear.

The normal metabolism of chylomicrons involves the rapid conversion to chylomicron remnants by the action of endothelial lipases. Lipoprotein lipase (LPL) requires apolipoprotein CII (apoCII) to catalyze the hydrolysis of TG and

\*To whom correspondence should be addressed at Department of Nutrition, Dietetics and Food Science, Curtin University, GPO Box U1987, Western Australia, 6845. E-mail: mamo.j@health.curtin.edu.au

Abbreviations: apoB<sub>48</sub>, -B-100, -C, -CII, -CIII, -E, apolipoproteins B<sub>48</sub>, B-100, C, CII, CIII, E; HL, hepatic lipase; LPL, lipoprotein lipase.

is responsible for approximately 70% of chylomicron TG lipolysis. Chylomicron remnants are subsequently removed from circulation primarily by the liver *via* the apoB<sub>100</sub>/E receptor. The processes of lipolysis and high-affinity uptake of chylomicrons are critically regulated by the size, lipid composition, and apolipoprotein composition of the particles (26,27). Given that dietary oxidized cholesterols increase the cholesterol content and size of chylomicrons, it was hypothesized that these sterols may modulate the clearance of chylomicrons from plasma. Therefore, the objective of this study was to investigate the effect of oxidized cholesterol on chylomicron metabolism *in vivo*. The mechanism of how oxysterols may alter chylomicron metabolism was studied by determining the effect of oxysterols on apolipoprotein composition, lipolysis, and receptor-mediated uptake processes.

## MATERIALS AND METHODS

**Materials.** Cholesterol (>99% purity) and triolein (>99% purity) were purchased from Sigma (St. Louis, MO). Cholesterol (catalog no. TR13015; Trace Scientific, Melbourne, Australia) and TG (Wako, Osaka, Japan) were determined colorimetrically. Bis(trimethylsilyl)-trifluoroacetamide was purchased from Sigma. Radiolabeled lipids, [<sup>14</sup>C]palmitate and [<sup>3</sup>H]cholesterol, were purchased from Amersham Pharmacia Pty. Ltd. (Piscataway, NJ).

**Preparation of lipid emulsions.** The purified and autooxidized cholesterol emulsions were prepared as previously described (9). Briefly, aliquots of radiolabeled TG ([<sup>14</sup>C]palmitate) and cholesterol ([<sup>3</sup>H]cholesterol) were placed into a glass vial, and the solvent was evaporated under N<sub>2</sub>. The pure or heat-treated cholesterol (50 mg) predissolved in chloroform and triolein (600 mg) was added, and the solvent was evaporated under N<sub>2</sub> in a water bath at 37°C for both cholesterol treatments. The control treatment consisted of triolein (600 mg) alone. The GC-MS analysis of the purified cholesterol emulsion showed 99.9% purity. The GC-MS analysis of the oxidized cholesterol emulsion was cholesterol (69.3%), 7β-hydroxycholesterol (6.9%), 5α,6α-epoxycholesterol (4.8%), 5β,6β-epoxycholesterol (4.83%), 7-ketocholesterol (8.6%), 6-hydroxycholesterol (1.0%), cholest-4-ene-3-one (0.4%), 4,6-cholestadiene-3-one (1.4%), cholestane-3,6-dione (1.0%), and unknown oxysterols (1.5%) (9).

**Chylomicron isolation.** The isolation of lymph chylomicrons has been described previously (9,28). Approval for experimental procedures was obtained from the University of Western Australia Ethics Committee, and procedures followed recommendations of the National Health and Medical Research Council of Australia. Briefly, 300 g male Wistar nonfasted rats were anesthetized with phenobarbital (0.05 mg/kg), and the superior mesenteric lymph duct was cannulated and the duodenum cannulated *via* a gastrostomy. The triolein vehicle alone (control) and cholesterol emulsions (50 mg autooxidized cholesterol or purified cholesterol) were administered *via* the gastric cannula. Chylomicrons were then isolated from lymph by density ultracentrifugation as previ-

ously described (29). Chylomicron cholesterol and TG were measured, and oxysterol analysis was done by GC-MS as reported previously (9,30,31). The size of chylomicrons was also determined using an automated particle sizer.

**Kinetic studies with radiolabeled chylomicrons.** Nonfasted recipient male Wistar rats weighing 300 ± 10 g were anesthetized with ketamine/xylazine (2:1, 1 mL/kg), and the right carotid artery and left jugular vein were cannulated as reported previously (28). Chylomicrons were injected into the external jugular vein at a dose of 7–10 mg of TG in 0.4–0.5 mL, and blood samples were taken from the carotid artery into heparinized tubes after injection of doubly labeled chylomicrons. At the end of the clearance study, rats were given a lethal dose of phenobarbital *via* the jugular vein, and the liver and spleen were removed. Blood volume was calculated as 4% of body weight (28). The radioactivity of plasma and tissues was measured using a Wallac 1410 Liquid Scintillation Counter in dual-label mode with autoquench correction (28).

**Chylomicron TG lipolysis with postheparin plasma lipases.** The lipoprotein TG lipolysis studies were carried out *in vitro* using techniques previously described (32). The enzyme activities of LPL and hepatic lipase (HL) were determined for chylomicrons isolated from rats given the triolein vehicle alone (control), autooxidized cholesterol, or purified cholesterol. The assay quantitates the [<sup>14</sup>C]FFA after liberation from chylomicron TG ([<sup>14</sup>C]palmitate) by the action of LPL and HL. TG hydrolysis was expressed as the appearance of radiolabeled FA released (μmol FA/mL/h) (32).

**Preparation of chylomicron remnants.** Chylomicron remnants were generated in functionally hepatectomized rats as previously described (33). Briefly, male Wistar rats were anesthetized with ketamine/xylazine (1 mL/kg) and a hepatectomy was performed. Chylomicrons isolated from the control, autooxidized cholesterol, and purified cholesterol-treated donor rats were infused into the femoral vein. After 30 min blood was taken from the abdominal aorta, and chylomicron remnants were isolated by density ultracentrifugation as previously described (29).

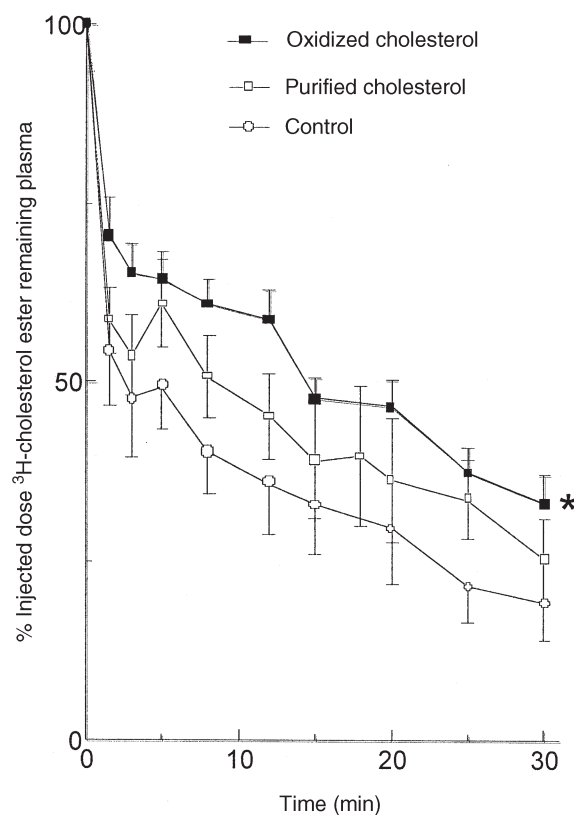
**Apolipoprotein analysis.** Chylomicrons and chylomicron remnants were delipidated according to the method of Herbert *et al.* (34). Chylomicrons and chylomicron remnant apolipoproteins were separated by SDS-PAGE and by isoelectric focusing to separate the isoforms of the apolipoproteins as described previously (32). Chylomicrons and chylomicron remnants were pooled from each treatment group to ensure there was sufficient protein after delipidation of samples for visualization and quantitation of apolipoproteins. The area of apolipoprotein bands was standardized to apoB<sub>48</sub> to enable determination of apolipoprotein changes per particle, as one chylomicron contains one apoB<sub>48</sub>.

**Statistical analysis.** The chylomicron kinetics, organ uptake, and rates of lipolytic activity were compared between treatments by one-way ANOVA with a Bonferroni correction for multiple comparisons testing for significance at α = 0.05 (GraphPad InStat, San Diego, CA). Chylomicron TG and cholesterol clearance from plasma were determined as the area above the curve (GraphPad Prism 1.00).

**RESULTS**

Chylomicrons isolated from rats given oxysterols were approximately 100 nm larger compared to those from purified cholesterol and control animals owing to increased TG and cholesterol incorporation (Table 1). In the postprandial phase (2–4 h) there was an increase in size as well as changes in chylomicron composition compared to fasted chylomicrons in all treatment groups due to absorption of lipid from the infusate. Therefore, for the kinetic studies, chylomicrons isolated *in vivo* during this period were pooled.

The metabolism of chylomicrons is a twofold process involving lipolysis of chylomicron TG to form cholesteryl ester-rich remnant particles and rapid removal of chylomicron remnants from circulation primarily by the liver *via* receptor-mediated processes. The clearance from plasma of chylomicron cholesteryl ester represents the uptake of chylomicron remnants by tissues and organs and is predominantly an indicator of high-affinity uptake *via* hepatic receptors. The clearance from plasma of cholesterol in chylomicrons containing oxysterols and purified cholesterol is shown in Figure 1. The clearance of chylomicron remnants was reduced by approximately 33%, based on the greater percentage of cholesteryl ester radioactivity remaining in plasma (area below the curve,  $1569.2 \pm 87.22$ ) compared to control chylomicrons ( $1067.6 \pm 179.52$ ,  $P = 0.014$ ). Chylomicrons isolated from rats given purified cholesterol also had delayed clearance, which was intermediate compared to control and oxidized cholesterol-containing chylomicrons, but the removal of these particles was not significantly different from that of the other two treatment groups ( $1334.77 \pm 152.10$ ). In all three groups studied, chylomicron clearance from plasma was characterized by a rapid phase (0–5 min) followed by a slower metabolic rate (5–30 min), which is consistent with previous studies on chylomicron metabolism *in vivo* (23,26,28,33). The rate of clearance of chylomicrons isolated from oxysterol-fed rats was reduced by approximately 10% compared to the purified and control



**FIG. 1.** The clearance from plasma of chylomicron cholesteryl ester is shown as a percentage of the dose of radioactive <sup>3</sup>H-cholesterol ester injected. Chylomicrons were isolated from lymph-cannulated rats given an infusate of either oxidized cholesterol or purified cholesterol in a vehicle of triolein or triolein (control) alone *via* a gastric cannula. Chylomicrons were then injected into the external jugular vein of recipient conscious rats. Data are mean  $\pm$  SEM ( $n = 9$ ),  $P < 0.05$ . \*The chylomicrons containing oxidized cholesterol products had a significantly delayed clearance from the plasma compared to the control ( $P = 0.014$ ) but not the purified cholesterol containing chylomicrons.

chylomicrons during the initial rapid phase but was similar in the slower phase of catabolism.

The clearance of chylomicron TG from plasma for chylomicrons containing oxysterols, purified cholesterol, and control particles is shown in Figure 2. The plasma clearance profile observed for chylomicron TG typifies the initial rapid phase, in which chylomicrons bind to endothelial lipases on infusion of particles into the circulation, and the slower phase, which represents release of chylomicrons from lipases and subsequent particle uptake (23,28,33). Both oxysterol and purified cholesterol incorporation into chylomicrons resulted in a similar and delayed TG clearance from plasma compared to chylomicrons containing TG alone (area below the curve, oxysterols  $948.3 \pm 76.71$ ,  $P = 0.0068$ ; purified cholesterol  $904.89 \pm 97.31$ ,  $P = 0.0025$ ; controls  $489.8 \pm 129.88$ ). The impaired TG clearance was marked in the first 5 min after chylomicron infusion in which both the oxidized and purified cholesterol-containing chylomicrons had only 50% of the TG cleared compared to 75% in the control.

There was no significant difference in the hepatic uptake of chylomicrons as a consequence of oxysterol or cholesterol

**TABLE 1**  
The Composition and Size<sup>a</sup> of Lymph Chylomicrons Isolated from Rats Given Control<sup>b</sup>, Oxidized Cholesterol, or Purified Cholesterol Infusates (mean  $\pm$  SEM)

	Chylomicrons		
	Control ( $n = 3$ )	Purified ( $n = 3$ )	Oxidized ( $n = 3$ )
Cholesterol ( $\mu\text{g/mL}$ )	$294 \pm 52$	$652 \pm 100$	$949 \pm 74^c$
TG ( $\mu\text{g/mL}$ )	$9.8 \pm 2.4$	$11.9 \pm 1.9$	$22.2 \pm 4.2^c$
Particle size (nm)	$127 \pm 10$	$176 \pm 11$	$264 \pm 15^c$
Oxysterols <sup>d</sup> ( $\mu\text{g/mL}$ )	—	—	$476 \pm 12^c$

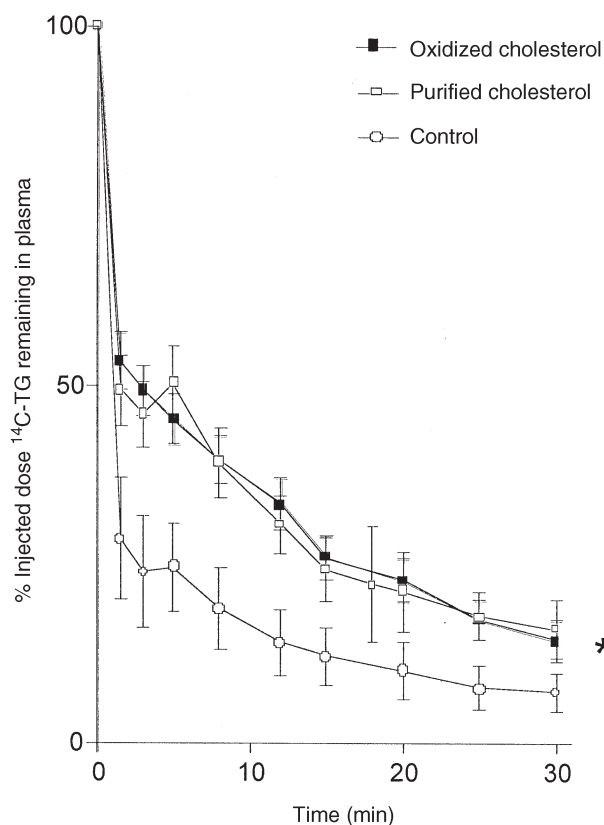
<sup>a</sup>Characterization of chylomicrons at 2–6 h following gastric delivery of infusate.

<sup>b</sup>Controls are chylomicrons isolated from animals given an infusate of the TG vehicle alone.

<sup>c</sup>The composition and size of lymph chylomicrons isolated from rats given oxidized cholesterol compared to both control and purified cholesterol-treated rats,  $P < 0.05$ .

<sup>d</sup>The major oxysterols in the oxidized cholesterol chylomicrons include 7 $\beta$ -hydroxycholesterol, 5 $\alpha$ ,6 $\alpha$ -epoxycholesterol, 5 $\beta$ ,6 $\beta$ -epoxycholesterol, and 7-ketocholesterol.





**FIG. 2.** The clearance from plasma of chylomicron TG is shown as a percentage of the dose of radioactive  $^{14}\text{C}$ -TG injected. See Figure 1 for experimental procedures. Chylomicrons were then injected into the carotid artery of conscious recipient rats. Data are mean  $\pm$  SEM ( $n = 9$ ),  $P < 0.05$ . \*There was no difference in the plasma clearance of TG between chylomicrons containing oxidized cholesterol or purified cholesterol. Chylomicrons containing both oxidized and purified cholesterol had a significant delay in clearance of TG compared to the control ( $P = 0.0068$  and  $P = 0.0025$ , respectively).

feeding as shown in Table 2. The splenic uptake of chylomicrons is representative of the reticuloendothelial system and was shown to be similar for chylomicrons isolated from rats given oxysterols or purified cholesterol.

To elucidate whether the delayed clearance of chylomicrons containing oxysterols or purified cholesterol was a con-

sequence of impaired remnant formation, the lipolytic process was assessed using the *in vivo* lipolytic index and by measuring lipase-mediated hydrolysis *in vitro*. The rate of chylomicron remnant formation can be estimated by the difference in TG clearance (lipolysis plus particle uptake) and cholesteryl ester clearance (particle uptake alone) and is called the lipolytic index (34,35). The delayed clearance of chylomicrons containing oxysterols did not appear to be due to slower remnant formation. Rather, the chylomicrons containing oxysterols had a higher mean lipolytic index (area above the curve,  $620.88 \pm 64.67$ ), but this was not significantly greater than either the control or purified cholesterol chylomicrons (area above the curve,  $577.80 \pm 251.99$  and  $429.88 \pm 64.67$ , respectively).

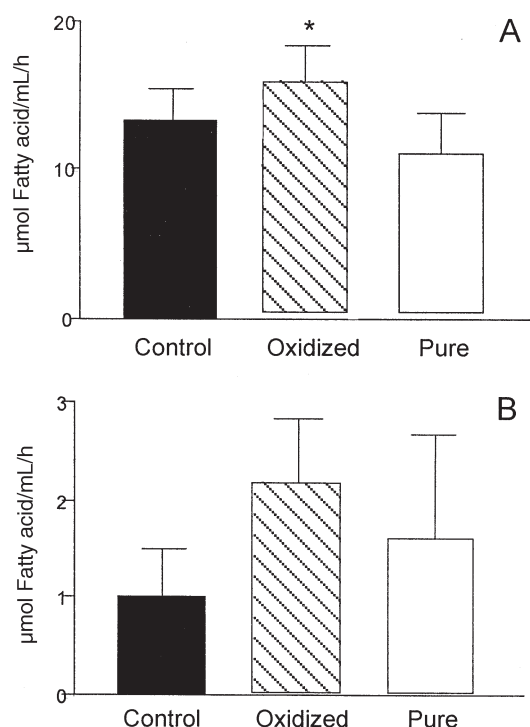
To further explore changes in the lipolytic process, the extent of lipolysis of chylomicron TG was measured to assess the activity of lipases. Chylomicrons used for the *in vitro* lipolysis measurements were isolated from rats given lipid emulsions containing oxidized cholesterol, purified cholesterol, or TG alone (control). In chylomicrons containing oxysterols, the total lipolysis of TG substrate was greater compared to the purified cholesterol-containing chylomicrons and control chylomicrons by 30 and 20%, respectively. The increase in rate of substrate lipolysis in chylomicrons containing oxysterols was attributable to LPL, which account for 90% of chylomicron TG cleavage (Fig. 3A). Chylomicron TG lipolysis occurred at a faster rate in rats fed oxysterols ( $15.85 \pm 2.39 \mu\text{mol FA/mL/h}$ ) compared to control and purified cholesterol-fed rats ( $11.14 \pm 2.72 \mu\text{mol FA/mL/h}$ ,  $P = 0.048$ , and  $13.24 \pm 2.15 \mu\text{mol FA/mL/h}$ ,  $P = 0.041$ ). HL accounted for a small increase in substrate lipolysis in the chylomicrons containing oxysterols, but this was not significant compared to the other chylomicrons, as shown in Figure 3B.

The apolipoprotein complement of chylomicrons and chylomicron remnants is critical in the regulation of their metabolism because the apolipoproteins serve as cofactors for lipases and ligands for receptors. The apolipoproteins of chylomicrons and chylomicron remnants are shown in Table 3. The ratio of total apoE/apoC was approximately 60% lower in chylomicrons isolated from rats given oxidized (0.115) and purified cholesterol (0.121) compared to controls (0.305), as shown in Table 3. Oxysterol incorporation into chylomicrons also reduced the mass of apoE by 38% per particle (as normal-

**TABLE 2**  
**Hepatic and Splenic Uptake of Chylomicrons Isolated from Rats Given Oxidized Cholesterol, Purified Cholesterol, and Control Infusates<sup>a</sup>**

Infusate	n	Organ uptake (% injected dose, mean $\pm$ SEM)			
		TG ( $^{14}\text{C}$ )palmitic acid)		Cholesterol ( $^3\text{H}$ )cholesterol)	
		Liver	Spleen	Liver	Spleen
Control (triolein)	5	11.45 $\pm$ 2.84	0.39 $\pm$ 0.18	30.72 $\pm$ 2.84	1.57 $\pm$ 0.18
Oxidized cholesterol	9	9.86 $\pm$ 0.79	0.82 $\pm$ 0.07	29.31 $\pm$ 3.53	1.50 $\pm$ 0.23
Purified cholesterol	9	13.16 $\pm$ 1.41	0.87 $\pm$ 0.07	30.80 $\pm$ 3.58	1.57 $\pm$ 0.10

<sup>a</sup>Nascent chylomicrons were isolated from rats given infusates of either oxidized cholesterol or purified cholesterol in a vehicle of triolein or triolein (control) alone *via* a gastric cannula. Chylomicrons were then injected into the external jugular of conscious recipient rats, and arterial blood was sampled to monitor the clearance of chylomicrons from plasma. Following the final arterial blood sample at 30 min, rats were sacrificed and the liver and spleen removed.



**FIG. 3.** The rate of lipoprotein lipase activity (A), and hepatic lipase (B) in postheparin plasma of chylomicron TG isolated from rats given oxidized ( $n = 4$ ) or purified ( $n = 4$ ) cholesterol in a vehicle of triolein and vehicle alone (control,  $n = 4$ ). TG substrate hydrolysis was expressed as the appearance of radiolabeled FA released ( $\mu\text{mol FA/mL/h}$ ). \*The rate of lipase activity in oxidized cholesterol postheparin plasma was significantly different compared to that of purified cholesterol and control ( $P < 0.05$ ).

ized for apoB<sub>48</sub>) compared to 21% for purified cholesterol-containing chylomicrons (see Table 3). The decreased apoE content was subsequently confirmed in posthydrolyzed remnants enriched with oxysterols and purified cholesterol, in which they had an 18 and 12% lower apoE per particle, respectively, compared to control chylomicron remnants. The chylomicron remnants from oxysterol-fed rats also contained a greater amount of apoC compared to the control and purified cholesterol chylomicron remnants, which expressed only

traces of this apolipoprotein. Further to the changes in total apoE content, the apoE isoform expression was also altered in chylomicrons derived from oxidized cholesterol, showing half the apoE<sub>4</sub> (4% of total apoC and apoE) compared to the control (8%) or purified cholesterol chylomicron (9%), as shown in Table 3. In addition, the chylomicron apoC isoforms CIII<sub>1+2</sub> and CIII<sub>3</sub> were also shown to be elevated in oxysterol-fed rats.

**DISCUSSION**

We proposed that oxidized cholesterol incorporation into lymph chylomicrons may modulate chylomicron metabolism based on previous observations showing that oxidized cholesterol alter chylomicron structure and composition (9). The results reported here are the first experiments using *in vivo*-synthesized lymph chylomicrons isolated after intestinal absorption of oxidized cholesterol and purified cholesterol to study the kinetics of these particles *in vivo*. It has been demonstrated in this study that cholesterol enrichment of lymph chylomicrons retards the clearance of chylomicrons from circulation. Moreover, oxidized cholesterol exacerbate the reduced clearance of chylomicron remnants from circulation compared to purified cholesterol.

The kinetics of both oxidized cholesterol- and purified cholesterol-enriched chylomicrons displayed a biphasic mode of clearance with an initial rapid phase followed by a slower rate of clearance, which is consistent with the established catabolism of chylomicrons *in vivo* (26,28). The initial, rapid phase is indicative of the binding of chylomicrons to endothelial lipases. The second, slower phase primarily represents sequestration of particles onto extracellular matrices, and the internalization of chylomicrons and remnants *via* receptor-mediated processes by the liver and other tissues. Chylomicrons isolated from rats given oxidized cholesterol showed a moderate impairment of tissue uptake as reflected in the decreased removal from plasma of the chylomicron cholesterol ester, but this was not significantly different from the purified cholesterol-containing chylomicrons. Similarly, chylomicrons isolated from rats given purified cholesterol displayed impaired removal from plasma but to a lesser degree than

**TABLE 3**  
**The Apolipoprotein Ratio and Isoform Content of Chylomicrons and Chylomicron Remnants<sup>a</sup>**

	E/B <sub>48</sub>	C/B <sub>48</sub>	E/C	E <sub>4</sub> <sup>b</sup>	E <sub>3</sub> <sup>b</sup>	E <sub>2</sub> <sup>b</sup>	CII <sup>c</sup>	CIII <sub>0</sub> <sup>c</sup>	CIII <sub>1+2</sub> <sup>c</sup>	CIII <sub>3</sub> <sup>c</sup>
Chylomicrons										
Control	3.36	11.01	0.305	8	2	—	T	41	25	23
Oxidized	2.09	18.20	0.115	4	2	—	T	41	30	36
Pure	2.65	21.89	0.121	9	4	—	T	48	19	20
Chylomicron remnants										
Control	1.51	T	T	19	18	5	—	49	—	8
Oxidized	1.24	0.45	2.77	20	16	8	—	34	—	12
Pure	1.34	T	T	22	28	6	—	40	—	4

<sup>a</sup>Samples were pooled from each treatment group to provide sufficient protein for apolipoprotein analysis. Apolipoproteins were separated using SDS-PAGE (5–20% polyacrylamide) and apolipoprotein isoforms were separated using isoelectric focusing (1% polyacrylamide/8 M urea). Apolipoprotein content was expressed per particle (one chylomicron contains one apoB<sub>48</sub>). Apolipoprotein isoforms were expressed as a percentage of the total apolipoprotein content, respectively. T, trace.

<sup>b</sup>Percent total apoE.

<sup>c</sup>Percent total apoC.

those animals given oxysterols. The delay in removal of chylomicrons containing oxidized cholesterol was particularly evident in the initial phase of clearance compared to both the control and purified cholesterol containing chylomicrons. Therefore, these results suggest that oxidized cholesterol may impair the initial binding or interaction of particles with extracellular matrices and receptors that enable rapid sequestration and removal of chylomicrons from the circulation.

TG clearance from the plasma is normally indicative of the extent of lipolysis, which is obligatory for chylomicron remnant formation and thereafter for uptake by tissues, predominantly the liver. The clearance of chylomicron TG from plasma was found to be impaired in both the oxidized cholesterol- and purified cholesterol-enriched particles. The delayed clearance of chylomicrons isolated from rats given oxidized cholesterol was not a result of delayed conversion to the remnant form because lipolysis *in vivo* did not appear to be impaired. Rather, the *in vitro* lipolytic studies showed that chylomicrons isolated from rats given oxidized cholesterol had increased TG lipolysis compared to control and purified cholesterol-containing chylomicrons.

The lipolysis of chylomicron TG is regulated by the apolipoprotein complement of the particles. The ratio and mass of apolipoproteins play a key role in determining the lipolytic rate. ApoCII is an important cofactor for the action of LPL, whereas apoCIII and apoE inhibit LPL activity (35,36). Interestingly, both the oxidized cholesterol- and purified cholesterol-containing chylomicrons had a reduced total apoE/C ratio, which is consistent with the finding that chylomicrons enriched with oxidized cholesterol had increased LPL TG hydrolysis. In the purified cholesterol-containing chylomicrons, no effect on LPL activity was observed. A lower apoE/C ratio has been associated with larger particle size (37) and may account for the preferential hydrolysis of the larger TG-enriched particles isolated from rats given oxidized cholesterol.

The inhibitory action of apoCIII may have influenced the complete lipolysis of oxidized cholesterol-containing chylomicron remnants, however, which is necessary for the internalization of particles by tissues (38). The hydrolysis of TG from larger chylomicron particles has previously been shown in the rat model to be relatively incomplete compared to smaller particles (23). However, the size of particles does not appear to inhibit the sequestration of particles by the liver (23). Chylomicrons that are partially hydrolyzed have reduced binding affinity for uptake by receptor-mediated pathways and may require further hydrolysis by hepatic lipases before actual internalization by hepatocytes (27).

ApoE is associated with the sequestration and uptake of chylomicron remnants by tissues. The confirmation of apoE has been reported to be altered by the particle size of lipoproteins, whereby as the particle size of TG-rich lipoproteins increases, the  $\alpha$ -helical conformation of apoE unfolds, which is unfavorable in terms of the interaction of particles with the apoB-100/E receptor at least (37). Hence, the greater size of chylomicrons containing oxidized cholesterol may prevent

the apoE-associated uptake of these particles by tissues other than the liver. Particle size can also alter the molecular order of lipid constituents, which may affect the conformation of apoE (39). The hydroxyl, epoxide, and keto groups associated with oxysterols may disturb the order of lipid packing in the chylomicrons, as observed in phospholipid bilayer models (40). In the chylomicrons containing oxidized cholesterol, this may affect particle surface structure, apoE conformation, and interaction with apoE ligands. However, it should be noted that the removal of larger particles from circulation is thought to be less dependent on interaction with the apoB-100/E receptor specifically and more reliant on other mechanisms of sequestration, including interaction with extracellular matrices and other receptor proteins (37).

Collectively, the findings of this study suggest that the impaired clearance of chylomicrons containing oxidized cholesterol may be associated with extra-hepatic tissues. The hepatic sequestration of chylomicrons enriched with oxysterols was not altered compared to the control or purified cholesterol-containing chylomicrons. The splenic uptake of chylomicrons rich in oxidized cholesterol showed that these particles were not preferentially removed by the reticuloendothelial system. However, splenic uptake does only account for less than 2% of chylomicron remnant uptake. The impaired uptake of chylomicrons enriched with oxidized sterols by tissues other than the liver and spleen warrants further investigation. However, it would appear that the delayed clearance of these particles may be due to a combined effect of the observed reduction in apoE and elevated apoCIII content, and potential effects on complete lipolysis, receptor-mediated, and nonspecific mechanisms of removal of these particles from plasma.

The impaired clearance of chylomicrons containing oxidized cholesterol and the associated accumulation in plasma of these particles may be mechanisms whereby oxidized cholesterol exacerbate cholesterol deposition in the arterial wall and the development of atherosclerosis in animal models (16–18) and perhaps humans (19). The accumulation of chylomicron remnants in plasma results in increased delivery and retention of these particles by the arterial wall leading to accelerated lesion development, as evidenced in type III hyperlipoproteinemia (41) and familial hypercholesterolemia (42). Indeed, in animal models of impaired chylomicron remnant and LDL clearance, such as apoE- and LDL-receptor-deficient mice, feeding diets containing oxidized cholesterol leads to accelerated atherosclerotic lesion development compared to mice fed cholesterol alone (43). Rong and coworkers (44) have shown that repeated arterial exposure of emulsions containing oxidized cholesterol results in vascular injury and enhanced permeability of the arterial endothelium to macromolecules in the rabbit model. Modulation of vascular integrity and permeability by dietary oxysterols may further influence the uptake of cholesterol-rich remnant particles such as postprandial remnants and LDL into the arterial wall (44).

In summary, the impaired removal of oxidized cholesterol-containing chylomicrons from plasma appears to be associated with modulation of the size and apolipoprotein composition of

chylomicrons upon incorporation of dietary-derived oxidized cholesterol into these particles. Although further investigations in humans are required, the results of this study suggest that the consumption of cholesterol-rich processed foods may adversely modulate postprandial metabolism with the potential to exacerbate the development of cardiovascular disease.

**ACKNOWLEDGMENTS**

This project was funded by the Royal Perth Hospital Medical Research Foundation and the National Heart Foundation, Australia.

**REFERENCES**

1. Hulten, L.M., Lindmark, H., Diczfalusy, U., Bjorkhem, I., Ottosson, M., Yani, L., Bondjers, G., and Wiklund O. (1996) Oxysterols Present in Atherosclerotic Tissue Decrease the Expression of Lipoprotein Lipase Messenger RNA in Human Monocyte-Derived Macrophages, *J. Clin. Invest.* 97, 461–468.
2. Carpenter, K.L., Taylor, S.E., van der Veen, C., Williamson, B.K., Ballantine, J.A., and Mitchinson, M.J. (1995) Lipids and Oxidized Lipids in Human Atherosclerotic Lesions at Different Stages of Development, *Biochim. Biophys. Acta.* 1256, 141–150.
3. Van der Bovenkamp, P., Kosmeijer-Schuil, T.G., and Katan, M.B. (1988) Quantification of Oxysterols in Dutch Foods: Egg Products and Mixed Diets, *Lipids* 23, 1079–1085.
4. Larkeson, B., Dutta, P.C., and Hansson, I. (2000) Effects of Frying and Storage on Cholesterol Oxidation in Minced Meat Products, *J. Am. Oil. Chem. Soc.* 77, 675–680.
5. Przygonski, K., Jelen, H., and Wasowicz, E. (2000) Determination of Cholesterol Oxidation Products in Milk Powder and Infant Formulas by Gas Chromatography and Mass Spectrometry, *Nahrung-Food* 44, 122–125.
6. Addis, P.B. (1986) Occurrence of Lipid Oxidation Products in Foods, *Food Chem. Toxicol.* 24, 1021–1030.
7. Sander, B.D., Smith, D.E., Addis, P.B., and Park, S.W. (1989) Effects of Prolonged and Adverse Storage Conditions on Levels of Cholesterol Oxidation Products in Dairy Products, *J. Food Sci.* 54, 874–879.
8. Park, S.W., and Addis P.B. (1987) Cholesterol Oxidation Products in Some Muscle Foods, *J. Food Sci.* 52, 1504–1505.
9. Vine, D.F., Croft, K.D., Beilin, L.J., and Mamo, J.C.L. (1997) Absorption of Dietary Cholesterol Oxidation Products and Incorporation into Lymph Chylomicrons, *Lipids* 32, 887–893.
10. Osada, K., Sasaki, E., and Sugano, M. (1994) Lymphatic Absorption of Oxidized Cholesterol in Rats, *Lipids* 29, 555–559.
11. Emanuel, H.A., Hassel, C.A., Addis, P.B., Bergmann, S.D., and Zavoral, J.H. (1991) Plasma Cholesterol Oxidation Products in Human Subjects Fed a Meal Rich in Oxysterols, *J. Food Sci.* 56, 843–847.
12. Linseisen, J., and Wolfram, G. (1998) Absorption of Cholesterol Oxidation Products from Ordinary Foodstuff in Humans, *Ann. Nutr. Metab.* 42, 221–230.
13. Imai, H., Werthessen, N.T., Taylor, C.B., and Lee, K.T. (1976) Angiotoxicity and Atherosclerosis due to Contaminants of U.S.P. Grade Cholesterol, *Arch. Pathol. Lab. Med.* 100, 565–572.
14. Taylor, C.B., Peng, S.K., Werthessen, N.T., Tham, P., and Lee, K.T. (1979) Spontaneously Occurring Angiotoxic Derivatives of Cholesterol, *Am. J. Clin. Nutr.* 32, 40–45.
15. Fornas, E., Fortea, A., Renau, J., and Camanas, A. (1987) Cholesterol Oxidation Products Induce Erythrocyte Accumulation and Endothelium Alterations in the Aorta of Rats. Turnover of Endothelial Cells in the Apparently Intact Areas Remains Unchanged, *Exp. Pathol.* 31, 105–112.

16. Vine, D.F., Mamo, J.C.L., Beilin, L.J., and Croft, K.D. (1998) Dietary Oxysterols Are Incorporated in Plasma Triglyceride-Rich Lipoproteins, Increase Their Susceptibility to Oxidation and Increase Aortic Cholesterol Concentration of Rabbits, *J. Lipid Res.* 39, 1995–2004.
17. Rong, J.X., Shen, L.J., Chang, Y.H., Richters, A., Hodis, H.N., and Sevanian, A. (1999) Cholesterol Oxidation Products Induce Vascular Foam Cell Lesion Formation in Hypercholesterolemic New Zealand White Rabbits, *Arterioscler. Thromb. Vasc. Biol.* 19, 2179–2188.
18. Staprans, I., Pan, X.M., Rapp, J.H., and Feingold, K.R. (1998) Oxidized Cholesterol in the Diet Accelerates the Development of Aortic Atherosclerotic Lesions in Cholesterol-Fed Rabbits, *Arterioscler. Thromb. Vasc. Biol.* 18, 977–983.
19. Jacobson, M.S. (1987) Cholesterol Oxides in Indian Ghee: Possible Cause of Unexplained High Risk of Atherosclerosis in Indian Immigrant Populations, *Lancet* 2 (Sept. 19), 656–658.
20. Proctor, S.D., and Mamo, J.C.L. (1996) Arterial Fatty Lesions Have Increased Uptake of Chylomicron Remnants but Not Low-Density Lipoproteins, *Coron. Artery Dis.* 7, 239–245.
21. Redgrave, T.G., Dunne, K.B., Roberts, D.C., and West, C.E. (1976) Chylomicron Metabolism in Rabbits Fed Diets With or Without Added Cholesterol, *Atherosclerosis* 24, 501–508.
22. Juhel, C., Dubois, C., Senft, M., Levy, E., Lafont, H., and Lairon, D. (1997) Postprandial Lipaemia Is Exacerbated in Fat-Cholesterol-Fed Rabbits: Relationship to Atheroma Deposition, *Brit. J. Nutr.* 78, 301–311.
23. Martins, I.J., Mortimer, B.C., Miller, J., and Redgrave, T.G. (1996) Effects of Particle Size and Number on the Plasma Clearance of Chylomicrons and Remnants, *J. Lipid Res.* 37, 2696–2705.
24. Hussain, M.M., Innerarity, T.L., Brecht, W.J., and Mahely, R.W. (1995) Chylomicron Metabolism in Normal, Cholesterol-Fed, and WHHL Rabbits, *J. Biol. Chem.* 270, 8578–8587.
25. Mortimer, B.-C., Tso, P., Phan, C.T., Beveridge, D.J., Wen, J., and Redgrave, T.G. (1995) Features of Cholesterol Structure that Regulate the Clearance of Chylomicron-like Lipid Emulsions, *J. Lipid Res.* 36, 2038–2053.
26. Redgrave, T.G. (1983) Formation and Metabolism of Chylomicrons, *Int. Rev. Physiol.* 28, 103–130.
27. Hussain, M.M., Kancha, R.K., Zhou, Z., Luchoomun, J., Zu, H., and Baakillah, A. (1996) Chylomicron Assembly and Catabolism: Role of Apolipoprotein Receptors, *Biochim. Biophys. Acta* 1300, 151–170.
28. Umeda, Y., Redgrave, T.G., Mortimer, B.C., and Mamo, J.L. (1995) Kinetics and Uptake *in vivo* of Oxidatively Modified Lymph Chylomicrons, *Am. J. Physiol.* 268 (Gastrointest. Liver Physiol. 37), 709–716.
29. Redgrave, T.G., Roberts, D.C., and West, C.E. (1975) Separation of Plasma Lipoproteins by Density Gradient Ultracentrifugation, *Anal. Chem.* 65, 42–49.
30. Mori, T.A., Croft, K.D., Puddey, I.B., and Beilin, L.J. (1996) Analysis of Native and Oxidized Low-Density Lipoprotein Oxysterols Using Gas-Chromatography–Mass Spectrometry with Selective Ion Monitoring, *Redox Rep.* 1, 5–34.
31. Folch, J., Lees, M., and Sloane-Stanley, G.H. (1959) A Simple Method for the Isolation and Purification of Total Lipids from Animal Tissues, *J. Biol. Chem.* 226, 497–509.
32. Mamo, J.C., Hirano, T., Sainsbury, A., Fitzgerald, A.K., and Redgrave, T.G. (1992) Hypertriglyceridemia Is Exacerbated by Slow Lipolysis of Triacylglycerol-Rich Lipoproteins in Fed but Not Fasted Streptozotocin Diabetic Rats, *Biochim. Biophys. Acta* 1128, 132–138.
33. Jeffrey, F., and Redgrave, T.G. (1982) Chylomicron Metabolism Differs Between Hooded and Albino Laboratory Rats, *J. Lipid Res.* 23, 154–60.
34. Herbert, P.N., Shulman, R.S., Levy, R.S., and Fredrickson, D.S.



- (1973) Fractionation of the C-Apoproteins from Human Plasma Very Low Density Lipoproteins, *J. Biol. Chem.* 248, 4941–4946.
35. Rensen, P.C., and van Berkel, T.J. (1996) Apolipoprotein E Effectively Inhibits Lipoprotein Lipase-Mediated Lipolysis of Chylomicron-like Triglyceride-rich Emulsions *in vitro* and *in vivo*, *J. Biol. Chem.* 271, 14791–14799.
  36. Jong, M.C., Hofker, M.H., and Havekes, L.M. (1999) Role of apoC's in Lipoprotein Metabolism: Functional Differences Between ApoCI, ApoCII and ApoCIII, *Arterioscler. Thromb. Vasc. Biol.* 19, 472–484.
  37. Rensen, P.C., Herijgers, N., Netscher, M.H., Meskers, C.J., van Eck, M., and van Berkel, T.J. (1997) Particle Size Determines the Specificity of Apolipoprotein E-Containing Triglyceride-rich Emulsions for the LDL Receptor Versus Hepatic Remnant Receptor *in vivo*, *J. Lipid Res.* 38, 1070–1084.
  38. Mann, C.J., Troussard, A.A., Yen, F.T., Hannouche, N., Najib, J., Fruchart, J.C., Lotteau, V., Andre, P., and Bihain, B.E. (1997) Inhibitory Effects of Specific Apolipoprotein C-III Isoforms on the Binding of Triglyceride-rich Lipoproteins to the Lipolysis-Stimulated Receptor, *J. Biol. Chem.* 272, 31348–31354.
  39. Mims, M.P., Soma, M.R., and Morrisett, J.D. (1990) Effect of Particle Size and Temperature on the Conformation and Physiological Behaviour of ApoE Bound to Model Lipoprotein Particles, *Biochemistry* 29, 6639–6647.
  40. Verhagen, J.C., ter Braake, P., Teunissen, J., van Ginkel, G., and Sevanian, A. (1996) Physical Effects of Biologically Formed Cholesterol Oxidation Products on Lipid Membranes Investigated with Fluorescence Depolarization Spectroscopy and Electron Spin Resonance, *J. Lipid Res.* 37, 1488–1502.
  41. Breslow, J.L., Zannis, V.I., Sangiacomo, T.R., Third, J.L., Tracy, T., and Glueck, C.J. (1982) Studies of Familial Type III Hyperlipoproteinemia Using as a Genetic Marker the ApoE Phenotype E2/2, *J. Lipid Res.* 23, 1224–1235.
  42. Mamo, J.C., Smith, D., Yu, K.C., Kawaguchi, A., Harada-shiba, M., Yamamura, T., and Yamamoto, A. (1998) Accumulation of Chylomicrons and Chylomicron-Remnants in Homozygous Subjects with Familial Hypercholesterolaemia, *Euro. J. Clin. Invest.* 28, 379–384.
  43. Staprans, I., Pan, X.M., Rapp, J.H., Grunfeld, C., and Feingold, K.R. (2000) Oxidized Cholesterol in the Diet Accelerates the Development of Atherosclerosis in LDL Receptor- and Apolipoprotein E-Deficient Mice, *Arterioscler. Thromb. Vasc. Biol.* 20, 708–714.
  44. Rong, J.X., Rangasawamy, S., Shen, L.J., Dave, R., Chang, Y.H., Peterson, H., Hodis, H.N., Chisolm, G.M., and Sevanian, A. (1998) Arterial Wall Injury by Cholesterol Oxidation Products Causes Endothelial Dysfunction and Arterial Wall Cholesterol Accumulation, *Arterioscler. Thromb. Vasc. Biol.* 18, 1885–1894.
- [Received January 2, 2002, and in revised form April 7, 2002; revision accepted April 9, 2002]

# Changes in the Chemical Composition of Surfactant-like Particles Secreted by Rat Small Intestine in Response to Different Dietary Fats

Seema Kalra<sup>a</sup>, Safrun Mahmood<sup>b</sup>, J.P. Nagpaul<sup>a</sup>, and Akhtar Mahmood<sup>a,\*</sup>

<sup>a</sup>Department of Biochemistry, Panjab University, Chandigarh-160014, India, and

<sup>b</sup>Department of Experimental Medicine, Post Graduate Institute of Medical Education and Research, Chandigarh-160012, India

**ABSTRACT:** Consumption of dietary oil, *viz.*, corn, fish, coconut, or olive, induced the secretion of surfactant-like particles (SLP) in rat intestine. These lipoprotein particles differ in (i) levels of alkaline phosphatase activity, (ii) lipid composition, and (iii) FA composition in response to feeding of different oils. The secreted particles had similar buoyancy (1.07–1.08 g/mL) and cholesterol/phospholipid molar ratios (0.61–0.72) except that feeding coconut oil to rats produced SLP with a low (0.18) cholesterol/phospholipid molar ratio compared to control animals. It is concluded from these observations that feeding different oils induces the secretion of lipoprotein particles in rat intestine with different chemical compositions.

Paper no. L8629 in *Lipids* 37, 463–468 (May 2002).

Fat feeding increases intestinal alkaline phosphatase (IAP) in serum, but the mechanism responsible for this phenomenon is unclear. The role of surfactant-like particles (SLP) has been implicated in the delivery of this membrane-bound enzyme into lumen and serum (1). These particles, secreted by enterocytes, exhibit morphologic and surface-active properties resembling pulmonary surfactants and are enriched for IAP and PC (2). Chemical analysis of SLP revealed that they consist of four to six major proteins having molecular sizes of the order of 30–120 kDa (3). These lipoprotein particles were associated with fat droplets and have been implicated in transepithelial transport of TAG (4) in rat intestine. Previous studies on the characterization of SLP have been based on corn oil feeding (3). However, feeding different dietary fats induces different changes in chemical composition of the brush border membrane (BBM) in rat intestine (5). Changing the saturation of dietary fats produces substantial differences in the FA composition of the membranes of intact viable cells and tissues (6,7). Changes in the FA composition of membranous proteins may be responsible for altered enzyme activities, as many enterocyte plasma membrane enzymes are in-

trinsic proteins whose activities depend on the fluidity and physical state of the membrane lipids (8,9). Therefore, the objectives of this study were to determine (i) whether the choice of dietary oil affects the quality and quantity of SLP production in rat intestine and (ii) whether the lipid and enzyme activity profile of these lipoprotein membranes varied under these conditions.

## MATERIALS AND METHODS

Adult male Wistar rats (150–170 g) were used. The animals were obtained from Central Animal Facility of Panjab University, Chandigarh, and were maintained on a commercial rat pellet diet (Hindustan Lever Ltd., India) with free access to water until they attained the required weight. All procedures done on animals were approved by the Ethical Committee Board of Panjab University, Chandigarh, India. Animals were divided into five groups and were fed corn (group 2), fish (group 3), coconut (group 4), or olive (group 5) oil. Rats were fasted overnight with free access to water. On the following day, animals were given 2.0 mL of the respective oil intragastrically *via* an infant feeding tube and were killed 5 h after fat feeding. Animals in the control group received saline alone (group 1).

**Tissue sampling.** Animals were sacrificed under ether anesthesia. Blood was collected by introducing a needle in the left ventricle of the heart, and perfusion was done with 0.9% saline until the liver was blanched to minimize contamination of tissue samples with blood. Blood samples were then incubated at 37°C for 30 min and then centrifuged at 5,000 × *g* for 15 min at 4°C to separate serum. Serum was then frozen at –20°C in aliquots until further analysis. Starting from the ligament of Treitz, 20 cm of proximal intestine was removed. The intestine was opened longitudinally, and the mucosal surface was lightly scraped using Whatman no. 3 paper and suspended in solution A [5mM Tris (hydroxymethyl) amino methane buffer, pH 7.4, containing 5 mM CaCl<sub>2</sub>] as described by Eliakim *et al.* (2).

**Gradient centrifugation.** SLP were isolated from the light mucosal scrapings by passing them through a gradient that separated membrane-bound phosphatase (density 1.07–1.08

\*To whom correspondence should be addressed at Department of Biochemistry, Panjab University, Sector 14, Chandigarh 160014, India.  
E-mail: akhtarmah@yahoo.com

Abbreviations: BBM, brush border membrane; Chl, cholesterol; IAP, intestinal alkaline phosphatase; LPC, lysophosphatidylcholine; PL, phospholipid; SLP, surfactant-like particle.

g/L) from free IAP (density 1.057 g/L). The mucosal scrapings from each of the five groups were fractionated on continuous NaBr gradients (0.49–1.46 M in solution A) as described for the isolation of human lung surfactant (10). A visible white band of density 1.07–1.08 g/L was formed against clear solution after centrifugation at  $100,000 \times g$  for 16 h at 5°C using an SW-41 rotor (Beckman Instruments). These conditions were identical to those used by Eliakim *et al.* (2) to isolate rat intestinal SLP. One-milliliter fractions were removed from the top of the gradient by siphoning and used for biochemical analyses. Fractions 3 and 4, exhibiting maximal IAP activity, were pooled from several gradients, dialyzed, and concentrated using an Amicon filter (XM-10) assembly (Millipore Corp., Bedford, MA).

**Enzyme assays.** Alkaline phosphatase activity was assayed by the method of Bergmeyer (11). Disaccharidases were determined by the method of Dahlqvist (12). Protein was determined by the method of Lowry *et al.* (13) using BSA as the standard.

**Lipid extraction and analysis.** Total lipids from SLP were extracted by the method of Folch *et al.* (14). Various phospholipid (PL) fractions were estimated following the method of Marinetti (15). Total cholesterol (Chl) was determined by the method of Zlatkis *et al.* (16). TG were estimated by the method of Van Handel *et al.* (17).

**TLC.** PL were fractionated by TLC using  $\text{CHCl}_3/\text{CH}_3\text{OH}/7\text{N NH}_3$  (65:25:4, by vol) as the resolving solvent and quantified. Synthetic PL (Sigma Chemical Co., St. Louis, MO) were used as standards in parallel lanes.

Individual spots were identified by exposing the plates to iodine vapors in a glass chamber. Yellowish-brown spots seen were scraped off the plates, and PL were estimated as described by Marinetti (15). Individual PL fractions were determined as percentage of the total PL.

**FA analysis.** FA from total lipid extract were methylated using boron trifluoride/methanol reagent as described by Metcalfe and Schmitz (18). FA were analyzed by GC–MS (Shimadzu QP-5000) using a DB 23 capillary column (J&W Scientific, Folsom, CA; 30 m length, 0.25 mm i.d.). FAME were detected by GC with an FID, followed by mass determination. The carrier gas used was helium at a pressure of 72.3 kPa.

**Statistical analysis.** Statistical analysis of the data was done using Student's *t*-test and two-way ANOVA. Values having  $P < 0.05$  were considered to be statistically significant.

**BCIP staining.** Purified SLP proteins (100  $\mu\text{g}$ ) were separated on 10% polyacrylamide-SDS gels under nondenaturing conditions and stained with 5-bromo-4-chloro-3-indolyl phosphate (BCIP) for the detection of alkaline phosphatase activity in the gels. The gels were incubated in BCIP (1 mg/mL in 50 mM Tris-HCl, pH 7.6) solution at 37°C. After the bands of desired intensity were visible, the reaction was stopped by transferring the gel to 10% acetic acid and then the gel was rinsed in distilled water and dried.

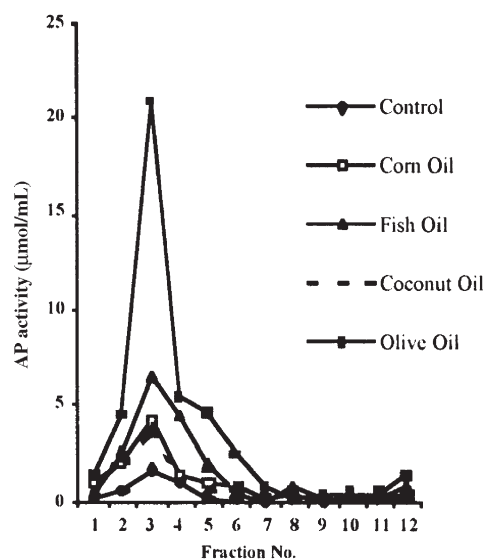
**Western blotting.** SLP (100  $\mu\text{g}$  protein) from rats fed fats 5 h previously were subjected to electrophoresis under denatur-

ing conditions in 10% polyacrylamide-SDS gels, and Western blotting was performed as described (3). Briefly, the proteins were transferred onto an Immobilon P membrane (Millipore) at 30 volts for 16 h at 4°C. Anti-SLP (1:1000) was used as primary antibody, and color was developed using peroxidase-linked secondary anti-immunoglobulin, 2,4-diaminobenzene, and  $\text{H}_2\text{O}_2$ .

## RESULTS

The activity profile of IAP in various NaBr gradient fractions after centrifugation of light scrapings from intestine of control and fat-fed rats is shown in Figure 1. As expected from Eliakim *et al.* (2), the activity of IAP peaked in fraction 3, corresponding to a density of 1.07–1.08 g/L. However, the level of IAP activity varied considerably in animals fed different oils. It followed the pattern olive oil > fish oil > corn oil > coconut oil > saline-treated animals.

Although IAP constitutes the major enzyme in SLP, it also contains small amounts of various brush border enzymes (2). Thus, the activities of various disaccharidases in purified SLP were also analyzed and expressed on a protein basis. These results are shown in Table 1. SLP from olive oil-fed animals showed a threefold increase in IAP activity ( $P < 0.001$ ) as compared to the controls, whereas the increases in enzyme activity induced by corn oil or fish oil feeding were 1.6- ( $P < 0.001$ ) and 1.3-fold ( $P < 0.01$ ), respectively. IAP activity in SLP was slightly increased upon coconut oil treatment ( $P < 0.05$ ) compared to control rats. Thus, specific activities of AP were as maximal in animals fed olive oil, followed by corn oil, fish oil, and coconut oil with respect to control animals. Sucrase, lactase, and trehalase activities in SLP either declined



**FIG. 1.** Profile of alkaline phosphatase (AP) activity in NaBr gradient fractions of intestinal scrapings from rats fed dietary oils. Crude surfactant-like particle (SLP) scrapings were applied on NaBr gradient and centrifuged at  $100,000 \times g$  for 16 h at 4°C. One-milliliter fractions were subsequently collected for AP estimation.

**TABLE 1**  
Effect of Feeding Different Oils to Rats on Various Enzymes in Purified Surfactant-Like Particles in Intestine<sup>a</sup>

Treatment	AP	Sucrase	Trehalase	Lactase
	(nmol/min/mg protein)			
Saline	2.60 ± 0.07	0.14 ± 0.01	0.13 ± 0.01	11.91 ± 1.01
Corn oil	4.26 ± 0.08 <sup>c</sup>	0.11 ± 0.02	0.02 ± 0.01 <sup>c</sup>	4.28 ± 0.61 <sup>c</sup>
Fish oil	3.46 ± 0.04 <sup>b</sup>	0.13 ± 0.03	0.04 ± 0.01 <sup>c</sup>	6.92 ± 0.90 <sup>c</sup>
Coconut oil	2.78 ± 0.06 <sup>a</sup>	0.08 ± 0.02 <sup>b</sup>	0.05 ± 0.01 <sup>c</sup>	3.90 ± 0.29 <sup>c</sup>
Olive oil	7.58 ± 0.10 <sup>c</sup>	0.07 ± 0.01 <sup>c</sup>	0.03 ± 0.01 <sup>c</sup>	2.53 ± 0.31 <sup>c</sup>

<sup>a</sup>Values are mean ± SD (*n* = 5). <sup>b</sup>*P* < 0.05; <sup>c</sup>*P* < 0.01; <sup>c</sup>*P* < 0.001 compared to the controls.

or remained unaltered upon oil feeding to the animals, compared to the control group.

The role of SLP in IAP transport has been described (19); thus, IAP activity was also determined in serum after fat feeding (Table 2). Serum AP activity was increased 4.3-fold (*P* < 0.001) after feeding olive oil as compared to the controls, whereas a 3.5-fold increase in the enzyme activity was observed in fish oil- and corn oil-fed animals (*P* < 0.001). Serum from coconut oil-fed animals showed 3.0-fold increase in AP activity as compared to the control animals (*P* < 0.001). Serum from olive oil-fed animals exhibited significantly higher activity compared to corn oil-fed rats (*P* < 0.001). Total TG levels were also elevated in serum after feeding of different fats to rats, compared to control group (Table 2).

Data on the lipid composition of SLP (Table 3) revealed that PL content was significantly enhanced in corn, fish, or olive oil-fed rats (*P* < 0.001) but was unaffected by coconut oil feeding to rats compared to controls. Corn or olive oil feeding enhanced total Chl (*P* < 0.001), but coconut oil feeding significantly reduced the Chl content of SLP in rat (76%, *P* < 0.001). The Chl/PL molar ratio was essentially unaffected and varied between 0.61 and 0.68 in SLP isolated from intestines of rats fed different oils. However, animals given coconut oil had a considerably lower Chl/PL molar ratio (0.18). Thus, the PL and Chl contents of SLP secreted by gut are modified by feeding different oils.

As shown in Table 4, PL composition of SLP also showed considerable variations in response to feeding of different oils to rats. In all four experimental groups examined, PS was not detected in isolated SLP. However, PC and lysophosphatidylcholine (LPC) constituted 60–80% of the PL of SLP except in the coconut oil-fed group, which contained 86% of PC, whereas LPC was only 4%. Sphingomyelin content of SLP from corn

oil- or coconut oil-fed animals decreased compared to the control group (*P* < 0.001). All the oil-fed rats except those given coconut oil showed an appreciable increase in PE content of SLP.

The FA composition of SLP showed that feeding different dietary fats also modified the fatty acyl group composition of membranous SLP lipids (Table 5). In the control group, the major FA was palmitic acid (91%); only 9% was stearic acid. Feeding corn oil reduced palmitic acid to 63%; other FA detected included oleic (27%) stearic (8%), and myristic (2%). Feeding animals with fish oil produced SLP with 81% palmitic and 14% oleic acid; stearic acid content (5%) was low compared to that in corn oil-fed animals. SLP from olive oil-fed rats had 64% palmitic and 36% palmitoleic acid. In SLP from coconut oil-fed animals, palmitic acid constituted about 92% while the remaining 8% was stearic and myristic acids.

Since IAP constitutes the major marker of SLP produced by the gut, activity of the enzyme in nondenaturing SDS-PAGE gel was also analyzed under various experimental conditions. Figure 2 shows the BCIP staining of SLP preparations from animals fed different oils. Feeding of olive oil (lane 3) resulted in the maximal IAP activity (121%) compared to the control (lane 1), followed by fish oil (lane 5; 85%), corn oil (lane 2; 30%) and coconut oil (lane 4; 25%).

Western blot analysis of SLP proteins from animals fed different oils showed six to eight protein bands, but four major proteins of molecular sizes 116, 99, 66, and 35 kDa were quite conspicuous in SLP isolated from corn-, fish-, coconut-, or olive oil-fed animals (Fig. 3). Relative densities obtained from the scan of various protein bands in SLP from animals fed different oils are shown in Figure 3A. Feeding of different oils induced different proteins. Olive oil feeding maximally induced 116 kDa protein compared to other

**TABLE 2**  
Effect of Feeding Different Oils on Serum AP Activity (nmol/mL) and Total TG Levels (mg/dL) in Rats<sup>a</sup>

Treatment	AP	TG
Saline	22.90 ± 1.10	155.36 ± 12.40
Corn oil	80.90 ± 2.61 <sup>c</sup>	277.24 ± 18.28 <sup>c</sup>
Fish oil	83.73 ± 3.67 <sup>c</sup>	249.65 ± 30.12 <sup>c</sup>
Coconut oil	68.24 ± 2.12 <sup>c</sup>	185.13 ± 15.38 <sup>b</sup>
Olive oil	98.41 ± 4.37 <sup>c</sup>	229.59 ± 23.00 <sup>c</sup>

<sup>a</sup>Values are mean ± SD (*n* = 6). <sup>b</sup>*P* < 0.01; <sup>c</sup>*P* < 0.001 compared to the control. AP, alkaline phosphatase.

**TABLE 3**  
Effect of Different Dietary Oils on Phospholipid and Cholesterol Contents of SLP Secreted by Rat Intestine<sup>a</sup>

Treatment	Total phospholipids (mg/g protein)	Total cholesterol (mg/g protein)	Chl/PL (mol/mol)
Saline	68.16 ± 3.13	26.08 ± 2.80	0.72
Corn oil	224.62 ± 7.12 <sup>c</sup>	71.74 ± 3.41 <sup>c</sup>	0.61
Fish oil	84.04 ± 4.80 <sup>c</sup>	27.51 ± 1.93	0.62
Coconut oil	64.13 ± 4.18	6.21 ± 0.50 <sup>c</sup>	0.18
Olive oil	153.51 ± 4.01 <sup>c</sup>	55.08 ± 0.69 <sup>c</sup>	0.68

<sup>a</sup>Values are mean ± SD (*n* = 6). <sup>c</sup>*P* < 0.001 compared to the controls. SLP, surfactant-like particle; PL, phospholipid; Chl, cholesterol.



**TABLE 4**  
Effect of Dietary Oils on Phospholipid Composition (percentage of total PL content) of SLP Secreted by Rat Intestine<sup>a</sup>

Treatment	LPC	SM	PC	PI	PS	PE
Saline	33.36 ± 1.23	19.19 ± 1.23	35.02 ± 0.56	11.68 ± 2.16	ND	0.75 ± 0.07
Corn oil	39.20 ± 0.23 <sup>b</sup>	1.10 ± 0.72 <sup>c</sup>	46.69 ± 1.73 <sup>c</sup>	8.79 ± 1.23	ND	3.79 ± 0.36 <sup>c</sup>
Fish oil	19.48 ± 4.36 <sup>a</sup>	19.49 ± 4.23	40.32 ± 2.06 <sup>a</sup>	17.11 ± 0.76 <sup>a</sup>	ND	3.60 ± 0.16 <sup>c</sup>
Coconut oil	4.30 ± 1.32 <sup>c</sup>	2.89 ± 1.16 <sup>c</sup>	86.40 ± 8.13 <sup>c</sup>	6.05 ± 2.34	ND	0.35 ± 0.03 <sup>b</sup>
Olive oil	23.26 ± 2.16 <sup>b</sup>	14.36 ± 6.41	46.58 ± 0.63 <sup>c</sup>	13.65 ± 1.56	ND	2.15 ± 0.76 <sup>a</sup>

<sup>a</sup>Values are mean ± SD (*n* = 3). <sup>a</sup>*P* < 0.05; <sup>b</sup>*P* < 0.01; <sup>c</sup>*P* < 0.001 compared to the controls. ND, not detected; LPC, lysophosphatidylcholine; SM, sphingomyelin; for other abbreviations see Table 3.

groups. Feeding coconut oil maximally induced a 99-kDa protein, whereas corn oil feeding induced a 66-kDa protein. The 35-kDa protein was maximally induced in rats fed fish oil. However, the 35-kDa protein was reduced below the control level in SLP from coconut oil-fed rats. Thus, different oils induced various proteins in SLP to different extents in rat intestine.

## DISCUSSION

These results indicate that different dietary fats induced the secretion of SLP in rats with different (i) chemical composition, (ii) IAP activity, and (iii) qualitatively similar but quantitatively varying protein patterns as revealed by SDS-PAGE gels. However, the isolated SLP exhibited similar buoyant density (1.07–1.08 g/L) and Chl/PL molar ratios in response to feeding corn, fish, and olive oil to rats. These findings are essentially similar those of Eliakim *et al.* (2). Among the different oils studied, feeding olive oil induced maximal production of IAP-rich SLP. Animals fed coconut oil showed a slight increase in IAP activity compared to the controls but coconut oil had a minimal effect among the four oils studied.

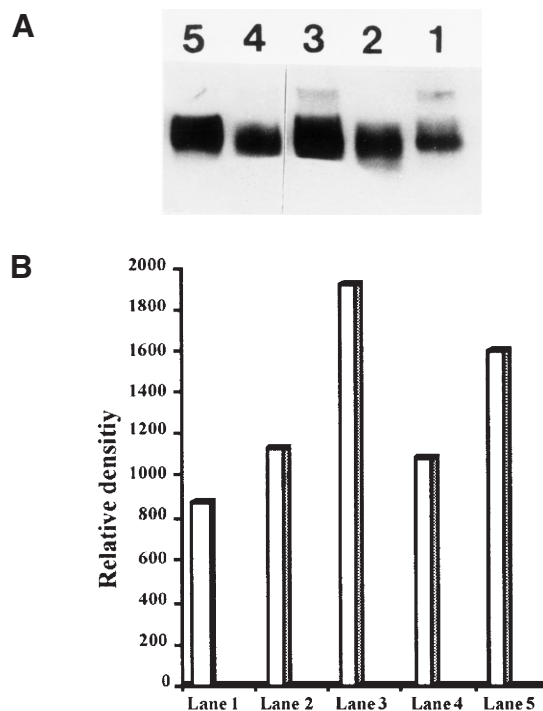
The observed changes in IAP activity were further confirmed by analysis of IAP activity in SLP run on SDS-PAGE under nonreduced conditions, as determined by staining with BCIP for IAP activity. These findings indicate differential effects of dietary fats on the production of SLP in the rat intestine having different enzyme and chemical compositions. These results could be related to different levels and degrees of saturation of these oils (20). Kaur *et al.* (5) found changes in chemical composition of BBM in rat intestine in response to different fats. Similar changes also occur in SLP secreted by the intestine upon feeding different oils. These may affect the stability and turnover rate of the particle proteins in the intestine.

**TABLE 5**  
Effect of Dietary Oils on the FA Composition (percentage of total FA content) of Surfactant-like Particles Secreted by Rat Intestine<sup>a</sup>

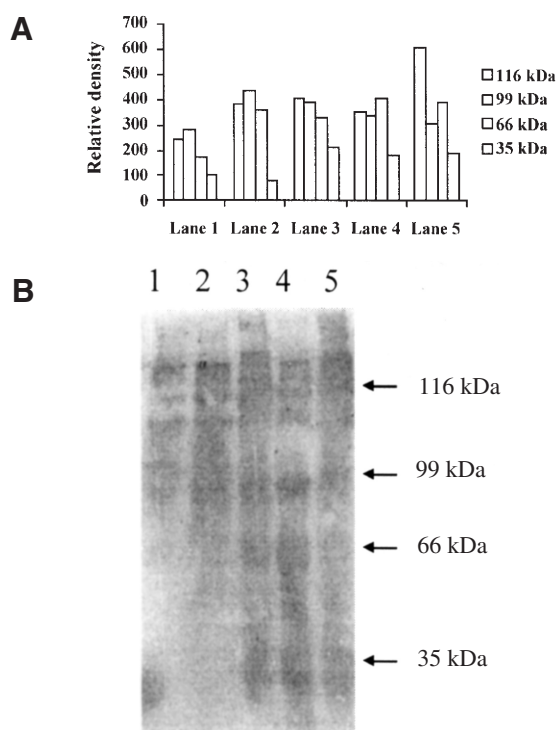
Treatment	14:0	16:0	16:1	18:0	18:1
Saline	—	91.10	—	8.90	—
Corn oil	1.87	62.69	—	8.51	26.93
Fish oil	—	81.01	—	5.34	13.65
Coconut oil	2.21	92.18	—	5.61	—
Olive oil	—	63.96	36.04	—	—

<sup>a</sup>Values are mean of two observations.

Changes in enzyme activities in response to different dietary oils also may be due to changes in the lipid microenvironment of SLP, which are accompanied by shifts in transition temperatures and values of energies of activation (21). In the present data changes in lipid composition of SLP with different dietary fats are evident. Differences in the orientation of these enzymes in the lipid milieu may also be responsible for the differential effects in particle proteins seen with various oils (22,23). Also, much higher IAP/sucrase ratios of SLP (18–108) were observed in different experimental groups as compared to the reported value of 0.99 in BBM by Young *et al.* (24), thus indicating highly enriched IAP in these particles as compared



**FIG. 2.** (A) BCIP staining of AP activity in SLP proteins separated on polyacrylamide gel electrophoresis (PAGE) from rats fed dietary oils (100 µg). Protein was applied in each lane on 10% acrylamide gel under nonreducing conditions. The gel was stained for AP by transferring the gel in 1 mg/mL BCIP in 50 mM Tris-HCl, pH 7.6, and the reaction was stopped with 10% acetic acid. (B) Relative densities of AP bands identified by BCIP staining of SLP proteins on PAGE as determined by densitometric scanning (lane 1—control, lane 2—corn oil, lane 3—olive oil, lane 4—coconut oil, lane 5—fish oil). BCIP, 5-bromo-4-chloro-3-indolyl phosphate; for other abbreviations see Figure 1.



**FIG. 3.** (A) Western blot analysis of SLP isolated from intestinal scrapings in rats fed different dietary oils. Protein (100  $\mu$ g) was subjected to PAGE, and anti-SLP (1:1000) was used as described in the Materials and Methods section. (B) Scan of protein bands identified by Western blotting of SLP isolated from rat intestine (lane 1—control, lane 2—coconut oil, lane 3—fish oil, lane 4—corn oil, lane 5—olive oil). The bands were scanned by densitometry, and the relative density of the various bands was obtained in the form of peaks. The area under each peak was determined to obtain the intensity of the protein band.

to brush borders. Similar results have been reported by DeSchryver-Kecsckemeti *et al.* (25). The maximal ratio (108) was observed in our work in SLP from olive oil-fed animals, thus indicating maximal induction of SLP in this group.

The increase in alkaline phosphatase activity observed in serum upon feeding dietary oils (except for coconut oil) is in agreement with the role of SLP as a vehicle that delivers IAP into the serum and also to the lumen (25). A marked increase in the levels of total TG in serum may be due to association of SLP with TAG transport (4). The lipid composition of SLP was considerably modified in response to fat feeding, which was quite distinct from the response reported for BBM. This further suggested that these lipoprotein particles are not derived from the underlying plasma membrane but constitute a distinct membranous entity (2) and thus may have distinct regulation.

PL and Chl contents increased in response to feeding different oils containing unsaturated FA, *viz.*, corn, fish, and olive oils. The PL content of SLP remained unaltered, while the amount of Chl was decreased in response to feeding coconut oil. These changes are presumably related to the saturation index of the dietary fat. The decrease in Chl/PL molar ratio in SLP from coconut oil-fed animals seems similar to that ob-

served by Brasitus *et al.* (26) and Wahnon *et al.* (27) in BBM, who reported an increase in Chl/PL molar ratio in animals maintained on a PUFA-rich diet as compared to those on a saturated fat-rich diet. This may represent a compensatory response to the diet. Mahmood *et al.* (3) reported a Chl/PL ratio of 1.49 for BBM and 0.68 for SLP. In the present study SLP had Chl/PL molar ratios of 0.61–0.68 except for coconut oil, which had a ratio of 0.18, thus indicating the distinct nature of these structures from underlying BBM. Furthermore, a different composition was observed for SLP at the level of individual PL fractions and FA composition as compared to BBM. PS was undetectable, and major phospholipids were PC and LPC as reported earlier by Eliakim *et al.* (2). Coconut oil feeding enhanced PC up to 86% but appreciably decreased other PL. It has been shown in animal models and cultured cells that the uptake of LPC leads to an increase in the transport of TAG (28). In this context the observed decrease of LPC in SLP of coconut oil-fed animals might affect their ability to transport TAG. The functional role in the gut of such changes in PL composition of SLP, however, remains to be identified.

FA in SLP from coconut oil-fed animals were entirely saturated, 92% being 16:0 and the rest being 14:0 and 18:0. However, SLP from unsaturated oil-fed animals had 63–81% palmitic acid (16:0). Other FA, including unsaturated ones, were found. Corn oil had 27% of 18:1, fish oil had 14% of 18:1, and olive oil had 36% of 16:1. Thus, the saturation index declined in response to feeding unsaturated fats to animals. These findings may suggest that the FA composition of the secreted SLP membranes is derived from *de novo* synthesis. Regulation of release of FA by decreasing the rate of esterification or secretion or both in response to dietary n-3 FA by enterocytes has been reported by Murthy *et al.* (29). Also  $\Delta^9$ - $\Delta^6$ -desaturase activities have been demonstrated in intestinal mucosa of rats (30) and in the human CaCo-2 cell line (31). Intestinal desaturases, unlike their counterparts in liver, did not respond to changes in dietary levels of n-3 FA. SLP contains proteins that are distinct and thus may be related to fat metabolism (32).

Feeding of dietary fats, *viz.*, olive, fish, and corn oil, induced formation of SLP in the rat intestine with different lipid and IAP activity. As determined by IAP assay, feeding olive oil produced greater amounts of SLP than feeding corn oil. Composition of these particles varied with type of fat given to rats. Considerable changes were observed in Chl and PL contents of SLP from coconut oil-fed animals. Thus, induction of SLP in response to a high-fat diet may be related to the degree of saturation/unsaturation and type of fat consumed by the animals. The physiological significance of these observations needs to be established.

#### ACKNOWLEDGMENTS

We are grateful to Prof. David H. Alpers of Washington University School of Medicine (St. Louis, MO) for providing the rat SLP antibody used in these experiments. Seema Kalra was the recipient of a research fellowship from the Council of Scientific and Industrial Research (New Delhi, India).

## REFERENCES

1. Alpers, D.H., Mahmood, A., Engle, M., Yamagishi, F., and DeSchryver-Kecsckemeti, K. (1994) The Secretion of Intestinal Alkaline Phosphatase (IAP) from the Enterocytes, *J. Gastroenterol.* 29 (Suppl.) 63–67.
2. Eliakim, R., DeSchryver-Kecsckemeti, K., Noguee, L., Stenson, W.F., and Alpers, D.H. (1989) Isolation and Characterization of a Small Intestinal Surfactant-like Particle Containing Alkaline Phosphatase and Other Digestive Enzymes, *J. Biol. Chem.* 264, 20614–20619.
3. Mahmood, A., Mahmood, S., DeSchryver-Kecsckemeti, K., and Alpers, D.H. (1993) Characterization of Proteins in Rat and Human Surfactant-like Particles, *Arch. Biochem. Biophys.* 300, 280–286.
4. Mahmood, A., Yamagishi, F., Eliakim, R., DeSchryver-Kecsckemeti, K., Gramlich, T.L., and Alpers, D.H. (1994) A Possible Role of Rat Intestinal Surfactant-like Particles in Transepithelial Triacylglycerol Transport, *J. Clin. Invest.* 93, 70–80.
5. Kaur, M., Kaur, J., Ojha, S., and Mahmood, A. (1996) Dietary Fat Effects on Brush Border Membrane Composition and Enzyme Activities in Rat Intestine, *Ann. Nutr. Metab.* 40, 269–276.
6. Spector, A.A. (1989) Polyunsaturated Fatty Acids in Membrane Function, in *Biomembranes and Nutrition* (Leger, C.L., and Bereziat, G., eds.), *Colloq. INSERM* 195, 11–19.
7. Stubbs, C.D. (1989) Physico-chemical Responses of Cell Membranes to Dietary Manipulation, in *Biomembranes and Nutrition* (Leger, C.L., and Bereziat, G., eds.), *Colloq. INSERM* 195, 125–133.
8. Brasitus, T.A., and Dudeja, P.K. (1988) Small and Large Intestinal Plasma Membranes: Structure and Function, in *Advances in Membrane Fluidity* (Aloia, R.C., Curtaina, C.C., and Gordon, L.M., eds.), Alan R. Liss, New York, pp. 227–254.
9. Proulx, P. (1991) Structure–Function Relationships in Intestinal Brush Border Membranes, *Biochim. Biophys. Acta* 1071, 255–271.
10. Phelps, D.S., Tausch, H.W., Jr., Benson, B., and Hagwood, S. (1984) An Electrophoretic and Immunochemical Characterization of Human Surfactant-Associated Proteins, *Biochim. Biophys. Acta* 791, 226–238.
11. Bergmeyer, H.U. (1965) Determination in Serum with *p*-Nitrophenyl Phosphate, in *Methods of Enzymatic Analysis* (Bergmeyer, H.U., ed.), pp. 783–785, Academic Press, New York.
12. Dahlqvist, A. (1964) Method for Assay of Intestinal Disaccharidases, *Anal. Biochem.* 7, 18–25.
13. Lowry, O.H., Rosebrough, N.J., Farr, A.L., and Randall, R.J. (1951) Protein Measurement with the Folin Phenol Reagent, *J. Biol. Chem.* 193, 265–275.
14. Folch, J., Lees, M. and Sloane-Stanley, G.H. (1957) A Simple Method for the Isolation and Purification of Total Lipids from Animal Tissues, *J. Biol. Chem.* 266, 479–509.
15. Marinetti, G.V. (1962) Chromatographic Separation, Identification and Analysis of Phosphatides, *J. Lipid Res.* 3, 1–20.
16. Zlatkis, A., Zak, B., and Boyle, A.J. (1953) A New Method for Direct Determination of Serum Cholesterol, *J. Lab. Clin. Med.* 41, 486–492.
17. Van. Handel, E., Zilversmit, D.B., and Bowman, K. (1957) Determination of Serum Triglycerides, *J. Lab. Clin. Med.* 50, 152–157.
18. Metcalfe, L.D., and Schmitz, A.A. (1961) The Rapid Preparation of Fatty Acid Esters for Gas Chromatographic Analysis, *Anal. Chem.* 33, 363–364.
19. Zhang, Y., Shao, J.S., Xie, Q.M., and Alpers, D.H. (1996) Immunolocalization of Alkaline Phosphatase and Surfactant-like Particle Proteins in Rat Duodenum During Fat Absorption, *Gastroenterology* 110, 478–488.
20. Takase, S., and Goda, T. (1990) Effects of Medium Chain Triglycerides on Brush Border Membrane-Bound Enzyme Activity in Rat Small Intestine, *J. Nutr.* 120, 969–976.
21. Linden, C.D., Keith, A.D., and Fox, C.F. (1973) Correlations Between Fatty Acid Distribution in Phospholipids and the Temperature Dependence of Membrane Physical State, *J. Supramol. Struct.* 1, 523–534.
22. Brasitus, T.A., and Schachter, D. (1980) Lipid Dynamics and Lipid–Protein Interactions in Rat Enterocyte Basolateral and Microvillus Membranes, *Biochemistry* 19, 2763–2769.
23. Mahmood, A., and Ansari, S. (1981) Solubilization of Sucrase and Alkaline Phosphatase from Microvillus Membrane of Guinea Pig Intestine Using Papain and Detergents, *Indian J. Biochem. Biophys.* 18, 198–201.
24. Young, G.P., Friedman, S., Yedlin, S.T., and Alpers, D.H. (1981) Effect of Fat Feeding on Intestinal Alkaline Phosphatase Activity in Tissue and Serum, *Am. J. Physiol.* 241, G461–G468.
25. DeSchryver-Kecsckemeti, K., Eliakim, R., Green, K., and Alpers, D.H. (1991) A Novel Intracellular Pathway for Rat Intestinal Digestive Enzymes (alkaline phosphatase and sucrase) via a Lamellar Particle, *Lab. Invest.* 65, 365–373.
26. Brasitus, T.A., Davidson, N.O., and Schachter, D. (1985) Variations in Dietary Triacylglycerol Saturation Alter the Lipid Composition and Fluidity of Rat Intestinal Plasma Membranes, *Biochim. Biophys. Acta.* 812, 460–472.
27. Wahnou, R., Cogan, U., and Mokady, S. (1992) Dietary Fish Oil Modulates the Alkaline Phosphatase Activity and Not the Fluidity of Rat Intestinal Microvillus Membrane, *J. Nutr.* 122, 1077–1084.
28. Muir, L.V., Born, E., Mathur, S.N., and Field, F.J. (1996) Lysophosphatidylcholine Increases 3-Hydroxy-3-methylglutaryl-coenzyme A Reductase Gene Expression in CaCo-2 Cells, *Gastroenterology* 110, 1068.
29. Murthy, S., Albright, E., Mathur, S.N., and Field, F.J. (1990) Effect of Eicosapentaenoic Acid on Triacylglycerol Transport in CaCo-2 Cells, *Biochim. Biophys. Acta.* 1045, 147–155.
30. Garg, M.L., Keelan, M., Thomson, A.B.R., and Clandinin, M.T. (1988) Fatty Acid Desaturation in the Intestinal Mucosa, *Biochim. Biophys. Acta* 958, 139–141.
31. Chen, Q., and Nilsson, A. (1993) Desaturation and Chain Elongation of n-3 and n-6 Polyunsaturated Fatty Acids in the Human CaCo-2 Cell Line, *Biochim. Biophys. Acta.* 1166, 193–201.
32. Yamagishi, F., Komoda, T., and Alpers, D.H. (1994) Secretion and Distribution of Rat Intestinal Surfactant-like Particles Following Fat Feeding, *Am. J. Physiol.* 266, G944–G952.

[Received September 18, 2000, and in final revised form March 18, 2002; revision accepted March 26, 2002]

# *In vitro* Effects of Fat, FA, and Cholesterol on Sphingomyelin Hydrolysis Induced by Rat Intestinal Alkaline Sphingomyelinase

Jian-Jun Liu<sup>a</sup>, Åke Nilsson<sup>b</sup>, and Rui-Dong Duan<sup>a,\*</sup>

<sup>a</sup>Cell Biology B, Biomedical Center B11, Lund University, S-221 84 Lund, Sweden, and <sup>b</sup>Institute of Medicine, Lund University Hospital, S-221 85 Lund, Sweden

**ABSTRACT:** Dietary sphingomyelin (SM) may have regulatory effects on cell proliferation and tumorigenesis in the colon. Alkaline sphingomyelinase (SMase) is the major enzyme responsible for hydrolysis of SM in the gut. Previously we purified the enzyme and showed that the presence of glycerophospholipids inhibited SM hydrolysis induced by alkaline SMase *in vitro*. In the present work, we studied the effects of TG, DG, FA, ceramide, and cholesterol on SM hydrolysis catalyzed by purified alkaline SMase. The results showed that both TG (triolein and tristearin) and DG (1,2-dioleoyl-*sn*-glycerol and 1,2-distearoyl-*rac*-glycerol) inhibited the activity of alkaline SMase. 1-Monooleoyl-*rac*-glycerol, 1-monostearoyl-*rac*-glycerol, stearic acid, oleic acid, linoleic acid, linolenic acid, and arachidonic acid stimulated the activity of alkaline SMase at 0.4–0.8 mM concentrations but inhibited the enzyme at higher concentrations. There was no difference between the effects induced by saturated and unsaturated FA. A short-chain FA such as lauric acid had a stronger stimulatory effect at low concentrations and weaker inhibitory effect at high concentrations than long-chain FA. Choosing linoleic acid as an example, we found that FA had similar effects on both alkaline SMase and neutral SMase. Cholesterol and ceramide when mixed with FA to increase its solubility in bile salt micelles inhibited SMase activity. In conclusion, glycerides, FA, ceramide, and cholesterol influence SM hydrolysis catalyzed by intestinal alkaline SMase. The presence of lipids in the diet may thus influence the course of SM digestion in the gut and thereby the exposure of colon to SM metabolites.

Paper no. L8978 in *Lipids* 37, 469–474 (May 2002).

Sphingomyelin (SM) is an important constituent of most cell membranes and is present in many dietary products including milk, meat, egg, and fish (1–3). Digestion of SM in the gut may have implications in colonic tumorigenesis. Recent studies have shown that when SM was given to mice treated with dimethylhydrazine, the number of colonic aberrant crypt foci was reduced by 70% (4). Dietary SM also reduced the proportion of malignant carcinomas to benign adenomas in di-

methylhydrazine-treated mice (5). We previously found that the activities of sphingomyelinase (SMase) in human colonic adenoma, carcinoma, and adenomatous polyposis were significantly decreased, indicating a potential chemopreventive effect of SMase on colon cancer (6,7).

Several types of SMase that are responsible for the catabolism of SM in different organs and cellular locations have been identified (8,9). In the intestinal tract, there is a specific SMase termed alkaline SMase, which is present in both intestinal mucosa and lumen, with peak activity in the middle of small intestine (10,11). Animal studies have shown that digestion of dietary SM occurs mainly in the middle and lower part of the small intestine where alkaline SMase is abundant, indicating an important role of the enzyme for the digestion of SM in the gut (12).

Digestion and absorption of dietary SM is characterized as a slow and incomplete process (12–14). The factors that influence the activity of alkaline SMase in the intestinal tract are still unclear. In our previous study, we found that other phospholipids, including PC, PI, PE, PS, and some of their metabolites had an inhibitory effect on SM hydrolysis induced by intestinal alkaline SMase (15). In this paper, we examined the effects of the major dietary lipids in the gut, i.e., TG, its hydrolysis products, and cholesterol on the hydrolysis of SM *in vitro* as catalyzed by purified rat intestinal alkaline SMase.

## MATERIALS AND METHODS

**Materials.** Triolein, tristearin, lauric acid, palmitic acid, arachidic acid, and arachidonic acid were purchased from Labora Chemicon (Stockholm, Sweden). 1,2-Dioleoyl-*sn*-glycerol, 1,2-distearoyl-*rac*-glycerol, 1-monooleoyl-*rac*-glycerol, 1-monostearoyl-*rac*-glycerol, stearic acid, oleic acid, linoleic acid, linolenic acid, and arachidonic acid, cholesterol, ceramide, and taurocholate (TC) were from Sigma-Aldrich AB (Stockholm, Sweden). Rat intestinal alkaline SMase was purified from rat intestinal mucosa as described previously (16), and bacterial neutral SMase was purchased from Sigma-Aldrich AB. SM was purified from bovine milk and was provided by Lena Nyberg of Skane Dairies' Association of Sweden. The purified SM was labeled with

\*To whom correspondence should be addressed.

E-mail: rui-dong.duan@med.lu.se

Abbreviations: SM, sphingomyelin; [<sup>14</sup>C-SM], <sup>14</sup>C-choline-labeled sphingomyelin; SMase, sphingomyelinase; TC, taurocholate.



$^{14}\text{C}$ -choline [ $^{14}\text{C}$ -SM] according to the method of Stoffel (17), with its specific activity being 56  $\mu\text{Ci}/\text{mg}$ .

**Preparation of TG, FA, ceramide, and cholesterol solution.** Glycerides, FFA, ceramide, and cholesterol were dissolved in chloroform/methanol (2:1) as 1 mg/mL stock solutions and stored at  $-20^\circ\text{C}$ . At the beginning of each experiment, lipids of different amounts were added to the test tubes and dried under a blowing stream of nitrogen. The lipids were then suspended in bile salt containing buffers after sonication, and their effects on SM hydrolysis were examined as described below.

**Assay of SM hydrolysis by alkaline and neutral SMase.** The assay of SM hydrolysis induced by alkaline SMase has been described previously (18). Briefly, to each test tube with the lipids tested was added 75  $\mu\text{L}$  of assay buffer containing 30 mM Tris, 0.15 M NaCl, 2 mM EDTA, 10 mM TC, pH 9.0, followed by sonication for 10 s. Five microliters of purified rat intestinal alkaline SMase (5 ng) in 20 mM Tris buffer, pH 8.2, was then added, and the reaction was started by the addition of 10,000 dpm [ $^{14}\text{C}$ -SM] in 20  $\mu\text{L}$  0.15 M NaCl solution containing 10 mM TC. The incubation was performed at  $37^\circ\text{C}$  for 30 min and then stopped by adding 0.4 mL chloroform/methanol (2:1). Phase partitioning was obtained by centrifugation at  $6,000 \times g$  for 3 s and a 100  $\mu\text{L}$  aliquot of the upper phase containing the cleaved  $^{14}\text{C}$ -phosphocholine was taken for liquid scintillation counting. As for the assay of SM hydrolysis induced by neutral SMase, a similar procedure was performed except for the assay buffer, which contained 30 mM Tris-HCl, 0.15 M NaCl, 4 mM  $\text{MgCl}_2$ , and 10 mM TC, pH 7.4.

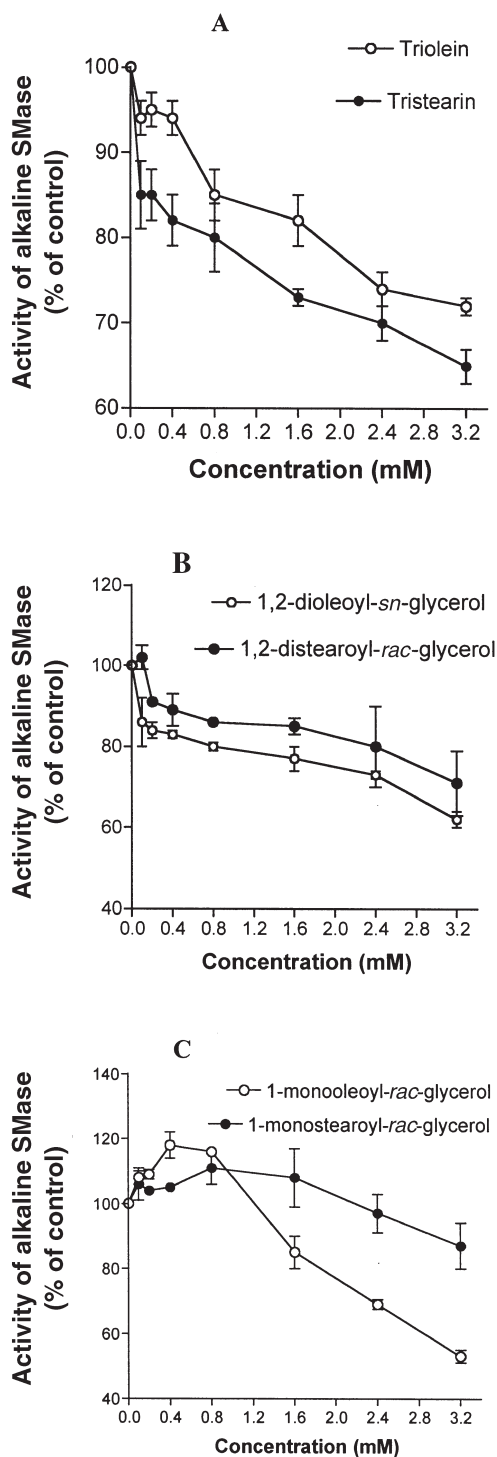
**Statistical analysis.** The data were expressed as mean  $\pm$  SEM. Two-way ANOVA and Student's *t*-test were used when available to compare the differences between two groups.  $P < 0.05$  was considered statistically significant.

## RESULTS

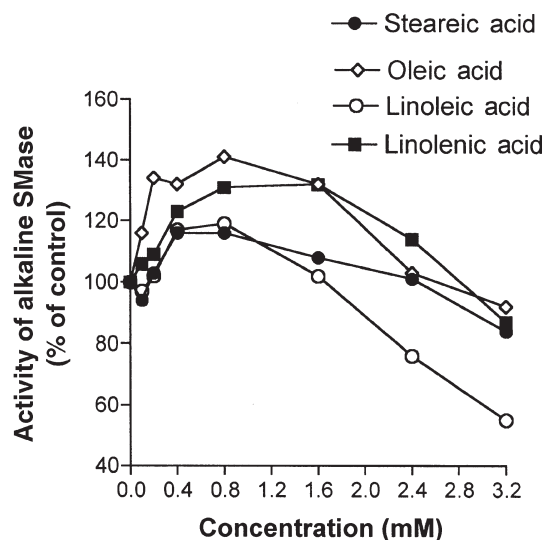
**Inhibitory effect of TG and TG metabolites on alkaline SMase activity.** As shown in Figure 1 (panels A and B), the presence of TG and DG reduced SM hydrolysis induced by rat intestinal alkaline SMase in a dose-dependent manner. The effect of tristearin was stronger than that of triolein, and that of distearin was slightly stronger than that of diolein. The effects of monoolein and monostearin are more or less biphasic, stimulating SM hydrolysis at low concentrations but inhibiting it at high concentrations (panel C).

**Effects of FA on the activity of alkaline SMase.** The effects of stearic, oleic, linoleic, and linolenic acids on the activity of alkaline SMase are shown in Figure 2. All of these  $\text{C}_{18}$  FA showed stimulatory effects, with peak effect at concentrations around 0.4 to 0.8 mM. The stimulatory effect decreased when the concentration was over 0.8 mM, and the inhibitory effect became evident when the concentration reached 3.2 mM. Oleic acid was the most effective, whereas linolenic acid was the least effective acid tested in stimulating SM hydrolysis by alkaline SMase.

The effects of FA on alkaline SMase with carbon chain length are shown in Figure 3. When the efficacies of lauric



**FIG. 1.** Effects of TG, DG, and MG on intestinal alkaline sphingomyelinase (SMase) activity. Different amounts of TG and partial glycerides dissolved in chloroform/methanol (2:1) were added to the test tubes and dried under nitrogen. Alkaline SMase assay buffer (pH 9.0) was added, followed by sonication for 10 s. Alkaline SMase and  $^{14}\text{C}$ -choline-labeled sphingomyelinase were then added, and the enzyme activity was measured. The activity in the absence of any glycerolipids was taken as 100%. The specific activity in the enzyme preparation is about 160 nmol/h/mL. Results are mean  $\pm$  SE obtained from three experiments. The differences between triolein and tristearin and between diolein and distearin are statistically significant ( $P < 0.05$ , ANOVA test).



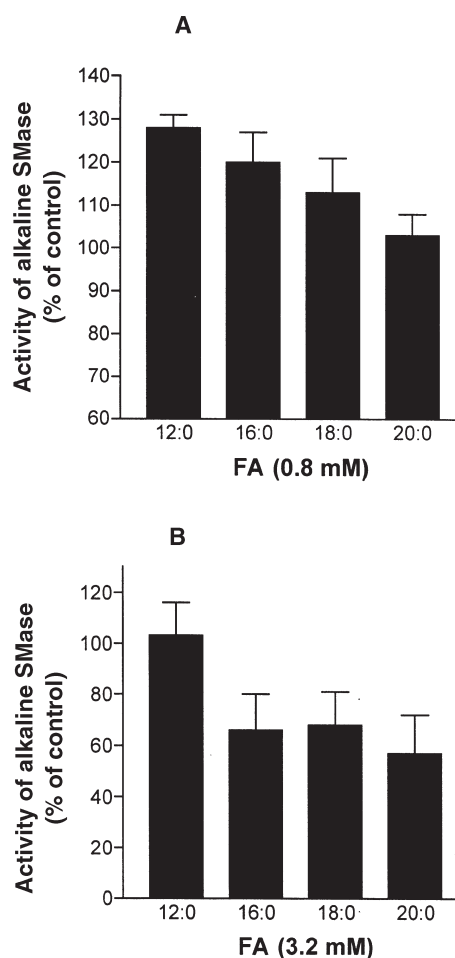
**FIG. 2.** Effects of stearic acid, oleic acid, linoleic acid, and linolenic acid on the activity of alkaline SMase. Different amounts of FA were added in the test tubes and dried by nitrogen, followed by adding the assay buffer and sonication. The reaction was started by adding alkaline SMase and  $^{14}\text{C}$ -choline-labeled sphingomyelin [ $^{14}\text{C}$ -SM]. The activity of the enzyme was determined, and the activity in the absence of any FA was regarded as 100%. The results are means from three experiments. For other abbreviation see Figure 1.

acid (12:0), palmitic acid (16:0), stearic acid (18:0), and arachidic acid (20:0) were compared at 0.8 mM, the stimulatory effect of FA was found to decrease with increasing carbon chain length (panel A). At a concentration of 3.2 mM (Fig. 3B), palmitic, stearic, and arachidic acids all reduced the activity to same extent (about 50%), whereas lauric acid inhibited the activity of this enzyme only slightly.

**Effects of arachidonic acid on alkaline SMase activity.** It has been reported previously that arachidonic acid activates membrane-bound neutral SMase (19). We studied the *in vitro* effect of arachidonic acid on the activity of alkaline SMase. As shown in Figure 4, arachidonic acid dose-dependently stimulated the activity of alkaline SMase up to 0.8 mM and inhibited it at higher concentrations. At a concentration of 3.2 mM, the activity of alkaline SMase fell to about 50% of the control.

**Comparison of the effects of FA on alkaline and neutral SMase activities.** To find out whether the effect of FA on alkaline SMase was specific, we compared the effect of linoleic acid on the activity of alkaline SMase at pH 9.0 and the activity of neutral SMase at pH 7.4. Linoleic acid was found to have similar biphasic effects on both alkaline and neutral SMase (Fig. 5). However, the dose-dependent curve for neutral SMase shifted to the right, and the extent of changes was greater than those for alkaline SMase, indicating neutral SMase is more sensitive than alkaline SMase in response to the FA.

**Effect of cholesterol and ceramide on the activity of alkaline SMase.** Owing to the low solubility of cholesterol and ceramide in pure TC micelles, their effects on SM hydrolysis cannot be studied in ways similar to those used for other lipids.

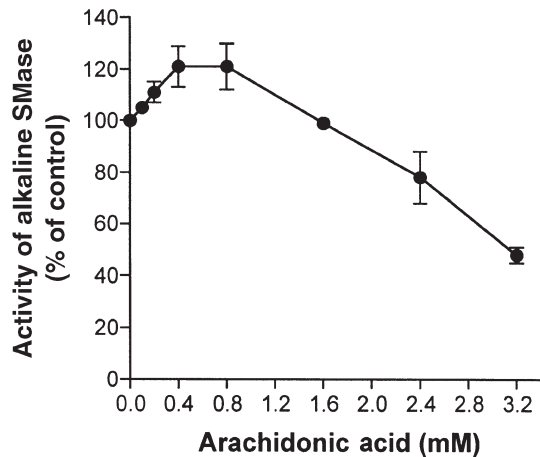


**FIG. 3.** Effects of FA with different chain lengths on the activity of alkaline SMase. Lauric acid, palmitic acid, stearic acid, and arachidic acid at 0.8 (A) and 3.2 mM (B) final concentration were mixed with [ $^{14}\text{C}$ -SM] and alkaline SMase in the assay buffer. The activity of the alkaline SMase was determined, and the activity in the absence of any FA was taken as 100%. The results are mean  $\pm$  SE obtained from three experiments. For abbreviations see Figures 1 and 2.

However, the solubility can be increased in mixed TC-FFA micelles. We therefore mixed 0.4 mM linoleic acid with different amounts of cholesterol or ceramide and examined the effects of the ratio of cholesterol or ceramide, to linoleic acids on alkaline SMase activity. As shown in Figure 6, both cholesterol and ceramide inhibited the hydrolysis of SM in the presence of linoleic acid. The maximal inhibitory effect for cholesterol was at a ratio of cholesterol/linoleic acid about 1:1, and that for ceramide at a ratio of ceramide/linoleic acid about 2:1.

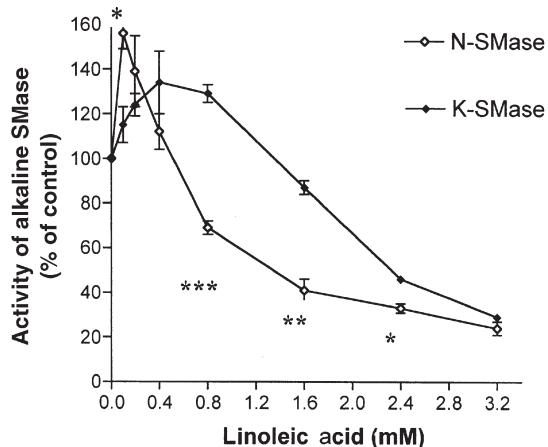
## DISCUSSION

The present study examined the role of glycerides, FA, and cholesterol on SM hydrolysis induced by purified intestinal alkaline SMase. Our results demonstrate that TG, DG, ceramide, and cholesterol have inhibitory effects on hydrolysis of SM, whereas MG and FA have biphasic effects, stimulating it at low concentrations and inhibiting it at higher concentrations. When

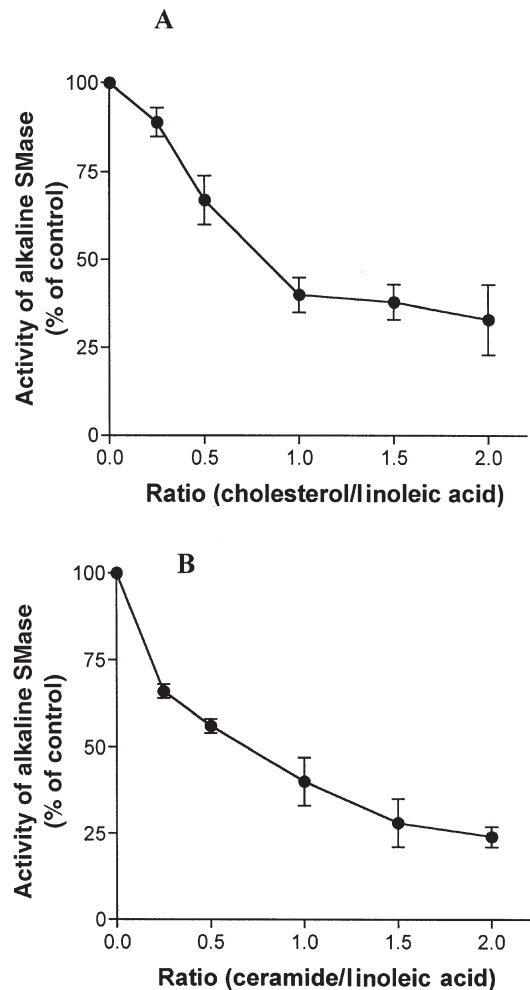


**FIG. 4.** Effect of arachidonic acid on the activity of alkaline SMase. Different amounts of arachidonic acid were added to the test tubes and dried by nitrogen. The assay buffer was added followed by sonication. Alkaline SMase activity was determined and the activity in the absence of arachidonic acid was taken as 100%. The results are mean  $\pm$  SE obtained from three separate experiments. For abbreviation see Figure 1.

the effects of FA with different chain lengths were compared, a medium-chain FA (12:0, lauric acid) was more effective than the 16–20 carbon FA in stimulating alkaline SMase at 0.8 mM concentration, and was less effective in inhibiting the enzyme



**FIG. 5.** Comparison of the effects of linoleic acid on the activity of alkaline SMase (K-SMase) and neutral SMase (N-SMase). Different amounts of linoleic acid were added in the tubes and dried under nitrogen. Neutral assay buffer (pH 7.4) and alkaline assay buffer (pH 9.0) were added, respectively, followed by sonication. After adding neutral and alkaline SMase, respectively, the reaction was started by adding 10,000 dpm [ $^{14}$ C-SM]. The activities of neutral and alkaline SMase were determined, and the activities in the absence of linoleic acid were taken as 100%. The results (mean  $\pm$  SEM) were obtained from three separate experiments. \* $P < 0.05$ , \*\* $P < 0.05$ , and \*\*\* $P < 0.05$ , compared with K-SMase of the same concentration. For abbreviations see Figures 1 and 2.



**FIG. 6.** Effect of cholesterol (A) and ceramide (B) on the activities of alkaline SMase. Linoleic acid (final concentration 0.4 mM) was mixed with different amounts of cholesterol or ceramide and dried under nitrogen. The assay buffer was added followed by sonication. The alkaline SMase was assayed in the assay buffer. Activity in the absence of cholesterol or ceramide was taken as 100%. The results (mean  $\pm$  SEM) were obtained from three separate experiments. For abbreviation see Figure 1.

at 3.2 mM concentration. Arachidonic acid stimulated alkaline SMase, similar to what was previously reported for neutral SMase in cultured cells (19).

Lipid hydrolysis in the intestinal tract depends on the sequential interactions of various lipolytic enzymes, substrates, and products present in the gut. For example, hydrolysis of Intralipid (an intravenous lipid emulsion) is significantly enhanced by short- and medium-chain FA produced by gastric lipase (20), and hydrolysis of the FA ester at position 2 of glycerophospholipids by phospholipase  $A_2$  accelerates the hydrolysis of TG in a similar emulsion (21). Whereas the concerted actions among gastric lipase, bile-salt stimulated lipase, pancreatic lipase  $A_2$ , and classic pancreatic lipase have been intensively studied, little is known about the influence of other lipases and lipolytic products on hydrolysis of SM. Digestion of SM in the gut is drawing more attention recently, as it may have implica-

tions in intestinal tumorigenesis and atherosclerosis (23,24). Therefore, to study the influence of lipids on SM hydrolysis not only is of nutritional importance but also has clinical implications.

Although the intestinal lumen contains SMase and ceramidase, not all of the ingested SM is hydrolyzed and absorbed (12–14). The rate-limiting factors for SM hydrolysis have not been clarified, although the localization of the alkaline SMase, the high concentration of bile salts, and the relatively low pH in the gut may be implicated (18). We recently demonstrated that glycerophospholipids and their metabolites had an inhibitory effect on the activity of alkaline SMase activity *in vitro* (15). In the present *in vitro* study, we extended our previous study by showing that TG and DG inhibit SM hydrolysis catalyzed by alkaline SMase. It appears that before digestion and absorption of both dietary TG and the phospholipids, SM hydrolysis in the intestinal tract cannot be effective until both dietary TG and phospholipids are digested and absorbed. As for cholesterol, an earlier *in vivo* experiment showed that feeding cholesterol together with SM inhibited digestion and absorption of SM in the rat intestinal tract (25). In the present study, we examined the possibility that cholesterol in the presence of 0.4 mM linoleic acid would facilitate the solubilization of cholesterol in the micelles and found that cholesterol caused significant inhibition of the SM hydrolysis. Similar to cholesterol, ceramide also reduced SM hydrolysis caused by alkaline SMase. As the absorption of ceramide is slow and ceramide can be identified along the intestinal tract including the colon, it may exert inhibitory roles along the gut. However, in the gut, hydrolysis of ceramide is catalyzed by neutral ceramidase, whose distribution in the intestine is parallel to that of alkaline SMase (26). Thus, intestinal neutral ceramidase could play a role in limiting the inhibitory effects of ceramide on alkaline SMase activity.

The mechanism by which TG, partial glycerides, FA, and cholesterol influence SM hydrolysis catalyzed by alkaline SMase may be related to their effects on the physical form of the substrate or on the enzyme. The finding that linoleic acid had similar effects on the activity of both intestinal alkaline SMase and bacterial neutral SMase indicated that the effects of FA were not enzyme-specific. The presence of glycerides and FA could change the size, surface charge, or the conformational structure of the mixed micelles formed by bile salts and SM. The solubility limit of MG and FA such as oleate in 10-mM TC solution can reach over 10 mM (27,28). The addition of glycerides to the micelle may influence the affinity of this enzyme for its substrate or change the diffusion intensity, thus facilitating or interfering with the hydrolysis of SM.

The solubility of cholesterol in a bulk system containing TC and SM is low (29). Even in the presence of oleate and 10 mM TC, its solubility limit is only about 0.4 mM (27). When the concentration of cholesterol reached 0.4 mM, with a ratio of linoleic acid to cholesterol of 1:1 in this study, more cholesterol could not be incorporated into micelles. This may explain why no further inhibition of the SM hydrolysis was seen at higher cholesterol concentrations.

On the basis of the present study and earlier studies both *in vivo* and *in vitro*, we postulate that the rate of hydrolysis of dietary SM in the upper part of the small intestine is low because of the low level of alkaline SMase (11) and the presence of TG, partial glycerides, and glycerophospholipids that tend to inhibit SM hydrolysis. In the middle and lower parts of the small intestine, the alkaline SMase levels are higher, and most of the glycerolipids have been hydrolyzed and absorbed; thus, the inhibitory effects of other lipids on SM hydrolysis become less effective. As a consequence, digestion of dietary SM occurs mainly in this part of small intestine (12). However, endogenous and dietary cholesterol still remain in the gut lumen and may decrease the rate of SM hydrolysis in this part of the intestine. Although the physiological concentrations of these lipids in different parts of the intestine are unknown, it is reasonable to suspect that the inhibitors of alkaline SMase are present along the whole length of the small intestine. The presence of multiple inhibitors, on one hand, results in a low rate of SM digestion, and on the other hand, results in the exposure of the colon to intact SM and its hydrolytic products such as ceramide. This may have implications for the antitumorigenic effect of SM metabolism in the colon.

#### ACKNOWLEDGMENT

This work was supported by grants from the Swedish Medical Research Council (12156 and 03969), Swedish Cancer Foundation (000307), Albert Pahlsson Foundation, and University Hospital of Lund.

#### REFERENCES

- Blank, M., Cress, E.A., Smith, Z.L., and Snyder, F. (1992) Meats and Fish Consumed in the American Diet Contain Substantial Amounts of Ether-Linked Phospholipids, *J. Nutr.* 122, 1656–1661.
- Holmes-McNary, M.Q., Cheng, W.L., Mar, M.H., Fussell, S., and Zeisel, S.H. (1996) Choline and Choline Esters in Human and Rat Milk and in Infant Formulas, *Am. J. Clin. Nutr.* 64, 572–576.
- Zeisel, S.H., Char, D., and Sheard, N.F. (1986) Choline Phosphatidylcholine and Sphingomyelin in Human and Bovine Milk and Infant Formulas, *J. Nutr.* 116, 50–58.
- Dillehay, D.L., Webb, S.K., Schmelz, E.-M., and Merrill, A.H. (1994) Dietary Sphingomyelin Inhibits 1,2-Dimethylhydrazine-Induced Colon Cancer in CF1 Mice, *J. Nutr.* 124, 615–620.
- Schmelz, E.M., Dillehay, D.L., Webb, S.K., Reiter, A., Adams, J., and Merrill, A.H., Jr. (1996) Sphingomyelin Consumption Suppresses Aberrant Colonic Crypt Foci and Increases the Proportion of Adenomas Versus Adenocarcinomas in CF1 Mice Treated with 1,2-Dimethylhydrazine: Implications for Dietary Sphingolipids and Colon Carcinogenesis, *Cancer Res.* 56, 4936–4941.
- Hertvig, E., Nilsson, Å., Nyberg, L., and Duan, R.-D. (1996) Alkaline Sphingomyelinase Activity Is Decreased in Human Colorectal Carcinoma, *Cancer* 79, 448–453.
- Hertvig, E., Nilsson, Å., Björk, J., Hultkrantz, R., and Duan, R.-D. (1999) Familial Adenomatous Polyposis Is Associated with a Marked Decrease in Alkaline Sphingomyelinase Activity: A Key Factor to the Unrestrained Cell Proliferation, *Br. J. Cancer* 81, 232–236.



8. Quintern, L.E., Weitz, G., Nehrkorn, H., Tager, J.M., Schram, A.W., and Sandhoff, K. (1987) Acid Sphingomyelinase from Human Urine: Purification and Characterization, *Biochim. Biophys. Acta* 922, 323–336.
9. Chatterjee, S. (1993) Neutral Sphingomyelinase, *Adv. Lipid Res.* 26, 25–48.
10. Nilsson, Å. (1969) The Presence of Sphingomyelin- and Ceramide-Cleaving Enzymes in the Small Intestinal Tract, *Biochim. Biophys. Acta* 176, 339–347.
11. Duan, R.-D., Nyberg, L., and Nilsson, Å. (1995) Alkaline Sphingomyelinase Activity in Rat Gastrointestinal Tract: Distribution and Characterization, *Biochim. Biophys. Acta* 1259, 49–55.
12. Nyberg, L., Nilsson, Å., Lundgren, P., and Duan, R.-D. (1997) Localization and Capacity of Sphingomyelin Digestion in the Rat Intestinal Tract, *J. Nutr. Biochem.* 8, 112–118.
13. Nilsson, Å. (1968) Metabolism of Sphingomyelin in the Intestinal Tract of the Rat, *Biochim. Biophys. Acta* 164, 575–584.
14. Schmelz, E.-M., Crall, K.J., Larocque, R., Dillehay, D.L., and Merrill, A.H. (1994) Uptake and Metabolism of Sphingolipids in Isolated Intestinal Loops of Mice, *J. Nutr.* 124, 702–712.
15. Liu, J.J., Nilsson, Å., and Duan, R.-D. (2000) Effects of Phospholipids on Sphingomyelin Hydrolysis Induced by Intestinal Alkaline Sphingomyelinase: An *in vitro* Study, *J. Nutr. Biochem.* 11, 192–197.
16. Cheng, Y., Nilsson, Å., Tömquist, E., and Duan, R.-D. (2002) Purification, Characterization and Expression of Rat Intestinal Alkaline Sphingomyelinase, *J. Lipid Res.* 43, 316–324.
17. Stoffel, W. (1975) Chemical Synthesis of Choline-Labeled Lecithins and Sphingomyelin, *Methods Enzymol.* 36, 533–541.
18. Duan, R.-D., and Nilsson, Å. (1999) Sphingolipid Hydrolyzing Enzymes in the Gastrointestinal Tract, *Methods Enzymol.* 311, 276–286.
19. Jayadev, S., Linaudic, C.M., and Hannun, Y.A. (1994) Identification of Arachidonic Acid as a Mediator of Sphingomyelin Hydrolysis in Response to Tumor Necrosis Factor Alpha, *J. Biol. Chem.* 269, 5757–5763.
20. Gargouri, Y., Pieroni, G., Riviere, C., Lowe, P.A., Saunier, J.F., Sarda, L., and Verger, R. (1986) Importance of Human Gastric Lipase for Intestinal Lipolysis: An *in vitro* Study, *Biochim. Biophys. Acta* 879, 419–423.
21. Borgström, B. (1980) Importance of Phospholipids, Pancreatic Phospholipase A<sub>2</sub> and Fatty Acid for Digestion of Dietary Fat, *Gastroenterology* 78, 954–962.
22. Duan, R.-D. (1998) Hydrolysis of Sphingomyelin in the Gut and Clinical Implications in Colorectal Tumorigenesis and Other Gastrointestinal Diseases, *Scand. J. Gastroenterol.* 33, 673–683.
23. Chatterjee, S. (1998) Sphingolipids in Atherosclerosis and Vascular Biology, *Arterioscler. Thromb. Vasc. Biol.* 18, 1523–1533.
24. Jiang, X.C., Paultre, F., Pearson, T.A., Reed, R.G., Francis, C.K., Lin, M., Berglund, L., and Tall, A.R. (2000) Plasma Sphingomyelin Level as a Risk Factor for Coronary Artery Disease, *Arterioscler. Thromb. Vasc. Biol.* 20, 2614–2618.
25. Nyberg, L., Duan, R.-D., and Nilsson, Å. (2000) A Mutual Inhibitory Effect on Absorption of Sphingomyelin and Cholesterol, *J. Nutr. Biochem.* 11, 244–249.
26. Lundgren, P., Nilsson, Å., and Duan, R.-D. (2001) Distribution and Properties of Neutral Ceramidase Activity in Rat Intestinal Tract, *Dig. Dis. Sci.* 46, 765–772.
27. Reynier, M.O., Crotte, C., Montet, J.C., Sauve, P., and Gerolami, A. (1987) Intestinal Cholesterol and Oleic Acid Uptake from Solutions Supersaturated with Lipids, *Lipids* 22, 28–32.
28. Reynier, M., Sari, H., D'Anglebermes, M., Kye, E.A., and Pasero, L. (1991) Differences in Lipid Characteristics of Undifferentiated and Enterocytic-Differentiated HT 29 Human Colonic Cells, *Cancer Res.* 51, 1270–1277.
29. Young, S.C., and Hui, D.Y. (1999) Pancreatic Lipase/Colipase-Mediated Triacylglycerol Hydrolysis Is Required for Cholesterol Transport from Lipid Emulsions to Intestinal Cells, *Biochem. J.* 339, 615–620.

[Received January 7, 2002, and in revised form April 4, 2002; revision accepted April 7, 2002]

# Albumin Stimulates Lysophosphatidic Acid Acyltransferase Activity in T-Lymphocyte Membranes

Christopher A. Jolly\* and Latha Kannan

Division of Nutritional Sciences and Institute for Cellular and Molecular Biology,  
The University of Texas at Austin, Austin, Texas 78712

**ABSTRACT:** Phosphatidic acid (PtdOH) and lysophosphatidic acid (lysoPtdOH) have been shown to enhance T-lymphocyte function. However, the FA preference and influence of acyl-CoA binding proteins on lysoPtdOH and PtdOH biosynthesis are not known. Therefore, we determined glycerol-3-phosphate acyltransferase (GPAT) and lysophosphatidic acid acyltransferase (LAT) activity in rat T-lymphocyte and liver membrane preparations in the presence of palmitoyl-CoA and oleoyl-CoA with or without BSA. We found two different properties of GPAT and LAT in whole T-lymphocyte membrane preparations relative to liver. First, T-lymphocyte basal GPAT and LAT activities were similar, whereas in liver membranes LAT activity was 10-fold higher than GPAT. Second, T-lymphocyte LAT, but not GPAT, activity was inducible (fivefold) by the addition of albumin in the presence of palmitoyl-CoA but not oleoyl-CoA. In contrast, albumin stimulated GPAT, but not LAT, activity in liver membranes in the presence of palmitoyl-CoA. These results show, for the first time, that T-lymphocyte LAT activity can be increased by the presence of an acyl-CoA binding protein, which may indicate a new important control mechanism for regulating intracellular lysoPtdOH and PtdOH levels in T-lymphocytes.

Paper no. L8922 in *Lipids* 37, 475–480 (May 2002).

Phosphatidic acid (PtdOH) is a key intermediate in generating most glycerophospholipids (1) and can serve directly as a lipid signaling molecule (2). For example, PtdOH has been shown to stimulate raf-1 kinase activity (3,4) and increase intracellular calcium levels (2). Recently, lysophosphatidic acid (lysoPtdOH) has also been shown to be a potent mitogen involved in mediating the effects of several hormones such as epidermal growth factor (5). PtdOH is synthesized *de novo* by the sequential acylation of glycerol-3-phosphate to lysoPtdOH then to PtdOH *via* glycerol-3-phosphate acyltransferase (GPAT) and lysophosphatidic acid acyltransferase (LAT), respectively. GPAT is thought to be the rate-limiting enzyme in PtdOH formation, as liver GPAT activity is approximately 10-fold less than that of LAT (6,7). Furthermore, several recent studies have shown that liver GPAT, but not LAT, activity can be enhanced in membrane preparations

*in vitro* using proteins that bind the substrate acyl-CoA, including albumin (6,8–11).

T-lymphocytes are key immune regulatory cells influencing both the type and extent of immune response. Both PtdOH and lysoPtdOH have been implicated in regulating the response of T-lymphocytes to various mitogens, including cytokines (12). Several recent lines of evidence have further added to the potentially critical role of PtdOH and/or lysoPtdOH in T-lymphocyte function by showing that the LAT gene is located in the same chromosomal region as the major histocompatibility complex III gene (13), that lysoPtdOH stimulates T-lymphocyte migration (14), and that the addition of exogenous lysoPtdOH can enhance T-lymphocyte proliferation (15,16) and wound healing (17). On the other hand, PtdOH generation has been linked to the function of interleukin-2 (18), which is a potent autocrine and paracrine T-lymphocyte growth factor. The increased PtdOH production may be important in lowering cyclic AMP levels, which are antimitogenic in T-lymphocytes (19).

Although PtdOH and lysoPtdOH have been implicated as important regulators of T-lymphocyte function, the relative activities of GPAT and LAT and their ability to incorporate saturated vs. unsaturated FA and the influence of proteins that bind acyl-CoA have not been examined in T-lymphocytes. Therefore, we examined GPAT and LAT activities in T-lymphocyte and liver whole-membrane preparations and determined the influence of palmitic vs. oleic acid containing acyl-CoA in the presence or absence of albumin on PtdOH biosynthesis. Herein, we find different properties of GPAT and LAT in T-lymphocytes relative to liver, which may play an important role in lysoPtdOH- and PtdOH-dependent functions in T-lymphocytes.

## MATERIALS AND METHODS

**Materials.** ESA-free BSA, palmitoyl-CoA, and oleoyl-CoA were purchased from Sigma (St. Louis, MO). The [<sup>14</sup>C]palmitoyl-CoA and [<sup>14</sup>C]oleoyl-CoA were purchased from NEN Life Sciences (Boston, MA).

**T-lymphocyte isolation and membrane preparation.** Male, 3-mon-old Sprague–Dawley rat splenic T-lymphocytes were isolated as described by the manufacturer using negative selection Immulan columns (Biotex, Inc., Houston, TX). All animal procedures were approved by the University of Texas Animal Use and Care Committee. Negative selection prevents the confounding variable of perturbing T-lymphocyte receptors,

\*To whom correspondence should be addressed at Division of Nutritional Sciences, The University of Texas at Austin, Gearing Rm 117/A2700, Austin, TX 78712. E-mail: jolly@mail.utexas.edu

Abbreviations: ACBP, acyl CoA binding protein; GPAT, glycerol-3-phosphate acyltransferase; LAT, lysophosphatidic acid acyltransferase; L-FABP, liver FA binding protein; lysoPtdOH, lysophosphatidic acid; PtdCho, phosphatidylcholine; PtdIns, phosphatidylinositol; PtdOH, phosphatidic acid; PtdSer, phosphatidylserine; Spm, sphingomyelin.

as with positive selection, and of potentially altering intracellular metabolism. T-lymphocytes were counted and viability (>92%) was determined by trypan blue exclusion (20). We routinely obtain approximately 90% pure T-lymphocytes using this technique. Whole-membrane preparations from liver and purified T-lymphocytes were prepared essentially as described previously (21). Briefly, T-lymphocytes and liver membranes were homogenized and passed through a syringe to disrupt cells in a buffer containing 300 mM mannitol, 15 mM Tris, 5 mM EGTA, and 0.1 mM PMSF. The supernatant was centrifuged at  $48,000 \times g$  for 30 min, and the pellet was resuspended in cold reaction buffer. Protein concentrations were determined using the BioRad Protein Assay.

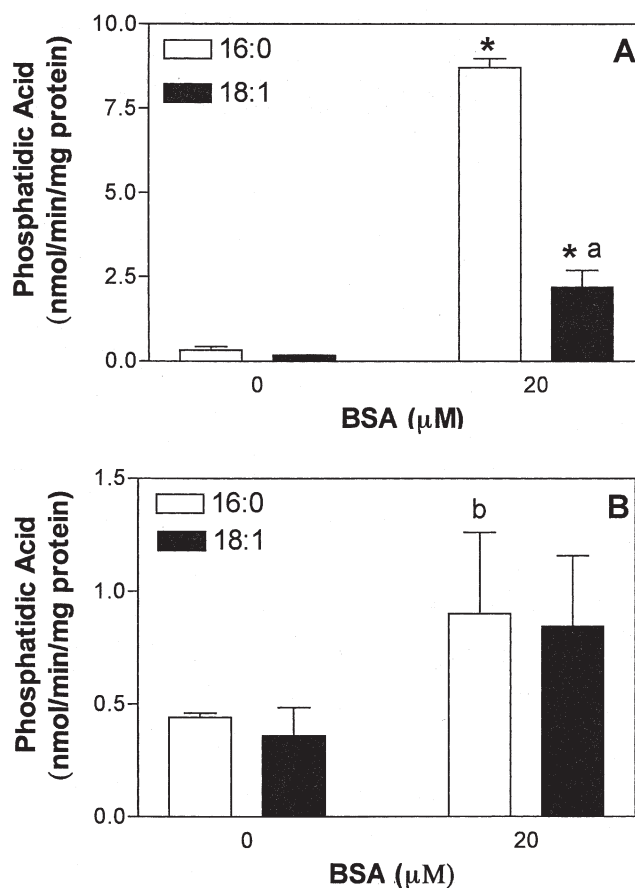
**PtdOH biosynthesis.** Phosphatidic acid biosynthesis was carried out essentially as described previously (8) using 10  $\mu$ g of membrane protein incubated for 30 min at 37°C with the following modifications: Twenty micromolar essential fatty acid-free BSA and 40  $\mu$ M [ $^{14}$ C]palmitoyl-CoA or [ $^{14}$ C]oleoyl-CoA was used. Both palmitoyl-CoA and oleoyl-CoA were chosen, because we had used the two acyl-CoA in liver and wished to remain consistent with our previously published observations (8,22). Purified bovine albumin was chosen rather than rat albumin for consistency with previously published observations (11). Preliminary experiments were carried out to determine the optimal concentration (20  $\mu$ M) of albumin to use. The first reaction used glycerol-3-phosphate as the substrate and measured GPAT activity. The second reaction involved the substitution of glycerol-3-phosphate with lysoPtdOH to determine LAT activity. Individual phospholipids were separated by TLC using Silica Gel 60 plates with a solvent system containing chloroform/methanol/acetic acid/ddH<sub>2</sub>O (50:37.5:3.5:0.5, vol/vol). The bands corresponding to PtdOH, as determined by simultaneously running an authentic standard, were scraped and counted by scintillation counting. GPAT activity was determined by multiplying the cpm by two (two radiolabeled FA incorporated into PtdOH from glycerol-3-phosphate) then dividing by the specific activity of the [ $^{14}$ C]acyl-CoA solution to obtain nmol of synthesized PtdOH. The nmol of PtdOH formed was then divided by the incubation time (30 min) and the amount of membrane protein used in the reaction (0.010 mg) to obtain nmol/min/mg protein. For LAT activity, the calculation was the same except that the cpm value was not multiplied by two, as only one radiolabeled FA was incorporated per PtdOH molecule using lysoPtdOH as substrate.

**Phospholipid FA transacylation.** The GPAT assay was carried out as described previously (6) except that isolated T-lymphocyte membranes were incubated in the presence or absence of 20  $\mu$ M EFA-free BSA with either [ $^{14}$ C]palmitoyl-CoA or [ $^{14}$ C]oleoyl-CoA. Following phospholipid subclass isolation by TLC, the bands corresponding to phosphatidylcholine (PtdCho), phosphatidylinositol (PtdIns), phosphatidylserine (PtdSer), and sphingomyelin (Spm) were identified using authentic standards, scraped, and counted by scintillation counting. Incorporation of radiolabeled FA was calculated as described above for the LAT assay and expressed as nmol/min/mg protein.

**Statistical analysis.** Data were analyzed with the unpaired Student's *t*-test using GraphPad Prism software (San Diego, CA). A *P* value less than 0.05 was considered significantly different.

## RESULTS

**PtdOH biosynthesis.** To assess the PtdOH biosynthetic capability of T-lymphocytes, liver whole-membrane preparations were used in parallel as a control. Liver membranes were chosen as the control because the influence of multiple acyl-CoA binding proteins on PtdOH biosynthesis has previously been shown (10,11). Additionally, using liver membranes allowed the researchers to determine whether the albumin effects were similar in different cell populations, such as the T-lymphocyte. Figure 1 shows that basal GPAT activity was similar between



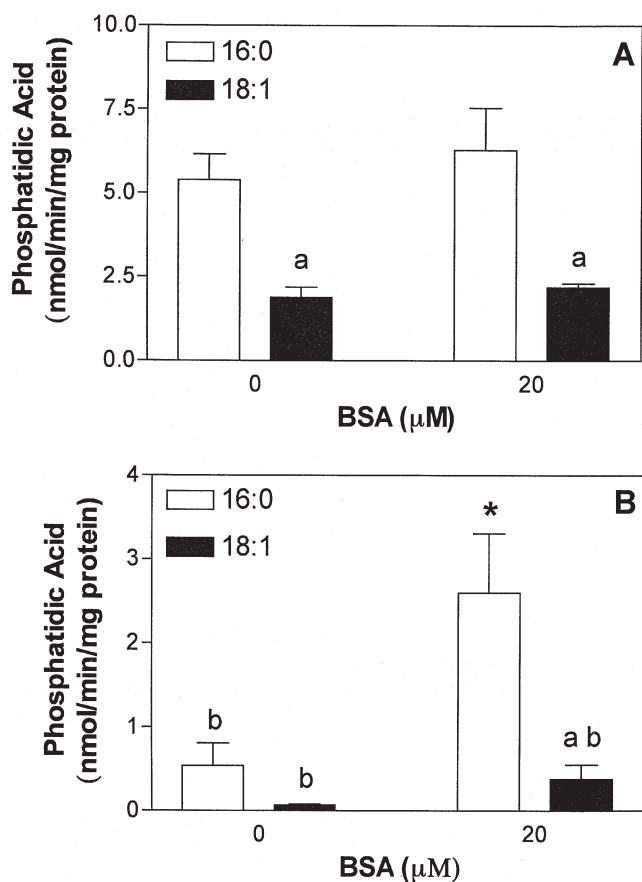
**FIG. 1.** Glycerol-3-phosphate acyltransferase activity is marginally induced by albumin in T-lymphocyte membranes. Whole membranes from liver (A) and T-lymphocytes (B) were isolated as described in the Materials and Methods section. Reactions were carried out in the presence of glycerol-3-phosphate, with or without albumin, and palmitoyl-CoA (open bars) or oleoyl-CoA (solid bars). Values represent the mean  $\pm$  SEM of 3–4 separate animals. Bars with an asterisk are significantly different ( $P < 0.05$ ) compared to the bars with the same acyl-CoA and no albumin stimulation. The bar with the roman letter a is significantly different ( $P < 0.05$ ) between palmitoyl-CoA and oleoyl-CoA within the no-albumin or with-albumin groups. The bar in panel B with a roman letter b is significantly different ( $P < 0.05$ ) from the corresponding bar in panel A.

T-lymphocyte and liver membranes in the presence of palmitoyl-CoA or oleoyl-CoA. Similar to previous observations, addition of albumin stimulated liver membrane GPAT activity 25- and 13-fold in the presence of palmitoyl-CoA and oleoyl-CoA, respectively (Fig. 1A), whereas albumin did not have a significant effect in T-lymphocyte membranes in the presence of either palmitoyl-CoA or oleoyl-CoA (Fig. 1B).

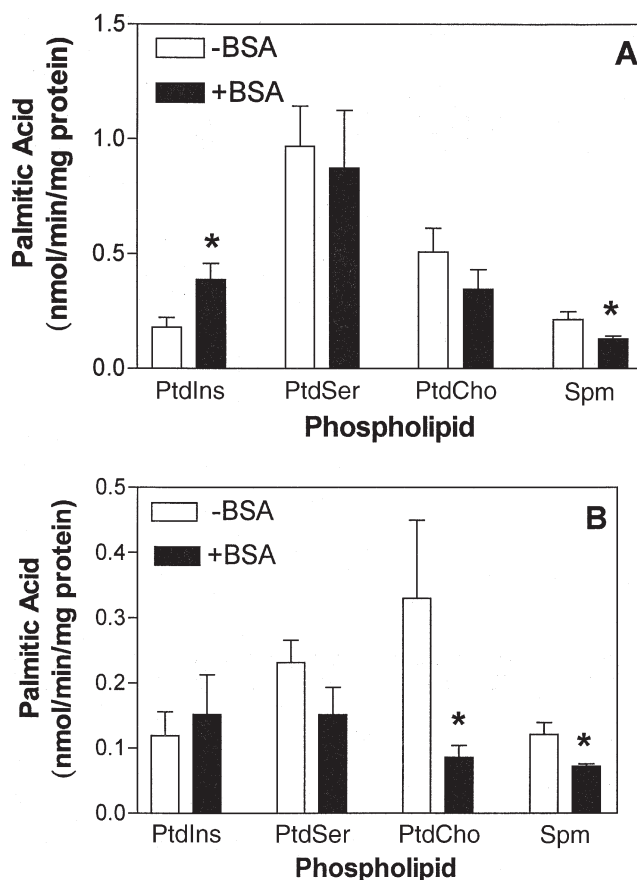
Figure 2A shows that basal liver membrane LAT activity is threefold higher in the presence of palmitoyl-CoA compared to oleoyl-CoA. The LAT activity was 17- and 11-fold higher than GPAT activity in the presence of palmitoyl-CoA and oleoyl-CoA, respectively. The LAT activity in T-lymphocyte membranes was similar to that of GPAT in the presence of palmitoyl-CoA (Fig. 2B). Interestingly, basal LAT activity in the presence of oleoyl-CoA was approximately sixfold less than the GPAT activity. Liver membrane LAT activity was 10- and 29-fold higher compared to the T-lymphocyte for palmi-

toyl-CoA and oleoyl-CoA, respectively. Albumin did not significantly induce liver membrane LAT activity in the presence of either palmitoyl-CoA or oleoyl-CoA (Fig. 2A). However, albumin significantly induced T-lymphocyte LAT activity fivefold in the presence of either palmitoyl-CoA or oleoyl-CoA (Fig. 2B). Even in the presence of albumin, T-lymphocyte LAT activity was only approximately 50 and 20% that of basal liver membrane LAT activity in the presence of palmitoyl-CoA and oleoyl-CoA, respectively.

*Phospholipid FA transacylation.* The FA composition of phospholipids can also be influenced by the nonenzymic transacylation of FA into preexisting phospholipids in addition to PtdOH biosynthesis (9). Therefore, the influence of albumin on the incorporation of palmitoyl-CoA into liver and T-lymphocyte membrane phospholipid subclasses was determined and is shown in Figure 3. Incorporation of palmitic acid into PtdSer was greater than into PtdIns, PtdCho, or Spm in liver membranes (Fig. 3A), whereas in the T-lymphocytes palmitic acid was incorporated primarily into PtdSer and

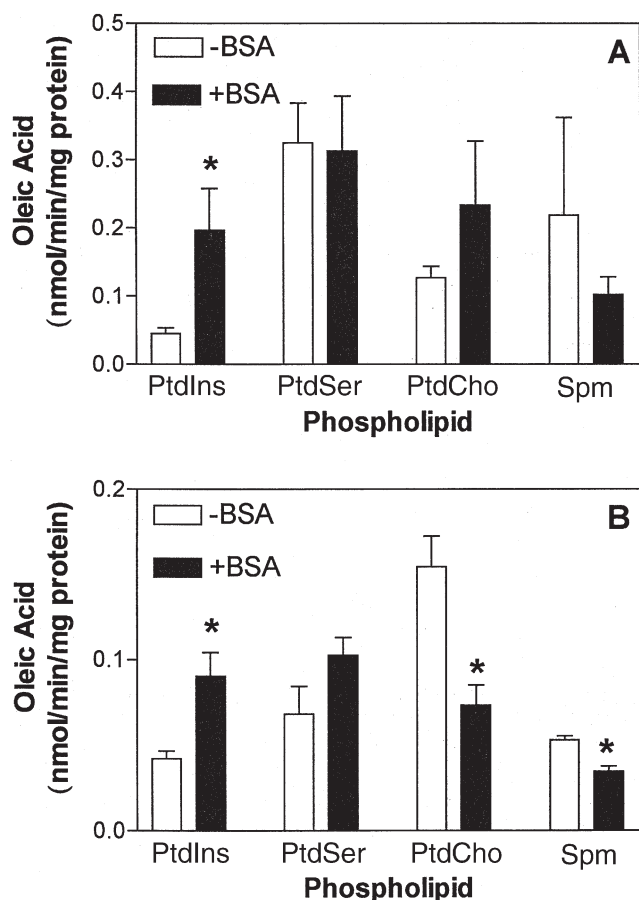


**FIG. 2.** Lysophosphatidic acid acyltransferase activity is low in T-lymphocyte membranes and enhanced by albumin. Whole membranes from liver (A) and T-lymphocytes (B) were isolated as described in Figure 1. Reactions were carried out in the presence of lysophosphatidic acid, with or without albumin, and palmitoyl-CoA (open bars) or oleoyl-CoA (solid bars). Values represent the mean ± SEM of 3–4 separate animals. Bars with an asterisk are significantly different ( $P < 0.05$ ) compared to the bars with the same acyl-CoA and no albumin stimulation. Bars with the roman letter a are significantly different ( $P < 0.05$ ) between palmitoyl-CoA and oleoyl-CoA within the no-albumin or with-albumin groups. Bars in panel B with a roman letter b are significantly different ( $P < 0.05$ ) from the corresponding bar in panel A.



**FIG. 3.** Palmitic acid transacylation into phosphatidylcholine (PtdCho) is reduced by albumin in T-lymphocyte membranes. Whole membranes from liver (A) and T-lymphocytes (B) were isolated, and reactions were carried out as described in Figure 1 in the presence of palmitoyl-CoA with (solid bars) or without (open bars) albumin. Values represent the mean ± SEM of 3–4 separate animals. Bars with an asterisk are significantly different ( $P < 0.05$ ) compared to the unstimulated bars with the same acyl-CoA. PtdIns, phosphatidylinositol; PtdSer, phosphatidylserine; Spm, sphingomyelin.





**FIG. 4.** Oleic acid transacylation into PtdIns is enhanced by albumin. Whole membranes from liver (A) and T-lymphocytes (B) were isolated and reactions were carried out as described in Figure 1 in the presence of oleoyl-CoA with (solid bars) or without (open bars) albumin. Values represent the mean  $\pm$  SEM of 3–4 separate animals. Bars with an asterisk are significantly different ( $P < 0.05$ ) compared to the bars with the same acyl-CoA and no albumin stimulation. For abbreviations see Figure 3.

PtdCho and, to a lesser extent, into PtdIns and Spm (Fig. 3B). The addition of albumin significantly reduced the incorporation of palmitic acid into Spm in both liver and T-lymphocyte membranes. In contrast, albumin significantly reduced the incorporation of palmitic acid into PtdCho in T-lymphocyte membranes but did not have a significant effect in liver membranes. Furthermore, albumin significantly enhanced palmitic acid incorporation into liver PtdIns by twofold while having no effect in T-lymphocyte membranes.

Similar to palmitic acid, oleic acid was preferentially incorporated into PtdSer compared to PtdIns, PtdCho, and Spm in liver membranes (Fig. 4A). In contrast, oleic acid was preferentially incorporated into PtdCho in T-lymphocyte membranes (Fig. 4B). Addition of albumin significantly enhanced the incorporation of oleic acid into PtdIns in liver membranes while not significantly influencing the other phospholipid subclasses examined (Fig. 4A). Similar effects of albumin were seen in T-lymphocytes except that oleic acid incorporation into PtdCho was reduced by 50% (Fig. 4B).

## DISCUSSION

Although albumin is always present physiologically, it was important to perform the assays in the absence of albumin to determine the relative contribution of albumin vs. the enzyme itself on cellular GPAT and LAT activity as well as on acyl-CoA preference. The most striking observation presented in this investigation was the increase in LAT activity in T-lymphocyte membranes in the presence of albumin, whereas GPAT activity was not significantly affected. In contrast, liver membrane GPAT and not LAT activity was induced by the addition of albumin. The reason for this difference is unknown but may be related to the expression of different LAT isoforms in spleen and liver. Recently, two LAT isoforms ( $\alpha$  and  $\beta$ ) have been cloned. The  $\beta$  isoform was primarily located in liver and muscle, whereas the  $\alpha$  isoform was found in all tissues tested including spleen (12). However, other factors such as membrane composition cannot be ruled out. Our results in the liver showed that basal GPAT activity was approximately 25-fold less than LAT activity and were similar to those published previously (6). However, the 25-fold induction of GPAT activity with albumin was twice as high as that reported by Jolly *et al.* (6). The reason for this discrepancy is most likely due to the use of whole-membrane preparations in this study rather than isolated microsomes as reported previously. Both GPAT and LAT are located in several organelles, including mitochondria and microsomes (7); thus, the inclusion of all organelles in a membrane preparation may result in higher PtdOH biosynthetic capacity. We chose to examine PtdOH biosynthesis in whole membrane preparations to determine the total biosynthetic capability of T-lymphocytes, since multiple organelles may be involved under *in vivo* conditions. The lower basal activity of LAT in T-lymphocytes is significant given the recent results showing that the substrate lysoPtdOH is a potent T-lymphocyte mitogen (15,16). Thus, the lower basal LAT activity as compared to that of liver would prevent lysoPtdOH from being quickly converted to PtdOH prior to exerting its biological activity. However, showing that LAT activity is inducible, as we found for albumin addition, indicates that potential mechanism(s) exist which can quickly eliminate lysoPtdOH when necessary. Furthermore, this suggests a novel biological function for proteins that bind acyl-CoA (i.e., remove lysoPtdOH).

The exact mechanism(s) by which albumin stimulates GPAT in liver membranes and LAT in T-lymphocyte membranes is not known. Enhanced activity due to a potential contaminant in the albumin preparation is not likely, because a multitude of other highly purified proteins that bind acyl-CoA can enhance GPAT activity in membrane preparations (10). Similarly, the preference of albumin in stimulating LAT activity in the presence of palmitoyl-CoA, but not oleoyl-CoA, is not known. However, several possibilities exist, including the preference for albumin to extract (i.e., solubilize) palmitoyl-CoA over oleoyl-CoA from membranes, preferably preventing the hydrolysis of palmitoyl-CoA to palmitate and coenzyme or by direct interaction of albumin with the LAT

enzyme. Future studies examining the influence of other proteins that bind acyl-CoA are needed to elucidate the potential mechanism(s) by which albumin stimulates PtdOH biosynthesis, as different acyl-CoA binding proteins have different numbers of acyl-CoA binding sites and vary in their affinity for acyl-CoA. However, this will be difficult, because most proteins that bind acyl-CoA are not commercially available in a highly purified form, requiring the proteins to be purified by individual investigators. It is tempting to speculate, however, that the mechanism involves direct interaction between the enzyme and acyl-CoA-bound albumin. This speculation is derived from two recent reports. First, it has been shown that acyl-CoA bound to acyl-CoA binding protein (ACBP) is preferred over free acyl-CoA to enhance carnitinepalmitoyl-acyltransferase activity in mitochondria (23). Second, both liver FA binding protein (L-FABP) and ACBP can stimulate PtdOH biosynthesis to a similar degree in the presence of oleoyl-CoA, even though L-FABP has two acyl-CoA binding sites and ACBP has only one (6). Whereas these studies examined the influence of albumin on GPAT and LAT in unstimulated T-lymphocytes, determining whether T-lymphocyte activation using mitogens may somehow change the ability of albumin or other acyl-CoA binding proteins to influence PtdOH biosynthesis requires further investigation.

The transacylation of palmitic and oleic acids into phospholipid subclasses also differed between liver and T-lymphocyte membranes. Oleic acid was preferentially incorporated into PtdCho in T-lymphocytes, whereas PtdSer appeared to be the major site of incorporation in liver. Additionally, albumin enhanced the incorporation of oleic acid into PtdIns both in liver and T-lymphocyte membranes and reduced palmitic acid incorporation in T-lymphocyte membrane PtdCho. This is significant because both PtdIns and PtdCho are important sources of DAG, which activates protein kinase C and is an important signal for appropriate T-lymphocyte proliferation (24,25). Furthermore, DAG containing unsaturated FA are thought to be more potent activators of protein kinase C.

## ACKNOWLEDGMENT

This work was supported in part by startup funds from The University of Texas at Austin (C.A.J.).

## REFERENCES

- Athenstaedt, K., and Daum, G. (1999) Phosphatidic Acid, a Key Intermediate in Lipid Metabolism, *Eur. J. Biochem.* 266, 1–16.
- English, D., Cui, Y., and Siddiqui, R.A. (1996) Messenger Functions of Phosphatidic Acid, *Chem. Phys. Lipids* 80, 117–132.
- Rizzo, M.A., Shome, K., Watkins, S.C., and Romero, G. (2000) The Recruitment of Raf-1 to Membranes Is Mediated by Direct Interaction with Phosphatidic Acid and Is Independent of Association with Ras, *J. Biol. Chem.* 275, 23911–23918.
- Ghosh, S., and Bell, R.M. (1997) Regulation of Raf-1 Kinase by Interaction with the Lipid Second Messenger, Phosphatidic Acid, *Biochem. Soc. Trans.* 25, 561–565.
- Swarthout, J.T., and Walling, H.W. (2000) Lysophosphatidic Acid: Receptors, Signaling and Survival, *Cell Mol. Life Sci.* 57, 1978–1985.
- Jolly, C.A., Wilton, D.C., and Schroeder, F. (2000) Microsomal Fatty Acyl-CoA Transacylation and Hydrolysis: Fatty Acyl-CoA Species Dependent Modulation by Liver Fatty Acyl-CoA Binding Proteins, *Biochim. Biophys. Acta* 1483, 185–197.
- Dircks, L., and Sul, H.S. (1999) Acyltransferases of *de novo* Glycerophospholipid Biosynthesis, *Prog. Lipid Res.* 38, 461–479.
- Jolly, C.A., Hubbell, T., Behnke, W.D., and Schroeder, F. (1997) Fatty Acid Binding Protein: Stimulation of Microsomal Phosphatidic Acid Formation, *Arch. Biochem. Biophys.* 341, 112–121.
- Gossett, R.E., Edmondson, R.D., Jolly, C.A., Cho, T.H., Russell, D.H., Knudsen, J., Kier, A.B., and Schroeder, F. (1998) Structure and Function of Normal and Transformed Murine Acyl-CoA Binding Proteins, *Arch. Biochem. Biophys.* 350, 201–213.
- Gossett, R.E., Frolov, A.A., Roths, J.B., Behnke, W.D., Kier, A.B., and Schroeder, F. (1996) Acyl-CoA Binding Proteins: Multiplicity and Function, *Lipids* 31, 895–918.
- Daae, L.N., and Bremer, J. (1970) The Acylation of Glycerophosphate in Rat Liver. A New Assay Procedure for Glycerophosphate Acylation, Studies on Its Subcellular and Submitochondrial Localization and Determination of the Reaction Products, *Biochim. Biophys. Acta* 210, 92–104.
- West, J., Tompkins, C.K., Balantac, N., Nudelman, E., Meengs, B., White, T., Bursten, S., Coleman, J., Kumar, A., Singer, J.W., and Leung, D.W. (1997) Cloning and Expression of Two Human Lysophosphatidic Acid Acyltransferase cDNAs That Enhance Cytokine-Induced Signaling Responses in Cells, *DNA Cell Biol.* 16, 691–701.
- Aguado, B., and Campbell, R.D. (1998) Characterization of a Human Lysophosphatidic Acid Acyltransferase That Is Encoded by a Gene Located in the Class III Region of the Human Major Histocompatibility Complex, *J. Biol. Chem.* 273, 4096–4105.
- Zheng, Y., Kong, Y., and Goetzl, E.J. (2001) Lysophosphatidic Acid Receptor-Selective Effects on Jurkat T Cell Migration Through a Matrigel Model Basement Membrane, *J. Immunol.* 166, 2317–2322.
- Zheng, Y., Voice, J.K., Kong, Y., and Goetzl, E.J. (2000) Altered Expression and Functional Profile of Lysophosphatidic Acid Receptors in Mitogen-Activated Human Blood T Lymphocytes, *FASEB J.* 14, 2387–2389.
- Hooks, S.B., Santos, W.L., Im, D.S., Heise, C.E., Macdonald, T.L., and Lynch, K.R. (2000) Lysophosphatidic Acid-Induced Mitogenesis Is Regulated by Lipid Phosphate Phosphatases and Is Edg-Receptor Independent, *J. Biol. Chem.* 276, 4611–4621.
- Balazs, L., Okolicany, J., Ferrebee, M., Tolley, B., and Tigyi, G. (2001) Topical Application of the Phospholipid Growth Factor Lysophosphatidic Acid Promotes Wound Healing *in vivo*, *Am. J. Physiol.: Regul. Integr. Comp. Physiol.* 280, R466–R472.
- Flores, I., Casaseca, T., Martinez, A.C., Kanoh, H., and Merida, I. (1996) Phosphatidic Acid Generation Through Interleukin 2(IL-2)-Induced Alpha-Diacylglycerol Kinase Activation Is an Essential Step in IL-2-Mediated Lymphocyte Proliferation, *J. Biol. Chem.* 271, 10334–10340.
- Marcoz, P., Nemoz, G., Prigent, A.F., and Lagarde, M. (1993) Phosphatidic Acid Stimulates the Rolipram-Sensitive Cyclic Nucleotide Phosphodiesterase from Rat Thymocytes, *Biochim. Biophys. Acta* 1176, 129–136.
- Jolly, C.A., Jiang, Y.H., Chapkin, R.S., and McMurray, D.N. (1997) Dietary (n-3) Polyunsaturated Fatty Acids Suppress Murine Lymphoproliferation, Interleukin-2 Secretion, and the Formation of Diacylglycerol and Ceramide, *J. Nutr.* 127, 37–43.
- Ando, S., Tomita-Yamaguchi, T., and Santoro, T.J. (1993) Long Chain Fatty Acid Utilization of T-cells from Autoimmune MRL-lpr/lpr Mice, *Biochim. Biophys. Acta* 1181, 141–147.
- Jolly, C.A., Murphy, E.J., and Schroeder, F. (1998) Differential

- Influence of Rat Liver Fatty Acid Binding Protein Isoforms on Phospholipid Fatty Acid Composition: Phosphatidic Acid Biosynthesis and Phospholipid Fatty Acid Remodeling, *Biochim. Biophys. Acta* 1390, 258–268.
23. Abo-Hashema, K.A., Cake, M.H., Lukas, M.A., and Knudsen, J. (2001) The Interaction of Acyl-CoA with Acyl-CoA Binding Protein and Carnitine Palmitoyltransferase I, *Int. J. Biochem. Cell Biol.* 33, 807–815.
24. Nishizuka, Y. (1992) Intracellular Signaling by Hydrolysis of Phospholipids and Activation of Protein Kinase C, *Science* 258, 607–614.
25. Fernandes, G., and Jolly, C.A. (1998) Nutrition and Autoimmune Disease, *Nutr. Rev.* 56, S161–S169.

[Received September 24, 2001, and in revised form February 14, 2002; revision accepted April 19, 2002]

# Comparison of the Effects of Dietary $\alpha$ -Linolenic, Stearidonic, and Eicosapentaenoic Acids on Production of Inflammatory Mediators in Mice

Kenji Ishihara<sup>a,\*</sup>, Wataru Komatsu<sup>b</sup>, Hiroaki Saito<sup>a</sup>, and Kazuki Shinohara<sup>c</sup>

<sup>a</sup>Functional Biochemistry Section, Marine Biochemistry Division, National Research Institute of Fisheries Science, Yokohama 236-8648, Japan, <sup>b</sup>Department of Food and Nutrition, Toita Women's College, Hachioji 193-0802, Japan, and <sup>c</sup>Food Function Division, National Food Research Institute, Tsukuba 305-8642, Japan

**ABSTRACT:** The effects of dietary stearidonic acid (18:4n-3) on inflammatory mediator release in whole blood and splenocytes was investigated in Balb/c mice, and the effects were compared with those of two other n-3 PUFA:  $\alpha$ -linolenic acid (18:3n-3) and EPA (20:5n-3). TAG mixtures containing 10% of 18:4n-3, 18:3n-3, or 20:5n-3 as the respective sole n-3 PUFA were enzymatically synthesized. Diets containing synthesized TAG mixtures were fed to Balb/c mice for 3 wk. The release of prostaglandin E<sub>2</sub> (PGE<sub>2</sub>) and tumor necrosis factor (TNF) were measured in whole blood and splenocytes stimulated with lipopolysaccharide. In whole blood, the production of TNF was suppressed by all dietary n-3 PUFA (18:3n-3, 18:4n-3, and 20:5n-3) as compared with the control diet, which contained TAG prepared from safflower oil. PGE<sub>2</sub> production was not significantly changed. Differences among the n-3 PUFA (18:3n-3, 18:4n-3, and 20:5n-3) were not observed. In splenocytes, PGE<sub>2</sub> production was suppressed by dietary n-3 PUFA, but TNF production was not. GC analysis of plasma and splenocyte FA profiles showed an increase in the levels of 20:4n-3, 20:5n-3, and 22:6n-3 in mice fed the diet containing 18:4n-3.

Paper no. L8944 in *Lipids* 37, 481–486 (May 2002).

Since the discovery of a low incidence of heart disease in Eskimos by Dyerberg *et al.* (1–3), the nutritional, physiological, and pharmacological effects of n-3 PUFA on humans have been recognized. Many studies showed vegetable and fish oils rich in n-3 PUFA, such as EPA (20:5n-3), DHA (22:6n-3) and  $\alpha$ -linolenic acid (18:3n-3), to have beneficial effects on pathophysiological states such as coronary heart disease, hyperlipidemia, and inflammation, and the contribution of these PUFA to the beneficial effects has been studied (4,5).

The major n-3 PUFA in seafood are 20:5n-3 and 22:6n-3. In addition to these, some seafoods contain various n-3 PUFA such as hexadecatetraenoic acid (16:4n-3), stearidonic acid (18:4n-3), and tetracosahexaenoic acid (24:6n-3) (6,7). We have studied the physiological activities of these FA *in vitro*

Presented in part at the 17th International Congress of Nutrition, October 27–31, 2001, Wien, Austria.

\*To whom correspondence should be addressed at Marine Biochemistry Division, National Research Institute of Fisheries Science, Fisheries Research Agency, 2-12-4 Fukuura, Kanazawaku, Yokohama 236-8648, Japan. E-mail: hplc@affrc.go.jp

Abbreviations: LPS, lipopolysaccharide; PGE<sub>2</sub>, prostaglandin E<sub>2</sub>; TNF, tumor necrosis factor.

and found a suppressing effect of these PUFA on eicosanoid production (8,9).

Stearidonic acid (18:4n-3) is an intermediate in the metabolism from 18:3n-3 to longer n-3 PUFA (10). Stearidonic acid is contained in significant amounts in fish oils (11), in plant oils (12,13), and in edible algae (7). *In vivo* metabolism of 18:4n-3 has been studied in rats (10) and mice (14). Iritani *et al.* (15) showed a suppressive effect of 18:4n-3 on liver lipogenic enzyme activity in rats. Recently, Hansen Petrik *et al.* (16) reported that dietary 18:4n-3 strongly suppressed tumorigenesis in Apc<sup>Min/+</sup> mice and that the suppression was correlated with the inhibition of prostaglandin (PG) biosynthesis. Thus, interest in the nutritional and physiological activity of 18:4n-3 is increasing.

Dietary oils containing n-3 PUFA have anti-inflammatory activity in animals and humans (4,5,17). In this work, we studied the effect of dietary 18:4n-3 on inflammatory mediator release from the whole blood and splenocytes in mice (to assess the anti-inflammatory effect of 18:4n-3) and compared this effect with that of other common n-3 PUFA (18:3n-3 and 20:5n-3). We measured prostaglandin E<sub>2</sub> (PGE<sub>2</sub>) and tumor necrosis factor (TNF) release. Both are well known as mediators of inflammation, and both play important roles in many pathological processes (18–22). PGE<sub>2</sub> also has been reported to be closely related to intestinal carcinogenesis in Apc<sup>Min/+</sup> mice (23), and TNF has been considered to act as an internal promoter of carcinogenesis (18). This study gives information about not only anti-inflammatory but also the anticarcinogenic effects of dietary 18:4n-3.

## EXPERIMENTAL PROCEDURES

**Animals and diets.** Twenty-eight male Balb/c mice (3 wk of age, Tokyo Experimental Animals, Tokyo, Japan) were housed individually in stainless steel cages and fed a commercial pellet diet (CE-2; Japan CLEA, Tokyo, Japan) for 3 d before starting the experimental diets. Mice were maintained in an air-conditioned room (temperature: 20–22°C; relative humidity: 55–65%; lighting: 0700–1900). All animal procedures were in accordance with the National Research Institute of Fisheries Science guidelines for the ethical treatment of laboratory animals. The mice were divided into four dietary groups (seven mice/group): control, 18:3n-3, 18:4n-3,



and 20:5n-3. Each group was fed the experimental diet *ad libitum* for 3 wk. This period and dose of PUFA were based on the study of Yamazaki *et al.* (10). They studied the incorporation and metabolism of dietary 18:4n-3 in rats and found that feeding for 3 wk at a dose of 1% of the diet significantly affected tissue FA profiles.

The composition of the experimental diet was as follows (g/kg diet): casein, 230; cornstarch, 410; sucrose, 200; AIN-76 mineral mixture, 35; AIN-76 vitamin mixture, 10; cellulose powder, 20; maltodextrin, 20; DL-methionine, 3; choline bitartrate, 2; test oil, 100. Sucrose was purchased from Maruha Corp. (Tokyo, Japan). DL-Methionine and choline bitartrate were from Wako Pure Chemical Industry (Osaka, Japan). Maltodextrin was a generous gift from Matsutani Chemical Industry (Hyogo, Japan). The test oils were prepared as described below.

**Preparation of test oils.** Stearidonic acid (purity > 95%) was purified from the brown alga *Undaria pinnatifida* as previously described (24).  $\alpha$ -Linolenic acid was obtained from Wako Pure Chemical Industry. EPA was generously donated by Nissui Corp. (Tokyo, Japan). Safflower oil (Ajinomoto Corp., Tokyo, Japan) was saponified in ethanolic-KOH, and FFA were extracted as previously described (24). TAG containing n-3 PUFA were enzymatically synthesized essentially according to the method of Kosugi and Azuma (25). Briefly, the n-3 FA and safflower FFA were mixed 1:1 (w/w); 20 g of the FFA mixture was then added along with 1.8 g of glycerol (approximate molecular ratio, 3:1) and 1.3 g of Novozyme 435 (kind gift from Novozymes Japan, Chiba, Japan). The mixture was reacted at 60°C under vacuum conditions (~10 Torr) on a magnetic stirrer (500 rpm) for 24 h. After the reaction, lipid was extracted by the method of Folch *et al.* (26), and TAG were purified by Florisil column chromatography using hexane/diethyl ether (7:3, vol/vol) as solvent. Purified TAG were diluted with safflower oil and purified by the same method as that for synthesized TAG to give a composition of n-3 PUFA at 10% (w/w), and DL- $\alpha$ -tocopherol was added to the mixture at a level of 0.2% (w/w). The FA composition of the test oils is shown in Table 1. With this method, we obtained TAG which contained 18:3n-3, 18:4n-3, or 20:5n-3 as almost the sole n-3 PUFA. This allowed us to evaluate the effect of single dietary n-3 PUFA.

**Measurement of inflammatory mediator release in whole blood.** Inflammatory mediator release in whole blood was assayed essentially according to the report of Di Santo *et al.* (27). At the end of the experimental period, mice were fasted for 5 h and anesthetized with i.p. injection of Nembutal (1 mL/kg body weight; Dainippon Pharmaceutical, Osaka, Japan). Whole blood was collected from heart in a syringe that contained 7 U of heparin/0.1 mL of saline. Aliquots (100  $\mu$ L) of whole blood were dispensed into a 96-well microtiter plate to which was added 10  $\mu$ L of PBS containing 0.1  $\mu$ g of lipopolysaccharide (LPS, from *Escherichia coli* O26:B6; Wako Pure Chemical Industry). Six hours later, blood was recovered and plasma was collected after centrifugation at 1,000  $\times$  g for 15 min. Plasma TNF activity was measured as cytotoxicity against L929 fibroblasts as described by Komatsu *et al.* (28). Plasma PGE<sub>2</sub>

**TABLE 1**  
**FA Composition of Test Oils<sup>a</sup>**

FA	Dietary group			
	Control	18:3n-3	18:4n-3	20:5n-3
	g/100 g total FA			
14:0	0.1	0.0	0.1	0.1
16:0	4.6	4.0	4.4	4.1
16:1n-7	0.2	0.2	0.2	0.2
18:0	1.8	1.6	1.6	1.6
18:1n-9	75.5	66.2	66.3	67.9
18:2n-6	16.9	17.1	14.9	15.2
18:3n-6	0.0	0.0	0.1	0.0
18:3n-3	0.3	10.2	0.6	0.2
18:4n-3	0.0	0.0	10.0	0.0
20:0	0.4	0.3	0.3	0.3
20:1n-9	0.3	0.2	0.2	0.3
20:1n-7	0.1	0.1	0.1	0.1
20:4n-6	0.0	0.0	0.3	0.0
20:5n-3	0.0	0.0	0.7	10.0

<sup>a</sup>Test oils were synthesized as described in the Experimental Procedures section.

concentration was measured with PGE<sub>2</sub> enzyme immunoassay kit (Cayman Chemical Company, Ann Arbor, MI; cross-reactivity: PGE<sub>2</sub> 100%, PGE<sub>3</sub> 43%, PGE<sub>1</sub> 18.7%, 6-keto PGF<sub>1 $\alpha$</sub>  1%, PGD<sub>2</sub> <0.01%). In a preliminary experiment, PGE<sub>2</sub> production in whole blood incubated without LPS was less than 5% of that incubated with LPS.

**Measurement of inflammatory mediator release by splenocytes.** The spleen was excised and splenocytes were isolated as described by Hayek *et al.* (29) and suspended in RPMI-1640 medium supplemented with 5% FCS (Biological Industry Inc., Beit Haemek, Israel). Splenocyte suspension was seeded into 24-well plates (10<sup>6</sup> cells/0.5 mL/well). Following the preincubation for 2 h, splenocytes were stimulated by adding of 50  $\mu$ L of PBS containing 0.5  $\mu$ g of LPS (final concentration: 1  $\mu$ g/mL). This concentration of LPS was confirmed to fully stimulate splenocyte TNF production (data not shown). After 6 h stimulation, the supernatant was collected, and TNF activity and PGE<sub>2</sub> concentration were measured as detailed above. Cellular protein content was measured with Bio-Rad protein assay reagent (Bio-Rad Laboratory, Hercules, CA).

**FA analysis.** Lipids of plasma and splenocytes were extracted by the method of Folch *et al.* (26). Total lipids of plasma and splenocytes were methyl-esterified and analyzed by GC using the previously reported method (9).

**Statistical analysis.** Statistical analyses were done using StatPartner version 3 (NEC software, Tokyo, Japan). Data obtained in this report were analyzed by one-way ANOVA. If significant, data were further analyzed by Duncan's multiple range test. Significance level was set at  $P < 0.05$ .

## RESULTS

**Growth, food intake, and relative organ weight.** Initial body weight, body weight gain, total food intake, and relative liver weight were not different among the dietary groups (Table 2).

**TABLE 2**  
**Initial Body Weight, Body Weight Gain, Total Food Intake, and Relative Weight of Liver<sup>a</sup>**

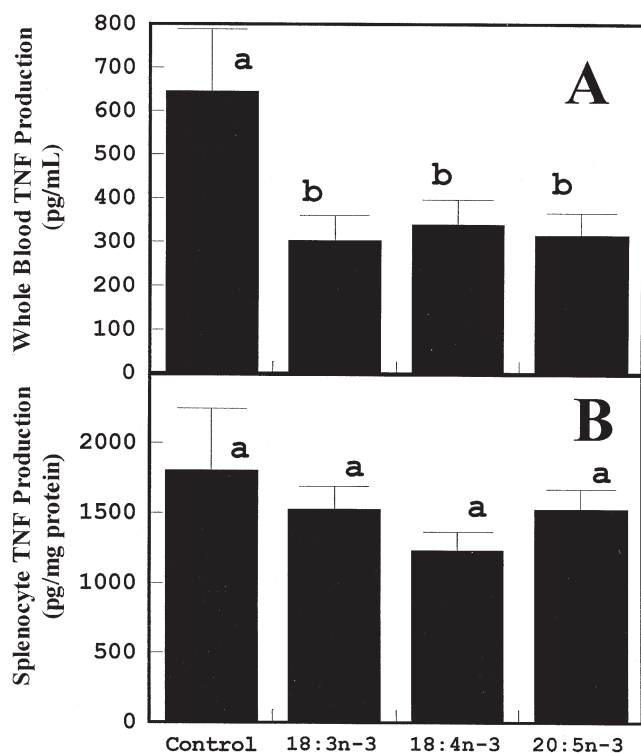
Diet group	Initial body weight (g)	Body weight gain (g/3 wk)	Total food intake (g/3 wk)	Relative liver weight (% of body weight)
Control	18.0 ± 0.3	5.5 ± 0.4	83.2 ± 1.4	4.03 ± 0.09
18:3n-3	18.0 ± 0.3	5.1 ± 0.1	79.2 ± 1.9	4.08 ± 0.12
18:4n-3	18.0 ± 0.3	5.3 ± 0.4	79.7 ± 1.9	3.64 ± 0.18
20:5n-3	17.9 ± 0.4	5.5 ± 0.3	86.0 ± 2.0	3.74 ± 0.10

<sup>a</sup>Data are expressed as the mean ± SEM of seven mice. Data were analyzed by one-way ANOVA, and no significant differences were observed ( $P > 0.05$ ).

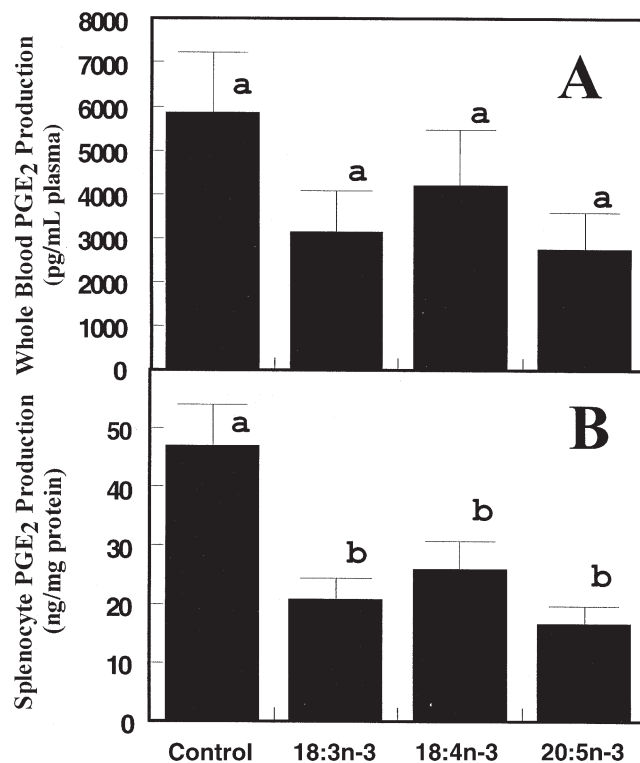
**TNF production in whole blood and splenocytes.** TNF production in whole blood was significantly decreased by dietary n-3 PUFA compared to the control group (59% for 18:3n-3, 59% for 18:4n-3, and 61% for 20:5n-3, Fig. 1A). There was no difference among the dietary n-3 PUFA. In splenocytes (Fig. 1B), no significant difference was found between the dietary groups, but there was a tendency for TNF production to be reduced by dietary n-3 PUFA.

**PGE<sub>2</sub> release in whole blood and splenocytes.** PGE<sub>2</sub> synthesis in whole blood and splenocytes is shown in Figure 2. Splenocyte PGE<sub>2</sub> synthesis was significantly suppressed in n-3 PUFA-fed mice (56, 45, and 64% compared to the control in 18:3n-3, 18:4n-3, and 20:5n-3 fed groups, respectively). There was no difference among the dietary n-3 PUFA. Whole blood PGE<sub>2</sub> production revealed the same trend as for splenocytes, but it was not significant.

**FA profile.** FA profiles of the total lipid of plasma and splenocytes were analyzed (Fig. 3). The proportion of arachidonic acid (20:4n-6) was decreased in serum and splenocytes by dietary n-3 PUFA. Dietary 20:5n-3 more effectively decreased the composition of 20:4n-6 than 18:4n-3 and 18:3n-3. The influence of dietary n-3 PUFA on the composition of n-3 PUFA differed between plasma and splenocytes (Fig. 3). In plasma, dietary n-3 PUFA increased the composition of 22:6n-3 to the same extent. Dietary 18:3n-3 only increased 22:6n-3, but 18:4n-3 and 20:5n-3 increased the composition of 18:4n-3 and 20:5n-3 as well as 22:6n-3 (Fig. 3A). In splenocytes, the 22:6n-3 level was raised only by dietary 18:4n-3. Dietary 18:3n-3 did not change the levels of n-3 PUFA significantly. Dietary 18:4n-3 elevated the proportion of 18:4n-3, 20:4n-3, 20:5n-3, 22:5n-3, and 22:6n-3. EPA increased 20:5n-3 and 22:5n-3 (Fig. 3B).



**FIG. 1.** Tumor necrosis factor (TNF) production from whole blood (A) and splenocytes (B) in mice fed n-3 PUFA. Vertical bars indicate SEM of seven mice. Values not sharing a common letter are significantly different at  $P < 0.05$  by Duncan's multiple range test.



**FIG. 2.** Prostaglandin (PG) E<sub>2</sub> production from whole blood (A) and splenocytes (B) in mice fed n-3 PUFA. Vertical bars indicate SEM of seven mice. Values not sharing a common letter are significantly different at  $P < 0.05$  by Duncan's multiple range test.

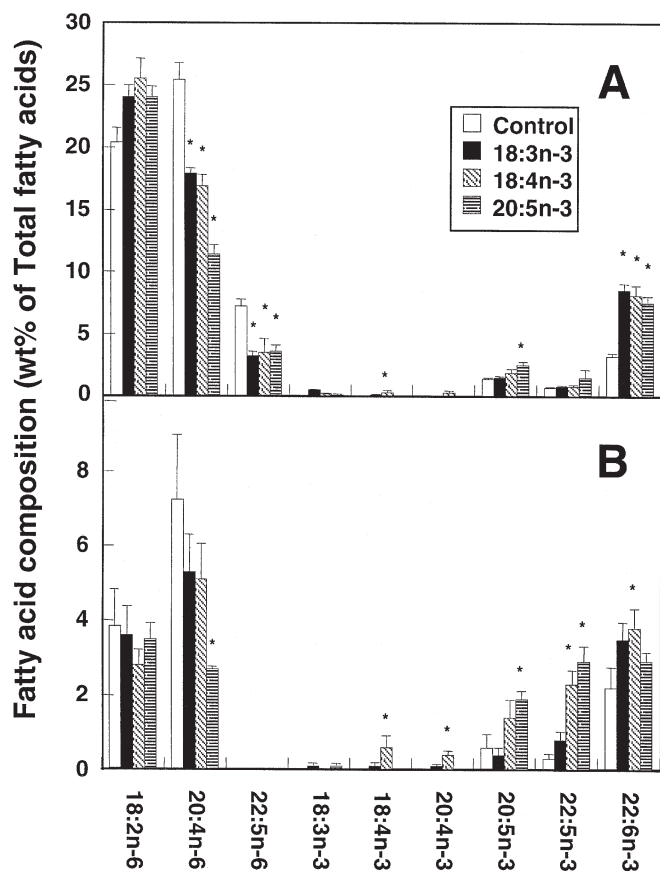


FIG. 3. n-6 and n-3 PUFA composition of total lipid in serum (A) and splenocytes (B) in mice fed n-3 PUFA. Vertical bars indicate SEM of seven mice. Asterisk (\*) indicates significant difference from control by Duncan's multiple range test.

## DISCUSSION

In this study, we synthesized TAG that contained 18:4n-3 as the almost sole n-3 PUFA by using the lipase reaction reported by Kosugi and Azuma (25). TAG containing 18:3n-3 and 20:5n-3 were also synthesized. This allowed us to investigate the nutritional effect of dietary 18:4n-3 while avoiding influences of the chemical form of the FA and the co-occurrence of other PUFA. Several reports describe nutritional studies of diets containing 18:4n-3 (10,12,14–16). Some of these studies used black currant seed oil, which has a high percentage composition of  $\gamma$ -linolenic acid (18:3n-6) and 18:3n-3, and a relatively low percentage composition of 18:4n-3. Yamazaki *et al.* (10) and Huang *et al.* (14) studied the metabolic uptake of 18:4n-3 by using pure 18:4n-3 ethyl ester although digestion and absorption of FA reportedly differ between the ethyl ester form and the TAG form (30). Therefore, this is the first report studying nutritional effects of 18:4n-3 as a sole n-3 PUFA and in TAG form. The method used in this report for preparing the test oils may be applicable to the nutritional study of other FA.

In this study, we examined the effect of dietary 18:4n-3 on the release of inflammatory mediators (TNF and PGE<sub>2</sub>) in whole blood and splenocytes in response to LPS *ex vivo*.

These mediators are known to be produced and play important roles in the inflammation process (19). LPS is a component of gram-negative bacterial cell walls and induces many inflammatory reactions and leads to the production of inflammatory mediators when administered into animals (31). Thus, inflammatory mediator release in response to LPS exposure *ex vivo* will reflect the intensity of inflammatory response in the animal. Dietary n-3 PUFA are known to reveal beneficial effects *via* suppressing the production of these mediators in inflammation and other disease models (20–22).

Eicosanoids (PG and leukotrienes) are synthesized from 20:4n-6. n-3 PUFA such as 18:3n-3, 20:5n-3, and 22:6n-3 can suppress their synthesis (17). Hansen Petrik *et al.* (16) measured PG levels in the small intestine of mice fed diets supplemented with various FA ethyl esters. They showed that dietary n-3 PUFA (18:3n-3, 18:4n-3, 20:5n-3, and 22:6n-3) decreased the PGE<sub>2</sub> level, and the decrement did not differ among the n-3 PUFA. This result is in agreement with our results. However, Kockmann *et al.* (32) reported that the inhibition of the production of cyclooxygenase pathway products by 18:4n-3 in isolated human platelets *in vitro* was less than the inhibitory activity of 20:5n-3. In our unpublished results, 18:4n-3 had only a weaker inhibitory activity than 20:5n-3 on PGE<sub>2</sub> synthesis in cultured murine macrophage cell line. Thus, suppressive activity of dietary 18:4n-3 on PGE<sub>2</sub> synthesis may be exerted not only by 18:4n-3 itself but also by its metabolites, such as 20:5n-3 and 22:6n-3. In this study, metabolism of 18:4n-3 to 20:5n-3 and 22:6n-3 was observed in plasma and splenocytes (Fig. 3). In whole blood, the effect of n-3 PUFA on PGE<sub>2</sub> production was not significant but was similar to that of splenocytes. However, FA profiles of serum and splenocytes were different (Fig. 3). The reasons for the difference in response of PGE<sub>2</sub> production to dietary n-3 PUFA is not clear. There might be real FA pools, not reflected in the FA profile of total lipids that influence PGE<sub>2</sub> production.

Calder (21) and Blok *et al.* (22) reviewed reports of studies of the effect of dietary n-3 PUFA on inflammatory cytokine production in animals *ex vivo*. In their reviews, there are reports showing inconsistent results: decreasing, no, and increasing effects of dietary n-3 PUFA on cytokine production. Most human *ex vivo* and animal *in vivo* studies revealed a suppression of cytokine production by dietary n-3 PUFA (21,22). Blok *et al.* (22) and Calder (21) suggested the detailed conditions of the experiments (cell type used, methods of stimulation, incubation time, etc.) may have produced the contradictory results. Most of the studies that have shown an enhancing effect of n-3 PUFA on cytokine production used peritoneal macrophages as cytokine sources. In this study, a significant suppression of TNF production was observed in whole blood. From these results, it is suggested that interactions of different types of cells are required for the expression of a suppressive effect on cytokine production of dietary n-3 PUFA. The experiment that used thioglycolate-elicited macrophages showed an inhibition of cytokine production by dietary n-3 PUFA. In this case, it was possible that these macrophages had interactions with other cells during stimulation with thioglycolate *in vivo*. Our present results



showed suppression of TNF production by dietary n-3 PUFA in whole blood but not in splenocytes. Whole blood is a complex system and consists of many types of cells; on the other hand, the isolated splenocyte system is relatively simple. Thus, cellular interactions in both systems seem to be different. It might explain the difference in the effect of n-3 PUFA on TNF production in the two systems. Hansen Petrik *et al.* (16) revealed an anticarcinogenic activity of dietary n-3 PUFA, and the activity of 18:4n-3 and 20:5n-3 was stronger than that of 18:3n-3 and 22:6n-3. They suggested their activity was in part due to the suppression of PGE<sub>2</sub> synthesis. It was reported that TNF could act as an endogenous tumor promoter (18). Thus, the possibility is suggested that dietary 18:4n-3 may exert its anticarcinogenic effect not only by suppression of PGE<sub>2</sub> synthesis but also by the suppression of TNF production.

Stearidonic acid (18:4n-3) is a  $\Delta$ 6-desaturase metabolite of 18:3n-3.  $\Delta$ 6-Desaturation is known as a rate-limiting step of the metabolism of 18:3n-3 to longer n-3 PUFA (10). Thus, 18:4n-3 is expected to be more readily metabolized than 18:3n-3. This was reported in mouse liver and intestine lipids (14,16) and in rat liver and plasma lipids (10). In the present results, we found 18:4n-3 was metabolized more readily than 18:3n-3 only in splenocytes. The reason is not clear. Differences in the chemical form of PUFA, tissue enzyme activities, and co-occurring FA may influence the metabolism of n-3 PUFA. Dietary n-3 PUFA reduced the 20:4n-6 concentration in serum and splenocytes (Fig. 3). EPA reduced the level of arachidonic acid (20:4n-6) more effectively than 18:3n-3 and 18:4n-3. Arachidonic acid is a precursor of PG biosynthesis. PG are known to influence cytokine production, inflammation reaction, and carcinogenesis (16,17,19–22). Tissue 20:4n-6 level has been shown to influence PG biosynthesis (16,17,23). Thus, dietary n-3 PUFA may be important due to their ability to reduce tissue level of 20:4n-6.

In this study, we compared the effects of dietary 18:3n-3, 18:4n-3, and 20:5n-3 on the production of TNF and PGE<sub>2</sub> in mice and found that all three n-3 PUFA had suppressive activity on the production of TNF in whole blood and PGE<sub>2</sub> in splenocytes. Differences in activity among dietary groups were not observed. However, differences in the rate of incorporation and metabolism of n-3 PUFA were suggested in some tissues. Therefore, it is possible that the differences in the activity of n-3 PUFA will be found in some physiological functions.

## ACKNOWLEDGMENT

We thank Dr. Kazuhiko Hata (Central Research Institute, Nissui Corporation) for providing us 20:5n-3 ethyl ester, Novozymes Japan Ltd. for giving us Novozyme 435, and Matsunami Chemical Industry for the donation of maltodextrin. We thank Kazuhiko Yamamoto for his skillful technical assistance.

## REFERENCES

- Dyerberg, J., Bang, H.O., and Hjorne, N. (1975) Fatty Acid Composition of the Plasma Lipids in Greenland Eskimos, *Am. J. Clin. Nutr.* 192, 433–435.
- Bang, H.O., and Dyerberg, J. (1972) Plasma Lipids and Lipoproteins in Greenlandic West Coast Eskimos, *Acta Med. Scand.* 192, 85–94.
- Bang, H.O., and Dyerberg, J. (1980) The Bleeding Tendency in Eskimos, *Dan. Med. Bull.* 27, 202–205.
- Stansby, M.E. (1990) Nutritional Properties of Fish Oil for Human Consumption—Modern Aspects, in *Fish Oils in Nutrition* (Stansby, M.E., ed.), pp. 289–308, Van Nostrand Reinhold, New York.
- Cunnane, S.C. (1992) What Is the Nutritional and Clinical Significance of  $\alpha$ -Linolenic Acid in Humans? in *Essential Fatty Acids and Eicosanoids—Invited Papers from the Third International Congress* (Sinclair, A., and Gibson, R., eds), pp. 379–382, American Oil Chemists' Society, Champaign.
- Ota, T., Chihara, Y., Itabashi, Y., and Takagi, T. (1994) Occurrence of All-*cis*-6,9,12,15,18,21-Tetracosahexaenoic Acid in Flatfish Lipids, *Fish. Sci.* 60, 171–175.
- Takagi, T., Asahi, M., and Itabashi, Y. (1985) Fatty Acid Composition of Twelve Algae from Japanese Waters, *Yukagaku* 34, 1008–1012.
- Ishihara, K., Murata, M., Kaneniwa, M., Saito, H., Shinohara, K., and Maeda-Yamamoto, M. (1998) Inhibition of Icosanoid Production in MC/9 Mouse Mast Cells by n-3 Polyunsaturated Fatty Acids Isolated from Edible Marine Algae, *Biosci. Biotechnol. Biochem.* 62, 1412–1415.
- Ishihara, K., Murata, M., Kaneniwa, M., Saito, H., Shinohara, K., Maeda-Yamamoto, M., Kawasaki, K., and Oozumi, T. (1998) Effect of Tetracosahexaenoic Acid on the Content and Release of Histamine, and Eicosanoid Production in MC/9 Mouse Mast Cell, *Lipids* 33, 1107–1114.
- Yamazaki, K., Fujikawa, M., Hamazaki, T., Yano, S., and Shono, T. (1992) Comparison of the Conversion Rates of alpha-Linolenic Acid [18:3(n-3)] and Stearidonic Acid [18:4(n-3)] to Longer Polyunsaturated Fatty Acids in Rats, *Biochim. Biophys. Acta* 1123, 18–26.
- Stansby, M.E., Schlenk, H., and Gruger, E.H., Jr. (1990) Fatty Acid Composition of Fish, in *Fish Oils in Nutrition* (Stansby, M.E., ed.) pp. 289–308, Van Nostrand Reinhold, New York.
- Crozier, G.L., Fleith, M., Traitler, H., and Finot, P.A. (1989) Black Currant Seed Oil Feeding and Fatty Acids in Liver Lipid Classes of Guinea Pigs, *Lipids* 24, 460–466.
- Guil-Guerrero, J.L., Gomez-Mercado, F., Garcia-Maroto, F., and Campra-Madrid, P. (2000) Occurrence and Characterization of Oils Rich in gamma-Linolenic Acid Part I: *Echium* Seeds from Macaronesia, *Phytochemistry* 53, 451–456.
- Huang, Y.S., Smith, R.S., Redden, P.R., Cantrill, R.C., and Horrobin, D.F. (1991) Modification of Liver Fatty Acid Metabolism in Mice by n-3 and n-6  $\Delta$ 6-Desaturase Substrates and Products, *Biochim. Biophys. Acta* 1082, 319–327.
- Iritani, N., Inoguchi, K., Endo, M., Fukuda, E., and Morita, M. (1980) Identification of Shellfish Fatty Acids and Their Effects on Lipogenic Enzymes, *Biochim. Biophys. Acta* 618, 378–382.
- Hansen Petrik, M.B., McEntee, M.F., Johnson, B.T., Obukowicz, M.G., and Whelan, J. (2000) Highly Unsaturated (n-3) Fatty Acids, but Not alpha-Linolenic, Conjugated Linoleic or gamma-Linolenic Acids, Reduce Tumorigenesis in Apc<sup>Min/+</sup> Mice, *J. Nutr.* 130, 2434–2443.
- Hwang, D. (2000) Fatty Acids and Immune Response—A New Perspective in Searching for Clues to Mechanism, *Annu. Rev. Nutr.* 20, 431–456.
- Fujiki, H., Suganuma, M., Okabe, S., Sueoka, E., Suga, K., Imai, K., and Nakachi, K. (2000) A New Concept of Tumor Promotion by Tumor Necrosis Factor-alpha, and Cancer Preventive Agents (–)Epigallocatechin Gallate and Green Tea—A Review, *Cancer Detect. Prev.* 24, 91–99.
- James, M.J., Gibson, R.A., and Cleland, L.G. (2000) Dietary Polyunsaturated Fatty Acids and Inflammatory Mediator Production, *Am. J. Clin. Nutr.* 71, 343S–348S.



20. Sperling, R.I. (1991) Dietary Omega-3 Fatty Acids: Effects on Lipid Mediators of Inflammation and Rheumatoid Arthritis, *Rheum. Dis. Clin. North Am.* 17, 373–389.
21. Calder, P.C. (1997) n-3 Polyunsaturated Fatty Acids and Cytokine Production in Health and Disease, *Ann. Nutr. Metab.* 41, 203–234.
22. Blok, W.L., Katan, M.B., and van der Meer, J.W.M. (1996) Modulation of Inflammation and Cytokine Production by Dietary (n-3) Fatty Acids, *J. Nutr.* 126, 1515–1533.
23. Hansen Petrik, M.B., McEntee, M.F., Chiu, C.-H., and Whelan, J. (2000) Antagonism of Arachidonic Acid Is Linked to the Antitumorigenic Effect of Dietary Eicosapentaenoic Acid in *Apc<sup>Min/+</sup>* Mice, *J. Nutr.* 130, 1153–1158.
24. Ishihara, K., Murata, M., Kaneniwa, M., Saito, H., Komatsu, W., and Shinohara, K. (2000) Purification of Stearidonic [18:4(n-3)] and Hexadecatetraenoic Acid [16:4(n-3)] from Algal Fatty Acid with Lipase and Medium Pressure Liquid Chromatography, *Biosci. Biotech. Biochem.* 64, 2454–2457.
25. Kosugi, Y., and Azuma, N. (1994) Synthesis of Triacylglycerol from Polyunsaturated Fatty Acid by Immobilized Lipase, *J. Am. Oil Chem. Soc.* 71, 1397–1403.
26. Folch, J., Lees, M., and Sloane Stanley, G.H. (1957) A Simple Method for the Isolation and Purification of Total Lipids from Animal Tissues, *J. Biol. Chem.* 226, 497–509.
27. Di Santo, E., Meazza, C., Sironi, M., Fruscella, P., Mantovani, A., Sipe, J.D., and Ghezzi, P. (1997) IL-13 Inhibits TNF Production but Potentiates That of IL-6 *in vivo* and *ex vivo* in Mice, *J. Immunol.* 159, 379–382.
28. Komatsu, W., Yagasaki, K., Miura, Y., and Funabiki, R. (1997) Stimulation of Tumor Necrosis Factor and Interleukin-1 Productivity by the Oral Administration of Cabbage Juice to Rats, *Biosci. Biotechnol. Biochem.* 61, 1937–1938.
29. Hayek, M.G., Han, S.N., Wu, D., Watkins, B.A., Meydani, M., Dorsey, J.L., Smith, D.E., and Meydani, S.N. (1999) Dietary Conjugated Linoleic Acid Influences the Immune Response of Young and Old C57BL/6NCrIBR Mice, *J. Nutr.* 129, 32–38.
30. Lawson, L.D., and Hughes, B.G. (1988) Absorption of Eicosapentaenoic Acid and Docosahexaenoic Acid from Fish Oil Triacylglycerols or Fish Oil Ethyl Esters Co-ingested with a High-Fat Meal, *Biochem. Biophys. Res. Commun.* 156, 960–963.
31. Sadeghi, S., Wallace, F.A., and Calder, P.C. (1999) Dietary Lipids Modify the Cytokine Response to Bacterial Lipopolysaccharide in Mice, *Immunology* 96, 404–410.
32. Kockmann, V., Spielmann, D., Traitler, H., and Lagarde, M. (1989) Inhibitory Effect of Stearidonic Acid (18:4n-3) on Platelet Aggregation and Arachidonate Oxygenation, *Lipids* 24, 1004–1007.

[Received November 1, 2001, and in revised form February 14, 2002; revision accepted March 26, 2002]

# Peroxisome Proliferator-Activated Receptor $\alpha,\gamma$ Coagonist LY465608 Inhibits Macrophage Activation and Atherosclerosis in Apolipoprotein E Knockout Mice

Steven H. Zuckerman\*, Raymond F. Kauffman, and Glenn F. Evans

Division of Cardiovascular Research, Lilly Research Laboratories, Indianapolis, Indiana 46285

**ABSTRACT:** The apolipoprotein E (apoE) knockout mouse has provided an approach to the investigation of the effect of both cellular and humoral processes on atherosclerotic lesion progression. In the present study, pharmacologic modulation of both interferon gamma (IFN $\gamma$ )-inducible macrophage effector functions, and atherosclerotic lesions in the apoE knockout mouse were investigated using the peroxisome proliferator-activated receptor (PPAR)  $\alpha,\gamma$  coagonist LY465608. LY465608 inhibited, in a concentration-dependent manner, IFN $\gamma$  induction of both nitric oxide synthesis and the  $\beta$  2 integrin CD11a in elicited peritoneal macrophages from apoE knockout mice. Similar effects were observed *ex vivo* following 10 d of treating mice with 10 mg/kg of LY465608. Treatment of apoE knockout mice for 18 wk with LY465608 resulted in a statistically significant 2.5-fold reduction in atherosclerotic lesion area in en face aorta preparations. These effects were apparent in the absence of any reduction in total serum cholesterol or in lipoprotein distribution. Finally, treatment of apoE knockout mice with established atherosclerotic disease resulted in a modest but not statistically significant decrease in aortic lesional surface area. These results demonstrate the utility of PPAR coagonists in reducing the progression of the atherosclerotic lesion.

Paper no. L8986 in *Lipids* 37, 487–494 (May 2002).

Novel therapeutic approaches to the prevention and mitigation of atherosclerotic disease include strategies in which more specific interventions toward the inflammatory response are being considered. The macrophage is involved in all aspects of the pathobiology of the atherosclerotic lesion and mediates its effects through both cellular and humoral processes including the elaboration of cytokines and oxidants (1–3). Macrophage activation has been observed within the atheroma and is believed to be due to the autocrine and

paracrine effects of cytokines as well as to the binding and ingestion of oxidized LDL (4–6). Interferon  $\gamma$  (IFN $\gamma$ ) represents one such macrophage-activating cytokine whose effects on apolipoprotein (apoE) secretion, ABC-1 and ACAT expression, cholesterol efflux, and metalloprotease production could contribute to the pathology associated with atherosclerosis (7–12). Inhibiting IFN $\gamma$  signaling, for example, by crossing apoE knockout (KO) mice with mice lacking the IFN $\gamma$  receptor, results in reduced atherosclerosis (13). These *in vivo* results suggest that pharmacologic agents that inhibit macrophage activation through IFN $\gamma$  signaling could be useful in slowing or reversing lesion progression.

The peroxisome proliferator-activated receptors (PPAR) represent nuclear receptors that function as ligand-activated transcription factors. PPAR subtypes include PPAR $\alpha$ , PPAR $\delta$ , and PPAR $\gamma$ ; upon ligand activation, PPAR form heterodimeric structures with the retinoid X receptor to bind to and activate specific gene transcription through PPAR response elements (14–16). Anti-inflammatory effects both *in vitro* and *in vivo* have been reported for both PPAR $\alpha$ - and PPAR $\gamma$ -specific agonists (17–21). PPAR $\gamma$  agonists, for example, have been reported to inhibit IFN $\gamma$ -induced inducible nitric oxide synthetase (iNOS) activity, gelatinase, and scavenger receptor activity *in vitro* in mouse macrophages, matrix metalloprotease 9 (MMP 9) activity in human monocyte-derived macrophages, and both phorbol ester and lipopolysaccharide induction of tumor necrosis factor (TNF) and interleukin 6 (IL-6) production (17,22–25). PPAR $\gamma$  agonists also have been reported to increase both scavenger receptor class B type I (SR-BI) and CD36 expression in macrophages, thereby contributing to the process of reverse cholesterol transport (26–30).

Similarly, PPAR $\alpha$  agonists also have been reported to have anti-inflammatory effects including inhibiting the production of MMP 9 activity, IL-6 and endothelin-1 secretion, and cyclooxygenase 2 and iNOS expression (19–21). PPAR activation appears to inhibit inflammatory processes by antagonizing both nuclear factor  $\kappa$ B (NF- $\kappa$ B) and activator protein-1 (AP-1) pathways (20,21,31). Therefore, it would be expected that PPAR $\alpha$  or  $\gamma$  agonists should be beneficial in preclinical models of atherosclerosis. To this extent, the recent reports demonstrating that activation of the retinoid X receptor

\*To whom correspondence should be addressed.  
E-mail: Zuckerman\_Steven@Lilly.com

Abbreviations: ABC-1, ATB-binding cassette transporter-1; AP-1, activator protein-1; apo, apolipoprotein; CD11a, integrin  $\alpha_L$ ; CD11b, integrin  $\alpha_M$ ; CD36, member of the scavenger receptor family; CMC, carboxymethylcellulose; FITC, fluorescein isothiocyanate; FPLC, fast protein liquid chromatography; IFN $\gamma$ , interferon  $\gamma$ ; IL, interleukin; iNOS, inducible nitric oxide synthetase; KO, knockout; LDLR, LDL receptor; LY465608, 2-[4-[2-(2-biphenyl-4-yl-5-methyl-oxazol-4-yl)-ethoxy]-phenoxy]-2-methyl-propionic acid; MMP 9, matrix metalloprotease 9; NF- $\kappa$ B, nuclear factor  $\kappa$ B; PPAR, peroxisome proliferator-activated receptor; SR-BI, scavenger receptor class B, type I; TNF, tumor necrosis factor.

through the administration of rexinoids or a PPAR $\alpha,\gamma$  coagonist reduced lesion development in the apoE KO mouse (32) suggest the utility of this approach. Separate studies with the PPAR $\gamma$  agonist troglitazone, rosiglitazone, or GW7845 also reported reductions in lesional areas in both apoE and LDL receptor KO mice as well as increases in CD36 and lipoprotein lipase message (33–35).

LY465608 (2-[4-[2-(2-biphenyl-4-yl-5-methyl-oxazol-4-yl)-ethoxy]-phenoxy]-2-methyl-propionic acid) represents a new class of PPAR $\alpha,\gamma$  coagonists in which the pharmacophores of known PPAR $\gamma$  and PPAR $\alpha$  selective agents were combined into a single compound. IC<sub>50</sub> values for human PPAR $\alpha,\gamma$  of 174 and 548 nM, respectively, were determined (36). Cotransfection studies demonstrated that this compound is an effective agonist against both receptors as well as the mouse PPAR $\alpha$ . The specificity of this compound was also determined in transfection studies where it was demonstrated that the  $K_i$  for retinoid and rexinoid receptors, glucocorticoid, and thyroid receptors was greater than 10  $\mu$ M. Finally, this compound has been demonstrated to lower both plasma glucose and TG levels in a diabetic mouse model at 30 mg/kg (36). These results as well as the nuclear receptor specificity of LY465608 suggested a potential therapeutic role for this PPAR coagonist in reducing atherosclerosis in the apoE KO mouse.

The present study was initiated to evaluate the impact of LY465608 on macrophage effector functions *in vitro* systematically, to evaluate its effects on macrophage responses to IFN $\gamma$  *ex vivo*, and to determine whether there would be any beneficial effect on lesion development and/or progression. LY465608 was demonstrated both *in vitro* and *ex vivo* to inhibit the ability of IFN $\gamma$  to induce both iNOS and CD11a expression. Furthermore, when administered at the initiation of exposure of apoE KO mice to an atherogenic diet, LY465608 significantly reduced the extent of atherosclerotic lesion development. Finally, similar studies were performed on older apoE KO mice with established lesions to determine whether a similar beneficial effect could be observed in lesional surface area. These latter results, however, failed to achieve statistical significance. Collectively, the results provide further evidence for the therapeutic value of a PPAR coagonist in the treatment of atherosclerosis in a model in which a vascular effect is observed in the absence of a significant beneficial impact on serum lipoprotein profiles.

## MATERIALS AND METHODS

**Macrophage cultures and reagents.** Peritoneal macrophages were obtained from thymoglobulin-primed apoE KO mice (C57BL/6Tac-Apo<sup>tm1Unc</sup>N11, male; Taconic Laboratories, Germantown, NY) and maintained in culture in RPMI 1640 supplemented with 2% FCS (Hyclone Laboratories, Logan, UT). Macrophages were activated with the designated concentrations of recombinant murine IFN $\gamma$  (BioSource International, Camarillo, CA) for 48 h, and supernatants were quantified for nitrites and cells processed for flow cytometry. LY465608 at final concentrations between 1 nM and 10  $\mu$ M

were added to the macrophage cultures at the time of IFN $\gamma$  addition.

**Flow cytometry and nitric oxide measurements.** Following 48 h of stimulation with IFN $\gamma$ , macrophage cultures were stained with a phycoerythrin-conjugated antibody against CD11a (integrin  $\alpha$ L) or fluorescein isothiocyanate (FITC)-conjugated antibody against CD11b (integrin  $\alpha$ M) (Pharmin-gen, San Diego, CA). All flow cytometry experiments were evaluated on 10,000 individual cells gated for macrophages based on their forward and side light-scatter profiles. The mean fluorescence intensity was measured using a Becton Dickinson FacSort with Cellquest software (Becton Dickinson, San Jose, CA). Supernatants were quantified for nitric oxide levels using the Griess reaction as previously described (30). The optic density change at 10 min was measured at 550 nm and converted to micromoles of nitrites based on a sodium nitrite standard curve.

**Atherosclerosis model.** Male apoE KO mice were shifted to a high-fat diet (21% milkfat, 0.15% cholesterol; Harlan Teklad, Madison, WI) and were dosed orally by gavage with 10 mg/kg of LY465608 [prepared in 1% carboxymethylcellulose (CMC) plus 1% Tween 80] daily. Mice were treated with LY465608, 10 mg/kg/d, for 18 wk starting at 8 wk of age when they were shifted to a high-fat diet. At the end of the 18 wk of treatment both vehicle and LY465608 mice were evaluated for lipoprotein profiles and atherosclerotic lesions. In studies designed to investigate the effect of LY465608 on established lesions, mice were maintained on the high-fat diet for 16 wk and then treated for an additional 12 wk with 10 mg/kg LY465608 prior to sacrifice. The control animals in all experiments were dosed with the CMC vehicle. All animal studies were in compliance with institutional guidelines.

**Lesion analysis.** At sacrifice, animals were prepared for en face aorta evaluation by cutting the aorta below the bifurcation in the lower abdomen as previously described (37). Briefly, the aortas were perfused with PBS, cleaned of external fat, opened, flattened on a microscope slide, and covered with a coverglass. All samples were fixed in 4% formalin and kept at 4°C in humidified chambers until imaging. Samples were visualized using a Microtek ScanMaker 9600 XL (Microtek Lab, Inc., Redondo Beach, CA) and Adobe Photoshop LE (Adobe Systems, San Jose, CA). The images were analyzed using a custom-written macro (Mike Esterman, Jeff Hanson, Lilly Research Labs) in Image Pro Plus (Media Cybernetics, L.P., Silver Spring, MD) that uses the threshold tool to select lesion sites based on image intensity contrasted to the normal translucent arterial wall. Lesion area and total aortic area were expressed in square mm. Approximately 45 mm square of total aortic surface was evaluated per aorta for lesion quantification.

**Serum cholesterol and lipoprotein analysis.** Total serum cholesterol levels were measured using the Cholesterol CII kit from Wako Pure Chemicals (Richmond, VA). Sera from each group at the designated times were pooled, and 25–100  $\mu$ L aliquots were resolved by fast protein liquid chromatography (FPLC; Pharmacia, Bromma, Sweden) using tandem-linked Superose

6 columns as previously described (38). Total cholesterol was quantified enzymatically (Wako Chemicals USA, Richmond, VA) from 100- $\mu$ L aliquots of the FPLC fractions. The relative amount of cholesterol within each peak was determined by area quantification under the curves using the appropriate baseline modifications from the FPLC cholesterol tracings. Serum TG levels were measured by enzymatic assay (Sigma Chemicals, St. Louis, MO).

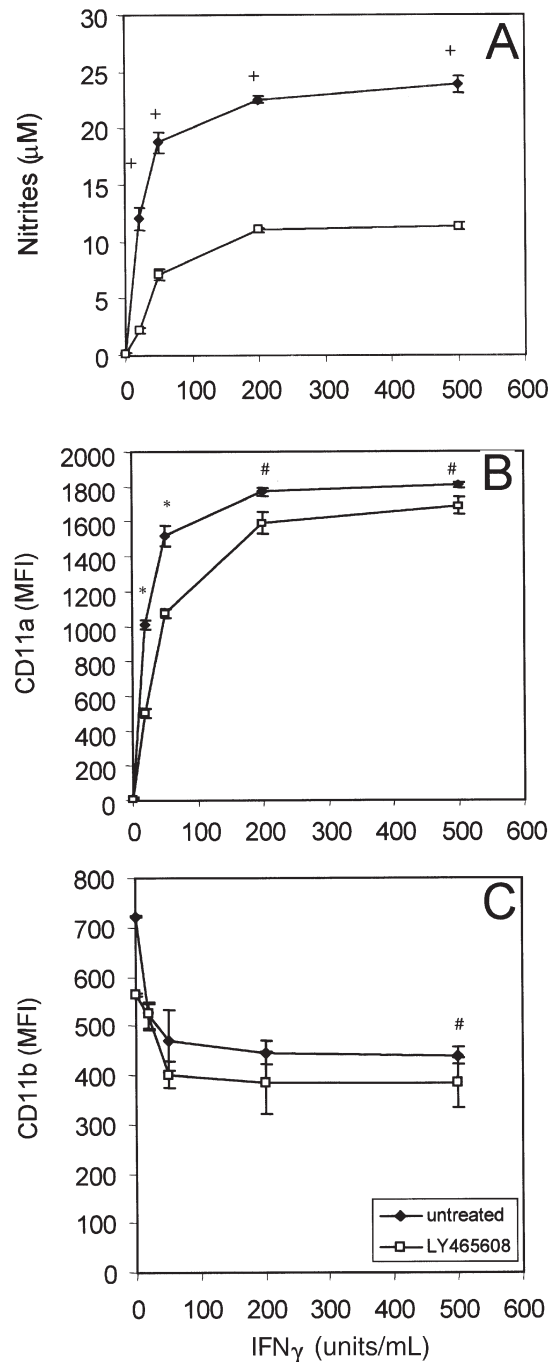
**Statistics.** Statistical analysis was performed by unpaired (two-tailed) *t*-test. Values are reported as means  $\pm$  SD. The 95% confidence limit was taken as significant ( $P < 0.05$ ). Additional statistical analysis was by a Dunnett's multiple comparisons test. Analysis of the lesion area data was performed using chi square and Tukey's biweight function robust method as well as by a Mann-Whitney U test, a nonparametric test.

## RESULTS

Activation of primary peritoneal macrophages with IFN $\gamma$  results in an increase in macrophage effector functions including the generation of nitric oxide through the induction of iNOS and the upregulation of the  $\beta$  2 integrin CD11a. Consistent with previous studies using the less-specific PPAR $\gamma$  agonist 15-deoxy- $\Delta^{12,14}$ -prostaglandin J<sub>2</sub> (30), 100 nM LY465608 resulted in a significant reduction both in nitric oxide production (Fig. 1A) and in CD11a induction (Fig. 1B) at all concentrations of IFN $\gamma$  used for macrophage activation. In contrast, CD11b, which is already expressed on the macrophage surface, was only significantly modulated by LY465608 at the highest IFN $\gamma$  concentration (Fig. 1C). The effects of the coagonist were concentration dependent, with significant effects apparent at 100 nM for both iNOS activity (Fig. 2A) and CD11a induction without any effect on CD11b expression until the highest concentration of 10  $\mu$ M (Fig. 2B). These results suggested that a PPAR $\alpha,\gamma$  coagonist was able to mitigate the macrophage effector functions induced by IFN $\gamma$ .

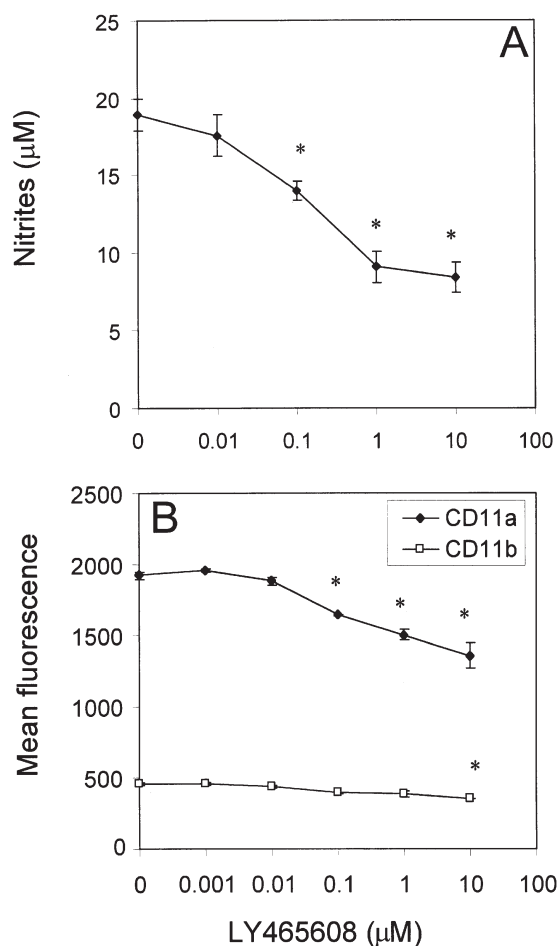
To determine whether a similar impact on macrophage effector functions could be demonstrated *in vivo*, apoE KO mice on standard laboratory chow were dosed at 10 mg/kg orally with LY465608 for up to 10 d. At day 10, elicited macrophages were harvested and stimulated *in vitro* with varying concentrations of IFN $\gamma$  for an additional 48 h. In comparison with the vehicle group, elicited macrophages from LY465608-treated mice showed a reduced induction of CD11a at both optimal (500 units/mL) and suboptimal (50 units/mL) concentrations of IFN $\gamma$  (Fig. 3A), and at optimal IFN $\gamma$  concentrations, they showed an approximate 50% reduction in nitric oxide formation (Fig. 3B). There was also, in the LY465608-treated animals, an overall increase in total serum cholesterol; in the control cholesterol was  $412 \pm 89$  vs. coagonist  $591 \pm 186$  mg/dL. This increase in the coagonist group was statistically significant by a two-tailed unpaired *t*-test ( $P < 0.03$ ).

The demonstration *ex vivo* that LY465608 was able to modulate IFN $\gamma$ -mediated macrophage effector functions



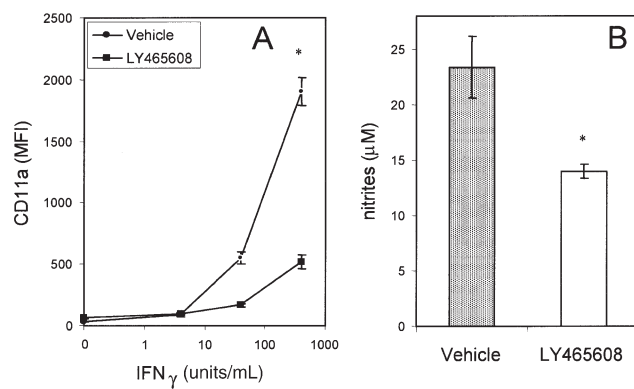
**FIG. 1.** Effects of LY465608 (2-[4-[2-(2-biphenyl-4-yl-5-methyl-oxazol-4-yl)-ethoxy]-phenoxy]-2-methyl-propionic acid) on interferon  $\gamma$  (IFN $\gamma$ )-mediated induction of nitric oxide and CD11a in murine peritoneal macrophages. Macrophages from apoE KO mice were treated *in vitro* in triplicate, with 0–500 units/mL IFN $\gamma$  with or without 100 nM LY465608 for 40–60 h. Cell supernatants were assayed for nitrites (A), and cells for the membrane integrins CD11a (B) and CD11b (C) by flow cytometry measuring the mean fluorescence intensity (MFI). Brackets represent the standard deviation of the mean from triplicate cultures. The difference between the untreated and LY465608-treated macrophages was significant by a two-tailed unpaired Student's *t* test at  $P < 0.05$  (#),  $P < 0.01$  (\*), or  $P < 0.001$  (+). A standard two-way ANOVA was also performed, followed by a Bonferroni adjusted multiple comparison of treated vs. untreated at each IFN $\gamma$  concentration. Significance was at the  $P < 0.001$  (+,\*) or  $P < 0.05$  (#) levels.





**FIG. 2.** LY465608 in a concentration-dependent manner inhibited nitric oxide and CD11a induction by IFN $\gamma$ . Triplicate cultures of macrophages were treated with 1 nM to 10  $\mu$ M LY465608 with 200 units/mL IFN $\gamma$ . After 48 h incubation, supernatants were assayed for nitrites (A), and cells were evaluated for expression of CD11a and CD11b (B). \*Difference from the control was significant by a two-tailed unpaired Student's *t*-test ( $P < 0.01$ ). A one-way ANOVA analysis was also performed, followed by a Dunnett's multiple comparison of each concentration of LY465608 compared to vehicle. Significance was also at the  $P < 0.01$  level. For abbreviations see Figure 1.

suggested it could have a favorable impact on atherosclerotic disease progression in the apoE KO mouse. Accordingly, mice were treated with LY465608, 10 mg/kg/d, for 18 wk starting at 8 wk of age, when they were shifted to a high-fat diet. At the end of the 18 wk of treatment, both vehicle and LY465608 mice were evaluated for cholesterol and lipoprotein profiles, and quantitation of aortic lesions was performed on the en face preparations. As demonstrated (Fig. 4A), LY465608 treatment reduced the rate of weight gain compared to the vehicle group. This decrease in weight gain was not due to a reduction in food consumption, which remained relatively constant in both groups through the duration of the study (approximately 25 g/mouse/wk). Interestingly, the LY465608-treated animals had a statistically significant ( $P < 0.01$ ) increase in serum cholesterol relative to the vehicle group at sacrifice ( $996 \pm 217$  vs.  $808 \pm 208$  mg/dL) which

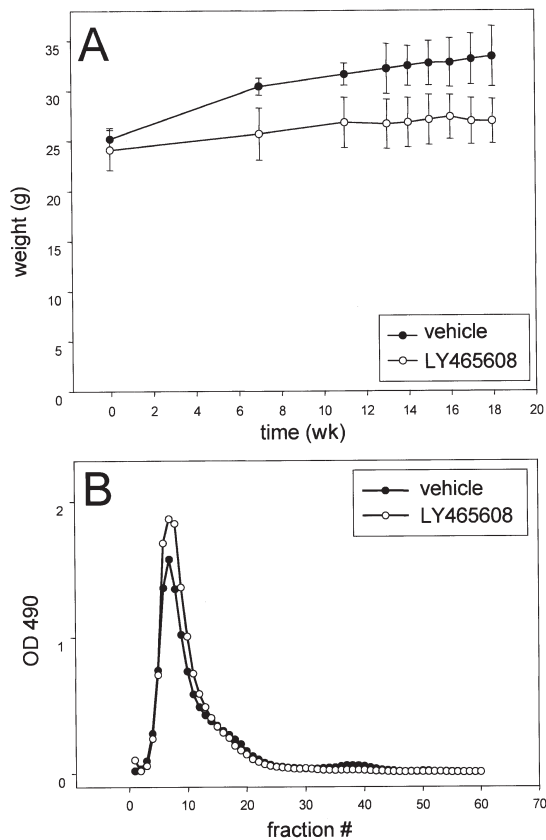


**FIG. 3.** Ex vivo effects of LY465608 on murine peritoneal macrophages. ApoE KO mice were dosed orally for 10 d with LY465608 or vehicle alone; and elicited peritoneal macrophages were collected, plated in 24-well plates, and evaluated for IFN $\gamma$ -induced CD11a expression (A) and nitric oxide production (B). CD11a expression was measured following induction of macrophages with varying concentrations of IFN $\gamma$  (5, 50, and 500 units/mL) and for nitric oxide production at 500 units/mL of IFN $\gamma$ . Macrophages were not exposed to exogenous LY465608 during the 48–72 h *in vitro* phase of the experiment. Cells from three animals for each treatment were pooled before plating. Representative experiment of five; brackets indicate the SD of the mean. \*Difference from the control was significant by a two-tailed unpaired Student's *t*-test ( $P < 0.01$ ). For abbreviations see Figures 1 and 2.

was evident in the VLDL peak of the lipoprotein profile (Fig. 4B). Serum TG were reduced in the LY465608 group ( $521 \pm 191$  vs.  $591 \pm 217$  mg/dL); however, this reduction was not statistically significant.

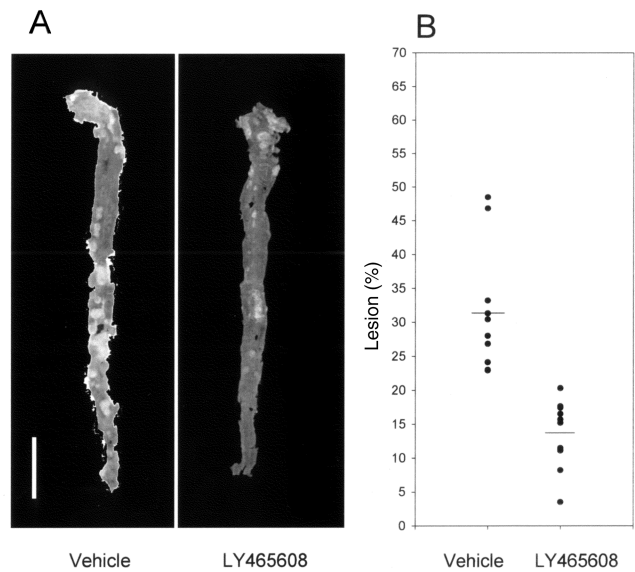
Although there were no significant reductions in the VLDL or LDL lipoproteins, and in fact there was a consistent increase in the former, there were significant reductions in aortic lesions in the LY465608-treated animals. En face evaluation of the lesion distribution revealed that the atherosclerotic lesions were primarily localized to the aortic arch and the surfaces around the bifurcations. Representative aortas en face (Fig. 5A) clearly demonstrate a decrease in the lesion surface area in the LY465608-treated animals that was statistically significant and apparent when the lesion distribution for each animal was quantified (Fig. 5B). The mean lesion area in the vehicle group was  $31.5 \pm 9.2$  vs.  $13.5 \pm 4.9\%$ , and this difference was significant ( $P < 0.0001$ ). Furthermore, the vehicle group had 8 of 9 animals with  $>25\%$  lesion area, whereas the LY465608 group had 0 of 10 animals with greater than 25% of the surface area containing lesions. These results demonstrate a significant reduction in lesion progression when apoE KO mice were treated with LY465608 at the time that they were shifted to the high-fat atherogenic diet.

To determine whether the PPAR coagonist LY465608 could have a similar effect in apoE KO mice with established lesions, a final series of experiments was performed in which mice were allowed to consume the high-fat diet for 16 wk. Following 16 wk on diet, mice were randomized to receive either LY465608 at 10 mg/kg or vehicle and were continued on diet and treatments for an additional 12 wk prior to



**FIG. 4.** Effect of LY465608 on weight gain and serum cholesterol profile. ApoE KO mice, 10 per group, were placed on “western” high-fat diets and dosed with LY465608 or the vehicle for 18 wk. Body weights and food consumption were measured weekly. Body weights (A) and total serum cholesterol fast protein liquid chromatography profile (B) were determined on pooled serum samples at the termination of the study. Brackets represent the SD of the mean. The difference in weight between the vehicle- and LY465608-treated mice was significant by a two-tailed unpaired Student’s *t*-test ( $P < 0.01$ ) by 6 wk treatment and remained so through the remainder of the study. The changes in weight were also analyzed by a repeated measures ANOVA, and the LY465608 group was compared to vehicle at each week using a Bonferroni adjusted multiple comparison test. By this analysis significance after week 0 was  $P < 0.0001$ . OD, optical density; for other abbreviations see Figure 1.

sacrifice. As demonstrated (Fig. 6A), apoE KO mice treated with the PPAR coagonist demonstrated a significant reduction in weight, which was apparent by 2 wk. As in the previous study, this reduction in weight gain was not due to a decrease in food consumption. Furthermore, serum cholesterol levels between the two groups were indistinguishable ( $1517 \pm 503$  vehicle and  $1518 \pm 590$  mg/dL for LY465608) as were the lipoprotein profiles, which consisted primarily of a VLDL fraction with an LDL shoulder (data not shown). There was, however, a significant increase in serum TG in the LY465608 animals  $884 \pm 442$  vs.  $418 \pm 130$  mg/dL ( $P < 0.003$ ). Quantification of lesion surface area revealed that 11 of 15 animals treated with LY465608 had less than 25% lesion area compared to the vehicle group with 6 of 15. The chi-squared test for the significance of this change in ratio, however, did not achieve statistical significance ( $P < 0.065$ ). Although there

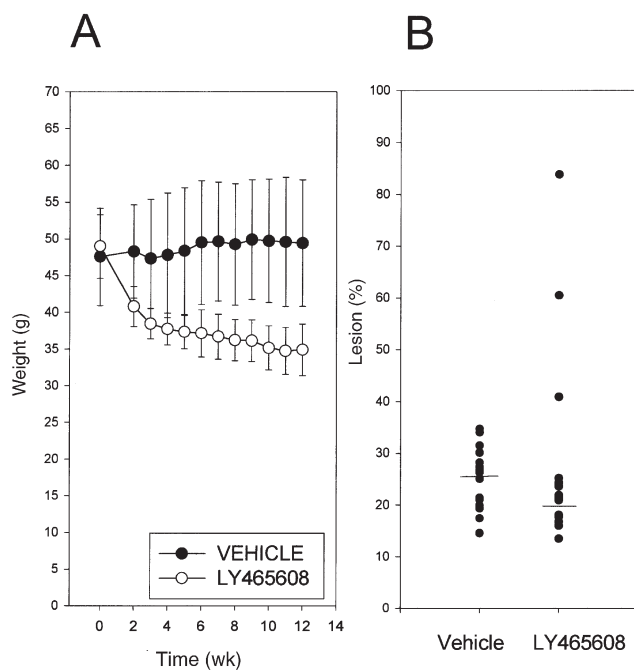


**FIG. 5.** Effect of LY465608 on aortic lesion formation in apoE KO mice on “western” diet. Mice at 8 wk of age were placed on a high-fat diet and randomized to vehicle or 10 mg/kg LY465608 groups. After 18 additional weeks on the diet the animals were sacrificed, and the aortas were dissected and placed on microscope slides. Representative en face images of the aorta from control and LY465608-treated aortas (A) and the percentage of the aortic surface area covered with lesions are presented for each animal ( $n = 10$  per group) (B). Note reduction in the lesion surface area from the LY465608-treated animals. This difference was significant by a two-tailed unpaired Student’s *t*-test ( $P < 0.0001$ ). Scale bar represents 5 millimeters.

appeared to be a nonsignificant reduction in lesion area in this study on established lesions, there was one animal in the LY465608 group that had greater than 80% of the aortic surface area covered with lesion. Whereas this animal did have other problems detected at autopsy, i.e., fluid in the lungs, there was no apparent reason to treat this animal as an outlier and hence it was included in the data set. These results, however, do suggest that intervention fairly late in the process of lesion development can in fact reduce further increases in lesion accumulation through effects independent of serum cholesterol levels or lipoprotein profiles.

## DISCUSSION

PPAR $\alpha$ , $\gamma$  agonists as well as coagonists are clearly demonstrating additional biologic responses beyond HDL elevation and insulin sensitization that would suggest a broader therapeutic role in the management of chronic inflammatory diseases (39–42). To explore these potential roles further, the PPAR $\alpha$ , $\gamma$  coagonist LY465608 was evaluated in a model of atherosclerosis where HDL represents a minor component of the lipoprotein profile and where insulin sensitivity is not recognized as part of the disease process. The apoE KO model represents such a model and is characterized by extremely high serum cholesterol (>1000 mg/dL when placed on a high-fat diet), primarily carried on VLDL and remnant particles, and significant lesions throughout the aortas (43).



**FIG. 6.** Therapeutic intervention with LY465608 on mice after 16 wk on a high-fat diet. ApoE KO mice were placed on the “western” diet for 16 wk and then randomized ( $n = 15$  per group) to receive LY465608 orally at 10 mg/kg or vehicle alone for an additional 12 wk. The high-fat diet was continued during this treatment phase. Weight (A) and food consumption were monitored weekly. At the termination of the experiment, the aortic surface area covered with atherosclerotic lesions was quantified and the distribution was presented for each animal (B). The difference in weight between the two groups was significant by a two-tailed unpaired Student’s  $t$ -test ( $P < 0.01$ ) as early as 2 wk on LY465608. The changes in weight were also analyzed by a repeated measures ANOVA, and the LY465608 group was compared to vehicle at each week using a Bonferroni adjusted multiple comparison test. By this analysis, significance after week 0 was  $P < 0.01$ . (B) Robust mean estimates are presented (horizontal bars) and were 26.3% in the vehicle and 21.6% for the LY465608 group. The chi-squared test for the significance of the difference in lesion surface area did not achieve statistical significance ( $P < 0.065$ ).

The present study was designed to determine whether LY465608 treatment *in vitro* would mitigate the macrophage response to IFN $\gamma$  using both iNOS and CD11a induction as indicators of macrophage activation. These two parameters can be linked to the pathology associated within the atherosclerotic lesion by inducing oxidant stress with the former and by promoting macrophage adherence and migration through the  $\beta 2$  integrin pathway with the latter (44,45). The results of this study demonstrated a direct inhibitory effect of this coagonist on these parameters of macrophage activation. Furthermore, similar effects were also apparent *ex vivo* when apoE KO mice were pretreated with LY465608 for 10 d prior to harvesting elicited macrophages and subjecting them to *in vitro* stimulation with IFN $\gamma$ . In additional studies, 4–5 d of oral treatment with LY465608 exhibited similar *ex vivo* results (data not shown).

The ability of the coagonist to influence these effector functions suggested that LY465608 should favorably reduce

atherosclerotic lesion progression, and, in fact, lesional surface area was reduced 2.5-fold in the experimental group. The extent of lesion reduction in the apoE KO mouse compares favorably with similar studies recently reported for the PPAR $\gamma$  agonist troglitazone (35), with troglitazone, rosiglitazone, or GW7845 in the LDL receptor KO (33, 34), and with a retinoid X receptor agonist LG100364 (32). This latter study reported a lesser effect on lesion reduction with the PPAR coagonist GW2331, and still lesser efficacy with the PPAR $\gamma$  agonist rosiglitazone.

Although the results in reducing total lesional area were similar across these studies, some differences were observed. In the present study we detected a reduction in weight gain with chronic administration without an impact on food consumption. These effects were consistent with PPAR $\alpha$  activity of the coagonist, as PPAR $\alpha$  agonists have been reported to reduce body weight increase in other rodent models (46,47). It is, however, noteworthy that in one study troglitazone did reduce total body weight in the LDL receptor (LDLR) KO mice fed a high-fat diet (34). Chen *et al.* (35) reported a doubling in HDL cholesterol but no effect on total cholesterol or TG, whereas Claudel *et al.* (32) reported increases in total serum cholesterol and TG, primarily in the VLDL and remnant peak. In the present study we did not detect any increase in HDL cholesterol but did observe a significant increase in total cholesterol, through the VLDL and remnant peak, but no increase in serum TG as seen in the second study which had been designed to evaluate the effect of LY465608 on lesion development.

Finally, to reflect the clinical situation more closely, we designed studies to determine whether LY465608 would have an effect on established lesions rather than initiating treatment at the time of exposure to the atherogenic diet. Accordingly, apoE KO mice were maintained on the atherogenic diet for 16 wk prior to initiating treatment with LY465608 for an additional 12 wk. These results, although failing to achieve statistical significance, did suggest reduced lesional surface areas in the LY465608 group when compared to the controls. This represents, to the best of our knowledge, the first study in which intervention with a potential anti-atherosclerotic compound was evaluated in apoE KO mice with established lesions. Whereas the precise mechanism(s) by which PPAR coagonists may limit the development of new lesions and affect established lesional mass remains unclear, it is likely to involve the inhibition of both NF- $\kappa$ B and AP-1 dependent transcriptional pathways (20,21). PPAR expression within atherosclerotic lesions in monocytes, macrophages, foam cells, and smooth muscle and endothelial cells provides a pathway for limiting lesion progression (45). PPAR $\alpha$  agonists, for example, reportedly induce apoptosis of TNF-activated macrophages and limit monocyte recruitment in early lesions by inhibiting TNF induction of vascular cell adhesion molecule expression, presumably by serving as negative regulators of NF- $\kappa$ B (48,49). One such mechanism of inhibiting NF- $\kappa$ B activation is through the induction of I $\kappa$ B $\alpha$  by PPAR $\alpha$  agonists and thus keeping the NF- $\kappa$ B complex inactive within



the cytoplasm (21). However, whereas many of the NF- $\kappa$ B and AP-1 dependent regulated genes are thought to be proinflammatory, such as MMP-9, IL-6, and TNF, there is some evidence that PPAR agonists may have confounding effects on lesion development. Lee *et al.* (50), for example, reported that the PPAR $\alpha$  agonist Wy14643 stimulated the synthesis of IL-8 and monocyte chemoattractant protein-1 in human aortic endothelial cells, whereas the PPAR $\gamma$  agonist troglitazone suppressed production of these chemokines. Furthermore, although PPAR agonists have been reported to upregulate CD36 and consequently the uptake of oxidized LDL (28,29), further studies have implicated a PPAR $\gamma$  pathway for promoting cholesterol efflux through the increase in ABC-1 expression *via* induction (26). These authors further demonstrated that PPAR $\gamma$ -null bone marrow cells transplanted into LDLR KO mice resulted in significant increases in atherosclerotic lesion mass. Collectively, these studies suggest that PPAR coagonists should favorably affect atherosclerotic disease through anti-inflammatory processes as well as by stimulating reverse cholesterol transport.

The results of the *in vitro* and *in vivo* studies clearly demonstrate that the PPAR coagonist LY465608 can favorably affect atherosclerotic disease progression through processes unrelated to changes in serum lipoprotein profiles. These data demonstrate a clear role and direction for the next generation of agents to treat atherosclerosis, namely, targeting the vascular component.

## ACKNOWLEDGMENTS

The authors wish to acknowledge Dr. Mary K. Peters for providing LY465608, and Mark Farman for statistical support. The technical assistance of Pat Forlor, Jack Cochran, Phyllis A. Cross, Brian K. McKenney, Martin S. Cramer, Richard L. Tielking, Courtney Burch, Kat Andrzejewski, and Renee L. Grubbs is also gratefully acknowledged.

## REFERENCES

- Ross, R. (1999) Atherosclerosis—An Inflammatory Disease, *N. Engl. J. Med.* 340, 115–126.
- Berliner, J.Z., Navab, M., Fogelman, A.M., Frank, J.S., Deme, L.L., Edwards, P.A., Watson, A.D., and Lusis, A.J. (1995) Atherosclerosis: Basic Mechanisms, Oxidation, Inflammation, and Genetics, *Circulation* 91, 2488–2496.
- Libby, P., Geng, Y., Aikawa, M., Schoenbeck, U., Mach, F., Clinton, S., Sukhova, G., and Lee, R. (1996) Macrophages and Atherosclerotic Plaque Stability, *Curr. Opin. Lipidol.* 7, 330–335.
- Geng, Y., Holm, J., Nygren, S., Bruzelius, M., Stemme, S., and Hansson, G.K. (1995) Expression of Macrophage Scavenger Receptor in Atherosclerosis: Relationship Between Scavenger Receptor Isoforms and the T Cell Cytokine, Interferon- $\gamma$ , *Arterioscler. Thromb. Vasc. Biol.* 15, 1995–2002.
- Erren, M., Reinecke, H., Junker, R., Fobker, M., Schulte, H., Schurek, J.O., Kropf, J., Kerber, S., Brethardt, G., Assman, G., and Cullen, P. (1999) Systemic Inflammatory Parameters in Patients with Atherosclerosis of the Coronary and Peripheral Arteries, *Arterioscler. Thromb. Vasc. Biol.* 19, 2355–2363.
- Hansson, G.K. (1997) Cell-Mediated Immunity in Atherosclerosis, *Curr. Opin. Lipidol.* 8, 301–311.
- Brand, K., Mackman, N., and Curtiss, L.K. (1993) Interferon- $\gamma$  Inhibits Macrophage Apolipoprotein E Production by Posttranslational Mechanisms, *J. Clin. Invest.* 91, 2031–2039.
- Zuckerman, S.H., Evans, G.F., and O'Neal, L. (1992) Cytokine Regulation of Macrophage Apo E Secretion: Opposing Effects of GM-CSF and TGF- $\beta$ , *Atherosclerosis* 96, 203–214.
- Panousis, C.G., and Zuckerman, S.H. (2000) Interferon-gamma Induces Downregulation of Tangier Disease Gene (ATP-binding-cassette transporter 1) in Macrophage-Derived Foam Cells, *Arterioscler. Thromb. Vasc. Biol.* 20, 1565–1571.
- Panousis, C.G., and Zuckerman, S.H. (2000) Regulation of Cholesterol Distribution in Macrophage-Derived Foam Cells by Gamma Interferon (IFN- $\gamma$ ), *J. Lipid Res.* 41, 75–83.
- Whitman, S.C., Ravisankar, P., Elam, H., and Daugherty, A. (2000) Exogenous Interferon-gamma Enhances Atherosclerosis in Apolipoprotein E-/- Mice, *Am. J. Pathol.* 157, 1819–1824.
- Boehm, U., Clamp, T., Groot, M., and Howard, J.C. (1997) Cellular Responses to Interferon- $\gamma$ , *Annu. Rev. Immunol.* 15, 749–795.
- Gupta, S., Pablo, A.M., Jiang, X.C., Wang, N., Tall, A.R., and Schindler, C. (1997) IFN- $\gamma$  Potentiates Atherosclerosis in ApoE Knockout Mice, *J. Clin. Invest.* 91, 1219–1224.
- Mangelsdorf, D.J., Thummel, C., Beato, M., Herrlich, P., Schütz, G., Umesono, K., Blumberg, B., Kastner, P., Mark, M., Chambon, P., and Evans, R.M. (1995) The Nuclear Receptor Superfamily: The Second Decade, *Cell* 83, 835–839.
- Chambon, P. (1995) The Molecular and Genetic Dissection of the Retinoid Signaling Pathway, *Recent Prog. Horm. Res.* 50, 317–332.
- Gearing, K.L., Gottlicher, M., Teboul, M., Widmark, E., and Gustafsson, J.A. (1993) Interaction of the Peroxisome-Proliferator-Activated Receptor and Retinoid X Receptor, *Proc. Natl. Acad. Sci. USA* 90, 1440–1444.
- Ricote, M., Huang, J.T., Welch, J.S., and Glass, C.K. (1999) The Peroxisome Proliferator-Activated Receptor  $\gamma$  (PPAR $\gamma$ ) as a Regulator of Monocyte/Macrophage Function, *J. Leuk. Biol.* 66, 733–739.
- Yang, X.Y., Wang, L.H., Chen, T., Hodge, D.R., Resau, J.H., DaSilva, L., and Farrar, W.L. (2000) Activation of Human T Lymphocytes Is Inhibited by Peroxisome Proliferator-Activated Receptor  $\gamma$  (PPAR $\gamma$ ) Agonists, *J. Biol. Chem.* 275, 4541–4544.
- Shu, H., Wong, B., Zhou, G., Li, Y., Berger, J., Woods, J.W., Wright, S., and Cai, T-Q. (2000) Activation of PPAR $\alpha$  or  $\gamma$  Reduces Secretion of Matrix Metalloproteinase 9 but Not Interleukin 8 from Human Monocytic THP-1, *Biochem. Biophys. Res. Comm.* 267, 345–349.
- Delerive, P., DeBosscher, K., Besnard, S., Berghe, W.V., Peters, J.M., Gonzalez, F.J., Fruchart, J.-C., Tedgui, A., Haegeman, G., and Staels, B. (1999) Peroxisome Proliferator-Activated Receptor  $\alpha$  Negatively Regulates the Vascular Inflammatory Gene Response by Negative Cross-Talk with Transcription Factors NF- $\kappa$ B and AP-1, *J. Biol. Chem.* 274, 32048–32054.
- Delerive, P., Gervois, P., Fruchart, J.-C., and Staels, B. (2000) Induction of I $\kappa$ B $\alpha$  Expression as a Mechanism Contributing to the Anti-inflammatory Activities of Peroxisome Proliferator-Activated Receptor- $\alpha$  Activators, *J. Biol. Chem.* 275, 36703–36707.
- Ricote, M., Li, A.C., Willson, T.M., Kelly, C.J., and Glass, C.K. (1998) The Peroxisome Proliferator-Activated Receptor- $\gamma$  Is a Negative Regulator of Macrophage Activation, *Nature* 391, 79–82.
- Colville-Nash, P.R., Qureshi, S.S., Willis, D., and Willoughby, D.A. (1998) Inhibition of Inducible Nitric Oxide Synthase by Peroxisome Proliferator-Activated Receptor Agonists: Correlation with Induction of Heme Oxygenase 1, *J. Immunol.* 161, 978–984.
- Jiang, C., Ting, A.T., and Seed, B. (1998) PPAR- $\gamma$  Agonists Inhibit Production of Monocyte Inflammatory Cytokines, *Nature* 391, 82–86.



25. Marx, N., Sukhova, G., Murphy, C., Libby, P., and Plutzky, J. (1998) Macrophages in Human Atheroma Contain PPAR $\gamma$ . Differentiation-Dependent Peroxisomal Proliferator-Activated Receptor  $\gamma$  (PPAR $\gamma$ ) Expression and Reduction of MMP-9 Activity Through PPAR $\gamma$  Activation in Mononuclear Phagocytes *in vitro*, *Am. J. Pathol.* 153, 17–23.
26. Chawla, A., Boisvert, W.A., Lee, C.-H., Laffitte, B.A., Barak, Y., Joseph, S.B., Liao, D., Nagy, L., Edwards, P.A., Curtiss, L.K., *et al.* (2001) A PPAR $\gamma$ -LXR-ABCA1 Pathway in Macrophages Is Involved in Cholesterol Efflux and Atherogenesis, *Molecular Cell* 7, 161–171.
27. Chinetti, G., Gbaguidi, F.G., Griglio, S., Mallat, Z., Antonucci, M., Poulain, P., Chapman, J., Fruchart, J.-C., Tedgui, A., Najib-Fruichart, J., and Staels, B. (2000) CLA-1/SR-BI Is Expressed in Atherosclerotic Lesion Macrophages and Regulated by Activators of Peroxisome Proliferator-Activated Receptors, *Circulation* 101, 2411–2417.
28. Tontonoz, P., Nagy, L., Alvarez, J.G.A., Thomazy, V.A., and Evans, R.M. (1998) PPAR $\gamma$  Promotes Monocyte/Macrophage Differentiation and Uptake of Oxidized LDL, *Cell* 93, 241–252.
29. Nagy, L., Tontonoz, P., Alvarez, J.G.A., Chen, H., and Evans, R.M. (1998) Oxidized LDL Regulates Macrophage Gene Expression Through Ligand Activation of PPAR $\gamma$ , *Cell* 93, 229–240.
30. Zuckerman, S.H., Panousis, C.G., Mizrahi, J., and Evans, G.F. (2000) The Effect of  $\gamma$ -Interferon to Inhibit Macrophage-High Density Lipoprotein Interactions Is Reversed by 15-Deoxy- $\Delta^{12,14}$ -Prostaglandin J<sub>2</sub>, *Lipids* 35, 1239–1247.
31. Delerive, P., Martin-Nizard, F., Chinetti, G., Trottein, F., Fruchart, J.-C., Duriez, P., and Staels, B. (1999) PPAR Activators Inhibit Thrombin Induced Endothelin-1 Production in Human Vascular Endothelial Cells by Inhibiting the AP-1 Signaling Pathway, *Circ. Res.* 85, 394–402.
32. Claudel, T., Leibowitz, M.D., Fievet, C., Tailleux, A., Wagner, B., Repa, J.J., Torpier, G., Lobaccaro, J.-M., Paterniti, J.R., Mangelsdorf, D.J., Heyman, R.A., and Auwerx, J. (2001) Reduction of Atherosclerosis in Apolipoprotein E Knockout Mice by Activation of the Retinoid X Receptor, *Proc. Natl. Acad. Sci. USA* 98, 2610–2615.
33. Li, A.C., Brown, K.K., Silvestre, M.J., Willson, T.M., Palinski, W., and Glass, C.K. (2000) Peroxisome Proliferator-Activated Receptor  $\gamma$  Ligands Inhibit Development of Atherosclerosis in LDL Receptor-Deficient Mice, *J. Clin. Invest.* 106, 523–531.
34. Collins, A.R., Meehan, W.P., Kintscher, U., Jackson, S., Wakino, S., Noh, G., Palinski, W., Hsueh, W.A., and Law, R.E. (2001) Troglitazone Inhibits Formation of Early Atherosclerotic Lesions in Diabetic and Nondiabetic Low Density Lipoprotein Receptor-Deficient Mice, *Arterioscler. Thromb. Vasc. Biol.* 21, 365–371.
35. Chen, Z., Ishibashi, S., Perrey, S., Osuga, J.-I., Gotoda, T., Kitamine, T., Tamura, Y., Okazaki, H., Yahagi, N., Iizuka, Y., *et al.* (2001) Troglitazone Inhibits Atherosclerosis in Apolipoprotein E-Knockout Mice. Pleiotropic Effects on CD36 Expression and HDL, *Arterioscler. Thromb. Vasc. Biol.* 21, 372–377.
36. Brooks, D.A., Etgen, G.J., Rito, C.J., Shuker, A.J., Dominianni, S.J., Warshawsky, A.M., Ardecky, R., Paterniti, J.R., Tyhonas, J., Karanewsky, D.S., *et al.* (2001) The Design and Synthesis of 2-Methyl-2-[4-[2-(5-methyl-2-aryloxazol-4-yl)ethoxy]phenoxy]propionic Acids: A New Class of PPAR $\alpha,\gamma$  Agonists, *J. Med. Chem.* 44, 2061–2064.
37. Zuckerman, S.H., Evans, G.F., Schelm, J.A., Eacho, P.I., and Sandusky, G. (1999) Estrogen-Mediated Increases in LDL Cholesterol and Foam Cell-Containing Lesions in Human ApoB100  $\times$  CETP Transgenic Mice, *Arterioscl., Thromb., Vasc. Biol.* 19, 1476–1483.
38. Evans, G.F., Bensch, W.R., Apelgren, L.D., Bailey, D., Kauffman, R.F., Bumol, T.F., and Zuckerman, S.H. (1994) Inhibition of Cholesteryl Ester Transfer Protein in Normocholesterolemic and Hypercholesterolemic Hamsters: Effects on HDL Subspecies, Quantity, and Apoprotein Distribution, *J. Lipid Res.* 35, 1634–1645.
39. Keller, H., Dreyer, C., Medin, J., Mahfoudi, A., Ozato, K., and Wahli, W. (1993) Fatty Acids and Retinoids Control Lipid Metabolism Through Activation of Peroxisome Proliferator-Activated Receptor-Retinoid X Receptor Heterodimers, *Proc. Natl. Acad. Sci. USA* 90, 2160–2164.
40. Forman, B.M., Chen, J., and Evans, R.M. (1997) Hypolipidemic Drugs, Polyunsaturated Fatty Acids, and Eicosanoids Are Ligands for Peroxisome Proliferator-Activated Receptors  $\alpha$  and  $\gamma$ , *Proc. Natl. Acad. Sci. USA* 94, 4318–4323.
41. Lehmann, J., Moore, L., Smith-Oliver, A., Wilkison, W., Willson, T., and Kliewer, S. (1995) An Antidiabetic Thiazolidinedione Is a High Affinity Ligand for Peroxisome Proliferator-Activated Receptor  $\gamma$ , *J. Biol. Chem.* 270, 12953–12956.
42. Schoonjans, K., Staels, B., and Auwerx, J. (1996) Role of the Peroxisome Proliferator-Activated Receptor in Mediating the Effects of Fibrates and Fatty Acids on Gene Expression, *J. Lipid Res.* 37, 907–925.
43. Smith, J.D., and Breslow, J.L. (1997) The Emergence of Mouse Models of Atherosclerosis and Their Relevance to Clinical Research, *J. Int. Med.* 242, 99–109.
44. Keane, J.F., Jr. (2000) Atherosclerosis: from Lesion Formation to Plaque Activation and Endothelial Dysfunction, *Mol. Aspects Med.* 21, 99–166.
45. Neve, B.P., Fruchart, J.-C., and Staels, B. (2000) Role of the Peroxisome Proliferator-Activated Receptor (PPAR) in Atherosclerosis, *Biochem. Pharm.* 60, 1245–1250.
46. Guerre-Millo, M., Gervois, P., Raspe, E., Madsen, L., Poulain, P., Derudas, B., Herbert, J.-M., Winegar, D.A., Willson, T.M., Fruchart, J.-C., *et al.* (2000) Peroxisome Proliferator-Activated Receptor  $\alpha$  Activators Improve Insulin Sensitivity and Reduce Adiposity, *J. Biol. Chem.* 275, 16638–16642.
47. Chaput, E., Saladin, R., Silvestre, M., and Edgar, A.D. (2000) Fenofibrate and Rosiglitazone Lower Serum Triglycerides with Opposing Effects on Body Weight, *Biochem. Biophys. Res. Commun.* 271, 445–450.
48. Staels, B., Koenig, W., Habib, A., Chinetti, G., Fruchart, J.-C., Najib, J., Maclouf, J., and Tedgui, A. (1998) Activation of Human Aortic Smooth-Muscle Cells Is Inhibited by PPAR $\alpha$  but Not PPAR $\gamma$  Activators, *Nature* 393, 790–793.
49. Chinetti, G., Griglio, S., Antonucci, M., Torra, I.P., Delerive, P., Majdt, Z., Fruchart, J.-C., Chapman, J., Najib, J., and Staels, B. (1998) Activation of Proliferator-Activated Receptors  $\alpha$  and  $\gamma$  Induces Apoptosis of Human Monocyte-Derived Macrophages, *J. Biol. Chem.* 273, 25573–25580.
50. Lee, H., Shi, W., Tontonoz, P., Wang, S., Subbanagounder, G., Hedrick, C.C., Hama, S., Borromeo, C., Evans, R.M., Berliner, J.A., and Nagy, L. (2000) Role for Peroxisome Proliferator-Activated Receptor  $\alpha$  in Oxidized Phospholipid-Induced Synthesis of Monocyte Chemotactic Protein-1 and Interleukin-8 by Endothelial Cells, *Circ. Res.* 87, 516–521.

[Received January 22, 2002, and in revised form March 29, 2002; revision accepted April 9, 2002]

# Targeted Disruption of Peroxisomal Proliferator-Activated Receptor $\beta$ ( $\delta$ ) Results in Distinct Gender Differences in Mouse Brain Phospholipid and Esterified FA Levels

Thad A. Rosenberger<sup>a,\*</sup>, Jonathan T. Hovda<sup>a</sup>, and Jeffrey M. Peters<sup>b</sup>

<sup>a</sup>Brain Physiology and Metabolism Section, National Institute on Aging, National Institutes of Health, Bethesda, Maryland 20892, and <sup>b</sup>Department of Veterinary Science and Center for Molecular Toxicology and Carcinogenesis, Pennsylvania State University, University Park, Pennsylvania 16802

**ABSTRACT:** The peroxisomal proliferator-activated receptor  $\beta$  ( $\delta$ ) (PPAR $\beta$ ) is a nuclear hormone receptor that is ubiquitously expressed and that regulates the transcription of genes involved in lipid metabolism. A homozygous PPAR $\beta$ -null mouse has been developed in which the ligand-binding domain of the PPAR $\beta$  receptor is disrupted. Analysis of brains from these animals shows that female null mice have 24 and 17% increases in plasmalogen ethanolamine and phosphatidylserine and a 9% decrease in the level of phosphatidylinositol when compared to controls. The phospholipid changes found in female null mice were associated with increased levels of esterified 18:1n-9, 20:1n-9, 20:4n-6, and 22:5n-3 FA in plasmalogen ethanolamine, 20:1n-9 in phosphatidylinositol, and 18:0, 18:1n-9, 18:3n-6, 20:1n-9, and 20:4n-6 in phosphatidylserine. Increased levels of esterified 18:1n-9, 18:2n-6, 18:3n-6, and 20:1n-9 were also found in the phosphatidylethanolamine fraction despite its cellular content remaining unchanged. Brain phospholipid content in male PPAR $\beta$ -null mice did not differ from controls, but increased levels of 20:1n-9 in the phosphatidylinositol and 18:1n-9 in the phosphatidylserine fractions were observed. No changes were found in the content of brain cholesterol, TAG, and FFA in either female or male PPAR $\beta$ -null mice. These data suggest that PPAR $\beta$  is involved in maintaining FA and phospholipid levels in adult female mouse brain and provide strong evidence that suggests a role for PPAR $\beta$  in brain peroxisomal acyl-CoA utilization.

Paper no. L8920 in *Lipids* 37, 495–500 (May 2002).

The peroxisome proliferator-activated receptors (PPAR) are regulatory transcriptional factors that constitute a subfamily of nuclear hormone receptors that are classified into three types:  $\alpha$ ,  $\beta$  (also called  $\delta$  or nuc 1), and  $\gamma$  (1). PPAR maintain lipid homeostasis by regulating the expression of enzymes involved in peroxisomal and mitochondrial  $\beta$ -oxidation, FA mobilization, and adipocyte differentiation in response to differential ligand activation and gene expression (1).

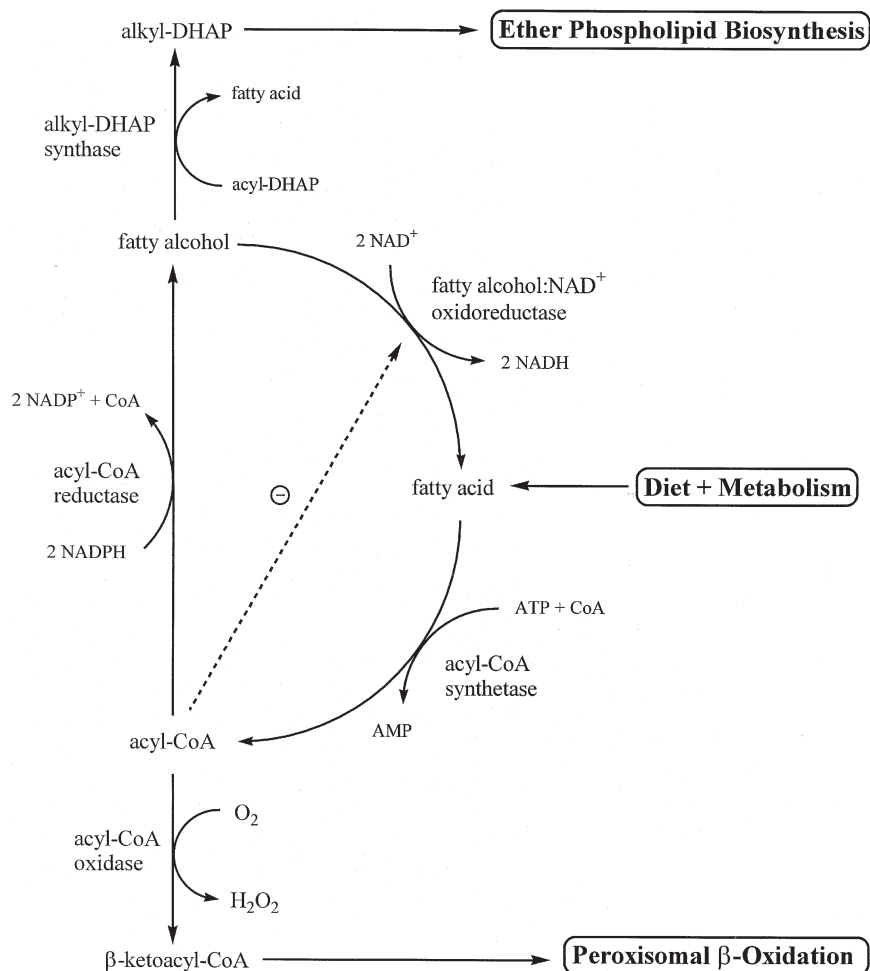
\*To whom correspondence should be addressed at Brain Physiology and Metabolism Section, National Institute on Aging, NIH, Building 10, Room 6N202, Bethesda, MD 20892-1582. E-mail: plsetn@mail.nih.gov

Abbreviations: ACS-2, acyl-CoA synthetases 2; CerPCho, sphingomyelin; plasmalogen, 1-*O*-alk-1'-enyl-2-acyl-*sn*-glycero-3-phosphocholine; plasmalogen ethanolamine, 1-*O*-alk-1'-enyl-2-acyl-*sn*-glycero-3-phosphoethanolamine; phosphatidylcholine, 1,2-diacyl-*sn*-glycero-3-phosphocholine; phosphatidylethanolamine, 1,2-diacyl-*sn*-glycero-3-phosphoethanolamine; phosphatidylinositol, 1,2-diacyl-*sn*-glycero-3-phosphoinositol; phosphatidylserine, 1,2-diacyl-*sn*-glycero-3-phosphoserine; PPAR, peroxisomal proliferator-activated receptors.

Although the functions of both PPAR $\alpha$  and  $\gamma$  are well documented, the role of PPAR $\beta$  remains elusive. It has been shown that PPAR $\beta$  can modulate the expression of brain acyl-CoA synthetases 2 (ACS-2) in reaggregated brain cell culture (2), which suggests that the activation of this nuclear transcription factor can affect the utilization of FA by modulating the levels of acyl-CoA. However, the expression of ACS-2 is not altered by the targeted disruption of PPAR $\beta$  in the adult mouse (3). That the first three committed steps in ether phospholipid metabolism occur in the peroxisome (4), and acyl-CoA synthase-2 mRNA expression is unaffected by the absence of PPAR $\beta$ , suggest that the decreased myelin content found in the female PPAR $\beta$ -null mice (3) may be the result of altered peroxisomal acyl-CoA utilization. To begin to examine this idea, phospholipid and FA composition of brains from PPAR $\beta$ -null mice were determined. Since female PPAR $\beta$ -null mice exhibited a more pronounced constitutive phenotype, it was hypothesized that female PPAR $\beta$ -null mice might also show significant alterations in brain phospholipid composition.

Whereas most of the functions known to occur in peroxisomes involve lipid metabolism, the  $\beta$ -oxidation of FA and the biosynthesis of ether phospholipids are central to their role (5,6). In the peroxisome, unsaturated FA are converted into coenzyme A (CoA) esters by peroxisomal acyl-CoA synthetases unique to this organelle (7) and then  $\beta$ -oxidized into acetyl-CoA and shorter FA, or are oxidized to fatty alcohol (Fig. 1). The preliminary steps of ether phospholipid biosynthesis also occur in the peroxisome and involve the formation of both fatty alcohol and acyl-dihydroxyacetone phosphate (Fig. 1). Studies using liver peroxisomes show that lignoceric acid, and not hexadecanol or hexadecanoic acid, is the principal source of the 1-*O*-alkyl group found in ether phospholipids (8) and suggest that the formation of fatty alcohol is coupled to peroxisomal  $\beta$ -oxidation. That the activity of fatty alcohol:NAD<sup>+</sup> oxidoreductase is inhibited by palmitoyl-CoA and NADH in a concentration-dependent manner suggests that the utilization of acyl-CoA in the peroxisome can regulate fatty alcohol levels by inhibiting the oxidation of peroxisomal FA (Fig. 1) (9).

However, the involvement of PPAR $\beta$  and its influence on peroxisomal gene products that modulate peroxisomal FA and ether phospholipid metabolism in brain are uncertain. Therefore, to assess the potential role of PPAR $\beta$  in the maintenance



**FIG. 1.** The utilization of FA and acyl-CoA in the peroxisome showing the balance between peroxisomal  $\beta$ -oxidation and ether phospholipid biosynthesis. Outlined are the initial and committed steps and cofactors involved in the utilization of peroxisomal FA and acyl-CoA. Reactions involved in the formation of acyl-CoA from FA, the initial step in peroxisomal  $\beta$ -oxidation of acyl-CoA, the reduction of acyl-CoA to fatty alcohol, the initial step in the formation of ether phospholipid, and the oxidation of fatty alcohol to FA are represented. The dashed line represents the postulated inhibition of fatty alcohol: $\text{NAD}^+$  oxidoreductase by acyl-CoA (9). Acyl-DHAP, acyl-dihydroxyacetone phosphate.

of brain FA and ether phospholipid synthesis, we performed analyses of brains from PPAR $\beta$ -null mice. We found that distinct membrane phospholipid changes occur in the female PPAR $\beta$ -null mouse that are associated with increased levels plasmeneylethanolamine and phosphatidylserine, decreased levels of phosphatidylinositol, and altered levels of esterified FA. These data suggest that PPAR $\beta$  is involved in the maintenance of brain FA and phospholipid levels in adult female mouse brain and provide strong evidence that suggests a role for PPAR $\beta$  in brain peroxisomal acyl-CoA utilization.

## EXPERIMENTAL PROCEDURES

Phospholipid, neutral lipid, and FAME standards were purchased from Nu-Chek-Prep (Elysian, MN), TLC plates were from Analtech (Deerfield, IL), and HPLC-grade *n*-hexane and 2-propanol were from EM Science (Gibbstown, NJ). Reagent-grade chloroform, methanol, and other chemicals were from Mallinckrodt (Paris, KY). All samples and extracts

were stored in *n*-hexane/2-propanol (3:2, vol/vol) + 5.5%  $\text{H}_2\text{O}$  under  $\text{N}_2$  at  $-80^\circ\text{C}$ .

**Tissue and extraction.** The homozygous wild-type control and PPAR $\beta$ -null mice used for this work have been described previously (3) and were maintained in accordance with the National Institutes of Health Guidelines for the Care and Use of Laboratory Animals (NIH Publication No. 80-23). Brains from female and male control and PPAR $\beta$ -null mice between the ages of 9 and 12 mon were snap-frozen following cervical dislocation. Whole frozen brains were extracted using *n*-hexane/2-propanol (3:2, vol/vol) in a glass Tenbroeck homogenizer as previously described (10).

**Phospholipid and neutral lipid separation.** Standards and samples in chloroform were applied to  $20 \times 20$  cm Whatman silica gel 60A LK6 TLC plates and separated as previously described (11). Bands corresponding to ethanolamine glycerophospholipids, phosphatidylinositol, phosphatidylserine, choline glycerophospholipids, sphingomyelin, and neutral lipids were scraped from the TLC plate and stored. The

ethanolamine and choline glycerophospholipid fractions were extracted off the silica gel using *n*-hexane/2-propanol (3:2, vol/vol) + 5.5% H<sub>2</sub>O, combined, and concentrated under N<sub>2</sub> at 55°C. The glycerophospholipid fractions were subjected to mild acid hydrolysis to cleave the vinyl ether linkage of the plasmalogens and the phosphatidylethanolamine; lysoplasmylethanolamine, phosphatidylcholine, and lysoplasmylethanolamine fractions were purified using HPLC (12). Half of the samples were used to quantify FA and other half were used to assay for lipid phosphorus (13).

**Neutral lipid separation.** The neutral lipid fractions were extracted from the silica gel by using *n*-hexane/2-propanol (3:2, vol/vol) + 5.5% H<sub>2</sub>O, concentrated under N<sub>2</sub> at 55°C, and dissolved in *n*-hexane/2-propanol/acetic acid (98.7:1.2:0.1, by vol). The individual neutral lipid fractions were separated by HPLC (14) using a Selectosil 5 $\mu$  silica column (250  $\times$  4.6 mm; Phenomenex, Torrance, CA). Fractions corresponding to cholesterol, TAG, and FFA were collected in separate screw-top test tubes and stored at -80°C. The esterified FA in the TAG and the FFA were quantified by GC. Cholesterol was quantified by colorimetric assay (15).

**Methylation of esterified FA and FFA.** The esterified FA found in the different phospholipids and the TAG fractions were methylated using 0.5 M methanolic KOH at 37°C for 30 min. The reaction was stopped with methylformate, and the FAME were extracted using *n*-hexane. The FFA and esterified FA in the sphingomyelin fractions were methylated using 2% sulfuric acid in toluene/methanol (1:1, vol/vol) at 65°C for 2 h. The reaction was stopped with H<sub>2</sub>O, and the FAME were extracted in petroleum ether. The FAME were quantified by GC.

**GC of FAME.** FAME were separated using a gas chromatograph (Trace 2000; ThermoQuest, Houston, TX) equipped with a capillary column (30 m  $\times$  0.32 mm i.d.; SP 2330, Supelco, Bellefonte, PA) and an FID. Methyl heptadecanoate was used as an internal standard, and the individual FA were quantified by peak area analysis. The flow rate of the helium carrier gas was constant and set at 2.5 mL·min<sup>-1</sup>. Injection and detection ports were set at 250°C. Sample runs were initiated at 90°C with a temperature gradient to 230°C over 20.0 min. FAME standards were used to establish the relative retention times and concentration factors. The detector response was linear, with correlation coefficients of 0.998 or greater within the sample concentration range for all FA standards of differing chain length and degree of saturation.

**Data and statistics.** Unpaired *t*-tests were performed on the averaged means using the GraphPad InStat® statistical program (GraphPad, San Diego, CA). Unpaired *t*-tests were used to test the statistical significance between control and PPAR $\beta$ -null female and male groups. Statistical significance was taken as  $P \leq 0.05$ .

## RESULTS

**Brain phospholipid levels.** Table 1 shows the brain phospholipid composition of female and male control and PPAR $\beta$ -null mice along with statistical comparisons. The levels of plasmenyl-

**TABLE 1**  
Brain Phospholipid Levels of Control and PPAR $\beta$ -null Female and Male Mice<sup>a</sup>

	Female		Male	
	Control	PPAR $\beta$ -null	Control	PPAR $\beta$ -null
PtdEtn	11.1 $\pm$ 1.4	12.4 $\pm$ 1.3	10.6 $\pm$ 1.5	11.7 $\pm$ 1.4
PlsEtn	7.4 $\pm$ 1.3	9.8 $\pm$ 0.7**	6.6 $\pm$ 1.1	7.3 $\pm$ 0.9
PtdIns	2.2 $\pm$ 0.1	2.0 $\pm$ 0.1*	2.1 $\pm$ 0.2	2.4 $\pm$ 0.6
PtdSer	5.8 $\pm$ 0.6	7.0 $\pm$ 0.5*	6.1 $\pm$ 0.4	7.2 $\pm$ 2.4
PtdCho	22.6 $\pm$ 0.7	21.7 $\pm$ 2.0	19.9 $\pm$ 2.5	21.6 $\pm$ 1.9
PlsCho	1.1 $\pm$ 0.2	0.9 $\pm$ 0.5	0.8 $\pm$ 0.3	0.8 $\pm$ 0.1
CerPCho	3.4 $\pm$ 0.4	3.2 $\pm$ 0.1	3.1 $\pm$ 0.1	3.6 $\pm$ 1.0
Total	52.6 $\pm$ 4.9	57.0 $\pm$ 3.3	49.2 $\pm$ 4.9	54.5 $\pm$ 4.3

<sup>a</sup>Values represent the mean  $\pm$  SD in units of  $\mu$ mol·g brain<sup>-1</sup> ( $n = 5$ ). \* $P < 0.02$ ; \*\* $P < 0.01$ . PPAR $\beta$ , peroxisomal proliferator-activated receptor  $\beta$ ; PtdEtn, phosphatidylethanolamine; PlsEtn, plasmenylethanolamine; PtdIns, phosphatidylinositol; PtdSer, phosphatidylserine; PtdCho, phosphatidylcholine; PlsCho, plasmenylcholine; CerPCho, sphingomyelin.

ethanolamine and phosphatidylserine were significantly increased from 7.4  $\pm$  1.3 to 9.8  $\pm$  0.7 and 5.8  $\pm$  0.6 to 7.0  $\pm$  0.5  $\mu$ mol·g brain<sup>-1</sup> in female PPAR $\beta$ -null mice as compared to controls, respectively. The level of phosphatidylinositol also decreased in female PPAR $\beta$ -null mice from 2.2  $\pm$  0.1 to 2.0  $\pm$  0.1  $\mu$ mol·g brain<sup>-1</sup>. No changes in the amount of total brain phospholipid were detected in either genotype of female or male mice. The changes in the female PPAR $\beta$ -null mice represent an increase of 24 and 14% in the levels of plasmenylethanolamine and phosphatidylserine, respectively, and a 9% decrease in the level of phosphatidylinositol. No changes were found in the phospholipid composition of male PPAR $\beta$ -null mice. The compositional changes in the female PPAR $\beta$ -null mouse brains show that there is a significant mole percentage increase of plasmenylethanolamine and a subsequent decrease in the percentages of phosphatidylinositol and phosphatidylcholine (data not shown). Consistent with the phospholipid levels, the male PPAR $\beta$ -null mice had no apparent change in the composition of brain phospholipid as compared to controls.

**FA composition of the phospholipid classes.** Tables 2–6 show the esterified FA composition of the brain phospholipid classes in units of nmol·g brain<sup>-1</sup> with statistical comparisons. As expected, there were large increases in the levels of esteri-

**TABLE 2**  
FA Levels of Brain PtdEtn in Control and PPAR $\beta$ -null Male and Female Mice<sup>a</sup>

	Female		Male	
	Control	PPAR $\beta$ -null	Control	PPAR $\beta$ -null
16:0	2,199 $\pm$ 269	2,502 $\pm$ 255	2,133 $\pm$ 323	2,321 $\pm$ 399
18:0	8,865 $\pm$ 812	9,217 $\pm$ 730	7,658 $\pm$ 1,011	8,090 $\pm$ 1,440
18:1n-9	3,554 $\pm$ 867	4,669 $\pm$ 595*	3,406 $\pm$ 672	4,169 $\pm$ 906
18:2n-6	139 $\pm$ 18	176 $\pm$ 14**	145 $\pm$ 27	169 $\pm$ 37
18:3n-3	28 $\pm$ 2	43 $\pm$ 13*	47 $\pm$ 10	43 $\pm$ 12
20:1n-9	535 $\pm$ 202	781 $\pm$ 103*	583 $\pm$ 112	675 $\pm$ 128
20:3n-6	114 $\pm$ 13	124 $\pm$ 15	105 $\pm$ 28	105 $\pm$ 24
20:4n-6	3,056 $\pm$ 537	2,952 $\pm$ 379	1,785 $\pm$ 571	1,874 $\pm$ 626
22:6n-3	5,120 $\pm$ 846	5,174 $\pm$ 990	3,099 $\pm$ 1,239	3,210 $\pm$ 1,160

<sup>a</sup>Values represent the mean  $\pm$  SD in units of nmol·g brain<sup>-1</sup> ( $n = 5$ ). \* $P < 0.05$ ; \*\* $P < 0.01$ . For abbreviations see Table 1.



**TABLE 3**  
FA Levels of Brain PlsEtn in Control and PPAR $\beta$ -null Male and Female Mice<sup>a</sup>

	Female		Male	
	Control	PPAR $\beta$ -null	Control	PPAR $\beta$ -null
16:0	523 $\pm$ 144	487 $\pm$ 41	393 $\pm$ 47	443 $\pm$ 26
18:0	723 $\pm$ 213	603 $\pm$ 235	694 $\pm$ 166	748 $\pm$ 103
18:1n-9	2,029 $\pm$ 637	3,257 $\pm$ 886*	1,639 $\pm$ 378	1,794 $\pm$ 362
18:3n-3	22 $\pm$ 15	33 $\pm$ 19	33 $\pm$ 16	19 $\pm$ 13
20:1n-9	928 $\pm$ 441	1,640 $\pm$ 305*	917 $\pm$ 207	986 $\pm$ 183
20:3n-6	43 $\pm$ 40	85 $\pm$ 22	75 $\pm$ 22	60 $\pm$ 7
20:4n-6	742 $\pm$ 145	1,015 $\pm$ 241*	455 $\pm$ 178	412 $\pm$ 175
22:5n-3	632 $\pm$ 249	1,048 $\pm$ 275*	466 $\pm$ 251	351 $\pm$ 213
22:6n-3	1,420 $\pm$ 280	2,120 $\pm$ 695	895 $\pm$ 466	778 $\pm$ 429

<sup>a</sup>Values represent the mean  $\pm$  SD in units of nmol-g brain<sup>-1</sup> ( $n = 5$ ). \* $P < 0.05$ . For abbreviations see Table 1.

**TABLE 4**  
FA Levels of Brain PtdIns in Control and PPAR $\beta$ -null Male and Female Mice<sup>a</sup>

	Female		Male	
	Control	PPAR $\beta$ -null	Control	PPAR $\beta$ -null
16:0	187 $\pm$ 19	179 $\pm$ 8	158 $\pm$ 41	193 $\pm$ 35
18:0	1,123 $\pm$ 108	1,095 $\pm$ 87	939 $\pm$ 259	1,013 $\pm$ 147
18:1n-9	191 $\pm$ 15	196 $\pm$ 13	155 $\pm$ 40	210 $\pm$ 40
20:1n-9	10 $\pm$ 4	16 $\pm$ 3*	9 $\pm$ 4	16 $\pm$ 6*
20:4n-6	1,318 $\pm$ 140	1,327 $\pm$ 85	1,110 $\pm$ 297	1,080 $\pm$ 156
22:6n-3	188 $\pm$ 22	201 $\pm$ 23	161 $\pm$ 36	153 $\pm$ 29

<sup>a</sup>Values represent the mean  $\pm$  SD in units of nmol-g brain<sup>-1</sup> ( $n = 5$ ). \* $P < 0.05$ . For abbreviations see Table 1.

fied FA in the plasmeneylethanolamine and phosphatidylserine phospholipids of female PPAR $\beta$ -null mice. These changes were associated with increased levels of 18:1n-9, 20:1n-9, 20:4n-6, and 22:5n-3 FA in plasmeneylethanolamine (Table 3) and increased levels of 18:0, 18:1n-9, 18:3n-6, 20:1n-9, and 20:4n-6 in phosphatidylserine (Table 5). A significant increase in 18:1n-9 was also found in the phosphatidylserine fraction of male PPAR $\beta$ -null mice. Both female and male PPAR $\beta$ -null mice had significant increases in the level of 20:1n-9 in the phosphatidylinositol fraction (Table 4), despite

**TABLE 5**  
FA Levels of Brain PtdSer in Control and PPAR $\beta$ -null Male and Female Mice<sup>a</sup>

	Female		Male	
	Control	PPAR $\beta$ -null	Control	PPAR $\beta$ -null
16:0	251 $\pm$ 21	269 $\pm$ 38	256 $\pm$ 44	246 $\pm$ 16
18:0	5,981 $\pm$ 424	7,667 $\pm$ 1,125*	6,215 $\pm$ 1,060	6,350 $\pm$ 636
18:1n-9	2,600 $\pm$ 544	3,894 $\pm$ 489**	2,847 $\pm$ 585	3,429 $\pm$ 428*
18:2n-6	41 $\pm$ 6	44 $\pm$ 6	42 $\pm$ 5	51 $\pm$ 6
18:3n-3	47 $\pm$ 11	75 $\pm$ 12**	70 $\pm$ 15	70 $\pm$ 9
20:1n-9	227 $\pm$ 49	358 $\pm$ 55**	295 $\pm$ 53	308 $\pm$ 30
20:3n-6	54 $\pm$ 10	68 $\pm$ 15	63 $\pm$ 8	67 $\pm$ 8
20:4n-6	406 $\pm$ 46	544 $\pm$ 95*	383 $\pm$ 61	430 $\pm$ 65
22:6n-3	4,337 $\pm$ 439	4,974 $\pm$ 1,005	4,475 $\pm$ 696	3,870 $\pm$ 376

<sup>a</sup>Values represent the mean  $\pm$  SD in units of nmol-g brain<sup>-1</sup> ( $n = 5$ ). \* $P < 0.05$ ; \*\* $P < 0.01$ . For abbreviations see Table 1.

**TABLE 6**  
FA Levels of Brain CerPCho in Control and PPAR $\beta$ -null Male and Female Mice<sup>a</sup>

	Female		Male	
	Control	PPAR $\beta$ -null	Control	PPAR $\beta$ -null
16:0	276 $\pm$ 75	257 $\pm$ 83	185 $\pm$ 14	247 $\pm$ 16**
18:0	1,799 $\pm$ 101	1,691 $\pm$ 116	1,360 $\pm$ 237	1,349 $\pm$ 194
18:1n-9	105 $\pm$ 17	85 $\pm$ 12	63 $\pm$ 6	92 $\pm$ 24*
20:0	41 $\pm$ 8	49 $\pm$ 5	38 $\pm$ 9	35 $\pm$ 6
22:0	44 $\pm$ 5	29 $\pm$ 11	45 $\pm$ 14	33 $\pm$ 9
24:0	37 $\pm$ 20	64 $\pm$ 19	51 $\pm$ 12	37 $\pm$ 13
24:1n-9	345 $\pm$ 144	473 $\pm$ 83	359 $\pm$ 96	344 $\pm$ 70
26:1n-9	44 $\pm$ 7	25 $\pm$ 11*	20 $\pm$ 6	13 $\pm$ 14

<sup>a</sup>Values represent the mean  $\pm$  SD in units of nmol-g brain<sup>-1</sup> ( $n = 5$ ). \* $P < 0.05$ ; \*\* $P < 0.01$ . For abbreviations see Table 1.

the fact that the female PPAR $\beta$ -null mice had a 9% decrease in the amount of this phospholipid. Analysis of the female PPAR $\beta$ -null mouse brain phosphatidylethanolamine fraction also revealed significant increases in the levels of 18:1n-9, 18:n-6, 18:3n-6, and 20:1n-9 with no changes in the male phosphatidylethanolamine fraction (Table 2) or the female and male phosphatidylcholine, plasmeneylcholine, and sphingomyelin fractions (data not shown).

**Brain cholesterol, TAG, and FFA.** Analysis of brain neutral lipids shows that the absence of a functional PPAR $\beta$  did not affect the levels of total brain cholesterol, TAG, FFA, or the cholesterol to phospholipid ratio in both female and male PPAR $\beta$ -null mice (Table 7).

## DISCUSSION

In this study we found that the female PPAR $\beta$ -null mouse brain, consistent with the constitutive phenotype, showed elevated levels of plasmeneylethanolamine and phosphatidylserine and decreased levels of phosphatidylinositol. However, no changes were found in the phospholipid content in the male PPAR $\beta$ -null mouse brain. Analysis of the esterified FA content in the membrane phospholipids showed an overall trend toward increased levels of esterified long-chain n-9 and n-6 FA with a more pronounced phenotype being present in the female null mouse. The PPAR $\beta$ -null mouse phenotype showed no changes in the levels of cellular cholesterol or TAG in either female or male mice.

These data suggest that PPAR $\beta$  is involved in maintaining FA and phospholipid levels in adult mouse brain that result in distinct gender-related differences when PPAR $\beta$  is disrupted. Although the presence of gender-related differences in lipid metabolism is not unusual, the molecular basis responsible for this phenomenon is not completely understood. It is known that circulating levels of estrogen can modulate the fasting activity of both TAG lipase and neutral cholesteryl ester hydrolase activity, alter lipoprotein metabolism at subcellular sites in the liver, and increase the plasma clearance of LDL and HDL (16). The hepatic uptake of long-chain FA from plasma is also nearly twofold faster for females than males in both humans (17,18) and rats (19–21) because of gender-related differences in intra-

**TABLE 7**  
**Neutral Lipid Levels (A) and Cholesterol-to-Phospholipid Ratio (B) of Control and PPAR $\beta$ -null Female and Male Mice<sup>a</sup>**

	Female		Male	
	Control	PPAR $\beta$ -null	Control	PPAR $\beta$ -null
A: Triacylglyceride	120 $\pm$ 21	121 $\pm$ 19	90 $\pm$ 13	122 $\pm$ 31
FFA	585 $\pm$ 121	489 $\pm$ 84	474 $\pm$ 54	544 $\pm$ 117
B: Cholesterol	44,121 $\pm$ 8,031	45,634 $\pm$ 4,704	43,500 $\pm$ 1,833	49,461 $\pm$ 2,729
Chol/lipid	0.834 $\pm$ 0.085	0.801 $\pm$ 0.078	0.888 $\pm$ 0.063	0.910 $\pm$ 0.071

<sup>a</sup>Values represent the mean  $\pm$  SD in units of nmol·g brain<sup>-1</sup> ( $n = 5$ ). Chol, cholesterol; lipid, phospholipid. For other abbreviation see Table 1.

cellular FA transport and binding proteins (22) and in the larger sinusoidal volume (23). However, the metabolic rates for [<sup>3</sup>H]palmitate utilization in female and male liver are similar, as determined by using the traditional multiple-indicator dilution model to measure apparent influx, efflux, and cytoplasmic diffusion constants (23). Thus, whereas the plasma clearance rate of palmitate in female is faster, the rate of metabolism is not. Therefore, the altered phospholipid and FA composition found in the female PPAR $\beta$ -null mouse may be due to both the gender-related alterations in metabolism and a disruption in the transport and utilization of brain FA.

Indeed, the altered brain FA and phospholipid composition found in the PPAR $\beta$ -null female mice can be the result of several mechanisms. However, the presence of increased amounts of esterified long-chain FA is indicative of either reduced oxidation or increased metabolism. Increased levels of brain plasmenylethanolamine, coupled with the fact that the first committed steps in ether phospholipid synthesis occur in the peroxisome, suggest that PPAR $\beta$  may function to modulate the enzymes involved in peroxisomal FA and acyl-CoA metabolism (Fig. 1). Because the rate-limiting and committed step in ether phospholipid metabolism is the formation of the fatty alcohol (24), accumulation of PUFA and acyl-CoA may indirectly influence the levels of ether phospholipid by increasing the levels of the committed substrate, fatty alcohol (Fig. 1). Although FA transport may be affected in the female PPAR $\beta$ -null mouse, it is more likely that the increased levels of plasmenylethanolamine found in the female PPAR $\beta$ -null mouse brain are due to altered peroxisomal FA and acyl-CoA utilization.

In the female PPAR $\beta$ -null mouse, there were multiple changes in both brain phospholipid and esterified FA, which suggest that PPAR $\beta$  may play a role in maintaining membrane structure and may influence bulk membrane dynamics. However, the cholesterol to phospholipid ratio, an indicator of bulk membrane dynamic changes (25,26), in both female and male PPAR $\beta$ -null mice did not differ significantly from the controls owing to the lack of significant differences in the levels of total brain cholesterol and total brain phospholipid. Although the female PPAR $\beta$ -null mouse displayed multiple changes in membrane phospholipid and FA content, gross changes in membrane dynamics were not present. However, the chain length and degree of saturation of esterified FA do participate in membrane organization (27–29) and are important in the proper function of membrane-bound protein (30).

Even though bulk membrane dynamic changes were not present in the PPAR $\beta$ -null mice, alterations in the FA composition could affect the physical properties of the membrane in terms of the rate and range of acyl chain motion, lateral diffusion of lipid and proteins, as well as alterations in protein–lipid interactions (25,31). The increased levels of esterified n-9 and n-6 FA in the PPAR $\beta$ -null mice, despite a lack of bulk membrane dynamic changes, can alter the membrane phase transition and hence influence brain function.

In this regard, the displacement of acylated proteins from membrane rafts, which are specialized regions within the plasma membrane that contain high levels of plasmenylethanolamine, phosphatidylserine, and phosphatidylinositol and are important to intracellular signaling and vesicular trafficking (32–35), are dependent on phospholipid and FA composition (33,36). The formation of these lipid rafts is also involved in signal transduction and is thought to influence the turnover of inositol-containing phospholipids (37). Therefore, alteration in the phospholipid and FA composition of lipid rafts not only can influence protein–lipid interactions but also may influence the turnover of inositol-containing phospholipid. Therefore, the increase in 20:1n-9 in phosphatidylinositol despite its overall decrease in brain may be a result of changes in the turnover rate of inositol-containing phospholipid due to altered membrane dynamics and, indirectly, to the loss of PPAR $\beta$  function.

These data suggest that PPAR $\beta$  is involved in maintaining FA and phospholipid levels in adult mouse brain that result in distinct gender-related differences when PPAR $\beta$  is disrupted. The alterations in the levels of brain plasmenylethanolamine and the changes in esterified FA composition provide strong evidence of a role for PPAR $\beta$  in brain peroxisomal acyl-CoA utilization. However, further studies are needed to identify target genes of PPAR $\beta$ , how they regulate the gender-related lipid changes found in PPAR $\beta$ -null mice, the influence PPAR $\beta$  has on peroxisomal acyl-CoA utilization, and its effect on ether phospholipid metabolism in the brain.

## REFERENCES

- Desvergne, B., and Wahli, W. (1999) Peroxisome Proliferator-Activated Receptors: Nuclear Control of Metabolism, *Endocr. Rev.* 20, 649–688.
- Basu-Modak, S., Braissant, O., Escher, P., Desvergne, B., Honegger, P., and Wahli, W. (1999) Peroxisome Proliferator-

- Activated Receptor Beta Regulates Acyl-CoA Synthetase 2 in Reaggregated Rat Brain Cell Cultures, *J. Biol. Chem.* 274, 35881–35888.
3. Peters, J.M., Lee, S.S., Li, W., Ward, J.M., Gavrilo, O., Everett, C., Reitman, M.L., Hudson, L.D., and Gonzalez, F.J. (2000) Growth, Adipose, Brain, and Skin Alterations Resulting from Targeted Disruption of the Mouse Peroxisome Proliferator-Activated Receptor Beta(delta), *Mol. Cell Biol.* 20, 5119–5128.
  4. Lee, T.C. (1998) Biosynthesis and Possible Biological Functions of Plasmalogens, *Biochim. Biophys. Acta* 1394, 129–145.
  5. Wanders, R.J., and Tager, J.M. (1998) Lipid Metabolism in Peroxisomes in Relation to Human Disease, *Mol. Aspects Med.* 19, 69–154.
  6. Paltauf, F. (1983) Biosynthesis of 1-O-(1'-alkenyl)Glycerolipids (plasmalogens), in *Ether Lipids: Biochemical and Biomedical Aspects* (Mangold, H.K., and Paltauf, F., eds.), pp. 107–128, Academic Press, New York.
  7. Kunau, W.H., Dommès, V., and Schulz, H. (1995) Beta-Oxidation of Fatty Acids in Mitochondria, Peroxisomes, and Bacteria: A Century of Continued Progress, *Prog. Lipid Res.* 34, 267–342.
  8. Hayashi, H., and Hara, M. (1997) 1-Alkenyl Group of Ethanolamine Plasmalogen Derives Mainly from *de novo*-Synthesized Fatty Alcohol Within Peroxisomes, but Not Extraperoxisomal Fatty Alcohol or Fatty Acid, *J. Biochem. (Tokyo)* 121, 978–983.
  9. Rizzo, W.B., Craft, D.A., Dammann, A.L., and Phillips, M.W. (1987) Fatty Alcohol Metabolism in Cultured Human Fibroblasts. Evidence for a Fatty Alcohol Cycle, *J. Biol. Chem.* 262, 17412–17419.
  10. Radin, N.S. (1981) Extraction of Tissue Lipids with a Solvent of Low Toxicity, *Methods Enzymol.* 72, 5–7.
  11. Jolly, C.A., Hubbell, T., Behnke, W.D., and Schroeder, F. (1997) Fatty Acid Binding Protein: Stimulation of Microsomal Phosphatidic Acid Formation, *Arch. Biochem. Biophys.* 341, 112–121.
  12. Murphy, E.J., Stephens, R., Jurkowitz-Alexander, M., and Horrocks, L.A. (1993) Acidic Hydrolysis of Plasmalogens Followed by High-Performance Liquid Chromatography, *Lipids* 28, 565–568.
  13. Rouser, G., Siakotos, A.N., and Fleischer, S. (1966) Quantitative Analysis of Phospholipids by Thin-Layer Chromatography and Phosphorus Analysis of Spots, *Lipids* 1, 85–86.
  14. Murphy, E.J., Rosenberger, T.A., and Horrocks, L.A. (1996) Separation of Neutral Lipids by High-Performance Liquid Chromatography: Quantification by Ultraviolet, Light Scattering and Fluorescence Detection, *J. Chromatogr. B Biomed. Appl.* 685, 9–14.
  15. Bowman, R.E., and Wolf, R.C. (1962) A Rapid and Specific Ultramicro Method for Total Serum Cholesterol, *Clin. Chem.* 8, 302–309.
  16. Fu, D., and Hornick, C.A. (1995) Modulation of Lipid Metabolism at Rat Hepatic Subcellular Sites by Female Sex Hormones, *Biochim. Biophys. Acta* 1254, 267–273.
  17. Knutson, T.W., Knutson, L.F., Hogan, D.L., Koss, M.A., and Isenberg, J.I. (1995) Human Proximal Duodenal Ion and Water Transport. Role of Enteric Nervous System and Carbonic Anhydrase, *Dig. Dis. Sci.* 40, 241–246.
  18. Pond, S.M., Gordon, R.A., and Bass, L. (1996) Sex Differences in Initial Clearance of Palmitate by Human Hepatocytes, *Eur. J. Clin. Invest.* 26, 76–81.
  19. Kushlan, M.C., Gollan, J.L., Ma, W.L., and Ockner, R.K. (1981) Sex Differences in Hepatic Uptake of Long Chain Fatty Acids in Single-Pass Perfused Rat Liver, *J. Lipid Res.* 22, 431–436.
  20. Soler-Argilaga, C., and Heimberg, M. (1976) Comparison of Metabolism of Free Fatty Acid by Isolated Perfused Livers from Male and Female Rats, *J. Lipid Res.* 17, 605–615.
  21. Ockner, R.K., Burnett, D.A., Lysenko, N., and Manning, J.A. (1979) Sex Differences in Long Chain Fatty Acid Utilization and Fatty Acid Binding Protein Concentration in Rat Liver, *J. Clin. Invest.* 64, 172–181.
  22. Luxon, B.A., and Weisiger, R.A. (1993) Sex Differences in Intracellular Fatty Acid Transport: Role of Cytoplasmic Binding Proteins, *Am. J. Physiol.* 265, G831–G841.
  23. Luxon, B.A., Holly, D.C., Milliano, M.T., and Weisiger, R.A. (1998) Sex Differences in Multiple Steps in Hepatic Transport of Palmitate Support a Balanced Uptake Mechanism, *Am. J. Physiol.* 274, G52–G61.
  24. Snyder, F., Lee, T., and Wykle, R.L. (1985) Ether-Linked Glycerolipids and Their Bioactive Species: Enzymes and Metabolic Regulation, in *The Enzymes of Biological Membranes* (Martonosi, A.N., ed.), pp. 1–58, Plenum Press, New York.
  25. Stubbs, C.D., and Smith, A.D. (1984) The Modification of Mammalian Membrane Polyunsaturated Fatty Acid Composition in Relation to Membrane Fluidity and Function, *Biochim. Biophys. Acta* 779, 89–137.
  26. Ohvo-Rekila, H., Ramstedt, B., Leppimäki, P., and Slotte, J.P. (2002) Cholesterol Interactions with Phospholipids in Membranes, *Prog. Lipid Res.* 41, 66–97.
  27. Holte, L.L., Peter, S.A., Sinnwell, T.M., and Gawrisch, K. (1995) <sup>2</sup>H Nuclear Magnetic Resonance Order Parameter Profiles Suggest a Change of Molecular Shape for Phosphatidylcholines Containing a Polyunsaturated Acyl Chain, *Biophys. J.* 68, 2396–2403.
  28. Saiz, L., and Klein, M.L. (2001) Influence of Highly Polyunsaturated Lipid Acyl Chains of Biomembranes on the NMR Order Parameters, *J. Am. Chem. Soc.* 123, 7381–7387.
  29. Saiz, L., and Klein, M.L. (2001) Structural Properties of a Highly Polyunsaturated Lipid Bilayer from Molecular Dynamics Simulations, *Biophys. J.* 81, 204–216.
  30. Palczewski, K., Kumasaka, T., Hori, T., Behnke, C.A., Motoshima, H., Fox, B.A., Le Trong, I., Teller, D.C., Okada, T., Stenkamp, R.E., et al. (2000) Crystal Structure of Rhodopsin: A G Protein-Coupled Receptor, *Science* 289, 739–745.
  31. Schroeder, F. (1984) Role of Membrane Lipid Asymmetry in Aging, *Neurobiol. Aging* 5, 323–333.
  32. Simons, K., and Toomre, D. (2000) Lipid Rafts and Signal Transduction, *Nat. Rev. Mol. Cell Biol.* 1, 31–39.
  33. Thai, T.P., Rodemer, C., Jauch, A., Hunziker, A., Moser, A., Gorgas, K., and Just, W.W. (2001) Impaired Membrane Traffic in Defective Ether Lipid Biosynthesis, *Hum. Mol. Genet.* 10, 127–136.
  34. Pike, L.J., Han, X., Chung, K.N., and Gross, R.W. (2002) Lipid Rafts Are Enriched in Arachidonic Acid and Plasmalogen Ethanolamine and Their Composition Is Independent of Caveolin-1 Expression: A Quantitative Electrospray Ionization/Mass Spectrometric Analysis, *Biochemistry* 41, 2075–2088.
  35. Zajchowski, L.D., and Robbins, S.M. (2002) Lipid Rafts and Little Caves, *Eur. J. Biochem.* 269, 737–752.
  36. Stulnig, T.M., Huber, J., Leitinger, N., Imre, E.M., Angelisova, P., Nowotny, P., and Waldhausl, W. (2001) Polyunsaturated Eicosapentaenoic Acid Displaces Proteins from Membrane Rafts by Altering Raft Lipid Composition, *J. Biol. Chem.* 276, 37335–37340.
  37. Laux, T., Fukami, K., Thelen, M., Golub, T., Frey, D., and Caroni, P. (2000) GAP43, MARCKS, and CAP23 Modulate PI(4,5)P<sub>2</sub> at Plasmalemmal Rafts, and Regulate Cell Cortex Actin Dynamics Through a Common Mechanism, *J. Cell Biol.* 149, 1455–1472.

[Received September 21, 2001, and in revised form February 19, 2002; revision accepted February 23, 2002]



# Pancreatic $\beta$ -Cell $\alpha_{2A}$ Adrenoceptor and Phospholipid Changes in Hyperlipidemic Rats

L. Clément<sup>a,\*</sup>, K.-A. Kim-Sohn<sup>a</sup>, C. Magnan<sup>a</sup>, N. Kassis<sup>a</sup>, P. Adnot<sup>b</sup>, M. Kergoat<sup>b</sup>,  
F. Assimacopoulos-Jeannet<sup>c</sup>, L. Pénicaud<sup>d</sup>, F.-F. Hsu<sup>e</sup>, J. Turk<sup>e</sup>, and A. Ktorza<sup>a</sup>

<sup>a</sup>Laboratoire de Physiopathologie de la Nutrition, CNRS UMR 7059, Université Paris 7, 75251 Paris cedex 05, <sup>b</sup>Merck-Lipha, Chilly Mazarin, France, <sup>c</sup>Département de Biochimie Médicale, Centre Médical Universitaire, CH1211 Genève 4, Switzerland, <sup>d</sup>Laboratoire de Neurobiologie, Plasticité Tissulaire et Métabolisme Énergétique, CNRS UMR 5018, Université Paul Sabatier, CHU Rangueil, 31000 Toulouse, France, and <sup>e</sup>Mass Spectrometry Resource, Department of Medicine, Washington University School of Medicine, St. Louis, Missouri 63110

**ABSTRACT:** We previously showed that a 48-h intravenous lipid infusion in rats induces pancreatic  $\beta$ -cell hypersensitivity to catecholamines. Our aim was to study the lipid-related changes that may account for such hypersensitivity in pancreatic islets. We show here that a 48-h increase in plasma FFA alters the binding characteristics of  $\beta$ -cell  $\alpha_2$  adrenoceptors in rats. Lipid infusion decreases pancreatic norepinephrine (NE) turnover rate by 28%, reflecting a reduction of pancreatic NE stores. Following lipid infusion, the density of  $\alpha_2$  adrenoceptor binding sites is significantly lower and receptor affinity higher, both in islet homogenates (by three- and fivefold, respectively) and isolated whole  $\beta$ -cells (by two- and sixfold, respectively). These changes correlate with the elevated insulin response to glucose found in lipid-infused rats. We also found a modification of islet phospholipid content, particularly in phosphoethanolamine species containing infused FA such as palmitate, oleate, stearate, and linoleate. This may account for the modifications in receptor affinity. These results suggest that hyperlipidemia-associated pathologies such as diabetes and obesity not only may result from alterations of metabolic pathways but also may be a consequence of early modifications in nervous firing rates and signal transduction pathways.

Paper no. L8993 in *Lipids* 37, 501–506 (May 2002).

Among the many signals modulating islet insulin response to glucose, the autonomic nervous system plays a determinant role (reviewed in Refs. 1,2). Acetylcholine, released by parasympathetic neurons, has a potentiating effect on glucose-induced insulin secretion (GIIS), as opposed to the inhibiting effect of the sympathetic neurotransmitter, norepinephrine (NE) (3). In a previous study, we showed that a 48-h increase in plasma FFA concentration in rats lowers sympathetic nervous activity and leads to increased  $\beta$ -cell responsiveness to glucose with no concomitant alteration of either basal glycemia or insulinemia (4). Changes in sympathetic activity have been associated with dyslipidemia in both humans (5–7) and rats (8,9).

\*To whom correspondence should be addressed at Université Paris 7, CNRS ESA 7059, case 7126, 2 place Jussieu, 75251 Paris cedex 05, France. E-mail: clement@paris7.jussieu.fr

Abbreviations: ESI, electrospray ionization; FACS, fluorescence-activated cell sorting; FAD, flavin adenine dinucleotide; GIIS, glucose-induced insulin secretion; IL, Intralipid; KRBH buffer, Krebs-Ringer-bicarbonate-Hepes; NE, norepinephrine; POPE, palmitoyl-oleoyl-PE; RT-PCR, reverse transcription-PCR; [<sup>3</sup>H]RX821002, 2-(2-methoxy-1,4-benzodioxan-2-yl)-2-imidazole, a benzodioxane derivative that exhibits high affinity for  $\alpha_2$ -adrenergic receptors; TM buffer, Tris-HCl/MgCl<sub>2</sub> buffer.

Taken together, these results suggest that the sympathetic nervous system may have a determinant role in lipid-associated metabolic diseases such as type 2 diabetes and obesity.

In both rats and humans, catecholaminergic inhibition of insulin secretion is mediated by  $\alpha_{2A}$  adrenergic receptors (3), which are the predominant forms of  $\beta$ -cell adrenoceptors. Paradoxically, we found that  $\beta$ -cell sensitivity to oxymetazoline, a relatively selective  $\alpha_{2A}$ -adrenoceptor agonist, was elevated by lipid infusion (4). Thus, the aim of our study was to identify the mechanisms implicated in this  $\beta$ -cell hypersensitivity. We show here that hyperlipidemia alters the binding characteristics of  $\beta$ -cell  $\alpha_2$  adrenoceptors; the density of  $\alpha_2$  adrenoceptor binding sites is significantly lowered and receptor affinity is increased after lipid infusion. As there is no difference in mRNA levels, the reduced number of receptors may result from lipid-related posttranslational modifications. The changes in islet phospholipid composition and in pancreatic NE content may account for the higher receptor affinity. These results suggest that hyperlipidemia-associated pathologies such as diabetes and obesity not only may result from alterations of metabolic pathways but also may be a consequence of early modifications in nervous firing rates and signal transduction pathways.

## EXPERIMENTAL PROCEDURES

**Animal experiments.** All rats were treated in accordance with the European Community guidelines, and the experimentation was approved by our local institution. Male Wistar rats weighing 240–270 g were used. They were allowed free access to standard laboratory chow pellets (UAR, Villemoisson-sur-Orge, France) and water.

Operations were performed under pentobarbital anesthesia (50 mg/kg intraperitoneally; Sanofi, Libourne, France). For intravenous infusion, a catheter was implanted in the right atrium *via* the jugular vein. Rats were infused either with a 20% TG emulsion (Intralipid KabiVitrum 2,000 kcal/L, Stockholm, Sweden) mixed with heparin 20 U/mL (IL rats) or with a saline/heparin solution as described previously (4). The percentage composition of the 20% Intralipid emulsion was: 10 palmitate, 4 stearate, 23 oleate, 53 linoleate, and 8 linolenate.

**Hormone and substrate concentrations.** Blood samples obtained from caudal vessels were used for measurement of



substrate (FFA, TG, glucose) and insulin concentrations. Glucose was measured using a glucose monitor (Roche Diagnostic, Meylan, France). Enzymatic assay kits were used to determine plasma FFA (NEFA C; Wako Chemical, Marburg, Germany) and TG and glycerol concentrations (Boehringer Mannheim Biochemica, Mannheim, Germany). Insulin was measured by radioimmunoassay (DiaSorin, Antony, France). Plasma and organ NE levels were determined by HPLC with C<sub>18</sub> reversed-phase material (150 × 2 mm Beckman column packed with Ultrasphere ODS C (Beckman/Altex, San Antonio, TX; 18.5 μm average particle size) and electrochemical detection (Kontron 402) after alumina extraction. Calibration curves were made with spiked plasma or homogenate. Recoveries were calculated on the basis of peak heights measured by an integrator (Shimadzu System, Yakanike, Japan).

**In vivo GIIS studies.** After 48 h of infusion, a single injection of glucose (0.5 mg/kg) was administered in rats *via* the intracardiac catheter. Blood samples were collected before and 1, 3, 5, 10, 15, 20, and 30 min after glucose injection. Plasma was obtained after centrifugation, and glucose concentration was immediately determined using a glucose monitor (Boehringer). The remaining plasma was stored at -20°C until insulin assay.

**Pancreatic NE turnover.** We used the synthesis inhibition method by Brodie *et al.* (10). Two hours after lights on, rats were injected with  $\alpha$ -methyl-DL-*p*-tyrosine, a tyrosine hydroxylase inhibitor (250 mg/kg *i.p.*; Sigma Chemical). Three hours after injection, one group of rats (T<sub>3</sub>h) was killed, and the pancreata were rapidly removed and frozen in liquid nitrogen. The other group (T<sub>6</sub>h) received an additional 125 mg/kg *i.p.* of  $\alpha$ -methyl-DL-*p*-tyrosine. These rats were killed 3 h later and the pancreata were also removed and frozen. Rats from a third group (T<sub>0</sub>h) were not injected with the inhibitor, and they were killed at the beginning of the experiment.

**Pancreatic islet and  $\beta$ -cell isolation.** Islets of Langerhans were isolated after collagenase digestion of the pancreas as previously described (11). For cellular dissociation, the isolated islets were pooled in 15 mL chelation saline buffer (PBS, 5 mM EGTA) and incubated for 5–6 min at 37°C in buffer supplemented with 0.1 mg/mL trypsin (Difco, Draveil, France), with occasional mixing with a Pasteur pipette. The digestion was stopped by adding cold KRBH buffer (Krebs-Ringer-bicarbonate-Hepes; 140 mM NaCl, 3.6 mM KCl, 0.5 mM NaH<sub>2</sub>PO<sub>4</sub>, 0.5 mM MgSO<sub>4</sub>, 2 mM NaHCO<sub>3</sub>, 1.5 mM CaCl<sub>2</sub>, 10 mM Hepes, 5.6 mM glucose, 0.5% BSA). The isolated islet cells were washed twice in cold KRBH buffer. This procedure yielded on average 0.5 × 10<sup>6</sup> islet cells per pancreas. Islets and sorted  $\beta$ -cells were used either for binding experiments or for RNA extraction.

**Fluorescence-activated cell sorting (FACS).** Islet cells were sorted using a FACSTAR Plus (Becton Dickinson, San Jose, CA). An argon laser (model 163, Spectra Physics, Mountain View, CA) illuminated the cells at 488 nm. An interference filter detected the light emitted at 510–540 nm, which was taken as the flavin adenine nucleotide (FAD) cell content. The discrimination between  $\beta$ -cells and non- $\beta$ -cells was done using autofluorescence for FAD (FL-1) and cell size (forward size scatter).  $\beta$ -Cells displayed a 50% higher FAD content (12) and

were 50% larger (13) than non- $\beta$ -cells. Cell sorting was done using Normal-R mode, ensuring 90% purity with a 2 drop-envelope. The quality of the sorting was verified by a subsequent cell FACS analysis of a sample of the purified cells.

**Radioligand binding studies.**  $\alpha_2$ -Adrenergic receptors were quantified by radioligand binding using [<sup>3</sup>H]RX821002 [2-(2-methoxy-1,4-benzodioxan-2-yl)-2-imidazoline; 59 Ci/mmol; Amersham, Saclay, France], a benzodioxane derivative that exhibits high affinity for  $\alpha_2$ -adrenergic receptors, either on freshly isolated and sonicated islets of Langerhans or on whole pancreatic  $\beta$ -cells. In the first case, 600 to 800 freshly isolated islets were resuspended in 2.6 mL of TM buffer (50 mM Tris-HCl, 5 mM MgCl<sub>2</sub>, pH 7.5), and sonicated for 5 s. Total binding was measured by incubating 75 to 100 μg of islet homogenate proteins [as determined by the method of Lowry *et al.* (14)] with increasing concentrations of [<sup>3</sup>H]RX821002, in a total volume of 400 μL of TM buffer. After a 1-h incubation at 25°C, bound radioligand was separated from free radioligand by rapid filtration over glass fiber filters (Millipore) under vacuum and was measured in a Packard Tri-Carb 460C liquid scintillation system. Nonspecific binding was measured using 10<sup>-4</sup> M epinephrine (Sigma). On whole pancreatic  $\beta$ -cells, the study was carried out as above, with 20,000 to 30,000 cells per tube and 2 h incubation at 4°C. Data from binding experiments were analyzed using a nonlinear curve-fitting GraphPad Prism® program (GraphPad Software, San Diego, CA).

**Competitive standard RNA synthesis for quantitative PCR.** For a precise quantitation of  $\alpha_{2A}$  adrenoceptor RNA, we synthesized a 219 bp standard RNA containing the same sequence as the rat  $\alpha_{2A}$  adrenoceptor RNA from positions 196 to 396, plus a 3' end constituted of the 487 to 506  $\alpha_{2A}$  adrenoceptor RNA sequence. Hence, the standard RNA has the same, but shorter, sequence as the target RNA and can still be amplified with the same primers. Total cellular RNA (250 ng) was reverse-transcribed and amplified using One-Step RT-PCR Kit (Qiagen, Courtaboeuf, France) with the following primers: 5'-AAT TCT AAT ACG ACT CAC TAT AGG GAG AAG CGC CCC AGA ACC TCT TCC T-3' (forward) and 5'-AGT GGC GGG AAG GAG ATG ACG TAG CGG TCA AGG CTG ATG G-3' (reverse). Forty microliters of the 248bp cDNA PCR product was transcribed *in vitro* in a 100-μL reaction volume and incubated for 2 h at 37°C, using T7 RNA polymerase according to the manufacturer's instructions (Roche-Boehringer Mannheim, Mannheim, Germany). At the end of the reaction, T7 RNA polymerase was heat-inactivated (5 min, 65°C), and the transcription product was treated with 100 U of DNase I–RNase free for 15 min at 37°C. Standard RNA was purified using Qiagen's RNeasy® Mini Kit, with an on-column DNase digestion. Standard RNA solution was tested for contamination by cDNA in a PCR assay.

**Reverse transcription-PCR (RT-PCR) assay.** Total cellular RNA from frozen cells were extracted using the method of Chomczynski and Sacchi (15). The primers used for the  $\alpha_{2A}$  adrenergic receptor subtype were chosen as described in (16): 5'-GCG CCC CAG AAC CTC TTC CT-3' (forward) and 5'-AGT GGC GGG AAG GAG ATG AC-3' (reverse) and

provided amplification of a 311-bp fragment, from positions 196 to 506. In each reaction, 200 ng of total cellular RNA was co-reverse transcribed and amplified with 10<sup>5</sup> to 10<sup>8</sup> standard RNA molecules in a single reaction using One-Step RT-PCR Kit (Qiagen) including a hot start PCR, in 27 cycles of 1 min denaturation at 94°C, 1 min annealing at 60°C, and 1 min extension at 72°C. Negative controls were performed by omitting RNA from the RT-PCR reaction. Band intensities were quantified by densitometry using National Institutes of Health Image software. The logarithmic value of the ratio of standard RNA to α<sub>2A</sub> adrenergic receptor RNA was plotted against the logarithmic value of standard RNA molecule number. Thus, an equimolar point was determined where the starting number of α<sub>2A</sub> adrenergic receptor RNA equaled the starting number of standard RNA molecules (logarithmic value of the ratio equals 0).

**Electrospray ionization (ESI) MS.** ESI/MS analyses were performed on a Finnigan (San Jose, CA) TSQ-7000 triple stage quadrupole mass spectrometer equipped with an electrospray ion source and controlled by Finnigan ICIS software operated on a DEC alpha station (computer). Phospholipids were dissolved in methanol/chloroform (9:1, vol/vol) at final concentrations of about 1–5 pmol/μL. To facilitate formation of anionic species for negative ion analyses and to form lithiated adducts of PC for positive ion analyses, methanolic LiOH (0.1 μM/μL) was added to a final concentration of 2–5 nmol/μL (17,18). Samples were infused (1 μL/min) into the ESI source with a Harvard syringe pump. The electrospray needle and the skimmer were at ground potential, and the electrospray chamber and the entrance of the glass capillary were at 4.5 kV. The heated capillary temperature was 250°C. For collisionally activated dissociation and tandem MS, precursor ions were selected in the first quadrupole (Q1) and collided with Ar (2.3 mtorr) in the rf (radio frequency)-only second quadrupole (Q2) using a collision energy of 30–35 eV, and mass-analyzed in the third quadrupole (Q3). Both the Q1 and Q3 were tuned to unit resolution, and the mass spectra were obtained in the profile mode. Typically, a 1-min period of signal averaging was employed for scanned spectra, and 1 to 10 min was employed for tandem mass spectra. The product-ion spectra of the [M + Li]<sup>+</sup> ion of PC and the [M – H]<sup>–</sup> ions of PE and PI were used for the structural assignments of the phospholipid species (19,20).

**Statistics.** Results are given as means ± SEM. Statistical analyses were performed using ANOVA. Results from binding experiments were statistically analyzed using the Mann–Whitney U test.

**RESULTS**

**Plasma FFA, TG, glycerol, and catecholamine concentrations.** As shown in Table 1, after a 48-h intravenous lipid infusion, there was a fourfold increase in plasma FFA concentration as well as a twofold increase in plasma glycerol. As heparin was infused with the intralipid emulsion, thus stimulating lipoprotein-lipase activity, the level of TG remained similar to that of control rats throughout the lipid infusion. There was a 60% reduction in plasma NE in IL rats as compared to control rats. Plasma glucose and insulin were similar in all rats.

**TABLE 1**  
**Time Course of Plasma TG, FFA, Glycerol, and NE Concentrations During Lipid Intravenous Infusion<sup>a</sup>**

	Infusion time (h)		
	0	24	48
TG (mg/L)	0.92 ± 0.11	1.04 ± 0.16	1.10 ± 0.31
FFA (μM)	311 ± 35	1012 ± 173**	1222 ± 119**
Glycerol (μM)	0.32 ± 0.06	0.61 ± 0.10**	0.68 ± 0.29**
NE (ng/L)	1.53 ± 0.12	1.17 ± 0.10*	0.63 ± 0.07**

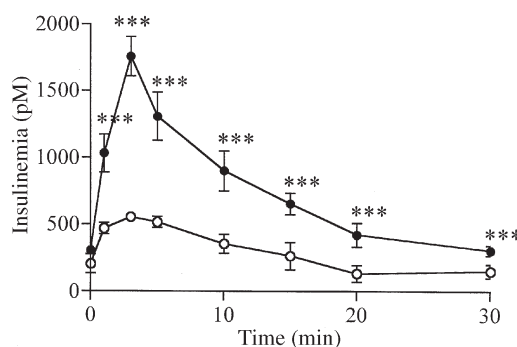
<sup>a</sup>Values are mean ± SEM. \*P < 0.05; \*\*P < 0.01, significantly different from time 0. NE, norepinephrine.

**Effect of lipid infusion on in vivo GIIS.** The *in vivo* time course of plasma insulin concentrations are depicted in Figure 1. At time 0, plasma insulin was similar in both groups. After glucose injection, insulin level was significantly higher at all time points in lipid-infused compared to control rats. Changes in glucose concentration were similar in both groups (data not shown).

**Pancreatic NE turnover.** We found a significant reduction of the endogenous pancreatic stores (control: 419 ± 3 ng; IL: 293 ± 4 ng; Table 2) as well as a 28% decrease in turnover rate of NE in the pancreas of IL rats as compared to control rats (control: 63.2 ± 0.5 ng/h; IL: 45.5 ± 0.6 ng/h), with no significant changes in NE half-life.

**Islet and β-cell α<sub>2</sub> adrenoceptor binding characteristics.** The 48-h intravenous lipid infusion resulted in a threefold decrease in sonicated islet α<sub>2</sub> adrenoceptor number (control: 38.8 ± 7.6 fmol/mg of proteins vs. 13.9 ± 2.2 fmol/mg of proteins in IL rats; Fig. 2A) and a twofold decrease in whole β-cell binding sites number (control: 112.3 ± 26.8 fmol/10<sup>6</sup> cells; IL: 61.3 ± 10.9 fmol/10<sup>6</sup> cells; Fig. 3A). The dissociation constant (K<sub>d</sub>) is significantly reduced in IL rats compared to controls, thus reflecting a higher affinity, as measured on islet homogenates (control: 2.53 ± 0.41 nM; IL: 0.51 ± 0.19 nM; Fig. 2B) as well as on whole isolated β-cells (control: 1.22 ± 0.37 nM; IL: 0.24 ± 0.08 nM; Fig. 3B).

**β-Cell α<sub>2A</sub> adrenoceptor mRNA concentration.** Using competitive quantitative RT-PCR, we found no difference in the concentration of α<sub>2A</sub> adrenoceptor mRNA between IL and control rats (data not shown).



**FIG 1.** Time course of plasma insulin during glucose-induced insulin secretion after intravenous lipid infusion. Control rats (○) and IL (●) rats. Values are mean ± SEM. \*\*\*P < 0.001, significantly different from control rats. IL, Intralipid-infused, where IL is supplied by KabiVitrum (Stockholm, Sweden).

**TABLE 2**  
Pancreatic NE Levels ( $NE_0$ ), Fractional Turnover Constants ( $k$ ), and Turnover Rates<sup>a</sup> (TR)

	$NE_0$ (ng)	$k$ ( $h^{-1}$ )	TR (ng/h)
Control	419 ± 3	0.151	63.2 ± 0.5
IL	293 ± 4**	0.156	45.5 ± 0.6**

<sup>a</sup>Values are mean ± SEM. \*\* $P < 0.01$ , significantly different from control rats. IL, Intralipid-infused rats. Intralipid source: KabiVitrum (Stockholm, Sweden).

**Islet phospholipid composition.** There was no significant difference in PC and PI relative intensities in islets of IL rats compared to controls (data not shown). In PE species, we found a significant 47% elevation in the relative intensity of palmitoyl-oleoyl-PE (POPE: 16:0/18:1 and 18:1/16:0; control rats: 8.8 ± 1.3%; IL rats: 16.5 ± 1.3%, Fig. 4) and a 28% increase in stearyl-linoleyl-PE (18:0/18:2; control rats: 24 ± 0.9%; IL rats: 33.5 ± 3.2%, Fig. 4).

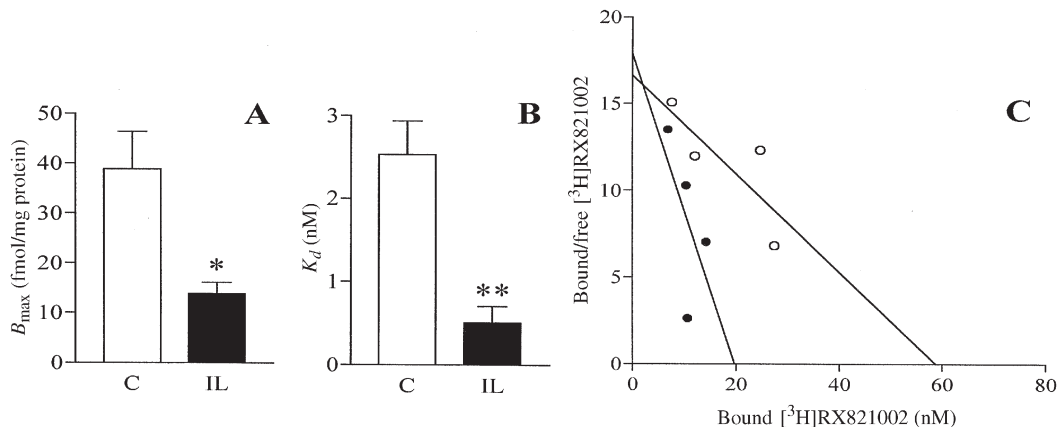
## DISCUSSION

Our aim was to understand how lipids induced islet catecholamine hypersensitivity. In this study, we report that a

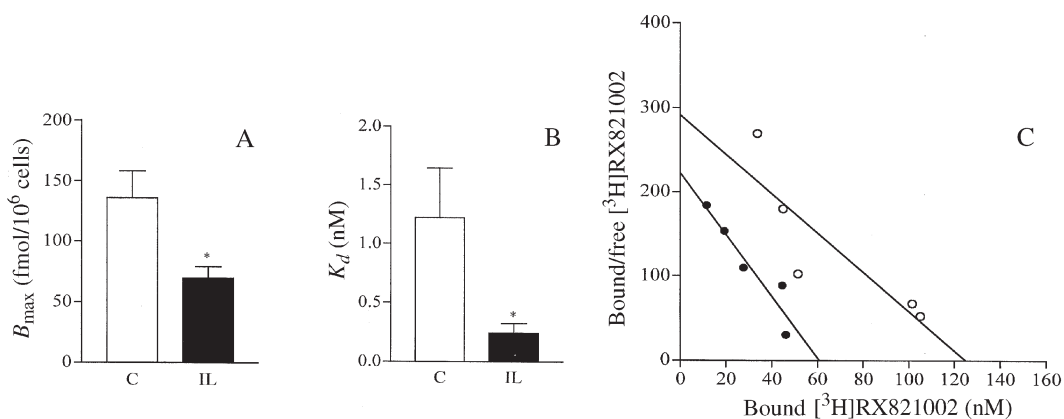
48-h increase in plasma FFA alters the binding characteristics of  $\beta$ -cell  $\alpha_2$  adrenoceptors.

We confirmed that a 48-h lipid infusion leads to an increased GIIS (4). We had previously established that this was partly the result of a reduced sympathetic nervous activity, as measured at the cervical sympathetic ganglion level (4). Consequently, plasma NE concentrations were significantly lower in IL rats, reflecting changes in global sympathetic nervous activity. To assess local changes in sympathetic firing rates, we measured pancreatic NE turnover rate and found a 28% reduction following lipid infusion. Thus, the attenuation in sympathetic activity was also found at the level of the pancreas, concordant with the increased GIIS in IL rats (4). A similar reduction in pancreatic NE turnover was described in diet-induced and genetically obese rats (8,21–23), suggesting that changes in pancreatic catecholamine content may therefore be a consequence of the main metabolic abnormality related to obesity, i.e., chronic elevation of plasma FFA concentration.

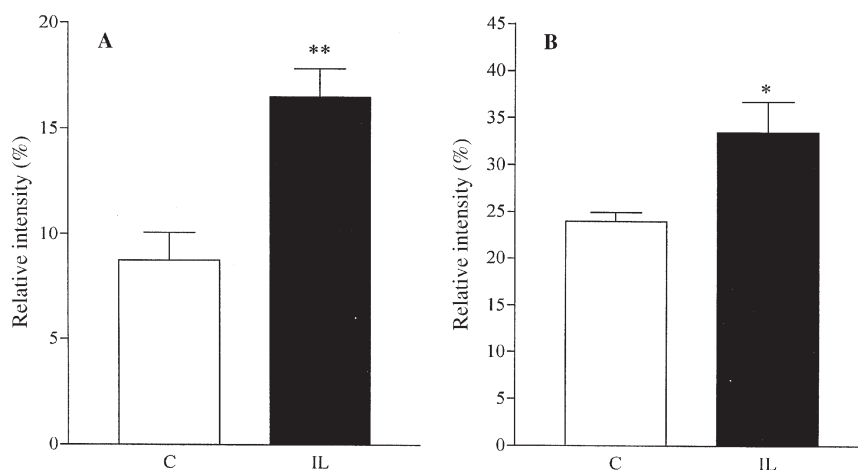
Using radioligand binding assay, we showed that hyperlipidemia induced a fivefold decrease in  $\beta$ -cell  $\alpha_2$  adrenoceptor dissociation constant ( $K_d$ ), reflecting an enhanced affinity for the radioligand. Because  $\alpha_{2A}$  adrenoceptors are the pre-



**FIG. 2.** Islet  $\alpha_2$  adrenoceptor characteristics after intravenous lipid infusion. (A) Maximal binding; (B) dissociation constant ( $K_d$ ); (C) Scatchard representation: control (C) rats (○) and IL rats (●). Values are mean ± SEM. \* $P < 0.05$ ; \*\* $P < 0.01$ , significantly different from control rats. [<sup>3</sup>H]RX821002, a benzodioxane derivative that exhibits high affinity for  $\alpha_2$ -adrenergic receptors; for other abbreviation see Figure 1.



**FIG. 3.**  $\beta$ -Cell  $\alpha_2$  adrenoceptor characteristics after intravenous lipid infusion. (A) Maximal binding; (B) dissociation constant ( $K_d$ ); (C) Scatchard representation: C rats (○) and IL rats (●). Values are mean ± SEM. \* $P < 0.05$ , significantly different from control rats. For abbreviations see Figures 1 and 2.



**FIG. 4.** Islet phospholipid composition after intravenous infusion. Percentage of relative intensity of *m/z* 700 (16:0/18:1 and 18:1/16:0) and 742 (18:0/18:2) PE species in isolated islets from C (open bars) and IL rats (solid bars). Values are mean ± SEM. \**P* < 0.05, \*\**P* < 0.01, significantly different from controls.

dominant form of β-cell α<sub>2</sub> adrenoceptors, this result could also account for the islet hypersensitivity to oxymetazoline in IL rats (4). Other studies have demonstrated that hyperlipidemia is associated with a higher adrenoceptor sensitivity (24). The lower pancreatic NE stores may account for the higher β-cell α<sub>2A</sub> adrenoceptor affinity in IL rats, since ligand depletion stabilizes high-affinity forms of the receptor, as shown in ventromedial hypothalamic nucleus-lesioned rats (25). However, we cannot exclude a direct effect of FFA on the pancreatic β-cell, as shown in other cell types (24). High extracellular lipid levels can alter the FA profile of membranes, changing membrane fluidity, as shown both *in vivo* (26) and *in vitro* (27). It is established that changes in receptor lipid environment change G-protein-coupled receptor ligand affinity (28), and this may be enhanced in adrenoceptors where the ligand binding site is a hydrophobic region located inside the plasma membrane. Our evidence suggests that intravenous lipid infusion changes islet phospholipid content. Particularly, we found an increase in phosphoethanolamine species containing infused FA such as palmitate (10% of the infused emulsion), oleate (23%), stearate (4%), and linoleate (53%). Such changes may be partly responsible for the increased β-cells' α<sub>2A</sub> adrenoceptor affinity in hyperlipidemic rats.

Another important result in our study is the threefold decrease in the number of islet α<sub>2</sub> adrenoceptor binding sites in IL rats, as compared to controls. The α<sub>2A</sub> adrenoceptor being the predominant α<sub>2</sub> subtype in pancreatic β-cells (29), these changes likely reflect modifications in islet α<sub>2A</sub> adrenoceptors. We measured α<sub>2</sub> adrenoceptor binding sites on whole β-cells and found a similar decrease. The lower number of α<sub>2A</sub> adrenoceptors was particularly surprising considering the reduction in pancreatic NE content in these rats, which, in normal physiological states, is coupled to an upregulation of adrenoceptors (30). However, several other studies have described a similar defect in α<sub>2</sub> adrenoceptor regulation in response to NE release in obesity-related states (21,31,32). Par-

ticularly, Levin (21,31) found that in hypothalamic nuclei of obesity-prone rats, both α<sub>2</sub> adrenoceptor number and NE turnover were decreased when compared to obesity-resistant rats.

The α<sub>2A</sub> adrenoceptor mRNA concentration in isolated β-cells is not attenuated in IL rats, as shown using quantitative competitive RT-PCR. Thus, we conclude that lipids affect islet adrenoceptor density by acting at the posttranslational level. One hypothesis is receptor palmitoylation, which is a dynamic process regulating α<sub>2A</sub> adrenoceptor function (33). In favor of this hypothesis, we found that IL rat islets display a higher islet POPE content, reflecting a greater palmitate availability for receptor palmitoylation. α<sub>2A</sub> adrenoceptors contain a potential site for palmitoylation, i.e., Cys 442, in the carboxyterminal region. It is now established that α<sub>2A</sub> adrenoceptor downregulation is palmitoylation-dependent (34). Receptor downregulation may thus occur in response to lower catecholamine levels than in controls, resulting in a reduced α<sub>2A</sub> adrenoceptor number with no concomitant increase in NE pancreatic content. These results, although preliminary, suggest that hyperlipidemia may alter β-cell signal transduction pathways, explaining the defective islet response to regulators such as NE, as described in other hyperlipidemic models (21,31).

Lower pancreatic sympathetic output and α<sub>2A</sub> adrenoceptor number may account for enhanced GIIS in IL rats. In addition, the higher α<sub>2A</sub> adrenoceptor affinity may explain the pancreatic hypersensitivity to oxymetazoline. As shown in humans in the very early stages of obesity, sympathetic tone is low and, as reported here, may be associated with islet hypersensitivity to catecholamine (35). Later, if the sympathetic tone were to increase, as is the case in obese individuals, such a hypersensitivity would become deleterious for pancreatic function and would account for the abnormal GIIS in obese, prediabetic subjects. The lipid-related changes in islet catecholamine receptor and metabolism reported here provide new insights into the perturbations of islet responsiveness to glucose due to chronic elevation of FFA concentration.



## ACKNOWLEDGEMENTS

We would like to thank Géraldine Bienvenu (INSERM U515, Paris, France; director: Professor Yves le Bouc) and the rest of the staff for their helpful technical support.

## REFERENCES

- Ahren, B., Taborsky, G.J., Jr., and Porte, D., Jr. (1986) Neuropeptidergic Versus Cholinergic and Adrenergic Regulation of Islet Hormone Secretion, *Diabetologia* 29, 827–836.
- Bentham, L., Mundinger, T.O., and Taborsky, G.J., Jr. (2001) Parasympathetic Inhibition of Sympathetic Neural Activity to the Pancreas, *Am. J. Physiol. Endocrinol. Metab.* 280, E378–E381.
- Ahrén, B. (2000) Autonomic Regulation of Islet Hormone Secretion—Implications for Health and Disease, *Diabetologia* 43, 393–410.
- Magnan, C., Collins, S., Berthault, M.F., Kassis, N., Vincent, M., Gilbert, M., Pénicaud, L., Ktorza, A., and Assimacopoulos-Jeannet, F. (1999) Lipid Infusion Lowers Sympathetic Nervous Activity and Leads to Increased  $\beta$ -Cell Responsiveness to Glucose, *J. Clin. Invest.* 103, 413–419.
- Troisi, R.J., Weiss, S.T., Parker, D.R., Sparrow, D., Young J.B., and Landsberg, L. (1991) Relation of Obesity and Diet to Sympathetic Nervous System Activity, *Hypertension* 5, 669–677.
- Scherrer, U., Owlya, R., and Lepori, M. (1996) Body Fat and Sympathetic Nerve Activity, *Cardiovasc. Drugs Ther.* 10, 215–222.
- Peterson H.R., Rothschild, M., Weinberg, C.R., Fell, R.D., McLeish, K.R., and Pfeifer, M.A. (1988) Body Fat and the Activity of the Autonomic Nervous System, *N. Engl. J. Med.* 318, 1077–1083.
- Levin, B.F., Triscari, J., and Sullivan, A.C. (1983) Altered Sympathetic Activity During Development of Diet-Induced Obesity in Rat, *Am. J. Physiol.* 244, R347–R355.
- Young, J.B., and Walgren, M.C. (1994) Differential Effects of Dietary Fats on Sympathetic Nervous Activity in the Rat, *Metabolism* 43, 51–60.
- Brodie, B.B., Costa, E., Dlabac A., Neff, N.H., and Smookler, H.H. (1966) Application of Steady State Kinetics to the Estimation of Synthesis Rate and Turnover Time of Tissue Catecholamines, *J. Pharmacol. Exp. Ther.* 154, 493–498.
- Pralong, W.F., Bartley, C., and Wollheim, C.B. (1990) Single Islet  $\beta$ -Cell Stimulation by Nutrients: Relationship Between Pyridine Nucleotide, Cytosolic  $Ca^{2+}$  and Secretion, *EMBO J.* 9, 53–60.
- Van de Winkel, M., Maes, E., and Pipeleers, D. (1982) Islet Cell Analysis and Purification by Light Scatter and Autofluorescence, *Biochem. Biophys. Res. Comm.* 107, 525–532.
- Nielsen, D.A., Lernmark, A., Berelowitz, M., Bloom, G.D., and Steiner, D.F. (1982) Sorting of Pancreatic Islet Subpopulation by Light Scattering Using a Fluorescence-Activated Cell Sorter, *Diabetes* 31, 299–306.
- Lowry, O.H., Rosebrough, N.J., Farr, A.L., and Randall, A.J. (1951) Protein Measurement with the Folin Phenol Reagent, *J. Biol. Chem.* 193, 265–275.
- Chomczynski, P., and Sacchi, N. (1987) Single-Step Method of RNA Isolation by Acid Guanidium Thiocyanate-Phenol-Chloroform Extraction, *Anal. Biochem.* 162, 156–159.
- Chan, S.L., Perrett, C.W., and Morgan, N.G. (1997) Differential Expression of  $\alpha_2$ -Adrenoceptor Subtypes in Purified Rat Pancreatic Islet A- and B-Cells, *Cell. Signal.* 9, 71–78.
- Ramanadham, S., Hsu, F.F., Bohrer, A., Nowatzke, W., Ma, Z., and Turk, J. (1998) Electrospray Ionization Mass Spectrometric Analyses of Phospholipids from Rat and Human Pancreatic Islets and Subcellular Membranes: Comparison to Other Tissues and Implications for Membrane Fusion in Insulin Exocytosis, *Biochemistry* 37, 4553–4567.
- Hsu, F.F., Bohrer, A., and Turk, J. (1998) Formation of Lithiated Adducts of Glycerophosphocholine Lipids Facilitates Their Identification by Electrospray Ionization Tandem Mass Spectrometry, *J. Am. Soc. Mass Spectrom.* 9, 516–526.
- Hsu, F.F., and Turk, J. (2000) Characterization of Phosphatidylinositol, Phosphatidylinositol-4-phosphate, and Phosphatidylinositol-4,5-bisphosphate by Electrospray Ionization Tandem Mass Spectrometry: A Mechanistic Study, *J. Am. Soc. Mass Spectrom.* 11, 986–999.
- Hsu, F.F., and Turk, J. (2000) Charge-Remote and Charge-Driven Fragmentation Processes in Diacyl Glycerophosphoethanolamine upon Low-Energy Collisional Activation. A Mechanistic Proposal, *J. Am. Soc. Mass Spectrom.* 11, 892–899.
- Levin, B.E. (1995) Reduced Norepinephrine Turnover in Organs and Brains of Obesity-Prone Rats, *Am. J. Physiol.* 268, R389–R394.
- Levin, B.E., Triscari, J., and Sullivan, A.C. (1983) Relationship Between Sympathetic Activity and Diet-Induced Obesity in Two Rat Strains, *Am. J. Physiol.* 245, R364–R371.
- Levin, B.E., Triscari, J., and Sullivan, A.C. (1982) Sympathetic Activity in Thyroid-Treated Zucker Rats, *Am. J. Physiol.* 243, R170–R178.
- Bordoni, A., Lorenzini, A., Horrobin, D.F., Biagi, P.L., and Hrelia, S. (1997) Manipulation of Lipid Composition of Rat Heart Myocytes Aged in Culture and Its Effect on  $\alpha_1$ -Adrenoceptor Stimulation, *Biochim. Biophys. Acta* 1348, 339–345.
- Campfield, L.A., Smith, F.J., and Larue-Achagiotis, C. (1986) Temporal Evolution of Altered Islet Neurotransmitter Sensitivity After VMH Lesion, *Am. J. Physiol.* 251, R63–R69.
- Heshka, J.T., and Jones, P.J. (2001) A Role for Dietary Fat in Leptin Receptor, OB-Rb, Function, *Life Sci.* 69, 987–1003.
- Renaud, G., Bouma, M.E., Foliot, A., and Infante, R. (1985) Free Fatty-Acid Uptake by Isolated Rat Hepatocytes, *Arch. Int. Physiol. Biochim.* 93, 313–319.
- Litman, B.J., Niu, S.-L., Polozova, A., and Mitchell, D.C. (2001) The Role of Docosahexaenoic Acid Containing Phospholipids in Modulating G Protein-Coupled Signaling Pathways: Visual Transduction, *J. Mol. Neurosci.* 16, 237–242.
- Chan, C.B., and MacPhail, R.M. (1992) Functional Characterization of  $\alpha$ -Adrenoceptors on Pancreatic Islets of fa/fa Zucker Rats, *Mol. Cell. Endocrinol.* 84, 33–37.
- Cooper, J., Bloom, F., and Roth, R. (1991) Norepinephrine and Epinephrine, in *The Biochemical Basis of Neuropharmacology*, pp. 220–284, Oxford University Press, Oxford, United Kingdom.
- Levin, B.E. (1990) Obesity-Prone and -Resistant Rats Differ in Their Brain [ $^3H$ ]Praminoclonidine Binding, *Brain Res.* 512, 54–59.
- Boundy, V., and Cincotta, A. (2000) Hypothalamic Adrenergic Receptor Changes in the Metabolic Syndrome of Genetically Obese (ob/ob) Mice, *Am. J. Physiol. Regul. Integr. Comp. Physiol.* 279, R505–R514.
- Morello, J.P., and Bouvier, M. (1996) Palmitoylation: A Post-translational Modification That Regulates Signalling from G-Protein Coupled Receptors, *Biochem. Cell Biol.* 74, 449–457.
- Eason, M.G., Jacinto, M.T., Theiss C.T., and Liggett, S.B. (1994) The Palmitoylated Cysteine of the Cytoplasmic Tail of  $\alpha_{2A}$ -Adrenergic Receptors Confers Subtype-Specific Agonist-Promoted Downregulation, *Proc. Natl. Acad. Sci. USA* 91, 11178–11182.
- Ravussin, E., and Gautier J.-F. (1999) Metabolic Predictors of Weight Gain, *Intl. J. Obes. Relat. Metab. Disord.* 23, 37–41.

[Received January 28, 2002, and in revised form March 26, 2002; revision accepted April 10, 2002]

# Evidence of a Tetradocosahexaenoic Cardiolipin in Some Marine Bivalves

Edouard Kraffe<sup>a</sup>, Philippe Soudant<sup>b</sup>, Yanic Marty<sup>a,\*</sup>,  
Nelly Kervarec<sup>c</sup>, and Philippe Jehan<sup>d</sup>

<sup>a</sup>Unité Mixte CNRS 6521, Université de Bretagne Occidentale, Brest, France, <sup>b</sup>Unité Mixte CNRS 6539, IUEM, Université de Bretagne Occidentale, Plouzané, France, <sup>c</sup>Laboratoire de RMN, Université de Bretagne Occidentale, Brest, France, and <sup>d</sup>CRMPO, Université de Rennes 1, Rennes, France

**ABSTRACT:** Separation of phospholipid classes in lipid extracts from the scallop *Pecten maximus*, the Pacific oyster *Crassostrea gigas*, and the blue mussel *Mytilus edulis* was conducted using HPLC. An isolated polar lipid fraction was found to contain a very high level of DHA, up to 80 mol% of the total FA. MS with electrospray ionization in the positive-ion mode, tandem MS (MS-MS) and multidimensional NMR spectroscopy were used to analyze the detailed chemical structure of this polar lipid fraction. The isolated fraction contained exclusively cardiolipin (CL) molecules, predominantly in a form with four docosahexaenoyl chains (Do<sub>4</sub>CL). To the best of our knowledge, this is the first time that such a CL form has been analytically characterized and described in these three bivalve species. This tetradocosahexaenoic CL is presumed to reflect a specific adaptation in bivalves that enhances the structural and functional mechanisms of biomembranes in response to variations in environmental conditions (temperature, salinity, emersion).

Paper no. L8989 in *Lipids* 37, 507–514 (May 2002).

In a previous study, we described a polar lipid fraction containing a high amount of DHA (22:6n-3) ester residue from the scallop *Pecten maximus* (1). By analyzing the polar lipid composition of larvae and male and female gonads of *P. maximus*, the specific composition of this fraction was confirmed (2–4). It was also demonstrated that though the 22:6n-3 level changed slightly with dietary modification (2,3), the overall

22:6n-3 FA molar percentage was maintained between 60 and 90 mol% of the total FA of the fraction. However, based on the retention times of standards obtained from the HPLC, the isolated fraction, initially designated as GLY, was not directly related to any of the less common phospholipid classes [PA, phosphatidylglycerol (PG); cardiolipin (CL), and glycolipids] that eluted nearby (1). Furthermore, attempts using HPLC and high-performance TLC (HPTLC), methods commonly utilized for lipid identification (5,6), produced contradictory results and failed to clearly identify this DHA-rich lipid class. As this point, we propose two hypotheses: (i) marine bivalves contain an unidentified polar lipid class, and (ii) the high DHA content of this lipid class changes the chromatographic retention time, thus leading to a previous mistaken identification. To clearly elucidate the molecular structure of this compound, further purification and use of conventional spectroscopic methods are required. MS is usually used in combination with NMR spectroscopy to determine molecular structure of purified unknown compounds (7,8). The recent development of “soft” ionization techniques for MS, such as electrospray ionization (ESI), provides the advantage of characterizing a wider variety of biological compounds including phospholipids (9,10). Particularly, the negative-ion mode ESI–MS system gives information about the molecular weight of the acyl constituents (10). Additionally, the positive-ion mode ESI+/MS is known to provide more information on the nature of the glycerol backbone (9). NMR has also been proven to be a valuable additional approach for the determination of structure and configuration of the core of some glycolipids and phospholipids (11,12). The present paper reports (i) the isolation and characterization of a previously described DHA-rich lipid fraction employing HPLC, HPTLC, and GC, and (ii) the determination of the structure and purity of this DHA-rich compound by the combination of ESI+/MS and ESI+/tandem MS (ESI+/MS-MS) in the positive-ion mode with NMR. The putative functions of this phospholipid in marine bivalves are also discussed.

## MATERIALS AND METHODS

**Materials.** Mammalian CL standard (MamCL) [CL from bovine heart, with four linoleoyl chains (L<sub>4</sub>CL) content

\*To whom correspondence should be addressed at Unité Mixte CNRS 6521, Université de Bretagne Occidentale, BP809, 29285 Brest Cedex, France. E-mail: Yanic.Marty@univ-brest.fr

Abbreviations: CL, cardiolipin, common name of diphosphatidylglycerol; DQF-COSY, double-quantum filter correlated spectroscopy; DG, diacylglycerol; DGDG, digalactosyldiacylglycerols; DorCL, docosahexaenoic-rich cardiolipin fraction; Do<sub>4</sub>CL, 1',3'-bis[1,2-didocosahexaenoyl-*sn*-glycero-3-phospho]-glycerol, cardiolipin with four docosahexaenoyl chains; also named tetradocosahexaenoic cardiolipin; Do<sub>3</sub>PCL, cardiolipin with three docosahexaenoyl and one palmitoyl chains; ESI, electrospray ionization; HMQC, heteronuclear multiple quantum coherence; HPTLC, high-performance thin-layer chromatography; L<sub>4</sub>CL, 1',3'-bis[1,2-dilinoleoyl-*sn*-glycero-3-phospho]-*rac*-glycerol, cardiolipin with four linoleoyl chains; M<sub>2</sub>PG, 1,2-dimyristoyl-*sn*-glycero-3-phosphoglycerol; M<sub>4</sub>CL, 1',3'-bis[1,2-dimyristoyl-*sn*-glycero-3-phospho]-*rac*-glycerol; MamCL, mammalian cardiolipin standard; MGDG monogalactosyldiacylglycerols; MS-MS, tandem MS; O<sub>2</sub>PA, 1,2-dioleoyl-*sn*-glycero-3-phosphoric acid; O<sub>4</sub>CL, 1',3'-bis[1,2-dioleoyl-*sn*-glycero-3-phospho]-*rac*-glycerol; P<sub>2</sub>PA, 1,2-dipalmitoyl-*sn*-glycero-3-phosphoric acid; PG, phosphatidylglycerol; SAPG, 1-stearoyl-2-arachidonoyl-*sn*-glycero-3-phosphoglycerol; TOF, time of flight.

>98%, sodium salt]; phosphatidic acids [di-oleic ( $O_2PA$ ) and di-palmitic ( $P_2PA$ )]; phosphatidylglycerols (PG) [stearic-arachidonic (SAPG) and dimyristic ( $M_2PG$ )]; glycolipid standards [monogalactosyldiacylglycerols (MGDG) and digalactosyldiacylglycerols (DGDG) (from whole wheat flour)] and PE (from bovine brain) were obtained from Sigma (St. Quentin Fallavier, France). CL standards (sodium salts) with four oleoyl ( $O_4CL$ ) and four myristoyl chains ( $M_4CL$ ) were obtained from Avanti Polar Lipids (Alabaster, AL). Boron trifluoride ( $BF_3$ , 10% by wt in methanol) was obtained from Supelco (St. Quentin Fallavier, France). Other described reagents and solvents were purchased from Merck (Darmstadt, Germany).

**Sample preparation and lipid extraction.** Adult *P. maximus* scallops were collected from the Bay of Brest in September 2000. The muscles of 10 individual scallops were removed and homogenized with a Danguomeau homogenizer at  $-180^\circ C$ . Lipid extraction was conducted on muscle homogenates according to the method described by Folch *et al.* (13). The organic phase containing total lipids was washed twice by addition of methanol/water as described by Nelson (14). Then 0.01 wt% BHT (antioxidant) was added, and the extract was stored at  $-20^\circ C$  under nitrogen. Total lipids were also extracted from whole body tissues of Pacific oyster (*Crassostrea gigas*) and blue mussel (*Mytilus edulis*) as indicated above (four individuals of each species collected from the Bay of Best in September 2000, were pooled and homogenized).

**Separation of polar lipids by silica gel microcolumn.** An aliquot of the lipid extracts was evaporated to dryness, and lipids were recovered with three washings of 500  $\mu L$  of  $CHCl_3/MeOH$  (98:2, vol/vol) and deposited at the top of a silica gel microcolumn [30  $\times$  5 mm i.d., packed with Kieselgel 60 (70–230 mesh, Merck) previously heated at  $450^\circ C$  and deactivated with 5 wt%  $H_2O$ ] (15). Neutral lipids were eluted with 10 mL of  $CHCl_3/MeOH$  (98:2, vol/vol). The polar lipid fraction was recovered with 15 mL of MeOH and stored at  $-20^\circ C$  for later phospholipid class separation by HPLC and FA composition analysis by GC.

**Isolation of DHA-rich CL fraction (DorCL) by silica gel liquid chromatography (LC) column.** To obtain high quantities of the DorCL fraction, an aliquot of *P. maximus* muscle lipid extract was evaporated to dryness, recovered with three washings of 1 mL of  $CHCl_3/MeOH$  (98:2, vol/vol), and deposited at the top of a silica gel column (40  $\times$  25 mm i.d., same packing as the one described above). The neutral lipids were first eluted with 160 mL of  $CHCl_3/MeOH$  (98:2, vol/vol), and then 160 mL of acetone was passed through the column to elute glycolipids. The DorCL fraction was recovered by rinsing the column with 160 mL of  $CHCl_3/MeOH$  (90:10, vol/vol). An aliquot of this isolated fraction was taken to determine the purity by HPLC and GC. The rest was further analyzed using NMR and MS.

**Separation of phospholipid classes and FA analysis.** Separation of the phospholipid classes was achieved, based on the method previously described (1), on a Waters (Milford, MA) HPLC system (UV detection at 206 nm). For a better identifi-

cation within the low-polarity phospholipid area, this method was modified as follows. Only the diol column (OH-bound silica gel column, Lichrosorb Diol 5  $\mu m$ , 250  $\times$  4 mm i.d.; Merck) was employed, and a binary mobile phase was used. A linear gradient of 15 min was performed from 100% solvent A (acetonitrile) to an 8:2 ratio of solvent A and solvent B (acetonitrile/methanol/phosphoric acid, 93:5:1.5, by vol). This solvent ratio was maintained for 5 min, and followed by a linear gradient to 100% solvent B in 10 min. The column was maintained on solvent B for 30 min, and then switched to 100% solvent A during 15 min to reactivate the column. Solvent flow rate was 1 mL/min. The DorCL fraction was identified, collected, and analyzed for FA composition using GC after transesterification ( $MeOH/BF_3$ ) (4).

**Characterization of DorCL isolated from LC by HPTLC.** HPTLC (Silica gel 60, 10  $\times$  10 cm; Merck) was pre-run with a mixture of hexane/diethyl ether (1:1, vol/vol). The plate was then dried and activated for 1 h at  $160^\circ C$ . First, the isolated DorCL fraction and phospholipid standards (SAPG, MamCL, PE, DGDG, and MGDG) were dissolved in chloroform/methanol (2:1, vol/vol), then deposited in separate lanes of the plate and developed with the solvent system methyl acetate/isopropanol/chloroform/methanol/3 M KCl (10:10:10:4:3.6, by vol). Second, to evidence the possible influence of the FA chain unsaturation on the chromatographic behaviors of CL and PG, equivalent concentrations of DorCL and lipid standards ( $M_4CL$ ,  $O_4CL$ , MamCL, SAPG,  $M_2PG$ ) were converted into a single salt form by dissolving them, in a solution of chloroform/methanol/1 M  $CaCl_2$  (65:25:3 by vol), before spotting them onto HPTLC plates. This approach eliminated the influence due to the cations with which acidic phospholipids are associated (5). Then they were developed using a solvent system containing the same cation (chloroform/methanol/0.5 M  $CaCl_2$ ; 65:40:4, by vol) to prevent any ion exchange during chromatography (5). To visualize the lipid bands, HPTLC plates were charred 20 min at  $160^\circ C$  after dipping in a solution containing 8% (by vol) orthophosphoric acid and 3% (by wt) cupric sulfate.

**ESI-MS.** ESI-MS analyses were performed on a high-resolution tandem mass spectrometer ZABSpec TOF (Micromass, Manchester, United Kingdom) with an EBE time of flight (TOF) geometry equipped with a micro-ESI source. High-resolution masses were obtained from ions of a known internal standard, polyethyleneglycol, added to the sample before injection. Mass measurement accuracy was usually less than 5 ppm. Mass spectra were obtained in the positive mode over the  $m/z$  range of 100 to 3,000 (ESI accelerating potential: +4.0 kV). All samples were dissolved in chloroform/methanol (1:1, vol/vol). This solvent mixture was found to give stable electrospray conditions and optimal parent quasi-molecular ion peaks. Samples were then continuously injected into the system at a flow rate of 10  $\mu L/min$  (0.3  $\mu L/min$  in nanospray mode) by a syringe pump. MS/MS of cardiolipins after ESI was obtained by passage of the mass-selected precursor ion in the TOF analyzer. Kinetic energy of ions before collision was 500 eV, and dissociation was induced through collision activation with methane gas.



**NMR spectroscopy.** All NMR analyzes were conducted on a Bruker DRX-500 Avance Spectrometer (Wissembourg, France) equipped with a triple inverse 5-mm  $^1\text{H}/\{^1\text{H}\}/^{13}\text{C}$  gradient probehead. The probe temperature was 298°K. Prior to analysis, lipid samples (DorCL and standards) were dissolved in  $\text{CDCl}_3/\text{CD}_3\text{OD}$  (1:2.5, vol/vol), except for MGDG, which was dissolved in  $\text{CDCl}_3$ . All samples were warmed and sonicated at about 30°C for about 5 min. 2-D NMR spectra were acquired with nonspinning samples with deuterium frequency locking.  $^1\text{H}$ - $^1\text{H}$  double-quantum filter correlated spectroscopy (DQF-COSY) and heteronuclear multiple quantum coherence (HMQC) were employed to assign signals and were performed according to standard pulse sequences with a delay of 60 ms. DQF-COSY and HMQC measurements on DorCL in the area 3.5–4.5 ppm were recorded by collecting 512 (F2)  $\times$  200 (F1) data points zero-filled to 512 (F1) using spectral width of 500 Hz (500 MHz) with a repetition time of 2 s.  $^1\text{H}$  and  $^{13}\text{C}$  NMR chemical shifts were expressed in ppm by reference to tetramethylsilane as external standard.

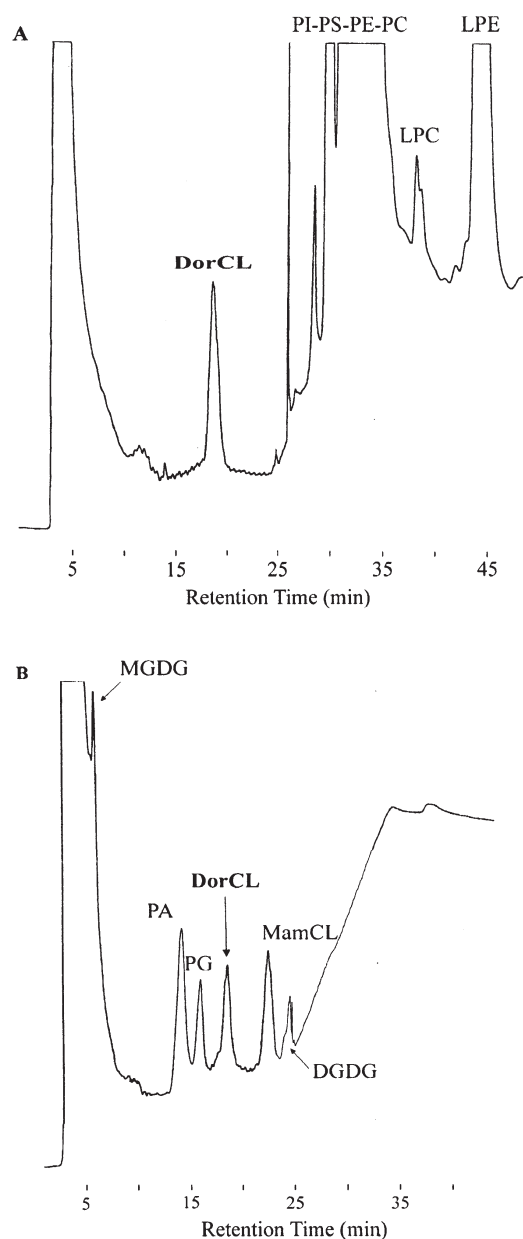
## RESULTS

**Analyzes of phospholipid classes by HPLC.** The previously unidentified DorCL peak eluted first, before all the identified phospholipid classes (Fig. 1A). Similar elution patterns were obtained when polar lipid fractions from the other two bivalve species, *C. gigas* and *M. edulis*, were analyzed. When the isolated DorCL fraction was co-injected with commercial phospholipid and glycolipid standards of similar polarity ( $\text{O}_2\text{PA}$ , SAPG, MamCL, MGDG, DGDG), it was eluted between the mammalian cardiolipin (MamCL) and PG (Fig. 1B).

**Analyzes of phospholipid classes by HPTLC.** HPTLC analysis of DorCL fraction together with the foregoing lipid standards also showed that the DorCL fraction had an  $R_f$  value 0.5 different from those lipid standards [SAPG (0.42); MamCL (0.45); PE (0.47); DGDG (0.57); MGDG (0.88)] (Fig. 2A). When the DorCL fraction and lipid standards (PG and CL with different unsaturation of acyl chains) were all converted to a single salt form prior to HPTLC analyses, results (Fig. 2B) revealed that elution differences existed between the CL standards and DorCL fraction, whereas SAPG and  $\text{M}_2\text{PG}$  were eluted together.

**FA composition of DorCL.** GC analysis of FAME derived from the isolated DorCL fraction of the three bivalve species showed a FA profile with 83–94 mol% of 22:6n-3 (DHA) (Table 1). Three other FA, 16:0, 22:5n-3 and 20:5n-3, are important minor components. The DorCL class contributed 0.6 to 1.0 mol% of the total phospholipids. In terms of polar lipids, 6.2 to 13.6 mol% of the total DHA content was found in the DorCL fraction.

**Isolation of DorCL by LC.** The proportion 90:10 (chloroform/methanol, vol/vol) was found to be the best solvent mixture to isolate the DorCL fraction for mass production. Although the controls [phospholipid standards: PA ( $\text{P}_2\text{PA}$ ,  $\text{O}_2\text{PA}$ ), PG ( $\text{M}_2\text{PG}$ , SAPG), and CL ( $\text{M}_4\text{CL}$ ,  $\text{O}_4\text{CL}$ , MamCL)] were found to elute using this solvent mixture, for all the

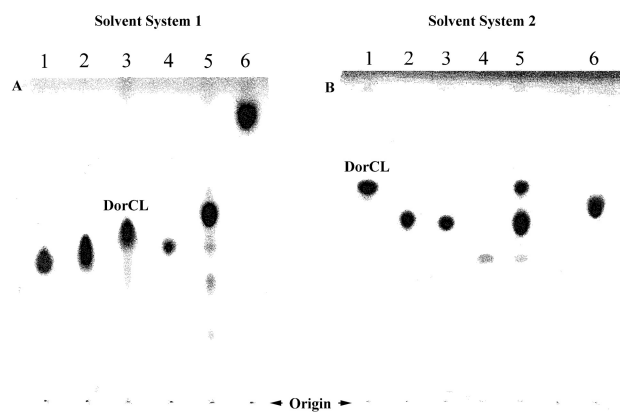


**FIG. 1.** HPLC separations of phospholipid classes. (A) Polar lipid extract of *Pecten maximus* muscle. (B) Co-injection of the isolated DHA-rich cardiolipin (DorCL) with standards of acidic phospholipids. Chromatographic conditions used are indicated in Materials and Methods section. LPC and LPE = 2-acyl-*sn*-glycero-3-phosphorylcholine and 2-acyl-*sn*-glycero-3-phosphorylethanolamine (resulting principally from the hydrolysis of plasmalogens by the mobile acid phase used); MGDG, monogalactosyldiacylglycerol; PA, phosphatidic acid; PG, phosphatidylglycerol; MamCL, mammalian cardiolipin standard; DGDG, digalactosyldiacylglycerol.

analyzed samples only the DorCL peak was detected when this 90:10 solvent fraction was analyzed by HPLC.

**ESI/MS.** Parent quasi-molecular ion peaks obtained for the DorCL mass spectrum (Fig. 3A) and for the MamCL sodium





**FIG. 2.** High-performance TLC analysis of the isolated DorCL and phospholipid standards. (A) SAPG = Lane 1, MamCL = 2, DorCL = 3, PE = 4, DGDG = 5, and MGDG = 6 were dissolved in chloroform/methanol solution (2:1, vol/vol) and subjected to solvent system 1 (methyl acetate/isopropanol/chloroform/methanol/3 M KCl, 10:10:10:4:3.6, by vol). (B) The polar solvent system 2 (chloroform/methanol/0.5 M CaCl<sub>2</sub>, 65:40:4, by vol) was used for the TLC analysis of CL (DorCL = Lane 1, MamCL = 2, O<sub>4</sub>CL = 3, M<sub>4</sub>CL = 4, CL mixture = 5) and PG [(SAPG + M<sub>2</sub>PG) = 6] with different acyl chain compositions; the compounds were applied in chloroform/methanol/1 M CaCl<sub>2</sub> (65:25:3, by vol) solution at equivalent concentrations. Developed compounds were visualized by cupric acid treatment and charring. SAPG, 1-stearoyl-2-arachidonoyl-*sn*-glycero-3-phosphoglycerol; O<sub>4</sub>CL, 1',3'-bis[1,2-dioleoyl-*sn*-glycero-3-phospho]-*rac*-glycerol; M<sub>4</sub>CL, 1',3'-bis[1,2-dimyristoyl-*sn*-glycero-3-phospho]-*rac*-glycerol; CL, cardiolipin; M<sub>2</sub>PG, 1,2-dimyristoyl-*sn*-glycero-3-phosphoglycerol. For other abbreviations see Figure 1.

salt form mass spectrum (Fig. 3B) revealed the mass difference between these two CL. For MamCL, the mass-to-charge ( $m/z$ ) 1515.9 corresponds to the Na<sup>+</sup> adduct of the sodium salt form of a CL with four linoleoyl chains (L<sub>4</sub>CL). There is a 192 u difference between a sodiated ion at  $m/z$  1707.9 in the DorCL mass spectrum and the quasi-molecular ion of MamCL at  $m/z$  1515.9. This value corresponds exactly to the mass difference between a CL (DorCL) with four 22:6n-3 acyl chains and a CL (MamCL) with four 18:2n-6 chains. Moreover, the comparison between the two positive ion mass spectra shows that a similar fragmentation occurred. Indeed, there are differences of 144 u between the fragment at 1357.4 of DorCL and the fragment at 1213.5 of MamCL, 96 u between fragments at 995.5, 893.4, and 735.6 of DorCL, and fragments at 899.4, 797.5, and 639.5 of MamCL, or 48 u between the fragment at 373.2 of DorCL and the fragment at 325.2 of MamCL. These differences correspond to the mass differences between three, two, or one chains of 22:6n-3 and 18:2n-6. A comparison of M<sub>4</sub>CL and O<sub>4</sub>CL standard spectra (data not shown) gave the same results.

The collision-induced dissociation study (MS-MS) of the quasi-molecular ion of DorCL produced an equivalent product-ion pattern as the ESI+/MS analysis, except for the fragments at  $m/z$  735.6 and 1967.9. The minor sodiated fragment ion at  $m/z$  1357.8 may correspond to a complex fragmentation that resulted in a loss of one FA chain plus Na<sup>+</sup>. Fragment ions at 995.6 and 893.4 were shown to correspond,

**TABLE 1**

**FA Tissue Composition of the DorCL Fraction of *C. gigas*, *M. edulis*, and *P. maximus* (mol% of the total FA of the fraction)**

FA	Bivalve		
	<i>C. gigas</i> , whole	<i>M. edulis</i> , whole	<i>P. maximus</i> , muscle
16:0	4.3	1.6	3.2
18:0	2.5	3.3	2.5
18:1n-9	1.4	Trace	Trace
18:1n-7	Trace <sup>a</sup>	Trace	Trace
20:1n-9	Trace	1.9	0.0
20:1n-7	1.2	0.8	0.0
18:2n-6	0.0	1.7	0.0
18:3n-3	0.0	5.9	0.0
20:4n-6	Trace	Trace	0.0
20:5n-3	2.3	1.9	Trace
21:5n-3	1.4	Trace	Trace
22:5n-6	Trace	0.0	0.0
22:5n-3	1.4	0.4	4.1
22:6n-3	85.5	82.6	90.1
Total PUFA	90.6	92.5	94.1
Portion of 22:6n-3 in DorCL (%) <sup>b</sup>	13.6	6.2	7.4
DorCL (mol%) <sup>c</sup>	0.9	0.6	1.0

<sup>a</sup>Trace, <0.1%.

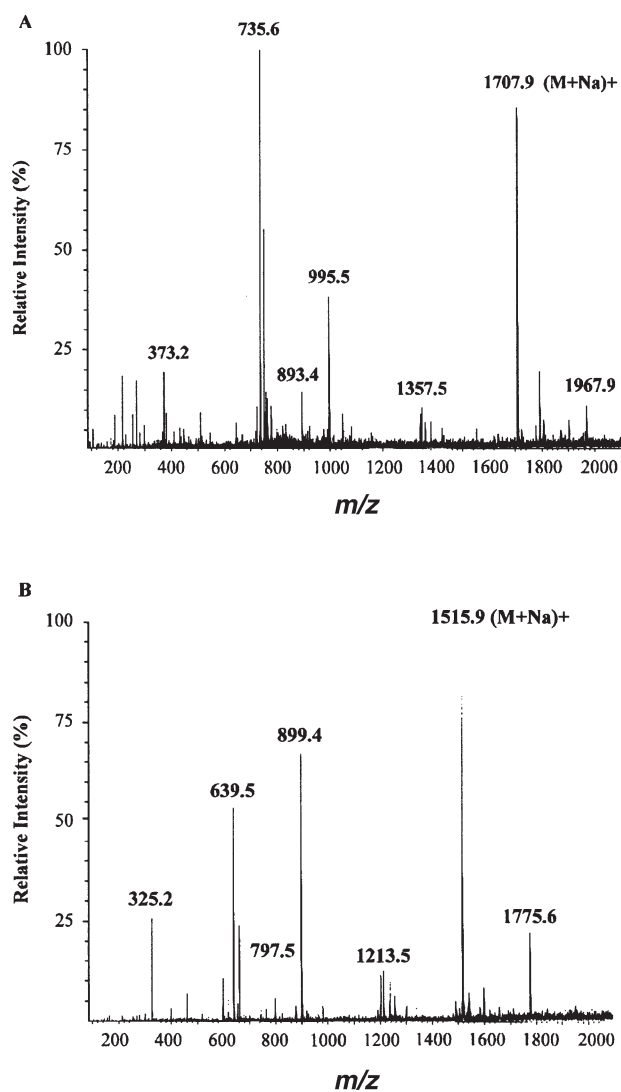
<sup>b</sup>Percentage of 22:6n-3 in the DorCL class relatively to total 22:6n-3 content.

<sup>c</sup>Percentage of the DorCL class relative to other PL classes. Organisms: *Crasostrea gigas*, *Mytilus edulis*, *Pecten maximus*. Abbreviation: DorCL, DHA-rich cardiolipin fraction.

respectively, to the analogs of PG, [(PG-H + PO<sub>3</sub>Na) + Na]<sup>+</sup> and [PG-H + Na]<sup>+</sup>, resulting from a loss of one diacylglycerol fragment (DG) and one PA fragment, respectively. There was also a peak at  $m/z$  645.3, which was believed to be from the fragment ion  $m/z$  995.6 with the loss of one FA chain plus Na<sup>+</sup>. The fragment at  $m/z$  735.6, which was absent from the positive-ion MS-MS, corresponds to a didocosaheptaenoyl-glycerol sodiated ion [DG + Na]<sup>+</sup>. The peak at  $m/z$  1967.9 for DorCL (also absent in the positive-ion MS-MS) shows a 192 u difference, with the corresponding peak at  $m/z$  1775.8 for MamCL. These particular ions were confirmed to be the dimer of a fragment ion [2(PG-H + PO<sub>3</sub>Na) + Na]<sup>+</sup> detected at  $m/z$  995.5 for DorCL and  $m/z$  899.4 for MamCL.

Finally, the exact mass of the quasi-molecular ion of 1707.9270 (Fig. 4), compared to the value of 1707.9259 calculated for a molecular formula C<sub>97</sub>H<sub>140</sub>O<sub>17</sub>P<sub>2</sub>Na<sub>3</sub>, further supports the assignment of this four-22:6n-3 O-acyl cardiolipin structure (Do<sub>4</sub>CL). The presence of a minor peak corresponding to the quasi-molecular ion of Do<sub>3</sub>PCL (tridocosaheptaenoyl-palmitoyl CL) was also noticed at  $m/z$  1636.9.

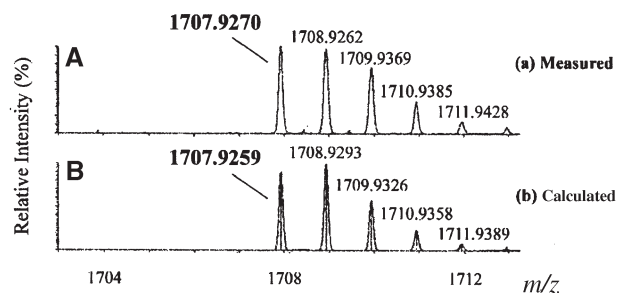
**NMR spectrometry.** Characteristic resonances of the sugar proton region of MGDG (3.5–4 ppm) or of the <sup>+</sup>NCH<sub>2</sub> multiplet (3.65 ppm) of a choline derivative were not apparent in the <sup>1</sup>H resonance spectrum (Fig. 5). This excluded the presence of carbohydrate moieties or of nitrogen in the DorCL fraction. The presence of unsaturated acyl chains was character-



**FIG. 3.** Positive ion electrospray ionization (ESI) mass spectra. (A) DorCL. (B) MamCL. Compounds dissolved in chloroform/methanol solution (1:1, vol/vol) before submission to ESI/MS, conditions as described in the Materials and Methods section. M-dissociated molecular form. For other abbreviations see Figure 1.

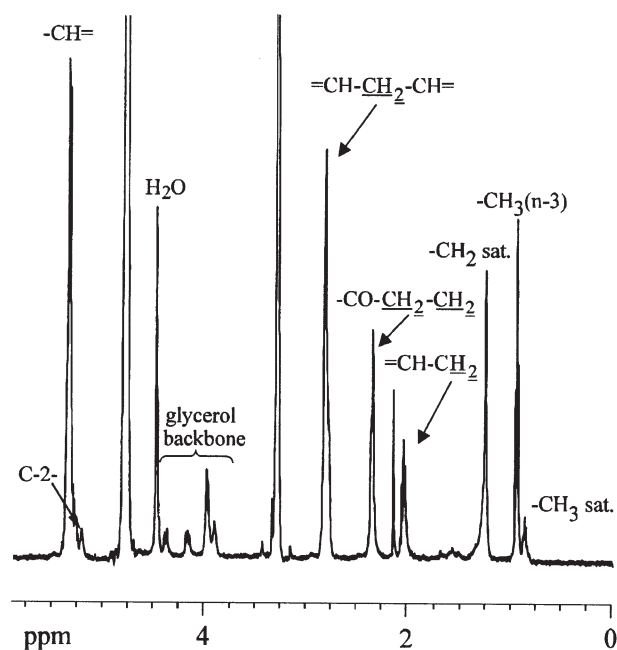
ized by the  $^1\text{H}$  and  $^{13}\text{C}$  resonances of olefinic  $-\text{CH}=\text{CH}-$ , bis-allylic and allylic methylene protons (Table 2) and validated by the  $^1\text{H}$  DQF-COSY and HMQC measurements (data not shown). Protons from terminal methyl groups show one triplet at 0.95 ppm (from unsaturated n-3 acyl chains) and one of weaker intensity at 0.88 ppm (mainly from 16:0 acyl chains). The integral ratio of these two triplets indicates a proportion of 82 mol% of n-3 PUFA. The integral ratio of triplet at 0.95 ppm and multiplet at 2.36 ppm ( $-\text{C}_\alpha\text{H}_2$  and  $-\text{C}_\beta\text{H}_2$ ) (where  $\alpha$  and  $\beta$  positions are relative to the carbonyl group) confirms that most of unsaturated n-3 acyl chains are constituted by 22:6n-3.

In considering the phospholipid backbone, the high-field single proton of C-2 outer glycerols resonated typically at 5.21 ppm ( $^1\text{H}$ ) and 71.56 ppm ( $^{13}\text{C}$ ). The other glycerol protons of the two quasi-equivalent outer glycerols and of the



**FIG. 4.** High-resolution ESI+MS measurement of  $(\text{M} + \text{Na})^+$ . (A) Experimental isotopic distribution. (B) Theoretical isotopic distribution.

central glycerol could be assigned from a comprehensive set of NMR data in the area 3.5–4.5 ppm (for details see the Materials and Methods section) (Fig. 5, Table 2). The eight-line multiplet at 4.38 and 4.16 ppm ( $^1\text{H}$ ), corresponding to an AB part of an ABX type system, was assigned to the magnetically inequivalent methylene protons ( $\text{C}-1-\text{H}_1$ ,  $\text{C}-1-\text{H}'_1$ ) of outer glycerols C-1. When the integral ratio of the proton signals of outer glycerols C-2 + C-1 to the remaining resonances at 3.98 and around 3.9 ppm ( $^1\text{H}$ ) (outer glycerols C-3 plus central glycerol protons) was calculated, it indicated a ratio of 0.62 ( $\approx 6:9$ ) corresponding to a CL. This is in good agreement with the ratio of 0.646 ( $\approx 6:9$ ) calculated for the MamCL standard. The corresponding integral ratios for PG and PA were 0.411 ( $\approx 3:7$ ) and 1.5 (3:2), respectively. The HMQC spectrum of DorCL (Fig. 6) allows the specific assignments of the nine protons from the two equivalent outer glycerols C-3 and from the C'-1, C'-2 and C'-3 of central glycerol. The methylene



**FIG. 5.**  $^1\text{H}$  resonance spectrum of DorCL. Detailed NMR data are depicted in Table 2. For abbreviation see Figure 1.

**TABLE 2**  
 **$^1\text{H}$  and  $^{13}\text{C}$  NMR Data of DorCL**

Component moiety	C numbering <sup>a</sup>	System	$^1\text{H}$ $\delta$ (ppm)	Multiplicity	$^{13}\text{C}$ $\delta$ (ppm)
Outer glycerols	C-1	$\text{CH}_2\text{O}$	4.16	<i>dd</i>	63.36
			4.38	<i>dd</i>	
	C-2	CHO	5.21	<i>m</i>	71.56
Central glycerol	C-3	$\text{CH}_2\text{OP}^b$	3.98	<i>m</i>	64.42
	C'-1 + C'-3	$\text{CH}_2\text{OP}^b$	3.89	<i>m</i>	66.55
			3.98	<i>m</i>	
Fatty acyl chains	C'-2	CHO	3.90	<i>m</i>	70.50
		$-\text{CH}=\text{CH}-$	5.35	<i>m</i>	128
	$-\text{CH}_2-(\text{CH}=\text{CH})^c$	2.06	<i>q</i>	21.23	
	$(=\text{CH})-\text{CH}_2-(\text{CH}=\text{CH})^d$	2.80	<i>m</i>	26.29	
	$-\text{C}_\alpha\text{H}_2^e$	2.36	<i>m</i>	34.80	
	$-\text{C}_\beta\text{H}_2^e$	2.36	<i>m</i>	23.39	
	$-\text{CH}_3$ (n-3) <sup>f</sup>	0.95	<i>t</i>	14.50	
	$-\text{CH}_3$ (sat) <sup>g</sup>	0.86	<i>t</i>	14.50	
	$-\text{CH}_2-$ (sat) <sup>h</sup>	1.25	<i>m</i>	30.53	

<sup>a</sup>Carbons of the cardiolipin backbone are designated as: C-1 (*sn*-1 O-acyl chain), C-2 (*sn*-2 O-acyl chain), or C-3 (-phosphate group) for the two outer glycerols and C'-1 (-phosphate group), C'-2 (-OH), or C'-3 (-phosphate group) for central glycerol.

<sup>b</sup>The protons of the methylene group show couplings to  $^{31}\text{P}$  (which shows a single resonance at +0.15 ppm relative to external  $\text{H}_3\text{PO}_4$ ).

<sup>c</sup>Allylic protons.

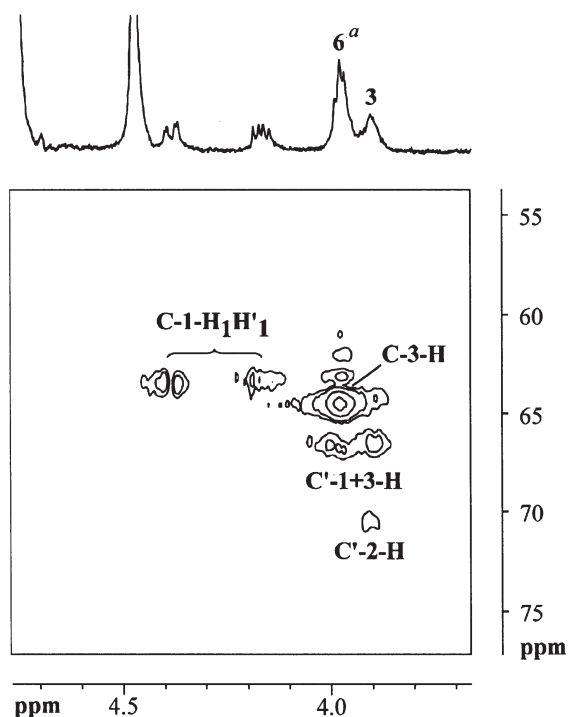
<sup>d</sup>Bis-allylic protons.

<sup>e</sup>Relatively to carbonyl group.

<sup>f</sup>From unsaturated (n-3) acyl chains.

<sup>g</sup>From saturated or unsaturated >(n-3) acyl chains.

<sup>h</sup>Non-desielding methylene protons. Hydrogen/carbon assignment was validated by  $^1\text{H}$  DQF-COSY double-quantum filter correlated spectroscopy and heteronuclear multiple quantum coherence.



**FIG. 6.** Heteronuclear multiple quantum coherence of the glycerol backbone region of DorCL. C' = central glycerol; C = phosphatidylglycerols. Assignments between H1 and H'1 may have to be reversed. <sup>a</sup>Proportion of hydrogen atoms in each signal, based on signal integration, are calculated relatively to  $\text{CH}_3$  peak integral [ $\text{CH}_3$ (n-3) for DorCL = 12]. For abbreviation see Figure 1.

protons from both C-3 outer glycerols at 64.42 ppm ( $^{13}\text{C}$ ) appear as a multiplet at 3.98 ppm ( $^1\text{H}$ ) ( $^1\text{H}$  DQF-COSY not represented). Part of the 3.98 ppm ( $^1\text{H}$ ) resonances and the most shielded resonances around 3.90 ppm have been assigned to the central glycerol protons. All these resonances are nearly synchronous and show a complex multiplet from spin-spin interactions between phosphorus  $^{31}\text{P}$  vicinal and geminal protons. However, two carbon resonances are clearly resolved at 66.55 and 70.5 ppm ( $^{13}\text{C}$ ). The signal at 66.55 ppm ( $^{13}\text{C}$ ) has been assigned to both phosphorylated C'-1 and C'-3 methylene groups. The other has been attributed to the C'-2 proton. Consequently, in DorCL (Fig. 6), the integral ratio of the multiplet (resonances at 3.98 ppm) to the nearby resonances (around 3.90 ppm) gave a ratio of  $\approx 6:3$ .

## DISCUSSION

Through isolation and chemical and structural analyses using a combination of HPLC, HPTLC, LC, GC, ESI+/MS, ESI+/MS-MS, and NMR, the present study provides evidence of the existence of a DHA-rich (22:6n-3 > 80 mol%) CL, in the three bivalve species *C. gigas*, *M. edulis*, and *P. maximus*. Although DorCL accounted for no more than 1 mol% of the total phospholipids in these three bivalve species, it contains up to 13.6 mol% of total DHA content of the polar lipids.

As shown from the results of the present study and from previous investigations (1–4), employing HPLC (Fig. 1B) or HPTLC (Fig. 2A,B) alone was unable to link the DorCL to any phospholipid class because chromatographic behaviors

of the former differed from the common CL. Chromatographic properties of acidic phospholipids on adsorption chromatography are, to some extent, dependent on the cations with which they are associated (5,6). In taking this into account, the results from HPTLC analysis of phospholipid extracts and standards after converting into a single salt form confirmed that the higher mobility of DorCL shown in HPTLC is more likely due to the presence of fatty acyl chains with higher degrees of unsaturation (i.e., 4 DHA) rather than the effects of associated cations.

Information on the analysis of CL by ESI is limited, and the reported analyses were conducted solely in the negative ion mode (16,17). The present study provides information about the fragmentation processes of CL generated in the positive ion mode. Furthermore, the use of MS-MS allowed the structural interpretation of most ions obtained by ESI+/MS and confirmed that they were the results of Na<sup>+</sup> adduct fragment ions from a Do<sub>4</sub>CL. Surprisingly, MS-MS did not detect the main [DG + Na]<sup>+</sup> fragment ion, despite its presence in all of the ESI+/MS CL spectra. This ion was thought to be generated by a protonation process in the ionization chamber when using CHCl<sub>3</sub> as solvent. It was also noted that fragment ions were able to form dimers in ESI+. Although dimers of parent quasi-molecular ions have been noted previously (8), formation of dimers from fragment ions was first described in ESI+. Also, there are only a few studies analyzing CL using NMR (7,18). Results from the present study provide additional interpretations in the most interesting region, 3.9–4.5 ppm (<sup>1</sup>H) corresponding to proton resonances from the glycerol backbone.

In bacteria and fungi, CL contain mostly saturated and monoenoic FA with 14–18 carbon chain lengths (19,20). CL from mammalian species, which have been studied extensively (see Ref. 20 for review), are essentially restricted to 18-carbon chain length and dominated by 18:2n-6 (linoleic acid; >80 mol%). In marine animals, minor phospholipid classes such as CL have not received as much attention as other phospholipid classes (21); thus, there is little available information in this area. A CL with a relatively high content of 22:6n-3 (53.8 mol% of 22:6n-3) in the eastern oyster, *C. virginica*, had been previously reported (22). However, the results reported differed from a later study conducted on the same species and other bivalve species, the hard clam, *Mercentaria mercenaria* (total n-3 PUFA < 43% in CL of both species) (23). High amounts of both n-3 and n-6 PUFA in CL were reported in marine animals although no specific PUFA was found to be predominant in CL (10,24,25). In the three bivalve species analyzed, the DorCL mass spectrum, showed that the molecular form with four docosahexaenoyl chains (Do<sub>4</sub>CL) was the main peak. There was only a minor quantity of the Do<sub>3</sub>PCL form. With respect to the few molecular species compositions of CL from other organisms analyzed, (7,19,26), the presence of a molecular form with four identical acyl chains has regularly been reported.

Bivalves have low, limited, or no ability for synthesis of C<sub>20</sub>–C<sub>22</sub> PUFA with more than three double bonds. They must

acquire these *via* diet (27,28). In fact, molluscan phytoplanktonic diets are rich in C<sub>20</sub>–C<sub>22</sub> PUFA, including 22:6n-3, particularly 20:5n-3 (EPA) (29). Interestingly, in *P. maximus*, a relatively constant 22:6n-3 content in the DorCL fraction was found in both female and male gonads despite the possibility of drastic changes in the 22:6n-3 contents of their diets (2,3). In mammals, 18:2n-6 was replaceable by up to 30 mol% 22:6n-3 when rats were fed with DHA-enriched diets (30,31). Moreover, rats fed on a diet containing sardine oil, with EPA >> DHA, preferentially incorporated DHA rather than EPA in CL (32). Thus, for mammals, when DHA is bioavailable its incorporation into CL is favored among PUFA. Consequently, a common and beneficial effect likely could explain this 22:6n-3 selectivity.

CL is exclusively found in the inner mitochondrial membrane (33). It is required for maintenance of the mitochondrial structural integrity and for proper respiratory functioning (electron transport chain) and ATP-synthesizing enzyme complexes (20,33,34). Although most isolated membrane lipids are known to form bilayer aggregates, CL have been shown to promote phase transition from bilayer (lamellar, L<sub>α</sub>) to nonbilayer aggregate structures (inverted hexagonal phase, H<sub>II</sub>) (35). The unique pattern with four 22:6n-3 acyl chains, increasing the volume of the hydrophobic moiety of CL, may make it more prone to form nonbilayer H<sub>II</sub> phases (36). In addition it was shown that increase of 22:6n-3 residue in CL reduced cytochrome *c* oxidase activity (31) and increased the activity of the oligomycin-sensitive ATPase complex (32). Thus, it is speculated that this DorCL may reflect a specific adaptation in bivalves by enhancing the functionality of mechanisms of membrane phase transformation or/and allowing an optimal activity of the oxidative phosphorylation in response to fluctuation in environmental conditions (temperature, salinity, emersion).

In summary, results from the present study provide the first evidence of the existence of a specific CL with the main molecular form constituted with four 22:6n-3 acyl chains in *P. maximus*, *M. edulis*, and *C. gigas*. The dominance of 22:6n-3 acyl chains in CL from these three bivalve species renders the general opinion that “eukaryotic cardiolipins are mostly restricted to C<sub>18</sub> acyl chains” debatable. Future studies should look into whether this DHA-dominant CL is also present in other bivalve species.

## ACKNOWLEDGMENTS

The authors would like to thank Dr. Fu-Lin Chu, Virginia Institute of Marine Science (Gloucester Point, VA), for the critical review of the first draft of the manuscript. We thank Dr. Pierre Guenot for expert MS assistance and Dr. Roger Pichon for help in NMR interpretation. This work was supported by a grant from Ministère de l'Éducation Nationale de la Recherche et de la Technologie (M.E.N.R.T., France).

## REFERENCES

1. Soudant, P., Marty, Y., Moal, J., and Samain, J.F. (1995) Separation of Major Polar Lipids in *Pecten maximus* by High-Performance Liquid Chromatography and Subsequent Determination



- of Their Fatty Acids Using Gas Chromatography, *J. Chromatogr. B* 673, 15–26.
2. Soudant, P., Moal, J., Marty, Y., and Samain, J.F. (1996) Impact of the Quality of Dietary Fatty Acids on Metabolism and the Composition of Polar Lipid Classes in Female Gonads of *Pecten maximus* (L.), *J. Exp. Mar. Biol. Ecol.* 205, 149–163.
  3. Soudant, P., Moal, J., Marty, Y., and Samain, J.F. (1997) Composition of Polar Lipid Classes in Male Gonads of *Pecten maximus* (L.). Effect of Nutrition, *J. Exp. Mar. Biol. Ecol.* 215, 103–114.
  4. Soudant, P., Marty, Y., Moal, J., Masski, H., and Samain, J.F. (1998) Fatty Acid Composition of Polar Lipid Classes During Larval Development of Scallop *Pecten maximus* (L.), *Comp. Biochem. Phys. A* 121, 279–288.
  5. Nielsen, H. (1974) Silica Gel Thin-Layer Chromatography of Acidic Phospholipids. I. Effect of Metal Ions of the Adsorbent and Phospholipid on the Chromatographic Mobility of Cardiolipin and Phosphatidylinositol, *J. Chromatogr.* 89, 275–285.
  6. Tocher, D., and Harvie, D. (1988) Fatty Acid Composition of the Major Phosphoglycerides from Fish Neural Tissues; (n-3) and (n-6) Polyunsaturated Fatty Acids in Rainbow Trout (*Salmo gairdneri*) and Cod (*Gadus morhua*) Brains and Retinas, *Fish. Physiol. Biochem.* 5, 229–239.
  7. Corcelli, A., Colella, M., Mascolo, G., Fanizzi, F.P., and Kates, M. (2000) A Novel Glycolipid and Phospholipid in the Purple Membrane, *Biochemistry* 39, 3318–3326.
  8. Orådd, G., Andersson, A.S., Rilfors, L., Lindblom, G., Strandberg, E., and André, P. (2000)  $\alpha$ -Methylene Ordering of Acyl Chains Differs in Glucolipids and Phosphatidylglycerol from *Acholeplasma laidlawii* Membranes:  $^2\text{H}$ -NMR Quadrupole Splittings from Individual Lipids in Mixed Bilayers, *Biochim. Biophys. Acta* 1468, 329–344.
  9. Khim, H.-Y., Wang, T.-C.L., and Ma, Y.-C. (1994) Liquid Chromatography/Mass Spectrometry of Phospholipids Using Electrospray Ionization, *Anal. Chem.* 66, 3977–3982.
  10. MacPherson, J.C., Pavlovich, J.G., and Jacobs, R.S. (1998) Phospholipid Composition of the Granular Amebocyte from the Horseshoe Crab, *Limulus polyphemus*, *Lipids* 33, 931–940.
  11. Gunstone, F.D. (1992) High-Resolution  $^1\text{H}$  and  $^{13}\text{C}$  NMR, in *Lipid Analysis. A Practical Approach* (Hamilton, R.J., and Hamilton, S., eds.), pp. 244–262, Oxford University Press, New York.
  12. Bonzom, P.M.A., Nicolaou, A., Zloh, M., Baldeo, W., and Gibbons, W.A. (1999) NMR Lipid Profile of *Agaricus bisporus*, *Phytochemistry* 50, 1311–1321.
  13. Folch, J., Lees, M., and Sloane-Stanley, G.H. (1957) A Simple Method for the Isolation and Purification of Total Lipids from Animal Tissues, *J. Biol. Chem.* 226, 497–509.
  14. Nelson, G.J. (1993) Isolation and Purification of Lipids from Biological Matrices, in *Analyses of Fats, Oils and Lipoproteins*. (Perkins, E.G., ed.), pp. 20–59, American Oil Chemists' Society, Champaign.
  15. Marty, Y., Delaunay, F., Moal, J., and Samain, J.F. (1992) Changes in the Fatty Acid Composition of the Scallop *Pecten maximus* (L.) During Larval Development, *J. Exp. Mar. Biol. Ecol.* 163, 221–234.
  16. Han, X., and Gross, R.W. (1995) Structural Determination of Picomole Amounts of Phospholipids via Electrospray Ionization Tandem Mass Spectrometry, *J. Am. Soc. Mass. Spectrom.* 6, 1202–1210.
  17. Hoischen, C., Ihn, W., Gura, K., and Gumpert, J. (1997) Structural Characterization of Molecular Phospholipid Species in Cytoplasmic Membranes of the Cell Wall-Less *Streptomyces hygroscopicus* L. Form by Use of Electrospray Ionization Coupled with Collision-Induced Dissociation Mass Spectrometry, *J. Bacteriol.* 179, 3437–3442.
  18. Adosraku, R.K., Smith, J.D., Nicolaou, A., and Gibbons, W.A. (1996) *Tetrahymena thermophila*: Analysis of Phospholipids and Phosphonolipids by High-Field  $^1\text{H}$ -NMR, *Biochim. Biophys. Acta* 1299, 167–174.
  19. Schlame, M., Brody, S., and Hostetler, K. (1993) Mitochondrial Cardiolipin in Diverse Eukaryotes. Comparison of Biosynthetic Reactions and Molecular Acyl Species, *Eur. J. Biochem.* 212, 727–735.
  20. Schlame, M., Rua, D., and Greenberg, M.L. (2000) The Biosynthesis and Functional Role of Cardiolipin, *Prog. Lipid Res.* 39, 257–288.
  21. Vaskovsky, V.E. (1989) Phospholipids, in *Marine Biogenic Lipids, Fats, and Oils* (Ackman, R.G., ed.), pp. 199–242, CRC Press, Boca Raton.
  22. Glémet, H.C., and Ballantyne, J.S. (1995) Influences of Environmental Salinity on the Structure and Function of Gill Mitochondria Membranes of an Osmoconforming Invertebrate, *Crassostrea virginica*, *Mar. Biol.* 121, 673–683.
  23. Gillis, T.E., and Ballantyne, S.J. (1999) Influences of Subzero Thermal Acclimation on Mitochondrial Membrane Composition of Temperate Zone Marine Bivalve Mollusks, *Lipids* 34, 59–66.
  24. Glémet, H.C., Gerrits, M.F., and Ballantyne, J.S. (1997) Membrane Lipids of Red Muscle Mitochondria from Land-Locked and Sea Urchin Arctic Char, *Salvelinus alpinus*, *Mar. Biol.* 129, 673–679.
  25. Mita, M., and Ueta, N. (1989) Fatty Chain Composition of Phospholipids in Sea Urchin Spermatozoa, *Comp. Biochem. Phys. B* 92B, 319–322.
  26. Schlame, M., Shanske, S., Doty, S., König, T., Sculco, T., DiMauro, S., and Blanck, T.J.J. (1999) Microanalysis of Cardiolipin in Small Biopsies Including Skeletal Muscle from Patients with Mitochondrial Disease, *J. Lipid Res.* 40, 1585–1592.
  27. Chu, F.L.E., and Webb, K.L. (1984) Polyunsaturated Fatty Acids and Neutral Lipids in Developing Larvae of the Oyster, *Crassostrea virginica*, *Lipids* 19, 815–820.
  28. Waldock, M.J., and Holland, D.L. (1984) Fatty Acid Metabolism in Young Oysters, *Crassostrea gigas*: Polyunsaturated Fatty Acids, *Lipids* 19, 332–336.
  29. Ackman, R.G. (1983) Fatty Acid Metabolism of Bivalves, *Proc. 2nd Int. Conf. Publ.* 2, 358–375.
  30. Berger, A., Gershwin, M.E., and German, J.B. (1992) Effects of Various Dietary Fats on Cardiolipin Acyl Composition During Ontogeny of Mice, *Lipids* 27, 605–612.
  31. Watkins, S.M., Lin, T.Y., Davis, R.M., Ching, J.R., DePeters, E.J., Halpern, G.M., Walzem, R.L., and German, J.B. (2001) Unique Phospholipid Metabolism in Mouse Heart in Response to Dietary Docosahexaenoic or  $\alpha$ -Linoleic Acids, *Lipids* 36, 247–254.
  32. Yamaoka, S., Urade, R., and Kito, M. (1988) Mitochondrial Function in Rats Is Affected by Modification of Membrane Phospholipids with Dietary Sardine Oil, *J. Nutr.* 118, 290–296.
  33. Hatch, G.M., and McClarty, G. (1998) Cardiolipin Remodeling in Eukaryotic Cells Infected with *Chlamydia trachomatis* Is Linked to Elevated Mitochondrial Metabolism, *Biochem. Biophys. Res. Commun.* 243, 356–360.
  34. Robinson, N.C. (1982) Specificity and Binding Affinity of Phospholipids to the High-Affinity Cardiolipin Sites of Beef Heart Cytochrome C Oxidase, *Biochemistry* 21, 184–188.
  35. Powell, G.L., and Marsh, D. (1985) Polymorphic Phase Behaviour of Cardiolipin Derivatives Studied by  $^{31}\text{P}$  NMR and X-Ray Diffraction, *Biochemistry* 24, 2902–2908.
  36. Sankaram, M.B., Powell, G.L., and Marsh, D. (1989) Effect of Acyl Chain Composition on Salt-Induced Lamellar to Inverted Hexagonal Phase Transitions in Cardiolipin, *Biochim. Biophys. Acta* 980, 389–392.

[Received January 23, 2002, and in revised form April 5, 2002; revision accepted April 18, 2002]

# Analysis of Vitamin E and Its Oxidation Products by HPLC with Electrochemical Detection

Ryo Yamauchi<sup>a,\*</sup>, Hiroki Noro<sup>b</sup>, Makoto Shimoyamada<sup>a</sup>, and Koji Kato<sup>b</sup>

Departments of <sup>a</sup>Bioprocessing and <sup>b</sup>Food Science, Faculty of Agriculture, Gifu University, Gifu 501-1193, Japan

**ABSTRACT:** A sensitive HPLC procedure with postcolumn reduction and electrochemical detection was developed for the analysis of vitamin E and its oxidation products,  $\alpha$ -tocopherylquinone, epoxy- $\alpha$ -tocopherylquinones, and 8a-(lipid-dioxy)- $\alpha$ -tocopherones. After the separation on a reversed-phase column, on-line zinc-catalyzed reduction allowed the detection of  $\alpha$ -tocopherylquinone and epoxy- $\alpha$ -tocopherylquinones, whereas platinum-catalyzed reduction allowed the detection of 8a-(lipid-dioxy)- $\alpha$ -tocopherones. The lowest detectable level of each compound was about 0.2 pmol at the signal-to-noise ratio of 3. This method was applied to the detection of  $\alpha$ -tocopherol products in peroxidized human plasma. When the plasma was peroxidized by the addition of a free radical initiator, peaks corresponding to  $\alpha$ -tocopherylquinone, epoxy- $\alpha$ -tocopherylquinones, and the addition products of  $\alpha$ -tocopherol with peroxy radicals derived from cholesteryl ester hydroperoxides and PC hydroperoxides were observed. The amount of these oxidation products in the plasma increased with the depletion of endogenous  $\alpha$ -tocopherol. The results indicate that the method is useful to detect the oxidation products formed by the peroxy radical-trapping reactions of  $\alpha$ -tocopherol in biological systems. Paper no. L8957 in *Lipids* 37, 515–522 (May 2002).

Lipid peroxidation in biological tissues and fluids is implicated in a variety of damaging pathological events (1,2).  $\alpha$ -Tocopherol ( $\alpha$ -TH), the most active form of vitamin E in biological systems, inhibits peroxidation of unsaturated lipids by trapping peroxy radicals (3).  $\alpha$ -TH efficiently transfers a hydrogen atom to a peroxy radical, giving a hydroperoxide

and an  $\alpha$ -tocopheroxyl radical. The  $\alpha$ -tocopheroxyl radical then reacts with a second peroxy radical to form a nonradical product. The peroxy radical-trapping reaction of  $\alpha$ -TH yields 8a-substituted tocopherones and isomeric epoxytocopherones as the primary oxidation products (4,5). Therefore, the formation of these products is consistent with the behavior of  $\alpha$ -TH as a chain-breaking antioxidant in biological systems. In most biological samples, the amount of  $\alpha$ -TH is very small compared with the lipid contents. Therefore, we need a highly sensitive and specific methodology to analyze the oxidation products of  $\alpha$ -TH in biological samples. We previously reported the chemiluminescence-based HPLC method for the analysis of the addition products of  $\alpha$ -TH with peroxy radicals of PC, 8a-(phosphatidylcholine-dioxy)- $\alpha$ -tocopherones (TOO-PC) (6). This HPLC technique was found advantageous for the sensitive and specific determination of TOO-PC in biological samples. However, other  $\alpha$ -TH products such as  $\alpha$ -tocopherylquinone ( $\alpha$ -TQ) could not be detected by this chemiluminescence-based assay.

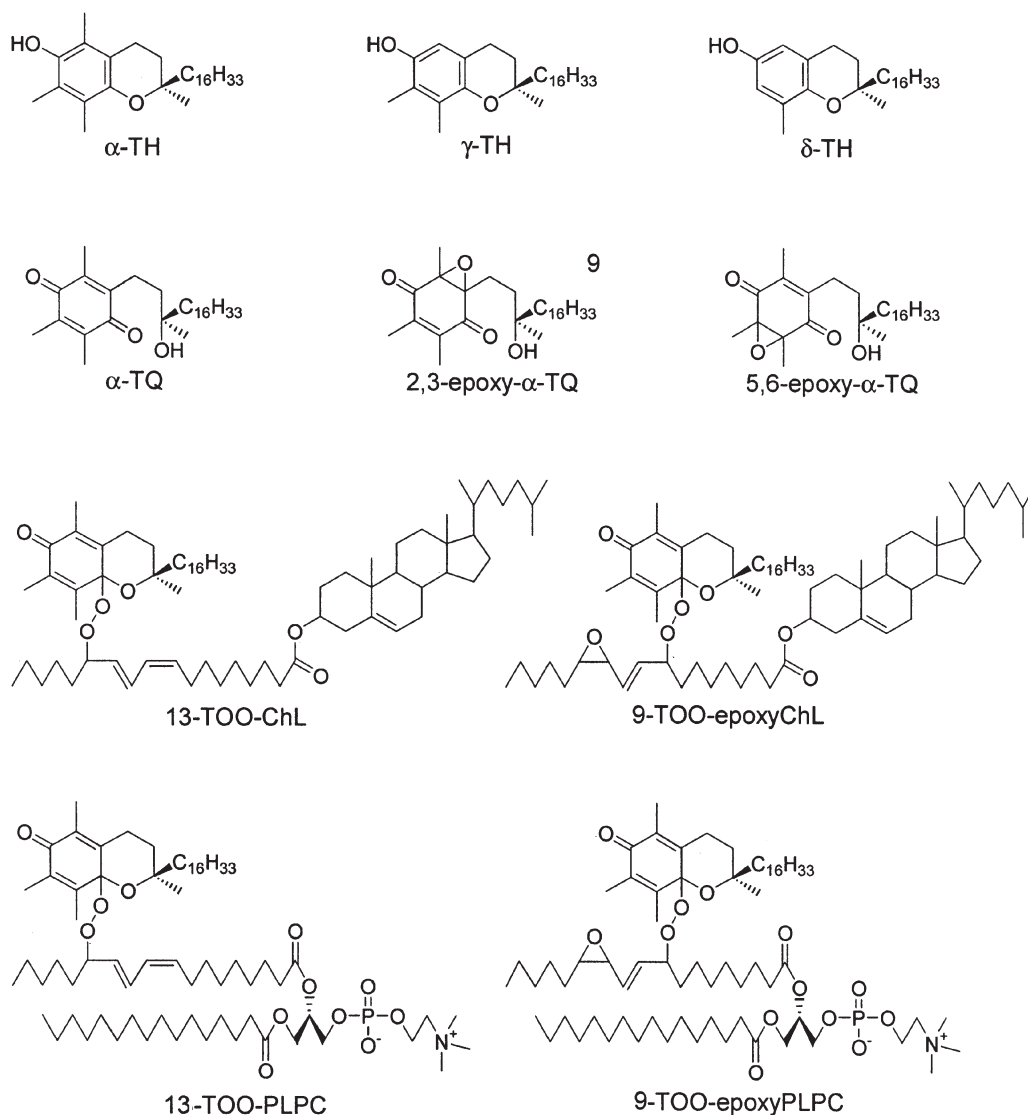
Electrochemical detection provides the most sensitive measurement of compounds that undergo redox reactions. On-line reduction by a postcolumn reactor (7–9) or by a coulometric method (10–12) has been reported for the parallel electrochemical detection of TH,  $\alpha$ -TH oxidation products, ubiquinols, and ubiquinones, in which the quinone ring was reduced to give the corresponding hydroquinone. In the present study, we developed a sensitive method for the assay of  $\alpha$ -TH and its oxidation products (see Fig. 1) in biological samples using an HPLC separation, postcolumn zinc or platinum reduction, and electrochemical detection. We applied this method for the detection of  $\alpha$ -TH products in peroxidized human blood plasma. The main lipids in human plasma are cholesteryl esters (ChE) and phospholipids (13). Particularly, cholesteryl linoleate (ChL) is the major oxidizable lipid substrate in LDL and other lipoproteins. Therefore, we expected the formation of the addition products of  $\alpha$ -TH with peroxy radicals of ChL during the peroxidation of human plasma.

## MATERIALS AND METHODS

**Chemicals.** *RRR*- $\alpha$ -TH was purchased from Sigma Chemical Co. (St. Louis, MO) and purified by reversed-phase HPLC (14). *RRR*- $\gamma$ - and *RRR*- $\delta$ -TH were prepared from mixed isomers of

\*To whom correspondence should be addressed at Department of Bioprocessing, Faculty of Agriculture, Gifu University, 1-1 Yanagido, Gifu City, Gifu 501-1193, Japan. E-mail: yamautir@cc.gifu-u.ac.jp

Abbreviations: AAPH, 2,2'-azobis(2-amidinopropane) dihydrochloride; APCI-MS, atmospheric pressure chemical ionization mass spectrometry; ChE-OOH, cholesteryl ester hydroperoxides; ChL-OOH, cholesteryl linoleate hydroperoxides; ECD, electrochemical detector; LC-MS, HPLC coupled with on-line mass spectrometry; PC-OOH, phosphatidylcholine hydroperoxides; PLPC, 1-palmitoyl-2-linoleoyl-3-*sn*-phosphatidylcholine; 13-PLPC-OOH, 1-palmitoyl-2-[(9Z,11E)-(S)-13-hydroperoxy-9,11-octadecadienyl]-3-*sn*-phosphatidylcholine; TH, tocopherol; TOO-ChE, 8a-(cholesterylester-dioxy)- $\alpha$ -tocopherones; TOO-ChL, cholesteryl (8a-dioxy- $\alpha$ -tocopherone)-octadecadienoates; TOO-epoxyChL, cholesteryl (8a-dioxy- $\alpha$ -tocopherone)-epoxyoctadecenoates; TOO-epoxyPLPC, 1-palmitoyl-2-[(8a-dioxy- $\alpha$ -tocopherone)-epoxyoctadecenyl]-3-*sn*-phosphatidylcholines; TOO-PC, 8a-(phosphatidylcholine-dioxy)- $\alpha$ -tocopherones; TOO-PLPC, 1-palmitoyl-2-[8a-dioxy- $\alpha$ -tocopherone)-octadecadienyl]-3-*sn*-phosphatidylcholines; TQ, tocopherylquinone.



**FIG. 1.** Structures of tocopherols (TH),  $\alpha$ -tocopherylquinone ( $\alpha$ -TQ), and epoxy- $\alpha$ -tocopherylquinones (epoxy- $\alpha$ -TQ), and typical structures of 8a-(lipid-dioxy)- $\alpha$ -tocopherones, cholesteryl (9*Z*,11*E*)-13-(8a-dioxy- $\alpha$ -tocopherone)-(9,11)-octadecadienoate (13-TOO-ChL), cholesteryl (*E*)-9-(8a-dioxy- $\alpha$ -tocopherone)-12,13-epoxy-10-octadecenoate (9-TOO-epoxyChL), 1-palmitoyl-2-[(9*Z*,11*E*)-13-(8a-dioxy- $\alpha$ -tocopherone)-(9,11)-octadecadienoyl]-3-*sn*-phosphatidylcholine (13-TOO-PLPC), and 1-palmitoyl-2-[(*E*)-9-(8a-dioxy- $\alpha$ -tocopherone)-12,13-epoxy-10-octadecenoyl]-3-*sn*-phosphatidylcholine (9-TOO-epoxyPLPC).

TH (Hohnen Oil Co., Tokyo, Japan) (15). Authentic  $\alpha$ -TQ, 2,3-epoxy- $\alpha$ -TQ, and 5,6-epoxy- $\alpha$ -TQ were prepared as described previously (16). Cholesteryl linoleate hydroperoxides (ChL-OOH) were prepared by autoxidation of ChL in the presence of  $\alpha$ -TH (17). Cholesteryl (8a-dioxy- $\alpha$ -tocopherone)-octadecadienoates (TOO-ChL) and cholesteryl (8a-dioxy- $\alpha$ -tocopherone)-epoxyoctadecenoates (TOO-epoxyChL) were prepared by the iron-catalyzed reaction of  $\alpha$ -TH with ChL-OOH (18). 1-Palmitoyl-2-[(9*Z*,11*E*)-(*S*)-13-hydroperoxy-9,11-octadecadienoyl]-3-*sn*-phosphatidylcholine (13-PLPC-OOH) was prepared by the oxidation of 1-palmitoyl-2-linoleoyl-3-*sn*-PC (PLPC) with soybean lipoxygenase-1 (Sigma Chemical Co.) in the presence of deoxycholate (19).

1-Palmitoyl-2-[(8a-dioxy- $\alpha$ -tocopherone)-octadecadienoyl]-3-*sn*-phosphatidylcholines (TOO-PLPC) were prepared by reacting  $\alpha$ -TH with PLPC (20). 1-Palmitoyl-2-[(8a-dioxy- $\alpha$ -tocopherone)-12,13-epoxy-octadecenoyl]-3-*sn*-phosphatidylcholines (TOO-epoxyPLPC) were prepared by the iron-catalyzed reaction of  $\alpha$ -TH with 13-PLPC-OOH in methanol (21). The structures of these  $\alpha$ -TH products were characterized using MS and NMR spectrometry (16–21). 2,2'-Azobis(2-amidinopropane) dihydrochloride (AAPH) was obtained from Wako Pure Chemical Co. (Osaka, Japan). All solvents used were of HPLC grade.

**HPLC system.** The HPLC system used in the present study was essentially the same as that reported by Yamashita and



Yamamoto (8) and Leray *et al.* (9). HPLC was carried out with a Waters Model 600E system connected to a Waters Model 486 UV/Vis detector and an ED623 electrochemical detector. For the simultaneous analysis of TH and  $\alpha$ -TQ, the mobile phase of methanol/water (95:5, vol/vol) containing 10 mM lithium acetate and 5 mM trifluoroacetate was passed through a J'sphere ODS-H80 column (150  $\times$  4.6 mm i.d., carbon content of 22%; YMC Co., Kyoto, Japan) at a flow rate of 1.0 mL/min. The mobile phase was maintained oxygen-free by continuous bubbling with helium gas. The column eluate was monitored at 280 nm and subsequently passed to a solid-phase postcolumn reactor (10  $\times$  4.0 mm i.d.), which was made by dry-packing of zinc particles (particle size of <75  $\mu$ m; Wako Pure Chemical Co.) under vibration (9). Then TH and the reduced  $\alpha$ -TQ were detected by an amperometric electrochemical detector (ECD) with a glassy carbon working electrode and an Ag/AgCl reference electrode. The applied oxidation potential was set at +700 mV (9). For the analysis of 8a-(lipid-dioxy)- $\alpha$ -tocopherones, a mobile phase of methanol/water (98.5:1.5, vol/vol) containing 10 mM lithium acetate [for the analysis of 8a-(cholesterylester-dioxy)- $\alpha$ -tocopherones (TOO-ChE)] or methanol/water (97.5:2.5, vol/vol) containing 20 mM choline chloride (for the analysis of TOO-PC) was passed through a J'sphere ODS-L80 column (150  $\times$  4.6 mm i.d., carbon content of 9%) at a flow rate of 1.0 mL/min. The column eluate was monitored at 240 nm and subsequently passed to a solid-phase postcolumn reactor (50  $\times$  4.0 mm i.d.), which was made by dry-packing of platinum catalyst (5% platinum on alumina, -325 mesh; Aldrich Chemical Co., Milwaukee, WI) (7). The reduced tocopherones were detected by an amperometric ECD at the oxidation potential of +700 mV. Chromatographic data were recorded by a MacLab data acquisition system with a Peaks application program (AD Instruments Pty. Ltd., Castle Hill, Australia).

**Peroxidation of human plasma.** The fresh, heparinized blood from a healthy 24-old male was centrifuged at 1000  $\times$  g for 10 min to separate plasma. The plasma (4.0 mL) was kept for 5 min at 37°C in a shaking water bath under air, and then 1.0 mL of 100 mM AAPH in 10 mM sodium phosphate buffer (pH 7.4, containing 125 mM NaCl) was added to start lipid peroxidation (the final concentration of AAPH was 20 mM).

**Quantification.** At specific intervals, a 0.5-mL aliquot of the reaction mixture was taken for lipid extraction. Total lipids were extracted by the method of Bligh and Dyer (22). The extraction solvents (methanol and chloroform) contained 0.03% BHT. The lipid extracts were evaporated to dryness under a stream of nitrogen gas, dissolved in 0.5 mL of chloroform, and applied on a Supelclean LC-NH2 (Supelco, Bellefonte, PA) minicolumn made from Pasteur pipettes (filling height of 4 cm). The column was eluted with chloroform (4 mL) and then with methanol (4 mL). The chloroform and methanol fractions were pooled, respectively, and each solvent was evaporated under nitrogen gas. The chloroform fraction was dissolved in 100  $\mu$ L of 2-propanol and analyzed for TH,  $\alpha$ -TQ, ChE-OOH, and TOO-ChE; the methanol fraction was dissolved in 100  $\mu$ L of ethanol and analyzed for PC-OOH

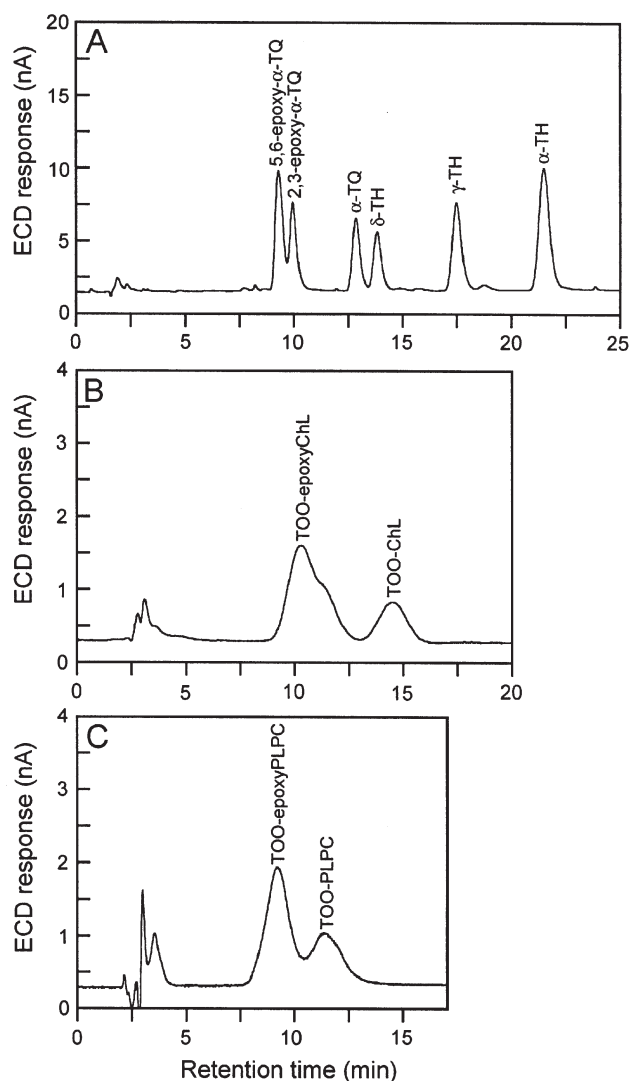
and TOO-PC, respectively. TH,  $\alpha$ -TQ, TOO-ChE, and TOO-PC were quantified by the established HPLC method described in the present study. To determine the percentage recovery of compounds, authentic compounds were spiked into the diluted plasma sample (0.5 mL) and then extracted with chloroform/methanol followed by the solid-phase extraction as described above. ChE-OOH and PC-OOH were quantified by chemiluminescent-based HPLC (6). The concentration of each hydroperoxide was calculated from the standard curve of authentic ChL-OOH or 13-PLPC-OOH. For isolation of the product peak, the sample solution was injected into a J'sphere ODS-M80 column (150  $\times$  4.6 mm i.d., carbon content of 14%) with a solvent system of methanol (for the isolation of TH and  $\alpha$ -TQ), methanol/2-propanol/hexane (50:35:15, by vol; for the isolation of TOO-ChE), or methanol/ethanol (2:3, vol/vol; for the isolation of TOO-PC) at 1.0 mL/min and detected at 240 or 285 nm.

**HPLC coupled with on-line MS (LC-MS).** LC-MS was carried out using a Shimadzu LCMS-QP8000 $\alpha$  quadrupole instrument equipped with an atmospheric pressure chemical ionization (APCI) source. Sample lipids were separated isocratically on a Luna 3- $\mu$ m C18(2) column (150  $\times$  2.0 mm i.d.; Phenomenex, Torrance, CA) with methanol/water (98:2, vol/vol) for TH and  $\alpha$ -TQ, methanol/2-propanol/hexane (50:35:15, by vol) for TOO-ChE, or methanol/ethanol (2:3, vol/vol) for TOO-PC at 0.2 mL/min. The separation sample was introduced into the APCI source. The APCI probe was maintained at 4.5 kV with a temperature of 400°C. Nebulizing gas (nitrogen) was delivered at a flow rate of 2.5 L/min. The curved desolvation line voltage was at -40 V with a temperature of 250°C. The deflector voltage was maintained at +40 V for the analysis of TH and  $\alpha$ -TQ or at +80 V for the analysis of TOO-ChE and TOO-PC. Ionization was performed in the positive mode, and mass spectra were acquired between  $m/z$  100 and 500 at a scan rate of 2 s per spectrum (for TH and  $\alpha$ -TQ) or between  $m/z$  300 and 1300 at a scan rate of 4 s (for TOO-ChE or TOO-PC).

## RESULTS AND DISCUSSION

HPLC techniques have been widely accepted and applied for the analysis of TH and  $\alpha$ -TQ in biological samples (9,10,12,23,24). The combination of UV or fluorescent detection with HPLC separation lacks sufficient sensitivity for biological samples (23,24). On the other hand, electrochemical detection provides the most sensitive measurement of TH and  $\alpha$ -TQ (9,10,12,24). Therefore, we examined the HPLC system with a postcolumn reactor and electrochemical detection to measure the oxidation products of  $\alpha$ -TH. The system consisted of a pump, an injector, a separation column, a solid-phase postcolumn reactor containing zinc or platinum catalyst, and an ECD. Figure 2A shows a typical chromatogram of the standard TH,  $\alpha$ -TQ, and  $\alpha$ -TQ using postcolumn zinc reduction and electrochemical detection. A standard mixture of  $\alpha$ -,  $\gamma$ -, and  $\delta$ -TH,  $\alpha$ -TQ, and epoxy- $\alpha$ -TQ was well separated, and very intense peaks appeared on the chromatogram. On





**FIG. 2.** HPLC of TH and  $\alpha$ -TH products using postcolumn reduction and electrochemical detection. (A) A standard mixture of  $\alpha$ -TH (100 pmol),  $\gamma$ -TH (100 pmol),  $\delta$ -TH (100 pmol),  $\alpha$ -TQ (93 pmol), 2,3-epoxy- $\alpha$ -TQ (68 pmol), and 5,6-epoxy- $\alpha$ -TQ (71 pmol) was injected into a J'sphere ODS-80H column developed with 95% methanol containing 10 mM lithium acetate and 5 mM trifluoroacetate followed by postcolumn zinc reduction. (B) A standard mixture of TOO-ChL (25 pmol) and TOO-epoxyChL (74 pmol) was injected into a J'sphere ODS-80L column developed with 98.5% methanol containing 10 mM lithium acetate followed by postcolumn platinum reduction. (C) A standard mixture of TOO-PLPC (21 pmol) and TOO-epoxyPLPC (36 pmol) was injected into a J'sphere ODS-80L column developed with 97.5% methanol containing 20 mM choline chloride followed by postcolumn platinum reduction. Each eluate was monitored by an electrochemical detector (ECD) at +700 mV. See Figure 1 for abbreviations.

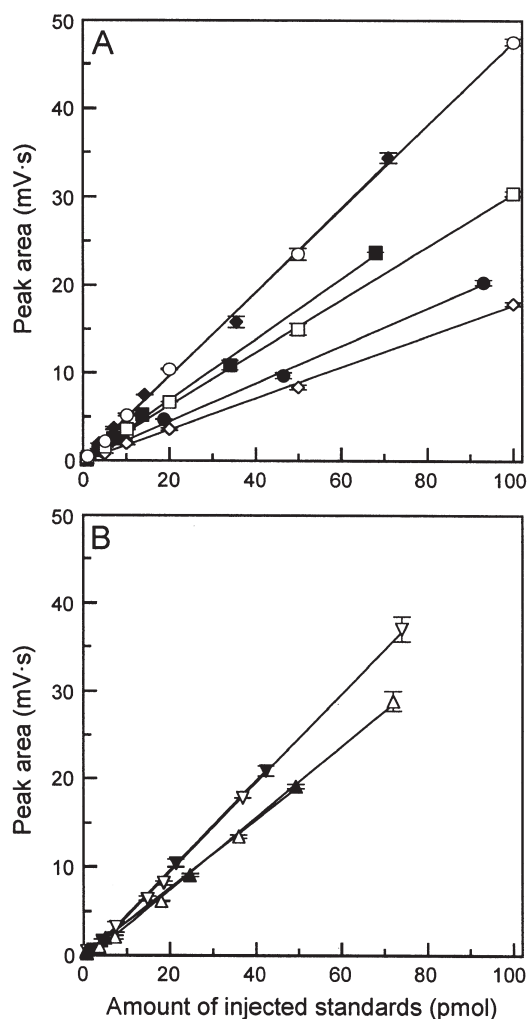
the other hand, peaks of only weak intensity were observed by the UV detection (data not shown). The zinc catalyst was useful for reducing both  $\alpha$ -TQ and epoxy- $\alpha$ -TQ to  $\alpha$ -tocopherylhydroquinone under the acidic solvent condition, and the resulting hydroquinone could be detected at an applied oxidation potential of +700 mV (9). The zinc catalyst was more effective in reducing  $\alpha$ -TQ at a column length of 10 mm,

compared with 50 mm. The longer reducing column resulted in peak broadening.

The 8 $\alpha$ -substituted  $\alpha$ -tocopherone products hydrolyze to  $\alpha$ -TQ immediately in the presence of acid (16,25). Therefore, it is impossible to analyze these products with the above HPLC condition using postcolumn zinc reduction. Alternatively, a postcolumn reactor containing platinum catalyst can reduce quinone compounds to the corresponding hydroquinones in the absence of acid (7,8). Using the platinum column reactor, we analyzed two types of 8 $\alpha$ -(lipid-dioxy)- $\alpha$ -tocopherone compounds: TOO-ChL and TOO-epoxyChL from the reaction between  $\alpha$ -TH and ChL-derived peroxy radicals, and TOO-PLPC and TOO-epoxyPLPC from the reaction between  $\alpha$ -TH and PLPC-derived peroxy radicals. Typical chromatograms of authentic compounds are shown in Figures 2B and 2C. On each chromatogram, very intense peaks corresponding to the 8 $\alpha$ -(lipid-dioxy)- $\alpha$ -tocopherone compounds were observed. The platinum catalyst was most effective in reducing 8 $\alpha$ -(lipid-dioxy)- $\alpha$ -tocopherones at a column length of 50 mm. If the shorter column was used, the reduction ability of the platinum catalyst went down with successive injections of sample solutions. On the contrary, the platinum catalyst did not reduce epoxy- $\alpha$ -TQ under the present conditions (data not shown).

Figure 3 shows the standard curves for the determination of TH,  $\alpha$ -TQ, epoxy- $\alpha$ -TQ, TOO-ChL, TOO-epoxyChL, TOO-PLPC, and TOO-epoxyPLPC. Each standard curve showed a good correlation between the peak area measured by electrochemical detection and the amount of each compound, with the regression equations of  $y = 0.469x + 0.626$  ( $r = 0.999$ ) for  $\alpha$ -TH,  $y = 0.297x + 0.251$  ( $r = 0.998$ ) for  $\gamma$ -TH,  $y = 0.175x + 0.152$  ( $r = 0.995$ ) for  $\delta$ -TH,  $y = 0.214x + 0.250$  ( $r = 0.999$ ) for  $\alpha$ -TQ,  $y = 0.343x + 0.117$  ( $r = 0.998$ ) for 2,3-epoxy- $\alpha$ -TQ,  $y = 0.474x + 0.203$  ( $r = 0.999$ ) for 5,6-epoxy- $\alpha$ -TQ,  $y = 0.381x + 0.075$  ( $r = 0.999$ ) for TOO-ChL,  $y = 0.407x - 0.743$  ( $r = 0.999$ ) for TOO-epoxyChL,  $y = 0.504x - 0.435$  ( $r = 0.999$ ) for TOO-PLPC, and  $y = 0.503x - 0.499$  ( $r = 0.999$ ) for TOO-epoxyPLPC. The lowest detectable level of each compound as a signal-to-noise ratio was estimated to be about 0.2 pmol, respectively. We have previously reported that the detection limit for TOO-PC by the chemiluminescence-based HPLC method is about 1 pmol (6). Thus, the present method using electrochemical detection is very highly sensitive for the detection of  $\alpha$ -TH products.

We applied the above HPLC system for the analysis of the oxidative fate of endogenous  $\alpha$ -TH in human blood plasma. Before the HPLC analysis, the plasma lipids extracted with chloroform/methanol were treated with a solid-phase extraction on silica-NH<sub>2</sub>. TH,  $\alpha$ -TQ, and TOO-ChE were eluted in the chloroform fraction, and then TOO-PC were eluted in the methanol fraction. In using this sample treatment, the recoveries of TH and  $\alpha$ -TH products were checked by the addition of known amounts of the standards into the diluted human plasma (Table 1). TH and  $\alpha$ -TQ were recovered almost satisfactorily, but the recoveries of the 8 $\alpha$ -substituted tocopherone



**FIG. 3.** Calibration curves for standard compounds. (A)  $\alpha$ -TH ( $\circ$ ),  $\gamma$ -TH ( $\square$ ),  $\delta$ -TH ( $\diamond$ ),  $\alpha$ -TQ ( $\bullet$ ), 2,3-epoxy- $\alpha$ -TQ ( $\blacksquare$ ), and 5,6-epoxy- $\alpha$ -TH ( $\blacklozenge$ ). (B) TOO-ChL ( $\blacktriangle$ ), TOO-epoxyChL ( $\triangle$ ), TOO-PLPC ( $\blacktriangledown$ ), and TOO-epoxyPLPC ( $\nabla$ ). Each data point represents the mean  $\pm$  SD of three determinations. See Figure 1 for abbreviations.

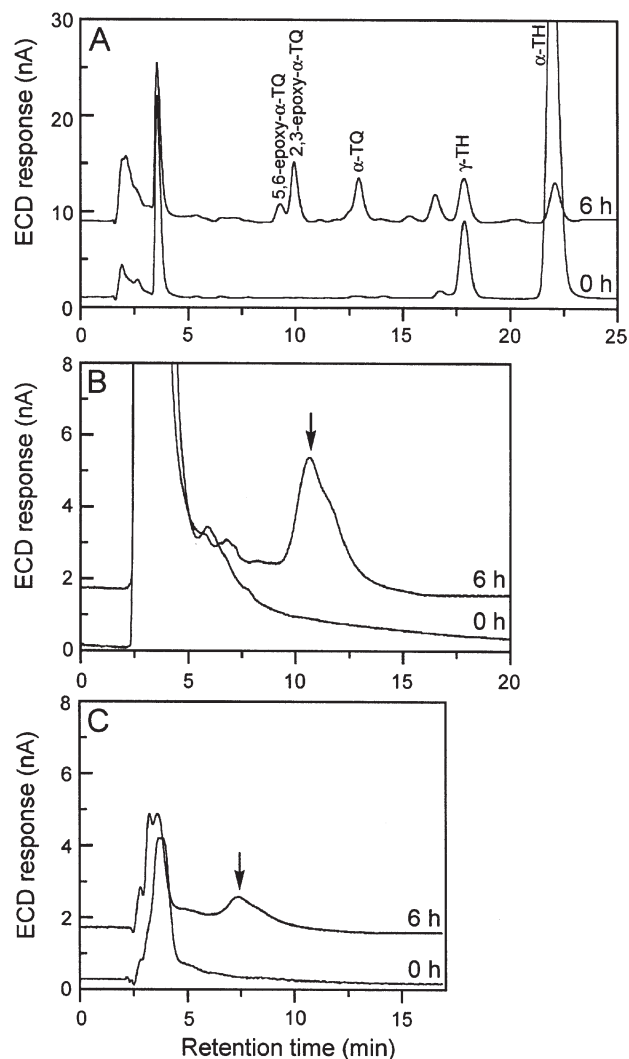
**TABLE 1**  
Recovery of Spiked Standards Added to Diluted Human Plasma<sup>a,b</sup>

Compound <sup>c</sup>	Human plasma (pmol)	Added standard (pmol)	Found (pmol)	Recovery (%)
$\alpha$ -TH	393 $\pm$ 19	200	586 $\pm$ 8	98.9 $\pm$ 3.4
$\gamma$ -TH	63 $\pm$ 5	200	244 $\pm$ 17	93.0 $\pm$ 7.6
$\alpha$ -TQ	ND	186	176 $\pm$ 3	94.6 $\pm$ 1.8
2,3-epoxy- $\alpha$ -TQ	ND	136	123 $\pm$ 5	90.1 $\pm$ 3.4
5,6-epoxy- $\alpha$ -TQ	ND	142	134 $\pm$ 2	94.1 $\pm$ 1.4
TOO-ChL	ND	247	214 $\pm$ 15	86.7 $\pm$ 6.1
TOO-epoxyChL	ND	149	106 $\pm$ 2	71.3 $\pm$ 1.6
TOO-PLPC	ND	212	167 $\pm$ 6	78.9 $\pm$ 3.1
TOO-epoxyPLPC	ND	310	237 $\pm$ 8	76.5 $\pm$ 2.6

<sup>a</sup>The diluted human plasma was made by the addition of 9 vol of 10 mM sodium phosphate buffer (pH 7.4, containing 125 mM NaCl) with 1 vol of human plasma.

<sup>b</sup>Each value is expressed as mean  $\pm$  SD ( $n = 3$ ).

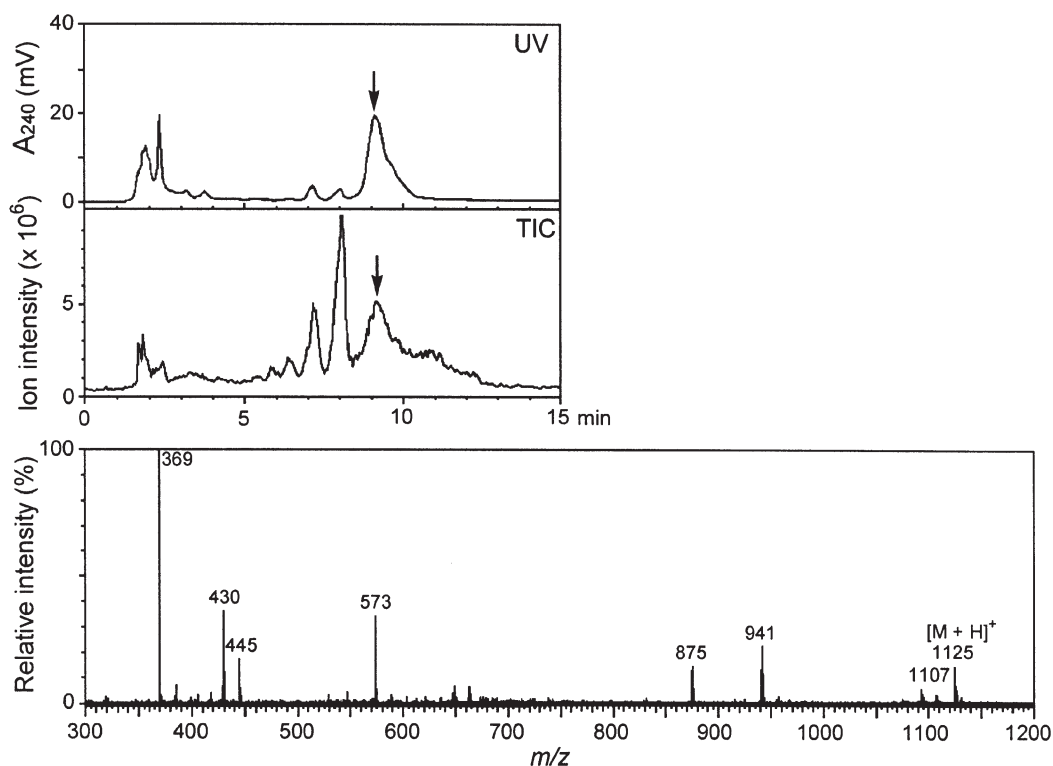
<sup>c</sup>See Figure 1 for abbreviations; ND, not detectable.



**FIG. 4.** HPLC of TH and  $\alpha$ -TH products from the peroxidized human plasma using postcolumn reduction and electrochemical detection. The human plasma (4.0 mL) was incubated at 37°C for 0 and 6 h by the addition of 1.0 mL of 100 mM 2,2'-azobis(2-amidinopropane) dihydrochloride (AAPH; final concentration, 20 mM). The reaction mixture was extracted with chloroform/methanol, and the total lipid fraction was passed through a silica-NH<sub>2</sub> column using chloroform and methanol. The chloroform and methanol fractions were injected into HPLC and detected by an ECD at +700 mV after postcolumn zinc or platinum reduction. The HPLC conditions are the same as described in Figure 2. (A) The chloroform fraction was injected into HPLC followed by postcolumn zinc reduction. (B) The chloroform fraction was injected into HPLC followed by postcolumn platinum reduction. The arrow indicates the elution position of authentic TOO-epoxyChL. (C) The methanol fraction was injected into HPLC followed by postcolumn platinum reduction. The arrow indicates the elution position of authentic TOO-epoxyPLPC. See Figures 1 and 2 for abbreviations.

products were somewhat poorer due to their instability during the sample preparation process.

The human plasma was reacted with peroxy radicals that had been generated in the aqueous phase by the thermal decomposition of AAPH. The starting plasma sample contained

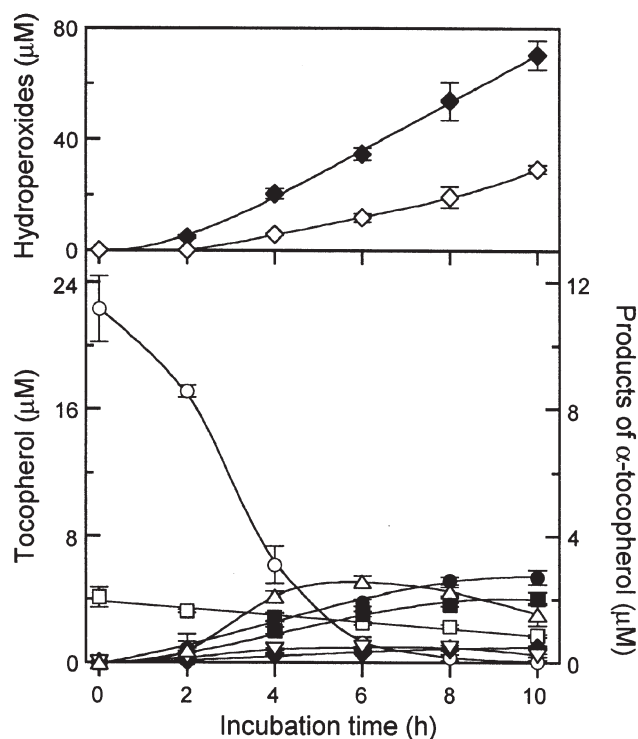


**FIG. 5.** HPLC coupled with on-line MS analysis of 8a-(cholesteryl ester-dioxy)- $\alpha$ -tocopherones (TOO-epoxyChE) fraction from the peroxidized human plasma. The peak corresponding to TOO-epoxyChE, as shown in Figure 4B, was collected and injected into a Luna C18 column ( $2 \times 150$  mm i.d.; Phenomenex, Torrance, CA) developed with methanol/2-propanol/hexane (50:35:15, by vol) at 0.2 mL/min. UV detection at 240 nm, the total ion chromatogram (TIC) of atmospheric pressure chemical ionization-MS, and mass spectrum of the peak indicated by arrows are shown. See Figure 2 for abbreviations.

endogenous  $\alpha$ -TH ( $22.3 \pm 2.1$   $\mu$ M) and  $\gamma$ -TH ( $4.1 \pm 0.6$   $\mu$ M). Figure 4A shows the HPLC chromatogram of the TH and  $\alpha$ -TQ compounds during the AAPH-initiated peroxidation of human plasma. A peak corresponding to  $\alpha$ -TH decreased after the 6-h reaction, and peaks corresponding to  $\alpha$ -TQ and epoxy- $\alpha$ -TQ appeared as the oxidation products of  $\alpha$ -TH. The identity of each peak was confirmed by co-elution against the authentic standards and by LC-MS analysis: two isomeric epoxy- $\alpha$ -TQ, APCI-MS  $m/z$  463 ( $[M + H]^+$ , 6%) and 445 ( $[M - OH]^+$ , 100%);  $\alpha$ -TQ, APCI-MS  $m/z$  445 ( $[M + H]^+$ , 1%) and 429 ( $[M - OH]^+$ , 100%);  $\gamma$ -TH, APCI-MS  $m/z$  417 ( $[M + H]^+$ , 70%) and 151 (100%); and  $\alpha$ -TH, APCI-MS  $m/z$  431 ( $[M + H]^+$ , 100%) and 165 (63%). The HPLC chromatograms of the product fractions of ChE and PC are shown in Figures 4B and 4C. An intense peak corresponding to TOO-epoxyChE appeared around 10.7 min of retention time as the ChE products (Fig. 4B). This peak was collected by preparative HPLC and analyzed by LC-MS (Fig. 5). The APCI-MS showed a protonated molecular ion at  $m/z$  1125 ( $[M + H]^+$ , 14%) and significant ions at  $m/z$  1107 ( $[M - OH]^+$ , 4%), 942 (22%), 875 (13%), 573 (34%), 445 ( $[\alpha$ -tocopherone + O] $^+$ , 17%), 430 ( $[\alpha$ -tocopherone] $^+$ , 36%), and 369 ( $[\text{cholesterol} - OH]^+$ , 100%). Thus, this peak was identified as TOO-epoxyChL, the addition products of  $\alpha$ -TH with cholesteryl epoxy-

linoleate-peroxyl radicals. On the analysis of PC products, only a smaller peak corresponding to TOO-epoxyPC appeared around 7.5 min of retention time after the 6-h reaction (Fig. 4C). This peak was also collected by preparative HPLC and analyzed by LC-MS. The APCI-MS indicated the presence of the  $\alpha$ -tocopherone structure at  $m/z$  430 together with the presence of some other unknown compounds (data not shown). Therefore, we could not identify its structure from the APCI-MS. This peak was assigned as TOO-epoxyPC only by comparison of the HPLC behavior with that of authentic TOO-epoxyPLPC.

The disappearance of endogenous antioxidants in human blood plasma has been reported in relation to the appearance of various lipid hydroperoxides (26). In the present study, the consumption of endogenous  $\alpha$ -TH was observed with the formation of lipid hydroperoxides, ChE-OOH and PC-OOH, when the peroxidation was initiated by AAPH (Fig. 6). The oxidation products of  $\alpha$ -TH,  $\alpha$ -TQ, epoxy- $\alpha$ -TQ, TOO-epoxyChL, and TOO-epoxyPC appeared with depletion of  $\alpha$ -TH. The oxidation products formed in the 4-h plasma sample accounted for 32% of the consumed  $\alpha$ -TH. A similar product distribution has been reported in the AAPH-initiated peroxidation of PLPC liposomes containing  $\alpha$ -TH, although the type of 8a-substituted tocopherones was different (20).



**FIG. 6.** Changes of cholesteryl ester hydroperoxides (ChE-OOH), PC hydroperoxides (PC-OOH), endogenous TH, and  $\alpha$ -TH products during the AAPH-initiated peroxidation of human plasma. The human plasma (4.0 mL) was incubated at 37°C by the addition of 1.0 mL of 100 mM AAPH (final concentration, 20 mM). Formation of ChE-OOH ( $\blacklozenge$ ) and PC-OOH ( $\diamond$ ), the consumption of  $\alpha$ -TH ( $\circ$ ) and  $\gamma$ -TH ( $\square$ ), and the formation of  $\alpha$ -TQ ( $\bullet$ ), 2,3-epoxy- $\alpha$ -TQ ( $\blacksquare$ ), 5,6-epoxy- $\alpha$ -TQ ( $\blacklozenge$ ), TOO-epoxyPC ( $\triangle$ ), and TOO-epoxyChE ( $\nabla$ ) are shown. Each value is expressed as mean  $\pm$  SD of three different experiments. See Figures 1 and 4 for abbreviations.

The classical action of  $\alpha$ -TH is that of a chain-breaking antioxidant that reflects its ability to react rapidly with chain-carrying lipid peroxy radicals (3–5). Alternatively,  $\alpha$ -TH can directly scavenge the radical that initiates peroxidation (27). In both cases, the relatively nonreactive  $\alpha$ -tocopheroxyl radical is formed. This radical rapidly reacts with another available radical to yield nonradical products. If the  $\alpha$ -tocopheroxyl radical traps the chain-propagating peroxy radicals formed from ChE or PC directly, the primary products are 8a-(ChE-dioxy)- $\alpha$ -tocopherones or 8a-(PC-dioxy)- $\alpha$ -tocopherones (20). However, we could not detect such 8a-substituted tocopherone products in the peroxidized plasma. Instead, the products we detected were the addition products of  $\alpha$ -TH with epoxy lipid-peroxy radicals, TOO-epoxyChL, and TOO-epoxyPC, in addition to  $\alpha$ -TQ and epoxy- $\alpha$ -TQ (Fig. 4). The epoxy lipid-peroxy radicals can be produced from the metal ion-catalyzed decomposition of lipid hydroperoxides such as ChE-OOH and PC-OOH (28,29). Thus, the  $\alpha$ -TH in human plasma may react only with such secondary produced peroxy radicals. Frei *et al.* (26) demonstrated that  $\alpha$ -TH in plasma was considerably less effective in preventing peroxidative damage to lipids induced by aqueous oxidants. Moreover,

$\alpha$ -TH can exert prooxidant activity on lipoprotein lipids, and a model of TH-mediated peroxidation has been developed to explain such prooxidant activity of  $\alpha$ -TH during lipoprotein peroxidation (30,31). Therefore, the accumulation of hydroperoxides before the depletion of  $\alpha$ -TH and the formation of 8a-(epoxy lipid-dioxy)- $\alpha$ -tocopherones indicates that  $\alpha$ -TH is less effective in preventing lipid peroxidation in human plasma.

Liebler *et al.* (32) have developed the most sensitive methodology of a stable isotope dilution GC-MS for analyzing  $\alpha$ -TH,  $\alpha$ -TQ, and epoxy- $\alpha$ -TQ in biological samples. They concluded that 8a-substituted  $\alpha$ -tocopherones and epoxytocopherones, rather than their hydrolyzed products, were the principal oxidation products of  $\alpha$ -TH in biological systems (32,33). However, this was only assumed from the evidence that the additional release of  $\alpha$ -TQ was observed in the acid-treated samples. The HPLC with electrochemical detection described in the present study could detect such tocopherone products in biological samples directly.

In conclusion, the HPLC technique presented here is found advantageous for the sensitive and specific determination of the 8a-substituted  $\alpha$ -tocopherones in biological samples. The oxidation products of  $\alpha$ -TH might be useful markers for the antioxidant and prooxidant reactions in biological samples. We are studying further application of the present HPLC methodology to some biological samples.

## REFERENCES

- Slater, T.F. (1984) Free-Radical Mechanisms in Tissue Injury, *Biochem. J.* 222, 1–15.
- Sevanian, A., and Hochstein, P. (1985) Mechanisms and Consequences of Lipid Peroxidation in Biological Systems, *Annu. Rev. Nutr.* 5, 365–390.
- Burton, G.W., and Traber, M.G. (1990) Vitamin E: Antioxidant Activity, Biokinetics, and Bioavailability, *Annu. Rev. Nutr.* 10, 357–3382.
- Liebler, D.C. (1993) The Role of Metabolism in the Antioxidant Function of Vitamin E, *Crit. Rev. Toxicol.* 23, 147–169.
- Kamel-Eldin, A., and Appelqvist, L.-Å. (1996) The Chemistry and Antioxidant Properties of Tocopherols and Tocotrienols, *Lipids* 31, 671–701.
- Yamauchi, R., Hara, Y., Murase, H., and Kato, K. (2000) Analysis of the Addition Products of  $\alpha$ -Tocopherol with Phosphatidylcholine-Peroxy Radicals by High-Performance Liquid Chromatography with Chemiluminescent Detection, *Lipids* 35, 1405–1410.
- Wakabayashi, H., Yamato, S., Nakajima, M., and Shimada, K. (1994) Simultaneous Determination of Oxidized and Reduced Coenzyme Q and  $\alpha$ -Tocopherol in Biological Samples by High Performance Liquid Chromatography with Platinum Catalyst Reduction and Electrochemical Detection, *Biol. Pharm. Bull.* 17, 997–1002.
- Yamashita, S., and Yamamoto, Y. (1997) Simultaneous Determination of Ubiquinol and Ubiquinone in Human Plasma as a Marker of Oxidative Stress, *Anal. Biochem.* 250, 66–73.
- Leray, C., Andriamampandry, M.D., Freund, M., Gachet, C., and Cazenave, J.-P. (1998) Simultaneous Determination of Homologues of Vitamin E and Coenzyme Q and Products of  $\alpha$ -Tocopherol Oxidation, *J. Lipid Res.* 39, 2099–2105.
- Murphy, M.E., and Kehrer, J.P. (1987) Simultaneous Measurement of Tocopherols and Tocopheryl Quinones in Tissue Fractions



- Using High-Performance Liquid Chromatography with Redox-Cycling Electrochemical Detection, *J. Chromatogr.* 421, 71–82.
11. Edlund, P.O. (1988) Determination of Coenzyme Q<sub>10</sub>,  $\alpha$ -Tocopherol and Cholesterol in Biological Samples by Coupled-Column Liquid Chromatography with Coulometric and Ultraviolet Detection, *J. Chromatogr.* 425, 87–97.
  12. Takeda, H., Shibuya, T., Yanagawa, K., Kanoh, H., and Takasaki, M. (1996) Simultaneous Determination of  $\alpha$ -Tocopherol and  $\alpha$ -Tocopherolquinone by High-Performance Liquid Chromatography and Coulometric Detection in the Redox Mode, *J. Chromatogr.* 722, 287–294.
  13. Thomas, S.R., Neuzil, J., Mohr, D., and Stocker, R. (1995) Coantioxidants Make  $\alpha$ -Tocopherol an Efficient Antioxidant for Low-Density Lipoprotein, *Am. J. Clin. Nutr.* 62 (Suppl.), 1357S–1364S.
  14. Yamauchi, R., Yagi, Y., and Kato, K. (1994) Isolation and Characterization of Addition Products of  $\alpha$ -Tocopherol with Peroxyl Radicals of Dilinoleoylphosphatidylcholine in Liposomes, *Biochim. Biophys. Acta* 1212, 43–49.
  15. Yamauchi, R., and Matsushita, S. (1977) Quenching Effect of Tocopherols on the Methyl Linoleate Photooxidation and Their Oxidation Products, *Agric. Biol. Chem.* 41, 1425–1430.
  16. Yamauchi, R., Yagi, Y., and Kato, K. (1996) Oxidation of  $\alpha$ -Tocopherol During the Peroxidation of Dilinoleoylphosphatidylcholine in Liposomes, *Biosci. Biotechnol. Biochem.* 60, 616–620.
  17. Yamamoto, Y., Brodsky, M.H., Baker, J.C., and Ames, B.N. (1987) Detection and Characterization of Lipid Hydroperoxides at Picomole Levels by High-Performance Liquid Chromatography, *Anal. Biochem.* 160, 7–13.
  18. Yamauchi, R., Kamatani, Y., Shimoyamada, M., and Kato, K. (2002) Preparation of the Addition Products of  $\alpha$ -Tocopherol with Cholesteryl Linoleate-Peroxyl Radicals, *Biosci. Biotechnol. Biochem.* 66, 670–673.
  19. Brash, A.R., Ingram, C.D., and Harris, T.M. (1987) Analysis of a Specific Oxygenation Reaction of Soybean Lipoxygenase-1 with Fatty Acids Esterified in Phospholipids, *Biochemistry* 26, 5465–5471.
  20. Yamauchi, R., Mizuno, H., and Kato, K. (1998) Preparation and Characterization of 8a-(Phosphatidylcholine-dioxy)- $\alpha$ -tocopherones and Their Formation During the Peroxidation of Phosphatidylcholine in Liposomes, *Biosci. Biotechnol. Biochem.* 62, 1293–1300.
  21. Yamauchi, R., Ozaki, K., Shimoyamada, M., and Kato, K. (2002) Iron-Catalyzed Reaction Products of  $\alpha$ -Tocopherol with 1-Palmitoyl-2-linoleoyl-3-*sn*-phosphatidylcholine (13S)-Hydroperoxide, *Chem. Phys. Lipids* 114, 193–201.
  22. Blich, E.G., and Dyer, W.J. (1959) A Rapid Method of Total Lipid Extraction and Purification, *Can. J. Biochem. Physiol.* 37, 911–917.
  23. Bieri, J.G., and Tolliver, T.J. (1981) On the Occurrence of  $\alpha$ -Tocopherolquinone in Rat Tissue, *Lipids* 16, 777–779.
  24. Vatassery, G.T. (1994) Determination of Tocopherols and Tocopherolquinone in Human Red Blood Cell and Platelet Samples, *Methods Enzymol.* 234, 327–331.
  25. Liebler, D.C., and Burr, J.A. (1992) Oxidation of Vitamin E During Iron-Catalyzed Lipid Peroxidation: Evidence for Electron-Transfer Reactions of the Tocopheroxyl Radical, *Biochemistry* 31, 8278–8284.
  26. Frei, B., Stocker, R., and Ames, B.N. (1988) Antioxidant Defenses and Lipid Peroxidation in Human Blood Plasma, *Proc. Natl. Acad. Sci. USA* 85, 9748–9752.
  27. Evans, C., Scaiano, J.C., and Ingold, K.U. (1992) Absolute Kinetics of Hydrogen Abstraction from  $\alpha$ -Tocopherol by Several Reactive Species Including an Alkyl Radical, *J. Am. Chem. Soc.* 114, 4589–4593.
  28. Gardner, H.W. (1989) Oxygen Radical Chemistry of Polyunsaturated Fatty Acids, *Free Radic. Biol. Med.* 7, 65–86.
  29. Wilcox, A.L., and Marnett, L.J. (1993) Polyunsaturated Fatty Acid Alkoxy Radicals Exist as Carbon-Centered Epoxyallylic Radicals: A Key Step in Hydroperoxide-Amplified Lipid Peroxidation, *Chem. Res. Toxicol.* 6, 413–416.
  30. Bowry, V.W., and Stocker, R. (1993) Tocopherol-Mediated Peroxidation. The Prooxidant Effect of Vitamin E on the Radical-Initiated Oxidation of Human Low-Density Lipoprotein, *J. Am. Chem. Soc.* 115, 6029–6044.
  31. Thomas, S.R., and Stocker, R. (2000) Molecular Action of Vitamin E in Lipoprotein Oxidation: Implications for Atherosclerosis, *Free Radic. Biol. Med.* 28, 1795–1805.
  32. Liebler, D.C., Burr, J.A., Philips, L., and Ham, A.J.L. (1996) Gas Chromatography–Mass Spectrometry Analysis of Vitamin E and Its Oxidation Products, *Anal. Biochem.* 236, 27–34.
  33. Ham, A.J.L., and Liebler, D.C. (1997) Antioxidant Reactions of Vitamin E in the Perfused Rat Liver: Product Distribution and Effect of Dietary Vitamin E Supplementation, *Arch. Biochem. Biophys.* 339, 157–164.

[Received November 27, 2001, and in revised form February 19, 2002; revision accepted April 12, 2002]

# A Convenient Method for Determination of the C<sub>20-22</sub> PUFA Composition of Glycerolipids in Blood and Breast Milk

Ken'ichi Ichihara<sup>a,\*</sup>, Kanako Waku<sup>a</sup>, Chiaki Yamaguchi<sup>a</sup>, Kazumi Saito<sup>a</sup>,  
Akira Shibahara<sup>b</sup>, Shuichi Miyatani<sup>b</sup>, and Kohei Yamamoto<sup>c</sup>

<sup>a</sup>Biological Chemistry, Faculty of Agriculture, Kyoto Prefectural University, Shimogamo, Kyoto 606-8522, Japan,

<sup>b</sup>Department of Clinical Nutrition, Osaka Prefecture College of Health Sciences, Habikino 583-8555, Japan,

and <sup>c</sup>General Testing Research Institute of Japan Oil Stuff Inspectors' Corporation, Kobe 658-0044, Japan

**ABSTRACT:** A convenient method was developed for preparation of FAME in small amounts from glycerolipids of blood or breast milk. Initially, 0.04–0.06 mL blood or breast milk was spotted onto a small piece of filter paper (1.5 × 1.5 cm) that had been washed with acetone containing 0.05% 2,6-di-*tert*-butyl-*p*-cresol (BHT). Each piece, once it had dried, was put in a small test tube, to which 2 mL hexane and 0.2 mL 2 M KOH/methanol were added. After vigorous mixing or sonication for 2 min at room temperature, the solution was neutralized or acidified by the addition of a few drops of acetic acid. To the solution was added 2 mL H<sub>2</sub>O, and then the hexane layer that separated was concentrated to dryness *in vacuo*. The FAME obtained were analyzed by GC. The method was applicable to the analysis of a large number of blood and breast milk samples, and the arachidonate/(eicosapentaenoate + docosahexaenoate) ratios could be determined rapidly.

Paper no. L8916 in *Lipids* 37, 523–526 (May 2002).

Arachidonic acid (ARA, 20:4n-6), EPA (20:5n-3), and DHA (22:6n-3) are major C<sub>20-22</sub> long-chain PUFA in humans and are ubiquitous components of membrane phospholipids that make up the structural matrix of cellular membranes. ARA and EPA are utilized for eicosanoid synthesis and involved in signal transduction (1); there is also increasing recognition that some diseases may be associated with an imbalance of the ratio of n-6/n-3 PUFA in the human diet (2–7). DHA is also an important structural component of photoreceptor and cortical neuronal membranes (8). Since the human brain grows rapidly between the sixth month of gestation and the first month after birth (8) and the vision of human infants develops for several months after birth (9), the FA composition of breast milk can affect the retinal and brain development of breast-fed infants (10,11). Analyses of the FA compositions of human blood and breast milk therefore have increasing nutritional and health implications (12,13), and they will be used more widely for indications of nutritional conditions in the near future.

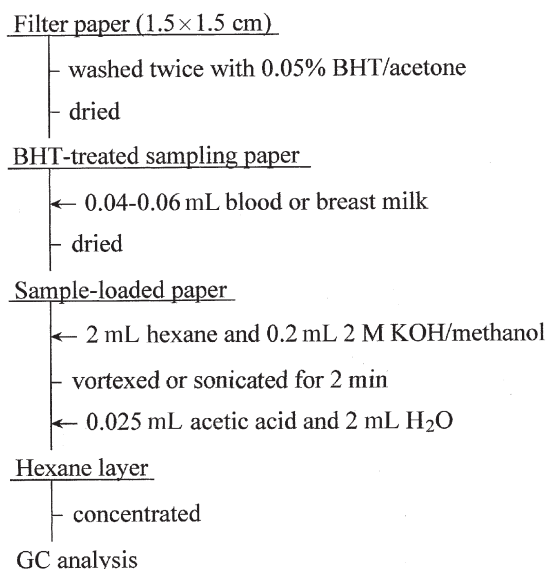
The composition of FA is determined by using GC to analyze their methyl esters. However, many preparative methods for FAME from blood or breast milk include time-consuming procedures. Some methods require more than 1 mL of blood or breast milk. Here, we report a convenient method for preparation of FAME from a few drops of blood or breast

milk; the method also can be used in analyzing a large number of samples. The procedure includes the direct transesterification of samples on filter papers with KOH/methanol.

## MATERIALS AND METHODS

**Reagents.** Authentic FA were purchased from Avanti Polar Lipids (Alabaster, AL), Cayman Chemical (Ann Arbor, MI), Doosan Serdary Research Laboratories (Englewood Cliffs, NJ), Larodan Fine Chemicals AB (Malmö, Sweden), Nacalai Tesque (Kyoto, Japan), Nu-Chek-Prep (Elysian, MN), Sigma (St. Louis, MO), and Wako Pure Chemical Industries (Osaka, Japan). Organic solvents and other chemicals including BHT were of reagent grade and were used without further purification.

**Preparation of sampling papers.** Sheets of filter paper, Whatman 3MM (Whatman Inc., Clifton, NJ), were cut into small pieces (1.5 × 1.5 cm) and then soaked for a few minutes in acetone that contained 0.05% BHT so as to wash out contaminants in the filter paper and to impregnate it with the antioxidant (Scheme 1). This treatment was repeated with a fresh BHT-containing acetone solution without drying between immersions. The sampling papers thus prepared were air-dried and stored at room temperature until use.



SCHEME 1

\*To whom correspondence should be addressed. E-mail: ichihara@kpu.ac.jp  
Abbreviations: 18:2, linoleic acid; 18:3,  $\alpha$ -linolenic acid; ARA, arachidonic acid.

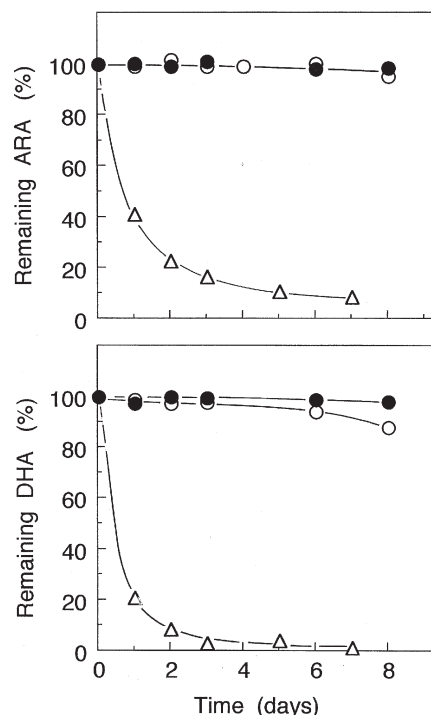
**Preparation of FAME from blood or breast milk.** Sampling papers were spotted with 0.04–0.06 mL blood, serum, or breast milk and were air-dried overnight or dried for 30 min *in vacuo*. They were inserted individually into small test tubes, and 2 mL hexane and 0.2 mL 2 M KOH/methanol per test tube were added. The tubes were vigorously mixed with a vortex mixer for 2 min at 25°C (room temperature) or above. When the methanolysis was thus completed, the alkaline solution was neutralized with a few drops (0.025 mL or more) of acetic acid. To each tube was added 2–3 mL H<sub>2</sub>O without vigorous mixing, which causes gelatinization of the contents of blood samples. An aliquot (1.5–1.8 mL) of the hexane layer was transferred to a vial, and the hexane solution was evaporated to dryness *in vacuo*.

**GC analysis.** For rapid analysis, we used a glass column (4 mm × 2 m) packed with a thermostable liquid phase, 10% SP-2340 on 100–120 mesh Chromosorb WAW (Supelco, Bellefonte, PA). FAME obtained were dissolved in 0.02 mL methyl acetate or hexane and were analyzed by GC (220°C, N<sub>2</sub> 30 mL/min; or 235°C, N<sub>2</sub> 55 mL/min). Methyl acetate was somewhat better than hexane to minimize the tailing of injection solvent. Although fast-eluting peaks in GC analysis were not completely separated from each other under the above conditions, the C<sub>20–22</sub> PUFA composition was determined with a data-processor, CHROMATOPAC C-R1B (Shimadzu, Kyoto, Japan).

## RESULTS AND DISCUSSION

In an alcoholic solution of the hydroxide of an alkali metal, the hydroxide–alkoxide equilibrium greatly favors alkoxide formation [ROH + OH<sup>−</sup> ⇌ RO<sup>−</sup> + H<sub>2</sub>O], and most of the total base is the alkoxide, but not the hydroxide (14). When esters are treated with alcoholic alkali/hydroxide solutions, alcoholysis of the esters therefore proceeds much faster than saponification. The relative difference in rates is of the order of 1,500-fold (15). This reaction, alkali-catalyzed alcoholysis, has been used for preparation of FAME from glycerolipids (16), and the FA components of glycerolipids are almost quantitatively converted to their methyl esters within 1–2 min at room temperature (17). The data presented here demonstrate that the rapid and convenient methanolysis previously reported (17) can be applied to small amounts of blood and breast milk and also to a large number of the samples.

**Prevention of autoxidation of PUFA.** Small pieces of filter paper were used as blood- or breast milk-sampling papers. Pieces of filter paper that have been spotted can easily be transported by mail, for example, from hospitals to laboratories for analysis. A large number of spotted papers can also be stored compactly. Nishio *et al.* (18) proposed a method for the diagnosis of a disease using blood spot samples. However, when spots of dried blood or breast milk are exposed to the air, the oxidation of PUFA will probably proceed rapidly. In fact, when authentic PUFA were stored on filter paper at room temperature in the dark, more than 60% of each PUFA disappeared after 1 d (Fig. 1). The order of oxidation rates was DHA > EPA > ARA. To prevent autoxidation of PUFA during storage, small pieces of filter paper were soaked twice in



**FIG. 1.** Effects of BHT on autoxidation of PUFA on filter paper. Each PUFA, along with 11-eicosenoic acid as an internal standard, were applied on sampling papers that had been treated with 0% (Δ), 0.025% (○), or 0.05% (●) BHT in acetone. The spotted sampling papers were allowed to stand at room temperature for autoxidation, and then the remaining amount of the PUFA was followed by GC. Methylation for GC analysis was carried out on the spotted sampling papers with 10% BF<sub>3</sub> in methanol for 30 min at room temperature, and the methyl esters formed were extracted with hexane. Data on EPA are not presented, but they were similar to those for ARA and DHA.

acetone containing 0.025 or 0.05% BHT as an antioxidant. Impurities that had been adsorbed by the filter paper were simultaneously washed out with the solvent. A hexane solution of authentic ARA, EPA, or DHA was dropped onto the BHT-impregnated sampling papers. 11-Eicosenoic acid was used as the internal standard, because the monounsaturated FA was not apparently oxidized during the period of subsequent exposure. When the filter paper was washed with 0.05% BHT-containing acetone, none of the PUFA tested were significantly oxidized within 8 d (Fig. 1). With 0.025% BHT, DHA slightly decreased at day 8. When spotted sampling papers were air-dried overnight or dried *in vacuo* for 30 min before methanolysis, no significant differences in the PUFA composition were found between the two methods of drying.

**Quality of filter paper.** Autoxidation of PUFA in blood was measured on various kinds of filter paper (Whatman No. 2, No. 42, 3MM, and Advantec No. 131) for 5 d. Of the filter papers tested, Whatman 3MM gave the most reliable data (Table 1). ARA, EPA, and DHA did not apparently decrease for 5 d. Because Whatman 3MM is the thickest among the filter papers tested, it is probable that blood was well absorbed by the thick filter paper and that blood lipids and BHT could consequently come into intimate contact.

The analysis of serum for FA content confirmed that appli-

**TABLE 1**  
Dependence of Autoxidation of Blood C<sub>20-22</sub> PUFA on the Quality of Filter Paper<sup>a</sup>

FA	Remaining FA (%)			
	(filter paper)			
	No. 2	No. 42	3MM	No. 131
ARA	90.9	101.0	96.2	91.4
EPA	68.7	71.6	96.3	68.5
DHA	80.8	96.3	95.2	68.5

<sup>a</sup>The sampling papers treated with 0.025% BHT in acetone were spotted with 0.04 mL blood. They were stored at room temperature for 5 d, and the remaining PUFA were determined. ARA, arachidonic acid.

cation of sample volumes in the range of 0.04–0.12 mL did not affect the analytical data on the PUFA compositions (Table 2).

**Mixing for reaction.** When many samples were to be treated, vortexing was replaced by sonication. Spotted sampling papers and the reagents were placed in small test tubes and sonicated in a water bath of an ultrasonic cleaner at 25°C or above. The reaction time of 2 min was the same as that for vortexing. The efficiency of methanolysis under sonication was the same as that for vortexing (data not shown).

**Accuracy.** The C<sub>20-22</sub> PUFA composition of blood was determined by the present filter paper/KOH/methanol method, and it was compared with that determined according to the following conventional procedure. To 2 mL blood were added 1 mL water, 4 mL methanol, 4 mL chloroform, and a trace amount of BHT. The mixture was vortexed for 2 min and then centrifuged at 1,500 × g for 3 min. The chloroform layer was washed with an equal volume of water. After centrifugation, the chloroform solution was dried with anhydrous sodium sulfate and concentrated *in vacuo*. The lipids obtained were converted into FAME by the KOH/methanol method previously described (17) and analyzed by GC (Table 3). There was no significant difference between the FA composition determined by the filter paper/KOH/methanol method and that determined by the conventional extraction/methanolysis method.

**Application of the present method and measurement of ARA/(EPA + DHA) ratios in blood.** Unsaturated FA of the n-3

**TABLE 2**  
Effects of the Amounts of Serum Applied to Sampling Papers on the C<sub>20-22</sub> PUFA Analysis

Serum sample	Applied volume (mL)	C <sub>20-22</sub> PUFA (%) <sup>a</sup>			ARA/(EPA + DHA)
		ARA	EPA	DHA	
A	0.04	4.6	0.5	2.0	1.8
	0.08	4.9	0.5	2.3	1.8
	0.12	5.0	0.5	2.2	1.9
B	0.04	5.3	1.0	4.5	1.0
	0.08	5.7	1.0	4.8	1.0
	0.12	5.3	0.7	4.3	1.1
C	0.04	5.2	3.0	5.9	0.6
	0.08	5.7	2.7	6.3	0.6
	0.12	5.0	2.6	6.5	0.5

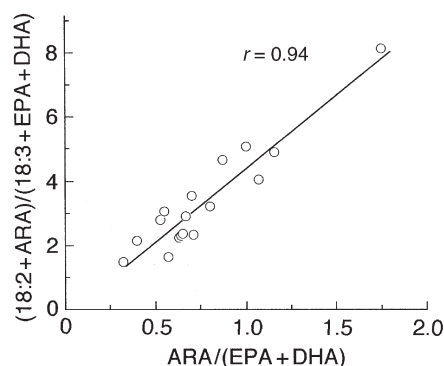
<sup>a</sup>For abbreviation see Table 1.

**TABLE 3**  
Determination of the C<sub>20-22</sub> PUFA Compositions of Blood by the Different Methods

Method	C <sub>20-22</sub> PUFA (%) <sup>a</sup>			
	ARA	EPA	DHA	ARA/(EPA + DHA)
Filter paper/KOH/ methanol method	10.5 ± 0.4	2.6 ± 0.2	6.6 ± 0.5	1.1 ± 0.1
Extraction/KOH/ methanol method	9.7 ± 0.1	2.3 ± 0.1	7.2 ± 0.2	1.0 ± 0.1

<sup>a</sup>Values represent mean ± SD (n = 3). For abbreviation see Table 1.

and n-6 series have biological functions different from each other (1,2). They also compete with each other in regulation of cellular functions. Blood or breast milk contains 18:2 and ARA as the major n-6 PUFA and also contains 18:3, EPA, and DHA as the major n-3 PUFA. In GC analysis of FAME, the C<sub>18</sub> PUFA (18:2 and 18:3) are eluted faster than the C<sub>20-22</sub> PUFA (ARA, EPA, and DHA). However, GC analysis restricted to the C<sub>20-22</sub> PUFA is much faster than that of all of the FA components including both the C<sub>18</sub> and C<sub>20-22</sub> PUFA. The C<sub>18</sub> PUFA *in vivo* were elongated and desaturated to the corresponding C<sub>20-22</sub> PUFA, which physiologically function or are further metabolized to eicosanoids. Because ARA, EPA, and DHA are thus the major functional PUFA, the ARA/(EPA + DHA) ratios of blood glycerolipids were determined and compared with the ratios of (18:2 + ARA)/(18:3 + EPA + DHA). The latter ratios essentially represent those of n-3/n-6. As a model experiment, blood samples of 17 humans practicing a fasting cure were analyzed. Figure 2 shows that the ARA/(EPA + DHA) ratio correlates strongly with the (18:2 + ARA)/(18:3 + EPA + DHA) ratio. This means that the measurement of n-6/n-3 ratio can be replaced by the measurement of ARA/(EPA + DHA) ratio, although other n-3 and n-6 PUFA are also present in blood and breast-milk lipids. Taking these into consideration, we routinely measure ARA/(EPA + DHA) ratios instead of n-6/n-3 ratios, and we recommend the use of the ARA/(EPA + DHA) ratio as a practical index of the n-6/n-3 ratio. Figure 3 is a typical gas chromatogram focused on C<sub>20-22</sub> PUFA methyl esters derived from blood and breast milk by the present method. Although



**FIG. 2.** Relationship between the ARA/(EPA + DHA) ratio and the (18:2 + ARA)/(18:3 + EPA + DHA) ratio in blood glycerolipids. For details, see text.



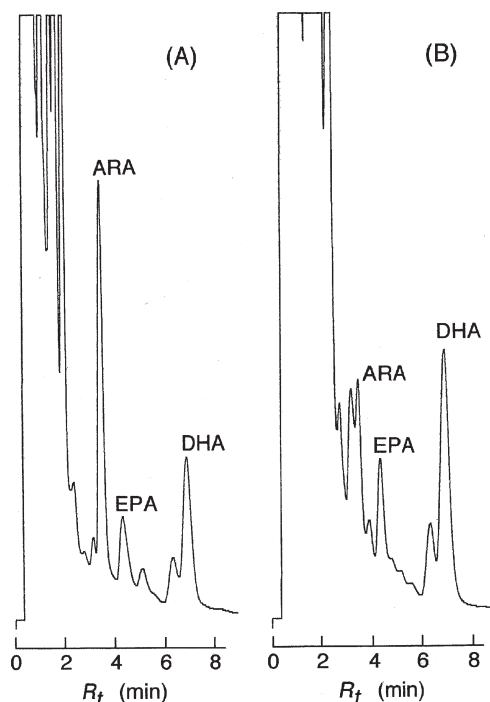


FIG. 3. GC analyses of the C<sub>20-22</sub> PUFA methyl esters prepared from blood (A) and breast milk (B). Column temperature, 235°C; N<sub>2</sub> gas, 55 mL/min.

packed-column GC is inferior to capillary GC in resolution, the former possesses the advantage of long column-life for injection of crude FAME samples. Capillary GC requires a purification procedure, such as TLC or column chromatography with small silica gel cartridges, of FAME prepared from crude samples, whereas FAME prepared from blood or breast milk can be directly injected onto a packed column without purification as described here. In general, retention times in packed-column GC are also shorter than those in capillary GC. In our laboratories, more than 600 samples have been successively analyzed on a packed column of SP-2340. Probably, it is possible to analyze more than a thousand samples with one column. Packed-column GC is therefore suitable for routine FAME analyses of a large number of crude lipid samples.

The two major merits of the method—it requires only small amounts of samples, and the procedure is simple and rapid—permitted us to follow the successive changes in the C<sub>20-22</sub> PUFA composition of blood lipids taken from subjects after they had eaten (data not shown).

FAME can be prepared from many samples of small amounts of blood or breast milk by alkaline methanolysis on small pieces of filter paper. The method requires neither sophisticated apparatus nor expensive reagents. Although the FA components of steryl esters and sphingomyelins do not react and FFA are not esterified under the conditions employed here, the present method will be useful for analysis of the PUFA composition of glycerolipids in blood and breast milk. This is the case especially for analysis of breast milk, because more than 97% of lipids in breast milk are TAG (19).

## ACKNOWLEDGMENTS

We thank Associate Professor Kumiko Morikawa (Osaka Prefecture College of Health Sciences, Habikino, Japan) for providing samples of breast milk and Nippon Oil & Fats Co. (Amagasaki, Japan) for supplying oleic and linoleic acids.

## REFERENCES

1. Spector, A.A. (1999) Essentiality of Fatty Acids, *Lipids* 34 (Suppl.), S1–S3.
2. Lands, W.E.M. (1993) Eicosanoids and Health, *Ann. NY Acad. Sci.* 676, 46–59.
3. Adams, P.B., Lawson, S., Sanigorski, A., and Sinclair, A.J. (1996) Arachidonic Acid to Eicosapentaenoic Acid Ratio in Blood Correlates Positively with Clinical Symptoms of Depression, *Lipids* 31 (Suppl.), S157–S161.
4. Kalmijin, S., Launer, L.J., Ott, A., Witteman, J.C.M., Hofman, A., and Breteler, M.M.B. (1997) Dietary Fat Intake and the Risk of Incident Dementia in the Rotterdam Study, *Ann. Neurol.* 42, 776–782.
5. Leonard, E.C. (1999) Dietary Fatty Acids: Effect of n-6/n-3 Balance on Human Nutrition and Disease, *Lipid Technol.* 11, 110–114.
6. Connor, W.E. (2000) Importance of n-3 Fatty Acids in Health and Disease, *Am. J. Clin. Nutr.* 71 (Suppl.), 171S–175S.
7. O'Keefe, J.H., Jr., and Harris, W.S. (2000) From Inuit to Implementation: Omega-3 Fatty Acids Come of Age, *Mayo Clin. Proc.* 75, 607–614.
8. Koletzko, B. (1992) Fats for Brains, *Eur. J. Clin. Nutr.* 46 (Suppl. 1), S51–S62.
9. Teller, D.Y. (1997) First Glances: The Vision of Infants, *Invest. Ophthalmol. Vis. Sci.* 38, 2183–2203.
10. Williams, C., Birch, E.E., Emmett, P.M., Northstone, K., and the Avon Longitudinal Study of Pregnancy and Childhood Study Team (2001) Stereoacuity at Age 3.5 y in Children Born Full-Term Is Associated with Prenatal and Postnatal Dietary Factors: A Report from a Population-Based Cohort Study, *Am. J. Clin. Nutr.* 73, 316–322.
11. Sattar, N., Berry, C., and Greer, I.A. (1998) Essential Fatty Acids in Relation to Pregnancy Complications and Fetal Development, *Br. J. Obstet. Gynaecol.* 105, 1248–1255.
12. Jensen, C.L., Maude, M., Anderson, R.E., and Heird, W.C. (2000) Effect of Docosahexaenoic Acid Supplementation of Lactating Women on the Fatty Acid Composition of Breast Milk Lipids and Maternal and Infant Plasma Phospholipids, *Am. J. Clin. Nutr.* 71 (Suppl.), 292S–299S.
13. Fidler, N., Sauerwald, T., Pohl, A., Demmelmair, H., and Koletzko, B. (2000) Docosahexaenoic Acid Transfer into Human Milk After Dietary Supplementation: A Randomized Clinical Trial, *J. Lipid Res.* 41, 1376–1383.
14. Caldin, E.F., and Long, G. (1954) The Equilibrium Between Ethoxide and Hydroxide Ions in Ethanol and in Ethanol–Water Mixtures, *J. Chem. Soc.*, 3737–3742.
15. Pardee, A.M., and Reid, E.E. (1920) The Influence of Ester Transposition in the Determination of Saponification Numbers, *J. Ind. Eng. Chem.*, 129–133.
16. Glass, R.L. (1971) Alcoholysis, Saponification and the Preparation of Fatty Acid Methyl Esters, *Lipids* 6, 919–925.
17. Ichihara, K., Shibahara, A., Yamamoto, K., and Nakayama, T. (1996) An Improved Method for Rapid Analysis of the Fatty Acids of Glycerolipids, *Lipids* 31, 535–539; 31, 889 (erratum).
18. Nishio, H., Kodama, S., Yokoyama, S., Matsuo, T., Mio, T., and Sumino, K. (1986) A Simple Method to Diagnose Adrenoleukodystrophy Using a Dried Blood Spot on Filter Paper, *Clin. Chim. Acta* 159, 77–82.
19. Jensen, R.G. (1999) Lipids in Human Milk, *Lipids* 34, 1243–1271.

[Received September 10, 2001; and in revised form March 4, 2002; revision accepted March 8, 2002]

# Base-Catalyzed Derivatization Methodology for FA Analysis. Application to Milk Fat and Celery Seed Lipid TAG

Frédéric Destailats and Paul Angers\*

Department of Food Science and Nutrition, and Dairy Research Center (STELA),  
Université Laval, Sainte-Foy, Québec, Canada, G1K 7P4

**ABSTRACT:** In this paper, an alternative base-catalyzed methodology for the facile derivatization in mild conditions of lipid TAG prior to FA analysis is proposed. Reagents were prepared by proton exchange between potassium *tert*-butoxide and either ethanol, *n*-propanol, *n*-butanol, or 2-methoxyethanol and used for the synthesis, at 40°C for 15 min, of the corresponding derivatives, which were directly analyzed by GC. This methodology can be used on a routine basis and has been applied to standard and complex natural lipid samples. Tripalmitin was used to determine optimal reaction conditions; and bovine milk fat, containing C<sub>4</sub> to C<sub>22</sub> acids, and celery (*Apium graveolens*) seed oil, characterized by a high level of petroselinic acid, were comparatively analyzed as their ethyl, *n*-propyl, *n*-butyl, and 2-methoxyethyl esters.

Paper no. L8924 in *Lipids* 37, 527–532 (May 2002).

Derivatization of FA esterified to glycerol is a prerequisite step for their analysis by GC, TLC, and HPLC. FAME are the derivatives most widely used by lipid analysts. Various methodologies have been developed for their synthesis from glycerides, which were reviewed by Christie (1,2). Acid-catalyzed methylation is usually performed in methanol using either boron trifluoride (3,4), hydrochloric acid, or sulfuric acid as catalysts, and at temperatures of 80 to 100°C for 30 to 60 min. Although FAME derivatives are well suited for most analytical needs, other ester derivatives have been synthesized in acidic conditions for specific purposes, such as conferring lower volatility to short-chain FA or improving peak resolution of isomeric FA. Isopropyl esters were initially used successfully to enhance resolution of complex lipid samples such as bovine or human milk fat (5–8), oil samples containing petroselinic acid (9–11), and geometrical isomers of  $\alpha$ -linolenic acid (11–15). CLA isomers from French cheeses were also analyzed using isopropyl ester derivatives (16), whereas *n*-butyl esters were used for studies on FA composition of butterfat and cheeses (17,18). Moreover, both FA *n*-butyl and phenylethyl esters have been used for analysis of petroselinic acid in seed oils (19,20).

The use of strong acidic reagents such as boron trifluoride, hydrochloric or sulfuric acids, and of moderate to high temperature conditions may, however, result in the presence of some artifact peaks of degradation products on the chromatograms that compromise the accuracy of GC analysis (21).

\*To whom correspondence should be addressed at Department of Food Science and Nutrition, Université Laval, Sainte-Foy (Québec) Canada, G1K 7P4. E-mail: paul.angers@al.n.ulaval.ca

Base-catalyzed methylation of glyceride FA is, like its acid counterpart, an equilibrium reaction that can be driven to near completion by the use of an excess of the derivatizing alcohol. Sodium methoxide in methanol is the usual reagent for the synthesis of FAME derivatives from glycerides (2,22). This transesterification reaction is performed at room to moderately elevated temperatures for 5 to 15 min for TAG, and at 40 to 50°C for 15 min for samples containing cholesteryl esters, in order to ensure complete derivatization. Unlike the acidic derivatization procedures, literature reporting on either the practical disadvantages resulting from the mild reaction conditions used in base-catalyzed methylation of acylated FA or base-catalyzed formation of other FA derivatives than methyl esters is scarce (23,24).

The present paper proposes a general mild methodology for the synthesis of ethyl, *n*-propyl, *n*-butyl, and 2-methoxyethyl FA derivatives by base-catalyzed transesterification of glycerides, and their use for high-resolution GC analysis of bovine milk fat and celery seed oil.

## MATERIALS AND METHODS

**Reference compounds and reagents.** Dipalmitin, monopalmitin, tributyrin, tricaprin, tricaproin, tricapylin, trilaurin, trilinolenin, trimyristin, triolein, tripalmitin, and tristearin were obtained from Sigma Chemicals (St. Louis, MO). *n*-Butanol, ethanol, 2-methoxyethanol, potassium *tert*-butoxide (1.0 M in THF), and *n*-propanol were obtained from Aldrich Chemicals (Milwaukee, WI).

**Bovine milk fat.** The winter milk fat was a sample from Parmalat (Montréal, Québec, Canada). A 25-kg block was tempered and then divided into samples of 100 g, which were rapidly melted, washed with deionized water, dried over anhydrous sodium sulfate and filtered in a heated (60°C) oven, and kept under N<sub>2</sub> in closed vials at –35°C until utilization.

**Oil extraction.** Mature dry seeds (10 g) of celery (*Apium graveolens*), purchased from a local seed retailer, were washed and finely grounded in a mortar. Oil was extracted with hexane on a Soxhlet apparatus and then recovered by filtering and drying the extract over anhydrous sodium sulfate and evaporating the solvent under vacuum at 30°C on a rotary evaporator (21% yield). The oil was stored under N<sub>2</sub> at –35°C until further use.

**General TAG derivatization methodology.** A solution of potassium *tert*-butoxide in THF (100  $\mu$ L, 1.0 M) was added to

anhydrous ethanol, *n*-propanol, *n*-butanol, or 2-methoxyethanol (200  $\mu$ L each) in closed vials for the preparation of the corresponding potassium alkoxides. After homogenization, a solution of a lipid sample (10 mg) in hexane (1 mL) was added to one of the reagent solutions (300  $\mu$ L), and the mixture was held at 40°C for 15 min. After cooling to room temperature, water (1 mL) and hexane (2 mL) were successively added. For milk fat samples, FA esters were extracted with 3  $\times$  1 mL of hexane to ensure complete extraction of short-chain FA. The tube was vortexed for *ca.* 5 s and allowed to stand for 1 min. If necessary, addition of a droplet of a saturated aqueous solution of sodium chloride usually broke up any emulsions that formed. The organic phase was dried over anhydrous sodium sulfate and filtered. FA ester solutions were kept under N<sub>2</sub> in closed vials, at -18°C, until analysis. Stock solutions of the reagents were also prepared and proved stable for weeks at 5°C.

**Optimization of reaction conditions.** A solution of tripalmitin (10 mg) in hexane (1 mL) was added to a solution of either potassium ethoxide, *n*-propoxide, *n*-butoxide, or 2-methoxyethoxide in THF (300  $\mu$ L), and rates of transesterification were monitored at different temperatures by GC on a 6890 Series II gas chromatograph (Hewlett-Packard, Palo Alto, CA), equipped with a fused-silica RTX-65 TG capillary column (30 m  $\times$  0.25 mm i.d., 0.10  $\mu$ m film thickness; Restek, Bellefonte, PA) and connected to a ChemStation (Hewlett-Packard, Palo Alto, CA). The injection (split mode) and detection (FID) were performed at 400°C, with an oven temperature of 190°C isothermal for 8 min, increased to 360°C at 10°C min<sup>-1</sup>, and isothermal for 5 min at 360°C. The inlet pressure of the carrier gas (H<sub>2</sub>) was 100 kPa. Under these conditions, FA esters, MAG, DAG, and TAG are fully resolved.

**FA ester analysis.** Analysis of FA esters was performed on the same apparatus. The injector (split mode) and detector temperatures were maintained at 250°C. Celery seed oil was analyzed on a DB-225 capillary column (30 m  $\times$  0.25 mm i.d., 0.25  $\mu$ m film thickness; J&W, Folsom, CA) at 190°C isothermal for 30 min, with H<sub>2</sub> as carrier gas (140 kPa). Butterfat analysis was performed on a BPX-70 capillary column (SGE, Melbourne, Australia; 60 m  $\times$  0.25 mm i.d., 0.25  $\mu$ m film thickness) with temperature programming from 60 to 210°C at 5°C min<sup>-1</sup> and isothermal for 30 min at this temperature. H<sub>2</sub> was also used as carrier gas with a head pressure of 130 kPa. Determination of response factors was performed by derivatization of simple acid TAG standards from C<sub>4</sub> to C<sub>18</sub>.

## RESULTS AND DISCUSSION

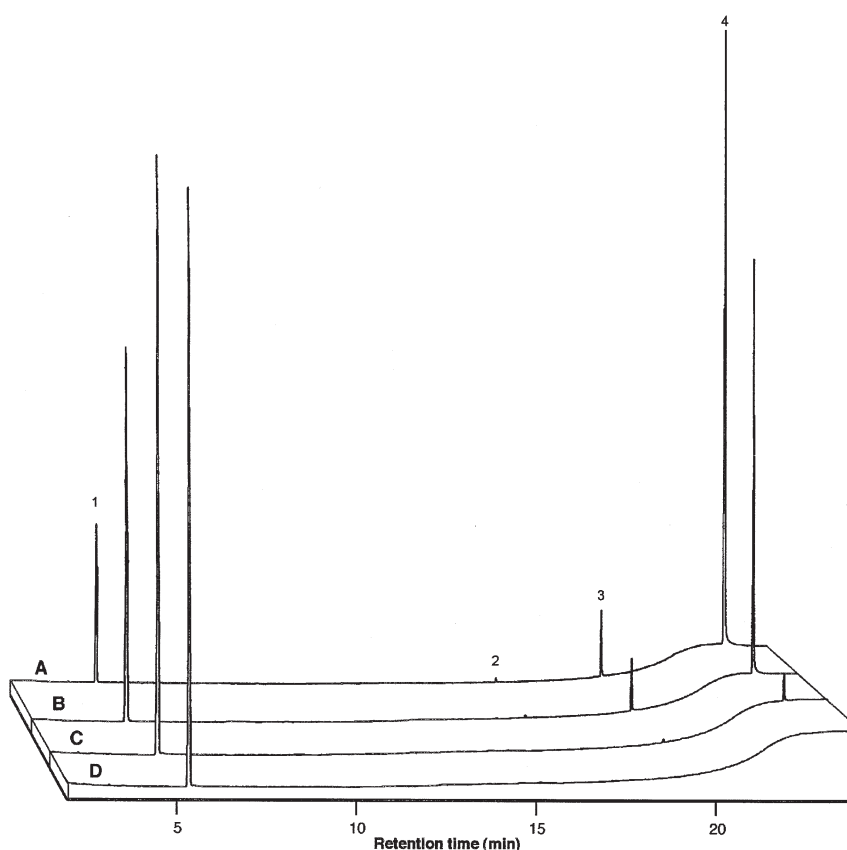
**Formation of catalysts.** In base-catalyzed transesterification reactions, the conjugated base of an alcohol acts as a nucleophile to form the new derivative. However, only a limited number of alkoxides that can form FA derivatives suitable for GC analysis are commercially available. To overcome this limitation, we readily synthesized conjugated bases of primary alcohols (ethanol, *n*-propanol, *n*-butanol, and 2-methoxyethanol) by proton exchange with a stronger base, potassium *tert*-butoxide, the conjugated base of *tert*-butanol, a tertiary alcohol. It is well

known that pK<sub>a</sub> values for tertiary alcohols are 2 to 3 units higher than those for primary alcohols, thus resulting in an almost exclusive formation of the desired base. This strategy proved itself more convenient for the formation of primary alkoxides than the use of metallic sodium or potassium, since solutions of potassium *tert*-butoxide are commercially available.

**FA derivatization.** Solutions of tripalmitin in hexane were added to solutions of potassium ethoxide, *n*-propoxide, *n*-butoxide, and 2-methoxyethoxide in THF, and rates of transesterification were monitored at different temperatures by GC. Complete derivatization was observed after 10 to 20 min at room temperature for all derivatives (Fig. 1), while at 40°C, the reaction was complete in less than 10 min. As expected, owing to increasing chelating character from TAG to DAG to MAG, the latter species was transesterified at a higher rate than both DAG and TAG, as shown by the very low levels of MAG on the chromatograms at 30 s and at 3 min (Fig. 1), while DAG were transesterified more rapidly than TAG. Although transesterification of TAG can be efficiently performed at room temperature, to ensure complete derivatization of all O-acyl species, reactions should be carried out at a temperature of 40°C for 15 min, reserving the lower temperatures for more heat-sensitive samples.

**GC analysis.** With respect to GC analysis of the different FA derivatives, two parameters were considered; response factors and resolution of positional isomers of unsaturated FA. Response factors for FA ester derivatives were determined from results of transesterification of standard solutions of simple TG in the range of 4:0 to 18:3 in order to ensure that transesterification proceeded equally well on different TG, because somewhat bulky alkoxides can act both as nucleophiles, which would result in the desired transesterification reaction, or as a base, thus leading to condensation products. As expected, in the mild conditions used, the latter reaction was not detected for any of the alkoxides tested. These results from derivatization of standards confirmed that only minor corrections to area percentage values were required to obtain accurate quantitative results for esters of medium- to long-chain FA with *n*-propyl, *n*-butyl, and 2-methoxyethyl ester derivatives (Table 1) (23). However, 2-methoxyethyl esters, which exhibited the lowest overall FID signal (*ca.* 40% lower), were least affected by the presence of carbon-carbon double bonds. *n*-Butyl esters were the most sensitive to the presence of such unsaturations. Differences between theoretical and experimental values in FA quantitation by FID are not unusual and have previously been detailed (23). Obviously, losses of short-chain FA were limited during the derivatization step because vapor pressures and hydrophilic characteristics were reduced compared to methyl ester derivatives. These observations correspond to results from studies on milk fat analysis using isopropyl (7) and *n*-butyl (17,18,23) ester derivatives.

Milk fat was analyzed for its FA composition after derivatization with potassium alkoxides of ethanol, *n*-propanol, *n*-butanol, and 2-methoxyethanol in the corresponding alcohols (Fig. 2). Results are in agreement with literature data (7,25), which make obvious the reliability and the accuracy of the new procedures



**FIG. 1.** Gas-liquid chromatogram of products from transesterification at 25°C of tripalmitin by potassium 2-methoxyethoxide in 2-methoxyethanol and THF after (A) 30 s reaction time, (B) 3 min reaction time, (C) 10 min reaction time, and (D) 20 min reaction time, on a 30-m RTX-65TG capillary column (Restek, Bellefonte, PA) on temperature-programming mode (see Materials and Methods section for detailed procedure). Peak identification: (1) 2-methoxyethyl palmitate; (2) monopalmitin (mixture of isomers); (3) dipalmitin (mixture of isomers); and (4) tripalmitin.

(Table 2). In addition, results for all FA, among the different derivatives, are close, with only small observed differences.

GC separation of petroselinic acid (*cis*-6 18:1), as found in *Apiaceae* seed oils, from oleic acid (*cis*-9 18:1) requires alternative FA derivatives to FAME, which either co-elute or show only a partial resolution (10) on long (e.g., 50- or 100-m) polar

capillary columns. These acids have, however, been resolved as isopropyl (9–11), *n*-butyl (19), and phenylethyl (20) esters, and as dibutyrate derivatives of MAG (26). Using the new derivatization procedures, we performed GC FA analysis of celery seed oil as ethyl, *n*-propyl, *n*-butyl, and 2-methoxyethyl derivatives on a 25-m 50% cyanopropyl phenyl methyl silicone open tubular capillary column (Fig. 3). Resolution between petroselinic and oleic acid isomers increased with increasing chain length of the alcohol moiety, resulting in  $R_S$  (resolution) values for ethyl, *n*-propyl, and *n*-butyl of 0.40, 0.55 and 0.90, respectively. Resolution was also enhanced by increasing the polarity of the derivative, as a baseline resolution ( $R_S = 1.57$ ) was obtained with the new 2-methoxyethyl derivative. However, *cis* and *trans* isomers of 18:1 acid were not fully resolved with the latter. Celery seed oil was mainly composed of palmitic (6.9%), stearic (1.4%), petroselinic (64.3%), oleic (8.1%), and linoleic (18.0%) acids; minor FA included hexadecenoic (0.1%),  $\alpha$ -linolenic (0.6%), and *cis*-vaccenic (0.5%) acids.

In this paper, we have demonstrated that different ester derivatives of FA may be easily prepared by transesterification of TAG using base catalysts. In the proposed reaction conditions, sample degradations were minimized, and the procedure gave good quantitative and qualitative results on com-

**TABLE 1**  
Experimental Response Factors for Ethyl, *n*-Propyl, *n*-Butyl and 2-Methoxyethyl Ester Derivatives of FA, Relative to Palmitate<sup>a</sup>

FA	FAEE <sup>b</sup>	FAPE	FABE	FAMOE
4:0	1.146	1.114	1.013	1.078
6:0	0.941	0.991	0.942	0.929
8:0	0.862	0.885	0.923	0.872
10:0	0.859	0.929	0.980	0.882
12:0	0.918	0.985	0.992	0.937
14:0	0.965	0.973	1.000	0.978
16:0	1.000	1.000	1.000	1.000
18:0	1.057	0.976	0.977	0.992
18:1	0.919	0.947	1.148	0.989
18:3	0.920	0.987	1.170	1.007

<sup>a</sup>Values are means of triplicate analysis.

<sup>b</sup>FAEE, FA ethyl ester; FAPE, FA *n*-propyl ester; FABE, FA *n*-butyl ester; FAMOE, FA 2-methoxyethyl ester.



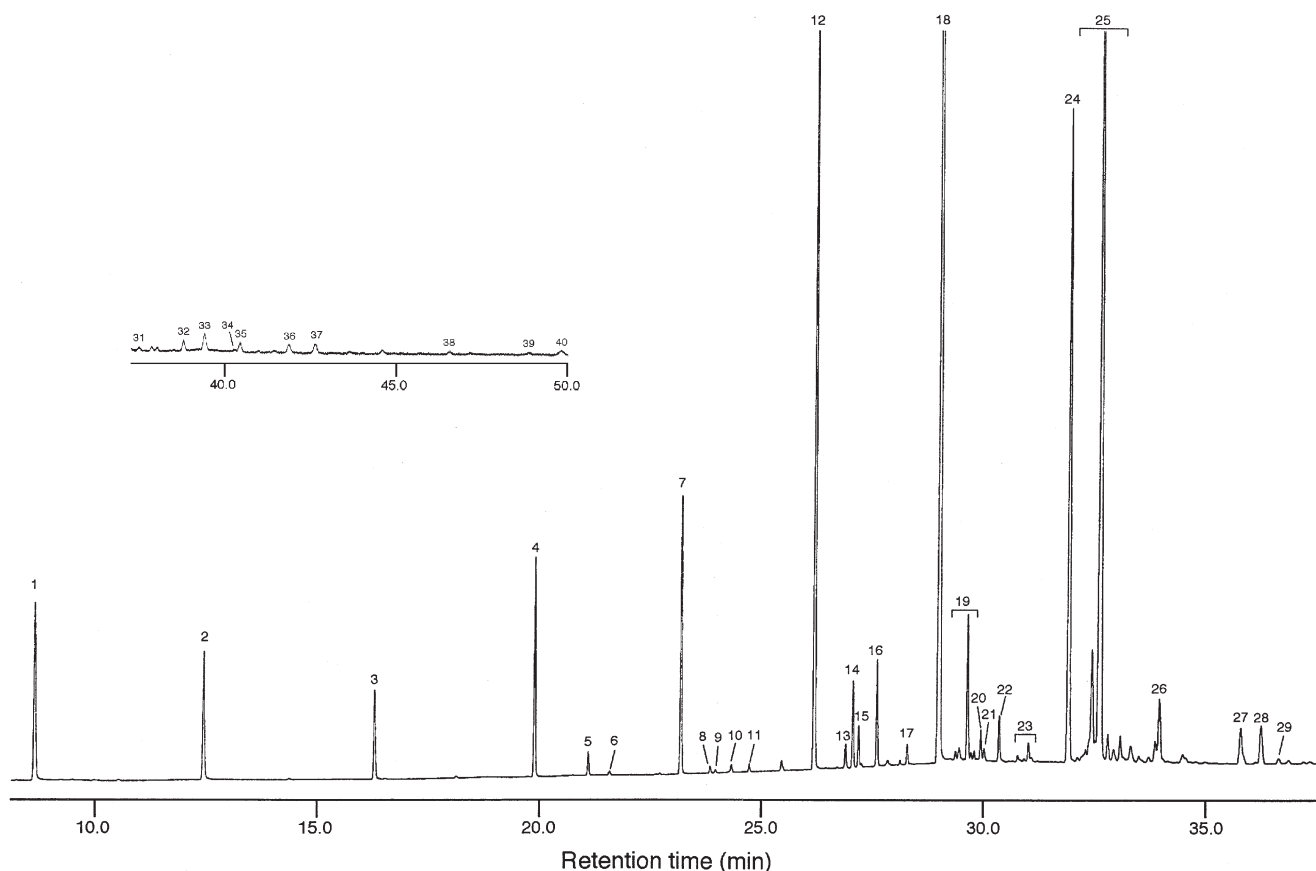


FIG. 2. Gas-liquid chromatogram of FA 2-methoxyethyl esters of butterfat, obtained using a 60-m BPX-70 capillary column (SGE, Melbourne, Australia) on temperature-programming mode (see Materials and Methods section for detailed analytical conditions). Peak identification is as shown in Table 2.

plex lipid samples. The use of alkoxides prepared by proton exchange with potassium *tert*-butoxide or other strong bases is not limited to the primary alcohols presented in this paper, as numerous other derivatives can be prepared by following the same procedure.

## ACKNOWLEDGMENTS

We acknowledge financial support of Natural Sciences and Engineering Research Council of Canada and Fonds FCAR. The authors are also grateful to R.L. Wolff for discussion and revision of the manuscript, and to Fondation de l'Université Laval for a Ph.D. scholarship to F. Destailats.

## REFERENCES

- Christie, W.W. (1990) Preparation of Methyl Esters—Part 1, *Lipid Technol.* 2, 48–49.
- Christie, W.W. (1990) Preparation of Methyl Esters—Part 2, *Lipid Technol.* 2, 79–80.
- Metcalfe, L.D., and Schmitz, A.A. (1961) The Rapid Preparation of Fatty Acid Esters for Gas Chromatography Analysis, *Anal. Chem.* 33, 363–364.
- Morrison, W.R., and Smith, L.M. (1964) Preparation of Fatty Acid Methyl Esters and Dimethyl Acetals from Lipids with Boron Fluoride–Methanol, *J. Lipid Res.* 5, 600–608.
- Wolff, R.L., and Castera-Rossignol, A.M.F. (1987) Mise au Point et Évaluation d'une Méthode d'Extraction de la Matière Grasse de Fromage de Type Emmenthal, *Rev. Fr. Corps Gras* 34, 123–132.
- Wolff, R.L., and Fabien, R.J. (1989) Utilisation de l'Isopropanol pour l'Extraction de la Matière Grasse de Produits Laitiers et Pour l'Estérification Subséquent des Acides Gras, *Lait* 69, 33–46.
- Wolff, R.L., Bayard, C.C., and Fabien, R.J. (1995) Evaluation of Sequential Methods for the Determination of Butterfat Fatty Acid Composition with Emphasis on *trans*-18:1 Acids. Application to the Study of Seasonal Variations in French Butters, *J. Am. Oil Chem. Soc.* 72, 1471–1483.
- Wolff, R.L. (1995) Content and Distribution of *trans*-18:1 Acids in Ruminant Milk and Meat Fats. Their Importance in European Diets and Their Effect on Human Milk, *J. Am. Oil Chem. Soc.* 72, 259–272.
- Wolff, R.L., and Vandamme, F.F. (1992) Separation of Petroselinic (*cis*-6 18:1) and Oleic (*cis*-9 18:1) Acids by Gas-Liquid Chromatography of Their Isopropyl Esters, *J. Am. Oil Chem. Soc.* 69, 1228–1231.
- Wolff, R.L. (1998) Comments on the Methodology for the Separation and Quantification of *cis*-6 (Petroselinic) and *cis*-9 (Oleic) Acids, *J. Am. Oil Chem. Soc.* 75, 893–894.
- Wolff, R.L. (1995) Recent Applications of Capillary Gas-Liquid Chromatography to Some Difficult Separations of Positional or Geometrical Isomers of Unsaturated Fatty Acids, in *New Trends in Lipid and Lipoprotein Analysis* (Sébastien, J.L., and Perkins, R.G., eds.), pp. 147–180, AOCS Press, Champaign.
- Wolff, R.L. (1992) Resolution of Linolenic Acid Geometrical Isomers by Gas-Liquid Chromatography on a Capillary Column

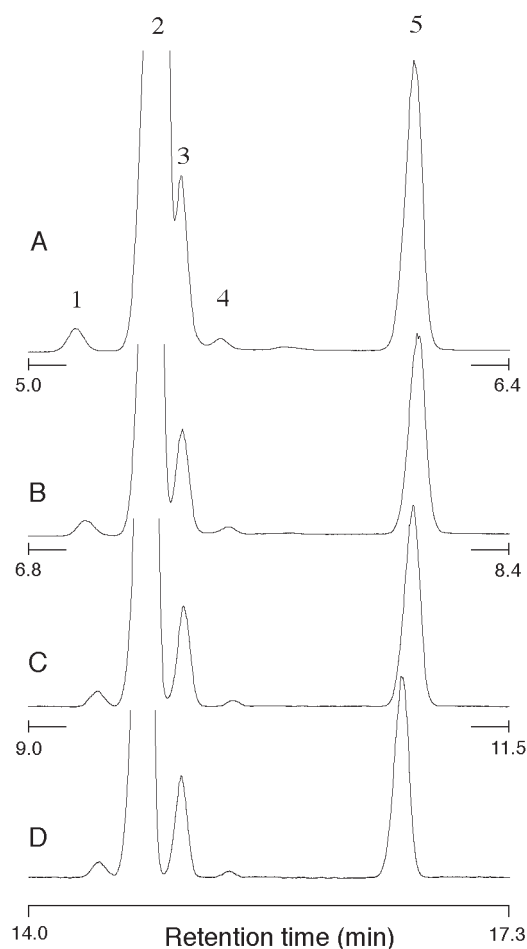
**TABLE 2**  
**FA Composition (FA wt%) of Québec Winter Butterfat**  
**by GLC Analysis Using Ethyl, *n*-Propyl, *n*-Butyl,**  
**and 2-Methoxyethyl Ester Derivatives<sup>a</sup>**

Peak no.	FA	FAEE <sup>b</sup>	FAPE	FABE	FAMOE
1	4:0	3.63	3.82	3.80	3.55
2	6:0	2.15	2.17	2.19	2.18
3	8:0	1.26	1.12	1.26	1.29
4	10:0	2.75	2.68	2.93	2.95
5	10:1	0.30	0.18	0.32	0.31
6	11:0	0.05	0.16	0.06	0.06
7	12:0	3.23	3.33	3.44	3.27
8	12:1	0.08	0.09	0.09	0.08
9	13:0 <i>iso</i>	0.04	0.04	0.05	0.04
10	13:0 <i>aiso</i>	0.09	0.09	0.09	0.10
11	13:0	0.09	0.09	0.09	0.11
12	14:0	10.88	10.94	11.22	10.59
13	14:1	1.30 <sup>c</sup>	1.30 <sup>c</sup>	1.34 <sup>c</sup>	0.98
14	15:0 <i>iso</i>				0.28
15	15:0 <i>aiso</i>	0.50	0.51	0.51	0.49
16	15:0	1.23	1.23	1.25	1.22
17	16:0 <i>iso</i>	0.24	0.27	0.27	0.10
18	16:0	31.82	31.33	30.87	31.40
19	16:1 <i>cis</i> + <i>trans</i>	2.17	2.19	2.28	2.44
20	17:0 <i>iso</i>	0.39	0.38	0.37	0.37
21	17:0 <i>aiso</i>	0.40	0.40	0.39	0.43
22	17:0	0.63	0.60	0.60	0.65
23	17:1	0.32	0.31	0.31	0.38
24	18:0	10.10	10.34	10.07	10.57
25	18:1 <i>cis</i> + <i>trans</i>	22.35	22.37	22.20	22.76
26	18:2 <i>cis</i> -9, <i>cis</i> -12	1.59	1.64	1.59	1.25
27	18:3 <i>cis</i> -9, <i>cis</i> -12, <i>cis</i> -15	0.75	0.75	0.74	0.79
28	20:0	0.13	0.13	0.15	0.13
29	18:2 <i>cis</i> -9, <i>trans</i> -11	0.89	0.88	0.84	0.87
30	20:1	0.09	0.11	0.10	0.12
31	20:2	0.02	0.03	0.03	0.03
32	20:3 <i>cis</i> -8, <i>cis</i> -11, <i>cis</i> -14	0.08	0.06	0.08	0.07
33	20:3 <i>cis</i> -11, <i>cis</i> -14, <i>cis</i> -17	0.09	0.08	0.14	0.12
34	20:4	0.02	0.03	0.02	0.02
35	20:5	0.07	0.07	0.07	0.05
36	22:0	0.05	0.07	0.05	0.06
37	22:1	0.09	0.08	0.07	0.07
38	22:2	0.03	0.04	0.02	0.03
39	22:4	0.02	0.02	0.02	0.02
40	22:5	0.05	0.04	0.07	0.07

<sup>a</sup>Values are means of triplicate analyses. Results were normalized to 100% for comparison.

<sup>b</sup>For abbreviations see Table 1.

<sup>c</sup>Values for 14:1 and 15:0 *iso*.



**FIG. 3.** Partial gas-liquid chromatograms of the C<sub>18</sub> region for FA (A) ethyl; (B) *n*-propyl; (C) *n*-butyl; and (D) 2-methoxyethyl esters, prepared from celery seed oil, and analyzed on a 30-m DB-225 capillary column (J&W, Folsom, CA) in isothermal mode at 190°C (see Materials and Methods section for detailed analytical conditions). Peak identification: (1) 18:0; (2) *cis*-6 18:1; (3) *cis*-9 18:1; (4) *cis*-11 18:1; (5) *cis*-9, *cis*-12 18:2.

- Coated with a 100% Cyanopropyl Polysiloxane Film (CP Sil 88), *J. Chromatogr. Sci.* 30, 17–22.
- Wolff, R.L. (1992) Applications Récentes de la Colonne Capillaire CP Sil 88 à la Séparation par CPG d'Isomères Positionnels ou Géométriques d'Acides Gras Polyinsaturés d'Origine Biologique ou Alimentaire, *Spectra* 2000 165, 41–46.
  - Wolff, R.L. (1993) Further Studies on Artificial Geometrical Isomers of  $\alpha$ -Linolenic Acid in Edible Linolenic Acid-Containing Oils, *J. Am. Oil Chem. Soc.* 70, 219–224.
  - Wolff, R.L. (1993) Heat-Induced Geometrical Isomerization of  $\alpha$ -Linolenic Acid: Effect of Temperature and Heating Time on the Appearance of Individual Isomers, *J. Am. Oil Chem. Soc.* 70, 425–430.
  - Lavillonière, F., Martin, J.C., Bougnoux, P., and Sébédio, J.L.

- (1998) Analysis of Conjugated Linoleic Acid Isomers and Content in French Cheeses, *J. Am. Oil Chem. Soc.* 75, 343–352.
- Iverson, J.L., and Sheppard, A.J. (1977) Butyl Ester Preparation for Gas-Liquid Chromatographic Determination of Fatty Acid in Butter, *J. Assoc. Off. Anal. Chem.* 60, 248–258.
- Ackman, R.G., and Macpherson, E.J. (1994) Coincidence of *cis*- and *trans*-Monoethylenic Fatty Acids Simplifies the Open-Tubular Gas-Liquid Chromatography of Butyl Esters of Butter Fatty Acids, *Food Chem.* 50, 45–52.
- Thies, W. (1995) Determination of the Petroselinic Acid in Seeds of *Coriandrum sativum* by Gas-Liquid Chromatography as *n*-Butyl Esters, *Fat Sci. Technol.* 97, 411–413.
- Liu, L., and Hammond, E.G. (1995) Phenylethyl Esters of Fatty Acids for the Analytical Resolution of Petroselinic and Oleate, *J. Am. Oil Chem. Soc.* 72, 749–751.
- Christie, W.W. (1994) Why I Dislike Boron Trifluoride-Methanol, *Lipid Technol.* 6, 66–68.
- Christopherson, S.W., and Glass, R.L. (1969) Preparation of Milkfat Methyl Esters by Alcoholysis in an Essentially Non-alcoholic Solution, *J. Dairy Sci.* 52, 1289–1290.
- Ulberth, F., Gabernig, R.G., and Schrammel, F. (1995) Flame-Ionization Detector Response to Methyl, Ethyl, Propyl, and Butyl Esters of Fatty Acids, *J. Am. Oil Chem. Soc.* 76, 263–266.

24. Kramer, J.K.G., Fellner, V., Dugan, M.E.R., Sauer, F.D., Mossoba, M.M., and Yurawecz, M.P. (1997) Evaluating Acid and Base Catalysts in the Methylation of Milk and Rumen Fatty Acids with Special Emphasis on Conjugated Dienes and Total *trans* Fatty Acids, *Lipids* 32, 1219–1228.
25. Precht, D., and Molkenin, J. (1996) Rapid Analysis of the Isomers of *trans*-Octadecenoic Acid in Milk Fat, *Int. Dairy J.* 6, 791–809.
26. Destailats, F., Arul, J., Simon, J.E., Wolff, R.L., and Angers, P. (2002) Dibutyrate Derivatization of Monoacylglycerols for the Resolution of Regioisomers of Oleic, Petroselinic, and *cis*-Vaccenic Acids, *Lipids* 37, 111–116.

[Received September 28, 2001, and in final revised form April 2, 2002; revision accepted April 9, 2002]

# Stereochemistry of the Hydroperoxides Formed During Autoxidation of CLA Methyl Ester in the Presence of $\alpha$ -Tocopherol

Taina I. Hämäläinen<sup>a,\*</sup>, Susanna Sundberg<sup>b,c</sup>, Tapio Hase<sup>a</sup>, and Anu Hopia<sup>b</sup>

<sup>a</sup>Department of Chemistry, Laboratory of Organic Chemistry, <sup>b</sup>Department of Applied Chemistry and Microbiology, Food Chemistry Division, and <sup>c</sup>Department of Chemistry, Laboratory of Analytical Chemistry, 00014 University of Helsinki, Finland

**ABSTRACT:** The initial steps in the autoxidation of CLA methyl ester are poorly understood. The aim of this study was to determine the stereochemistry of the hydroperoxides formed during autoxidation of CLA methyl ester in the presence of a good hydrogen atom donor. For this purpose, 9-*cis*,11-*trans* CLA methyl ester was autoxidized in the presence of  $\alpha$ -tocopherol under atmospheric oxygen at 40°C in the dark. The CLA methyl ester hydroperoxides were isolated, reduced to the corresponding hydroxy derivatives, and separated by HPLC. The stereochemistry of seven hydroxy-CLA methyl esters was investigated. The position of the hydroxy group was determined by GC-MS. The geometry as well as the position of the double bonds in the alkyl chain was determined by NMR. In addition, the <sup>13</sup>C NMR spectra of six hydroxy-CLA methyl esters were assigned using COSY, gradient heteronuclear multiple bond correlation, gradient heteronuclear single quantum correlation, and total correlation spectroscopy experiments. The autoxidation of 9-*cis*,11-*trans* CLA methyl ester in the presence of a good hydrogen atom donor is stereoselective in favor of one geometric isomer, namely the 13-(*R,S*)-hydroperoxy-9-*cis*,11-*trans*-octadecadienoic acid methyl ester. Three types of conjugated diene hydroperoxides are formed as primary hydroperoxides: *trans,trans* hydroperoxides (12-OOH-8*t*,10*t* and 9-OOH-10*t*,12*t*), a *cis,trans* hydroperoxide with the *trans* double bond adjacent to the hydroperoxide-bearing carbon atom (13-OOH-9*c*,11*t*), and a new type of *cis,trans* lipid hydroperoxide with the *cis* double bond adjacent to the hydroperoxide-bearing carbon atom (8-OOH-9*c*,11*t*). In addition, three nonkinetic hydroperoxides (13-OOH-9*t*,11*t*, 8-OOH-9*t*,11*t*, and 9-OOH-10*t*,12*c*) are formed. This study supports the theory that CLA methyl ester autoxidizes at least partly through an autocatalytic

free radical reaction. The complexity of the hydroperoxide mixture is due to formation of two different pentadienyl radicals. Moreover, the stereoselectivity in favor of one geometric isomer can be explained by the selectivity of the two previous steps: the preferential formation of a *W*-conformer of the pentadienyl radical over the *Z*-conformer, and regioselectivity of the oxygen addition to the pentadienyl radical.

Paper no. L9005 in *Lipids* 37, 533–540 (June 2002).

The hydroperoxide theory of autoxidation was developed and successfully applied to FA by Farmer and co-workers in the early 1940s (1). The hydroperoxides formed in the autoxidation of methyl oleate and methyl linoleate, the two model compounds in the FA autoxidation studies, were fully characterized after the development of appropriate analytical techniques in the late 1970s and early 1980s (reviewed in Refs. 2,3). Today, the hydroperoxide theory is generally accepted in explaining the autoxidation of monounsaturated and nonconjugated PUFA. However, the autoxidation mechanism of conjugated PUFA has been less studied. Moreover, the autoxidation mechanism of conjugated FA is thought to be different from that of the nonconjugated FA and to produce different reaction products (1,4). For example, the initial steps in the autoxidation of CLA, which has been the subject of an increasing number of scientific studies owing to its beneficial physiological effects, are still poorly understood (4,5). Very recently, we were able to provide evidence that hydroperoxides are also formed during the autoxidation of CLA methyl ester (6). Furthermore, it was shown, contrary to earlier beliefs, that the main isomers of CLA methyl ester hydroperoxides have a conjugated diene monohydroperoxide structure similar to the methyl linoleate hydroperoxides.

In continuation of our previous work (6), we now report on an investigation into the autoxidation of pure 9-*cis*,11-*trans* CLA methyl ester performed in the presence of  $\alpha$ -tocopherol (20% per weight) under atmospheric oxygen at 40°C in the dark. The primary objective was to determine the stereochemistry of the main CLA methyl ester hydroperoxides. The hydroperoxides were separated as their hydroxy derivatives by HPLC and characterized by UV; GC-MS; and <sup>1</sup>H, <sup>13</sup>C, and 2-D NMR techniques. With well-characterized products it was possible to propose a mechanism for the autoxidation

\*To whom correspondence should be addressed at University of Helsinki, Department of Chemistry, Laboratory of Organic Chemistry, P.O. Box 55 (A.I. Virtasen aukio 1), 00014 University of Helsinki, Finland. E-mail: taina.hamalainen@helsinki.fi

Abbreviations: BSTFA, bis(trimethylsilyl)-trifluoroacetamide; gHMBC, gradient heteronuclear multiple bond correlation; gHSQC, gradient heteronuclear single quantum correlation; methyl linoleate, 9-*cis*,12-*cis*-octadecadienoic acid methyl ester; 8-OH-9*c*,11*t*, 8-(*R,S*)-hydroxy-9-*cis*,11-*trans*-octadecadienoic acid methyl ester; 8-OH-9*t*,11*t*, 8-(*R,S*)-hydroxy-9-*trans*,11-*trans*-octadecadienoic acid methyl ester; 9-OH-10*t*,12*c*, 9-(*R,S*)-hydroxy-10-*trans*,12-*cis*-octadecadienoic acid methyl ester; 9-OH-10*t*,12*t*, 9-(*R,S*)-hydroxy-10-*trans*,12-*trans*-octadecadienoic acid methyl ester; 12-OH-8*t*,10*t*, 12-(*R,S*)-hydroxy-8-*trans*,10-*trans*-octadecadienoic acid methyl ester; 13-OH-9*c*,11*t*, 13-(*R,S*)-hydroxy-9-*cis*,11-*trans*-octadecadienoic acid methyl ester; 13-OH-9*t*,11*t*, 13-(*R,S*)-hydroxy-9-*trans*,11-*trans*-octadecadienoic acid methyl ester; TMCS, trimethylchlorosilane; TOCSY, total correlation spectroscopy.



of CLA methyl ester in the presence of a good hydrogen atom donor.

## EXPERIMENTAL PROCEDURES

**Materials.** 9-*cis*,11-*trans* CLA methyl ester was purchased from Matreya Inc. (Pleasant Gap, PA). The presence of only one CLA methyl ester isomer was confirmed by  $^{13}\text{C}$  NMR (7).  $\alpha$ -Tocopherol was obtained from Merck (Darmstadt, Germany). Isopropanol was purchased from Fisher Scientific (Loughborough, United Kingdom) and it was dried by distillation over calcium hydride before use. Calcium hydride and sodium borohydride were obtained from Fluka (Buchs, Switzerland). *t*-Butyl methyl ether and heptane were from Rathburn Chemicals (Walkerburn, Scotland), bis(trimethylsilyl)-trifluoroacetamide (BSTFA) and trimethylchlorosilane (TMCS) from Merck, and platinum(IV) oxide from Fluka.

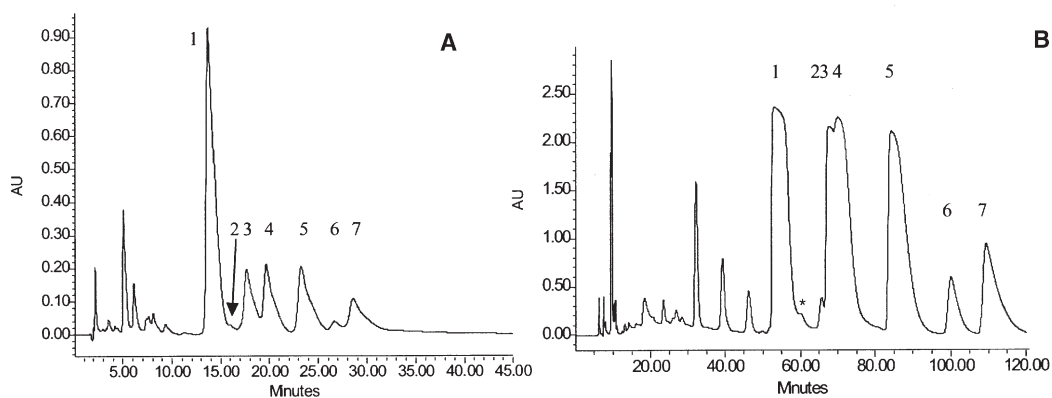
**Autoxidation.** The 9-*cis*,11-*trans* CLA methyl ester ( $3 \times 0.5$  g/20 mL glass vial) was autoxidized for 19 d in the presence of  $\alpha$ -tocopherol (20% per weight) under atmospheric oxygen at 40°C in the dark. The extent of oxidation measured as consumption of the 9-*cis*,11-*trans* CLA methyl ester by GC was 13%. The yield of hydroperoxides was approximately 9% based on peroxide value (PV = 586 meq/kg), which was measured by the ferric thiocyanate method (8). Nonoxidized 9-*cis*,11-*trans* CLA methyl ester (approx. 1.2 g) was recovered.

**Preparation of the hydroxy-CLA methyl esters.** The CLA methyl ester hydroperoxides were isolated from the autoxidation reaction mixture by silica gel column (2 g; Varian, Harbor City, CA) chromatography followed by TLC and reduced to the corresponding hydroxy derivatives using  $\text{NaBH}_4$  in dry isopropanol at 0°C as reported previously (6). The hydroper-

oxides and the hydroxy derivatives were stored as dilute heptane solutions at -20°C under nitrogen.

**Isocratic normal-phase HPLC.** The mixture of the hydroxy-CLA methyl esters was analyzed by HPLC using a Supelco silica column (Supelcosil LC-SI, 25.0 cm  $\times$  2.1 mm i.d., particle size 5  $\mu\text{m}$ ; Bellefonte, PA) and 7% *t*-butyl methyl ether in heptane as an eluent at 0.4 mL/min flow rate (Fig. 1A). The isomers were separated using a semipreparative Merck silica column (LiChrospher Si 60, 25.0  $\times$  1.0 cm i.d., particle size 5  $\mu\text{m}$ ) and 8% *t*-butyl methyl ether in heptane as an eluent at 2.0 mL/min flow rate. Approximately 4 mg of the mixture of the hydroxy-CLA methyl esters was repeatedly injected, and seven fractions were collected (Fig. 1B). Fractions 2, 3, and 4 were further purified using the analytical column, and fraction 6 was purified using the semipreparative column. The columns were equipped with a Waters 501 HPLC pump, Waters Pump Control Module, Waters WISP 710B, and Waters 996 Photodiode Array Detector (from 200 to 400 nm; Milford, MA) set at 234 nm.

**Derivatization to trimethylsilyl ethers and GC-MS.** Analysis of the different hydroxy isomers as corresponding hydroxystearates enables the unambiguous determination of the positional isomers (9). Hydrogenation of the separated hydroxy-CLA methyl esters to the corresponding hydroxystearates was performed using platinum(IV) oxide (5 mg) as a catalyst in methanol (5 mL). A slow stream of  $\text{H}_2$  was introduced into the mixture for 30 min while stirring. Chloroform (2 mL) was added. The reaction mixture was filtered and the solvent was removed under a stream of nitrogen gas. The residue was silylated by adding anhydrous pyridine (100  $\mu\text{L}$ ) and the derivatization reagent (100  $\mu\text{L}$ ) containing 99% of BSTFA and 1% of TMCS. The reaction mixture was allowed



**FIG. 1.** (A) HPLC analysis of the hydroxy-CLA methyl esters using Supelco silica column (Supelcosil LC-SI, 25.0 cm  $\times$  2.1 mm i.d., particle size 5  $\mu\text{m}$ ; Bellefonte, PA) and 7% *t*-butyl methyl ether in heptane (Rathburn Chemicals, Walkerburn, Scotland) as an eluent at a 0.4 mL/min flow rate with UV detection at 234 nm. (B) Semipreparative (4 mg) HPLC separation of the hydroxy-CLA methyl esters using a Merck silica column (LiChrospher So 60, 25.0 cm  $\times$  1.0 cm i.d., particle size 5  $\mu\text{m}$ ; Darmstadt, Germany) and 8% *t*-butyl methyl ether in heptane (Rathburn Chemicals) as an eluent at a 2.0 mL/min flow rate with UV detection at 234 nm. Peaks: 1 = 13-(*R,S*)-hydroxy-9-*cis*,11-*trans*-octadecadienoic acid methyl ester (13-OH-9*c*,11*t*); 2 = 13-(*R,S*)-hydroxy-9-*trans*,11-*trans*-octadecadienoic acid methyl ester (13-OH-9*t*,11*t*); 3 = 12-(*R,S*)-hydroxy-8-*trans*,10-*trans*-octadecadienoic acid methyl ester (12-OH-8*t*,10*t*); 4 = 9-(*R,S*)-hydroxy-10-*trans*,12-*cis*-octadecadienoic acid methyl ester (9-OH-10*t*,12*c*); 5 = 9-(*R,S*)-hydroxy-10-*trans*,12-*trans*-octadecadienoic acid methyl ester (9-OH-10*t*,12*t*); 6 = 8-(*R,S*)-hydroxy-9-*cis*,11-*trans*-octadecadienoic acid methyl ester (8-OH-9*c*,11*t*); 7 = 8-(*R,S*)-hydroxy-9-*trans*,11-*trans*-octadecadienoic acid methyl ester (8-OH-9*t*,11*t*). \*Unidentified compound.

to stand overnight in the dark at room temperature. The trimethylsilyl ethers were analyzed on an Agilent 5973 mass spectrometer connected to a Hewlett-Packard gas chromatograph (HP 6890 Series GC System). The gas chromatograph was equipped with an Rtx-5MS (crossbond 5% diphenyl polysiloxane, 95% dimethyl polysiloxane) capillary column (Restek Corporation, Bellefonte, PA), 60 m × 0.25 mm i.d., film thickness 0.1 μm; carrier gas: helium, 1.2 mL/min. Samples (0.5–1 μL) were injected using on-column injection. Column temperature program: 70°C (1 min), 40°C min<sup>-1</sup> to 170°C; 170°C (2 min), 5°C min<sup>-1</sup> to 250°C; 250°C (20 min); interface temperature: 280°C; ion source temperature: 230°C; ionization: electron impact 70 eV; mass range: 100–400 u; sampling rate: 4.72 scans/s; scan threshold: 150.

**UV spectroscopy.** The hydroxy-CLA methyl esters with conjugated diene chromophores were quantified by UV spectroscopy (λ = 234 nm). UV spectra were recorded in ethanol solution on a PerkinElmer UV/vis spectrometer Lambda Bio. Molar absorbance (ε) values used in calculations were from Reference 10. The ε value of 13-(*R,S*)-hydroxy-9-*trans*,11-*trans*-octadecadienoic acid methyl ester (13-OH-9*t*,11*t*) was used in calculations for the 12-(*R,S*)-hydroxy-8-*trans*, 10-*trans*-octadecadienoic acid methyl ester (12-OH-8*t*,10*t*) and the ε values of the 9-hydroxy isomers for the 8-hydroxy isomers.

**NMR spectroscopy.** <sup>1</sup>H, <sup>13</sup>C, and 2-D NMR spectra were recorded on a Bruker 500 Avance spectrometer with ν (<sup>1</sup>H) = 500 MHz and ν (<sup>13</sup>C) = 125 MHz in deuteriochloroform [Aldrich, Milwaukee, WI; contains 0.1% (vol/vol) tetramethylsilane, 99.8% <sup>2</sup>H] at 27°C. Chemical shifts (δ) are given in parts per million (ppm) relative to tetramethylsilane (δ 0.00).

13-(*R,S*)-Hydroxy-9-*cis*,11-*trans*-octadecadienoic acid methyl ester (13-OH-9*c*,11*t*) (99%, 69 mM) <sup>1</sup>H NMR δ 6.48 (*dddd*, 1 H, H-11, <sup>3</sup>J<sub>11,12</sub> = 15.2 Hz, <sup>3</sup>J<sub>11,10</sub> = 11.1 Hz, <sup>4</sup>J<sub>11,9</sub> ≈ <sup>4</sup>J<sub>11,13</sub> ≈ 1.1 Hz), 5.97 (*ddtd*, 1 H, H-10, <sup>3</sup>J<sub>10,9</sub> ≈ 11.0 Hz, <sup>4</sup>J<sub>10,8</sub> ≈ 1.4 Hz, <sup>4</sup>J<sub>10,12</sub> ≈ 0.6 Hz), 5.67 (*dd*, 1 H, H-12, <sup>3</sup>J<sub>12,13</sub> = 6.9 Hz), 5.43 (*dt*, 1 H, H-9, <sup>3</sup>J<sub>9,8</sub> = 7.7 Hz), 4.16 (*dt*, 1 H, H-13, <sup>3</sup>J<sub>13,14</sub> ≈ 6.6 Hz), 3.66 (*s*, 3 H, OCH<sub>3</sub>), 2.30 (*t*, 2 H, H-2, <sup>3</sup>J<sub>2,3</sub> = 7.5 Hz), 2.17 (*dt*, 2 H, H-8, <sup>3</sup>J<sub>8,7</sub> ≈ 7.4 Hz), 1.60 (*quintet*, 2 H, H-3, <sup>3</sup>J<sub>3,4</sub> = 7.3 Hz), 1.57 (*m*, 1 H, H-14), 1.51 (*m*, 1 H, H-14'), 1.45 – 1.35 (*m*, 2 H, H-7), 1.35 – 1.25 (*m*, 12 H, H-4, H-5, H-6, H-15, H-16, H-17), 0.89 (*t*, 3 H, H-18, <sup>3</sup>J<sub>18,17</sub> = 6.9 Hz).

13-(*R,S*)-Hydroxy-9-*trans*,11-*trans*-octadecadienoic acid methyl ester (13-OH-9*t*,11*t*) (92%, 1 mM) <sup>1</sup>H NMR δ 6.17 (*dd*, 1 H, H-11, <sup>3</sup>J<sub>11,12</sub> = 15.2 Hz, <sup>3</sup>J<sub>11,10</sub> = 10.5 Hz), 6.02 (*dd*, 1 H, H-10, <sup>3</sup>J<sub>10,9</sub> = 15.1 Hz), 5.69 (*dt*, 1 H, H-9, <sup>3</sup>J<sub>9,8</sub> = 6.8 Hz), 5.57 (*dd*, 1 H, H-12, <sup>3</sup>J<sub>12,13</sub> = 7.0 Hz), 4.11 (*dt*, 1 H, H-13, <sup>3</sup>J<sub>13,14</sub> ≈ 6.5 Hz), 3.67 (*s*, 3 H, OCH<sub>3</sub>), 2.30 (*t*, 2 H, H-2, <sup>3</sup>J<sub>2,3</sub> = 7.5 Hz), 2.07 (*td*, 2 H, H-8, <sup>3</sup>J<sub>8,7</sub> ≈ 7.1 Hz), 1.66 – 1.47 (*m*, 4 H, H-3, H-14), 1.44 – 1.22 (*m*, 14 H, H-4, H-5, H-6, H-7, H-15, H-16, H-17), 0.91 – 0.80 (*m*, 3 H, H-18).

12-(*R,S*)-Hydroxy-8-*trans*,10-*trans*-octadecadienoic acid methyl ester (12-OH-8*t*,10*t*) (92%, 16 mM) <sup>1</sup>H NMR δ 6.17 (*dd*, 1 H, H-10, <sup>3</sup>J<sub>10,11</sub> = 15.2 Hz, <sup>3</sup>J<sub>10,9</sub> = 10.4 Hz), 6.01 (*dd*, 1 H, H-9, <sup>3</sup>J<sub>9,8</sub> = 15.1 Hz), 5.68 (*dt*, 1 H, H-8, <sup>3</sup>J<sub>8,7</sub> = 7.0 Hz), 5.57 (*dd*, 1 H, H-11, <sup>3</sup>J<sub>11,12</sub> = 7.0 Hz), 4.11 (*dt*, 1 H, H-12,

<sup>3</sup>J<sub>12,13</sub> ≈ 6.6 Hz), 3.67 (*s*, 3 H, OCH<sub>3</sub>), 2.30 (*t*, 2 H, H-2, <sup>3</sup>J<sub>2,3</sub> = 7.5 Hz), 2.07 (*ddd*, 2 H, H-7, <sup>3</sup>J<sub>7,6</sub> ≈ 7.0 Hz, <sup>4</sup>J<sub>7,9</sub> ≈ 1.0 Hz), 1.62 (*quintet*, 2 H, H-3, <sup>3</sup>J<sub>3,4</sub> = 7.4 Hz), 1.53 (*m*, 1 H, H-13), 1.48 (*m*, 1 H, H-13'), 1.45 – 1.35 (*m*, 2 H, H-6), 1.35 – 1.22 (*m*, 12 H, H-4, H-5, H-14, H-15, H-16, H-17), 0.88 (*t*, 3 H, H-18, <sup>3</sup>J<sub>18,17</sub> = 6.9 Hz).

9-(*R,S*)-Hydroxy-10-*trans*,12-*cis*-octadecadienoic acid methyl ester (9-OH-10*t*,12*c*) (92%, 13 mM) <sup>1</sup>H NMR δ 6.49 (*dddd*, 1 H, H-11, <sup>3</sup>J<sub>11,10</sub> = 15.2 Hz, <sup>3</sup>J<sub>11,12</sub> = 11.1 Hz, <sup>4</sup>J<sub>11,9</sub> ≈ <sup>4</sup>J<sub>11,13</sub> ≈ 1.1 Hz), 5.97 (*ddtd*, 1 H, H-12, <sup>3</sup>J<sub>12,13</sub> = 10.8 Hz, <sup>4</sup>J<sub>12,14</sub> ≈ 1.5 Hz, <sup>4</sup>J<sub>12,10</sub> ≈ 0.7 Hz), 5.66 (*dd*, 1 H, H-10, <sup>3</sup>J<sub>10,9</sub> = 6.9 Hz), 5.45 (*dt*, 1 H, H-13, <sup>3</sup>J<sub>13,14</sub> = 7.6 Hz), 4.15 (*dt*, 1 H, H-9, <sup>3</sup>J<sub>9,8</sub> ≈ 6.4 Hz), 3.66 (*s*, 3 H, OCH<sub>3</sub>), 2.30 (*t*, 2 H, H-2, <sup>3</sup>J<sub>2,3</sub> = 7.5 Hz), 2.18 (*ddd*, 2 H, H-14, <sup>3</sup>J<sub>14,15</sub> ≈ 7.4 Hz), 1.62 (*quintet*, 2 H, H-3, <sup>3</sup>J<sub>3,4</sub> = 7.2 Hz), 1.57 (*m*, 1 H, H-8), 1.51 (*m*, 1 H, H-8'), 1.39 (*quintet*, 2 H, H-15, <sup>3</sup>J<sub>15,16</sub> = 7.1 Hz), 1.36 – 1.24 (*m*, 12 H, H-4, H-5, H-6, H-7, H-16, H-17), 0.89 (*t*, 3 H, H-18, <sup>3</sup>J<sub>18,17</sub> = 6.9 Hz).

9-(*R,S*)-Hydroxy-10-*trans*,12-*trans*-octadecadienoic acid methyl ester (9-OH-10*t*,12*t*) (94%, 21 mM) <sup>1</sup>H NMR δ 6.17 (*dd*, 1 H, H-11, <sup>3</sup>J<sub>11,10</sub> = 15.2 Hz, <sup>3</sup>J<sub>11,12</sub> = 10.4 Hz), 6.02 (*dd*, 1 H, H-12, <sup>3</sup>J<sub>12,13</sub> = 15.1 Hz), 5.70 (*dt*, 1 H, H-13, <sup>3</sup>J<sub>13,14</sub> = 7.0 Hz), 5.57 (*dd*, 1 H, H-10, <sup>3</sup>J<sub>10,9</sub> = 7.0 Hz), 4.10 (*dt*, 1 H, H-9, <sup>3</sup>J<sub>9,8</sub> = 6.6 Hz), 3.66 (*s*, 3 H, OCH<sub>3</sub>), 2.30 (*t*, 2 H, H-2, <sup>3</sup>J<sub>2,3</sub> = 7.5 Hz), 2.07 (*ddd*, 2 H, H-14, <sup>3</sup>J<sub>14,15</sub> = 7.0 Hz, <sup>4</sup>J<sub>14,12</sub> ≈ 1.4 Hz), 1.61 (*quintet*, 2 H, H-3, <sup>3</sup>J<sub>3,4</sub> = 7.2 Hz), 1.58 (*m*, 1 H, H-8), 1.50 (*m*, 1 H, H-8'), 1.37 (*quintet*, 2 H, H-15, <sup>3</sup>J<sub>15,16</sub> = 7.3 Hz), 1.35 – 1.23 (*m*, 12 H, H-4, H-5, H-6, H-7, H-16, H-17), 0.89 (*t*, 3 H, H-18, <sup>3</sup>J<sub>18,17</sub> = 7.0 Hz).

8-(*R,S*)-Hydroxy-9-*cis*,11-*trans*-octadecadienoic acid methyl ester (8-OH-9*c*,11*t*) (99%, 1 mM) <sup>1</sup>H NMR δ 6.31 (*ddd*, 1 H, H-11, <sup>3</sup>J<sub>11,12</sub> = 15.0 Hz, <sup>3</sup>J<sub>11,10</sub> = 11.1 Hz, <sup>4</sup>J<sub>11,9</sub> ≈ <sup>4</sup>J<sub>11,13</sub> ≈ 1.2 Hz), 6.02 (*pt*, 1 H, H-10, <sup>3</sup>J<sub>10,9</sub> ≈ 9.9 Hz), 5.74 (*dt*, 1 H, H-12, <sup>3</sup>J<sub>12,13</sub> = 7.0 Hz), 5.27 (*t*, 1 H, H-9, <sup>3</sup>J<sub>9,8</sub> ≈ 8.3 Hz), 4.56 (*dt*, 1 H, H-8, <sup>3</sup>J<sub>8,9</sub> ≈ 6.7 Hz), 3.66 (*s*, 3 H, OCH<sub>3</sub>), 2.30 (*t*, 2 H, H-2, <sup>3</sup>J<sub>2,3</sub> = 7.5 Hz), 2.05 (*dt*, 2 H, H-13, <sup>3</sup>J<sub>13,14</sub> ≈ 7.0 Hz), 1.66 – 1.58 (*m*, 2 H, H-3), 1.58 – 1.42 (*m*, 2 H, H-7), 1.42 – 1.35 (*m*, 2 H, H-14), 1.35 – 1.22 (*m*, 12 H, H-4, H-5, H-6, H-15, H-16, H-17), 0.89 (*t*, 3 H, H-18, <sup>3</sup>J<sub>18,17</sub> = 6.9 Hz). A sample containing 77% of 8-OH-9*c*,11*t* (4 mM) was used for the 2-D NMR experiments.

8-(*R,S*)-Hydroxy-9-*trans*,11-*trans*-octadecadienoic acid methyl ester (8-OH-9*t*,11*t*) (95%, 9 mM) <sup>1</sup>H NMR δ 6.17 (*dd*, 1 H, H-10, <sup>3</sup>J<sub>10,9</sub> = 15.2 Hz, <sup>3</sup>J<sub>10,11</sub> = 10.4 Hz), 6.02 (*dd*, 1 H, H-11, <sup>3</sup>J<sub>11,12</sub> = 15.1 Hz), 5.70 (*dt*, 1 H, H-12, <sup>3</sup>J<sub>12,13</sub> = 7.0 Hz), 5.56 (*dd*, 1 H, H-9, <sup>3</sup>J<sub>9,8</sub> = 7.0 Hz), 4.10 (*dt*, 1 H, H-8, <sup>3</sup>J<sub>8,7</sub> ≈ 6.6 Hz), 3.66 (*s*, 3 H, OCH<sub>3</sub>), 2.30 (*t*, 2 H, H-2, <sup>3</sup>J<sub>2,3</sub> = 7.5 Hz), 2.07 (*dt*, 2 H, H-13, <sup>3</sup>J<sub>13,14</sub> ≈ 7.0 Hz), 1.62 (*quintet*, 2 H, H-3, <sup>3</sup>J<sub>3,4</sub> = 7.2 Hz), 1.53 (*m*, 1 H, H-7), 1.47 (*m*, 1 H, H-7'), 1.38 (*quintet*, 2 H, H-14, <sup>3</sup>J<sub>14,15</sub> = 7.1 Hz), 1.40 – 1.23 (*m*, 12 H, H-4, H-5, H-6, H-15, H-16, H-17), 0.88 (*t*, 3 H, H-18, <sup>3</sup>J<sub>18,17</sub> = 6.9 Hz).

## RESULTS AND DISCUSSION

**Autoxidation and HPLC of the hydroxy-CLA methyl esters.** The autoxidation of 9-*cis*,11-*trans* CLA methyl ester was

performed in the presence of a large amount of  $\alpha$ -tocopherol in order to produce a sufficient amount of primary hydroperoxides for characterization and to simplify the mixture of hydroperoxides formed, as has been observed for the autoxidation of methyl linoleate (11). The autoxidation was stopped when the extent of oxidation was 13%. At this oxidation level under the conditions of the investigation, hydroperoxides are formed but are not yet degraded to secondary oxidation products to a degree that would cause problems during purification. The hydroperoxides were isolated by column chromatography. In the  $^1\text{H}$  NMR spectrum of the mixture of CLA methyl ester hydroperoxides, the hydroperoxide protons appear as partly overlapping singlets at  $\delta$  7.89–7.73. Unlike the linoleate hydroperoxides, the CLA methyl ester hydroperoxides are formed in unequal amounts judging from the integrals of the hydroperoxide proton signals. In particular, one isomer (resolved OOH singlet at  $\delta$  7.87) accounted for approximately 42% of all the different hydroperoxide protons. Since the primary objective was not to investigate the properties of the hydroperoxides but rather the stereochemical distribution of the isomers formed, the hydroperoxides were converted chemoselectively (12) to the corresponding hydroxy compounds. Furthermore, as reported for the methyl hydroxylinoleates, this was expected to reduce the risk of isomerization under HPLC conditions (13) and to improve the HPLC separation of the different isomers (10).

Separation and analysis of the mixture of the hydroxy-CLA methyl esters into seven components using 7–8% *t*-butyl methyl ether in heptane is depicted in Figure 1. As expected, based on the  $^1\text{H}$  NMR spectrum of the CLA methyl ester hydroperoxides, the HPLC chromatogram revealed an unequal distribution of the hydroxy isomers. HPLC analysis of the mixture at  $\lambda = 234$  nm gave the following elution order and area percentage composition of the hydroxy-CLA methyl esters: 13-OH-9*c*,11*t* (50%), 13-OH-9*t*,11*t* (<1%), 12-OH-8*t*,10*t* (12%), 9-OH-10*t*,12*c* (13%), 9-OH-10*t*,12*t* (15%), 8-OH-9*c*,11*t* (2%), and 8-OH-9*t*,11*t* (8%).

*Characterization of the hydroxy-CLA methyl ester isomers by UV, GC-MS, and NMR.* The separated hydroxy-CLA methyl esters were analyzed by HPLC, and UV spectra were recorded. Three different  $\lambda_{\text{max}}$  values for the three different types of isomers were recorded. The absorption maximum of the *cis,trans* isomers (allylic methine is adjacent to the *trans* double bond) (fractions 1 and 4) was at 234.4 nm, that of the *cis,trans* isomer (allylic methine is adjacent to the *cis* double bond) (fraction 6) at 232.1 nm, and that of the *trans,trans* isomers (fractions 2, 3, 5, and 7) at 230.9 nm.

The position of the hydroxy group of the individual hydroxy-CLA methyl esters was determined by GC-MS using trimethylsilyl ethers of the corresponding hydroxystearates, which gave two characteristic fragment ions in MS. The results are summarized in Table 1.

*Methyl 13-hydroxy-9-cis,11-trans octadecadienoate (fraction 1).* Easily recognizable groups in the  $^1\text{H}$  NMR spectrum of the 13-hydroxy isomer were the olefinic, allylic methine, methoxy, H-2, allylic methylene, and H-18 proton signals.

**TABLE 1**  
Fragment Ions from Trimethylsilyl Ethers of Stearic Acid Methyl Esters Prepared by  $\text{PtO}_2$ -Catalyzed Hydrogenation of the Fractions Containing Hydroxy-CLA Methyl Esters

Fraction	Fragment ions ( <i>m/z</i> )	Corresponding hydroxystearate
1	173, 315	13-OH
2	173, 315	13-OH
3	187, 301	12-OH
4	229, 259	9-OH
5	229, 259	9-OH
6	243, 245	8-OH
7	243, 245	8-OH

The four multiplets in the olefinic region are characteristic of a conjugated diene structure with two lower-field “inner” protons at  $\delta$  6.48 (*dddd*, H-11) and 5.97 (*dddd*, H-10) and two higher-field “outer” protons at  $\delta$  5.67 (*dd*, H-12) and 5.43 (*dt*, H-9). The geometry of the double bonds was determined based on the vicinal coupling constants ( $^3J = 15.2$  Hz for a *trans* and  $^3J \approx 11.0$  Hz for a *cis* double bond) and was further confirmed by characteristic chemical shifts of allylic methine and methylene carbons in the  $^{13}\text{C}$  NMR spectrum. The chemical shift at  $\delta$  72.90 (C-13) was characteristic of an allylic methine carbon atom adjacent to a *trans* double bond (14) and the chemical shift at  $\delta$  27.68 (C-8) confirmed that the allylic methylene carbon was adjacent to a *cis* double bond (15,16).

An H-H-COSY experiment confirmed the assignments of the  $^1\text{H}$  NMR spectrum and was used to identify the signals of the methylene groups adjacent to the allylic protons (H-7 and H-14) as well as the H-3 signal. In addition, based on the cross-peak signals in the COSY spectrum, the diastereotopic protons (H-14 and H-14') adjacent to the allylic methine group resonated at different frequencies ( $\delta$  1.57 and 1.51). Since geminal couplings are generally  $-10$  to  $-20$  Hz and  $|\Delta\nu| \approx 30$  Hz, the signals are higher-order multiplets. Owing to rapid tumbling of the molecule in solution at room temperature, the coupling constants of the diastereotopic protons to the allylic methine proton were averaged to 6.6 Hz (measured from the allylic methine multiplet).

Windowing [the acquired free induction decay data were zero-filled and multiplied by a negative exponential function ( $\text{lb} = -0.10$  Hz) before Fourier transformation] was used to improve the resolution of the  $^1\text{H}$  NMR spectrum, and it enabled the determination of some coupling constants between nuclei that were four bonds apart ( $^4J$ ). A long-range COSY experiment was used to determine the coupled nuclei.

The position of the double bond system in the alkyl chain was determined using a 2-D total correlation spectroscopy (TOCSY) experiment by establishing which allylic resonance was closest to the methyl group. The TOCSY spectrum showed the protons belonging to the same coupled spin system; and by using a suitable mixing time in the pulse program, it was possible to control how far the magnetization was transferred within the spin system. Figure 2A shows an expanded plot of a portion of the 2-D TOCSY spectrum for the 13-hydroxy isomer run with the relatively long mixing

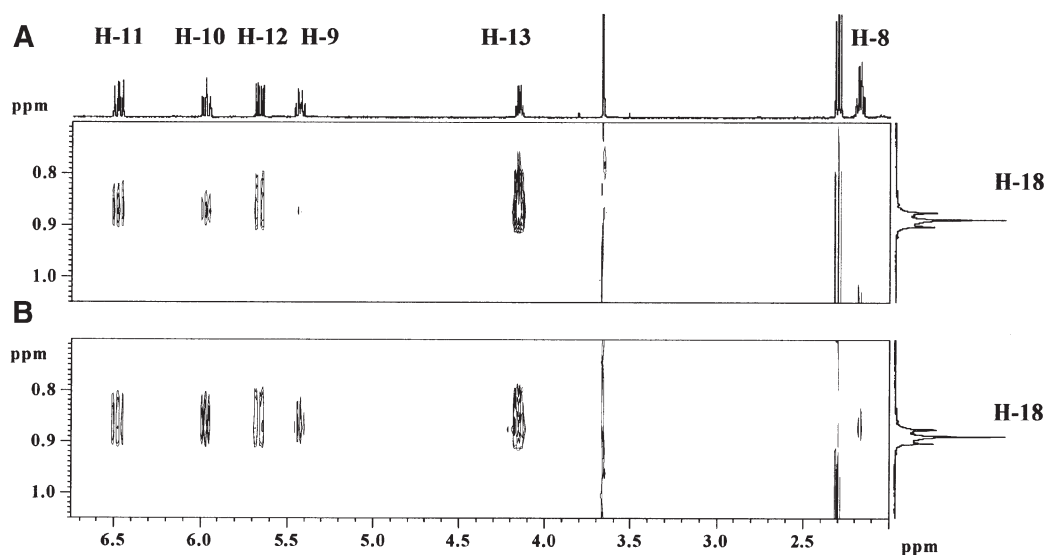


FIG. 2. Expanded plots of the 2-D total correlation spectroscopy spectra of the 13-OH-9*c*,11*t* isomer (69 mM); (A) mixing time 140 ms; (B) mixing time 180 ms.

time of 140 ms. The methyl group protons correlate with the allylic methine proton but not with the allylic methylene protons; thus, the position of the double bond system must be 9-*cis*,11-*trans*. This is in accord with the methyl group resonance correlating more strongly with the protons in the *trans* double bond than with the more remote protons in the *cis* double bond. When the TOCSY spectrum was run using a mixing time of 180 ms, the correlation cross-peaks between the methyl group protons and the different olefinic protons became more intense, and the interaction of the methyl group with the allylic methylene protons started to appear (Fig. 2B).

The previously identified protons could be correlated with the carbons directly attached in a gradient heteronuclear single quantum correlation (gHSQC) spectrum, allowing the identification of olefinic (C-9 to C-12), allylic methine (C-13), allylic methylene (C-8) and methylene carbons adjacent to the allylic positions (C-7 and C-14), C-2, C-3, and C-18. Further assignments could be made by observing the correlations between protons and carbons over two and three bonds in a gradient heteronuclear multiple bond correlation (gHMBC) spectrum. In particular, the H-18 methyl group protons had two strong correlation cross-peaks, which allowed the distinction of carbons C-16 from C-17 on chemical shift grounds. C-15 could be identified based on correlations to the previously assigned protons H-14 and H-13. More importantly, the position of the double bond system was confirmed by the correlation of C-16 to H-14, which in turn was correlated to the allylic methine carbon C-13.

**Other isomers.** The 13-hydroxy isomer of fraction 2 was characterized based on  $^1\text{H}$  NMR alone, owing to the small amount of compound. By using a combination of 2-D NMR techniques (COSY, gHSQC, gHMBC, and TOCSY), the  $^1\text{H}$  and  $^{13}\text{C}$  NMR spectra of the other hydroxy-CLA methyl esters (fractions 3–7) were assigned in a manner similar to that

of the 13-OH-9*c*,11*t* isomer. The proton assignments are listed in the Experimental Procedures section, and the carbon data collected are shown in Table 2. The assignments of the  $^{13}\text{C}$  NMR spectra of the 13-hydroxy isomer and the 9-hydroxy isomers are in agreement with the results of Frankel *et al.* (14).

It should be noted that in the  $^{13}\text{C}$  NMR spectrum of the 8-hydroxy-9-*cis*,11-*trans* isomer (fraction 6), the chemical shift at  $\delta$  67.94 is characteristic of an allylic methine adjacent to a *cis* double bond (12). This hydroxy compound corresponds to a new type of allylic monohydroperoxide conjugated diene isomer formed in the autoxidation of polyunsaturated FA esters. The related 2-hydroperoxy-3-*cis*,5-*trans*-heptadiene is known to be formed in the autoxidation of 2-*cis*,5-*trans*-heptadiene (17).

**Mechanism.** The most striking feature in the autoxidation of the 9-*cis*,11-*trans* CLA methyl ester is that under the conditions used in this study, the reaction was clearly stereoselective in favor of one geometric isomer (as a pair of enantiomers). The most feasible mechanism for an autoxidation reaction, that proceeds through hydroperoxide intermediates is the autocatalytic free radical pathway. The initial step in the autoxidation of the 9-*cis*,11-*trans* CLA methyl ester can be envisaged as an abstraction of one of the four allylic hydrogens. In the  $^1\text{H}$  NMR spectrum of the 9-*cis*,11-*trans* CLA methyl ester, the methylene protons adjacent to the *cis* double bond resonated at a slightly lower field ( $\delta$  2.15) compared to the methylene protons adjacent to a *trans* double bond ( $\delta$  2.09). This implies that the chemical surroundings of the two allylic groups are slightly different. Furthermore, the allylic position, in the conformations that are most likely to undergo fragmentation (the C–H bond undergoing fragmentation perpendicular to the diene  $\pi$  system), is sterically more crowded when adjacent to a *cis* double bond than to a *trans* double



**TABLE 2**  
<sup>13</sup>C NMR Chemical Shift Values of Hydroxy-CLA Methyl Esters<sup>a</sup>

Carbon nucleus	13-OH-9 <i>c</i> ,11 <i>t</i>	12-OH-8 <i>t</i> ,10 <i>t</i>	9-OH-10 <i>t</i> ,12 <i>c</i>	9-OH-10 <i>t</i> ,12 <i>t</i>	8-OH-9 <i>c</i> ,11 <i>t</i>	8-OH-9 <i>t</i> ,11 <i>t</i>
C-1	174.34	174.27	174.31	174.31	174.28	174.28
C-2	34.08	34.08	34.09	34.09	34.08	34.08
C-3	24.90	24.88	24.92	24.92	24.88	24.88
C-4	29.06–28.96	29.00–28.78	29.35–29.07	29.35–28.92	29.20–28.90	29.21–28.89
C-5	29.06–28.96	29.00–28.78	29.35–29.07	29.35–28.92	29.20–28.90	29.21–28.89
C-6	29.06–28.96	29.00–28.78	29.35–29.07	29.35–28.92	25.16	25.25
C-7	29.48	32.53	25.35	25.36	37.40	37.23
C-8	27.68	135.26	37.31	37.29	67.94	72.85
C-9	132.79	129.59	72.91	72.87	131.34	133.50
C-10	127.84	130.88	135.76	133.57	130.62	131.06
C-11	125.74	133.76	125.89	131.02	125.01	129.38
C-12	135.97	72.90	127.67	129.41	137.53	135.70
C-13	72.90	37.36	133.10	135.65	32.85	32.66
C-14	37.34	25.41	27.76	32.62	29.20–28.90	29.21–28.89
C-15	25.13	29.24	29.35–29.07	29.35–28.92	29.20–28.90	29.21–28.89
C-16	31.79	31.80	31.47	31.42	31.71	31.73
C-17	22.61	22.61	22.55	22.53	22.62	22.62
C-18	14.05	14.08	14.05	14.04	14.09	14.09
OCH <sub>3</sub>	51.47	51.46	51.45	51.45	51.45	51.46

<sup>a</sup>13-OH-9*c*,11*t*, 13-(*R,S*)-hydroxy-9-*cis*,11-*trans*-octadecadienoic acid methyl ester; 12-OH-8*t*,10*t*, 12-(*R,S*)-hydroxy-8-*trans*,10-*trans*-octadecadienoic acid methyl ester; 9-OH-10*t*,12*c*, 9-(*R,S*)-hydroxy-10-*trans*,12-*cis*-octadecadienoic acid methyl ester; 9-OH-10*t*,12*t*, 9-(*R,S*)-hydroxy-10-*trans*,12-*trans*-octadecadienoic acid methyl ester; 8-OH-9*c*,11*t*, 8-(*R,S*)-hydroxy-9-*cis*,11-*trans*-octadecadienoic acid methyl ester; 8-OH-9*t*,11*t*, 8-(*R,S*)-hydroxy-9-*trans*,11-*trans*-octadecadienoic acid methyl ester.

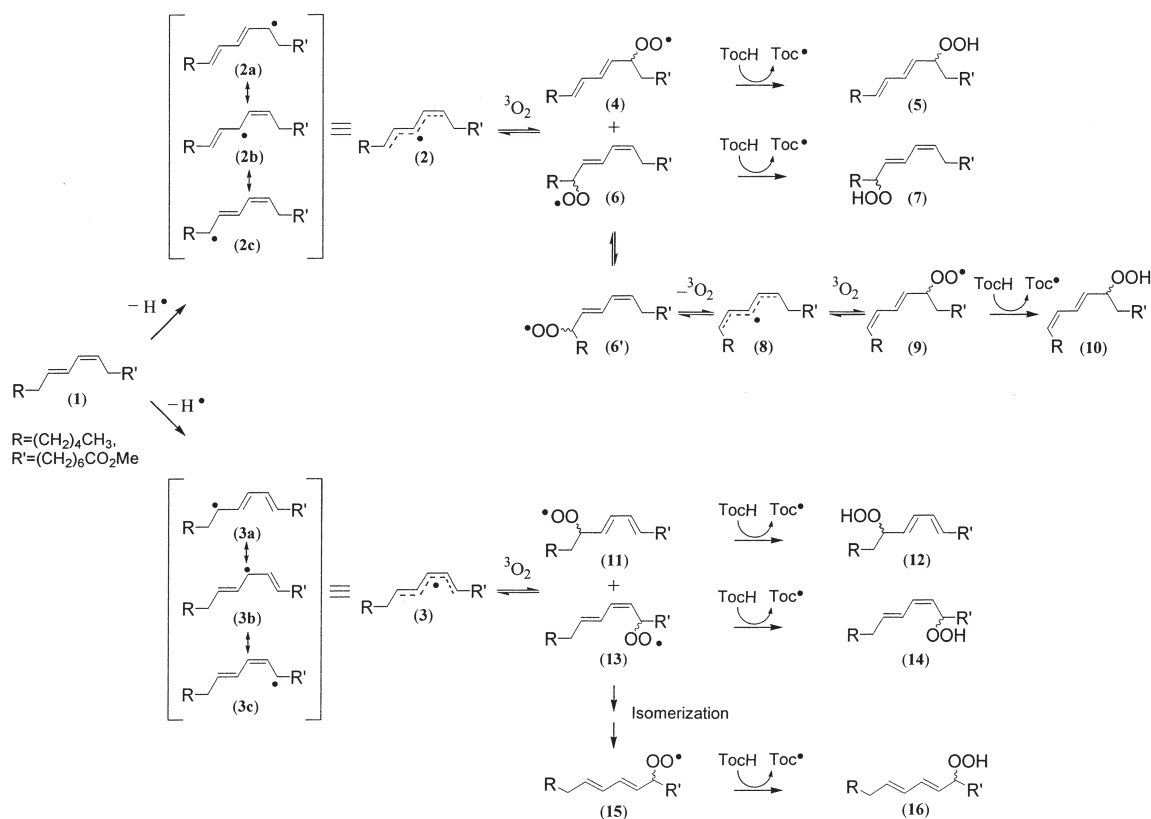
bond. However, the electronic or the steric factors alone at the two allylic positions are hardly large enough to account for the observed stereoselectivity.

Abstraction of a hydrogen atom from the allylic positions adjacent to a *trans* double bond leads to the formation of a pentadienyl radical delocalized between carbons 9 and 13 (**2**), whereas hydrogen abstraction from the alternative allylic position leads to the formation of a pentadienyl radical delocalized between carbons 8 and 12 (**3**) (Scheme 1, where TocH =  $\alpha$ -tocopherol and Toc• =  $\alpha$ -tocopherol radical). The delocalization of the pentadienyl radicals **2** and **3** is represented by three resonance structures (**a** to **c**). The resonance structures (**2b** and **3b**) in which the double bonds are not conjugated are energetically less favorable, and thus the contribution to the resonance hybrids is smaller than that of the other conjugated resonance structures. The spatial arrangement of the double bonds in both of the conjugated resonance structures, **2a** and **2c**, that contribute to the pentadienyl radical **2** is *s-trans*, whereas that of the conjugated resonance structures **3a** and **3c** that contributes to the pentadienyl radical **3** is such that only one is *s-trans* and the other *s-cis*. Thus, the radical **2** (*W*-shaped conformation) is energetically more stable than radical **3** (*Z*-shaped conformation). Invoking the Hammond postulate, we can assume that the geometry of the transition state resembles that of the pentadienyl radical. Hence, the transition state leading to radical **2** should be more stable than the one leading to radical **3**, and thereby the activation energy ( $\Delta G^\ddagger$ ) for the formation of radical **2** is smaller than it is for the formation of radical **3**; and thus radical **2** is formed faster.

The propagation step consists of the radical–radical coupling reaction between the pentadienyl radical and molecular

oxygen. Since this reaction proceeds under normal oxygen pressures at or near the diffusion control rate (18), the geometry of the double bonds is not expected to change through isomerization of the pentadienyl radical. Furthermore, the isomerization of the *W*-conformer **2** is energetically unfavorable based on the analogy with the pentadienyl radical itself (19). The resonance-stabilized pentadienyl radicals are essentially planar, and the new chiral center is formed without stereoselection. However, the studies performed with methyl oleate (20) and with four different geometric isomers of methyl linoleate (21) under kinetic conditions show that the attack of oxygen on the carbons of the allylic or the pentadienyl radical is regioselective. In particular, as indicated in the methyl linoleate study (21), the pentadienyl radical terminus having a partial *trans* double bond character reacts faster than the terminus having a partial *cis* double bond character. Thus, addition of oxygen to the pentadienyl radical **2**, which is the same radical as the one formed from methyl 9-*cis*,12-*trans*-linoleate, leads to the preferential formation of the 13-peroxyl radical **6** having a *cis,trans* geometry over the 9-peroxyl radical **4**, which has the more stable *trans,trans* configuration. When the oxidation occurs in the presence of the good hydrogen atom donor,  $\alpha$ -tocopherol, the next step is relatively fast and selectively produces 13-OOH-9*c*,11*t* (**7**). Smaller amounts of the other three primary or kinetic hydroperoxides, **5**, **12**, and **14**, are also expected to form.

Because the high level of a strong hydrogen donor was expected to stabilize the kinetic autoxidation products, the formation of the nonkinetic hydroperoxides, **10** and **16**, was unexpected and is not easily explained. The autoxidation under the conditions employed in this investigation was selective, leading



SCHEME 1

to preferential formation of the 13-peroxyl radical **6**, which is involved in competing hydrogen atom abstraction and  $\beta$ -scission reactions. Hydrogen atom abstraction occurs rapidly in the presence of a good hydrogen atom donor compared to  $\beta$ -scission. However, isomerization of the peroxyl radical **6** through  $\beta$ -scission of the conformer **6'** would ultimately lead to the formation of 9-OOH-10*t*,12*c* (**10**) as has been demonstrated previously (22–24). Furthermore, it has been suggested that at high  $\alpha$ -tocopherol concentration the hydrogen atom abstraction reaction between the  $\alpha$ -tocopherol and peroxyl radical is reversible (2). The  $\beta$ -scission pathway also explains the formation of a small amount of the 13-OOH-9*t*,11*t* from the peroxyl radical **4**. More of this isomer was expected to form in the absence of  $\alpha$ -tocopherol, which is the topic of further studies.

Presuming that under normal oxygen pressures the pentadienyl radical *Z*-conformation does not isomerize before it is trapped by oxygen, 8-OOH-9*t*,11*t* (**16**) should be formed by isomerization of the primary peroxyl radicals **11** or **13**. Isomerization through the  $\beta$ -scission pathway of the radical **11** would initially lead to the formation of an 8-peroxy-9-*trans*,11-*cis* radical, and that of the radical **13** would lead to a 12-peroxy-8-*cis*,10-*trans* radical. Since neither of the hydroperoxides was found from the reaction mixture, this pathway seems unlikely. Because both termini of the pentadienyl radical **3** have a partial *trans* double bond character, we would expect about the same amount of the radical **13** to be formed as the radical **11**. However, significantly less 8-OOH-9*c*,11*t*

(**14**) than 12-OOH-8*t*,10*t* (**12**) was formed based on the HPLC analysis of the corresponding hydroxy esters. Therefore, if the hydroperoxide **12** is not formed by some other mechanism, the peroxyl radical **13** isomerizes and/or decomposes to secondary autoxidation products faster than the peroxyl radical **11**. The origin of the lability of the radical **13** could be that, unlike the other peroxyl isomers, the carbon atom bearing the peroxy group is adjacent to a *cis* double bond. Moreover, the isomerization of the radical **13** by two successive [2,3] allylperoxyl rearrangements, proceeding through a cyclic transition state as the oleate allylperoxyl rearrangement (25), leads, after hydrogen atom abstraction, to the formation not only of hydroperoxide **16** but also of **12**.

Although the isomerization of the peroxyl radical **13** by addition of oxygen at C-10 is feasible, the autoxidation conditions used are not purely kinetic, and this study does not provide evidence ruling out direct isomerization of the *Z*-conformation pentadienyl radical (**3**). With the pentadienyl radical itself, isomerization of the *Z*-conformation to the *W*-conformation is expected to be diffusion-controlled, and at above  $-63^\circ\text{C}$  the *Z*-conformer is fully converted into the *W*-conformer (26). The direct isomerization of the *Z*-conformer **3** leads to the more stable *W*-conformer, which is, at least in theory, a precursor of hydroperoxides **16** and **12**. However, this alternative pathway is possible only if the conformational isomerization occurs at a rate that competes successfully with the diffusion-controlled peroxidation of the radical **3**.

The autoxidation of conjugated FA has been suggested to differ from the autoxidation of nonconjugated PUFA. In the light of the results of this investigation, it can be concluded that the eminent feature of the autoxidation of 9-*cis*,11-*trans* CLA methyl ester in the presence of a good hydrogen atom donor is that one hydroperoxide (as a pair of enantiomers) is formed predominantly at the expense of other isomers. When methyl linoleate is autoxidized in the presence of  $\alpha$ -tocopherol at 40°C, the formation of two kinetic *cis,trans* hydroperoxides in 1:1 ratio is favored over the two thermodynamic *trans,trans* hydroperoxides (11), whereas the autoxidation of CLA methyl esters leads to the formation of a more complex isomeric mixture. There are four instead of two different positional isomers owing to the formation of two different pentadienyl radicals. Furthermore, conjugated diene hydroperoxides with *trans,trans* geometry and a new type of *cis,trans* hydroperoxide with a *cis* double bond adjacent to the hydroperoxide-bearing carbon atom are formed as kinetic hydroperoxides. Since oxidation reactions and formation of hydroperoxides of specific stereochemistry play an important role in many biological reactions, these differences in hydroperoxide formation may partly explain the unique bioactive properties of CLA.

#### ACKNOWLEDGMENT

The authors wish to acknowledge funding support from the Research Council for Environment and Natural Resources of Academy of Finland.

#### REFERENCES

- Swern, D. (1961) Primary Products of Olefinic Autoxidations, in *Autoxidation and Antioxidants* (Lundberg, W.O., ed.), Vol. 1, pp. 1–54, John Wiley & Sons, New York.
- Porter, N.A., Caldwell, S.E., and Mills, K.A. (1995) Mechanisms of Free Radical Oxidation of Unsaturated Lipids, *Lipids* 30, 277–290.
- Chan, H.W.-S., and Coxon, D.T. (1987) Lipid Hydroperoxides, in *Autoxidation of Unsaturated Lipids* (Chan, H.W.S., ed.), pp. 17–50, Academic Press, London.
- Yurawecz, M.P., Sehat, N., Mossoba, M.M., Roach, J.A.G., and Ku, Y. (1997) Oxidation Products of Conjugated Linoleic Acid and Furan Fatty Acids, in *New Techniques and Applications in Lipid Analysis* (McDonald, R.E., and Mossoba, M.M., eds.), pp. 183–215, AOCS Press, Champaign.
- Eulitz, K., Yurawecz, M.P., and Ku, Y. (1999) The Oxidation of Conjugated Linoleic Acid, in *Advances in Conjugated Linoleic Acid Research* (Yurawecz, M.P., Mossoba, M.M., Kramer, J.K.G., Pariza, M.W., and Nelson, G.J., eds.), Vol. 1, pp. 55–63, AOCS Press, Champaign.
- Hämäläinen, T.I., Sundberg, S., Mäkinen, M., Kaltia, S., Hase, T., and Hopia, A. (2001) Hydroperoxide Formation During Autoxidation of Conjugated Linoleic Acid Methyl Ester; *Eur. J. Lipid Sci. Technol.* 103, 588–593.
- Lie Ken Jie, M.S.F., Pasha, M.K., and Alam, M.S. (1997) Synthesis and Nuclear Magnetic Resonance Properties of All Geometrical Isomers of Conjugated Linoleic Acids, *Lipids* 32, 1041–1044.
- Ueda, S., Hayashi, T., and Namiki, M. (1986) Effect of Ascorbic Acid on Lipid Autoxidation in a Model Food System, *Agric. Biol. Chem.* 50, 1–7.
- Frankel, E.N., Neff, W.E., Rohwedder, W.K., Khambay, B.P.S., Garwood, R.F., and Weedon, B.C.L. (1977) Analysis of Autoxidized Fats by Gas Chromatography–Mass Spectrometry: I. Methyl Oleate, *Lipids* 12, 901–907.
- Chan, H.W.-S., and Levett, G. (1977) Autoxidation of Methyl Linoleate. Separation and Analysis of Isomeric Mixtures of Methyl Linoleate Hydroperoxides and Methyl Hydroxylinoates, *Lipids* 12, 99–104.
- Peers, K.E., Coxon, D.T., and Chan, H.W.-S. (1981) Autoxidation of Methyl Linolenate and Methyl Linoleate: The Effect of  $\alpha$ -Tocopherol, *J. Sci. Food Agric.* 32, 898–904.
- Frankel, E.N., Garwood, R.F., Khambay, B.P.S., Moss, G.P., Weedon, B.C.L. (1984) Stereochemistry of Olefin and Fatty Acid Oxidation. Part 3. The Allylic Hydroperoxides from the Autoxidation of Methyl Oleate, *J. Chem. Soc., Perkin Trans 1*, 2233–2240.
- Chan, H.W.-S., Costaras, C.T., Prescott, F.A.A., and Swoboda, P.A.T. (1975) Thermal Isomerisations of Linoleate Hydroperoxides, a Phenomenon Affecting the Determination of Isomeric Ratios, *Biochim. Biophys. Acta* 398, 347–350.
- Frankel, E.N., Neff, W.E., and Weisleder, D. (1990) Determination of Methyl Linoleate Hydroperoxides by  $^{13}\text{C}$  Nuclear Magnetic Resonance Spectroscopy, in *Methods in Enzymology* (Parker, L., and Glazer, A.N., eds.), Vol. 186, pp. 380–387, Academic Press, New York.
- Bus, J., Sies, I., and Lie Ken Jie, M.S.F. (1976)  $^{13}\text{C}$ -NMR of Methyl, Methylene, and Carbonyl Carbon Atoms of Methyl Alkenoates and Alkynoates, *Chem. Phys. Lipids* 17, 501–518.
- Gunstone, F.D., Pollard, M.R., Scrimgeour, C.M., and Vedanayagam, H.S. (1977) Fatty Acids. Part 50.  $^{13}\text{C}$  Nuclear Magnetic Resonance Studies of Olefinic Fatty Acids and Esters, *Chem. Phys. Lipids* 18, 115–129.
- Frankel, E.N., Garwood, R.F., Vinson, J.R., and Weedon, B.C.L. (1982) Stereochemistry of Olefin and Fatty Acid Oxidation. Part 1. Autoxidation of Hexene and Hepta-2,5-diene Isomers, *J. Chem. Soc., Perkin Trans 1*, 2707–2713.
- Ingold, K.U. (1969) Peroxy Radicals, *Acc. Chem. Res.* 2, 1–9.
- MacInnes, I., and Walton, J.C. (1985) Rotational Barriers in Pentadienyl and Pent-2-en-4-ynyl Radicals, *J. Chem. Soc., Perkin Trans. 2*, 1073–1076.
- Porter, N.A., Mills, K.A., and Carter, R.L. (1994) A Mechanistic Study of Oleate Autoxidation: Competing Peroxyl H-Atom Abstraction and Rearrangement, *J. Am. Chem. Soc.* 116, 6690–6696.
- Porter, N.A., and Wujek, D.G. (1984) Autoxidation of Polyunsaturated Fatty Acids, an Expanded Mechanistic Study, *J. Am. Chem. Soc.* 106, 2626–2629.
- Chan, H.W.-S., Levett, G., and Matthew, J.A. (1978) Thermal Isomerization of Methyl Linoleate Hydroperoxides. Evidence of Molecular Oxygen as a Leaving Group in a Radical Rearrangement, *J. Chem. Soc. Chem. Comm.*, 756–757.
- Chan, H.W.-S., Levett, G., and Matthew, J.A. (1979) The Mechanism of the Rearrangement of Linoleate Hydroperoxides, *Chem. Phys. Lipids* 24, 245–256.
- Porter, N.A., Lehman, L.S., Weber, B.A., and Smith, K.J. (1981) Unified Mechanism for Polyunsaturated Fatty Acid Autoxidation. Competition of Peroxy Radical Hydrogen Atom Abstraction,  $\beta$ -Scission, and Cyclization, *J. Am. Chem. Soc.* 103, 6447–6455.
- Porter, N.A., and Wujek, J.S. (1987) Allylic Hydroperoxide Rearrangement:  $\beta$ -Scission or Concerted Pathway? *J. Org. Chem.* 52, 5085–5089.
- Davies, A.G., Griller, D., Ingold, K.U., and Lindsay, D.A. (1981) An Electron Spin Resonance Study of Pentadienyl and Related Radicals: Homolytic Fission of Cyclobut-2-enylmethyl Radicals, *J. Chem. Soc., Perkin Trans. 2*, 633–641.

[Received February 11, 2002; in revised form and accepted May 14, 2002]

# Regiospecific Enzymatic Oxygenation of *cis*-Vaccenic Acid During Aerobic Senescence of the Halophilic Purple Sulfur Bacterium *Thiohalocapsa halophila*

Daphné Marchand<sup>a</sup>, Vincent Grossi<sup>a</sup>, Agnès Hirschler-Rea<sup>b</sup>, and Jean-François Rontani<sup>a,\*</sup>

<sup>a</sup>Laboratoire d'Océanographie et de Biogéochimie (UMR 6535), 13288 Marseille, France, and <sup>b</sup>Laboratoire de Microbiologie, IMEP, 13397 Marseille, France

**ABSTRACT:** A regiospecific oxygenation of the allylic carbon 10 of *cis*-vaccenic acid has been observed in senescent cells of the halophilic purple sulfur bacterium *Thiohalocapsa halophila* incubated under aerobic conditions in darkness. The results obtained strongly suggest that these enzymatic processes involve the initial dioxygenase-mediated formation of 10-hydroperoxy-octadec-*cis*-11-enoic acid, which is not accumulated in the cells of *T. halophila* owing to its high cytotoxic properties. Deuterium labeling and GC-MS analyses enabled us to demonstrate that subsequent enzymatic conversions of this allylic hydroperoxide involved reduction, cleavage, isomerization, and saturation reactions. Some of the specific oxidation products thus formed could constitute potential *T. halophila* biomarkers.

Paper no. L8991 in *Lipids* 37, 541–548 (June 2002).

Lipoxygenases (formerly called lipoxidases in plants) are a family of related nonheme iron-containing enzymes that are widely distributed in humans, animals, and plants (1). Although lipoxygenase was originally discovered in leguminous plants, it soon became clear that lipoxygenases are widespread throughout the plant kingdom, including algae (2,3) and bryophytes (4). These enzymes dioxygenate PUFA containing all-*cis*-methylene-interrupted double bonds such as octadeca-9,12-all-*cis*-dienoic acid (linoleic acid), octadeca-9,12,15-all-*cis*-trienoic acid (linolenic acid), eicosa-5,8,11,14-all-*cis*-tetraenoic acid (arachidonic acid), or eicosa-5,8,11,14,17-all-*cis*-pentaenoic acid, yielding unsaturated hydroperoxy FA with one pair of conjugated double bonds (5). The dioxygenation of PUFA by a lipoxygenase formally consists of three steps: (i) removal of one hydrogen atom from the double allylic methylene carbon atom forming a FA radical, (ii) conjugation of the double bonds with a *trans*-isomerization of the shifted double bond (the conjugation being accompanied by a rearrangement of the radical electron), and (iii) insertion of dioxygen (5). Lipoxygenases may also catalyze the oxygenation of monounsaturated FA such as oleic (6–9) and octadec-*cis*-12-enoic (9) acids, these processes mainly affording hydroxy-, hydroperoxy-, or oxoacids.

The reactive properties attributed to hydroperoxides have

\* To whom correspondence should be addressed at Laboratoire d'Océanographie et de Biogéochimie (UMR 6535), Centre d'Océanologie de Marseille (OSU), campus de Luminy case 901, 13288-Marseille, France. E-mail: rontani@com.univ-mrs.fr

Abbreviations: BSTFA, bis(trimethylsilyl) trifluoroacetamide; DMDS, dimethyl disulfide; TMS, trimethylsilyl.

led to speculation that lipoxygenase participates in the senescence process in plants (10). However, conflicting experimental evidence leaves this question unanswered for the moment (11,12).

During aerobic incubation of senescent cells of the halophilic purple sulfur bacterium *Thiohalocapsa halophila* in darkness, we observed a regiospecific peroxidation of the allylic carbon 10 of octadec-11-*cis*-enoic acid (*cis*-vaccenic acid), which was attributed to the involvement of a dioxygenase. The subsequent enzymatic conversions of the 10-hydroperoxyoctadec-11-*cis*-enoic acid thus formed have been studied by deuterium labeling and involve reduction, cleavage, isomerization, and saturation reactions.

## EXPERIMENTAL PROCEDURES

*Source of strain.* *Thiocapsa halophila* strain SG 3202 was isolated from the red layer occurring all year around in the laminar microbial mat at the sediment surface of hypersaline ponds in the saltern of Salin-de-Giraud (Camargue, France) (13) and was renamed *Thiohalocapsa halophila* DSM 6210 by Imhoff *et al.* (14) after examination of its 16S rDNA.

*Culture conditions.* The final synthetic medium for maintenance and growth of *T. halophila* was prepared according to the method of Pfennig and Trüper (15), and contained (per litre of distilled water): KH<sub>2</sub>PO<sub>4</sub> (0.3 g), KCl (0.3 g), NH<sub>4</sub>Cl (0.5 g), NaCl (100 g), MgSO<sub>4</sub>·7H<sub>2</sub>O (3 g), MgCl<sub>2</sub>·6H<sub>2</sub>O (6 g), and CaCl<sub>2</sub> (0.05 g). After sterilization, the liquid medium was supplemented with Na<sub>2</sub>S<sub>2</sub>O<sub>3</sub> (0.08 g), NaHCO<sub>3</sub> (1.5 g), Na<sub>2</sub>S·9H<sub>2</sub>O (0.48 g), CH<sub>3</sub>COONa (0.16 g), trace element solution [SL12 (16)] (1 mL), and vitamin solution [VA (17)] (1 mL) under a mixture of gas (N<sub>2</sub>/CO<sub>2</sub>, 90:10). The pH was finally adjusted between 7.2 and 7.4, and the medium was distributed in 250-mL sterile screwcap bottles. To minimize the gaseous volume, the flasks were brimmed. Cultures were incubated at 20°C under an illumination of 110 μmol photons m<sup>-2</sup> s<sup>-1</sup> (12 h light and dark cycle) provided by a mix of 30 W fluorescent (Osram, fluora) and 60 W tungsten lamps (one of each). Aerobic incubations were carried out in 250-mL Erlenmeyer flasks under the same conditions with magnetic stirring.

*Experiments with senescent cells.* After growth, cultures were distributed in 250-mL Erlenmeyer flasks and taken through several freeze-thaw cycles to provide some disruption



of cellular structure. The flasks were then incubated at 20°C under aerobic and anaerobic conditions in darkness.

**Treatment.** After incubation, the content of each flask was filtered on GF/F (Whatman) paper, and the filters were saponified directly or after reduction.

**Reduction of hydroperoxides to alcohols.** Hydroperoxides were reduced to the corresponding alcohols in methanol (25 mL) by excess NaBH<sub>4</sub> or NaBD<sub>4</sub> (10 mg/mg of extract) using magnetic stirring (15 min at 0°C) (18). During this treatment ketones are also reduced, and the possibility of some ester cleavage cannot be excluded.

**Alkaline hydrolysis.** Saponification was carried out on both reduced and nonreduced samples. After reduction, 25 mL of water and 2.8 g of potassium hydroxide were added, and the mixture was directly saponified by refluxing for 2 h. In the case of nonreduced samples, an additional 25 mL of methanol was added before saponification. After cooling, the contents of the flask were extracted three times with *n*-hexane. The combined *n*-hexane extracts were dried over anhydrous Na<sub>2</sub>SO<sub>4</sub>, filtered, and concentrated by using a rotary evaporator to give the unsaponified fraction. The aqueous phase was then acidified with hydrochloric acid (pH 1) and subsequently extracted three times with dichloromethane. Treatment of the combined dichloromethane extracts as described above gave the saponified fraction.

**Derivatization.** After evaporation of solvents, the residues were taken up in 400 µL of a mixture of pyridine and bis(trimethylsilyl) trifluoroacetamide (BSTFA) (Supelco, St Quentin Fallavier, France) (3:1, vol/vol) and silylated for 1 h at 50°C. After evaporation to dryness under nitrogen, the residues were taken up in a mixture of ethyl acetate and BSTFA and analyzed by GC–EIMS.

**Dimethyldisulfide (DMDS) treatment.** Following the procedure initially described by Vincenti *et al.* (19), the extract to be derivatized was dissolved in 250 µL of hexane, 250 µL of DMDS, and 125 µL of an iodine solution (60 mg of iodine in 1 mL of diethyl ether). The reaction mixture was held at 50°C for 24 h and then diluted with hexane. The reaction was quenched with 2 mL of 5% Na<sub>2</sub>S<sub>2</sub>O<sub>3</sub>, and the hexane layer was pipetted off. The solution was extracted twice with hexane; the hexane extracts were combined, dried on Na<sub>2</sub>SO<sub>4</sub>, filtered, and the solvent was evaporated by using a rotary evaporator. The residue was then silylated as described above and analyzed by GC–EIMS.

**Hydrogenation.** Lipid extracts were hydrogenated overnight under magnetic stirring in methanol with Pd/CaCO<sub>3</sub> (10–20 mg/mg of extract) (Aldrich, St Quentin Fallavier, France) as a catalyst. After hydrogenation, the catalyst was removed by filtration, and the filtrate was concentrated by rotary evaporation.

**Identification of FA and their oxidation products.** These compounds were identified by comparison of retention times and mass spectra with those of standards and quantified (calibration with external standards) by GC–EIMS. Derivatives of regioisomeric hydroxy compounds, which often coeluted, can be distinguished by their EI mass spectra to a great extent,

since the main fragments are caused by α-cleavage at the site of the functional group. These isomers could thus be detected and quantified by measurement of the ion currents of these specific fragment ions. Characterization of *cis* and *trans* allylic hydroxyacids was based on comparison of their retention times with those of standard compounds.

GC–EIMS analyses were carried out with an HP 5890 series II plus gas chromatograph connected to an HP 5972 mass spectrometer. The following conditions were used: 30 m × 0.25 mm (i.d.) fused-silica capillary column coated with HP5 (Hewlett-Packard; film thickness, 0.25 µm); oven temperature programmed from 60 to 130°C at 30°C min<sup>-1</sup> and then from 130 to 300°C at 4°C min<sup>-1</sup>; carrier gas (He) maintained at 1.04 bar until the end of the temperature program and then programmed from 1.04 bar to 1.5 bar at 0.04 bar min<sup>-1</sup>; injector (splitless) temperature, 300°C; electron energy, 70 eV; source temperature, 170°C; cycle time, 1.5 s.

**Standard compounds.** Palmitoleic, oleic, and *cis*- and *trans*-vaccenic acids were purchased from Sigma (St Quentin Fallavier, France). Fe<sup>2+</sup>/ascorbate-induced autoxidation (20) of *cis*-vaccenic acid produced a mixture of allylic hydroperoxides containing significant amounts of *cis*- and *trans*-10-hydroperoxyoctadec-11-enoic acids (21). Subsequent reduction of these different hydroperoxides in methanol with excess NaBH<sub>4</sub> afforded the corresponding hydroxyacids. Oxoacids were obtained by dehydration of the corresponding hydroperoxides in a mixture of pyridine and acetic anhydride (22). Hydrogenation of hydroxyacids and oxoacids was carried out in methanol with Pd/CaCO<sub>3</sub> as catalyst. A mixture of diastereoisomeric 10,11-, 9,10-, and 8,9-dihydroxyoctadecanoic acids was obtained after (i) photosensitized oxidation of oleic acid (in pyridine in the presence of hematoporphyrin as sensitizer) (23), (ii) NaBH<sub>4</sub> reduction of the resulting 9-hydroperoxyoctadec-*trans*-10-enoic and 10-hydroperoxyoctadec-*trans*-8-enoic acids, (iii) hydrogenation of the corresponding allylic hydroxyacids, (iv) dehydration (overnight) of the mixture of 9- and 10-hydroxyoctadecanoic acids thus formed in benzene with *p*-toluenesulfonic acid as catalyst, and (v) subsequent OsO<sub>4</sub> treatment (24).

## RESULTS AND DISCUSSION

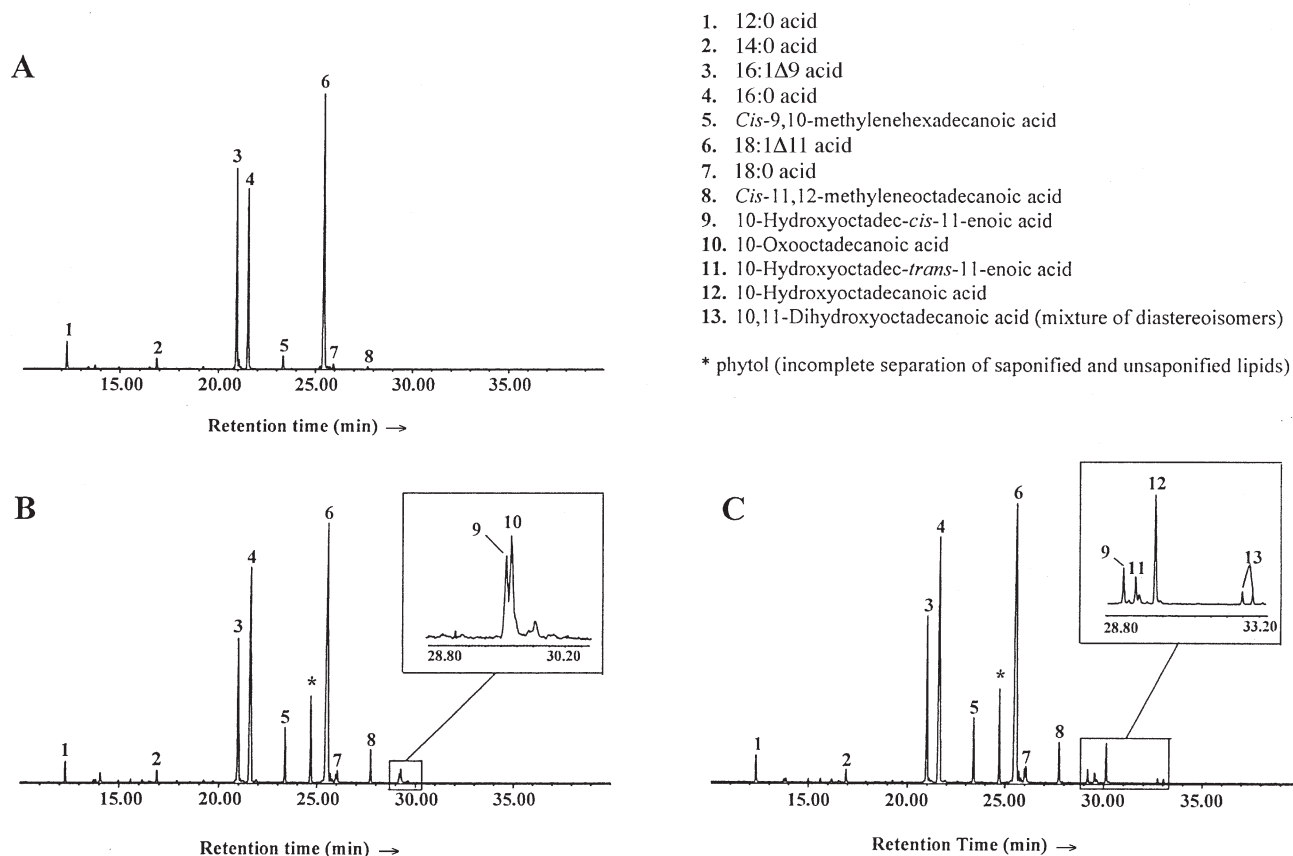
Purple sulfur bacteria generally constitute the most prominent anoxygenic phototrophs in microbial mats. Because of the fluctuating gradients of oxygen and sulfide in the mats, these organisms may be exposed to oxygen. It is well established that purple sulfur bacteria resident in microbial mats not only are oxygen tolerant but can also continue anoxygenic photosynthesis even under fully aerobic conditions. Some species are even capable of performing an aerobic mode of metabolism, either as chemoorganotrophs or chemolithotrophs (25,26). Consequently, we have compared the lipidic composition of healthy and senescent cells of *T. halophila* incubated under aerobic and anaerobic conditions.

The unsaponified lipidic fraction obtained after alkaline hydrolysis of cells of *T. halophila* grown under anaerobic

conditions is dominated by a single component, assigned by GC-EIMS as phytol. This isoprenoid alcohol arises from the hydrolysis of bacteriochlorophyll *a*, which constitutes with okenone the major photosynthetic pigments of this purple sulfur bacterium (13). Okenone, which was thought to be present in large amounts in this fraction, was not amenable to GC with the operating conditions described in the Experimental Procedures section. GC-EIMS analysis of the corresponding saponifiable fraction revealed the presence of 12:0, 14:0, 16:0, 16:1, 18:0, and 18:1 FA (Fig. 1A). To establish the position of the double bond in the monounsaturated FA, the saponified fraction was treated with DMDS (19). The position of the double bond was determined from the mass spectra of the DMDS derivatives on the basis of the fragments formed by cleavage between the carbons bearing the thioether groups. The main monounsaturated FA present in *T. halophila* are 16:1 $\Delta$ 9 and 18:1 $\Delta$ 11 FA. Comparison of their retention times with those of standards showed that these compounds are, respectively, palmitoleic and *cis*-vaccenic acids. This saponified fraction also contains small amounts of *cis*-9,10-methylenehexadecanoic and *cis*-11,12-methyleneoctadecanoic acids (Fig. 1A), formed by the addition of a methylene group across the double bond of palmitoleic and *cis*-vaccenic acids, respectively (27). These cyclopropane FA have been

differentiated from their corresponding olefinic isomers after catalytic hydrogenation (28).

The saponified and unsaponified fractions of healthy cells of *T. halophila* remained practically unchanged after incubation under aerobic conditions. In contrast, aerobic and anaerobic incubations of senescent cells of *T. halophila* resulted in a significant increase in the amounts of cyclopropane FA (Fig. 1). In most bacteria, the amount of cyclopropane FA depends very much on the growth conditions, and the level generally increases when the growth rate decreases (27). This statement is in good agreement with the increasing amounts of *cis*-9,10-methylenehexadecanoic and *cis*-11,12-methyleneoctadecanoic acids observed during the senescence of *T. halophila*. After aerobic incubation of senescent cells of *T. halophila*, some interesting additional peaks appeared in the total ion current chromatograms of the NaBH<sub>4</sub> reduced and nonreduced saponified fractions (peaks 9–13; Fig. 1). These new compounds were unambiguously identified by comparison of their retention times and EI mass spectra with those of suitable standards. Peaks 9 and 11 were, respectively, attributed to *cis*- and *trans*-10-hydroxyoctadec-11-enoic acids. The EI mass spectra of these silylated compounds exhibit a strong fragment ion at *m/z* 213 corresponding to the cleavage at the carbon bearing the –OSiMe<sub>3</sub> group (Fig. 2). Characterization



**FIG. 1.** Total ion chromatograms obtained after injection of saponified lipids of (A) healthy cells of *Thiohalocapsa halophila* incubated under anoxic conditions, (B) senescent cells of *T. halophila* incubated under oxic conditions for 10 d, and (C) senescent cells of *T. halophila* incubated under oxic conditions for 10 d and reduced with NaBH<sub>4</sub>.

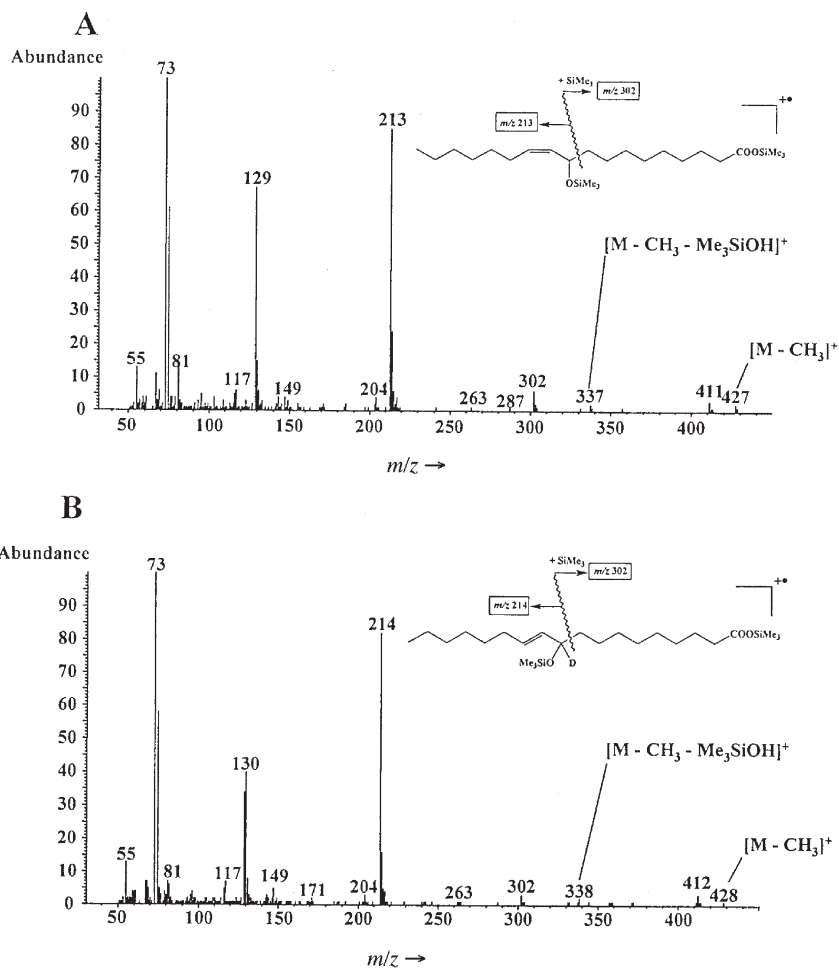


FIG. 2. Electron impact mass spectra of (A) 10-hydroxyoctadec-*cis*-11-enoic and (B) NaBD<sub>4</sub>-reduced 10-oxooctadec-*trans*-11-enoic acids (silylated).

of *cis* and *trans* isomers was based on comparison of their retention times with those of standard compounds. 10-Hydroxyoctadec-*trans*-11-enoic acid only appears if the samples are reduced with NaBH<sub>4</sub> before the alkaline hydrolysis (Fig. 1C), whereas the amount of 10-hydroxyoctadec-*cis*-11-enoic acids

increases slightly (25%) after this treatment (Figs. 1B,1C). Some attempts at reduction with NaBD<sub>4</sub> instead of NaBH<sub>4</sub> have been carried out in order to determine whether the additional production of hydroxyacids results from the reduction of the corresponding hydroperoxy- or oxoacids (Fig. 3). The

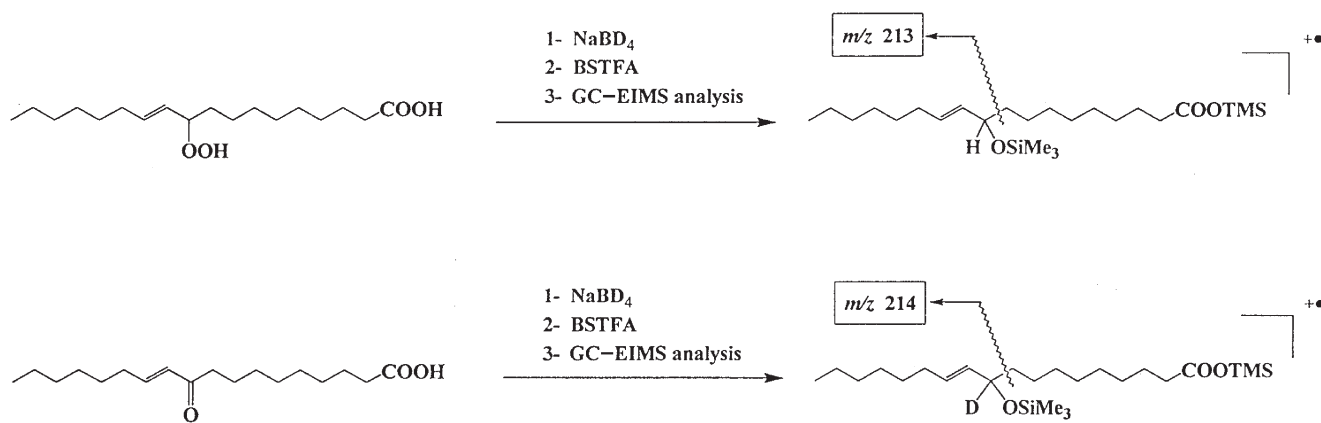


FIG. 3. Mass spectrometric characterization of hydroperoxy- and oxoacids after NaBD<sub>4</sub> reduction. BSTFA, bis(trimethylsilyl) trifluoroacetamide; TMS, trimethylsilyl.

results obtained with this deuterium labeling demonstrate that this additional production results from the reduction of the corresponding oxoacids (Fig. 2B). These oxoacids could not be directly characterized in nonreduced samples since they do not survive alkaline hydrolysis and are cleaved after hydration and retro-aldol reactions (21). Surprisingly, the original extracts of senescent cells of *T. halophila* contained 10-oxooctadec-*trans*-11-enoic, 10-oxooctadec-*cis*-11-enoic, and 10-hydroxy-octadec-*cis*-11-enoic acids.

Peak 10 (Fig. 1B) has been attributed to 10-oxooctadecanoic acid. The EI mass spectrum of this silylated compound (Fig. 4A) shows odd-electron fragment ions arising

from McLafferty rearrangement ( $m/z$  272, 156, and 58) and a prominent ion corresponding to  $\beta$ -cleavage relative to the keto group ( $m/z$  215) (28). This compound (which is not affected by alkaline hydrolysis) is quantitatively reduced to the corresponding hydroxyacid (peak 12; Fig. 1C) after  $\text{NaBD}_4$  treatment (Fig. 4B). It is interesting to note that peak 12 was lacking in the nonreduced extract (Fig. 1B).

Two peaks corresponding to diastereoisomeric 10,11-dihydroxyoctadecanoic acids appeared after  $\text{NaBH}_4$  reduction of the samples (peaks 13; Fig. 1C). The mass spectra of these compounds obtained after reduction with  $\text{NaBD}_4$  instead of  $\text{NaBH}_4$  provided a basis for demonstrating that they arise

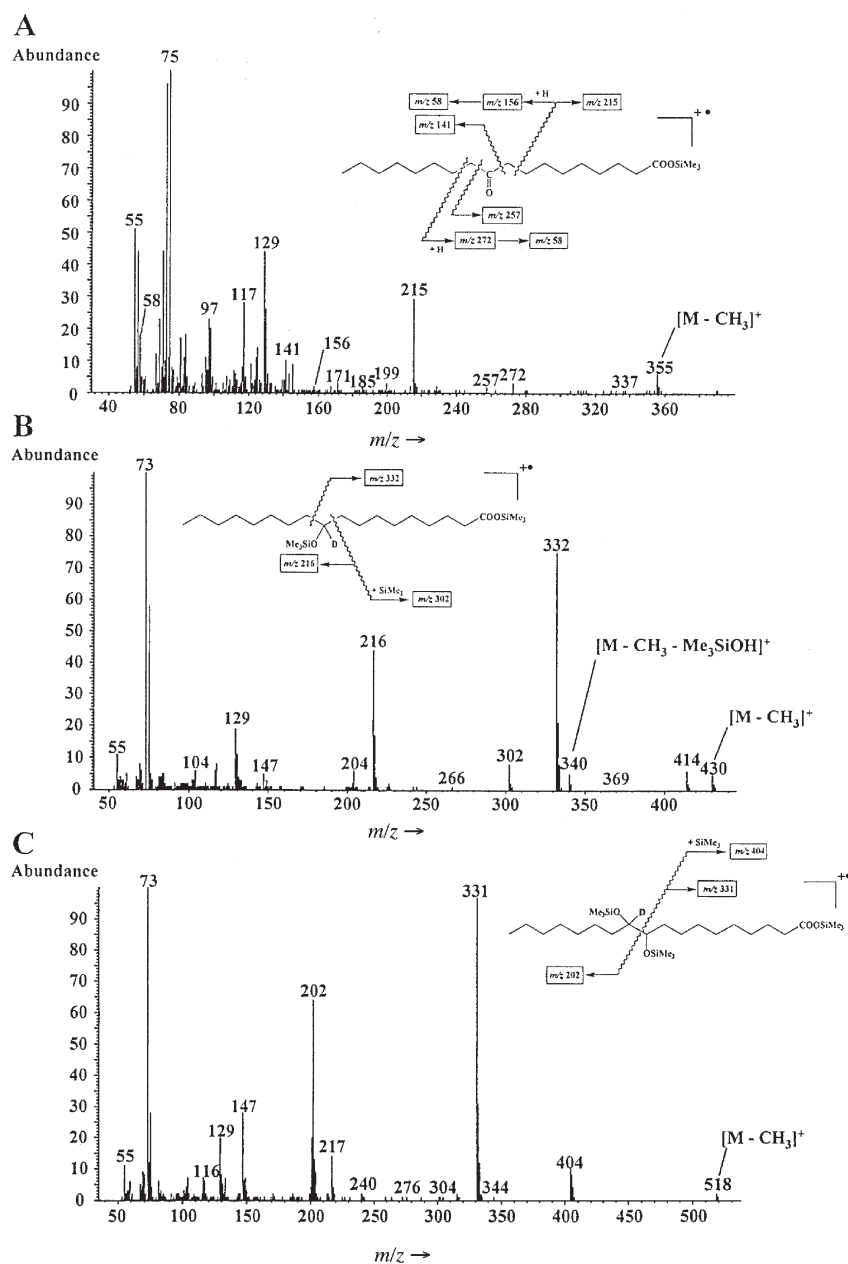


FIG. 4. Electron impact mass spectra of (A) 10-oxooctadecanoic, (B)  $\text{NaBD}_4$ -reduced 10-oxooctadecanoic, and (C)  $\text{NaBD}_4$ -reduced 10-hydroxy-11-oxooctadecanoic acids (silylated).



from the reduction of 10-hydroxy-11-oxooctadecanoic acid (Fig. 4C), which does not survive alkaline hydrolysis. It was previously demonstrated that an enzyme named hydroperoxide dehydrase catalyzes the conversion of 13- or 9-hydroperoxide of linoleic or linolenic acids to allene oxides (29), whose spontaneous nonenzymatic hydrolysis afforded  $\alpha$ -ketols (30). Although hydroperoxide dehydrase generally acts on hydroperoxides having a pair of conjugated double bonds (30), the specific formation of 10-hydroxy-11-oxooctadecanoic acid observed in the cells of *T. halophila* can be attributed to the dehydration of 10-hydroperoxyoctadec-11-enoic acid by a similar enzyme, followed by the nonenzymatic hydrolysis of the allene oxide thus formed (Fig. 5). This further suggests that the different oxidation products detected result from an initial peroxidation at C10 of *cis*-vaccenic acid.

Autoxidation of this acid yields mainly a mixture of *trans* 10-, *cis* 10-, *trans* 11-, *trans* 12-, *trans* 13- and *cis* 13-hydroperoxides, with minor amounts of *cis* 11- and *cis* 12-hydroperoxides (21), while its photosensitized oxidation produces a mixture of *trans* 11- and *trans* 12-hydroperoxides (31). Consequently, the specific oxidation at C10 of *cis*-vaccenic acid observed in senescent cells of *T. halophila* can be attributed to enzymatic peroxidation. It is generally considered that dioxygenases are not expressed in bacteria or yeast (32). However, Guerrero *et al.* (7) reported oxidation of oleic acid to 10-hydroperoxyoctadec-*trans*-8-enoic and 10-hydroxyoctadec-*trans*-8-enoic acids by *Pseudomonas* sp. 42A2. These authors also demonstrated that the conversion enzyme has dioxygenase activity. Our results suggest that such enzymes may also be present in some strains of purple sulfur bacteria.

A kinetic study of the production of *cis*-vaccenic acid oxidation products allowed us to show that this enzymatic process initially produces 10-hydroperoxyoctadec-*cis*-11-enoic acid, which in turn is converted to the different oxida-

tion products identified (Fig. 6). These compounds constitute 16% of the parent *cis*-vaccenic acid after incubation for 10 d. The dioxygenase catalyzing this peroxidation appeared to be highly regiospecific. Although the configuration of the carbon 10 of 10-hydroperoxyoctadec-*cis*-11-enoic acid has not been determined, one would expect that this enzyme introduces oxygen stereospecifically, forming only one of the possible optical isomers. Indeed, the formation of racemic products by dioxygenases is always accompanied by the occurrence of positional isomers (5), and such isomers are lacking in the different extracts analyzed. We could not find evidence of high amounts of intact hydroperoxides in the cells of *T. halophila*; this is not surprising since these compounds are not generally found in healthy plant cells. They are extremely cytotoxic and cause damage to membranes and proteins in particular (33). Several enzymatic processes causing further reactions of the hydroperoxides and inhibiting their accumulation have been previously described. These processes involve: (i) reduction to the corresponding hydroxyacids (33), (ii) homolytic cleavage of the O–O bond resulting in the formation of oxoacids (1), (iii) dehydration to allene oxides and subsequent hydrolysis of these unstable intermediates (29), and (iv) direct cleavage of the hydroperoxides to aldehydes and oxoacids (34).

The reduction of hydroperoxides of linoleic or linolenic acids to the corresponding hydroxyacids has been attributed to dioxygenase itself (33). The production of 10-hydroxyoctadec-*cis*-11-enoic acid in *T. halophila* cells may result from the reduction of the corresponding hydroperoxyacid by a similar enzyme (Fig. 5). The breakdown of hydroperoxy-polyenoic FA *via* the lipohydroperoxidase reaction affords oxopolyenoic FA (1). It is interesting to note that Clapp *et al.* (9) reported the soybean lipoxygenase-mediated oxygenation of monounsaturated FA to allylic oxoacids. These authors assume that the formation of such products may involve a typical

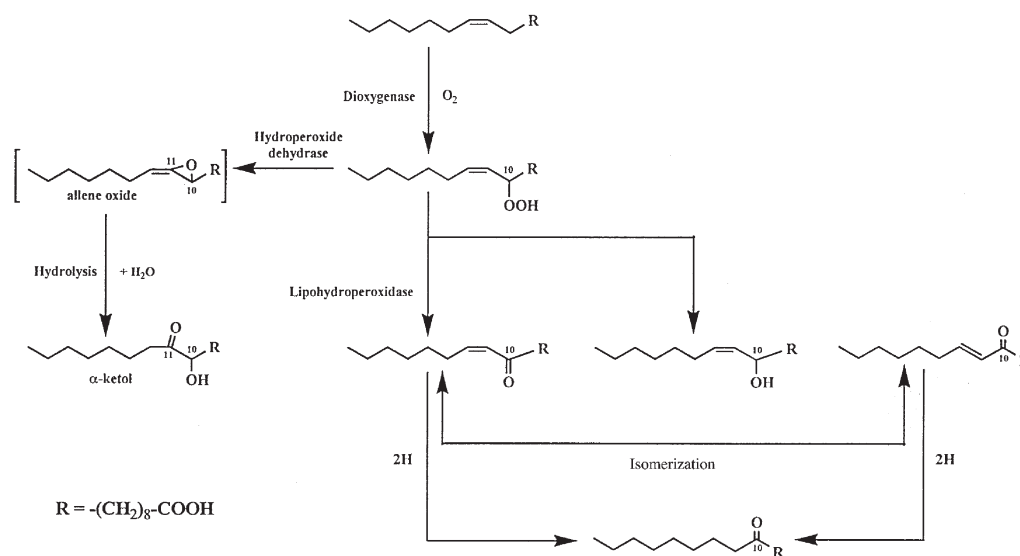
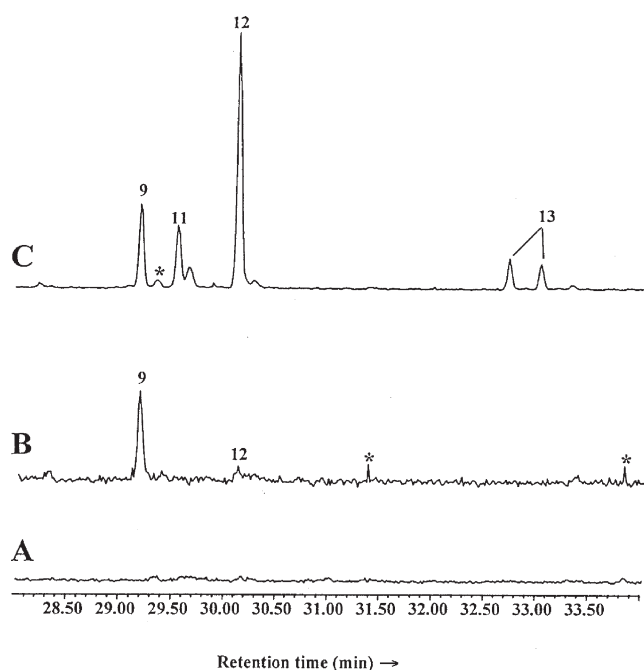


FIG. 5. Proposed pathways for the enzymatic oxygenation of *cis*-vaccenic acid in senescent cells of *T. halophila* incubated under aerobic conditions. For name see Figure 1.



**FIG. 6.** Partial total ion chromatograms obtained after injection of  $\text{NaBH}_4$ -reduced saponified lipids of (A) healthy cells of *T. halophila* incubated under oxic conditions for 10 d, (B) senescent cells of *T. halophila* incubated under oxic conditions for 2 d, and (C) senescent cells of *T. halophila* incubated under oxic conditions for 10 d (\* represents contaminants). The numbers refer to structures given in Figure 1. For name see Figure 1.

dioxygenation reaction to form an allylic hydroperoxide and its subsequent conversion to a ketone by loss of water. A similar conversion of 10-hydroperoxyoctadec-*cis*-11-enoic acids to the corresponding oxoacid seems to intervene in *T. halophila* cells (Fig. 5). As stated above, a small part of the 10-hydroperoxyoctadec-*cis*-11-enoic acid undergoes dehydration to allene oxide and spontaneous hydrolysis to 10-hydroxy-11-oxooctadecanoic acid. Hydroperoxide lyase catalyzes the cleavage of FA hydroperoxides into aldehydes and oxoacid fragments (35). Such an enzyme does not intervene in cells of *T. halophila*, since we failed to detect significant amounts of octanal and  $\text{C}_{10}$  oxoacid corresponding to the fragmentation of 10-hydroperoxyoctadec-*cis*-11-enoic acid.

As well as enzymatic conversion, the hydroperoxides formed may also undergo chemical decomposition under mild conditions. The majority of these decomposition reactions involve free radicals and are promoted by heat, photolysis, metal ions, and metalloproteins. The products of these reactions are similar to those of enzymatic transformations or are either homologs or isomers of the enzymatically produced compounds (33). The involvement of such abiotic processes during the degradation of 10-hydroperoxyoctadec-*cis*-11-enoic acid cannot be totally excluded.

The 10-oxooctadec-*cis*-11-enoic acid formed undergoes subsequent saturation to 10-oxooctadecanoic acid (Fig. 5). The saturation of unsaturated FA in the gut of some animals has long been recognized (36). This biohydrogenation is brought about by the mixed culture of rumen bacteria and

involves several enzyme-catalyzed steps. In the present case, the formation of 10-oxooctadecanoic acid can be attributed to the involvement of similar enzymatic processes. It was previously demonstrated that anaerobic incubation of oleic and elaidic acids with strained rumen contents lead to the formation of their saturated counterpart (stearic acid) and to a lesser extent to the isomerization of each monounsaturated FA to its geometric isomer (37). Consequently, the formation of 10-oxooctadec-*trans*-11-enoic acid may be attributed to the isomerization of its geometrical isomer during the biohydrogenation (Fig. 5).

The enzymatic oxygenation of PUFA is very specific with respect to the double bond position in the FA that is oxygenated (32,38). Although palmitoleic and *cis*-vaccenic acids both possess a *cis*-double bond located in position n-7, we detected only trace amounts of compounds resulting from the oxidation of the carbon 8 of palmitoleic acid after aerobic incubation of senescent cells of *T. halophila*. The enzyme catalyzing the oxygenation of monounsaturated FA seems to have a strong affinity toward the *cis*-vaccenic acid. This process, which is induced during senescence, acts during dark and illuminated aerobic incubation of cells of *T. halophila*.

It is interesting to note that we failed to detect the different compounds deriving from the enzymatic oxygenation of the allylic carbon 10 of *cis*-vaccenic acid in senescent cells of *Halochromatium glycolicum* DSM 11080 and *Halochromatium salexigens* DSM 4395, which constitute the halophilic *Chromatiaceae* most closely related phylogenetically to *T. halophila* (39). These compounds could thus constitute potential *T. halophila* biomarkers. Some of these markers could notably facilitate determining the presence of this purple sulfur bacterium in modern and perhaps also in ancient ecosystems.

## ACKNOWLEDGMENTS

Thanks are due to Drs. Pierre Caumette and Robert Matheron for their generous gift of the strains *H. glycolicum* DSM 11080, *H. salexigens* DSM 4395, and *T. halophila* DSM 6210. We also thank Michael Paul for his careful reading of the English. This work was supported by grants from the MATBIOPOL European Project (contract EVK3-CT-1999-00010).

## REFERENCES

- Schewe, T., Rapoport, S.M., and Kühn, H. (1986) Enzymology and Physiology of Reticulocyte Lipoxygenase: Comparison with Other Lipoxygenases, *Adv. Enzymol. Relat. Areas Mol. Biol.* 58, 191–272.
- Zimmerman, D.C., and Vick, B.A. (1973) Lipoxygenase in *Chlorella pyrenoidosa*, *Lipids* 8, 264–266.
- Beneytout, J.L., Andrianarison, R.H., Rakotoarisoa, Z., and Tixier, M. (1989) Properties of a Lipoxygenase in Blue-Green Algae (*Oscillatoria* sp.), *Plant Physiol.* 91, 367–372.
- Matsui, K., Narahara, H., Kajiwara, T., and Hatanaka, A. (1991) Purification and Properties of Lipoxygenase in *Marchantia polymorpha* Cultured Cells, *Phytochemistry* 30, 1499–1502.
- Kühn, H., Schewe, T., and Rapoport, S.M. (1986) The Stereochemistry of the Reactions of Lipoxygenases and Their Metabolites. Proposed Nomenclature of Lipoxygenases and Related Enzymes, *Adv. Enzymol.* 58, 273–311.

6. Wang, T., Yu, W.G., and Powell, W.S. (1992) Formation of Monohydroxy Derivatives of Arachidonic Acid, Linoleic Acid, and Oleic Acid During Oxidation of Low Density Lipoprotein by Copper Ions and Endothelial Cells, *J. Lipid Res.* **33**, 525–537.
7. Guerrero, A., Casals, I., Busquets, M., Leon, Y., and Manresa, A. (1997) Oxidation of Oleic Acid to (*E*)-10-Hydroperoxy-8-octadecenoic and (*E*)-10-Hydroxy-8-octadecenoic Acids by *Pseudomonas* sp. 42A2, *Biochim. Biophys. Acta* **1347**, 75–81.
8. Oliw, E.H., Su, C., Skogström, T., and Benthin, G. (1998) Analysis of Novel Hydroperoxides and Other Metabolites of Oleic, Linoleic, and Linolenic Acids by Liquid Chromatography–Mass Spectrometry with Ion Trap MS<sup>n</sup>, *Lipids* **33**, 843–852.
9. Clapp, C.H., Senchak, S.E., Stover, T.J., Potter, T.C., Findeis, P.M., and Novak, M.J. (2001) Soybean Lipoxygenase-Mediated Oxygenation of Monounsaturated Fatty Acids to Enones, *J. Am. Chem. Soc.* **123**, 747–748.
10. Thompson, J.E., Froese, C.D., Madey, E., Smith, M.D., and Hong, Y. (1998) Lipid Metabolism During Plant Senescence, *Prog. Lipid Res.* **37**, 119–141.
11. Prakash, T.R., Swamy, P.M., Suguna, P., and Reddanna, P. (1990) Characterization and Behaviour of 15-Lipoxygenase During Peanut Cotyledonary Senescence, *Biochem. Biophys. Res. Commun.* **172**, 462–470.
12. Berger, S., Weichert, H., Porzel, A., Wasternack, C., Kühn, H., and Feussner, I. (2001) Enzymatic and Non-enzymatic Lipid Peroxidation in Leaf Development, *Biochim. Biophys. Acta* **1533**, 266–276.
13. Caumette, P., Baulaigue, R., and Matheron, R. (1991) *Thiocapsa halophila* sp. nov., a New Halophilic Phototrophic Purple Sulfur Bacterium, *Arch. Microbiol.* **155**, 170–176.
14. Imhoff, J.F., Süling, J., and Petri, R. (1998) Phylogenetic Relationships Among the *Chromatiaceae*, Their Taxonomic Reclassification and Description of the New Genera *Allochromatium*, *Halochromatium*, *Isochromatium*, *Marichromatium*, *Thiococcus*, *Thiohalocapsa* and *Thermochromatium*, *Int. J. Syst. Bacteriol.* **48**, 1129–1143.
15. Pfennig, N., and Trüper, H.G. (1992) The Family *Chromatiaceae*, in *The Prokaryotes* (Balows, A., Trüper, H.G., Dworkin, M., Harder, W., and Schleifer, K.H., eds.), pp. 3200–3221, Springer, New York.
16. Caumette, P., Baulaigue, R., and Matheron, R. (1988) Characterization of *Chromatium salexigens* sp. nov., a Halophilic *Chromatiaceae* Isolated from Mediterranean Salinas, *System Appl. Microbiol.* **10**, 284–292.
17. Imhoff, J.F., and Trüper, M. (1992) The Genus *Rhodospirillum* and Related Genera, in *The Prokaryotes* (Balows, A., Trüper, H.G., Dworkin, M., Harder, W., and Schleifer, K.H., eds.), pp. 2141–2155, Springer, New York.
18. Teng, J.I., Kulig, M.J., Smith, L.L., Kan, G., and van Lier, J.E. (1973) Sterol Metabolism XX. Cholesterol 7 $\beta$ -Hydroperoxide, *J. Org. Chem.* **38**, 119–123.
19. Vincenti, M., Guglielmetti, G., Cassani, G., and Tonini, C. (1987) Determination of Double Bond Position in Diunsaturated Compounds by Mass Spectrometry of Dimethyl Disulfide Derivatives, *Anal. Chem.* **59**, 694–699.
20. Loidl-Stahlhofen, A., and Spiteller, G. (1994)  $\alpha$ -Hydroxyaldehydes, Products of Lipid Peroxidation, *Biochim. Biophys. Acta* **1211**, 156–160.
21. Marchand, D., and Rontani, J.-F. (2001) Characterisation of Photooxidation and Autoxidation Products of Phytoplanktonic Monounsaturated Fatty Acids in Marine Particulate Matter and Recent Sediments, *Org. Geochem.* **32**, 287–304.
22. Mihara, S., and Tateba, H. (1986) Photosensitized Oxygenation Reactions of Phytol and Its Derivatives, *J. Org. Chem.* **51**, 1142–1144.
23. Frankel, E.N., Neff, W.E., and Bessler, T.R. (1979) Analysis of Autoxidized Fats by Gas Chromatography–Mass Spectrometry: V. Photosensitized Oxidation, *Lipids* **14**, 961–967.
24. MacCloskey, J.A., and MacClelland, M.J. (1965) Mass Spectra of *O*-Isopropylidene Derivatives of Unsaturated Fatty Esters, *J. Am. Chem. Soc.* **87**, 5090–5093.
25. Kämpf, C., and Pfennig, N. (1980) Capacity of *Chromatiaceae* for Chemotrophic Growth. Specific Respiration Rates of *Thiocystis violacea* and *Chromatium vinosum*, *Arch. Microbiol.* **127**, 125–135.
26. De Wit, R., and Van Gemerden, H. (1990) Growth of the Phototrophic Purple Sulfur Bacterium *Thiocapsa roseopersicina* Under Oxic/Anoxic Regimens in the Light, *FEMS Microbiol. Ecol.* **73**, 69–76.
27. Harwood, J.L., and Russell, N.L. (1984) *Lipids in Plants and Microbes*, 162 pp., Georges Allen and Unwin, London.
28. MacCloskey, J.A. (1969) Mass Spectrometry of Lipids and Steroids, *Methods Enzymol.* **14**, 382–450.
29. Hamberg, M. (1987) Mechanism of Corn Hydroperoxide Isomerase: Detection of 12,13(*S*)-Oxido-9(*Z*),11-octadecadienoic Acid, *Biochim. Biophys. Acta* **920**, 76–84.
30. Hamberg, M., and Fahlstadius, P. (1990) Allene Oxide Cyclase: A New Enzyme in Plant Lipid Metabolism, *Arch. Biochem. Biophys.* **276**, 518–526.
31. Rontani, J.-F. (1998) Photodegradation of Unsaturated Fatty Acids in Senescent Cells of Phytoplankton: Photoproduct Structural Identification and Mechanistic Aspects, *J. Photochem. Photobiol.* **114A**, 37–44.
32. Kühn, H., and Thiele, B.J. (1999) The Diversity of the Lipoxygenase Family. Many Sequence Data but Little Information on Biological Significance, *FEBS Lett.* **449**, 7–11.
33. Galliard, T., and Chan, H.W.-S. (1980) Lipoxygenases, in *The Biochemistry of Plants: A Comprehensive Treatise* (Stumpf, P.K., and Conn, E.E., eds.), Vol. 4, pp. 131–161, Academic Press, New York.
34. Galliard, T., Matthew, J.A., Fishwick, M.J., and Wright, A.J. (1976) The Enzymatic Degradation of Lipids Resulting from Physical Disruption of Cucumber (*Cucumis sativus*) Fruit, *Phytochemistry* **15**, 1647–1650.
35. Vick, B.A. (1993) Oxygenated Fatty Acids of the Lipoxygenase Pathway, in *Lipid Metabolism in Plants* (Moore, T.S., ed.), pp. 168–191, CRC Press, Boca Raton.
36. Hammond, R.C. (1988) Enzymatic Modification at the Mid-chain of Fatty Acids, *Fat Sci. Technol.* **1**, 18–27.
37. Morris, L.J. (1970) Mechanism and Stereochemistry in Fatty Acid Metabolism, *Biochem. J.* **118**, 681–693.
38. Hamberg, M., and Samuelsson, B. (1967) On the Specificity of the Oxygenation of Unsaturated Fatty Acids Catalyzed by Soybean Lipoxidase, *J. Biol. Chem.* **242**, 5329–5335.
39. Imhoff, J.F. (2001) True Marine and Halophilic Anoxygenic Phototrophic Bacteria, *Arch. Microbiol.* **176**, 243–254.

[Received January 28, 2002, and in revised form April 4, 2002; revision accepted April 25, 2002]

# Dietary Fish Oil and Vitamin E Enhance Doxorubicin Effects in P388 Tumor-Bearing Mice

Qi-Yuan Liu and Benny K.H. Tan\*

Department of Pharmacology, Faculty of Medicine, National University of Singapore, Singapore 117597, Republic of Singapore

**ABSTRACT:** In this study, four kinds of rodent diets, CO, FO, CVe, and FVe, were used by addition of canola oil, oil mixture (fish oil + canola oil), canola oil plus vitamin E, and oil mixture plus vitamin E, respectively, to a basic diet, AIN-93G, to investigate the influence of dietary fish oil and vitamin E on doxorubicin (DOX) treatment in P388 ascitic mice. Animal life span (LS) and heart damage were recorded in mice fed the four different diets and treated with different doses of DOX. The optimal doses of DOX for antitumor effect as manifested by increased LS were 6.0 and 9.0 mg/kg. Both fish oil and vitamin E significantly enhanced this effect. On the other hand, DOX at 12.0 mg/kg induced severe heart damage, which was also significantly aggravated by both fish oil and vitamin E, as shown by both decreased LS and increased serum creatine phosphokinase activity. Fish oil and vitamin E appeared to enhance the antitumor effect of optimal doses of DOX but to aggravate cardiotoxicity owing to DOX overdose.

Paper no. L8891 in *Lipids* 37, 549–556 (June 2002).

The effects of PUFA on tumor development and tumor growth have been intensively investigated in both animal models and humans in the past two decades. Although rigid scientific proof has yet to be obtained, it is generally believed that n-6 PUFA in terrestrial plant oils enhance tumor growth, but n-3 PUFA in fish oil have a protective effect (1). Furthermore, two long-chain n-3 PUFA that are found in significant amounts in fish oil, *viz.*, EPA (20:5n-3) and DHA (22:6n-3), may exert multiple activities to retard the growth of tumor cells and xenografts (2,3). On the other hand, it is known that certain physical and functional properties of cell membranes can be modified when PUFA content is changed, and lipid nutrition directed at producing this modification has been suggested in cancer therapy (4). By altering the properties of membrane lipids, FA-based diets may provide a new approach for enhancing the effectiveness of certain antineoplastic therapies.

Vitamin E (vit E) includes eight naturally occurring compounds of two classes, tocopherols and tocotrienols, with different biological activities. Tocopherols are the most important chain-breaking antioxidants within cellular membranes, mainly owing to their ability to donate phenolic hydrogens to lipid free radicals (5). They are present in oily seeds, leaves, and other

\*To whom correspondence should be addressed at Dept. of Pharmacology, Faculty of Medicine, National University of Singapore, MD2, 18 Medical Dr., Singapore 117597, Republic of Singapore.  
E-mail: phctankh@nus.edu.sg

Abbreviations: CPK, creatine phosphokinase; DOX, doxorubicin; HNE, 4-hydroxynonenal; LS, life span; MDA, malondialdehyde, vit E, vitamin E.

green parts of higher plants. It is generally agreed that the relative antioxidant activity of the tocopherols *in vivo* is in the order of  $\alpha > \beta > \gamma > \delta$  (6). In addition to their antioxidant property, tocopherols and their derivatives have been reported to have pro-oxidant properties in some biological systems (7,8).

Doxorubicin (DOX) has been widely used in the treatment of a variety of solid tumors and hematological malignancies. Several of its biological effects are supposedly derived from its quinone moiety acting as an alkylating/aryllating electrophile or a pro-oxidant. The quinone structure permits DOX to act as an electron acceptor in reactions mediated by oxoreductases, such as cytochrome P450 reductase (9), NADH dehydrogenase (10), and xanthine oxidase (11), to convert the quinone to a semiquinone free radical. Under anaerobic conditions, the semiquinone undergoes further reduction accompanied by reductive cleavage of the sugar residue to generate a quinone methide, which binds covalently to nucleophiles and is known to form adducts with DNA (12). In the presence of O<sub>2</sub>, however, this semiquinone radical is spontaneously and rapidly reoxidized in a process that generates a superoxide radical (13). The superoxide radical and its dismutation product, hydrogen peroxide, undergo Haber–Weiss and Fenton reactions, respectively, to form the hydroxyl radical, which is able to extract a doubly allylic hydrogen atom from PUFA and thus initiate lipid peroxidation (14). The nonenzymatic formation of reactive oxygen species is mediated by the formation of complexes between DOX and iron, which can either react with O<sub>2</sub> to yield superoxide radical and hydrogen peroxide or bind O<sub>2</sub> in a superoxo- or peroxo-like form (15). Despite its antitumor effect, clinical effectiveness of DOX is hindered by its unique dose-limiting cardiotoxicity (16), possibly because of the sensitivity of the heart to reactive free radicals, due to a low activity of antioxidant enzymes (17). Separate studies, however, have found both effectiveness (18,19) and ineffectiveness (20) of vit E in cardioprotection in DOX-treated animals.

In this study, we prepared four experimental diets by adding natural oils to the basic components of AIN-93G, a purified diet for laboratory rodent growth (21). These diets differed in their contents of n-3 PUFA and tocopherols. We tested their effects on the therapeutic efficacy of various doses of DOX in mice induced with P388 ascitic tumor [which is the standard transplantable murine tumor most sensitive to DOX (18)], recording life span (LS) of the tumor-bearing mice, and examining animal heart damage by measurement of serum creatine phosphokinase (CPK) level (a biochemical marker of animal myocardial damage).



## EXPERIMENTAL PROCEDURES

**Cell lines and chemicals.** The P388 cell line was obtained from ATCC (American Type Culture Collection, Manassas, VA), and the cells were grown in DBA/2 mice for one generation before use in the following animal experiments. All chemicals were purchased from Sigma-Aldrich (St. Louis, MO) unless otherwise stated.

**Diets.** Four experimental diets with AIN-93G as a base food were prepared by Specialty Feed Service (Glen Forest, Australia) as follows: (i) CO: AIN-93G + 10% canola oil; (ii) FO: AIN-93G + 8.5% fish oil + 1.5% canola oil; (iii) CVe: AIN-93G + 500 mg/kg natural vit E + 10% canola oil; (iv) FVe: AIN-93G + 500 mg/kg natural vit E + 8.5% fish oil + 1.5% canola oil.

Canola oil, a favorable dietary oil, is an appropriate control to use to study the effect of long-chain n-3 PUFA in fish oil because it contains a relatively high proportion of linoleic acid (18:2n-6) and  $\alpha$ -linolenic acid (18:3n-6), and a low proportion of EPA and DHA. Canola oil (1.5%) was added to fish oil (8.5%) in FO and FVe diets in order to increase linoleic acid content to above 1%, which is the requirement for optimal rodent growth. The FA composition of the four diets is shown in Table 1. Total n-6 PUFA content was similar in the four diets, whereas n-3 PUFA contents, particularly EPA and DHA, were greater in FO and FVe than in CO and CVe. On the other hand,

**TABLE 1**  
**FA Composition in Four Experimental Diets<sup>a</sup>**

FA (%)	CO	FO	CVe	FVe
Individual				
14:0	ND	4.3	ND	4.5
16:0	5.6	19.8	4.6	19.2
18:0	1.3	2.2	2.0	5.0
16:1	ND	5.1	ND	4.1
18:1	60.1	19.3	60.3	18.4
20:1	1.5	ND	1.5	ND
18:2n-6	20.3	16.6	20.1	13.5
18:3n-3	10.2	ND	10.5	ND
18:4n-3	0.6	1.3	0.6	1.7
20:4n-6	ND	1.9	ND	1.9
20:5n-3	0.5	8.7	0.5	9.1
22:6n-3	ND	20.9	ND	22.5
Total	100	100	100	100
Class <sup>b</sup>				
$\Sigma$ SFA	6.9	26.3	6.6	28.7
$\Sigma$ MUFA	61.6	24.4	61.8	22.5
$\Sigma$ PUFA	31.6	49.4	31.7	48.7
$\Sigma$ n-3 PUFA	11.3	30.9	11.6	33.3
$\Sigma$ n-6 PUFA	20.3	19.8	20.7	17.1
$\Sigma$ n-3 PUFA/ $\Sigma$ n-6 PUFA	0.56	1.56	0.56	1.95
Average double bond <sup>c</sup>	1.4	2.4	1.4	2.4

<sup>a</sup>Diet CO, AIN-93G + 10% canola oil; FO, AIN-93G + 8.5% fish oil + 1.5% canola oil; CVe, AIN-93G + 500 mg/kg natural vitamin E + 10% canola oil; FVe, AIN-93G + 500 mg/kg natural vitamin E + 8.5% fish oil + 1.5% canola oil; ND, not detected.

<sup>b</sup>SFA, saturated FA; MUFA, monounsaturated FA.

<sup>c</sup>"Average double bond" means average number of double bonds per molecule of FA.

AIN-93G basic diet contains 75 mg/kg *d*- $\alpha$ -tocopherol acetate (21). The natural vit E used in our experiments is a mixed tocopherol concentrate, Covi-ox<sup>®</sup> T-70 (Cognis Nutrition & Health, Broadmeadows, Victoria, Australia), with relative amounts of  $\alpha$ - (14%),  $\beta$ - (1%),  $\gamma$ - (62%), and  $\delta$ -tocopherols (23%). Five hundred milligrams of Covi-ox<sup>®</sup> T-70 contains 350 mg of total tocopherols. According to the manufacturer (Specialty Feed Service, Glen Forest, Australia), canola oil contained 330, 16, 846 and 56 mg/kg of  $\alpha$ -,  $\beta$ -,  $\gamma$ -, and  $\delta$ -tocopherols, respectively, whereas fish oil contained 340 mg/kg of  $\alpha$ -tocopherol only. The calculated contents of individual vit E species in four diets are shown in Table 2, indicating that CVe and FVe contained a significantly higher content of all tocopherol species compared to CO and FO, respectively.

Comparisons between CO and FO and between CVe and FVe were made to evaluate the effect of fish oil, whereas comparisons between CO and CVe and between FO and FVe were made to examine the effect of vit E on tumor-bearing or normal mice with or without DOX treatment.

**Measurements of LS.** All experiments with animals were conducted according to guidelines in "International Guiding Principles for Animal Research," *WHO Chronicles*, Vol. 39, 1985. Male BDF1 mice purchased from Animal Resources Center (Canning Vale, Western Australia) were used at 6–8 wk of age when their body weights ranged between 19.0 and 21.0 g. The animals were kept in filter-covered plastic cages, housed in a temperature-controlled room with a diurnal 12 h light cycle, and provided with tap water and the assigned experimental diets *ad libitum* for 10 d prior to experimentation and continuously thereafter. This period of time was found to be sufficient to modify the PUFA composition of phospholipids in most organs to stable levels in mice (22). The animals were inoculated intraperitoneally on day 0 with P388 cells ( $10^6$  cells/mouse), followed by injection of DOX or saline also intraperitoneally on days 1 and 6. Deaths among the experimental animals were recorded at least twice a day.

**Determination of DOX cardiotoxicity.** In the second experiment, the BDF1 mice were maintained, fed, and administered DOX or saline as described above without the inoculation of tumor cells. The animals were killed on day 7 by cervical dislocation, blood was collected by cardiac puncture, and serum was obtained after the clotting of blood at room temperature for 1 h. Serum was kept frozen ( $-76^{\circ}\text{C}$ ) until analysis. Cardiotoxicity was determined by measuring serum CPK activity, calculated according to the Sigma Diagnostics Procedure No. 47-UV. A

**TABLE 2**  
**Vitamin E Content (mg/kg) in Four Experimental Diets<sup>a</sup>**

Species of vitamin E	CO	FO	CVe	FVe
$\alpha$ -Tocopherol acetate	75	75	75	75
$\alpha$ -Tocopherol	33	33.9	82	82.9
$\beta$ -Tocopherol	1.6	0.2	5.1	3.7
$\gamma$ -Tocopherol	84.6	12.7	301.6	229.7
$\delta$ -Tocopherol	5.6	0.8	86.1	81.3
Total	200	122.2	549.8	472.6

<sup>a</sup>For description of diets see Table 1.

CPK Test kit (CK-20; Sigma Chemical Co.) based on the method described by Szasz *et al.* (23) was used in the study.

*Lipid analysis of P388 ascitic tumor cells and cardiac tissue.* In the third experiment, BDF1 mice were fed experimental diets 10 d prior to the experimentation and thereafter. P388 cells ( $10^7$  cells/mouse) were intraperitoneally inoculated into animals on day 0. On day 7, the mice were killed by cervical dislocation. The hearts were collected and ascitic tumor cells obtained by lavage of the peritoneum with ice-cold saline. The tumor cells were pelleted at  $700 \times g$  for 5 min and washed twice with the same buffer solution. Total lipid was extracted using a method described by Folch *et al.* (24). The phospholipid fraction was separated by silicic acid chromatography (25), saponified in alkali (26), and methylated with  $\text{BF}_3/\text{methanol}$  (27). The fractions of FAME with different chain lengths and unsaturations were separated in a Hewlett-Packard 5890 gas chromatograph using a DB-225 column (J&W Scientific, Folsom, CA). Peaks were identified by comparison with the retention times of known standards and peak areas quantified.

*Statistical analysis.* Data were analyzed by Student's *t*-test or ANOVA as shown in the text and the legends for the tables and figures. Experimental data are shown as mean  $\pm$  SD.  $P < 0.05$  was set as the level of significance throughout the study.

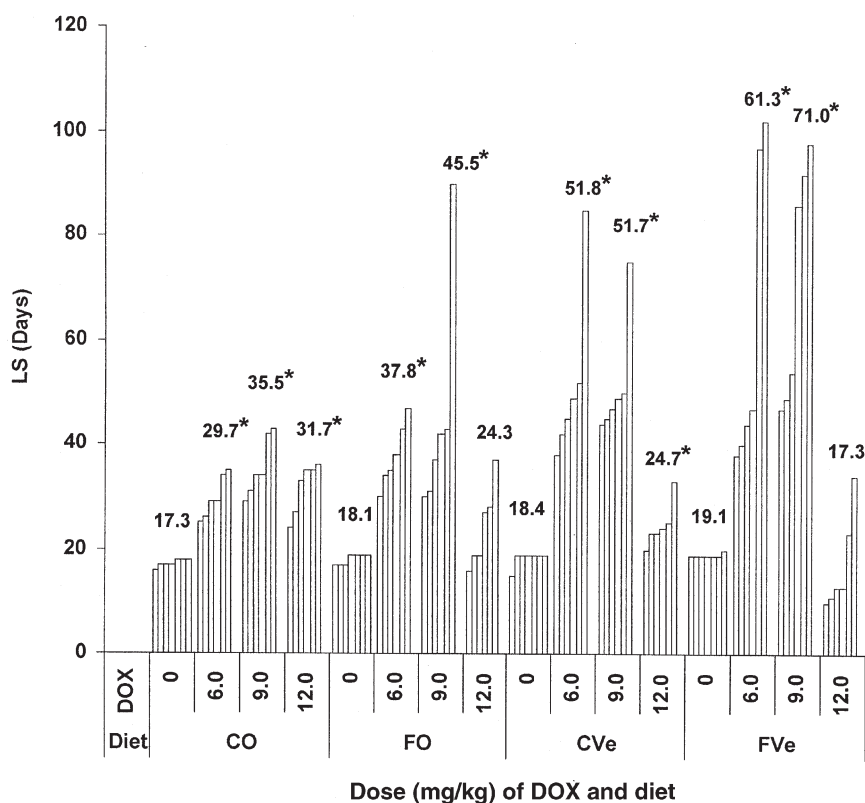
**TABLE 3**  
ANOVA on Life Span (LS) of P388 Ascitic Mice<sup>a</sup>

Two-way ANOVA		
Source	P0 (n = 28)	P12 (n = 24)
Fish oil	0.052	0.018
Vit E	0.010	0.023
Fish oil $\times$ vit E	0.854	1.000
Multiway ANOVA		
Source	P6,9 (n = 48)	
DOX	0.262	
Fish oil	0.025	
Vit E	<0.001	
DOX $\times$ fish oil	0.567	
DOX $\times$ vit E	0.844	
Fish oil $\times$ vit E	0.601	

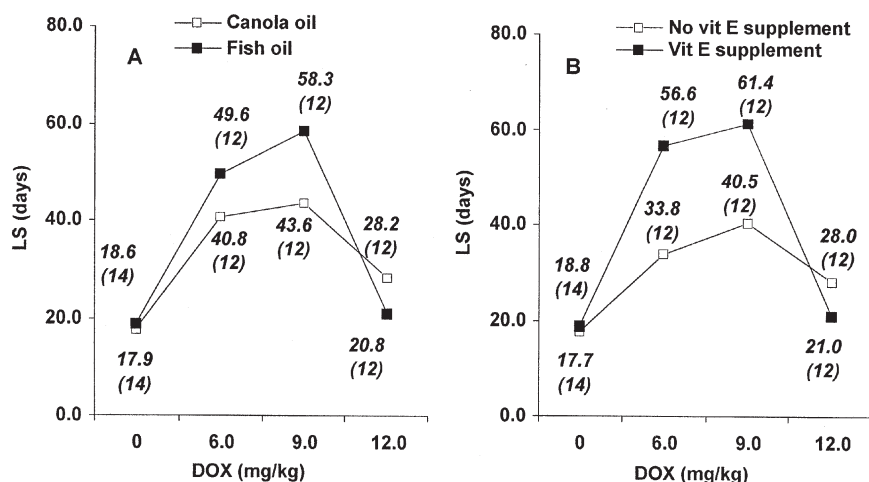
<sup>a</sup>Canola oil served as the control for fish oil. Column P0 considers data on the LS of animals without doxorubicin (DOX) treatment; P12, with 12.0 mg/kg DOX treatment; and P6,9, with 6.0 and 9.0 mg/kg DOX treatment; n, number of mice; vit E, vitamin E.

## RESULTS

*LS of P388 ascitic mice.* The individual LS of P388 ascitic mice fed the four experimental diets and administered vari-



**FIG. 1.** Effects of different doses of doxorubicin (DOX) and experimental diets on life span (LS) of P388 ascitic mice. Each column represents the LS of one animal, whereas the value above the cluster of columns represents the mean LS in each group. \* $P < 0.05$  represents the difference between the saline and DOX-treated groups on the same diet (Student's *t*-test). Diets: CO, AIN-93G + 10% canola oil; FO, AIN-93G + 8.5% fish oil + 1.5% canola oil; CVe, AIN-93G + 500 mg/kg natural vitamin E + 10% canola oil; FVe, AIN-93G + 500 mg/kg natural vitamin E + 8.5% fish oil + 1.5% canola oil.



**FIG. 2.** Effects of fish oil and vitamin E (vit E) on LS of P388 ascitic mice treated with various doses of DOX. The values outside and inside the parentheses at each point represent the mean LS and number of animals, respectively, in the group. (A) Effect of fish oil; (B) effect of vit E. Canola oil served as the control for fish oil. For abbreviations see Figure 1.

ous doses of DOX are shown in Figure 1. The results of statistical analyses of the data are shown in Figures 1 and 2 and Table 3. In the absence of DOX treatment, vit E supplement increased the mean LS from 17.7 to 18.8 d ( $P = 0.010$ , two-way ANOVA) (Fig. 2B, Table 3). Both 6.0 and 9.0 mg/kg DOX significantly increased animal LS in all diet groups ( $P < 0.05$ , Student's *t*-test) (Fig. 1), but there was no significant difference ( $P = 0.262$ , multiway ANOVA) in therapeutic efficacy between these two doses (Table 3). Both fish oil and vit E, however, were found to significantly enhance the effect of DOX at these doses ( $P = 0.025$  and  $<0.001$ , respectively, multiway ANOVA) (Table 3). Fish oil increased the mean LS from 40.8 to 49.6 d in mice treated with 6.0 mg/kg DOX and from 43.6 to 58.3 d in mice treated with 9.0 mg/kg DOX (Fig. 2A). Vit E increased the mean LS from 33.8 to 56.6 d in mice treated with 6.0 mg/kg DOX and from 40.5 to 61.4 d in mice treated with 9.0 mg/kg DOX (Fig. 2B). When DOX dose was increased to 12.0 from 9.0 mg/kg, animal LS was significantly decreased ( $P < 0.001$ , multiway ANOVA followed by Tukey's test for DOX only), suggesting the negative effect of DOX at this high dose. Both fish oil and vit E significantly aggravated this negative effect ( $P = 0.018$  and  $0.023$ , respectively, two-way ANOVA) (Table 3), with fish oil decreasing the mean LS from 28.2 to 20.8 d (Fig. 2A), and vit E decreasing the mean LS from 28.0 to 21.0 d (Fig. 2B).

**DOX-induced CPK activity.** The experimental data of plasma CPK levels in mice fed the four experimental diets and treated with various doses of DOX are shown in Table 4, part A. The results of statistical analysis on the data are shown in Table 4, part B, and Figure 3. DOX increased plasma CPK activity dose-dependently (Table 4). Two-way ANOVA (Table 4) showed that vit E inhibited plasma CPK activity in mice without DOX (decrease of 0.3 unit/mL serum;  $P < 0.001$ ) or with 6.0 mg/kg DOX (decrease of 0.3 unit/mL serum;  $P = 0.007$ ) but did not significantly modify CPK activity with 9.0 mg/kg DOX. In contrast, vit E enhanced CPK activity in the presence

of 12.0 mg/kg DOX (increase of 0.7 unit/mL serum;  $P = 0.002$ , two-way ANOVA). On the other hand, fish oil increased DOX-induced CPK activity to an extent proportional to DOX dose (increases of 0, 0.3, 0.6, and 1.5 unit/mL serum in 0, 6.0, 9.0, and 12.0 mg/kg DOX-treated mice with  $P = 0.935$ , 0.005,  $<0.001$ , and  $<0.001$ , respectively, two-way ANOVA) (Fig. 3).

**FA composition of ascitic tumors and animal hearts.** Lipid analysis of the FA composition in phospholipids indicated that n-6 PUFA content was comparable in both P388 ascitic tumor and mouse heart of all four groups, whereas n-3 PUFA as well as total PUFA content was significantly larger in both tissues of FO- and FVe-fed mice than those in CO- and CVe-fed mice

**TABLE 4**  
Effects of Fish Oil and Vit E on CPK Activity in Mice Treated with Various Doses of DOX<sup>a</sup>

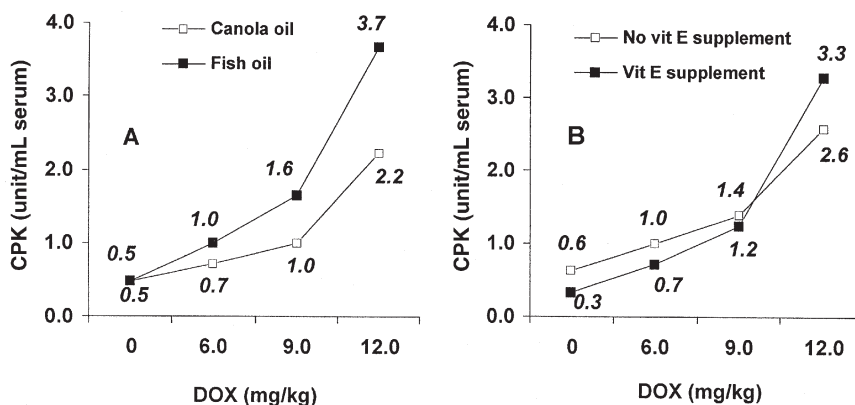
Diet	DOX (mg/kg)			
	0	6.0	9.0	12.0
CO	0.6 ± 0.1	0.8 ± 0.1	1.1 ± 0.2	1.9 ± 0.2
FO	0.7 ± 0.1	1.1 ± 0.3	1.7 ± 0.3	3.3 ± 0.1
CVe	0.4 ± 0.1	0.6 ± 0.2	0.9 ± 0.2	2.5 ± 0.3
FVe	0.3 ± 0.1	0.8 ± 0.2	1.6 ± 0.2	4.1 ± 0.7

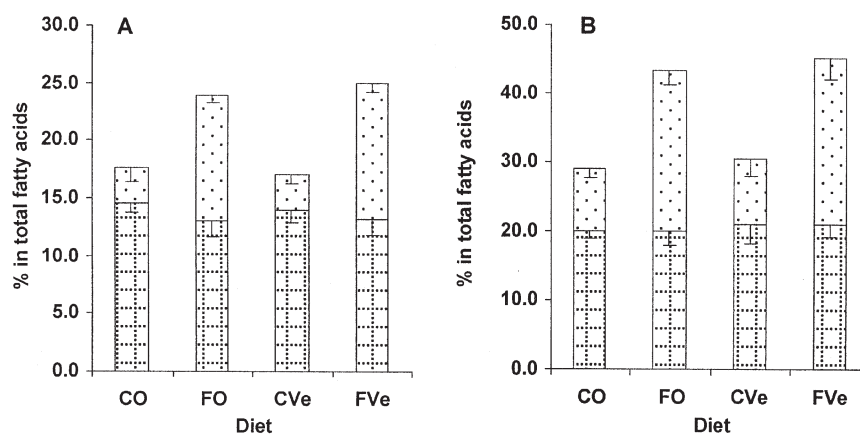
Source	<i>P</i> 0 ( <i>n</i> = 24)	<i>P</i> 6 ( <i>n</i> = 24)	<i>P</i> 9 ( <i>n</i> = 24)	<i>P</i> 12 ( <i>n</i> = 24)
Fish oil	0.935	0.005	<0.001	<0.001
Vit E	<0.001	0.007	0.095	0.002
Fish oil × vit E	0.142	0.456	0.965	0.687

<sup>a</sup>The experimental data are shown as mean ± SD of six determinations on the samples obtained from four mice in each diet group. Canola oil served as the control of fish oil. Column *P*0 considers the data on groups given saline treatment; *P*6, with 6.0 mg/kg DOX treatment; *P*9, with 9.0 mg/kg DOX treatment; and *P*12, with 12.0 mg/kg DOX treatment. *n*, number of determinations.

<sup>b</sup>Multiway ANOVA followed by Tukey's test for DOX only,  $P < 0.001$  for 0 vs. 6.0 mg/kg,  $P < 0.001$  for 6.0 vs. 9.0 mg/kg, and  $P < 0.001$  for 9.0 vs. 12.0 mg/kg. For description of diets see Table 1. For abbreviations see Table 3.



**FIG. 3.** Effects of fish oil/vit E interactions with DOX on CPK activity in normal mice. The value at each point represents the mean CPK activity from 12 determinations on the samples from eight mice in each group. (A) Effect of fish oil; (B) effect of vit E. Canola oil served as the control for fish oil. CPK, creatine phosphokinase; for other abbreviations see Figures 1 and 2.



**FIG. 4.** Effects of experimental diets on PUFA in phospholipids of P388 ascitic tumor and mouse heart. (A) P388 ascitic tumor; (B) animal heart. The columns represent mean  $\pm$  SD from five separate determinations on samples from three mice in each group. For diets see Figure 1. Key: n-3 PUFA, bars with stippling; n-6 PUFA, bars with vertical and horizontal lines.

(Fig. 4). The increased content of n-3 PUFA in FO and FVe groups can be attributed largely to EPA and DHA (data not shown), both of which were present in large amounts in FO and FVe diets.

## DISCUSSION

Four AIN-93G-based rodent diets, CO, FO, CVe, and FVe, were designed for this study. CO and CVe contained 10% canola oil, whereas FO and FVe contained 8.5% fish oil plus 1.5% canola oil. CVe and FVe additionally included 500 mg/kg natural vit E. FO and FVe with CO and CVe as their respective controls were used to investigate the effect of fish oil, and CVe and FVe with CO and FO as their respective controls were applied to assess the effect of vit E.

This study demonstrated the therapeutic effect of vit E in P388 mice (6.2% increase in mean LS;  $P = 0.010$ , two-way ANOVA). This was consistent with the previous reports of tumor inhibitory and chemopreventive effects of tocopherols

(28–30). Vit E may inhibit tumor growth *via* the cytotoxic effects of tocopherols and their derivatives (31–33), induction of apoptosis through activation of P21<sup>WAF1/CIP1</sup> (34), reduction of prostaglandin E<sub>2</sub> production (35), and abatement of muscle wasting in cancer cachexia (36).

In the present study, the optimal DOX antitumor effect was observed at 6.0 and 9.0 mg/kg doses. When DOX dose was increased to 12.0 mg/kg, the animal LS significantly decreased, indicating that DOX at this high dose produced a severe negative effect. The major negative effect of DOX might be its cardiotoxicity, as it was shown that serum CPK activity increased dose-dependently. Transmission electron microscopy also demonstrated that DOX at 12.0 mg/kg induced myofibrillar fragmentation and damaged mitochondria in the heart (data not shown).

The effects of DOX at various doses were modified by both fish oil and vit E. Fish oil not only significantly enhanced 6.0 and 9.0 mg/kg DOX therapeutic efficacy in P388 ascitic mice (21.6 and 33.7% increases in mean LS, respectively;



$P = 0.025$ , multiway ANOVA) but also elevated mouse plasma CPK level to an extent proportional to the DOX dose administered, implying that fish oil might enhance DOX cytotoxicity in both tumor cells and heart. The chemistry of DOX lends itself to enzymatic and nonenzymatic generation of superoxide radical and the secondary reactive oxygen species derived from superoxide, including hydrogen peroxide and hydroxyl radical (10,14). The hydroxyl radical is able to extract a doubly allylic hydrogen atom from the unsaturated lipids to form lipid radicals (37), which may react quickly with  $O_2$  to form lipid peroxy radicals that in turn produce lipid endoperoxides (37), or else initiate the lipid peroxidation cycle, converting other unsaturated lipids into lipid hydroperoxides (38). A number of lipid endoperoxides and hydroperoxides and their aldehyde derivatives have been implicated as causative agents for cytotoxic processes in cells (39). Lipid peroxidation has been suggested to be the cause of DOX cytotoxicity in both tumor (40) and heart tissue (41). The increased membrane lipid unsaturation would consequently provide more targets for peroxidative events generated by the metabolism of DOX, thus increasing the cytotoxicity to tissues. On the other hand, the interaction between fish oil and DOX cytotoxicity might also occur through the enhancement of DOX accumulation owing to the increased membrane lipid unsaturation and thus fluidity (4,42). The lipid analysis in the present study showed that PUFA content (an index of cell membrane unsaturation) was increased in both ascitic tumor and animal heart in mice fed FO and FVE, suggesting the possibility that dietary fish oil could directly enhance DOX-induced lipid peroxidation as well as elevate intracellular DOX accumulation in both tumors and heart. Although fish oil markedly exacerbated 12.0 mg/kg DOX cardiotoxicity and abolished the DOX therapeutic effect, the increased LS was achieved when DOX was administered at optimal doses, i.e., tumor inhibition could be achieved with DOX at optimal doses while deleterious effects on the heart occurred only with DOX overdose. This suggests that heart and tumor may have differential responses to the interaction of fish oil and DOX and/or differential sensitivities to the cytotoxicity induced by DOX combined with fish oil.

Vit E seemed to have an inhibitory effect on 6.0 mg/kg DOX-induced CPK release. Many studies found that vit E injection protected against DOX cardiotoxicity (18,19). The cardioprotective effect was achieved in the present study by dietary vit E. The scavenging activity of vit E on lipid peroxidation has been proposed to account for the cardioprotective effect of DOX in DOX-treated animals (18,19), although mechanism(s) other than its antioxidant activity might also contribute to the cardioprotection (43). On the other hand, vit E has been reported to directly enhance the inhibitory effect of DOX on tumor growth (34), and this may partly explain the enhanced therapeutic effectiveness of 9.0 mg/kg DOX. It is thus possible that vit E might enhance the therapeutic efficacy of DOX at optimal doses *via* cardioprotection and/or enhancement of tumor growth inhibition.

Through a synergistic interaction between tocopherols and

overdose DOX, vit E supplement aggravated 12.0 mg/kg DOX cardiotoxicity and thus decreased animal LS (25%;  $P = 0.023$  in two-way ANOVA). Tocopherols transform to chromanoxyl radicals in the scavenging of lipid radicals. In the absence of adequate reductants, such as ascorbic acid, the chromanoxyl radicals will be irreversibly degraded to tocopheryl quinones (44), which are able to initiate and/or enhance lipid peroxidation (6). Owing to the potential pro-oxidant activity of vit E, it may interact synergistically with DOX to produce reactive free radicals and induce lipid peroxidation. Overdose DOX treatment produces oxidative stress, which may overwhelm and/or reduce the antioxidant capability in cells. In the absence of an efficient antioxidant apparatus, such as in the heart, the reactive oxygen metabolites of tocopherols, together with DOX, engender the production of vast amounts of oxygen free radicals, thereby causing extreme cytotoxicity to cells through drastically increased lipid peroxidation.

It thus seems that, at least in animals, vit E may express antioxidant or other activities to protect against heart damage when combined with DOX at optimal doses, but produce a pro-oxidant effect to enhance DOX-induced cardiotoxicity when combined with overdose DOX. This may explain why, in some studies, vit E was reported to be ineffective in cardioprotection (20) or even to be deleterious to the heart of DOX-treated animals (45). Another point to note is that, although  $\alpha$ -tocopherol content was similar between fish oil and canola oil, the latter had a greater  $\gamma$ -tocopherol content than fish oil. However, fish oil but not canola oil enhanced the therapeutic efficacy of DOX, implying that  $\alpha$ -tocopherol, but not  $\gamma$ -tocopherol, may be the dominant species of vit E with respect to its activity. This is consistent with the fact that  $\alpha$ -tocopherol has both a higher (absolute value) tissue distribution (46) and a higher antioxidant activity (6) than  $\gamma$ -tocopherol.

In addition, the function of both PUFA and tocopherols as alkylating/aryllating agents is known to account for some of their biological effects. The electrophiles generated from lipid peroxidation, such as malondialdehyde (MDA) and 4-hydroxynonenal (HNE), may react with DNA bases. MDA modifies purine bases to generate a tricyclic adduct with guanine (47) and an acyclic adduct with adenine (48). HNE reacts directly with 2'-deoxyguanosine to produce a tricyclic substituted propane adduct and is readily oxidized to the epoxide derivative, which can covalently modify both 2'-deoxyguanosine and 2'-deoxyadenosine to form etheno adducts (49). Failure to repair these DNA lesions can lead to apoptosis (50). On the other hand,  $\gamma$ - and  $\delta$ -tocopherol quinones generated from  $\gamma$ - and  $\delta$ -tocopherols, respectively, are cytotoxic aryllating electrophiles because they contain an  $\alpha,\beta$  unsaturated carbonyl structure that forms Michael adducts with compounds containing a thiol nucleophilic group, such as glutathione and proteins (51). Whether treatment with PUFA, tocopherols, and DOX leads to the interactions through their alkylating/aryllating activities and thereby enhances therapeutic efficacy remains to be studied.

Animal xenograft studies found that human lung cancer (52) and mammary carcinoma (53) in nude mice showed a greater sensitivity to DOX when the mice were fed fish oil.

Furthermore, the present work comprehensively investigated the influence of dietary fish oil and vit E, individually and in combination, on the therapeutic efficacy of DOX and has shown their additively enhancing effects on optimal doses of DOX in P388 ascitic mice. Increasing DOX dose, however, led to severe heart damage, which was exacerbated by fish oil and vit E. Thus overall, it appears that both fish oil and vit E modulate the effects of DOX in the laboratory mouse like a double-edged sword, on the one hand enhancing its antitumor effect and on the other, aggravating its cardiotoxicity.

## ACKNOWLEDGMENTS

This work was supported by a Research Grant from the National University of Singapore (No. R-184-000-018-112). The authors thank Annie Hsu for technical assistance in animal experiments and Frances Lim for her help in the use of the gas chromatograph for the estimation of FAME.

## REFERENCES

- Fay, M.P., Freedman, L.S., Clifford, C.K., and Midthune, D.N. (1997) Effect of Different Types and Amounts of Fat on the Development of Mammary Tumors in Rodents: A Review, *Cancer Res.* 57, 3979–3988.
- Gonzalez, M.J. (1992) Lipid Peroxidation and Tumor Growth: An Inverse Relationship, *Med. Hypotheses* 38, 106–110.
- Calviello, G., Palozza, P., Nicuolo, F.E., Maggiano, N., and Bartoli, G.M. (2000) n-3 PUFA Dietary Supplementation Inhibits Proliferation and Store-Operated Calcium Influx in Thymoma Cells Growing in Balb/c Mice, *J. Lipid Res.* 41, 182–188.
- Burns, C.P., and North, J.A. (1986) Adriamycin Transport and Sensitivity in Fatty Acid-Modified Leukemic Cells, *Biochim. Biophys. Acta* 888, 10–17.
- Frei, B. (1994) Reactive Oxygen Species and Antioxidant Vitamins: Mechanisms of Action, *Am. J. Med.* 97 (Supp. 13A), 5S–12S.
- Kamal-Eldin, A., and Appelqvist, L. (1996) The Chemistry and Antioxidant Properties of Tocopherols and Tocotrienols, *Lipids* 31, 671–701.
- Terao, J., and Matsushita, S. (1986) The Peroxidizing Effect of  $\alpha$ -Tocopherol on Autoxidation of Methyl Linoleate in Bulk Phase, *Lipids* 21, 255–260.
- Mukai, K. (1993) Synthesis and Kinetic Study of Antioxidant and Prooxidant Actions of Vitamin E Derivatives, in *Vitamin E in Health and Disease* (Packer, L., and Fuchs J., eds.), pp. 97–120, Marcel Dekker, New York.
- Berlin, V., and Haseltine, W.A. (1981) Reduction of Adriamycin to a Semiquinone Free Radical by NADPH Cytochrome P450 Reductase Produces DNA Cleavage in a Reaction Mediated by Molecular Oxygen, *J. Biol. Chem.* 256, 4747–4756.
- Doroshov, J.H. (1983) Anthracycline Antibiotic-Stimulated Superoxide, Hydrogen Peroxide and Hydroxyl Radical Production by NADH Dehydrogenase, *Cancer Res.* 43, 4543–4551.
- Pan, S.S., and Bachur, N.R. (1980) Xanthine Oxidase Catalyzed Reductive Cleavage of Anthracycline Antibiotics and Free Radical Formation, *Mol. Pharmacol.* 17, 95–99.
- Cullinane, C., and Phillips, D.R. (1990) Induction of Stable Transcriptional Blockage Sites by Adriamycin: GpC Specificity of Apparent Adriamycin-DNA Adducts and Dependence on Iron(III) Ions, *Biochemistry* 29, 5638–5646.
- Lown, J.W., Chen, H.H., Plambeck, J.A., and Acton, E.M. (1982) Further Studies on the Generation of Reactive Oxygen Species from Activated Anthracyclines and the Relationship to Cytotoxic Action and Cardiotoxic Effects, *Biochem. Pharmacol.* 31, 575–581.
- Gutteridge, J.M. (1984) Lipid Peroxidation and Possible Hydroxyl Radical Formation Stimulated by the Self-Reduction of a Doxorubicin-Iron(III) Complex, *Biochem. Pharmacol.* 33, 1725–1728.
- Gianni, L., Zweier, J.L., Abraham, L., and Myers, C.E. (1985) Characterization of the Cycle of Iron-Mediated Electron Transfer from Adriamycin to Molecular Oxygen, *J. Biol. Chem.* 260, 6820–6826.
- Lefrak, E.A., Pitha, J., Rosenheim, S., and Gottlieb, J.A. (1973) A Clinicopathologic Analysis of Adriamycin Cardiotoxicity, *Cancer* 32, 302–314.
- Doroshov, J.H., Locker, G.Y., and Myers, C.E. (1980) Enzymatic Defenses of the Mouse Heart Against Reactive Oxygen Metabolites, *J. Clin. Invest.* 65, 128–135.
- Myers, C.E., McGuire, W.P., Liss, R.H., Ifrim, I., Grotzinger, K., and Young, R.C. (1977) Adriamycin: The Role of Lipid Peroxidation in Cardiac Toxicity and Tumor Response, *Science* 197, 165–167.
- Wang, Y.M., Madanat, F.F., Kimball, J.C., Gleiser, C.A., Ali, M.K., Kaufman, M.W., and van Eys, J. (1980) Effect of Vitamin E Against Adriamycin-Induced Toxicity in Rabbits, *Cancer Res.* 40, 1022–1027.
- Breed, J.G., Zimmerman, A.N., Dormans, J.A., and Pinedo, H.M. (1980) Failure of the Antioxidant Vitamin E to Protect Against Adriamycin-Induced Cardiotoxicity in the Heart, *Cancer Res.* 40, 2033–2038.
- Reeves, P.G., Nielsen, F.H., and Fahey, G.C.J., Jr. (1993) AIN-93 Purified Diets for Laboratory Rodents: Final Report of the American Institute of Nutrition *ad hoc* Writing Committee on the Reformulation of the AIN-76A Rodent Diet, *J. Nutr.* 123, 1939–1951.
- Swanson, J.E., Black, J.M., and Kinsella, J.E. (1988) Dietary Menhaden Oil: Effects on the Rate and Magnitude of Modification of Phospholipid Fatty Acid Composition of Mouse Heart and Brain, *Br. J. Nutr.* 59, 535–545.
- Szasz, G., Gruber, W., and Bernt, E. (1976) Creatine Kinase in Serum I: Determination of Optimum Reaction Conditions, *Clin. Chem.* 22, 650–656.
- Folch, J., Lee, M., and Sloane Stanley, G.H. (1957) A Simple Method for the Isolation and Purification of Total Lipids from Animal Tissues, *J. Biol. Chem.* 226, 497–509.
- Wilder, P.J., Overman, D.K., Tenenholz, T.C., and Gutierrez, P.L. (1990) Differences in Myristic Acid Synthesis and in Metabolic Rate for P388 Cells Resistant to Doxorubicin, *J. Lipid Res.* 31, 1973–1982.
- Browse, J., McCourt, P.J., and Somerville, C.R. (1986) Fatty Acid Composition of Leaf Lipids Determined After Combined Digestion and Fatty Acid Methyl Ester Formation from Fresh Tissue, *Anal. Biochem.* 152, 141–145.
- Morrison, W.R., and Smith, L. (1964) Preparation of Fatty Acid Methyl Esters and Dimethylacetals from Lipids with Boron Fluoride-Methanol, *J. Lipid Res.* 5, 600–608.
- Fleshner, N., Fair, W.R., Huryk, R., and Heston, W.D. (1999) Vitamin E Inhibits the High-Fat Diet Promoted Growth of Established Human Prostate LNCaP Tumors in Nude Mice, *J. Urol.* 161, 1651–1654.
- Factor, V.M., Laskowska, D., Jensen, M.R., Woitach, J.T., Popescu, N.C., and Thorgeirsson, S.S. (2000) Vitamin E Reduces Chromosomal Damage and Inhibits Hepatic Tumor Formation in a Transgenic Mouse Model, *Proc. Natl. Acad. Sci. USA* 97, 2196–2201.
- Decensi, A., and Costa, A. (2000) Recent Advances in Cancer Chemoprevention, with Emphasis on Breast and Colorectal Cancer, *Eur. J. Cancer* 36, 694–709.
- Ramanathan, R., Das, N.P., and Tan, C.H. (1994) Effects of  $\gamma$ -Linolenic Acid, Flavonoids, and Vitamins on Cytotoxicity and Lipid Peroxidation, *Free Radic. Biol. Med.* 16, 43–48.

32. Thornton, D.E., Jones, K.H., Jiang, Z., Zhang, H., Liu, G., and Cornwell, D.G. (1995) Antioxidant and Cytotoxic Tocopheryl Quinones in Normal and Cancer Cells, *Free Radic. Biol. Med.* 18, 963–976.
33. Cornwell, D.G., Jones, K.H., Jiang, Z., Lantry, L.E., Southwell-Keely, P., Kohar, I., and Thornton, D.E. (1998) Cytotoxicity of Tocopherols and Their Quinones in Drug-Sensitive and Multidrug-Resistant Leukemia Cells, *Lipids* 33, 295–301.
34. Chinery, R., Brockman, J.A., Peeler, M.O., Shyr, Y., Beauchamp, R.D., and Coffey, R.J. (1997) Antioxidants Enhance the Cytotoxicity of Chemotherapeutic Agents in Colorectal Cancer: A p53-Independent Induction of P21<sup>WAF1/CIP1</sup> via C/EBP $\beta$ , *Nature Med.* 3, 1233–1241.
35. Jiang, Q., Elson-Schwab, I., Courtemanche, C., and Ames, B.N. (2000)  $\gamma$ -Tocopherol and Its Major Metabolite, in Contrast to  $\alpha$ -Tocopherol, Inhibit Cyclooxygenase Activity in Macrophages and Epithelial Cells, *Proc. Natl. Acad. Sci. USA* 97, 11494–11499.
36. Buck, M., and Chojkier, M. (1996) Muscle Wasting and Dedifferentiation Induced by Oxidative Stress in a Murine Model of Cachexia Is Prevented by Inhibitors of Nitric Oxide Synthesis and Antioxidants, *EMBO J.* 15, 1753–1765.
37. Pryor, W.A., and Stanley, J.P. (1975) A Suggested Mechanism for the Production of Malonaldehyde During the Autoxidation of Polyunsaturated Fatty Acids. Nonenzymatic Production of Prostaglandin Endoperoxides During Autoxidation, *J. Org. Chem.* 40, 3615–3617.
38. Buege, J.A., and Aust, S.D. (1978) Microsomal Lipid Peroxidation, *Methods Enzymol.* 52, 302–310.
39. Esterbauer, H., and Cheeseman, K.H. (1990) Determination of Aldehydic Lipid Peroxidation Products: Malonaldehyde and 4-Hydroxynonenal, *Methods Enzymol.* 186, 407–421.
40. Benchekroun, M.N., Pourquier, P., Schott, B., and Robert, J. (1993) Doxorubicin-Induced Lipid Peroxidation and Glutathione Peroxidase Activity in Tumor Cell Lines Selected for Resistance to Doxorubicin, *Eur. J. Biochem.* 211, 141–146.
41. Powell, S.R., and McCay, P.B. (1995) Inhibition of Doxorubicin-Induced Membrane Damage by Thiol Compounds: Toxicologic Implications of a Glutathione-Dependent Microsomal Factor, *Free Radic. Biol. Med.* 18, 159–168.
42. Liu, Q.-Y., and Tan, B.K.H. (2000) Effects of *cis*-Unsaturated Fatty Acids on Doxorubicin Sensitivity in P388/DOX Resistant and P388 Parental Cell Lines, *Life Sci.* 67, 1207–1218.
43. Carrasquedo, F., Glanc, M., and Fraga, C.G. (1999) Tissue Damage in Acute Myocardial Infarction: Selective Protective by Vitamin E, *Free Radic. Biol. Med.* 26, 1587–1590.
44. Liebler, D.C., and Burr, J.A. (1992) Oxidation of Vitamin E During Iron-Catalyzed Lipid Peroxidation: Evidence for Electron-Transfer Reactions of the Tocopheroxyl Radical, *Biochemistry* 31, 8278–8284.
45. Shinozawa, S., Gomita, Y., and Araki, Y. (1988) Effect of High Dose Alpha-Tocopherol and Alpha-Tocopherol Acetate Pretreatment on Adriamycin (Doxorubicin) Induced Toxicity and Tissue Distribution, *Physiol. Chem. Phys. Med. NMR* 20, 329–335.
46. Podda, M., Weber, C., Traber, M.G., and Packer, L. (1996) Simultaneous Determination of Tissue Tocopherols, Tocotrienols, Ubiquinol, and Ubiquinone, *J. Lipid Res.* 37, 893–901.
47. Marnett, L.J., Basu, A.K., O'Hara, S.M., Weller, P.E., Rahman, A.F.M.M., and Oliver, J.P. (1986) Reaction of Malondialdehyde with Guanine Nucleosides: Formation of Adducts Containing Oxadiazabicyclonene Residues in the Base-Pairing Region, *J. Am. Chem. Soc.* 108, 1348–1350.
48. Stone, K., Ksebati, M.B., and Marnett, L.J. (1990) Investigation of the Adducts Formed by Reaction of Malondialdehyde with Adenosine, *Chem. Res. Toxicol.* 3, 33–38.
49. Lee, S.H., Rindgen, D., Bible, R.H., Jr., Hajdu, E., and Blair, I.A. (2000) Characterization of 2'-Deoxyadenosine Adducts Derived from 4-Oxo-2-nonenal, a Novel Product of Lipid Peroxidation, *Chem. Res. Toxicol.* 13, 565–574.
50. Johnson, T.M., Yu, Z.X., Ferrans, V.J., Lowenstein, R.A., and Finkel, T. (1996) Reactive Oxygen Species Are Downstream Mediators of p53-Dependent Apoptosis, *Proc. Natl. Acad. Sci. USA* 93, 11848–11852.
51. Jones, K.H., Liu, J.J., Roehm, J.S., Eckel, J.J., Eckel, T.T., Stichrath, C.R., Triola, C.A., Jiang, Z., Bartoli, G.M., and Cornwell, D.G. (2002)  $\gamma$ -Tocopheryl Quinone Stimulates Apoptosis in Drug-Sensitive and Multidrug-Resistant Cancer Cells, *Lipids* 37, 173–184.
52. Hardman, W.E., Moyer, M.P., and Cameron, I.L. (2000) Dietary Fish Oil Sensitizes A549 Lung Xenografts to Doxorubicin Chemotherapy, *Cancer Lett.* 151, 145–151.
53. Hardman, W.E., Avula, C.P., Fernandes, G., and Cameron, I.L. (2001) Three Percent Dietary Fish Oil Concentrate Increased Efficacy of Doxorubicin Against MDA-MB 231 Breast Cancer Xenografts, *Clin. Cancer Res.* 7, 2041–2049.

[Received August 13, 2001, and in revised form May 15, 2002; revision accepted May 16, 2002]



# Effect of Palm Oil Carotene on Breast Cancer Tumorigenicity in Nude Mice

Kalanithi Nesaretnam<sup>a,\*</sup>, Ammu Radhakrishnan<sup>b</sup>, Kanga Rani Selvaduray<sup>a</sup>, Karin Reimann<sup>a</sup>, Jayalakshmi Pailoor<sup>c</sup>, Ghazali Razak<sup>a</sup>, Mina Mustafa Mahmood<sup>d</sup>, and Jasbir Singh Dahliwal<sup>e</sup>

<sup>a</sup>Malaysian Palm Oil Board, Bandar Baru Bangi, 43000 Kajang, Selangor, Malaysia, <sup>b</sup>International Medical University, Bukit Jalil, 57000 Kuala Lumpur, Malaysia, <sup>c</sup>Department of Pathology, Faculty of Medicine, University of Malaya, 50603 Kuala Lumpur, Malaysia, <sup>d</sup>Faculty of Medicine and Health Sciences, University Putra Malaysia, 43400 Serdang, Malaysia, and <sup>e</sup>Institute for Medical Research, 50588 Kuala Lumpur, Malaysia

**ABSTRACT:** Biological therapies are new additions to breast cancer treatment. Among biological compounds,  $\beta$ -carotene has been reported to have immune modulatory effects, in particular, enhancement of natural killer cell activity and tumor necrosis factor- $\alpha$  production by macrophages. The objective of this study was to investigate the effect of palm carotene supplementation on the tumorigenicity of MCF-7 human breast cancer cells injected into athymic nude mice and to explore the mechanism by which palm carotenes suppress tumorigenesis. Forty-eight 4-wk-old mice were injected with  $1 \times 10^6$  MCF-7 cells into their mammary fat pad. The experimental group was supplemented with palm carotene whereas the control group was not. Significant differences were observed in tumor incidence ( $P < 0.001$ ) and tumor surface area and metastasis to lung ( $P < 0.005$ ) between the two groups. Natural killer (NK) cells and B-lymphocytes in the peripheral blood of carotene-supplemented mice were significantly increased ( $P < 0.05$  and  $P < 0.001$ , respectively) compared with controls. These results suggest that palm oil carotene is able to modulate the immune system by increasing peripheral blood NK cells and B-lymphocytes and suppress the growth of MCF-7 human breast cancer cells.

Paper no. L8967 in *Lipids* 37, 557–560 (June 2002).

Cancer of the breast is the most common cancer and cause of death from cancer in women. An estimated 570,000 cases occurred in 1999, accounting for 9% of all new cases of cancer (1). The development of effective biological agents for prevention and treatment of breast cancer is under intense investigation. Naturally occurring agents such as carotenoids and retinoids and their derivatives are appealing biological agents. Unrefined palm oil represents the richest natural source of carotenoids with  $\alpha$ - and  $\beta$ -carotene being the major components (2). Carotenoids have been proposed as cancer-preventive agents (3). *In vitro* studies showed that carotenoids, especially lycopene and  $\alpha$ -carotene, have antioxidant and antiproliferative properties that are thought to be responsible for the anticancer effects of carotenoids (4,5). Carotenoid-induced enhancement of immune functions has been investigated in some experimental studies using animal models. Beneficial

\*To whom correspondence should be addressed at Malaysian Palm Oil Board, 6 Persiaran Institusi, Bandar Baru Bangi, 43000 Kajang, Selangor, Malaysia. E-mail: sarnesar@mpob.gov.my

Abbreviations: FACS, Fluorescence activated cell sorter; IFN, interferon; mfp, mammary fat pad; NK, natural killer; TCR, T-cell receptor; TNF, tumor necrosis factor.

effects of  $\beta$ -carotene have been demonstrated on T- and B-cell proliferation, number of T-helper cells, and cytotoxicity of natural killer cells (6). Fernandes *et al.* (7) studied the effects of  $\beta$ -carotene on the activity of natural killer (NK) cells in athymic nude mice. The results showed a significant modulation of NK cell activity in these mice.

This study was designed to explore the effect of palm carotene supplementation on breast cancer tumorigenicity and changes in the immune status of nude mice.

## MATERIALS AND METHODS

Female athymic nude mice (NCRnu/nu), 3- to 4-wk old, were housed under pathogen-free conditions in microisolators. The care and treatment of the experimental animals conformed to the guidelines of the Institute for Medical Research for the ethical treatment of laboratory animals. Mice were obtained from the Institute for Medical Research, Kuala Lumpur. Both the control and the experimental groups were fed a commercial mouse pellet diet; the only difference in their diets was that mice in the experimental group were supplemented with 1000 ppm of carotene emulsion, which was provided daily as drinking water for the 20 wk of the experiment.

*Experimental procedure.* The mice were anesthetized with Phenobarbital and a 50- $\mu$ L volume of inoculum containing  $1 \times 10^6$  MCF-7 (human breast cancer) cells was injected into a right-sided thoracic mammary fat pad (mfp) that had been exposed by a small incision (5 mm). The mice were weighed and palpated at weekly intervals. At necropsy, body and tumor weights were determined, and the extent of lung metastases was assessed.

*Isolation of mouse peripheral blood leukocytes.* Mice were sacrificed and blood was collected through heart puncture in heparinized tubes. The blood was spun at  $900 \times g$  for 5 min at 4°C. The plasma was removed, and the red blood cells were lysed by addition of 900  $\mu$ L of sterile water for 30 s followed by addition of  $10 \times$  PBS. The tubes were inverted three or four times and leukocytes were recovered by centrifugation at  $900 \times g$  for 5 min. The cells were resuspended with 1 mL of cold fluorescence-activated cell sorter (FACS 1% BSA in PBS with 0.1% sodium azide; Becton Dickinson, San Jose, CA) blocking buffer. The tubes were again centrifuged at  $900 \times g$  for 5 min. The supernatant was discarded, and the cells



were resuspended in cold FACS blocking buffer and aliquoted appropriately for staining with conjugated antibodies for flow cytometer analysis.

**Flow cytometer assay.** Appropriately diluted conjugated antibodies [antimouse CD2 (stains T-cells and NK cells), antimouse CD19 (stains B-lymphocytes), antimouse  $\gamma\delta$  T-cell receptor (TCR: stains T-lymphocytes), and antimouse Pan NK (stains NK cells); Pharmingen, San Diego, CA] were added to the corresponding blood samples and mixed. After 45 min incubation on ice in the dark, 1 mL of FACS (0.1% BSA and 0.1% sodium azide) wash buffer was added to each tube. The cells were recovered by centrifugation ( $900 \times g$  for 5 min at  $4^\circ\text{C}$ ) and resuspended in 400  $\mu\text{L}$  of FACS fix Solution 1 (1% BSA and 0.1% sodium azide), and 400  $\mu\text{L}$  of FACS fix Solution 2 (4% formalin in PBS) was added. The cells were mixed thoroughly and analyzed on Becton-Dickinson cell sorter Cell-Quest software. For each sample 10,000 cells were collected for analysis.

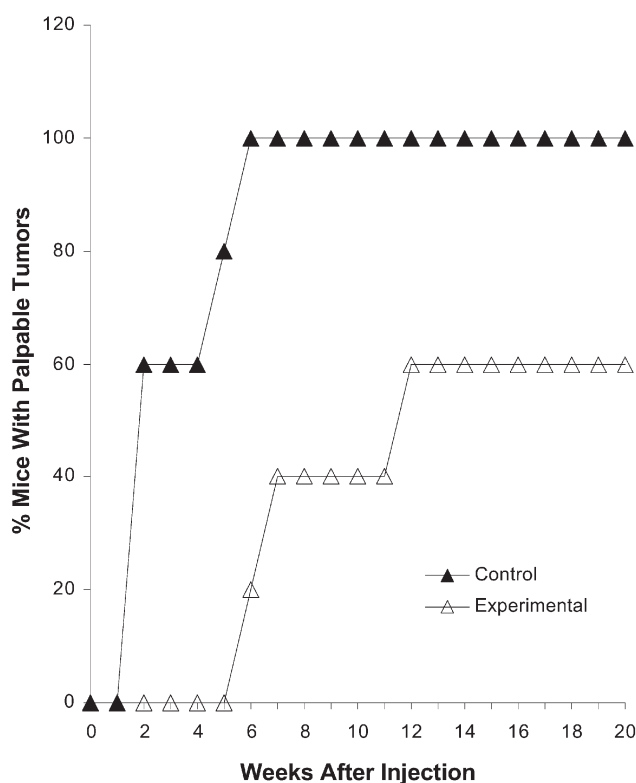
**Carotene analysis.** The  $\alpha$ - and  $\beta$ -carotene were analyzed by HPLC. The system used was a Shimadzu LC-10AT HPLC coupled with a Shimadzu Model SPD 10A UV-vis detector, Shimadzu class VP data acquisition software, and Crestpak C18S metaphase column (Biosains, Kuala Lumpur, Malaysia). The eluting solvent (mobile phase) was a mixture of 89% acetonitrile and 11% dichloromethane. The flow rate was 1.0 mL/min. The detector was set at a wavelength of 450 nm. A standard solution of a mixture of  $\alpha$ - and  $\beta$ -carotene was loaded onto the HPLC column before loading the samples.

**Statistical analysis.** Statistical analysis was performed using the SPSS (Chicago, IL) program. Fisher's exact test was used to test for a significant difference in the tumor incidence between experimental and control mice. An independent-sample *t*-test was used to test for a difference in the tumor surface and carotene deposition between experimental and control mice.

## RESULTS

**Effect of palm oil carotene supplementation on mammary fat pad tumorigenesis.** The cumulative incidence of mfp tumorigenesis in control and experimental mice is summarized in Figure 1. Tumors in experimental mice first appeared 6 wk after injection with MCF-7 cells with a cumulative incidence of 20% compared to controls; the latter developed tumors in the second week after injection. The cumulative incidence of tumors in the experimental animals was 60% at 20 wk. The difference in the tumor incidence rate over the 20 wk of the study in the experimental and control groups was statistically significant ( $P < 0.001$ ).

**Tumor growth and metastases.** Tumor surface area (Fig. 2) in experimental mice with primary tumors was significantly lower ( $P < 0.05$ ) than that of control mice. Three (12.5%) of the 24 mice in the control group and one (4.1%) in the carotene-supplemented group had visible pulmonary metastatic nodules. There was a significant difference ( $P < 0.05$ ) in the total metastatic incidence of control (50%) and experimental mice (17%) at autopsy (Table 1).



**FIG. 1.** Rate of appearance of palpable tumors at MCF-7 inoculation site in athymic nude mice. Data points show the percentage of mice with palpable primary tumors in mice supplemented with 1000 ppm palm oil carotene (experimental) vs. control over the 20 wk ( $n = 24$  for each group).

**TABLE 1**  
Effect of Palm Oil Carotene Supplementation on the Incidence of Grossly Visible Pulmonary Metastatic Nodules and Micrometastases from MCF-7 Human Breast Cancer Solid Tumor in Mammary Fat Pads of Nude Mice<sup>a</sup>

Animal groups	Grossly visible nodules	Micrometastases	Total metastatic incidence
Control	3/24 (12.5)	9/24 (37.5)	12/24 (50)
Experimental <sup>b</sup>	1/24 (4.2)	3/24 (12.5)	4/24 (17) <sup>c</sup>

<sup>a</sup>Numbers in parentheses indicate percentages.

<sup>b</sup>Carotene-supplemented mice.

<sup>c</sup>Significantly different from control group ( $P < 0.05$ ).

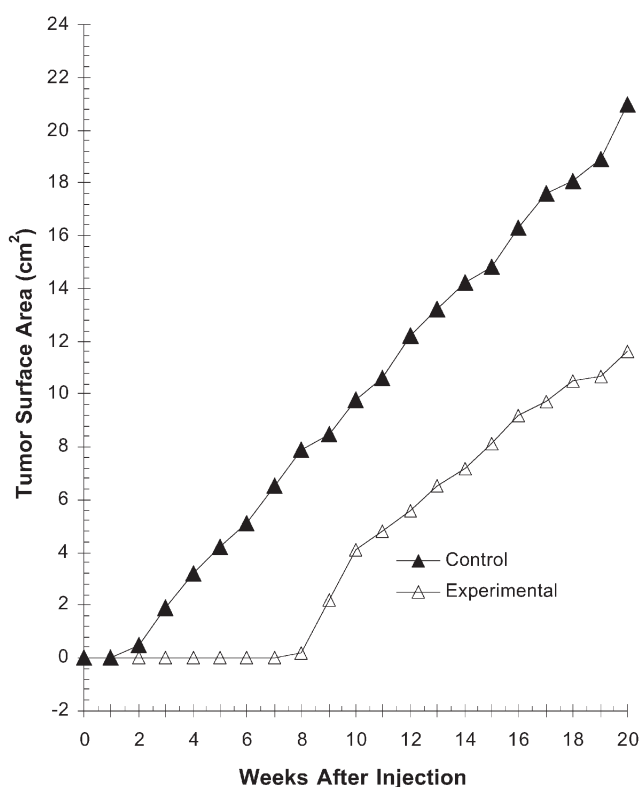
**TABLE 2**  
Flow Cytometry Analysis of Peripheral Blood Leukocytes of Experimental and Control Mice

Animal groups	Percentage of leukocyte count $\pm$ SD <sup>a</sup>		
	NK cells	$\gamma\delta$ -TCR T-lymphocytes	B-Lymphocytes
Control	27 $\pm$ 4.5	19.8 $\pm$ 3.6	26.9 $\pm$ 5.4
Experimental <sup>b</sup>	45 $\pm$ 4.2 <sup>c</sup>	19.97 $\pm$ 3.9	57.8 $\pm$ 7.0 <sup>c</sup>

<sup>a</sup>Results are expressed as mean percentage  $\pm$  SD of the respective leukocytes present in the 10,000 cells that were collected for analysis. Each sample was done in duplicate. TCR, T-cell receptor; NK, natural killer.

<sup>b</sup>Carotene-supplemented mice.

<sup>c</sup>Significantly different ( $P < 0.05$ ) from control.



**FIG. 2.** Tumor surface area of palpable primary tumors in athymic nude mice. Data points show the mean tumor surface area as calculated from weekly external measurements over a 20-wk period. The primary tumors in control mice grew faster than those in mice supplemented with palm oil carotenes (experimental). The difference in tumor surface area between the two groups was found to be statistically significant ( $P < 0.05$ ).

#### *Effect of carotene supplementation on the immune system.*

Twenty weeks of palm oil carotene supplementation in nude mice resulted in an increase of peripheral blood NK cell population compared with control mice (Table 2). Mice supplemented with carotene had a mean NK cell population of  $45 \pm 4.25\%$  (mean  $\pm$  SD) of the leukocyte population, whereas the mean NK population in control mice was only  $27 \pm 4.15\%$  ( $P < 0.05$ ). The B-lymphocyte population in the carotene-treated mice ( $57.8 \pm 7.0\%$ ) was also increased when compared with the control ( $26.98 \pm 5.4\%$ ).

**HPLC analysis of mice adipose tissue and liver.** HPLC analysis of fat extracted from adipose tissue of experimental mice revealed deposition of  $0.78 \pm 0.15$  ppm ( $\mu\text{g/g}$  tissue)  $\alpha$ -carotene and  $1.35 \pm 0.23$  ppm  $\beta$ -carotene (total carotene =  $2.13 \pm 0.17$  ppm). Similarly, for liver  $\alpha$ -carotene reached  $2.78 \pm 0.45$  ppm and  $\beta$ -carotene averaged  $5.52 \pm 0.92$  ppm (total carotene =  $8.30 \pm 0.34$  ppm). No  $\alpha$ - or  $\beta$ -carotene was found in adipose or liver tissues of control animals.

## DISCUSSION

In this study, the time to appearance of palpable tumors at the inoculation site increased in the carotene-supplemented group, and these animals also had a significantly lower tumor

incidence compared to the control group. In addition, the mean tumor surface area and lung metastases in experimental mice with primary tumors were significantly lower than those of control mice. These findings suggest that palm oil carotene can induce anticancer and antimetastatic effects against MCF-7 cells injected into nude mice.

The results also showed a significant increase in the peripheral blood NK cell population and B-lymphocytes in nude mice supplemented with palm oil carotene compared with untreated control mice. It might be possible to connect these observations with what previous studies have shown about retinoid-induced enhancement of the immune system: that  $\beta$ -carotene derived from palm oil may stimulate or enhance the immune system through local conversion to retinoic acid at the tissue level (8). Based on the findings of the present study together with previous study results (9), it is possible that  $\beta$ -carotene from palm oil is converted to retinoic acid by the oxidative cleavage of  $\beta$ -apocarotenoid acid, formed by asymmetric cleavage of  $\beta$ -carotene in the intestinal mucosa, as reviewed by Wang *et al.* (10). Interestingly, analysis of  $\beta$ -carotene deposition in the adipose tissue and liver of carotene-supplemented mice showed only trace amounts of  $\beta$ -carotene deposited in their adipose tissue although a substantial amount of carotenes was supplemented to these mice over the 20 wk of the study. A possible explanation for this observation is that most of the  $\beta$ -carotene was converted to retinoic acid and/or its derivatives.

The binding of retinoic acid to its receptors results in an autocrine production of interferon (IFN) (9): IFN- $\alpha$  and IFN- $\beta$  will potentiate the activity of NK cells, and IFN- $\gamma$  will activate macrophages. Activated macrophages produce interleukin-12, which stimulates the proliferation of and IFN- $\gamma$  production by NK cells. We speculate that increased numbers of NK cells elicited by palm oil carotene may play a crucial role in the suppression of the growth of injected MCF-7 cells. B-cells increased in number in the peripheral blood of carotene-supplemented mice. However, Boven *et al.* (11) found that B-cells in nude mice do not play an important immune function because their production of immunoglobulins is limited only to the immunoglobulin M isotype. The number of  $\gamma\delta$ -TCR T-lymphocytes did not differ significantly between control and experimental mice. This finding may indicate that these cells do not play an important role in mediating the immune surveillance against malignancy, at least in nude mice.

## REFERENCES

1. Bundred, N.J. (2001) Prognostic and Predictive Factors in Breast Cancer, *Cancer Treat. Rev.* 27, 137–142.
2. Cottrell, R. (1991) Nutritional Aspects of Palm Oil, *Am. J. Clin. Nutr.* 53, 989S–1009S.
3. Meyskens, F.L. (1990) Coming of Age—The Chemoprevention of Cancer, *N. Engl. J. Med.* 323, 825–827.
4. Nesaretnam, K., Jin Lim, E., Reimann, K., and Lai, L.C. (2000) Effect of a Carotene Concentrate on the Growth of Human Breast Cancer Cells and pS2 Gene Expression, *Toxicology* 151, 117–126.

5. Singh, D.K., Scott, M., and Lippman, K. (1998) Cancer Chemoprevention Part 1: Retinoids and Carotenoids and Other Classic Antioxidants, *Oncogene* 2, 774–780.
6. Bendich, A. (1991) Beta-Carotene and the Immune Response, *Proc. Nutr. Soc.* 50, 263–274.
7. Fernandes-Carlos, T., Riondel, J., Glise, D., Guiraud, P., and Favier, A. (1997) Modulation of Natural Killer Cell Functional Activity in Athymic Nude Mice by  $\beta$ -Carotene, Oestrone and Their Association, *Anticancer Res.* 17, 2523–2527.
8. Kolla, V., Weihua, X., and Kalvakolanu, D.V. (1997) Modulation of Interferon Action by Retinoids. Induction of Murine STAT 1 Gene Expression by Retinoic Acid, *J. Biol. Chem.* 272, 9742–9758.
9. Niikura, T., Hirata, R., and Weil, S.C. (1997) A Novel Interferon-Inducible Gene Expressed During Myeloid Differentiation, *Blood Cells Mol. Dis.* 23, 337–349.
10. Wang, X.D., Russell, R.M., Liu, C., Stickel, F., Smith, D.D., and Krinsky, N.I. (1996) Beta-Oxidation in Rabbit Liver *in vitro* and in the Perfused Ferret Liver Contributes to Retinoic Acid Biosynthesis from Beta-Apocarotenoic Acids, *J. Biol. Chem.* 271, 26490–26498.
11. Boven, E., and Winograd, B. (1991) *The Nude Mouse in Oncology Research*, CRC Press, Boca Raton.

[Received December 14, 2001, and in revised form March 6, 2002; revision accepted May 30, 2002]

# Antihypertensive Effects of a Dietary Unsaturated FA Mixture in Spontaneously Hypertensive Rats

S. Bellenger-Germain, J.-P. Poisson, and M. Narce\*

UPRES Lipides et Nutrition, Faculté des Sciences Gabriel, Université de Bourgogne, Dijon, France

**ABSTRACT:** The aim of the present study was to investigate whether a mixture of dietary n-6 and n-3 PUFA could lower blood pressure in spontaneously hypertensive rats (SHR) of different ages. In addition, we studied how such a treatment could normalize the FA composition of plasma TAG and cholesterol esters (CE), and of red blood cell (RBC) total lipids. SHR (ages 4, 19, and 50 wk) were fed a normal diet (control groups) or a semi-synthetic diet containing a mixture of  $\gamma$ -linolenic acid (GLA), EPA, and DHA (experimental groups). Systolic blood pressure was measured at regular intervals. After 11 wk of consuming this diet, plasma TAG and CE were separated by TLC and analyzed for their FA composition. Total FA composition of RBC was also determined. The degree to which blood pressure was elevated was reduced in SHR after 11 wk of diet. The largest decrease was obtained with the oldest animals. In RBC, EPA and DHA contents increased. In plasma TAG and CE, EPA, DHA, and GLA increased whereas arachidonic acid decreased. The n-6 and n-3 unsaturated FA mix slowed the development of hypertension in young SHR and decreased blood pressure in adult and aged SHR. In addition, the present treatment altered the n-3 and n-6 PUFA content of SHR lipids to that seen in normotensive rats.

Paper no. L8626 in *Lipids* 37, 561–567 (June 2002).

The hypotensive effects of dietary n-3 PUFA have been observed with marine oil supplementations, both in humans (1–3) and spontaneously hypertensive rats (SHR) (4,5). Experiments using purified forms of the major components of these oils—EPA (20:5n-3) and DHA (22:6n-3)—have shown a decrease in blood pressure in patients suffering from hypertension (6) and in SHR (7,8). Contradictory reports show no protective effect of the consumption of fish oil—or of its derivatives—on hypertension (9–11), if used at low doses. These discrepancies can also be explained by study design differences, as for example the composition and doses of administered fats, the balance between n-6 and n-3 PUFA, the age of animals, and the duration of the treatment.

In earlier work, we showed that treatment of SHR with a dietary EPA and DHA combination (EPA30) did not decrease blood pressure (12). Moreover, it is well known that prolonged supplementation with only n-3 PUFA is accompanied by

changes in FA composition of various organs and tissues (13–15). These FA, incorporated at the expense of n-6 FA (16), can induce n-6 PUFA reduction in same-cell types (17). Evidence has been found for a competition between these two families of FA for entry into and release from cellular phospholipids and for a competition for the desaturase enzymes that catalyze their bioconversion into longer and more unsaturated FA, precursors of eicosanoids (18,19). Such changes can lead to a deficit in n-6 PUFA derivatives (17,20) and possibly alter the influence of such lipid mediators on blood pressure regulation, vasodilation, and platelet aggregation (21,22). Blood dihomo- $\gamma$ -linolenic acid (DGLA, 20:3n-6) level is a strong predictor of both coronary heart disease and stroke (23,24). On the other hand, the hypotensive effect of evening primrose oil, rich in  $\gamma$ -linolenic acid (GLA, 18:3n-6), has been described (25,26), and a similar effect has been shown with purified GLA, administered by peritoneal injection (27).

In a preliminary study we observed that a mixture of n-3 FA (EPA30) failed to decrease adult SHR blood pressure. The aim of the present investigation was to evaluate the possible effect of a dietary GLA/EPA/DHA combination (GLA80/EPA30) on blood pressure in SHR at three different ages, corresponding to prehypertensive, hypertensive, and aged hypertensive rats. Such a mixture would bypass the  $\Delta 6$  desaturation step in the process of EFA metabolism, which has been shown to be inhibited in SHR (28). Thus, the metabolic products from n-6 EFA, known to be involved in membrane fluidity and to be precursors of second messengers regulating blood pressure, would be maintained. In addition, plasma lipid derangement is known to be one of the primary factors associated with developing and maintaining hypertension (29,30). Consequently, we have determined the impact of such a treatment on the FA profiles of plasma lipids and red blood cell (RBC) membranes.

## MATERIALS AND METHODS

**Animals and diets.** All aspects of the animal experiments were approved by the Ethics Committee for Experimental Animals of the University of Burgundy, Dijon. Forty-two SHR were provided by IFFA-Credo (Domaine des Oncins, L'Arbresle, France). On arrival, rats were fed commercial standard pellets (Souriffarat, U.A.R A04, Villemoisson sur Orge, France) for 1 wk. During the whole experiment, animals were kept in individual metabolic cages. The room was maintained at  $22 \pm 2^\circ\text{C}$ ,  $60 \pm 5\%$  RH, and with a day/night alternation of 12 h/12 h. Animals had free access to food and tap water. Next, twelve

Part of this study was presented at the 90th Annual Meeting of the American Oil Chemist's Society (Orlando, Florida, May 9–12, 1999).

\*To whom correspondence should be addressed at UPRES Lipides et Nutrition, Faculté des Sciences Mirande, Université de Bourgogne, 6 blvd Gabriel, 21000 Dijon, France. E-mail: Michel.Narce@u-bourgogne.fr

Abbreviations: CE, cholesterol ester; DGLA, dihomo- $\gamma$ -linolenic acid; GLA,  $\gamma$ -linolenic acid; RBC, red blood cells; SHR, spontaneously hypertensive rat; WKY, Wistar Kyoto rat.



**TABLE 1**  
**FA Composition of EPA30, GLA80, and ISIO4 Oil and of Control and Experimental Diets<sup>a</sup> (g/100 g)**

	EPA30	GLA80	ISIO4	Control diet	Experimental diet
16:0	—	—	6.2	6.2	3.8
18:0	—	—	3.3	3.3	2.0
20:0	—	—	0.3	0.3	0.2
22:0	—	0.6	0.8	0.8	0.6
24:0	—	—	0.3	0.3	0.2
Total saturated	—	0.6	10.9	10.9	6.8
16:1n-7	15.1	—	—	—	3.9
<b>18:1n-9</b>	6.1	3.0	<b>40.0</b>	<b>40.0</b>	<b>26.6</b>
20:1n-9	—	—	0.2	0.2	0.1
Total monounsaturated	21.2	3.0	40.2	40.2	30.6
<b>18:2n-6</b>	3.7	15.6	<b>45.9</b>	<b>45.9</b>	<b>31.2</b>
<b>18:3n-6</b>	2.4	<b>79.8</b>	1.3	1.3	<b>11.4</b>
20:2n-6	—	0.4	—	—	Trace
20:4n-6	1.7	—	—	—	0.4
Total n-6 PUFA	7.8	95.8	47.2	47.2	43.0
18:3n-3	—	0.6	1.6	1.6	1.0
18:4n-3	7.4	—	—	—	1.9
<b>20:5n-3</b>	<b>37.7</b>	—	0.1	0.1	<b>9.9</b>
22:5n-3	5.5	—	—	—	1.4
<b>22:6n-3</b>	<b>20.4</b>	—	—	—	<b>5.3</b>
Total n-3 PUFA	71.0	0.6	1.7	1.7	19.5

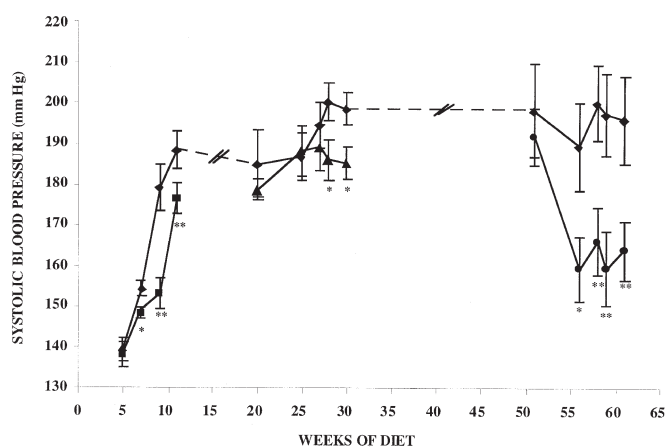
<sup>a</sup>Values were determined by GLC. Boldface used to emphasize certain FA in mixture.

4-wk-old, sixteen 19-wk-old, and fourteen 50-wk-old SHR (groups A, B, and C, respectively) were adapted for 1 wk to a semisynthetic diet (used as control diet and stored at 4°C) containing (g/100 g): 58.7 cornstarch, 20 casein, 5 cellulose powder, 5 saccharose, 4 minerals, 2 vitamins (Usine d'Alimentation Rationnelle), 0.3 methionine (Sigma Chemical Co., St. Louis, MO) and 5 lipids (ISIO 4 oil; Lesieur, Boulogne Billancourt, France). As human diets are generally high in linoleic acid, we chose as the control a commercial oil recommended by nutritionists that is high in n-6 PUFA as compared to the diet usually provided to rodents. The animals of each age group were then randomly assigned to groups of 6–8 rats each to either the control diet (containing 5% of lipids as ISIO 4 oil) or the semisynthetic diet containing 5% of lipids including a mixture composed of 26% EPA30 and 12.5% GLA80 (Callanish Ltd. Breasclate, Isle of Lewis, United Kingdom) and 61.5% ISIO 4 oil for 11 wk. The FA composition of EPA30, GLA80, and ISIO4 oils and control and experimental diets is presented in Table 1. The fresh mixture of GLA80/EPA30, prepared daily, was added to the diet in the form of ethyl esters just before being given to animals. The stability of the ethyl esters of the mixture, under these conditions, after exposure to air was confirmed by GLC. In order to administer the same amounts of GLA/EPA/DHA mixture to each experimental animal, the diet was given as follows: 13 g of the experimental diet was administered during the evening, and the ration was complemented the following morning with the control diet, *ad libitum*. Control animals (normotensive Wistar Kyoto rats: WKY) were fed the control diet under the same conditions as the experimental animals. Food intake was

measured daily and body weight weekly. Indirect systolic blood pressure was determined as follows: The rats were prewarmed for half an hour in a warming cupboard at 35°C, in order to prepare the rat's tail for the measurement with a plethysmographic method (BP Recorder 8005; M+M Electronic Inc., Basel-Müchensee, Switzerland). Four blind readings were obtained from each rat and averaged, after the highest and the lowest values were excluded.

At the end of the feeding period, animals were anesthetized with 0.1 mL/100 g body weight sodium pentobarbital (Sanofi, Paris, France). Blood from the abdominal aorta was collected in heparinized tubes and centrifuged at 1,700 × g for 10 min (Janetzki, T32c; Bioblock, Strasbourg, France) to separate plasma. RBC and plasma were then frozen (−20°C) under nitrogen before analysis.

*Plasma and RBC lipid analyses.* RBC were washed three times at 4°C (12,100 × g for 3 min) (J-21B, rotor JA20; Beckman Instruments, Fullerton, CA) with isotonic Tris buffer (NaCl 150 mmol/L, EDTA 1 mmol/L, Tris 10 mmol/L), pH 7.8. RBC membranes were prepared by centrifugation (12,100 × g for 10 min) in a hypotonic Tris buffer (NaCl 7 mmol/L, EDTA 1 mmol/L, Tris 5 mmol/L), pH 7.8 at 4°C and washed in distilled water at 4°C during 10 min at 12,100 × g. RBC and plasma lipids were extracted (31). TAG were separated from cholesterol esters (CE) by TLC using hexane/ethyl ether/acetic acid/methanol (180:40:4:6, by vol) as solvent system. Areas corresponding to TAG and CE were immediately scraped off the plates, extracted with chloroform/methanol (9:1, vol/vol) and then analyzed for FA composition. FAME were prepared by transmethylation using 14%



**FIG. 1.** Effect of experimental diet on blood pressure of groups A–C: systolic blood pressure from control rats (◆) and experimental rats (group A: ■, group B: ▲, and group C: ●). Results are shown as mean  $\pm$  SEM for  $n = 6$  (group A),  $n = 8$  (group B), and  $n = 7$  (group C). Each blood pressure is the mean of four measurements, after exclusion of the highest and the lowest values. Significantly different from control rats: \* $P < 0.05$ , \*\* $P < 0.01$ .

boron trifluoride in methanol (32), then separated by GLC (Packard model 417 gas–liquid chromatograph; Packard, Downers Grove, IL) equipped with an FID and a 30-m capillary glass column coated with Carbowax 20M (Applied Science Labs, State College, PA), and identified by their relative retention times (FA standards; Nu-Chek-Prep, Elysian, MN).

**Statistical analyses.** Results are expressed as the arithmetic mean for each group with their standard error (mean  $\pm$  SEM). Unpaired Student's *t*-test was used to determine significant differences between experimental and control groups for each age. Statistical difference was accepted at  $P < 0.05$  (\*) and  $P < 0.01$  (\*\*). For each diet, the means from groups A, B, and C were classified after ANOVA using Duncan's multiple range test. In each line, means assigned different superscript letters (b, c, d, e) were significantly different ( $P < 0.05$ ).

## RESULTS

**Food intake and body weight.** Food intake ( $16.9 \pm 0.7$  g/d) and body weights of experimental groups A and B were similar to controls during the whole experiment. Before killing, body weights were  $354 \pm 9$  g and  $388 \pm 3$  g in groups A and B, respectively. Moreover, the food intake of group C was significantly increased in the experimental group during the last 3 wk of the experiment ( $19.0 \pm 0.4$  vs.  $17.0 \pm 0.3$  g/d). The body weight was also significantly increased in this group during the last weeks of diet ( $476 \pm 13$  vs.  $439 \pm 12$  g).

**Blood pressure.** Results related to the blood pressure are presented in Figure 1. No difference was observed between SHR control groups at the end of the experiment. In the three age groups, the treatment with GLA80/EPA30 decreased blood pressure in SHR ( $-19$ ,  $-14$ , and  $-32$  mm Hg for groups A, B, and C, respectively). The duration required to lower systolic blood pressure was different according to the age: 5 wk of treatment for groups A and C and 8 wk for group B. In the three treated groups, systolic blood pressure remained at the lowest level until the end of the experiment.

**Total FA composition of RBC membranes.** The FA composition of RBC membranes from groups A and B is presented in Table 2. Compared to control group A, the levels of 18:0 and 22:5n-3 were higher in control group B, whereas 18:1 was lower. After treatment, we observed a significant increase of GLA, EPA, and DHA in the animals fed the GLA80/EPA30 mixture. The acid 22:4n-6 decreased in the two experimental groups compared to controls. However, 18:2n-6 and 20:4n-6, which are EFA of the n-6 family, remained unchanged after treatment.

**TAG and CE FA composition of plasma.** Table 3 shows the FA composition of plasma TG. When comparing SHR control groups with each other, plasma TAG of group C had increased 18:3 n-6 (about threefold vs. the two other groups) and 20:4n-6 (+50% vs. group A). In each age group, treatment increased the levels of 20:5n-3, 22:6n-3, and 18:3n-6. In

**TABLE 2**  
Total FA Composition<sup>a</sup> of Red Blood Cells from Control and Experimental Spontaneously Hypertensive Rats (SHR)

FA	Weight %			
	Group A 4 wk-old SHR		Group B 19 wk-old SHR	
	Control	Experimental	Control	Experimental
18:0	13.4 $\pm$ 1.0	12.9 $\pm$ 1.2	25.0 $\pm$ 1.5 <sup>b</sup>	24.0 $\pm$ 3.0 <sup>c</sup>
18:1n-7 + n-9	14.6 $\pm$ 0.5	14.2 $\pm$ 0.8	10.9 $\pm$ 0.5 <sup>b</sup>	12.2 $\pm$ 0.5
18:2n-6	8.0 $\pm$ 0.7	7.0 $\pm$ 0.5	6.2 $\pm$ 0.4 <sup>b</sup>	7.2 $\pm$ 0.4 <sup>c</sup>
<b>18:3n-6</b>	<b>0.03 <math>\pm</math> 0.02</b>	<b>0.2 <math>\pm</math> 0.05**</b>	<b>0.03 <math>\pm</math> 0.02</b>	<b>0.2 <math>\pm</math> 0.05**</b>
20:4n-6	12.7 $\pm$ 1.7	13.8 $\pm$ 3.3	10.3 $\pm$ 0.8	11.8 $\pm$ 1.3
<b>20:5n-3</b>	<b>0.02 <math>\pm</math> 0.01</b>	<b>0.9 <math>\pm</math> 0.3*</b>	—	<b>0.3 <math>\pm</math> 0.1*<sup>c</sup></b>
22:4n-6	1.4 $\pm$ 0.3	0.7 $\pm$ 0.1*	2.1 $\pm$ 0.5	1.0 $\pm$ 0.03 <sup>***c</sup>
22:5n-6	1.1 $\pm$ 0.08	0.8 $\pm$ 0.2	1.8 $\pm$ 0.3	1.0 $\pm$ 0.09*
22:5n-3	0.3 $\pm$ 0.1	1.9 $\pm$ 0.7*	1.2 $\pm$ 0.3 <sup>b</sup>	2.0 $\pm$ 0.3*
<b>22:6n-3</b>	<b>0.5 <math>\pm</math> 0.4</b>	<b>1.5 <math>\pm</math> 0.7*</b>	<b>0.7 <math>\pm</math> 0.08</b>	<b>1.8 <math>\pm</math> 0.2**</b>

<sup>a</sup>Results are shown as mean  $\pm$  SEM for groups A ( $n = 6$ ) and B ( $n = 8$ ). \* $P < 0.05$  and \*\* $P < 0.01$  when compared with corresponding control. Boldface used to emphasize certain FA in mixture.

<sup>b,c</sup> $P < 0.05$  for groups A and B inside each diet (control or experimental).

**TABLE 3**  
**TAG FA Composition<sup>a</sup> (wt%) of Plasma from Control and Experimental SHR**

FA	Group A 4 wk-old SHR		Group B 19 wk-old SHR		Group C 50 wk-old SHR	
	Control	Experimental	Control	Experimental	Control	Experimental
16:0	22.0 ± 1.8	26.5 ± 1.0*	22.0 ± 2.1	26.1 ± 2.7	20.6 ± 1.2	21.2 ± 2.0
16:1n-7	4.6 ± 0.6	8.2 ± 0.8**	6.1 ± 1.1	7.6 ± 1.2	6.5 ± 1.6	7.4 ± 0.7
18:0	3.1 ± 0.2 <sup>b</sup>	5.3 ± 0.6*, <sup>d,e</sup>	4.5 ± 1.0 <sup>b</sup>	6.2 ± 0.6 <sup>d</sup>	2.8 ± 0.3	3.4 ± 0.9 <sup>e</sup>
18:1n-7 + n-9	36.5 ± 1.4	31.2 ± 1.4*	34.1 ± 1.7	32.9 ± 2.1	34.1 ± 1.2	28.2 ± 1.3**
18:2n-6	22.4 ± 2.1	15.4 ± 0.7**	22.0 ± 2.5	17.8 ± 2.6	21.5 ± 1.6	19.3 ± 3.8
<b>18:3n-6</b>	<b>0.6 ± 0.1</b>	<b>1.9 ± 0.8</b>	<b>0.4 ± 0.1</b>	<b>0.9 ± 0.6</b>	<b>1.7 ± 0.7<sup>b</sup></b>	<b>2.4 ± 1.0</b>
20:4n-6	5.0 ± 0.4 <sup>b</sup>	2.6 ± 0.3**	5.5 ± 1.0 <sup>b,c</sup>	2.5 ± 0.7*	7.5 ± 0.7 <sup>c</sup>	3.0 ± 0.2**
<b>20:5n-3</b>	—	<b>2.1 ± 0.6**,<sup>d,e</sup></b>	—	<b>1.5 ± 0.7*,<sup>d</sup></b>	<b>0.07 ± 0.05<sup>b</sup></b>	<b>4.0 ± 1.0**,<sup>e</sup></b>
22:4n-6	1.5 ± 0.3	—**	0.9 ± 0.2	—**	1.7 ± 0.5	—*
22:5n-6	0.8 ± 0.1	—**	0.6 ± 0.2	—**	0.6 ± 0.02	—*
22:5n-3	0.30 ± 0.02	1.6 ± 0.5*	0.20 ± 0.08	0.6 ± 0.4	0.10 ± 0.08	2.1 ± 0.6**
<b>22:6n-3</b>	<b>0.06 ± 0.06</b>	<b>2.9 ± 0.3**</b>	<b>0.30 ± 0.09</b>	<b>1.1 ± 0.7</b>	<b>0.10 ± 0.08</b>	<b>7.4 ± 1.2**,<sup>d</sup></b>

<sup>a</sup>Results are shown as mean ± SEM for control group A ( $n = 4$ ) and for groups B and C and experimental group A ( $n = 5$ /group). \* $P < 0.05$  and \*\* $P < 0.01$  when compared with the corresponding control. Boldface used to emphasize certain FA in mixture. See Table 2 for abbreviation.

<sup>b-e</sup> $P < 0.05$  for groups A–C compared inside each diet (control or experimental).

group C, 20:5n-3 increased in greater proportion than in groups A and B (+90 and +166%, respectively). In the same way, the increase of 22:6n-3 was higher in group C than in groups B and A (6.7-fold vs. group B and 2.5-fold vs. group A). Compound 20:4n-6 was decreased in all treated groups (–48, –55, and –60% in groups A, B, and C, respectively), whereas 22:4n-6 and 22:5n-6 were not detectable in treated animals. Linoleic acid (18:2n-6) decreased in all groups, and significantly in group A. As for the other FA, 16:0 increased in treated groups A and B and 16:1n-7 and 18:0 increased in treated group A. Acid 18:1 decreased in all groups, significantly in groups A and C.

Table 4 shows the FA composition of plasma CE. There is no significant difference between control groups except for 16:1n-7, which was higher for group B. In the three treated SHR groups, 18:3n-6, 20:5n-3, and 22:6n-3 increased significantly. A marked decrease of 20:4n-6 and a slight decrease of 18:2n-6 appeared in the three experimental groups. Compounds 18:1 and 16:1n-7 increased in groups A and B but remained unchanged in group C. Compounds 16:0 and 18:0 in-

creased whatever the age of animals, but less so in group C. We did not detect any 22:4n-6, 22:5n-6, or 22:5n-3, whatever the group of rats.

## DISCUSSION

To our knowledge, this study is the first to compare the effects of a specific FA mixture from vegetable and fish origin in SHR at different ages. The treatment has been administered to young rats (group A) during the development of the pathogenesis of hypertension; to adults (group B) when hypertension is well established; and to aging rats (group C). Body weights of experimental groups A and B remained similar to controls during the treatment. These observations indicate good acceptance by SHR of the treatment. However, in group C, the body weights of experimental rats increased significantly compared to controls after 8 and 10 wk of diet. This phenomenon was associated with an increased food intake after 10 wk of treatment although the treatment mode was identical in the three groups. Surprisingly, the animals from group C ate more and

**TABLE 4**  
**Cholesterol Ester FA Composition<sup>a</sup> (wt%) of Plasma from Control and Experimental SHR**

FA	Group A 4 wk-old SHR		Group B 19 wk-old SHR		Group C 50 wk-old SHR	
	Control	Experimental	Control	Experimental	Control	Experimental
16:0	10.2 ± 1.0	16.0 ± 0.6**	10.2 ± 0.8	14.7 ± 0.2*, <sup>c</sup>	9.3 ± 0.8	10.6 ± 1.1 <sup>d</sup>
16:1n-7	4.6 ± 0.7	7.8 ± 1.3*	5.7 ± 1.3 <sup>b</sup>	8.4 ± 1.3	4.3 ± 0.3	5.0 ± 0.4
18:0	1.5 ± 0.3	4.2 ± 1.0*, <sup>c</sup>	1.7 ± 0.3	3.7 ± 0.5**, <sup>d</sup>	1.0 ± 0.2	1.4 ± 0.2
18:1n-7 + n-9	7.7 ± 0.3	10.1 ± 0.8*	8.3 ± 0.6	10.1 ± 0.8*	8.4 ± 0.5	8.5 ± 1.0
18:2n-6	13.1 ± 0.8	11.1 ± 0.7	13.0 ± 0.2	10.7 ± 0.5*	12.8 ± 0.1	11.9 ± 0.3
<b>18:3n-6</b>	<b>0.4 ± 0.3</b>	<b>4.6 ± 0.4**</b>	<b>0.8 ± 0.1</b>	<b>5.2 ± 1.1**</b>	<b>0.9 ± 0.3</b>	<b>5.2 ± 0.1**</b>
20:4n-6	60.9 ± 1.7	39.7 ± 2.2**	58.8 ± 2.4	39.0 ± 2.7**	61.0 ± 1.1	45.1 ± 2.4**
<b>20:5n-3</b>	—	<b>3.4 ± 0.4**</b>	—	<b>5.1 ± 0.6**,<sup>c</sup></b>	<b>0.7 ± 0.7</b>	<b>9.1 ± 0.6**,<sup>d</sup></b>
<b>22:6n-3</b>	<b>0.5 ± 0.2</b>	<b>1.4 ± 0.4*</b>	<b>0.3 ± 0.1</b>	<b>1.5 ± 0.2**</b>	<b>0.6 ± 0.2</b>	<b>2.2 ± 0.3**</b>

<sup>a</sup>Results are shown as mean ± SEM for control groups A–C ( $n = 5$ /group) and experimental group A ( $n = 5$ ). \* $P < 0.05$  and \*\* $P < 0.01$  when compared with corresponding control. Boldface used to emphasize certain FA in mixture. See Table 2 for abbreviation.

<sup>b-d</sup> $P < 0.05$  for groups A–C compared inside each diet (control or experimental).

gained more weight than their controls, especially at the end of the feeding period. In this group, the lowering of blood pressure started earlier than in groups A and B—from week 5 to week 11 of the treatment. As SHR are usually smaller than the nonhypertensive control rats (WKY) used in these experiments once hypertension has been stabilized (33), we can hypothesize that the blood pressure-lowering effect of the treatment leads to a long-range weight compensation.

Based on our findings, this treatment with GLA80/EPA30 attenuated the development of elevated blood pressure in SHR. The greatest reduction of blood pressure was obtained with the oldest animals. For young (group A) and aged (group C) rats, the treatment effect was evident after 5 wk of administration of the experimental diet, while 8 wk were needed for adults (group B). Using purified PUFA, other authors have shown the ability of GLA (27) and EPA/DHA (7,8,34,35) to decrease blood pressure. Until now, the only studies that have reported GLA reduced blood pressure involved GLA administration by peritoneal injection (27) or by force-feeding (36); other studies have found no effect or opposite effects (9–11). It has been considered that DHA is the principal n-3 FA responsible for lowering blood pressure in humans (37). None of these studies included GLA, EPA, and DHA combined together, nor did they include investigations from young to aged rats. In an earlier part of this work, using the same control diet and the same strain, we investigated the effect of EPA30 alone and found no decrease in blood pressure in the experimental SHR group (12). Indeed, we showed that EPA30 increased the level of trienoic prostaglandin precursors and decreased the level of dienoic prostaglandin precursors. In the present work, we added GLA80 to EPA30 because the low cardiovascular morbidity of Greenland Eskimos has been linked to their unique diet of seafood rich in n-3 PUFA, and to their accumulation of GLA and DGLA (38), thus suggesting an inhibition of  $\Delta 5$  desaturase. The mixture used in the present experiment mimics such physiological conditions.

We showed that elevated blood pressure was related to changes in cell membrane lipids and fluidity (39), which could induce changes in receptor–effector coupling (40). The FA composition of RBC also has been studied, since membrane PUFA influence some transmembrane ion transport systems and since membrane cation fluxes in RBC may be altered in essential hypertension. We did not observe any decrease of 18:2n-6, as reported in the literature (14), when, consistent with a previous study (41), increased EPA and DHA levels were induced by the treatment. This can be explained by the addition of GLA, which is the  $\Delta 6$  desaturated product of 18:2n-6, in the treatment and by the fact that ISIO4 oil contains a high level of 18:2n-6. Arachidonic acid (20:4n-6) content was not affected by the age of the animals and the treatment. Therefore, a GLA supply appears required to avoid a decrease of 20:4n-6 in erythrocyte membranes, a phenomenon that is usually observed in essential hypertension (42). All together, the GLA80/EPA30 diet induced the positive expected effects of EPA and DHA, i.e., it prevented the reduction of n-6 PUFA.

The plasma PUFA composition reflects the treatment with GLA80/EPA30, in agreement with previous studies showing increased n-3 PUFA levels with marine oil dietary supplementation (15). The decrease of 20:4n-6 and of its elongation/desaturation products (22:4n-6 and 22:5n-6) indicates that the n-3 FA increased at the expense of n-6 PUFA. In young rats, the level of 18:2n-6 decreased, as previously observed with dietary fish oil supplementation (5). Indeed, this decrease was smaller in adults, and no difference was observed in the oldest rats. Although GLA is a 20:4n-6 precursor, we found a decrease of plasma 20:4n-6. This result is probably due to a partial inhibition of  $\Delta 6$  n-6 and/or  $\Delta 5$  n-6 desaturation steps by n-3 PUFA, as described by Christiansen *et al.* (43). These changes in arachidonic acid content could, as a consequence, induce a decrease of thromboxane A<sub>2</sub>, a strong vasoconstrictor and pro-aggregant lipid mediator, as observed in platelets of mice consuming a diet supplemented with n-3 PUFA (44).

Serum n-3 PUFA have been inversely correlated with cardiovascular disease (29), and n-3 FA intake may reduce not only blood pressure but also platelet aggregability (1,42) and consequently lower the risk of atherosclerosis (45). We found an increase of serum n-3 PUFA in both TAG and CE that was associated with reduced blood pressure, whatever the age of the animals, counterbalancing the high levels of 20:4n-6 in plasma CE generally described in hypertension (46). The present treatment appears to be efficient in decreasing the level of this plasma FA in all groups.

In summary, in contrast to what we observed with EPA30 alone (12), the treatment of SHR with GLA80/EPA30 reduced blood pressure, particularly in the oldest animals. The treatment appeared also to be active when administered during the prehypertensive phase. In light of the current findings, if such a FA mixture is relevant for laboratory studies involving experimental models of hypertension, given the different fat and FA metabolism in SHR vs. humans, how relevant these observations are to humans remains to be determined.

## ACKNOWLEDGMENTS

This investigation was supported by Ministère de l'Éducation Nationale, de la Recherche et de la Technologie and Région de Bourgogne, France. Sandrine Bellenger-Germain was recognized for this work at the 91st Annual Meeting of the AOCS (San Diego, CA, April 25–28, 2000). The authors are indebted to Callanish Ltd. Breaslete for providing purified EPA30 and GLA80, to Joseph Gresti for technical advice, and to Jérôme Bellenger for technical assistance.

## REFERENCES

1. Lorenz, R., Spengler, U., Fischer, S., Duhm, J., and Weber, P.C. (1983) Platelet Function, Thromboxane Formation and Blood Pressure Control During Supplementation of the Western Diet with Cod Liver Oil, *Circulation* 67, 504–511.
2. Morris, M.C., Sacks, F., and Rosner, B. (1993) Does Fish Oil Lower Blood Pressure? A Meta-analysis of Controlled Trials, *Circulation* 88, 523–533.



3. Bao, D.Q., Mori, T.A., Burke, V., Puddey, I.B., and Beilin, L.J. (1998) Effects of Dietary Fish and Weight Reduction on Ambulatory Blood Pressure in Overweight Hypertensives, *Hypertension* 32, 710–717.
4. Howe, P.R.C., Rogers, P.F., and Lungershausen, Y. (1991) Blood Pressure Reduction by Fish Oil in Adult Rats with Established Hypertension—Dependence on Sodium Intake, *Prostaglandins Leukot. Essent. Fatty Acids* 44, 113–117.
5. Yin, K., Chu, Z.M., and Beilin, L.S. (1991) Blood Pressure and Vascular Reactivity Changes in Spontaneously Hypertensive Rats Fed Fish Oil, *Br. J. Pharmacol.* 102, 991–997.
6. Bonaa, K.H., Bjerve, K.S., Straume, B., Gram, I.T., and Thelle, D. (1990) Effect of Eicosapentaenoic and Docosahexaenoic Acids on Blood Pressure in Hypertension. A Population-Based Intervention Trial from the Tromsø Study, *N. Engl. J. Med.* 322, 795–801.
7. Sasaki, S., Nakamura, K., Uchida, A., Fujita, H., Itoh, H., Nakata, T., Takeda, K., and Nakagawa, M. (1995) Effects of Gamma-Linolenic and Eicosapentaenoic Acids on Blood Pressure in SHR, *Clin. Exp. Pharmacol. Physiol.* (Suppl. 1), S306–S307.
8. Yin, K., Chu, Z.M., and Beilin, L.J. (1990) Effect of Fish Oil Feeding on Blood Pressure and Vascular Reactivity in Spontaneously Hypertensive Rats, *Clin. Exp. Pharmacol. Physiol.* 17, 235–239.
9. Flaten, H., Hostmark, A.T., Kierulf, P., Lystad, E., Trygg, K., Bjerkedal, T., and Osland, A. (1990) Fish-Oil Concentrate: Effects on Variables Related to Cardiovascular Disease, *Am. J. Clin. Nutr.* 52, 300–306.
10. Wing, L.M., Nestel, P.J., Chalmers, J.P., Rouse, I., West, M.J., Bune, A.J., Tonkin, A.L., and Russell, A.E. (1990) Lack of Effect of Fish Oil Supplementation on Blood Pressure in Treated Hypertensives, *J. Hypertens.* 8, 339–343.
11. Cobiac, L., Clifton, P.M., Abbey, M., Belling, G.B., and Nestel, P.J. (1991) Lipid, Lipoprotein, and Hemostatic Effects of Fish vs. Fish-Oil n-3 Fatty Acids in Mildly Hyperlipidemic Males, *Am. J. Clin. Nutr.* 53, 1210–1216.
12. Narce, M., Frenoux, J.M., Dardel, V., Foucher, C., Germain, S., Delachambre, M.C., and Poisson, J.P. (1997) Fatty Acid Metabolism, Pharmacological Nutrients and Hypertension, *Biochimie* 79, 135–138.
13. Hamazaki, T., Urakaze, M., Makuta, M., Ozawa, A., Soda, Y., Tatsumi, H., Yano, S., and Kumagai, A. (1987) Intake of Different Eicosapentaenoic Acid-Containing Lipids and Fatty Acid Pattern of Plasma Lipids in the Rats, *Lipids* 22, 994–998.
14. Rao, C.V., Zang, E., and Reddy, B.S. (1993) Effect of High Corn Oil, Olive Oil and Fish Oil on Phospholipid Fatty Acid Composition in Male F344 Rats, *Lipids* 28, 441–447.
15. Prisco, D., Filippini, M., Francalanci, I., Paniccia, R., Gensini, G.F., Abbate, R., and Neri Serneri, G.G. (1996) Effect of n-3 Polyunsaturated Fatty Acid Intake on Phospholipid Fatty Acid Composition in Plasma Erythrocytes, *Am. J. Clin. Nutr.* 63, 925–932.
16. McLennan, P., Howe, P., Abeywardena, M., Muggli, R., Raederstorff, D., Mano, M., Rayner, T., and Head, R. (1996) The Cardiovascular Protective Role of Docosahexaenoic Acid, *Eur. J. Pharmacol.* 300, 83–89.
17. Schoene, N.W., and Fiore, D. (1981) Effect of a Diet Containing Fish Oil on Blood Pressure in Spontaneously Hypertensive Rats, *Prog. Lipid Res.* 20, 569–570.
18. Rubin, D., and Laposata, M. (1992) Cellular Interactions Between n-6 and n-3 Fatty Acids: A Mass Analysis of Fatty Acid Elongation/Desaturation, Distribution Among Complex Lipids, and Conversion to Eicosanoids, *J. Lipid Res.* 33, 1431–1440.
19. Lands, W.E., Libelt, B., Morris, A., Kramer, N.C., Prewitt, T.E., Bowen, P., Schmeisser, D., Davidson, M.H., and Burns, J.H. (1992) Maintenance of Lower Proportions of (n-6) Eicosanoid Precursors in Phospholipids of Human Plasma in Response to Added Dietary (n-3) Fatty Acids, *Biochim. Biophys. Acta* 1180, 147–162.
20. Watanabe, Y., Huang, Y.-S., Simmons, V.A., and Horrobin, D.F. (1989) The Effect of Dietary n-6 and n-3 Polyunsaturated Fatty Acids on Blood Pressure and Tissue Fatty Acid Composition in Spontaneously Hypertensive Rats, *Lipids* 24, 638–644.
21. Kirtland, S.J. (1988) Prostaglandin E<sub>1</sub>: A Review, *Prostaglandins Leukot. Essent. Fatty Acids* 32, 165–174.
22. Mtabaji, J.P., Manku, M.S., and Horrobin, D.F. (1993) Abnormalities in Dihomo- $\gamma$ -Linolenic Acid: Release in the Pathogenesis of Hypertension, *Am. J. Hypertens.* 6, 458–462.
23. Miettinen, T.A., Naukkarinen, V., Huttunen, J.K., Mattilas, J., and Kumlin, T. (1982) Fatty Acid Composition of Serum Predicts Myocardial Infarction, *Br. Med. J.* 285, 993–996.
24. Dyerberg, J., Bang, H.O., and Hjörne, N. (1975) Fatty Acid Composition of the Plasma Lipids in Greenland Eskimos, *Am. J. Clin. Nutr.* 28, 958–966.
25. Engler, M.M., Engler, M.B., Erickson, S.K., and Paul, S.M. (1992) Dietary Gamma-Linolenic Acid Lowers Blood Pressure and Alters Aortic Reactivity and Cholesterol Metabolism in Hypertension, *J. Hypertens.* 10, 1197–1204.
26. Hoffmann, P., Block, H.U., Beitz, J., Taube, C., Forster, W., Wortha, P., Singer, P., Naumann, E., and Heine, H. (1986) Comparative Study of the Blood Pressure Effects of Four Different Vegetable Fats on Young, Spontaneously Hypertensive Rats, *Lipids* 21, 733–737.
27. St. Louis, C., Lee, R.M.K.W., Rosenfeld, J., and Fargas-Babjak, A. (1992) Antihypertensive Effect of  $\gamma$ -Linolenic Acid in Spontaneously Hypertensive Rats, *Hypertension* 19 (2 Suppl.), II-111–II-115.
28. Narce, M., and Poisson, J.-P. (1995) Age-Related Depletion of Linoleic Acid Desaturation in Liver Microsomes from Young Hypertensive Rats, *Prostaglandins Leukotr. Essent. Fatty Acids* 53, 59–63.
29. Simon, J.A., Hodgkins, M.L., Browner, W.S., Neuhaus, J.M., Bernert, J.T., and Hulley, S.B. (1995) Serum Fatty Acids and the Risk of Coronary Heart Disease, *Am. J. Epidemiol.* 142, 469–476.
30. Bonaa, K.H., and Thelle, D.S. (1991) Association Between Blood Pressure and Serum Lipids in a Population. The Tromsø Study, *Circulation* 83, 1305–1315.
31. Folch, J., Lees, M., and Sloane-Stanley, G.H. (1957) A Simple Method for Isolation and Purification of Total Lipids from Animal Tissues, *J. Biol. Chem.* 226, 497–509.
32. Slover, H.T., and Lanza, E. (1979) Quantitative Analysis of Food Fatty Acids by Capillary Gas Chromatography, *J. Am. Oil Soc.* 56, 933–943.
33. Narce, M., Asdrubal, P., Delachambre, M.-C., Gresti, J., and Poisson, J.-P. (1995) Influence of Spontaneous Hypertension on n-3  $\Delta$ 6-Desaturase Activity and Fatty Acid Composition of Rat Hepatocytes, *Mol. Cell. Biochem.* 152, 7–12.
34. Yosefy, C., Viskoper, J.R., Varon, D., Ilan, I., Pilpel, D., Lugassy, G., Schneider, R., Savyon, N., Adan, Y., and Raz, A. (1996) Repeated Fasting and Refeeding with 20:5n-3 Eicosapentaenoic Acid (EPA): A Novel Approach for Rapid Fatty Acid Exchange and Its Effect on Blood Pressure, Plasma Lipids and Hemostasis, *J. Hum. Hypertens.* 10 (Suppl. 3), S135–S139.
35. Engler, M.M., Engler, M.B., Goodfriend, T.L., Ball, D.L., Yu, Z., Su, P., and Kroetz, D.L. (1999) Docosahexaenoic Acid Is an Antihypertensive Nutrient That Affects Aldosterone Production in SHR, *Proc. Soc. Exp. Biol. Med.* 221, 32–38.
36. Lam, B.J., Marcinkiewicz, E., Quilley, J., Hirai, A., Yoshida, S., Tamura, Y., and Wong, P.Y.K. (1986) Hypotensive Effects of Eicosapentaenoic Acid (EPA) and Its Influence on Eicosanoid Metabolism in Spontaneously Hypertensive Rats, *J. Hypertens.* 4 (Suppl.), S453–S455.
37. Mori, T.A., Bao, D.Q., Burke, V., Puddey, I.A., and Beilin, L.J. (1999) Docosahexaenoic Acid but Not Eicosapentaenoic Acid

- Lowers Ambulatory Blood Pressure and Heart Rate in Humans, *Hypertension* 34, 253–260.
38. Dyeberg, J., and Jorgensen, K.A. (1982) Marine Oils and Thrombogenesis, *Prog. Lipid Res.* 21, 255–269.
  39. Foucher, C., Narce, M., Nasr, L., Delachambre, M.-C., and Poisson, J.-P. (1997) Liver Microsomal Membrane Fluidity and Microsomal Desaturase Activities in Adult Spontaneously Hypertensive Rats, *J. Hypertens.* 15, 863–869.
  40. Spector, A.A., and Yorek, M.A. (1985) Membrane Lipid Composition and Cellular Function, *J. Lipid Res.* 26, 1015–1035.
  41. Van den Boom, M.A.P., Groot Wassink, M., Roelofsen, B., De Fouw, N.J., and Op Den Kamp, J.A.F. (1996) The Influence of a Fish-Oil-Enriched Diet on the Phospholipid Fatty Acid Turnover in the Rabbit Red Cell Membrane *in vivo*, *Lipids* 31, 285–293.
  42. Russo, C., Olivieri, O., Guarini, P., Pasqualini, R., Azzini, M., and Corrocher, R. (1997) Increased Membrane Ratios of Metabolite to Precursor Fatty Acid in Essential Hypertension, *Hypertension* 29, 1058–1063.
  43. Christiansen, E.N., Lund, J.S., Rortveit, T., and Rustan, C.R. (1991) Effect of Dietary n-3 and n-6 Fatty Acids on Fatty Acid Desaturation in Rat Liver, *Biochim. Biophys. Acta* 1082, 57–62.
  44. Li, B., Birdwell, C., and Whelan, J. (1994) Antithetic Relationship of Dietary Arachidonic Acid and Eicosapentaenoic Acid on Eicosanoid Production *in vivo*, *J. Lipid Res.* 35, 1869–1877.
  45. Leaf, A., and Weber, P.C. (1988) Cardiovascular Effects of n-3 Fatty Acids, *N. Engl. J. Med.* 318, 549–557.
  46. Zheng, Z.J., Folsom, A.R., Ma, J., Arnett, D.K., McGovern, P.G., and Eckfeldt, J.H. (1999) Plasma Fatty Acid Composition and 6-Year Incidence of Hypertension in Middle-Aged Adults: The Atherosclerosis Risk in Communities (ARIC) Study, *Am. J. Epidemiol.* 150, 492–500.

[Received September 15, 2002, and in final revised form and accepted May 23, 2002]

# Lauric Acid Is Desaturated to 12:1n-3 by Hepatocytes and Rat Liver Homogenates

Philippe Legrand<sup>a,\*</sup>, Daniel Catheline<sup>a</sup>, Vincent Rioux<sup>a</sup>, and Georges Durand<sup>b</sup>

<sup>a</sup>Laboratoire de Biochimie INRA-ENSA, 35042 Rennes, France,

and <sup>b</sup>Laboratoire de Nutrition INRA, 78352 Jouy-en-Josas, France

**ABSTRACT:** Lauric acid desaturation was investigated and described in liver homogenates and in cultured rat hepatocytes. The identification of the desaturated product of lauric acid has been performed using the oxidative cleavage method, and we showed that the obtained monoene was mainly 12:1n-3. This result suggests that lauric acid desaturation could be the first step in the biosynthesis of  $\alpha$ -linolenic acid in animal cells.

Paper no. L8861 in *Lipids* 37, 569–572 (June 2002).

Desaturation of saturated FA is well known and documented for stearic acid (18:0) and palmitic acid (16:0). Concerning myristic acid (14:0), the presence of myristoleic acid has been detected in several tissues (1,2) as well as in a muscular cell line (3), and we have recently shown the biosynthesis and identification of 14:1n-5 by a  $\Delta 9$ -desaturation in cultured rat hepatocytes (4). Conversely, lauric acid desaturation has not yet been investigated although small amounts of lauroleic acid (12:1) are known to be present in milk lipids (5,6). The aim of this report was to study the desaturation of lauric acid in homogenates of fresh liver and in cultured rat hepatocytes. We demonstrated that, in the absence of competing substrate, lauric acid is desaturated at the  $\Delta 9$ -position, producing 12:1n-3.

## MATERIALS AND METHODS

**Chemicals.** BSA, HEPES, Williams' medium E (catalog no. W 4125), insulin (bovine), dexamethasone, collagenase, and unlabeled FA were purchased from Sigma (St Quentin Fallavier, France). Penicillin–streptomycin antibiotic mixture was provided by GIBCO BRL (Eragny, France). FBS was purchased from J. Boy S.A. (Reims, France). [1-<sup>14</sup>C]Lauric acid was purchased from Amersham-Pharmacia-Biotech (Orsay, France). [1-<sup>14</sup>C]Myristic acid, [1-<sup>14</sup>C]palmitic acid, and [1-<sup>14</sup>C]stearic acid were purchased from DuPont NEN (Le Blanc Mesnil, France). Solvent and other chemicals were obtained from Prolabo (Paris, France) or Merck (Darmstadt, Germany), except high-purity reagents for HPLC application, which were from Fisher (Elancourt, France). Falcon Primaria petri culture dishes, 60 mm in diameter (AES, Combourg, France), were used.

**Animals and diet.** Male Sprague–Dawley rats (body weight 250 g) obtained from the R. Janvier breeding center

(Le Genest-St Isle, France) were freely fed rat chow. They were food-deprived 12 h prior to sacrifice, liver removal, or hepatocyte preparation. The experimental protocol was in compliance with applicable guidelines from the French Ministry of Agriculture.

**Desaturase assay in rat liver.** Immediately after each rat was killed, the liver was removed and utilized for postmitochondrial supernatant preparation (7). A 4-g sample of liver was minced and homogenized in 16 mL of 50 mmol/L phosphate buffer (pH 7.4) containing 0.25 mol/L sucrose. The homogenate was centrifuged for 30 min at 10,000  $\times$  g. The resulting postmitochondrial supernatant was collected, diluted threefold with the phosphate buffer, and used for  $\Delta 9$ -desaturase assay as previously described (8). Enzymatic activity was determined using a 1-mL assay mixture that contained the following: 100  $\mu$ L supernatant (containing 100 to 500  $\mu$ g protein), 150 mmol/L phosphate buffer (pH 7.16), 6 mmol/L MgCl<sub>2</sub>, 7.2 mmol/L ATP, 0.54 mmol/L CoA, and 0.8 mmol/L NADH. The reaction was started with the addition of various amounts (usually 80 nmol) of [1-<sup>14</sup>C]lauric acid (660 MBq/mmol). Comparative  $\Delta 9$ -desaturase assays were also performed with 80 nmol [1-<sup>14</sup>C]myristic acid, [1-<sup>14</sup>C]palmitic acid, and [1-<sup>14</sup>C]stearic acid. The incubation was carried out in a shaking water bath at 37°C for 20 min. The reaction was stopped by adding 1 mL 2 mol/L KOH in ethanol. Each assay mixture was then heated for 30 min at 70°C. The FA were liberated by acidification, extracted with diethylether, and dried. For each desaturase assay, a control was performed whereby the reaction was stopped by addition of KOH before addition of the radiolabeled lauric acid. The percentage of apparent conversion in the control was subtracted from the one in the assay.

**Incubation of cultured rat hepatocytes with radiolabeled lauric acid.** Hepatocytes were obtained by collagenase perfusion *in situ*, as previously described (4). The culture medium (Williams' E) was supplemented with 26 mM NaHCO<sub>3</sub>, 12.5 mM HEPES, 15  $\mu$ M BSA, antibiotic mixture (50,000 IU/L penicillin, 50 mg/L streptomycin), 1  $\mu$ M insulin, and 1  $\mu$ M dexamethasone. For plating only (1.5  $\cdot$  10<sup>6</sup> cells/dish), the culture medium was supplemented with 7% (by vol) FBS. After plating, the cells were maintained in a humidified incubator at 37°C under 5% CO<sub>2</sub> in air. After 4 h, the plating medium was changed to a serum-free culture medium.

[1-<sup>14</sup>C]Lauric acid, diluted with the nonradiolabeled lauric acid to the final specific activity (183 MBq/mmol), was

\*To whom correspondence should be addressed at Laboratoire de Biochimie, INRA-ENSA, 65 rue de Saint Briec, CS 84215, 35042 Rennes Cedex, France. E-mail: Philippe.Legrand@agrennes.educagri.fr

incubated for 30 min at 70°C with 300  $\mu\text{L}$  KOH (2 mol/L) in ethanol. The FA salt obtained was dissolved at pH 10 in Williams' medium E containing 0.15 mmol/L BSA. The FA/albumin molar ratio was equal to 0.67:1. After 24 h of gentle shaking, the pH was adjusted to 7.35 and the medium was filtered through a medium with average pore size of 0.2  $\mu\text{m}$ . The solution obtained was used as incubation medium (4). The final FA concentration was 0.1 mmol/L. At 24 h of culture, incubation was initiated by replacing the culture medium with 2 mL (per dish) of [1- $^{14}\text{C}$ ]lauric acid-containing medium. Incubation was carried out for 12 h at 37°C in a 5%  $\text{CO}_2$  atmosphere.

At the end of the incubation, the medium was removed, the cells were washed twice with ice-cold PBS (150 mmol/L NaCl, 0.94 mmol/L  $\text{NaH}_2\text{PO}_4$ , 4 mmol/L  $\text{Na}_2\text{HPO}_4$ , pH 7.4) and harvested with a rubber policeman in PBS. The cell suspension was centrifuged at  $800 \times g$  for 4 min. The supernatant was discarded and the cell pellet kept for lipid extraction. Cellular lipids were extracted twice with 4 and 2 mL each hexane/isopropanol (3:2, by vol) (4). Lipid extracts were then saponified for 30 min at 70°C by 1 mL of 2 mol/L KOH in ethanol. The FA were liberated by acidification and extracted twice with diethylether. Cellular FA were then converted to FA naphthacyl esters as described below and separated on HPLC.

**FA analysis by HPLC separation.** FA from either desaturase assay or cultured hepatocyte incubation were converted to FA naphthacyl esters as recently described (9). The derivatization procedure was started by addition of 500  $\mu\text{L}$  2-bromo-2'-acetonaphthone (0.04 mol/L in acetone) and 500  $\mu\text{L}$  triethylamine (0.1 mol/L in acetone) to the FA extracts. After 15 min in a boiling water bath, 1 mL of acetic acid solution (0.033 mol/L in acetone) was added for an additional 10 min at 100°C. After evaporation, naphthacyl derivatives were dissolved with 200  $\mu\text{L}$  of a mixture of methanol/dichloromethane (3:1, by vol.). Twenty microliters of the derivative solution was used for analysis. FA naphthacyl esters were separated on HPLC (Alliance integrated system; Waters, St Quentin en Yvelines, France) using a Nova-Pak C18 column ( $4.6 \times 250$  mm; Waters) and a guard column (Nova-Pak C18;  $3.9 \times 20$  mm; Waters). The separation was performed by elution (1 mL/min) with a gradient of methanol/acetonitrile/water starting at 10:80:10 (by vol) and increasing to 0:90:10 (by vol) over a period of 50 min. Elution of naphthacyl derivatives was monitored by UV absorbance at 246 nm (tunable absorbance detector 486; Waters). Peaks corresponding to radiolabeled FA (substrate and product of the desaturase assays) were collected (fraction collector, Waters) and subjected to liquid scintillation counting (Packard Tri-Carb 1600 TR, Meriden, CT).

Preliminary identification of FA naphthacyl esters was based on retention times obtained for naphthacyl esters prepared from radiolabeled and nonradiolabeled FA standards (9).

From the amount of radioactivity found in the monoene product vs. the radioactivity recovered in the saturated sub-

strate, the enzyme activity could be determined and expressed as pmol substrate converted to product/mg protein/min.

**Identification of radiolabeled monounsaturated FA by oxidative cleavage.** To identify the radiolabeled monounsaturated FA derived from [1- $^{14}\text{C}$ ]lauric acid, the position of the double bond was determined according to the method of Von Rudloff (10), adapted in this laboratory for FA naphthacyl esters (9). Unsaturated FA naphthacyl esters separated by HPLC were collected. They were then submitted to oxidative cleavage by a mixture of permanganate-periodate for 6 h. The mono- and dicarboxylic acids obtained were extracted by addition of diethylether, converted to naphthacyl esters as previously described, and separated by HPLC first with an isocratic elution (1 mL/min) of acetonitrile/water (50:50, vol/vol) for 10 min, then by increasing linearly to (100:0, vol/vol) for 40 min. Retention times of mono- and dicarboxylic acids were previously determined by standard analysis (Fluka, St Quentin Fallavier, France). Radiolabeled dicarboxylic acids were collected and subjected to liquid scintillation counting. The radioactivity recovered in dicarboxylic acids and the chain length indicate the double-bond position on the monounsaturated FA.

**Protein measurement.** Protein was determined by a modified Lowry procedure (11), either in the supernatant used for the  $\Delta 9$ -desaturase assays or in the cells as total cellular protein.

**Expression of results and statistical analysis.** The values reported are means  $\pm$  SD. *P*-values were calculated by using Student's test for two-group comparisons. The differences were considered significant at a *P*-value of less than 0.05.

## RESULTS AND DISCUSSION

Lauric acid desaturation activity was first obtained using a post-mitochondrial supernatant of rat liver. The routinely used  $\Delta 9$ -desaturase assay was adapted for [1- $^{14}\text{C}$ ]lauric acid as substrate: we incubated 80 nmol of [1- $^{14}\text{C}$ ]lauric acid (660 MBq/mmol), i.e., about  $3 \cdot 10^6$  dpm/assay with the postmitochondrial fraction from rat liver. Only 10% of the total FA extracted from the assay was injected and analyzed by HPLC so that the column was not overloaded (i.e., about  $3 \cdot 10^5$  dpm/injection). We usually recovered about 6,000 dpm in the monounsaturated product after HPLC separation. The percentage of desaturation was obtained from these two values (about 2%). Moreover, for each  $\Delta 9$ -desaturase assay, a control was performed where by the reaction was stopped by addition of KOH before addition of the radiolabeled lauric acid. This control was also analyzed by HPLC in order to measure the background value of dpm in the collected fraction corresponding to the 12:1 peak (less than 500 dpm), showing the presence of impurities (12:1) in the 12:0 radiolabeled preparation.

The desaturation activity was measured with different substrate concentrations (Fig. 1). We showed a curve reaching a plateau at about 80  $\mu\text{M}$  lauric acid concentration. At this substrate concentration, lauric acid desaturase activity was measured in six animals, and we obtained a mean value of 120



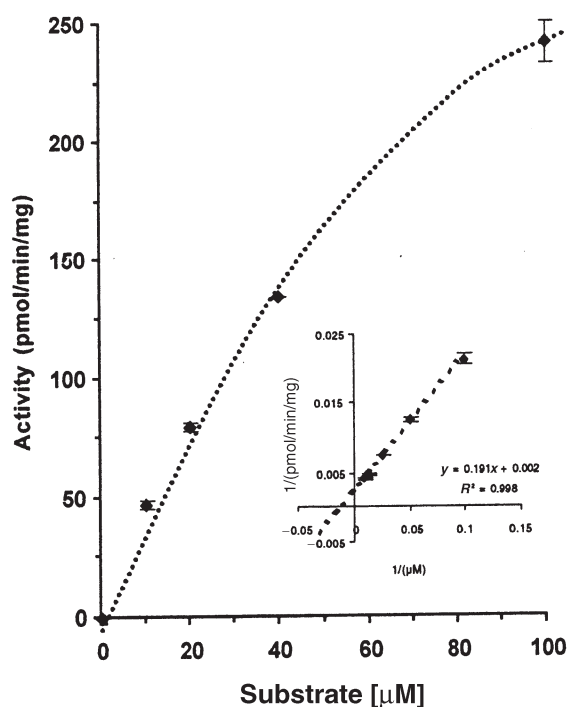


FIG. 1.  $\Delta 9$ -Desaturase activity as a function of lauric acid concentration. Each point is the mean of three measurements  $\pm$  SD. The insert presents the Lineweaver-Burke plot of the desaturase activity (estimated apparent  $K_m \approx 75 \mu\text{M}$ ).

pmol/min/mg protein. The comparison with the  $\Delta 9$ -desaturation activity of the other substrates (myristic, palmitic, and stearic acids) was performed on three animals, showing a clear increase in activity as a function of the chain length of the substrate (Fig. 2).

Identification of the desaturated product of lauric acid has been performed on the  $C_{12}$  monoene using the oxidative cleavage method described above (see the Materials and Methods section). After the oxidative cleavage of the  $C_{12}$  monoene, we obtained a  $C_9$  dicarboxylic acid carrying 70% of the radioactivity (Fig. 3). We thus demonstrated that the product of lauric desaturation was mainly 12:1n-3, obtained by a  $\Delta 9$ -desaturase.

A second experiment was performed using a cultured rat hepatocyte system. [ $1\text{-}^{14}\text{C}$ ]Lauric acid substrate was added to the culture medium in the form of an albuminic complex, and analysis of the different labeled FA after 12 h incubation demonstrated the presence of a labeled 12:1 monoene (Fig. 4). Its identification using the oxidative cleavage method (see above) and analysis of labeled dicarboxylic fragments showed that this monoene was mainly 12:1n-3. The desaturation of lauric acid was quantitatively low compared to other metabolic fats: Only 35% of the initial radioactivity was still in FA form after 12 h incubation, suggesting a high  $\beta$ -oxidation level. Thus, besides  $\beta$ -oxidation, we could observe that lauric acid was mainly converted to myristic and palmitic acids.

Our results indicate for the first time that lauric acid is desaturated in rat liver homogenate and in cell culture. This is

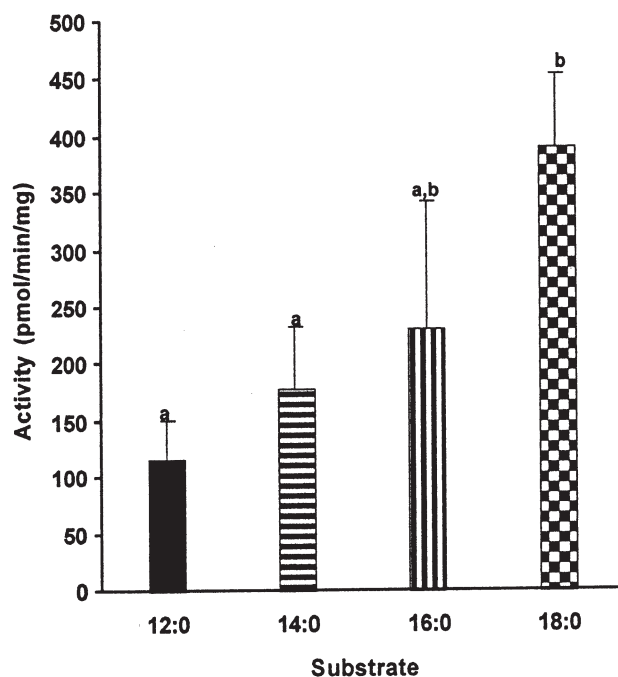


FIG. 2. Comparative desaturation activity of lauric, myristic, palmitic, and stearic acids in rat liver. Postmitochondrial supernatant from liver homogenate (same amount of protein) was used for desaturase assay as described in the Materials and Methods section. Each point is the mean of three measurements  $\pm$  SD. Significant differences ( $P < 0.2$ ) are indicated by differing letters. The apparent  $K_m$  are 34, 22, and 10  $\mu\text{M}$  for myristic, palmitic, and stearic acids, respectively, in our experimental conditions.

in agreement with an observation (12) reported in 1976 that dodecanoyl-CoA was the substrate (very low activity) of a reconstructed desaturase system.

The principal interest of the present work is to show that the main product of lauric acid desaturation under our condi-

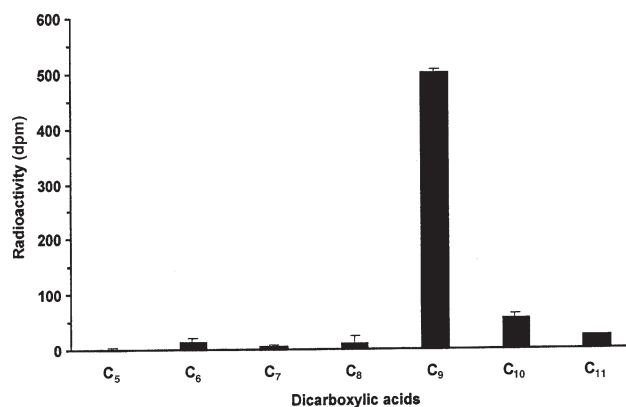
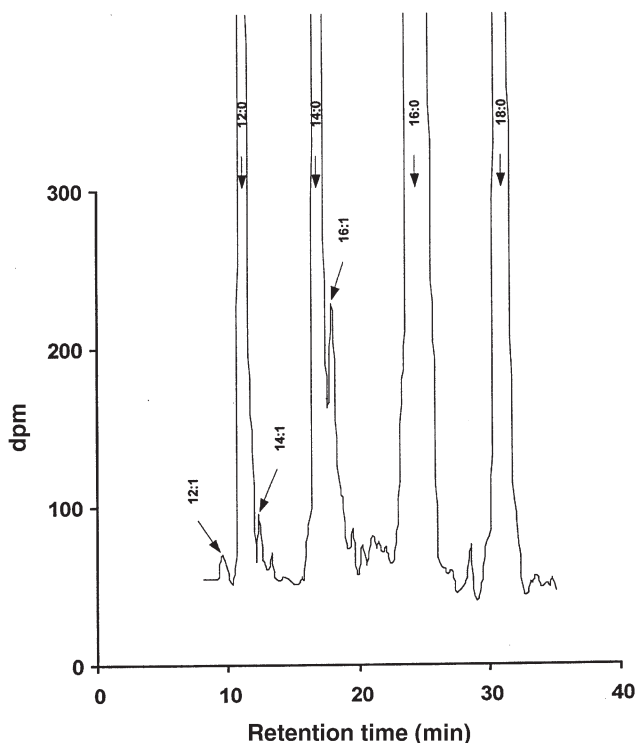


FIG. 3. Radioactivity recovered in dicarboxylic acids following the oxidative cleavage of 12:1. The identification of the 12:1 produced by lauric acid desaturation was performed by oxidative cleavage by a permanganate-periodate mixture for 6 h and by HPLC separation of the obtained dicarboxylic acids (identified by retention time) as described in the Materials and Methods section. Each value is the mean of three measurements  $\pm$  SD.



**FIG. 4.** Radioactivity of the FA obtained after a 12-h incubation of [ $^{14}\text{C}$ ]lauric acid with cultured rat hepatocytes (see the Materials and Methods section). FA were separated by HPLC and collected every 10 s. They were identified by comparison of retention times with those of standard FA. Each fraction was submitted to liquid scintillation counting, and the radioactivity vs. retention time was plotted.

tions is a member of the n-3 series. We propose a possible pathway that requires neither  $\Delta 12$ -desaturase nor  $\Delta 15$ -desaturase. Indeed, from successive conversion of 12:0 by  $\Delta 9$ -desaturation,  $\Delta 6$ -desaturation, elongation,  $\Delta 5$ -desaturation, and two final elongations, 18:3n-3 could be obtained. We may bear in mind here that the last elongation step of our putative pathway was described by Klenk in 1965 (13) and confirmed by Cunnane *et al.* (14), who obtained 18:3n-3 from 16:3n-3.

Although, in the present conditions, we did not observe biosynthesis of 12:1n-6 from 12:0, we suggest that 18:2n-6 biosynthesis from 12:0 might be possible using exclusively  $\Delta 6$ - and  $\Delta 5$ -desaturations and elongations. The two last steps of this putative pathway have been demonstrated in the past by Sprecher in 1968 (15), who showed a biosynthesis of 18:2n-6 from 14:2n-6 and 16:2n-6 in fat-deficient rats. Later, Cunnane *et al.* (14) confirmed these results using 16:2n-6 as a precursor. In the experimentation by Sprecher (15), neither 10:1n-6 nor 12:2n-6 was transformed into linoleic acid. Using rats fed a fat-free diet would be of great interest to further investigate our putative pathway. We have already observed (data not shown) 30 generations of a lineage of lipid-deprived rats that were healthy and exhibited only a reduction in pup growth, described up to the fifth generation (16).

In conclusion, the present results showing the  $\Delta 9$ -desaturation of lauric acid into 12:1n-3 in cultured cells and liver homogenates have led us to ask whether a possible biosynthesis of "essential" FA could exist under some circumstances in animals.

## REFERENCES

- Schenck, P.A., Rakoff, H., and Emken, E.A. (1996)  $\Delta 8$ -Desaturation *in vivo* of Deuterated Eicosatrienoic Acid by Mouse Liver, *Lipids* 31, 593–600.
- Hamosh, M., and Bitman, J. (1992) Human Milk in Disease: Lipid Composition, *Lipids* 27, 848–857.
- Wang, L., Kaduce, T.L., and Spector, A.A. (1991) Myristic Acid Utilization and Processing in BC3H1 Muscle Cells, *J. Biol. Chem.* 266, 13883–13890.
- Rioux, V., Lemarchal, P., and Legrand, P. (2000) Myristic Acid, Unlike Palmitic Acid, Is Rapidly Metabolized in Cultured Rat Hepatocytes, *J. Nutr. Biochem.* 11, 198–207.
- Balcao, V.M., Kemppinen, A., Malcata, F.X., and Kalo, P.J. (1998) Modification of Butterfat by Selective Hydrolysis and Interesterification by Lipase: Process and Product Characterization, *J. Am. Oil Chem. Soc.* 75, 1347–1358.
- Jensen, R.G., and Newburg, D.S. (1995), Milk Lipids, Part B: Bovine Milk Lipids, in *Handbook of Milk Composition* (Jensen, R.G., ed.), pp. 543–575, Academic Press, San Diego.
- Legrand, P., and Hermier, D. (1992) Hepatic  $\Delta 9$ -Desaturation and Plasma VLDL Level in Genetically Lean and Fat Chickens, *Int. J. Obes.* 16, 289–294.
- Legrand, P., Catheline, D., Fichot, M.-C., and Lemarchal, P. (1997) Inhibiting  $\Delta 9$ -Desaturase Activity Impairs Triacylglycerol Secretion in Cultured Chicken Hepatocytes, *J. Nutr.* 127, 249–256.
- Rioux, V., Catheline, D., Bouriel, M., and Legrand, P. (1999) High-Performance Liquid Chromatography of Fatty Acids as Naphthacyl Derivatives, *Analisis* 27, 186–193.
- Von Rudloff, E. (1956) Oxidation of Lipids in Media Containing Organic Solvents, *Can. J. Chem.* 34, 1413–1418.
- Bensadoun, A., and Weinstein, D. (1976) Assay of Proteins in the Presence of Interfering Materials, *Anal. Biochem.* 70, 241–250.
- Enoch, H.G., Catala, A., and Strittmatter, P. (1976) Mechanism of Rat Liver Microsomal Stearoyl-CoA Desaturase, *J. Biol. Chem.* 251, 5095–5103.
- Klenk, E. (1965) The Metabolism of Polyenoic Fatty Acids, *Adv. Lipid Res.* 3, 1–23.
- Cunnane, S.C., Ryan, M.A., Craig, K.S., Brookes, S., Koletzko, B., Demmelair, H., Singer, J., and Kyle, D.J. (1995) Synthesis of Linoleate and  $\alpha$ -Linolenate by Chain Elongation in the Rat, *Lipids* 30, 781–783.
- Sprecher, H. (1968) The Total Synthesis and Metabolism of 4-Decenoate, Dodeca-3,6-dienoate, Tetradeca-5,8-dienoate, and Hexadeca-7,10-dienoate in the Fat-Deficient Rat, *Lipids* 3, 14–20.
- Ollivier-Bousquet, M., Lavialle, F., Guesnet, P., Rainteau, D., and Durand, G. (1997) Lipid-Depleted Diet Perturbs Membrane Composition and Intracellular Transport in Lactating Mammary Cells, *J. Lipid Res.* 38, 913–925.

[Received June 20, 2001; and in revised form May 2, 2002; accepted May 2, 2002]

# LDL Binding to Lipid Emulsion Particles: Effects of Incubation Duration, Temperature, and Addition of Plasma Subfractions

Nathalie F. Chanson<sup>a</sup>, Jean-François Lontie<sup>1,a</sup>, Annette Gulik<sup>b</sup>,  
Jacqueline Férézou<sup>c,\*</sup>, and Yvon A. Carpentier<sup>a</sup>

<sup>a</sup>L. Deloyers Laboratory for Experimental Surgery, Université Libre de Bruxelles, Brussels, Belgium,

<sup>b</sup>Centre de Génétique Moléculaire, CNRS, Gif sur Yvette, France,

and <sup>c</sup>Laboratoire de Physiologie de la Nutrition, Université Paris-Sud, Orsay, France

**ABSTRACT:** Lipid emulsions used in parenteral nutrition interact with lipoproteins leading to exchanges of lipids and acquisition of several apolipoproteins (apo). It has been previously observed that, during *in vitro* incubation of emulsions with purified LDL, a variable fraction of LDL binds to TG-rich emulsion particles. The purpose of this study was to better characterize such an interaction. Two emulsions containing 20% soybean oil (Endolipid®, B. Braun AG, Melsungen, Germany) or fish oil were incubated with LDL, either alone or in the presence of various plasma subfractions, for different durations and at different temperatures. The fraction named M-LE (containing TG-rich particles modified after incubation) was separated by ultracentrifugation or gel filtration chromatography, and the apoB content was measured as an index of LDL binding to TG-rich emulsion particles. The formation of such complexes was visualized by freeze-fracture electron microscopy. LDL binding was not influenced by the method used for M-LE isolation. Binding occurred quickly, did not increase with prolonged incubation, was inversely related to increasing incubation or ultracentrifugation temperature, and withstood 40 h of ultracentrifugation at 163,000 × *g*. The presence of glycerol or excess phospholipids in the emulsion did not markedly affect the formation of the complexes. In contrast, adding very small amounts of lipoprotein-poor plasma (*d* > 1.210 g/mL) or HDL markedly reduced the process, and albumin had no effect. The TG composition of the emulsion influenced the binding of LDL to TG-rich particles, since more apoB was found in M-LE from fish oil than from soybean oil emulsion.

Paper no. L8965 in *Lipids* 37, 573–580 (June 2002).

Lipid emulsions used in parenteral nutrition contain a majority of TG-rich particles that resemble endogenous chylomicrons with respect to size and structural assembly. They differ from chylomicrons mainly by the absence of structural apolipoproteins (apo) such as apoB-48 and apoA-1. These particles are suspended in a mesophase, containing glycerol and an excess of phospholipid (PL) emulsifier, that can be isolated by ultracentrifugation as a fraction of PL-rich particles (1).

Like TG-rich lipoproteins (TRL), infused emulsion particles interact with endogenous lipoproteins and acquire sev-

<sup>1</sup>Deceased.

\*To whom correspondence should be addressed at Laboratoire de Physiologie de la Nutrition, Bâtiment 447, Université Paris-Sud, F-91 405 Orsay, France. E-mail: jacqueline.ferezou@ibaic.u-psud.fr

Abbreviations: apo, apolipoproteins; CE, cholesteryl esters; CETP, cholesteryl ester transfer protein; M-LE, modified-lipid emulsion particles; PL, phospholipids; TRL, TG-rich lipoproteins.

eral exchangeable apo, namely, apoC and apoE, from HDL (2–6). They also transfer some of the exogenous PL to plasma lipoproteins (7). In addition, cholesteryl ester (CE) and TG exchanges, regulated by the cholesteryl ester transfer protein (CETP), take place between TG-rich particles and CE-rich lipoproteins (8–10). Exchanges of lipids, apo, and other proteins also take place during *in vitro* incubations of emulsions with lipoproteins (3,4,11). More specifically, inverse changes in the overall fluidity of both TG-rich particles and LDL have been observed after incubation (12).

Preliminary studies showed that the incubation of various emulsions with purified LDL resulted in the enrichment of emulsion TG-rich particles with both CE and apoB, despite the absence of CETP (13). Since apoB is a nontransferable structural apo deeply anchored in LDL (14,15), this finding suggested some binding of LDL to emulsion particles and the formation of complexes. As could be expected, adding lipoprotein-poor plasma as a source of CETP (16) to the incubation mixture increased the CE transfer to TG-rich particles but markedly reduced apoB binding (17). This binding process could display some analogy with the phenomenon of fusion or attachment of LDL to artificial microemulsion particles that occurs *in vitro*, as previously reported (18,19).

The purpose of the present study was to better characterize LDL binding to TG-rich particles of lipid emulsions by using various incubation conditions. LDL binding was assessed by measuring the apoB content in the fraction containing the TG-rich particles modified by incubation (named M-LE), and was visualized by electron microscopy after cryofracture. The effects on the binding process of duration and temperature for incubation or ultracentrifugation were also studied. The potential role of other emulsion components, such as glycerol and PL-rich particles, was also examined, as well as the effect of adding albumin or other plasma components, such as the lipoprotein-poor subfraction or various lipoprotein subfractions, to the incubation mixture. The influence of the emulsion TG content was addressed by incubating LDL with emulsions manufactured with long-chain TG from soybean oil (Endolipid®) or with long- and very long chain TG from fish oil.

## EXPERIMENTAL PROCEDURES

**Plasma pool.** Sixteen healthy overnight-fasted subjects (2 males and 14 females, 25–50 yr old) volunteered for the study

and signed an informed consent. Blood samples were collected in tubes containing EDTA (1 mg/mL) and  $\text{NaN}_3$  (0.2 mg/mL) and immediately placed in iced water. Plasma samples were separated at 4°C in a Beckman J2.21 centrifuge (Beckman Instruments Inc., Fullerton, CA) at  $2,000 \times g$  for 10 min. Plasma samples were pooled, and the various lipoprotein subfractions were immediately separated.

**Preparation of plasma subfractions.** Different plasma subfractions were separated by sequential ultracentrifugation in a Beckman L8-55 ultracentrifuge using an angular Beckman 50.2Ti rotor (16). The TRL-free subfraction was obtained at  $d > 1.019$  g/mL (20 h; 5°C;  $227,000 \times g$ ). LDL subfraction was separated at  $1.030 < d < 1.055$  g/mL (20 h; 5°C;  $227,000 \times g$ ) to obtain a homogeneous population of mid-sized LDL particles (17). HDL ( $1.063 < d < 1.210$  g/mL) and the lipoprotein-poor ( $d > 1.210$  g/mL) plasma subfraction were also separated (48 h; 5°C;  $227,000 \times g$ ). After isolation, each subfraction was dialyzed in the dark against 40 vol of saline solution (0.19 M NaCl with 0.02% EDTA,  $\text{NaN}_3$  0.02%, pH 7.4) with three changes of dialysis solution over a 24-h period (18). The LDL and the TRL-free subfractions were enriched with sucrose to obtain final concentrations of 5 and 1% sucrose, respectively (19). Aliquots of TRL-free ( $d > 1.019$  g/mL), LDL, HDL, and lipoprotein-free ( $d > 1.210$  g/mL) plasma subfractions were frozen at -70°C for a maximum of 5 mon. Immediately prior to each experiment, aliquots of LDL and of other plasma subfractions were thawed by immersion in a 37°C water bath. Sucrose was removed from LDL and from the TRL-free subfraction by dialysis (three changes of 100  $\times$  sample volume over a 1-h period) in the same saline solution as described above (18).

**Intact and fractionated lipid emulsions.** Intact emulsions (B. Braun Melsungen AG, Melsungen, Germany) contained 200 g/L TG, 12 g/L egg yolk PL emulsifier, and 25 g/L glycerol. They consisted of a commercially available emulsion containing long-chain TG from soybean oil (20% Endolipid®) and of an experimental emulsion containing long- and very long chain TG from fish oil. The commercial soybean oil emulsion was used either intact, or after dialysis (as described above for the plasma subfractions) to remove glycerol, or after fractionation to isolate TG-rich particles from the mesophase, as previously reported (12,24). In brief, a 40-mL sample was ultracentrifuged (1 h; 15°C;  $20,000 \times g$ ) using a Beckman 50.2Ti rotor. The tube was cut with a Beckman tube-slicer just under the limit of the lipid cake (which contains TG-rich particles), and the mesophase (glycerol and PL-rich particles) was discarded. The lipid cake was resuspended in a KBr solution of  $d = 1.006$  g/mL and washed by a second ultracentrifugation run (1 h; 15°C;  $20,000 \times g$ ). TG-rich particles were then resuspended to the initial volume with a KBr solution of  $d = 1.006$  g/mL at a TG concentration of 200 g/L. According to previous experiments using this procedure, 75–80% of the total PL content of the soybean emulsion is distributed in TG-rich particles and the rest in the mesophase PL-rich particles (24).

**Incubation protocol.** Aliquots of the plasma subfractions were thawed and the sucrose was removed as described above. Samples of LDL ( $1.030 > d > 1.055$  g/mL) containing 0.58 mg

apoB, or samples of TRL-free plasma subfraction ( $d > 1.019$  g/mL) containing 44 mg protein, were incubated with soybean or fish oil emulsion samples in sealed Beckman polyallomer Opti-Seal tubes, using a fixed emulsion-TG/LDL-apoB ratio of 12:1 (w/w). In most of the assays, 0.2 mL of native or fractionated emulsion was incubated with 2.5–3.5 mL of LDL either alone or in the presence of other plasma subfractions or protein components. Briefly, lipoprotein-poor plasma, BSA, or HDL was added to the incubation mixture at protein concentrations ranging from 0 up to four times the usual mean normal plasma concentration of the lipoprotein-poor plasma subfraction (70 g/L), serum albumin (40 g/L), or HDL (1.2 g/L apoA-1). These conditions were defined to ensure that TG, plasma apoB, apoA-1, total protein, and albumin concentrations were below, at, or above those currently found in physiological conditions. Incubations were carried out in a shaking water bath at 4, 20, or 37°C for 0, 1, 4, or 20 h. In routine assays, incubations were performed at 37°C for 4 h.

**Separation of postincubation modified emulsion TG-rich particles (M-LE).** After incubation, the M-LE fraction, containing the modified emulsion TG-rich particles, was separated by ultracentrifugation ( $163,000 \times g$ ) at  $d = 1.006$  g/mL using a Beckman 50.4Ti rotor. Different ultracentrifugation durations (3, 20, or 40 h) and temperatures (5 or 20°C) were used for specific assays, but M-LE fractions were routinely obtained after ultracentrifugation for 20 h at 5°C. The tubes were cut at 1.5 cm from the bottom, and M-LE was recovered in the supernatant.

Alternatively, to check that the binding process was not an artifact due to the ultracentrifugation procedure, postincubation TG-rich particles were separated from the other components of the incubation mixture by gel filtration chromatography on a 2% agarose column (Sephacose CL-2B,  $1.6 \times 90$  cm; Pharmacia, Uppsala, Sweden). The column was eluted with a phosphate buffer (containing 0.15 M NaCl, 0.01% EDTA, and 0.01%  $\text{NaN}_3$ ; pH 7.4) at a flow rate of 0.6 mL/min for 340 min. Sixty minutes after the start of the run, fractions were collected every 5 min; TG was measured in each fraction. The TG-rich fractions eluting in the void volume of the column were pooled to obtain the M-LE fraction for subsequent analyses.

**Freeze-fracture electron microscopy.** After incubation of the soybean oil emulsion with LDL alone (4 h at 37°C), both the intact incubation mixture and the M-LE fraction isolated by ultracentrifugation (20 h at 5°C) were examined by freeze-fracture electron microscopy and compared to the intact emulsion. The method has been described previously (25), and the LDL particles were identified according to Gulik-Krzywicki *et al.* (26). In brief, a small drop of each sample, containing 30% glycerol as a cryoprotectant, was set down on a conventional copper planchet and rapidly frozen in liquid propane. Fracturing and replication were done with Balzers BAF 301 freeze-etching unit (Balzers, Balzers, Liechtenstein) using platinum carbon shadowing. Organic material was digested with 20% SDS and thereafter with sulfochromic acid. Replicas were then washed with distilled water and observed using a Philips 410 electron microscope (Philips, Eindhoven, The Netherlands).



**Analytical procedures.** All assays were performed in duplicate. Lipid analyses were performed on LDL; on intact, washed, and dialyzed emulsions; and on M-LE fractions obtained by ultracentrifugation or by gel filtration chromatography. TG were measured enzymatically using a commercial test kit (Triglycerides GPO-PAP, Roche Diagnostic, Mannheim, Germany). ApoB and apoA-1 were determined using a specific ELISA as previously described (27). Total protein content was measured in the lipoprotein and plasma fractions as described by Lowry *et al.* (28). All reagents, including KBr, were analytical grade products.

**Statistical analysis.** The results are expressed as mean values  $\pm$  SEM. Statistical differences between results obtained with different emulsion fractions under various conditions were determined by multivariate analysis (ANOVA) followed by a Fisher multiple comparison test. A value of  $P < 0.05$  was the criterion of significance.

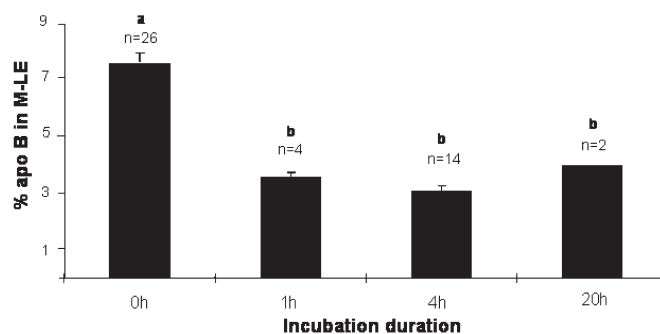
## RESULTS

**Separation of M-LE by ultracentrifugation vs. gel filtration chromatography.** After incubation of soybean oil emulsion with LDL alone (4 h at 37°C), TG-rich particles were isolated by ultracentrifugation (20 h at 5°C) or by HPLC. The two methods gave comparable results, since  $6.16 \pm 1.70\%$  of the initial apoB amount in LDL was recovered in M-LE separated by centrifugation vs.  $5.50 \pm 0.63\%$  ( $n = 12$ ) in M-LE isolated by chromatography ( $n = 12$ ) (a nonsignificant difference).

**Effect of incubation, ultracentrifugation duration, and temperature on LDL binding to TG-rich particles.** When soybean oil emulsion was incubated with LDL alone for different durations at 37°C, apoB recovery in M-LE separated by ultracentrifugation (20 h at 5°C) was significantly higher when TG-rich particles were isolated immediately after mixing LDL and emulsion (0 h incubation duration) than after prolonged (1, 4, or 20 h) incubation, as illustrated in Figure 1. Various ultracentrifugation durations to separate the postincubation emulsion TG-rich particles did not significantly modify apoB recovery in M-LE, which averaged  $8.67 \pm 1.18$  ( $n = 3$ ),  $7.41 \pm 0.64$  ( $n = 4$ ), and  $9.86\%$  ( $n = 2$ ) of the initial LDL apoB content after 3, 20, and 40 h, respectively.

Incubations of soybean oil emulsion with LDL alone were carried out to test the effect of different temperatures for incubation (4, 20, or 37°C) and for ultracentrifugation (5 or 20°C), and different incubation durations (0, 1, or 4 h) on apoB recovery in M-LE (Fig. 2). Regardless of the incubation conditions, apoB recovery was significantly higher in M-LE separated by ultracentrifugation at 5°C than at 20°C. Moreover, a significant effect of incubation temperature was found, with the lowest apoB recovery observed at 37°C and the highest at 4°C.

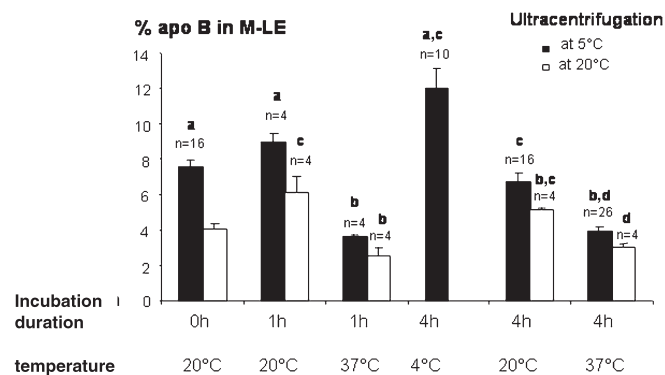
**Effect of emulsion components on LDL binding to TG-rich particles.** The effect of emulsion glycerol and PL-rich particles on the LDL binding process was studied by incubating the native or fractionated soybean oil emulsion with LDL alone, or after adding the lipoprotein-poor plasma fraction, at a protein concentration similar to that usually found in human plasma



**FIG. 1.** Effect of incubation duration on apolipoprotein (apo)B recovery in modified emulsion TG-rich particles. Soybean oil emulsion was incubated with LDL alone at 37°C for 0, 1, 4, or 20 h. The modified emulsion TG-rich particles (M-LE fraction) were separated by ultracentrifugation (20 h; 5°C;  $163,000 \times g$ ) at  $d = 1.006$  g/mL, and apoB recovery in M-LE was expressed in percent of the initial LDL apoB content (mean  $\pm$  SEM for  $n > 2$ ). Different roman letter superscripts indicate significant differences at  $P < 0.05$ , by ANOVA and the Fisher *post hoc* test. ApoB recovery was significantly higher when M-LE was isolated immediately after mixing emulsion and LDL (0 h) than after prolonged incubations for 2, 4, or 20 h.

(Table 1). In both conditions, removing glycerol by dialysis significantly increased apoB recovery in M-LE, whereas removing the whole mesophase (glycerol plus PL-rich particles) by washing had no effect, compared with the intact emulsion. Whatever the treatment of the emulsion (intact, dialyzed, or washed), adding lipoprotein-poor plasma to the incubation mixture markedly reduced LDL binding to TG-rich particles.

**Effect of adding different plasma subfractions or protein components on LDL binding to TG-rich particles. (i) Lipoprotein-poor ( $d > 1.210$  g/mL) subfraction.** The inhibitory effect of lipoprotein-poor plasma on the LDL binding process was investigated by adding increasing amounts of this plasma



**FIG. 2.** Effect of incubation and ultracentrifugation temperatures on LDL binding to emulsion TG-rich particles. TG-rich particles from soybean oil emulsion were incubated with LDL alone for 0, 1, or 4 h, at 4, 20, or 37°C. The M-LE fraction was separated by ultracentrifugation at  $d = 1.006$  g/mL (20 h,  $163,000 \times g$ ) at 5 or 20°C, and apoB recovery in M-LE was expressed as percentage of the initial LDL apoB content (mean  $\pm$  SEM). Different roman letter superscripts indicate significant differences at  $P < 0.05$ , by ANOVA and the Fisher *post hoc* test. The effect of ultracentrifugation (5 vs. 20°C) was significant at  $P < 0.001$ , and the effect of incubation temperature was significant at  $P < 0.0001$  (20 vs. 37°C),  $P = 0.0001$  (20 vs. 4°C) or  $P = 0.028$  (37 vs. 4°C). Incubation duration had no significant effect. For abbreviations, see Figure 1.

**TABLE 1**  
**ApoB Recovery in Modified Emulsion TG-rich Particles According to the Treatment of the Lipid Emulsion and Incubation Without or With Lipoprotein-poor Plasma<sup>a</sup>**

Incubation conditions	Percent recovery of apoB	
	Without LPP	With LPP
Intact	9.19 ± 1.55 <sup>a</sup> (n = 6)	0.77 ± 0.26 <sup>c</sup> (n = 6)
Dialyzed	14.76 ± 2.76 <sup>b</sup> (n = 4)	0.93 ± 0.10 <sup>c</sup> (n = 4)
Washed	7.99 ± 1.22 <sup>a</sup> (n = 9)	0.50 ± 0.12 <sup>c</sup> (n = 7)

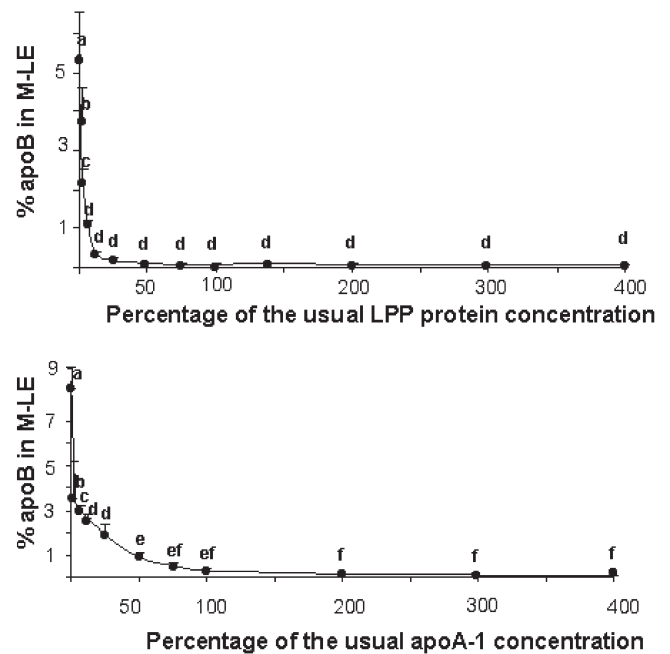
<sup>a</sup>Soybean oil emulsion was used intact, dialyzed (to eliminate glycerol), or washed (to eliminate glycerol and phospholipid-rich particles). After incubation (4 h; 37°C) of emulsion samples with LDL alone or in the presence of lipoprotein-poor plasma (LPP), the fraction containing the modified emulsion TG-rich particles (M-LE) was separated by ultracentrifugation (20 h; 5°C; 163,000 × g) at  $d = 1.006$  g/mL. Results are expressed as percentage of the initial LDL apolipoprotein B (apoB) amount recovered in M-LE (mean ± SEM). Different roman letter superscripts indicate significant differences, by ANOVA and the Fisher *post hoc* test. The effect of adding LPP is significant at  $P < 0.0001$ , and the effect of dialysis, at  $P = 0.046$ .

( $d > 1.210$  g/mL) subfraction to the incubation mixture. When the concentration was above (from one to four times) the usual protein concentration of this fraction in human plasma, apoB recovery in M-LE remained very low (Fig. 3A). Reducing this concentration had no effect on the LDL binding until very low concentrations were reached (lower than 0.10 of the usual protein concentration). Indeed, apoB recovery in M-LE sharply decreased from the highest value ( $5.38 \pm 0.51\%$ ,  $n = 9$ ) found when the emulsion was incubated with LDL alone, to  $3.75 \pm 0.50$ ,  $2.22 \pm 0.0.13$ ,  $1.07 \pm 0.07$ ,  $0.38 \pm 0.02$ , and  $0.17 \pm 0.04\%$  ( $n = 7$ ) when the protein concentration of the added subfraction increased from 2 to 3, 6, 13, and 25%, respectively, of the usual value in human plasma.

(ii) HDL ( $1.063 < d < 1.210$  g/mL) subfraction. Increasing the HDL protein concentration in the incubation mixture (from zero to four times the usual apoA-1 concentration in human plasma) reduced apoB recovery in M-LE (Fig. 3B). At protein concentrations below the usual HDL plasma concentration, the inhibitory effect of HDL on LDL binding to TG-rich particles was less pronounced than that of lipoprotein-poor plasma (Fig. 3A). ApoB recovery in M-LE ( $n = 4$ ), which reached  $8.16 \pm 0.56\%$  when no HDL was added to the mixture, decreased to  $3.51 \pm 0.37$ ,  $3.26 \pm 0.09$ ,  $2.96 \pm 0.17$ ,  $2.58 \pm 0.15$ , and  $1.94 \pm 0.25\%$  when the HDL concentration increased to 2, 3, 6, 13, and 25% of the normal plasma apoA-1 concentration, respectively.

(iii) TRL-free ( $d > 1.019$  g/mL) subfraction. While apoB recovery in M-LE was markedly lower in the presence than in the absence of lipoprotein-poor plasma ( $0.24 \pm 0.04$  vs.  $6.36 \pm 0.93\%$ ,  $P < 0.0001$ ,  $n = 25$ ), it was further reduced when the whole TRL-free plasma subfraction was used instead of LDL plus lipoprotein-free plasma ( $0.05 \pm 0.01$  vs.  $0.24 \pm 0.04\%$ ,  $P < 0.0001$ ,  $n = 25$ ).

(iv) BSA. When soybean oil emulsion was incubated with LDL in the presence of BSA at concentrations ranging from



**FIG. 3.** Effect of increasing amounts of lipoprotein-poor plasma (LPP) subfraction (A) or HDL (B) on emulsion TG-rich particles. TG-rich particles from soybean oil emulsion were incubated (4 h; 37°C) with LDL in the presence of increasing amounts of LPP subfraction or of HDL (ranging from zero to four times their respective usual total protein or apoA-1 concentration in human plasma) in the incubation mixture. The M-LE fraction was separated by ultracentrifugation, and apoB recovery in M-LE was calculated as percentage of initial LDL apoB content (mean ± SEM). Different roman letter superscripts indicate significant differences ( $P < 0.05$ ) by ANOVA and the Fisher *post hoc* test. ApoB recovery was highest and significantly different from all the other values when emulsion was incubated with LDL alone. The lowest apoB recoveries were observed for LPP or HDL concentrations above 0.1 and 2 times their usual protein concentrations, respectively. For abbreviations and technical details, see Figure 1.

zero to four times the usual albumin concentration in human plasma, apoB recovery in M-LE remained relatively stable (between 5 and 12% of the initial LDL content), with no correlation to BSA concentration (results not shown).

*Effect of the emulsion TG composition on LDL binding to TG-rich particles, according to the method used for protein measurement in M-LE.* After incubation of soybean or fish oil emulsion with LDL alone, the M-LE fractions were separated by ultracentrifugation and assayed for apoB content by ELISA and for total protein content by the method of Lowry *et al.* (28) (Table 2). Regardless of the technique used for protein measurement, a striking difference in LDL binding to TG-rich particles was observed between the two emulsions, since the recovery of either apoB or total proteins in M-LE was about threefold higher for fish oil than for soybean oil emulsion. However, for the two emulsions tested, the total protein amount measured by the method of Lowry *et al.* was about fourfold higher than the apoB amount routinely assessed by ELISA, a difference that was highly significant. The two techniques, however, were checked on LDL prior to incubation and gave comparable values for apoB and protein content (data not shown).

**TABLE 2**  
**Effect of Emulsion TG Composition on LDL Binding to TG-Rich Particles Calculated on the Basis of the Recovery of the Initial LDL ApoB or Total Protein Content<sup>a</sup>**

Emulsion	Percent recovery of LDL	
	ApoB	Total proteins
Soybean oil ( <i>n</i> = 3)	3.03 ± 0.38 <sup>a</sup>	13.70 ± 5.74 <sup>a</sup>
Fish oil ( <i>n</i> = 9)	9.52 ± 0.64 <sup>a</sup>	39.94 ± 5.19 <sup>b</sup>

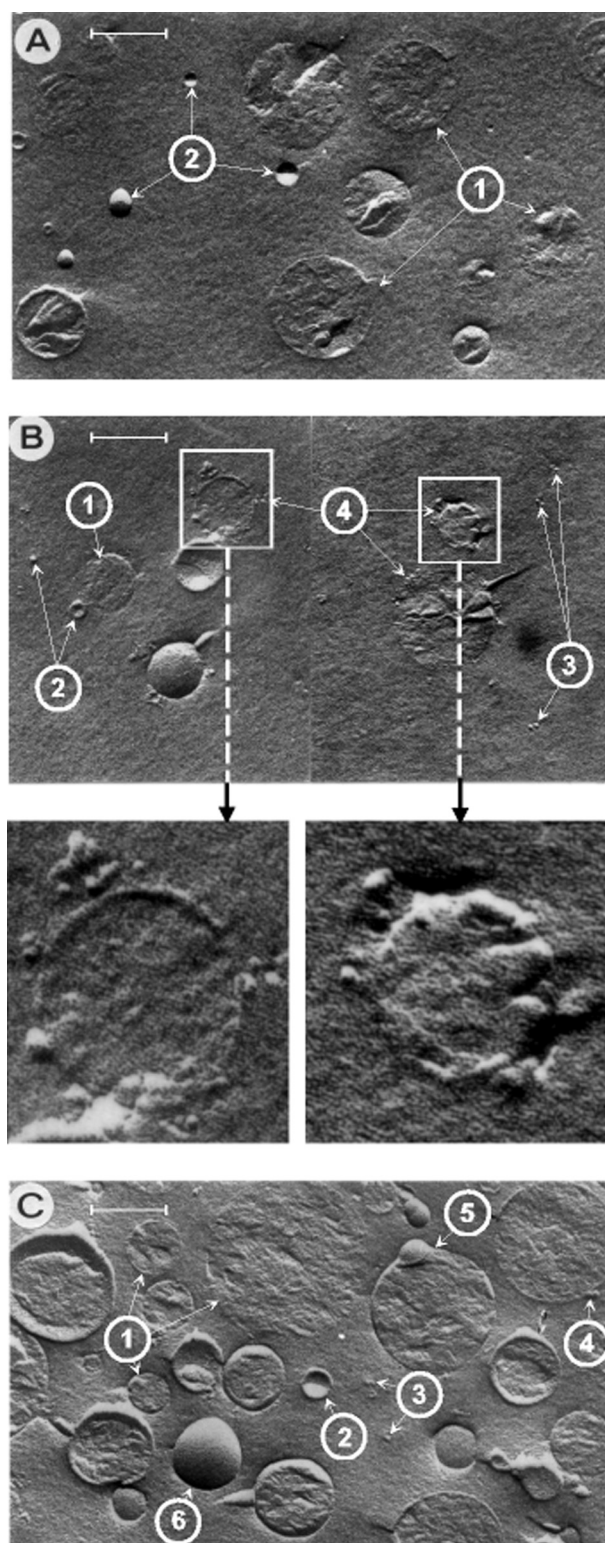
<sup>a</sup>After incubation (4 h; 37°C) of soybean or fish oil emulsion with LDL alone, the fraction containing M-LE was separated by ultracentrifugation (20 h; 5°C; 163,000 × *g*) at *d* = 1.006 g/mL. ApoB was measured by ELISA and total protein content according to Lowry *et al.* (28). Results are expressed as percentage of the initial LDL apoB or total protein amount recovered in M-LE (mean ± SEM). Different roman letter superscripts indicate significant differences by ANOVA and the Fisher *post hoc* test. The effect of TG composition of emulsions is significant at *P* = 0.003 and the effect of the method used to assess the protein contents at *P* < 0.0001.

**Freeze-fracture electron microscopy analysis.** Freeze-fracture electron microscopy of intact 20% Endolipid® showed a majority of TG-rich particles (typical cross fracture) together with a small number of liposomes or PL-rich particles (typical concave or convex fracture surface) (Fig. 4A). After incubating the emulsion with LDL, examination of the intact mixture revealed the presence of LDL particles tightly bound to TG-rich particles (Fig. 4B). Similarly, LDL particles were also found on the surface of TG-rich particles separated by ultracentrifugation from the incubation mixture (Fig. 4C). Fused liposomes, large liposomes, and fused structures of liposomes and TG-rich particles were also present, probably generated by the ultracentrifugation process.

## DISCUSSION

Our preliminary results strongly suggested that a binding process can occur *in vitro* between purified LDL and emulsion particles (13). The aim of the present study was to better characterize this interaction between LDL and emulsion particles, which was shown to be independent of CETP present in the lipoprotein-poor plasma fraction (19). An *in vitro* model was used to incubate purified LDL with two emulsions (20% Endolipid® or a 20% fish oil emulsion) under various conditions but to keep an emulsion-TG/LDL-apoB ratio close to that currently observed in clinical conditions during parenteral infusion of lipid emulsions. After ultracentrifugation, the amount of apoB recovered in the M-LE fraction was used as an index of LDL binding to TG-rich particles.

In contrast to CETP-mediated enrichment of TG-rich lipoproteins with esterified cholesterol, which increases with incubation duration (29), LDL binding to TG-rich particles is a very rapid process, since apoB was detected in the M-LE fraction isolated immediately after putting LDL in presence of the emulsion (Fig. 1). Moreover, the extent of LDL binding appeared to be inversely related to both incubation and ultracentrifugation temperatures (Fig. 2). Indeed, the strongest interactions between the particles took place at incubation temperatures below 37°C, and apoB recovery was higher when M-LE was separated by ultracentrifugation at 5



**FIG. 4.** Freeze-fracture electron microscopy of intact and postincubation lipid emulsion. After incubating (4 h; 37°C) soybean oil emulsion with LDL alone, the M-LE fraction was separated by ultracentrifugation. (A) The intact emulsion contains large TG-rich particles (cross fracture) and smaller liposomes (concave or convex surface); (B) the incubation mixture shows TG-rich lipoproteins (1), liposomes (2), very small free LDL particles (3), LDL bound to the surface of TG-rich particles (4); (C) the M-LE fraction contains TG-rich particles (1), liposomes (2), free LDL (3), LDL bound to the surface of TG-rich particles (4), and liposomes fused with TG-rich particles (5) or with other liposomes (6). The scale bars correspond to 200 nm.



than at 20°C. These observations suggest that LDL binding to TG-rich particles is favored by lipid-protein interactions, which are stronger at temperatures below 37°C.

That apoB recovery in M-LE was not influenced by the method used to isolate modified TG-rich particles after incubation (ultracentrifugation or chromatography) indicates that the formation of complexes between LDL and artificial particles is not an artifact of ultracentrifugation. Furthermore, the cohesive forces stabilizing these complexes must be very high, since they were not dissociated after ultracentrifugation for 20 or 40 h at  $163,000 \times g$ , whereas such ultracentrifugation can pull some apo (such as apoE, apoC, or apoA-1) out of the lipoprotein particle surface (30,31).

Freeze-fracture electron microscopic analysis of the incubation mixture and of the M-LE fraction showed LDL particles tightly associated with the surface of TG-rich particles in crude incubation mixtures (Fig. 4B). The mechanism by which such an interaction takes place may be analogous to the process described for endogenous TG-rich lipoprotein formation, involving the fusion of a large TG-rich particle with a smaller apoB-containing particle (32). It is noteworthy that *in vitro* fusion of LDL to artificial microemulsion particles has also been observed by electron microscopy (18,19).

We have previously reported that emulsion TG-rich particles are substantially more fluid than LDL and that incubation modifies the fluidity of reisolated particles (12). Indeed, the fluidity of TG-rich particles is decreased, but that of LDL is increased, owing to lipid and protein exchanges between the particles. Moreover, the TG core composition, which influences the physical properties of the PL surface of TG-rich particles (33,34), markedly affects LDL binding to TG-rich particles (35). After incubation, TG-rich particles from the fish oil emulsion acquired larger amounts of ordering components (cholesterol and protein) from LDL than TG-rich particles from soybean oil emulsion, which displayed a relatively lower increase in structural order (12). As a confirmation, apoB recovery was significantly higher in M-LE from fish oil than from soybean oil emulsion. These results suggest that the extent of LDL binding may depend on the initial fluidity of emulsion TG-rich particles, which is related to the TG composition of lipid emulsions (12).

Earlier observations indicated that many plasma proteins (namely, albumin present in large amounts in lipoprotein-poor plasma) are able to bind to emulsion TG-rich particles *in vitro* (36). In the present study, even very small amounts of the plasma lipoprotein-poor ( $d > 1.210$  g/mL) subfraction (which contains the bulk of plasma proteins, including CETP) inhibited the binding process without abolishing it completely. Indeed, after incubation of soybean oil emulsion with LDL in the presence of lipoprotein-poor plasma (at and above the usual concentration in human plasma), less than 1% of the initial apoB amount was recovered in M-LE, vs. 5% or more when LDL were incubated alone. Similarly, adding HDL to the incubation mixture efficiently reduced LDL binding with a concentration-dependent effect. Likewise, apoA-1 has been reported to inhibit LDL fusion to microemulsion particles

(19). In the present study, LDL binding to TG-rich particles was even more markedly reduced when both LDL and lipoprotein-poor plasma were replaced by the whole TRL-free ( $d > 1.019$  g/mL) subfraction (containing LDL + HDL + lipoprotein-poor fraction). This confirms the inhibitory role of HDL and of other plasma components on the binding process. However, albumin probably does not play a prominent part in LDL binding to TG-rich particles, confirming previous studies on LDL binding to microemulsion particles (19). In contrast to other results (4), some apoA-1 was detected (by ELISA and by electrophoresis) in M-LE isolated from lipid emulsion incubated with LDL in the presence of HDL or lipoprotein-poor plasma (data not shown). Unexpectedly, after incubation of soybean or fish oil emulsion with LDL alone, the amount of total protein measured in M-LE according to Lowry *et al.* (28) was about fourfold higher than the apoB amount estimated by ELISA, while apoB represents more than 95% of the protein content of LDL (37). Such discrepancy suggests that ELISA may underestimate LDL binding to TG-rich particles (38,39). We speculate that LDL interaction with large TG-rich particles may have hidden some apoB epitopes, either by masking them or by inducing modifications in their structure, thereby reducing their recognition by antibodies raised against intact LDL. If this was the case, the amount of LDL bound to TG-rich particles would be substantially higher than that estimated by ELISA.

Thus, LDL may quickly bind to emulsion TG-rich particles *in vitro*. The complexes formed between LDL and TG-rich particles can be visualized by electron microscopy, even in a crude incubation mixture. The binding process is influenced by the TG composition of the emulsion, since it is particularly marked for fish oil compared with soybean oil emulsion. In contrast, LDL binding to TG-rich particles is reduced by several denser plasma subfractions, such as HDL and the lipoprotein-poor ( $d > 1.21$  g/mL) plasma subfraction, but not by albumin. The formation of complexes between LDL and emulsion particles seems to be reduced when incubation conditions mimic *in vivo* conditions. Taking into account the fact that the extent of the LDL-binding could be underestimated by ELISA apoB measurements in M-LE, our results raise the question of the actual magnitude, as well as the metabolic relevance, of such binding process *in vivo*. However, detecting the complexes formed by LDL and exogenous lipid particles in the serum of infused patients may be difficult because of the presence of other circulating TG-rich lipoproteins containing apoB. The formation of such complexes could be influenced not only by the composition of infused emulsions but also by the LDL composition specific to each patient. The possible consequences on the metabolism of circulating emulsion particles and LDL are currently unknown.

## ACKNOWLEDGMENTS

We would like to dedicate this paper to the memory of Jean-François Lontie, Ph.D. We would like to express our appreciation to Patricia D'Hont, Annie Louche, Ingrid Laurent, Jean-Claude Dedieu, and Marc Moqué for their excellent technical assistance. We also wish



to thank Prof. Richard J. Deckelbaum (Institute of Human Nutrition, Columbia University, New York) and Prof. Jacques Winand (Laboratory of Biochemistry and Nutrition, Université Libre de Bruxelles, Brussels, Belgium) for helpful advice. The emulsions were kindly provided by B. Braun Medical (Melsungen, Germany). Part of this work was presented at the Congress of the Société Francophone de Nutrition Entérale et Parentérale (SFNEP) (Paris, 1997) and was awarded the 1997 Annual Prize. Nathalie F. Chanson was supported by a CIFRE fellowship from B. Braun Medical (France).

## REFERENCES

- Groves, M.J., Wineberg, M., and Brain, A.P.R. (1985) The Presence of Liposomal Material in Phosphatide Stabilized Emulsions, *J. Dispersion Sci. Technol.* 6, 237–243.
- Havel, R.J., Kane, J.P., and Kashyap, M.L. (1973) Interchange of Apolipoproteins Between Chylomicrons and High Density Lipoproteins During Alimentary Lipemia in Man, *J. Clin. Invest.* 52, 32–38.
- Lontie, J.-F., Deckelbaum, R.J., and Carpentier, Y.A. (1997) Triglyceride Core of Lipid Emulsions Modulates the Acquisition of Exchangeable Plasma Apolipoproteins (apos) *in vitro*, *Clin. Nutr.* 16 (Suppl. 2), 5 (abstract).
- Weinberg, R.B., and Scanu, A.M. (1982) *In vitro* Reciprocal Exchange of Apoproteins and Nonpolar Lipids Between Human High Density Lipoproteins and an Artificial Triglyceride-Phospholipid Emulsion (Intralipid), *Atherosclerosis* 44, 141–152.
- Iriyama, K., and Carpentier, Y.A. (1994) Clinical Significance of Transfer of Apolipoproteins Between Triacylglycerol-Rich Particles in Lipid Emulsions and Plasma Lipoproteins, *Nutrition* 10, 252–254.
- Connelly, P.W., and Kuksis, A. (1981) Effect of Core Composition and Particle Size of Lipid Emulsions on Apolipoprotein Transfer of Plasma Lipoproteins *in vivo*, *Biochim. Biophys. Acta* 666, 80–89.
- Kuksis, A., Breckenridge, W.C., Myher, J.J., and Kakis, G. (1978) Replacement of Endogenous Phospholipids in Rat Plasma Lipoproteins During Intravenous Infusion of an Artificial Lipid Emulsion, *Can. J. Biochem.* 56, 630–639.
- Tall, A.R. (1993) Plasma Cholesteryl Ester Transfer Protein, *J. Lipid Res.* 34, 1255–1274.
- Barter, P.J. (1990) Enzymes Involved in Lipid and Lipoprotein Metabolism, *Curr. Opin. Lipidol.* 1, 518–523.
- Granot, E., Deckelbaum, R.J., Eisenberg, S., Oschry, Y., and Bengtsson-Olivecrona, G. (1985) Core Modification of Human Low-Density Lipoprotein by Artificial Triacylglycerol Emulsion, *Biochim. Biophys. Acta* 833, 308–315.
- Connelly, P.W., and Kuksis, A. (1983) Influence of Divalent Cations on Rat Apolipoprotein Transfer to Synthetic Lipoproteinlike Lipid Emulsions *in vitro*, *Can. J. Biochem. Cell Biol.* 61, 63–71.
- Chanson, N.F., Lontie, J.-F., Carpentier, Y.A., and Motta, C. (2001) Incubation of Lipid Emulsions with Plasma Lipoproteins Modifies the Fluidity of Each Particle, *Lipids* 36, 819–825.
- Chanson, N.F., Vanweyenberg, V., Deckelbaum, R.J., and Carpentier, Y.A. (1996) Interactions Between LDL and Lipid Emulsion Particles: Influence of Core Triglyceride (TG) Composition, *Clin. Nutr.* 15 (Suppl. 1), 23 (abstract).
- Phillips, M.L., and Schumaker, V.N. (1989) Conformation of Apolipoprotein B After Lipid Extraction of Low Density Lipoproteins Attached to an Electron Microscope Grid, *J. Lipid Res.* 30, 415–422.
- Chatterton, J.E., Phillips, M.L., Curtiss, L.K., Milne, R.W., Marcel, Y.L., and Schumaker, V.N. (1991) Mapping Apolipoprotein B on the Low Density Lipoprotein Surface by Immunoelectron Microscopy, *J. Biol. Chem.* 266, 5955–5962.
- Quig, D.W., and Zilversmit, D.B. (1990) Plasma Lipid Transfer Activities, *Annu. Rev. Nutr.* 10, 169–193.
- Chanson, N.F., Lontie, J.-F., and Carpentier, Y. A. (1997) Facteurs intervenant pour inhiber la liaison des lipoprotéines de densité légère (LDL) aux particules d'une émulsion intraveineuse dérivée du soja, *Nutr. Clin. Métabol.* 11 (Suppl. 4), 304 (abstract).
- Parks, J.S., Martin, J.A., Johnson, F.L., and Rudel, L.L. (1985) Fusion of Low Density Lipoproteins with Cholesterol Ester-Phospholipid Microemulsions. Prevention of Particle Fusion by Apolipoprotein A-I, *J. Biol. Chem.* 260, 3155–3163.
- Chun, P.W., Brumbaugh, E.E., and Shiremann, R.B. (1986) Interaction of Human Low Density Lipoprotein and Apolipoprotein B with Ternary Lipid Microemulsion. Physical and Functional Properties, *Biophys. Chem.* 25, 223–241.
- Havel, R.J., Eder, H.A., and Bragdon, J.H. (1955) The Distribution and Chemical Composition of Ultracentrifugally Separated Lipoproteins in Human Serum, *J. Clin. Invest.* 34, 1345–1353.
- Lee, D.M., and Alaupovic, P. (1974) Physicochemical Properties of Low-Density-Lipoproteins of Normal Human Plasma, *Biochem. J.* 137, 155–167.
- Deckelbaum, R.J., Shipley, G.G., Small, D.M., Lees, R.S., and George, P.K. (1975) Thermal Transitions in Human Plasma Low Density Lipoproteins, *Science* 190, 392–394.
- Rumsey, S.C., Galeano, N.F., Arad, Y., and Deckelbaum, R.J. (1992) Cryopreservation with Sucrose Maintains Normal Physical and Biological Properties of Human Plasma Low Density Lipoproteins, *J. Lipid Res.* 33, 1551–1561.
- Férézou, J., Lai, N.-T., Lerai, C., Hajri, T., Frey, A., Cabaret, Y., Courtieu, J., Lutton, C., and Bach, A.C. (1994) Lipid Composition and Structure of Commercial Parenteral Emulsions, *Biochim. Biophys. Acta* 1312, 149–158.
- Aggerbeck, L.P., and Gulik-Krzywicki, T. (1986) Studies of Lipoproteins by Freeze-Fracture and Etching Electron Microscopy, *Methods Enzymol.* 128, 457–472.
- Gulik-Krzywicki, T., Yates, M., and Aggerbeck, P. (1979) Structure of Serum Low-Density Lipoprotein, *J. Mol. Biol.* 131, 475–484.
- Dubois, D.Y., Cantraine, F., and Malmendier, C.L. (1987) Comparison of Different Sandwich Enzyme Immunoassays for the Quantitation of Human Apolipoprotein A-I and A-II, *Immunol. Methods* 96, 115–120.
- Lowry, O.H., Rosebrough, N.J., Farr, A.L., and Randall, R.J. (1951) Protein Measurement with the Folin Phenol Reagent, *J. Biol. Chem.* 193, 265–275.
- Lagrost, L. (1994) Regulation of Cholesterol Ester Transfer Protein (CETP) Activity: Review of *in vitro* and *in vivo* Studies, *Biochim. Biophys. Acta* 1215, 209–236.
- Herbert, P.N., Forte, T.M., Shulman, R.S., La Piana, M.J., Gong, E.L., Levy, R.I., Fredrickson, D.S., and Nichols, A.V. (1975) Structural and Compositional Changes Attending the Ultracentrifugation of Very Low Density Lipoproteins, *Prep. Biochem.* 5, 93–129.
- Liang, H.-Q., Rye, K.A., and Barter, P.J. (1994) Dissociation of Lipid-Free Apolipoprotein A-I from High Density Lipoproteins, *J. Lipid Res.* 35, 1187–1199.
- Hamilton, R.L., Wong, J.S., Cham, C.M., Nielsen, L.B., and Young, S.G. (1998) Chylomicron-Sized Lipid Particles Are Formed in the Setting of Apolipoprotein B Deficiency, *J. Lipid Res.* 39, 1543–1557.
- Deckelbaum, R.J., Hamilton, J.A., Moser, A., Bengtsson-Olivecrona, G., Butbul, E., Carpentier, Y.A., Gutman, A., and Olivecrona, T. (1990) Medium-Chain versus Long-Chain Triacylglycerol Emulsion Hydrolysis by Lipoprotein Lipase and Hepatic Lipase: Implications for the Mechanisms of Lipase Action, *Biochemistry* 29, 1136–1142.
- Hamilton, J.A., Vural, J.M., Carpentier, Y.A., and Deckelbaum,

- R.J. (1996) Incorporation of Medium Chain Triacylglycerols into Phospholipid Bilayers: Effect of Long Chain Triacylglycerols, Cholesterol, and Cholesteryl Esters, *J. Lipid Res.* 37, 773–782.
35. Chanson, N.F., Férézou, J., Gulik, A., Lontie, J.F., and Carpentier, Y.A. (1998) LDL Binding to Lipid Emulsions Is Markedly Influenced by the Triglyceride Fatty Acid Pattern of Exogenous Particles, *Clin. Nutr.* 17 (Suppl. 1), 58–59 (abstract).
36. Carlson, L.A. (1980) Studies on the Fat Emulsion Intralipid. I. Association of Serum Proteins to Intralipid Triglyceride Particles (ITP), *Scand. J. Clin. Lab. Invest.* 40, 139–144.
37. Chan, L. (1992) Apolipoprotein B, the Major Protein Component of Triglyceride-Rich and Low Density Lipoproteins, *J. Biol. Chem.* 267, 25621–25624.
38. Beghin, L., Duhal, N., Lacroix, B., Bonte, J.P., Fruchart, J.C., and Luc, G. (1997) Measurements of VLDL-, IDL-, and LDL-Apo B Levels by a Combination of Isopropanol Precipitation and Mass Spectrometry, *Int. Atheroscler. Soc.* 1, 395 (abstract).
39. Beghin, L., Duhal, N., Poulain, P., Hauw, P., Lacroix, B., Lecerf, J.P., Bonte, J.P., Fruchart, J.C., and Luc, G. (2000) Measurements of Apolipoprotein B Concentration in Plasma Lipoproteins by Combining Selective Precipitation and Mass Spectrometry, *J. Lipid Res.* 41, 1172–1176.

[Received December 10, 2001, and in revised form April 30, 2002; revision accepted May 13, 2002]

# Transfer of Lipids Between Hemolymph and Hepatopancreas in the Shrimp *Macrobrachium borellii*

Fernando García, María González-Baró, and Ricardo Pollero\*

Instituto de Investigaciones Bioquímicas de La Plata (INIBIOLP), Consejo Nacional de Investigaciones Científicas y Técnicas (CONICET)—Universidad Nacional de La Plata (UNLP), La Plata, Argentina

**ABSTRACT:** Crustacean lipids are transported in the hemolymph by an HDL. The hepatopancreas is the most important and active organ regarding lipid metabolism, so we studied the interchange of FA and acylglycerols between both components of the hepatopancreas–hemolymph system in the decapod crustacean *Macrobrachium borellii*. The hepatopancreas and a sole plasma lipoprotein were labeled by *in vivo* incubations with  $^{14}\text{C}$  palmitic acid injected into the hemolymph. Then they were incubated *in vitro* with unlabeled hepatopancreas and hemolymph, and the transfer of lipids between them was measured by radiochromatographic techniques. It was determined *in vivo* that more than 80% of the circulating palmitic acid was taken up by the hepatopancreas and incorporated into PC and TAG. Both classes of lipids, but mainly PC, were transferred back from tissues to the hemolymph. Lipid transfer was also demonstrated *in vitro*. The transfer of PC (30% of labeling) as well as that of FFA (48% of labeling) from hemolymph to hepatopancreas was determined. On the other hand, FFA were released more efficiently than the acylglycerols from intact hepatopancreas to hemolymph, and they were the only lipid transferred when the hepatopancreas had been previously washed.

Paper no. L8959 in *Lipids* 37, 581–585 (June 2002).

For several years, we have carried out certain metabolic studies using the hepatopancreas of the shrimp *Macrobrachium borellii* as a model. We first reported that the seasonal distribution of lipids was closely related to the diet (1). Afterward, we explored the consumption of lipids under stressful conditions (2), the effect of temperature upon the FA  $\beta$ -oxidation system (3), and the metabolism of palmitic acid as a precursor of TAG (4). We therefore postulated that the hepatopancreas is the main organ in *M. borellii* responsible for the synthesis and the degradation of TAG. Liver and fat body are the organs analogous to the hepatopancreas in vertebrates and insects, respectively. The hepatopancreas also performs digestive functions, enzyme secretion, and excretion of waste materials (5,6).

Although the occurrence of very high density lipoproteins (VHDL) has been reported in hemolymph of some crab and shrimp species (7,8), plasma lipid transport in crustaceans is mainly carried out by HDL. These lipoproteins are structurally much simpler than the ones present in vertebrates, and up to now there has been no evidence for the presence of any

LDL in crustacean plasma (9). Recently, we characterized the plasma lipoproteins of *M. borellii* and found that their compositions are similar to those of other crustaceans (García, F., unpublished results). We observed two different lipoproteins: one HDL found in animals of both sexes, and another HDL, found exclusively in the hemolymph of females during the reproductive season, that is involved in vitellogenesis.

These studies led to the hypotheses that the hepatopancreas, as a biosynthetic organ, transfers lipids to the hemolymph HDL for distribution among other tissues and that the hemolymph transfers to the hepatopancreas the lipids resulting from absorption across the digestive tract. In this way, biochemical interactions must be involved. The mechanism of interchange of lipids between hemolymph lipoproteins and tissues in crustaceans is still unknown. The results reported here deal with investigations performed *in vitro* on the transfer of FFA and other lipids between plasma HDL and the hepatopancreas of *M. borellii*, as well as between isolated lipoprotein and artificial membranes.

## MATERIALS AND METHODS

**Biological and chemical materials.** Male and nonovogenic female adult specimens of *M. borellii* were collected in summer from a water course close to the Río de la Plata, Argentina. They were kept in glass aquaria containing tap water at room temperature (20–25°C) until used for the experiments.  $1\text{-}^{14}\text{C}$  Palmitic acid (57.0 mCi/mmol, 99% radiochemically pure) and PC, L- $\alpha$ -dipalmitoyl (dipalmitoyl- $1\text{-}^{14}\text{C}$ , 111 mCi/mmol, 97% radiochemically pure) were purchased from New England Nuclear Corp. (Boston, MA). All chemicals were of analytical grade.

**In vivo labeling with radioactive FA.** Radioactive palmitic acid was administered to groups of 4–8 shrimp. They were maintained in aquaria at room temperature for 1, 4, 7, or 16 h. The cephalic sinus of each animal was injected with 5  $\mu\text{L}$  of an aqueous solution containing 2  $\mu\text{Ci}$  (35 nmol) radioactive FA as the ammonium salt. A syringe with a needle designed for animal injection (Hamilton Co.) was used. After incubations, hepatopancreas and hemolymph were separated. Labeled hepatopancreas were used either for radioactive lipid analysis or for the transference studies between hepatopancreas and hemolymph. Hemolymph was obtained by puncturing the cephalic sinus using a syringe containing 0.1 N sodium citrate as anticoagulant. Hematic cells were separated by centrifugation at  $100 \times g$  for 10 min. Labeled plasma was used for lipid

\*To whom correspondence should be addressed at INIBIOLP, Fac. Medicina, UNLP, Calles 60 y 120, La Plata (1900), Argentina.  
E-mail: pollero@atlas.med.unlp.edu.ar

analysis in the experiments of transference between plasma and hepatopancreas as well as for lipoprotein isolation.

**Plasma lipoprotein isolation.** Plasma lipoprotein was isolated by density gradient ultracentrifugation. Aliquots of plasma were overlaid on sodium bromide solutions (density 1.25 g/mL) containing 0.01% sodium azide and centrifuged at  $178,000 \times g$  for 24 h in a Beckman L8 70M centrifuge, using an SW 60 Ti rotor. The total volume of the tubes was fractionated from top to bottom into 0.2-mL aliquots. The protein content of each fraction was monitored spectrophotometrically at 280 nm. Radioactivity in each fraction was measured by liquid scintillation counting in Wallac 1214 Rack Beta equipment. One tube containing a NaCl solution (density 1.04 g/mL) instead of plasma was centrifuged simultaneously and fractionated in order to determine the density of the fractions by monitoring the refractive indices. Fractions corresponding to densities of 1.10–1.14 g/mL and showing increases in absorbance at 280 nm and in radioactivity were pooled, and the protein content was determined colorimetrically (10).

**Lipid extraction and analysis.** Lipids from hepatopancreas and hemolymph plasma were extracted following the procedure of Folch *et al.* (11), and the extracts were utilized for lipid separation by TLC. Lipid classes were separated by high-performance-TLC on Merck plates (Darmstadt, Germany), using hexane/diethyl ether/acetic acid (80:20:1.5 by vol) for neutral lipids and chloroform/methanol/acetic acid/water (65:25:4:4 by vol) for phospholipids.

Radioactivity distribution in different lipid classes was detected by scanning proportional counting using a Berthold LB-2723 Dunnschicht Scanner II apparatus (Wildbad, Germany). Appropriate standards, run simultaneously, were visualized by exposure to iodine vapors.

**Lipid transfer assays between hepatopancreas and hemolymph.** To explore the transfer of lipids from the hepatopancreas to the hemolymph, the palmitic acid-labeled hepatopancreas (donor) was incubated with unlabeled hemolymph plasma (acceptor). Incubations were done in 50 mM potassium phosphate buffer pH 7.4, 0.25 M sucrose, with the addition of 5  $\mu$ L aprotinin as protease inhibitor in a final volume of 330  $\mu$ L. Assays were carried out at 27°C for 30 min, with shaking. The donor/acceptor ratio was a whole hepatopancreas (70–90 mg) /125  $\mu$ L hemolymph. On the other hand, palmitic acid-labeled plasma (donor) was incubated under similar conditions with unlabeled hepatopancreas (acceptor). In another series of experiments, labeled hepatopancreas extensively rinsed with 3% albumin in 50 mM potassium phosphate buffer pH 7.4, were incubated with unlabeled hemolymph. After incubations, tissue and medium were separated, and lipids were extracted and analyzed as described above. All transfer experiments were done at least in triplicate.

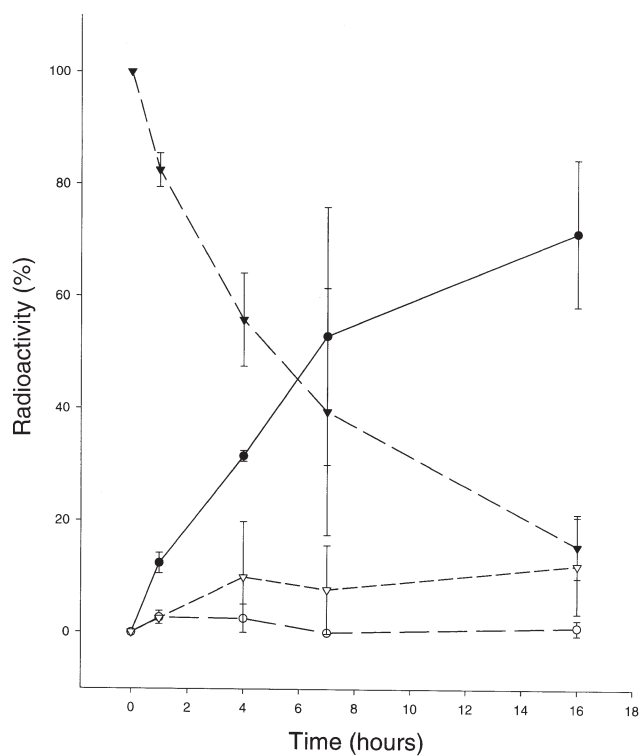
Data collected from the transfer experiments were analyzed by a Mann–Witney nonparametric test. It was applied to radioactivity values in original and remaining lipids. Differences were considered with a significance level of 0.05.

**Lipid transfer between liposomes and HDL.** Liposome (multilamellar vesicle) preparations were done basically as

described previously (12). A stock solution of radioactive (45 nCi) and unlabeled (1 mg) PC in chloroform/methanol (2:1 vol/vol) was placed in round-bottomed flasks, and the solvent was completely evaporated. Dry phospholipid was hydrated with 1 mL 50 mM Tris-HCl buffer, pH 8.4, and thoroughly vortexed for 30 s 10 times in a bath at 60°C. Liposomes (donor) and isolated plasma lipoprotein (acceptor) in a ratio of 500  $\mu$ g phospholipid/450  $\mu$ g protein were incubated in a final volume of 1 mL at 27°C for 2 h. After incubation, the liposomes were pelleted by centrifuging the sample twice at  $167,000 \times g$  for 90 min in a 70.1 Ti rotor as above. Lipoprotein remained in the supernatant. A tube containing labeled liposomes and buffer was centrifuged simultaneously as a blank.

## RESULTS

**Palmitic acid uptake and incorporation into the hepatopancreas and hemolymph.** Different classes of circulating radioactive lipids in hemolymph were detected after having injected labeled palmitic acid into the cephalic sinus and sacrificing the animals after different incubation times. The results obtained are shown in Figure 1. A marked decrease of the label detected in FFA was observed that, after 16 h, reached less than 20% of its initial values. At the same time, radioactivity in the PC frac-



**FIG. 1.** Distribution of radioactivity into lipid classes after injection of  $^{14}\text{C}$  palmitate into the hemolymph of *Macrobrachium borellii*. Radioactive palmitate as ammonium salt (2  $\mu\text{Ci}$ : 35 nmol) was injected into the cephalic sinus and incubated *in vivo* for different times. Error bars indicate SD of the mean ( $n = 3$ ). ●, PC; ○, DAG; ▼, FFA; ▽, TAG.



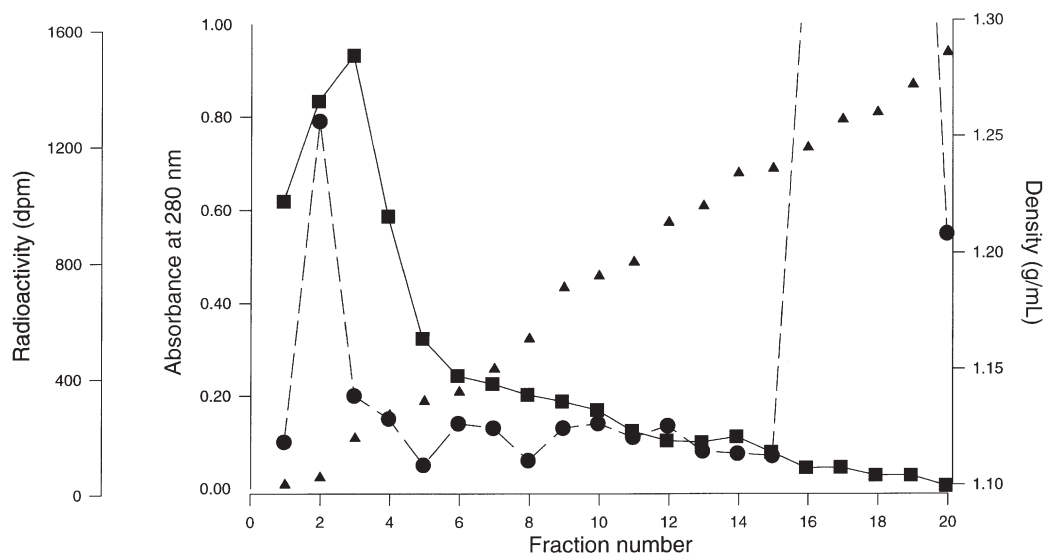


FIG. 2. Total proteins (●, absorbance at 280 nm), radioactivity (■), and density (▲) distribution in plasma fractions of *M. borellii*. Shrimp were incubated *in vivo* with 2  $\mu\text{Ci}$  (35 nmol)  $^{14}\text{C}$ -palmitate for 5 h. Plasma was ultracentrifuged in a NaBr gradient and fractionated. For abbreviation see Figure 1.

tion increased with the incubation time, whereas the labeling in neutral lipids remained nearly constant.

To elucidate the role of the plasma lipoprotein in the uptake of lipids, the plasma was fractionated by ultracentrifugation in a density gradient. Radioactivity and protein content were measured in each fraction. The results are shown in the profiles in Figure 2, in which the highest labeling correlates with a protein peak at a density of 1.10–1.14 g/mL. This corresponded to the sole plasma lipoprotein present in the hemolymph of the specimens of *M. borellii* that we analyzed and is consistent with the density of the HDL.

Palmitic acid injected into the hemolymph was rapidly taken up by the hepatopancreas and then incorporated into several acylglycerols. The percentage of the label incorporated into different lipid classes as a function of time is presented in Figure 3. An even distribution of radioactivity between the neutral and glycerophospholipids occurred with short-time incubations, whereas at longer times, the label accumulated mainly in PC and to a lesser proportion in neutral acylglycerols. It is evident that DAG, with the minimal labeling concentration, are only intermediates in the synthesis of the other lipids.

*Lipid transfer between the hemolymph and the hepatopancreas.* When unlabeled hepatopancreas was incubated for 30 min with hemolymph labeled mainly in the FFA fraction, around one-half of the radioactivity was transferred to the tissue (Fig. 4A). At longer *in vivo* incubation times (16 h), the hemolymph contained the label distributed in PC as well as in FFA and TAG. When it was used as donor in incubations with unlabeled hepatopancreas, only the transfer of PC was observed (Fig. 4B).

Figure 5 shows the results from experiments in which radioactive hepatopancreas was incubated *in vitro* with unla-

beled hemolymph under two different experimental conditions. After 30 min of incubation, a substantial amount of PC, most of the labeled FFA, and a small amount of TAG were transferred from intact hepatopancreas to hemolymph (Fig. 5A). In another set of experiments, labeled hepatopancreas were washed prior to incubation with BSA, which removes the FA associated with the external face of the hepatopancreas membrane. Figure 5B shows that the FFA is the only lipid transferred to hemolymph, whereas the total radioactivity of

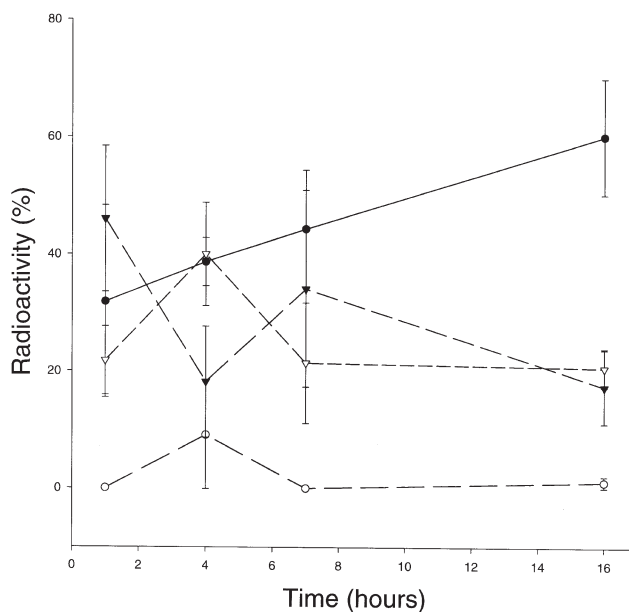
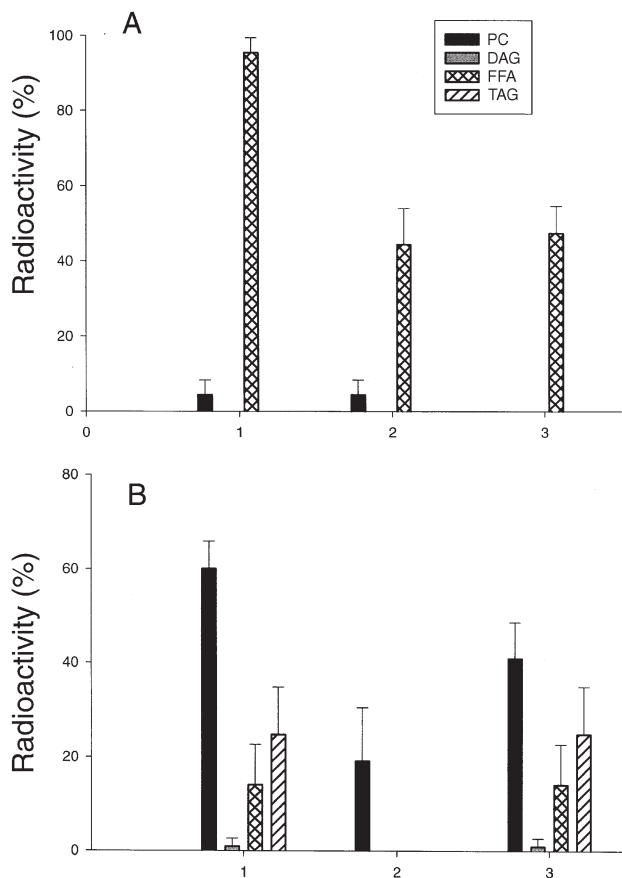


FIG. 3. The distribution of radioactivity into lipid classes in the hepatopancreas of *M. borellii* under the conditions indicated in Figure 1 ( $n = 3$ ). Error bars represent SD. For abbreviation and key for lipid classes see Figure 1.

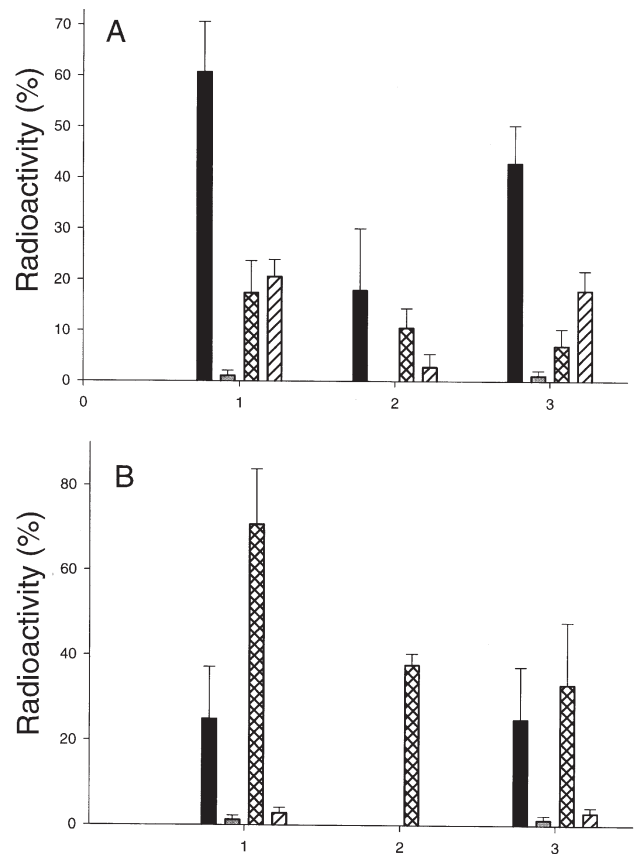


**FIG. 4.** *In vitro* transfer of labeled lipids from the hemolymph to the hepatopancreas. Whole unlabeled hepatopancreas were exposed to labeled hemolymph for 30 min. (A) Transfer from hemolymph mainly labeled in the FFA ( $P < 0.05$ ). (B) Transfer from hemolymph labeled in the FFA and acylglycerols (PC:  $P < 0.05$ ). 1, Labeled lipids in original hemolymph. 2, Labeled lipids transferred to the hepatopancreas. 3, Labeled lipids remaining in hemolymph. Error bars indicate SD of the mean ( $n = 3$ ).

phospholipids and neutral lipids remains in the tissue. In another experimental model, an artificial liposome preparation containing labeled PC was used as donor of lipids to the hemolymph. Under these conditions, no transfer of phospholipid from the liposomes to the lipoprotein was observed; in fact when we reisolated the lipoprotein after the incubation with labeled liposomes, no radioactivity was detected in the lipoprotein fraction.

## DISCUSSION

The decrease of the FFA circulating in the hemolymph during the incubation, together with an increase of phospholipids and neutral lipids, clearly indicates that the precursor injected into hemolymph is rapidly incorporated into tissues that synthesize acylglycerols, which then release them back to circulation. The increase in total circulating lipids is mainly attributable to PC, whereas the content of TAG and DAG remains unaltered. It may be inferred that the phospholipid synthesis



**FIG. 5.** *In vitro* transfer of labeled lipids from the hepatopancreas to the hemolymph. Whole labeled hepatopancreas were exposed to unlabeled hemolymph for 30 min. (A) Transfer from hepatopancreas without treatment (FFA and PC:  $P < 0.05$ ). (B) Transfer from hepatopancreas extensively rinsed with albumin-buffer solution (FFA:  $P < 0.05$ ). For key see Figure 4. Error bars represent SD of the mean ( $n = 3$ ).

in tissues is more active than that of neutral lipids. However, the radioactivity distribution among hepatopancreas lipids after *in vivo* FFA incorporation suggests that this organ is active in PC synthesis at longer times, although at shorter times it is able to synthesize both lipids. A similar observation was previously reported when we studied the lipid metabolism of *M. borellii* hepatopancreas (4). Also, the tissues are likely to retain the TAG synthesized, preferentially transferring PC to hemolymph. This fact is coincident with the results obtained from studies on the lipid composition of this and some other crustaceans, where PC was found to be the predominant circulating lipid (13) and TAG are accumulated by the hepatopancreas (1). These observations led us to suggest that those phospholipids synthesized in the hepatopancreas could be easily transferred to hemolymph. The presence of the circulating label only in the high-density plasma fraction demonstrated the role of HDL in taking up lipids from tissues. All the animals used in these experiments were males and nonvitellogenic females; thus, plasma did not contain any vitellogenin, but only the HDL common to both sexes (14).

The study of the *in vitro* transfer of lipids from hemolymph

to the hepatopancreas showed a clear trend of hemolymph to supply the tissue with FFA as well as PC, depending on their relative labeling in hemolymph. The transfer of FFA corroborates the preceding observations dealing with the components of the hemolymph–hepatopancreas system, where hemolymph is likely to provide the FA necessary for the synthesis of acylglycerols, a task that is performed by a tissue of greater activity like the hepatopancreas. *In vitro* experiments were carried out for short times in order to avoid the possibility of lipid synthesis within the hepatopancreas masking the transfer results. In other organisms, the release of the circulating FFA to tissues is produced by HDL structures that are poor in lipids. This is the case of the albumin–FFA complex in vertebrates or the VHDL in certain molluscs (15) and in insects (16). It is evident that this role in *M. borellii* is done by the HDL since it is the only circulating lipoprotein.

*In vivo*-labeled hepatopancreas, where radioactivity was mainly accumulated in PC and also in smaller amounts in TAG and FFA, were used for *in vitro* experiments. The transfer of these lipids to the hemolymph was demonstrated. In this case, the FFA were comparatively the most efficiently transferred lipid group. Even though PC was highly labeled, it was less efficiently transferred than FFA, whereas the transference of TAG was slight. This also shows a markedly different behavior between glycerophospholipids and neutral lipids, coincident with a large amount of PC in the circulating lipoprotein and an accumulation of TAG in the hepatopancreas under natural conditions. There is a marked change when the experiments are performed using washed hepatopancreas since only the FFA are transferred. As a consequence, it appeared that no carrier would be involved in the FFA transfer, whereas that of glycerophospholipids could be mediated by a transfer factor. If this is the case, this factor could be associated with the hepatopancreas membrane, and it could be removed by the albumin buffer used for washing the tissue. These results led us to another experiment using an artificial membrane as donor. Thus, we tried to transfer labeled PC from liposomes to hemolymph; we found plasma HDL was not able to take up the phospholipid under our experimental conditions. This result reinforces the above assumption about the occurrence of a carrier that would transport lipids from tissue membranes to circulation.

## ACKNOWLEDGMENTS

This work was supported by grants from CONICET, CICBA, and UNLP, Argentina. M. G-B. is a member of Carrera del Investigador CONICET, Argentina. R.P. is a member of Carrera del Investigador CICBA, Argentina.

## REFERENCES

- González-Baró, M.R., and Pollero, R.J. (1988) Lipid Characterization and Distribution Among Tissues of the Freshwater Crustacean *Macrobrachium borellii* During an Annual Cycle, *Comp. Biochem. Physiol.* 91B, 711–715.
- Pollero, R.J., González-Baró, M.R., and Irazú, C.E. (1991) Lipid Classes' Consumption Related to Fasting and Thermal Stress in the Shrimp *Macrobrachium borellii*, *Comp. Biochem. Physiol.* 99B, 233–238.
- Irazú, C.E., González-Baró, M.R., and Pollero, R.J. (1992) Effect of Environmental Temperature on Mitochondrial  $\beta$ -Oxidation Activity in Gills and Hepatopancreas of the Freshwater Shrimp *Macrobrachium borellii*. *Comp. Biochem. Physiol.* 102B, 721–725.
- González-Baró, M.R., and Pollero, R.J. (1993) Palmitic Acid Metabolism in Hepatopancreas of the Freshwater Shrimp *Macrobrachium borellii*, *Comp. Biochem. Physiol.* 106B, 71–75.
- O'Connor, J.D., and Gilbert, L.I. (1968) Aspects of Lipid Metabolism in Crustaceans, *Am. Zool.* 8, 529–539.
- Al-Mohanna, S.Y., and Nott, J.A. (1986) B-Cells and Digestion in the Hepatopancreas of *Penaeus semisulcatus* (Crustacea: Decapoda), *J. Mar. Biol. Assoc. UK* 66, 403–414.
- Komatsu, M., Ando, S., and Teshima, S.I. (1993) Comparison of Hemolymph Lipoproteins from Four Species of Crustacea, *J. Exp. Zool.* 266, 257–265.
- Hall, M., Vanheusden, M.C., and Söderhäll, K. (1995) Identification of the Major Lipoproteins in Crayfish Hemolymph as Proteins Involved in Immune Recognition and Clotting, *Biochem. Biophys. Res. Commun.* 216, 939–946.
- Yepiz-Placencia, G., Vargas-Albores, F., and Higuera-Ciajara, I. (2000) Penaeid Shrimp Hemolymph Lipoproteins, *Aquaculture* 191, 177–189.
- Lowry, O.H., Rosebrough, N.J., Farr, A., and Randall, R.J. (1951) Protein Measurement with the Folin Phenol Reagent, *J. Biol. Chem.* 193, 265–275.
- Folch, J., Lees, M., and Sloane-Stanley, G.H. (1957) A Simple Method for the Isolation and Purification of Total Lipids from Animal Tissues, *J. Biol. Chem.* 226, 497–509.
- González-Baró, M.R., Garda, H., and Pollero, R.J. (2000) Effect of Fenitrothion on Dipalmitoyl and 1-Palmitoyl-2-oleoylphosphatidylcholine Bilayers, *Biochim. Biophys. Acta* 1468, 304–310.
- Lee, R.F., and Puppione, D.L. (1988) Lipoproteins I and II from the Hemolymph of the Blue Crab *Callinectes sapidus*: Lipoprotein II Associated with Vitellogenesis, *J. Exp. Zool.* 248, 278–289.
- Lee, R.F. (1991) Lipoproteins from the Hemolymph and Ovaries of Marine Invertebrates, in *Advances in Comparative and Environmental Physiology* (Gilles, R., ed.), Vol. 7, pp. 187–208, Springer-Verlag, London.
- Heras, H., and Pollero, R. (1990) Occurrence of Plasma Lipoproteins in Octopods. Partial Characterization and Interorgan Transport of Lipids, *J. Exp. Mar. Biol. Ecol.* 140, 29–38.
- González, M.S., Rimoldi, O.J., and Brenner, R.R. (1995) Studies on Very-High-Density Lipoprotein of *Triatoma infestans* Hemolymph in Relation to Its Function as Free Fatty Acid Carrier, *Comp. Biochem. Physiol.* 110B, 767–775.

[Received December 3, 2001; accepted May 17, 2002]

# Lipid, FA, and Sterol Composition of New Zealand Green Lipped Mussel (*Perna canaliculus*) and Tasmanian Blue Mussel (*Mytilus edulis*)

Karen J. Murphy<sup>a,\*</sup>, Ben D. Mooney<sup>b</sup>, Neil J. Mann<sup>a</sup>, Peter D. Nichols<sup>b</sup>, and Andrew J. Sinclair<sup>a</sup>

<sup>a</sup>RMIT University, Melbourne, Victoria 3001, Australia, and <sup>b</sup>CSIRO Marine Research, Hobart, Tasmania 7001, Australia

**ABSTRACT:** The lipid, FA, and sterol composition of the New Zealand green lipped mussel (NZGLM, *Perna canaliculus*) and of the Tasmanian blue mussel (TBM, *Mytilus edulis*) were compared using TLC-FID and GC-MS. The respective mussel species were obtained from three different sites in both New Zealand (NZ) and Tasmania. Lipid class distribution of both mussel species was characterized by a high proportion of phospholipid (PL, 57–79%) and TG (10–25%), FFA (7–12%), and sterols (ST, 12–18%). The NZGLM had higher proportions of TG, FFA, and ST ( $P < 0.01$ ), whereas the TBM had a higher proportion of PL ( $P < 0.01$ ). There were higher proportions of total PUFA, saturated FA, n-3 FA, and hydroxy and nonmethylene-interrupted FA ( $P < 0.05$ ) in the TBM compared with the NZGLM. The major FA in the NZGLM were 16:0 (15–17%), 20:5n-3 (14–20%), and 22:6n-3 (11–17%). The same FA dominated lipids in the TBM, although there were significantly higher proportions of 16:0 ( $P = 0.000$ ) and 22:6 n-3 ( $P = 0.003$ ) and lower proportions of 20:5n-3 ( $P = 0.0072$ ) in the TBM. A novel PUFA, 28:8n-3, was detected in both mussels with higher amounts in the TBM, which probably reflects a greater dietary contribution of dinoflagellates for this species. Cholesterol was the dominant sterol in both mussels. Other major sterols included brassicasterol, 22-methylcholesterol, *trans*-22-dehydrocholesterol, and desmosterol. There were significant differences ( $P < 0.05$ ) between the NZGLM and TBM for 12 of the 20 sterols measured. Six sterols showed significant site differences for the NZGLM, and 10 for the TBM. The differences in the FA and sterol composition between the two species may be due to the diet of the NZGLM being more diatom-derived and the diet of the TBM having a greater dinoflagellate component.

Paper no. L8863 in *Lipids* 37, 587–595 (June 2002).

Molluscs are divided into seven classes; however, literature on their lipid composition is only available for a select group, one being the bivalvia (1). The New Zealand green lipped mussel (NZGLM), *Perna canaliculus* [not to be confused with the green lipped mussel *Perna viridis* from the region of

Hong Kong as investigated by Ching *et al.* (2), Li *et al.* (3), and Chong *et al.* (4)], is a bivalve marine mussel native to New Zealand (NZ), from the molluscan family Mytilidae, found in the deep-sea beds in the Hauraki Gulf in NZ's North Island waters (5,6). It is distinguished from other bivalve species by the presence of a bright green stripe around the posterior ventral margin of the shell and its distinctive green lip, which is visible on the inside of the shell. The flesh and ligaments of the NZGLM tend to be larger than those of the common blue mussel found in Tasmanian waters and referred to in this study as the Tasmanian blue mussel (TBM). It possesses a shape similar to the common blue mussel (*Mytilus edulis*) and can exceed 120 mm in size (6). The external color of the TBM can vary from blue to purple or black. It is found in coastal waters off the southern coast of Australia, spreading from the lower west to the lower east coast and into Tasmanian waters. TBM vary in size up to 130 mm; however, they are more commonly found to be less than 90 mm in size (7).

Lipid constitutes around 2% of the wet weight in the blue mussel (7–9) of which approximately 75% is structural lipids (10). Depending on season and/or the life cycle of the mussel, lipid content and composition may vary. During various stages of the life cycle, particularly in female mussels, the blue mussel is able to synthesize 16:0 and 18:0 and their derivatives *de novo* (10). Other biochemical changes in the mussel may result from variability in metabolic activity, location, sex, and spawning (11).

*Mytilus edulis* and *P. canaliculus*, like several other marine organisms such as molluscs in general and fish, not only are low in dietary cholesterol but also contain cholesterol-lowering phytosterols (12) and abundant n-3 PUFA, particularly the long-chain FA such as 22:6n-3 and 20:5n-3 (1); this is unlike most terrestrial organisms, which are rich in n-6 FA (13). The n-3 PUFA from marine sources have been linked with reducing certain risk factors for cardiovascular disease, such as lowering plasma TG (14) and reducing potential thrombosis as well as alleviating the symptoms of inflammatory conditions such as arthritis and skin disorders (15–19). Literature has not reported any research conducted on defining the similarities and or differences in lipid composition of the NZGLM and the TBM, and to our knowledge this is the first study that compares the lipid composition of both mussels.

\*To whom correspondence should be addressed at Department of Food Science, RMIT University, GPO Box 2476V, Melbourne, Victoria, 3001, Australia. E-mail: karen.murphy@rmit.edu.au

Abbreviations: 20:5n-3, EPA; 22:6n-3, DHA; HC, hydrocarbon; i18:0, isomer of 18:0 FA; MUFA, monounsaturated FA; NMI, nonmethylene interrupted; NZ, New Zealand; NZGLM, New Zealand green lipped mussel; PL, phospholipid; SFA, saturated FA; ST, sterol; TBM, Tasmanian blue mussel; 4,8,12-TMTD, 4,8,12-trimethyl tetradecanoic acid; WE, wax ester.



## MATERIALS AND METHODS

NZGLM were obtained from three sites in NZ (South Island, Marlborough Sound, Coromandel, with water temperatures of 14.6, 16.5, and 16°C, respectively) and transported frozen by air to CSIRO Marine Research in Hobart, Tasmania, Australia, and stored at -20°C for 3–5 d, until analysis. Upon harvest, mussels were chilled and frozen within 24–36 h of collection. TBM were collected from three sites in Tasmania, Australia (Deep Bay 1, Deep Bay 2, Great Oyster Bay; water temperatures unknown) and stored at -20°C for 3–5 d until analysis. Upon harvest, mussels were chilled and frozen within 24 h of collection. Both species of mussels were collected in late spring (October). Data relating to food sources and availability and water quality are unknown; however, it is known that TBM from Deep Bay were collected during a dinoflagellate bloom. Lipids were extracted overnight from three individual animals from each site using a modification of the one-phase chloroform/methanol/water (2:1:0.8, by vol) Bligh and Dyer extraction (20). After phase separation by the addition of chloroform and water (final solvent ratio, 1:1:0.9, by vol), the lipids were recovered in the lower chloroform phase and the total solvent extract was evaporated *in vacuo* at 40°C. Lipid content to a constant weight was determined under a stream of nitrogen gas. Lipid class analyses were conducted immediately and, where other analyses were to be performed, samples were stored at -20°C for no more than 3 d in a known volume of chloroform.

A portion of the lipid extract for each mussel was analyzed using an Iatroscan MK V TH10 TLC-FID analyser (Iatron Laboratories, Tokyo, Japan) to determine the amounts of individual lipid classes. Samples were analyzed in duplicate using silica gel SIII Chromarods (5 µm particle size) (Drummond Scientific Company, Broomall, PA) and applied by 1-µL disposable micropipettes. Separation was achieved using a polar solvent system of hexane/diethyl ether/glacial acetic acid (60:17:0.1, by vol) to resolve nonpolar components including wax ester (WE), TG, FFA, and sterols (ST). A second nonpolar solvent system (hexane/diethyl ether, 96:4, vol/vol) was used for selected samples to resolve nonpolar components such as hydrocarbon (HC) from WE and TG from diacylglycerol ether. After development, the Chromarods were dried at 80°C to evaporate all remaining solvent and scanned immediately, thus minimizing adsorption of atmospheric contaminants. The TLC-FID unit was calibrated using known standards for each lipid class (21). Peaks were quantified using an IBM PC using DAPA software (Kalamunda, Western Australia, Australia).

An aliquot of the total lipid extract, including methyl ester internal standards (19:0 and 23:0), was transmethylated using a mild acid methylation to obtain FAME and fatty aldehydes (21). ST were obtained by alkaline saponification of another aliquot of the lipid extract and were then converted to their corresponding trimethylsilyl ethers by the addition of 150 µL of *N,O*-bis(trimethylsilyl) trifluoroacetamide and heating overnight at 60°C. GC analyses were performed using a

Hewlett-Packard 5890 GC on HP7673 A Autosampler, a split/splitless injector, with an FID and an HP5 nonpolar 50-m cross-linked methyl (5% phenyl) silicone fused-silica capillary column with an i.d. of 0.32 mm and 0.17 µm film thickness (Hewlett-Packard). Samples were injected at 50°C and held for 1 min. The oven temperature was increased at 30°C/min to 150°C, then at 2°C/min to 250°C, and then 5°C/min to a final temperature of 300°C, which was held for 15 min. The injector and detector were maintained at 290 and 310°C, respectively, and hydrogen was used as the carrier gas. Peak areas were quantified on an IBM-compatible computer using Millennium 32 V.3.05.01 software (Waters Corporation, Milford, MA).

GC-MS analyses were performed on a ThermoQuest GCQ system (Thermoquest, Austin, TX) fitted with an on-column injector. The GC was fitted with a capillary column similar to that described above, and GC conditions were the same as described above.

Statistical analyses were conducted using Minitab Version 12.0 for Windows (State College, PA). Where mussel groups were compared, a two-sample *t*-test and confidence interval were conducted. Where sites were compared within mussel groups, a one-way ANOVA was used. Data are reported as mean ± SD ( $n = 9$ , three animals from three sites for each species) in both text and tables, and  $P < 0.05$  was considered significantly different.

## RESULTS

**Lipid composition.** Total lipid on a wet weight basis was 17.9 mg/g (4.4 SD) in the NZGLM and 12.3 mg/g (4.0 SD) in the TBM ( $P = 0.013$ ). The predominant lipid class in both the NZGLM and TBM was PL, 60 and 74% (of total lipid), respectively, followed by TG (22 and 13%, respectively), with lower levels of FFA (12 and 7%, respectively) (Table 1). Both mussel species had a low percentage of WE (<0.3%). There was a significantly higher percentage of TG ( $P = 0.038$ ), FFA ( $P = 0.016$ ), and ST ( $P = 0.0085$ ) in the NZGLM compared with the TBM, and a significantly higher proportion of PL in the TBM ( $P = 0.010$ ). There were no significant differences in the lipid class composition between sites for the TBM. However, there was a significant difference for FFA in the NZGLM between sites ( $P = 0.042$ ).

**FA.** Fifty individual FA and fatty aldehydes were identified in the mussels (Table 2; data in table not in order of elution shown in Fig. 1). The predominant FA were palmitic acid (16:0), 20:5n-3 (EPA), and 22:6n-3 (DHA) in both mussels, with 16:0 in significantly higher proportions in the TBM. There were significantly higher percentages of 14:0, 16:1n-7c, 16:1n-7t, 16:1n-9c, 17:0, 18:1n-7c, 18:2n-6, 20:1n-7c, 20:2 nonmethylene interrupted (NMI), 20:3n-6, 20:4n-6, 20:5n-3, 21:5n-3, 22:0, 22:4n-6, 22:5n-6, and 22:5n-3 in the NZGLM ( $P < 0.05$ ). The TBM had significantly higher percentages of 15:0, 16:0,  $\alpha$ -hydroxy 16:0 FA, 4,8,12-trimethyl tetradecanoic acid (4,8,12-TMTD), isomer of 18:0 FA (i18:0), 19:1, 20:2n-6, 22:2 NMI, 22:5n-6, and 22:6n-3 ( $P < 0.05$ ).

**TABLE 1**  
**Lipid Class Composition (%) and Total Lipid Content for the New Zealand Green Lipped Mussel (NZGLM) and the Tasmanian Blue Mussel (TBM)**

	Percent composition <sup>a</sup>								P value between species
	NZGLM				TBM				
	Site 1	Site 2	Site 3	Mean	Site 1	Site 2	Site 3	Mean	
Wax ester	ND	0.4 ± 0.6	ND	0.1 ± 0.4	0.5 ± 0.9	ND	ND	0.2 ± 0.1	—
TG	25.3 ± 8.9	17.8 ± 5.1	22.2 ± 5.0	21.8 ± 6.6 <sup>b</sup>	17.2 ± 15.7	12.7 ± 3.1	10.5 ± 2.9	13.5 ± 8.6	P = 0.038
FFA	10.7 ± 1.6	14.9 ± 2.4 <sup>d</sup>	9.6 ± 2.1	11.7 ± 3.0 <sup>b</sup>	9.7 ± 6.4	7.0 ± 1.7	5.4 ± 0.7	7.3 ± 3.8	P = 0.016
Sterol	6.8 ± 1.2	5.5 ± 0.3	6.6 ± 0.5	6.3 ± 0.9 <sup>b</sup>	4.9 ± 1.2	4.9 ± 1.2	5.1 ± 0.7	5.0 ± 0.9	P = 0.008
Phospholipid	57.1 ± 7.8	61.4 ± 5.4	61.7 ± 3.5	60.1 ± 5.5	67.1 ± 20.8	75.1 ± 4.2	78.7 ± 4.1	73.6 ± 12.0 <sup>c</sup>	P = 0.010
Total lipid (mg/g wet weight)	19.7 ± 5.4	19.1 ± 4.2	14.9 ± 3.4	17.9 ± 4.4 <sup>b</sup>	16.0 ± 5.3	10.6 ± 1.7	10.3 ± 1.3	12.3 ± 4.0	P = 0.013

<sup>a</sup>Data for each species, as determined by Iatroscan, are the mean of nine individual animals, representing three animals from each of three sites (values are expressed as mean ± SD). ND, not detectable

<sup>b</sup>Significantly higher than the TBM based on paired *t*-tests ( $P < 0.05$ ).

<sup>c</sup>Significantly higher than the NZGLM based on paired *t*-tests ( $P < 0.05$ ).

<sup>d</sup>Site significantly different from other sites (NZGLM) based on ANOVA ( $P < 0.05$ ).

The novel very long chain PUFA 28:8n-3 was detected in both the NZGLM (0.2%) and TBM (0.8%), with significantly higher levels ( $P < 0.0001$ ) in the TBM.

Pseudo iso 16:0 and 18:0 were recognized as degradation products of dimethylacetals formed from the original corresponding aldehydes.

There were several significant differences between sites for the percent FA composition in both the NZGLM and TBM. The differences between sites for the NZGLM were between 15:0, 16:1n-7c, 18:3n-6, 18:1n-9c, 20:5n-3, 20:1n-11c, 21:5n-3, 22:5n-6, and 22:6n-3 ( $P < 0.05$ ) and between sites for the TBM for 20:3n-6, i18:0, 4,8,12-TMTD, and 28:8n-3 ( $P < 0.05$ ).

PUFA were the dominant class of FA in both mussels (Table 3). Saturated FA (SFA) were the next most abundant group, with a higher proportion in the TBM, followed by mono-unsaturated FA (MUFA). The NZGLM had a significantly higher percentage of MUFA ( $P < 0.0001$ ), whereas the TBM had a significantly higher percentage of SFA, total n-3 PUFA, fatty aldehydes, NMI FA,  $\alpha$ -hydroxy FA, and several unidentified PUFA ( $P < 0.05$ ) compared with the NZGLM. There were no significant differences found between sites in the proportions of SFA, MUFA, and PUFA for either mussel species.

**Sterols.** Twenty sterols were identified in the TBM and NZGLM (Table 4, Fig. 2). Relative levels of individual sterols ranged from <0.5 to 32% (of total sterols). Cholesterol was the major sterol in both mussels (30% TBM and 29% NZGLM). The other sterols common to both the NZGLM and TBM were brassicasterol, 24-methylcholesterol, *trans*-22-dehydrocholesterol, desmosterol, and isofucosterol. The NZGLM had a significantly higher amount of brassicasterol, 24-nordehydrocholesterol, ocellasterol, lathosterol, 24-methylcholesterol, 23,24-dimethylcholesta-5,22E-dien-3 $\beta$ -ol, and isofucosterol ( $P < 0.05$ ). The TBM had significantly higher amounts of cholestanol, desmosterol, 24-methylenecholesterol, 24-ethylcholesterol ( $P < 0.05$ ), and an unidentified sterol (peak 14). Both mussel types contained around 2% of the C<sub>30</sub> sterol dinosterol, and a second C<sub>30</sub> sterol, 4,23,24-

trimethyl-5 $\alpha$ -cholest-7-en-3 $\beta$ -ol, was also present in the NZGLM. In the NZGLM, animals from site 3 (Coromandel) had significantly higher proportions of 23,24-dimethylcholesta-5,22E-dien-3 $\beta$ -ol ( $P = 0.002$ ), 24-methylenecholesterol, isofucosterol, and 4,23,24-trimethyl-5 $\alpha$ -cholest-7-en-3 $\beta$ -ol ( $P < 0.05$ ). Mussels from site 1 (South Island) had a significantly higher amount of dinosterol ( $P = 0.047$ ) and site 2 animals (Marlborough Sound) had a significantly higher amount of 22-*trans*-dehydrocholesterol ( $P = 0.015$ ).

For the TBM, site 1 mussels (Deep Bay 1) had significantly higher amounts of 24-nordehydrocholesterol, 22-*trans*-dehydrocholesterol, brassicasterol, 24-methylenecholesterol, and an unidentified sterol ( $P < 0.05$ ). Site 2 animals (Deep Bay 2) had a significantly higher amount of 24-methylcholesterol, and Site 3 animals (Great Oyster Bay) had significantly higher amounts of cholesterol, cholestanol, lathosterol, and 23,24-dimethylcholesterol ( $P < 0.05$ ).

## DISCUSSION

**Lipid composition.** Lipid contents in the TBM and NZGLM (1.2 to 1.8%) were similar to values reported in a study investigating the lipid composition of marine invertebrates of the Pacific Northwest (8). That study found the common blue mussel to have a lipid content of 1.8% in comparison to clams (1.5–1.7%), cockles (0.9–1.7%), horse clams (2%), and fresh oysters (2.5–4%), with crustacea such as crab and shrimp at around 1 and 1.5%, respectively. Yearsley *et al.* (7) and Nichols *et al.* (9) reported a lipid content in the TBM of 1.7% wet weight. Perry (22) investigated the lipid content of various mollusca and found the lipid content varied from 1.5% in a female mollusc *Subnina undulata* to 4% in the limpet *Cellana transerica*. The lipid content results for the TBM and the NZGLM in this study are in agreement with earlier studies of the blue mussel and other molluscs. The main lipid class of NZGLM and TBM was PL (up to 74%), which is consistent with other data for molluscs (7–9,22).

**TABLE 2**  
**FA Composition (%) for the NZGLM and the TBM**

FA <sup>b</sup>	Percent composition <sup>a</sup>								P value between species
	NZGLM				TBM				
	Site 1	Site 2	Site 3	Mean	Site 1	Site 2	Site 3	Mean	
14:0	3.7 ± 1.0	3.5 ± 1.0	3.2 ± 0.4	3.5 ± 0.8 <sup>c</sup>	1.5 ± 1.1	1.4 ± 0.4	1.1 ± 0.1	1.3 ± 0.6	P = 0.0000
4,8,12-TMTD	0.5 ± 0.1	0.6 ± 0.1	0.6 ± 0.1	0.5 ± 0.1	0.5 ± 0.1	1.3 ± 0.4	1.3 ± 0.1 <sup>f</sup>	1.0 ± 0.4 <sup>d</sup>	P = 0.0110
15:0	0.5 ± 0.1	0.6 ± 0.1	0.7 ± 0.0 <sup>e</sup>	0.1 ± 0.03	0.5 ± 0.2	0.3 ± 0.1	0.3 ± 0.1	0.2 ± 0.1 <sup>d</sup>	P = 0.0002
16:1n-7c <sup>g</sup>	8.6 ± 0.6	7.4 ± 0.1	8.6 ± 0.6 <sup>e</sup>	8.2 ± 0.7 <sup>c</sup>	4.2 ± 3.7	3.2 ± 0.8	2.5 ± 0.5	3.3 ± 2.0	P = 0.0001
16:1n-7t/16:2	0.7 ± 0.1	0.8 ± 0.2	0.9 ± 0.1	0.8 ± 0.1 <sup>c</sup>	0.2 ± 0.1	0.2 ± 0.1	0.1 ± 0.1	0.1 ± 0.1	P = 0.0000
16:1n-9c	0.1 ± 0.0	0.2 ± 0.1	0.2 ± 0.1	0.1 ± 0.0 <sup>c</sup>	0.1 ± 0.1	0.1 ± 0.1	0.1 ± 0.1	0.1 ± 0.1	P = 0.0330
16:0	16.3 ± 0.7	16.8 ± 0.4	16.5 ± 0.1	16.5 ± 0.5	20.1 ± 0.7	20.1 ± 2.1	20.1 ± 0.4	20.6 ± 1.1 <sup>d</sup>	P = 0.0000
i17:0	0.5 ± 0.2	0.6 ± 0.1	0.5 ± 0.1	0.6 ± 0.1	0.7 ± 0.3	0.6 ± 0.2	0.7 ± 0.1	0.7 ± 0.2	P = 0.0950
17:0	1.2 ± 0.1	1.0 ± 0.1	1.2 ± 0.1	1.1 ± 0.1 <sup>c</sup>	0.8 ± 0.3	0.6 ± 0.1	0.6 ± 0.1	0.7 ± 0.2	P = 0.0000
i18:0	0.5 ± 0.2	0.6 ± 0.1	0.4 ± 0.0	0.5 ± 0.1	0.6 ± 0.2	0.9 ± 0.1	1.1 ± 0.1 <sup>f</sup>	0.9 ± 0.3 <sup>d</sup>	P = 0.0014
18:0	4.4 ± 1.0	4.6 ± 0.5	3.9 ± 0.3	4.3 ± 0.6	3.7 ± 1.5	4.5 ± 0.8	5.1 ± 0.3	4.4 ± 1.1	P = 0.7900
18:1n-9c/18:3	1.9 ± 0.2	2.2 ± 0.1	2.2 ± 0.1 <sup>e</sup>	2.1 ± 0.2	2.7 ± 1.4	1.5 ± 0.2	1.5 ± 0.1	1.9 ± 0.9	P = 0.4800
18:1n-7c	3.1 ± 0.1	3.3 ± 0.2	3.2 ± 0.2	3.2 ± 0.2 <sup>c</sup>	1.9 ± 0.0	2.1 ± 0.2	2.0 ± 0.3	2.0 ± 0.2	P = 0.0000
18:1n-7t	0.5 ± 0.0	0.5 ± 0.1	0.5 ± 0.1	0.5 ± 0.04 <sup>c</sup>	0.1 ± 0.0	0.1 ± 0.1	0.1 ± 0.0	0.1 ± 0.0	P = 0.0000
18:2n-6	1.4 ± 0.1	1.6 ± 0.1	1.6 ± 0.2	1.5 ± 0.1 <sup>c</sup>	1.3 ± 0.3	1.0 ± 0.1	1.0 ± 0.1	1.1 ± 0.2	P = 0.0001
18:3n-6	0.1 ± 0.1	ND	0.2 ± 0.0 <sup>e</sup>	0.1 ± 0.1	ND	1.8 ± 3.2	ND	0.6 ± 1.8	P = 0.4200
18:4n-3	1.7 ± 0.4	2.1 ± 0.1	1.7 ± 0.2	1.8 ± 0.3	2.4 ± 1.3	1.4 ± 0.3	1.2 ± 0.1	1.6 ± 0.9	P = 0.5500
18:5n-3	0.3 ± 0.1	0.2 ± 0.1	0.2 ± 0.1	0.2 ± 0.1	0.3 ± 0.1	0.2 ± 0.2	0.2 ± 0.1	0.3 ± 0.3	P = 0.3600
α-OH 16:0	0.4 ± 0.0	0.4 ± 0.1	0.5 ± 0.1	0.5 ± 0.1	0.6 ± 0.1	0.8 ± 0.2	0.7 ± 0.1	0.7 ± 0.2 <sup>d</sup>	P = 0.0007
19:1	0.0 ± 0.1	0.1 ± 0.1	0.03 ± 0.1	0.1 ± 0.1	0.3 ± 0.2	0.1 ± 0.0	0.1 ± 0.0	0.2 ± 0.1 <sup>d</sup>	P = 0.0440
20:2n-6	0.3 ± 0.1	0.5 ± 0.1	0.4 ± 0.1	0.4 ± 0.1	0.7 ± 0.3	0.6 ± 0.1	0.6 ± 0.1	0.7 ± 0.1 <sup>d</sup>	P = 0.0006
20:2NMI	1.0 ± 0.3	1.0 ± 0.2	1.1 ± 0.2	1.1 ± 0.2 <sup>c</sup>	0.5 ± 0.2	0.3 ± 0.0	0.3 ± 0.1	0.7 ± 0.3	P = 0.0450
20:4n-6	2.3 ± 0.5	2.1 ± 0.4	2.7 ± 0.3	2.4 ± 0.5 <sup>c</sup>	1.5 ± 0.7	1.9 ± 0.2	1.8 ± 0.2	1.7 ± 0.4	P = 0.0060
20:5n-3	20.0 ± 1.0 <sup>e</sup>	19.1 ± 0.2	14.9 ± 0.9	17.9 ± 2.4 <sup>c</sup>	13.3 ± 3.5	15.1 ± 0.9	15.4 ± 0.8	14.6 ± 2.1	P = 0.0072
20:3n-6	0.1 ± 0.0	0.2 ± 0.0	0.2 ± 0.0	0.5 ± 0.0 <sup>c</sup>	0.5 ± 0.1 <sup>f</sup>	0.3 ± 0.1	0.3 ± 0.1	0.4 ± 0.1	P = 0.0026
20:4n-3/20:2NMI	1.7 ± 0.6	2.5 ± 0.5	2.0 ± 0.3	2.1 ± 0.5	2.5 ± 0.8	2.0 ± 0.4	1.8 ± 0.4	2.1 ± 0.6	P = 0.9700
20:1n-11c	0.6 ± 0.4	3.5 ± 0.4 <sup>e</sup>	2.4 ± 1.6	2.2 ± 1.5	2.9 ± 1.7	1.6 ± 1.7	2.5 ± 1.4	2.4 ± 1.5	P = 0.8300
20:1n-9c	2.2 ± 0.6	0.0 ± 0.0	0.8 ± 1.4	1.0 ± 1.3	1.1 ± 1.9	1.7 ± 1.5	0.9 ± 1.5	1.2 ± 1.5	P = 0.7200
20:1n-7c	1.7 ± 0.4	1.8 ± 0.3	1.1 ± 0.1 <sup>e</sup>	1.5 ± 0.4 <sup>c</sup>	0.8 ± 0.1	0.9 ± 0.1	0.8 ± 0.2	0.8 ± 0.1	P = 0.0004
21:5n-3	0.5 ± 0.1 <sup>e</sup>	0.4 ± 0.1	0.4 ± 0.1	0.9 ± 0.2 <sup>c</sup>	0.2 ± 0.1	0.2 ± 0.0	0.2 ± 0.0	0.4 ± 0.1	P = 0.0000
22:5n-6	0.3 ± 0.1	0.2 ± 0.1	0.4 ± 0.1 <sup>e</sup>	0.3 ± 0.1	0.2 ± 0.1	0.2 ± 0.0	0.2 ± 0.1	1.1 ± 0.1 <sup>d</sup>	P = 0.0120
22:6n-3	12.5 ± 0.4	12.3 ± 0.9	15.8 ± 1.3 <sup>e</sup>	13.5 ± 1.9	18.2 ± 5.5	21.3 ± 2.0	24.2 ± 0.8	21.2 ± 3.9 <sup>d</sup>	P = 0.0003
22:4n-6	0.3 ± 0.1	0.4 ± 0.1	0.4 ± 0.1	0.4 ± 0.1 <sup>c</sup>	0.1 ± 0.1	0.2 ± 0.1	0.2 ± 0.1	0.2 ± 0.0	P = 0.0000
22:5n-3	1.5 ± 0.3	1.6 ± 0.2	1.3 ± 0.1	1.5 ± 0.2	1.1 ± 0.2	1.1 ± 0.1	1.1 ± 0.1	1.1 ± 0.1	P = 0.0007
22:2NMI	1.0 ± 0.3	1.0 ± 0.2	1.1 ± 0.2	2.1 ± 0.4	1.4 ± 0.4	1.4 ± 0.2	1.2 ± 0.3	2.6 ± 0.5 <sup>d</sup>	P = 0.0320
22:0	0.1 ± 0.0	0.1 ± 0.1	0.1 ± 0.1	0.1 ± 0.04 <sup>c</sup>	0.0 ± 0.1	0.0 ± 0.1	ND	ND	P = 0.0032
C <sub>23</sub> PUFA	0.2 ± 0.1	0.1 ± 0.1	0.1 ± 0.0	0.2 ± 0.1	0.2 ± 0.1	0.1 ± 0.1	0.2 ± 0.0	0.2 ± 0.1	P = 0.0360
28:8n-3	0.4 ± 0.3	0.1 ± 0.1	0.2 ± 0.1	0.2 ± 0.2	0.6 ± 0.1	0.9 ± 0.1	0.9 ± 0.2 <sup>f</sup>	0.8 ± 0.2 <sup>d</sup>	P = 0.0000
Other	0.7 ± 1.1	0.4 ± 0.3	0.7 ± 0.5	3.1 ± 1.7	1.5 ± 0.7	0.8 ± 1.0	0.7 ± 0.6	5.0 ± 2.6	P = 0.0870

<sup>a</sup>Data for each species are the mean of nine individual animals, representing three animals from each of three sites (values are expressed as mean ± SD).

<sup>b</sup>4,8,12-TMTD, 4,8,12-trimethyl tetradecanoic acid; NMI, nonmethylene interrupted; α-OH 16:0, α-hydroxy 16:0 FA. Other (includes 17:2 and C<sub>22</sub> PUFA, and pseudo iso 16:0 and 18:0 degradation products of dimethylacetal). For other abbreviations see Table 1.

<sup>c</sup>Significantly higher than the TBM based on paired *t*-tests (*P* < 0.05).

<sup>d</sup>Significantly higher than the NZGLM based on paired *t*-tests (*P* < 0.05).

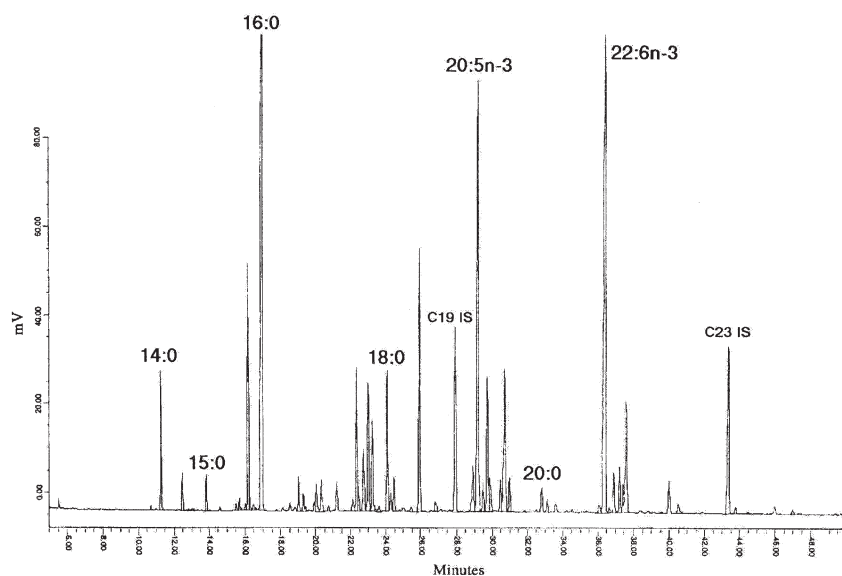
<sup>e</sup>Site significantly different from other sites (NZGLM) based on ANOVA (*P* < 0.05).

<sup>f</sup>Site significantly different from other sites (TBM) based on ANOVA (*P* < 0.05).

<sup>g</sup>16:1n-7c is clearly separated from 16:1n-13t on the HP5 capillary column (Hewlett-Packard).

Depending on the length of storage, temperature, and climatic conditions, marine invertebrates such as molluscs can undergo various changes in their lipid profiles owing to the activity of various enzymes. Jeong *et al.* (23) and Jeong (24) studied the effect of temperature and storage on lipid oxidation and composition of total lipid and lipid fractions of the oyster *Crassostrea gigas* and the giant ezo scallop *Patinopecten yessoensis*. In any marine source containing unsaturated FA, particularly long-chain n-3 PUFA, there is the risk of lipid de-

terioration during storage. Both studies showed that with increased storage time and with an increase in temperature of up to 35°C, there was a significant increase in oxidation as measured by TBARS, a significant decrease in total lipids, polar lipids, and PUFA, and a significant increase in nonpolar lipids and FFA. These data suggest the activity of various lipases and lipolytic enzymes responsible for enzymatic hydrolysis. In the study by Jeong *et al.* (23), after 12 mon of frozen storage there was a decrease in PL leading to an accu-



**FIG. 1.** Typical FAME profile of Tasmanian blue mussel. Samples were separated on an HP5 (nonpolar) 50-m cross-linked methyl (5% phenyl) silicone fused-silica capillary column, using a Hewlett-Packard 5890 gas chromatograph with FID. IS, internal standard.

mulation of FFA, causing an increase in the relative proportion of neutral lipids. This study reports the presence of significant proportions of FFA in both the NZGLM and TBM. Since these were not present in lipid extracts for mussels that were placed into extraction solvents within 10 min of harvesting, it is likely that the FFA represent hydrolytic degradation as reported by others (23,24). Generally, FFA are quite low in concentration; however, as Jeong *et al.* (23) and Jeong (24) showed in their studies with decreasing temperature and during storage, there is an increase in nonpolar lipids and FFA due to the action of lipolytic enzymes. Perhaps in the present study lipid hydrolysis had occurred during storage, which would account for the high levels of FFA in both mussels.

The differences in lipid content and lipid class composition between the NZGLM and TBM may be due to seasonal variation, as there are differences in climate between New Zealand and Tasmania. Differences may also reflect the stage

of development of the mussel, particularly the gonadal development (1). In addition, the sex of the mussel can alter lipid content and lipid class composition, since female mussels tend to have lower levels of total lipid (1). The dietary intake of the mussels and the availability of food may also reflect the differences seen between species. Perry (22) reported that HC in molluscs are derived mainly from environmental pollution such as fuel oil, crude oil, or motorboat oil; however, uncontaminated scallops were found to have a limited range of naturally occurring HC. HC profiles characteristic of pollution, such as a lack of odd-chain dominance and the presence of unresolved complex material and other specific biomarkers, were not observed in our samples. These observations are consistent with the pristine nature of the sampling locations from which all mussels were collected.

*FA.* Nearly half of the FA in each mussel species were PUFA, and up to 42% of the FA in both mussels were n-3

**TABLE 3**  
FA (% of total FA) for the NZGLM and the TBM

	Percent composition <sup>a</sup>								P value between species
	NZGLM				TBM				
	Site 1	Site 2	Site 3	Mean	Site 1	Site 2	Site 3	Mean	
Saturated FA	27.8 ± 1.2	28.6 ± 0.7	27.6 ± 0.2	28.0 ± 0.9	28.9 ± 1.2	29.5 ± 2.7	30.4 ± 0.6	29.6 ± 1.6 <sup>c</sup>	P = 0.023
PUFA	44.6 ± 0.4	44.5 ± 0.6	43.7 ± 2.3	44.2 ± 1.3	44.0 ± 7.4	49.2 ± 4.6	50.1 ± 1.2	47.8 ± 5.2	P = 0.086
Monounsaturated FA	18.2 ± 0.8	18.2 ± 0.8	18.4 ± 0.5 <sup>b</sup>	18.2 ± 0.6	11.9 ± 4.4	10.4 ± 1.0	9.6 ± 0.8	10.6 ± 2.5	P = 0.000
Total n-3 FA	37.5 ± 0.4	37.8 ± 0.6	36.1 ± 2.2	37.1 ± 1.4	38.2 ± 7.2	41.7 ± 1.8	44.6 ± 1.4	41.5 ± 4.7 <sup>c</sup>	P = 0.025
Total n-6 FA	5.1 ± 0.4	5.2 ± 0.4	6.0 ± 0.5	5.4 ± 0.6	4.6 ± 0.4	6.1 ± 3.0	4.3 ± 0.2	5.0 ± 1.8	P = 0.550
Other	7.5 ± 2.2	6.5 ± 0.5	8.1 ± 1.9	7.4 ± 1.6	12.4 ± 2.8	9.5 ± 2.8	8.4 ± 2.3	10.1 ± 2.9 <sup>c</sup>	P = 0.030

<sup>a</sup>Data for each species are the mean of nine individual animals, representing three animals from each of three sites (values are expressed as mean ± SD).

<sup>b</sup>Significantly higher than the TBM based on paired *t*-tests ( $P < 0.05$ ).

<sup>c</sup>Significantly higher than the NZGLM based on paired *t*-tests ( $P < 0.05$ ).

<sup>d</sup>Other includes hydroxy, isobranched, NMI FA, fatty aldehydes, and unidentified PUFA. For abbreviations see Tables 1 and 2.



**TABLE 4**  
**Sterol Composition (%) for the NZGLM and the TBM**

Peak number	Percent composition <sup>a</sup>										P value between species		
	NZGLM					TBM							
	Site 1	Site 2	Site 3	Mean	Site 1	Site 2	Site 3	Mean	Site 1	Site 2		Site 3	Mean
24-Nordehydrocholesterol	3.5 ± 0.2	4.2 ± 0.4	3.7 ± 0.1	3.8 ± 0.4 <sup>b</sup>	3.4 ± 0.1 <sup>c</sup>	2.1 ± 0.4	2.1 ± 0.3	2.5 ± 0.7	2.1 ± 0.4	2.1 ± 0.4	2.1 ± 0.3	2.5 ± 0.7	P = 0.0040
Occlasterol	4.0 ± 1.3	3.2 ± 1.6	2.8 ± 0.5	3.3 ± 1.2 <sup>b</sup>	1.7 ± 0.2	1.5 ± 0.2	1.3 ± 0.2	1.5 ± 0.2	1.7 ± 0.2	1.5 ± 0.2	1.3 ± 0.2	1.5 ± 0.2	P = 0.0019
<i>Trans</i> -22-dehydrocholesterol	10.6 ± 0.3	14.0 ± 2.1 <sup>d</sup>	10.0 ± 0.3	11.5 ± 2.2	12.0 ± 2.2 <sup>c</sup>	8.6 ± 0.8	8.7 ± 0.7	9.8 ± 2.0	12.0 ± 2.2 <sup>c</sup>	8.6 ± 0.8	8.7 ± 0.7	9.8 ± 2.0	—
Cholesterol	28.4 ± 1.2	31.9 ± 5.6	27.7 ± 1.1	29.3 ± 3.5	26.6 ± 1.3	31.2 ± 1.0	32.1 ± 1.8 <sup>c</sup>	30.0 ± 2.7	26.6 ± 1.3	31.2 ± 1.0	32.1 ± 1.8 <sup>c</sup>	30.0 ± 2.7	—
Cholestanol	0.6 ± 0.1	0.9 ± 0.2	0.8 ± 0.1	0.8 ± 0.2	1.6 ± 0.3	2.9 ± 0.4	3.5 ± 0.5 <sup>c</sup>	2.7 ± 0.9 <sup>e</sup>	1.6 ± 0.3	2.9 ± 0.4	3.5 ± 0.5 <sup>c</sup>	2.7 ± 0.9 <sup>e</sup>	P = 0.0003
Desmosterol	8.2 ± 0.4	8.5 ± 2.5	7.6 ± 0.5	8.1 ± 1.3	10.8 ± 2.4	10.3 ± 1.3	8.9 ± 0.5	10.0 ± 1.5 <sup>e</sup>	10.8 ± 2.4	10.3 ± 1.3	8.9 ± 0.5	10.0 ± 1.5 <sup>e</sup>	P = 0.0140
Brassicasterol	14.7 ± 0.4	14.2 ± 2.0	14.7 ± 0.4	14.6 ± 1.1 <sup>b</sup>	11.0 ± 0.5 <sup>c</sup>	9.1 ± 0.4	8.6 ± 0.7	9.6 ± 1.1	11.0 ± 0.5 <sup>c</sup>	9.1 ± 0.4	8.6 ± 0.7	9.6 ± 1.1	P = 0.0000
Lathosterol	0.9 ± 0.6	1.0 ± 1.1	0.7 ± 0.2	0.9 ± 0.6 <sup>b</sup>	0.1 ± 0.1	0.3 ± 0.0	0.5 ± 0.1 <sup>c</sup>	0.3 ± 0.2	0.1 ± 0.1	0.3 ± 0.0	0.5 ± 0.1 <sup>c</sup>	0.3 ± 0.2	P = 0.0320
Lophenol/ergosterol	ND	ND	ND	ND	2.0 ± 0.5	1.4 ± 0.3	1.3 ± 1.2	1.5 ± 0.4	2.0 ± 0.5	1.4 ± 0.3	1.3 ± 1.2	1.5 ± 0.4	—
24-Methylenecholesterol	ND	ND	1.6 ± 0.3 <sup>d</sup>	0.5 ± 0.8	6.6 ± 0.7 <sup>c</sup>	4.4 ± 0.8	4.7 ± 0.4	5.2 ± 1.1 <sup>e</sup>	6.6 ± 0.7 <sup>c</sup>	4.4 ± 0.8	4.7 ± 0.4	5.2 ± 1.1 <sup>e</sup>	P = 0.0000
24-Methylcholesterol	16.7 ± 0.6	13.6 ± 6.8	10.3 ± 0.5	13.6 ± 4.4 <sup>b</sup>	6.0 ± 1.2	11.7 ± 0.1 <sup>c</sup>	11.2 ± 1.0	9.6 ± 2.7	6.0 ± 1.2	11.7 ± 0.1 <sup>c</sup>	11.2 ± 1.0	9.6 ± 2.7	P = 0.0420
23,24-Dimethylcholesta-5,22E-dien-3β-ol	2.7 ± 0.3	1.8 ± 1.0	4.8 ± 0.1 <sup>d</sup>	3.1 ± 1.5 <sup>b</sup>	1.4 ± 0.2	1.9 ± 0.1	2.1 ± 0.1 <sup>c</sup>	1.8 ± 0.3	1.4 ± 0.2	1.9 ± 0.1	2.1 ± 0.1 <sup>c</sup>	1.8 ± 0.3	P = 0.0320
Porifasterol	ND	ND	ND	Tr <sup>f</sup>	ND	ND	ND	Tr <sup>f</sup>	ND	ND	ND	Tr <sup>f</sup>	—
Unidentified	1.3 ± 0.2	1.4 ± 0.8	1.5 ± 0.0	1.4 ± 0.4	3.1 ± 0.4	3.5 ± 0.6	3.2 ± 0.3	3.3 ± 0.4 <sup>e</sup>	3.1 ± 0.4	3.5 ± 0.6	3.2 ± 0.3	3.3 ± 0.4 <sup>e</sup>	P = 0.0000
24-Ethylcholesterol	ND	ND	0.2 ± 0.3	0.1 ± 0.2	1.5 ± 0.1	1.3 ± 0.1	1.2 ± 0.1	1.3 ± 0.1 <sup>e</sup>	1.5 ± 0.1	1.3 ± 0.1	1.2 ± 0.1	1.3 ± 0.1 <sup>e</sup>	P = 0.0000
Isotucosterol	3.9 ± 0.3	2.3 ± 1.3	10.8 ± 1.1 <sup>d</sup>	5.7 ± 4.0 <sup>b</sup>	2.7 ± 0.6	2.4 ± 0.2	2.5 ± 0.2	2.5 ± 0.3	2.7 ± 0.6	2.4 ± 0.2	2.5 ± 0.2	2.5 ± 0.3	P = 0.0480
Dinosterol	3.6 ± 0.5 <sup>d</sup>	2.7 ± 1.7	1.0 ± 0.2	2.4 ± 1.5	1.9 ± 0.3	1.9 ± 0.5	2.2 ± 0.3	2.0 ± 0.3	1.9 ± 0.3	1.9 ± 0.5	2.2 ± 0.3	2.0 ± 0.3	—
Unidentified	ND	ND	ND	ND	2.4 ± 0.2	1.9 ± 0.5	2.0 ± 0.1	2.1 ± 0.3	2.4 ± 0.2	1.9 ± 0.5	2.0 ± 0.1	2.1 ± 0.3	—
4,23,24-Trimethyl-5α-cholest-7-en-3β-ol	ND	ND	1.6 ± 0.2 <sup>d</sup>	0.5 ± 0.8	ND	ND	ND	ND	ND	ND	ND	ND	—
Unidentified	ND	ND	ND	ND	0.9 ± 0.4 <sup>c</sup>	ND	ND	0.3 ± 0.5	0.9 ± 0.4 <sup>c</sup>	ND	ND	0.3 ± 0.5	—

<sup>a</sup>Data for each species are the mean of nine individual animals, representing three animals from each of three sites (values are expressed as mean ± SD).

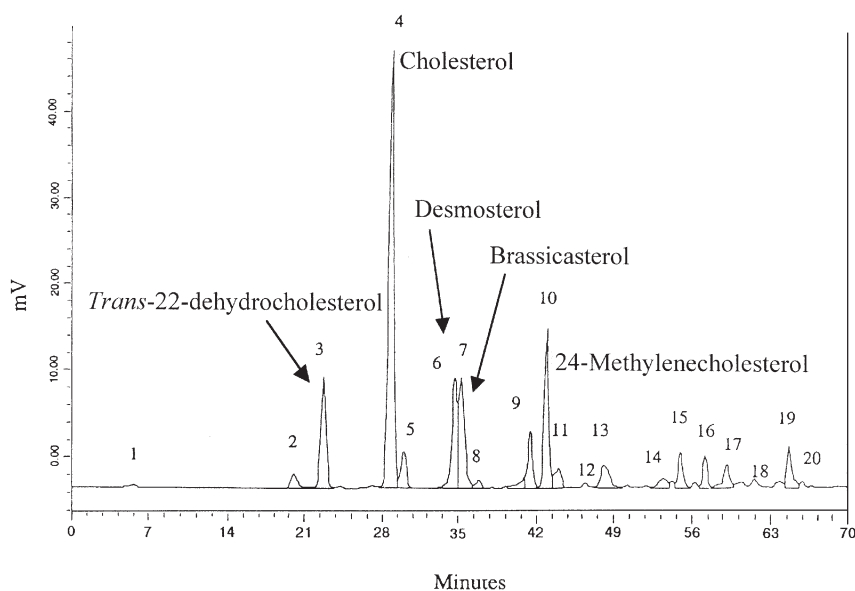
<sup>b</sup>Significantly higher than the TBM based on paired *t*-tests ( $P < 0.05$ ).

<sup>c</sup>Site significantly different from other sites (TBM) based on ANOVA ( $P < 0.05$ ).

<sup>d</sup>Site significantly different from other sites (NZGLM) based on ANOVA ( $P < 0.05$ ).

<sup>e</sup>Significantly higher than the NZGLM based on paired *t*-tests ( $P < 0.05$ ).

<sup>f</sup>Trace, less than 0.1%, for other abbreviations see Table 1.



**FIG. 2.** Typical sterol profile of New Zealand green lipped mussel. Separated on an HP5 (nonpolar) 50-m cross-linked methyl (5% phenyl) silicone fused-silica capillary column, using a Hewlett-Packard 5890 GC with FID.

PUFA, while approximately 5% were n-6 PUFA. The predominant n-3 PUFA were 20:5n-3 and 22:6n-3. The NZ mollusc *M. canaliculus* contains a similar FA profile, dominated by 20:5n-3 and 22:6n-3 PUFA (9). Many marine species of molluscs are rich in 20:5n-3, with lower levels of 22:5n-3 and 22:6n-3. Other bivalvia species, such as *Ostrea lutaria* and *C. gigas*, have also been found to contain high levels of 20:5n-3 and 22:6n-3, with the former being the predominant PUFA. In the present study, there was a significantly higher amount of 22:6n-3 (14–20%), particularly in the TBM. In contrast to previous studies, the high proportion of 22:6n-3 in the NZGLM and TBM probably largely reflects the composition of the planktonic diet. Various algal species are known to contain elevated levels of 22:6n-3, including dinoflagellates, cryptomonads, and certain thraustochytrids as well as zooplankton (25,26).

Mollusc FA profiles usually contain about 30–40% SFA (1,8,21), a level which was found in the present study. The SFA profiles were similar for both species and also to profiles for other molluscs.

The presence of 28:8n-3, along with the C<sub>30</sub> sterol dinosterol, indicates a strong dietary influence, in particular for the TBM. The TBM were collected during an algal bloom of the dinoflagellate *Gymnodinium catenatum* that occurs in southern Tasmanian waters. *Gymnodinium catenatum* recently has been reported to contain 28:8n-3 and cholesterol as a major sterol (27). Van Pelt *et al.* (28) reported the presence of 28:8n-3 in the dinoflagellate *Cryptocodinium cohnii*. This dietary link is further supported by the presence of 24-methyl-5 $\alpha$ -cholest-7-en-3 $\beta$ -ol in the TBM. This sterol is also found in *G. catenatum* (29). The higher amounts of 28:8n-3 in the TBM than in the NZGLM suggest a greater dietary dinoflagellate contribution with this species.

The fatty acid 18:5n-3 has also been used as a marker for dinoflagellate ingestion (29), although it is also present in a few other algal species (25). The dinoflagellate biomarkers dinosterol and C<sub>28</sub> PUFA were present in the TBM at higher levels than in the NZGLM, whereas 18:5n-3 was only a minor component in both mussels and in similar proportions (0.2 to 0.3%).

The anti-inflammatory properties of fish oils are thought to be due to the presence of 20:5n-3 and 22:6n-3 (15); correspondingly, Whitehouse *et al.* (18) have reported that the anti-inflammatory activity in an oil extract of lipids from the NZGLM is associated with PUFA, which have 4, 5, and 6 double bonds. In the present study the total proportion of PUFA with 4, 5, and 6 double bonds was 40% in the NZGLM and 43% in the TBM ( $P = 0.92$ ), indicating little difference between species.

The 20:2 and 22:2 NMI FA were found in similar concentrations (3–5%) to levels occurring in a variety of marine molluscs such as gastropods (30). Zhukova and Svetashev (31) reported similar proportions of these FA in *M. edulis* (4.6%), the oyster *C. virginica* (5.8%), and the northern quahog *Merccenaria mercenaria* (2.9%). The presence of these NMI indicates a dietary contribution, as they may be derived from algae and zooplanktonic pteropods such as *Limacina helicina* and result from desaturation of 20:1n-9 and 20:1n-7 (22,31,32). In the study of oysters by Abad *et al.* (32), NMI were present in concentrations from 2 to 10%, depending on the season.

The presence of 4,8,12-TMTD has also been previously reported in various molluscs (30). The American oyster *C. virginica* contained small amounts of 4,8,12-TMTD and NMI dienoic acids (31). The NMI 20:2 and 22:2 are constituents of red algae; thus, their presence may also indicate direct dietary contribution.

**Sterols.** Compared with other marine invertebrates, molluscs are unique, as they contain a wide range of sterols besides cholesterol (8). Both mussels in the current study contained a similar range of sterols, however, in differing proportions, with cholesterol the most prominent sterol ranging from 27 to 32%. Another NZ mussel, *M. planulatus*, has been reported to contain at least eight of the sterols identified in our mussels (22). It may be difficult to compare sterol profiles due to varying extraction techniques and sensitivity of analytical methods. Sterols in *M. planulatus* included *trans*-22-dehydrocholesterol (10%), cholesterol (46%), desmosterol (6%), 24-methylenecholesterol (10%), 24-methylcholesterol (4%), 24-ethylcholesterol (4%), and stigmaterol (1%). Perry (22) also reported similar sterol composition in the BM. Plant sterols such as sitosterol and stigmaterol as identified in both mussel species are believed to aid in cholesterol-lowering in humans (12). Cholesterol was the main sterol (46%) followed by brassicasterol (13%), 24-methylcholesterol and 24-ethylcholesterol (both 4%), and *trans*-22-dehydrocholesterol (2%). Cholesterol was also identified in scallops, up to 60% (22), with some additional more complex C<sub>28</sub> and C<sub>29</sub> sterols.

Gordon (8) reported desmosterol and brassicasterol in similar amounts in the BM. Desmosterol is thought to be an intermediate in cholesterol biosynthesis. The clam *Saxidomus giganteus* has the ability to bioconvert 24-methylenecholesterol and 7-cholestenol, but it is not known if sterols other than cholesterol are synthesized by the mussels.

Teshima and Kanazawa (11) found sterols in the BM and abalone to be predominantly composed of cholesterol (30 and 93%, respectively), followed by 22-dehydrocholesterol (25 and 6%, respectively) and 24-methylenecholesterol (12% and a trace, respectively). The BM contained desmosterol,  $\beta$ -sitosterol, and three unidentified sterols (7%). Gordon (8) reported cholesterol as the dominant sterol in oysters (50%) followed by brassicasterol/desmosterol (25%) and 24-methylenecholesterol (25%). Teshima and Kanazawa (11) showed that molluscs have the ability to synthesize cholesterol; however, this ability is dependent on the mussel's life cycle, sexual maturation, and sex.

This study provides data for the whole tissue of the NZGLM, about which considerable interest exists due to the reported bioactivity in the oil from this species (18,19). The NZGLM had similar lipid content and lipid class composition to the TBM. Differences observed between the two species were probably due to dietary differences and also may reflect seasonal variation, the development of the mussel, particularly the gonads, and/or the sex of the mussel, which can alter the lipid content and lipid class composition.

## ACKNOWLEDGMENTS

This study was funded in part by the Fisheries Research and Development Corporation (99/331). We thank Danny Holdsworth for his assistance with GC-MS, in particular CI/GC-MS experiments; John Croft, MacFarlane Laboratories New Zealand; Dr. Vicky Wadley; and the Mussel and Fish Co-op. Taseas, kindly provided the mussels used in this study.

## REFERENCES

- Joseph, J.D. (1982) Lipid Composition of Marine and Estuarine Invertebrates. Part II Mollusca, *Prog. Lipid Res.* 21, 109–153.
- Ching, E.W.K., Siu, W.H.L., Lam, P.K., Xu, L., Zhang, Y., Richardson, B.J., and Wu, R.S.S. (2001) DNA Adduct Formation and DNA Strand Breaks in Green-Lipped Mussels (*Perna viridis*) Exposed to Benzo[a]pyrene: Dose- and Time-Dependent Relationships, *Mar. Pollut. Bull.* 42, 603–610.
- Li, S.C., Wang, W.X., and Hsieh, D.P. (2002) Effects of Toxic Dinoflagellate *Alexandrium tamarens* on the Energy Budgets and Growth of Two Marine Bivalves, *Mar. Environ. Res.* 53, 145–160.
- Chong, K., and Wang, W.X. (2001) Comparative Studies on the Biokinetics of Cd, Cr and Zn in the Green Mussel *Perna viridis* and the Manila Clam *Ruditapes philippinarum*, *Environ. Pollut.* 115, 107–121.
- Goode, J., and Willson, C. (1990) *Seafood of Australia and New Zealand. A Comprehensive Guide to Its Preparation and Cooking*, Angus and Robertson, North Ryde, New South Wales, Australia.
- Creber, A. (1987) *The Complete Australian and New Zealand Fish and Seafood Cookbook*, William Heinemann, Richmond, Victoria, Australia.
- Yearsley, G.K., Last, P.R., and Ward, R.D. (1998) Australian Seafood Domestic Species, FRDC Project 95/122, pp. 335–409, CSIRO Marine Research, Hobart, Australia.
- Gordon, D.T. (1982) Sterols in Mollusks and Crustacea of the Pacific Northwest, *J. Am. Oil Chem. Soc.* 59, 536–545.
- Nichols, P.D., Virtue, P., Mooney, B.D., Elliott, N.G., and Yearsley, G.K. (1998) Seafood the Good Food. The Oil Content and Composition of Australian Commercial Fishes, Shellfishes and Crustaceans. FRDC Project 95/122. Guide Prepared for the Fisheries Research and Development Corporation, CSIRO, Hobart, Australia.
- Kluytmans, J.H., Boot, J.H., Oudejans, R.C.H.M., and Zandee, D.I. (1985) Fatty Acid Synthesis in Relation to Gametogenesis in the Mussel *Mytilus edulis*, *Comp. Biochem. Physiol.* 81, 959–963.
- Teshima, S., and Kanazawa, A. (1974) Biosynthesis of Sterols in Abalone, *Haliotis gurneri* and Mussel, *Mytilus edulis*, *Comp. Biochem. Physiol.* 47, 555–561.
- Gylling, H., and Miettinen, T.A. (1999) Cholesterol Reduction by Different Plant Stanol Mixtures and with Variable Fat Intake, *Metabolism* 48, 575–580.
- Naughton, J.M., O'Dea, K., and Sinclair, A.J. (1986) Animal Foods in Traditional Australian Aboriginal Diets: Polyunsaturated and Low Fat, *Lipids* 21, 684–690.
- Nestel, P.J. (2000) Fish Oil and Cardiovascular Disease: Lipids and Arterial Function, *Am. J. Clin. Nutr.* 71, 228S–231S.
- James, M.J., and Cleland, L.G. (1997) Dietary n-3 Fatty Acids and Therapy for Rheumatoid Arthritis, *Sem. Arth. Rheum.* 27, 85–97.
- James, M.J., Gibson, R.A., and Cleland, L.G. (2000) Dietary Polyunsaturated Fatty Acids and Inflammatory Mediator Production, *Am. J. Clin. Nutr.* 71, 343S–348S.
- Lorenz, R., Weber, P.C., Szimnau, P., Heldwein, W., Strasser, T., and Loeschke, K. (1989) Supplementation with n-3 Fatty Acids from Fish Oil in Chronic Inflammatory Bowel Disease—A Randomized, Placebo-Controlled, Double-Blind Cross-over Trial, *J. Intern. Med.* 225, 225–232.
- Whitehouse, M.W., Macrides, T.A., Kalafitis, N., Betts, W.H., Haynes, D.R., and Broadbent, J. (1997) Anti-inflammatory Activity of a Lipid Fraction (lyprinol) from the NZ Green-Lipped Mussel, *Inflammopharmacology* 5, 237–246.
- Rainsford, K.D., and Whitehouse, M.W. (1980) Gastroprotective and Anti-inflammatory Properties of Green Lipped Mussel

- (*Perna canaliculus*) Preparation, *Arzneimittelforschung/Drug Res.* 30, 2128–2132.
20. Bligh, E.G., and Dyer, W.J. (1959) A Rapid Method of Total Lipid Extraction and Purification, *Can. J. Biochem. Physiol.* 37, 911–917.
  21. Phleger, C.F., Nelson, M.M., Mooney, B.D., and Nichols, P.D. (2001) Interannual Variations in the Lipids of the Antarctic Pteropods *Clione limacina* and *Clio pyramidata*, *Comp. Biochem. Physiol. B* 128, 553–564.
  22. Perry, G.J. (1977) Lipids in the Marine Environment, Ph.D. Thesis, Melbourne University, Victoria Australia.
  23. Jeong, B.Y., Ohshima, T., Koizumi, C., and Kanou, Y. (1990) Lipid Deterioration and Its Inhibition of Japanese Oyster *Crassostrea gigas* During Frozen Storage, *Nippon Suisan Gakkaishi* 56, 2083–2091.
  24. Jeong, B.Y. (1999) Changes in Molecular Species Compositions of Glycerophospholipids in the Adductor Muscle of the Giant Ezo Scallop *Patinopecten yessoensis* During Frozen Storage, *J. Food Lipids* 6, 131–147.
  25. Volkman, J.K., Jeffrey, S.W., Nichols, P.D., Rogers, G.I., and Garland, C.D. (1989) Fatty Acid and Lipid Composition of 10 Species of Microalgae Used in Mariculture, *J. Exp. Mar. Biol. Ecol.* 128, 219–240.
  26. Lewis, T.E., Nichols, P.D., and McMeekin, T.A. (1999) The Biotechnological Potential of Thraustochytrids, *Mar. Biotechnol.* 1, 580–587.
  27. Mansour, M.P., Volkman, J., and Holdsworth, D.G. (1999) Very-Long Chain C<sub>28</sub> Highly Unsaturated Fatty Acids in Marine Dinoflagellates, *Phytochemistry.* 50, 541–548.
  28. Van Pelt, C.K., Huang, M.C., Tschanz, C.L., and Brenna, J.T. (1999) An Octane Fatty Acid, 4,7,10,13,16,19,22,25-Octacosaoctanoic Acid (28:8n-3), Found in Marine Oils, *J. Lipid Res.* 40, 1501–1505.
  29. Hallegraff, G., Nichols, P.D., Volkman, J.K., Blackburn, S., and Everitt, D. (1991) Pigments, Sterols and Fatty Acids of the Toxic Dinoflagellate *Gymnodinium catenatum*, *J. Phycol.* 27, 591–599.
  30. Ackman, R.G., Hooper, S.N., and Ke, P.J. (1971) The Distribution of Saturated and Isoprenoid Fatty Acids in the Lipids of Three Species of Molluscs, *Littorina litorea*, *Crassostrea virginica*, and *Venus mercenaria*, *Comp. Biochem. Physiol. B* 39, 579–587.
  31. Zhukova, N.V., and Svetashev, V.I. (1986) Non-methylene Interrupted Dienoic Fatty Acids in Molluscs from the Sea of Japan, *Comp. Biochem. Physiol. B* 83, 643–646.
  32. Abad, M., Ruiz, C., Martinez, D., Mosquera, G., and Sanchez, J.L. (1995) Seasonal Variations of Lipid Classes and Fatty Acids in Flat Oyster, *Ostrea edulis*, from San Cibrao (Galicia, Spain), *Comp. Biochem. Physiol. C* 110, 109–118.

[Received June 27, 2001, and in revised form April 30, 2002; revision accepted May 1, 2002]



# Two Novel Glucosylceramides from Gonads and Body Walls of the Patagonian Starfish *Allostichaster inaequalis*

María E. Díaz de Vivar<sup>a</sup>, Alicia M. Seldes<sup>b</sup>, and Marta S. Maier<sup>b,\*</sup>

<sup>a</sup>Facultad de Ciencias Naturales (Sede Puerto Madryn), Universidad Nacional de la Patagonia "San Juan Bosco," 9120 Chubut, Argentina, and <sup>b</sup>Departamento de Química Orgánica, Facultad de Ciencias Exactas y Naturales, Universidad de Buenos Aires, 1428 Buenos Aires, Argentina

**ABSTRACT:** From the water-insoluble lipid fraction of the chloroform/methanol/water extract of the gonads and body walls of the Patagonian starfish *Allostichaster inaequalis*, two new glucosylceramides (**4** and **7**) were isolated together with the known phalluside-1 (**1**) and two glucosylceramides (**2** and **3**) previously isolated from the starfish *Cosmasterias lurida*. The new compounds were characterized as (2*S*,3*R*,4*E*,8*E*,10*E*)-1-(β-D-glucopyranosyloxy)-3-hydroxy-2-[(*R*)-2-hydroxy-15-tetracosenoyl] amino-4,8,10-octadecatriene (**4**) and (2*S*,3*R*,4*E*,15*Z*)-1-(β-D-glucopyranosyloxy)-3-hydroxy-2-[(*R*)-2-hydroxyhexadecanoyl] amino-4,15-docosadiene (**7**) by means of spectroscopic and chemical methods.

Paper no. L8958 in *Lipids* 37, 597–603 (June 2002).

Glucosylceramides and related compounds have been isolated from several marine invertebrates, such as echinoderms (1–10), sponges (11–13), ascidians (14), sea anemones (15), bryozoa (16), and gorgonians (17). These compounds have shown a variety of biological activities, such as cytotoxicity against L1210 leukemia cells *in vitro* (8), histidine decarboxylase (1) and DNA topoisomerase I (16) inhibition, and moderate wound-healing activity (9). These biological activities may be related to the amphipathic nature of the molecule (18).

As part of our investigation on polar metabolites from cold-water echinoderms of the South Atlantic, we previously reported the isolation and structural elucidation of glucosylceramides from the starfish *Cosmasterias lurida* Philippi (19). The present paper deals with the isolation and structural elucidation of glucosylceramides from gonads and body walls of *Allostichaster inaequalis* Koehler, a starfish of the Patagonian coast of Argentina. This is the first report on the comparative study of glucosylceramides of gonads and body walls from a dissected starfish.

## EXPERIMENTAL PROCEDURES

*Chromatographic and instrumental methods.* Preparative HPLC was carried out in a Spectra Physics chromatograph

\*To whom correspondence should be addressed at Departamento de Química Orgánica, Facultad de Ciencias Exactas y Naturales, Universidad de Buenos Aires, Pabellón 2, Ciudad Universitaria, 1428 Buenos Aires, Argentina. E-mail: maier@qo.fcen.uba.ar

Abbreviations: Ac<sub>2</sub>O, acetic anhydride; BW, glucosylceramide mixture from body walls of the starfish; CC, column chromatography; DMDS, dimethyl disulfide; G, glucosylceramide mixture from gonads of the starfish; LCB, long-chain bases; RP-TLC, reversed-phase TLC; TFA, trifluoroacetic acid.

(Fremont, CA) with a solvent delivery system Spectra Series P100, a Thermo Separation Products refractive index detector (Fremont, CA), and a Spectra Series UV100 UV detector (Fremont, CA) using a Phenomenex Ultracarb ODS 20 column (250 × 10 mm, 5 μm) (Torrance, CA) at a flow rate of 2.0 mL/min, eluting with MeOH/H<sub>2</sub>O (99:1, vol/vol) for the glucosylceramide mixture from the body walls (BW) and MeOH/H<sub>2</sub>O (98:2, vol/vol) for the glucosylceramide mixture from the gonads (G). GC was performed on a Hewlett-Packard 5890 A chromatograph (Avondale, PA) equipped with a FID. An Ultra-2 column (0.2 mm i.d. × 50 m) (Hewlett-Packard) was used with nitrogen as the carrier gas. The column temperature was programmed from 160 to 280°C at a rate of 10°C/min. GC-MS analyses were performed on a VG Trio-2 instrument (Manchester, United Kingdom) employing the electron impact (EI) mode (ionizing potential 70 eV). Helium was used as carrier gas, a capillary column (CP-Sil 5 CB, 0.25 mm i.d. × 50 m length; Chrompack, Middleburg, The Netherlands) (column temperature: 100–290°C; rate: 10°C/min) was used for FAME and long-chain base (LCB) analyses, and an SP 2340 fused-silica column (0.32 mm i.d. × 30 m) (column temperature: 80–270°C; rate: 12°C/min, and then isothermic at 270°C for 20 min) was used for the dimethyl disulfide (DMDS) derivative analyses. Optical rotations were measured on a PerkinElmer 343 polarimeter (Überlingen, Germany). Melting points were measured on a Fisher-Johns m.p. apparatus model 2572 A and are uncorrected.

<sup>1</sup>H and <sup>13</sup>C NMR and 2-D NMR spectra were recorded in a Bruker AM 500 spectrometer (Karlsruhe, Germany) at 500 MHz for <sup>1</sup>H and 125 MHz for <sup>13</sup>C NMR; tetramethylsilane was used as internal standard, and coupling constants (*J*) were represented in Hz. FABMS spectra were registered in a VG-ZAB BEQ spectrometer.

*Materials.* Dry flash-column chromatography (flash-CC) was performed on silica gel H (230–400 mesh; Merck, Darmstadt, Germany) with the solvents indicated in each case. Normal-phase TLC was performed on silica gel F<sub>254</sub> (Merck) with CH<sub>2</sub>Cl<sub>2</sub>/MeOH/AcOEt/H<sub>2</sub>O (8.5:1.5:2:0.1, by vol). Reversed-phase (RP)-TLC was performed on C<sub>18</sub> silica gel 60 F<sub>254</sub> (Merck) with MeOH. CC was performed on silica gel (70–230 mesh; Merck) with CH<sub>2</sub>Cl<sub>2</sub>/MeOH/H<sub>2</sub>O (8:1.3:0.1, by vol).

Fresh specimens of *A. inaequalis* were collected in Bahía Nueva (Puerto Madryn, Chubut, Argentina) and identified by Dr. Alejandro Tablado from the Museo Argentino de Ciencias

**TABLE 1**  
**<sup>1</sup>H NMR Data for Compounds 1–7 in CD<sub>3</sub>OD<sup>a</sup>**

H	1–3, 5, 6	4	7
1a	3.70 ( <i>dd</i> , 10.3, 3.6)	3.70 ( <i>dd</i> , 10.2, 3.6)	3.71 ( <i>dd</i> , 10.5, 3.3)
1b	4.10 ( <i>dd</i> , 10.3, 5.4)	4.09 ( <i>dd</i> , 10.2, 5.4)	4.11 <i>m</i>
2	3.99 <i>m</i>	3.98 <i>m</i>	3.97 <i>m</i>
3	4.13 ( <i>bt</i> , 7.5)	4.14 ( <i>bt</i> , 7.3)	4.11 <i>m</i>
4	5.48 ( <i>dd</i> , 15.2, 7.0)	5.48 ( <i>dd</i> , 15.4, 7.5)	5.47 ( <i>dd</i> , 15.3, 7.3)
5	5.74 ( <i>dt</i> , 15.2, 6.3)	5.73 ( <i>dt</i> , 15.0, 6.4)	5.72 ( <i>dt</i> , 15.0, 6.6)
6	2.20 <i>m</i>	2.15 <i>m</i>	2.04 <i>m</i>
7	2.07 <i>m</i>	2.03 <i>m</i>	2.04 <i>m</i>
8	5.35 ( <i>t</i> , 6.8)	5.56 <i>m</i> <sup>a</sup>	
9		5.96 <i>m</i> <sup>b</sup>	
10	6.02 ( <i>d</i> , 15.4)	5.99 <i>m</i> <sup>b</sup>	
11	5.56 ( <i>dt</i> , 15.4, 7.1)	5.54 <i>m</i> <sup>a</sup>	
18	0.89 ( <i>t</i> , 6.6)	0.89 ( <i>t</i> , 6.6)	0.89 ( <i>t</i> , 6.2)
19	1.70 <i>s</i>		
(CH <sub>2</sub> )	1.24–1.30 <i>bs</i>	1.24–1.30 <i>bs</i>	1.24–1.30 <i>bs</i>
2'	3.98 <i>m</i>	3.98 <i>m</i>	3.97 <i>m</i>
C=C-H		5.35 ( <i>t</i> , 4.8, H-15' and H-16')	5.35 ( <i>t</i> , 5.85, H-15, H-16)
1''	4.26 ( <i>d</i> , 7.7)	4.26 ( <i>d</i> , 7.75)	4.26 ( <i>d</i> , 7.7)
2''	3.19 ( <i>dd</i> , 9.1, 7.7)	3.18 ( <i>dd</i> , 9.1, 7.8)	3.19 <i>bd</i>
3''	3.38 <i>m</i>	3.38 <i>m</i>	3.38 <i>m</i>
4''	<i>b</i>	<i>b</i>	<i>b</i>
5''	3.26 <i>m</i>	3.26 <i>m</i>	3.26 <i>m</i>
6''a	3.66 ( <i>dd</i> , 12.5, 5.4)	3.64 ( <i>dd</i> , 11.9, 5.0)	3.66 ( <i>dd</i> , 11.8, 5.2)
6''b	3.86 ( <i>bd</i> , 12.0)	3.87 ( <i>bd</i> , 10.7)	3.87 ( <i>bd</i> , 12.0)

<sup>a</sup>Assignments with the same superscript (a,b) may be reversed.

<sup>b</sup>Signals superimposed with the solvent.

Naturales “Bernardino Rivadavia,” Buenos Aires, Argentina, where a voucher specimen is preserved (MACN 34396).

**Extraction and isolation.** Animals (45 specimens, 910 g wet weight) were collected and dipped in sea water. Gonads of both sexes and body walls were dissected out. Body walls (649 g) and gonads (148.5 g) were extracted twice by the method of Bligh and Dyer (20) with a solvent mixture of CHCl<sub>3</sub>/MeOH/H<sub>2</sub>O (1:2:0.8, by vol) (2 L/kg) for 72 h at room temperature. The solvent mixture was then diluted to CHCl<sub>3</sub>/MeOH/H<sub>2</sub>O (2:2:1.8, by vol) by addition of CHCl<sub>3</sub> and H<sub>2</sub>O. After filtration *in vacuo*, each chloroformic layer was evaporated to dryness under reduced pressure, thus rendering total lipids (11.9 g from body walls and 4.0 g from gonads). The extracts were fractionated into lipid classes by flash-CC eluting with CHCl<sub>3</sub>; CHCl<sub>3</sub>/AcOEt (80:20, vol/vol); acetone and MeOH. The eluted fractions were analyzed by TLC; spots were revealed with specific reagents (21). Acetone eluates (1.32 g from body walls and 729.6 mg from gonads) contained glycolipids and were repurified by CC, yielding BW (563 mg) and G (534.5 mg).

**Separation of glucosylceramides.** A part of each mixture of glucosylceramides was repeatedly submitted to RP-HPLC. Mixture BW (320.4 mg) (solvent MeOH/H<sub>2</sub>O 99:1, vol/vol) rendered six major fractions: **1**, *R<sub>t</sub>* = 38.0 min, 16.7 mg; **2**, *R<sub>t</sub>* = 44.4 min, 8.2 mg; **3**, *R<sub>t</sub>* = 53.2 min, 8.7 mg; **4**, *R<sub>t</sub>* = 94.8 min, 8.1 mg; **5**, *R<sub>t</sub>* = 110.8 min, 12.3 mg; **6**, *R<sub>t</sub>* = 114.0 min, 4.1 mg. Mixture G (165.0 mg) (solvent MeOH/H<sub>2</sub>O 98:2, vol/vol) furnished three major fractions: **1**, *R<sub>t</sub>* = 50.0 min, 7.1 mg; **7**, *R<sub>t</sub>* = 85.0 min, 8.9 mg; **4**, *R<sub>t</sub>* = 127.0 min, 9.4 mg.

(2S,3R,4E,8E,10E)-1-(β-D-Glucopyranosyloxy)-3-hy-

droxy-2-[(R)-2-hydroxydecanoyl]amino-9-methyl-4,8,10-octadecatriene (**1**). White solid, m.p. 123°C; [α]<sub>D</sub> = -21.4° (*c* = 0.3, CHCl<sub>3</sub>); FABMS (-) *m/z* 724 [M - H]<sup>-</sup>, 562 [M - 162]<sup>-</sup>; <sup>1</sup>H and <sup>13</sup>C NMR (CD<sub>3</sub>OD), see Tables 1 and 2.

(2S,3R,4E,8E,10E)-1-(β-D-Glucopyranosyloxy)-3-hydroxy-2-[(R)-2-hydroxyheptadecanoyl]amino-9-methyl-4,8,10-octadecatriene (**2**). White solid, m.p. 125°C; [α]<sub>D</sub> = -14.3° (*c* = 0.2, CHCl<sub>3</sub>); FABMS (-): *m/z* 738 [M - H]<sup>-</sup>, 576 [M - 162]<sup>-</sup>; <sup>1</sup>H and <sup>13</sup>C NMR (CD<sub>3</sub>OD), see Tables 1 and 2.

(2S,3R,4E,8E,10E)-1-(β-D-Glucopyranosyloxy)-3-hydroxy-2-[(R)-2-hydroxydecanoyl]amino-9-methyl-4,8,10-octadecatriene (**3**). White solid, m.p. 132°C; [α]<sub>D</sub> = -12.3° (*c* = 0.3, CHCl<sub>3</sub>); FABMS (-): *m/z* 752 [M - H]<sup>-</sup>, 590 [M - 162]<sup>-</sup>; <sup>1</sup>H and <sup>13</sup>C NMR (CD<sub>3</sub>OD), see Tables 1 and 2.

(2S,3R,4E,8E,10E)-1-(β-D-Glucopyranosyloxy)-3-hydroxy-2-[(R)-2-hydroxy-15-tetracosenoyl]amino-4,8,10-octadecatriene (**4**). White solid, m.p. 182°C; [α]<sub>D</sub> = -12.5° (*c* = 0.3, *n*-propanol); FABMS (-): *m/z* 820 [M - H]<sup>-</sup>, 658 [M - 162]<sup>-</sup>, λ<sub>max</sub> 224 nm (MeOH), <sup>1</sup>H and <sup>13</sup>C NMR (CD<sub>3</sub>OD), see Tables 1 and 2.

(2S,3R,4E,15Z)-1-(β-D-Glucopyranosyloxy)-3-hydroxy-2-[(R)-2-hydroxyhexadecanoyl]amino-4,15-docosadiene (**7**). White solid, m.p. 175°C; [α]<sub>D</sub> = -31.2° (*c* = 0.2, CHCl<sub>3</sub>); FABMS (-): *m/z* 768 [M - H]<sup>-</sup>, 606 [M - 162]<sup>-</sup>; <sup>1</sup>H and <sup>13</sup>C NMR (CD<sub>3</sub>OD), see Tables 1 and 2.

**Synthesis of DMDS derivatives.** Sample (5 mg) was dissolved in carbon disulfide (0.5 mL), and DMDS (0.5 mL) and iodine (2.5 mg) were added to the solution. The mixture was kept at 60°C for 40 h in a small-volume sealed vial. The reaction was quenched with aqueous Na<sub>2</sub>S<sub>2</sub>O<sub>3</sub> 5%, and the mixture

**TABLE 2**  
**<sup>13</sup>C NMR Data for Compounds 1–7 in CD<sub>3</sub>OD**

C	1–3, 5, 6	4	7
1	69.7	69.7	69.9
2	54.6	54.6	54.6
3	72.8	72.8	72.9
4	131.3	131.4	131.1
5	134.4	134.2	134.8
6	33.9	33.6	33.1
7	35.5	35.5	35.9
8	128.5 <sup>a</sup>	132.0 <sup>c</sup>	
9	135.0	131.7 <sup>b</sup>	
10	136.1	132.3 <sup>b</sup>	
11	130.3 <sup>a</sup>	133.5 <sup>c</sup>	
(CH <sub>2</sub> ) <sub>n</sub>	30.3–33.0	30.3–33.2	30.4–30.7
CH <sub>3</sub> –CH <sub>2</sub>	14.4	14.4	14.4
14			28.2 <sup>e</sup>
15			130.4 <sup>f</sup>
16			131.2 <sup>f</sup>
17			27.9 <sup>e</sup>
19	12.8		
1'	177.0	177.2	177.2
2'	73.1	73.1	73.1
14', 17'		28.1	
15'		130.8 <sup>d</sup>	
16'		131.0 <sup>d</sup>	
1''	104.7	104.7	104.7
2''	74.9	75.0	75.0
3''	77.9	78.0	78.0
4''	71.3	71.6	71.6
5''	77.9	78.0	77.9
6''	62.5	62.7	62.7

<sup>a</sup>Assignments with the same superscript (a–f) may be reversed.

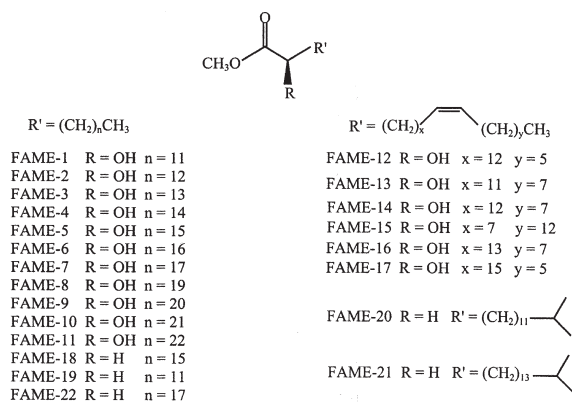
was extracted with cyclohexane (1.0 mL). The extract was evaporated to dryness under reduced pressure, and the residue (DMDS derivative) was redissolved in CH<sub>2</sub>Cl<sub>2</sub> and analyzed by GC–MS.

## RESULTS AND DISCUSSION

Two water-insoluble lipid fractions were obtained from the chloroform/methanol/water extracts of gonads and body walls of the Patagonian starfish *A. inaequalis*. These extracts were subjected to flash-CC and CC to render glycosylceramide mixtures BW and G. Both fractions exhibited the characteristic signals of a sphingosine-type glycosylceramide possessing 2-hydroxy FA and β-glucopyranose moieties in their <sup>1</sup>H NMR spectra: two terminal methyls at δ 0.95 ppm (*d*, *J* = 7.5 Hz) and 0.89 ppm (*d*, *J* = 7.5 Hz), methylenes at δ 1.24–1.30 ppm (*brs*), a singlet at δ 1.70 ppm, due to a methyl group attached to an olefinic carbon, and olefinic signals at δ 5.48 ppm (*dd*, *J* = 14.1, 7.1 Hz), δ 5.56 ppm (*dt*, *J* = 15.7, 6.8 Hz), δ 5.76 ppm (*dt*, *J* = 15.3, 6.2 Hz) and δ 6.04 ppm (*d*, *J* = 15.5 Hz), together with one anomeric doublet at δ 4.26 ppm (*d*, *J* = 7.8 Hz) and hexose proton signals between δ 3.6 and 4.0 ppm. FABMS (negative ion mode) spectra of each mixture showed several [M]<sup>−</sup> or [M – H]<sup>−</sup> peaks, revealing the presence of complex mixtures of monohexosylceramides. Before separation of the mixtures BW and G into individual glyco-

sylceramides, the FA constituents and LCB moieties of these molecular species were investigated. BW and G were methanolized (22) with 1 N HCl in 82% (by vol) aqueous MeOH to yield each a mixture of FAME and a mixture of LCB together with methyl-D-glucopyranose. GC analysis of the peracetylated alditol derivative (23) confirmed glucose as the hexosyl moiety (*R*<sub>t</sub> = 10.31 min, *R*<sub>t</sub> of reference peracetylated D-glucitol = 10.33 min).

Analysis of the FAME mixture of BW by GC–MS showed the presence of 18 compounds (FAME 1–18) (Scheme 1), which were characterized by comparing their spectral data with those reported previously (5,7). The 2-hydroxy-substituted saturated FAME were characterized as methyl-(2*R*)-hydroxy-tetradecanoate (FAME-1) (*R*<sub>t</sub> = 14.20 min, *m/z* 258 [M]<sup>+</sup>, 199 [M – 59]<sup>+</sup>), -pentadecanoate (FAME-2) (*R*<sub>t</sub> = 15.30 min, *m/z* 272 [M]<sup>+</sup>, 213 [M – 59]<sup>+</sup>), -hexadecanoate (FAME-3) (*R*<sub>t</sub> = 16.43 min, *m/z* 286 [M]<sup>+</sup>, 227 [M – 59]<sup>+</sup>), -heptadecanoate (FAME-4) (*R*<sub>t</sub> = 17.20 min, *m/z* 300 [M]<sup>+</sup>, 241 [M – 59]<sup>+</sup>), -octadecanoate (FAME-5) (*R*<sub>t</sub> = 18.43 min, *m/z* 314 [M]<sup>+</sup>, 255 [M – 59]<sup>+</sup>), -nonadecanoate (FAME-6) (*R*<sub>t</sub> = 19.05 min, *m/z* 328 [M]<sup>+</sup>, 269 [M – 59]<sup>+</sup>), -eicosanoate (FAME-7) (*R*<sub>t</sub> = 20.18 min, *m/z* 342 [M]<sup>+</sup>, 284 [M – 59]<sup>+</sup>), -docosanoate (FAME-8) (*R*<sub>t</sub> = 22.15 min, *m/z* 370 [M]<sup>+</sup>, 311 [M – 59]<sup>+</sup>), -tricosanoate (FAME-9) (*R*<sub>t</sub> = 23.17 min, *m/z* 384 [M]<sup>+</sup>, 326 [M – 59]<sup>+</sup>), -tetracosanoate (FAME-10) (*R*<sub>t</sub> = 24.47 min, *m/z* 398 [M]<sup>+</sup>, 339 [M – 59]<sup>+</sup>), and -pentacosanoate (FAME-11)



SCHEME 1

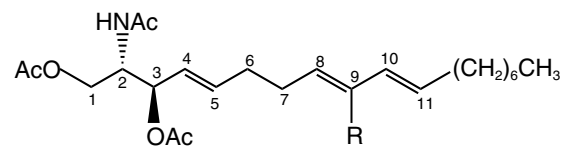
( $R_t = 25.67$  min,  $m/z$  412  $[M]^+$ , 353  $[M - 59]^+$ ). Four unsaturated and one nonsubstituted FAME were identified as methyl-(2*R*)-hydroxy-docosenoate (FAME-12) ( $R_t = 21.87$  min,  $m/z$  369  $[M + H]^+$ , 309  $[M - 59]^+$ ), -tricosenoate (FAME-13) ( $R_t = 22.85$  min,  $m/z$  382  $[M]^+$ , 323  $[M - 59]^+$ ), -tetracosenoate (FAME-14 and FAME-15) ( $R_t = 24.13$  min,  $m/z$  396  $[M]^+$ , 337  $[M - 59]^+$ ), -pentacosenoate (FAME-16 and FAME-17) ( $R_t = 25.38$  min,  $m/z$  410  $[M]^+$ , 352  $[M - 59]^+$ ). The position of the double bond in the unsaturated methyl-(2*R*)-hydroxyacids (FAME 12–17) was determined by GC–MS analysis of the DMDS derivatives (24). The following unsaturated FAME were identified: methyl-(2*R*)-hydroxy-15-docosenoate (FAME-12) ( $R_t = 19.53$  min,  $m/z$  392  $[M - 60]^+$ , 247  $[392 - 145]^+$ , 145  $[CH_3(CH_2)_5CH=SCH_3]^+$ ), -14-tricosenoate (FAME-13) ( $R_t = 22.58$  min,  $m/z$  418  $[M - 59 + H]^+$ , 245  $[418 - 173]^+$ , 173  $[CH_3(CH_2)_7-CH=SCH_3]^+$ ), -15-tetracosenoate (FAME-14) ( $R_t = 24.12$  min,  $m/z$  432  $[M - 59 + H]^+$ , 259  $[432 - 173]^+$ , 173), -10-tetracosenoate (FAME-15) ( $R_t = 24.12$  min,  $m/z$  432  $[M - 59 + H]^+$ , 243  $[CH_3-(CH_2)_{12}-CH=SCH_3]^+$ , 189  $[432 - 243]^+$ ), -16-pentacosenoate (FAME-16) ( $R_t = 26.55$  min,  $m/z$  446  $[M - 59 + H]^+$ , 273  $[446 - 173]^+$ , 173), and -18-pentacosenoate (FAME-17) ( $R_t = 26.73$  min,  $m/z$  446  $[M - 59 + H]^+$ , 301  $[446 - 145]^+$ , 145). The only nonsubstituted FAME was identified as methyl-ocotadecanoate (FAME-18) ( $R_t = 15.15$  min,  $m/z$  298  $[M]^+$ , 239  $[M - 59]^+$ , 74). The main FAME were the 2-hydroxy-substituted saturated ones: FAME-4 (17.9%), FAME-5 (5.6%), FAME-6 (7.8%), FAME-9 (10.4%), FAME-10 (12.2%), and FAME-11 (22.8%).

Analysis of the FAME mixture of G by GC–MS allowed identification of eight 2-hydroxy-substituted saturated FAME (1–5 and 8–10), methyl-(2*R*)-hydroxy-tetracosenoate (FAME-15) ( $R_t = 24.12$  min,  $m/z$  396  $[M]^+$ , 339  $[M - 59]^+$ ), and four nonsubstituted FAME: methyltetradecanoate (FAME-19) ( $R_t = 12.80$  min,  $m/z$  242  $[M]^+$ , 211  $[M - 31]^+$ ), -14-methylpentadecanoate (FAME-20) ( $R_t = 15.10$  min,  $m/z$  270  $[M]^+$ , 239  $[M - 31]^+$ , 227  $[M - 43]^+$ ), -16-methylheptadecanoate (FAME-21) ( $R_t = 17.17$  min,  $m/z$  298  $[M]^+$ , 267  $[M - 31]^+$ , 255  $[M - 43]^+$ , 74), and -eicosanoate (FAME-22)

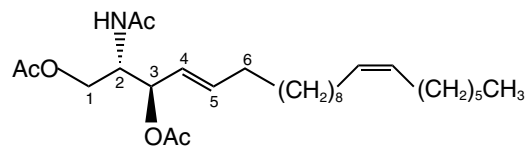
( $R_t = 19.02$  min,  $m/z$  326  $[M]^+$ , 295  $[M - 31]^+$ , 267  $[M - 59]^+$ , 74) (Scheme 1). The main FAME was FAME-4 (28.4%) along with smaller proportions of FAME-3 (6.6%) and FAME-6 (7.4%). Optical rotations of FAME mixtures from BW ( $[\alpha]_D = -2.4^\circ$  ( $c = 1.3$ ,  $CHCl_3$ )) and G ( $[\alpha]_D = -16.4^\circ$  ( $c = 0.73$ ,  $CHCl_3$ )) are in good agreement with the data reported in the literature (25); therefore, the absolute stereochemistry at C-2' is suggested to be *R*.

LCB mixtures derived from methanolysis of BW and G were acetylated with acetic anhydride ( $Ac_2O$ )/pyridine at  $70^\circ C$  and analyzed by GC–MS, showing the presence of 2-acetamido-1,3-diacetoxy-9-methyl-4,8,10-octadecatriene (acetylated LCB-1) ( $R_t = 20.5$  min,  $m/z$  375  $[M - CH_3COOH]^+$ , 316  $[M - CH_3COOH - CH_3COO]^+$ , 256, 178, 85), 2-acetamido-1,3-diacetoxy-4,8,10-octadecatriene (acetylated LCB-2) ( $R_t = 19.87$  min,  $m/z$  361  $[M - CH_3COOH]^+$ , 302  $[M - CH_3COOH - CH_3COO]^+$ , 256, 164, 85), and 2-acetamido-1,3-diacetoxy-4,15-docosadiene (acetylated LCB-3) ( $R_t = 23.3$  min,  $m/z$  421  $[M - CH_3COO + H]^+$ , 376  $[M - 43 - CH_3COOH]^+$ , 316  $[M - 43 - 2 \times CH_3COOH]^+$ , 281  $[M - CH_3COO - C_{10}H_{39}]^+$ , 207  $[M - 43 - C_9H_{17}]^+$  (Scheme 2). The relative stereochemistry at C-2 and C-3 was proposed as 2*S*,3*R* from optical rotation data of the acetylated LCB mixtures ( $[\alpha]_D = -17.2^\circ$  ( $c = 0.3$ ,  $Cl_3CH$ ), in good agreement with data for synthetic 1-*O*-2-*N*-3-*O*-triacetyl-*D*-erythro-sphingosine (26).

Fraction BW (320.4 mg) was separated repeatedly by RP-HPLC into six major fractions (1–6), whereas fraction G (165.0 mg) yielded three fractions (1, 4, and 7). Each fraction displayed a single peak on RP-HPLC. Fractions 1–4 and 7 revealed single molecular ion peaks in their negative FAB mass spectra, but fractions 5 and 6 exhibited two and three molecular ions, respectively.

Acetylated LCB-1 R = CH<sub>3</sub>

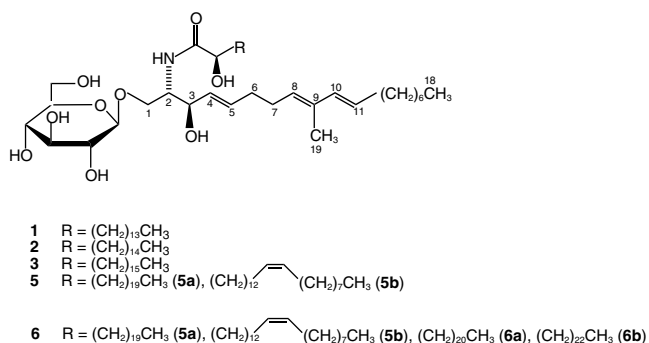
Acetylated LCB-2 R = H



Acetylated LCB-3

SCHEME 2





SCHEME 3

Fractions **1–3**, **5**, and **6** (Scheme 3) showed the same characteristic <sup>1</sup>H and <sup>13</sup>C NMR signals due to C-1-C-11, C-1', C-2', C-1''-C-6'' of a 1-*O*-β-glucopyranoside of a (2*S*,3*R*,4*E*,8*E*,10*E*)-2-amino-1,3-dihydroxy-9-methyl-4,8,10-octadecatriene ceramide possessing a (2*R*)-hydroxy FA (Tables 1 and 2). The presence of a singlet at δ 1.71 ppm in the <sup>1</sup>H NMR spectrum and of the corresponding signal at δ 12.8 ppm in the <sup>13</sup>C NMR spectrum was diagnostic for the presence of a methyl group (C-19) attached to an olefinic carbon. <sup>13</sup>C NMR spectra (Table 2) confirmed the ceramide nature of the compounds (δ 177.0 ppm, C=O) with normal-chain bases and FA (terminal methyl at δ 14.4 ppm) and a (2*S*,3*R*,4*E*)-sphingosine-type base indicated by C-2 and C-3 chemical shifts at δ 54.6 and 72.8 ppm (5).

These spectra were almost superimposable with those of ophidiacerebroside C (8) and of glucosylceramides isolated from *C. lurida* (20) containing (2*S*,3*R*,4*E*,8*E*,10*E*)-2-amino-9-methyl-4,8,10-octadecatrien-1,3-diol as the LCB moiety.

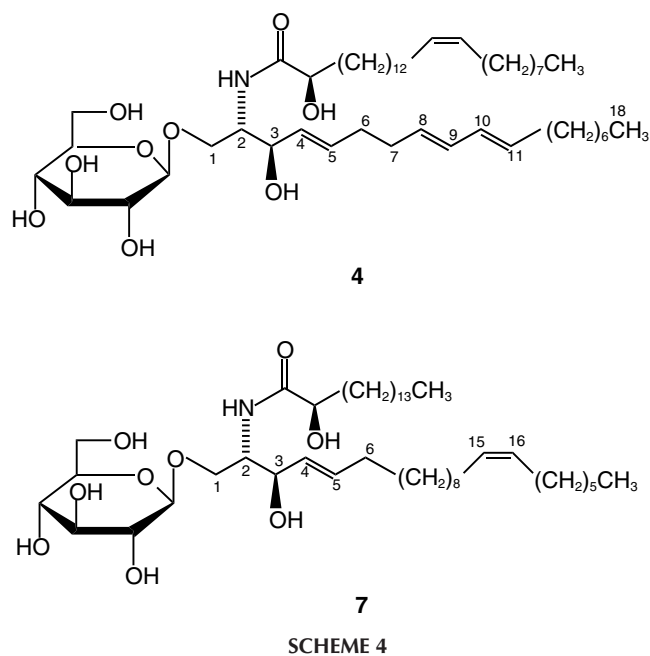
Fractions **1–3**, **5**, and **6** were methanolized (23) and the FAME analyzed by GC-MS; a single FAME was detected for fractions **1** (FAME-3), **2** (FAME-4), and **3** (FAME-5), two kinds of FAME were obtained for fraction **5** (FAME-8 and FAME-14) and four kinds of FAME for fraction **6** (FAME-8, FAME-9, FAME-14, and FAME-11). Double-bond position in FAME-14 was determined from the GC-MS analysis of the DMDS derivative (24) according to ions at *m/z* 490 [M]<sup>+</sup>, 317 [M - 173]<sup>+</sup>, and 173.

LCB obtained from methanolysis of **1–3**, **5**, and **6** were acetylated and analyzed by GC-MS. Results showed the presence of 2-acetamido-1,3-diacetoxy-9-methyl-4,8,10-octadecatriene as evidenced by the ions at *m/z* 435 [M]<sup>+</sup>, 375 [M - CH<sub>3</sub>COOH]<sup>+</sup>, 315 [M - 2 × CH<sub>3</sub>COOH]<sup>+</sup> and 256 (β-cleavage from Δ<sup>4</sup>).

Taking into account the FABMS spectra and the methanolysis products of each fraction, one can determine that three fractions are homogeneous. These fractions are assigned to compounds **1**, **2**, and **3** (Scheme 3). Glucosylceramide **1** was identified as phalluside-1, previously isolated from the ascidian *Phallusia fumigata* (14), whereas **2** and **3** are also known compounds previously isolated from *C. lurida* (20). Fraction **5** (Scheme 3) is a mixture of glucosylceramide **5a**, previously isolated from *Ophidiaster ophidiamus* (ophidiacerebroside C)

(8) and *C. lurida* (19) and the new **5b** {(2*S*,3*R*,4*E*,8*E*,10*E*)-1-(β-D-glucopyranosyloxy)-3-hydroxy-2-[(*R*)-2-hydroxy-15-tetracosenoyl]amino-9-methyl-4,8,10-octadecatriene}. Fraction **6** (Scheme 3) is a mixture of the known glucosylceramides ophidiacerebroside C (**5a**) and **6a**, previously isolated from *O. ophidiamus* (8), and the new glucosylceramides **5b** and **6b** (2*S*,3*R*,4*E*,8*E*,10*E*)-1-(β-D-glucopyranosyloxy)-3-hydroxy-2-[(*R*)-2-hydroxypentacosanoyl]amino-9-methyl-4,8,10-octadecatriene. Scarcity of material prevented our attempt to isolate new glucosylceramides **5b** and **6b** as pure compounds.

Compound **4** (Scheme 4) was obtained as a white amorphous powder. The FABMS (negative ion mode) spectrum showed a single [M - H]<sup>-</sup> peak at *m/z* 820 and the corresponding [M - 162]<sup>-</sup> ion at *m/z* 658 due to the loss of the hexose unit. The <sup>13</sup>C NMR spectrum (Table 2) of **4** was similar to that of glucosylceramides **1–3**, **5**, and **6** except that its structure lacked the methyl group at C-9 as reflected by the absence of the signal at δ 12.8 ppm and the singlet at δ 1.70 ppm in the <sup>1</sup>H NMR spectrum (Table 1). Signals at δ 73.1 (C-2') and 25.1 ppm (C-3'), shifted downfield compared with those of an unsubstituted acid, indicated the presence of a 2-hydroxyacid moiety (27). The unsaturation pattern in the <sup>1</sup>H NMR spectrum showed a double doublet at δ 5.48 ppm (*J* = 15.4, 7.5 Hz, H-4) and a double triplet at δ 5.73 ppm (*J* = 15.1, 6.4 Hz, H-5), characteristic of a Δ<sup>4</sup> sphingosine with *trans* configuration and multiplets at δ 5.54, 5.56, 5.96, and 5.99 ppm. This pattern differed from the olefinic pattern observed for glucosylceramides **1–3**, **5**, and **6** with the methyl group at C-9 in the LCB moiety (Table 1). The COSY <sup>1</sup>H-<sup>1</sup>H spectrum of **4** showed correlations between the H-4 signal (δ 5.48 ppm), the broad triplet at δ 4.14 ppm (H-3), and the double triplet at δ 5.73 ppm (H-5). The latter signal also correlated with a multiplet at δ 2.15 ppm (H-6). Further correlations



SCHEME 4

between olefinic signals at  $\delta$  5.54, 5.56, 5.96, and 5.99 ppm and vicinal methylene groups at positions 7 and 12 allowed us to establish the olefinic pattern of the LCB unit as a 4,8,10-triene. The conjugated diene structure was also supported by a UV absorbance band at 224 nm. The same LCB moiety was identified for the first time in a mixture of LCB obtained by hydrolysis of the glucosylceramide mixture isolated from the spermatozoa of the starfish *Asterias amurensis* (28) and further in a ceramide isolated from the gorgonian *Acabaria undulata* (17). A LCB also containing a 4,8,10-triene but whose structure was not completely defined was reported in a glucosylceramide isolated from the ascidian *P. fumigata* (14).

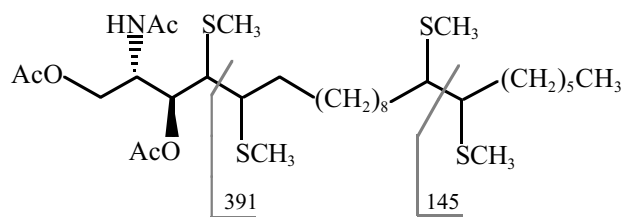
The isolated olefinic triplet at  $\delta$  5.35 ppm ( $J = 4.8$  Hz), which correlated only with a methylene signal at  $\delta$  1.98 ppm, was therefore assigned to the acid moiety. *Z* geometry was deduced from the  $J$  value and the triplet shape of the signal (5) in the  $^1\text{H}$  NMR spectrum and was confirmed by the chemical upfield shift of allylic methylene carbon signals at  $\delta$  28.1 ppm (27). The presence of eight olefinic signals in the  $^{13}\text{C}$  NMR spectrum of **4** confirmed the presence of three unsaturations in the base and one in the acid moiety. Assignment of these signals was derived from  $^1\text{H}$ - $^1\text{H}$  COSY and bidimensional NMR experiments.

Acidic methanolysis of **4** yielded a FAME, a methyl glycoside, and a LCB. GC analysis of the peracetylated alditol derivative (23) confirmed glucose as the hexosyl moiety. GC-MS analysis of the FAME showed a single peak at  $R_t = 23.90$  min. The molecular ion peak at  $m/z$  396  $[\text{M}]^+$  and fragment ion peaks at  $m/z$  365  $[\text{M} - 31]^+$  and 338  $[\text{M} - \text{CH}_3\text{COO} + \text{H}]^+$  confirmed the presence of methyl-2-hydroxytetra-cosenoate (FAME-14, Scheme 1). The double-bond position in FAME-14 was determined by GC-MS analysis of the DMDS derivative (24) according to peaks at  $m/z$  490  $[\text{M}]^+$ , 431  $[\text{M} - \text{CH}_3\text{COO}]^+$ , 384  $[431 - \text{SCH}_3]^+$ , 257  $[431 - 173 - \text{H}]^+$ , and 173.

Acetylation of LCB derived from methanolysis of **4** and GC-MS analysis of the acetylated LCB showed the presence of a C-18 sphingosine-type base (acetylated LCB-2, Scheme 2) on the basis of peaks at  $m/z$  421  $[\text{M}]^+$ , 243 (C-5/C-6 cleavage), and 85 ( $\beta$ -cleavage to  $\Delta^{10}$ ).

All these data allowed us to determine the structure of the new glucosylceramide **4** as (2*S*,3*R*,4*E*,8*E*,10*E*)-1-( $\beta$ -D-glucopyranosyloxy)-3-hydroxy-2-[(*R*)-2-hydroxy-15-tetra-cosenoyl]amino-4,8,10-octadecatriene. The LCB and FA moieties of **4** have been detected in the LCB and FAME mixtures isolated from the glucosylceramide mixture of *A. amurensis* (28), but because no attempt was made in the reference work to obtain the pure cerebrosides, it cannot be inferred whether glucosylceramide **4** was present in spermatozoa of *A. amurensis*.

The  $^1\text{H}$  NMR spectrum of **7** (Table 1) showed characteristic signals at  $\delta$  3.71 (H-1), 4.11 (H-1, H-3), 3.97 (H-2, H-2'), 5.47 (H-4), and 5.72 ppm (H-5) for a glucosylceramide containing a sphingosine-type LCB moiety and a 2-hydroxy FA. The monosaccharide signals in the  $^1\text{H}$  and  $^{13}\text{C}$  NMR spectra (Tables 1 and 2) confirmed glucose as the hexose unit. Glu-



SCHEME 5

cosylceramide **7** (Scheme 4) showed the presence of an additional disubstituted double bond on the basis of a triplet at  $\delta$  5.35 ppm in the  $^1\text{H}$  NMR spectrum and two olefinic carbon signals at  $\delta$  130.4 and 131.2 ppm in the  $^{13}\text{C}$  NMR spectrum. In determining the identities of the FA and the LCB, compound **7** was methanolized with 1 N HCl in 82% (by vol) aqueous MeOH. FAME analysis of **7** allowed identification of methyl-2-hydroxyhexadecanoate (FAME-3) on the basis of ions at  $m/z$  286  $[\text{M}]^+$  and 227  $[\text{M} - \text{CH}_3\text{COO}]^+$ . GC-MS analysis of the acetylated LCB showed ions at  $m/z$  361  $[479 - 2 \times \text{CH}_3\text{COO}]^+$  and 216 (cleavage at C-3/C-4), suggesting the presence of a sphingosine-type base with 22 carbons and one isolated double bond in the chain. *Z* geometry of the double bond was deduced from the  $J$  value (5.9 Hz) and the shape of the signal at  $\delta$  5.35 ppm (5) in the  $^1\text{H}$  NMR spectrum and confirmed by the chemical upfield shift of allylic methylene carbon signals at  $\delta$  27.9 and 28.2 ppm (29). The position of the additional double bond in the LCB was determined to be  $\Delta^{15}$  from the CG-MS analysis of the DMDS derivative of the acetylated LCB (24), on the basis of the peaks shown in Scheme 5.

All these data allowed identification of **7** as (2*S*,3*R*,4*E*,15*Z*)-1-( $\beta$ -D-glucopyranosyloxy)-3-hydroxy-2-[(*R*)-2-hydroxyhexadecanoyl]amino-4,15-docosadiene, a new compound. Related glucosylceramides with  $\Delta^9$  and  $\Delta^{13}$  LCB moieties were isolated from the starfish *A. amurensis versicolor* (5).

A comparative analysis of the composition of both mixtures (BW and G) showed differences in the FA and LCB moieties. LCB-1 was the most frequent LCB found in BW, whereas LCB-1, LCB-2, and LCB-3 were equally distributed in G. As for the FAME composition, BW showed FAME-11 as the main component, but FAME-4 was the component in greater proportion in G. All FAME detected in BW had *normal* chains, whereas G showed FAME with *iso* chains as minor components.

## ACKNOWLEDGMENTS

This work was supported by the International Foundation for Science, Stockholm, Sweden, and the Organization for the Prohibition of Chemical Weapons, The Hague, The Netherlands, through a grant to M.S. Maier. We also wish to thank Consejo Nacional de Investigaciones Científicas y Técnicas (CONICET), Agencia Nacional de Promoción Científica y Tecnología, and the Universidad de Buenos Aires (UBA) for financial support of this work. We are indebted to Unidad de Servicio de Microanálisis y Métodos Físicos Aplicados

Organicos [CONICET-Facultad de Ciencias Exactas y Naturales (FCEN), UBA] for NMR spectra and Laboratorio Nacional de Análisis y Servicios-Espectrometría de masa de alta resolución (CONICET-FCEN, UBA) for mass spectra. We are also grateful to Dr. Alejandro Tablado from the Museo de Ciencias Naturales "Bernardino Rivadavia" for the taxonomic identification of the starfish. M.S.M. and A.M.S. are Research Members of the National Research Council of Argentina (CONICET).

## REFERENCES

- Kawano, Y., Higuchi, R., Isobe, R., and Komori, T. (1988) Isolation and Structure of Six New Cerebrosides, *Liebigs Ann. Chem.*, 19–24.
- Kawano, Y., Higuchi, R., Isobe, R., and Komori, T. (1988) Isolation and Structure of Two New Ceramide Lactosides, *Liebigs Ann. Chem.*, 1181–1183.
- Higuchi, R., Natori, T., and Komori, T. (1990) Isolation and Characterization of Acanthocerebroside B and Structure Elucidation of Related, Nearly Homogeneous Cerebrosides, *Liebigs Ann. Chem.*, 51–55.
- Higuchi, R., Kagoshima, M., and Komori, T. (1990) Structures of Three New Cerebrosides, Astrocerebroside A, B, and C, and of Related Nearly Homogeneous Cerebrosides, *Liebigs Ann. Chem.*, 659–663.
- Higuchi, R., Zhou, J.X., Inukai, K., and Komori, T. (1991) Isolation and Structure of Six New Cerebrosides, Astrocerebrosides A–F, and Two Known Cerebrosides, Astrocerebroside A and Acanthocerebroside C, *Liebigs Ann. Chem.*, 745–752.
- Higuchi, R., Inagaki, M., Togawa, K., Miyamoto, T., and Komori, T. (1994) Isolation and Structure of Three New Cerebrosides, CE-2b, CE-2c, and CE-2d, from the Sea Cucumber *Cucumaria echinata*, *Liebigs Ann. Chem.*, 79–81.
- Higuchi, R., Inagaki, M., Togawa, K., Miyamoto, T., and Komori, T. (1994) Isolation and Structure of Cerebrosides from the Sea Cucumber *Pentacta australis*, *Liebigs Ann. Chem.*, 653–658.
- Jin, W., Rinehart, K.L., and Jares-Erijman, E.A. (1994) Ophidiocerebrosides: Cytotoxic Glycosphingolipids Containing a Novel Sphingosine from a Sea Star, *J. Org. Chem.* 59, 144–147.
- Venkannababu, U., Bhandari, S.P.S., and Garg, H.S. (1997) Regulosides A–C: Glycosphingolipids from the Starfish *Pentacaster regulus*, *Liebigs Ann./Recueil* 1245–1247.
- Babu, U.V., Bhandari, S.P.S., and Garg, H.S. (1997) Temnosides A and B, Two New Glycosphingolipids from the Sea Urchin *Temnopleurus toreumaticus* of the Indian Coast, *J. Nat. Prod.* 60, 732–734.
- Agrawal, S., and Garg, H.S. (1994) A Novel Sphingosine Derivative from the Sponge *Spirastrella inconstans*, *J. Nat. Prod.* 58, 442–445.
- Li, H., Matsunaga, S., and Fusetani, N. (1995) Halicylindrosides, Antifungal and Cytotoxic Cerebrosides from the Marine Sponge *Halichondria cylindrata*, *Tetrahedron* 51, 2273–2280.
- Natori, T., Morita, M., Akimoto, K., and Koezuka, Y. (1994) Agelasphins, Novel Antitumor and Immunostimulatory Cerebrosides from the Marine Sponge *Agelas mauritanus*, *Tetrahedron* 50, 2771–2784.
- Durán, R., Zubía, E., Ortega, M.J., Naranjo, S., and Salvá, J. (1998) Phallusides, New Glucosphingolipids from the Ascidian *Phallusia fumigata*, *Tetrahedron* 54, 14597–14602.
- Chakrabarty, M., Balabyal, A., and Barua, A. (1994) New Ceramides from the Hypotensive Extract of a Sea Anemone, *Paracondylactis indicus*, *J. Nat. Prod.* 57, 393–395.
- Ojika, M., Yoshino, G., and Sakagami, Y. (1997) Novel Ceramide 1-Sulfates, Potent DNA Topoisomerase I Inhibitors Isolated from the Bryozoa *Watersipora cucullata*, *Tetrahedron Lett.* 38, 4235–4238.
- Shin, J., and Seo, Y. (1995) Isolation of New Ceramides from the Gorgonian *Acabaria undulata*, *J. Nat. Prod.* 58, 948–953.
- Schmidt, R.R. (1989) Recent Developments in the Synthesis of Glycoconjugates, *Pure Appl. Chem.* 61, 1257–1270.
- Maier, M.S., Kuriss, A., and Seldes, A.M. (1998) Isolation and Structure of Glucosylceramides from the Starfish *Cosmasterias lurida*, *Lipids* 33, 825–827.
- Bligh, E.G., and Dyer, W.J. (1959) A Rapid Method of Total Lipid Extraction and Purification, *Can. J. Biochem. Physiol.* 37, 911–917.
- Kates, M. (1986) *Techniques of Lipidology*, 2nd edn., pp. 239–244, Elsevier Science Publishers, Oxford.
- Gaver, R.C., and Sweeley, C.C. (1965) Methods for Methanolysis of Sphingolipids and Direct Determination of Long-Chain Bases by Gas Chromatography, *J. Am. Oil Chem. Soc.* 42, 294–298.
- Maier, M.S., Roccatagliata, A.J., Kuriss, A., Chludil, H., Seldes, A.M., Pujol, C.A., and Damonte, E.B. (2001) Two New Cytotoxic and Virucidal Trisulfated Triterpene Glycosides from the Antarctic Sea Cucumber *Staurocucumis liouvillei*, *J. Nat. Prod.* 64, 732–736.
- Vincenti, M., Guglielminetti, G., Cassani, G., and Tonini, C. (1987) Determination of Double Bond Position in Diunsaturated Compounds by Mass Spectrometry of Dimethyl Disulfide Derivatives, *Anal. Chem.* 59, 694–699.
- Pretorius, Y.Y., and Horn, D. (1954) The Synthesis and Stereochemistry of the Straight-Chain  $\alpha$ -Hydroxy-acids, *J. Chem. Soc.* 1460–1464.
- Julina, R., Herzig, T., Bernet, B., and Vasella, A. (1986) Enantioselective Synthesis of D-erythro-Sphingosine and of Ceramide, *Helv. Chim. Acta* 69, 368–373.
- Kim, S.Y., Choi, Y., Huh, H., Kim, J., Kim, Y., and Lee, H.S. (1997) New Antihepatotoxic Cerebrosides from *Lycium chinense* Fruits, *J. Nat. Prod.* 60, 274–276.
- Irie, A., Kubo, H., and Hoshi, M. (1990) Glucosylceramide Having a Novel Tri-unsaturated Long-Chain Base from the Spermatozoa of the Starfish, *Asterias amurensis*, *J. Biochem.* 107, 578–586.
- Breitmaier, E. (1987) *Carbon-13 NMR Spectroscopy*, 3rd edn., pp. 108–116, VCH, Weinheim.

[Received November 28, 2001, and in revised form April 16, 2002; revision accepted April 26, 2002]



# Positional Distribution of CLA in TAG of Lamb Tissues

Lyn J. Paterson<sup>a</sup>, Randall J. Weselake<sup>a,\*</sup>, Priya S. Mir<sup>b</sup>, and Zahir Mir<sup>b</sup>

<sup>a</sup>Department of Chemistry and Biochemistry, University of Lethbridge, Lethbridge, Alberta, T1K 3M4 Canada, and <sup>b</sup>Agriculture and Agri-Food Canada, Lethbridge Research Centre, Lethbridge, Alberta, T1J 4B1 Canada

**ABSTRACT:** The content and positional distribution of CLA in TAG fractions of lamb tissues was examined with either preformed CLA or the linoleic acid precursor of CLA in the diet as experimental treatments. The CLA content of phospholipid (PL) from these tissues was also examined. Thirteen lambs were randomized to the following dietary treatments: (i) control diet (no supplement); (ii) CLA supplementation (0.33 g d<sup>-1</sup> for 21 d prior to weaning) to milk-replacer of pre-ruminating lambs, or (iii) feeding linoleic acid-rich oil (6% safflower oil on a dry matter basis) to weaned ruminating lambs. At slaughter, tissue samples were procured from diaphragm, rib muscle, and subcutaneous (SC) adipose tissue. Safflower oil supplementation in the diet resulted in an increase in CLA content of the TAG from diaphragm, rib muscle, and SC adipose tissue by about threefold ( $P < 0.05$ ) on a mol% basis. CLA was localized to the *sn*-1/3 positions of TAG. Animals that received pre-formed CLA, however, had increased proportions of CLA at the *sn*-2 position of TAG from SC adipose tissue, suggesting that there were tissue-specific dietary effects and possible age-related effects on the mode of FA incorporation into TAG. Safflower oil supplementation in the diet had no effect on the CLA content of PL from diaphragm, rib muscle, and SC adipose tissue, suggesting that CLA was preferentially incorporated into the TAG of these tissues.

Paper no. L8792 in *Lipids* 37, 605–611 (June 2002).

CLA isomers are intermediary metabolites in the bioconversion of dietary linoleic acid (18:2) to stearic acid (18:0) by the microorganism *Butyrivibrio fibrisolvens* in ruminants (1). CLA includes several positional and geometric isomers of 18:2 with double bonds predominantly at the 9- and 11-, 10- and 12-, or 11- and 13-carbon atoms, with various combinations of *cis* and *trans* configuration at each double bond. CLA represents a relatively minor component of the total FA composition of foods, but ingestion of the isomers results in strong fat-to-lean repartitioning effects in rats (2), protection against the effects of carcinogens when present in the diet (in the range of 0.1–1%) (3,4), and stimulation of the immune system (5). Furthermore, CLA in milk has been implicated as a factor responsible for the inverse relationship between high milkfat consumption and low incidence of mammary cancer in humans (6).

In general, meat and dairy products from ruminants contain more CLA than products from nonruminants (7,8). The

concentration of CLA in beef ranges from 1.7 to 8.5 mg CLA g<sup>-1</sup> of fat and is affected by the nature of the feed (9,10). Canola oil or full-fat rapeseed supplementation of goat or dairy cow diets, respectively, increased CLA content in milk (11,12). A diet that included 5% free 18:2 significantly increased the CLA concentration of both the neutral lipid (NL) and phospholipid (PL) fractions of liver tissue samples from rats (2). As well, inclusion of preformed CLA in rat diets has been shown to result in a sixfold increase in the CLA content of the PL fraction compared to controls (13). In a more recent study using mice, a dose-dependent increase in CLA content was observed in epidermal NL and PL as CLA in the diet was increased from 0 to 1.5% (14). CLA and other conjugated diene intermediates also have been found in the PL fraction from lamb liver (15). A recent study with lactating dairy cows has indicated that *trans*-11 18:1 represents the major precursor of CLA in milk fat (16). The CLA was produced by the catalytic action of an endogenous  $\Delta 9$  desaturase. In another recent study, pigs were shown to produce back fat CLA by endogenous  $\Delta 9$  desaturation of dietary *trans*-11 18:1 (17).

Recently, we demonstrated that dietary safflower or sunflower oil supplementation enhanced the CLA content of various lamb tissues through provision of the 18:2 precursor of CLA (18,19). The current study extends our investigations on the inclusion of 18:2 in the diet of lambs to gain insight into the pathway of incorporation of CLA into the major glycerolipid classes of muscle and adipose tissue. Lipid samples were isolated from diaphragm, rib muscle and subcutaneous (SC) adipose tissue obtained at slaughter from lambs fed CLA as a free acid pre-weaning (pre-ruminating) and those fed a high-18:2 diet post-weaning (ruminating) to investigate effects on the CLA content of TAG and PL. Incorporation of CLA into TAG was further investigated through analyses of the positional distribution of CLA on the glycerol backbone.

## MATERIALS AND METHODS

**Lambs and dietary regimes.** The management protocol and diets fed to the crossbred (Suffolk  $\times$  Dorset) lambs (*Ovis aries*) used as a source of tissue in this study have been reported previously (18). Thirteen 4-wk-old lambs with an average weight of  $12.5 \pm 3.4$  kg ( $\pm$  SEM) were removed from ewes and then maintained in two pens with ready access to milk replacer from an artificial ewe feeding apparatus for 21 d. The lambs also had access to a pelleted creep feed composed of barley grain, alfalfa, and soybean meal. Five lambs in the control treatment and four lambs designated to receive

\*To whom correspondence should be addressed at Dept. of Chemistry and Biochemistry, University of Lethbridge, 4401 University Dr., Lethbridge, Alberta, T1K 3M4 Canada. E-mail: weselake@uleth.ca

Abbreviations: 16:0, palmitic acid; 18:0, stearic acid; 18:1, oleic acid; 18:2, linoleic acid;  $\alpha$ -18:3,  $\alpha$ -linolenic acid; NL, neutral lipid; PL, phospholipid; SC, subcutaneous; TL, total lipid.



6% safflower oil upon weaning were given 50 mL of milk replacer containing 5 mL of olive oil as a carrier on a daily basis by bottle. Four lambs constituting the CLA treatment group received 50 mL of milk replacer containing 0.33 g CLA (free acid) (catalog # 05507; Sigma-Aldrich Canada Ltd., Oakville, Ontario, Canada) dissolved in 5 mL of olive oil on a daily basis. The lambs were weaned off the artificial ewe after 21 d at an average weight of  $18.9 \pm 3.4$  kg ( $\pm$  SEM) and were then transferred to individual pens and provided a pelleted diet *ad libitum*. Control lambs and those that received CLA-supplemented milk replacer were supplied with the pelleted diet, whereas the lambs in the safflower oil treatment were administered a pelleted diet supplemented with 6% oil on a dry matter basis.

Safflower oil bought from a commercial source contained 78% 18:2. Commercial safflower oil has been reported to contain 0.7 mg CLA/g (20). The CLA from Sigma-Aldrich consisted of about 50% *trans*-9,*cis*-11 and *cis*-9,*trans*-11 combined, 40% *trans*-10,*cis*-12, and 10% *cis*-10,*cis*-12 CLA. The pelleted diet consisted of the following ingredients: barley, 56.2%; dehydrated alfalfa, 29.5%; soybean meal, 9.0%; molasses, 2.0%; mineral mixture, 1.05%; maxi-pel (a binder used to keep the pellet intact), 1.0%; calcium phosphate, 0.5%; ammonium chloride, 0.5%; dicalcium phosphate, 0.2%; 0.2% vitamin A (10 million IU  $\text{kg}^{-1}$ ); vitamin E (100,000 IU  $\text{kg}^{-1}$ ), 0.033%; and Deccox (to prevent coccidiosis) pre-mix, 0.018%. The diet had a crude protein content of 16.6%. The pelleted diet was low in fat content. Collectively, the dried alfalfa and barley contained less than 2% lipid (21). This diet was fed to the lambs for  $80 \pm 1.8$  d. The average weight of the animals at slaughter was  $45 \pm 2.9$  kg ( $\pm$  SEM).

**Tissue samples.** At the time of slaughter, samples were procured from diaphragm and SC adipose tissue. A double chop from the 12th and 13th ribs was sampled from each animal at the time of cutting. All tissue samples were obtained from the same half of the carcass. Tissue samples were stored in sterile plastic bags with as little air as possible, kept on ice for approximately 30 min and then frozen in liquid  $\text{N}_2$ . Tissues were stored at  $-20^\circ\text{C}$  until used. Samples were thawed at  $4^\circ\text{C}$ , and subsamples were ground with a hand grinder until completely blended and then refrozen and stored at  $-20^\circ\text{C}$ .

**Lipid extraction.** Lipids were extracted using  $\text{CHCl}_3/\text{CH}_3\text{OH}$  (2:1, vol/vol) (22). Stored tissue was thawed at  $4^\circ\text{C}$ , and 500 mg of tissue was weighed into a test tube and homogenized in 5 mL of  $\text{CHCl}_3/\text{CH}_3\text{OH}$  (2:1, vol/vol), using a Kinematica homogenizer model PT-10-35 (Brinkmann Instruments, Rexdale, Ontario, Canada) at speed setting 6 for 30 s. The probe was rinsed with 5 mL  $\text{CHCl}_3/\text{CH}_3\text{OH}$  (2:1, vol/vol), and the rinse and homogenate were combined and centrifuged at  $1600 \times g$  for 30 min. The supernatant was washed two times with 2 mL 0.29% NaCl (wt/vol), and the final organic phase was passed through a small column of anhydrous  $\text{Na}_2\text{SO}_4$ . The dehydrated lipid extract was then evaporated to dryness at 37 to  $40^\circ\text{C}$  under a gentle stream of  $\text{N}_2$ . The total lipid (TL) was dissolved in  $\text{CHCl}_3$  to a final concentration of  $150 \text{ mg mL}^{-1}$  and stored at  $-20^\circ\text{C}$  under  $\text{N}_2$ .

**Separation of lipid classes.** TL was fractionated into NL and PL fractions using a modification (2) of a previously described method (23). TL ( $30\text{--}60 \text{ mg}$  in  $500\text{--}1000 \mu\text{L}$   $\text{CHCl}_3$ ) was applied to a silica cartridge (Sep-Pak Classic; Waters Limited, Mississauga, Ontario, Canada) followed by a three-step elution procedure. The NL fraction was eluted with 20 mL  $\text{CHCl}_3$  injected by syringe at a flow rate of approximately  $25 \text{ mL min}^{-1}$ . MAG was eluted with 10 mL  $\text{CHCl}_3/\text{CH}_3\text{OH}$  (98:2, vol/vol) at a flow rate of approximately  $20 \text{ mL min}^{-1}$ . The PL fraction was eluted with 30 mL  $\text{CH}_3\text{OH}$  at a flow rate of  $25 \text{ mL min}^{-1}$ . The PL and NL fractions were evaporated to dryness under  $\text{N}_2$  gas and dissolved in  $\text{CHCl}_3$  to a final concentration  $10 \text{ mg mL}^{-1}$ , then stored under  $\text{N}_2$  at  $-20^\circ\text{C}$ .

**TAG isolation.** Two hundred microliters of  $150 \text{ mg TL mL}^{-1}$  ( $30 \text{ mg TL}$ ) were applied to a pre-run EM Science HPTLC-Fertigplatten Kieselgel 60 plate ( $10 \times 20 \text{ cm}$ , 0.25 mm thick) (VWR Canlab, Mississauga, Ontario, Canada). Fifty microliters of  $10 \text{ mg}$  trioleoylglycerol  $\text{mL}^{-1}$  were applied as a reference standard (Sigma-Aldrich Canada, Oakville, Ontario, Canada). Lipids were separated with one ascension of hexane/diethyl ether/acetic acid (80:20:1, by vol) (24). The isolated TAG were dissolved in  $\text{CHCl}_3$  to a concentration of  $10 \text{ mg mL}^{-1}$  and stored under  $\text{N}_2$  at  $-20^\circ\text{C}$ .

**Digestion of TAG using pancreatic lipase.** Pancreatic lipase was used to generate *sn*-2-MAG from TAG (25). Two milligrams of dried TAG was suspended in  $500 \mu\text{L}$  of pancreatic lipase buffer [1 M Tris-HCl, pH 8, containing 10% gum arabic (wt/vol) and 0.23 M  $\text{CaCl}_2$  (wt/vol)] by sonication. Five hundred microliters of pancreatic lipase buffer containing  $8 \text{ mg}$  pancreatic lipase  $\text{mL}^{-1}$  was added to the TAG suspension; the mixture was vortexed briefly and incubated at  $37^\circ\text{C}$  for 1 h in a shaking water bath. The reaction was stopped with  $500 \mu\text{L}$  of 0.1 N acetic acid, and the lipid was extracted three times with 2 mL diethyl ether. Each extract was passed through a small column of anhydrous  $\text{Na}_2\text{SO}_4$ , combined, and then evaporated to dryness under  $\text{N}_2$ . The extracted lipid was redissolved in  $100\text{--}200 \mu\text{L}$   $\text{CHCl}_3$  and applied to boric acid TLC plates (see below). Fifty microliters of a  $10 \text{ mg mL}^{-1}$  solution of *sn*-2-monooleoylglycerol (Sigma-Aldrich) was applied as a reference standard. Lipids were separated by one ascension of  $\text{CHCl}_3/\text{CH}_3\text{COCH}_3$  (88:12, vol/vol) (26).

**Elution of TAG and MAG from silica gel.** TAG and *sn*-2-MAG standards were visualized with iodine vapor. The silica containing the fraction of interest was removed from the TLC plate with a glass microscope slide onto glassine paper and transferred to a methanol-washed test tube. Lipids were eluted from silica by extracting twice with 5 mL and once with 2 mL of  $\text{CHCl}_3$ . The slurry was shaken vigorously and centrifuged at  $400 \times g$  for 5 min. Each eluent was passed through a column of anhydrous  $\text{Na}_2\text{SO}_4$ . The combined lipid fractions were stored at  $-20^\circ\text{C}$  under  $\text{N}_2$ .

**Preparation of boric acid TLC plates.** Boric acid TLC plates were prepared using a slurry of 60 g Silica Gel G (Sigma-Aldrich) and 160 mL 0.4 M boric acid to make five  $20 \times 20 \text{ cm}$ , 0.5 mm thick, TLC plates. The plates were air-

dried, heated for 2 h at 120°C, and then stored at room temperature in the presence of desiccant until use.

**Analysis of FA composition.** Tetramethylguanidine was used to transmethylate lipid samples (27,28). Lipid samples were dried under N<sub>2</sub> with 2 µL of 20 mg 21:0 methyl ester mL<sup>-1</sup> added as an internal standard. The dried lipid was suspended in 500 µL methanol/tetramethylguanidine (4:1, vol/vol) and incubated in a boiling water bath for 30 min. Five milliliters of saturated NaCl solution were added after cooling to room temperature, and the lipids were extracted three times with 2 mL of petroleum ether. The extracts were combined and passed through a column of anhydrous Na<sub>2</sub>SO<sub>4</sub>. The lipid extract was evaporated to dryness under N<sub>2</sub> and redissolved in 100 µL hexane. Analysis of FAME was carried out using a Supelcowax-10, 30 m × 0.25 mm × 0.25 µm column (Sigma-Aldrich) installed in a HP5890 Series Plus II gas chromatograph equipped with a FID and splitless injection (10). The initial temperature was 50°C. This was increased to 200°C at a rate of 25°C per minute. Following this, the temperature was then increased, sequentially, from 200 to 220°C and 220 to 240°C at a rate of 1°C per min and 15°C per min, respectively. Identification of FA was by comparison to retention times of known standards (Sigma-Aldrich), and quantification of the peaks was done by determining the area under each peak. Individual FA were calculated as a mol% of the following combined FA: 16:0, 18:0, 18:1, 18:2, α-18:3, and CLA. In the case of CLA, GLC peaks for all isomers were pooled and reported as mol% of 16:0, 18:0, 18:1, 18:2, α-18:3, and CLA.

**Calculations and statistical analysis.** The FA composition of the *sn*-1/3 positions of the TAG (29) was calculated from the mean values obtained from the TAG (combined *sn*-1, *sn*-2, and *sn*-3) and *sn*-2-MAG FA analysis as follows:

$$\text{sn-1/3 mol\%} = (\text{TAG mol\%} \times 3 - \text{sn-2-MAG mol\%})/2 \quad [1]$$

The methods used for determining positional distribution of FA were tested with standard TAG. FA composition data were analyzed using the JMP IN Version 3.2.1 statistical package (SAS Institute Inc., 1989–1997, Cary, NC). ANOVA was followed by a pairwise comparison of treatments to the control using Dunnett's test (30).

## RESULTS

**FA composition of TAG.** The FA compositions of the TAG fractions of diaphragm, rib muscle, and SC adipose tissue are shown in Tables 1–3. Long-chain PUFA (>C<sub>18</sub>) were not included in the analyses, and the isomers of CLA were not fully resolved. The mole percent of CLA in TAG was significantly higher ( $P < 0.05$ ) in animals fed 6% safflower oil compared to the controls. In general, the CLA content of the TAG fraction of diaphragm, rib muscle, and SC adipose tissue increased by about threefold in animals that received the safflower oil dietary treatment. No significant differences in the CLA content of TAG were observed between tissues of the CLA-supplemented group and controls. Regardless of diet, oleic acid (18:1) was the major component of the TAG

**TABLE 1**  
Effect of Diet on FA Composition of TAG and Positional Distribution of FA in TAG from Diaphragm

Fraction	Diet	FA (mol%) <sup>a</sup>						<i>n</i>
		16:0	18:0	18:1	18:2	α-18:3	CLA	
TAG	CLA	26.8	16.7	50.9	4.3	1.0	0.4	3
	Control	24.7	18.2	51.2	4.7	0.8	0.3	5
	Safflower	28.1	17.0	47.4	5.7	0.9	0.8*	4
	SEM	1.17	1.08	1.05	0.27	0.22	0.04	
<i>sn</i> -2	CLA	39.7	28.6	21.7	9.9	0	0	3
	Control	34.2	25.4	30.4	9.7	0.16	0.15	5
	Safflower	36.2	27.5	24.4	12.1	0	0	4
	SEM	3.00	2.16	3.41	2.55	0.06	0.06	
<i>sn</i> -1/3	CLA	20.4	10.7	65.4	1.5	1.5	0.5	3
	Control	20.0	14.6	61.6	2.2	1.1	0.3	5
	Safflower	24.1	11.7	59.0	2.6	1.4	1.2*	4
	SEM	2.97	1.91	2.75	1.33	0.33	0.06	

<sup>a</sup>Mol% of the total FA listed. \* $P < 0.05$  by Dunnett's test compared to control; CLA, conjugated linoleic acid in diet as free acid pre-weaning; safflower, 6% safflower oil in diet post-weaning; control, no dietary treatment.

(46.2–54.5 mol%) in these three tissues. This was followed by palmitic acid (16:0) (24.7–33.1 mol%), stearic acid (18:0) (9.5–18.2 mol%), 18:2 (4.1–6.4 mol%), CLA (0.2–1.6 mol%) and α-linolenic acid (α-18:3) (0.5–1.1 mol%). The 16:0 content of TAG from the rib muscle of lambs fed safflower oil was significantly lower ( $P < 0.05$ ) than the control (27.6 vs. 31.5 mol%). This decrease was apparently compensated for by increases in the proportions of 18:0, 18:1, and 18:2. The proportion of α-18:3 also decreased significantly ( $P < 0.05$ ), from 1.0 mol% of the TAG in the control to 0.5 mol% of the TAG in the safflower oil-fed group.

**TABLE 2**  
The Effect of Diet on FA Composition of TAG and Positional Distribution of FA in TAG from Rib Muscle

Fraction	Diet	FA (mol%) <sup>a</sup>						<i>n</i>
		16:0	18:0	18:1	18:2	α-18:3	CLA	
TAG	CLA	33.1	14.8	46.2	4.6	1.1	0.2	4
	Control	31.5	16.2	46.4	4.7	1.0	0.3	5
	Safflower	27.6*	17.6	47.9	5.6	0.5*	0.8*	4
	SEM	0.87	0.85	1.2	0.44	0.09	0.04	
<i>sn</i> -2	CLA	37.2	24.3	31.6	7.0	0	0	4
	Control	39.6	25.5	31.1	3.4	0.16	0.2	5
	Safflower	40.0	24.0	31.4	4.4	0	0.2	4
	SEM	1.71	2.49	2.11	1.75	0.06	0.14	
<i>sn</i> -1/3	CLA	31.0	10.0	53.5	3.4	1.7	0.3	4
	Control	27.5	11.6	54.0	5.3	1.4	0.3	5
	Safflower	21.4	14.4	56.1	6.2	0.8*	1.1*	4
	SEM	1.7	2.0	1.5	1.7	0.14	0.08	

<sup>a</sup>Mol% of the total FA listed. \* $P < 0.05$  by Dunnett's test compared to control; CLA, conjugated linoleic acid in diet as free acid pre-weaning; safflower, 6% safflower oil in diet post-weaning; control, no dietary treatment.

**TABLE 3**  
The Effect of Diet on FA Composition of TAG and Positional Distribution of FA in TAG from Subcutaneous Adipose Tissue

Fraction	Diet	FA (mol%) <sup>a</sup>						n
		16:0	18:0	18:1	18:2	$\alpha$ -18:3	CLA	
TAG	CLA	30.8	9.5	54.5	4.1	0.7	0.5	4
	Control	30.0	11.1	52.0	5.5	0.9	0.5	5
	Safflower	32.2	10.8	48.3	6.4	0.7	1.6*	4
	SEM	1.26	1.03	2.26	0.59	0.81	0.16	
<i>sn</i> -2	CLA	15.3	9.7	64.8	5.3	1.4	4	4
	Control	19.8	11.7	60.5	7.9	0	0	5
	Safflower	28.9	19.9	47.4	3.7	0	0	4
	SEM	2.73	2.40	4.40	1.80	0.46	1.05	
<i>sn</i> -1/3	CLA	38.5	9.4	49.3	3.5	0.3	-0.9 <sup>b</sup>	4
	Control	35.1	10.8	47.7	4.3	1.3	0.8	5
	Safflower	33.8	6.3	48.7	7.8	1.1	2.3*	4
	SEM	2.85	2.28	4.99	1.05	0.36	0.70	

<sup>a</sup>Mol% of the total FA listed. \* $P < 0.05$  by Dunnett's test compared to control.

<sup>b</sup>Negative value due to low abundance of FA. CLA, conjugated linoleic acid in diet as free acid pre-weaning; safflower, 6% safflower oil in diet post-weaning; control, no dietary treatment.

**Positional distribution of CLA and other FA in TAG.** The FA compositions of the *sn*-2 and *sn*-1/3 positions of diaphragm, rib muscle, and SC adipose tissue TAG as determined by pancreatic lipase digestion are also shown in Tables 1–3. No significant differences in the proportions of FA in the *sn*-2 position of TAG from the diaphragm, rib muscle, or SC adipose tissue were seen, and CLA was more abundant in *sn*-1/3 positions of TAG than in the *sn*-2 position. The proportion of CLA detected at the *sn*-2 position was 0.2 mol% or lower in all categories with the exception of SC adipose tissue, where the proportion of CLA in the *sn*-2 position was 4 mol% (Table 3). The proportion of CLA present in the *sn*-1/3 positions of TAG from the three tissues of lambs that were fed the safflower oil-supplemented diet was significantly higher ( $P < 0.05$ ) than in *sn*-1/3 positions of TAG from controls. The proportion of CLA increased by about three- to fourfold at this position over the three tissue types. In general, the FA composition at the *sn*-2 position of TAG in the muscle tissues (diaphragm and rib) differed considerably from the TAG isolated from SC adipose tissue. For example, the proportion of 18:1 at the *sn*-2 position of TAG from SC adipose tissue ranged from 47.4 to 64.8 mol%, whereas the proportion of this FA ranged from 21.7 to 31.6 mol% in the two muscle types. In rib muscle, the proportion of  $\alpha$ -18:3 at the *sn*-1/3 position of TAG was significantly lower ( $P < 0.05$ ) in animals fed a diet supplemented with safflower oil than in the control (0.8 vs. 1.4 mol%) (Table 2).

**FA composition of PL.** CLA content ranged from 0–1.8 mol% in the PL of diaphragm, rib muscle, and SC adipose tissue (Table 4). The only significant changes ( $P < 0.05$ ) attributable to diet were for safflower oil-fed animals, which showed a decrease of over twofold in mol% of  $\alpha$ -18:3 in the PL of both diaphragm and rib. The major FA of diaphragm

**TABLE 4**  
The Effect of Diet on FA Composition of Phospholipid from Diaphragm, Rib Muscle, and Subcutaneous Adipose Tissue

Fraction	Diet	FA (mol%) <sup>a</sup>						n
		16:0	18:0	18:1	18:2	$\alpha$ -18:3	CLA	
Diaphragm	CLA	19.6	23.6	22.4	32.5	1.8	0.01	3
	Control	17.7	25.1	20.8	34.8	1.6	0.03	5
	Safflower	14.0	26.0	16.0	43.3	0.7*	0	4
	SEM	1.41	1.09	1.63	2.70	0.16	0.01	
Rib	CLA	22.5	13.5	34.3	24.0	2.5	0.05	4
	Control	22.1	14.9	33.3	26.3	2.3	1.2	5
	Safflower	15.3	12.4	25.3	44.2	0.9*	1.8	4
	SEM	1.71	1.45	3.02	5.1	0.20	0.5	
SC fat	CLA	25.6	17.0	47.7	8.3	0.4	1.1	4
	Control	28.0	18.4	45.6	6.1	0.6	1.1	5
	Safflower	19.7	13.7	54.7	10.7	0.2	1.0	4
	SEM	3.04	1.98	4.95	2.34	0.19	0.50	

<sup>a</sup>Mol% of the total FA listed. \* $P < 0.05$  by Dunnett's test compared to control; CLA, conjugated linoleic acid in diet as free acid pre-weaning; safflower, 6% safflower oil in diet post-weaning; control, no dietary treatment; SC, subcutaneous.

PL was 18:2 (32.5–43.3 mol%). The CLA content in the diaphragm was lower than in any of the other tissue PL, ranging from 0 to 0.03 mol%. The major FA of rib muscle PL were 18:1 (25.3–34.3 mol%) and 18:2 (24.0–44.2 mol%). The CLA content of rib muscle PL ranged from 0.05 to 1.8 mol%. The major FA of SC adipose tissue PL was 18:1 (45.6–54.7 mol%). The CLA content of SC adipose tissue PL ranged from 1.0 to 1.1 mol%. The 18:2 content of PL of SC adipose tissue was the lowest of all tissues studied at 6.1–10.7 mol%.

## DISCUSSION

Basal diets supplemented by unprotected polyunsaturated fats in vegetable oils have been shown to have little effect on FA composition of adipose tissue and skeletal muscle sampled from various sites in steers (31). For example, supplementation with 6% safflower oil resulted in a slight increase in the proportion of 16:0 and 18:0. Because dietary lipids are extensively hydrogenated in the rumen to produce saturated FA, incorporation of higher levels of polyunsaturated fats in ruminant tissues is usually accomplished by feeding protected fat supplements that pass through the rumen and are absorbed in the small intestine unchanged. The 18:2 present in safflower oil is biohydrogenated in the rumen ultimately to produce 18:0. Intermediates of the biohydrogenation of 18:2 are CLA and *trans*-11 18:1 (1). A recent investigation of the duodenal flow of FA in ewes has shown that CLA and *trans*-11 18:1 are equally abundant (32). In the current study, lambs fed a diet supplemented with 6% safflower oil showed a significant increase ( $P < 0.05$ ) in the proportion of CLA in the TAG fraction of diaphragm, rib muscle, and SC adipose tissue. No significant change in the content of other major FA components was observed. Increases of two- to fourfold in the CLA con-



tent of TL of tissues from lambs fed a diet supplemented with 6% safflower oil have been observed (18).

The polyunsaturated FA content in tissues of young ruminants has been shown to increase following feeding with milk replacers supplemented with 12.5–70 g sunflower oil d<sup>-1</sup> for up to 16 wk (31). The muscle and adipose tissue from animals on this supplemented diet contained up to 40% of 18:2 in the TAG fraction after 30 d. This increase in 18:2 content was accomplished owing to the bypass of the rumen when the esophageal groove was closed while suckling. In this way, the components of the diet were absorbed in the small intestine as in nonruminants. In the current study, the direct feeding of CLA to pre-weaned lambs for 21 d prior to weaning did not increase the CLA content of the TAG fraction of any of the tissues studied. The CLA may have been oxidized in the liver. The increased CLA content observed in the TAG of the animals receiving the safflower oil diet resulted in the incorporation and storage of CLA in the TAG fraction of diaphragm, rib muscle, and SC adipose tissue. The higher proportion of CLA in the TAG of the SC adipose tissue, which was twofold that of diaphragm and rib muscle (see Tables 1–3), suggested that CLA was preferentially stored in this fat depot. Since CLA was apparently oxidized in pre-ruminant animals fed pre-formed CLA, it is possible that the increased levels of tissue CLA observed with the diet supplemented with 6% safflower oil may be the result of endogenous  $\Delta^9$  desaturation of *trans*-11 18:1 produced in the rumen from 18:2.

In mammalian fat depots, unsaturated FA have a tendency to be localized to the *sn*-2 position of TAG, whereas saturated FA tend to be localized to the *sn*-1 and *sn*-3 positions (33). Recently, it was reported that TAG from human breast adipose tissue contained higher percentages of CLA at the *sn*-2 position and lower percentages of CLA at the *sn*-1/3 positions relative to TAG from adipose tissue from benign breast tumors (34). Changes in FA positional distribution as affected by diet also have been shown in bovine and ovine adipose tissues (35–37) and ovine liver (36), but the mechanism responsible for these diet-induced changes is unknown. In previous studies with ruminants fed a protected supplement, high proportions of additional 18:2 were incorporated into adipose tissues with preferential esterification to the *sn*-2 position and to a lesser extent the *sn*-3 position (31,36).

In the present study, the positional distribution analyses of the FA of TAG from the three tissues showed an increased proportion of CLA in the *sn*-1/3 positions in the safflower oil diet group that may be linked to the selectivity of the acyltransferases of TAG bioassembly. In contrast, CLA was detected in the *sn*-2 position of TAG of SC adipose tissue from the CLA-supplemented animals (Table 3). This observation indicated that feeding CLA to pre-weaning lambs had an effect on the placement of the CLA within TAG from SC adipose tissue. CLA supplied through duodenal flow from the rumen or conversion of duodenal *trans*-11 18:1 to CLA later in animal life, however, resulted in preferential incorporation of CLA at the *sn*-1/3 positions of TAG from this tissue. The availability of new molecular tools for TAG-biosynthetic enzymes is having a substantial

effect on investigations into the regulation of TAG bioassembly by nutrients, hormones, and physiological conditions (38). These molecular tools could prove useful in increasing our understanding of the mode of CLA incorporation into TAG.

*sn*-1,2-DAG produced during TAG biosynthesis can also be diverted to the biosynthesis of nitrogenous PL (38–40). Previous studies on incorporation of CLA have shown that CLA is readily incorporated into the PL fraction of the mammary gland and forestomach tissues of rodents (13,41). There is also evidence that CLA is preferentially incorporated into the NL fraction in mice (42). In the current study, safflower oil supplementation in the diet had no effect on the CLA content of PL from diaphragm, rib muscle, and SC adipose tissue, suggesting that CLA was preferentially incorporated into the TAG of these tissues. These observations suggested that there could be a threshold of CLA incorporation into the PL of ruminants. It has been suggested that the biological activity of CLA may be related more to deposition of fat rather than through effects on PL alteration (37). The relatively low levels of  $\alpha$ -18:3 in the PL of SC adipose tissue (Table 4) may have been due to the competitive metabolism of CLA vs. 18:2 to produce a conjugated form of 18:3 (15), which was not quantified in this study. Since *sn*-1,2-DAG is also a precursor of nitrogenous PL, the CLA composition of TAG at the *sn*-1/2 positions might be expected to reflect that of the PL to some extent, although deacylation–acylation mechanisms are known to further alter the fatty acyl composition of PL (43). The PL from muscle tissue, however, represented a combination of PL from both intramuscular adipocytes and muscle fibers. TAG biosynthesis has also been reported to occur in muscle fibers (40,44). Therefore, there may be differences in the incorporation of CLA into the TAG of adipocytes from that of muscle fibers.

Supplementation of lamb feedlot diet with safflower oil as a source of unprotected 18:2 resulted in a significant increase in the CLA content of TAG from various tissues. Dietary manipulation had no significant effect on the CLA content of the PL suggesting that the FA isomers were preferentially incorporated into TAG. The highest mol% CLA was observed in SC adipose tissue, indicating that CLA was preferentially stored in this fat depot. CLA was not detected in significant quantities at the *sn*-2 position of the TAG molecule in any of the tissues examined. There was, however, an increased amount of CLA in the *sn*-2 position of the SC adipose tissue from animals supplemented with pre-formed CLA prior to weaning. Although feeding CLA to pre-weaning lambs had no effect on the total CLA content of the TAG, it influenced the positional distribution of CLA on the TAG molecule. The described ruminant feeding model may be useful for investigating the enzymology of CLA production and incorporation into glycerolipids of ruminants. In addition to investigating endogenous production of CLA from *trans*-11 18:1, studies on the specificity and selectivity for CLA of the acyltransferases involved in TAG and PL biosynthesis should provide further insight into the mechanism of CLA incorporation into glycerolipids. In recent studies, we have characterized DAG acyltransferase involved in TAG biosynthesis in bovine muscle tissue using the diaphragm as a source of enzyme



because this is the only muscle tissue that is available within 30 min of slaughter in a commercial abattoir (45,46). The use of the diaphragm in our current study of the positional distribution of CLA in TAG will provide background knowledge for designing future experiments that will focus on the enzymology of CLA incorporation using this tissue. It will also be important to examine the relative contributions of intramuscular adipocytes vs. muscle fibers to CLA incorporation into glycerolipids.

## ACKNOWLEDGMENTS

The authors thank Tara Furukawa-Stoffer, Christopher Gregg, Chris Kazala, and Brenda Pink for technical help, and the farm staff at the sheep barn of the Lethbridge Research Centre for animal care. The authors also thank The Canada-Alberta Livestock Trust Fund for providing the animals, and Dr. Fred Lozeman and Chris Kazala for critical evaluations of the manuscript.

## REFERENCES

- Kepler, C.R., Hirons, K.P., McNeill, J.J., and Tove, S.B. (1966) Intermediates and Products of the Biohydrogenation of Linoleic Acid by *Butyrivibrio fibrisolvens*, *J. Biol. Chem.* 241, 1350–1354.
- Chin, S.F., Storkson, J.M., Liu, W., Albright, K.J., and Pariza, M.W. (1994) Conjugated Linoleic Acid (9,11- and 10,12-octadecadienoic acid) Is Produced in Conventional but Not Germ-Free Rats Fed Linoleic Acid, *J. Nutr.* 124, 694–701.
- Ip, C. (1997) Review of the Effect of *trans* Fatty Acids, Oleic Acid, n-3 Polyunsaturated Fatty Acids, and Conjugated Linoleic Acid on Mammary Carcinogenesis in Animals, *Am. J. Clin. Nutr.* 66, 1523S–1529S.
- Ha, Y.L., Grimm, N.K., and Pariza, M.W. (1989) Newly Recognized Anticarcinogenic Fatty Acids: Identification and Quantification in Natural and Processed Cheeses, *J. Agric. Food Chem.* 37, 75–81.
- Cook, M.E., Miller, C.C., Park, Y., and Pariza, M. (1993) Immune Modulation by Altered Nutrient Metabolism: Nutritional Control of Immune-Induced Growth Depression, *Poult. Sci.* 72, 1301–1305.
- Knekt, P., Jarvinen, R., Seppanen, R., Pukkala, E., and Aromaa, A. (1996) Intake of Dairy Products and the Risk of Breast Cancer, *Br. J. Cancer* 73, 687–691.
- Fogerty, A.C., Ford, G.L., and Svoronos, D. (1988) Octadeca-9,11-dienoic Acid in Foodstuffs and in the Lipids of Human Blood and Breast Milk, *Nutr. Rep. Int.* 38, 937–944.
- Jiang, J., Bjoerck, L., Fonden, R., and Emanuelson, M. (1996) Occurrence of Conjugated *cis*-9,*trans*-11-Octadecadienoic Acid in Bovine Milk: Effect of Feed and Dietary Regimen, *J. Dairy Sci.* 79, 438–445.
- Shantha, N.C., Crum, A.D., and Decker, E.A. (1994) Evaluation of Conjugated Linoleic Acid Concentrations in Cooked Beef, *J. Agric. Food Chem.* 42, 1757–1760.
- Mir, Z., Paterson, L.J., and Mir, P.S. (2000) Fatty Acid Composition and Conjugated Linoleic Acid (CLA) Content of Intramuscular Fat in Crossbred Cattle With and Without Wagyu Genetics Fed a Barley Based Diet, *Can. J. Anim. Sci.* 80, 195–197.
- Mir, Z., Goonewardene, L.A., Okine, E., Jaegar, S., and Scheer, H.D. (1999) Effect of Feeding Canola Oil on Constituents, Conjugated Linoleic Acid (CLA) and Fatty Acid Profiles in Goat's Milk, *Small Rum. Res.* 33, 137–143.
- Stanton, C., Lawless, F., Kjellmer, G., Harrington, D., Devery, R., Connolly, J.F., and Murphy, J. (1997). Dietary Influence on Bovine Milk *cis*-9,*trans*-11 Conjugated Linoleic Acid Content, *J. Food Sci.* 62, 1083–1086.
- Ip, C., Chin, S.F., Scimeca, J.A., and Pariza, M.W. (1991) Mammary Cancer Prevention by Conjugated Dienoic Derivative of Linoleic Acid, *Cancer Res.* 51, 6118–6124.
- Kavanaugh, C.J., Liu, K.L., and Belury, M.A. (1999) Effect of Dietary Conjugated Linoleic Acid on Phorbol Ester-Induced PGE<sub>2</sub> Production and Hyperplasia in Mouse Epidermis, *Nutr. Cancer* 33, 132–138.
- Banni, S., Carta, G., Contini, M.S., Angioni, E., Deiana, M., Dessi, M.A., Melis, M.P., and Corongiu, F.P. (1996) Characterization of Conjugated Diene Fatty Acids in Milk, Dairy Products, and Lamb Tissues, *Nutr. Biochem.* 7, 150–155.
- Griinari, J.M., Corl, B.A., Lacy, S.H., Chouinard, P.Y., Nurmela, K.V., and Bauman, D.E. (2000) Conjugated Linoleic Acid Is Synthesized Endogenously in Lactating Dairy Cows by  $\Delta^9$ -Desaturase, *J. Nutr.* 130, 2285–2291.
- Gläser, K.R., Scheeder, M.R.L., and Wenk, C. (2000) Dietary C18:1 *trans* Fatty Acids Increase Conjugated Linoleic Acid in Adipose Tissue of Pigs, *Eur. J. Lipid Sci. Technol.* 102, 684–686.
- Mir, Z., Rushfeldt, M.L., Mir, P.S., Paterson, L.J., and Weslake, R.J. (2000) Effect of Dietary Supplementation with Either Conjugated Linoleic Acid (CLA) or Linoleic Acid Rich Oil on the CLA Content of Lamb Tissues, *Small Rum. Res.* 36, 25–31.
- Ivan, M., Mir, P.S., Koenig, K., Rode, L.M., Neill, L., Entz, T., and Mir, Z. (2001) Effects of Dietary Sunflower Seed Oil on Protozoal Population in the Rumen, Growth, and the Tissue Concentrations of Fatty Acids Including Conjugated Linoleic Acid in Sheep, *Small Rum. Res.* 41, 215–227.
- Chin, S.F., Liu, W., Storkson, J.M., Ha, Y.L., and Pariza, M.W. (1992) Dietary Sources of Conjugated Dienoic Isomers of Linoleic Acid, a Newly Recognized Class of Anticarcinogens, *J. Food Comp. Anal.* 5, 185–197.
- Palmquist, D.L. (1988) The Feeding Value of Fats, in *Feed Science* (Orskov, E.R., ed.), pp. 293–311, Elsevier, Amsterdam.
- Folch, J., Lees, M., and Sloane-Stanley, G.H. (1957) A Simple Method for the Isolation and Purification of Total Lipids from Animal Tissues, *J. Biol. Chem.* 226, 497–509.
- Juaneda, P., and Rocquelin, G. (1985) Rapid and Convenient Separation of Phospholipids and Nonphosphorus Lipids from Rat Heart Using Silica Cartridges, *Lipids* 20, 40–41.
- Pomeroy, M.K., Kramer, J.K.G., Hunt, D.J., and Keller, W.A. (1991) Fatty Acid Changes During Development of Zygotic and Microspore-Derived Embryos of *Brassica napus*, *Physiol. Plant.* 81, 447–454.
- Myher, J.J., and Kuksis, A. (1979) Stereospecific Analysis of Triacylglycerols via Racemic Phosphatidylcholines and Phospholipase C, *Can. J. Biochem.* 57, 117–124.
- Myher, J.J., Kuksis, A., Geher, K., Park, P.W., and Diersen-Schade, D.A. (1996) Stereospecific Analysis of Triacylglycerols Rich in Long-Chain Polyunsaturated Fatty Acids, *Lipids* 31, 207–215.
- Shantha, N.C., Decker, E.A., and Hennig, B. (1993) Comparison of Methylation Methods for the Quantitation of Conjugated Linoleic Acid Isomers, *J. AOAC Int.* 73, 644–649.
- Schuchardt, U., and Lopes, O.C. (1988) Tetramethylguanidine Catalyzed Transesterification of Fats and Oils a Method for Rapid Determination of Their Composition, *J. Am. Oil Chem. Soc.* 65, 1940–1941.
- Kagawa, M., Matsubara, K., Kimura, K., Shiono, H., and Fukui, Y. (1996) Species Identification by the Positional Analysis of Fatty Acid Composition in Triacylglyceride of Adipose and Bone Tissues, *Forensic Sci. Int.* 79, 215–226.
- Dunnett, C.W. (1955) A Multiple Comparison Procedure for Comparing Several Treatments with a Control, *J. Am. Stat. Assoc.* 50, 1096–1121.
- Christie, W.W. (1979) The Effects of Diet and Other Factors on the Lipid Composition of Ruminant Tissues and Milk, *Prog. Lipid Res.* 17, 245–277.

32. Kucuk, O., Hess, B.W., Ludden, P.A., and Rule, D.C. (2001) Effect of Forage: Concentrate Ratio on Ruminal Digestion and Duodenal Flow of Fatty Acids in Ewes, *J. Anim. Sci.* 79, 2233–2240.
33. Brockerhoff, H., Hoyle, R.J., and Wolmark, N. (1966) Positional Distribution of Fatty Acids in Triglycerides of Animal Depot Fats, *Biochim. Biophys. Acta* 116, 67–72.
34. Lavillonniere, F., and Bougnoux, P. (1999) Conjugated Linoleic Acid (CLA) and the Risk of Breast Cancer, in *Advances in CLA Research* (Yurawecz, M.P., Mossoba, M.M., Kramer, J.K.G., Pariza, M.W., and Nelson, G.J., eds.), pp. 276–282, AOCS Press, Champaign.
35. Hawke, J.C., Morrison, I.M., and Wood, P. (1977) Structures of Triacylglycerols in Lamb Fat with Elevated Levels of Linoleic Acid, *J. Sci. Food Agric.* 28, 293–300.
36. Mills, S.C., Cook, L.J., and Scott, T.W. (1975) Effect of Dietary Fat Supplementation on the Composition and Positional Distribution of Fatty Acids in Ruminant and Porcine Glycerides, *Lipids* 11, 49–60.
37. Smith, S.B., Yang, A., Larsen, T.W., and Tume, R.K. (1998) Positional Analysis of Triacylglycerols from Bovine Adipose Tissue Lipids Varying in Degree of Unsaturation, *Lipids* 33, 197–207.
38. Coleman, R.A., Lewin, T.M., and Muoio, D.M. (2000) Physiological and Nutritional Regulation of Enzymes of Triacylglycerol Synthesis, *Annu. Rev. Nutr.* 20, 77–103.
39. Lehner, R., and Kuksis, A. (1996) Biosynthesis of Triacylglycerols, *Prog. Lipid Res.* 35, 169–201.
40. Cortright, R.N., Muoio, D.M., and Dohm, G.L. (1997) Skeletal Muscle Lipid Metabolism: A Frontier for New Insights into Fuel Homeostasis, *Nutr. Biochem.* 8, 228–245.
41. Ha, Y.L., Storkson J., and Pariza M.W. (1990) Inhibition of Benzo(a)pyrene-Induced Mouse Forestomach Neoplasia by Conjugated Dienoic Derivatives of Linoleic Acid, *Cancer Res.* 50, 1097–1101.
42. Belury, M.A., Nickel, K.P., Bird, C.E., and Wu, Y. (1996) Dietary Conjugated Linoleic Acid Modulation of Phorbol Ester Skin Tumor Promotion, *Nutr. Cancer* 26, 149–157.
43. Farooqui, A.A., Horrocks, L.A., and Farooqui, T. (2000) Deacylation and Reacylation of Neural Membrane Glycerophospholipids, *J. Mol. Neurosci.* 14, 123–135.
44. Guo, Z. (2001) Triglyceride Content in Skeletal Muscle: Variability and the Source, *Anal. Biochem.* 296, 1–8.
45. Middleton, C.K., Kazala, E.C., Lozeman, F.J., Hurly, T.A., Mir, P.S., Bailey, D.R.C., Jones, S.D.M., and Weselake, R.J. (1998) Evaluation of Diacylglycerol Acyltransferase as an Indicator of Intramuscular Fat Content in Beef Cattle, *Can. J. Anim. Sci.* 78, 265–270.
46. Lozeman, F.J., Middleton, C.K., Deng, J., Kazala, E.C., Verhaege, C., Mir, P.S., Bailey, D.R.C., and Weselake, R.J. (2001) Characterization of Diacylglycerol Acyltransferase in Bovine Adipose and Muscle Tissue, *Comp. Biochem. Physiol. Part B* 130, 105–115.

[Received April 18, 2001, and in revised form April 25, 2002; revision accepted May 17, 2002]

# Analysis of Diastereomeric DAG Naphthylethylurethanes by Normal-Phase HPLC with On-line Electrospray MS

J.J. Ågren<sup>a,b,\*</sup> and A. Kuksis<sup>a</sup>

<sup>a</sup>Banting and Best Department of Medical Research, University of Toronto, Toronto, Ontario M5G 1L6, Canada, and <sup>b</sup>Department of Physiology, University of Kuopio, FIN-70211 Kuopio, Finland

**ABSTRACT:** Normal-phase HPLC resolution of *sn*-1,2(2,3)- and *x*-1,3-DAG generated by partial Grignard degradation from natural TAG was carried out with both (*R*)-(-) and (*S*)-(+)-1-(1-naphthyl)ethylurethane derivatives. The diastereomeric *sn*-1,2- and *sn*-2,3-DAG derivatives were resolved using two Supelcosil LC-Si (5  $\mu$ m, 25 cm  $\times$  4.6 mm i.d.) columns in series and an isocratic elution with 0.37% isopropanol in hexane at a flow rate of 0.7 mL/min. The DAG were detected by UV absorption at 280 nm and were identified by electrospray ionization MS in the positive ion mode following postcolumn addition of chloroform/methanol/30% ammonium hydroxide (75:24.5:0.5, by vol) at 0.6 mL/min. Application of the method to a stereospecific analysis of the molecular species of TAG of rat VLDL showed that the TAG composition of VLDL circulating under basal conditions differs markedly from that of VLDL secreted by the liver during inhibition of serum lipases. The inhibition of serum lipases resulted in a significant proportional decrease in 16:0 and PUFA and an increase in 18:0 and oligoenoic FA in the *sn*-1-position, whereas the FA compositions in the *sn*-2- and *sn*-3-positions were much less affected.

Paper no. L8997 in *Lipids* 37, 613–619 (June 2002).

Stereospecific normal-phase HPLC analysis of natural TAG via the diastereomeric naphthylethylurethanes (NEU) of the DAG derived by Grignard degradation has been proposed (1–4) as an inexpensive substitute for the more costly chiral-phase HPLC analyses (5–7). However, the method does not give a complete resolution of the diastereomeric DAG derivatives when applied to TAG with a wide range of FA (2,3). Partial overlaps among enantiomers during chiral-phase HPLC of the dinitrophenylurethanes (DNPU) of DAG have been successfully dealt with by combining it with on-line MS (5,6) or by resolving the enantiomers as bis-DNPU derivatives of the *sn*-1- and *sn*-3-MAG (7,8). The present study reports that a combination of normal-phase HPLC of the diastereomeric NEU of DAG with on-line electrospray ionization MS (ESI-MS) also permits an accurate determination of the positional distribution of FA in the acylglycerols, as indicated by stereospecific analyses of rat VLDL TAG. The quan-

tification of any remaining incompletely resolved molecular species of DAG was facilitated by utilizing both *R*-(-)- and *S*-(+)-forms of the derivatives. The study shows that a combination of normal-phase HPLC resolution of the diastereomeric *sn*-1,2- and *sn*-2,3-DAG NEU with on-line MS provides an effective alternative to chiral-phase HPLC resolution of the enantiomeric 3,5-DNPU.

## MATERIALS AND METHODS

**Materials.** All solvents were HPLC or reagent grade and were purchased from Caledon Chemicals (Toronto, Canada) or Aldrich Chemical Co. (Milwaukee, WI). Ethyl magnesium bromide and *R*-(-)- and *S*-(+)-1-(1-naphthyl)ethylisocyanate were also from Aldrich Chemical Co. Sep-Pak® C18-cartridges were purchased from Waters Corporation (Milford, MA). Tripalmitoylglycerol (99%) was obtained from Sigma (St. Louis, MO).

**Animal procedure.** Male Wistar rats weighing 300–350 g and maintained on standard chow were used. Rats were fasted for 4 h before they were anesthetized with Somnatol (pentobarbital, 50 mg/kg; M.T.C. Pharmaceuticals, Cambridge, Canada). A cannula was inserted into the femoral vein and Triton WR1339 (600 mg/kg, Tyloxapol; Sigma, St. Louis, MO) or saline was injected. Two hours after injection, blood was drawn and rats were killed by heart puncture. The blood samples were taken into 5% EDTA, and plasma was immediately separated by centrifugation. Plasma was overlain with a NaCl solution ( $d = 1.006$  g/mL), and VLDL were separated by ultracentrifugation at  $125,000 \times g$  in a 70.1 Ti rotor (Beckman Instruments, Palo Alto, Ca) for 16 h at 16°C. Livers were removed and frozen in  $-70^\circ\text{C}$ . These studies were approved by the Animal Care Committee of the University of Toronto.

**Isolation of TAG.** Rat plasma VLDL and rat liver were extracted with chloroform/methanol (2:1, vol/vol) (9). Liver samples (300–400 mg) were thoroughly minced with a scalpel and extracted twice. The TAG were isolated by TLC on silica gel H plates using heptane/isopropyl ether/acetic acid (60:40:4, by vol) as the developing solvent (10). The TAG band was located by spraying the plate with dichlorofluorescein, scraping off the spot, extracting the TAG with chloroform/methanol, and, after solvent evaporation, redissolving it in chloroform for storage at  $-20^\circ\text{C}$ .

**Preparation of DAG.** The plasma VLDL and liver TAG were partially deacylated to *sn*-1,2-, *sn*-2,3-, and *sn*-1,3-DAG by Grignard reaction (3). The TAG (about 1 mg) were dissolved in

\*To whom the correspondence should be addressed at Department of Physiology, University of Kuopio, P.O. Box 1627, FIN-70211 Kuopio, Finland. E-mail: Jyrki.Agren@uku.fi

Abbreviations: CapEx, capillary exit voltage; DNPU, dinitrophenylurethane; HPLC/ESI-MS, HPLC with on-line electrospray ionization MS; NEU, 1-(1-naphthyl)ethylurethane; 14:0, myristic acid; 16:0, palmitic acid; 18:0, stearic acid; 18:1, oleic acid; 18:2, linoleic acid; 18:3, linolenic acid; 20:4, arachidonic acid; 20:5, eicosapentaenoic acid; 22:4, docosatetraenoic acid; 22:5, docosapentaenoic acid; 22:6, docosahexaenoic acid.

dry diethyl ether (1 mL) and 3 M ethyl magnesium bromide in dry diethyl ether (40  $\mu$ L) was added. The mixture was shaken for 1 min before glacial acetic acid (50  $\mu$ L) in hexane (5 mL) and water (2 mL) were added to terminate the reaction. The organic layer was washed with 0.5% sodium bicarbonate (2 mL) and water (2 mL) and dried by passing through two Pasteur pipettes containing anhydrous sodium sulfate. The solvent was evaporated in a stream of dry nitrogen at room temperature, and the products were immediately derivatized.

**Preparation of NEU derivatives.** The Grignard products were dissolved in dry toluene (0.3 mL), and *R*-(-)- or *S*-(+)-1-(1-naphthyl)ethyl isocyanate (10  $\mu$ L) and 4-pyrrolidinopyridine (4 mg) were added. The derivatization was performed by heating the mixture at 50°C overnight (3). After evaporation of solvents in a stream of nitrogen, the reaction products were dissolved in methanol/water (95:5, vol/vol) and applied to a Sep-Pak C18 column, which had been solvated with the same solvent. An additional 15 mL of this solvent was passed through the column, and NEU derivatives were then eluted with acetone (10 mL).

**HPLC resolution of diastereomers.** The diastereomeric NEU derivatives of *sn*-1,2- and *sn*-2,3-DAG were separated (2) by normal-phase HPLC using in series two Supelcosil LC-Si columns (5  $\mu$ m, 25 cm  $\times$  4.6 mm i.d., Supelco Inc., Bellefonte, PA). The columns were installed in a Waters 550 liquid chromatograph connected to a Waters 990 photodiode array detector. The samples were injected in hexane (10  $\mu$ L). The columns were eluted with 0.37% isopropanol in hexane at a flow rate of 0.7 mL/min, and peaks were detected at 280 nm.

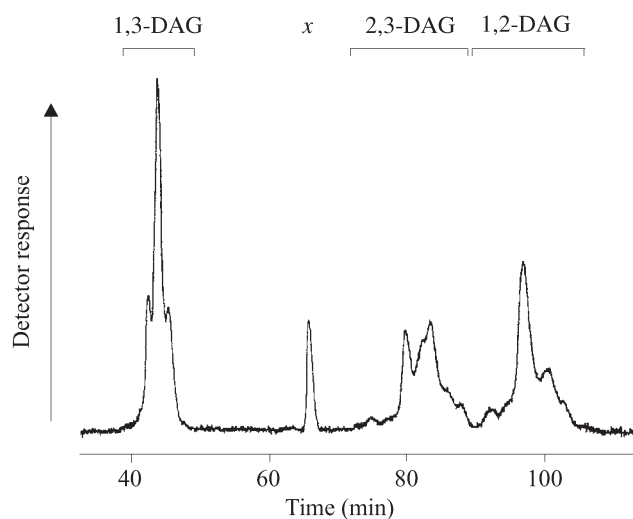
**HPLC/ESI-MS.** The molecular species of DAG were identified by passing the effluent of the normal-phase HPLC columns into a Hewlett-Packard 5989A single quadrupole mass spectrometer equipped with a Hewlett-Packard Model 59987A nebulizer-assisted ESI interface. Nitrogen gas was used as both nebulizing gas (60 psi) and drying gas (60 psi, 270°C). Positive ESI spectra were taken following postcolumn addition of chloroform/methanol/30% ammonium hydroxide (75:24.5:0.5, by vol) at 0.6 mL/min. The capillary exit voltage (CapEx) was 220 V (unless indicated otherwise), and the mass range scanned was 500–720 (200–1000 in test runs). Capillary, endplate, and cylinder voltages were –4, –3.5, and –5 kV, respectively, in the positive ion mode. The CapEx, which determines the extent of fragmentation by means of a collision-induced dissociation process, was varied between +90 and +270 V. Identification of the various unknown species was performed on the basis of retention time of standards, averaged full mass spectra, and the fragmentation patterns. The relative proportions of the molecular species of the DAG were calculated from the areas of the peaks obtained by single ion plots extracted from the total ion current spectra. The masses given in text and figures refer to protonated nominal, ammoniated, and sodiated ions.

**FA analysis.** FAME of NEU derivatives of DAG and TAG were prepared by acidic methanolysis using 6% H<sub>2</sub>SO<sub>4</sub> in methanol in sealed vials at 80°C for 2 h. The methyl esters were extracted with hexane and analyzed by GLC (Hewlett-Packard, Model 5890 Series II gas chromatograph) using a 15 m  $\times$  0.32 mm i.d. (film thickness 0.20  $\mu$ m) SP 2380 capillary column

(Supelco, Bellefonte, PA). The carrier gas was hydrogen at an inlet pressure of 3 psi. The column was held at 100°C for 0.5 min and then programmed at 20°C/min to 130°C and then at 5°C/min to 240°C (11). The FA were identified by comparing retention times of any peaks with those of standards.

## RESULTS

**Optimization of HPLC separations.** Previous work (2,3) had established isooctane with 0.33% isopropanol (containing 2% water) as an optimal mobile phase (flow rate 1 mL/min) for the resolution of the diastereomeric *sn*-1,2- and *sn*-2,3-DAG made up of the common FA. Under these conditions, the *sn*-1,3-DAG emerged as an early peak followed by *sn*-1,2- and *sn*-2,3-DAG in the case of the *S*-derivative, or *sn*-2,3- and *sn*-1,2-DAG in the case of the *R*-derivative. Usually, two to three peaks of approximately equal intensity were seen for each of the *sn*-1,2- and *sn*-2,3-diastereomers. Figure 1 shows the normal-phase separation of *R*-derivatives in the present study and demonstrates that a somewhat greater resolution of the *sn*-1,2- and *sn*-2,3-diastereomers may be obtained by the combination of slower flow rate (0.7 mL/min) and greater proportion (0.37%) of isopropanol in the eluant. As shown below, a complete resolution between the *sn*-1,2- and *sn*-2,3-diastereomers was not obtained. Thus, the species of the *sn*-2,3-diastereomers retained longest overlapped with the molecular species of the *sn*-1,2-diastereomers emerging earliest. The order of elution was reversed for the *S*-derivative. As shown below, ESI-MS can complement this resolution by allowing minor, unresolved components to be identified under these conditions. Other ratios and flow rates of isopropanol and hexane, and other polar modifiers (e.g., methanol and ethanol) failed to improve the resolution or significantly shorten the elution time without loss of resolution of the wide range of DAG derivatives analyzed here. A minor unknown peak (peak *x*, Fig. 1) appeared in the UV profile before the *sn*-2,3-



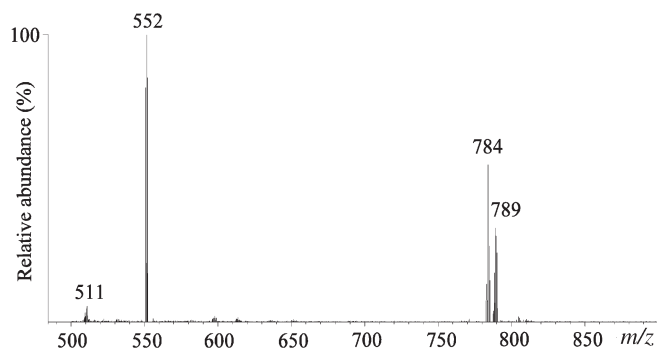
**FIG. 1.** Normal-phase HPLC separation of *sn*-1,3-, *sn*-2,3-, and *sn*-1,2-DAG prepared from rat plasma VLDL TAG (*x* = unknown peak). Chromatographic conditions were as described in text.



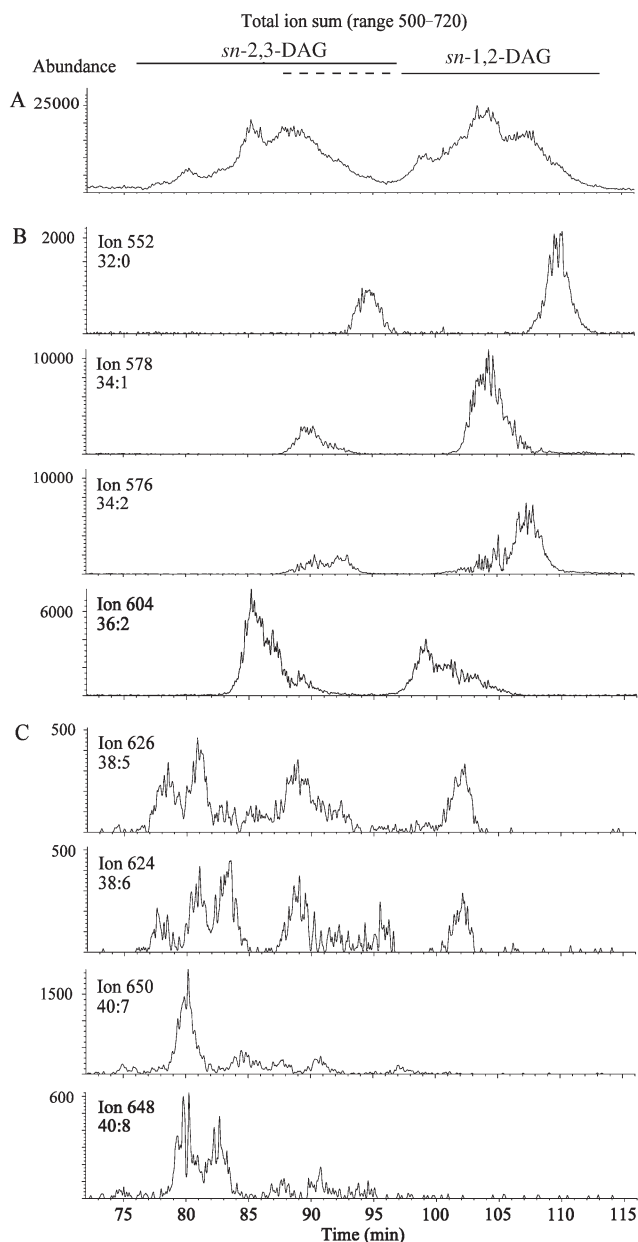
DAG peak. It had insufficient mass to be detected by positive ion MS, and FA were not found in the eluant.

**Optimization of HPLC/ESI-MS conditions.** Having optimized the HPLC resolution of the diastereomeric naphthylethylurethanes, we proceeded to optimize the ESI-MS detection and identification of the molecular species of the DAG derivatives. To take advantage of the positive ionization of the NEU, it was necessary to supplement the HPLC column flow with a polar solvent. Several combinations of solvents and different flow rates were tested, and the highest response at the normal ESI operating voltage of 170 V was obtained with chloroform/methanol/30% ammonium hydroxide (75:24.5:0.5, by vol) at 0.6 mL/min. This resulted in the near exclusive formation of the ammonia  $[M + 18]^+$  and sodium  $[M + 23]^+$  adducts, however, which complicated the identification of the molecular species of DAG using the single quadrupole mass spectrometer. This problem was resolved by increasing the CapEx voltage to 220 V. Under these conditions, proportionally correct yields were obtained for the DAG-like ions  $[M - NEU]^+$  without any reduction in the sensitivity of detection of the molecular species of the DAG derivatives. The formation of  $[M - NEU]^+$  ions was estimated on the basis of parallel analyses of standard mixtures of 14:0/16:0-, 16:0/16:0-, 16:0/18:1-, and 18:0/18:1-glycerol NEU derivatives and on the basis of test samples (NEU derivatives of liver DAG) analyzed using different CapEx levels. The  $[M - NEU]^+$  ions were extracted from the total ion current spectra by the computer. A mass spectrum of the NEU derivative of *sn*-1,2-dipalmitoylglycerol, derived from tripalmitoylglycerol by Grignard degradation, is shown in Figure 2. Both ammonia and sodium adducts ( $m/z$  784 and 789, respectively) are seen as well as a DAG-like ion ( $m/z$  552) along with a NEU derivative of monopalmitoylglycerol ( $m/z$  511), which can be depicted as  $[(M - RCOO) + H]^+$ .

**Application to natural TAG.** Figure 3A shows the total positive ion current profile recorded by HPLC/ESI-MS for the diastereomeric NEU (*R*-form) of the DAG derived from plasma VLDL TAG, along with the single ion mass chromatograms recorded for the selected *sn*-2,3- and *sn*-1,2-DAG species. Since the ions are plotted on an abridged time scale (70 to 115 min), the base widths of the peaks appear wider than those recorded for the same sample (30 to 115 min) by



**FIG. 2.** Mass spectra of naphthylethylurethane (NEU) derivative of *sn*-1,2-dipalmitoylglycerol prepared from tripalmitoylglycerol and separated by HPLC as described in text.



**FIG. 3.** HPLC/electrospray ionization (ESI)-MS analysis of *sn*-2,3-DAG (70–96 min) and *sn*-1,2-DAG (96–115 min, with some exceptions; see text) of rat plasma VLDL TAG. (A) Total positive ion chromatogram (ion sum from  $m/z$  500 to 720). (B) and (C), single ion mass chromatograms of some selected molecular species indicated by protonated nominal mass and carbon number/number of double bonds. HPLC/ESI-MS conditions were as described in text.

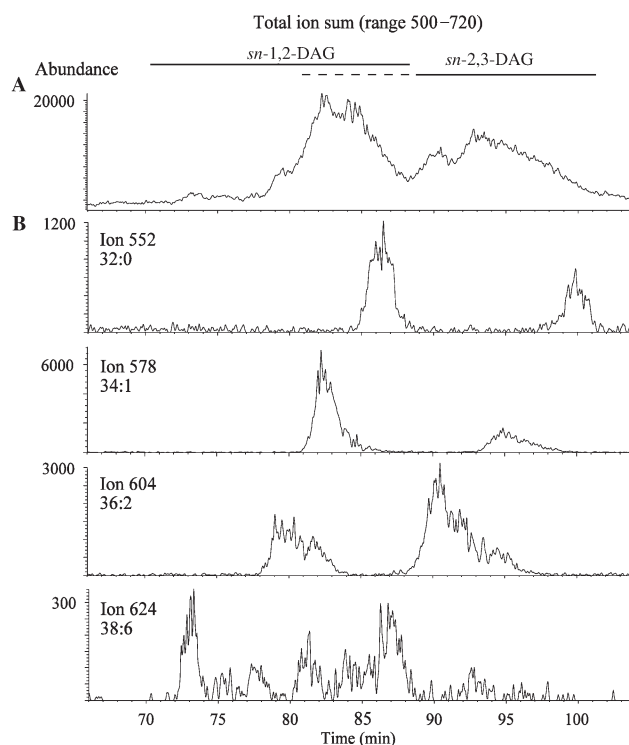
the UV detector (Fig. 1). True widening of the base widths of the peaks resulted from the postcolumn addition of the polar ionization solvent. However, almost baseline separation between the diastereomers was obtained. All molecular species of acyl carbons of 36 or less were completely resolved (Fig. 3B), whereas those with higher numbers of acyl carbons showed very minor overlaps (Fig. 3C). This was largely due to the shorter retention time of the higher molecular species and not to a lack of resolution of isobaric diastereomers. Although the oligoenoic (having few sites of unsaturation) species with the longest carbon chains were always eluted first

within each diastereomer, the number of double bonds affected the elution order in a rather irregular manner, which could nevertheless be sorted out by MS. Although the presence of monoenoic FA in 34 and 36 acyl carbon species decreased the retention time relative to the saturated species of the same carbon number, the presence of FA with two or more double bonds resulted in a delayed elution of the species. The HPLC separation of the diastereomeric NEU derivatives of DAG containing 20 and 22 acyl carbon PUFA was much more complicated than that observed for the other species. Thus, part of the *sn*-1,2-DAG species containing 22:4, 22:5, and 22:6 FA were eluted with the tail end of the *sn*-2,3-DAG species. Specifically, the *sn*-1,2-DAG species 38:5, 38:6, and 38:7, made up of combinations of 16- and 22-carbon FA, overlapped with the *sn*-2,3-DAG containing combinations of 18- and 20-carbon FA. These mixtures of species were eluted between 87 and 95 min and were represented by ions 624, 626, and 628. In addition, the *sn*-2,3-DAG species eluted between 75 and 87 min contained other major polyunsaturated species with *m/z* 626 (e.g., 16:0/22:5), 624 (e.g., 16:1/22:5; 16:0/22:6), 650 (e.g., 18:1/22:6; 18:2/22:5), and 648 (e.g., 18:2/22:6; 18:3/22:5). The elution order of species with 16 and 22 or 18 and 20 acyl carbon FA was determined on the basis of the fragment ion distribution  $\{[(M - RCOO) + H]^+$  and  $[RCO + 74]^+$  ions having 20:4, 22:5, or 22:6 as a single FA}. To obtain an accurate estimate of the quantities of the individual species emerging between 87 and 95 min, it was necessary to perform the analysis using the *S*-form of the NEU derivatives (Fig. 4), which reversed the order of elution of the diastereomers without changing the order of elution of the molecular species within the *sn*-1,2- and *sn*-2,3-species. As a result, the *sn*-1,2-DAG species, such as 16:0/22:6, was now eluted first without any overlapping with the oligoenoic species of the other diastereomer. In general, the separation of the *S*-form derivatives was not as good as that obtained for the *R*-form because the *sn*-2,3-DAG moieties of VLDL TAG contained much more of the long-chain polyunsaturated species, which as the *S*-derivatives eluted with the tail end of the *sn*-1,2-DAG.

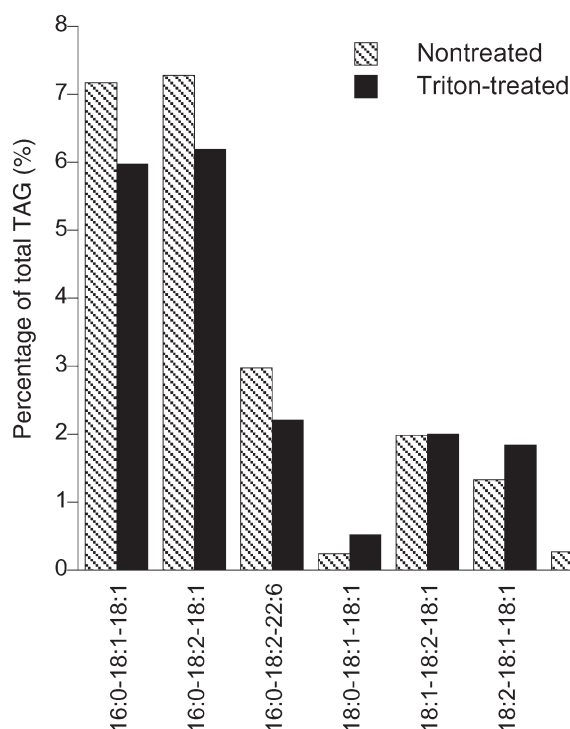
Table 1 gives the composition of the *sn*-1,2- and *sn*-2,3-DAG moieties of the TAG of normal rat plasma VLDL and liver, whereas Table 2 gives the stereospecific distribution of the FA calculated for VLDL TAG from the *sn*-1,2- and *sn*-2,3-DAG given in Table 1. The stereospecific distribution of the FA was calculated according to Brockerhoff (12). The overall accuracy of the stereospecific analysis is indicated by the good reconstitution of the FA composition of the original TAG. Figure 5 shows the quantitative distribution of the molecular species of VLDL TAG from the Triton-treated and control rats. There is a significant change in the TAG composition of the plasma VLDL because of the inhibition of the serum lipases by the detergent, which resulted in a preservation of the FA composition in the *sn*-1-position of the TAG secreted by the liver.

## DISCUSSION

The present study demonstrates the advantages of combining MS with normal-phase HPLC resolution of diastereomeric



**FIG. 4.** Total positive ion chromatogram (A) and single ion chromatograms (B) of some selected molecular species of *sn*-1,2- and *sn*-2,3-DAG prepared from rat plasma VLDL TAG and separated as their (*S*-form NEU derivatives. HPLC/ESI-MS conditions were as described in text. For abbreviations see Figures 2 and 3.



**FIG. 5.** Content of some selected calculated TAG species in circulating (nontreated) and newly secreted (Triton-treated) VLDL. The FA in the *sn*-1 position is on the left in the abbreviated notation of molecular species.

**TABLE 1**  
**The Proportions of *sn*-1,2- and *sn*-2,3-DAG from Rat Plasma VLDL and Liver TAG<sup>a</sup>**

C/DB	DAG species	<i>sn</i> -1,2-DAG		<i>sn</i> -2,3-DAG	
		VLDL	Liver	VLDL	Liver
30:0	14:0-16:0	0.4 ± 0.0	0.4 ± 0.0	0.3 ± 0.0	0.1 ± 0.0
30:1	14:0-16:1	0.4 ± 0.0	0.3 ± 0.0	0.2 ± 0.0	0.1 ± 0.0
32:0	16:0-16:0	4.4 ± 0.2	8.5 ± 0.3	1.7 ± 0.2	2.3 ± 0.2
32:1	16:0-16:1	3.6 ± 0.0	5.2 ± 0.1	2.0 ± 0.1	1.8 ± 0.2
32:2	16:1-16:1	1.4 ± 0.1	0.9 ± 0.0	0.8 ± 0.0	0.5 ± 0.1
33:0	16:0-17:0 + 15:0-18:0	0.5 ± 0.0	1.0 ± 0.0	0.3 ± 0.0	0.3 ± 0.0
33:1	16:1-17:0 + 15:0-18:1	1.0 ± 0.1	1.1 ± 0.0	0.6 ± 0.0	0.4 ± 0.0
34:0	16:0-18:0	1.6 ± 0.3	3.5 ± 0.1	1.2 ± 0.1	1.9 ± 0.0
34:1	16:0-18:1 + 16:1-18:0	21.9 ± 0.8	22.4 ± 0.1	6.1 ± 0.3	10.3 ± 0.7
34:2	16:0-18:2 + 16:1-18:1	22.5 ± 0.2	17.9 ± 0.7	7.8 ± 0.1	9.0 ± 0.2
34:3	16:1-18:2 + 16:0-18:3	6.3 ± 0.4	4.3 ± 0.3	3.4 ± 0.1	2.9 ± 0.1
34:4	16:1-18:3 + 14:0-20:4	0.4 ± 0.0	0.1 ± 0.0	0.3 ± 0.0	0.1 ± 0.0
35:1	17:0-18:1 + 15:0-20:1	1.0 ± 0.1	1.1 ± 0.1	0.5 ± 0.1	0.6 ± 0.1
35:2	17:0-18:2 + 15:0-20:2	1.2 ± 0.0	1.0 ± 0.1	0.9 ± 0.0	0.9 ± 0.1
35:3	17:0-18:3 + 15:0-20:3	0.6 ± 0.0	0.3 ± 0.0	0.6 ± 0.0	0.3 ± 0.0
36:0	18:0-18:0	0.4 ± 0.0	0.5 ± 0.0	0.5 ± 0.0	0.4 ± 0.0
36:1	18:0-18:1	2.1 ± 0.0	3.5 ± 0.0	1.7 ± 0.2	4.2 ± 0.2
36:2	18:1-18:1 + 18:0-18:2	6.8 ± 0.4	9.3 ± 0.2	14.2 ± 0.5	16.5 ± 0.3
36:3	18:1-18:2	7.7 ± 0.2	8.2 ± 0.2	17.2 ± 0.4	17.2 ± 0.7
36:4	18:2-18:2 + 18:1-18:3	2.2 ± 0.1	2.4 ± 0.0	3.7 ± 0.2	3.9 ± 0.2
36:4	16:0-20:4	1.1 ± 0.0	0.7 ± 0.0	4.0 ± 0.1	3.1 ± 0.4
36:5	16:0-20:5	0.7 ± 0.1	0.2 ± 0.0	1.7 ± 0.1	1.2 ± 0.1
38:2	18:0-20:2 + 18:1-20:1	0.8 ± 0.1	0.6 ± 0.0	1.4 ± 0.1	1.2 ± 0.1
38:3	18:0-20:3 + 18:1-20:2 + 18:2-20:3	1.4 ± 0.2	1.0 ± 0.1	2.3 ± 0.2	1.9 ± 0.1
38:4	16:0-22:4	0.6 ± 0.0	0.5 ± 0.0	1.0 ± 0.0	0.9 ± 0.0
38:4	18:0-20:4 + 18:1-20:3 + 18:2-20:2	1.0 ± 0.0	0.9 ± 0.0	2.0 ± 0.0	1.6 ± 0.0
38:5	16:0-22:5 + 16:1-22:4	0.9 ± 0.0	0.7 ± 0.0	2.1 ± 0.0	2.0 ± 0.1
38:5	18:0-20:5 + 18:1-20:4 + 18:2-20:3	0.9 ± 0.0	0.8 ± 0.0	1.1 ± 0.1	0.9 ± 0.0
38:6	16:0-22:6 + 16:1-22:5	0.9 ± 0.0	0.8 ± 0.0	2.0 ± 0.0	1.5 ± 0.0
38:6	18:1-20:5 + 18:2-20:4	0.4 ± 0.0	0.3 ± 0.0	0.8 ± 0.1	0.3 ± 0.0
38:7	16:1-22:6	0.7 ± 0.1	0.2 ± 0.0	0.8 ± 0.1	0.4 ± 0.1
40:4	18:0-22:4	0.2 ± 0.0	0.1 ± 0.0	0.4 ± 0.0	0.3 ± 0.0
40:5	18:0-22:5 + 18:1-22:4	0.4 ± 0.0	0.2 ± 0.0	1.4 ± 0.1	1.5 ± 0.0
40:6	18:0-22:6 + 18:1-22:5	0.9 ± 0.1	0.5 ± 0.0	3.8 ± 0.1	3.4 ± 0.1
40:7	18:1-22:6 + 18:2-22:5	1.5 ± 0.1	0.4 ± 0.0	6.6 ± 0.2	4.1 ± 0.2
40:8	18:2-22:6 + 18:3-22:5	1.1 ± 0.0	0.2 ± 0.0	3.6 ± 0.2	1.8 ± 0.2
40:9	18:3-22:6	0.3 ± 0.0	0.0 ± 0.0	0.8 ± 0.0	0.2 ± 0.2
42:11	20:5-22:6	ND	ND	0.3 ± 0.0	ND

<sup>a</sup>Results are expressed as average ± range/2 from two rats. The variations of ranges are less than 6% for major components (>2% of total mixture) and less than 17% for minor components. C, carbon number; DB, number of double bonds.

DAG for stereospecific analysis of natural TAG. To minimize co-elution of diastereomeric groups, it is necessary to utilize both (*R*)-(–)- and (*S*)-(+)–NEU derivatives, although ESI–MS with appropriate fragmentation can provide sufficient information to assign identities to unresolved species of DAG. The NEU derivatives of DAG yield characteristic  $[M - \text{NEU}]^+$ ,  $[(M - \text{RCOO}) + \text{H}]^+$ , and  $[\text{RCO} + 74]^+$  ions for each DAG species from which the molecular weight and exact pairing of FA can be unequivocally obtained. The characteristic ions appear to be generated in nearly correct mass proportions, as indicated by the quantitative comparisons of the reconstitution data.

The normal-phase HPLC described by Christie and co-workers (3) provides a rapid and complete resolution of the diastereomeric NEU derivatives of *sn*-1,2- and *sn*-2,3-DAG with identical FA, but separation of diastereomers containing different FA results in overlap or interdigitation of many molecular species, and identification of individual diastereomers becomes difficult or impossible. Furthermore, the solvent sys-

tems thus far employed for the normal phase HPLC of diastereomeric DAG fail to provide a complete separation of molecular species within either diastereomer class. In fact, previous work by Christie and co-workers (3) has led to the conclusion that no sensible pattern is discernible for the NEU derivatives containing 20- and 22-carbon PUFA species of fish oil TAG. In the present study, part of the *sn*-1,2-DAG species containing 22:4, 22:5, and 22:6 FA were eluted with the tail end of the *sn*-2,3-DAG derivatives. Specifically, the *sn*-1,2-DAG species 38:5, 38:6, and 38:7, made up of combinations of 16- and 22-carbon acids, overlapped with the *sn*-2,3-DAG containing combinations of 18- and 20-carbon FA, when run as the *R*-derivative. In order to obtain an accurate estimate of the quantities of the individual species, it was necessary to complete another HPLC analysis using the *S*-form of the NEU derivatives, which were eluted in the reverse order. As a result, the *sn*-1,2-DAG species, such as 16:0/22:6, were eluted first without any overlap.

**TABLE 2**  
**FA Composition of Rat Plasma VLDL TAG, and of *sn*-1,2- and *sn*-2,3-DAG Prepared from TAG, and Positional Distribution of FA in TAG (mean of two experiments)**

FA	TAG	<i>sn</i> -1,2-DAG	<i>sn</i> -2,3-DAG	<i>sn</i> -1	<i>sn</i> -2	<i>sn</i> -3
14:0	0.9	1.0	0.7	1.5	0.4	1.0
15:0	0.6	0.6	0.5	0.8	0.5	0.5
16:0	27.7	37.2	12.8	57.6	16.8	8.8
17:0	0.4	0.5	0.4	0.4	0.7	0.1
18:0	2.4	2.8	2.6	1.9	3.6	1.5
16:1n-9	0.5	0.6	0.5	0.6	0.6	0.4
16:1n-7	2.4	1.6	2.3	2.6	0.5	4.0
18:1n-9	25.4	22.9	32.2	11.9	34.0	30.4
18:1n-7	3.3	2.1	3.1	3.8	0.3	5.9
20:1n-9 + 11	0.4	0.5	0.7	-0.2	1.1	0.2
18:2n-6	21.4	22.7	26.7	10.7	34.8	18.6
18:3n-3	1.0	1.3	1.2	0.6	2.1	0.4
20:2n-6	0.4	0.3	0.6	0.0	0.6	0.6
20:3n-6	0.6	0.3	0.7	0.5	0.2	1.1
20:4n-6	1.6	1.1	2.3	0.2	2.0	2.5
20:5n-3	1.8	0.8	2.0	1.3	0.3	3.8
22:4n-6	0.4	0.3	0.7	-0.2	0.9	0.6
22:5n-3	2.2	0.9	2.4	1.7	0.2	4.7
22:6n-3	6.6	2.5	7.6	4.5	0.4	14.8

An examination of the order of elution of the molecular species within each diastereomer group revealed that the species were actually eluted in an orderly fashion within each homologous series represented. The impression of a lack of discernible order had arisen from the complex mixture of homologous series represented in each diastereomer group. For any specific homologous series, the molecular species were resolved in a reproducible order arising from both polar and nonpolar interactions with the solid phase of the column, although the overall range of elution times was rather limited. Furthermore, the order of elution of the members of the various homologous series was the same for both diastereomer groups obtained with the same reagent.

The fully saturated species were resolved in the following order of increasing retention times: 18:0/18:0 < 16:0/18:0 < 16:0/17:0 < 16:0/16:0 < 14:0/16:0. Thus, the longer-chain saturates, being less polar, are eluted earlier than the shorter-chain saturates. Similarly, the monoenoic species were resolved in the following order of increasing retention times: 18:0/18:1 < 17:0/18:1 < 16:0/18:1 < 16:0/16:1. The dienoic species were eluted in the following order of increasing retention times: 18:0/20:2 < 18:0-18:2 < 16:0/18:2. The 16:0/18:2 species was retained slightly longer than the 16:0/18:1 species, indicating a somewhat higher polarity. Likewise, the 18:1/18:2 and 18:2/18:2 species were retained longer than the 18:1/18:1 species, which was also eluted slightly faster than 18:0/18:0. This is in accordance with results obtained with standard lipids (3). Within 36:4 species, 18:2/18:2 eluted before 16:0/20:4, and within species with a combination of 18 and 20 acyl carbon FA, species with 20:1, 20:2, and 20:3 eluted slightly earlier than species with 20:4 and 20:5, indicating increased polarity of species with 20:4 and 20:5.

Polyunsaturated species containing 22:4, 22:5, and 22:6

eluted before oligoenoic species, and they often produced more than one peak. For example, *sn*-2,3-DAG species with *m/z* 648 (40:8) were divided into two peaks with about equal size (Fig. 3C). This could have indicated a separation between the 18:2/22:6 and 18:3/22:5 species or a resolution of the reverse isomers (*sn*-2-18:2/*sn*-3-22:6 and *sn*-2-22:6/*sn*-3-18:2). A reverse isomer resolution for the DNPU derivatives of *sn*-1,2-DAG containing combinations of medium- and long-chain FA has recently been reported by Itabashi *et al.* (13) using RP-HPLC or silver ion HPLC. The small number of fragment ions of minor DAG species and the overlapping of different species giving the same fragment ions, however, made it impossible to definitely identify all such species in the present study.

Knowing the exact identity and quantity of all significant species of both *sn*-1,2- and *sn*-2,3-DAG greatly increases the accuracy of calculating the stereospecific distribution of the FA, although minor discrepancies may remain owing to limited isomerization of the DAG during Grignard degradation and subsequent sample workup. Nevertheless, it was possible to demonstrate significant differences in the composition of the molecular species of VLDL TAG between Triton-treated and control rats. The differences could be rationalized on the basis of the known FA and stereospecificity of plasma lipoprotein and hepatic lipases and on the inhibitory effects of the detergent, as reviewed elsewhere (Ågren, J.J., Ravandi, A., Kuksis, A., and Steiner, G., unpublished data). The normal-phase HPLC/ESI-MS method should be applicable to stereospecific analyses of TAG from other sources, including bovine milk fat and fish oils, which contain a wider range of FA than those found in plasma VLDL. Both of these fats have already been successfully analyzed following chiral-phase separation of the enantiomeric *sn*-1,2- and *sn*-2,3-DAG (6,14). A stereospecific analysis of TAG *via* the NEU derivatives of DAG derived from Grignard degradation provides an economic alternative to chiral-phase HPLC of the DNPU.

## ACKNOWLEDGMENT

This research was supported by funds from the Finnish Cultural Foundation.

## REFERENCES

1. Michelson, P., Aronsson, E., Odham, G., and Akesson, B. (1985) Diastereomeric Separations of Natural Glycero Derivatives as Their 1-(Naphthyl)ethyl Carbamates by High-Performance Liquid Chromatography, *J. Chromatogr.* 350, 417-426.
2. Laakso, P., and Christie, W.W. (1990) Chromatographic Resolution of Chiral Diacylglycerol Derivatives: Potential in the Stereospecific Analysis of Triacyl-*sn*-glycerols, *Lipids* 25, 349-353.
3. Christie, W.W., Nikolova-Damyanova, B., Laakso, P., and Herslof, B. (1991) Stereospecific Analysis of Triacyl-*sn*-glycerols *via* Resolution of Diastereomeric Diacylglycerol Derivatives by High-Performance Liquid Chromatography on Silica, *J. Am. Oil Chem. Soc.* 68, 695-701.
4. Damiani, P., Santinelli, F., Simonetti, M.S., Castellini, M., and Rosi, M. (1994) Comparison Between Two Procedures for



- Stereospecific Analysis of Triacylglycerols from Vegetable Oils—I: Olive Oil, *J. Am. Oil Chem. Soc.* 71, 1157–1162.
5. Takagi, T., and Itabashi, Y. (1987) Rapid Separations of Diacyl- and Dialkylglycerol Enantiomers by High-Performance Liquid Chromatography on a Chiral Stationary Phase, *Lipids* 22, 596–600.
  6. Itabashi, Y., Kuksis, A., Marai, L., and Takagi, T. (1990) HPLC Resolution of Diacylglycerol Moieties of Natural Triacylglycerols on a Chiral Phase Consisting of Bonded (*R*)-(+)-1-(1-Naphthyl)ethylamine, *J. Lipid Res.* 31, 1711–1717.
  7. Takagi, T., and Ando, Y. (1991) Stereospecific Analysis of Triacyl-*sn*-glycerols by Chiral High-Performance Liquid Chromatography, *Lipids* 26, 542–547.
  8. Taylor, D.C., MacKenzie, S.L., McCurdy, A.R., McVetty, P.B.E., Giblin, E.M., Pass, E.W., Stone, S.J., Scarth, R., Rimmer, S.R., and Pickard, M.D. (1994) Stereospecific Analysis of Seed Triacylglycerols from High Erucic Acid Brassicaceae: Detection of Erucic Acid at the *sn*-2 Position in *Brassica oleracea* L. Genotypes, *J. Am. Oil Chem. Soc.* 71, 163–167.
  9. Folch, J., Lees, M., and Sloane Stanley, G.H. (1957) A Simple Method for the Isolation and Purification of Total Lipides from Animal Tissues, *J. Biol. Chem.* 226, 497–509.
  10. Yang, L.Y., and Kuksis, A. (1991) Apparent Convergence (at 2-monoacylglycerol level) of Phosphatidic Acid and 2-Monoacylglycerol Pathways of Synthesis of Chylomicron Triacylglycerols, *J. Lipid Res.* 32, 1173–1186.
  11. Yang, L.Y., Kuksis, A., Myher, J.J., and Steiner, G. (1995) Origin of Triacylglycerol Moiety of Plasma Very Low Density Lipoproteins in the Rat: Structural Studies, *J. Lipid Res.* 36, 125–136.
  12. Brockerhoff, H. (1971) Stereospecific Analysis of Triglycerides, *Lipids* 6, 942–956.
  13. Itabashi, Y., Myher, J.J., and Kuksis, A. (2000) High-Performance Liquid Chromatographic Resolution of Reverse Isomers of 1,2-Diacyl-*rac*-glycerols as 3,5-Dinitrophenylurethanes, *J. Chromatogr. A* 893, 261–279.
  14. Itabashi, Y., Myher, J.J., and Kuksis, A. (1993) Determination of Positional Distribution of Short-Chain Fatty Acids in Bovine Milk Fat on Chiral Columns, *J. Am. Oil Chem. Soc.* 71, 1177–1181.

[Received February 4, 2002; in revised form and accepted May 24, 2002]

# Method for Analysis of 4-Hydroxy-2-(*E*)-nonenal with Solid-Phase Microextraction

Tatsuhiko Uchida, Naohiro Gotoh, and Shun Wada\*

Department of Food Science and Technology, Tokyo University of Fisheries, Tokyo 108-8477, Japan

**ABSTRACT:** A simple analytical method for 4-hydroxy-2-(*E*)-nonenal (HNE) using solid-phase microextraction (SPME) fiber was developed. HNE or the derivative of HNE formed by reaction with 2,4-dinitrophenylhydrazine (DNPH) was extracted from the sample solution by immersing the SPME fiber into the solution, and the amount of HNE was quantified by HPLC. The extraction conditions of HNE and HNE-DNPH were examined, using standard solutions, with respect to fiber coating, NaCl concentration, rate of stirring, adsorption temperature, and adsorption time. The recovery of HNE reached 80%, and the quantification limits of HNE and HNE-DNPH using standard compounds were 14.1 pmol/10 mL and 486.5 fmol/10 mL, respectively. This method can be applied to the detection of HNE in oxidized oil or samples of porcine liver.

Paper no. L8956 in *Lipids* 37, 621–626 (June 2002).

4-Hydroxy-2-(*E*)-nonenal (HNE) is one of the secondary oxidation products formed from n-6 PUFA and is found in many biological systems (1). HNE is cytotoxic, genotoxic, and mutagenic, and these properties are related to human diseases such as Alzheimer's (2), atherosclerosis (3), and Parkinson's (4). Thus, HNE is now regarded as a stress marker in biological systems (5).

A number of methods have been developed to detect and quantify HNE in lipids, cells, or tissues. Originally, HNE was analyzed by using an HPLC-spectrophotometric detector (SP) system with monitoring at 223 nm (6). However, HNE is not stable, and many compounds absorb near 220 nm; therefore, derivatives of HNE have also been used to detect and quantify HNE. Derivatization of HNE with 2,4-dinitrophenylhydrazine (DNPH) is the most common method, with measurement by an HPLC-SP system at 370 nm (6,7). HNE and HNE-DNPH also have been measured by an HPLC-electrochemical detector (ECD) system (8). Other derivatives have been also utilized. Derivatization of HNE with 1,3-cyclohexanedione (CHD) was detected with an HPLC-fluorescence detector (FL) system (9). A pentafluorobenzyl hydroxylamine hydrochloride derivative was determined by an HPLC-MS

system (10). Other chromatographic methods, such as GC (11–13), TLC (14), and micellar electrokinetic chromatography (15), also have been used for the analysis of HNE or derivatives of it. In measuring HNE levels in tissue, ELISA has been utilized (16). ELISA detects conjugation products of HNE with protein by use of monoclonal antibodies. However, the experimental procedures that these methods require are complex, and sample preparation requires several steps before analysis can begin.

Solid-phase microextraction (SPME) is a technique to concentrate volatile or nonvolatile components from a liquid, solid, or gas for GC or HPLC analysis. The SPME fiber is exposed in the sample to adsorb the component of interest and injected directly into the GC or HPLC (17). The SPME fiber is exposed in the sample to adsorb the components of interest. It is then injected directly into the GC or HPLC (17). That is, for GC the SPME fiber is directly injected into the injection port, where it is then exposed to the flowing gas; the exposure time depends on the sample species. For HPLC, the fiber is injected into the HPLC, which acts as a desorption chamber, and also is exposed to the solvent under the injection mode.

The SPME method can concentrate analytes without the use of any solvent and does not require any complicated apparatus. Furthermore, the SPME-GC or SPME-HPLC method can quantify the component at a level of parts per trillion. The SPME method has been used recently to extract kerosene from soil (18), flavor substances from air, organic compounds from water (18), alcohol from blood (19), and to analyze food (20). Since there has been no study of the HNE analysis by the SPME method, the aim of this study was to develop a facile and rapid method for the detection and quantification of HNE in oil and biological samples by the SPME method.

## EXPERIMENTAL PROCEDURES

**Chemicals and materials.** HNE was purchased from Calbiochem (Los Angeles, CA). DNPH was obtained from Aldrich Chemical Company, Inc. (Milwaukee, WI). All other chemicals and solvents were of reagent grade and were from common commercial sources. Direct immersion-SPME fused-silica fiber coated with polydimethylsiloxane (PDMS) (thickness of coating: 100  $\mu$ m), polyacrylate (85  $\mu$ m), polydimethylsiloxane/divinylbenzene (PDMS/DVB) (60  $\mu$ m), and carbowax/templated resin (50  $\mu$ m) were purchased from

\*To whom correspondence should be addressed at Department of Food Science and Technology, Tokyo University of Fisheries, 4-5-7 Konan, Minato-ku, Tokyo 108-8477, Japan. E-mail: wada@tokyo-u-fish.ac.jp

Abbreviations: CW/TPR, carbowax/templated resin; CHD, 1,3-cyclohexanedione; DNPH, 2,4-dinitrophenylhydrazine; ECD, electrochemical detector; FL, fluorescence detector; HNE, 4-hydroxy-2-(*E*)-nonenal; PDMS, polydimethylsiloxane; PDMS/DVB, polydimethylsiloxane/divinylbenzene; SP, spectrophotometric detector; SPME, solid-phase microextraction.

Supelco (Bellefonte, PA). The polarities of the fibers increase in this order.

**DNPB derivatization.** Standard HNE-DNPB derivative was prepared by the reaction of HNE and DNPB (8). An HNE–water solution was mixed with an equal volume of DNPB solution (3.5 mg of DNPB dissolved in 10 mL of 1 M HCl) and stored in the dark at room temperature for 2 h. HNE-DNPB was extracted twice from the mixture with  $\text{CH}_2\text{Cl}_2$  and concentrated under nitrogen. HNE-DNPB was separated from the reaction mixture by TLC using  $\text{CH}_2\text{Cl}_2$  as developing solvent (14). The HNE-DNPB band was scraped off and extracted with methanol. The extract was filtered, dried under a nitrogen stream, and re-dissolved in methanol. The concentration of HNE-DNPB was measured by spectrophotometer at 370 nm and calculated by using the molar absorptivity  $\epsilon_{370\text{ nm}} = 28,000\text{ M}^{-1}\text{cm}^{-1}$ .

**HPLC analysis.** HNE and HNE-DNPB were detected and quantified by an RP-HPLC system comprising a pump (Type LC-6A, Shimadzu Co., Kyoto, Japan), spectrophotometric detector (Type SPD-10A, Shimadzu Co.), injector (SPME/HPLC interface, rheodyne valve version; Supelco, Bellefonte, PA), ODS column (4.6 × 250 mm; Kakoki Shouji Co., Tokyo, Japan), and Chromatopac integrator (Type C-R6A, Shimadzu Co). HNE was detected at 223 nm using acetonitrile/water (40:60, vol/vol) as mobile phase. HNE-DNPB was detected at 370 nm using 50 mM pH 4.6 acetate buffer/methanol (1:3, vol/vol) as elution solvent. Flow rates for both conditions were 1.0 mL/min. The fiber used was washed in the desorption chamber, SPME/HPLC interface rheodyne valve version, under the injection mode for 30 min.

**Evaluation of fibers.** Ten milliliters of standard HNE dissolved in distilled water was prepared in the range of 0.1–8 nmol/10 mL. The HNE concentration was calculated by using a molar absorptivity  $\epsilon_{223\text{ nm}} = 13,750\text{ M}^{-1}\text{cm}^{-1}$ . SPME fiber was introduced into the standard solution at 40°C for 10 min without agitation. Desorption of HNE or HNE-DNPB from fiber was conducted in the desorption chamber, SPME/HPLC interface rheodyne valve version, under static mode for 20 min. A calibration curve of HNE with each fiber was made, and the best fiber for analysis was determined by the slope of the calibration curve. Evaluation of fibers for HNE-DNPB analysis was conducted in the same manner at pH 7.0.

**Improvement of adsorbing condition.** The effects of temperature (30–60°C), rate of stirring (0–200 rpm), ionic strength (0–20% NaCl), and time on adsorption of HNE on fiber were investigated. The effect of adsorption time was evaluated under the optimal conditions of temperature, rate of stirring, and NaCl concentration.

**Recovery of HNE.** HNE extraction from soybean oil samples (100 mg) was investigated using the procedure of Lang *et al.* (21). An HNE-methanol solution (2.91 nmol and 0.29 nmol) was added to the oil sample in 1% volume. Methanol was removed from the oil sample under a nitrogen stream, and the sample was then extracted twice with 2 mL of distilled water containing 0.1% BHT. The two extracts were combined and centrifuged at 3,000 × *g* for 10 min. The water phase was transferred to a vial and made up to 10 mL with

NaCl solution. SPME fiber was introduced into the vial. HNE was adsorbed under the improved conditions determined in the previous paragraph and the recovery of HNE was analyzed with HPLC. In HNE-DNPB analysis, the extracts from oil samples were combined and immediately reacted with an equal volume of DNPB reagent (3.5 mg of DNPB dissolved in 10 mL of 1 M HCl). The mixture was stored in the dark at room temperature for 2 h. After the reaction, the pH of the reaction mixture was adjusted to 7.0 with 1 N NaOH and made to 10 mL with NaCl solution. HNE-DNPB was measured by the same procedure used in HNE analysis.

Porcine liver sample (1 g) was cut into small pieces, and HNE–methanol solution (2.91 nmol and 0.29 nmol) was added to it. The sample was homogenized with 2 mL of methanol containing 0.1% BHT for 2 min. The homogenate was centrifuged at 3000 × *g* for 10 min, and the supernatant was collected. The residue was re-extracted by the same procedure, and the supernatant was collected. The supernatants were combined and made to 10 mL with NaCl solution. The recovery of HNE was measured by the same method used for the oil sample. In HNE-DNPB analysis, the extract was reacted with an equal volume of DNPB solution (the same solution used in the oil sample) and stored in the dark at room temperature for 2 h. HNE-DNPB was measured by the same method carried out in the oil sample.

The recovery rate for HNE, or  $([\text{HNE found}]/[\text{HNE added}]) \times 100$ , is calculated by Equation 1 as

$$[\text{HNE found}] = [\text{HNE}]_{\text{measured}} - [\text{HNE}]_{\text{originally contained}} \quad [1]$$

where [HNE] added is the concentration of HNE added in soybean oil or porcine liver.

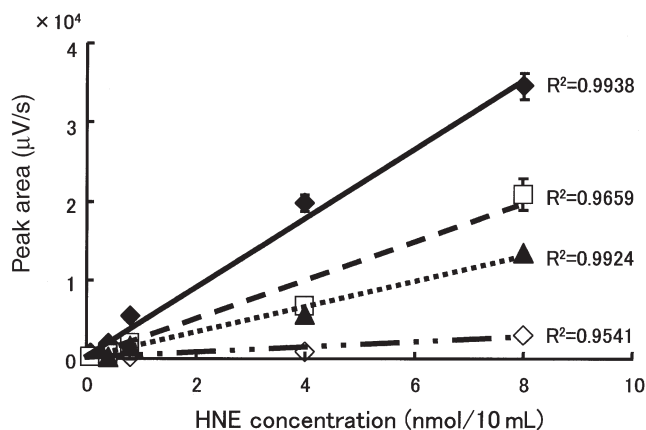
**Detection of HNE in oxidized oil and oxidized porcine liver sample.** Soybean oil was oxidized at 45°C in the dark for 24 h, and porcine liver (1 g) homogenate was oxidized with 1 μmol  $\text{Fe}_2\text{SO}_4$  at 40°C in the dark for 4 h. The HNE contents of these oxidized samples were analyzed by using the SPME-HPLC method.

**Statistical analysis.** Each analysis was conducted at least five times. ANOVA procedures were performed. The differences were determined by Fisher's least significant difference tests, and the significance level was set at  $P < 0.05$ . Regressions of the calibration curves were examined with the test for regression slope, and significance levels were set at  $P < 0.05$ . Furthermore, the two regression slopes were compared and significant differences were set at  $P < 0.05$ .

## RESULTS AND DISCUSSION

All the analyses were examined by two analysts on separate days, and each experiment was conducted at least five times. Physical limits of the fibers were about 50 uses; however, the reproducibility was maintained after 50 uses (data not shown).

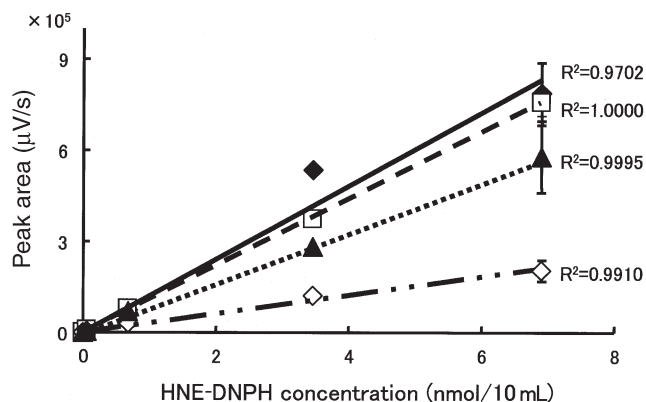
Figure 1 shows the calibration curves of HNE using four kinds of fibers. All the calibration curves were drawn by regression line. The regressions were examined by test for



**FIG. 1.** Calibration curves for standard 4-hydroxy-2-(*E*)-nonenal (HNE) by polydimethylsiloxane/divinylbenzene (PDMS/DVB) (◆), polyacrylate (□), carbowax/templated resin (CW/TPR) (▲), and PDMS (◇) fiber. Conditions were as follows: adsorption time, 10 min; adsorption temperature, 40°C; stirring, none; NaCl, none added. The error bars indicate SD of at least five experiments. The regressions were examined by test for regression slope and were significant ( $P < 0.001$ ).

regression slope and they were significant ( $P < 0.001$ ). The best linearity ( $R^2 = 0.9938$ ) and the greatest slope were associated with the PDMS/DVB fiber. On the other hand, the PDMS fiber, which is nonpolar, could not adsorb HNE compared with other fibers. PDMS/DVB fiber has been used for the analysis of polar compounds (22), aromatic amines (23), and the like. It has also been used to adsorb volatile lipid oxidation products for GC analysis (24,25). The results of the present study show that PDMS/DVB fiber is suitable for analysis of HNE with the SPME-HPLC method.

The calibration curves for HNE-DNPH using four kinds of fibers were also drawn by regression line. The regressions were examined by the test for significance of the regression and were found to be different ( $P < 0.001$ ). PDMS/DVB fiber



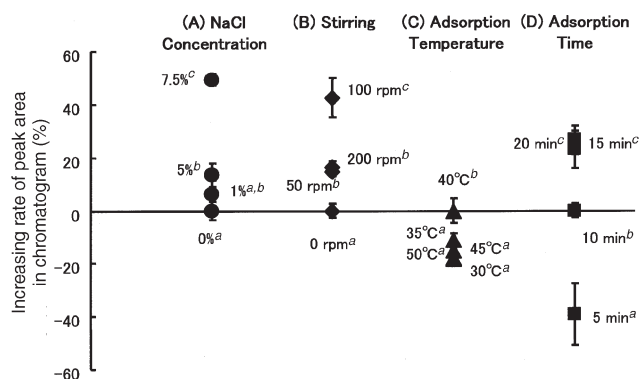
**FIG. 2.** Calibration curves of standard HNE-2,4-dinitrophenylhydrazine (DNPH) derivative by PDMS/DVB (◆), polyacrylate (□), CW/TPR (▲), and PDMS (◇) fiber. Conditions were as follows: adsorption time, 10 min; adsorption temperature, 40°C; stirring, none; NaCl, none added. The error bars indicate SD of at least five experiments. The regressions were examined by test for regression slope and were significant ( $P < 0.001$ ).

was again the most sensitive fiber for HNE-DNPH analysis (Fig. 2). However, the linearity of the calibration curve was the worst among the four fibers ( $R^2 = 0.9702$ ). Polyacrylate fiber, having almost the same polarity as PDMS/DVB fiber, was also a sensitive fiber for the detection of HNE-DNPH, and the linearity of the calibration curve was the best ( $R^2 = 1.000$ ). A comparison of the regression slopes between calibration curves of PDMS/DVB fiber and polyacrylate fiber found no significant difference. Accordingly, polyacrylate fiber was employed for HNE-DNPH analysis.

SPME is an equilibrium sampling method. Therefore, to increase the distribution constant one must increase the amount of HNE or HNE-DNPH adsorbed on the SPME fiber. The distribution constant is affected by both the polarity of the fiber (Figs. 1 and 2) and the ionic strength (17). Normally, increasing the ionic strength of the solvent can increase the distribution constant of the organic compound between solvent and fiber coating and decrease the solubility of the organic compound in water. The amount of HNE adsorbed on the fiber increased with increasing NaCl concentration and reached a plateau at 7.5% NaCl (Fig. 3A), where the amount of HNE adsorbed was 50% higher than that with no added NaCl. The solubility of HNE in water is high (6.6 mg/mL), but increasing the NaCl concentration reduces its solubility and enhances the transfer of HNE from sample solution to the fiber.

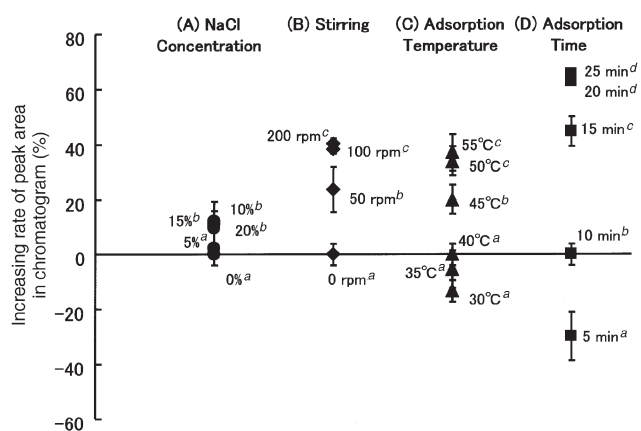
The effect of adding NaCl on the adsorption of HNE-DNPH on SPME fiber was less than that of HNE. In the HNE-DNPH experiment, the concentration of NaCl was varied from 0 to 20% (Fig. 4A). However, the increase in the amount adsorbed onto the fiber was only 10% in 20% NaCl solution compared with 0% NaCl solution. Since the solubility of HNE-DNPH in pure water is less than that of HNE, the addition of NaCl would not affect the solubility of HNE-DNPH to the same extent as HNE.

Increasing the mobility of dissolved HNE or HNE-DNPH enhances the amounts absorbed on SPME fiber. Both stirring



**FIG. 3.** Improvement of adsorbing conditions of HNE on PDMS/DVB fiber as related to NaCl concentration (A), rate of stirring (B), adsorption temperature (C), and adsorption time (D). The error bars indicate SD of at least five experiments. In each column, means with different italic letters are significantly different at  $P < 0.05$ . For abbreviations see Figure 1.





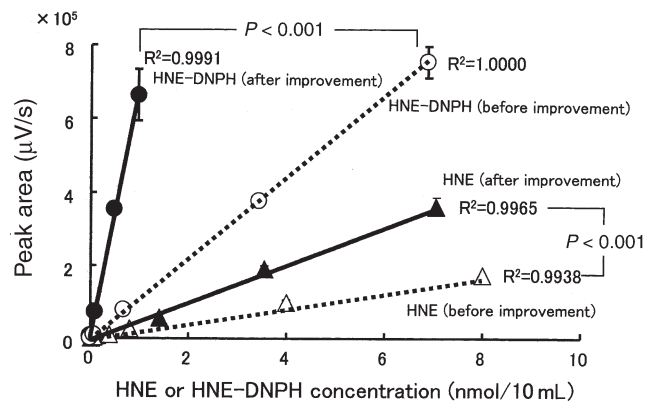
**FIG. 4.** Improvement of adsorbing conditions of HNE-DNPH on polyacrylate fiber as related to NaCl concentration (A), rate of stirring (B), adsorption temperature (C), and adsorption time (D). The error bars indicate SD of at least five experiments. In each column, means with different italic letters are significantly different at  $P < 0.05$ . For abbreviations see Figures 1 and 2.

and increased temperature impart kinetic energy to the molecules. In our experiments, the stirring rate was varied from 0 to 200 rpm; the best agitation speeds were 100 (Fig. 3B, HNE) and 200 rpm (Fig. 4B, HNE-DNPH). For HNE-DNPH, the temperature was varied from 30 to 55°C (Fig. 4C); the greatest adsorption occurred at 55°C. On the other hand, the optimal temperature in the range of 30–50°C for adsorption of HNE was 40°C (Fig. 3C). These phenomena can be ascribed to the vaporization of HNE, a semivolatile compound (b.p. 84–87°C), into the headspace above the sample after acquisition of energy. This idea is supported by the results shown in Figure 4 where the amount of HNE-DNPH adsorbed increased with higher stirring rates and temperatures. HNE-DNPH has a large M.W. compared with HNE (336 vs. 156) and therefore is only very slightly volatile. As a result, HNE-DNPH would be efficiently adsorbed on the fiber without any loss to the headspace.

The adsorption time was also considered in our attempts to maximize the amount adsorbed on the fiber. For HNE, adsorption reached a plateau at 15 min (Fig. 3D), whereas for HNE-DNPH maximal adsorption was at 20 min (Fig. 4D).

The optimal conditions for adsorption of HNE and HNE-DNPH are summarized in Table 1. Calibration curves using these conditions are shown in Figure 5. A comparison of the regression slopes was conducted between calibration curves after and before optimization for HNE or HNE-DNPH analysis, and they were significantly different ( $P < 0.001$ ).

Calibration curves of both HNE and HNE-DNPH were



**FIG. 5.** Comparison of calibration curves before and after improvement of conditions. The initial conditions were: NaCl, 0%; no stirring; temperature, 40°C; adsorption time, 10 min. The improved conditions are listed in Table 1. The error bars indicate SD of at least five experiments. The regressions were examined by test for regression slope and were significant ( $P < 0.001$ ). The comparison of the regression slopes between calibration curves for HNE and HNE-DNPH before and after improvement revealed a significant difference ( $P < 0.001$ ).

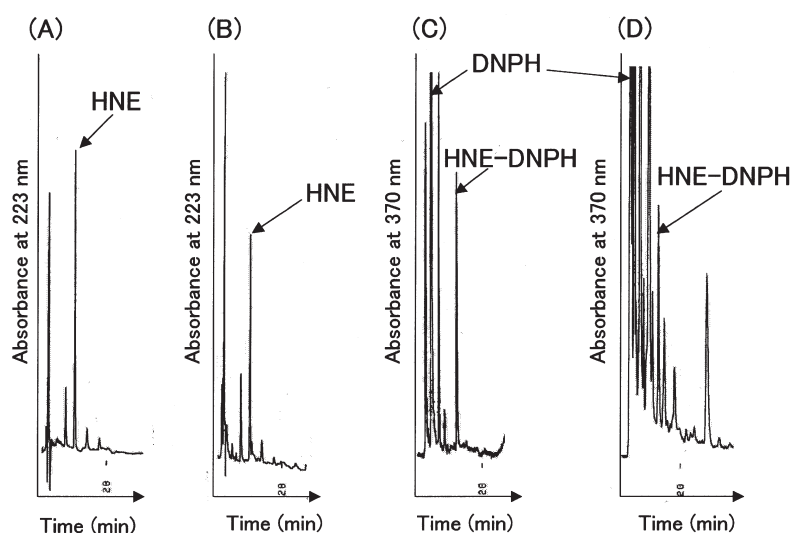
more sensitive than the original calibration curves. The quantification limit was set as a signal-to-noise ratio of 3 (8,9). The quantification limit of HNE was 14.1 pmol/10 mL and that of HNE-DNPH was 486.5 fmol/10 mL. The quantification limits of the HNE-HPLC-SP and HNE-DNPH-HPLC-SP methods, the conventional methods for HNE detection, were reported for HNE as 2 pmol/20  $\mu$ L (1000 pmol/10 mL) (6) and for HNE-DNPH as 1 pmol/20  $\mu$ L (500 pmol/10 mL) (6), respectively. Both the HNE-DNPH-HPLC-ECD (8) and HNE-CHD-HPLC-FL (9) methods are known as sensitive methods for the quantification of HNE, and the quantification limits are 15 and 50 fmol, respectively. The quantification limit of the HNE-DNPH-HPLC-ECD method was also calculated as 25 pmol/10 mL because the injection volume was 6  $\mu$ L. Similarly, the quantification limit of HNE-CHD-HPLC-FL was 25 pmol/10 mL because the injection volume was 20  $\mu$ L. These results indicate that the quantification limit of HNE with the SPME-HPLC method was better than with these other methods.

In Figure 6 the HPLC chromatogram of HNE standard sample (A) can be compared with that of an oil sample (B) mixed with HNE. The HPLC chromatogram of an HNE-DNPH standard sample (Fig. 6C) can also be compared with that of HNE-DNPH extracted from a DNPH-derived porcine liver sample containing HNE (Fig. 6D). Peak identification was based on retention time. Recovery of HNE was calculated (Table 2). Average recovery was about 80%. SPME is an equilibrium sampling method. That is, 100% recovery is

**TABLE 1**  
Improved Conditions of HNE and HNE-DNPH Analysis on Each Factor<sup>a</sup>

	Fiber	NaCl conc.	Stirring	Adsorption temp.	Adsorption time
HNE analysis	PDMS/DVB	7.5%	100 rpm	40°C	15 min
HNE-DNPH analysis	Polyacrylate	10.0%	100 rpm	50°C	20 min

<sup>a</sup>HNE, 4-hydroxy-2-(E)-nonenal; HNE-DNPH, HNE-2,4-dinitrophenylhydrazine; PDMS/DVB, polydimethylsiloxane/divinylbenzene.



**FIG. 6.** Chromatograms of (A) 3.5 nmol/10 mL HNE solution and (B) soybean oil mixed with 2.91 nmol HNE detected by HPLC-SP. Chromatograms of (C) 0.41 nmol/10 mL HNE-DNPH solution and (D) DNPH derivative of porcine liver mixed with 0.35 nmol HNE and detected by HPLC-SP. SP, spectrophotometric detector; for other abbreviations see Figures 1 and 2.

**TABLE 2**

**Recovery Rate of HNE from Soybean or Porcine Liver Mixed with Standard HNE Solution ( $n = 5$ )**

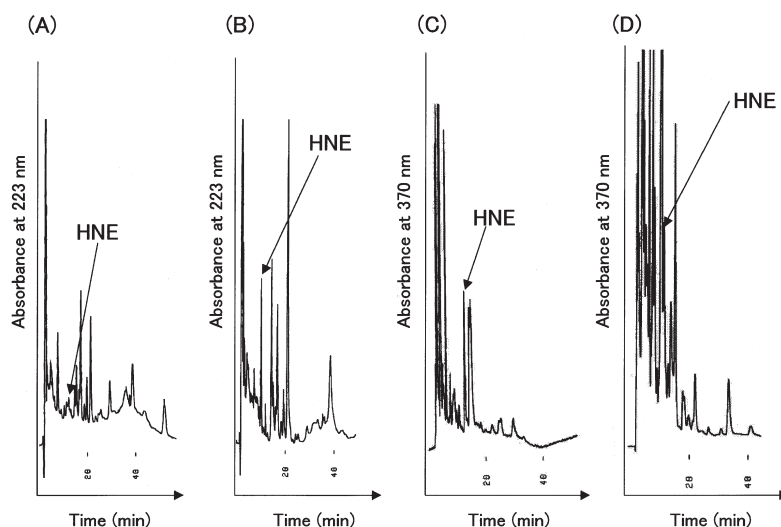
Sample	HNE present (nmol) <sup>a</sup>	Method	HNE added (nmol)	HNE found (nmol) <sup>b</sup>	Recovery of added HNE (%)
Soybean oil <sup>c</sup>	0.38 ± 0.09	HNE	2.91	2.53 ± 0.33	87
			0.29	0.18 ± 0.09	62
		HNE-DNPH	2.91	2.57 ± 0.15	88
			0.29	0.28 ± 0.08	76
Porcine liver <sup>d</sup>	0.88 ± 0.12	HNE	3.52	2.47 ± 0.52	70
			0.35	Trace	—
		HNE-DNPH	3.52	2.86 ± 0.53	81
			0.35	0.23 ± 0.05	66

<sup>a</sup>"HNE present" was analyzed by the HNE-DNPH method.

<sup>b</sup>"HNE found" was determined by subtracting the concentration of HNE originally contained in the sample, "HNE present," from the concentration of HNE measured in the sample to which HNE was added.

<sup>c</sup>Oil sample (100 mg) was extracted twice with 2 mL of distilled water.

<sup>d</sup>Porcine liver sample (1 g) was extracted twice with 2 mL of methanol. For abbreviations see Table 1.



**FIG. 7.** Chromatograms of HNE in (A) soybean oil and (B) oxidized soybean oil as detected by HPLC-SP, and of HNE in (C) porcine liver and (D) oxidized porcine liver derivatized with DNPH and detected by HPLC-SP. For abbreviations see Figures 1, 2, and 6.

impossible; thus, 80% recovery is a fairly high value. Recoveries of HNE by direct HNE analysis were lower in samples with trace additions of HNE (0.29 nmol). In particular, HNE was not detected in porcine liver samples to which trace amounts of HNE were added. HNE reacts primarily with amino acids such as histamine and lysine (3), and this reactivity is thought to be one of the causes of high toxicity of HNE in biological systems. This reaction also may interrupt the adsorption of HNE on the fiber in this system. On the other hand, the recovery of HNE by the HNE-DNPH method was almost constant, and the trace amount of HNE in the porcine liver sample could be detected.

Chromatograms of oxidized soybean oil analyzed directly for HNE (B) and of oxidized porcine liver samples analyzed by HNE-DNPH (D) are shown in Figure 7. The formation of HNE was observed in both samples. These results indicate that the method developed in this study also can be used to detect HNE in oxidized samples.

Conventional methods for HNE require the purification of the sample using TLC (26), solid-phase extraction (21), or column extraction (7) before analysis by GC or HPLC because the sample normally contains lipids, oxidized lipids, and oxidized protein, which interfere with HNE or HNE-DNPH analysis. In this experiment, HNE analysis using SPME was developed. SPME fibers can adsorb target molecules and the method is fast, sensitive, and quantitative. In addition, complicated apparatus is not needed. This methodology is available for not only fat and oil samples but also biological samples.

## REFERENCES

- Esterbauer, H., Schaur, R.J., and Zollner, H. (1991) Chemistry and Biochemistry of 4-Hydroxynonenal, Malonaldehyde and Related Aldehydes, *Free Radical Biol. Med.* 11, 81–128.
- Mattson, M.P. (2000) Free Radical-Mediated Disruption of Cellular Ion Homeostasis, Mitochondrial Dysfunction, and Neuronal Degeneration in Sporadic and Inherited Alzheimer's Disease, in *Free Radicals in Brain Pathophysiology* (Poli, G., Cadenas, E., and Packer, L., eds.), pp. 323–357, Marcel Dekker, New York.
- Uchida, K. (2000) Role of Reactive Aldehyde in Cardiovascular Diseases, *Free Radical Biol. Med.* 28, 1685–1696.
- Selly, M.L. (1998) (E)-4-hydroxy-2-nonenal may be involved in the pathogenesis of Parkinson's disease, *Free Radical Biol. Med.* 25, 169–174.
- Poli, G., and Schaur, R.J. (2000) 4-Hydroxynonenal in the Pathomechanisms of Oxidative Stress, *Life* 50, 315–321.
- Esterbauer, H., and Cheeseman, K.H. (1990) Determination of Aldehydic Lipid Peroxidation Products: Malonaldehyde and 4-Hydroxynonenal, *Meth. Enzymol.* 186, 407–421.
- Strohmaier, H., Helmut, H.S., and Schaur, R.J. (1995) Detection of 4-Hydroxynonenal (HNE) as a Physiological Component in Human Plasma, *J. Lipid Mediat., Cell Signal.*, 11, 51–61.
- Goldring, C., Casini, A.F., Maellaro, E., Del Bello, B., and Comporti, M. (1993) Determination of 4-Hydroxynonenal by High-Performance Liquid Chromatography with Electrochemical Detection, *Lipids* 28, 141–145.
- Holley, A.E., Walker, M.K., Cheeseman, K.H., and Slater, T.F. (1993) Measurement of *n*-Alkenals and Hydroxyalkenals in Biological Samples, *Free Radical Biol. Med.* 15, 281–289.
- Blanchflower, W.J., Walsh, D.M., Kennedy, S., and Kennedy, D.G. (1993) A Thermospray Mass Spectrometric Assay for Fe-Induced 4-Hydroxynonenal in Tissues, *Lipids* 28, 261–264.
- Tamura, H., and Shibamoto, T. (1991) Gas Chromatographic Analysis of Malonaldehyde and 4-Hydroxy-2-(E)-nonenal Produced from Arachidonic Acid and Linoleic Acid in a Lipid Peroxidation Model System, *Lipids* 26, 170–173.
- Thomas, M.J., Robinson, T.W., Samuel, M., and Forman, H.J. (1995) Detecting and Identifying Volatile Aldehydes as Dinitrophenylhydrazones Using Gas Chromatography Mass Spectrometry, *Free Radical Biol. Med.* 18, 553–557.
- Rosiers, C.D., Rivest, M.J., Boily, M.J., Jette, M., Ayala, C.C., and Kumar, A. (1993) Gas Chromatographic–Mass Spectrometric Assay of Tissue Malondialdehyde, 4-Hydroxynonenal, and Other Aldehydes After Their Reduction to Stable Alcohols, *Anal. Biochem.* 208, 161–170.
- Beckman, J.K., Morley, S.A., Jr., and Greene, H.L. (1991) Analysis of Aldehydic Lipid Peroxidation Products by TLC/Densitometry, *Lipids* 26, 155–161.
- Claeson, K., Thorsen, G., and Karlberg, B. (2001) Micellar Electrokinetic Chromatography Separation and Laser-Induced Fluorescence Detection of the Lipid Peroxidation Products 4-Hydroxynonenal, *J. Chromatogr. B.* 763, 133–138.
- Toyokuni, S., Miyake, N., Hiai, H., Hagiwara, M., Kawakishi, S., Osawa, T., and Uchida, K. (1995) The Monoclonal Antibody Specific for the 4-Hydroxy-2-nonenal Histidine Adduct, *FEBS Lett.* 359, 189–191.
- Lord, H., and Pawliszyn, J. (2000) Evolution of Solid-Phase Microextraction Technology, *J. Chromatogr. A.* 885, 153–193.
- Penalver, A., Pocurull, E., Borrull, F., and Marce, R.M. (1999) Trends in Solid-Phase Microextraction for Determining Organic Pollutants in Environmental Samples, *Trends Anal. Chem.* 18, 557–568.
- Lee, Z., Kumazawa, T., Sato, K., Seno, H., Ishii, A., and Suzuki, O. (1998) Improved Extraction of Ethanol from Human Body Fluids by Headspace SPME with a Carboxen/PDMS Fiber, *Chromatographia* 47, 593–595.
- Kataoka, H., Lord, H.L., and Pawliszyn, J. (2000) Applications of Solid Phase Microextraction in Food Analysis, *J. Chromatogr. A.* 800, 35–62.
- Lang, J., Celotto, C., and Esterbauer, H. (1985) Quantitative Determination of the Lipid Peroxidation Products 4-Hydroxynonenal by High-Performance Liquid Chromatography, *Anal. Biochem.* 150, 369–378.
- Kelly, M., and Larroque, M. (1999) Trace Determination of Diethylphthalate in Aqueous Media by SPME-HPLC, *J. Chromatogr. A.* 841, 177–185.
- Wu, Y.-C., and Huang, S.-D. (1999) SPME Coupled with HPLC for the Determination of Aromatic Amines, *Anal. Chem.* 71, 310–318.
- Brunton, N.P., Cronin, D.A., Monahan, F.J., and Durcan, R. (2000) A Comparison of Solid-Phase Microextraction (SPME) Fibers for Measurement of Hexanal and Pentanal in Cooked Turkey, *Food Chem.* 68, 339–345.
- Stashenko, E.E., Puertas, M.A., Salgar, W., Delgado, W., and Martinez, J.R. (2000) Solid-Phase Microextraction with On-Fibre Derivatisation Applied to the Analysis of Volatile Carbonyl Compounds, *J. Chromatogr. A.* 886, 175–182.
- Esterbauer, H., Benedetti, A., Lang, J., Fulceri, R., Fauler, G., and Comporti, M. (1986) Studies on the Mechanism of Formation of 4-Hydroxynonenal During Microsomal Lipid Peroxidation, *Biochim. Biophys. Acta* 876, 154–166.

[Received November 27, 2001, and in revised form May 2, 2002; revision accepted May 24, 2002]

## A Critique of 50-m CP-Sil 88 Capillary Columns Used Alone to Assess *trans*-Unsaturated FA in Foods: The Case of the TRANSFAIR Study

Sir:

The industry-sponsored TRANSFAIR study, conducted by more than 70 participants, was aimed at determining reliable data on the total as well as on clusters of *trans*-unsaturated FA (*trans*-UFA) contents of several hundred food items purchased in 14 European countries (1–6). We wish here to comment on the results obtained in that study, particularly those for France and Germany, for which a wealth of detailed and accurate data on individual *trans* isomers has been accumulated by other authors for practically all kinds of major foods (7–17).

In the TRANSFAIR study, FA and *trans*-UFA in particular were determined on (a) 50-m CP-Sil 88 capillary column(s) (commercial source not mentioned; operated isothermally at 195°C). This column, however, is known to present several drawbacks, whether operated isothermally or with temperature programming, that preclude any complete separation of *trans*-UFA if a preliminary fractionation, e.g., by silver nitrate TLC, is not performed. We will describe, in this letter, the main limitations of this kind of column when used alone for the assessment of *trans* isomers.

First of all, the *trans*-16:1 isomers [present in rather low amounts in ruminant fats (18), human milk fat (19), and partially hydrogenated fish oils (18)] are not fully resolved from the *cis*-16:1 isomers and also overlap with branched-17:0 acids. In particular, the *trans*-9 16:1 acid (palmitelaidic acid, the single commercially available standard) may coincide with iso-17:0 acid (19,20) under most analytical conditions. The proportion of the latter FA in ruminant milk fat is considerably higher than that of palmitelaidic acid (8,19), which resulted in overestimates in the TRANSFAIR study by as much as 2,000% in some instances [1,200% on average (7)].

Second, the 50-m CP-Sil 88 column is known to give access to only the  $\Delta 4$  to  $\Delta 11$  *trans*-18:1 isomers (or to the  $\Delta 12$  and part of the  $\Delta 13/14$  isomers in the most favorable case with relatively low contents of oleic acid, and when the  $\Delta 4$  and  $\Delta 5$  isomers are taken into account by the integrator) while the other unsaturated *trans* isomers with a  $\Delta 12$ ,  $\Delta 13$ ,  $\Delta 14$ ,  $\Delta 15$ , and  $\Delta 16$  double bond are eluting under the main oleic ( $\Delta 9$  *cis*-18:1) acid peak, or even after it (21). It could be calculated that data from the TRANSFAIR study for all dairy products that were analyzed were indeed underestimated by an average of *ca.* 35% (9). However, this value is by no means applicable to individual analyses of ruminant fats for the

following reasons. The underreporting of *trans*-18:1 isomers from ruminant milk depends on the operating temperature of the column (being somewhat lower at higher temperatures), on the nature of the carrier gas and its linear velocity, and on the feed of the cattle (pasture vs. barn feeding: greater underreporting in the former conditions as compared to the latter). Note that in the TRANSFAIR study, the operating temperature of the column was 195°C, which precluded integration of the 4:0 to 7:0 acids. Together they represent *ca.* 6% of total FA in bovine milk lipids, implying that data for FA determined in the TRANSFAIR study must be divided by 1.06, thus contributing to underestimation of total *trans* isomers. Also, aging of the column appreciably modifies the resolution (skewing of peaks). This is important in view of the facts (i) that the group of *trans*-18:1 isomers represents the greatest part of dietary *trans*-UFA (more than 80% of total *trans*-UFA in ruminant fats and 90% in partially hydrogenated vegetable oils) (16,17), and (ii) that ruminant fats are the main source of dietary *trans*-18:1 acids in many European countries (12). Another consequence is that data for oleic acid in the TRANSFAIR study are overestimates. Unfortunately, no corrections can be made for other food items containing partially hydrogenated vegetable oils, as the correction factors for such oils are variable (21). However, approximations can be deduced for several categories of French and German foods from data in Reference 10.

Third, *trans*-18:3 isomers that are formed during the deodorization of  $\alpha$ -linolenic acid-containing vegetable oils (22) were likely mixed with 20:0 and/or *cis*- and/or *trans*-20:1 acids. The resolution of these FA is highly dependent on the operating temperature and the length of the CP-Sil 88 column and requires that special analytical precautions be taken (23). Oils containing  $\alpha$ -linolenic acid (mostly rapeseed and soybean oils) from France and Germany (and a few other European countries) have been described in detail in this respect and have been shown to present similar geometrical isomers in practically equal relative proportions (24–27). It is impossible to make any sound comments or to draw any conclusions regarding *trans* isomers of linoleic acid since no chromatograms were published in any of the many papers discussing the TRANSFAIR study (1–6,28). *Trans* isomers of linoleic acid are naturally present in ruminant fats and are otherwise found in vegetable oils after either deodorization or partial hydrogenation. Here too, depending on the column temperature, these isomers may interfere with other components in that complex chromatographic region, particularly in



ruminant fats (16,29). In brief, owing to the large uncertainties in clusters of *trans*-UFA (16:1, 18:1, 18:2, and 18:3 isomers) described above, the calculated total *trans*-UFA in foods in the TRANSFAIR study, based on inappropriate methodology, should not be considered accurate measurements of *trans* FA content of foods (7). The reader who is particularly interested in regulatory matters on food composition may now decide on the usefulness of such data.

Finally, in the concluding papers of the TRANSFAIR study (6,28), estimates of the daily individual intake of total *trans*-UFA by men and women separately (6), or by whole populations (29), were made for the 14 countries under investigation. These were 2.1 and 1.9 grams per person per day (g/p/d) for French and German women, respectively, and were slightly higher for men. These values are in contradiction with detailed data on human milk fat established for the two populations. The milk fat of German women contains *ca.* 3.8 g of total *trans*-UFA per 100 g of FA (30), whereas the corresponding value for French women is only *ca.* 2.3 g (12,31). Based solely on the TRANSFAIR study data, one would have to conclude that German women are able to concentrate considerably more *trans*-UFA in their milk, whereas French women are not. More seriously, we prefer to conclude that the TRANSFAIR study estimates are erroneous and unreliable because of a faulty analytical procedure applied to all foods under investigation. If there is a relationship between the quantity of dietary *trans*-UFA and that present in human milk, the consumption of *trans*-UFA by German women should then be at least 4 g/p/d, which is twice the value calculated in the TRANSFAIR study.

In conclusion, it should be added that because each individual *trans*-UFA has its own metabolic fate (32,33), mixing all categories of *trans*-UFA is of little use for nutritionists. Methods are presently available to clearly separate, identify, and quantify individual *trans*-UFA (14,34), which also permit rather accurate estimates of the relative contributions of ruminant fats and partially hydrogenated vegetable oils to the total per capita daily *trans*-UFA intake (12,30,35,36). These include an obligatory preliminary step, e.g., silver ion TLC, in order to suppress overlaps of *trans*-UFA with interfering FA, as described above. An alternative procedure, which has been less frequently used, is RP-HPLC, which allows simplified GC analyses of *trans*-PUFA (31), including CLA (not reported in the TRANSFAIR study). Also, 100-m or even longer columns should be preferred to improve the resolution of isomers. However, if the GC operating temperatures are not optimal, the separations will not be very different from those obtained with 50-m columns [compare, e.g., chromatograms displayed in Refs. 12 (50-m CP-Sil 88 column) and 37 (100-m CP-Sil 88 column)]. With these combinations of analytical methods, provided the operating conditions are optimized (generally, rather low temperatures), additional data on most individual isomers can be collected (38,39). This critique of the TRANSFAIR study obviously is applicable to all data on *trans*-UFA in the literature not obtained by the combinations of methods described above. The use of long to very long capillary columns coated with 100% cyanopropyl poly-

siloxane polymer still requires complementary fractionation techniques. This should be kept in mind when considering food FA labeling, including that of the so-called "*trans*-fatty acids."

## REFERENCES

1. Van Poppel, G., Van Erp-Baart, M.-A., Leth, T., Gevers, E., Van Amelsvoort, J., Lanzmann-Petithory, D., Kafatos, A., and Aro, A. (1998) *Trans Fatty Acids in Foods in Europe: The TRANSFAIR Study*, *J. Food Compos. Anal.* 11, 112–136.
2. Aro, A., Van Amelsvoort, J., Becker, W., Van Erp-Baart, M.-A., Kafatos, A., Leth, T., and Van Poppel, G. (1998) *Trans Fatty Acids in Dietary Fats and Oils from 14 European Countries: The TRANSFAIR Study*, *J. Food Compos. Anal.* 11, 137–148.
3. Aro, A., Antoine, J.M., Pizzoferrato, L., Reykdal, O., and Van Poppel, G. (1998) *Trans Fatty Acids in Dairy and Meat Products from 14 European Countries: The TRANSFAIR Study*, *J. Food Compos. Anal.* 11, 150–160.
4. Aro, A., Amaral, E., Kesteloot, H., Rimestad, A., Thamm, M., and Van Poppel, G. (1998) *Trans Fatty Acids in French Fries, Soups and Snacks from 14 European Countries: The TRANSFAIR Study*, *J. Food Compos. Anal.* 11, 170–177.
5. Van Erp-Baart, M.-A., Couet, C., Cuadrado, C., Kafatos, A., Stanley, J., and Van Poppel, G. (1998) *Trans Fatty Acids in Bakery Products from 14 European Countries: The TRANSFAIR Study*, *J. Food Compos. Anal.* 11, 161–169.
6. Hulshof, K.F.A.M., Van Erp-Baart, M.A., Anttolainen, M., Becker, W., Church, S.M., Couet, C., Hermann-Kunz, E., Kesteloot, H., Leth, T., Martins, I., *et al.* (1999) Intake of Fatty Acids in Western Europe with Emphasis on *trans* Fatty Acids: The TRANSFAIR Study, *Eur. J. Clin. Nutr.* 53, 143–157.
7. Wolff, R.L., Precht, D., and Molquentin, J. (1998) Occurrence and Distribution Profiles of *trans*-18:1 Acids in Edible Fats of Natural Origin, in *Trans Fatty Acids in Human Nutrition* (Sébédo, J.L., and Christie, W.W., eds.), pp. 1–33, Oily Press, Dundee, Scotland.
8. Destailats, F., Wolff, R.L., Precht, D., and Molquentin, J. (2000) Study of Individual *trans*- and *cis*-16:1 Isomers in Cow, Goat, and Ewe Cheese Fats by Gas–Liquid Chromatography with Emphasis on the *trans*- $\Delta$ 3 Isomer, *Lipids* 35, 1027–1032.
9. Precht, D., Molquentin, J., Destailats, F., and Wolff, R.L. (2001) Comparative Studies on Individual Isomeric 18:1 Acids in Cow, Goat, and Ewe Milk Fats by Low-Temperature High-Resolution Capillary Gas–Liquid Chromatography, *Lipids* 36, 827–832.
10. Wolff, R.L., Combe, N.A., Destailats, F., Boué, C., Precht, D., Molquentin, J., and Entressangles, B. (2000) Follow-up of the  $\Delta$ 4 to  $\Delta$ 16 *trans*-18:1 Isomer Profile and Content in French Processed Foods Containing Partially Hydrogenated Vegetable Oils During the Period 1995–1999. Analytical and Nutritional Implications, *Lipids* 35, 815–825.
11. Wolff, R.L. (1994) Contribution of *trans*-18:1 Acids from Dairy Fat to European Diets, *J. Am. Oil Chem. Soc.* 71, 277–283.
12. Wolff, R.L. (1995) Content and Distribution of *trans*-18:1 Acids in Ruminant Milk and Meat Fats. Their Importance in European Diets and Their Effect on Human Milk, *J. Am. Oil Chem. Soc.* 72, 259–272.
13. Wolff, R.L., Bayard, C.C., and Fabien, R.J. (1995) Evaluation of Sequential Methods for the Determination of Butterfat Fatty Acid Composition with Emphasis on *trans*-18:1 Acids. Application to the Study of Seasonal Variations in French Butters, *J. Am. Oil Chem. Soc.* 72, 1471–1483.
14. Precht, D., and Molquentin, J. (1996) Rapid Analysis of the Isomers of *trans* Octadecenoic Acids in Milk Fat, *Int. Dairy J.* 6, 791–809.

15. Molquentin, J., and Precht, D. (1996) Isomeric Distribution and Rapid Determination of *trans*-Octadecenoic Acids in German Brands of Partially Hydrogenated Edible Fats, *Nahrung-Food* 40, 297–304.
16. Precht, D., and Molquentin, J. (1997) *Trans*-Geometrical and Positional Isomers of Linoleic Acid Including Conjugated Linoleic Acid (CLA) in German Milk and Vegetable Fats, *Fett/Lipid* 99, 319–326.
17. Precht, D., and Molquentin, J. (2000) Recent Trends in the Fatty Acid Composition of German Sunflower Margarines, Shortenings, and Cooking Fats with Emphasis on Individual C16:1, C18:1, C18:2, C18:3, and C20:1 *trans* Isomers, *Nahrung-Food* 44, 222–228.
18. Molquentin, J., and Precht, D. (1997) Occurrence of *trans*-Hexadecenoic Acids in Bovine Milkfats and Partially Hydrogenated Fats, *Milchwissenschaft* 52, 380–385.
19. Precht, D., and Molquentin, J. (2000) Identification and Quantitation of *cis/trans*-C16:1 and C17:1 Fatty Acid Positional Isomers in German Human Milk Lipids by Thin-Layer Chromatography and Gas Chromatography/Mass Spectrometry, *Eur. J. Lipid Sci. Technol.* 102, 102–113.
20. Precht, D. (1990) Quantitativer Nachweis von Milchlipp in Schokolademischungen. I. Bestimmung von Milchlippanteilen in Kakaobutter, *Fat Sci. Technol.* 92, 153–161.
21. Wolff, R.L., Combe, N.A., Precht, D., Molquentin, J., and Ratnayake, W.M.N. (1998) Accurate Determination of *trans*-18:1 Isomers by Capillary Gas-Liquid Chromatography on Cyanoalkyl Polysiloxane Stationary Phases, *Oléagineux Corps gras Lipides* 5, 295–299.
22. Ackman, R.G., Hooper, S.N., and Hooper, D.I. (1974) Linolenic Acid Artifacts from the Deodorization of Oils, *J. Am. Oil Chem. Soc.* 51, 42–49.
23. Wolff, R.L. (1994) Analysis of Alpha-Linolenic Acid Geometrical Isomers in Deodorized Oils by Capillary Gas-Liquid Chromatography on Cyanoalkyl Polysiloxane Stationary Phases: A Note of Caution, *J. Am. Oil Chem. Soc.* 71, 907–909.
24. Wolff, R.L. (1992) *Trans*-Polyunsaturated Fatty Acids in French Edible Rapeseed and Soybean Oils, *J. Am. Oil Chem. Soc.* 69, 106–110.
25. Wolff, R.L. (1993) Further Studies on Artificial Geometrical Isomers of  $\alpha$ -Linolenic Acid in Linolenic Acid Containing Oils, *J. Am. Oil Chem. Soc.* 70, 219–224.
26. Wolff, R.L. (1993) Occurrence of Artificial *trans*-Polyunsaturated Fatty Acids in Refined (deodorized) Walnut Oils, *Sci. Aliments* 13, 155–163.
27. Wolff, R.L. (1997) *Trans* Isomers of  $\alpha$ -Linolenic Acid in Deodorized Oils, *Lipid Technol. Newslett.* 3, 3639.
28. Van Poppel, G. (1998) Intake of *trans* Fatty Acids in Western Europe: The TRANSFAIR Study, *Lancet* 351, 1099.
29. Precht, D., Molquentin, J., McGuire, M.A., McGuire, M.K., and Jensen, R.G. (2001) Overestimates of Oleic and Linoleic Acid Contents in Materials Containing *trans* Fatty Acids and Analyzed with Short Packed Gas Chromatographic Columns, *Lipids* 36, 213–216.
30. Precht, D., and Molquentin, J. (1999) C18:1, C18:2 and C18:3 *trans* and *cis* Fatty Acid Isomers Including Conjugated *cis*  $\Delta^9,trans$   $\Delta^{11}$  Linoleic Acid (CLA) as Well as Total Fat Composition of German Human Milk Lipids, *Nahrung-Food* 43, 233–244.
31. Chardigny, J.M., Wolff, R.L., Mager, E., Sébédio, J.-L., Martine, L., and Juanéda, P. (1995) *Trans* Mono- and Polyunsaturated Fatty Acids in Human Milk, *Eur. J. Clin. Nutr.* 49, 523–531.
32. Hølmer, G. (1998) Biochemistry of *trans* Monoenoic Acids, in *Trans Fatty Acids in Human Nutrition* (Sébédio, J.L., and Christie, W.W., eds.), pp. 163–189, Oily Press, Dundee, Scotland.
33. Sébédio, J.L., and Chardigny, J.M. (1998) Biochemistry of *trans* Polyunsaturated Acids, in *Trans Fatty Acids in Human Nutrition* (Sébédio, J.L., and Christie, W.W., eds.), pp. 192–215, Oily Press, Dundee, Scotland.
34. Wolff, R.L. (1999) Simple Methods for the Identification and Quantification by GLC of Most Individual *trans*-18:1 Isomers Present in Foods and Human Tissues, *Lipid Technol.* 11, 16–18.
35. Boué, C., Combe, N., Billeaud, C., Mignerot, C., Entressanges, B., They, G., Geoffrion, H., Brun, J.L., Dally, O., and Leng, J.J. (2000) *Trans* Fatty Acids in Adipose Tissue of French Women in Relation to Their Dietary Origin, *Lipids* 35, 561–566.
36. Wolff, R.L., Precht, D., and Molquentin, J. (1998) *Trans*-18:1 Acid Content and Profile in Human Milk Lipids: Critical Survey of Data in Connection with Analytical Methods, *J. Am. Oil Chem. Soc.* 75, 661–671.
37. Alonso, L., Fontecha, J., Lozada, L., Fraga, M.J., and Juarez, M. (1999) Fatty Acid Composition of Caprine Milk: Major, Branched-Chain, and *trans* Fatty Acids, *J. Dairy Sci.* 82, 876–884.
38. Wolff, R.L., and Bayard, C.C. (1995) Improvement in the Resolution of Individual *trans*-18:1 Isomers by Capillary Gas-Liquid Chromatography: Use of a 100-m CP-Sil 88 Column, *J. Am. Oil Chem. Soc.* 72, 1197–1201.
39. Molquentin, J., and Precht, D. (1995) Optimized Analysis of *trans*-Octadecenoic Acids in Edible Fat, *Chromatographia* 41, 267–272.

Robert L. Wolff<sup>a,\*</sup> and Dietz Precht<sup>b</sup>  
<sup>a</sup>INRA, UNL, 21065 Dijon Cedex, France,  
 and <sup>b</sup>Institute of Dairy Chemistry and Technology,  
 Federal Dairy Research Center,  
 24121 Kiel, Germany

[Received September 9, 2001, and in revised form and accepted May 17, 2002]

\*To whom correspondence should be addressed at INRA, UNL, 17, rue Sully, B.P. 86510, 21065 Dijon Cedex, France. E-mail: wolff@dijon.inra.fr

# Action of 1-(11-Selenadodecyl)-glycerol and 1-(11-Selenadodecyl)-3-Trolox-glycerol Against Lipid Peroxidation

Violeta Raneva<sup>a,b,\*</sup>, Hiroyuki Shimasaki<sup>a</sup>, Yumi Furukawa<sup>a</sup>, Nobuo Ueta<sup>a</sup>,  
Nedyalka Yanishlieva<sup>b</sup>, Jon Erik Aaseng<sup>c</sup>, Vassilia Partali<sup>c</sup>, Hans-Richard Sliwka<sup>c</sup>,  
Yasukazu Yoshida<sup>d</sup>, and Etsuo Niki<sup>d</sup>

<sup>a</sup>First Department of Biochemistry, Teikyo University School of Medicine, Tokyo 173-8605, Japan, <sup>b</sup>Lipid Chemistry Department, Institute of Organic Chemistry, Bulgarian Academy of Sciences, Sofia 1113, Bulgaria, <sup>c</sup>Department of Chemistry, Norwegian University of Science and Technology, N-7491 Trondheim, Norway, and <sup>d</sup>Human Stress Signal Research Center, Advanced Institute for Science and Technology, Ikeda 563-8577, Japan

**ABSTRACT:** The antioxidant action on lipid peroxidation of the synthesized selenium compounds 1-(11-selenadodecyl)-glycerol (SeG) and 1-(11-selenadodecyl)-3-Trolox-glycerol (SeTrG, where Trolox = 6-hydroxy-2,5,7,8-tetramethylchroman-2-carboxylic acid) was investigated. We compared the reactivity of the selenium compounds toward peroxy radicals and their inhibitory effect on lipid peroxidation, induced by several kinds of initiating species such as azo compounds, metal ions, and superoxide/nitric oxide in solution, micelles, membranes, and rat plasma. SeTrG, but not SeG, scavenged peroxy radicals. SeG reduced methyl linoleate hydroperoxides in organic solution and in methyl linoleate micelles oxidized by ferrous ion (Fe<sup>2+</sup>)/ascorbic acid. In rat plasma SeG and SeTrG decreased the formation of lipid hydroperoxides generated by hydrophilic azo compounds. SeG and SeTrG spared  $\alpha$ -tocopherol ( $\alpha$ -TOH) consumption in multilamellar vesicle membranes oxidized by hydrophilic or lipophilic initiators, and only SeTrG spared  $\alpha$ -TOH in superoxide/nitric oxide oxidized membranes. In rat plasma oxidized by radical initiators (either hydrophilic or lipophilic) or superoxide/nitric oxide, SeTrG suppressed  $\alpha$ -TOH consumption, but SeG had no effect. The two selenium-containing compounds showed inhibitory effects on lipid peroxidation that depended on their structure, the medium where they acted, and the oxidant used.

Paper no. L9010 in *Lipids* 37, 633–640 (July 2002).

The trace element selenium, constituent of selenoproteins, protects against viral (HIV and hepatitis) infections, cardiovascular diseases, and cancer. Selenium may stimulate the immune

\*To whom correspondence should be addressed at First Department of Biochemistry, Teikyo University School of Medicine, 2-11-1 Kaga, Itabashi-ku, Tokyo 173-8605, Japan. E-mail: villy@med.teikyo-u.ac.jp

Abbreviations: A, absorbance; AA, ascorbic acid; AAPH, 2,2'-azobis(2-amidinopropane) dihydrochloride; AMVN, 2,2'-azobis(2,4-dimethylvaleronitrile); CA, caffeic acid; DOPAC, 3,4-dihydroxyphenylacetic acid; DPBQ, *N,N'*-diphenyl-*p*-benzoquinone diimine; DPPD, *N,N'*-diphenyl-*p*-phenyldiamine; ebselen, 2-phenyl-1,2-benzoselenazol-3(2H)-one; MeO-AMVN, 2,2'-azobis(4-methoxy-2,4-dimethylvaleronitrile); MeLOH, methyl linoleate alcohols; MeLOOH, methyl linoleate hydroperoxides; MLV, multilamellar vesicles; PMC, 2,2,5,7,8-pentamethyl-6-chromanol; SeG, 1-(11-selenadodecyl)-glycerol; SeTrG, 1-(11-selenadodecyl)-3-Trolox-glycerol; SIN-1, 3-morpholinolonylamine hydrochloride; Trolox, 6-hydroxy-2,5,7,8-tetramethylchroman-2-carboxylic acid;  $\alpha$ -TOH,  $\alpha$ -tocopherol; Toc-3, tocotrienols.

system and benefit thyroid function, reproduction, and mood (1,2). As a functional center of the glutathione peroxidases, selenium catalyzes the reduction of hydrogen peroxide and of lipid and phospholipid hydroperoxides to water and alcohols. It prevents the formation of free radicals and defends against oxidative stress (1,2). The antiatherogenic and anticancer potentials of selenium are related to its antioxidative properties (2). The biological potentials of organoselenium compounds have been extensively reviewed (3,4).

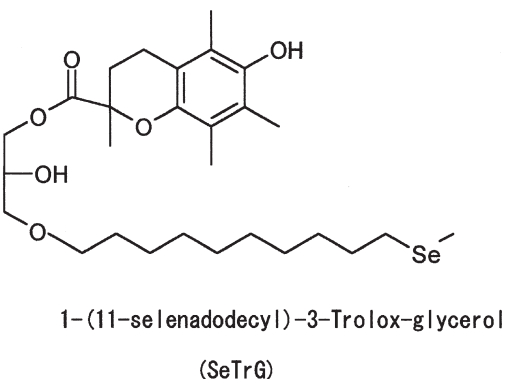
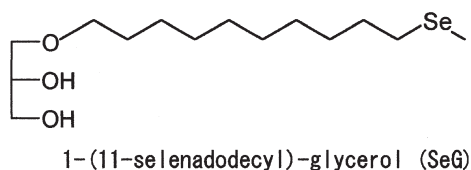
Sodium selenate, sodium selenite, selenourea, and selenomethionine (5), ebselen (6–8), tetradecylselenoacetic acid (9), the monoglyceride 1-(11-selenadodecyl)-glycerol (SeG) (10), and the triglyceride 1-( $\beta$ -apo-8'-carotenoyl)-2-(7-selenaocanoyl)-3-(6-hydroxy-2,5,7,8-tetramethylchroman-2-acyl)-glycerol (11) show antioxidant capacity. Selenoproteins and organoselenium compounds protect against pro-oxidants and peroxynitrite (12). Ebselen reduces the extent of hemolysis of human erythrocytes incubated with peroxynitrite (13) and the frequency of transformation of mouse embryo fibroblasts exposed to 2,2'-azobis(2-amidinopropane) dihydrochloride (AAPH) and 3-morpholinolonylamine hydrochloride (SIN-1) (14).

Nutritional sources of selenium are brazil nuts, kidney, crab, liver, fish, and meat (1). Selenium is one of the antioxidant components in garlic extract (15) and green tea (16).

Mixtures of selenium and vitamin E show a synergistic antioxidant effect *in vitro* (17). The effects of vitamin E and selenium against prostate cancer (18), radiation-induced injury (19), and fungal toxin (20) are related to their antioxidative action against lipid peroxidation.

The purpose of this work is to elucidate the relationship between the structure of the selenium compounds SeG and the recently synthesized 1-(11-selenadodecyl)-3-Trolox-glycerol (SeTrG) (Scheme 1), their reactivity toward oxidants, and antioxidant activity in various lipid systems. SeTrG combines two antioxidants chemically: selenium and the vitamin E derivative Trolox (6-hydroxy-2,5,7,8-tetramethylchroman-2-carboxylic acid). The radical-scavenging activity of SeG and SeTrG was tested in *N,N'*-diphenyl-*p*-phenyldiamine (DPPD) oxidation. Organic solutions, micelles, multilamellar





SCHEME 1

liposomes, and rat plasma were used as lipid substrates. Metal ions, hydrophilic initiators, or lipophilic radical initiators were used as oxidants. The reactions were performed at 37°C in air.

## MATERIALS AND METHODS

**Synthesis of SeG and SeTrG.** The synthesis of SeG was previously described (21). SeTrG was prepared by esterifying SeG with Trolox, 4-dimethylaminopyridine, and *N,N'*-dicyclohexylcarbodiimide at room temperature (21). After reaction, the product was purified by preparative TLC (32% yield). The structures of SeG and SeTrG were verified by MS and by <sup>1</sup>H and <sup>13</sup>C NMR (21).

**Materials.** Ascorbic acid (AA), AAPH, 2,2'-azobis(2,4-dimethylvaleronitrile) (AMVN), DPPD, 2,2'-azobis(4-methoxy-2,4-dimethylvaleronitrile) (MeO-AMVN), 2,2,5,7,8-pentamethyl-6-chromanol (PMC),  $\alpha$ -tocopherol ( $\alpha$ -TOH), and Trolox were purchased from Wako Pure Chemical Industries Ltd. (Osaka, Japan). Methyl linoleate and SIN-1 were obtained from Sigma Chemical Co. (St. Louis, MO). Tocotrienols (Toc-3) were from Fuji Chemical Co., Ltd. (Toyama, Japan). Soybean PC was purchased from Nichiyu Liposome Co., Inc. (Tokyo, Japan) and purified by column chromatography. Ethanol and 2-propanol were from Wako Pure Chemical Industries Ltd., and methanol and *n*-hexane from Kanto Chemical Co., Inc. (Tokyo, Japan). The *n*-hexane and 2-propanol were of HPLC grades. All other reagents were of analytical grade.

**Animals and diets.** All experimental procedures were conducted in compliance with the Teikyo University's policy on animal care and use. Several male rats, Sprague-Dawley strain, 5 wk old, were purchased from Saitama Experimental Animals Supply Co., Ltd. (Saitama, Japan). They were fed Certified-1 Diet (CRF-1), Oriental Yeast Co. (Tokyo, Japan)

for several weeks. During this period, a blood sample from the retro-ocular plexus of each animal was taken at certain intervals. The  $\alpha$ -TOH content in the plasma, obtained by centrifugation of rat blood, was in the range of 20–24  $\mu$ M.

**Estimation of antioxidant reactivity toward peroxy radicals.** DPPD reacts with free radicals to form *N,N'*-diphenyl-*p*-benzoquinone diimine (DPBQ), which has a strong absorbance at 440 nm (22). DPPD (100  $\mu$ M final concentration), mixed with SeG or SeTrG (500  $\mu$ M) in acetonitrile, was preincubated at 37°C for 3 min. AMVN (50 mM final concentration) was added to start the reaction under air at 37°C. DPPD oxidation was traced at 440 nm by means of a U-3310 Hitachi spectrophotometer (Tokyo, Japan).

**Inhibition of oxidation of lipids by SeG and SeTrG.** Methyl linoleate hydroperoxides (MeLOOH), synthesized from methyl linoleate by lipoxidase in methanol, at a concentration of 99  $\mu$ M, were incubated at 37°C under air with 200  $\mu$ M SeG. The MeLOOH and the corresponding methyl linoleate alcohols (MeLOH) were detected by an HPLC system (Shimadzu Corp., Kyoto, Japan), equipped with a UV detector and Wakosil-II 5C18 RS (4.6  $\times$  250 mm) column (Wako Pure Chemical Industries Ltd.). Acetonitrile/distilled water (9:1, vol/vol) at a flow rate of 0.7 mL/min was used as an eluent.

Methyl linoleate micelles were prepared by vigorously mixing with a vortex mixer for 2 min methyl linoleate (25 mM for measuring UV absorbance or 75 mM for measuring O<sub>2</sub> consumption) and SDS (0.5 M) in PBS (10 mM, pH 7.4). For measurement of UV absorbance at 234 nm (A<sub>234</sub>), 3 mL of the methyl linoleate micelle dispersion (25 mM in 0.5 M SDS containing PBS) was placed in a quartz cell of a U-3310 Hitachi spectrophotometer (Tokyo, Japan). Adding 5  $\mu$ L of 40 mM Fe<sup>2+</sup>/400 mM AA (final concentration 5  $\mu$ M Fe<sup>2+</sup>/50  $\mu$ M AA) induced the oxidation. The reaction was performed at 37°C under air. When SeG was used as antioxidant, 400  $\mu$ M SeG was added to the methyl linoleate micelle dispersion before oxidation. A<sub>234</sub> was scanned with time. A dispersion of unoxidized methyl linoleate micelles was used as a reference. The O<sub>2</sub> consumption was measured with a Galvani-type oxygen electrode, MD-1000 (Iijima Electronics Corp., Tokyo, Japan). The O<sub>2</sub>-concentration was set at 0  $\mu$ M with the meter in water containing 5% sodium bisulfite and at 220  $\mu$ M in water saturated with air at 35°C. The methyl linoleate micelle dispersion (75 mM in 0.5 M SDS containing PBS) was placed in the cell of the O<sub>2</sub> electrode having a volume of 2.25 mL. After 10 min, the addition of 5  $\mu$ L of 4 mM Fe<sup>2+</sup>/40 mM AA (final concentration 0.6  $\mu$ M Fe<sup>2+</sup>/6  $\mu$ M AA) induced the oxidation, which was performed at 35.8°C under air. After another 10 min, SeTrG (100  $\mu$ M final concentration) or SeG (500  $\mu$ M final concentration) was added, and the O<sub>2</sub> consumption was recorded.

In multilamellar vesicle (MLV) oxidations, SeG or SeTrG were externally added (i) or incorporated (ii) in the multilamellar liposomes.

(i) *SeG and SeTrG externally added to MLV suspensions.* When MLV suspensions were oxidized by AAPH, soybean PC (2.8 mM), and  $\alpha$ -TOH (15  $\mu$ M) were dissolved in chloroform



and mixed, and the solvent was evaporated completely under nitrogen ( $N_2$ ). PBS containing EDTA (0.1 mM) was added, and the mixture was treated with a vortex mixer to form an MLV suspension. The MLV suspension was divided into three tubes. SeG and SeTrG at concentration of 100  $\mu$ M were added to two of them. The MLV suspensions were placed in a water bath shaker (37°C, 150 oscillations per minute) and AAPH (20 mM final concentration) was added to start the oxidation. When MLV suspensions were oxidized by the internally incorporated AMVN, AMVN (6 mM) was mixed together with soybean PC and  $\alpha$ -TOH, and the same procedure as described above was used. The oxidation was started by placing the MLV suspensions in a water bath shaker (37°C, 150 oscillations per minute).

(ii) *SeG and SeTrG incorporated in MLV.* The same procedure as described above was used, but SeG or SeTrG, each 100  $\mu$ M, was added to a mixture of soybean PC,  $\alpha$ -TOH, and AMVN (when used) in the beginning of the preparation of MLV suspensions. In SIN-1 oxidation, 0.4 mL of MLV suspension, without or with externally added SeG or SeTrG at a concentration of 300  $\mu$ M, was oxidized at 37°C for 60 min by externally added SIN-1 (0.3–1 mM) in 1 mM EDTA solution. Aliquots of 0.2 mL of the oxidized MLV suspensions were withdrawn at measured time intervals and processed for measuring  $\alpha$ -TOH concentration. The oxidation was stopped by the addition of EDTA (100  $\mu$ M) and freezing (23).

Rat plasma was obtained by mixing the plasma from several rat blood samples, followed by centrifugation twice at  $950 \times g$  for 5 min. Fresh rat plasma (2 mL), without or with SeG or SeTrG in ethanol solution added beforehand at appropriate concentration, was incubated for 2–3 min at 37°C in a water bath shaker before the oxidants AAPH (20 mM) in 1 mM EDTA solution or MeO-AMVN (2 mM) in methanol solution were added to start the oxidation. The final concentrations of methanol and ethanol were 1 and 0.5 vol%, respectively. In SIN-1 oxidation, 0.4 mL rat plasma, without or with 300  $\mu$ M SeG or SeTrG, was oxidized at 37°C for 60 min by SIN-1 (0.3–1.2 mM) in 1 mM EDTA solution. Aliquots of 0.2 mL of oxidized rat plasma were withdrawn at measured time intervals and handled as described above. The samples were processed for measuring  $\alpha$ -TOH concentration.

*$\alpha$ -TOH extraction.*  $\alpha$ -TOH was extracted from rat plasma or MLV suspension by the modified method of Abe and Katsui (24), and Abe *et al.* (25) as described by Shabit *et al.* (26). A volume of 10  $\mu$ L ethanol containing 2  $\mu$ g 2,2,5,7,8-pentamethyl-6-chromanol (PMC) as an internal standard was added to oxidized rat plasma or MLV suspension (0.2 mL). The sample was diluted with distilled water (2.0 mL) and ethanol (2.0 mL) after consecutive mixings for 1 min with a vortex mixer. The  $\alpha$ -TOH was extracted with *n*-hexane (5.0 mL). A 0.9% NaCl water solution (2.0 mL) was added and mixed 2–3 min with a vortex mixer at which time rat plasma was used (for precipitation of the proteins). The mixture was centrifuged at  $1,500 \times g$  for 10 min at 4°C. The upper layer, containing  $\alpha$ -TOH, the internal standard, and the lipids, was pipetted. All procedures were performed at 4°C in an ice bath.

The *n*-hexane was evaporated under  $N_2$ . The residue was then dissolved in *n*-hexane (1.6 mL), and a volume of 20  $\mu$ L of the solution was injected into the column of the HPLC system.

*$\alpha$ -TOH detection by HPLC.* The HPLC system contained an injector (Rheodyne Incorporated, Cotati, CA), DGU-4A Shimadzu degasser (Shimadzu Corp., Kyoto, Japan), NH<sub>2</sub>-1251-N,  $4.6 \times 250$  mm, Senshu Pak column (Senshu Scientific Co., Ltd., Tokyo, Japan), LC-10 AD Shimadzu liquid chromatograph, RF-10 A Shimadzu spectrofluorometric detector, and C-R6A Shimadzu Chromatopac recorder. The  $\alpha$ -TOH was detected at an excitation wavelength of 298 nm and an emission wavelength of 325 nm. The mobile phase was *n*-hexane/2-propanol (98:2, vol/vol) at flow rate 1.0 mL/min.

*UV analysis of conjugated diene hydroperoxides.* Oxidized rat plasma, without or with antioxidants, was diluted with distilled water 80 times and was analyzed by a U-3310 Hitachi spectrophotometer by scanning from 300 to 200 nm at a rate of 60 nm/min. Unoxidized rat plasma, 80 times diluted, was used as a reference.

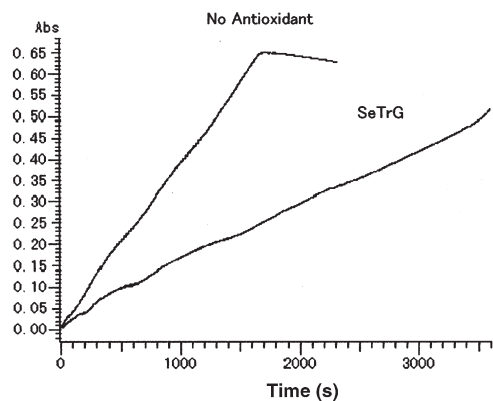
## RESULTS AND DISCUSSION

Antioxidants act by different mechanisms such as radical scavenging, hydroperoxide reduction, and metal ion sequestration (27). We examined the antioxidative properties of SeG and SeTrG mechanisms of action as antioxidants in different systems: organic solution, MeLOOH in methanol solution, methyl linoleate micelles, PC liposomes membranes, and rat plasma.

*SeG and SeTrG peroxy radical-scavenging activity.* The peroxy radicals act as chain-carrying species in lipid peroxidation. We investigated if SeG and SeTrG can act as chain-breaking antioxidants and compared their ability to scavenge peroxy radicals competing with DPPD in organic solution (acetonitrile). One molecule of DPPD rapidly scavenges two radicals and forms DPBQ (22), which has a strong absorbance at 440 nm. The absorbance increased with time due to the formation of DPBQ from DPPD by the reaction with the radicals generated by AMVN (Fig. 1). The addition of SeTrG decreased the rate of DPPD oxidation as compared with the control reaction because SeTrG scavenged radicals in competition with DPPD. SeTrG had no induction period. The curve for variation of the absorbance upon addition of SeG coincided with that of the control reaction, where no antioxidant was added. The results from DPPD oxidation showed that SeTrG was able to scavenge peroxy radicals, whereas SeG was not able to compete with DPPD in scavenging peroxy radicals.

*Reduction of lipid hydroperoxides.* Selenium compounds act as antioxidants by reducing lipid hydroperoxides. Hydroperoxide formation in sunflower oil was retarded by SeG (10). Ebselen, which exerts glutathione-peroxidase activity, also acts as antioxidant by reducing FA and lipid hydroperoxides (7,8). We examined the ability of SeG and SeTrG to reduce hydroperoxides in solution, micelles, and rat plasma.

SeG reduced MeLOOH to the corresponding alcohols in a time-dependent manner (Fig. 2). SeG also suppressed the

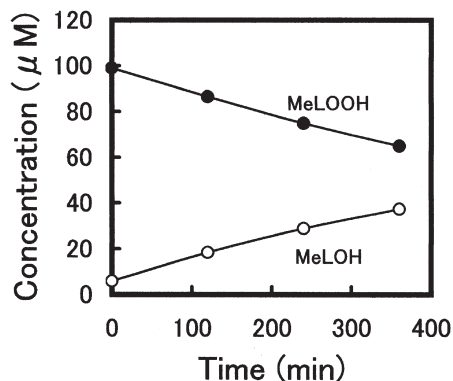


**FIG. 1.** Effect of 1-(11-selenadodecyl)-3-Trolox-glycerol (SeTrG) on the formation of *N,N'*-diphenyl-*p*-benzoquinone diimine (DPBQ) ( $\lambda_{\max} = 440$  nm) as a result of *N,N'*-diphenyl-*p*-phenylenediamine (DPPD) oxidation under air at 37°C. 2,2'-Azobis(2,4-dimethylvaleronitrile) (AMVN) (50 mM) was added to DPPD in acetonitrile or to a mixture of DPPD (100  $\mu$ M) and antioxidant (500  $\mu$ M) in acetonitrile. The increase in absorbance at 440 nm was monitored.

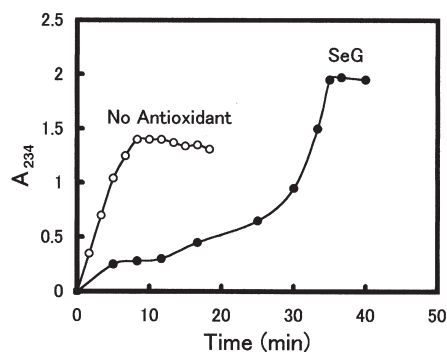
formation of hydroperoxides generated by metal ion-induced peroxidation of methyl linoleate micelles (Fig. 3). We conclude that (i) SeG reduces hydroperoxides, which are required for metal-ion catalyzed oxidation, and (ii) SeG cannot scavenge peroxy radicals. This behavior is similar to the antihypertensive drug carvedilol (28), which is effective against ferric ion-induced oxidation but fails to scavenge radicals.

We compared the activity of SeG and SeTrG against  $\text{Fe}^{2+}/\text{AA}$  oxidation by measuring  $\text{O}_2$  consumption (Fig. 4). SeTrG (100  $\mu$ M) showed much greater activity than SeG (500  $\mu$ M) because SeTrG incorporates the potent antioxidant Trolox group.

We examined the activity of SeG and SeTrG as antioxidants in the oxidation of rat plasma induced by the hydrophilic initiator AAPH. The change in absorbance  $A$  at 234 nm of oxidized rat plasma in the absence and presence of SeG or SeTrG is shown in Figure 5. The two selenium-containing



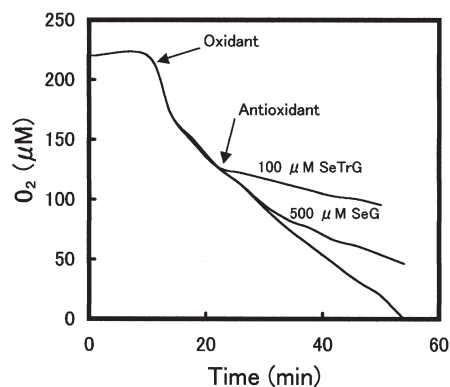
**FIG. 2.** Reduction of methyl linoleate hydroperoxides (MeLOOH) (initial concentration 99  $\mu$ M in methanol) to the corresponding methyl linoleate alcohols (MeLOH) by 200  $\mu$ M 1-(11-selenadodecyl)-glycerol (SeG) under air at 37°C.



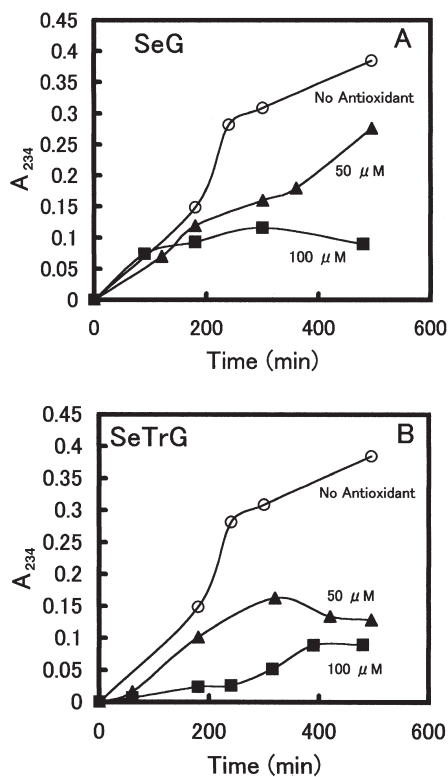
**FIG. 3.** Inhibitory effect of SeG at concentration 400  $\mu$ M (●) on the formation of conjugated diene hydroperoxides, measured by the time-dependent variation in absorbance at 234 nm ( $A_{234}$ ), in methyl linoleate micelle dispersion [25 mM methyl linoleate in 0.5 mM SDS-PBS (10 mM), pH = 7.4] oxidized by 5  $\mu$ M  $\text{Fe}^{2+}/50$   $\mu$ M AA ( $\text{FeSO}_4/\text{ascorbic acid}$ ) under air at 37°C. (○) Change in  $A_{234}$  with time without the addition of antioxidant. For abbreviation see Figure 2.

compounds suppressed the formation of conjugated diene hydroperoxides at concentrations of 50 and 100  $\mu$ M in rat plasma. SeTrG showed a greater effect than SeG.

*Inhibitory effect of SeG and SeTrG on  $\alpha$ -TOH consumption in MLV suspensions and rat plasma.* Antioxidants can act cooperatively or synergistically with other antioxidants. The synergistic action between vitamin E and vitamin C is well known (23,29).  $\alpha$ -TOH is the most abundant lipophilic antioxidant in LDL. It is located predominantly in the outer PC monolayer of organized LDL structures, and it places its active phenolic groups at the surface (23). The rate of lipid oxidation,  $\alpha$ -TOH consumption, and conjugated peroxide diene formation are correlated (29). Liposomes are widely used as models for biomembranes. We used multilamellar soybean PC liposomes, containing  $\alpha$ -TOH (Fig. 6). As oxidants we used the hydrophilic radical initiators AAPH or SIN-1 added to MLV suspensions (Figs. 6A, 6C, 7) or the lipophilic AMVN incorporated into membranes (Figs. 6B, 6D). SeG



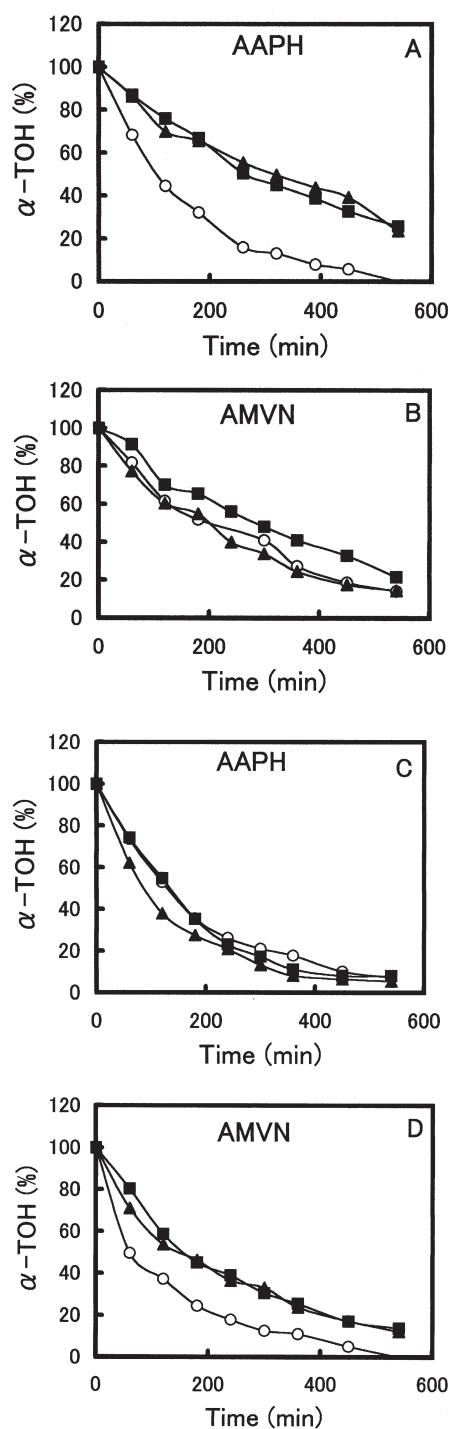
**FIG. 4.** Inhibitory effect of SeG (500  $\mu$ M) and SeTrG (100  $\mu$ M) on oxygen ( $\text{O}_2$ ) consumption in the oxidation under air at 35.8°C of methyl linoleate micelle dispersion (75 mM methyl linoleate in 0.5 M SDS PBS (10 mM), pH = 7.4) by 0.6  $\mu$ M  $\text{Fe}^{2+}/6$   $\mu$ M AA. For abbreviations see Figures 1–3.



**FIG. 5.** Inhibitory effect of SeG (A) and SeTrG (B) on the formation of conjugated diene hydroperoxides measured by time-dependent variation in  $A_{234}$  in rat plasma oxidized by 2,2'-azobis(2-amidinopropane) dihydrochloride (AAPH). SeG (A) and SeTrG (B) at concentrations of 50 ( $\blacktriangle$ ) and 100 ( $\blacksquare$ )  $\mu$ M were added to rat plasma (2 mL) before AAPH (20 mM) was finally added to start the oxidation under air at 37°C. Oxidized plasma (0.05 mL) was diluted with distilled water 80 times, and  $A_{234}$  was monitored. The spectrum was scanned from 300 to 200 nm at a speed of 60 nm/min. (○) Change in  $A_{234}$  with oxidation time without the addition of antioxidants. For abbreviations see Figures 1–3.

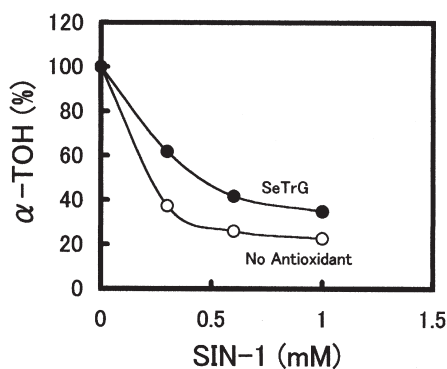
and SeTrG were externally added to MLV suspensions (Figs. 6A, 6B, 7) or incorporated into PC layers (Figs. 6C, 6D). The results from Figure 6 can be explained considering the structure of the selenium-containing compounds, their localization, and the character of the oxidant used—hydrophilic or lipophilic. SeG and SeTrG added externally to MLV oxidized by AAPH (Fig. 6A) are situated in the aqueous medium. They decompose the lipid hydroperoxides produced by the hydrophilic AAPH and protect  $\alpha$ -TOH. SeG and SeTrG externally added to MLV oxidized by internally incorporated AMVN (Fig. 6B) are situated in the aqueous phase, but the radicals are produced inside the PC layers. SeG and SeTrG cannot interact with lipid hydroperoxides due to dimensional restrictions. SeTrG shows some effect due to the presence of the Trolox group having radical-scavenging activity.

Incorporated in MLV oxidized by AAPH (Fig. 6C), SeG and SeTrG do not show antioxidant protection. The selenium compounds cannot act with the lipid hydroperoxides produced out of the vesicles by the water-soluble AAPH. SeTrG cannot scavenge peroxy radicals. It is known that the efficiency of vitamin E for radical scavenging decreases as the



**FIG. 6.** Inhibitory effects on  $\alpha$ -tocopherol ( $\alpha$ -TOH) consumption of SeG ( $\blacktriangle$ ) and SeTrG ( $\blacksquare$ ) at a concentration of 100  $\mu$ M externally added (A,B) or incorporated (C,D) in soybean PC multilamellar vesicles (MLV), containing 15  $\mu$ M  $\alpha$ -TOH, and oxidized under air at 37°C by 20 mM AAPH (A,C) or by incorporated 6 mM AMVN (B,D) (○)  $\alpha$ -TOH consumption without the addition of antioxidant. For abbreviations see Figures 1, 2, and 5.

radical goes deeper into the interior of the LDL structures (23). SeG showed slight prooxidative effect. The hydroxyl groups of SeG are oriented toward the aqueous phase and most probably are attacked by the hydrophilic initiators, thus

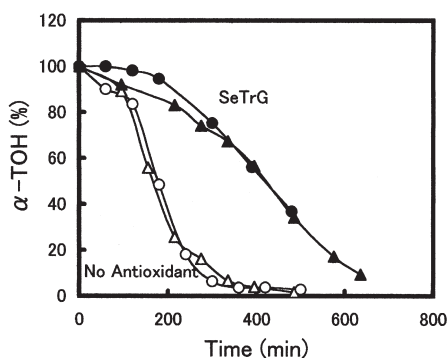


**FIG. 7.** Inhibitory effect of SeTrG at concentration of 300  $\mu\text{M}$  (●) on  $\alpha$ -TOH consumption in soybean PC MLV, containing 20  $\mu\text{M}$   $\alpha$ -TOH, oxidized for 60 min under air at 37°C by externally added 3-morpholinodisnonylamine hydrochloride (SIN-1) at concentrations of 0.3–1 mM. (○)  $\alpha$ -TOH consumption without the addition of antioxidant. For abbreviations see Figures 1 and 6.

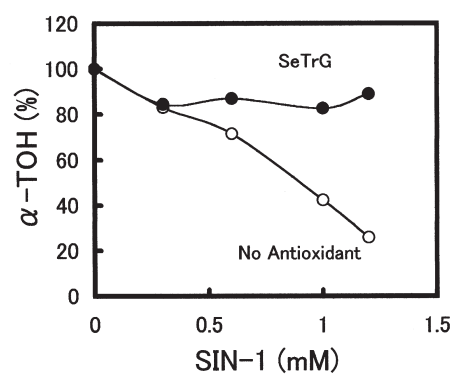
propagating the oxidation. Incorporated in MLV and oxidized by internally incorporated AMVN (Fig. 6D), SeG and SeTrG can decompose the lipid hydroperoxides produced inside the PC layers, and SeTrG can scavenge radicals. SeTrG in the beginning of the process shows greater effect than SeG due to the presence of the potent antioxidant Trolox group.

We studied the inhibitory effect of SeG and SeTrG on  $\alpha$ -TOH consumption in MLV suspensions oxidized by the hydrophilic initiator SIN-1 (Fig. 7). Under air, SIN-1 thermally decomposes to nitric oxide and superoxide, which rapidly combine to peroxyntirite, which initiates lipid peroxidation (30). In MLV oxidation by SIN-1, SeTrG slightly spared  $\alpha$ -TOH. SeG did not show an effect.

The inhibitory effect of SeTrG on  $\alpha$ -TOH consumption in rat plasma oxidized by the hydrophilic initiator AAPH or MeO-AMVN, producing radicals both in the aqueous and the lipid phases, is shown in Figure 8. The kinetic curves of  $\alpha$ -



**FIG. 8.** Comparison of the effect of SeTrG at concentration 100  $\mu\text{M}$  (●,▲) on  $\alpha$ -TOH consumption in rat plasma oxidation under air at 37°C induced by 20 mM AAPH (●) or by 2 mM 2,2'-azobis(4-methoxy-2,4-dimethylvaleronitrile) (MeO-AMVN) (▲). Open symbols:  $\alpha$ -TOH consumption without the addition of SeTrG in rat plasma oxidation induced by 20 mM AAPH (○) or by 2 mM MeO-AMVN (△). For abbreviations see Figures 1, 5, and 6.

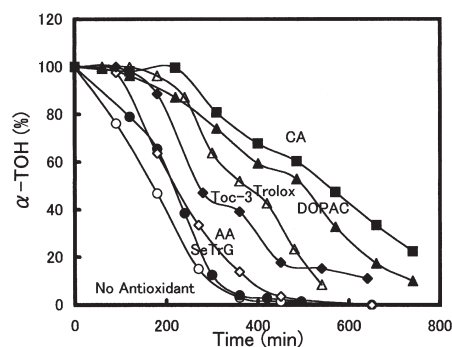


**FIG. 9.** Inhibitory effect of SeTrG (●) at concentration of 300  $\mu\text{M}$  on  $\alpha$ -TOH consumption in rat plasma oxidized for 60 min under air at 37°C by SIN-1 in the range of concentrations 0.3–1.2 mM. (○)  $\alpha$ -TOH consumption without the addition of SeTrG. For abbreviations see Figures 1, 6, and 7.

TOH consumption in AAPH and MeO-AMVN oxidations (open symbols) are almost identical. The presence of 100  $\mu\text{M}$  SeTrG (black symbols) induced a pronounced lag phase and delayed the oxidation rate. SeG did not spare  $\alpha$ -TOH in AAPH nor in MeO-AMVN rat plasma oxidations.

The effect of SeTrG on  $\alpha$ -TOH consumption against SIN-1 oxidation of rat plasma is shown in Figure 9. The presence of 300  $\mu\text{M}$  SeTrG spared the endogenous  $\alpha$ -TOH in plasma oxidized by SIN-1 at concentrations 0.3–1.2 mM (Fig. 9). In AAPH and MeO-AMVN oxidation of rat plasma, all of the endogenous  $\alpha$ -TOH was consumed, but in SIN-1 oxidation a considerable amount remained and was unchanged after 30 min of oxidation (data not shown). The same was seen in the erythrocyte hemolysis induced by SIN-1 (13). SeG was not effective against SIN-1 oxidation in rat plasma.

The efficiency of an antioxidant is dependent on the oxidant and model used. We showed that SeG reduced lipid hydroperoxides (Figs. 2, 3, 5) and protected  $\alpha$ -TOH in AAPH- or



**FIG. 10.** Comparison of the inhibitory effect of the antioxidants SeTrG (●), ascorbic acid (AA) (◇), tocotrienols (Toc-3) (◆), Trolox (△), 3,4-dihydroxyphenylacetic acid (DOPAC) (▲), and caffeic acid (CA) (■) at concentrations of 50  $\mu\text{M}$  on  $\alpha$ -TOH consumption in rat plasma oxidized by 20 mM AAPH under air at 37°C. (○)  $\alpha$ -TOH consumption without the addition of antioxidant. For abbreviations see Figures 1, 5, and 6.



AMVN-oxidized MLV suspensions, but not in rat plasma. Ebselen also reduced lipid hydroperoxides but had no radical-scavenging activities (7) and could not suppress the oxidations of LDL induced by AAPH (33). Ebselen spared  $\alpha$ -TOH during the initial stages of LDL oxidation initiated by a low flux of aqueous peroxy radicals (8). Both SeG and SeTrG inhibited the formation of lipid hydroperoxides (Fig. 5), but only SeTrG spared  $\alpha$ -TOH in plasma. We showed that only SeTrG had radical scavenging ability (Fig. 1). Also, in comparing the kinetic curves of  $\alpha$ -TOH consumption in rat plasma (Fig. 8) and in a liposome system (Fig. 6), it can be seen that in rat plasma  $\alpha$ -TOH is consumed with a pronounced lag phase, but in the MLV system without a lag phase. The same effect was seen in rat plasma oxidized by AAPH and explained "as a result of the reaction of the aqueous peroxy radicals with the aqueous antioxidants ascorbate, sulfhydryls, bilirubin and urate" (31). Rat plasma is a complex biological environment, containing lipids, proteins, and hydrophilic and lipophilic antioxidants (23,31). The relative importance of the different antioxidants may be influenced by factors such as mobility, reactivity with other antioxidants, and reactivity with oxidant radicals. This may explain why SeG did not spare  $\alpha$ -TOH in rat plasma but spared it in an MLV system when oxidized by the hydrophilic initiators AAPH or the lipophilic AMVN or MeO-AMVN. It was found previously that SeG reacts synergistically with tocopherols in sunflower oil (10). The presence of two hydroxyl groups in SeG may have an undesirable prooxidative effect (10). It is also possible that SeG has lower mobility in the membranes due to hydrogen bonding between the hydroxyl groups and the water (32).

In SIN-1 oxidations we showed that SeG did not spare  $\alpha$ -TOH, whereas ebselen suppressed erythrocyte hemolysis induced by peroxynitrite (13). Trolox does not effectively suppress erythrocyte hemolysis (13), but SeTrG, containing both Trolox and selenium, spared  $\alpha$ -TOH. SeTrG was more effective in rat plasma than in MLV. This could be explained by the fact that rat plasma contains micromolar concentrations of glutathione. Glutathione recycles the oxidized seleno-oxides (12). For example, the cellular selenium-containing enzymes glutathione peroxidases, phospholipid glutathione peroxidases, and selenoprotein P protect against peroxynitrite. They degrade peroxynitrite to nitric dioxide and water at the expense of glutathione, which is converted to glutathione disulfide (12).

To elucidate the structural role of the selenium compounds in the antioxidant properties, we compared the effects on  $\alpha$ -TOH consumption of SeTrG, Toc-3, and Trolox at a concentration of 50  $\mu$ M in rat plasma oxidized by 20 mM AAPH (Fig. 10). For comparison, the effects of the antioxidants AA, caffeic acid (CA), and 3,4-dihydroxyphenylacetic acid (DOPAC) (34) are shown in the same figure. SeTrG showed lower inhibitory effect than Toc-3 and Trolox, and Toc-3 had a lower inhibitory effect than Trolox. The phytol chain of chromanols has only a small effect on the inhibition of peroxidation, but is significant for the mobility of chromanols between membranes (23,32). Trolox, without a phytol chain,

can easily move between the membranes and shows potent antioxidant action. The glycerol part of SeTrG with the selenium-containing long hydrocarbon chain lowers its mobility in the membranes, which weakens the antioxidant activity of SeTrG compared to Trolox. The same comparison is valid for Toc-3 with their isoprenoid chain. Toc-3 are potent in decreasing rat plasma and LDL oxidizability (31,35).  $\alpha$ -Toc-3 activity is comparable to that of  $\alpha$ -TOH (31). CA and DOPAC show the strongest antioxidant effects owing to the presence of two hydroxyl groups in the *ortho* position (34).

In this paper we compared the inhibitory effect of the organic selenium compounds SeG and SeTrG *in vitro* on lipid peroxidation in organic solution, MeLOOH solution, methyl linoleate micelles, MLV suspensions, and rat plasma. SeTrG scavenged peroxy radicals. SeG reduced MeLOOH in methanol solution and in Fe<sup>2+</sup>/AA-catalyzed methyl linoleate micelle oxidation. SeTrG was more effective than SeG against Fe<sup>2+</sup>/AA-catalyzed methyl linoleate micelle oxidation. In rat plasma the two organoselenium compounds suppressed the formation of conjugated diene hydroperoxides in the AAPH-induced oxidation. In MLV suspensions SeG and SeTrG spared  $\alpha$ -TOH in AAPH- or AMVN-induced oxidations; SeTrG was effective in sparing  $\alpha$ -TOH during SIN-1 oxidation, but not SeG. In rat plasma SeTrG spared  $\alpha$ -TOH consumption in the AAPH-, MeO-AMVN-, or SIN-1-induced oxidations, but SeG was not effective. In conclusion, SeG and SeTrG showed antioxidant protection *in vitro*. They contain bound selenium, which is not available for the selenium pool, and are expected to be nontoxic to mammals.

## ACKNOWLEDGMENTS

The Japan Society for the Promotion of Science Postdoctoral Fellowship Program for Foreign Researchers supported this work. The authors are grateful to Dr. Ryota Maeba, Teikyo University School of Medicine, for advice on the preparation of the MLV suspensions and the experiments measuring the O<sub>2</sub> consumption.

## REFERENCES

1. Rayman, M.P. (2000) The Importance of Selenium to Human Health, *Lancet* 356, 233–241.
2. Flohe, L., Andreesen, J.R., Brigelius-Flohe, R., Maiorino, M., and Ursini, F. (2000) Selenium, the Element of the Moon, in *Life on Earth, IUBMB Life* 49, 411–420.
3. Parnham, M.J. (1996) The Pharmaceutical Potential of Seleno-organic Compounds, *Exp. Opin. Invest. Drugs* 5, 861–870.
4. Muges, G., du Mont, W.W., and Sies, H. (2000) Chemistry of Biologically Important Synthetic Organoselenium Compounds, *Chem. Rev.* 7, 2125–2179.
5. Feroci, G., and Fini, A. (1998) Study on the Antioxidant Effect of Several Selenium and Sulphur Compounds, *J. Trace Elem. Med. Biol.* 12, 96–100.
6. Müller, A., Cadenas, E., Graf, P., and Sies, H. (1984) A Novel Biologically Active Seleno-Organic Compound—I. Glutathione Peroxidase-like Activity *in vitro* and Antioxidant Capacity of PZ 51 (ebselen), *Biochem. Pharmacol.* 33, 3235–3239.
7. Noguchi, N., Yoshida, Y., Kaneda, H., Yamamoto, Y., and Niki, E. (1992) Action of Ebselen as an Antioxidant Against Lipid Peroxidation, *Biochem. Pharmacol.* 44, 39–44.

8. Lass, A., Witting, P., Stocker, R., and Esterbauer, H. (1996) Inhibition of Copper- and Peroxyl Radical-Induced LDL Lipid Oxidation by Ebselen: Antioxidant Actions in Addition to Hydroperoxide-Reducing Activity, *Biochim. Biophys. Acta* 1303, 111–118.
9. Muna, Z.A., Bolann, B.J., Chen, X., Songstad, J., and Berge, R.K. (2000) Tetradecylthioacetic Acid and Tetradecylselenoacetic Acid Inhibit Lipid Peroxidation and Interact with Superoxide Radical, *Free Radic. Biol. Med.* 28, 1068–1078.
10. Yanishlieva, N., Raneva, V., Marinova, E., Houte, H., Partali, V., and Sliwka, H.R. (2001) 11-Selenadodecylglyceryl-1-ether in Lipid Autoxidation, *J. Am. Oil Chem. Soc.* 78, 691–696.
11. Naalsund, T., Malterud, K.E., Partali, V., and Sliwka, H.R. (2001) Synthesis of a Triantioxidant Compound: Combination of  $\beta$ -Apo-8'-carotenoic Acid, Selenacapyroic Acid and Trolox in a Triglyceride, *Chem. Phys. Lipids* 112, 59–65.
12. Arteel, G.E., and Sies, H. (2001) The Biochemistry of Selenium and the Glutathione System, *Environm. Toxicol. Pharmacol.* 10, 153–158.
13. Kondo, H., Takahashi, M., and Niki, E. (1997) Peroxynitrite-Induced Hemolysis of Human Erythrocytes and Its Inhibition by Antioxidants, *FEBS Lett.* 413, 236–238.
14. Takabe, W., Niki, E., Uchida, K., Yamada, S., Satoh, K., and Noguchi, N. (2001) Oxidative Stress Promotes the Development of Transformation: Involvement of a Potent Mutagenic Lipid Peroxidation Product, Acrolein, *Carcinogenesis* 22, 935–941.
15. Borek, C. (2001) Antioxidant Health Effects of Aged Garlic Extract, *J. Nutr.* 131, 1010S–1015S.
16. Pillai, S.P., Mitscher, L.A., Menon, S.R., Pillai, C.A., and Shankel, D.M. (1999) Antimutagenic/Antioxidant Activity of Green Tea Components and Related Components, *J. Environ. Pathol. Toxicol. Oncol.* 18, 147–158.
17. Maiorino, M., Coassin, M., Roveri, A., and Ursini, F. (1989) Microsomal Lipid Peroxidation: Effect of Vitamin E and Its Functional Interaction with Phospholipid Hydroperoxide Glutathione Peroxidase, *Lipids* 24, 721–726.
18. Helzlsouer, K.J., Huang, H.Y., Alberg, A.J., Hoffman, S., Burke, A., Norkus, E.P., Morris, J.S., and Comstock, G.W. (2000) Association Between  $\alpha$ -Tocopherol,  $\gamma$ -Tocopherol, Selenium, and Subsequent Prostate Cancer, *J. Natl. Cancer Inst.* 92, 2018–2023.
19. Mutlu-Türkoglu, Ü., Erbil, Y., Öztezcan, S., Olgaç, V., Toker, G., and Uysal, M. (2000) The Effect of Selenium and/or Vitamin E Treatments on Radiation-Induced Intestinal Injury in Rats, *Life Sci.* 66, 1905–1913.
20. Shokri, F., Heidari, M., Gharagozloo, S., and Ghazi-Khansari, M. (2000) *In vitro* Inhibitory Effects of Antioxidants on Cytotoxicity of T-2 Toxin, *Toxicol.* 146, 171–176.
21. Houte, H., Partali, V., Sliwka, H.R., and Quartey, E.G.K. (2000) Synthesis of Structured Lipids and Ether Lipids with Antioxidants: Combination of a Seleno Fatty Acid and a Seleno Fatty Alcohol with a Carotenoid Acid in Glyceride Molecule, *Chem. Phys. Lipids* 105, 105–114.
22. Noguchi, N., Yamashita, H., Gotoh, N., Yamamoto, Y., Numano, R., and Niki, E. (1998) 2,2'-Azobis(4-Methoxy-2,4-dimethylvaleronitrile), a New Lipid-Soluble Azo Initiator: Application to Oxidations of Lipids and Low-Density Lipoprotein in Solution and in Aqueous Dispersions, *Free Radic. Biol. Med.* 24, 259–268.
23. Gotoh, N., Noguchi, N., Tsuchiya, J., Morita, K., Sakai, H., Shimasaki, H., and Niki, E. (1996) Inhibition of Oxidation of Low Density Lipoprotein by Vitamin E and Related Compounds, *Free Rad. Res.* 24, 123–134.
24. Abe, K., and Katsui, G. (1975) Determination of Tocopherols in Serum by High Speed Liquid Chromatography, *Vitamins (Japan)* 49, 259–263.
25. Abe, K., Ohmae, M., and Katsui, G. (1976) Rapid and Micro-Method for Determination of Tocopherols in Liver, *Vitamins (Japan)* 50, 453–457.
26. Shabit, J., Ishida, Y., Shimasaki, H., and Ueta, N. (1998) Biological Tissue Damage Induced by AMVN [2,2'-Azobis-(2,4-dimethylvaleronitrile)] and Its Inhibition by  $\alpha$ -Tocopherol in Rats, *Teikyo Medical Journal* 21, 211–218.
27. Niki, E., Noguchi, N., Tsuchihashi, H., and Gotoh, N. (1995) Interaction Among Vitamin C, Vitamin E, and  $\beta$ -Carotene, *Am. J. Clin. Nutr.* 62, 1322S–1326S.
28. Noguchi, N., Nishino, K., and Niki, E. (2000) Antioxidant Action of the Antihypertensive Drug, Carvedilol, Against Lipid Peroxidation, *Biochem. Pharmacol.* 59, 1069–1076.
29. Niki, E., Saito, T., Kawakami, A., and Kamiya, Y. (1984) Inhibition of Oxidation of Methyl Linoleate in Solution by Vitamin E and Vitamin C, *J. Biol. Chem.* 259, 4177–4182.
30. Darley-Usmar, V.M., Hogg, N., O'Leary, V.J., Wilson, M.T., and Moncada, S. (1992) The Simultaneous Generation of Superoxide and Nitric Oxide Can Initiate Lipid Peroxidation in Human Low Density Lipoproteins, *Free Rad. Res. Commun.* 17, 9–20.
31. Suarna, C., Hood, R.L., Dean, R.T., and Stocker, R. (1993) Comparative Antioxidant Activity of Tocotrienols and Other Natural Lipid-Soluble Antioxidants in a Homogeneous System, and in Rat and Human Lipoproteins, *Biochim. Biophys. Acta* 1166, 163–170.
32. Niki, E. (1987) Inhibition of Oxidation of Liposomal- and Biomembranes by Vitamin E, in *Clinical and Nutritional Aspects of Vitamin E* (Hayashi, O., and Mino, M., eds.), pp. 3–13, Elsevier Science Publishers, Amsterdam.
33. Noguchi, N., Gotoh, N., and Niki, E. (1994) Effects of Ebselen and Probucol on Oxidative Modifications of Lipid and Protein of Low Density Lipoprotein Induced by Free Radicals, *Biochim. Biophys. Acta* 1213, 176–182.
34. Raneva, V., Shimasaki, H., Ishida, Y., Ueta, N., and Niki, E. (2001) Antioxidative Activity of 3,4-Dihydroxyphenylacetic Acid and Caffeic Acid in Rat Plasma, *Lipids* 36, 1111–1116.
35. O'Byrne, D., Grundy, S., Packer, L., Devaraj, S., Baldenius, K., Hoppe, P.P., Kraemer, K., Jialal, I., and Traber, M.G. (2000) Studies of LDL Oxidation Following  $\alpha$ -,  $\gamma$ -, or  $\delta$ -Tocotrienyl Acetate Supplementation of Hypercholesterolemic Humans, *Free Rad. Biol. Med.* 29, 834–845.

[Received February 18, 2002, and in revised form June 27, 2002; revision accepted July 15, 2002]

# Interaction of CETP Inhibitory Peptide and Lipoprotein Substrates in Cholesteryl Ester Transfer Assay: Relationship Between Association Properties and Inhibitory Activities

Kyung-Hyun Cho<sup>a</sup>, Ju-Young Lee<sup>b</sup>, Myung-Sook Choi<sup>c</sup>, Song-Hae Bok<sup>a</sup>, and Yong Bok Park<sup>b,\*</sup>

<sup>a</sup>Cardiovascular Research Laboratory, Korea Research Institute of Bioscience and Biotechnology, Yuseong, Daejeon, 305-333, Korea, <sup>b</sup>Department of Genetic Engineering, College of Natural Sciences, and <sup>c</sup>Department of Food Science and Nutrition, College of Human Ecology, Kyungpook National University, Taegu, 702-701, Korea

**ABSTRACT:** In a previous study, CETP inhibitory peptide (3 kDa) was isolated from hog plasma. The peptide, synthesized chemically according to the amino acid sequence of the 3-kDa peptide (designated P<sub>28</sub>), showed CETP inhibitory activity both *in vitro* and *in vivo* [Cho *et al.* (1998) *Biochim. Biophys. Acta* 1391, 133–144]. We report herein further unique features of P<sub>28</sub> when it was associated with the cholesteryl ester (CE)-donor and -acceptor lipoproteins. Lipoprotein substrates with P<sub>28</sub> present in both HDL (as a CE-donor) and LDL (as a CE-acceptor) served as poor substrates, with CE-transfer activity decreased up to 60% compared to normal substrates without P<sub>28</sub>. P<sub>28</sub> was found to be located in HDL fractions of hog plasma and showed the same electromobility as that visualized by PAGE on 7% polyacrylamide gel under nondenaturing conditions. Addition of apolipoprotein A-1 (apoA-1) or apoB antibody to a normal CE-transfer mixture did not alter CE-transfer activity. However, addition of apoA-1 or -B antibody to a CETP-inhibition mixture decreased the inhibitory activity of P<sub>28</sub> by *ca.* 20%. Western blot analysis revealed that P<sub>28</sub> was associated only with human and hog HDL among several lipoproteins purified from human, hog, and rabbit. CETP-inhibition assays with various lipoprotein substrates revealed that P<sub>28</sub> exhibited substrate-specific inhibitory activity. The inhibitory activity of P<sub>28</sub> was highly dependent on the type of lipoprotein substrate (whether CE-donor or -acceptor); P<sub>28</sub> inhibited CE transfer from HDL to LDL, but it did not inhibit CE transfer from HDL to HDL.

Paper no. L8941 in *Lipids* 37, 641–646 (July 2002).

Human CETP redistributes cholesteryl ester (CE) and TAG between nonequilibrated lipoproteins in plasma. CETP, a 70–74 kDa hydrophobic glycoprotein (1,2), regulates the concentration of HDL-cholesterol in the blood stream (3,4). Even though the role of CETP in atherosclerosis is still controversial, many reports have concluded that CETP plays an atherogenic role in reversing cholesterol transport. Inhibition of CETP activity in animals having normal levels of CETP (5–7) and introduction of human CETP into CETP-deficient animals (8–12) have demonstrated that CETP accelerates the accumulation of CE in LDL, resulting in a retardation of cholesterol

removal from the blood stream. In addition, transgenic expression of simian CETP cDNA in mice (13) led to a decrease in HDL-cholesterol and a subsequent appearance of atherosclerotic lesions after prolonged feeding of a cholesterol-rich diet (14). Reduced plasma CETP activity induced by CETP vaccination resulted in an improved lipoprotein profile and a reduction in aortic lesions in a rabbit model (15). Recently, a chemical CETP inhibitor treatment with human subjects raised HDL-cholesterol levels in phase II clinical trial (16).

Although the precise mechanism of CE transfer by CETP has not been fully elucidated, it is generally accepted that neutral lipid exchange involves at least two key steps: (i) the interaction of CETP with lipoprotein particles, from which (ii) it picks up or deposits neutral lipid molecules (17). Three general models have been proposed in the light of data from kinetic studies (18–20). The first suggests that CETP could act as a shuttle carrying CE and TAG between distinct lipoprotein fractions (18). The second indicates that CETP could also mediate the formation of a ternary collision complex involving one lipoprotein donor, one lipoprotein acceptor, and CETP (19). The third model is similar to the second but includes the presence of dimeric CETP (20).

A few proteins from animal plasma have been used as modulators of CETP or lipid transfer inhibitor proteins (LTIP). Apolipoprotein F (apoF) was purified from human lipoprotein-deficient serum, associated with LDL (21). A peptide with high homology to the amino terminus of apoC-1 was purified from baboon plasma associated with HDL<sub>1</sub> (22). Those reports indicate that association characteristics of the CETP inhibitor and lipoprotein substrate are variable depending on their individual properties.

In a previous study, we purified CETP inhibitory peptide from hog plasma by ultracentrifugation, sequential column chromatographies, and finally electroelution from polyacrylamide gel (23). M.W. of the peptide was approximately 3 kDa. A peptide synthesized chemically according to the amino acid sequence of the 3-kDa peptide (designated P<sub>28</sub>) showed approximately the same degree of CETP inhibitory activity as the purified 3-kDa peptide. The sequence of P<sub>28</sub> was as follows: N-Glu-Asp-Thr-Ser-Pro-Glu-Asp-Lys-Met-Gln-Asp-Tyr-Val-Lys-Gln-Ala-Thr-Arg-Thr-Ala-Gln-Asp-Ala-Leu-Thr-Ser-Val-Lys-C.

In this study, we investigated the association properties of the synthesized peptide (P<sub>28</sub>) with lipoproteins, especially in

\*To whom correspondence should be addressed at Department of Genetic Engineering, College of Natural Sciences, Kyungpook National University, Taegu, 702-701, Korea. E-mail: parkyb@knu.ac.kr

Abbreviations: ApoA-1, apolipoprotein A-1; apoB, apolipoprotein B; BCA, biconchonic acid; CE, cholesteryl ester; HDL<sub>R</sub>, reconstituted HDL; LDL<sub>R</sub>, reconstituted LDL; LTIP, lipid transfer inhibitor protein; PVDF, polyvinylidene difluoride.



HDL and LDL, to determine accurately its properties in the lipoprotein–substrate complex and extended effects on the degree of CETP inhibition activity among various substrates.

## EXPERIMENTAL PROCEDURES

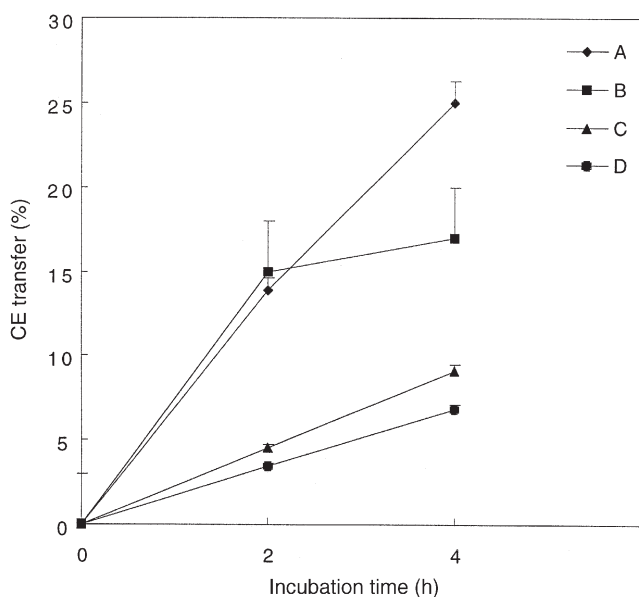
**Materials.** Radioactive  $1\alpha,2\alpha$ - $n$ - $[^3\text{H}]$ cholesteryl oleate was purchased from Amersham Life Sciences (Amersham, United Kingdom). CNBr-activated Sepharose 4B was obtained from Pharmacia (Uppsala, Sweden). Immobilon-P<sup>SQ</sup> membrane was purchased from Millipore (Bedford, MA). Antihuman apoA-1 IgG, antihuman apoB IgG, and enzyme-coupled secondary reagents were purchased from Boehringer Mannheim Biochemicals (Mannheim, Germany). All other reagents were obtained from Sigma (St. Louis, MO).

Human plasma was obtained from fresh EDTA-containing blood (donated by healthy male volunteers who had fasted for 16 h) by low-speed centrifugation ( $5,000 \times g$ ) for 15 min at  $4^\circ\text{C}$ . Hog and rabbit blood were collected in bottles containing  $\text{Na}_2\text{-EDTA}$  (final concentration = 1 mg/mL), and plasma was isolated by the same method as for human plasma. Aliquots of fresh plasma were placed in tubes containing sodium azide (0.02% wt/vol), phenyl-methyl-sulfonyl fluoride (1 mM in the final concentration), and chloramphenicol (50  $\mu\text{g}/\text{mL}$  in the final concentration), and stored at  $-70^\circ\text{C}$  until use.

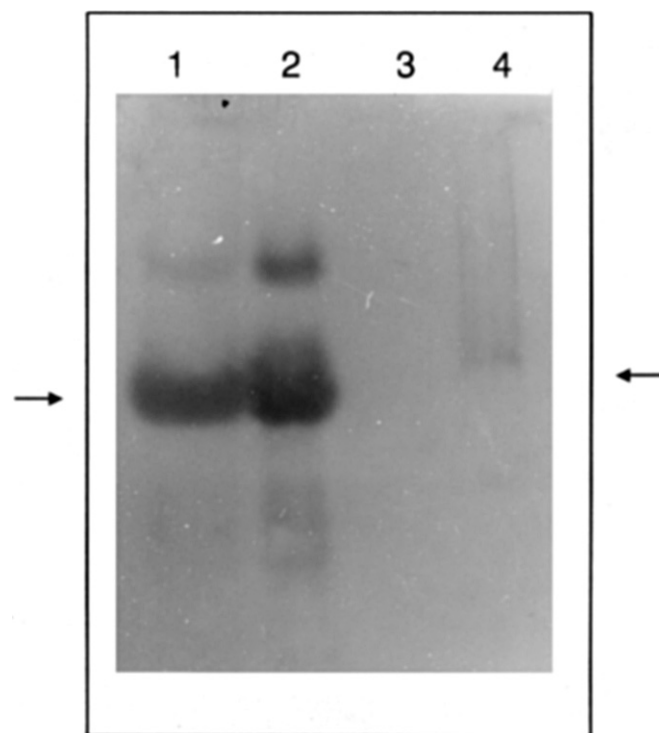
**Isolation of lipoproteins and partial purification of CETP.** HDL ( $d = 1.063\text{--}1.21$ ), LDL ( $d = 1.019\text{--}1.063$ ), and VLDL

( $d = 0.95\text{--}1.006$ ) were isolated from normolipidemic human, rabbit, or hog plasma by a standard protocol including ultracentrifugation (24) and gel filtration column chromatography (25). The isolated lipoproteins were dialyzed against 10 mM ammonium bicarbonate/5 mM EDTA to remove excessive potassium bromide. The purified human LDL and HDL were used individually as CE-acceptors in the CE-transfer assays. Human CETP was partially purified to about 80% purity by ammonium sulfate precipitation (15% in the final concentration, wt/vol) and phenyl-Sepharose column chromatography, as previously described by Albers *et al.* (26). Purity of the CETP and its activity were determined by SDS-PAGE and CE-transfer assays. Protein concentration was determined by using the Pierce bicinchoninic acid (BCA) protein assay reagent (Rockford, IL) with BSA as a standard.

**Preparation of reconstituted HDL and LDL.** Reconstituted lipoproteins were used as artificial substrates for the CE-transfer assay, where tritiated reconstituted HDL ( $[^3\text{H}]\text{HDL}_R$ ) containing apoA-1 and reconstituted LDL ( $\text{LDL}_R$ ) containing apoB were used as the CE-donor and CE-acceptor, respectively, in the CETP assay. They were prepared by the sodium cholate dialysis method as described previously (27,28). For synthesis of both  $\text{HDL}_R$  and  $\text{LDL}_R$  lipoproteins containing



**FIG. 1.** Effect of lipoprotein substrates on cholesteryl ester (CE)-transfer activities in the presence or absence of  $\text{P}_{28}$ . Final concentration of  $\text{P}_{28}$  in reconstituted lipoproteins was 10  $\mu\text{M}$ . Lipoprotein reconstitution and CETP assay were carried out as described in the Experimental Procedures section. Line A, CE transfer from  $\text{HDL}_R$  (where R = reconstituted) to  $\text{LDL}_R$ ; line B, CE transfer from  $\text{P}_{28}\text{-HDL}_R$  to  $\text{LDL}_R$ ; line C, CE transfer from  $\text{HDL}_R$  to  $\text{P}_{28}\text{-LDL}_R$ ; line D, CE transfer from  $\text{P}_{28}\text{-HDL}_R$  to  $\text{P}_{28}\text{-LDL}_R$ . The substrates containing  $\text{P}_{28}$  (line D) showed CE-transfer activity diminished up to 60% compared to the normal substrates (line A). Data are expressed as mean  $\pm$  SD from triplicate determinations. For  $\text{P}_{28}$  sequence see text.



**FIG. 2.** Immunodetection of the 3-kDa peptide after SDS-PAGE with 7% nondenaturing polyacrylamide gel. Proteins were loaded onto the gel without denaturation. Immunoreacted bands were visualized by alkaline phosphatase conjugate (nitro blue tetrazolium/5-bromo-4-chloro-3-indolylphosphate; Sigma, St. Louis, MO). Lane 1, lipid transfer complex containing hog HDL (50  $\mu\text{g}$  of apolipoproteins),  $\text{LDL}_R$  (50  $\mu\text{g}$  of apoB), partially purified CETP (300  $\mu\text{g}$ ), and  $\text{P}_{28}$  (90  $\mu\text{g}$ ); lane 2,  $\text{P}_{28}$  (90  $\mu\text{g}$ ); lane 3,  $\text{LDL}_R$  (50  $\mu\text{g}$  of apoB); lane 4, hog HDL (50  $\mu\text{g}$  of apolipoproteins). Arrows indicate immunodetected band by anti- $\text{P}_{28}$ -IgG. For  $\text{P}_{28}$  sequence see text.



$P_{28}$ , concentrations of  $P_{28}$  in the reconstituted lipoproteins were adjusted to 10  $\mu$ M (final concentration).

**CETP and its inhibition assay.** A CE-transfer assay was carried out using tritiated HDL<sub>R</sub> as the CE-donor substrate for CETP. The HDL<sub>R</sub> was covalently immobilized on agarose for easy separation of [<sup>3</sup>H]HDL<sub>R</sub>-agarose after CE-transfer incubation, as described previously (23).

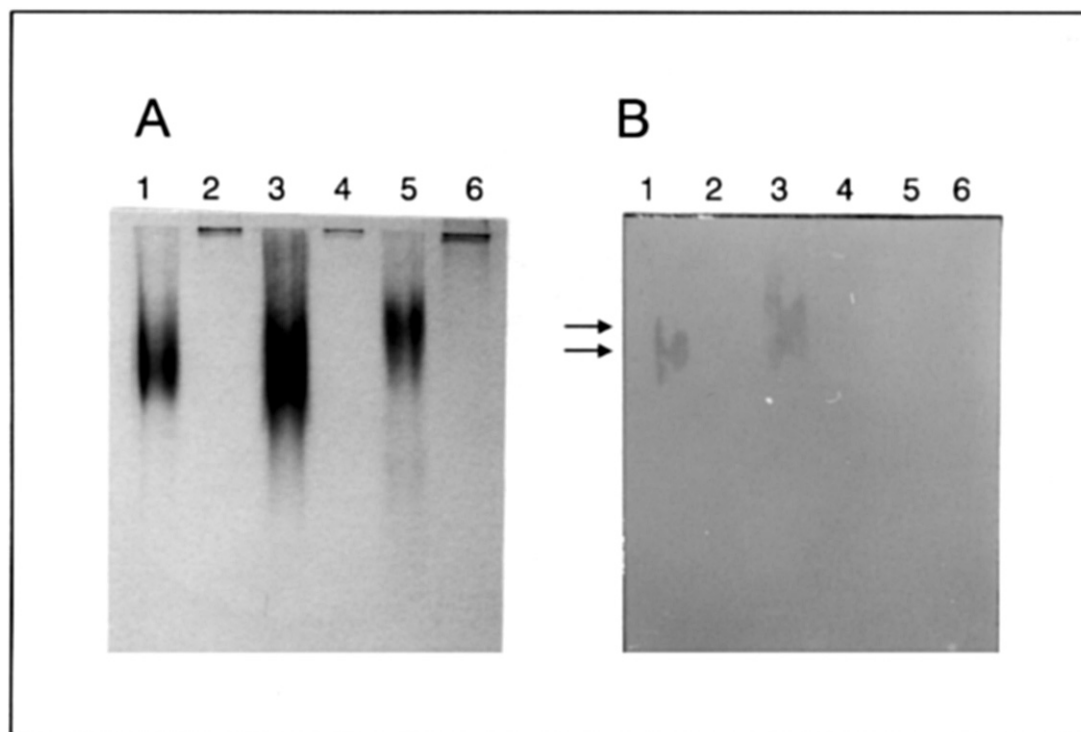
To determine the effect of apoA-1 or apoB antibody addition on CETP inhibition activity of  $P_{28}$ , antihuman apoA-1 or apoB IgG was pre-incubated with partially purified CETP for 30 min at 37°C to inactivate the CETP source. After pre-incubation,  $P_{28}$  was added to the mixture as an inhibitor source, and the total mixture was re-incubated for 1 h at 37°C. After incubation, normal substrates (LDL<sub>R</sub> and HDL<sub>R</sub>) were added to the mixture and incubated for another 2 h at 37°C with shaking. After incubation, the supernatant of the mixture was removed and counted in a scintillation analyzer (Packard Tri-carb 1600TR) to calculate specific CE-transfer activity compared to a control group without antibody addition during pre-incubation.

**Preparation of antibodies against  $P_{28}$  and immunoblotting.** Antibodies against the  $P_{28}$  were produced and IgG was isolated according to a standard method, described elsewhere (29). For immunoblotting experiments, protein samples to be tested were electrophoresed in two gel slabs in parallel: Pro-

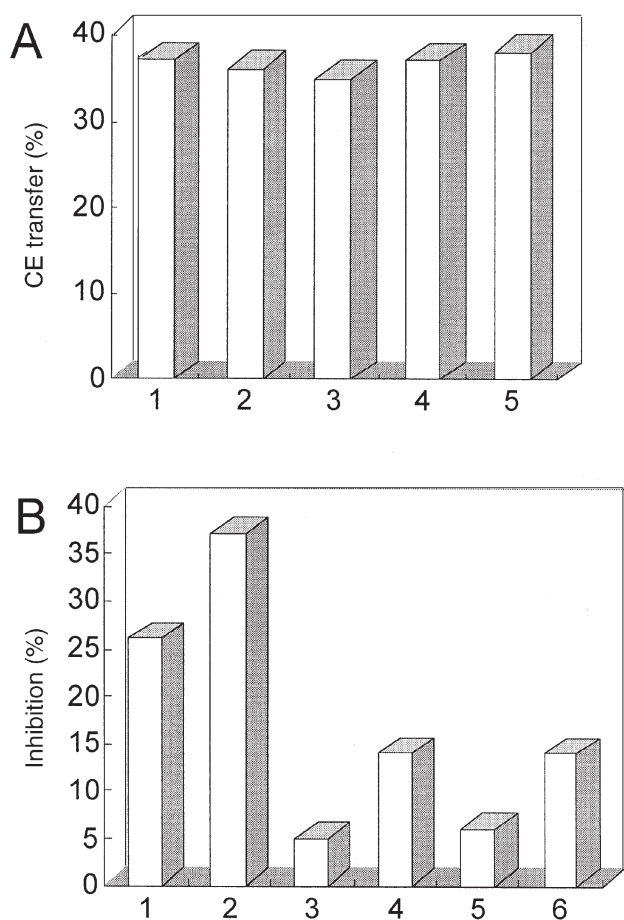
teins on one gel were stained with 0.125% Coomassie brilliant blue R-250 and the other gel was electroblotted onto the Immobilon-P<sup>SQ</sup> membrane using a Semi-Phor transfer unit (Hoefer Scientific Instruments, San Francisco, CA) at 50 mA for 90 min. The blotted membrane was incubated with the antibody against the  $P_{28}$  (diluted 1:10<sup>4</sup>) in the presence of 1% BSA/0.1% Tween-20 in PBS (pH 7.4). Immunoreacted bands were visualized as described by Towbin and Gordon (29).

To identify the original location of the 3 kDa peptide and the effect of  $P_{28}$  in the lipid transfer complex, we incubated 9  $\mu$ g of  $P_{28}$ , 300  $\mu$ g of partially purified CETP, 50  $\mu$ g of hog HDL, and 320  $\mu$ g of hog LDL at 37°C for 16 h to allow them to bind completely with the lipoproteins. After incubation, the mixture was loaded onto 7% polyacrylamide gel without SDS-treatment and boiled to allow migration with its native charge. After electrophoresis, proteins on the gel were blotted onto the PVDF membrane to analyze with anti- $P_{28}$  IgG to compare the preferential binding properties between lipoproteins and the  $P_{28}$ .

**Association properties of  $P_{28}$  and lipoproteins.** The purified LDL (10  $\mu$ g) and HDL (6  $\mu$ g) from human, hog, and rabbit were incubated individually with  $P_{28}$  (10  $\mu$ g) for 1 h at 37°C, and the incubation mixtures were concentrated completely by a SpeedVac<sup>®</sup> Plus (Savant Instruments, Farmingdale, NY). The concentrated mixtures were redissolved in 10



**FIG. 3.** Different association patterns of  $P_{28}$  with various lipoproteins. Ten micrograms of the  $P_{28}$  was incubated with 6  $\mu$ g of HDL or 10  $\mu$ g of LDL from hog, human, and rabbit, individually, in a shaking incubator for 1 h at 37°C. The mixtures were concentrated and electrophoresed in 8% polyacrylamide gel without SDS-treatment and sample boiling to allow migration with its native charge. Electrophoretic patterns were visualized by Coomassie staining (A) and immunodetection (B) using  $P_{28}$ -IgG. Incubation mixtures of each lane are as follows. Lane 1,  $P_{28}$  and hog HDL; lane 2,  $P_{28}$  and hog LDL; lane 3,  $P_{28}$  and human HDL; lane 4,  $P_{28}$  and human LDL; lane 5,  $P_{28}$  and rabbit HDL; lane 6,  $P_{28}$  and rabbit LDL. Arrows indicate immunodetected bands detected in lanes 1 and 3. For  $P_{28}$  sequence see text.



**FIG. 4.** Effect of adding apolipoprotein antibody on CE-transfer (A) and CETP-inhibition (B) assays. Data were expressed as a mean value from triplicate determinations. (A), Partially purified human CETP (30  $\mu$ L, 300  $\mu$ g) was pre-incubated with apoA-1 or -B IgG for 1 h at 37°C. The mixtures were incubated with assay substrates (LDL<sub>R</sub> and HDL<sub>R</sub>) for 2 h at 37°C to allow the CE-transfer reaction from HDL<sub>R</sub> to LDL<sub>R</sub>. 1, CETP source + TBS (50  $\mu$ L); 2, CETP source + apoA-1 IgG (1.5  $\mu$ g); 3, CETP source + apoA-1 IgG (15  $\mu$ g); 4, CETP source + apoB IgG (1.5  $\mu$ g); 5, CETP source + apoB IgG (15  $\mu$ g). (B), Partially purified human CETP (30  $\mu$ L, 300  $\mu$ g) was pre-incubated with P<sub>28</sub> for 30 min at 37°C. After pre-incubation, the mixture was incubated with apoA-1 or apoB IgG for 1 h at 37°C. The mixtures were re-incubated with the assay substrates (LDL<sub>R</sub> and HDL<sub>R</sub>) for 2 h at 37°C to allow the CE-transfer reaction. 1, CETP source + TBS (50  $\mu$ L) + P<sub>28</sub> (5  $\mu$ M); 2, CETP source + TBS (50  $\mu$ L) + P<sub>28</sub> (50  $\mu$ M); 3, CETP source + apoA-1 IgG (1.5  $\mu$ g) + P<sub>28</sub> (5  $\mu$ M); 4, CETP source + apoA-1 IgG (15  $\mu$ g) + P<sub>28</sub> (50  $\mu$ M); 5, CETP source + apoB IgG (1.5  $\mu$ g) + P<sub>28</sub> (5  $\mu$ M); 6, CETP source + apoB IgG (15  $\mu$ g) + P<sub>28</sub> (50  $\mu$ M). For other abbreviations see Figure 1. TBS, Tris-buffered saline; for P<sub>28</sub> sequence see text.

$\mu$ L of electrophoresis sample buffer without SDS. The mixtures were electrophoresed in 7% polyacrylamide gel under native conditions and the gel was blotted onto the PVDF membrane for immunodetection.

## RESULTS AND DISCUSSION

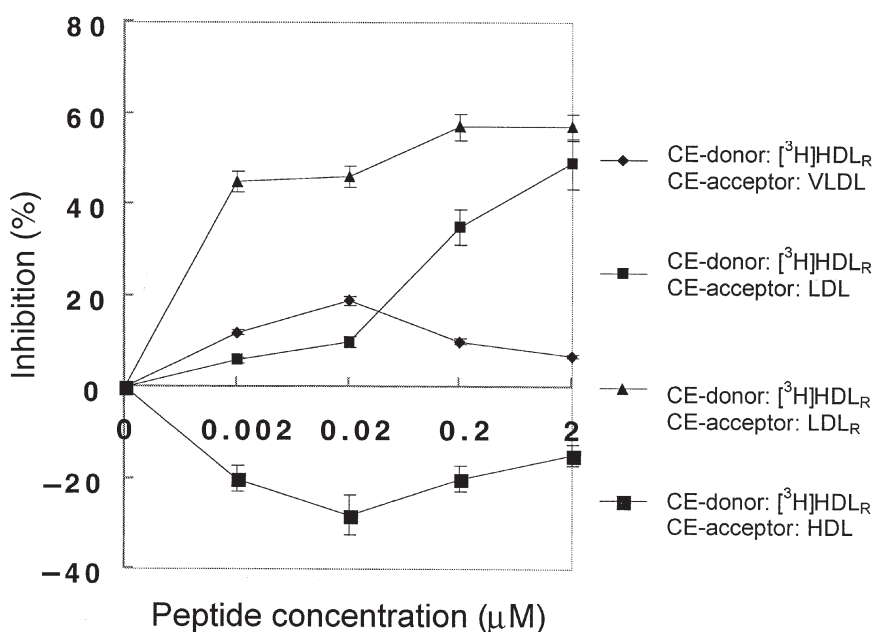
**Role of P<sub>28</sub> in the lipid-transfer complex.** The CE-donor (trinitated HDL<sub>R</sub>) and CE-acceptor (LDL<sub>R</sub>), both synthesized with

P<sub>28</sub> (designated P<sub>28</sub>-HDL<sub>R</sub> and P<sub>28</sub>-LDL<sub>R</sub>, respectively) according to previously described methods (23,25), were used to test the effect of P<sub>28</sub> in lipoprotein substrates, whether HDL<sub>R</sub> (CE-donor) or LDL<sub>R</sub> (CE-acceptor), in the CE-transfer mechanism of the lipid-CETP complex. As shown in Figure 1, normal substrates (from HDL<sub>R</sub> to LDL<sub>R</sub>) yielded 23.7  $\pm$  1% (mean  $\pm$  SD) of CE-transfer activity, and P<sub>28</sub>-containing substrates (from P<sub>28</sub>-HDL<sub>R</sub> to P<sub>28</sub>-LDL<sub>R</sub>) yielded only 6.8  $\pm$  2% of CE-transfer activity in the same condition. As shown in Figure 1, the presence of P<sub>28</sub> in lipoproteins (both HDL<sub>R</sub> and LDL<sub>R</sub>) decreased CE-transfer activity of the lipid-transfer complex by up to 60%. This result suggests that CE-transfer activity was altered by the presence of P<sub>28</sub> in substrates of both LDL and HDL. In human plasma, most of the CETP was associated with HDL particles (31,32), and kinetic studies revealed that either a carrier-mediated mechanism of transfer (19) or the formation of a ternary collision complex consisting of CETP and donor and acceptor lipoproteins was involved (18). The P<sub>28</sub> appears to interfere with the binding of CETP and lipoproteins by forming a lipid-transfer complex, as with other apolipoproteins, and this effect is equal in both HDL and LDL.

**Immunodetection of the 3 kDa in hog HDL fraction.** To determine the location of the 3-kDa peptide in the circulation of hog blood as well as the preferential binding properties of P<sub>28</sub> in the formation of a ternary collision complex, we incubated P<sub>28</sub>, the CETP source (human plasma), hog HDL, and hog LDL for 2 h at 37°C. After incubation, the mixture was electrophoresed on 7% polyacrylamide gel without sample denaturation. Proteins on the gel were blotted onto the PVDF membrane and immuno-detected with anti-P<sub>28</sub> IgG. Figure 2 illustrates that the mixture (lane 1) and the P<sub>28</sub> (lane 2) showed the same migration mobility on the gel, and a protein band was detected in the hog HDL fraction (lane 4) with the same band position as P<sub>28</sub> (lane 2). The mixture (lane 1) and the P<sub>28</sub> (lane 2) seemed to have similar electromobility, whereas the purified hog LDL did not show the same mobility. From this result, it is possible to predict that the 3-kDa peptide is associated with the hog HDL fraction in *in vivo* circulation.

**Association capabilities of P<sub>28</sub> and animal lipoproteins.** HDL and LDL fractions from normolipidemic animals (hog, human, and rabbit) were individually incubated with P<sub>28</sub> for 1 h at 37°C. The mixtures were concentrated completely and electrophoresed in 8% native polyacrylamide gel. As shown in panel B of Figure 3, the band detected in lanes 1 and 3 suggests that P<sub>28</sub> could form an association complex with hog and human HDL but not with rabbit HDL. On the contrary, the association of P<sub>28</sub> and LDL from the three species was not detected by the same immunoblotting analysis with P<sub>28</sub>-IgG (lanes 2, 4, and 6 of panel B). These results indicate that P<sub>28</sub> formed a lipoprotein complex with only hog and human HDL. Neither rabbit HDL nor LDL of the three species was associated with a lipoprotein complex, indicating that binding tendencies might be somewhat different in rabbit lipoproteins.

**Influence of apo antibodies on CE inhibition by P<sub>28</sub>.** Addition of the apoA-1 or -B antibody on the lipid-transfer com-



**FIG. 5.** CETP inhibition assay with various CE-acceptors. Reconstituted HDL (HDL<sub>R</sub>, 0.05 mL, 64 μg apolipoprotein, 30,000 dpm) was used as a CE-donor and reconstituted LDL (LDL<sub>R</sub>, 0.3 mL, 240 μg apolipoprotein), intact LDL (0.3 mL, 243 μg apolipoprotein), VLDL (0.3 mL, 56 μg apolipoprotein), or HDL (0.3 mL, 390 μg apolipoprotein) was used as a CE-acceptor. The CETP assay was carried out according to the method described by Cho *et al.* (23) using human plasma (0.05 mL) as a CETP source. The data were expressed as a mean ± SD of triplicate determinations. For other abbreviation see Figure 1.

plex involving HDL<sub>R</sub>, LDL<sub>R</sub>, and CETP did not reduce CE-transfer activity, as shown in panel A of Figure 4. This result suggests that the apoA-1 or apoB antibody did not affect normal transfer of CE from HDL to LDL. However, the inhibitory activity of P<sub>28</sub> decreased to 20% of the control value by adding the apoA-1 or apoB antibody to the incubation mixture, as shown in panel B of Figure 4. The P<sub>28</sub> showed 37% inhibition in the absence of the IgG (apoA-1 or -B), whereas it showed approximately 12% inhibition in the presence of apoA-1 or apoB IgG. These results indicate that the apoA-1 or apoB antibody might be effective in the CE-inhibition of P<sub>28</sub> by either association or interaction.

**Differential influence of CE-acceptors on CETP inhibition by P<sub>28</sub>.** CETP inhibition by P<sub>28</sub> in human plasma was shown to depend on the lipoprotein substrate, especially in CE-acceptors. The inhibitory activity was highly specific, depending on the type of substrate. When P<sub>28</sub> was incubated with LDL<sub>R</sub> as a CE-acceptor (Fig. 5), more than 40% of the CETP activity was inhibited. However, no inhibitory activity was shown when HDL was used as a CE-acceptor, indicating that P<sub>28</sub> could selectively inhibit CE-transfer from HDL to LDL. Under the same conditions, P<sub>28</sub> even facilitated CE transfer from donor to acceptor HDL.

Results of this study suggest that CETP, P<sub>28</sub>, and HDL operate together in the lipid transfer complex, as explained by others (32,33). The Morton group reported that CETP-VLDL and CETP-LDL complexes were much less stable than CETP-HDL complexes *in vitro* and that LTIP disrupts CETP

activity by binding to lipoproteins, interfering in the association of CETP with lipoproteins (32,34). The most acceptable hypothesis is that the formation of CETP-lipoprotein complexes is mediated by an electrostatic interaction between positively charged groups of CETP (35) and negatively charged lipoprotein surface components (33). Those reports strongly support the role of an electrostatic interaction in the formation of a lipid-transfer complex between CETP and lipoproteins. Since P<sub>28</sub> has a negatively charged group in its amino terminus, one possible hypothesis is that the presence of P<sub>28</sub> in lipoproteins may interfere with binding of CETP and lipoproteins, as demonstrated by Morton and Zilversmit (32). The presence of P<sub>28</sub> in HDL or LDL can alter CETP inhibition, and the effect is specific to the CE-acceptor.

#### ACKNOWLEDGMENT

This research was supported by a grant (no. KRF-2001-015-FP0066) from the Korea Research Foundation (KRF).

#### REFERENCES

1. Jarnagin, A.S., Kohr, W., and Fielding, C. (1987) Isolation and Specificity of a Mr 74,000 Cholesteryl Ester Transfer Protein from Human Plasma, *Proc. Natl. Acad. Sci. USA* 84, 1854–1857.
2. Hesler, C.B., Swenson T.L., and Tall, A.R. (1987) Purification and Characterization of a Human Plasma Cholesteryl Ester Transfer Protein, *J. Biol. Chem.* 262, 2275–2282.

3. Morton, R.E., and Zilversmit, D. B. (1983) Inter-relationship of Lipids Transferred by the Lipid-Transfer Protein Isolated from Human Lipoprotein-Deficient Plasma, *J. Biol. Chem.* *258*, 11751–11757.
4. Inazu, A., Brown, M.L., Hesler, C.B., Agellon, L.B., Koizumi, J., Takata, K., Maruhama, Y., Mabuchi, H., and Tall, A.R. (1990) Increased High-Density Lipoprotein Caused by a Common Cholesteryl Ester Transfer Protein Gene Mutation, *N. Engl. J. Med.* *323*, 1234–1238
5. Whitlock, M.E., Swenson, T.L., Ramakrishnan, R., Leonard, M.T., Marcel, Y.L., Milne, R.W., and Tall, A.R. (1989) Monoclonal Antibody Inhibition of Cholesteryl Ester Transfer Protein Activity in the Rabbit: Effects on Lipoprotein Composition and High Density Lipoprotein Cholesteryl Ester Metabolism, *J. Clin. Invest.* *84*, 129–137.
6. Abbey, M., and Calvert, G.D. (1989) Effects of Blocking Plasma Lipid Transfer Protein Activity in the Rabbit, *Biochim. Biophys. Acta* *1003*, 20–29.
7. Gaynor, B.J., Sand, T., Clark, R.W., Aiello, R.J., Bamberger, M.J., and Moberly, J.B. (1994) Inhibition of Cholesteryl Ester Transfer Protein Activity in Hamsters Alters HDL Lipid Composition, *Atherosclerosis* *110*, 101–109.
8. Ha, Y.C., Chang, L.B.F., and Barter, P.J. (1985) Effects of Injecting Exogenous Lipid Transfer Protein into Rats, *Biochim. Biophys. Acta* *833*, 203–210.
9. Quig, D.W., and Zilversmit, D.B. (1986) Disappearance and Effects of Exogenous Lipid Transfer Activity in Rats, *Biochim. Biophys. Acta* *879*, 171–178.
10. Ha, Y.C., and Barter, P.J. (1986) Effects of Sucrose Feeding and Injection of Lipid Transfer Protein on Rat Plasma Lipoproteins, *Comp. Biochem. Physiol. B* *83*, 463–466.
11. Gavish, D., Oschry, Y., and Eisenberg, S. (1987) *In vivo* Conversion of Human HDL3 to HDL2 and ApoE-rich HDL1 in the Rat: Effects of Lipid Transfer Protein, *J. Lipid Res.* *28*, 257–267.
12. Groener, J.E.M., van Gent, T., and van Tol, A. (1989) Effect of Lipid Transfer Protein on Plasma Lipids, Apolipoproteins and Metabolism of High-Density Lipoprotein Cholesteryl Ester in the Rat, *Biochim. Biophys. Acta* *1002*, 93–100.
13. Marotti, K.R., Castle, C.K., Murray, R.W., Rehberg, E.F., Polites, H.G., and Melchior, G.W. (1992) The Role of Cholesteryl Ester Transfer Protein in Primate Apolipoprotein A-I Metabolism: Insights from Studies with Transgenic Mice, *Arterioscler. Thromb.* *12*, 736–744.
14. Marotti, K.R., Castle, C.K., Boyle, T.P., Lin, A.H., Murray, R.W., and Melchior, G.W. (1993) Severe Atherosclerosis in Transgenic Mice Expressing Simian Cholesteryl Ester Transfer Protein, *Nature* *364*, 73–75.
15. Rittershaus, C.W., Miller, D.P., Thomas, L.J., Picard, M.D., Honan, C.M., Emmett, C.D., Pettey, C.L., Adari, H., Hammond, R.A., Beattie, D.T., et al. (2000) Vaccine-Induced Antibodies Inhibit CETP Activity *in vivo* and Reduce Aortic Lesions in a Rabbit Model of Atherosclerosis, *Arterioscler. Thromb. Vasc. Biol.* *20*, 2106–2112.
16. de Grooth, G.J., Kuivenhoven, J.A., Stalenhoef, A.F.H., de Graff, J., Zwinderman, A.H., Posma, J.L., van Tol, A., and Kastelein, J.J.P. (2002) Efficacy and Safety of a Novel Cholesteryl Ester Transfer Protein Inhibitor, JTT-705, in Humans: A Randomized Phase II Dose-Response Study, *Circulation* *105*, 2159–2165.
17. Barter, P.J., Hopkins, G.J., Gorjatschko, L., and Jones, M.E. (1982) A Unified Model of Esterified Cholesterol Exchanges Between Human Plasma Lipoproteins, *Atherosclerosis* *44*, 27–40.
18. Ihm, J., Quinn, D.M., Busch, S.J., Chataing, B., and Harmony, J.A.K. (1982) Kinetics of Plasma Protein-Catalyzed Exchange of Phosphatidylcholine and Cholesteryl Ester Between Plasma Lipoproteins, *J. Lipid Res.* *23*, 1328–1341.
19. Barter, P.J., and Jones, M.E. (1980) Kinetic Studies of the Transfer of Esterified Cholesterol Between Human Plasma Low and High Density Lipoproteins, *J. Lipid Res.* *21*, 238–249.
20. Tall, A.R. (1993) Plasma Cholesteryl Ester Transfer Protein, *J. Lipid Res.* *34*, 1255–1274.
21. Wang, X., Driscoll, D.M., and Morton, R.E. (1999) Molecular Cloning and Expression of Lipid Transfer Inhibitor Protein Reveals Its Identity with Apolipoprotein F, *J. Biol. Chem.* *274*, 1814–1820.
22. Kushwaha, R.S., Hasan, S.Q., McGill, H.C., Jr., Getz, G.S., Dunham, R.G., and Kanda, P. (1993) Characterization of Cholesteryl Ester Transfer Protein Inhibitor from Plasma of Baboons (*Papio* sp.), *J. Lipid Res.* *34*, 1285–1297.
23. Cho, K.H., Lee, J.Y., Choi, M.S., Cho, J.M., Lim, J.S., and Park, Y.B. (1998) A Peptide from Hog Plasma That Inhibits Human Cholesteryl Ester Transfer Protein, *Biochim. Biophys. Acta* *1391*, 133–144.
24. Havel, R.J., Eder, H.A., and Bragdon, J.H. (1955) The Distribution and Chemical Composition of Ultracentrifugally Separated Lipoproteins in Human Serum, *J. Clin. Invest.* *34*, 1345–1353.
25. Chen, C.H., and Albers, J.J. (1982) Characterization of Proteoliposomes Containing Apolipoprotein A-I: A New Substrate for the Measurement of Lecithin:Cholesterol Acyltransferase Activity, *J. Lipid Res.* *23*, 680–691.
26. Albers, J.J., Tollefson, J.H., Cheng, C.-H., and Steinmetz, A. (1984) Isolation and Characterization of Human Plasma Lipid Transfer Proteins, *Arteriosclerosis* *4*, 49–58.
27. Batzri, S., and Korn, E.D. (1973) Single Bilayer Liposomes Prepared Without Sonication, *Biochim. Biophys. Acta* *298*, 1015–1019.
28. Allen, T.M., Romans, A.Y., Kercret, H., and Segrest, J.P. (1980) Detergent Removal During Membrane Reconstitution, *Biochim. Biophys. Acta* *601*, 328–342.
29. Dunbar, B.S., and Schwoebel, E.D. (1990) Preparation of Polyclonal Antibodies, *Methods Enzymol.* *182*:663–670.
30. Towbin, H., and Gordon, J. (1984) Immunoblotting and Dot Immunobinding—Current Status and Outlook, *J. Immunol. Methods* *72*, 313–340.
31. Pattnaik, N.M., and Zilversmit, D.B. (1979) Interaction of Cholesteryl Ester Exchange Protein with Human Plasma Lipoproteins and Phospholipid Vesicles, *J. Biol. Chem.* *254*, 2782–2786.
32. Morton, R.E. (1985) Binding of Plasma-Derived Lipid Transfer Protein to Lipoprotein Substrates. The Role of Binding in the Lipid Transfer Process, *J. Biol. Chem.* *260*, 12593–12599.
33. Sammett, D., and Tall, A.R. (1985) Mechanisms of Enhancement of Cholesteryl Ester Transfer Protein Activity by Lipolysis, *J. Biol. Chem.* *260*, 6687–6697.
34. Morton, R.E., and Zilversmit, D.B. (1981) A Plasma Inhibitor of Triglyceride and Cholesteryl Ester Transfer Activities, *J. Biol. Chem.* *256*, 11992–11995.
35. Wang, S., Deng, L., Brown, M.L., Agellon, L.B., and Tall, A.R. (1991) Structure–Function Studies of Human Cholesteryl Ester Transfer Protein by Linker Insertion Scanning Mutagenesis, *Biochemistry* *30*, 3484–3490.

[Received October 24, 2001, and in revised form May 5, 2002; revision accepted June 3, 2002]



# Intestinal Apolipoprotein B Secretion Is Inhibited by the Flavonoid Quercetin: Potential Role of Microsomal Triglyceride Transfer Protein and Diacylglycerol Acyltransferase

Adele Casaschi, Qi Wang, Ka'ohimanu Dang, Alison Richards, and Andre Theriault\*

Division of Medical Technology, John A. Burns School of Medicine, University of Hawaii at Manoa, Honolulu, Hawaii

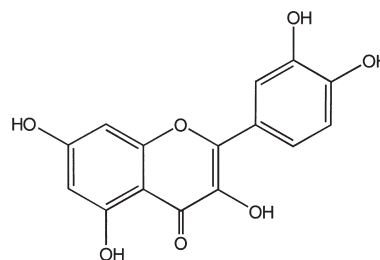
**ABSTRACT:** Recent studies have yielded evidence that plant flavonoids reduce hepatic lipid and apolipoprotein B (apoB) secretion. However, the possible role of flavonoids in regulating lipid and apoB secretion by the intestine has not been studied. The purpose of our study was to examine the effects of quercetin, a common dietary flavonoid, on TAG and apoB secretion in a human intestinal cell-line, CaCo-2. Differentiated postconfluent CaCo-2 cells grown on filters and pretreated with quercetin for 8 h were shown by ELISA to inhibit basolateral apoB secretion in a dose-dependent manner. At 15  $\mu$ M, the secretion of both apoB-100 and apoB-48 were inhibited similarly. This effect was shown to be specific, as quercetin did not affect the incorporation of [ $^{35}$ S]methionine/cysteine into secreted TCA-precipitable proteins. To determine the mechanism underlying this inhibitory effect, we examined two regulatory points: TAG availability and lipid transfer to the lipoprotein particle. Quercetin inhibited TAG synthesis under both basal and lipid-rich conditions, indicating that lipid availability is a determining factor in the regulation of apoB secretion by quercetin. The reduction was due at least in part to a decrease in diacylglycerol acyltransferase activity. We next examined lipid transfer or lipidation of the lipoprotein particle by analyzing microsomal TAG transfer protein (MTP) activity. Quercetin decreased MTP activity moderately. In summary, the data demonstrated that pharmacological concentrations of quercetin are a potent inhibitor of intestinal apoB secretion and that reduced lipid availability and lipidation in the lipoprotein assembly step are the mechanism for the suppression of apoB-containing lipoprotein secretion by quercetin in CaCo-2 cells.

Paper no. L9011 in *Lipids* 37, 647–652 (July 2002).

Several epidemiological studies have demonstrated an association of a quercetin-rich diet with a lowered risk of developing cardiovascular disease (CVD) (1–3). Abundant in onions, apples, red wine, and tea, quercetin (Scheme 1) has been shown to be protective against CVD by influencing several processes, including a decrease in LDL oxidation (4), a decrease in platelet aggregation (5), and an improved endothelial function (6). Furthermore, researchers have recently

\*To whom correspondence should be addressed at Division of Medical Technology, John A. Burns School of Medicine, University of Hawaii at Manoa, 1960 East-West Road, Biomed C-206, Honolulu, Hawaii 96822. E-mail: andret@hawaii.edu

Abbreviations: apoB, apolipoprotein B; apoB-Lp, apoB-containing lipoprotein; ACAT, acyl CoA:cholesterol acyltransferase; CVD, cardiovascular disease; DMEM, Dulbecco's modified Eagle's medium; DGAT, diacylglycerol acyltransferase; HMG, hydroxymethylglutaryl; IgG, immunoglobulin G; LDH, lactate dehydrogenase; MTP, microsomal TAG transfer protein; PVDF, polyvinylidene difluoride; SF, serum-free.



SCHEME 1

claimed that quercetin (7) and other plant flavonoids (8–10) possess lipid-lowering action. Among Japanese women, quercetin intake was inversely correlated with both total cholesterol and LDL-cholesterol (7). This lipid-lowering activity has obvious clinical significance. Consequently, there has been an increased interest in the investigation of plant flavonoids with respect to their lipid-lowering activity.

The mechanism of action of plant flavonoids on lipoprotein production has been the subject of recent study. Work from Huff's laboratory has shown that the citrus flavonoids naringenin and hesperetin reduced apolipoprotein B-containing lipoprotein (apoB-Lp) secretion in the human hepatoma cell line, HepG2, *via* reduced activity and expression of acyl CoA:cholesterol acyltransferase (ACAT) and microsomal TAG transfer protein (MTP) (11). ACAT is responsible for the synthesis of cholesterol ester in lipoprotein assembly, whereas MTP plays a role in lipoprotein assembly by catalyzing the transfer of lipids to nascent apoB molecules. Our laboratory also showed similar results in HepG2 cells with the flavonoid taxifolin, which was also shown to reduce hydroxymethylglutaryl (HMG) CoA reductase activity (12) and diacylglycerol acyltransferase (DGAT) activity (13). HMG CoA reductase and DGAT are considered to be the rate-limiting enzyme in the synthesis of cholesterol and TAG, respectively.

Lipid availability and lipid transfer to the nascent apoB molecule are acknowledged to be key factors in regulating apoB-Lp secretion (reviewed in Ref. 14). Particularly, the availability and transfer of TAG and cholesterol esters are thought to be primarily involved in the regulation of apoB-Lp secretion. Although progress has been made in understanding the regulation of hepatic apoB-Lp secretion by plant flavonoids, the contribution of these compounds in regulating lipid and apoB production by the intestine, an important lipogenic organ, has not been studied. Since the intestine has several characteristics that differ

from the liver, it is probable that the regulatory mechanism may differ. Structural differences are apparent as the liver produces a full-length apoB molecule (apoB-100), whereas the intestine produces a shortened, edited apoB molecule (apoB-48). Also, hepatic apoB is used for assembly of VLDL, while intestinal apoB is used for chylomicron assembly. The purpose of the present study is to examine the role of quercetin, a common flavonoid of the human diet, on lipid and apoB synthesis and secretion using a well-established human colon cancer cell line, CaCo-2, as the model system. Our hypothesis tested whether quercetin can suppress intestinal apoB-Lp secretion *via* lipid synthesis and/or lipid transfer. Since the intestine is an important site of lipid synthesis and lipoprotein production, this study could contribute to our understanding of the therapeutic action of flavonoids in hyperlipidemia.

## MATERIALS AND METHODS

**Materials.** Quercetin (3,5,7,3',4'-pentahydroxyflavone) dihydrate was purchased from Sigma Chemical Co. (St. Louis, MO) and dissolved in ethanol. An appropriate amount of stock solution was diluted with culture medium to give a final ethanol concentration of 0.1%. CaCo-2 cells (HTB-37) were obtained from American Type Culture Collection (ATCC; Rockville, MD). Cell culture media, FBS (certified grade), antibiotic-antimycotic mixture, and other tissue culture reagents were from InVitrogen Life Technologies Corp. (Carlsbad, CA). Transwell filters were obtained from Corning Costar Corp. (Cambridge, MA). Electrophoresis reagents and polyvinylidene difluoride (PVDF) membranes were from Bio-Rad Laboratories (Hercules, CA). [<sup>35</sup>S]Protein labeling mix (1175 Ci/mmol), [2-<sup>3</sup>H]glycerol (5–20 Ci/mmol), [palmitoyl-1-<sup>14</sup>C]palmitoyl coenzyme A (40–60 mCi/mmol), and Reflection™ autoradiography films were purchased from Perkin-Elmer Life Science Research Products (Boston, MA). Monospecific goat anti-human apoB antiserum was obtained from Alexon-Trend (Ramsey, MN). Plastic-backed TLC plates (Silica Gel 60) were from Alltech Associates Inc. (Deerfield, IL). Cell toxicity lactate dehydrogenase (LDH) assay was purchased from Promega Corp. (Madison, WI). Sodium oleate, 1,2-dioleoyl-*sn*-glycerol, BSA, EDTA, horseradish peroxidase conjugate anti-goat IgG, and other common laboratory reagents were from Sigma Chemical Co. MTP activity kit was from Roar Biomedical (New York, NY).

**Cell culture.** Differentiated CaCo-2 cell cultures were maintained in Dulbecco's modified Eagle's medium (DMEM) with 20% FBS and 0.1 mM nonessential amino acids at 37°C with 5% CO<sub>2</sub> and 95% air and subcultured in 24-mm diameter Transwell filters and grown to about 2 wk postconfluent. In experiments without oleate, cells were treated with quercetin in 20% FBS-DMEM. In studies with oleate, a serum-free (SF) medium (15) consisting of DMEM/F-12, 0.1 mM nonessential amino acids, 35 mg/L human transferrin, 5 mg/L bovine insulin, 20 μM ethanolamine, and 25 μM sodium selenite was used. Quercetin was added to both apical and basolateral media. We chose an 8-h incubation and added a nontoxic con-

centration of EDTA (0.5 mM) to the cell culture medium to minimize chemical instability of the compound (16). Untreated control cells received 0.1% (vol/vol) ethanol and EDTA without quercetin.

**ApoB ELISA.** ApoB mass in the basolateral media was determined using a competitive-binding ELISA as previously described (17).

**Lipid analysis.** To measure the rate of TAG synthesis and secretion, postconfluent treated and untreated cells were labeled with 80 μCi/mL [<sup>3</sup>H]glycerol for 8 h. After labeling, basolateral media and cells were harvested, and radiolabeled lipids were extracted and measured using TLC as described by Theriault *et al.* (12). After lipid extraction, cell proteins were digested in 1 mL of 0.1 N NaOH and measured as described below.

**Protein synthesis analysis.** Total protein synthesis was measured by the incorporation of [<sup>35</sup>S]methionine/cysteine (50 μCi/mL) into proteins and quantitated by TCA precipitation as described by Theriault *et al.* (12).

**Western blotting.** Equal amounts of basolateral media proteins were loaded and separated by SDS-PAGE (6% gel). Transfer of apoB molecules onto PVDF membrane was performed at 45 mA for 18 h in a cooled blotting buffer [25 mM Tris pH 7.7, 192 mM glycine, 0.1% (wt/vol) SDS, and 20% (vol/vol) methanol]. Immunoblotting was carried out as follows: The membrane was blocked in a blocking buffer (1 M Tris pH 7.5, 0.15 M NaCl, 0.1% Tween 20, and 5% nonfat dry milk) for 1 h; incubated with goat anti-human apoB antiserum (1:5,000) in rinsing buffer (1 M Tris pH 7.5, 0.15 M NaCl, 0.1% Tween 20) containing 10% BSA for 1 h; washed three times with rinsing buffer; incubated with horseradish peroxidase conjugate anti-goat IgG (1:16,000) in rinsing buffer containing 10% BSA for 1 h; and washed as described above. All incubations were performed on a shaker at room temperature. ApoB-antibody complexes were visualized with ECL™ chemiluminescence blotting reagents according to the manufacturer's instructions (Amersham Pharmacia Biotech, Piscataway, NJ). Quantification of the apoB bands was performed on an AMBIS Radioanalytic System (San Diego, CA) within the linear range of detection.

**DGAT activity assay.** Treated and untreated cells were harvested into a Tris buffer (175 mM, pH 7.8) and homogenized with a sonicator. Esterification of DAG was measured by using labeled palmitoyl-CoA as described by Grigor and Bell (18). The assay was performed in a total volume of 250 μL of Tris buffer (175 mM, pH 7.8) containing FA-free BSA (1 mg/mL), MgCl<sub>2</sub> (4 mM), and [1-<sup>14</sup>C]palmitoyl-CoA (0.25 μCi/mL). After a 10-min pre-incubation at 23°C, the reaction was started by adding homogenized cells (100 μg cell protein/mL) and 1,2-DAG (400 μM) for 10 min. The reaction was terminated by the addition of hexane, and the TAG formed was extracted and subjected to TLC in chloroform/acetic acid (96:4). The assay was linear up to 200 μg/mL of cell protein.

**Other methods.** Cell protein content was measured according to Bradford (19) (i.e. Bio-Rad) using BSA as the standard. The activity of LDH released into the media was measured spectrophotometrically using the CytoTox 96 nonradioactive

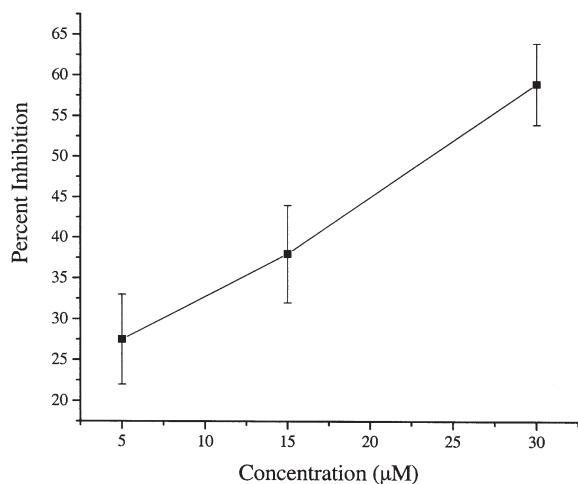
cytotoxicity assay according to the manufacturer's protocol (Promega Corp.). MTP activity in cell extracts was measured by a fluorescent assay according to the manufacturer's protocol (Roar Biomedical).

**Statistics.** All results with apoB and lipids were normalized to the amount of cellular protein. Statistical differences were analyzed by using Student's *t*-test with the level of significance set at 0.05.

## RESULTS

**Quercetin inhibits apoB secretion in a dose-dependent manner.** We initially based our concentration and incubation time on an earlier study investigating the fate of quercetin in CaCo-2 cells (16). Quercetin is known to be labile and undergo considerable catabolism during prolonged exposure in cell culture conditions. The above study showed that a concentration of 15  $\mu$ M for up to 8 h in the presence of FBS and a nontoxic concentration of EDTA inhibited the main pathway for chemical degradation of quercetin. The study indicated the degradation pathway was dependent on the presence of ferrous ions and EDTA chelated this iron. Therefore, this information was taken into account when evaluating its biological properties on apoB metabolism.

As shown in Figure 1, quercetin added in concentrations of 5, 15, and 30  $\mu$ M to the culture medium and held for 8 h decreased apoB mass into the basolateral media in a dose-dependent manner. Percent inhibition was  $27 \pm 5\%$  at 5  $\mu$ M,  $38 \pm 6\%$  at 15  $\mu$ M, and  $59 \pm 5\%$  at 30  $\mu$ M. At or below 30  $\mu$ M, there was no significant release of LDH into the media, indicating no cytotoxicity effect (data not shown). As a control to determine whether the effect of quercetin was specific to apoB, the amount of proteins secreted in the presence and ab-

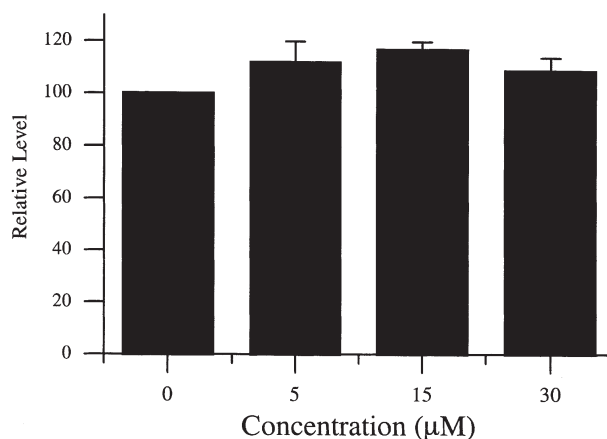


**FIG. 1.** Quercetin inhibits apolipoprotein B (apoB) secretion dose-dependently. CaCo-2 cells were treated with various concentrations of quercetin in 20% FBS-Dulbecco's modified Eagle's medium (DMEM) for 8 h. Untreated control cells received 0.1% ethanol without quercetin. The amount of apoB present in the basolateral media was determined by ELISA. Data are expressed as percent inhibition of untreated control cells (set as 100%). Values represent the mean  $\pm$  SD of two independent experiments performed in duplicate.

sence of quercetin was also analyzed by TCA-precipitation with cells labeled with [ $^{35}$ S]methionine/cysteine. As indicated in Figure 2, TCA-precipitable radioactivity from media incubated with up to 30  $\mu$ M quercetin remained essentially unchanged vs. the untreated control, indicating that the flavonoid did not alter protein secretion and that the effect on apoB secretion was specific. Subsequently, we chose the 15  $\mu$ M concentration in the following experiments since we felt this dose was well studied for its chemical stability in CaCo-2 cells. We consider this dose to be a pharmacological dose.

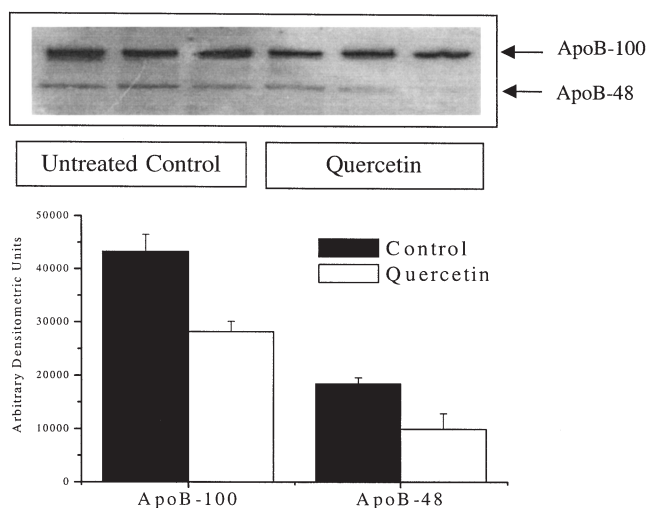
**Quercetin inhibits apoB-100 and -48 secretion.** CaCo-2 cells, unlike primary enterocytes, are known to synthesize two forms of apoB, which, together with lipids, assemble into a LDL/VLDL-sized lipoprotein particle (20). To further characterize the effect of quercetin on the secretion of the two M.W. forms of apoB (i.e., apoB-100 and apoB-48), we differentiated them by SDS-PAGE and immunoblotting. As shown in Figure 3, the secretion of apoB-100 and apoB-48 into the basolateral medium was inhibited by 35% ( $28,214 \pm 1,942$  vs.  $43,270 \pm 3,262$  arbitrary densitometric units) and 46% ( $18,395 \pm 1,193$  vs.  $9,950 \pm 2,934$  arbitrary densitometric units), respectively. The data suggest that quercetin is able to inhibit the assembly and secretion of intestinally derived lipoproteins, and the mechanism involved in the assembly of both forms of apoB in CaCo-2 cells may be similar.

**Quercetin inhibits apoB and TAG secretion under oleate treatment.** Oleate treatment is known to increase the secretion of apoB and a VLDL/chylomicron-sized lipoprotein in CaCo-2 cells (21). To investigate whether oleate can overcome the inhibitory effect of quercetin, we measured total apoB secretion by ELISA with cells treated with 15  $\mu$ M quercetin in the presence or absence of 0.8 mM oleic acid. In the presence of oleic acid, apoB secretion nearly doubled (Fig. 4). In the presence of quercetin, the inhibition of apoB secretion from oleate-treated cells was greater than non-oleate-treated cells (51% inhibition in the presence vs. 30% inhibition in the absence of oleate),

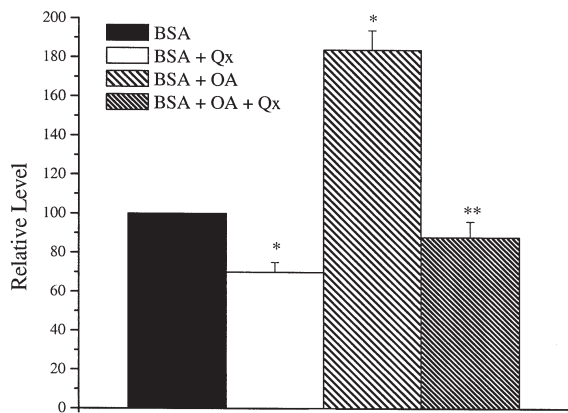


**FIG. 2.** Effect of quercetin on apoB secretion is specific. CaCo-2 cells were treated with and without quercetin for 6 h. Incubations were continued in the presence of [ $^{35}$ S]methionine/cysteine for 2 h. Total protein secretion was determined by TCA precipitation. Data are expressed relative to control (set as 100%). Values represent the mean  $\pm$  SD of two independent experiments performed in duplicate. For abbreviation see Figure 1.





**FIG. 3.** Quercetin inhibits apoB-100 and apoB-48 secretion. CaCo-2 cells were treated with and without quercetin (15  $\mu$ M) in 20% FBS-DMEM for 8 h. The amount of apoB-100 and apoB-48 present in the basolateral media was determined by Western blotting. The bottom figure is the data obtained from the densitometric scanning of the X-ray film (top figure) and is expressed as arbitrary densitometric units  $\pm$  SD. The figure is a representation of a typical experiment performed in triplicate. For abbreviations see Figure 1.



**FIG. 4.** Quercetin inhibits apoB secretion under lipid-rich condition. CaCo-2 cells were treated with and without quercetin (Qx) at 15  $\mu$ M in serum-free (SF) media containing BSA  $\pm$  oleic acid (OA) (0.81 mM) for 8 h. The amount of apoB secreted was analyzed by ELISA. Data are expressed relative to the BSA control (set as 100%). Values represent the results of two independent experiments performed in triplicate. \* $P$  < 0.05 vs. BSA control, \*\* $P$  < 0.05 vs. OA control. For abbreviation see Figure 1.

suggesting that quercetin can inhibit apoB secretion under lipid-rich conditions.

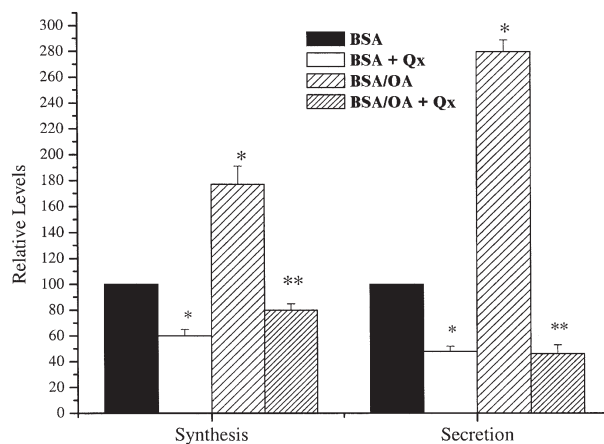
It has been reported that nascent TAG are preferentially used for the assembly of chylomicrons (20). Therefore, the effect of oleate and quercetin on TAG synthesis and secretion were assessed. As expected, oleate increased TAG synthesis and secretion by one- to twofold (Fig. 5). With respect to secretion, addition of quercetin resulted in a  $84 \pm 7\%$  inhibition in the presence of oleate and  $52 \pm 4\%$  in the absence of oleate ( $P$  < 0.05,  $n$  = 2). Quercetin inhibited TAG synthesis from oleate-treated cells by a similar percentage as in non-oleate-treated cells ( $40 \pm 5\%$

inhibition in the absence of oleate vs.  $55 \pm 5\%$  inhibition in the presence of oleate,  $P$  < 0.05,  $n$  = 2). Thus, it appears that supplementation of CaCo-2 cells with oleic acid is associated with a greater effect on apoB and TAG secretion by quercetin.

**Quercetin decreases DGAT and MTP activity.** The assembly process of intestinally derived lipoproteins depends on both the availability of TAG and the transfer of this lipid to apoB to form a primordial lipoprotein particle (20,21). DGAT is a critical enzyme for the synthesis of TAG for lipoprotein assembly, and MTP plays a role in lipoprotein assembly by catalyzing the transfer of lipids to nascent apoB molecules. Therefore, we examined the effect of quercetin on these two lipogenic enzymes, involved in TAG synthesis and secretion, in the presence of oleic acid. First, we tested the effect of quercetin on human CaCo-2 MTP activity by using fluorogenic-labeled donor liposomes and phospholipid acceptor liposomes. As shown in Figure 6, quercetin reduced MTP activity moderately ( $22 \pm 4\%$ ,  $P$  < 0.05,  $n$  = 2), but significantly, in oleate-treated cells. To determine the underlying mechanism of action of quercetin on TAG synthesis, we measured DGAT activity by means of the rate of incorporation of [ $^{14}$ C]palmitoylCoA into TAG. As shown in Figure 6, quercetin decreased DGAT activity by  $47 \pm 9\%$  ( $P$  < 0.05,  $n$  = 2). In combination, these results suggest that quercetin inhibited TAG-rich, apoB-48-containing lipoprotein secretion, in part through the reduction of both DGAT and MTP activity.

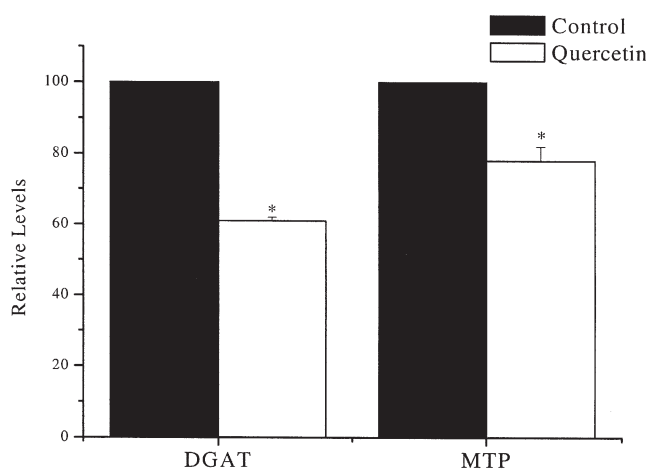
## DISCUSSION

Various dietary FA have been shown to exert effects on plasma TAG levels as a result of the altered assembly of intestinally derived lipoproteins (22,23). Like FA, a sizeable fraction of most flavonoids is absorbed by the small intestine (24). As a consequence, there is considerable interest in their biological



**FIG. 5.** Quercetin inhibits TAG synthesis and secretion. CaCo-2 cells were treated with and without quercetin (15  $\mu$ M) in SF media containing BSA  $\pm$  oleic acid (0.81 mM) in the presence of [ $^3$ H]glycerol for 8 h. Incorporation of glycerol into TAG was measured by TLC. Data are expressed as a percentage of BSA control (set as 100%). Values represent the mean  $\pm$  SD of two independent experiments performed in duplicate. \* $P$  < 0.05 BSA control; \*\* $P$  < 0.05 OA control. For abbreviations see Figure 4.





**FIG. 6.** Quercetin decreases diacylglycerol acyltransferase (DGAT) and microsomal TAG transfer protein (MTP) activity. CaCo-2 cells were treated with and without quercetin (15  $\mu$ M) in SF media containing BSA + oleic acid (0.81 mM) for 8 h. DGAT and MTP activities in whole cells were measured. Data are expressed as a percentage of the control (set as 100%). Values represent the mean  $\pm$  SD of two independent experiments performed in duplicate. \* $P < 0.05$  control.

effect on intestinal lipid metabolism. Despite recent reports on hepatic lipoprotein production (11,12), the effect of plant flavonoids on intestinal lipoprotein production has not been investigated previously. In this study, we examined the effect of quercetin, a common dietary flavonoid, on apoB and lipid synthesis and secretion using CaCo-2 cells as the model system. Our study showed that cells treated with quercetin for 8 h inhibited apoB secretion into the basolateral medium in a dose-dependent manner. The effect was shown to be specific, as general protein secretion remained essentially unchanged. We attributed this inhibitory action to quercetin and not its metabolites. A previous study indicated that, under our experimental conditions, quercetin was protected from metabolism and chemical degradation (15). The 50% inhibition concentration ( $IC_{50}$ ) was about 24  $\mu$ M, a concentration representing a pharmacological dose. Since CaCo-2 secretes two forms of apoB (i.e., apoB-100 and apoB-48), we examined whether quercetin exerted its effect on either form. It has been reported that MTP inhibitors added to CaCo-2 cells inhibited apoB-100, and not apoB-48 (15,25). In contrast, our results indicated a similar decrease in both forms of apoB, suggesting that mechanisms other than lipidation may be involved. To simulate postprandial conditions, cells were challenged with oleic acid. We have shown that apoB secretion can be stimulated by oleate supplementation. Addition of quercetin reversed the stimulatory effect of oleate, indicating that quercetin can inhibit apoB secretion under lipid-rich conditions. Consistent with the apoB studies, quercetin also inhibited the basolateral secretion of radiolabeled TAG in the absence and presence of oleic acid. These effects were more pronounced with oleate treatment.

To investigate the mechanism of action for the decrease in apoB-Lp secretion, we examined two possible regulatory points. First, we examined TAG availability, a major determining factor in the assembly and secretion of intestinally derived apoB-Lp. Upon addition of quercetin, *de novo* TAG synthesis

was markedly inhibited under basal and lipid-rich conditions, indicating TAG may be less available for the assembly of an apoB-Lp particle. This result is in agreement with our earlier report regarding a similar flavonoid of a different plant origin, taxifolin (12). In HepG2 cells taxifolin was shown to inhibit TAG synthesis; however, the molecular mechanism for this remained unresolved. In this study, we attempted to examine this question more closely. We chose to analyze the activity of DGAT, a key enzyme in TAG synthesis. It catalyzes the final reaction in the glycerol phosphate pathway, considered to be the main pathway for TAG synthesis (26). Supplementation of quercetin in the presence of oleic acid markedly reduced DGAT activity. This finding is novel as flavonoids have never been reported to decrease DGAT activity. Only a few naturally occurring compounds have been reported to inhibit DGAT activity (27–29). Thus, the inhibition of apoB-Lp secretion may be accounted for, in part, by low availability of TAG *via* reduced DGAT activity.

Transfer of lipids to the nascent apoB molecule to form the primordial lipoprotein is a second major determining factor in the assembly and secretion of intestinally derived apoB-Lp (25,30). Transfer of lipids, primarily TAG and cholesterol esters, is catalyzed by MTP. Since flavonoids reportedly inhibit MTP activity in HepG2 cells (11), we chose to examine this enzyme in CaCo-2 cells. Quercetin, in the presence of oleic acid, reduced MTP activity in CaCo-2 cells but to a lesser extent than was observed in HepG2 cells. A mildly inhibitory effect on the secretion of apoB also has been reported with BMS-200150, a specific MTP inhibitor, in CaCo-2 cells (25) and is consistent with our data. The moderate decrease in MTP activity caused by quercetin likely contributes to the reduction in apoB secretion. However, we cannot rule out that other steps in lipoprotein assembly and secretion may be involved with quercetin. Particularly, the marked reduction in apoB and TAG secretion under oleate treatment may not account for the modest decrease in both MTP and DGAT activity. ACAT activity and cholesterol ester availability may also be involved, as has been previously reported in HepG2 cells (11). However, since TAG is thought to be the preferentially used lipid for the assembly of intestinally-derived lipoprotein (20), we chose to examine only TAG synthesis in our CaCo-2 study.

The reduction of both DGAT and MTP activity by quercetin suggests that reduced availability and transfer of TAG to apoB may account for its lowering action on apoB-Lp secretion in CaCo-2 cells. These data are consistent with previous observations that flavonoids can inhibit TAG synthesis and MTP activity in HepG2 cells (11,12). Our data may have clinical relevance in the treatment of hypertriglyceridemia. However, the concentrations used in our study are not likely to be achieved by consuming quercetin-containing fruits and vegetables since flavonoids in general are considered micronutrients. Rather, our study allows for the identification of foods that could be genetically engineered to increase levels of specific flavonoids. Such metabolic engineering has recently been published with specific reference to flavonoids found in tomatoes (31). Our study also allows for new drug development in the area of hypertriglyceridemia.

## ACKNOWLEDGMENTS

Supported by the American Heart Association of Hawaii (0051329Z). K.D. is a recipient of a fellowship from the National Institute of Health (NIH) MARC U Star Biomedical Research (MBRS) Program (GMO7684).

## REFERENCES

1. Renaud, S., and de Lorgeril, M. (1992) Wine, Alcohol, Platelets, and the French Paradox for Coronary Heart Disease, *Lancet* 339, 1523–1526.
2. Hertog, M.G., Kromhout, D., Aravanis, C., Blackburn, H., Buzina, R., Fidanza, F., Giampaoli, S., Jansen, A., Menotti, A., Nedeljkovic, S., et al. (1995) Flavonoid Intake and Long-Term Risk of Coronary Heart Disease and Cancer in the Seven Countries Study, *Arch. Intern. Med.* 155, 381–386.
3. Keli, S.O., Hertog, M.G., Feskens, E.J., and Kromhout, D. (1996) Dietary Flavonoids, Antioxidant Vitamins, and Incidence of Stroke: The Zutphen Study, *Arch. Intern. Med.* 156, 637–642.
4. Frankel, E.N., Kanner, J., German, J.B., Parks, E., and Kinsella, J.E. (1993) Inhibition of Oxidation of Human Low-Density Lipoprotein by Phenolic Substances in Red Wine, *Lancet* 341, 454–457.
5. Gryglewski, R.J., Korbut, R., Robak, J., and Swies, J. (1987) On the Mechanism of Antithrombotic Action of Flavonoids, *Biochem. Pharmacol.* 36, 317–322.
6. Stein, J.H., Keevil, J.G., Wiebe, D.A., Aeschlimann, S., and Folts, J.D. (1999) Purple Grape Juice Improves Endothelial Function and Reduces the Susceptibility of LDL Cholesterol to Oxidation in Patients with Coronary Artery Disease, *Circulation* 100, 1050–1055.
7. Arai, Y., Watanabe, S., Kimira, M., Shimoi, K., Mochizuki, R., and Kinae, N. (2000) Dietary Intakes of Flavonols, Flavones and Isoflavones by Japanese Women and the Inverse Correlation Between Quercetin Intake and Plasma LDL Cholesterol Concentration, *J. Nutr.* 130, 2243–2250.
8. Nassuato, G., Iemmolo, R.M., Strazzabosco, M., Lirussi, F., Deana, R., Francesconi, M.A., Muraca, M., Passera, D., Fraggaso, A., Orlando, R., et al. (1991) Effect of Silibinin on Biliary Lipid Composition. Experimental and Clinical Study, *J. Hepatol.* 12, 290–295.
9. Kurowska, E.M., Spence, J.D., Jordan, J., Wetmore, S., Freeman, D.J., Piche, L.A., and Serratore, P. (2000) HDL-Cholesterol-Raising Effect of Orange Juice in Subjects with Hypercholesterolemia, *Am. J. Clin. Nutr.* 72, 1095–1100.
10. Merz-Demlow, B.E., Duncan, A.M., Wangen, K.E., Xu, X., Carr, T.P., Phipps, W.R., and Kurzer, M.S. (2000) Soy Isoflavones Improve Plasma Lipids in Normocholesterolemic, Premenopausal Women, *Am. J. Clin. Nutr.* 71, 1462–1469.
11. Wilcox, L.J., Borradaile, N.M., de Dreu, L.E., and Huff, M.W. (2001) Secretion of Hepatocyte apoB Is Inhibited by the Flavonoids, Naringenin and Hesperetin, via Reduced Activity and Expression of ACAT2 and MTP, *J. Lipid Res.* 42, 725–734.
12. Theriault, A., Wang, Q., Van Iderstine, S.C., Chen, B., Franke, A.A., and Adeli, K. (2000) Modulation of Hepatic Lipoprotein Synthesis and Secretion by Taxifolin, a Plant Flavonoid, *J. Lipid Res.* 41, 1969–1979.
13. Theriault, A., Casaschi, A., and Ota, D. (2002) Secretion of Hepatic Triglyceride-Rich Lipoprotein Is Inhibited by the Flavonoid, Taxifolin, via Reduced DGAT and MTP Activity, *Arterioscler. Thromb. Vasc. Biol.* 22, a-74 (abstract).
14. Olofsson, S.O., Asp, L., and Boren, J. (1999) The Assembly and Secretion of Apolipoprotein B-Containing Lipoproteins, *Curr. Opin. Lipidol.* 10, 341–346.
15. Haghpassand, M., Wilder, D., and Moberly, J.B. (1996) Inhibition of Apolipoprotein B and Triglyceride Secretion in Human Hepatoma Cells (HepG2), *J. Lipid Res.* 37, 1468–1480.
16. Boulton, D.W., Walle, U.K., and Walle, T. (1999) Fate of the Flavonoid Quercetin in Human Cell Lines: Chemical Instability and Metabolism, *J. Pharm. Pharmacol.* 51, 353–359.
17. Yee, W.L., Wang, Q., Agdinaoay, T., Dang, K., Chang, H., Grandinetti, A., Franke, A.A., and Theriault, A. (2002) Green Tea Catechins Decrease Apolipoprotein B-100 Secretion from HepG2 Cells, *Mol. Cell. Biochem.* 229, 85–92.
18. Grigor, M.R., and Bell, R.M. (1982) Separate Monoacylglycerol and Diacylglycerol Acyltransferases Function in Intestinal Triacylglycerol Synthesis, *Biochim. Biophys. Acta* 712, 464–472.
19. Bradford, M.M. (1976) A Rapid and Sensitive Method for the Quantitation of Microgram Quantities of Protein Utilizing the Principle of Protein-Dye Binding, *Anal. Biochem.* 72, 248–254.
20. Levy, E., Mehran, M., and Seidman, E. (1995) Caco-2 Cells as a Model for Intestinal Lipoprotein Synthesis and Secretion, *FASEB J.* 9, 626–635.
21. Luchoomun, J., and Hussain, M.M. (1999) Assembly and Secretion of Chylomicrons by Differentiated Caco-2 Cells. Nascent Triglycerides and Preformed Phospholipids Are Preferentially Used for Lipoprotein Assembly, *J. Biol. Chem.* 274, 19565–19572.
22. van Greevenbroek, M.M., van Meer, G., Erkelens, D.W., and de Bruin, T.W. (1996) Effects of Saturated, Mono-, and Polyunsaturated Fatty Acids on the Secretion of Apo B Containing Lipoproteins by Caco-2 Cells, *Atherosclerosis* 121, 139–150.
23. Cartwright, I.J., and Higgins, J.A. (1999) Increased Dietary Triacylglycerol Markedly Enhances the Ability of Isolated Rabbit Enterocytes to Secrete Chylomicrons: An Effect Related to Dietary Fatty Acid Composition, *J. Lipid Res.* 40, 1858–1866.
24. Gee, J.M., and Johnson, I.T. (2001) Polyphenolic Compounds: Interactions with the Gut and Implications for Human Health, *Curr. Med. Chem.* 8, 1245–1255.
25. van Greevenbroek, M.M., Robertus-Teunissen, M.G., Erkelens, D.W., and de Bruin, T.W. (1998) Participation of the Microsomal Triglyceride Transfer Protein in Lipoprotein Assembly in Caco-2 Cells: Interaction with Saturated and Unsaturated Dietary Fatty Acids, *J. Lipid Res.* 39, 173–185.
26. Farese, R.V., Jr., Cases, S., and Smith, S.J. (2000) Triglyceride Synthesis: Insights from the Cloning of Diacylglycerol Acyltransferase, *Curr. Opin. Lipidol.* 11, 229–234.
27. Rustan, A.C., Nossen, J.O., Christiansen, E.N., and Drevon, C.A. (1988) Eicosapentaenoic Acid Reduces Hepatic Synthesis and Secretion of Triacylglycerol by Decreasing the Activity of Acyl-Coenzyme A:1,2-Diacylglycerol Acyltransferase, *J. Lipid Res.* 29, 1417–1426.
28. Tomoda, H., Ohyama, Y., Abe, T., Tabata, N., Namikoshi, M., Yamaguchi, Y., Masuma, R., and Omura, S. (1999) Roselipins, Inhibitors of Diacylglycerol Acyltransferase, Produced by *Gliocladium roseum* KF-1040, *J. Antibiot. (Tokyo)* 52, 689–694.
29. Tabata, N., Ito, M., Tomoda, H., and Omura, S. (1997) Xanthohumols, Diacylglycerol Acyltransferase Inhibitors, from *Humulus lupulus*, *Phytochemistry* 46, 683–687.
30. Gordon, D.A., and Jamil, H. (2000) Progress Towards Understanding the Role of Microsomal Triglyceride Transfer Protein in Apolipoprotein-B Lipoprotein Assembly, *Biochim. Biophys. Acta* 1486, 72–83.
31. Muir, S.R., Collins, G.J., Robinson, S., Hughes, S., Bovy, A., Ric De Vos, C.H., van Tunen, A.J., and Verhoeven, M.E. (2001) Overexpression of Petunia Chalcone Isomerase in Tomato Results in Fruit Containing Increased Levels of Flavonols, *Nat. Biotechnol.* 19, 470–474.

[Received February 19, 2002, and in revised form June 7, 2002; revision accepted June 10, 2002]

# Distinction Between Esterases and Lipases: A Kinetic Study with Vinyl Esters and TAG

Henri Chahinian<sup>a</sup>, Lylia Nini<sup>b</sup>, Elisabeth Boitard<sup>c</sup>, Jean-Paul Dubès<sup>c</sup>,  
Louis-Claude Comeau<sup>b</sup>, and Louis Sarda<sup>d,\*</sup>

<sup>a</sup>Laboratoire de Lipolyse Enzymatique, CNRS, 13402 Marseille, Cedex 20, <sup>b</sup>Laboratoire de Biochimie Appliquée, Faculté de St-Jérôme, 13397 Marseille, Cedex 20, <sup>c</sup>Laboratoire de Thermochimie, Université de Provence, Faculté St-Charles, 13331 Marseille, Cedex 3, and <sup>d</sup>Laboratoire de Biochimie, Université de Provence, Faculté St-Charles, 13331 Marseille, Cedex 3, France

**ABSTRACT:** The better to characterize enzymes hydrolyzing carboxyl ester bonds (carboxyl ester hydrolases), we have compared the kinetic behavior of various lipases and esterases against solutions and emulsions of vinyl esters and TAG. Short-chain vinyl esters are hydrolyzed at comparable rates by esterases and lipases and have higher limits of solubility in water than corresponding TAG. Therefore, they are suited to study the influence of the physical state of the substrate on carboxyl ester hydrolase activity within a large concentration range. Enzymes used in this study are TAG lipases from microorganisms, lipases from human and guinea pig pancreas, pig liver esterase, and acetylcholinesterase. This study also includes cutinase, a fungal enzyme that displays functional properties between esterases and lipases. Esterases display maximal activity against solutions of short-chain vinyl esters (vinyl acetate, vinyl propionate, and vinyl butyrate) and TAG (triacetin, tripropionin, and tributyrin). Half-maximal activity is reached at ester concentrations far below the solubility limit. The transition from solution to emulsion at substrate concentrations exceeding the solubility limit has no effect on esterase activity. Lipases are active on solutions of short-chain vinyl esters and TAG but, in contrast to esterases, they all display maximal activity against emulsified substrates and half-maximal activity is reached at substrate concentrations near the solubility limit of the esters. The kinetics of hydrolysis of soluble substrates by lipases are either hyperbolic or deviate from the Michaelis–Menten model and show no or weak interfacial activation. The presence of molecular aggregates in solutions of short-chain substrates, as evidenced by a spectral dye method, likely accounts for the activity of lipases against soluble esters. Unlike esterases, lipases hydrolyze emulsions of water-insoluble medium- and long-chain vinyl esters and TAG such as vinyl laurate, trioctanoin, and olive oil. In conclusion, comparisons of the kinetic behavior of carboxyl ester hydrolases against solutions and emulsions of vinyl esters and TAG allows the distinction between lipases and esterases. In this respect, it clearly appears that guinea pig pancreatic lipase and cutinase are unambiguously classified as lipases.

Paper no. L8990 in *Lipids* 37, 653–662 (July 2002).

Lipases (EC 3.1.1.3.) and esterases (EC 3.1.1.1.) both catalyze the hydrolysis of carboxyl ester bonds. For many years,

\*To whom correspondence should be addressed at Laboratoire de Biochimie, Université de Provence, Faculté St-Charles, Case Postale 65, 3 Place Victor Hugo, 13331 Marseille, Cedex 3, France. E-mail: sarda@newsup.univ-mrs.fr

the distinction between lipases and esterases has been based on their substrate specificity and their capacity to hydrolyze esters in solution and emulsion, respectively (1–4). It is generally considered that lipases hydrolyze water-insoluble medium- and long-chain TAG, such as trioctanoin and triolein, although they also display high activity against emulsions of somewhat (slightly) water-soluble short-chain TAG such as tripropionin and tributyrin.

Esterases are defined as enzymes acting on solutions of short-chain fatty acyl esters such as methyl butyrate, ethyl butyrate and triacetin, which are poorly hydrolyzed by lipases. In contrast to classical lipases, typical esterases are not interfacially activated, i.e., they show no abrupt increase in activity at substrate concentrations exceeding the solubility limit. Esterases are inactive against emulsions of long-chain TAG.

During the past 10 yr, the determination of the 3-D structure of several lipases, including lipases secreted by microorganisms and by the pancreas of higher mammals, has revealed that the active site, which contains the same Ser-His-Asp/Glu catalytic triad as that found in serine proteases, is covered by a peptide loop (lid) that has to move away to give access to substrate (5–12). A correlation has been made between the existence of the lid structure and the specific action of lipases on aggregated forms of esters although it is not known whether the change in conformation corresponding to the opening of the lid is triggered by lipase–substrate interaction at lipid–water interfaces.

More recently, results of kinetic and structural studies carried out with cutinase (13) and lipase from guinea pig pancreas (14) have challenged the classical distinction between lipases and esterases. These enzymes, in which the lid domain is deleted or restricted to a small number of amino acid residues, were found to hydrolyze water-insoluble long-chain TAG as well as solution in tributyrin without showing interfacial activation. These observations have led to the conclusion that lipases may act on monomeric substrates and that the distinction between esterases and lipases should no longer be correlated with the physical state of the substrate and/or the presence of a lid domain in enzyme molecule. As a consequence, it is proposed that lipases should be simply classified as carboxyl ester hydrolases having the capacity to act on water-insoluble long-chain TAG (15).



Recently, we investigated the kinetic behavior of a large variety of well-characterized lipases of known 3-D structure in solutions and emulsions of vinyl esters so as to directly compare the biochemical properties of lipases acting on TAG and partial acylglycerols, respectively (16,17). As shown earlier by Brockerhoff, emulsions of vinyl esters are good substrates for porcine pancreatic lipase (18,19). Short-chain vinyl esters, whose solubility largely exceeds that of TAG such as tripropionin and tributyrin, are suited for studying the influence of the physical state of the substrate on activity by comparing the rates of hydrolysis of soluble and emulsified esters within a large range of concentrations. We have found that lipases from *Rhizomucor miehei*, *Rhizopus oryzae*, *Thermomyces lanuginosa*, *Penicillium camembertii*, *P. cyclopium* (lipases I and II), *Candida rugosa*, *C. antarctica* (lipase A), human pancreas, and guinea pig pancreas display different kinetic behavior against solutions of vinyl propionate and vinyl butyrate although they all expressed maximal activity against emulsions. Actually, some of these lipases hydrolyze solutions of vinyl esters at high relative rates compared to emulsions and follow Michaelis–Menten kinetics, while others, which are less active against soluble substrates, deviate from the Michaelis–Menten model. It was clear from these studies that interfacial activation could not be taken as the unique criterion to characterize lipases. In the present study, we compared the kinetic behavior of lipases and esterases against solutions and emulsions of vinyl esters and TAG for the purpose of better differentiating between the two classes of carboxyl ester-hydrolyzing enzymes. Esterases used in this study are pig liver esterase and acetylcholinesterase from *Electrophorus electricus*. Cutinase from *Fusarium solani pisi*, which, functionally speaking, is considered as a link between esterases and lipases, is included in this study.

## MATERIALS AND METHODS

**Enzymes and substrates.** Pig liver esterase and acetylcholinesterase from *Electrophorus electricus* were purchased from Sigma-Aldrich-Fluka (F-38297 St Quentin Fallavier, France). Human pancreatic lipase and colipase, guinea pig pancreatic lipase, and cutinase were kindly provided by Dr. R. Verger and Dr. F. Carrière (CNRS, Marseille, France). Lipase from *R. oryzae* was prepared in the laboratory as described previously (20). Lipases from *R. miehei* and *T. lanuginosa* were kindly provided by Dr. S. Patkar (Novo Nordisk A/S, Copenhagen, Denmark). The protein concentration of enzyme samples was estimated by the colorimetric method of Lowry *et al.* (21) using BSA as standard protein for calibration. Methyl butyrate, ethyl butyrate, vinyl acetate, vinyl propionate, vinyl butyrate, vinyl laurate, and benzopurpurin 4B were obtained from Sigma-Aldrich-Fluka. Triacetin, tripropionin, tributyrin, and trioctanoin were supplied by Acros Organics (F-93166 Noisy-le-Grand, France). Olive oil was from local origin. The solubility limit of vinyl acetate in 2.5 mM Tris-HCl buffer pH 7.0 containing 0.1 M NaCl was determined by the turbidimetric method, as reported before (17). The solubility limit of vinyl acetate is 315 mM, which corresponds to 0.9 mL of ester in 30

mL. The solubility limits of vinyl propionate and vinyl butyrate are 86 and 22 mM, respectively, which corresponds to 280 and 85  $\mu$ L of ester in 30 mL. The solubility limits of triacetin and tripropionin are 330 and 10 mM, which corresponds to 1.86 mL and 70  $\mu$ L in 30 mL, respectively. The solubility limit of tributyrin has been determined by different methods. Values ranging from 0.41 (22) to 0.8 mM (23) have been reported.

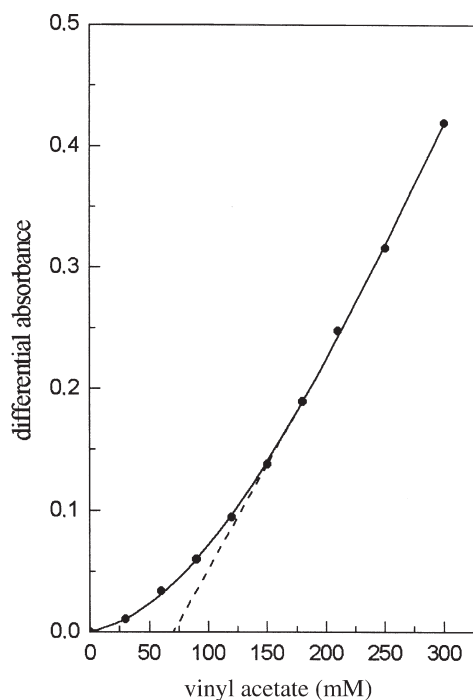
**Determination of enzymatic activity.** The enzymatic hydrolysis of solutions and emulsions of esters was followed potentiometrically at 25°C and pH 7.0 with a pH-stat (TTT 80 Radiometer, Copenhagen, Denmark). Assays with vinyl laurate and olive oil were carried out at pH 8.0 and 9.0, respectively. Assays were performed in 30 mL of 2.5 mM Tris-HCl buffer pH 7.0 containing 0.1 M NaCl. Standard conditions for measuring enzyme activity at increasing concentrations of substrate have been described previously (16). No detergent or emulsifier was added to measure activity against supersaturated solutions of partially soluble esters (vinyl acetate, vinyl propionate, and vinyl butyrate; triacetin, tripropionin, and tributyrin) and emulsions of water-insoluble vinyl laurate and trioctanoin. Released FA were titrated with 0.1 M NaOH. In the case of vinyl laurate, correction was made for partial dissociation of lauric (dodecanoic) acid at pH 8.0 assuming a  $pK_a$  of 7.4. Olive oil was emulsified with gum arabic (24). The amount of enzyme used in assays corresponds to 5–10 units measured at a substrate concentration ensuring maximal activity. The concentration of ester in solution or emulsion was arbitrarily expressed as millimoles per liter. Enzymatic activity was expressed as units. One enzyme unit corresponded to the liberation of one microequivalent of acid per minute under standard assay conditions. Specific activity was expressed as units per milligram of enzyme protein.

**Detection of molecular aggregates in solutions of vinyl acetate.** The existence of molecular aggregates in a solution of vinyl acetate was detected by the same spectral dye method as previously used in kinetic studies with vinyl propionate and vinyl butyrate (16) and with short-chain TAG (25). The experimental procedure was as follows: The dye solution was prepared in 25 mM Tris-HCl buffer pH 7.0 containing 0.05 M NaCl at a concentration of 50 mg benzopurpurin/L. A solution of vinyl acetate was prepared by adding 1.4 mL of vinyl acetate to 50 mL of the solution of benzopurpurin 4B (final concentration 304 mM, corresponding to 96.5% saturation). The solution of vinyl acetate was mixed with increasing volumes of the solution of benzopurpurin in stoppered vials, and absorbance was measured against the solution of benzopurpurin after 15 min at 510 nm in 1-cm cells. Differential absorbance was plotted against vinyl acetate concentration. As indicated by the curve shown in Figure 1, an apparent CMC around 70 mM was estimated for vinyl acetate.

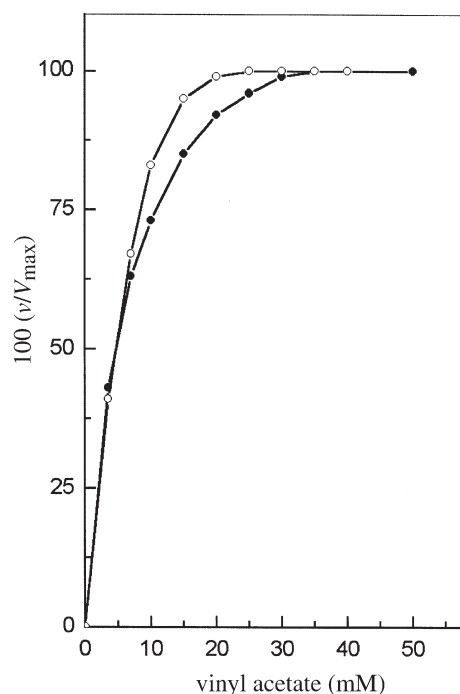
## RESULTS

**Hydrolysis of vinyl acetate by pig liver esterase and acetylcholinesterase.** The kinetic behavior of pig liver esterase and acetylcholinesterase against vinyl acetate is shown in Figure 2.





**FIG. 1.** Differential absorbance of a solution of benzopurpurin 4B in the presence of vinyl acetate. The solution of benzopurpurin is prepared in 25 mM Tris-HCl buffer pH 7.0 with 0.05 M NaCl with increasing amounts of vinyl acetate at concentration below the solubility limit (315 mM). Absorbance is measured at 510 nm. A CMC of 70 mM is estimated for vinyl acetate from the intercept of the curve with the x axis.



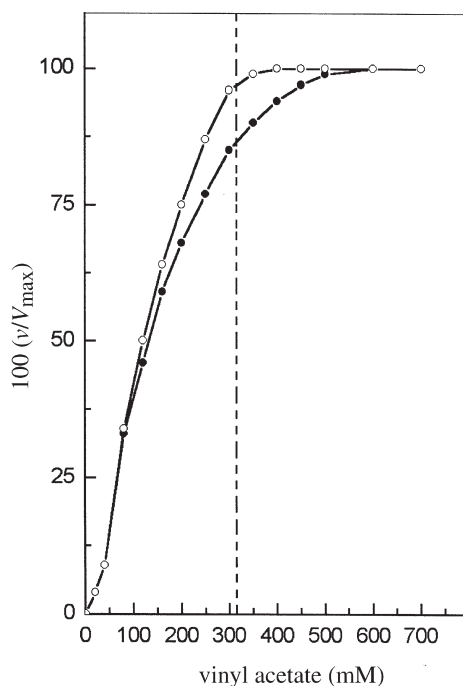
**FIG. 2.** Effect of ester concentration on the rate of hydrolysis of solutions of vinyl acetate ( $v$ ) by pig liver esterase (open circles) and acetylcholinesterase (solid circles). Assays were performed at pH 7.0 and 25°C in Tris-HCl buffer with 0.1 M NaCl. Activity is expressed as percentage of maximal activity ( $V_{\max}$ ). The solubility limit of vinyl acetate (315 mM) is not indicated.

In both cases, the shape of the curves representative of the variation of the initial rate of hydrolysis of vinyl acetate ( $v$ ) as a function of substrate concentration ( $S$ ) is hyperbolic. Esterases display maximal activity ( $V_{\max}$ ) against soluble vinyl acetate. The ester concentration corresponding to half-maximal activity ( $K_{0.5}$ ) is around 4 mM. Specific activities, estimated from values of  $V_{\max}$ , are 320 and 970 units  $\text{mg}^{-1}$  for pig liver esterase and acetylcholinesterase, respectively. These values are in the same range as those found with esters commonly used to assay pig liver esterase activity, such as methyl butyrate and ethyl butyrate. The values of  $K_{0.5}$ , estimated from the hyperbolic  $v/S$  curves obtained with pig liver esterase on methyl butyrate and ethyl butyrate (not shown), are around 2 (specific activity: 190 units  $\text{mg}^{-1}$ ) and 1 mM (specific activity: 310 units  $\text{mg}^{-1}$ ), respectively.

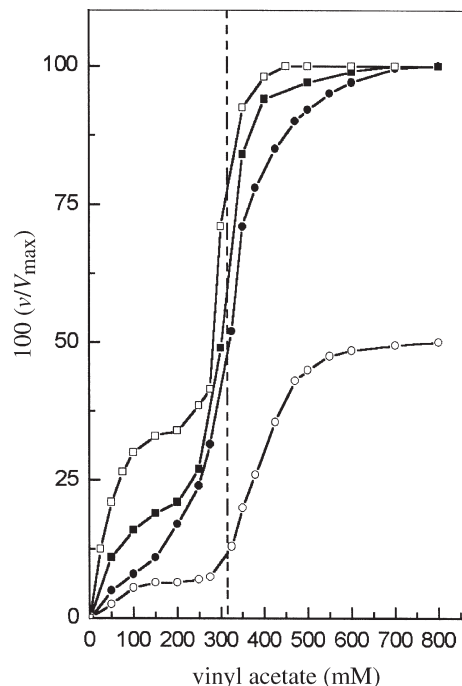
*Hydrolysis of vinyl acetate by lipases from R. oryzae, R. miehei, T. lanuginosa, human pancreas, and guinea pig pancreas.* The substrate concentration dependency of the initial rate of hydrolysis of vinyl acetate by lipases from *R. oryzae* and *R. miehei* is shown in Figure 3. The shape of the curves representing the kinetic behavior of the lipases is similar to that of the curves obtained with pig liver esterase and acetylcholinesterase except that, at low concentration of substrate, the curves are sigmoidal. Likely, this is related to the low amount and/or type of molecular aggregates formed in the 0–0.75 mM range of concentration of vinyl acetate (see Fig.

1). It can be further observed that the two lipases are highly active against solutions of vinyl acetate as compared to emulsions. Activity continuously increases at ester concentration beyond the solubility limit and reaches its maximal value in the presence of emulsified particles. The values of  $K_{0.5}$  estimated from the  $v/S$  curves are as high as 130 (specific activity: 640 units  $\text{mg}^{-1}$ ) and 120 mM (specific activity: 1940 units  $\text{mg}^{-1}$ ) for lipases from *R. oryzae* and *R. miehei*, respectively.

Figure 4 shows the kinetic behavior of lipases from *T. lanuginosa*, human pancreas, and guinea pig pancreas against vinyl acetate. The three lipases display low activity against soluble vinyl acetate as compared to lipases from *R. miehei* and *R. oryzae*, and enzymatic activity sharply increases at ester concentrations near the solubility limit of the substrate. All lipases express maximal activity at a substrate concentration exceeding the solubility limit. Colipase, the protein co-factor of pancreatic lipase that forms a specific complex with lipase at the lipid–water interface, has a marked effect on activity against soluble vinyl acetate as well as ester in emulsion. Colipase enhances pancreatic lipase activity by enabling the enzyme to interact with aggregates formed in the 100–300 mM range of concentration of vinyl acetate and by stabilizing lipase adsorbed at the micelle–water interface in its open active conformation. Although it is difficult to estimate the values of  $K_{0.5}$  from the irregular kinetic curves of Figure 4, it appears that, in all cases, half-maximal activity is reached at



**FIG. 3.** Effect of vinyl acetate concentration on the rate of hydrolysis by lipases from *Rhizopus oryzae* (open circles) and *Rhizomucor miehei* (solid circles). Assays were performed as described in the legend of Figure 2. The solubility limit of vinyl acetate (315 mM) is indicated by the dotted line. The concentration of vinyl acetate is expressed as millimoles per liter below and above the solubility limit of the substrate. For experimental conditions, see Figure 2.



**FIG. 4.** Effect of vinyl acetate concentration on the rate of hydrolysis by lipases from *Thermomyces lanuginosa* (open squares), guinea pig pancreas (solid squares) and human pancreas. Assays with human pancreatic lipase were performed in the absence (open circles) and presence (solid circles) of colipase in fivefold molar excess to lipase. The dotted line represents the solubility limit of vinyl acetate. For experimental conditions, see Figure 2.

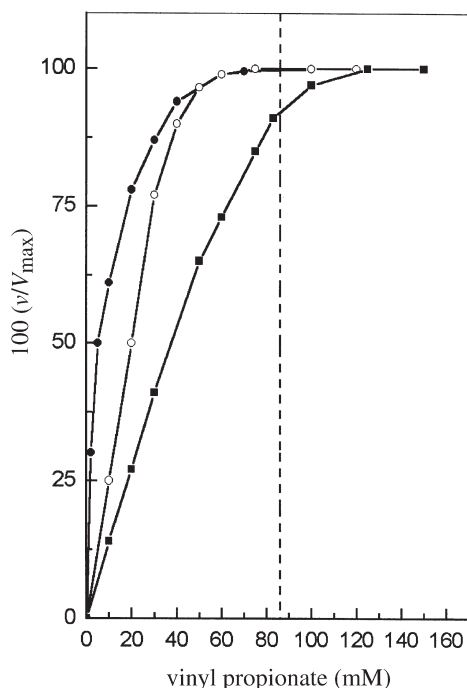
ester concentrations in the range 280–320 mM, near the solubility limit of vinyl acetate. The specific activities of lipases from *T. lanuginosa*, human pancreas, and guinea pig pancreas, measured against vinyl acetate, are 700, 200, and 90 units  $\text{mg}^{-1}$ , respectively.

*Hydrolysis of vinyl propionate, vinyl butyrate, and vinyl laurate by pig liver esterase and acetylcholinesterase. Comparison with TAG lipases.* Both pig liver esterase and acetylcholinesterase hydrolyze solutions of vinyl propionate (Fig. 5). The  $v/S$  curves are hyperbolic, and maximal activity is reached at low ester concentrations. The values of  $K_{0.5}$  for pig liver esterase and acetylcholinesterase are 5 (specific activity: 300 units  $\text{mg}^{-1}$ ) and 18 mM (specific activity: 210 units  $\text{mg}^{-1}$ ), respectively. Vinyl butyrate is hydrolyzed by pig liver esterase (Fig. 6) but not by acetylcholinesterase. The value of  $K_{0.5}$  is 2 mM, and the specific activity of the enzyme is 470 units  $\text{mg}^{-1}$ .

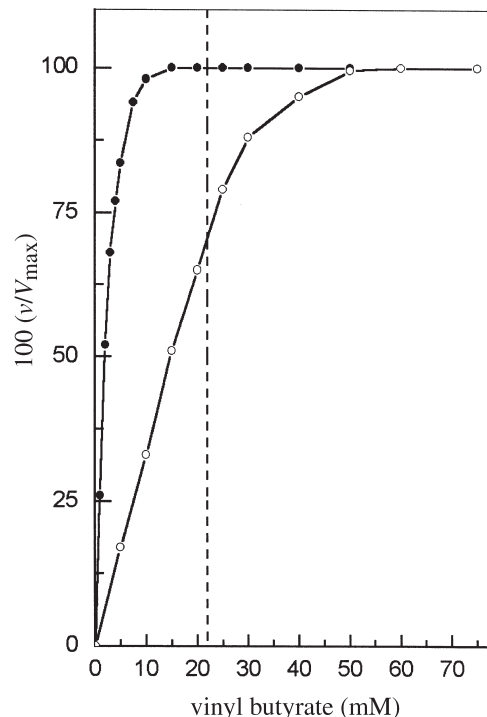
The kinetic curves obtained with *R. oryzae* lipase and human pancreatic lipase against vinyl propionate and vinyl butyrate have been reported previously (17). Values of  $K_{0.5}$  estimated from the  $v/S$  curves obtained with *R. oryzae* lipase and vinyl propionate or vinyl butyrate are 25 and 12 mM, respectively, with specific activities of 1600 and 3300  $\text{mg}^{-1}$ . The values of  $K_{0.5}$  for human pancreatic lipase against vinyl propionate and vinyl butyrate are 75 and 25 mM with specific activities of 960 and 750 units  $\text{mg}^{-1}$ , respectively. In Figures

5 and 6, the  $v/S$  curves of *R. miehei* lipase against vinyl propionate and vinyl butyrate are presented. Values of  $K_{0.5}$ , estimated from the curves, are 35 and 15 mM, and the specific activities are 7500 and 11,000 units  $\text{mg}^{-1}$ , respectively. As observed with vinyl acetate, vinyl propionate and vinyl butyrate, the values of  $K_{0.5}$  estimated for lipases are higher than those for esterases. Unlike human pancreatic lipase and other classical TAG lipases, pig liver esterase and acetylcholinesterase are inactive against emulsions of water-insoluble vinyl laurate. The specific activities of human pancreatic lipase and lipases from *R. oryzae* and *R. miehei* against vinyl laurate are 450, 2700, and 11,000 units  $\text{mg}^{-1}$  with  $K_{0.5}$  as low as 4, 2, and 2 mM, respectively (16).

*Hydrolysis of TAG by esterases. Comparison with lipases.* The activities of pig liver esterase and acetylcholinesterase were determined against short-, medium-, and long-chain TAG including triacetin, tripropionin, tributyrin, trioctanoin, and olive oil. The enzymes are totally devoid of activity against trioctanoin and olive oil, which are insoluble in water. The  $v/S$  curves obtained with pig liver esterase against triacetin, tripropionin, and tributyrin are shown in Figures 7A and 7B. Again, esterase activity against all substrates is maximal at low substrate concentrations, far below the solubility limit of the TAG. Specific activities of pig liver esterase against triacetin, tripropionin, and tributyrin are 60, 50, and 70 units  $\text{mg}^{-1}$ , with  $K_{0.5}$  of 3, 0.3, and 0.15 mM, respectively.



**FIG. 5.** Effect of vinyl propionate concentration on the rate of hydrolysis by pig liver esterase (solid circles), acetylcholinesterase (open circles), and lipase from *Rhizomucor miehei* (solid squares). The dotted line indicates the solubility limit of vinyl propionate (86 mM). For experimental conditions see Figure 2.



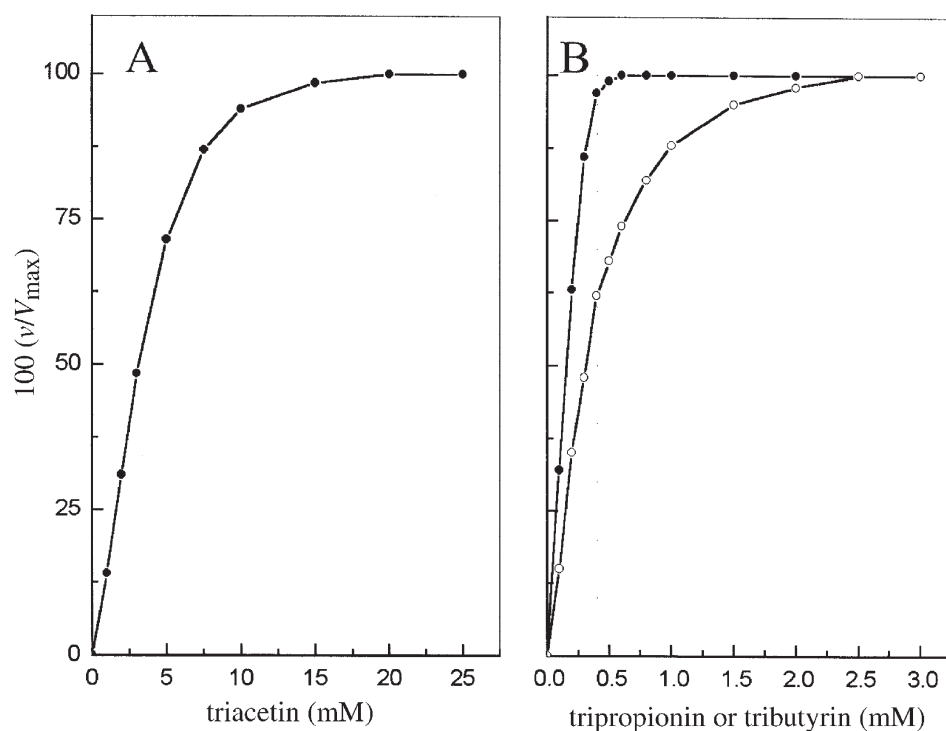
**FIG. 6.** Effect of vinyl butyrate concentration on the rate of hydrolysis by pig liver esterase (solid circles) and lipase from *Rhizomucor miehei* (open circles). The dotted line indicates the solubility limit of vinyl butyrate (22 mM). For experimental conditions see Figure 2.

Acetylcholinesterase hydrolyzes triacetin (specific activity: 450 units  $\text{mg}^{-1}$ ;  $K_{0.5}$ : 30 mM) but not tripropionin or tributyrin (Table 1). Results of kinetic studies carried out with TAG lipases under the same conditions have been presented in previous reports (16,17). For example, the specific activity of *R. oryzae* lipase against tripropionin is 110 units  $\text{mg}^{-1}$  with  $K_{0.5}$  of 4 mM, and that of human pancreatic lipase is 4,000 units  $\text{mg}^{-1}$  with  $K_{0.5}$  of 8 mM (17). As observed with vinyl esters, values of  $K_{0.5}$  for the hydrolysis of short-chain TAG by classical lipases are higher than those found for pig liver esterase.

*Hydrolysis of vinyl esters and TAG by cutinase.* Cutinase is an extracellular lipolytic enzyme of small molecular mass, secreted by the fungus *F. solani pisi*, which hydrolyzes TAG as efficiently as lipases. Kinetic studies carried out with tributyrin as substrate pointed out that cutinase differs from classical lipases in that it hydrolyzes soluble as well as emulsified substrate showing no interfacial activation. Longhi and Cambillau (13) concluded that cutinase had the capacity to hydrolyze monomeric substrates and showed function properties between esterases and lipases. This conclusion found support from the determination of the 3-D structure of the enzyme (13). Cutinase belongs to the family of proteins containing the  $\alpha/\beta$  hydrolase fold and the Ser-His-Asp/Glu catalytic triad found in serine hydrolases. Unlike other lipases, cutinase does not possess a lid domain, and, therefore, the active site is accessible to solvent. It seems that interpretation of the kinetics of hydrolysis of tributyrin by cutinase and the lack of interfacial activa-

tion should be reconsidered in the light of the data showing that solutions of short-chain vinyl esters or tripropionin are also readily hydrolyzed by classical lipases such as lipases from *R. oryzae* and *R. miehei* and that, as reported previously (17,25), solutions of short-chain esters contain not only monomers but also multimolecular aggregates. Unfortunately, the very low solubility of tributyrin (0.4 mM) does not allow assessment of the physical state of ester molecules dispersed in the aqueous phase. It is likely that, as previously shown for triacetin and tripropionin, molecules of tributyrin associate in solution in the presence of 0.1 M NaCl and that small aggregates present in the aqueous phase may account for the activity of cutinase on soluble tributyrin.

Here, we compared the kinetic behavior of cutinase with solutions and emulsions of vinyl esters and short-chain TAG with that of esterases and lipases. As can be seen from the  $v/S$  curves shown in Figure 8, the relative activity of cutinase against solutions of vinyl acetate, vinyl propionate, and vinyl butyrate is high compared with the maximal activity measured against emulsified esters. Specific activities are 650, 700, and 1375 units  $\text{mg}^{-1}$  with  $K_{0.5}$  values of 150, 40, and 12 mM, respectively. The kinetics of the hydrolysis of short-chain TAG by cutinase are illustrated in Figure 9. Specific activities measured against triacetin, tripropionin, and tributyrin are 320, 570, and 360 units  $\text{mg}^{-1}$  with  $K_{0.5}$  of 70, 10, and 0.25 mM, respectively. The kinetic behavior of cutinase with solutions and emulsions of partially water-soluble vinyl esters and TAG is comparable to that of lipases from *R. oryzae* and



**FIG. 7.** Hydrolysis of short-chain TAG by pig liver esterase. (A) Effect of triacetin concentration on the rate of hydrolysis by pig liver esterase. (B) Effect of the concentration of tripropionin (open circles) and tributyrin (solid circles) on the rate of hydrolysis by pig liver esterase. The solubility limits of triacetin (330 mM), tripropionin (10 mM), and tributyrin (0.41 mM) are not indicated. For experimental conditions see Figure 2.

*R. miehei* and markedly differs from that of typical esterases. Furthermore, cutinase, in contrast to pig liver esterase and acetylcholinesterase, hydrolyzes emulsions of water-insoluble vinyl laurate (specific activity: 775 units  $\text{mg}^{-1}$ ;  $K_{0.5}$ : 5 mM) and trioctanoin (specific activity: 830 units  $\text{mg}^{-1}$ ;  $K_{0.5}$ : 5 mM). Values of  $K_{0.5}$  are in the same range as those found

for classical lipases. For example, the value of  $K_{0.5}$  is 3.75 mM for the hydrolysis of vinyl laurate (specific activity: 450 units  $\text{mg}^{-1}$ ) and 3.25 mM for the hydrolysis of trioctanoin by *R. oryzae* lipase (specific activity: 7000 units  $\text{mg}^{-1}$ ). Specific activities of carboxyl ester-hydrolyzing enzymes used in this kinetic study are reported in Table 1.

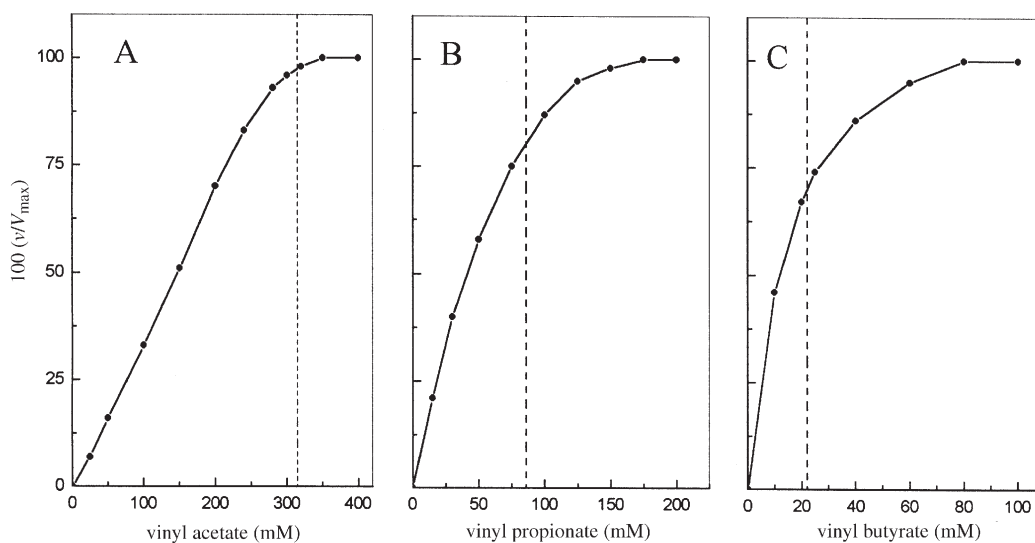
**TABLE 1**  
**Specific Activities<sup>a</sup> of Esterases and Lipases Measured Against Vinyl Esters and TAG**

	Vinyl acetate	Vinyl propionate	Vinyl butyrate	Vinyl laurate	Triacetin	Tripropionin	Tributyrin	Trioctanoin	Olive oil
Pig liver esterase	320	300	470	0	60	50	70	0	0
Acetylcholinesterase	970	210	0	0	450	0	0	0	0
Cutinase	650	700	1,375	775	320	570	360	830	670 <sup>b</sup>
Guinea pig pancreatic lipase	90	360	270	160	740	1,000	2,000	175	500
<i>Rhizopus oryzae</i> Lipase	640	1,600	3,300	2,700	60	110	900	7,000	1,000
<i>Rhizomucor miehei</i> lipase	1,940	7,500	11,000	11,000	20	400	2,200	9,200	3,300
<i>Thermomyces lanuginosa</i> lipase	700	3,000	3,700	12,000	0	225	2,250	9,250	2,900
Human pancreatic lipase	200	960	750	450	10	4,000	9,500	6,500	4,000

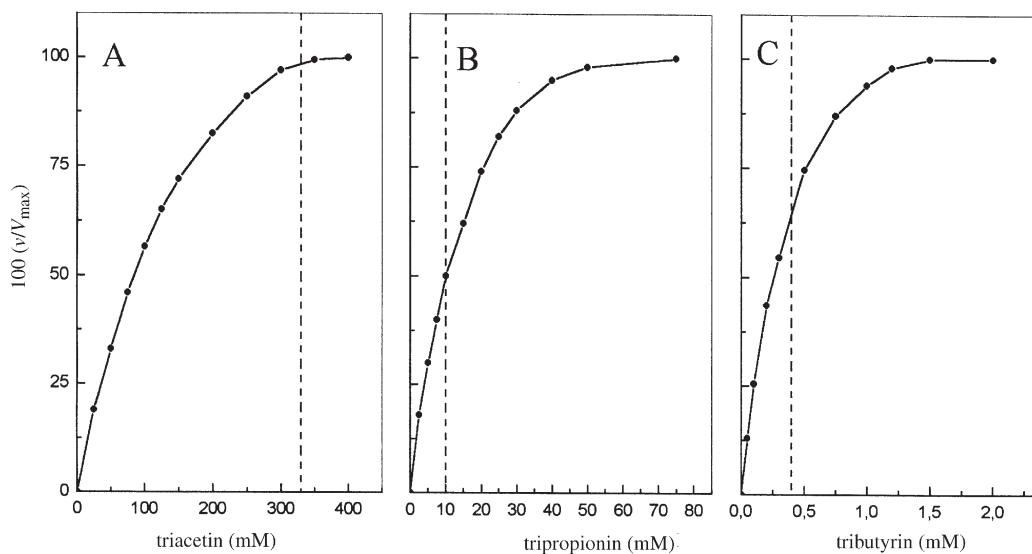
<sup>a</sup>Activity is measured at optimal substrate concentration and expressed as enzyme units. Specific activity is expressed as units  $\text{mg}^{-1}$ .

<sup>b</sup>From Reference 13.





**FIG. 8.** Hydrolysis of short-chain vinyl esters by cutinase. Effect of ester concentration on the rate of hydrolysis of (A) vinyl acetate, (B) vinyl propionate, and (C) vinyl butyrate. The dotted lines indicate the solubility limits of vinyl acetate (315 mM), vinyl propionate (86 mM), and vinyl butyrate (22 mM), respectively. For experimental conditions see Figure 2.



**FIG. 9.** Hydrolysis of short-chain TAG by cutinase. Effect of ester concentration on the rate of hydrolysis of (A) triacetin, (B) tripropionin, and (C) tributyrin. The dotted lines indicate the solubility limits of triacetin (330 mM), tripropionin (10 mM), and tributyrin (0.41 mM), respectively. For experimental conditions see Figure 2.

## DISCUSSION

In early comparative studies of the hydrolysis of methyl butyrate and triacetin by horse liver esterase and porcine pancreatic lipase, large differences were found between the kinetic behaviors of the two classes of enzymes (26). Under the conditions used for assaying carboxyl ester hydrolase activity, pancreatic lipase displayed low activity against esters at concentration below the solubility limit, and hydrolysis sharply increased in the presence of emulsified particles, in

supersaturated solutions. In contrast to pancreatic lipase, the activity of liver esterase was maximal against solutions of methyl butyrate and triacetin and was not enhanced at ester concentrations beyond the point of saturation of the solution. Consequently, the increase in activity shown by pancreatic lipase in a heterogeneous assay system (interfacial activation) was considered as a typical feature of the mode of action of lipases at a lipid-water interface. It was further hypothesized that interfacial activation of lipases would result from a change in the conformation of enzymes specifically bound to

**TABLE 2**  
**Hydrolysis<sup>a</sup> of Vinyl Acetate and Tripropionin by Esterases and Lipases**

	Pig liver esterase	Acetylcholinesterase	Cutinase	Guinea pig pancreatic lipase	<i>R. oryzae</i> lipase	<i>R. miehei</i> lipase	<i>T. lanuginosa</i> lipase	Human pancreatic lipase
Vinyl acetate	4	4	140	295	130	120	280	315
Tripropionin	0.3	—	10	10.5	4	8	15	8.5

<sup>a</sup> $K_{0.5}$ , the ester concentration that corresponds to half-maximal activity ( $V_m/2$ ), is estimated from the  $v/S$  curves and expressed as millimoles per liter. The substrate concentration is arbitrarily expressed as millimoles per liter both in the soluble and emulsified concentration range of substrate. The solubility limits of vinyl acetate and tripropionin are 315 and 10 mM, respectively. For abbreviations see Table 1.

large-size particles of the emulsion (26,27). Later, this hypothesis found support from the determination of the 3-D structure of human pancreatic lipase (6) and lipases from the fungi *R. miehei* (7) and *Geotrichum candidum* (10). In these lipases, the active site is covered by a peptide loop (lid), which has to move away to give access to the substrate. It was proposed to correlate the interfacial activation with the transition between the closed (inactive) form and the open (active) form of lipase (7,15).

During the past decade, a large number of lipases have been isolated and characterized. Studies of their molecular and catalytic properties have challenged the classical distinction between lipases and esterases based on interfacial activation. Lipases from *Pseudomonas glumae* (28,29), *P. aeruginosa* (30,31), *C. antarctica* (lipase B) (32), and pancreatic lipase from coypu (*Myocastor coypus*) (33), which possess a lid domain; cutinase, a lipolytic enzyme from *F. solani pisi* (13); and lipase from guinea pig pancreas (14), in which the lid domain is absent or restricted to a few amino acid residues, hydrolyzed solutions of esters showing no or weak interfacial activation. In some cases, such as lipase from *Staphylococcus hyicus*, typical interfacial activation was found only with some substrates (34). Then, it was concluded that lipases had the capacity to act on monomeric solutions as well as emulsions and that lipases should simply be considered as a particular class of carboxyl ester hydrolases having, unlike esterases, the capacity to act on water-insoluble long-chain TAG (15). The possible existence of small aggregates (micelles) in solutions of esters was not taken into account and, from a mechanistic point of view, the possibility that lipases could be interfacially activated by micelles was not systematically considered.

Recently, we used vinyl esters as substrates to compare the kinetic properties of several lipases from filamentous fungi (*R. oryzae*, *R. miehei*, *T. lanuginosa*, *P. camembertii*), yeasts (*C. rugosa*, *C. antarctica*) and guinea pig and human pancreas (16,17). Studies of the kinetics of hydrolysis of vinyl propionate and vinyl butyrate clearly showed that lipases were active to some extent against solutions of short-chain vinyl esters although they all displayed maximal activity against emulsions. In some cases, enzyme kinetics did not follow the classical Michaelis–Menten model, suggesting that substrate concentration was not the only parameter governing enzyme activity against soluble substrates.

In the present study, we compared the kinetic behavior of classical lipases and typical esterases, namely, pig liver esterase and acetylcholinesterase, against vinyl esters and TAG

in solution and in emulsion. Lipolytic enzymes having functional properties between lipases and esterases, such as guinea pig pancreatic lipase and cutinase from *F. solani pisi*, were included in this study. In addition to vinyl propionate, vinyl butyrate, and vinyl laurate, we investigated the kinetics of enzymatic hydrolysis of vinyl acetate, whose solubility limit (315 mM) greatly exceeds that of vinyl propionate (86 mM), vinyl butyrate (22 mM), tripropionin (10 mM), and tributyrin (0.4 mM).

Our results show that classical lipases, together with pig liver esterase, cutinase, and guinea pig pancreatic lipase, hydrolyze slightly water-soluble short-chain vinyl esters (vinyl acetate, vinyl propionate, and vinyl butyrate). Acetylcholinesterase is active on vinyl acetate and vinyl propionate but, as expected, does not hydrolyze vinyl butyrate (Table 1). In comparing the kinetic behaviors of the enzymes with vinyl acetate, it appears that esterases express maximal activity in the soluble concentration range. The substrate concentration corresponding to half-maximal activity ( $K_{0.5}$ ) of esterases is around 4 mM (Table 2). In contrast, classical lipases, guinea pig pancreatic lipase and cutinase, which show limited activity against soluble vinyl acetate, display maximal activity against emulsions.  $K_{0.5}$  values of 120, 130, and 140 mM are found for lipases from *R. miehei* and *R. oryzae* and for cutinase, respectively (Table 2). Values of  $K_{0.5}$  for lipases from *T. lanuginosa*, human pancreas, and guinea pig pancreas are in the 280–315 mM range, near the solubility limit of vinyl acetate (315 mM). Similar observations can be made with vinyl propionate, vinyl butyrate, and short-chain TAG. Esterases are inactive against water-insoluble medium- and long-chain esters such as vinyl laurate, trioctanoin, and olive oil, which are hydrolyzed by classical lipases, guinea pig pancreatic lipase, and cutinase (Table 1). Consequently, guinea pig pancreas lipase and cutinase have to be classified unambiguously as lipases. It appears that the capacity of the enzymes to hydrolyze emulsions of vinyl laurate or trioctanoin, on the one hand, and the determination of the  $K_{0.5}$  values with short-chain vinyl esters, in particular vinyl acetate, on the other hand, should help to characterize carboxyl ester hydrolases and to distinguish between lipases and esterases (35).

Comparison of the specific activities (Table 1) and  $K_{0.5}$  values (Table 2) of lipases and esterases, measured against vinyl esters and TAG, clearly indicates that esterases show preference for short-chain vinyl esters and do not hydrolyze medium- and long-chain esters. In contrast, classical lipases preferentially act on emulsions of tripropionin and tributyrin,

which are slightly soluble in water, and on water-insoluble vinyl laurate, trioctanoin, and olive oil. Cutinase and guinea pig pancreatic lipase, in contrast to other carboxyl ester hydrolases, hydrolyze all types of esters at comparable rates. It is interesting to notice that lipases from *R. miehei*, *T. lanuginosa*, and human pancreas possess a full-length lid domain, whereas the lid structure is restricted to five amino acid residues in the guinea pig lipase and is absent in cutinase. In cutinase, however, the highly flexible peptide region around the active site is involved in substrate binding and plays the same role as the lid domain in other lipases (36,37). Taken together, these observations suggest, from an evolutionary point of view, that the presence of the lid domain in classical lipases is directly related to their capacity to specifically hydrolyze long-chain TAG. This conclusion is in accordance with results of earlier crystallographic studies of the 3-D structure of the lipase-colipase complex co-crystallized with mixed micelles of PC showing that the lid domain is an essential component of the active site as it interacts with an acyl chain of the phospholipid (12). It is expected that further studies of the physical state of ester molecules dispersed in water, together with studies of enzyme structures, will contribute to understanding the mode of action of lipases and to a better distinction between esterases and lipases.

## ACKNOWLEDGMENTS

The authors wish to thank Drs. Robert Verger and Frédéric Carrière (CNRS, Marseille) for their interest in this study, helpful advice, and stimulating discussions during the preparation of the manuscript.

## REFERENCES

1. Tsujita, T., Shirai, K., Saito, Y., and Okuda, H. (1990) Relationship Between Lipase and Esterase, in *Isozymes: Structure, Function, and Use in Biology and Medicine*, pp. 915–933, Wiley-Liss, New York.
2. Jaeger, K.E., Ransac, S., Dijkstra, B.W., Colson, C., Van Heuvel, M., and Misset, O. (1994) Bacterial Lipases, *FEMS Microbiol. Rev.* 15, 29–63.
3. Rosenstein, R., and Götz, F. (2000) Staphylococcal Lipases: Biochemical and Molecular Characterization, *Biochimie* 82, 1005–1014.
4. Fojan, P., Jonson, P.H., Petersen, M.T.N., and Petersen, S.B. (2000) What Distinguishes an Esterase from a Lipase: A Novel Structural Approach, *Biochimie* 82, 1033–1041.
5. Brady, L., Brzozowski, A.M., Derewenda, Z.S., Dodson, E., Dodson, G.G., Tolley, S., Turkenburg, J.P., Christiansen, L., Høge-Jensen, B., Nørskov, L., et al. (1990) A Serine Protease Triad Forms the Catalytic Centre of a Triacylglycerol Lipase, *Nature* 343, 767–770.
6. Winkler, F.K., D'Arcy, A., and Hunziker, W. (1990) Structure of Pancreatic Lipase, *Nature* 343, 771–774.
7. Derewenda, Z.S., Derewenda, U., and Dodson, G.G. (1992) The Crystal and Molecular Structure of the *Rhizomucor miehei* Triglyceride Lipase at 1.9 Å Resolution, *J. Mol. Biol.* 227, 818–839.
8. Brzozowski, A.M., Derewenda, U., Derewenda, Z.S., Dodson, G.G., Lawson, D.M., Turkenburg, J.P., Bjorkling, F., Høge-Jensen, B., Patkar, S.A., and Thim, L. (1991) A Model for Interfacial Activation in Lipases from the Structure of a Fungal Lipase-Inhibitor Complex, *Nature* 351, 761–764.
9. Schrag, J.D., Yunge, L., Shan, W., and Cygler, M. (1991) Ser-His-Glu Forms the Catalytic Site of a Lipase from *Geotrichum candidum*, *Nature* 351, 761–764.
10. Schrag, J.D., and Cygler, M. (1993) A Refined Structure of the Lipase from *Geotrichum candidum*, *J. Mol. Biol.* 230, 575–591.
11. Van Tilbeurgh, H., Sarda, L., Verger, R., and Cambillau, C. (1992) Structure of the Lipase-Procolipase Complex, *Nature* 359, 159–162.
12. Van Tilbeurgh, H., Egloff, M.P., Martinez, C., Rugani, N., Verger, R., and Cambillau, C. (1993) Interfacial Activation of the Lipase-Procolipase Complex by Mixed Micelles Revealed by X-ray Crystallography, *Nature* 362, 814–820.
13. Longhi, S., and Cambillau, C. (1999) Structure-Activity of Cutinase, a Small Lipolytic Enzyme, *Biochim. Biophys. Acta* 1441, 185–196.
14. Hjorth, A., Carrière, F., Cudrey, C., Woldike, H., Boel, E., Lawson, D.M., Ferrato, F., Cambillau, C., Dodson, G.G., Thim, L., and Verger, R. (1993) A Structural Domain (the lid) Found in Pancreatic Lipases Is Absent in the Guinea Pig (phospho)Lipase, *Biochemistry* 32, 4702–4707.
15. Verger, R. (1997) Interfacial Activation of Lipases: Facts and Artifacts, *TIBTECH.* 15, 32–38.
16. Chahinian, H., Nini, L., Boitard, E., Dubès, J.P., Sarda, L., and Comeau, L. (2000) Kinetic Properties of *Penicillium cyclopium* Lipase Studied with Vinyl Esters, *Lipids* 35, 919–926.
17. Nini, L., Sarda, L., Comeau, L.C., Boitard, E., Dubès, J.P., and Chahinian, H. (2001) Lipase-Catalysed Hydrolysis of Short-Chain Substrates in Solution and in Emulsion: A Kinetic Study, *Biochim. Biophys. Acta* 1534, 34–44.
18. Brockerhoff, H. (1968) Substrate Specificity of Pancreatic Lipase, *Biochim. Biophys. Acta* 159, 296–303.
19. Brockerhoff, H. (1970) Substrate Specificity of Pancreatic Lipase. Influence of the Structure of the Fatty Acids on the Reactivity of Esters, *Biochim. Biophys. Acta* 212, 92–101.
20. Hiol, A., Jonzo, M.D., Rugani, N., Druet, D., Sarda, L., and Comeau, L.C. (2000) Purification and Characterization of an Extracellular Lipase from a Thermophilic *Rhizopus oryzae* Strain Isolated from Palm Fruit, *Enzyme Microb. Technol.* 26, 421–430.
21. Lowry, O.H., Rosebrough, N.J., Farr, A.L., and Randall, R.J. (1951) Protein Measurement with the Folin Phenol Reagent, *J. Biol. Chem.* 193, 265–275.
22. Ferrato, F., Carrière, F., Sarda, L., and Verger, R. (1997) A Critical Reevaluation of the Phenomenon of Interfacial Activation, *Methods Enzymol.* 286, 327–347.
23. Berg, O.G., Cajal, Y., Butterfoss, G.L., Grey, R.L., Alsina, M.A., Yu, B.Z., and Jain, M.K. (1998) Interfacial Activation of Triglyceride Lipase from *Thermomyces (Humicola) lanuginosa*: Kinetic Parameters and a Basis for the Control of the Lid, *Biochemistry* 37, 6615–6627.
24. Canioni, P., Julien, R., Rathelot, J., and Sarda, L. (1977) Pancreatic and Microbial Lipases: A Comparison of the Interaction of Pancreatic Colipase with Lipases of Various Origins, *Lipids* 12, 393–397.
25. Entressangles, B., and Desnuelle, P. (1968) Action of Pancreatic Lipase on Aggregated Glyceride Molecules in an Isotropic System, *Biochim. Biophys. Acta* 159, 285–295.
26. Sarda, L., and Desnuelle, P. (1958) Action de la lipase pancréatique sur les esters en émulsion, *Biochim. Biophys. Acta* 30, 513–521.
27. Desnuelle, P., Ailhaud, G., and Sarda, L. (1960) Inhibition de la lipase pancréatique par le diéthyl-*p*-nitrophénylphosphate en émulsion, *Biochim. Biophys. Acta* 37, 570–571.
28. Deever, A.M. (1992) Mechanism of Activation of Lipolytic Enzymes, Ph.D. Thesis, University of Utrecht, The Netherlands, 192 pp.
29. Noble, M.E.M., Cleasby, A., Johnson, L.N., Egmond, M.R., and Frenken, L.G. (1993) The Crystal Structure of Triacylglycerol Lipase from *Pseudomonas glumae* Reveals a Partially Redundant Catalytic Aspartate, *FEBS Lett.* 331, 123–128.

30. Jaeger, K.E., Ransac, S., Koch, H.B., Ferrato, F., and Dijkstra, B.W. (1993) Topological Characterization and Modeling of the 3D Structure of Lipase from *Pseudomonas aeruginosa*, *FEBS Lett.* 332, 143–149.
31. Jaeger, K.E., Ransac, S., Dijkstra, B.W., Colson, C., Vanheuver, M., and Misset, O. (1994) Bacterial Lipases, *FEMS Microbiol. Rev.* 15, 29–63.
32. Martinelle, M., Holmquist, M., and Hult, K. (1995) On the Interfacial Activation of *Candida antarctica* Lipase A and B as Compared with *Thermomyces lanuginosa* Lipase, *Biochim. Biophys. Acta* 1258, 272–276.
33. Thirstrup, K., Verger, R., and Carrière, F. (1994) Evidence for a Pancreatic Lipase Subfamily with New Kinetic Properties, *Biochemistry* 33, 2748–2756.
34. Van Oort, M.G., Deever, A.M., Dijkman, R., Tjeenk, M.L., Vereij, H.M., De Haas, G.H., Wenzig, E., and Götz, F. (1989) Purification and Substrate Specificity of *Staphylococcus hyicus* Lipase, *Biochemistry* 28, 9278–9285.
35. Arpigny, J.L., and Jaeger, K.E. (1999) Bacterial Lipolytic Enzymes: Classification and Properties, *Biochem. J.* 343, 177–183.
36. Prompers, J.J., Groenewegen, A., Hilbers, C.W., and Pepermans, H.A.M., (1999) Backbone Dynamics of *Fusarium solani pisi* Cutinase Probed by NMR. The Lack of Interfacial Activation Revisited, *Biochemistry* 38, 5315–5327.
37. Egmond, M.R., and de Vlieg, J. (2000) *Fusarium solani pisi* Cutinase, *Biochimie* 82, 1015–1021.

[Received January 24, 2002, and in revised form May 28, 2002; revision accepted June 10, 2002]



# PC and PE Synthesis: Mixed Micellar Analysis of the Cholinephosphotransferase and Ethanolaminephosphotransferase Activities of Human Choline/Ethanolamine Phosphotransferase 1 (CEPT1)

Marcia M. Wright and Christopher R. McMaster\*

Atlantic Research Centre, Departments of Pediatrics and Biochemistry & Molecular Biology, IWK Health Centre, Dalhousie University, Halifax, Nova Scotia, B3H 4H7, Canada

**ABSTRACT:** The human choline/ethanolamine phosphotransferase 1 (CEPT1) gene codes for a dual-specificity enzyme that catalyzes the *de novo* synthesis of the two major phospholipids through the transfer of a phosphobase from CDP-choline or CDP-ethanolamine to DAG to form PC and PE. We used an expression system devoid of endogenous cholinephosphotransferase and ethanolaminephosphotransferase activities to assess the diradylglycerol specificity of CEPT1. A mixed micellar assay was used to ensure that the diradylglycerols delivered were not affecting the membrane environment in which CEPT1 resides. The CEPT1 enzyme displayed an apparent  $K_m$  of 36  $\mu\text{M}$  for CDP-choline and 4.2 mol% for di-18:1 DAG with a  $V_{\text{max}}$  of 14.3  $\text{nmol min}^{-1} \text{mg}^{-1}$ . When CDP-ethanolamine was used as substrate, the apparent  $K_m$  was 98  $\mu\text{M}$  for CDP-ethanolamine and 4.3 mol% for di-18:1 DAG with a  $V_{\text{max}}$  of 8.2  $\text{nmol min}^{-1} \text{mg}^{-1}$ . The preferred diradylglycerol substrates used by CEPT1 with CDP-choline as the phosphobase donor were di-18:1 DAG, di-16:1 DAG, and 16:0/18:1 DAG. A major difference between previous emulsion-based assay results and the mixed micelle results was a complete inability to use 16:0(O)/2:0 as a substrate for the *de novo* synthesis of platelet-activating factor when the mixed micelle assay was used. When CDP-ethanolamine was used as the phosphobase donor, 16:0/18:1 DAG, di-18:1 DAG, and di-16:1 DAG were the preferred substrates. The mixed micelle assay also allowed the lipid activation of CEPT to be measured, and both the cholinephosphotransferase and ethanolaminephosphotransferase activities displayed the unusual property of product activation at 5 mol%, implying that specific lipid activation binding sites exist on CEPT1. The protein kinase C inhibitor chelerythrine and the human DAG kinase inhibitor R59949 both inhibited CEPT1 activity with  $\text{IC}_{50}$  values of 40  $\mu\text{M}$ .

Paper no. L9042 in *Lipids* 37, 663–672 (July 2002).

PC and PE are the major membrane phospholipids found in eukaryotic cells, constituting approximately 50 and 25% of membrane mass, respectively. PC is synthesized by a

cholinephosphotransferase activity that forms a phosphoester bond through the transfer of phosphocholine from CDP-choline to DAG (1–8). PE is synthesized through an analogous reaction that substitutes CDP-ethanolamine as the phosphobase donor (1,3,9–11). An accurate determination of specificity with respect to fatty acyl chain length is of great interest in lipid enzymology, as this can explain the molecular mechanism by which these enzymes contribute to the distribution of FA within phospholipids of the lipid bilayer. The fatty acyl groups of PC and PE govern the membrane structure and function of the phospholipids and also serve as reservoirs for numerous signaling molecules. For example, highly saturated PC molecules are the major component of lung surfactant (12,13), and arachidonic acid is released from PC for the production of prostaglandins and leukotrienes (14,15). In addition, a cholinephosphotransferase reaction has been implicated in the synthesis of a platelet-activating factor (PAF) precursor and the inflammatory mediator PAF itself (16). The PAF precursor is identical in structure to PC except that it contains an ether-linked FA at the *sn*-1 position of the glycerol backbone, with arachidonic acid as the preferred FA at the *sn*-2 position. PAF itself also contains an ether-linked *sn*-1 FA, but the *sn*-2 group is an acetyl moiety (17,18). Metabolism of the PAF precursor to PAF is initiated by a  $\text{Ca}^{2+}$ -activated phospholipase  $\text{A}_2$  that will hydrolyze arachidonic acid containing PC or the PAF precursor for the release of arachidonic acid from both lipids (19), as well as to produce PAF from lysoPAF through the action of PAF acetyltransferase (20).

One of the major obstacles to characterizing integral membrane lipid-metabolizing enzymes is that essentially water-insoluble, exogenous lipid substrates are delivered to membrane fractions containing the enzyme of interest in an aqueous solution with water-soluble substrates and cofactors. A second complication is that the membrane fraction used as enzyme source may contain more than one isoform of an enzyme catalyzing the same reaction, thus complicating the interpretation of enzymatic kinetics and substrate specificities. One solution to the assay of several enzyme isoforms that reside in a particular membrane is to purify the enzyme to homogeneity; however, most integral membrane-bound enzymes are difficult

\*To whom correspondence should be addressed at Atlantic Research Centre, 5849 University Ave., Room C-302, Dalhousie University, Halifax, Nova Scotia, B3H 4H7, Canada. E-mail: cmcmaste@is.dal.ca

Abbreviations: CEPT1, choline/ethanolamine phosphotransferase 1; CPT1, choline phosphotransferase 1; PAF, platelet-activating factor.

to purify because they must be removed from their membrane environment by solubilization with detergents to be amenable to column chromatography. This process often inactivates the enzyme, and indeed a cholinephosphotransferase has yet to be purified to homogeneity. A second solution is to isolate a cDNA coding for the enzyme and its expression in a cell type devoid of its activity. Recently, two human genes/cDNA were isolated that encode cholinephosphotransferase and ethanolaminephosphotransferase activities, and that appear to provide the entire complement of these enzyme activities in humans, were expressed in a *Saccharomyces cerevisiae* strain devoid of its endogenous cholinephosphotransferase and ethanolaminephosphotransferase activities (1,2,21). Results showed the human choline phosphotransferase 1 (CPT1) gene encodes a CDP-choline-specific enzyme for the synthesis of PC, whereas the human choline/ethanolamine phosphotransferase 1 (CEPT1) gene codes for an enzyme that can use either CDP-choline or CDP-ethanol-amine as substrates to synthesize PC or PE, respectively. The diradylglycerol substrate specificity of CPT1 and CEPT1 were also determined in these studies, with a broad range of diradylglycerols being utilized. Most notably, both enzymes were found to be capable of *de novo* synthesis of PAF and the PAF precursor (2,16).

In these analyses the diradylglycerol substrate species specificity of CPT1 and CEPT1 was determined using an emulsion-based assay in which a small amount of detergent was used to solubilize the diradylglycerol substrates. This assay type is the major method by which cholinephosphotransferase activity has previously been characterized (4,6,8–11,16,22,23), and our use of this assay allowed the activities of the CPT1- and CEPT1-encoded cholinephosphotransferase activities to be compared to these previous studies. However, this assay method does suffer from two major disadvantages. First, the delivery of the different lipophilic diradylglycerol substrates variously alters the physical parameters of the membrane in which the cholinephosphotransferase enzyme resides, and the activity measurements for the different diradylglycerol substrates possibly reflect alterations in the physical parameters of the membrane rather than true substrate specificity of the active sites of the enzyme. Second, because the enzyme cannot be studied independent of its native lipid environment, lipid activation and lipophilic inhibitor studies cannot be performed, as these molecules can also affect the physical parameters of the membrane. Therefore, it is difficult to interpret whether alterations in activity are due to membrane perturbations or accurately reflect the effect of the lipid on the activity of the enzyme. Mammalian cholinephosphotransferase appears to be exquisitely sensitive to its membrane environment, as demonstrated by the various attempts to purify the enzyme (6,9,10,22,23). It was rapidly inactivated by most detergents, and its activity was partially reconstituted by the addition of specific phospholipids (22,23).

The use of mixed micelle surface-dilution kinetic assay systems has resulted in the accurate portrayal of acyl group specificity for several integral membrane lipid-metabolizing

enzymes (3,5,24–34). The mixed micelle method presents the lipid substrate in a uniform matrix and resolves the problem of the differing lipophilic substrates, activators, or inhibitors physically altering the membrane structure in which the enzyme resides (24). In this study, we have characterized the specificity of the diradylglycerol substrate, as well as the effects of soluble and lipophilic activators and inhibitors, on the cholinephosphotransferase and ethanolaminephosphotransferase activities of human CEPT1 using a mixed micelle assay method.

## MATERIALS AND METHODS

**Materials.** All materials used in the preparation of yeast media were purchased from Difco Laboratories (Detroit, MI). [Methyl-<sup>14</sup>C]cytidine 5'-diphosphocholine and [ethanolamine-1,2-<sup>14</sup>C]cytosine 5'-diphosphoethanolamine were purchased from American Radiolabeled Chemicals (St. Louis, MO). Lipids, di-8:0 ethylene glycol, di-10:0 ethylene glycol, and di-18:1 ethylene glycol were purchased from Avanti Polar Lipids (Alabaster, AL). Inhibitors used were products of BioMol (Plymouth Meeting, PA).

**Membrane isolation.** Yeast cells devoid of their endogenous cholinephosphotransferase activity (HJ091—a *ura3 his3 leu2 trp1 cpt1::LEU2 ept1*<sup>-</sup>) were transformed with pAH9 (CEPT1), pAH12 (CPT1), or p416GPD (vector control), which express the human cDNA from the constitutive glyceraldehyde dehydrogenase promoter; transformants were selected on minimal medium containing the required nutritional supplements to allow for plasmid maintenance (1–3). The yeast cells were grown to midlog phase, and cultures were centrifuged at 1000 × *g* for 10 min, decanted, and resuspended in 25 mL of ice-cold membrane isolation buffer that contained 20% glycerol, 50 mM Tris-HCl pH 7.4, and 1 mM EDTA. Cells were centrifuged at 1000 × *g* for 10 min, decanted, and resuspended in 0.7 mL isolation buffer, which was then transferred to a test tube containing 0.5 mL of 0.5-mm glass beads. This mixture was vortexed at high speed five times for 30 s each with 30 s on ice between each mixing. The resulting homogenate was transferred to a new tube and the beads were rinsed twice with 0.5 mL isolation buffer, with each rinse being added to the homogenate. To pellet unbroken cells, nuclei, and mitochondria, the homogenate was centrifuged at 15,000 × *g* for 15 min at 4°C. The supernatant was transferred to an ultracentrifuge tube and spun at 450,000 × *g* for 15 min at 4°C. The microsomal membrane pellet was resuspended by Teflon pestle homogenization in 0.5 mL isolation buffer. Protein concentration in the microsomal membranes was determined by the method of Lowry *et al.* (35).

**Enzyme assays.** In the mixed micelle assay to determine cholinephosphotransferase and ethanolaminephosphotransferase activities, the diradylglycerol substrates and lipid activators were dried under nitrogen gas and resuspended by sonication in an assay mixture that contained 50 mM Tris-HCl (pH 8.0), 20 mM MgCl<sub>2</sub>, 20% glycerol, 10 mol% diradylglycerol, and 10 mol% lipid activator (PC unless

otherwise noted) or lipophilic inhibitor in 1% sodium cholate. To the micelle were added 10–25  $\mu\text{g}$  of membrane protein as enzyme source, and the mixture was incubated at 25°C for 5 min to allow for mixed micelle formation. Soluble inhibitors were added to the assay mix at this stage, and the assay was initiated by the addition of [ $^{14}\text{C}$ ]CDP-choline (0.4 mM, 2000 dpm/nmol) or [ $^{14}\text{C}$ ]CDP-ethanolamine (0.4 mM, 2000 dpm/nmol) to a final volume of 100  $\mu\text{L}$ . Assays were incubated at 25°C for 20 min and terminated by the addition of 3 mL  $\text{CHCl}_3/\text{CH}_3\text{OH}$  (2:1, vol/vol) and 1.5 mL 0.9% (wt/vol) KCl. Tubes were vortexed, and phase separation was facilitated by centrifugation at  $2000 \times g$  for 10 min. The aqueous phase was aspirated, and the organic phase was washed twice with 2 mL 40%  $\text{CH}_3\text{OH}/\text{H}_2\text{O}$  (vol/vol). A sample of the organic phase was dried in a scintillation vial, and radioactivity was determined by scintillation counting. The organic phase was analyzed by TLC using the solvent  $\text{CHCl}_3/\text{CH}_3\text{OH}/\text{NH}_4\text{OH}/\text{H}_2\text{O}$  (70:30:2:2, by vol) to ensure that PC or PE were the products. The mixed micellar assay described above satisfied the criteria of enzyme activities being dependent on the mole fraction of the lipid substrate and not dependent on micelle concentration at a fixed mole fraction of lipid components.

## RESULTS

**Kinetic analysis of CEPT1.** The human CEPT1 enzyme was expressed in an *S. cerevisiae* strain devoid of its endogenous cholinephosphotransferase and ethanolaminephosphotransferase activities by genetic inactivation of the genes coding for the yeast enzymes (1–3). This expression system ensured that all measurable activity was due to the expressed human CEPT1 enzyme. The mixed micelle system has previously been used to accurately assess the acyl specificity and lipid activation profiles of a number of integral membrane lipid-metabolizing enzymes (24–34). Hence, we sought to establish a mixed micelle method amenable to analysis of the human cholinephosphotransferase enzymes CPT1 and CEPT1. Surprisingly, both enzymes were completely inactive when the Triton X-100 micelle assay was used to characterize the yeast Cpt1p and Ept1p cholinephosphotransferase and choline/ethanolaminephosphotransferase enzymes (3). When searching for a detergent that could be used with the mixed micelle method for analysis of the mammalian enzymes, the researchers found that sodium cholate resulted in surface dilution kinetics (including complete dependence on the addition of exogenous DAG substrate) and bulk lipid concentration appropriate for a kinetic analysis of CEPT1. Surprisingly, sodium cholate micelles did not support the activity of human CPT1 despite the very high degree of primary amino acid and predicted similarities in secondary structure between CPT1 and CEPT1.

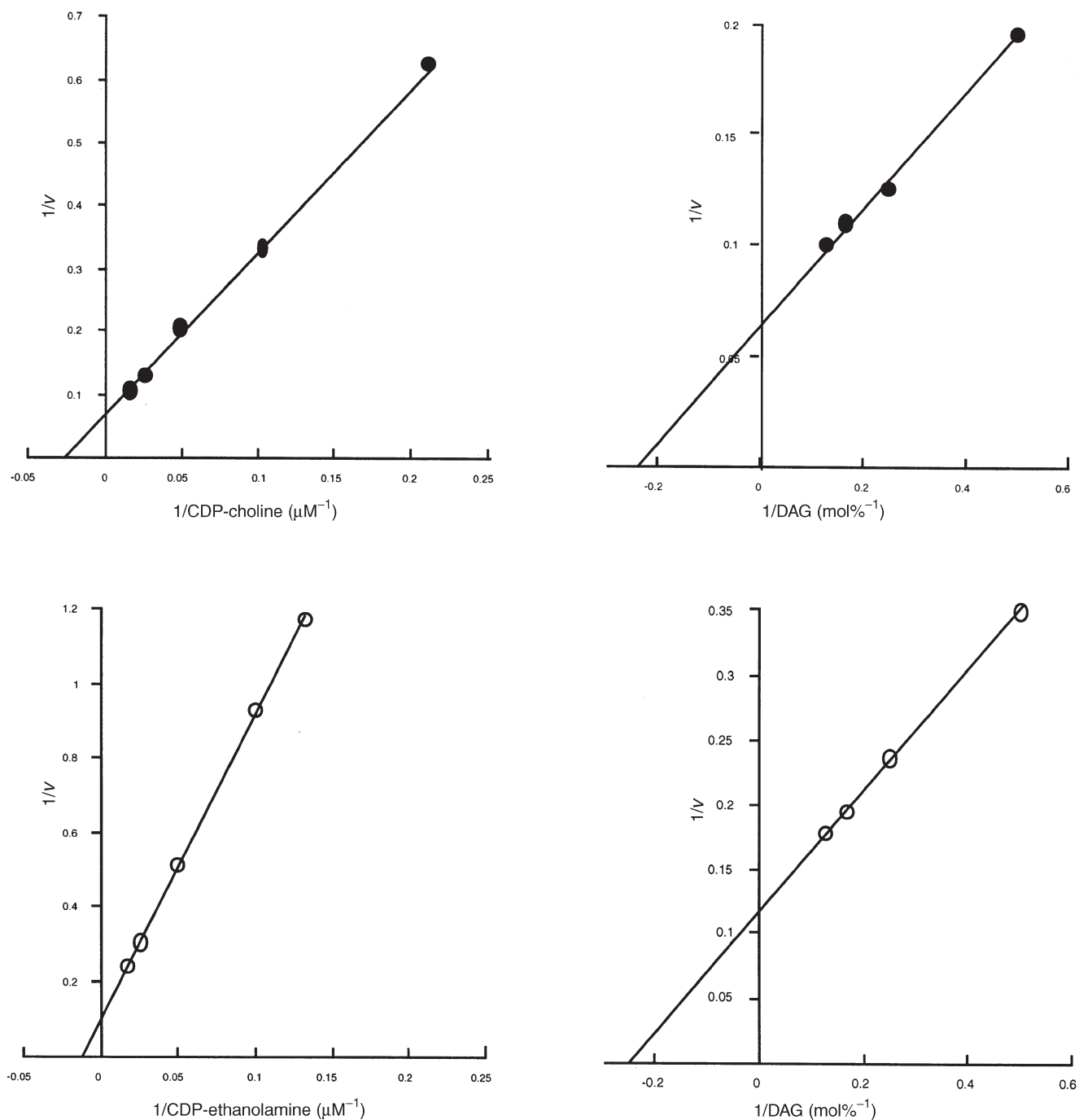
The kinetic parameters of apparent  $K_m$  and  $V_{\max}$  values were previously measured for CEPT1 using a Tween 20-based emulsion assay with CDP-choline and di-18:1 DAG as substrates. These results revealed an apparent  $K_m$  for CDP-

choline of 37  $\mu\text{M}$  and 850  $\mu\text{M}$  for di-18:1 DAG with a  $V_{\max}$  of 10.5  $\text{nmol min}^{-1} \text{mg}^{-1}$ . Using the mixed micelle assay, we determined that the apparent  $K_m$  for CDP-choline was 36  $\mu\text{M}$ , and for di-18:1 DAG it was 4.2 mol% with a  $V_{\max}$  of 14.3  $\text{nmol min}^{-1} \text{mg}^{-1}$ . The kinetic parameters of apparent  $K_m$  and  $V_{\max}$  values for CEPT1 using the Tween 20-based emulsion assay using CDP-ethanolamine and di-18:1 DAG as substrates previously revealed an apparent  $K_m$  of 101  $\mu\text{M}$  for CDP-ethanolamine and 890  $\mu\text{M}$  for di-18:1 DAG with a  $V_{\max}$  of 4.4  $\text{nmol min}^{-1} \text{mg}^{-1}$ . Using the mixed micelle assay, the apparent  $K_m$  for CDP-ethanolamine was 98  $\mu\text{M}$  and for di-18:1 DAG was 4.3 mol% with a  $V_{\max}$  of 8.2  $\text{nmol min}^{-1} \text{mg}^{-1}$  (Fig. 1). (Results are means of at least three separate experiments. SEM was less than 15% of the mean for each point.)

**Diradylglycerol specificity of CEPT1.** A comparison of the species specificity of various diradylglycerols for the cholinephosphotransferase activity of CEPT1 between the emulsion-based and mixed micelle assays revealed extreme differences. In our previous work using the emulsion-based assay, a very small amount of detergent was added to the diradylglycerol substrate to allow its solubilization, which can result in the various substrates altering the membrane environment in which CEPT1 resides (1). In that case, cholinephosphotransferase activity of CEPT1 preferred di-10:0 DAG = 16:0(O)/2:0  $\gg$  di-16:1 = di-8:0 = di-18:1 = 16:0/22:6  $>$  di-12:0  $>$  di-14:0 = di-16:0. When compared to the mixed micelle assay results, one of the most obvious differences was the inability to use 16:0(O)/2:0 as a substrate in the mixed micelle assay, revealing an inability to synthesize PAF *de novo* by CEPT1 (Table 1). In the mixed micelle assay, di-18:1 DAG, di-16:1 DAG, and 16:0/18:1 DAG were the preferred substrates, and CEPT1 could also use 16:0(O)/20:4 for *de novo* synthesis of the PAF precursor.

The diradylglycerol specificity of the ethanolaminephosphotransferase activity of CEPT1 was also assessed using the mixed micelle system and compared to the emulsion-based delivery of the diradylglycerol substrates. In the emulsion-based assay with CDP-ethanolamine as a substrate, the number of DAG species was limited, with di-18:1 DAG  $>$  16:0/18:1 = di-16:1  $>$  16:0/22:6, and the levels of ethanol-aminephosphotransferase activity were undetectable using any other diradylglycerol substrate (1). With the mixed micelle assay, the profile of DAG species that could be used as substrates by the ethanolaminephosphotransferase activity of CEPT1 was expanded, with 16:0/18:1 DAG = di-18:1 = di-16:1  $>$  18:0/20:4 = 16:0/22:6  $>$  di-16:0 used as substrates (Table 1).

**Lipid cofactor requirement of CEPT1.** The mixed micelle assay system is unique in that lipids can be added to the micelles without dramatically affecting the physical state of the environment in which CEPT1 resides. Thus, various lipid activators can be directly compared (3,24). In an emulsion-based system, on the other hand, very little or no detergent is added to the membrane in which CEPT1 resides such that the excess lipid added as either substrate or activator can dramatically alter the membrane environment and vary the physical



**FIG. 1.** Lineweaver–Burke analysis of human choline/ethanolamine phosphotransferase 1 (CEPT1)-catalyzed cholinephosphotransferase and ethanolaminephosphotransferase activities. Human CEPT1 was expressed in *Saccharomyces cerevisiae* cells devoid of their endogenous cholinephosphotransferase and ethanolaminephosphotransferase activities. CEPT1 cholinephosphotransferase (●) and ethanolaminephosphotransferase (○) activities were determined using the mixed micelle method, as described in the Materials and Methods section, with di-18:1 DAG as phosphobase acceptor and 10 mol% PC as lipid activator. The results represent the means of three separate experiments. SEM were less than 15% for each point.

state of the membrane. This makes it difficult to interpret whether the alterations in enzyme activity are due to specific lipid binding to CEPT1 or to gross alterations in the physical characteristics of the membrane.

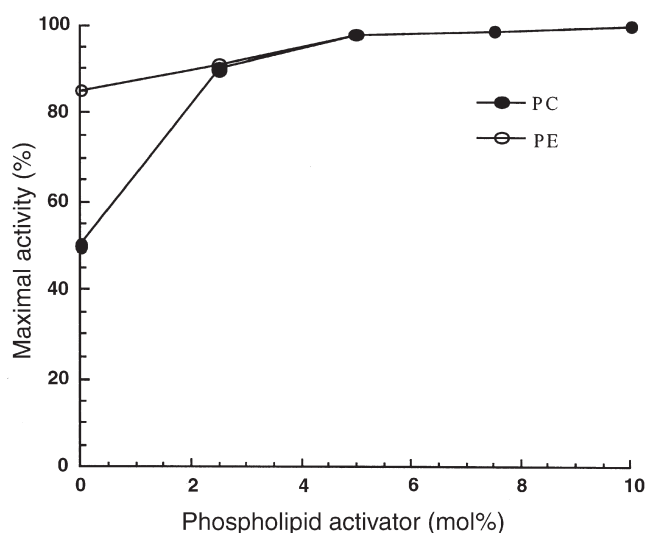
Various lipid activators were tested at 10 mol% using the mixed micelle assay. This analysis revealed that several phospholipids were capable of altering both the cholinephosphotransferase and ethanolaminephosphotransferase activities of



**TABLE 1**  
**Diradylglycerol Specificity of Human CEPT1<sup>a</sup>**

Diradylglycerol substrate	CDP-alcohol substrate (%)	
	CDP-choline	CDP-ethanolamine
Di-8:0	0	0
Di-10:0	72	0
Di-12:0	12	0
Di-14:0	12	0
Di-16:0	6	37
Di-16:1	95	90
Di-18:1	100	100
16:0/18:1	82	118
16:0/22:6	73	58
18:0/20:4	65	60
16:0/2:0	0	0
16:0(O)/2:0	0	0
16:0(O)/20:4	69	0

<sup>a</sup>A mixed micelle assay was performed using CDP-choline or CDP-ethanolamine with the DAG indicated above as substrate and 10 mol% PC as activating lipid, as described in the Materials and Methods section. Di-18:1 DAG was chosen as the 100% control and possessed enzyme activity of 12.5 nmol min<sup>-1</sup> mg<sup>-1</sup> using CDP-choline and 7.6 nmol min<sup>-1</sup> mg<sup>-1</sup> for CDP-ethanolamine as substrates. The results are means of at least three separate experiments. SEM was less than 15% of the mean for each point. CEPT1, choline/ethanolamine phosphotransferase 1.



**FIG. 2.** Product activation of CEPT1. Human CEPT1 was expressed in *S. cerevisiae* cells devoid of their endogenous cholinephosphotransferase and ethanolaminephosphotransferase activities. CEPT1 cholinephosphotransferase activity (●) for the synthesis of PC and ethanolaminephosphotransferase activity (○) for the synthesis of PE was assayed using the mixed micelle method, as described in the Materials and Methods section. The mixed micelle assay for the synthesis of cholinephosphotransferase was supplemented with the indicated mol% of PC, and the ethanolaminephosphotransferase assay was supplemented with PE. The results are means of three separate experiments. SEM were less than 15% for each point. For abbreviations see Figure 1.

**TABLE 2**  
**Lipid Activation of CEPT1 Activity<sup>a</sup>**

Lipid activator	CDP-alcohol substrate (%)	
	CDP-choline	CDP-ethanolamine
No lipid	51	85
PC	100	100
LPC	113	47
PE	78	98
PA	78	82
PI	118	95
PS	77	49
PG	102	70
CL	17	12
TAG	18	28

<sup>a</sup>A mixed micelle assay was performed using CDP-choline or CDP-ethanolamine with di-18:1 DAG as substrate at 10 mol% activating lipid as described in the Materials and Methods section. Enzyme activity was 12.5 nmol min<sup>-1</sup> mg<sup>-1</sup> using CDP-choline and 7.6 nmol min<sup>-1</sup> mg<sup>-1</sup> for CDP-ethanolamine with PC as lipid activator. The results are means of at least three separate experiments. SEM was less than 15% of the mean for each point. LPC, lysophosphatidylcholine; PG, phosphatidylglycerol; CL, cardiolipin. For other abbreviation see Table 1.

**CEPT1.** CEPT1 did not absolutely require a lipid activator, since activity was noted in the absence of exogenously added phospholipid. Of the lipids that could activate CEPT1, the product of the CEPT1 cholinephosphotransferase reaction, PC, was one of the best activators of the cholinephosphotransferase activity of the enzyme, and the product of the ethanolaminephosphotransferase activity of CEPT1, PE, was one of the best activators of the ethanolaminephosphotransferase reaction (Table 2). PC and PE concentrations of approximately 5 mol% were required to fully activate CEPT1 (Fig. 2). The acyl specificity of the PC molecules required to activate the cholinephosphotransferase activity of CEPT1 was also analyzed: PC molecules with physiologic chain lengths were all equally capable of activation, whereas short-chain PC species were poor activators (Table 3). The ability of a broad range of long-chain PC molecular species to support CEPT1 activity in a mixed micelle assay was also observed for the yeast Cpt1p and Ept1p enzymes (3).

**TABLE 3**  
**Acyl Specificity of Activation of CEPT1 by PC<sup>a</sup>**

PC species	Activity (% control)
PC (egg)	100
Di-4:0 PC	11
Di-6:0 PC	10
Di-14:0 PC	69
Di-16:0 PC	85
Di-16:1 PC	88
Di-18:1 PC	95
16:0/20:4 PC	92
16:0(O)/20:4 PC	85

<sup>a</sup>A mixed micelle assay was performed using CDP-choline with di-18:1 DAG as substrate and 10 mol% PC as activating lipid as described in the Materials and Methods section. Enzyme activity was 12.5 nmol min<sup>-1</sup> mg<sup>-1</sup> using CDP-choline as substrate and PC (egg) as lipid activator. The results are means of at least three separate experiments. SEM was less than 15% of the mean for each point.

**TABLE 4**  
**Potential CEPT1 Inhibitors<sup>a</sup>**

Inhibitor	Concentration	Activity (% control)
Protein kinase C inhibitors		
Di-8:0 ethylene glycol	10 mol%	60
Di-10:0 ethylene glycol	10 mol%	75
Di-18:0 ethylene glycol	10 mol%	72
Chelerythrine	100 $\mu$ M	25
DAG kinase inhibitor		
R59949	200 $\mu$ M	16
Phospholipase A <sub>2</sub> inhibitor		
Oleyloxyethylphosphocholine	200 $\mu$ M	85
Farnesyltransferase inhibitors		
N-Acetyl-S-farnesyl-L-cysteine	100 $\mu$ M	71
Manumycin A	100 $\mu$ M	77
L-744,832	100 $\mu$ M	101

<sup>a</sup>A mixed micelle assay was performed using CDP-choline with di-18:1 DAG as substrate and 10 mol% PC as activating lipid as described in the Materials and Methods section. Lipophilic inhibitors are expressed as mol% and essentially soluble inhibitors as mM. Enzyme activity was 12.5 nmol min<sup>-1</sup> mg<sup>-1</sup> using CDP-choline as substrate and PC (egg) as lipid activator in the absence of inhibitor. The results are means of at least three separate experiments. SEM was less than 15% of the mean for each point. di-8:0 Ethylene glycol, di-10:0 ethylene glycol, and di-18:1 ethylene glycol were purchased from Avanti Polar Lipids (Alabaster, AL). All other inhibitors were from BioMol (Plymouth Meeting, PA).

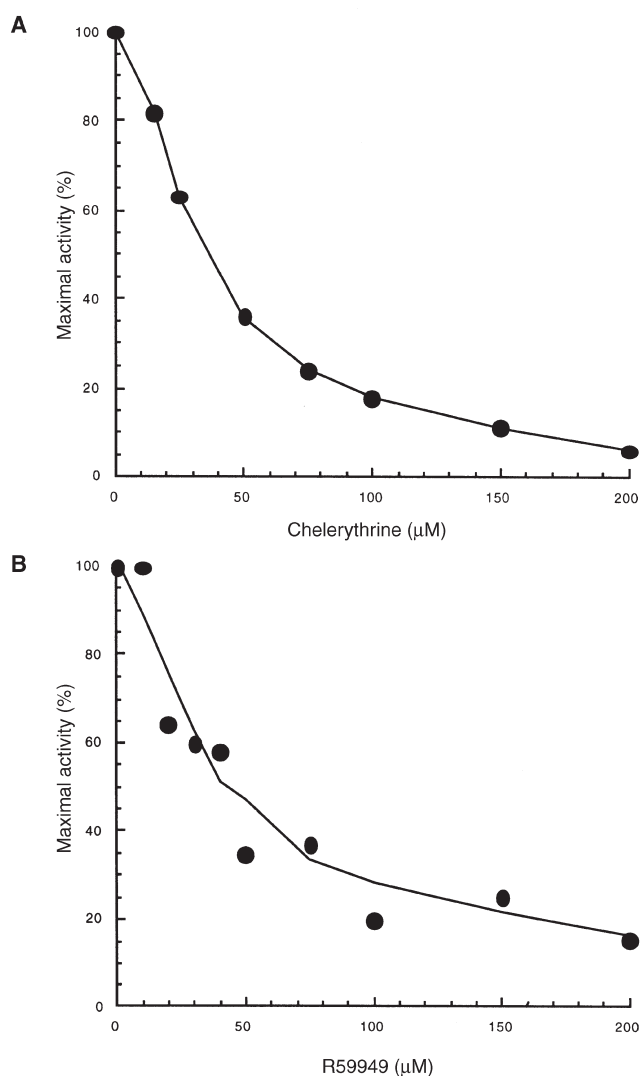
**Inhibitors of CEPT1 activity.** Previous reports using an emulsion-based assay (36,37) identified farnesol as an *in vitro* inhibitor of cholinephosphotransferase activity. Using a mixed micelle assay, we demonstrated that farnesol did not inhibit CEPT1 activity (21). The addition of large concentrations of farnesol apparently compromised the structure of the membrane in which CEPT1 resides, resulting in its inactivation rather than its inhibition (21,38). We investigated compounds that could be used in the mixed micelle assay as efficient inhibitors of CEPT1 that would not alter the physical parameters in which the CEPT1 enzymes resides when the lipophilic molecules were added. Compounds were chosen based on their ability to inhibit other DAG-utilizing enzymes (such as DAG kinase), alter the activity of DAG-responsive enzymes (such as proteins kinase C), inhibit PC phospholipases (which could work either by binding to the active site where PC is formed or by preventing the activation of CEPT1 by PC), or affect the attachment of lipophilic molecules to proteins. Of the compounds tested, cholinephosphotransferase activity was inhibited most efficiently by the protein kinase C inhibitor chelerythrine and the mammalian DAG kinase inhibitor R59949 (Table 4). To establish the efficacy of inhibition, the concentration dependence of these two inhibitors was examined. Both chelerythrine and R59949 exhibited an IC<sub>50</sub> of 40  $\mu$ M (Fig. 3).

## DISCUSSION

One of the major obstacles to accurately assessing the properties of mammalian cholinephosphotransferase enzymes has been the use of cellular membranes as the enzyme source. Our

recent isolation of two separate human cDNAs, CEPT1 coding for a dual-specificity choline/ethanolaminephosphotransferase enzyme (1) and CPT1 coding for a cholinephosphotransferase-specific enzyme (2), has complicated the interpretation of previous analyses of these enzyme activities. It is not known if one or both of these enzymes were present in the preparations used as the cholinephosphotransferase enzyme source (4,6,8–11,22,23,28,39,40). Previously, we developed an expression system in *S. cerevisiae* that was devoid of its endogenous cholinephosphotransferase and ethanolamine-phosphotransferase activities; mutational inactivation of the respective encoding genes allowed for the individual assessment of heterologously expressed cholinephosphotransferase and ethanolaminephosphotransferase enzymes. We also used this system to examine the kinetic properties and substrate specificities of the human CEPT1- and CPT1-encoded enzymes (1,2). In these studies a small amount of detergent was used to solubilize the diradylglycerol substrate to aid its delivery to the isolated membranes in an aqueous solution. This was the most popular method of assaying cholinephosphotransferase and ethanolaminephosphotransferase activities of these enzymes, and it allowed the properties of human CEPT1 and CPT1 to be compared to those in the literature. However, delivery of an excess of the CEPT1 lipophilic substrates in the presence of a small amount of detergent dramatically altered the physical state in which the enzyme resides. Thus, it was difficult to determine whether the observed differences in activity reflected true enzymatic and substrate specificity parameters or alterations in the membrane environment in which the integral membrane protein resides, which ultimately determine the activity of the enzyme. To circumvent this problem, a mixed micellar system was developed to study CEPT1. The current system solubilizes the membrane in which the enzyme resides (in the presence of excess detergent) such that exogenously added lipids represent 10 mol% or less of the detergent added to solubilize the membranes; thus, the physical parameters on the membrane are not altered by the exogenous lipids (24–34). This allows for a more accurate assessment of substrate specificity and lipid activation. The mixed micellar enzyme assay was used to determine kinetic parameters, diradylglycerol substrate specificity, lipid activation, and inhibition by both lipophilic and soluble compounds that were previously known to alter the activity of other DAG-utilizing or responsive enzymes toward the human CEPT1-encoded choline/ethanolaminephosphotransferase.

When mixed micelle conditions were established to examine CEPT1 properties, we discovered that neither human CEPT1 nor CPT1 was active when assayed using the Triton X-100-based mixed micelle assay we had previously used to characterize the yeast Cpt1p and Ept1p enzymes (3). This was surprising based on the high degree of predicted conservation of primary and secondary structures between the yeast and human enzymes. The ability to catalyze a CDP-alcohol phosphotransferase reaction using sodium cholate was found with



**FIG. 3.** Inhibition of CEPT1 activity by chelerythrine and R59949 (Bio-Mol, Plymouth Meeting, MA). Human CEPT1 was expressed in *S. cerevisiae* cells devoid of their endogenous cholinephosphotransferase and ethanolaminephosphotransferase activities. CEPT1 cholinephosphotransferase activity for the synthesis of PC was assayed using the mixed micelle method, as described in the Materials and Methods section, with the indicated concentrations of (A) chelerythrine or (B) R59949. The results are means of three separate experiments. SEM were less than 15% for each point. For abbreviations see Figure 1.

mammalian CEPT1 but not human CPT1. Based on this observation, we predicted that when assaying mammalian cellular membranes we could use the sodium cholate assay to measure enzyme activity for specific determination of CEPT1-dependent cholinephosphotransferase activity.

The kinetic parameters for substrate CDP-alcohol substrate affinity were similar for the emulsion (1,2) and the mixed micellar-based assay using di-18:1 DAG as the phosphobase acceptor. Apparent  $K_m$  values were 36–37  $\mu\text{M}$  for CDP-choline and 98–101  $\mu\text{M}$  for CDP-ethanolamine. Apparent  $V_{\text{max}}$  values were also similar. The cholinephosphotrans-

ferase reaction catalyzed at a rate of 10.5  $\text{nmol min}^{-1} \text{mg}^{-1}$  using the emulsion-based assay and 14.3  $\text{nmol min}^{-1} \text{mg}^{-1}$  for the mixed micelle assay, whereas the ethanolaminephosphotransferase reaction catalyzed at a rate of 4.4  $\text{nmol min}^{-1} \text{mg}^{-1}$  when the di-18:1 DAG was delivered as an emulsion and at 8.2  $\text{nmol min}^{-1} \text{mg}^{-1}$  when di-18:1 DAG was presented in mixed micelle form.

A comparison of the diradylglycerol substrate specificity of CEPT1 using emulsion-based vs. mixed micelle assays revealed major differences in substrate specificity. One of the main differences was in the ability of the cholinephosphotransferase reaction of CEPT1 to synthesize PAF *de novo*; it was very efficient in the emulsion assay but was undetectable in the mixed micelle assay (2,16). Indeed, with regard to the cholinephosphotransferase reaction of CEPT1 using the emulsion-based assay, the diradylglycerol substrate specificity by and large reflected the solubility of the lipophilic substrate in aqueous solutions. Using the mixed micelle assay, the preferred diradylglycerols reflected those normally found within cellular membranes. The differences in ethanolaminephosphotransferase activity of CEPT1 were not as drastic as for the cholinephosphotransferase activity, as the emulsion-based assay for ethanolaminephosphotransferase activity had a much narrower DAG species profile. A similar profile, although with a moderately expanded DAG substrate species capability, was observed for the ethanolaminephosphotransferase of CEPT1 using the mixed micelle assay.

The mixed micelle substrate specificity preferences were consistent with previous analyses of metabolic labeling of hepatocytes in cell cultures. Analysis of the DAG cellular specificity for PC that had been synthesized *de novo* through the CDP-choline pathway revealed that DAG containing saturated and monounsaturated FA were the preferred substrates (41). However, this same study revealed that PE synthesized *de novo* and catalyzed by ethanolaminephosphotransferase contained a higher percentage of polyunsaturated double bonds. A more recent study using deuterated precursors and MS analysis of the lipids synthesized in a hepatocyte cell line predicted that 16:0/18:1 DAG and di-18:1 DAG were the preferred substrates for the *de novo* synthesis of PC by cholinephosphotransferase and also that 16:0/18:1 DAG and di-18:1 DAG were the preferred substrates for *de novo* ethanolaminephosphotransferase synthesized PE (42). The results from this study closely parallel the DAG fatty acyl species specificity determined in our mixed micellar analysis of CEPT1 cholinephosphotransferase and ethanolaminephosphotransferase activities.

Similar to the yeast Cpt1p and Ept1p enzymes (3), human CEPT1 were activated by phospholipids. However, the yeast enzymes displayed an absolute requirement for phospholipid activation, whereas the human CEPT1 enzyme was active without the addition of exogenous phospholipids but could be further activated by including phospholipids in the micelle. In the mixed micelle assay, detergent was added in excess such that the lipid present in the enzyme source was diluted to negli-

gible levels. Similar to the yeast Cpt1p and Ept1p enzymes, human CEPT1 appears to possess distinct binding sites on the enzyme for phospholipid, and occupation of these site(s) alters enzyme activity. However, unlike the yeast enzyme activities, human CEPT1 activity was not completely dependent on exogenous phospholipid. At a fixed concentration of 10 mol%, several membrane phospholipids were capable of fully supporting CEPT1-derived cholinephosphotransferase and ethanolaminephosphotransferase activity. TAG was not an activator of CEPT1, implying that a phosphobase was required for activation. Interestingly, PC was one of the best activators of CEPT1, which implies that a form of product activation may exist *in vivo*. The local microconcentration of PC at the site of CEPT1 in the cell was expected to be high, as CEPT1 continually synthesizes PC. This was also true for PE activation of the ethanolaminephosphotransferase property of CEPT1, although it was far less pronounced than for the cholinephosphotransferase activity. As the cholinephosphotransferase and ethanolaminephosphotransferase steps are generally not rate limiting in the synthesis of PC and PE in cells, product activation might be a mechanism by which CEPT1 does not impinge on the rate of synthesis for PC and PE, as determined by the upstream rate-limiting enzymes (43–45).

Using an emulsion-based assay, farnesol was previously identified as an *in vitro* inhibitor of human CEPT1 activity (36,37). Further work with this assay demonstrated farnesol does not inhibit the CEPT1 enzyme but instead appears to inhibit CEPT1 over time by providing a membrane environment in which it is progressively inactivated (21,28). Using a mixed micelle method in which the added lipid did not dramatically alter the environment in which the enzyme resides, we were unable to detect significant inhibition of CEPT1 activity by farnesol (21). Using our method we investigated inhibitors of CEPT1 cholinephosphotransferase activity by using compounds previously identified as either inhibiting the activity of enzymes that also metabolize DAG or compounds that are known to interfere with DAG activation of proteins. Of the compounds tested, the human DAG kinase inhibitor R59949 (46) and the protein kinase C inhibitor chelerythrine (47) were the best inhibitors of CEPT1 activity. The  $IC_{50}$  concentrations required for *in vitro* inhibition of CEPT1 cholinephosphotransferase activity were 40  $\mu$ M for both compounds. This was dramatically higher than those for *in vitro* human DAG kinase inhibition by R59949 (0.3  $\mu$ M) and chelerythrine inhibition of protein kinase C (0.66  $\mu$ M). However, chelerythrine has been shown to inhibit PC synthesis and cause apoptosis in cells at concentrations that effectively inhibit CEPT1 activity *in vitro* (36). Induction of apoptosis by chelerythrine could be altered by the addition of exogenous PC, implying that PC metabolism may play a role in chelerythrine-mediated apoptosis (36). The role of CEPT1 inhibition by chelerythrine in the regulation of chelerythrine-induced apoptosis is currently under study.

An accurate determination of the fatty acyl specificity of lipid-metabolizing enzymes is of great interest, as this can de-

fine the molecular mechanism by which the enzyme contributes to the apportionment of FA within phospholipids. All of the characteristics observed in this study can be attributed to human CEPT1, as the expression system used resulted in human CEPT1 as the sole cholinephosphotransferase and ethanolaminephosphotransferase encoding activity being expressed. We characterized human CEPT1 using a mixed micellar assay system as a means to separate the physical effects of lipid substrates and activators on the membranes in which CEPT1 resides from true enzymatic effects of the added lipids. The results presented are more reflective of those observed in cell cultures for CEPT1 substrate specificity through metabolic labeling analyses than those in previous emulsion-based analyses of CEPT1. Notably, PAF could not be synthesized *de novo* by CEPT1 using the mixed micelle method even though it was synthesized in abundance when using the emulsion-based assay (2,16). As PAF is a very potent inflammatory mediator, a precise knowledge of its possible biosynthetic routes is essential.

## ACKNOWLEDGMENTS

This work was supported by operating and group grants from the CIHR to CRM. CRM is an IWK senior clinical research scholar. MMW is supported by a CaRE Nova Scotia Ph.D. studentship. The authors thank Annette Henneberry and Jason Williams for initial characterization of CEPT1 using the mixed micelle assay and Harold Cook, David Byers, and Neale Ridgway for helpful discussions throughout the course of this study.

## REFERENCES

1. Henneberry, A.L., and McMaster, C.R. (1999) Cloning and Expression of a Human Choline/Ethanolaminephosphotransferase: Synthesis of Phosphatidylcholine and Phosphatidylethanol-amine, *Biochem. J.* 339, 291–298.
2. Henneberry, A.L., Wistow, G., and McMaster, C.R. (2000) Cloning, Genomic Organization, and Characterization of a Human Cholinephosphotransferase, *J. Biol. Chem.* 275, 29808–29815.
3. Hjelmstad, R.H., and Bell, R.M. (1991) *sn*-1,2-Diacylglycerol Choline- and Ethanolaminephosphotransferases in *Saccharomyces cerevisiae*. Mixed Micellar Analysis of the *CPT1* and *EPT1* Gene Products, *J. Biol. Chem.* 266, 4357–4365.
4. Weiss, S.B., Smith, S.W., and Kennedy, E.P. (1958) The Enzymatic Formation of Lecithin from Cytidine Diphosphate Choline and D-1,2-Diglyceride, *J. Biol. Chem.* 233, 53–64.
5. Williams, J.G., and McMaster, C.R. (1998) Scanning Alanine Mutagenesis of the CDP-Alcohol Phosphotransferase Motif of *Saccharomyces cerevisiae* Cholinephosphotransferase, *J. Biol. Chem.* 273, 13482–13487.
6. O, K.M., and Choy, P.C. (1990) Solubilization and Partial Purification of Cholinephosphotransferase from Hamster Tissues, *Lipids* 25, 122–124.
7. McMaster, C.R., and Bell, R.M. (1997) CDP-choline:1,2-Diacylglycerol Cholinephosphotransferase, *Biochim. Biophys. Acta* 1348, 100–110.
8. Mantel, C.R., Schulz, A.R., Miyazawa, K., and Broxmeyer, H.E. (1993) Kinetic Selectivity of Cholinephosphotransferase in Mouse Liver: The  $K_m$  for CDP-choline Depends on Diacylglycerol Structure, *Biochem. J.* 289, 815–820.



9. O, K.M., Siow, Y.L., and Choy, P.C. (1989) Hamster Liver Cholinephosphotransferase and Ethanolaminephosphotransferase Are Separate Enzymes, *Biochem. Cell Biol.* 67, 680–686.
10. Mancini, A., Del Rosso, F., Roberti, R., Orvietani, P., Coletti, L., and Binaglia, L. (1999) Purification of Ethanolaminephosphotransferase from Bovine Liver Microsomes, *Biochim. Biophys. Acta* 1437, 80–92.
11. Ford, D.A., Rosenbloom, K.B., and Gross, R.W. (1992) The Primary Determinant of Rabbit Myocardial Ethanolamine Phosphotransferase Substrate Selectivity Is the Covalent Nature of the *sn*-1 Aliphatic Group of Diradylglycerol Acceptors, *J. Biol. Chem.* 267, 11222–11228.
12. Rooney, S.A., Young S.L., and Mendelson, C.R. (1994) Molecular and Cellular Processing of Lung Surfactant, *FASEB J.* 8, 957–967.
13. Osanai, K., Mason R.J., and Voelker, D.R. (2001) Pulmonary Surfactant Phosphatidylcholine Transport Bypasses the Brefeldin A Sensitive Compartment of Alveolar Type II Cells, *Biochim. Biophys. Acta* 1531, 222–229.
14. Funk, C.D. (2001) Prostaglandins and Leukotrienes: Advances in Eicosanoid Biology, *Science* 294, 1871–1875.
15. Samuelsson, B., and Funk, C.D. (1989) Enzymes Involved in the Biosynthesis of Leukotriene B<sub>4</sub>, *J. Biol. Chem.* 264, 19469–19472.
16. Woodard, D.S., Lee, T.C., and Snyder, F. (1987) The Final Step in the *de novo* Biosynthesis of Platelet Activating Factor, *J. Biol. Chem.* 262, 2520–2527.
17. Tokumura, A., Sumida, T., Toujima, M., Kogure, K., and Fukuzawa, K. (2000) Platelet-Activating Factor (PAF)-like Oxidized Phospholipids: Relevance to Atherosclerosis, *Biofactors* 13, 29–33.
18. Prescott, S.M., Zimmerman, G.A., Stafforini, D.M., and McIntyre, T.M. (2000) Platelet-Activating Factor and Related Lipid Mediators, *Annu. Rev. Biochem.* 69, 419–445.
19. Hirabayashi, T., and Shimizu, T. (2000) Localization and Regulation of Cytosolic Phospholipase A<sub>2</sub>, *Biochim. Biophys. Acta* 1488, 124–138.
20. Tjoelker, L.W., and Stafforini, D.M. (2000) Platelet-Activating Factor Acetylhydrolases in Health and Disease, *Biochim. Biophys. Acta* 1488, 102–123.
21. Wright, M.M., Henneberry, A.L., Lagace, T.A., Ridgway, N.D., and McMaster, C.R. (2001) Uncoupling Farnesol Induced Apoptosis from Its Inhibition of Phosphatidylcholine Synthesis, *J. Biol. Chem.* 276, 25254–25261.
22. Mancini, A., Roberti, R., Binaglia, L., Missiri, A.E., and Freyz, L. (1993) Factors Affecting the Stability of Detergent Solubilized Cholinephosphotransferase and Ethanolaminephosphotransferase, *Membrane Biochem.* 10, 43–52.
23. Cornell, R., and MacLennan, D.H. (1985) Solubilization and Reconstitution of Cholinephosphotransferase from Sarcoplasmic Reticulum: Stabilization of Solubilized Enzyme by Diacylglycerol and Glycerol, *Biochim. Biophys. Acta* 821, 97–105.
24. Carman, G.M., Deems, R., and Dennis, E.A. (1995) Lipid Signaling Enzymes and Surface Dilution Kinetics, *J. Biol. Chem.* 270, 18711–18714.
25. Ellis, M.V., James, S.R., Perisic, O., Downes, C.P., Williams, R.L., and Katan, M. (1998) Catalytic Domain of Phosphoinositide-specific Phospholipase C (PLC). Mutational Analysis of Residues Within the Active Site and Hydrophobic Ridge of PLC $\delta$ 1, *J. Biol. Chem.* 273, 11650–11659.
26. Carman, G.M., and Dowhan, W. (1979) Phosphatidylserine Synthase from *Escherichia coli*. The Role of Triton X-100 in Catalysis, *J. Biol. Chem.* 254, 8391–8397.
27. Lin, Y.P., and Carman, G.M. (1990) Kinetic Analysis of Yeast Phosphatidate Phosphatase Toward Triton X-100/Phosphatidate Mixed Micelles, *J. Biol. Chem.* 265, 166–170.
28. Bru, R., Blochliger, E., and Luisi, P.L. (1993) *sn*-1,2-Diacylglycerol Cholinephosphotransferase from Pig Liver: Mixed Micellar Assay and Kinetic Analysis of the Partially Pure Enzyme, *Arch. Biochem. Biophys.* 307, 295–303.
29. Kucera, G.L., Miller, C., Sisson, P.J., Wilcox, R.W., Wiemer, Z., and Waite, M. (1988) Hydrolysis of Thioester Analogs by Rat Liver Phospholipase A<sub>1</sub>, *J. Biol. Chem.* 263, 12964–12969.
30. Ridgway, N.D., and Vance, D.E. (1988) Kinetic Mechanism of Phosphatidylethanolamine *N*-Methyltransferase, *J. Biol. Chem.* 263, 16864–16871.
31. MacDonald, M.L., Mack, K.F., Williams, B.W., King, W.C., and Glomset, J.A. (1988) A Membrane-bound Diacylglycerol Kinase That Selectively Phosphorylates Arachidonoyl-diacylglycerol. Distinction from Cytosolic Diacylglycerol Kinase and Comparison with the Membrane-bound Enzyme from *Escherichia coli*, *J. Biol. Chem.* 263, 1584–1592.
32. Walsh, J.P., Fahrner, L., and Bell, R.M. (1990) *sn*-1,2-Diacylglycerol Kinase of *Escherichia coli*. Diacylglycerol Analogues Define Specificity and Mechanism, *J. Biol. Chem.* 265, 4374–4381.
33. Horrevoets, A.J., Hackeng, T.M., Verheij, H.M., Dijkman, R., and de Haas, G.H. (1989) Kinetic Characterization of *Escherichia coli* Outer Membrane Phospholipase A Using Mixed Detergent–Lipid Micelles, *Biochemistry* 28, 1139–1147.
34. Lewis, K.A., Garigapati, V.R., Zhou, C., and Roberts, M.F. (1993) Substrate Requirements of Bacterial Phosphatidylinositol-specific Phospholipase C, *Biochemistry* 32, 8836–8841.
35. Lowry, O.H., Rosebrough, N.J., Farr, A.L., and Randall, R.J. (1951) Protein Measurement with the Folin Phenol Reagent, *J. Biol. Chem.* 193, 265–275.
36. Anthony, M.L., Zhao, M., and Brindle, K.M. (1999) Inhibition of Phosphatidylcholine Biosynthesis Following Induction of Apoptosis in HL-60 cells, *J. Biol. Chem.* 274, 19686–19692.
37. Miquel, K., Pradines, A., Terce, F., Selmi, S., and Favre, G. (1998) Competitive Inhibition of Cholinephosphotransferase by Geranylgeraniol and Farnesol Inhibits Phosphatidylcholine Synthesis and Induces Apoptosis in Human Lung Adenocarcinoma A549 Cells, *J. Biol. Chem.* 273, 26179–26186.
38. Meigs, T.E., Roseman, D.S., and Simoni, R.D. (1996) Regulation of 3-Hydroxy-3-methylglutaryl-coenzyme A Reductase Degradation by the Nonsterol Mevalonate Metabolite Farnesol *in vivo*, *J. Biol. Chem.* 271, 7916–7922.
39. Ishidate, K., Matsuo, R., and Nakazawa, Y. (1993) CDP-choline:1,2-Diacylglycerol Cholinephosphotransferase from Rat Liver Microsomes. I. Solubilization and Characterization of the Partially Purified Enzyme and the Possible Existence of an Endogenous Inhibitor, *Lipids* 28, 89–96.
40. Kanoh, H., and Ohno, K. (1976) Solubilization and Purification of Rat Liver Microsomal 1,2-Diacylglycerol:CDP-choline Cholinephosphotransferase and 1,2-Diacylglycerol:CDP-ethanolamine Ethanolaminephosphotransferase, *Eur. J. Biochem.* 66, 201–210.
41. Samborski, R.W., Ridgway, N.D., and Vance, D.E. (1990) Evidence That Only Newly Made Phosphatidylethanolamine Is Methylated to Phosphatidylcholine and That Phosphatidylethanolamine Is Not Significantly Deacylated–Reacylated in Rat Hepatocytes, *J. Biol. Chem.* 265, 18322–18329.
42. DeLong, C.J., Shen, Y.J., Thomas, M.J., and Cui, Z. (1999) Molecular Distinction of Phosphatidylcholine Synthesis Between the CDP-choline Pathway and Phosphatidylethanolamine Methylation Pathway, *J. Biol. Chem.* 274, 29683–29688.

43. Kent, C. (1995) Eukaryotic Phospholipid Biosynthesis, *Annu. Rev. Biochem.* 64, 315–343.
44. Tabas, I. (2000) Cholesterol and Phospholipid Metabolism in Macrophages, *Biochim. Biophys. Acta* 1529, 164–174.
45. Ridgway, N.D., Byers, D.M., Cook, H.W., and Storey, M.K. (1999) Integration of Phospholipid and Sterol Metabolism in Mammalian Cells, *Prog. Lipid Res.* 38, 337–360.
46. Jiang, Y., Sakane, F., Kanoh, H., and Walsh J.P. (2000) Selectivity of the Diacylglycerol Kinase Inhibitor 3-[2-(4-[bis-(4-fluorophenyl)methylene]-1-piperidiny)ethyl]-2,3-dihydro-2-thioxo-4(1H)quinazolinone (R59949) Among Diacylglycerol Kinase Subtypes, *Biochem. Pharmacol.* 59, 763–772.
47. Herbert, J.M., Augereau, J.M., Gleye, J., and Maffrand, J.P. (1990) Chelerythrine Is a Potent and Specific Inhibitor of Protein Kinase C, *Biochem. Biophys. Res. Commun.* 172, 993–999.

[Received April 3, 2002, and in revised form May 4, 2002; accepted May 6, 2002]

# Effect of Fenitrothion on the Physical Properties of Crustacean Lipoproteins

C.F. Garcia, M. Cunningham, M.R. González-Baró, H. Garda\*, and R. Pollero

Instituto de Investigaciones Bioquímicas de La Plata (INIBIOLP), Consejo Nacional de Investigaciones Científicas y Técnicas (CONICET)-Universidad Nacional de La Plata (UNLP), (1900) La Plata, Argentina

**ABSTRACT:** The effect of the liposoluble organophosphorus insecticide fenitrothion (FS) on lipid packing and rotation of two crustacean plasma HDL was investigated. These lipoproteins, HDL-1 and HDL-2, differed in their lipid composition, but their lipid/protein ratios were similar. The rotational behavior of the fluorescent probes 1,6-diphenyl-1,3,5-hexatriene (DPH) and 3-(*p*-(6-phenyl)-1,3,5-hexatrienyl) phenylpropionic acid (DPH-PA) was used to obtain information about the lipid dynamics in the outer and inner regions, respectively, of the lipid phase of the lipoproteins. Fluorescent steady-state anisotropy ( $r_s$ ), lifetime ( $\tau$ ), rotational correlation time ( $\tau_r$ ), and the limiting anisotropy ( $r_\infty$ ) of these probes were measured in the lipoproteins exposed to different concentrations of FS *in vitro*. The results showed the penetration of FS into both plasma lipoproteins, altering the lipid dynamics of the inner as well as the outer regions. The overall effect of the insecticide was to induce an increase in the lipid order in a concentration-dependent fashion. DPH and DPH-PA fluorescence-lifetime shortening indicated that FS increased the polarity of the probe environment, suggesting an enhanced water penetration into the lipoprotein lipid phase, may be due to the induction of failures in the lipid packing. Even in the absence of FS, a higher ordering of the lipid phase was found in HDL-2 compared to HDL-1, a fact that might be attributed to a higher percentage of sphingomyelin in HDL-2.

Paper no. L8954 in *Lipids* 37, 673–679 (July 2002).

The toxic effects of organophosphorus insecticides on target and nontarget organisms have been described in several studies, although only a few have reported the effects of these xenobiotics on the lipid metabolism. These insecticides are known to cause neurotoxic effects by inhibiting acetylcholinesterase and other enzymes (1,2). The proper function of integral membrane proteins depends on the environment, specifically, the membrane structure. This fact prompted several groups to investigate the alterations in the physicochemical properties of membranes produced when these insecticides, which are mostly liposoluble, are inserted into the lipid bilayers. In this regard, studies done in natural membranes from mammals and some other vertebrates (3–5), an invertebrate (6), and in artificial membranes (7,8) have shown the

\*To whom correspondence should be addressed at INIBIOLP, Fac. de Cs. Médicas, UNLP, Calles 60 y 120, La Plata (1900), Argentina.  
E-mail: hagarada@isis.unlp.edu.ar

Abbreviations:  $\Delta$ , polarized phase shift; DPH, 1,6-diphenyl-1,3,5-hexatriene; DPH-PA, 3-(*p*-(6-phenyl)-1,3,5-hexatrienyl) phenylpropionic acid; FPLC, fast-flow protein liquid chromatography; FS, fenitrothion;  $r_0$ , fundamental anisotropy;  $r_s$ , steady-state anisotropy;  $r_\infty$ , limiting anisotropy;  $\tau$ , lifetime;  $\tau_M$ , modulation lifetime;  $\tau_p$ , phase lifetime;  $\tau_r$ , rotational correlation time.

overall alterations on membrane lipid dynamics produced by organophosphorous insecticides.

We hypothesized that these liposoluble xenobiotics might also alter other lipoprotein systems such as the circulating lipoproteins, so we carried out the present work using as models the insecticide fenitrothion (FS) and two high-density hemolymphatic lipoproteins from the decapod crustacean *Macrobrachium borellii*. Lipids in crustaceans are transported by HDL-1 and HDL-2 (9). HDL-1 is present in the plasma of both males and females. In *M. borellii* it is a particle of 295 kDa composed of three apolipoproteins of 124, 26, and 23 kDa that transport exogenous and endogenous lipids. HDL-2, also called vitellogenin, is only present in females during the vitellogenic periods; its function is to carry the yolk precursors from extra-ovarian synthesis sites to the ovocyte. The *M. borellii* native lipoprotein (440 kDa) has three apolipoprotein subunits (94, 26, and 23 kDa) (Garcia, C.F., unpublished results). Although both serum lipoproteins have high phospholipid contents, their lipid compositions are different. Taking into account the different functions and phospholipid contents of HDL-1 and HDL-2, and their similar lipid/protein ratio, we considered them as an appropriate model to study the effect of insecticides on the physicochemical properties of lipoproteins, correlating their structural and functional characteristics with FS sensitivity. This may be of physiological interest since alterations in the physical properties of these lipoproteins affect lipid transport *in vitro*, and they may influence the lipid exchange among tissues.

The rotational behavior of 1,6-diphenyl-1,3,5-hexatriene (DPH) and 3-(*p*-(6-phenyl)-1,3,5-hexatrienyl) phenylpropionic acid (DPH-PA) was studied to investigate the effect of FS on the dynamics of the lipoprotein lipid phase. Whereas the neutral DPH senses mainly the hydrophobic deep interior of the lipoprotein lipid phase, the anionic DPH-PA is anchored to the interface through its carboxylate group, and it locates its fluorescent moiety more externally. Fluorescence lifetime, and steady-state and frequency-resolved anisotropy measurements were made. They allowed us to evaluate the polarity of the probe's environments, as well as to resolve the probe rotation in terms of rate and amplitude, which are indicative of the lipid phase fluidity and ordering, respectively.

## MATERIALS AND METHODS

*Sampling and isolation of lipoproteins.* Male and ovogenic female adult specimens of *M. borellii* were collected in a

watercourse close to the Rio de la Plata, Argentina. After severing their heads, the shrimps were placed in a tube and centrifuged at low speed to obtain hemolymph. The lipoproteins under study were isolated by density gradient ultracentrifugation. Aliquots of plasma were overlaid on 3 mL NaBr solution (density 1.26 g/mL) containing 0.01% sodium azide and centrifuged at  $178,000 \times g$  at  $10^\circ\text{C}$  for 24 h in a Beckman L8 70-M centrifuge, using a SW60 Ti rotor. The total volume of the tubes was fractionated from top to bottom into 0.2-mL aliquots. The protein content of each fraction was monitored spectrophotometrically at 280 nm. One tube containing a NaCl solution (density 1.04 g/mL) instead of plasma was centrifuged simultaneously and fractionated in order to determine the density of the fractions by monitoring the refraction indexes.

**Lipid and protein analysis.** Lipids were extracted following the method of Folch *et al.* (10). Quantitative determinations of lipid classes were performed by TLC coupled to an FID in an Iatroscan apparatus Model TH-10, after separation on Chromarods SIII, using a triple development solvent system as described previously (11). All lipid classes were quantified using MAG as internal standard. Total protein concentration in each fraction isolated from the density gradient was measured colorimetrically by the method of Lowry *et al.* (12).

**In vitro determination of FA binding to HDL-1.** Total serum of *M. borellii* was incubated with 0, 20, and 40 ppm FS for 2 h. Afterward, the FA-binding capacity was assayed with 0.5  $\mu\text{Ci}$  (9 nmol) of  $[1-^{14}\text{C}]$ palmitic acid (NEN, Boston, MA) as ammonium salt for 30 min. To isolate the labeled HDL-1, plasma hemolymph was analyzed under nondenaturing conditions by preparative gel filtration fast-flow protein liquid chromatography (FPLC) on a Superdex 200 HR 10/30 column (Amersham-Pharmacia, Uppsala, Sweden) using 0.1 M Tris-HCl pH 8.0 at a flow rate of 0.4 mL/min. Protein was detected at 280 nm. The column was calibrated with thyroglobulin, ferritin, BSA, and ribonuclease A (Amersham-Pharmacia) as protein markers. The HDL fraction was collected based on the retention time and relative mass ratio. The identity of HDL-1 was corroborated by PAGE, the protein concentration was determined (12), and the radioactivity of the palmitic acid bound to each protein peak was quantified by liquid scintillation counting.

**Fluorescent measurement.** All measurements were made in a SLM 4800 C phase-modulation spectrofluorometer (SLM Instruments Inc., Urbana, IL). For labeling, 3 mL of buffer solution lipoproteins (100  $\mu\text{g}/\text{mL}$ ) were mixed with a few microliters of concentrated DMSO solutions of DPH or DPH-PA (final concentration 4  $\mu\text{M}$ ). Blanks were prepared in the same way as samples, without the fluorescent probes but with addition of the same volume of DMSO as reference in order to correct fluorescence intensities for nonspecific fluorescence and light-scattering. Samples were gently swirled at  $20^\circ\text{C}$  for at least 2 h, in the absence of light, to allow a complete equilibration of the probes with the lipoproteins. FS from ethanolic concentrated solutions (1, 10, and 20 ppm) was added to samples prior to equilibration.

*Lifetime, steady-state, and dynamic polarization measure-*

*ments.* Polarized phase shift ( $\Delta$ ), steady-state anisotropy ( $r_s$ ), and lifetime ( $\tau$ ) were measured according to Lakowicz *et al.* (13,14) with modifications (15,16). The excitation wavelength was 361 nm, and the emitted light passed through a sharp cut-off filter at 389 nm to eliminate light of wavelengths below 389 nm.

Measurements of  $\tau$  were obtained with the exciting light amplitude-modulated at 18 and 30 MHz by a Debye-Sears modulator and vertically polarized by a Glan-Thompson polarizer. The emission light passed through the filter and then through a Glan-Thompson polarizer oriented  $55^\circ$  to the vertical to eliminate effects of Brownian motion (17). The phase shift and demodulation of the emitted light relative to a reference of known  $\tau$  were determined and used to compute the phase lifetime ( $\tau_p$ ), and the modulation lifetime ( $\tau_M$ ) of the sample (17). POPOP (1,4-bis(5-phenyloxazol-2-yl)benzene) in ethanol, which has a  $\tau$  of 1.35 ns (14–19) was used as reference. The differential polarized phase shift ( $\Delta$ ) was determined according to Lakowicz *et al.* (13,14) by exciting with light modulated at 18 and 30 MHz and vertically polarized, and by measuring the phase difference between the parallel and perpendicular components of the emitted light.

The measured values of  $r_s$ ,  $\tau$ , and  $\Delta$ , and the fundamental anisotropy ( $r_0$ ), which had previously been estimated as 0.390 (20), were used to calculate the limiting anisotropy ( $r_\infty$ ) and the rotational correlation time ( $\tau_r$ ), which is the inverse of the rotational rate, as previously described (15,16) in accordance with the theory developed by Weber (21).

## RESULTS

**Separation and analysis of lipoproteins.** Plasma hemolymph was separated by density gradient ultracentrifugation into HDL-1 (hydrated density 1.13 g/mL), which is found in animals of both sexes, and HDL-2 (hydrated density 1.18 g/mL), which is found only in females at the vitellogenic stage.

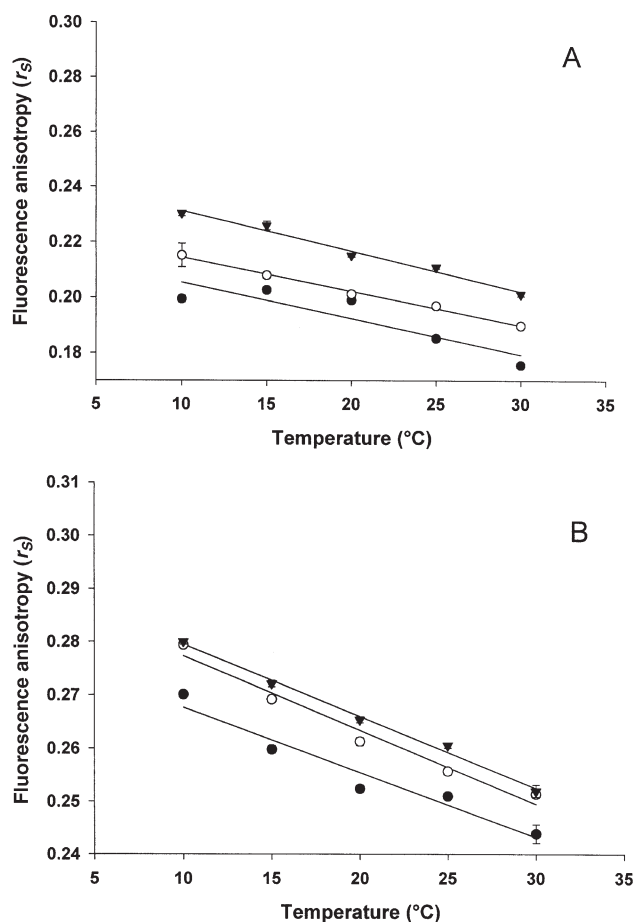
Lipid composition, determined by TLC-FID, is shown in Table 1. The predominant lipid class in both lipoproteins is PC, which is found in a higher proportion in HDL-1, whereas

**TABLE 1**  
Lipid Composition<sup>a</sup> and Lipid/Protein Ratio of Lipoproteins Isolated from Plasma of *Macrobrachium borellii*

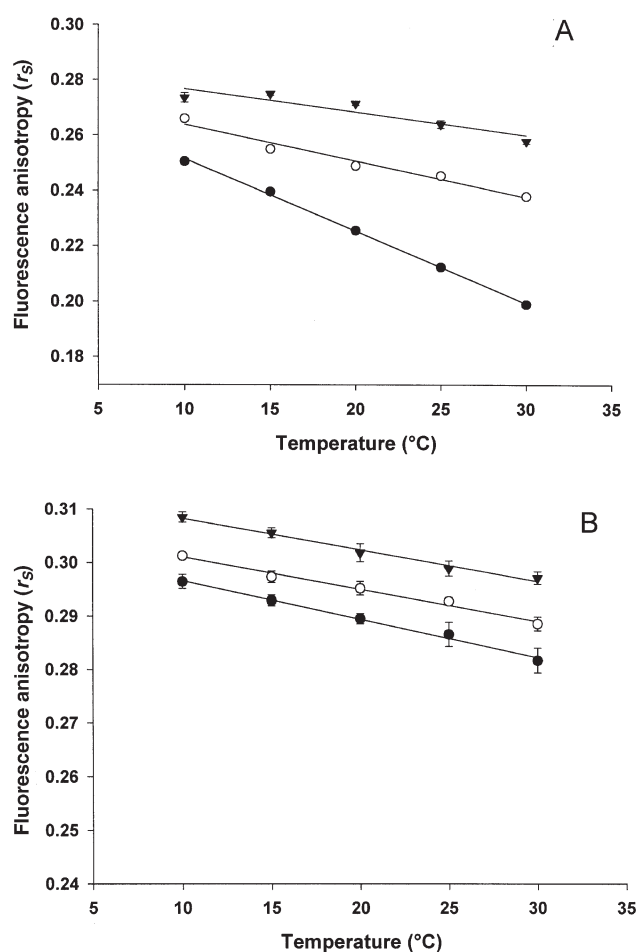
Lipid classes	Fraction	
	HDL-1	HDL-2
TAG (%)	15.2 $\pm$ 2.3	16.3 $\pm$ 0.8
FFA (%)	11.7 $\pm$ 0.6	12.3 $\pm$ 0.7
Cholesterol (%)	14.6 $\pm$ 2.0	12.3 $\pm$ 2.0
PE (%)	19.5 $\pm$ 0.3	16.9 $\pm$ 1.9
PC (%)	38.8 $\pm$ 4.5	22.1 $\pm$ 2.3
Sphingomyelin (%)	Trace	18.8 $\pm$ 1.7
Total lipids (mg/mL hemolymph)	3.3 $\pm$ 0.4	4.67 $\pm$ 0.4
Total proteins (mg/mL hemolymph)	2.9 $\pm$ 0.3	4.45 $\pm$ 0.2
Lipid/protein ratio	1.13	1.04
Hydrated density (g/mL)	1.11–1.13	1.16–1.19

<sup>a</sup>Data on lipid classes are expressed as weight percentage as determined and quantified by TLC-FID. Values represent the mean  $\pm$  SD of three independent analyses.





**FIG. 1.** Effect of fenitrothion (FS) on HDL-1. 1,6-Diphenyl-1,3,5-hexatriene (DPH) (A) and 3-(*p*-(6-phenyl)-1,3,5-hexatrienyl) phenylpropionic acid (DPH-PA) (B) fluorescence anisotropy ( $r_s$ ) vs. temperature, in the absence (●) and the presence of 10 (○) and 20 (▼) ppm of FS. Values represent the average of five different determinations  $\pm$  SD. The linear correlation coefficients ranged between 0.790 and 0.999.



**FIG. 2.** Effect of FS on HDL-2. DPH (A) and DPH-PA (B) fluorescence anisotropy ( $r_s$ ) vs. temperature, in the absence (●) and the presence of 10 (○) and 20 (▼) ppm of FS. Values represent the average of five different determinations  $\pm$  SD. The linear correlation coefficients ranged between 0.850 and 0.999. For abbreviations see Figure 1.

the percentages of PE, TAG, cholesterol, and FFA did not show significant differences between HDL-1 and HDL-2. A relatively high content of sphingomyelin was evident in HDL-2, but it was not present in HDL-1.

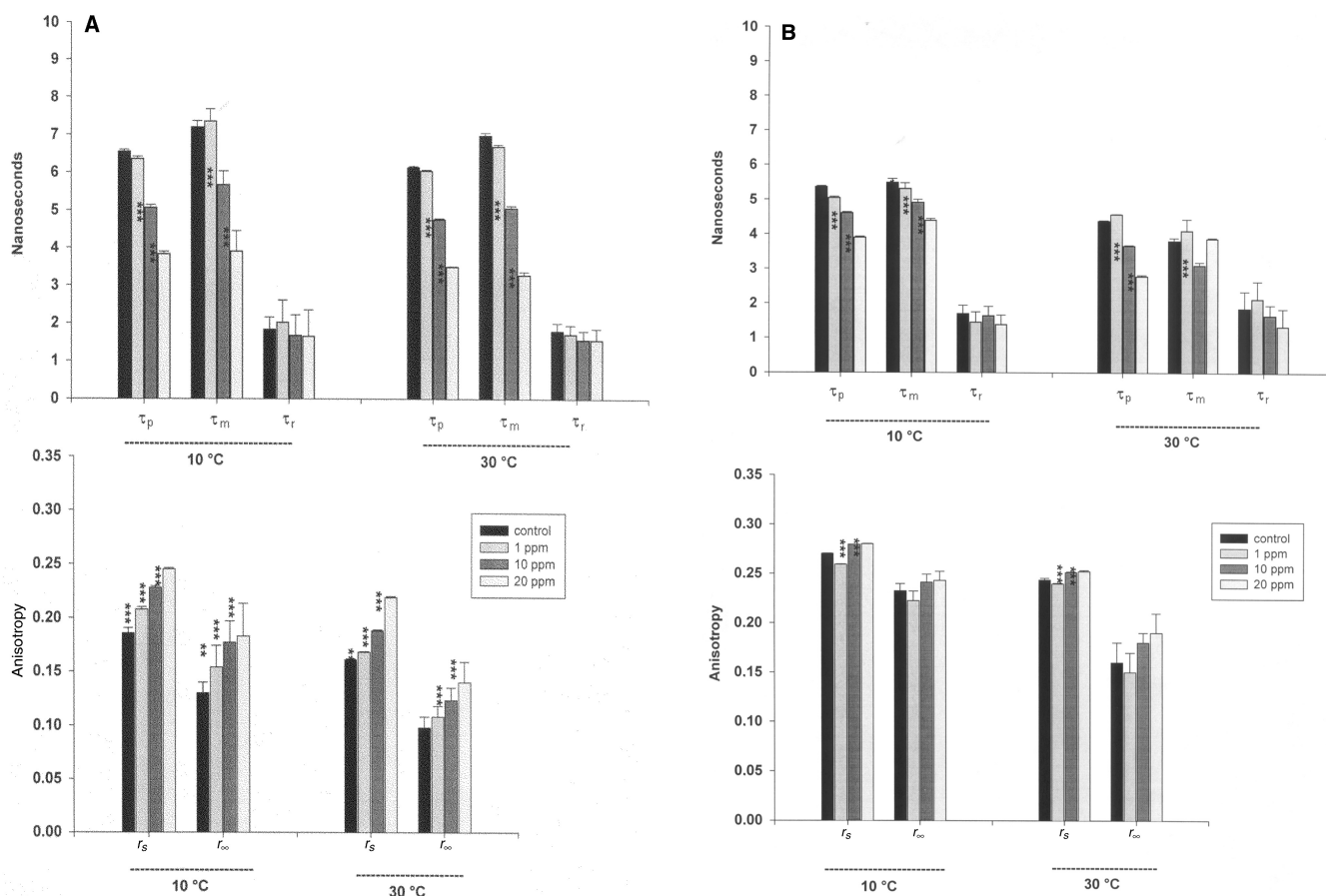
The lipid/protein ratio (lower in HDL-2) was consistent with the hydration densities (higher in HDL-2).

*FS increases steady-state anisotropy of DPH-derived fluorophores in HDL-1 and HDL-2.* Different concentrations (1–20 ppm) of FS affect the microenvironment of the fluorescent probes in HDL-1 (Fig. 1) and HDL-2 (Fig. 2). FS increases  $r_s$  either in the hydrophobic core of the lipoproteins, probed with DPH (Fig. 2A), or in the outer regions of the lipoproteins, probed with DPH-PA (Fig. 2B). The observed effect is dependent on the concentration of the pesticide, and it is constant within the temperature range 10–30°C. We used that temperature range because it represents the extremes of temperature recorded in the stream where these animals live.

*Effect of FS on the lifetimes of DPH and DPH-PA and on the lipid order of HDL-1 and HDL-2.* To better understand the effect of FS on the rotational behavior of DPH and DPH-PA,

lifetime and differential polarized phase shifts ( $\Delta$ ) were measured. They were used to calculate  $\tau_r$  and  $r_\infty$  in HDL-1 (Fig. 3) and HDL-2 (Fig. 4). These measurements were made at 18 and 30 MHz. Since the values obtained at both frequencies were similar, only the values of 18 MHz are shown. It is notable that calculation of  $\tau_r$  and  $r_\infty$  from measurements at discrete frequencies requires homogeneity in the rotamer fluorescence lifetime (15,16). For both probes, but especially for DPH (Figs. 3A and 4A), modulation lifetimes ( $\tau_M$ ) are somewhat higher than phase lifetimes ( $\tau_p$ ), indicating some heterogeneity in the fluorophore population. However, the fact that the values of  $\tau_r$  and  $r_\infty$  obtained are relatively independent of the frequency indicates that they are essentially correct average values of the different rotamer populations.

A significant shortening was observed in the fluorescence lifetime ( $\tau_p$  and  $\tau_M$ ) of DPH and DPH-PA incorporated into HDL-1 (Fig. 3) or HDL-2 (Fig. 4) in which different concentrations of FS were added at 10 or 30°C. In the case of HDL-1, FS incorporation did not alter the rotational correlation time ( $\tau_r$ ) of DPH or DPH-PA (Fig. 3). FS also evoked a concentration-



**FIG. 3.** Steady-state fluorescence anisotropy ( $r_s$ ), phase lifetime ( $\tau_p$ ), modulation lifetime ( $\tau_M$ ), rotational correlation time ( $\tau_r$ ), and limiting anisotropy ( $r_\infty$ ) of (A) DPH and (B) DPH-PA in HDL-1 of *Macrobrachium borellii*, measured in the absence or presence of 1, 10, and 20 ppm FS at 10 and 30°C. Student's *t*-test was used to compare the significance of the differences with respect to the sample without FS: \*\*\* $P < 0.001$ , \*\* $P < 0.01$ , \* $P < 0.05$ .

dependent increase in the steady-state and limiting anisotropy of both probes in HDL-1, at both temperatures.

Figure 4(A and B) shows the effect of FS incorporation on HDL-2. A decrease of  $\tau_r$  for DPH after the addition of the toxin was found at both temperatures, whereas for DPH-PA, it was observed only at 30°C. As was found for HDL-1, FS increased  $r_\infty$  significantly for both probes in HDL-2. These results indicate that FS incorporation generated a strong effect on the lipid phase dynamics of HDL-1 and HDL-2 at both temperatures.

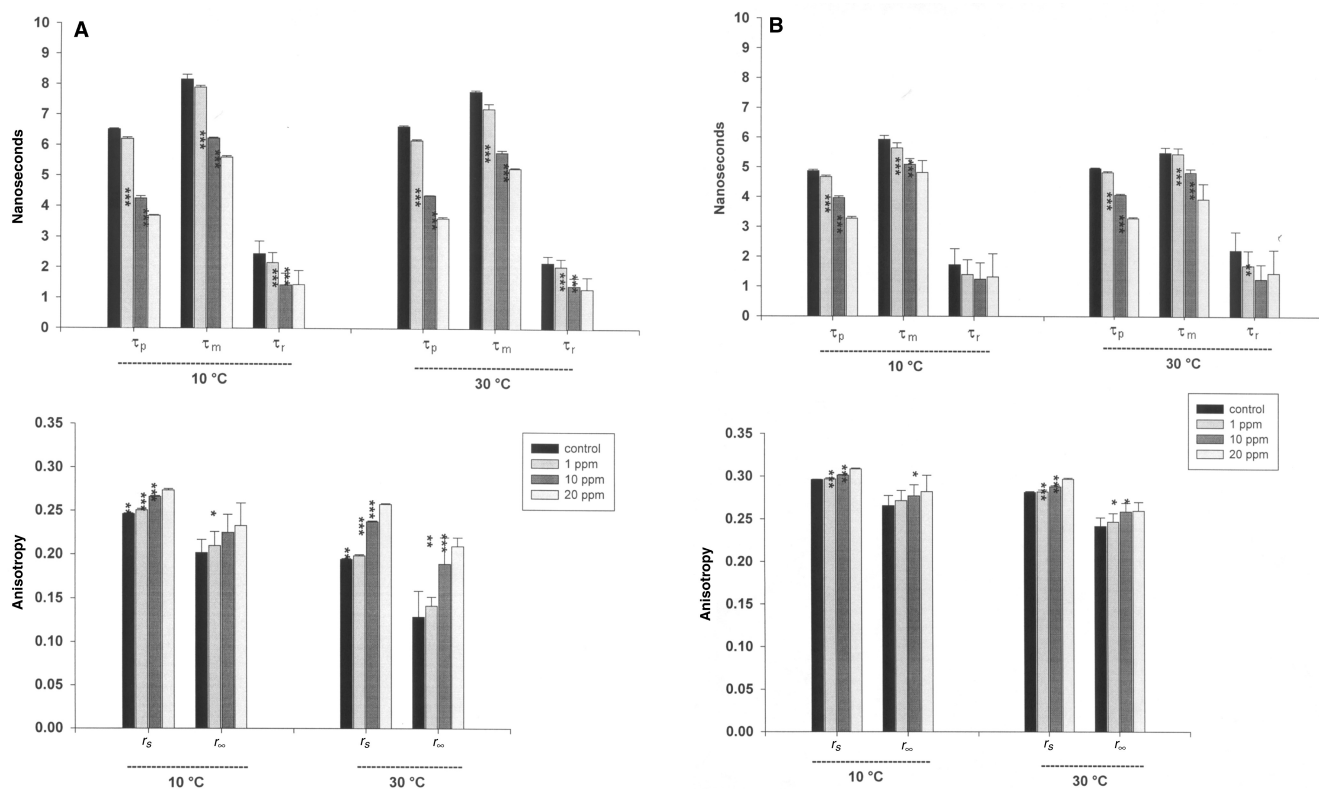
From comparison of both lipoproteins (Figs. 3 and 4), it is evident that for both probes, higher  $r_s$  and  $r_\infty$  values were obtained in HDL-2 than in HDL-1. This fact indicates that HDL-2 has a more ordered lipid phase than HDL-1. On the other hand, the fluorescence lifetimes and  $\tau_r$  of both probes were similar in both lipoproteins.

*FS decreases palmitic acid binding to HDL-1.* In the presence of  $^{14}\text{C}$ -labeled palmitic acid, the only radioactive fraction detected in nonvitellogenic *M. borellii* hemolymph was the one corresponding to the HDL-1. The FPLC retention time and PAGE of the eluted fractions corroborated its identity. When exposed to FS, palmitic acid bound to HDL-1 decreased 1.6-

(20 ppm FS) and 12.6-fold (40 ppm FS), i.e., the radioactivity was 64 and 9% compared to the control, respectively.

## DISCUSSION

Several organophosphorus, chlorinated, and pyrethroid insecticides were reported to affect the fluidity of native and model membranes (22–34). In previous studies using the same insecticide, we demonstrated on the basis of fluorescent anisotropy measurements that FS increases the lipid order in the bilayer of *M. borellii* microsomal membranes, but it does not alter the rotational rate of the DPH and DPH-PA (6). In the present study, the spectroscopic properties of two fluorescent probes located in different regions of the lipoprotein were used to investigate the influence of the insecticide FS, at different concentrations, on the physical state of the lipid phase of two *M. borellii* lipoproteins. One of the probes, DPH, is an elongated molecule, which is a useful fluorophore for studying alterations in the lipid packing and ordering. It penetrates the hydrophobic core of membranes and locates in the acyl chain region. The carboxylate group of the other fluorophore, DPH-PA, interacts with the polar headgroups of the phospholipids,



**FIG. 4.** Steady-state fluorescence anisotropy ( $r_s$ ), phase lifetime ( $\tau_p$ ), modulation lifetime ( $\tau_m$ ), rotational correlation time ( $\tau_r$ ), and limiting anisotropy ( $r_\infty$ ) of (A) DPH and (B) DPH-PA in HDL-2 of *M. borellii*, measured in the absence or presence of 1, 10, and 20 ppm FS at 10, and 30°C. Student's *t*-test was used to compare the significance of the differences with respect to the sample without FS: \*\*\* $P < 0.001$ , \*\* $P < 0.01$ , \* $P < 0.05$ .

locating the fluorescent moiety more outwardly than in the case of DPH. Both probes are preferentially oriented with their long axis parallel to the acyl chains, and the motion that causes depolarization is the wobbling that displaces this long axis.

The increase in  $r_s$  of DPH and DPH-PA generated by FS addition demonstrated that this insecticide modifies the physical properties of the lipid phases in the hydrophobic core as well as in the outer region of both lipoproteins. A rigidifying effect of FS is suggested by the increased  $r_s$  values, although this general parameter depends not only on the rotational behavior but also on the fluorescent lifetime. The shortening in the fluorescent lifetime produced by FS is one of the facts causing the increase in  $r_s$ . However, the results of the differential polarization phase measurements confirm that FS produces a rigidifying effect on these lipoproteins by increasing the lipid phase ordering, evoked through the hindering of the probes' wobbling amplitude resulting in an increased  $r_\infty$ . On the other hand, the rotational rate of these probes is not restricted by the incorporation of FS. At least at 30°C, FS seems to increase the rotational rate of both fluorophores slightly, as indicated by the decrease in  $\tau_r$ , in HDL-2, but  $\tau_r$  remained unchanged in HDL-1 after FS addition. We can therefore assume that the main parameter modified by FS is the lipid order.

The interaction of pyrethroids with liposomal phospholipids evidenced a lower lipid order and a shortening in the DPH lifetime (23). On the contrary, the present results showed that FS decreased DPH and DPH-PA fluorescence lifetime but increased the lipid order in HDL-1 and HDL-2. It is unlikely that this lifetime decrease is due to the direct quenching by FS of the probes' fluorescence, since as previously demonstrated the fluorescence intensity and lifetime of DPH in ethanol were not affected by a large excess of FS (6). Then, the observed decrease in the fluorescence lifetime of these probes is caused by the alterations produced by FS within the structure of the lipoprotein lipid phase. Defects caused by FS in the lipid packing can allow increased water penetration into the hydrophobic interior of these systems, consistent with observations in natural (6) and artificial membranes of 1-palmitoyl-2-oleoyl and dipalmitoyl PC (8).

The action of organophosphorus insecticides on membranes has been related to cholesterol content in those membranes (5). Thus, high proportions of cholesterol preclude the insecticide insertion into the membrane. Although cholesterol content is relatively high in both lipoproteins of *M. borellii*, this does not seem entirely to hinder FS insertion into the lipid phase.

The present results also indicate that HDL-2 has a higher ordering of the lipid phase than HDL-1, a fact that can be at-

tributed to the different lipid compositions of both lipoproteins. The main difference in composition is the presence of sphingomyelin in HDL-2 but not in HDL-1. It is well-known that sphingomyelin has a rigidifying effect on membranes (35), lipid monolayers (36), liposomes (37), and some human lipoproteins (38), but its physiological function in plasma is still controversial. It was postulated that sphingomyelin may act as an inhibitor of lipoprotein peroxidation because of its rigidifying effect, which may hinder the lateral propagation of the lipid-peroxy radicals (39). In this way, the presence of sphingomyelin in HDL-2 rather than in HDL-1 could be important for yolk synthesis. DNA damage in the embryo could be minimized if the precursor is peroxide-poor. This fact would explain the higher  $r_s$  and  $r_\infty$  values found in HDL-2. Thus, FS is able to penetrate the lipid phase of HDL-2 and produce a further ordering increase; this effect is especially noticeable at 30°C.

In brief, these results show that FS can be a perturbing agent to the circulating lipoproteins of *M. borellii*, increasing their lipid phase order, producing packing defects, and thus affecting their structures and functions. In HDL-1, a decrease in the binding of palmitic acid was observed, implying that the proper structure of the lipoprotein is essential for the lipid-binding capacity. Although PC is the major lipid class in HDL-1, we have previously observed in *in vivo* studies that HDL-1 can exchange FA with the hepatopancreas in *M. borellii* (40). In this regard, insecticide actions can be important from both the physiological and toxicological points of view.

## ACKNOWLEDGMENTS

This work was supported by grants from CONICET, Comisión de Investigaciones Científicas de la Provincia de Buenos Aires (CICBA), Fondo para la Investigación Científica y Tecnológica-Agencia Nacional de Promoción Científica y Tecnológica (FONCYT), and UNLP, Argentina. M.R.G-B. and H.G. are members of Carrera del Investigador CONICET, Argentina. R.P. is member of Carrera del Investigador CICBA, Argentina.

## REFERENCES

- Narahashi, T. (1982) Cellular and Molecular Mechanisms of Action of Insecticides: Neurophysiological Approach, *Neurotoxicol. Teratol.* 4, 753–758.
- Omkar, and Shukla, G.S. (1985) Nature of Dichlorvos Intoxication in a Freshwater Prawn, *Macrobrachium Lamarrei* (H. Milne Edwards), *Environ. Research* 37, 349–354.
- Antunes-Madeira, M.C., And Madeira, V.M.C. (1984) Partition of Parathion in Synthetic and Native Membranes, *Biochim. Biophys. Acta* 778, 49–56.
- Purshottam, T., and Srivastava, R.K. (1987) Parathion Toxicity in Relation to Liver Microsomal Oxidases, Lipid Composition and Fluidity, *Pharmacology* 35, 227–233.
- Antunes-Madeira, M.C., Videira, R.A., and Madeira, V.M. (1994) Effects of Parathion on Membrane Organization and Its Implications for the Mechanisms of Toxicity, *Biochim. Biophys. Acta* 1190, 149–154.
- González-Baró, M.R., Garda, H., and Pollero, R.J. (1997) Effect of Fenitrothion on Hepatopancreas Membrane Fluidity in *Macrobrachium Borellii*, *Pest. Biochem. Physiol.* 58, 133–143.
- Blasiak, J. (1993) Changes in the Fluidity of Model Lipid Membranes Evoked by the Organophosphorus Insecticide Methylbromfeninfos, *Acta Biochim. Pol.* 40, 39–41.
- González-Baró, M.R., Garda, H., and Pollero, R.J. (2000) Effect of Fenitrothion on Dipalmitoyl and 1-Palmitoyl-2-oleoylphosphatidylcholine Bilayers, *Biochim. Biophys. Acta* 1468, 304–310.
- Lee, R.F. (1991) Lipoproteins from the Hemolymph and Ovaries of Marine Invertebrates, in *Advances in Comparative and Environmental Physiology* (Gilles, R., ed.), Vol. 7, pp. 187–208, Springer-Verlag, London.
- Folch, J., Lees, M., and Sloane-Stanley, G.H. (1957) A Simple Method for the Isolation and Purification of Total Lipids from Animal Tissues, *J. Biol. Chem.* 226, 497–509.
- Cunningham, M., And Pollero, R.J. (1996) Characterization of Lipoprotein Fractions with High Content of Hemocyanin in the Hemolymphatic Plasma of *Polybetes Pythagoricus*, *J. Exp. Zool.* 274, 275–280.
- Lowry, O.H., Rosebrough, N.J., Farr, A.L., and Randall, R.J. (1951) Protein Measurement with the Folin Phenol Reagent, *J. Biol. Chem.* 193, 265–275.
- Lakowicz, J.R., Prendergast, F.G., and Hogen, D. (1979) Differential Polarized Phase Fluorometric Investigations of Diphenylhexatriene in Lipid Bilayers. Quantitation of Hindered Depolarizing Rotations, *Biochemistry* 18, 508–519.
- Lakowicz, J.R. (1983) *Principles of Fluorescence Spectroscopy*, pp. 52–95, 156–188, Plenum Press, New York.
- Tricerri, M.A., Garda, H.A., and Brenner, R.R. (1994) Lipid Chain Order and Dynamics at Different Bilayer Depths in Liposomes of Several Phosphatidylcholines Studied by Differential Polarized Phase Fluorescence, *Chem. Phys. Lipids* 71, 61–72.
- Garda, H.A., Bernasconi, A.M., and Brenner, R.R. (1994) Possible Compensation of Structural and Viscotropic Properties in Hepatic Microsomes and Erythrocyte Membranes of Rats with Essential Fatty Acid Deficiency, *J. Lipid Res.* 35, 1367–1377.
- Spencer, R.D., and Weber, G. (1970) Influence of Brownian Rotations and Energy Transfer upon the Measurements of Fluorescence Lifetime, *J. Chem. Phys.* 52, 1654–1663.
- Lakowicz, J.R., and Cherek, H. (1980) Dipolar Relaxation in Proteins on the Nanosecond Timescale Observed by Wavelength-Resolved Phase Fluorometry of Tryptophan Fluorescence, *J. Biol. Chem.* 255, 831–834.
- Lakowicz, J.R., Cherek, H., and Bevan, D.R. (1980) Demonstration of Nanosecond Dipolar Relaxation in Biopolymers by Inversion of the Apparent Fluorescence Phase Shift and Demodulation Lifetimes, *J. Biol. Chem.* 255, 4403–4406.
- Garda, A., Bernasconi, A.M., and Brenner, R.R. (1994) Influence of Membrane Proteins on Lipid Matrix Structure and Dynamics. A Differential Polarized Phase Fluorescence Study in Rat Liver Microsomes and Erythrocyte Membranes, *An. Asoc. Quim. Arg.* 82, 305–323.
- Weber, G. (1978) Limited Rotational Motion: Recognition by Differential Phase Fluorometry, *Acta Phys. Pol. A* 54, 173–179.
- Omann, G.M., and Lakowicz, J.R. (1982) Interactions of Chlorinated Hydrocarbon Insecticides with Membranes, *Biochim. Biophys. Acta* 684, 83–95.
- Stelzer, K.J., and Gordon, M.A. (1985) Interactions of Pyrethroids With Phosphatidylcholine Liposomal Membranes, *Biochim. Biophys. Acta* 812, 361–368.
- Perez-Albarsanz, M.A., Lopez-Aparicio, P., Senar, S., and Recio, M.N. (1991) Effects of Lindane on Fluidity and Lipid Composition in Rat Renal Cortex Membranes, *Biochim. Biophys. Acta* 1066, 124–130.
- Lopez-Aparicio, P., Recio, M.N., Prieto, J.C., Carmena, M.J., and Perez-Albarsanz, M.A. (1991) Effect of Lindane upon the Beta-Adrenergic Stimulation of Cyclic AMP Accumulation in Rat Renal Cortical Tubules Caused by Alterations in Membrane Fluidity, *Life Sci.* 49, 1141–1154.



26. Sarkar, S.N., Balasubramanian, S.V., and Sikdar, S.K. (1993) Effect of Fenvalerate, a Pyrethroid Insecticide, on Membrane Fluidity, *Biochim. Biophys. Acta* 1147, 137–142.
27. Moya-Quiles, M.R., Munoz-Delgado, E., and Vidal, C.J. (1994) Interactions of the Pyrethroid Insecticide Allethrin with Liposomes, *Arch. Biochem. Biophys.* 312, 95–100.
28. Antunes-Madeira, M.C., and Madeira, V.M. (1986) Partition of DDT in Synthetic and Native Membranes, *Biochim. Biophys. Acta* 861, 159–164.
29. Antunes-Madeira, M.C., and Madeira, V.M. (1989) Membrane Fluidity as Affected by the Insecticide Lindane, *Biochim. Biophys. Acta* 982, 161–166.
30. Antunes-Madeira, M.A., and Madeira, V.M. (1990) Membrane Fluidity as Affected by the Organochlorine Insecticide DDT, *Biochim. Biophys. Acta* 1023, 469–474.
31. Antunes-Madeira, M.C., Almeida, L.M., and Madeira, V.M. (1990) Effects of Lindane on Membrane Fluidity: Intramolecular Excimerization of a Pyrene Derivative and Polarization of Diphenylhexatriene, *Biochim. Biophys. Acta* 1022, 110–114.
32. Antunes-Madeira, M.C., Almeida, L.M., and Madeira, V.M. (1993) Depth-Dependent Effects of DDT and Lindane on the Fluidity of Native Membranes and Extracted Lipids. Implications for Mechanisms of Toxicity, *Bull. Environ. Contam. Toxicol.* 51, 787–794.
33. Antunes-Madeira, M.C., and Madeira, V.M. (1993) Effects of DDE on the Fluidity of Model and Native Membranes: Implications for the Mechanisms of Toxicity, *Biochim. Biophys. Acta* 1149, 86–92.
34. Videira, R.A., Antunes-Madeira, M.C., Custodio, J.B., and Madeira, V.M. (1995) Partition of DDE in Synthetic and Native Membranes Determined by Ultraviolet Derivative Spectroscopy, *Biochim. Biophys. Acta* 1238, 22–28.
35. Barenholz, Y. (1984) Sphingomyelin-Lecithin Balance in Membranes, in *Physiology of Membrane Fluidity* (Shinitzky, M., ed.), Vol. 1, pp. 131–173, CRC Press, Boca Raton.
36. Lund-Katz, S., Laboda, H.M., McLean, L.R., and Phillips, M.C. (1988) Influence of Molecular Packing and Phospholipid Type on Rates of Cholesterol Exchange, *Biochemistry* 27, 3416–3423.
37. Sommer, A., Prenner, E., Gorges, R., Stutz, H., Grillhofer, H., Kostner, G.M., Paltauf, F., and Hermetter, A. (1992) Organization of Phosphatidylcholine and Sphingomyelin in the Surface Monolayer of Low Density Lipoprotein and Lipoprotein (a) as Determined by Time-Resolved Fluorometry, *J. Biol. Chem.* 267, 24217–24222.
38. Lottin, H., Motta, C., and Simard, G. (1996) Differential Effects of Glycero- and Sphingo-phospholipolysis on Human High-Density Lipoprotein Fluidity, *Biochim. Biophys. Acta* 1301, 127–132.
39. Subbaiah, P., Subramanian, V., and Wang, K. (1999) Novel Physiological Function of Sphingomyelin in Plasma, *J. Biol. Chem.* 274, 36409–36414.
40. Garcia, F., Gonzalez-Baro, M., and Pollero, R. (2002) Transfer of Lipids Between Hemolymph and Hepatopancreas in the Shrimp *Macrobrachium borelli*, *Lipids* 37, 581–585.

[Received November 26, 2001, and in revised form May 15, 2002; revision accepted June 6, 2002]

# *Trans*-7,*cis*-9 CLA Is Synthesized Endogenously by $\Delta^9$ -Desaturase in Dairy Cows

Benjamin A. Corl<sup>a</sup>, Lance H. Baumgard<sup>a,1</sup>, J. Mikko Griinari<sup>b</sup>, Pierluigi Delmonte<sup>c</sup>,  
Kim M. Morehouse<sup>c</sup>, Martin P. Yurawecz<sup>c</sup>, and Dale E. Bauman<sup>a,\*</sup>

<sup>a</sup>Department of Animal Science, Cornell University, Ithaca, New York, <sup>b</sup>Department of Animal Science, University of Helsinki, Helsinki, Finland, and <sup>c</sup>U.S. Food and Drug Administration, Center for Food Safety and Applied Nutrition, Washington, DC

**ABSTRACT:** *Cis*-9,*trans*-11 and *trans*-7,*cis*-9 CLA are the most prevalent CLA isomers in milkfat. The majority of *cis*-9,*trans*-11 CLA is synthesized endogenously by  $\Delta^9$ -desaturase. We tested the hypothesis that *trans*-7,*cis*-9 CLA originates from endogenous synthesis by inhibiting  $\Delta^9$ -desaturase with a source of cyclopropene FA (sterculic oil: SO) or with a *trans*-10,*cis*-12 CLA supplement. Experiment 1 (four cows; Latin square) involved four treatments: control, SO, partially hydrogenated vegetable oil (PHVO), and PHVO + SO. Milk, plasma, and rumen fluid were collected. Experiment 2 treatments (four cows) were 0 or 14.0 g/d of 10,12 CLA supplement; milk and plasma were collected. Samples were analyzed by GC and Ag<sup>+</sup>-HPLC to determine FA. In Experiment 1, SO decreased milkfat content of *trans*-7,*cis*-9 CLA by 68 to 71% and *cis*-9,*trans*-11 CLA by 61 to 65%. In Experiment 2, the 10,12 CLA supplement decreased milkfat content of *trans*-7,*cis*-9 CLA and *cis*-9,*trans*-11 by 44 and 25%, respectively. Correcting for the extent of treatment-induced inhibition of  $\Delta^9$ -desaturase based on changes in myristic and myristoleic acids, endogenous synthesis of *trans*-7,*cis*-9 CLA represented 85 and 102% in Experiments 1 and 2, respectively. Similar corrected values were 77 and 58% for endogenous synthesis of *cis*-9,*trans*-11 CLA. Thus, milkfat *cis*-9,*trans*-11 CLA was primarily from endogenous synthesis with a minor portion from rumen escape. In contrast, *trans*-7,*cis*-9 CLA was not present in rumen fluid in significant amounts. Results indicate this isomer in milkfat is derived almost exclusively from endogenous synthesis *via*  $\Delta^9$ -desaturase.

Paper no. L9018 in *Lipids* 37, 681–688 (July 2002).

CLA have been reported to have many positive health effects in biomedical studies with animal models (1). Given that CLA are simply positional and geometric isomers of octadecadienoic acid, many combinations of double bond positions and conformations are theoretically possible, and several have been detected in ruminant fat using highly selective methods. CLA were thought to be somewhat unique to ruminants because of ruminal biohydrogenation; at present, 19 isomers have been identified in milkfat (2), and 14 have been reported in beef fat (3). *Cis*-9,*trans*-11 CLA and *trans*-7,*cis*-9 CLA are the most prevalent isomers; together they generally account for 75 to 80% of the CLA found in food products derived from ruminants (2,4).

<sup>1</sup>Present address: University of Arizona, Department of Animal Sciences, 228 Shantz Bldg., P.O. Box 210038, Tucson, AZ 85721-0038.

\*To whom correspondence should be addressed at Department of Animal Science, 262 Morrison Hall, Cornell University, Ithaca, NY 14853-4801. E-mail: deb6@cornell.edu

Abbreviations: PHVO, partially hydrogenated vegetable oil; SO, sterculic oil.

The overwhelmingly predominant CLA isomer found in foods of ruminant origin is *cis*-9,*trans*-11 CLA (2,4,5). This CLA isomer is an intermediate in ruminal biohydrogenation of linoleic acid. Initially, it was thought that the *cis*-9,*trans*-11 CLA in ruminant fats was of rumen origin (see Griinari and Bauman, Ref. 6). By using sterculic acid, a specific inhibitor of  $\Delta^9$ -desaturase, we recently demonstrated that the majority of *cis*-9,*trans*-11 CLA in milkfat is derived from endogenous synthesis *via*  $\Delta^9$ -desaturase with ruminally derived *trans*-11 18:1 as the substrate (7,8). *Trans*-11 18:1 is the only *trans* FA isomer currently described as an intermediate in biohydrogenation. However, many other *trans*-18:1 isomers are found in rumen fluid (9) and milkfat (10), and these are believed to originate from double bond migration or alternative pathways of biohydrogenation (6).

Under certain dietary conditions, *trans*-10,*cis*-12 CLA is found in milkfat, and it represents a contrast to the *cis*-9, *trans*-11 CLA isomer. *Trans*-10,*cis*-12 CLA appears to be exclusively ruminally derived and is a product of ruminal biohydrogenation in which the initial isomerization takes place at the *cis*-9 position of linoleic acid rather than at the *cis*-12 position, as in the more typical pathway (6). The *trans*-10,*cis*-12 CLA isomer causes a reduction in milkfat synthesis and a decrease in  $\Delta^9$ -desaturase in dairy cows (11,12), the latter resulting in a decrease in endogenous synthesis of *cis*-9,*trans*-11 CLA. In growing rodents, *trans*-10,*cis*-12 CLA also reduces body fat accretion (13) and has been shown to reduce the gene expression and enzyme activity for  $\Delta^9$ -desaturase (14–16).

The origin of *trans*-7,*cis*-9 CLA found in ruminant fat has not been established. Given ruminal production of *trans*-7 18:1, we hypothesized that *trans*-7,*cis*-9 CLA would be derived from endogenous synthesis *via*  $\Delta^9$ -desaturase. Our objective was to test this hypothesis using two different *in vivo* approaches to inhibit  $\Delta^9$ -desaturase in lactating dairy cows, one involving the use of cyclopropenoid FA and the other involving a dietary supplement of *trans*-10,*cis*-12 CLA.

## EXPERIMENTAL PROCEDURES

Study protocols and procedures for these experiments were approved by the Cornell University Institutional Animal Care and Use Committee. Studies utilized lactating Holstein cows fitted with rumen fistulae and housed in metabolic tie stalls at the Large Animal Research and Teaching Unit at Cornell University. Cows were fed a total mixed ration formulated using the Cornell Net Carbohydrate and Protein System (17) to meet or exceed predicted nutrient requirements (18). Cows

were given *ad libitum* access to feed with equal portions of fresh feed offered before milking at 0600 and 1800 h.

**Cows and experimental design.** Details of Experiment 1 have been described previously (8). Briefly, four cows ( $115 \pm 9$  d in milk) were used in a  $4 \times 4$  Latin square design. The four treatments were: skim milk (500 mL/d; control), partially hydrogenated vegetable oil (250 g/d; PHVO), sterculic oil (8.8 g/d; SO), and PHVO + SO. Treatments were abomasally infused *via* polyvinyl chloride tubing (0.5 cm i.d.) that passed through the rumen fistula and sulcus omasi into the abomasum (19). One-fourth of the daily treatment dose was infused every 6 h for 4 d with a 6-d interval between treatment periods. Milk samples, collected at both milkings on the last day of treatment, and a plasma sample, collected after the evening milking on the last day of the treatment period, were stored at  $-20^{\circ}\text{C}$  until further analyses. Rumen fluid samples were collected on the last day of each treatment period at 1, 2, and 4 h after the morning feeding. Sampling times were chosen to coincide with maximal rates of biohydrogenation to optimize detection of CLA isomers normally produced in very low amounts (20,21). Rumen samples were centrifuged at  $1,200 \times g$  for 10 min, and the pellet was saved and frozen at  $-20^{\circ}\text{C}$  until further analysis. This fraction represents the fine particles and associated bacteria; the FA intermediates have been shown to be bound to the fine particulate matter in the rumen (22,23).

Details of Experiment 2 have been described previously (24). Briefly, four cows ( $228 \pm 54$  d in milk) were used in a  $4 \times 4$  Latin square design. Treatments were abomasal infusion of four doses of *trans*-10,*cis*-12 CLA. For the present study, only the low-dose (0 g/d; control) and high-dose (14.0 g/d; 10,12 CLA supplement) treatments were utilized. The 10,12 CLA supplement was emulsified in skim milk and infused continuously for 5 d with 7 to 8 d between treatment periods. Milk samples were collected at both milkings on the last day of treatment and stored at  $-20^{\circ}\text{C}$  until further analysis. On day 5 of infusion, seven blood samples were obtained *via* jugular catheter over a 45 min interval at 0900 and 1400 h. Plasma was harvested immediately and stored at  $-20^{\circ}\text{C}$ . Prior to analysis, plasma samples were thawed and pooled by individual animal.

**GC analysis.** Extraction of lipid from milk and plasma samples and preparation of FAME by base-catalyzed transmethylation have been described previously (8,25). The FA of SO were transmethylated by the same procedure used for milkfat. For analysis, the PHVO and the *trans*-10,*cis*-12 CLA supplements were methylated using 1% sulfuric acid in methanol as described by Christie (26).

Rumen sample pellets were freeze-dried and then ground in liquid nitrogen using a mortar and pestle. A composite (0.5 g) was made for individual animals and transferred to a screw-top extraction tube. Water (0.5 mL) was added and the tube was vortexed for 30 s. The sample was acidified by adding 3–4 drops of 2 M HCl and then vortexed for 30 s, sonicated for 5 min, and extracted twice with 4.0 mL hexane/isopropanol (3:2) according to Hara and Radin (27). The combined organic phases were washed with 2.0 mL distilled water

and dried over 1 g sodium sulfate for 30 min. Solvent was evaporated under a stream of  $\text{N}_2$ , and the lipid was stored at  $-20^{\circ}\text{C}$ . FFA were separated from other lipids using 1 g aminopropyl columns (Mega Bond-Elut; Varian Corp.) as described by Bateman and Jenkins (28). Columns were prepared with 6 mL hexane, and lipid samples were dissolved in 1.0 mL hexane and applied to the column. Neutral lipids were eluted from the column with 8.0 mL hexane/isopropanol (3:1). FFA were eluted with 9.0 mL 2% acetic acid in ether and collected. The solvent was then evaporated under a stream of  $\text{N}_2$ , and the lipid was stored at  $-20^{\circ}\text{C}$ . Rumen FFA were methylated using trimethylsilyldiazomethane according to the procedure of Hashimoto *et al.* (29) with modifications. Briefly, FFA were dissolved in 0.4 mL methanol and 1.6 mL toluene. One mL 30 mM trimethylsilyldiazomethane was added and the solution was incubated at room temperature for 30 min. The reaction was stopped using 5–10 drops acetic acid. Five milliliters of water and 1 mL hexane were added and the solution was vortexed. The organic phase was dried over 1 g sodium sulfate for 30 min. The organic phase was transferred to a new tube, and the solvent was evaporated under a stream of  $\text{N}_2$ . The FAME were then dissolved in 0.45 mL hexane for GC analysis.

The FAME from milkfat, plasma, rumen samples, and infused supplements were quantified by GC (Hewlett-Packard GC system 6890+ with an FID) using a SP-2560 capillary column (100 m  $\times$  0.25 mm i.d. with 0.2  $\mu\text{m}$  film thickness; Supelco Inc., Bellefonte, PA). GC parameters for milkfat, plasma, and infused supplements were described previously (8,24). GC parameters for rumen samples were similar except for temperature programming, where the oven temperature was initially held at  $160^{\circ}\text{C}$  for 28 min and then increased at  $5^{\circ}\text{C}/\text{min}$  to  $220^{\circ}\text{C}$  and held at this temperature for 10 min. Each peak was identified and quantified using pure methyl ester standards (Nu-Chek-Prep, Elysian, MN). A butter reference standard (CRM 164; Commission of the European Communities, Community Bureau of Reference, Brussels, Belgium) was used to determine recoveries and correction factors for individual FA.

**HPLC.** The FAME prepared from the samples were also analyzed using an HPLC system consisting of a Waters 996 photodiode array detector, a Waters 2690 separations module (Alliance), and the Millennium<sup>32</sup> chromatography manager, version 3.20 (Waters Corporation, Milford, MA). Three silver ion columns (ChromSpher 5 Lipids,  $250 \times 4.6$  mm; Varian Analytical Supplies, Harbor City, CA) were used in series for the separation of the lipids. The solvent consisted of UV-grade hexane with 0.1% acetonitrile and 0.5% ethyl ether, prepared fresh daily. Ethyl ether was used to reduce analysis time and minimize retention volume drift, which is a well-known problem encountered in working with  $\text{Ag}^+$  HPLC. The column was pretreated daily by eluting with 1% acetonitrile/hexane for 30–60 min prior to sample analysis. A commercial CLA FAME reference was injected two or three times before test portion injections commenced. Typical injections of test portion volumes were 5–15  $\mu\text{L}$ , representing  $<250 \mu\text{g}$

lipid. Identifications were made by co-injection with a reference material or by confirming the retention volume relative to both toluene (0.5% was added to each sample prior to injection) and *cis-9,trans-11* CLA. All the CLA isomers were available commercially, synthesized by isomerization of a commercially available reference with I<sub>2</sub>, or synthesized by conjugation of partially hydrogenated linolenic acids ( $\alpha$  or  $\gamma$ ; Refs. 30,31).

**Calculations and statistical analyses.** The *cis-9,trans-11* CLA peak in the GC analysis method co-elutes with two other CLA isomers—*trans-7,cis-9* CLA and *trans-8,cis-10* CLA (32). Using data from the HPLC analysis, areas for *trans-7,cis-9* CLA, *trans-8,cis-10* CLA, and *cis-9,trans-11* CLA were summed, and the percentage of each isomer contained in the three isomer peak from GC analysis was used to calculate the content of each isomer in a sample. The content of other CLA isomers in samples was then calculated based on their area from HPLC analysis relative to the area for the three isomer peak.

Statistical analysis of Experiment 1 was as a 4 × 4 Latin square using the mixed procedure of SAS (33). The model included effects for period, cow, and treatment. Treatment effects were determined to be significant at  $P < 0.05$  and when this occurred, individual treatments were compared for significant differences using a *t*-test. For Experiment 2, data were analyzed statistically using a two-factor ANOVA for effects of cow and treatment. Treatment effects were determined to be significant at  $P < 0.05$ .

## RESULTS

**Experiment 1.** PHVO was infused to supply additional *trans-11* 18:1 for endogenous synthesis of *cis-9,trans-11* CLA, but it also contained substantial amounts of other *trans-18:1* FA (Table 1). Although no CLA was detectable in the PHVO by GC analysis, isomers were detected by the more sensitive HPLC method. Of the CLA isomers detected, 67% were *trans,trans*, 27% were *cis/trans*, and 4% were *cis,cis*. For the SO supplement, sterculic acid was the major cyclopropenoic FA, but lesser amounts of malvalic acid were also present (Table 1). The SO supplement contained no CLA isomers as determined by GC analysis and was not further analyzed for CLA isomers by more sensitive methods.

Supplements were abomasally infused as an experimental means to bypass possible modification by rumen bacteria. Milk yield was unaffected by treatment, although treatments did modestly reduce milkfat yield and the fat content of milk (8 to 17%; Table 2). Additional details on infusions and performance data, including milk FA composition, have been presented elsewhere (8).

The concentration of *trans-7,cis-9* CLA in FA extracted from rumen fluid samples did not statistically differ from zero ( $P > 0.2$ ), although trace levels were detected in an occasional sample (Table 3). *Trans-7,cis-9* CLA was present in plasma lipids, but no treatment effects were observed (Table 3). In contrast, treatment effects were obvious in milkfat with *trans-7,cis-9* CLA, decreasing 71% when SO and control treatments

**TABLE 1**  
Composition of FA in Sterculic Oil (SO) and Partially Hydrogenated Vegetable Oil (PHVO)

FA	Content (wt%)
SO	
16:0	22.95
18:1, cyclo <sup>a</sup>	6.33
18:0	1.87
18:1, <i>cis-9</i>	5.08
18:1, <i>cis-9,cis-12</i>	5.03
19:1, cyclo <sup>a</sup>	55.86
Other	2.88
PHVO	
12:0	1.18
14:0	0.61
16:0	11.70
18:0	5.61
18:1, <i>trans-6,7,8</i>	3.61
18:1, <i>trans-9</i>	12.80
18:1, <i>trans-10</i>	12.15
18:1, <i>trans-11</i>	9.40
18:1, <i>trans-12</i>	6.09
Other	36.85

<sup>a</sup>Cyclo refers to presence of a cyclopropene ring. In 18:1, cyclo is 7-(2-octyl-1-cyclopropenyl) heptanoic acid (malvalic acid) and in 19:1, cyclo is 8-(2-octyl-1-cyclopropenyl) octanoic acid (sterculic acid).

were compared and 68% when PHVO + SO with PHVO treatments were compared. Relative to the control treatment, infusion of PHVO increased milk content of *trans-7,cis-9* CLA by 26%.

*Cis-9,trans-11* CLA was the most abundant CLA isomer present in rumen fluid, plasma, and milk (Table 3). Treatment effects were observed on the content of this CLA isomer in milk, but not for rumen fluid or plasma. In milk, infusion PHVO increased *cis-9,trans-11* CLA, whereas SO infusion markedly decreased *cis-9,trans-11* CLA by 65% (SO vs. control treatments) and 61% (PHVO + SO vs. PHVO treatments).

*Trans-10,cis-12* CLA was present in FA extracted from rumen fluid, plasma, and milk (Table 3). Treatments that included infusion of PHVO resulted in small increases in the milkfat content of *trans-10,cis-12* CLA, but no changes were observed in rumen fluid or plasma. Small amounts of several other *cis/trans* CLA isomers were also present in plasma and milkfat and there were minor quantitative differences related to treatment (data not presented). However, these isomers were detected at extraordinarily low levels in a region of the chromatogram with known interferences and inadequate confirmation. In rumen fluid, other *cis/trans* CLA isomers were detected only in an occasional sample and the means for these isomers were not statistically different from zero. Several *trans,trans* CLA isomers were also detected, and these minor components were summed into total *trans,trans* CLA isomers (Table 3). Treatments that involved abomasal infusion of PHVO resulted in a small increase in the milkfat content of total *trans,trans* CLA isomers.

The ratio of *cis-9,trans-11* to *trans-11* 18:1 was evaluated because they are intermediates in ruminal biohydrogenation and are related as product and substrate for endogenous



**TABLE 2**  
**Performance of Lactating Dairy Cows During Abomasal Infusion of PHVO, SO,**  
**and *trans*-10,*cis*-12 CLA Supplement**

	Milk yield (kg/d)	Milkfat	
		Content (wt%)	Yield (g/d)
Experiment 1 <sup>a</sup>			
Treatments			
Control	39.8	3.32 <sup>a</sup>	1329 <sup>a</sup>
SO	38.6	3.03 <sup>b,c</sup>	1169 <sup>b</sup>
PHVO	37.8	2.90 <sup>b</sup>	1107 <sup>b</sup>
PHVO + SO	38.4	3.24 <sup>a,c</sup>	1253 <sup>a,b</sup>
SEM	0.7	0.08	52
<i>p</i> <sup>b</sup>	0.27	0.01	0.03
Experiment 2 <sup>c</sup>			
Treatments			
Control	26.4	3.00	772
10,12 CLA supplement	23.5	1.61	383
SEM	1.0	0.07	26
<i>p</i> <sup>b</sup>	0.20	0.001	0.001

<sup>a</sup>Cows were abomasally infused with skim milk (control), SO, PHVO, or PHVO + SO. For abbreviations see Table 1.

<sup>b</sup>Statistical probability of treatment effects. When a treatment effect was significant ( $P < 0.05$ ), differences among treatments were compared by *t*-test as indicated by lowercase roman superscripts (a,b,c) within a column ( $P < 0.05$ ).

<sup>c</sup>Cows were abomasally infused with skim milk (control) or *trans*-10,*cis*-12 CLA (10,12 CLA supplement).

synthesis by  $\Delta^9$ -desaturase. No treatment effects were observed for rumen fluid or plasma, but the ratio in milk was affected (Fig. 1). The SO and PHVO + SO treatments reduced the ratio by 70 and 75% as compared to the control and PHVO treatments, respectively, and PHVO caused a 19% reduction in the ratio as compared to the control treatment. The

ratios of *trans*-7,*cis*-9 CLA to *trans*-6,7,8 18:1 were also evaluated; they followed a similar pattern for the different biological samples and treatments. No treatment differences were observed in the ratio for FA from rumen fluid or plasma. However, SO and PHVO + SO treatments reduced the ratio by 75 and 80%, respectively, when compared with the con-

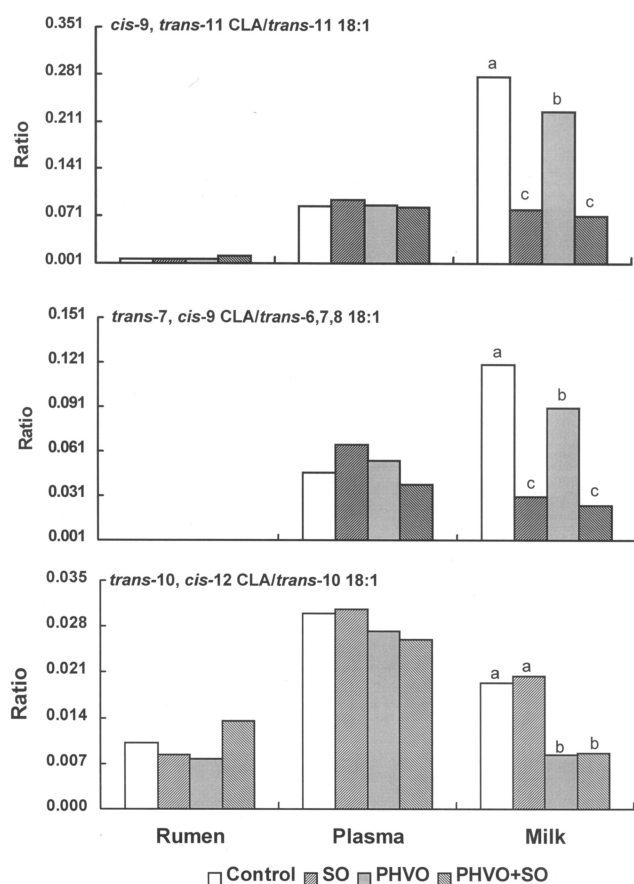
**TABLE 3**  
**CLA Isomers Present in Rumen Fluid, Plasma, and Milk During Abomasal Infusion of PHVO**  
**and SO in Lactating Dairy Cows**

FA	Treatment <sup>a</sup> (mg/g FA)				SEM	<i>p</i> <sup>b</sup>
	Control	SO	PHVO	PHVO + SO		
Rumen fluid						
<i>Trans</i> -7, <i>cis</i> -9 CLA <sup>c</sup>	ND	ND	ND	ND	—	—
<i>Cis</i> -9, <i>trans</i> -11 CLA	0.383	0.361	0.315	0.607	0.132	0.47
<i>Trans</i> -10, <i>cis</i> -12 CLA	0.153	0.130	0.125	0.227	0.039	0.32
Other <i>cis/trans</i> CLA <sup>c</sup>	ND	ND	ND	ND	—	—
Total <i>trans,trans</i> CLA	0.858	0.711	0.577	0.953	0.200	0.59
Plasma						
<i>Trans</i> -7, <i>cis</i> -9 CLA	0.043	0.065	0.051	0.037	0.011	0.37
<i>Cis</i> -9, <i>trans</i> -11 CLA	0.475	0.594	0.514	0.501	0.047	0.38
<i>Trans</i> -10, <i>cis</i> -12 CLA	0.051	0.048	0.047	0.038	0.010	0.81
Other <i>cis/trans</i> CLA	0.098	0.085	0.095	0.087	0.022	0.97
Total <i>trans,trans</i> CLA	0.254	0.330	0.319	0.282	0.031	0.37
Milkfat						
<i>Trans</i> -7, <i>cis</i> -9 CLA	0.519 <sup>a</sup>	0.149 <sup>b</sup>	0.655 <sup>c</sup>	0.209 <sup>d</sup>	0.012	0.001
<i>cis</i> -9, <i>trans</i> -11 CLA	5.884 <sup>a</sup>	2.051 <sup>b</sup>	6.817 <sup>c</sup>	2.690 <sup>d</sup>	0.217	0.001
<i>Trans</i> -10, <i>cis</i> -12 CLA	0.131 <sup>a</sup>	0.141 <sup>a</sup>	0.177 <sup>b</sup>	0.187 <sup>b</sup>	0.006	0.001
Other <i>cis/trans</i> CLA	0.172 <sup>a,b</sup>	0.120 <sup>b</sup>	0.221 <sup>a</sup>	0.143 <sup>b</sup>	0.016	0.002
Total <i>trans,trans</i> CLA	0.599 <sup>a</sup>	0.548 <sup>a</sup>	0.776 <sup>b</sup>	0.796 <sup>b</sup>	0.024	0.001

<sup>a</sup>Cows were abomasally infused with skim milk (control), SO, PHVO, or PHVO + SO. For abbreviations see Table 1.

<sup>b</sup>Statistical probability of treatment effects. When a treatment effect was significant ( $P < 0.05$ ), differences among treatments were compared by *t*-test as indicated by lowercase roman superscripts (a–d) within a row ( $P < 0.05$ ).

<sup>c</sup>These CLA isomers were not detected (ND) in all samples analyzed, and means for these isomers were not statistically different from zero ( $P > 0.2$ ).



**FIG. 1.** Ratios of *cis-9,trans-11* CLA/*trans-11* 18:1; *trans-7,cis-9* CLA/*trans-6,7,8* 18:1; and *trans-10,cis-12* CLA/*trans-10* 18:1 in FA from rumen fluid, plasma, and milk. Cows were abomasally infused with skim milk (control), stercularic oil (SO), partially hydrogenated vegetable oil (PHVO), or partially hydrogenated vegetable oil plus stercularic oil (PHVO + SO). For ratios of *cis-9,trans-11* CLA/*trans-11* 18:1, the respective SEM were 0.003, 0.012, and 0.005 for rumen fluid, plasma, and milkfat. For ratios of *trans-7,cis-9* CLA/*trans-6,7,8* 18:1, the SEM were 0.013 and 0.006 for plasma and milkfat, respectively. Ratios for *trans-7,cis-9* CLA/*trans-6,7,8* 18:1 are not shown for rumen fluid because the concentrations were not significantly different from zero ( $P > 0.2$ ). For ratios of *trans-10,cis-12* CLA/*trans-10* 18:1, the respective SEM were 0.003, 0.006, and 0.001 for rumen fluid, plasma, and milkfat. When a treatment effect was significant ( $P < 0.05$ ), differences among treatments were compared by *t*-test as indicated by letters above columns (a,b,c).

control and PHVO treatments. In contrast, the infusion of PHVO reduced the ratio of *trans-7,cis-9* CLA to *trans-6,7,8* 18:1 by 24% when compared to the control (Fig. 1). Endogenous synthesis of CLA involves addition of a *cis* double bond between carbons 9 and 10 of the substrate FA, either *trans-11* 18:1 or *trans-7* 18:1. Thus, ratio changes for both *cis-9,trans-11* CLA and *trans-7,cis-9* CLA are consistent with endogenous synthesis in the mammary gland via  $\Delta^9$ -desaturase.

The ratio of *trans-10,cis-12* CLA to *trans-10* 18:1 serves as a reference for comparison; both of these FA are intermediates in an alternative pathway in the rumen biohydrogenation of linoleic acid, but there is no known pathway for the endogenous synthesis of *trans-10,cis-12* CLA (6). Infusions of SO had no effect on the ratio in rumen fluid, plasma FA, or milk. Consis-

tent with the presence of *trans-10* 18:1 in PHVO, the treatments involving abomasal infusion of PHVO reduced the ratio in milk (Fig. 1).

**Experiment 2.** To inhibit  $\Delta^9$ -desaturase with *trans-10,cis-12* CLA, the 10,12 CLA supplement was abomasally infused to avoid modification by rumen microbes. Of the CLA isomers present in the supplement, 98.3% was *trans-10,cis-12* CLA and 1.4% was *cis-9,trans-11* CLA. Additional details about the infusion and performance data, including milk FA composition, have been presented (24). Infusion of the 10,12 CLA supplement reduced milkfat content and yield by 46 and 50%, respectively (Table 2).

The CLA compositions of plasma and milk are shown in Table 4; rumen fluid was not sampled. Infusion of the 10,12 CLA supplement resulted in the expected increase in plasma lipid and milkfat content of *trans-10,cis-12* CLA (Table 4). In the case of *trans-7,cis-9* CLA and *cis-9,trans-11* CLA, treatment had no effect on the concentration of these isomers in plasma. However, milk content of *trans-7,cis-9* CLA and *cis-9,trans-11* CLA was decreased by 44 and 25%, respectively, with infusion of 10,12 CLA supplement. Small amounts of other *cis/trans* CLA isomers were detected in plasma lipids and milkfat, and the 10,12 CLA supplement increased their concentration. However, these CLA isomers were detected at very low levels and eluted in a region of the chromatogram with known interferences (data not presented).

The effect of the 10,12 CLA supplement on the ratios of *cis-9,trans-11* CLA to *trans-11* 18:1 and *trans-7,cis-9* CLA to *trans-6,7,8* 18:1 are compared in Figure 2. The ratio of *cis-9,trans-11* CLA to *trans-11* 18:1 was slightly greater in plasma but was markedly reduced in milk (a 46.9% decrease). The ratio of *trans-7,cis-9* CLA to *trans-6,7,8* 18:1 in plasma was not affected by the 10,12 CLA supplement treatment, but was decreased by 64.0% in milkfat (Fig. 2). As expected, infusion of the 10,12 CLA supplement dramatically increased the ratio of *trans-10,cis-12* CLA to *trans-10* 18:1 in both plasma and milk (Fig. 2).

## DISCUSSION

CLA isomers have received a great deal of attention because of the health benefits observed in biomedical studies with animal models (1). Most research with pure isomers has been related to *cis-9,trans-11* CLA with its anticarcinogenic effects and *trans-10,cis-12* CLA for its effects on lipid metabolism. The biological effects of these isomers have been characterized more completely because of their availability in relatively pure form, but it is reasonable that other CLA isomers will also have biological effects. Synthetically produced CLA often contains significant quantities of several isomers and minor quantities of many others. Even ruminant food products, in which the predominant CLA isomer is *cis-9,trans-11*, contain minor quantities of several other CLA isomers (2,4). We have previously shown that *cis-9,trans-11* CLA found in milkfat from dairy cows originates predominantly from endogenous synthesis by  $\Delta^9$ -desaturase (7,8). The second-most

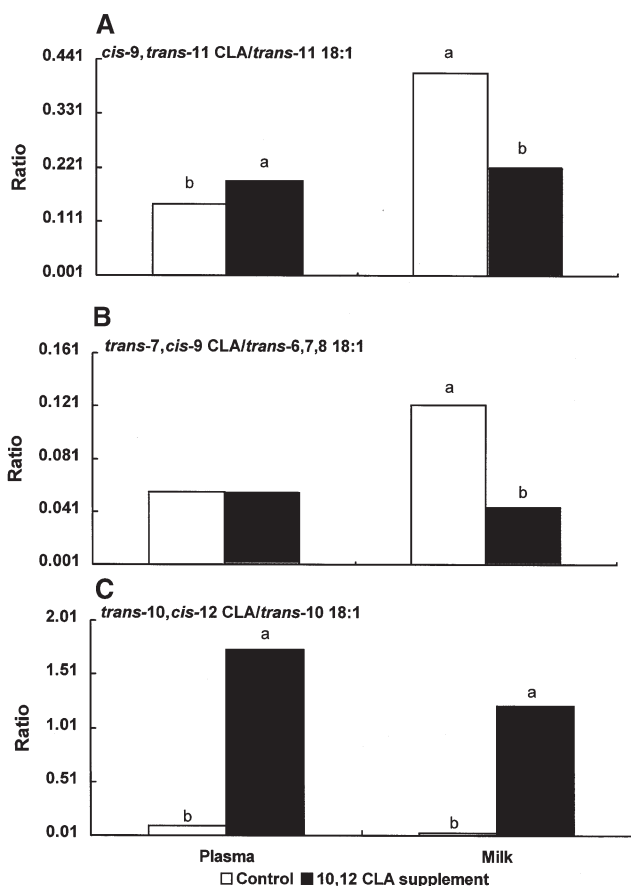
**TABLE 4**  
**CLA Isomers Present in Plasma and Milk During Abomasal Infusion of *trans*-10,*cis*-12 CLA in Lactating Dairy Cows**

FA	Treatment <sup>a</sup> (mg/g FA)		SEM	<i>P</i> <sup>b</sup>
	Control	10,12 CLA supplement		
Plasma				
<i>Trans</i> -7, <i>cis</i> -9 CLA	0.030	0.039	0.003	0.13
<i>Cis</i> -9, <i>trans</i> -11 CLA	0.559	0.845	0.125	0.20
<i>Trans</i> -10, <i>cis</i> -12 CLA	0.092 <sup>c</sup>	1.680	0.245	0.02
Other <i>cis/trans</i> CLA	0.118	0.215	0.042	0.20
Total <i>trans,trans</i> CLA	0.301	0.368	0.020	0.10
Milkfat				
<i>Trans</i> -7, <i>cis</i> -9 CLA	0.417	0.234	0.019	0.001
<i>Cis</i> -9, <i>trans</i> -11 CLA	6.047	4.532	0.334	0.01
<i>Trans</i> -10, <i>cis</i> -12 CLA	0.119	6.169	0.486	0.001
Other <i>cis/trans</i> CLA	0.080	0.103	0.004	0.002
Total <i>trans,trans</i> CLA	0.515	0.786	0.054	0.01

<sup>a</sup>Cows were abomasally infused with skim milk (control) or *trans*-10,*cis*-12 CLA (10,12 CLA supplement).

<sup>b</sup>Statistical probability of treatment effects.

<sup>c</sup>Mean not statistically different from zero ( $P > 0.7$ ).



**FIG. 2.** Ratios of *cis*-9,*trans*-11 CLA/*trans*-11 18:1; *trans*-7,*cis*-9 CLA/*trans*-6,7,8 18:1; and *trans*-10,*cis*-12 CLA/*trans*-10 18:1 in FA from plasma and milk. Cows were abomasally infused with skim milk (control) or *trans*-10,*cis*-12 CLA (10,12 CLA supplement). For ratios of *cis*-9,*trans*-11 CLA/*trans*-11 18:1; *trans*-7,*cis*-9 CLA/*trans*-6,7,8 18:1; and *trans*-10,*cis*-12 CLA/*trans*-10 18:1, the respective SEM were 0.002, 0.006, and 0.242 (plasma); and 0.003, 0.013, and 0.099 (milkfat). A significant treatment effect ( $P < 0.05$ ) is indicated by letters above columns (a,b).

prevalent CLA isomer found in the milkfat of dairy cows is *trans*-7,*cis*-9 (2,4). Given that this isomer also contains a *cis*-9 double bond, our objective was to examine the extent to which *trans*-7,*cis*-9 CLA originates *via* endogenous synthesis involving  $\Delta^9$ -desaturase.

Endogenous synthesis of *trans*-7,*cis*-9 CLA would utilize the *trans*-7 18:1 that originates from the metabolism of PUFA by rumen bacteria (6,9). To quantify *trans*-7,*cis*-9 CLA endogenous synthesis, we conducted *in vivo* studies with two inhibitors of  $\Delta^9$ -desaturase, cyclopropenoid FA and *trans*-10,*cis*-12 CLA. *In vivo* studies with chickens, rats, mice, pigs, and cows (see review, Ref. 34) and *in vitro* experiments with cellular extracts (e.g., 35,36) have established that cyclopropenoid FA are potent inhibitors of  $\Delta^9$ -desaturase. Cook *et al.* (37) demonstrated that feeding SO that was formulated to bypass rumen fermentation inhibited  $\Delta^9$ -desaturase and modified milk FA composition in lactating dairy cows. Bickerstaffe and Johnson (38) showed similar results with intravenous infusions of SO to a lactating goat. Experiment 1 utilized SO that was isolated from seeds of the *Sterculia foetida* tree. Two cyclopropenoid FA constituted 62% of the oil: sterculic acid with a ring at the 9-10 position, and malvalic acid with the ring at the 8-9 position. The second method to inhibit  $\Delta^9$ -desaturase used a *trans*-10,*cis*-12 CLA supplement. This specific CLA isomer has been shown to reduce gene expression and inhibit enzyme activity for  $\Delta^9$ -desaturase in hepatic tissue from rodents (14–16). We similarly demonstrated that *trans*-10,*cis*-12 CLA was a very potent inhibitor of  $\Delta^9$ -desaturase activity in lactating cows based on alterations in milk FA composition (11), and it also markedly reduced mRNA abundance for  $\Delta^9$ -desaturase in mammary tissue (12). However, use of *trans*-10,*cis*-12 CLA presents some complications because, in addition to effects on  $\Delta^9$ -desaturase, *trans*-10,*cis*-12 CLA also causes a reduction in milkfat yield (11,24,39).

We observed that the milkfat content of *trans-7,cis-9* CLA was affected by both inhibitors of  $\Delta^9$ -desaturase. The *trans-7,cis-9* CLA concentration was reduced by 70% with the SO infusion (Experiment 1) and by 44% with infusion of the 10,12 CLA supplement (Experiment 2). Quantitatively, this represents a minimal estimate of endogenous synthesis because the inhibition of  $\Delta^9$ -desaturase is not complete. A correction factor for the extent of  $\Delta^9$ -desaturase inhibition can be calculated based on changes in the milkfat content of myristic and myristoleic acids. Milk FA with 14 carbons are almost exclusively synthesized *de novo* by the mammary gland of the dairy cow. Therefore, the magnitude of the reduction in milk content of *cis-9* 14:1 provides a correction factor for the extent of the treatment-induced inhibition of  $\Delta^9$ -desaturase (7,8). Milk content of *cis-9* 14:1 was reduced 84% in response to SO infusion and 43% in response to 10,12 supplement infusion. In applying these correction factors, endogenous synthesis accounted for 85 and 102% of the *trans-7,cis-9* CLA in milkfat for Experiments 1 and 2, respectively. Thus, the *trans-7,cis-9* CLA in milkfat would appear to originate predominantly from endogenous synthesis.

Consistent with *trans-7,cis-9* CLA originating almost exclusively from endogenous synthesis, this CLA isomer was not detected in FA extracted from rumen fluid whereas *cis-9,trans-11* CLA was readily detected. Trace levels of *trans-7,cis-9* CLA were detected in plasma, and this probably relates to *trans-7,cis-9* CLA originating from endogenous synthesis in the small intestine and adipose tissue. We have previously shown that some *cis-9,trans-11* CLA in milkfat is formed from desaturation of *trans-11* 18:1 by tissues other than the mammary gland (8). Approximately 50% of the FA found in milkfat of ruminants are taken up from circulating FA (40). A portion of the circulating lipids originates from FA absorbed from the digestive tract, and  $\Delta^9$ -desaturase has been reported in the small intestine of ruminants (41). The other portion of circulating FA are derived from the mobilization of body fat reserves. In a well-fed lactating cow, approximately 8% of milk FA originate from body reserves, and this percentage increases if intake is inadequate to meet requirements (42,43). The presence of  $\Delta^9$ -desaturase in adipose tissue from sheep and cattle has been established (44,45), and *trans-7* 18:1 of dietary origin is most likely desaturated to *trans-7,cis-9* CLA in this tissue. Indeed, Fritsche *et al.* (3) reported that *trans-7,cis-9* CLA was the second-most prevalent CLA isomer in body fat of cattle. However,  $\Delta^9$ -desaturase is very active in mammary tissue of ruminants (44,46,47), and based on our data, the mammary gland must be the major site for the endogenous synthesis of *trans-7,cis-9* CLA. This is clearly evident by the substantial increase in the ratios of  $\Delta^9$ -desaturase products to substrates when plasma lipids and milkfat (mammary gland) are compared (Figs. 1 and 2). As expected,  $\Delta^9$ -desaturase was also implicated in the endogenous synthesis of *cis-9,trans-11* CLA in both experiments. In applying the correction factor based on myristic and myristoleic acids, endogenous synthesis accounted for 77% of the *cis-9,trans-11* CLA in milkfat in Experiment 1. Likewise, the corrected estimate for Experiment 2 was 58% of *cis-9,trans-11* CLA from

endogenous synthesis, although this estimate was complicated by the marked reduction (50%) in milkfat yield that also occurred. These estimates for endogenous synthesis of *cis-9,trans-11* CLA agree with our previous analysis of the data in Experiment 1 using less sophisticated analytical techniques (8) and other published studies (7).

This is the first investigation to specifically examine the origin of *trans-7,cis-9* CLA found in milkfat of dairy cows. Through the use of two different inhibitors of  $\Delta^9$ -desaturase, we demonstrated that the *trans-7,cis-9* CLA found in the milkfat of dairy cows originates almost exclusively *via* endogenous synthesis by  $\Delta^9$ -desaturase. Consistent with this result, the *trans-7,cis-9* CLA isomer was not present in FA isolated from rumen fluid. Results for *cis-9,trans-11* CLA indicate that endogenous synthesis is also the major source of this isomer in milkfat, but in this case a portion of the *cis-9,trans-11* CLA originates as an intermediate formed in rumen biohydrogenation of linoleic acid.

#### ACKNOWLEDGMENTS

The contributions of Debra A. Dwyer and Dottie I. Ceuter are greatly appreciated. The assistance of Laxminarayan Venkat Ratnam and Kandukuri V. Raman for acquiring *S. foetida* seeds is also gratefully acknowledged. These investigations were supported in part by the National Dairy Council (Rosemont, IL), Valio Ltd. (Helsinki, Finland), the Cornell Northeast Dairy Foods Research Center and the Cornell Agricultural Experiment Station (Ithaca, NY).

#### REFERENCES

1. Whigham, L.D., Cook, M.E., and Atkinson, R.L. (2000) Conjugated Linoleic Acid: Implications for Human Health, *Pharm. Res.* 42, 503–510.
2. Sehat, N., Kramer, J.K.G., Mossoba, M.M., Yurawecz, M.P., Roach, J.A.G., Eulitz, K., Morehouse, K.M., and Ku, Y. (1998) Identification of Conjugated Linoleic Acid Isomers in Cheese by Gas Chromatography, Silver Ion High Performance Liquid Chromatography, and Mass Spectral Reconstructed Ion Profiles. Comparison of Chromatographic Elution Sequences, *Lipids* 33, 963–971.
3. Fritsche, J., Fritsche, S., Solomon, M.B., Mossoba, M.M., Yurawecz, M.P., Morehouse, K., and Ku, Y. (2000) Quantitative Determination of Conjugated Linoleic Acid Isomers in Beef Fat, *Eur. J. Lipid Sci.* 102, 667–672.
4. Yurawecz, M.P., Roach, J.A.G., Sehat, N., Mossoba, M.M., Kramer, J.K.G., Fritsche, J., Steinhart, H., and Ku, Y. (1998) A New Conjugated Linoleic Acid Isomer, 7 *trans*,9 *cis*-Octadecadienoic Acid, in Cow Milk, Cheese, Beef, and Human Milk and Adipose Tissue, *Lipids* 33, 803–809.
5. Parodi, P.W. (1977) Conjugated Octadecadienoic Acids of Milk Fat, *J. Dairy Sci.* 60, 1550–1553.
6. Griinari, J.M., and Bauman, D.E. (1999) Biosynthesis of Conjugated Linoleic Acid and Its Incorporation into Meat and Milk in Ruminants, in *Advances in Conjugated Linoleic Acid Research* (Yurawecz, M.P., Mossoba, M.M., Kramer, J.K.G., Pariza, M.W., and Nelson, G.J., eds.), Vol. 1, pp. 180–200, AOCS Press, Champaign.
7. Griinari, J.M., Corl, B.A., Lacy, S.H., Chouinard, P.Y., Nurmela, K.V.V., and Bauman, D.E. (2000) Conjugated Linoleic Acid Is Synthesized Endogenously in Lactating Dairy Cows by  $\Delta^9$ -Desaturase, *J. Nutr.* 130, 2285–2291.
8. Corl, B.A., Baumgard, L.H., Dwyer, D.A., Griinari, J.M., Phillips, B.S., and Bauman, D.E. (2001) The Role of  $\Delta^9$ -Desaturase in the Production of *cis-9,trans-11* CLA, *J. Nutr. Biochem.* 12, 622–630.



9. Katz, I., and Keeney, M. (1966) Characterization of the Octadecenoic Acids in Rumen Digesta and Rumen Bacteria, *J. Dairy Sci.* 49, 962–966.
10. Parodi, P.W. (1976) Distribution of Isomeric Octadecenoic Fatty Acids in Milk Fat, *J. Dairy Sci.* 59, 1870–1873.
11. Baumgard, L.H., Corl, B.A., Dwyer, D.A., and Bauman, D.E. (2000) Identification of the Conjugated Linoleic Acid Isomer That Inhibits Milk Fat Synthesis, *Am. J. Physiol.* 278, R179–R184.
12. Baumgard, L.H., Matitashvili, E., Corl, B.A., Dwyer, D.A., and Bauman, D.E. (2002) *Trans*-10,*cis*-12 CLA Decreases Lipogenic Rates and Expression of Genes Involved in Milk Lipid Synthesis in Dairy Cows, *J. Dairy Sci.* 85, in press.
13. Park, Y., Albright, K.J., Liu, W., Storkson, J.M., and Pariza, M.W. (1999) Evidence That the *trans*-10,*cis*-12 Isomer of Conjugated Linoleic Acid Induces Body Composition Changes in Mice, *Lipids* 34, 235–241.
14. Lee, K.N., Pariza, M.W., and Ntambi, J.M. (1998) Conjugated Linoleic Acid Decreases Hepatic Stearoyl-CoA Desaturase mRNA Expression, *Biochem. Biophys. Res. Comm.* 248, 817–821.
15. Bretillon, L., Chardigny, J.M., Grégoire, S., Berdeaux, O., and Sébédio, J.-L. (1999) Effects of Conjugated Linoleic Acid Isomers on the Hepatic Microsomal Desaturation Activities *in vitro*, *Lipids* 34, 965–969.
16. Park, Y., Storkson, J.M., Ntambi, J.M., Cook, M.E., Sih, C.J., and Pariza, M.W. (2000) Inhibition of Hepatic Stearoyl-CoA Desaturase Activity by *trans*-10,*cis*-12 Conjugated Linoleic Acid and Its Derivatives, *Biochim. Biophys. Acta* 1486, 285–292.
17. Fox, D.G., Sniffen, C.J., O'Connor, J.D., Russell, J.B., and Van Soest, P.J. (1992) A Net Carbohydrate and Protein System for Evaluating Cattle Diets: III. Cattle Requirements and Diet Adequacy, *J. Anim. Sci.* 70, 3578–3596.
18. National Research Council (1989) *Nutrient Requirements of Dairy Cattle*, 6th rev. edn., National Academy of Sciences, Washington, DC.
19. Spires, H.R., Clark, J.H., Derrig, R.G., and Davis, C.L. (1975) Milk Production and Nitrogen Utilization in Response to Post-ruminal Infusion of Sodium Caseinate in Lactating Cows, *J. Nutr.* 105, 1111–1115.
20. Harfoot, C.G., Noble, R.C., and Moore, J.H. (1973) Food Particles as a Site for Biohydrogenation of Unsaturated Fatty Acids in the Rumen, *Biochem. J.* 132, 829–832.
21. Singh, S., and Hawke, J.C. (1979) The *in vitro* Lipolysis and Biohydrogenation of Monogalactosyldiglyceride by Whole Rumen Contents and Its Fractions, *J. Sci. Food Agr.* 30, 603–612.
22. Harfoot, C.G., Noble, R.C., and Moore, J.H. (1975) The Role of Plant Particles, Bacteria and Cell-Free Supernatant Fractions of Rumen Contents in the Hydrolysis of Trilinolein and the Subsequent Hydrogenation of Linoleic Acid, *Antonie van Leeuwenhoek* 41, 533–542.
23. Harfoot, C.G., and Hazlewood, G.P. (1988) Lipid Metabolism in the Rumen, in *The Rumen Microbial Ecosystem* (Hobson, P.N., ed.), pp. 285–322, Elsevier Applied Science, London.
24. Baumgard, L.H., Sangster, J.K., and Bauman, D.E. (2001) Milk Fat Synthesis in Dairy Cows Is Progressively Reduced by Increasing Supplemental Amounts of *trans*-10,*cis*-12 Conjugated Linoleic Acid (CLA), *J. Nutr.* 131, 1764–1769.
25. Chouinard, P.Y., Corneau, L., Saebø, A., and Bauman, D.E. (1999) Milk Yield and Composition During Abomasal Infusion of Conjugated Linoleic Acid, *J. Dairy Sci.* 82, 2737–2745.
26. Christie, W.W. (1989) *Gas Chromatography and Lipids: A Practical Guide*, p. 68, The Oily Press, Ayr, Scotland.
27. Hara, A., and Radin, N.S. (1978) Lipid Extraction of Tissues with a Low-Toxicity Solvent, *Anal. Biochem.* 90, 420–426.
28. Bateman, H.G., and Jenkins, T.C. (1997) Method for Extraction and Separation by Solid Phase Extraction of Neutral Lipid, Free Fatty Acids, and Polar Lipid from Mixed Microbial Cultures, *J. Agric. Food Chem.* 45, 132–134.
29. Hashimoto, N., Aoyama, T., and Shiori, T. (1981) New Methods and Reagents in Organic Synthesis. 14. A Simple Efficient Preparation of Methyl Esters with Trimethylsilyldiazomethane (TM-SCHN<sub>2</sub>) and Its Application to Gas Chromatographic Analysis of Fatty Acids, *Chem. Pharm. Bull.* 29, 1475–1478.
30. Yurawecz, M.P., Delmonte, P., Kataoka, A., Morehouse, K.M., Corl, B., Baumgard, L., and Bauman, D.E. (2002) Determination of Conjugated Octadecadienoic Fatty Acid Methyl Esters by Silver-Ion HPLC Using Relative Retention Volumes, *Abstracts of the 93rd AOCS Annual Meeting*, AOCS Press, Champaign (Abstract S6).
31. Yurawecz, M.P., Delmonte, P., Roach, J.A.G., Morehouse, K.M., Weisz, A., Ito, Y., Nyman, P., and Lehmann, L. (2002) Synthesis and Isolation of *trans*-7,*cis*-9 Octadecadienoic Acid and Other CLA Isomers by Base Conjugation of Partially Hydrogenated Octadecatrienoic Fatty Acids, *Abstracts of the 93rd AOCS Annual Meeting*, AOCS Press, Champaign (Abstract S4).
32. Fritsche, J., Rickert, R., Steinhart, H., Yurawecz, M.P., Mossoba, M.M., Sehat, N., Roach, J.A.G., Kramer, J.K.G., and Ku, Y. (1999) Conjugated Linoleic Acid (CLA) Isomers: Formation, Analysis, Amounts in Foods, and Dietary Intake, *Fett/Lipid* 101, 272–276.
33. SAS Institute, Inc. (1989) *SAS/STAT User's Guide, Version 6*, 4th edn., SAS Institute, Cary, NC.
34. Phelps, R.A., Shenstone, F.S., Kemmerer, A.R., and Evans, R.J. (1965) A Review of Cyclopropenoid Compounds: Biological Effects of Some Derivatives, *Poult. Sci.* 44, 358–394.
35. Jeffcoat, R., and Pollard, M.R. (1977) Studies on the Inhibition of the Desaturases by Cyclopropenoid Fatty Acids, *Lipids* 12, 480–485.
36. Raju, P.K., and Reiser, R. (1967) Inhibition of Fatty Acyl Desaturase by Cyclopropene Fatty Acids, *J. Biol. Chem.* 242, 379–384.
37. Cook, L.J., Scott, T.W., Mills, S.C., Fogerty, A.C., and Johnson, A.R. (1976) Effects of Protected Cyclopropene Fatty Acids on the Composition of Ruminant Milk Fat, *Lipids* 11, 705–711.
38. Bickerstaffe, R., and Johnson, A.R. (1972) The Effect of Intravenous Infusions of Sterculic Acid on Milk Fat Synthesis, *Br. J. Nutr.* 27, 561–570.
39. Peterson, D.G., Baumgard, L.H., and Bauman, D.E. (2002) Milk Fat Response to Low Doses of *trans*-10,*cis*-12 Conjugated Linoleic Acid (CLA), *J. Dairy Sci.* 85, 1764–1766.
40. Bauman, D.E., and Davis, C.L. (1974) Biosynthesis of Milk Fat, in *Lactation: A Comprehensive Treatise* (Larson, B.L., and Smith V.R., eds.), Vol. 2, pp. 31–75, Academic Press, New York.
41. Bickerstaffe, R., and Annison, E.F. (1969) Glycerokinase and Desaturase Activity in Pig, Chicken and Sheep Intestinal Epithelium, *Comp. Biochem. Physiol.* 31, 47–54.
42. Palmquist, D.L., and Mattos, W. (1978) Turnover of Lipoproteins and Transfer to Milk Fat of Dietary (1-<sup>14</sup>C)Linoleic Acid in Lactating Cows, *J. Dairy Sci.* 61, 561–565.
43. Bauman, D.E., and Griinari, J.M. (2001) Regulation and Nutritional Manipulation of Milk Fat: Low-Fat Milk Syndrome, *Livest. Prod. Sci.* 70, 15–29.
44. Ward, R.J., Travers, M.T., Richards, S.E., Vernon, R.G., Slater, A.M., Buttery, P.J., and Barber, M.C. (1998) Stearoyl-CoA Desaturase mRNA Is Transcribed from a Single Gene in the Ovine Genome, *Biochim. Biophys. Acta* 1391, 145–156.
45. St. John, L.C., Lunt, D.K., and Smith, S.B. (1991) Fatty Acid Elongation and Desaturation Enzyme Activities of Bovine Liver and Subcutaneous Adipose Tissue Microsomes, *J. Anim. Sci.* 69, 1064–1073.
46. Kinsella, J.E. (1972) Stearyl CoA as a Precursor of Oleic Acid and Glycerolipids in Mammary Microsomes from Lactating Bovine: Possible Regulatory Step in Milk Triglyceride Synthesis, *Lipids* 7, 349–355.
47. McDonald, T.M., and Kinsella, J.E. (1973) Stearyl-CoA Desaturase of Bovine Mammary Microsomes, *Arch. Biochem. Biophys.* 156, 223–231.

[Received March 8, 2002, and in revised form June 10, 2002; revision accepted June 28, 2002]

# High Intake, but Not Low Intake, of CLA Impairs Weight Gain in Growing Mice

Ann Hayman<sup>a</sup>, Alastair MacGibbon<sup>b</sup>, Rodger J. Pack<sup>c,\*</sup>, Kay Rutherford<sup>c</sup>, and J. Hilary Green<sup>a</sup>

<sup>a</sup>Milk and Health Research Centre, <sup>b</sup>Fonterra Research Centre, and <sup>c</sup>Institute of Food, Nutrition and Human Health, Massey University, Palmerston North, New Zealand

**ABSTRACT:** CLA has a range of biological properties, including effects on lipid metabolism and body composition in experimental animals. The prevalent isomer of CLA found in the human diet is 9*c*,11*t*-CLA, and it is predominantly found in products containing fat from ruminant animals. This study investigated the effect of dietary CLA on energy balance in mice. Synthetic CLA reduced body fat in growing male BALB/c mice in a dose-dependent manner over the range 0.25–1.0% w/w CLA in the diet. Weight gain was also reduced at the highest levels of dietary CLA, being only 5.88 ± 2.68 g/4 mice (mean ± 1 SD) after 4 wk of 2.0% CLA in the diet, compared with weight gains of 7.51 ± 2.22 to 8.17 ± 2.34 g/4 mice in the 0–0.5% CLA groups. There was no significant effect on weight gain if diets contained 0.5% synthetic CLA or less. These results suggest that high levels of a synthetic mixture of CLA isomers modify energy metabolism and body composition and that high levels of synthetic CLA impair weight gain and reduce body fat pad mass in growing mice.

Paper no. L8693 in *Lipids* 37, 689–692 (July 2002).

CLA comprises a mixture of positional and geometric isomers of linoleic acid (18:2). Because the major isomer found in tissue is 9*c*,11*t*, it has been suggested that this isomer is the most biologically active. CLA in the human diet comes predominantly from food derived from ruminant animals, especially dairy products. Milkfat typically provides 3–6 mg CLA/g fat, in which the predominant isomer is 9*c*,11*t*. However, recent research indicates that 10*t*,12*c*-CLA is the isomer that most influences body composition (1). By using semipurified CLA isomers or CLA isomer mixtures enriched with 9*c*,11*t*-CLA or 10*t*,12*c*-CLA, Park *et al.* (1) concluded that body composition changes in mice (reduced body fat and increased body water, protein, and body ash) were associated with dietary 10*t*,12*c*-CLA. They found no effects with semipurified 9*c*,11*t*-CLA. Nevertheless, these results are consistent with previous reports that dietary supplementation with synthetic CLA reduces the amount of body fat in experimental mice, rats, and pigs (2–9).

The present study investigated the effect of a range of dietary levels of synthetic CLA, containing a mixture of 9*c*,11*t*-CLA (37%) and 10*t*,12*c*-CLA (46%), on energy balance and body fat mass in mice.

\*To whom correspondence should be addressed at Institute of Food, Nutrition and Human Health, Massey University, Private Bag 11-222, Palmerston North, New Zealand.  
E-mail: R.J.Pack@massey.ac.nz

## EXPERIMENTAL PROCEDURES

**Animals and diets.** All the experiments had the prior approval of the Massey University Animal Ethics Committee.

One hundred twenty male weaned but growing BALB/c mice aged 7–8 wk were used. They were kept in stainless steel cages with a mesh front and floor. A sliding tray collected spilled food and waste 2 cm beneath the floor. The animals were maintained at 22 ± 2°C, with a regular 12-h light/dark cycle. For 1 wk prior to the study the mice were fed a standard, milk-free rodent chow pellet (Sharpes Grain and Seed, Palmerston North, New Zealand). The mice were divided into six equal groups that were fed standard isoenergetic diets supplemented with 0.0, 0.1, 0.25, 0.5, 1.0, and 2.0% w/w synthetic CLA (Tonalin; Pharmanutrients, Lake Bluff, IL) for a period of 4 wk.

The aspects of energy balance measured in this study were: (i) food and energy intake; (ii) energy expenditure, by both indirect calorimetry and observed physical activity; (iii) stored energy, obtained from total carcass mass, chemical analysis of body fat, and the mass of dissectible adipose tissue deposits (fat pads).

The diet consisted of approximately 54% bovine skim milk powder, 30% corn flour, and 5% corn oil. In addition, it contained 5% of a mineral and vitamin supplement and 1% cellulose. In mixes where Tonalin was added, the quantity of corn oil included was reduced *pro rata*. Gross energy content of the diet was determined by bomb calorimetry (Gallenramp Autobomb; Watson Victor Ltd., Wellington, New Zealand). The fat content of the diets was determined by the Soxhlet method, using diethyl ether for fat extraction. The protein content was determined by measuring total nitrogen using the Leco® auto-analysis technique (10). In addition, ash was measured by overnight burning in a muffle furnace at 500°C, and dry matter was assessed by drying samples for 16 h at 105°C. CLA was analyzed following accelerated solvent extraction and conversion to methyl esters using boron trifluoride (11). FAME samples were analyzed using a Shimadzu GC-17A gas chromatograph (Shimadzu Corporation, Kyoto, Japan) equipped with an FID, BPX70 capillary column (50 m × 0.22 mm i.d. × 0.25 μm film thickness), and a pre-column (1 m × 0.53 mm i.d., deactivated fused-silica open tubular). Samples were injected on-column, and the FAME separated using a temperature gradient (80–150–220°C) with hydrogen as the carrier gas. Tridecanoic acid was added to the sample before extraction as an internal standard as well as BHT to protect CLA from oxidation.

**Energy intake.** Energy intake was calculated from measurements of the gross energy content of the diet and weekly

measurements of food intake. Since the mice were housed in pairs, energy intake was derived per pair of mice.

**Energy expenditure.** Energy expenditure was calculated from measurements of respiratory gas exchange using an indirect calorimeter. The indirect calorimeter consisted of a Perspex™ box 280 × 350 mm side and 160 mm in height with an open base, under which the caged animals were placed. Gas was drawn from the calorimeter using a Jun ACO 5503 air pump and passed through a Fleisch head (size 00; OEM Medical, Richmond, VA), heated to prevent condensation. A Validyne differential pressure transducer (DP45-16; VacuMed, Ventura, CA) across the Fleisch head measured gas flow through the system. A rotameter in the system was used to calibrate the Fleisch head and provided visual evidence of airflow during the experiment. A flow rate of 500 mL/min was used, and this resulted in a CO<sub>2</sub> concentration in the calorimeter of approximately 1%. Gas passed to a mixing chamber with an internal volume of approximately 200 mL where the temperature was measured using a thermistor previously calibrated against a mercury-in-glass thermometer. Gases were desiccated (Drierite; Hammond Drierite Co., Xenia, OH) and analyzed by a Servomex OA 137 oxygen analyzer (Servomex Controls, Crowborough, England) and a Datex Normcap carbon dioxide analyzer (Datex Medical, Helsinki, Finland). Both gas analyzers had been modified to have an analog output accurate to ±0.01% and were calibrated using room air, nitrogen, and a beta standard gas (BOC Gases, Inc.) of known composition. The output from the analyzers, temperature, and airflow were captured using a MacLab 8/s A/D converter (ADI Instruments, Sydney, Australia) using MacLab Chart software (Version 3.5.6/s; ADI Instruments) and VO<sub>2</sub>, VCO<sub>2</sub>, and the respiratory exchange ratio were calculated on-line.

Measurements of metabolic rate were made at the end of each 4-wk dietary intervention. Mice were studied in groups of four, from both the same diet treatment and the same group, to ensure that the gas leaving the calorimeter had an oxygen concentration in the order of 20%. On each occasion the mice were in the calorimeter for 45 min, and recordings were made during the last 10 min to allow the gas concentrations to stabilize, and for the animals to become accustomed to being in the calorimeter.

**Physical activity.** Visual, subjective observations of mouse activity were recorded at 5-min intervals during calorimetry. For each mouse these were scored as: 1 = asleep; 2 = drowsy, shuffling feet, not moving, cleaning, grooming; 3 = a little movement around cage, feeding, tunneling in wood shavings; 4 = moderate movement around cage, climbing on feeder, playing vigorously with wood shavings, picking up and moving shavings; 5 = vigorous movement around cage, running, jumping, climbing/hanging with all four feet on roof bars. The data for each calorimeter run could, therefore, range between 4 and 20, and this figure was divided by 4 to give a single value of individual murine activity.

**Stored energy.** (i) *Live weight.* Individual animals were weighed before and after the dietary interventions to the nearest 0.01 g (Watson-Victor Mettler Ltd., PM6000), and weight gain over 4 wk was calculated.

(ii) *Body composition by dissection.* Immediately after euthanasia by isoflurane, the intestine was cut below the stomach between the pylorus and duodenum, and the remaining gastrointestinal tract removed. The small amount of adipose tissue adhering to the intestine was removed by dissection and kept with the carcass, and the intestine was discarded.

Carcasses were frozen and subsequently analyzed for body composition. Each carcass was weighed, the stomach removed, and the carcass weighed again. This carcass weight, which had the stomach, intestine, and 1–2 mL of blood removed, was used in subsequent calculations of percentage body fat by dissection (fat pad mass) of individual mice.

The upper body fat was removed and weighed. It comprised interscapular brown adipose tissue, that is, any subcutaneous adipose tissue located on the upper back and where the thoracic limbs insert. The lower body fat located in the abdominal region, the genital region, surrounding the kidneys, and lining the anterior of the abdominal cavity and on the pelvic limbs was similarly treated. The total body fat by dissection was the sum of the upper and lower body fat. Body fat percentage by dissection was calculated relative to the carcass weight at the start of dissection. The dissected adipose deposits and the carcass (without stomach and intestine) were recombined and weighed again for subsequent chemical analysis.

*Body composition by chemical analyses.* Samples were prepared for chemical analysis in the groups of four that were used for indirect calorimetry. The four carcasses were homogenized in a food blender (Waring), weighed, frozen, and then freeze-dried (Cuddon Model 0610 Freeze Drier; W.G.G. Cuddon Ltd., Blenheim, New Zealand). The freeze-dried material was ground in a rotating hammer mill (Thomas Scientific, Swedesboro, NJ) and passed through a 2-mm screen before it was chemically analyzed.

*Chemical determination of body composition.* The energy, fat, protein, ash, and moisture content of the animal bodies were determined using the same procedures described for the diets.

*Statistics.* Differences between diet groups were initially analyzed using a one-way ANOVA, and means were compared using the Tukey test (MINITAB, version 12.1). Each data point represented either individual mice or cages of mice, as appropriate. A second analysis using two-way ANOVA and regression equations was carried out using the statistical packages in GraphPad Prism (version 2.01, GraphPad Software, San Diego, CA). All results are shown as the mean ± 1 SD.

## RESULTS

**Diet composition.** The control rodent diet provided 16.40 kJ/g of energy and comprised 18.4% protein, 2.7% fat, 5.5% ash, 11.3% moisture (w/w) with the balance being carbohydrate (w/w). Ingredient composition of the experimental diets is shown in Table 1. The Tonalin used to supply the CLA contained 59.14% CLA as well as oleic (22.19%), palmitic (6.47%), linoleic (4.53%), and stearic (4.14%) acids.

**Food and energy intake.** Food intake between groups ranged from 8.12 ± 0.75 (1% CLA group) to 9.5 ± 0.73



**TABLE 1**  
Added Fat Composition of CLA-Modified Mouse Diets (ingredient g/100 g diet)

	CLA concentration					
	Control	0.1%	0.25%	0.5%	1.0%	2.0%
Corn oil	5.300	5.146	4.915	4.531	3.762	2.223
Tonalin <sup>a</sup>	—	0.154	0.385	0.769	1.538	3.077

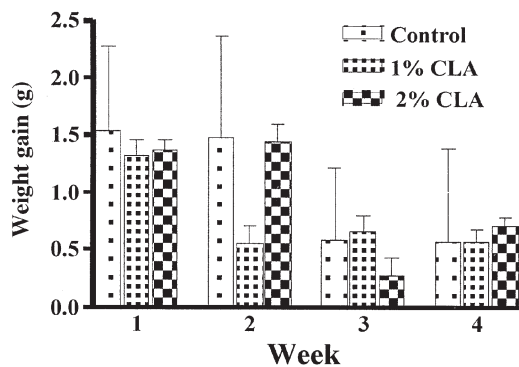
<sup>a</sup>Tonalin (Pharmanutrients, Lake Bluff, IL), in FFA form (approximately 60% CLA).

g/d/pair of mice (0.25% CLA group). This was equivalent to a range of 140 ± 13 to 163 ± 13 kJ/d. The food and energy intake of the 0.25% group was significantly higher than that of the zero CLA and 1% CLA groups (*P* < 0.05).

All the mice gained weight during the study. Although it appeared that weight gain was markedly reduced after either the first or second week of the study (Fig. 1), this was not the case. Linear regression of the data from all diet groups, with a *post hoc* runs test, indicated that the reduction in weight gain was linear. The 4-wk weight gain of the animals fed 2.0% CLA in the diet was 5.88 ± 2.68 g/pair. This was significantly less than the weight gain of pairs of mice fed no CLA (7.81 ± 2.01 g; *P* < 0.05), 0.1% CLA (7.75 ± 2.03 g; *P* < 0.01), 0.25% CLA (7.51 ± 2.22 g; *P* < 0.05), and 0.5% CLA (8.17 ± 2.34 g; *P* < 0.001). The 4-wk weight gain of the pairs of mice fed 1% CLA was 7.15 ± 1.17 g, which was not significantly different from any other group.

**Energy expenditure and physical activity.** There was no difference in energy expenditure or activity between the groups of mice as measured by indirect calorimetry or observation of activity. Metabolic rate ranged from 0.12 ± 0.03 in the 0.25 and 0.50% CLA groups to 0.14 ± 0.01 kJ/min/4 mice. There was no significant difference in respiratory exchange ratio between groups, which varied between 0.92 and 0.96. Physical activity scores ranged from 1.97 ± 0.9 in the 0.5% CLA group to 2.84 ± 1.17 in the 0.1% CLA group. There was a strong positive linear correlation between metabolic rate and the subjective physical activity score (*R*<sup>2</sup> = 0.79).

**Body composition.** Tables 2–4 show body composition



**FIG. 1.** Weekly weight gain during the experiment. All diet groups appeared to show a rapid reduction in growth at the end of the first (1% CLA) or second week (control and 2% CLA). However linear regression of the data from all groups indicated the reduction in weight gain was progressive. (Mean ± SD; only three groups are shown for clarity.)

**TABLE 2**  
Live Weight at the End of Trial and Weight Gain During Experiment; Comparison of Group Means

Diet CLA %	<i>n</i>	Live weight after 4 wk on diet (g)	Weight gain during trial (g)
0.0	20	25.88 ± 1.57	3.90 ± 1.07
0.1	20	25.49 ± 2.02	3.88 ± 1.20
0.25	18	24.88 ± 1.30	3.76 ± 1.20
0.5	16	25.72 ± 1.77	4.09 ± 1.19
1.0	18	24.55 ± 1.53	3.57 ± 0.74
2.0	14	24.69 ± 2.12	2.94 ± 1.43

data. There was a highly significant (*P* < 0.001) dose-dependent reduction in body fat pad mass as measured by weighing dissected fat with increasing dietary CLA (Fig. 2). The total body energy content of the mice obtained by chemical analysis of the carcass also decreased (Table 4). Conversely, the percentage of lean body mass (derived from chemical analyses of body protein, moisture, and ash) appeared to increase as body fat pad mass decreased. However, this observation did not reach statistical significance in the current study.

**DISCUSSION**

Synthetic CLA fed to 6-wk-old, male BALB/c mice in a 4-wk trial (0.0, 0.1, 0.25, 0.5, 1.0, and 2.0% w/w CLA) reduced body fat pad mass in a dose-dependent manner. It was effective in reducing body fat over the range 0.25 to 1.0%. The observed reduction in body fat in mice has been reported in previous studies (2–5). The dose/response pattern of body fat reduction seen in this feeding trial indicated an effective CLA intake range (0.5–1.0%) over which CLA supplementation could influence body composition. Furthermore, no additional body fat reduction could be obtained by feeding above this level (>1.0% synthetic CLA in the diet). The reduction in non-fat pad lean

**TABLE 3**  
Body Fat Pad Mass, Relative and Absolute, Obtained by Dissection and Comparison of Group Means

Diet CLA %	<i>n</i>	Body fat pad mass as % carcass weight <sup>a</sup>	Total body fat pad mass <sup>a</sup> (g)
0.0	20	5.60 ± 1.27	1.19 ± 0.32
0.1	20	5.44 ± 1.27	1.14 ± 0.34
0.25	18	4.38 ± 0.92	0.88 ± 0.19
0.5	16	2.96 ± 0.68	0.61 ± 0.15
1.0	18	2.23 ± 0.82	0.42 ± 0.16
2.0	14	2.37 ± 0.64	0.45 ± 0.14

Statistical significance <sup>b</sup>	0.1	0.25	0.5	1.0	2.0	0.1	0.25	0.5	1.0	2.0
0.0	NS	***	***	***	***	NS	***	***	***	***
0.1	—	***	***	***	***	—	***	***	***	***
0.25	—	—	***	***	***	—	—	***	***	***
0.5	—	—	—	*	NS	—	—	—	**	*
1.0	—	—	—	—	NS	—	—	—	—	NS
2.0	—	—	—	—	—	—	—	—	—	—

<sup>a</sup>Mean ± SD. Based on individual carcass weight at start of dissection.

<sup>b</sup>Significance level: \* < 0.05; \*\* < 0.01; \*\*\* < 0.001; NS, not significant (i.e., no significant difference between means of the groups).



**TABLE 4**  
**Body Fat Obtained from Chemical Analysis of the Carcass and Total Carcass Energy Content**

Diet CLA %	n <sup>a</sup>	Body fat (chemical) <sup>b</sup>					Gross energy <sup>b</sup>				
		%					kJ/g				
0.0	5	8.65 ± 0.82					8.45 ± 0.28				
0.1	5	8.13 ± 1.18					8.24 ± 0.42				
0.25	4	6.79 ± 1.28					7.66 ± 0.35				
0.5	3	4.77 ± 0.14					7.18 ± 0.08				
1.0	4	2.90 ± 0.16					6.42 ± 0.10				
2.0	3	2.70 ± 0.60					6.56 ± 0.13				

Statistical significance <sup>c</sup>	0.1	0.25	0.5	1.0	2.0	0.1	0.25	0.5	1.0	2.0
0.0	NS	NS	***	***	***	NS	*	***	***	***
0.1	—	NS	***	***	***	—	NS	***	***	***
0.25	—	—	NS	***	***	—	NS	***	***	***
0.5	—	—	—	NS	NS	—	—	*	NS	NS
1.0	—	—	—	—	NS	—	—	—	—	NS
2.0	—	—	—	—	—	—	—	—	—	—

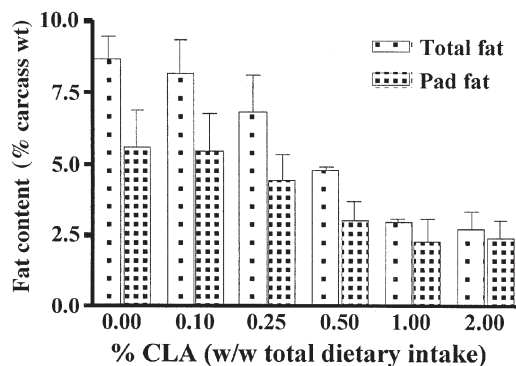
<sup>a</sup>Mean ± SD. Carcasses analyzed in groups of four.

<sup>b</sup>Based on weight of group of four combined homogenized carcasses prior to freeze drying.

<sup>c</sup>Significance level: \* $<0.05$ ; \*\* $<0.01$ ; \*\*\* $<0.001$ ; NS, not significant (i.e., no significant difference between means of the group).

body mass at the higher levels of dietary CLA has previously been reported in one study (4), but not in others (2,5).

Although a graded reduction in total body fat and energy was seen in mice fed 0.25 to 1.0% w/w synthetic CLA, this was not balanced by measurable reductions in feed intake or increased energy expenditure. The mechanism by which equivalent energy intakes from diets differing only in a small portion of their total FA profile can result in a change in body fat from 8.65 (control) to 2.90% (1.0% CLA) is not clear from the present study. However, a recent study indicated that CLA may, in part, act by preventing energy absorption by the gut, not only from fat but also from other components, such as protein and carbohydrate (12).



**FIG. 2.** Reduction in fat content with increasing levels of dietary CLA. Increasing the dietary intake of CLA up to 1% w/w of the diet produced a progressive decrease in both the fat pad mass and the fat content obtained by chemical analysis of the carcass after the abdominal viscera had been removed (total fat). A further increase of dietary CLA to 2% produced no further decrease in either fat pool. (Data = mean ± SD.)

The results from this study suggest that reasonable levels of a synthetic mixture of CLA isomers are biologically active and influence energy metabolism and body composition. Body fat, both fat pad mass and carcass fat content, was reduced in a dose-related manner over the range 0.25 to 1.0% CLA. There was no significant further body fat reduction in the group of mice fed more than 1.0% synthetic CLA. In addition, levels of 1.0 and 2.0% synthetic CLA fed to growing mice reduced weight gain.

## ACKNOWLEDGMENTS

The New Zealand Dairy Board supported this study. We are grateful to Bertram Fong, John Pedley, Neil Ward, Maggie Zhou, and Hian Voon for valuable technical assistance.

## REFERENCES

- Park, Y., Storkson, J.M., Albright, K.J., Liu, W. and Pariza, M.W. (1999). Evidence That the *trans*-10,*cis*-12 Isomer of Conjugated Linoleic Acid Induces Body Composition Changes in Mice, *Lipids* 34, 235–241.
- Park, Y., Albright, K.J., Liu, W., Storkson, J. M., Cook, M.E., and Pariza, M.W. (1997). Effect of Conjugated Linoleic Acid on Body Composition in Mice, *Lipids* 32, 853–857.
- Sugano, M., Tsujita, A., Yamasaki, M., Noguchi, M., and Yamada, K. (1998) Conjugated Linoleic Acid Modulates Tissue Levels of Chemical Mediators and Immunoglobulins in Rats, *Lipids* 33, 521–527.
- West, D.B., Delany, J.P., Camet, P.M., Blohm, F., Truett, A.A., and Scimeca, J. (1998) Effects of Conjugated Linoleic Acid on Body Fat and Energy Metabolism in the Mouse, *Proc. Amer. Physiol. Soc.* 275, R667–R672.
- Delany, J.P., Blohm, F., Truett, A.A., Scimeca J.A., and West, D.B. (1999) Conjugated Linoleic Acid Rapidly Reduced Body Fat Content in Mice Without Affecting Energy Intake, *Am. J. Physiol.* 276, 1172–1179.
- Dugan, M.E.R., Aalhus, J.L., Schaefer, A.L., and Kramer, J.K.G. (1997) The Effects of Conjugated Linoleic Acid on Fat to Lean Repartitioning and Feed Conversion in Pigs, *Can. J. Anim. Sci.* 77, 723–725.
- Cook, M.E., Jerome, D.L., Crenshaw, T.D., Buege, D.R., Pariza, M.W., Albright, K.J., Schmidt, S.P., Scimeca, J.A., Lofgren, P.A., and Hentges, E.J. (1998) Feeding Conjugated Linoleic Acid Improves Feed Efficiency and Reduces Whole Body Fat in Pigs, *FASEB J.* 12, A836.
- Dunshea, F.R., Ostrowka, E., Muralitharan, M., Cross, R., Bauman, D.E., Pariza, M.W., and Skarie, C. (1998) Dietary Conjugated Linoleic Acid Decreases Back Fat in Finisher Gilts, *J. Anim. Sci.* 76 (Suppl. 1), 131.
- Choi, Y., Kim, Y.-C., Han, Y.-B., Park, Y., Pariza, M.W., and Ntambi, J.M. (2000) The *trans*-10,*cis*-12 Isomer of Conjugated Linoleic Acid Downregulates Stearoyl-CoA Desaturase 1 Gene Expression in 3T3-L1 Adipocytes, *J. Nutr.* 130, 1920–1924.
- Anon. (1994) The Dumas Technique, *Food Rev.* 21(4), 39–41.
- Christie, W.W. (1990). Preparation of Methyl Esters—Part 1. *Lipid Technol.* 2, 48–49.
- Terstra, A.H.M., Beynen, A.C., Everts, H., Kocsis, S., Katan, M.B., and Zock, P.L. (2002) The Decrease in Body Fat in Mice Fed Conjugated Linoleic Acid Is Due to Increases in Energy Expenditure and Energy Loss in the Excreta, *J. Nutr.* 132, 940–945.

[Received November 27, 2000, and in final revised form June 4, 2002; revision accepted June 28, 2002]

# Interaction Between Dietary Protein and Fat in Triglyceride Metabolism in the Rat: Effects of Soy Protein and Menhaden Oil

Isabelle Demonty<sup>a,c</sup>, Yves Deshaies<sup>b</sup>, Benoît Lamarche<sup>a,c</sup>, and Hélène Jacques<sup>a,c,\*</sup>

<sup>a</sup>Human Nutrition Research Group, Department of Food Sciences and Nutrition, <sup>b</sup>Department of Anatomy and Physiology, and <sup>c</sup>The Nutraceutical and Functional Food Institute, Laval University, Québec, Canada, G1K 7P4

**ABSTRACT:** The objective of the present study was to determine the mechanisms by which dietary proteins interact with dietary lipids in the regulation of triglyceridemia in rats. Male Sprague-Dawley rats ( $n = 56$ ) were subjected to 28-d experimental diets containing different combinations of proteins (20% w/w) and lipid sources (14% w/w): (i) casein–menhaden oil, (ii) casein–beef tallow, (iii) soy protein–menhaden oil, and (iv) soy protein–beef tallow. Significant protein–lipid interactions were observed on triglyceridemia and hepatic cholesterol in fasted rats. The combination of casein and beef tallow was associated with high plasma TG and hepatic cholesterol concentrations, which were reduced by substitution either of soy for casein or of menhaden oil for beef tallow. Therefore, triglyceridemia and liver cholesterol remained low with soy protein feeding, independently of the lipid source, as well as with menhaden oil feeding, regardless of the protein source. The menhaden oil diets reduced plasma cholesterol, hepatic TG, and TG secretion compared with beef tallow diets independently of the dietary protein source. Modifying the source of dietary proteins and lipids had no effect on post-heparin plasma lipoprotein lipase activity. These results demonstrate that soy protein can lower rat triglyceridemia relative to casein when associated with beef tallow consumption, whereas menhaden oil can attenuate hypertriglyceridemia when rats are fed casein. The data further suggest that part of the hypotriglyceridemic effect of soy protein in the rat may be mediated by reduced hepatic lipid synthesis, as is the case for menhaden oil.

Paper no. L9050 in *Lipids* 37, 693–699 (July 2002).

Both dietary proteins and fish oil have been shown to influence plasma lipid concentrations. The hypocholesterolemic effect of soy protein compared with animal proteins is well known (1–4). Several mechanisms have been proposed to explain the hypocholesterolemic effect of soy protein. These include a reduction in intestinal absorption of cholesterol and bile acids (5), a decrease in the insulin-to-glucagon ratio (6), a rise in thyroid hormone concentrations (7), and an increase in the activity of apolipoprotein (apo) B/E receptors (5,8). However, the effect of soy protein on triglyceridemia is less well documented. A diminution of plasma TG concentrations has been observed in some rat (1,9) and human studies (3).

\*To whom correspondence should be addressed at Department of Food Sciences and Nutrition, Paul-Comtois Bldg., Laval University, Sainte-Foy (Québec) G1K 7P4, Canada. E-mail: helene.jacques@aln.ulaval.ca

Abbreviations: apoB, apolipoprotein B; HTGL, hepatic TG lipase; LPL, lipoprotein lipase; PHP-LPL, post-heparin lipoprotein lipase.

The protein itself and its amino acid composition, as well as nonprotein constituents naturally present in soy protein isolate, such as isoflavones, may be implicated (8).

Omega (n)-3 PUFA present in fish oil also have potent hypotriglyceridemic effects (10). The mechanisms responsible for the decrease in plasma TG concentrations associated with consumption of n-3 FA of fish oil involve a reduction in hepatic TG and VLDL synthesis (11,12), and an increase in VLDL and chylomicron degradation by lipoprotein lipase (LPL) (13).

Little is known so far on the effects and mechanisms involved in the interactions between dietary proteins and lipids on the modulation of plasma lipid concentrations. Our previous study (9) demonstrated that dietary proteins may modify the effects of fish oil on triglyceridemia in the rat. Indeed, the hypotriglyceridemic effect of fish oil was more pronounced in rats fed soy protein than in rats fed casein (9). The present study was thus undertaken to understand the mechanisms by which dietary proteins interact with dietary lipids in regulating plasma TG levels. The distinct and interactive effects of two dietary proteins (soy protein and casein) and two dietary lipids (menhaden oil and beef tallow) on plasma and hepatic lipid concentrations, TG secretion rates, post-heparin lipoprotein lipase (PHP-LPL), and hepatic TG lipase (HTGL) activity were investigated in rats.

## MATERIALS AND METHODS

**Experimental animals.** Sprague-Dawley rats (Charles River) initially weighing approximately 200 g were housed in individual stainless-steel wire-bottom mesh cages. The temperature ( $20 \pm 2^\circ\text{C}$ ) and relative humidity (45–55%) of the animal room were constant, and the rats were kept under a daily inverted light-dark cycle (light: 2100 to 0900). During an adaptation period of 2–6 d, rats were fed a nonpurified commercial diet (Purina, St. Louis, MO). They were then randomly assigned to one of four dietary groups ( $n = 14$  per group). For a 28-d period, purified diets and water were provided once daily on an *ad libitum* basis. Records of food intake were taken daily, and body weight was monitored three times a week. The protocol was approved by the Animal Care Committee of Laval University according to the guidelines of the Canadian Council on Animal Care.

**Purified diets.** Diets were similar except for the protein (20%) and the lipid (14%) source (Table 1). The four experi-

**TABLE 1**  
**Composition (g/kg) of the Purified Diets**

Ingredients	Ca-Mo <sup>a</sup>	Ca-Bt	Sp-Mo	Sp-Bt
Casein	228.25	228.25	—	—
Soy protein	—	—	231.25	231.25
Cornstarch	522.67	522.67	519.67	519.67
Cellulose	50	50	50	50
Menhaden oil	100	—	100	—
Beef tallow	—	100	—	100
Soybean oil	40	40	40	40
Cholesterol	10	10	10	10
Minerals	35	35	35	35
Vitamins	10	10	10	10
Choline bitartrate	2.5	2.5	2.5	2.5
$\alpha$ -Tocopherol	1.2	1.2	1.2	1.2
BHA	0.2	0.2	0.2	0.2
BHT	0.2	0.2	0.2	0.2

<sup>a</sup>Ca-Mo = Casein–Menhaden oil, Ca-Bt = Casein–Beef tallow, Sp-Mo = Soy protein–Menhaden oil, Sp-Bt = Soy protein–Beef tallow.

mental diets were composed of the following protein–lipid mixtures: casein–menhaden oil, casein–beef tallow, soy protein–menhaden oil, or soy protein–beef tallow. Beef tallow and menhaden oil were supplied by ICN Biomedicals Inc. (Aurora, OH), and soybean oil was purchased from a local supermarket. According to manufacturer information, the composition of menhaden oil was (by weight): saturated FA 28.2%, monounsaturated FA 23.0%, EPA 16.0%, DHA 10.8%, linoleic acid 1.8%, and arachidonic acid 2.3%. Beef tallow contained (by weight): saturated FA 49.8%, mainly from palmitic (24.9%) and stearic (18.9%) acids; monounsaturated FA 41.8%, mainly from oleic acid (36.0%); and PUFA 4.0%. The cholesterol content of menhaden oil and beef tallow was 5.23 and 1.09 mg/g, respectively. Therefore, menhaden oil provided only 0.5 g cholesterol/kg in menhaden oil diets, and beef tallow provided only 0.1 g cholesterol/kg in beef tallow diets. These amounts were considered as negligible. As proposed by Fritsche and Johnston (14),  $\alpha$ -tocopherol, BHA, and BHT (ICN Biomedicals Inc.) were added to the diets to minimize the oxidation of n-3 and n-6 FA in menhaden oil, and n-6 PUFA in soybean oil and beef tallow. Highly purified casein, soybean protein isolate, cornstarch, cellulose (Alphacel), cholesterol, rat AIN-93 mineral mix, AIN-93 vitamin mix, and choline bitartrate were purchased from ICN Biomedicals Inc. The protein content ( $N \times 6.25$ ) of casein (87.6% protein) and soybean protein isolate (86.5% protein) was determined using a Kjeldahl–Foss autoanalyzer (Model 16216; Foss Co., Hillerod, Denmark). The level of protein in the diets was adjusted at the expense of cornstarch on an isonitrogenous basis. The residual lipid content of casein (0.05%) and soy protein (0.45%) was assayed using a Goldfish Lipid Extractor (Model 35001; Labconco Corp., Kansas City, MO). The energy content of the diets was measured in an automatic adiabatic calorimeter (Model 1241; Parr Instruments, Moline, IL), and the diets were found to be isoenergetic with values ranging from 19.4 to 19.9 kJ/g.

*Experimental procedures and measurement of post-heparin lipoprotein and hepatic lipase activities.* On day 23 of the

experimental period, rats were cannulated *via* the jugular vein under isoflurane anesthesia. They were allowed to recover for 3 d before being subjected to the following procedure. On day 26, after a 12-h fast, the rats were administered 200 IU/kg body weight of heparin through the jugular catheter. A 0.25-mL blood sample was collected 10 min later and centrifuged (1,500  $\times g$ , 4°C) to obtain plasma, which was stored at –80°C for subsequent determination of lipoprotein lipase (LPL) and HTGL activities. Post-heparin plasma LPL and HTGL activities were determined by measuring the amount of *in vitro* hydrolysis by post-heparin plasma samples of a labeled triolein emulsion in the presence of 0.1 or 1 mol/L NaCl (15).

*Determination of TG secretion rate.* On day 28, TG secretion rate was measured according to the method of Otway and Robinson (16). After a 12-h fast, rats were injected through the jugular catheter with 300 mg/kg body weight of Triton WR-1339, a detergent that prevents intravascular TG catabolism. Blood samples (0.15 mL) were taken before (0 min) and 20, 40, and 60 min after Triton injection, centrifuged (1,500  $\times g$ , 4°C, 10 min) to obtain plasma, and stored at –80°C for subsequent determination of TG concentrations. Fasting plasma lipid levels were determined in the pre-Triton (0 min) samples. Rats were then killed by CO<sub>2</sub> after O<sub>2</sub>/CO<sub>2</sub> anesthesia. Rates of VLDL TG secretion were determined from regression analysis of TG accumulation in plasma vs. time and adjusted for plasma volume.

*Plasma, lipoprotein, and hepatic lipid analyses.* Total plasma TG concentrations were determined in all blood samples by an enzymatic method using the Triglycerides/GB kit provided by Roche Diagnostics (Laval, Québec, Canada). Total plasma cholesterol concentrations were measured by an enzymatic method (CHOD-PAP kit of Boehringer Mannheim provided by Roche Diagnostics) only in blood samples collected before Triton injection. The liver of rats was removed after sacrifice and stored at –80°C. Hepatic lipids were extracted with chloroform/methanol (2:1, vol/vol) according to Folch *et al.* (17), and cholesterol and TG were determined enzymatically as described above.

**Statistical analyses.** The results are expressed as mean  $\pm$  SEM. To determine the main protein and lipid effects, as well as interactions between dietary proteins and lipids, data were subjected to an ANOVA according to a  $2 \times 2$  factorial arrangement, using the general linear model (GLM) procedure of the Statistical Analysis System (SAS Institute, Cary, NC). A  $P$  value  $<0.05$  was considered significant. When statistically significant protein–lipid interactions were detected, Duncan's New Multiple Range test was performed to identify differences among diet groups.

## RESULTS

**Food consumption and weight gain.** Table 2 shows the mean food consumption and body weight gain of rats fed the experimental diets. Food intake was similar for all dietary groups. Weight gain was slightly lower in rats fed soy protein than in those fed casein and in rats fed beef tallow compared to those fed menhaden oil, but these differences were not statistically significant ( $P = 0.30$ ). Likewise, food efficiency (g body weight gain/g food ingested) tended to be lower in rats fed soy protein compared to those given casein, but the difference was not significant.

**Plasma and hepatic cholesterol.** Total plasma cholesterol concentrations are presented in Table 3. The overall ANOVA and multiple comparisons are shown in the bottom half of the table. The lipid source had a significant effect ( $P = 0.002$ ) on

plasma cholesterol concentrations, which were lower in menhaden oil-fed than in beef tallow-fed rats. The two protein sources had a similar impact on plasma cholesterol levels.

Diet effects on hepatic cholesterol concentrations are shown in Table 3 and Figure 1. A significant ( $P = 0.02$ ) protein–lipid interaction was observed. The combination of casein and beef tallow resulted in high liver cholesterol concentrations, which were reduced by substitution either of soy for casein or of menhaden oil for beef tallow. Hence, liver cholesterol remained low with soy protein feeding, independently of the lipid source, as well as with menhaden oil consumption, regardless of the protein source.

**Plasma and hepatic TG concentrations, TG secretion rates, and lipase activities.** Plasma and hepatic TG concentrations and TG secretion rates are presented in Table 4. A significant ( $P = 0.05$ ) protein–lipid interaction was observed on fasting triglyceridemia (Fig. 2). The combination of casein and beef tallow was associated with high plasma TG concentrations, which were reduced by substitution either of soy protein for casein or of menhaden oil for beef tallow. Triglyceridemia therefore remained low with soy protein feeding, independently of the lipid source, as well as with menhaden oil feeding, regardless of the protein source.

The protein and lipid sources independently affected hepatic TG concentrations (Table 4). Soy protein feeding resulted in lower hepatic TG content compared with casein feeding ( $P = 0.01$ ). TG concentrations in the liver were also

**TABLE 2**  
Food Intake and Weight Gain of Rats Fed the Purified Diets<sup>a</sup>

Dietary group	<i>n</i>	Food intake (g/d)	Weight gain (g/28 d)	Food efficiency (g gained/g food)
Ca-Mo	13	19.2 $\pm$ 0.4	135 $\pm$ 10	6.84 $\pm$ 0.28
Ca-Bt	12	18.6 $\pm$ 0.6	127 $\pm$ 8	6.82 $\pm$ 0.35
Sp-Mo	12	19.6 $\pm$ 0.5	122 $\pm$ 7	6.56 $\pm$ 0.33
Sp-Bt	14	18.1 $\pm$ 0.4	110 $\pm$ 7	5.85 $\pm$ 0.30

<sup>a</sup>Values are means  $\pm$  SEM. For abbreviations see Table 1.

**TABLE 3**  
Total Plasma and Hepatic Cholesterol Levels of Rats Fed the Purified Diets<sup>a</sup>

Dietary group	<i>n</i>	Plasma cholesterol (mmol/L)	Hepatic cholesterol ( $\mu$ mol/g of liver)
Ca-Mo	6	1.4 $\pm$ 0.2	69 $\pm$ 5
Ca-Bt	7	2.2 $\pm$ 0.2	102 $\pm$ 10
Sp-Mo	7	1.4 $\pm$ 0.1	80 $\pm$ 8
Sp-Bt	6	2.9 $\pm$ 0.3	86 $\pm$ 9
Source of variation		ANOVA ( $P$ values) <sup>b</sup>	
Protein		0.29	0.40
Lipid		0.002	0.05
Protein $\times$ lipid		0.22	0.02
Comparisons			
Protein		Sp = Ca	See Figure 1
Lipid		Mo < Bt	

<sup>a</sup>Values are means  $\pm$  SEM. For abbreviations see Table 1.

<sup>b</sup> $P < 0.05$  indicates significant protein and lipid effects and their interactions.



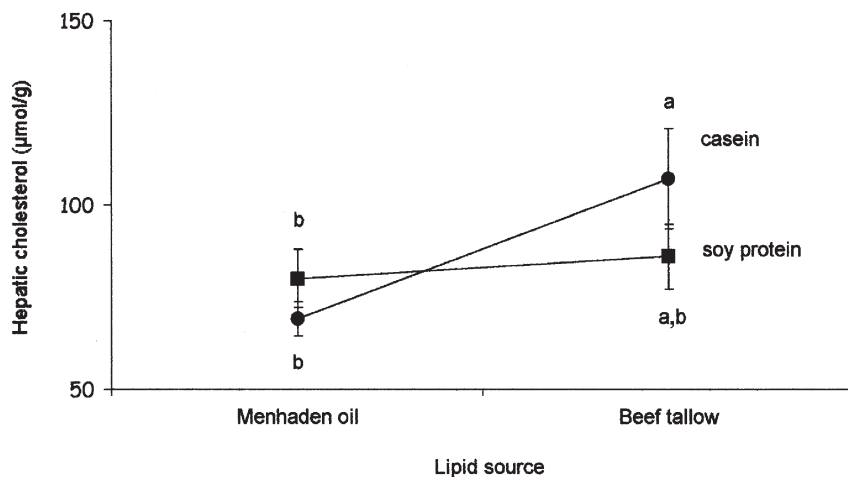


FIG. 1. Interaction between dietary proteins and lipids on total hepatic cholesterol concentrations ( $P = 0.02$ ). Groups bearing different letters are significantly different at  $P < 0.05$ .

decreased after menhaden oil consumption compared with beef tallow consumption ( $P = 0.0001$ ). The lowest values of hepatic TG content were thus observed in soy protein–menhaden oil-fed rats, whereas the highest hepatic TG concentrations were noted in casein–beef tallow-fed animals. In menhaden oil-fed rats, TG secretion rates were lower than in those fed beef tallow ( $P = 0.008$ ) regardless of the protein source. Hepatic TG ( $r = 0.51$ ,  $P = 0.02$ ,  $n = 22$ ) and cholesterol ( $r = 0.47$ ,  $P = 0.026$ ,  $n = 22$ ) concentrations were positively correlated with TG secretion rates.

No significant difference was observed in LPL activity between the four experimental groups. On the other hand, the lipid source had an independent effect on HTGL activity ( $P = 0.02$ ), which was lower in menhaden oil-fed rats than in beef tallow-fed rats. Soy protein strongly ( $P = 0.06$ ) tended to lower HTGL activity when compared with casein. There was

also a trend ( $r = 0.37$ ,  $P = 0.07$ ,  $n = 25$ ) for a positive correlation between HTGL activities and plasma TG concentrations in fasted rats.

## DISCUSSION

The results of this study support the concept, previously described (9), of an interaction between dietary proteins and fish oil in the modulation of triglyceridemia in rats. The findings show that soy protein exerted a hypotriglyceridemic effect similar to that of menhaden oil in the rat, which may be related in part to the reduction in hepatic lipid concentrations consequent to soy protein and menhaden oil consumption.

In the present study, menhaden oil feeding resulted in low plasma TG concentrations in both casein- and soy protein-fed rats, whereas beef tallow resulted in high triglyceridemia

TABLE 4  
Total Plasma and Hepatic TG Concentrations, TG Secretion Rates, and Lipase Activities in Rats Fed the Purified Diets<sup>a</sup>

Dietary group	n	Plasma TG (mmol/L)	TG			HTGL activity (µU/mL/h) <sup>c</sup>
			secretion rates (µmol/min)	Hepatic TG (µmol/g of liver)	PHP-LPL <sup>b</sup> activity (µU/mL/h) <sup>c</sup>	
Ca-Mo	6	0.18 ± 0.03	4.1 ± 0.2	32 ± 3	22 ± 2	24 ± 3
Ca-Bt	6	0.39 ± 0.04	5.3 ± 0.4	63 ± 9	27 ± 3	33 ± 6
Sp-Mo	7	0.25 ± 0.03	4.3 ± 0.6	20 ± 4	24 ± 2	18 ± 2
Sp-Bt	5	0.25 ± 0.05	5.1 ± 0.6	45 ± 6	23 ± 2	21 ± 3
Source of variation			ANOVA ( $P$ values) <sup>d</sup>			
Protein		0.38	0.50	0.01	0.63	0.06
Lipid		0.02	0.008	0.0001	0.60	0.02
Protein × lipid		0.05	0.19	0.30	0.37	0.44
Comparisons						
Protein		See Figure 2	Sp = Ca	Sp < Ca	Sp = Ca	Sp = Ca
Lipid			Mo < Bt	Mo < Bt	Mo = Bt	Mo < Bt

<sup>a</sup>Values are means ± SEM.

<sup>b</sup>PHP-LPL = post-heparin lipoprotein lipase; HTGL = hepatic TG lipase; for other abbreviations see Table 1.

<sup>c</sup>1 µU/mL/h = 1 µmol nonesterified FA released per mL of plasma per hour of incubation.

<sup>d</sup> $P < 0.05$  indicates significant protein and lipid effects and their interactions.

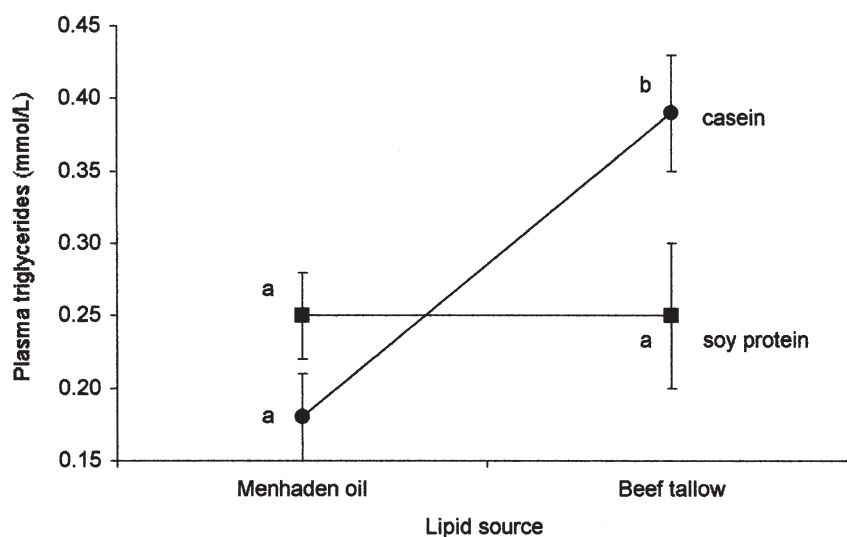


FIG. 2. Interaction between dietary proteins and lipids on total plasma TG concentrations ( $P = 0.05$ ). Groups bearing different letters are significantly different at  $P < 0.05$ .

when combined with casein but low triglyceridemia when combined with soy protein. The lowering effect of fish oil in comparison with saturated FA on triglyceridemia has previously been observed in the rat (11). The results of the present study suggest that the hypotriglyceridemic impact of fish oil may not be affected by the dietary source of proteins. This is in accordance with the data reported by Sakono *et al.* (18) showing in the rat a hypotriglyceridemic effect of fish oil (compared with safflower oil) when combined with either casein or soy protein. In the present study, the lowering effect of fish oil on triglyceridemia was associated with a concomitant reduction in hepatic TG concentrations. A reduced TG synthesis by the liver previously reported in several studies (12,19,20) may be responsible for this effect. Moreover, in the present study TG secretion rates were lower in menhaden oil-fed rats than in those fed beef tallow, and a positive correlation was observed between hepatic TG concentrations and TG secretion rates. Therefore, it is very likely that menhaden oil reduced TG synthesis and their incorporation into VLDL, resulting in a diminished secretion of VLDL by the liver.

Soy protein consumption maintained low plasma TG concentrations relative to casein and attenuated the hypertriglyceridemic effect associated with beef tallow consumption. A hypotriglyceridemic effect of soy protein has been reported previously in rats (1) and in hamsters (21). In humans, the impact of soy protein on triglyceridemia remains unclear. A meta-analysis of 38 controlled clinical studies concluded that substituting soy protein for animal protein significantly lowered total cholesterol, LDL cholesterol, and TG (the latter by approximately 11%) without affecting HDL cholesterol (3). Our own study in children with familial hypercholesterolemia found a 22% decrease in plasma TG, with no change in plasma or LDL cholesterol, following the consumption of a soy-protein beverage compared to cow's milk, either of which

replaced 35% of the energy from protein (4). In contrast, other studies reported an absence of effect of soy protein on triglyceridemia, either when compared to casein in normolipidemic men (22) or to milk protein in hypercholesterolemic postmenopausal women (23). Differences in experimental design or in baseline lipemia may explain such discrepancies, but, taken together, the data suggest that at least in some conditions soy protein also can lower triglyceridemia in humans.

Recent results from our laboratory suggested that the isoflavones naturally present in soy protein isolate may be involved in the hypotriglyceridemic effect of soy protein (24). In the present study, a reducing effect of soy protein compared with casein on hepatic TG concentrations and a correlation between hepatic TG levels and TG secretion rates were observed. This is consistent with the results obtained by Iritani *et al.* (25) showing a lower activity of lipogenic enzymes associated with lower hepatic and plasma TG levels in rats fed soy protein compared with casein. It is therefore likely that the hypotriglyceridemic effect of soy protein observed in the present study was consequent to a reduction in hepatic TG concentrations resulting from a diminution in TG synthesis.

Although soy protein diets resulted in low plasma and hepatic TG concentrations, they had no significant effect on TG secretion rates in the present study. This is in accordance with the results of another study undertaken in our laboratory showing a hypotriglyceridemic effect of soy protein in cornstarch-fed rats but no effect on TG secretion rates (24). Pfeuffer and Barth (26) demonstrated that the lowering effect of soy protein consumption on TG secretion rates was observed in rats fed a high-sucrose diet but was not detected in rats whose triglyceridemia was lowered by a high-cornstarch soy protein diet. Therefore, the possibility remains that the hypotriglyceridemic effect of soy protein in the rat may be mediated in part by changes in TG secretion rates by the liver, as

previously observed in sucrose-fed rats (26), but that this effect is below detectability levels when cornstarch is the carbohydrate source.

A major determinant of triglyceridemia is the intravascular hydrolysis of TG by LPL (27). In the present study, diets had no significant effect on PHP-LPL activity, suggesting that the hypotriglyceridemic effects of soy protein and menhaden oil were not due to changes in LPL activity. HTGL activity was significantly lowered in menhaden oil-fed rats compared with beef tallow-fed rats. This is in accordance with the results of a recent study that showed reduced plasma TG concentrations and hepatic lipase activity when the degree of saturation of the lipid sources fed to rats was decreased (28). As proposed by Benhizia *et al.* (20), the decrease in intravascular hepatic lipase activity observed in the present study after menhaden oil consumption may have been consequent to the decrease in plasma concentrations of TG-rich lipoproteins. The decrease in triglyceridemia observed in soy protein-fed rats may have contributed in the same way to the diminution of HTGL activity ( $P = 0.06$ ) in this group.

In addition to its hypotriglyceridemic effect, the hypocholesterolemic effect of n-3 PUFA from fish oil in comparison with saturated FA frequently has been observed in the rat (9,20,29,30). This effect was reproduced in the present study: Menhaden oil consumption significantly lowered plasma cholesterol concentrations in comparison with beef tallow consumption. The mechanism for this effect may involve an increase in the activity of LDL receptors in the liver and in the transport of apoB-containing lipoproteins by these receptors (29,30). An inhibition of hepatic TG synthesis and cholesterol esterification, leading to a reduced secretion of VLDL-cholesterol by the liver, also may be implicated (29). In the present study, a significant protein-lipid interaction was observed on hepatic cholesterol concentrations. Beef tallow maintained a high hepatic cholesterol content when combined with casein but not when combined with soy protein, whereas menhaden oil maintained low hepatic cholesterol concentrations in the presence of either soy protein or casein. Although no correlation between hepatic and plasma cholesterol concentrations was detected, it remains possible that decreased hepatic cholesterol concentrations may have contributed in part to lower cholesterolemia in menhaden oil-fed rats. Interestingly, Avramoglu *et al.* (31) have shown that VLDL secretion correlates with total mass of cholesterol esters within HepG2 cells. In the present study, TG secretion rates were positively correlated with hepatic cholesterol concentrations ( $P = 0.026$ ,  $r = 0.47$ ,  $n = 12$ ). Therefore, the lower hepatic cholesterol levels observed in menhaden oil-fed rats may have contributed in part to the reduction of TG secretion rates and the hypotriglyceridemic effect observed after menhaden oil consumption.

The hypocholesterolemic effect of soy protein relative to casein is fairly well established, particularly in hypercholesterolemic human subjects (3,32–34), and has been reproduced in some, but not all, studies in the rat model (1,32,35). In the present experiment, there was no significant effect of dietary

proteins on plasma cholesterol concentrations. This may be due in part to the use of cornstarch as a carbohydrate source. Indeed, it has previously been shown that the effects of dietary proteins on cholesterolemia are less pronounced in rats when fed with cornstarch than with sucrose (26,36).

The highest cholesterol concentrations in the liver were observed in casein-beef tallow-fed rats. These data are in good agreement with those showing that saturated FA increase hepatic cholesterol content in comparison with PUFA (39). Casein, compared to soy protein, also increased hepatic cholesterol concentrations in the rat (37,38). The mechanism for the protein effect may involve a rise in intestinal absorption of cholesterol (28,34), which leads to an increased cholesterol transport from gut to liver and a consequent rise in hepatic cholesterol concentrations. The present results suggest that the effect of casein may be additive to that of beef tallow, resulting in high hepatic cholesterol concentrations in casein-beef tallow-fed rats. On the other hand, although soy protein did not modify cholesterolemia overall in the present study, it did result in lower hepatic cholesterol concentrations, compared to casein, in beef tallow-fed rats. Earlier studies also showed that soy protein compared to casein reduced hepatic cholesterol concentrations in the rat (9,39). Therefore, the present results indicate that soy protein may prevent the increasing effect of beef tallow on hepatic cholesterol levels.

The present results support the concept of an interaction between dietary proteins and lipids in the modulation of triglyceridemia in the rat. The present study also demonstrates that soy protein can lower triglyceridemia relative to casein when associated with beef tallow consumption in the rat. On the other hand, menhaden oil can attenuate hypertriglyceridemia induced by casein feeding. Although the mechanisms may differ somewhat, decreased hepatic TG and cholesterol concentrations in rats fed soy protein and menhaden oil suggest that the lowering effect of soy protein on triglyceridemia may be partly mediated by a reduced hepatic lipid synthesis, as is the case for menhaden oil. Studies on liver lipid synthesis should help to clarify the mechanisms by which dietary proteins interact with dietary lipids in the modulation of triglyceridemia in the rat.

## ACKNOWLEDGMENTS

The authors wish to thank Josée Lalonde, Geneviève Asselin, and Julie Goulet for their technical help. This research was supported by the Natural Sciences and Engineering Research Council of Canada.

## REFERENCES

1. Horigome, T., and Cho, Y.S. (1992) Dietary Casein and Soybean Protein Affect the Concentrations of Serum Cholesterol, Triglycerides and Free Amino Acids in Rats, *J. Nutr.* 122, 2273–2282.
2. Carroll, K.K., and Kurowska, M.E. (1995) Soy Consumption and Cholesterol Reduction: Review of Animal and Human Studies, *J. Nutr.* 125, 594S–597S.
3. Anderson, J.W., Johnstone, B.M., and Cook-Newell, M.E. (1995) Meta-Analysis of the Effects of Soy Protein Intake on

- Serum Lipids, *N. Engl. J. Med.* 333, 276–282.
4. Laurin, D., Jacques, H., Moorjani, S., Steinke, F.H., Gagné, C., Brun, D., and Lupien, J. (1991) Effects of Soy-Protein Beverage on Plasma Lipoproteins in Children with Familial Hypercholesterolemia, *Am. J. Clin. Nutr.* 54, 98–103.
  5. Beynen, A.C. (1990) Mode of Cholesterolemic Action of Dietary Proteins, *Monogr. Atheroscler.* 16, 153–159.
  6. Sanchez, A., and Hubbard, R.W. (1991) Plasma Amino Acids and the Insulin/Glucagon Ratio as an Explanation for the Dietary Protein Modulation of Atherosclerosis, *Med. Hypotheses* 36, 27–32.
  7. Forsythe, W.A., 3rd (1990) Dietary Proteins, Cholesterol and Thyroxine: A Proposed Mechanism, *J. Nutr. Sci. Vitaminol.* 36 (Suppl.), S101–S104.
  8. Potter, S.M. (1998) Soy Protein and Cardiovascular Disease: The Impact of Bioactive Components in Soy, *Nutr. Rev.* 56, 231–235.
  9. Demonty, I., Deshaies, Y., and Jacques, H. (1998) Dietary Proteins Modulate the Effects of Fish Oil on Triglyceridemia in the Rat, *Lipids* 33, 913–921.
  10. Connor, W.E., DeFrancesco, C.A., and Connor, S.L. (1993) n-3 Polyunsaturated Fatty Acids from Fish Oil. Effects on Plasma Lipoproteins and Hypertriglyceridemic Patients, *Ann. N.Y. Acad. Sci.* 683, 16–34.
  11. Haug, A., and Hostmark, A.T. (1987) Lipoprotein Lipases, Lipoproteins and Tissue Lipids in Rats Fed Fish Oil or Coconut Oil, *J. Nutr.* 117, 1011–1017.
  12. Wang, H., Chen, X., and Fisher, E.A. (1993) n-3 Fatty Acids Stimulate Intracellular Degradation of Apoprotein B in Rat Hepatocytes, *J. Clin. Invest.* 91, 1380–1389.
  13. Kinsella, J.E., Lokesh, B., and Stone, R.A. (1990) Dietary n-3 Polyunsaturated Fatty Acids and Amelioration of Cardiovascular Diseases: Possible Mechanisms, *Am. J. Clin. Nutr.* 52, 1–28.
  14. Fritsche, K.L., and Johnston, P.V. (1988) Rapid Autoxidation of Fish Oil in Diets Without Added Antioxidants, *J. Nutr.* 118, 425–426.
  15. Belahsen, R., and Deshaies, Y. (1993) Involvement of Insulinemia in the Postprandial Hypotriacylglycerolemia Induced by Prazosin in the Rat, *Metabolism* 42, 1301–1309.
  16. Otway, B.S., and Robinson, D.S. (1967) The Use of a Non-ionic Detergent (Triton WR 1339) to Determine Rates of Triglyceride Entry into the Circulation of the Rat Under Different Physiological Conditions, *J. Physiol.* 190, 321–332.
  17. Folch, J., Lees, M., and Sloane Stanley, G.H. (1957) A Simple Method for the Isolation and Purification of Total Lipids from Animal Tissues, *J. Biol. Chem.* 226, 497–508.
  18. Sakono, M., Yoshida, K., and Yahiro, M. (1993) Combined Effects of Dietary Protein and Fat on Lipid Metabolism in Rats, *J. Nutr. Sci. Vitaminol.* 39, 335–343.
  19. Chiang, M.T., and Tsai, M.L. (1995) Effect of Fish Oil on Plasma Lipoproteins, Liver Glucose-6-phosphate Dehydrogenase and Glucose-6-phosphatase in Rats, *Int. J. Vitamin. Nutr. Res.* 65, 276–282.
  20. Benhizia, F., Hainault, I., Serouge, C., Lagrange, D., Hajduch, E., Guichard, C., Malewiak, M.I., Quignard-Boulangé, A., Lavau, M., and Griglio, S. (1994) Effects of Fish Oil–Lard Diet on Rat Plasma Lipoproteins, Liver FAS, and Lipolytic Enzymes, *Am. J. Physiol.* 267 (6Pt1), E975–E982.
  21. Terpstra, A.H.M., Holmes, J.C., and Nicolosi, J. (1991) The Hypocholesterolemic Effect of Dietary Soybean Protein vs. Casein in Hamsters Fed Cholesterol-Free or Cholesterol-Enriched Semipurified Diets, *J. Nutr.* 121, 944–947.
  22. Nilausen, K., and Meinertz, H. (1999) Lipoprotein(a) and Dietary Proteins: Casein Lowers Lipoprotein(a) Concentrations as Compared with Soy Protein, *Am. J. Clin. Nutr.* 69, 419–425.
  23. Gardner, C.D., Newell, K.A., Cherin, R., and Haskell, W.L. (2001) The Effect of Soy Protein With or Without Isoflavones Relative to Milk Protein on Plasma Lipids in Hypercholesterolemic Postmenopausal Women, *Am. J. Clin. Nutr.* 73, 728–735.
  24. Demonty, I., Lamarche, B., Deshaies, Y., and Jacques, H., Role of Soy Isoflavones in the Hypotriglyceridemic Effect of Soy Protein in the Rat, *J. Nutr. Biochem.*, in press.
  25. Iritani, N., Nagashima, K., Fukuda, H., Katsurada, A., and Tanaka, T. (1986) Effects of Dietary Proteins on Lipogenic Enzymes in Rat Liver, *J. Nutr.* 116, 190–197.
  26. Pfeuffer, M., and Barth, C.A. (1992) Dietary Sucrose but Not Starch Promotes Protein-Induced Differences in Rates of VLDL Secretion and Plasma Lipid Concentrations in Rats, *J. Nutr.* 122, 1582–1586.
  27. Eckel, R.H. (1989) Lipoprotein Lipase. A Multifunctional Enzyme Relevant to Common Metabolic Diseases, *N. Engl. J. Med.* 320, 1060–1068.
  28. Terpstra, A.H.M., van den Berg, P., Jasen, H., Beynen, A.C., and van Tol, A. (2000) Decreasing Dietary Fat Saturation Lowers HDL-Cholesterol and Increases Hepatic HDL Binding in Hamsters, *Br. J. Nutr.* 83, 151–159.
  29. Spady, D.K., Horton, J.D., and Cuthbert, J.A. (1995) Regulatory Effects of n-3 Polyunsaturated Fatty Acids on Hepatic LDL Uptake in the Hamster and Rat, *J. Lipid Res.* 36, 1009–1020.
  30. Spady, D.K., and Woolett, L.A. (1990) Interaction of Dietary Saturated and Polyunsaturated Triglycerides in Regulating the Processes That Determine Plasma Low Density Lipoprotein Concentrations in the Rat, *J. Lipid Res.* 31, 1809–1819.
  31. Avramoglu, R.K., Cianflone, K., and Sniderman, A.D. (1996) Role of the Neutral Lipid Accessible Pool in the Regulation of apoB-100 Lipoprotein Particles by HepG2 Cells, *J. Lipid Res.* 36, 2513–2528.
  32. Forsythe, W.A., Green, M.S., and Anderson, J.J. (1986) Dietary Protein Effects on Cholesterol and Lipoprotein Concentrations: A Review, *J. Am. Coll. Nutr.* 5, 533–549.
  33. Erdman, J.W., Jr. (2000) AHA Science Advisory: Soy Protein and Cardiovascular Disease: A Statement for Healthcare Professionals from the Nutrition Committee of the AHA, *Circulation* 102, 2555–2559.
  34. Tonstad, S., Smerud, K., and Hoie, L. (2002) A Comparison of the Effects of 2 Doses of Soy Protein or Casein on Serum Lipids, Serum Lipoproteins, and Plasma Total Homocysteine in Hypercholesterolemic Subjects, *Am. J. Clin. Nutr.* 76, 78–84.
  35. Pfeuffer, M., and Barth, C.A. (1986) Modulation of Very Low-Density Lipoprotein Secretion by Dietary Protein Is Age-Dependent in Rats, *Ann. Nutr. Metab.* 30, 281–288.
  36. Hurley, C., Galibois, I., and Jacques, H. (1995) Fasting and Postprandial Lipid and Glucose Metabolisms Are Modulated by Dietary Proteins and Carbohydrates: Role of Plasma Insulin Concentrations, *J. Nutr. Biochem.* 6, 540–546.
  37. Hennessy, L.K., Osada, J., Ordovas, J.M., Nicolosi, R.J., Stucchi, A.F., Brousseau, M.E., and Schaefer, E.J. (1992) Effects of Dietary Fats and Cholesterol on Liver Lipid Content and Hepatic Apolipoprotein A-1, B, and E and LDL Receptor mRNA Levels in Cebus Monkeys, *J. Lipid Res.* 33, 351–360.
  38. Horton, J.D., Cuthbert, J.A., and Spady, D.K. (1995) Dietary Fatty Acids Regulate Low-Density-Lipoprotein-Cholesterol Metabolism, *Am. J. Clin. Nutr.* 60 (Suppl. 6), 991S–996S.
  39. Terpstra, A.H.M., van Tintelen, G., and West, C.E. (1982) The Effect of Semipurified Diets Containing Different Proportions of Either Casein or Soybean Protein on the Concentration of Cholesterol in Whole Serum, Serum Lipoproteins and the Liver in Male and Female Rats, *Atherosclerosis* 42, 85–95.

[Received April 16, 2002, and in revised form July 11, 2002; revision accepted July 12, 2002]



# Correlation Between Fatty Acyl Composition in Neutral and Polar Lipids and Enzyme Activities from Various Tissues of Calcium-Deficient Rats

Carlos A. Marra\*, Omar Rimoldi, and María J.T. de Alaniz

Instituto de Investigaciones Bioquímicas de La Plata, Consejo Nacional de Investigaciones Científicas y Técnicas (CONICET)—Universidad Nacional de La Plata (UNLP), Facultad de Ciencias Médicas, UNLP, La Plata, Argentina

**ABSTRACT:** In this study we investigated the changes induced by feeding rats a calcium-deficient diet (0.5 g Ca/kg diet) during 65 d after weaning. Phospholipase A<sub>2</sub>, acyl-Co synthetase and FA  $\Delta$ 9-,  $\Delta$ 6-, and  $\Delta$ 5-desaturase activities were also determined. Calcium deficiency evoked a general alteration in the quality and proportion of the FA chains acylated to neutral and polar lipids from liver, lungs, spleen, brain, kidneys, fat, articular cartilage, erythrocyte ghosts, and plasmas, characterized by an increment of saturated FA and a significant depletion of polyunsaturated acids derived from linoleate and  $\alpha$ -linolenate. Several interlipid and lipid/protein relationships were also modified in microsomes from calcium-deprived rats, with a concomitant reduction in the rotational mobility of the probe diphenylhexatriene. Phospholipase A<sub>2</sub> and acyl-CoA synthetase activities were also decreased and increased, respectively, in some tissues from calcium-deficient rats, whereas  $\Delta$ 9-,  $\Delta$ 6- and  $\Delta$ 5-desaturases were significantly depressed. We conclude that changes in tissue fatty acyl composition evoked by calcium deprivation are due to alterations in the acylation/deacylation cycles *via* inhibition of the phospholipase A<sub>2</sub>. These changes were reflected in the physicochemical properties of the membranes, which in turn inhibits desaturase activities. A possible failure in the transcription rate for desaturase-mRNA was also discussed.

Paper no. L8980 in *Lipids* 37, 701–714 (July 2002).

Previous works from our laboratory have documented that the content of dietary calcium plays an important role in PUFA metabolism since a calcium-deficient (CaD) diet fed to rats for 65 d caused a significant inhibition of  $\Delta$ 5-,  $\Delta$ 6-, and  $\Delta$ 9-desaturase activities in liver microsomes (1). It was also reported by Huang *et al.* (2) that deprivation of calcium may cause a decrease in the rate of elongation of  $\gamma$ -linolenic acid (18:3n-6) (2). The authors supported this conclusion by the analysis of microsomal fatty acyl composition obtained from calcium-deprived rats whose diets were supplemented—or not—with 18:3n-6 acid. Previously, Bierenbaum *et al.* (3) suggested that calcium may limit the availability of 18:3n-6 for the elongase system by forming insoluble complexes with this cation. We also demonstrated that a CaD diet was able to produce a marked stimulation in acyl-CoA synthetase activ-

ity (4) and a significant reduction in phospholipase A<sub>2</sub> activity that evokes permanent alterations in the physicochemical properties of the liver microsomal membranes (1). The picture that emerges from those results is that the changes in the desaturase activities correlate well with both the rotational mobility of the diphenylhexatriene probe and the analytical changes produced on the microsomal lipids by the CaD diet. Whether these changes were completely developed in liver tissue or whether they were the consequence of a general alteration in the lipid metabolism that, in fact, involved various tissues of the animal is not clear. In addition, the importance of the inhibition of FA desaturase activities induced by calcium depletion on the FA composition of lipids from tissues other than liver still remains unexplored. The central role of liver FA desaturases in supplying PUFA for the rest of the body prompted us to investigate the possible correlation between calcium content and lipid composition among several tissues from both sufficient (S) and CaD rats. The aim of the present study was to obtain a general description of the changes induced by calcium deficiency and to evaluate the contribution of some key enzyme activities—involved in FA metabolism—to changes observed under the CaD condition.

## MATERIALS AND METHODS

**FA and other chemicals.** The unlabeled FA used as standards for GLC or employed in the enzymatic determinations were obtained from Nu-Chek-Prep (Elysian, MN). ATP (disodium salt), NADH, *N*-acetylcysteine, CoA (lithium salt), snake venom (*Crotalus atrox*) Western Diamondback Rattlesnake, and sodium deoxycholate (grade II) were purchased from Sigma Chemicals Co. (St. Louis, MO). Unlabeled phospholipids were obtained from Serdary Research Laboratories (London, Ontario, Canada). The procedure to obtain labeled PC was developed in our laboratory after assaying different experimental conditions (1). The following radioactive FA were supplied by Amersham International (Buckinghamshire, UK) (specific activity as mCi/mmol and percent degree of radiochemical purity are indicated, respectively, in parentheses: [1-<sup>14</sup>C]palmitic (58.0, 99), [1-<sup>14</sup>C]linoleic (55.5, 99), and [1-<sup>14</sup>C]jeicosa-8,11,14-trienoic (58.5, 99). The concentration and degree of purity of the FA were routinely checked by liquid scintillation counting and GLC of their FAME prepared by using 14% boron trifluoride in methanol (Alltech Associ-

\*To whom correspondence should be addressed at Facultad de Medicina, Universidad Nacional de La Plata, 60 y 120 (1900) La Plata, Argentina. E-mail: camarra@atlas.med.unlp.edu.ar

Abbreviations: 18:3n-6,  $\gamma$ -linolenic acid; 20:4n-6, arachidonic acid; CaD, calcium-deficient; DBI, double bond index; DPH, 1,6-diphenyl-1,3,5-hexatriene; ED, elongation-desaturation index; PDIA, palmitoyl desaturase index activity; S, sufficient (control); SDIA, stearoyl desaturase activity index.

ates Inc., Deerfield, IL). Eicosa-11-monoenoic acid was used as internal standard. FA were appropriately diluted in absolute ethanol (Riedel-de-Haen, Seelze, Germany) and stored in the dark at  $-20^{\circ}\text{C}$  under an atmosphere of  $\text{N}_2$  until used. Solvents for HPLC were provided by Carlo Erba (Milano, Italy). 1,6-Diphenyl-1,3,5-hexatriene (DPH) probe was obtained from Fluka Chemie AG GmbH & Co. (Buenos Aires, Argentina). Other chemicals used were supplied by commercial sources.

**Animal treatment.** Female Wistar rats from Comisión Nacional de Energía Atómica (Buenos Aires, Argentina) weighing  $170 \pm 10$  g were bred and maintained on a control diet (Cargill type "C," Rosario, Argentina) throughout gestation and lactation. The dams were housed in plastic cages (one animal per cage) in a vivarium kept at  $22 \pm 1^{\circ}\text{C}$  with a 12-h light/dark cycle and a RH of  $60 \pm 10\%$ . After weaning, 24 female pups (weighing  $47 \pm 4$  g/animal) were randomly divided into two groups of 12 animals each and fed *ad libitum* either on a CaD diet (group CaD) or on a balanced one (group S). The composition of the CaD diet prepared in our laboratory was reported in detail in a previous paper (4). The  $\text{Ca}^{2+}$  content of the diet (0.5 g/kg) was determined in a Shimadzu Atomic Absorption Spectrophotometer AA-630-12 (Shimadzu Corp., Kyoto, Japan) following the mineralization procedure described elsewhere (5). Control animals were fed a standard balanced diet supplemented with 5.0 g/kg calcium in order to supply the mineral at a level equivalent to that recommended by The American Institute of Nutrition for the Formulation of the AIN-93 Purified Diets for Laboratory Rodents (6). The content of  $\text{Ca}^{2+}$  in drinking water (given *ad libitum*) was determined either by atomic absorption or by calcium-selective electrode (Orion model 93-20; Orion Research Inc., Cambridge, MA), and it was generally below 15 ppm. During the feeding period, body weight, water consumption, and food intake were determined every day. Samples of blood (100 to 150  $\mu\text{L}$ ) were collected from the tail vein once a week in order to determine plasma calcium levels. Animals were sacrificed on day 65 after feeding. In order to avoid individual differences among animals that might result from an *ad libitum* feeding, on day 64 all the rats were fasted for 24 h, re-fed with the corresponding diet for 2 h, and then killed by decapitation without prior anesthesia 12 h after the refeeding period. All the diet components used were purchased from Carlo Erba (Milano, Italy) or Mallinckrodt Chem. Works (Oneonta, NY). The casein was depleted of calcium by EGTA treatment and then defatted with boiling acetone. The calcium content in the extracted casein was negligible. Animal maintenance and handling were in accordance with the NIH guide for the care and use of laboratory animals (7).

**Collection of samples and preparation of microsomal suspensions.** Liver, heart, kidneys, skeletal muscle (psoas major and quadriceps), lungs, brain, and spleen from S and CaD rats were rapidly excised and immediately placed in an ice-cold homogenizing medium (8). The homogenates were processed individually at  $1^{\circ}\text{C}$ , and the microsomal fractions were separated by differential centrifugation at  $110,000 \times g$  as described previously (8). Microsomal pellets were resuspended in cold

homogenizing solution up to a final protein concentration of 30–40 mg/mL. Other tissues such as perirenal fat, large bones (femur and tibiotarsal), and articular cartilage from S and CaD rats were also used to obtain homogenates from whole tissue samples because, in these cases, microsomal suspensions were not prepared. Cortical (parietal) and tibiotarsal bones—with intact articular and epiphyseal cartilages—were carefully excised; chilled on ice; and thoroughly cleaned of connective tissues, fatty inclusions, and vessels; weighed; and stored at  $-80^{\circ}\text{C}$  under  $\text{N}_2$  atmosphere until further use. Thin-sliced cartilage samples were prepared as shavings from the articular surfaces of femoral condyles and tibial plateaus from six S or CaD rats. They were processed and assayed separately. Epiphyseal and diaphyseal zones of one femur per rat were also excised and processed independently. They were carefully rinsed in ice-cold saline to remove adherent tissues and/or body fluids and homogenized using a powerful homogenizer with a rotating blade (Ultra-Turrax Type TP 18/10; Janke & Kunkel, Staufen, Germany). Blood was also collected after killing the rats by decapitation. Samples were individually dispensed into heparinized tubes and fractionated by centrifugation at  $50 \times g$  for 10 min. Plasmas were immediately processed for calcium determination and lipid analysis. Erythrocyte ghosts were prepared by hypotonic lysis according to the procedure of Dodge *et al.* (9), as modified by Berlin *et al.* (10). An aliquot from the erythrocyte membranes was processed for steady-state fluorescence anisotropy determinations ( $r_s$ ) following the procedure described in Reference 11. The rest was employed for lipid analysis.

**Lipid analysis.** Product identification and quantification after FA desaturase activity assays were performed by RP-HPLC according to previously described methods (1,12). GLC of the FAME was performed as indicated in a previous paper (13) except that in this case we used a capillary column mounted in a Hewlett-Packard HP 6890 Series GC System Plus (Avondale, PA) equipped with a terminal computer integrator. The FAME were identified by comparison of their relative retention times with authentic standards, and the mass distribution was calculated electronically by quantification of the peak areas. Total lipids were extracted from S and CaD samples by the method of Folch *et al.* (14). Phospholipid and neutral lipid fractions were separated from the Folch extracts by a micro-column chromatography method described elsewhere (15). Cholesterol content was enzymatically measured according to Allain *et al.* (16). Total lipids and neutral lipids were estimated gravimetrically after evaporation of an aliquot of the corresponding lipid extract (Folch or silicic acid subfraction, respectively) up to constant weight (17). Phospholipids were measured as phosphorus content (18) after mineralization of an aliquot from the silicic acid partition.

**Enzymatic determinations.** Phospholipase  $\text{A}_2$  activity was determined in microsomal fractions from various tissues with [ $^{14}\text{C}$ ]PC (24.0 mCi/mmol, 99% pure) as substrate according to the method of Hirata *et al.* (19) with the modifications described in a previous paper (1). To determine the FA desaturase activities in microsomal suspensions from various tissues of S

and CaD rats, each FA used as substrate ( $[1-^{14}\text{C}]16:0$ ,  $[1-^{14}\text{C}]18:2n-6$ , or  $[1-^{14}\text{C}]20:3n-3$ ) was diluted to a specific activity of 0.20 to 0.25  $\mu\text{Ci/mol}$  with the respective pure unlabeled FA. In order to compare results, the enzymatic assays were conducted at saturated substrate concentrations. Each assay was performed by incubation of 1.25 mg of liver microsomal protein or 5 mg of brain, kidney, lung, heart, or spleen microsomal protein in an open test tube with  $5 \cdot 10^3$  pmol of diluted labeled substrate for liver or  $10^4$  pmol for the other tissues, in a Dubnoff shaker at  $37^\circ\text{C}$  for 10 min. The total volume of the incubation medium was 0.8 mL. Details of the assay procedure were described in previous papers (1,20,21). Acyl-CoA activity assays were performed on cytosol fractions obtained as supernatants of  $110,000 \times g$ , according to the method of Tanaka *et al.* (22) as modified previously (4).

**Measurement of  $\Delta 6$ -desaturase mRNA.** Total liver RNA of six S or CaD animals were isolated by means of Wizard RNA Isolation System (Promega, Madison, WI) according to the manufacturer's instructions. Total RNA (20  $\mu\text{g}$ ) was size-fractionated on a 1% formaldehyde gel and then transferred to a Zeta-Probe nylon membrane (Bio-Rad, Hercules, CA). The  $\Delta 6$ -desaturase and  $\beta$ -actin probes were prepared by incorporating  $[^{32}\text{P}]\text{dCTP}$  by random primer labeling. Northern blot hybridization analysis was performed as described by Sambrook *et al.* (23). The autoradiographic signal for  $\Delta 6$ -desaturase mRNA was quantified and normalized to mRNA for  $\beta$ -actin, with all mRNA probed on the same gel.

**Other analytical determinations.** Calcium content in liver microsomal suspensions was determined after mineralization (5) by atomic absorption or calcium-sensitive electrode as described elsewhere (1,4). The protein content was determined by the micro-method of Lowry *et al.* (24) with crystalline serum albumin as standard. Fluorescence anisotropy measurements 352 nm excitation, 435 nm emission were done at  $37^\circ\text{C}$  following the procedure of Shinitzky and Barenholz (25,26). The apparatus used, a detailed description of the method employed, and the calculations/corrections made appeared in a previous paper (11).

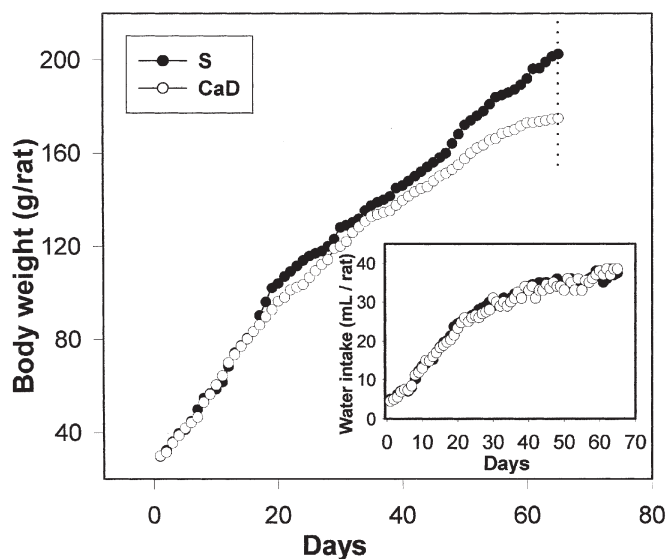
**Graphic software and statistical treatment of the data.** All values represent the mean of 3 to 6 individual determinations (assayed in duplicate or triplicate)  $\pm 1$  SEM. To test the statistical significance of numerical differences in results, data were analyzed by either the Student *t*-test or by ANOVA, with the aid of Systat (version 8.0 for Windows) from SPSS Science (Chicago, IL). Data were also plotted and analyzed using Sigma Scientific Graphing Software (version 8.0) from Sigma Chemical Co. and/or GB-STAT Professional Statistics Program (version 4.0) from Dynamic Microsystems Inc. (Silver Spring, MD). The autoradiographic signal for  $\Delta 6$ -desaturase mRNA was quantified using 1-D Image Analysis Software (Kodak, Rochester, NY) from multiple exposures. It was normalized to mRNA for  $\beta$ -actin, with all mRNA probed on the same gel.

## RESULTS

In our experimental model of calcium deficiency, we observed that both S and CaD rats grew at a similar rate for the initial

15 d after feeding. Then, the CaD group grew at a rate that was reduced—but not statistically significant—until day 65, when differences between groups became significant (Fig. 1). Water intake expressed as mL/rat was very similar in both groups of animals throughout the entire experimental period (Fig. 1, inset). As shown in Figure 2, food intakes, expressed as grams of food per rat or relative to body weight (inset), were not significantly different between both groups of rats despite the fact that in the initial 10 d of feeding, CaD animals exhibited an increased food intake compared to that of S ones. After the first week of feeding, a progressive decline in plasma calcium concentration was observed in CaD rats (from  $2.63 \pm 0.10$  mM at day 0 to  $2.11 \pm 0.15$ ,  $1.73 \pm 0.12$ , or  $1.58 \pm 0.07$  mM at days 8, 16, and 24, respectively) up to day 28 in which the values remained essentially constant and significantly lower ( $1.50 \pm 0.08$  mM) than those from the S group ( $2.63 \pm 0.10$  mM). Table 1 shows calcium content determinations in various tissues on the day of sacrifice.

With the exception of fat, brain, and lung, the rest of the tissue homogenates showed an important decrease in Ca content. In large bones the loss of calcium represented *ca.* 60% decrease with respect to control samples. Liver, kidney, erythrocytes, cortical bone, and articular cartilage showed 30 to 50% decreases in calcium content, but heart and skeletal muscle were affected to a minor extent (20%). When the microsomal suspension of some tissues was examined for their calcium content, only liver, kidney, and spleen showed significant decrease in the concentration of this cation (a loss of 42 to 47% with respect to control determinations). These findings were reflected in the total calcium content of plasma, which decreased 43% with respect to that of S rats. The proportion of ionic calcium in the plasma of CaD animals also decreased 66% with respect



**FIG. 1.** Body weight (expressed as g per rat) and water intake (mL/rat, inset) were registered during the entire experimental period. Each datum is the mean of six rats per group. SEM, omitted for simplicity, never exceeded 6% of the corresponding mean value. The vertical dotted line represents the first significant difference between control (S) and calcium-deficient (CaD) rats.

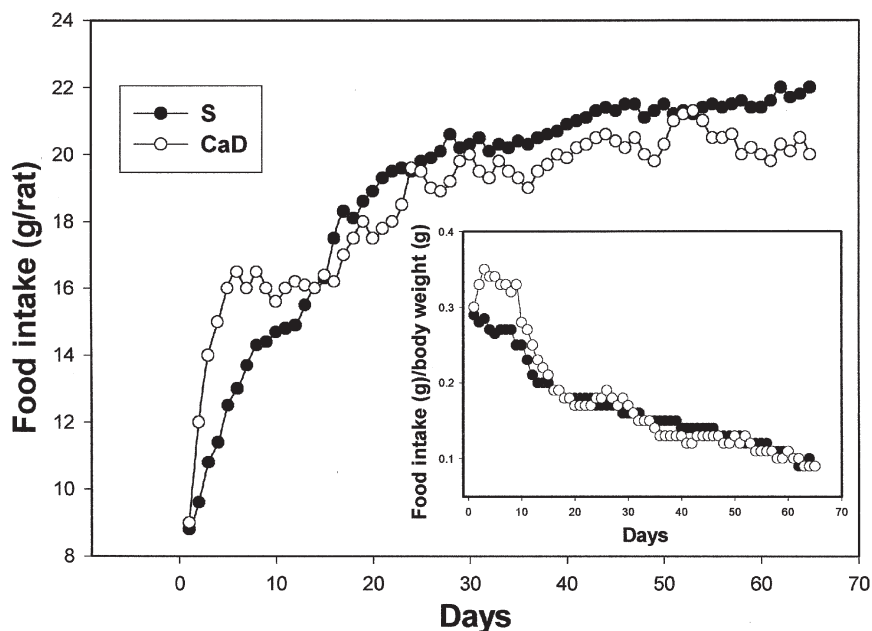


FIG. 2. Food intake was registered during the entire experimental period and expressed as g of aliment per rat or as the ratio g of food/g of body weight (insert). Each datum is the mean of six rats per group. SEM, omitted for simplicity, never exceeded 8% of the corresponding mean value. Points from days 2 to 9 (inclusive) were significantly different between S and CaD groups. For abbreviations see Figure 1.

to control ones, and the percentage of bound calcium in the blood of treated animals ( $78.0 \pm 2.1$ ) was significantly higher than that found in the control group ( $62.2 \pm 1.8$ ).

The fatty acyl composition of neutral and polar lipids was profoundly modified under CaD conditions. The most important changes were found in liver, followed by kidney, spleen, and cartilage. Table 2 shows the result obtained when we analyzed microsomal neutral lipids from liver, brain, kidney, and heart. Neutral lipids from brain microsomes exhibited a

decreased content of arachidonate and docosahexaenoate (n-3). By contrast, heart microsomes showed no significant changes. Palmitate and stearate content were increased in microsomal neutral lipids from both liver and kidney, with no concomitant modifications in the proportion of the corresponding monoenoates. In liver, the content of linoleate was diminished by 47% with respect to control values, and the proportion of 20:4n-6 (arachidonate) was dramatically reduced with a simultaneous increase in the level of its direct

TABLE 1  
Calcium<sup>a</sup> Content in Tissues<sup>b</sup> from Control (S) or Calcium-Deficient (CaD) Rats

	Whole tissue		Microsomes	
	S	CaD	S	CaD
Liver <sup>a</sup>	1.51 ± 0.05	0.90 ± 0.02*	2.62 ± 0.04	1.51 ± 0.05*
Heart <sup>a</sup>	2.22 ± 0.05	1.80 ± 0.04*	5.53 ± 0.11	5.10 ± 0.20
Skeletal muscle <sup>a</sup>	3.10 ± 0.12	2.55 ± 0.08*	6.06 ± 0.20	5.74 ± 0.31
Brain <sup>a</sup>	2.30 ± 0.08	2.15 ± 0.10	4.12 ± 0.07	3.60 ± 0.15
Kidney <sup>a</sup>	1.23 ± 0.02	0.77 ± 0.03*	1.74 ± 0.05	0.92 ± 0.06*
Fat <sup>a</sup>	0.95 ± 0.04	0.80 ± 0.10	ND	ND
Erythrocytes <sup>a</sup>	1.88 ± 0.11	1.10 ± 0.07*	ND	ND
Lung <sup>a</sup>	2.12 ± 0.06	1.93 ± 0.11	3.05 ± 0.09	2.68 ± 0.13
Spleen <sup>a</sup>	1.76 ± 0.05	0.84 ± 0.03*	1.97 ± 0.06	1.15 ± 0.08*
Cortical bone <sup>b</sup>	18.6 ± 0.7	11.7 ± 0.5*	ND	ND
Epiphyseal bone <sup>b</sup>	15.9 ± 0.4	7.4 ± 0.6*	ND	ND
Diaphyseal bone <sup>b</sup>	21.5 ± 0.5	10.1 ± 0.3*	ND	ND
Articular cartilage <sup>b</sup>	6.3 ± 0.4	4.2 ± 0.1*	ND	ND
Plasma (total) <sup>c</sup>	2.63 ± 0.10	1.50 ± 0.08*	ND	ND
Plasma (ionic) <sup>c</sup>	0.98 ± 0.03	0.33 ± 0.02*	ND	ND

<sup>a</sup>Calcium contents were determined by atomic absorption from samples collected on day 65 after feeding. For technical details see the Materials and Methods section.

<sup>b</sup>Results were expressed as <sup>a</sup>nmol/mg of protein; <sup>b</sup>percentage of total wet weight; or <sup>c</sup>mM. Each value is the mean ± 1 SEM of four to six independent determinations assayed in duplicate. \*Significantly different ( $P < 0.01$ ) with respect to the corresponding S value.



**TABLE 2**  
**Fatty Acyl Composition<sup>a</sup> of Microsomal Neutral Lipids from Tissues of Control (S) or Calcium-Deficient (CaD) Rats**

FA	Liver		Brain		Kidney		Heart	
	S	CaD	S	CaD	S	CaD	S	CaD
14:0	0.6 ± 0.1	0.6 ± 0.1	0.2 ± 0.0	0.3 ± 0.0	0.8 ± 0.1	0.5 ± 0.1	1.6 ± 0.2	2.2 ± 0.1
16:0	38.9 ± 1.2	45.9 ± 1.5*	30.3 ± 2.0	31.5 ± 3.1	25.9 ± 1.3	33.0 ± 2.0*	40.1 ± 3.0	39.0 ± 2.5
16:1n-7	3.3 ± 0.1	4.2 ± 0.2	6.5 ± 0.2	7.2 ± 0.3	4.0 ± 0.5	3.9 ± 0.1	2.4 ± 0.2	1.5 ± 0.1
18:0	7.8 ± 0.2	11.6 ± 0.9*	7.1 ± 0.1	6.8 ± 0.2	18.4 ± 2.5	24.3 ± 1.9*	36.1 ± 2.1	38.7 ± 1.9
18:1n-9	16.5 ± 0.6	18.5 ± 1.8	39.8 ± 2.7	41.0 ± 3.5	21.2 ± 1.4	20.7 ± 1.3	13.2 ± 0.7	14.3 ± 0.7
18:2n-6	25.4 ± 1.3	13.6 ± 0.7*	20.1 ± 1.6	19.5 ± 1.5	17.0 ± 1.8	15.0 ± 1.0	6.4 ± 0.3	5.8 ± 0.1
18:3n-6	0.1 ± 0.0	Trace	0.1 ± 0.0	0.2 ± 1.5	0.1 ± 0.0	0.1 ± 0.0	0.1 ± 0.0	0.2 ± 0.0
18:3n-3	0.1 ± 0.0	Trace	0.2 ± 0.0	0.1 ± 0.0	0.1 ± 0.0	Trace	0.1 ± 0.0	0.2 ± 0.0
18:4n-3	0.1 ± 0.0	Trace	0.3 ± 0.1	0.2 ± 0.0	Trace	Trace	0.1 ± 0.0	Trace
20:3n-6	0.3 ± 0.1	1.1 ± 0.1*	0.8 ± 0.1	0.5 ± 0.1	0.4 ± 0.1	0.5 ± 0.1	0.3 ± 0.1	0.1 ± 0.0
20:4n-6	4.5 ± 0.1	Trace*	5.5 ± 0.2	4.0 ± 0.1*	6.3 ± 0.1	3.5 ± 0.1*	2.9 ± 0.1	2.1 ± 0.1
20:5n-3	0.1 ± 0.0	Trace	0.1 ± 0.0	0.1 ± 0.0	0.1 ± 0.0	Trace	0.1 ± 0.0	0.1 ± 0.0
22:0	Trace	0.2 ± 0.0*	0.1 ± 0.0	Trace	0.1 ± 0.0	Trace	0.3 ± 0.0	0.1 ± 0.0
22:1n-9	0.1 ± 0.0	Trace	0.1 ± 0.0	Trace	0.1 ± 0.0	Trace	0.1 ± 0.0	Trace
22:2n-6	0.2 ± 0.0	Trace	0.2 ± 0.0	Trace	0.1 ± 0.0	0.1 ± 0.0	0.1 ± 0.0	0.1 ± 0.0
22:3n-3	0.1 ± 0.0	Trace	0.2 ± 0.0	Trace	Trace	0.1 ± 0.0	Trace	Trace
22:4n-6	0.1 ± 0.0	Trace	0.1 ± 0.0	Trace	Trace	Trace	Trace	Trace
22:5n-6	0.2 ± 0.0	Trace	0.1 ± 0.0	0.1 ± 0.0	0.1 ± 0.0	0.1 ± 0.0	Trace	Trace
22:4n-3	0.1 ± 0.0	0.1 ± 0.0	0.1 ± 0.0	0.1 ± 0.0	0.1 ± 0.0	0.2 ± 0.0	Trace	Trace
22:5n-3	Trace	Trace	0.3 ± 0.1	0.1 ± 0.0	Trace	0.1 ± 0.0	Trace	Trace
22:6n-3	0.1 ± 0.0	0.1 ± 0.0	0.8 ± 0.1	0.3 ± 0.1*	0.1 ± 0.0	0.2 ± 0.0	0.2 ± 0.0	Trace
24:1	Trace	0.1 ± 0.0	0.1 ± 0.0	0.1 ± 0.0	Trace	Trace	Trace	Trace

<sup>a</sup>GLC of the FAME was performed as indicated in the Materials and Methods section. Each value is expressed as  $\mu\text{g}/\text{mg}$  protein and corresponds to the mean  $\pm 1$  SEM of three independent determinations performed on randomly selected samples. Other FA not listed in the table are present in minor amounts. \*Significantly different ( $P < 0.01$ ) with respect to the corresponding control value. Amounts below 0.1  $\mu\text{g}/\text{mg}$  protein are indicated as "Trace." SEM below 0.1 are indicated as "0.0."

precursor (20:3n-6). The fall in 20:4n-6 was also observed in neutral lipids from kidney microsomes, but it was of lesser extent (44%) than that of liver (98%). Within the C<sub>22</sub> FA homologs, we observed in liver microsomes a minor increase in the proportion of 22:0. Phospholipid fatty acyl composition was also modified by calcium deficiency (Table 3). The composition of brain and heart microsomes showed no significant modifications, whereas liver and kidney exhibited an altered pattern. The extent of these changes, especially in liver microsomes, was more pronounced in both number and extension than that observed in neutral lipids. The saturated FA 14:0, 16:0, 18:0, and 22:0 were increased in liver phospholipids from CaD rats, whereas kidney phospholipids contained elevated levels of palmitate and stearate relative to those found in S rats. The most striking difference between the phospholipid fatty acyl composition from CaD and S animals was the higher proportion of linoleate in liver and kidney (72 and 40% over control data, respectively). Arachidonate was decreased *ca.* 60% in liver without any modification in the proportion of its metabolic precursor (20:3n-6). In contrast, the content of 20:4n-6 in phospholipids from kidney microsomes remained unchanged. In phospholipids of microsomes from CaD rats, the highest homologs derived from  $\alpha$ -linolenate, such as 20:5n-3 and 22:6n-3, were decreased 75 and 48%, respectively, with a concomitant increase of 50% in their metabolic precursor (18:3n-3).

Tables 4 and 5 summarize analytical data of fatty acyl composition from neutral and polar lipids of spleen and lung microsomes, fat, and articular cartilage. In neutral lipids from

spleen microsomes (Table 4), saturated FA were increased but arachidonate was decreased *ca.* 83% with respect to the values obtained in S rats. An important increase of 20:3n-6 (400%) was also observed. Neutral lipids of fat from CaD rats showed an increased proportion of arachidonate that was the only change associated with dietary manipulation. Lung microsomes evidenced no significant changes under calcium restriction, but in the case of articular cartilage, an increase in 20:3n-9 and 22:1n-9 FA with a simultaneous decrease in 20:4n-6 and 22:2n-6 were observed (Table 4). The phospholipid fraction from spleen microsomes (Table 5) showed alterations similar to those described for the neutral lipids, that is, an increased proportion of 16:0, 18:0, and 20:3n-6 with a reduced relative amount of 20:4n-6. Contrary to what was seen with neutral lipids, in phospholipids of fat from CaD rats an 86% reduction in arachidonate content was observed. Table 5 also shows that phospholipids from both lung and articular cartilage exhibited a marked decrease in arachidonate proportion. It is also important to remark that, in articular cartilage, we found a large amount of 20:3n-9 FA and low levels of n-6 PUFA (<10%), as previously reported by other authors (27,28). This particular composition is more evident in phospholipids than in neutral lipids of S rats. Interestingly, 20:3n-9 accumulated in neutral and polar lipids of articular cartilage under the CaD condition (Table 5).

The composition of fatty acyl chains in neutral lipids from erythrocyte ghosts or plasmas obtained from CaD animals remained unchanged with respect to that of S rats (Table 6). However, in phospholipids from erythrocyte ghosts a

**TABLE 3**  
**Fatty Acyl Composition<sup>a</sup> of Microsomal Phospholipids from Tissues of Control (S) or Calcium-Deficient (CaD) Rats**

FA	Liver		Brain		Kidney		Heart	
	S	CaD	S	CaD	S	CaD	S	CaD
14:0	0.2 ± 0.0	0.9 ± 0.1*	0.2 ± 0.0	0.3 ± 0.1	0.1 ± 0.0	0.4 ± 0.1	1.1 ± 0.2	1.9 ± 0.2
16:0	17.5 ± 1.3	24.6 ± 1.3*	33.7 ± 1.9	35.4 ± 2.0	18.7 ± 0.9	25.5 ± 0.7*	14.0 ± 0.9	17.0 ± 1.3
16:1n-7	1.0 ± 0.1	0.7 ± 0.1	7.8 ± 0.1	8.1 ± 0.4	1.8 ± 0.1	1.3 ± 0.1	3.2 ± 0.1	3.0 ± 0.2
18:0	20.2 ± 0.9	28.8 ± 1.3*	28.5 ± 2.0	32.1 ± 3.1	16.2 ± 0.7	22.2 ± 1.1*	21.7 ± 1.6	25.4 ± 2.1
18:1n-9	5.5 ± 0.3	5.7 ± 0.2	22.3 ± 1.2	20.3 ± 2.0	9.3 ± 0.5	10.3 ± 0.8	5.8 ± 0.2	4.9 ± 0.2
18:2n-6	4.6 ± 0.2	7.9 ± 0.2*	14.5 ± 0.2	15.9 ± 1.0	9.6 ± 0.4	13.4 ± 0.3*	12.6 ± 1.1	11.7 ± 0.9
18:3n-6	0.3 ± 0.1	0.4 ± 0.1	0.3 ± 0.1	0.3 ± 0.1	0.2 ± 0.0	0.1 ± 0.0	0.1 ± 0.0	0.2 ± 0.0
18:3n-3	0.2 ± 0.0	0.4 ± 0.0*	0.2 ± 0.0	0.1 ± 0.0	0.4 ± 0.1	0.3 ± 0.0	0.2 ± 0.0	0.2 ± 0.0
18:4n-3	0.1 ± 0.0	0.1 ± 0.0	0.5 ± 0.1	0.3 ± 0.0	0.3 ± 0.1	0.4 ± 0.1	0.3 ± 0.0	0.2 ± 0.0
20:3n-6	2.7 ± 0.1	2.0 ± 0.2*	1.7 ± 0.1	2.2 ± 0.1	1.5 ± 0.1	0.6 ± 0.1	0.8 ± 0.1	0.7 ± 0.1
20:4n-6	27.4 ± 1.5	11.8 ± 2.0*	6.9 ± 0.2	6.0 ± 0.2	24.7 ± 0.8	21.5 ± 1.3	18.7 ± 0.3	15.5 ± 0.4
20:5n-3	0.4 ± 0.1	0.1 ± 0.0*	0.2 ± 0.0	0.3 ± 0.1	0.3 ± 0.1	0.2 ± 0.0	0.3 ± 0.1	0.2 ± 0.0
22:0	0.2 ± 0.0	0.5 ± 0.0*	0.1 ± 0.0	0.1 ± 0.0	0.4 ± 0.1	0.2 ± 0.0	0.2 ± 0.0	Trace
22:1n-9	0.2 ± 0.0	0.1 ± 0.0	0.2 ± 0.0	0.1 ± 0.0	0.2 ± 0.0	Trace	0.2 ± 0.0	0.3 ± 0.1
22:2n-6	0.3 ± 0.1	Trace	0.5 ± 0.1	0.3 ± 0.1	0.1 ± 0.0	Trace	0.1 ± 0.0	0.1 ± 0.0
22:3n-3	0.1 ± 0.0	Trace	0.3 ± 0.0	0.2 ± 0.0	0.2 ± 0.0	Trace	Trace	Trace
22:4n-6	0.3 ± 0.0	0.1 ± 0.0	0.4 ± 0.1	0.2 ± 0.0	0.3 ± 0.1	0.1 ± 0.0	Trace	Trace
22:5n-6	0.2 ± 0.0	Trace	1.1 ± 0.2	0.9 ± 0.1	0.2 ± 0.0	0.1 ± 0.0	0.1 ± 0.0	0.1 ± 0.0
22:4n-3	0.2 ± 0.0	Trace	0.3 ± 0.1	0.2 ± 0.0	0.3 ± 0.1	0.1 ± 0.0	0.1 ± 0.0	0.1 ± 0.0
22:5n-3	0.1 ± 0.0	Trace	0.8 ± 0.1	1.1 ± 0.1	0.3 ± 0.0	0.1 ± 0.0	0.2 ± 0.0	0.1 ± 0.0
22:6n-3	10.1 ± 0.3	5.3 ± 0.2*	9.2 ± 0.3	10.2 ± 0.2	2.6 ± 0.2	2.0 ± 0.1	7.0 ± 0.2	6.3 ± 0.2
24:1	Trace	0.1 ± 0.0	0.2 ± 0.0	0.3 ± 0.1	Trace	Trace	0.2 ± 0.0	0.1 ± 0.0

<sup>a</sup>GLC of the FAME was performed as indicated in the Materials and Methods section. Each value is expressed as µg/mg protein and corresponds to the mean ± 1 SEM of three independent determinations performed on randomly selected samples. Other FA not listed in the table are present in minor amounts. \*Significantly different ( $P < 0.01$ ) with respect to the corresponding control value. Amounts below 0.1 µg/mg protein are indicated as "Trace." SEM below 0.1 are indicated as "0.0."

**TABLE 4**  
**Fatty Acyl Composition<sup>a</sup> of Microsomal Neutral Lipids from Tissues of Control (S) or Calcium-Deficient (CaD) Rats**

FA	Spleen		Lung		Fat		Cartilage	
	S	CaD	S	CaD	S	CaD	S	CaD
14:0	0.8 ± 0.1	0.6 ± 0.1	1.6 ± 0.3	1.0 ± 0.1	1.5 ± 0.2	1.1 ± 0.2	2.0 ± 0.2	2.3 ± 0.3
16:0	33.5 ± 1.2	39.7 ± 1.3*	47.0 ± 2.5	40.5 ± 1.8	22.4 ± 1.0	21.2 ± 1.1	30.4 ± 1.9	29.6 ± 2.0
16:1n-7	2.5 ± 0.1	3.1 ± 0.2	4.0 ± 0.1	4.7 ± 0.2	7.2 ± 0.2	6.8 ± 0.2	6.1 ± 0.2	5.7 ± 0.4
18:0	13.3 ± 0.3	16.9 ± 0.7*	11.8 ± 0.4	13.4 ± 0.3	6.9 ± 0.3	9.0 ± 0.2	7.3 ± 0.2	8.6 ± 0.4
18:1n-9	28.0 ± 1.7	22.2 ± 2.3	12.5 ± 0.4	10.0 ± 0.5	35.7 ± 2.0	33.1 ± 2.0	47.4 ± 2.5	45.0 ± 1.9
18:2n-6	15.0 ± 1.0	15.3 ± 0.9	10.0 ± 0.5	14.3 ± 0.5	22.1 ± 1.7	23.5 ± 2.5	2.6 ± 0.1	3.0 ± 0.2
18:3n-6	0.1 ± 0.0	0.1 ± 0.0	0.1 ± 0.0	0.2 ± 0.0	0.1 ± 0.0	0.2 ± 0.0	0.1 ± 0.0	0.1 ± 0.0
18:3n-3	0.2 ± 0.0	0.1 ± 0.0	0.1 ± 0.0	0.1 ± 0.0	0.1 ± 0.0	0.2 ± 0.0	0.1 ± 0.0	0.2 ± 0.0
18:4n-3	0.1 ± 0.0	0.1 ± 0.0	Trace	0.1 ± 0.0	0.2 ± 0.0	0.3 ± 0.0	0.2 ± 0.0	0.3 ± 0.0
20:3n-9	Trace	Trace	Trace	0.1 ± 0.0	Trace	Trace	2.2 ± 0.3	3.8 ± 0.2*
20:3n-6	0.2 ± 0.1	1.0 ± 0.1*	1.5 ± 0.1	1.8 ± 0.2	0.5 ± 0.1	0.9 ± 0.1	0.1 ± 0.0	0.1 ± 0.0
20:4n-6	5.3 ± 0.2	0.9 ± 0.2*	7.0 ± 0.2	9.7 ± 0.6	1.5 ± 0.1	2.7 ± 0.1*	0.3 ± 0.0	Trace*
20:5n-3	Trace	Trace	0.1 ± 0.0	0.1 ± 0.0	0.1 ± 0.0	0.2 ± 0.0	0.1 ± 0.0	0.2 ± 0.0
22:0	Trace	Trace	0.3 ± 0.0	0.2 ± 0.0	0.3 ± 0.0	0.4 ± 0.1	0.4 ± 0.1	0.5 ± 0.1
22:1n-9	Trace	Trace	0.1 ± 0.0	0.1 ± 0.0	0.1 ± 0.0	0.2 ± 0.1	0.2 ± 0.0	0.5 ± 0.1*
22:2n-6	0.2 ± 0.0	Trace	0.1 ± 0.0	0.1 ± 0.0	0.1 ± 0.0	0.1 ± 0.0	0.5 ± 0.1	0.1 ± 0.0*
22:3n-3	Trace	Trace	0.1 ± 0.0	0.2 ± 0.0	Trace	Trace	Trace	Trace
22:4n-6	0.1 ± 0.0	Trace	1.5 ± 0.2	1.3 ± 0.1	0.1 ± 0.0	0.1 ± 0.0	Trace	Trace
22:5n-6	0.4 ± 0.1	Trace	1.0 ± 0.1	0.9 ± 0.1	0.1 ± 0.0	Trace	Trace	Trace
22:4n-3	Trace	Trace	0.2 ± 0.0	0.2 ± 0.0	Trace	Trace	Trace	Trace
22:5n-3	Trace	Trace	0.3 ± 0.0	0.1 ± 0.0	0.2 ± 0.0	Trace	Trace	Trace
22:6n-3	0.3 ± 0.0	Trace	0.7 ± 0.1	0.8 ± 0.1	0.7 ± 0.1	Trace	Trace	Trace
24:1	Trace	Trace	Trace	0.1 ± 0.0	0.1 ± 0.0	Trace	Trace	Trace

<sup>a</sup>GLC of the FAME was performed as indicated in the Materials and Methods section. Each value is expressed as µg/mg protein and corresponds to the mean ± 1 SEM of three independent determinations performed on randomly selected samples. Other FA not listed in the table are present in minor amounts. \*Significantly different ( $P < 0.01$ ) with respect to the corresponding control value. Amounts below 0.1 µg/mg protein are indicated as "Trace." SEM below 0.1 are indicated as "0.0."

**TABLE 5**  
**Fatty Acyl Composition<sup>a</sup> of Microsomal Phospholipids from Tissues of Control (S) or Calcium-Deficient (CaD) Rats**

FA	Spleen		Lung		Fat		Cartilage	
	S	CaD	S	CaD	S	CaD	S	CaD
14:0	Trace	0.1 ± 0.0	1.0 ± 0.1	0.9 ± 0.1	1.2 ± 0.2	1.1 ± 0.1	0.3 ± 0.0	0.3 ± 0.1
16:0	21.5 ± 1.1	27.2 ± 0.8*	23.2 ± 2.2	24.5 ± 2.1	25.4 ± 0.9	27.3 ± 1.5	12.5 ± 0.3	15.4 ± 0.3*
16:1n-7	3.0 ± 0.1	2.7 ± 0.1	6.1 ± 0.5	7.2 ± 0.3	4.5 ± 0.2	4.9 ± 0.2	9.5 ± 0.2	8.0 ± 0.4
18:0	12.0 ± 0.5	14.8 ± 0.6*	10.0 ± 0.4	8.8 ± 0.2	12.0 ± 0.3	13.4 ± 0.4	17.0 ± 0.5	19.8 ± 0.6*
18:1n-9	18.7 ± 0.6	16.3 ± 1.0	15.5 ± 0.6	17.3 ± 0.6	24.1 ± 1.0	26.5 ± 2.1	40.4 ± 2.0	31.8 ± 1.3*
18:2n-6	14.6 ± 0.5	15.7 ± 0.8	13.1 ± 0.7	14.0 ± 0.4	17.5 ± 0.4	17.0 ± 0.9	3.5 ± 0.1	4.0 ± 0.1
18:3n-6	0.5 ± 0.1	0.6 ± 0.1	0.3 ± 0.0	0.5 ± 0.1	0.2 ± 0.0	0.3 ± 0.0	0.1 ± 0.0	0.1 ± 0.0
18:3n-3	0.3 ± 0.0	0.2 ± 0.0	0.2 ± 0.0	0.2 ± 0.0	0.3 ± 0.0	0.4 ± 0.1	0.2 ± 0.0	0.1 ± 0.0
18:4n-3	0.2 ± 0.0	0.2 ± 0.0	0.2 ± 0.0	0.2 ± 0.0	0.1 ± 0.0	0.3 ± 0.0	0.1 ± 0.0	0.2 ± 0.0
20:3n-9	Trace	0.1 ± 0.0	0.2 ± 0.0	0.2 ± 0.0	0.1 ± 0.0	0.1 ± 0.0	8.5 ± 0.2	13.0 ± 0.5*
20:3n-6	2.4 ± 0.1	3.6 ± 0.1*	2.6 ± 0.2	3.0 ± 0.2	2.2 ± 0.1	2.6 ± 0.1	0.5 ± 0.1	1.0 ± 0.1*
20:4n-6	18.5 ± 0.3	12.1 ± 0.3*	14.1 ± 0.8	10.0 ± 0.2*	7.4 ± 0.1	1.0 ± 0.1*	4.8 ± 0.1	2.3 ± 0.1*
20:5n-3	0.2 ± 0.0	0.1 ± 0.0	0.4 ± 0.0	0.5 ± 0.1	0.3 ± 0.0	0.3 ± 0.0	0.3 ± 0.0	0.4 ± 0.1
22:0	0.1 ± 0.0	0.1 ± 0.0	0.2 ± 0.0	0.2 ± 0.0	0.4 ± 0.1	0.5 ± 0.1	0.3 ± 0.0	0.3 ± 0.0
22:1n-9	0.2 ± 0.0	0.2 ± 0.0	0.2 ± 0.0	0.4 ± 0.1	0.2 ± 0.0	0.2 ± 0.0	1.6 ± 0.1	2.9 ± 0.1*
22:2n-6	0.3 ± 0.0	0.2 ± 0.0	0.5 ± 0.1	0.4 ± 0.1	0.4 ± 0.1	0.3 ± 0.0	Trace	Trace
22:3n-3	0.1 ± 0.0	0.1 ± 0.0	0.2 ± 0.0	0.3 ± 0.0	0.2 ± 0.0	0.3 ± 0.1	0.3 ± 0.0	0.4 ± 0.1
22:4n-6	3.3 ± 0.1	2.5 ± 0.2	4.3 ± 0.2	3.8 ± 0.1	0.3 ± 0.0	0.2 ± 0.0	0.1 ± 0.0	Trace
22:5n-6	1.5 ± 0.1	1.1 ± 0.3	3.5 ± 0.1	3.0 ± 0.1	0.2 ± 0.0	0.3 ± 0.0	Trace	Trace
22:4n-3	0.2 ± 0.0	0.1 ± 0.0	0.4 ± 0.1	0.5 ± 0.1	0.2 ± 0.0	0.2 ± 0.0	Trace	Trace
22:5n-3	1.0 ± 0.1	0.8 ± 0.1	0.8 ± 0.1	0.9 ± 0.1	0.8 ± 0.1	0.7 ± 0.1	Trace	Trace
22:6n-3	1.3 ± 0.1	1.1 ± 0.2	2.9 ± 0.1	3.1 ± 0.1	1.8 ± 0.2	1.9 ± 0.1	Trace	Trace
24:1	0.1 ± 0.0	0.1 ± 0.0	0.1 ± 0.0	0.1 ± 0.0	0.2 ± 0.0	0.2 ± 0.0	Trace	Trace

<sup>a</sup>GLC of the FAME was performed as indicated in the Materials and Methods section. Each value is expressed as µg/mg protein and corresponds to the mean ± 1 SEM of three independent determinations performed on randomly selected samples. Other FA not listed in the table are present in minor amounts. \*Significantly different ( $P < 0.01$ ) with respect to the corresponding control value. Amounts below 0.1 µg/mg protein are indicated as "Trace." SEM below 0.1 are indicated as "0.0."

**TABLE 6**  
**Fatty Acyl Composition<sup>a</sup> of Neutral and Polar Lipids from Erythrocyte Ghosts and Plasmas from Control (S) or Calcium-Deficient (CaD) Rats**

FA	Neutral lipids				Phospholipids			
	Erythrocyte ghosts		Plasmas		Erythrocyte ghosts		Plasmas	
	S	CaD	S	CaD	S	CaD	S	CaD
14:0	0.7 ± 0.1	0.5 ± 0.1	0.1 ± 0.0	0.1 ± 0.0	Trace	0.1 ± 0.0	0.3 ± 0.1	0.3 ± 0.1
16:0	48.8 ± 3.1	47.2 ± 4.4	37.5 ± 2.2	41.0 ± 3.9	30.1 ± 2.0	29.8 ± 3.0	23.1 ± 0.8	26.9 ± 0.5*
16:1n-7	0.5 ± 0.1	0.7 ± 0.1	1.6 ± 0.1	1.3 ± 0.2	2.1 ± 0.1	1.7 ± 0.2	2.5 ± 0.1	2.3 ± 0.1
18:0	45.1 ± 4.2	48.1 ± 4.0	12.6 ± 1.7	13.2 ± 1.0	16.4 ± 0.8	17.5 ± 1.1	23.0 ± 2.2	24.4 ± 1.1
18:1n-9	10.9 ± 1.1	9.7 ± 0.4	8.9 ± 1.5	9.0 ± 0.5	10.6 ± 0.5	11.3 ± 0.7	6.6 ± 0.2	5.9 ± 0.3
18:2n-6	3.0 ± 0.3	4.5 ± 0.4	32.8 ± 2.6	33.3 ± 4.0	16.8 ± 1.1	15.0 ± 0.9	11.3 ± 0.2	19.8 ± 0.3*
18:3n-6	0.1 ± 0.0	0.2 ± 0.0	0.1 ± 0.0	0.2 ± 0.0	0.2 ± 0.0	0.1 ± 0.0	0.4 ± 0.1	0.3 ± 0.0
18:3n-3	0.2 ± 0.0	0.1 ± 0.0	0.1 ± 0.0	0.1 ± 0.0	0.1 ± 0.0	0.3 ± 0.1	0.2 ± 0.0	0.1 ± 0.0
18:4n-3	0.1 ± 0.0	0.1 ± 0.0	0.2 ± 0.0	0.1 ± 0.0	0.1 ± 0.0	0.2 ± 0.0	0.3 ± 0.0	0.2 ± 0.0
20:3n-6	0.1 ± 0.0	0.1 ± 0.0	0.2 ± 0.0	0.2 ± 0.0	1.0 ± 0.1	0.8 ± 0.1	1.0 ± 0.1	0.3 ± 0.0
20:4n-6	0.8 ± 0.1	0.5 ± 0.1	5.1 ± 0.1	4.7 ± 0.1	7.6 ± 0.1	4.2 ± 0.1*	14.9 ± 0.2	8.8 ± 0.3*
20:5n-3	0.1 ± 0.0	0.1 ± 0.0	0.1 ± 0.0	0.1 ± 0.0	0.3 ± 0.1	0.1 ± 0.0	0.1 ± 0.0	0.1 ± 0.0
22:0	Trace	0.1 ± 0.0	Trace	Trace	0.1 ± 0.0	0.1 ± 0.0	0.1 ± 0.0	Trace
22:1n-9	Trace	0.1 ± 0.0	Trace	Trace	0.1 ± 0.0	0.1 ± 0.0	0.3 ± 0.0	0.2 ± 0.0
22:2n-6	0.1 ± 0.0	Trace	Trace	Trace	0.2 ± 0.0	Trace	0.2 ± 0.0	0.1 ± 0.0
22:3n-3	Trace	Trace	Trace	Trace	0.1 ± 0.0	Trace	0.3 ± 0.1	0.2 ± 0.0
22:4n-6	0.1 ± 0.0	Trace	0.1 ± 0.0	Trace	0.3 ± 0.0	Trace	0.2 ± 0.0	Trace
22:5n-6	0.1 ± 0.0	Trace	0.1 ± 0.0	Trace	0.2 ± 0.0	Trace	0.1 ± 0.0	0.1 ± 0.0
22:4n-3	Trace	Trace	Trace	Trace	0.3 ± 0.0	Trace	0.1 ± 0.0	0.1 ± 0.0
22:5n-3	Trace	Trace	Trace	Trace	0.1 ± 0.0	Trace	0.1 ± 0.0	Trace
22:6n-3	0.1 ± 0.0	Trace	0.3 ± 0.1	0.1 ± 0.0	7.9 ± 0.1	5.0 ± 0.1*	3.2 ± 0.1	1.9 ± 0.2
24:1	Trace	Trace	0.1 ± 0.0	Trace	0.1 ± 0.0	Trace	Trace	0.1 ± 0.0

<sup>a</sup>GLC of the FAME was performed as indicated in the Materials and Methods section. Each value is expressed as µg/mg protein and corresponds to the mean ± 1 SEM of three independent determinations performed on randomly selected samples. Other FA not listed in the table are present in minor amounts. \*Significantly different ( $P < 0.01$ ) with respect to the corresponding control value. SEM below 0.1 are indicated as "0.0." Amounts below 0.1 µg/mg protein are indicated as "Trace."

decrease of 45% in the relative content of arachidonate and a 37% reduction in the 22:6n-3 level were observed. In the plasma phospholipid fraction we found much increased percentages of palmitate and  $\alpha$ -linoleate and decreased arachidonate levels relative to those of control animals (Table 6).

The analytical changes described above correlate well with various metabolic indicators that account for the rate of supply and/or utilization of the different FA chains acylated to lipids (29,30). In Table 7 are summarized some of these parameters for liver and kidney, calculated from the results in Tables 2 and 3. The double-bond index (DBI), obtained as PUFA/saturated FA ratio, was significantly decreased (50 to 60%) in neutral and polar lipids from both liver and kidney microsomes. One possible explanation is that this result may be the consequence of a general failure in FA desaturation capacity together with an accumulation of saturated FA. In all fractions studied, the decrease in the PUFA relative content was evoked through a similar contribution of the n-3 and n-6 FA, resulting in a very similar n-3/n-6 ratio for control and treated animals. However, it was not the same with the essential/nonessential FA ratio. This parameter was significantly diminished in both neutral and polar lipids from the liver and kidney of CaD rats. This alteration may be produced through both a selective loss of unsaturated FA derived from linoleate and/or  $\alpha$ -linolenate and the increment in the FA members of the n-7 and n-9 series. In fact, results from Table 7 indicate that these two possibilities are in agreement with the results obtained. The inhibition in the metabolic transformation of linoleate was clearly indicated through the decreased values of the ED (elongation-desaturation) 18:2n-6 index. Moreover, comparison between this index and ED 20:4n-6 also indicates that the impairment for linoleate utilization was greater in the  $\Delta 6$  desaturation step than in the  $\Delta 5$  one.

Similar conclusions can be derived from comparison between the sum of the desaturase index activity— $\Delta 6 + \Delta 5$  DIA—and the individual index for  $\Delta 6$  and  $\Delta 5$  desaturase enzymes. With regard to this metabolic pathway in kidney phospholipids,  $\Delta 5$ -desaturase activity not only remained at control levels under CaD conditions but also was stimulated (Table 7). The significant decrease in the palmitoyl- and stearoyl-desaturase activity indexes indicates that calcium deficiency also evoked an impairment in the metabolic utilization of both palmitate and stearate, the precursors of the n-7 and n-9 FA series, respectively.

Lipid relationships and data from fluorescence anisotropy measurement of various tissues from CaD rats are shown in Tables 8 and 9. Cholesterol/phospholipid ratio was diminished in heart and kidney microsomes and also in erythrocyte ghosts, articular cartilage, and plasmas. With the sole exception of brain microsomes, in all samples studied a significant reduction in the cholesterol/protein ratio was observed. In most of the tissues, the total lipid/cholesterol ratio was also diminished, indicating that the reduction in the proportion of total lipids was greater than that of cholesterol. The total lipid/protein ratio was significantly reduced in spleen, erythrocyte ghosts, cartilage, and plasmas from CaD rats. Articular cartilage was the only tissue that exhibited a significant decrease in the proportion of total lipids to phospholipids, whereas all the other examined tissues showed an important increase in neutral lipid content relative to polar lipids. Measurements of neutral and polar lipid contents relative to the amount of total protein demonstrated that the general increase observed in the neutral lipid/polar lipid ratio was evoked primarily by the reduction in the phospholipid/protein ratio rather than the increase in the neutral lipid/protein ratio (Table 7).

Steady-state DPH fluorescence anisotropy determinations

**TABLE 7**  
**Analytical Parameters from Fatty Acyl Composition of Microsomal Lipids**

Analytical parameters	Phospholipids <sup>a</sup>				Neutral lipids <sup>a</sup>			
	Liver		Kidney		Liver		Kidney	
	S	CaD	S	CaD	S	CaD	S	CaD
Saturated acids	38.1 ± 1.1	54.6 ± 0.8*	35.4 ± 1.4	48.1 ± 3.1*	47.3 ± 2.1	57.3 ± 1.8*	45.2 ± 1.8	57.8 ± 2.5*
PUFA	47.0 ± 2.0	27.9 ± 0.7*	41.2 ± 2.6	38.9 ± 2.9	31.4 ± 3.3	15.2 ± 2.0*	24.5 ± 2.4	19.9 ± 1.1*
DBI <sup>a</sup>	1.23 ± 0.03	0.51 ± 0.02*	1.16 ± 0.10	0.80 ± 0.02*	0.66 ± 0.05	0.32 ± 0.02*	0.54 ± 0.04	0.34 ± 0.03*
Total n-3	11.1 ± 0.2	5.90 ± 0.06*	4.20 ± 0.10	3.10 ± 0.10*	0.50 ± 0.02	0.20 ± 0.01*	0.70 ± 0.01	0.50 ± 0.02*
Total n-6	35.9 ± 1.9	22.2 ± 0.5*	36.8 ± 3.3	35.8 ± 4.0	30.9 ± 1.9	14.7 ± 2.4*	24.0 ± 2.0	19.4 ± 1.4*
(n-3)/(n-6)	0.31 ± 0.03	0.27 ± 0.03	0.11 ± 0.02	0.09 ± 0.01	0.02 ± 0.01	0.02 ± 0.01	0.03 ± 0.0	0.03 ± 0.0
EFA/non-EFA <sup>b</sup>	7.01 ± 0.2	4.28 ± 0.1*	0.88 ± 0.02	0.65 ± 0.01*	0.47 ± 0.02	0.18 ± 0.01*	0.35 ± 0.01	0.24 ± 0.01*
ED 18:2n-6 <sup>c</sup>	6.59 ± 0.2	1.75 ± 0.1*	2.75 ± 0.03	1.66 ± 0.02*	4.81 ± 0.5	0.08 ± 0.01*	0.40 ± 0.03	0.27 ± 0.02*
ED 20:4n-6 <sup>d</sup>	0.02 ± 0.0	0.01 ± 0.0	0.02 ± 0.0	0.01 ± 0.0	0.07 ± 0.02	—*	0.02 ± 0.0	0.02 ± 0.0
( $\Delta 6 + \Delta 5$ ) DIA <sup>e</sup>	5.96 ± 0.10	1.49 ± 0.11*	2.57 ± 0.10	1.60 ± 0.10*	0.18 ± 0.04	—*	0.37 ± 0.02	0.23 ± 0.01*
( $\Delta 6$ ) DIA <sup>f</sup>	0.59 ± 0.02	0.25 ± 0.01*	0.16 ± 0.02	0.04 ± 0.0*	0.01 ± 0.0	0.08 ± 0.01*	0.02 ± 0.0	0.03 ± 0.0
( $\Delta 5$ ) DIA <sup>g</sup>	10.2 ± 0.3	5.90 ± 0.2*	16.4 ± 1.5	35.8 ± 2.9*	15.0 ± 0.9	—*	15.8 ± 1.7	7.00 ± 0.9*
PDIA <sup>h</sup>	0.06 ± 0.003	0.03 ± 0.0*	0.10 ± 0.01	0.05 ± 0.01*	0.08 ± 0.01	0.09 ± 0.02	0.15 ± 0.02	0.12 ± 0.02
SDIA <sup>i</sup>	0.27 ± 0.02	0.20 ± 0.0*	0.57 ± 0.01	0.46 ± 0.0*	2.12 ± 0.1	1.68 ± 0.1*	1.15 ± 0.03	0.85 ± 0.01*

<sup>a</sup>Results are expressed as the mean ± 1 SEM of three independent determinations obtained from data in Tables 2 and 3. Parameters a, b, f, h, and i were calculated according to Lepage *et al.* (30). Calculations for parameters c and d were done according to Martínez and Ballabriga (29). <sup>a</sup>PUFA/saturated, <sup>b</sup>[(n-6) + (n-3)]/[(n-7) + (n-9) + saturated], <sup>c</sup>[20:3n-6 + 20:4n-6 + 22:5n-6]/18:2n-6, <sup>d</sup>[22:4n-6 + 22:5n-6]/20:4n-6, <sup>e</sup>20:4n-6/18:2n-6, <sup>f</sup>20:3n-6/18:2n-6, <sup>g</sup>20:4n-6/20:3n-6, <sup>h</sup>16:1n-7/16:0, <sup>i</sup>18:1n-9/18:0. DBI, double bond index; ED, elongation-desaturation index; DIA, desaturase index activity; PDIA, palmitoyl desaturase index activity; SDIA, stearoyl desaturase index activity; for other abbreviations see Table 1. \*Significantly different with respect to the corresponding control values. Amounts below 0.01 are indicated as "—." SEM <0.01 are indicated as "0.0."



**TABLE 8**  
**Interlipid Relationships and Fluorescence Anisotropy of Microsomal Membranes from Liver, Heart, Kidney, and Brain of Control (S) or Calcium-Deficient (CaD) Rats<sup>a</sup>**

	Liver		Heart		Kidney		Brain	
	S	CaD	S	CaD	S	CaD	S	CaD
Cholesterol/phospholipids (μmol/μmol)	0.32 ± 0.02	0.23 ± 0.01	0.29 ± 0.02	0.15 ± 0.02*	0.41 ± 0.02	0.26 ± 0.01*	0.52 ± 0.02	0.63 ± 0.04
Total lipids/phospholipids (mg/μmol)	0.79 ± 0.03	0.98 ± 0.04	0.96 ± 0.03	1.11 ± 0.10	0.56 ± 0.02	0.64 ± 0.03	1.25 ± 0.11	1.32 ± 0.20
Total lipids/cholesterol (mg/μmol)	2.48 ± 0.02	3.00 ± 0.03*	3.31 ± 0.04	7.40 ± 0.26*	1.37 ± 0.01	2.46 ± 0.02*	2.40 ± 0.15	2.09 ± 0.10
Phospholipids/protein (μmol/mg)	0.45 ± 0.03	0.30 ± 0.01*	0.40 ± 0.02	0.37 ± 0.03	0.60 ± 0.02	0.41 ± 0.01*	0.51 ± 0.05	0.32 ± 0.03*
Neutral lipids/protein (μg/mg)	0.06 ± 0.003	0.11 ± 0.01*	0.04 ± 0.005	0.06 ± 0.01	0.05 ± 0.004	0.13 ± 0.005*	0.03 ± 0.002	0.03 ± 0.005
Cholesterol/protein (μmol/mg)	0.14 ± 0.01	0.07 ± 0.01*	0.12 ± 0.01	0.06 ± 0.01*	0.25 ± 0.01	0.10 ± 0.01*	0.27 ± 0.02	0.20 ± 0.05
Total lipids/protein (mg/mg)	0.36 ± 0.03	0.29 ± 0.02*	0.38 ± 0.02	0.41 ± 0.03	0.34 ± 0.01	0.26 ± 0.03*	0.65 ± 0.05	0.42 ± 0.20
Neutral lipids/polar lipids (μg/μg)	0.13 ± 0.01	0.37 ± 0.02*	0.10 ± 0.01	0.16 ± 0.02*	0.08 ± 0.005	0.32 ± 0.01*	0.06 ± 0.01	0.09 ± 0.01
DPH fluorescence anisotropy	0.1405 ± 0.0010	0.1012 ± 0.0008*	0.2314 ± 0.0020	0.2001 ± 0.0015*	0.1971 ± 0.0012	0.1355 ± 0.0009*	0.1113 ± 0.0007	0.1204 ± 0.0011

<sup>a</sup>Results are expressed as the mean ± 1 SEM of three independent determinations. For details see the Materials and Methods section. Diphenylhexatriene (DPH) steady-state fluorescence anisotropy in membrane suspensions was measured at 37°C using the probe DPH as described in the Materials and Methods section. Results for DPH determinations are expressed as the mean ± 1 SEM of six independent determinations assayed in duplicate. \*Significantly different ( $P < 0.01$ ) from the respective control value.

**TABLE 9**  
**Interlipid Relationships and Fluorescence Anisotropy of Erythrocyte Ghosts, Whole Articular Cartilage, Plasma, and Microsomal Membranes from Spleen of Control (S) or Calcium-Deficient (CaD) Rats<sup>a</sup>**

	Spleen		Erythrocyte ghosts		Articular cartilage		Plasma	
	S	CaD	S	CaD	S	CaD	S	CaD
Cholesterol/phospholipids (μmol/μmol)	0.55 ± 0.03	0.43 ± 0.04	0.86 ± 0.05	0.54 ± 0.02*	2.0 ± 0.1	0.32 ± 0.03	2.33 ± 0.08	2.05 ± 0.11*
Total lipids/phospholipids (mg/μmol)	0.61 ± 0.02	0.70 ± 0.03	0.52 ± 0.03	0.60 ± 0.04	7.6 ± 0.2	1.4 ± 0.1*	2.11 ± 0.09	2.34 ± 0.11
Total lipids/cholesterol (mg/μmol)	1.07 ± 0.06	1.64 ± 0.03*	0.60 ± 0.04	0.35 ± 0.03*	4.6 ± 0.1	4.4 ± 0.1*	0.80 ± 0.04	1.00 ± 0.03
Phospholipids/protein (μmol/mg)	0.50 ± 0.03	0.33 ± 0.03*	0.35 ± 0.03	0.12 ± 0.01*	0.03 ± 0.01	5.0 ± 0.2	0.04 ± 0.01	0.01 ± 0.00*
Neutral lipids/protein (μg/mg)	0.06 ± 0.004	0.10 ± 0.01	0.04 ± 0.003	0.06 ± 0.01	0.06 ± 0.01	0.01 ± 0.00*	0.02 ± 0.001	0.03 ± 0.001
Cholesterol/protein (μmol/mg)	0.28 ± 0.02	0.14 ± 0.01*	0.30 ± 0.03	0.19 ± 0.02*	0.05 ± 0.01	0.01 ± 0.00*	0.10 ± 0.02	0.02 ± 0.00*
Total lipids/protein (mg/mg)	0.30 ± 0.02	0.23 ± 0.03*	0.18 ± 0.01	0.07 ± 0.01*	0.23 ± 0.03	0.04 ± 0.01*	0.08 ± 0.01	0.02 ± 0.00*
Neutral lipids/polar lipids (μg/μg)	0.12 ± 0.01	0.30 ± 0.03*	0.11 ± 0.01	0.49 ± 0.04*	2.1 ± 0.2	3.7 ± 0.2*	0.50 ± 0.03	1.76 ± 0.05*
DPH fluorescence anisotropy	0.1202 ± 0.0005	0.1051 ± 0.0003*	0.1077 ± 0.0005	0.0831 ± 0.0006*	ND	ND	ND	ND

<sup>a</sup>Results are expressed as the mean ± 1 SEM of three independent determinations randomly selected from both experimental groups, whether S or CaD. For details see the Materials and Methods section. Diphenylhexatriene (DPH) steady-state fluorescence anisotropy in membrane suspensions was measured at 37°C using the probe DPH as described in the Materials and Methods section. Results for DPH determinations are expressed as the mean ± 1 SEM of six independent determinations assayed in duplicate. \*Significantly different ( $P < 0.01$ ) from the respective control value. ND, not determined.

were carried out in microsomal suspensions from both S and CaD rats (Tables 8 and 9). Experimental data show that calcium deficiency produces microsomal membranes in which acyl chain packing is disordered relative to the membranes of the S group. A similar conclusion was obtained from plasma membranes of erythrocyte ghosts from CaD rats. Fluorescence anisotropy determinations in suspensions from CaD brain microsomes showed no significant changes with respect to the control, as expected from the minor alterations observed in the proportion of membrane lipids under calcium deficiency (Tables 2, 3, and 8).

Some enzyme activities closely related to lipid metabolism were determined in various tissues from S and CaD rats (Table 10). As regards FA desaturases, the most striking difference observed was the very low levels of activities that all tissues studied exhibited with respect to that of liver microsomes. These differences were observed irrespective of the substrate assayed. Kidney and heart microsomes were more active than spleen, lung, or brain. However, specific activity in liver was much greater than that determined in kidney or heart microsomes. The CaD diet evoked an important reduction (54 to 59% respect to control values) in  $\Delta 5$ ,  $\Delta 6$ , and  $\Delta 9$  liver desaturase activities. This reduction was also observed for the rest of the tissues studied except for heart, in which only  $\Delta 9$ -desaturase capacity was affected (Table 10). Basal activity for phospholipase A<sub>2</sub> varied from a maximum for kidney microsomes to a minimum for spleen ones. Lung, heart, and liver displayed similar activities. Calcium deficiency did not modify phospholipase A<sub>2</sub> activity of brain, lung, or heart, but the activities in microsomes from kidney, liver, and spleen were significantly reduced: *ca.* 80% for the former tissues and 35% for the latter (Table 10). The most active tissue acylating free FA to CoA-SH was the liver, which exhibited a basal acyl-CoA synthetase activity three times greater than that of kidney, lung, or heart. Brain and spleen were the least active

tissues studied, with a basal enzyme activity that was almost 80% smaller than that of control liver. In microsomes from CaD rats, an increased acyl-CoA synthetase activity was determined in both kidney and liver (32 and 76% higher, respectively, than that of controls).

Finally, we found a significant reduction in the transcription rate for mRNA that encodes for liver  $\Delta 6$ -desaturase (Fig. 3). The ratio mRNA ( $\Delta 6$ -desaturase)/mRNA ( $\beta$ -actin) was reduced from  $1.62 \pm 0.17$  for S rats to  $0.93 \pm 0.06$  for CaD ones (-43% with respect to control values).

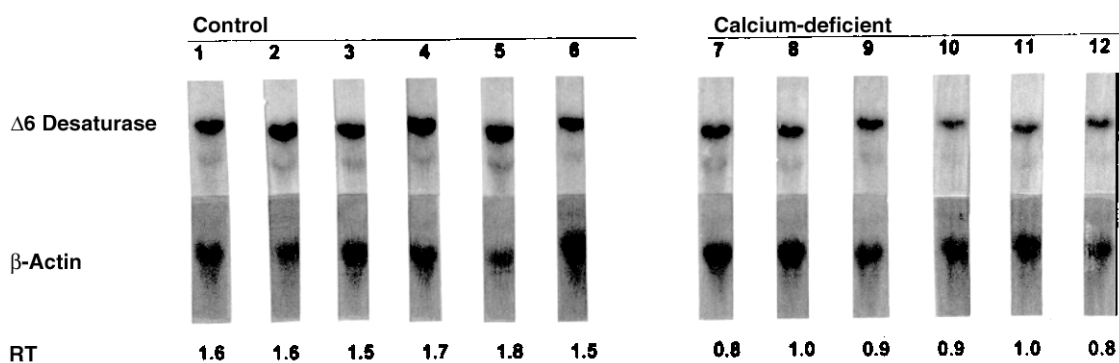
## DISCUSSION

From these results it is evident that calcium levels are, indeed, involved in FA metabolism, and that its deficiency evoked many alterations in several tissues from CaD rats. Taking into account that desaturases are key enzymes in FA metabolism, the main question arising from our findings is whether the analytical changes are the cause or the consequence of the altered desaturase activities. Several studies from this and other laboratories have extensively documented that alterations in desaturase activities, evoked by hormonal and/or dietary manipulations, are usually reflected in the acyl composition of cellular lipids (1,31-36). On the other hand, previous studies from our laboratory demonstrated that fasting and/or energy restriction profoundly modifies desaturase activities, and the gain in body weight is directly involved in this regulatory effect (31,32,37,38). It is generally accepted that desaturase activities determine the final FA profile of a tissue and, in turn, its particular lipid metabolism (31,32,34-36). As stated before, a modified desaturase activity can be ascribed to a change in the body weight gain under certain dietary conditions; therefore, subsequent alterations in the FA profile may be considered as a natural consequence of such a modification. However, in our experimental conditions changes ob-

**TABLE 10**  
Enzyme Activities<sup>a</sup> in Various Tissues from Control (S) or Calcium-Deficient (CaD) Rats

Microsome source	Treatment	Desaturase activities <sup>a</sup>			Phospholipase A <sub>2</sub> <sup>b</sup>	Acyl-CoA-synthetase <sup>c</sup>
		$\Delta 9$ (16:0)	$\Delta 5$ (20:3)	$\Delta 6$ (18:2)		
Brain	S	16 ± 1	23 ± 2	15 ± 2	3,112 ± 124	27.6 ± 0.9
	CaD	ND*	Trace*	ND*	3,410 ± 137	33.3 ± 1.5
Kidney	S	25 ± 3	34 ± 3	26 ± 4	7,241 ± 153	40.1 ± 2.6
	CaD	ND*	8 ± 2*	ND*	2,099 ± 111*	53.2 ± 1.9*
Lung	S	31 ± 3	16 ± 1	18 ± 3	2,114 ± 85	43.4 ± 2.8
	CaD	ND*	Trace*	Trace*	1,309 ± 94*	69.7 ± 3.2*
Heart	S	31 ± 4	48 ± 2	55 ± 3	2,485 ± 76	54.1 ± 3.0
	CaD	ND*	40 ± 3	49 ± 4	2,102 ± 127	57.7 ± 2.5
Liver	S	168 ± 7	402 ± 11	205 ± 12	3,501 ± 143	148.7 ± 3.9
	CaD	96 ± 5*	237 ± 8*	111 ± 9*	686 ± 75*	256.1 ± 4.4*
Spleen	S	15 ± 1	19 ± 3	17 ± 2	1,609 ± 90	29.8 ± 0.7
	CaD	ND*	Trace*	ND*	1,051 ± 107*	54.6 ± 1.4*

<sup>a</sup>Results are expressed as <sup>a</sup>pmol of substrate transformed/min-mg protein, <sup>b</sup>dpm/mg protein, or <sup>c</sup>nmol/min-mg protein. Data are given as the mean ± 1 SEM of four independent determinations performed on samples randomly selected from both experimental groups, whether S or CaD. \*Significantly different with respect to the corresponding control value ( $P < 0.01$ ). For technical details see the Materials and Methods section. Trace, below 5 pmol/min/mg protein; ND, nondetectable amount.



**FIG. 3.** Amount of mRNA of  $\Delta 6$  desaturase from livers of S and CaD rats as measured by blot hybridization. Total mRNA isolated from livers was processed independently and subjected to electrophoresis in 1% formaldehyde gel. Blot hybridization was performed as described in the text with the indicated  $^{32}\text{P}$ -labeled probe. The amount of radioactivity in each band was quantified and normalized by means of an image analysis software system. "RT" indicates the relative content of mRNA for  $\Delta 6$ -desaturase gene with respect to the mRNA for  $\beta$ -actin; the latter was chosen to normalize the results for loading differences. Individual ratios are shown below each blot. Means  $\pm$  1 SEM were  $1.62 \pm 0.12$  and  $0.93 \pm 0.06$  for S and CaD rats, respectively. For abbreviations see Figure 1.

served in both the FA profile of several tissues (Tables 2 to 5) and the activities of the desaturase enzymes (Table 10) can be ascribed to calcium deprivation (Table 1) rather than to a difference in food intake (Fig. 1) and/or body weight gain (Fig. 2) between CaD and S rats. Dietary calcium is known to make calcium soaps with FA in the gut, resulting in increased excretion of dietary fats. In the CaD diet group, fat absorption can be expected to be greater than in the S group, thus providing another possible mechanism for the observed differences in tissue FA composition. However, we think the diet employed in our experiments contained standard (normal) amounts of lipids, as previously demonstrated (7). If the phenomenon of low fat absorption plays a particular role in the changes we observed, the analytical and enzymatic modifications would be expected to result from a general lack of availability of calories from fat (or a simultaneous depletion in saturated FA and PUFA as diet precursors). On the contrary, our observations suggest a PUFA deficiency with a selective depletion of FA keeping constant the ratio (n-3)/(n-6). Moreover, previous works from this and other laboratories have demonstrated that low-fat diets evoked a stimulation of  $\Delta 9$ - and  $\Delta 6$ -desaturase activities rather than an inhibition (32,39,40).

Previous experiments clearly demonstrated that the regulatory step in the desaturation mechanism is located at the level of the desaturase protein itself (41,42). Additional evidence from our laboratory led us to discard, rather confidently, a direct effect of calcium ions on the desaturase enzyme itself or on another component involved in the transport of electrons to the terminal component of the desaturase system (1). At present, no experimental evidence that relates to the possible role of a calcium as a desaturase cofactor and/or any other function of this cation as an essential component during the catalytic process has been presented. The results of our previous experiments, performed on the  $\Delta 9$  and  $\Delta 5$  liver microsomal desaturase activities in CaD rats, also led us to discard the idea of the involvement of a soluble (cytosolic) factor or of a problem related to the activation of the substrate

by acylation to CoA-SH (1). Moreover, in the present study we found a significant increase in the acyl-CoA synthetase activity in various tissues from CaD rats (Table 10) in which desaturase activities were simultaneously depressed. A similar conclusion was obtained in the case of the acyl-CoA synthetase activity from livers of CaD rats (1,4). From these considerations, it seems that the effect of calcium deficiency on the desaturase activities may result from an indirect modification that would be produced through a common metabolic disturbance that involves the three desaturase systems we have studied.

The CaD diet clearly induced important modifications in the quality and/or quantity of the FA chains acylated to neutral and polar lipid fractions from microsomal membranes of several tissues (Tables 2 to 5). These changes were closely related to the measured Ca level in tissues (Table 1), and they were observed even in tissues with FA profiles generally considered very stable, such as brain (Table 2) and cartilage (Tables 4 and 5), in which there is not much metabolic diversity owing to their very specialized functions. They were also reflected, though in minor extension, in lipids from erythrocyte ghosts and plasmas from CaD rats (Table 6). Calculations made from the analytical data demonstrated in general that these changes are characterized by an increased saturated FA proportion and a significant decrease in PUFA and DBI (Table 7). All the analytical parameters calculated for the estimation of the metabolic conversion of the saturated and unsaturated FA precursors (29,30) suggest a general loss of desaturation capacity in microsomes from CaD rats (Table 7). In all the tissues studied from CaD rats, we found a significant decrease in the membrane packing order with respect to S rats that was closely associated with several changes in the interlipid and lipid/protein ratios (Tables 8 and 9). It is generally accepted that the main factors that determine the fluidity of membrane lipids are the cholesterol/phospholipid molar ratio and the degree of unsaturation of the phospholipid acyl chains (43–45). In relation to this, the proportion of cholesterol—usually associated with a diminished membrane

fluidity—was significantly reduced in CaD rats with respect to S ones (1,2; Tables 8 and 9). We also found a decrease in those indices determined by the PUFA and DBI. The data presented in Tables 2 to 7 compared to those from Tables 8 and 9 may indicate an apparent contradiction since the CaD condition caused a large decrease in PUFA and an increase in saturated FA, while acyl packing order decreased as a result.

As is well known, the cholesterol/phospholipid ratio, together with DBI values, is the main determinant of acyl chain packing order in membranes (41–43). Tables 8 and 9 show a significant decrease in  $r_s$  values that directly correlates with a decrease of more than 40% in the cholesterol/phospholipid ratio. Apparently, two different changes in membrane composition produce opposite effects on acyl chain packing order: One of them decreases this physicochemical parameter and the other one increases it. The resulting DPH data show that the reduction in cholesterol drives the change measured in the packing state of the membrane. Previous work has documented that, in microsomes from animals fed a fat-deficient diet, the common feature is a depletion in the FA derived from the precursor linoleic and  $\alpha$ -linolenic acids (46,47). The physicochemical state of the membrane is well-known as a key question in determining the activities of the desaturase systems (31,32,41,48–51). As was previously suggested (52), an increased fluidity leads to a depletion in PUFA biosynthesis, and vice versa. This is one aspect of a general regulatory mechanism that controls several membrane functions and that has been designated “viscotropic regulation” (47,52).

Additional experimental support for a central role of the decreased desaturase activities in the effects evoked by calcium deprivation was obtained by determining the transcriptional rate of the mRNA that encodes for rat liver  $\Delta 6$ -desaturase enzyme. In recent reports by Kan *et al.* (53) and Xing and Insel (54), it was demonstrated that a calcium increase in cytosol gives rise to the release of arachidonic acid into the nucleus by means of phospholipase  $A_2$  translocation to the nuclear envelope. This fact is related to the stimulated transcription of desaturase genes described by Landschulz *et al.* (55). Thus, a decrease in calcium availability would imply a reduced transcription rate of FA desaturase from CaD rats.

We think that at least two different mechanisms leading to the same biochemical effect exist. In one, calcium deprivation in rats evoked an important alteration in acylation/deacylation cycles through the inhibition of the calcium-dependent phospholipase  $A_2$ . This primary effect results in a significant modification of the physicochemical properties of the microsomal membranes that, in turn, leads to a subsequent inhibition of the desaturase activities by viscotropic effect. In the other postulated mechanism, deprivation of calcium leads to a general failure in the transcriptional rate for the corresponding FA desaturase mRNA. As a result of these two mechanisms, the modifications in the analytical FA pattern and membrane composition would be the consequence of the adaptation to the CaD condition, which seems to be of general influence rather than limited to a central organ such as liver.

The relationship between FA metabolism in humans and calcium deprivation was recently reviewed (56). Especially in elderly people, calcium loss is related to altered membrane functions and several changes in lipid composition (57). Although this field of study has received some attention during recent years, we think that the interactions between FA metabolism and calcium availability deserve more investigation since they offer novel approaches for understanding human illnesses of increasing incidence such as osteoporosis (56).

## ACKNOWLEDGMENTS

The authors are grateful to Norma Cristalli for her excellent technical assistance. This study was supported in part by grants from CONICET, Agencia Nacional de Promoción Científica y Tecnológica, and Comisión de Investigaciones Científicas, Argentina.

## REFERENCES

1. Marra, C.A., and Alaniz, M.J.T. de (2000) Calcium Deficiency Modifies Polyunsaturated Fatty Acid Metabolism in Growing Rats, *Lipids* 35, 983–990.
2. Huang, Y.S., McAdoo, K.R., Mitchell, J., and Horrobin, D.F. (1983) Effects of Calcium Deprivation on n-6 Fatty Acid Metabolism in Growing Rats, *Biochem. Med. Metab. Biol.* 40, 61–67.
3. Bierenbaum, M.L., Fleischman, A.I., and Rachelson, R.I. (1972) Long-Term Human Studies on the Lipid Effects of Oral Calcium, *Lipids* 7, 202–206.
4. Marra, C.A., and Alaniz, M.J.T. de (1999) Acyl-CoA Synthetase Activity in Liver Microsomes from Calcium-Deficient Rats, *Lipids* 34, 343–354.
5. Alto, L., and Dhalla, N.S. (1979) Myocardial Cation Contents During Induction of Calcium Paradox, *Am. J. Physiol.* 237, H713–H719.
6. Reeves, P.G., Nielsen, F.H., and Fahey, G.C., Jr. (1993) AIN-93 Purified Diets for Laboratory Rodents: Final Report of the American Institute of Nutrition *ad hoc* Writing Committee on the Reformulation of the AIN-76A Rodent Diet, *J. Nutr.* 123, 1939–1951.
7. National Research Council (1985) *Guide for the Care and Use of Laboratory Animals*, Publication No. 85-23 (rev.), National Institutes of Health, Bethesda, MD.
8. Marra, C.A., Alaniz, M.J.T. de, and Brenner, R.R. (1986) Modulation of  $\Delta 6$  and  $\Delta 5$  Rat Liver Microsomal Desaturase Activities by Dexamethasone-Induced Factor, *Biochim. Biophys. Acta* 879, 388–393.
9. Dodge, J.T., Mitchell, C., and Hanahan, D.J. (1963) The Preparation and Chemical Characteristics of Hemoglobin-Free Ghosts of Human Erythrocytes, *Arch. Biochem. Biophys.* 100, 119–130.
10. Berlin, E., Bhathara, S.J., Judd, J.T., Nair, P.P., Jones, D.Y., and Tayler, P.R. (1989) Dietary Fat and Hormonal Effects on Erythrocyte Membrane Fluidity and Lipid Composition in Adult Women, *Metabolism* 8, 790–796.
11. Marra, C.A., Mangioni, J.O., Tavella, M., Alaniz, M.J.T. de, Ortiz, D., and Sala, C. (1998) Hormonal-Induced Changes on the Lipid Composition and DPH-Fluorescence Anisotropy of Erythrocyte Ghosts from Pre- and Postmenopausal Women, *Acta Physiol. Pharmacol. Toxicol. Latinoam.* 17, 8–17.
12. Garda, H.A., Leikin, A.I., and Brenner, R.R. (1992) Determination of Fatty Acid Desaturase Activities by RP-HPLC, *An. Asoc. Quim. Argent.* 80, 365–371.
13. Marra, C.A., and Alaniz, M.J.T. de (1989) Influence of Testosterone Administration on the Biosynthesis of Unsaturated Fatty Acids in Male and Female Rats, *Lipids* 24, 1014–1019.
14. Folch, J., Lees, M., and Sloane Stanley, G.A. (1957) A Simple



- Method for the Isolation and Purification of Total Lipids from Animal Tissues, *J. Biol. Chem.* 226, 497–509.
15. Hanahan, D.J., Dittnar, J.C., and Warashima, E. (1957) A Column Chromatographic Separation of Classes of Phospholipids, *J. Biol. Chem.* 228, 685–690.
  16. Allain, C.C., Poon, L.S., Chen, C.S.G., Richmond, W., and Fu, P.C. (1974) Enzymatic Determination of Total Serum Cholesterol, *Clin. Chem.* 20, 470–475.
  17. Marra, C.A., and Alaniz, M.J.T. de (1990) Mineralocorticoids Modify Rat Liver  $\Delta 6$  Desaturase Activity and Other Parameters of Lipid Metabolism, *Biochem. Int.* 22, 483–493.
  18. Chen, P.S., Toribara, T.Y., and Warner, H. (1956) Microdetermination of Phosphorus, *Anal. Chem.* 33, 1405–1406.
  19. Hirata, F., Schiffmann, E., Venkatasubramanian, K., Salomon, D., and Exelrod, J. (1980) A Phospholipase A<sub>2</sub> Inhibitory Protein in Rabbit Neutrophils Induced by Glucocorticoids, *Proc. Natl. Acad. Sci. USA* 77, 2533–2536.
  20. Irazú, C.E., González-Rodríguez, S., and Brenner, R.R. (1993)  $\Delta 5$  Desaturase Activity in Rat Kidney Microsomes, *Mol. Cell. Biochem.* 129, 31–37.
  21. López Jiménez, J., Bordón, A., Hrelia, S., Rossi, C.A., Turchetto, E., Zamora Navarro, S., and Biagi, P.L. (1993) Evidence for a Detectable  $\Delta 6$ -Desaturase Activity in Rat Heart Microsomes: Aging Influence on Enzyme Activity, *Biochem. Biophys. Res. Comm.* 192, 1037–1041.
  22. Tanaka, T., Hosaka, K., Hoshimaru, M., and Numa, S. (1979) Purification and Properties of Long-Chain Acyl-Coenzyme-A Synthetase from Rat Liver, *Eur. J. Biochem.* 98, 165–172.
  23. Sambrook, J., Fritsch, E., and Maniatis, T. (1989) *Molecular Cloning: A Laboratory Manual*, Cold Spring Harbor Laboratory Press, New York.
  24. Lowry, O.H., Rosebrough, M.J., Farr, A.J., and Randall, R.J. (1951) Protein Measurement with the Folin Phenol Reagent, *J. Biol. Chem.* 193, 275–295.
  25. Shinitzky, M., and Barenholz, Y. (1974) Dynamics of the Hydrocarbon Layer in Liposomes of Lecithin and Sphingomyelin Containing Diacetylphosphate, *J. Biol. Chem.* 249, 2652–2657.
  26. Shinitzky, M., and Barenholz, Y. (1978) Fluidity Parameters of Lipid Regions Determined by Fluorescence, *Biochim. Biophys. Acta* 515, 367–394.
  27. Xu, H., Watkins, B.A., and Adkisson, H. (1994) Dietary Lipids Modify the Fatty Acid Composition of Cartilage, Isolated Chondrocytes and Matrix Vesicles, *Lipids* 29, 619–625.
  28. Cleland, K.A., James, M.J., Neumann, M.A., Gibson, R.A., and Cleland, L.G. (1995) Differences in Fatty Acid Composition of Immature and Mature Articular Cartilage in Humans and Sheep, *Lipids* 30, 949–953.
  29. Martínez, M., and Ballabriga, A. (1987) Effect of Parenteral Nutrition with High Doses of Linoleate on the Developing Human Liver and Brain, *Lipids* 22, 133–138.
  30. Lepage, G., Levy, E., Ronco, N., Galeano, N., and Roy, C. (1989) Direct Transesterification of Plasma Fatty Acids for Diagnosis of Essential Fatty Acid Deficiency in Gastric Fibrosis, *J. Lipid Res.* 30, 1483–1490.
  31. Brenner, R.R. (1981) Nutritional and Hormonal Factors Influencing Desaturation of Essential Fatty Acids, *Prog. Lipid Res.* 20, 41–48.
  32. Brenner, R.R. (1987) Polyunsaturated Fatty Acid Metabolism and Its Regulation, in *Recent Advances in Essential Fatty Acid Research* (Das, V.N., ed.), Vol. I, pp. 5–18, Academic Publication, Gandhinagar, India.
  33. Marra, C.A., and Alaniz, M.J.T. de (1997) Role of Calcium Ionophore and Phospholipase A<sub>2</sub> Inhibitors on the Fatty Acid Composition of Hepatoma Tissue Culture Cells and Lipid Secretion, *Med. Sci. Res.* 25, 59–62.
  34. Garg, M.L., Keelan, M., Thomson, A.B.R., and Clandinin, M.T. (1992) Desaturation of Linoleic Acid in the Small Bowel Is Increased by Short-Term Fasting and by Dietary Content of Linoleic Acid, *Biochim. Biophys. Acta* 1126, 17–25.
  35. De Antueno, R.J., Cantrill, R.C., Huang, Y.S., Elliot, M., and Horrobin, D.F. (1993) Relationship Between Mouse Liver  $\Delta 9$  Desaturase Activity and Plasma Lipids, *Lipids* 28, 285–290.
  36. Alaniz, M.J.T. de, and Marra, C.A. (1994) Role of  $\Delta 9$  Desaturase Activity in the Maintenance of High Levels of Monoenoic Fatty Acids in Hepatoma Cultured Cells, *Mol. Cell. Biochem.* 137, 85–90.
  37. Marín, M.C., De Tomás, M.E., Serres, C., and Mercuri, O. (1995) Protein–Energy Malnutrition During Gestation and Lactation in Rats Affects Growth Rate, Brain Development, and Essential Fatty Acid Metabolism, *J. Nutr.* 125, 1017–1024.
  38. Marín, M.C., and Alaniz, M.J.T. de (1998) Relationship Between Dietary Oil During Gestation and Lactation and Biosynthesis of Polyunsaturated Fatty Acids in Control and in Malnourished Dam and Pup Rats, *J. Nutr. Biochem.* 9, 388–395.
  39. Brenner, R.R. (1981) Nutritional and Hormonal Factors Influencing Desaturation of Essential Fatty Acids, *Prog. Lipid Res.* 20, 41–48.
  40. Sprecher, H. (1983) The Mechanism of Fatty Acid Chain Elongation and Desaturation in Animals, in *High and Low Erucic Acid Rapeseed Oil* (Kramer, J.D.G., Souer, F.D., and Pidgen, W.J., eds.), pp. 385–411, Academic Press, New York.
  41. Brenner, R.R., Garda, H., Leikin, A.I., and Pezzano, H. (1980) Effect of Temperature on the Structure of Rat Liver Microsomes Studied by Electron Spin Resonance, Fluorescence and Activity of Enzymes Involved in Fatty Acid Biosynthesis, *Acta Physiol. Latinoam.* 30, 225–238.
  42. Garda, H., and Brenner, R.R. (1982) Effect of Induced Phase Transitions on the Glucose-6-phosphate Activity and Electron Transport of Rat Liver Microsomes, *Acta Physiol. Latinoam.* 32, 31–52.
  43. Virtanen, J.A., Ruonala, M., Vauhkonen, M., and Sonerharju, P. (1995) Lateral Organization of Liquid-Crystalline Cholesterol-dimyristoylphosphatidylcholine Bilayers. Evidence for Domains with Hexagonal and Centered Rectangular Cholesterol Superlattices, *Biochemistry* 34, 11568–11581.
  44. Rietveld, A., and Simons, K. (1998) The Differential Miscibility of Lipids as the Basis for the Formation of Functional Membrane Rafts, *Biochim. Biophys. Acta* 1376, 467–479.
  45. Nagle, J.F., and Nagle, S.T. (2000) Structure of Lipid Bilayers, *Biochim. Biophys. Acta* 1469, 159–195.
  46. Mandon, E.C., Gómez Dumm, I.N.T. de, and Brenner, R.R. (1986) Effect of Dietary Columbinic Acid on the Fatty Acid Composition and Physical Membrane Properties of Different Tissues of EFA-Deficient Rats, *Arch. Latinoam. Nutr.* 36, 401–414.
  47. Soulages, J.L., and Brenner, R.R. (1989) Interactions Among Phospholipids of Guinea Pig Rough Microsomes, Effect of Fat Deficiency, *Mol. Cell. Biochem.* 90, 127–136.
  48. Garda, H.A., and Brenner, R.R. (1984) Short-Chain Aliphatic Alcohols Increase Rat-Liver Microsomal Membrane Fluidity and Affect the Activities of Some Microsomal Membrane-Bound Enzymes, *Biochim. Biophys. Acta* 769, 160–170.
  49. Garda, H.A., and Brenner, R.R. (1985) *In vitro* Modification of Cholesterol Content of Rat Liver Microsomes. Effects upon Membrane “Fluidity” and Activities of Glucose-6-phosphatase and Fatty Acid Desaturation Systems, *Biochim. Biophys. Acta* 819, 45–54.
  50. Leikin, A.I., and Brenner, R.R. (1987) Cholesterol-Induced Microsomal Changes Modulate Desaturase Activities, *Biochim. Biophys. Acta* 922, 294–303.
  51. Garg, M.L., Wierzbicki, A.A., Thomson, A.B.R., and Clandinin, M.T. (1988) Dietary Cholesterol and/or n-3 Fatty Acid Modulate  $\Delta^9$ -Desaturase Activity in Rat Liver Microsomes, *Biochim. Biophys. Acta* 962, 330–336.

52. Brenner, R.R. (1984) Effect of Unsaturated Acids on Membrane Structure and Enzyme Kinetics, *Prog. Lipid Res.* 23, 69–96.
53. Kan, H., Ruan, Y., and Malik, K.U. (1996) Involvement of Mitogen-Activated Protein Kinase and Translocation of Cytosolic Phospholipase A<sub>2</sub> to the Nuclear Envelope in Acetylcholine-Induced Prostacyclin Synthesis in Rabbit Coronary Endothelial Cells, *Mol. Pharmacol.* 50, 1139–1147.
54. Xing, M., and Insel, P.A. (1996) Protein Kinase C-Dependent Activation of Cytosolic Phospholipase A<sub>2</sub> and Mitogen-Activated Protein Kinase by Alpha 1-Adrenergic Receptors in Madin-Darby Canine Kidney Cells, *J. Clin. Invest.* 97, 1302–1310.
55. Landschulz, K.T., Jump, D.B., MacDougald, O.A., and Lane, M.D. (1994) Transcriptional Control of the Stearoyl-CoA Desaturase-1 Gene by Polyunsaturated Fatty Acids, *Biochem. Biophys. Res. Commun.* 200, 763–768.
56. Kruger, M.C., and Horrobin, D.F. (1997) Calcium Metabolism, Osteoporosis, and Essential Fatty Acids: A Review, *Prog. Lipid Res.* 36, 131–151.
57. Alisio, A., Canas, F., De Bronia, D.H., Pereira, R., and Tolosa de Talamoni, N. (1997) Effect of Vitamin D Deficiency on Lipid Composition and Calcium Transport in Basolateral Membrane Vesicles from Chick Intestine, *Biochem. Mol. Biol. Int.* 42, 339–347.

[Received January 8, 2002, and in final revised form July 1, 2002; revision accepted July 3, 2002]

# Positional and Geometric Isomer Separation of FAME by Comprehensive 2-D GC

Robert J. Western<sup>a</sup>, Sally S.G. Lau<sup>a</sup>, Philip J. Marriott<sup>a,\*</sup>, and Peter D. Nichols<sup>b</sup>

<sup>a</sup>Australian Centre for Research on Separation Science, Department of Applied Chemistry, RMIT University, Melbourne, Victoria 3001, Australia, and <sup>b</sup>Commonwealth Scientific and Industrial Research Organisation (CSIRO) Marine Research, Hobart, Tasmania, Australia

**ABSTRACT:** The technique of comprehensive GC (GC × GC) was applied to the analysis of a standard mixture of FAME. The methodology involved the use of two directly coupled capillary GC columns providing different retention mechanisms, with a pulsing modulator located near their union. The first column was chosen to elute analytes based on b.p. variations, and the second column was based on polarity. Thus, the separation in the two dimensions was orthogonal, since solutes delivered simultaneously to the second column had similar b.p., and the second column separated these primarily on their differentiating mechanisms of polarity. Greater sensitivity of detection and narrower peak widths were obtained; here, peak response increases of about 20-fold were obtained, with pulsed peak widths of about 150 ms. Peaks were displayed in a 2-D contour plot to allow the complexity of the compounds to be seen and their b.p. and polarity properties to be readily recognized. Chromatographic separation of geometric and positional isomers of FAME in the 2-D space is possible. Since retention can be related to the degree and manner of unsaturation and isomerization, and as peak positions are highly reproducible in the 2-D retention map, this is a useful aid for component identification in the absence of appropriate standards. In this work, two column combinations were used to examine the effects of polarity changes on component separation. Improved quantitation based on FID area measurement was demonstrated. A sample of marine oil gave 49 resolved, identified peaks, with at least an additional 20 peaks resolved but not identified.

Paper no. L8946 in *Lipids* 37, 715–724 (July 2002).

For dietary, nutritional, and therapeutic reasons, the analysis of FA contained in animal fats and vegetable and other oils has been of considerable interest for some time (1). Analysis of these carboxylic acids has generally been achieved by the formation of the FAME, followed by GC separation and identification. Maximizing the efficiency of separation is now required because of the increasing awareness that these individual compounds may play an important role in human and animal health and because of the structural significance of the compounds. Complex samples comprising components of similar physicochemical properties may make complete reso-

lution difficult or impossible. The need to separately identify individual FAME must therefore increasingly rely on the use of the highest-resolution separation methods available. The ability to separate and uniquely identify such isomers in complex samples is a basic requirement to support their accurate quantitation.

FAME are relatively simple to prepare by established methods, their elution temperatures are lower than the underivatized FA, their GC elution characteristics are more favorable, and a large body of retention index data is available. GC separation of FAME geometric and positional isomers by utilizing the subtle differences between these compounds and specific solute/stationary phase interaction is possible to some degree, but rarely will all peaks be resolved to baseline (2) even when exceedingly long, highly polar (100 m CP Sil 88) columns are used. The increased length requires slow programming rates (<1°C/min) for maximum efficiency; consequently, analysis times are longer. An added complication is that the polar columns required for single-dimension separation can cause the polyunsaturated FAME (PUFA) to elute at similar times as the more saturated higher-M.W. FAME (3), requiring higher resolution (longer columns and slower temperature programming) than would otherwise be necessary (2–6). This increases the complexity of component identification. Good component separation through increased chromatographic column length also enhances identification of components using the retention index.

The most effective (precise and accurate) analysis of any mixture using chromatographic techniques arises when all relevant components are fully resolved from both the other analytes of interest and matrix interferences. In order to minimize the effects of the latter, it is often necessary to perform complex sample cleanup, often decreasing the PUFA yield or recovery.

Multidimensional GC may offer a solution to the resolution and time limitations imposed by single-column analysis, but it cannot be readily applied to an analysis of the total sample. However, the comprehensive 2-D GC (GC × GC) method overcomes this limitation, and a complete 2-D resolution map of a sample may be realized. The present report investigates the possibilities of using GC × GC to maximize the separation efficiency by molecular size, degree of unsaturation, and positional and geometric isomerization of FAME through the significant increase in resolution that can be obtained by using this technique. Furthermore, chemical properties may be deduced from the position of the components in the 2-D separa-

\*To whom correspondence should be addressed at Australian Centre for Research on Separation Science, Department of Applied Chemistry, RMIT University, GPO Box 2476V, Melbourne, Victoria 3001, Australia. E-mail: philip.marriott@rmit.edu.au

Abbreviations: D1, dimension 1; D2, dimension 2;  $d_f$ , film thickness; GC × GC, comprehensive 2-D GC; LMCS, longitudinally modulated cryogenic system.

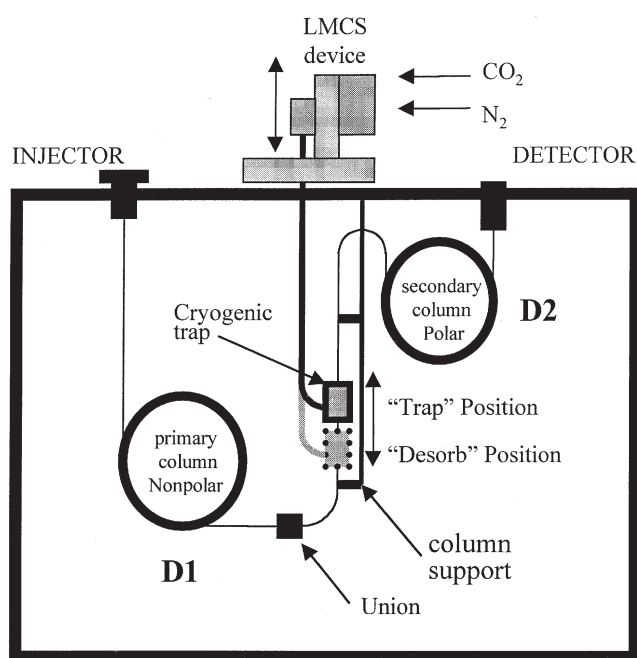
tion, where the location of a compound in the 2-D space may be related to structural features of the molecule. The standard mixtures examined were chosen to demonstrate the application of this technique. Use of a marine oil illustrates the possibilities of the method for complex sample analysis.

## MATERIALS AND METHODS

**Gas chromatography.** All GC analyses were performed on an Agilent 6890 gas chromatograph (Agilent Technologies, Little Falls, DE) equipped with a split/splitless injector, an Agilent 6890 autosampler, and an FID. The data collection rate from the FID was performed at 20 Hz for “normal” GC and either at 100 or 200 Hz for GC  $\times$  GC studies. Chromatographic analyses used a single-temperature program ramp. Hydrogen carrier gas was used at an initial nominal pressure of 100 kPa, and pressure was programmed to maintain a constant average linear velocity. Two column sets were used: column set 1: 30 m  $\times$  0.25 mm i.d.  $\times$  0.25  $\mu$ m film thickness ( $d_f$ ) BPX5 (5% phenyl-equivalent polysilphenylene phase) coated column connected to a 0.8 m  $\times$  0.1 mm i.d.  $\times$  0.1  $\mu$ m  $d_f$  BP20 (polyethylene glycol phase) column. Column set 2: 25 m  $\times$  0.22 mm i.d.  $\times$  0.2  $\mu$ m  $d_f$  BP1 (100% polydimethylsiloxane) coated column connected to a 1.0 m  $\times$  0.1 mm i.d.  $\times$  0.2  $\mu$ m  $d_f$  BPX70 (cyanopropyl polysilphenylene—equivalent to 70% cyanopropyl siloxane). All columns were obtained from SGE International (Ringwood, Victoria, Australia). Temperature program conditions are given in figure legends.

**Description of cryogenic modulation and the GC  $\times$  GC technique.** GC  $\times$  GC is a relatively new technique (7,8), in which effluent from a primary analysis column (dimension 1, or D1) is compressed and/or pulsed as a narrow “re-injection” band onto a second column (dimension 2, or D2). For most applications, the primary column is a conventional nonpolar b.p. separation column, with solutes separated based on dispersion forces. The second column is chosen for its ability to separate those overlapping components from D1 that show differences in D2 sufficient to afford separation. Each re-injection step gives an individual chromatogram on the second column, normally of a few seconds duration, and each of these is contiguous with its neighboring pulsed chromatogram. Since the primary column separation is carried out on a nonpolar phase, the elution temperature is lower than would be expected on a polar column. This aids in extending the molar mass analysis range, since the maximal operating temperature is largely controlled by the upper temperature limit of the polar (second) column. The short second column does not add significantly to the total retention.

Scheme 1 is a diagram of the GC  $\times$  GC arrangement incorporating a longitudinally modulated cryogenic system (LMCS, Everest model; Chromatography Concepts, Doncaster, Australia) (9). A variety of applications of the technique have been reported (10–16). A cryotrap is mounted inside the oven around one of the columns (normally D2) near the union connecting D1 and D2. Expanding liquid CO<sub>2</sub> is used to cool the trap to approximately 100°C or more less than the oven temperature.



SCHEME 1

The movement of the trap is initiated by Agilent Chemstation software. The trap can be moved between the “trap” and “release” (desorb) positions in one of two modes. The most commonly used is the “modulation” mode, where, after a predetermined time, the sequence is initiated by the external events controller of the Agilent Chemstation. The trap then moves in an accurately controlled repetitive sequence of alternate trapping and releasing. Modulation can be varied from 1.5 to 9.9 s in steps of 0.1 s. A 3-s modulation period was used for all GC  $\times$  GC chromatograms in this research. Targeted trapping is an alternative mode. Here, each step is directly controlled by the Chemstation event controller. This mode maximizes solute sensitivity, because an individual component can be completely trapped (zone compressed) into a single cryogenic event before being released as a single narrow band onto the second column. This mode can also be used to determine absolute D2 retention time. Data processing of the resultant digital data stream is detailed elsewhere (16). The GC  $\times$  GC result is effectively a 2-D plot of b.p. separation in one (horizontal) dimension and polarity separation in the (vertical) second. The nonpolar/polar column arrangement allows coeluting solutes (of different polarities) on D1 to be separated by polar interactions on D2. The converse arrangement would mean that coeluting solutes of different polarities would then have to be separated on a nonpolar D2 column, which is less easily achieved.

Refocusing the solute stream near the end of the column set results in zone-compressed components whose sensitivity is significantly increased over the corresponding conventional, single-column analysis. This is a major benefit of the cryogenic modulation process used here (17). The dimensions of D2 must be chosen to complete each individual D2 separation in a relatively few (e.g., one or two) modulation cycles. D1 dimensions and operating conditions are similar to those



of normal single-capillary GC analysis. The D2 column is usually a short, narrow bore column of a thin stationary phase coating operating under fast, pseudo-isothermal conditions. It may be considered isothermal because of the short analysis time compared to the oven ramp rate (i.e., the temperature increment may be only 0.2°C for a 4-s elution time on D2 with a temperature program of 3°C/min).

de Geus *et al.* (18) showed the feasibility of characterizing FAME by 2-D GC. This group used a thermal sweeper modulator to resolve the analytes in FA mixtures contained in fish and vegetable oils. Separation of linear saturated and unsaturated compounds by size, degree of unsaturation, and positional isomerization was shown.

The cryotrapping modulation mechanism is shown in Scheme 2. With the cryomodulator resting in the trap position, solute molecules traveling in the carrier gas encounter the cooled zone and are sorbed in or on the stationary phase as a narrow band (Scheme 2A).

Movement of the trap a sufficient (short) distance along the column to its desorb position (Scheme 2C) causes it to pass over the trapped solutes (Scheme 2B). It travels far enough to clear the trapping section of the column, with that section now raised to the prevailing oven temperature through the forced air flow of the oven, and the trapped solute(s) are then remobilized (Scheme 2C). The bandwidth of the solute (when remobilized) at this point is estimated to be approximately 15 ms, and the trapped solute zone will be of the order of mm length.

At Scheme 2C, any solute that reaches the cooled section of column while the trap is in the desorb position condenses out into a narrow band at this new trap position. As the trap moves back to the start position (Scheme 2D), the condensed solute is again mobilized, moving with the carrier gas until it recondenses, along with any additional incoming solute,

ready for release in the next cycle (Scheme 2E). The process is repeated continually (modulation) or as required (targeted) over the required time segment of the chromatogram.

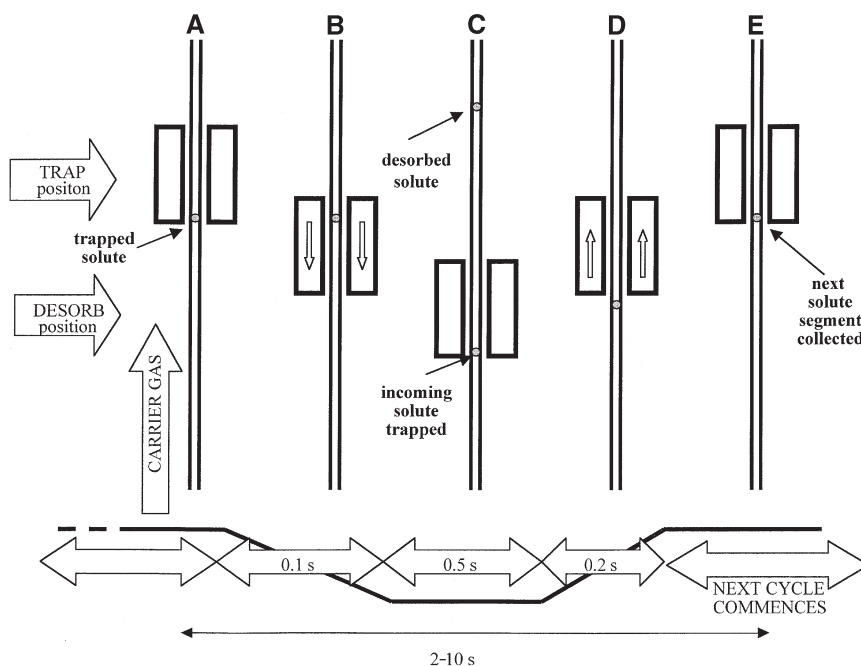
**Standards and sample.** All studies were carried out using the commercially available FAME mixture GLC 87 supplied by Nu-Chek-Prep Inc. (Elysian, MN) as pure standard material to aid in technique development. The GLC 87 mixture contains saturated and unsaturated FAME and a range of  $C_{16}$ ,  $C_{18}$ ,  $C_{20}$ ,  $C_{22}$ , and  $C_{24}$  mono- and polyunsaturated FAME. The concentration (by mass) of each compound present was as follows: 12:0 (3.0%); 13:0 (3.0%); 14:0 (3.0%); 15:0 (3.0%); 16:0 (18.5%); 17:0 (1.0%); 18:0 (6.5%); 19:0 (0.5%); 20:0 (0.5%); 22:0 (1.2%); 14:1n-5 (0.5%); 16:1n-7 (1.5%); 16:1n-7*t* (0.5%); 18:1n-9 (16.0%); 18:1n-9*t* (2.0%); 18:2n-6 (23.0%); 18:2n-6*t,t* (3.0%); 18:3n-3 (3.0%); 18:3n-6 (0.5%); 20:1n-9 (0.4%); 20:3n-3 (0.5%); 20:3n-6 (1.5%); 20:4n-6 (5.0%); 22:1n-6 (0.4%); 22:2n-6 (0.5%); 22:6n-3 (1.0%); 24:1n-9 (0.5%). The FAME mixture was diluted with analytical grade acetone and injected using split injection with a suitable split ratio.

The marine oil (blue mussel)-derived FAME sample was prepared by using standard procedures (19).

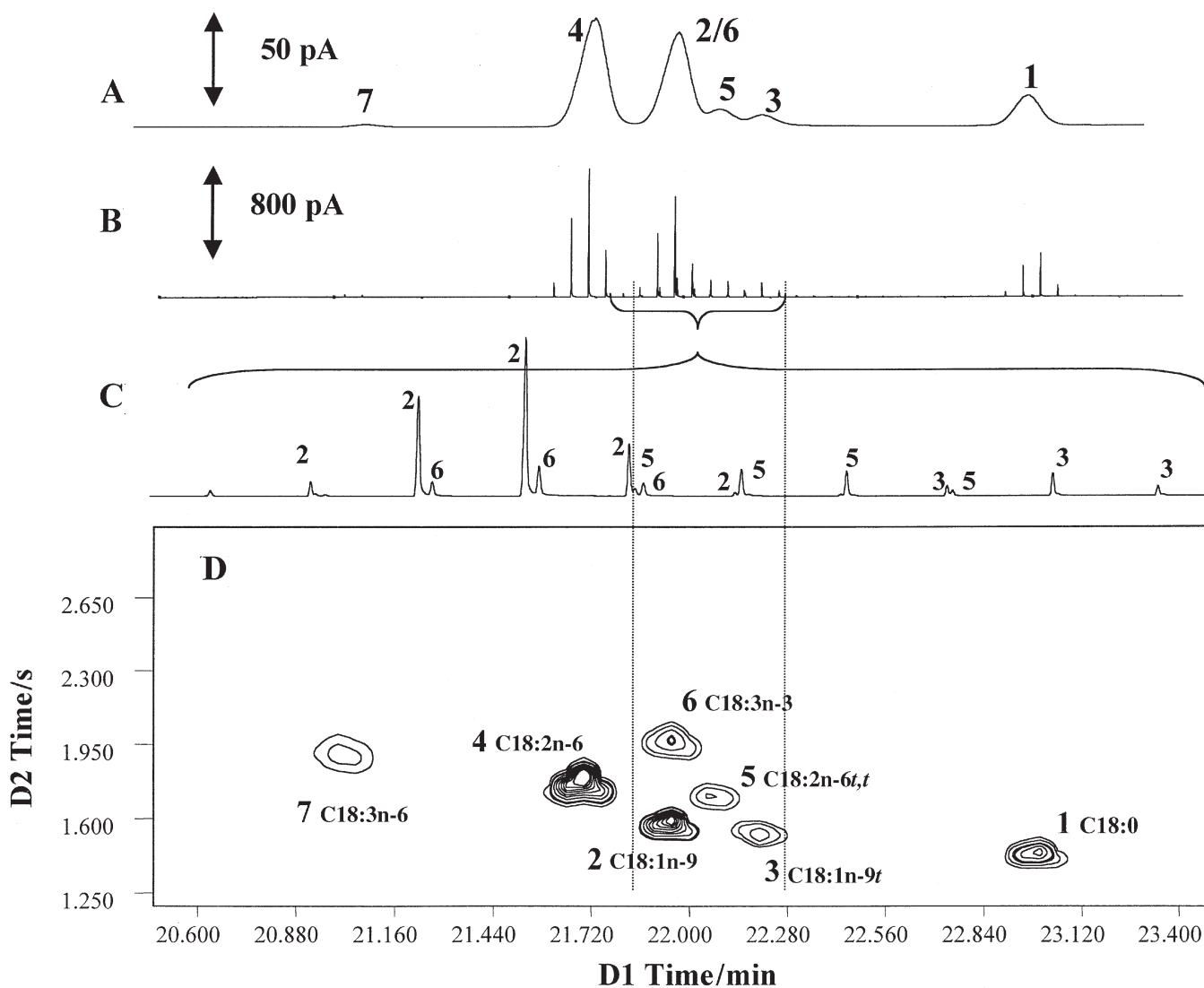
## RESULTS AND DISCUSSION

In this study, the interpretation of isomeric separations focused on the  $C_{18}$  and  $C_{20}$  FAME present in the mixture. The  $C_{18}$  region comprised the seven components 18:0, 18:1n-9, 18:1n-9*t*, 18:2n-6, 18:2n-6*t,t*, 18:3n-3, and 18:3n-6, having different degrees of unsaturation. The  $C_{20}$  region comprised 20:0, 20:1n-9, 20:3n-3, 20:3n-6, and 20:4n-6.

**BPX5/BP20 column set. (i)  $C_{18}$  region.** Figure 1 shows results of the  $C_{18}$  region obtained with column set 1. Figure 1A is a normal GC analysis obtained on the two-column set with-



SCHEME 2



**FIG. 1.** Comparative chromatograms of  $C_{18}$  FAME on column set 1. (A) Normal GC; (B) modulated GC  $\times$  GC chromatogram; (C) expanded region of (B); (D) GC  $\times$  GC 2-D contour plot. (A), (B), and (D) are aligned by dimension 1 (D1) retention times. The temperature program was 150 to 250°C at 2°C/min at a constant flow rate of 1.2 mL/min. The detector and injector temperatures were 260 and 250°C, respectively. A split ratio of 100:1 and a modulation period of 3 s were used. D2, dimension 2.

out using the modulator and shows a chromatogram with only three well-resolved peaks over the 20.50–23.50-min elution region; significant peak overlaps were observed with only six distinct peak maxima seen. Peak widths ( $4\sigma$ ) of about 9 s wide and maximal peak response of about 63 pA were observed. Figure 1B is the same sample run under the same conditions but with the modulator,  $CO_2$  coolant, and nitrogen shield gas operating. Peak widths are now about 0.14 s, and the height of the maximal pulse is 1370 pA (about 20 $\times$  taller than its normal GC peak response). Comparison of the two figures shows a similar overall peak profile; however, each compound in the modulated chromatogram (Fig. 1B) is now a sequence of about five pulses. Figures 1A, B, and D are arranged so that the peaks are aligned vertically, whereas Figure 1C shows an expansion of peaks 2, 3, 5, and 6 to illustrate the successive pulsed D2 chromatograms that eventually formed the 2-D contour plot.

Figure 1D shows a 2-D presentation of the GC  $\times$  GC chromatogram in the  $C_{18}$  region. All seven components are fully resolved; their individual presence is quite clearly seen on the 2-D contour plot. The full separation of these compounds took only 2.2 min in the first dimension, and 0.3 s in the second.

Manipulating the contour plot parameters can often disclose hidden peaks, as can varying the scaling contour. If the contour baseline used for peak plotting is too high, some partial overlap of peaks may be concealed. FAME with greater unsaturation, being more polar, appear with longer retention times in the second dimension. Increased resolution in the first (time-determining) dimension is only required for improved selectivity of positional isomers. The 18:1 component set here is simpler than might be present in regular samples, and as complexity increases, improvements in chromatography are required. An increase in the D2 column length would be sufficient to achieve this.

Figure 2 is the 2-D contour plot of the complete GLC 87 mixture, where complete separation of this mixture was achieved in 40 min. As an indication of the amount of separation required for high PUFA separation, the difference in D2 retention times between 22:0 and 22:6n-3 was approximately 1 s. Increased sample complexity, requiring an increase in D2 resolution, can be achieved by increasing the D2 column length.

Concentrations of the compounds in the original mixture are known, so it is possible to identify the positions of the various  $C_{18}$  isomers in the 2-D space based on their relative peak areas. Peak relative retentions were otherwise supported by GC-MS data using a column similar to that for GC analyses. Thus, the peaks in Figure 1 were identified (as shown in Table 1). For GC  $\times$  GC, peak abundances showed excellent correlation with expected amounts, where the summed areas of peak pulses for each component were compared with the total peak areas for all FAME. Component 6 was not observed as a separate peak in the normal GC analysis, so it could not be quantified. Likewise, some component areas were determined by peak skimming or vertical line drops at peak valleys. These could have led to the inaccurate peak area assignments noted. Where peaks were clearly individual components, GC  $\times$  GC and normal GC gave equivalent peak area percentage results in the present application.

(ii)  $C_{20}$  region. A similar comparison may be made for the  $C_{20}$  region. The unmodulated chromatogram gave peaks about 9.1 s wide ( $4\sigma$ ) and were of reasonably low response (*ca.* 12 pA). Run under modulated conditions, each peak was again a sequence of about five to six pulses, with the expected increases in peak height. Figure 3 shows the 27.5–31.0 min (the  $C_{20}$ ) region, with two separate sets of peak pulses (marked a and b) eluting between 29.5 and 29.9 min. Note that while their D1 retention time is the same, they are well separated in the D2 dimension. The 20:1/20:3n-3 peaks are located in a relative relationship in the 2-D space similar to that shown for 18:1/18:3n-3, suggesting that the relative location of peaks in the 2-D space may be correlated with molecular structure.

(iii) Homologous series trend and unsaturation retention trend. Figure 4 illustrates elution positions in the 2-D space, related by trends in degree of unsaturation (or iso-structural) lines and structure variation for FAME of particular carbon numbers. Positions enclosed by oval zones superimposed on the plot are similar to the lines proposed by de Geus *et al.* (18). Based on this model, it should be possible to identify, to a first approximation, the structure of other FAME eluting elsewhere in the chromatogram. Thus, on Figure 4 the curved lines refer to the trend in homologous series, with  $C_x$  representing the chain length and  $y$  showing an undifferentiated variable (at this

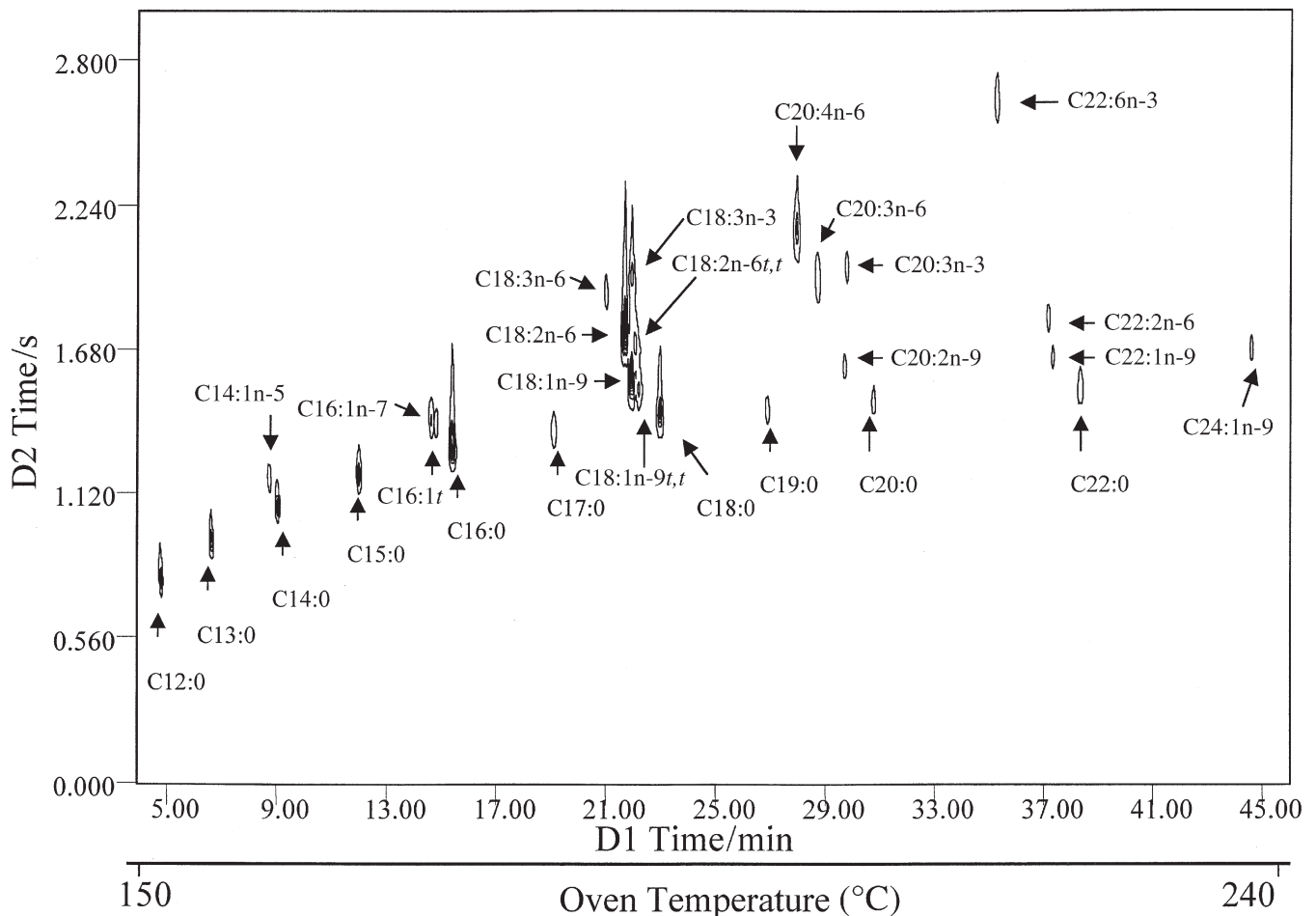


FIG. 2. 2-D contour of GLC 87 FAME mixture (Nu-Chek-Prep, Elysian, MN) under conditions given in Figure 1. For abbreviations see Figure 1.

**TABLE 1**  
**Identification of C<sub>18</sub> Peaks Using Relative Peak Areas<sup>a</sup>**

Peak	GC × GC peak area (pA·s) <sup>b</sup>	Concentration (% by mass) <sup>c</sup>	Expected (% mass)	Peak identity	Normal GC peak area (pA·s) <sup>d</sup>	Mass <sup>e</sup> (%)
1	101.0	6.7	6.5	18:0	96.4	6.5
2	248.4	16.5	16.0	18:1n-9	296.2	20.0
3	32.3	2.1	2.0	18:1n-9 <i>t</i>	34.1	2.3
4	355.7	23.7	23.0	18:2n-6	348.2	23.5
5	47.3	3.1	3.0	18:2n-6 <i>t,t</i>	46.6	3.1
6	47.4	3.1	3.0	18:3n-3	NQ <sup>e</sup>	NQ <sup>e</sup>
7	8.03	0.53	0.5	18:3n-6	7.1	0.5
Total	840.1				828.6	

<sup>a</sup>Refer to Figures 1A and 1B.

<sup>b</sup>GC × GC results giving sum of all pulses (Fig. 1B results).

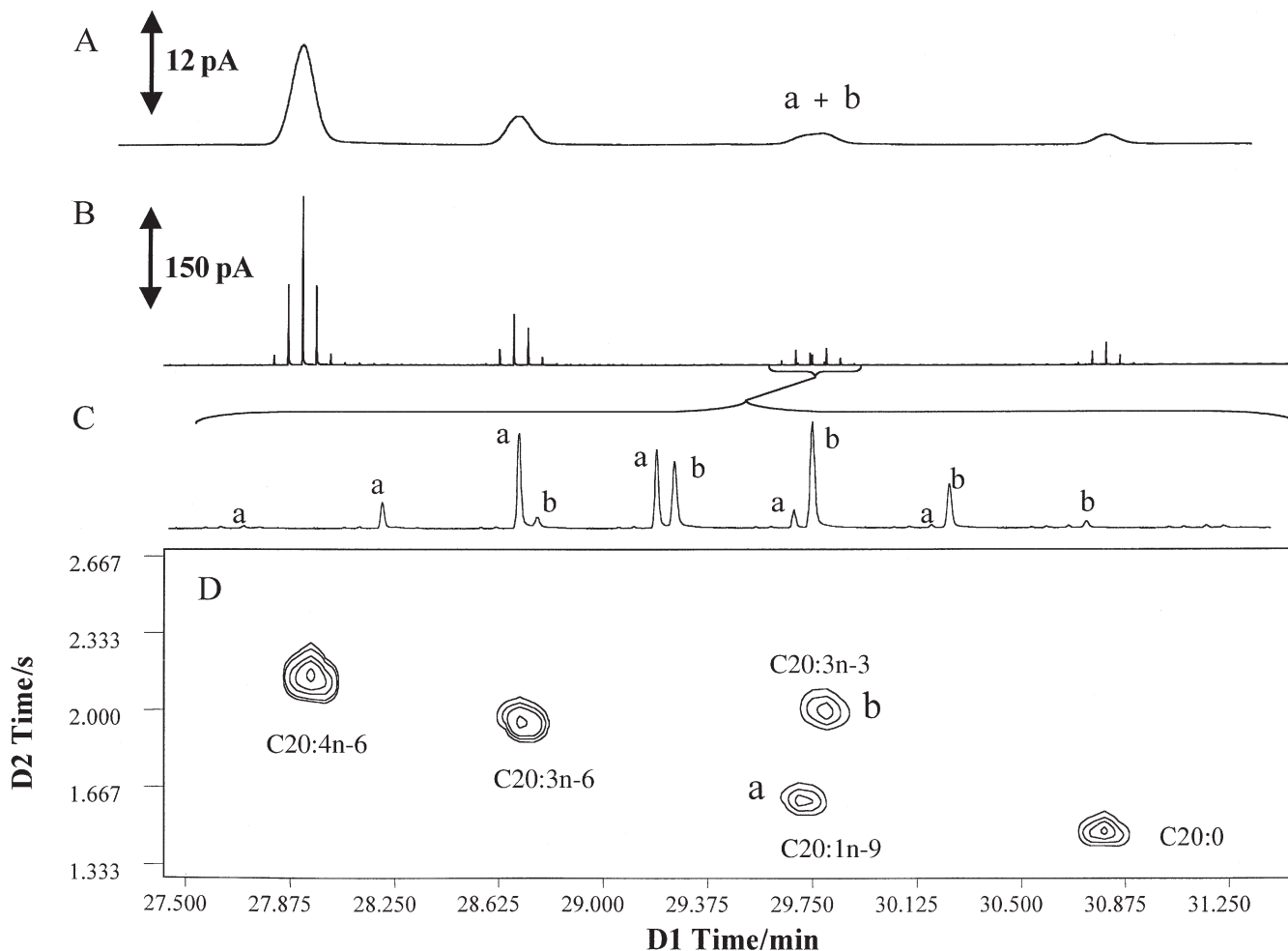
<sup>c</sup>Percentages based on total integrated peak areas for all FAME (= 1503.7 pA·s).

<sup>d</sup>Figure 1A results.

<sup>e</sup>NQ, not quantified; peak not observable. This peak is incorporated into the peak 2 area, which shows an elevated area percentage.

stage) included for completeness of definition. The zones marked C<sub>14</sub> through C<sub>22</sub> refer to trends for different isomers and components within a given carbon number set. Variations in the trend are somewhat variable depending on the nature of

the individual FAME, although one might anticipate that the fine detail of the relative positions of different FAME might be correlated with structural features, as is indicated to some extent in the pattern within the C<sub>18</sub> and C<sub>20</sub> compound sets.



**FIG. 3.** Comparative 2-D chromatogram of C<sub>20</sub> FAME on column set 1 under the conditions given in Figure 1. (A) Normal GC; (B) modulated GC × GC chromatogram; (C) expanded region of (B); (D) GC × GC 2-D contour plot. (a) C<sub>20</sub>:1n-9; (b) C<sub>20</sub>:3n-3. For abbreviations see Figure 1.



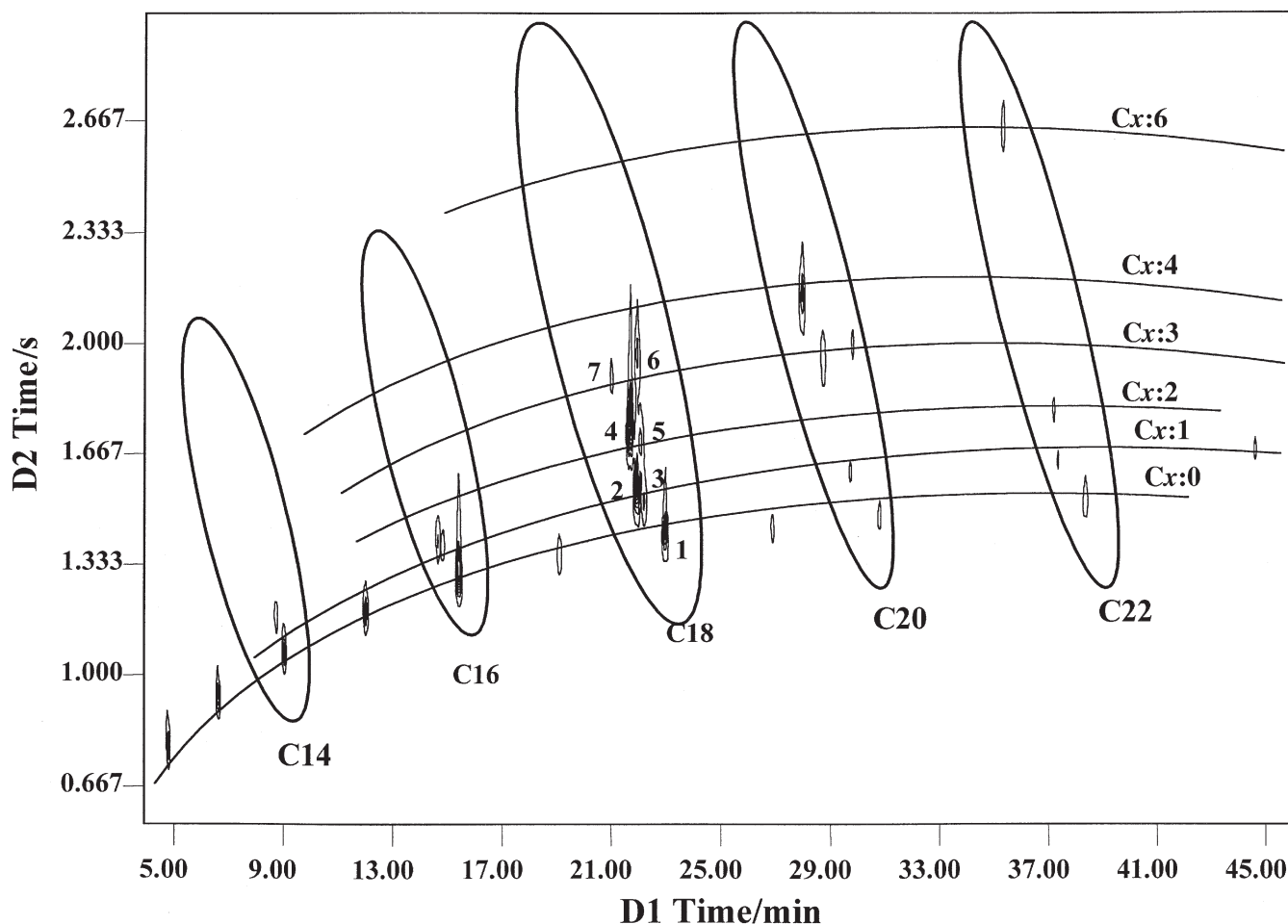


FIG. 4. Correlated trends showing the degree of unsaturation retention and homologous series (curved lines are numbered according to the degree of unsaturation) in the 2-D space. For abbreviations see Figure 1.

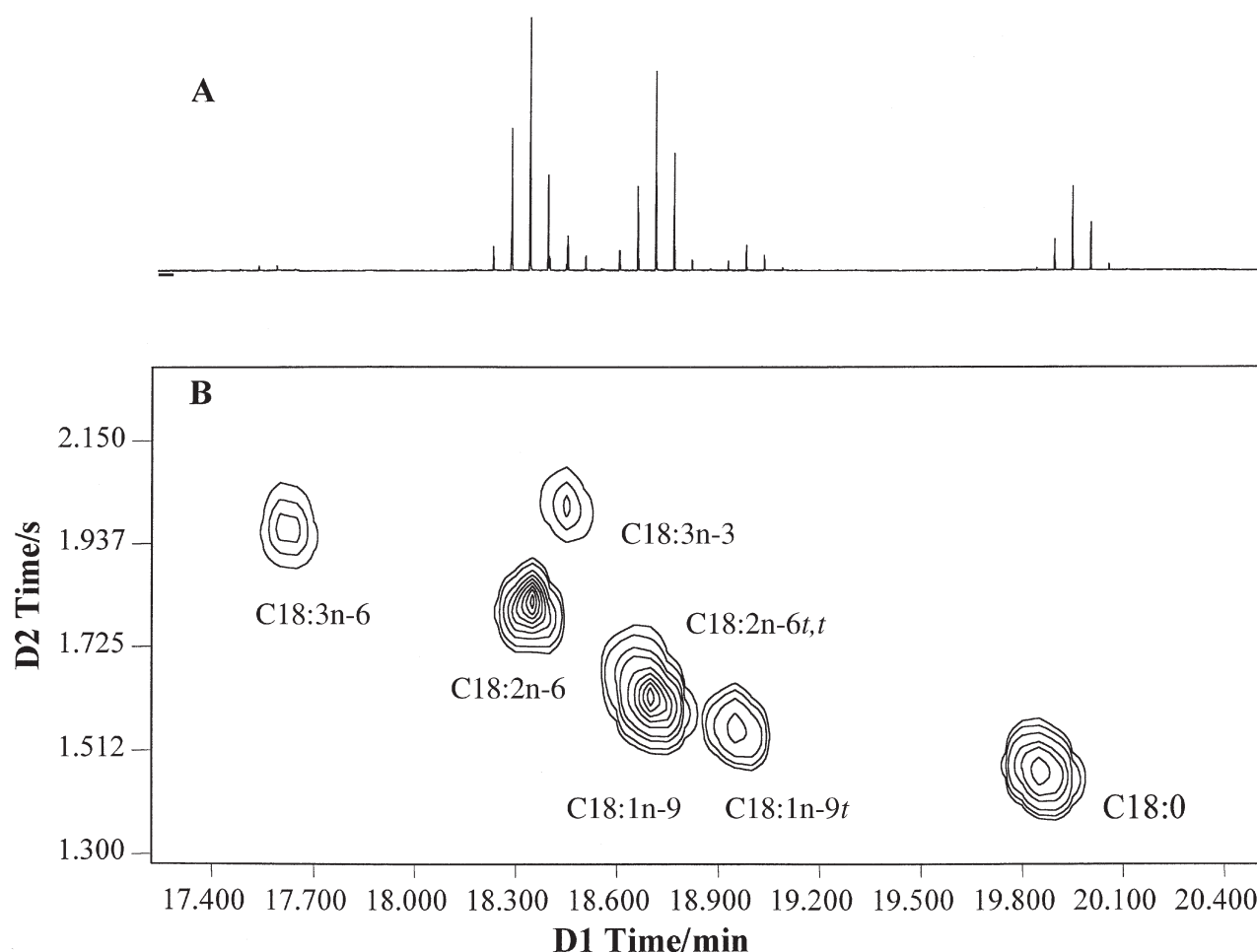
Such data presentation may then be used to facilitate the identification of FAME, especially under a situation where a standard is not available for confirmation purposes.

**BP1/BPX70 column set.** In order to increase resolution of the FAME mixture in the  $C_{18}$  isomer region, the study was repeated with column set 2. It was chosen to maximize the available difference in polarity between the BPX70 D2 column and the low-polarity BP1 D1 column. Along with CP Sil 88, BPX70 is sometimes reported to be the column phase of choice for FAME analysis. Figure 5 shows the modulated chromatogram and the 2-D contour plot of  $C_{18}$  FAME isomers. The compound 18:2n-6,t was not well resolved, being obscured by 18:1n-9, which is present in high abundance. It appears that the less polar BP20 column had better selectivity for these FAME. Figure 6 compares the 2-D plots for the two different column sets for  $C_{18}$  FAME, indicating the relative 2-D positions of 18:3n-3 and 18:2n-6,t; both these components shifted to shorter  $t_R$  compared with the other FAME in this region, which appear to have good pattern matching. In Figure 6B, 18:2n-6,t was placed at an approximate position based on the observation of a shoulder on the pulses of the main peak 18:1n-9. Therefore, 18:2n-6,t could not be seen as

a separate peak in Figure 5 and now co-elutes with 18:1n-9 on D1; these two peaks are vertically aligned in Figure 6B. This contributes to its lower resolution compared with Figure 6A, where 18:2n-6,t is offset from 18:1n-9. As with any chromatographic separation, a change in chromatographic conditions would overcome this problem.

The structural similarity of 18:3n-3 and 18:3n-6 should mean they do not have a large difference in their polarity. Thus, in both Figures 6A and 6B they have only a small difference in their D2 retention times but have a considerable difference in the D1 (b.p.) retention times. Compounds 18:2n-6 and 18:3n-3 have a greater D2 retention difference; this can be interpreted as showing a larger difference in polarity, corresponding to more double bonds in the latter species. However, the difference is larger in column set 2 (approximately 0.187 s) than in column set 1 (approximately 0.169 s), and the different elution temperatures may account for this.

**Marine oil sample.** Figure 7 shows the GC  $\times$  GC separation of a marine oil derived from blue mussel (19). The components were identified by both matching retention times from the present work, and manual spectral deconvolution of GC-MS analysis on a column with properties similar to the



**FIG. 5.** Comparative chromatograms of  $C_{18}$  FAME on column set 2. Conditions are as shown in Figure 1. (A) Modulated GC  $\times$  GC chromatogram; (B) GC  $\times$  GC 2-D contour plot. For abbreviations see Figure 1.

D1 column used in the GC  $\times$  GC studies reported here. The compounds identified are listed in Table 2. It should be noted that the FAME are separated from alkanes (identified by injection of alkane standards) and a suspected plasticizer peak, which are potential causes of interference in single-column chromatography. About 50 peaks are identified or tentatively identified in Figure 7, with an additional  $\sim 20$  peaks showing good resolution but for which identity is unknown. The precision of peak positions in the 2-D space means that the identification of given components in each sample may be as simple as comparing or overlaying the 2-D plots. In addition, identifying the difference between samples involves comparing the differences in peak positions in the 2-D plots.

GC  $\times$  GC separation using LMCS is a powerful technique for analyzing complicated FAME mixtures. Both resolution and sensitivity are increased compared with nonmodulated (conventional) GC. By use of the 2-D contour plot, the presence of all peaks can be detected and also peaks can be easily recognized. Furthermore, trends in both homologous series and unsaturation retention can be identified on the 2-D contour plot. This should aid in identifying unknowns. The approach should now be validated with increasingly complex FAME samples, especially those known to present difficulties

**TABLE 2**  
FAME Components Identified in a Marine Oil Sample

Peak no.	Identity <sup>a</sup>	Peak no.	Identity
1	14:0	25	19:0
2	i15:0	26	19:1
3	a15:0	27	19:1
4	4,8,12 TMTD <sup>b</sup>	28	20:5n-3
5	15:0	29	20:4n-6
6	i16:0	30	20:3n-6
7	16:1n-7	31	20:2NMI <sup>c</sup>
8	16:1n-7 <i>t</i>	32	20:2NMI <sup>c</sup>
9	16:2	33	20:2n-6
10	16:0	34 + 35	20:1n-11 + 20:1n-9
11	i17:0	36	22:1n-7
12	a17:0	37	20:0
13	17:2	38	22:6n-3
14	17:0	39	22:5n-3
15	i18:0	40	22:3
16	18:5n-6	41	22:2n-11
17	18:5n-3	42	22:2n-9
18	18:3n-3	43	22:2n-7
19	18:2n-6	44	22:2n-7 <i>t</i>
20	18:1n-9	45	22:1n-9
21	18:1n-7	46	22:0
22	18:1n-7 <i>t</i>	47	23:0
23	18:1n-5	48	24:1
24	18:0	49	24:0

<sup>a</sup>i, iso; a, anteiso.

<sup>b</sup>TMTD, trimethyltetradecanoic acid.

<sup>c</sup>NMI, nonmethylene interrupted.

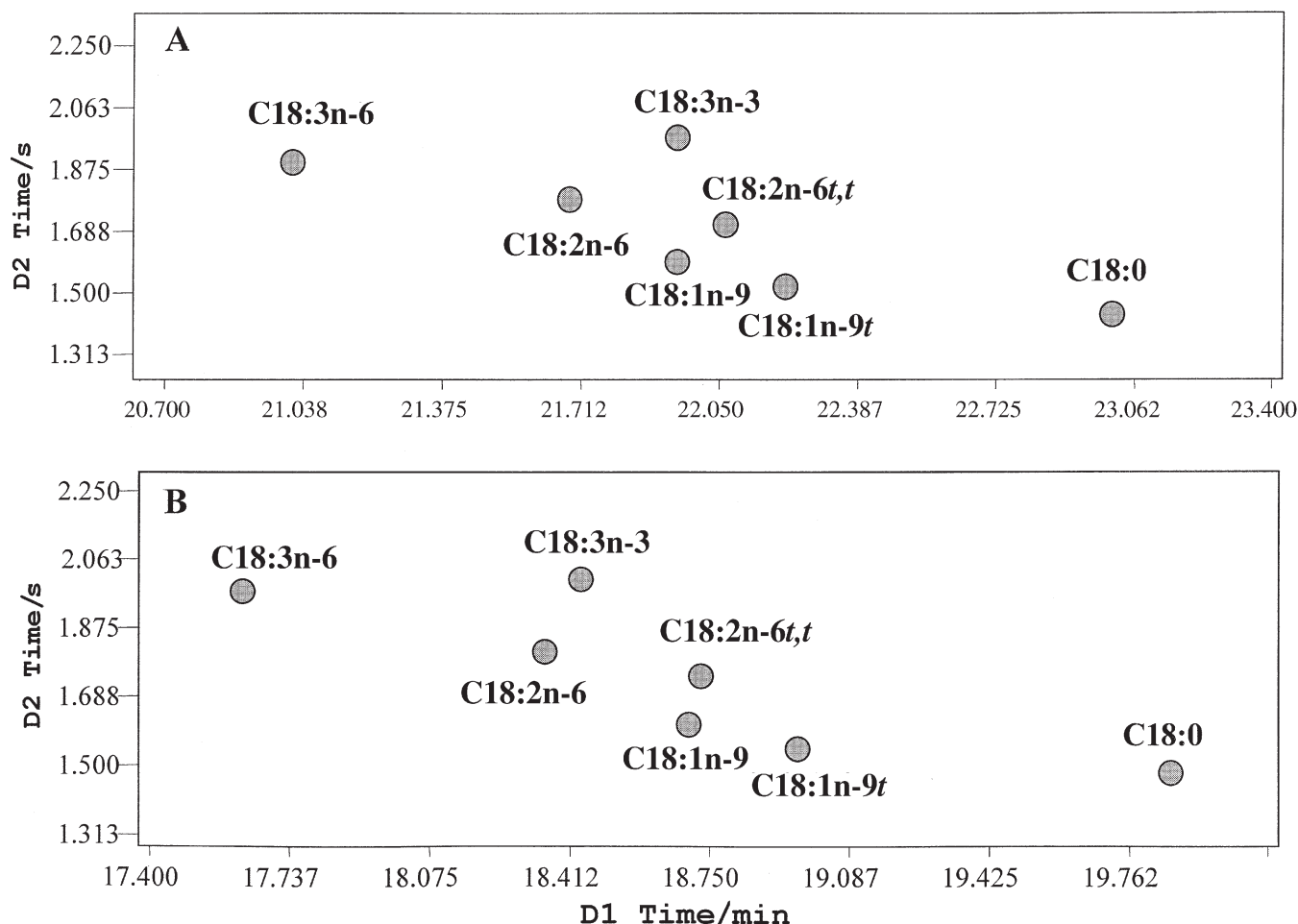


FIG. 6. Comparison of C<sub>18</sub> FAME peak elution patterns for (A) column set 1, and (B) column set 2. For abbreviations see Figure 1.

in separation of key components. This will then permit refinement of the choice of column set, column dimensions, and operating conditions, if required, to maximize 2-D resolution.

#### ACKNOWLEDGMENTS

The authors acknowledge Agilent Technologies for provision of GC facilities; SGE International for the supply of columns; Prof. Andrew Sinclair, RMIT Food Science, for some standards used in this study; and Paul Morrison for his technical assistance.

#### REFERENCES

- Paquot, C. (1979) *IUPAC Standard Methods for the Analysis of Fats, Oils, and Derivatives*, 6th edn., Part 1, Sections 1 and 2, Pergamon Press, New York.
- Wolff, R.L. (1992) Resolution of Linoleic Acid Geometrical Isomers by Gas-Liquid Chromatography on a Capillary Column Coated with a 100% Cyanopropyl Polysiloxane Film (CP™ Sil 88), *J. Chromatogr. Sci.* 30, 17–22.
- Precht, D., and Molquentin, J. (2000) Recent Trends in the Fatty Acid Composition of German Sunflower Margarines, Shortenings and Cooking Fats with Emphasis on Individual C16:1, C18:1, C18:2, C18:3 and C20:1 *trans* Isomers, *Nahrung* 44, 222–228.
- Precht, D., and Molquentin, J. (1999) Influence of the Heating Temperature on the Fat Composition of Milk Fat with the Emphasis on *cis/trans* Isomerization, *Nahrung* 43, 25–33.
- Fritsche, J., and Steinhart, H. (1998) Analysis, Occurrence, and Physiological Properties of *trans* Fatty Acids (TFA) with Particular Emphasis on Conjugated Linoleic Acid Isomers (CLA)—A Review, *Fett/Lipid* 6, 190–210.
- Yurawecz, M., Sehat, N., Mossoba, M., Roach, J., Kramer, J., and Ku, Y. (2000) Variations in Isomer Distribution in Commercially Available Conjugated Linoleic Acid, *Fett/Lipid* 8, 277–282.
- Venkatramani, C., Xu, J., and Phillips, J. (1996) Separation Orthogonality in Temperature Programmed Comprehensive Two-Dimensional Chromatography, *Anal. Chem.* 66, 1486–1492.
- Bruckner, C., Prazen, B., and Synovec, R. (1998) Comprehensive Two-Dimensional High-Speed Gas Chromatography with Chemometric Analysis, *Anal. Chem.* 70, 2796–2804.
- Marriott, P.J., and Kinghorn, R.M. (1997) Longitudinally Modulated Cryogenic System. A Generally Applicable Approach to Solute Trapping and Mobilization in Gas Chromatography, *Anal. Chem.* 69, 2582–2588.
- Kinghorn, R.M., and Marriott, P.J. (1998) Comprehensive Two-Dimensional Gas Chromatography Using a Modulating Cryogenic Trap, *J. High Resolut. Chromatogr.* 21, 620–622.
- Kinghorn, R.M., Marriott, P.J., and Dawes, P.A. (1998) Longitudinal Modulation Studies for Augmentation of Injection and Detection in Capillary Gas Chromatography, *J. Microcolumn Sep.* 10, 611–616.

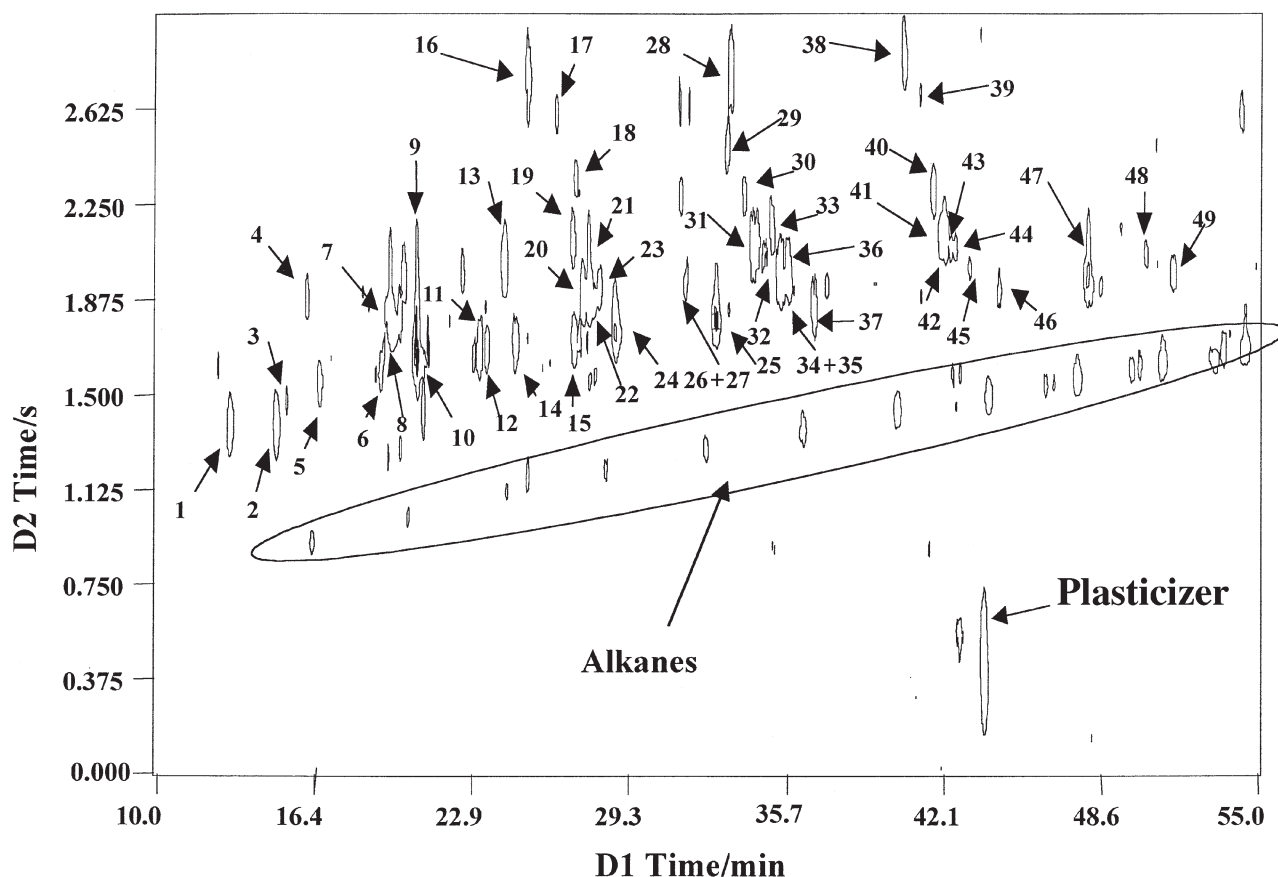


FIG. 7. Comprehensive 2-D GC analysis of marine oil on a BP1/BPX70 column set (SGE International, Ringwood, Victoria, Australia). GC conditions are similar to those shown in Figure 1. Identified compounds are reported in Table 2. For abbreviations see Figure 1.

12. Kinghorn, R.M., and Marriott, P.J. (1999) High Speed Cryogenic Modulation—A Technology Enabling Comprehensive Multidimensional Gas Chromatography, *J. High Resolut. Chromatogr.* 22, 235–238.
13. Marriott, P.J., and Kinghorn, R.M. (2000) Longitudinal Cryogenic Modulation in Gas Chromatography—A New Technology for Separation Science, *LC.GC Europe* 13, 428–436.
14. Shellie, R., Marriott, P.J., and Cornwell, C. (2000) Characterization and Comparison of Tea Tree and Lavender Oils by Using Comprehensive Gas Chromatography, *J. High Resolut. Chromatogr.* 23, 554–560.
15. Truong, T., Marriott, P.J., and Porter, N.A. (2001) Analytical Study of Comprehensive and Targeted Multidimensional Gas Chromatography Incorporating Modulated Cryogenic Trapping, *J. AOAC Int.* 84, 323–335.
16. Shellie, R.A. (2000) Natural Product (especially fragrance) Characterisation and Classification Using Novel Gas Chromatographic Methods, Honours Thesis, RMIT University, Melbourne, Australia, p. 31.
17. Phillips, J.B., and Beens, J. (1999) Comprehensive Two-Dimensional Gas Chromatography: A Hyphenated Method with Strong Coupling Between the Two Dimensions, *J. Chromatogr. A* 856, 331–347.
18. de Geus, H.-J., Aidos, I., de Boer, J., Luten, J.B., and Brinkman, U.A.Th. (2001) Characterisation of Fatty Acids in Biological Oil Samples Using Comprehensive Multidimensional Gas Chromatography, *J. Chromatogr. A* 910, 95–103.
19. Murphy, K.J., Mooney, B.D., Mann, N.J., Nichols, P.D., and Sinclair, A.J. (2002) Lipid, FA, and Sterol Composition of New Zealand Green Lipped Mussel (*Perna canaliculus*) and Tasmanian Blue Mussel (*Mytilus edulis*), *Lipids* 37, 587–595.

[Received November 5, 2001, and in revised form May 20, 2002; revision accepted June 28, 2002]



## Similar Effects of *c9,t11*-CLA and *t10,c12*-CLA on Immune Cell Functions in Mice

D.S. Kelley<sup>a,\*</sup>, J.M. Warren<sup>a</sup>, V.A. Simon<sup>a</sup>, G. Bartolini<sup>a</sup>, B.E. Mackey<sup>b</sup>, and K.L. Erickson<sup>c</sup>

<sup>a</sup>Western Human Nutrition Research Center, ARS, USDA, and Department of Nutrition, University of California, Davis, California, <sup>b</sup>Western Regional Research Center, Albany, California, and <sup>c</sup>Department of Cell Biology and Human Anatomy, University of California, Davis, California

**ABSTRACT:** Published results regarding the effects of CLA on immune cell functions have ranged from stimulation to inhibition. In those studies, a mixture of CLA isomers were used, and food intake was not controlled. We have examined whether the discrepancies in the results of earlier studies may be due to the lack of controlled feeding and whether the two isomers of CLA may differ in their effects on immune cell functions. Three groups of C57BL/6 female mice were fed either a control, *c9,t11*-CLA-, or *t10,c12*-CLA (0.5 wt%)-supplemented diet, 5 g/d, for 56 d. At the end of the study, the number of immune cells in spleens, bone marrows, or in circulation; proliferation of splenocytes in response to T and B cell mitogens; and prostaglandin secretion *in vitro* did not differ among the three groups. Both CLA isomers significantly increased *in vitro* tumor necrosis factor  $\alpha$  and interleukin (IL)-6 secretion and decreased IL-4 secretion by splenocytes compared to those in the control group. Thus, the two CLA isomers had similar effects on all response variables tested. The discrepancies among the results from previous studies did not seem to be caused by the differences in the isomer composition of CLA used.

Paper no. L9027 in *Lipids* 37, 725–728 (July 2002).

CLA is a collective term for isomers of linoleic acid that have conjugated double bonds. Depending on the position and geometry of the double bonds, several isomers of CLA have been reported (1). Feeding a mixture of these isomers altered several indices of immune cell functions in animal models (2–11) but not in humans (12,13). Even in the animal models, the effects of dietary CLA on immune cell functions have been modest and variable. Thus, in one study splenocyte proliferation in response to the T cell mitogen phytohemagglutinin (PHA) was enhanced 3 wk after supplementing mouse diets with CLA, but not after 6 wk (4). Proliferation in response to another T cell mitogen, Concanavalin A (Con A), was not altered at 3 and 6 wk after CLA supplementation. In another study, 8 wk of CLA supplementation of young mice enhanced splenocyte proliferation at Con A concentrations of

0.5 and 5.0 mg/L, but not at 1.5 mg/L; CLA supplementation did not alter splenocyte proliferation in response to PHA (5). Similar inconsistencies were found regarding the effects of CLA feeding on cytokine secretion, delayed hypersensitivity skin response, and other indices of immune response (2–11). None of these studies controlled food intake or fed purified isomers of CLA, which may be partially responsible for some of the discrepancies. This study examined the effects of two purified isomers of CLA on immune cell functions under conditions of controlled food intake. Isomers used in our study were the *cis*-9 and *trans*-11 (*c9,t11*-CLA), and *trans*-10 and *cis*-12 (*t10,c12*-CLA), which are among the most abundant isomers found in the mixtures used in previous studies. We used a single concentration (0.5 wt%) of each isomer, which is equivalent to the concentrations of these isomers present in the CLA mixtures (0.1 to 1.5%) used in previous studies.

### MATERIALS AND METHODS

**Diets and animals.** Highly enriched *c9,t11*-CLA, and *t10,c12*-CLA isomers as FFA were a kind gift from Natural ASA (Hovdebygda, Norway). Both preparations contained more than 85% of the isomer of interest. AIN-93G mouse diet was used as the basal diet. Fat source in the diet was corn oil, 50 g/kg. CLA isomers were added at 5 g/kg by replacing an equivalent amount of corn oil. Diets were constantly flushed with nitrogen gas while being gently mixed in a blender and then stored at  $-20^{\circ}\text{C}$ . Fresh dietary packets were served each day.

Thirty-five 8-wk-old, pathogen-free C57BL/6N female mice were purchased from Charles River (Raleigh, NC) and divided into three groups (11 or 12/group). Animals were maintained in a sterile air curtain isolator at  $25^{\circ}\text{C}$ , with light and dark cycles of 12 h each. Based on our previous experience with food required by the mice in this age range (14), they were offered fresh food every day (5 g/animal/d) for 56 d. All food was consumed within 4–6 h in all groups. This avoided the need for paired feeding and reduced the possibility of CLA oxidation. At the end of the study, body weight of the mice fed the diet containing *t10,c12*-CLA was significantly lower than that of the other two groups, which did not differ from each other. All conditions and handling of the animals were approved by the Animal Care and Use Committee at the University of California–Davis.

\*To whom correspondence should be addressed at USDA/ARS/WHNRC, Department of Nutrition, University of California–Davis, One Shields Ave., Davis, CA 95616. E-mail: dkelley@whnrc.usda.gov

Abbreviations: BrdU, 5-bromo-2-deoxyuridine; *c*, *cis*; Con A, Concanavalin A; DME, Dulbecco's modified Eagle medium; IL, interleukin; LPS, lipopolysaccharide; PGE<sub>2</sub>, prostaglandin E<sub>2</sub>; PHA, phytohemagglutinin; *t*, *trans*; TNF $\alpha$ , tumor necrosis factor  $\alpha$ .

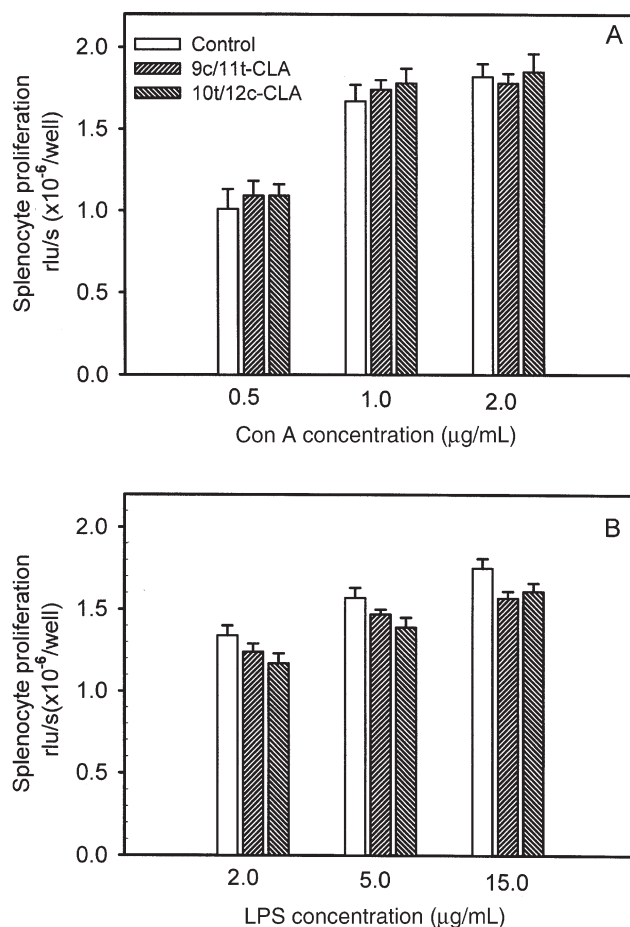
**Tissue collection and cell culture.** Mice were anesthetized, and blood was collected into EDTA-containing syringes by heart puncture. Spleens were aseptically removed, weighed, and placed in 5 mL Dulbecco's modified Eagle medium (DME; Sigma Chemical Co., St. Louis, MO) containing 5% FCS, 25 mmol Hepes, 8 mmol glutamine, penicillin 10 KU/L, and streptomycin 10 mg/L. Splenocytes were prepared as previously reported (15) and suspended in the DME medium containing 5% FCS. For cell proliferation assays, splenocyte concentrations were adjusted to 2 million/mL and 100  $\mu$ L cell suspensions were added to each well of 96-well plates (Falcon Labware, Gaithersburg, MD). This was followed by the addition of an extra 100  $\mu$ L media containing either the T cell mitogen, Con A (final concentrations 0, 0.5, 1.0, and 2.0 mg/L), or the B cell mitogen, lipopolysaccharide (LPS) (final concentrations 0, 2.0, 5.0, and 15.0 mg/L). Three wells were used for each mitogen concentration. Plates were then incubated at 37°C, 5% CO<sub>2</sub>, and 100% humidity for 72 h. Proliferation was determined by incorporation of 5-bromo-2-deoxyuridine (BrdU) into the DNA (16,17); the Proliferation ELISA BrdU chemiluminescence kit was purchased from Roche (Mannheim, Germany) and used as described by the manufacturer. Results are expressed as relative light units (rlu)/s/well; one rlu is equivalent to one million photons/s/well.

For cytokine and eicosanoid secretion assays, 2 million splenocytes in duplicates were incubated in 1.0 mL of media containing LPS (0, 1, and 10 mg/L) or Con A (0, 1, and 5 mg/L) in 24-well plates for 4, 24, and 48 h. The cell culture media were collected following centrifugation and stored frozen at -70°C. Media from LPS-treated cultures were used to monitor tumor necrosis factor  $\alpha$  (TNF $\alpha$ ), interleukin (IL)-6, and prostaglandin (PG) E<sub>2</sub>, while those from Con A-treated cells were used to determine IL-2 and IL-4 using ELISA assays. Mitogen concentrations and incubation times were selected based on preliminary experiments. ELISA kits for TNF $\alpha$ , IL-2, IL-4, and IL-6 were purchased from BD Pharmingen (San Diego, CA) and those for PGE<sub>2</sub> from Cayman (Ann Arbor, MI).

**Statistical analysis.** The data were subjected to one-way ANOVA between and within diets, using the SAS software (18). The one-tailed version of Dunnett's test was used to make comparisons of the test diet means with the control diet. Levene's test was used to examine the homogeneity of variance assumption. When heterogeneity was encountered, it was incorporated into the model using the SAS PROC MIXED.

## RESULTS

**Effect of CLA on cell numbers and splenocyte proliferation.** Both CLA isomers did not alter the total number of circulating white blood cells or their percentages as neutrophils, lymphocytes, monocytes, eosinophils, and basophils; nor did they alter the number of splenocytes or bone marrow cells (not shown). Figure 1 shows that neither of the CLA isomers altered splenocyte proliferation in response to both the T and B cell mitogens, although the proliferation was increased with increase in mitogen concentration in all groups.



**FIG. 1.** Effect of CLA on splenocyte proliferation in response to Concanavalin A (Con A) (A) and lipopolysaccharide (LPS) (B). Splenocytes were cultured with the indicated mitogen concentrations for 72 h. Lymphocyte proliferation was examined by the incorporation of 5-bromo-2-deoxyuridine into the cellular DNA during the last 24 h in culture. Results are expressed as mean  $\pm$  SEM of rlu (relative light units)/s/well. Neither of the CLA isomers altered splenocyte proliferation in response to both the mitogens.

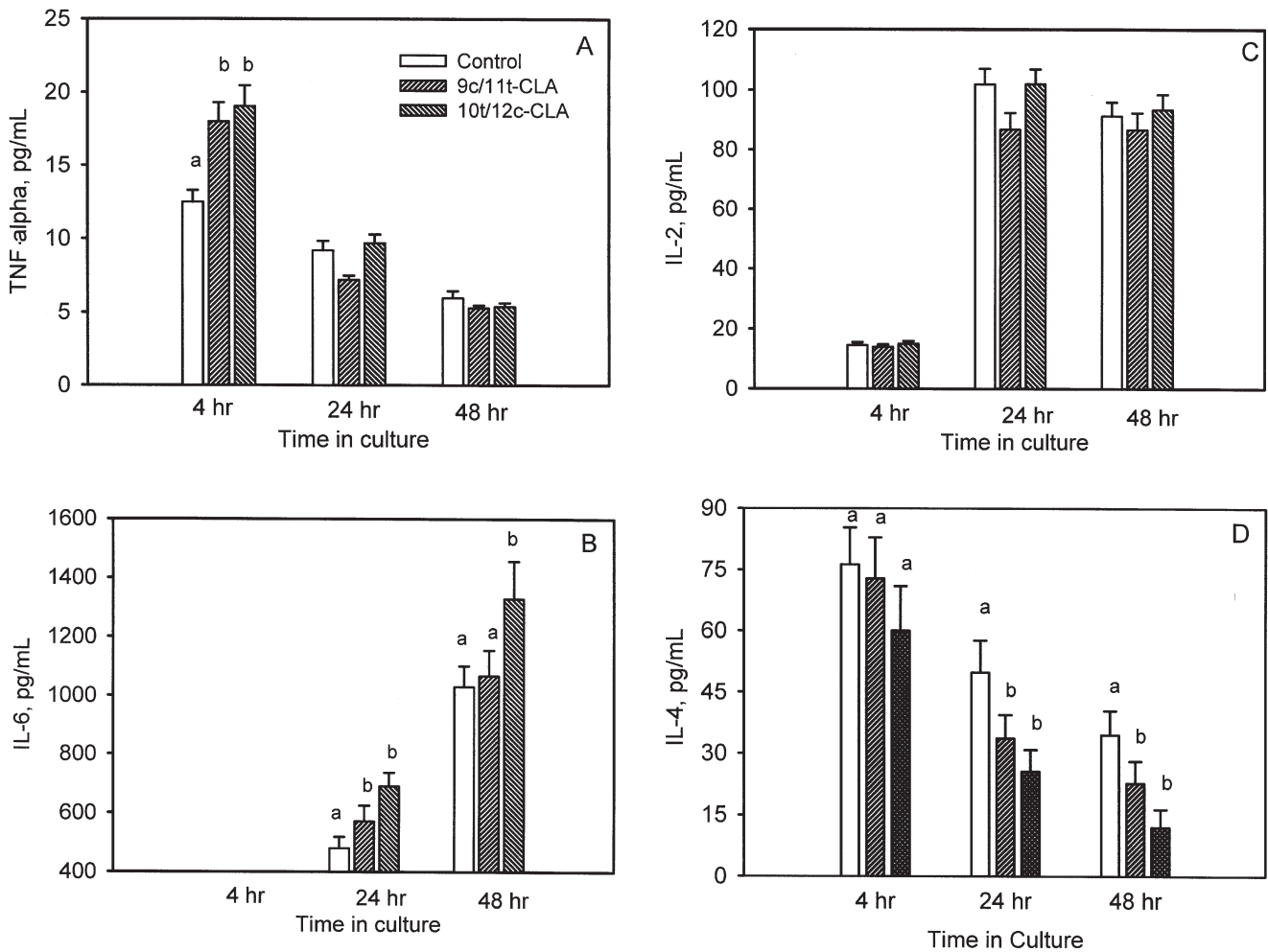
**Effect of CLA on eicosanoid and cytokine secretion.** We examined the effects of CLA feeding on markers for inflammation (PGE<sub>2</sub>, TNF $\alpha$ , and IL-6) and on representative cytokines for Th1 (IL-2) and Th2 (IL-4) cells. Treatment effects at the two mitogen concentrations were similar, but results are shown only for the higher mitogen concentrations (LPS, 10  $\mu$ g/mL, for PGE<sub>2</sub>, TNF $\alpha$ , and IL-6; Con A, 5  $\mu$ g/mL for IL-2 and IL-4). Concentrations of PGE<sub>2</sub> in the medium collected at 4, 24, and 48 h from the splenocytes isolated from the mice fed control diet were 5.0  $\pm$  0.6, 5.4  $\pm$  0.5, 5.3  $\pm$  0.6 pg/mL, respectively. The PGE<sub>2</sub> concentrations in the two CLA groups did not differ from those in the control group (not shown). Medium concentrations of TNF $\alpha$  and IL-4 decreased between 4 and 48 h, whereas those of IL-2 and IL-6 increased (Figs. 2A–D). TNF $\alpha$  secreted within 4 h of mitogen stimulation was significantly greater ( $P < 0.001$ ) in both the CLA groups than in the control group. Medium concentration of TNF $\alpha$  did not differ among the three groups at 24 and 48 h, and also

between the two CLA isomers at all three time points. IL-6 secreted into the medium after 4 h of LPS treatment was non-detectable in all three groups. Twenty-four hours after LPS treatment, secreted IL-6 was significantly ( $P < 0.01$ ) greater in both the CLA groups than in the control group, whereas after 48 h, the difference was significant only for *t10,c12*-CLA ( $P < 0.01$ ) (Fig. 2B).

The concentration of secreted IL-2 increased six- to seven-fold from 4 to 24 h in all three groups of cells but did not change between 24 and 48 h; there was no difference in its concentration among the three groups at all three time points (Fig. 2C). Neither of the CLA isomers altered the concentration of IL-4 secreted within 4 h of mitogen treatment, but it was significantly reduced by both the isomers at 24 and 48 h after mitogen treatment (Fig. 2D). There was no difference in IL-4 concentrations in the two CLA groups at all three time points.

## DISCUSSION

We compared the effects of feeding two purified isomers of CLA on several indices of immune and inflammatory responses in mice maintained on a controlled feeding regime. Effects of the two isomers on immune cell functions did not differ. Both the *c9,t11*-CLA and *t10,c12*-CLA did not alter the number of immune cells in circulation, in spleens, or in bone marrows. Neither of the isomers affected splenocyte proliferation in response to T and B cell mitogens, or the secretion of PGE<sub>2</sub> and IL-2. We had found similar results with feeding of a mixture of CLA isomers to healthy women (12,13). These results are in part consistent with those of earlier reports in mice (4,5). In one of these reports, 8 wk of CLA supplementation resulted in a modest increase in splenocyte proliferation at Con A concentrations of 0.5 and 5.0, but not



**FIG. 2.** Effect of dietary CLA on *in vitro* secretion of tumor necrosis factor  $\alpha$  (TNF $\alpha$ ) (A), interleukin (IL)-6 (B), IL-2 (C), and IL-4 (D) by splenocytes stimulated with 10  $\mu$ g/mL LPS (A and B) and 5  $\mu$ g/mL Con A (C and D). Bars with different letters are significantly different. Secreted TNF $\alpha$  at 4 h was significantly ( $P < 0.001$ ) greater in both CLA groups than in the control group; at 24 and 48 h there was no significant difference among all three groups. Secreted IL-6 at 24 h was significantly ( $P < 0.01$ ) greater in both CLA groups than the control group; at 48 h the difference was significant only for the *t10,c12*-CLA group. At all times, secreted IL-2 was not significantly different among the three groups. Secreted IL-4 was significantly less in both CLA groups than in the control group at 24 and 48 h ( $P < 0.03$ ) but not at 4 h.



at 1.5 mg/L (5). In the other report, 6 wk of CLA supplementation did not affect splenocyte proliferation (4). IL-2 secretion was increased in one (5) but not in the other study (4). Results regarding splenocyte proliferation differ from those of another study that found increased proliferation in response to both Con A and PHA in splenocytes isolated from mice fed a CLA-containing diet (2).

Both CLA isomers increased the secretion of TNF $\alpha$  and IL-6 and decreased that of IL-4 (Figs. 2A–D). These changes could have been easily missed if we had tested all cytokines only at a single time point. Our results regarding TNF $\alpha$  and IL-6 differ from those obtained with rat peritoneal macrophages, where feeding a mixture of CLA isomers decreased the secretion of both these cytokines (6). Those investigators reported that the effect of CLA varied with the n-6/n-3 FA ratio of the experimental diets. Results of our current study also differ from those found in humans (12,13), which most likely are due to the amount of CLA fed; the amount of CLA/kg body weight was 20 times greater in the mouse than in the human study. The amount of CLA needed in humans to match that used in the mice will require 75 g/d/60 kg person; this is greater than or equal to the total daily fat consumed by most humans and cannot be considered as a nutritional supplement.

Published effects of CLA on immune cell functions varied not only for the functions tested in this study but also for other functions including delayed type hypersensitivity response, ratios between helper and suppressor T cells, and serum immunoglobulin levels (4–10) as well. The results have ranged from stimulation to inhibition or no effect. These discrepancies do not seem to be due to the differences in isomer composition of the CLA mixtures used, because the effects of two isomers in the present study were similar. These may be due to lack of controlled feeding or other factors, including culture conditions (serum type and concentration, mitogen concentration and culture period), cell type (peritoneal vs. splenocyte vs. blood cells) composition, and storage of the diets, species, and age of the animals.

In conclusion, both CLA isomers have similar effects on several aspects on immune cell functions in mice; many indices were not altered by both isomers, whereas others were modestly affected by both isomers. Because of only modest effects, even at high concentrations of CLA intake, any clinical benefit to enhance immune status with nutritional supplements of CLA seems unlikely.

## REFERENCES

- Eulitz, K., Yurawecz, M.P., Sehat, N., Fritsche, J., Roach, J.A.G., Mossoba, M.M., Kramer, J.K.G., Adlof, R.O., and Ku, Y. (1999) Preparation, Separation, and Confirmation of the Eight Geometrical *cis/trans* Conjugated Linoleic Acid Isomers, 8,10- Through 11,13-18:2, *Lipids* 34, 873–877.
- Miller, C.C., Park, Y., Pariza, M., and Cook, M.E. (1994) Feeding Conjugated Linoleic Acid to Animals Partially Overcame the Catabolic Responses Due to Endotoxin Injection, *Biochem. Biophys. Res. Commun.* 198:1107–1112.
- Cook, M.E., Miller, C.C., Park, Y., and Pariza, M. (1993)

- Immune Modulation by Altered Nutrient Metabolism: Nutritional Control of Immune-Induced Growth Depression, *Poul. Sci.* 72, 1301–1305.
- Wong, M.W., Chew, B.P., Wong, T.S., Hosick, H.L., Boylston, T.D., and Schultz, T.D. (1997) Effects of Dietary Conjugated Linoleic Acid on Lymphocyte Function and Growth of Mammary Tumors in Mice, *Anticancer Res.* 17:987–994.
- Hayek, M.J., Han, S.N., Wu, D., Watkins, B.A., Meydani, M., Dorsey, J.L., Smith, D.E., and Meydani, S.K. (1999) Dietary Conjugated Linoleic Acid Influences the Immune Response of Young and Old C57BL/6NCrIBR Mice, *J. Nutr.* 129:32–38.
- Turek, J.J., Li, Y., Schoenlein, I.A., Allen, K.G.D., and Watkins B.A. (1998) Modulation of Macrophage Cytokine Production by Conjugated Linoleic Acid Is Influenced by the Dietary n-6:n-3 Fatty Acid Ratio, *J. Nutr. Biochem.* 9:258–266.
- Sugano, M., Tsujita, A., Yamasaki, M., Noguchi, M., and Yamada, K. (1998) Conjugated Linoleic Acid Modulates Tissue Levels of Chemical Mediators and Immunoglobulins, *Lipids* 33:521–527.
- Yamasaki, M., Kishihara, K., Mansho, K., Ogino, Y., Kasai, M., Sugano, M., Tachibana, H., and Yamada, K. (2000) Dietary Conjugated Linoleic Acid Increases Immunoglobulin Productivity of Sprague-Dawley Rat Splenocytes, *Biosci. Biotechnol. Biochem* 64: 2159–2164.
- Bassaganya-Riera, J., Hontecillas-Margarzo, R., Bregendahl, K., Wannemuehler, M.J., and Zimmerman, D.R. (2001) Effects of Dietary Conjugated Linoleic Acid in Nursery Pigs of Dirty and Clean Environments on Growth, Empty Body Composition, and Immune Competence, *J. Anim. Sci.* 79:714–721.
- Bassaganya-Riera, J., Hontecillas, R., Zimmerman, D.R., and Wannemuehler, M.J. (2001) Dietary Conjugated Linoleic Acid Modulates Phenotype and Effector Functions of Porcine CD8+ Lymphocytes, *J. Nutr.* 131: 2370–2377.
- Turnock, L., Cook, M., Steinberg, H., Czuprynski, C. (2001) Dietary Supplements with Conjugated Linoleic Acid Does Not Alter the Resistance of Mice to *Listeria monocytogenes* Infection, *Lipids* 36, 135–138.
- Kelley, D.S., Taylor, P.C., Rudolph, I.L., Benito, P., Nelson, G.J., Mackey, B.E., and Erickson, K. (2000) Dietary Conjugated Linoleic Acid Did Not Alter Immune Status in Young Healthy Women, *Lipids* 35, 1065–1071.
- Kelley, D.S., Simon, V.A., Taylor, P.C., Rudolph, I.L., Benito, P., Nelson, G.J., Mackey, B.E., and Erickson, K. (2001) Dietary Supplementation with Conjugated Linoleic Acid Increased Its Concentration in Human Peripheral Blood Mononuclear Cells, but Did Not Alter Their Function, *Lipids* 36, 1–6.
- Chapkins, R.S., Somers, S.D., Schumacher L.S., and Erickson, K.L. (1988) Fatty Acid Composition of Macrophage Phospholipids in Mice Fed Fish or Borage Oil, *Lipids* 23, 380–383.
- Kelley, D.S., Nelson, G.J., Serrato, C.M., Schmidt, P.C., and Branch, L.B. (1988) Effect of Type of Dietary Fat on the Indices of Immune Status of Rabbits, *J. Nutr.* 118:1376–1384.
- Porstmann, T., Ternyck, T., and Avrameas, S. (1985) Quantitation of 5-Bromo-2-deoxyuridine Incorporation into DNA: An Enzyme Immunoassay for the Assessment of the Lymphoid Cell Proliferation Response, *J. Immunol. Methods* 82, 169–179.
- Huong, P.L.T., Kolk, A.H.J., Eggelte, T.A., Verstijnen, C.P.H.J., Gilis, H., and Hendriks, J.T. (1991) Measurement of Antigen Specific Lymphocyte Proliferation Using 5-Bromo-2-deoxyuridine Incorporation, *J. Immunol. Methods* 140, 243–248.
- SAS Institute Inc. (1997) *SAS/STAT Software: Changes and Enhancement Through Release 6.12*, SAS Institute Inc., Cary, NC, p. 1167.

[Received March 18, 2002, and in revised form June 19, 2002; revision accepted July 1, 2002]



# Identification and Expression of Mammalian Long-Chain PUFA Elongation Enzymes

Amanda E. Leonard<sup>a</sup>, Bruce Kelder<sup>b</sup>, Emil G. Bobik<sup>a</sup>, Lu-Te Chuang<sup>a</sup>, Christopher J. Lewis<sup>b</sup>, John J. Kopchick<sup>b</sup>, Pradip Mukerji<sup>a</sup>, and Yung-Sheng Huang<sup>a,\*</sup>

<sup>a</sup>Ross Products Division, Abbott Laboratories, Columbus, Ohio 43215, and

<sup>b</sup>Department of Biomedical Sciences, Ohio University, Athens, Ohio 45701

**ABSTRACT:** In mammalian cells, Sprecher has proposed that the synthesis of long-chain PUFA from the 20-carbon substrates involves two consecutive elongation steps, a  $\Delta 6$ -desaturation step followed by retroconversion (Sprecher, H., *Biochim. Biophys. Acta* 1486, 219–231, 2000). We searched the database using the translated sequence of human elongase ELOVL5, whose encoded enzyme elongates monounsaturated and polyunsaturated FA, as a query to identify the enzyme(s) involved in elongation of very long chain PUFA. The database search led to the isolation of two cDNA clones from human and mouse. These clones displayed deduced amino acid sequences that had 56.4 and 58% identity, respectively, to that of ELOVL5. The open reading frame of the human clone (ELOVL2) encodes a 296-amino acid peptide, whereas the mouse clone (Elov12) encodes a 292-amino acid peptide. Expression of these open reading frames in baker's yeast, *Saccharomyces cerevisiae*, demonstrated that the encoded proteins were involved in the elongation of both 20- and 22-carbon long-chain PUFA, as determined by the conversion of 20:4n-6 to 22:4n-6, 22:4n-6 to 24:4n-6, 20:5n-3 to 22:5n-3, and 22:5n-3 to 24:5n-3. The elongation activity of the mouse Elov12 was further demonstrated in the transformed mouse L cells incubated with long-chain ( $C_{20}$ - and  $C_{22}$ -carbon) n-6 and n-3 PUFA substrates by the significant increase in the levels of 24:4n-6 and 24:5n-3, respectively. This report demonstrates the isolation and identification of two mammalian genes that encode very long chain PUFA specific elongation enzymes in the Sprecher pathway for DHA synthesis.

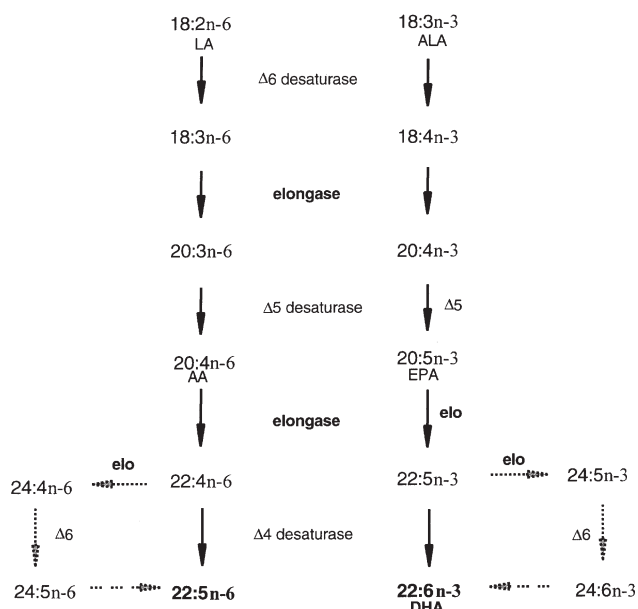
Paper no. L9060 in *Lipids* 37, 733–740 (August 2002).

PUFA are involved in many biological functions including inflammatory response (1), fetal growth and development (2), retinal function, and brain development (3,4). The 20-carbon PUFA also serve as precursors to eicosanoids, such as prostaglandins, prostacyclins, thromboxanes, and leukotrienes (5). Small amounts of very long chain PUFA with a chain length of 22 carbons or more are also present in many animal tissues, especially in the testis, retina, brain, and liver (6).

PUFA of the n-6 and n-3 families are either obtained directly from the diet or derived from biosynthesis of dietary

\*To whom correspondence should be addressed at Strategic-Discovery Research, Ross Products Division, Abbott Laboratories, 625 Cleveland Ave., Columbus, OH 43215. E-mail: vic.huang@abbott.com

Abbreviations: AA, arachidonic acid (20:4n-6); ALA,  $\alpha$ -linolenic acid (18:3n-3); LA, linoleic acid (18:2n-6); m-ELO, mouse L cells cloned with mouse elongase gene Elov12.



**FIG. 1.** Metabolic pathway of long-chain PUFA. The dashed arrows indicate the Sprecher pathway (Ref. 11).

EFA, linoleic acid (LA, 18:2n-6) and  $\alpha$ -linolenic acid (ALA, 18:3n-3). The biosynthesis of n-6 and n-3 long-chain PUFA requires several desaturation and elongation enzymes (Fig. 1). The  $\Delta 6$ -desaturase converts LA and ALA to  $\gamma$ -linolenic acid (18:3n-6) and stearidonic acid (18:4n-3), respectively. An elongation system adds two carbons to synthesize 20:3n-6 from 18:3n-6 and 20:4n-3 from 18:4n-3. The  $\Delta 5$ -desaturase then converts 20:3n-6 and 20:4n-3 to form arachidonic acid (AA, 20:4n-6) and EPA (20:5n-3), respectively. A second elongation system converts AA to 22:4n-6 and converts EPA to 22:5n-3. It was generally believed that 22:5n-6 and DHA (22:6n-3) were formed from 22:4n-6 and 22:5n-3 by the action of  $\Delta 4$ -desaturase. However, results from several studies have indicated that such a  $\Delta 4$ -desaturase does not exist in mammalian tissues (7–10). Sprecher and others have shown that DHA is produced in mammalian cells through a pathway involving two consecutive elongation steps (from 20:4n-6 to 22:4n-6 and from 22:4n-6 to 24:4n-6 in the n-6 metabolic pathway, and from 20:5n-3 to 22:5n-3 and from 22:5n-3 to 24:5n-3 in the n-3 metabolic pathway) (11–16), followed by a

$\Delta 6$ -desaturation (from 24:4n-6 to 24:5n-6 in the n-6 pathway and from 24:5n-3 to 24:6n-3 in the n-3 pathway) and retro-conversion (from 24:5n-6 to 22:5n-6 and from 24:6n-3 to DHA, by  $\beta$ -oxidation in the peroxisomes) (Fig. 1) (17).

According to Sprecher's pathway, synthesis of long-chain PUFA (i.e., DHA from ALA and 22:5n-6 from LA) requires at least three different elongation steps. Since recent evidence has suggested that chain length-specific PUFA-elongating enzymes are present in rat microsomes (16–18), it is possible that the three elongation steps in Sprecher's pathway are regulated by different elongation enzymes. Previously, we isolated ELOVL5 from human liver and demonstrated the ability of the encoded enzyme to elongate C<sub>18</sub>- and C<sub>20</sub>-PUFA when expressed in baker's yeast, *Saccharomyces cerevisiae* (19). However, no enzyme that is involved in the elongation of 22:4n-6 to 24:4n-6 and 22:5n-3 to 24:5n-3, respectively, has been identified (17).

Recently, Tvrdik *et al.* (20) isolated a series of mouse elongation genes (Elovl1, Elovl2, and Elovl3). They showed that Elovl1 and Elovl3 genes are homologs of yeast ELO3 and ELO2 genes, respectively (21), and that their encoded proteins are involved in the elongation of a broad group of saturated and monounsaturated FA up to 24 carbons, but not long-chain PUFA (21). The specific activity of Elovl2, on the other hand, had not been established. Since the level of expression of Elovl2 is high in testis, which is also rich in long-chain PUFA, it is possible that Elovl2 is involved in the metabolism of long-chain PUFA species (20). In this report, we describe the isolation of Elovl2 from mouse and its homolog ELOVL2 from human, and demonstrate the involvement of their respective encoded enzymes in elongation of very long chain PUFA when expressed in baker's yeast and mammalian cells. This is the first report of mammalian genes encoded for very long chain PUFA-specific elongation enzymes involved in the biosynthesis pathway proposed by Sprecher (11).

## EXPERIMENTAL PROCEDURES

**Identification and cloning of the Elovl2 and ELOVL2 cDNA.** A Basic Local Alignment Search Tool (BLAST) search of the databases through the National Center for Biotechnology Information (NCBI) (<http://ncbi.nlm.nih.gov>) was carried out using the DNA sequence of human ELOVL5 as a query. The search resulted in identifying the mouse and human expressed sequence tag (EST) sequences with high homology to the ELOVL5 sequence. Primers were designed to PCR-amplify the protein coding regions of Elovl2 and ELOVL2 from mouse and human brain Marathon-Ready™ cDNA (Clontech, Palo Alto, CA), respectively. Primers RO819 (5'-ATG ATG CCA TGG AGC AGC TGA AGG CCT TTG-3') and RO820 (5'-CAG TCT CTG CTT TAA AAC AAG CTC GTC-3') were designed based on the putative Elovl2 sequence, and primers RO869 (5'-TGC GGA CCA TGG AAC ATC TAA AGG CCT TTG-3') and RO870 (5'-TTA CTC AAG CTT ATT GTG CTT TCT TGT TC-3') were designed based on the putative ELOVL2 sequence. The DNA frag-

ments were then ligated into the pYX242(*NcoI/HindIII*) vector (Novagen, Madison, WI) to form plasmids designated as pRAE-84 (Elovl2) and pRAE-90 (ELOVL2), respectively.

**Expression of the mouse and human cDNA in baker's yeast.** The plasmid DNA, pRAE-84 and pRAE-90, were transformed into *S. cerevisiae* 334, and the resulting clones were screened for elongase activity (22). *S. cerevisiae* 334, which contains only the pYX242 vector, was used as the negative control. The cultures were grown for 44 h at 30°C in selective media containing saturated FA (16:0, 18:0, 20:0, 22:0), monounsaturated FA (16:1, 18:1, 20:1), and different PUFA (e.g., LA, ALA, 18:3n-6, 18:4n-3, 20:4n-6, 20:5n-3, 22:4n-6, and 22:5n-3) as substrates.

**Cloning and expression of the mouse cDNA in L cells.** In this study, the mouse L cells used to generate the cell lines were derivatives of the fibroblast-like LtK cells (23). The mouse Elovl2 DNA fragment was ligated into the pMET vector to form the plasmid pMET-mELONGASE-bGHpA. Mouse L cells were then transfected with this plasmid by the calcium phosphate precipitation procedure to generate stable cell lines (24). The presence of the integrated elongation enzyme sequences in individual L-cell clones was verified by DNA slot blot hybridization analysis using an [ $\alpha$ -<sup>32</sup>P]dCTP-labeled *SmaI/EcoRI* fragment from pRAE-84. The resulting clones were screened for elongating activity in the serum-free medium with or without the added substrate. Mouse L cells without the mouse elongation enzyme cDNA were used as the negative control. The cells were grown in T25 cm<sup>2</sup> flasks to 80% confluency in DMEM (High Glucose; Gibco, Grand Island, NY) containing 10% Nu-Serum, 50  $\mu$ g/mL gentamicin sulfate, 15  $\mu$ g/mL hypoxanthine, 1  $\mu$ g/mL aminopterin, and 5.15  $\mu$ g/mL thymidine. The cells were then washed two times with 6 mL of serum-free DMEM and incubated for 18 h in 10 mL DMEM, 50  $\mu$ g/mL gentamicin sulfate, 15  $\mu$ g/mL hypoxanthine, 1  $\mu$ g/mL aminopterin, and 5.15  $\mu$ g/mL thymidine with or without substrate. In this study, 100  $\mu$ M of long-chain PUFA (20:4n-6, 22:4n-6, 20:5n-3, and 22:5n-3) were used as substrates for determination of the expressed cDNA activity. Following incubation, the cells were isolated by trypsin treatment, resuspended in 1 mL serum-free DMEM and pelleted by low-speed centrifugation. The supernatant was removed and the cells were stored at -80°C until FA analysis.

**Distribution of Elovl2 in mouse tissues.** Male (C57 Black) mice were fed a normal diet for 24 wk. Total RNA was isolated from fresh tissues using RNA STAT-60™ (Tel-Test Inc., Friendswood, TX). Ten micrograms of total RNA was resolved on a 1% agarose gel containing 1% formaldehyde and then transferred to GeneScreen Plus (NEN, Boston, MA). Membranes were hybridized overnight in ULTRAhyb™ solution (Ambion, Inc., Austin, TX). The cDNA probe for Elovl2 was the *SmaI/EcoRI* fragment from pRAE-84. The probe was labeled with [ $\alpha$ -<sup>32</sup>P]dCTP using the Random Primed DNA Labeling Kit (Roche, Palo Alto, CA).

**FA analysis.** The FA distribution (as percentage of total FA) of recombinant yeast cells containing pRAE-84, pRAE-90, pYX242, and mouse L cells inoculated with pMET-

mELONGASE-bGHPA, in the presence of various substrates, was analyzed following the method described previously (24–26). Briefly, the rinsed cell pellet was extracted with 20 mL of chloroform/methanol (2:1, vol/vol) containing 16 µg triheptadecanoin (used as the internal standard). After extraction, the total cell lipids were saponified and methylated. FAME were then analyzed by GC using a Hewlett-Packard gas-liquid chromatograph (model 6890) equipped with an FID and a 30-m fused-silica capillary column (0.32 mm, i.d.) coated with 0.25 µm Omegawax (Supleco, Bellefonte, PA). The injector and detector temperatures were 230°C. The FAME were identified by comparison of their retention times with authentic standards. The identity of novel FA was verified by GC-MS using a Hewlett-Packard mass selective detector (model 5972) operating at an ionization voltage of 70 eV with a scan range of 20–500 Da. The mass spectra of new peaks obtained were compared with those of a standard prepared by H. Sprecher. The percent conversion was calculated as  $[\text{product}/(\text{substrate} + \text{product})] \times 100$ .

## RESULTS

*Isolation of putative mouse and human cDNA sequences.* The human ELOVL5 translated sequence was used as a query to search the database for a putative mammalian protein sequence involved in the long-chain PUFA elongation of the retroconversion pathway. The search resulted in two full-length sequences, mouse Elovl2 and human ELOVL2. Mouse Elovl2 consisted of 876 bp, which encoded for 292 amino acids. The translated sequence of Elovl2 exhibited 58% iden-

tity with that of human ELOVL5 (Fig. 2). The sequence of human ELOVL2 consisted of 888 bp, which encoded for 296 amino acids. The putative human elongase had 56.4% identity with the human ELOVL5 protein (Fig. 2).

*Expression of the mouse and human cDNA in yeast.* To examine the substrate specificity of Elovl2 and ELOVL2, the recombinant yeast strains 334(pRAE-84) containing Elovl2 and 334(pRAE-90) containing ELOVL2 were grown in minimal media supplemented with 25 µM of different FA substrates. In yeast strains incubated with either saturated FA (16:0, 18:0, 20:0, and 22:0), or monounsaturated FA (16:1, 18:1, and 20:1), no elongation of these substrates was detected (data not shown). To examine if Elovl2 and ELOVL2 had the ability to elongate long-chain n-6 PUFA, the recombinant yeast strains 334(pRAE-84) and 334(pRAE-90) were grown in minimal media supplemented with 25 µM of 18:2n-6, 18:3n-6, 20:4n-6, or 22:4n-6. No elongation products were observed in 334(pRAE-84) and 334(pRAE-90) yeasts incubated with 18:2n-6 (data not shown). When 18:3n-6 was added as the substrate, a small level of 20:3n-6 (0.43% by weight of total yeast FA), the elongation product of 18:3n-6, was found in yeast strain 334(pRAE-84) but not in 334(pRAE-90) (Table 1). When both yeast strains were incubated with the 20- and 22-carbon long-chain n-6 PUFA, significant proportions of these substrates were converted to their respective elongated products. For example, when 20:4n-6 was added as the substrate, a considerable amount of 20:4n-6 was converted to 22:4n-6: 3.29% in strain 334(pRAE-84) and 1.18% in strain 334(pRAE-90). In addition to 22:4n-6, a novel FA was also observed in yeast lipid

ELOVL5	1	- - - MEHFDASLSTYFKALLGPRDTRVKGWFLLDNYIPT
ELOVL2	1	MEHLKAFDDEINAFLDNMFGRDPSRVRGWFTLDSYLP
Elovl2	1	MEQLKAFDNEVNAFLDNMFGPRDPSRVRGWFLLDYSYLP
ELOVL5	36	FICSVIYLLIVWLGPKYMRNKQPFSCRGILVVYNLGLT
ELOVL2	39	FFLTVMYLLSIWLGKMKYMRNRPALSLRGILTLYNLGIT
Elovl2	39	FILTIYLLSIWLGKMKYMRNRPALSLRGILTLYNLAIT
ELOVL5	74	LLSLYMFCELVTVGVEGKYNFFCQGTTRTAGESDMKIIIR
ELOVL2	77	LLSAYMLAELILSTWEGGYNLQCCDLTSAGEADIRVAK
Elovl2	77	LLSAYMLVELILSSWEGGYNLQCCNLD SAGEGDVIRVAK
ELOVL5	112	VLWWYYFSKLIIEFMDTFFFILRKNNHQITVLHVYHHAS
ELOVL2	115	VLWWYYFSKSVFELDTIFFVLRKKTSTQITFLHVYHHAS
Elovl2	115	VLWWYYFSKLVFELDTIFFVLRKKTSTQITFLHVYHHAS
ELOVL5	150	MLNIWWFVMNWPVPCGHSYFGATLNSFIHVLMSYYGLS
ELOVL2	153	MFNIWWCVLNIWIPCGQSFFFGPTLNSFVHILMSYYGLS
Elovl2	153	MFNIWWCVLNIWIPCGQSFFFGPTLNSFIHILMSYYGLS
ELOVL5	188	SVPSMRPYLWWKKYITQGGQLLQFVLTIIQTSCGVIWPC
ELOVL2	191	VFP SMHKYLWWKKYLTQAQLVQFVLTITHTMSAVVKPC
Elovl2	191	VFP SMHKYLWWKKYLTQAQLVQFVLTITHTLSAVVKPC
ELOVL5	226	TFPLGWLYFYQIGYMSLIALFTNFYIQTYNKKGASRRK
ELOVL2	229	GFPFGCLIFQSSYMLTLVILFLNFYVQTYRKKPM - - - K
Elovl2	229	GFPFGCLIFQSSYMMTLVILFLNFYIQTYRKKPM - - - K
ELOVL5	264	DHLKDHQNGSMAAVNGHTNSFSPLENNVKPRKLRKD
ELOVL2	264	KDMQEPAGK - EVKNGFSKAYFTAANGVMNKKAK
Elovl2	264	KELQE - - - K - EVKNGFPKAHLIVANGMTDKKAK

FIG. 2. Comparison of the deduced amino acid sequence of ELOVL5, ELOVL2, and Elovl2. The histidine box is underlined.



**TABLE 1**  
**FA Profiles (% by weight of total lipids) of Yeast Strains Containing pRAE-84, pRAE-90, or Vector Incubated with 25  $\mu$ M of Long-Chain n-6 PUFA (mean of four determinations)**

	18:3n-6			20:4n-6			22:4n-6		
	Control	pRAE-84	pRAE-90	Control	pRAE-84	pRAE-90	Control	pRAE-84	pRAE-90
18:3n-6	2.03	2.49	4.16	—	—	—	—	—	—
20:3n-6	—	0.43	—	—	—	—	—	—	—
20:4n-6	—	—	—	14.94	12.24	10.50	—	—	—
22:4n-6	—	—	—	—	3.29	1.18	11.44	16.60	20.34
24:4n-6	—	—	—	—	3.22	0.53	—	1.30	0.67

<sup>a</sup>pRAE-84, mouse ELOVL2 elongation enzyme gene; pRAE-90, human ELOVL2 elongation enzyme gene.

extracts. This FA had a retention time by GC and ion fragmentation pattern by GC–MS identical to those of the authentic 24:4n-6 standard (a gift from H. Sprecher) (Fig. 3). Thus, this novel FA was identified as 24:4n-6, an elongation product of 22:4n-6. The level of 24:4n-6 accounted for 3.22% in strain 334(pRAE-84), and 0.53% in strain 334(pRAE-90). Incubation with 22:4n-6 also resulted in an increase in the level of 24:4n-6 in both yeast strains (Table 1).

The recombinant yeast strains 334(pRAE-84) and 334(pRAE-90) were also grown in minimal media supplemented with 25  $\mu$ M of different n-3 long-chain PUFA substrates (e.g., 18:3n-3, 18:4n-3, 20:5n-3, and 22:5n-3). In yeasts incubated with 18:3n-3, no detectable amounts of 20:3n-3 (the elongation product of 18:3n-3) were found (data not shown). When incubated with 18:4n-3, a small portion of this FA (0.30%) in yeast strain 334(pRAE-84), but not 334(pRAE-90), was converted to its elongation product, 20:4n-3 (Table 2). When incubated with 20:5n-3 and 22:5n-3, both yeast strains showed the ability to elongate both n-3 PUFA (Table 2). Specifically, incubation with 20:5n-3 resulted in an increase in the levels of 22:5n-3, the direct elongation product of 20:5n-3. A novel FA was also detected in the yeast lipid extracts. The identity of this novel FA was confirmed to be 24:5n-3 based on its identical retention time and fragmentation pattern to that of the authentic 24:5n-3 standard (a gift from H. Sprecher) (Fig. 4). The levels of 24:5n-3 were found to be 3.38% in strain 334(pRAE-84) and 1.94% in strain 334(pRAE-90). Incubation with 22:5n-3 also significantly increased the levels of 24:5n-3: 2.02% in 334(pRAE-84) and 1.51% in 334(pRAE-90).

*Expression of the mouse cDNA in mouse L cells.* Control and Elov12-cloned mouse L cells (m-ELO) were incubated in serum-free medium containing 100  $\mu$ M of n-6 FA (i.e., 20:4n-6 and 22:4n-6). Results in Table 3 show that the FA profile of m-ELO cells was significantly different from that of the control cells. When 20:4n-6 was added as the substrate, the level of 24:4n-6 was significantly higher (3.01%) in cells inoculated with the Elov12 gene than that (0.59%) in the controls, an increase of more than fivefold. When 22:4n-6 was added as the substrate, the levels of 24:4n-6 in the m-ELO cells were significantly increased to 1.44% (vs. 0.06% in the controls). This represented a 24-fold increase.

Similar results were also seen in the control and m-ELO cells incubated in serum-free medium supplemented with two

different n-3 substrates, 20:5n-3 or 22:5n-3 (Table 4). In cells incubated with 20:5n-3, the level of 24:5n-3 was 1.69% in the m-ELO cells. When compared with the control cells (0.55%), there was a greater than threefold difference. When 22:5n-3 was added as the substrate, the level of 24:5n-3 was increased to 4.66% in the m-ELO cells. In comparison with the control cells (1.72%), this represents a threefold difference.

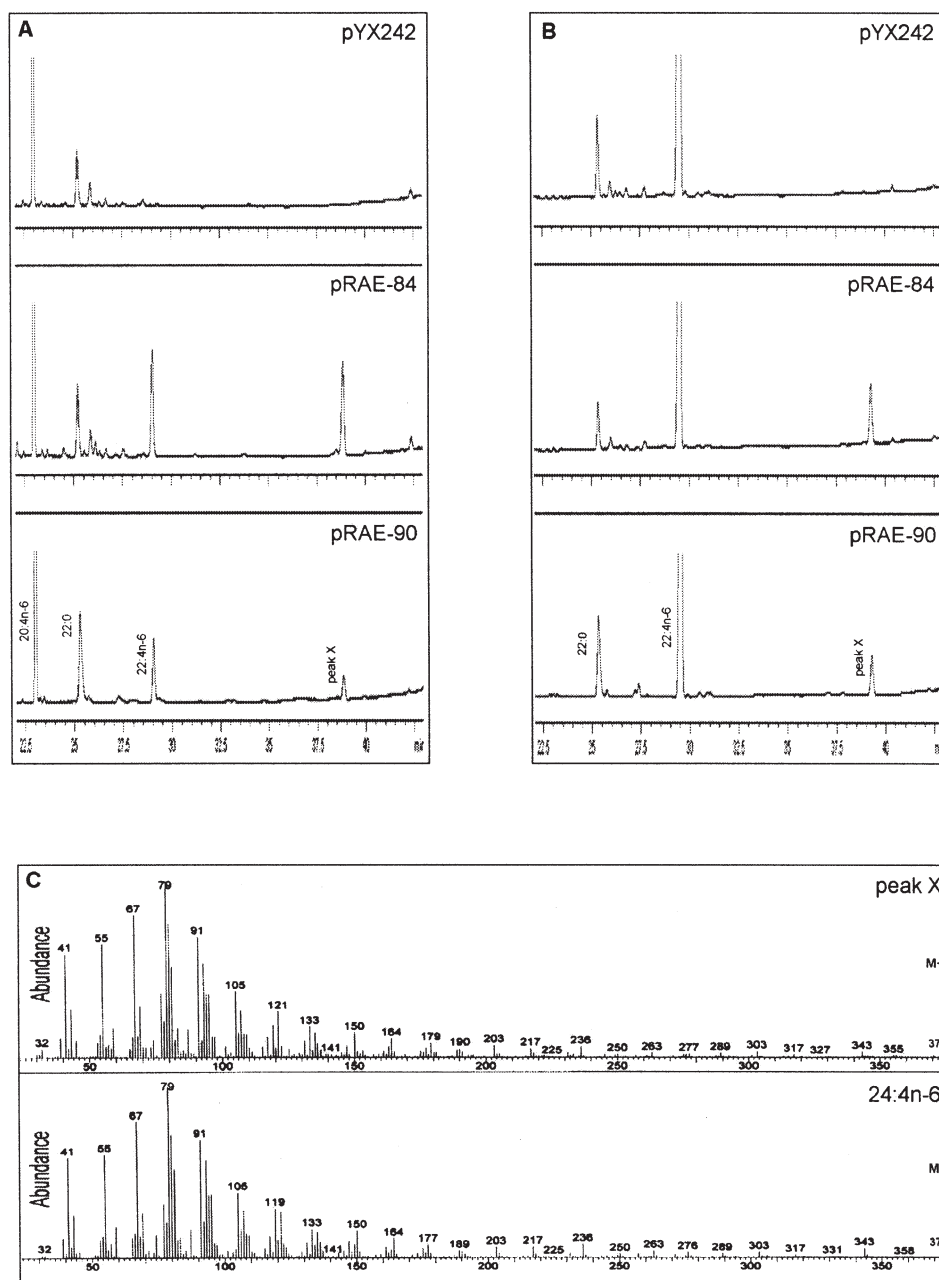
*Distribution of Elov12 mRNA in mouse tissues.* Northern blot analysis of Elov12 expression in several mouse tissues revealed that the highest levels of Elov12 mRNA were found in the testis and liver followed by brain and kidney (Fig. 5). A larger additional mRNA (5 Kb) was also found in the liver, and a smaller additional mRNA (1.3 Kb) in the testis of all mice.

## DISCUSSION

It was believed that DHA and 22:5n-6 were synthesized through the conversion of 22:5n-3 and 22:4n-6, respectively, by  $\Delta$ 4-desaturase. However, recent studies in mammalian cells by Sprecher and others (14,17) have shown that DHA and 22:5n-6 are produced from EPA and AA through a pathway involving two consecutive elongation steps, followed by a  $\Delta$ 6-desaturation and retroconversion by  $\beta$ -oxidation in the peroxisomes (7). Numerous elongation enzymes specific for saturated and monounsaturated FA (20,21), and a human enzyme, ELOVL5, responsible for the elongation of C<sub>18</sub>- and C<sub>20</sub>-PUFA, have previously been identified (19); however, the enzyme that elongates C<sub>20</sub>- and C<sub>22</sub>-PUFA, which is involved in Sprecher's pathway of long-chain PUFA synthesis, has not been identified. In this study, by comparing the identity of the known human PUFA elongation enzyme, ELOVL5, and mouse and human EST sequences, we have successfully identified the mouse Elov12 and human ELOVL2 cDNA sequences involved in long-chain PUFA biosynthesis.

When the mouse Elov12 cDNA was expressed in yeast cells, its encoded enzyme was actively involved in elongation of the added C<sub>20</sub>- to C<sub>22</sub>-PUFA and C<sub>22</sub>- to C<sub>24</sub>-PUFA. The encoded enzyme could also convert C<sub>18</sub>- to C<sub>20</sub>-PUFA to a lesser extent, but converted no saturated and monounsaturated FA substrates to their respective elongated products. This finding indicates that this mouse enzyme exhibits substrate specificity for both n-6 and n-3 long-chain PUFA.





**FIG. 3.** Gas chromatogram of long-chain FA in control yeast cells and yeast cells transformed with only the vector (pYX242), or with mouse Elov12 (pRAE-84) or human ELOVL2 (pRAE-90) elongation enzyme genes. The yeasts were incubated in 25  $\mu$ M of the substrate, either 20:4n-6 (panel A) or 22:4n-6 (panel B), for 44 h at 30°C. The GC-MS fragmentation pattern of peak X in yeast lipids was compared with that of the authentic 24:4n-6 (panel C).

When human ELOVL2 cDNA was expressed in yeast cells, its encoded elongation enzyme also converted the added C<sub>20</sub>- to C<sub>22</sub>-PUFA and C<sub>22</sub>- to C<sub>24</sub>-PUFA to their respective elongated products, but had no effect on C<sub>18</sub>-PUFA, saturated FA, or monounsaturated FA. This finding indicates that this human enzyme exhibited a substrate specificity for long-chain PUFA (C<sub>20</sub>- and C<sub>22</sub>-PUFA). However, unlike the mouse Elov12-encoded enzyme, this human enzyme had no effect on C<sub>18</sub>-PUFA. This suggests, in spite of high homology between

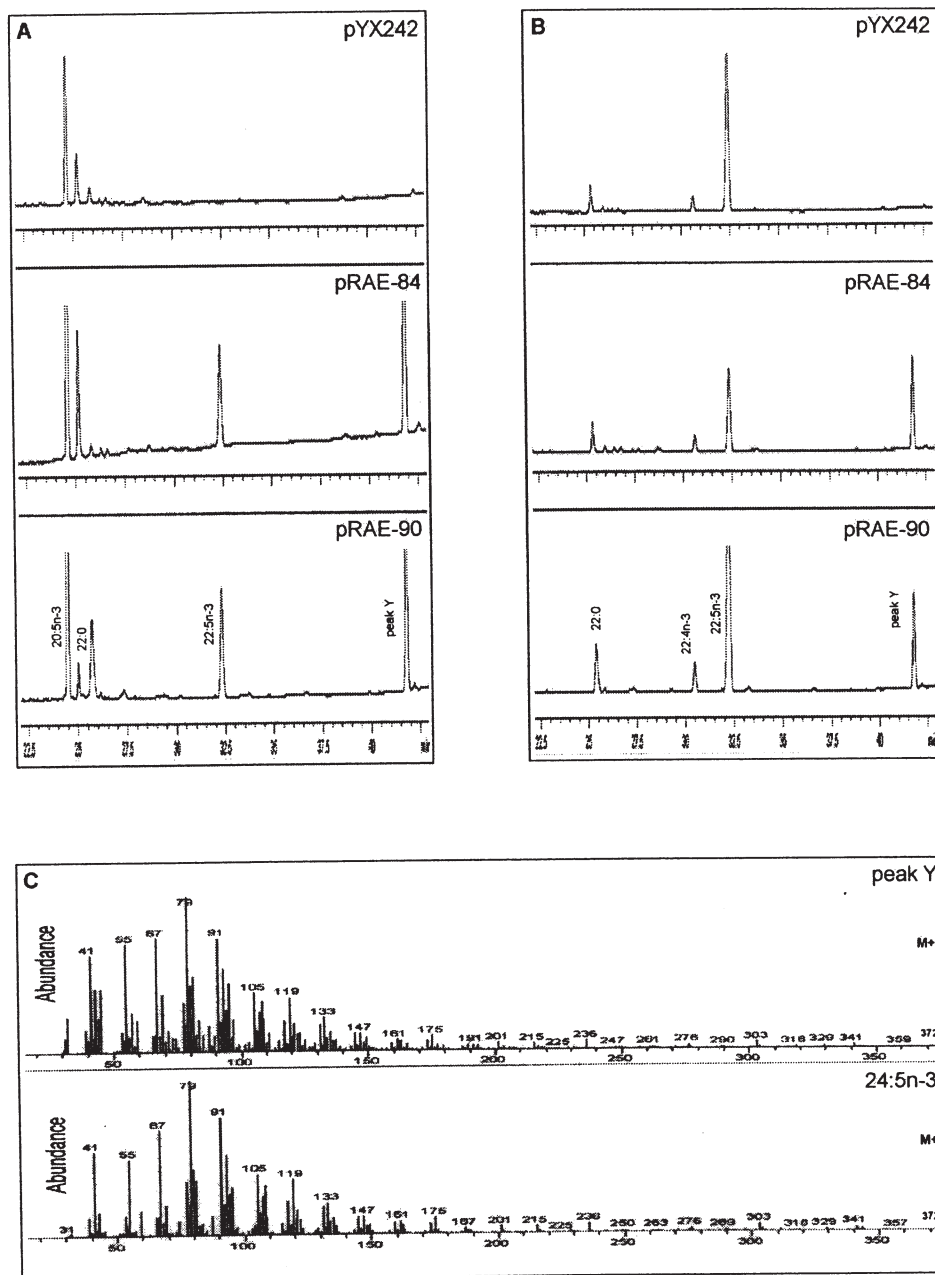
the human and mouse enzymes, there exists a species difference in substrate specificity. Nevertheless, our findings indicate that Elov12 and ELOVL2 are the enzymes responsible for the elongation of the long-chain PUFA in Sprecher's pathway in mouse and human tissues, respectively.

In a separate study, the mouse Elov12 cDNA was overexpressed in m-ELO cells. Results in Tables 3 and 4 show that when C<sub>20</sub>-PUFA were added as the substrate, there were marked accumulations of C<sub>22</sub>-PUFA and variable amounts of

**TABLE 2**  
**FA Profiles (% by weight of total lipids) of Yeast Strains Containing pRAE-84, pRAE-90, or Vector Incubated with 25  $\mu$ M of Long-Chain n-3 PUFA (mean of four determinations)<sup>a</sup>**

	18:4n-3			20:5n-3			22:5n-3		
	Control	pRAE-84	pRAE-90	Control	pRAE-84	pRAE-90	Control	pRAE-84	pRAE-90
18:4n-3	2.28	2.39	2.84	—	—	—	—	—	—
20:4n-3	—	0.30	—	—	—	—	—	—	—
20:5n-3	—	—	—	9.97	3.84	5.10	—	—	—
22:5n-3	—	—	—	—	1.21	1.64	8.79	5.87	8.36
24:5n-3	—	—	—	—	3.38	1.94	—	2.02	1.51

<sup>a</sup>For abbreviations see Table 1.



**FIG. 4.** Gas chromatogram of long-chain FA in control yeast cells and yeast cells transformed with only the vector (pYX242), or with mouse Elov12 (pRAE-84) or human ELOVL2 (pRAE-90) elongation enzyme genes. The yeasts were incubated in 25  $\mu$ M of the substrate, either 20:5n-3 (panel A) or 22:5n-3 (panel B), for 44 h at 30°C. The GC-MS fragmentation pattern of peak Y in yeast lipids was compared with that of the authentic 24:5n-3 (panel C).

**TABLE 3**  
**FA Profiles (% by weight of total lipids) of m-ELO or Control Cells Grown in the Presence of 100  $\mu$ M of Different n-6 FA (mean  $\pm$  SD of four determinations)<sup>a</sup>**

	No substrate		20:4n-6		22:4n-6	
	Control	m-ELO	Control	m-ELO	Control	m-ELO
20:4n-6	0.59 $\pm$ 0.02	1.06 $\pm$ 0.03	14.25 $\pm$ 0.22	22.71 $\pm$ 0.33	ND	ND
22:4n-6	0.02 $\pm$ 0.01	0.09 $\pm$ 0.01	7.78 $\pm$ 0.34	10.66 $\pm$ 0.50	4.40 $\pm$ 0.19	5.20 $\pm$ 0.45
24:4n-6	ND	ND	0.59 $\pm$ 0.06	3.01 $\pm$ 0.17	0.06 $\pm$ 0.04	1.44 $\pm$ 0.23

<sup>a</sup>ND, not detected. M-ELO, mouse L cells cloned with mouse elongase gene Elov12.

**TABLE 4**  
**FA Profiles (% by weight of total lipids) of m-ELO or Control Cells Grown in the Presence of 100  $\mu$ M of Different n-3 FA (mean  $\pm$  SD of four determinations)<sup>a</sup>**

	No substrate		20:5n-3		22:5n-3	
	Control	m-ELO	Control	m-ELO	Control	m-ELO
20:5n-3	0.05 $\pm$ 0.00	0.01 $\pm$ 0.01	5.59 $\pm$ 0.33	13.45 $\pm$ 1.12	ND	ND
22:5n-3	0.09 $\pm$ 0.01	0.13 $\pm$ 0.02	14.46 $\pm$ 0.14	14.78 $\pm$ 0.55	29.84 $\pm$ 0.98	36.04 $\pm$ 1.11
24:5n-3	ND	ND	0.55 $\pm$ 0.04	1.69 $\pm$ 0.15	1.72 $\pm$ 0.25	4.66 $\pm$ 0.12

<sup>a</sup>For abbreviations see Table 3.

C<sub>24</sub>-PUFA in both control and m-ELO cells. This finding suggests that the endogenous elongation enzyme in mouse cells was involved in elongation of C<sub>20</sub>-PUFA to C<sub>22</sub>-PUFA, and to a lesser extent the elongation of C<sub>22</sub>-PUFA to C<sub>24</sub>-PUFA. As results showed that the endogenous enzyme elongated C<sub>20</sub>-PUFA at a higher rate than the C<sub>22</sub>-PUFA, this step appeared to be rate-limiting. Nevertheless, the level of C<sub>24</sub>-PUFA of both n-3 and n-6 families was significantly higher in the m-ELO cells than in the control cells, whether the substrate was a C<sub>20</sub>- or a C<sub>22</sub>-PUFA, indicating an enhanced elongation of C<sub>22</sub>- to C<sub>24</sub>-PUFA in the m-ELO cells.

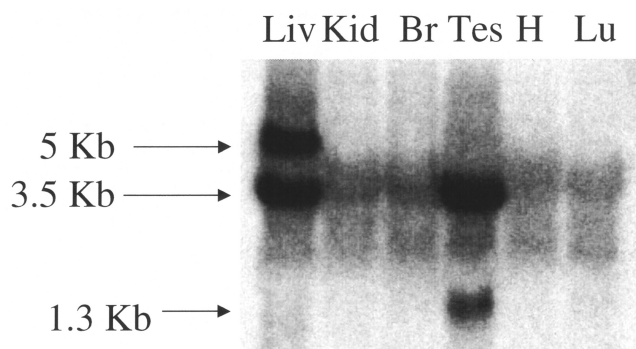
We have also examined the distribution of the Elov12 transcript in various mouse tissues and found that the levels of mRNA in the testis and liver were significantly higher than in other tissues examined (Fig. 5). These results parallel the higher levels of C<sub>22</sub> and C<sub>24</sub> FA detected in these tissues (6,27). Previously, Tvrđik *et al.* (20) hypothesized that due to high level in testis, Elov12 may be involved in long-chain

PUFA elongation. It is also noteworthy that a larger additional mRNA was found in the liver, and a smaller additional mRNA was found in the testis of all mice. The larger and smaller transcripts may express spliced variants of the Elov12 enzyme, which may be involved in the regulation of gene expression.

In summary, we have identified mouse and human genes that are homologs to the human ELOVL5 gene. Expression of Elov12 and ELOVL2 cDNA in baker's yeast and expression of Elov12 in mouse L cells produced an active enzyme involved in the elongation of C<sub>20</sub>- and C<sub>22</sub>-PUFA, but not saturated or monounsaturated FA. Our findings provide direct evidence of the existence of an elongation enzyme in mammalian cells that is involved in the biosynthesis pathway of long-chain PUFA (i.e., DHA and 22:5n-6), as proposed by Sprecher (11).

## REFERENCES

1. Samuelsson, B. (1983) From Studies of Biochemical Mechanism to Novel Biological Mediators: Prostaglandin Endoperoxides, Thromboxanes, and Leukotrienes. Nobel Lecture, 8 December 1982, *Biosci. Rep.* 3, 791–813.
2. Carlson, S.E., Werkman, S.H., Peeples, J.M., Cooke, R.J., and Tolley, E.A. (1993) Arachidonic Acid Status Correlates with First Year Growth in Preterm Infants, *Proc. Natl. Acad. Sci. USA* 90, 1073–1077.
3. Crawford, M.A., Costeloe, K., Ghebremeskel, K., Phylactos, A., Skirvin, L., and Stacey, F. (1997) Are Deficits of Arachidonic and Docosahexaenoic Acids Responsible for the Neural and Vascular Complications of Preterm Babies? *Am. J. Clin. Nutr.* 66, 1032S–1041S.
4. Uauy, R., Peirano, P., Hoffman, D., Mena, P., Birch, D., and Birch, E. (1996) Role of Essential Fatty Acids in the Function of the Developing Nervous System, *Lipids* 31, S167–S176.
5. Horrobin, D.F. (1992) Nutritional and Medical Importance of gamma-Linolenic Acid, *Prog. Lipid Res.* 31, 163–194.
6. Poulos, A. (1995) Very Long Chain Fatty Acids in Higher Animals—A Review, *Lipids* 30, 1–14.



**FIG. 5.** Tissue distribution of Elov12. The abundance of Elov12 transcript in various mouse tissues was determined by Northern analysis. Ten micrograms of total RNA was used for each tissue. Liv, liver; Kid, kidney; Br, brain; Tes, testis; H, heart; Lu, lung.

7. Voss, A., Reinhart, M., Sankarappa, S., and Sprecher, H. (1991) The Metabolism of 7,10,13,16,19-Docosapentaenoic Acid to 4,7,10,13,16,19-Docosahexaenoic Acid in Rat Liver Is Independent of a 4-Desaturase, *J. Biol. Chem.* **266**, 19995–20000.
8. Wang, N., and Anderson, R.E. (1993) Synthesis of Docosahexaenoic Acid by Retina and Retinal Pigment Epithelium, *Biochemistry* **32**, 13703–13709.
9. Mohammad, B.S., Sankarappa, S., Geiger, M., and Sprecher, H. (1995) Reevaluation of the Pathway for the Metabolism of 7,10,13,16-Docosatetraenoic Acid to 4,7,10,13,16-Docosapentaenoic Acid in Rat Liver, *Arch. Biochem. Biophys.* **317**, 179–184.
10. Moore, S.A., Hurt, E., Yoder, E., Sprecher, H., and Spector, A.A. (1995) Docosahexaenoic Acid Synthesis in Human Skin Fibroblasts Involves Peroxisomal Retroconversion of Tetracosahexaenoic Acid, *J. Lipid Res.* **36**, 2433–2443.
11. Sprecher, H. (2000) Metabolism of Highly Unsaturated n-3 and n-6 Fatty Acids, *Biochim. Biophys. Acta* **1486**, 219–231.
12. Delton-Vandenbroucke, I., Grammas, P., and Anderson, R.E. (1997) Polyunsaturated Fatty Acid Metabolism in Retinal and Cerebral Microvascular Endothelial Cells, *J. Lipid Res.* **38**, 147–159.
13. Caruso, D., Risé, P., Galella, G., Regazzoni, C., Toia, A., Galli, G., and Galli, C. (1994) Formation of 22 and 24 Carbon 6-Desaturated Fatty Acids from Exogenous Deuterated Arachidonic Acid Is Activated in THP-1 Cells at High Substrate Concentrations, *FEBS Lett.* **343**, 195–199.
14. Sprecher, H. (1996) New Advances in Fatty-Acid Biosynthesis; *Nutrition* **12**, S5–S7.
15. Marzo, I., Alava, M.A., Piñeiro, A., and Naval, J. (1996) Biosynthesis of Docosahexaenoic Acid in Human Cells: Evidence That Two Different  $\Delta 6$ -Desaturase Activities May Exist, *Biochim. Biophys. Acta* **1301**, 263–272.
16. Luthria, D.L., and Sprecher, H. (1997) Studies to Determine if Rat Liver Contains Multiple Chain Elongating Enzymes, *Biochim. Biophys. Acta* **1346**, 221–230.
17. Sprecher, H., Luthria, D.L., Mohammed, B.S., and Baykoucheva, S.P. (1995) Reevaluation of the Pathways for the Biosynthesis of Polyunsaturated Fatty Acids, *J. Lipid Res.* **36**, 2471–2477.
18. Su, H.-M., Moser, A.B., Moser, H.W., and Watkins, P.A. (2001) Peroxisomal Straight-Chain Acyl-CoA Oxidase and D-Bifunctional Protein Are Essential for the Retroconversion Step in Docosahexaenoic Acid Synthesis, *J. Biol. Chem.* **276**, 38115–38120.
19. Leonard, A.E., Bobik, E.G., Dorado, J., Kroeger, P.E., Chuang, L.-T., Thurmond, J.M., Parker-Barnes, J.M., Das, T., Huang, Y.-S., and Mukerji, P. (2000) Cloning of a Human cDNA Encoding a Novel Enzyme Involved in the Elongation of Long-Chain Polyunsaturated Fatty Acids, *Biochem. J.* **350**, 765–770.
20. Tvrđik, P., Westerberg, R., Silve, S., Asadi, A., Jakobsson, A., Cannon, B., Loison, G., and Jacobsson, A. (2000) Role of a New Mammalian Gene Family in the Biosynthesis of Very Long Chain Fatty Acids and Sphingolipids, *J. Cell Biol.* **149**, 707–717.
21. Oh, C.-S., Toke, D.A., Mandala, S., and Martin, C.E. (1997) *ELO2* and *ELO3*, Homologues of the *Saccharomyces cerevisiae ELO1* Gene, Function in Fatty Acid Elongation and Are Required for Sphingolipid Formation, *J. Biol. Chem.* **272**, 17376–17384.
22. Knutzon, D.S., Thurmond, J.M., Huang, Y.-S., Chaudhary, S., Bobik, E.G., Jr., Chan, G.M., Kirchner, S.J., and Mukerji, P. (1998) Identification of  $\Delta 5$ -Desaturase from *Mortierella alpina* by Heterologous Expression in Bakers' Yeast and Canola, *J. Biol. Chem.* **273**, 29360–29366.
23. Wigler, M., Pellicer, A., Silverstein, S., and Axel, R. (1978) Biochemical Transfer of Single-Copy Eucaryotic Genes Using Total Cellular DNA as Donor, *Cell* **14**, 725–731.
24. Kelder, B., Richmond, C., Stavnezer, E., List, E.O., and Kopchick, J.J. (1997) Production, Characterization, and Functional Activities of v-Ski in Cultured Cells, *Gene* **202**, 15–21.
25. Huang, Y.-S., Chaudhary, R., Thurmond, J.M., Bobik, E.G., Jr., Yuan, L., Chan, G.M., Kirchner, S., Mukerji, P., and Knutzon, D.S. (1999) Cloning of  $\Delta 12$ - and  $\Delta 6$ -Desaturases from *Mortierella alpina* and Recombinant Production of  $\gamma$ -Linolenic acid in *Saccharomyces cerevisiae*, *Lipids* **34**, 649–659.
26. Kelder, B., Mukerji, P., Kirchner, S., Hovanec, G., Leonard, A.E., Chuang, L.-T., Kopchick, J.J., and Huang, Y.-S. (2001) Expression of Fungal Desaturase Genes in Cultured Mammalian Cells, *Mol. Cell. Biochem.* **219**, 7–11.
27. Innis, S.M., Sprecher, H., Hachey, D., Edmond, J., and Anderson, R.E. (1999) Neonatal Polyunsaturated Fatty Acid Metabolism, *Lipids* **34**, 139–149.

[Received May 1, 2002, and in revised form July 22, 2002; revision accepted July 24, 2002]



# Effect of Dietary Conjugated Linoleic Acid (CLA) on Metabolism of Isotope-Labeled Oleic, Linoleic, and CLA Isomers in Women

E.A. Emken<sup>a,\*</sup>, R.O. Adlof<sup>a</sup>, S. Duval<sup>a</sup>, G. Nelson<sup>b</sup>, and P. Benito<sup>b</sup>

<sup>a</sup>USDA, ARS, National Center for Agricultural Utilization Research, Food & Industrial Oils, Peoria, Illinois 61604, and

<sup>b</sup>USDA, ARS, Western Human Nutritional Research Center, University of California, Davis, California 95616

**ABSTRACT:** The purpose of this study was to investigate the effect of dietary CLA on accretion of 9*c*-18:1, 9*c*,12*c*-18:2, 10*t*,12*c*-18:2, and 9*c*,11*t*-18:2 and conversion of these FA to their desaturated, elongated, and chain-shortened metabolites. The subjects were six healthy adult women who had consumed normal diets supplemented with 6 g/d of sunflower oil or 3.9 g/d of CLA for 63 d. A mixture of 10*t*,12*c*-18:2-*d*<sub>4</sub>, 9*c*,11*t*-18:2-*d*<sub>6</sub>, 9*c*-18:1-*d*<sub>8</sub>, and 9*c*,12*c*-18:2-*d*<sub>2</sub>, as their ethyl esters, was fed to each subject, and nine blood samples were drawn over a 48-h period. The results show that dietary CLA supplementation had no effect on the metabolism of the deuterium-labeled FA. These metabolic results were consistent with the general lack of a CLA diet effect on a variety of physiological responses previously reported for these women. The <sup>2</sup>H-CLA isomers were metabolically different. The relative percent differences between the accumulation of 9*c*,11*t*-18:2-*d*<sub>6</sub> and 10*t*,12*c*-18:2-*d*<sub>4</sub> in plasma lipid classes ranged from 9 to 73%. The largest differences were a fourfold higher incorporation of 10*t*,12*c*-18:2-*d*<sub>4</sub> than 9*c*,11*t*-18:2-*d*<sub>6</sub> in 1-acyl PC and a two- to threefold higher incorporation of 9*c*,11*t*-18:2-*d*<sub>6</sub> than 10*t*,12*c*-18:2-*d*<sub>4</sub> in cholesterol esters. Compared to 9*c*-18:1-*d*<sub>8</sub> and 9*c*,12*c*-18:2-*d*<sub>2</sub>, the 10*t*,12*c*-18:2-*d*<sub>4</sub> and 9*c*,11*t*-18:2-*d*<sub>6</sub> isomers were 20–25% less well absorbed. Relative to 9*c*-18:1, incorporation of the CLA isomers into 2-acyl PC and cholesterol ester was 39–84% lower and incorporation of 10*t*,12*c*-18:2 was 50% higher in 1-acyl PC. This pattern of selective incorporation and discrimination is similar to the pattern generally observed for *trans* and *cis* 18:1 positional isomers. Elongated and desaturated CLA metabolites were detected. The concentration of 6*c*,10*t*,12*c*-18:3-*d*<sub>4</sub> in plasma TG was equal to 6.8% of the 10*t*,12*c*-18:2-*d*<sub>4</sub> present, and TG was the only lipid fraction that contained a CLA metabolite present at concentrations sufficient for reliable quantification. In conclusion, no effect of dietary CLA was observed, absorption of CLA was less than that of 9*c*-18:1, CLA positional isomers were metabolically different, and conversion of CLA isomers to desaturated and elongated metabolites was low.

Paper no. L9030 in *Lipids* 37, 741–750 (August 2002).

The geometrical and positional isomers of conjugated octa-decadienoic acid are commonly referred to as CLA and have been reported to produce a variety of physiological effects.

\*To whom correspondence should be addressed at Midwest Research Consultants, 11422 Princeville-Jubilee Rd., Princeville, IL 61559. E-mail: eaemken@npoint.net

Abbreviations: AUC, area under the curve; CE, cholesterol ester; Chylo-TL, chylomicron total lipid; PC-1, 1-acyl phosphatidylcholine; PC-2, 2-acyl phosphatidylcholine; PL Total, total phospholipid; THP, tetrahydropyranyl; TL, total lipid.

Examples include body fat loss, increased lean body mass, anticarcinogenic activity, antiatherogenic effects, reduced glucose levels, and enhanced immune function. Studies related to these and other physiological and health effects of CLA have recently been reviewed (1–3). The metabolism of CLA isomers in rats and yeast cells has been investigated (4–8), but no definitive data are available on the metabolism of CLA isomers in human subjects.

Three recent human studies have reported that supplementation with 0.36 to 3.2 g/d of CLA reduced the percent body fat compared to the control group (9–11). Differences in plasma lipid FA composition following dietary CLA supplementation suggested that CLA decreased Δ-6 and Δ-9 desaturase and increased Δ-5 desaturase activity (11). The results from a fourth study with adult women receiving 3.9 g/d of CLA for 63 d have been reported recently in a series of papers (12–18). In this study, CLA supplementation did not produce measurable effects on body composition, energy expenditure, lipolysis, plasma leptin concentrations, appetite, platelet function, blood coagulation, immune response, and mononuclear cell function (12–15). Diet did not influence cytokines and eicosanoid secretion *in vitro* and did not alter plasma cholesterol, LDL, HDL, or TG levels (16,18). An almost fourfold increase in the weight percentage of CLA in plasma lipid occurred, but there was no change in the CLA content of adipose tissue (18).

The purpose of this study was to address the following questions that relate to the metabolism of CLA isomers in a subgroup of adult women from the above dietary study. Does dietary CLA supplementation influence accretion and turnover of oleic acid, linoleic acid, and CLA isomers in plasma lipids? To what degree does conjugation of a *trans* double bond with a *cis*-9 or a *cis*-12 double bond influence unsaturated FA metabolism? Are there significant differences between the metabolism of the two CLA isomers (9*c*,11*t*-18:2 and 10*t*,12*c*-18:2) most prevalent in diets?

## EXPERIMENTAL PROCEDURES

**Study design.** Six Caucasian female subjects enrolled in a CLA diet study volunteered to participate in this stable isotope study. Three of the women were from the control group that had received a sunflower oil supplement (6 g/d), and three were from the experimental group that had received 6

**TABLE 1**  
**Physical Characteristics and Plasma Lipid Profiles of Female Subjects<sup>a</sup>**

Diet group <sup>b</sup>	Subject number	Body wt (kg)	BMI <sup>c</sup> (kg/m <sup>2</sup> )	Plasma lipids (mg/dL) <sup>d</sup>		
				TG	Cholesterol	Total lipid <sup>e</sup>
Cntrl	1	63.6	21.32	67	174	139
	2	87.2	28.39	46	212	177
	3	54.0	20.43	53	211	214
Exp	4	55.6	21.71	64	200	214
	5	65.1	23.16	44	155	167
	6	54.5	21.98	77	216	231

<sup>a</sup>Nonsmokers, ages 23 to 41, normal hypertensive.

<sup>b</sup>Cntrl, control diet. Exp, experimental CLA diet.

<sup>c</sup>BMI, body mass index.

<sup>d</sup>Fasting plasma lipid concentrations at end of 60 d diet period.

<sup>e</sup>mg of total lipid FA per 100 mL of plasma.

g/d of a commercially produced CLA supplement for 60 d. The CLA supplement contained 65% CLA (3.9 g/d of CLA). The subjects were between the ages of 23 and 41 yr and were housed in a metabolic ward. Physical examinations and clinical blood profile data indicated that all subjects were in good health. Medical histories indicated no evidence of congenital ailments. The subjects' height/weight ratios, blood pressures, and fasting serum cholesterol and TG concentrations were within normal ranges. Physical characteristics and plasma lipid profiles for the subjects participating in this isotope study are summarized in Table 1. Plasma lipid data are for blood samples drawn at the end of the diet study. Institutional ethical approval was obtained for the study protocol from the Agricultural Research Service's Human Studies Institutional Review Committee and the University of California at Davis, Human Subjects Committee. Informed consent was obtained from each subject before initiation of the study. Complete information on the study design, diet compositions, and other details has been described previously (12,14).

**Deuterated FA.** The synthesis of deuterium-labeled methyl *cis*-9,*cis*-12-octadecadienoate-12,13-*d*<sub>2</sub> (9*c*,12*c*-18:2-*d*<sub>2</sub>) and methyl *trans*-10,*cis*-12-octadecadienoate-15,15,16,16-*d*<sub>4</sub> (10*t*,12*c*-18:2-*d*<sub>4</sub>) were synthesized and purified as previously reported (19,20). Methyl *cis*-9-octadecenoate-11,11,12,12,17,17,18,18-*d*<sub>8</sub> (9*c*-18:1-*d*<sub>8</sub>) was prepared in a manner analogous to that described for 9*c*-18:1-14,14,15,15,17,18-*d*<sub>6</sub> (21). To prepare the -*d*<sub>8</sub> analog, 5-hexyn-1-ol was converted to the tetrahydropyranyl (THP) ether, reduced (<sup>2</sup>H<sub>2</sub>; Wilkinson's catalyst) to yield the THP ether of hexanol-5,5,6,6-*d*<sub>4</sub>, and the THP ether was converted to the iodide (H<sub>3</sub>PO<sub>4</sub>/P<sub>2</sub>O<sub>5</sub>/KI). The C6 iodide was coupled (lithium metal/liquid NH<sub>3</sub>) with 2-propyn-1-ol to yield 2-nonyn-1-ol-8,8,9,9-*d*<sub>4</sub>. The nine-carbon acetylenic alcohol-*d*<sub>4</sub> was converted to the THP ether and reduced (Wilkinson's catalyst; <sup>2</sup>H<sub>2</sub>) to form the THP ether of nonanol-2,2,3,3,8,8,9,9-*d*<sub>8</sub>. The THP ether of nonanol-*d*<sub>8</sub> was converted to 1-iodononane-*d*<sub>8</sub> (H<sub>3</sub>PO<sub>4</sub>/P<sub>2</sub>O<sub>5</sub>/KI), then to 1-nonyl-*d*<sub>8</sub>-triphenylphosphonium iodide, and the phosphonium salt was coupled with methyl 9-oxononanoate (Wittig reaction) to yield 9*c*-18:1-*d*<sub>8</sub>. The synthesis of methyl *cis*-9,*trans*-11-octadecadienoate-14,14,15,15,17,18-*d*<sub>6</sub> (9*c*,11*t*-18:2-*d*<sub>6</sub>) was analogous to preparation of 9*c*,11*t*-18:2-17,17,18,18-*d*<sub>4</sub>

(20) except that the THP ether of hexanol-2,2,3,3,5,6-*d*<sub>6</sub> [2-(hexyloxy-2,2,3,3,5,6-*d*<sub>6</sub>) tetrahydropyran] was utilized as the deuterium-containing fragment. The hexanol-*d*<sub>6</sub> was prepared by reduction (Wilkinson's catalyst/D<sub>2</sub> gas) of the THP ether of 2-hexyn-5-ene-1-ol. The "ene-yne-ol" THP ether was prepared by coupling (Grignard) 1-bromo-prop-2-ene with the THP ether of 2-propyn-1-ol. The THP ether of hexanol-2,2,3,3,5,6-*d*<sub>6</sub> was converted to the iodide (H<sub>3</sub>PO<sub>4</sub>/P<sub>2</sub>O<sub>5</sub>/KI), then coupled with 2-propyn-1-ol to yield 2-nonyn-1-ol-*d*<sub>6</sub>, which was reduced (lithium metal/liquid NH<sub>3</sub>) to *trans*-2-nonen-1-ol-*d*<sub>6</sub>, converted to 1-bromo-*trans*-2-nonen-*d*<sub>6</sub> (with Ph<sub>3</sub>PBr<sub>2</sub>). This triphenylphosphonium salt was subsequently coupled (Wittig reaction) with methyl 9-oxononanoate to yield 9*c*,11*t*-18:2-*d*<sub>6</sub>. The deuterated FAME were converted to their ethyl esters using sodium metal in ethanol as previously described (22). The isotopic purity of the deuterated FA was: 85.8% for 9*c*-18:1-*d*<sub>8</sub>, 73.4% for 9*c*,12*c*-18:2-*d*<sub>2</sub>, 83.5% for 9*c*,11*t*-18:2-*d*<sub>6</sub>, and 83.7% for 10*t*,12*c*-18:2-*d*<sub>4</sub>. Chemical purity was 90.6% for 9*c*-18:1-*d*<sub>8</sub>, 78.9% for 9*c*,12*c*-18:2-*d*<sub>2</sub>, 91.6% for 9*c*,11*t*-18:2-*d*<sub>6</sub>, and 89.9% for 10*t*,12*c*-18:2-*d*<sub>4</sub>. Impurities were small amounts (1 to 5%) of deuterated odd chain-length and *trans* FA isomers. Nondeuterated 16:0, 18:0, and 9*c*-18:1 (13% total) were also present in 9*c*,12*c*-18:2-*d*<sub>2</sub>.

**Stable isotope study design.** A mixture of deuterated ethyl esters (62.4 g) containing 9*c*-18:1-*d*<sub>8</sub>, 9*c*,12*c*-18:2-*d*<sub>2</sub>, 9*c*,11*t*-18:2-*d*<sub>6</sub>, and 10*t*,12*c*-18:2-*d*<sub>4</sub> was blended for 1 min with 950 g of no-fat yogurt and 92.7 g of powdered sugar in a blender blanketed with nitrogen. The six subjects were fasted overnight (12 h), and each subject was fed a one-sixth portion of the deuterated ethyl ester mixture. The first subject was fed at 7:00 A.M. and the remaining subjects were fed at 10-min intervals in order to allow time for blood draws. The amount of deuterated ethyl esters fed to each subject was 1.77 g 9*c*-18:1-*d*<sub>8</sub>, 3.30 g 9*c*,12*c*-18:2-*d*<sub>2</sub>, 2.66 g 9*c*,11*t*-18:2-*d*<sub>6</sub>, and 2.68 g 10*t*,12*c*-18:2-*d*<sub>4</sub> after adjusting the actual weights for chemical and isotopic purity. Subjects were provided a no-fat breakfast at 8:00 A.M. A low-fat (ca.15% fat calories) lunch was provided at 12:00 noon. Following the noon meal, subjects returned to their respective control or CLA diet schedule.

**Sample collection.** Blood samples (14 mL each) were collected by venipuncture at 0, 2, 4, 6, 8, 12, 24, 36, and 48 h and

used for isolation of plasma lipid classes. Additional blood samples (*ca.* 14 mL) were collected at 2, 4, and 6 h and used for isolation of chylomicron total lipid (Chylo-TL). Chylomicron fractions were isolated by conventional preparative ultracentrifuge methods (23). Representative chylomicron samples were analyzed by electrophoresis to confirm the purity of the chylomicron fractions (24).

**Analysis of plasma lipid FA.** Plasma lipids were extracted with 2:1 chloroform/methanol (25). Preparative TLC was used to isolate TG, cholesterol ester (CE), and phospholipid fractions from plasma total lipid (TL) (26). Known weights of triheptadecanoin, cholesterol heptadecanoate, and diheptadecanyl-*sn*-phosphatidylcholine (Applied Science, State College, PA) were added as internal standards to the TL extract. Methanolic sodium methoxide was used to prepare methyl esters from the isolated lipid classes (22). The FA at the 1-acyl and 2-acyl positions of PC were determined by isolation and analysis of products produced following treatment of PC with *Ophiophagus hannah* venom (Kentucky Reptile Zoo, Slade, KY) (27).

The percentages of labeled and unlabeled FA in the plasma lipid classes were obtained by GC-MS analysis of their methyl esters (28). Weights of the 17:0 internal standards added were used to determine the concentrations (mg/mL) of each deuterated and nondeuterated FA. A Hewlett-Packard model 5988A quadrupole mass spectrometer operated in a positive CI mode with isobutane as the ionization reagent was used to analyze the methyl ester samples. The GC-MS methodology utilized selected ion monitoring of the appropriate ion masses for the FA in each GC peak. The areas for each of the ion masses monitored were obtained by integration of the selected ion peaks. The gas chromatograph-mass spectrometer was equipped with a SUPELCOWAX 10 fused-silica column (30 m  $\times$  0.25 mm; Supelco Inc., Bellefonte, PA). The column was temperature-programmed from 165 to 265°C at 5°C/min with a 20-min final hold. The specific operating conditions and computer-assisted storage and processing of the MS data have been described previously (28,29). Response factors were determined by analysis of standard mixtures containing weighed amounts of pure fatty methyl esters purchased from Nu-Chek- Prep Inc. (Elysian, MN) and Applied Science. The accuracy of the GC-MS data was determined by analysis of plasma TG, phospholipid, and CE samples containing known weights of 9*c*,18:1-*d*<sub>8</sub>, 9*c*,12*c*-18:2-*d*<sub>2</sub>, 9*c*,11*t*-18:2-*d*<sub>6</sub>, and 10*t*,12*c*-18:2-*d*<sub>4</sub>. The weight for each of the deuterated fatty esters added was equal to about 0.3% of the total unlabeled FA in the samples. SD were based on three replicate analyses. The SD for 9*c*,18:1-*d*<sub>8</sub>, 9*c*,12*c*-18:2-*d*<sub>2</sub>, 9*c*,11*t*-18:2-*d*<sub>6</sub>, and 10*t*,12*c*-18:2-*d*<sub>4</sub> in the TG, phospholipid, and CE-spiked samples ranged from  $\pm$ 0.002 to 0.004.

The accuracy of the GC-MS data for unlabeled methyl esters was confirmed by analysis of a subset of samples using a Varian model 3400 gas chromatograph. The GC was equipped with a 100 m  $\times$  0.25 mm SP2560 fused-silica capillary column (Supelco) and an FID. Operating conditions were: split ratio, 1:100; linear velocity of helium, 21 cm/s;

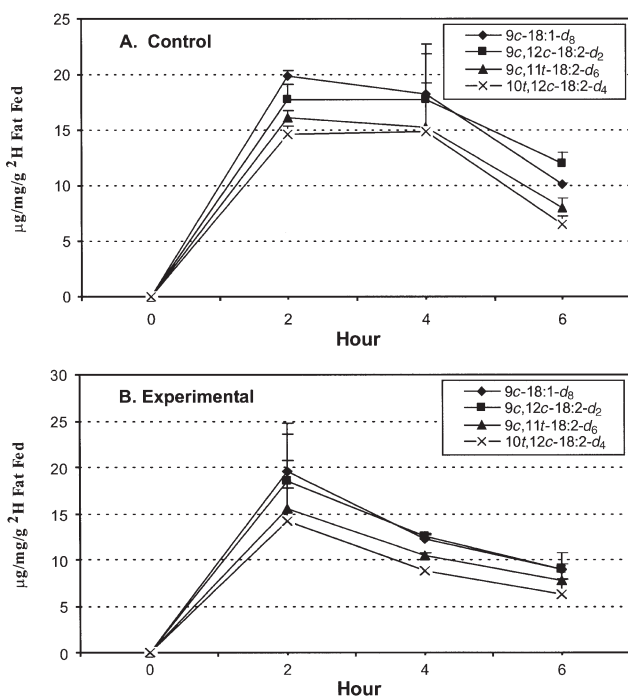
detector and injection temperature, 235°C. The identification and accuracy of the GC peaks areas were confirmed by comparison to data for authentic standards and mixtures of known composition.

**Statistical analysis and calculations.** A two-tailed, unpaired *t*-test was used to test for significant differences between control and experimental diet group data for the same FA. A two-tailed, paired *t*-test was used to test for significant differences between data for different deuterium-labeled FA (30). For comparisons of different labeled FA, the data for the individual control and experimental samples were pooled since the data for the two groups were not significantly different. The concentration data ( $\mu$ g/mL) for the deuterated FA and their metabolites were normalized to compensate for differences in plasma lipid concentrations of the subjects and for differences between the weights of <sup>2</sup>H-FA in the fed mixture. Normalization of the data to a per gram of deuterated FA fed basis was achieved by dividing the mg of deuterated FA per mL plasma data by the total concentration (mg/mL plasma) of the sample. The  $\mu$ g of deuterated FA per mg of TL data were then divided by the weights for the deuterated FA in the fed mixture. Time-course curves were produced by plotting the normalized  $\mu$ g deuterated FA/mg of TL data for the nine samples collected over the 48-h study period. The total area-under-curve (AUC) data were obtained by calculating the total area under the time-course curve, as described previously (31,32), and are similar to weighted-average data.

## RESULTS

**Absorption.** The time-course curves for Chylo-TL are shown in Figure 1 for 9*c*,11*t*-18:2-*d*<sub>6</sub>, 10*t*,12*c*-18:2-*d*<sub>4</sub>, 9*c*,12*c*-18:2-*d*<sub>2</sub> and 9*c*-18:1-*d*<sub>8</sub>. These curves provide a comparison of the relative absorption and clearance of these FA. Clearance of the labeled FA appears to be faster for the CLA diet group, but there were no significant differences between AUC data from the control and experimental groups. The Chylo-TL results show that 10*t*,12*c*-18:2-*d*<sub>4</sub> was about 10% less well absorbed than 9*c*,11*t*-18:2-*d*<sub>6</sub> ( $P < 0.001$  for pooled control plus experimental data) and that both CLA isomers were 20–25% less well absorbed than oleic and linoleic acid ( $P < 0.001$ ).

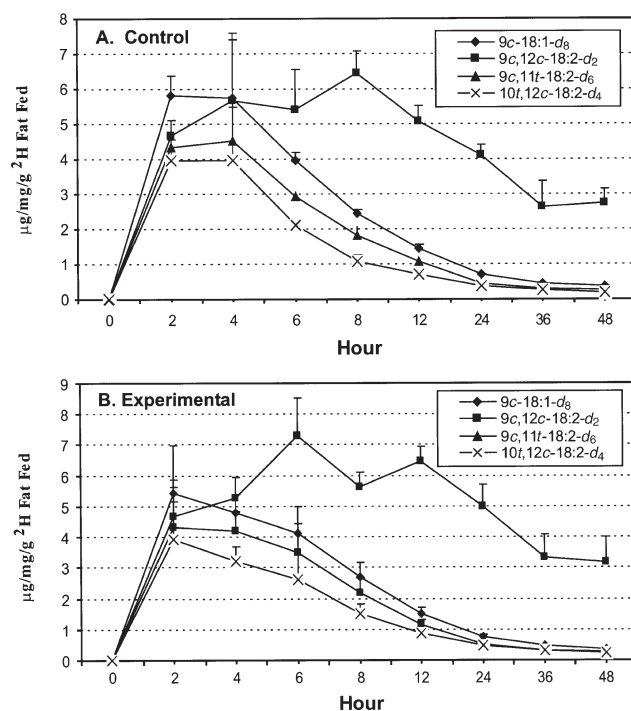
**Effect of diet.** Time-course curves for the major lipid classes in plasma are shown in Figures 2–6. Comparison of data plots from women fed the control and CLA-supplemented experimental diets show that dietary CLA had little influence on incorporation of the deuterium-labeled FA used in this study. The total areas for these curves are summarized in Table 2. The control vs. experimental diet data were not significantly different except for 9*c*,11*t*-18:2-*d*<sub>6</sub> CE and 9*c*-18:1-*d*<sub>8</sub> PE data. Accumulation of 9*c*,11*t*-18:2-*d*<sub>6</sub> in CE was low, but it was 65.5% higher ( $P < 0.02$ ) for subjects fed the control diet than for the experimental group subjects. In contrast, control vs. experimental group CE data for the 10*t*,12*c*-18:2-*d*<sub>4</sub> CLA isomer are not significantly different. The concentration of 9*c*-18:1-*d*<sub>8</sub> in PE was 6.5  $\mu$ g/mg/g higher for the CLA-supplemented diet than for the control diet ( $P < 0.02$ ),



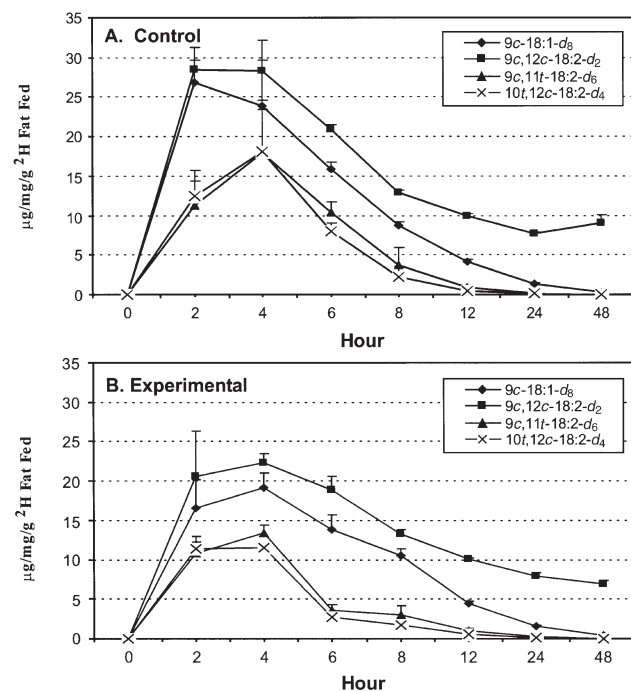
**FIG. 1.** Time-course plots for uptake and clearance of  $9c$ - $18:1$ - $d_8$ ,  $9c,12c$ - $18:2$ - $d_2$ ,  $9c,11t$ - $18:2$ - $d_6$  and  $10t,12c$ - $18:2$ - $d_4$  in chylomicron total lipids of subjects fed the control and experimental diets. Each data point is the average for data from three subjects. Error bars equal SE. Error bars are not shown when less than the size of the symbol.

but the time-course curves show this minor difference was due to the 8-h sample data. Overall, the effect of dietary supplementation with 3.9 g/d of CLA on the accumulation and turnover of  $9c,11t$ - $18:2$ - $d_6$ ,  $10t,12c$ - $18:2$ - $d_4$ ,  $9c,12c$ - $18:2$ - $d_2$  and  $9c$ - $18:1$ - $d_8$  in plasma lipids was limited and consistent with the absence of a dietary supplementation effect.

**Comparisons of FA accretion in plasma lipid classes.** An overview of differences between the lipid class data is provided by the percent  $^2H$ -FA data in Figure 7. The percentage data illustrate the relative difference between incorporation of  $9c,11t$ - and  $10t,12c$ - $18:2$ , the general overall discrimination against incorporation of the CLA isomers, and the obvious (expected) preference for  $9c,12c$ - $18:2$ - $d_2$  incorporation. The differences between the percentages shown for Chyl-TL and the other lipid classes are a reflection of enzyme specificity for incorporation of the deuterated FA. For example, 78% of all the deuterated FA incorporated in total PC was  $9c,12c$ - $18:2$ - $d_2$ , which is consistent with the high  $9c,12c$ - $18:2$ - $d_2$  content observed for human plasma PC. The percentages for  $9c$ - $18:1$ - $d_8$  (7.5%) and  $9c,11t$ - $18:2$ - $d_6$  (6.0%) were not significantly different, but the percentage for  $10t,12c$ - $18:2$ - $d_4$  (8.4%) was significantly higher ( $P < 0.001$ ) than  $9c$ - $18:1$ - $d_8$  and  $9c,11t$ - $18:2$ - $d_6$  due to its selective incorporation in the 1-acyl PC (PC-1) position (34% of total deuterated FA). The lower percentage for the CLA isomers in plasma TL and TG than for  $9c$ - $18:1$ - $d_8$  suggests that the  $\beta$ -oxidation rates for the CLA isomers were higher than for  $9c$ - $18:1$ .

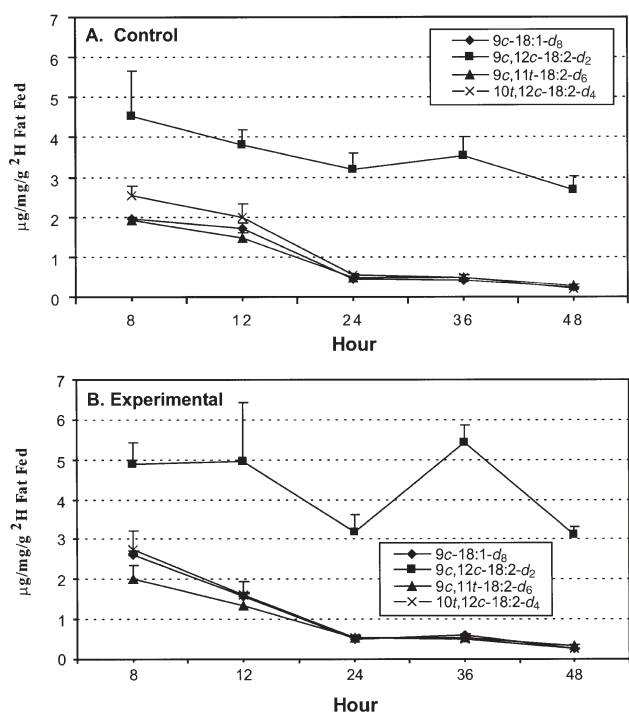


**FIG. 2.** Time-course plots for uptake and clearance of  $9c$ - $18:1$ - $d_8$ ,  $9c,12c$ - $18:2$ - $d_2$ ,  $9c,11t$ - $18:2$ - $d_6$  and  $10t,12c$ - $18:2$ - $d_4$  in plasma total lipid of subjects fed the control and experimental diets. Each data point is the average for data from three subjects. Error bars equal SE. Error bars are not shown when less than the size of the symbol.



**FIG. 3.** Time-course plots for uptake and clearance of  $9c$ - $18:1$ - $d_8$ ,  $9c,12c$ - $18:2$ - $d_2$ ,  $9c,11t$ - $18:2$ - $d_6$ , and  $10t,12c$ - $18:2$ - $d_4$  in plasma TG of subjects fed the control and experimental diets. Each data point is the average for data from three subjects. Error bars equal SE. Error bars are not shown when less than the size of the symbol.

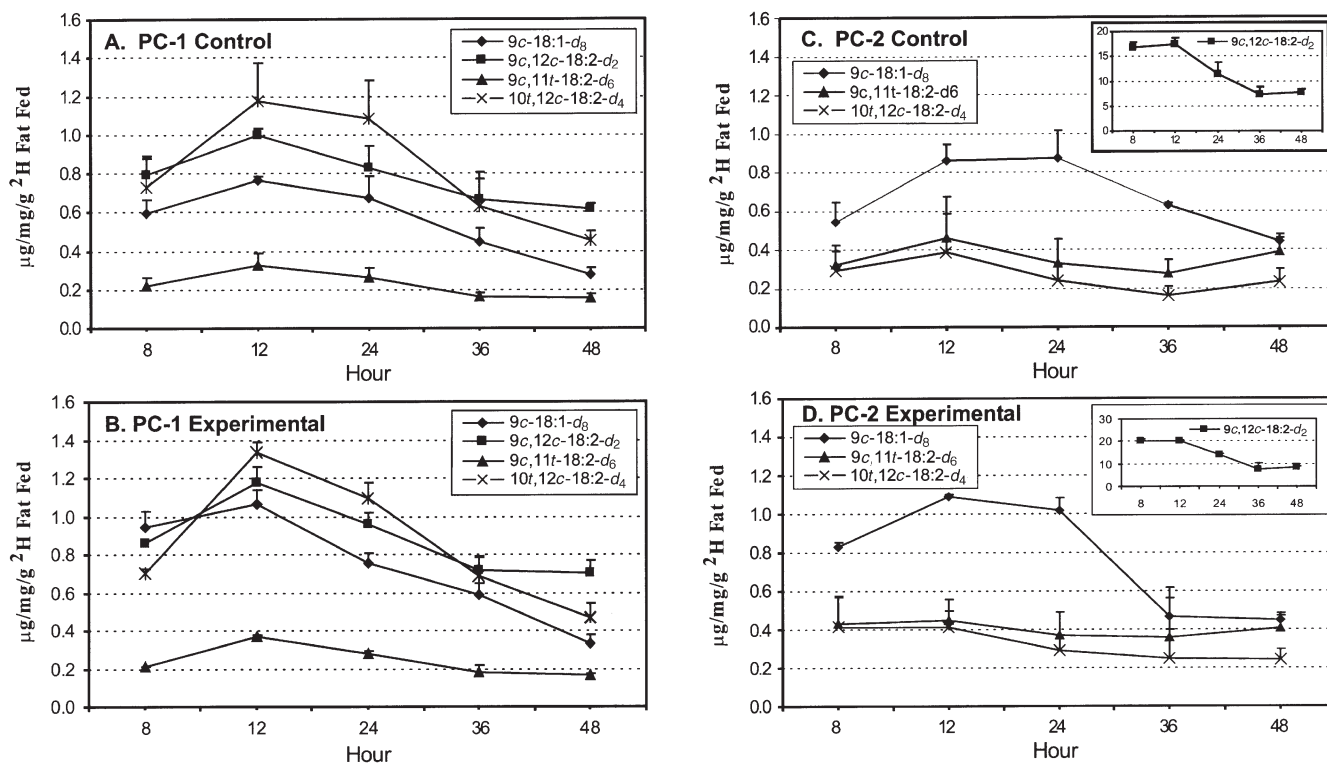




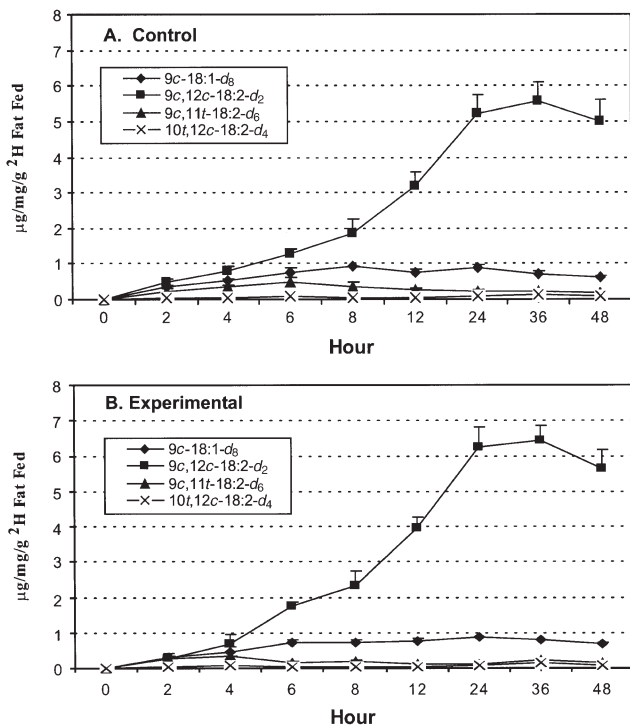
**FIG. 4.** Time-course plots for uptake and clearance of  $9c$ - $18:1-d_8$ ,  $9c,12c$ - $18:2-d_2$ ,  $9c,11t$ - $18:2-d_6$ , and  $10t,12c$ - $18:2-d_4$  in plasma PE of subjects fed the control and experimental diets. Each data point is the average for data from three subjects. Error bars equal SE. Error bars are not shown when less than the size of the symbol.

The selectivity ratios shown in Table 3 for  $9c,11t$ - $18:2-d_6$ ,  $10t,12c$ - $18:2-d_4$ , and  $9c,12c$ - $18:2-d_2$  are a measure of the acyltransferase selectivity for incorporation of these FA into the various plasma lipid classes. Previously reported (33–38) selectivity values for *trans*- and *cis*- $18:1$  positional isomers and  $18:0$  were recalculated as simple ratios and are included for comparison. Note that  $9c$ - $18:1$  is the reference FA and has a selectivity value of 1.0. Values less than 1.0 indicate discrimination and values greater than 1.0 indicate preferential incorporation. The selectivity values within a specific lipid class for  $9c,11t$ - $18:2-d_6$  and  $10t,12c$ - $18:2-d_4$  are in the same range as values listed for the positional  $18:1$  isomers. The exception is the PC-1 value for  $9c,11t$ - $18:2-d_6$  (0.46), which is much smaller than values listed for other isomers. The selectivity value of 0.46 for  $9c,11t$ - $18:2-d_6$  indicates that  $9c,11t$ - $18:2-d_6$  incorporation at the PC-1 position was about 50% lower than for  $9c$ - $18:1-d_8$  and 5–9 times less than for the other  $18:1$  isomers listed in Table 3. These results suggest that, compared to most other FA isomers,  $9c,11t$ - $18:2-d_6$  has an atypical configuration and is not a good substrate for PC transferase. However, a comparison of the selectivity values for accretion of  $9c,11t$ - $18:2-d_6$  and  $10t,12c$ - $18:2-d_4$  into all other plasma lipid classes shows that both CLA isomers are more metabolically characteristic of *trans*- and *cis*- $18:1$  positional isomers than of  $18:0$ ,  $9c$ - $18:1$ , or  $9c,12c$ - $18:2$ .

AUC data for the control and experimental diet groups listed in Table 2 were not significantly different and were



**FIG. 5.** Time course plots for uptake and clearance of  $9c$ - $18:1-d_8$ ,  $9c,12c$ - $18:2-d_2$ ,  $9c,11t$ - $18:2-d_6$ , and  $10t,12c$ - $18:2-d_4$  in plasma 1-acyl phosphatidylcholine (PC-1) and 2-acyl phosphatidylcholine (PC-2) of subjects fed the control and experimental diets. The plots for the  $9c,12c$ - $18:2-d_2$  PC-2 data are shown as inserts. Each data point is the average for data from three subjects. Error bars equal SE. Error bars are not shown when less than the size of the symbol.



**FIG. 6.** Time-course plots for uptake and clearance of  $9c$ - $18:1$ - $d_8$ ,  $9c$ , $12c$ - $18:2$ - $d_2$ ,  $9c$ , $11t$ - $18:2$ - $d_6$ , and  $10t$ , $12c$ - $18:2$ - $d_4$  in plasma cholesterol ester of subjects fed the control and experimental diets. Each data point is the average for data from three subjects. Error bars equal SE. Error bars are not shown when less than the size of the symbol.

therefore combined to test for statistical differences between individual FA within a lipid class. The following are some selected comparisons.

(i) *TG*. Incorporation of  $9c$ - $18:1$ - $d_8$  was 50–70% higher ( $P < 0.001$ ) than for the labeled CLA isomers, and the difference between the  $9c$ , $11t$ - $18:2$ - $d_6$  and  $10t$ , $12c$ - $18:2$ - $d_4$  isomers was small (13%) but significant ( $P < 0.001$ ).

(ii) *CE*. Incorporation of  $9c$ , $12c$ - $18:2$ - $d_2$  was about 7.7 times higher than  $9c$ - $18:1$ - $d_8$ , 33 times higher than  $9c$ , $11t$ - $18:2$ - $d_6$ , and 70 times higher than  $10t$ , $12c$ - $18:2$ - $d_4$  ( $P$  values all  $< 0.001$ ). The concentration of  $^2H$ -CLA in CE was the lowest for any plasma lipid class. AUC data for  $10t$ , $12c$ - $18:2$ - $d_4$  are 48 to 65% lower than for  $9c$ , $11t$ - $18:2$ - $d_6$  ( $P < 0.001$ ). This difference is both a reflection of LCAT selectivity and the lower concentrations of  $10t$ , $12c$ - $18:2$  in 2-acylphosphatidylcholine (PC-2).

(iii) *PC-1*. Accumulation of  $10t$ , $12c$ - $18:2$ - $d_4$  in PC-1 was three to four times higher than  $9c$ , $11t$ - $18:2$ - $d_6$  but was not different from  $9c$ , $12c$ - $18:2$ - $d_2$ . More (25–30%)  $10t$ , $12c$ - $18:2$ - $d_4$  than  $9c$ - $18:1$ - $d_8$  ( $P < 0.001$ ) was incorporated. In contrast, incorporation of  $9c$ , $11t$ - $18:2$ - $d_6$  in PC-1 was 60–70% less than  $9c$ - $18:1$ - $d_8$  ( $P < 0.001$ ). The striking difference between the incorporation in PC-1 for these two CLA isomers is evidence to support the suggestion that these CLA isomers have different physiological effects (39,40). The results are consistent with cultured cell and yeast studies that found these CLA isomers have different effects on apolipoprotein B secretion, TG levels, and stearyl-CoA desaturase activity (39–41).

**TABLE 2**  
Total Area-Under-Curve Data for Deuterium-Labeled FA in Plasma Lipids of Adult Female Subjects<sup>a</sup>

Lipid class	Diet group <sup>b</sup>	Deuterium-labeled FA			
		$9c$ - $18:1$ - $d_8$ $\mu\text{g}/\text{mg}/\text{g} \pm \text{SD}^c$	$9c$ , $12c$ - $18:2$ - $d_2$ $\mu\text{g}/\text{mg}/\text{g} \pm \text{SD}$	$9c$ , $11t$ - $18:2$ - $d_6$ $\mu\text{g}/\text{mg}/\text{g} \pm \text{SD}$	$10t$ , $12c$ - $18:2$ - $d_4$ $\mu\text{g}/\text{mg}/\text{g} \pm \text{SD}$
Chylo-TL <sup>d</sup>	Cntrl	86.5 $\pm$ 17.1	83.2 $\pm$ 13.9	70.7 $\pm$ 16.7	65.5 $\pm$ 18.0
	Exp	81.3 $\pm$ 7.5	82.2 $\pm$ 7.0	67.0 $\pm$ 2.0	59.0 $\pm$ 2.1
TG	Cntrl	207.1 $\pm$ 18.1	502.6 $\pm$ 20.6	98.1 $\pm$ 25.1	87.7 $\pm$ 23.7
	Exp	188.0 $\pm$ 29.7	460.8 $\pm$ 49.0	73.8 $\pm$ 11.4	59.6 $\pm$ 10.5
CE	Cntrl	33.6 $\pm$ 6.5	193.9 $\pm$ 34.4	11.2 $\pm$ 1.1 <sup>e</sup>	4.0 $\pm$ 1.1
	Exp	34.9 $\pm$ 3.9	230.4 $\pm$ 30.6	8.0 $\pm$ 0.4	4.1 $\pm$ 0.6
Total PL <sup>d</sup>	Cntrl	2.1 $\pm$ 0.6	15.7 $\pm$ 3.1	1.9 $\pm$ 0.6	2.6 $\pm$ 0.9
	Exp	2.2 $\pm$ 0.2	21.3 $\pm$ 2.0	2.0 $\pm$ 0.3	3.1 $\pm$ 0.01
PCf	Cntrl	34.2 $\pm$ 4.2	370.0 $\pm$ 34.5	26.6 $\pm$ 2.2	38.6 $\pm$ 5.2
	Exp	38.6 $\pm$ 0.7	383.0 $\pm$ 6.9	31.6 $\pm$ 4.9	42.0 $\pm$ 5.0
PC-1	Cntrl	21.6 $\pm$ 3.4	30.1 $\pm$ 3.8	8.8 $\pm$ 2.0	33.2 $\pm$ 7.4
	Exp	27.9 $\pm$ 3.8	34.9 $\pm$ 0.9	9.8 $\pm$ 0.9	35.9 $\pm$ 0.3
PC-2	Cntrl	27.8 $\pm$ 2.6	423.9 $\pm$ 25.5	13.5 $\pm$ 2.0	9.4 $\pm$ 2.5
	Exp	26.5 $\pm$ 7.3	438.6 $\pm$ 96.3	13.8 $\pm$ 4.0	10.6 $\pm$ 3.2
PE	Cntrl	26.6 $\pm$ 2.2	130.4 $\pm$ 13.5	26.4 $\pm$ 0.2	31.0 $\pm$ 1.2
	Exp	33.1 $\pm$ 1.9	171.2 $\pm$ 36.8	29.6 $\pm$ 3.8	32.4 $\pm$ 2.8
TL	Cntrl	65.5 $\pm$ 8.8	189.1 $\pm$ 3.3	48.1 $\pm$ 9.8	37.3 $\pm$ 9.2
	Exp	65.6 $\pm$ 9.1	222.0 $\pm$ 50.8	51.5 $\pm$ 9.8	41.7 $\pm$ 6.2

<sup>a</sup>For comparisons of individual FA in a lipid class, data for Cntrl and Exp subjects are combined ( $n = 6$ ). All FA comparisons are significantly different at  $P < 0.001$  except for PC ( $9c$ , $11t$ - $18:2$ - $d_6$  vs.  $9c$ - $18:1$ - $d_8$ ), PE ( $9c$ , $11t$ - $18:2$ - $d_6$  vs.  $9c$ - $18:1$ - $d_8$ ), PE ( $10t$ , $12c$ - $18:2$ - $d_4$  vs.  $9c$ - $18:1$ - $d_8$ ) and PE ( $10t$ , $12c$ - $18:2$ - $d_4$  vs.  $9c$ , $11t$ - $18:2$ - $d_6$ ).

<sup>b</sup>Cntrl = control diet group; Exp = experimental diet group.

<sup>c</sup> $\mu\text{g}/\text{mg}/\text{g}$  =  $\mu\text{g}$  deuterated FA per mg of total FA in lipid class per g of deuterated fat fed ( $n = 3$ ).

<sup>d</sup>Chylomicron total lipid (Chylo-TL) and total phospholipid (Total PL) values represent area-under-curve data for 0-, 2-, 4-, and 6-h samples.

<sup>e</sup>Cntrl vs. Exp diet group for cholesterol esters  $9c$ , $11t$ - $18:2$ - $d_6$  ( $P < 0.01$ ). No other diet group comparisons for the same deuterium-labeled FA are significantly different.

<sup>f</sup>Values for PC represent area-under-curve data for the 8-, 12-, 24-, 36-, and 48-h samples. PC-1, 1-acyl phosphatidylcholine; PC-2, 2-acyl phosphatidylcholine; TL, total lipid.

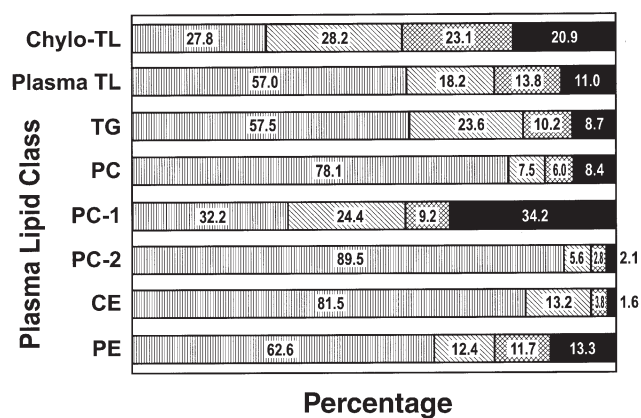


FIG. 7. Percentage of 9c-18:1-d<sub>8</sub> (diagonal lines), 9c,12c-18:2-d<sub>2</sub> (vertical lines), 9c,11t-18:2-d<sub>6</sub> (cross-hatched), and 10t,12c-18:2-d<sub>4</sub> (solid) in human plasma lipid classes. Percentages are calculated from the combined average of area concentration data for subjects fed the control and experimental diets. Chylo-TL, chylomicron total lipid; TL, total lipid; PC-1, 1-acyl PC; PC-2, 2-acyl PC; CE, cholesterol ester.

(iv) *PC-2*. The concentration of 9c-18:1-d<sub>8</sub> was 2.0 to 2.7 times higher than that of the CLA isomers (*P* < 0.001), and 9c,11t-18:2-d<sub>6</sub> was 25% higher than 10t,12c-18:2-d<sub>4</sub> (*P* < 0.001). The concentration of 9c,12c-18:2-d<sub>2</sub> in the PC-2 position is about 16 times greater than 9c-18:1-d<sub>8</sub> and is typical of the high selectivity previously observed for linoleic acid (31,32,42).

(v) *PE*. Data for the CLA isomers were not significantly different, and 9c,12c-18:2-d<sub>2</sub> concentrations were about five times higher than for any other labeled FA. PE is the only lipid class where accumulation of 9c-18:1-d<sub>8</sub> was not significantly greater than that for 9c,11t-18:2-d<sub>6</sub> or 10t,12c-18:2-d<sub>4</sub>.

(vi) *TL*. Accumulation and turnover of 9c,12c-18:2-d<sub>2</sub> in plasma TL were significantly higher (*P* < 0.001) than for the CLA isomers and reflect the marked difference in the shapes of the time-course curves for plasma TL (Fig. 2). AUC TL values for 9c,12c-18:2-d<sub>2</sub> are four to five times larger (*P* < 0.001) than for the CLA isomers and three times larger than for 9c-18:1-d<sub>8</sub> (*P* < 0.001). Curve shape for 9c-18:1-d<sub>8</sub> incorporation and disappearance was similar to those of the CLA

isomers, but total curve area for 9c-18:1-d<sub>8</sub> was 25% higher than for 9c,11t-18:2-d<sub>6</sub> (*P* < 0.001) and 40% higher than for 10t,12c-18:2-d<sub>4</sub> (*P* < 0.001). The 9c,11t-18:2-d<sub>6</sub> data were 21% higher than for 10t,12c-18:2-d<sub>4</sub> (*P* < 0.001).

*Metabolites*. Only two deuterium-labeled FA metabolites were present at levels sufficient for accurate measurement. The chain-shortened 9c-18:1-d<sub>8</sub> metabolite (16:1-d<sub>8</sub>) was 1.8% in TL and 1.3% in TG of the 9c-18:1-d<sub>8</sub> present. The Δ6-desaturated 10t,12c-18:2 metabolite (6c,10t,12c-18:3-d<sub>4</sub>) was equal to 5% in TL and 6.8% in TG of the 10t,12c-18:2-d<sub>4</sub> present. Little or no 6c,10t,12c-18:3-d<sub>4</sub> was detected in the samples of other plasma lipid classes, and the Δ6-desaturated 9c,11t-18:2-d<sub>6</sub> metabolite (6c,9c,11t-18:3-d<sub>6</sub>) was not detected. Trace amounts of labeled 20:2, 20:3, and 20:4 containing a conjugated diene structure were present in a few (<5%) samples. Elongated and desaturated 9c,12c-18:2-d<sub>2</sub> metabolites were present in all plasma lipid classes, but concentrations of the dideuterated n-6 metabolites were not sufficiently higher than the m + 2 natural <sup>13</sup>C background levels to allow accurate quantification.

DISCUSSION

Accumulations of labeled FA in all plasma lipid classes were not significantly different for women receiving the control and CLA-supplemented diets, with one exception. The concentrations of 9c,11t-18:2-d<sub>6</sub> in CE were statistically different, but the difference probably does not indicate a biologically important effect of diet because the absolute difference is very small. Comparison of the control and experimental diet results shows that dietary CLA does not alter oleic acid or linoleic acid metabolism and suggests that dietary CLA would not produce physiological effects associated with oleic and linoleic acid metabolism. The lack of a measurable effect of dietary CLA on 9c-18:1-d<sub>8</sub> and 9c,12c-18:2-d<sub>2</sub> metabolism contrasts with results for 20:4n-6- and 22:6n-3-supplemented diets that showed both 20:4n-6 and 22:6n-3 have a major influence on the metabolism of deuterium-labeled 9c-18:1 and 9c,12c-18:2 (31,32,43). The results from this study are consistent with results from a study that found incorporation of

TABLE 3 Selectivity Values for Incorporation of CLA Isomers Relative to Oleic Acid in Plasma Lipid Classes of Adult Women<sup>a</sup>

Lipid class	FA selectivity values										
	9c,11t-18:2	10t,12c-18:2	9c,12c-18:2	9t-18:1	10t-18:1	10c-18:1	11t-18:1	11c-18:1	12t-18:1	12c-18:1	18:0
TG	0.53	0.50	2.48	0.89	0.87	0.79	0.66	0.85	0.51	0.71	0.96
CE	0.34	0.16	6.26	0.19	0.29	0.18	0.06	0.45	0.20	0.69	0.01
PC	0.97	1.50	10.54	1.35	0.54	1.29	1.00	1.15	1.48	3.8	4.56
PC-1	0.46	1.90	1.34	3.63	2.19	3.98	3.89	1.62	5.37	3.80	13.13
PC-2	0.61	0.50	16.14	0.61	0.23	0.71	0.14	0.85	0.13	4.47	0.04
PE	1.15	1.44	5.11	1.95	0.91	0.89	1.41	1.26	1.02	1.29	ND <sup>b</sup>

<sup>a</sup>Area-under-curve (AUC; μg/mg/g) data used for calculation of selectivity values. Selectivity values equal FA AUC data divided by the AUC data for 9c-18:1. Reference value for 9c-18:1 = 1.00. CLA and 9c,12c-18:2 selectivity values are the average of control plus experimental groups. All selectivity ratios are adjusted for reduced absorption of FA if appropriate. Selectivity values for *cis*- and *trans*-18:1 positional isomers and for 18:0 are from previously published studies.

<sup>b</sup>ND, not data; for other abbreviations see Table 2.

nonconjugated unsaturated FA in rat liver was not altered by dietary CLA (8).

The apparent lower absorption for the  $^2\text{H}$ -CLA isomers compared to  $9c$ -18:1- $d_8$  was unexpected. Previous studies showed absorption of  $^2\text{H}$ -20:3n-6 and  $^2\text{H}$ -20:4n-6 was lower than  $^2\text{H}$ -18:1 (43,44), but significantly lower absorption of 18-carbon FA was not observed for labeled *cis*- and *trans*-18:1 FA isomers (45) nor for  $^2\text{H}$ -18:0 (38). A possible explanation for this result is that 20–30% of the  $^2\text{H}$ -CLA was absorbed *via* the portal transport and is consistent with human jejunum data for linolenic acid (46). Alternatively, one or both of the pathways (MAG and glycerol-3-phosphate) responsible for FA incorporation into TG during absorption may partially discriminate against CLA isomers. Hydrolysis of CLA TG by pancreatic lipase *in vitro* was reported to be lower than for trilinolein (47), and may have been a factor with the deuterated CLA ethyl esters used in the present study. However, rat data showed that CLA and  $9c$ ,12*c*-18:2 TG were equally well absorbed (47), which is not consistent with the results from this study in humans.

Comparison of incorporation data shows that metabolism of the  $^2\text{H}$ -CLA isomers is clearly different from that for oleic and linoleic acids. These results suggest that conjugation of the *cis*-9 and the *cis*-12 double bonds with a *trans* double bond has a major impact on the selectivity of the acylation enzymes that are responsible for incorporation. Conjugation does not appear to influence turnover rates since all plasma lipid class time-course curves show that disappearance of the CLA isomers is similar to  $9c$ -18:1. The selectivity values listed in Table 3 show that there was discrimination against incorporation of the  $^2\text{H}$ -CLA isomers in TG and CE and preferential incorporation in phospholipid, PC, and PE relative to  $9c$ -18:1- $d_8$  and  $9c$ ,12*c*-18:2- $d_2$ . Comparison of selectivity values for the CLA isomers to  $9c$ ,12*c*-18:2- $d_2$  values and values previously reported for *cis*- and *trans*-18:1 positional isomers and 18:0 (34–39) shows that  $9c$ ,11*t*-18:2 and  $10t$ ,12*c*-18:2 are metabolized more like *trans*-18:1 isomers than 18:0,  $9c$ -18:1, or  $9c$ ,12*c*-18:2. For example, the selectivity ratio of 1.90 for  $10t$ ,12*c*-18:2 is between the values for 11*c*- and  $10t$ -18:1 and indicates preferential incorporation at the PC-1 position. The PC-1 selectivity ratio of 0.46 indicates discrimination against  $9c$ ,11*t*-18:2 incorporation and is unusual because  $9c$ ,11*t*-18:2 is the only *trans* FA in which discrimination has been observed to occur at the PC-1 position. The CE selectivity values for  $9c$ ,11*t*-18:2 (0.34) and  $10t$ ,12*c*-18:2 (0.16) reflect a strong discrimination against acylation of cholesterol, which is a consistent characteristic of *trans*- and *cis*-18:1 positional isomers.

The lower concentrations of CLA isomers in TG and TL compared to oleic acid are generally consistent with the selectivity ratios for 18:1 isomers. The  $10t$ ,12*c*-18:2/ $9c$ ,11*t*-18:2 in human plasma TL was 0.78 and indicated an overall 22% preferential accretion of  $9c$ ,11*t*-18:2. The TL selectivity values of 0.81 for  $10t$ ,12*c*-18:2 and 0.92 for  $9c$ ,11*t*-18:2 represent the entire plasma lipid pool and suggest that, like  $^{13}\text{C}$ -

labeled  $9t$ -18:1 (48), a larger portion of the CLA isomers than oleic acid are  $\beta$ -oxidized. This suggestion is supported by results from rats, where  $\beta$ -oxidation of  $^{14}\text{C}$ -CLA isomers was about 17% higher than  $9c$ ,12*c*-18:2 (49). Overall, the results for the metabolism of CLA isomers showed many similarities to our previously reported results for *trans*-18:1 positional isomers. This observation is an interesting anomaly since a plethora of positive health benefits have been reported for CLA (1–3) but *trans*-18:1 isomers are considered to have a negative effect on serum cholesterol and to constitute a risk for coronary heart disease (45).

Studies in rats and yeast cell models have reported chain-shortened, elongated, and desaturated metabolites of CLA (4–8). In rat liver, the two main metabolites of  $10t$ ,12*c*-18:2 were  $8t$ ,10*c*-16:2 and  $6c$ ,10*t*,12*c*-18:3, and the main metabolite of  $9c$ ,11*t*-18:2 was  $8c$ ,11*c*,13*t*-20:3 (5). In this study with adult women,  $6c$ ,10*t*,12*c*-18:3- $d_4$  was the only CLA metabolite present in measurable amounts, and it does not appear to be elongated to  $8c$ ,12*t*,14*c*-20:3. The detection of  $6c$ ,10*t*,12*c*-18:3 in plasma TG but not in phospholipid samples is consistent with results for rat liver lipids (5). The importance of the *cis*-12 double bond is well recognized, but conjugation of the *cis*-12 double bond with a *trans* double bond would reduce the  $\pi$  electron density of the *cis*-12 double bond and alter its spatial arrangement or conformation compared to  $9c$ ,12*c*-18:2. Thus, the relatively high conversion of  $10t$ ,12*c*-18:2- $d_4$  is an unexpected result.

For these women,  $9c$ ,11*t*-18:2- $d_6$  clearly was not a good substrate for  $\Delta 6$ -desaturation, and neither CLA isomer was a good substrate for elongation, but why CLA metabolite concentrations were much lower than reported for rats was not clear. The higher amount of dietary CLA fed per kilogram of body weight in the rat studies and the higher desaturase activity of rats compared to humans would account for some of the observed difference. A possible contributing factor is that desaturase and elongase activities for women appear to be considerably lower than for men. For example, in comparable previous studies with adult men, the concentrations of  $9c$ ,12*c*-18:2- $d_2$  desaturation and elongation products were sufficient for accurate measurements (31,32,42). In this study with adult females, levels of elongated and desaturated  $9c$ ,12*c*-18:2- $d_2$  metabolites were usually too low for accurate quantification.

We found no effect of dietary CLA supplementation on the metabolism of the  $^2\text{H}$ -FA investigated. CLA isomers were not as well absorbed as oleic and linoleic acids. The  $9c$ ,11*t*-18:2 and  $10t$ ,12*c*-18:2 isomers were metabolically different, and their accretion in plasma lipids was characteristic of *cis*- and *trans*-18:1 positional isomers. Conversion of the  $^2\text{H}$ -CLA isomers to 18- and 20-carbon PUFA was negligible, except for the conversion of  $10t$ ,12*c*-18:2 to  $6c$ ,10*t*,12*c*-18:2.

## ACKNOWLEDGMENTS

Lynne C. Copes and Erin L. Walter for assistance with laboratory procedures and sample analyses.



## REFERENCES

- Yurawecz, M.P., Mossoba, M.M., Kramer, J.K.G., Pariza, M.W., and Nelson, G.J. (1999) *Advances in Conjugated Linoleic Acid Research*, Vol. 1, 480 pp., AOCS Press, Champaign.
- Banni, S., and Martin, J.C. (1998) Conjugated Linoleic Acid and Metabolites, in *Trans Fatty Acids in Human Nutrition* (Sebedio, J.L., and Christie, W.W., eds.), pp. 261–302, Oily Press, Dundee, Scotland.
- MacDonald, H.B. (2000) Conjugated Linoleic Acid and Disease Prevention: A Review of Current Knowledge, *J. Am. Coll. Nutr.* 19, 111S–118S.
- Sebedio, J.-L., Juaneda, P., Dobson, G., Ramilison, I., Martin, J.C., Chardigny, J.M., and Christie, W.W. (1997) Metabolites of Conjugated Isomers of Linoleic Acid (CLA) in the Rat, *Biochim. Biophys. Acta* 1345, 5–10.
- Sebedio, J.-L., Angioni, E., Chardigny, J.M., Gregoire, S., Juaneda, P., and Berdeaux, O. (2001) The Effect of Conjugated Linoleic Acid Isomers on Fatty Acid Profiles of Liver and Adipose Tissues and Their Conversion to Isomers of 16:2 and 18:3 Conjugated Fatty Acids in Rats, *Lipids* 36, 575–582.
- Chuang, L.-T., Thurmond, J.M., Liu, J.-W., Kirchner, S.J., Mukerji, P., Bray, T.M., and Huang, Y.S. (2001) Effect of Conjugated Linoleic Acid on Fungal  $\Delta 6$ -Desaturase Activity in a Transformed Yeast System, *Lipids* 36, 139–143.
- Chuang, L.-T., Leonard, A.E., Liu, J.-W., Mukerji, P., Bray, T.M., and Huang, Y.S. (2001) Inhibitory Effect of Conjugated Linoleic Acid on Linoleic Acid Elongation in Transformed Yeast with Human Elongase, *Lipids* 36, 1099–1103.
- Banni, S., Carta, G., Angioni, E., Murru, E., Scanu, P., Melis, M.P., Bauman, D.E., Fischer, S.M., and Ip, C. (2001) Distribution of Conjugated Linoleic Acid and Metabolites in Different Lipid Fractions in the Rat Liver, *J. Lipid Res.* 42, 1056–1061.
- Mougiou, V., Matsakas, A., Petridou, A., Ring, S., Sagredos, A., Melissopoulou, A., Tsigilis, N., and Nikolaidis, M. (2001) Effect of Supplementation with Conjugated Linoleic Acid on Human Serum Lipids and Body Fat, *J. Nutr. Biochem.* 12, 585–594.
- Thom, E., Wadstein, J., and Gudmundsen, O. (2001) Conjugated Linoleic Acid Reduces Body Fat in Healthy Exercising Humans, *J. Int. Med. Res.* 29, 392–396.
- Smedman, A., and Vessby, B. (2001) Conjugated Linoleic Acid Supplementation in Humans—Metabolic Effects, *Lipids* 36, 773–781.
- Zambell, K.L., Keim, N.L., Van Loan, M.D., Gale, B., Benito, P., Kelly, D.S., and Nelson, G.J. (2000) Conjugated Linoleic Acid Supplementation in Humans: Effects on Body Composition and Energy Expenditure, *Lipids* 35, 777–782.
- Medina, E.A., Horn, W.F., Keim, N.L., Havel, P.J., Benito, P., Kelly, D.S., Nelson, G.J., and Erickson, K.L. (2000) Conjugated Linoleic Acid Supplementation in Humans: Effects on Circulating Leptin Concentrations and Appetite, *Lipids* 35, 783–788.
- Kelly, D.S., Taylor, P.C., Rudolph, I.L., Benito, P., Nelson, G.J., Mackey, B.E., and Erickson, K.L. (2000) Dietary Conjugated Linoleic Acid Did Not Alter Immune Status in Healthy Young Women, *Lipids* 35, 1065–1071.
- Benito, P., Nelson, G.J., Kelly, D.S., Bartolini, G., Schmidt, P.C., and Simon, V. (2001) The Effect of Conjugated Linoleic Acid on Platelet Function, Platelet Fatty Acid Composition, and Blood Coagulation in Humans, *Lipids* 36, 221–227.
- Kelly, D.S., Simon, V., Taylor, P.C., Rudolph, I.L., Benito, P., Nelson, G.J., Mackey, B.E., and Erickson, K.L. (2001) Dietary Supplementation with Conjugated Linoleic Acid Increased Its Concentration in Human Peripheral Blood Mononuclear Cells, but Did Not Alter Their Function, *Lipids* 36, 669–674.
- Zambell, K.L., Horn, W.F., and Keim, N.L. (2001) Conjugated Linoleic Acid Supplementation in Humans: Effects on Fatty Acid and Glycerol Kinetics, *Lipids* 36, 767–772.
- Benito, P., Nelson, G.J., Kelly, D.S., Bartolini, G., Schmidt, P.C., and Simon, V. (2001) The Effect of Conjugated Linoleic Acid on Plasma Lipoproteins and Tissue Fatty Acid Composition in Humans, *Lipids* 36, 229–236.
- Adlof, R.O., and Emken, E.A. (1993) Large-Scale Preparation of Linoleic Acid- $d_2$  Enriched Triglycerides from *Crepis alpina* Seed Oil, *J. Am. Oil Chem. Soc.* 70, 817–819.
- Adlof, R.O., Walter, E.L., and Emken, E.A. (1997) Synthesis of Five Conjugated Linoleic Acid Isomers Labelled with Deuterium Atoms, *Proceedings, International Symposium on the Synthesis and Applications of Isotopes and Isotopically Labelled Compounds* 6, pp. 387–390, John Wiley & Sons, New York.
- Adlof, R.O., and Emken, E.A. (1978) Synthesis of Methyl *cis*-9-Octadecenoate-14,14,15,15,17,18-D $_6$ , *J. Labelled Compd. Radiopharm.* 15, 97–104.
- Christie, W.W. (1973) *Lipid Analysis*, pp. 89–90, Pergamon Press, New York.
- Lindgren, F.T., Jensen, L.C., and Hatch, F.T. (1972) The Isolation and Quantitative Analysis of Serum Lipoproteins, in *Blood Lipids and Lipoproteins* (Nelson, G.J., ed.), pp. 186–188, Wiley-Interscience, New York.
- Narayan, K.A. (1975) Electrophoresis Methods for the Separation of Serum Lipoproteins, in *Analysis of Lipids and Lipoproteins*. (Perkins, E.G., ed.), pp. 225–249, American Oil Chemists' Society, Champaign.
- Folch, J., Lees, M., and Sloane-Stanley, G.E. (1957) A Simple Method for the Isolation and Purification of Total Lipids from Animal Tissues, *J. Biol. Chem.* 226, 497–509.
- French, J.A., and Anderson, D.W. (1973) Separation and Quantitative Recovery of Lipid Classes: A Convenient Thin-Layer Chromatographic Method, *J. Chromatogr.* 80, 133–136.
- Robertson, A.F., and Lands, W.E.M. (1962) Positional Specificities in Phospholipid Hydrolyses, *Biochemistry* 1, 804–810.
- Rohwedder, W.K., Emken, E.A., and Wolf, D.J. (1985) Analysis of Deuterium-Labeled Blood Lipids by Chemical Ionization Mass Spectrometry, *Lipids* 20, 303–311.
- Schenck, P.A., Rakoff, H., and Emken, E.A. (1996)  $\Delta 8$  Desaturation *in vivo* of Deuterated Eicosatrienoic Acid by Mouse Liver, *Lipids* 31, 593–600.
- Statistical Analysis System Institute (1987) *SAS Guide for Personal Computers*, 6th edn., SAS Institute, Cary, NC.
- Emken, E.A., Adlof, R.O., Duval, S.M., and Nelson, G.J. (1998) Effect of Dietary Arachidonic Acid on Metabolism of Deuterated Linoleic Acid by Adult Male Subjects, *Lipids* 33, 471–480.
- Emken, E.A., Adlof, R.O., Duval, S.M., and Nelson, G.J. (1999) Effect of Dietary Docosahexaenoic Acid on Desaturation and Uptake *in vivo* of Isotope-Labeled Oleic, Linoleic, and Linolenic Acids by Male Subjects, *Lipids* 34, 785–791.
- Emken, E.A., Adlof, R.O., Rohwedder, W.K., and Gulley, R.M. (1989) Incorporation of *trans*-8- and *cis*-8-Octadecenoic Acid Isomers in Human Plasma and Lipoprotein Lipids, *Lipids* 24, 61–69.
- Emken, E.A., Rohwedder, W.K., Dutton, H.J., DeJarlais, W.J., Adlof, R.O., Macklin, J.F., Dougherty, R.M., and Iacono, J.M. (1979) Incorporation of Deuterium-Labeled *cis*- and *trans*-9-Octadecenoic Acids in Humans: Plasma, Erythrocyte, and Platelet Phospholipids, *Lipids* 14, 547–554.
- Emken, E.A., Rohwedder, W.K., Adlof, R.O., DeJarlais, W.J., and Gulley, R.M. (1985) *In vivo* Distribution and Turnover of *trans*- and *cis*-10-Octadecenoic Acid Isomers in Human Plasma Lipids, *Biochim. Biophys. Acta* 836, 233–245.
- Emken, E.A., Rohwedder, W.K., Adlof, R.O., DeJarlais, W.J., and Gulley, R.M. (1986) Absorption and Distribution of Deuterium-Labeled *trans*- and *cis*-11-Octadecenoic Acid in Human Plasma and Lipoprotein Lipids, *Lipids* 21, 589–595.
- Emken, E.A., Dutton, H.J., Rohwedder, W.K., Rakoff, H., Adlof, R.O., Gulley, R.M., and Canary, J.J. (1980) Distribution of

- Deuterium-Labeled *cis*- and *trans*-12-Octadecenoic Acids in Human Plasma and Lipoprotein Lipids, *Lipids* 15, 864–871.
38. Emken, E.A., Adlof, R.O., Rohwedder, W.K., and Gulley, R.M. (1993) Influence of Linoleic Acid on Desaturation and Uptake of Deuterium-Labeled Palmitic and Stearic Acids in Humans, *Biochim. Biophys. Acta* 1170, 173–181.
  39. Yotsumoto, H., Hara, E., Naka, S., Adlof, R.O., Emken, E.A., and Yanagita, T. (1999) 10*trans*, 12*cis*-Linoleic Acid Reduces Apolipoprotein B Secretion in HepG2 Cells, *Food Res. Intl.* 31, 403–409.
  40. Evans, M., Park, Y., Pariza, M., Curtis, L., Kuebler, B., and McIntosh, M. (2001) *Trans*-10,*Cis*-12 Conjugated Linoleic Acid Reduces Triglyceride Content While Differently Affecting Peroxisome Proliferator Activated Receptor Y2 and aP2 Expression in 3T3-L1 Preadipocytes, *Lipids* 36, 1223–1232.
  41. Choi, Y., Park, Y., Pariza, M.W., and Ntambi, J.M. (2001) Regulation of Stearoyl-CoA Desaturase Activity by the *trans*-10, *cis*-12 Isomer of Conjugated Linoleic Acid in HepG2 Cells, *Biochem. Biophys. Res. Comm.* 284, 689–693.
  42. Emken, E.A., Adlof, R.O., Rohwedder, W.K., and Gulley, R.M. (1994) Dietary Linoleic Acid Influences Desaturation and Acylation of Deuterium-Labeled Linoleic and Linolenic Acids in Young Adult Males, *Biochim. Biophys. Acta* 1213, 277–288.
  43. Emken, E.A., Adlof, R.O., Duval, S.M., and Nelson, G.J. (1997) Influence of Dietary Arachidonic Acid on Metabolism *in vivo* of 8*c*,11*c*,14*c*-Eicosatrienoic Acid in Humans, *Lipids* 32, 441–448.
  44. Emken, E.A., Adlof, R.O., Duval, S.M., and Nelson, G.J. (1996) Influence of Dietary Arachidonic Acid on Human Metabolism of Deuterium-Labeled Dihomo- $\gamma$ -linoleic Acid (20:3n-6) and Arachidonic Acid (20:4n-6), in *PUFA in Infant Nutrition: Consensus and Controversies*, p. 25, Meeting Abstracts, AOCS, Champaign.
  45. Emken, E.A. (1995) Physiological Properties, Intake and Metabolism, in *Trans Fatty Acids and Coronary Heart Disease Risk* (Kris-Etherton, P.M., ed.) *Am. J. Clin. Nutr.* 62, 655S–708S.
  46. Surawicz, C.M., Saunders, D.R., Sillery, J., and Rubin, C.E. (1981) Linolenate Transport By Human Jejunum: Presumptive Evidence for Portal Transport at Low Absorption Rates, *Am. J. Physiol.* 240, G157–G162.
  47. Martin, J.-C., Sebedio, J.-L., Caselli, C., Pimont, C., Martine, L., and Bernard, A. (2000) Lymphatic Delivery and *in vitro* Pancreatic Lipase Hydrolysis of Glycerol Esters of Conjugated Linoleic Acids in Rats, *J. Nutr.* 130, 1108–1114.
  48. DeLany, J.P., Windhauser, M.M., Champagne, C.M., and Bray, G.A. (2000) Differential Oxidation of Individual Dietary Fatty Acids in Humans, *Am. J. Clin. Nutr.* 72, 905–911.
  49. Sergiel, J.-P., Chardigny, J.-M., Sebedio, J.-L., Berdeaux, O., Juaneda, P., Loreau, O., Pasquis, B., and Noel, J.-P. (2001)  $\beta$ -Oxidation of Conjugated Linoleic Acid Isomers and Linoleic Acid in Rats, *Lipids* 36, 1327–1329.

[Received March 20, 2002, and in final revised form July 25, 2002; revision accepted July 29, 2002]

# Dietary CLA Alters Yolk and Tissue FA Composition and Hepatic Histopathology of Laying Hens

Gita Cherian<sup>a,\*</sup>, Troy B. Holsonbake<sup>a</sup>, Mary P. Goeger<sup>a</sup>, and Rob Bildfell<sup>b</sup>

<sup>a</sup>Department of Animal Sciences and <sup>b</sup>College of Veterinary Medicine, Oregon State University, Corvallis, Oregon 97331

**ABSTRACT:** The effect of dietary CLA along with n-3 PUFA on yolk FA profile and hepatic lipid accumulation was investigated. Laying hens ( $n = 40$ ) were randomly assigned to four experimental diets containing 0, 0.5, 1.0, or 2.0% CLA. Menhaden oil was used as the source of n-3 PUFA. Dietary CLA did not affect the total lipid content of egg yolk ( $P > 0.05$ ). The amounts of CLA isomers (*cis*-9 *trans*-11, *trans*-10 *cis*-12) in the egg yolk were proportional to the levels of CLA in the diet ( $P < 0.05$ ). The total CLA content in the egg yolk was 0, 0.97, 2.4, and 5.3 wt%, respectively ( $P < 0.05$ ). Addition of CLA resulted in an increase in saturated FA ( $P < 0.05$ ) with a concomitant reduction in monounsaturated FA ( $P < 0.05$ ) in the yolk, liver, abdominal fat, breast, and thigh muscle. No difference in saturated and monounsaturated FA content in heart and spleen tissue was noted. Dietary CLA at all concentrations resulted in an increase ( $P < 0.05$ ) in the total number of fat vacuoles and lipid infiltration in hepatocytes. The number of cells with 75% or higher lipid vacuolation in the cytoplasm was also increased ( $P < 0.05$ ) by 2.0% CLA. Dietary CLA at 0.5% levels resulted in an increase ( $P < 0.05$ ) in the total lipid content of hepatic tissue. The total lipid content in leg muscle was lower ( $P < 0.05$ ) in CLA-fed birds. However, no effect of CLA on lipid content of breast muscle, heart, spleen and adipose tissue was observed ( $P > 0.05$ ). The current study used CLA in a FFA form. The effects of using CLA in other form such as TG on avian hepatic tissue need to be investigated.

Paper no. L9044 in *Lipids* 37, 751–757 (August 2002).

Because of the controversy concerning dietary animal fat and potential links to human health problems such as cardiovascular disease and certain types of cancer, consumers are very interested in functional foods that can prevent or ameliorate disease processes. Several different strategies have been adopted by the animal food industry to enhance the nutritional value of animal foods. The major emphasis has been focused on modification of lipid and PUFA composition. Among the different PUFA, longer-chain n-3 PUFA and CLA have received considerable attention for their health-enhancing properties (1,2). These include the TG-lowering and antiatherosclerotic and antiarrhythmic properties of n-3 PUFA (3,4) as well as the anticarcinogenic and antiatherogenic properties of CLA (2). Other beneficial effects of CLA include body fat reduction, immunomodulation, and antioxidant properties (5,6).

\*To whom correspondence should be addressed at 122 Withycombe Hall, Dept. of Animal Science, Oregon State University, Corvallis, OR 97331-6702. E-mail: Gita.Cherian@orst.edu

Abbreviations: FLS, fatty liver syndrome; MUFA, monounsaturated FA; SFA, saturated fatty acid.

Animal products contribute 70% of total FA in typical Western diets. This includes CLA and n-3 PUFA, which are supplied predominantly by food lipids of ruminant animals and marine products. Current intake of CLA is estimated to be several hundred milligrams/day (7). Based on animal data, approximately 3 g/d of CLA would be required to produce beneficial effects in humans (8). However, as Americans are opting for low-fat dairy and beef products and choosing more poultry-based foods than beef, it is likely that the dietary contribution of CLA and n-3 PUFA will further be reduced in a typical U.S. diet. When associated with food, CLA reportedly has higher tissue retention and better anticancer effects than commercially available supplements (9). In this respect, CLA and n-3 PUFA-enriched chicken eggs may be an alternative vehicle for delivering health-promoting FA to consumers.

In chickens, the lymphatic system is rudimentary, and liver is the first tissue to be exposed to dietary lipids. The major route of fat absorption is by mixed micelle formations. The chylomicrons are absorbed directly into the portal blood for transport to the liver for further synthesis and subsequent tissue deposition. Such a feature also predisposes birds to a pathological condition called fatty liver syndrome (FLS). A high percentage of commercial layers in the United States develop FLS, causing the hepatocytes to distend with fat vacuoles and resulting in rupture and death (10). The ability of CLA to reduce body fat, increase lean body mass, and increase feed efficiency may have important implications for FLS. The use of CLA as a means to reduce fat deposition may be a method to control or reverse this process. The objectives of the present study were to investigate the effect of feeding CLA along with n-3 PUFA on the yolk and tissue FA incorporation and to assess the hepatic histopathology, lipid infiltration, and performance parameters of hens.

## MATERIALS AND METHODS

These experiments were reviewed by the Oregon State University Animal Care Committee to ensure adherence to Animal Care Guidelines.

**Birds and diets.** Thirty-two-week-old single Comb White Leghorn laying hens ( $n = 40$ ) were kept in individual cages and were fed a corn-soybean meal-based diet with added CLA at 0 (Diet 1), 0.5 (Diet 2), 1.0 (Diet 3), and 2.0% (Diet 4) (Table 1). All diets contained 3% menhaden oil, and the CLA source in Diets 2, 3, and 4 was substituted for menhaden oil on a weight/weight basis. The CLA source, which contained

**TABLE 1**  
**Composition and Calculated Analysis of the Laying Hen Diets**

Ingredients <sup>a</sup>	Added dietary CLA (%)			
	0	0.5	1.0	2.0
Corn	60.6	60.6	60.6	60.6
Soybean meal	24.6	24.6	24.6	24.6
Limestone	6.0	6.0	6.0	6.0
Biophos <sup>TM</sup>	1.5	1.5	1.5	1.5
Layer premix <sup>b</sup>	0.3	0.3	0.3	0.3
Fish oil	3.0	2.5	2.0	1.0
CLA	0.0	0.50	1.0	2.0
Salt	0.35	0.35	0.35	0.35
Methionine DL	0.1	0.1	0.1	0.1
Calculated analyses				
Crude protein	16.5	16.5	16.5	16.5
ME (kcal/kg)	2938.5	2938.5	2938.5	2938.5
Calcium	3.7	3.7	3.7	3.7
Available phosphorus	0.8	0.8	0.8	0.8

<sup>a</sup>Values expressed as wt% except where indicated; ME, metabolizable energy.

<sup>b</sup>Supplied per kg of the diet the following: vitamin A, 8250 IU; vitamin D, 2640 IU; vitamin E, 16.5 IU; riboflavin, 5.28 mg; niacin, 26.4 mg; vitamin B<sub>12</sub>, 8.91 µg; biotin, 0.099 mg; pyridoxine, 1.32 mg; thiamine, 1.155 mg; selenium, 0.264 mg; manganese, 90.4 mg; zinc, 92.4 mg.

75% FFA) was obtained from a commercial source and contained 34.9% *c9,t11*- and 35.9% *t10,c12*-CLA isomers (PharmaNutrients, Lake Bluff, IL). All the diets were isocaloric and isonitrogenous (Table 1). The diets were prepared biweekly and kept in a cold room (4°C) in air-tight containers. Hens were fed the experimental diet for a period of 42 d. Total feed consumption and daily egg production were monitored. Initial and final body weights of birds were recorded.

**Sample collection.** Hens were fed the experimental diet shown in Table 1 for 2 wk before eggs were collected for this study. Six eggs from each treatment were randomly selected for FA analysis ( $n = 6$ ). The eggs were weighed, and yolks were separated using an egg separator and weighed. The albumen weight was calculated by subtracting yolk and shell weight from total egg weight. The yolks were stored in freezer bags at -20°C until extraction. On day 42 of feeding, 6 birds per treatment were randomly selected. The birds were killed, and liver tissue was collected by a veterinary pathologist at the Oregon State University Veterinary Hospital. The liver tissue was weighed and recorded. The spleen, heart, breast, and leg muscle and abdominal fat were collected and were kept frozen (-20°C) until analysis.

**Lipid and FA analyses.** Total lipids were extracted from egg yolk and tissues with chloroform/methanol (2:1, vol/vol) by the method of Folch *et al.* (11). One gram of sample was weighed into a screw-capped test tube with 20 mL of chloroform/methanol (2:1, vol/vol) and homogenized with a Polytron for 5 to 10 s at high speed. The homogenate was filtered through Whatman #1 filter paper into a 100-mL graduated cylinder, and 5 mL of 0.88% sodium chloride solution was added and mixed. After phase separation, the volume of the lipid layer was recorded, and the top layer was completely siphoned off. Three milliliters of the lipid extracts was dried in a block heater under nitrogen and used for FA analyses. The dried lipids were redissolved in 2 mL of a boron trifluoride/

methanol methylation solution and were incubated in a boiling water bath for 1 h at 90–100°C (12). After cooling to room temperature, the FAME were separated by hexane and distilled water. Total lipids were determined gravimetrically.

Analysis of FA composition was performed with a HP 6890 gas chromatograph (Hewlett-Packard) equipped with an autosampler, FID, and a fused-silica capillary column, 100 m × 0.25 mm × 0.2 µm film thickness (Sp-2560; Supelco, Bellefonte, PA). Sample (1 µL) was injected with helium as a carrier gas onto the column programmed for ramped oven temperatures (initial temperature was 110°C, held for 1.0 min, then ramped at 15.0°C/min to 190°C and held for 55.0 min, then ramped at 5.0°C/min to 230°C and held for 5.0 min). Inlet and detector temperatures were both 220°C. Peak areas and percentages were calculated using Hewlett-Packard ChemStation software. FAME were identified by comparison with retention times of authentic standards (Matreya, Pleasant Gap, PA). FA values and total lipids are expressed as weight percentages.

**Hepatic histopathology and criteria for fat scoring.** A slice of liver about 1 × 1 × 0.5 cm thick was taken from the right lobe of each hen, fixed in 10% neutral buffered formalin for 48 h, embedded in paraffin, sectioned (8 µm), and stained with hematoxylin and eosin stain prior to microscopic examination. For each section of the liver, three randomly located areas were graded at 40× magnification using a grid within a 10× ocular piece. Approximately 20 hepatocytes would be expected to fall within the limits of the grid. Fat content of each grid was assessed in two patterns: (i) total number of fat vacuoles in the grid, (ii) number of cells within the grid having >75% lipid vacuolation of cytoplasm. For each method, the sum total from each bird was divided by three to give an average value per grid. A fat vacuole was considered to be any nonstaining area of cytoplasm with a sharply defined border. The two methods were used, as it is common for lipid-laden cells to be largely occupied by only one or two vacuoles in severe fatty metamorphosis. A single section from each bird was assessed in this manner. A final average for each group was then calculated.

**Statistical analysis.** The effect of dietary CLA on egg quality, production performance, tissue FA, and hepatic histopathology were analyzed by ANOVA using SAS (version 8.2) (SAS Institute, Cary, NC). Student-Newmann-Keuls multiple range test (13) was used to compare differences among treatment means ( $P < 0.05$ ). Mean values and SEM are reported.

## RESULTS AND DISCUSSION

The FA composition of the diet is shown in Table 2. Performance of hens was measured for 42 d (test period). No significant difference ( $P > 0.05$ ) was observed in feed consumption, initial and final body weights of birds, egg production, egg weight, yolk weight or total edible portion, yolk color and haugh unit (data not shown).

**Gross necropsy findings.** No significant abnormalities were noted in any of the birds examined with the exception of hepatic changes. When compared to Diet 1, livers from birds fed CLA-added diets were pale, with Diet 4 having the most



**TABLE 2**  
Major FA Composition (%) of Laying Hen<sup>a</sup> Diet

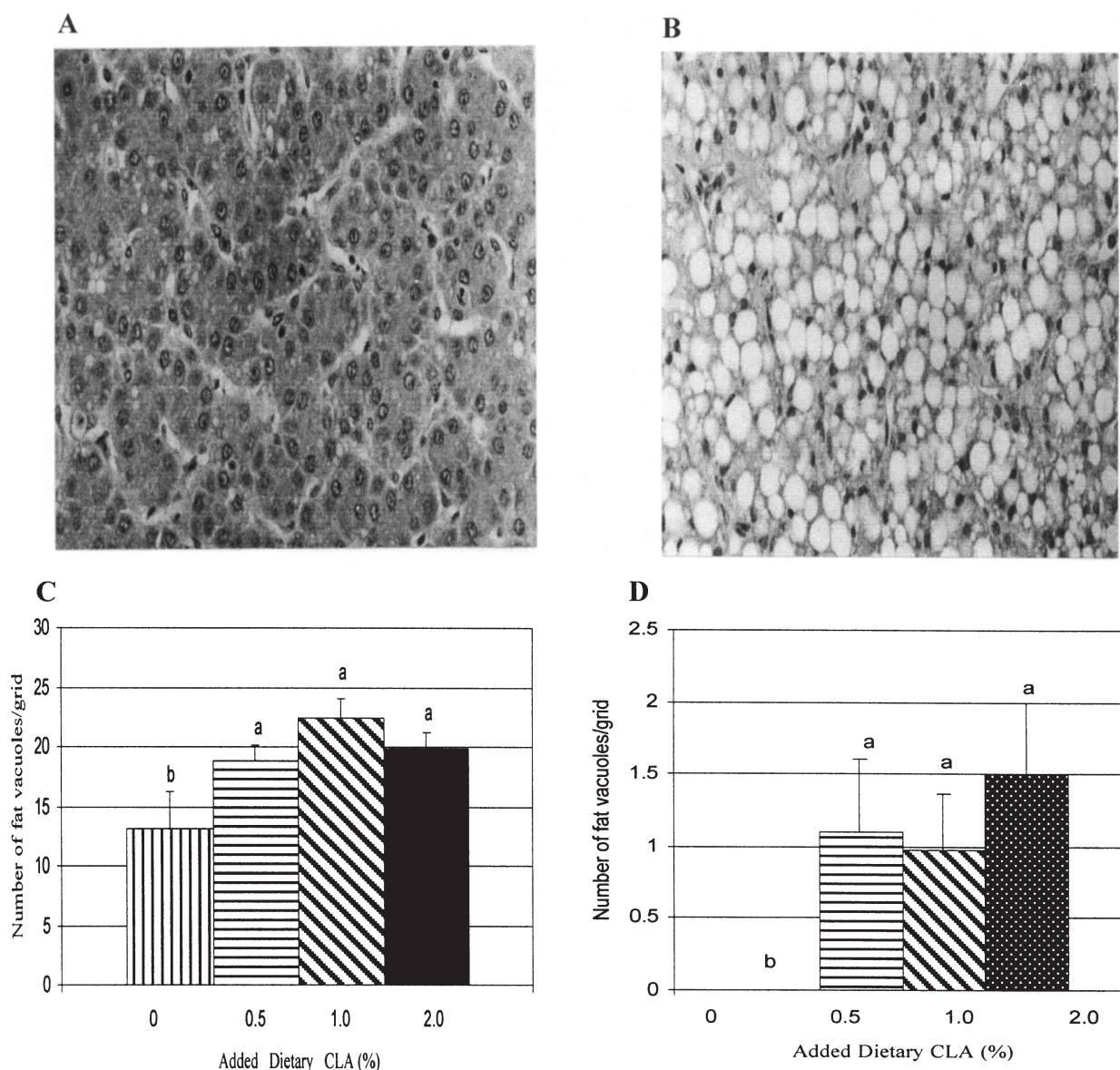
FA	Added dietary CLA (%)			
	0	0.5	1.0	2.0
16:0	16.8	15.1	13.0	11.4
18:0	3.6	3.6	3.2	3.2
18:1n-9	18.7	18.8	18.2	18.8
18:2n-6	35.4	30.4	28.1	25.2
20:4n-6	0.3	0.2	0.2	0.1
20:5n-3	5.1	4.1	3.4	1.4
22:6n-3	3.4	3.0	2.4	0.9
<i>cis</i> -9, <i>trans</i> -11 CLA	0.0	4.9	8.9	15.9
<i>trans</i> -10, <i>cis</i> -12 CLA	0.0	4.2	9.1	14.9
Total CLA	0.0	9.2	18.1	30.7
Total SFA	25.5	23.2	19.7	15.8
Total MUFA	19.3	19.5	18.7	18.7

<sup>a</sup>n = 6. SFA, saturated FA. MUFA, monounsaturated FA.

severe hepatic pallor. Grossly visible hepatic hemorrhages were noticed in some birds fed Diet 4.

**Hepatic histopathology.** The liver tissue from hens fed Diet 4 had the most significant pathology, including the most extensive fat deposition, and number of cells with 75% vacuolation (Fig. 1). Fine droplets of fat were distributed diffusely through hepatocytes of birds fed Diet 1. However, more extensive hepatocytic vacuolation due to fat deposition was observed in the CLA-fed birds. Large vacuoles containing fat distended many hepatocytes. The total number of fat vacuoles per grid and the number of hepatocytes with greater than 75% cytoplasmic vacuolation was higher ( $P < 0.05$ ) in CLA-fed hens than controls.

In addition to scoring the liver for fat deposition, the sections were examined for other lesions. Abnormalities associated with fatty liver such as dilated sinusoids and intrasinusoidal fibrin deposition were noted in birds fed Diet 4. Single-cell necrosis



**FIG. 1.** Histopathology of liver tissues from hens fed diets containing CLA. (A) Typical histological section of liver tissue from hens fed 0% CLA; (B) hens fed 2.5% CLA; (C) number of fat vacuoles/grid; (D) number of cells with 75% or higher fat vacuolation. Means with no common superscript (a,b) differ ( $P < 0.05$ );  $n = 6$ .

was more common in liver tissue of Diet 4 hens. Although no difference was found in liver weight as percentage of body weight, total fat content and lipid infiltration were significantly altered in hens fed with added CLA. A similar effect of CLA in enhancing liver lipid content in mice has been reported (14).

**Liver total lipids and FA.** When liver lipids were extracted and the lipid content was determined gravimetrically, a significant effect of dietary CLA and total lipid extract per gram liver tissue was noted (Table 3). Livers of hens fed even 0.5% CLA (Diet 2) contained approximately twice the amount of lipids compared to Diet 1. Increasing CLA to 1.0 and 2.0% did not result in further increase in hepatic total lipid content when compared to 0.5% (Table 3). A recent study by Twibell *et al.* (15) reported a decrease in liver total lipids in perch when diets contained CLA. However, Belury and Kempa-Stecko (14) reported that feeding CLA to rats increased the liver total lipid. Therefore, it appears that the effect of dietary CLA on hepatic lipid content is species-specific.

Liver FA concentrations were significantly affected by dietary lipids (Table 3). The increase in CLA isomers was higher ( $P < 0.05$ ) in birds fed Diets 2, 3, and 4. No CLA was detected in the control birds. Total CLA concentrations of birds fed 0.5, 1.0, and 2.0% CLA were 0.77, 1.35, and 2.67%, compared to 0% in the control birds. The *cis* 9,*trans* 11 isomer was the major CLA in liver tissue. The increase in CLA was at the expense of oleic acid. The saturated FA content increased significantly in liver of birds fed CLA. Even a minor increase in CLA (0.5%) resulted in a dramatic change in the concentration of palmitic (16:0) and stearic acids (18:0). No difference was observed for the content of total n-3 FA. Although fish oil

was at the highest concentration in Diet 1, no differences were observed in the 22:6n-3 and 20:5n-3 content in liver.

To our knowledge, effects of dietary CLA on lipid concentrations and infiltrations in hens have not been reported previously. Whether the enhanced liver lipid infiltration is a specific effect of CLA remains to be determined. The current study used CLA in a FFA form. The effects of using CLA in other forms such as TG need to be investigated. Positive energy balance has been reported to cause FLS and associated hepatic lipidosis in hens. In the current study, the experimental diets were isocaloric, and the total fat in the laying hen ration was within the ranges for laying chickens. No differences in body weight, liver weight as percentage of body weight, and feed consumption were noted among birds. The significant changes in hepatic histopathology observed in Diet 4 suggest that dietary CLA may influence hepatic lipid metabolism and subsequently may contribute to hepatic lipidosis.

**Egg yolk total lipids and FA.** The total fat content of the egg yolk was not affected by dietary treatment ( $P > 0.05$ ). However, the FA content was significantly altered by dietary CLA. The CLA content of the egg yolk increased significantly in a dose-dependent manner with the dietary CLA content (Table 4). At 2% inclusion levels (Diet 4), yolks showed the highest incorporation of CLA. The total yolk CLA constituted 5.3% in Diet 4 compared to 0% in Diet 1 ( $P < 0.05$ ). The major CLA isomer in the yolk lipids was *c9,t11* and constituted 0, 0.8, 1.6, and 3.6% in the yolk lipids of hens fed Diets 1, 2, 3, and 4, respectively. The content of *t10,c12* constituted 0, 0.16, 0.8, and 1.6% in yolk lipids from hens fed Diets 1, 2, 3, and 4, respectively. CLA added at a 2% level resulted in over 50% reduction of monounsaturated FA (MUFA) and replacement by saturated FA (SFA). These results corroborate Chamrusspollert and Sell (16), Du *et al.* (17), and Raes *et al.* (18). The  $\Delta^9$ -desaturase enzyme is responsible for the conversion of stearic acid (18:0) to oleic acid (18:1). Dietary CLA may have an inhibitory action on desaturases, thereby

**TABLE 3**  
Liver Tissue FA Composition of Hens' Diets  
Containing Different Levels of CLA<sup>a</sup>

Fatty acids	Added dietary CLA (%)				SEM
	0	0.5	1.0	2.0	
	(% of total lipids)				
14:0	0.60 <sup>b</sup>	0.91 <sup>a</sup>	0.88 <sup>a</sup>	0.62 <sup>b</sup>	0.08
16:0	25.17 <sup>b</sup>	31.02 <sup>a</sup>	33.23 <sup>a</sup>	32.63 <sup>a</sup>	0.30
16:1	4.03 <sup>a</sup>	3.31 <sup>b</sup>	2.64 <sup>c</sup>	2.04 <sup>d</sup>	0.13
18:0	11.75 <sup>c</sup>	19.11 <sup>b</sup>	22.92 <sup>a</sup>	21.20 <sup>a,b</sup>	0.27
18:1	37.09 <sup>a</sup>	27.05 <sup>b</sup>	22.91 <sup>c</sup>	21.77 <sup>c</sup>	0.35
18:2n-6	10.95 <sup>a,b</sup>	10.47 <sup>a,b</sup>	9.13 <sup>b</sup>	12.01 <sup>a</sup>	0.23
18:3n-3	0.27	0.32	0.24	0.25	0.04
18:4n-3	0.40	0.10	0.08	0.12	0.12
20:4n-6	2.17 <sup>a</sup>	1.10 <sup>b</sup>	0.99 <sup>b</sup>	1.59 <sup>a,b</sup>	0.16
CLA, <i>c9,t11</i>	0.00 <sup>d</sup>	0.53 <sup>c</sup>	0.88 <sup>b</sup>	1.84 <sup>a</sup>	0.09
CLA, <i>t10,c12</i>	0.00 <sup>c</sup>	0.21 <sup>b,c</sup>	0.39 <sup>b</sup>	0.71 <sup>a</sup>	0.09
CLA, others	0.00 <sup>d</sup>	0.03 <sup>c</sup>	0.07 <sup>b</sup>	0.11 <sup>a</sup>	0.02
22:4n-6	0.10	0.05	0.05	0.07	0.04
22:5n-3	0.39	0.47	0.41	0.40	0.10
22:6n-3	5.11	3.96	3.38	3.27	0.64
20:5n-3	0.12 <sup>a</sup>	0.05 <sup>b</sup>	0.04 <sup>b</sup>	0.06 <sup>b</sup>	0.04
TSFA	38.74 <sup>c</sup>	51.97 <sup>b</sup>	57.79 <sup>a</sup>	55.09 <sup>a,b</sup>	0.36
TMUFA	41.26 <sup>a</sup>	30.51 <sup>b</sup>	25.67 <sup>c</sup>	23.91 <sup>c</sup>	0.37
Total CLA	0.00 <sup>d</sup>	0.77 <sup>c</sup>	1.35 <sup>b</sup>	2.67 <sup>a</sup>	0.12
Total lipids	7.5 <sup>b</sup>	13.2 <sup>a</sup>	12.3 <sup>a,b</sup>	10.4 <sup>a,b</sup>	1.44

<sup>a</sup>Means within a row with no common superscript (a-d) differ ( $P < 0.05$ );  $n = 6$ . TSFA, total saturated FA; TMUFA, total monounsaturated FA.

**TABLE 4**  
Major FA Composition (%) of Egg Yolk as Influenced by Hen Diets  
Containing Different Levels of CLA<sup>a</sup>

FA	Added dietary CLA (%)				SEM
	0	1.0	1.5	2.0	
	(% of total lipids)				
16:0	28.5 <sup>b</sup>	33.8 <sup>a</sup>	34.7 <sup>a</sup>	35.3 <sup>a</sup>	0.46
18:0	8.7 <sup>c</sup>	16.2 <sup>b</sup>	19.7 <sup>a</sup>	20.7 <sup>a</sup>	0.52
18:1n-9	38.2 <sup>a</sup>	24.7 <sup>b</sup>	20.9 <sup>c</sup>	17.4 <sup>d</sup>	0.58
18:2n-6	11.6	12.2	12.0	12.9	0.52
20:4n-6	0.7 <sup>a,b</sup>	0.5 <sup>b</sup>	0.7 <sup>a,b</sup>	0.8 <sup>a</sup>	0.06
22:6n-3	3.0 <sup>c</sup>	4.2 <sup>a</sup>	3.8 <sup>b</sup>	2.5 <sup>d</sup>	0.10
<i>cis</i> -9, <i>trans</i> -11-CLA	0.0 <sup>d</sup>	0.8 <sup>c</sup>	1.6 <sup>b</sup>	3.6 <sup>a</sup>	0.06
<i>trans</i> -10, <i>cis</i> -12-CLA	0.0 <sup>c</sup>	0.16 <sup>c</sup>	0.8 <sup>b</sup>	1.6 <sup>a</sup>	0.08
Total CLA	0.0 <sup>d</sup>	0.97 <sup>c</sup>	2.4 <sup>b</sup>	5.3 <sup>a</sup>	0.13
Total SFA	38.3 <sup>c</sup>	51.3 <sup>b</sup>	55.5 <sup>a</sup>	56.8 <sup>a</sup>	0.67
Total MUFA	41.4 <sup>a</sup>	26.8 <sup>b</sup>	22.4 <sup>c</sup>	18.7 <sup>d</sup>	0.40
Total lipids	16.0	18.1	17.7	17.6	0.57

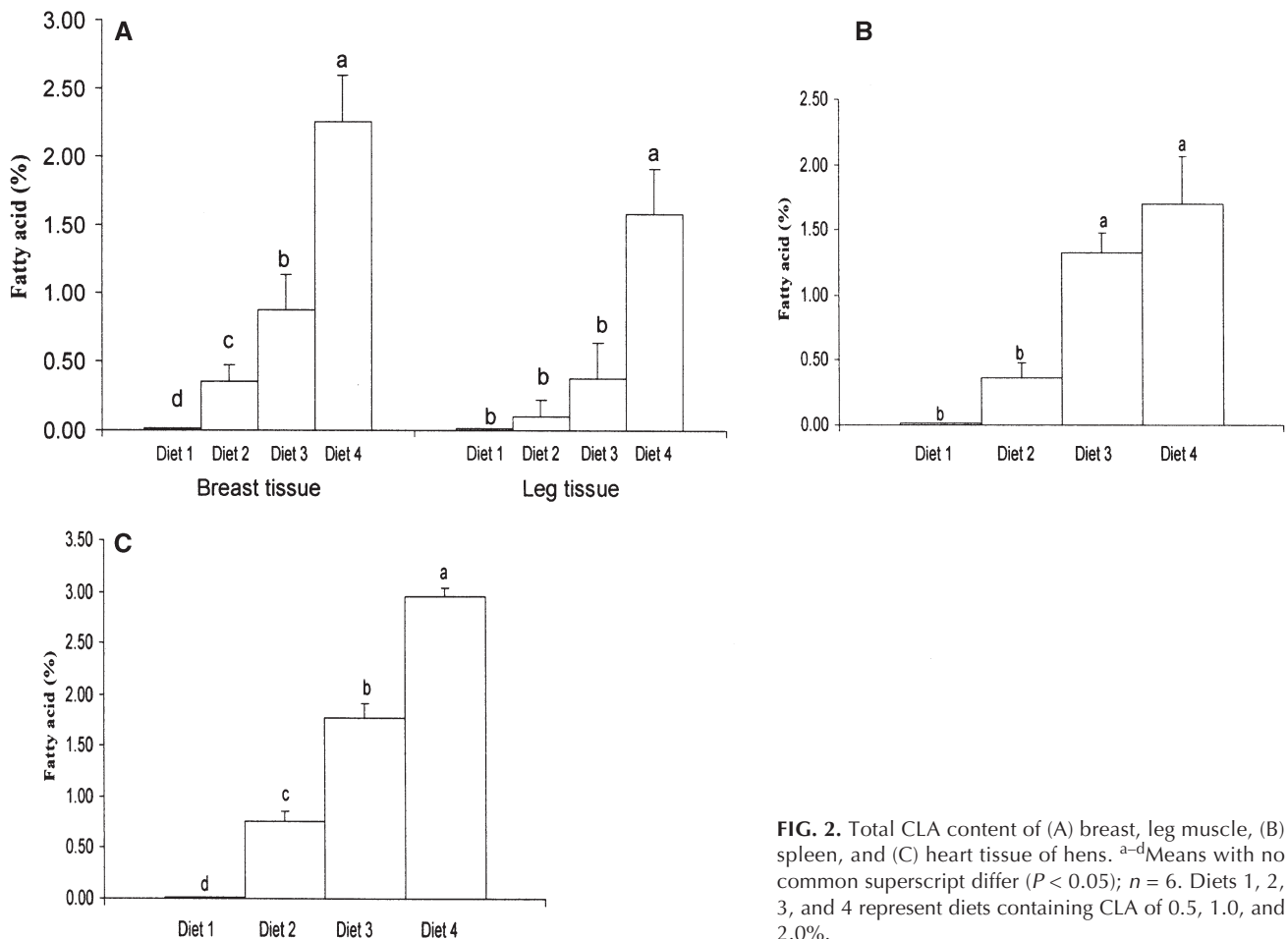
<sup>a</sup>Means within a row with no common superscript (a-d) differ ( $P < 0.05$ );  $n = 6$ . SFA, saturated FA; MUFA, monounsaturated FA.

leading to the reduction of MUFA. A recent study also reported a decrease in mRNA expression of stearoyl CoA in CLA-fed rats, affecting the synthesis of MUFA and accumulation of SFA (19). The SFA contents of the eggs from hens fed Diets 3 and 4 were higher ( $P < 0.05$ ) than for hens fed Diets 1 and 2. A twofold increase in stearic acid was also observed in hens fed Diet 2. Higher levels of SFA in yolk lipids may be a health concern owing to the association of 14:0 and 16:0 FA with plasma cholesterol and cardiovascular diseases. No effect of CLA on linoleic acid was observed in the yolk. However, 20:4n-6 was reduced in birds fed Diet 2. These results suggest an inhibitory action of CLA on enzymes responsible for MUFA synthesis resulting in an accumulation of SFA. Dietary CLA did not alter the total n-6 and n-3 PUFA content of yolk. Although Diet 1 contained low CLA and high fish oil, Diets 2 and 3 incorporated higher percentages of 22:6n-3 than Diet 1 ( $P < 0.05$ ). The reason for this high incorporation of 22:6n-3 is not clear. The low content of 22:6n-3 in Diet 4 may be due to the low level of menhaden oil in these diets.

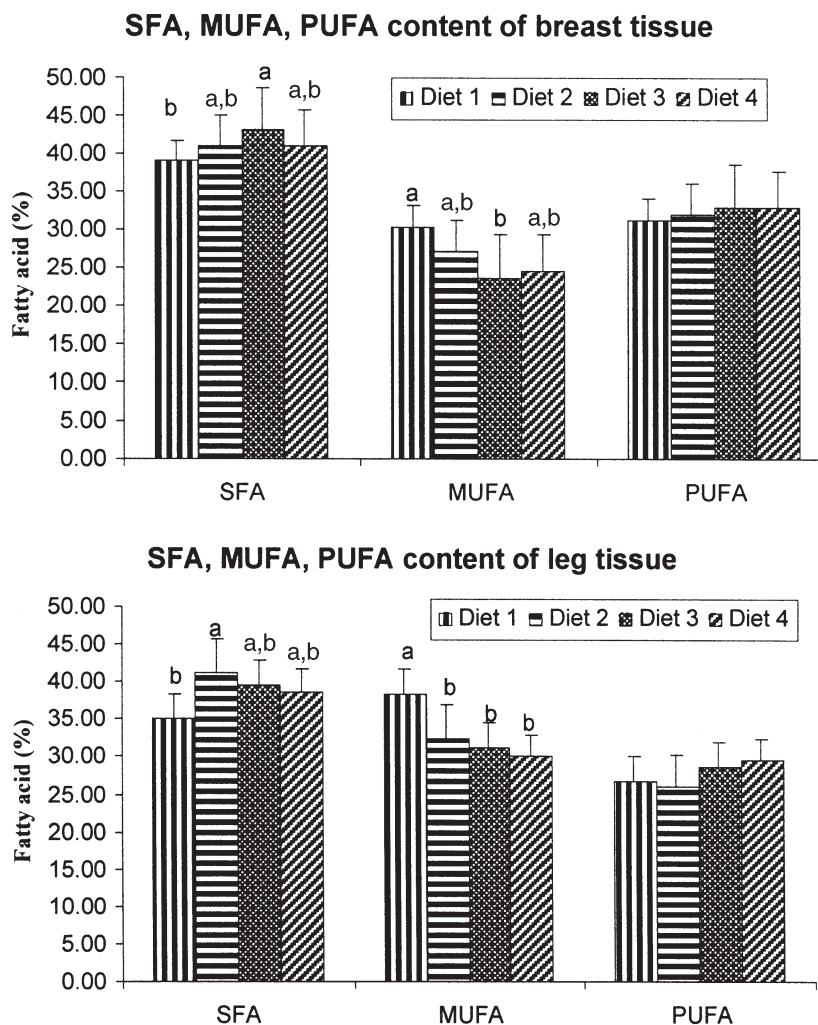
**Muscle tissue total lipids and FA.** Addition of CLA resulted in a significant increase in total CLA in the thigh and breast muscles (Fig. 2). The breast muscle incorporated more CLA than leg muscle. The total MUFA were reduced by feeding CLA (Fig. 3), which confirmed previous reports in poultry

(19). No difference was observed in the total PUFA. The total SFA was increased ( $P < 0.05$ ) by feeding CLA in Diets 3 and 2 in the breast and thigh muscle, respectively. Addition of CLA did not affect the incorporation of 20:5n-3 or 22:6n-3 in the thigh meat. However, the content of 20:4n-6 was significantly reduced in birds fed Diet 1. The concentrations in breast meat of 22:6n-3 and 20:5n-3 were highest in hens fed Diet 3. No difference was observed in the content of 20:4n-6 in the breast meat. The fat content of breast muscle was not affected by dietary CLA. The total fat was 1.1, 1.07, 0.88, and 0.88% for hens fed Diets 1, 2, 3, and 4, respectively. However, a significant decrease in thigh meat total fat was observed. The total fat varied from 5.1 to 1.9, 1.6, and 1.7% for hens fed Diets 1, 2, 3, and 4, respectively. The significant reduction in fat content observed in thigh meat from hens fed CLA is of importance in producing CLA-enriched low-fat chicken meat for human consumption. Although the meat from laying chickens is not sold commercially, these results may have implications in developing value-added FA-modified further processed products. However, further research on the sensory attributes of such meat products is needed.

The increased dietary intake of CLA was reflected in the FA composition of abdominal fat (Table 5). The total CLA constituted 3.0% in hens fed Diet 4 when compared to 0% in Diet 1. The percentage of oleic acid (18:1) was reduced by



**FIG. 2.** Total CLA content of (A) breast, leg muscle, (B) spleen, and (C) heart tissue of hens. <sup>a-d</sup>Means with no common superscript differ ( $P < 0.05$ );  $n = 6$ . Diets 1, 2, 3, and 4 represent diets containing CLA of 0.5, 1.0, and 2.0%.



**FIG. 3.** Saturated, monounsaturated, and polyunsaturated fatty acid content of breast and leg muscle of hens' diets containing different levels of CLA. <sup>a-d</sup>Means with no common superscript differ ( $P < 0.05$ );  $n = 6$ . Diets 1, 2, 3, and 4 represent hen diets containing CLA at 0.5, 1.0, and 2.0%. SFA = saturated FA; MUFA = monounsaturated FA. Error bars represent SEM.

feeding CLA, with a concomitant increase in stearic acid (18:0). The content of long-chain n-3 and n-6 FA was minimal in the abdominal fat and was not affected by the dietary treatment. No difference was observed in the total lipid content in the abdominal fat. Body fat reduction properties of CLA are controversial. At a 0.5% level, CLA has been reported to increase the abdominal fat in broiler birds (20). However, Delany *et al.* (21) reported a marked and rapid reduction in fat accumulation in rats. It appears that birds are not as sensitive to dietary CLA as mice.

The increase in CLA concentration resulting from feeding CLA to hens was observed in other hen tissues such as the spleen and heart. A dose-dependent increase ( $P < 0.05$ ) in CLA was observed in the heart and spleen (Fig. 2). However, the dramatic changes in SFA and MUFA content observed in yolk or liver was not noticed in heart or spleen. Feeding CLA did not alter the SFA, MUFA, or n-6 FA in these tissues. Therefore, it appears that the FA-modifying effect of CLA in

the hen is tissue-specific. Hens rely on spleen and lymph nodes for immune responses, as thymus and bursa wither as the birds mature. Therefore, the alteration in CLA content in these tissues and its effect on the long-term health of birds needs to be evaluated.

In conclusion, the results of these studies demonstrate the role of dietary CLA and n-3 PUFA in modulating CLA and PUFA concentration in different tissues of the hen. Consumption of chicken eggs enriched with CLA and n-3 PUFA would be an alternative vehicle for providing these FA to the human diet. Whether the dietary CLA-associated hepatic lipidosis observed in this study is a phenomenon peculiar to laying hens or one that may occur in any situation in which the metabolic activity of the liver is enhanced or chronically stressed is not known. The present findings indicate that specific dietary protocols instituted for the purpose of enriching shell eggs with CLA must be evaluated under commercial conditions for impact on FLS prior to large-scale adoption. The ef-



**TABLE 5**  
**Abdominal Tissue FA Composition (%) of Hens' Diets**  
**Containing Different Levels of CLA<sup>a</sup>**

FA	Added dietary CLA (%)				SEM
	0	0.5	1.0	2.0	
	(% total lipids)				
14:0	1.63 <sup>a</sup>	1.70 <sup>a</sup>	1.58 <sup>a</sup>	0.99 <sup>b</sup>	0.09
16:0	23.69 <sup>c</sup>	26.10 <sup>b</sup>	27.28 <sup>a</sup>	25.52 <sup>b</sup>	0.20
16:1	6.18 <sup>a</sup>	5.31 <sup>b</sup>	4.90 <sup>b,c</sup>	4.30 <sup>c</sup>	0.17
18:0	5.61 <sup>c</sup>	7.78 <sup>a,b</sup>	9.00 <sup>a</sup>	7.28 <sup>b</sup>	0.22
18:1	39.29 <sup>a</sup>	34.89 <sup>b</sup>	33.39 <sup>b</sup>	35.51 <sup>b</sup>	0.29
18:2n-6	21.10	21.17	20.19	21.45	0.23
18:3n-3	1.04	1.02	0.95	0.91	0.06
18:4n-3	0.20	0.29	0.29	0.31	0.10
20:4n-6	0.01	0.00	0.00	0.00	0.02
CLA, c9,t11	0.00 <sup>c</sup>	0.48 <sup>c</sup>	1.05 <sup>b</sup>	1.68 <sup>a</sup>	0.13
CLA, t10,c12	0.00 <sup>c</sup>	0.28 <sup>c</sup>	0.72 <sup>b</sup>	1.22 <sup>a</sup>	0.11
CLA, others	0.00 <sup>b</sup>	0.00 <sup>b</sup>	0.00 <sup>b</sup>	0.06 <sup>a</sup>	0.03
22:4n-6	0.00	0.00	0.00	0.00	0.00
22:5n-3	0.01	0.01	0.00	0.00	0.03
22:6n-3	0.02	0.05	0.00	0.00	0.05
20:5n-3	0.00	0.00	0.00	0.00	0.00
TSFA	31.93 <sup>c</sup>	36.28 <sup>a,b</sup>	38.37 <sup>a</sup>	34.27 <sup>b</sup>	0.27
TMUFA	45.65 <sup>a</sup>	40.37 <sup>b</sup>	38.43 <sup>b</sup>	39.97 <sup>b</sup>	0.31
Total CLA	0.00 <sup>c</sup>	0.76 <sup>c</sup>	1.77 <sup>b</sup>	2.97 <sup>a</sup>	0.18
Total lipids	81.4	78.8	81.7	75.7	2.51

<sup>a</sup>Means within a row with no common superscript (a–d) differ ( $P < 0.05$ );  $n = 6$ . For abbreviations see Table 3.

fects of CLA on liver lipid metabolism in the chicken require further investigation.

**ACKNOWLEDGMENTS**

The Ott Professorship awarded to G. Cherian is acknowledged. The CLA used in this study was kindly supplied by PharmaNutrients, Lake Bluff, IL 60044. The assistance of Oregon State University Poultry Farm staff is acknowledged. The generous donation of menhaden oil from Omega Protein Inc, Reedville, VA 22539 is appreciated. Journal paper No. 11882 of the Oregon State University Extension and Experiment Station Communications, Corvallis, OR 97331-6702.

**REFERENCES**

1. Simopoulos, A.P. (1991) Omega-3 Fatty Acids in Health and Disease and in Growth and Development, *Am. J. Clin. Nutr.* 54, 438–463.
2. Pariza, M.W., Park, Y., and Cook, M.E. (2001) The Biologically Active Isomers of Conjugated Linoleic Acid, *Prog. Lipid Res.* 40, 283–298.
3. Kang, J.X., and Leaf, F.A. (1996) The Cardiac Antiarrhythmic Effects of Dietary Polyunsaturated Fatty Acid, *Lipids* 31, S41–S44.
4. Nair, S.D.S., Leitch, J.W., Falconer, J., and Garg, M.L. (1997) Prevention of Cardiac Arrhythmia by Dietary (n-3) Polyunsaturated Fatty Acids and Their Mechanism of Action, *J. Nutr.* 127, 383–393.
5. Cook, M.E., Miller, C.C., Park, Y., and Pariza, M.W. (1993) Immune Modulation by Altered Nutrient Metabolism: Nutri-

- tional Control of Immune-Induced Growth Depression, *Poult. Sci.* 72, 1301–1305.
6. Cantwell, H.R., O'Shea, D.M., and Stanton, C. (1999) The Effect of Conjugated Linoleic Acid on the Antioxidant Enzyme Defense System in Rat Hepatocytes, *Lipids* 34, 833–839.
7. Fritsche, J., Rickert, R., Steinhart, H., Yurawecz, M.P., Mossoba, M.M., Sehat, N., Roach, J.A.G., Kramer, J.K.G., and Ku, Y. (1999) Conjugated Linoleic Acid (CLA) Isomers: Formation, Analysis, Amounts in Foods and Dietary Intake, *Fett Lipid* 101, 272–276.
8. Ha, Y.L., Grimm, N.K., and Pariza, M.W. (1989) Newly Recognized Anticarcinogenic Fatty Acids: Identification and Quantification in Natural and Processed Cheeses, *J. Agric. Food Chem.* 37, 75–81.
9. Ip, C., Banni, S., Angioni, E., Carta, G., McGinley, J., Thompson, H.J., Barbano, D., and Bauman, D. (1999) Conjugated Linoleic Acid-Enriched Butterfat Alters Mammary Gland Morphogenesis and Reduces Cancer Risk in Rats, *J. Nutr.* 129, 2135–2142.
10. Squires, J., and Leeson, S. (1998) Etiology of Fatty Liver Syndrome in Laying Hens. *Br. J. Vet. Med.* 144, 602–609.
11. Folch, J., Lees, M., and Sloane Stanley, G.H. (1957) A Simple Method for the Isolation and Purification of Total Lipids from Animal Tissues, *J. Biol. Chem.* 226, 497–507.
12. Cherian, G., Wolfe, F.H., and Sim, J.S. (1996) Dietary Oils with Added Tocopherols: Effects on Egg or Tissue Tocopherols, Fatty Acids and Oxidative Stability, *Poult. Sci.* 75, 423–432.
13. Steel, R.G.D., and Torrie, J.H. (1980) *Principles and Procedures of Statistics: A Biometrical Approach*, 2nd edn., McGraw-Hill Book Co., Toronto.
14. Belury, M.M., and Kempa-Steczko, A. (1997) Conjugated Linoleic Acid Modulates Hepatic Lipid Composition in Mice, *Lipids* 32, 199–204.
15. Twibell, R.G., Watkins, B.A., and Brown, P.B. (2001) Dietary Conjugated Linoleic Acids and Lipid Source Alter Fatty Acid Composition of Juvenile Yellow Perch, *J. Nutr.* 131, 2322–2328.
16. Chamruspollert, M., and Sell, J.L. (1999) Transfer of Dietary Conjugated Linoleic Acid to Egg Yolks of Chickens, *Poult. Sci.* 78, 1138–1150.
17. Du, M., Ahn, D.U., and Sell, J.L. (1999) Effect of Dietary Conjugated Linoleic Acid on the Composition of Egg Yolk Lipids, *Poult. Sci.* 78, 1639–1645.
18. Raes, K., Huyghebaert, G., Smet, S.D., Nollet, L., Arnouts, S., and Demeyer, D. (2002) The Deposition of Conjugated Linoleic Acids in Eggs of Laying Hens Fed Diets Varying in Fat and Fatty Acid Profile, *J. Nutr.* 132, 182–189.
19. Choi, Y., Kim, Y.C., Han, Y.B., Park, Y., Pariza, M.W., and Ntambi, J.M. (2000) The *trans*-10,*cis*-2 Isomer of Conjugated Linoleic Acid Downregulates Stearoyl-CoA Desaturase 1 Gene Expression in 3T3-L1 Adipocytes, *J. Nutr.* 130, 1920–1924.
20. Du, M., and Ahn, D.U. (2002) Effect of Dietary Conjugated Linoleic Acid on the Growth Rate of Live Birds and on the Abdominal Fat Content and Quality of Broiler Meat, *Poult. Sci.* 81, 428–433.
21. DeLany, J.P., Blohm, P., Truett, A.A., Scimeca, J.A., and West, D.B. (1999) Conjugated Linoleic Acid Rapidly Reduces Body Fat Content in Mice Without Affecting Energy Intake, *Am. J. Physiol.* 276, R1172–R1179.

[Received April 8, 2002, and in revised form August 8, 2002; revision accepted August 9, 2002]

# Retinal Sensitivity Loss in Third-Generation n-3 PUFA-Deficient Rats

Harrison S. Weisinger<sup>a,b,c,\*</sup>, James A. Armitage<sup>a</sup>, Brett G. Jeffrey<sup>d</sup>, Drake C. Mitchell<sup>b</sup>, Toru Moriguchi<sup>b</sup>, Andrew J. Sinclair<sup>c</sup>, Richard S. Weisinger<sup>a</sup>, and Norman Salem, Jr.<sup>b</sup>

<sup>a</sup>Howard Florey Institute of Experimental Physiology and Medicine, University of Melbourne, 3010, Victoria, Australia; <sup>b</sup>Laboratory of Membrane Biochemistry and Biophysics, National Institute on Alcohol Abuse and Alcoholism (NIAAA), National Institutes of Health (NIH), Rockville, Maryland 20852; <sup>c</sup>Department of Food Science, Royal Melbourne Institute of Technology University, Melbourne, 3000, Victoria, Australia; and <sup>d</sup>Department of Paediatrics and Child Health, Flinders Medical Centre, The Flinders University of South Australia, Bedford Park, Adelaide, 5042, South Australia, Australia

**ABSTRACT:** A previous study conducted in guinea pigs suggested that ingestion of diets high in EPA and DHA may result in suboptimal retinal function. The aim of the present study was to evaluate retinal function in pigmented (Long-Evans) rats, raised to a third generation on diets that were either deficient in n-3 PUFA or adequate (with the addition of DHA). Electroretinographic assessment employed full-field white flash stimulation. Photoreceptor responses were evaluated in terms of peak amplitudes and implicit times (a-wave, b-wave), intensity–response functions (Naka–Rushton), and the parameters of a model of transduction (P3). Retinal phospholipid FA composition was measured by capillary GLC. DHA levels were reduced by 55% in n-3-deficient animals compared with the n-3-adequate group, whereas the levels of docosapentaenoic acid n-6 were 44 times higher in n-3-deficient animals. The level of arachidonic acid was marginally higher (12.8%) in n-6-adequate animals. The n-3-deficient animals exhibited significantly reduced retinal sensitivity ( $\sigma$  and  $S$  values were both affected by 0.29 log units) and increased b-wave implicit times compared with those fed the n-3-adequate diet. These data suggest that n-3 PUFA are required for development of retinal sensitivity, more so than other indices of retinal function assessed by current methods, such as maximal response amplitude. However, the benefit for retinal function of adding preformed DHA to diets already replete in n-3 PUFA remains unclear.

Paper no. L8999 in *Lipids* 37, 759–765 (August 2002).

The retinal photoreceptors contain the highest levels of n-3 long-chain PUFA (LCPUFA) in the body (1,2). The major product of n-3 PUFA metabolism is DHA, which is found at concentrations approximating 50 mol% in the rod outer segment membranes (3,4).

The relevance of n-3 FA for the development of the ner-

This study was conducted at the Laboratory of Membrane Biochemistry and Biophysics, National Institute on Alcohol Abuse and Alcoholism, National Institutes of Health.

\*To whom correspondence should be addressed at Section of Neurobiology, Howard Florey Institute of Experimental Physiology and Medicine, University of Melbourne, 3010, Victoria, Australia.  
E-mail: h.weisinger@hfi.unimelb.edu.au

Abbreviations: AA, 20:4n-6 (arachidonic acid); ALA, 18:3n-3 ( $\alpha$ -linolenic acid); DPA, 22:5 (docosapentaenoic acid); ERG, electroretinogram; F3, third generation; FO, fish oil; LCPUFA, long-chain polyunsaturated fatty acid; n-3, omega-3; n-6, omega-6; P3, fast P3 model of phototransduction; RAS, renin–angiotensin system; RMS, root mean, squared (error term).

vous system is evident from the fact that human breast milk contains on the order of 0.6% of its total fat as n-3 FA, half of which is DHA (5). Furthermore, there is much evidence to suggest that an even slightly reduced n-3 FA status during infancy can have a measurable impact on development and subsequent function, particularly vision (6–11).

The first study to report the effect of dietary FA on retinal function was that of Benolken *et al.* (12) in which rats were fed a fat-free diet, resulting in a 60% reduction in retinal DHA. This was associated with reductions in electroretinographic (ERG) response amplitudes, attributed to anomalous photoreceptor activity. In a later study, the same authors (13) studied the effects of feeding rats a diet free of fat, or those associated with supplementation using either n-9, n-6, or n-3 substrate. They determined that the diets containing 2% 18:3n-3 ( $\alpha$ -linolenic acid, ALA) led to the greatest ERG amplitudes and concluded that n-3 FA are the most critical for the development of normal retinal function.

In a more recent study, Weisinger *et al.* (8) found that third-generation albino guinea pigs raised on diets adequate in n-3 PUFA substrate with the addition of fish oil [FO; containing the preformed LCPUFA (20:5n-3) EPA and DHA] displayed reduced ERG amplitudes compared with those raised on an n-3 adequate diet without FO. Moreover, FO-fed animals were found to perform no better than those fed an n-3-deficient diet. This finding is inconsistent with *in vitro* reconstituted membrane studies indicating that DHA-containing phospholipids are most effective at promoting the activity of membrane-bound proteins, such as those found in the retinal outer segments (14).

There are several possible explanations for the rather surprising findings. First, FO-fed animals may have suffered oxidative damage subsequent to elevated LCPUFA levels. Indeed, it has been demonstrated that animals raised on diets high in n-3 PUFA were more susceptible to retinal light damage (15) and that animals exposed to bright illuminations exhibited a selective loss of DHA in the retina (16,17). However, data for oxidative status and retinal histology were not obtained. Alternatively, since the FO contained high levels of EPA, retinal integrity or function may have been compromised by the resulting competitive reduction in arachidonic acid (AA) metabolism.

In a subsequent study, also performed in guinea pigs fed either safflower oil (n-3-deficient)- or canola oil (n-3-adequate)-based diets, Weisinger *et al.* (9) reported that depletion of n-3 PUFA in the retina affected the sensitivity [a parameter related to the amplification process of a fast P3 phototransduction (P3); Ref. 18] of the photoreceptor response far more than it did the response amplitude [i.e., a-wave, peak-to-peak, or the Naka–Rushton maximal response amplitude ( $R_{max}$ )]. This suggests that photoreceptor sensitivity is more susceptible to n-3 PUFA deficiency than is response amplitude, and supports the proposal that DHA influences membrane biophysical properties and thus its interactions with membrane-bound proteins [such as rhodopsin and transducin (19)]. Furthermore, it appears that direct provision of DHA and EPA by FO may be less consistent with optimal retinal function than provision of n-3 LCPUFA substrate (i.e., ALA) alone.

Bourre and coworkers (20) found that the functional differences observed between infant rats raised on diets either deficient or adequate in n-3 PUFA did not persist into adulthood. However, as previously argued by Vingrys *et al.* (21), the conclusions drawn by Bourre *et al.* need to be reconsidered in light of their age-related response reductions, which were more pronounced in the n-3-adequate group.

In the present study, we considered the retinal function of pigmented rats, raised through three generations on diets either deficient or adequate in n-3 FA; the latter diet contained both ALA and preformed DHA. The study differed from previous studies in rats in two important ways. First, the rats were tested at a later age to assess the purported reversibility of effects relating to n-3 PUFA deficiency. Second, the n-3-adequate diet was designed to minimize the reduction in neural AA accretion. Both diets contained antioxidant protection through the addition of vitamin E. This is the first study to assess retinal sensitivity in third-generation rats raised on diets that were deficient or adequate (with DHA) in n-3 PUFA.

## MATERIALS AND METHODS

**Animals and diets.** All procedures involving animals were conducted in accordance with the Association for Research in Vision and Ophthalmology (ARVO) Statement for the Use of Animals in Ophthalmic and Vision Research. They were approved by the NIAAA Animal Care Committee.

Animals in this experiment were raised on one of two semipurified diets (Table 1). Dietary fats were supplied by the supplementary oils added to the diets, thus creating one diet deficient in n-3 FA (n-3 Def) and the other n-3 adequate with the addition of preformed DHA (n-3 Adq). The assayed FA compositions of both experimental diets are given in Table 2. The diets contained vitamin E (75 IU/kg diet). Other details regarding the composition of the salt and vitamin mixes have been described previously (22).

Animals were raised for three generations (F3) to amplify the FA changes, as previously reported by this and other laboratories (23–25). Twelve F3 male, hooded rats (Long-Evans) were used for the study ( $n = 6$  per diet). Animals were fed

**TABLE 1**  
Diet Compositions (expressed as g/kg diet)<sup>a</sup>

Component	g/kg	
Casein, vitamin-free	200	
Carbohydrate	600	
Cornstarch	150	
Sucrose	100	
Dextrose	199	
Maltose-dextrin	150	
Cellulose	50	
Salt mix	35	
Vitamin mix	10	
L-Cystine	3	
Choline bitartrate	2.5	
TBHQ	0.02	
Fat	100	
Fat sources	n-3 Adq	n-3 Def
Coconut oil	74.49	81
Safflower oil	17.7	19
Flaxseed oil	4.81	—
DHASCO	3	—

<sup>a</sup>See Reference 22 for details of diet composition. DHASCO was obtained from Martek Bioscience Corp. (Columbia, MD). n-3 Adq, diet adequate in n-3 PUFA; n-3 Def, diet deficient in n-3 PUFA.

once per day with dietary pellets and water *ad libitum*. The ambient light (300 lux) was cycled in the animal room (12 h/12 h light/dark cycle), with temperature maintained at 21°C. Animals were matched for body weight at the time of testing [i.e., at 33 wk of age; mean (g) ± SEM; n-3 Def: 878.0 ± 19.6; n-3 Adq: 881.2 ± 40].

**TABLE 2**  
FA Composition of Diets (expressed as percentage of total lipid)<sup>a</sup>

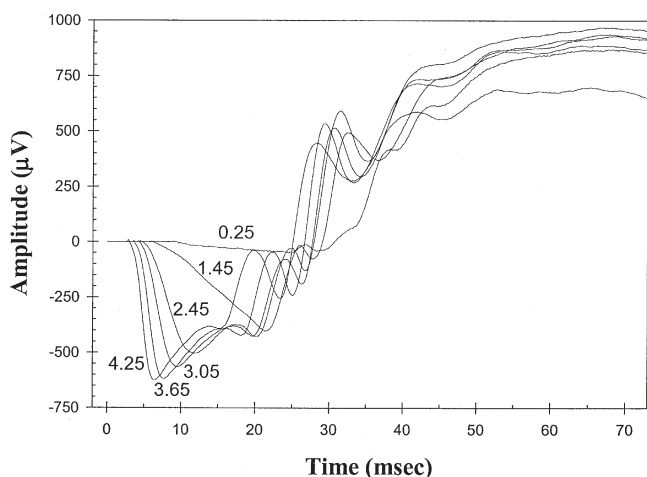
FA	n-3 Adq	n-3 Def
8:0	2.1	0.8
10:0	3.9	3.8
12:0	35.3	39.7
14:0	15.5	16.7
16:0	9.5	9.8
18:0	9.0	9.7
20:0	0.2	0.2
22:0	0.1	0.1
24:0	0.1	0.1
Total saturated	75.7	80.8
16:1n-7	0.03	0.03
18:1n-9	4.4	3.5
18:1n-7	0.3	0.3
20:1	0.1	0.1
22:1	0.02	0.01
Total monounsaturated	4.8	3.9
18:2n-6	15.7	15.1
20:2n-6	0.06	0.05
Total n-6	15.8	15.1
18:3n-3	2.5	0.04
22:6n-3	1.3	—
Total n-3	3.8	0.04
18:2n-6/18:3n-3	6	345
n-6/n-3	4	346
Total PUFA	20	15

<sup>a</sup>See Reference 22 for other details. For abbreviations see Table 1.

**ERG assessment.** Rats were dark-adapted overnight before deep anesthesia was induced by injection of ketamine (80 mg/kg, i.p.; Ketaset, Wyeth, Madison, NJ) and xylazine (20 mg/kg; Phoenix Pharmaceuticals, St. Joseph, MO). These doses resulted in effective anesthesia for a period of 60 min. Pupillary mydriasis was induced by instillation of one drop of tropicamide 0.5% (Mydracyl; Alcon, Ft. Worth, TX), and local anesthesia was achieved using proparacaine HCl 0.5% (Alcaine; Alcon).

Animals were positioned on a platform placed in the center of a Ganzfeld dome (LKC Technologies, Gaithersburg, MD) that provided full-field stimulation. Electrodes (Ag/AgCl) were positioned (+ve, cornea; -ve, buccal cavity; grnd, subcutaneous at the tail) and animals moved into place *via* the platform. Corneal contact was optimized by regular application of sterile saline. The light source (Vivitar 283; Vivitar, Newbury Park, CA) was mounted on the Ganzfeld dome such that neutral density filters (Wratten; Eastman Kodak, Rochester, NY) could be used to attenuate light passing into the dome. Flash energies spanned 4 log units; the unattenuated flash provided 3.5 log cd-sec-m<sup>-2</sup>. As previously described for the guinea pig (9), retinal illuminance (scot td-sec), was determined by integrating the spectral output of the unattenuated light source and the scotopic spectral sensitivity function for the rat (26). The highest retinal illuminance used in this study was 4.25 log scot td-sec. ERG assessment proceeded from lowest to highest flash intensity to preserve adaptation.

Two responses were averaged for each intensity with a variable interstimulus interval that ranged from 2 to 5 min, again to avoid light adaptation. ERG were amplified, filtered (gain × 1000, 3 dB at 1 Hz), digitized (8 bit, 6.7 kHz), and stored (internal gain, 4×) using a Neuroscientific recording system and analytical interface (Neuroscientific, New York, NY). The Ganzfeld dome, electrodes, and pre-amplifier were electrically shielded by a Faraday cage. Figure 1 shows a representative family of ERG curves, following on-line filtering and averaging.



**FIG. 1.** Representative electroretinographic (ERG) response family (diet adequate in n-3, n-3 Adq) for stimuli ranging from 0.25 to 4.25 log scot td-sec. Each wave form represents the average of two responses. Interstimulus intervals ranged from 2 to 5 min. Oscillatory potentials were filtered prior to analysis of the principal components.

(i) **Intensity-response characteristics—Naka–Rushton relationship.** Stimulation of the visual system results in a sigmoid response as a function of intensity (27,28). The Naka–Rushton plot can be used to describe this relationship as given by Equation 1,

$$R = R_{\max} \cdot \frac{I^n}{I^n + \sigma^n} \quad [1]$$

where  $R$  ( $\mu$ V) is the response amplitude and  $I$  (log scot td-sec) is the retinal illuminance. The derived parameters are:  $R_{\max}$  ( $\mu$ V), the maximal response amplitude;  $\sigma$  (log scot td-sec), the illuminance required to elicit a response equal to half  $R_{\max}$ ; and  $n$  (dimensionless), the slope of the curve.

(ii) **Photoreceptor response model—fast P3 (P3).** A measure of the photoreceptor contribution to the full-field flash ERG response was determined by applying the model described in Equation 2, in which P3 amplitude ( $\mu$ V) is a function of retinal illuminance ( $i$ , scot td-sec) and time after flash onset ( $t$ , sec).  $S$  [(scot td-sec)<sup>-1</sup>sec<sup>-2</sup>] is a sensitivity parameter that is scaled by retinal illuminance (18),  $R_{mP3}$  ( $\mu$ V) is the maximal photoreceptor response arising from the rods, and  $t_d$  (sec) is a brief delay, comprising several short delays inherent in the activation processes of phototransduction (29) or within the recording system itself (30). This model also takes account of the membrane capacitative time constant,  $\tau$ (sec), which enables more reliable fitting for responses to high-stimulus intensities (30).

$$P3(i,t) \equiv \left\{ 1 - \exp[-i \cdot S \cdot (t - t_d)^2] \right\} \otimes \left[ \exp\left(\frac{-t}{\tau}\right) \cdot \tau^{-1} \right] \cdot R_{mP3} \quad [2]$$

where  $t_d > t$ , and  $\otimes$  represents the convolution integral. The digital solution of Equation 2, described by Smith and Lamb (30), was used during ensemble fitting.

Optimization of the model was achieved by using a spreadsheet solver module (Microsoft Excel, Microsoft, Redmond, WA) to minimize the least-square error derived from a Levenberg–Marquardt routine, given by Equation 3 (31).

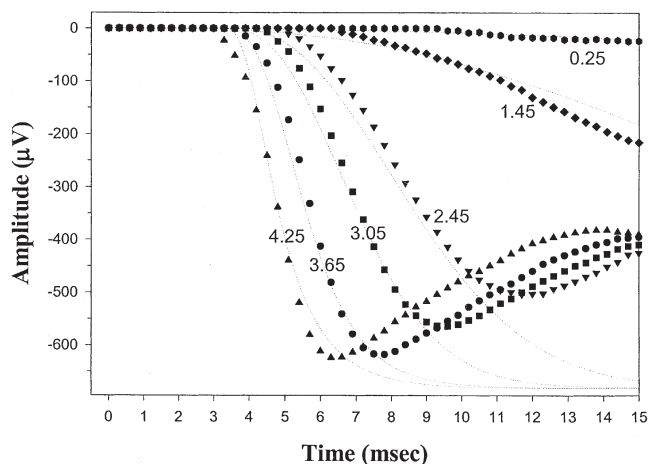
$$\text{Minimize over } R_{mP3}, S, t_d, \tau : \sum \sqrt{[y_i - y(x_i; R_{mP3}, S, t_d, \tau)]^2} \quad [3]$$

In this equation, the variables  $R_{mP3}$ ,  $S$ ,  $t_d$  and  $\tau$  were floated (simultaneously for all six a-waves) to optimize the least-square error term (RMS) for the fit of 1 to  $N$  data points ( $x_p$ ,  $y_i$ ), where  $y_i$  is the observed amplitude,  $x_i$  is the time,  $y$  is the predicted value from the fit, and  $N$  is the data point corresponding to the first local minimum or 15 msec, whichever came first. Since responses to brighter flashes contain fewer data points prior to b-wave intrusion, calculation of RMS was adjusted such that each response carried an equal weight.

Figure 2 illustrates ensemble analysis of the P3, performed on the leading edges of the a-waves.

**FA analysis.** Following all experiments, rats were killed by decapitation. Retinae were dissected into PBS prior to determination of lipid composition (modified after Folch *et al.*) (32). The total lipid extracts were transmethylated with 14% BF<sub>3</sub>-methanol at 100°C for 60 min. Methyl esters were then analyzed on a Hewlett-Packard 5890/Series II gas chromato-





**FIG. 2.** Representative ERG response family (n-3 Adq; truncated at 15 msec) for stimuli ranging from 0.25 to 4.25 log scot td-sec. Raw data are indicated by the symbols; fitted phototransduction model (P3) values are indicated by fine solid lines. For abbreviations see Figure 1.

graph equipped with an FID and fused-silica capillary column (DB-FFAP, 30 m × 0.25 mm × 0.25 µm; J&W, Folsom, CA) with carrier gas (hydrogen) at a linear velocity of 50 cm/sec. Injector and detector temperatures were set to 250°C and oven temperature program was as follows: 130 to 175°C at 4°C/min, 175 to 210°C at 1°C/min, and then to 245°C at 30°C/min, with a final hold for 15 min. The FAME from 10:0 to 24:1n-9 were identified by comparison to the retention times of a standard mixture (Nu-Chek-Prep 462; Nu-Chek-Prep, Elysian, MN).

**Statistical analysis.** Data were checked for normality and homogeneity of variances. Differences in retinal FA composition, Naka–Rushton values, and modeled P3 parameters were analyzed with a *t*-test, whereas peak amplitude and implicit times were analyzed using a two-way repeated measures ANOVA (Statview, SAS Institute, Cary, NC; Statistica, Statsoft, Tulsa, OK).

## RESULTS

**Animals.** The rats used in this study were normal in all respects. No differences in general appearance or activity were observed. However, animals in both groups were obese compared with animals of this species raised on standard chow diets, which contain only one-third of the lipid content.

**Retinal FA analysis.** The results of the FA analysis are provided in Table 3. There were no differences in the amounts of saturated FA, nor in the majority of monounsaturates found in retinal tissues. Animals in the n-3 Def group had very low levels of DHA (14.8% of total phospholipid FA) and high levels of docosapentaenoic acid (DPA) n-6 (17.5%). This finding was the opposite for the n-3 Adq group, in which DHA levels were 32.7% and DPA n-6 levels were 0.4% (Table 3). There was a small but significant change in AA between the two groups (n-3 Adq: 7.65 ± 0.15; n-3 Def: 8.78 ± 0.18). Thus, although the ratio of n-6/n-3 was different, the combined n-6 + n-3 were no different for the two groups.

**TABLE 3**  
Retinal Phospholipid FA Composition (g FA/100 g phospholipid FA ± SEM) for Rats Fed Diets That Differ in FA Composition

FA	n-3 Adq (n = 6)	n-3 Def (n = 6)
14:0	0.23 ± 0.02	0.23 ± 0.01
16:0	15.68 ± 0.12	15.47 ± 0.2
18:0	22.65 ± 0.28	22.41 ± 0.22
20:0	0.34 ± 0.01	0.30 ± 0.01
22:0	0.12 ± 0.01	0.09 ± 0.01
24:0	ND	ND
Total saturated	40.69 ± 0.30	40.55 ± 0.20
16:1n-7	0.37 ± 0.03	0.40 ± 0.02
18:1n-9	6.69 ± 0.07	6.39 ± 0.05*
18:1n-7	1.63 ± 0.02	1.86 ± 0.03*
20:1	0.18 ± 0.004	0.17 ± 0.003*
22:1	ND	ND
24:1	ND	ND
Total monounsaturated	9.05 ± 0.14	9.03 ± 0.09
18:2n-6	0.39 ± 0.04	0.25 ± 0.04*
18:3n-6	0.06 ± 0.01	0.05 ± 0.01*
20:3n-6	0.16 ± 0.004	0.12 ± 0.01*
20:4n-6	7.65 ± 0.15	8.78 ± 0.18*
22:4n-6	1.27 ± 0.03	2.30 ± 0.09*
22:5n-6	0.40 ± 0.05	17.53 ± 0.83**
Total n-6	10.00 ± 0.15	29.08 ± 0.96**
18:3n-3	ND	ND
20:5n-3	0.11 ± 0.003	ND*
22:5n-3	0.38 ± 0.01	0.06 ± 0.01**
22:6n-3	32.74 ± 0.27	14.85 ± 0.98**
Total n-3	33.23 ± 0.27	14.91 ± 0.98**
20:3n-9	ND	ND
22:5n-6/22:6n-3	0.01 ± 0.002	1.22 ± 0.13**
22:5n-6 + 22:6n-3	33.13 ± 0.22	32.38 ± 0.33
n-6/n-3	0.30 ± 0.04	1.95 ± 0.13**
n-6 + n-3	43.23 ± 0.30	43.99 ± 0.43

<sup>a</sup>ND, not detected; \**P* < 0.05; \*\**P* < 0.01. For abbreviations see Table 1.

**ERG.** Data for peak amplitude and implicit times are given in Table 4. Animals fed the n-3 Def diet exhibited increased b-wave implicit times (mean increase = 3.2 ± 0.9 msec, *P* < 0.05) compared with those fed the n-3 Adq diet. However, there were no statistically significant differences between the two diet groups for a-wave amplitude (*P* = 0.23), b-wave (peak-to-peak) amplitude (*P* = 0.19), or a-wave implicit time (*P* = 0.10). Owing to high intragroup variability and noise inherent to the ERG procedure, the power of the test was low ( $\beta$  = 0.95).

**Naka–Rushton analysis.** Response kinetics of the a-wave amplitude were different for animals in the two diet groups (Table 5). The semisaturation constant ( $\sigma$ ) was significantly increased (*P* < 0.05) by 0.29 log units in the n-3 Def group compared with the n-3 Adq group. There was no significant difference in  $R_{max}$  (*P* = 0.58) between the two diet groups.

**P3 fitting and analysis.** The phototransduction sensitivity parameter (*S*) was significantly decreased (*P* < 0.05) by 0.29 log units in n-3 Def animals compared with the n-3 Adq group. There were no significant differences in the values between animals in the n-3 Adq and n-3 Def groups for  $t_d$  (2.9 ± 0.1 vs. 2.8 ± 0.2, *P* = 0.58) or  $\tau$  (1.3 ± 0.2 vs. 1.2 ± 0.4, *P* = 0.80). There was also no significant difference in fitted  $R_{mp3}$  amplitude (504.1 ± 50.2 vs. 492.2 ± 38.6, *P* = 0.85) (Table 5).

**TABLE 4**  
**Peak (a-wave and b-wave) Amplitude and Implicit Time Measures (mean  $\pm$  SEM) as a Function of Flash Energy for Animals Fed Diets That Differ in FA Composition**

Flash energy (log scot td-sec)	a-Wave amplitude ( $\mu$ V)		Peak-to-peak amplitude ( $\mu$ V)		a-Wave implicit time (msec)		b-Wave implicit time <sup>a</sup> (msec)	
	n-3 Adq (n = 6)	n-3 Def (n = 6)	n-3 Adq (n = 6)	n-3 Def (n = 6)	n-3 Adq (n = 6)	n-3 Def (n = 6)	n-3 Adq (n = 6)	n-3 Def (n = 6)
0.25	60.0 $\pm$ 14.1	35.6 $\pm$ 6.8	690.6 $\pm$ 67.2	621.2 $\pm$ 50.1	26.0 $\pm$ 1.2	27.2 $\pm$ 0.7	64.9 $\pm$ 1.9	69.7 $\pm$ 1.4
1.45	245.4 $\pm$ 40.0	176.9 $\pm$ 29.0	1003.1 $\pm$ 120.7	684.7 $\pm$ 136.1	21.7 $\pm$ 0.3	23.1 $\pm$ 0.7	67.3 $\pm$ 1.4	70.6 $\pm$ 1.8
2.45	355.8 $\pm$ 42.7	290.6 $\pm$ 15.6	1126.9 $\pm$ 114.5	884.1 $\pm$ 65.6	12.0 $\pm$ 0.3	12.1 $\pm$ 0.2	65.8 $\pm$ 1.3	71.0 $\pm$ 1.5
3.05	395.8 $\pm$ 47.1	319.5 $\pm$ 30.4	1127.7 $\pm$ 118.6	915.7 $\pm$ 103.3	9.7 $\pm$ 0.2	9.9 $\pm$ 0.2	68.3 $\pm$ 1.2	70.3 $\pm$ 1.9
3.65	439.1 $\pm$ 51.3	393.7 $\pm$ 34.3	1141.9 $\pm$ 115.9	1036.7 $\pm$ 91.9	7.5 $\pm$ 0.1	7.8 $\pm$ 0.2	64.7 $\pm$ 1.1	68.1 $\pm$ 2.2
4.25	469.7 $\pm$ 43.4	379.7 $\pm$ 66.6	1023.1 $\pm$ 90.3	795.9 $\pm$ 139.1	6.3 $\pm$ 0.1	6.7 $\pm$ 0.1	55.3 $\pm$ 2.1	59.0 $\pm$ 2.6

<sup>a</sup>n-3 Adq < n-3 Def;  $P < 0.05$ . For abbreviations see Table 1.

**TABLE 5**  
**Fitted Electretinographic (ERG) Response Parameters for Animals Fed Diets That Differ in FA Composition**

Fitted parameter	n-3 Adq	n-3 Def
Naka-Rushton		
$\sigma$ (log cd-sec·m <sup>-2</sup> )	1.79 $\pm$ 0.13 <sup>a</sup>	2.08 $\pm$ 0.12
$R_{max}$ ( $\mu$ V)	476.4 $\pm$ 40.4	440.7 $\pm$ 46.7
Phototransduction (P3)		
$R_{mp3}$ ( $\mu$ V)	504.1 $\pm$ 50.2	492.2 $\pm$ 38.6
$t_d$ (sec)	2.9 $\pm$ 0.1	2.8 $\pm$ 0.2
$\tau$ (sec)	1.3 $\pm$ 0.2	1.2 $\pm$ 0.4
$\log S$ [(scot td-sec) <sup>-1</sup> sec <sup>-2</sup> ]	2.13 $\pm$ 0.10 <sup>a</sup>	1.84 $\pm$ 0.08

<sup>a</sup>Significantly different from n-3 Def animals;  $P < 0.05$ . For other abbreviations see Table 1.

## DISCUSSION

In agreement with previous studies utilizing dietary FA manipulation over three generations (23–25), animals showed alterations in their tissue FA compositions (Table 3). The well-established (inverse) relationship between the level of retinal DHA and DPA n-6 was also observed (33), i.e., there was no mean difference in the total amounts of n-3 + n-6 PUFA for the two groups. The elimination of high levels of EPA in the n-3 Adq diet ensured that retinal AA levels were slightly higher than those typically associated with the ingestion of diets high in n-3 PUFA (25).

The results of this study demonstrate that photoreceptor sensitivity ( $\sigma$ ) is affected by dietary manipulation, with animals in the n-3 Def group 0.29 log units less sensitive than those fed the n-3 Adq diet. From this result, it is inferred that n-3 PUFA-deficient animals require approximately twice as much light to reach a given response compared with those supplied adequate n-3 PUFA.

The reduction in photoreceptor sensitivity indicated by the Naka-Rushton analysis precisely reflected the results of the P3 analysis, in which the intensity scaling parameter ( $S$ ) was also significantly reduced by 0.29 log units. According to the model of Hood and Birch (34), a change in the sensitivity parameter is equivalent to a change in flash energy. Sensitivity is therefore determined by the quantal catch of the receptor that is, in turn, affected by structural parameters such as rod-packing density, receptor alignment, and pigment content.

However, following light capture, it is the amplification within the rhodopsin–transducin–phosphodiesterase cascade that determines sensitivity. As gross receptor morphology is reportedly unaffected by n-3 PUFA deficiency (35), it is likely that the reduction in sensitivity lies in the elements of the transduction cascade. This is consistent with our previous work in guinea pigs (9), in which we observed large losses in sensitivity (0.7 log units) independent of changes in  $R_{mp3}$ . The difference in sensitivity loss (i.e., 0.7 log units in n-3-deficient guinea pigs vs. n-3 Def rats in the present study) may be accounted for by interspecies differences, or by the fact that the control diet in the guinea pig study was canola oil-based and hence lacked DHA.

One way in which n-3 PUFA deficiency may affect retinal function is by modulating the function of membrane bound proteins in the retina. It is known that changes in the phospholipid FA profile alter the biophysical properties of reconstructed cell membranes (19,36,37). One mechanism by which n-3 deficiency may lead to diminished signal transduction in the retina is by decreasing the conversion of rhodopsin to its active isoform (metarhodopsin II) following light stimulation (19). In addition, new biophysical data (Niu, S.L., and Litman, B.J., personal communication) indicate that slower phosphodiesterase activation occurs in reconstituted membranes composed of PC-DPA n-6 compared with PC-DHA. As Bush *et al.* (38) found rhodopsin levels to be moderately increased subsequent to n-3 PUFA deficiency, reduced transductional efficiency may be coupled to increased expression of rhodopsin. This is consistent with the work of Calvert *et al.* (39), who demonstrated that a reduction in the amount of rhodopsin contained per lipid within the outer segment membranes resulted in faster G-protein to rhodopsin coupling and increased retinal sensitivity. It appears that a reduction in n-3 PUFA within the rod outer segment membrane and an increase in rhodopsin/lipid both slow transduction, thereby reducing sensitivity without affecting the maximal response amplitude.

One other possibility is that n-3 deficiency exerts its effect on retinal function by affecting the activity of the renin–angiotensin system (RAS). Recent investigations of the effects of n-3 PUFA deficiency on body fluid and metabolite homeostasis (40) and on blood pressure (41) suggest that functional

development of the RAS is affected by the neural phospholipid FA profile. Furthermore, Jacobi *et al.* (42) reported that the RAS has a neuromodulatory effect on the electroretinogram, in that pharmacological blockade of the RAS results in increased sensitivity measures.

Numerous studies have found differences in visual function between animals (or human infants) fed diets low in n-3 PUFA and those fed diets containing preformed DHA (6,11, 43,44). The failure of the present study to detect differences in the maximal response amplitudes is difficult to interpret owing to the low statistical power resulting from small sample size and highly variable data (the number of animals required for a power of 0.8 was calculated to be approximately 30 per group). It would, however, be consistent with an earlier study (8) in which electroretinographic response amplitudes recorded from guinea pigs raised on FO-based diets were no different from those from an n-3 PUFA-deficient group.

The finding of a delayed b-wave peak (i.e., increased implicit time) in n-3 Def animals is consistent with previous dietary FA manipulation studies in rats, cats, and monkeys but has not been observed in guinea pigs (for a review, see Jeffrey *et al.*, Ref. 11). It has been proposed that delays in ERG implicit times (11) may result from slower diffusion of transduction proteins through retinal photoreceptor membranes that are depleted of DHA (14). Furthermore, an increased b-wave implicit time may represent a delay in the transmission of the neural signal at the level of retinal bipolar cells. However, the interpretation of delayed b-waves is difficult, as they can be artifacts of an increase in amplitude of the underlying negatively directed voltage (i.e., slow P3).

These data do not support the notion that ERG deficits subsequent to n-3 deficiency subside with age, and suggest that P3 sensitivity is more susceptible to n-3 PUFA depletion than to other more conventionally used measures of retinal function, such as peak amplitude. The observed decrease in *S* is most likely due to modulation of the kinetics of one or more of the proteins involved in the P3 cascade, although possibly through another membrane-dependent receptor system such as the RAS. The way in which this translates to changes in visual perception or adaptation remains to be elucidated.

## ACKNOWLEDGMENTS

The authors acknowledge the assistance of Dr. Lee Chedester (logistics and animal care), Jim Loewke (biochemical analyses), Toni Calzone and Kevin Powell (technical support), and the support of Australian Academy of Science (HSW). Dr. Weisinger is supported by a National Health and Medical Research Council Australian Postdoctoral Fellowship 007103.

## REFERENCES

- Daemen, F.J. (1973) Vertebrate Rod Outer Segment Membranes, *Biochim. Biophys. Acta* 300, 255–288.
- Salem, N., Jr. (1989) Omega-3 Fatty Acids: Molecular and Biochemical Aspects, in *New Protective Roles for Selected Nutrients* (Spiller, G.A., and Scala, J., eds.), pp. 109–228, Alan R. Liss, New York.
- Fliesler, S.J., and Anderson, R.E. (1983) Chemistry and Metabolism of Lipids in the Vertebrate Retina, *Prog. Lipid Res.* 22, 79–131.
- Penn, J.S., and Anderson, R.E. (1987) Effect of Light History on Rod Outer-Segment Membrane Composition in the Rat, *Exp. Eye Res.* 44, 767–778.
- Rodriguez-Palmero, M., Koletzko, B., Kunz, C., and Jensen, R. (1999) Nutritional and Biochemical Properties of Human Milk: II. Lipids, Micronutrients, and Bioactive Factors, *Clin. Perinatol.* 26, 335–359.
- Uauy, R.D., Birch, E.E., Birch, D.G., and Hoffman, D.R. (1994) Significance of  $\omega$ -3 Fatty Acids for Retinal and Brain Development of Preterm and Term Infants, *World Rev. Nutr. Diet.* 75, 52–62.
- Neuringer, M. (1993) The Relationship of Fatty Acid Composition to Function in the Retina and Visual System, in *Lipids, Learning, and the Brain: Fats in Infant Formulas, Report of the 103rd Ross Conference on Paediatric Research* (Dobbing, J., ed.), pp. 134–163, Ross Laboratories, Columbus.
- Weisinger, H.S., Vingrys, A.J., and Sinclair, A.J. (1996) The Effect of Docosahexaenoic Acid on the Electroretinogram of the Guinea Pig, *Lipids* 31, 65–70.
- Weisinger, H.S., Vingrys, A.J., Bui, B.V., and Sinclair, A.J. (1999) Effects of Dietary n-3 Fatty Acid Deficiency and Repletion in the Guinea Pig Retina, *Invest. Ophthalmol. Vis. Sci.* 40, 327–338.
- Makrides, M., Neumann, M., Simmer, K., Pater, J., and Gibson, R. (1995) Are Long-Chain Polyunsaturated Fatty Acids Essential Nutrients in Infancy? *Lancet* 345, 1463–1468.
- Jeffrey, B.G., Weisinger, H.S., Neuringer, M., and Mitchell, D.C. (2001) The Role of Docosahexaenoic Acid in Retinal Function, *Lipids* 36, 859–871.
- Benolken, R.M., Anderson, R.E., and Wheeler, T.G. (1973) Membrane Fatty Acids Associated with the Electrical Response in Visual Excitation, *Science* 182, 1253–1254.
- Wheeler, T.G., Benolken, R.M., and Anderson, R.E. (1975) Visual Membranes: Specificity of Fatty Acid Precursors for the Electrical Response to Illumination, *Science* 188, 1312–1314.
- Mitchell, D.C., Niu, S.L., and Litman, B.J. (2001) Optimization of Receptor-G Protein Coupling by Bilayer Lipid Composition I: Kinetics of Rhodopsin–Transducin Binding, *J. Biol. Chem.* 276, 42801–42806.
- Organisciak, D.T., Darrow, R.M., Jiang, Y.L., and Blanks, J.C. (1996) Retinal Light Damage in Rats with Altered Levels of Rod Outer Segment Docosahexaenoate, *Invest. Ophthalmol. Vis. Sci.* 37, 2243–2257.
- Wiegand, R.D., Giusto, N.M., Rapp, L.M., and Anderson, R.E. (1983) Evidence for Rod Outer Segment Lipid Peroxidation Following Constant Illumination of the Rat Retina, *Invest. Ophthalmol. Vis. Sci.* 24, 1433–1435.
- Wiegand, R.D., Joel, C.D., Rapp, L.M., Nielsen, J.C., Maude, M.B., and Anderson, R.E. (1986) Polyunsaturated Fatty Acids and Vitamin E in Rat Rod Outer Segments During Light Damage, *Invest. Ophthalmol. Vis. Sci.* 27, 727–733.
- Hood, D.C., and Birch, D.G. (1997) Assessing Abnormal Rod Photoreceptor Activity with the a-Wave of the Electroretinogram: Applications and Methods, *Doc. Ophthalmol.* 92, 253–267.
- Litman, B.J., and Mitchell, D.C. (1996) A Role for Phospholipid Polyunsaturation in Modulating Membrane Protein Function, *Lipids* 31, S-193–S-197.
- Bourre, J.M., Francois, M., Youyou, A., Dumont, O., Piciotti, M., Pascal, G., and Durand, G. (1989) The Effects of Dietary Alpha-Linolenic Acid on the Composition of Nerve Membranes, Enzymatic Activity, Amplitude of Electrophysiological Parameters, Resistance to Poisons and Performance of Learning Tasks in Rats, *J. Nutr.* 119, 1880–1892.

21. Vingrys, A.J., Weisinger, H.S., and Sinclair, A.J. (1998) The Effect of Age and n-3 PUFA Level on the ERG in the Guinea Pig, in *Lipids and Infant Nutrition* (Sinclair, A., and Huang, Y., eds.), pp. 85–99, AOCS Press, Champaign.
22. Reeves, P., Neilsen, F., and Fahey, G. (1993) Committee Report on the AIN-93 Purified Rodent Diet, *J. Nutr.* 123, 1939–1951.
23. Leat, W.M.F., Curtis, R., Millichamp, N.J., and Cox, R.W. (1986) Retinal Function in Rats and Guinea Pigs Reared on Diets Low in Essential Fatty Acids and Supplemented with Linoleic or Linolenic Acids, *Ann. Nutr. Metab.* 30, 166–174.
24. Wainwright, P.E., Huang, Y.S., Coscina, D.V., Levesque, S., and McCutcheon, D. (1994) Brain and Behavioral Effects of Dietary n-3 Deficiency in Mice: A Three Generational Study, *Dev. Psychobiol.* 27, 467–487.
25. Weisinger, H.S., Vingrys, A.J., and Sinclair, A.J. (1995) Dietary Manipulation of Long-Chain Polyunsaturated Fatty Acids in the Retina and Brain of Guinea Pigs, *Lipids* 30, 471–473.
26. Birch, D., and Jacobs, G.H. (1975) Behavioral Measurements of Rat Spectral Sensitivity, *Vision Res.* 15, 687–691.
27. Fulton, A.B., Hansen, R.M., and Findl, O. (1995) The Development of the Rod Photoresponse from Dark-Adapted Rats, *Invest. Ophthalmol. Vis. Sci.* 36, 1038–1045.
28. Severns, M.L., and Johnson, M.A. (1993) The Care and Fitting of Naka–Rushton Functions to Electretinographic Intensity-Response Data, *Doc. Ophthalmol.* 85, 135–150.
29. Lamb, T.D., and Pugh, E.N., Jr. (1992) A Quantitative Account of the Activation Steps Involved in Phototransduction in Amphibian Photoreceptors, *J. Physiol.* 449, 719–758.
30. Smith, N.P., and Lamb, T.D. (1997) The a-Wave of the Human Electretinogram Recorded with a Minimally Invasive Technique, *Vision Res.* 37, 2943–2952.
31. Press, W.H., Teukolsky, S.A., Vetterling, W.T., and Flannery, B.P. (1992) *Numerical Recipes in C. The Art of Scientific Computing*, Cambridge University Press, New York.
32. Schwertner, H.A., and Mosser, E.L. (1993) Comparison of Lipid Fatty Acids on a Concentration Basis vs. Weight Percentage Basis in Patients With and Without Coronary Artery Disease or Diabetes, *Clin. Chem.* 39, 659–663.
33. Galli, C., White, H.B., Jr., and Paoletti, R. (1971) Lipid Alterations and Their Reversion in the Central Nervous System of Growing Rats Deficient in Essential Fatty Acids, *Lipids* 6, 378–387.
34. Hood, D.C., and Birch, D.G. (1993) Light Adaptation of Human Rod Receptors: The Leading Edge of Human a-Wave and Models of Rod Receptor Activity, *Vision Res.* 33, 1605–1618.
35. Futterman, S., Downer, J.L., and Hendrickson, A. (1971) Effect of Essential Fatty Acid Deficiency on the Fatty Acid Composition, Morphology, and Electretinographic Response of the Retina, *Invest. Ophthalmol.* 10, 151–156.
36. Litman, B.J., Niu, S.L., Polozova, A., and Mitchell, D.C. (2001) The Role of Docosahexaenoic Acid Containing Phospholipids in Modulating G Protein-Coupled Signaling Pathways: Visual Transduction, *J. Mol. Neurosci.* 16, 237–242; discussion 279–284.
37. Brown, M.F. (1994) Modulation of Rhodopsin Function by Properties of the Membrane Bilayer, *Chem. Phys. Lipids* 73, 159–180.
38. Bush, R.A., Malnoe, A., Reme, C.E., and Williams, T.P. (1994) Dietary Deficiency of n-3 Fatty Acids Alters Rhodopsin Content and Function in the Rat Retina, *Invest. Ophthalmol. Vis. Sci.* 35, 91–100.
39. Calvert, P.D., Govardovskii, V.I., Krasnoperova, N., Anderson, R.E., Lem, J., and Makino, C.L. (2001) Membrane Protein Diffusion Sets the Speed of Rod Phototransduction, *Nature* 411, 90–94.
40. Armitage, J.A., Burns, P.L., Sinclair, A.J., Weisinger, H.S., Vingrys, A.J., and Weisinger, R.S. (2001) Perinatal Omega-3 Fatty Acid Deprivation Alters Thirst and Sodium Appetite in Adult Rats, *Appetite* 37, 258.
41. Weisinger, H.S., Armitage, J.A., Sinclair, A.J., Vingrys, A.J., Burns, P.L., and Weisinger, R.S. (2001) Perinatal Omega-3 Fatty Acid Deficiency Affects Blood Pressure Later in Life, *Nat. Med.* 7, 258–259.
42. Jacobi, P.C., Osswald, H., Jurklics, B., and Zrenner, E. (1994) Neuromodulatory Effects of the Renin–Angiotensin System on the Cat Electretinogram, *Invest. Ophthalmol. Vis. Sci.* 35, 973–980.
43. Neuringer, M., Connor, W.E., Lin, D.S., and Anderson, G.J. (1993) Effects of n-3 Fatty Acid Deficiency on Retinal Physiology and Function, in *The Third International Congress on Essential Fatty Acids and Eicosanoids* (Sinclair, A.J., and Gibson, R.A., eds.), pp. 161–164, AOCS Press, Champaign.
44. Pawlosky, R.J., Denkins, Y., Ward, G., and Salem, N., Jr. (1997) Retinal and Brain Accretion of Long-Chain Polyunsaturated Fatty Acids in Developing Felines: The Effects of Corn Oil-Based Maternal Diets, *Am. J. Clin. Nutr.* 65, 465–472.

[Received February 8, 2002, and in revised form and accepted July 16, 2002]



# n-3 FA Increase Liver Uptake of HDL-Cholesterol in Mice

Valérie le Morvan, Marie-France Dumon, Antonio Palos-Pinto, and Annie M. Béard\*

Laboratoire de Biochimie et de Biologie Moléculaire, Université Victor Ségalen Bordeaux 2, 33076 Bordeaux, France

**ABSTRACT:** In humans, diets rich in fish oil (containing n-3 FA) decrease the incidence of coronary artery diseases. This is thought to be caused by the induction in liver and skeletal muscle of genes involved in lipid oxidation, and to the repression in liver and adipose tissue of genes responsible for lipogenesis. n-3 FA are known to reduce the synthesis of FA and TG in the liver, resulting in a decrease of plasma concentrations of TG-rich lipoproteins. On the other hand, little is known of a possible effect of n-3 FA on HDL metabolism. To investigate this question, female C57Bl/6J mice were fed an n-3 FA-enriched diet for 16 wk. As expected from previous studies, we found that total cholesterol, TG, and phospholipids were reduced in the plasma of treated mice. We also found that HDL-cholesterol decreased after this treatment and that the *in vivo* fractional catabolic rate of HDL-cholesteryl ester was significantly higher in treated mice than in control mice fed a standard diet. Consistent with these results, treated mice exhibited increased uptake of HDL-cholesteryl ester in the liver. Moreover, quantitative reverse transcriptase-PCR analysis showed a two- to threefold increase in scavenger receptor B-1 gene expression. Taken together, these results suggest that an n-3 FA-enriched diet stimulates one step in the reverse cholesterol transport in mice, probably by increasing the amount of the scavenger receptor class B-1. These effects of n-3 FA on HDL metabolism may contribute to their beneficial effects on the vasculature.

Paper no. L9028 in *Lipids* 37, 767–772 (August 2002).

Interest in dietary fish oil has been stimulated by the observation that Greenland Eskimo populations, whose consumption of fish is high, have a decreased incidence of coronary artery disease compared to a Danish control population despite their high-fat diet (1). The components conferring such protective properties to fish oil are the n-3 FA, mainly EPA and DHA (2), long-chain highly polyunsaturated FA of 20 or 22 carbons with five or six double bonds (20:5- and 22:6n-3), respectively.

The beneficial effects of n-3 FA on coronary artery disease are best exemplified by a reduced frequency of reinfarction (3). The physiological response seems to include decreased platelet aggregation (4), reduced production of inflammatory and chemotactic substances by the endothelium (5–7), and modification of plasma lipid levels. Fish oil has been shown to lower fasting TG plasma concentrations, possibly by reducing TG synthesis in the liver (8–11). In addition, fish oil increases lipoprotein lipase activity leading to an accelerated

catabolism of VLDL (12) and chylomicrons, which contributes to the decrease in postprandial triglyceridemia (13,14). The molecular mechanism(s) of action of n-3 FA have remained speculative until recently, when evidence showed that these substances control the transcription of specific genes in the liver such as FA synthase, S14 protein, and lipoprotein lipase. One pathway seems to depend on the direct binding of these compounds to peroxisome proliferator-activated receptor  $\alpha$  (PPAR $\alpha$ ), while another might be due to a decrease in sterol regulatory element binding protein (SREBP-1c) mRNA (15,16).

Although the effects of fish oils on the metabolism of TG-rich lipoproteins are now well documented and can be explained in molecular terms, their potential effects on HDL metabolism are still unclear. Several epidemiological studies have shown that HDL-cholesterol concentrations tend to increase when the diet is rich in n-3 FA (12), but we are not aware of studies reporting an effect of n-3 FA on HDL-cholesterol transport to the liver. HDL are known to participate in a regulatory process called reverse cholesterol transport (17), by which peripheral cells transfer their excess cholesterol to circulating HDL before being taken up by the liver for excretion. Since HDL play a pivotal role in the transport of plasma cholesterol, it seemed promising to explore the possibility that some of the beneficial effects of n-3 FA could be due to an increase in reverse cholesterol transport and, if so, by which biochemical mechanism(s).

## MATERIALS AND METHODS

**Animals.** Normal female C57Bl/6 mice were obtained from Iffa Credo (L'Arbresle, France). They were housed in a full-barrier animal facility on a 12 h light/dark cycle, with free access to food and water. Since n-3 FA can be considered as a possible supplement or treatment in the human diet for their beneficial roles, we decided in this study to add these FA to the standard mouse diet. Mice were thus placed either on a regular diet or on a regular diet enriched in n-3 FA. The regular diet was rodent diet (no. 113; UAR, Epinay-sur-Orge, France). Its composition was (w/w) 5% fat; 51% carbohydrate; 22% protein; 4% fiber; 6% minerals; and added vitamins A, B, D, and E. The basal rodent diet was supplemented with 3.33% n-3 FA. The n-3 FA (w/w; 60% EPA and 40% DHA) were kindly provided by Pierre Fabre Santé Laboratoires (MAXEPA® capsules; Pierre Fabre Santé, Castres, France). The n-3-supplemented food was made each week, stored in individual packages at +4°C under nitrogen, and changed twice a day in order to avoid oxidation. FA composition of diets was measured by GC. The n-3 enriched diet con-

\*To whom correspondence should be addressed at Université Victor Ségalen Bordeaux 2, Laboratoire de Biochimie et de Biologie Moléculaire, Zone Nord—Case 49–146, Rue Léo Saignat, 33076 Bordeaux Cedex, France. E-mail: annie.berard@biomemohv.u-bordeaux2.fr

Abbreviations: FPLC, fast protein liquid chromatography; MEM, Eagle's minimal essential medium; PPAR $\alpha$ , peroxisome proliferator-activated receptor  $\alpha$ ; RT-PCR, reverse transcriptase-PCR; SR, scavenger receptor.

tained 19% EPA (20:5n-3) and 13% DHA (22:6n-3) from total FA. Mice were fed the diet for 16 wk. They did not lose weight and had normal hepatic tests (alanine aminotransferase, aspartate aminotransferase, lactate dehydrogenase) throughout the experiment. The use of the research protocol was in accordance with the French Ministry of Agriculture, section on Health and Animal Protection (approval 04476).

**Plasma lipid and lipoprotein analysis.** Mice were fasted 4 h and blood was drawn in tubes containing 4 mmol/L EDTA. Plasma was obtained by centrifugation at  $3,000 \times g$  for 20 min at 4°C. Plasma samples were separated, divided into aliquots, and stored frozen (-80°C) until analyzed. Total cholesterol and TG concentrations were measured in 10- $\mu$ L aliquots of plasma by using commercial enzymatic kits (Dade, Paris La Défense, France) and the Paramax automated chemistry analyzer (Dade). Free cholesterol and phospholipid concentrations were measured in 10- $\mu$ L aliquots of plasma by using commercial enzymatic kits (bioMérieux, Marcy l'Etoile, France) and the Uvikon 922 spectrophotometer (Kontron Instruments, Milano, Italy). Cholesteryl ester values were calculated as the difference between total cholesterol and free cholesterol concentrations. HDL were isolated from the supernatant obtained after selective precipitation of apolipoprotein B-containing lipoproteins with phosphotungstic acid in the presence of magnesium ions and centrifugation. HDL-cholesterol was then quantified by enzymatic determination (bioMérieux).

**Gel filtration chromatography.** After centrifugation of pooled fresh mouse plasmas at  $22,000 \times g$  for 20 min at 4°C, 200  $\mu$ L of clear supernatant was applied to a fast protein liquid chromatography (FPLC) system with two Superose columns connected in series (Pharmacia LKB, Orsay, France). Lipoproteins were eluted at 0.3 mL/min with PBS, pH = 7.4, containing 1 mmol/L EDTA and 0.02% sodium azide. After the first 10 mL was eluted, 60 fractions (0.51 mL each) were collected. Total cholesterol was quantified in each fraction to establish an FPLC profile. Since the FPLC were performed with pools, we have no direct information on the interindividual variability of the profiles. However, determination of cholesterol into HDL, the major lipoprotein in mice, could reflect variability.

**LCAT activity.** Plasma LCAT activity was determined as described previously (18) using 4  $\mu$ L of mouse plasma.

**FA determination.** Blood drawn from mice was collected into tubes containing 4 mmol/L EDTA and was centrifuged. HDL lipoproteins were isolated by sequential ultracentrifugation in 1.063 g/mL, followed by 1.210 g/mL (5 h) KBr solutions, at  $436,000 \times g$ , 4°C, in a TL100 rotor (Beckman Instruments, Gagny, France), and were kept at -80°C until analysis. Lipid extraction was done with hexane/isopropanol, and classes of lipids were separated by TLC (Merck-Clévenot, Nogent-sur-Marne, France) in diethyl ether/petroleum ether/acetic acid (270:30:3, by vol), associated with iodine detection. Phospholipids and cholesteryl esters were extracted with hexane/isopropanol. Isopropyl ester preparation of FA and their separation for further analysis by a fused-silica capillary column (CP Sil 88 column; Chrompack, Les

Ulis, France) with a Carlo Erba model 5160 gas chromatograph equipped with an FID were done as previously described (19). FA were identified by retention times obtained from various standards and from FA extracted from the diet and chromatographed under the same conditions.

**Cell culture and cholesterol efflux.** Normal human embryonic lung fibroblasts (MRC-5 cells; Bioproducts, BioWhittaker, Gagny, France) were grown in 24-well plates containing Eagle's minimal essential medium (MEM; Gibco BRL, Cergy-Pontoise, France) supplemented with 10% bovine calf serum, 2 mmol/L glutamine, 100 IU/mL penicillin, and 100  $\mu$ g/mL streptomycin (Gibco BRL). When subconfluent, the cells were incubated with MEM-10% bovine calf serum and 1  $\mu$ Ci/well of radiolabeled unesterified cholesterol ([1,2-<sup>3</sup>H]cholesterol; Dupont-New England Nuclear, Paris, France) until confluent monolayers were obtained. The cells were then washed three times with MEM/BSA and incubated with MEM/BSA for 24 h prior to performance of efflux assays in the presence of mouse plasmas prepared in 5% MEM/BSA. After the efflux period, media were collected and centrifuged to remove any detached cells. An aliquot of the medium was then counted by liquid scintillation. The radioactivity remaining in the cell pellet was determined after overnight extraction with isopropanol. Cholesterol efflux from the cells was determined as described previously (20). Efflux results are expressed in percentages after dividing the cpm in media by the sum of the cpm in media plus cells (21). At least three culture wells were incubated with each plasma sample. Mouse plasmas used as cholesterol acceptors were kept at -80°C until use. MEM/1% BSA without acceptor was used as a blank. To standardize the cellular response obtained with different batches of cells and labeling media, at least five aliquots of a standard plasma prepared from a pool of human plasmas were always included as test samples.

**HDL-cholesteryl ester metabolic studies.** Liposomes were generated by sonicating L- $\alpha$ -phosphatidylcholine (Sigma, L'Isle d'Abeau Chesnes, France), [<sup>3</sup>H]cholesteryl ester (Dupont-NEN), and butylated hydroxytoluene (Sigma) as described (22) and incubating for 18 h at 37°C with HDL (2 mg total protein) isolated from mice fed a regular diet or an n-3-enriched diet. Labeled lipoproteins were isolated by sequential ultracentrifugation in 1.063 g/mL (5 h) followed by 1.210 g/mL (12 h) KBr solution at 4°C and  $436,000 \times g$  in a TL100 rotor and analyzed as described previously (21). Isolated labeled HDL ( $10^6$  cpm) was injected in the saphenous vein of mice fed either a regular diet or an n-3-enriched diet. Mice were pre-anesthetized with ketamine (50 mg/kg) and xylazine (14 mg/kg). Injected radiolabeled HDL-cholesterol represented <5% of the pool sizes of recipient mice HDL-cholesteryl esters. Blood sampling was performed at 5, 15, 30, 60, 120, 240, 480, and 600 min after injection, and samples were counted in a Packard Tri-Carb liquid scintillation counter. The fractional catabolic rate for HDL-cholesteryl esters was calculated from the plasma decay curves of [<sup>3</sup>H]cholesteryl oleyl ester. To establish the rate of liver uptake, livers were harvested 2 h after injection, minced, extracted according to the

method of Folch *et al.* (23), and counted in a Packard Tri-Carb liquid scintillation counter.

**RNA isolation and analysis.** Mouse livers were obtained from mice on a standard diet or an n-3 FA-rich diet. All samples were immediately placed into a Trizol® solution (Gibco BRL) and stored at  $-80^{\circ}\text{C}$  pending RNA isolation. Total RNA were isolated according to the method of Chomczynski and Sacchi (24). The amount of RNA was determined by measuring absorption at 260 nm. Quality of the isolated RNA was controlled by the 260:280 nm ratio (1.8–2.0) and by denaturing gel electrophoresis. Tissue RNA were analyzed by Northern blot after fractionation on a 1.2% formaldehyde/agarose gel, and transferred to a Nylon Nitran Plus membrane (Schleicher & Schuell, Dassel, Germany) using the Turbo-blotter transfer system (Schleicher & Schuell). Hybridization was performed with  $^{32}\text{P}$ -labeled probes for mouse scavenger receptor (SR)-B1 (detecting both SR-B1 and SR-B2 transcripts) and  $\beta$ -actin. Autoradiographs were obtained by exposing Biomax MS films (Pharmacia-Amersham, Orsay, France) with two intensifying screens at  $-80^{\circ}\text{C}$ . The blots were analyzed using a PhosphorImager (Molecular Dynamics, Sunnyvale, CA). Northern blots were performed twice with pools of livers taken from four or five mice in each study group of mice maintained on specific diets for 16 wk. A second independent experiment was performed using an equal number of mice maintained on their respective diets for 6 wk.

For quantitative polymerase chain reaction (PCR) analysis, RNA were first reverse-transcribed to cDNA using random primers and a GeneAmp® RNA PCR kit (PE Biosystems, Courtaboeuf, France). The specific primers and TaqMan® probe were designed using Primer Express software (PE Biosystems) and synthesized by Genset (Paris, France). Each probe was double-labeled with the fluorescent reporter dye 6-carboxyfluorescein covalently linked to the 5' end of the probe and the quencher dye 6-carboxytetramethylrhodamine attached to the 3' end. Quantitative PCR was performed for SR-B1 transcripts in 96-well reaction plates with optical caps. Fluorescence was followed continuously for each reaction. Gene expression was normalized for the 18S amount. Quantitative PCR were performed three times with individual livers from four mice on an n-3-enriched diet for 16 wk and from five control mice. Data are expressed as a fold change in gene expression in treated mice compared to untreated mice.

**Statistical analysis.** A paired Student's *t*-test was used to compare values in groups of animals fed different diets. Statistical significance was defined as  $P < 0.05$ . Results are expressed as mean  $\pm$  SEM.

## RESULTS

**Characterization of plasma lipids and LCAT activity in C57Bl/6J mice fed an n-3-enriched diet.** Analysis of plasma lipids and lipoproteins in mice fed a regular diet or an n-3 FA-supplemented diet for 16 wk is shown in Table 1. Plasma concentrations of TG were significantly reduced in treated mice ( $P < 0.0003$ ), consistent with previous reports (25). In addition,

these mice showed a significant decrease in plasma concentrations of total cholesterol, phospholipids, and HDL-cholesterol. At 3 wk, TG concentrations decreased ( $0.62 \pm 0.01$  vs.  $0.40 \pm 0.07$  mg/dL,  $n = 20$  in each study group,  $P < 0.01$ ), whereas total cholesterol and HDL-cholesterol concentrations did not change significantly ( $P = 0.26$  and  $0.49$ , respectively). These results suggested that the long-term n-3-enriched diet was necessary to find changes in HDL-cholesterol concentrations in our study. A new batch of mice ( $n = 10$ ) was analyzed after 6 wk on the n-3-enriched diet. These data confirmed the 16-wk data. We found a decrease in the following plasma lipid concentrations: TG ( $52.4 \pm 4.4$  vs.  $56.8 \pm 5.9$  mg/dL,  $P < 0.02$ ), total cholesterol ( $62.2 \pm 3.7$  vs.  $79.1 \pm 7.6$  mg/dL,  $P < 0.0005$ ), free cholesterol ( $13.5 \pm 1.6$  vs.  $16.4 \pm 1.3$  mg/dL,  $P < 0.004$ ), phospholipids ( $110.3 \pm 7.7$  vs.  $139.1 \pm 10.0$  mg/dL,  $P < 0.0002$ ), and HDL-cholesterol ( $53.0 \pm 7.9$  vs.  $67.1 \pm 7.7$  mg/dL,  $P < 0.003$ ). Moreover, determination of LCAT activity in mouse plasma showed no effect from the diets ( $27.5 \pm 1.4$  vs.  $28.3 \pm 0.4$  nmol/mL/h in treated vs. untreated animals, respectively,  $P > 0.05$ ).

Analysis of plasma lipoproteins was also performed by FPLC (Fig. 1). In agreement with plasma lipoprotein determinations, FPLC analysis revealed a decrease in HDL-cholesterol. In addition, the size of the HDL particles present in the plasma of the mice on an n-3-enriched diet was increased compared to untreated mice, indicating an enrichment in cholesteryl ester. These results were confirmed by a second experiment with a new batch of mice treated for 6 wk (data not shown).

The above results, which showed that mice respond to n-3 FA by a series of changes also found in humans, encouraged us to continue to use mice as a model for further studies.

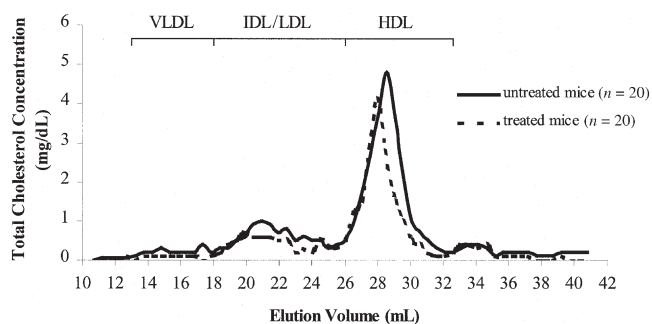
**An n-3-enriched diet modifies the FA composition of plasma HDL.** Analysis of the FA composition of plasma HDL by GC demonstrated that, although the concentration of n-3 FA-containing phospholipids increased from 22 to 26% of the total FA in treated mice, the concentration of n-3 FA in cholesteryl esters did not exceed 6 to 8% of the total FA (data not shown). We confirm here (26,27) that, quantitatively, EPA was distributed equally between plasma phospholipids and cholesteryl esters, whereas a greater concentration of DHA was present in phospholipids. The EPA/DHA ratio was much

**TABLE 1**  
Lipids in C57Bl6/J Female Mice on an n-3 FA-Enriched Diet for 16 wk<sup>a</sup>

	Untreated mice ( $n = 20$ )	Treated mice ( $n = 20$ )
TC (mg/dL)	$62.9 \pm 1.8$	$56.0 \pm 1.3^{***}$
TG (mg/dL)	$61.9 \pm 0.2$	$33.4 \pm 1.4^*$
PL (mg/dL)	$144.7 \pm 1.2$	$92.5 \pm 3.6^*$
FC (mg/dL)	$18.7 \pm 0.2$	$15.2 \pm 0.4^{**}$
CE (mg/dL)	$44.2 \pm 1.6$	$40.7 \pm 1.2$
CE/TC	$0.70 \pm 0.01$	$0.73 \pm 0.01$
HDL-c (mg/dL)	$45.8 \pm 2.1$	$39.0 \pm 1.1^{***}$
TC/HDL-c	$1.38 \pm 0.04$	$1.44 \pm 0.04$

<sup>a</sup>Results are expressed as mean  $\pm$  SEM; \* $P < 0.0003$ , \*\* $P < 0.002$ , \*\*\* $P < 0.04$ . TC, total cholesterol; PL, phospholipids; FC, free cholesterol; CE, cholesteryl esters; HDL-c, HDL-cholesterol.





**FIG. 1.** Fast protein liquid chromatography analysis of plasma lipoproteins in mice. Figure shows the cholesterol distribution in the plasma lipoproteins from untreated mice (bold line,  $n = 20$ ) and mice treated with n-3 FA for 16 wk (dotted line,  $n = 20$ ) after analysis by FPLC. The elution positions of VLDL, IDL (intermediate density lipoprotein)/LDL, and HDL lipoproteins are indicated.

higher in cholesteryl esters than in the precursor phospholipids, showing a marked difference in the utilization of EPA by mouse LCAT.

**Analysis of changes in cholesterol efflux.** To evaluate the functional properties of n-3 FA-enriched HDL, we performed efflux studies in fibroblasts. MRC-5 cells were loaded with unesterified cholesterol and incubated with mouse plasma at 5%. Plasmas from treated mice ( $n = 6$ ) were not more efficient in stimulating cholesterol efflux than those from mice on a regular diet ( $n = 6$ ) even after correction of the cholesterol efflux data for plasma HDL-cholesterol concentrations (Table 2).

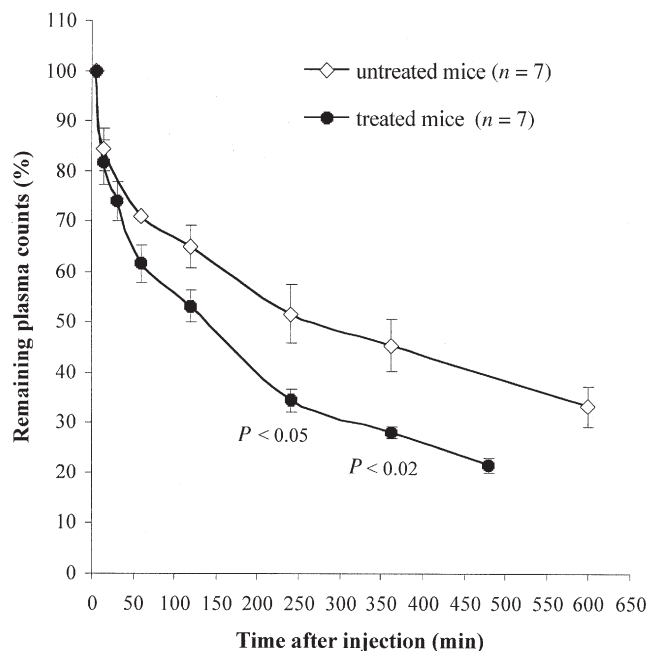
**n-3 FA increase HDL-cholesterol uptake by the liver.** The transfer of cholesteryl esters to the liver by HDL was significantly higher in mice fed an n-3-enriched diet compared to mice on a standard diet. The plasma decay of [ $^3$ H]cholesteryl ester of HDL from treated mice was faster than that of control HDL (Fig. 2): The fractional catabolic rate for HDL cholesteryl esters was increased 1.5-fold in treated mice compared to untreated mice (Table 2). In addition, accumulation of [ $^3$ H]cholesteryl esters derived from HDL in the liver was significantly increased by 23% in treated animals (Table 2).

**TABLE 2**  
**Effects of an n-3 Diet (16 wk) on HDL Metabolism in Female C57B16/J Mice<sup>a</sup>**

	Without treatment ( $n = 6$ )	With treatment ( $n = 6$ )
Cholesterol efflux (%)	17.7 $\pm$ 2.0	12.2 $\pm$ 1.3
Corrected cholesterol efflux <sup>b</sup> (%)	17.7 $\pm$ 2.0	14.3 $\pm$ 1.0
	Without treatment ( $n = 7$ )	With treatment ( $n = 7$ )
FCR (d <sup>-1</sup> )	4.8 $\pm$ 0.3	7.1 $\pm$ 0.2*
Liver uptake (total cpm)	224015 $\pm$ 7916	275630 $\pm$ 7675**
Total hepatic lipids (10 <sup>-3</sup> mg/mg of tissue)	37 $\pm$ 4	43 $\pm$ 6

<sup>a</sup>Results are expressed as mean  $\pm$  SEM;  $P < 0.02$ , \*\* $P < 0.05$ . FCR, fractional catabolic rate.

<sup>b</sup>Corrected cholesterol efflux values were obtained from plasma HDL-cholesterol concentration values.



**FIG. 2.** Plasma decay of [ $^3$ H]cholesteryl ester HDL from control and treated mice. Plasma decay of [ $^3$ H]cholesteryl ester HDL from control ( $\diamond$ ,  $n = 7$ ) and treated mice ( $\bullet$ ,  $n = 7$ ) were evaluated after injection of radiolabeled lipoproteins in mice.

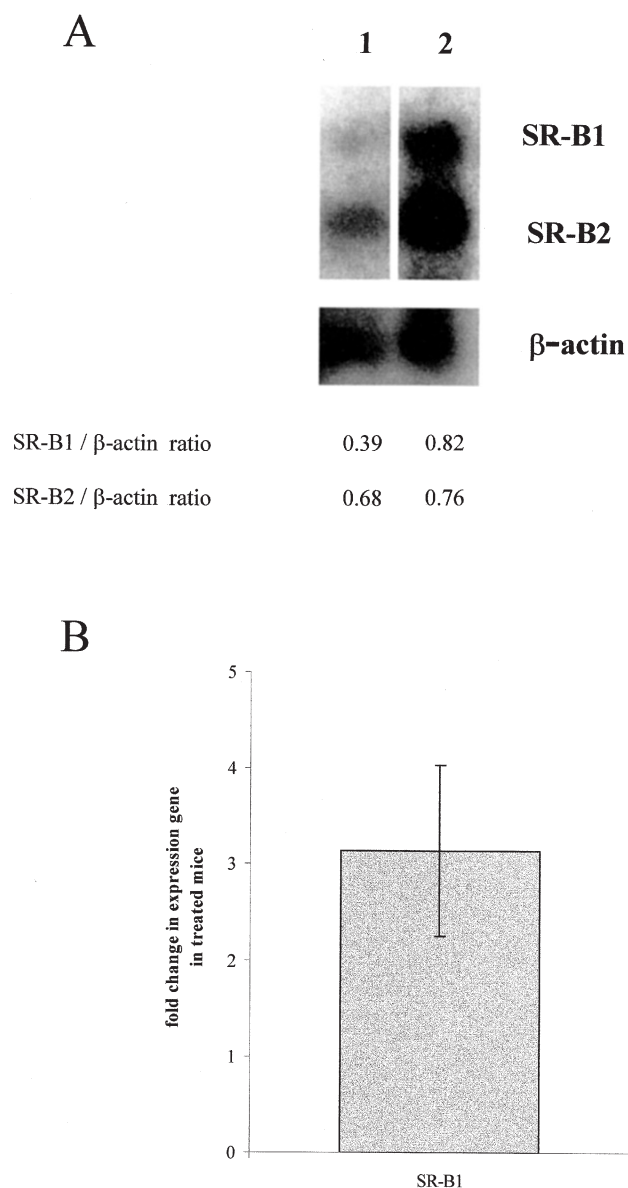
The above results show for the first time that an n-3 FA-enriched diet in the mouse accelerates the removal of HDL-cholesteryl esters from the plasma.

**n-3 FA increase hepatic SR-B1 mRNA in mice.** Since uptake of HDL-cholesteryl esters was increased in mice fed an n-3-rich diet, we explored liver SR-B1 mRNA levels by Northern blot and quantitative reverse transcriptase (RT)-PCR analysis. Compared to  $\beta$ -actin mRNA, which served as a control for message amounts for the tissue analyzed by Northern blot, SR-B1 transcripts markedly increased in livers from treated mice while changes in SR-B2 mRNA was not significant (Fig. 3A). Quantitative PCR analysis showed a threefold increase in SR-B1 mRNA ( $3.14 \pm 0.89$ -fold increase) in liver from mice on the omega-3 FA-enriched diet (Fig. 3B). Thus, an n-3 FA-enriched diet may increase SR-B1 protein expression, as suggested by the increase in its mRNA, and may explain the increased removal of HDL-cholesteryl esters from the plasma of treated mice.

## DISCUSSION

Evidence (28,29) is accumulating that cold-water fish or commercially available preparations of fish oil exert a protective effect against atherosclerosis, hypertension, thrombosis, and inflammation. This effect is thought to be due to the role of EPA and DHA of the n-3 FA family. Current interest in the effects of long-term ingestion of n-3 FA in lowering coronary artery disease risk has been stimulated by epidemiologic and clinical studies. These effects may include altered lipid metabolism. In this study using a murine model, EPA and DHA decreased TG and total cholesterol concentrations. The





**FIG. 3.** Scavenger receptor (SR)-B1 mRNA analysis in control and treated mice. (A) Northern blot analysis of RNA isolated from liver of untreated mice (lane 1,  $n = 5$ ) and mice treated with n-3 FA for 16 wk (lane 2,  $n = 4$ ). The autoradiograph for the hybridization with mouse SR-B1 cDNA is presented in the top panel and shows the two transcripts of SR-B1; mouse  $\beta$ -actin cDNA hybridization is presented in the bottom panel. The experiment was conducted with two batches of mice. (B) Quantitative PCR analysis shows the relative quantity of SR-B1 mRNA from individual livers of four mice on an n-3 FA-enriched diet compared to livers from five control mice. Target and endogenous control (18S) amplifications were done in separate tubes and results were normalized to 18S (three experiments). Data are expressed as the mean of the fold change in gene expression in treated mice compared to untreated mice. For other abbreviation see Figure 2.

decrease in total cholesterol level was due mainly to a decrease in HDL-cholesterol but also to that of LDL-cholesterol concentrations. The reduction of HDL-cholesterol in mice by n-3 FA may seem paradoxical because of the protective effect of HDL in humans and the fact that n-3 FA generally tend to

increase HDL concentrations in humans (12). However, a decrease in HDL does not necessarily imply that reverse cholesterol transport is impaired (30,31).

To study the impact of an n-3-enriched diet on reverse cholesterol transport, we first analyzed cholesterol efflux in a tissue culture model. We found that plasmas from mice being fed an n-3-enriched diet took up cellular cholesterol to a lesser degree than those from mice on a standard diet. However, since the HDL particle number was lower in treated mice, as shown by FPLC results, it is possible that on a per-particle basis, HDL from the treated mice were not impaired in their ability to extract cholesterol from cells. In the study plasmas, HDL particles were enriched in n-3 FA: EPA and DHA were incorporated into phospholipids and cholesteryl esters of HDL prepared from treated mice. Hence, we can conclude that the enrichment of HDL in n-3 FA does not provoke a modification in HDL function during the first step of reverse cholesterol transport. Gillotte *et al.* (32) also demonstrated that plasma from African green monkeys on a diet enriched in n-3 polyunsaturated fats did not influence cholesterol efflux. On the other hand, Dusserre *et al.* (33) demonstrated that cholesterol efflux from the cell membrane into the phospholipid bilayer of an artificial acceptor particle increased when EPA and DHA concentrations in cell phospholipids were higher. They hypothesized that alterations in plasma membrane fluidity or lipid domain structure might be responsible for the effects observed.

Cholesteryl esterification in HDL is another step in reverse cholesterol transport that can be evaluated by LCAT activity determination. However, LCAT activity values showed no change when mice were placed on an n-3-enriched diet, and the ratio of cholesteryl ester to total cholesterol did not increase significantly in mouse plasma.

To investigate the last step of reverse cholesterol transport, we quantified the hepatic uptake of HDL-cholesteryl esters and found that it was accelerated by n-3 FA. The fact that n-3 FA are ligands of PPAR $\alpha$  (15) is indicative of an effect of these substances at the gene level. In the mouse, the removal of HDL-cholesteryl esters from the plasma is thought to be mainly due to SR-B1 present on cells of different organs, including liver. We report here for the first time that n-3 FA induce a two- to threefold increase in SR-B1 mRNA, suggesting an increase in the amount of SR-B1 at the surface of liver cells. This effect on the last step of reverse cholesterol transport—an important mechanism by which HDL are thought to reduce the development of atherosclerosis—could account, at least in part, for the beneficial effect of diets rich in n-3 FA reported in epidemiological studies. We are presently using transcriptional arrays to identify other genes that could be targets for n-3 FA.

#### ACKNOWLEDGMENTS

We thank Prof. Yves Michel Darmon for reviewing our article and Prof. M. Clerc for discussions. We thank Dr. Dominique Breilh for providing assistance in kinetic study analysis, Anne Dupoirion for technical assistance, and H el ene Seguy for the preparation of the manuscript. This work was supported by Pierre Fabre Sant e and the P ole M edicament-GBM-Conseil R egional-Aquitaine, France.

## REFERENCES

- Dyerberg, J., and Bang, H.O. (1982) A Hypothesis on the Development of Acute Myocardial Infarction in Greenlanders, *Scand. J. Clin. Invest.* 42 (Suppl. 161), 7–13.
- Bang, H.O., and Dyerberg, J. (1973) The Composition of Food Consumed by Greenland Eskimos, *Acta Med. Scand.* 200, 69–73.
- Sangor, R., and Gillott, T. (1991) Long-Term Reduction in Reinfarction Rate, Blood Fibrinogen, Triglyceride and Total Cholesterol in Patients Taking Omega-3 Fatty Acids for Ischaemic Heart Disease, in *Fish Oil and Blood Vessel Wall Interactions* (Vanhoutte, P.M., and Douste-Blazy, Ph., eds.), pp. 149–160, John Libbey Eurotext, Paris, France.
- Nieuwenhuys, C.M., and Hornstra, G. (1998) The Effects of Purified Eicosapentaenoic and Docosahexaenoic Acids on Arterial Thrombosis Tendency and Platelet Function in Rats, *Biochim. Biophys. Acta* 1390, 313–322.
- Heller, A., Koch, T., Schmeck, J., and van Ackern, K. (1998) Lipid Mediators in Inflammatory Disorders, *Drugs* 55, 487–496.
- Fox, P.L., and Dicorleto, P.E. (1988) Fish Oils Inhibit Endothelial Cell Production of Platelet-Derived Growth Factor-like Protein, *Science* 241, 453–456.
- Weber, C., Erl, W., Pietsch, A., Danesch, U., and Weber, P. (1995) Docosahexaenoic Acid Selectively Attenuates Induction of Vascular Cell Adhesion Molecule-1 and Subsequent Monocytic Cell Adhesion to Human Endothelial Cells Stimulated by Tumor Necrosis Factor-alpha, *Arterioscler. Thromb. Vasc. Biol.* 15, 622–628.
- Phillipson, B.E., Rothrock, D.W., Connor, W.E., Harris, W.S., and Illingworth, D.R. (1985) Reduction of Plasma Lipids, Lipoproteins, and Apoproteins by Dietary Fish Oils in Patients with Hypertriglyceridemia, *N. Engl. J. Med.* 312, 1210–1216.
- Harris, W.S., Connor, W.E., Illingworth, D.R., Rothrock, D.W., and Foster, D.M. (1990) Effects of Fish Oil on VLDL Triglyceride Kinetics in Humans, *J. Lipid Res.* 31, 1549–1558.
- Rustan, A.C., Nossen, J.O., Christiansen, E.N., and Drevon, C.A. (1988) Eicosapentaenoic Acid Reduces Hepatic Synthesis and Secretion of Triacylglycerol by Decreasing the Activity of Acyl-coenzyme A:1,2-Diacylglycerol Acyltransferase, *J. Lipid Res.* 29, 1417–1426.
- Hebbachi, A.M., Seelaender, M.C., Baker, B.W., and Gibbons, G.F. (1997) Decreased Secretion of Very-Low-Density Lipoprotein Triacylglycerol and Apolipoprotein B Is Associated with Decreased Intracellular Triacylglycerol Lipolysis in Hepatocytes Derived from Rats Fed Orotic Acid or n-3 Fatty Acids, *Biochem. J.* 325, 711–719.
- Harris, W.S. (1997) n-3 Fatty Acids and Serum Lipoproteins: Human Studies, *Am. J. Clin. Nutr.* 65 (Suppl.), 1645S–1654S.
- Hansen, J.B., Grimsgaard, S., Nilsen, H., Nordoy, A., and Bonna, K.H. (1998) Effects of Highly Purified Eicosapentaenoic Acid and Docosahexaenoic Acid on Fatty Acid Absorption, Incorporation into Serum Phospholipids and Postprandial Triglyceridemia, *Lipids* 33, 131–138.
- Roche, H.M., and Gibney, M.J. (1999) Long-Chain n-3 Polyunsaturated Fatty Acids and Triacylglycerol Metabolism in the Postprandial State, *Lipids* 34 (Suppl.), S259–S265.
- Ren, B., Thelen, A.P., Peters, J.M., Gonzalez, F.J., and Jump, D.B. (1997) Polyunsaturated Fatty Acid Suppression of Hepatic Fatty Acid Synthase and S14 Gene Expression Does Not Require Peroxisome Proliferator-Activated Receptor Alpha, *J. Biol. Chem.* 272, 26827–26832.
- Kim, H.J., Takahashi, M., and Ezaki, O. (1999) Fish Oil Feeding Decreases Mature Sterol Regulatory Element-Binding Protein 1 (SREBP-1) by Down-regulation of SREBP-1c mRNA in Mouse Liver. A Possible Mechanism for Down-regulation of Lipogenic Enzyme mRNAs, *J. Biol. Chem.* 274, 25892–25898.
- Eisenberg, S. (1984) High Density Lipoprotein Metabolism, *J. Lipid Res.* 25, 1017–1058.
- Chen, C.H., and Albers, J.J. (1982) Characterization of Proteoliposomes Containing Apoprotein A-I: A New Substrate for the Measurement of Lecithin:Cholesterol Acyltransferase Activity, *J. Lipid Res.* 23, 680–691.
- Peuchant, E., Wolff, R., Salles, C., and Jensen, R. (1989) One-Step Extraction of Human Erythrocyte Lipids Allowing Rapid Determination of Fatty Acid Composition, *Anal. Biochem.* 181, 341–344.
- de la Llera Moya, M., Atger, V., Paul, J.L., Fournier, N., Moatti, N., Giral, P., Friday, K.E., and Rothblat, G. (1994) A Cell Culture System for Screening Human Serum for Ability to Promote Cellular Cholesterol Efflux. Relations Between Serum Components and Efflux, Esterification, and Transfer, *Arterioscler. Thromb.* 14, 1056–1065.
- Bérard, A., Foger, B., Remaley, A., Shamburek, R., Vaisman, B.L., Talley, G., Paigen, B., Hoyt, R.F., Jr., Marcovina, S., Brewer, H.B., Jr., and Santamarina-Fojo, S. (1997) High Plasma HDL Concentrations Associated with Enhanced Atherosclerosis in Transgenic Mice Overexpressing Lecithin-Cholesteryl Acyltransferase, *Nat. Med.* 3, 744–749.
- Morton, R.E., and Silversmit, D.B. (1981) A Plasma Inhibitor of Triglyceride and Cholesteryl Ester Transfer Activities, *J. Biol. Chem.* 256, 11992–11995.
- Folch, J., Lees, M., and Sloane Stanley, G.H. (1957) A Simple Method for the Isolation and Purification of Total Lipides from Animal Tissues, *J. Biol. Chem.* 226, 497–509.
- Chomczynski, P., and Sacchi, N. (1987) Single-Step Method of RNA Isolation by Acid Guanidinium Thiocyanate-Phenol-Chloroform Extraction, *Anal. Biochem.* 162, 156–159.
- Yoshida, H., Mawatari, M., Ikeda, I., Imaizumi, K., Seto, A., and Tsuji, H. (1999) Effect of Dietary Seal and Fish Oils on Triacylglycerol Metabolism in Rats, *J. Nutr. Sci. Vitaminol.* 45 (Tokyo), 411–421.
- Holub, B.J., Bakker, D.J., and Skeaff, C.M. (1987) Alterations in Molecular Species of Cholesterol Esters Formed via Plasma Lecithin-Cholesterol Acyltransferase in Human Subjects Consuming Fish Oil, *Atherosclerosis* 66, 11–18.
- Leaf, D.A., Connor, W.E., Barstad, L., and Sexton, G. (1995) Incorporation of Dietary n-3 Fatty Acids into the Fatty Acids of Human Adipose Tissue and Plasma Lipid Classes, *Am. J. Clin. Nutr.* 62, 68–73.
- Leaf, A., and Weber, P.C. (1988) Cardiovascular Effects of n-3 Fatty Acids, *N. Engl. J. Med.* 318, 1349–1357.
- Kromhout, D., Bosscheiter, E.B., and DeLozenne Coulander, C. (1985) The Inverse Relation Between Fish Consumption and 20-Year Mortality from Coronary Heart Disease, *N. Engl. J. Med.* 312, 1205–1209.
- Hayek, T., Chajek-Shaul, T., Walsh, A., Azrolan, N., and Breslow, J.L. (1991) Probucol Decreases Apolipoprotein A-I Transport Rate and Increases High Density Lipoprotein Cholesteryl Ester Fractional Catabolic Rate in Control and Human Apolipoprotein A-I Transgenic Mice, *Arterioscler. Thromb.* 11, 1295–1302.
- Plump, A.S., Azrolan, N., Odaka, H., Wu, L., Jiang, X., Tall, A., Eisenberg, S., and Breslow, J.L. (1997) ApoA-I Knockout Mice: Characterization of HDL Metabolism in Homozygotes and Identification of a Post-RNA Mechanism of ApoA-I Up-regulation in Heterozygotes, *J. Lipid Res.* 38, 1033–1047.
- Gillotte, K.L., Lundkatz, S., de la Llera-Moya, M., Parks, J.S., Rudel, L.L., Rothblat, G.H., and Phillips, M.C. (1998) Dietary Modification of High Density Lipoprotein Phospholipid and Influence on Cellular Cholesterol Efflux, *J. Lipid Res.* 39, 2065–2075.
- Dusserre, E., Pulcini, T., Bourdillon, M.C., Ciavatti, M., and Berthezene, F. (1995) Omega-3 Fatty Acids in Smooth Muscle Cell Phospholipids Increase Membrane Cholesterol Efflux, *Lipids* 30, 35–41.

[Received March 18, 2002, and in revised form June 28, 2002; revision accepted July 24, 2002]

# Impaired Lipoprotein Metabolism in Obese Offspring of Streptozotocin-Induced Diabetic Rats

Hafida Merzouk<sup>a</sup>, Sihem Madani<sup>b</sup>, Aziz Hichami<sup>b</sup>, Josiane Prost<sup>b</sup>, Kabirou Moutairou<sup>c</sup>, Jacques Belleville<sup>b</sup>, and Naim Akhtar Khan<sup>b,\*</sup>

<sup>a</sup>Laboratory of Animal Physiology, Tlemcen University, Algeria, <sup>b</sup>UPRES 2422, Lipids and Nutrition, Bourgogne University, Dijon 21000 France, and <sup>c</sup>FAST, University of Abomey Calavi, Cotonou, Benin

**ABSTRACT:** The time course of changes in lipoprotein metabolism of obese offspring of mildly diabetic rats was studied with respect to serum lipoprotein composition as well as LCAT and tissue lipoprotein lipase (LPL) activities. Mild hyperglycemia in pregnant rats was induced by intraperitoneal injection of streptozotocin on day 5 of gestation. Control pregnant rats were injected with citrate buffer. At birth, obese pups had higher serum glucose, insulin, and lipoprotein (VLDL, LDL-HDL<sub>1</sub>, HDL<sub>2,3</sub>) levels than control pups. After 1 mon of life, all of these parameters in obese rats became similar to those of controls. However, LCAT, adipose tissue LPL, and hepatic triacylglycerol lipase activities were high. At 2 mon of age, VLDL-TAG levels were higher in obese females than in controls. By the age of 3 mon, obese offspring had developed insulin resistance with hyperglycemia, hyperinsulinemia, and higher serum lipoprotein concentrations. Indeed, qualitative abnormalities of lipoproteins were seen and were typical of obese and diabetic human beings. Fetal hyperinsulinemia should be considered as a risk factor for later metabolic diseases, including dyslipoproteinemia.

Paper no. L9012 in *Lipids* 37, 773–781 (August 2002).

Considerable interest has been generated over the last decade on the potential role of factors that disturb fetal growth in the development of chronic diseases including obesity, diabetes mellitus, and atherosclerosis in adulthood. Previous studies have found that fetal undernutrition as well as fetal overnutrition was associated with the acquisition of later risk factors for chronic diseases (1–4).

Maternal diabetes during pregnancy is an important risk factor for fetal overnutrition leading to fetal obesity, resulting from the combined effects of excessive transfer of maternal nutrients (glucose, amino acids, nonesterified FA) to fetal hyperinsulinemia (4–6). Fetal hyperinsulinemia was associated with the development of glucose intolerance, obesity, and diabetes during childhood and adulthood (1,3,7).

Obesity and diabetes mellitus are associated with compositional changes in serum lipoproteins (8–10). Plasma lipoprotein concentrations and compositions are determined

by many factors. Both secretion by liver and intestine and uptake and degradation by specific or nonspecific pathways are involved. In addition, the combined action of several enzymes, such as lipoprotein lipase (LPL), hepatic triacylglycerol lipase (HTGL) and LCAT, on lipoproteins and movements of lipids and apolipoproteins (apo) in plasma also control the lipoprotein levels. It is of interest to determine if fetal hyperinsulinemia is a risk factor for later dyslipoproteinemia. In humans, follow-up studies are difficult to carry out, in part because of long periods and multiple factors affecting growth performance. Therefore, there is a need to establish an animal model for investigation of this issue. Previous studies reported that induction of hyperglycemia in pregnant rats, by streptozotocin injection on day 5 of gestation, resulted in fetal hyperglycemia, hyperinsulinemia, and fetal obesity (11–13). The obese rat pups of diabetic dams maintained accelerated body weight gain, had increased fat storage, and developed glucose intolerance by 12 wk of age (11–13), which reflected an interesting analogy to human observations. Although most of the authors have focused on altered glucose homeostasis in obese hyperinsulinemic offspring of diabetic mothers, lipoprotein profiles that might be indicative of metabolic diseases remain to be discovered.

The purpose of the present investigation was to determine the time course of changes in serum lipoprotein (VLDL, LDL-HDL<sub>1</sub>, HDL<sub>2,3</sub>) concentrations and compositions as well as serum LCAT and tissue lipolytic activities (liver, adipose tissue, muscle) in obese offspring of streptozotocin-induced mildly hyperglycemic rats. This study would advance our knowledge on the adverse consequences of maternal diabetes, on the offspring.

## MATERIALS AND METHODS

*Animals and experimental protocol.* Adult Wistar rats were obtained from Iffa Credo (Lyon, France). After mating, the first day of gestation was estimated by the presence of spermatozooids in vaginal smears. Pregnant rats were housed individually in wood-chip bedded plastic cages at constant temperature (25°C) and humidity (60 ± 5%) with a 12-h light-dark cycle. They had free access to water and a commercial diet (UAR, Villemoisson-sur-Orge, France) containing 21% (w/w) protein, 4% (w/w) lipid, 53.5% (w/w) carbohydrate, 4.5% (w/w)

\*To whom correspondence should be addressed at UPRES 2422, Lipids and Nutrition, 6 Bd. Gabriel, Bourgogne University, Dijon 21000 France. E-mail: Naim.Khan@u-bourgogne.fr

Abbreviations: Apo, apolipoproteins; EC, esterified cholesterol; HTGL, hepatic triacylglycerol lipase; LPL, lipoprotein lipase; PL, phospholipid; TAG, triacylglycerol; UC, unesterified cholesterol.



fiber, 5% (w/w) minerals, and 2% (w/w) vitamins. A total of 30 pregnant rats were made diabetic by intraperitoneal injection of streptozotocin (40 mg/kg body weight) in 0.1 M citrate buffer, pH 4.5, on the fifth day of gestation. Twelve pregnant dams were injected with citrate buffer alone as a control group. On days 13, 16, 18, and 20 of gestation, maternal blood was collected for plasma glucose concentrations by cutting off the tip of tail and squeezing it gently. Pregnant rats with plasma glucose levels between 5.55 and 16.65 mmol/L (compared with 5 mmol/L in controls) were designated as mildly hyperglycemic (13) and were included in the study. The success rate in obtaining these mildly hyperglycemic dams in the current series was 60%, or 18 of 30 streptozotocin-treated rats. A total of 150 pups from the 18 streptozotocin-treated dams and 110 pups from the 12 control dams were delivered spontaneously and weighed within 12 h. Pups from the streptozotocin-treated dams whose birth weights were 1.7 SD (above the 90th percentile) greater than the mean birth weight of the control pups were classified as obese pups (13) and included in the study. The mean birth weight of the control pups was  $5.95 \pm 0.45$  g. Therefore, experimental pups with birth weights greater than 6.8 g were included as obese in the study. The success rate of obtained obese pups was 60% (90 out of 150). The mean birth weight of the obese pups was  $8.10 \pm 0.50$  g. These obese pups were hyperglycemic and hyperinsulinemic at birth. The normal-sized offspring of diabetic mothers (60 out of 150) were excluded, as maternal diabetes related to fetal obesity was the criterion of our experimental population selection.

Twenty newborn rats of each group (control and experimental) were killed by decapitation, and blood was collected. To obtain sufficient serum samples for lipid and lipoprotein determinations, blood was pooled.

The remaining obese and control pups were left with their own mothers. Litter sizes were kept between six and eight pups per nursing dam to maintain a similar postnatal intake during the suckling period. Pups were weighed weekly up to 12 wk of age. The genders of the pups were identified at 3 wk by examining the external genitalia. Pups were weaned at 4 wk of age. Male and female rats were housed separately, two or three rats per cage, and allowed food (commercial diet, UAR) and water *ad libitum*. The general guidelines for the care and use of laboratory animals recommended by the Council of European Communities were followed.

**Blood and tissue samples.** At 4, 8, and 12 wk of age, after overnight fasting, eight rats from each group were anesthetized with pentobarbital (60 mg/kg body weight) and then bled from the abdominal aorta. Serum was obtained by low-speed centrifugation ( $1000 \times g$ , 20 min) and preserved with 0.26 mmol/L EDTA and 3 mmol/L sodium azide. Liver, gastrocnemius muscle, and fat tissue surrounding the kidney and epididymal areas for the male rats or ovary and fallopian tubes for the female rats were removed, washed with cold saline, quickly blotted, and weighed. For lipolytic activity determination, tissue homogenates in 0.9% NaCl containing heparin (Sigma, St. Louis) were prepared as described by

Mathe *et al.* (14) for liver, and by Inadera *et al.* (15) for adipose tissue and muscle.

**Isolation of lipoprotein fractions.** Serum lipoproteins of density  $<1.21$  kg/L were isolated by single ultracentrifugation flotation (Model L8-55 ultracentrifuge, 50 Ti rotor; Beckman Instruments, Palo Alto, CA), according to Havel *et al.* (16). The three fractions (VLDL, LDL-HDL<sub>1</sub>, HDL<sub>2-3</sub>) were isolated from total lipoproteins by a single-spin discontinuous gradient according to the method of Redgrave *et al.* (17) as modified by Meghelli-Bouchenak *et al.* (18). Purified fractions of VLDL ( $d < 1.006$ ), LDL-HDL<sub>1</sub> ( $1.006 < d < 1.06$ ), and HDL<sub>2-3</sub> ( $1.06 < d < 1.21$ ) were dialyzed against 0.15 mol/L NaCl and 1 mmol/L disodium EDTA, pH 7.4, at 4°C in spectra/por 2 dialysis tubing (Spectrum Laboratories, Rancho Dominguez, CA).

**Apo electrophoresis.** After partial delipidation, VLDL and HDL<sub>2-3</sub> apo were estimated by using a SDS-PAGE system with 2.5–20% acrylamide at 25 V for 18 h, according to Irwin *et al.* (19). After staining with Coomassie brilliant blue (G-250; Sigma, L'Isle d'Abeau, France), destained gels were scanned at 600 nm with a densitometer (model profil 26; Sébia, Issy les Moulineaux, France). Proportions of the various apo were determined from the densitometry tracings. Concentrations of each apo were calculated, based on the percentage of the area for each apo, relative to the total area for each serum sample. Data are expressed as arbitrary units (AU)/L serum. The apo samples for all groups of the rats were electrophoresed in parallel, but the staining affinity of each peptide was not determined. However, when 50–200 µg total protein was applied, the chromogenicity of each major band was shown to change linearly relative to the total amount of protein applied to the gel. To check the validity of our calculations, immunoelectrophoresis according to Laurell (20) was also used for apoA-I and B-100 quantitation.

**Chemical analysis.** Serum glucose was determined by glucose oxidase method using a glucose analyzer (Beckman Instruments, Fullerton, CA). Serum insulin was analyzed by radioimmunoassay kit (Serono Diagnostic, Braintree, MA) using rat insulin standards.

Lipoprotein-TAG, phospholipid (PL), total cholesterol, and unesterified cholesterol (UC) contents were determined by Boehringer Mannheim (Mannheim, Germany) kits, using enzymatic methods. Esterified cholesterol (EC) concentrations were obtained as the difference between total cholesterol and UC values. Total apo contents of each lipoprotein fraction were determined according to Lowry *et al.* (21).

**Assay for LCAT activity.** Serum LCAT activity was assayed by conversion of <sup>3</sup>H-UC to <sup>3</sup>H-EC, according to the method of Glomset and Wright (22), modified by Knipping (23), as previously described (24). Serum LCAT activity was expressed as nanomoles esterified cholesterol per hour per milliliter of serum.

**Lipolytic activities determination.** Tissue homogenates were centrifuged at  $1500 \times g$  for 5 min, and the supernatants containing heparin-releasable lipase were assayed for LPL or HTGL activities according to the method of Nilsson-Ehle and



Ekman (25). For HTGL assay, the concentration of NaCl in 100  $\mu$ L of liver supernatant (the enzyme source) was adjusted to 1 mol/L NaCl, and the solution was incubated at 37°C, for 1 h, with 100  $\mu$ L of [<sup>3</sup>H]triolein emulsion substrate (final concentrations: 1.42 mmol/L triolein, 0.1 mmol/L lysophosphatidylcholine, 0.2% (wt/vol) albumin, 0.1 mmol/L Tris-HCl, pH 9, 0.5 mol/L NaCl). For adipose tissue or muscle LPL determinations, the incubation medium contained 1.42 mmol/L triolein, 0.1 mmol/L lysophosphatidylcholine, 0.2% (wt/vol) albumin, 5% (vol/vol) heart-inactivated serum (providing apoC-II, an activator of LPL), 0.1 mol/L Tris-HCl (pH 8), 0.15 mol/L NaCl. At the end of the incubation period, the FA released were extracted with chloroform/methanol/heptane (1.25:1.41:1, by vol) followed by 0.1 mol/L potassium carbonate/borate buffer, pH 10.5. <sup>3</sup>H radioactivity in 1.5-mL aliquots of the methanol/water upper phase was measured in 10 mL of scintillation liquid (Ready Solv. HP/6; Beckman) in a 7500 LS scintillation counter (Beckman, Palo Alto, CA). Enzyme activity was expressed as nanomoles of FA released per minute per milligram protein.

**Statistical analysis.** Results are expressed as means  $\pm$  SD. The significance of differences among groups was analyzed statistically by ANOVA, followed by Duncan's multiple-range test (26) for parameter changes with age. The significance of differences between obese and control rats at each age was assessed using Student's *t*-test. These calculations were performed using Statistica, Version 4.1 (Statsoft, Tulsa,

OK). Differences were considered statistically significant at *P* < 0.05.

## RESULTS

**Serum glucose and insulin concentrations, and body weight.** At birth, serum glucose and insulin concentrations were higher in obese pups than in controls (1.10  $\pm$  0.20 vs. 0.64  $\pm$  0.11 g/L and 95.3  $\pm$  13.2 vs. 48  $\pm$  10.6 pmol/L, respectively). These values were similar for obese and control rats at 30 and 60 d (results not shown). At day 90, however, obese rats, both males and females, showed higher glucose and insulin levels compared to controls (1.59  $\pm$  0.24 vs. 0.91  $\pm$  0.25 g/L and 284.5  $\pm$  55.7 vs. 187.6  $\pm$  35.6 pmol/L, respectively).

In addition, obese offspring of diabetic dams (both males and females) had significantly higher body weights than controls throughout the first 12 wk of life (results not shown). However, the normal-sized offspring of diabetic mothers (excluded from the present study) were not hyperinsulinemic at birth, had normal growth rates, and showed no significant differences from controls for all parameters studied (results not shown).

**VLDL mass and lipid concentrations.** VLDL mass and lipid contents increased with age in all groups with marked variations during the first month of life. At birth, VLDL mass and VLDL TAG were higher in obese pups than in controls (Table 1). At day 30 and day 60, VLDL mass and lipid contents were similar in control and obese male rats. However, at day 60,

**TABLE 1**  
Postnatal Changes in VLDL Mass and Lipid Contents of Obese and Control Rats<sup>a</sup>

	Male rats		Female rats	
	Control	Obese	Control	Obese
VLDL mass (g/L)				
D0	0.26 $\pm$ 0.14 <sup>c</sup>	0.38 $\pm$ 0.05 <sup>d,*</sup>	0.26 $\pm$ 0.14 <sup>c</sup>	0.38 $\pm$ 0.05 <sup>d,*</sup>
D30	1.04 $\pm$ 0.42 <sup>b</sup>	1.14 $\pm$ 0.44 <sup>c</sup>	0.99 $\pm$ 0.16 <sup>b</sup>	1.08 $\pm$ 0.33 <sup>c</sup>
D60	1.26 $\pm$ 0.22 <sup>a</sup>	1.36 $\pm$ 0.19 <sup>b</sup>	1.21 $\pm$ 0.36 <sup>a</sup>	1.68 $\pm$ 0.16 <sup>b,*</sup>
D90	1.28 $\pm$ 0.47 <sup>a</sup>	2.08 $\pm$ 0.16 <sup>a,**</sup>	1.28 $\pm$ 0.39 <sup>a</sup>	2.40 $\pm$ 0.16 <sup>a,**</sup>
TAG (mmol/L)				
D0	0.10 $\pm$ 0.02 <sup>c</sup>	0.16 $\pm$ 0.05 <sup>d,*</sup>	0.10 $\pm$ 0.02 <sup>c</sup>	0.16 $\pm$ 0.05 <sup>c,*</sup>
D30	0.60 $\pm$ 0.33 <sup>b</sup>	0.58 $\pm$ 0.39 <sup>c</sup>	0.46 $\pm$ 0.16 <sup>b</sup>	0.44 $\pm$ 0.19 <sup>b</sup>
D60	0.80 $\pm$ 0.44 <sup>a</sup>	0.78 $\pm$ 0.19 <sup>b</sup>	0.64 $\pm$ 0.08 <sup>a</sup>	1.15 $\pm$ 0.11 <sup>a,**</sup>
D90	0.81 $\pm$ 0.05 <sup>a</sup>	1.12 $\pm$ 0.11 <sup>a,*</sup>	0.66 $\pm$ 0.33 <sup>a</sup>	1.17 $\pm$ 0.16 <sup>a,**</sup>
Phospholipids (mmol/L)				
D0	0.06 $\pm$ 0.05 <sup>c</sup>	0.09 $\pm$ 0.08 <sup>c</sup>	0.06 $\pm$ 0.05 <sup>c</sup>	0.09 $\pm$ 0.08 <sup>c</sup>
D30	0.27 $\pm$ 0.05 <sup>b</sup>	0.36 $\pm$ 0.19 <sup>b</sup>	0.26 $\pm$ 0.08 <sup>b</sup>	0.40 $\pm$ 0.22 <sup>b</sup>
D60	0.32 $\pm$ 0.08 <sup>a</sup>	0.37 $\pm$ 0.11 <sup>b</sup>	0.31 $\pm$ 0.05 <sup>a</sup>	0.36 $\pm$ 0.16 <sup>b</sup>
D90	0.36 $\pm$ 0.11 <sup>a</sup>	0.52 $\pm$ 0.11 <sup>a,*</sup>	0.34 $\pm$ 0.11 <sup>a</sup>	0.54 $\pm$ 0.02 <sup>a,*</sup>
Unesterified cholesterol (mmol/L)				
D0	0.03 $\pm$ 0.02 <sup>b</sup>	0.04 $\pm$ 0.02 <sup>c</sup>	0.03 $\pm$ 0.02 <sup>b</sup>	0.04 $\pm$ 0.02 <sup>c</sup>
D30	0.06 $\pm$ 0.02 <sup>a</sup>	0.08 $\pm$ 0.05 <sup>b</sup>	0.05 $\pm$ 0.02 <sup>a</sup>	0.07 $\pm$ 0.02 <sup>b</sup>
D60	0.07 $\pm$ 0.02 <sup>a</sup>	0.08 $\pm$ 0.08 <sup>b</sup>	0.06 $\pm$ 0.02 <sup>a</sup>	0.10 $\pm$ 0.14 <sup>a</sup>
D90	0.08 $\pm$ 0.05 <sup>a</sup>	0.13 $\pm$ 0.02 <sup>a,*</sup>	0.08 $\pm$ 0.08 <sup>a</sup>	0.14 $\pm$ 0.02 <sup>a,*</sup>
Esterified cholesterol (mmol/L)				
D0	0.03 $\pm$ 0.02 <sup>b</sup>	0.03 $\pm$ 0.02 <sup>c</sup>	0.03 $\pm$ 0.02 <sup>c</sup>	0.03 $\pm$ 0.02 <sup>c</sup>
D30	0.12 $\pm$ 0.08 <sup>a</sup>	0.20 $\pm$ 0.16 <sup>b</sup>	0.09 $\pm$ 0.14 <sup>b</sup>	0.18 $\pm$ 0.08 <sup>b</sup>
D60	0.13 $\pm$ 0.11 <sup>a</sup>	0.21 $\pm$ 0.16 <sup>b</sup>	0.11 $\pm$ 0.16 <sup>b</sup>	0.24 $\pm$ 0.15 <sup>b</sup>
D90	0.15 $\pm$ 0.05 <sup>a</sup>	0.30 $\pm$ 0.02 <sup>a,*</sup>	0.20 $\pm$ 0.11 <sup>a</sup>	0.65 $\pm$ 0.22 <sup>a,*</sup>

<sup>a</sup>Values are means  $\pm$  SD of eight rats from each group. Males and females constitute separate groups. At day 0, the values for both control and obese rats are the same in both males and females, as gender could not be identified at this stage. Significant differences between obese and control rats at each age are indicated as: \**P* < 0.05; \*\**P* < 0.01. Means within the same group with different superscript letters (a–d) are significantly different according to age for each group (*P* < 0.05).

**TABLE 2**  
**Postnatal Changes in LDL-HDL<sub>1</sub> Mass and Lipid Contents of Obese and Control Rats<sup>a</sup>**

	Male rats		Female rats	
	Control	Obese	Control	Obese
LDL-HDL <sub>1</sub> mass (g/L)				
D0	0.86 ± 0.08 <sup>a</sup>	1.30 ± 0.11 <sup>b,**</sup>	0.86 ± 0.08 <sup>a</sup>	1.30 ± 0.11 <sup>b,**</sup>
D30	0.68 ± 0.22 <sup>b</sup>	0.74 ± 0.25 <sup>c</sup>	0.74 ± 0.16 <sup>b</sup>	0.73 ± 0.08 <sup>d</sup>
D60	0.66 ± 0.42 <sup>b</sup>	0.83 ± 0.30 <sup>c</sup>	0.75 ± 0.36 <sup>b</sup>	0.98 ± 0.22 <sup>c</sup>
D90	0.69 ± 0.14 <sup>b</sup>	1.54 ± 0.22 <sup>a,**</sup>	0.76 ± 0.11 <sup>b</sup>	1.48 ± 0.16 <sup>a,**</sup>
TAG (mmol/L)				
D0	0.13 ± 0.05 <sup>a</sup>	0.23 ± 0.08 <sup>a,*</sup>	0.13 ± 0.05 <sup>a</sup>	0.23 ± 0.08 <sup>a,*</sup>
D30	0.04 ± 0.02 <sup>b</sup>	0.03 ± 0.02 <sup>c</sup>	0.06 ± 0.05 <sup>b</sup>	0.05 ± 0.05 <sup>b</sup>
D60	0.02 ± 0.02 <sup>b</sup>	0.02 ± 0.02 <sup>c</sup>	0.03 ± 0.02 <sup>b</sup>	0.02 ± 0.02 <sup>c</sup>
D90	0.02 ± 0.02 <sup>b</sup>	0.06 ± 0.02 <sup>b,*</sup>	0.02 ± 0.02 <sup>b</sup>	0.06 ± 0.02 <sup>b,*</sup>
Phospholipids (mmol/L)				
D0	0.26 ± 0.08	0.37 ± 0.11 <sup>b,*</sup>	0.26 ± 0.08	0.37 ± 0.11 <sup>b,*</sup>
D30	0.26 ± 0.16	0.36 ± 0.28 <sup>b</sup>	0.30 ± 0.22	0.31 ± 0.16 <sup>b</sup>
D60	0.28 ± 0.28	0.27 ± 0.25 <sup>b</sup>	0.28 ± 0.16	0.40 ± 0.14 <sup>b</sup>
D90	0.31 ± 0.11	0.78 ± 0.33 <sup>a,*</sup>	0.31 ± 0.28	0.60 ± 0.16 <sup>a,*</sup>
Unesterified cholesterol (mmol/L)				
D0	0.21 ± 0.02	0.30 ± 0.05 <sup>b,*</sup>	0.21 ± 0.02	0.30 ± 0.05 <sup>b,*</sup>
D30	0.19 ± 0.16	0.24 ± 0.14 <sup>b</sup>	0.18 ± 0.05	0.26 ± 0.08 <sup>b</sup>
D60	0.19 ± 0.14	0.31 ± 0.16 <sup>b</sup>	0.17 ± 0.22	0.32 ± 0.16 <sup>b</sup>
D90	0.16 ± 0.08	0.42 ± 0.16 <sup>a,*</sup>	0.20 ± 0.08	0.47 ± 0.11 <sup>a,*</sup>
Esterified cholesterol (mmol/L)				
D0	0.14 ± 0.05 <sup>c</sup>	0.22 ± 0.05 <sup>d,*</sup>	0.14 ± 0.05 <sup>c</sup>	0.22 ± 0.05 <sup>d,*</sup>
D30	0.30 ± 0.08 <sup>b</sup>	0.32 ± 0.14 <sup>c</sup>	0.28 ± 0.11 <sup>b</sup>	0.34 ± 0.16 <sup>c</sup>
D60	0.41 ± 0.28 <sup>a</sup>	0.49 ± 0.16 <sup>b</sup>	0.55 ± 0.42 <sup>a</sup>	0.59 ± 0.28 <sup>b</sup>
D90	0.36 ± 0.11 <sup>a</sup>	0.60 ± 0.16 <sup>a,*</sup>	0.46 ± 0.22 <sup>a</sup>	0.79 ± 0.16 <sup>a,*</sup>

<sup>a</sup>For footnote see Table 1.

VLDL mass and TAG were significantly higher in obese females than in control females (+40 and +100, respectively). At day 90, VLDL levels and all components of VLDL were significantly greater in obese rats, both males and females, compared to controls. In terms of percentage, the relative composition of VLDL in obese males was close to that of control males, suggesting an increase in VLDL particles at day 90. However, in obese females, the surface to core components [(protein + PL + UC)/(TG + EC)] and EC to triacylglycerols (EC/TG) ratios were higher than control values ( $1.38 \pm 0.05$  and  $0.42 \pm 0.05$ , respectively, in obese females vs.  $1.20 \pm 0.04$  and  $0.22 \pm 0.06$ , respectively in control females). These data suggested an increase in VLDL particles that were enriched in EC in obese females at day 90.

**LDL-HDL<sub>1</sub> mass and lipid concentrations.** Serum LDL-HDL<sub>1</sub> levels showed a significant decrease in the course of the first month of life in both control and obese rats, accompanied by compositional changes (Table 2). In fact, LDL-HDL<sub>1</sub> particles became enriched in EC and depleted in TAG. Afterward, LDL-HDL<sub>1</sub> levels and composition remained constant in control males and females. In contrast, a significant increase in all lipid contents of LDL-HDL<sub>1</sub> was observed between day 30 and day 90 in obese offspring, both males and females.

At birth, LDL-HDL<sub>1</sub> amounts were significantly higher in obese pups compared to control values (+50%), as a result of an increase in all LDL-HDL<sub>1</sub> components. At day 30 and day 60, no significant differences in LDL-HDL<sub>1</sub> particles were observed among rat groups. At day 90, all lipid contents of

LDL-HDL<sub>1</sub> were greater in obese rats than in controls. As the relative composition of these fractions was not modified, the results suggested an increase in LDL-HDL<sub>1</sub> particles in adult obese rats.

**HDL<sub>2-3</sub> mass and lipid concentrations.** During the first month of life, HDL<sub>2-3</sub> levels increased in both obese and control rats due to a rise in PL, UC, and EC contents (Table 3). Afterward, the rise in HDL<sub>2-3</sub> amounts was reflected mainly by higher PL in control rats, by TAG and PL in obese males, and by TAG, PL, UC, and EC in obese females.

At birth, obese pups had higher HDL<sub>2-3</sub> amounts compared to controls (+39%). In addition, all apo and lipids of HDL<sub>2-3</sub> were increased, suggesting an increase in HDL particles in obese pups. At day 30 and day 60, HDL<sub>2-3</sub> lipid and apo levels became similar in control and obese rats. However, at day 90, HDL<sub>2-3</sub> amounts were significantly higher in obese males and females than in controls (32 and 33%, respectively). Indeed, HDL<sub>2-3</sub>-PL, TAG, and EC levels were higher in obese males and females than in their respective controls at day 90. The surface to core components ratio was higher in obese than in control males ( $0.32 \pm 0.04$  vs.  $0.24 \pm 0.03$ ) and in obese than in control females ( $0.35 \pm 0.05$  vs.  $0.26 \pm 0.04$ ), suggesting a modification of HDL relative composition in adult obese rats.

**VLDL and HDL<sub>2-3</sub> apo.** (i) **VLDL apo.** A significant age-related increase in VLDL-apo concentrations was observed in all groups (Table 4). There were no significant differences in VLDL-apo between obese and control groups at day 0, and

**TABLE 3**  
**Postnatal Changes in HDL<sub>2-3</sub> Mass and Lipid Contents of Obese and Control Rats<sup>a</sup>**

	Male rats		Female rats	
	Control	Obese	Control	Obese
HDL <sub>2-3</sub> mass (g/L)				
D0	1.12 ± 0.05 <sup>c</sup>	1.56 ± 0.14 <sup>d,**</sup>	1.12 ± 0.05 <sup>c</sup>	1.56 ± 0.14 <sup>d,**</sup>
D30	2.86 ± 0.44 <sup>b</sup>	3.04 ± 0.42 <sup>c</sup>	2.80 ± 0.53 <sup>b</sup>	2.90 ± 0.72 <sup>c</sup>
D60	3.36 ± 1.09 <sup>a</sup>	3.68 ± 0.67 <sup>b</sup>	3.25 ± 0.95 <sup>a</sup>	3.75 ± 0.42 <sup>b</sup>
D90	3.40 ± 0.44 <sup>a</sup>	4.48 ± 0.25 <sup>a,**</sup>	3.48 ± 0.30 <sup>a</sup>	4.62 ± 0.67 <sup>a,**</sup>
TAG (mmol/L)				
D0	0.09 ± 0.02 <sup>a</sup>	0.16 ± 0.05 <sup>a,*</sup>	0.09 ± 0.02 <sup>a</sup>	0.16 ± 0.05 <sup>a,*</sup>
D30	0.06 ± 0.02 <sup>b</sup>	0.06 ± 0.02 <sup>b</sup>	0.05 ± 0.05 <sup>b</sup>	0.08 ± 0.05 <sup>b</sup>
D60	0.05 ± 0.02 <sup>b</sup>	0.08 ± 0.02 <sup>b</sup>	0.05 ± 0.02 <sup>b</sup>	0.07 ± 0.05 <sup>b</sup>
D90	0.05 ± 0.02 <sup>b</sup>	0.13 ± 0.05 <sup>a,**</sup>	0.04 ± 0.05 <sup>b</sup>	0.14 ± 0.08 <sup>a,**</sup>
Phospholipids (mmol/L)				
D0	0.39 ± 0.14 <sup>c</sup>	0.50 ± 0.05 <sup>d,*</sup>	0.39 ± 0.14 <sup>c</sup>	0.50 ± 0.05 <sup>d,*</sup>
D30	0.93 ± 0.14 <sup>b</sup>	1.01 ± 0.08 <sup>b</sup>	1.00 ± 0.11 <sup>b</sup>	0.92 ± 0.30 <sup>c</sup>
D60	1.34 ± 0.44 <sup>a</sup>	1.37 ± 0.53 <sup>b</sup>	1.20 ± 0.28 <sup>a</sup>	1.32 ± 0.33 <sup>b</sup>
D90	1.39 ± 0.53 <sup>a</sup>	2.02 ± 0.44 <sup>a,*</sup>	1.40 ± 0.39 <sup>a</sup>	1.82 ± 0.42 <sup>a,*</sup>
Unesterified cholesterol (mmol/L)				
D0	0.28 ± 0.05 <sup>b</sup>	0.38 ± 0.05 <sup>b,*</sup>	0.28 ± 0.05 <sup>b</sup>	0.38 ± 0.05 <sup>d,*</sup>
D30	0.53 ± 0.44 <sup>a</sup>	0.68 ± 0.30 <sup>a</sup>	0.50 ± 0.39 <sup>a</sup>	0.48 ± 0.08 <sup>c</sup>
D60	0.63 ± 0.33 <sup>a</sup>	0.83 ± 0.36 <sup>a</sup>	0.65 ± 0.50 <sup>a</sup>	0.67 ± 0.28 <sup>b</sup>
D90	0.71 ± 0.44 <sup>a</sup>	0.87 ± 0.42 <sup>a</sup>	0.80 ± 0.44 <sup>a</sup>	0.91 ± 0.39 <sup>a</sup>
Esterified cholesterol (mmol/L)				
D0	0.10 ± 0.05 <sup>b</sup>	0.22 ± 0.02 <sup>c,*</sup>	0.10 ± 0.05 <sup>b</sup>	0.22 ± 0.02 <sup>d,*</sup>
D30	0.93 ± 0.36 <sup>a</sup>	0.96 ± 0.28 <sup>b</sup>	0.75 ± 0.50 <sup>a</sup>	0.70 ± 0.30 <sup>c</sup>
D60	1.18 ± 1.03 <sup>a</sup>	1.22 ± 0.44 <sup>a</sup>	0.96 ± 0.30 <sup>a</sup>	1.27 ± 0.61 <sup>b</sup>
D90	0.95 ± 0.33 <sup>a</sup>	1.42 ± 0.72 <sup>a,**</sup>	1.08 ± 0.25 <sup>a</sup>	1.71 ± 0.39 <sup>a,**</sup>

<sup>a</sup>For footnote see Table 1.

also at day 30 and day 60 (results not shown). At day 90, VLDL-apoB-100, -apoB-48, -apoE, -apoC-II and -apoC-III were markedly increased in both male and female obese rats, compared with controls. In addition, the apoC-II to apoC-III ratio in VLDL was higher in obese rats than in controls ( $0.50 \pm 0.03$  vs.  $0.37 \pm 0.02$  in males and  $0.52 \pm 0.04$  vs.  $0.38 \pm 0.02$  in females).

(ii) *HDL<sub>2-3</sub> apo*. HDL<sub>2-3</sub> apoA-I, -A-II, -A-IV, -C-II, and -C-III increased with age in both obese and control pups (Table 4). HDL<sub>2-3</sub> apoE levels did not vary significantly with age in any group. At birth, HDL<sub>2-3</sub> apoA-I, -A-II, -A-IV, -C-II, -C-III, and -E concentrations were higher in obese pups than in controls. At day 30 and day 60, no significant differences in HDL<sub>2-3</sub> apo profiles were observed between obese and control rats (results not shown). At day 90, HDL<sub>2-3</sub> apoC-II concentrations were greater in obese males and females compared to their respective controls (+91 and +90%, respectively). Indeed, the apoC-II/apoC-III ratio in HDL<sub>2-3</sub> was increased in obese offspring compared with controls ( $0.74 \pm 0.03$  vs.  $0.39 \pm 0.04$  in males and  $0.65 \pm 0.04$  vs.  $0.42 \pm 0.02$  in females).

*Serum LCAT activity*. LCAT activity increased gradually with age in both obese and control rats (Fig. 1). At birth, LCAT activity was significantly greater in obese pups than in controls (+57%). At days 30, 60, and 90, this activity was about 1.5-fold higher in both male and female obese rats compared with controls.

*Tissue lipolytic activities*. Because tissue lipolytic activities are low at birth, developmental changes in LPL activities were monitored after 1 mon of life. Adipose tissue LPL, as well as HTGL activities, decreased gradually with age in all groups (Fig. 2). Adipose tissue LPL activity, expressed as nmol FFA·min<sup>-1</sup>·mg<sup>-1</sup>protein), was significantly greater in both male and female obese rats than in their respective controls at day 30 and day 60. However, at day 90, values were similar in all groups. No difference in muscle LPL activity was observed between obese and control rats, whatever the age (results not shown). In contrast, HTGL activity was significantly greater in obese rats at all ages.

## DISCUSSION

Offspring of mildly diabetic rats were obese, hyperinsulinemic, and hyperlipidemic at birth and gained significantly more weight than control offspring (results not shown). The increased body weight was reflected by increased adipose tissue weight in these offspring (both males and females) at all ages (results not shown). Thus, the increase in adiposity seen in either male or female offspring of diabetic mothers was maintained throughout adulthood. However, the postnatal metabolic changes varied according to sex and age.

Our results showed that at birth, obese rats had higher VLDL amounts, which were accompanied by higher VLDL-TAG concentrations than control values, suggesting an

**TABLE 4**  
**Postnatal Changes in VLDL and HDL<sub>2-3</sub> Apolipoproteins of Obese and Control Rats<sup>a,b</sup>**

	Male rats		Female rats	
	Control	Obese	Control	Obese
VLDL apoproteins				
ApoB-100 D0	40.31 ± 11.48 <sup>b</sup>	48.90 ± 13.96 <sup>b</sup>	40.31 ± 11.48 <sup>b</sup>	48.90 ± 13.96 <sup>b</sup>
D90	90 ± 12.43 <sup>a</sup>	140 ± 11.68 <sup>a,**</sup>	101.60 ± 14.42 <sup>a</sup>	181.12 ± 12.15 <sup>a,**</sup>
ApoB-48 D0	16.40 ± 4.63 <sup>b</sup>	18.90 ± 5.18 <sup>b</sup>	16.40 ± 4.63 <sup>b</sup>	18.90 ± 5.18 <sup>b</sup>
D90	43.12 ± 8.90 <sup>a</sup>	91.92 ± 9.81 <sup>a,**</sup>	48.83 ± 7.53 <sup>a</sup>	95.33 ± 8.93 <sup>a,**</sup>
ApoE D0	21.30 ± 6.77 <sup>b</sup>	26.92 ± 5.63 <sup>b</sup>	21.30 ± 6.77 <sup>b</sup>	26.92 ± 5.63 <sup>b</sup>
D90	62.15 ± 8.15 <sup>a</sup>	108.40 ± 11.53 <sup>a,**</sup>	62.10 ± 6.61 <sup>a</sup>	110.21 ± 9.30 <sup>a,**</sup>
ApoC-II D0	4.80 ± 1.57 <sup>b</sup>	6.70 ± 2.64 <sup>b</sup>	4.80 ± 1.57 <sup>b</sup>	6.70 ± 2.64 <sup>b</sup>
D90	19.01 ± 3.15 <sup>a</sup>	39.42 ± 7.66 <sup>a,**</sup>	18.22 ± 3.08 <sup>a</sup>	36.40 ± 5.94 <sup>a,**</sup>
ApoC-III D0	4.80 ± 1.97 <sup>b</sup>	7.73 ± 2.89 <sup>b</sup>	4.80 ± 1.97 <sup>b</sup>	7.73 ± 2.89 <sup>b</sup>
D90	45.93 ± 6.75 <sup>a</sup>	80.30 ± 9.48 <sup>a,**</sup>	49.27 ± 5.11 <sup>a</sup>	81.01 ± 6.32 <sup>a,**</sup>
HDL <sub>2-3</sub> apoproteins				
ApoA-I D0	181.31 ± 11.42 <sup>b</sup>	246.90 ± 22.64 <sup>b,*</sup>	181.31 ± 11.42 <sup>b</sup>	246.90 ± 22.64 <sup>b,*</sup>
D90	564.81 ± 60.11 <sup>a</sup>	609.88 ± 58.70 <sup>a</sup>	589.70 ± 70.18 <sup>a</sup>	646.87 ± 80.20 <sup>a</sup>
ApoA-II D0	22.40 ± 3.18 <sup>b,*</sup>	40.61 ± 6.43 <sup>b,*</sup>	22.40 ± 3.18 <sup>b</sup>	40.61 ± 6.43 <sup>b,*</sup>
D90	61.10 ± 21.43 <sup>a</sup>	64.80 ± 19.11 <sup>a</sup>	69.31 ± 24.78 <sup>a</sup>	96.47 ± 35.16 <sup>a</sup>
ApoA-IV D0	63.54 ± 11.14 <sup>b</sup>	117.38 ± 21.38 <sup>b,*</sup>	63.54 ± 11.14 <sup>b</sup>	117.38 ± 21.38 <sup>b,*</sup>
D90	251.80 ± 50.64 <sup>a</sup>	250.55 ± 42.33 <sup>a</sup>	201.10 ± 38.64 <sup>a</sup>	234.81 ± 55.36 <sup>a</sup>
ApoE D0	201.68 ± 8.11	237.24 ± 9.48 <sup>*</sup>	201.68 ± 8.11	237.24 ± 9.48 <sup>*</sup>
D90	244.78 ± 30.14	247.70 ± 20.10	229.60 ± 30.26	269.50 ± 40.50
ApoC-II D0	30.20 ± 4.15 <sup>b</sup>	41.76 ± 5.98 <sup>b,*</sup>	30.20 ± 4.15 <sup>b</sup>	41.76 ± 5.98 <sup>b,*</sup>
D90	81.30 ± 10.06 <sup>a</sup>	155.60 ± 14.11 <sup>a,**</sup>	86.70 ± 15.64 <sup>a</sup>	165.31 ± 18.11 <sup>a,**</sup>
ApoC-III D0	50.87 ± 4.14 <sup>b</sup>	61.11 ± 5.73 <sup>b,*</sup>	50.87 ± 4.14 <sup>b</sup>	61.11 ± 5.73 <sup>b,*</sup>
D90	206.20 ± 25.38 <sup>a</sup>	211.40 ± 30.14 <sup>a</sup>	213.58 ± 36.95 <sup>a</sup>	256.90 ± 47.86 <sup>a</sup>

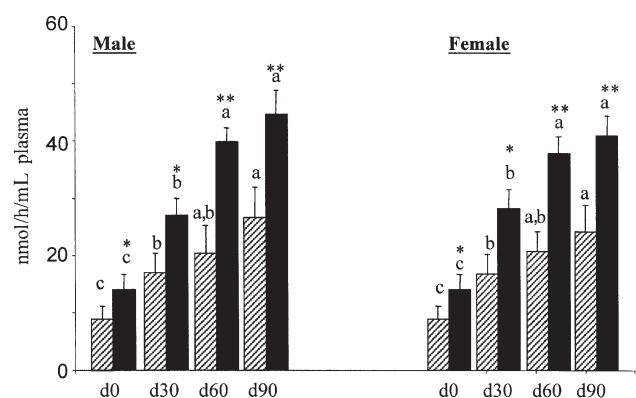
<sup>a</sup>Values are means ± SD of eight rats from each group. Males and females constitute separate groups. At day 0, the values for both control and obese rats are the same in both males and females as gender could not be identified at this stage. Significant differences between obese and control rats at each age are indicated as: \* $P < 0.05$ ; \*\* $P < 0.01$ . Means within the same group with different superscript letters (a,b) are significantly different according to age for each group ( $P < 0.05$ ).

<sup>b</sup>Expressed as AU/L (arbitrary units/L serum).

increase in hepatic TAG synthesis and secretion. Combined effects of fetal hyperinsulinemia and an enhancement in glucose and FFA transfer in the diabetic mother could explain elevated fetal hepatic VLDL secretion and hypertriglyceridemia, as reported by previous studies (27–29). At birth, obese offspring of diabetic dams also presented higher LDL-HDL<sub>1</sub> and HDL<sub>2-3</sub> levels, accompanied by higher lipid and apo contents of these fractions, suggesting an increase in the number of LDL-HDL<sub>1</sub> and HDL<sub>2-3</sub> particles, resulting probably from their enhanced synthesis. Since the HDL fraction is primarily responsible for lipid transport during fetal life in humans (30) and in rats (31), elevated HDL contents might reflect an increase in the requirement for cholesterol and PL for plasma membrane, hormone, and surfactant synthesis in obese fetuses. It is well known that high insulin levels lead to enhanced growth of fetal tissues (6). We have previously described similar results in human macrosomic newborns of type 1 diabetic mothers (32,33).

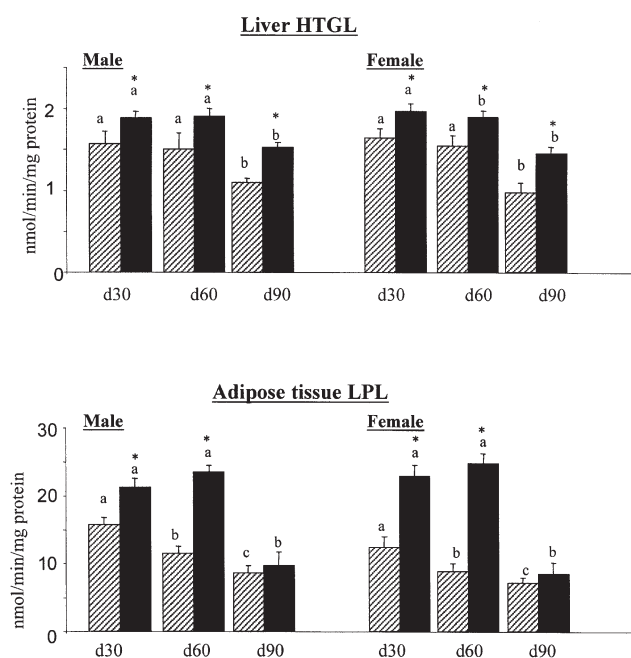
In this study, after 1 mon of life (day 30), which corresponded to the suckling period, serum glucose, insulin, and lipoprotein concentrations and compositions in male and female obese offspring of diabetic dams became similar to those of their respective controls. However, serum LCAT, adipose tissue LPL, and HTGL activities were higher in obese than in control rats. The early elevation of adipose tissue LPL activity associated with normal muscle LPL activity was a

contributory factor to the maintenance of obesity in offspring of diabetic rats. High LPL and HTGL activities are normally associated with enhanced lipoprotein and remnant catabolism, resulting especially in low TAG and VLDL levels, and



**FIG. 1.** LCAT activity of rat sera. Values are means ± SD of eight rats from each group. Males and females constitute separate groups. At day 0 (d0), the values for both control and obese rats are the same in both males and females as gender could not be identified at this stage. Significant differences between obese and control rats at each age are indicated as: \* $P < 0.05$ , \*\* $P < 0.01$ . Means within the same group with different superscript letters (a–c) are significantly different according to age for each group ( $P < 0.05$ ). Hatched and filled histograms represent, respectively, control and obese rats.





**FIG. 2.** Adipose tissue lipoprotein lipase (LPL) and hepatic TG lipase (HTGL) activities in obese and control rats. Values are means  $\pm$  SD of eight rats from each group. Males and females constitute separate groups. Significant differences between obese and control rats at each age are indicated as: \* $P < 0.05$ , \*\* $P < 0.01$ . Means within the same group with different superscript letters (a–c) are significantly different according to age for each group ( $P < 0.05$ ). Hatched and filled histograms represent, respectively, control and obese rats.

in high LDL and HDL<sub>1</sub> levels in the rats (14). These correlations were not found in our obese rats at day 30. On the other hand, the well-known correlation between LCAT activity and HDL levels also was not seen in these rats. These findings suggest that an increased rate of lipoprotein synthesis combined with an enhanced lipoprotein catabolism in obese offspring of diabetic rats might contribute to maintaining a normal lipoprotein profile at day 30. A higher demand for lipid during the phase of rapid growth could explain high lipoprotein turnover, knowing that most of the obese rats tissues were hypertrophic. Indeed, an increased insulin sensitivity could be envisaged, as suggested by other works (6,7). Therefore, persistence of a higher number of insulin receptors and/or greater insulin-binding affinity in the target tissue may contribute to enhanced anabolic effects despite normal serum insulin levels in these obese rats at day 30.

After 2 mon of life (day 60), which corresponded to 1 mon postweaning period, the obese rats again showed serum glucose, insulin, and lipoprotein levels similar to those in controls, except for VLDL-TAG levels, which were enhanced in obese females compared to control females. This could be the result of increased estrogen levels in obese females, since estrogen enhances hepatic TAG production and secretion (34).

After 3 mon of life (day 90), a period reflecting adulthood, the situation was different. Some metabolic alterations that had disappeared at birth and that had subsequently disap-

peared at day 30 and day 60 were present and were worsened. Adult obese offspring (both males and females) had elevated glucose, insulin, and lipoprotein levels compared to controls. They also displayed significant increases in LCAT and HTGL activities. In these adult obese rats, adipose tissue LPL activity became similar to that found in adult control rats. Taken together, the results strongly suggested that obese offspring of diabetic dams developed insulin resistance in adulthood, in agreement with other studies (11,13). It is well known that the development of obesity is linked with insulin sensitivity, whereas weight maintenance in the obese state is associated with insulin resistance (35). In several animal models, obesity and adipocyte hypertrophy precede the development of insulin resistance (36,37). At day 90, adult obese offspring of diabetic dams presented both quantitative and qualitative abnormalities of different lipoproteins. Compositional changes were more apparent when composition was expressed as the percentage of total lipoprotein mass rather than absolute concentration of the components. Adult obese rats showed high VLDL concentrations, accompanied by a concomitant increase in all VLDL-apo and lipid components, suggesting elevated VLDL particle numbers. Overproduction of VLDL, a common feature of human and various experimental obesities, is a direct consequence of hyperinsulinemia and hepatic hyperlipogenesis (8,9,36,38). Indeed, in obese females, VLDL particles were enriched in EC at day 90. This compositional abnormality is well documented in human diabetes and results from increased lipid transfer between VLDL and HDL (8,9). However, in the rat, which has low EC transfer protein activity, HDL concentrations would not be directly affected by interactions between HDL and TAG-rich lipoproteins. Thus, the increased cholesterol content in the VLDL fraction could reflect VLDL hepatic synthesis rich in cholesterol. These adult obese rats also presented enhanced HDL<sub>2-3</sub> levels. In contrast to reduced HDL concentrations observed in obesity and diabetes in man (9,10,39), a positive correlation between adiposity and HDL levels was seen in several animal models of obesity (40,41). Adult obese offspring of diabetic dams also presented compositional changes of HDL<sub>2-3</sub> particles, including enrichment in TAG, cholesterol, and PL.

In our study, adult obese offspring had high HDL-apoC-II contents compared to control values. Indeed, they also had high VLDL-apoC-II and -apoC-III concentrations. The apoC-II to apoC-III ratio was increased in both VLDL and HDL particles of these adult obese rats compared to control values. Since apoC-II is an activator of LPL and apoC-III is an inhibitor of LPL, high proportions of apoC-II compared to apoC-III in obese offspring at day 90 could be a physiological compensatory mechanism to establish TAG homeostasis during a period related to insulin resistance. In conclusion, obese offspring of mildly diabetic rats presented altered lipoprotein metabolism at birth and at adulthood.

Developmental lipoprotein profile changes in offspring of diabetic dams were characterized by two periods. A first period (days 0–60), with increased insulin sensitivity, was

associated with increased fat storage and high lipoprotein turnover leading to a normalization of lipoprotein profiles. A second period (day 90), with decreased insulin sensitivity and the appearance of insulin resistance, was associated with circulating lipoprotein abnormalities. Fetal hyperinsulinemia in diabetic pregnancy should then be considered as one of the potential risk factors for later metabolic diseases, including adult dyslipoproteinemia. Attention needs to be focused on the disordered lipoprotein profile in offspring of diabetic mothers.

## ACKNOWLEDGMENT

This work was supported by the French Foreign Office (International Research Extension grants 01 MDU 531).

## REFERENCES

- Dörner, G., and Plagemann, A. (1994) Perinatal Hyperinsulinism as Possible Predisposing Factor for Diabetes Mellitus, Obesity and Enhanced Cardiovascular Risk in Later Life, *Horm. Metab. Res.* 26, 213–221.
- Barker, D.J.P. (1995) Fetal Origins of Coronary Heart Disease, *Br. Med. J.* 311, 171–174.
- Weiss, P., Scholz, H.S., Haas, J., Tamussino, K.F., Seissler, J., and Borkenstein, M.H. (2000) Long-Term Follow-up of Infants of Mothers with Type 1 Diabetes: Evidence for Hereditary and Nonhereditary Transmission of Diabetes and Precursors, *Diabetes Care* 23, 905–911.
- Schwartz, R., and Teramo, K.A. (2000) Effects of Diabetic Pregnancy on the Fetus and Newborn, *Semin. Perinatol.* 2, 120–135.
- Kalkhoff, R.K. (1991) Impact of Maternal Fuels and Nutritional State on Fetal Growth, *Diabetes* 40, 61–65.
- Fowden, A.L. (1989) The Role of Insulin in Prenatal Growth, *J. Dev. Physiol.* 12, 173–182.
- Plagemann, A., Harder, T., Kohlhoff, R., Rohde, W., and Dörner, G. (1997) Glucose Tolerance and Insulin Secretion in Children of Mothers with Pregestational IDDM or Gestational Diabetes, *Diabetologia* 40, 1094–1100.
- Bioletto, S., Golay, A., Munger, R., Kalix, B., and James, R.W. (2000) Acute Hyperinsulinemia and Very Low Density and Low Density Lipoprotein Subfractions in Obese Subjects, *Am. J. Clin. Nutr.* 71, 443–449.
- Verges, B.L. (1999) Dyslipidaemia in Diabetes Mellitus. Review of the Main Lipoprotein Abnormalities and Their Consequences on the Development of Atherogenesis, *Diabetes Metab.* 25, 32–40.
- Syvanne, M., and Taskinen, M.R. (1997) Lipids and Lipoproteins as Coronary Risk Factors in Non-Insulin-Dependent Diabetes Mellitus, *Lancet* 350 (Suppl. 1), S120–S123.
- Oh, W., Gelardi, N.L., and Cha, C.J. (1988) Maternal Hyperglycemia in Pregnant Rats: Its Effect on Growth and Carbohydrate Metabolism in the Offspring, *Metabolism* 37, 1146–1151.
- Gelardi, N.L., Cha, C.J., and Oh, W. (1991) Evaluation of Insulin Sensitivity in Obese Offspring of Diabetic Rats by Hyperinsulinemic-Euglycemic Clamp Technique, *Pediatr. Res.* 30, 40–44.
- Gelardi, N.L., Cha, C.J., and Oh, W. (1990) Glucose Metabolism in Adipocytes of Obese Offspring of Mild Hyperglycemic Rats, *Pediatr. Res.* 28, 641–645.
- Mathe, D., Serougne, C., Ferezou, J., and Lecuyer, B. (1991) Lipolytic Activities in Rats Fed a Sucrose-rich Diet Supplemented with Either Cystine or Cholesterol: Relationships with Lipoprotein Profiles, *Ann. Nutr. Metab.* 35, 165–173.
- Inadera, H., Tashiro, J., Okubo, Y., Ishikawa, Y., Shirai, K., Saito, Y., and Yoshida, S. (1992) Response of Lipoprotein Lipase to Calorie Intake in Streptozotocin-Induced Diabetic Rats, *Scand. J. Lab. Invest.* 52, 797–802.
- Havel, R.J., Eder, H.A., and Bragdon, J.H. (1955) The Distribution and Chemical Composition of Ultracentrifugally Separated Lipoproteins in Human Serum, *J. Clin. Invest.* 34, 1345–1353.
- Redgrave, T.G., Robert, D.C.K., and West, C.E. (1975) Separation of Plasma Lipoproteins by Density-Gradient Ultracentrifugation, *Anal. Biochem.* 65, 42–49.
- Meghelli-Bouchenak, M., Boquillon, M., and Belleville, J. (1989) Serum Lipoprotein Composition and Amounts During the Consumption of Two Different Low Protein Diets Followed by a Balanced Diet, *Nutr. Rep. Int.* 39, 323–343.
- Irwin, D., O'lonney, P.A., Quinet, E., and Vahouny, G.V. (1984) Application of SDS Gradient Polyacrylamide Gel Electrophoresis to Analysis of Apolipoprotein Mass and Radioactivity of Lipoproteins, *Atherosclerosis* 53, 163–172.
- Laurell, C.B. (1966) Quantitative Estimation of Protein by Electrophoresis in Agarose Gel Containing Antibodies, *Anal. Biochem.* 15, 45–50.
- Lowry, O.H., Rosebrough, N.J., Farr, A.L., and Randall, R.I. (1951) Protein Measurement with Folin Phenol Reagent, *J. Biol. Chem.* 193, 265–275.
- Glomset, J.A., and Wright, J.L. (1964) Some Properties of Cholesterol Esterifying Enzyme in Human Plasma, *Biochim. Biophys. Acta.* 89, 266–271.
- Knipping, G. (1986) Isolation and Properties of Porcine Lecithin: Cholesterol Acyltransferase, *Eur. J. Biochem.* 154, 289–294.
- Merzouk, H., Lamri, M.Y., Meghelli-Bouchenak, M., Korso, N., Prost, J., and Belleville, J. (1997) Serum Lecithin:Cholesterol Acyltransferase Activity and HDL<sub>2</sub> and HDL<sub>3</sub> Composition in Small for Gestational Age Newborns, *Acta Paediatr.* 86, 528–532.
- Nilsson-Ehle, P., and Ekman, R. (1977) Rapid, Simple and Specific Assay for Lipoprotein Lipase and Hepatic Lipase, *Artery* 3, 194–209.
- Duncan, D.B. (1955) Multiple Range and Multiple *F* Tests, *Biometrics* 11, 1–42.
- Vileisis, R.A., and Oh, W. (1983) Enhanced Fatty Acid Synthesis in Hyperinsulinemic Rat Fetuses, *J. Nutr.* 113, 246–252.
- Shafir, E., and Khassis, S. (1982) Maternal-Fetal Fat Transport vs. New Fat Synthesis in the Pregnant Diabetic Rat, *Diabetologia* 22:111–117.
- Shafir, E., and Barash, V. (1987) Placental Function in Maternal-Fetal Fat Transport in Diabetes, *Biol. Neonate* 51, 102–112.
- Rosseneu, M., Van Biervliet, J.P., Bury, J., and Vinamoint, N. (1983) Isolation and Characterization of Lipoprotein Profiles in Newborns by Density Gradient Ultracentrifugation, *Pediatr. Res.* 17, 788–794.
- Garcia-Molina, V., Aguilera, J.A., Gil, A., and Sanchez-Pozo, A. (1996) Changes in Plasma Lipoproteins and Liver Lipids in Neonatal Rats, *Comp. Biochem. Physiol.* 113B, 789–793.
- Merzouk, H., Bouchenak, M., Loukidi, B., Madani, S., Prost, J., and Belleville, J. (2000) Fetal Macrosomia Related to Maternal Poorly Controlled Type 1 Diabetes Strongly Impairs Serum Lipoprotein Concentrations and Composition, *J. Clin. Pathol.* 53, 917–923.
- Merzouk, H., Madani, S., Korso, N., Bouchenak, M., Prost, J., and Belleville, J. (2000) Maternal and Fetal Serum Lipid and Lipoprotein Concentrations and Compositions in Type 1 Diabetic Pregnancy: Relationship with Maternal Glycemic Control, *J. Lab. Clin. Med.* 136, 441–448.
- Schaefer, E.J., Foster, D.M., Zech, L.A., Lindgren, F.T., Brewer, H.B., and Levy, R.I. (1983) The Effects of Estrogen Administration on Plasma Lipoprotein Metabolism in Premenopausal Females, *J. Clin. Endocrinol. Metab.* 57, 262–267.

35. Frayn, K.N., and Coppack, S.W. (1992) Insulin Resistance, Adipose Tissue and Coronary Heart Disease, *Clin. Sci.* 82, 1–8.
36. Suckling, K.E., and Jackson, B. (1993) Animal Models of Human Lipid Metabolism, *Prog. Lipid. Res.* 32, 1–24.
37. Gruen, R., Hietanen, E., and Greenwood, M.R.C. (1978) Increased Adipose Tissue Lipoprotein Lipase Activity During the Development of Genetically Obese Rat (fa/fa), *Metabolism* 27, 1955–1966.
38. Boulange, A., Planche, E., and Gasquet, P. (1981) Onset and Development of Hypertriglyceridemia in the Zucker Rat (fa/fa), *Metabolism* 30, 1045–1052.
39. MacLean, P.S., Bower, J.F., Vadlamudi, S., Green, T., and Barakat, H.A. (2000) Lipoprotein Subpopulation Distributions in Lean, Obese, and Type 2 Diabetic Women: A Comparison of African and White Americans, *Obes. Res.* 8, 62–70.
40. Cohn, J.S., Nestel, P.J., and Turley, S.D. (1987) Metabolism of High Density Lipoprotein in the Hyperlipidemic Diabetic SHR/N-Corpulent Rat, *Metab. Clin. Exp.* 36, 230–236.
41. Mela, D.J., Cohen, R.S., and Kris-Etherton, P.M. (1987) Lipoprotein Metabolism in a Rat Model of Diet-Induced Adiposity, *J. Nutr.* 117, 1655–1662.

[Received February 19, 2002, and in revised form June 24, 2002; revision accepted July 24, 2002]

# High Oleic Acid Oil Suppresses Lung Tumorigenesis in Mice Through the Modulation of Extracellular Signal-Regulated Kinase Cascade

Tatsuya Yamaki<sup>a</sup>, Tomohiro Yano<sup>b,\*</sup>, Haruna Satoh<sup>b</sup>, Tatsuo Endo<sup>a</sup>,  
Chinami Matsuyama<sup>a</sup>, Hitomi Kumagai<sup>a</sup>, Mitsuyoshi Miyahara<sup>a</sup>, Hidetoshi Sakurai<sup>a</sup>,  
Jan Pokorný<sup>c</sup>, Sung Jae Shin<sup>b</sup>, and Kiyokazu Hagiwara<sup>b</sup>

<sup>a</sup>College of Bioresource Sciences, Nihon University, Fujisawa, Kanagawa 252-8510, Japan, <sup>b</sup>Department of Food Science Research for Health, National Institute of Health and Nutrition, Tokyo 162-8636, Japan, and <sup>c</sup>Faculty of Food and Biochemical Technology, Institute of Chemical Technology, CZ-16628 Prague 6, Czech Republic

**ABSTRACT:** This study was undertaken to estimate the effect of dietary high oleic acid oil (OA) on 4-(methylnitrosamino)-1-(3-pyridyl)-1-butanone (NNK)-induced lung tumorigenesis in mice. Diet containing 10% oil was fed to mice through experimental periods. On day 30 after NNK injection (100 mg/kg body weight, i.p.), the treatment increased the level of prostaglandin E<sub>2</sub> (PGE<sub>2</sub>) as well as proliferating cell nuclear antigen, a marker of cell proliferation in a high linoleic acid oil (LA)-fed group but not in an OA-fed group. The NNK treatment also induced the activation of an extracellular signal-regulated kinase (Erk) cascade (Erk, Mek and Raf-1) in an LA-fed group. On the other hand, OA feeding abolished the NNK-induced activation of the Erk cascade. In conjugation with these events, OA feeding reduced lung tumor incidence and tumor multiplicity (percentage of mice with tumors) in mice compared with LA feeding at the 20th experimental week. These results suggest that OA suppresses lung tumorigenesis and that this suppression is correlated with the inhibition of PGE<sub>2</sub> production and inactivation of the Erk cascade.

Paper no. L9013 in *Lipids* 37, 783–788 (August 2002).

Cigarette smoking is the leading cause of lung cancer. A tobacco-specific nitrosamine, 4-(methylnitrosamino)-1-(3-pyridyl)-1-butanone (NNK), is formed from the nitrosation of nicotine during tobacco processing and cigarette smoking and has been suggested to play an important role in human tobacco-related cancers (1,2). In laboratory animals, NNK is the most potent lung carcinogen of tobacco-specific nitrosamines (3). In mouse lung tumors induced by NNK, mutational activation of *K-ras* gene caused by GC→AT transitions in the second base of codon 12 have been detected (4,5). The mutational activation of *K-ras* gene is then followed by proliferation and progression to a malignant tumor (5). From the similarity of the mutational activation of *K-ras* gene observed in human lung cancer and mouse lung tumors, the induction of lung tumors by NNK in mice is a

\*To whom correspondence should be addressed at Department of Food Science Research for Health, National Institute of Health and Nutrition, 1-23-1 Toyama, Shinjuku-ku, Tokyo 162-8636, Japan. E-mail: yano@nih.go.jp

Abbreviations: Erk, extracellular signal-regulated kinase; LA, high linoleic acid sunflower oil; NNK, 4-(methylnitrosamino)-1-(3-pyridyl)-1-butanone; OA, high oleic acid peanut oil; PCNA, proliferating cell nuclear antigen; PGE<sub>2</sub>, prostaglandin E<sub>2</sub>; RIPA, radioimmunoprecipitation assay.

well-established model for studying lung carcinogenesis and its modulating factors in humans (6).

Epidemiological and experimental studies suggest that an increased dietary intake of olive oil plays a beneficial role in the prevention of certain cancers (7–10). Although the proportion of smokers and total intake of dietary fat were the same between southern and northern Italy, the mortality rate for lung cancer was lower in the former (11). In southern Italy, the traditional diet is rich in olive oil, whereas in northern Italy the diet is rich in red meat and butter (11). This increased intake of olive oil may partly account for the low lung cancer mortality rate. A previous report indicates that oleic acid, a major component of olive oil, contributes to the oil-dependent inhibition of lung tumorigenesis (12). Other olive oil components, such as squalene, may have an antitumor-promoting effect (13). In order to establish the usefulness of oleic acid as a preventive component against lung cancer, it is necessary to further investigate an exact role of the FA in regulating the development of lung cancers.

Prostaglandin E<sub>2</sub> (PGE<sub>2</sub>) from n-6 FA acts as a promoter in several types of cancers (14). On the other hand, other FA (n-3 and n-9) like oleic acid attenuate proliferation of colon cancer cells through the reduction of PGE<sub>2</sub> level (15). In previous reports, we demonstrated that pulmonary PGE<sub>2</sub> levels positively correlated with the development of lung tumors in mice treated with chemical carcinogens (16). The activation of the extracellular signal-regulated kinase (Erk) cascade based on the mutation of *K-ras* gene is required for the lung tumor promotion (17). Also, a recent report showed that PGE<sub>2</sub> stimulates the activation of Erk cascade in some tumor cells (18). Overall, it is likely that oleic acid attenuates the activation of Erk cascade in lung tumorigenesis *via* the suppression of PGE<sub>2</sub> levels and subsequently inhibits the development of lung tumors. In this context, the present study was designed to clarify the foregoing hypothesis. To avoid the influence of anticarcinogenic components other than oleic acid involved in olive oil, pure high oleic acid peanut oil (OA) from SunOleic Peanut was used in this study instead of olive oil (19). The composition of oleic acid in this peanut oil was fairly similar to that in olive oil (20). The composition of FA in pure OA, olive oil, and high linoleic acid sunflower oil (LA) is shown in Table 1.



**TABLE 1**  
**Composition of FA in Each Oil**

FA	High oleic acid peanut oil	Olive oil	High linoleic acid sunflower oil
14:0	0.0	0.0	1.5
16:0	5.3	0.0	7.2
16:1	0.0	0.8	0.0
18:0	2.3	3.6	2.6
18:1	81.5	83.2	12.2
18:2	3.4	11.5	76.5
18:3	0.0	0.9	0.0
20:0	1.2	0.0	0.0
20:1	2.2	0.0	0.0
22:0	2.5	0.0	0.0
24:0	1.6	0.0	0.0

## MATERIALS AND METHODS

**Animals and treatment.** Animal experiments were approved by our Academic Committee on Animal Experiments prior to the onset of the studies. Specific pathogen-free *AJ* strain female mice (SLC, Shizuoka, Japan) were used. The mice were maintained under a clean-rack system at  $22 \pm 1^\circ\text{C}$  and  $55 \pm 5\%$  RH with a 12-h diurnal system. Sterilized water was given *ad libitum*. The mice were fed AIN-76A diet containing 10% LA or OA for 2 wk. After that, the mice were given NNK (Chem-syn Science Laboratory, Shawnee Mission, KS) dissolved in saline at a dose of 100 mg/kg body weight or vehicle by a single i.p. injection. On day 30 after the injection, four mice for PGE<sub>2</sub> assay, three mice for proliferating cell nuclear antigen (PCNA) assay, three mice for Raf-1 kinase assay, and three mice for Mek and Erk assay were killed under anesthesia with pentobarbital. We have already shown that several tumor promotion and cell proliferation markers drastically increase on day 30 after the NNK injection and that the elevations closely relate to the development of lung tumors (16,17,21), so we selected this point to determine biochemical parameters in order to estimate the tumor promotion stage. At week 20 after the injection, 12 mice in each group were sacrificed to confirm the development of lung tumors according to the previous report (21).

**Determination of PGE<sub>2</sub> levels.** A 20% lung homogenate was prepared in 0.1 M Tris-HCl buffer (pH 7.4) containing 0.15 M azide for PGE<sub>2</sub> assay. After centrifugation at  $100,000 \times g$  for 1 h, the supernatant was acidified to pH 3.0, and PGE<sub>2</sub> from the supernatant was extracted with ethyl acetate. The extracted sample was passed through a SEP-PAK C<sub>18</sub> column (Waters Associates, Milford, MA), and the methanol eluate was then evaporated (22). PGE<sub>2</sub> level in the residue was estimated by an ELISA system (Cayman Chemical, Ann Arbor, MI).

**Raf-1 kinase activity assay.** Raf-1 kinase activity was determined using a single-step assay for the kinase based on phosphorylation of recombinant Mek-1, detected using an activation-specific Mek antibody (New England Biolabs, Beverly, MA) that recognized Mek only when specifically phosphorylated by Raf (23). A 20% lung homogenate was prepared in radioimmunoprecipitation assay (RIPA) buffer (25 mM Hepes,

pH 7.5, 150 mM NaCl, 1% Triton X-100, 10% glycerol, 10 mM MgCl<sub>2</sub>, 25 mM NaF, 10 mM Na<sub>3</sub>VO<sub>4</sub>, 1 mM phenylmethyl sulfonyl fluoride, 1 mM EDTA, 10 μg/mL leupeptin, 10 μg/mL aprotinin, and 0.1% deoxycholate). After the supernatant was prepared by centrifugation at  $100,000 \times g$  for 1 h, Raf-1 was immunoprecipitated from 500 μg of the supernatant protein using sheep polyclonal anti-c-Raf antibody (UBI, Lake Placid, NY). An *in vitro* kinase assay was performed using recombinant Mek-1 substrate (Santa Cruz Biotechnology, Santa Cruz, CA) at 30°C for 30 min. The reaction mixture contained Raf-1 immunocomplex, 20 μM ATP, 500 ng of Mek-1 substrate, 20 mM NaCl, 1 mM DTT, 10 mM MgCl<sub>2</sub>, 1 mM MnCl<sub>2</sub>, and 20 mM Tris-HCl buffer (pH 7.4). The samples were resolved by 10% SDS-PAGE and probed with polyclonal antiphosphorylated Mek (New England Biolabs), polyclonal anti-Raf (Santa Cruz Biotechnology) and monoclonal anti-Mek-1 (Transduction Labs, Lexington, KY) antibodies. Detection was accomplished using ECL (Amersham, Piscataway, NJ) and a cooled CCD camera-linked Cool Saver system (Atto, Tokyo, Japan). A 2-D densitometric evaluation of each band was performed using Atto Image Analysis Software (Atto). Molecular sizing was done using Rainbow M.W. marker (Amersham). Protein concentrations were determined using DC Protein Assay (BioRad, Hercules, CA).

**The assay of PCNA level.** The supernatant was prepared from 20% homogenate in RIPA buffer as described in the assay of Raf-1 kinase activity. The supernatant containing 100 μg protein was incubated overnight with p13suc1-agarose (UBI). The pellet was resolved by 10% SDS-PAGE and probed with monoclonal anti-PCNA antibody (Dako, Denmark). β-Actin was used as an internal standard, and this protein was separated on 10% SDS-PAGE and probed with anti-β-actin antibody (Sigma, St. Louis, MO). Each protein band was detected as mentioned above. PCNA-p13 complex was useful as a marker of cell proliferation during carcinogenesis (24), and we confirmed the level of PCNA-p13 complex is positively associated with PCNA labeling index in alveolar epithelial cells (a main progenitor cell of mouse lung tumor) (25). Thus, the level is a good marker to estimate proliferation of alveolar epithelial cells during lung tumorigenic process.

**The assay of Mek and Erk activations.** The activations of Mek and Erk were estimated by immunoblot analysis using antiphosphorylated Mek (Mek-P), phosphorylated Erk (Erk-P), and Mek and Erk antibodies (New England Biolabs). The supernatant containing 20 μg protein was resolved in 10% SDS-PAGE, and subsequently each protein band was detected as mentioned above.

**The estimation of lung tumors.** At autopsy, the lungs were fixed by intratracheal instillation of 10% buffered formalin. After separation of each pulmonary lobe, the number of induced tumors was counted under a dissecting microscope (21). These tumors were embedded in paraffin, sectioned, and stained with hematoxylin and eosin for histological analysis.

**Statistical analysis.** Comparisons were performed by the chi-square test for the percentage of tumor-bearing mouse, and other data were analyzed by one-way ANOVA followed

by Duncan's multiple-range test. *P* values of 0.05 or less were considered significant.

## RESULTS

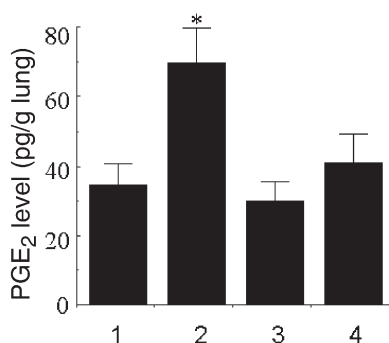
The ratios of body weight final/initial were 1.30 in LA + vehicle-treated group (LA-vehicle), 1.29 in LA + NNK-treated group (LA-NNK), 1.31 in OA + vehicle-treated group (OA-vehicle), and 1.30 in OA + NNK-treated group (OA-NNK), respectively. There were no significant differences among these groups.

The level of PGE<sub>2</sub> in mouse lung on day 30 after NNK injection is shown in Figure 1. The level of PGE<sub>2</sub> in the LA-NNK group was about twofold greater than that in the LA-vehicle group, and the difference was statistically significant. On the other hand, the level of PGE<sub>2</sub> in the OA-NNK group showed only a slight insignificant increase compared with the OA-vehicle group.

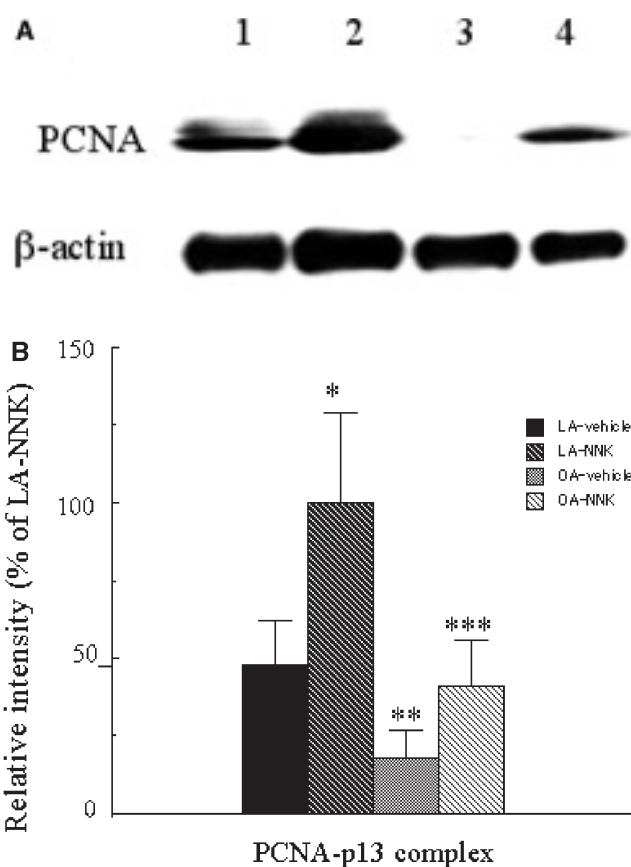
Levels of PCNA-p13 complex (a marker of cell proliferation) and the densitometric evaluation are shown in Figures 2A and 2B, respectively. The level of the PCNA in the LA-NNK group showed a significant increase compared with that in the LA-vehicle group. Also, the difference in the PCNA level between the OA-vehicle and OA-NNK groups was similar to that between the LA-vehicle and the LA-NNK groups, but the level of PCNA-p13 in the OA-fed groups was much lower (*P* ≤ 0.05) than that in the LA-fed groups.

Changes in the activation of the Erk cascade on day 30 after NNK injection are shown in Figure 3. The activated level of the Erk cascade (Raf-1, and phosphorylated Mek and Erk) in the LA-NNK group was much higher than that in the other three groups (Figs. 3A–C), and this difference was statistically significant (Fig. 3D). There was no difference in the activated level of the Erk cascade among the three groups except for the LA-NNK group (Fig. 3D).

The effect of LA and OA feeding on NNK-induced lung tumorigenesis is summarized in Table 2. In the LA-NNK group lung tumors were found in 100% of the mice, with an



**FIG. 1.** The change of pulmonary prostaglandin E<sub>2</sub> (PGE<sub>2</sub>) level in mice treated with 4-(methylnitrosoamino)-1-(3-pyridyl)-1-butanone (NNK). 1, High linoleic acid sunflower oil (LA)-vehicle; 2, LA-NNK; 3, high oleic acid peanut oil (OA)-vehicle; 4, OA-NNK. Each column represents the mean from four samples, and bars indicate SE. \*Significantly different from LA-vehicle, OA-vehicle, and OA-NNK. This experiment was carried out twice.



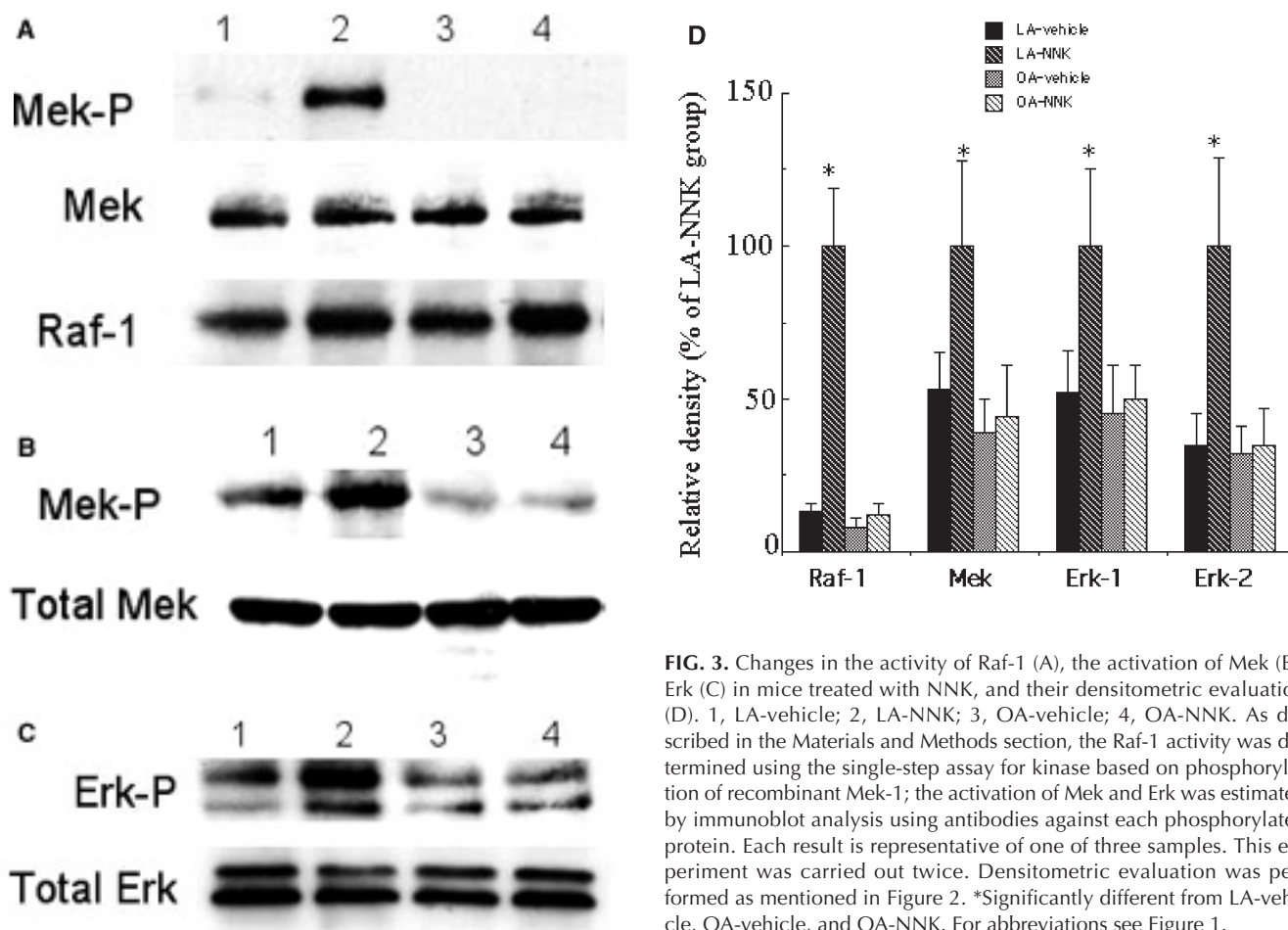
**FIG. 2.** The change of proliferating cell nuclear antigen (PCNA) level in mice treated with NNK (A) and its densitometric analysis (B). Immunoblot analysis of the level of PCNA precipitated with p13suc1-agarose and  $\beta$ -actin were carried out as detailed in the Materials and Methods section. This result is representative of one of three samples. This experiment was carried out twice. Densitometric evaluation was performed as discussed in the Materials and Methods section. Each intensity shown is the mean of three samples; vertical lines indicate SE. Each value is expressed as a relative ratio against the LA-NNK group, and the value in the group is shown as 100. \*Significantly different from LA-vehicle, OA-vehicle, and OA-NNK. \*\*Significantly different from LA-vehicle, LA-NNK and OA-NNK. \*\*\*Significantly different from LA-NNK and OA-vehicle. For abbreviations see Figure 1.

average of 6.3 tumors per mouse. Compared to the LA-NNK group, the OA-NNK group had a 25% lower incidence of lung tumors and a 31% reduced lung tumor level (4.8 tumors per mouse). These differences between the two groups were statistically significant. Furthermore, no difference between the LA-vehicle and OA-vehicle groups in the development of lung tumors was observed.

## DISCUSSION

The present study demonstrates that LA feeding compared with OA feeding reduced the development of lung tumors in mice treated with NNK. Changes in PGE<sub>2</sub> levels correlated with FA-induced changes in tumorigenesis.

During the carcinogenic process, at the initiation stage, the fixation of DNA damage induced by carcinogen exposure occurs (the appearance of the initiated cells). Subsequently, the



initiated cells begin to proliferate in response to various stimuli such as a promoter, finally leading to the development of tumors (26). In the murine NNK-induced lung tumorigenesis model, a high percentage of the lung tumors have mutational activation of the *K-ras* gene (4,5). We have also detected *K-ras* gene activation in lung with the same mutation as seen in NNK-induced lung tumors before the appearance of microscopically observable tumors (27). These reports suggest that NNK-initiated cells having a mutation of the *K-ras* gene appear to remain latent within pulmonary normal cells and require additional events (such as exposure to growth-promoting agents) to trigger neoplastic development. The present study indicates that the difference in the development of lung tumors between OA-NNK and LA-NNK groups is based on

the difference in cell proliferation at the promotion stage. On the other hand, we confirmed that there was no difference in the fixation of DNA injury at the initiation stage between the two groups (Yamaki, T., Yano, T., and Sakurai, H., unpublished data). These results suggest that promoter(s)-stimulated proliferation of the initiated cells in the OA-NNK group during the promotion stage is less than that in the LA-NNK group. We have observed that the level of pulmonary arachidonic acid as a main precursor of PGE<sub>2</sub> in the LA-fed group was higher than that in the OA-fed group (Yamaki, T., Yano, T., and Sakurai, H., unpublished data). Thus, we postulate that a difference in PGE<sub>2</sub> levels occurring between the two groups is due to the difference in the precursor level, and that the difference is key to regulating the development of lung tumors

**TABLE 2**  
Tumor Multiplicity of the 20th Experimental Week in the Lungs of Mice

Group	No. of mice	No. of mice with tumors	% of mice with tumors	No. of total tumors	No. of tumors/mouse (mean ± SE)
LA + vehicle	12	0	0	0	0
OA + vehicle	12	0	0	0	0
LA + NNK	12	12	100	75	6.25 ± 2.15
OA + NNK	12	9	75 <sup>a</sup>	43	4.78 ± 2.80 <sup>a</sup>

<sup>a</sup>Significantly different from LA + NNK group ( $P < 0.05$ ). Abbreviations: LA, high linoleic acid sunflower oil; OA, high oleic acid peanut oil; NNK, 4-(methylnitrosoamino)-1-(3-pyridyl)-1-butanone.



in this model. In fact, we found that PGE<sub>2</sub> levels correlated with the development of lung tumors in mice treated with NNK.

In lung cancer cells with *K-ras* mutations, the constitutive activation of Erk cascade based on the mutations induces phospholipase A<sub>2</sub> and cyclooxygenase-2, and this induction is associated with a high generation of PGE<sub>2</sub> in the cells (28). Also, this study shows that the reduction of PGE<sub>2</sub> production by cyclooxygenase inhibitors contributes to negative growth control of the lung cancer cells. In a recent study, we demonstrated that PGE<sub>2</sub> stimulates proliferation of lung cancer cells with *K-ras* mutations by reinforcing the activation of the Erk cascade (29). In *in vivo* studies, we showed that the activation of the Erk cascade based on *K-ras* mutations and the induction of cyclooxygenase and oxygenase-mediated PGE<sub>2</sub> production are necessary for cell proliferation at the promotion stage of lung tumorigenesis in mice (16,17,21). It seems that high generation of PGE<sub>2</sub> associated with the induction of cyclooxygenase during the carcinogenic process in the lung contributes to the constitutive activation of the Erk cascade, abnormal cell proliferation, and the development of lung tumors. Thus, as we have shown, the regulation of PGE<sub>2</sub> production by OA feeding, perhaps owing to a reduction in the precursor FA levels, actually reduces the risk of lung carcinogenesis. Furthermore, our present results support the possibility that an increased intake of olive oil and oleic acid contributes to reduction of lung cancer mortality.

Although the level of PGE<sub>2</sub> in the LA-vehicle group was almost the same as that in the OA-vehicle group, cell proliferation in the former was significantly higher than that in the latter. These results suggest that other factors in addition to PGE<sub>2</sub> contribute to OA feeding-dependent suppression of cell proliferation in lung.

In previous reports FFA were demonstrated to influence cell growth directly through the induction of proto-oncogenes like *c-fos* via Ca<sup>2+</sup> and protein kinase C signaling (30). Different effects on cell growth were observed depending on the type of FFA (31). Thus, this effect of FFA may relate to the OA feeding-dependent decrease in cell proliferation. In comparing the relation of the PGE<sub>2</sub> level and cell proliferation between LA-NNK and OA-NNK groups, it is clear that the reduction in the level of PGE<sub>2</sub> by OA feeding correlates with the suppression of cell proliferation at the promotion stage. On the other hand, in comparing vehicle treatment, NNK-induced elevation of cell proliferation in the OA-fed group was higher than that of the NNK-induced increase of PGE<sub>2</sub> levels, suggesting that promoters other than PGE<sub>2</sub> stimulated the cell proliferation at the promotion stage. However, cell proliferation in the OA-NNK group was almost equal to that in the LA-vehicle group and was much lower than that in the LA-NNK group. Thus, a beneficial effect of OA feeding, the suppression of lung carcinogenesis, presumably depends on both the reduction of PGE<sub>2</sub> levels and other effects that are independent of PGE<sub>2</sub>.

#### ACKNOWLEDGMENT

This study was supported in part by a grant-in-aid for Cancer Research from the Ministry of Health, Labor and Welfare of Japan.

#### REFERENCES

1. Hecht, S.S. (1994) Metabolic Activation and Detoxification of Tobacco-Specific Nitrosamines—A Model for Cancer Prevention Strategies, *Drug. Metab. Rev.* 26, 373–390.
2. Hoffmann, D., Brunnemann, K.D., Prokopczyk, B., and Djordjevic, M.V. (1994) Tobacco-Specific *N*-Nitrosamines and Areca-Derived *N*-Nitrosamines: Chemistry, Biochemistry, Carcinogenicity, and Relevance to Humans, *J. Toxicol. Environ. Health* 41, 1–52.
3. Hoffman, D., and Hecht, S.S. (1985) Nicotine-Derived *N*-Nitrosamines and Tobacco-Related Cancer: Current Status and Future Directions, *Cancer Res.* 4, 935–944.
4. Belinsky, S.A., Devereux, T.R., Maronpot, R.R., Stoner, G.D., and Anderson, M.W. (1989) Relationship Between the Formation of Promutagenic Adducts and the Activation of the *K-ras* Protooncogene in Lung Tumors from A/J Mice Treated with Nitrosamines, *Cancer Res.* 49, 5305–5311.
5. Jackson, E.L., Willis, N., Mercer, K., Bronson, R.T., Crowley, D., Montoya, R., Jacks, T., and Tuveson, D. (2001) Analysis of Lung Tumor Initiation and Progression Using Conditional Expression of Oncogenic *K-ras*, *Gene Develop.* 15, 3243–3248.
6. Malkinson, A.M. (1992) Primary Lung Tumors in Mice: An Experimentally Manipulable Model of Human Adenocarcinoma, *Cancer Res.* 52, 2670s–2676s.
7. Cohen, L.A., Thompson, D.O., Maeura, Y., Choi, K., Blank, M.E., and Rose, D.P. (1986) Dietary Fat and Mammary Cancer. I. Promoting Effects of Different Dietary Fats on *N*-Nitrosomethylurea-Induced Rat Mammary Tumorigenesis, *J. Natl. Cancer Inst.* 77, 43–51.
8. Reddy, B.S. (1994) Chemoprevention of Colon Cancer by Dietary Fatty Acids, *Cancer Metastasis Rev.* 13, 285–302.
9. Fortes, C., Forastiere, F., Anatra, F., and Schmid, G. (1995) Consumption of Olive Oil and Specific Food Groups in Relation to Breast Cancer Risk in Greece, *J. Natl. Cancer Inst.* 87, 1020–1021.
10. Landa, M., Frago, N., and Tres, A. (1994) Diet and the Risk of Breast Cancer in Spain, *Eur. J. Cancer Prev.* 3, 313–320.
11. Taioli, E., Nicolosi, A., and Wynder, E.L. (1991) Possible Role of Diet as a Host Factor in the Aetiology of Tobacco-Induced Lung Cancer: An Ecological Study in Southern and Northern Italy, *Int. J. Epidemiol.* 20, 611–614.
12. Smith, T.J., Yang, G.Y., Seril, D.N., Liao, J., and Kim, S. (1998) Inhibition of 4-(methylnitrosamino)-1-(3-pyridyl)-1-Butanone-Induced Lung Tumorigenesis by Dietary Olive Oil and Squalene, *Carcinogenesis* 19, 703–706.
13. Newmark, H.L. (1997) Squalene, Olive Oil, and Cancer Risk: A Review and Hypothesis, *Cancer Epidemiol. Biomarkers Prev.* 6, 1101–1103.
14. Bennett, A., Del Tacca, M., Stamford, I.F., and Zebro, T. (1977) Prostaglandins from Tumors of Human Large Bowel, *Br. J. Cancer* 35, 881–884.
15. Reddy, B.S., and Sugie, S. (1998) Effect of Different Levels of Omega-3 and Omega-6 Fatty Acids on Azoxymethane-Induced Colon Carcinogenesis in F344 Rats, *Cancer Res.* 48, 6642–6647.
16. Yano, T., Yano, Y., Uchida, M., Murakami, A., Hagiwara, K., Otani, S., and Ichikawa, T. (1997) The Modulation Effect of Vitamin E on Prostaglandin E<sub>2</sub> Level and Ornithine Decarboxylase Activity at the Promotion Stage of Lung Tumorigenesis in Mice, *Biochem. Pharmacol.* 53, 1757–1759.
17. Yano, T., Yano, Y., Nagashima, Y., Yuasa, M., Yajima, S., Horikawa, S., Hagiwara, K., Kishimoto, M., Ichikawa, T., and Otani, S. (1999) Activation of Extracellular Signal-Regulated Kinase in Lung Tissues of Mice Treated with Carcinogen, *Life Sci.* 64, 229–236.
18. Englaro, W., Rezzonico, R., Durand-Clement, M., Lallemand, D., Ortonne, J.P., and Ballotti, R. (1995) Mitogen-Activated Protein Kinase Pathway and AP-1 Are Activated During cAMP-Induced Melanogenesis in B-16 Melanoma Cells, *J. Biol. Chem.* 270, 24315–24320.



19. Hauman, B.F. (1998) Peanuts Find Niche in Healthy Diet, *inform 9*, 746–752.
20. Knauff, D.A., Gorbet, D.W., and Norden, A.J. (1995) SunOleic 95R Peanut, *Florida Agricultural Experiment Station Circular*, Miami, S400.
21. Yano, Y., Yano, T., Uchida, M., Murakami, M., Ogita, T., Ichikawa, T., Otani, S., and Hagiwara, K. (1997) The Inhibitory Effect of Vitamin E on Pulmonary Polyamine Biosynthesis, Cell Proliferation and Carcinogenesis in Mice, *Biochim. Biophys. Acta* 1356, 35–42.
22. Yamaki, K., and Oh-Ishi, S. (1989) Fluorometric High-Performance Liquid Chromatographic Analysis of Prostaglandin (PG) Metabolites: Application to the Catabolism of PGE<sub>2</sub> and PGF<sub>2α</sub> in Rat and Rabbit Kidney Homogenates, *J. Pharmacobiodyn.* 12, 74–79.
23. Bondzi, C., Grant, S., and Krystal, G.W. (2000) A Novel Analysis for the Measurement of Raf-1 Kinase Activity, *Oncogene* 19, 5030–5033.
24. Said, T.K., and Medina, D. (1995) Cell Cyclins and Cyclin-Dependent Kinase Activities in Mouse Mammary Tumor Development, *Carcinogenesis* 16, 823–830.
25. Yano, T., Yajima, S., Hagiwara, K., Kumadaki, I., Yano, Y., Otani, S., Uchida, M., and Ichikawa, T. (2000) Vitamin E Inhibits Cell Proliferation and the Activation of Extracellular-Regulated Kinase During the Promotion Phase of Lung Tumorigenesis Irrespective of Antioxidative Effect, *Carcinogenesis* 21, 2129–2133.
26. Kumar, R., Sukumar, S., and Barbacid, M. (1990) Activation of *ras* Oncogenes Preceding the Onset of Neoplasia, *Science* 248, 1101–1104.
27. Yano, T., Yajima, S., Nakamura, T., Horikawa, S., Kishimoto, M., and Ichikawa, T. (1998) The Inhibitory Effect of Vitamin E on 4-(methylnitrosamino)-1-(3-pyridyl)-1-Butanone-Induced DNA Injury and the Fixation of the DNA Injury in Mouse Lungs. *Naunyn Schmiedebergs Arch. Pharmacol.* 358, 275–278.
28. Heasley, L.E., Thaler, S., Nicks, M., Price, B., Skorecki, K., and Nemenoff, R.A. (1997) Induction of Cytosolic Phospholipase A<sub>2</sub> by Oncogenic *ras* in Human Non-Small Cell Lung Cancer, *J. Biol. Chem.* 272, 14501–14504.
29. Yano, T., Zissel, G., Muller-Qernheim, J., Shin, S.J., Satoh, H., and Ichikawa, T. (2002) Prostaglandin E<sub>2</sub> Reinforces the Activation of Ras Signal Pathway in Lung Adenocarcinoma Cells via EP<sub>3</sub>, *FEBS Lett.* 518, 154–158.
30. Roche, E., Buteau, J., Aniento, I., Reig, J.A., Soria, B., and Prentki, M. (1999) Palmitate and Oleate Induce the Immediate-Early Response Genes *c-fos* and *nur-77* in the Pancreatic β-Cell Line INS-1, *Diabetes* 48, 2007–2014.
31. Wickramasinghe, N.S., Jo, H., McDonald, J.M., and Hardy, R.W. (1996) Stearate Inhibition of Breast Cancer Cell Proliferation. A Mechanism Involving Epidermal Growth Factor Receptor and G-Proteins, *Am. J. Pathol.* 148, 987–995.

[Received February 19, 2002, and in revised form July 22, 2002; revision accepted July 27, 2002]

# Enrichment of LDL with EPA and DHA Decreased Oxidized LDL-Induced Apoptosis in U937 Cells

Tianying Wu, Cissy Geigerman, Ye-Sun Lee, and Rosemary C. Wander\*

Human Nutrition Research Laboratory, University of North Carolina at Greensboro, Greensboro, North Carolina 27402-6170

**ABSTRACT:** Oxidized LDL (oxLDL) may contribute to the accumulation of apoptotic cells in atherosclerotic plaques. Although it is well established in monophasic chemical systems that the highly unsaturated EPA and DHA will oxidize more readily than FA that contain fewer double bonds, our previous studies showed that enrichment of LDL, which has discrete polar and nonpolar phases, with these FA did not increase oxidation. The objective of this study was to compare the extent of apoptosis induced by EPA/DHA-rich oxLDL to that induced by EPA/DHA-non-rich oxLDL in U937 cells. LDL was obtained from one healthy subject three times before and after supplementation for 5 wk with 15 g/d of fish oil (FO), an amount easily obtainable from a diet that contains fatty fish. After supplementation, an EPA/DHA-rich LDL was obtained. Oxidative susceptibility of LDL, as determined by measuring the formation of conjugated dienes and the accumulation of cholesteryl ester hydroperoxides, was not higher in EPA/DHA-rich LDL. The oxLDL-induced cell apoptosis was detected by the activation of caspase-3, the translocation of PS to the outer surface of the plasma membrane using the Annexin V-fluorescein isothiocyanate binding assay, and the presence of chromatin condensation and nuclear fragmentation using the 4,6-diamidino-2-phenylindole staining assay. All three measures showed that after FO supplementation, EPA/DHA-rich oxLDL-induced cell apoptosis decreased. The decrease was not related to the concentration of lipid hydroperoxides. This study suggests that a possible protective effect of EPA/DHA-rich diets on atherosclerosis may be through lessening cell apoptosis in the arterial wall.

Paper no. L8943 in *Lipids* 37, 789–796 (August 2002).

Recent findings show that apoptosis is responsible for much of the cell death seen during atherosclerosis. Indeed, apoptosis has been positively correlated with the localization and severity of atherosclerosis (1). Macrophages, smooth muscle cells, and lymphocytes undergoing apoptosis all have been found in human atherosclerotic lesions (2–4). Of the three cell types, macrophages appear to be the preferred cell population in atherosclerotic lesions to undergo apoptosis (2,5,6). Apoptotic macrophages have been implicated in the initiation and

enlargement of the cellular lipid-core in the advanced atherosclerotic lesion (7–9). Furthermore, this process can lead to the activation of thrombosis (7–9).

Oxidized LDL (oxLDL) plays a critical role in the development of atherosclerosis (10,11). Recently, oxLDL has been shown to induce apoptosis in human umbilical vein endothelial cells (12,13), smooth muscle cells and fibroblasts (14), and macrophages (15,16).

It is conceivable that the role of oxLDL in the development of atherosclerosis could be through induction of apoptosis. The mechanisms by which oxLDL induce apoptosis are not well understood. Lipid hydroperoxides (17), decomposition products (i.e., 4-hydroxynonenal) (18), and cholesterol oxidation products (oxysterols) (i.e., 25-hydroxycholesterol or 7- $\beta$  hydroxycholesterol) (13,19–21) are generated during oxidation of LDL and have been shown to induce apoptosis. However, the relative potencies of these different products are not yet known. Furthermore, upregulated Fas and Fas-ligand (22), the release of cytochrome *c* from mitochondria (21), the activation of caspase-8 (22), caspase-3 (13,15,21), and an increase in cellular calcium concentrations (23) have all been implicated in oxLDL-induced cell apoptosis.

Current research has attempted to identify those factors that regulate the oxidation of LDL and the production of its decomposition products. It is believed that an improved understanding of these factors may provide a therapeutic tool for controlling the development and progression of atherosclerosis. For example, dietary FA influence the rate and extent of LDL oxidation. EPA and DHA are FA mainly from fish that are associated with a decreased risk of cardiovascular disease. In a recent clinical trial, results showed that enriching LDL with EPA/DHA produced a lower concentration of lipid hydroperoxides compared to the LDL enriched with linoleic acid (24), when LDL was subjected to oxidation. Given that lipid hydroperoxides are the predominant lipid oxidation products found in atherosclerotic lesions (25), our findings support a role of EPA/DHA in reducing the severity of atherosclerosis. Moreover, reduced production of lipid hydroperoxides may lessen the formation of secondary oxidation products such as 4-hydroxynonenal, thereby reducing apoptosis.

The effect of oxidized LDL that has been enriched with EPA/DHA on cell apoptosis has not been investigated. In order to evaluate this, the oxidative susceptibility of EPA/DHA-rich LDL was compared to that of EPA/DHA-non-rich LDL. The extent of apoptosis of U937 cells induced by

\*To whom corresponding should be addressed at Dept. of Nutrition, P.O. Box 26170, University of North Carolina at Greensboro, Greensboro, NC 27402-6170. E-mail: rcwander@uncg.edu

Abbreviations: AMC, aminomethyl coumarin; CE18:200H, cholesteryl linoleate hydroperoxide; CEOOH, cholesteryl ester hydroperoxides; DAPI, 4,6-diamidino-2-phenylindole; FITC, fluorescein isothiocyanate; FO, fish oil; HDL-C, HDL-cholesterol; LDL-C, LDL-cholesterol; nLDL, native LDL; oxLDL, oxidized low-density lipoprotein; PI, propidium iodide.

EPA/DHA-rich oxLDL was compared to that of EPA/DHA-non-rich oxLDL. U937 cells are human pro-monocytic cells and share many characteristics with macrophages. Additionally, they are one of the easiest cell models in which to study apoptosis. EPA/DHA-rich oxLDL contained less or equivalent concentrations of lipid hydroperoxides as did EPA/DHA-non-rich oxLDL. Apoptosis of U937 cells was induced after 6–7 h of incubation with oxLDL, and was lower in cells treated with EPA/DHA-rich oxLDL compared to cells treated with EPA/DHA-non-rich oxLDL.

## MATERIALS AND METHODS

**Supplementation and experimental design.** The University of North Carolina at Greensboro Institutional Review Board approved the current study, and the subject signed informed consent prior to entering the study. A healthy, nonsmoking male (37 yr) was supplemented with 15 g/d fish oil (FO) for 5 wk. Plasma was collected on three separate days before and after supplementation. The FA profile of the oil was measured by GC using heptadecanoic acid (Nu-Chek-Prep, Elysian, MN) as an internal standard as previously described (26). The supplement (15 g) provided 1.26 g EPA and 1.08 g DHA. This amount (2.34 g) of n-3 FA is similar to that found in two servings (200 g) of Chinook salmon (27). FO supplements were kindly provided by OmegaPure™ (Houston, TX) in bulk and were then encapsulated by Banner Pharmacaps, Inc. (High Point, NC). A mixture of  $\alpha$ -,  $\gamma$ -, and  $\delta$ -tocopherols (courtesy of ADM Nutraceuticals, Decatur, IL) and TBHQ (Eastman Chemical Company, Kingsport, TN) were added to the oil. The vitamin E content of the oil was measured by HPLC (Agilent Technologies 1100 series, Palo Alto, CA) using a fluorometric detector set at 292 nm for excitation and 330 nm for emission (28). Recovery of  $\alpha$ -tocopherol added to the sample was 92%, and the interassay coefficient of variation was 5.6%. After these additions, the oil contained 0.540 mg  $\alpha$ -tocopherol/g oil, 0.689 mg  $\gamma$ -tocopherol/g oil, 0.177 mg  $\delta$ -tocopherol/g oil, and 0.02% TBHQ.

**Cell culture and treatment.** A week before the experiments, U937 cells (ATCC, Rockville, MD) were thawed from the frozen vials and maintained at  $1\text{--}5 \times 10^5/\text{mL}$  cells in T-75 culture flasks in RPMI 1640 medium supplemented with 10% FBS, 1% glutamine (200 mmol/L), 1% penicillin-streptomycin (10,000 IU/mL), and 0.2% amphotericin B (250  $\mu\text{g}/\text{mL}$ ) at 37°C in a 95% air/5% CO<sub>2</sub> humidified incubator. These cells were used in subsequent experiments.

**Preparation of lipoproteins and determination of LDL oxidative susceptibility.** Blood samples were collected into Vacutainer® tubes (Beckton Dickinson, Franklin Lakes, NJ) containing Na<sub>2</sub>EDTA (1 g/L) after an overnight fast ( $\geq 10$  h). Plasma was immediately isolated by centrifugation at  $1200 \times g$  for 15 min at 4°C (Jouan GR 4-12, Winchester, VA). An aliquot of plasma was stored at  $-80^\circ\text{C}$  for later measurement of the lipid profile. The lipid profile, including plasma concentrations of cholesterol, triacylglycerol (TAG), HDL-cholesterol (HDL-C), and LDL-cholesterol (LDL-C), were measured

to ensure that the subject was normolipemic. Plasma concentrations of cholesterol and TAG were measured as previously described (29). The cholesterol concentration of the HDL fraction was measured by an enzymatic method in samples after the precipitation of the LDL and VLDL fractions with phosphotungstic acid in conjunction with MgCl<sub>2</sub> (Sigma Kit #352-4, St. Louis, MO) (30). LDL-C concentration was calculated using the following formula: total cholesterol – HDL-C – TAG/5 (31). LDL was isolated from plasma by centrifugation using a modification of the method of Chung *et al.* (32) as modified by Chen and Loo (33). Briefly, 28 mL of NaCl (0.195 M) was carefully overlaid on 11.5 mL of plasma in a 39.5 mL tube (Beckman, Quick-seal, Palo Alto, CA). The ultracentrifuge tube was placed in a 50.2 Ti rotor (Beckman) and centrifuged at  $190,000 \times g$  (40,000 rpm) for 2 h in a Beckman L7-65 ultracentrifuge.

An aliquot of the isolated LDL was stored at  $-80^\circ\text{C}$  for measurement of the FA profile. The FA profile was measured by GC as previously described (26) using heptadecanoic acid (Nu-Chek-Prep) as an internal standard. Following removal of EDTA and KBr from a second aliquot of LDL by using a 10 DG disposable column (Bio-Rad Laboratories, Hercules, CA), the cholesterol concentration was determined enzymatically as previously described (29) and is referred to as LDL-C.

The EDTA/KBr-free LDL was oxidized; and cholesteryl ester hydroperoxide (CEOOH) concentration, apoptotic events, and conjugated diene formation were measured. CEOOH and apoptosis were measured in aliquots taken from the same oxidized solution. In this system 0.4 mg LDL-C/mL was oxidized with 5  $\mu\text{M}$  Cu<sup>2+</sup>. The formation of conjugated dienes was measured in a separate system by continuously monitoring their production at 234 nm in a Beckman DU-640 spectrophotometer, as we have previously reported (34), at 37°C over a 6-h time period. The concentration of conjugated dienes was calculated using the molar extinction coefficient 29,500 M<sup>-1</sup>cm<sup>-1</sup> (35). The three variables—lag time, rate of oxidation, and maximal concentration of conjugated dienes—were determined. Maximal rate was determined to be the slope of the line of best fit through the points that defined the steepest slope of the curve. The length of the lag phase was determined to be the time (value for  $x$ ) at the intersection of the line describing the maximal rate and the line describing the initial rate. The maximal concentration was determined from the maximum absorption measured during the 6-h oxidation. The absorption at 234 nm plateaued at about 5 h and then began to decrease, indicating that secondary oxidation products were being formed as the conjugated dienes degraded. As many products are formed during this time and their absorptivity is unknown, monitoring the absorbance at 234 nm would yield ambiguous results and was terminated at 6 h. The maximal rate of formation and the concentration of conjugated dienes were expressed relative to the protein content of the EDTA/KBr-free LDL. The protein content of the LDL was determined using a kit obtained from Bio-Rad Laboratories. It was previously determined that optimal performance for the measurement of conjugated dienes was obtained

when 55  $\mu\text{g}$  LDL protein/mL (0.25 mg LDL/mL) was used (34). However, to make comparisons between the system in which CEOOH and apoptosis were measured and that in which conjugated dienes were measured, the ratio of  $\text{Cu}^{2+}$  to LDL-C had to be constant. This was accomplished by measuring the protein content of the EDTA/KBr-free LDL and diluting it to 55  $\mu\text{g}$  protein/mL. Because the dilution factor was known, the concentration of cholesterol in this diluted solution could be calculated. Once the cholesterol concentration was known, the concentration of  $\text{CuSO}_4$  needed to maintain consistency across both systems could be calculated. This calculation was made for each sample.

To measure CEOOH concentration and apoptosis in the EDTA/KBr-free LDL sample before oxidation was initiated by the addition of  $\text{CuSO}_4$ , a sample of LDL was removed and EDTA (1.5 mg/mL) was immediately added to prevent oxidation. This sample is identified as native LDL (nLDL). The remaining EDTA/KBr-free LDL was oxidized. An aliquot was removed after 6 h, and EDTA (1.5 mg/mL) was added immediately to halt the oxidation reactions. The remaining EDTA/KBr-free LDL sample was oxidized four more hours (a total of 10 h), and again EDTA was added to terminate the oxidation reactions. HPLC with an isoluminol-dependent chemiluminescence detection method, as previously reported (24), with slight modification was used to analyze nLDL, 6-h oxLDL, and 10-h oxLDL for CEOOH formation. Briefly, nLDL and oxLDL were extracted with hexane, evaporated, and dissolved in ethanol. Samples were injected onto a C-18 column (Supelcosil LC-18, 5  $\mu\text{m}$ , 250  $\times$  4.6 mm; Supelco, Bellefonte, PA) using a mobile phase of methanol/*tert*-butanol (1:1, vol/vol) at a flow rate of 1.0 mL/min. A postcolumn chemiluminescence reagent consisting of 3:7 (vol/vol) methanol to 100 mM sodium borate buffer (pH 10) containing 1 mM isoluminol (6-amino-2,3-dihydro-1,4-phthalazine-dione; Sigma), and 3 mg/L microperoxidase (MP-11; Sigma) at a flow rate of 1.5 mL/min was added to the eluent. Cholesteryl linoleate hydroperoxide (CE18:2OOH) (Cayman Chemicals, Ann Arbor, MI) was used as an external standard to quantify the amount of CE18:2OOH present in the samples. The modifications gave a single peak from CEOOH rather than several peaks, each associated with a different CEOOH, as reported previously (24). Thus, a more global assessment of the oxidation of core lipids was obtained.

**Apoptosis assays.** Apoptosis was assessed by three methods: caspase-3 activity, translocation of PS, and condensed chromatin and nuclear fragmentation. In the caspase-3 method, acetyl-asp-glu-val-asp-aminomethyl coumarin (Ac-DEVD-AMC), a synthetic tetrapeptide fluorogenic substrate, was added to the samples. This substrate is cleaved in the presence of caspase-3, releasing the fluorescent AMC moiety, which can be quantified by fluorescence intensity spectrophotometrically (36) (PharMingen #6332K, San Diego, CA). For the second method, translocation of PS from the inner to the outer leaflet of the plasma membrane was measured by the Annexin V binding assay. In this assay Annexin V conjugated to fluorescein isothiocyanate (FITC) binds to the translocated PS, and the

amount of the conjugate can be quantified fluorometrically. This assay can be used as a marker of early apoptosis (37). In addition, in this assay cells were costained with propidium iodide (PI). This is used as a marker for cell membrane permeability, a change that occurs during the latter stages of apoptosis and in necrosis. Viable and early apoptotic cells, which have intact membranes, exclude PI, but necrotic cells do not. Apoptotic cells are FITC-positive and PI-negative, whereas necrotic cells are both FITC- and PI-positive. In the third assay, condensed chromatin and nuclear fragmentation were visualized microscopically after staining the cells with the fluorescent dye 4,6-diamidino-2-phenylindole (DAPI).

All three measures of apoptosis were made before and after supplementation with FO. Each treatment was performed in triplicate. The cells were incubated with unoxidized LDL (nLDL), LDL that was oxidized for 6 h (6-h oxLDL), and LDL that was oxidized for 10 h (10-h oxLDL). The concentration of LDL-C was maintained at 66  $\mu\text{g}/\text{mL}$  for caspase-3 activity and DAPI staining measurements and 133  $\mu\text{g}/\text{mL}$  for PS translocation. Incubations with the LDL were 6–7 h long. All experiments included positive and negative controls. For the negative control, cells were incubated in LDL-free medium. Two positive controls were used. One positive control was to treat the cells with 25-hydroxycholesterol (62.5–66.7  $\mu\text{g}/\text{mL}$ ) (Sigma-Aldrich, St. Louis, MO) for 6 h. The other one was to treat them with (1.5  $\mu\text{g}/\text{mL}$ ) camptothecin (Sigma-Aldrich) for 4 h. A shorter incubation was used for the camptothecin because it induced apoptosis more quickly. Since the supplementation lasted about 5 wk, the LDL that was enriched with EPA/DHA was obtained later than the LDL that was not enriched with these FA. The use of these two positive controls allowed us to establish that the U937 cells behaved in a similar fashion at both times.

For the measurement of caspase-3 activity,  $5 \times 10^5$  cells were incubated with the negative and two positive controls, nLDL, 6-h oxLDL, and 10-h oxLDL. Cells were harvested and washed 2 $\times$  with PBS (pH 7.4, 10 mmol/L), resuspended in lysis buffer (100  $\mu\text{L}$  buffer/L  $\times 10^6$  cells), and stored at  $-20^\circ\text{C}$  for batch analysis. Samples were analyzed using a fluorescence spectrophotometer (PerkinElmer LS 50B, Norwalk, CT) set at 380 nm for excitation and 420 nm for emission. Data are expressed as relative fluorescent intensity per  $10^5$  cells.

For the measurement of translocation of PS,  $2.5 \times 10^5$  cells were incubated in the same six systems: the negative and positive controls, nLDL, 6-h oxLDL, and 10-h oxLDL. After incubation, 0.3 mL of the cell suspension was removed from each well and washed 2 $\times$  with ice-cold PBS ( $\text{Ca}^{2+}$ : $\text{Mg}^{2+}$ -free). The resulting cell pellet was suspended in 0.1 mL binding buffer [10 mmol/L HEPES/NaOH (pH 7.4), 140 mmol/L NaCl, 2.5 mmol/L  $\text{CaCl}_2$ ], 5  $\mu\text{L}$  of Annexin V-FITC (as supplied by PharMingen #65874x, San Diego, CA), and 10  $\mu\text{L}$  of PI stock solution (50  $\mu\text{g}/\text{mL}$ ) and then incubated in the dark for 15 min. After incubation, an additional 0.4 mL aliquot of binding buffer was added to the cell solution. Cells were analyzed with a FACS Calibur flow cytometer (Becton Dickinson, San Jose, CA) using the FL1 channel to detect the



signal generated by Annexin V-FITC and the FL2 channel to detect the signal generated by PI. Data are expressed as the percentage of cells positively stained with Annexin V-FITC but negatively stained with PI.

For the DAPI staining assay  $2.5 \times 10^5$  cells were incubated with native LDL, 10-h oxLDL, and the controls. Cells were harvested and washed 2× with PBS (pH 7.4, 10 mmol/L) before being resuspended in 200  $\mu$ L of PBS and loaded on poly-L-lysine slides (Sigma #P-0425) in Cytospin Chambers (StatSpin, Inc. #CC03, Norwood, MA) for 10 min. Slides were cytospun in a Cytofuge<sup>®</sup>2 (StatSpin, Inc.) for 4 min at 850 rpm (40 × g), immersed in fresh 3.7% formaldehyde solution for 20 min at 4°C, and subsequently stored at least one night in ice-cold 70% ethanol at -20°C. Following storage, slides were washed 3× with PBS, immersed into a diluted DAPI solution (1  $\mu$ g/mL) for 10 min, and then viewed on an Olympus BX-60 fluorescence microscope (Melville, NY) equipped with a SPOT digital camera (Sterling Heights, MI). The excitation wavelength was 358 nm, and the emission wavelength was 461 nm. The apoptotic cells were identified by a bright blue nucleus, characteristic of either condensed or fragmented chromatin, whereas normal cells were characterized by a faint blue nucleus. At least 80 cells were counted from three randomly selected fields on each slide. Slides were examined for each sample. The percentage of apoptotic cells was calculated by dividing the number of apoptotic cells by the total number of cells × 100%.

**Statistical analysis.** The significance of supplementation with FO on the lipid profile, the FA profile, and LDL oxidative susceptibility was determined using a two-sample *t*-test (38). The repeated measure's procedure was used to determine statistically significant differences between time points as well as the FO supplements on CEOOH concentration (38). To determine the influence of the length of time that LDL was oxidized on the extent of apoptosis, the data were analyzed using a one-way ANOVA (38). When a significant difference was found, pair-wise comparisons were performed using the Tukey-Kramer test to determine significant differences among treatments (38). To determine the effect of FO supplementation on extent of apoptosis, a two-sample *t*-test was used (38). All experiments were repeated three times before and after supplementation. Analyses were completed using the SAS general linear model procedure (version 8; SAS Institute Inc., Cary, NC). A value of  $P < 0.05$  was considered significant.

## RESULTS

The TAG concentration in plasma was reduced ( $P = 0.02$ ) from baseline by 51% after FO supplementation. The FO supplementation did not significantly ( $P > 0.05$ ) alter the concentration of cholesterol, HDL-C, or calculated cholesterol in LDL. The LDL FA profile changed after supplementation with FO (Fig. 1). The concentration of EPA (20:5n-3) and DHA (22:6n-3) in LDL was 1100 and 110% higher after supplementation, respectively, compared to baseline ( $P < 0.05$  for both FA).

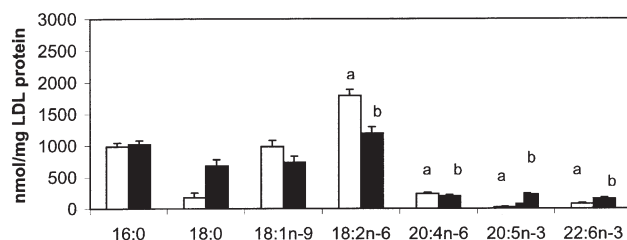
The lag time and maximal rate of production for conjugated dienes were significantly ( $P < 0.05$ ) different from baseline after FO supplementation (Table 1). The lag time was reduced by 32 min, and the maximal rate of production for conjugated dienes was reduced by 37%. However, the maximal amount of conjugated dienes produced in the LDL was similar ( $P > 0.05$ ) after FO supplementation compared to baseline.

The concentration of CEOOH in LDL both before and after supplementation with fish oil, i.e., the concentration in nLDL, was less than 180 pmol/mg LDL-C, the lower limit of detection of this assay (Fig. 2). The concentration of CEOOH produced in LDL oxidized for 6 h was 35% lower ( $P = 0.007$ ) after FO supplementation than before FO supplementation. In contrast, the concentration of CEOOH in the LDL before and after FO supplementation was statistically equivalent in the samples oxidized for 10 h ( $P > 0.05$ ) (Fig. 2).

For all measures of apoptosis, the response seen in the negative controls, i.e., those cells incubated in LDL-free medium (Fig. 3), was similar to the response seen in U937 cells treated with nLDL, suggesting that LDL did not initiate apoptosis. There were no significant differences ( $P > 0.05$ ) before and after FO supplementation for U937 cells treated with either 25-hydroxycholesterol or camptothecin, regardless of which measure of apoptosis was used. This suggests that the apoptotic response of the U937 cells was similar even when measures were separated by the 5-wk supplementation interval.

Two statistical assessments of the data were performed. One was to determine if the extent of apoptosis was influenced by the length of time that LDL was oxidized. This comparison was made separately for the samples obtained before and after supplementation with FO. The second evaluation was to determine if the supplementation with FO influenced the extent of apoptosis induced by LDL after the LDL was oxidized for a defined time.

**Influence of length of time that LDL was oxidized on extent of apoptosis.** For all three measures of apoptosis, oxidation of LDL increased the extent of apoptosis (Fig. 3). Both before and after supplementation with FO, the activity of caspase-3 was higher in cells treated with LDL oxidized for 6 or 10 h compared to cells treated with nLDL ( $P = 0.0001$  in all comparisons except for cells treated with LDL oxidized for 6 h after FO supplementation, where it was 0.0324). However, although



**FIG. 1.** FA concentration in LDL before (open bars) and after (solid bars) supplementation with fish oil. Data are least square means (LSM)  $\pm$  SEM. Bars with different letters above them for each FA are significantly different,  $P \leq 0.05$ .

TABLE 1

Lag Time, Rate of Formation of Conjugated Dienes, and Maximum Production of Conjugated Dienes in LDL Before and After Supplementation with Fish Oil<sup>a</sup>

	Lag time (min)	Maximum rate (nmol/mg LDL protein/min)	Maximum production (nmol/mg LDL protein)
Before FO	140 ± 2	1.87 ± 0.08	186 ± 17
After FO	108 ± 2	1.17 ± 0.08	171 ± 17
Before FO vs. after FO ( <i>P</i> values) <sup>b</sup>	0.0002	0.0032	0.5749

<sup>a</sup>Least square means (LSM) ± SEM calculated for triplicate determinations made from three independent experiments.

<sup>b</sup>*P* value from two-sample *t*-test.

the activity of caspase-3 was higher in the cells treated with LDL oxidized for 10 h compared to those treated with LDL oxidized for 6 h before supplementation with FO ( $P = 0.0001$ ), its activity was statistically equivalent in those cells treated with LDL oxidized for 6 and 10 h after supplementation with FO.

In using the Annexin V assay, both before and after supplementation with FO, the percentage of apoptotic cells was higher in cells treated with LDL oxidized for 6 and 10 h ( $P = 0.0001$ ) compared to cells treated with nLDL. However, in contrast to the caspase-3 assay, the extent of apoptosis was significantly higher in the cells treated with LDL oxidized for 10 h compared to LDL oxidized for 6 h both before ( $P = 0.0001$ ) and after FO supplementation ( $P = 0.0033$ ).

In using the DAPI staining assay both before and after FO supplementation, the percentage of apoptotic cells was higher in cells treated by LDL oxidized for 10 h compared to cells treated with nLDL ( $P = 0.0001$ ).

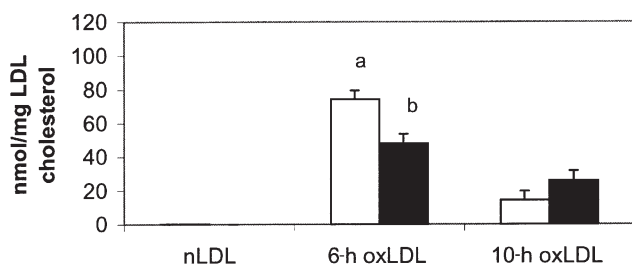
**Influence of FO supplementation on extent of apoptosis.** Apoptosis induced by oxLDL, regardless of assay used, was decreased by FO supplementation. The activity of caspase-3 in U937 cells treated with LDL oxidized for 6 and 10 h after supplementation with FO was reduced by 13 ( $P = 0.0053$ ) and 22% ( $P = 0.0001$ ), respectively, compared to treatment with LDL oxidized for the same length of time but obtained before

supplementation with FO (Fig. 3A). On the basis of the Annexin V assays, only after the LDL had been oxidized for 10 h was a significant difference measured in the extent of apoptosis before and after FO supplementation. It was 30% lower ( $P < 0.0001$ ) in U937 cells treated with EPA/DHA-rich LDL compared to EPA/DHA-non-rich LDL oxidized for 10 h (Fig. 3B). Results from the DAPI staining assays showed a 61% reduction ( $P = 0.0001$ ) in apoptosis for U937 cells treated with LDL oxidized for 10 h after FO supplementation compared to before supplementation (Fig. 3C).

## DISCUSSION

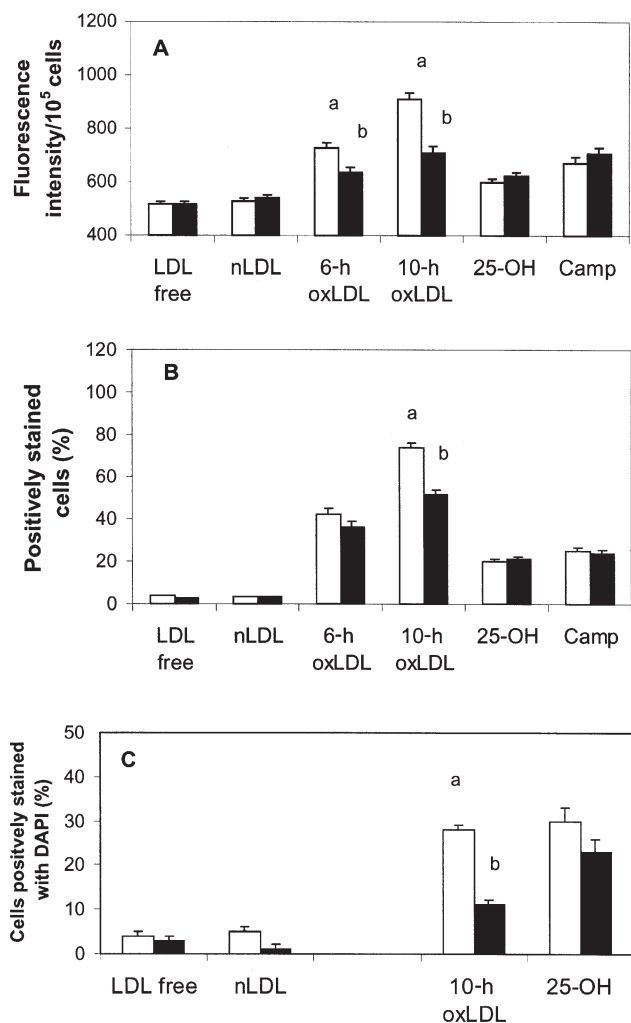
Apoptotic vascular cells have been found in atherosclerotic lesions (2–4). Since oxLDL has been reported to induce apoptosis of endothelial cells (12,13), smooth muscle cells and fibroblasts (14), and macrophages (15,16) *in vitro*, it may be a candidate for the induction of apoptosis of vascular cells *in vivo*. The oxidized lipids in oxLDL are thought to be responsible for apoptosis. Thus, events that modify the bioactive lipid profile of oxLDL may affect its ability to induce apoptosis. We showed in this study and previously (24,34) that LDL enriched with EPA and DHA has the intuitively predicted shorter lag time, suggesting increased oxidative susceptibility, but a paradoxical decrease in rate of formation of conjugated dienes, suggesting decreased oxidative susceptibility. The explanation that we have offered is that bicycloendoperoxides are formed in the presence of EPA and DHA and that they rapidly migrate to the surface of the LDL particle because of their polarity. Thus, since radicals are removed from the system, the rate of the propagation is slowed. These reactions would alter the lipid entities present in oxLDL that would induce apoptosis. Thus, the purpose of this study was to determine if EPA/DHA-rich oxLDL, obtained after FO supplementation, altered the extent of apoptosis as compared to the LDL obtained prior to FO supplementation. Several standard apoptotic markers were used to provide a better confirmation of apoptosis. The results showed that oxLDL induced apoptosis in U937 cells, as characterized by the activation of caspase-3, translocation of PS, and chromatin condensation and nuclear fragmentation. However, LDL obtained after supplementation with FO and then oxidized induced less apoptosis than LDL obtained before supplementation with FO.

LDL enriched with EPA/DHA and oxidized for 10 h in-



**FIG. 2.** Lipid peroxidation before (open bars) and after (solid bars) supplementation with fish oil as indicated by the concentration of cholesterol ester hydroperoxides in LDL. Each of the labels on the x-axis are defined as follows: nLDL, native LDL, is the LDL sample before any oxidation has occurred; 6-h oxLDL represents LDL oxidized for 6 h with copper; 10-h oxLDL represents LDL oxidized for 10 h. Data are least square means (LSM) ± SEM. Bars with different letters above them at each time for LDL oxidation are significantly different,  $P \leq 0.05$ .

duced significantly less apoptosis in U937 cells by all three measures used. However, when the U937 cells were treated with LDL oxidized for 6 h, the decrease was significant only



**FIG. 3.** Measurement of apoptosis in U937 cells induced by LDL. Cells were incubated with nLDL; 6-h oxLDL; and 10-h oxLDL. Cells were incubated without LDL (free LDL) as a negative control. They were incubated with 25-hydroxycholesterol (25-OH) or camptothecin (Camp) as positive controls. Two statistical assessments of the data were performed. One was to determine if the extent of apoptosis was influenced by the length of time that the LDL was oxidized. This comparison is discussed in the text. The second evaluation was to determine if the supplementation with fish oil influenced the extent of apoptosis induced by LDL oxidized for a defined length of oxidation (open bars, before supplementation with fish oil; solid bars, after supplementation). The results from this comparison are represented here. (A) Measurement of activity of caspase-3. The activity of caspase-3 was expressed as fluorescence intensity per 10<sup>5</sup> cells. (B) Measurement of U937 cells positively stained with Annexin V–fluorescein isothiocyanate (FITC), negatively stained with propidium iodide. Data are displayed as the percentage of 10<sup>4</sup> cells stained with Annexin V–FITC. (C) Measurement of 4,6-diamidino-2-phenylindole (DAPI) staining of U937 cells. Apoptotic cells were characterized by a bright blue nucleus and condensed and fragmented chromatin. Data are least square means (LSM)  $\pm$  SEM. Bars with different letters above them have a significant effect produced by the fish oil supplementation,  $P \leq 0.05$ . For other abbreviations see Figure 2.

when measured by caspase-3 activity. Caspase-3 causes the proteolysis of several substrates (39) and thereby brings about the characteristic morphological changes seen in apoptosis, such as the alteration of the cellular membranes and nuclei (40). Thus, the activation of caspase-3 occurs before the translocation of PS, chromatin condensation, or nuclear fragmentation. That the EPA/DHA-rich LDL oxidized for a shorter period of time (6 h) did not cause significant differences in the changes of the translocation of PS suggests that the changes in translocation of PS induced by the presence of these FA may require the activation of caspase-3 and occur after the activation of caspase-3 (41). It does not eliminate the possibility that other pathways are also associated with the translocation of PS and are triggered by oxLDL containing EPA/DHA. The release of cytochrome *c* from mitochondria (21), the activation of caspase-8 (22) and caspase-3 (13,15,21), and an increase in cellular calcium concentrations (23) all have been implicated in oxLDL-induced cell apoptosis. Whether they work together with caspase-3 or independently is not known.

Although the extent of apoptosis was higher in the cells treated with LDL oxidized for 10 h than LDL oxidized for 6 h, the concentration of CEOOH was higher in the LDL oxidized for 6 h than that in LDL oxidized for 10 h. This divergence suggests that CEOOH were not the causative agents. In this study, the concentration of conjugated dienes reached its maximum value after approximately 5 h of oxidation. It is well-established (35) that by the time the concentration of conjugated dienes plateaus, secondary oxidation products have begun to form. However, since secondary oxidation products were not measured in this study, it cannot be concluded that they were the causative factor.

The suggestion that the CEOOH generated by oxLDL were not responsible for mediating cell apoptosis is indirectly supported by Lizard *et al.* (19) and Harada-Shiba *et al.* (13). Both of these groups of investigators showed that oxysterols induced apoptosis in smooth muscle and endothelial cells. Liu *et al.* (18) also showed that a different form of secondary products, i.e., 4-hydroxynonenal, induced apoptosis in smooth muscle cells. However, Siow *et al.* (14) reported more apoptotic events in smooth muscle cells at the point of greatest lipid hydroperoxide production compared with secondary lipid oxidation products, i.e., aldehydes and ketones. The divergence among the above findings may reflect differences in the degree of LDL oxidation and/or the fact that a thorough evaluation of secondary oxidation products was not done.

A strength of this study is that the concentration of lipid hydroperoxides, CEOOH, was measured directly *via* HPLC with an isoluminol-dependent chemiluminescence detection method. This is among the most sensitive methods for detecting lipid hydroperoxides directly, rather than their presence being inferred, as is done with other measures. It clearly showed CEOOH was not the major compound responsible for apoptosis.

In conclusion, we have demonstrated that enrichment of oxLDL with EPA/DHA, obtained after supplementing a



human with FO, protected U937 cells against oxLDL-induced apoptosis and was not related to the concentration of CEOOH. However, the oxLDL used in these studies may not simulate oxLDL *in vivo*. Thus, the relevance of the data collected in this study to explain the bioactivity of oxLDL *in vivo* is unknown. Although copper is frequently used to mediate LDL oxidation, it may not be a physiologically relevant initiator for LDL oxidation. LDL oxidized *ex vivo* with copper may provide insight into the impact on the oxidation of LDL and vascular walls *in vivo* that occurs when individuals consume diets rich in EPA and DHA. This study suggests that an increased concentration of EPA/DHA in LDL may influence its oxidative susceptibility and subsequent pathology and that the major compounds responsible for apoptosis are not CEOOH.

## ACKNOWLEDGMENTS

This study was supported in part by the North Carolina Agriculture Experimental Station and the Linus Pauling Institute (Corvallis, OR). We would like to thank Dr. George Loo in the Department of Nutrition and Foodservice Systems at the University of North Carolina at Greensboro and Dr. Mark L. Failla in the Department of Human Nutrition and Foodservice Management at the Ohio State University for their invaluable advice.

## REFERENCES

- Stehbens, W.E. (2000) The Significance of Programmed Cell Death or Apoptosis and Matrix Vesicles in Atherogenesis, *Cell. Mol. Biol.* 46, 99–110.
- Björkerud, S., and Björkerud, B. (1996) Apoptosis Is Abundant in Human Atherosclerotic Lesions, Especially in Inflammatory Cells (macrophages and T cells), and May Contribute to the Accumulation of Gruel and Plaque Instability, *Am. J. Pathol.* 149, 367–380.
- Han, D.K.M., Haudenschild, C.C., Hong, M.K., Tinkle, B.T., Leon, M.B., and Liau, G. (1995) Evidence for Apoptosis in Human Atherogenesis and in a Rat Vascular Injury Model, *Am. J. Pathol.* 147, 267–277.
- Mitchinson, M.J., Hardwick, S.J., and Bennett, M.R. (1996) Cell Death in Atherosclerotic Plaques, *Curr. Opin. Lipidol.* 7, 324–329.
- Hegy, L., Skepper, J.N., Cary, N.R., and Mitchinson, M.J. (1996) Foam Cell Apoptosis and the Development of the Lipid Core of Human Atherosclerosis, *J. Pathol.* 180: 423–429.
- Isner, J.M., Kearney, M., Bortman, S., and Passeri, J. (1995) Apoptosis in Human Atherosclerosis and Restenosis, *Circulation* 91, 2703–2711.
- Ball, R.Y., Stowers, E.C., Burton, J.H., Cary, N.R., Skepper, J.N., and Mitchinson, M.J. (1995) Evidence That the Death of Macrophage Foam Cells Contributes to the Lipid Core of Atheroma, *Atherosclerosis* 114: 45–54.
- Hegy, L., Hardwick, S.J., Siow, R.C., and Skepper, J.N. (2001) Macrophage Death and the Role of Apoptosis in Human Atherosclerosis, *J. Hematother. Stem Cell. Res.* 10, 27–42.
- Kockx, M.M., and Knaapen, M.W. (2000) The Role of Apoptosis in Vascular Disease, *J. Pathol.* 190, 267–280.
- Witztum, J.L., and Steinberg, D. (1991) Role of Oxidized LDL in Atherogenesis, *J. Clin. Invest.* 88, 1785–1792.
- Berliner, J.A., and Heinecke, J.W. (1996) The Role of Oxidized Lipoproteins in Atherosclerosis, *Free Radic. Biol. Med.* 20, 707–727.
- Dimmeler, S., Haendeler, J., Galle, J., and Zeiher, A.M. (1997) Oxidized Low-Density Lipoprotein Induces Apoptosis of Human Endothelial Cells by Activation of CPP32-like Proteases. A Mechanistic Clue to the ‘Response to Injury’ Hypothesis, *Circulation* 95, 1760–1763.
- Harada-Shiba, M.K., Kinoshita, M.K., Kamido, H.S., and Shimokado, K.T. (1998) Oxidized Low Density Lipoprotein Induces Apoptosis in Cultured Human Umbilical Vein Endothelial Cells by Common and Unique Mechanisms, *J. Biol. Chem.* 273, 9681–9687.
- Siow, R.C., Richards, J.P., Pedley, K.C., Leake, D.S., and Mann, G.E. (1999) Vitamin C Protects Human Vascular Smooth Muscle Cells Against Apoptosis Induced by Moderately Oxidized LDL Containing High Levels of Lipid Hydroperoxides, *Arterioscler. Thromb. Vasc. Biol.* 19, 2387–2394.
- Wintergerst, E.S., Jelk, J., Rahner, C., and Asmis, R. (2000) Apoptosis Induced by Oxidized Low Density Lipoprotein in Human Monocyte-Derived Macrophages Involves CD36 and Activation of Caspase-3, *Eur. J. Biochem.* 267, 6050–6059.
- Hardwick, S.J., Hegyi, L., Clare, K., Law, N.S., Carpenter, K.L., Mitchinson, M.J., and Skepper, J.N. (1996) Apoptosis in Human Monocyte-Macrophages Exposed to Oxidized Low Density Lipoprotein, *J. Pathol.* 179, 294–302.
- Wang, T.G., Gotoh, Y., Jennings, M.H., Rhoads, C.A., and Aw, T.Y. (2000) Lipid Hydroperoxide-Induced Apoptosis in Human Colonic CaCo-2 Cells Is Associated with an Early Loss of Cellular Redox Balance, *FASEB J.* 14, 1567–1576.
- Liu, W., Kato, M., Akhand, A.A., Hayakawa, A., Suzuki, H., Miyata, T., Kurokawa, K., Hotta, Y., Ishikawa, N., and Nakashima, I. (2000) 4-Hydroxynonenal Induces a Cellular Redox Status-Related Activation of the Caspase Cascade for Apoptotic Cell Death, *J. Cell. Sci.* 113, 635–641.
- Lizard, G., Monier, S., Cordelet, C., Gesquiere, L., Deckert, V., Guedry, S., Lagrost, L., and Gambert, P. (1999) Characterization and Comparison of the Mode of Cell Death, Apoptosis Versus Necrosis, Induced by 7 $\beta$ -Hydroxycholesterol and 7-Ketocholesterol in the Cells of the Vascular Wall, *Arterioscler. Thromb. Vasc. Biol.* 19, 1190–2000.
- Spyridopoulos, I., Wischhusen, J., Rabenstein, B., Mayer, P., Axel, D.I., Frohlich, K.U., and Karsch, K.R. (2001) Alcohol Enhances Oxysterol-Induced Apoptosis in Human Endothelial Cells by a Calcium-Dependent Mechanism, *Arterioscler. Thromb. Vasc. Biol.* 21, 439–444.
- Yang, L., and Sinensky, M.S. (2000) 25-Hydroxycholesterol Activates a Cytochrome *c* Release-Mediated Caspase Cascade, *Biochem. Biophys. Res. Commun.* 278, 557–563.
- Lee, T., and Chau, L. (2001) Fas/Fas Ligand-Mediated Death Pathway Is Involved in OxLDL-Induced Apoptosis in Vascular Smooth Muscle Cells, *Am. J. Cell. Physiol.* 280, C709–C718.
- Vieira, O., Escargueil-Blanc, I., Meilhac, O., Basile, J.P., Laranjinha, J., Almeida, L., Salvayre, R., and Negre-Salvayre, A. (1998) Effect of Dietary Phenolic Compounds on Apoptosis of Human Cultured Endothelial Cells Induced by Oxidized LDL, *Br. J. Pharmacol.* 123: 565–573.
- Higdon, J.V., Du, S.H., Lee, Y.S., Wu, T., and Wander, R.C. (2001) Supplementation of Postmenopausal Women with Fish Oil Does Not Increase Overall Oxidation of LDL *ex vivo* Compared to Dietary Oils Rich in Oleate and Linoleate, *J. Lipid Res.* 42, 407–418.
- Suarna, C., Dean, R.T., May, J., and Stocker, R. (1995) Human Atherosclerotic Plaque Contains Both Oxidized Lipids and Relatively Large Amounts of  $\alpha$ -Tocopherol and Ascorbate, *Arterioscler. Thromb. Vasc. Biol.* 15, 1616–1624.
- Song, J., and Wander, R.C. (1991) Effects of Dietary Selenium and Fish Oil (MaxEPA) on Arachidonic Acid Metabolism and Hemostatic Function in the Rat, *J. Nutr.* 121, 284–292.
- Wander, R.C., and Patton, B.D. (1991) Lipids and Fatty Acids



- of Three Species of Northeast Pacific Finfish Harvested in Summer, *Food Composition Anal.* 4, 128–135.
28. Arnaud, J., Fortis, I., Blachier, S., Kia, D., and Favier, A. (1991) Simultaneous Determination of Retinol,  $\alpha$ -Tocopherol and  $\beta$ -Carotene in Serum by Isocratic High-Performance Liquid Chromatography, *J. Chromatogr.* 572, 103–116.
  29. Wander, R.C., Du, S.H., and Thomas, D.R. (1998) Influence of Long-Chain Polyunsaturated Fatty Acids on Oxidation of Low Density Lipoprotein, *Prostaglandins Leukotrienes Essent. Fatty Acids* 59, 143–151.
  30. Marz, W., and Gross, W. (1986) Analysis of Plasma Lipoproteins by Ultracentrifugation in a New Fixed Angle Rotor: Evaluation of a Phosphotungstic Acid/MgCl<sub>2</sub> Precipitation and a Quantitative Lipoprotein Electrophoresis Assay, *Clin Chim. Acta* 160, 1–18.
  31. Friedewald, W.T., Levy, R.I., and Fredrickson, D.S. (1972) Estimation of the Concentration of Low-Density Lipoprotein Cholesterol in Plasma, Without Use of the Preparative Ultracentrifuge, *Clin. Chem.* 18, 499–502.
  32. Chung, B.H., Segrest, J.P., Ray, M.J., Brunzell, J.D., Hokanson, J.E., Krauss, R.M., Beaudrie, K., and Cone, J.T. (1986) Single Vertical Spin Density Gradient Ultracentrifugation, *Methods Enzymol.* 128, 181–209.
  33. Chen, C., and Loo, G. (1995) Cigarette Smoke Extract Inhibits Oxidative Modification of Low Density Lipoprotein, *Atherosclerosis* 112, 177–185.
  34. Wander, R.C., Du, S.-H., Ketchum, S.O., and Rowe, K.E. (1996) Interaction of Vitamin E and Fish Oil on LDL Oxidation in Postmenopausal Women With and Without Hormone Replacement Therapy, *Am. J. Clin. Nutr.* 63, 184–193.
  35. Esterbauer, H., Striegl, G., Puhl, H., and Rotheneder, M. (1989) Continuous Monitoring of *in vitro* Oxidation of Human Low Density Lipoprotein, *Free Radic. Res. Commun.* 6, 67–75.
  36. Stennicke, H.R., and Salvesen, G.S. (1997) Biochemical Characteristics of Caspases-3, -6, -7, and -8, *J. Biol. Chem.* 272, 25719–25723.
  37. Martin, S.J., Reutelingsperger, C.P., McGahon, A.J., Rader, J.A., van Schie, R.C., LaFace, D.M., and Green, D.R. (1995) Early Redistribution of Plasma Membrane Phosphatidylserine Is a General Feature of Apoptosis Regardless of the Initiating Stimulus: Inhibition by Overexpression of Bcl-2 and Abl, *J. Exp. Med.* 182, 1545–1556.
  38. Ramsey, F., and Schafer, D. (1999) *Statistical Sleuth: A Course in Methods of Data Analysis*, Duxbury Press, Boston.
  39. Kuida, K., Haydar, T.F., Kuan, C.Y., Gu, Y., Taya, C., Karasuyama, H., Su, M.S., Rakic, P., and Flavell, R.A. (1998) Reduced Apoptosis and Cytochrome *c*-Mediated Caspase Activation in Mice Lacking Caspase 9, *Cell* 94, 325–337.
  40. Song, Z., and Steller, H. (1999) Death by Design: Mechanism and Control of Apoptosis, *Trends Cell Biol.* 9, M49–M52.
  41. Belloc, F., Belaud-Rotureau, M.A., Lavignolle, V., Bascans, E., Braz-Pereira, E., Durrieu, F., and Lacombe, F. (2000) Flow Cytometry Detection of Caspase 3 Activation in Preapoptotic Leukemic Cells, *Cytometry* 40, 151–160.

[Received October 29, 2001, and in final revised form August 9, 2002; revision accepted August 22, 2002]

# Eicosapentaenoic Acid Promotes Apoptosis in Ramos Cells *via* Activation of Caspase-3 and -9

Hilde Heimli<sup>a</sup>, Camilla Giske<sup>a</sup>, Soheil Naderi<sup>b</sup>, Christian A. Drevon<sup>a,\*</sup>, and Kristin Hollung<sup>a</sup>

<sup>a</sup>Institute for Nutrition Research and <sup>b</sup>Institute for Medical Biochemistry, University of Oslo, Norway

**ABSTRACT:** Eicosapentaenoic acid (EPA; 20:5n-3) may reduce the cell number in cultured leukemia/lymphoma cells owing to reduced cell proliferation, induction of cell death, or a combination of these processes. EPA has been shown to promote apoptosis in Ramos cells, and our present study was focused on a possible cell cycle arrest and the pathways by which the apoptotic process is induced. Apoptosis may proceed along the intrinsic (mitochondrial) or the extrinsic (death receptor) pathway, which are mediated *via* different caspases. Caspases are a class of homologous cysteine proteases recognized as pivotal mediators of apoptosis. We investigated whether EPA affects progression of the cell cycle or promotes apoptosis directly. By incorporation of [<sup>3</sup>H]thymidine and [<sup>3</sup>H]valine, we showed that DNA, as well as protein synthesis, was reduced after incubation of Ramos cells with EPA for 6 h. We monitored cell cycle distribution by 5-bromo-2'-deoxyuridine staining and observed no cell cycle arrest in the EPA-incubated cells. Incubation of cells with EPA caused PS-flipping, as demonstrated by annexin V-binding (flow cytometry), and cleavage of poly(ADP-ribose) polymerase measured by Western blot analysis. Furthermore, we observed increased activity of caspase-3 and -9, but not of caspase-8. Whereas inhibitors of caspase-3 and -9 reduced EPA-induced apoptosis, inhibition of caspase-8 did not. This suggests that EPA may promote apoptosis *via* the intrinsic pathway in Ramos cells. Thus, the reduction in cell number can be explained by a direct apoptotic effect of EPA rather than *via* cell cycle arrest.

Paper no. L9077 in *Lipids* 37, 797–802 (August 2002).

Cancer is a major cause of morbidity and mortality in developed societies. Observations in several cancer cell lines, animal models, and epidemiological studies suggest that n-3 PUFA may decrease cell proliferation and viability of cancer cells (1–6). We have previously reported that EPA induces apoptosis in Ramos cells and necrosis in Raji cells (7). The necrotic death mode is associated with oxidative stress as evaluated by an enhanced level of superoxide anion and by the protective effect of different antioxidants, whereas antioxidants had no protective effect on apoptotic cell death. We have also observed that n-3 as well as n-6 PUFA cause reduced

cell numbers after 48–72 h incubation in several leukemia/lymphoma cell lines (3,7). The reason for diminished cell numbers might be due to reduced cell proliferation, induction of cell death, or a combination of these processes. Albino and coworkers (1) have shown that PUFA-induced reduction in cell number corresponds with cell cycle arrest in malignant melanoma cell lines.

Apoptosis was first described by Kerr and coworkers in 1972 (8) and is characterized by cell shrinkage, membrane blebbing, chromatin condensation, and fragmentation of DNA. Repression of apoptosis is one of the main underlying problems in the development of cancer, and disruption of the apoptotic program can promote tumor initiation, progression, and resistance to treatment (9). The two major apoptotic pathways in mammalian cells use different initiator caspases in response to stimuli. Members of the death receptor superfamily, such as CD95R and tumor necrosis factor receptor, trigger the extrinsic pathway (10–12). Binding of ligand to the death receptors then induces formation of the death-inducing signaling complex, which recruits procaspase-8, leading to activation of initiator caspase-8. The other major apoptotic pathway is the intrinsic pathway (13,14), which is activated in response to other extracellular signals and intracellular insults such as DNA damage. Pro- and anti-apoptotic Bcl-2-like proteins may be located in the mitochondrial membrane, where they compete to regulate exit of cytochrome c (15,16). Excess of pro-apoptotic molecules causes release of cytochrome c, which is necessary for activation of caspase-9. The extrinsic and intrinsic pathways converge by activation of caspase-3. Downstream of caspase-3, the apoptotic pathway branches into a multitude of subpathways, which *in vivo* results in the ordered dismantling and removal of the cell (17). One of the first proteins identified as being cleaved by caspase-3 during apoptosis was poly(ADP-ribose) polymerase (PARP) (18). PARP is a nuclear enzyme that binds to DNA ends and catalyzes adenosine 5'-diphosphate (ADP)-ribosylation of nuclear proteins to facilitate DNA repair. PARP is cleaved at a single site by caspase-3, causing formation of a small fragment containing the DNA-binding domain and an 89 kDa catalytic domain (19). The small fragment retains its DNA-binding capacity, and by competing with full-length PARP for binding it prevents the repair enzymes from accessing damaged DNA (20).

In the present study, we observed apoptotic events in the lymphoma cell line Ramos as early as 4 h after addition of

\*To whom correspondence should be addressed at Institute for Nutrition Research, University of Oslo, P.O. Box 1046, Blindern, 0316 Oslo, Norway.  
E-mail: c.a.drevon@basalmed.uio.no

Abbreviations: AnV, annexin V; BrdU, 5-bromo-2'-deoxyuridine; FACS, fluorescence-activated cell sorter; FCS, fetal calf serum; FITC, fluorescein isothiocyanate; HO342, Hoechst 33342; HRP, horseradish peroxidase; PARP, poly(ADP-ribose) polymerase; PI, propidium iodide.

EPA. This is shown by activation of caspase-9 and caspase-3, followed by cleavage of PARP. However, no cell cycle arrest was detected. Our study provides new insight into the primary mechanisms by which a specific EFA promotes apoptosis.

## MATERIALS AND METHODS

**Materials.** EPA, FA-free BSA, propidium iodide (PI), Hoechst 33342 (HO342), 5-bromo-2'-deoxyuridine (BrdU), cytochrome c, L-glutamine, streptomycin/penicillin, and staurosporine were purchased from Sigma Chemical Co. (St. Louis, MO). PBS, RPMI-1640, and fetal calf serum (FCS) were from BioWhittaker (Walkersville, MD). Fujichrome Provia 400 professional color reversal film was supplied by Fuji (Tokyo, Japan). The In Situ Cell Death Detection Kit, Fluorescein, was purchased from Boehringer Mannheim (Mannheim, Germany). Bicinchoninic acid Protein Assay Reagent was bought from Pierce (Rockford, IL). Fluorescein isothiocyanate (FITC)-labeled anti-BrdU and annexin V (AnV) were from BD PharMingen (San Diego, CA). Cleaved PARP (Asp214) antibody (Human Specific) and anti-rabbit IgG secondary antibody [horseradish peroxidase (HRP)-conjugated] for Western blot analysis were obtained from Cell Signaling (Beverly, MA). ECL Plus Western blotting detection reagents were bought from Amersham Biosciences (Piscataway, NJ). Caspase-9 inhibitor (Z-LEHD-FMK), caspase-3 inhibitor (Z-DEVD-FMK), and caspase-8 inhibitor (Z-IETD-FMK) were purchased from R & D Systems Inc. (Minneapolis, MN). Polyacrylamide gels were bought from Bio-Rad Laboratories (Hercules, CA). Nitrocellulose membranes were purchased from Schleicher & Schuell (Dassel, Germany). Other chemicals were of analytical grade from commercial suppliers.

**Cell cultures.** Ramos and Jurkat cells were purchased from BioWhittaker. The cell lines were cultured in RPMI medium supplemented with 10% heat-inactivated FCS, L-glutamine (2 mM), and streptomycin/penicillin (0.1 mg/mL). Cells were incubated with FA complexed to FA-free BSA at a molar ratio of 2.5:1, whereas control cells were incubated with FA-free BSA. FA-BSA complexes were added to cells immediately prior to seeding the cells in 96-well plates. Cells were routinely kept in logarithmic growth at  $0.3\text{--}1.2 \times 10^6$  cells/mL. For experiments, cells were seeded at a density of  $0.3 \times 10^6$  cells/mL.

**Incorporation of [ $^3\text{H}$ ]thymidine and [ $^3\text{H}$ ]valine.** For measurement of DNA and protein synthesis, 200  $\mu\text{L}$  of Ramos cell suspension ( $0.6 \times 10^6$  cells) was incubated in the absence or presence of 30  $\mu\text{M}$  EPA in 96-well microtiter plates from Costar (Cambridge, MA). For the last 60 min of incubation, 0.5  $\mu\text{Ci}$  [ $^3\text{H}$ ]thymidine or [ $^3\text{H}$ ]valine was added to each well. Cells were harvested and ice-cold ethanol was added to the [ $^3\text{H}$ ]thymidine-incubated cells, whereas 10% trichloroacetic acid was added to the [ $^3\text{H}$ ]valine-incubated cells. The precipitates were resuspended in 200  $\mu\text{L}$  0.2 M NaOH or 70 mM SDS with 10% Triton X-100. Cell lysates (100  $\mu\text{L}$ ) were then counted in a scintillation counter.

**DNA staining with PI and HO342.** For microscopic analyses of cell viability, 1 mL of the cell cultures was first incubated with 10  $\mu\text{L}$  of PI (0.5 mg/mL) in the dark for 20 min. Thereafter, 10  $\mu\text{L}$  of HO342 (1 mg/mL) was added to the same cultures and incubated for another 20 min in the dark. After staining, the cell pellets were resuspended in 10  $\mu\text{L}$  of FCS. Drops of the cell suspensions were placed on a microscope slide and air-dried before at least 200 cells were counted in a Leitz Ortholux II fluorescence microscope (Leica, Wetzlar, Germany). The cells were photographed with an MPS 48/52 camera (Leica Mikroskopie und Systeme, Wetzlar, Germany). The film was exposed as 800 ISO but developed as 400 ISO.

**Cell cycle distribution.** For analysis of cell cycle distribution after incubation with EPA, Ramos cells were incubated with 10  $\mu\text{M}$  of BrdU for the last 60 min. Cells ( $3 \times 10^6$ ) were fixed in 70% ethanol, stored at  $-20^\circ\text{C}$ , and then digested in a suspension of 0.2% pepsin dissolved in 2 M HCl. After 30 min of incubation in the dark at room temperature, the HCl was neutralized by 0.1 M tetraborate (pH 8.5). The pellets were then washed in 10 mM HEPES buffer containing 4% FCS and 0.5% Tween-20. After incubation with FITC-anti-BrdU for 30 min, the pellets were resuspended in PBS to which were added 20  $\mu\text{g}/\text{mL}$  of PI and 40  $\mu\text{g}/\text{mL}$  of RNase A. The samples were filtered through a 30- $\mu\text{m}$  nylon mesh, and 10,000 cells were analyzed by flow cytometry (Becton Dickinson FACScan; Becton Dickinson, Franklin Lakes, NJ) to assess cell cycle distribution patterns (G0/G1, S, and G2/M phases).

**PS translocation.** AnV-FITC binding and PI staining were performed according to the recommended protocol, and the cells were analyzed by flow cytometry (Becton Dickinson FACScan). Briefly, aliquots of cells were washed in PBS, resuspended in binding buffer supplied by the manufacturer, and mixed with AnV-FITC and PI. After 5 min of incubation in the dark at room temperature, 10,000 cells at each time point were analyzed by flow cytometry. The percentage of AnV-positive cells was calculated based on the fraction of PI-negative cells. Each data point represents fluorescence analysis of  $10^4$  cells from three independent experiments.

**Immunoblot analysis of PARP degradation.** Cell lysates were prepared in a buffer containing 20 mM HEPES, 250 mM NaCl, 2 mM EDTA, 0.1% Nonidet P-40, 2  $\mu\text{g}/\text{mL}$  leupeptin, 2  $\mu\text{g}/\text{mL}$  aprotinin, 0.5  $\mu\text{g}/\text{mL}$  benzamidin, 1 mM DTT, and 1 mM PMSF. Cellular proteins (40  $\mu\text{g}/\text{mL}$ ) were separated on a 7.5% SDS/polyacrylamide gel and electrotransferred onto a nitrocellulose membrane. The membrane was probed with cleaved-PARP (Asp214) antibody, which detects only the large fragment of human PARP (89 kDa) produced by caspase cleavage, and then with anti-mouse antibody conjugated to HRP. Protein bands were detected by chemiluminescence (ECL-plus). The positive control was prepared from a Jurkat cell lysate, which was incubated with 4 mM  $\text{MgCl}_2$ , 10 mM KCl, 1 mM EGTA, 2 mM dATP, and 250  $\mu\text{g}/\text{mL}$  cytochrome c for 60 min at  $30^\circ\text{C}$ .

**Caspase activity assays.** Activity of the caspase-3, -8, and -9 cysteine proteases was determined by colorimetric activation

assays according to the manufacturer's protocol (R & D Systems Inc.). Ability of the cell lysate to cleave the reporter molecule was quantified spectrophotometrically at a wavelength of 405 nm using a microplate reader (Bio-Rad). The time-dependent change in absorbance at 405 nm was converted to caspase activity (pmol/h/ $\mu$ g of total protein) according to the manufacturer's protocol (Promega Corp., Madison, WI). Pure *p*-nitroaniline was used for a standard curve.

**Caspase-3, -8, and -9 inhibitors.** For inhibition of caspase-3, -8, and -9 activities, Ramos cells were incubated with 50  $\mu$ M Z-DEVD-FMK, 100  $\mu$ M Z-IETD-FMK, or 4  $\mu$ M Z-LEHD-FMK, respectively (21,22), in combination with EPA. After 24 h the cells were stained with PI and HO342 and harvested for microscopic analysis.

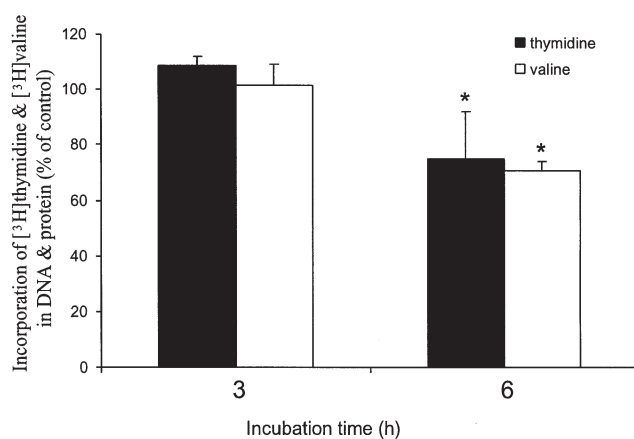
**Statistics.** Results are presented as means  $\pm$  SD. Unless otherwise specified, a Student's *t*-test analysis was used to determine the significance level of differences among sample groups, with a significance criterion of  $P \leq 0.05$ . All reported *P*-values are two sided.

## RESULTS

**EPA induces reduction in synthesis of DNA and proteins, but no cell cycle arrest.** Previously, we have reported that EPA reduced the number of Ramos cells after 48 h incubation (7). Before that time point, we could not detect any effect of EPA on cell numbers. To clarify the events preceding the reduction in cell number, we measured the synthesis of DNA and proteins. Ramos cells were incubated with 30  $\mu$ M EPA for 3 and 6 h and assessed for [ $^3$ H]thymidine incorporation into DNA or for [ $^3$ H]valine incorporation into proteins. Figure 1 shows that [ $^3$ H]thymidine- and [ $^3$ H]valine-incorporation were reduced by  $33 \pm 13$  and  $39 \pm 16\%$ , respectively, after 6 h incubation, whereas there were no significant changes after 3 h. Apoptosis was not observed after 3 or 6 h by staining with PI and HO342 (data not shown).

We have also previously performed dose-response experiments and found that up to a 24-h incubation period, there were marginal differences between 30 and 60  $\mu$ M EPA regarding cell numbers (7). Therefore, in all the following experiments, 60  $\mu$ M EPA was used. To examine whether the reduced incorporation of [ $^3$ H]thymidine and [ $^3$ H]valine was caused by cell cycle arrest, Ramos cells were incubated for 0, 3, 6, 9, and 12 h with EPA, stained with FITC-antiBrdU, and analyzed by fluorescence-activated cell sorter (FACS). At all time points, no significant effect on cell cycle distribution was observed (Table 1).

**EPA induces apoptosis via the intrinsic apoptotic pathway.** During the apoptotic process, PS is translocated from the inner to the outer leaflet of the plasma membrane. FITC-labeled AnV is a membrane-impermeable protein that binds to cells only if PS is present on the outer leaflet of the plasma membrane. To examine whether the reduced incorporation of [ $^3$ H]thymidine and [ $^3$ H]valine at 6 h could be explained by induction of apoptosis rather than by cell cycle arrest, we assayed Ramos cells incubated with EPA for AnV binding.



**FIG. 1.** DNA and protein synthesis. Incorporation of [ $^3$ H]thymidine and [ $^3$ H]valine was measured in Ramos cells incubated with 30  $\mu$ M EPA for 3 or 6 h. Data represent means  $\pm$  SD of incorporated [ $^3$ H]thymidine or [ $^3$ H]valine as the percentage of control in three separate experiments performed in triplicate. \* $P \leq 0.05$ .

FITC-AnV binding was significantly increased at 14 h and increased during further EPA incubation, with 25% AnV-positive cells appearing after 24 h (Fig. 2).

To further investigate the time point for onset of apoptosis, Ramos cells were incubated with EPA up to 24 h. We detected cleaved PARP in Ramos cells 8–24 h after adding EPA (Fig. 3). Thus, our observations indicated that PS-flipping occurred concomitantly with cleavage of PARP in Ramos cells incubated with EPA.

Because PARP is one of the downstream targets of caspase-3, we assayed EPA-supplemented Ramos cells for caspase-3 activity. Caspase-3 activity was detected 4 h after EPA supplementation and reached a maximum after 10 h (Fig. 4A). Caspases are synthesized as inactive enzymes, and once activated by proteolytic cleavage, the apoptotic processes are switched on. Caspase activity was not detected in control cells (data not shown).

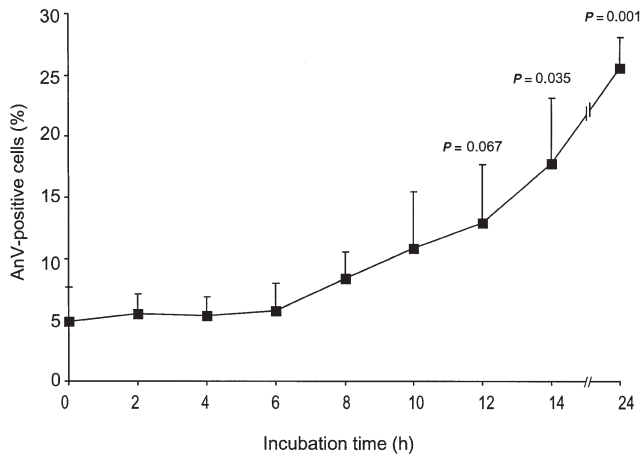
The activities of caspase-8 and -9 were assayed to elucidate whether EPA activates the extrinsic or the intrinsic pathway in Ramos cells. The cells were incubated with EPA for up to 24 h. Caspase-9 activity was first observed after 4 h incubation, and the activity was markedly above background for at least 12 h (Fig. 4B). Up to 24 h incubation, no significant activity of caspase-8 was observed (Fig. 4C). Jurkat cells incubated with 1  $\mu$ M staurosporine for 6 h were used as positive controls for caspase-8 activity (23). Our data indicate that EPA induces apoptosis *via* the intrinsic pathway rather than the extrinsic pathway in Ramos cells. To further challenge

**TABLE 1**  
Cell Cycle Distribution in Ramos Cells After 0–12 h of EPA Incubation<sup>a</sup>

	0 h	3 h	6 h	9 h	12 h
G0/G1	66.2 $\pm$ 4.4	66.2 $\pm$ 2.4	67.3 $\pm$ 6.6	69.6 $\pm$ 7.5	70.2 $\pm$ 4.3
S	22.5 $\pm$ 2.4	23.3 $\pm$ 2.9	21.9 $\pm$ 3.2	21.5 $\pm$ 2.2	19.6 $\pm$ 2.6
G2/M	11.3 $\pm$ 2.7	10.7 $\pm$ 3.2	10.9 $\pm$ 3.2	8.9 $\pm$ 6.2	10.4 $\pm$ 2.6

<sup>a</sup>Data represent means  $\pm$  SD from three separate experiments.



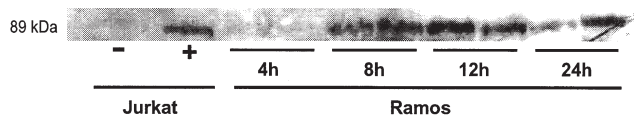


**FIG. 2.** EPA-induced PS translocation. Flipping of PS in Ramos cells incubated with 60  $\mu$ M EPA was measured by flow cytometry. Data represent the percentage of AnV-binding cells, given as means  $\pm$  SD from three separate experiments.

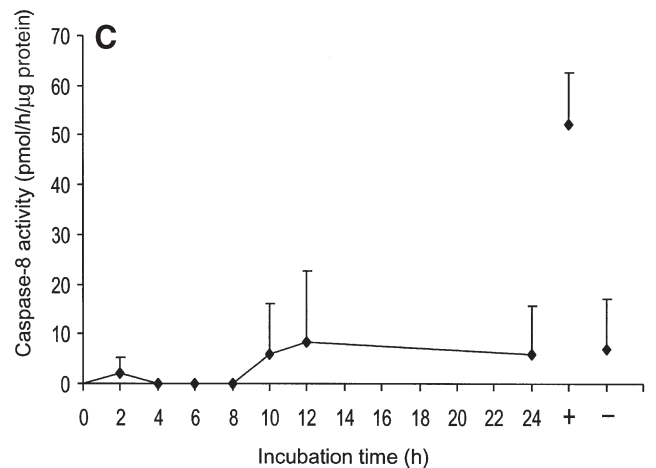
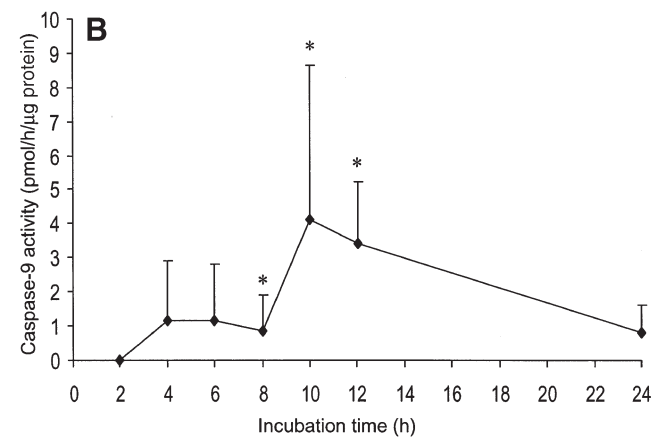
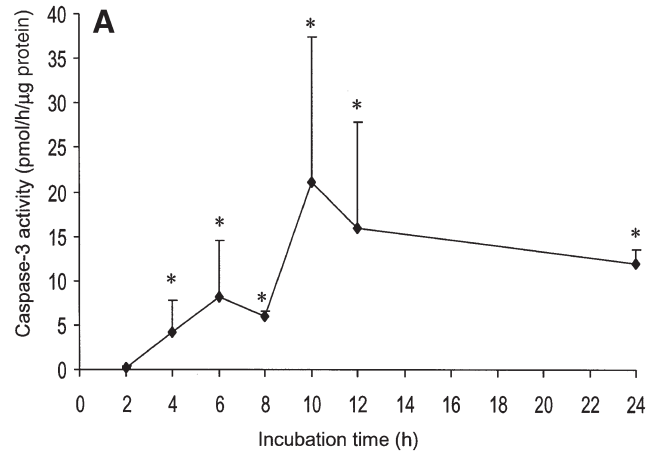
these findings, Ramos cells were incubated with specific inhibitors for caspase-9, caspase-3, or caspase-8 and exposed to EPA for 24 h. After 24 h incubation, EPA-induced apoptosis was microscopically detectable after staining with HO342 and PI (data not shown). Both caspase-9 and caspase-3 inhibitors significantly reduced EPA-induced apoptosis, whereas no significant reduction was observed by inhibition of caspase-8 (Fig. 5A). None of the applied inhibitors induced apoptosis *per se* (data not shown). The set of photographs shown in Figure 5B provides a qualitative impression of cell membrane integrity and nuclear structure. Staining with PI (red) indicates leaky plasma membranes since this dye cannot cross intact cell membranes. HO342, however, crosses intact as well as distorted plasma membranes and stains the nuclei in all cells (blue). When HO342 associates with condensed chromatin found in apoptotic cells, the blue color becomes more intense.

## DISCUSSION

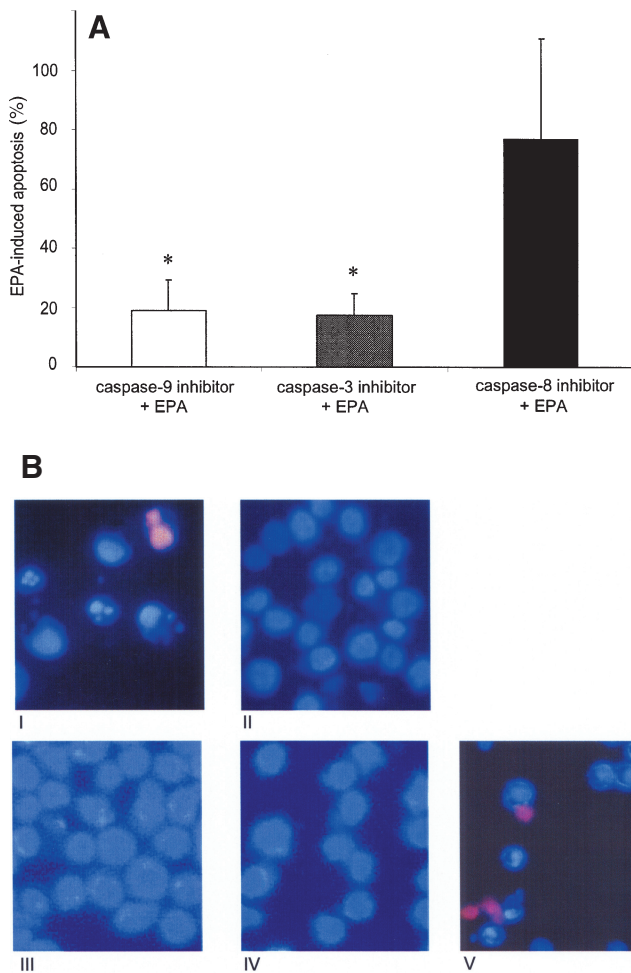
In the present study we have shown that EPA reduced cell numbers by induction of apoptosis *via* activation of caspases, rather than by causing cell cycle arrest in Ramos cells. Cas-



**FIG. 3.** Cleavage of poly(ADP-ribose) polymerase (PARP). Cells were incubated with 60  $\mu$ M of EPA for the indicated time points, lysed, and 100  $\mu$ g protein was loaded in each lane. Cleaved PARP (89 kDa fragment) was detected with anti-PARP polyclonal antibody. The lanes labeled with - and + refer to untreated and cytochrome c-treated (positive control) Jurkat cell lysate, respectively. Two individual parallels are shown for each time point. One of three experiments is presented.



**FIG. 4.** Caspase-3, -9, and -8 activity. Cells were incubated with 60  $\mu$ M EPA, and caspase activity was measured by a colorimetric assay as cleavage of the caspase-3 specific peptide DEVD-pNA (A), of the caspase-9 specific peptide LEHD-pNA (B), or of the caspase-8 specific peptide IETD-pNA (C). The lane labeled with + refers to staurosporine-treated Jurkat cells (1  $\mu$ M, 6 h), whereas the lane labeled - refers to untreated Jurkat cells. Data represent three separate experiments performed in duplicate (means  $\pm$  SD). A Mann-Whitney analysis was used to determine significance level of differences related to the zero time point, \* $P \leq 0.05$ .



**FIG. 5.** Effect of specific caspase inhibitors. Ramos cells were incubated for 24 h with 60  $\mu$ M of EPA and either 4  $\mu$ M of the caspase-9 inhibitor Z-LEHD-FMK, 50  $\mu$ M of the caspase-3 inhibitor Z-DEVD-FMK or 100  $\mu$ M of the caspase-8 inhibitor Z-IETD-FMK. Propidium iodide and Hoechst 33342 (HO342) associate with DNA and emit red and blue light, respectively, when exposed to UV light. Data are presented as the percentage of apoptotic cells induced by EPA (means  $\pm$  SD) and represent three separate experiments performed in duplicate  $*P \leq 0.05$  (A). One set of photographs is shown to provide qualitative information about cell viability after 24 h incubation with EPA (I), BSA control (II), or EPA in addition to caspase-9 inhibitor (III), caspase-3 inhibitor (IV), or caspase-8 inhibitor (V) (B).

pase-3 was significantly activated as early as 4 h after addition of EPA, which may explain the reduced synthesis of DNA and protein. We previously reported that 12 h incubation of 60  $\mu$ M EPA induced DNA fragmentation in Ramos cells ( $16 \pm 10\%$ , mean  $\pm$  SD), detected by the terminal deoxynucleotidyl transferase-mediated dUTP nick-end labeling (TUNEL) technique (3). To clarify early events during the induction of apoptosis, we assessed the effect of EPA on PS-flipping, which is suggested to be an early signal in the apoptotic process (24–26). We did not detect EPA-induced translocation of PS earlier than the previously observed DNA fragmentation monitored by TUNEL (3). This observation is in accordance with recent data from Span and coworkers (25),

showing that PS translocation is followed rapidly (within 1 h) by oligonucleosomal DNA fragmentation.

In addition to PS-flipping and DNA fragmentation, activation of caspases is of crucial importance in the apoptotic process. Usually, an active caspase molecule may activate an inactive procaspase by proteolytic cleavage. The downstream effector caspase-3 may be activated either by caspase-9 or caspase-8, representing the intrinsic and the extrinsic apoptotic pathways, respectively. The active form of caspase-9 is generated by association with a protein cofactor (Apaf), as well as cytochrome c (27), which may be released from the mitochondrial membrane by a Bcl-2-regulated process (15,28–30). To investigate by which pathway EPA initiates apoptosis in Ramos cells, we measured the activity of caspase-3 and caspase-9 and found that they were both activated, whereas caspase-8 activity was not significantly activated at any time point. We detected caspase-3 activated as early as 4 h after addition of EPA, and caspase-9 activity was also observed at 4 h, but no significant activation of caspase-9 was detected until 8 h. During the apoptotic process, caspase-3 activity increased relatively more than caspase-9 activity. Despite the statistically insignificant increase of caspase-9 activity at 4 h, we suggest that the activity is sufficient to transduce the apoptotic signal to the effector caspase-3. This would be in agreement with other observations reporting low activity of initiator caspases as compared to the activity of effector caspases (31–33). To challenge the involvement of the intrinsic, rather than the extrinsic, apoptotic pathway, we incubated Ramos cells with specific inhibitors of caspase-3, -8, and -9 in combination with EPA. The inhibitors of caspase-3 and -9 reduced the number of apoptotic cells toward the control level, whereas inhibition of caspase-8 did not. This is in agreement with increased caspase-3 and caspase-9 activities during EPA-induced apoptosis. Thus, our data indicate that EPA-induced apoptosis is mediated *via* the intrinsic apoptotic pathway rather than *via* the extrinsic pathway in Ramos cells. Based on our data we still cannot explain how EPA activates the first, most upstream caspases. Previous data from our laboratory have indicated that eicosanoids and reactive oxygen species are not involved in the EPA-induced reduction of Ramos cell proliferation (3,7,34). Further characterization of the initial mechanisms involved in EPA-induced apoptosis is important because PUFA might play a role in the prevention and treatment of certain types of cancer.

## ACKNOWLEDGMENTS

We thank Anne Randi Alvestad for excellent technical assistance, Hege Henriksen and Siv Kjølrsrud Bøhn for help with statistics and figures. This work was supported by grants from the Norwegian Cancer Society, Throne Holst Fond for Ernæringsforskning, Freia Medicinske Fond, and Eckbos Legat.

## REFERENCES

1. Albino, A.P., Juan, G., Traganos, F., Reinhart, L., Connolly, J., Rose, D.P., and Darzynkiewicz, Z. (2000) Cell Cycle Arrest and

- Apoptosis of Melanoma Cells by Docosahexaenoic Acid: Association with Decreased pRb Phosphorylation, *Cancer Res.* 60, 4139–4145.
2. Caygill, C.P., Charlett, A., and Hill, M.J. (1996) Fat, Fish, Fish Oil and Cancer, *Br. J. Cancer* 74, 159–164.
  3. Finstad, H.S., Myhrstad, M.C., Heimli, H., Lomo, J., Blomhoff, H.K., Kolset, S.O., and Drevon, C.A. (1998) Multiplication and Death-type of Leukemia Cell Lines Exposed to Very Long-Chain Polyunsaturated Fatty Acids, *Leukemia* 12, 921–929.
  4. Kaizer, L., Boyd, N.F., Kriukov, V., and Tritchler, D. (1989) Fish Consumption and Breast Cancer Risk: An Ecological Study, *Nutr. Cancer* 12, 61–68.
  5. Petrik, M.B., McEntee, M.F., Johnson, B.T., Obukowicz, M.G., and Whelan, J. (2000) Highly Unsaturated (n-3) Fatty Acids, but Not alpha-Linolenic, Conjugated Linoleic or gamma-Linolenic Acids, Reduce Tumorigenesis in Apc(Min/+) Mice, *J. Nutr.* 130, 2434–2443.
  6. Rao, C.V., Hirose, Y., Indranie, C., and Reddy, B.S. (2001) Modulation of Experimental Colon Tumorigenesis by Types and Amounts of Dietary Fatty Acids, *Cancer Res.* 61, 1927–1933.
  7. Heimli, H., Finstad, H.S., and Drevon, C.A. (2001) Necrosis and Apoptosis in Lymphoma Cell Lines Exposed to Eicosapentaenoic Acid and Antioxidants, *Lipids* 36, 613–621.
  8. Kerr, J.F., Wyllie, A.H., and Currie, A.R. (1972) Apoptosis: A Basic Biological Phenomenon with Wide-Ranging Implications in Tissue Kinetics, *Br. J. Cancer* 26, 239–257.
  9. Lowe, S.W., and Lin, A.W. (2000) Apoptosis in Cancer, *Carcinogenesis* 21, 485–495.
  10. Ashkenazi, A., and Dixit, V.M. (1998) Death Receptors: Signaling and Modulation, *Science* 281, 1305–1308.
  11. Salvesen, G.S., and Dixit, V.M. (1997) Caspases: Intracellular Signaling by Proteolysis, *Cell* 91, 443–446.
  12. Wallach, D., Boldin, M., Varfolomeev, E., Beyaert, R., Vandenaebelle, P., and Fiers, W. (1997) Cell Death Induction by Receptors of the TNF Family: Towards a Molecular Understanding, *FEBS Lett.* 410, 96–106.
  13. Li, P., Nijhawan, D., Budihardjo, I., Srinivasula, S.M., Ahmad, M., Alnemri, E.S., and Wang, X. (1997) Cytochrome c and dATP-Dependent Formation of Apaf-1/Caspase-9 Complex Initiates an Apoptotic Protease Cascade, *Cell* 91, 479–489.
  14. Zou, H., Henzel, W.J., Liu, X., Lutschg, A., and Wang, X. (1997) Apaf-1, a Human Protein Homologous to *C. elegans* CED-4, Participates in Cytochrome c-Dependent Activation of Caspase-3, *Cell* 90, 405–413.
  15. Adams, J.M., and Cory, S. (1998) The Bcl-2 Protein Family: Arbiters of Cell Survival, *Science* 281, 1322–1326.
  16. Green, D.R., and Reed, J.C. (1998) Mitochondria and Apoptosis, *Science* 281, 1309–1312.
  17. Hengartner, M.O. (2000) The Biochemistry of Apoptosis, *Nature* 407, 770–776.
  18. Kaufmann, S.H., Desnoyers, S., Ottaviano, Y., Davidson, N.E., and Poirier, G.G. (1993) Specific Proteolytic Cleavage of Poly(ADP-ribose) Polymerase: An Early Marker of Chemotherapy-Induced Apoptosis, *Cancer Res.* 53, 3976–3985.
  19. Lazebnik, Y.A., Kaufmann, S.H., Desnoyers, S., Poirier, G.G., and Earnshaw, W.C. (1994) Cleavage of Poly(ADP-ribose) Polymerase by a Proteinase with Properties like ICE, *Nature* 371, 346–347.
  20. Yung, T.M., and Satoh, M.S. (2001) Functional Competition Between Poly(ADP-ribose) Polymerase and Its 24-kDa Apoptotic Fragment in DNA Repair and Transcription, *J. Biol. Chem.* 276, 11279–11286.
  21. Gastman, B.R., Yin, X.M., Johnson, D.E., Wieckowski, E., Wang, G.Q., Watkins, S.C., and Rabinowich, H. (2000) Tumor-Induced Apoptosis of T Cells: Amplification by a Mitochondrial Cascade, *Cancer Res.* 60, 6811–6817.
  22. Schempp, C.M., Simon-Haarhaus, B., Termeer, C.C., and Simon, J.C. (2001) Hypericin Photo-Induced Apoptosis Involves the Tumor Necrosis Factor-Related Apoptosis-Inducing Ligand (TRAIL) and Activation of Caspase-8, *FEBS Lett.* 493, 26–30.
  23. Takahashi, A., Hirata, H., Yonehara, S., Imai, Y., Lee, K.K., Moyer, R.W., Turner, P.C., Mesner, P.W., Okazaki, T., Sawai, H., et al. (1997) Affinity Labeling Displays the Stepwise Activation of ICE-Related Proteases by Fas, Staurosporine, and CrmA-Sensitive Caspase-8, *Oncogene* 14, 2741–2752.
  24. Bratton, D.L., Fadok, V.A., Richter, D.A., Kailey, J.M., Guthrie, L.A., and Henson, P.M. (1997) Appearance of Phosphatidylserine on Apoptotic Cells Requires Calcium-Mediated Nonspecific Flip-Flop and Is Enhanced by Loss of the Aminophospholipid Translocase, *J. Biol. Chem.* 272, 26159–26165.
  25. Span, L.F., Pennings, A.H., Vierwinden, G., Boezeman, J.B., Raymakers, R.A., and de Witte, T. (2002) The Dynamic Process of Apoptosis Analyzed by Flow Cytometry Using Annexin-V/Propidium Iodide and a Modified *in situ* End Labeling Technique, *Cytometry* 47, 24–31.
  26. Zhuang, J., Ren, Y., Snowden, R.T., Zhu, H., Gogvadze, V., Savill, J.S., and Cohen, G.M. (1998) Dissociation of Phagocyte Recognition of Cells Undergoing Apoptosis from Other Features of the Apoptotic Program, *J. Biol. Chem.* 273, 15628–15632.
  27. Cain, K., Brown, D.G., Langlais, C., and Cohen, G.M. (1999) Caspase Activation Involves the Formation of the Aposome, a Large (approximately 700 kDa) Caspase-Activating Complex, *J. Biol. Chem.* 274, 22686–22692.
  28. Antonsson, B., and Martinou, J.C. (2000) The Bcl-2 Protein Family, *Exp. Cell Res.* 256, 50–57.
  29. Gross, A., McDonnell, J.M., and Korsmeyer, S.J. (1999) BCL-2 Family Members and the Mitochondria in Apoptosis, *Genes Dev.* 13, 1899–1911.
  30. Reed, J.C. (1997) Double Identity for Proteins of the BCL-2 Family, *Nature* 387, 773–776.
  31. Glazyrin, A.L., Adsay, V.N., Vaitkevicius, V.K., and Sarkar, F.H. (2001) CD95-Related Apoptotic Machinery Is Functional in Pancreatic Cancer Cells, *Pancreas* 22, 357–365.
  32. Herrera, B., Fernandez, M., Alvarez, A.M., Roncero, C., Benito, M., Gil, J., and Fabregat, I. (2001) Activation of Caspases Occurs Downstream from Radical Oxygen Species Production, Bcl-xL Down-Regulation, and Early Cytochrome C Release in Apoptosis Induced by Transforming Growth Factor beta in Rat Fetal Hepatocytes, *Hepatology* 34, 548–556.
  33. Kiyokawa, N., Mori, T., Taguchi, T., Saito, M., Mimori, K., Suzuki, T., Sekino, T., Sato, N., Nakajima, H., Katagiri, Y.U., et al. (2001) Activation of the Caspase Cascade During Stx1-Induced Apoptosis in Burkitt's Lymphoma Cells, *J. Cell Biochem.* 81, 128–142.
  34. Finstad, H.S., Drevon, C.A., Kulseth, M.A., Synstad, A.V., Knudsen, E., and Kolset, S.O. (1998) Cell Proliferation, Apoptosis and Accumulation of Lipid Droplets in U937-1 Cells Incubated with Eicosapentaenoic Acid, *Biochem. J.* 336, 451–459.

[Received May 28, 2002, and in revised form and accepted August 12, 2002]



# Positional Distribution of FA in TAG of Enzymatically Modified Borage and Evening Primrose Oils

S.P.J. Namal Senanayake and Fereidoon Shahidi\*

Department of Biochemistry, Memorial University of Newfoundland, St. John's, Newfoundland, Canada A1B 3X9

**ABSTRACT:** Stereospecific analysis was carried out to establish positional distribution of FA in the TAG of DHA, EPA, and (EPA + DHA)-enriched oils. In this study, TAG of enzymatically modified oils were purified using a silicic acid column. The TAG were then subjected to positional distribution analysis using a modified procedure involving reductive cleavage with Grignard reagent. The results showed that in DHA-enriched borage oil (BO), DHA was randomly distributed over the three positions of TAG, whereas  $\gamma$ -linolenic acid (GLA) was mainly esterified at the *sn*-2 and -3 positions. In DHA-enriched evening primrose oil (EPO), however, DHA and GLA were concentrated in the *sn*-2 position. In EPA-enriched BO, EPA was randomly distributed over the three positions of TAG, similar to that observed for DHA. In EPA-enriched EPO, however, this FA was mainly located at the primary positions (*sn*-1 and *sn*-3) of TAG. In both oils, GLA was preferentially esterified at the *sn*-2 position. In (EPA + DHA)-enriched BO, EPA and DHA were mainly esterified at the *sn*-1 and -3 positions of TAG, whereas GLA was mainly located at the *sn*-2 position. In (EPA + DHA)-enriched EPO, GLA was mainly located at the *sn*-2 and -3 positions; EPA was preferentially esterified at the *sn*-1 and -3 positions, and DHA was found mainly at the *sn*-3 position.

Paper no. L8998 in *Lipids* 37, 803–810 (August 2002).

Borage oil (BO) and evening primrose oil (EPO) are major sources of  $\gamma$ -linolenic acid (18:3n-6; GLA), an essential n-6 polyunsaturated fatty acid (PUFA). GLA is an important intermediate in the bioconversion of linoleic acid (18:2n-6) to arachidonic acid (AA; 20:4n-6). GLA-rich oils have been used in the treatment of certain skin-related diseases, hypertension, premenstrual syndrome, diabetes, and cancer (1). Therefore, many research groups have actively pursued investigations on concentrating GLA from borage, evening primrose, blackcurrant, and fungal oils (2-5) for pharmaceutical and dietetic applications.

The n-3 PUFA, such as EPA (20:5n-3) and DHA (22:6n-3), have also gained recognition for their vital role in human health and nutrition. EPA has several health benefits related to cardiovascular disease, arthritis, thrombosis, psoriasis, inflammation, and renal and auto-immune disorders (6). DHA is important in the development of the central nervous system and visual acuity of infants (7).

The beneficial effects of both GLA (n-6) and n-3 FA are associated with the production of eicosanoids. Incorporation of n-3 PUFA from marine sources into BO and EPO may provide specialty oils for specific nutritional and clinical appli-

cations. This may be possible *via* lipase-catalyzed reactions. Lipase-assisted reactions, such as transesterification of plant oils with n-3 PUFA, have been successfully used for preparation of structured lipids (SL) (8–10). SL are TAG that contain mixtures of short-, medium- and long-chain FA in the same glycerol molecule and are believed to be effective in delivering desired FA to target specific diseases and certain pathological conditions.

The structure of the TAG molecule exerts a major impact on its nutritional and biochemical properties. Intestinal absorption of FA is reportedly dependent on their arrangement in the TAG molecules. Investigation of the absorption of FA in a canine model suggested that the positional distribution of FA within the TAG molecules might affect the metabolic fate of FA (11). During digestion, lipases hydrolyze TAG into FFA, predominantly from the *sn*-1 and -3 positions and 2-MAG (12), which will be absorbed into the intestinal mucosal cells of the small intestine. Although most dietary lipids are in the TAG form, relatively little is known about the importance of stereospecific composition of TAG on the biological activity of dietary FA (13). Differences in the positional distribution of FA have also been shown to have specific effects on the profile, structure, and composition of the lipoproteins (13).

Stereospecific analysis determines how the FA of TAG are distributed over the three different positions of the glycerol molecule (14). Differences in the distributions of FA among different positions in TAG from natural fats and oils were first demonstrated systematically by enzymatic hydrolysis procedures, especially pancreatic lipase hydrolysis for the analysis of the FA of position *sn*-2, before complex stereospecific hydrolysis procedures were developed that permitted determination of complete positional distributions of FA to be determined. Because of this historical analytical procedure development, there has been a tendency to assume that the composition of FA esterified to the sole secondary hydroxyl group must have greater importance than those of the two primary positions. It is certainly true that the composition of the *sn*-2 position is of great importance when TAG are consumed and digested by animals, since *sn*-2-MAG so produced can be absorbed by the intestine and utilized as such (15). On the other hand, the results of stereospecific analyses have shown that the compositions of all three positions in certain fats can be distinctive and can highlight important aspects of the biosynthetic processes.

The positional distribution of FA in TAG of both BO and EPO has previously been determined (16,17). In the present study, stereospecific analyses of TAG have been carried out for DHA-, EPA-, and (EPA + DHA)-enriched BO and EPO.

\*To whom correspondence should be addressed. E-mail: fshahidi@mun.ca  
Abbreviations: AA, arachidonic acid, 20:4n-6; BO, borage oil; EPO, evening primrose oil; GLA,  $\gamma$ -linolenic acid, 18:3n-6; LA, linoleic acid; SL, structured lipids.



## EXPERIMENTAL PROCEDURES

**Materials.** BO was obtained from Bioriginal Food and Science Corporation (Saskatoon, Saskatchewan, Canada), and evening primrose oil was provided by Efamol, Inc. (Kentville, Nova Scotia, Canada). Algal oil containing 47.4% DHA was obtained from Martek Biosciences Corporation (Columbia, MD). EPA concentrate (93.1% EPA) was provided by Dr. T. Ohshima (Tokyo, Japan). Immobilized lipase from *Candida antarctica* (Novozym-435) was provided by Novo Nordisk Biochem North America, Inc. (Franklinton, NC). The nonspecific lipase from *Pseudomonas* sp. (PS-30) was supplied by Amano Enzymes U.S.A. Co., Ltd, (Troy, VA).

**Preparation of DHA concentrate from algal oil by urea-FA complexation.** DHA concentrate (up to 97.1%) was obtained from the hydrolyzed algal oil using the urea-FA complexation method as described by Senanayake and Shahidi (18).

**Determination of enzyme activity.** Lipase activity was measured as described by Senanayake and Shahidi (8). One unit (U) of lipase activity was defined as nanomoles of FA (oleic acid equivalents) produced per minute per gram of enzyme. Lipase activities of Novozym-435 and lipase PS-30 were 554 and 11,936 U, respectively.

**Enzymatic synthesis of DHA-enriched oils.** BO (300 mg) or EPO (297 mg) was mixed with DHA concentrate (120 mg) at a mole ratio of 1:1 in a screw-capped test tube, and then immobilized Novozym-435 lipase (250 enzyme activity units) and water (2% by weight of substrates plus enzyme) were added in hexane (3 mL). The mixture was stirred in an orbital shaker at 250 rpm and 45°C. Individual sample vials were removed and analyzed after 24 h. All reactions were performed in triplicate (9).

**Enzymatic synthesis of EPA-enriched oils.** Modified oils containing EPA were produced by acidolysis reactions using nonimmobilized lipase PS-30 from *Pseudomonas* sp. In this study, BO (300 mg) or EPO (297 mg) was mixed with EPA (115 mg) in a screw-capped test tube, and then lipase (250 enzyme activity units) and water (2% by weight of substrates plus enzyme) were added in hexane (3 mL). The mixture was stirred in an orbital shaker at 250 rpm and 45°C. Individual sample vials were removed and analyzed after 24 h. All reactions were performed in triplicate.

**Enzymatic synthesis of (EPA + DHA)-enriched oils.** BO (300 mg) or EPO (297 mg) was mixed with EPA (53.5 mg) and DHA (58.2 mg) at a mole ratio of 1:0.5:0.5, in a screw-capped test tube, and then lipase PS-30 preparation (250 enzyme activity units) and water (2% by weight of substrates plus enzyme) were added in hexane (3 mL). The mixture was stirred in an orbital shaker at 250 rpm and 45°C. Individual sample vials were removed and analyzed after 24 h. All reactions were performed in triplicate (8).

**Analysis of products.** The enzymes were removed by passing the reaction mixture through a bed of anhydrous sodium sulfate. Samples were placed in 250-mL conical flasks, to which 20 mL of a mixture of acetone/ethanol (1:1, vol/vol) were added. The reaction mixture was titrated with 0.5 N

NaOH to a phenolphthalein endpoint. The mixture was transferred to a separatory funnel and thoroughly mixed with 25 mL hexane. The lower aqueous layer was separated and discarded. The upper hexane layer containing acylglycerols was passed through a bed of anhydrous sodium sulfate. The acylglycerol fraction was subsequently recovered following hexane removal at 45°C using a rotary evaporator.

**Removal of non-TAG constituents from enzymatically modified oils.** Removal of non-TAG constituents from enzymatically modified BO and EPO was carried out using column chromatography (1.25 cm internal diameter and 10 cm height) on silicic acid (100–200 mesh size; Sigma, St. Louis, MO). The column was first washed with hexane, and then 1.25 g modified oil was introduced onto it. Hexane (50 mL) was added to the column, which was then eluted with 10% (vol/vol) diethyl ether in hexane (250 mL). The solvent was removed under vacuum at 40°C using a rotary evaporator. The recovered oil was then passed through a layer of anhydrous sodium sulfate. To prevent oxidation of purified oils, a few crystals of BHT were added to the mixture.

**Stereospecific analyses of enzymatically modified BO and EPO.** Stereospecific analysis was performed on purified modified oils according to the method described by Brockerhoff (14) and Brockerhoff *et al.* (19) with some modifications. The purified TAG (1.0 g) was dissolved in anhydrous diethyl ether (50 mL) and mixed with methyl magnesium bromide (3.5 mL, 3.0 M CH<sub>3</sub>MgBr; Sigma). The Grignard reaction was allowed to proceed with continuous stirring until a clear solution was obtained. To stop the reaction, glacial acetic acid (1.0 mL) was slowly added to the mixture followed by 10% (wt/vol) boric acid solution (10 mL; to minimize acyl migration). Stirring of the reaction mixture was continued for another 2 to 3 min. The whole mixture was then transferred to a separatory funnel and allowed to separate into two layers. The top ether layer was removed, and the lower aqueous layer was washed twice with diethyl ether. The combined ether layers were washed successively with 10 mL of water, 10 mL of 2% (wt/vol) aqueous sodium bicarbonate, and 10 mL of water, and then dried over anhydrous sodium sulfate.

**Separation of individual lipids after Grignard reaction.** Products of the Grignard reaction were dissolved in a minimum amount of chloroform and applied to several TLC plates (20 × 20 cm; silica gel, 60Å mean pore diameter, 2–25 µm mean particle size, 500 µm thickness, with dichlorofluorescein; Sigma) impregnated with 5% (wt/vol) boric acid. The plates were developed in two different solvent systems of diethyl ether/petroleum ether (boiling point 30–60°C) (8:92, vol/vol) and diethyl ether/petroleum ether (40:60, vol/vol), respectively. After drying, the bands were located by viewing under short (254 nm)- and long (356 nm)-wavelength UV lights (Spectraline, Model ENF-240C; Spectronics Co., Westbury, NY). From the separated bands of TAG ( $R_f = 0.99$ ), tertiary alcohol ( $R_f = 0.72$ ), 1,2-DAG and 2,3-DAG ( $R_f = 0.32$ ), 1,3-DAG ( $R_f = 0.41$ ), and MAG ( $R_f = 0.05$ ), 1,2- and 2,3-DAG bands were scraped off and then extracted with diethyl ether. The ether layer was evaporated under nitrogen to obtain 1,2- and 2,3-DAG. After re-

moving a small amount of sample for FA analysis, the DAG fractions were used to prepare synthetic phospholipids.

**Preparation of synthetic phospholipids from DAG fraction.** The 1,2- and 2,3-DAG were dissolved in 1.0 mL of diethyl ether and mixed with 2.5 mL pyridine/diethyl ether/phenyl dichlorophosphate (1:1:0.5, by vol). The reaction mixture was then allowed to stand at room temperature for 1 h, after which 5 mL of pyridine, 3.0 mL of diethyl ether, and a few drops of water were added while cooling in an ice bath. The content of flask was subsequently mixed with 86 mL of methanol/water/chloroform/triethylamine (30:25:30:1, by vol). After standing, the lower chloroform layer containing synthetic phospholipids (1,2-diacyl-3-phosphophenol and 2,3-diacyl-1-phosphophenol) was separated and the solvent removed at 40°C using a rotary evaporator. The recovered synthetic phospholipids were used for stereospecific hydrolysis by the phospholipase A<sub>2</sub> enzyme.

**Stereospecific hydrolysis of synthetic phospholipids by phospholipase A<sub>2</sub>.** The synthetic phospholipids (1,2-diacyl-3-phosphophenol and 2,3-diacyl-1-phosphophenol) obtained were dissolved in 3.0 mL of diethyl ether and transferred to a solution containing 15 mL of 0.1 M triethylammonium bicarbonate (pH 7.5), 100 µL of 0.1 M calcium chloride, and 2.0 mg of phospholipase A<sub>2</sub> (EC 3.1.1.4; Sigma) obtained from snake venom (*Crotalus adamantus*). The mixture was then shaken gently overnight in a Gyrotory water bath shaker (Model G76; New Brunswick Scientific Co., Inc., New Brunswick, NJ), and water in the mixture was evaporated at 40°C using a rotary evaporator. To prevent foaming during evaporation, 15 mL of isobutanol was added to the mixture.

The hydrolyzed products were dissolved in 1.0 mL of chloroform/methanol (1:1, vol/vol) containing one drop of glacial acetic acid. The dissolved hydrolytic products were

applied to silica gel TLC plates (20 × 20 cm; 60Å mean pore diameter, 2–25 µm mean particle size, 500 µm thickness, with dichlorofluorescein, Sigma) impregnated with 5% (wt/vol) boric acid. The plates were developed in diethyl ether/petroleum ether (40:60, vol/vol), dried in a fumehood, and then kept over concentrated aqueous ammonia for 10 min and subsequently redeveloped in aqueous ammonia/methanol/diethyl ether (2:15:83, by vol). After drying, the bands were located by viewing under short (254 nm)- and long (356 nm)-wavelength UV lights (Spectraline, Model ENF-240C; Spectronics Co.). The separated bands—FFA (hydrolyzed from *sn*-2 position of 1,2-diacyl-3-phosphophenol;  $R_f = 0.72$ ), unhydrolyzed 2,3-diacyl-1-phosphophenol ( $R_f = 0.49$ ), lysophosphatide ( $R_f = 0.08$ ), and small amounts of 1,2- and 2,3-DAG ( $R_f = 0.91$ )—were scraped off and extracted into chloroform/methanol (1:1, vol/vol). The L-lysophosphatide fraction permitted identification of the FA composition at the *sn*-1 position of TAG of modified oils. These results are reported in Tables 1–6. After having removed a small amount of sample for FA analysis, the unhydrolyzed 2,3-diacyl-1-phosphophenol fraction was subjected to porcine pancreatic lipase hydrolysis using the procedure described below in order to obtain 2-monoacyl-1-phosphatide and FFA (hydrolyzed from *sn*-3 position). All separated lipid fractions were analyzed for their FA composition by employing the GC procedure (18).

**Hydrolysis of enzymatically modified oils by pancreatic lipase.** Hydrolysis of purified oils as well as separated 2,3-diacyl-1-phosphophenol by pancreatic lipase was carried out according to the method described by Christie (20). Tris-hydrochloric buffer (5 mL; 1.0 M, pH 8.0), 0.5 mL of calcium chloride (2.2%, wt/vol), and 1.25 mL of sodium taurocholate (0.05%, wt/vol) were added to 25 mg of oil in a glass test tube. The whole mixture was allowed to equilibrate at 40°C

**TABLE 1**  
Positional Distribution of FA in DHA-Enriched Borage Oil (BO)<sup>a</sup>

FA (mol%)	TAG <sup>b</sup>	<i>sn</i> -1 <sup>b</sup>	<i>sn</i> -2 <sup>b</sup>	<i>sn</i> -3 <sup>b</sup>
8:0	0.04 ± 0.01	0.08 ± 0.03	ND	0.05 ± 0.02
10:0	0.15 ± 0.02	0.17 ± 0.02	0.07 ± 0.02	0.30 ± 0.02
12:0	0.16 ± 0.03	0.12 ± 0.06	0.10 ± 0.05	0.19 ± 0.08
14:0	0.09 ± 0.01	0.05 ± 0.03	0.08 ± 0.04	0.11 ± 0.03
14:1	0.04 ± 0.01	0.02 ± 0.01	ND	0.06 ± 0.02
16:0	4.33 ± 0.57	3.90 ± 0.33	4.52 ± 0.05	3.50 ± 0.05
16:1	0.19 ± 0.03	0.12 ± 0.08	0.17 ± 0.05	0.23 ± 0.10
17:0	ND	0.02 ± 0.01	ND	0.04 ± 0.02
17:1	0.21 ± 0.07	0.45 ± 0.08	ND	0.15 ± 0.01
18:0	2.09 ± 0.15	1.12 ± 0.21	2.92 ± 0.07	1.95 ± 0.30
18:1	12.3 ± 0.50	12.3 ± 0.56	11.7 ± 0.82	8.24 ± 0.40
18:2n-6	24.7 ± 0.90	23.9 ± 1.08	22.8 ± 1.57	25.3 ± 0.37
18:3n-6	16.1 ± 0.26	13.2 ± 0.38	18.4 ± 0.85	19.2 ± 0.51
18:3n-3	0.19 ± 0.09	0.27 ± 0.08	0.17 ± 0.06	0.20 ± 0.07
20:0	ND	0.11 ± 0.04	0.22 ± 0.05	ND
20:1	2.12 ± 0.20	2.79 ± 0.46	2.70 ± 0.10	1.09 ± 0.31
20:2	0.13 ± 0.07	0.23 ± 0.10	0.12 ± 0.30	0.08 ± 0.04
22:1	1.24 ± 0.08	1.77 ± 0.14	1.90 ± 0.09	0.72 ± 0.07
22:6n-3	35.3 ± 1.50	34.6 ± 0.85	33.5 ± 0.25	35.9 ± 0.74
24:1	0.47 ± 0.09	0.89 ± 0.12	0.11 ± 0.06	0.41 ± 0.09

<sup>a</sup>DHA-enriched BO was synthesized using Novozym-435 from *Candida antarctica* (Novo Nordisk Biochem North America, Franklinton, NC) as the biocatalyst.

<sup>b</sup>Mean ± SD of triplicate stereospecific analyses. ND, not detected.

**TABLE 2**  
**Positional Distribution of FA in DHA-Enriched Evening Primrose Oil (EPO)<sup>a</sup>**

FA (mol%)	TAG <sup>b</sup>	<i>sn</i> -1 <sup>b</sup>	<i>sn</i> -2 <sup>b</sup>	<i>sn</i> -3 <sup>b</sup>
12:0	0.12 ± 0.08	0.15 ± 0.02	0.13 ± 0.02	0.08 ± 0.04
14:0	0.12 ± 0.05	0.09 ± 0.02	0.13 ± 0.04	0.17 ± 0.04
14:1	0.08 ± 0.02	0.12 ± 0.01	0.08 ± 0.05	0.07 ± 0.03
16:0	7.55 ± 0.17	7.81 ± 0.35	3.74 ± 0.41	10.6 ± 0.73
16:1	0.06 ± 0.02	0.08 ± 0.04	0.17 ± 0.04	ND
18:0	2.31 ± 0.42	2.90 ± 0.51	1.47 ± 0.26	3.97 ± 0.59
18:1	4.63 ± 0.35	7.81 ± 0.16	1.49 ± 0.54	3.20 ± 0.61
18:2n-6	43.4 ± 0.64	45.1 ± 0.97	44.9 ± 0.59	41.5 ± 0.88
18:3n-6	7.05 ± 0.15	5.48 ± 0.56	7.49 ± 0.82	4.79 ± 0.51
18:3n-3	0.21 ± 0.06	0.29 ± 0.03	0.23 ± 0.05	0.08 ± 0.04
20:0	0.50 ± 0.12	0.42 ± 0.08	0.32 ± 0.04	0.59 ± 0.11
20:1	0.29 ± 0.16	0.14 ± 0.05	0.36 ± 0.06	0.36 ± 0.17
22:1	0.13 ± 0.04	0.15 ± 0.05	0.17 ± 0.03	0.12 ± 0.06
22:6n-3	33.1 ± 0.70	24.5 ± 0.72	38.2 ± 0.52	33.1 ± 0.87

<sup>a</sup>DHA-enriched EPO was synthesized using Novozym-435 from *C. antarctica* as the biocatalyst. For manufacturer and abbreviations see Table 1.

<sup>b</sup>Mean ± SD of triplicate stereospecific analyses.

in a water bath for 1 min; subsequently, 5.0 mg of porcine pancreatic lipase (EC 3.1.1.3; Sigma) was added to it. The mixture was then placed in a Gyrotory water bath shaker (Model G76; New Brunswick Scientific Co. Inc.) at 200 rpm under nitrogen for 8 to 10 min at 40°C. Ethanol (5 mL) was added to stop the enzymatic hydrolysis followed by addition of 5.0 mL of 6.0 M HCl. The hydrolytic products were extracted three times with 50 mL of diethyl ether, and the ether layer was washed twice with distilled water and dried over anhydrous sodium sulfate. After removal of the solvent under vacuum at 30°C, the hydrolytic products were separated on

silica gel TLC plates (20 × 20 cm; 60Å mean pore diameter, 2–25 µm mean particle size, 500 µm thickness, with dichlorofluorescein; Sigma) impregnated with 5% (wt/vol) boric acid. The plates were developed using hexane/diethyl ether/acetic acid (70:30:1, by vol). After drying, the bands were located by viewing under short (254 nm)- and long (356 nm)-wavelength UV lights (Spectraline, Model ENF-240C; Spectronics Co.). The bands were scraped off and their lipids extracted into chloroform/methanol (1:1, vol/vol) or diethyl ether and subsequently used for FA analysis by the GC procedure described by Senanayake and Shahidi (18). It should

**TABLE 3**  
**Positional Distribution of FA in EPA-Enriched BO<sup>a</sup>**

FA (mol%)	TAG <sup>b</sup>	<i>sn</i> -1 <sup>b</sup>	<i>sn</i> -2 <sup>b</sup>	<i>sn</i> -3 <sup>b</sup>
8:0	0.03 ± 0.01	0.09 ± 0.04	ND	ND
10:0	0.03 ± 0.01	0.02 ± 0.01	0.04 ± 0.02	0.04 ± 0.02
12:0	0.16 ± 0.05	0.19 ± 0.06	ND	0.28 ± 0.09
14:0	0.13 ± 0.07	0.05 ± 0.02	0.05 ± 0.03	0.33 ± 0.14
14:1	0.02 ± 0.01	0.04 ± 0.02	ND	0.06 ± 0.02
16:0	6.45 ± 0.21	4.31 ± 0.15	8.82 ± 0.18	4.75 ± 0.46
16:1	0.47 ± 0.07	0.58 ± 0.13	0.08 ± 0.05	0.69 ± 0.11
18:0	1.85 ± 0.23	0.84 ± 0.15	1.95 ± 0.43	0.69 ± 0.21
18:1	11.6 ± 0.52	10.3 ± 0.52	10.8 ± 0.35	14.5 ± 0.74
18:2n-6	22.2 ± 0.91	23.6 ± 0.91	21.2 ± 0.42	20.2 ± 0.83
18:3n-6	15.1 ± 0.82	11.5 ± 0.34	18.6 ± 0.63	13.4 ± 0.12
18:3n-3	0.17 ± 0.05	0.14 ± 0.09	ND	0.30 ± 0.15
20:0	0.27 ± 0.06	0.54 ± 0.16	ND	0.13 ± 0.06
20:1	3.00 ± 0.09	2.15 ± 0.38	3.80 ± 0.04	3.18 ± 0.38
20:2	0.18 ± 0.02	0.39 ± 0.16	ND	0.17 ± 0.09
20:4	0.14 ± 0.05	0.08 ± 0.03	ND	0.45 ± 0.05
20:5n-3	32.7 ± 1.28	33.4 ± 0.86	32.5 ± 0.79	30.9 ± 1.05
22:0	0.17 ± 0.09	0.04 ± 0.02	0.11 ± 0.06	0.38 ± 0.06
22:1	2.05 ± 0.11	3.58 ± 0.15	1.20 ± 0.28	1.04 ± 0.34
22:5	0.07 ± 0.01	0.07 ± 0.04	ND	0.19 ± 0.06
24:0	0.05 ± 0.01	ND	ND	0.29 ± 0.13
24:1	1.22 ± 0.08	0.24 ± 0.05	0.58 ± 0.24	2.77 ± 0.47

<sup>a</sup>EPA-enriched BO was synthesized using lipase PS-30 from *Pseudomonas* sp. (Amano Enzymes, U.S.A. Co. Ltd., Troy, VA) as the biocatalyst. For abbreviations see Table 1.

<sup>b</sup>Mean ± SD of triplicate stereospecific analyses.

**TABLE 4**  
**Positional Distribution of FA in EPA-Enriched EPO<sup>a</sup>**

FA (mol%)	TAG <sup>b</sup>	<i>sn</i> -1 <sup>b</sup>	<i>sn</i> -2 <sup>b</sup>	<i>sn</i> -3 <sup>b</sup>
8:0	ND	0.08 ± 0.03	ND	0.10 ± 0.04
10:0	0.03 ± 0.01	0.09 ± 0.02	0.03 ± 0.02	0.04 ± 0.03
12:0	ND	ND	0.40 ± 0.08	ND
14:0	0.06 ± 0.02	0.09 ± 0.04	0.05 ± 0.05	0.08 ± 0.04
14:1	ND	0.04 ± 0.03	0.03 ± 0.01	ND
16:0	4.55 ± 0.36	2.94 ± 0.14	5.98 ± 0.15	3.18 ± 0.52
16:1	0.12 ± 0.05	0.11 ± 0.08	0.12 ± 0.04	0.08 ± 0.05
18:0	1.65 ± 0.49	0.08 ± 0.04	3.60 ± 0.27	1.43 ± 0.28
18:1	6.92 ± 0.58	6.48 ± 0.67	8.54 ± 0.44	5.31 ± 0.40
18:2n-6	43.7 ± 1.71	39.1 ± 0.59	48.4 ± 0.61	37.5 ± 0.75
18:3n-6	5.43 ± 0.29	4.39 ± 0.54	7.16 ± 0.37	4.84 ± 0.46
18:3n-3	0.16 ± 0.07	0.08 ± 0.04	0.10 ± 0.04	0.28 ± 0.08
20:0	0.31 ± 0.05	0.49 ± 0.17	0.20 ± 0.04	0.26 ± 0.12
20:1	0.27 ± 0.04	0.22 ± 0.08	0.19 ± 0.06	0.34 ± 0.07
20:2	ND	ND	0.03 ± 0.02	0.05 ± 0.02
20:4	0.11 ± 0.02	0.21 ± 0.04	0.10 ± 0.04	0.27 ± 0.05
20:5n-3	35.1 ± 0.78	39.5 ± 0.86	23.2 ± 0.58	42.1 ± 1.55
22:0	ND	0.04 ± 0.03	ND	0.03 ± 0.02
22:1	0.11 ± 0.04	0.20 ± 0.06	ND	0.24 ± 0.07
24:1	ND	ND	0.08 ± 0.05	ND

<sup>a</sup>EPA-enriched EPO was synthesized using lipase PS-30 from *Pseudomonas* sp. For abbreviations see Table 1; for manufacturer see Table 3.

<sup>b</sup>Mean ± SD of triplicate stereospecific analyses.

be noted that the FA profiles of 2-MAG fractions were used to give the results (FA distribution at the *sn*-2 position) in Tables 1–6. The hydrolytic products of 2,3-diacyl-1-phosphophenol provided the FA composition of the *sn*-3 position of TAG of modified oils. These results are also reported in Tables 1–6.

**Preparation of FAMES.** FA composition of the lipid fractions was determined following conversion to methyl esters. About 15 mg of each oil was weighed into a 6-mL well-cleaned Teflon-lined, screw-capped conical vial. The internal standard (250 ng/100 µL chloroform, methyl tricosanoate,

C<sub>23:0</sub>) was added to the vial, and the solvent in the oil–internal standard mixture was evaporated under a stream of nitrogen. Transmethylation reagent (2 mL; freshly prepared 6 mL of concentrated sulfuric acid made up to 100 mL with spectral grade methanol and 15 mg of hydroquinone as an antioxidant) was added to the sample vial and mixed by vortexing. The mixture was incubated overnight at 60°C and subsequently cooled (18). Distilled water (1 mL) was added to the mixture after thorough mixing, and it was extracted three times with 1.5 mL of pesticide-grade hexane. A few crystals

**TABLE 5**  
**FA Distribution in Different Positions of TAG of (EPA + DHA) Enriched BO<sup>a</sup>**

FA (mol%)	TAG <sup>b</sup>	<i>sn</i> -1 <sup>b</sup>	<i>sn</i> -2 <sup>b</sup>	<i>sn</i> -3 <sup>b</sup>
8:0	0.02 ± 0.01	ND	0.03 ± 0.02	0.40 ± 0.04
10:0	0.02 ± 0.01	ND	0.05 ± 0.03	1.41 ± 0.20
12:0	0.05 ± 0.02	0.59 ± 0.10	0.08 ± 0.03	1.38 ± 0.51
14:0	0.07 ± 0.05	0.69 ± 0.20	0.09 ± 0.06	0.89 ± 0.20
16:0	5.06 ± 0.50	7.15 ± 0.80	1.05 ± 0.06	5.99 ± 0.80
16:1	ND	ND	0.21 ± 0.02	1.99 ± 0.30
17:0	0.02 ± 0.01	ND	0.05 ± 0.02	0.22 ± 0.05
17:1	0.20 ± 0.05	ND	0.30 ± 0.06	ND
18:0	2.21 ± 0.05	5.15 ± 0.70	1.02 ± 0.50	2.76 ± 0.50
18:1	11.5 ± 0.40	12.8 ± 0.80	14.1 ± 1.20	8.85 ± 1.00
18:2n-6	20.5 ± 2.00	22.9 ± 1.00	26.2 ± 2.60	15.3 ± 1.25
18:3n-6	16.9 ± 0.70	4.12 ± 1.00	32.9 ± 1.50	15.1 ± 0.80
18:3n-3	ND	3.71 ± 0.85	0.45 ± 0.04	0.64 ± 0.50
20:1	2.94 ± 0.50	3.06 ± 0.60	1.40 ± 0.08	2.43 ± 0.60
20:2	0.20 ± 0.04	ND	0.12 ± 0.06	ND
20:4	0.63 ± 0.05	ND	1.43 ± 0.50	0.14 ± 0.05
20:5n-3	25.9 ± 2.30	26.1 ± 1.50	15.2 ± 0.30	30.8 ± 2.50
22:1	1.24 ± 0.40	3.49 ± 0.80	0.77 ± 0.05	1.07 ± 0.50
22:6n-3	8.50 ± 0.85	8.33 ± 1.01	3.77 ± 0.80	9.81 ± 0.80

<sup>a</sup>(EPA + DHA)-enriched BO was synthesized using lipase PS-30 from *Pseudomonas* sp. as the biocatalyst. For abbreviations see Table 1; for manufacturer see Table 3.

<sup>b</sup>Mean ± SD of triplicate stereospecific analyses.



**TABLE 6**  
**FA Distribution in Different Positions of TAG of (EPA + DHA)-Enriched EPO<sup>a</sup>**

FA (mol%)	TAG <sup>b</sup>	<i>sn</i> -1 <sup>b</sup>	<i>sn</i> -2 <sup>b</sup>	<i>sn</i> -3 <sup>b</sup>
8:0	0.02 ± 0.01	0.35 ± 0.10	ND	0.89 ± 0.04
10:0	0.04 ± 0.01	0.81 ± 0.03	0.03 ± 0.01	0.44 ± 0.20
12:0	0.04 ± 0.01	0.49 ± 0.06	0.03 ± 0.01	0.18 ± 0.51
16:0	3.75 ± 0.40	3.43 ± 0.30	1.61 ± 0.05	4.10 ± 0.80
16:1	ND	1.06 ± 0.20	0.07 ± 0.01	0.32 ± 0.30
18:0	1.15 ± 0.50	1.49 ± 0.40	1.28 ± 0.40	2.00 ± 0.05
18:1	6.22 ± 0.80	2.14 ± 0.70	2.53 ± 0.60	14.2 ± 0.70
18:2n-6	45.6 ± 1.50	40.1 ± 2.40	61.0 ± 2.80	32.6 ± 1.50
18:3n-6	8.59 ± 0.50	4.22 ± 0.70	10.8 ± 0.90	9.04 ± 1.10
18:3n-3	0.13 ± 0.05	2.71 ± 0.50	0.33 ± 0.02	1.02 ± 0.50
20:0	ND	0.82 ± 0.50	ND	ND
20:1	0.40 ± 0.20	1.38 ± 0.41	0.23 ± 0.08	0.32 ± 0.20
20:2	0.20 ± 0.03	ND	ND	ND
20:4	0.58 ± 0.02	ND	ND	ND
20:5n-3	25.0 ± 1.00	31.5 ± 2.00	17.2 ± 0.30	24.1 ± 0.60
22:1	0.37 ± 0.03	0.92 ± 0.06	ND	ND
22:6n-3	7.91 ± 0.91	5.80 ± 0.70	4.82 ± 0.55	10.5 ± 1.00

<sup>a</sup>(EPA + DHA)-enriched EPO was synthesized using lipase PS-30 from *Pseudomonas* sp. as the biocatalyst. For abbreviations see Table 1; for manufacturer see Table 3.

<sup>b</sup>Mean ± SD of triplicate stereospecific analyses.

of hydroquinone were added to each vial prior to extraction with hexane. Hexane layers were separated, combined, and transferred to a clean tube and then washed two times with 1.5 mL of distilled water. In the first wash, the aqueous layer was removed, and in the second wash, the hexane layer was separated and evaporated under a stream of nitrogen. FAME were then dissolved in 1 mL of carbon disulfide and used for GC analysis.

**Analysis of FAME by GC.** A Hewlett-Packard 5890 Series II gas chromatograph (Hewlett-Packard, Toronto, Canada) equipped with a SUPELCOWAX 10 column (0.25 mm diameter, 30 m length, 0.25 µm film thickness; Supelco Canada Ltd., Oakville, Ontario) was used for analyzing FAME. The oven temperature was initially set at 220°C for 10.25 min and then ramped to 240°C at 30°C/min and then held there for 9 min. The injector and detector (FID) temperatures were both at 270°C. Ultra-high-purity helium was used as a carrier gas (15 mL/min). HP 3365 Series II ChemStation software (Hewlett-Packard, Toronto, Canada) was used for data handling. The relative content of FAME as mole percentages was calculated using methyl tricosanoate (C<sub>23:0</sub>) as an internal standard.

## RESULTS AND DISCUSSION

In the first step of stereospecific analyses, TAG of modified BO and EPO were hydrolyzed by porcine pancreatic lipase in order to split FA at the *sn*-1 and -3 positions, yielding 2-MAG. This reaction accurately provides the FA composition of the *sn*-2 position of the TAG. In the second step, the TAG of both oils were modified by Grignard degradation using methyl magnesium bromide (CH<sub>3</sub>MgBr). Laakso and Christie (21) and Nwosu and Boyd (22) used the Grignard reaction to obtain partially deacylated acylglycerols. The products of the Grignard degradation of TAG consist of MAG, 1,2- and 2,3-DAG, 1,3-DAG, and a tertiary alcohol. Among these, 1,2- and 2,3-DAG were isolated and used to prepare synthetic racemic phosphatides *via* the re-

action with dichlorophenyl-phosphate. This reaction produced 1,2-diacylglycero-3-phosphophenol and 2,3-diacylglycero-1-phosphophenol, which were subsequently hydrolyzed by stereospecific phospholipase A<sub>2</sub>.

Tables 1–6 show the FA compositions and positional distributions of FA in the modified TAG used in this study. The reproducibility of the stereospecific analysis was examined by triplicate analyses of modified product FA compositions. The CV was 1.5–4.2% for selected FA, such as linoleic acid (LA; 18:2n-6), GLA (18:3n-6) and DHA (22:6n-3), in the DHA-enriched oils. In EPA (20:5n-3)-enriched oils, the CV for LA, GLA, and EPA were in the range of 2.2–5.4%. The CV for the same FA (LA, GLA, EPA, and DHA) in the (EPA + DHA)-enriched oils were 3.2–11.5%.

Tables 1 and 2 show the positional distribution of FA in TAG of DHA-enriched oils examined. The results of this study showed that DHA was fairly evenly distributed over all three positions (34.6% at *sn*-1, 33.5% at *sn*-2, and 35.9% at *sn*-3) of the TAG molecules of DHA-enriched BO (Table 1). In DHA-enriched EPO, however, this FA was preferentially esterified at the *sn*-2 position (38.2%), followed by *sn*-3 (33.1%) and *sn*-1 (24.5%) positions (Table 2). In this study, DHA-enriched oils were synthesized using Novozym-435 from *C. antarctica* as the biocatalyst. The positional specificity of *C. antarctica* depends on the type of reactants employed. In some reactions, this enzyme functions as a nonspecific lipase, whereas in others it exhibits *sn*-1,3 positional specificity (24). The results showed that under assay conditions employed in this study, this enzyme acts as a nonspecific lipase. In DHA-enriched BO, the saturated FA 16:0 and 18:0 favored the *sn*-2 position (Table 1). However, in DHA-enriched EPO, these FA were concentrated in the *sn*-1 and -3 positions (Table 2).

The stereospecific distributions of FA in the native BO and EPO have previously been determined (16,17). In native BO, GLA was distributed asymmetrically and preferentially ester-

ified at the *sn*-2 (32.2–40.4%) and *sn*-3 (17.4–30.1%) positions (16,17). The *sn*-1 position of native BO contained 4% GLA (16). In native EPO, GLA was found to be concentrated in the *sn*-2 and -3 positions of TAG (16). The *sn*-2 and -3 positions of native EPO contained 10.3–10.7 and 10.2–13.5%, GLA, respectively (16,17). The *sn*-1 position of native EPO also had 3.5–4.9% GLA (16,17). LA was nearly evenly distributed in all positions of native EPO (73.3% at *sn*-1, 78.9% at *sn*-2, and 74.2% at *sn*-3), but was concentrated in the *sn*-1 (54.3%) and *sn*-2 (42.5%) positions of native BO (16). The *sn*-3 position of native BO also contained 17.6% LA (16). The results of our study showed that in DHA-enriched BO, GLA was mainly located in the *sn*-2 (18.4%) and *sn*-3 (19.2%) positions of TAG (Table 1). In DHA-enriched EPO, however, GLA was concentrated in the *sn*-2 (7.5%) position (Table 2). LA was randomly distributed over all three positions of TAG in both oils.

Lee and Akoh (25) performed pancreatic lipase hydrolysis on an SL synthesized *via* interesterification reaction between medium-chain TAG and EPA ethyl ester using *C. antarctica* lipase as the biocatalyst. Their results showed that EPA was mainly incorporated in the *sn*-2 position of the TAG. This demonstrated that *C. antarctica* lipase has a high specificity for the *sn*-2 position under experimental conditions employed in their work.

In another study, the positional distribution of FA in TAG of EPA-enriched oils was determined, and the corresponding results are shown in Tables 3 and 4. It should be noted that EPA-enriched oils were produced using lipase PS-30 from *Pseudomonas* sp. as the biocatalyst. The saturated FA 16:0 and 18:0 were concentrated at the *sn*-2 position of TAG of EPA-enriched oils (Tables 3 and 4). The EPA of EPA-enriched BO was randomly distributed in the TAG (33.4% at *sn*-1; 32.5% at *sn*-2; 30.9% at *sn*-3) (Table 3). In EPA-enriched EPO, however, this FA was mainly esterified at the primary positions (39.5% at *sn*-1 and 42.1% at *sn*-3) of TAG (Table 4) and was also present in appreciable amounts (23.2%) at the *sn*-2 position. Therefore, it is assumed that *Pseudomonas* sp. lipase shows no specificity and may incorporate EPA in all three positions of TAG of the oils. In both oils, GLA was esterified preferentially at the *sn*-2 position (18.6 and 7.2% in EPA-enriched BO and EPO, respectively), followed by the *sn*-3 position (4.8–13.4%). In EPA-enriched BO, LA in TAG was distributed randomly (23.6% at *sn*-1, 21.2% at *sn*-2, and 20.2% at *sn*-3) whereas in EPA-enriched EPO it was mainly located at the *sn*-2 (48.4%) position followed by *sn*-1 (39.1%) and *sn*-3 (37.5%) positions (Tables 3 and 4).

The positional distributions of FA in TAG of (EPA + DHA)-enriched oils were also determined, and the results are assembled in Tables 5 and 6. In this study, (EPA + DHA)-enriched oils were synthesized using lipase PS-30 from *Pseudomonas* sp. as the biocatalyst. In (EPA + DHA)-enriched BO and EPO, saturated FA such as 16:0 and 18:0 occurred mainly at the *sn*-1 and -3 positions of TAG. However, these modified oils were different in the dominancy and distribution of n-3 and n-6 PUFA in their TAG molecules. In (EPA + DHA)-enriched BO,

GLA was mainly located at the *sn*-2 position (32.9%), followed by the *sn*-3 position (15.1%) (Table 5). However, EPA and DHA were preferentially esterified at the *sn*-1 and -3 positions of TAG molecules (Table 5); and their quantities were EPA, 26.1 and 30.8% and DHA, 8.3 and 9.8%, respectively. In (EPA + DHA)-enriched EPO, GLA was located mainly at the *sn*-2 (10.8%) and *sn*-3 (9.0%) positions of TAG (Table 6). EPA was preferentially esterified at the *sn*-1 (31.5%) and *sn*-3 (24.1%) positions, but approximately half of the DHA was located in the *sn*-3 position (10.5%) of the TAG molecules (Table 6). Therefore, lipase from *Pseudomonas* sp., under the conditions employed in this study, has the ability to incorporate n-3 FA (EPA and DHA) preferentially at the *sn*-1 and -3 positions of the TAG molecules.

Brockerhoff *et al.* (26) reported that in fish oils the long-chain PUFA tend to be concentrated in the *sn*-2 position whereas in marine mammals they favored the *sn*-1 and -3 positions of TAG. Recently, Wanasundara and Shahidi (27) reported similar results for seal blubber and menhaden oils. Aursand *et al.* (28) investigated the positional distribution of n-3 PUFA in fish and marine mammal oils using high-resolution <sup>13</sup>C NMR spectroscopy. These authors found that in fish oils DHA was concentrated in the *sn*-2 position whereas EPA was more randomly distributed over the three positions of TAG. In seal oil, DHA was predominantly present in the *sn*-1 and -3 positions (27,29). Ando *et al.* (30) also determined the positional distribution of FA in the TAG of fish oils (capelin, herring, menhaden, sardine, and saury) by HPLC using a chiral stationary phase and found that in these oils DHA was present predominantly in the *sn*-2 position. Shimada *et al.* (31) synthesized a SL by acidolysis of tripalmitin with AA (20:4n-6) using 1,3-specific *Rhizopus delemar* lipase. They reported that in the SL so produced AA was predominantly present at the *sn*-1,3 positions (56.9%) of TAG.

Stereospecific analysis of TAG and hydrolysis products provides some useful information about the mechanism of gastric digestion. Intestinal absorption of FA reportedly depends on the arrangement of FA in the TAG molecules. The influence of FA specificity on intestinal absorption in adults has recently been reviewed and positively correlated with the TAG structure in chylomicrons (32). During digestion, FA in the *sn*-1 and -3 positions of TAG are liberated by a positionally specific enzyme such as pancreatic lipase, but the FA attached to the *sn*-2 position of the TAG are absorbed and distributed in the body in the chylomicron form (33). However, clinical studies need to be carried out to verify this latter assumption.

BO and EPO have been used as GLA-rich specialty oils. Enzymatic preparation of DHA and/or EPA-rich TAG from these oils is of recent interest (8–10). It is expected that synthesis of SL containing GLA, EPA, and DHA will provide optimal health benefits. Both n-3 and n-6 PUFA have been recognized for their salient roles in human health and nutrition (6,7). The special positional distribution of GLA, DHA, and EPA in these modified TAG may confirm the potential benefits in certain health and nutritional applications.

## ACKNOWLEDGMENTS

This research financially was supported by a research grant from the Natural Sciences and Engineering Research Council (NSERC) of Canada to the corresponding author. The supply of algal oil from Martek Biosciences Corporation (Columbia, MD), BO from Bioriginal Food and Science Corporation (Saskatoon, Canada), EPO from Efamol, Inc. (Kentville, Nova Scotia, Canada) and the enzymes from Amano Enzymes U.S.A. Co. Ltd. (Troy, VA) and Novo Nordisk Biochem North America, Inc. (Franklinton, NC) are gratefully acknowledged. We also thank Dr. T. Ohshima (Tokyo, Japan) for his generous supply of the EPA concentrate.

## REFERENCES

- Horrobin, D.F. (1990) Gamma Linolenic Acid: An Intermediate in Essential Fatty Acid Metabolism with Potential as an Ethical Pharmaceutical and as a Food, *Rev. Contemp. Pharmacother.* 1, 1–41.
- Rahmatullah, M.S.K.S., Shukla, V.K.S., and Mukherjee, K.D. (1994)  $\gamma$ -Linolenic Acid Concentrates from Borage and Evening Primrose Oil Fatty Acids via Lipase-Catalyzed Esterification, *J. Am. Oil Chem. Soc.* 71, 563–569.
- Rahmatullah, M.S.K.S., Shukla, V.K.S., and Mukherjee, K.D. (1994) Enrichment of  $\gamma$ -Linolenic Acid from Evening Primrose Oil and Borage Oil via Lipase-Catalyzed Hydrolysis, *J. Am. Oil Chem. Soc.* 71, 569–573.
- Yokochi, T., Usita, M.T., Kamisaka, Y., Nakahara, T., and Suzuki, O. (1990) Increase in the  $\gamma$ -Linolenic Acid Content by Solvent Winterization of Fungal Oil Extracted from *Mortierella* Genus, *J. Am. Oil Chem. Soc.* 67, 846–851.
- Mukherjee, K.D., and Kiewitt, I. (1991) Enrichment of  $\gamma$ -Linolenic Acid from Fungal Oil by Lipase-Catalyzed Reactions, *Appl. Microbiol. Biotechnol.* 35, 579–584.
- Weaver, B.J., and Holub, B.J. (1988) Health Effects and Metabolism of Dietary Eicosapentaenoic Acid, *Prog. Food Nutri. Sci.* 12, 111–150.
- Lauritzen, L., Hansen, H.S., Jorgensen, M.H., and Michaelsen, K.F. (2001) The Essentiality of Long Chain n-3 Fatty Acids in Relation to Development and Function of the Brain and Retina, *Prog. Lipid Res.* 40, 1–94.
- Senanayake, S.P.J.N., and Shahidi, F. (1999) Enzyme-Assisted Acidolysis of Borage (*Borago officinalis* L.) and Evening Primrose (*Oenothera biennis* L.) Oils: Incorporation of Omega-3 Polyunsaturated Fatty Acids, *J. Agric. Food Chem.* 47, 3105–3112.
- Senanayake, S.P.J.N., and Shahidi, F. (1999) Enzymatic Incorporation of Docosahexaenoic Acid into Borage Oil, *J. Am. Oil Chem. Soc.* 76, 1009–1015.
- Senanayake, S.P.J.N., and Shahidi, F. (2000) Structured Lipids Containing Long-Chain Omega-3 Polyunsaturated Fatty Acids, in *Seafood in Health and Nutrition. Transformation in Fisheries and Aquaculture: Global Perspectives*. Shahidi, F. (ed.), pp. 29–44, ScienceTech Publishing, St. John's, Newfoundland, Canada.
- Jensen, G.L., McGarvey, N., Taraszewski, R., Wixon, S.K., Seidner, D.L., Pai, T., Yeh, Y.Y., Lee, T.W., and DeMichele, S.J. (1994) Lymphatic Absorption of Enterally Fed Structured Triacylglycerol Versus Physical Mix in a Canine Model, *Am. J. Clin. Nutr.* 60, 518–524.
- Mattson, F.H., and Volpenhein, R.A. (1962) Rearrangement of Glyceride Fatty Acids During Digestion and Absorption, *J. Biol. Chem.* 237, 53–55.
- Kubow, S. (1996) The Influence of Positional Distribution of Fatty Acids in Native, Interesterified and Structure-Specific Lipids on Lipoprotein Metabolism and Atherogenesis, *J. Nutr. Biochem.* 7, 530–541.
- Brockerhoff, H. (1971) Stereospecific Analysis of Triglycerides, *Lipids* 6, 943–956.
- Carey, M.C., Small, D.M., and Bliss, C.M. (1983) Lipid Digestion and Absorption, *Annu. Rev. Physiol.* 45, 651–677.
- Lawson, L.D., and Hughes, B.G. (1988) Triacylglycerol Structure of Plant and Fungal Oils Containing  $\gamma$ -Linolenic Acid, *Lipids* 23, 313–317.
- Redden, R.P., Lin, X., Fahey, J., and Horrobin, D.F. (1995) Stereospecific Analysis of the Major Triacylglycerol Species Containing  $\gamma$ -Linolenic Acid in Evening Primrose Oil and Borage Oil, *J. Chromatography* 704, 99–111.
- Senanayake, S.P.J.N., and Shahidi, F. (2000) Concentration of Docosahexaenoic Acid (DHA) from Algal Oil via Urea Complexation, *J. Food Lipids* 7, 51–61.
- Brockerhoff, H., Ackman, R.G., and Hoyle, R.J. (1963) Specific Distribution of Fatty Acids in Marine Lipids, *Arch. Biochem. Biophys.* 100, 9–12.
- Christie, W.W. (1982) Structural Analysis of Lipids by Means of Enzymatic Hydrolysis, in *Lipid Analysis*. (Christie, W.W., ed.), pp. 155–166, Pergamon Press, New York.
- Laakso, P., and Christie, W.W. (1990) Chromatographic Resolution of Chiral Diacylglycerol Derivatives: Potential in the Stereospecific Analysis of Triacyl-*sn*-glycerols, *Lipids* 25, 349–353.
- Nwosu, C.V., and Boyd, L.C. (1997) Positional Distribution of Fatty Acids on Triacylglycerols of Menhaden (*Brevoortia tyrannus*) and Salmon (*Salmo salar*) Oils, *J. Food Lipids* 4, 65–74.
- Verheij, H.M., and Dijkstra, B.W. (1994) Phospholipase A<sub>2</sub>: Mechanism and Structure, in *Lipases* (Woolley, P., and Petersen, B., eds.), pp. 119–138, Cambridge University Press, Cambridge.
- Novo Nordisk Biochem North America, Inc., Product Sheet B 606c-GB, Franklinton, NC, 1999.
- Lee, K., and Akoh, C.C. (1996) Immobilized Lipase-Catalyzed Production of Structured Lipids with Eicosapentaenoic Acid at Specific Positions, *J. Am. Oil Chem. Soc.* 73, 611–615.
- Brockerhoff, H., Hoyle, R.J., Hwang, P.C., and Litchfield, C. (1968) Positional Distribution of Fatty Acids in Depot Triglycerides of Aquatic Animals, *Lipids* 3, 24–29.
- Wanasundara, U.N., and Shahidi, F. (1997) Positional Distribution of Fatty Acids in Triacylglycerols of Seal Blubber Oil, *J. Food Lipids* 4, 51–64.
- Aursand, M., Jorgensen, L., and Grasdalen, H. (1995) Positional Distribution of  $\omega$ 3 Fatty Acids in Marine Lipid Triacylglycerols by High-Resolution <sup>13</sup>C Nuclear Magnetic Resonance Spectroscopy, *J. Am. Oil Chem. Soc.* 72, 293–297.
- Ikeda, I., Yoshida, H., Tomooka, M., Yosef, A., Imaizumi, K., Tsuji, H., and Seto, A. (1998) Effects of Long-Term Feeding of Marine Oils with Different Positional Distribution of Eicosapentaenoic and Docosahexaenoic Acids on Lipid Metabolism, Eicosanoid Production, and Platelet Aggregation in Hypercholesterolemic Rats, *Lipids* 33, 897–904.
- Ando, Y., Nishimura, K., Aoyanagi, N., and Takagi, T. (1992) Stereospecific Analysis of Fish Oil Triacyl-*sn*-glycerols, *J. Am. Oil Chem. Soc.* 69, 417–424.
- Shimada, Y., Nagao, T., Hamasaki, Y., Akimoto, K., Sugihara, A., Fujikawa, S., Komemushi, S., and Tominaga, Y. (2000) Enzymatic Synthesis of Structured Lipid Containing Arachidonic and Palmitic Acids, *J. Am. Oil Chem. Soc.* 77, 89–93.
- Phan, C.T., and Tso, P. (2001) Intestinal Lipid Absorption and Transport, *Front. Bioscience* 6, D299–D319.
- Nelson, C.M., and Innis, S.M. (1999) Plasma Lipoprotein Fatty Acids Are Altered by the Positional Distribution of Fatty Acids in Infant Formula Triacylglycerols and Human Milk, *Am. J. Clin. Nutr.* 70, 62–69.

[Received February 5, 2002, and in revised form July 16, 2002; revision accepted August 8, 2002]



# Characterization of *trans*-Monounsaturated Alkenyl Chains in Total Plasmalogens (1-*O*-alk-1'-enyl-2-acyl glycerophospholipids) from Sheep Heart

Robert L. Wolff\*

INRA, Unité de Nutrition Lipidique, 21065 Dijon Cedex, France

**ABSTRACT:** In the present study, we investigated the alkenyl chains from sheep heart plasmalogens (1-*O*-alk-1'-enyl-2-acyl glycerophospholipids) after their conversion into trimethylene dioxyalkanyl (TMDOA) derivatives. Particular attention was given to monounsaturated alkenyl chains (C<sub>18</sub> mainly). For this purpose, a combination of silver ion TLC and GLC on highly polar, very long capillary columns was applied to TMDOA derivatives. Approximately 30 different alkenyl chains could be separated, and the main observation was that the component previously reported as a *cis*-9 18:1 alkenyl chain in plasmalogens embraces in fact a wide range of *trans* and *cis* isomers, in amounts equal to 7.9 and 5.6%, respectively, of total alkenyl chains. Concerning the *trans*-monoenoate fraction, isomers with their ethylenic bond spanning from  $\Delta 6$ – $\Delta 8$  to  $\Delta 16$  were tentatively identified on the basis of their distribution profile, which was similar to that of *trans*-18:1 acids prepared and isolated from sheep adipose tissue. The main *trans*-monoenoic C<sub>18</sub> alkenyl chain in sheep heart plasmalogens would thus have its double bond in position 11, which seems logical, as alkenyl chains are derived from the corresponding alcohols, themselves issued from the corresponding FA, and in this particular case, vaccenic (*trans*-11 18:1) acid. *cis*-Monoenoic C<sub>18</sub> alkenyl chains also appear more complex than realized earlier, showing in particular isomers with their ethylenic bond farther than the  $\Delta 9$  position, in addition to the main isomer derived from oleic acid. Several *trans*-16:1 alkenyl chains could be observed (totaling ca. 1%), but *cis*-16:1 isomers were present in trace amounts only.

Paper no. L8968 in *Lipids* 37, 811–816 (August 2002).

In the many studies devoted to the biochemical effects of dietary *trans*-monounsaturated FA (MUFA), plasmalogens (1-*O*-alk-1'-enyl-2-acyl-glycerophospholipids) seem to have been little investigated. In neither the monograph on *trans* FA edited in 1979 by Emken and Dutton (1) nor in that edited in 1998 by Sébédio and Christie (2) was the word “plasmalogen” indexed. However, a few observations on plasmalogens in relation to *trans*-MUFA were made in the past. Dietary *trans*-MUFA were shown to be incorporated, after their *in vivo* conversion to the corresponding alcohols, into rat heart plasmalogen alkenyl chains (3), and into rat heart and kidney

mitochondria plasmalogens (4–6). In the latter case, elaidic (*trans*-9 18:1) acid was used as a model for *trans*-MUFA, and both alkenyl and acyl chains were analyzed. It was also demonstrated that L-M cultured cells could accumulate elaidyl alcohol (a precursor in the biosynthesis of plasmalogens) when the medium was supplemented with elaidic acid (7,8). Cell-free systems from mouse preputial gland tumors are able to promote alcohol synthesis from elaidic acid when adequate cofactors are present (9). Moreover, addition of a mixture of radioactive *trans*-octadecenols to cultured L1210 or S180 ascite cells resulted in the incorporation of these components into plasmalogens (10). The same observation was made when the mixture was injected intracranially into rat brain (10).

Plasmalogens, mostly of the ethanolamine and choline forms, are common components of cellular membranes. Their proportions relative to total phospholipids, however, depend on the organ considered. Their alkenyl chain composition is generally considered a simple one, being essentially limited to 16:0, 18:0, and 18:1 chains, and to some minor branched and odd-numbered saturated chains in the case of ruminant organs. In considering 18:1 chains, there is little information regarding the position of the ethylenic bond, but it is generally admitted that it is principally located at the  $\Delta 9$  position, with a *cis* configuration (derived from oleic acid).

Plasmalogens in ruminant organs may be different, because the rumen microflora synthesizes *trans*-MUFA from PUFA present in the feed. Thus, ruminants may be considered as naturally consuming *trans*-MUFA and are a model of choice to study the metabolic fate of these components. In earlier studies on the rat (4–6), we observed that dietary elaidic acid (fed as trielaidin) could replace, after its conversion into elaidyl alcohol, an important proportion of the saturated alkenyl chains without affecting the percentage of the *cis*-9 18:1 chains. We thus suspected that *trans*-18:1 alkenyl chains might be present naturally in ruminant plasmalogens, which contain an important proportion of saturated alkenyl chains. We present evidence here that total plasmalogens from sheep heart, taken as a natural model, do contain *trans*-monounsaturated alkenyl chains with a distribution profile similar to that generally found in TAG from ruminant milk and adipose tissue lipids. Because plasmalogen alkenyl chains are derived from the corresponding alcohols, themselves produced from the corresponding FA, we also analyzed the FA from sheep adipose tissue.

\*Address correspondence at INRA, Unité de Nutrition Lipidique, 17, rue Sully, B.P. 86510, 21065 DIJON Cedex, France. E-mail: wolff@dijon.inra.fr  
Abbreviations: DCF, 2',7'-dichlorofluorescein; MUFA, monounsaturated fatty acids; TMDOA, trimethylene dioxyalkanyl.



## EXPERIMENTAL PROCEDURES

**Samples.** The heart of a sheep aged less than 6 mon was obtained from a local slaughterhouse and freed from apparent fatty tissues; the auricles were then removed. The ventricles were next divided into two parts (approximately 70 g each) and kept at  $-80^{\circ}\text{C}$  until use. Additionally, approximately 100 g of adipose tissue was taken off the animal and also stored at  $-80^{\circ}\text{C}$ .

**Lipid extraction and fractionation.** After thawing for 24 h at  $4^{\circ}\text{C}$ , one-half of the heart muscle was minced with scissors and homogenized with a household electric grinder. Fifteen grams of the homogenate was dispersed for 1 min in 80 mL methanol with an UltraTurrax T25 (Janke & Kunkel GmbH & Co. KG, Staufen, Germany) before adding 160 mL chloroform and performing a second 1-min homogenization with the UltraTurrax. The suspension was filtered on paper into a separatory funnel and washed with 50 mL of a 0.8% aqueous solution of NaCl (11). After standing for 1 h, the lower phase was withdrawn and the solvents were evaporated. The residue (775 mg) was dissolved in 7.7 mL of chloroform (*ca.* 100 mg/mL) and kept at  $-18^{\circ}\text{C}$  until use. Similarly, 5 g of adipose tissue was extracted with 20 mL of methanol, followed by 40 mL of chloroform. The final lipid extract (3.57 g) was dissolved in enough chloroform to make a 0.5 g lipid/mL solution.

An aliquot of the heart lipid solution (0.5 mL) was fractionated into neutral and polar lipids using a Sep-Pak<sup>®</sup> Plus silica cartridge (Waters Corporation, Milford, MA) eluted with 20 mL chloroform followed by 30 mL methanol. Polar lipids were dissolved in 1.5 mL of chloroform.

**Preparation of trimethylene dioxyalkanyl (TMDOA) derivatives.** A portion (250  $\mu\text{L}$ ) of the polar lipid solution was evaporated to dryness under a stream of  $\text{N}_2$  in a round-bottomed tube. The tube was inverted over a test tube cap containing 1 mL concentrated HCl for 5 min. The fumes cause complete hydrolysis of the alkenyl ether bond of the plasmalogens without affecting 1,2-diacyl- or 1-*O*-alkanyl-2-acyl glycerophospholipids (12,13). After flushing the tube with  $\text{N}_2$  to remove residual HCl vapors, the lipids were dissolved in 5 mL chloroform. Transformation of the released aldehydes into TMDOA was performed according to a modification of the method devised by Palmer *et al.* (14). To the preceding solution were added 10 mg of *p*-toluenesulfonic acid (Sigma-Aldrich Chimie S.à.r.l., Saint Quentin Fallavier, France) and 500  $\mu\text{L}$  of 1,3-propanediol (Sigma-Aldrich). The tube was tightly capped and the reaction was allowed to proceed for 3 h at  $80^{\circ}\text{C}$  with constant magnetic stirring. At the end of the reaction, the tube was cooled and the chloroform phase was washed with 5 mL distilled water. The chloroform phase was taken to dryness, and the residue dissolved in 0.5 mL of chloroform and fractionated into TMDOA and unreacted polar lipids on a Sep-Pak<sup>®</sup> cartridge as described above for neutral and polar lipids. TMDOA derivatives were further purified by TLC on precoated silica gel H plates (Merck, Darmstadt, Germany) with the solvents hexane/diethyl ether (80:20, vol/vol). TMDOA derivatives were visualized under UV light

(366 nm) after spraying a 0.2% ethanolic solution of 2',7'-dichlorofluorescein (DCF). The intense band with  $R_f = 0.66$  was scraped, and TMDOA derivatives were eluted with diethyl ether (three 2.5-mL portions). After filtration, the solvent was removed under a stream of  $\text{N}_2$ , and the residue was dissolved in 1 mL of hexane for further processing. A faint band observed near the origin was attributed to unreacted aldehydes or to residual 1,3-propanediol.

**FAME preparation.** To 250  $\mu\text{L}$  of the solution of lipids extracted from sheep adipose tissue was added 2.75 mL hexane, followed by 300  $\mu\text{L}$  of a 0.5 N solution of sodium methoxide in methanol. The mixture was thoroughly vortexed for 1 min and further heated for 10 min at  $50^{\circ}\text{C}$ . The reaction mixture was washed with 3 mL water, and the supernatant was withdrawn, evaporated to dryness, and dissolved in 1 mL of hexane.

**Fractionation of TMDOA derivatives and FAME.** TMDOA derivatives were fractionated according to the number and the configuration of ethylenic bonds by silver ion TLC as described elsewhere for FAME (15). The solvent was hexane/diethyl ether (75:25, vol/vol). The three bands ( $R_f = 0.50, 0.63,$  and  $0.75$ ) that were revealed as described above were scraped, and TMDOA derivatives were extracted with a biphasic solvent system that allowed removal of the DCF (15). FAME prepared from adipose tissue were processed in the same way, except that the proportions of solvents were 90:10 (vol/vol). Here too, the three main FAME bands with  $R_f = 0.82, 0.64,$  and  $0.45$  were scraped and the FAME eluted from the gel (15).

**GLC.** Unfractionated as well as fractionated TMDOA derivatives or FAME were analyzed on a HP 4890A chromatograph (Hewlett-Packard, Palo Alto, CA) equipped with a 100-m CP-Sil 88 capillary column [0.20 mm i.d., 0.25  $\mu\text{m}$  film (cyanopropyl siloxane polymer); Chrompack, Middelburg, The Netherlands]. Unless otherwise stated, the oven operating temperatures were:  $60^{\circ}\text{C}$  for 1 min, increase at  $20^{\circ}\text{C}/\text{min}$  to  $190^{\circ}\text{C}$  (TMDOA) or  $160^{\circ}\text{C}$  (FAME), then isothermal for 60 min, second increase at  $20^{\circ}\text{C}/\text{min}$  to  $210^{\circ}\text{C}$ , isothermal for 5 min. The injector (splitless; purge time set at 30 s) and the FID were maintained at 250 and  $280^{\circ}\text{C}$ , respectively. Hydrogen was the carrier gas, with a head pressure of 210 kPa. Injections (1  $\mu\text{L}$ ) were made automatically by an Agilent 6890 Series Injector (Hewlett-Packard). Alternatively, fractionated TMDOA were analyzed in a Hewlett-Packard 5890 Series II chromatograph, also equipped with an automatic injection system (same as above). The chromatograph was equipped with a 120-m BPX 70 capillary column [0.25 mm i.d., 0.20  $\mu\text{m}$  film (biscyanopropylsiloxane-silphenylene polymer); SGE, Melbourne, Australia] with  $\text{H}_2$  as a carrier gas (head pressure, 200 kPa). The injector and detector were maintained at 250 and  $280^{\circ}\text{C}$ , respectively. The column was operated under the same temperature programs as the CP-Sil 88 column. For specific purposes (separation of critical pairs), the temperature of the first plateau was lowered to  $140^{\circ}\text{C}$  (TMDOA and FAME).

**Identification and quantification of TMDOA derivatives and FAME.** Individual peaks of isomeric 18:1 FAME were

identified according to Wolff and Bayard (16). Identification of TMDOA was made by analogy with FAME isolated in comparable bands after silver ion TLC. Peaks were integrated and quantified with the Diamir software (© 1999 JMBS Inc., Fontaine, France; version 1.5.302.2). No correction factors were applied, and data are given as area percentages. Calculations of total *trans*- as well as *cis*-18:1 isomers were made through the use of *trans*-11 18:1 acid for *trans*-18:1 isomers, and of *cis*-9 18:1 acid, after subtraction of the *trans*-13 plus *trans*-14 critical pair, for *cis*-18:1 isomers.

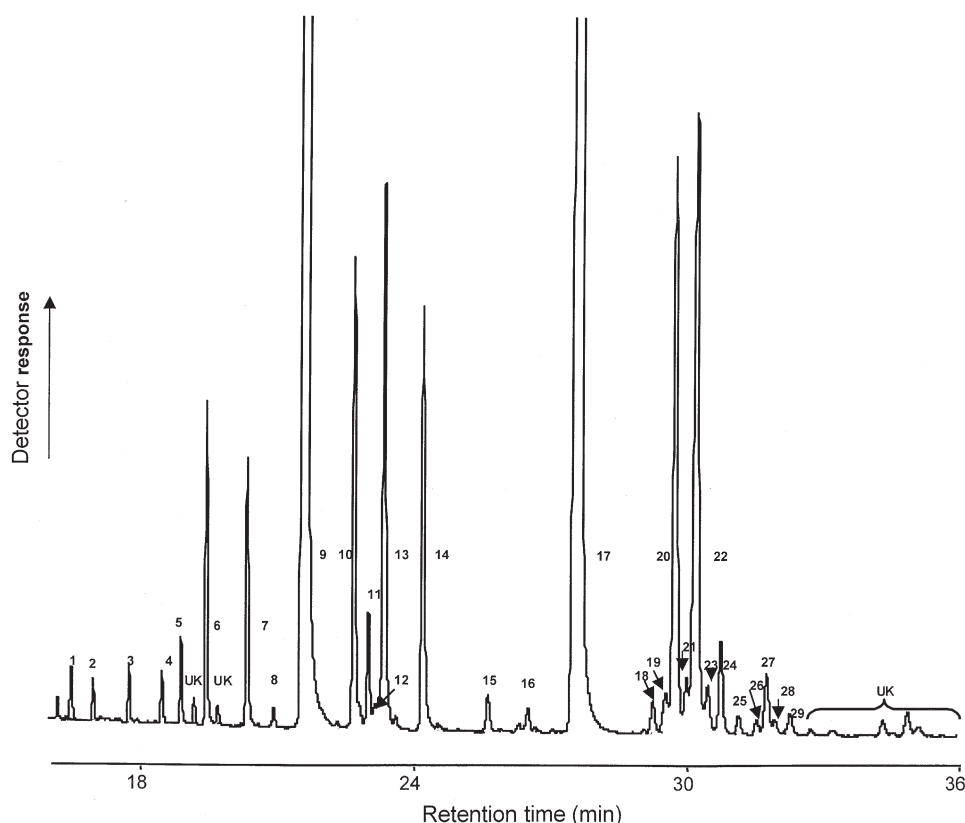
**GLC-MS.** The analysis of TMDOA, either unfractionated or fractionated, was performed using an HP6890 chromatograph coupled to an HP5973 mass spectrometer (Hewlett-Packard). A BPX 70 capillary column (50 m × 0.33 i.d., 0.25 μm film; SGE) was used with a temperature program from 50 to 190°C at a rate of 15°C/min. Helium was the carrier gas at a velocity of 36 m·s<sup>-1</sup>. The splitless injector was maintained at 250°C. The electron impact mass spectra were recorded at 70 eV between 30 and 350 amu.

## RESULTS AND DISCUSSION

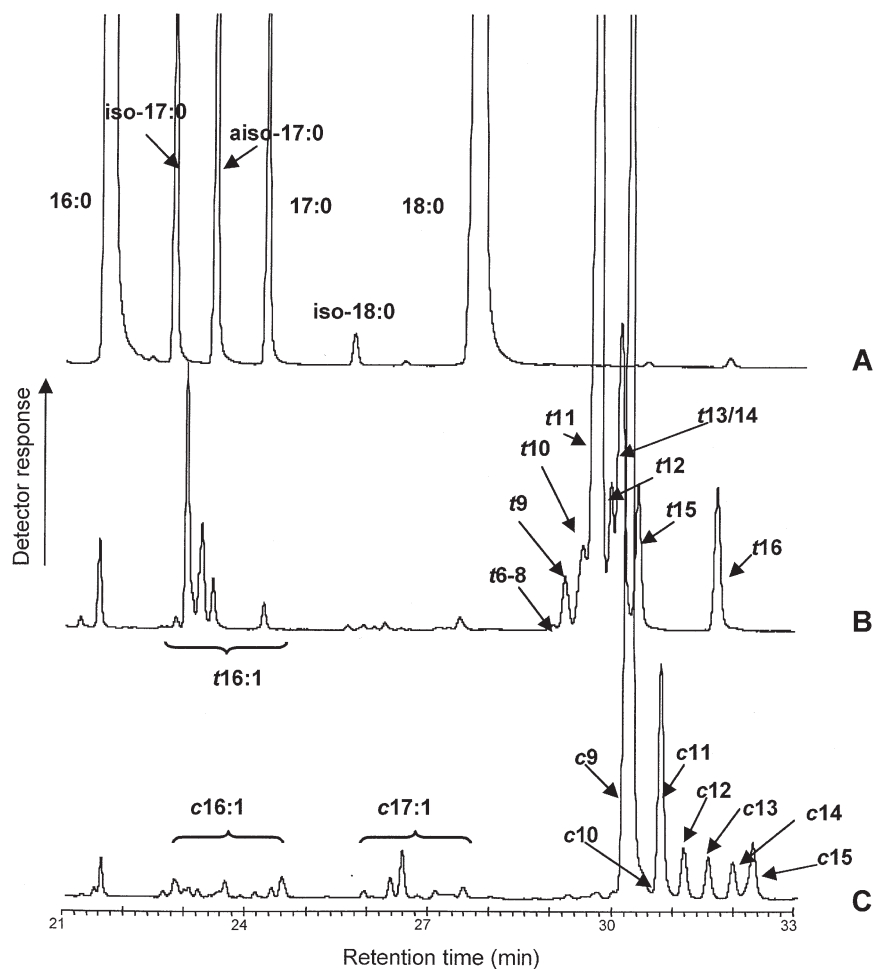
**Determination of alkenyl chain structures.** Recent information for sheep heart phospholipid composition unfortunately is lacking. However, in older studies (17,18), it was established that plasmalogens of the ethanolamine and choline

forms represent 31–41% (depending on the study), that is roughly one-third of total phospholipids in sheep heart. Sheep heart thus represents an interesting starting material for the study of plasmalogen alkenyl chains. Additionally, information on the composition of these alkenyl chains is lacking. However, it can be hypothesized that this composition should not be very different from that of beef heart, for which some compositions were published earlier (see Ref. 16). As indicated in the introductory statement, the alkenyl moieties are composed mostly of 16:0, 18:0, and 18:1 chains, to which minor amounts of branched (iso and anteiso forms) chains (odd- and even-numbered) should be added (19). Trials were made to use free aldehydes or dimethylacetals, but we could not obtain as good a resolution as with TMDOA by GLC at any operating temperature (results not shown).

As can be seen from the chromatogram of unfractionated TMDOA derivatives (Fig. 1), the profile of total plasmalogen alkenyl chains is more complex than recognized thus far. This undoubtedly results from the use of highly efficient polar capillary columns of great length. In most earlier studies, short packed columns with moderately polar stationary phases were used and obviously could not give such details. To simplify the identification of peaks, TMDOA derivatives fractionated by silver ion TLC were also analyzed under the same conditions (Fig. 2). The fraction with an  $R_f$  of 0.75 contained two main peaks, identified as 16:0 and 18:0. Three relatively



**FIG. 1.** Chromatogram of total trimethylene dioxyalkanyl derivatives of alkenyl chains from sheep heart plasmalogens. Analysis on a 100-m CP-Sil 88 capillary column operated under conditions described in the Experimental Procedures section (plateau at 190°C). Identification of peaks is given in Table 1 (UK, unknown structure).



**FIG. 2.** Partial chromatograms ( $C_{16}$  to  $C_{18}$  regions) of (A) saturated, (B) *trans*- and (C) *cis*-monoenoic trimethylene dioxyalkanyl derivatives of alkenyl chains from sheep heart plasmalogens fractionated by silver ion TLC. Analyses on a 100-m CP-Sil 88 capillary column operated under conditions described in the Experimental Procedures section (same as in Fig. 1).

minor peaks eluting between them were assigned the structures iso-17:0, anteiso-17:0, and 17:0. No peaks were found eluting after 18:0. Of the peaks eluting before 16:0, the identifications were based on those by Schmid *et al.* (19) for bovine heart plasmalogens: iso-14:0, 14:0, iso-15:0, anteiso-15:0, 15:0, and iso-16:0, in this elution order. The saturated FAME fraction ( $R_f = 0.82$ ) prepared from sheep adipose tissue showed exactly the same chain structure distribution (results not shown), with, however, different proportions (e.g., 18:0  $\gg$  16:0 in adipose tissue, instead of 16:0  $\gg$  18:0 in heart alkenyl chains).

The intermediate fraction of TMDOA with an  $R_f$  of 0.63 showed a GLC profile similar to that presented by *trans*-18:1 FAME prepared from milk or adipose tissue lipids from several ruminants (20–22), in particular to FAME prepared from sheep adipose tissue (results not shown), thus allowing the tentative identifications indicated in Figure 2. These identifications are also based on the principle that isomeric 18:1 isomers, such as FAME, FA isopropyl esters (16), or 2-alkenyl-4,4-dimethyloxazoline derivatives (23), are sequentially eluted as a function of the position of the ethylenic bond from

$\Delta 4$  to  $\Delta 16$ . With respect to the peak identified as  $\Delta 13/\Delta 14$  on the CP-Sil 88 column, the two isomers could be almost baseline-resolved with the BPX 70 column operated at low temperature (140°C; results not shown). The main peak is likely the  $\Delta 11$  isomer, biosynthetically derived from vaccenic (*trans*-11 18:1) acid through an intermediary alcohol. In addition to *trans*-monounsaturated  $C_{18}$  TMDOA derivatives, several minor *trans*-16:1 isomers could be observed in the same fraction (Fig. 2). According to a recent study on *trans*-16:1 isomers in ruminant milk fat, including ewes (24), the main *trans*-16:1 isomer would have its double bond in position  $\Delta 9$ . A *trans*-16:1 alkenyl chain was characterized in heart and kidney mitochondria of rats fed trielaidin (6), which would suggest possible chain-shortening of *trans*-octadecenoates to *trans*-hexadecenoates.

The slowest-moving TMDOA band collected after silver ion TLC corresponds to *cis*-monounsaturated TMDOA. This band contained one main *cis*-18:1 chain, likely the  $\Delta 9$  one. In addition, several minor peaks eluted after this peak are tentatively assigned the structures given in Figure 2, by analogy with the structures determined for FAME from ruminant fats

(20–22), in particular from sheep adipose tissue. Surprisingly, only traces of *cis*-16:1 isomers could be observed in the monounsaturated TMDOA fraction, in contrast to its FAME counterpart. On the other hand, *cis*-17:1 isomers were present in significant amounts.

GLC–MS of both unfractionated and fractionated TMDOA derivatives showed for all peaks a major fragment at  $m/z = 87$ , characteristic of the dioxane ring, as well as the molecular ion  $[M - 1]^+$  for each peak (Table 1). Unfortunately, no characteristic ions allowing determination of the position of the ethylenic bond are produced with these derivatives, and GC–MS could not confirm our tentative identifications of monounsaturated alkenyl chains.

**Quantitative aspects.** The proportions of the different alkenyl chains are given in Table 1. Total saturated chains account for *ca.* 85% of total alkenyl chains, with two components, 16:0 and 18:0, constituting the bulk of this group. As observed earlier by Schmid *et al.* (19) in alkenyl chains from beef heart, several odd-numbered as well as iso and anteiso forms occur in sheep heart plasmalogens. In particular, such chains with 17 carbon atoms represent 8.6% of total alkenyl chains (10% of saturated chains). Among the remaining

alkenyl chains, total *trans*-18:1 and *trans*-16:1 isomers account for 7.9 and 1%, respectively, whereas *cis*-18:1 isomers account for only 4.8% of the total. Thus, *cis*-18:1 isomers represent only slightly more than one-third of total 18:1 isomers.

In Table 2 are displayed the relative distributions of individual *trans*- and *cis*-18:1 isomers in heart plasmalogen alkenyl chains and in adipose tissue acyl chains (determined after silver ion TLC). The two earliest-eluting *trans* isomers ( $\Delta 4$  and  $\Delta 5$ ), present in adipose tissue, were not observed in heart plasmalogens. In both TMDOA and FAME fractions, one component is predominant: for FAME, it corresponds to vaccenic acid (*ca.* 74%), and it is inferred that the double bond in the major TMDOA (*ca.* 60%) similarly is at the  $\Delta 11$  position. The  $\Delta 13/\Delta 14$  pair (either in TMDOA or in FAME), not resolved at 190°C on the CP-Sil 88 column, could easily be split at 140°C on the BPX 70 column, allowing quantification of both isomers (they are present in almost similar amounts in both TMDOA and FAME). Isomers with their ethylenic bond between the  $\Delta 12$  and  $\Delta 16$  positions are present in higher proportions in heart plasmalogens than in adipose tissue TAG. This would suggest that some discrimination may exist between the utilization of isomeric *trans*-18:1 acids for their deposition in depot fats and their incorporation (after their reduction to fatty alcohols) into plasmalogens.

Regarding the *cis*-18:1 fraction, some differences also are visible between TMDOA (heart plasmalogens) and FAME

**TABLE 1**  
Alkenyl Chain Composition of Total Plasmalogens from Sheep Heart Analyzed as Trimethylene Dioxyalkanyl (TMDOA) Derivatives

Peak number <sup>a</sup>	Structure of the alkyl chain of TMDOA <sup>b</sup>	$[M - 1]^+$ <sup>c</sup>	Area % <sup>d</sup>
1	13:0	255	0.23
2	iso-14:0	269	0.14
3	14:0	269	0.21
4	iso-15:0	283	0.19
5	anteiso-15:0	283	0.35
6	15:0	283	1.33
7	iso-16:0	297	1.26
8	anteiso-16:0	297	0.11
9	16:0	297	45.30
10	iso-17:0	311	2.66
11	<i>t</i> -16:1	295	0.64
12	<i>t</i> -16:1	295	0.16
13	anteiso-17:0	311	3.35
14	17:0	311	2.56
15	iso-18:0	325	0.26
16	<i>c</i> -17:1	309	0.18
17	18:0	325	26.72
18	<i>t</i> $\Delta$ 9 18:1	323	0.26
19	<i>t</i> $\Delta$ 10 18:1	323	0.38
20	<i>t</i> $\Delta$ 11 18:1	323	4.63
21	<i>t</i> $\Delta$ 12 18:1	323	0.44
22	<i>t</i> $\Delta$ 13, <i>t</i> $\Delta$ 14, <i>c</i> $\Delta$ 9 18:1	323	5.46
23	<i>t</i> $\Delta$ 15, <i>c</i> $\Delta$ 10 18:1	323	0.45
24	<i>c</i> $\Delta$ 11 18:1	323	0.76
25	<i>c</i> $\Delta$ 12 18:1	323	0.16
26	<i>c</i> $\Delta$ 13 18:1	323	0.12
27	<i>t</i> $\Delta$ 16 18:1	323	0.53
28	<i>c</i> $\Delta$ 14 18:1	323	0.13
29	<i>c</i> $\Delta$ 15 18:1	323	0.21

<sup>a</sup>Peak numbers refer to Figure 1.

<sup>b</sup>*t*, *trans*; *c*, *cis*.

<sup>c</sup>Determined by GLC coupled to MS.

<sup>d</sup>Means of two analyses on a CP-Sil 88 column (plateau at 190°C; see the Experimental Procedures section for other operating conditions).

**TABLE 2**  
Relative Composition of *cis* and *trans* Monounsaturated Alkenyl Chains of Total Plasmalogens from Sheep Heart Analyzed as TMDOA. Comparison with FAME Prepared from Sheep Adipose Tissue<sup>a</sup>

Double bond position <sup>b</sup>	TMDOA (area %)	FAME (area %)
<i>t</i> $\Delta$ 4	— <sup>c</sup>	0.4
<i>t</i> $\Delta$ 5	—	0.2
<i>t</i> $\Delta$ 6– $\Delta$ 8	0.2	2.3
<i>t</i> $\Delta$ 9	2.4	1.4
<i>t</i> $\Delta$ 10	4.6	2.8
<i>t</i> $\Delta$ 11	59.3	73.6
<i>t</i> $\Delta$ 12	5.6	3.3
<i>t</i> $\Delta$ 13	7.5	4.4
<i>t</i> $\Delta$ 14	8.2	4.4
<i>t</i> $\Delta$ 15	6.0	3.2
<i>t</i> $\Delta$ 16	6.1	4.0
<i>c</i> $\Delta$ 6/ <i>c</i> $\Delta$ 8	Trace <sup>d</sup>	0.2
<i>c</i> $\Delta$ 9/ <i>c</i> $\Delta$ 10	76.5 <sup>e</sup>	92.4
<i>c</i> $\Delta$ 11	12.8	4.1
<i>c</i> $\Delta$ 12	2.6	1.1
<i>c</i> $\Delta$ 13	2.3	0.3
<i>c</i> $\Delta$ 14	2.1	0.4
<i>c</i> $\Delta$ 15	3.7	1.5

<sup>a</sup>Data were obtained by a combination of analyses of TMDOA and FAME on 100-m CP-Sil 88 and BPX 70 capillary columns operated as indicated in the Experimental Procedures section. The critical pair *t* $\Delta$ 13/*t* $\Delta$ 14, not separated under routine analytical conditions, was almost baseline-resolved at 140°C on the BPX 70 column.

<sup>b</sup>For abbreviations see Table 1.

<sup>c</sup>Not detected.

<sup>d</sup>Less than 0.2%.

<sup>e</sup>With both TMDOA and FAME, the *c* $\Delta$ 10 isomer could only be separated as a small shoulder at the base of the descending edge of the main *c* $\Delta$ 9 isomer and could not be correctly integrated.



(adipose tissue TAG) (Table 2). In FAME, the proportion of the  $\Delta 9$  isomer is higher than that in TMDOA, whereas the  $\Delta 11$  isomer is higher in TMDOA than in FAME. More generally, the proportions of isomers with their ethylenic bond between  $\Delta 11$  and  $\Delta 15$  are higher in TMDOA than in FAME. Here too, some discrimination may exist in targeting individual *cis*-18:1 isomers to plasmalogens or to TAG.

## ACKNOWLEDGMENTS

The author is much indebted to Mariannick Darbois and Pierre Juanéda for their invaluable assistance.

## REFERENCES

- Emken, E.A., and Dutton, H.J., eds. (1979) *Geometrical and Positional Fatty Acid Isomers*, American Oil Chemists' Society, Champaign.
- Sébédio, J.L., and Christie, W.W., eds. (1998) *Trans Fatty Acids in Human Nutrition*, Oily Press, Dundee, Scotland.
- Mukherjee, K.D., and Kiewitt, I. (1980) Incorporation of Isomeric Octadecenoic Acids into Alk-1-enyl Moieties of Cardiac Glycerophospholipids of the Rat, *FEBS Lett.* 122, 133–134.
- Wolff, R.L., Combe, N.A., and Entressangles, B. (1985) Modification of Alkenyl Chain Profile in Plasmalogens of Rat Heart Mitochondria by Dietary Trielaidin, *Lipids* 20, 367–372.
- Wolff, R.L., Combe, N.A., and Entressangles, B. (1987) Effets Comparés de l'Acide Elaïdique Alimentaire sur les Chaînes Alkényles et Acyles des Glycerophospholipides de Mitochondries de Reins de Rats, *Rev. Fr. Corps Gras* 34, 525–532.
- Wolff, R.L., Combe, N.A., and Entressangles, B. (1988) Evolution au Cours du Temps de la Composition en Chaînes Alkényles et Acyles des Plasmalogènes de Mitochondries de Cœur et de Reins chez des Rats Ingérant de la Triélaïdine, *Reprod. Nutr. Develop.* 28, 603–615.
- Lee, T.C., Hougland, A.E., and Stephens, S. (1979) Perturbation of Lipid Metabolism in L-M Cultured Cells by Elaïdic Acid Supplementation: Formation of Fatty Alcohols, *Biochem. Biophys. Res. Commun.* 91, 299–304.
- Lee, T.C., and Stephens, S. (1982) The Modification of Lipid Composition in L-M Cultured Cells Supplemented with Elaïdate. Increased Formation of Fatty Alcohol, *Biochim. Biophys. Acta* 712, 299–304.
- Wykle, R.L., Malone, B., and Snyder, F. (1979) Acyl-CoA Reductase Specificity and Synthesis of Wax Esters in Mouse Preputial Gland Tumors, *J. Lipid Res.* 20, 890–896.
- Weber, N., and Richter, I. (1982) Formation of Ether Lipids and Wax Esters in Mammalian Cells. Specificity of Enzymes with Regard to Carbon Chains of Substrates, *Biochim. Biophys. Acta* 711, 197–207.
- Folch, J., Lees, M., and Sloane-Stanley, G.M. (1957) A Simple Method for the Isolation of Total Lipids from Animal Tissues, *J. Biol. Chem.* 226, 497–509.
- Oshima, T., Wada, S., and Koizumi, C. (1989) 1-*O*-Alk-1'-enyl-2-acyl and 1-*O*-Alkyl-2-acyl Glycerophospholipids in White Muscle of Bonito *Euthynnus pelamis* (Linnaeus), *Lipids* 24, 363–370.
- Murphy, E.J., Stephens, R., Jurkowitz-Alexander, M., and Horrocks, L.A. (1993) Acidic Hydrolysis of Plasmalogens Followed by High-Performance Liquid Chromatography, *Lipids* 28, 565–568.
- Palmer, J.W., Schmid, P., Pfeiffer, D.R., and Schmid, H.H.O. (1981) Lipids and Lipolytic Enzyme Activities of Rat Heart Mitochondria, *Arch. Biochem. Biophys.* 211, 674–682.
- Wolff, R.L. (1994) Contribution of *trans*-18:1 Acids from Ruminant Fats to European Diet, *J. Am. Oil Chem. Soc.* 71, 277–283.
- Wolff, R.L., and Bayard, C.C. (1995) Improvement in the Resolution of *trans*-18:1 Isomers by Capillary Gas–Liquid Chromatography: Use of a 100-m CP-Sil 88 Column, *J. Am. Oil Chem. Soc.* 72, 1197–1201.
- White, D.A. (1973) The Phospholipid Composition of Mammalian Tissues, in *Form and Function of Phospholipids* (Ansell, G.B., Dawson, R.M.C., and Hawthorne, J.N., eds.), Elsevier, Amsterdam, pp. 441–482.
- Getz, G.S., Bartley, W., Lurie, D., and Notton, B.M. (1968) The Phospholipids of Various Sheep Organs, Rat Liver and of Their Subcellular Fractions, *Biochim. Biophys. Acta* 152, 325–339.
- Schmid, H.H.O., Bandi, P.C., and Sun, K.K. (1971) The Structures of the Branched-Chain Alk-1-enyl Ethers of Bovine Heart Muscle, *Biochim. Biophys. Acta* 152, 270–273.
- Precht, D., Molkenin, J., Destailats, F., and Wolff, R.L. (2001) Comparative Studies on Individual Isomeric 18:1 Acids in Cow, Goat, and Ewe Milk Fats by Low-Temperature High-Resolution Capillary Gas–Liquid Chromatography, *Lipids* 36, 827–832.
- Wolff, R.L., Precht, D., Nasser, B., and El Kebbij, M.S. (2001) *Trans*- and *cis*-Octadecenoic Isomers in the Hump and Milk Lipids from *Camelus dromedarius*, *Lipids* 36, 1175–1178.
- Wolff, R.L., Precht, D., and Molkenin, J. (1998) Occurrence and Distribution Profiles of *trans*-18:1 Acids in Edible Fats of Natural Origin, in *Trans Fatty Acids in Human Nutrition* (Sébédio, J.L., and Christie, W.W., eds.), pp. 1–33, Oily Press, Dundee, Scotland.
- Mossoba, M.M., McDonald, R.E., Roach, J.A.G., Fingerhut, D.D., Yurawecz, M.P., and Sehat, N. (1997) Spectral Confirmation of *Trans* Monounsaturated C<sub>18</sub> Fatty Acid Positional Isomers, *J. Am. Oil Chem. Soc.* 74, 125–130.
- Destailats, F., Wolff, R.L., Precht, D., and Molkenin, J. (2000) Study of Individual *trans*- and *cis*-16:1 Isomers in Cow, Goat, and Ewe Cheese Fats by Gas–Liquid Chromatography with Emphasis on the *trans*- $\Delta 3$  Isomer, *Lipids* 35, 1027–1032.

[Received December 18, 2001; accepted June 26, 2002]

# A Direct Method for Regiospecific Analysis of TAG Using $\alpha$ -MAG

F. Turon<sup>a,\*</sup>, P. Bachain<sup>b</sup>, Y. Caro<sup>b</sup>, M. Pina<sup>b</sup>, and J. Graille<sup>b</sup>

<sup>a</sup>Sea Oil, Beaumont-Hague, France, and <sup>b</sup>Lipotech Laboratory, CIRAD-AMIS, Montpellier, France

**ABSTRACT:** An analytical procedure was developed for regiodistribution analysis of TAG using  $\alpha$ -MAG prepared by an ethyl magnesium bromide deacylation. In the present communication, the deacylation procedure is shown to lead to representative  $\alpha$ -MAG, allowing the composition of the native TAG in the  $\alpha$ -position to be determined directly. The composition in the  $\beta$ -position can then be estimated from the composition of the  $\alpha$ -MAG and TAG according to the formula  $3 \times \text{TAG} - 2 \times \alpha\text{-MAG}$ . The estimates are superior to those obtained using the  $\alpha,\beta$ -DAG and Brockerhoff calculations as they come closer to the theoretical value and have smaller SD. The present procedure, first demonstrated on a synthetic TAG, was then successfully applied to the analysis of borage oil, milkfat, and tuna oil.

Paper no. L8939 in *Lipids* 37, 817–821 (August 2002).

Much work has been done to simplify the regiodistribution analysis of TAG using a chemical deacylation (1–4). Since the chemical deacylation makes most of the TAG accessible to a regiodistribution analysis (5–8), difficulties are due to the occurrence of some unavoidable acyl migration, which naturally changes analysis results (9). In order to improve the accuracy of analysis, suitable conditions need to be found to minimize the incidence of isomerization and, therefore, for the Grignard deacylation to produce acylglycerols representative of the original TAG structure. Accordingly, methods in the literature generally make use of  $\alpha,\beta$ -DAG (9–13) or  $\beta$ -MAG (2), with appropriate calculations. A shortcoming is that the FA composition of the  $\alpha$ -position is not analyzed directly but obtained by calculation and is therefore subject to cumulative errors of GC analysis (10,13). Some recent methods using both the  $\alpha$ - and  $\beta$ -MAG produced from TAG by a Grignard deacylation involve their analysis by HPLC on chiral columns (1,3). However, use of these methods on a routine basis is laborious, since they require special and expensive analytical equipment rather than the standard GC equipment.

In the present communication, we have examined the possibility of producing representative  $\alpha$ -MAG, i.e., with a random FA distribution, by an ethyl magnesium bromide deacylation of TAG. The classical procedure of deacylation is modified to (i) find suitable conditions for decreasing isomerization, (ii) determine the regiospecific distribution through the GC analysis of  $\alpha$ -MAG, and (iii) corroborate the results obtained with the pancreatic lipase hydrolysis (standardized procedure ISO 6800).

The method was first demonstrated by the regiodistribution analysis of a racemic *sn*-1,3-dipalmitoleyl-*sn*-2-oleoyl-glycerol (POP), then by the analysis of borage oil, milkfat, and tuna oil.

## EXPERIMENTAL PROCEDURES

**Materials.** Borage oil was obtained from Bertin (Lagny-lesec, France). Tuna oil was an industrial product from Sea Oil (Beaumont-Hague, France). Milkfat was obtained from Bel (Vendome, France). The racemic synthetic POP (99%+), a crude lipase from porcine pancreas, and a 0.2% solution of 2',7'-dichlorofluorescein in ethanol (DCF solution) were purchased from Sigma Chemical Company (St. Louis, MO). A 3.0-M solution of ethyl magnesium bromide ( $\text{C}_2\text{H}_5\text{MgBr}$ ) in diethyl ether was obtained from Aldrich (Milwaukee, WI). A methanolic solution of boron trifluoride (10%, wt/vol) was obtained from Fluka (Hauptpauge, New York). Silicic acid 60 F<sub>254</sub> TLC plates were obtained from Merck (Darmstadt, Germany). Anhydrous  $\text{NaHCO}_3$ , boric acid, and all organic solvents were also from Merck.

**Pancreatic lipase hydrolysis.** The standard pancreatic lipase hydrolysis procedure used to determine the FA composition in the  $\beta$ -position of TAG was modified from Luddy *et al.* (14).

**Chemical deacylation of TAG.** Forty milligrams of pure TAG was dissolved in 2 mL of dry diethyl ether. A  $\text{C}_2\text{H}_5\text{MgBr}$  solution (670  $\mu\text{L}$ ) was added directly using a pipette equipped with a positive displacement mechanism that isolated the aspirated liquid from the air (Gilson, Middleton, WI). The mixture was shaken for 15 s, then 300  $\mu\text{L}$  of glacial acetic acid was added, followed by 5 mL of a 0.4-M boric acid solution in water to stop the reaction. The lipid products (newly formed partial acylglycerols, tertiary alcohols, and residual TAG) were then extracted with the diethyl ether. This extract was washed with a 5-mL solution of aqueous boric acid (0.4 M)/aqueous  $\text{NaHCO}_3$  (2%), 50:50 (vol/vol) then resolved by TLC without further treatment.

The MAG were quickly isolated by preparative TLC on precoated silicic acid that was impregnated with a 5% boric acid solution in methanol (wt/vol) to prevent isomerization (15). The plates were developed with a chloroform/acetone/acetic acid solution (85:15:1, by vol) to isolate the *sn*-1(3)- from the *sn*-2-MAG. After development, bands were revealed and visualized with the DCF solution under UV light (366 nm). The following bands were observed:  $\alpha$ -MAG ( $R_f = 0.26$ );  $\beta$ -MAG ( $R_f = 0.38$ );  $\alpha,\beta$ -DAG ( $R_f = 0.76$ );  $\alpha,\alpha'$ -DAG ( $R_f = 0.85$ ); tertiary alcohols of the deacylated FA and residual TAG ( $R_f = 0.95$ ). The silica gel of corresponding bands

\*To whom correspondence should be addressed at Danone Vitapole, RD 128, F 91767 Palaiseau Cedex, France.

E-mail: fturon@danone.com

Abbreviations: DCF, 2',7'-dichlorofluorescein; POP, *sn*-1,3-dipalmitoleyl-*sn*-2-oleoyl-glycerol.

was scraped off and transferred to Teflon-lined screw-capped tubes for methyl ester preparation.

**Methyl ester preparation and analysis.** Methyl esters were prepared according to Morrison and Smith (16). A methanolic solution (0.5 to 0.8 mL) of boron trifluoride was added directly to the silica gel, and methylation was performed at 100°C for 60 min.

FAME were analyzed by GLC with a Carlo Erba GC 8000 Top apparatus (Erba Science, Paris, France) equipped with an FID. Methyl esters were separated in a glass capillary column (30 m × 0.32 mm i.d.) coated with CARBOWAX 20M, programmed from 185 to 210°C (4°C/min), and held isothermally for 10 min. Peak areas and percentages were calculated by a Merck D2000 integrator. Areas obtained with the integrator were divided by chain length to yield the mole percentage of FA.

## RESULTS

**Regiodistribution analysis of POP.** The degree of purity of the POP was first verified. Pancreatic lipase hydrolysis confirmed that the β-position was occupied almost entirely by oleic acid (98.5%) and that the α-position was occupied by palmitic acid (99.3%). Results of the analysis of partial acylglycerols obtained from the Grignard degradation of POP are detailed in Table 1. Results of the analysis of the α,β-DAG agreed well with the lipase hydrolysis, certainly within the limits of analysis errors. The α,α'-DAG was contaminated with isomerized α,β-DAG, as evidenced by the content of oleic acid (4.5%). The β-MAG were strongly contaminated with 5.6% palmitic acid that had migrated from the α-position. We observed only 1.8% contamination of α-MAG. Con-

sequently, the results from the α-MAG analysis were closer to the reference value and provided direct analysis of the α-position. The FA distribution in the β-position could then be analyzed by direct determination through the β-MAG or by calculation based on the composition of the different acylglycerols, as demonstrated at the bottom of Table 1. The most accurate estimate was obtained by calculation from  $3 \times \text{TAG} - 2 \times \alpha\text{-MAG}$ . The estimates were  $96.3 \pm 0.9\%$  (mean ± SD) oleic acid.

Although the FA profile of the α,β-DAG was closer to the FA distribution of the original TAG, the estimates based on the α,β-DAG composition gave negative values. This reflects the larger factors of the equation  $4 \times \alpha, \beta\text{-DAG} - 3 \times \text{TAG}$  than the equations used with α-MAG. The positional analysis obtained by calculation from the α,β-DAG was therefore subject to cumulative experimental errors of GC analysis.

**Regiodistribution analysis of borage oil.** The method was then applied to determine the regiospecific distribution of borage oil. First, pancreatic lipase hydrolysis was used to determine the composition at the β-position through the β-MAG. To verify the validity of the lipase hydrolysis, the TAG composition was recalculated from the composition of α,β-DAG and β-MAG through the equation  $3 \times \text{TAG} = 4 \times \alpha, \beta\text{-DAG} - \beta\text{-MAG}$  (Table 2). Results showed excellent agreement with the data for the composition of TAG (multiple correlation coefficient  $R = 0.993$ , with a confidence interval of 95%), confirming that the enzymatic deacylation generated a random mixture of representative acylglycerols. Table 2 gives the analysis of partial acylglycerols from the Grignard deacylation compared with the results obtained with pancreatic lipase. Nonreproducible results were obtained for the β-MAG analysis; the FA composition disagreed within 3% (absolute) for the minor component (palmitic acid). The composition in the β-position could then be estimated from the composition of α-MAG and TAG. The estimates compared favorably to those found using the pancreatic lipase procedure, as they came closer to the theoretical value and had smaller SD (Table 3). The composition of the FA at the α-position could be calculated from data for α,β-DAG and TAG or from TAG minus β-MAG. However, a direct analysis of α-MAG was preferable, since the results obtained were more accurate and showed smaller SD than those obtained by calculations from the α,β-DAG (Table 4).

**Regiodistribution analysis of tuna oil and milkfat.** The results obtained by the modified regiodistribution analysis of milkfat and tuna oil, respectively, are presented in Tables 5 and 6. These confirm previously published work on the FA regiodistribution of these substrates for the short- or medium-chain FA ( $C_{10}$  or less) (17,18) or for very long chain PUFA (19,20).

Regiodistribution analysis on the basis of the classical procedures involving α,β-DAG or β-MAG is often complicated for fats and oils with a widely diverse FA spectrum, such as milkfat or fish oils. The superposition of elution bands in the TLC technique is the main problem, so this analytical limitation was eliminated in our approach of using boric acid coated

**TABLE 1**  
Regiospecific Analysis of Synthetic  
*sn*-1,3-Dipalmitoleyl-*sn*-2-oleoyl-glycerol

Method	Compound	Positions	FA composition <sup>a</sup> (mol% <sup>b</sup> )	
			16:0	18:1
Pancreatic lipase	TAG	α, β, α'	66.7	33.3 ± 0.2
	β-MAG	β	1.5	98.5 ± 0.9
	α,β-DAG	α, β, α'	49.8	50.2 ± 0.4
	α FA <sup>c</sup>	α, α'	99.3	0.7 ± 0.4
C <sub>2</sub> H <sub>5</sub> MgBr	β-MAG	β	5.6	94.4 ± 3.5
	α,β-DAG	α, β, α'	49.4	50.6 ± 0.1
	α,α'-DAG	α, α'	95.5	4.5 ± 1.2
	α-MAG	α, α'	98.2	1.8 ± 0.4
	$4 \times \alpha, \beta\text{-DAG} - 3 \times \text{TAG}$	β	-2.5	102.5 ± 0.5
	$3 \times \text{TAG} - 2 \times \alpha\text{-MAG}$	β	3.7	96.3 ± 0.9
	Direct β-MAG	β	5.6	94.4 ± 3.5
	$3 \times \text{TAG} - 2 \times \alpha, \beta\text{-DAG}$	α, α'	101.3	-1.3 ± 0.2
	$(3 \times \text{TAG} - \beta\text{-MAG})/2$	α, α'	97.3	2.7 ± 1.8
	Direct α-MAG	α, α'	98.2	1.8 ± 0.4

<sup>a</sup>Values are means ± SD of two GC analyses of products from four hydrolysis experiments.

<sup>b</sup>Areas obtained with the integrator were divided by chain length to yield the mole percentage of FA.

<sup>c</sup>Calculated from the equation  $2 \times \alpha\text{-MAG} = 3 \times \text{TAG} - \beta\text{-MAG}$ .

**TABLE 2**  
**Regiospecific Analysis of Borage Oil Obtained by Hydrolysis with Pancreatic Lipase and Deacylation with Ethyl Magnesium Bromide**

	Compound	Position	FA composition <sup>a</sup> (mol%)						
			16:0	18:0	18:1	18:2	18:3	20:1	22:1
Pancreatic lipase	TAG	$\alpha$ , $\beta$ , $\alpha'$	11.7 (0.2)	4.0 (0.1)	18.7 (0.1)	38.2 (0.1)	21.5 (0.1)	3.7 (0.1)	2.1 (0.1)
	$\beta$ -MAG	$\beta$	1.3 (0.1)	0.4 (0.1)	18.2 (0.3)	42.6 (0.5)	37.0 (0.3)	0.4 (0.1)	0.0 (0.0)
	$\alpha$ , $\beta$ -DAG	$\alpha$ , $\beta$	10.4 (0.2)	3.2 (0.1)	17.1 (0.1)	38.7 (0.1)	27.0 (0.5)	2.4 (0.1)	1.2 (0.2)
	TAG <sup>b</sup>	$\alpha$ , $\beta$ , $\alpha'$	13.3 (0.4)	4.1 (0.1)	16.7 (0.3)	37.5 (0.7)	23.7 (0.7)	3.1 (0.1)	1.6 (0.3)
C <sub>2</sub> H <sub>5</sub> MgBr	$\alpha$ , $\beta$ -DAG	$\alpha$ , $\beta$ , $\alpha'$	9.2 (0.2)	3.1 (0.1)	18.1 (0.2)	39.4 (0.2)	26.0 (0.3)	2.7 (0.1)	1.4 (0.1)
	$\beta$ -MAG	$\beta$	4.0 (3.0)	2.1 (2.1)	18.0 (1.5)	39.8 (2.3)	35.5 (1.9)	0.4 (0.3)	0.1 (0.2)
	$\alpha$ -MAG	$\alpha$ , $\alpha'$	16.9 (0.9)	6.0 (0.1)	19.5 (0.2)	36.9 (0.5)	12.7 (0.3)	5.2 (0.2)	2.8 (0.3)
	TAG <sup>c</sup>	$\alpha$ , $\beta$ , $\alpha'$	12.6 (1.5)	4.7 (0.9)	19 (1.0)	37.9 (1.6)	20.3 (1.1)	3.6 (0.8)	1.9 (0.3)

<sup>a</sup>Values are means  $\pm$  SD of two GC analyses of products from four hydrolysis experiments.<sup>b</sup>Recalculated from the equation  $3 \times \text{TAG} = 4 \times \alpha$ , $\beta$ -DAG  $- \beta$ -MAG.<sup>c</sup>Recalculated from the equation  $3 \times \text{TAG} = \beta$ -MAG  $+ 2 \times \alpha$ -MAG.**TABLE 3**  
**Results of Regiospecific Analysis of Borage Oil According to the Pancreatic Lipase Hydrolysis and Ethyl Magnesium Bromide Deacylation:  $\beta$ -Position**

Compound	FA composition <sup>a</sup> (mol%)						
	16:0	18:0	18:1	18:2	18:3	20:1	22:1
$\beta$ -MAG <sup>b</sup>	1.3 (0.1)	0.4 (0.1)	18.2 (0.3)	42.6 (0.5)	37.0 (0.3)	0.4 (0.1)	0.0 (0.0)
$4 \times \alpha$ , $\beta$ -DAG $- 3 \times \text{TAG}$	1.7 (1.0)	0.2 (0.2)	16.3 (0.8)	42.8 (0.8)	39.7 (1.3)	-0.2 (0.1)	-0.5 (0.2)
$\beta$ -MAG <sup>c</sup>	4.0 (3.0)	2.1 (2.1)	18.0 (1.5)	39.8 (2.3)	35.5 (1.9)	0.4 (0.3)	0.1 (0.2)
$3 \times \text{TAG} - 2 \times \alpha$ -MAG	1.3 (1.7)	0.1 (0.2)	17.2 (0.4)	41.1 (1.1)	39.0 (0.6)	0.7 (0.5)	0.7 (0.6)

<sup>a</sup>Values are means  $\pm$  SD of two GC analyses of products from four hydrolysis experiments.<sup>b</sup>From Table 2, Pancreatic lipase.<sup>c</sup>From Table 2, C<sub>2</sub>H<sub>5</sub>MgBr.**TABLE 4**  
**Results of Regiospecific Analysis of Borage Oil According to the Pancreatic Lipase Hydrolysis and Ethyl Magnesium Bromide Deacylation:  $\alpha$ -Position**

Compound	FA composition <sup>a</sup> (mol%)						
	16:0	18:0	18:1	18:2	18:3	20:1	22:1
$(3 \times \text{TAG} - \beta$ -MAG)/2 <sup>b</sup>	16.9 (0.1)	5.8 (0.1)	18.9 (0.2)	36.2 (0.2)	13.8 (0.2)	5.3 (0.0)	3.1 (0.0)
$3 \times \text{TAG} - 2 \times \alpha$ , $\beta$ -DAG	16.7 (0.5)	5.9 (0.1)	19.9 (0.4)	36.0 (0.4)	12.4 (0.7)	5.6 (0.1)	3.4 (0.1)
$\alpha$ -MAG <sup>c</sup>	16.9 (0.9)	6.0 (0.1)	19.5 (0.2)	36.9 (0.5)	12.7 (0.3)	5.2 (0.2)	2.8 (0.3)
$(3 \times \text{TAG} - \beta$ -MAG)/2	15.6 (1.5)	4.9 (1.0)	19.0 (0.7)	37.5 (1.2)	14.5 (0.9)	5.3 (0.2)	3.1 (0.1)

<sup>a</sup>Values are means  $\pm$  SD of two GC analyses of products from four hydrolysis experiments.<sup>b</sup>From Table 2, Pancreatic lipase.<sup>c</sup>From Table 2, C<sub>2</sub>H<sub>5</sub>MgBr.**TABLE 5**  
**Experimental<sup>a</sup> and Literature<sup>b</sup> Values for Principal FA Distribution Between  $\alpha$ - and  $\beta$ -Positions of Milkfat**

Position	FA composition (mol%)									
	4:0	6:0	8:0	10:0	12:0	14:0	16:0	18:0	18:1	18:2
$\alpha$ -Position	11.4 (10.2–17.5)	6.1 (5.5–7.4)	2.2 (2.0–3.3)	3.3 (3–4)	3.6 (3–3.7)	9.7 (8–10.2)	27.1 (19.5–28)	11.5 (5.5–11.9)	15.1 (14.6–26.5)	1.2 (0.4–2.0)
$\beta$ -Position	— <sup>c</sup> (—)	0.4 (0.1–1)	1.9 (1–2.9)	6.9 (3–7.8)	7.6 (6–8.1)	20.3 (18–23)	42.9 (32–36.7)	6.2 (3–10)	9.6 (7.2–19)	1.1 (0.6–4.0)

<sup>a</sup>Values are means  $\pm$  SD of five replicate analyses.<sup>b</sup>Literature data are in parentheses.<sup>c</sup>Concentrations lower than 0.1% are not reported.



**TABLE 6**  
**Experimental<sup>a</sup> and Literature<sup>b</sup> Values for FA Distribution**  
**Between  $\alpha$ - and  $\beta$ -Positions of Tuna Oil**

FA	FA composition (mol%)	
	$\beta$ -Position	$\alpha$ -Position
14:0	6.4 ± 0.7 (3.5–7.6)	4.3 ± 0.6 (3.0–4.7)
15:0	0.9 ± 0.4 (0.7–1.5)	1.9 ± 0.5 (0.9–1.5)
16:0	18.5 ± 1.8 (8.9–16.7)	18.5 ± 1.8 (13.5–22.3)
16:1n-7	5.7 ± 0.9 (5.5–7.1)	5.7 ± 0.7 (5.5–7.8)
16:2	2.8 ± 0.2 (2.7–3.1)	1.3 ± 0.2 (1.4–1.6)
17:0	0.3 ± 0.0 (0.2–0.5)	1.2 ± 0.0 (0.7–1.4)
18:0	0.1 ± 0.0 (0.4–1.3)	7.3 ± 0.1 (2.3–7.5)
18:1n-9	5.9 ± 0.4 (6.1–7.8)	20.2 ± 0.4 (16.7–24.9)
18:1n-7	1.0 ± 0.1 (1.1–2.1)	3.2 ± 0.5 (3–3.5)
18:2n-6	1.4 ± 0.2 (1.1–2.5)	1.6 ± 0.1 (1.7–2.5)
18:3n-6	— <sup>c</sup> (—)	0.5 ± 0.0 (—)
18:3n-3	0.5 ± 0.0 (0.6–0.7)	0.6 ± 0.1 (0.6–0.8)
18:4n-3	0.9 ± 0.1 (1.4–1.7)	0.6 ± 0.1 (0.7–0.9)
20:1n-11, n-13	0.3 ± 0.0 (0.2–0.4)	0.2 ± 0.1 (0.1–0.5)
20:1n-9	0.5 ± 0.0 (0.4–0.5)	2.1 ± 0.2 (1.1–1.3)
20:2n-6	0.1 ± 0.0 (0.1–0.3)	0.5 ± 0.1 (0.3–0.4)
20:3n-6	0.2 ± 0.1 (0.1–0.2)	0.1 ± 0.1 (0.0–0.1)
20:4n-6	2.4 ± 0.2 (2.3–2.6)	1.6 ± 0.2 (1.5–2)
20:5n-3	8.9 ± 0.9 (6.7–8.1)	6.3 ± 0.5 (6.0–8.2)
22:0	— (—)	0.4 ± 0.0 (—)
22:1n-11, n-13	0.1 ± 0.0 (0.1–0.3)	0.6 ± 0.1 (0.5–0.7)
22:4n-6	0.3 ± 0.0 (0.2–0.3)	0.6 ± 0.2 (0.2–0.4)
22:5n-6	2.0 ± 0.3 (1.9–2.3)	1.3 ± 0.3 (1.3–1.5)
22:5n-3	1.4 ± 0.3 (1.4–1.8)	1.5 ± 0.1 (0.9–1.4)
22:6n-3	38.4 ± 2.5 (32.7–46.3)	13.5 ± 1.9 (12.4–24.9)
Others	1.0	4.4

<sup>a</sup>Values are means ± SD of five replicate analyses.

<sup>b</sup>Literature data are in parentheses.

<sup>c</sup>Concentrations lower than 0.1% are not reported.

silica plates in isolating the  $\alpha$ -MAG fraction. The strong affinity of the hydroxyl groups in the  $\alpha$ -MAG fraction—independent of their compositions—resulted in the lowest  $R_f$  values, which allowed an easy separation and contamination-free recovery of the  $\alpha$ -MAG.

## DISCUSSION

The present method gives an accurate analysis of the  $\alpha$ -position in the original TAG. The  $\alpha$ -MAG are present in sufficient quantities and a random FA distribution is obtained. This point deserves particular attention. As early as 1966, Yurkowski and Brockerhoff (9) reported that the MAG ( $\alpha$ - and  $\beta$ -MAG) from the Grignard deacylation reaction could not be used for analytical purposes, since their FA compositions were not representative of the original TAG structure. Extensive acyl migration took place during the deacylation procedure. In 1993, Becker *et al.* (2) discussed the positive effect of an excess amount of allyl magnesium bromide reagent to produce representative  $\beta$ -MAG.

Based on these observations, we modified deacylation conditions from the usual procedure by using a higher ratio of ethyl magnesium bromide to TAG for a shorter reaction time. Under these conditions, more acyl shifting was observed from the  $\alpha$ - to  $\beta$ -position (5.6% contamination of  $\beta$ -MAG) than

from the  $\beta$ - to  $\alpha$ -position (1.8% contamination of  $\alpha$ -MAG). These results are opposite those usually observed for this type of analysis (2,9,11) and for chemical equilibrium between the  $\alpha$ - and  $\beta$ -positions (21). However, as reported in the literature (4,22), deacylation is not random with regard to FA position on the glycerol molecule. Ethyl magnesium bromide exhibited a higher selectivity toward the  $\alpha$ -position than did allyl magnesium bromide, and the Grignard reagents generated opposite results regarding MAG production. Thus, the proportion of  $\alpha$ -MAG (30–35%) produced by ethyl magnesium bromide may have been overemphasized with a higher ratio of reagent and a shorter reaction time, leading to the formation of minute amounts of  $\beta$ -MAG (less than 10%).

The present procedure allows oils and fats that are not amenable to analysis with pancreatic lipase to be directly accessible to a regiodistribution analysis, without resorting to calculations. This method is particularly useful with TAG containing short-chain FA ( $C_{10}$  or less) or very long chain PUFA, as no significant selectivity was observed with respect to chain length or unsaturation of FA in the partial deacylation of TAG (2,22).

## REFERENCES

1. Takagi, T., and Ando, Y. (1991) Stereospecific Analysis of Triacyl-*sn*-glycerols by Chiral High-Performance Liquid Chromatography, *Lipids* 26, 542–547.
2. Becker, C.C., Rosenquist, A., and Holmer, G. (1993) Regiospecific Analysis of Triacylglycerols Using Allyl Magnesium Bromide, *Lipids* 28, 147–149.
3. Ando, Y., and Takagi, T. (1999) Micro Method for Stereospecific Analysis of Triacyl-*sn*-glycerols by Chiral-Phase High-Performance Liquid Chromatography, *J. Am. Oil Chem. Soc.* 70, 1047–1049.
4. Angers, P., and Arul, J. (1999) A Simple Method for Regiospecific Analysis of Triacylglycerols by Gas Chromatography, *J. Am. Oil Chem. Soc.* 76, 481–484.
5. Entressangles, B., Pasero, L., Savary, P., Sarda, L., and Desnuelle, P. (1961) Influence de la nature des chaînes sur la vitesse de leur hydrolyse par la lipase pancréatique, *Bull. Soc. Chim. Biol.* 43, 581–585.
6. Lawson, L.D., and Hughes, B.G. (1988) Triacylglycerol Structure of Plant and Fungal Oils Containing  $\gamma$ -Linolenic Acid, *Lipids* 23, 313–317.
7. Brockerhoff, H. (1965) Stereospecific Analysis of Triglycerides: An Analysis of Human Depot Fat, *Arch. Biochem. Biophys.* 110, 586–590.
8. Bottino, N.R., Vandenburg, G.A., and Reiser, R. (1967) Resistance of Certain Long-Chain Polyunsaturated Fatty Acids of Marine Oils to Pancreatic Lipase Hydrolysis, *Lipids* 2, 489–493.
9. Yurkowski, M., and Brockerhoff, H. (1966) Fatty Acid Distribution of Triglycerides Determined by Deacylation with Methyl Magnesium Bromide, *Biochim. Biophys. Acta* 125, 55–59.
10. Brockerhoff, H. (1967) Stereospecific Analysis of Triglycerides: An Alternative Method, *J. Lipid Res.* 8, 167–169.
11. Christie, W.W., and Moore, J.H. (1969) A Semimicro Method for the Stereospecific Analysis of Triglycerides, *Biochim. Biophys. Acta* 176, 445–452.
12. Christie, W.W. (1982) *Lipid Analysis*, pp. 155–161, Pergamon Press, Oxford.
13. Brockerhoff, H. (1971) Stereospecific Analysis of Triglycerides, *Lipids* 6, 942–956.
14. Luddy, F.E., Barfield, R.A., Herb, S.F., Magidman, P., and

- Riemenschneider, R.W. (1963) Pancreatic Lipase Hydrolysis of Triglycerides by a Semimicro Technique, *J. Am. Oil Chem. Soc.* 41, 693–696.
15. Thomas, A.E., III, Scharoun, J.E., and Ralston, H. (1965) Quantitative Estimation of Isomeric Monoglycerides by Thin-Layer Chromatography, *J. Am. Oil Chem. Soc.* 42, 789–792.
  16. Morrison, W.R., and Smith, L.M. (1964) Preparation of Fatty Acid Methyl Esters and Dimethylacetals from Lipids with Boron Fluoride–Methanol, *J. Lipid Res.* 5, 600–608.
  17. Christie, W.W., and Claperton, J.L. (1982) Structures of the Triglycerides of Cow's Milk, Fortified Milks (including infant formulae), and Human Milk, *J. Soc. Dairy Technol.* 35, 22–24.
  18. Ozenne, C. (1993) Biofaçonnement de la matière grasse laitière, Ph.D. Thesis, University of Montpellier II, France, pp. 119–132.
  19. Ando, Y., Ota, T., and Yazawa, K. (1996) Stereospecific Analysis of Triacyl-*sn*-glycerols in Docosahexaenoic Acid-rich Fish Oils, *J. Am. Oil Chem. Soc.* 73, 483–487.
  20. Ando, Y., Satake, M., and Takahashi, Y. (2000) Reinvestigation of Positional Distribution of Fatty Acids in Docosahexaenoic Acid-rich Fish Oil Triacyl-*sn*-glycerols, *Lipids* 35, 579–582.
  21. Larsson, K., and Quinn, P.J. (1994) Physical Properties: Structural and Physical Characteristics, in *The Lipid Handbook*, 2nd edn., pp. 443–446, Chapman and Hall, London.
  22. Angers, P., and Arul, J. (2000) Determination of Selectivity of Grignard Reagents in Partial Deacylation Reactions of Triacylglycerols by Gas Chromatography, *inform* 11, S58.

[Received October 23, 2001, and in final revised form July 31, 2002; revision accepted August 22, 2002]

# Evaluation of Two GC Columns (60-m SUPELCOWAX 10 and 100-m CP Sil 88) for Analysis of Milkfat with Emphasis on CLA, 18:1, 18:2 and 18:3 Isomers, and Short- and Long-Chain FA

John K.G. Kramer\*, C. Brian Blackadar, and Jianqiang Zhou

Food Research Program, Agriculture and Agri-Food Canada, Guelph, Ontario, Canada N1G 5C9

**ABSTRACT:** Milkfat is a complex mixture of many diverse FA, some of which have demonstrated health benefits including anticancer properties. Attempts are under way to enrich milkfats with long-chain n-3 PUFA and CLA. It has been recommended that the analysis of these milkfats requires gas chromatography (GC) equipped with long, highly polar capillary columns. However, many analyses have been reported using CARBOWAX™ type (polyethylene glycol) capillary columns, such as SUPELCOWAX 10, even though the separation characteristics of many of the FA and their isomers present in milkfats have not been described in detail. This includes the isomers of CLA, *cis*- and *trans*-octadecenoic acid (18:1), linoleic acid (18:2n-6), and linolenic acid (18:3n-3), and the long-chain PUFA. On the other hand, the resolution of these FA and their isomers has been more fully described using the highly polar capillary columns, such as CP Sil 88 and SP2560 because of the improved resolution obtained using these polar columns. The present study was undertaken to characterize the separation of these FA present in milkfats using a 60-m SUPELCOWAX 10 column, to compare the results to those from a 100-m CP Sil 88 column, and to determine if these two columns could possibly serve to complement each other for the analysis of total milkfat. The advantages of the SUPELCOWAX 10 column were a better resolution of the short-chain saturated from their monounsaturated FA (MUFA) analogs, and a complete separation of the  $\alpha$ -linolenic (18:3n-3) and eicosadecenoic acid (20:1) isomers. It also provided an alternative elution order of the linoleic (18:2n-6), 18:3n-3 and  $\gamma$ -linolenic (18:3n-6) acid isomers. On the other hand, the CP Sil 88 column provided a better resolution of the CLA isomers, MUFA, the isolated *cis* and *trans* MUFA fractions, the PUFA, and many the 18:2n-6 and 18:3n-3 isomers. A complete analysis of milk lipids using the CP Sil 88 column required the prior separation of total FAME using silver ion-TLC. The results of the present study confirm that the 100-m highly polar capillary GC columns are mandatory for the analysis of milk lipids, and at best, the 60 m SUPELCOWAX 10 capillary column serves as a

complementary GC column to provide different separations in certain regions based on its intermediate polarity.

Paper no. L9065 in *Lipids* 37, 823–835 (August 2002).

The analysis of milkfats and fats from ruminant animals has taken on new importance in the last decade since the identification of CLA in these fats that possess anticarcinogenic, antiatherosclerotic, immune-stimulating, and fat-partitioning properties (1,2). At first the emphasis on the analysis was the resolution and identification of the CLA isomers (3–7). Now the analysis has been extended to include the complex mixture of *trans*-octadecenoic acids (*t*-18:1), since it was shown that 11*t*-18:1 converts to CLA by  $\Delta$ 9-desaturase in animals (8–11) and humans (12,13). In addition, there have been efforts to increase the contents of n-3 PUFA in milkfats for health reasons in adults (14) as well infants (15).

GC is by far the most widely used method for the analysis of FA, and the FA are generally analyzed as their FAME. Flexible fused silica columns coated with the highly polar cyanoalkyl polysiloxane stationary phases (marketed under such names as CP Sil 88, SP 2380, SP2560, and BPX-70) have been recommended for the analyses of milkfats that contain complex mixtures of geometric and positional isomers of monounsaturated FA (MUFA) (16–23) and CLA isomers (23–26), plus a range of FA from 4:0 to long-chain PUFA (23). These columns are generally available in 100 m length.

Flexible fused-silica capillary columns coated with CARBOWAX™ type (polyethylene glycol) stationary phases (i.e., SUPELCOWAX 10, DB-WAX, etc.) have been (7), and continue to be, used for the analyses of milkfats (27–29). The manufacturers claims that these columns have a low bleed, and lower minimum and higher upper temperature limits. However, we suspect that the main reason for the selection of these columns is their intermediate polarity, which is helpful in the identification of complex FAME mixtures, since the more common unsaturated FAME of even chain length *X* elute before the next saturated even FAME [(*X* + 2*C*):0]; i.e., 18:3 elute before 20:0, 20:5n-3 before 22:0, and 22:5n-3 before 24:0 (30–32). The exception is 22:6n-3, which elutes either before (31,32) or between 24:0 and 24:1 (30,32). Odd chain

\*To whom correspondence should be addressed at Food Research Program, Agriculture and Agri-Food Canada, 93 Stone Road West, Guelph, Ontario, Canada, N1G 5C9. E-mail: kramerj@agr.gc.ca

Abbreviations: Ag<sup>+</sup>-TLC, silver ion-thin layer chromatography; MUFA, monounsaturated fatty acids. The  $\Delta$  nomenclature for double bond position is used throughout the text except for identification of most methylene-interrupted PUFA in which the terminal n position is identified.

length FA cause minimal interference since their content in milk products is generally low. Although these properties of the CARBOWAX-type stationary phases are rather helpful, the lack of polarity to resolve closely related geometric and positional isomers of FAME is a marked disadvantage.

Systematic characterizations of the different regions of the GC separation of total milk FAME using the highly polar cyanoalkyl polysiloxane capillary columns have been intensively investigated for their resolution of *cis* and *trans* MUFA (16–23,33,34), CLA (4–7,23–26), 18:2/18:3 (19,35–39), and 18:3/20:1 (38) regions. On the other hand, a similar evaluation of the same regions of milk FAME has not been reported using a capillary column coated with a CARBOWAX-type stationary phase, such as SUPELLOWAX 10. Several reports have detailed the elution order of selected FAME on CARBOWAX-type stationary phases under isothermal conditions (31,32,40–42). Even though these values are not strictly comparable, they can be helpful to predict the possible structure of unknown FAME.

The present study was therefore undertaken to evaluate the resolution characteristics of a typical CARBOWAX-type column, such as the 60-m SUPELLOWAX 10 column (Supelco Inc., Bellefonte, PA). The FA investigated are those typically found in milkfat, such as short-chain FA, branched chain FA, MUFA, and long-chain PUFA, including the geometric and positional isomers of 18:1, 18:2, 18:3, and CLA. In addition, hydrogen and helium were evaluated as carrier gases. The complex FAME standard #463 available from Nu-Chek-Prep (Elysian, MN) was used as a GC standard because it provided the spectrum of FAME from 4:0 to 22:6n-3 generally found in milkfats. Furthermore, the separations on the 60-m SUPELLOWAX 10 column were compared to those on a 100-m CP Sil 88 column to determine if these two columns could possibly serve to complement each other for the analysis of milkfats.

## MATERIALS AND METHODS

Bovine milk was purchased locally or was available from cooperative studies with Arthur R. Hill and Brian W. McBride, University of Guelph, Guelph, Ontario, Canada. Methyl ester

standards, GC reference standard FAME mixture #463, and a mixture of four positional CLA isomers (#UC-59M) were purchased from Nu-Chek-Prep Inc. (Elysian, MN). Pure 9*c*,11*t*-CLA and 10*t*,12*c*-CLA were obtained from Matreya Inc. (Pleasant Gap, PA). *p*-Toluenesulfonic acid, sodium salt was purchased from Sigma-Aldrich Ltd. (St. Louis, MO). All chemicals and solvents were of analytical grade.

Two identical gas chromatographs (Model 5890 Series II, Hewlett-Packard, Palo Alto, CA) were used that were equipped with FID, split/splitless injection ports, autosamplers (Hewlett-Packard, Model 7673), and a Hewlett-Packard ChemStation software data system (Version A.07; Hewlett-Packard, Avondale, PA). The injector and detector temperatures were set at 250°C. One GC was fitted with a SUPELLOWAX 10 flexible fused column (60 m × 0.25 mm i.d. × 0.2 μm film thickness) kindly donated by Len Sidisky, Supelco Inc. (Bellefonte, PA). The other was a CP Sil 88 flexible fused column (100 m × 0.25 mm i.d. × 0.2 μm film thickness; manufactured by Chrompack, Middelburg, The Netherlands, and available from Varian Inc., Mississauga, Canada). Both hydrogen and helium were evaluated as the carrier gas with each column. The column inlet pressure was set at 175 kPa for both columns, resulting in carrier gas flow rates of about 1 mL/min. Samples were dissolved in either hexane or isooctane containing about 1 to 2 μg/μL of total FAME, and 1 μL (CP Sil 88 column) or 3 μL volumes (SUPELLOWAX 10 column) were injected. A splitless injection system was used that was flushed after 0.3 s. The typical temperature programs used for the analysis of total milk FAME were from 45 to 215°C for the CP Sil 88 column and from 65 to 240°C for the SUPELLOWAX 10 column. To maximize the separation of the *trans* MUFA, a low-temperature stepwise isothermal program was selected for the CP Sil 88 column to separate the 16:1 isomers at 120°C, the 18:1 isomers just after increasing the temperature to 150°C, the 20:1 isomers at 175°C, and the 22:1 and 24:1 isomers at 220°C. The temperature settings were chosen to elute the MUFA during each of the isothermal steps to help sharpen the peaks. A similar stepwise temperature program was designed for the SUPELLOWAX 10 column. Details on the different temperature programs are listed in Table 1. Low temperature isothermal GC conditions have

**TABLE 1**  
Temperature Program Used for the Analysis of Milkfats, Standards and Lipid Fractions

Carrier gas	Sample	Temperature program	Total time (min)
SUPELLOWAX 10 column			
H <sub>2</sub>	Total FAME	65°C (1 min)—13°C/min—195°C (50 min)—15°C/min—240°C (50 min)	87.7
He	Total FAME	65°C (1 min)—13°C/min—195°C (20 min)—15°C/min—240°C (80 min)	114
H <sub>2</sub> or He	<i>trans</i> -18:1 and CLA	Stepwise isothermal program: 130°C (200 min)—15°C/min—160°C (75 min)—15°C/min—185°C (60 min)—15°C/min—240°C (50 min). Also starting at 140 or 150°C	392
CP Sil 88 column			
H <sub>2</sub>	Total FAME	45°C (4 min)—13°C/min—175°C (27 min)—4°C/min—215°C (35 min)	86
He	Total FAME	45°C (4 min)—13°C/min—175°C (27 min)—4°C/min—215°C (60 min)	111
H <sub>2</sub> or He	<i>trans</i> -18:1 and CLA	Stepwise isothermal program: 120°C (200 min)—15°C/min—150°C (70 min) 15°C/min—175°C (60 min)—15°C/min—240°C (50 min)	386.7



been used successfully in the separation of *cis* and *trans* 16:1, 18:1 and 20:1 isomers from dairy fats (16–23).

The reference standard FAME mixture #463 from Nu-Chek-Prep (Elysian, MN) was found to be very useful to evaluate both the column characteristics and the FA range present in milkfat. The standard #463 consisted of 53 FAME from 4:0 to 22:6n-3 including several geometric isomers, but it lacked CLA. For this reason, a 5:1 mixture was prepared consisting of the GC reference FAME standard (#463) and CLA (#UC-59M); the latter consisted of four positional CLA isomers (8*t*,10*c*-, 9*c*,11*t*-, 10*t*,12*c*-, and 11*c*,13*t*-CLA). This mixture was often used as the FAME reference in this study.

Total milk FAME, which includes both neutral and phospholipids, were prepared using Na methoxide as catalyst (21–24,43,44). Total milk FAME were fractionated by silver ion TLC (Ag<sup>+</sup>-TLC) into three bands, i.e., saturates, mono *trans*, and mono *cis* plus CLA, by using a combination of previously described procedures (17,19,45). Briefly, precoated silica gel G glass plates (20 × 20 cm × 0.25 mm thickness; Fisher Scientific, Ottawa, Canada) were washed with chloroform/methanol (1:1), air-dried, and heated for 1 h at 110°C. After cooling, the plates were dipped into a solution of 5% AgNO<sub>3</sub> in acetonitrile (wt/vol) for 20 min. Next the plates were air-dried, then activated at 110°C for 1 h before use. Total milk FAME in hexane were applied onto the TLC plates using a TLC streaker (Applied Science, State College, PA) at a concentration of 0.4 mg/cm, and developed in a solvent mixture of hexane/diethyl ether (90:10). Bands were visualized under UV light after spraying with 2',7'-dichlorofluorescein and then scraped off, and the FAME were recovered from the silica after addition of 1.5 mL methanol, 1.5 mL 1 N aqueous NaCl, and 2 mL of hexane. Hexane extraction was repeated once more, and the combined hexane layers were dried over anhydrous Na<sub>2</sub>SO<sub>4</sub>, reduced appropriately with a stream of nitrogen, and analyzed by GC.

Pure 9*c*,11*t*- and 10*t*,12*c*-CLA were isomerized in hexane at room temperature and room light for 1 h using a dilute solution of iodine in hexane as a catalyst (26). The mixture of four positional CLA isomers was also isomerized to yield all eight possible *cis/trans* CLA isomers. Methyl linoleate (9*c*,12*c*-18:2; 18:2*n*-6),  $\alpha$ -linolenate (9*c*,12*c*,15*c*-18:2; 18:3*n*-3) and  $\gamma$ -linolenate (6*c*,9*c*,12*c*-18:2; 18:3*n*-6) were isomerized in dioxane at 100°C using *p*-toluenesulfinic acid as catalyst (46; Adlof, R., personal communication). Briefly, an aqueous solution of *p*-toluenesulfinic acid, sodium salt (2 g in 12 mL of water) was acidified with 6 N H<sub>2</sub>SO<sub>4</sub>. The precipitate was washed and filtered twice with 15 mL cold water, dissolve in 15 mL diethyl ether, and precipitated by adding 10 mL of hexane. The white crystals were filtered and dried under vacuum. Separate solutions of *p*-toluenesulfinic acid (10 mg in 2 mL) and PUFA (20 mg in 20 mL) were prepared in dioxane. Isomerizations were carried out in 5-mL culture tubes fitted with Teflon-lined screw caps by adding 1 mg of the PUFA in 1 mL and one drop of the *p*-toluenesulfinic acid solutions in dioxane. The tubes were flushed with nitrogen, mixed, and heated at 100°C for 7, 15, or 30 min. The tubes were cooled,

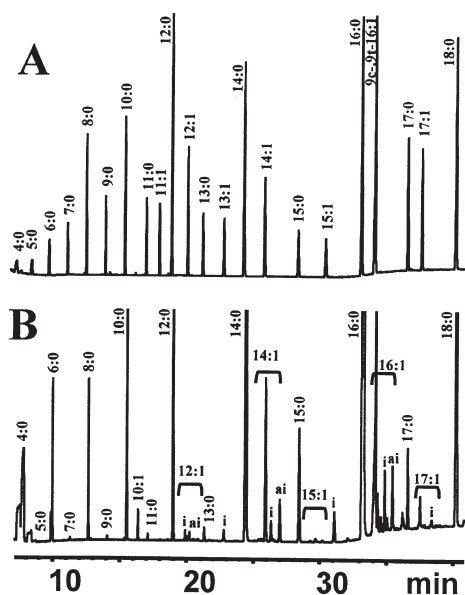
and 1 mL of 1 N NaOH and 2 mL of hexane were added and then mixed. The hexane layer was removed, dried over Na<sub>2</sub>SO<sub>4</sub>, and analyzed by GC. Various reaction times were selected to provide different ratios of the all-*trans* isomer, mixed *cis/trans* intermediates, and all-*cis* starting material for identification of isomers by GC. The isomerized product of 9*c*,12*c*-18:2 contained about equal proportions of the *cis/trans* intermediates, as were the three mono-*trans* and three di-*trans* intermediates from methyl  $\alpha$ - and  $\gamma$ -linolenate. To differentiate the individual *cis/trans* intermediates, the isomerized products of both 18:2 and 18:3 were separated by Ag<sup>+</sup>-TLC, and the *cis/trans* regions were split into an upper and a lower band, to obtain fractions containing unequal proportions of the *cis/trans* isomers that were used to differentiate the individual *cis/trans* isomers on the two GC columns.

## RESULTS AND DISCUSSION

Analyses of total milk FAME using the 60-m SUPELCOWAX 10 flexible fused-silica capillary column, and hydrogen as carrier gas, required a temperature program from 65°C to 240°C to elute all FAME from 4:0 to long-chain PUFA present in total milkfat in about 90 min (Table 1). Analyses of total milk FAME terminated at 190 to 225°C using the SUPELCOWAX 10 column, as is often the practice, would not allow for the complete elution of long-chain saturated FA and PUFA. The long-chain FAME will accumulate in the column and often cause interferences in subsequent analyses. The use of helium as carrier gas instead of hydrogen, increased the analysis time for total milk FAME from about 90 to 110 min using the same temperature program, but the relative elution order of the FAME was generally similar. No attempt was made to increase the temperature of this program to avoid altering the relative elution sequence of several FAME. Temperature effects on the relative elution patterns among isomers are well recognized; see effects of 18:3 isomers relative to 11*c*-20:1 (38), and mixtures of *trans*- and *cis*-18:1 isomers (17).

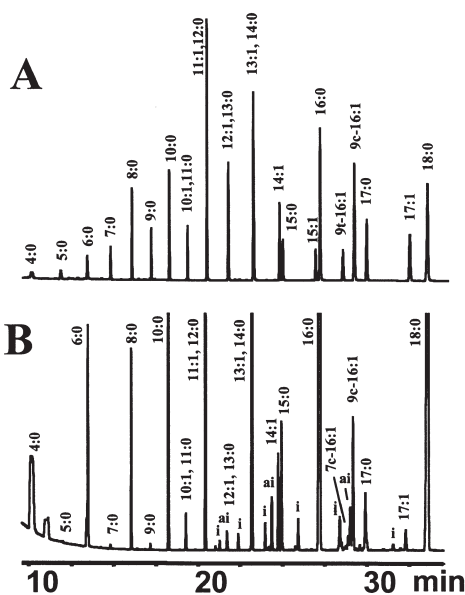
On the other hand, total milk FAME were resolved in about 90 min using a 100-m CP Sil 88 flexible fused-silica capillary column, hydrogen as the carrier gas, and a temperature program from 45 to 215°C (Table 1). Using helium as carrier gas increased the analysis time from about 90 to 110 min (Table 1), but the separations were not always as good as observed using hydrogen.

*The 4:0 to 18:0 FAME region.* Figure 1 shows a partial GC profile from 4:0 to 18:0 for the standard FAME mixture #463 (Fig. 1A) and total milk FAME (Fig. 1B) obtained by using the SUPELCOWAX 10 column and a typical temperature program (Table 1). The comparable GC regions for the standard FAME mixture #463 and for total milk FAME using the CP Sil 88 column are shown in Figures 2A and 2B, respectively. The SUPELCOWAX 10 column with its medium polarity effectively separated the saturated FAME from their MUFA analogs, whereas by using the CP Sil 88 column, the 10:1 to 13:1 FAME coeluted with their next higher saturated



**FIG. 1.** Partial gas chromatogram of the 4:0 to 18:0 FAME region using a 60-m SUPELCOWAX 10 capillary column, helium as carrier, and a typical temperature program from 65 to 240°C. (A) FAME standard #463 from Nu-Chek-Prep (Elysian, MN), (B) total milk FAME from cows fed a control diet. i, iso; ai, anteiso.

FAME. For example, the presence of 10:1 in milk lipids was clearly identified using the SUPELCOWAX 10 column (Fig. 1B), but this FA coeluted with 11:0 when using the CP Sil 88 column (Fig. 2B). At a low sample load, 10:1 and 11:0 FAME occasionally could be separated on the CP Sil 88 column. The structure of 10:1 in dairy fat was previously identified as



**FIG. 2.** Partial gas chromatogram of the 4:0 to 18:0 FAME region using a 100-m CP Sil 88 capillary column, hydrogen as carrier, and a typical temperature program from 45 to 215°C. (A) FAME standard #463 from Nu-Chek-Prep (Elysian, MN); (B) total milk FAME from cows fed a control diet. i, iso; ai, anteiso.

10:1n-1 (47). For a more definitive identification of the saturated FA and MUFA of less than 15 carbons with the CP Sil 88 column, a prior fractionation of the *cis* and *trans* fractions by  $\text{Ag}^+$ -TLC was required. Analyzing milk FAME solutions in hexane or isooctane by GC resulted in a “chair-like” appearance of the 4:0 and 6:0 FAME peaks, as reported previously (48). A mass spectral analysis was performed, which showed that the entire chair-like peak consisted only of the FAME in question. Ulberth and Henniger (48) showed that the peak shapes of 4:0 and 6:0 could be improved by using polar solvents, such as diethyl ether or dichloromethane, but quantification was not affected. Replacing the hexane of milk FAME after methylation with a more polar solvent is not recommended since this would result in loss of 4:0 FAME.

On the SUPELCOWAX 10 column there was no separation of the geometric isomers of 14:1, 15:1 and 16:1, as evidenced by the coelution of 9*c*- and 9*t*-16:1 in both the standard #463 and milk FAME (Fig. 1). There was a partial separation of the positional isomers of MUFA on this column. On the other hand, there was a clear resolution of both the geometric (9*t*-16:1 before 9*c*-16:1; Fig. 2A) and positional MUFA isomers (7*c*-16:1 before 9*c*-16:1; Fig. 2B) on the CP Sil 88 column (Fig. 2).

Milkfats also contain branched-chain FA with odd-chain (iso and anteiso 13:0, 15:0, and 17:0) and even-chain lengths (iso 14:0, 16:0, and 18:0). The branched-chain FAME can easily be misidentified as MUFA isomers on both the SUPELCOWAX 10 and the CP Sil 88 columns from 12:1 to 17:1. The branched-chain iso and anteiso FAME eluted among the *cis* and *trans* MUFA isomers that elute over a wide range on both columns. Comparing the results from both columns may help to clarify a number of co-eluting peaks, but an unequivocal identification requires a prior  $\text{Ag}^+$ -TLC separation of the saturated, mono-*trans*, and mono-*cis* FAME. Overestimation of *trans*-16:1 content in human tissue as a consequence of including iso-17:0 led to the erroneous association of *trans*-16:1 intake and coronary heart disease (20).

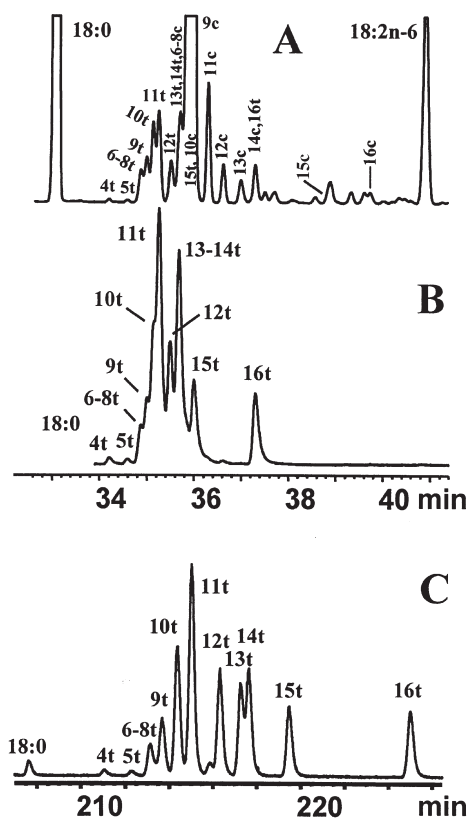
In this study we restricted ourselves to the analysis of FAME. Isopropyl (45,49), butyl (47), and *tert*-butyl esters (50,51) have been used for the analysis of milk lipids. These derivatives have the benefit of not requiring correction factors to quantitate the area response of the FID of the short-chain FAME from 4:0 to 12:0 (45,52). Their use has been limited because the esterification solutions are not commercially available, the catalysts employed are strong acids that isomerize CLA, and the separation characteristics of all these esters have not been as well documented as FAME. A base-catalyzed method has just been reported that permits the preparation of longer-chain FA esters by using potassium *tert*-butoxide to prepare the potassium alkoxides of different alcohols (53).

*Resolution of the 18:1 cis and trans isomers and overlap with other FAME.* On the CP Sil 88 column there was a partial resolution of *trans*- and *cis*-18:1 isomers. The retention times for both the *cis*- and *trans*-18:1 isomers increased with increasing  $\Delta$  values. The *trans* 18:1 isomers 4*t*- to 11*t*-18:1

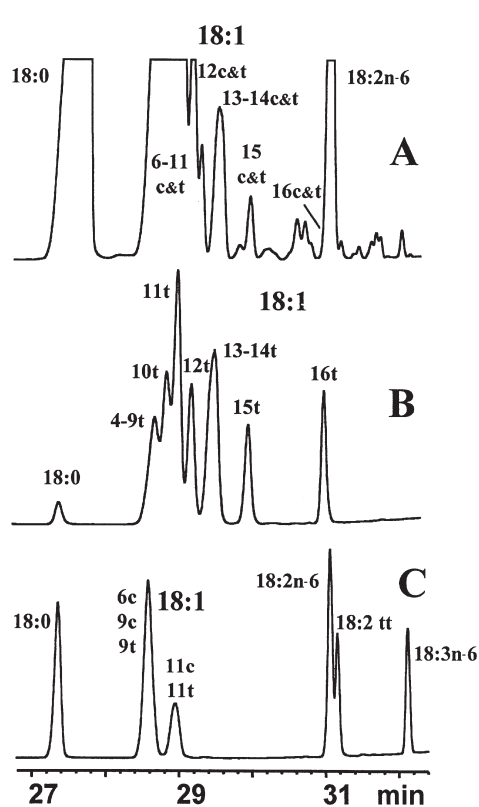
eluted before the *cis*- and remaining *trans*-18:1 isomers (Fig. 3A,B). Similar results were reported previously for a CP Sil 88 (16,17,23,54–56), SP-2560 (24,25,56), and SP-2340 (33) columns. The near-baseline resolution between 11*t*- and 12*t*-18:1 (see Fig. 3A) was used to quantify the total *trans*-18:1 content after separation of the *cis*- and *trans*-18:1 fractions by Ag<sup>+</sup>-TLC and analyses by GC using isothermal temperature operations (23). The isolated *trans*-18:1 fractions could then be completely resolved on the CP Sil 88 column starting at 120°C, except for 6*t*- to 8*t*-18:1 (19–23,34,49; see Fig. 3C). Attempts have been made to analyze all the 18:1 isomers at 165 to 190°C isothermal conditions (17,32,56), without the need for a prior Ag<sup>+</sup>-TLC fractionation. Under these isothermal conditions, many of the 18:1 *cis* and *trans* isomers could be identified, whereas other isomers were only partially resolved, or not resolved. The separations are dependent on temperature (32,56), and somewhat less so on the column make (56). Below 180°C there was a better resolution of the 4*t*- to 11*t*-18:1 region (17), but above 180°C this region was not as well resolved (56). The lack of separation of 4*t*- to 11*t*-18:1 may not pose a problem if only the total *trans* content is to be determined, but it is unsuitable for milk analyses in

which these 18:1 isomers are of biological interest. In fact, all of these isothermal operations are not practical for total milkfat analysis, since 4:0 to 10:0 FAME will elute with the solvent, and the low sample load required to give a good separation of the 18:1 isomers will make the detection and analysis of many minor long-chain PUFA difficult, if not impossible. A prior Ag<sup>+</sup>-TLC fractionation was mandatory. It should be noted that even when using a stepwise isothermal temperature condition starting at 120°C, there was no resolution of all the 18:1 isomers of total milk FAME. With this low-temperature stepwise isothermal condition, the pair 11*t*-18:1 and 6*c*- to 8*c*-18:1 were not resolved, nor were the pairs 9*c*- and 12*t*-18:1, 15*t*- and 12*c*-18:1, and 16*t* and 14*c*-18:1 (data not shown).

On the SUPELCOWAX 10 column there was no separation of the *cis*- and *trans*-18:1 isomers with either hydrogen or helium as carrier gas, and with a typical temperature program (Fig. 4A). The lack of separation was evident by comparing total milk FAME (Fig. 4A) to the isolated *trans*- (Fig. 4B) and *cis*-18:1 fractions (data not shown) isolated from total milk FAME by Ag<sup>+</sup>-TLC, and to the standard FAME mixture #463 (Fig. 4C). However, the elution sequence of the



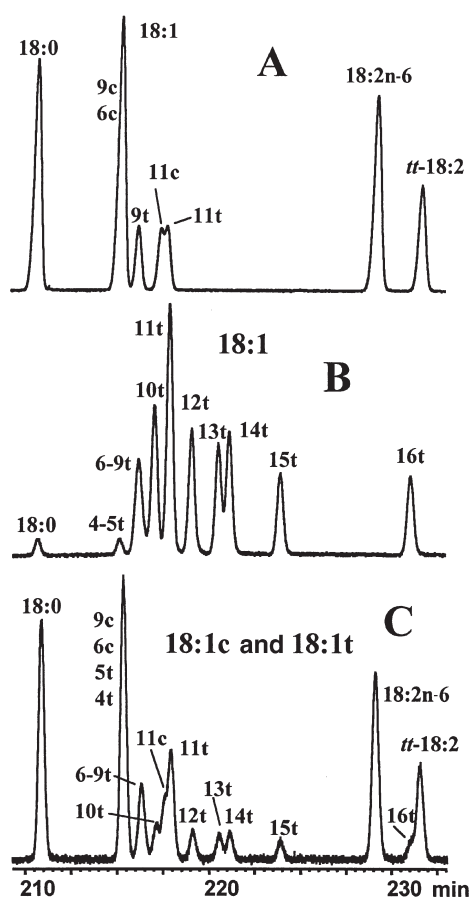
**FIG. 3.** Partial gas chromatogram of the 18:0 to 18:2n-6 FAME region using a 100-m CP Sil 88 capillary column, hydrogen as carrier, and a typical temperature program from 45 to 215°C. (A) Total milk FAME from cows fed a control diet; (B) *trans* fraction isolated from the same milkfat FAME as (A) using Ag<sup>+</sup>-TLC; (C) the same *trans* fraction as (B) but resolved using the stepwise isothermal GC program starting at 120°C.



**FIG. 4.** Partial gas chromatogram of the 18:0 to 18:2n-6 FAME region using a 60-m SUPELCOWAX 10 capillary column, hydrogen as carrier, and a typical temperature program from 65 to 240°C. (A) Total milk FAME from cows fed a control diet; (B) *trans* fraction isolated from the same milkfat FAME as (A) using Ag<sup>+</sup>-TLC; (C) FAME standard #463 from Nu-Chek-Prep (Elysian, MN).

individual *trans*- (Fig. 4B) and *cis*-18:1 positional isomers (data not shown) increased with increasing  $\Delta$ 18:1 values, similar to the results on the highly polar columns (Fig. 3B). With this temperature program, 4*t*- to 9*t*-18:1 and 13*t*- plus 14*t*-18:1 eluted as single peaks (Fig. 4B).

In an attempt to improve the resolution of the 18:1 region on the SUPELLOWAX 10 column, low-temperature stepwise isothermal separations were conducted starting at 130, 140, and 150°C; both 130 and 140°C provided good separations. The standard FAME mixture #463 (Fig. 5A) was compared to the *trans* fraction isolated from total milk FAME by Ag<sup>+</sup>-TLC (Fig. 5B). The identity of several *trans*-18:1 isomers and the relative elution of the *trans*-18:1 FA to that of other FA was established by co-injection of #463 with the total *trans* fraction isolated by Ag<sup>+</sup>-TLC (Fig. 5C). The results in Figure 5 were taken from a GC separation in which helium was the carrier gas, and the gas chromatograph was operated under a low-temperature stepwise isothermal condition; similar results were obtained using hydrogen as carrier gas.



**FIG. 5.** Partial gas chromatogram of the 18:0 to 9*t*,12*t*-18:2 FAME region using a 60 m SUPELLOWAX 10 capillary column, helium as carrier, and an isothermal temperature program of 130°C for 200 min followed by 75 min at 160°C. (A) FAME standard #463 from Nu-Chek-Prep (Elysian, MN); (B) *trans* fraction isolated from total milk FAME of cows fed a control diet; (C) FAME standard #463 from Nu-Chek-Prep spiked with the *trans* fraction in (B).

The results from this isothermal operation condition indicated that for a given positional isomer, *cis* eluted just before *trans* on the SUPELLOWAX 10 column (Fig. 5A), which was opposite to that observed using the highly polar capillary columns. Bannon *et al.* (40) also observed the reversed elution of geometric *cis*- and *trans*-18:1 isomer pairs, but noted that their relative elution changed depending on the isothermal column temperature and on the positional isomer. At lower temperatures (200°C), many *cis* isomers eluted just before *trans*, but slightly after *trans* at higher temperatures (240°C). However, the elution sequence of the *trans* 18:1 isomers was similar to that observed for the polar capillary columns, i.e., the retention times increased with increasing  $\Delta$ 18:1 values for both the SUPELLOWAX 10 (Fig. 5B) and CP Sil 88 columns (Fig. 3C). The separation distance between the geometric isomers was small. The *trans* isomer eluted about halfway to the next higher *cis* isomer. There were also differences in the resolution of the *trans* isomers between these two GC columns. On the SUPELLOWAX 10 column 4*t*- to 9*t*-18:1 coeluted, whereas 13*t*- and 14*t*-18:1 were resolved (Fig. 5B). This latter resolution appeared rather surprising since that pair of isomers provided such a challenge using the highly polar capillary columns (17–19). With the CP Sil 88 column, only 6*t*- to 8*t*-18:1 still remain unresolved at 120°C (Fig. 3C). The *trans*-18:1 isomers on the SUPELLOWAX 10 column were identified based on quantitative comparison of all the peaks in several *trans* fractions analyzed by both the SUPELLOWAX 10 and CP Sil 88 capillary columns. Analysis of the *cis* fraction of total milk FAME isolated by Ag<sup>+</sup>-TLC showed that the retention times of the *cis* isomers also increased with increased  $\Delta$  values (results not shown).

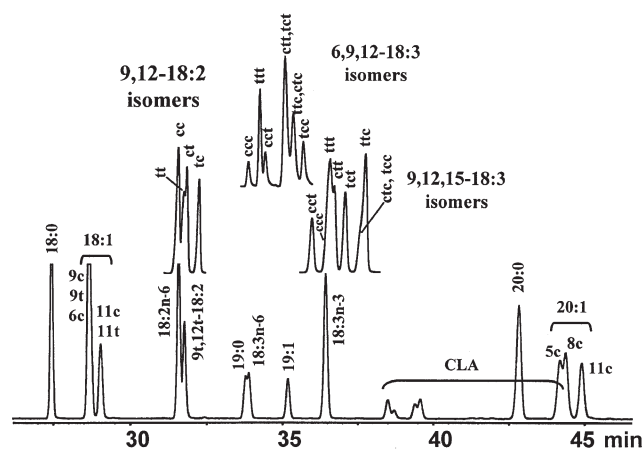
Of particular concern was the elution position of 16*t*-18:1 (a component generally found in milkfat) relative to the 18:2 FAME when using the SUPELLOWAX 10 column in either temperature operation. With a typical temperature program, 16*c*- and 16*t*-18:1 coeluted with 18:2*n*-6 (Fig. 4A,B), but during isothermal operation it eluted at the leading edge of 9*t*,12*t*-18:2 (Fig. 5C). By contrast, on the CP Sil 88 column, all *cis*- and *trans*-18:1 isomers eluted well before 18:2*n*-6 (Fig. 3A,B). Therefore, at best the SUPELLOWAX 10 column could provide an alternative total *cis*- plus *trans*-18:1 content by summing up all peaks from 18:0 up to and including 15*c*-/15*t*-18:1, except for 16*c*- plus 16*t*-18:1, since these geometric isomers eluted with (Fig. 4) or after 18:2*n*-6 (Fig. 5), depending on the temperature program chosen. By contrast, there was no overlap of 16*c*- and 16*t*-18:1 with 18:2*n*-6 during isothermal operations when using a 50-m SUPELLOWAX 10 column at either 200, 220, or 240°C (40).

*Separation of the synthetic geometric isomers of 18:2 and 18:3.* Many of the geometric and positional 18:2 and 18:3 isomers in milkfat have not been identified, and standards are not available. Therefore, we prepared all four geometric isomers of 9,12-18:2, and eight isomers of 9,12,15-18:3 and 6,9,12-18:3 from methyl linoleate (9*c*,12*c*-18:2; 18:2*n*-6),  $\alpha$ -linolenate (9*c*,12*c*,15*c*-18:3; 18:3*n*-3) and  $\gamma$ -linolenate (6*c*,9*c*,12*c*-18:3;



18:3n-6), respectively (see Materials and Methods). The elution sequences of the geometric isomers of these three FA using highly polar GC columns were previously characterized (19,35–39). On the other hand, the elution order of all these geometric isomers, and their possible interference with other FAME on the SUPELCOWAX 10 column, have received limited attention (36,39,40,42). To help in the identification, several reaction times were selected to obtain different ratios of the all-*trans*, to *cis/trans* intermediates, to all-*cis* starting material. To further distinguish the *cis/trans* intermediates, the isomerized mixtures were separated by  $\text{Ag}^+$ -TLC, and the *cis/trans* bands were divided into an upper and lower part in order to obtain *cis/trans* fractions of unequal distribution of the different mono-*trans* or di-*trans* isomers that could then be used to identify and compare the isomers on the two GC columns. The methylene-interrupted geometric isomers of all three PUFA were separated on the CP Sil 88 (Fig. 6) and the SUPELCOWAX 10 column (Fig. 7), using the typical temperature programs. The FAME mixture #463 was spiked with the CLA mixture and served as reference standard.

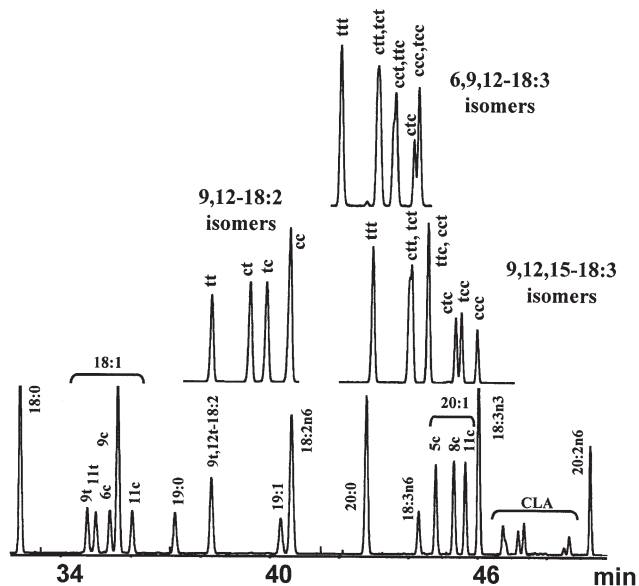
In general, all the isomerized products eluted before the all-*cis* isomer on the CP Sil 88 column (Fig. 6), but most of these isomers eluted after the all-*cis* isomer on SUPELCOWAX 10 column (Fig. 7). The elution order of the four 9,12-18:2 FAME isomers on the CP Sil 88 column was  $tt < ct < tc < cc$  (Fig. 6), and these isomers all eluted after the *cis*- and *trans*-18:1 isomers, except 15*c*- and 16*c*-18:1. On the SUPELCOWAX 10 column, the elution order was  $cc < tt < ct <$



**FIG. 7.** Partial gas chromatogram of the 18:0 to 20:1 FAME region using a 60-m SUPELCOWAX 10 capillary column, hydrogen as carrier, and a typical temperature program from 65 to 240°C. Lower panel: FAME standard #463 spiked with the CLA mixture #UC-59M, both from Nu-Chek-Prep; the isomeric mixture of linoleic (9,12-18:2),  $\alpha$ -linolenic (9,12,15-18:3), and  $\gamma$ -linolenic acid (6,9,12-18:3) are placed above the lower chromatogram in the appropriate elution positions.

(Fig. 7), but some isomers were not well resolved. When the column was operated isothermally, all four 18:2 isomers were resolved, but the relative elution sequence changed to  $cc < ct < tt < tc$  (Table 2). Based on the separation of the 9,12-18:2 isomers on the SUPELCOWAX 10 column several peaks eluting after 18:2n-6 in milk FAME could be accounted for, but none before 18:2n-6. Without standards, or GC/MS analyses as their 4,4-dimethyloxazoline derivatives, it remains unclear what FAME eluted between the 15*c*-/15*t*-18:1 peak and the 18:2n-6 of total milk FAME on this column and temperature program (Fig. 4A). We suspect that some non-methylene-interrupted 18:2 isomers eluted in this region, such as 9-*trans*,15-*cis*-18:2, a non-methylene-interrupted 18:2 isomer identified in milkfats (37). The elution order of the four 9,12-18:2 FAME [or 20:2 FAME (42)] isomers on polar (33–38,40,42) and CARBOWAX-type columns (36,40,42) is generally in agreement with our present findings. Occasionally, the *ct* isomers on the CARBOWAX-type columns may be reversed (42), which could be related to column type, column length, temperature program (40), and/or chain length.

The elution order of the isomers of 9,12,15-18:3 and 6,9,12-18:3 FAME on the CP Sil 88 column was generally  $tft < di\text{-}trans < mono\text{-}trans < ccc$  (Fig. 6). On the other hand, the elution order on the SUPELCOWAX 10 column was generally  $ccc < tft < di\text{-}trans < mono\text{-}trans$ , with minor exceptions (Fig. 7). The elution sequence within the di-*trans* ( $ctt < tct < ttc$ ) and mono-*trans* ( $cct < ctc < tcc$ ) 18:3 isomers was consistent and the same for both 18:3 FAME on both columns (Figs. 6 and 7). Among the di-*trans* isomers of both 18:3 FAME and both columns, there was little separation between *ctt* and *tct* (except for 9,12,15-18:3 on the SUPELCOWAX 10 column), while *ttc* was well resolved. All the mono-*trans* isomers of both 18:3 FAME were resolved on both columns,



**FIG. 6.** Partial gas chromatogram of the 18:0 to 20:2n-6 FAME region using a 100-m CP Sil 88 capillary column, hydrogen as carrier, and a typical temperature program from 45 to 215°C. Lower panel: FAME standard #463 spiked with the CLA mixture #UC-59M, both from Nu-Chek-Prep (Elysian, MN); the isomeric mixture of linoleic (9,12-18:2),  $\alpha$ -linolenic (9,12,15-18:3) and  $\gamma$ -linolenic acid (6,9,12-18:3) are placed above the lower chromatogram in the appropriate elution positions.

**TABLE 2**  
**Elution Order of CLA, 18:1, 9,12-18:2, and 9,12,15-18:3 Geometric and Positional Isomers on the CP Sil 88 and SUPELCOWAX 10 Capillary Column Using Typical Temperature Programs<sup>a</sup>**

FA	Isomers	CP Sil 88	SUPELCOWAX 10
Elution order using a temperature program <sup>a</sup>			
CLA	All isomers	$c/t < cc < tt$	The same
	$c, t$ or $t, c$	$8, 10 < 9, 11 < 10, 12 < 11, 13$	The same
	$c, c$	$8, 10 < 9, 11 < 10, 12$ etc.	The same
	$t, t$	$12, 14 < 11, 13 < (10, 12 = 9, 11 = 8, 10 \leq 7, 9)$	$(11, 13 = 10, 12 = 9, 11 \leq 8, 10)$
	Geometric $c/t$	$Xc, (X + 2)t < Xt, (X + 2)c$	The same
	Positional $c/t$	$(X - 2)t, Xc < Xc, (X + 2)t$	The same
18:1	Positional $c$ or $t$	$4 < 5 < (6-8) < 9 < 10 < 11 < 12 < 13 < 14 < 15 < 16$	$(4-9) < 10 < 11 < 12 < 13 < 14 < 15 < 16$
	$c$ vs. $t$	$t < c; (X + 5.5)t = Xc$	$c < t; (X + 0.5)c = Xt$
9,12-18:2	All isomers	$tt < ct < tc < cc$	$c, c < (tt < ct) < tc$
9,12,15-18:3	All isomers	$ttt < (ctt \leq tct) < (ttc = cct) < ctc < tcc < ccc$	$cct < (ccc \leq ttt \leq ctt) < tct < (ctc \leq tcc \leq ttc)$
	Mono- <i>trans</i>	$cct < ctc < tcc$	$cct < (ctc \leq tcc)$
	Di- <i>trans</i>	$(ctt \leq tct) < ttc$	$ctt < tct < ttc$
6,9,12-18:3	All isomers	$ttt < (ctt \leq tct) < (ttc = cct) < ctc < (tcc = ccc)$	$ccc < ttt < cct < (ctt \leq tct) < (ttc = ctc) < tcc$
	Mono- <i>trans</i>	$cct < ctc < tcc$	$cct < ctc \leq tcc$
	Di- <i>trans</i>	$(ctt \leq tct) < ttc$	$(ctt < tct) < ttc$
Elution order using stepwise isothermal temperature conditions <sup>c</sup>			
9,12-18:2	All isomers	$tt < ct < tc < cc$	$cc < ct < tt < tc$
9,12,15-18:3	All isomers	$ttt < (ctt < tct) < cct < ttc < ctc < tcc < ccc$	$cct < ccc < ctt < (ttt < tct < ctc) < tcc < ttc$
6,9,12-18:3	All isomers	$ttt < (ctt < tct < cct) < (ctc < ttc) < (tcc < ccc)$	$ccc < cct < ctc < (ctt < tcc) < (tct = ttt) < ttc$

<sup>a</sup>The results of long stepwise isothermal GC programs are given only if the elution order was different.

<sup>b</sup>Temperature programs for the CP Sil 88 and the SUPELCOWAX 10 columns are given in Table 1.

<sup>c</sup>The stepwise isothermal temperature programs used for the CP Sil 88 and the SUPELCOWAX 10 columns are given in Table 1.  $c$ , *cis*;  $t$ , *trans*;  $c/t$  could be either  $c, t$  or  $t, c$ ; isomers that were not resolved are given in parentheses.

except for *ctc*- and *tcc*-9,12,15-18:3 on the SUPELCOWAX 10 column. Overlaps of the mono- and di-*trans* 18:3 FAME are shown in Figures 6 and 7 and listed in Table 2. The elution order of the eight 18:3 FAME [or 20:3 FAME (42)] isomers on polar (33,36,39,42) and CARBOWAX-type columns (39,42) is generally in agreement with our present findings. However, the relative elution sequence of the individual isomers, or their assignments, on the CARBOWAX-type columns may be reversed (39). Again this may be due to differences in column type, column length, temperature program used, and/or chain length. We based our geometric assignments on comparison with the demonstrated elution order on the polar GC columns (36).

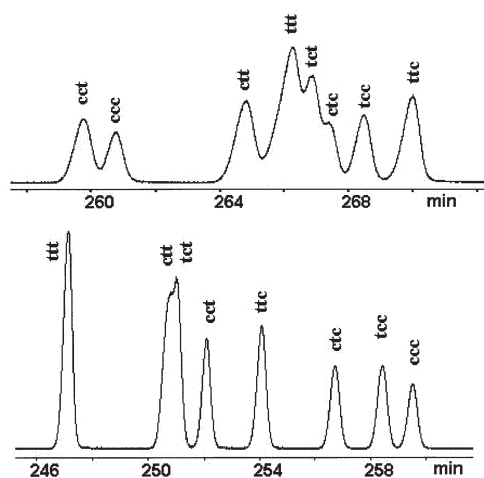
On the CP Sil 88 column, many of the isomers from methyl  $\alpha$ -linolenate (9,12,15-18:3) eluted in the region of the 20:1 isomers present in milkfats (Fig. 6). Wolff (38) showed that the elution order of 11*c*-20:1 relative to the 9,12,15-18:3 isomers could be reversed when using these polar columns by decreasing the column temperature from 180°C to 155°C. However, this would not be a solution for the analysis of milkfats, since these fats contain many positional *cis*- and *trans*-20:1 isomers (23,34), several of which would overlap with the isomers of 9,12,15-18:3. By contrast, the SUPELCOWAX 10 column resulted in a marked separation of the isomers of 9,12,15-18:3 and 20:1 (Fig. 7), thus making this column particularly suited for their identification. Furthermore, on the SUPELCOWAX 10 column the 9,12,15-18:3 isomers eluted before the CLA region (Fig. 7). To identify the 9,12,15-18:3 and 20:1 isomers definitively using the CP Sil 88 column, the isolated Ag<sup>+</sup>-TLC fractions need to be examined.

Under isothermal conditions all eight isomers of 9,12,15-18:3 were separated on either the SUPELCOWAX 10 (Fig. 8A) or the CP Sil 88 columns (Fig. 8B), although the isomers were better resolved using the latter column. The elution order of a few mono-*trans* to di-*trans* 9,12,15-18:3 isomers changed slightly using the isothermal conditions compared to using the typical temperature program, but the order within these two groups was not affected (Fig. 8).

The resolution of all eight isomers of 6,9,12-18:3 (18:3n-6) under isothermal conditions was more successful using the SUPELCOWAX 10 column (Fig. 9A) than the CP Sil 88 column (Fig. 9B). However, several isomers remained unresolved when using either one of the GC columns, and the elution order of a number of mono-*trans* to di-*trans* 6,9,12-18:3 isomers changed relative to the separation using temperature programming. A complete list of the elution order of all the 18:2 and 18:3 isomers on both columns is summarized in Table 2.

*Separation of CLA isomers and overlap with other FAME.* On a CP Sil 88 column, all the CLA isomers eluted in a GC region between 18:3n-3 and 20:2n-6 (Fig. 10A, B). This region was shown to be rather free of interfering FAME except for 21:0, a minor component present in total milk FAME except in the sphingomyelin fraction (25,57), and trace amounts of some 20:2 isomers that were present at an order of magnitude less than the minor CLA isomers (57).

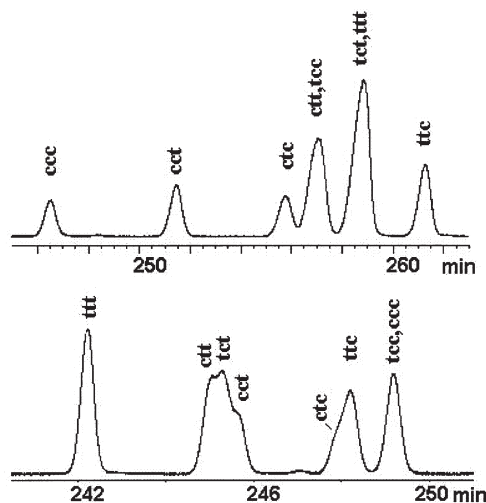
The elution order of the CLA isomers using the CP Sil 88 column was:  $c/t < c, c < t, t$  (Fig. 10B), as determined previously (7,23-26). The polar column completely resolved 10*t*, 12*c*- and 11*c*, 13*t*-CLA, but 9*c*, 11*t*- and 8*t*, 10*c*- were unresolved. All four



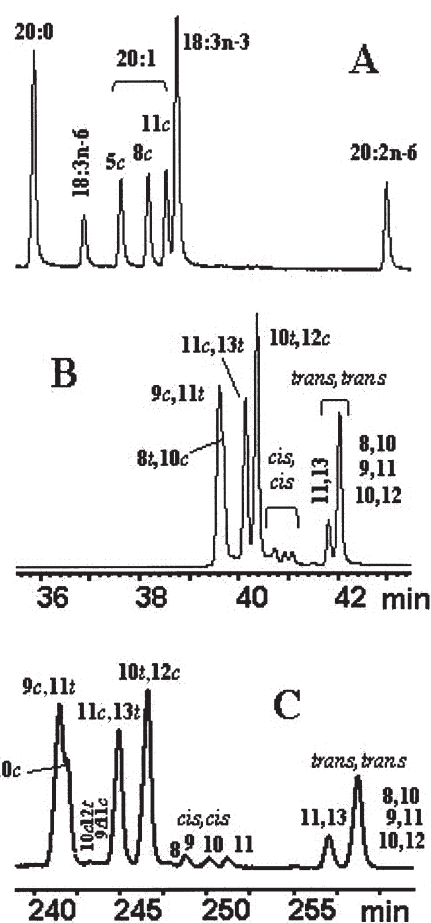
**FIG. 8.** Separation of isomerized methyl  $\alpha$ -linolenate (9,12,15-18:3) at 100°C for 7 min. Upper panel: a 60-m SUPELCOWAX 10 capillary column was operated isothermally at 130°C for 200 min followed by 75 min at 160°C. Lower panel: a 100-m CP Sil 88 capillary column operated isothermally at 120°C for 200 min followed by 70 min at 150°C. Hydrogen was used as carrier gas for both separations.

*cis,cis*-CLA isomers resolved in the elution order of 8,10-, 9,11-, 10,12-, and 11,13-CLA, whereas the *trans,trans*-CLA isomers gave rise to two peaks consisting of 11,13-CLA followed by a mixture of the remaining three positional isomers (7,23–26). A total separation of all the CLA isomers could not be achieved by GC, even by performing the analysis isothermally at 125°C and using the 100-m CP Sil 88 column (23; Fig. 10C).

On the SUPELCOWAX 10 column, the CLA isomers eluted after 18:3n-3 and stretched into the 20:1 isomer region when using helium or hydrogen as carrier gas and a typical



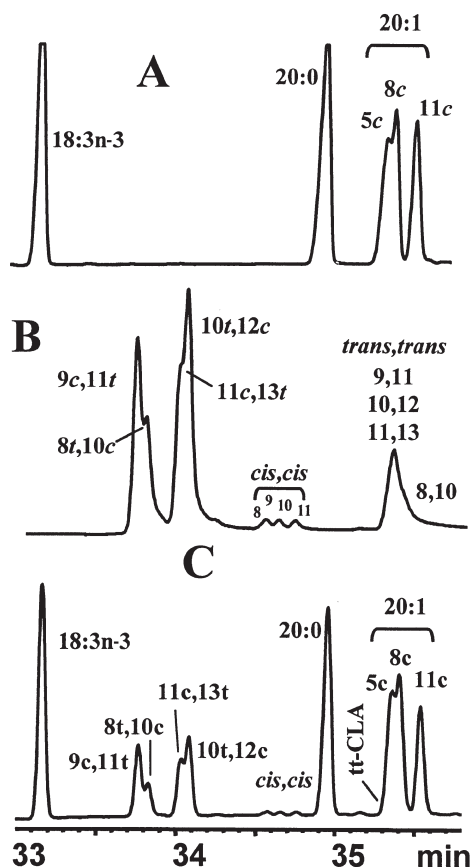
**FIG. 9.** Separation of isomerized methyl  $\gamma$ -linolenate (6,9,12-18:3) at 100°C for 15 min. Upper panel: a 60-m SUPELCOWAX 10 capillary column was operated isothermally at 130°C for 200 min followed by 75 min at 160°C. Lower panel: a 100-m CP Sil 88 capillary column operated isothermally at 120°C for 200 min followed by 70 min at 150°C. Hydrogen was used as carrier gas for both separations.



**FIG. 10.** Partial gas chromatogram of the 20:0 to 20:2n-6 FAME region using a 100-m CP Sil 88 capillary column, hydrogen as carrier, and a typical temperature program from 45 to 215°C. (A) FAME standard #463 from Nu-Chek-Prep (Elysian, MN); (B) CLA mixture #UC-59M from Nu-Chek-Prep; (C) CLA mixture #UC-59M from Nu-Chek-Prep separated isothermally at 120°C for 200 min followed by 70 min at 150°C.

temperature program (Fig. 11). However, the elution order was the same as on the CP Sil 88 column, *c/t* < *c,c* < *t,t* (Fig. 11B). There was only a limited resolution of the four positional *cis/trans*-CLA isomers; both 9*c*,11*t*- and 8*t*,10*c*-CLA, and 10*t*,12*c*- and 11*c*,13*t*-CLA were only partially separated (Fig. 11B). All four *cis,cis*-CLA isomers separated and eluted just before 20:0. The *trans,trans*-CLA isomers eluted as one broad peak with 8*t*,10*c*-CLA concentrated in the trailing edge, and all the *trans,trans*-CLA isomers eluted together with the 20:1 isomers (Fig. 11A, B). This was confirmed by co-injection of #463 and the CLA isomers (Fig. 11C).

The elution of the *trans,trans*-CLA isomers in the 20:1 region on the SUPELCOWAX 10 column was of particular concern, since milkfats are known to contain many 20:1 isomers and small amounts of *trans,trans*-CLA isomers (7,23,24,58). This interference is rather critical when evaluating methylation procedures. We showed that acid catalysts, but not base catalysts, increased the *trans,trans*-CLA content and produced methoxy artifacts (24). Therefore, the CP Sil

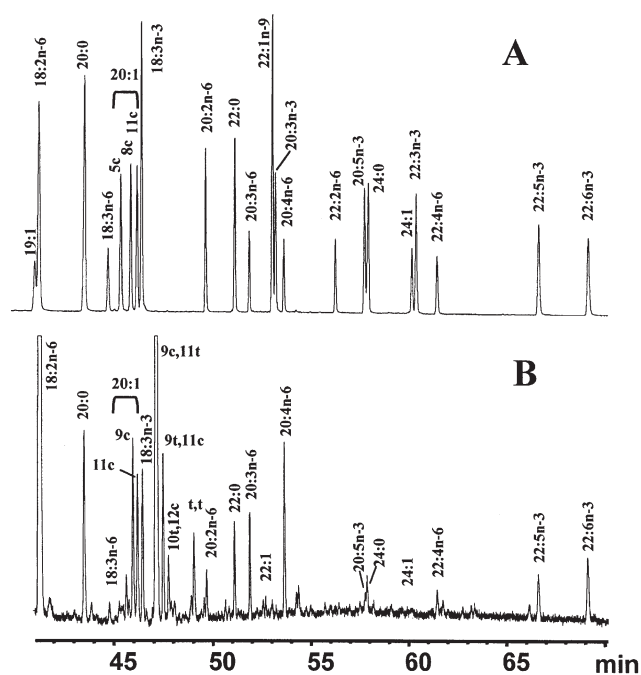


**FIG. 11.** Partial gas chromatogram of the 18:3n-3 to 20:1 FAME region using a 60-m SUPELCOWAX 10 capillary column, hydrogen as carrier, and a typical temperature program from 65 to 240°C. (A) FAME standard #463 from Nu-Chek-Prep (Elysian, MN); (B) CLA mixture #UC-59M from Nu-Chek-Prep; (C) FAME standard #463 spiked with the CLA mixture #UC-59M, both from Nu-Chek-Prep.

88 column, or similar polar columns (SP-2560 or BPX-70), are preferred since there is no interference in the *trans,trans*-CLA region. In two recent reports the methylation of CLA was re-evaluated (59,60), and, unfortunately, in both cases a SUPELCOWAX 10 column was used.

**The polyunsaturated FAME region.** Milkfats contain small amounts of C<sub>20</sub> and C<sub>22</sub> PUFA, which are identified by using both the CP Sil 88 (Fig. 12B) and the SUPELCOWAX 10 (Fig. 13B) columns. The analyses of the PUFA are important considering present-day efforts to increase the n-3 PUFA content in milkfats for health reasons through feeding cow diets containing fish meal (61), fish oil (62), or algae (50). The more prominent of the PUFA present in milkfats are: 20:3n-6, 20:4n-6 (arachidonic acid), 20:5n-3 (EPA), 22:4n-6, and 22:5n-3. DHA (22:6n-3) is present only in trace amounts in milkfat unless the cow's diet contained some fish or algal products (50,61,62); Figure 12B represents a milk from cows fed a fish meal diet, and Figure 13B a milk from cows fed a control diet.

All the long-chain C<sub>20</sub> and C<sub>22</sub> PUFA were well resolved



**FIG. 12.** Partial gas chromatogram of the 18:2n-6 to 22:6n-3 FAME region using a 100-m CP Sil 88 capillary column, hydrogen as carrier, and a typical temperature program from 45 to 215°C. (A) FAME standard #463 from Nu-Chek-Prep (Elysian, MN); (B) total milk FAME from cows fed a diet containing fish meal.

on the CP Sil 88 column by using the typical temperature program (Fig. 12). By programming the temperature to 215°C, all the long-chain PUFA eluted in about 70 min. However, a note of caution is appropriate. There may be slight differences between GC columns from the same supplier even when using identical GC conditions. In our case we observed that the elution order of 20:5n-3 and 24:0 was opposite on two different 100-m CP Sil 88 columns, even though all other parameters were kept the same. Closely eluting peaks would be most susceptible to minor column differences and to known column temperature effects that alter the relative elution sequence (32).

The SUPELCOWAX 10 column was programmed to 240°C to elute the long-chain PUFA that would otherwise accumulate in the column and cause interferences in subsequent GC analyses. The separation of the long-chain PUFA on the 60-m SUPELCOWAX 10 column provided a greater challenge, since 20:5n-3 coeluted with 22:0, 22:5n-3 with 24:0, and 22:6n-3 eluted after 24:1n-9 (Fig. 13A). In a previous study using a 30-m SUPELCOWAX 10 column, we showed that 20:5n-3 eluted before 22:0, 22:5n-3 before 24:0, and 22:6n-3 eluted between 24:0 and 24:1n-9 (30). This increase in the relative retention time of the long-chain PUFA relative to the saturated FAME was attributed to the longer column length. All the coeluting pairs of FAME could be resolved on the 60 m SUPELCOWAX 10 column by isothermal GC operations at 140°C (data not shown), but routine 6 h analyses are not practical.



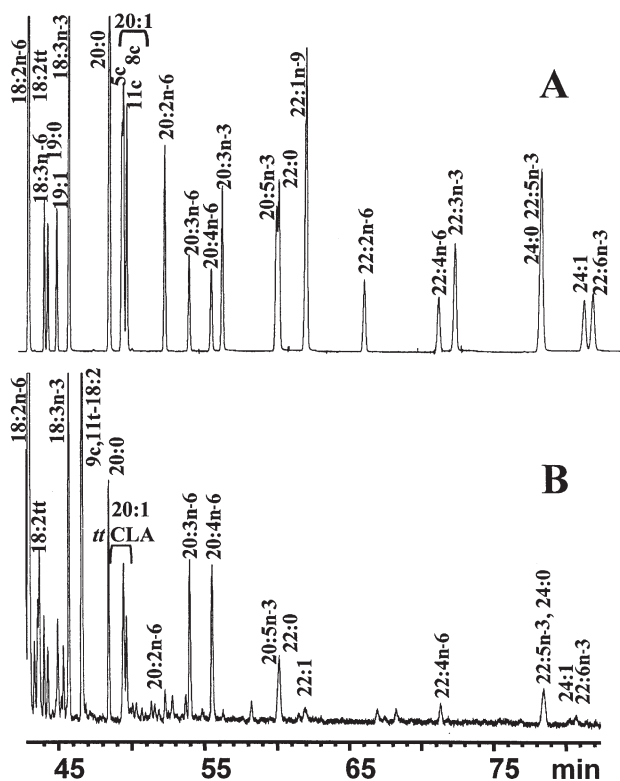


FIG. 13. Partial gas chromatogram of the 18:2n-6 to 22:6n-3 FAME region using a 60-m SUPELCOWAX 10 capillary column, hydrogen as carrier, and a typical temperature program from 65 to 240°C. (A) FAME standard #463 from Nu-Chek-Prep (Elysian, MN); (B) total milk FAME from cows fed a control diet.

In the present study the separation of the different FA regions of milkfats were evaluated using a 60-m SUPELCOWAX 10 column, and compare to that of a 100-m CP Sil 88 column whose separations are better characterized. The SUPELCOWAX 10 column was shown to give a better resolution of the short-chain saturated FA and their MUFA analogs, and it gave a complete separation of the 18:3n-3 and 20:1 isomers. The SUPELCOWAX 10 column provided an alternative approach to obtain the total 18:1 content, and to separate the isomers of 18:2n-6 and 18:3n-3. This column could also serve to confirm the identity of individual FA by comparison of the two columns. On the other hand, the CP Sil 88 column provided a better resolution of the CLA isomers, MUFA, the isolated *trans* and *cis* isomer fractions, the PUFA, and the 18:2n-6 and 18:3n-3 isomers. The lack of separation of the short-chain saturated FA and MUFA, and the overlap of the 9,12,15-18:3 and 20:1 isomers can be overcome by analyzing the isolated Ag<sup>+</sup>-TLC fractions. In conclusion it would appear that a 100-m highly polar capillary GC column is mandatory for the analysis of milk lipids, whereas the 60-m SUPELCOWAX 10 capillary column at best can serve as a complementary GC column mainly because of its intermediate polarity that often provides different separation characteristics.

## ACKNOWLEDGMENTS

Contribution number S111 from the Food Research Program, Agriculture and Agri-Food Canada.

## REFERENCES

1. Yurawecz, M.P., Mossoba, M.M., Kramer, J.K.G., Pariza, M.P., and Nelson, G.J. (eds.) (1999) *Advances in Conjugated Linoleic Acid Research*, Vol. 1, AOCS Press, Champaign.
2. Pariza, M.P., Park, Y., and Cook, M.E. (2001) The Biologically Active Isomers of Conjugated Linoleic Acid, *Progr. Lipid Res.* 40, 283–298.
3. Ha, Y.L., Grimm, N., and Pariza, M.W. (1989) Newly Recognized Anticarcinogenic Fatty Acids: Identification and Quantitation in Natural and Processed Cheeses, *J. Agric. Food Chem.* 37, 75–81.
4. Sehat, N., Yurawecz, M.P., Roach, J.A.G., Mossoba, M.M., Kramer, J.K.G., and Ku, Y. (1998) Silver-Ion High-Performance Liquid Chromatographic Separation and Identification of Conjugated Linoleic Acid Isomers, *Lipids* 33, 217–221.
5. Lavillonnière, F., Martin, J.C., Bougnoux, P. and Sébédio, J.-L. (1999) Analysis of Conjugated Linoleic Acid Isomers and Content in French Cheeses, *J. Am. Oil Chem. Soc.* 75, 343–352.
6. Sehat, N., Rickert, R., Mossoba, M.M., Kramer, J.K.G., Yurawecz, M.P., Roach, J.A.G., Adlof, R.O., Morehouse, K.M., Fritsche, J., Eulitz, K., et al. (1999) Improved Separation of Conjugated Linoleic Acid Methyl Esters by Silver-Ion High-Performance Liquid Chromatography, *Lipids* 34, 407–413.
7. Kramer, J.K.G., Sehat, N., Fritsche, J., Mossoba, M.M., Eulitz, K., Yurawecz, M.P., and Ku, Y. (1999) Separation of Conjugated Linoleic Acid Isomers, in *Advances in Conjugated Linoleic Acid Research* (Yurawecz, M.P., Mossoba, M.M., Kramer, J.K.G., Pariza, M.P., and Nelson, G.J., eds.), Vol. 1, pp. 83–109, AOCS Press, Champaign.
8. Mahfouz, M.M., Valicenti, A.J., and Holman, R.T. (1980) Desaturation of Isomeric *trans*-Octadecenoic Acids by Rat Liver Microsomes, *Biochim. Biophys. Acta* 618, 1–12.
9. Griinari, J.M., and Bauman, D.E. (1999) Biosynthesis of Conjugated Linoleic Acid and Its Conversion into Meat and Milk in Ruminants, in *Advances in Conjugated Linoleic Acid Research*, (Yurawecz, M.P., Mossoba, M.M., Kramer, J.K.G., Pariza, M.P., and Nelson, G.J., eds.), Vol. 1, pp. 180–200, AOCS Press, Champaign.
10. Griinari, J.M., Corl, B.A., Lacy, S.H., Chouinard, P.Y., Nurmela, K.V.V., and Bauman, D.E. (2000) Conjugated Linoleic Acid Is Synthesized Endogenously in Lactating Dairy Cows by  $\Delta^9$ -Desaturase, *J. Nutr.* 130, 2285–2291.
11. Santora, J.E., Palmquist, D.L., and Rohrig, K.L. (2000) *Trans*-Vaccenic Acid Is Desaturated to Conjugated Linoleic Acid in Mice, *J. Nutr.* 130, 208–215.
12. Salminen, I., Mutanen, M., Jauhiainen, M., and Aro, A. (1998) Dietary *trans* Fatty Acids Increase Conjugated Linoleic Acid Levels in Human Serum, *Nutr. Biochem.* 9, 93–98.
13. Adlof, R.O., Duval, S., and Emken, E.A. (2000) Biosynthesis of Conjugated Linoleic Acid in Humans, *Lipids* 35, 131–135.
14. Prevention and Treatment of Vascular Disease—A Nutritional-Based Approach, Part III: n-3 Fatty Acids (2001) *Lipids* 36 (Suppl.) S65–S129.
15. A Symposium on PUFA in Maternal and Child Health, September 10–13, 2000, Kansas City, Missouri (2001) *Lipids* 36, 859–1076.
16. Wolff, R.L., and Bayard, C.C. (1995) Improvement in the Resolution of Individual *trans*-18:1 Isomers by Capillary Gas-Liquid Chromatography: Use of a 100-m CP Sil 88 Column, *J. Am. Oil Chem. Soc.* 72, 1197–1201.
17. Molkenin, J., and Precht, D. (1995) Optimized Analysis of

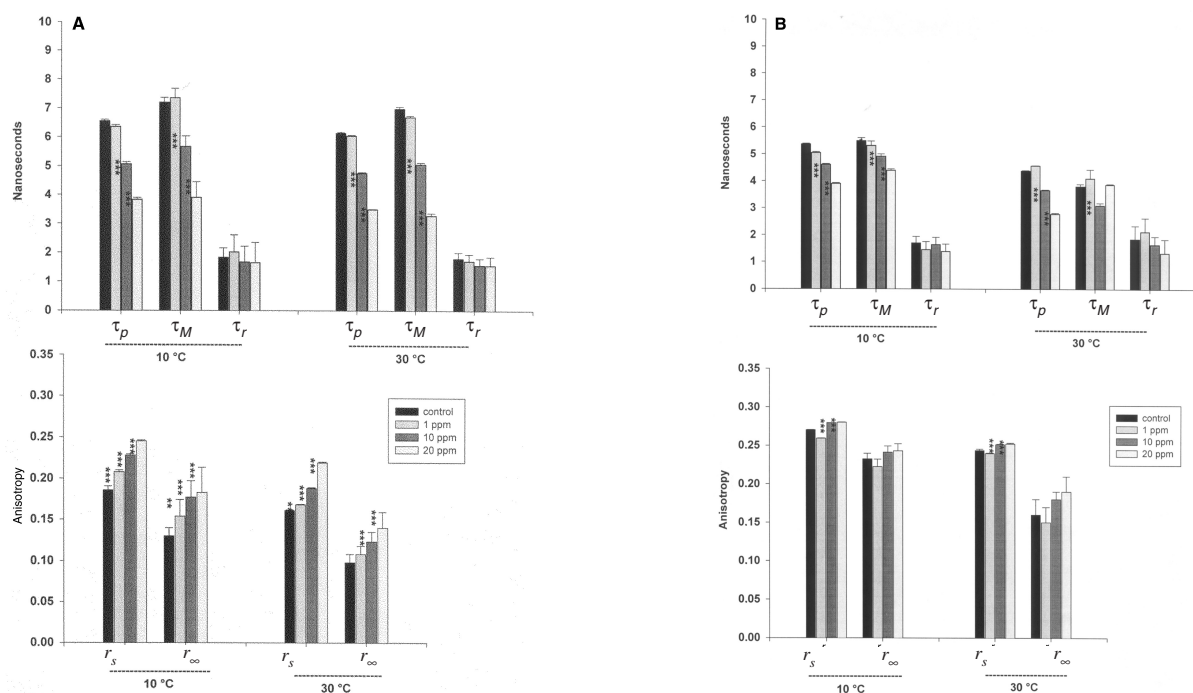
- trans*-Octadecenoic Acids in Edible Fats, *Chromatographia* 41, 267–272.
18. Mossoba, M.M., McDonald, R.E., Roach, J.A.G., Fingerhut, D.D., Yurawecz, M.P., and Sehat, N. (1997) Spectral Confirmation of *trans* Monounsaturated C<sub>18</sub> Fatty Acid Positional Isomers, *J. Am. Oil Chem. Soc.* 74, 125–130.
  19. Precht, D., and Molckentin, J. (1999) C18:1, C18:2 and C18:3 *trans* and *cis* Fatty Acid Isomers Including Conjugated *cis* Δ9, *trans* Δ11 Linoleic Acid (CLA) as Well as Total Fat Composition of German Human Milk Lipids, *Nahrung* 43, 233–244.
  20. Precht, D., and Molckentin, J. (2000) Identification and Quantitation of *cis/trans* C16:1 and C17:1 Fatty Acid Positional Isomers in German Human Milk Lipids by Thin-Layer Chromatography and Gas Chromatography/Mass Spectrometry, *Eur. J. Lipid Sci. Technol.* 102, 102–113.
  21. Wolff, R.L., Precht, D., Nasser, B., and El Kebbij, M.S. (2001) *Trans*- and *Cis*-Octadecenoic Acid Isomers in the Hump and Milk Lipids from *Camelus dromedarius*, *Lipids* 36, 1175–1178.
  22. Precht, D., Molckentin, J., Destailats, F., and Wolff, R.L. (2001) Comparative Studies on Individual Isomeric 18:1 Acids in Cow, Goat, and Ewe Milk Fats by Low-Temperature High-Resolution Capillary Gas–Liquid Chromatography, *Lipids* 36, 827–832.
  23. Kramer, J.K.G., Cruz-Hernandez, C., and Zhou, J. (2001) Conjugated Linoleic Acids and Octadecenoic Acids: Analysis by GC, *Eur. J. Lipid Sci. Technol.* 103, 600–609.
  24. Kramer, J.K.G., Fellner, V., Dugan, M.E.R., Sauer, F.D., Mossoba, M.M., and Yurawecz, M.P. (1997) Evaluating Acid and Base Catalysts in the Methylation of Milk and Rumen Fatty Acids with Special Emphasis on Conjugated Dienes and Total *trans* Fatty Acids, *Lipids* 32, 1219–1228.
  25. Kramer, J.K.G., Sehat, N., Dugan, M.E.R., Mossoba, M.M., Yurawecz, M.P., Roach, J.A.G., Eulitz, K., Aalhus, J.L., Schaefer, A.L., and Ku, Y. (1998) Distribution of Conjugated Linoleic Acid (CLA) Isomers in Tissue Lipid Classes of Pigs Fed a Commercial CLA Mixture Determined by Gas Chromatography and Silver Ion-High Performance Liquid Chromatography, *Lipids* 33, 549–558.
  26. Eulitz, K., Yurawecz, M.P., Sehat, N., Fritsche, J., Roach, J.A.G., Mossoba, M.M., Kramer, J.K.G., Adlof, R.O., and Ku, Y. (1999) Preparation, Separation, and Confirmation of the Eight Geometrical *cis/trans* Conjugated Linoleic Acid Isomers 8,10- Through 11,13-18:2, *Lipids* 34, 873–877.
  27. Dhiman, T.R., Anand, G.R., Satter, L.D., and Pariza, M.W. (1999) Conjugated Linoleic Acid Content of Milk from Cows Fed Different Diets, *J. Dairy Sci.* 82, 2146–2156.
  28. Baumgard, L.H., Corl, B.A., Dwyer, D.A., Saebø, A., and Bauman, D.E. (2000) Identification of the Conjugated Acid Isomer That Inhibits Milk Fat Synthesis, *Am. J. Physiol. Regulatory Integrative Comp. Physiol.* 278, R179–R184.
  29. Chouinard, P.Y., Corneau, L., Butler, W.R., Chilliard, Y., Drackley, J.K., and Bauman, D.E. (2001) Effect of Dietary Lipid Source on Conjugated Linoleic Acid Concentrations in Milk Fat, *J. Dairy Sci.* 84, 680–690.
  30. Kramer, J.K.G., Fouchard, R.C., and Jenkins, K.J. (1985) Differences in Chromatographic Properties of Fused Silica Capillary Columns, Coated, Crosslinked, Bonded, or Crosslinked and Bonded with Polyethylene Glycols (CARBOWAX 20M) Using Complex Fatty Acid Methyl Ester Mixtures, *J. Chromatogr. Sci.* 23, 54–56.
  31. Ackman, R.G. (1986) WCOT (Capillary) Gas-Liquid Chromatography, in *Analysis of Oils and Fats* (Hamilton, R.J., and Rossell, J.B., eds.), pp. 137–206, Elsevier Applied Science Publishers, New York.
  32. Thompson, R.H. (1996) Simplifying Fatty Acid Analyses in Multicomponent Foods with a Standard Set of Isothermal GLC Conditions Coupled with ECL Determinations, *J. Chromatogr. Sci.* 34, 495–504.
  33. Ratnayake, W.M.N., and Beare-Rogers, J.L. (1990) Problems of Analyzing C<sub>18</sub> *cis* and *trans*-Fatty Acids of Margarine on the SP-2340 Capillary Column, *J. Chromatogr. Sci.* 28, 633–639.
  34. Precht, D., and Molckentin, J. (2000) Recent Trends in the Fatty Acid Composition of German Sunflower Margarines, Shortenings and Cooking Fats with Emphasis on Individual C16:1, C18:1, C18:2 C18:3, and 20:1 *trans* Isomers, *Nahrung* 44, 222–228.
  35. Wolff, R.L. (1992) Resolution of Linolenic Acid Geometrical Isomers by Gas–Liquid Chromatography on a Capillary Column Coated with a 100% Cyanopropyl Polysiloxane Film (CP™ Sil 88), *J. Chromatogr. Sci.* 30, 17–22.
  36. Wolff, R.L. (1995) Recent Applications of Capillary Gas–Liquid Chromatography to Some Difficult Separations of Positional or Geometrical Isomers of Unsaturated Fatty Acids, in *New Trends in Lipid and Lipoprotein Analyses* (Sébédio, J.-L., and Perkins, E.G., eds.), pp. 147–180, AOCS Press, Champaign.
  37. Precht, D., and Molckentin, J. (1997) *Trans*-Geometrical and Positional Isomers of Linoleic Acid Including Conjugated Linoleic Acid (CLA) in German Milk and Vegetable Fats, *Fett/Lipid* 99, 319–326.
  38. Wolff, R.L. (1994) Analysis of α-Linolenic Acid Geometrical Isomers in Deodorized Oils by Capillary Gas–Liquid Chromatography on Cyanoalkyl Polysiloxane Phases: A Note of Caution, *J. Am. Oil Chem. Soc.* 71, 907–909.
  39. Juaneda, P., Sébédio, J.-L., and Christie, W.W. (1994) Complete Separation of the Geometrical Isomers of Linolenic Acid by High-Performance Liquid Chromatography with a Silver Ion Column, *J. High Res. Chromatogr.* 17, 321–324.
  40. Bannon, C.D., Craske, J.D., and Norman, L.M. (1988) Effects of Overload of Capillary Gas–Liquid Chromatographic Columns on the Equivalent Chain Lengths of C<sub>18</sub> Unsaturated Fatty Acid Methyl Esters, *J. Chromatogr.* 447, 43–52.
  41. Christie, W.W. (1988) Equivalent Chain-Lengths of Methyl Ester Derivatives of Fatty Acids on Gas–Liquid Chromatography, *J. Chromatogr.* 447, 305–314.
  42. Wijesundera, R.C., and Ackman, R.G. (1989) Evaluation of Calculation of ECL Values for *cis* and *trans* Isomers of Some Diethyleneic C<sub>20</sub> Fatty Acids: Mono- and Diethyleneic Capillary GLC Data for the Liquid Phases SP-2340, SUPELCOWAX 10, and SPB-1, *J. Chromatogr. Sci.* 27, 399–404.
  43. Christie, W.W. (1982) A Simple Procedure for Rapid Transmethylation of Glycerolipids and Cholesterol Esters, *J. Lipid Res.* 23, 1072–1075.
  44. Chouinard, P.Y., Corneau, L., Barbano, D.M., Metzger, L.E., and Bauman, D.E. (1999) Conjugated Linoleic Acids Alter Milk Fatty Acid Composition and Inhibit Milkfat Secretion in Dairy Cows, *J. Nutr.* 129, 1579–1584.
  45. Wolff, R.L. (1994) Contribution of *trans*-18:1 Acids from Dairy Fat to European Diets, *J. Am. Oil Chem. Soc.* 71, 277–283.
  46. Snyder, J.M., and Scholfield, C.R. (1982) *Cis-Trans* Isomerization of Unsaturated Fatty Acids with *p*-Toluenesulfonic Acid, *J. Am. Oil Chem. Soc.* 59, 469–470.
  47. Ackman, R.G., and Macpherson, E.J. (1994) Coincidence of *cis*- and *trans*-Monoethyleneic Fatty Acids Simplifies the Open-Tubular Gas–Liquid Chromatography of Butyl Esters of Butter Fatty Acids, *Food Chem.* 50, 45–52.
  48. Ulberth, F., and Henninger, M. (1992) On-Column Injection of Fatty Acid Methyl Esters onto Polar Capillary Columns Without Distortion of Early Eluting Peaks, *J. High Res. Chromatogr.* 15, 54–56.
  49. LeDoux, M., Rouzeau, A., Bas, P., and Sauvart, D. (2002) Occurrence of *trans*-C<sub>18:1</sub> Fatty Acid Isomers in Goat Milk: Effect of Two Dietary Regimens, *J. Dairy Sci.* 85, 190–197.
  50. Franklin, S.T., Martin, K.R., Baer, R.J., Schingoethe, D.J., and Hippen, A.R. (1999) Dietary Marine Algae (*Schizochytrium* sp.) Increases Concentrations of Conjugated Linoleic, Docosahexaenoic

- and *trans* Vaccenic Acids in Milk of Dairy Cows, *J. Nutr.* 129, 2048–2054.
51. Piperova, L.S., Teter, B.B., Bruckental, I., Sampugna, J., Mills, S.E., Yurawecz, M.P., Fritsche, J., Ku, K., and Erdman R.A. (2000) Mammary Lipogenic Enzyme Activity, *trans* Fatty Acids and Conjugated Linoleic Acids Are Altered in Lactating Dairy Cows Fed a Milk Fat-Depressing Diet, *J. Nutr.* 130, 2568–2574.
52. Ackman, R.G., and Sipos, J.C. (1964) Application of Specific Response Factors in the Gas Chromatographic Analysis of Methyl Esters of Fatty Acids with Flame Ionization Detectors, *J. Am. Oil Chem. Soc.* 41, 377–378.
53. Destailats, F., and Angers, P. (2002) Base-Catalyzed Derivatization Methodology for FA Analysis. Application to Milk Fat and Seed Lipid TAG, *Lipids* 37, 527–532.
54. Griinari, J.M., Dwyer, D.A., McGuire, M.A., Bauman, D.E., Palmquist, D.L., and Nurmela, K.V.V. (1998) *trans*-Octadecenoic Acids and Milk Fat Depression in Lactating Dairy Cows, *J. Dairy Sci.* 81, 1251–1261.
55. Precht, D., Molkentin, J., McGuire, M.A., McGuire, M.K., and Jensen, R.G. (2001) Overestimates of Oleic and Linoleic Acid Contents in Materials Containing *trans* Fatty Acids and Analyzed with Short Packed Gas Chromatographic Columns, *Lipids* 36, 213–216.
56. Ratnayake, W.M.N. (2001) Analysis of Dietary *trans* Fatty Acids, *J. Oleo Sci.* 50, 339–352.
57. Roach, J.A.G., Yurawecz, M.P., Kramer, J.K.G., Mossoba, M.M., Eulitz, K., and Ku, Y. (2000) Gas Chromatography–High Resolution Selected-Ion Mass Spectrometric Identification of Trace 21:0 and 20:2 Fatty Acids Eluting with Conjugated Linoleic Acid Isomers, *Lipids* 35, 797–802.
58. Sehat, N., Kramer, J.K.G., Mossoba, M.M., Yurawecz, M.P., Roach, J.A.G., Eulitz, K., Morehouse, K.M., and Ku, Y. (1998) Identification of Conjugated Linoleic Acid Isomers in Cheese by Gas Chromatography, Silver Ion High-Performance Liquid Chromatography and Mass Reconstructed Ion Profiles. Comparison of Chromatographic Elution Sequences, *Lipids* 33, 963–971.
59. Yamasaki, M., Kishihara, K., Ikeda, I., Sugano, M., and Yamada, K. (1999) A Recommended Esterification Method for Gas Chromatographic Measurement of Conjugated Linoleic Acid, *J. Am. Oil Chem. Soc.* 76, 933–938.
60. Park, Y., Albright, K.J., Cai, Z.Y., and Pariza, M.W. (2001) Comparison of Methylation Procedures for Conjugated Linoleic Acid and Artifact Formation by Commercial (Trimethylsilyl)Diazomethane, *J. Agric. Food Chem.* 49, 1158–1164.
61. Wright, T.S., Holub, B.J., and McBride, B.W. (1999) Apparent Transfer Efficiency of Docosahexaenoic Acid from Diet to Milk in Dairy Cows, *Can. J. Anim. Sci.* 79, 565–568.
62. Baer, R.J., Ryali, J., Schingoethe, D.J., Kasperson, K.M., Donovan, D.C., Hippen, A.R., and Franklin, S.T. (2001) Composition and Properties of Milk and Butter from Cows Fed Fish Oil, *J. Dairy Sci.* 84, 345–353.

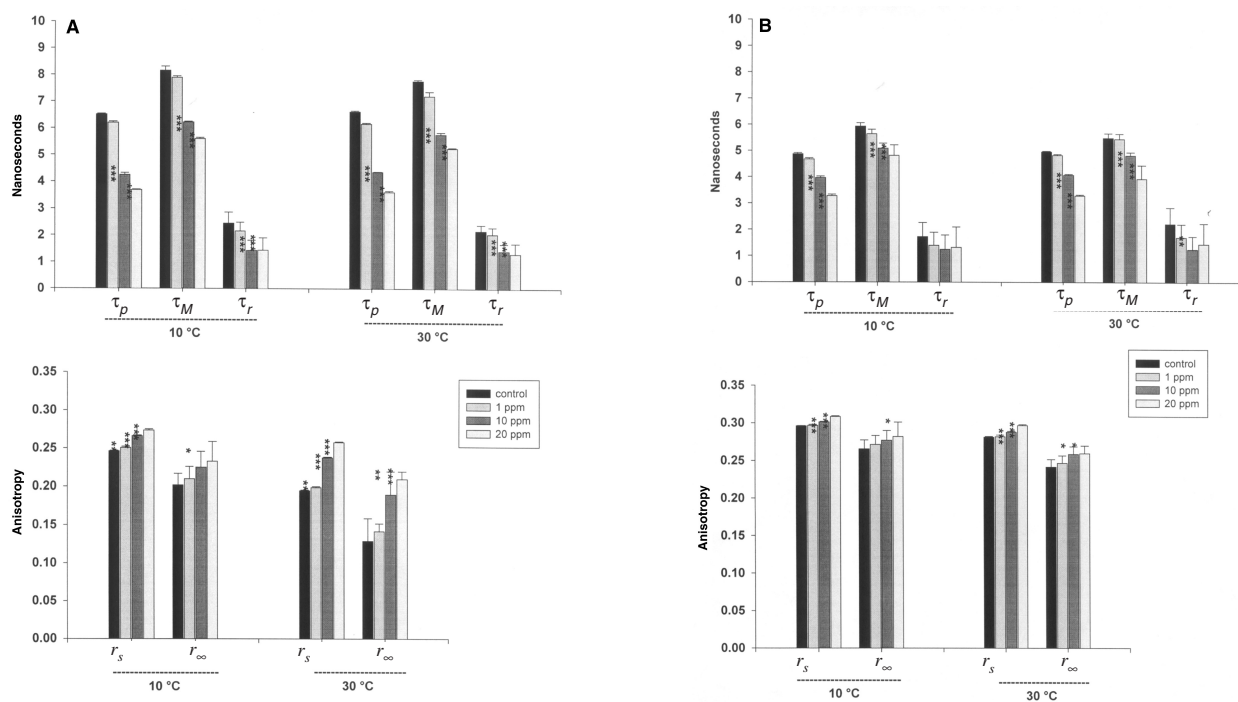
[Received May 6, 2002, and in revised form and accepted August 23, 2002]

## ERRATUM/CLARIFICATION

The authors of "Effect of Fenitrothion on the Physical Properties of Crustacean Lipoproteins (Garcia, C.F., Cunningham, M., González-Baró, M.R., Garda, H., and Pollero, R., *Lipids* 37, 673-679, 2002) have notified the Editor in Chief that axis labels in two figures presented in this article were incomplete. The revised versions of Figures 3 and 4 are reprinted below in their entirety.



**FIG. 3.** Steady-state fluorescence anisotropy ( $r_s$ ), phase lifetime ( $\tau_p$ ), modulation lifetime ( $\tau_M$ ), rotational correlation time ( $\tau_r$ ), and limiting anisotropy ( $r_{\infty}$ ) of (A) DPH and (B) DPH-PA in HDL-1 of *Macrobrachium borellii*, measured in the absence or presence of 1, 10, and 20 ppm FS at 10 and 30 °C. Student's *t*-test was used to compare the significance of the differences with respect to the sample without FS: \*\*\* $P < 0.001$ , \*\* $P < 0.01$ , \* $P < 0.05$ .



**FIG. 4.** Steady-state fluorescence anisotropy ( $r_s$ ), phase lifetime ( $\tau_p$ ), modulation lifetime ( $\tau_M$ ), rotational correlation time ( $\tau_r$ ), and limiting anisotropy ( $r_{\infty}$ ) of (A) DPH and (B) DPH-PA in HDL-2 of *M. borellii*, measured in the absence or presence of 1, 10, and 20 ppm FS at 10, and 30 °C. Student's *t*-test was used to compare the significance of the differences with respect to the sample without FS: \*\*\* $P < 0.001$ , \*\* $P < 0.01$ , \* $P < 0.05$ .



## Visual Acuity and Retinal Function in Infant Monkeys Fed Long-Chain PUFA

Brett G. Jeffrey<sup>a,1</sup>, Drake C. Mitchell<sup>b</sup>, Joseph R. Hibbeln<sup>b</sup>, Robert A. Gibson<sup>c</sup>,  
A. Lee Chedester<sup>d</sup>, and Norman Salem Jr.<sup>b,\*</sup>

<sup>a</sup>Department of Paediatrics and Child Health, Flinders Medical Centre, The Flinders University of South Australia, Bedford Park, Adelaide, SA 5042, Australia, <sup>b</sup>Laboratory of Membrane Biochemistry and Biophysics, National Institute on Alcohol Abuse and Alcoholism, National Institutes of Health, Rockville, Maryland 20852, <sup>c</sup>Child Nutrition Research Centre, Child Health Research Institute, Adelaide, SA 5000, Australia, and <sup>d</sup>Unit of Laboratory Animal Science, National Institute on Alcohol Abuse and Alcoholism, National Institutes of Health, Rockville, Maryland 20852

**ABSTRACT:** Previous randomized clinical trials suggest that supplementation of the human infant diet with up to 0.35% DHA may benefit visual development. The aim of the current study was to assess the impact of including arachidonic acid (AA) and a higher level of DHA in the postnatal monkey diet on visual development. Infant rhesus monkeys were fed either a control diet (2.0%  $\alpha$ -linolenic acid as the sole n-3 FA) or a supplemented diet (1.0% DHA and 1.0% AA) from birth. Visual evoked potential acuity was measured at 3 mon of age. Rod and cone function were assessed in terms of parameters describing phototransduction. Electroretinogram (ERG) amplitudes and implicit times were recorded over a wide intensity range ( $-2.2$  to  $4.0$  log scot td-sec) and assessed in terms of intensity response functions. Plasma DHA and AA were significantly increased ( $P < 0.001$ ) in the diet-supplemented monkeys compared with the control monkeys. There was an approximately equal effect of diet for the rod phototransduction parameters, sensitivity, and capacitance but in the opposite directions. Diet-supplemented monkeys had significantly shorter b-wave implicit times at low retinal illuminances ( $< -0.6$  log scot td-sec). There were no significant effects of diet for visual acuity or the other 23 ERG parameters measured. The results suggest that supplementation of the infant monkey diet with 1.0% DHA and 1.0% AA neither harms nor provides substantial benefit to the development of visual acuity or retinal function in the first four postnatal months.

Paper no. L9080 in *Lipids* 37, 839–848 (September 2002).

Randomized clinical trials in both term and preterm human infants have sought to determine whether a supply of preformed DHA is required in the neonatal diet to achieve normal retinal and visual acuity development (1–14). Differences in visual acuity that have persisted beyond 3 mon of age between infants fed a DHA-supplemented formula and infants

fed a formula containing  $\alpha$ -linolenic acid (ALA) as the sole n-3 FA, have been reported in some (2,4,8,10,13,14) but not all studies (3,5–7,9,11,12). Although there are numerous differences between study protocols, which may account for the varying results, one important factor may be the level of DHA used in the supplemented formulas. Over the range of DHA supplementation used (0.1 to 0.36% of total FA), differences in visual acuity have generally been reported when the level of DHA in the supplemented formula was at the upper end of the range. The level of DHA used in supplemented formula milks has typically been based on the level of DHA found in breast milk from the region of study. The majority of these human trials have originated in North America, with additional trials from Australia and Europe. In the United States and Australia, the level of DHA reported in breast milk is typically less than 0.35% of total FA, which is at the lower end of breast milk DHA concentrations reported from around the world (15,16). Much higher DHA levels in breast milk have been reported in Nigeria (0.93%), among the Canadian Inuit (1.4%), and in Asian countries such as Japan, China, Malaysia, and India (0.7–0.9%) (15,16).

Whether supplementing human infant formulas with DHA levels greater than 0.35% would provide any additional benefit to the development of visual acuity or retinal function during development is unknown. Alternatively, experiments in guinea pigs suggest that very high levels of n-3 long-chain PUFA (LCPUFA) may be deleterious to the development of retinal function. Guinea pigs fed a fish oil-based diet containing high concentrations of DHA (2.8%) and EPA (4.3%) had significant reductions in electroretinogram (ERG) a- and b-wave amplitudes in comparison with guinea pigs fed a diet containing a high level of ALA (8%) as the only n-3 FA (17). Although the levels of DHA and EPA used in the guinea pig were very high, the results highlight the importance of determining whether supplementation of infant formulas with higher levels of LCPUFA than those used in previous human studies could affect retinal development.

There has been little investigation into the effect of altering dietary n-3 FA levels on the function of the cone photoreceptors. Birch *et al.* (1) reported alterations in rod- but not cone-isolated ERG at 6 wk postnatal age in preterm infants fed a corn oil-based formula (0.5% ALA) compared with

\*To whom correspondence should be addressed at Laboratory of Membrane Biochemistry & Biophysics, NIAAA, 12420 Parklawn Dr., Rm. 1-14, Rockville, MD 20852. E-mail: nsalem@niaaa.nih.gov

<sup>1</sup>Current address: Department of Neuroscience, Oregon National Primate Research Center, Oregon Health and Science University, Beaverton, OR 97006. This study was conducted at the Laboratory of Membrane Biochemistry and Biophysics, National Institute on Alcohol Abuse and Alcoholism, National Institutes of Health, Rockville, MD 20852.

Abbreviations: AA, 20:4n-6, arachidonic acid; ALA, 18:3n-3,  $\alpha$ -linolenic acid; ERG, electroretinogram; LCPUFA, long-chain PUFA; OP, oscillatory potentials; P2, postreceptor response; P3, phototransduction response; PCA, postconceptual age; VEP, visual evoked potential.

infants fed a fish oil-supplemented formula (0.35% DHA, 0.65% EPA). Recent studies suggest that altered activation and inactivation of the phototransduction cascade within the rod photoreceptors appear to account for the altered rod-driven ERG in n-3-deficient animals (18,19). However, the structure and function of cones is quite different from that of rods, and further investigation is required to determine whether the two classes of photoreceptors have different susceptibility to the level of DHA in the diet during early development.

The rhesus monkey is an ideal model for the long-term study of the effect of altering the n-3 content of the diet on retinal function. Only higher primates, including humans, apes, and old-world monkeys, have a fovea that enables high visual acuity and three classes of cones that enable trichromatic vision (20). Other similarities between the structure, function, and development of the retina of macaque monkeys, such as the rhesus, and the human are well described (20–24). The aim of the current study was to assess visual acuity and the function of both the rod and cone photoreceptors in infant monkeys fed a diet containing a substantially higher level of DHA (1.0% of total FA) and AA (1.0%) than those used in previous randomized human infant studies.

## MATERIALS AND METHODS

**Animals and diets.** All experiments were reviewed and approved by the Institutional Animal Care and Use Committee of the National Institute on Alcohol Abuse and Alcoholism (NIAAA) of the National Institutes of Health (NIH; Rockville, MD). Twenty rhesus monkeys (*Macaca mulatta*) were separated from their mothers at birth and randomized to receive a control ( $N = 10$ ) or LCPUFA-supplemented formula ( $N = 10$ ). The control formula milk consisted of 6 scoops of powdered primate infant milk (Primalac; Bio-Serv, Frenchtown, NJ) mixed in 2100 mL of water and combined with 1300 mL of human infant formula (Similac; Ross Products, Columbus, OH). The supplemented formula milk was created by adding 1 mL of DHA/AA (46% DHASCO and 54% ARASCO; Martek Biosciences, Columbia, MD) to the control formula to provide approximately 100  $\mu\text{g}/\text{mL}$  of DHA and AA in the final solution. Supplemented formula was mixed as needed, at least once per day. The FA contents of both diets are listed in Table 1. Each diet group had an identical number of males and females and approximately equal mean birth weights. For the first 30 d, infants were provided with 50 mL of fresh formula every 2 h from 8 A.M. to 8 P.M. Infants were provided with another 50-mL bottle overnight. At 30 d of age, infants were switched to receiving 200 mL of formula twice daily until 4 mon of age. From 2 wk of age, infants were provided with 2–4 chow blocks (see Table 1 for FA analysis) every few days. Water was provided *ad libitum*.

**FA analysis.** A blood sample was taken at 2, 4, 8, 12, and 16 wk of age and plasma was analyzed for FA content using GC. The method of FA analysis has been described in detail elsewhere (25).

**TABLE 1**  
**FA Composition of Diets (wt% of total FA)<sup>a</sup>**

FA	Control formula	Supplemented formula	Monkey chow
8:0	1.9 $\pm$ 0.1	1.8 $\pm$ 0.05	0.1
10:0	1.6 $\pm$ 0.03	1.6 $\pm$ 0.03	1.0
12:0	13.6 $\pm$ 1.4	12.7 $\pm$ 0.9	0.1
14:0	5.9 $\pm$ 0.6	6.2 $\pm$ 1.4	1.8
16:0	11.5 $\pm$ 0.8	11.8 $\pm$ 2.2	19.7
18:0	4.2 $\pm$ 0.2	3.9 $\pm$ 0.9	9.3
20:0	0.3 $\pm$ 0.0	0.3 $\pm$ 0.0	0.2
22:0	0.3 $\pm$ 0.1	0.3 $\pm$ 0.0	0.1
16:1	1.0 $\pm$ 0.1	1.1 $\pm$ 0.1	2.7
18:1n-9	29.7 $\pm$ 5.0	28.2 $\pm$ 8.8	31.4
18:1n-7	0.9 $\pm$ 0.1	4.0 $\pm$ 0.9	3.5
20:1n-9	0.2 $\pm$ 0.01	0.2 $\pm$ 0.1	0.4
24:1n-9	0.1 $\pm$ 0.01	0.1 $\pm$ 0.003	ND
18:2n-6	27.4 $\pm$ 3.4	25.8 $\pm$ 2.4	20.4
18:3n-6	0.03 $\pm$ 0.008	0.1 $\pm$ 0.00	ND
20:2n-6	ND	ND	0.1
20:3n-6	ND	ND	0.1
20:4n-6	0.04 $\pm$ 0.006	1.0 $\pm$ 0.4	0.2
22:4n-6	ND	ND	0.1
22:5n-6	ND	ND	0.1
18:3n-3	2.0 $\pm$ 0.5	2.1 $\pm$ 0.7	1.5
20:5n-3	ND	0.1 $\pm$ 0.1	0.3
22:5n-3	ND	0.02 $\pm$ 0.01	0.1
22:6n-3	ND	1.0 $\pm$ 0.4	0.2

<sup>a</sup>Values represent the mean  $\pm$  SD based on 14 independent measurements. ND, not detected.

**Visual acuity measurement.** Visual acuity was measured at 3 mon of age using visual evoked potentials (VEP). VEP were recorded from two channels while the infant monkey watched a grating stimulus on a high-resolution grayscale monitor. During each recording session, an assistant held the alert monkey and the monkey's attention was attracted to the screen using a variety of small, bright, and jangly toys. If the monkey became distracted or looked away, the stimulus was paused and restarted when the monkey was again looking at the screen. Two active electrodes, one for each channel, were positioned on the scalp over the foveal projection areas, located 10 mm superior and 20 mm posterior to the aural canals. The positioning of the active electrodes was based on mapping of the central visual field to the skull of a rhesus monkey using single-cell recordings (Lamme, V., personal communication). The ground electrode (Cz) was positioned over the midline between the aural canals, and the reference electrode (Fz 10-20 system) was positioned 3 cm anterior to the ground. All electrodes were 6 mm Ag/AgCl cups held in place with collodion glue. A conductive gel was inserted into the cup of each electrode to ensure low contact impedance with the skin. The differential VEP signal was fed to isolation amplifiers (Bio Amp; ADInstruments, Sydney, Australia) amplified by a factor of 20,000 and filtered between 0.3 and 50 Hz ( $-3$  dB points). The amplified signal was sampled at 300 Hz and digitized via an eight-bit analog-to-digital (A/D) converter and stored on a computer disc for subsequent off-line analysis.

**VEP acuity recording stimuli.** Steady-state VEP were recorded in response to a square wave grating contrast reversed 12 times per second. The VEP was recorded for

11 spatial frequencies between 1 and 12 cycles per degree (cyc/deg), excluding 11 cyc/deg, in 1-cyc/deg increments. The VEP was recorded for a 3-s presentation of each spatial frequency. Each spatial frequency was presented between 3 and 12 times depending on the alertness and cooperation of the monkey. The test distance was 100 cm for all spatial frequencies with the exception of 5 and 9 cyc/deg, where the test distance was 75 cm. At a viewing distance of 100 cm, the stimulus grating formed a  $15 \times 19^\circ$  field. Gratings had a contrast of 80% and screen luminance was  $35 \text{ cd/m}^2$ .

*VEP acuity analysis.* A discrete Fourier transform (DFT) was performed over each 3-s record to obtain the amplitude and phase of the signal at 12 Hz, the reversal rate of the grating stimulus. For each spatial frequency, mean VEP amplitude was calculated from the vectorial average of the recorded responses. The 95% confidence interval of the vectorial mean was calculated using  $T_{\text{circ}}^2$  (26). Visual acuity was derived by fitting a linear regression through those points that met the following criteria: (i) Amplitude increased monotonically with decreasing spatial frequency, and (ii)  $T_{\text{circ}}^2$  did not cross the zero amplitude axis. Visual acuity in cyc/deg was determined from the extrapolation of the regression line to the spatial frequency axis (27). As visual acuity is distributed normally on a logarithmic scale, each acuity was converted to the log of minimal angle of resolution (logMAR) for comparison between groups.

*ERG recording protocol: animal preparation.* Monkeys were anesthetized with intramuscular injections of ketamine (15 mg/kg and then 7.5 mg/kg at 30- to 50-min intervals as required), xylazine (1 mg/kg and then 0.5 mg/kg), and atropine sulfate (0.2 mg/kg) at induction only. Rectal temperature was maintained between  $36.5$  and  $39.5^\circ\text{C}$  with water-circulated heating pads placed beneath and on top of the monkey. Heart rate was monitored by electrocardiogram and respiratory function monitored by pulse oximetry. Pupils were dilated with phenylephrine (2.5%) and tropicamide (1%), and the monkey was dark-adapted for 30 min before the beginning of ERG recording. Full-field ERG were recorded from an infant monkey bipolar Burian–Allen contact lens electrode (Hansen Ophthalmic Development Lab, Iowa City, IA). After the cornea had been anesthetized with proparacaine (0.5%), the Burian–Allen electrode was inserted into the eye with a drop of methylcellulose (1%) placed on the contact lens. A needle electrode inserted subcutaneously in the middle of the back served as ground.

*Conventional ERG: stimulus and recording.* Flash stimulation was provided by a PS22 stimulator (Astro-Med/Grass, West Warwick, RI). Rod-isolated ERG were recorded scotopically to a series of short-wavelength flashes (“blue,” Wratten 47B;  $\lambda_{\text{max}} = 449 \text{ nm}$ , half-bandwidth = 47 nm) that produced retinal illuminances from  $-2.3$  to  $1.5 \text{ log scot td-sec}$  in 0.2-log steps. Cone ERG were obtained from 30-Hz white (1.1 log scot td-sec) flicker presented photopically (background = 2.7 log phot td). Eight or 16 (intensity <  $-1.2 \text{ log scot td-sec}$ ) responses were averaged at each intensity. ERG

were amplified by a gain of 20,000 or 100,000 (intensity <  $-1.2 \text{ log scot td-sec}$ ) and filtered ( $-3 \text{ dB}$  points at 1 and 1000 Hz) before being digitized at 1 kHz using an eight-bit A/D converter and stored on computer for off-line analysis.

*Conventional ERG analysis.* Amplitude and implicit time measurements were made for the a- and b-wave responses at each retinal illuminance and for the 30-Hz response. ERG a-wave and b-wave amplitudes were plotted against log retinal illuminance, and the data of each were fitted to the Naka–Rushton function (28,29):

$$V = V_{\text{max}} \frac{I^n}{I^n + K^n} \quad [1]$$

where  $V$  is amplitude ( $\mu\text{V}$ ) and  $I$  is retinal illuminance (scot td-sec). The derived parameters are  $V_{\text{max}}$ , maximum response ( $\mu\text{V}$ );  $K$ , log retinal illuminance that elicits half of  $V_{\text{max}}$  (log scot td-sec); and  $n$ , slope of the curve (dimensionless). The Naka–Rushton function was fitted to the data by regression using a linearized form of Equation 1.

*Isolation of photoreceptor function and postreceptor response.* Conventional ERG analysis cannot identify particular retinal mechanisms underlying the reported changes in ERG a- and b-waves because of the nonspecificity of the cellular origins of these ERG components when generated by low to moderate flash intensities (30). In Granit’s classic analysis (31), the ERG a-wave and b-wave are formed by the addition of two cellular responses, the P3 response from the photoreceptors and P2, a single postreceptor response. A quantitative model (P3 model) that describes the G-protein phototransduction cascade in single photoreceptors has been described (32). The same P3 model, or slight variants of it, has been used to fit the leading edges of ERG a-waves recorded to high-intensity flashes (e.g., Refs. 33 and 34). The a-wave recorded to a high-intensity flash represents the massed response of the photoreceptors, and the P3 model thereby provides an *in vivo* method of quantifying the phototransduction process. The isolated P2 response can be obtained by subtracting the P3 model from the ERG (35). The P2 response provides a more accurate assessment of bipolar cell function than does the ERG b-wave for a wide range of flash intensities (35).

*P3 and P2 stimulus and recording.* Flash stimulation was provided by a high-intensity camera flash (283; Vivitar, Newbury Park, CA). The ERG was recorded to a series of high-intensity white flashes (1.8 to 4.1 log scot td-sec) presented scotopically and then photopically (background = 2.7 log phot td). Rod-isolated ERG were obtained by subtracting the cone-isolated photopic ERG from the scotopic ERG at each flash intensity (36). Two responses were averaged at each intensity with interflash intervals ranging from 15 to 60 s. ERG were amplified by a gain of 20,000, filtered ( $-3 \text{ dB}$  points at 1 and 1000 Hz), and then digitized at 5 kHz.

*P3 analysis.* The following P3 model (37) was used to fit the leading edges of both the rod- and cone-isolated ERG a-waves derived from the high-intensity white flashes:



$$P3(i, t) \equiv \left( \left\{ 1 - \exp \left[ -i \cdot S \cdot (t - t_d)^2 \right] \right\} \otimes \left[ \exp(-t/\tau) \cdot 1/\tau \right] \right) \cdot R_{\max P3} \quad t_d > t \quad [2]$$

where  $\otimes$  represents the convolution integral and P3 is the leading edge of the a-wave at time  $t$  s, in response to a flash with a retinal illuminance of  $i$  scot td-sec. The parameters derived to fit the model were:  $S$ , the sensitivity parameter that scales retinal illuminance [(scot td-sec) $^{-1}$  s $^{-2}$ ];  $t_d$ , the delay due to the filter and finite duration of the flash (s);  $\tau$ , the time constant due to membrane capacitances; and  $R_{\max P3}$ , the maximum photoreceptor response ( $\mu$ V) (37,38). For cone ERG a-waves, retinal illuminances were measured in photopic trolands.

The parameters of the P3 model for the two classes of photoreceptors were determined by fitting Equation 2 simultaneously to the leading edges of the rod- and cone-isolated ERG a-waves (ensemble analysis). All analyses were performed with NONLIN (39), which uses a modified Gauss–Newton nonlinear least-squares algorithm (40), with subroutines specifying the P3 model written by the authors. The numerical solution of Equation 2 for discrete data (37) was used during the fitting process.

**P2 analysis.** The isolated P2 responses were derived by subtracting the P3 responses from the rod-isolated ERG. The amplitudes of the P2 responses were also plotted against log retinal illuminance, and the data were fitted to the Naka–Rushton function of Equation 1.

**Oscillatory potentials (OP).** The method for isolating the OP from the rod-isolated ERG recorded to high-intensity flash (4.1 log scot td-sec) has been described in detail previously (41). Briefly, before isolating the OP, the a-wave, as determined by Equation 2, was digitally subtracted from the rod-isolated ERG. The OP were then isolated using a digital, anticausal, Chebyshev type II filter [–3 dB points at 100 and 300 Hz, >30 dB attenuation in the stopbands (<75 and >400 Hz)]. The advantage of the anticausal filter is that the filtered response will have zero phase shift over the pass band.

**Statistical methods.** One of the authors (B.J.) was blinded to both the diets and groupings of monkeys during recording and analysis of all visual acuity and ERG results. Data were checked for normality and homogeneity of variance using either the Shapiro–Wilk test (for <50 observations, i.e., number of monkeys  $\times$  number of parameter measurements used in comparison) or the Kolmogorov–Smirnov test with a Lillifores correction (for number of observations >50). Implicit time data were compared using a two-way repeated-measures ANOVA. All other parameters were compared using a  $t$ -test for independent samples.

## RESULTS

**FA.** The results of plasma FA analysis at 4 mon of age are shown in Table 2. The diet-supplemented group had a slightly lower level of nonessential FA, but there were no significant differences in the amounts of saturated FA between the two

**TABLE 2**  
Plasma FA Composition at 4 mon of Age (wt% of total FA)

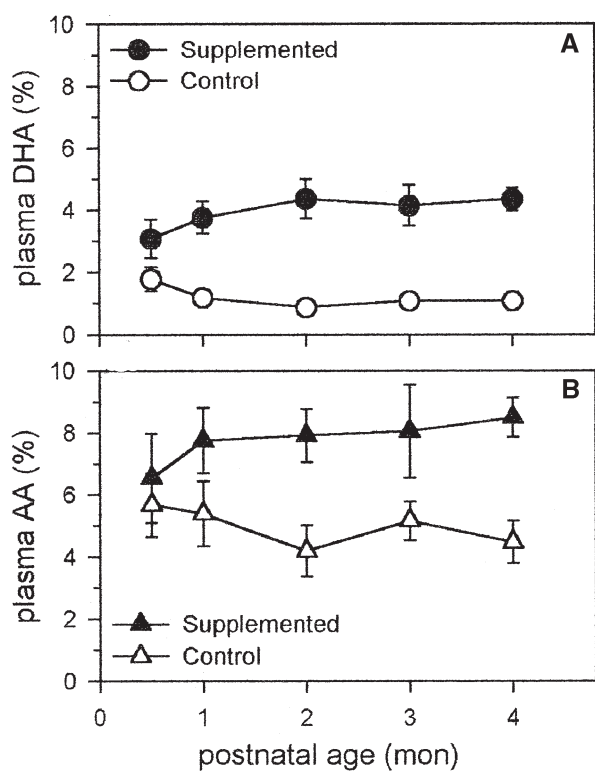
FA	Control formula	Supplemented formula	Significance <sup>a</sup>
14:0	1.34 $\pm$ 0.15	1.22 $\pm$ 0.10	NS
16:0	14.57 $\pm$ 0.50	14.49 $\pm$ 0.32	NS
18:0	10.64 $\pm$ 0.46	10.62 $\pm$ 0.41	NS
20:0	0.10 $\pm$ 0.00	0.10 $\pm$ 0.00	NS
22:0	0.10 $\pm$ 0.00	0.12 $\pm$ 0.01	NS
24:0	0.13 $\pm$ 0.02	0.14 $\pm$ 0.02	NS
Total saturated	26.89 $\pm$ 0.90	26.69 $\pm$ 0.80	NS
16:1	0.59 $\pm$ 0.03	0.46 $\pm$ 0.03	*
18:1n-9	15.88 $\pm$ 0.74	13.95 $\pm$ 0.39	*
18:1n-7	1.18 $\pm$ 0.08	1.05 $\pm$ 0.06	NS
20:1n-9	0.19 $\pm$ 0.01	0.17 $\pm$ 0.01	NS
20:3n-9	0.08 $\pm$ 0.02	0.07 $\pm$ 0.07	NS
24:1n-9	3.17 $\pm$ 0.20	3.46 $\pm$ 0.18	NS
Total nonessential	21.03 $\pm$ 0.60	19.08 $\pm$ 0.47	*
18:2n-6	34.58 $\pm$ 0.74	30.53 $\pm$ 0.70	**
18:3n-6	0.19 $\pm$ 0.02	0.10 $\pm$ 0.00	**
20:2n-6	0.37 $\pm$ 0.03	0.24 $\pm$ 0.02	**
20:3n-6	1.37 $\pm$ 0.12	0.65 $\pm$ 0.05	**
20:4n-6	4.67 $\pm$ 0.25	8.44 $\pm$ 0.20	**
22:4n-6	0.35 $\pm$ 0.02	0.25 $\pm$ 0.02	**
22:5n-6	0.26 $\pm$ 0.03	0.06 $\pm$ 0.02	**
Total n-6	41.78 $\pm$ 1.00	40.28 $\pm$ 0.81	NS
18:3n-3	0.60 $\pm$ 0.05	0.49 $\pm$ 0.03	NS
20:5n-3	0.25 $\pm$ 0.05	0.35 $\pm$ 0.04	NS
22:5n-3	0.55 $\pm$ 0.05	0.33 $\pm$ 0.02	**
22:6n-3	1.30 $\pm$ 0.16	4.35 $\pm$ 0.13	**
Total n-3	2.72 $\pm$ 0.25	5.48 $\pm$ 0.13	**
Total polyunsaturated	44.53 $\pm$ 1.23	45.78 $\pm$ 0.85	NS

<sup>a</sup>NS, not significant; \* $P$  < 0.05; \*\* $P$  < 0.01.

groups. As expected, DHA and AA were significantly elevated in the LCPUFA-supplemented group, but there was no significant difference in the total amount of polyunsaturates. Figure 1 shows plasma DHA and AA levels from 2 to 16 wk of age. Plasma DHA increased in the supplemented monkeys over the first two postnatal months before reaching a plateau of 4.4%, which was maintained until 4 mon of age. In the control group, plasma DHA fell postnatally to reach a low of 0.88% of total FA at 2 mon of age. At 3 and 4 mon of age, plasma DHA had increased to 1.08% of total FA, a 20% increase over the 2-mon low, probably reflecting that infants had started to consume some chow that contained 0.2% DHA. Plasma AA increased rapidly in diet-supplemented monkeys and remained high over the first four postnatal months but remained relatively constant in the control monkeys.

**Visual acuity.** Figure 2 shows the plot of 12-Hz amplitude and  $T_{\text{circ}}^2$  for each spatial frequency for a monkey fed the supplemented formula. When  $T_{\text{circ}}^2$  does not include the zero amplitude axis (solid circles), it can be said with 95% confidence that the signal is significantly different from zero. Visual acuity was determined from the extrapolation of the regression line to the spatial frequency axis (acuity = 11.3 cyc/deg = 0.24 logMAR). There was no significant difference ( $P$  = 0.74) in visual acuity between the supplemented (logMAR  $\pm$  SD = 0.31  $\pm$  0.08) and control monkeys (0.30  $\pm$  0.07). VEP acuity could not be measured in three monkeys from the control

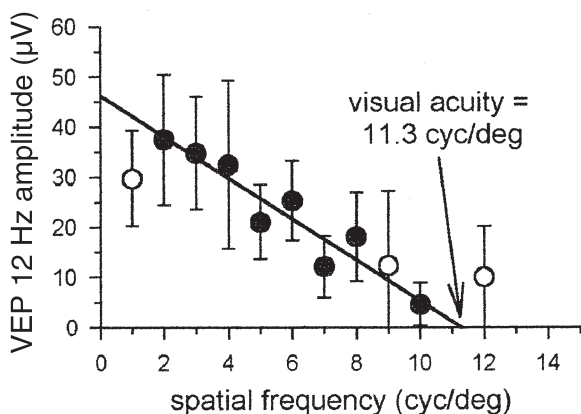




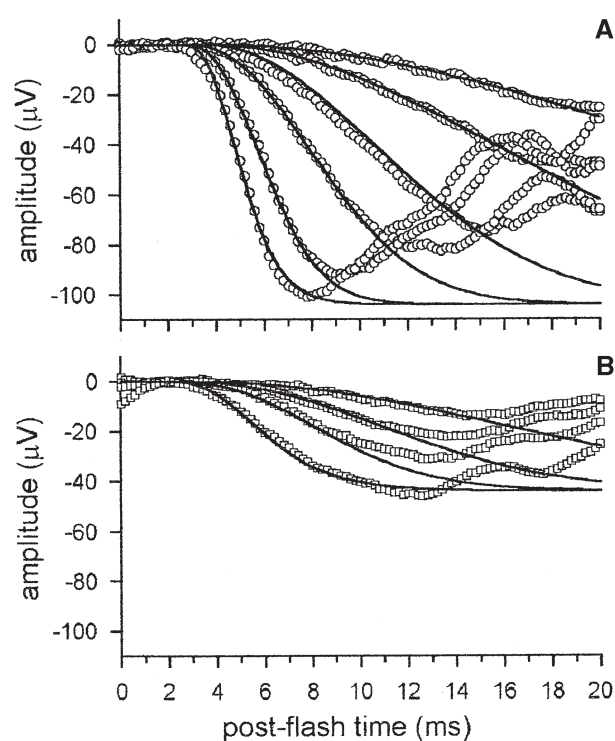
**FIG. 1.** (A) Plasma DHA expressed as a percentage of total FA plotted against postnatal age for the supplemented (solid circles) and control (open circles) monkeys. Error bars represent one SD. (B) Plasma arachidonic acid as a function of postnatal age (symbols are the same as for graph A).

group who became aggressive or uncooperative during testing. Detailed neurobehavioral assessment did not reveal any significant differences in temperament between the two dietary groups (42).

**Electroretinography.** Figure 3 shows representative rod (A) and cone-isolated ERG (B) from a DHA diet-supplemented monkey at 4 mon of age. The solid lines show the



**FIG. 2.** Visual evoked potential (VEP) amplitude at 12 Hz plotted against spatial frequency for a diet-supplemented monkey. Error bars indicate the 95% confidence interval of the vectorial mean calculated from  $T_{\text{circ}}^{-2}$ . The linear regression is applied to those points (solid circles) that lie on the linear portion of the graph and for which  $T_{\text{circ}}^{-2}$  does not cross the zero volt axis. A visual acuity of 11.3 cyc/deg was obtained from the extrapolation of the linear regression line to the spatial frequency axis.



**FIG. 3.** (A) Rod-isolated ERG (open circles) from a diet-supplemented monkey recorded to achromatic flashes that produced the retinal illuminances between 1.8 to 4.0 log scot td-sec (top to bottom). The dashed lines show the ensemble fit of Equation 2 (see text) to the leading edges of the rod-isolated ERG a-waves. The derived rod phototransduction parameters were  $S = 11.15$  (scot td-sec) $^{-1}$  s $^{-2}$ ,  $R_{\text{maxP3}} = 104$  μV,  $t_d = 2.65$  ms, and  $\tau = 0.89$  ms. (B) Cone-isolated ERG (open squares) from the same monkeys recorded to achromatic flashes that produced retinal illuminances of 1.8 to 3.3 log phot td-sec (top to bottom). The derived cone phototransduction parameters were  $S = 31.6$  (scot td-sec) $^{-1}$  s $^{-2}$ ,  $R_{\text{maxP3}} = 41.7$  μV,  $t_d = 1.79$  ms, and  $\tau = 1.92$  ms.

ensemble fits of Equation 2 to the leading edges of each set of a-waves.

Diet-supplemented monkeys had a significantly lower value of Rod $\tau$  ( $P < 0.05$ ) compared with the control monkeys, but there were no other significant differences in the rod phototransduction parameters between the two diet groups (Table 3). The parameter Rod $\tau$  represents the membrane capacitance time constant, and a lower value indicates that a shorter time is required for a change in the photocurrent following a flash. Supplemented monkeys also had a lower value for the rod phototransduction sensitivity parameter, Rod $S$ , compared with the control monkeys although the difference did not reach statistical significance ( $P = 0.07$ ). A lower value of Rod $S$  is considered poorer as it represents the gain of the phototransduction cascade (34).

There was no effect of diet for a-wave implicit times ( $P = 0.98$ ; Fig. 4A) or for any of the parameters describing rod or postphotoreceptor function derived from the fit of the Naka–Rushton function to the a-wave, b-wave, or P2 amplitudes (Table 3). There was also no effect of diet for the overall variation in b-wave implicit time with retinal illuminance ( $P = 0.2$ ; Fig. 4B). However, as can be seen in Figure 4B,

**TABLE 3**  
**Rod Parameters**

Parameter	Supplemented	Control	Power (%)
Rod P3 (N = 16)			
Rod $R_{\max P3}$ ( $\mu\text{V}$ )	161 $\pm$ 58	156 $\pm$ 59	85
Rod $S$ [(scot td-sec) $^{-1}$ s $^{-2}$ ]	5.9 $\pm$ 1.0	7.4 $\pm$ 1.8	99
Rod $t_d$ (ms)	2.6 $\pm$ 0.2	2.6 $\pm$ 0.2	100
Rod $\tau$ (ms)	0.79 $\pm$ 0.28 <sup>a</sup>	1.09 $\pm$ 0.26	94
Rod P2 (N = 14)			
P2 $V_{\max}$ ( $\mu\text{V}$ )	323 $\pm$ 123	339 $\pm$ 134	65
P2 $\log K$ (log scot td-sec)	0.82 $\pm$ 0.28	0.75 $\pm$ 0.23	54
P2 $n$	0.50 $\pm$ 0.04	0.53 $\pm$ 0.05	100
Rod a-wave (N = 14)			
a $V_{\max}$ ( $\mu\text{V}$ )	132 $\pm$ 55	151 $\pm$ 59	64
a $\log K$ (log scot td-sec)	2.33 $\pm$ 0.34	2.40 $\pm$ 0.23	45
a $n$	0.69 $\pm$ 0.11	0.59 $\pm$ 0.11	91
Rod b-wave (N = 18)			
b $V_{\max}$ ( $\mu\text{V}$ )	253 $\pm$ 120	232 $\pm$ 77	73
b $\log K$ (log scot td-sec)	0.20 $\pm$ 0.15	0.25 $\pm$ 0.19	94
b $n$	0.59 $\pm$ 0.04	0.58 $\pm$ 0.05	100

<sup>a</sup>Significantly different from control group,  $P < 0.05$ .

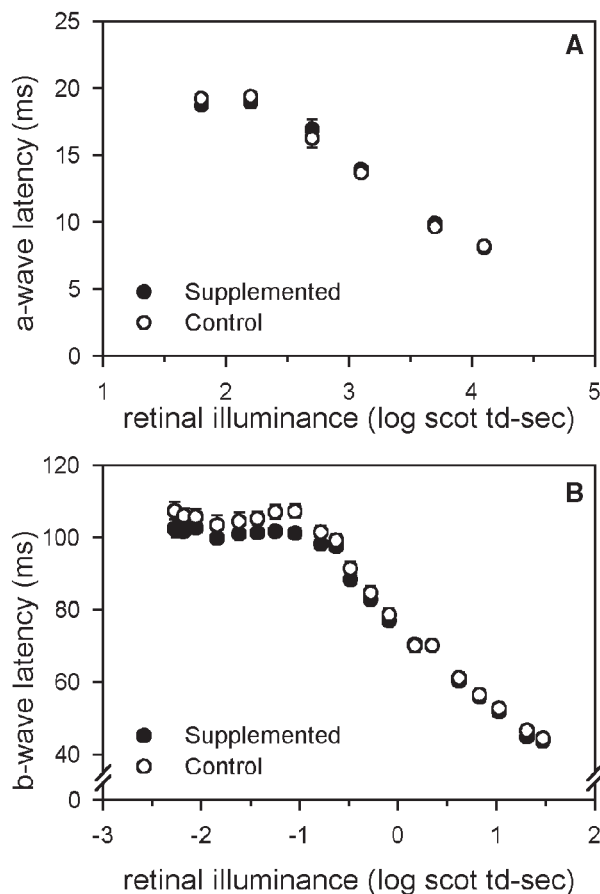
there was a tendency for diet-supplemented monkeys to have shorter b-wave implicit times as retinal illuminance decreased below  $-0.1$  log scot td-sec. For b-wave implicit times recorded to retinal illuminances of  $-0.6$  log scot td-sec and

**TABLE 4**  
**Cone Parameters**

Parameter	Supplemented	Control	Power (%)
Cone P3 (N = 16)			
Cone $R_{\max P3}$ ( $\mu\text{V}$ )	68.1 $\pm$ 26.9	59.0 $\pm$ 16.7	85
Cone $S$ [(scot td-sec) $^{-1}$ s $^{-2}$ ]	28.6 $\pm$ 9.5	30.4 $\pm$ 11.6	82
Cone $t_d$ (ms)	2.01 $\pm$ 0.24	2.07 $\pm$ 0.28	97
Cone $\tau$ (ms)	2.44 $\pm$ 1.16	1.98 $\pm$ 0.94	64
Cone 30 Hz flicker (N = 19)			
30 Hz amplitude ( $\mu\text{V}$ )	93.8 $\pm$ 30.3	95.0 $\pm$ 33.3	95
30 Hz latency (ms)	24.0 $\pm$ 1.5	24.1 $\pm$ 0.72	82

**TABLE 5**  
**Oscillatory Potentials (OP)**

Parameter	Supplemented	Control
OP amplitudes ( $\mu\text{V}$ )		
OP1	19.4 $\pm$ 11.3	17.4 $\pm$ 7.1
OP2	24.1 $\pm$ 18.3	21.8 $\pm$ 12.3
OP3	19.8 $\pm$ 14.1	16.6 $\pm$ 7.3
OP4	8.5 $\pm$ 5.7	6.4 $\pm$ 2.5
OP latencies (ms)		
OP1	10.9 $\pm$ 0.4	10.6 $\pm$ 0.6
OP2	16.3 $\pm$ 0.9	16.2 $\pm$ 1.2
OP3	22.6 $\pm$ 1.2	22.3 $\pm$ 1.6
OP4	29.0 $\pm$ 1.5	28.9 $\pm$ 1.8



**FIG. 4.** Mean a-wave (A) and b-wave (B) implicit times plotted as a function of retinal illuminance for the supplemented (closed circles) and control monkeys (open circles). Error bars indicate SEM.

lower, diet-supplemented monkeys had significantly shorter b-wave implicit times in comparison with those of the control monkeys ( $P < 0.007$ ).

There was no effect of diet for any of the parameters describing either cone phototransduction or cone flicker (Table 4). There was also no effect of diet for the implicit times ( $P = 0.98$ ) or amplitudes ( $P = 0.4$ ) of the OP (Table 5).

Calculations were done to determine if the present study had sufficient power to identify real differences between the two diet groups if they existed. The magnitude of a meaningful effect was estimated for each parameter as follows: a 0.5-octave difference in acuity, a 50% difference in amplitude parameters, an octave difference for log  $K$  parameters, a value of 0.2 for  $n$  parameters, 0.5 ms for phototransduction  $t_d$  parameters, and 2.0 ms for 30 Hz latency. For visual acuity and the majority of ERG parameters, there was at least 80% power to detect a meaningful difference between the diet groups if a true effect was present (Tables 3, 4, and 5).

## DISCUSSION

Of the 25 parameters measured, there was a significant effect of diet for only two parameters, Rod $\tau$  and b-wave implicit times at low retinal illuminances. The reason for the decrease in ERG b-wave implicit times in the diet-supplemented monkeys below retinal illuminances of  $-0.6$  log scot td-sec may be attributable to the presence of another ERG component whose presence becomes more influential on the b-wave at low retinal illuminances. The scotopic threshold response, a small, late corneal negative potential that originates from the

proximal retina (43), has a significant influence on b-wave amplitude for retinal illuminances below  $-1.5$  log scot td-sec in human adults (44). One possibility is that the decrease in b-wave implicit time could be due to an alteration in the amplitude and/or timing of the scotopic threshold response in the diet-supplemented monkeys. The OP also originate from the proximal retina (45), although from different sources than the scotopic threshold response. There were no alterations in OP in the present study, but in Birch's preterm human study (1), the only ERG abnormality to persist in the low-ALA infants at 57 wk postconceptional age (PCA) was a delay in the OP. One possibility is that the function of the proximal retina is more selectively or more greatly affected than the distal retina by alteration of the n-3 content of the diet. Delayed b-wave implicit times have also been reported in n-3-deficient monkeys compared with monkeys fed a high-ALA diet (19,46). However, the implicit time delay observed in the n-3-deficient monkeys occurred at substantially higher retinal illuminances ( $>1000$  brighter) than in the current experiment, suggesting a different retinal mechanism or different retinal origin.

The effect of diet on Rod $_S$  was approximately equal to that for Rod $_{\tau}$  but the effect was in the opposite direction. There was a significant negative correlation between Rod $_S$  and Rod $_{\tau}$  ( $r = -0.82$ ,  $P < 0.006$ ), suggesting that both parameters may not be necessary to provide adequate fits of the leading edges of the ERG a-waves. A form of the P3 model (Eq. 2), without the capacitance term, has also been used to fit the leading edge of the ERG a-wave (33,34). Therefore, Equation 2 was refitted to the ensemble of the ERG a-waves for each monkey, with the capacitance term held constant at the mean value for all monkeys (Rod $_{\tau} = 0.94$ ), and only  $R_{\max P3}$ ,  $S$ , and  $t_d$  were allowed to vary. Under these conditions, Rod $_S$  was significantly lower ( $P < 0.046$ ) in the diet-supplemented monkeys [mean  $\pm$  SD =  $5.8 \pm 1.2$  (scot td-sec) $^{-1}$  s $^{-2}$ ] compared with the control monkeys [ $7.5 \pm 1.9$  (scot td-sec) $^{-1}$  s $^{-2}$ ]. This result is inconsistent with a recent study in which rod phototransduction was not altered in adult monkeys maintained on an n-3-deficient diet compared with monkeys fed a control diet similar to the one used here (19). Given the overall number of parameters measured, it would be predicted that one parameter would reach statistical significance of  $P < 0.05$  by chance alone, making it possible that the differences in rod phototransduction between the two diet groups is coincidental.

The level of DHA (1.0%) included in the supplemented monkey infant formula was 2.8 to 10 times higher than that used in LCPUFA-supplemented formulas in randomized studies involving human infants. The results of the current study suggest that the higher level of DHA is neither beneficial nor harmful to the development of visual acuity or retinal function in infant primates. The deleterious effect of fish oil supplementation on retinal function in the guinea pig may be related to the very high levels of DHA (2.8%) and/or EPA (4.3%) included in the diet (17). High levels of EPA, in particular, may inhibit the accretion of n-6 LCPUFA such as AA into membrane phospholipids (47). Both EPA and AA are the

precursors of families of eicosanoids and prostaglandins that are thought to mediate a number of biological functions within the retina, including vascular responses, modulation of protein kinase C, and the modulation of calcium influx in retinal membranes (48,49). The altered retinal function in the fish oil-supplemented guinea pigs may be related to the levels of EPA and/or AA accreted to the retina.

No retinal FA compositional data are available for the infant monkeys described here, as they are part on an ongoing long-term study. However, it is of interest to compare the ERG results of the present study with previous studies that have similarly measured retinal function in monkey and human infants following manipulation of dietary LCPUFA intake. Direct comparison of human and monkey retinal function at the same chronological age is difficult given their differing rates of retinal development. However, it is clear that the rod outer segments continue to develop in both humans and monkeys at least through the first 4 mon of life (23,50). Birch *et al.* (1) reported reduced maximal amplitude, decreased retinal sensitivity, and elevated rod thresholds in preterm infants (born at 28–33 wk gestation) fed a formula containing just 0.5% ALA compared with infants fed a DHA (0.35%)-supplemented formula when ERG were recorded at 36 wk PCA. In a recent study by the same group, only retinal sensitivity was reduced at 6 wk postnatal age in term infants fed a formula with 1.5% ALA compared with infants fed a supplemented formula containing 0.35% DHA (10). The two major differences between the preterm and term studies were the levels of ALA used and the gestational ages at birth and testing. In humans the bulk of *in utero* DHA and AA accretion to the retina occurs during the last trimester of pregnancy (51). Therefore, the preterm infants likely had lower retinal LCPUFA concentrations at birth than did the term infants. A reduction in retinal LCPUFA at birth may make infants born prematurely more sensitive to the amount and type of n-3 FA such as DHA in the postnatal diet. Similar comparisons may be made across monkey studies. Neuringer *et al.* (46) reported that infants born to mothers fed an n-3-deficient diet from 2 mon before conception and throughout pregnancy (165 d) had only half the level of DHA in the retina as infants born to mothers fed a high-ALA diet. In the present study, all mothers received a normal chow diet containing LCPUFA and, as a result, all infants received the full complement of maternal FA. One of the clear differences between the present study and those involving preterm infants (1) and n-3-deficient monkeys (46) is that the monkeys in the present study were likely born with the full complement of retinal LCPUFA. The difference in results between the current monkey study and the study involving human infants born at term (10) may relate to species differences or may be related to the earlier age at ERG testing in the human infants.

Another important difference between the monkey and human infant studies is the postnatal fall in plasma DHA in the various groups. In preterm infants fed the low-ALA (0.5%) corn oil diet, plasma DHA fell to 0.6% at 36 wk PCA and to 0.4% by 57 wk PCA (52). Similarly, plasma DHA fell

to less than 0.4% DHA by 3 mon of age in n-3-deficient monkeys (46). For both the preterm infants fed the corn oil diet and the n-3-deficient monkeys, the ERG was altered at some time during the first postnatal months. In contrast, plasma DHA fell to 0.95% at 57 wk PCA in term infants fed the control formula that supplied 1.5% ALA as the sole n-3 FA, and in the present study plasma DHA did not fall below 0.88%. How the changes in plasma DHA affected retinal FA in either the human infants or monkeys in the current study is not easily determined. The levels of DHA in erythrocytes and plasma do not correlate well with retinal DHA levels (53,54), and substantial amounts of DHA can be found in the retina of n-3-deficient animals in the presence of extremely low erythrocyte or plasma DHA (55,56). The disparity between retinal and plasma DHA levels is likely due to the efficiency of the retina at sequestering DHA from circulating blood supply (57–59) and the ability of the retina to conserve DHA even during periods of prolonged dietary n-3 deficiency (60–62). However, the n-3-deficient monkey study and the preterm human study appear to suggest that the combination of lowered retinal DHA at birth and large fall in plasma DHA postnatally are associated with marked alterations in the ERG in the first postnatal months. The human infant studies also suggest that the level of plasma DHA alone does not predict ERG changes as the ERG normalized by 57 wk PCA despite the continued fall in plasma DHA. By comparison, the same human and monkey studies also suggest that plasma levels of up to 3.2–3.5% DHA in humans (1,10,52) and 4.4–8.8% in monkeys (current study, Ref. 19) are not deleterious to retinal function.

Comparison of the acuity results from the present study with human nutrition studies requires an adjustment for chronological age. The rates of acuity development are quite different between humans and monkeys as the rhesus monkey has a more developed fovea at birth, which also develops more rapidly during infancy than the human fovea. As a result, each week of visual acuity development in the macaque monkey is comparable to about 1 mon in the human (63). The results from the present study suggest no benefit from a diet with 1.0% DHA and 1.0% AA to acuity in the monkey at a developmental age equivalent to 12 mon in the human. Our acuity result is consistent with several studies in human infants (3,5–7,11,12) but conflicts with others (2,4,8,10,14).

The other independent variable to be considered is which AA was supplied in a concentration approximately equal to DHA in the supplemented formula. The AA was added because a reduction in growth has been reported in preterm human infants fed an EPA/DHA-supplemented formula that caused a significant reduction in the plasma AA level (64). Pigs fed a formula supplemented with approximately equal amounts of DHA and AA have significantly higher retinal DHA but not AA compared with pigs fed a control diet with moderate levels of the EFA but no LCPUFA (65–67). Given that the diet-supplemented monkeys received approximately equal amounts of DHA and AA, it is speculated that the retinal AA levels may not have been elevated in the diet-supple-

mented group compared with the control group of monkeys. If this is the case, then the level of retinal AA likely did not contribute to the results described here.

## ACKNOWLEDGMENTS

The authors acknowledge the assistance of Dr. Mark Haines, Alan Dodson, and Margro Purple for additional assistance with anesthesia and animal handling. B.G.J. was funded by a Ph.D. scholarship from Meadow Lea Foods Australia (Sydney, Australia) and a Flinders University Overseas Research Trip Award (Adelaide, Australia). Martek Biosciences Corporation (Columbia, MD) supplied the formula supplement and provided financial support.

## REFERENCES

1. Birch, D.G., Birch, E.E., Hoffman, D.R., and Uauy, R.D. (1992) Retinal Development in Very-Low-Birth-Weight Infants Fed Diets Differing in Omega-3 Fatty Acids, *Invest. Ophthalmol. Vis. Sci.* 33, 2365–2376.
2. Birch, E.E., Birch, D.G., Hoffman, D.R., and Uauy, R. (1992) Dietary Essential Fatty Acid Supply and Visual Acuity Development, *Invest. Ophthalmol. Vis. Sci.* 32, 3242–3253.
3. Carlson, S.E., Werkman, S.H., Rhodes, P.G., and Tolley, E.A. (1993) Visual-Acuity Development in Healthy Preterm Infants, Effect of Marine-Oil Supplementation, *Am. J. Clin. Nutr.* 58, 35–42.
4. Makrides, M., Neumann, M., Simmer, K., Pater, J., and Gibson, R. (1995) Are Long-Chain Polyunsaturated Fatty Acids Essential Nutrients in Infancy? *Lancet* 345, 1463–1468.
5. Carlson, S.E., Ford, A.J., Werkman, S.H., Peeples, J.M., and Koo, W.W.K. (1996) Visual Acuity and Fatty Acid Status of Term Infants Fed Human Milk and Formulas With and Without Docosahexaenoate and Arachidonate from Egg Yolk Lecithin, *Pediatr. Res.* 39, 882–888.
6. Carlson, S.E., Werkman, S.H., and Tolley, E.A. (1996) Effect of Long-Chain n-3 Fatty Acid Supplementation on Visual Acuity and Growth of Preterm Infants With and Without Bronchopulmonary Dysplasia, *Am. J. Clin. Nutr.* 63, 687–697.
7. Auestad, N., Montalto, M.B., Hall, R.T., Fitzgerald, K.M., Wheeler, R.E., Connor, W.E., Neuringer, M., Connor, S.L., Taylor, J.A., and Hartmann, E.E. (1997) Visual Acuity, Erythrocyte Fatty Acid Composition, and Growth in Term Infants Fed Formulas with Long Chain Polyunsaturated Fatty Acids for One Year, *Pediatr. Res.* 41, 1–10.
8. Birch, E.E., Hoffman, D.R., Uauy, R., Birch, D.G., and Prestidge, C. (1998) Visual Acuity and the Essentiality of Docosahexaenoic Acid and Arachidonic Acid in the Diet of Term Infants, *Pediatr. Res.* 44, 201–209.
9. Jorgensen, M.H., Holmer, G., Lund, P., Hernell, O., and Michaelsen, K.F. (1998) Effect of Formula Supplemented with Docosahexaenoic Acid and  $\gamma$ -Linolenic Acid on Fatty Acid Status and Visual Acuity in Term Infants, *J. Pediatr. Gastroenterol. Nutr.* 26, 412–421.
10. Hoffman, D.R., Birch, E.E., Birch, D.G., Uauy, R., Castaneda, Y.S., Lapus, M.G., and Wheaton, D.H. (2000) Impact of Early Dietary Intake and Blood Lipid Composition of Long-Chain Polyunsaturated Fatty Acids on Later Visual Development, *J. Pediatr. Gastroenterol. Nutr.* 31, 540–553.
11. Makrides, M., Neumann, M.A., Simmer, K., and Gibson, R.A. (2000) A Critical Appraisal of the Role of Dietary Long-Chain Polyunsaturated Fatty Acids on Neural Indices of Term Infants: A Randomized, Controlled Trial, *Pediatrics* 105, 32–38.
12. Auestad, N., Halter, R., Hall, R.T., Blatter, M., Bogle, M.L., Burks, W., Erickson, J.R., Fitzgerald, K.M., Dobson, V., Innis,



- S.M., *et al.* (2001) Growth and Development in Term Infants Fed Long-Chain Polyunsaturated Fatty Acids: A Double-Masked, Randomized, Parallel, Prospective, Multivariate Study, *Pediatrics* 108, 372–381.
13. O'Connor, D.L., Hall, R., Adamkin, D., Auestad, N., Castillo, M., Connor, W.E., Connor, S.L., Fitzgerald, K., Groh-Wargo, S., Hartmann, E.E., *et al.* (2001) Growth and Development in Preterm Infants Fed Long-Chain Polyunsaturated Fatty Acids: A Prospective, Randomized Controlled Trial, *Pediatrics* 108, 359–371.
  14. Birch, E.E., Hoffman, D.R., Castaneda, Y.S., Fawcett, S.L., Birch, D.G., and Uauy, R.D. (2002) A Randomized Controlled Trial of Long-Chain Polyunsaturated Fatty Acid Supplementation of Formula in Term Infants After Weaning at 6 Weeks of Age, *Am. J. Clin. Nutr.* 75, 570–580.
  15. Hamosh, M., and Salem, N., Jr. (1998) Long-Chain Polyunsaturated Fatty Acids, *Biol. Neonate* 74, 106–120.
  16. Jensen, R.G. (1999) Lipids in Human Milk, *Lipids* 34, 1243–1271.
  17. Weisinger, H.S., Vingrys, A.J., and Sinclair, A.J. (1996) The Effect of Docosahexaenoic Acid on the Electroretinogram of the Guinea Pig, *Lipids* 31, 65–70.
  18. Weisinger, H.S., Vingrys, A.J., Bui, B.V., and Sinclair, A.J. (1999) Effects of Dietary n-3 Fatty Acid Deficiency and Repletion in the Guinea Pig Retina, *Invest. Ophthalmol. Vis. Sci.* 40, 327–338.
  19. Jeffrey, B.G., Mitchell, D.C., Gibson, R.A., and Neuringer, M. (2002) n-3 Fatty Acid Deficiency Alters Recovery of the Rod Photoresponse in Rhesus Monkeys, *Invest. Ophthalmol. Vis. Sci.* 43, 2806–2814.
  20. Jacobs, G.H. (1996) Primate Photopigments and Primate Color Vision, *Proc. Natl. Acad. Sci. USA* 93, 577–581.
  21. Blough, D.S., and Schrier, A.M. (1963) Scotopic Spectral Sensitivity in the Monkey, *Science* 139, 493–494.
  22. Harwerth, R.S., and Smith, E.L. (1985) Rhesus Monkey as a Model for Normal Vision of Humans, *Am. J. Optom. Physiol. Opt.* 62, 633–641.
  23. Hendrickson, A.E. (1993) Morphological Development of the Primate Retina, in *Early Visual Development: Normal and Abnormal* (Simons, K., ed.), pp. 287–295, Oxford University Press, Oxford.
  24. Fulton, A., Hansen, R.M., Dorn, E., and Hendrickson, A. (1996) Development of Primate Rod Structure and Function, in *Infant Vision* (Vital-Durand, F., ed.), pp. 33–49, Oxford University Press, New York.
  25. Salem, N., Jr., Reyzer, M., and Karanian, J. (1996) Losses of Arachidonic Acid in Rat Liver After Alcohol Inhalation, *Lipids* 31 (Suppl.), S153–S156.
  26. Victor, J.D., and Mast, J. (1991) A New Statistic for Steady-State Evoked Potentials, *Electroencephalogr. Clin. Neurophysiol.* 78, 378–388 [published erratum appears in *Electroencephalogr. Clin. Neurophysiol.* 83, 270, 1992].
  27. Norcia, A.M., and Tyler, C.W. (1985) Spatial Frequency Sweep VEP: Visual Acuity During the First Year of Life, *Vision Res.* 25, 1399–1408.
  28. Massof, R.W., Wu, L., Finkelstein, D., Perry, C., Starr, S.J., and Johnson, M.A. (1984) Properties of Electroretinographic Intensity-Response Functions in Retinitis Pigmentosa, *Doc. Ophthalmol.* 57, 279–296.
  29. Hansen, R.M., and Fulton, A.B. (1993) Development of Scotopic Retinal Sensitivity, in *Early Visual Development Normal and Abnormal* (Simons, K., ed.), pp. 130–142, Oxford University Press, Oxford.
  30. Hood, D.C., and Birch, D.G. (1990) The a-Wave of the Human Electroretinogram and Rod Receptor Function, *Invest. Ophthalmol. Vis. Sci.* 31, 2070–2081.
  31. Granit, R. (1933) The Components of the Retinal Action Potential in Mammals and Their Relation to the Discharge in the Optic Nerve, *J. Physiol.* 77, 207–239.
  32. Lamb, T.D., and Pugh, E.N., Jr. (1992) A Quantitative Account of the Activation Steps Involved in Phototransduction in Amphibian Photoreceptors, *J. Physiol. (London)* 449, 719–758.
  33. Breton, M.E., Schueller, A.W., Lamb, T.D., and Pugh, E.N., Jr. (1994) Analysis of ERG a-Wave Amplification and Kinetics in Terms of the G-Protein Cascade of Phototransduction, *Invest. Ophthalmol. Vis. Sci.* 35, 295–309.
  34. Hood, D.C., and Birch, D.G. (1994) Rod Phototransduction in Retinitis Pigmentosa: Estimation and Interpretation of Parameters Derived from the Rod a-Wave, *Invest. Ophthalmol. Vis. Sci.* 35, 2948–2961.
  35. Hood, D.C., and Birch, D.G. (1992) A Computational Model of the Amplitude and Implicit Time of the b-Wave of the Human ERG, *Vis. Neurosci.* 8, 107–126.
  36. Hood, D.C., and Birch, D.G. (1997) Assessing Abnormal Rod Photoreceptor Activity with the a-Wave of the ERG: Applications and Methods, *Doc. Ophthalmol.* 92, 253–267.
  37. Smith, N.P., and Lamb, T.D. (1997) The a-Wave of the Human Electroretinogram Recorded with a Minimally Invasive Technique, *Vision Res.* 37, 2943–2952.
  38. Hood, D.C., and Birch, D.G. (1993) Human Cone Receptor Activity: The Leading Edge of the a-Wave and Models of Receptor Activity, *Vis. Neurosci.* 10, 857–871.
  39. Johnson, M.L., and Frasier, S.G. (1985) Nonlinear Least Squares Analysis, *Methods Enzymol.* 117, 301–342.
  40. Johnson, M.L., and Faunt, L.M. (1992) Parameters Estimation by Least-Squares Methods, *Methods Enzymol.* 210, 1–37.
  41. Jeffrey, B.G. (2000) The Role of Docosahexaenoic Acid in Retinal Function of the Rhesus Monkey (*Macaca mulatta*), Ph.D. Thesis, The Flinders University of South Australia, Adelaide, Australia, pp. 86–90.
  42. Champoux, M., Hibbeln, J.R., Shannon, C., Majchrzak, S., Suomi, S.J., Salem, N., Jr., and Higley, J.D. (2002) Fatty Acid Formula Supplementation and Neuromotor Development in Rhesus Monkey Neonates, *Pediatr. Res.* 51, 273–281.
  43. Sieving, P.A., Frishman, L.J., and Steinberg, R.H. (1986) Scotopic Threshold Response of Proximal Retina in Cat, *J. Neurophysiol.* 56, 1048–1061.
  44. Hood, D.C., and Birch, D.G. (1996) Beta Wave of the Scotopic (rod) Electroretinogram as a Measure of the Activity of Human On-Bipolar Cells, *J. Opt. Soc. Am. A* 13, 623–633.
  45. Karwoski, C., and Karwoski, K. (1991) Oscillatory Potentials, in *Principles and Practice of Clinical Electrophysiology of Vision* (Heckenlively, J.R., ed.), pp. 125–128, Mosby, New York.
  46. Neuringer, M., Connor, W.E., Lin, D.S., Anderson, G.J., and Barstad, L. (1991) Dietary  $\omega$ -3 Fatty Acids: Effects on Retinal Lipid Composition and Function in Primates, in *Retinal Degenerations* (R.E. Anderson, ed.), pp. 1–13, CRC Press, Boca Raton.
  47. Lands, W.E.M., Morris, A., and Libelt, B. (1990) Quantitative Effects of Dietary Polyunsaturated Fats on the Composition of Fatty Acids in Rat Tissues, *Lipids* 25, 505–516.
  48. Koutz, C.A., Wiegand, R.D., Rapp, L.M., and Anderson, R.E. (1995) Effect of Dietary Fat on the Response of the Rat Retina to Chronic and Acute Light Stress, *Exp. Eye Res.* 60, 307–316.
  49. Jeffrey, B.G., Weisinger, H.S., Neuringer, M., and Mitchell, D.C. (2001) The Role of Docosahexaenoic Acid in Retinal Function, *Lipids* 36, 859–871.
  50. Dorn, E.M., Hendrickson, L., and Hendrickson, A.E. (1995) The Appearance of Rod Opsin During Monkey Retinal Development, *Invest. Ophthalmol. Vis. Sci.* 36, 2634–2651.
  51. Martinez, M. (1992) Tissue Levels of Polyunsaturated Fatty Acids During Early Human Development, *J. Pediatr.* 120, S129–S138.
  52. Hoffman, D.R., and Uauy, R. (1992) Essentiality of Dietary

- Omega-3 Fatty Acids for Premature Infants: Plasma and Red Blood Cell Fatty Acid Composition, *Lipids* 27, 886–895.
53. Makrides, M., Neumann, M.A., Byard, R.W., Simmer, K., and Gibson, R.A. (1994) Fatty Acid Composition of Brain, Retina, and Erythrocytes in Breast- and Formula-Fed Infants, *Am. J. Clin. Nutr.* 60, 189–194.
54. Riesbick, S., Neuringer, M., and Connor, W.E. (1996) Effects of Omega-3 Fatty Acid Deficiency in Nonhuman Primates, in *Recent Developments in Infant Nutrition* (Bindels, J.G., ed.) pp. 157–172, Kluwer, Dordrecht.
55. Connor, W.E., Neuringer, M., and Lin, D.S. (1990) Dietary Effects on Brain Fatty Acid Composition: The Reversibility of n-3 Fatty Acid Deficiency and Turnover of Docosahexaenoic Acid in the Brain, Erythrocytes, and Plasma of Rhesus Monkeys, *J. Lipid Res.* 31, 237–247.
56. Wiegand, R.D., Koutz, C.A., Stinson, A.M., and Anderson, R.E. (1991) Conservation of Docosahexaenoic Acid in Rod Outer Segments of Rat Retina During n-3 and n-6 Fatty Acid Deficiency, *J. Neurochem.* 57, 1690–1699.
57. Sheaff Greiner, R.C., Zhang, Q., Goodman, K.J., Giussani, D.A., Nathanielsz, P.W., and Brenna, J.T. (1996) Linoleate,  $\alpha$ -Linolenate, and Docosahexaenoate Recycling into Saturated and Monounsaturated Fatty Acids Is a Major Pathway in Pregnant or Lactating Adults and Fetal or Infant Rhesus Monkeys, *J. Lipid Res.* 37, 2675–2686.
58. Sheaff Greiner, R.C., Winter, J., Nathanielsz, P.W., and Brenna, J.T. (1997) Brain Docosahexaenoate Accretion in Fetal Baboons: Bioequivalence of Dietary  $\alpha$ -Linolenic and Docosahexaenoic Acids, *Pediatr Res.* 42, 826–834.
59. Su, H.M., Bernardo, L., Mirmiran, M., Ma, X.H., Corso, T.N., Nathanielsz, P.W., and Brenna, J.T. (1999) Bioequivalence of Dietary  $\alpha$ -Linolenic and Docosahexaenoic Acids as Sources of Docosahexaenoate Accretion in Brain and Associated Organs of Neonatal Baboons, *Pediatr Res.* 45, 87–93.
60. Stinson, A.M., Wiegand, R.D., and Anderson, R.E. (1991) Recycling of Docosahexaenoic Acid in Rat Retinas During n-3 Fatty Acid Deficiency, *J. Lipid Res.* 32, 2009–2017.
61. Anderson, R.E., O'Brien, P.J., Wiegand, R.D., Koutz, C.A., and Stinson, A.M. (1992) Conservation of Docosahexaenoic Acid in the Retina, *Adv. Exp. Med. Biol.* 318, 285–294.
62. Bazan, N.G., Gordon, W.C., and Rodriguez de Turco, E.B. (1992) Docosahexaenoic Acid Uptake and Metabolism in Photoreceptors: Retinal Conservation by an Efficient Retinal Pigment Epithelial Cell-Mediated Recycling Process, *Adv. Exp. Med. Biol.* 318, 295–306.
63. Teller, D.Y., and Boothe, R.G. (1979) The Development of Vision in Infant Primates, *Trans. Ophthalmol. Soc. UK* 99, 333–337.
64. Carlson, S.E. (1996) Arachidonic Acid Status of Human Infants: Influence of Gestational Age at Birth and Diets with Very Long Chain n-3 and n-6 Fatty Acids, *J. Nutr.* 126, 1092S–1098S.
65. Craig Schmidt, M.C., Stieh, K.E., and Lien, E.L. (1996) Retinal Fatty Acids of Piglets Fed Docosahexaenoic and Arachidonic Acids from Microbial Sources, *Lipids* 31, 53–59.
66. Jiménez, J., Boza, J., Suárez, M.D., and Gil, A. (1997) The Effect of a Formula Supplemented with n-3 and n-6 Long-Chain Polyunsaturated Fatty Acids on Plasma Phospholipid, Liver Microsomal, Retinal, and Brain Fatty Acid Composition in Neonatal Piglets, *J. Nutr. Biochem.* 8, 217–223.
67. Alessandri, J.M., Goustard, B., Guesnet, P., and Durand, A. (1998) Docosahexaenoic Acid Concentrations in Retinal Phospholipids of Piglets Fed an Infant Formula Enriched with Long-Chain Polyunsaturated Fatty Acids: Effects of Egg Phospholipids and Fish Oils with Different Ratios of Eicosapentaenoic Acid to Docosahexaenoic Acid, *Am. J. Clin. Nutr.* 67, 377–385.

[Received May 30, 2002, and in revised form September 12, 2002; revision accepted September 20, 2002]

# FA Composition of Plasma, Red Blood Cell, and Liver Phospholipids of Newborn Piglets Fed *trans* Isomers of $\alpha$ -Linolenic Acid

Niyazi Acar, Jean-Michel Chardigny\*, Olivier Berdeaux, Simone Almanza, and Jean-Louis Sébédio

INRA, Unité de Nutrition Lipidique, 21065 Dijon Cedex, France

**ABSTRACT:** The effects of dietary *cis* and *trans*  $\alpha$ -linolenic acid (18:3n-3) on the FA composition of plasma, red blood cell, and liver phospholipids were studied in newborn piglets. Animals were fed for 14 d with one of three diets: a control diet (group A) containing *cis* 18:3n-3 at a level of 2.0% of total FA, a diet (group B) in which a part of the 18:3n-3 acid was isomerized (1.3% of *cis* 18:3n-3 and 0.7% of *trans* 18:3n-3), or a diet (group C) with 2.0% *cis* 18:3n-3 and 0.7% *trans* 18:3n-3. Feeding animals with diets containing *trans* 18:3n-3 resulted in the presence of *trans* isomers of 18:3n-3, *trans* isomers of EPA, and *trans* isomers of DHA in phospholipids; however, the level of total *trans* n-3 PUFA in tissues was less than 0.3% of total tissue FA. In group B, the reduction of dietary amounts of *cis* 18:3n-3 was associated with a decrease in individual and total *cis* n-3 PUFA. In contrast, in group C there was no decrease in tissue n-3 PUFA despite the increased dietary level of *trans* 18:3n-3. These results suggest that the isomerization of a part of dietary n-3 PUFA, leading to the reduction of their levels in the diet, could induce a decrease in n-3 PUFA in phospholipids. The physiological effects of *trans* PUFA are not known and should be considered in future studies.

Paper no. L9034 in *Lipids* 37, 849–852 (September 2002).

Lipids provide the major portion of food energy for infants fed breast milk or formula (1). They represent about 90% of all energy retained in the growing tissues of a full-term baby during the first 6 mon of life (2). Moreover, organ growth and development are closely related to dietary supply, metabolism, and physiological effects of EFA, including the precursors linoleic and  $\alpha$ -linolenic acids as well as their long-chain polyunsaturated metabolites with 20 or 22 carbon atoms (3). However, unusual lipids such as geometric isomers of unsaturated FA in *trans* configuration can be found in the diet of the newborn. Today, reliable quantitative data are available on the human milk and infant formula contents of *trans* FA (4–6).

Studies on rodents have shown that, after dietary intake, *trans* isomers of  $\alpha$ -linolenic acid can be elongated and desaturated into *trans* isomers of EPA (20:5n-3) and DHA (22:6n-3) (7,8). Since it is well known that *trans* FA can impair the

biosynthesis of PUFA (9,10), their effects on the metabolism and the bioavailability of EFA in the newborn is questioned.

The present study examines the FA composition of plasma, red blood cell (RBC), and liver phospholipids of newborn piglets receiving formulas differing in their levels of *trans* isomers of  $\alpha$ -linolenic acid. Three different formulas were studied: a control formula providing  $\alpha$ -linolenic acid in its natural isomeric form (diet A); a formula in which part of the  $\alpha$ -linolenic acid is given as geometrical isomers (diet B), and a formula that contains the same quantity of *cis*  $\alpha$ -linolenic acid as the control group and the same level of *trans*  $\alpha$ -linolenic acid as group B (diet C). This study was conducted for a relatively short time (14 d) in newborn piglets in order to examine acute effects in a rapidly growing animal fed only with the formulas studied.

## MATERIALS AND METHODS

**Animals and diets.** All animal use and care were conducted according to the French legislation (authorization no. 7676 delivered to I. Louveau). Pietrain piglets of term gestation were obtained from INRA–UMR Veau et Porc (Saint-Gilles, France). They were taken within 24 h after birth so that they still had passive immunity and were assigned randomly to one of the three groups ( $n = 6$ /group). Piglets were housed individually in a room controlled for temperature (28°C). Animals were bottle-fed every 2 h (from 7 to 21 h) until 15 d after birth with three standard formulas (in g/L: casein, 31; lactoserum, 21; lactose, 46; fat, 71; standard vitamin and mineral mix, 8). The formulas differed only in their contents of *cis* and *trans* isomers of  $\alpha$ -linolenic acid (Table 1). The three formulas were prepared by blédina sa (Steenvoorde, France) using oil mixtures provided by Lesieur (Coudekerque-Branche, France). Briefly, bleached canola oil was used after deodorization for 52.5 h at 205°C under 3 mbar (11) in order to provide *trans*  $\alpha$ -linolenic acid. In order to balance the *trans* linoleic acid levels in the mixtures, isomerized sunflower oil (270°C, 18 h, under nitrogen) was added (up to 0.2% of total oil).

**Tissue collection.** After 14 d of diet, piglets were killed by electrocution. The liver was removed and total blood was collected using EDTA as anticoagulant. Total blood was immediately centrifuged at  $1860 \times g$  at 4°C in order to separate plasma and RBC. The RBC pellet was then washed three times

\*To whom correspondence should be addressed at INRA, Unité de Nutrition Lipidique, 17 rue Sully, B.P. 86510, 21065 Dijon Cedex, France.  
E-mail: chardign@dijon.inra.fr  
Abbreviation: RBC, red blood cell.

**TABLE 1**  
**FA Composition<sup>a</sup> of the Dietary Lipids**

	Experimental groups		
	A	B	C
16:0	4.5	4.4	4.2
16:1	0.2	0.1	0.2
18:0	3.9	3.3	3.2
18:1	68.5	68.5	68.7
<i>trans</i> 18:1	0.7	0.7	0.5
18:2	18.9	19.0	19.0
<i>trans</i> 18:2	0.2	0.3	0.3
18:3	2.0	1.3	2.0
<i>trans</i> 18:3	0	0.7	0.7
20:0	0.3	0.3	0.3
20:1	0.3	0.8	0.4
22:0	0.5	0.6	0.5
Total 18:3	2.0	2.0	2.7

<sup>a</sup>Values expressed as percentage of total FAME.

with an isotonic saline solution. All samples were stored at  $-80^{\circ}\text{C}$  until lipid analysis.

**Lipid analysis.** Total lipids from liver and RBC were extracted according to the procedure of Folch *et al.* (12), whereas plasma total lipids were extracted by the method of Moilanen and Nikkari (13). Total phospholipids were separated from neutral lipids by the method of Juanéda and Rocquelin (14) and were transesterified with sodium methylate according to Christie *et al.* (15). The FAME were analyzed on a Hewlett-Packard (Palo Alto, CA) 5890 series II gas chromatograph equipped with a split/splitless injector, an FID, and a BPX 70-silica capillary column (120 m  $\times$  0.25 mm i.d.; film thickness 0.25  $\mu\text{m}$ ; SGE, Melbourne, Australia). The injector and the detector were maintained at 250 and 280 $^{\circ}\text{C}$ , respectively. Hydrogen was used as carrier gas (inlet pressure 300 kPa). The oven temperature was operated at 60 $^{\circ}\text{C}$  for 1 min, then increased from 60 to 175 $^{\circ}\text{C}$  at a rate of 20 $^{\circ}\text{C}/\text{min}$  and left at this point until the end of the analysis. FAME were identified by comparison with commercial or synthetic standards and quantified using the Diamir software (JMBS Inc., Portage, MI).

**Statistical analysis.** Results are expressed as means  $\pm$  SD. Statistical analyses were performed using the Statistical Analysis System (SAS Institute, Cary, NC). The ANOVA procedure

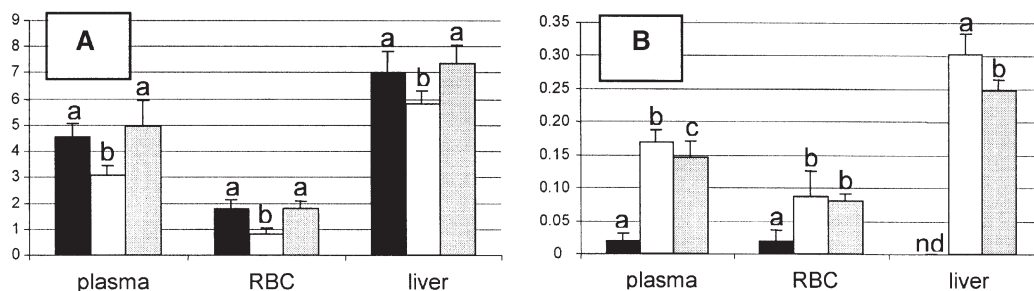
and the Newman-Keuls test were used between each group. *P* values of less than 0.05 were considered as significant.

## RESULTS AND DISCUSSION

The aim of this work was to study the effects of the partial isomerization of dietary  $\alpha$ -linolenic acid on the FA composition of plasma, RBC, and liver phospholipids in newborn piglets. This animal model constitutes an interesting model because of its resemblance to humans in terms of perinatal development. In our diets, isomerized sunflower oil (270 $^{\circ}\text{C}$  for 18 h) may have produced cyclic FA, polymers, hydroperoxides, and breakdown products of hydroperoxides. But since isomerized sunflower oil represented 200 g in the 100 kg of mix at the most, the relative proportions of these compounds may be insignificant compared to *trans* 18:3n-3.

Changing the levels of dietary *cis* and *trans* isomers of  $\alpha$ -linolenic acid did not result in any changes in saturated FA, monounsaturated FA, and n-6 PUFA (Table 2). Since the levels of arachidonic acid were unchanged, it seems that *trans*  $\alpha$ -linolenic did not compete with linoleic acid as suggested by Blond *et al.* (9). Only the levels of *cis* and *trans* n-3 PUFA were affected by the dietary treatments. Trace amounts of *trans* n-3 PUFA were detected in animals of the control group, whereas no *trans* FA were present in the control diet. This observation may be due to *trans* FA intake by the sow during the gestation period.

Isomerizing a part of the  $\alpha$ -linolenic acid in the diet (group B) resulted in the presence of *trans* isomers of  $\alpha$ -linolenic acid in all studied tissues. However, its incorporation into plasma, RBC, and liver phospholipids was low since it represented 0.2% of total FA at the most. The desaturation and elongation products of *trans*  $\alpha$ -linolenic acid, *trans* EPA, and *trans* DHA were also detected. Then, the amounts of total *trans* n-3 PUFA were significantly increased compared with the control group (Fig. 1B). However, the level of total *trans* PUFA was far lower than the level of total *cis* PUFA. On the other hand, the levels of *cis* n-3 PUFA were significantly decreased (Fig. 1A). This was particularly true for DHA, which was reduced by 20% in liver, by 40% in plasma, and by 60% in RBC phospholipids.



**FIG. 1.** Levels of total *cis* n-3 FA (A) and *trans* n-3 FA (B) (% of total FA) in plasma, red blood cell (RBC), and liver phospholipids of piglets fed 2.0% of *cis* 18:3n-3 (group A: solid bars), 1.3% of *cis* 18:3n-3 plus 0.7% of *trans* 18:3n-3 (group B: open bars), or 2.0% *cis* 18:3n-3 plus 0.7% *trans* 18:3n-3 (group C: gray bars); values are mean  $\pm$  SD; nd: not detected; a,b,c: significantly different between groups ( $P < 0.05$ ).



**TABLE 2**  
**FA Composition (as % of total FA) of Plasma, Red Blood Cell (RBC) Membrane, and Liver Phospholipids of Piglets Fed Formulas Containing cis or trans Isomers of  $\alpha$ -Linolenic Acid for 14 d<sup>a</sup> (n = 6)**

	Saturated FA (sat)			Monounsaturated FA (mono)									PUFA (poly)						trans FA		
	16:0	18:0	$\Sigma$ sat	18:1n-9	18:1n-7	20:1n-9	22:1n-9	$\Sigma$ mono	18:2n-6	20:4n-6	22:4n-6	22:5n-6	18:3n-3	20:5n-3	22:6n-3	$\Sigma$ poly	trans 18:3n-3	trans 20:5n-3	trans 22:6n-3	n-6/n-3	
<b>Plasma</b>																					
A	12.46 (1.11)	21.19 (1.59)	36.72 (1.13)	27.86 (1.14)	1.60 (0.09)	0.29 (0.04)	0.02 (0.00)	30.53 (1.28)	16.35 (1.45)	10.73 (1.00)	0.01 (0.01)	0.45 (0.10)	0.32 (0.03)	0.15 (0.02)	3.33 (0.34)	33.16 (1.06)	Trace <sup>b</sup>	Trace	Trace	6.22 (0.86)	
B	11.90 (1.39)	23.88 (1.48)	36.92 (1.62)	27.36 (1.48)	1.70 (0.15)	0.30 (0.06)	0.02 (0.00)	30.11 (1.35)	15.93 (2.97)	11.60 (1.95)	0.01 (0.00)	0.49 (0.19)	0.22 (0.06)	0.11 (0.03)	2.01 (0.32)	32.26 (1.40)	0.11 (0.01)	0.04 (0.00)	0.02 (0.00)	9.45 (1.39)	
C	11.28 (0.90)	24.12 (0.60)	36.34 (0.46)	27.24 (1.78)	1.78 (0.15)	0.30 (0.04)	0.02 (0.00)	30.02 (1.66)	16.48 (3.12)	10.87 (2.20)	0.01 (0.00)	0.40 (0.13)	0.38 (0.15)	0.17 (0.05)	3.58 (0.76)	33.92 (1.19)	0.09 (0.02)	0.04 (0.01)	0.01 (0.00)	5.94 (1.27)	
<b>RBC</b>																					
A	16.81 (0.54)	11.84 (0.90)	29.64 (1.03)	49.84 (3.09)	2.01 (0.12)	0.29 (0.05)	0.05 (0.01)	53.29 (2.90)	11.26 (1.73)	3.08 (1.28)	0.33 (0.08)	0.19 (0.09)	0.22 (0.08)	0.01 (0.00)	1.50 (0.25)	17.40 (3.40)	0.01 (0.00)	Trace	Trace	8.56 (1.12)	
B	17.24 (0.69)	12.29 (0.60)	30.57 (1.22)	49.87 (2.87)	1.80 (0.85)	0.29 (0.02)	0.04 (0.01)	53.10 (2.32)	11.27 (1.83)	2.74 (0.76)	0.33 (0.06)	0.19 (0.09)	0.16 (0.05)	0.01 (0.00)	0.61 (0.24)	16.17 (2.80)	0.06 (0.00)	0.01 (0.00)	0.02 (0.02)	19.62 (5.63)	
C	16.72 (0.71)	11.47 (0.29)	29.22 (0.56)	47.99 (1.89)	2.08 (0.14)	0.27 (0.01)	0.05 (0.02)	51.65 (1.71)	12.10 (1.09)	3.73 (0.58)	0.39 (0.07)	0.26 (0.04)	0.27 (0.05)	0.02 (0.01)	1.46 (0.26)	19.13 (1.65)	0.07 (0.00)	0.01 (0.00)	0.01 (0.01)	9.54 (1.32)	
<b>Liver</b>																					
A	8.96 (0.50)	24.79 (1.36)	35.99 (1.27)	20.82 (1.46)	1.50 (0.04)	0.29 (0.03)	0.04 (0.00)	23.79 (1.60)	13.51 (0.76)	16.88 (1.52)	0.48 (0.05)	0.98 (0.15)	0.23 (0.05)	0.21 (0.04)	5.44 (0.82)	40.13 (0.44)	Trace	Trace	Trace	4.82 (0.64)	
B	8.69 (0.79)	24.50 (1.54)	35.36 (1.40)	21.10 (0.98)	1.57 (0.09)	0.30 (0.02)	0.05 (0.00)	24.26 (1.16)	15.55 (0.74)	17.68 (0.91)	0.52 (0.10)	0.87 (0.14)	0.17 (0.03)	0.15 (0.03)	4.56 (0.50)	39.65 (0.47)	0.21 (0.02)	0.06 (0.01)	0.03 (0.01)	5.87 (0.63)	
C	8.86 (0.45)	24.73 (1.51)	35.46 (1.40)	19.90 (1.30)	1.64 (0.12)	0.30 (0.03)	0.04 (0.00)	23.15 (1.59)	14.20 (0.60)	16.99 (0.63)	0.44 (0.05)	0.83 (0.17)	0.26 (0.02)	0.26 (0.06)	5.72 (0.63)	41.09 (0.54)	0.18 (0.01)	0.05 (0.01)	0.02 (0.00)	4.66 (0.61)	

<sup>a</sup>Values are means, SD values are in parentheses.

<sup>b</sup>Trace, <0.01% of total FA; for a given tissue, values in columns followed by different letters are significantly different (P < 0.05).

To summarize, isomerizing a part of the dietary *cis*  $\alpha$ -linolenic acid into *trans*  $\alpha$ -linolenic reduced the amounts of *cis*  $\alpha$ -linolenic acid in the diet and led to a decrease in the levels of *cis* n-3 PUFA in phospholipids from plasma, liver, and RBC in animals. This is illustrated by the n-6/n-3 ratio, which was about twice as high as that in the control group for RBC phospholipids.

Correcting the levels of *cis*  $\alpha$ -linolenic acid in the diet by slightly increasing their levels (group C) succeeded in restoring *cis*  $\alpha$ -linolenic acid to levels equivalent to those of the control group in plasma, RBC, and liver phospholipids. The amounts of the longer-chain metabolites EPA and DHA were also recovered. As a consequence, the total *cis* n-3 PUFA levels and the n-6/n-3 ratio were restored. The geometrical isomers of  $\alpha$ -linolenic acid, EPA, and DHA were also present, but their levels were lower than those of group B. This is probably due to the increased dietary *cis* 18:3n-3/*trans* 18:3n-3 ratio in group C compared to group B. Even if the n-3 PUFA levels are restored, the physiological effects of *trans* PUFA have to be studied.

In conclusion, the main consequence of the isomerization of dietary  $\alpha$ -linolenic acid was a reduction of its levels in the diet, leading to an increase in the n-6/n-3 ratio, particularly in RBC. Since the FA composition of RBC membranes may reflect the neuronal membrane composition (16), the question of the effect of dietary EFA isomerization on brain composition and subsequently brain functioning is posed. An imbalanced diet may have several long-term consequences, particularly on major functions like vision or learning behavior (17,18).

## ACKNOWLEDGMENTS

The authors gratefully thank blédina sa and Lesieur for preparation of the formulas and the gift of the oils, respectively. The authors gratefully acknowledge Jean Le Dividich for supervising the nutritional experiment; Henri Renoult, Françoise Thomas, and Bruno Pasquis for technical assistance; and Pierre Juanéda and Jean-Pierre Sergiel for their help in bottle-feeding the animals. Niyazi Acar was funded by a fellowship from INRA and the Region of Burgundy (France).

## REFERENCES

- Koletzko, B., and Bremer, H.J. (1989) Fat Content and Fatty Acid Composition of Infant Formulae, *Acta Paediatr. Scand.* 78, 513–521.
- Fomon, S.J., Haschke, F., Ziegler, E.E., and Nelson, S.E. (1982) Body Composition of Reference Children from Birth to Age 10 Years, *Am. J. Clin. Nutr.* 35, 1169–1175.
- Koletzko, B. (1992) Fats for Brains, *Eur. J. Clin. Nutr.* 46 (Suppl. 1), S51–S62.
- Chardigny, J.M., Wolff, R.L., Mager, E., Sébédio, J.L., Martine, L., and Juanéda, P. (1995) Trans Mono- and Polyunsaturated Fatty Acids in Human Milk, *Eur. J. Clin. Nutr.* 49, 523–531.
- Chardigny, J.M., Wolff, R.L., Mager, E., Bayard, C.C., Sébédio, J.L., Martine, L., and Ratnayake, W.M.N. (1996) Fatty Acid Composition of French Infant Formulas with Emphasis on the Content and Detailed Profile of *trans* Fatty Acids, *J. Am. Oil Chem. Soc.* 73, 1595–1601.
- Ratnayake, W.M.N., Chardigny, J.M., Wolff, R.L., Bayard, C.C., Sébédio, J.L., and Martine, L. (1997) Essential Fatty Acids and Their *trans* Geometrical Isomers in Powdered and Liquid Infant Formulas Sold in Canada, *J. Pediatr. Gastr. Nutr.* 25, 400–407.
- Chardigny, J.M., Sébédio, J.L., Grandgirard, A., Martine, L., Berdeaux, O., and Vatièle, J.M. (1996) Identification of a Novel *trans* Isomer of 20:5n-3 in Liver Lipids of Rats Fed Heated Oil, *Lipids* 31, 165–168.
- Grandgirard, A., Piconneaux, A., Sébédio, J.L., O'Keefe, S.F., Sémon, E., and Le Quéré, J.L. (1989) Occurrence of Geometrical Isomers of Eicosapentaenoic and Docosahexaenoic Acids in Liver Lipids of Rats Fed Heated Linseed Oil, *Lipids* 24, 347–350.
- Blond, J.P., Henrichi, C., Precigou, P., Grandgirard, A., and Sébédio, J.L. (1990) Effect of 18:3n-3 Geometrical Isomers of Heated Linseed Oil on the Biosynthesis of Arachidonic Acid in the Rat, *Nutr. Res.* 10, 69–70.
- Blond, J.P., Chardigny, J.M., Sébédio, J.L., and Grandgirard, A. (1995) Effects of Dietary 18:3n-3 *trans* Isomers on the  $\Delta 6$  Desaturation of  $\alpha$ -Linolenic Acid, *J. Food Lipids* 2, 99–106.
- Hénon, G., Kemeny, Z., Recseg, K., Zwobada, F., and Kovari, K. (1999) Deodorization of Vegetable Oils. Part 1: Modeling the Geometrical Isomerization of Polyunsaturated Fatty Acids, *J. Am. Oil Chem. Soc.* 76, 73–81.
- Folch, J., Lees, M., and Sloane Stanley, G.M. (1957) A Simple Method for the Determination and the Purification of Total Lipids from Animal Tissues, *J. Biol. Chem.* 226, 497–509.
- Moilanen, T., and Nikkari, T. (1981) The Effect of Storage on the Fatty Acid Composition of Human Serum, *Clin. Chim. Acta* 114, 111–116.
- Juanéda, P., and Rocquelin, G. (1985) Rapid and Convenient Separation of Phospholipids and Non Phosphorus Lipids from Rat Heart Using Silica Cartridges, *Lipids* 20, 40–41.
- Christie, W.W., Sébédio, J.L., and Juanéda, P. (2001) A Practical Guide to the Analysis of Conjugated Linoleic Acid, *inform* 12, 147–152.
- Makrides, M., Simmer, K., Goggin, M., and Gibson, R. (1993) Erythrocyte Docosahexaenoic Acid Correlates with the Visual Response of Healthy, Term Infants, *Pediatr. Res.* 34, 425–427.
- Connor, W., Neuringer, M., and Reisbick, S. (1992) Essential Fatty Acids—The Importance of n-3 Fatty Acids in the Retina and Brain, *Nutr. Rev.* 50, 21–29.
- Bourre, J.M., François, M., Youyou, A., Dumont, O., Piciotti, M., Pascal, G., and Durand, G. (1989) The Effects of Dietary  $\alpha$ -Linolenic Acid on the Composition of Nerve Membranes, Enzymatic Activity, Amplitude of Electrophysiological Parameters, Resistance to Poisons and Performance of Learning Tasks in Rats, *J. Nutr.* 119, 1880–1892.

[Received March 25, 2002, and in revised form October 4, 2002; revision accepted October 8, 2002]

# Effects of Dietary Conjugated Linoleic Acid on the Expression of Uncoupling Proteins in Mice and Rats

Kafi N. Ealey, Ahmed El-Sohemy, and Michael C. Archer\*

Department of Nutritional Sciences, Faculty of Medicine, University of Toronto, Toronto, Canada M5S 3E2

**ABSTRACT:** CLA inhibits mammary cancer and reduces body fat accumulation in rodents. It is not known whether uncoupling proteins (UCP), which are modulators of energy balance and metabolism, play a role in these actions of CLA. To determine the effects of dietary CLA on the expression of UCP in various tissues, 5-wk-old Sprague-Dawley rats and C57Bl/6 mice were fed diets containing 1% CLA for 3 wk. CLA treatment reduced adipose depot weights in both rats and mice but had no significant effects on body weight. There was a species-specific effect of CLA on the expression of UCP. Whereas CLA did not affect the expression of UCP in most tissues in rats, mice fed CLA had increased expression of UCP2 in the mammary gland, brown adipose tissue (BAT), and white adipose tissue (WAT). Furthermore, UCP1 and UCP3 mRNA and protein levels in BAT were significantly lower in CLA-fed mice compared to controls. Skeletal muscle UCP3 mRNA was unchanged, but UCP3 protein levels were significantly increased in mice, suggesting translational or posttranslational regulation of this protein. Results from this study suggest that alterations in the expression of UCP in mice may be related to the previously reported effects of dietary CLA in lowering adiposity and increasing FA oxidation. In rats, however, induction of UCP is not likely to be responsible for fat reduction or for the inhibitory action of CLA on mammary carcinogenesis.

Paper no. L9087 in *Lipids* 37, 853–861 (September 2002).

Conjugated linoleic acid (CLA) is a collective term used to describe a group of geometric and positional isomers of linoleic acid that are found naturally in foods such as dairy products and meat (1). CLA has been shown to have a strong inhibitory effect on mammary tumorigenesis in rats (2,3). The mechanism responsible for this inhibition, however, is not known. Besides having anticarcinogenic properties, dietary CLA also has an effect on body composition and energy balance. Numerous studies have reported that feeding CLA to either rodents or humans decreases body fat accumulation and weight gain and increases FA oxidation and energy expenditure, often with no change in overall energy intake (4–6). It is possible that these effects on energy balance may mediate the effects of CLA on mammary cancer. The amount of usable energy available from the diet has a profound effect on the

development of mammary gland tumors in mice and rats (7). Diets rich in FA promote mammary tumorigenesis (8,9). This promoting effect may be due, in part, to the excess calories provided to the animal (7,10). Conversely, caloric restriction causes a marked inhibition of mammary tumorigenesis (11). Since uncoupling proteins (UCP) have been implicated in body composition changes and regulation of energy expenditure (12), it is possible that CLA regulates the expression of some or all of the UCP.

UCP are a class of transmembrane proteins found in the inner mitochondrial membrane. The first UCP discovered, UCP1, is expressed exclusively in brown adipose tissue (BAT) and functions by uncoupling ATP synthesis and mitochondrial electron transport, thereby allowing energy to be dissipated as heat (13). Recently identified homologs of UCP1 have raised the possibility that uncoupling of mitochondrial respiration in tissues other than BAT may play an important role in whole-body energy balance. UCP2 is expressed in most tissues (14), and UCP3 is expressed mainly in skeletal muscle and BAT (15). Although the physiological functions of UCP homologs in various tissues are not clear, proposed functions include mediation of cold- and diet-induced thermogenesis, regulation of energy expenditure, control of production of reactive oxygen species, and regulation of FA oxidation (12).

Dietary PUFA play a key role in regulating the expression of UCP genes (16–18). Rats fed fish oils rich in n-3 PUFA accumulate less body fat and have increased energy expenditure compared to rats fed diets rich in n-6 PUFA (19). These changes are accompanied by increased heat production and increased expression of UCP, suggesting that these mitochondrial proteins may play an important role in mediating the effects of fish oils on energy and lipid metabolism (19,20). Based on the similarity of the effects of CLA and fish oils on energy balance, we hypothesized that CLA may also increase expression of UCP in rodents.

An increase in UCP may increase metabolism at the whole-body level or in specific tissues such as the mammary gland. This has been demonstrated in UCP3 knockout mice that exhibit no changes in energy expenditure at the whole-body level, but have significantly altered mitochondrial energy metabolism in skeletal muscle (21). It is plausible that increased expression of UCP is an important mechanism by which dietary CLA regulates energy metabolism and inhibits mammary cancer in rodents. Like caloric restriction, a lack of

\*To whom correspondence should be addressed at 150 College St., Toronto, Ontario, Canada, M5S 3E2. E-mail: m.archer@utoronto.ca

Abbreviations: BAT, brown adipose tissue; PPAR, peroxisome proliferator-activated receptor; SNS, sympathetic nervous system; SSC, sodium chloride/sodium citrate; UCP, uncoupling protein; WAT, white adipose tissue.

energy available to normal mammary tissue caused by a loss of energy as heat might affect mammary tumorigenesis.

Two studies to date in mice have reported different results in different strains on the effect of CLA on the expression of UCP (22,23). The only study to date in rats showed that a CLA-supplemented diet improved glucose tolerance, reduced adiposity, and increased UCP2 expression in muscle and adipose tissue in obese Zucker rats that develop type II diabetes (24). It is not known, however, whether CLA affects the expression of UCP in normal rats with no metabolic imbalances. Furthermore, the effects of CLA on UCP protein levels in mice and rats have not been examined. The main objective of this study therefore was to determine the effects of dietary CLA on the expression of UCP in various tissues, including the mammary glands of mice and rats, and to relate the findings to the protective effect of CLA on cancer development.

## MATERIALS AND METHODS

**Animals and diets.** All animal treatment protocols were reviewed by and were in compliance with the Animal Care and Use Committee of the University of Toronto. Forty 4-wk-old female C57BL/6 mice and eighteen 4-wk-old Sprague-Dawley rats were obtained from Charles River Laboratories (St. Constant, Quebec City, Canada). They were housed at  $22 \pm 2^\circ\text{C}$  and 50% RH with a 12-h light/dark cycle and acclimatized for 1 wk on the control AIN-93G diet (Dyets, Bethlehem, PA) with free access to food and water. The experimental diet was formulated by replacing the 7% soybean oil in the AIN-93G diet with 6% soybean oil + 1% CLA (Nu-Chek-Prep, Elysian, MN); approximate composition: 43% *c-9,t-11-* and *t-9,c-11-CLA*, 45% *t-10,c-12-CLA*, 6% *c-9,c-11-*, *c-10,c-12-*, *t-9,t-11-*, *t-10,t-12-CLA* with 2% linoleate and 4% unidentified material. The diets were stored under nitrogen at  $-20^\circ\text{C}$ , and the animals were given fresh diet every 2–3 d.

**Study protocol.** At 5 wk of age, the rats and mice were randomized into two groups each. One group was maintained on the AIN-93G diet while the other group was fed the 1% CLA diet. Body weights and food intake were measured twice weekly. After 3 wk of feeding, animals were killed by cervical dislocation, and livers, BAT, retroperitoneal and abdominal white adipose tissue (WAT), gastrocnemius muscles, and whole mammary glands were excised. All tissues were immediately frozen in liquid nitrogen for subsequent determination of UCP gene expression and UCP mitochondrial protein levels.

**Northern blot analysis.** Total RNA was isolated from frozen tissues using Trizol reagent (Life Technologies Inc., Gaithersburg, MD), and 10–20  $\mu\text{g}$  of RNA was electrophoresed in 1.0% agarose gels containing formaldehyde. RNA was transferred overnight to nylon membranes (Ambion, Austin, TX) and UV-cross-linked. Prehybridization and hybridization were carried out at  $42^\circ\text{C}$  using Northern Max (Ambion) hybridization buffer. Blots were hybridized overnight using UCP1, UCP2, and UCP3 probes labeled with  $\alpha$ - $^{32}\text{P}$ -dCTP by random prime labeling. All probes were synthesized by reverse transcription-polymerase chain reaction

as described (15,25,26). For UCP1, forward and reverse primer sequences were 5'-CGGACTTTGGCGGTGTCCAGCGGAAGGTGAT-3' and 5'-AGCACACAAACATGATGACGTTCC-3', which correspond to conserved domains 279–298 and 1021–1044 of rat UCP1, respectively (15). For UCP2, primers used were 5'-TTAGAGAAGCTTGACCTTGC-3' and 5'-CGTTCCAGGATCCCAAGCGG-3', which correspond to positions 145–164 and 1148–1129, respectively, of the mouse UCP2 (25). For UCP3, primers used were 5'-GGGAAATCCTGCTGCTACCT-3' and 5'-TTCTTGTGATGTTGGGCCAA-3', corresponding to positions 1–20 and 703–723 of the mouse UCP3. Northern blots were washed twice in a solution of sodium chloride/sodium citrate (SSC) and SDS ( $2\times$  SSC/0.1% SDS) for 5 min at  $42^\circ\text{C}$  and twice in  $0.1\times$  SSC/0.1% SDS at  $50^\circ\text{C}$ . To quantify the signal, total  $^{32}\text{P}$  counts were determined using a Packard Instant Imager (Canberra Packard Canada, Mississauga, Canada) and normalized to counts obtained after hybridization of the membrane with a 28S rRNA probe.

**Isolation of mitochondria.** For isolation of mitochondria, tissues were homogenized in 4–6 mL of buffer containing 250 mM sucrose, 10 mM HEPES, 0.5 mM EDTA, and 0.1% BSA, pH 7.2, and kept on ice (27). The homogenate was centrifuged at  $600\times g$  for 5 min at  $4^\circ\text{C}$ . The supernatant was collected and centrifuged at  $8000\times g$  for 10 min at  $4^\circ\text{C}$ . The mitochondrial pellet was washed twice and finally resuspended in buffer without BSA. Mitochondrial protein concentrations were determined using the BioRad Protein Assay (Bio-Rad Laboratories, Hercules, CA).

**Western blot analysis.** Mitochondrial proteins solubilized in Laemmli buffer containing  $\beta$ -mercaptoethanol were heated for 5 min at  $95^\circ\text{C}$ , separated by electrophoresis on 13% polyacrylamide gels under denaturing conditions, and transferred to polyvinylidene difluoride membranes. Membranes were incubated overnight at  $4^\circ\text{C}$  in blocking buffer (5% nonfat dry milk in Tris-buffered saline/0.1% Tween 20). UCP1 was detected with a goat polyclonal antibody to a conserved amino-terminal peptide sequence of mouse UCP1 (Santa Cruz Biotechnology, Inc., Santa Cruz, CA). UCP3 was detected with a rabbit polyclonal antibody to a human UCP3 carboxy-terminal peptide (Chemicon International Inc., Temecula, CA). We showed that the UCP1 antibody did not cross-react with UCP2 or UCP3 in Western blots using muscle mitochondrial protein (data not shown). Furthermore, the UCP3 antibody did not cross-react with UCP2 when mitochondrial protein isolated from liver or mammary gland tissue was used (data not shown). After extensive washing in Tris-buffered saline/0.1% Tween 20, membranes were incubated with anti-goat (UCP1) or anti-rabbit (UCP3) horseradish peroxidase-conjugated secondary antibodies (Santa Cruz Biotechnology, Inc.) and developed with a standard ECL kit (Santa Cruz Biotechnology, Inc.). Chemiluminescence was detected on Biomax MR Kodak film, and bands were quantified using a FluorChem Imaging System (Alpha Innotech Corp., San Leandro, CA). We were unable to perform Western blot analysis of UCP2 owing to the unavailability of a reliable commercial antibody.



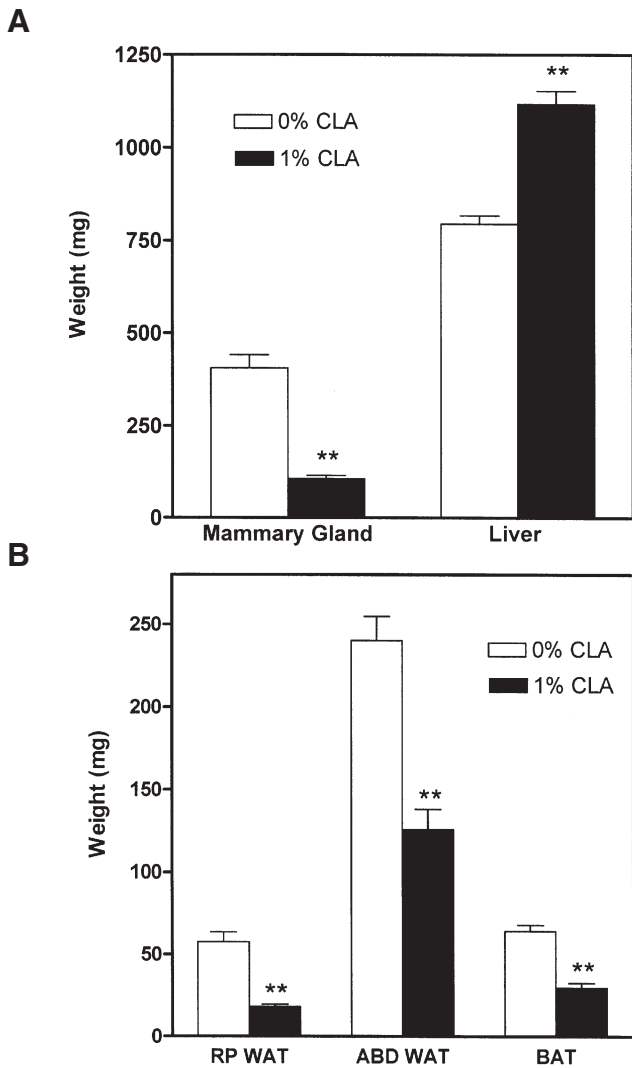
**Statistical analysis.** Results are expressed as means  $\pm$  SEM. Differences were determined by Student's unpaired *t*-test. Differences with  $P \leq 0.05$  were considered significant.

## RESULTS

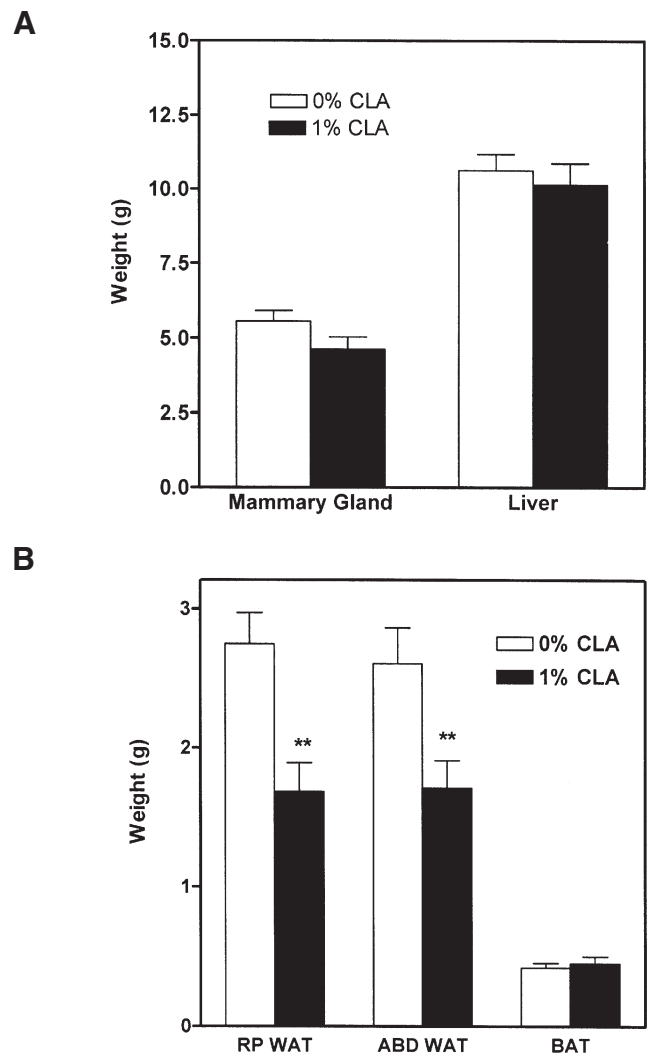
After 3 wk of feeding the AIN-93G control diet or the diet containing 1% CLA to C57BL/6 mice, food intake and body weights did not differ between the two groups ( $18.4 \pm 0.3$  g vs  $18.6 \pm 0.4$  g for control and CLA-fed mice, respectively). There was, however, a significant difference in weights of specific WAT depots and major organs. As shown in Figure 1A, mammary glands of CLA-fed mice weighed significantly less than those of control animals, and mice fed CLA had significantly larger livers that were also paler in color than the controls. Mice fed CLA also had significant decreases in wet

weights of several adipose depots (Fig. 1B). Retroperitoneal WAT was reduced by 68%, and the abdominal fat depot was reduced by approximately 50% in CLA-fed mice compared to those fed the control diet. A 50% reduction in BAT was observed in CLA-fed mice relative to controls.

Food intakes and body weights of female Sprague-Dawley rats fed diets containing CLA did not differ from rats fed the control diets ( $234.9 \pm 6.3$  vs.  $222.9 \pm 7.4$  g for control and CLA-fed rats, respectively). Unlike the mice, however, the wet weights of mammary glands and livers did not differ between the two groups of rats (Fig. 2A). As shown in Figure 2B, rats fed CLA had significantly lower wet weights of WAT depots. Retroperitoneal WAT was reduced by 40% in CLA-fed rats compared to those fed the control diet. A 35% reduction in weight was also observed in the abdominal WAT depots of CLA-fed rats compared to controls. The weight of the BAT depot in rats did not differ between the two dietary groups.



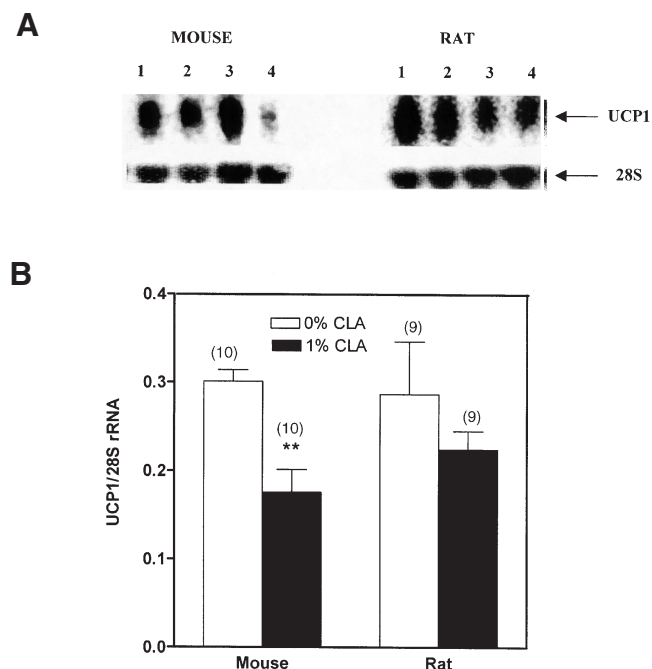
**FIG. 1.** Tissue weights of C57BL/6 mice fed a control or CLA-supplemented diet for 3 wk. (A) Wet weights of mammary glands and livers. (B) Wet weights of retroperitoneal (RP) white adipose tissue (WAT), abdominal (ABD) WAT, and brown adipose tissue (BAT) depots. (Means  $\pm$  SEM,  $n = 20$ /group, \*\* $P < 0.05$ .)



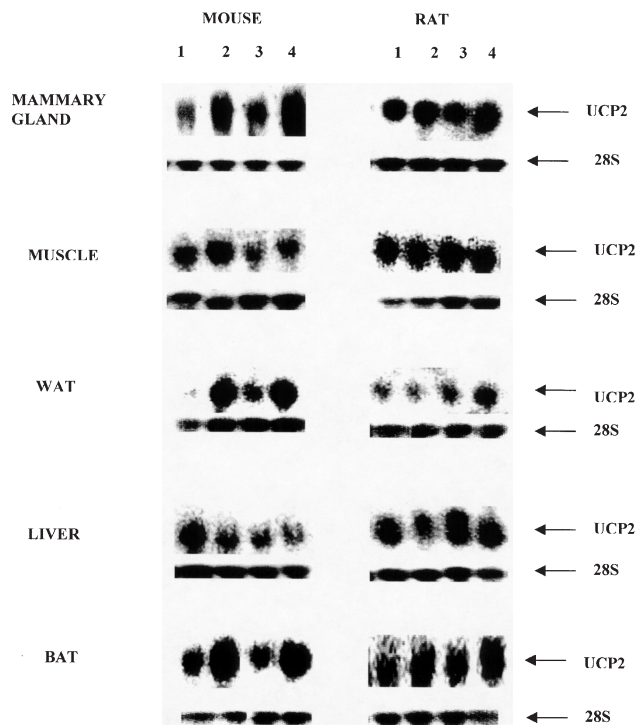
**FIG. 2.** Tissue weights of Sprague-Dawley rats fed a control or CLA-supplemented diet for 3 wk. (A) Wet weights of mammary glands and livers. (B) Wet weights of RP WAT, ABD WAT, and BAT depots. (Means  $\pm$  SEM,  $n = 9$ /group, \*\* $P < 0.05$ .) For abbreviations see Figure 1.

Northern blots were performed to determine the effects of CLA on the expression of various UCP genes. Representative blots showing mRNA from two animals in each experimental group are shown in Figures 3, 4, and 6. In addition, mean transcript levels from all of the animals in each group normalized to the 28S ribosomal band are shown graphically.

Figure 3 demonstrates the effects of dietary CLA on mRNA levels of UCP1 in both mice and rats. UCP1, expressed exclusively in BAT, was significantly decreased in CLA-fed mice compared to controls ( $P < 0.05$ ). There were no differences, however, in mRNA levels of UCP1 in rats fed the control diet compared to those fed the 1% CLA diet. UCP2 is expressed ubiquitously in rodent tissues. In this study, levels of UCP2 mRNA were examined in the mammary glands, livers, WAT, BAT, and skeletal muscle of mice and rats fed the control and experimental diets. Representative Northern blots of UCP2 in various tissues are shown in Figure 4. As shown in Figure 5A, in which bands from the Northern blots were quantified, UCP2 mRNA levels were significantly increased in the mammary gland, WAT, and BAT of mice fed CLA ( $P < 0.05$ ). In contrast, dietary CLA had no effect on the mRNA levels of UCP2 in any of the tissues studied in rats (Fig. 5B). UCP3 is expressed in the BAT and skeletal muscle of both mice and rats, as depicted in the representative Northern blots for UCP3 (Fig. 6). mRNA levels of UCP3 were decreased in BAT of CLA-fed mice ( $P = 0.05$ ) compared to controls, but expression of UCP3 in muscle



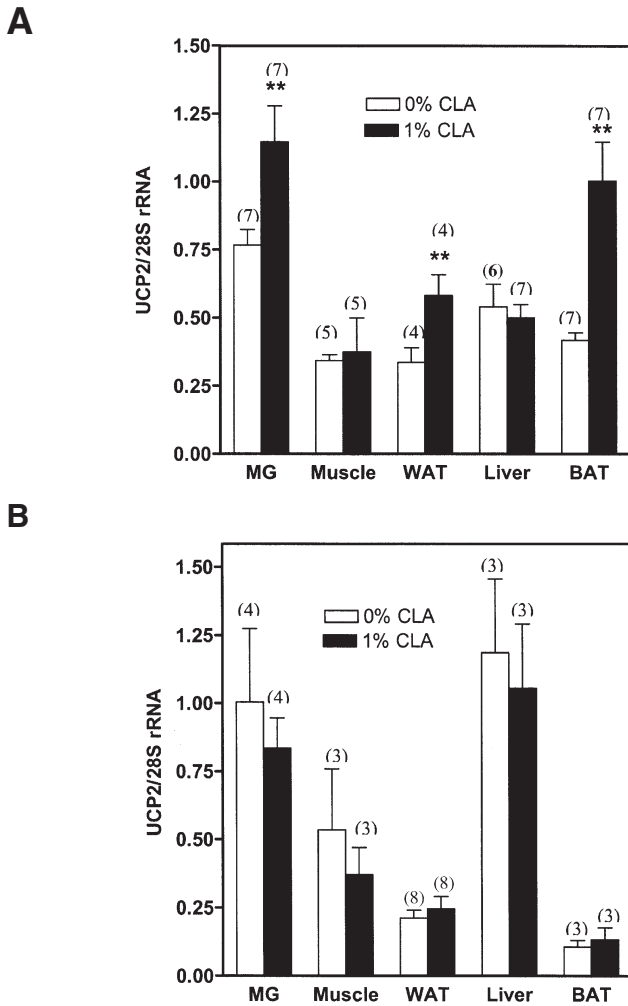
**FIG. 3.** Representative Northern blots showing the effects of a 1% CLA diet on uncoupling protein 1 (UCP1) mRNA levels in BAT from mice and rats. (A) Lanes 1 and 3 correspond to mRNA from controls, and lanes 2 and 4 correspond to mRNA from CLA-fed animals. Each lane is from a different animal. (B) Levels of UCP1 mRNA relative to 28S rRNA are shown. Numbers in parentheses indicate the number of animals/group for each tissue. (Means  $\pm$  SEM, \*\* $P < 0.05$ .) For abbreviations see Figure 1.



**FIG. 4.** Representative Northern blots showing the effects of a 1% CLA diet on UCP2 mRNA levels in various tissues in mice and rats. Lanes 1 and 3 correspond to mRNA from controls, and lanes 2 and 4 correspond to mRNA from CLA-fed animals. Each lane is from a different animal. For abbreviations see Figures 1 and 3.

tissue did not differ between the two groups (Fig. 7A). In rats, dietary CLA did not affect the mRNA levels of UCP3 in either BAT or muscle tissue (Fig. 7B).

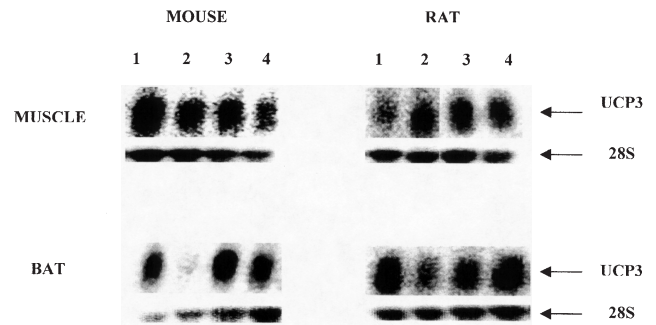
To investigate whether the effects of CLA on UCP gene expression corresponded to changes in immunoreactive protein levels, we determined the UCP content of isolated mitochondria by Western blot analysis. Consistent with the effects on gene expression, CLA-fed mice had significantly lower UCP1 protein levels in BAT compared to controls ( $P < 0.05$ ), but UCP1 protein levels in CLA-fed rats were higher than the controls ( $P = 0.05$ ) (Fig. 8). UCP3 protein levels were also significantly decreased in the BAT of CLA-fed mice ( $P < 0.05$ ) compared to controls, but no differences were observed in rats. Skeletal muscle UCP3 protein levels were significantly increased in CLA-fed mice ( $P < 0.05$ ) compared to controls. In rats, there was no difference in skeletal muscle UCP3 protein content between the control and CLA groups. As mentioned in the Materials and Methods section, UCP2 protein levels were not determined in this study. We showed that an antibody we purchased to detect UCP2 reacted with proteins of similar size and was not useful for Western blot analysis. It has recently been shown that other commercially available antibodies for UCP2 are not specific for this protein and produce other bands of similar M.W. (28).



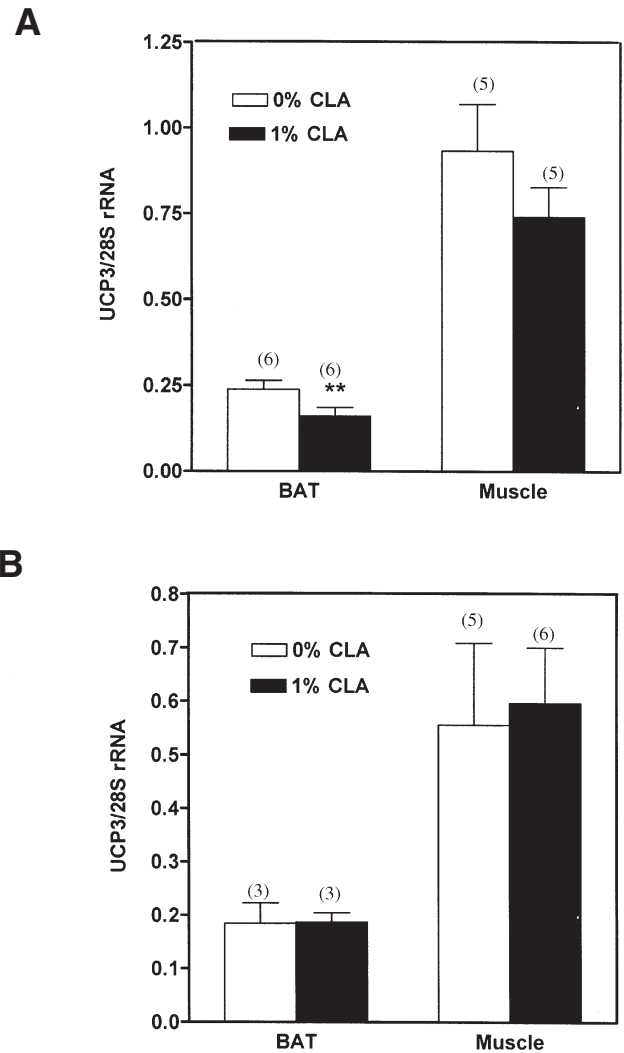
**FIG. 5.** Levels of mouse (A) and rat (B) mammary gland, muscle, WAT, liver, and BAT UCP2 mRNA relative to 28S rRNA. Numbers in parentheses indicate the number of animals/group for each tissue. (Means  $\pm$  SEM, \*\* $P < 0.05$ .) MG, mammary gland; for other abbreviations see Figures 1 and 3.

## DISCUSSION

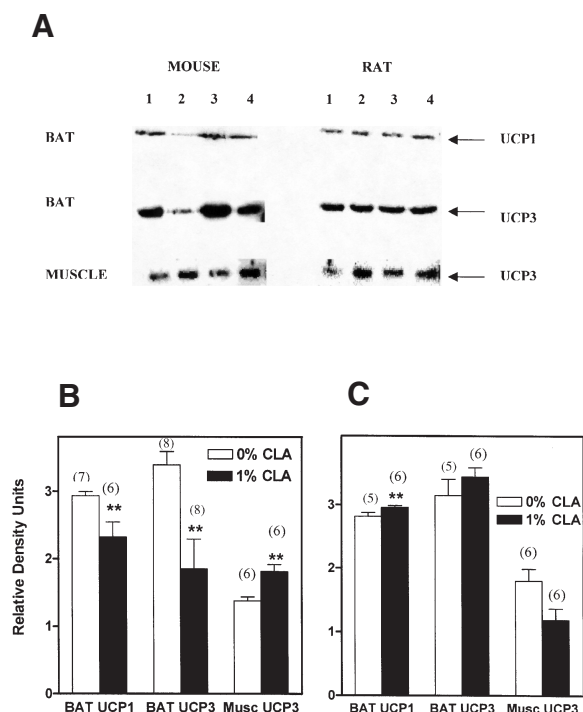
The objectives of this work were to investigate the effects of dietary CLA on the expression of UCP in rats and mice and to determine whether increased expression of UCP is a plausible mechanism by which CLA could directly or indirectly exert a protective effect on mammary gland tumorigenesis. We hypothesized that by regulating available energy, increased expressions of UCP, particularly UCP2, which is expressed in the mammary gland, could affect susceptibility to carcinogen-induced tumorigenesis in a manner similar to caloric restriction. It is likely that induction of UCP2 would reduce the efficiency of ATP synthesis, leading to global loss of cell membrane integrity and finally cell death by necrosis and/or apoptosis (23). A loss of epithelial cells in the mammary gland in this way could reduce the population of target cells for the carcinogen or, postinitiation, lead to a loss of pre-neoplastic cells.



**FIG. 6.** Representative Northern blots showing the effects of a 1% CLA diet on UCP3 mRNA levels in muscle and BAT of mice and rats. Lanes 1 and 3 correspond to mRNA from controls, and lanes 2 and 4 correspond to mRNA from CLA-fed animals. Each lane is from a different animal. For abbreviations see Figures 1 and 3.



**FIG. 7.** Levels of mouse (A) and rat (B) BAT and muscle UCP3 mRNA relative to 28S rRNA. Numbers in parentheses indicate the number of animals/group for each tissue. (Means  $\pm$  SEM, \*\* $P < 0.05$ .) For abbreviations see Figures 1 and 3.



**FIG. 8.** Representative Western blots of mitochondrial UCP1 and UCP3 from BAT and muscle of mice and rats. (A) Lanes 1 and 3 correspond to protein from controls, and lanes 2 and 4 correspond to protein from CLA-fed animals. Each lane is from a different animal. (B and C) Relative densities of UCP protein in mice (B) and rats (C). Numbers in parentheses indicate the number of animals/group for each tissue. (Means  $\pm$  SEM, \*\* $P < 0.05$ .) For abbreviations see Figures 1 and 3.

The rationale for investigating the effects of dietary CLA on UCP expression in both rats and mice in the present study was twofold. First, Sprague-Dawley rats initiated with 7,12-dimethylbenz[a]-anthracene or *N*-methyl-*N*-nitrosourea have been used to demonstrate the inhibitory effects of CLA on mammary carcinogenesis. Second, CLA has already been shown to increase energy expenditure in mice significantly (29), thus allowing mice to be used as controls for studies on UCP regulation. The mouse, however, is a poor model in which to study mammary tumorigenesis (30,31) and has not therefore been used to study the effects of CLA on cancer development.

As summarized in Table 1, our results show that regulation of UCP by CLA occurs in a different manner in rats and mice. Rats fed CLA had significantly reduced weights of WAT depots compared to controls, but no changes in total body weight. This lack of a change in body weight in rats, however, most likely reflects the fact that the WAT depots we measured represent only ~2% of total body weight. Thus, significant changes in the weights of these depots would not result in significant changes in body weight. There were no differences in the weights of any of the other tissues we analyzed in rats. Although previous studies in mice indicate that decreased body fat is associated with increased expression of UCP2 (32), this is not what we observed in rats. Indeed, CLA did not affect the expression of UCP2 in any of the tissues

**TABLE 1**  
Summary of the Effects of Dietary CLA on Uncoupling Proteins (UCP) in Mouse and Rat<sup>a</sup>

	Mouse		Rat	
	mRNA	Protein	mRNA	Protein
UCP1				
BAT	↓	↓	↔	↑
UCP2				
MG	↑	N/A	↔	N/A
WAT	↑	N/A	↔	N/A
BAT	↑	N/A	↔	N/A
Muscle	↔	N/A	↔	N/A
Liver	↔	N/A	↔	N/A
UCP3				
BAT	↓	↓	↔	↔
Muscle	↔	↑	↔	↔

<sup>a</sup>↓ (decrease), ↑ (increase), ↔ (no significant change), N/A = not available; BAT, brown adipose tissue; MG, mammary gland; WAT, white adipose tissue.

studied in rats, including the mammary gland. The expression of the other UCP homologs also was unaffected by CLA treatment in most of the tissues studied in rats. Dietary CLA given at the dose used in the current study (1%) and at levels 10-fold lower (0.1%) results in significant inhibition of mammary carcinogenesis in rats (2,3). Since the biochemical properties of early preneoplastic cells are likely to be similar to normal cells, the lack of an effect of 1% dietary CLA on UCP expression that we observed in the normal mammary gland of the rat suggests that it is unlikely that these proteins play a significant role in the inhibitory effect of CLA on cancer development.

In the present study, mice fed CLA had significantly lower weights of WAT, BAT, and whole mammary glands compared to controls, without any changes in total body weight. Our observations that the livers of CLA-fed mice weighed significantly more and were paler in color than livers from control animals are consistent with the reports of others that CLA-fed mice develop fatty livers (23,33). One reason for the lack of change in body weight of mice fed CLA may be that the loss of mass of the adipose depots is partially offset by the increase in the weight of the liver. Furthermore, although we did not measure total lean body mass in this study, it has been reported by others that dietary CLA significantly increases body protein accretion in mice (34). Despite the similarity in the effect of CLA on fat accumulation in rats and mice, our data indicate that the metabolic effect of CLA on UCP expression is quite different in the two species.

Consistent with studies in mice and humans suggesting that increased expression of UCP is associated with decreased body fat (32,35), in the present study, expression of UCP2 mRNA in WAT and BAT was significantly increased with CLA feeding. Indeed, our results confirm those from a recent study showing increased UCP2 in adipose tissues of mice fed CLA (23). In the liver there was no difference in UCP2 expression between either of the dietary groups. In the mouse mammary gland (including adipocytes, epithelial cells, and stromal cells) we showed increased UCP2 mRNA with CLA



feeding. It has been reported that, compared to animals fed a control diet, a diet containing CLA significantly decreases the growth rate of human breast cancer cells injected into the mammary fat pads of mice (36). Based on our data, a possible mechanism for this effect is through increased UCP2 expression, leading to reduced energy availability to the transplanted cells. Although we did not separate the mammary glands into individual cell types, a recent paper provides evidence that the stromal compartment within the mouse mammary gland expresses UCP1 and other genes involved in FA oxidation (37). These authors suggested that the coordinate regulation of genes involved in the  $\beta$ -oxidation of FA indicates the presence of BAT in the mammary gland. This suggests, in turn, a functional role for the mammary gland in adaptive thermogenesis (37). Tsuboyama-Kasaoka *et al.* reported that CLA induces apoptosis and increases UCP2 mRNA expression in adipose tissues of mice, suggesting that this may be a mechanism responsible for the reduced adipose tissue mass observed in CLA-fed mice.

The altered expression of UCP we observed in the BAT of mice may be involved in mechanisms of thermoregulation. BAT in rodents plays a major role in controlling body weight through diet-induced thermogenesis. This is primarily mediated by the uncoupling of mitochondrial respiration resulting from the marked oxidative capacity of the brown adipocytes (13,38). We hypothesized that the expression of UCP in BAT would be increased, corresponding to the increased energy expenditure and reduced adiposity that has been reported in mice fed CLA (29,39). Unexpectedly, mRNA and protein levels of UCP1 and UCP3 in BAT were significantly lower in CLA-fed mice compared to controls. One reason for these decreases could be an adaptive mechanism to compensate for increased UCP2 expression. In the BAT of UCP1-null mice, there is a fivefold elevation in the expression of UCP2 mRNA (40). Increased BAT UCP2 may be the reason that the UCP1-null mice do not have increased susceptibility to obesity (38). These observations suggest that these null mice have a compromised capacity to thermoregulate, such that they need to use other mechanisms to increase energy expenditure (38). Thus, UCP in BAT that are under control of the sympathetic nervous system (SNS) may function coordinately to enable the animal to maintain body weight and energy balance. In contrast to mice, in CLA-fed rats we observed a small but significant increase in UCP1 protein levels in BAT compared to controls. The physiological significance of this effect, however, is not clear.

Of all tissues, skeletal muscle plays the largest role in energy utilization owing to its size and has long been proposed to be the major site for adaptive thermogenesis in large mammals (12). There has been much interest recently in the UCP3 gene since its expression in skeletal muscle could potentially regulate fat metabolism and the development of obesity in humans (41). Expression of UCP in skeletal muscle, unlike BAT, is not under the control of the SNS (42). Results from *in vitro* studies in cells transfected with UCP3, as well as *ex vivo* and *in vivo*

studies in knockout and transgenic mice, suggest that UCP3 is thermogenic (43). Accumulating evidence, however, has led some investigators to conclude that UCP3 in skeletal muscle is primarily associated with the regulation of lipids as fuel substrate (42) and increased FA oxidation (44).

In the present study in mice, UCP3 was regulated differently in skeletal muscle than in BAT. We observed no changes in the mRNA levels of UCP3 in skeletal muscle isolated from mice fed CLA, but Western blot analysis showed that UCP3 protein was increased significantly, suggesting that this protein is under posttranslational control. These findings are consistent with a recent report suggesting UCP2 is regulated posttranslationally (28). In that study, while UCP2 mRNA levels remained unchanged, protein levels increased dramatically after stimulation with liposaccharide (28). Other studies that have investigated the effects of CLA on UCP have reported either that expression of UCP3 in the skeletal muscle of mice is not affected by CLA feeding (22,23) or that UCP3 mRNA levels are decreased (45). These studies, however, investigated only mRNA expression. Our results highlight the importance of analyzing both mRNA and protein levels to determine whether dietary or physiological stimuli influence these proteins at the transcriptional or translational level. Dietary CLA has been shown to increase FA oxidation in skeletal muscle (39). Our results indicate that induction of UCP3 may play a role in this effect since increased expression of UCP3 is associated with increased FA oxidation (44).

One reason for the different effects of CLA on UCP expression in mice and rats could be the known species-specific role of CLA in the activation of peroxisome proliferator-activated receptors (PPAR). CLA functions as a PPAR activator in mice (46) but in Sprague-Dawley rats it exerts little or no effect on PPAR-responsive genes. (47,48). Recent studies have shown that expression of UCP is regulated directly and indirectly by activated PPAR (49–52). Thus, it is possible that increased UCP2 expression in mice by CLA is a result of activation of PPAR.

In summary, dietary CLA caused a significant lowering of body fat accumulation in both rats and mice. In rats, however, CLA did not affect the expression of UCP in most of the tissues studied including the mammary gland, suggesting that induction of UCP is not a major mechanism responsible for fat reduction or for the known inhibitory action of CLA on mammary carcinogenesis. The alterations in UCP in mice observed in this study may be related to the previously reported effects of dietary CLA in lowering adiposity and increasing FA oxidation, and thus merit further investigation.

## ACKNOWLEDGMENTS

This research was supported by a grant from the Natural Sciences and Engineering Research Council (NSERC) with Dairy Farmers of Canada. M.C.A. is the recipient of an NSERC Industrial Research Chair and acknowledges support from the member companies of the Program in Food Safety, Nutrition and Regulatory Affairs (University of Toronto).

## REFERENCES

- Chin, S.F., Liu, W., Storkson, J.M., Ha, Y.L., and Pariza, M.W. (1992) Dietary Sources of Conjugated Dienoic Isomers of Linoleic Acid, a Newly Recognized Class of Anticarcinogens, *J. Food Comp. Anal.* 5, 185–197.
- Ip, C., Chin, S.F., Scimeca, J.A., and Pariza, M.W. (1991) Mammary Cancer Prevention by Conjugated Dienoic Derivative of Linoleic Acid, *Cancer Res.* 51, 6118–6124.
- Ip, C., Singh, M., Thompson, H., and Scimeca, J. (1994) Conjugated Linoleic Acid Suppresses Mammary Carcinogenesis and Proliferative Activity of the Mammary Gland in the Rat, *Cancer Res.* 54, 1212–1215.
- West, D.B., Delany, J.P., Camet, P.M., Blohm, F., Truett, A.A., and Scimeca, J. (1998) Effects of Conjugated Linoleic Acid on Body Fat and Energy Metabolism in the Mouse, *Am. J. Physiol.* 275, R667–R672.
- Whigham, L.D., Cook, M.E., and Atkinson, R.L. (2000) Conjugated Linoleic Acid: Implications for Human Health, *Pharmacol. Res.* 42, 503–510.
- Thom, E., Wadstein, J., and Gudmundsen, O. (2001) Conjugated Linoleic Acid Reduced Body Fat in Healthy Exercising Humans, *J. Int. Med. Res.* 29, 392–396.
- Freedman, L.S., Clifford, C., and Messina, M. (1990) Analysis of Dietary Fat, Calories, Body Weight, and the Development of Mammary Tumors in Rats and Mice: A Review, *Cancer Res.* 50, 5710–5719.
- Jackson, C.D., Weis, C., Chen, J.J., Bechtel, D.H., and Poirier, L.A. (1998) Relative Contribution of Calories from Dietary Fat, Carbohydrate, and Fiber in the Promotion of DMBA-Induced Mammary Tumors in Sprague-Dawley Rats, *Nutr. Cancer* 30, 194–200.
- Welsch, C.W. (1994) Interrelationship Between Dietary Lipids and Calories and Experimental Mammary Gland Tumorigenesis, *Cancer* 74, 1055–1062.
- Boissonneault, G.A., Elson, C.E., and Pariza, M.W. (1986) Net Energy Effects of Dietary Fat on Chemically Induced Mammary Carcinogenesis in F344 Rats, *J. Natl. Cancer Inst.* 76, 335–338.
- Gillette, C.A., Zhu, Z., Westerlind, K.C., Melby, C.L., Wolfe, P., and Thompson, H. (1997) Energy Availability and Mammary Carcinogenesis: Effects of Calorie Restriction and Exercise, *Carcinogenesis* 18, 1183–1188.
- Dulloo, A.G., and Samec, S. (2001) Uncoupling Proteins: Their Roles in Adaptive Thermogenesis and Substrate Metabolism Reconsidered, *Br. J. Nutr.* 86, 123–139.
- Ricquier, D., and Bouillaud, F. (2000) The Uncoupling Protein Homologues: UCP1, UCP2, UCP3, StUCP and AtUCP, *Biochem. J.* 345, 161–179.
- Fleury, C., and Sanchis, D. (1999) The Mitochondrial Uncoupling Protein-2: Current Status, *Int. J. Biochem. Cell Biol.* 31, 1261–1278.
- Boss, O., Samec, S., Paoloni-Giacobino, A., Rossier, C., Dulloo, A., Seydoux, J., Muzzin, P., and Giacobino, J.P. (1997) Uncoupling Protein-3: A New Member of the Mitochondrial Carrier Family with Tissue-Specific Expression, *FEBS Lett.* 408, 39–42.
- Clarke, S.D. (2000) Polyunsaturated Fatty Acid Regulation of Gene Transcription: A Mechanism to Improve Energy Balance and Insulin Resistance, *Br. J. Nutr.* 83, S59–S66.
- Armstrong, M.B., and Towle, H.C. (2001) Polyunsaturated Fatty Acids Stimulate Hepatic UCP-2 Expression via a PPAR $\alpha$ -Mediated Pathway, *Am. J. Physiol.* 281, E1197–E1204.
- Chevillotte, E., Rieusset, J., Roques, M., Desage, M., and Vidal, H. (2001) The Regulation of Uncoupling Protein-2 Gene Expression by  $\omega$ -6 Polyunsaturated Fatty Acids in Human Skeletal Muscle Cells Involves Multiple Pathways, Including the Nuclear Receptor Peroxisome Proliferator-Activated Receptor  $\beta$ , *J. Biol. Chem.* 276, 10853–10860.
- Baillie, R.A., Takada, R., Nakamura, M., and Clarke, S.D. (1999) Coordinate Induction of Peroxisomal Acyl-CoA Oxidase and UCP-3 by Dietary Fish Oil: A Mechanism for Decreased Body Fat Deposition, *Prostaglandins Leukot. Essent. Fatty Acids* 60, 351–356.
- Cha, S.H., Fukushima, A., Sakuma, K., and Kagawa, Y. (2001) Chronic Docosahexaenoic Acid Intake Enhances Expression of the Gene for Uncoupling Protein 3 and Affects Pleiotropic mRNA Levels in Skeletal Muscle of Aged C57BL/6NjCl Mice, *J. Nutr.* 131, 2636–2642.
- Cline, G.W., Vidal-Puig, A.J., Dufour, S., Cadman, K.S., Lowell, B.B., and Shulman, G.I. (2001) *In vivo* Effects of Uncoupling Protein-3 Gene Disruption on Mitochondrial Energy Metabolism, *J. Biol. Chem.* 276, 20240–20244.
- West, D.B., Blohm, F., Truett, A.A., and Delany, J.P. (2000) Conjugated Linoleic Acid Persistently Increases Total Energy Expenditure in AKR/J Mice Without Increasing Uncoupling Protein Gene Expression, *J. Nutr.* 130, 2471–2477.
- Tsuboyama-Kasaoka, N., Takahashi, M., Tanemura, K., Kim, H.-J., Tange, T., Okuyama, H., Kasai, M., Ikemoto, S., and Ezaki, O. (2000) Conjugated Linoleic Acid Supplementation Reduces Adipose Tissue by Apoptosis and Develops Lipodystrophy in Mice, *Diabetes* 49, 1534–1542.
- Ryder, J.W., Portocarrero, C.P., Song, X.M., Cui, L., Yu, M., Combatsiaris, T., Galuska, D., Bauman, D.E., Barbano, D.M., Charron, M.J., et al. (2001) Isomer-Specific Antidiabetic Properties of Conjugated Linoleic Acid: Improved Glucose Tolerance, Skeletal Muscle Insulin Action, and UCP-2 Gene Expression, *Diabetes* 50, 1149–1157.
- Carmona, M., Valmaseda, A., Brun, S., Vinas, O., Mampel, T., Iglesias, R., Giral, M., and Villarroya, F. (1998) Differential Regulation of Uncoupling Protein-2 and Uncoupling Protein-3 Gene Expression in Brown Adipose Tissue During Development and Cold Exposure, *Biochem. Biophys. Res. Commun.* 243, 224–228.
- Gong, D.W., Monemdjou, S., Gavrilova, O., Leon, L.R., Marcus-Samuels, B., Chou, C.J., Everrett, C., Kozak, L.P., Li, C., Deng, C., et al. (2000) Lack of Obesity and Normal Response to Fasting and Thyroid Hormone in Mice Lacking Uncoupling Protein-3, *J. Biol. Chem.* 275, 16251–16257.
- Vidal-Puig, A.J., Grujic, D., Zhang, C.-Y., Hagen, T., Boss, O., Ido, Y., Szczepanik, A., Wade, J., Mootha, V., Cortright, R., et al. (2000) Energy Metabolism in Uncoupling Protein 3 Gene Knockout Mice, *J. Biol. Chem.* 275, 16258–16266.
- Pecqueur, C., Alves-Guerra, M.-C., Gelly, C., Levi-Meyrueis, C., Couplan, E., Collins, S., Ricquier, D., Bouillaud, F., and Miroux, B. (2001) Uncoupling Protein 2, *in vivo* Distribution, Induction upon Oxidative Stress, and Evidence for Translation Regulation, *J. Biol. Chem.* 276, 8705–8712.
- Ohnuki, K., Haramizu, S., Oki, K., Ishihara, K., and Fushiki, T. (2001) A Single Oral Administration of Conjugated Linoleic Acid Enhanced Energy Metabolism in Mice, *Lipids* 36, 583–587.
- Medina, D. (1974) Mammary Tumorigenesis in Chemical Carcinogen-Treated Mice. I. Incidence in BALB/c and C57bl Mice, *J. Natl. Cancer Inst.* 53, 213–221.
- Medina, D., Butel, J.S., Socher, S.H., and Miller, F.L. (1980) Mammary Tumorigenesis in 7,12-Dimethylbenzanthracene-Treated C57BL  $\times$  DBA/2f F<sub>1</sub> Mice, *Cancer Res.* 40, 368–373.
- Surwit, R.S., Wang, S., Petro, A.E., Sanchis, D., Raimbault, S., Ricquier, D., and Collins, S. (1998) Diet-Induced Changes in Uncoupling Proteins in Obesity-Prone and Obesity-Resistant Strains of Mice, *Proc. Natl. Acad. Sci. USA* 95, 4061–4065.
- Belury, M.A., and Kempa-Steczko, A. (1997) Conjugated

- Linoleic Acid Modulates Hepatic Lipid Composition in Mice, *Lipids* 32, 199–204.
34. DeLany, J.P., Blohm, F., Truett, A.A., Scimeca, J.A., and West, D.B. (1999) Conjugated Linoleic Acid Rapidly Reduces Body Fat Content in Mice Without Affecting Energy Intake, *Am. J. Physiol.* 276, R1172–R1179.
35. Esterbauer, H., Schneitler, C., Oberkofler, H., Ebenbichler, C., Paulweber, B., Sandhofer, F., Ladurner, G., Hell, E., Strosberg, A.D., Patsch, J.R., *et al.* (2001) A Common Polymorphism in the Promoter of *UCP2* Is Associated with Decreased Risk of Obesity in Middle-Aged Humans, *Nature Gen.* 28, 178–183.
36. Hubbard, N.E., Lim, D., Summers, L., and Erickson, K.L. (2000) Reduction of Murine Mammary Tumor Metastasis by Conjugated Linoleic Acid, *Cancer Lett.* 150, 93–100.
37. Master, S.R., Hartman, J.L., D’Cruz, C.M., Moody, S.E., Keiper, E.A., Ha, S.I., Cox, J.D., Belka, G.K., and Chodosh, L.A. (2002) Functional Microarray Analysis of Mammary Organogenesis Reveals a Developmental Role in Adaptive Thermogenesis, *Mol. Endocrinol.* 16, 1185–1203.
38. Kozak, L.P., and Harper, M.-E. (2000) Mitochondrial Uncoupling Proteins in Energy Expenditure, *Annu. Rev. Nutr.* 20, 339–363.
39. Park, Y., Albright, K.J., Liu, W., Storkson, J.M., Cook, M.E., and Pariza, M.W. (1997) Effect of Conjugated Linoleic Acid on Body Composition in Mice, *Lipids* 32, 853–858.
40. Enerback, S., Jacobsson, A., Simpson, E.M., Guerra, C., Yamashita, H., Harper, M.-E., and Kozak, L.P. (1997) Mice Lacking Mitochondrial Uncoupling Protein Are Cold-Sensitive but Not Obese, *Nature* 387, 90–94.
41. Muzzin, P., Boss, O., and Giacobino, J. (1999) Uncoupling Protein 3: Its Possible Biological Role and Mode of Regulation in Rodents and Humans, *J. Bioenerg. Biomembr.* 31, 467–473.
42. Samec, S., Seydoux, J., and Dulloo, A.G. (1998) Role of UCP Homologues in Skeletal Muscles and Brown Adipose Tissue: Mediators of Thermogenesis or Regulators of Lipids as Fuel Substrate, *FASEB J.* 12, 715–724.
43. Giacobino, J.P. (2001) Uncoupling Protein 3 Biological Activity, *Biochem. Soc. Trans.* 29, 774–776.
44. Wolf, G. (2001) The Uncoupling Proteins UCP2 and UCP3 in Skeletal Muscle, *Nutr. Rev.* 59, 56–57.
45. Peters, J.M., Park, Y., Gonzalez, F.J., and Pariza, M.W. (2001) Influence of Conjugated Linoleic Acid on Body Composition and Target Gene Expression in Peroxisome Proliferator-Activated Receptor  $\alpha$ -Null Mice, *Biochim. Biophys. Acta* 1533, 233–242.
46. Belury, M.A., Moya-Camarena, S.Y., Liu, K.-L., and Vanden Heuvel, J.P. (1997) Dietary Conjugated Linoleic Acid Induces Peroxisome-Specific Enzyme Accumulation and Ornithine Decarboxylase Activity in Mouse Liver, *J. Nutr. Biochem.* 8, 579–584.
47. Moya-Camarena, S.Y., Vanden Heuvel, J.P., and Belury, M.A. (1998) Conjugated Linoleic Acid Activates Peroxisome Proliferator-Activated Receptor  $\alpha$  and  $\beta$  Subtypes but Does Not Induce Hepatic Peroxisome Proliferation in Sprague-Dawley Rats, *Biochim. Biophys. Acta* 1436, 331–342.
48. Moya-Camarena, S.Y., and Belury, M.A. (1999) Species Differences in the Metabolism and Regulation of Gene Expression by Conjugated Linoleic Acid, *Nutr. Rev.* 57, 336–340.
49. Moya-Camarena, S.Y., Vanden Heuvel, J.P., Blanchard, S.G., Leesnitzer, L.A., and Belury, M.A. (1999) Conjugated Linoleic Acid Is a Potent Naturally Occurring Ligand and Activator of PPAR $\alpha$ , *J. Lipid Res.* 40, 1426–1433.
50. McCarty, M.F. (2000) Activation of PPAR $\gamma$  May Mediate a Portion of the Anticancer Activity of Conjugated Linoleic Acid, *Med. Hypotheses* 55, 187–188.
51. Kelly, L.J., Vicario, P.P., Thompson, G.M., Candelore, M.R., Doebber, T.W., Ventre, J., Wu, M.S., Meurer, R., Forrest, M.J., Conner, M.W., *et al.* (1998) Peroxisome Proliferator-Activated Receptors  $\gamma$  and  $\alpha$  Mediate *in vivo* Regulation of Uncoupling Protein (UCP-1, UCP-2, UCP-3) Gene Expression, *Endocrinology* 139, 4920–4927.
52. Teruel, T., Smith, S.A., Peterson, J., and Clapham, J.C. (2000) Synergistic Activation of UCP-3 Expression in Cultured Fetal Rat Brown Adipocytes by PPAR $\alpha$  and PPAR $\gamma$  Ligands, *Biochem. Biophys. Res. Commun.* 273, 560–564.

[Received June 14, 2002, and in revised form September 18, 2002; revision accepted October 7, 2002]



# Isolation and Characterization of a $\Delta 5$ FA Desaturase from *Pythium irregulare* by Heterologous Expression in *Saccharomyces cerevisiae* and Oilseed Crops

Haiping Hong<sup>a</sup>, Nagamani Datla<sup>a</sup>, Samuel L. MacKenzie<sup>b</sup>, and Xiao Qiu<sup>a,\*</sup>

<sup>a</sup>Research & Development, Bioriginal Food and Science Corporation, Saskatoon, Saskatchewan, Canada S7J 0R1, and <sup>b</sup>National Research Council of Canada, Plant Biotechnology Institute, Saskatoon, Saskatchewan, Canada S7N 0W9

**ABSTRACT:** By using the polymerase chain reaction approach with two degenerate primers targeting the heme-binding and the third histidine-rich motifs in microsomal carboxyl-directed desaturases, we identified a cDNA *PiD5* from *Pythium irregulare* encoding a  $\Delta 5$  desaturase. The substrate specificity of the enzyme was studied in detail by expressing *PiD5* in a yeast (*Saccharomyces cerevisiae*) mutant strain, AMY-2 $\alpha$ , where *ole1*, a  $\Delta 9$  desaturase gene, is disrupted. The result revealed that the encoded enzyme could desaturate unsaturated FA from 16 to 20 carbons beginning with  $\Delta 9$  and  $\Delta 11$  as well as  $\Delta 8$  ethylenic double bonds. Introduction of *PiD5* into *Brassica juncea* under the control of a CaMV 35S constitutive promoter resulted in accumulation of several  $\Delta 5$ -unsaturated polymethylene-interrupted FA ( $\Delta 5$ -UPIFA) including 18:2-5,9, 18:2-5,11, 18:3-5,9,12, and 18:4-5,9,12,15 in vegetative tissues. The transgenic enzyme could also desaturate the exogenously supplied homo- $\gamma$ -linolenic acid (20:3-8,11,14) to arachidonic acid (20:4-5,8,11,14). Introduction of *PiD5* into *B. juncea* and flax under the control of seed-specific promoters resulted in production of  $\Delta 5$ -UPIFA, representing more than 10% of the total FA in the seeds.

Paper no. L9061 in *Lipids* 37, 863–868 (September 2002).

Long-chain PUFA (LCPUFA) such as arachidonic acid (AA, 20:4-5,8,11,14) and EPA (20:5-5,8,11,14,17) are  $\Delta 5$  desaturated FA with multiple double bonds in the acyl chains. They are essential components of cell membranes and intermediates for the biosynthesis of various eicosanoids, a series of biologically active compounds involved in regulation and mediation of cell homeostasis and physiological activities in mammals (1). Clinical research has shown that appropriate uses of these FA can provide protection against some chronic diseases such as cardiovascular disease and arterial thrombosis and can provide some beneficial effect on arthritis, renal disorders, diabetes, and various cancers (2,3).

Biosynthesis of  $\Delta 5$ -LCPUFA occurs through sequential desaturation and chain-elongation in most eukaryotic species.

\*To whom correspondence should be sent at National Research Council of Canada, Plant Biotechnology Institute, 110 Gymnasium Place, Saskatoon, SK, S7N 0W9, Canada. E-mail: Xiao.Qiu@nrc.ca

The sequence reported here (*PiD5*) has been deposited in GenBank under the accession number AF419297.

Abbreviations: AA, arachidonic acid; cyt, cytochrome; HGLA, homo- $\gamma$ -linolenic acid; LA, linoleic acid; LCPUFA, long-chain PUFA; ORF, open reading frame; PCR, polymerase chain reaction;  $\Delta 5$ -UPIFA,  $\Delta 5$ -unsaturated polymethylene-interrupted FA.

Starting with linoleic acid (LA, 18:2-9,12), biosynthesis of LCPUFA involves  $\Delta 6$  desaturation of LA to GLA (18:3-6,9,12), followed by elongation of GLA to homo- $\gamma$ -linolenic acid (HGLA, 20:3-8,11,14) and  $\Delta 5$  desaturation of HGLA to AA (20:4-5,8,11,14). The same set of desaturases and elongases can work on  $\alpha$ -linolenic acid (18:3-9,12,15), yielding the n-3 series of LCPUFA such as EPA (20:5-5,8,11,14,17).

Genes encoding  $\Delta 6$  FA desaturases have been cloned and characterized from various sources including higher plants (4), fungi (5), nematodes (6), moss (7), and mammals (8). More recently, genes encoding  $\Delta 5$  desaturase also have been identified from a slime mold (9), a nematode (10,11), *Mortierella alpina* (12,13), and humans (14,15). These studies have facilitated our understanding of the molecular mechanism underlying the biosynthesis as well as our application of this knowledge to the production of the EFA in heterologous systems.

In this report, we describe the identification of *PiD5*, a new cDNA from *Pythium irregulare* encoding a  $\Delta 5$  FA desaturase. *Pythium irregulare* is an oleaginous fungus that is unusual in that it contains a large amount of AA and EPA, both of which contain  $\Delta 5$  double bonds and show promise as dietary supplements. Expression of the desaturase in yeast and two different plants indicated that the *P. irregulare* enzyme might be useful for large-scale production of these  $\Delta 5$  FA in plants.

## MATERIALS AND METHODS

**Strains and culture conditions.** *Pythium irregulare* 10951 obtained from the American Type Culture Collection (Manassas, VA) was grown at 25°C for 6 d in a liquid medium consisting of yeast extract, 3.0 g/L; malt extract, 3 g/L; peptone, 5 g/L; glucose, 10 g/L; K<sub>2</sub>HPO<sub>4</sub>, 0.68 g/L, pH 6.0 (16). Biomass was harvested by filtration and washed three times with distilled water. The dried mass was ground with mortar and pestle into a fine powder in liquid nitrogen and stored at -70°C for use.

**Polymerase chain reaction (PCR)-based cloning.** Single-stranded cDNA was synthesized from total RNA using a First-Strand cDNA Synthesis Kit (Amersham Pharmacia Biotech, Piscataway, NJ) and used as a template for PCR amplification with two degenerate primers (the forward: GCN-RANGANCAYCCNGGNGG, and the reverse: ATNTKNG-GRAANARRTGRTG) (17).



**cDNA library construction and screening.** The mRNA was extracted from total RNA by using Dynabeads™ Oligo(dT)25 (DYNAL®; Dynal Biotech Inc., Lake Success, NY). The cDNA library was constructed and screened as described by Hong *et al* (17).

**Expression of *PiD5* in yeast (*Saccharomyces cerevisiae*).** The open reading frame (ORF) of *PiD5* was amplified by PCR using the high-fidelity *Pfu* polymerase (Stratagene, La Jolla, CA). After initial amplification, TAQ polymerase was added to the mixture to facilitate the TA cloning (PCR® 2.1; Invitrogen). Having confirmed that the PCR products were identical to the original cDNA by sequencing, the fragments were then released by BamHI-EcoRI double digestion and inserted into the yeast expression vector pYES2 (Invitrogen, Carlsbad, CA). Yeast strains InvSc2 (Invitrogen) and AMY-2 $\alpha$  (18) were transformed with the expression constructs using the lithium acetate method, and transformants were selected on minimal medium plates lacking Uracil (19). Minimal medium containing 2% galactose, either with or without 0.3 mM substrate FA in the presence of 0.1% NP-40 Tergitol (Sigma, St. Louis, MO), was inoculated with the yeast transformant cell suspension and incubated at 20°C for 3 d.

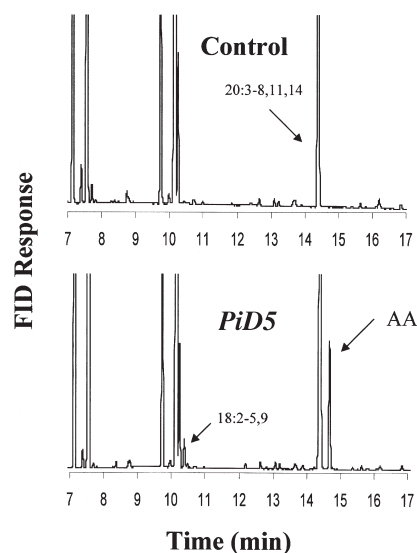
**Expression of *PiD5* in *Brassica juncea* and flax (*Linum usitatissimum*).** *Agrobacterium* transformation of *B. juncea* and flax was essentially according to our previous report (20).

**FA analysis.** Plant materials and yeast cells were harvested and washed twice with distilled water. Then 2 mL of methanolic KOH (7.5% wt/vol KOH in 95% methanol) was added to the materials and the mixture was sealed in a 12-mL glass culture tube and heated to 80°C for 60 min. Then 0.5 mL water was added and the sample was extracted twice with 2 mL hexane to remove the unsaponifiable lipids. The remaining aqueous phase was then acidified by adding 1 mL 6 N HCl and extracted twice with 2 mL hexane. The hexane phases were combined and dried under a stream of nitrogen. Next, 2 mL 3 N methanolic HCl (Supelco, Supelco Park, Bellefonte, PA) was added, and the mixture was heated at 80°C for 20 min. After cooling to room temperature, 1 mL 0.9% NaCl was added and the mixture was extracted twice with 2  $\times$  2 mL hexane.

Identity of the FA products was obtained by comparison of the retention time with standards or by GC-MS analysis of their derivatives. FA standards were purchased from Sigma (St. Louis, MO) and Nu-Chek-Prep (Elysian, MN). Fatty acyl diethylamine derivatives were prepared as described previously (17). GC-MS analysis was performed in standard EI mode using a Fisons VG TRIO 2000 mass spectrometer controlled by MassLynx version 2.0 software, coupled to a GC 8000 Series gas chromatograph. A DB-23 column (30 m  $\times$  0.25 mm i.d., 0.25  $\mu$ m film thickness; J&W Scientific, Folsom, CA) that was temperature-programmed at 180°C for 1 min, then 4°C/min to 240°C and held for 15 min, was used for the analysis (21).

## RESULTS

**Identification of *PiD5* from *P. irregulare*.** *Pythium irregulare* is an oleaginous fungus that is unusual in that it contains

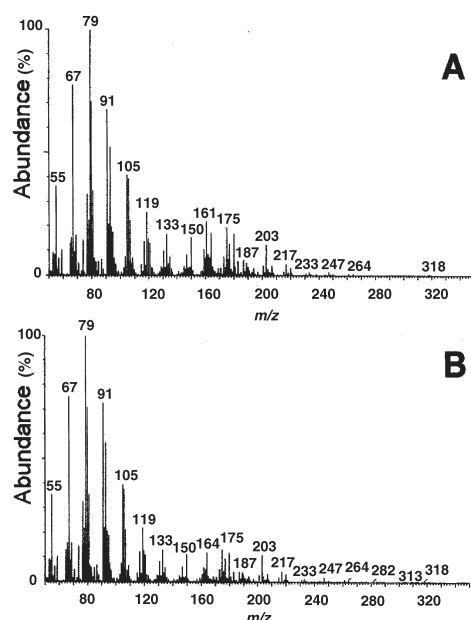


**FIG. 1.** GC analysis of FAME from yeast strain Invsc2 expressing *PiD5* with exogenous substrate homo- $\gamma$ -linolenic acid (HGLA, 20:3-8,11,14).

about 9% AA and 20% EPA. To identify genes coding for desaturases involved in the biosynthesis of these LCPUFA from *P. irregulare*, a PCR-based cloning strategy was adopted. Two degenerate primers were designed to target the heme-binding motif of cytochrome (cyt)  $b_5$ -like domain of so-called front-end desaturases (22) and the third conservative histidine motif in all microsomal desaturases, respectively. Using this strategy, we identified cDNA fragments from *P. irregulare* that encode a partial protein containing a cyt  $b_5$ -like domain in the N-terminus.

To isolate the full-length cDNA clone, the inserts were used as probes to screen a cDNA library of *P. irregulare*, which resulted in identification of several cDNA clones. Sequencing of all those clones identified a full-length cDNA that was named *PiD5*. The ORF of *PiD5* from *P. irregulare* is 1371 bp and codes for 456 amino acids (Genbank accession number AF419297). A homology search indicated *PiD5* shares high sequence similarity with the  $\Delta 5$  desaturases from *Dictyostelium discoideum* (9) and *M. alpina* (12,13). These results suggest the possible function of *PiD5* as a FA desaturase involved in AA and EPA biosynthesis.

**Expression of *PiD5* in yeast.** The *S. cerevisiae* Invsc2 was initially transformed with a plasmid, which contained the full-length ORF of the *PiD5* under the control of the galactose-inducible promoter. When the yeast transformant was induced by galactose in a medium containing HGLA (20:3-8,11,14), an extra peak was observed in the chromatogram of the FAME derived from the transformants compared with the control (Fig. 1). A comparison of the chromatogram with that of the standards revealed that the FAME had a retention time identical to AA (20:4-5,8,11,14) methyl ester. To confirm the regiochemistry of the products, the FAME was analyzed by GC-MS. The result indicated that the mass spectra of the new FA and the AA standard were identical (Fig. 2). These results



**FIG. 2.** GC-MS analysis of FAME of the new peak in Figure 1. (A) The PiD5 product; (B) the arachidonic standard (AA, 20:4-5,8,11,14).

demonstrate that PiD5 can convert HGLA into AA in yeast and indeed represents a new Δ5 desaturase from *P. irregulare*.

To study the substrate specificity of PiD5 further, we transferred the plasmid into another yeast strain, AMY-2α, where *ole1*, a Δ9 desaturase gene, is disrupted (18). The strain is unable to grow in minimal media without supplementation with monounsaturated FA. In our experiments, the strain was grown in minimal medium supplemented with 17:1(10Z), a nonsubstrate of PiD5, which enabled us to study the specificity of the enzyme toward various substrates, especially monounsaturates. A number of possible substrates including 16:1(9Z), 18:1(9Z), 18:1(11Z), 18:1(11E), 18:1(12E), 18:1(15Z), 18:2(9Z,12Z), 18:3(9Z,12Z,15Z), 20:2(11Z,14Z), and 20:3(11Z,14Z,17Z) were tested. Results indicated that PiD5 desaturated unsatu-

rated FA with Δ9 ethylenic and Δ11 ethylenic double bonds as well as the FA with a Δ8 ethylenic double bond (20:3-8,11,14). It could also desaturate *trans* FA such as 18:1(11E) and 18:1(12E).

Table 1 shows a comparison of the substrate preference of PiD5 for FA substrates tested in the yeast strain AMY-2α. As shown in Table 1, PiD5 appeared to prefer as substrate FA with a 20-carbon chain, such as 20:3(8Z,11Z,14Z), 20:3(11Z,14Z,17Z), and 20:2(11Z,14Z), whereas short-chain FA were relatively weaker substrates for the enzyme in yeast.

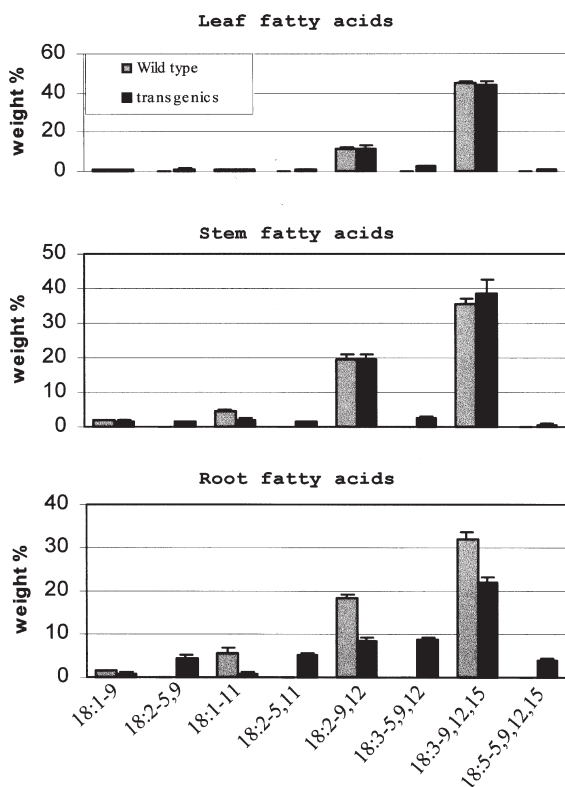
*Expression of PiD5 in B. juncea.* To determine whether PiD5 is functional in oilseed crops and whether its expression has any effect on their growth and development, we initially transformed *B. juncea* with a binary vector that contained PiD5 cDNA behind a constitutive promoter (a tandem cauliflower mosaic virus 35S promoter). Five independent primary transgenic plants were obtained, and the FA profile of lipids from different tissues was determined (Fig. 3). Compared with wild type, all transgenic plant tissues had an altered FA profile containing four additional peaks, which were identified as four different Δ5-unsaturated polymethylene-interrupted FA (Δ5-UPIFA), specifically, taxoleic (18:2-5,9); ephedrenic (18:2-5,11); pinolenic (18:3-5,9,12), and coniferonic acids (18:4-5,9,12,15). Thus, *B. juncea*, like yeast, can functionally express the *P. irregulare* Δ5 desaturase to convert the endogenous substrates 18:1-9, 18:1-11, 18:2-9,12, and 18:3-9,12,15 to the corresponding Δ5 desaturated FA. It appeared that roots produced the highest amount of the Δ5-UPIFA, representing more than 20% of the total FA, followed by 6% in stems and 5% in leaves.

In *B. juncea* there is no 20:3-8,11,14 substrate available, a preferred substrate for Δ5 desaturase. Thus, to examine whether the transgenic plant can produce AA, the substrate 20:3-8,11,14 was exogenously supplied. In this experiment, both wild type and transgenics were applied with an aqueous solution of sodium HGLA. It was found that exogenously applied substrates were readily taken up by plant tissues and converted into AA in transgenic plants (Fig. 4).

**TABLE 1**  
Conversion of Exogenous FA in Yeast AMY-2α/pPiD5<sup>a</sup>

Substrate	Substrate accumulation (wt%)	Product	Product accumulation (wt%)	Conversion (%)
16:1(9Z)	24.41	16:2(5Z,9Z)	0.47	1.89
18:1(9Z)	11.88	18:2(5Z,9Z)	1.26	9.59
18:1(11Z)	6.15	18:2(5Z,11Z)	0.85	12.14
18:1(11E)	4.57	18:2(5Z,11E)	0.08	1.72
18:1(12E)	4.77	18:2(5Z,12E)	0.09	1.85
18:1(15Z)	4.55	18:2(5Z,15Z)	0	0
18:2(9Z,12Z)	3.59	18:3(5Z,9Z,12Z)	0.09	2.44
18:3(9Z,12Z,15Z)	30.71	18:4(5Z,9Z,12Z,15Z)	0.07	0.23
20:2(11Z,14Z)	8.59	20:3(5Z,11Z,14Z)	2.08	19.49
20:3(8Z,11Z,14Z)	14.54	20:4(5Z,8Z,11Z,14Z)	2.68	15.56
20:3(11Z,14Z,17Z)	2.29	20:4(5Z,11Z,14Z,17Z)	1.08	32.04

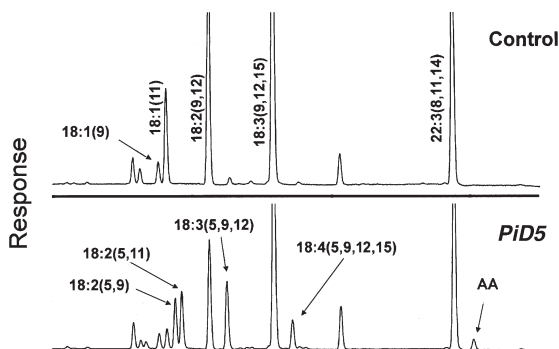
<sup>a</sup>Values are means of two duplicate samples. Products were identified by comparison of the retention times with standards or by GC-MS. pPiD5, plasma PiD5.



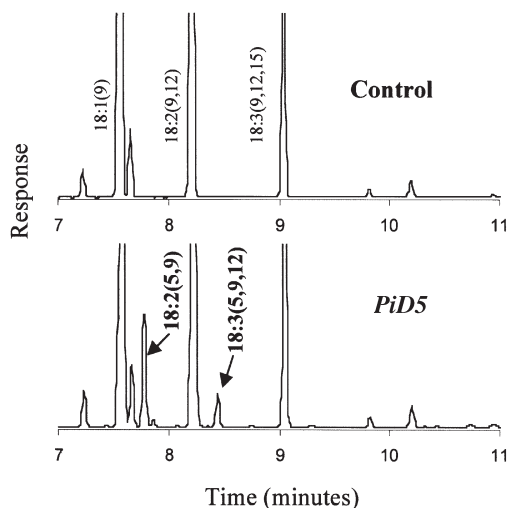
**FIG. 3.** FA composition of vegetative tissues (leaves, stems, and roots) expressing  $\Delta 5$  desaturase under the control of the 35S promoter. The FA levels are shown as the weight percentage of total FA in *Brassica juncea*.

Although the  $\Delta 5$ -UPIFA accumulated in all parts of the transgenic plant, there were no severe observable phenotypic changes except that the transgenic plant appeared slightly shorter than the corresponding wild type.

To produce  $\Delta 5$  desaturated FA in seeds, we transformed *B. juncea* with the construct containing *PiD5* cDNA behind a heterologous seed-specific promoter (*B. napus* napin promoter). Eight transgenic plants were produced, and the FA compositions of the primary transgenic seeds were deter-



**FIG. 4.** GC analysis of root FAME of *B. juncea* expressing *PiD5* with exogenous substrate HGLA (20:3-8,11,14). For abbreviations see Figures 1 and 3.



**FIG. 5.** Gas chromatogram of FAME prepared from seeds of *B. juncea* expressing *PiD5* under the control of the napin promoter. For abbreviation see Figure 3.

mined. FA analysis of transgenic seeds indicated that there were two new FA appearing in the gas chromatogram of transgenics compared with the wild-type control (Fig 5). These were identified as taxoleic acid (18:2-5,9) and pinolenic acid (18:3-5,9,12). Together they represent about 10% of the seed FA. Accumulation of  $\Delta 5$ -UPIFA has no significant effect on the oleic acid content compared with the untransformed control. This result is in contrast to the following result in flax transgenics expressing the same enzyme.

*Expression of PiD5 in flax.* To produce  $\Delta 5$  desaturated FA in flax seeds, we transformed flax with *PiD5* under the control of a flax seed-specific promoter (Truksa, M., and Qiu, X., unpublished data). As shown in Table 2, transgenic flax produced three  $\Delta 5$  desaturated FA: taxoleic, pinolenic, and coniferonic. Of these, taxoleic (18:2-5,9) was the most abundant and accounted for more than 9% of the total FA in an elite transgenic line, followed by coniferonic and pinolenic acids. Surprisingly, accumulation of  $\Delta 5$  desaturated FA in transgenic seeds had a significant impact on the composition of other FA, especially the oleic acid level. Accumulation of  $\Delta 5$  FA was accompanied by a huge increase in the oleic acids. The content of oleic acid in transgenic plants, on the average, reached 24.3% of the total FA, relative to the untransformed control at 17.4%.

**TABLE 2**  
Accumulation of  $\Delta 5$ -UPIFA in Seeds of Flax Transgenic Lines with the *PiD5* Desaturase Under the Control of a Seed-Specific Promoter<sup>a</sup>

FA	18:1 (9)	18:2 (5,9)	18:2 (9,12)	18:3 (5,9,12)	18:3 (9,12,15)	18:4 (5,9,12,15)
Wild type	17.4	0	14.9	0	56.6	0
Cnl-5-2	19.9	6.8	7.1	0.5	55.6	0.7
Cnl-10-1	29.1	9.3	5.1	0.4	47.6	0.4
Cnl-15-3	23.9	7.1	7.1	0.4	51.6	0.5

<sup>a</sup>The FA levels are shown as the weight percentage of total FA. UPIFA, unsaturated polymethylene-interrupted FA.

## DISCUSSION

In this report we describe isolation of a gene encoding  $\Delta 5$  desaturase from *P. irregulare*. Expression of the gene in *B. juncea* and flax resulted in production of  $\Delta 5$ -UPIFA, where the gene was expressed.

$\Delta 5$ -UPIFA occur widely in gymnosperms but less often in angiosperms (23). These FA are unusual in that two or more methylene units ( $\text{CH}_2$ ) separate the first double bond located at position 5 from the next double bond. Because of a structure similar to that of their counterparts, the usual  $\Delta 5$  desaturated PUFA,  $\Delta 5$ -UPIFA were reported to have beneficial effects on mammals, similar to those of  $\Delta 5$  EFA (24). In this study, we introduced the full-length *PiD5* into flax and *B. juncea* under the control of a seed-specific promoter, resulting in the accumulation of  $\Delta 5$ -UPIFA in oilseeds. In transgenic flax, taxoleic acid (18:2-5,9) represented more than 9% of the total FA. These findings suggest the possibility of producing a high level of  $\Delta 5$ -UPIFA in oilseed crops, which may increase the potential uses of these FA.

An interesting observation of this study was the changes in the seed FA composition of *PiD5* transgenic flax. It appeared that accumulation of  $\Delta 5$ -UPIFA in seeds was accompanied by an increase in the oleate content. A similar phenomenon was also observed with transgenic expression of *Fad2*-related enzymes, such as *Momordica charantia* conjugase (25) and castor and lesquerella oleate hydroxylases (26,27). It had been believed that a FA modified at the  $\Delta 12$  position interferes with the *FAD2* enzyme action, resulting in accumulation of a higher amount of oleic acid. Our data revealed that modification of FA at position 5 could also result in an increase in the oleate content in flax, but production of  $\Delta 5$ -UPIFA in *B. juncea* had little effect. It is not clear why the same transgene had different effects on the level of oleic acid in flax and *B. juncea*.

Biosynthesis of  $\Delta 5$ -UPIFA in gymnosperms was believed to involve two independent  $\Delta 5$  desaturases. One is specific for unsaturated FA with a  $\Delta 9$  ethylenic double bond, the other for unsaturated FA with a  $\Delta 11$  ethylenic double bond (28). Expression of *PiD5* in yeast and *B. juncea* revealed that the enzyme could effectively work on both 18:1-9 and 18:1-11, resulting in production of two corresponding products, taxoleic and ephedrenic acid, respectively. These data indicate that the  $\Delta 5$  desaturase from *P. irregulare* is quite flexible with respect to substrate requirement.

EPA and AA are both  $\Delta 5$  EFA. They form a unique class of food and feed constituents for humans and animals. Consequently, there is an increasing interest in the production in plants of AA- or EPA-containing oil for feed supplement and infant formula fortification. In this report we demonstrate that the  $\Delta 5$  desaturase isolated from *P. irregulare* is active in oilseed crops. The enzyme, when expressed in *B. juncea*, desaturated endogenous unsaturated substrates, resulting in several  $\Delta 5$  desaturated FA, and exogenously supplied substrate HGLA, resulting in production of AA in transgenic plants. These data suggest that this enzyme may be useful for large-

scale production of the  $\Delta 5$  EFA AA and EPA in oilseed crops. However, because of the promiscuous nature of the enzyme, the challenge for the production of AA and EPA in plants will be how to reduce or eliminate the undesirable FA such as  $\Delta 5$ -UPIFA. Co-expression of a  $\Delta 12$  desaturase and others in the LCPUFA pathway including  $\Delta 6$  desaturase,  $\Delta 6$  FA elongase, and  $\Delta 5$  desaturase may be a possible solution, by which the level of undesirable precursors would be reduced.

## ACKNOWLEDGMENTS

The authors thank Drs. Ed Kenaschuk, Gordon Rowland, and Derek Pots for providing flax and *B. juncea* germplasms; Drs. Andy Mitchell and Charles Martin for providing yeast mutant strains; Stephen Ambrose for performing mass spectrometry analysis; and Darwin Reed for preparing Figure 4.

## REFERENCES

- Gill, I., and Valivety, R. (1997) Polyunsaturated Fatty Acids, Part 1: Occurrence, Biological Activities and Applications, *TIBTECH* 15, 401–409.
- Das, U.N. (1990) Gamma-Linolenic Acid, Arachidonic Acid, and Eicosapentaenoic Acid as Potential Anticancer Drugs, *Nutrition* 6, 429–434.
- Babcock, T., Helton, W.S., and Espat, N.J. (2000) Eicosapentaenoic Acid (EPA): An Antiinflammatory  $\omega$ -3 Fat with Potential Clinical Applications, *Nutrition* 16, 1116–1118.
- Sayanova, O., Smith, M.A., Lapinskas, P., Stobart, A.K., Dobson, G., Christie, W.W., Shewry, P.R., and Napier, J.A. (1997) Expression of a Borage Desaturase cDNA Containing an N-Terminal Cytochrome *b5* Domain Results in the Accumulation of High Levels of  $\Delta 6$ -Desaturated Fatty Acids in Transgenic Tobacco, *Proc. Natl. Acad. Sci. USA* 94, 4211–4216.
- Huang, Y.S., Chaudhary, S., Thurmond, J.M., Bobik, E.G., Jr., Yuan, L., Chan, G.M., Kirchner, S.J., Mukerji, P., and Knutzon, D.S. (1999) Cloning of  $\Delta 12$ - and  $\Delta 6$ -Desaturases from *Mortierella alpina* and Recombinant Production of  $\gamma$ -Linolenic Acid in *Saccharomyces cerevisiae*, *Lipids* 34, 649–659.
- Napier, J.A., Hey, S.J., Lacey, D.J., and Shewry, P.R. (1998) Identification of a *Caenorhabditis elegans*  $\Delta 6$ -Fatty-Acid-Desaturase by Heterologous Expression in *Saccharomyces cerevisiae*, *Biochem. J.* 330, 611–614.
- Girke, T., Schmidt, H., Zahringer, U., Reski, R., and Heinz, E. (1998) Identification of a Novel  $\Delta 6$ -Acyl-Group Desaturase by Targeted Gene Disruption in *Physcomitrella patens*, *Plant J.* 15, 39–48.
- Cho, H.P., Takamura, M.T., and Clarke, S.D. (1999) Cloning, Expression, and Nutritional Regulation of the Mammalian  $\Delta 6$  Desaturase, *J. Biol. Chem.* 274, 471–477.
- Saito, T., and Ochiai, H. (1999) Identification of  $\Delta 5$  Fatty Acid Desaturase from the Cellular Slime Mold *Dictyostelium discoideum*, *Eur. J. Biochem.* 265, 809–814.
- Watts, J.L., and Browse, J. (1999) Isolation and Characterization of a  $\Delta 5$ -Fatty Acid Desaturase from *Caenorhabditis elegans*, *Arch. Biochem. Biophys.* 362, 175–182.
- Michaelson, L.V., Napier, J.A., Lazarus, C.M., Griffiths, G., and Stobart, A.K. (1998) Isolation of a  $\Delta 5$ -Desaturase Gene from *Caenorhabditis elegans*, *FEBS Lett.* 439, 215–218.
- Michaelson, L.V., Lazarus, C.M., Griffiths, G., Napier, J.A., and Stobart, A.K. (1998) Isolation of a  $\Delta 5$ -Fatty Acid Desaturase Gene from *Mortierella alpina*, *J. Biol. Chem.* 273, 19055–19059.
- Knutzon, D.S., Thurmond, J.M., Huang, Y.S., Chaudhary, S., Bobik, E.G., Jr., Chan, G.M., Kirchner, S.J., and Mukerji, P.



- (1998) Identification of  $\Delta 5$ -Desaturase from *Mortierella alpina* by Heterologous Expression in Baker's Yeast and Canola, *J. Biol. Chem.* 273, 29360–29366.
14. Cho, H.P., Takamura, M.T., and Clarke, S.D. (1999) Cloning, Expression, and Fatty Acid Regulation of the Mammalian  $\Delta 5$  Desaturase, *J. Biol. Chem.* 274, 37335–37339.
  15. Leonard, A.E., Kelder, B., Bobik, E.G., Chuan, L.T., Parker-Barnes, J.M., Thurmond, J.M., Kroeger, P.E., Kopchick, J.J., Huang, Y.S., and Mukerji, P. (2000) cDNA Cloning and Characterization of Human  $\Delta 5$ -Desaturase Involved in the Biosynthesis of Arachidonic Acid, *Biochem J.* 347, 719–724.
  16. Stinson, E.E., Kwoczek, R., and Kurantz, M.J. (1991). Effect of Cultural Conditions on Production of Eicosapentaenoic Acid by *Pythium irregulare*, *J. Ind. Microbiol.* 8, 171–178.
  17. Hong, H., Dalta, N., Reed, D.W., Covello, P.S., MacKenzie, S.L., and Qiu, X. (2002) High Level Production of  $\gamma$ -Linolenic Acid in *Brassica juncea* Using a  $\Delta$ -6 Desaturase from *Pythium irregulare*, *Plant Physiol.* 129, 354–362.
  18. Mitchell, A.G., and Martin, C.E. (1995) A Novel Cytochrome b5-Like Domain Is Linked to the Carboxyl Terminus of the *Saccharomyces cerevisiae*  $\Delta$ -9 Fatty Acid, *J. Biol. Chem.* 270, 29766–29772.
  19. Gietz, D., St. Jean, A., Woods, R.A., and Schiestl, R.H. (1992) Improved Method for High Efficiency Transformation of Intact Yeast Cells, *Nucleic Acids Res.* 20, 1425.
  20. Qiu, X., Hong, H.P., Datla, N., MacKenzie, S.L., Taylor, C.D., and Thomas, L.T. (2002) Expression of Borage  $\Delta$ -6 Desaturase in *Saccharomyces cerevisiae* and Oilseed Crops, *Can. J. Bot.* 80, 42–49.
  21. Qiu, X., Reed, D.W., Hong, H.P., Mackenzie, S.L., and Covello, P.S. (2001) Identification and Analysis of a Gene from *Calendula officinalis* Encoding a Fatty Acid Conjugase, *Plant Physiol.* 125, 847–855.
  22. Napier, J.A., Sayanova, O., Stobart, A.K., and Shewry, P.R. (1997). A New Class of Cytochrome b<sub>5</sub> Fusion Proteins, *Biochem. J.* 328, 717–720.
  23. Wolff, R.L., Christie, W.W., Pedrono, F., and Marpeau, A.M. (1999) Arachidonic, Eicosapentaenoic, and Biosynthetically Related Fatty Acids in the Seed Lipids from a Primitive Gymnosperm, *Agathis robusta*, *Lipids* 34, 1083–1097.
  24. Pasquier, E., Ratnayake, W.M.N., and Wolff, R.L. (2001) Effects of  $\Delta 5$  Polyunsaturated Fatty Acids of Maritime Pine (*Pinus pinaster*) Seed Oil on the Fatty Acid Profile of the Developing Brain of Rats, *Lipids* 36, 567–574.
  25. Cahoon, E.B., Carlson, T.J., Ripp, K.G., Schweiger, B.J., Cook, G.A., Hall, S.E., and Kinney, A.J. (1999) Biosynthetic Origin of Conjugated Double Bonds: Production of Fatty Acid Components of High-Value Drying Oils in Transgenic Soybean Embryos, *Proc. Natl. Acad. Sci. USA* 96, 12935–12940.
  26. Broun, P., and Somerville, C. (1997) Accumulation of Ricinoleic, Lesquerolic, and Densipolic Acids in Seeds of Transgenic *Arabidopsis* Plants That Express a Fatty Acyl Hydroxylase cDNA from Castor Bean, *Plant Physiol.* 113, 933–942.
  27. Broun, P., Boddupalli, S., and Somerville, C. (1998) A Bifunctional Oleate 12-Hydroxylase: Desaturase from *Lesquerella fendleri*, *Plant J.* 13, 201–210.
  28. Wolff, R.L., Christie, W.W., Pedrono, F., Marpeau, A.M., Tsevegsuren, N., Aitzetmüller, K., and Gunstone, F.D. (1999)  $\Delta 5$ -Olefinic Acids in the Seed Lipids from Four *Ephedra* Species and Their Distribution Between the  $\alpha$  and  $\beta$  Positions of Triacylglycerols. Characteristics Common to Coniferophytes and Cycadophytes, *Lipids* 34, 855–864.

[Received May 2, 2002, and in revised form and accepted September 23, 2002]

# Lipids and $\Delta 6$ -Desaturase Activity Alterations in Rat Liver Microsomal Membranes Induced by Fumonisin B<sub>1</sub>

W.C.A. Gelderblom<sup>a,\*</sup>, W. Moritz<sup>a</sup>, S. Swanevelder<sup>b</sup>, C.M. Smuts<sup>c</sup>, and S. Abel<sup>a</sup>

<sup>a</sup>PROMECC Unit, <sup>b</sup>Biostatistic Unit, and <sup>c</sup>NIRU, Medical Research Council, Tygerberg 7505, South Africa

**ABSTRACT:** Alterations in the membrane structure and function of hepatocyte membranes by fumonisin B<sub>1</sub> (FB<sub>1</sub>) have been proposed to play an important role in the disruption of growth regulatory effects and hence in the cancer-promoting ability of the mycotoxin. Detailed analyses of lipids in liver microsomal fractions of rats exposed to different dietary levels of FB<sub>1</sub> over a period of 21 d indicated an increase in PC, PE, PI, and cholesterol (Chol). These changes decreased the PC/PE and increased the total phospholipid/Chol ratios. When considering FA content, the quantities of total FA increased ( $P < 0.05$ ) in the major phospholipid fractions as a result of the increased phospholipid levels. However, when considering the relative levels (mg/100 mg of the total FA) of specific FA, the monounsaturated FA (16:1n-7 and 18:1n-9) and 18:2n-6 increased ( $P < 0.05$ ), whereas the long-chain PUFA decreased ( $P < 0.05$ ) in the main phospholipid fractions. Enzyme analyses indicated that the activity of the  $\Delta 6$ -desaturase was significantly reduced in liver microsomal preparations in a dose-dependent manner. An increase in the 20:3n-6/20:4n-6 ratio also suggested a decrease in the activity of the  $\Delta 5$ -desaturase. Disruption of microsomal lipid metabolism at different levels by FB<sub>1</sub> could play an important role in the alteration of growth regulatory effects in the liver.

Paper no. L9036 in *Lipids* 37, 869–877 (September 2002).

Fumonisin B<sub>1</sub> (FB<sub>1</sub>), a naturally occurring mycotoxin produced by *Fusarium verticillioides* in corn, alters growth regulatory responses in the liver. The inhibitory effect of FB<sub>1</sub> on growth-stimulating responses *in vitro* in different cell culture systems (1,2) and *in vivo* in rat liver has been related to the cancer-promoting activity of the compound (3,4). Studies in primary rat hepatocytes indicated that FB<sub>1</sub> increased the level of PC and PE, whereas sphingomyelin (SM) decreased (5). Total cholesterol (Chol) levels were decreased, and the relative levels of 18:2n-6 and 20:4n-6 increased. Sphingolipid metabolism was disrupted *via* the inhibition of ceramide synthase (6) resulting in the accumulation of sphinganine and to some extent sphingosine. The disruptions of lipid metabolism at different levels involving phospholipid, sphingolipid, and FA biosynthesis were suggested to be key events in the cytotoxicity of the fumonisins to hepatocytes (5). Subsequent investigations in primary hepatocytes indicated that FB<sub>1</sub> inhibited the epidermal growth factor (EGF) mitogenic

\*To whom correspondence should be addressed at PROMECC Unit/MRC, P.O. Box 19070, Tygerberg, 7505, South Africa.  
E-mail: wentzel.gelderblom@mrc.ac.za

Abbreviations: Chol, cholesterol; EGF, epidermal growth factor; FB<sub>1</sub>, fumonisin B<sub>1</sub>; LA, linoleic acid; PG, prostaglandin; SM, sphingomyelin; TFA, total FA; TPL, total phospholipid.

response, a common property of many cancer promoters in rat liver (1). This mitoinhibitory effect was not related to the disruption of sphingolipid metabolism; and events such as the disruption of Chol, phospholipid, and FA metabolism or combined effects seem to play a determining role. Recent findings indicated that the mitoinhibitory effect of FB<sub>1</sub> was counteracted by prostaglandin (PG) E<sub>2</sub>, suggesting that arachidonic acid (20:4n-6) metabolism is a key determinant affected by FB<sub>1</sub> (7). The modulation of FB<sub>1</sub> on 20:4n-6 and PG-induced effects on cell cycle progression and apoptosis have been reported (8,9).

When considering the FA profiles in hepatocytes exposed to FB<sub>1</sub>, it has been suggested that the rate-limiting enzyme in FA metabolism,  $\Delta 6$ -desaturase, is impaired (5). *In vivo* changes in the lipid profiles include increased Chol and PE levels and decreased SM in the liver of rats fed a dietary level of 250 mg FB<sub>1</sub>/kg for 21 d (10). A long-term feeding study in rats indicated an increased PE level at a dietary level as low as 1 ppm FB<sub>1</sub> (10). The relative level of 18:2n-6 was again significantly increased in PE, and 18:1n-9 was also markedly increased. The final FA of the n-6 pathway, 22:5n-6, was significantly decreased, indicating a disruption of the n-6 metabolic pathway, presumably owing to an impaired  $\Delta 6$ -desaturase enzyme. A similar effect was noticed in plasma PC, where the relative levels of 20:4n-6 and 22:5n-6 were reduced while 18:2n-6 accumulated.

It was proposed that changes in lipid metabolism in the liver, including phospho- and sphingolipids, Chol, and FA metabolism, play a determining role in the toxicological effects of the fumonisins (11,12). The interaction of these different lipid parameters is likely to be important in determining cell survival by altering cell proliferative and/or apoptotic pathways (13,14). The present study investigated lipid profiles of liver microsomal preparations of rats exposed to different dietary levels of FB<sub>1</sub> and the possible modulating effect on FA desaturation.

## MATERIALS AND METHODS

**Reagents.** [1-<sup>14</sup>C]Linoleic acid (LA; 18:2n-6) and [1-<sup>14</sup>C]-GLA (18:3n-6) were obtained from DuPont (Mechelen, Belgium). LA, GLA, NADH, ATP, nicotinamide, coenzyme A, and BHT [2,6-di-*tert*-butyl-*p*-cresol] were ordered from Sigma Chemical Corporation (St. Louis, MO). FB<sub>1</sub> was purified according to the method described by Cawood *et al.* (15) to a purity of 90–95%.

**Treatment of animals.** The Ethics Committee for Research on Animals approved this study, and it was conducted in compliance with policies and standards detailed in the South African Medical Research Council's principles and guidelines for the use of animals in biomedical research. Fischer 344 male rats were fed diets containing 10, 25, 50, 100, 250, and 500 mg FB<sub>1</sub>/kg diet over a period of 21 d, as described previously (3). Rats were terminated by decapitation and the livers collected in ice-cold saline and frozen at  $-70^{\circ}\text{C}$ .

**Preparation of microsomal preparations.** Liver homogenates were prepared by a modification of the methods described by Koba *et al.* (16) and De Antueno *et al.* (17). Liver was homogenized at  $4^{\circ}\text{C}$  with three parts of a homogenizing buffer consisting of a 0.1 M potassium phosphate buffer containing 0.25 M sucrose, 0.15 M KCl, 5 mM MgCl<sub>2</sub>, 1 mM EDTA, and 1.5 mM GSH using a Potter-Elvehjem homogenizer. The homogenate was first centrifuged at  $10,000 \times g$  for 20 min, then the supernatant was collected and centrifuged at  $105,000 \times g$  for 1 h. The microsomal pellet was resuspended in homogenizing buffer using a glass homogenizer to a level of 10 mg protein/mL and stored at  $-70^{\circ}\text{C}$ .

**Lipid analyses.** The microsomal preparations (2 mg protein/mL) were extracted with chloroform/methanol/BHT (2:1:0.01, vol/vol/%) according to the method of Smuts *et al.* (18). No lipid analyses were performed on the liver microsomal fraction of the rats fed the 500 mg FB<sub>1</sub>/kg diet. The phospholipid classes in the extracts were separated by TLC according to the method of Gilfillan *et al.* (19) using chloroform/methanol/petroleum ether/acetic acid/boric acid (40:20:30:10:1.8 g, by vol) as developing solvent. The spots corresponding with the major phospholipids were visualized under UV light and collected for phospholipid and FA analyses. Transmethylation of the FA was achieved by MeOH/H<sub>2</sub>SO<sub>4</sub> (95:5) treatment for 2 h at  $70^{\circ}\text{C}$  in glass-stoppered tubes. FAME were analyzed by GC on a Varian model 3700 gas chromatograph using fused-silica megabore DB-225 columns (J&W Scientific, Folsom, CA). The FA peaks were identified by comparison of retention times to those of a standard mixture of FFA 14:0 to 22:6 and quantified using an internal standard (17:0) and expressed as  $\mu\text{g}$  FA/mg protein.

Phospholipid analyses were carried out by the method of Itaya and Ui (20) using malachite green. The collected phospholipid fractions were digested in perchloric acid at  $170^{\circ}\text{C}$  for 2 h and diluted in an appropriate volume of H<sub>2</sub>O. Quantification was effected colorimetrically using phosphate as an external standard. The total Chol of the chloroform/methanol extracts was determined by the enzymatic iodine method using Chol oxidase and esterase enzyme preparations (18).

**$\Delta 6$ -desaturase assay.** Enzyme activity was monitored by the method of Koba *et al.* (16). Test tubes containing 0.5  $\mu\text{C}$  LA (ca. 100 nmol/mL = 100  $\mu\text{M}$ ; 20  $\mu\text{L}$  ethanol), 0.25 M sucrose, 0.15 M KCl, containing NaF (45 mM), NADH (1.0 mM), ATP (1.5 mM), CoA (0.25 mM), nicotinamide (0.5 mM), MgCl<sub>2</sub> (5 mM), GSH (1.5 mM), and 100 mM phosphate buffer (pH = 7.4) in a total incubation volume of 1 mL were preincubated at  $37^{\circ}\text{C}$  for 5 min. A 1-mL microsomal solution

(2 mg protein) was incubated separately for 5 min at  $37^{\circ}\text{C}$ , and 1 mL (2 mg protein) was added to the incubation mixture to obtain a final protein concentration of 1 mg/mL. This mixture was incubated for a further 30 min at  $37^{\circ}\text{C}$ . The assay was terminated by the addition of freshly prepared 10% KOH (1.8 N) in ethanol (2 mL), and the mixture was saponified at  $100^{\circ}\text{C}$  for 30 min. After acidifying with 0.4 mL of 11.6 N HCl (36%), the mixture was extracted with hexane ( $2 \times 5$  mL), the hexane was evaporated (N<sub>2</sub>), and the samples were transmethylated as described above. FAME were extracted with hexane/H<sub>2</sub>O ( $2 \times 2$  mL hexane + 1 mL H<sub>2</sub>O), and the hexane layer was evaporated to dryness under nitrogen. After addition of 80  $\mu\text{L}$  of hexane/chloroform (20:5, vol/vol) the methylated products were fractionated on AgNO<sub>3</sub>-TLC plates using chloroform/methanol (50:2, vol/vol) as developing solvent. For the preparation of the AgNO<sub>3</sub>-TLC plates, silica gel plates were impregnated with 10% AgNO<sub>3</sub> in acetonitrile for 15 min, dried at  $100^{\circ}\text{C}$  for 20 min, and kept desiccated in the dark prior to use. The spots were visualized under UV light after spraying with 0.1% dichlorofluorescein in chloroform/methanol (1:1 vol/vol). The spots corresponding with the substrate [ $1\text{-}^{14}\text{C}$ ]18:2n-6 (LA) and the product [ $1\text{-}^{14}\text{C}$ ]18:3n-6 (GLA) were scraped into scintillation vials; scintillation liquid was added, and the radioactivity determined. The control treatments consisted of incubations with heat-inactivated microsomes and microsomal preparations without the incubation mixture. Enzyme activity, which served to monitor the formation of GLA, was expressed as pmol GLA/min/mg protein.

**Statistical analyses.** Data were analyzed by a two-way ANOVA using the generalized linear model procedure, and Tukey's Studentized range test was used to determine whether the means differed statistically. Values were considered significant if  $P < 0.05$ .

## RESULTS

Details concerning the effects of the different dietary levels of FB<sub>1</sub> on the liver and body weight gains have been reported previously (3). In short, body weight gain was significantly reduced in rats fed the 250 mg FB<sub>1</sub>/kg diet ( $P < 0.01$ ) and markedly (although not significantly) affected in the animals that received the 100 mg FB<sub>1</sub>/kg diet.

**Chol and phospholipids.** The Chol content of the microsomes was significantly ( $P < 0.05$ ) and marginally ( $P < 0.1$ ) increased in the rats fed the 250 and 100 mg FB<sub>1</sub>/kg diets, respectively (Fig. 1A). Of the different phospholipid fractions analyzed, no significant effect on the concentration of PS was noticed as a result of the FB<sub>1</sub> treatment. In contrast, the levels of PC, PE, and PI were significantly increased ( $P < 0.05$  to  $P < 0.01$ ) in the 250 mg FB<sub>1</sub>/kg dietary group (Tables 1 and 2). In the case of PE, the concentration was also marginally ( $P < 0.1$ ) increased in the 100 mg FB<sub>1</sub>/kg dietary group. The total phospholipid (TPL) concentration was also significantly ( $P < 0.05$ ) increased from 100 mg FB<sub>1</sub>/kg, whereas it was marginally ( $P < 0.1$ ) increased at dietary levels of 10 and 50 mg FB<sub>1</sub>/kg diet (Fig. 1A). When considering the relative levels

**TABLE 1**  
**Concentration and FA Content (µg/mg protein) of the Major Liver Microsomal Phospholipids PC and PE of Rats Fed Different Dietary Levels of FB<sub>1</sub> for 21 d<sup>a</sup>**

Treatment (mg FB <sub>1</sub> /kg diet)	PC					PE				
	Control	10	50	100	250	Control	10	50	100	250
Phospholipids % of TPL	177.7 ± 27.1a 61.7a	226.0 ± 51.4a 63.3a	230.0 ± 44.2a 62.4a	254.3 ± 56.3a 60.5a	323.0 ± 40.5b 59.0a	69.8 ± 2.83a 21.6a	93.3 ± 17.2a 21.0a	87.9 ± 8.3a 21.9a	108.5 ± 9.1(b) 26.2(b)	153 ± 24.5A 28.3b
FA										
16:0	22.13 ± 0.54a	27.40 ± 1.62(b)	26.70 ± 2.68a	26.49 ± 2.63a	31.83 ± 2.27a	7.96 ± 1.42a	9.88 ± 1.00a	9.87 ± 0.36a	10.73 ± 1.82a	14.03 ± 1.08A
18:0	24.70 ± 1.97a	31.64 ± 2.55(b)	29.60 ± 3.46a	25.60 ± 3.28a	30.09 ± 2.18a	10.08 ± 2.57a	14.48 ± 2.16a	13.14 ± 0.56a	14.26 ± 1.18a	18.74 ± 1.73A
Total SFA	46.83 ± 2.48a	59.04 ± 0.94b	56.29 ± 5.87a	52.09 ± 5.19a	61.92 ± 4.45b	18.05 ± 3.99a	24.36 ± 3.15a	23.01 ± 0.65a	24.99 ± 2.85a	32.77 ± 2.82A
16:1	0.62 ± 0.15a	1.01 ± 0.31a	0.92 ± 0.25a	1.46 ± 0.28b	1.52 ± 0.28b	0.11 ± 0.01a	0.17 ± 0.03a	0.15 ± 0.03a	0.29 ± 0.06b	0.25 ± 0.05(b)
18:1	9.46 ± 0.42a	12.44 ± 1.42(b)	12.24 ± 0.82(b)	12.56 ± 0.61b	15.58 ± 2.20A	3.20 ± 0.58a	4.52 ± 0.08a	4.39 ± 0.65a	5.17 ± 0.38b	6.34 ± 0.89A
Total MUFA	10.08 ± 0.54a	13.46 ± 1.73(b)	13.16 ± 1.06(b)	14.03 ± 0.87b	17.10 ± 2.48A	3.31 ± 0.58a	4.69 ± 0.07a	4.54 ± 0.68a	5.46 ± 0.42b	6.60 ± 0.94A
18:2n-6	10.64 ± 1.52a	14.57 ± 1.06a	13.04 ± 0.20a	16.54 ± 2.00b	18.29 ± 4.19b	2.71 ± 0.94a	4.11 ± 0.60a	3.60 ± 0.41a	6.43 ± 1.10A	6.14 ± 0.80b
18:3n-6	0.34 ± 0.02a	0.50 ± 0.04a	0.40 ± 0.05a	0.72 ± 0.33a	0.81 ± 0.16(b)	0.08 ± 0.03a	0.14 ± 0.01a	0.10 ± 0.01a	0.22 ± 0.12a	0.19 ± 0.02a
20:3n-6	0.35 ± 0.01a	0.57 ± 0.03a	0.46 ± 0.12a	0.73 ± 0.29a	0.51 ± 0.34a	0.15 ± 0.02a	0.23 ± 0.04a	0.22 ± 0.05a	0.41 ± 0.13b	0.37 ± 0.01(b)
20:4n-6	36.12 ± 2.40a	48.88 ± 0.52A	47.52 ± 2.46A	37.80 ± 4.61a	40.73 ± 3.26a	13.32 ± 3.58a	19.99 ± 2.28(b)	18.22 ± 1.33a	20.70 ± 2.48b	21.38 ± 1.13b
22:4n-6	0.96 ± 0.20a	1.24 ± 0.14a	1.33 ± 0.23a	1.11 ± 0.30a	1.84 ± 0.11b	1.07 ± 0.21a	1.46 ± 0.03a	1.50 ± 0.05a	1.65 ± 0.48a	2.72 ± 0.05A
22:5n-6	4.59 ± 0.36a	4.74 ± 0.36a	5.73 ± 1.68a	3.33 ± 0.90a	6.64 ± 0.52a	4.06 ± 0.80a	4.29 ± 0.38a	4.85 ± 0.47a	3.33 ± 1.22a	8.08 ± 0.01A
Total n-6	53.01 ± 3.77a	70.50 ± 0.64A	68.48 ± 4.10b	60.23 ± 6.12a	68.81 ± 7.33b	21.39 ± 5.59a	30.22 ± 2.65(b)	28.48 ± 1.27a	32.72 ± 2.91b	38.87 ± 1.86A
22:5n-3	0.32 ± 0.11a	0.56 ± 0.06a	0.39 ± 0.15a	0.37 ± 0.03a	0.42 ± 0.11a	0.37 ± 0.12a	0.62 ± 0.02a	0.54 ± 0.06a	0.44 ± 0.13a	0.39 ± 0.16a
22:6n-3	3.16 ± 0.71a	4.51 ± 0.29b	4.01 ± 0.50a	2.56 ± 0.28a	2.98 ± 0.06a	3.14 ± 1.04a	4.82 ± 0.55(b)	4.17 ± 0.49a	2.60 ± 0.20a	3.84 ± 0.30a
Total n-3	3.60 ± 0.84a	5.24 ± 0.32b	4.57 ± 0.34a	3.12 ± 0.29a	3.60 ± 0.08a	3.54 ± 1.14a	5.53 ± 0.57b	4.78 ± 0.55a	3.14 ± 0.31a	4.37 ± 0.16a
PUFA	56.61 ± 4.60a	75.74 ± 0.86A	73.04 ± 4.28b	63.34 ± 6.40a	72.41 ± 7.41b	24.94 ± 6.73a	35.75 ± 3.16(b)	33.26 ± 1.76a	35.86 ± 3.13b	43.25 ± 2.02A
Total FA	113.5 ± 5.2a	148.2 ± 1.9b	142.5 ± 10.5b	129.5 ± 11.4a	154.8 ± 30.1b	46.4 ± 7.1a	64.8 ± 6.2a	60.8 ± 3.0a	66.3 ± 6.0a	84.0 ± 14.8b
n-6/n-3 ratio	15.12 ± 2.43a	13.49 ± 0.74a	15.02 ± 1.07a	19.31 ± 0.46b	19.10 ± 1.6(b)	6.13 ± 0.35a	5.48 ± 0.30a	6.00 ± 0.46a	10.46 ± 0.79A	8.87 ± 0.07A
P/S ratio	1.21 ± 0.11a	1.28 ± 0.02a	1.30 ± 0.06a	1.22 ± 0.01a	1.17 ± 0.04a	1.38 ± 0.08a	1.47 ± 0.09a	1.44 ± 0.04a	1.44 ± 0.07a	1.32 ± 0.05a

<sup>a</sup>Values are the means ± SD of triplicate determinations. FB<sub>1</sub>, fumonisin B<sub>1</sub>; TPL, total phospholipids; SFA, saturated FA; MUFA, monounsaturated FA; PUFA, polyunsaturated/saturated ratio. Means (rows) followed by the same letter do not differ statistically. If the letter differs, then  $P < 0.05$ . If the letters and cases differ (e.g., a vs. A), then  $P < 0.01$ . If the letter is in parentheses, then  $P < 0.1$ .



**TABLE 2**  
**Concentration and FA Content ( $\mu\text{g}/\text{mg}$  protein) of the Major Liver Microsomal Phospholipids PI and PS of Rats Fed Different Dietary Levels of  $\text{FB}_1$  for 21 d<sup>a</sup>**

Treatment (mg $\text{FB}_1/\text{kg}$ diet)	PS				PI				
	Control	10	50	250	Control	10	50	250	
Phospholipids % of TPL	9.63 $\pm$ 0.91a 3.7a	12.6 $\pm$ 1.3a 3.5a	13.1 $\pm$ 1.1a 3.3a	12.0 $\pm$ 3.2a 2.1b	39.8 $\pm$ 8.4a 13.0a	44.2 $\pm$ 6.0a 12.3a	46.9 $\pm$ 5.5a 12.4a	45.9 $\pm$ 5.0a 11.1b	59.1 $\pm$ 9.1b 10.6b
FA									
16:0	0.38 $\pm$ 0.03a	0.38 $\pm$ 0.07a	0.46 $\pm$ 0.11a	0.63 $\pm$ 0.14a	1.28 $\pm$ 0.08a	1.46 $\pm$ 0.37a	1.58 $\pm$ 0.17a	1.93 $\pm$ 0.21a	1.80 $\pm$ 0.13a
18:0	2.82 $\pm$ 0.83a	4.09 $\pm$ 0.29a	3.77 $\pm$ 0.15a	2.94 $\pm$ 0.59a	9.74 $\pm$ 1.00a	12.70 $\pm$ 0.53a	12.64 $\pm$ 0.63a	9.61 $\pm$ 0.38a	10.31 $\pm$ 0.76a
Total SFA	3.20 $\pm$ 0.86a	4.48 $\pm$ 0.36a	4.23 $\pm$ 0.26a	3.57 $\pm$ 0.73a	11.01 $\pm$ 1.04a	14.16 $\pm$ 0.70a	14.22 $\pm$ 0.75a	11.53 $\pm$ 0.58a	12.11 $\pm$ 0.90a
16:1	0.30 $\pm$ 0.02a	0.33 $\pm$ 0.03a	0.31 $\pm$ 0.06a	0.39 $\pm$ 0.12a	0.30 $\pm$ 0.02a	0.30 $\pm$ 0.03a	0.34 $\pm$ 0.03a	0.37 $\pm$ 0.12a	0.40 $\pm$ 0.17a
18:1	0.17 $\pm$ 0.04a	0.22 $\pm$ 0.01a	0.22 $\pm$ 0.02a	0.46 $\pm$ 0.15a	0.37 $\pm$ 0.06a	0.51 $\pm$ 0.11a	0.58 $\pm$ 0.09a	0.85 $\pm$ 0.11a	0.93 $\pm$ 0.15a
Total MUFA	0.47 $\pm$ 0.05a	0.56 $\pm$ 0.03a	0.54 $\pm$ 0.07a	0.85 $\pm$ 0.27b	0.67 $\pm$ 0.08a	0.81 $\pm$ 0.09a	0.92 $\pm$ 0.11a	1.22 $\pm$ 0.23b	1.33 $\pm$ 0.32b
18:2n-6	0.13 $\pm$ 0.04a	0.17 $\pm$ 0.01a	0.16 $\pm$ 0.02a	0.28 $\pm$ 0.07b	0.67 $\pm$ 0.08a	0.94 $\pm$ 0.06a	0.88 $\pm$ 0.14a	1.83 $\pm$ 0.65b	1.62 $\pm$ 0.31(b)
18:3n-6	0.02 $\pm$ 0.01a	0.04 $\pm$ 0.01a	0.03 $\pm$ 0.01a	0.02 $\pm$ 0.01a	0.02 $\pm$ 0.01a	0.03 $\pm$ 0.01a	0.03 $\pm$ 0.01a	0.07 $\pm$ 0.05a	0.06 $\pm$ 0.01a
20:4n-6	2.00 $\pm$ 0.71a	3.02 $\pm$ 0.08a	2.76 $\pm$ 0.09a	1.76 $\pm$ 0.37a	8.74 $\pm$ 0.42a	11.57 $\pm$ 0.76a	11.54 $\pm$ 0.28a	9.27 $\pm$ 0.19a	9.52 $\pm$ 0.11a
22:4n-6	0.12 $\pm$ 0.05a	0.17 $\pm$ 0.01a	0.16 $\pm$ 0.01a	0.25 $\pm$ 0.06b	0.29 $\pm$ 0.04a	0.39 $\pm$ 0.03a	0.44 $\pm$ 0.02b	0.29 $\pm$ 0.08a	0.42 $\pm$ 0.02(b)
22:5n-6	0.46 $\pm$ 0.13a	0.52 $\pm$ 0.11a	0.53 $\pm$ 0.06a	0.49 $\pm$ 0.10a	0.43 $\pm$ 0.07a	0.49 $\pm$ 0.05a	0.59 $\pm$ 0.03(b)	0.35 $\pm$ 0.07a	0.61 $\pm$ 0.05(b)
Total n-6	2.73 $\pm$ 0.93a	3.92 $\pm$ 0.12a	3.65 $\pm$ 0.11a	2.83 $\pm$ 0.62a	10.17 $\pm$ 0.31a	13.46 $\pm$ 0.67a	13.53 $\pm$ 0.37a	12.15 $\pm$ 0.70a	12.24 $\pm$ 0.37b
22:5	0.02 $\pm$ 0.02a	0.03 $\pm$ 0.00a	0.02 $\pm$ 0.00a	0.03 $\pm$ 0.01a	0.10 $\pm$ 0.03a	0.16 $\pm$ 0.01a	0.15 $\pm$ 0.11a	0.08 $\pm$ 0.02a	0.11 $\pm$ 0.02a
22:6	0.26 $\pm$ 0.10a	0.42 $\pm$ 0.05a	0.33 $\pm$ 0.04a	0.19 $\pm$ 0.04a	0.26 $\pm$ 0.04a	0.43 $\pm$ 0.02a	0.41 $\pm$ 0.04a	0.27 $\pm$ 0.03a	0.30 $\pm$ 0.01a
Total n-3	0.31 $\pm$ 0.12a	0.49 $\pm$ 0.05a	0.40 $\pm$ 0.04a	0.26 $\pm$ 0.06a	0.41 $\pm$ 0.04a	0.65 $\pm$ 0.02a	0.62 $\pm$ 0.06a	0.41 $\pm$ 0.01a	0.47 $\pm$ 0.03a
Total PUFA	3.04 $\pm$ 1.05a	4.41 $\pm$ 0.18a	4.04 $\pm$ 0.08a	2.54 $\pm$ 0.95a	10.58 $\pm$ 0.27a	14.11 $\pm$ 0.67a	14.15 $\pm$ 0.41a	12.56 $\pm$ 0.71a	12.71 $\pm$ 0.40b
Total FA	7.6 $\pm$ 2.2a	9.4 $\pm$ 0.5a	8.8 $\pm$ 0.2a	7.9 $\pm$ 2.6a	22.3 $\pm$ 1.3a	29.1 $\pm$ 0.8b	29.3 $\pm$ 1.0b	25.6 $\pm$ 1.3a	26.5 $\pm$ 4.8a
n-6/n-3 ratio	9.06 $\pm$ 0.33a	8.04 $\pm$ 0.61a	9.28 $\pm$ 1.22a	11.19 $\pm$ 0.01(b)	26.48 $\pm$ 4.16a	20.74 $\pm$ 0.98a	21.84 $\pm$ 1.51a	29.90 $\pm$ 1.41a	26.01 $\pm$ 0.66a
P/S ratio	0.93 $\pm$ 0.07a	0.99 $\pm$ 0.06a	0.95 $\pm$ 0.08a	0.87 $\pm$ 0.02a	0.97 $\pm$ 0.07a	1.00 $\pm$ 0.07a	1.00 $\pm$ 0.05a	1.09 $\pm$ 0.01a	1.06 $\pm$ 0.04a

<sup>a</sup>For footnote see Table 1.

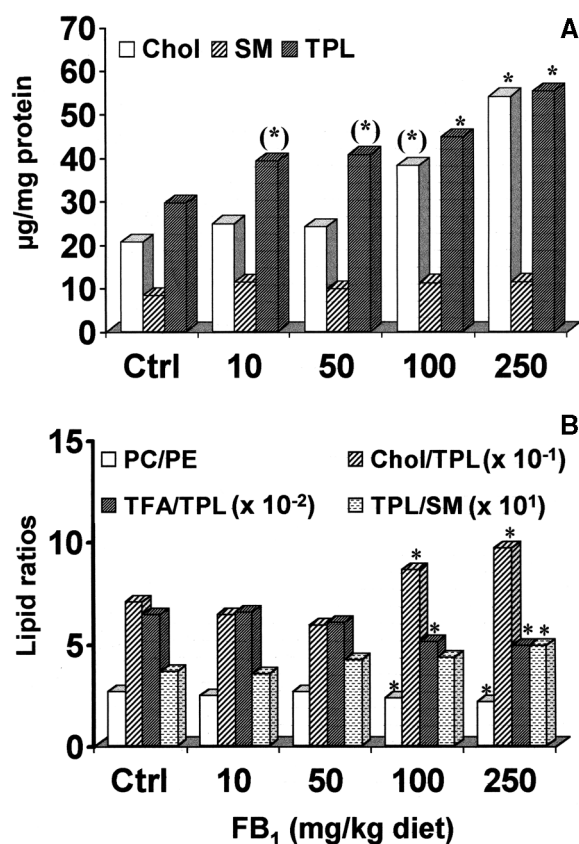


FIG. 1. (A) Effect of fumonisin B<sub>1</sub> (FB<sub>1</sub>) on the cholesterol (Chol), sphingomyelin (SM), and total phospholipid (TPL) levels in liver microsomes from rats exposed to different dietary levels over a period of 21 d. (B) Different lipid ratios that are possible factors modifying membrane fluidity. TFA, total FA. (\*) $P < 0.1$ , \*\* $P < 0.05$ .

of each phospholipid, expressed as a percentage of the TPL pool, the level of PC remained constant as PE increased marginally ( $P < 0.1$ ) and significantly ( $P < 0.05$ ) at 100 and 250 mg/kg dietary levels, respectively (Table 1). The relative levels of PI and PS significantly ( $P < 0.05$ ) decreased at the 100 and 250 mg FB<sub>1</sub>/kg dietary levels. As a result of the increase in the TPL pool, the total FA (TFA) were also increased marginally ( $P < 0.1$ ) to significantly ( $P < 0.05$ ) in the two high-dose groups, respectively. Owing to the changes in the lipid parameters of the microsomal membranes, the Chol/TPL ratio increased and the TFA/TPL and PC/PE ratios decreased in the 100 and 250 mg FB<sub>1</sub>/kg dietary groups (Fig. 1B).

**FA profiles.** The FA content, expressed as µg/mg protein, of the different phospholipids is summarized in Tables 1 and 2.

(i) **Saturated FA (16:0 and 18:0).** The total saturated fats increased significantly in the PC ( $P < 0.05$ ) and PE ( $P < 0.01$ ) phospholipid fractions in the 250 mg FB<sub>1</sub>/kg dietary group. In PC it was also significantly ( $P < 0.05$ ) increased in the 10 mg FB<sub>1</sub>/kg dietary group. Both 16:0 and 18:0 increased ( $P < 0.01$ ) in PE in the high-dose group whereas in PC only 16:0 increased significantly ( $P < 0.01$ ) in the high-dose group, and 18:0 was markedly increased in all FB<sub>1</sub>-treated groups. No changes were observed in PS and PI.

(ii) **Monounsaturated FA (16:1 and 18:1).** A marked to significant ( $P < 0.01$  to 0.05) increase in the monounsaturated

FA was noticed in all the phospholipid fractions in the livers of the two high-dose groups of rats (100 and 250 mg FB<sub>1</sub>/kg diet). In PC ( $P < 0.1$ ) and PE marked increases were also noticed at the 10 and 50 mg FB<sub>1</sub>/kg dietary levels. Both 16:1 and 18:1 contributed to the increased levels at the two high-dose levels; 18:1 was marginally ( $P < 0.1$ ) to significantly ( $P < 0.05$ ) increased in PC in all the FB<sub>1</sub>-treated groups.

(iii) **PUFA (n-6 PUFA: 18:2n-6, 20:4n-6, 22:4n-6, 22:5n-6).** LA (18:2n-6) was significantly ( $P < 0.1$  to 0.01) increased in all the phospholipid fractions in the 100 and 250 mg FB<sub>1</sub>/kg dietary groups, whereas it was markedly higher in PC and PE in the 10 and 50 mg FB<sub>1</sub>/kg groups. Arachidonic acid (20:4n-6) was significantly ( $P < 0.05$ ) increased in PC at dietary levels of 10 and 50 mg FB<sub>1</sub>/kg, but it was similar to the control levels in the two high-dose groups. No changes were observed in PS, whereas it was markedly to significantly ( $P < 0.1$  to 0.01) increased in PE and PI at all dose levels. The terminal FA in the n-6 pathway, 22:5n-6, was significantly ( $P < 0.01$ ) increased in PE at the high-dose level (250 mg FB<sub>1</sub>/kg). In PI, 22:5n-6 was significantly ( $P < 0.05$  to 0.01) increased at all the FB<sub>1</sub> dose levels. The total n-6 FA marginally to significantly increased in PC, PE, and PI at all the dose levels, whereas PS was not affected.

(iv) **PUFA (n-3 PUFA: 22:5n-3, 22:6n-3).** The level of 22:6n-3 was marginally ( $P < 0.1$ ) to significantly ( $P < 0.05$  to 0.01) increased in the PC, PE, and PI phospholipid fractions at the 10 mg FB<sub>1</sub>/kg dietary levels. At higher dietary levels it tended to mimic the level in the microsomes of the control rats despite the increase in the level of the respective phospholipid. The total n-3 FA tended to follow the same pattern in PC, PE, and PI, whereas PS was not affected.

**FA parameters.** Changes in the levels of the FA profiles presented above are related to the concentration of the respective phospholipid. As a result, PUFA were marginally ( $P < 0.1$ ) to significantly ( $P < 0.05$  to  $P < 0.01$ ) increased in the microsomal PC, PE, and PI phospholipid fractions of the FB<sub>1</sub>-treated animals. The n-6/n-3 FA ratio was also significantly ( $P < 0.05$ ) increased in PC and PE at the 100 and 250 mg FB<sub>1</sub>/kg dietary levels mainly due to an increase in the n-6 FA. The polyunsaturated/saturate FA ratio was not altered. The TFA increased markedly in the microsomes of the rats fed the 10 mg FB<sub>1</sub>/kg dietary level and significantly at the high-dose levels as a result of the increased levels of the individual phospholipids (Tables 1 and 2).

**FA desaturation.** When considering the activity of the FA  $\Delta$ -desaturases, the levels of the substrates and products of the enzyme are relevant. Since the concentration of phospholipids may vary, as in the case of the present study, the relative amount of each FA, expressed as a percentage of the TFA, needs to be considered. There was a significant increase in the relative levels of 16:1n-7, 18:1n-9, and 18:2n-6 and a significant decrease in the long-chain FA, 20:4n-6 and 22:6n-3, in PC (Fig. 2A) and PE (Fig. 2B) at a dietary level of 100 mg FB<sub>1</sub>/kg and above. The terminal FA of the n-6 metabolic pathway, 22:5n-6, significantly ( $P < 0.05$ ) decreased in both PE and PC in the 100 mg FB<sub>1</sub>/kg dietary

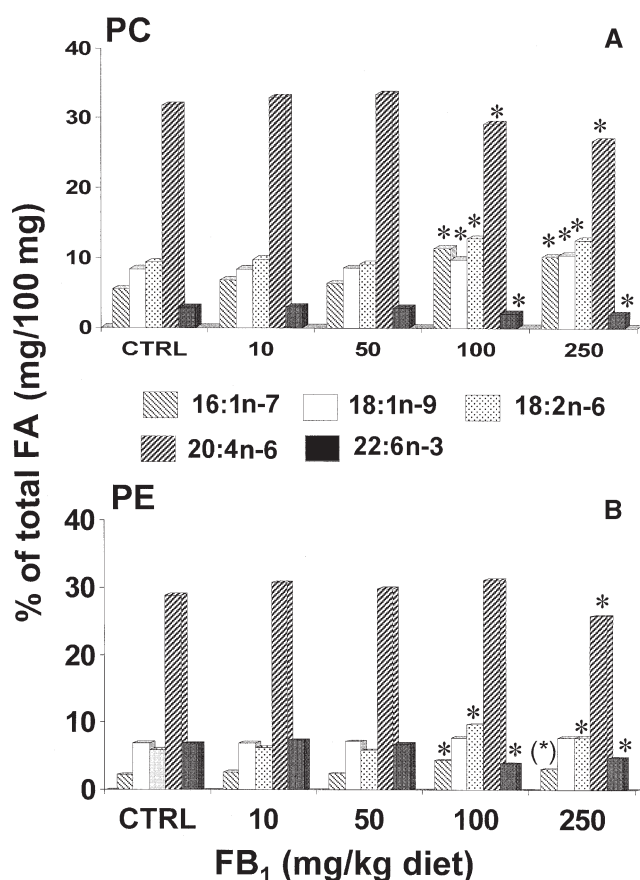


FIG. 2. The relative levels (% of total) of the FA in the major microsomal phospholipids PC (A) and PE (B) of the livers of rats fed different dietary levels of  $FB_1$  for 21 d. (\*) $P < 0.1$ , \* $P < 0.05$ . For abbreviation see Figure 1.

group while no decrease was noticed in the 250 mg  $FB_1$ /kg dietary group. A similar relative FA pattern was also noticed in PS and PI phospholipid fractions (data not shown). When considering specific FA ratios, using the relative concentration levels, the 18:2n-6/18:3n-6 ratio decreased significantly ( $P < 0.05$ ) in PC, whereas the 18:3n-6/20:4n-6 and 20:3n-6/20:4n-6 ratios increased significantly ( $P < 0.05$ ) in both PC and PE at the two high-dose  $FB_1$  dietary levels (Fig. 3A). No changes were observed in the 18:3n-6/20:3n-6 ratio in the PC and PE phospholipid fractions.

Enzyme analyses indicated that the conversion of  $^{14}C$ -LA to  $^{14}C$ -GLA, catalyzed by the  $\Delta 6$ -desaturase, was significantly reduced at dietary levels of 100 mg  $FB_1$  and higher (Fig. 3). The activity of the  $\Delta 5$ -desaturase was not determined.

## DISCUSSION

Lipid analyses of the livers of rats exposed to different dietary levels of  $FB_1$  indicated that the metabolism of Chol, phospholipid, FA, and sphingolipid is altered (10). The present study indicated that the phospholipids were significantly altered in the rat liver microsomal fraction due to elevated concentrations of PE, PC, and PI. When considering the relative contribution of each phospholipid to the TPL pool, PC remained constant at about

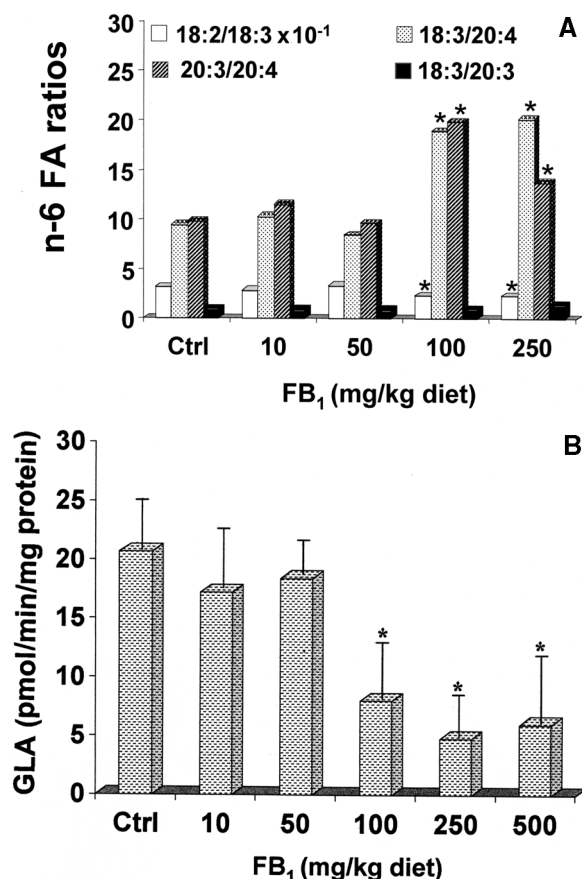


FIG. 3. Alterations of the relative FA ratios associated with changes in n-6 FA metabolism (A), and the effect of  $FB_1$  on the activity of the microsomal  $\Delta 6$ -desaturase enzyme as a function of different dietary doses fed to rats over a period of 21 d (B). Error bars represent the SD. \* $P < 0.05$ . For abbreviation see Figure 1.

60%, whereas PE increased significantly from 20 to 28%. The relative contribution of both PI and PS to the TPL pool tended to decrease, from 12 to 10% and from 4 to 2%, respectively. It appears that  $FB_1$  mainly altered the PE phospholipid compartment in rat liver microsomes, resulting in a significant decrease in the PC/PE ratio. Chol was also significantly increased (2.5 times) at the two higher dietary levels to the effect that, despite the increase in TPL, the Chol/TPL ratio increased significantly. The increase in the TPL also resulted in the increase in the TFA content. In this regard, the relative level of PUFA decreased significantly in PC, PE, and PI, and the saturated and monounsaturated FA compartment increased significantly.

The impact of these altered lipid parameters on membrane fluidity has been discussed in detail elsewhere (21). It was suggested that an increased Chol/TPL ratio decreased the PC/PE ratio, and the accumulation of the relative levels of the saturated FA together with the decrease in the long-chain PUFA could result in a more rigid microsomal membrane structure. It is not known to which extent the increase in the relative levels of the monounsaturated FA, 18:1n-9, and 18:2n-6 counteracted the impact of the other parameters in maintaining membrane fluidity. In this regard it was shown that, in persistent hepatocyte nodules, similar changes to the same lipid param-

ters were associated with an increase in fluidity (22). No changes in the concentration of the membrane sphingolipid, SM, were noticed as a result of the FB<sub>1</sub> treatment. Apparently, the disruption of sphingolipid metabolism, more specifically, the ceramide synthase by FB<sub>1</sub>, is not reflected in the microsomes. The TPL/SM ratio, however, increased significantly owing to the increase in the PC and PE concentration. As both phospholipids are involved in the synthesis of SM *via* PC:ceramide-phosphocholine and the PE:ceramide-phosphocholine transferases (23), the accumulation of PC and PE could be related to a decreased synthesis of SM owing to a reduced level of ceramide caused by the inhibition of ceramide synthase by FB<sub>1</sub>. Increased microsomal Chol is also known to induce the synthesis of SM by increasing the activities of the two phospholipid transferase enzymes (23). However, as the level of SM was not reduced, the above hypothesis does not explain the accumulation of PC and PE, and/or other mechanisms that regulate the level of SM in the microsomes may exist. Studies should be conducted on the modulating effect of FB<sub>1</sub> on Chol and phospholipid-metabolizing enzymes.

The increased TPL pool also resulted in an increase in the TFA concentrations in individual phospholipid fractions. This occurred at dietary levels as low as 10 mg FB<sub>1</sub>/kg. However, at the two higher levels the TFA/TPL ratio decreased mainly owing to an increase in TPL, whereas TFA levels did not increase to the same extent. The latter have been associated with the decrease in the relative values of PUFA, owing to the impaired  $\Delta 6$ -desaturase and/or increased lipid peroxidation induced by the hepatotoxic effects of FB<sub>1</sub> in the liver (4). Abel *et al.* (24) indicated that lipid peroxidation was significantly enhanced in rat liver microsomes after chronic feeding at a dietary level of 250 mg FB<sub>1</sub>/kg over a period of 21 d. Several other studies confirmed that FB<sub>1</sub> induces oxidation damage in membranal environments (25,26). Therefore, despite the increase in the concentration of the phospholipids, the PUFA levels, especially the relative levels of 20:4n-6 and 22:6n-3, which are prone to undergo lipid peroxidation, significantly decrease in both the PC and PE phospholipid fractions of the rats fed the high-dose FB<sub>1</sub> levels. It will not be possible to distinguish between the relative contribution of lipid peroxidation and an impaired FA desaturation toward the reduction of PUFA in the microsomes.

The activity of the  $\Delta 5$ - and  $\Delta 6$ -desaturase enzymes is affected by many factors including changes in the fluidity of the microsomal membrane (16), age (27–29), dietary status (30), different animal species, and different organs in the same species (16). Studies indicated that, with respect to dietary Chol and protein, altering the Chol/phospholipid and PC/PE ratios affects the fluidity of the microsomal membrane as well as the activity of the enzyme and hence the FA content of the microsomes (21,31). The FB<sub>1</sub>-induced alteration of FA patterns in the major phospholipid fractions in primary hepatocytes and in rat liver suggests an impaired  $\Delta 6$ -desaturase enzyme system (5,10). The present study indicates that FB<sub>1</sub> significantly decreased the activity of the  $\Delta 6$ -desaturase, resulting in the accumulation of 18:2n-6 in the major

phospholipids. When considering the 18:3n-6/20:4n-6 and 20:3n-6/20:4n-6 FA ratios, it appears that the activity of the  $\Delta 5$ -desaturase also is impaired. The increase in 18:3n-6 could explain the significant decrease in the 18:2n-6/18:3n-6 ratio, i.e., 18:3n-6 was proportionately higher than 18:2n-6. As no change was observed in the 18:3n-6/20:3n-6 ratio, it would appear that the activity of the elongase enzyme was not affected.

Whether the disruption of the activity of the FA  $\Delta$ -desaturases is related to a direct interaction with FB<sub>1</sub> or indirectly to a disruption of the membranal structure is unknown. The fact that Cawood *et al.* (32) indicated that FB<sub>1</sub> is tightly associated with hepatocyte membranes emphasizes the importance of monitoring the *in vitro* effects of FB<sub>1</sub> on the activity of the enzyme. Whatever the reason, the impairment of the FA  $\Delta$ -desaturases and the resultant disruption of FA metabolism are likely to disrupt the membrane integrity of the microsomes further. When considering the structural changes of the microsomal membranal environment, one must recognize that the activities of other important enzymes are also likely to be altered. Changes in the Chol and phospholipid membrane constituents have been shown to alter the activities of drug-metabolizing enzymes, such as cytochrome P450 (33–37). In this regard, recent studies indicated that the activity of certain isozymes of the hepatic P450 enzyme system are selectively inhibited and/or stimulated by FB<sub>1</sub> (38,39).

Structural changes with respect to Chol, phospholipids, and FA in the membrane environment of neoplastic cells have been reported to be important in the progression of these lesions into cancer (22). Membranal changes in hepatocyte nodules are associated with increased Chol and PE, resulting in an increased Chol/TPL ratio, a decrease in the PC/PE ratio, and changes in membrane fluidity. The  $\Delta 6$ -desaturase has been reported to be impaired in hepatocyte nodules and other cancerous tissue resulting in a specific FA pattern in the membranal phospholipids (22,40). The increased concentration of PE and subsequent increased level of 20:4n-6 have been implied to be important stimuli for the altered growth pattern in these lesions (22). A specific role for 20:4n-6 in the development of hepatocyte nodules has been proposed (22,41), suggesting a critical role of this FA in cancer development. Impairment of the  $\Delta 6$ -desaturase, presumably owing to structural changes in the membrane, is an early event in the genesis of hepatocyte nodules (22) and appears to be closely associated with the altered growth pattern of cancerous lesions. Recently, it was proposed that the disruption of the membrane structure by FB<sub>1</sub>, and more specifically the effect on PE and 20:4n-6 levels, could be important for the cancer-promoting ability of this compound in the liver (4,11). Addition of PG E<sub>2</sub> counteracts the mitoinhibitory effect of FB<sub>1</sub> on the EGF mitogenic response in primary hepatocytes, suggesting the disruption of 20:4n-6 metabolism (7). FB<sub>1</sub> also inhibits the effects of 20:4n-6, PG-E<sub>2</sub>, and PG-A<sub>2</sub> on apoptosis in esophageal cancer cells *in vitro* presumably related to decreased ceramide production (9).

Alterations in rat liver microsomal membrane lipid profiles and  $\Delta 6$ - and possibly  $\Delta 5$ -desaturase activity, leading to



altered FA metabolism, could have important implications regarding signaling pathways that determine cell survival and cancer development in the liver.

## ACKNOWLEDGMENTS

W.C.A. Gelderblom was a recipient of a Visiting Scientist Award from the International Agency for Research on Cancer, Lyon, France (1996).

## REFERENCES

- Gelderblom, W.C.A., Snyman, S.D., Van der Westhuizen, L., and Marasas, W.F.O. (1995) Mitoinhibitory Effect of Fumonisin B<sub>1</sub> on Rat Hepatocytes in Primary Culture, *Carcinogenesis* 16, 625–631.
- Tolleson, W.H., Melchior, W.B., Jr., Morris, S.M., McGarrity, L.J., Domon, O.E., Muskhelishvili, L., James, S.J., and Howard, P.C. (1996) Apoptotic and Anti-proliferative Effects of Fumonisin B<sub>1</sub> in Human Keratinocytes, Fibroblasts, Esophageal Epithelial Cells and Hepatoma, *Carcinogenesis* 17, 239–249.
- Gelderblom, W.C.A., Snyman, S.D., Lebepe-Mazur, S., van der Westhuizen, L., Kriek, N.P.J., and Marasas, W.F.O. (1996) The Cancer-Promoting Potential of Fumonisin B<sub>1</sub> in Rat Liver Using Diethylnitrosamine as Cancer Initiator, *Cancer Lett.* 109, 101–108.
- Gelderblom, W.C.A., Snyman, S.D., Abel, S., Lebepe-Mazur, S., Smuts, C.M., van der Westhuizen, L., Marasas W.F.O., Victor, T.C., Knasmuller, S., and Huber, W. (1996) Hepatotoxicity and -Carcinogenicity of the Fumonisin in Rats: A Review Regarding Mechanistic Implications for Establishing Risk in Humans, in *Fumonisin in Food* (Jackson, L.S., De Vries, J.W., and Bullerman L.B., eds.), Plenum, New York, pp. 279–296.
- Gelderblom, W.C.A., Smuts, C.M., Abel, S., Snyman, S.D., Cawood, M.E., van der Westhuizen, L., and Swanevelder, S. (1996) Effect of Fumonisin B<sub>1</sub> on Protein and Lipid Synthesis in Primary Rat Hepatocytes, *Food Chem. Toxicol.* 34, 361–369.
- Wang, E., Norred, W.P., Bacon, C.W., Riley, R.T., Merrill, A.H., Jr. (1991) Inhibition of Sphingolipid Biosynthesis by Fumonisin: Implications for Diseases Associated with *Fusarium moniliforme*, *J. Biol. Chem.* 266, 14486–14490.
- Gelderblom, W.C.A., Abel, S., Smuts, C.M., Swanevelder, S., and Snyman, S.D. (1999) Regulation of Fatty Acid Biosynthesis as a Possible Mechanism for the Mitoinhibitory Effect of Fumonisin B<sub>1</sub> in Primary Rat Hepatocytes, *Prostaglandins Leukot. Essent. Fatty Acids* 61, 225–234.
- Pinelli, E., Poux, N., Garren, L., Pipy, B., Castegnaro, M., Miller, D.J., and Pfohl-Leszkowicz, A. (1999) Activation of Mitogen-Activated Protein Kinase by Fumonisin B<sub>1</sub> Stimulates cPLA<sub>2</sub> Phosphorylation, the Arachidonic Acid Cascade and cAMP Production, *Carcinogenesis* 20, 1683–1688.
- Seegers, J.C., Joubert, A.M., Panzer, A., Lottering, M.L., Jordan, C.A., Joubert, F., Maree, J.L., Bianchi, P., de Kock, M., and Gelderblom, W.C.A. (2000) Fumonisin B<sub>1</sub> Influenced the Effects of Arachidonic Acid, Prostaglandins E<sub>2</sub> and A<sub>2</sub> on Cell Cycle Progression, Apoptosis Induction Tyrosine- and CDC2-Kinase Activity in Oesophageal Cancer Cells, *Prostaglandins Leukot. Essent. Fatty Acids* 62, 75–84.
- Gelderblom, W.C.A., Smuts, C.M., Abel, S., Snyman, S.D., van der Westhuizen, L., Huber, W.W., and Swanevelder, S. (1997) Effect of Fumonisin B<sub>1</sub> on the Level and Fatty Acid Composition of Selected Lipids in Rat Liver *in vivo*, *Food Chem. Toxicol.* 35, 647–656.
- Gelderblom, W.C.A., Abel, S., Smuts, C.M., Marnewick, J., Marasas, W.F.O., Lemmer, E.R., and Ramljak, D. (2001) Fumonisin-Induced Hepatocarcinogenesis: Mechanisms Related to Cancer Initiation and Promotion, *Environ. Health Perspect.* 109, 291–300.
- Riley, R.T., Enongene, E., Voss, K.A., Norred, W.P., Meredith, F.I., Sharma, R.P., Spitsbergen, J., Williams, D.E., Carlson, D.B., and Merrill, A.H., Jr. (2001) Sphingolipid Perturbations as Mechanisms for Fumonisin Carcinogenesis, *Environ. Health Perspect.* 109, 301–308.
- Ramljak, D., Calvert, R.J., Wiesenfeld, P.W., Diwan, B.A., Catipovic, B., Marasas, W.F.O., Victor, T.C., Anderson, L.M., and Gelderblom, W.C.A. (2000) A Potential Mechanism for Fumonisin B<sub>1</sub>-Mediated Hepatocarcinogenesis: Cyclin D1 Stabilization Associated with Activation of Akt and Inhibition of GSK-3 $\beta$  Activity, *Carcinogenesis* 21, 1537–1546.
- Lemmer, E.R., de la Motte Hall, P., Omori, N., Omori, M., Shephard, E.G., Gelderblom, W.C.A., Cruse, J.P., Barnard, R.A., Marasas, W.F.O., Kirsch, R.E., and Thorgeirsson, S.S. (1999) Histopathology and Gene Expression Changes in Rat Liver During Feeding of Fumonisin B<sub>1</sub>, a Carcinogenic Mycotoxin Produced by *Fusarium moniliforme*, *Carcinogenesis* 20, 817–824.
- Cawood, M.E., Gelderblom, W.C.A., Vlegaar, R., Behrend, Y., Thiel, P.G., and Marasas, W.F.O. (1991) Isolation of the Fumonisin Mycotoxins—A Quantitative Approach, *Appl. Environ. Microbiol.* 39, 1958–1962.
- Koba, K., Wakamatsu, K., Obata, K., and Sugano, M. (1993) Effects of Dietary Proteins on Linoleic Acid Desaturation and Membrane Fluidity in Rat Liver Microsomes, *Lipids* 28, 457–464.
- De Antueno, R.J., Elliot, M., and Horrobin, D.F. (1994) Liver  $\Delta 5$  and  $\Delta 6$  Desaturase Activity Differs Among Laboratory Rat Strains, *Lipids* 29, 327–331.
- Smuts, C.M., Kruger, M., van Jaarsveld, P.J., Fincham, J.E., Schall, R., van der Merwe, K.J., and Benadè, A.J.S. (1992) The Influence of Fish Oil Supplementation on Plasma Lipoproteins and Arterial Lipids in Vervet Monkeys with Established Artherosclerosis, *Prostaglandins Leukot. Essent. Fatty Acids* 47, 129–138.
- Gilfillan, A.M., Chu, A.J., Smart, D.A. and Rooney, S.A. (1983) Single Plate Separation of Lung Phospholipids Including Disaturated Phosphatidylcholine, *J. Lipid Res.* 24, 1651–1656.
- Itaya, K., and Ui, M. (1966) A New Micromethod for the Colorimetric Determination of Inorganic Phosphate, *Clin. Chim. Acta* 14, 361–366.
- Mahler, S.M., Wilce, P.A., and Shanley, B.C. (1988) Studies on Regenerating Liver and Hepatoma Plasma Membranes—I. Lipid and Protein Composition, *Int. J. Biochem.* 20, 605–611.
- Abel, S., Smuts, C.M., de Villiers, C., and Gelderblom, W.C.A. (2001) Changes in Essential Fatty Acid Patterns Associated with Normal Liver Regeneration and the Progression of Hepatocyte Nodules in Rat Hepatocarcinogenesis, *Carcinogenesis* 22, 795–804.
- Nikolova-Karakashian, M.N., Gravrilova, N.J., Petkova, D.H., and Setchenska, M.S. (1991) Sphingomyelin-Metabolizing Enzymes and Protein Kinase C Activity in Liver Plasma Membranes of Rats Fed with Cholesterol-Supplemented Diet, *Biochem. Cell Biol.* 70, 613–616.
- Abel, S., and Gelderblom, W.C.A. (1998) Oxidative Damage and Fumonisin B<sub>1</sub>-Induced Toxicity in Primary Rat Hepatocytes and Rat Liver *in vivo*, *Toxicology* 131, 121–131.
- Sahu, S.C., Eppley, R.M., Page, S.W., Gray, G.C., Barton, C.N., and O'Donnell, M.W. (1998) Peroxidation of Membrane Lipids and Oxidative DNA Damage by Fumonisin B<sub>1</sub> in Isolated Rat Liver Nuclei, *Cancer Lett.* 125, 117–121.
- Yin, J.-J., Smith, M.J., Eppley, R.M., Page, S.W., and Sphon, J.A. (1998) Effects of Fumonisin B<sub>1</sub> on Lipid Peroxidation in Membranes, *Biochim. Biophys. Acta* 1371, 134–142.
- Bourre, J.M., Piciotti, M., and Dumont, O. (1990)  $\Delta 6$  Desaturase

- in Brain and Liver During Development and Aging, *Lipids* 25, 354–356.
28. Blond, J.-P., Henchiri, C., and Bézard, J. (1989)  $\Delta 6$  and  $\Delta 5$  Desaturase Activities in Liver from Obese Zucker Rats at Different Ages, *Lipids* 24, 389–395.
  29. Maniongui, C., Blond, J.P., Ulmann, L., Durand, G., Poisson, J.P., and Bézard, J. (1993) Age-Related Changes in  $\Delta 6$  and  $\Delta 5$  Desaturase Activities in Rat Liver Microsomes, *Lipids* 28, 291–297.
  30. Ulmann, L., Blond, J.P., Maniongui, C., Poisson, J.P., Durand, G., Bézard, J., and Pascal, G. (1991) Effects of Age and Dietary Essential Fatty Acids on Desaturase Activities and on Fatty Acid Composition of Liver Microsomal Phospholipids of Adult Rats, *Lipids* 26, 127–133.
  31. Leiken, A.I., and Brenner, R.R. (1989) Fatty Acid Desaturase Activities Are Modulated by Phytosterol Incorporation in Microsomes, *Biochim. Biophys. Acta* 1005, 187–191.
  32. Cawood, M.E., Gelderblom, W.C.A., Alberts, J.F., and Snyman, S.D. (1994) Interaction of <sup>14</sup>C-Labelled Fumonisin B Mycotoxins with Primary Rat Hepatocyte Cultures, *Food Chem. Toxicol.* 32, 627–632.
  33. Lang, M. (1976) Dietary Cholesterol Caused Modification in the Structure and Function of Rat Hepatic Micromes Studied by Fluorescent Probes, *Biochim. Biophys. Acta* 455, 947–960.
  34. Narbonne, J.F., Pelissier, M.A., Bonnamour, D., Borin, C., and Albrecht, R. (1984) Lipid Composition and Monooxygenase Relationship in Liver Microsomal Membranes from Rats Fed Unbalanced Diets, *Toxicol. Lett.* 23, 73–77.
  35. Savolainen, M.J., Arranto, A.J., Hassinen, I.E., Luoma, P.V., Pelkonen, R.O., and Sotaniemi, E.A. (1985) Relationship Between Lipid Composition and Drug Metabolizing Capacity of Human Liver, *Eur. J. Pharmacol.* 27, 727–732.
  36. Wade, A.E. (1986) Effects of Dietary Fat on Drug Metabolism, *J. Pathol. Toxicol. Oncol.* 6, 161–189.
  37. Rikans, L.E., and Notley B.A. (1982) Age-Related Changes in Hepatic Microsomal Drug Metabolism Are Substrate Selective, *J. Pharmacol. Exp. Ther.* 220, 574–578.
  38. Spotti, M., Maas, R.F.M., de Nijs, C.M., and Fink-Gremmels, J. (2000) Effect of Fumonisin B<sub>1</sub> on Rat Hepatic P450 System, *Environ. Toxicol. Pharmacol.* 8, 197–204.
  39. Martinez-Larranaga, M.R., Anadon, A., Diaz, M.J., Fernandez, R., Sevil, B., Fernandez-Cruz, M.L., Fernandez, M.C., Martinez, M.A., and Anton, R.M. (1999) Induction of Cytochrome P-4501A1 and P-4504A1 Activities and Peroxisomal Proliferation by Fumonisin B<sub>1</sub>, *Toxicol. Appl. Pharmacol.* 141, 185–194.
  40. Horrobin, D.F. (1994) Unsaturated Lipids and Cancer, in *New Approaches to Cancer Treatment: Unsaturated Lipids and Photodynamic Therapy* (Horrobin, D.F., ed.), pp. 3–64, Churchill Communications Europe, London.
  41. Tang, Q., Denda, A., Tsujiuchi, T., Tsutsumi, M., Amanuma, T., Murata, Y., Maruyama, H., and Konishi, Y. (1993) Inhibitory Effects of Inhibitors of Arachidonic Acid Metabolism on the Evolution of Rat Liver Preneoplastic Foci into Nodules and Hepatocellular Carcinomas With or Without Phenobarbital Exposure, *Jpn. J. Cancer Res.* 84, 120–127.

[Received March 27, 2002, and in revised form September 12, 2002; revision accepted October 2, 2002]

# The Assembly of Hepatic Very Low Density Lipoproteins: Evidence of a Role for the Golgi Apparatus

Klara Valyi-Nagy, Carla Harris, and Larry L. Swift\*

Department of Pathology, Vanderbilt University School of Medicine, Nashville, Tennessee 37232-2561

**ABSTRACT:** Previous studies from our laboratory have suggested that the assembly of lipoproteins by the liver is not completed in the rough endoplasmic reticulum but continues while the particles are *en route* to or within the Golgi apparatus. To investigate further the role of the Golgi apparatus in lipoprotein assembly, mice were injected with [<sup>3</sup>H]glycerol and killed 7.5 to 45 min after injection. Microsomes and Golgi apparatus-rich fractions were isolated from the livers and separated into membrane and content fractions. TG within microsomal and Golgi membranes were labeled, rapidly reaching peak specific activity within 7.5 min of isotope injection. The specific activity of TG in microsomal membranes decreased to approximately 40% of peak values by 45 min, whereas the specific activity of TG in the Golgi membranes decreased to approximately 30% of peak values by 45 min. To determine whether the turnover of the Golgi membrane TG pool was dependent on microsomal TG transfer protein (MTP), mice were gavaged with an MTP inhibitor, and the labeling experiments were repeated. Inhibition of MTP attenuated the turnover of newly synthesized Golgi membrane TG by approximately 50% and the turnover of microsomal membrane TG by approximately 40%. Based on the rapid turnover of the Golgi membrane TG pool and the attenuation of the turnover of this pool by MTP inhibitor, we propose that lipid is transferred from the Golgi membrane to luminal lipoproteins in an MTP-dependent manner. The results support our hypothesis that assembly of VLDL continues within the Golgi apparatus.

Paper no. L8950 in *Lipids* 37, 879–884 (September 2002).

A number of studies have suggested that the assembly of VLDL by the liver occurs *via* a two-step process (1–3). In this model, lipoprotein assembly is initiated in the rough endoplasmic reticulum (ER) with the synthesis of apolipoprotein B (apoB). The first step involves the association of apoB with phospholipids and core material, primarily cholesterol ester, to form a small HDL-like particle. In the second step additional core material, primarily TG, is added to the HDL-like particle to form a VLDL.

The two-step model implies that assembly is completed within the ER of the cell. However, considerable evidence

suggests that the Golgi apparatus plays more than a passive role in the assembly process (4–7). For example, Bamberger and Lane (4), in studies with chick hepatocytes, concluded that assembly of TG with apoproteins occurs in the Golgi. Likewise Higgins' studies in rat liver suggested that the *trans*-Golgi regions appeared to be the major intracellular sites of assembly of apoB with TG (5). More recent studies by Stillemark *et al.* (8) suggest that assembly of apoB-48-containing VLDL is not completed in the rough ER. Pulse-chase studies combined with subcellular fractionation showed that apoB-48 VLDL did not accumulate in the rough ER, indicating either that completed apoB-48 VLDL was rapidly transferred out of the ER or that assembly steps occurred post-ER. Previous studies in our laboratory suggest a critical role for the Golgi apparatus in the assembly process. By comparing the composition of nascent VLDL ( $d < 1.006$  g/mL) recovered from the rough ER with VLDL recovered from the Golgi apparatus-rich fractions of rat livers, we concluded that an additional assembly step occurs while the particles are *en route* to the Golgi apparatus or within the Golgi apparatus (9). We estimated that up to 50% of the total VLDL TG and 30–40% of the phospholipid are added after the particle leaves the rough ER. The source of the lipid and the mechanism by which lipid is added to the particles is unknown. More recent studies in our laboratory (10) have documented size heterogeneity of nascent VLDL within the Golgi apparatus of mouse liver. We reported that approximately 50% of the apoB within the lumen of mouse liver Golgi apparatus was associated with particles recovered in the  $d$  1.006–1.210 g/mL fraction. Furthermore, using radioisotope tracer studies we found that more than 80% of the newly synthesized apoB found in the serum was recovered with the VLDL fraction. This suggested that lipid is added to the nascent particles within the Golgi apparatus before secretion.

This study was undertaken to investigate further the role of the Golgi apparatus in the assembly of VLDL by the liver. *In vivo* lipid labeling experiments with [<sup>3</sup>H]glycerol have led to the identification of a pool of newly synthesized TG within hepatic Golgi membranes. This pool, distinct from the pools in the rough and smooth ER, has a rapid turnover rate. Furthermore, the turnover of this pool is attenuated in the presence of a microsomal TG transfer protein (MTP) inhibitor. We hypothesize that this pool of TG is derived from the ER membranes and is used in the lipidation of VLDL within the Golgi apparatus in an MTP-dependent process.

\*To whom correspondence should be addressed at Department of Pathology, C 3321 Medical Center North, Vanderbilt University School of Medicine, Nashville, TN 37232-2561. E-mail: larry.swift@mcm.vanderbilt.edu

Abbreviations: apoB, apolipoprotein B; DGAT, DAG acyltransferase; ER, endoplasmic reticulum; MTP, microsomal TG transfer protein.



## EXPERIMENTAL PROCEDURES

**Animals.** Male ICR mice (approximately 30 g) were purchased from Harlan Industries (Indianapolis, IN). The animals were maintained in the Vanderbilt University Animal Care facility on food (Wayne Lab Blox; Allied Mills, Inc., Chicago, IL) and water *ad libitum* for at least 5 but no longer than 10 d prior to the experiments. All procedures using mice were approved by the Animal Care and Use Committee at Vanderbilt University.

**Isolation of subcellular fractions.** Golgi apparatus-rich fractions were isolated from the mouse livers by the method of Swift *et al.* (10). Livers (usually three, with a total mass of 5–6 g) were minced finely with scalpels, placed in homogenizing buffer (1.5 mL/g) consisting of 0.1 M phosphate buffer, pH 7.3; 0.25 M sucrose; 1% dextran; and 0.01 M MgCl<sub>2</sub> and homogenized at a setting of 45 for 20 s using a Virtishear homogenizer. The homogenate from three livers was placed in one tube and centrifuged in an SW40 rotor at 900 × *g* for 10 min, at which point the speed was increased to 6,000 × *g* and the samples centrifuged an additional 30 min. The supernatant was discarded except when used for the isolation of microsomes (see below). Homogenizing buffer (1.7 mL) was then added to the pellet. The top one-third of the pellet was gently dislodged from the remainder of the pellet, resuspended, and layered on 8 mL of 1.2 M sucrose. The samples were centrifuged in the SW40 rotor at 3,300 × *g* for 10 min, after which the speed was increased to 13,000 × *g* for 10 min and finally increased to 83,000 × *g* for 45 min. The material banding on the 1.2 M sucrose pad was carefully removed, diluted with ice-cold distilled water, and pelleted using the SW40 rotor (6,000 × *g* for 30 min). The pellet was resuspended in 15 mM Tris and 0.154 M NaCl, pH 7.4, and the content and membrane fractions were recovered by sodium carbonate treatment followed by centrifugation as described below.

Microsomes were isolated by centrifugation of the first supernatant at 114,000 × *g* for 60 min using an SW41 rotor. The pellet was washed by resuspending it in PBS; it was then pelleted under the same conditions. The final microsomal pellet was resuspended in PBS, quick-frozen, and stored at –80°C.

Cytosolic fat was defined as the fat that floated during the initial isolation of microsomes. It was recovered from the top of the tube after tube slicing and washed in PBS under the same conditions as used for isolation.

**Separation of membrane and luminal content fractions.** Golgi and microsomal fractions were incubated on ice with an equal volume of 0.2 M sodium carbonate, pH 11.0, for 60 min (11). The final concentration of protein in the sample was approximately 0.5–1.0 mg/mL. The membranes were pelleted using an Optima TLX tabletop ultracentrifuge with a TLA 120.2 rotor (511,000 × *g*, 30 min). The supernatant was dialyzed against 0.154 M NaCl and 0.01% EDTA, pH 7.4, and was used to isolate luminal lipoproteins.

**Isolation of nascent subcellular and serum lipoprotein fractions.** The *d* < 1.006 g/mL fraction was isolated using the TLA 120.2 rotor. The samples were centrifuged for 3 h at 511,000

× *g*, and the top 250–300 μL was removed after tube slicing. The density of the infranatant was raised to 1.210 g/mL using solid KBr, and the *d* 1.006–1.210 g/mL fraction was floated by centrifuging for 4.5 h at 511,000 × *g* in the TLA 120.2 rotor. The top 250–300 μL was removed after tube slicing, and both the *d* < 1.006 and the *d* 1.006–1.210 g/mL fractions were dialyzed against 0.01% EDTA, pH 7.4, with a final change against distilled water prior to lyophilization. Serum lipoproteins were isolated at the same densities using the same conditions with the final fractions being dialyzed and lyophilized.

**Radioisotope incorporation studies.** Mice were anesthetized with ketamine/xylazine and injected *via* the retroorbital plexus with 25–30 μCi [2-<sup>3</sup>H]glycerol (16.5 Ci/mmol; NEN Life Science Products, Inc., Boston, MA). At 7.5, 15, 30, and 45 min after injection, the animals were killed by exsanguination from the inferior vena cava. The livers were removed, trimmed of excess fat and connective tissue, and rinsed. Subcellular fractions and nascent lipoproteins were isolated as described above. Aliquots of serum (100 μL) were taken for isolation of serum lipoprotein fractions as described above.

**MTP inhibitor studies.** MTP inhibitor (BMS 197636, kindly provided by R. Gregg, Bristol Myers Squibb, Princeton, NJ) was dissolved in 10% M-Pyrol (*N*-methyl-2-pyrrolidone) 80% water, 5% Cremophor EL, and 5% ethanol at a concentration of 6.25 mg/mL. The inhibitor was administered to mice by gavage (20 μg/g) 60 min prior to injection of [<sup>3</sup>H]glycerol. The remainder of the experiment was as described above. To establish the effectiveness of the MTP inhibitor, hepatic VLDL TG production rates were assessed using Triton WR1339 (12).

**Isolation of lipids.** Membrane and cytosolic fat fractions were delipidated using the method of Folch *et al.* (13). Lipoprotein fractions were delipidated using ethanol/ether (14). Neutral and polar lipids were separated using small silicic acid columns (15). Neutral lipids were separated into individual lipid classes by TLC on silica gel 60A thin-layer plates (Whatman K-6; Fisher Scientific, Atlanta, GA) with petroleum ether/ethyl ether/acetic acid (80:20:1, by vol) as the developing solvent. TG were scraped from the plate into scintillation vials. Scintillation fluid (Bio-Safe II; Research Products International Corp., Mount Prospect, IL) was added, and radioactivity was determined using a Beckman LS6800 scintillation counter.

**Analytical and enzymatic assays.** Protein was determined by the bicinchoninic acid method (Pierce, Rockford, IL), modified to eliminate interference by lipid (16) and using BSA as standard. TG were quantified using an enzymatic assay (Raichem, San Diego, CA) adapted to microtiter plates. Aliquots of the lipid fractions were dissolved in isopropanol, and 20 μL was added to each well. Water (80 μL) was added followed by 100 μL of the color reagent. Plates were incubated at 37°C for 10 min and read at 520 nm using a BioRad Model 550 microplate reader. The assay was linear from 0.5 to 10.0 μg TG. Glycerol was used as a standard.

**Statistics.** Data are presented as the mean ± SEM and were analyzed by an unpaired Student's *t*-test using GraphPad InStat (GraphPad Software, San Diego, CA).

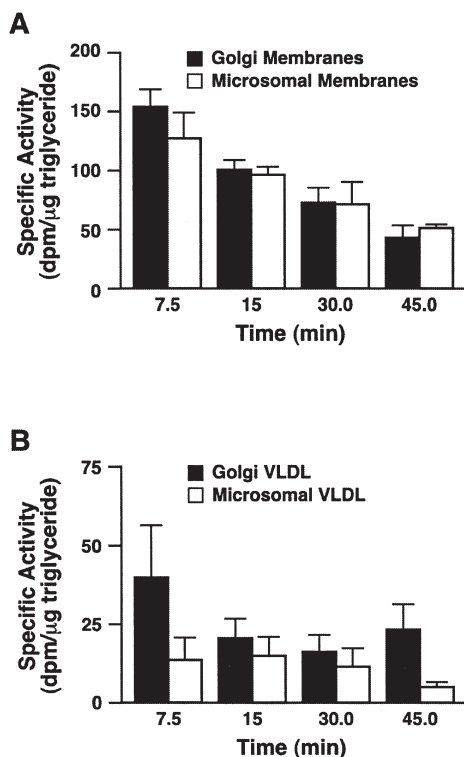


## RESULTS

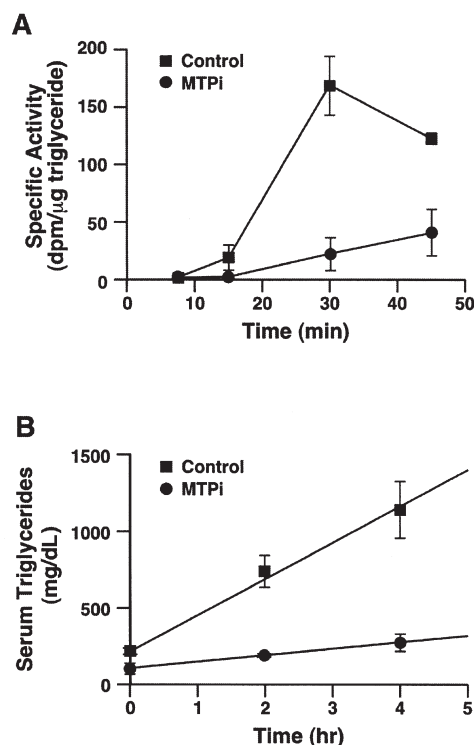
**[<sup>3</sup>H]Glycerol incorporation studies.** [<sup>3</sup>H]Glycerol was incorporated rapidly into Golgi and microsomal membrane TG, reaching peak specific activity in both membranes within 7.5 min of isotope injection (Fig. 1A). The specific activity of TG in the microsomal membranes decreased to approximately 40% of peak value by 45 min, while the specific activity of TG in Golgi membrane decreased to about 30% of peak value within the same time.

The appearance of labeled TG in Golgi VLDL followed a pattern similar to that of the TG within the Golgi membrane; however, the specific activity of Golgi VLDL TG was less than 50% of that in the Golgi membrane at each time point (Fig. 1B). The specific activity of TG in the  $d < 1.006$  g/mL lipoproteins recovered from the microsomal fraction remained relatively low with a peak near 15 to 30 min. The specific activity of the luminal TG was lower than in the membrane, similar to that observed in the Golgi. Labeled TG did not appear in the serum VLDL fraction until the 15-min time point, and increased to the 30-min time point, consistent with peak intracellular specific activity and its trafficking out of the cell (Fig. 2A).

**Incorporation of [<sup>3</sup>H]glycerol in MTP-inhibited animals.** The MTP inhibitor BMS 197636 was administered to mice



**FIG. 1.** Incorporation of [<sup>3</sup>H]glycerol into TG of mouse hepatic fractions. Mice were injected with 25–30 μCi [<sup>3</sup>H]glycerol, and hepatic fractions were isolated at different times after injection. Lipids were extracted, and TG mass and radioactivity were determined as described in the Experimental Procedures section. (A) Golgi and microsomal membranes; (B) Golgi and microsomal VLDL. Data represent the mean ± SEM. Golgi,  $n = 5$ ; microsomes,  $n = 4$ .

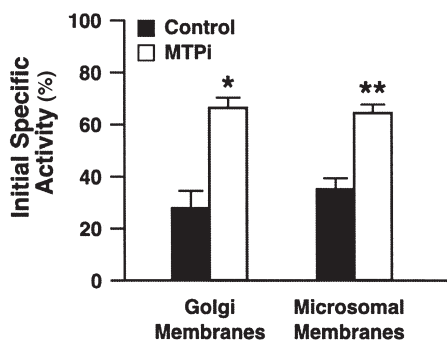


**FIG. 2.** Effects of the microsomal TG transfer protein (MTP) inhibitor BMS 197636 on hepatic TG production in mice. BMS 197636 was administered to mice by gavage (20 μg/g), and 60 min later [<sup>3</sup>H]glycerol was injected. The appearance of labeled TG in serum VLDL was monitored (A), and hepatic TG production was determined using the Triton method (B). Data represent the mean ± SEM. (A) Control,  $n = 3$ ; MTP inhibitor (MTPi),  $n = 3$ . (B) Control,  $n = 5$ ; MTPi,  $n = 3$ .

by gavage, and 60 min later hepatic TG production rates were determined. The MTP inhibitor decreased hepatic TG production rates by greater than 85% [ $127.4 \pm 4.7$  vs.  $17.1 \pm 5.9$  (mean ± SEM) μmol/kg/h,  $n = 3$ /group] (Fig. 2B). To verify the block in hepatic TG production, the inhibitor was given to mice and 60 min later [<sup>3</sup>H]glycerol was injected. Less than 5% of the radioactivity found in the serum VLDL of control animals was recovered in the MTP-inhibited mice, confirming the block of MTP activity and secretion of VLDL TG (Fig. 2A).

Inhibition of MTP did not affect the incorporation of newly synthesized TG into microsomal membranes, as the specific activity of the TG in these membranes at 7.5 min was identical to that found in the control (noninhibited) animals. However, inhibition of MTP did attenuate the turnover of newly synthesized TG in both the microsomal and Golgi membranes (Fig. 3). In microsomal membranes the turnover was reduced by approximately 40%, whereas in the Golgi membranes turnover was reduced nearly 50%.

The inhibitor dramatically altered the incorporation of newly synthesized TG into the cytosolic pool. In control animals the cytosolic TG pool reached peak specific activity approximately 30 min after [<sup>3</sup>H]glycerol injection (Fig. 4). In contrast, in animals given the inhibitor the specific activity of



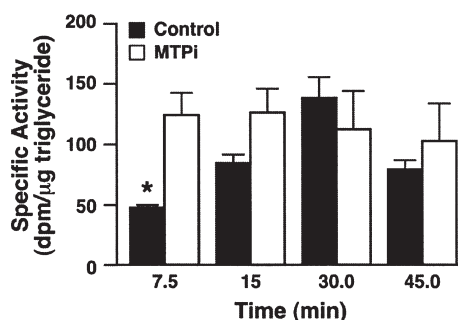
**FIG. 3.** Effects of the MTP inhibitor BMS 197636 on turnover of newly synthesized TG in microsomal and Golgi membranes. Control mice and mice given the BMS 197636 (20  $\mu\text{g/g}$ ) were injected with [ $2\text{-}^3\text{H}$ ]glycerol, and hepatic Golgi and microsomal membranes were isolated at 7.5 and 45 min postinjection. TG mass and radioactivity were determined as described in the Experimental Procedures section, and specific activity was calculated. The specific activity of TG at 45 min is expressed as percentage of specific activity at the 7.5-min time point. Data represent the mean  $\pm$  SEM. Control,  $n = 4$ ; MTPi  $n = 3$ . \* \*\*Significantly different from control at  $P = .007$  and  $.003$ , respectively. For abbreviations see Figure 2.

the cytosolic TG reached peak value within 7.5 min, and the specific activity at this time point was identical to the specific activity at 30 min in the control animals (Fig. 4). In addition, the specific activity of the cytosolic TG in the presence of the inhibitor remained constant over the experimental period, suggesting little movement out of this pool.

**Hepatic membrane and cytosol TG content.** Golgi membranes recovered after sodium carbonate treatment and release of luminal lipoproteins contained over twice as much TG as membranes recovered from microsomal fractions ( $P = 0.0004$ ) (Table 1). Inhibition of MTP led to a significant decrease in the amount of TG in the Golgi membrane and a slight, but not significant, increase in the amount of TG in the microsomal membrane. The cytosolic TG pool increased more than 130% when MTP was inhibited. It is important to note that in these studies MTP was inhibited from 67.5 to 105 min.

## DISCUSSION

A growing body of evidence suggests that the assembly of VLDL is not completed within the ER of the cell but continues *en route* to or within the Golgi apparatus (8,10,17). Previ-



**FIG. 4.** Incorporation of [ $^3\text{H}$ ]glycerol into TG in the cytosolic pool. Control mice and mice given the MTP inhibitor (BMS 197636, 20  $\mu\text{g/g}$ ) were injected with [ $2\text{-}^3\text{H}$ ]glycerol, and hepatic cytosolic fat was isolated at various times postinjection. TG mass and radioactivity were determined, and specific activity was calculated. Data are expressed as mean  $\pm$  SEM. Control,  $n = 4$ ; MTPi,  $n = 4$ . \*Significantly different from control at  $P < .005$ . For abbreviations see Figure 2.

ous studies from our laboratory have indicated that as much as 50% of the TG and 30% of the phospholipid may be added in the Golgi apparatus of the cell (9). More recent studies from our laboratory have identified a population of apoB-containing HDL within the Golgi apparatus of mouse liver that are apparently secreted as VLDL, suggesting that neutral lipid is added within the Golgi apparatus (10). The results presented here provide additional evidence for a direct role of the Golgi apparatus in the assembly process. Our studies demonstrate the presence of a pool of newly synthesized TG within the membranes of the Golgi apparatus. Based on membrane protein, the level of TG within this membrane is greater than that in the membrane of the ER (Table 1). The turnover of TG in the Golgi membrane pool is rapid and is similar to that found with the TG in the membrane of the microsomal fraction. Furthermore, the turnover of this Golgi membrane pool is attenuated by the MTP inhibitor BMS 197636. We suggest that this pool of TG is used in the lipidation of lipoproteins within the Golgi apparatus in an MTP-dependent process.

The presence of TG within Golgi membranes is not a new finding. Hebbachi and Gibbons (18) incubated rat hepatocytes for 4 h in the presence of labeled oleate and glycerol and reported that the membranes of both *cis*- and *trans*-Golgi were more heavily labeled with TG than those of the rough or smooth ER. The *trans*-Golgi membrane had nearly twice as

**TABLE 1**  
TG Content of Hepatic Fractions<sup>a</sup>

Group	Golgi membranes (mg/mg protein)	Microsomal membranes (mg/mg protein)	Cytosol ( $\mu\text{g/g}$ liver)
Control	0.062 $\pm$ 0.007 <sup>a,b</sup>	0.027 $\pm$ 0.003 <sup>a</sup>	198.0 $\pm$ 13.0 <sup>c</sup>
MTP inhibited	0.031 $\pm$ 0.004 <sup>b</sup>	0.032 $\pm$ 0.004	461.2 $\pm$ 42.9 <sup>c</sup>

<sup>a</sup>Data represent the mean  $\pm$  SEM from eight preparations. Values with the same roman superscript are significantly different at the following  $P$  values: <sup>a</sup>0.0004; <sup>b</sup>0.0007; <sup>c</sup><0.0001.

much labeled TG per mg subcellular vesicle protein as the smooth ER membrane and almost 10 times as much as the rough ER membrane. The *cis*-Golgi membrane contained about the same amount of labeled TG as the smooth ER membrane but eight times as much as the rough ER. Our studies demonstrate that the mass of TG in the Golgi membrane per mg protein is two to three times that found in the membranes of the rough and smooth ER (Table 1). Since TG is not a structural component of membranes and since the Golgi membrane is not recognized as a major site of TG synthesis, the presence of this amount of TG within the Golgi membrane led to questions about its origins and disposition. To address these questions, kinetic studies with radioisotopic tracers were performed.

The labeling kinetics of the Golgi membrane TG were similar to those found with microsomal membranes (Fig. 1). A number of studies have shown that TG is synthesized in the ER and trafficks primarily to the cytosol, although some may enter the VLDL assembly pathway (19,20). Our results suggest that newly synthesized TG also trafficks to the Golgi membrane, yet the pathway by which this occurs is unknown. It is unlikely that the Golgi membrane TG derives from the cytosolic pool since the specific activity of the Golgi pool is higher than that of the cytosol at the early time points. Furthermore, we have been unable to document significant level of DAG acyltransferase (DGAT) activity in Golgi membranes. The presence of DGAT in the Golgi membrane might be expected if TG were transported from the cytosolic pool *via* a process of hydrolysis and subsequent re-esterification analogous to that occurring with the ER (21). It seems most likely that the transfer of membrane TG from the ER to the Golgi occurs *via* vesicular transport (22,23). Moreau *et al.* (24), using an *in vitro* transfer assay, reported that little labeled TG was transferred to the Golgi fractions (24). However, their results were collected using an *in vitro* system in which lipid transfer was less than 1% of the total lipids. Transfer *in vivo* may be quite different.

Previous studies from our laboratory (9) led us to conclude that as much 50% of the VLDL TG may be added to nascent lipoproteins in the Golgi apparatus. The finding of newly synthesized TG within the Golgi membrane led us to hypothesize that this TG serves as a pool for addition to nascent lipoproteins. The mechanism by which this TG is added to nascent Golgi lipoproteins is unknown, but there is evidence that MTP may be present in *cis*- and *trans*-Golgi fractions of liver (18,25,26). In addition, a recent study demonstrates the presence of MTP in the Golgi apparatus of rat enterocytes (27).

We then studied the effects of MTP inhibition on the synthesis of TG and distribution of newly synthesized TG within the liver. Prior to initiating these studies, we demonstrated that rates of hepatic TG output, as measured using the Triton method, were reduced by more than 85% when mice were given the inhibitor at a dose of 20  $\mu\text{g/g}$  body weight (Fig. 2B). In addition, our radioisotope incorporation studies were consistent with the Triton studies, demonstrating a marked reduction in the amount of newly synthesized TG appearing in the serum pool over the 45-min time period (Fig. 2A).

The inactivation of MTP led to a doubling of the cytosolic TG pool and a slight, albeit statistically insignificant, increase in the microsomal membrane TG pool (Table 1). In contrast, the pool of TG in the Golgi membrane was decreased by nearly 40% when MTP was inactivated. As might be predicted, inhibition of MTP blocked the entry of newly synthesized TG into the lumen of the ER (data not shown). Surprisingly, in the presence of the inhibitor the specific activity of the cytosolic TG reached its peak more rapidly than in control samples, and the specific activity of this pool remained constant over the 45-min period (Fig. 4). These data suggest that inhibition of TG transfer to the lumen of the ER leads to more rapid transfer of newly synthesized TG into the cytosolic pool. Furthermore, the fact that the specific activity of this pool remained constant over the 45-min time period suggests that the inactivation of MTP blocks the transfer of TG from the cytosol to the ER membrane. Hebbachi and Gibbons (18) reported a similar result in studies with rat hepatocytes. They suggested that MTP inhibition blocks the transfer of cytosolic TG to the ER membrane by a route that involves the luminal leaflet of the ER membrane. As noted, this would cause an accumulation of TG not only in cytosol but also in the ER membrane. It is also possible that the inhibition of MTP affects the hydrolysis of TG in the cytosolic pool or even its re-esterification within the ER membrane. The decrease in TG in the Golgi membrane in relation to the increased TG in the ER membrane is an important finding. It suggests that if Golgi membrane TG does derive from ER membranes, this process is not a simple blebbing of the ER but must involve some sorting, as suggested by Moreau *et al.* (24), and the MTP alters or inhibits the sorting or transport in some manner.

Inhibiting MTP not only decreased the TG in the Golgi membrane but also attenuated the turnover of newly synthesized Golgi membrane TG (Fig. 3), which suggests that MTP may play a role in the transfer of TG from the Golgi membrane to its contents. Hebbachi *et al.* (25) reported that inhibiting MTP with BMS 200150 resulted in a delayed removal of apoB-100 and apoB-48 from the Golgi membranes, and Hebbachi and Gibbons (18) showed a delayed removal of newly synthesized TG from the membranes of *cis*- and *trans*-Golgi. Alternatively, inhibiting MTP could block the assembly of lipoprotein in the ER, leading to a decrease in lipoproteins in the Golgi apparatus. The transfer of TG from the Golgi membrane to nascent lipoproteins within the Golgi complex would then also be blocked because of a lack of acceptor lipoproteins within the lumen. In this case, the direct involvement of MTP within the Golgi apparatus would not be required. Regardless of the mechanism, the results support a role for the Golgi apparatus in adding lipid (TG) to nascent lipoproteins. Although our studies do not permit us to differentiate between occurrences in the *cis*- or *trans*-Golgi, it is possible that the lipidation occurs early within the Golgi apparatus as suggested by Cartwright and Higgins (7). Indeed, if MTP is located within the Golgi complex by way of escape from the ER, we might expect it to be found within the *cis* Golgi elements.

These studies provide additional evidence that the Golgi apparatus participates in the assembly of nascent lipoproteins by the liver. The finding of a pool of newly synthesized TG within the Golgi membrane fraction provides a plausible mechanism by which lipid is added to nascent lipoproteins. Our finding that the inhibition of MTP attenuates the turnover of the Golgi membrane TG pool further supports the hypothesis that this pool is involved in lipoprotein assembly within the Golgi. The pathway by which TG is delivered to the Golgi membranes and the precise mechanisms by which lipid is added to the particles being formed are under study.

## ACKNOWLEDGMENTS

This work was supported by National Institutes of Health grants, HL57984 and DK26657. We gratefully acknowledge Richard Gregg, Bristol Myers-Squibb, for the generous gift of MTP inhibitor and John Wetterau, Bristol Myers-Squibb, for helpful comments in the preparation of the manuscript.

## REFERENCES

- Alexander, C.A., Hamilton, R.L., and Havel, R.J. (1976) Subcellular Localization of B Apoprotein of Plasma Lipoproteins in Rat Liver, *J. Cell Biol.* 69, 241–263.
- Boren, J.S., Rustaeus, S., and Olofsson, S.-O. (1994) Studies on the Assembly of Apolipoprotein B-100 and B-48-Containing Very Low Density Lipoproteins in McA-RH7777 Cells, *J. Biol. Chem.* 269, 25879–25888.
- Olofsson, S.-O., Asp, L., and Borén, J. (1999) The Assembly and Secretion of Apolipoprotein B-Containing Lipoproteins, *Curr. Opin. Lipidol.* 10, 341–346.
- Bamberger, M., and Lane, M. (1990) Possible Role of the Golgi Apparatus in the Assembly of Very Low Density Lipoprotein, *Proc. Natl. Acad. Sci. USA* 87, 2390–2394.
- Higgins, J. (1988) Evidence That During Very Low Density Lipoprotein Assembly in Rat Hepatocytes Most of the Triacylglycerol and Phospholipid Are Packaged with Apolipoprotein B in the Golgi Complex, *FEBS Lett.* 232, 405–408.
- Boström, K., Borén, J., Wettsten, M., Sjöberg, A., Bondjers, G., Wiklund, O., Carlsson, P., and Olofsson, S.-O. (1988) Studies on the Assembly of ApoB-100-Containing Lipoproteins in HepG2 Cells, *J. Biol. Chem.* 263, 4434–4442.
- Cartwright, I., and Higgins, J. (1995) Intracellular Events in the Assembly of Very Low Density Lipoprotein Lipids with Apolipoprotein B in Isolated Rabbit Hepatocytes, *Biochem. J.* 310, 897–907.
- Stillemark, P., Borén, J., Andersson, M., Larsson, T., Rustaeus, S., Karlsson, K.-A., and Olofsson, S.-O. (2000) The Assembly and Secretion of Apolipoprotein B-48-Containing Very Low Density Lipoproteins in McA-RH7777 Cells, *J. Biol. Chem.* 275, 10506–10513.
- Swift, L.L. (1995) The Assembly of Very Low Density Lipoprotein in Rat Liver: A Study of Nascent Particles Recovered from the Rough Endoplasmic Reticulum, *J. Lipid Res.* 36, 395–406.
- Swift, L.L., Valyi-Nagy, K., Rowland, C., and Harris, C. (2001) Assembly of Very Low Density Lipoproteins in Mouse Liver: Evidence for Heterogeneity of Particle Density in the Golgi Apparatus, *J. Lipid Res.* 42, 218–224.
- Fujiki, Y., Hubbard, A.L., Fowler, S., and Lazarow, P.B. (1982) Isolation of Intracellular Membranes by Means of Sodium Carbonate Treatment: Application to Endoplasmic Reticulum, *J. Cell Biol.* 93, 97–102.
- Swift, L.L., Farkas, M.H., Major, A.S., Valyi-Nagy, K., Linton, M.F., and Fazio, S. (2001) A Recycling Pathway for Resecretion of Internalized Apolipoprotein E in Liver Cells, *J. Biol. Chem.* 276, 22965–22970.
- Folch, J., Lees, M., and Sloane Stanley, G.H. (1957) A Simple Method for the Isolation and Purification of Total Lipides from Animal Tissues, *J. Biol. Chem.* 226, 497–509.
- Bersot, T., Brown, W., Levy, R., Windmueller, H., Fredrickson, D., and LeQuire, V. (1970) Further Characterization of the Apolipoproteins of Rat Plasma Lipoproteins, *Biochemistry* 9, 3427–3433.
- Dittmer, J., and Wells, M. (1969) Quantitative and Qualitative Analysis of Lipids and Lipid Components, *Methods Enzymol.* 14, 482–530.
- Morton, R., and Evans, T. (1992) Modification of the Bicinchoninic Acid Protein Assay to Eliminate Lipid Interference in Determining Lipoprotein Protein Content, *Anal. Biochem.* 204, 332–334.
- Asp, L., Claesson, C., Borén, J., and Olofsson, S.-O. (2000) ADP-Ribosylation Factor 1 and Its Activation of Phospholipase D Are Important for the Assembly of Very Low Density Lipoproteins, *J. Biol. Chem.* 275, 26285–26292.
- Hebbachi, A.-M., and Gibbons, G. (1999) Inactivation of Microsomal Triglyceride Transfer Protein Impairs the Normal Redistribution but Not the Turnover of Newly Synthesized Glycerolipid in the Cytosol, Endoplasmic Reticulum and Golgi of Primary Rat Hepatocytes, *Biochim. Biophys. Acta* 1441, 36–50.
- Gibbons, G.F., and Wiggins, D. (1995) Intracellular Triacylglycerol Lipase: Its Role in the Assembly of Hepatic Very-Low-Density Lipoprotein (VLDL), *Adv. Enzyme Regul.* 35, 179–198.
- Salter, A.M., Wiggins, D., Sessions, V.A., and Gibbons, G.F. (1998) The Intracellular Triacylglycerol/Fatty Acid Cycle: A Comparison of Its Activity in Hepatocytes Which Secrete Exclusively Apolipoprotein (apo) B<sub>100</sub> Very-Low-Density Lipoprotein (VLDL) and in Those Which Secrete Predominantly apoB<sub>48</sub> VLDL, *Biochem. J.* 332, 667–672.
- Gibbons, G.F., Islam, K., and Pease, R.J. (2000) Mobilisation of Triacylglycerol Stores, *Biochim. Biophys. Acta* 1483, 37–57.
- Bannykh, S., and Balch, W. (1998) Selective Transport of Cargo Between the Endoplasmic Reticulum and Golgi Compartments, *Histochem. Cell Biol.* 109, 463–475.
- Palade, G.E. (1975) Intracellular Aspects of the Process of Protein Transport, *Science* 189, 347–354.
- Moreau, P., Rodriguez, M., Cassagne, C., Morré, D.M., and Morré, D.J. (1991) Trafficking of Lipids from the Endoplasmic Reticulum to the Golgi Apparatus in a Cell-Free System from Rat Liver, *J. Biol. Chem.* 266, 4322–4328.
- Hebbachi, A.-M., Brown, A.-M., and Gibbons, G. (1999) Suppression of Cytosolic Triacylglycerol Recruitment for Very Low Density Lipoprotein Assembly by Inactivation of Microsomal Triglyceride Transfer Protein Results in a Delayed Removal of apoB-48 from Microsomal and Golgi Membranes of Primary Rat Hepatocytes, *J. Lipid Res.* 40, 1758–1768.
- White, D., Bennett, A., Billett, M., and Salter, A. (1998) The Assembly of Triacylglycerol-Rich Lipoproteins: An Essential Role for the Microsomal Triacylglycerol Transfer Protein, *Br. J. Nutr.* 80, 219–229.
- Levy, E., Stan, S., Delvin, E., Menard, D., Shoulders, C., Garofalo, C., Slight, I., Seidman, E., Mayer, G., and Bendayan, M. (2002) Localization of Microsomal Triglyceride Transfer Protein in the Golgi, *J. Biol. Chem.* 277, 16470–16477.

[Received October 13, 2001, and in revised form June 13, 2002; revision accepted September 18, 2002]



# Destabilizing Effects of Fructose-1,6-bisphosphate on Membrane Bilayers

William D. Ehringer<sup>a,\*</sup>, Susan Su<sup>a</sup>, Benjamin Chiang<sup>b</sup>, William Stillwell<sup>c</sup>, and Sufan Chien<sup>b</sup>

Departments of <sup>a</sup>Physiology and Biophysics and <sup>b</sup>Surgery, University of Louisville, School of Medicine, Louisville, Kentucky 40292, and <sup>c</sup>Department of Biology, Purdue University School of Science, Indianapolis, Indiana 46254

**ABSTRACT:** Fructose-1,6-bisphosphate (FBP) is a high-energy glycolytic intermediate that decreases the effects of ischemia; it has been used successfully in organ perfusion and preservation. How the cells utilize external FBP to increase energy production and the mechanism by which the molecule crosses the membrane bilayer are unclear. This study examined the effects of FBP on membrane bilayer permeability, membrane fluidity, phospholipid packing, and membrane potential to determine how FBP crosses the membrane bilayer. Large unilamellar vesicles composed of egg phosphatidylcholine (Egg PC) were made and incubated with 50 mM FBP spiked with <sup>14</sup>C-FBP at 30°C. Uptake of FBP was significant ( $P < 0.05$ ) and dependent on the lipid concentration, suggesting that FBP affects membrane bilayer permeability. With added calcium (10 mM), FBP uptake by lipid vesicles decreased significantly ( $P < 0.05$ ). Addition of either 5 or 50 mM FBP led to a significant increase ( $P < 0.05$ ) in Egg PC carboxyfluorescein leakage. We hypothesized that the membrane-permeabilizing effects of FBP may be due to a destabilization of the membrane bilayer. Small unilamellar vesicles composed of dipalmitoyl pC (DPPC) were made containing either diphenyl-1,3,5-hexatriene (DPH) or trimethylammonia-DPH (TMA-DPH) and the effects of FBP on the fluorescence anisotropy (FA) of the fluorescent labels examined. FBP caused a significant decrease in the FA of DPH in the liquid crystalline state of DPPC ( $P < 0.05$ ), had no effect on FA of TMA-DPH in the liquid crystalline state of DPPC, but increased the FA of TMA-DPH in the gel state of DPPC. From phase transition measurements with DPPC/DPH or TMA-DPH, we calculated the slope of the phase transition as an indicator of the cooperativity of the DPPC molecules. FBP significantly decreased the slope, suggesting a decrease in fatty acyl chain interaction ( $P < 0.05$ ). The addition of 50 mM FBP caused a significant decrease ( $P < 0.05$ ) in the liquid crystalline/gel state fluorescence ratio of merocyanine 540, indicating increased head-group packing. To determine what effects these changes would have on cellular membranes, we labeled human endothelial cells with the membrane potential probe 3,3'-dipropylthiacarbocyanine iodide (DiSC<sub>3</sub>) and then added FBP. FBP caused a significant, dose-dependent decrease in DiSC<sub>3</sub> fluorescence, indicating membrane depolarization. We suggest that FBP destabilizes membrane bilayers by decreasing fatty acyl chain interaction, leading to significant increases in

membrane permeability that allow FBP to diffuse into the cell where it can be used as a glycolytic intermediate.

Paper no. L9024 in *Lipids* 37, 885–892 (September 2002).

Fructose-1,6-bisphosphate (FBP) has been proposed to enhance ATP production during ischemia and has shown its effectiveness in certain ischemic conditions, such as hemorrhagic, cardiogenic, and endotoxin shock (1,2), extremity ischemia (3), hypoxic brain and intestine injury (4–7), coronary occlusion (8), agent-induced tissue toxicity (9–11), isolated heart perfusion (12–15), left ventricular dysfunction (16,17), and hypothermic renal and liver preservation (18,19). Results from our laboratory indicated that when FBP was added to St. Thomas solution, rat heart preservation time was also increased (20,21). It is theorized that the mechanism by which FBP exerts its effects is by a direct metabolic enhancement. During periods of prolonged ischemia, glycolysis becomes the primary mechanism for ATP production. The reasoning behind the use of FBP for tissue protection during ischemia is that if FBP could cross the membrane bilayer, FBP would bypass the two ATP-depleting steps of glycolysis and thus double glycolytic ATP production. However, there is no known receptor for FBP (22), and the two phosphate groups of FBP have classically been thought to make the molecule unlikely to cross the membrane bilayer.

Recently, we showed that FBP can pass through membrane bilayers and cellular membranes (23). We also showed that FBP can increase the metabolism of cardiomyocytes once inside the cell (24). Several other studies have indicated that FBP can cross membrane bilayers. Hardin and Roberts (25) have shown by NMR spectroscopy of hog carotid artery segments that externally applied <sup>13</sup>C-FBP is metabolized. A similar finding was reported by Espanol *et al.* (26) using <sup>13</sup>C-FBP in neonatal rat brain slices. However, the permeability of FBP through the membrane bilayer has been questioned in several studies. For example, Roig *et al.* (27) suggested that FBP does not cross the cellular membrane but rather FBP alters potassium flux, which in turn decreases ATP demand by the cell. The decrease in potassium flux by FBP was also documented in a study by Galzigna and Rigobello (28). Clearly, there is no real consensus on how externally applied FBP can enter cells and supplement or preserve ATP levels.

The low permeability of FBP through cellular membrane bilayers is in part due to the high degree of hydration and the low solubility of FBP within the membrane interior. Thus, it is

\*To whom correspondence should be addressed at Department of Physiology and Biophysics, University of Louisville, HSC Bldg. A, Room 1110, 500 South Preston St., Louisville, KY 40292.

E-mail: wdehri01@gwise.louisville.edu

Abbreviations: DiSC<sub>3</sub>, 3,3'-dipropylthiacarbocyanine iodide; DPH, 1,6-diphenyl-1,3,5-hexatriene; DPPC, dipalmitoylphosphatidylcholine; Egg PC, egg phosphatidylcholine; FBP, fructose-1,6-bisphosphate; MC540, merocyanine 540; TMA-DPH, 1-(4-trimethylammoniumphenyl)-1,6-phenyl-1,3,5-hexatriene *p*-toluenesulfonate.

highly unlikely under normal circumstances that FBP would readily pass through the membrane bilayer by simple diffusive mechanisms. However, if the membrane bilayer were somehow destabilized, the hydrophobic barrier of the membrane bilayer would be changed and the permeability of water-soluble compounds would increase. One intriguing finding is that FBP is a potent calcium and divalent ion chelator (29). If high extracellular concentrations of FBP could chelate the counterbalancing ions that interact with the phospholipid head groups of the membrane bilayer, then this interaction could lead to substantial changes in membrane stability. In fact, substances that affect the counterbalancing ions that stabilize membrane bilayers previously have been shown to alter membrane stability (30). Thus, FBP could potentially destabilize membrane bilayers and allow the compound to cross the membrane bilayer by simple diffusive mechanisms. The goal of the following study is to examine how FBP destabilizes membrane bilayers and what effect the destabilization has on the diffusion of the compound across the membrane bilayer into the cytosol of the cell.

## MATERIALS AND METHODS

**Materials.** Dipalmitoylphosphatidylcholine (DPPC) and egg phosphatidylcholine (Egg PC) were purchased from Avanti Polar Lipids (Alabaster, AL) and used without further purification. The fluorescent probes, 1,6-diphenyl-1,3,5-hexatriene (DPH), 1-(4-trimethylammoniumphenyl)-1-6-phenyl-1,3,5-hexatriene *p*-toluenesulfonate (TMA-DPH), merocyanine 540 (MC540), carboxyfluorescein, and 3,3'-dipropylthiadicarbocyanine iodide (DiSC<sub>3</sub>) were purchased from Molecular Probes (Eugene, OR). Fructose, fructose-1-phosphate, fructose-6-phosphate, <sup>14</sup>C-FBP, and FBP were purchased from Sigma Chemical Company (St. Louis, MO). Human umbilical vein endothelial cells and EGM culture media were purchased from BioWhittaker Corp (Walkersville, MD).

**Lipid vesicle preparation.** DPPC, dissolved in chloroform, and lipid-soluble fluorescent probes (DPH and TMA-DPH) were dried under a stream of nitrogen gas onto the side of a glass test tube. Traces of chloroform were removed by vacuum pumping for a period of 12 h. The dried lipid material was hydrated in buffer above the phase transition of DPPC at 50°C for 30 min. The hydrated lipid material was vortexed for 5 min with two glass beads to form multilamellar vesicles. For the fluorescence anisotropy studies and carboxyfluorescein leakage studies, the multilamellar vesicles were sonicated using a Branson Sonifier 450 tip-type sonicator for 4 min at a 40% duty cycle, output level 6, creating small unilamellar vesicles. For the MC540 studies of lipid packing, the lipid vesicles were extruded through 0.2 μm Nucleopore filters using an Avanti Polar Lipids Extruder. The lipids were passed through the filters 20 times to create large unilamellar vesicles.

**Carboxyfluorescein leakage.** DPPC (20 mg/mL) small unilamellar vesicles were made in the presence of 60 mM carboxyfluorescein, 30 mM KCl, and 10 mM Na<sub>2</sub>HPO<sub>4</sub>; pH 7.4. The lipid vesicles were passed down a pre-swollen Sephadex column equilibrated with 90 mM KCl, 10 mM Na<sub>2</sub>HPO<sub>4</sub>, pH

7.4, to remove nonsequestered carboxyfluorescein. The eluted vesicles were kept on ice to minimize leakage of the carboxyfluorescein until experimentation. The vesicles were injected (25 μL) into 2 mL of one of three buffers: 0.5 mM FBP/89.5 mM KCl/10 mM Na<sub>2</sub>HPO<sub>4</sub>; 5 mM FBP/85 mM KCl/10 mM Na<sub>2</sub>HPO<sub>4</sub>; 50 mM FBP/40 mM KCl/10 mM Na<sub>2</sub>HPO<sub>4</sub> (all pH 7.4) at 50°C. In some experiments the FBP was replaced with an equivalent concentration of fructose-6-phosphate, fructose-1-phosphate, or fructose. The leakage of trapped carboxyfluorescein from the vesicles was monitored for a period of 7 min using a PerkinElmer LS50B Luminescence Spectrophotometer. The excitation was at 495 nm, and the emission was followed at 520 nm. The rate of carboxyfluorescein leakage, expressed as the change in fluorescent intensity over time, is directly proportional to the leakage of the carboxyfluorescein anion through the membrane bilayer. At the conclusion of each experiment, the vesicles were lysed with 2% Triton X-100 to release the remaining trapped carboxyfluorescein, and the final fluorescence after detergent addition was measured to achieve the percent carboxyfluorescein leakage.

**Fluorescence anisotropy.** Small unilamellar vesicles of DPPC containing DPH or TMA-DPH (800:1 lipid/probe ratio) were made in the presence of either 5 mM FBP/20 mM Na<sub>2</sub>HPO<sub>4</sub>, 50 mM FBP/20 mM Na<sub>2</sub>HPO<sub>4</sub>, 5 mM fructose/20 mM Na<sub>2</sub>HPO<sub>4</sub>, or 50 mM FBP/20 mM Na<sub>2</sub>HPO<sub>4</sub>, all pH 7.4. The vesicles were placed in quartz cuvettes with a small magnetic stir bar into a PerkinElmer LS50B. The cuvette chamber was thermally controlled by use of a Haak circulating water pump. The initial temperature of the chamber was 30°C. The G-factor, or grating factor, was calculated to correct for instrumental artifacts. Fluorescence anisotropy of the DPPC/DPH or DPPC/TMA-DPH solution was determined using horizontal and vertical polarizers mounted in a PerkinElmer Fast Filter Accessory using FL WinLab software. The temperature of the lipid vesicle solution was changed every 10 min in 2°C increments until the final temperature of 50°C was obtained. The heating ramp of the Haak circulator was kept constant during the experiment to ensure that the phase transition measurements were not an artifact of heating. The slope of the phase transition of DPPC was determined from the fluorescence anisotropy measurements. This value was calculated by measuring the change in anisotropy from 35 to 45°C.

**MC540 measurements of lipid packing.** DPPC large unilamellar vesicles were made in the presence of either 50 mM FBP/20 mM Na<sub>2</sub>HPO<sub>4</sub> or 50 mM fructose/20 mM Na<sub>2</sub>HPO<sub>4</sub> pH 7.4. The lipid vesicles were injected into a solution of MC540 (10 μg/mL) buffered with 20 mM Na<sub>2</sub>HPO<sub>4</sub>, pH 7.4. The lipids and MC540 were incubated above the phase transition temperature of DPPC (50°C) for a period of 1 h. The lipid/MC540 solution was placed into a PerkinElmer LS50B Luminescence Spectrophotometer. The DPPC/MC540 solution was excited at 540 nm, and the emission of the MC540 was measured from 570 to 650 nm. The temperature of the lipid solution was varied from 25 to 55°C, and at each temperature an emission scan of the MC540 was determined. The emission of MC540 at 593 nm is considered a measure of liq-

uid-crystalline-like lipid environment, whereas the emission of MC540 at 620 nm is a measure of gel state-like environment. Thus, the ratio of MC540 emission intensities at 593 nm/620 nm is indicative of the degree of lipid packing.

**Membrane potential measurements.** Human umbilical vein endothelial cells were grown on six-well culture plates for 3 d until confluence. The cells were gently trypsinized from the dish and washed 3× in Hank's Balanced Salt Solution (pH 7.4). The endothelial cells were incubated with the membrane potential-sensitive probe DiSC<sub>3</sub> for a period of 20 min. The cells were then exposed to increasing concentrations of FBP or fructose and the fluorescence of DiSC<sub>3</sub> followed.

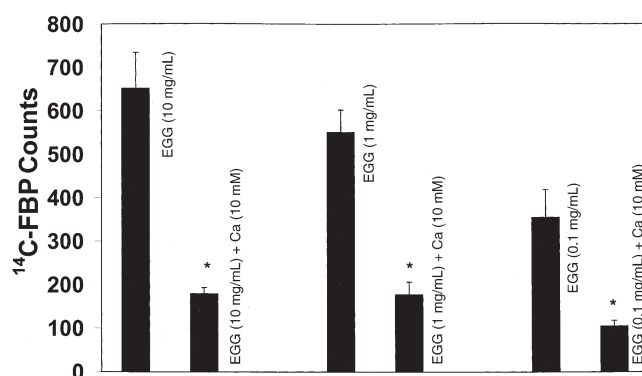
**Uptake of FBP by lipid vesicles.** Large unilamellar vesicles composed of Egg PC were made by lipid vesicle extrusion at 30°C. The final concentration of lipid was either 10, 1, or 0.1 mg/mL. The lipid vesicles were placed in an isosmotic solution containing 50 mM FBP spiked with 0.1 μCi <sup>14</sup>C-FBP. The vesicles were kept at 30°C by means of a circulating water bath. The vesicles and FBP were incubated for a period of 1 h, after which the vesicles were pelleted by ultracentrifugation. The pellet was washed 3× in an isosmotic buffer, and the radioactivity in the pellet was measured by liquid scintillation. In some experiments we added 10 mM calcium chloride to the FBP solution in order to examine the effects of calcium on the uptake of FBP.

**Statistical analysis.** The data in each experiment were first evaluated by ANOVA for repeated measurements using a two-factor analysis. When significant *F* values were encountered by ANOVA, the Student–Newman–Keuls' multiple-range test was used to determine which groups differed significantly from the others. Differences were considered statistically significant when *P* < 0.05. Statistical analysis was done with commercially available software (SigmaStat, Version 1.01; Jandel Corp., San Rafael, CA).

## RESULTS

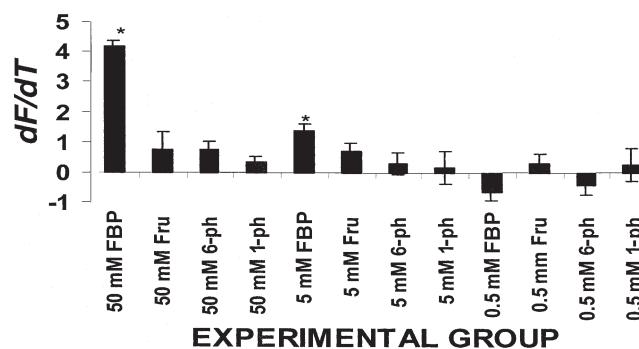
In the first experiment, we examined the uptake of <sup>14</sup>C-FBP by lipid vesicles composed of Egg PC at 30°C. The vesicles were incubated with 50 mM FBP for a period of 1 h, after which the radioactivity in the vesicles was measured. Increasing the lipid concentration of Egg PC resulted in increased uptake of the FBP inside the lipid vesicles (Fig. 1). Because FBP uptake might be affected by calcium, we examined how extravesicular calcium might alter the uptake of FBP. When the FBP was supplemented with 10 mM calcium chloride, the increase in FBP uptake in the Egg PC vesicles was significantly reduced.

In the next experiment, we examined the effects of FBP on membrane permeability. Small unilamellar vesicles composed of DPPC were made with a self-quenching concentration of carboxyfluorescein. In this assay, any change in membrane permeability causes the self-quenched carboxyfluorescein to leak out of the lipid vesicle into the external milieu where the carboxyfluorescein becomes highly fluorescent. The rate of fluorescence increase over time is indicative of heightened mem-



**FIG. 1.** The uptake of fructose-1,6-bisphosphate (FBP) by lipid vesicles composed of egg phosphatidylcholine (Egg PC: 0.1, 1, and 10 mg/mL) at 30°C. Large unilamellar vesicles were made and placed in a solution containing 50 mM FBP + <sup>14</sup>C-FBP (0.1 μCi). The vesicles were then exposed to 10 mM calcium chloride to determine how excess calcium affected uptake of FBP. FBP uptake was dependent on lipid concentration, and the uptake was significantly inhibited by the addition of calcium. The results are the mean radioactivity detected in 10 different samples. \*Significantly different from Egg PC at the same lipid concentration as tested by ANOVA (*P* < 0.05). Error bars represent SD.

brane permeability. The DPPC lipid vesicles containing carboxyfluorescein were exposed to increasing concentrations of FBP, fructose-6-phosphate, fructose-1-phosphate, or fructose (Fig. 2). The addition of 0.5 mM FBP had no effect on carboxyfluorescein leakage. However, 5 and 50 mM FBP caused significant changes in membrane permeability to carboxyfluorescein. In contrast, neither fructose-6-phosphate, fructose-1-phosphate, nor fructose had any effect on DPPC membrane bilayer permeability at any concentration examined. After completion of the experiment, Triton X-100 was mixed with the vesicles to determine percent leakage. The percent leakage for the 50 mM FBP group was 9.8% after Triton application.

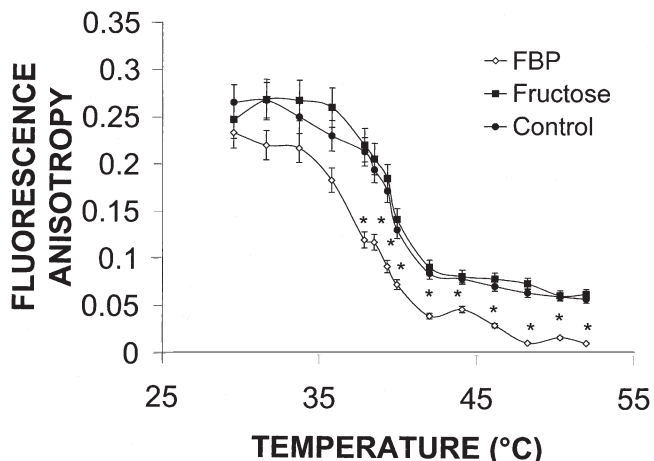


**FIG. 2.** FBP increases membrane permeability to carboxyfluorescein. Small unilamellar vesicles composed of dipalmitoylphosphatidylcholine (DPPC) were made in the presence of carboxyfluorescein. After removing the nonsequestered carboxyfluorescein, the vesicles were placed into cuvettes containing either FBP, fructose-1-phosphate (1-ph), fructose-6-phosphate (6-ph) or fructose (Fru) (45°C). The concentrations tested were 0.5, 5, and 50 mM, each osmotically balanced by addition of KCl. The addition of 5 and 50 mM FBP caused a significant increase in the leakage of trapped carboxyfluorescein. *dF/dT* = change in fluorescence/change in time (s). \*Significantly different from Fru, 1-ph, and 6-ph, as tested by ANOVA (*P* < 0.05). *n* = 7. Error bars represent SD. For abbreviation see Figure 1.

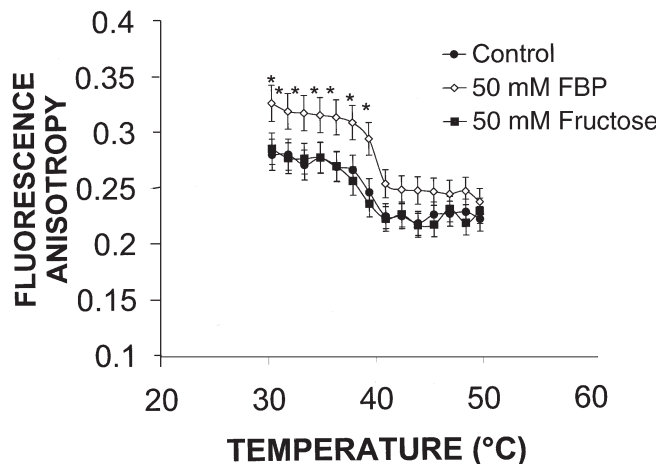


We hypothesized that the membrane permeability changes brought about by FBP could be the result of increased membrane fluidity (order). To examine this hypothesis, we made DPPC small unilamellar vesicles containing either DPH or TMA-DPH. DPH is a fluorescent probe that monitors membrane anisotropy changes in the fatty acyl chain region of the bilayer, whereas the amphipathic TMA-DPH measures anisotropy changes near the head group region of the bilayer. DPPC has a well-defined phase transition that occurs at 41.7°C. We measured fluorescence anisotropy of DPH in DPPC lipid vesicles from 28 to 50°C in the presence of either 50 mM FBP or 50 mM fructose (Fig. 3). The addition of FBP caused a significant decrease in membrane fluorescence anisotropy of DPH from 42 to 50°C (liquid crystalline state), indicating a more disordered lipid environment. FBP also broadened and lowered the phase transition of DPPC, which did not occur with an equimolar concentration of fructose. In contrast, fructose had no effect on DPPC membrane order within the same temperature span. We likewise examined the effects of 50 mM FBP and 50 mM fructose on DPPC membrane order using TMA-DPH (Fig. 4). Neither FBP nor fructose had any effect on the fluorescence anisotropy of TMA-DPH in the liquid crystalline state of DPPC. In the gel state of DPPC (28–40°C), FBP did cause a slight but significant increase in membrane order, which did not occur with fructose.

The slope of the phase transition, which is a measure of fatty acyl chain interaction during the main phase transition of DPPC, is derived by measuring the slope of the phase transition from 35 to 45°C. As the slope of the transition decreases, the degree of fatty acyl chain interaction decreases. From the phase transition measurements made in Figures 3 and 4, the slope of the transition was determined and plotted in Figure 5.



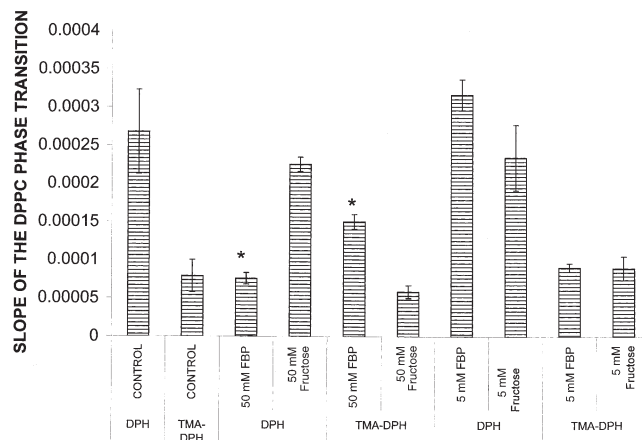
**FIG. 3.** FBP causes a decrease in fluorescence anisotropy of 1,6-diphenyl-1,3,5-hexatriene (DPH) in the liquid-crystalline state of DPPC. DPPC small unilamellar vesicles containing DPH were made in the presence of either 50 mM FBP, 50 mM fructose, or buffer (control). Fluorescence anisotropy measurements of DPH in DPPC were made from 28 to 50°C. The presence of FBP caused a significant decrease in the fluorescence anisotropy of DPH from 42 to 50°C. In contrast, fructose had no effect on DPH fluorescence anisotropy over the same temperature span. \*Significantly different from fructose and control as tested by ANOVA ( $P < 0.05$ ).  $n = 6$ . Error bars represent SD. For other abbreviations see Figures 1 and 2.



**FIG. 4.** FBP increases the fluorescence anisotropy of 1-(4-trimethylammoniumphenyl)-1,6-phenyl-1,3,5-hexatriene *p*-toluenesulfonate (TMA-DPH) in the gel state of DPPC. DPPC small unilamellar vesicles containing TMA-DPH were made in the presence of either 50 mM FBP, 50 mM fructose, or buffer (control). Fluorescence anisotropy of TMA-DPH in DPPC was made from 28 to 50°C. The presence of TMA-DPH caused a significant increase in the fluorescence anisotropy of TMA-DPH from 28 to 40°C. In contrast, neither fructose nor the control had any effect on the fluorescence anisotropy of TMA-DPH. \*Significantly different from fructose and control as tested by ANOVA ( $P < 0.05$ ).  $n = 6$ . Error bars represent SD. For abbreviations see Figures 1 and 2.

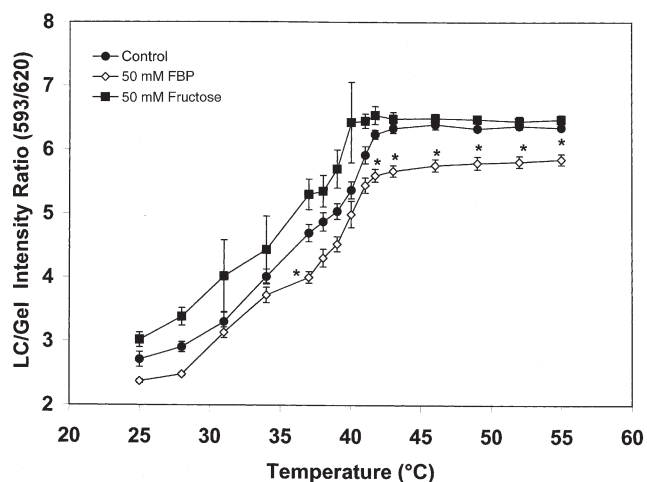
The presence of 50 mM FBP caused a significant decrease in the slope of the transition as measured by DPH. In contrast, 5 mM FBP had no effect on the slope of the DPPC transition. Furthermore, the slope of the phase transition as measured by TMA-DPH was unaffected by any concentration of FBP or fructose.

The changes in membrane bilayer parameters noted in Figures 2–5 suggest that the effects of FBP occur primarily in the



**FIG. 5.** The slope of the phase transition of DPPC suggests that 50 mM FBP decreases fatty acyl chain interaction. The slope of the phase transition of DPPC shown in Figures 3 and 4 was determined and is shown. The presence of 50 mM FBP decreased the slope of the transition in DPPC/DPH vesicles compared to fructose. In contrast, 50 mM FBP had no effect on the slope of the DPPC transition when monitored with TMA-DPH. Furthermore, 5 mM FBP had no effect on the slope of the phase transition. \*Significantly different from control and fructose as tested by ANOVA ( $P < 0.05$ ). Error bars represent SD. For abbreviations see Figures 1, 2, and 4.





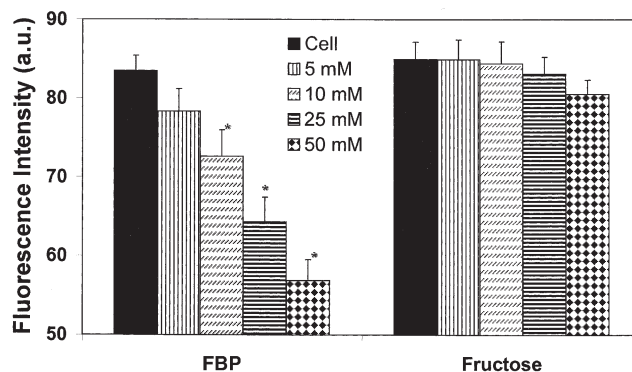
**FIG. 6.** FBP decreases the liquid crystalline (LC)/gel ratio of merocyanine 540 (MC540) in DPPC. DPPC large unilamellar vesicles were made in the presence of 50 mM FBP, 50 mM fructose, or buffer only (control). The fluorescence of MC540 at 593 nm (liquid-crystalline-like state) and at 620 nm (gel-like state) were measured from 25 to 55°C. FBP decreased the 593 nm/620 nm ratio, indicating a more densely packed membrane. In contrast, fructose had no effect on the MC540 593 nm/620 nm ratio. \*Significantly different from fructose and control as tested by ANOVA ( $P < 0.05$ ).  $n = 10$ . Error bars represent SD. For abbreviations see Figures 1 and 2.

fatty acyl chain region. To verify this finding, we utilized the phase-sensitive fluorescent probe MC540, which undergoes a shift in its emission maxima in response to changes in membrane phase. The emission of MC540 at 593 nm is indicative of a liquid crystalline environment, whereas the emission at 620 nm is indicative of a more gel-state membrane bilayer. DPPC lipid vesicles were made in the presence of FBP or fructose, incubated with MC540, and then the fluorescence emission maxima at 593 and 620 nm were determined (Fig. 6). The fluorescence ratio of 593 nm/620 nm (liquid crystalline/gel ratio) of MC540 in DPPC from 28 to 50°C is shown. The presence of FBP caused a significant decrease in the 593 nm/620 nm ratio.

If FBP causes significant changes in membrane permeability and destabilizes the membrane bilayer, it could have drastic effects on membrane potential. To examine this hypothesis, we grew human umbilical vein endothelial cells to confluence, and then removed them from their dishes by gentle trypsinization. The cells were incubated with the fluorescent membrane potential-sensitive dye DiSC<sub>3</sub>. The endothelial cells were placed in a cuvette, FBP or fructose was added to the cells, and the fluorescence of DiSC<sub>3</sub> was measured (Fig. 7). On addition of FBP, there was a concentration-dependent decrease in DiSC<sub>3</sub> fluorescence, indicating a decrease in membrane polarization. In contrast, fructose failed to achieve the same decreases in fluorescence of the DiSC<sub>3</sub>.

## DISCUSSION

FBP is a high-energy glycolytic intermediate that has been used with good success to supplement glycolysis during prolonged periods of ischemia. The theory that substantiates the



**FIG. 7.** FBP causes a significant decrease in membrane polarization of human umbilical vein endothelial cells as measured by 3,3'-dipropylthiadicarbocyanine iodide (DiSC<sub>3</sub>). Human umbilical vein endothelial cells were grown to confluence, removed from their dish, and incubated with the membrane potential fluorescent probe DiSC<sub>3</sub>. Upon addition of FBP, there was a stepwise decrease in DiSC<sub>3</sub> fluorescence, indicating a decrease in membrane polarization. \*Significantly different from fructose and control as tested by ANOVA ( $P < 0.05$ ).  $n = 8$ . Error bars represent SD. For other abbreviation see Figure 1.

use of FBP is that if the molecule could cross the membrane bilayer, it could double glycolytic ATP production. However, there has been a controversy within the literature regarding the mechanism responsible for the movement of FBP across the membrane bilayer. Since there is no known receptor for FBP (22), it is unlikely that the molecule moves across *via* a protein channel. Several theories have been suggested to explain how FBP crosses the membrane bilayer or supplements glycolysis. These have included the use of a dicarboxylate transporter (31), hydrolysis of the phosphate groups (26), and decrease in potassium flux and thus decreased ATP demand (27). However, what makes for an interesting argument is that when <sup>13</sup>C-FBP was added to cells, <sup>13</sup>C-lactate was detected (7), and that FBP crossed the membrane bilayer of lipid vesicles (23,24). Perhaps the most confusing issue regarding how FBP crosses the membrane bilayer is the widely held biochemical theory that phosphorylated sugars such as FBP do not readily diffuse through membrane bilayers. The purpose of this study was to examine the effects of FBP on membrane bilayers. The findings from this study show that FBP destabilizes the membrane bilayer by causing loss of fatty acyl chain interaction. We theorize that the loss of fatty acyl chain interaction is likely caused by the chelating effects of FBP on membrane calcium since FBP is a known divalent chelator (18). The destabilization of the membrane bilayer decreases hydrophobic interactions leading to increased membrane permeability, allowing FBP to diffuse down its concentration gradient into the cell.

No studies to date have examined the effects of FBP on membrane bilayer properties, mainly because the assumption is that FBP cannot pass through membrane bilayers. In fact, a number of studies have ignored the idea that FBP can directly have any effect on cellular ATP levels, mainly because it is assumed that FBP cannot cross the membrane bilayer (22). For example, Bickler and Buck (32) suggest that FBP cannot

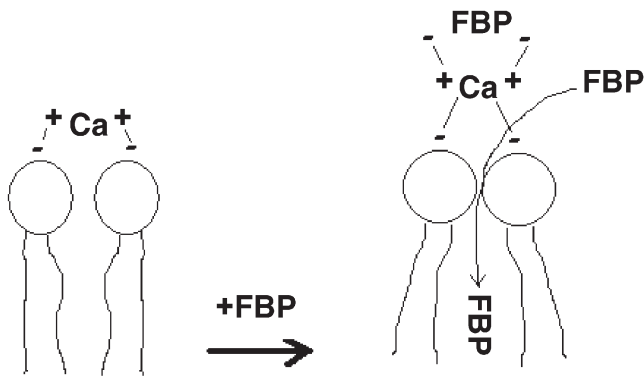
cross the membrane bilayer (although they show no evidence for this statement), but that exogenous FBP preserves ATP levels and decreases glutamate release. An earlier study by Galzigna and Rigobello (28) clearly states that the effects of FBP on proton and potassium flux "cannot, in fact, be explained on the basis of a penetration of the compound through the cell membranes, which is not possible," but affects these ions by some unknown mechanism. In support of the idea that FBP could have an effect on membrane bilayers, Hardin and Roberts (25) have shown that FBP crosses the cell membrane and is metabolized to lactate. They also theorized that FBP could cross the membrane bilayer by creating "polar discontinuities," allowing FBP to diffuse across the membrane bilayer. However, they offered no proof that would show that FBP creates polar discontinuities within the membrane bilayer, nor did they offer a mechanism to explain how FBP crosses the membrane bilayer.

When we examined the effects of FBP on the fluorescence anisotropy of DPH and TMA-DPH, we found that FBP caused some significant changes in the membrane bilayer (Figs. 3–5). Our studies indicate that FBP decreased the fluorescence anisotropy of DPH in DPPC vesicles in the liquid-crystalline state, whereas FBP had no effect on TMA-DPH fluorescence anisotropy in the liquid crystalline state of DPPC. One of the significant findings from this segment of the study was that FBP decreased the slope of the phase transition of DPPC, suggesting that DPPC fatty acyl chain interaction had decreased in the presence of FBP (Fig. 5). We also found that FBP caused the fluorescence of MC540 (a phase-sensitive fluorescent probe) to shift to a more predominant 620 nm reading (Fig. 6). This finding suggests that FBP causes the phospholipid head groups to become more condensed. One very plausible explanation of the data is that FBP causes the polar head groups to become more closely packed (MC540 data), which in turn increases the intramolecular distance between adjacent fatty acyl chains (DPH data). This drastic change in membrane structure could have significant effects on the barrier properties of the membrane bilayer to water-soluble substances such as FBP.

Cellular membrane bilayers are a complex mixture of lipids, proteins, and carbohydrates. The permeability of any substance through the membrane bilayer is a function of several different parameters including, but not limited to, M.W., lipid solubility of the agent, fatty acyl chain composition of the membrane bilayer, and the presence of integral membrane proteins. In the case of FBP, the M.W., charge, and degree of hydration would argue against the molecule passively diffusing through the membrane bilayer to any significant extent. In the case of glucose, the permeability (in the absence of any protein carrier) of the membrane bilayer to this substance is relatively small compared to more hydrophobic substances with similar M.W. (33). Thus, the long-held idea that FBP should not cross the membrane bilayer by diffusive mechanisms is substantiated by the literature. However, the idea that the permeability of the membrane bilayer to FBP should be relatively low does not take into account the chelating prop-

erties of FBP, especially when high external concentrations of FBP are utilized. Recently, it was shown that FBP could decrease the extracellular calcium concentration by up to 47% (29). Interestingly, when we exposed endothelial cells to histamine (a known intracellular calcium-elevating agent) we found an 80% decrease in intracellular calcium in the presence of 5 mM FBP (Ehringer, W.D., Chiang, B., and Chien, S., unpublished results). The chelation of calcium can have a measurable effect on cell membrane bilayer structure. For example, when extracellular calcium is elevated, nonbilayer structures can form as detected by  $^{31}\text{P}$  NMR (34). Trauble and Eibl found that only small changes in ionic environment can result in gross alterations in bilayer structure. Specifically, they found that divalent cations stabilized membrane bilayer structure. This same group has hypothesized that lowering extracellular cation levels could result in membrane destabilization, mainly because the tightly held counterbalancing ions help stabilize the membrane bilayer (35). Interestingly, removal of extracellular calcium can destabilize the membrane bilayer and cause loss of phospholipid head-group interaction (30). The loss of head-group interaction could lead to significant increases in membrane permeability as the destabilized phospholipids become less tightly packed. When we exposed lipid vesicles to FBP and extracellular calcium, we found a significant decrease in the uptake of FBP (Fig. 1). The fact that these vesicles lack any carrier protein argues strongly that the penetration of FBP into cells is likely the result of membrane destabilization, most likely due to chelation of membrane calcium. Furthermore, in the current study it was demonstrated that the uptake of FBP was increased by increasing the lipid concentration. This finding suggests that FBP alters membrane bilayer properties in proportion to the amount of lipid, which may explain how FBP can enter into cells.

One of the significant findings of this study is that FBP, a water-soluble molecule, can passively diffuse through membrane bilayers. The importance of this finding in the fields of organ preservation, tissue preservation, and ischemia needs to be addressed. The amount of FBP that can passively move through the membrane bilayers determined in the current study is relatively small (about 0.3% of the total FBP; see Fig. 1). However, the significance of the amount that is moving through when compared to the internal cellular concentration of FBP is considerable. It previously has been shown that FBP inside a cell is about 1.2  $\mu\text{M}$  (29). Thus, in our experiments with FBP we have demonstrated that as much as 75–150  $\mu\text{M}$  FBP can enter the cell. This is nearly a 60-fold increase in the normal level of FBP. For organ or tissue preservation during periods of low oxygen, this level of FBP would be more than sufficient to sustain glycolysis during low-oxygen periods. However, there appears to be a point of diminishing returns in terms of the amount of FBP that can be added, as evidenced by our membrane potential studies (Fig. 7). As the concentration of FBP is increased, there are significant changes in membrane depolarization. At doses above 10 mM FBP, the changes in membrane permeability



**FIG. 8.** Simplistic mechanism that may explain the calcium-chelating effects of FBP and the changes in membrane bilayer properties noted in the current study. Because FBP can compete with the phospholipid head groups for calcium, the head groups become stressed inward, resulting in increased head-group packing and decreased acyl chain interaction. The decrease in acyl chain group interaction leads to increased permeability to FBP. For abbreviation see Figure 1.

could result in the loss of substantial levels of intracellular ions and membrane potential.

Our findings indicate that FBP can increase acyl chain mobility in the liquid crystalline state (Fig. 3) and also increase head-group packing (Figs. 4, 6). When coupled with the ideas that the effects of FBP on membrane permeability are affected by calcium and that FBP is a known calcium chelator, the following model can be hypothesized (Fig. 8). FBP has been shown previously to chelate calcium (29). When FBP is added to cell membrane bilayers, the calcium that is used to stabilize phospholipid head groups is in direct competition with the chelating effects of FBP. In an attempt to compensate for the competition for calcium, the head groups bend inward to prevent the removal of calcium bound to the bilayer (Figs. 4, 6). This torque on the membrane head groups results in an increase in acyl chain area in the bilayer normal. Because the acyl chains are now more distant from one another, the disorder of the membrane increases, and hence the permeability increases (Figs. 1–3, 7).

The findings of the current study indicate that externally applied FBP can have dramatic effects on membrane bilayer stability. Externally applied FBP increases the fluorescence anisotropy of DPH and decreases the cooperativity of the phase transition. Since DPH mainly detects anisotropy changes in the membrane interior, it is hypothesized that fatty acyl chain interaction is decreased and the fluidity of the bilayer in this region is increased. Using the phase-sensitive fluorescent probe MC540, we have shown that FBP also causes the polar head groups of the membrane bilayer to become more closely spaced. These two pieces of data show that FBP affects membrane stability. The decrease in membrane stability in the presence of FBP allows the normally nonpermeant FBP to diffuse passively across the membrane bilayer. Once inside the cell, FBP could be used to increase glycolysis and thus decrease the effects of ischemia by doubling anaerobic ATP production.

## ACKNOWLEDGMENTS

This study was supported in part by grants from the National Institutes of Health (HL 64186); the American Heart Association, Ohio Valley Affiliate (9808447W); the University of Louisville Competitive Enhancement Grant (628404), and a grant from the Jewish Hospital Foundation of Louisville.

## REFERENCES

1. Markov, A.K., Turner, M.D., Oglethorpe, N., Neely, W.A., and Hellems, H.K. (1981) Fructose-1,6-bisphosphate: An Agent for Treatment of Experimental Endotoxin Shock, *Surgery* 90, 482–488.
2. Markov, A.K., Oglethorpe, N., Young, D.B., and Hellems, H.K. (1981) Irreversible Hemorrhagic Shock: Treatment and Cardiac Pathophysiology, *Circ Shock* 8, 9–19.
3. Cacioli, D., Clivati, A., Pelosi, P., Megevand, J., and Galeone, M. (1988) Hemorheological Effects of Fructose-1,6 Diphosphate in Patients with Lower Extremity Ischemia, *Curr. Med. Res. Opin.* 10, 668–674.
4. Farias, L.A., Smith, E.E., and Markov, A.K. (1990) Prevention of Ischemic-Hypoxic Brain Injury and Death in Rabbits with Fructose-1,6-diphosphate, *Stroke* 21, 606–613.
5. Sola, A., Berrios, M., Sheldon, R.A., Ferriero, D.M., and Gregory, G.A. (1996) Fructose-1,6-bisphosphate After Hypoxic Ischemic Injury Is Protective to the Neonatal Rat Brain, *Brain Res.* 741, 294–299.
6. Kelleher, J.A., Chan, T.Y.Y., Chan, P.H., and Gregory, G.A. (1996) Protection of Astrocytes by Fructose-1,6-bisphosphate and Citrate Ameliorates Neuronal Injury Under Hypoxic Conditions, *Brain Res.* 726, 167–173.
7. Juergens, T.M., and Hardin, C.D. (1996) Fructose-1,6-bisphosphate as a Metabolic Substrate in Hog Ileum Smooth Muscle During Hypoxia, *Mol. Cell Biochem.* 154, 83–93.
8. Janz, T.G., Leasure, J., and Olson, J.E. (1991) The Effects of Fructose-1,6-diphosphate on Myocardial Damage in Acute Coronary Artery Occlusion, *Resuscitation* 22, 45–54.
9. Danesi, R., Bernardini, N., Marchetti, A., Vernardini, M., Tacca, and M.D. (1990) Protective Effects of Fructose-1,6 Diphosphate on Acute and Chronic Doxorubicin Cardiotoxicity in Rats, *Cancer Chemother. Pharmacol.* 25, 326–332.
10. Cardoso, L.R., Santos, O.F.P., Boim, M.A., Barros, E.G., Ajzen, H., and Schor, N. (1996) Fructose-1,6 Diphosphate: Potential Protection in Cyclosporine-Induced Renal Impairment, *Nephron* 72, 67–71.
11. Rao, M.R., Olinde, K.D., and Markov, A.K. (1997) Protection from Amphotericin B-Induced Lipid Peroxidation in Rats by Fructose-1,6 Diphosphate, *Res. Commun. Mol. Pathol. Pharmacol.* 95, 217–220.
12. Starnes, J.W., Seiler, K.S., Bowles, D.K., Giardina, B., and Lazzarino, G. (1992) Fructose-1,6-bisphosphate Improves Efficiency of Work in Isolated Perfused Rat Hearts, *Am. J. Physiol.* 262, H380–H384.
13. Takeuchi, K., Hung, C.D., Friehs, I., Glynn, P., D'Agostino, D., Simplaceanu, E., McGowan, F.X., and del Nido, P.J. (1998) Administration of Fructose-1,6-diphosphate During Early Reperfusion Significantly Improves Recovery of Contractile Function in the Postischemic Heart, *J. Thorac. Cardiovasc. Surg.* 116, 335–343.
14. Nuutinen, E.M., Lazzarino, G., Giardina, B., and Hassinen, I.E. (1991) Effect of Exogenous Fructose-1,6-bisphosphate on Glycolysis in the Isolated Perfused Rat Heart, *Am. Heart J.* 122, 523–527.
15. Lazzarino, G., Nuutinen, M.E., Tavazzi, B., Cerroni, L., Di Piero, D., and Giardina, B. (1991) Preserving Effect of Fructose-1,6-bisphosphate on High-Energy Phosphate Compounds

- During Anoxia and Reperfusion in Isolated Langendorff-Perfused Rat Hearts, *J. Mol. Cell Cardiol.* 23, 13–23.
16. Munger, M.A., Botti, R.E., Grinblatt, M.A., and Kasmer, R.J. (1994) Effect of Intravenous Fructose-1,6-diphosphate on Myocardial Contractility in Patients with Left Ventricular Dysfunction, *Pharmacotherapy* 14, 522–528.
  17. Markov, A.K., Brumley, M.A., Figueroa, A., Skelton, T.N., and Lehan, P.H. (1997) Hemodynamic Effects of Fructose-1,6 Diphosphate in Patients with Normal and Impaired Left Ventricular Function, *Am. Heart J.* 133, 541–549.
  18. Herrero, I., Torras, J., Carrera, M., Castells, A., Pasto, L., Gil-Vernet, S., Alsina, J., and Grinyo, J.M. (1995) Evaluation of a Preservation Solution Containing Fructose-1,6-diphosphate and Mannitol Using the Isolated Perfused Rat Kidney. Comparison with Euro-Collins and University of Wisconsin Solutions, *Nephrol. Dial. Transplant.* 10, 519–526.
  19. Torras, J., Borobia, F.G., Herrero, I., Carrera, M., Riera, M., Bartrons, R.R., Figueras, J., Alsina, J., Cruzado, J.M., Jaurrieta, E., et al. (1995) Hepatic Preservation with a Cold-Storage Solution Containing Fructose-1,6-diphosphate and Mannitol: Evaluation with the Isolated Perfused Rat Liver and Comparison with University of Wisconsin Solution, *Transplant Proc.* 27, 2379–2381.
  20. Niu, W., Zhang, F., Ehringer, W., Tseng, M., Gray, L., and Chien, S. (1999) Enhancement of Hypothermic Heart Preservation with Fructose-1,6-diphosphate, *J. Surg. Res.* 85, 120–129.
  21. Chien, S., Zhang, F., Niu, W., Ehringer, W., Chiang, B., Shi, X., and Gray, L.A., Jr. (2000) Fructose-1,6-diphosphate and a Glucose-Free Solution Enhances Functional Recovery in Hypothermic Heart Preservation, *J. Heart Lung Transplant.* 19, 277–285.
  22. Rigobello, M.P., Bianchi, M., Deana, R., and Galzigna, L. (1982) Interaction of Fructose-1,6-diphosphate with Some Cell Membranes, *Agressologie* 23, 63–66.
  23. Ehringer, W.D., Niu, W., Chiang, B., Wang, O.L., Gordon, L., and Chien, S. (2000) Membrane Permeability of Fructose-1,6-diphosphate in Lipid Vesicles and Endothelial Cells, *Mol. Cell. Biochem.* 210, 35–45.
  24. Ehringer, W.D., Chiang, B., and Chien, S. (2001) The Uptake and Metabolism of Fructose-1,6-diphosphate in Rat Cardiomyocytes, *Mol. Cell. Biochem.* 221, 33–40.
  25. Hardin, C.D., and Roberts, T.M. (1994) Metabolism of Exogenously Applied Fructose-1,6-bisphosphate in Hypoxic Vascular Smooth Muscle, *Am. J. Physiol.* 267, H2325–H2332.
  26. Espanol, M.T., Litt, L., Hasegawa, K., Chang, L.H., Macdonald, J.M., Gregory, G., James, T.L., and Chan, P.H. (1998) Fructose-1,6-bisphosphate Preserves Adenosine Triphosphate but Not Intracellular pH During Hypoxia in Respiring Neonatal Rat Brain Slices, *Anesthesiology* 88, 461–472.
  27. Roig, T., Bartrons, R., and Bermudez, J. (1997) Exogenous Fructose-1,6-bisphosphate Reduces K<sup>+</sup> Permeability in Isolated Rat Hepatocytes, *Am. J. Physiol.* 273, C473–C478.
  28. Galzigna, L., and Rigobello, M.P. (1986) Proton and Potassium Fluxes in Rat Red Blood Cells Incubated with Sugar Phosphates, *Experientia* 42, 138–139.
  29. Hassinen, I.E., Nuutinen, E.M., Ito, K., Nioka, S., Lazzarino, G., Giardina, B., and Chance, B. (1991) Mechanism of the Effects of Exogenous Fructose-1,6-bisphosphate on Myocardial Energy Metabolism, *Circulation* 83, 584–593.
  30. Brasitus, T.A., and Dudeja, P.K. (1986) Modulation of Lipid Fluidity of Small- and Large-Intestinal Antipodal Membranes by Ca<sup>2+</sup>, *Biochem. J.* 239, 625–631.
  31. FINDER, D.R., and Hardin, C.D. (1999) Transport and Metabolism of Exogenous Fumarate and 3-Phosphoglycerate in Vascular Smooth Muscle, *Mol. Cell. Biochem.* 195, 113–121.
  32. Bickler, P.E., and Buck, L.T. (1996) Effects of Fructose-1,6-bisphosphate on Glutamate Release and ATP Loss from Rat Brain Slices During Hypoxia, *J. Neurochem.* 67, 1463–1468.
  33. Wheeler, T.J., Cole, D., and Hauck, M.A. (1998) Characterization of Glucose Transport Activity Reconstituted from Heart and Other Tissues, *Biochim. Biophys. Acta* 1414, 217–230.
  34. Cullis, P.R., and Verleij, A.J. (1979) Modulation of Membrane Structure by Ca<sup>2+</sup> and Dibucaine as Detected by <sup>31</sup>P NMR, *Biochim. Biophys. Acta* 552, 546–551.
  35. Trauble, H., and Eibl, H. (1974) Electrostatic Effects on Lipid Phase Transitions: Membrane Structure and Ionic Environment, *Proc. Natl. Acad. Sci.* 71, 214–219.

[Received March 13, 2002, and in revised form September 26, 2002; revision accepted October 8, 2002]



# Comparison of the Oxidizability of Various Glycerophospholipids in Bilayers by the Oxygen Uptake Method

Ryouta Maeba\*, Youltuz Yusuf, Hiroyuki Shimasaki, and Nobuo Ueta

Department of Biochemistry, Teikyo University School of Medicine, Tokyo 173-8605, Japan

**ABSTRACT:** The aims of this study were twofold: develop a convenient and rapid procedure for assessing the oxidizability of small quantities of glycerophospholipids in bilayers by the oxygen uptake method, and determine and compare the oxidizability of various glycerophospholipids in bilayers. Our purpose was to elucidate phospholipid oxidation characteristics in membranes. The quantitative autoxidation kinetics of dilinoleoyl phosphatidylcholine (DLPC) (18:2/18:2) was studied in large unilamellar vesicles (LUV) in aqueous dispersions with water-soluble initiator—2,2'-azobis(2-amidinopropane) dihydrochloride—and inhibitor 2-carboxy-2,5,7,8-tetramethyl-6-chromanol. The kinetic data indicated a high efficiency of free radical production, resulting in shortening of measuring time; the very low kinetic chain length, particularly in the induction period, suggested the possibility of including large errors in the kinetics data. Nevertheless, the autoxidation of DLPC obeyed the classic rate law:  $R_p = k_p[\text{LH}]R_i^{1/2}/(2k_t)^{1/2}$  (where  $R_p$  = rate of oxygen consumption,  $k_p$  = rate constant for chain propagation,  $[\text{LH}]$  = substrate concentration;  $R_i^{1/2}$  = square root of rate of chain initiation, and  $2k_t$  = rate constant for chain termination) in a mixed bilayer system with saturated dimyristoyl PC (14:0/14:0), which provided precise and reproducible data. Therefore, the system was used to assess the relative oxidizability of each glycerophospholipid DLPC (18:2/18:2), dilinolenoyl PC (18:3/18:3), 1-palmitoyl-2-linoleoyl PC (16:0/18:2), 1-palmitoyl-2-arachidonoyl PC (16:0/20:4), 1-palmitoyl-2-docosahexaenoyl PC (16:0/22:6), and dilinoleoyl PE (18:2/18:2) in bilayers. The results suggested that the oxidizability of glycerophospholipid in bilayers is substantially influenced by the number of intramolecular oxidizable acyl chains and the content of bis-allylic hydrogen in a structured environment, and showed deviation of the rate law for autoxidation in PC and PE mixed LUV, which possibly was due to non-homogeneous phospholipid distribution in vesicles.

Paper no. L9000 in *Lipids* 37, 893–900 (September 2002).

Lipid peroxidation mediated by free radicals *in vivo* has attracted growing attention because of its potential contribution to various diseases and the aging process (1). Oxidation in

\*To whom correspondence should be addressed at Department of Biochemistry, Teikyo University School of Medicine, 2-11-1 Kaga, Itabashi-Ku, Tokyo 173-8605, Japan. E-mail: maeba@med.teikyo-u.ac.jp

Abbreviations: AAPH, 2,2'-azobis(2-amidinopropane) dihydrochloride; DLPE, dilinoleoyl phosphatidylethanolamine; DLnPC, dilinolenoyl phosphatidylcholine; DLPC, dilinoleoyl phosphatidylcholine; DMPC, dimyristoyl phosphatidylcholine; DOPE, dioleoyl phosphatidylethanolamine; kcl, kinetic chain length;  $[\text{LH}]$ , substrate concentrations; LUV, large unilamellar vesicles; PAPC, 1-palmitoyl-2-arachidonoyl phosphatidylcholine; PDPC, 1-palmitoyl-2-docosahexaenoyl phosphatidylcholine; PLPC, 1-palmitoyl-2-linoleoyl phosphatidylcholine; Trolox, 2-carboxy-2,5,7,8-tetramethyl-6-chromanol.

biomembranes is one of the critical events leading to biomembrane dysfunction. Biomembranes basically consist of phospholipid bilayers; therefore, proper assessment of the oxidizability of phospholipid in bilayers is essential in understanding the oxidation of biomembranes. Among the available methods for assessing oxidizability, the oxygen uptake method is considered to be the most reliable and accurate.

Several investigators (2,3) have used the oxygen uptake method to determine the oxidizability of PC in vesicles as model membranes. In their quantitative kinetic studies on autoxidation, the kinetics of autoxidation in heterogeneous systems of bilayers and micelles has been shown to follow the classical rate law for autoxidation given by Equation 1 (4) as well as in homogeneous solution (5,6):

$$-d[\text{O}_2]/dt = R_p = k_p[\text{LH}]R_i^{1/2}/(2k_t)^{1/2} \quad [1]$$

where  $R_p$  is the rate of oxygen consumption;  $R_i$ , the rate of chain initiation;  $[\text{LH}]$ , the concentration of substrate; and  $k_p$  and  $2k_t$ , the rate constants for chain propagation and termination, respectively. The ratio of these rate constants,  $k_p/(2k_t)^{1/2}$ , is referred to as the susceptibility of a substrate to undergo autoxidation, that is, oxidizability. To allow quantitative studies on the kinetics of autoxidation, the rate of chain initiation  $R_i$  must be controlled and measurable. This is generally achieved by using thermally labile azo initiators (A–N=N–A), which decompose to give two radicals at a known and constant rate (7). The rate of initiation,  $R_i$ , is generally determined by the induction period method with a chain-breaking antioxidant as indicated by Equation 2:

$$R_i = n[\text{IH}]/t_{\text{inh}} \quad [2]$$

where IH is the antioxidant,  $t_{\text{inh}}$  the induction period produced by the addition of the antioxidant, and  $n$  the stoichiometric number of radicals trapped by each antioxidant. Since  $[\text{LH}]$  is known and  $R_p$  and  $R_i$  are determined experimentally, oxidizability,  $k_p/(2k_t)^{1/2}$ , can be calculated from Equation 3:

$$k_p/(2k_t)^{1/2} = R_p/[\text{LH}]R_i^{1/2} \quad [3]$$

Quantitative kinetic measurements can be made by using either water-soluble or lipid-soluble initiators with water-soluble or lipid-soluble inhibitors (8). Although the use of lipid-soluble initiator and inhibitor is the most reasonable for measuring the rate of initiation in the lipid phase, it is often

inconvenient and time-consuming. That is, (i) since it is sometimes difficult to incorporate the lipid-soluble initiator and inhibitor into vesicles in amounts that are known *a priori* by calculation, it is necessary to check their concentrations in some way after preparation of the vesicles. (ii) It is sometimes difficult to measure the induction period exactly, because the thermally labile initiator easily initiates autoxidation during preparation and pre-incubation of vesicles. (iii) Measurement with a lipid-soluble initiator is often more time-consuming than that with a water-soluble one because of the extremely low efficiency of free radical production in the lipid phase and the limited concentration of lipid-soluble initiator in vesicles. Accordingly, it was considered that water-soluble compounds that do not need to be incorporated into vesicles provide some advantages for measurement.

In the present study, a convenient procedure for assessing the oxidizability of glycerophospholipids in bilayers in a short experimental time and using a small quantity of test lipid was developed; the kinetic measurement was carried out on large unilamellar vesicles (LUV), which are more suitable model membranes for free radical oxidation *in vivo*, in the presence of the water-soluble initiator 2,2'-azobis(2-amidino-propane) dihydrochloride (AAPH) and the inhibitor 2-carboxy-2,5,7,8-tetramethyl-6-chromanol (Trolox) at a low molar ratio of substrate to initiator. The oxidizability values for each glycerophospholipid—dilinoleoyl phosphatidylcholine (DLPC; 18:2/18:2), dilinolenoyl phosphatidylcholine (DLnPC; 18:3/18:3), 1-palmitoyl-2-linoleoyl phosphatidylcholine (PLPC; 16:0/18:2), 1-palmitoyl-2-arachidonoyl phosphatidylcholine (PAPC; 16:0/20:4), 1-palmitoyl-2-docosa-hexaenoyl phosphatidylcholine (PDPC; 16:0/22:6), and dilinoleoyl phosphatidylethanolamine (DLPE; 18:2/18:2)—were determined, and their relationships to the peroxidation index were established in order to elucidate the characteristics of phospholipid oxidation in membranes.

## EXPERIMENTAL PROCEDURES

**Materials.** PLPC, PAPC, and PDPC were purchased from Sigma Chemicals (St. Louis, MO). DLPC and DLnPC were obtained from Doosan Serdary Research Laboratories (Englewood Cliffs, NJ). Dimyristoyl phosphatidylcholine (DMPC; 14:0/14:0) and dioleoyl phosphatidylethanolamine (DOPE, 18:1/18:1) were purchased from Nichiyu Liposome Co., Inc. (Tokyo, Japan). DLPE was obtained from Avanti Polar Lipids, Inc. AAPH was obtained from Wako Pure Chemical Industries (Osaka, Japan). Trolox was purchased from Aldrich Chemicals (Milwaukee, WI).

**Preparation of LUV.** Mixtures of saturated and unsaturated glycerophospholipids were dissolved in chloroform at a specified molar ratio. The solvent was evaporated completely in a stream of nitrogen ( $N_2$ ) gas. The dried lipids were dispersed in PBS (10 mM, pH 7.4) kept at 40°C (above the phase transition temperature for all lipids used) in the presence of 0.1 mM EDTA (Wako) in a vortex mixer to yield multilamellar vesicles. LUV were prepared from the multilamellar vesicles

with an extruder (Lipex Biomembranes Inc., Vancouver, Canada) as described previously (9). The concentration of phospholipids in the lipid dispersions and constituent molar ratio of phospholipids in vesicles was checked by TLC separation and phosphorus analysis for phospholipids after preparation of vesicles by extrusion.

**Autoxidation procedures.** Autoxidation of LUV was initiated with the water-soluble azo radical initiator AAPH, and oxygen consumption was measured in the aqueous dispersion. The rate of chain initiation  $R_i$  was determined by the induction period method with the water-soluble phenolic antioxidant Trolox. The dissolved oxygen in the reaction solvent was monitored with a Galvani-type oxygen electrode (MD-1000; Iijima Electronics Corp., Tokyo, Japan). The oxygen concentration was set at 0  $\mu$ M with the meter in water containing 5% sodium bisulfite (Wako) and at 220  $\mu$ M in water saturated with air at 37°C. Trolox (0.05–0.1  $\mu$ mol) was dissolved in ethanol (5  $\mu$ L) and added to the aqueous dispersion as an antioxidant before mixing the LUV with AAPH. In a typical experiment, 1.9 mL of a PBS dispersion of the appropriate LUV kept at 37°C was mixed with 0.35 mL of AAPH in PBS and put in a reaction vessel connected to an oxygen electrode. The reaction mixture was maintained at 37°C and stirred with a magnetic stirrer while measurements were taken.

## RESULTS

The kinetics of the autoxidation of DLPC in LUV in aqueous dispersions were measured by using variable amounts of vesicles, AAPH, and Trolox (Table 1). From the slope of the straight line obtained by plotting the induction period,  $t_{inh}$ , as a function of [Trolox]/[AAPH] (Fig. 1), the stoichiometric number of radicals trapped by Trolox,  $n$ , was found to be 1.8. This value is slightly lower than 2, the theoretical value for water-soluble vitamin E analog Trolox, which is known to trap two peroxy radicals. By using an  $n$  value of 1.8,  $R_i$  and the efficiency of free radical production,  $e$ , were calculated from Equations 2 and 4, respectively, where the concentrations of initiator, AAPH, and inhibitor, Trolox, are expressed in the lipid phase and  $2k_i$  for AAPH is taken as  $1.36 \times 10^{-6} s^{-1}$  at 37°C (10).

$$e = R_i / 2k_i [AAPH] \quad [4]$$

The kinetic chain length,  $kcl$ , is the number of substrate molecules oxidized per initiating radical and can be obtained from Equation 5:

$$kcl = (R_p \text{ or } R_{inh}) / R_i \quad [5]$$

where  $R_{inh}$  is the rate of oxygen consumption during the induction period.

The  $e$  values obtained, 0.71–1.00, show that free radicals were generated at very high efficiency, whereas the very low  $kcl$  values indicate insufficient progress of radical chain reactions in the present oxidizing system (Tables 1, 2). The effects

**TABLE 1**  
**The Kinetics of Autoxidation of DLPC in LUV, Initiated by AAPH at 37°C<sup>a</sup>**

DLPC (mM) <sup>b</sup>	AAPH (mM) <sup>b</sup>	Trolox (μM) <sup>b</sup>	$t_{inh}$ (s)	$10^6 R_i$ $= n^c [\text{Trolox}]^d / t_{inh}$ (M/s)	$10^3 R_i^{1/2}$ (M/s) <sup>1/2</sup>	$e = R_i / 2k_i [\text{AAPH}]^{d,e}$	$10^5 R_p^c$ (M/s)	kcl $= R_p / R_i$	$10^5 R_{inh}^d$ (M/s)	kcl $= R_{inh} / R_i$
1.28	23.3	22.2	1452	21.89	4.68	0.86	14.09	6	3.76	2
1.28	38.9	22.2	744	42.73	6.54	1.00	21.54	5	8.04	2
1.28	58.3	22.2	559	56.87	7.54	0.90	25.89	5	9.37	2
1.28	23.3	44.4	3312	19.20	4.38	0.76	10.03	5	2.97	2
1.28	38.9	44.4	1783	35.66	5.97	0.84	15.19	4	4.93	1
1.28	58.3	44.4	1145	55.53	7.45	0.88	19.43	3	7.15	1
2.14	23.3	33.3	2664	10.74	3.28	0.71	7.99	7	1.87	2
2.14	38.9	33.3	1464	19.54	4.42	0.77	12.74	7	3.23	2
2.14	58.3	33.3	924	30.96	5.56	0.81	16.91	5	4.68	2
2.56	23.3	22.2	1267	12.55	3.54	0.99	11.70	9	2.13	2
2.56	38.9	22.2	845	18.81	4.34	0.89	15.92	8	3.36	2
2.56	58.3	22.2	528	30.10	5.49	0.95	19.28	6	6.85	2
2.56	23.3	44.4	3074	10.34	3.22	0.81	7.84	8	1.59	2
2.56	38.9	44.4	1802	17.64	4.20	0.83	11.66	7	2.53	1
2.56	58.3	44.4	1109	28.67	5.35	0.90	15.59	5	3.82	1
4.05	23.3	22.2	1327	7.57	2.75	0.95	8.89	12	1.34	2
4.05	38.9	22.2	756	13.28	3.64	1.00	12.31	9	2.09	1
4.05	58.3	22.2	456	22.02	4.69	1.00	17.13	8	3.13	1
4.05	23.3	44.4	3180	6.32	2.51	0.79	6.17	10	0.98	2
4.05	38.9	44.4	1697	11.83	3.44	0.89	9.22	8	1.73	1
4.05	58.3	44.4	1195	16.81	4.10	0.84	11.99	7	2.28	1
5.05	23.3	33.3	2525	5.66	2.38	0.74	6.27	11	1.00	2
5.05	38.9	33.3	1344	10.64	3.26	0.84	10.46	10	1.68	2
5.05	58.3	33.3	936	15.28	3.91	0.80	12.20	8	2.34	2
6.76	23.3	33.3	2436	3.71	1.93	0.77	4.96	13	0.61	1
6.76	38.9	33.3	1234	7.33	2.71	0.92	8.16	11	1.06	1
6.76	58.3	33.3	888	10.18	3.19	0.85	10.44	10	1.41	1

<sup>a</sup>Abbreviations: DLPC, dilinoleoyl phosphatidylcholine; LUV, large unilamellar vesicle; DMPC, dimyristoyl phosphatidylcholine; AAPH, 2,2'-azobis(2-amidinopropane) dihydrochloride; Trolox, 2-carboxy-2,5,7,8-tetramethyl-6-chromanol; kcl, kinetic chain length.

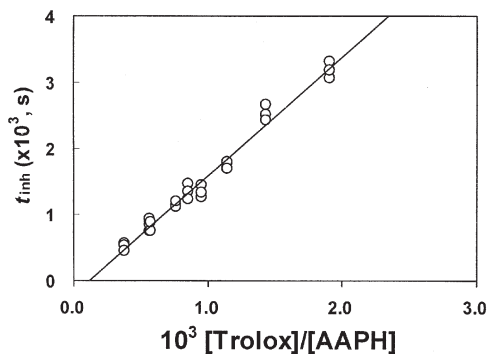
<sup>b</sup>The concentrations in the reaction solvent.

<sup>c</sup>The  $n$  value was taken as 1.8.

<sup>d</sup>The concentrations were calculated as per lipid volume, which was estimated by assuming that the density of phospholipid is 0.8.

<sup>e</sup>The  $k_i$  for AAPH was taken as  $6.8 \times 10^{-7} \text{s}^{-1}$ .

of the amounts of AAPH, Trolox, and vesicles on the kinetics data were explored by comparing the correlations between  $R_p$  and  $R_i^{1/2}$  (Figs. 2A–C). Measurements under a fixed concentration of Trolox (Fig. 2C) provided greater coefficient values,  $r_2 > 0.97$ , than those obtained under a fixed concentra-



**FIG. 1.** Plots of the induction period,  $t_{inh}$ , against  $[\text{Trolox}]/[\text{AAPH}]$  in the autoxidation kinetics of DLPC in LUV.  $y = 1.798x - 0.2069$ ,  $r^2 = 0.9805$ . Data from Table 1. Trolox, 2-carboxy-2,5,7,8-tetramethyl-6-chromanol; AAPH, 2,2'-azobis(2-amidinopropane) dihydrochloride; DLPC, dilinoleoyl phosphatidylcholine; LUV, large unilamellar vesicle.

tion of AAPH,  $r_2 > 0.90$  (Fig. 2B), or vesicles,  $r_2 > 0.91$  (Fig. 2A). Moreover, the  $R_p/R_i^{1/2}$  ratio was found to be influenced most by variation in the amount of Trolox (Fig. 2C). These results show that the measurement should be carried out with a fixed concentration of Trolox to obtain a more precise value. Therefore, the measurement was carried out hereafter with variable amounts of vesicles under fixed concentrations of AAPH and Trolox.

The oxidizability of DLPC in bilayers was determined by using three different mixed vesicles composed of various concentrations of oxidizable DLPC with an inert saturated DMPC (Table 2), because the concentration of substrate, [LH], for DLPC LUV composed of a single phospholipid shows a constant value independent of the amount of vesicles in the reaction solvent (11). Plots of  $R_p$  against  $R_i^{1/2}$  for each mixed LUV gave straight lines with  $r_2 > 0.96$  (Fig. 3A), which is evidence for a constant  $R_p/R_i^{1/2}$  ratio in each mixed LUV containing DLPC as an oxidizable substrate, at identical concentrations. A plot of  $R_p/R_i^{1/2}$  against [LH] gave an excellent linear correlation ( $r_2 = 0.99$ ) (Fig. 3B). The slope of the straight line obtained,  $R_p/[LH]R_i^{1/2} = 2.1 \cdot 10^{-2} (\text{Ms})^{-1/2}$ , corresponds to the oxidizability value for DLPC in bilayers. The

**TABLE 2**  
**The Kinetics of Autoxidation of DLPC in Mixed LUV with DMPC, Initiated by AAPH at 37°C<sup>a</sup>**

DLPC (mM) <sup>b</sup>	DMPC (mM) <sup>b</sup>	[DLPC] <sup>c</sup> (M)	$t_{inh}$ (s)	$10^6 R_i$ $= n^d [Trolox]^c / t_{inh}$ (M/s)	$10^3 R_i^{1/2}$ (M/s) <sup>1/2</sup>	$e = R_i / 2k_i [AAPH]^c$ <sup>e</sup>	$10^5 R_p^c$ (M/s)	kcl $= R_p / R_i$	$10^5 R_{inh}^c$ (M/s)	kcl $= R_{inh} / R_i$	$10^5 R_{p0}^{c,f}$ (M/s)	$10^5 (R_p - R_{p0})^c$ (M/s)
1.52	0	1.023	1296	49.06	7.00	0.81	19.03	4	6.72	1	4.17	14.86
3.03	0	1.023	1200	26.49	5.15	0.87	14.95	6	3.66	1	3.06	11.89
4.80	0	1.023	1200	16.74	4.09	0.87	12.85	8	2.15	1	2.43	10.42
1.01	0.51	0.714	1387	47.97	6.93	0.76	14.01	3	6.75	1	4.12	9.89
2.02	1.01	0.714	1260	26.40	5.14	0.83	11.79	4	3.60	1	3.06	8.73
3.20	1.60	0.714	1229	17.10	4.14	0.85	11.00	6	2.22	1	2.46	8.54
0.51	1.01	0.374	1356	51.44	7.17	0.77	9.84	2	7.37	1	4.27	5.57
1.01	2.02	0.374	1212	28.34	5.32	0.85	7.79	3	3.87	1	3.17	4.62
1.60	3.20	0.374	1212	18.18	4.26	0.87	6.77	4	2.36	1	2.53	4.24

<sup>a</sup>For abbreviations see Table 1.

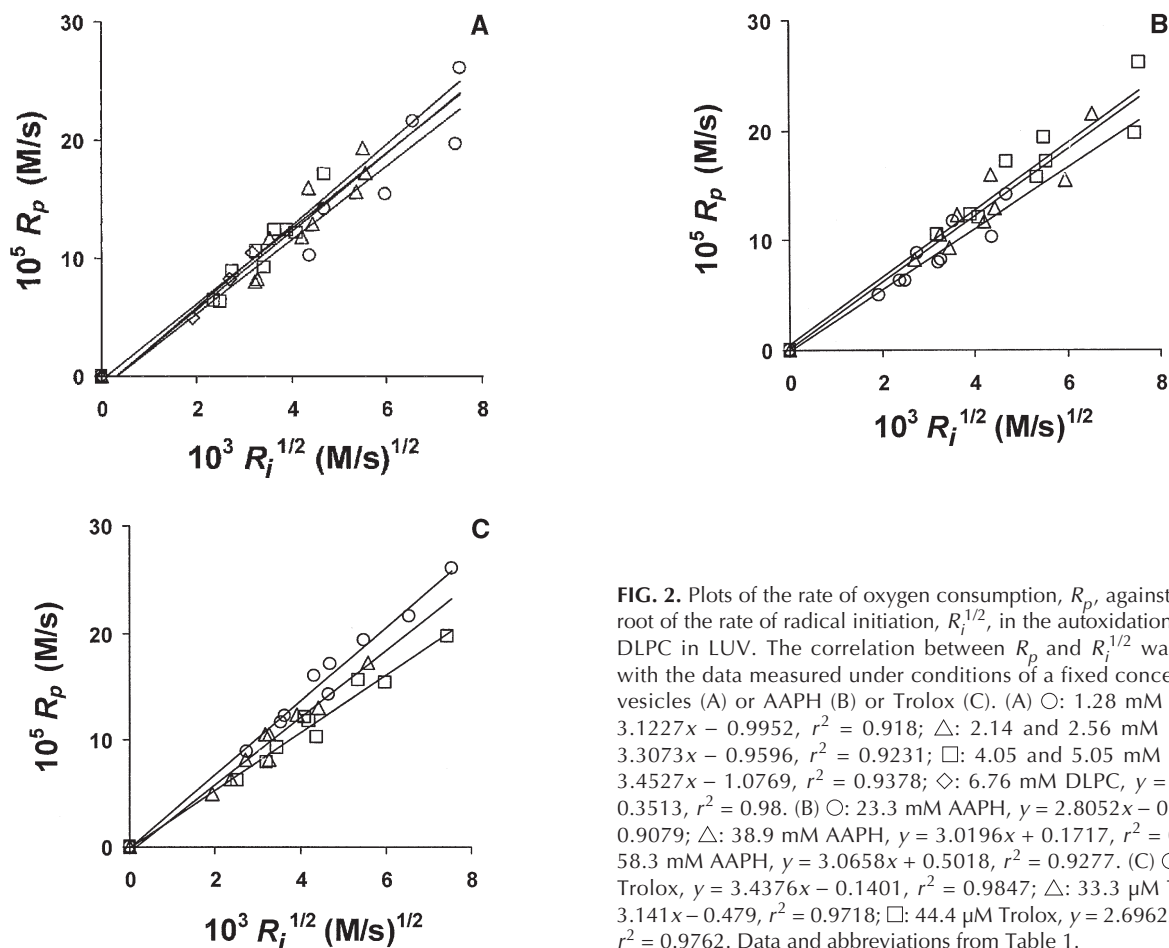
<sup>b</sup>See footnote b, Table 1.

<sup>c</sup>See footnote d, Table 1.

<sup>d</sup>See footnote c, Table 1.

<sup>e</sup>See footnote e, Table 1.

<sup>f</sup>The rate of oxygen consumption in the absence of oxidizable substrate, which was estimated from the intercept value,  $5.95 \times 10^{-3}$  (M/s)<sup>1/2</sup>, in Figure 3B.

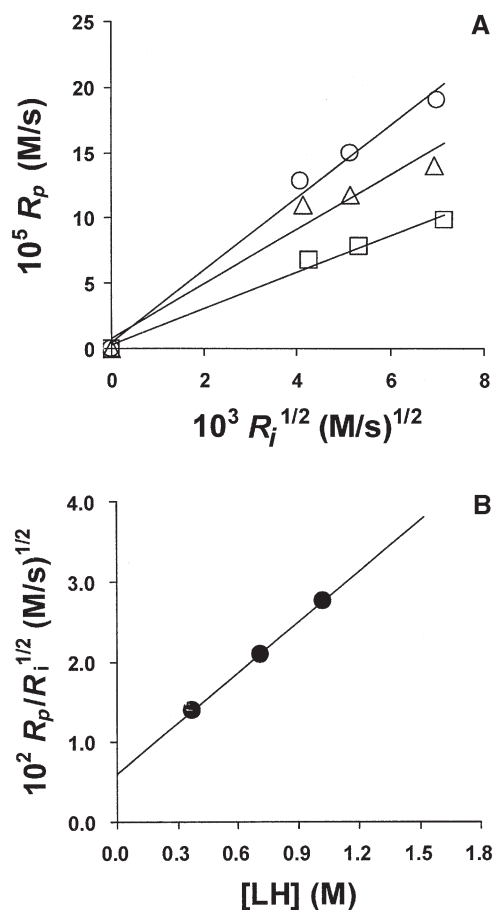


**FIG. 2.** Plots of the rate of oxygen consumption,  $R_p$ , against the square root of the rate of radical initiation,  $R_i^{1/2}$ , in the autoxidation kinetics of DLPC in LUV. The correlation between  $R_p$  and  $R_i^{1/2}$  was analyzed with the data measured under conditions of a fixed concentration of vesicles (A) or AAPH (B) or Trolox (C). (A)  $\circ$ : 1.28 mM DLPC,  $y = 3.1227x - 0.9952$ ,  $r^2 = 0.918$ ;  $\triangle$ : 2.14 and 2.56 mM DLPC,  $y = 3.3073x - 0.9596$ ,  $r^2 = 0.9231$ ;  $\square$ : 4.05 and 5.05 mM DLPC,  $y = 3.4527x - 1.0769$ ,  $r^2 = 0.9378$ ;  $\diamond$ : 6.76 mM DLPC,  $y = 3.2037x - 0.3513$ ,  $r^2 = 0.98$ . (B)  $\circ$ : 23.3 mM AAPH,  $y = 2.8052x - 0.1645$ ,  $r^2 = 0.9079$ ;  $\triangle$ : 38.9 mM AAPH,  $y = 3.0196x + 0.1717$ ,  $r^2 = 0.9222$ ;  $\square$ : 58.3 mM AAPH,  $y = 3.0658x + 0.5018$ ,  $r^2 = 0.9277$ . (C)  $\circ$ : 22.2  $\mu$ M Trolox,  $y = 3.4376x - 0.1401$ ,  $r^2 = 0.9847$ ;  $\triangle$ : 33.3  $\mu$ M Trolox,  $y = 3.141x - 0.479$ ,  $r^2 = 0.9718$ ;  $\square$ : 44.4  $\mu$ M Trolox,  $y = 2.6962x - 0.1149$ ,  $r^2 = 0.9762$ . Data and abbreviations from Table 1.

intercept, the  $R_p/R_i^{1/2}$  value when [LH] is zero (Fig. 3B), represents the ratio of the rate of oxygen consumption in the absence of the oxidizable substrate,  $R_{p0}$ , to the  $R_i^{1/2}$  value. Therefore, the rate of oxygen consumption involved in lipid peroxidation was corrected by subtracting each  $R_{p0}$  value, estimated from the intercept value,  $5.95 \cdot 10^{-3}$

(M/s)<sup>1/2</sup>, from the measured rate,  $R_p$  (Table 2). Plots of  $R_p - R_{p0}$  for each mixed LUV against  $R_i^{1/2}$  also gave straight lines with  $r_2 > 0.92$  (Fig. 4A). A plot of  $(R_p - R_{p0})/R_i^{1/2}$  against [LH] provided a straight line passing through zero (Fig. 4B). The slope of the straight line,  $(R_p - R_{p0})/[LH]R_i^{1/2} = 2.1 \cdot 10^{-2}$  (Ms)<sup>-1/2</sup>, was exactly equal to the value for

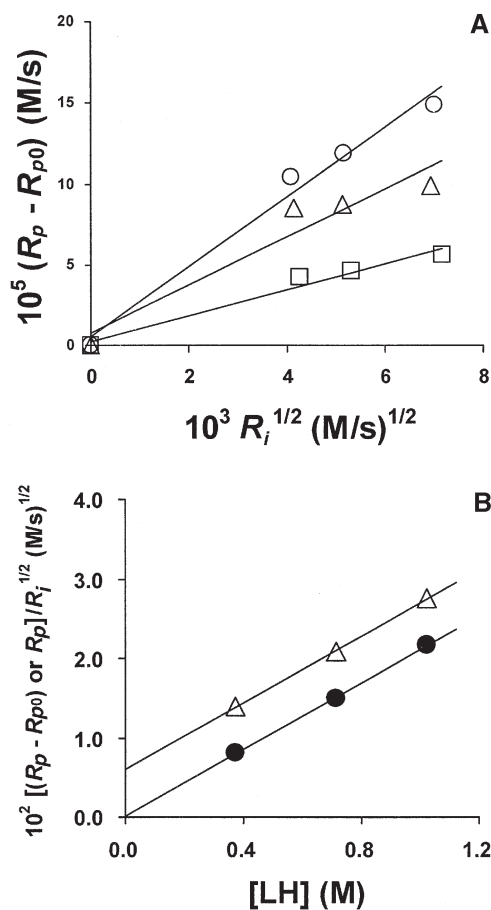




**FIG. 3.** Autoxidation kinetics of DLPC in mixed LUV with DMPC: (A) Plots of the rate of oxygen consumption,  $R_p$ , against the rate of radical initiation,  $R_i^{1/2}$ .  $\circ$ : [1.023] DLPC,  $y = 2.7599x + 0.5024$ ,  $r^2 = 0.9898$ ;  $\triangle$ : [0.714] DLPC,  $y = 2.0893x + 0.7332$ ,  $r^2 = 0.9601$ ;  $\square$ : [0.374] DLPC,  $y = 1.3948x + 0.2594$ ,  $r^2 = 0.9894$ . The kinetics data are shown in Table 2. (B) Plots of the ratio,  $R_p/R_i^{1/2}$ , obtained from Figure 3A, against [LH] in the autoxidation kinetics of DLPC in mixed LUV with DMPC. The concentration of substrate, [LH], is expressed as moles DLPC per liter of total lipid volume of vesicles and was changed by altering the relative amounts of DLPC and DMPC in vesicles.  $y = 2.1101x + 0.5952$ ,  $r^2 = 0.9998$ . DMPC, dimyristoyl phosphatidylcholine; for other abbreviations see Figure 1.

$R_p/[LH]R_i^{1/2}$ , which suggests that it may be unnecessary to correct the rate of oxygen consumption to obtain the oxidizability value. This inference was confirmed in all measurements for determination of the oxidizability of other glycerophospholipids (data not shown). Accordingly, the oxidizability values have been indicated using the uncorrected measured rates of oxygen consumption.

The oxidizability values for each glycerophospholipid were determined by using a mixed bilayer system with an inert saturated phospholipid. These are summarized in Table 3. The oxidizability values for PLPC, DLPC, and DLnPC were strongly correlated with their peroxidation indexes (Fig. 5A), but there was no linear correlation between the oxidizability value and peroxidation index among PC having a single oxidizable fatty acyl chain at the *sn*-2 position, such as PLPC, PAPC, and PDPC (Fig. 5B).



**FIG. 4.** Autoxidation kinetics of DLPC in mixed LUV with DMPC. (A) Plots of the corrected rate of oxygen consumption,  $R_p - R_{p0}$ , against the square root of the rate of radical initiation,  $R_i^{1/2}$ . The rates of oxygen consumption in the absence of oxidizable substrate,  $R_{p0}$ , are referred to in Table 2.  $\circ$ : [1.023] DLPC,  $y = 2.1645x + 0.5047$ ,  $r^2 = 0.9835$ ;  $\triangle$ : [0.714] DLPC,  $y = 1.4946x + 0.7332$ ,  $r^2 = 0.9248$ ;  $\square$ : [0.374] DLPC,  $y = 0.7992x + 0.2609$ ,  $r^2 = 0.9679$ . (B) Plots of the ratios,  $R_p/R_i^{1/2}$ , obtained from Figure 3A, and  $(R_p - R_{p0})/R_i^{1/2}$ , obtained from Figure 4A, against [LH] in the autoxidation kinetics of DLPC in mixed LUV with DMPC.  $\triangle$ :  $R_p/R_i^{1/2}$ ,  $y = 2.1101x + 0.5952$ ,  $r^2 = 0.9998$ ;  $\bullet$ :  $(R_p - R_{p0})/R_i^{1/2}$ ,  $y = 2.096x + 0.0081$ ,  $r^2 = 0.9997$ . For abbreviations see Figures 1 and 3.

The application of PC and PE mixed LUV to the determination of oxidizability was explored by measuring the oxidizability of DLPC in mixed LUV with DOPE instead of DMPC as an inert saturated phospholipid. Although  $r_2$  values between  $R_p$  and  $R_i^{1/2}$  were more than 0.98 in the autoxidations of each mixed LUV (Fig. 6A), plots of the  $R_p/R_i^{1/2}$  ratio against [LH] provided a curved line with a height at around 0.8 of [LH] (Fig. 6B). To confirm this phenomenon, the oxidizability of DLPE was measured in mixed LUV with DMPC. Although there were good correlations between  $R_p$  and  $R_i^{1/2}$  ( $r_2 > 0.98$ ) in each mixed LUV (Fig. 7A), plots of  $R_p/R_i^{1/2}$  against [LH] gave no linear correlation; again, the  $R_p/R_i^{1/2}$  value was beside the straight line over an [LH] value of 0.6 (Fig. 7B). The apparent oxidizability values of DLPC and DLPE were estimated as  $4.7 \times 10^{-2}$  and  $4.8 \times 10^{-2}$  (Ms) $^{-1/2}$ , respectively, from the slope of the straight

**TABLE 3**  
The Relative Oxidizability Values,  $R_p/[LH]R_i^{1/2}$ , for Various Glycerophospholipids Determined Using Mixed LUV with Inert Saturated Phospholipids

Test lipid <sup>a</sup>	Mixed LUV system <sup>a</sup>	$R_p/[LH]R_i^{1/2}$ $10^2$ (Ms) <sup>-1/2</sup>	$r^2$ <sup>b</sup>	Peroxidation index <sup>c</sup>
DLPC	DLPC/DMPC	2.1	0.999 (9)	100
DLPC	DLPC/DOPE	(4.7)	0.955 (9)	100
DLPE	DLPE/DMPC	(4.8)	0.962 (9)	100
PLPC	PLPC/DMPC	1.0	0.927 (9)	50
DlnPC	DlnPC/DMPC	4.7	0.998 (11)	200
PAPC	PAPC/DMPC	2.1	0.965 (8)	150
PDPC	PDPC/DMPC	2.1	0.988 (9)	250

<sup>a</sup>Abbreviations: DOPE, dioleoyl phosphatidylethanolamine; DLPE, dilinoleoyl phosphatidylethanolamine; PLPC, 1-palmitoyl-2-linoleoyl phosphatidylcholine; DlnPC, dilinolenoyl phosphatidylcholine; PAPC, 1-palmitoyl-2-arachidonoyl phosphatidylcholine; PDPC, 1-palmitoyl-2-docosahexaenoyl phosphatidylcholine. For other abbreviations see Table 1.

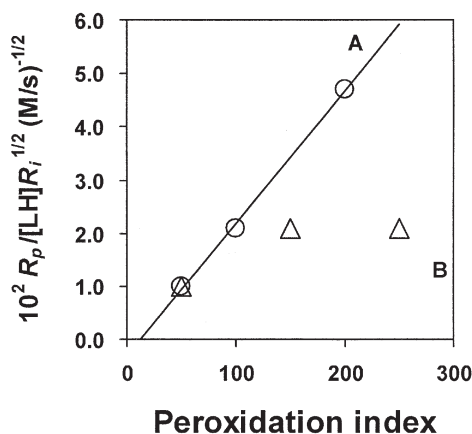
<sup>b</sup>The coefficient of correlation,  $r^2$ , was calculated based on the number of experiments (in parentheses).

<sup>c</sup>Peroxidation index (PI) was calculated according to the following equation: PI = (% dienoic  $\times$  1) + (% trienoic  $\times$  2) + (% tetraenoic  $\times$  3) + (% pentaenoic  $\times$  4) + (% hexaenoic  $\times$  5).

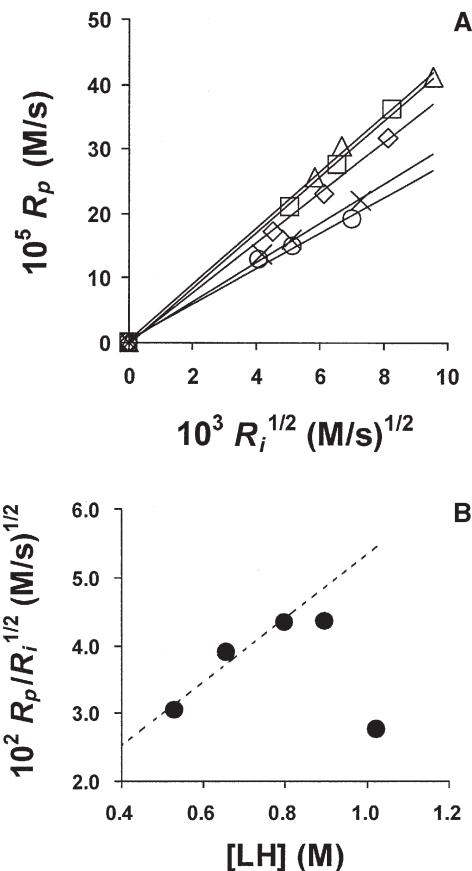
lines obtained by plotting  $R_p/R_i^{1/2}$  against [LH] within the range for which the correlation is linear (Figs. 6B, 7B).

## DISCUSSION

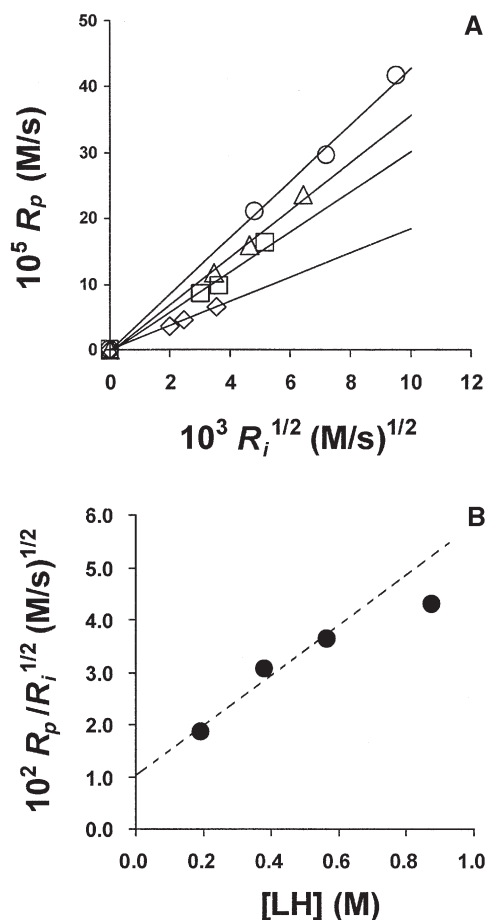
The present procedure, which used a water-soluble radical initiator and unilamellar vesicles with a small quantity of substrate, brought about a remarkable increase in the efficiency of free radical production ( $e > 0.6$  through all the experiments), resulting in shorter completion times (the dissolved oxygen was completely consumed in the reaction solvent within about 1 h). This oxidizing system is characterized by very low  $k_{cl}$  values, particularly in the induction period (Tables 1, 2), which indicates that possibly the initiating azo peroxy radicals are



**FIG. 5.** Relationship between peroxidation index and relative oxidizability value,  $R_p/[LH]R_i^{1/2}$ , of glycerophospholipids in bilayers. A (○): among PLPC, DLPC, and DlnPC; B (△): among PLPC, PAPC, and PDPC. PLPC, 1-palmitoyl-2-linoleoyl phosphatidylcholine; DlnPC, dilinolenoyl phosphatidylcholine; PLPC, 1-palmitoyl-2-linoleoyl phosphatidylcholine; PAPC, 1-palmitoyl-2-arachidonoyl phosphatidylcholine; PDPC, 1-palmitoyl-2-docosahexaenoyl phosphatidylcholine; DlnPC, dilinolenoyl phosphatidylcholine; for other abbreviations see Figure 1.



**FIG. 6.** (A) Plots of the rate of oxygen consumption,  $R_p$ , against the square root of the rate of radical initiation,  $R_i^{1/2}$ , in the autoxidation kinetics of DLPC in mixed LUV with dioleoyl phosphatidylethanolamine (DOPE). ○: [1.023] DLPC,  $y = 2.7599x + 0.5024$ ,  $r^2 = 0.9898$ ; △: [0.898] DLPC,  $y = 4.3583x + 0.2715$ ,  $r^2 = 0.9983$ ; □: [0.800] DLPC,  $y = 4.3322x - 0.3091$ ,  $r^2 = 0.9984$ ; ◇: [0.657] DLPC,  $y = 3.8911x - 0.1647$ ,  $r^2 = 0.9992$ ; ×: [0.530] DLPC,  $y = 3.047x + 0.2627$ ,  $r^2 = 0.9979$ . (B) Plots of the ratio,  $R_p/R_i^{1/2}$ , obtained from (A), against [LH] in the autoxidation kinetics of DLPC in mixed LUV with DOPE.  $y = 4.706x + 0.6397$ ,  $r^2 = 0.9554$ . For other abbreviations see Figures 1 and 3.



**FIG. 7.** Autoxidation kinetics of dilinoleoyl phosphatidylethanolamine (DLPE) in mixed LUV with DMPC. (A) Plots of the rate of oxygen consumption,  $R_p$ , against the square root of the rate of radical initiation,  $R_i^{1/2}$ .  $\circ$ : [0.877] DLPE,  $y = 4.3062x - 0.1531$ ,  $r^2 = 0.9971$ ;  $\triangle$ : [0.564] DLPE,  $y = 3.6176x - 0.4261$ ,  $r^2 = 0.9951$ ;  $\square$ : [0.382] DLPE,  $y = 3.0505x - 0.395$ ,  $r^2 = 0.9872$ ;  $\diamond$ : [0.194] DLPE,  $y = 1.8448x - 0.0227$ ,  $r^2 = 0.9998$ . (B) Plots of the ratio,  $R_p/R_i^{1/2}$ , obtained from (A), against [LH].  $y = 4.8013x + 1.0133$ ,  $r^2 = 0.9623$ . For other abbreviations see Figures 1 and 3.

trapped by the water-soluble inhibitor in the aqueous phase. This can lead to very large errors in determining the  $R_i$  for their lipid phase. It is quite possible that initiating azo peroxy radicals react with each other in the aqueous phase to terminate the initiating reaction, which also results in considerable errors in measuring both the  $R_i$  and  $R_p$  for their lipid phase. Accordingly, it was suggested that the present system may not be appropriate for determining an absolute oxidizability value for glycerophospholipids in bilayers.

Nevertheless, the kinetics data for autoxidation of DLPC, obtained in the mixed bilayer system with an inert saturated DMPC, were confirmed to follow the classical rate law closely for autoxidation,  $R_p = k_p[\text{LH}]R_i^{1/2}/(2k_t)^{1/2}$  (Figs. 3A,B). Furthermore, a combination of unilamellar vesicles and water-soluble initiator and inhibitor was found to give a clear induction period, which results in more precise and reproducible data. Therefore, the procedure was considered to be useful in assessing the relative oxidizability of glycerophospholipids in bilayers in identical systems.

Barclay *et al.* (12) and Yamamoto *et al.* (13) have reported that oxidizability values,  $k_p/(2k_t)^{1/2}$ , for DLPC in bilayers of  $4.6 \times 10^{-2}$  and  $9.2 \times 10^{-2}$  (Ms)<sup>-1/2</sup>. The value for DLPC obtained in the present procedure,  $2.1 \times 10^{-2}$  (Ms)<sup>-1/2</sup>, was less than half, but was within the same order of magnitude of these values despite possibly including large errors in the kinetics data. The errors in the rate of oxygen consumption may be neutralized by using a mixed bilayer system with inert saturated phospholipids as shown in Fig. 4B. But the rate of chain initiation,  $R_i$ , determined by the induction period method would give a large error in the oxidizability value, because the actual amount of initiating radicals involved in lipid peroxidation, in other words,  $R_i$ , is deduced to be smaller than the value estimated from the equation:  $R_i = n [\text{Trolox}]/t_{\text{inh}}$ . This overestimation of the  $R_i$  value may result in an oxidizability value lower than the true value.

The relative oxidizability values of various glycerophospholipids in bilayers have been determined in the system. The values of PLPC, DLPC, and DLnPC were linearly correlated with their peroxidation indexes, calculated on the basis of the numbers of bis-allylic hydrogens in the lipid molecules (Fig. 5A). There was no linear correlation between oxidizability and the peroxidation index among PC having a single oxidizable fatty acyl chain at the *sn*-2 position, such as PLPC, PAPC, and PDPC (Fig. 5B). The accuracy of our results cannot be confirmed, because the oxidizability values determined by the oxygen uptake method of other PC containing more unsaturated FA such as arachidonic acid (20:4) and docosahexaenic acid (22:6) have not been reported, and their relationships to the peroxidation index have not been discussed.

In a homogeneous solution, the existence of a positive relationship between the bis-allylic hydrogen number in the lipid molecule and the oxidizability is well known (14). In heterogeneous systems, the oxidizability in bilayers has been shown to depend on the bis-allylic hydrogen content by using multilamellar liposomes (15) or intact cells (16). On the other hand, the oxidizabilities of PUFA in aqueous micelles are inversely proportional to the bis-allylic hydrogen number (17,18). Interestingly, that molecular species of PC substantially affect oxidation kinetics has been shown by comparing the oxidizabilities of soybean PC and egg yolk PC in homogeneous solutions and in unilamellar vesicles (19,20). Our result with unilamellar vesicles appears to agree with their observations, because soybean PC contains mainly DLPC, whereas major molecular species of egg yolk PC have a single oxidizable acyl chain at the *sn*-2 position and an inert saturated acyl chain at the *sn*-1 position. This phenomenon may be explained in terms of "arm to arm autoxidation" theory (21), which is used to describe the increase in apparent oxidizability of glyceryl trilinoleate caused by decreasing its concentration in the reaction solvent (14).

When the oxidizability was measured with PC and PE mixed vesicles, there was no linear correlation between  $R_p/R_i^{1/2}$  and [LH] despite the excellent correlation between  $R_p$  and  $R_i^{1/2}$  ( $r_2 > 0.98$ ) for each mixed LUV (Figs. 6 and 7). This indicates the possibility of nonhomogeneous

distributions of PC and PE in unilamellar vesicles as observed in biomembranes (22), because the autoxidation reactions obey the rate law even in each mixed LUV. This causes an increase in the local concentration of oxidizable phospholipid in vesicles and so results in an increase in the apparent oxidizability of test lipid in bilayers. This inference may be supported by the greater oxidizability values for DLPC and DLPE determined in PC and PE mixed LUV,  $4.7 \times 10^{-2}$  and  $4.8 \times 10^{-2} \text{ (Ms)}^{-1/2}$ , respectively, than the value for DLPC determined in mixed vesicles with DMPC.

The present study describes a convenient and rapid procedure that would be useful in assessing the relative oxidizability of glycerophospholipids in bilayers. The results suggest that the oxidizability of phospholipids in bilayers is substantially influenced by the number of intramolecular oxidizable acyl chains, in addition to the content of bis-allylic hydrogen in a structured environment, and show deviation of the rate law for autoxidation in PC and PE mixed vesicles, possibly due to inhomogeneous phospholipid distribution in vesicles.

## REFERENCES

1. Armstrong, D., Sohol, R.S., Cutler, R.G., and Slater, T.F. (1984) *Free Radicals in Molecular Biology, Aging and Disease*, Raven Press, New York.
2. Barclay, L.R.C., and Ingold, K.U. (1981) Autoxidation of Biological Molecules. 2. The Autoxidation of a Model Membrane. A Comparison of the Autoxidation of Egg Lecithin Phosphatidylcholine in Water and in Chlorobenzene, *J. Am. Chem. Soc.* **103**, 6478–6485.
3. Yamamoto, Y., Niki, E., Kamiya, Y., and Shimasaki, H. (1984) Oxidation of Phosphatidylcholines in Homogeneous Solution and in Water Dispersion, *Biochim. Biophys. Acta* **795**, 332–340.
4. Barclay, L.R.C., Bailey, A.M.H., and Kong, D. (1985) The Antioxidant Activity of  $\alpha$ -Tocopherol–Bovine Serum Albumin Complex in Micellar and Liposome Autoxidations, *J. Biol. Chem.* **260**, 15809–15814.
5. Howard, J.A., and Ingold, K.U. (1967) Absolute Rate Constants for Hydrocarbon Autoxidation. VI. Alkyl Aromatic and Olefinic Hydrocarbons, *Can. J. Chem.* **45**, 793–802.
6. Howard, J.A. (1972) Absolute Rate Constants for Reactions of Oxyradicals, *Adv. Free Radical Chem.* **4**, 49–173.
7. Niki, E., Saito, M., Yoshikawa, Y., Yamamoto, Y., and Kamiya, Y. (1986) Oxidation of Lipids. XII. Inhibition of Oxidation of Soybean Phosphatidylcholine and Methyl Linoleate in Aqueous Dispersions by Uric Acid, *Bull. Chem. Soc. Jpn.* **59**, 471–477.
8. Barclay, L.R.C., Locke, S.J., MacNeil, J.M., VanKessel, J., Burton, G.W., and Ingold, K.U. (1984) Autoxidation of Micelles and Model Membranes. Quantitative Kinetic Measurements Can Be Made by Using Either Water-Soluble or Lipid-Soluble Initiators with Water-Soluble or Lipid-Soluble Chain-Breaking Antioxidants, *J. Am. Chem. Soc.* **106**, 2479–2481.
9. Maeba, R., Shimasaki, H., and Ueta, N. (2001) Generation of 7-Ketocholesterol by a Route Different from the Decomposition of Cholesterol 7-Hydroperoxide, *J. Oleo Sci.* **50**, 109–119.
10. Niki, E. (1990) Free Radical Initiators as Source of Water- or Lipid-Soluble Peroxyl Radicals, in *Methods in Enzymology* (Packer, L., ed.), Vol. 186, pp. 100–108, Academic Press, San Diego.
11. Barclay, L.R.C., Baskin, K.A., Kong, D., and Locke, S.J. (1987) Autoxidation of Model Membranes. The Kinetics and Mechanism of Autoxidation of Mixed Phospholipid Bilayers, *Can. J. Chem.* **65**, 2541–2550.
12. Barclay, L.R.C., Kong, D., and VanKessel, J. (1986) Autoxidation of Phosphatidylcholines Initiated with Dicumylhyponitrite in Solution and in Bilayers, *Can. J. Chem.* **64**, 2103–2108.
13. Yamamoto, Y., Niki, E., and Kamiya, Y. (1982) Quantitative Determination of the Oxidation of Methyl Linoleate and Methyl Linolenate, *Bull. Chem. Soc. Jpn.* **55**, 1548–1550.
14. Cosgrove, J.P., Church, D.F., and Pryor, W.A. (1987) The Kinetics of the Autoxidation of Polyunsaturated Fatty Acids, *Lipids* **22**, 299–304.
15. Mowri, H., Nojima, S., and Inoue, K. (1984) Effect of Lipid Composition of Liposomes on Their Sensitivity to Peroxidation, *J. Biochem.* **95**, 551–558.
16. Wagner, B.A., Buettner, G.R., and Burns, C.P. (1994) Free Radical-Mediated Lipid Peroxidation in Cells: Oxidizability Is a Function of Cell Lipid Bis-allylic Hydrogen Content, *Biochemistry* **33**, 4449–4453.
17. Miyashita, K., Nara, E., and Ota, T. (1993) Oxidative Stability of Polyunsaturated Fatty Acids in an Aqueous Solution, *Biosci. Biotechnol. Biochem.* **57**, 1638–1640.
18. Yazu, K., Yamamoto, Y., Ukegawa, K., and Niki, E. (1996) Mechanism of Lower Oxidizability of Eicosapentaenoate Than Linoleate in Aqueous Micelles, *Lipids* **31**, 337–340.
19. Koga, T., Takahashi, I., Yamauchi, R., Piskula, M., and Terao, J. (1997) Kinetic Studies on the Formation of Phosphatidylcholine Hydroperoxides in Large Unilamellar Vesicles by Azo Compounds, *Chem. Phys. Lipids* **86**, 85–93.
20. Nara, E., Miyashita, K., and Ota, T. (1997) Oxidative Stability of Liposomes Prepared from Soybean PC, Chicken Egg PC, and Salmon Egg PC, *Biosci. Biotechnol. Biochem.* **61**, 1736–1738.
21. Bowry, V.W. (1994) Arm-to-Arm Autoxidation in a Triglyceride: Remote Group Reaction Kinetics, *J. Org. Chem.* **59**, 2250–2252.
22. Zachowski, A. (1993) Phospholipids in Animal Eukaryotic Membranes: Transverse Asymmetry and Movement, *Biochem. J.* **294**, 1–14.

[Received February 8, 2002, and in revised form September 9, 2002; accepted September 17, 2002]



# Relationship Between Platelet Phospholipid FA and Mean Platelet Volume in Healthy Men

Duo Li<sup>a,c,\*</sup>, Alan Turner<sup>b</sup>, and Andrew J. Sinclair<sup>a</sup>

Departments of <sup>a</sup>Food Science and <sup>b</sup>Medical Laboratory Science, RMIT University, Melbourne 3001, Australia, and <sup>c</sup>Department of Food Science, Hangzhou University of Commerce, Hangzhou 310035, China

**ABSTRACT:** Increased mean platelet volume (MPV) has been suggested as an independent risk factor for acute myocardial infarction and the increased reactivity of large platelets. The aim of this study was to investigate the correlation between platelet phospholipid (PL) PUFA composition and MPV in 139 free-living healthy men ages 20–55 yr (vegans,  $n = 18$ ; ovo-lacto vegetarians,  $n = 43$ ; moderate meat-eaters,  $n = 60$ ; and high meat-eaters,  $n = 18$ ). Each subject completed a semiquantitative Food Frequency Questionnaire and gave a blood sample. Platelet PL FA composition and MPV were determined by standard methods. MPV was significantly greater in the vegans than in the ovo-lacto vegetarian, moderate, or high meat-eater groups ( $P < 0.01$ ). Both vegan and ovo-lacto vegetarian groups had significantly higher platelet PL 18:2n-6 and 22:4n-6, and lower 20:5n-3 and 22:6n-3 compared with the moderate and high meat-eater groups. The vegans demonstrated a significant reduction in 20:4n-6 and 22:5n-3 compared with the ovo-lacto vegetarian, high meat-eater, and moderate meat-eater groups. Bivariate analysis results showed that MPV was significantly positively correlated with platelet PL 18:2n-6 ( $P = 0.048$ ) and negatively correlated with 20:3n-6 ( $P = 0.02$ ), 20:5n-3 ( $P = 0.005$ ), and 22:5n-3 ( $P < 0.0001$ ), respectively. In a multiple linear regression analysis, after controlling for potential confounding factors such as dietary group, age, exercise, body mass index, and dietary polyunsaturated and saturated fat, cholesterol, carbohydrate, and fiber intake, the MPV was still strongly negatively correlated with platelet PL 20:3n-6 ( $P = 0.003$ ) and 22:5n-3 ( $P = 0.001$ ). The present data suggest that 22:5n-3 and 20:3n-6 may play a role in the structural function of the platelet membrane.

Paper no. L8755 in *Lipids* 37, 901–906 (September 2002).

Evidence from case control studies has indicated that an increased mean platelet volume (MPV) is an independent risk factor for acute myocardial infarction (MI) (1) and for acute and/or nonacute cerebral ischemia (2). Large platelets, in such cases, have been shown to have increased reactivity, leading to the potential for thrombus formation.

The major role of platelets is in maintaining vascular integrity and minimizing blood loss. The process is regulated

by a complex dynamic balance between factors released from both the endothelium and platelets, including prostacyclin (which inhibits platelet aggregation) and thromboxane (which potentiates aggregation). Platelets normally circulate in a quiescent disk-shaped state, but as they become activated, changes occur that cause them to undergo a disk-to-sphere transformation with the development of pseudopodia (3). This shape change leads to an increase in platelet size, as measured by MPV, and platelet aggregation is enhanced (4,5).

Flow cytometry techniques have demonstrated that this greater reactivity of larger platelets is associated with an increased exposure of fibrinogen receptors and the release of platelet granule contents (6). Platelet activation may be measured using more sophisticated tests of platelet function, such as platelet aggregation and release by platelet aggregometry, or by measurement of immunological markers of activation using flow cytometry. These techniques are time-consuming and labor-intensive, whereas measurement of platelet size (MPV) may be a useful rapid index of platelet activation in circumstances where production or loss is not impaired (7).

Dietary intervention and epidemiological studies have reported that increased levels of n-3 PUFA, relative to n-6 PUFA, in the platelet membrane may provide a protective effect against thrombus formation *via* reduced thromboxane A<sub>2</sub> formation (8). The consumption of purified 20:5n-3 ethyl esters (900 or 1800 mg/d) has been shown to decrease MPV significantly in patients with thrombotic or atherosclerotic diseases (9). Changes in the proportions of eicosapentaenoic and arachidonic acids of platelets have been reported to influence the structure, function, and fluidity (order) of the platelet membrane *via* eicosanoid metabolism (10); to bind to platelet membrane proteins *via* thioester bonds in place of saturated FA; and to modulate hydrophobic protein–membrane lipid and protein–protein interactions (11,12). However, there are no data in the literature on the correlation between the platelet phospholipid (PL) individual FA and MPV in either human or animal studies.

The aim of this study was to investigate the correlation between the composition of individual FA in platelet PL and MPV. We collected Food Frequency Questionnaires (FFQ) and blood samples from four groups of healthy men (vegans,  $n = 18$ ; ovo-lacto vegetarians,  $n = 43$ ; moderate meat-eaters,  $n = 60$ ; and high meat-eaters,  $n = 18$ ) ages 20–55 yr with widely varying intakes of long-chain PUFA. We hypothesized that the long-term intake of long-chain n-3 PUFA from their habitual diet would be negatively correlated with the MPV.

\*To whom correspondence should be addressed.

E-mail: duoli@mail.hzic.edu.cn

Abbreviations: BMI, body mass index; CTAD, citrate, theophylline, adenosine, and dipyridamole; CVD, cardiovascular disease; FFQ, Food Frequency Questionnaire; 12-HETE, 12-hydroxy-5,8,10,14-eicosatetraenoic acid; MI, myocardial infarction; MPV, mean platelet volume; MUFA, monounsaturated fatty acid; PG, prostaglandin; PL, phospholipid; PRP, platelet-rich plasma; SFA, saturated fatty acid.

## METHODS

**Subjects.** This study formed part of a large project investigating the association between diet and cardiovascular risk factors in Australian men (13). The project was approved by the Human Research Ethics Committee of RMIT University. One hundred thirty-nine healthy male nonsmokers between 20 and 50 yr of age were recruited through advertisements in university newsletters and local newspapers, and all subjects gave written informed consent for participation in the study. The exclusion criteria for this study were: evidence of cardiovascular disease (CVD), hypertension, renal disease, hyperlipemia, hematological disorders, diabetes, a family history of CVD, excess alcohol intake, and drug therapy. Subjects were asked to complete an FFQ (14) and were given detailed instructions on how to complete it. Each completed FFQ was checked by the same dietician. According to their habitual dietary intake (based on the FFQ), the subjects were divided into high meat-eaters ( $n = 18$ ), moderate meat-eaters ( $n = 60$ ), ovolacto vegetarians ( $n = 43$ ), and vegans ( $n = 18$ ). A high meat-eater was defined as someone consuming  $\geq 280$  g raw meat per day, and a moderate meat-eater was defined as one who consumed  $< 280$  g per day. A vegan was defined as someone who ate meat, eggs, and dairy products less than six times per year. An ovolacto vegetarian was defined as someone who ate meat no more than six times per year but consumed eggs and dairy products freely. For the subjects to be classified into these categories, they had to have been practicing their diets for at least 6 mon prior to the study.

**Dietary intake.** The dietary intake data of each subject were assessed using the FFQ and calculated using Diet/1 Version 4 software (Xyris Software, Pty. Ltd., Highgate Hill, QLD, Australia) with the NUTTAB 95 database based on Composition of Foods, Australia.

**Blood specimen collections.** Subjects came to the Medical Centre of RMIT University in the morning following an overnight fast. They were allowed to sit relaxed for 10 min, and then venous blood was drawn into CTAD (citrate, theophylline, adenosine, and dipyridamole) and citrate vacuum tubes with 21-gauge needles. After blood collection, the sub-

jects' weight, height, and blood pressure were measured. Two CTAD tubes of whole blood were spun at  $100 \times g$  for 10 min. Platelet-rich plasma (PRP) was removed, and platelets were isolated from PRP using the method of Castaldi and Smith (15).

**MPV.** MPV of citrate-preserved whole blood was measured on a Coulter STKR analyzer (Coulter Electronics Inc., Hialeah, FL).

**Platelet PL FA.** Total lipids of platelets were extracted with solvents, the platelet PL fraction was separated by TLC, and FAME of the platelet PL fraction were prepared and separated by GLC as described previously (16).

**Statistical analyses.** Data analyses were performed using a StatView software program (Abacus Concepts Inc., Berkeley, CA). An ANOVA was used to establish whether differences existed between the dietary groups for each parameter. If a significant difference was found, a further multiple comparison test was performed using Fisher's *post-hoc* tests to determine differences between each pair of dietary groups (13). Linear regressions were used to determine the relationship between MPV and platelet PL FA composition. Bivariate analyses were initially used to assess the relationship between MPV and platelet PL composition of individual FA, and dietary intake of micro- and macronutrients. In the multivariate linear regression analysis, MPV was used as a dependent variable, and platelet PL FA compositions were used as independent variables. Dietary intakes of PUFA, saturated fat, cholesterol, carbohydrate, and fiber were used as covariates and controlled for the following factors: exercise, dietary group, age, and body mass index (BMI) (17). The values are reported as mean  $\pm$  SD in Tables 1 and 2 and mean  $\pm$  SEM in Figure 1 unless otherwise specified. *P* values were two-sided, and  $< 0.05$  was considered significant.

## RESULTS

Table 1 reports the physiological characteristics and daily dietary intake of the four dietary groups. The mean BMI was significantly greater in both the high and moderate meat-eater groups than in both the ovolacto vegetarian and vegan groups.

**TABLE 1**  
**Physiological Characteristics and Daily Dietary Intake of the Four Dietary Groups (mean  $\pm$  SD)<sup>a</sup>**

	High meat ( $n = 18$ )	Moderate meat ( $n = 60$ )	Ovolacto ( $n = 43$ )	Vegan ( $n = 18$ )
Age (yr)	34.2 $\pm$ 9.4	38.3 $\pm$ 7.3	34.9 $\pm$ 9.0 <sup>b*</sup>	33.0 $\pm$ 7.7 <sup>b*</sup>
BMI	27.0 $\pm$ 3.4	26.4 $\pm$ 3.4	23.6 $\pm$ 2.8 <sup>a***,b***</sup>	23.3 $\pm$ 3.5 <sup>a***,b***</sup>
Energy (MJ)	1.64 $\pm$ 3.31	1.13 $\pm$ 2.48 <sup>a***</sup>	1.15 $\pm$ 2.46 <sup>a***</sup>	1.18 $\pm$ 2.44 <sup>a***</sup>
Protein (% of E)	19.4 $\pm$ 1.3	17.9 $\pm$ 2.2 <sup>a**</sup>	14.7 $\pm$ 2.2 <sup>a***,b***</sup>	14.1 $\pm$ 2.4 <sup>a***,b***</sup>
CHO (% of E)	40.3 $\pm$ 4.4	45.7 $\pm$ 6.8 <sup>a**</sup>	50.9 $\pm$ 6.4 <sup>a***,b***</sup>	57.4 $\pm$ 5.4 <sup>a***,b***,C***</sup>
Total fat (% of E)	37.8 $\pm$ 4.2	32.8 $\pm$ 6.1 <sup>a**</sup>	32.7 $\pm$ 6.2 <sup>a**</sup>	28.2 $\pm$ 4.3 <sup>a***,b***,C***</sup>
SFA (% of E)	17.4 $\pm$ 2.7	14.3 $\pm$ 3.2 <sup>a***</sup>	11.9 $\pm$ 4.0 <sup>a***,b***</sup>	6.6 $\pm$ 1.6 <sup>a***,b***,C***</sup>
MUFA (% of E)	14.9 $\pm$ 1.4	13.0 $\pm$ 2.8 <sup>a*</sup>	12.9 $\pm$ 3.2 <sup>a*</sup>	11.7 $\pm$ 2.7 <sup>a***</sup>
PUFA (% of E)	5.6 $\pm$ 1.4	5.6 $\pm$ 2.3	7.9 $\pm$ 2.5 <sup>a***,b***</sup>	9.8 $\pm$ 3.1 <sup>a***,b***,C**</sup>
Cholesterol (mg)	611 $\pm$ 150	332 $\pm$ 107 <sup>a***</sup>	197 $\pm$ 117 <sup>a***,b***</sup>	22 $\pm$ 22 <sup>a***,b***,C***</sup>
Fiber (g)	43 $\pm$ 12	33 $\pm$ 10 <sup>a</sup>	54 $\pm$ 18 <sup>a***,b***</sup>	77 $\pm$ 23 <sup>a***,b***,C***</sup>

<sup>a</sup>E, energy; CHO, carbohydrate; SFA, saturated FA; MUFA, monounsaturated FA; BMI, body mass index. Significance of differences for <sup>a</sup>high meat-eaters, <sup>b</sup>moderate meat-eaters, <sup>c</sup>ovolacto vegetarians: \* $P < 0.05$ , \*\* $P < 0.01$ , \*\*\* $P < 0.001$ .

The median age (range) was 35 yr (21 to 50) for the high meat-eater group, 38 (21 to 55) for the moderate meat-eater group, 31 (22 to 54) for the ovo-lacto vegetarian group, and 31 (22 to 50) for the vegan group. Energy intake was significantly higher in high meat-eaters than in the other three dietary groups. However, the energy sources were quite different between the four dietary groups. Protein, total fat, saturated FA (SFA), and monounsaturated FA (MUFA) as percentage of energy showed a significant decreasing tendency from high meat-eaters to moderate meat-eaters to ovo-lacto vegetarians and vegans. However, PUFA as percentage of energy was significantly increased from high meat-eaters to moderate meat-eaters to ovo-lacto vegetarians and vegans. Vegans do not eat dairy products and meats, and their fat intake was derived mostly from seeds, nuts, avocados, and vegetable oils. Cholesterol intake showed a significant decreasing tendency from high meat-eaters to moderate meat-eaters to ovo-lacto vegetarians to vegans. The small amount of cholesterol in the vegan diet was derived from egg-containing pastry.

There was a tendency for the MPV to increase from high meat-eaters to moderate meat-eaters to ovo-lacto vegetarians to vegans, and it was significantly greater in the vegan group than in the other three groups (Fig. 1).

Platelet PL PUFA compositions are shown in Table 2. There was no significant correlation between MPV and individual platelet SFA and MUFA, so only platelet PUFA data (% of total FA) are reported. The proportions of platelet PL 18:2n-6 and 22:4n-6 were significantly higher in both the ovo-lacto vegetarian and the vegan groups than in both the high and the moderate meat-eater groups. There was a significant tendency for 20:4n-6, 20:5n-3, and 22:6n-3 to decrease from the high and the moderate meat-eater groups to ovo-lacto vegetarian to vegan groups. The proportion of 22:5n-3 in the vegan group was significantly lower compared with other three dietary groups.

Bivariate analysis results showed that MPV was positively correlated with platelet PL 18:2n-6 ( $P = 0.048$ ) and negatively correlated with platelet PL 20:3n-6 ( $P = 0.02$ ), 20:5n-3

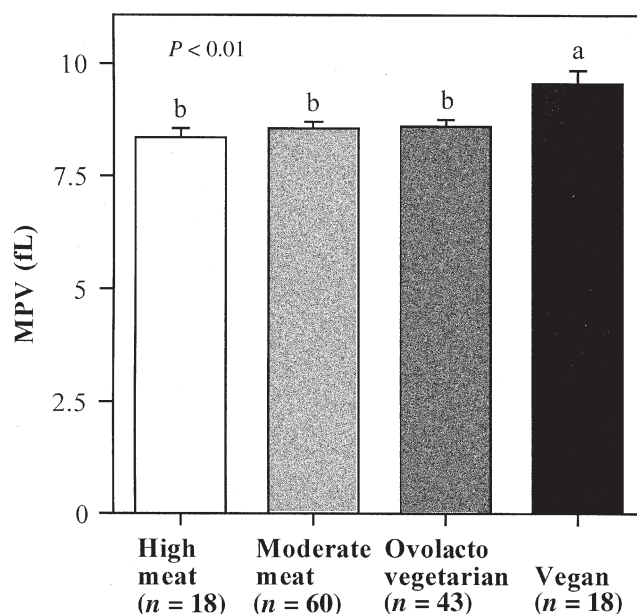


FIG. 1. Mean platelet volume (MPV) of four dietary groups. Lowercase a and b indicate a difference between dietary groups. Error bars represent mean  $\pm$  SEM.

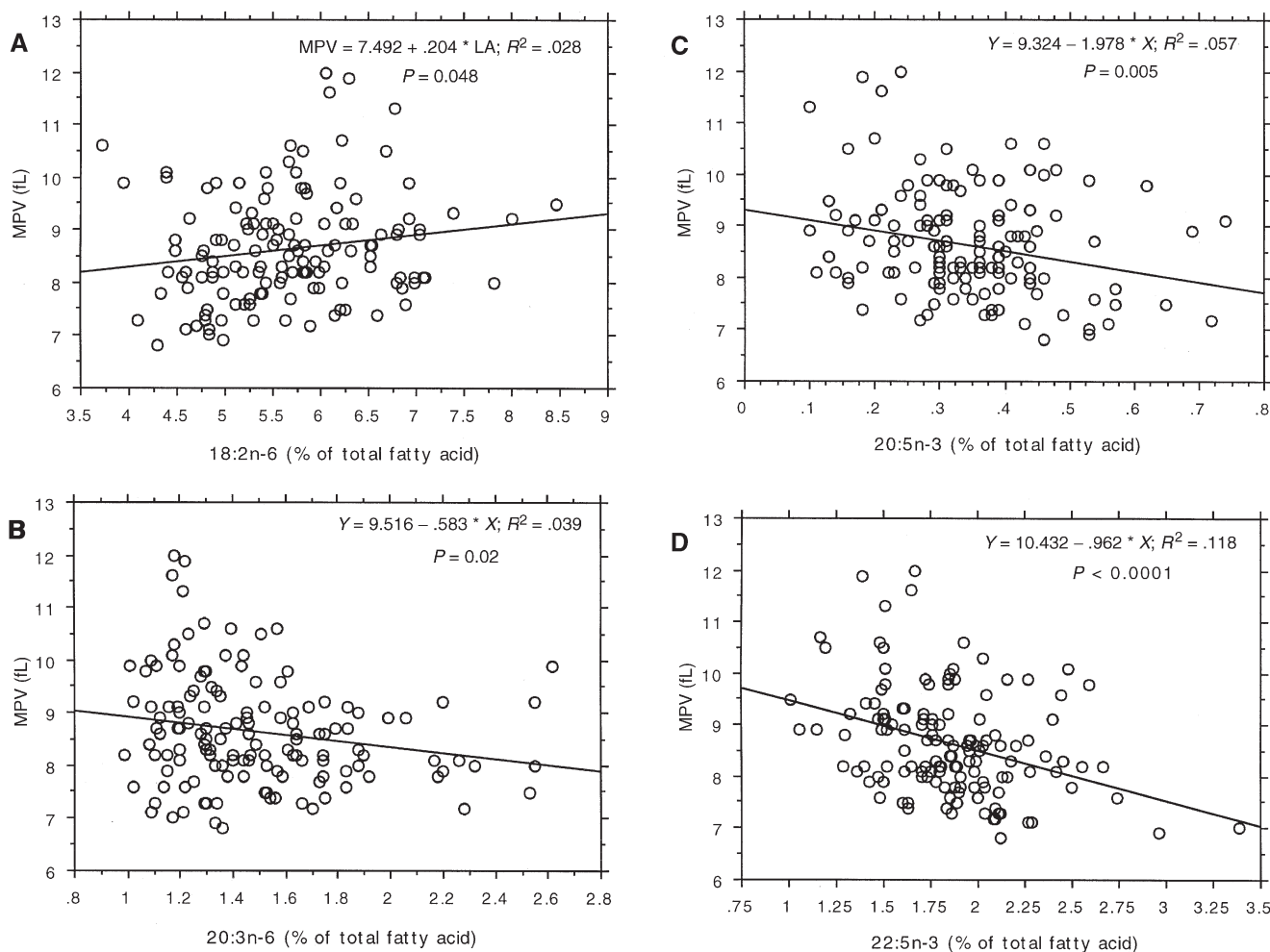
( $P = 0.005$ ), and 22:5n-3 ( $P < 0.0001$ ), respectively (Figs. 2 A–D). There was a significant negative correlation between MPV and platelet count ( $P < 0.001$ ). MPV was also positively correlated with dietary intake of carbohydrates ( $P = 0.043$ ), PUFA ( $P = 0.0146$ ), and fiber ( $P = 0.002$ ) and negatively correlated with dietary intake of SFA ( $P = 0.003$ ) and cholesterol ( $P = 0.002$ ).

Table 3 shows the results of the multiple linear regression, in which MPV was used as the dependent variable and platelet PL 22:5n-3, 18:2n-6, 20:3n-6, and 20:5n-3 were the independent variables. After controlling for confounding factors such as dietary group, age, BMI, dietary total saturated fat, total PUFA, cholesterol, carbohydrate, and fiber intake, the MPV was still strongly positively correlated with platelet PL 22:5n-3 ( $P = 0.0012$ ) and 20:3n-6 ( $P = 0.0034$ ).

TABLE 2  
Partial Platelet Phospholipid FA Composition of the Four Dietary Groups (% of total FA, mean  $\pm$  SD)<sup>a</sup>

FA	High meat (n = 18)	Moderate meat (n = 60)	Ovo-lacto (n = 43)	Vegan (n = 18)
18:2n-6	5.3 $\pm$ 0.7	5.2 $\pm$ 0.6	6.1 $\pm$ 0.9 <sup>a***,b***</sup>	6.3 $\pm$ 0.5 <sup>a***,b***</sup>
20:3n-6	1.5 $\pm$ 0.3	1.5 $\pm$ 0.3	1.5 $\pm$ 0.4	1.5 $\pm$ 0.4
20:4n-6	24.4 $\pm$ 1.4	24.5 $\pm$ 1.2	23.9 $\pm$ 1.3 <sup>b*</sup>	23.0 $\pm$ 1.7 <sup>a**,b***,c*</sup>
22:4n-6	2.3 $\pm$ 0.3	2.4 $\pm$ 0.3	2.6 $\pm$ 0.4 <sup>a**,b*</sup>	2.7 $\pm$ 0.5 <sup>a**,b**</sup>
22:5n-6	0.2 $\pm$ 0.0	0.3 $\pm$ 0.2	0.3 $\pm$ 0.1	0.2 $\pm$ 0.1
Total n-6	33.7 $\pm$ 1.9	33.9 $\pm$ 1.2	34.4 $\pm$ 1.5	33.8 $\pm$ 2.2
18:3n-3	0.0 $\pm$ 0.0	0.1 $\pm$ 0.1	0.1 $\pm$ 0.0	0.1 $\pm$ 0.2
20:5n-3	0.4 $\pm$ 0.1	0.4 $\pm$ 0.1	0.3 $\pm$ 0.1 <sup>a**,b***</sup>	0.2 $\pm$ 0.1 <sup>a***,b***,c*</sup>
22:5n-3	1.9 $\pm$ 0.3	1.9 $\pm$ 0.3	1.9 $\pm$ 0.5	1.5 $\pm$ 0.4 <sup>a**,b***,c***</sup>
22:6n-3	1.5 $\pm$ 0.4	1.6 $\pm$ 0.4	1.2 $\pm$ 0.4 <sup>a**,b***</sup>	0.9 $\pm$ 0.3 <sup>a***,b***,c**</sup>
Total n-3	3.7 $\pm$ 0.5	3.9 $\pm$ 0.5	3.3 $\pm$ 0.8 <sup>a**,b***</sup>	2.7 $\pm$ 0.5 <sup>a***,b***,c***</sup>
Total PUFA	37.4 $\pm$ 2.0	37.8 $\pm$ 1.1	37.8 $\pm$ 1.3	36.6 $\pm$ 2.3 <sup>b**,c**</sup>

<sup>a</sup>Significance of differences for <sup>a</sup>high meat-eaters, <sup>b</sup>moderate meat-eaters, <sup>c</sup>ovo-lacto vegetarians: \* $P < 0.05$ , \*\* $P < 0.01$ , \*\*\* $P < 0.001$ . The full FA composition can be found in Reference 13.



**FIG. 2.** Correlation of MPV with composition of platelet phospholipid 18:2n-6 (A), 20:3n-6 (B), 20:5n-3 (C), and 22:5n-3 (D). LA, 18:2n-6; for other abbreviation see Figure 1.

## DISCUSSION

The aim of this study was to investigate the correlation between MPV and individual FA composition in platelet PL. We hy-

**TABLE 3**  
**Relationships Between Mean Platelet Volume and Platelet Phospholipid FA Compositions, as Determined by Multiple Linear Regression, with Potential Confounding Factors as Covariates<sup>a</sup>**

Factors	Std. coeff.	P-Value
Platelet 18:2n-6	0.034	0.777
Platelet 20:3n-6	-0.281	0.003
Platelet 20:5n-3	-0.037	0.725
Platelet 22:5n-3	-0.319	0.001
CHO intake (% of E)	-0.072	0.542
Fiber intake (g/d)	0.205	0.088
Cholesterol intake (mg/d)	-0.095	0.574
PUFA intake (% of E)	0.010	0.960
SFA intake (% of E)	0.142	0.520
Age (yr)	-0.048	0.607
BMI	0.164	0.547
Exercise (h/d)	-0.058	0.120
Dietary group	0.207	0.247

<sup>a</sup>Std. Coeff., standardized regression coefficients; for other abbreviations see Table 1.

pothesized that the long-term intake of long-chain n-3 PUFA from the habitual diet would be negatively correlated with MPV, based on evidence from previous studies suggesting that n-3 PUFA reduce platelet aggregability (18,19).

In this study, the MPV was significantly positively correlated with platelet PL 18:2n-6 and negatively correlated with 20:3n-6, 20:5n-3, and 22:5n-3 in the bivariate analysis. In the multiple linear regression, after controlling for the confounding factors such as BMI, exercise, age, dietary groups, dietary intake of carbohydrates, fiber, cholesterol, PUFA, and SFA, the MPV was still significantly negatively correlated with platelet PL 20:3n-6 and 22:5n-3 ( $P < 0.01$ ). This result suggests that if it were possible to increase the levels of these particular PUFA in platelet membranes, this increase might be associated with a reduced MPV as discussed later. In the quiescent disk-like state associated with lower MPV values, platelets are less likely to be involved in thrombotic conditions (18) since they are not subject to activating stimuli that cause shape and behavioral changes. Although the main function of platelets is to arrest bleeding, they also have been implicated in the initiation and development of arterial thrombosis in circumstances where inappropriate activation occurs (19).



Reports of the effect of dietary intervention with n-3 PUFA on the MPV have been inconsistent. For example, the MPV showed a significant decrease when the diets of 34 patients (26 men and 8 women), ages 42 to 86 yr, with thrombotic or arteriosclerotic diseases were supplemented with 900 or 1800 mg of purified eicosapentaenoic acid ethyl ester for 12 wk (9). In contrast, the MPV showed significant increases when healthy subjects, ages 16 to 69 yr, consumed 15 mL of cod liver oil/olive oil (1:1, vol/vol) ( $n = 40$ ) and whale oil ( $n = 38$ ) daily for 12 wk (20); when 9 healthy men, ages 31 to 65 yr, consumed a salmon diet for 40 d (21); and when the diets of 34 healthy subjects (20 men and 14 women), ages 20 to 40 yr, were supplemented with 25 mL cod liver oil per day for 8 wk (22). The mean MPV was significantly reduced from 8.3 to 7.7 fL when 10 healthy men, ages 32 to 40 yr, consumed a high stearic acid diet (8% of energy), compared with a low stearic acid diet (2% of energy), for 40 d (23). In a similar study, the MPV decreased significantly from 8.9 to 8.4 fL when 13 healthy men, ages 20 to 55 yr, consumed a diet high in stearic acid (19.4 g/d) for 4 wk, compared with a baseline diet (7.3 g stearic acid/d); the latter was associated with an increase in the proportion of stearic acid (from 20.1 to 24.6%) in platelet PL (24). Platelet membrane 20:3n-6 was reported to decrease significantly ( $P < 0.01$ ) and MPV to increase significantly in postmenopausal women ( $n = 38$ ) who were given hormone replacement therapy for 6 wk (25).

MPV is influenced by body weight and physical exercise. MPV was shown to increase with age in a population study of 1065 subjects who ranged in age from 0 to 75 yr (27). The lightest subpopulation had the lowest MPV (26). MPV was shown to increase in obese patients who undertook weight loss therapy with either a hypocaloric diet or a nutritionally complete very low caloric diet for 40 wk (28). MPV also decreased significantly in 60 male and 18 female healthy subjects after 18 to 20 mon of physical exercise (29).

As discussed above, increased MPV in some cases is not necessarily a risk factor for CVD. As reported by others (30–32), we also found that MPV was significantly negatively correlated with platelet counts in healthy subjects. This indicates that in healthy subjects when MPV goes up, platelet count goes down to maintain a physiological platelet mass (33). Furthermore, the results of platelet size and shape studies carried out in patients with CVD cannot necessarily be extrapolated to healthy subjects. Results from the present study suggest that 22:5n-3 and 20:3n-6 play a role in the structural function of platelet membranes.

The results from this paper suggest that two PUFA found in platelets (20:3n-6 and 22:5n-3) may influence platelets by reducing their reactivity. The effects of these two PUFA on platelet function have rarely been studied, although they occur in platelets at about the same levels as 20:5n-3, perhaps because 22:5n-3 has only recently become available as a pure standard. Two reports, however, indicate that 22:5n-3 does influence platelet function. First, Careaga and Sprecher (34) reported that 22:5n-3 inhibited synthesis of both thromboxane  $B_2$  and 5,8,10-heptadecatrienoic acid from arachidonic

acid. They also reported that 12-hydroxy-5,8,10,14-eicosatetraenoic acid (12-HETE) synthesis increased due to substrate shunting to the lipoxygenase pathway when platelets were incubated with a high concentration of 22:5n-3 (20  $\mu$ M) and increasing levels of [ $1-^{14}C$ ]20:4n-6 (34). Second, Akiba *et al.* (35) reported that 22:5n-3, compared with 20:5n-3 or 22:6n-3, exhibited the most potent activity for inhibiting thromboxane  $A_2$  formation and for accelerating 12-HETE production by intact rabbit platelets. These authors suggested the effects may have been responsible for the marked inhibition of platelet aggregation by 22:5n-3. Oelz *et al.* (36) fed a large amount of 20:3n-6 to rabbits, and although considerable amounts of prostaglandin (PG)  $E_1$  and  $PGE_2$  were produced by their aggregating platelets, no changes in response to agonist ADP, collagen, and arachidonic acid were detected.

In conclusion, the data from this study support the need for further research on the role of different PUFA on platelet function using purified FA and various *ex vivo* techniques to probe the possible mechanisms of the action of PUFA on the platelet.

## ACKNOWLEDGMENT

This study was supported by a grant from the Meat Research Corporation of Australia, and an RMIT postgraduate scholarship for D.L. We acknowledge Neil Mann, Leeann Johnson, They Ng, Maureen Francis, Fiona Kelly, Lavinia Abedin, Alisa Wilson, and Sirithon Nakkote for their assistance in various aspects of the original large project.

## REFERENCES

1. Martin, J.F., Bath, P.M.W., and Burr, M.L. (1991) Influence of Platelet Size on Outcome After Myocardial Infarction, *Lancet* 338, 1408–1411.
2. O'Malley, T., Langhorne, P., Elton, R.A., and Stewart, C. (1995) Platelet Size in Stroke Patients, *Stroke* 26, 6995–6999.
3. Blockmans, D., Deckmyn, H., and Vermeylen, J. (1995) Platelet Activation, *Blood Rev.* 9, 143–156.
4. Laufer, N., Grover, N.B., Ben-Sasson, S., and Freund, H. (1979) Effects of Adenosine Diphosphate, Colchicine and Temperature on Size of Human Platelets, *Thromb. Haemost.* 41, 491–497.
5. Sharp, D.S., Bath, P.M.W., Martin, J.F., Beswick, A.D., and Sweetnam, P.M. (1994) Platelet and Erythrocyte Volume and Count: Epidemiological Predictors of Impedance Measured ADP-Induced Platelet Aggregation in Whole Blood, *Platelets* 5, 253–257.
6. Michelson, A.D. (1996) Flow Cytometry: A Clinical Test of Platelet Function, *Blood* 87, 4925–4963.
7. Bath, P.M., and Butterworth, R.J. (1996) Platelet Size: Measurement, Physiology and Vascular Disease, *Blood Coagul. Fibrinolysis* 7, 157–161.
8. Connor, S.L., and Connor, W.E. (1997) Are Fish Oils Beneficial in the Prevention and Treatment of Coronary Artery Disease? *Am. J. Clin. Nutr.* 66, 1020S–1031S.
9. Saga, T., Aoyama, T., and Takekoshi, T. (1994) Changes in Platelet Count and Mean Volume of Platelet After Administration of Eicosapentaenoic Acid Ethyl-Ester, and Factors That May Affect Those Changes, *Nippon Ronen. Igakkai Zasshi* 31, 538–547.
10. von Schacky, C., Fischer, S., and Weber, P.C. (1985) Long-Term Effects of Dietary Marine Omega-3 Fatty Acids upon

- Plasma and Cellular Lipids, Platelet Function, and Eicosanoid Formation in Humans, *J. Clin. Invest.* 76, 1626–1631.
11. Muszbek, L., and Laposata, M. (1993) Covalent Modification of Proteins by Arachidonate and Eicosapentaenoate in Platelets, *J. Biol. Chem.* 268, 18243–18248.
  12. Muszbek, L., Racz, E., and Laposata, M. (1997) Posttranslational Modification of Proteins with Fatty Acids in Platelets, *Prostaglandins Leukot. Essent. Fatty Acids.* 57, 359–366.
  13. Li, D., Sinclair, A.J., Mann, N., Turner, A., Kelly, F., Abedin, L., Wilson, A., and Ball, M. (1999) The Effect of Habitual Diet on the Thrombotic Risk Factors in Healthy Male Subjects, *Eur. J. Clin. Nutr.* 53, 612–619.
  14. Fidanza, F., Gentile, M.G., and Porrini, M. (1994) A Self-Administered Semiquantitative Food-Frequency Questionnaire with Optical Reading and Its Concurrent Validation, *Eur. J. Epidemiol.* 11, 1–8.
  15. Castaldi, P.A., and Smith, I.L. (1980) The Effect of Platelets on the *in vitro* Response to Prothrombin Complex Concentrates in F.VIII Inhibitor Plasma, *Pathology* 12, 111–118.
  16. Sinclair, A.J., O’Dea, K., Dunstan, G., Ireland, P.D., and Niall, M. (1987) Effect on Plasma Lipids and Fatty Acid Composition of Very Low Fat Diets Enriched with Fish or Kangaroo Meat, *Lipids* 22, 523–529.
  17. Cushman, M., Yanez, D., Psaty, B.M., Fried, L.P., Heiss, G., Lee, M., Polak, J.F., Savage, P.J., and Tracy, R.P. (1996) Association of Fibrinogen and Coagulation Factors VII and VIII with Cardiovascular Risk Factors in the Elderly, *J. Epidemiol.* 143, 665–676.
  18. Schoene, N.W. (1991) Dietary Fatty Acids and Platelet Function: Mechanisms, in *Health Effects of Dietary Fatty Acids* (Nelson, G., ed.), pp. 129–135, AOCS, Champaign.
  19. Farstad, M. (1998) The Role of Blood Platelets in Coronary Atherosclerosis and Thrombosis, *Scand. J. Clin. Lab. Invest.* 58, 1–10.
  20. Vognild, E., Elvevoll, E.O., Brox, J., Olsen, R.L., Barstad, H., Aursand, M., and Østerud, B. (1998) Effects of Dietary Marine Oils on Fatty Acid Composition, Platelet Membrane Fluidity, Platelet Responses, and Serum Lipids in Healthy Humans, *Lipids* 33, 427–436.
  21. Nelson, G.L., Schmidt, P.C., and Corash, L. (1991) The Effect of a Salmon Diet on Blood Clotting, Platelet Aggregation and Fatty Acids in Normal Adult Men, *Lipids* 26, 87–96.
  22. Hansen, J.B., Berge, L.N., Svensson, B., Lyngmo, V., and Nordoy, A. (1993) Effects of Cod Liver Oil on Lipids and Platelets in Males and Females, *Eur. J. Clin. Nutr.* 47, 123–131.
  23. Schoene, N.W., Allman, M.A., Dougherty, R.M., Denvir, E., and Iacono, J.M. (1992) Diverse Effects of Dietary Stearic and Palmitic Acids on Platelet Morphology, in *Essential Fatty Acids and Eicosanoids* (Gibson, R., and Sinclair, A.J., eds.), pp. 290–292, AOCS, Champaign.
  24. Kelly, F.D., Sinclair, A.J., Mann, N.J., Turner, A.H., Abedin, L., and Li, D. (2001) A Stearic Acid-Rich Diet Improves Thrombogenic and Atherogenic Risk Factor Profiles in Healthy Males, *Eur. J. Clin. Nutr.* 55, 88–96.
  25. Ranganath, L.R., Christofides, J., and Semple, M.J. (1996) Increased Mean Platelet Volume After Oestrogen Replacement Therapy, *Ann. Clin. Biochem.* 33, 555–560.
  26. Kabata, J., Raszeja-Specht, A., Steffek, I., and Angielski, S. (1995) Reference Values for Peripheral Blood Morphology in Countryside Population of Northern Poland, *Pol. Tyg. Lek.* 50, 62–65.
  27. Rososhansky, S., and Szymanski, I.O. (1994) PA-IgG on Platelet Subpopulations of Different Buoyant Densities: High Levels on the Low Density Population Is an Artifact, *Am. J. Hematol.* 47, 312–315.
  28. Toplak, H., and Wascher, T.C. (1994) Influence of Weight Reduction on Platelet Volume: Different Effects of a Hypocaloric Diet and a Very Low Calorie Diet, *Eur. J. Clin. Invest.* 24, 778–780.
  29. Van Wersch, J.W., Kaiser, V., and Janssen, G.M. (1989) Platelet System Changes Associated with a Training Period of 18–20 Months: A Transverse and a Longitudinal Approach, *Int. J. Sports Med.* 10, 181S–185S.
  30. Bessman, J.D., Williams, L.J., and Gilmer, P.R., Jr. (1981) Mean Platelet Volume Inverse Relation of Platelet Size and Count in Normal Subjects, and an Artifact of Other Particles, *Am. J. Clin. Pathol.* 76, 289–293.
  31. Bain, B.J. (1985) Platelet Count and Platelet Size in Males and Females, *Scand. J. Haematol.* 35, 77–79.
  32. Lozano, M., Narvaez, J., Faundez, Z., Mazzara, R., Cid, J., Jou, J.M., Marin, J.L., and Ordinas, A. (1998) Platelet Count and Mean Platelet Volume in the Spanish Population, *Med. Clin.* 110, 774–777.
  33. Li, D. (1998) The Influence of Diet on Atherosclerotic and Thrombotic Risk Factors in Healthy Men, Ph.D. Dissertation, RMIT University, Melbourne, Australia.
  34. Careaga, M.M., and Sprecher, H. (1984) Synthesis of Two Hydroxy Fatty Acids from 7,10,13,16,19-Docosapentaenoic Acid by Human Platelets, *J. Biol. Chem.* 259, 14413–14417.
  35. Akiba, S., Murata, T., Kitatani, K., and Sato, T. (2000) Involvement of Lipoxigenase Pathway in Docosapentaenoic Acid-Induced Inhibition of Platelet Aggregation, *Biol. Pharm. Bull.* 23, 1293–1297.
  36. Oelz, O., Seyberth, H.W., Knapp, H.R., Sweetman, B.J., Jr., and Oates, J.A. (1976) Effect of Feeding Ethyl-dihomo- $\gamma$ -linolenate on Prostaglandin Biosynthesis and Platelet Aggregation in the Rabbit, *Biochim. Biophys. Acta* 431, 268–277.

[Received February 26, 2001, and in revised form October 3, 2002; accepted October 4, 2002]

# Anandamide and Other *N*-Acylethanolamines in Human Tumors

Patricia C. Schmid<sup>a</sup>, Lester E. Wold<sup>b</sup>, Randy J. Krebsbach<sup>a</sup>,  
Evgueni V. Berdyshev<sup>a</sup>, and Harald H.O. Schmid<sup>a,\*</sup>

<sup>a</sup>The Hormel Institute, University of Minnesota, Austin, Minnesota 55912, and <sup>b</sup>Department of Laboratory Medicine and Pathology, Mayo Clinic and Mayo Foundation, Rochester, Minnesota 55905

**ABSTRACT:** Long-chain *N*-acylethanolamines (NAE), including the endocannabinoid, anandamide, accumulate in mammalian tissues under a variety of pathological conditions. They have also been shown to inhibit the growth of various cancer cell lines *in vitro*. Here, we report the presence, in widely differing amounts (3.88–254.46 pmol/μmol lipid P), of NAE and their precursor phospholipids in various human tumors and some adjacent unaffected tissues. Anandamide ranged from 1.5 to 48% of total NAE, and incubation of tissue homogenates suggested possible NAE biosynthesis by both the established transacylation-phosphodiesterase pathway *via N*-acyl PE and by direct *N*-acylation of ethanolamine.

Paper no. L9090 in *Lipids* 37, 907–912 (September 2002).

Long-chain *N*-acylethanolamines (NAE) and their precursors, *N*-acylethanolamine phospholipids (*N*-acyl PE), are ubiquitous constituents of mammalian cells, tissues, and certain body fluids. They can accumulate *post mortem* and under pathological conditions involving membrane degeneration (reviewed in Refs. 1,2). Relatively high amounts of these lipids have been identified in membranes of undifferentiated murine neuroblastoma C1300 N18 cells, but not after differentiation of these cells (3). Whereas the signaling activity of the major saturated and monounsaturated NAE has only recently become of interest (4,5), their polyunsaturated analogs, especially anandamide (20:4n-6 NAE), have received much more attention since they have been identified as endogenous cannabinoid receptor agonists (6; reviewed in Refs. 7,8). Because  $\Delta^9$ -tetrahydrocannabinol and other cannabinoids have been shown to inhibit the growth of various cancer cell lines and certain malignant tumors (9, reviewed in Ref. 10), the endocannabinoid, anandamide, was also tested for its potential antiproliferative effects. A dose-dependent anti-proliferative effect was observed in human breast cancer cells, but several other tumor cell lines were not similarly affected (11). The effect of anandamide was mediated by CB1-like cannabinoid receptors; inhibition occurred in the G1/S phase of the cell cycle and appeared to be due to

inhibition of prolactin-induced cell proliferation (11–13). Interestingly, the proliferative effect of nerve growth factor was also blocked by CB1 cannabinoid receptor agonists (13). The effect of anandamide was found to be enhanced by 16:0 NAE, which was shown to inhibit the expression of FA amide hydrolase (FAAH; 14). At this time it remains unclear what role anandamide and other cellular NAE may play in tumor cell proliferation *in vivo*.

Although it might be assumed that NAE, including anandamide, are present in human tumors, data regarding the presence of NAE in human neoplasms are not available. Such data are necessary before a possible correlation between NAE-mediated cell signaling and the malignant properties of human tumors can be postulated. In this communication, we report for the first time the levels and composition of NAE and their precursor phospholipids in a variety of human tumors, compared with adjacent normal tissues, obtained as surgical waste following surgery.

## MATERIALS AND METHODS

**Materials.** Anonymized samples of both malignant and adjacent benign human tissues were obtained following surgery and were placed on dry ice and kept frozen at  $-80^{\circ}\text{C}$  until analysis and/or incubation.

**Lipid extraction and fractionation.** The frozen tissues were weighed (typically 0.5–2.0 g), cut into small pieces, and homogenized with a Tissumizer (Tekmar, Cincinnati, OH) in 10 mL of ice-cold methanol; then 20 mL of chloroform was added and the mixture was homogenized again. The homogenate was transferred to a large screw-capped glass tube and 7.5 mL of 2.5% aqueous NaCl was added in order to separate phases (15). After centrifugation, the lower chloroform phase was transferred to a glass screw-capped tube, blown to dryness with  $\text{N}_2$ , and the residue redissolved in chloroform. Aliquots were taken for the determination of lipid phosphorus (16).

Internal standards of *N*-heptadecanoyl PE (0.6 μg) and deuterated NAE (16:0, 17:0, 18:0, 18:1, 18:2, and 20:4  $d_4$  NAE, 0.1 μg each) were added before the lipid extract (up to 3 μmol lipid P in chloroform) was applied to a 100 mg silica solidphase extraction (SPE) cartridge (Alltech). After elution of the neutral lipids with 4 mL of chloroform, NAE was eluted with 4 mL chloroform/methanol (98:2, vol/vol) and *N*-acyl PE with chloroform/methanol (8:2, vol/vol).

\*To whom correspondence should be addressed at the Hormel Institute, University of Minnesota, 801 16th Ave. NE, Austin, MN 55912.  
E-mail: hoschmid@hi.umn.edu

Abbreviations: *N*-acyl PE, *N*-acylphosphatidylethanolamine (possibly consisting of 1,2-diacyl, 1-*O*-alkyl-2-acyl, and 1-*O*-alk-1'-enyl-2-acyl-glycerol subclasses); FAAH, fatty acid amide hydrolase; NAE, *N*-acylethanolamine; SPE, solid-phase extraction.

**Assay of *N*-acyl PE and NAE.** Both *N*-acyl PE and NAE were derivatized and analyzed by GC-MS as described in detail previously (17). Briefly, the NAE fraction containing deuterated internal standards was converted to *t*-butyldimethylsilyl ethers and analyzed with a Hewlett-Packard 5890 gas chromatograph equipped with a 5972 mass selective detector and 7673 autosampler. The HP5MS column, 30 m by 0.25 mm i.d. (Hewlett-Packard, Palo Alto, CA), was programmed from 150 to 280°C at 50°C per min. The M – 57 ions were monitored in selected ion monitoring mode.

NAE derived from *N*-acyl PE by phospholipase D hydrolysis was isolated by SPE and processed as described above.

**Preparation and incubation of tissue.** Several tumors and one normal tissue sample were homogenized (Tissumizer) in 40 mM Hepes, pH 7.4. Aliquots of 0.5 mL, representing about 100 mg wet weight, were incubated in this buffer at 37°C for 1 h in the presence of either Ca<sup>2+</sup> or ethanolamine, 5 mM each, and lipids were then extracted and analyzed as described above.

## RESULTS

**Levels and compositions of *N*-acyl PE and NAE in human tumors and normal tissues.** Samples of human tumors and adjacent normal tissues were kept frozen until they were extracted and analyzed for *N*-acyl PE and NAE content. As summarized in Table 1, all tissues contained measurable amounts of both lipids. In general, tumor tissues contained

higher amounts of phospholipid on a wet weight basis than adjacent normal tissues. Hence, on a wet weight basis, tumor tissues contained substantially higher levels of both *N*-acyl PE and NAE, whereas NAE levels were either higher or lower than those of normal tissues when normalized to total phospholipid. Even on a phospholipid basis *N*-acyl PE levels in tumors were generally higher, with the notable exception of the malignant lymphoma of the terminal ileum (Table 1). This tumor had the lowest *N*-acyl PE level (30.92 pmol/μmol P), whereas a prostatic adenocarcinoma had the highest (381.09 pmol/μmol P).

The compositions (mol%) of the amide-linked FA of both *N*-acyl PE and NAE derived from the same tumor and benign tissues are listed in Table 2. The six *N*-acyl groups assayed represent the majority, but small amounts of other (polyunsaturated) FA may also have been present. As observed previously with animal tissues, 16:0 NAE was the main constituent of both NAE and the amide-linked FA of *N*-acyl PE. Interestingly, anandamide (20:4n-6 NAE) was relatively high in prostate, especially in prostate tumors, whereas the corresponding amide-linked arachidonate was low in the *N*-acyl PE of these tissues. Conversely, carcinoma of the bladder and soft tissue malignant fibrous histiocytoma, as well as adjacent normal skeletal muscle, exhibited relatively high *N*-arachidonate levels in *N*-acyl PE but low percentages of anandamide among NAE.

Assays of additional human tumors (Table 3) confirmed that they contained wide ranges of *N*-acyl PE, from 11.37

**TABLE 1**  
***N*-Acyl PE and NAE Levels of Human Tumors and Benign Tissues**

Tissue	Tumor type	Phospholipid (μmol P/g wet wt)	pmol/g wet wt			pmol/μmol P		
			<i>N</i> -Acyl PE	NAE	20:4 NAE	<i>N</i> -Acyl PE	NAE	20:4 NAE
Prostate tumor (no. 1)	Adenocarcinoma Gleason 3+4	16.84	4665.8	233.8	77.39	277.14	13.89	4.60
Benign prostate (no. 1)		11.30	1632.4	114.7	23.40	144.40	10.15	2.07
Prostate tumor (no. 2)	Adenocarcinoma Gleason 3+3	15.99	2942.9	142.2	18.34	183.99	8.89	1.15
Benign prostate (no. 2)		12.79	1828.7	108.4	9.65	143.02	8.48	0.75
Prostate tumor (no. 3)	Adenocarcinoma Gleason 4+4	17.69	6743.2	339.9	81.58	381.09	19.21	4.61
Benign seminal vesicle (no. 3)		7.34	1624.1	183.2	6.41	221.13	24.95	0.87
Bladder tumor	Grade 3 transitional cell carcinoma	13.21	2963.0	189.8	7.40	224.22	14.36	0.56
Benign bladder		4.97	866.3	137.7	4.82	174.17	27.68	0.97
Left anterior thigh tumor	Grade 4 malignant fibrous histiocytoma	19.24	6326.6	278.6	9.19	328.78	14.48	0.48
Benign thigh muscle		8.09	1141.0	112.8	1.92	141.12	13.95	0.24
Endometrial tumor	Grade 4 malignant carcinosarcoma <sup>a</sup>	14.81	2554.0	182.5	11.86	172.41	12.32	0.80
Benign cervix		4.04	691.9	91.8	3.86	171.18	22.71	0.95
Stomach tumor	Invasive grade 4 adenocarcinoma	14.41	3610.1	400.6	8.41	250.54	27.80	0.58
Benign stomach		19.06	405.2	154.2	5.71	21.26	8.09	0.30
Terminal ileum tumor	Malignant lymphoma <sup>b</sup>	15.93	492.6	181.8	5.64	30.92	11.41	0.35
Benign ileum (small bowel)		9.75	883.2	145.5	5.24	90.57	14.92	0.54

<sup>a</sup>Mixed müllerian tumor.

<sup>b</sup>With plasmacytic differentiation. *N*-Acyl PE, *N*-acylphosphatidylethanolamine; NAE, *N*-acylethanolamine.



**TABLE 2**  
**Composition (mol%) of Amide-Linked FA in *N*-Acyl PE and NAE<sup>a</sup> of Human Tumors and Benign Tissues**

Tissue	<i>N</i> -Acyl PE						NAE					
	Chain length: number of double bonds						Chain length: number of double bonds					
	16:0	18:0	18:1n-9	18:1n-7	18:2n-6	20:4n-6	16:0	18:0	18:1n-9	18:1n-7	18:2n-6	20:4n-6
Prostate tumor (no. 1)	69.3	11.8	8.8	4.9	3.5	1.8	16.7	14.7	11.7	5.9	17.9	33.1
Benign prostate (no.1)	49.7	16.4	11.2	7.7	6.2	8.8	35.9	22.6	8.2	7.3	5.6	20.4
Prostate tumor (no. 2)	53.3	15.1	14.3	9.3	4.6	3.5	36.0	23.9	12.0	6.4	8.9	12.9
Benign prostate (no. 2)	58.5	14.9	13.5	6.3	4.0	2.8	38.9	26.8	10.9	7.8	6.8	8.9
Prostate tumor (no. 3)	46.2	15.9	10.0	12.4	9.0	6.4	26.5	15.8	10.0	5.4	18.4	24.0
Benign seminal vesicle (no. 3)	53.8	17.6	12.6	4.9	5.6	5.5	42.6	28.6	9.6	8.5	7.3	3.5
Bladder tumor	40.7	22.9	11.5	6.1	9.3	9.5	42.0	30.0	10.3	9.0	4.8	3.9
Benign bladder	39.6	15.7	18.8	6.0	9.8	10.2	40.3	26.1	13.7	10.3	6.1	3.5
Left anterior thigh tumor	25.8	18.7	11.3	6.7	17.3	20.2	40.8	32.2	11.6	8.9	3.3	3.3
Benign thigh muscle	27.1	16.6	12.6	4.7	28.2	10.8	37.7	27.4	10.4	9.1	13.7	1.7
Endometrial tumor	72.8	11.4	7.2	3.5	3.9	1.2	35.1	24.4	12.2	14.4	7.4	6.5
Benign cervix	48.9	16.6	17.6	3.6	9.9	3.5	52.2	28.0	8.4	3.3	3.9	4.2
Stomach tumor	42.7	29.5	10.3	5.1	10.7	1.8	34.6	36.1	11.1	8.7	7.5	2.1
Benign stomach	35.0	12.8	15.8	5.7	26.6	4.2	36.3	25.0	9.2	17.4	8.5	3.7
Terminal ileum tumor	46.6	14.8	8.7	14.2	11.9	3.7	33.3	27.0	8.5	23.9	4.6	3.1
Benign ileum (small bowel)	41.3	19.1	17.4	5.1	15.4	1.7	43.1	30.6	11.1	4.7	7.1	3.6

<sup>a</sup>For abbreviations see Table 1.

pmol/ $\mu$ mol P in a lymph node metastatic melanoma to 1756.82 pmol/ $\mu$ mol P in a bladder carcinoma. These tumors also contained the lowest and highest levels of NAE, 3.88 and 254.46 pmol/ $\mu$ mol P, respectively. As a percentage of total amide-linked FA, 20:4n-6 ranged from 3.1 to 24.6% in *N*-acyl PE and from 1.5 to 48.0% in NAE.

*Generation of N-acyl PE and NAE in human tumors and normal tissues.* Although it is now generally accepted that NAE, including anandamide, are synthesized *via* *N*-acyl PE through the Ca<sup>2+</sup>-dependent transacylation-phosphodiesterase pathway (7,8), there is evidence that direct N-acylation of ethanolamine also occurs *in vitro* and in intact cells (17) in the presence of ethanolamine. Because the condensation of FA and ethanolamine could be selective for arachidonate, we tested preparations of human tumors and normal tissues for their capacity to synthesize *N*-acyl PE and NAE in the presence of Ca<sup>2+</sup> or ethanolamine. As shown in Figure 1, incubation in the presence of Ca<sup>2+</sup> resulted in the expected (but relatively minor) increases in *N*-acyl PE and NAE levels, whereas NAE levels were elevated dramatically in the presence of ethanolamine. In the case of a carcinoma of the bladder, NAE was increased about 47-fold over its level in unincubated tissue.

These data suggest that both transacylase and phospholipase D activity were present in these tissues, as in all other mammalian tissues examined so far (7,8), and that condensation of ethanolamine with endogenous FA occurred as well. Interestingly, this N-acylation of ethanolamine showed a

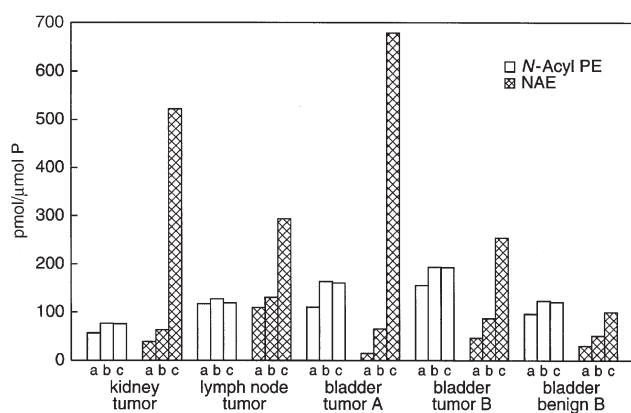
preference for arachidonate in both a bladder tumor and benign bladder tissue, leading to both an absolute (172-fold) and relative (from 4 to 15.2%) increase in anandamide (data not shown). Other tissues did not exhibit this effect. Whether such condensation reactions are relevant *in vivo* depends on the amounts of ethanolamine present in these tissues.

## DISCUSSION

We have shown here that malignant human tumors contain widely varying levels of *N*-acyl PE and NAE, whose compositions also varied widely. In most cases, cancer tissues contained substantially higher concentrations of these lipids than adjacent benign tissue, when normalized to wet weight, since most tumors also contained higher levels of phospholipids (Table 1). Such higher contents of phospholipids in tumors have been previously documented and suggested for use in the diagnosis of several types of cancer and for evaluating the efficacy of treatment (18–21). On a phospholipid basis, by far the highest levels of both *N*-acyl PE and NAE (1756 and 254 pmol/ $\mu$ mol lipid P, respectively) were seen in an invasive, grade 3 squamous cell carcinoma of the bladder (Table 3). In other cancers, *N*-acyl PE levels ranged from less than 20 to over 300 pmol/ $\mu$ mol P. NAE levels, which are commonly lower than those of *N*-acyl PE in the same tissue (1,8), ranged from less than 1 to over 60 pmol/ $\mu$ mol P (Tables 1 and 3). The concentration of the endocannabinoid anandamide (20:4n-6 NAE) was highest in prostate cancer (reaching 24

**TABLE 3**  
**N-Acyl PE and NAE in Human Tumors**

	N-Acyl PE (pmol/ $\mu$ mol P)					20:4n-6 (as % of total)					NAE (pmol/ $\mu$ mol P)					20:4n-6 (as % of total)						
	16:0	18:0	18:1n-9	18:1n-7	18:2n-6	20:4n-6	Total	16:0	18:0	18:1n-9	18:1n-7	18:2n-6	20:4n-6	Total	16:0	18:0	18:1n-9	18:1n-7	18:2n-6	20:4n-6	Total	
Right thyroid gr. 1 papillary carcinoma	56.13	8.71	17.10	6.10	18.15	5.64	111.84	6.97	2.03	2.17	0.87	3.70	1.60	18.04	8.9							
Endocervix, gr. 3 adenosquamous carcinoma	12.03	3.68	4.69	2.79	7.08	3.65	33.92	3.85	0.87	1.18	0.57	2.81	0.75	10.35	7.3							
Right axillary lymph node metastatic malignant melanoma	4.32	1.44	1.57	0.50	2.51	1.02	11.37	0.92	0.62	0.66	0.22	0.83	0.49	3.88	12.7							
Bladder, invasive gr. 3 squamous cell carcinoma	556.44	232.26	329.73	267.96	362.41	8.02	1756.82	76.17	12.36	36.47	28.11	95.81	3.72	254.46	1.5							
Prostate adenocarcinoma, Gleason 3+3	73.32	6.83	15.73	10.49	18.89	7.68	132.94	3.78	9.89	8.07	2.10	2.14	24.24	50.51	48.0							
Endometrium, mixed gr. 2 & 3 endometrioid adenocarcinoma	8.80	2.48	2.65	2.79	3.75	0.88	21.35	1.70	1.33	.128	1.10	1.24	1.05	7.80	13.4							
Endometrium, gr.1 endometrial adenocarcinoma	14.10	3.20	8.91	4.01	5.88	6.14	42.23	3.76	1.60	3.27	2.75	1.88	1.89	15.39	12.3							
Left breast, invasive gr. 4 ductal adenocarcinoma	14.25	6.02	7.67	2.92	7.64	7.79	46.29	2.62	0.95	1.16	0.56	1.59	0.46	7.60	6.1							
Left breast, infiltrating gr. 3 ductal adenocarcinoma	53.12	6.93	10.03	3.80	15.88	29.37	119.12	26.37	6.12	9.88	2.26	13.60	4.40	64.26	6.9							
Right breast, infiltrating gr. 4 lobular carcinoma	43.89	7.19	12.33	4.09	14.30	5.21	87.02	14.94	2.30	4.39	1.52	8.52	2.21	34.55	6.4							
Left breast, infiltrating gr. 4 ductal adenocarcinoma	96.33	3.78	17.20	15.50	39.49	5.42	177.72	5.31	0.51	1.47	1.47	3.59	0.70	13.30	5.3							
Colon, gr. 3 adenocarcinoma	27.20	8.23	11.02	3.45	10.67	3.88	64.44	6.38	4.09	3.68	1.43	3.86	2.21	21.91	10.1							



**FIG. 1.** Levels of total *N*-acylethanolamine (NAE) and *N*-acylphosphatidylethanolamine (*N*-acyl PE) in homogenates of tumor and normal tissues before incubation (a) or after incubation for 60 min in the presence of either 5 mM  $\text{Ca}^{2+}$  (b) or 5 mM ethanolamine (c).

pmol/ $\mu\text{mol P}$ ), where it also represented the highest percentage (48%) of NAE.

Because *N*-acyl PE is the direct precursor of NAE, including anandamide, the percentage distribution of their amide-linked FA tends to be similar (1,7,8). This was also the case with many of the human tumors and benign tissues analyzed. However, it is interesting to note that the percentage of the anandamide precursor, *N*-arachidonoyl PE, rather than of anandamide itself, was very high in breast cancer tissues (up to 25%). This may be relevant in view of the growth-inhibitory action of anandamide observed with human breast cancer cells (11–13). Although the turnover rates of *N*-acyl PE and NAE in these tumors are not yet known, they were shown to be very high in macrophages (22). In such a case, the high proportion of *N*-arachidonoyl PE could be an important source for the continuous production of anandamide in mammary tumors. Conversely, the very high percentage of anandamide in prostate cancer was not matched by an equally high percentage of *N*-arachidonoyl groups in its *N*-acyl PE precursor. These data are reminiscent of similar relationships seen in peri-implantation mouse uterus where anandamide was found to reach extremely high levels without a correspondingly high concentration of *N*-arachidonoyl PE (23).

Although the phospholipase D that hydrolyzes *N*-acyl PE to NAE does not exhibit any substrate selectivity with respect to *N*-acyl groups, anandamide could be formed under certain conditions by an alternative pathway. The FAAH that hydrolyzes NAE to FA and ethanolamine is known to act in reverse in the presence of high substrate concentrations (24–26). This reaction was shown to occur in intact cells in the presence of exogenous ethanolamine (22). Whether human tumors, such as prostate adenocarcinoma (Table 3), can produce significant concentrations of arachidonic acid and ethanolamine for selective anandamide production by this pathway remains to be investigated.

The data presented here were acquired over several years by a method that has been found to be highly accurate and

well reproducible. At this time, no comparable data are available in the literature. A recent study of NAE in human brain tumor (meningioma) and normal human brain, as well as neuroblastoma and lymphoma cells (27), reported levels several orders of magnitude higher (e.g., 50 nmol/g tissue of anandamide) than those reported by us and others. However, these data (27) must be accepted with caution because the internal standards were added to aqueous homogenates, which were subsequently centrifuged to obtain the membranes to be analyzed. The internal standards may have been discarded with the supernatants, resulting in a considerable overestimation of the compounds of interest. Thus, our present data represent the first reliable information on the presence of NAE and *N*-acyl PE in human cancer and will form the basis for further study on their potential role in carcinogenesis.

## ACKNOWLEDGMENTS

This work was supported in part by The Hormel Foundation and National Institutes of Health grant GM45741.

## REFERENCES

- Schmid, H.H.O., Schmid, P.C., and Natarajan, V. (1990) *N*-Acylated Glycerophospholipids and Their Derivatives, *Prog. Lipid Res.* 29, 1–43.
- Hansen, H.S., Moesgaard, B., Hansen, H.H., and Petersen, G. (2000) *N*-Acylethanolamines and Precursor Phospholipids—Relation to Cell Injury, *Chem. Phys. Lipids* 108, 135–150.
- Gulaya, N.M., Volkov, G.L., Klimashevskii, V.M., Govseeva, N.N., and Melnik, A.A. (1989) Changes in Lipid Composition of Neuroblastoma C1300 N18 Cell During Differentiation, *Neuroscience* 30, 153–164.
- Berdyshev, E.V., Schmid, P.C., Dong, Z., and Schmid, H.H.O. (2000) Stress-Induced Generation of *N*-Acylethanolamines in Mouse Epidermal JB6 P<sup>+</sup> Cells, *Biochem. J.* 346, 369–374.
- Berdyshev, E.V., Schmid, P.C., Krebsbach, R.J., Hillard, C.J., Huang, C., Chen, N., Dong, Z., and Schmid, H.H.O. (2001) Cannabinoid-Receptor-Independent Cell Signalling by *N*-Acylethanolamines, *Biochem. J.* 360, 67–75.
- Devane, W.A., Hanus, L., Breuer, A., Pertwee, R.G., Stevenson, L.A., Gibson, D., Mandelbaum, A., Etinger, A., and Mechoulam, R. (1992) Isolation and Structure of a Brain Constituent That Binds to the Cannabinoid Receptor, *Science* 258, 1946–1949.
- Di Marzo, V. (1998) ‘Endocannabinoids’ and Other Fatty Acid Derivatives with Cannabimimetic Properties: Biochemistry and Possible Physiopathological Relevance, *Biochim. Biophys. Acta* 1392, 153–175.
- Schmid, H.H.O. (2000) Pathways and Mechanisms of *N*-Acylethanolamine Biosynthesis: Can Anandamide Be Generated Selectively? *Chem. Phys. Lipids* 108, 71–87.
- Galve-Roperh, I., Sanchez, C., Cortes, M.L., del Pulgar, T.G., Izquierdo, M., and Guzman, M. (2000) Anti-tumoral Action of Cannabinoids: Involvement of Sustained Ceramide Accumulation and Extracellular Signal-Regulated Kinase Activation, *Nat. Med.* 6, 313–319.
- De Petrocellis, L., Melck, D., Bisogno, T., and Di Marzo, V. (2000) Endocannabinoids and Fatty Acid Amides in Cancer, Inflammation and Related Disorders, *Chem. Phys. Lipids* 108, 191–209.
- De Petrocellis, L., Melck, D., Palmisano, A., Bisogno, T., Laezza, C., Bifulco, M., and Di Marzo, V. (1998) The Endoge-

- nous Cannabinoid Anandamide Inhibits Human Breast Cancer Cell Proliferation, *Proc. Natl. Acad. Sci. USA* 95, 8375–8380.
12. Melck, D., Rueda, D., Galve-Roperh, I., De Petrocellis, L., Guzman, M., and Di Marzo, V. (1999) Involvement of the cAMP/Protein Kinase A Pathway and of Mitogen-Activated Protein Kinase in the Anti-proliferative Effects of Anandamide in Human Breast Cancer Cells, *FEBS Lett.* 463, 235–240.
  13. Melck, D., De Petrocellis, L., Orlando, P., Bisogno, T., Laezza, C., Bifulco, M., and Di Marzo, V. (2000) Suppression of Nerve Growth Factor Trk Receptors and Prolactin Receptors by Endocannabinoids Leads to Inhibition of Human Breast and Prostate Cancer Cell Proliferation, *Endocrinology* 141, 118–126.
  14. Di Marzo, V., Melck, D., Orlando, P., Bisogno, T., Zagoory, O., Bifulco, M., Vogel, Z., and De Petrocellis, L. (2001) Palmitoylethanolamide Inhibits the Expression of Fatty Acid Amide Hydrolase and Enhances the Anti-proliferative Effect of Anandamide in Human Breast Cancer Cells, *Biochem. J.* 358, 249–255.
  15. Folch, J., Lees, M., and Sloane Stanley, G.M. (1957) A Simple Method for the Isolation and Purification of Lipids from Animal Tissue, *J. Biol. Chem.* 226, 497–507.
  16. Bartlett, G.R. (1959) Phosphorus Assay in Column Chromatography, *J. Biol. Chem.* 234, 466–468.
  17. Schmid, P.C., Kuwae, T., Krebsbach, R.J., and Schmid, H.H.O. (1997) Anandamide and Other *N*-Acylethanolamines in Mouse Peritoneal Macrophages, *Chem. Phys. Lipids* 87, 103–110.
  18. Merchant, T.E., Diamantis, P.M., Lauwers, G., Haida, T., Kasimos, J.N., Guillem, J., Glonek, T., and Minsky, B.D. (1995) Characterization of Malignant Colon Tumors with <sup>31</sup>P Nuclear Magnetic Resonance Phospholipid and Phosphatic Metabolite Profiles, *Cancer* 76, 1715–1723.
  19. Ruggieri, S., Mugnai, G., Mannini, A., Calorini, L., Fallani, A., Barletta, E., Mannori, G., and Cecconi, O. (1999) Lipid Characteristics in Metastatic Cells, *Clin. Exp. Metastasis* 17, 271–276.
  20. Ronen, S.M., and Leach, M.O. (2001) Imaging Biochemistry: Applications to Breast Cancer, *Breast Cancer Res.* 3, 36–40.
  21. Merchant, T.E., Kasimos, J.N., Vroom, T., de Bree, E., Iwata, J.L., de Graaf, P.W., and Glonek, T. (2002) Malignant Breast Tumor Phospholipid Profiles Using <sup>31</sup>P Magnetic Resonance, *Cancer Lett.* 176, 159–167.
  22. Kuwae, T., Shiota, Y., Schmid, P.C., Krebsbach, R.J., and Schmid, H.H.O. (1999) Biosynthesis and Turnover of Anandamide and Other *N*-Acylethanolamines in Peritoneal Macrophages, *FEBS Lett.* 459, 123–127.
  23. Schmid, P.C., Paria, B.C., Krebsbach, R.J., Schmid, H.H.O., and Dey, S.K. (1997) Changes in Anandamide Levels in Mouse Uterus Are Associated with Uterine Receptivity for Embryo Implantation, *Proc. Natl. Acad. Sci. USA* 94, 4188–4192.
  24. Schmid, P.C., Zuzarte-Augustin, M.L., Krebsbach, R.J., and Schmid, H.H.O. (1985) Properties of Rat Liver *N*-Acylethanolamine Amidohydrolase, *J. Biol. Chem.* 260, 14145–14149.
  25. Ueda, N., Kurahashi, Y., Yamamoto, S., and Tokunaga, T. (1995) Partial Purification and Characterization of the Porcine Brain Enzyme Hydrolyzing and Synthesizing Anandamide, *J. Biol. Chem.* 270, 23823–23827.
  26. Ueda, N., Puffenbarger, R.A., Yamamoto, S., and Deutsch, D.G. (2000) The Fatty Acid Amide Hydrolase (FAAH), *Chem. Phys. Lipids* 108, 107–121.
  27. Maccarrone, M., Attinà, M., Cartoni, A., Bari, M., and Finazzi-Agrò, A. (2001) Gas Chromatography–Mass Spectrometry Analysis of Endogenous Cannabinoids in Healthy and Tumoral Human Brain and Human Cells in Culture, *J. Neurochem.* 76, 594–601.

[Received June 17, 2002, and in revised form and accepted September 18, 2002]



# Dolichol Levels in Younger and Older Rat Hearts Heterotopically Transplanted in Younger Recipients

Gabriella Cavallini<sup>a</sup>, Ilaria Parentini<sup>a</sup>, Rossella Di Stefano<sup>b</sup>, Marco Maccheroni<sup>c</sup>,  
Matilde Masini<sup>a</sup>, Maria Pollera<sup>a</sup>, Zina Gori<sup>a</sup>, Franco Mosca<sup>b</sup>, and Ettore Bergamini<sup>a,\*</sup>

<sup>a</sup>Dipartimento di Patologia sperimentale, Biotecnologie mediche, Infettivologia e Epidemiologia, University of Pisa, Italy, <sup>b</sup>Dipartimento di Oncologia, Trapianti e Tecnologie Avanzate in Medicina, University of Pisa, and <sup>c</sup>Azienda Ospedaliera Pisana, Pisa, Italy

**ABSTRACT:** Dolichol (D) levels increase dramatically in older tissue. An understanding of the exchangeability of D between tissues may be essential in order to understand the mechanism of the abnormal accumulation associated with aging. The question was investigated by the use of organ transplantation. D-poor hearts donated by 3-mon-old and D-rich by 22-mon-old male Lewis rats were transplanted heterotopically in 3-mon-old syngenic recipients, whose peripheral tissues and liver were poor in D. Native and transplanted hearts were taken 7 and 21 d after surgery. Native hearts of 3-mon- and 22-mon-old male Lewis rats served as control. D concentration and quantity were higher in older than in younger native hearts as expected. In the transplanted hearts, the quantity of D was unchanged, irrespective of the age of the donor and of the time of transplantation, whereas D concentration increased because of the remarkable disuse atrophy. No changes in D were observed in recipients' tissues. It is concluded that dolichol is not redistributed *via* circulation from the transplanted heart to the tissues and liver of the younger recipient.

Paper no. L9038 in *Lipids* 37, 913–916 (September 2002).

Dolichol is a long-chain polyisoprenoid widely distributed in the biological membranes of experimental systems and human tissues (1–3). Metabolism and functions of dolichol are largely unknown. Synthesis of dolichol has been demonstrated *in vitro* and *in vivo* in many tissues, but no enzymatic pathway for dolichol catabolism has been described so far (4). In view of the total dolichol content of the body, of the half-life of total body dolichol, and of the dolichol content in the extracellular space, it was concluded that the dolichol in tissues probably derives from biosynthesis in those tissues and that relocation of dolichol *via* circulation cannot be prominent *in vivo* (4,5). However, more recent evidence in a patient with abetalipoproteinemia reopened this question and invited the suggestion that the HDL-associated dolichols in serum could possibly be taken up at least in part and carried by HDL from peripheral tissues (6).

We thought that the clarification of the role of exchange between tissues in the metabolism of tissue dolichol might be essential in order to understand the mechanism underlying the

well-known, dramatic accumulation of dolichol in older animal tissues (7–10), and that transplantation experiments of older dolichol-rich tissues into younger recipients could give an answer to the question. In this research we report on the levels of dolichol in the heart of younger and older rat donors transplanted in younger recipients, and show that there is no net redistribution of dolichol from the old heart to the younger tissues.

## MATERIALS AND METHODS

**Animals.** Groups of male 2-mon-old rats of the Sprague-Dawley and Lewis strain were purchased from Harlan Italy (Corezzano, Italy) and maintained on a standard laboratory food (TEKLAD, Harlan) and water *ad libitum*. Rats were sacrificed 7 and 20 d after surgery; the grafted and the native hearts and kidney, liver, and extensor digitorum longus and soleus muscle were excised and weighed; and samples were taken for the extraction of lipid and the assay of cholesterol and dolichol by HPLC. Specimens for electron microscopy were taken from the left ventricular papillary muscle, and a quantitative analysis of ultracellular components (mitochondria, sarcoplasm, myofibrils, and dense bodies) was performed by morphometric techniques (11).

**Experimental model.** Three groups of Lewis rats were used. The first group consisted of age-matched heterotopic heart transplantation (HHTx) specimens in which donors and recipients were 3 mon old. The second group consisted of age-mismatched HHTx specimens in which the heart was taken from donors of 22 mon of age and transplanted into recipients of 3 mon of age. Hearts from the donor group (3-mon- or 22-mon-old rats) were excised under diethylether anesthesia and implanted into 3-mon-old Lewis anesthetized recipients heterotopically according to the Ono and Lindsay procedure (12). The beating activity of heart grafts was checked by daily palpation.

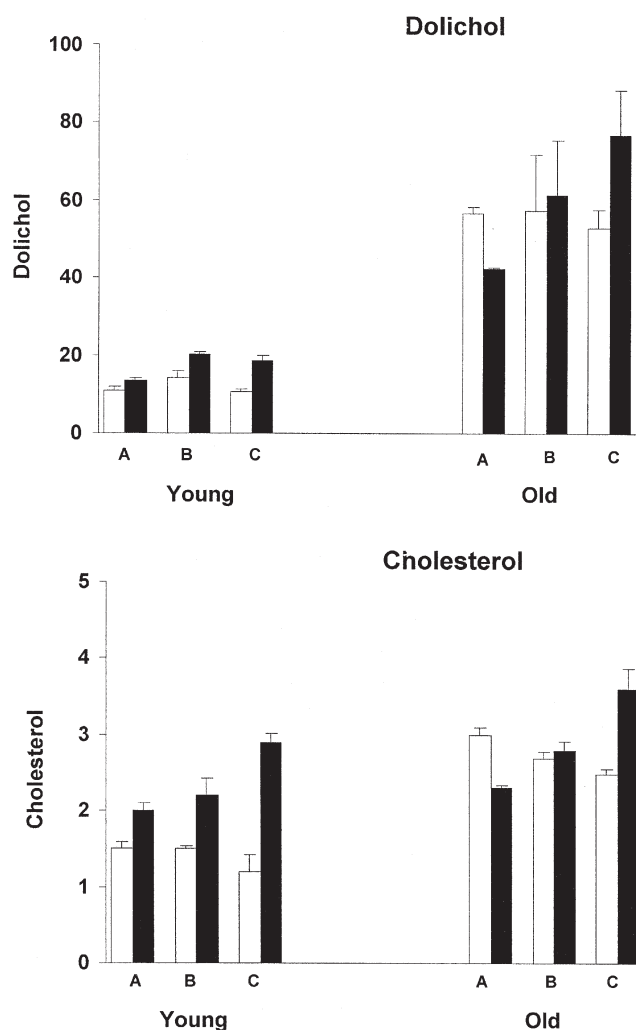
**Extraction and HPLC assay of cholesterol and dolichol.** The minced tissue (about 0.25 g) was hydrolyzed in 0.5 mL 0.25% pyrogallol in methanol and 0.5 mL 60% KOH at 100°C for 30 min; the mixture was extracted twice with diethyl ether/petroleum ether (1:1, vol/vol). The pooled extracts were washed with methanol/water (1:1, vol/vol) and dried under nitrogen. Cholesterol and isoprenoids were assayed by reversed-phase HPLC as described (13). The sensitivity of the method allowed us to measure a minimum of 50 ng chole-

\*To whom correspondence should be addressed at Dipartimento di Patologia sperimentale, Biotecnologie mediche, Infettivologia e Epidemiologia, Via Roma 55, 56126 Pisa, Italy. E-mail: ebergami@ipg.med.unipi.it  
Abbreviation: HHTx, heterotopic heart transplantation.

terol and 1.7 ng of total dolichol. Calibration curves of total peak height against quantity injected were linear in the 0.05–15  $\mu\text{g}$  (cholesterol) and in the 1.7–1000 ng (dolichol) range. Recovery of dolichol was determined by addition of internal standards to samples (10) and was 95%. Data are given as mg cholesterol and as  $\mu\text{g}$  dolichol in the organ and per g wet tissue.

**Statistical analysis.** The ANOVA test was used to evaluate differences among multiple conditions. Values of  $P > 0.05$  were considered not to be significant.

**Materials.** All reagents were of the highest quality commercially obtainable.



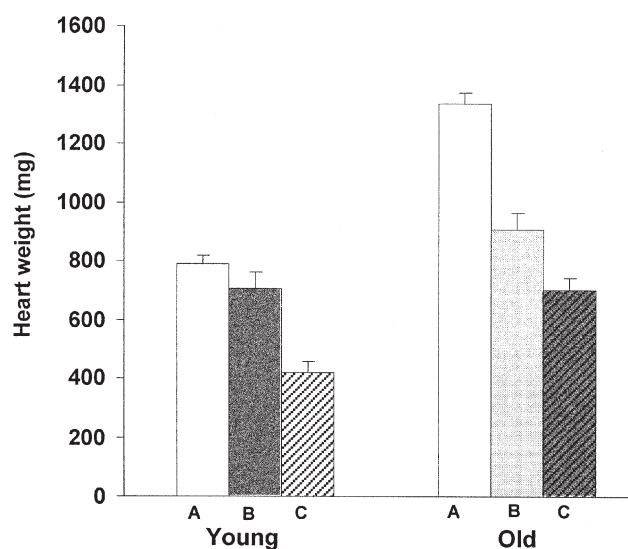
**FIG. 1.** Effect of transplantation on the accumulation of dolichol and cholesterol in the heart tissues of Lewis rats. Means  $\pm$  SEM of at least five cases are given. Open columns: quantity of dolichol ( $\mu\text{g}$ ) and cholesterol (mg) in the organ; solid columns, concentration of dolichol ( $\mu\text{g/g}$ ) and cholesterol (mg/g) in the heart tissue. (A) Native hearts; (B) passive hearts, 7 d after transplantation; (C) passive hearts, 20 d after transplantation. Statistical analysis (ANOVA) showed that the effects of age on dolichol quantity and concentration and on cholesterol quantity were significant ( $P < .01$  all); the effects of transplantation on the quantity of both lipids were not significant, and those on the concentration were significant (dolichol:  $P < .01$ ; cholesterol:  $P < .01$ ).

## RESULTS

Preliminary experiments on Sprague-Dawley rats showed that the levels of dolichol exhibited a similar, six- to sevenfold increase and that cholesterol levels did not change significantly with increasing age in several transplantable organs (14). The HHTx was considered to be the most suitable experimental model to investigate how much dolichol can be transferred between tissues because the liver and kidney may release part of their dolichol into bile and urine, respectively (2,5). The Lewis rat is the preferred rat strain for HHTx because of anatomy.

Figure 1 shows that, in the Lewis rat, the levels of dolichol in the older native hearts were almost fivefold higher than in younger native hearts, whereas the concentrations of cholesterol did not increase significantly with increasing age; that the quantities of dolichol and cholesterol in both the younger and the older transplanted hearts were not affected by organ transplantation (the slight decrease in the quantity of cholesterol was not significant); and that concentrations of the lipids increased significantly because of the remarkable disuse atrophy of the nonvolume-loaded HHTx. Atrophy was more rapid in the hearts from the older rats (Fig. 2). No changes in cholesterol and dolichol were found in the tissue of several recipients.

Disuse atrophy resulted in a significant increase in dolichol concentration in both younger and older HHTx. A morphometric quantitation of cell organelles in native and atrophic transplanted hearts showed that the volume density of mitochondria decreased substantially in transplanted younger and older hearts, whereas the volume density of the sarcoplasmic reticulum did not change significantly and the volume density of dense bodies increased (Fig. 3). The changes in the



**FIG. 2.** Heart weight of donor and recipient rats of the Lewis strain. Means  $\pm$  SEM of at least five cases are given. (A) Native hearts; (B) passive hearts, 7 d after transplantation; (C) passive hearts, 20 d after transplantation. Statistical analysis (ANOVA) showed that the effect of age ( $P < .01$ ) and of transplantation ( $P < .01$ ) and interaction age  $\times$  transplantation ( $P < .05$ ) were all significant.

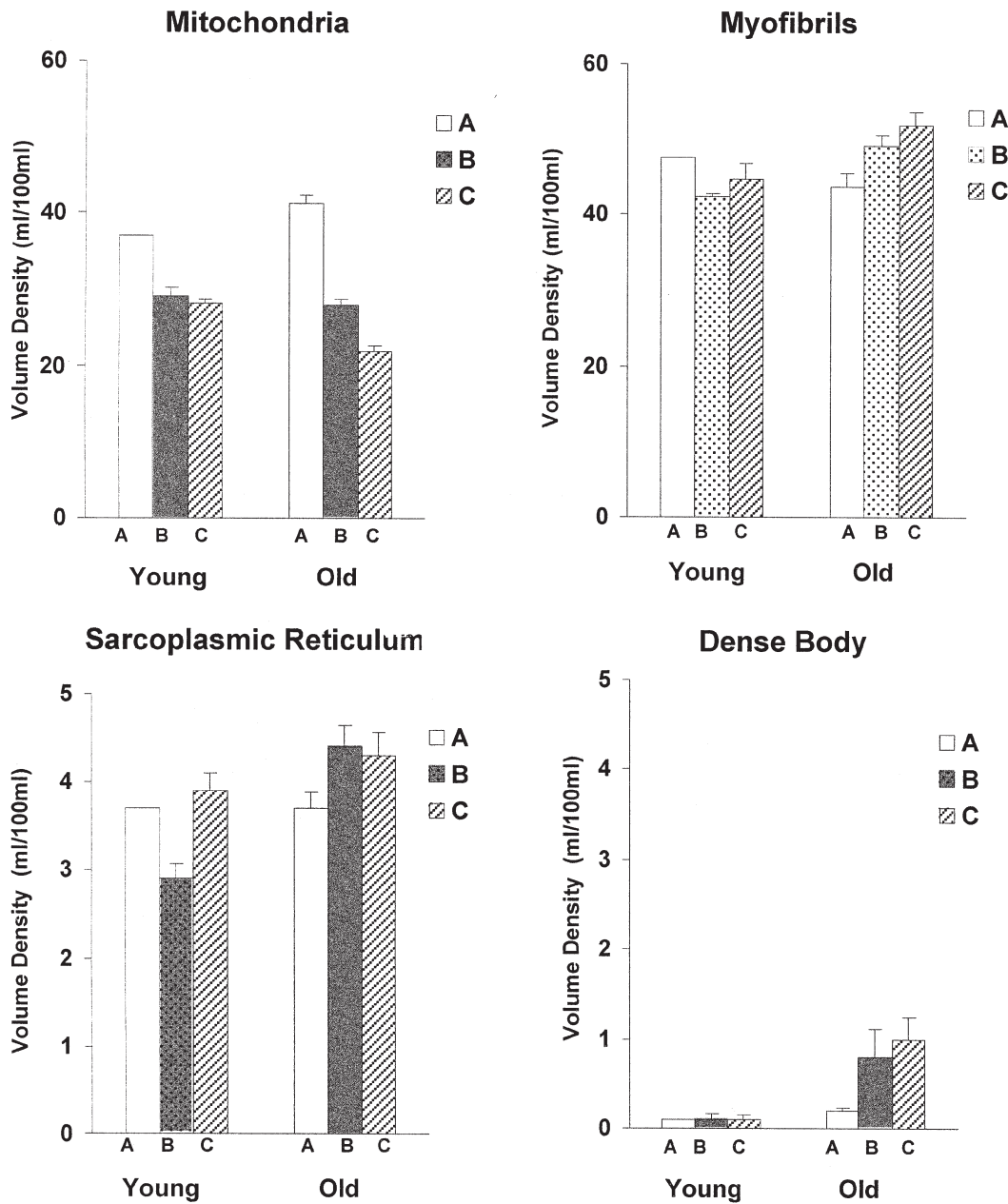


FIG. 3. Volume density of mitochondria, myofibrils, sarcoplasmic reticulum and dense body in the heart tissues of Lewis rats. Means  $\pm$  SEM of at least five cases are given. (A) Native hearts; (B) passive hearts, 7 d after transplantation; (C) passive hearts, 20 d after transplantation. Statistical analysis (ANOVA) showed that the effects of transplantation on mitochondria ( $P < .05$ ) and myofibrils ( $P < .05$ ) were significant both in younger and older heterotopic heart transplantation (HHTx); the effect on sarcoplasmic reticulum was not significant; and the effect on dense bodies was significant in older HHTx ( $P < .05$ ).

volume density of myofibrils were less than 10–20% but reached statistical significance.

## DISCUSSION

The transplanted hearts were volume-unloaded and became atrophic (15,16) but retained contractility. The faster loss of weight of the older HHTx might be attributed to a regression of the age-related hypertrophy of the left cardiomyocytes compensating for age-related cardiomyocyte loss (16). No

signs of underperfusion were visible in the cardiomyocytes of younger and older transplanted hearts by using the electron microscope. The concentrations of dolichol and cholesterol in younger native hearts were very close to those reported by Kalèn *et al.* (8) in young, adult, and mature male Sprague-Dawley rats. The present data show that dolichol accumulation continues until very old age in older native hearts. A major new finding is that the quantity of dolichol in the younger and older HHTx is similar to that in the native hearts of corresponding age, in spite of the loss of weight, and that

the quantity of dolichol in older HHTx, which is much larger than that in the tissues of the recipient rat, does not decrease with increased time post-transplantation. In conclusion, these results confirm that dolichol is not lost or transferred from the transplanted organ to the peripheral tissues or to the liver *via* circulation (4) and provide evidence that accumulation of dolichol in older tissues may be the consequence of an alteration of dolichol metabolism in those tissues. An age-dependent alteration in 3-hydroxy 3-methylglutaryl CoA reductase activity was reported in rat liver (17).

The increase in the concentration of cholesterol and dolichol in the atrophic HHTx may not necessarily imply a dramatic change in membrane composition. Shrinking of organelles and cytomembranes during atrophy is the consequence of autophagy and lysosomal degradation (18); indigestible lipids (like cholesterol and dolichol) in the degraded organelles and membranes may stay in the cells for a long time stored in the lysosomal compartment (residual bodies), which are enlarged (see also Refs. 18,19). In view of the way cells handle cholesterol, the small decrease in the quantity of this lipid in HHTx might have a physiological meaning (20).

#### ACKNOWLEDGMENTS

This work was cofunded by the Italian Ministry of University and Scientific Research. E. Bergamini is indebted to the Italian Consiglio Nazionale delle Ricerche for approval of the project (year 1995) even though the project could not be funded because of administrative delays.

#### REFERENCES

- Hemming, F.W. (1992) Dolichol: A Curriculum Cognitionis, *Biochem. Cell. Biol.* 70, 377–381.
- Rip, J.W., Rugar, A., Ravi, K., and Carroll, K.K. (1985) Distribution, Metabolism and Function of Dolichol and Polyprenols, *Prog. Lipid Res.* 24, 269–309.
- Choinacki, T., and Dallner, G. (1988) The Biological Role of Dolichol, *Biochem. J.* 251, 1–9.
- Carroll, K.K., Githrie, N., and Ravi, K. (1992) Dolichol: Function, Metabolism and Accumulation in Human Tissue, *Biochem. Cell. Biol.* 70, 382–384.
- Elmberger, P.G., Kalèn, A., Brunk, U.T., and Dallner, G. (1989) Discharge of Newly Synthesized Dolichol and Ubiquinone with Lipoprotein to Rat Perfusate and to the Bile, *Lipids* 24, 919–930.
- Kutiyama, M., Yashidone, H., Nakahara, K., Nakagawa, H., Fujiyama, J., Take, H., and Osame, M. (1999) Blood Dolichols in a Patient with Abetalipoproteinaemia, *Ann. Clin. Biochem.* 36, 176–179.
- Pullarkat, R.K., and Reha, H. (1982) Accumulation of Dolichols in Brain of Elderly, *J. Biol. Chem.* 257, 5991–5993.
- Kalèn, A., Appelkvist, A.L., and Dallner, G. (1989) Age-Related Changes in the Lipid Composition of Rat and Human Tissues, *Lipids* 24, 579–584.
- Daniels, I., and Hemming, F.W. (1990) Changes in Murine Tissue Concentrations of Dolichol and Dolichyl Derivatives Associated with Age, *Lipids* 25, 586–593.
- Marino, M., Dolfi, C., Paradiso, C., Cavallini, G., Masini, M., Gori, Z., Pollera, M., Trentalance, A., and Bergamini, E. (1998) Age-Dependent Accumulation of Dolichol in Rat Liver: Is Tissue Dolichol a Biomarker of Aging? *J. Gerontol. Biol. Sci.* 53A, B87–B93.
- Page, E., McCallister, L.P., and Power, B. (1971) Stereological Measurements of Cardiac Ultrastructures Implicated in Excitation–Contraction Coupling, *Proc. Nat. Acad. Sci. USA* 68, 1465–1466.
- Ono, K., and Lindsey, E.S. (1969) Improved Technique of Heart Transplantation in Rats, *J. Thorac. Cardiovasc. Surg.* 57, 225–229.
- Maltese, W.A., and Erdman, R.A. (1989) Characterization of Isoprenoid Involved in the Post-translational Modification of Mammalian Cell Proteins, *J. Biol. Chem.* 264, 18168–18172.
- Dini, B., Dolfi, C., Santucci, V., Cavallini, G., Donati, A., Gori, Z., Maccheroni, M., and Bergamini, E. (2001) Effects of Ageing and Increased Haemolysis on the Levels of Dolichol in Rat Spleen, *Exp. Gerontol.* 37, 99–105.
- Asfour, B., Hare, J.M., Kohl, T., Baba, H.A., Kass, D.A., Chen, K., Tjan, T.D., Hammel, D., Weyand, M., Hruban, R.H., et al. (1999) A Simple New Model of Physiologically Working Heterotopic Heart Transplantation Provides Hemodynamic Performance Equivalent to That of an Orthotopic Heart, *J. Heart Lung Transplant.* 18, 927–936.
- Rakusan, K., Cicutti, N., Spatenka, J., and Samanek, M. (1997) Geometry of the Capillary Net in Human Hearts, *Int. J. Microcir. Clin. Exp.* 17, 29–32.
- Marino, M., Pallottini, V., D'Eramo, C., Cavallini, G., Bergamini, E., and Trentalance, A. (2002) Age-Related Changes of Cholesterol and Dolichol Biosynthesis in Rat Liver, *Mech. Ageing Dev.* 123, 1183–1189.
- Stevens, A., and Lowe, J. (2000) *Pathology*, 2nd edn., p. 13, Mosby, London.
- Cutran, R.S., Kumar, V., and Collins, T. (1999) *Robbins Pathologic Basis of Diseases*, 6th edn., pp. 35–36, Saunders, Philadelphia.
- Simons, K., and Ikonen, E. (2000) How Cells Handle Cholesterol, *Science* 290, 1721–1726.

[Received March 28, 2002, and in revised form September 9, 2002; revision accepted September 20, 2002]



# Simultaneous Determination by GC-MS of Epoxy and Hydroxy FA as Their Methoxy Derivatives

R. Wilson\* and K. Lyall

Cardiovascular Research Unit, University of Edinburgh, Edinburgh EH8 9XF, Scotland, United Kingdom

**ABSTRACT:** We report on a capillary GC-MS method for the quantitative analysis of hydroxy and epoxy FA. Catalytic hydrogenation of lipid extracts produces stable saturated lipids. Saponification followed by methylation with boron trifluoride in the presence of methanol converts FA to methyl esters and epoxy groups to methoxy-hydroxy groups. These compounds are purified from nonoxidized methyl esters using solid phase extraction. Derivatization of the hydroxy group using tetramethylammonium hydroxide forms methoxy and vicinal dimethoxy FAME. When subjected to EI-MS, fragmentation gives two characteristic ion fragments for each epoxy and hydroxy positional isomer. Quantitative measurements were achieved using uniformly labeled hydroxy and epoxy  $^{13}\text{C}$  FA as internal standards. Epoxy and hydroxy FA were identified in both plasma and adipose tissue of men, and the levels of hydroxy and epoxy in these tissues were related. The levels of hydroxy isomers were typical of oxidation of linoleic acid, whereas epoxy isomers were characteristic of oxidation of oleic acid.

Paper no. L9071 in *Lipids* 37, 917-924 (September 2002).

Free radical damage of cellular components is believed to lead to the development of disease (1). Reactive oxygen species are formed during normal metabolic process and when homeostatic mechanisms are disrupted, damage occurs (2,3). Oxidative damage to lipids is one form of damage, but elucidating the involvement of lipid peroxidation in disease requires sensitive and specific techniques (4,5). Hydroperoxy FA are primary products of free radical damage but are short-lived and difficult to measure directly (5). The use of surrogate markers of lipid peroxidation (5) and their association with disease are now well documented (1). GC-MS provides unequivocal identification of metabolites and has become increasingly popular for the quantitative analysis of markers of lipid peroxidation in biological material (5-10). Epoxy FA are also formed during normal metabolic processes in the body (11-13) and, like hydroperoxy FA or their hydroxy derivatives, epoxy FA exhibit biological and toxicological behavior (1-3,5,11-13). The use of GC-MS for the quantitative analysis of epoxy FA is limited by the instability of the epoxy group at elevated temperatures. Although the mass spectrum gives limited structural information (14,15), the formation of

chlorohydrin adducts facilitates the identification of the epoxy group (15). Epoxy FA have been analyzed directly by GC-MS using less harsh on-column injection techniques (16,17) or by HPLC with MS detection (18). As intermediates in biosynthetic pathways, epoxy FA derived from arachidonic acid have been studied intensively (12,13,16-18). The identification of biologically active epoxy FA derived from linoleic acid has increased the interest in these compounds (11). Epoxy FA derived from  $\text{C}_{18}$  FA have been identified in blood, plasma, and urine from human volunteers (19-21), but that GC-MS technique requires reductive deuteration to discriminate epoxy from endogenous hydroxy FA (20,21). Although hydroxy and epoxy FA have been identified in heart tissue in pigs, quantitative measurements are limited (22). We previously described a GC-MS technique for the quantitative analysis of hydroxy FA from biological samples (23). In the present paper we describe a quantitative GC-MS method that simultaneously determines both epoxy and hydroxy FA in biological tissues.

## MATERIALS

All solvents were HPLC grade from Rathburn Chemicals (Walkerburn, Scotland). Platinum(IV) oxide was from Fluka (Gillingham, Dorset, United Kingdom). Tetramethylammonium hydroxide (TMAH) in methanol (25%, w/w), chloroperoxy benzoic acid, and deuterium gas were from Sigma-Aldrich (Gillingham, Dorset, United Kingdom). The suitability of boron trifluoride in methanol (14%, w/w) must be checked, as certain batches gave blanks with high 12-hydroxy and 9,10-epoxy. Uniformly labeled [ $^{13}\text{C}$ ]oleic acid was obtained from Nippon Sanso Europe GmbH (Plaisir, France). 10,13-Nonadecadienoate (19:2) methyl ester was from Nu-Chek-Prep (Elysian, MN) and other FAME were from Sigma-Aldrich (Poole, Dorset, United Kingdom). Solid-phase extraction (SPE) silica columns (500 mg) were obtained from IST (Hengoed, Mid-Glamorgan, United Kingdom). Hydroxy internal standards were synthesized from  $^{13}\text{C}$ -oleic methyl ester as detailed previously (23). Epoxy internal standards were synthesized from  $^{13}\text{C}$ -oleic methyl ester as detailed in *Lipid Analysis* (24). Citrated plasma collected in a clinical polyvinyl chloride (PVC) bag was obtained from the local blood transfusion service. To the plasma was added EDTA to a final concentration of 1.6 mg/mL. Aliquots of 1.2 mL were added to 1.5-mL Eppendorf tubes and then stored at  $-70^\circ\text{C}$ .

\*To whom correspondence should be addressed at Cardiovascular Research Unit, University of Edinburgh, George Square, Edinburgh EH8 9XF, Scotland, United Kingdom. E-mail: R.Wilson@ed.ac.uk

Abbreviations: amu, atomic mass units; SIM, selected ion monitoring; SPE, solid phase extraction; TMAH, tetramethylammonium hydroxide.

## METHODS

**Extraction of lipids from plasma.** Lipids were extracted from EDTA plasma as described previously (23). Briefly, to 10 mL dichloromethane/methanol (2:1, vol/vol) was added 100  $\mu$ L of standard (containing 1  $\mu$ g each of hydroxy and epoxy  $^{13}$ C-standard in chloroform), 100  $\mu$ L FA standard (containing 200  $\mu$ g 19:2 in methanol), 0.5 mL plasma, and 2 mL saline (0.88%, w/w). The samples were vortexed and then centrifuged at  $500 \times g$  for 5 min to separate the layers. The lower dichloromethane layer was transferred into a clean 7-mL screw-capped tube, and solvent was removed under argon at 35°C using a Techne DB3 3A Dri-Block apparatus (Duxford, Cambridge, United Kingdom). Dried lipid was immediately hydrogenated as described below.

**Hydrogenation (deuteration) and saponification.** Platinum catalyst was added to a solution of methanol/toluene (1:1, vol/vol) to give 5 mg of platinum catalyst per mL of solvent. The solvent was shaken to suspend the catalyst, and 1 mL was added to the dried plasma lipid. For adipose tissue, approximately 20 mg was teased with forceps to disrupt the tissue prior to addition of the platinum. The tube was purged with hydrogen for 20 s and capped using a Teflon seal. The tubes were then shaken at room temperature for 15 min on a Desaga shaker. Hydrogenation was rapid and quantitative. Hydrogenolysis is a side reaction that occurs during hydrogenation using active catalysts, such as platinum, leading to products other than those desired (25). In other experiments, hydroxy and epoxy standards were hydrogenated and products were determined by GC with FID detection. No major hydrogenolysis of epoxy or hydroxy standards was observed in these experiments.

Deuterium scrambling is a recognized phenomenon that occurs with active catalysts such as platinum (25,26); therefore, the amount of the deuterated isomers was not determined. In experiments to confirm the number of double bonds, cyclohexane was used as solvent and processed as follows to minimize deuterium scrambling. The tubes were purged with deuterium for 20 s and then shaken for 5 min to saturate the solvent with deuterium. The catalyst was added and the tube was again purged with deuterium and shaken for 5 min.

Hydrogenated lipid was then saponified (23,24) to release FA. To the tube was added 2 mL KOH (1 M) in methanol/water (95:5, vol/vol), and the sample was heated at 70°C for 30 min. After cooling, the sample was transferred to an 18-mL Quick-Fit tube to which 2 mL water and 3 mL hexane/ether (1:1, vol/vol) were added. The sample was vortexed and centrifuged if necessary at  $500 \times g$  for 2 min to separate the layers. The upper organic layer containing cholesterol was discarded, and the procedure was repeated using 3 mL hexane/ether (1:1, vol/vol). The sample was acidified with 0.5 mL HCl (5 M) and FA were recovered by extracting the aqueous layer twice using 3 mL hexane/ether (1:1, vol/vol). The extracts were pooled into a 7-mL screw-capped tube and solvent was removed under argon.

**Methylation and derivatization of epoxy groups.** To the

tube were added 0.5 mL toluene and 2 mL boron trifluoride in methanol (14%, w/w), and the sample was heated at 60°C for 10 min. After cooling, 2 mL water and 3 mL hexane/ether (1:1, vol/vol) were added, and the sample was vortexed and then centrifuged at  $500 \times g$  for 2 min to separate the layers. The upper organic layer was transferred to a clean tube, and the procedure was repeated by adding 3 mL hexane/ether (1:1, vol/vol). Solvent was removed under argon. During this procedure FA were methylated and epoxy groups were quantitatively converted into methoxy-hydroxy groups.

**Purification of methoxy and hydroxy FAME.** Because 9,10-epoxy stearate is found in plastic sources, the silica SPE columns were prewashed with chloroform to remove potential contaminants. Columns were air dried and then activated at 100°C for 20 min. Methoxy- and hydroxy-containing FAME were separated from saturated FAME as described previously (23). The SPE columns were conditioned using 5 mL hexane/ethyl acetate (98:2, vol/vol). The sample was transferred to the SPE column using  $2 \times 250 \mu$ L hexane/ethyl acetate (95:5, vol/vol) and nonoxidized saturated FAME were eluted using 5 mL hexane/ethyl acetate (95:5, vol/vol). Methoxy and hydroxy FAME were retained on the column and were then eluted using 5 mL hexane/ethyl acetate (50:50, by vol) and collected in 7-mL screw-capped tubes. Solvent was removed under argon.

**GC-MS.** The isolated FAME were transferred to vials using 250  $\mu$ L methanol/dichloromethane (1:1, vol/vol) containing TMAH (1%, w/w). This reagent methylates by pyrolysis in hot injection ports and converts hydroxy to methoxy FAME and methoxy-hydroxy FAME to vicinal dimethoxy FAME. Samples were analyzed using a Hewlett-Packard 6890 series II gas chromatograph equipped with a 5973 AMS mass spectrometer and a 6890 autosampler. For analysis, 2- $\mu$ L volumes were injected into a split/splitless injector set at 260°C under splitless mode. Analysis was performed using a 30 m  $\times$  0.25 mm i.d.  $\times$  0.25  $\mu$ m HP 5MS fused-silica capillary column (Hewlett-Packard, Cheadle Heath, United Kingdom) and the following temperature program: 3 min at 100°C, 25°C/min to 170°C, 2°C/min to 260°C, 5 min at 260°C. While the temperature was maintained at 260°C, two blank solutions of TMAH were injected at 5-min intervals to flush through the system. Helium, as carrier gas, was maintained at a constant flow rate of 0.9 mL/min.

EI (70 KeV)-MS of methoxy FAME produced two major ions with fragmentation on either side of the methoxy group. EI (70 KeV)-MS of vicinal dimethoxy FAME also gave two major ions with fragmentation occurring between the adjacent methoxy groups (Fig. 2C). Fragmentation of derivatized monoepoxy FA was similar to that of hydroxy FA; thus, both compounds were quantified simultaneously. A total of 23 ions were monitored for determination of hydroxy and epoxy isomers, with a dwell time of 30 ms and a cycle time of 0.96 cycle/s (Table 1). For each isomer, five-point dilution calibration curves were prepared. The abundance of the ion fragment representing the methoxy carboxylic methyl ester part of the molecule was used to calculate amounts (Fig. 2C).

**TABLE 1**  
**Characteristic Ion Fragments of Methoxy FAME and Vicinal Dimethoxy FAME Derived from Hydroxy and Epoxy FA**

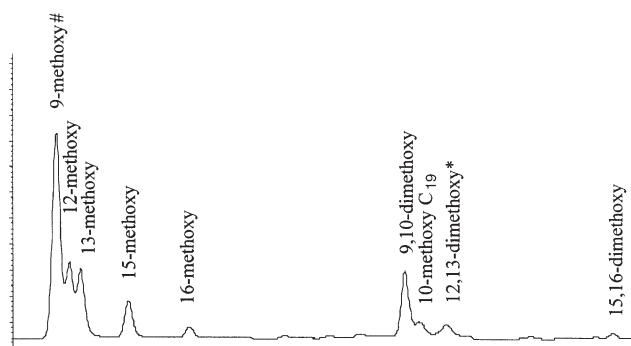
Methoxy and dimethoxy	RRT	Target ion	Qualifier ion	Ion ratio <sup>b</sup>
<sup>13</sup> C <sub>18</sub> 9-methoxy	1.000	210	181	1.74
<sup>13</sup> C <sub>18</sub> 10-methoxy	1.002	225	166	1.46
<sup>13</sup> C <sub>18</sub> 9,10-dimethoxy	1.108	210	166	3.15
C <sub>19</sub> 10-methoxy	1.113	215	171	1.70
C <sub>19</sub> 14-methoxy	1.122	271	115	1.52
C <sub>18</sub> 8-methoxy	1.000	187	185	2.19
C <sub>18</sub> 9-methoxy	1.001	201	171	1.70
C <sub>18</sub> 10-methoxy	1.002	215	157	1.44
C <sub>18</sub> 11-methoxy	1.004	229	143	0.87
C <sub>18</sub> 12-methoxy	1.005	243	129	0.78
C <sub>18</sub> 13-methoxy	1.009	257	115	0.58
C <sub>18</sub> 15-methoxy	1.032	285	87	0.35
C <sub>18</sub> 16-methoxy	1.060	299	73	0.29
C <sub>18</sub> 9,10-dimethoxy	1.109	201	157	2.96
C <sub>18</sub> 12,13-dimethoxy	1.119	243	115	1.34
C <sub>18</sub> 15,16-dimethoxy	1.173	285	73	1.04

<sup>a</sup>The above table gives the major ions from the fragmentation of methoxy and vicinal dimethoxy isomers derived from hydroxy and epoxy FA. The target ion representing the methoxy carboxylic methyl ester part of the molecule was used for the quantification. Relative retention times (RRT) are given in relation to the <sup>13</sup>C<sub>18</sub> 9-methoxy internal standard.

<sup>b</sup>The ion ratio (abundance of the target ion divided by that of the qualifier ion) was calculated from a scan chromatogram using standards.

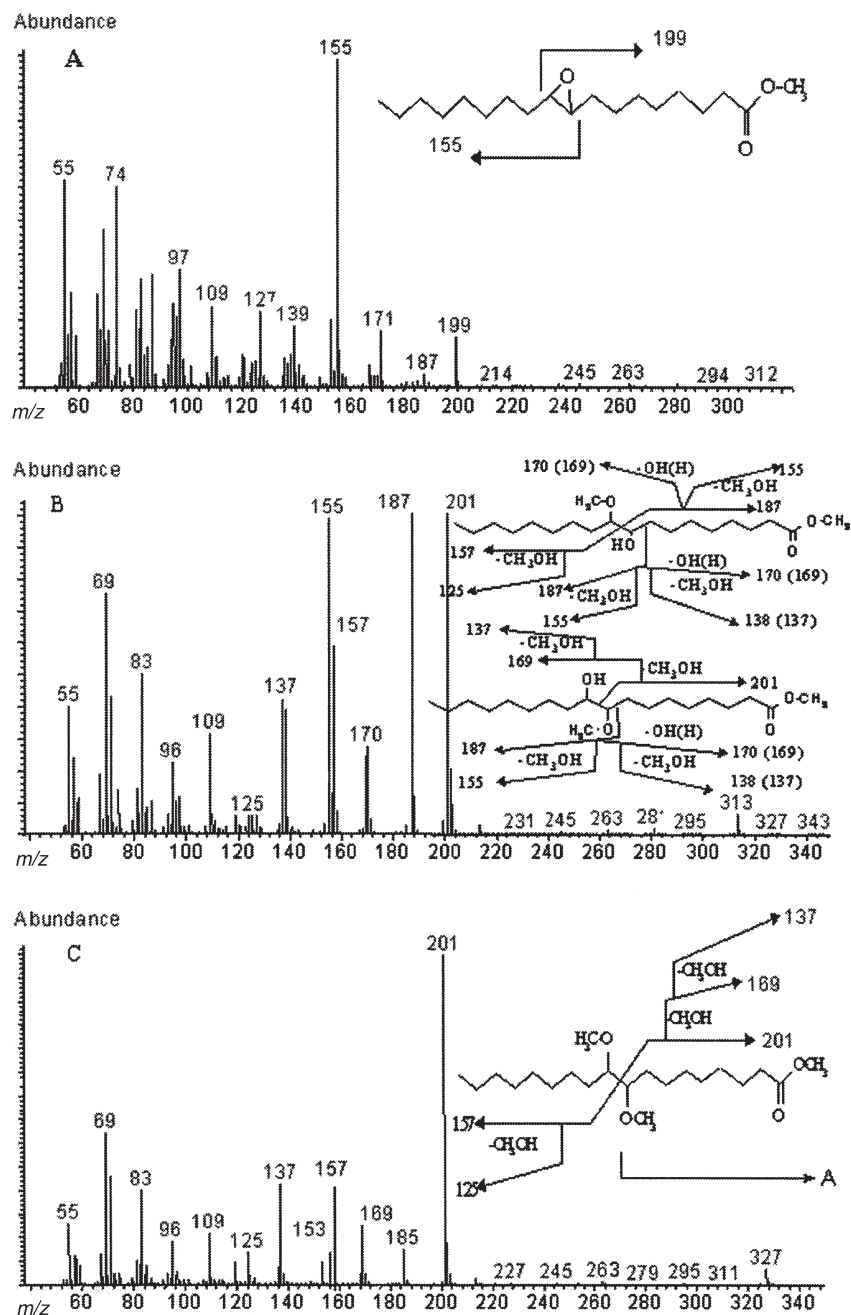
## RESULTS

The chromatographic separation of the methoxy and dimethoxy isomers is shown in Figure 1. The 8-, 9-, 10-, and 11-methoxy C<sub>18</sub> isomers were not resolved; the 12- and 13-methoxy C<sub>18</sub> were partially resolved, and the 15- and 16-methoxy C<sub>18</sub> are baseline resolved. The 9,10-dimethoxy C<sub>18</sub> was resolved from the 12,13-dimethoxy and 15,16-dimethoxy C<sub>18</sub> isomers. The 10-methoxy C<sub>19</sub> was partially resolved from



**FIG. 1.** Chromatogram of methoxy and dimethoxy isomers. A sample containing hydroxy and epoxy isomers was analyzed as detailed in the Methods section. The above figure shows the chromatographic separation of the methoxy and dimethoxy isomers. The 8-, 9-, 10-, and 11-methoxy (#) are not resolved, nor are the 12,13-dimethoxy C<sub>18</sub> and 14-methoxy C<sub>19</sub> (\*). However, the ions for each isomer are unique; therefore, these isomers can be determined by MS.

the 9,10-dimethoxy C<sub>18</sub>, whereas the 14-methoxy C<sub>19</sub> and the 12,13-dimethoxy C<sub>18</sub> were not resolved. The ions for these co-eluting isomers were unique; therefore, each could be determined by MS. The mass spectrum of 9,10-epoxy stearate was typical of that recorded in the literature (Fig. 2A). The interpretation of the mass spectra was relatively simple, with cleavage on either side of the epoxy group. Epoxy FAME, however, exhibited some degradation at high temperatures, giving multiple peaks, and it was considered necessary to convert epoxy FAME into derivatives that were stable in the hot injection port liner. Treatment with boron trifluoride in methanol converted the epoxy group to a vicinal hydroxy-methoxy group, and two isomers were formed. The two isomers from 9,10-epoxy stearate were not chromatographically resolved, whereas those from 15,16-epoxy stearate were baseline resolved (not shown) under the chromatographic conditions used. These compounds were stable at 260°C in the hot injection port liner. The mass spectra of these compounds were complex because of the loss of methoxy, hydroxy, and water (Fig. 2B). It was possible, however, to elucidate the structure of the two isomers from the mass spectrum (Fig. 2B). For the 9-hydroxy-10-methoxy isomer, fragmentation between these groups gave ions 157 and 187, and  $\alpha$ -fragmentation to the hydroxy group gave ion 187. Typical losses of CH<sub>3</sub>OH (32 amu), OH (17 amu), or H<sub>2</sub>O (18 amu) were identified, giving ions 170 (187 – 17), 169 (187 – 18), 155 (187 – 32), 138 (170 – 32), 137 (169 – 32), and 125 (157 – 32). For the 9-methoxy-10-hydroxy isomer, fragmentation between these groups gave ion 201 only, and  $\alpha$ -fragmentation



**FIG. 2.** Mass spectrum of 9,10-epoxy stearate and its derivatives. Figure A is the mass spectrum of 9,10-epoxy stearate. Conversion to hydroxy and methoxy stearate gives a simplified spectrum, and the fragments produced confirm the structure of the two isomers (Fig. B). However, the mass spectrum is further simplified, and for the dimethoxy derivative two ions, ions 201 and 157, can be used to identify and quantify 9,10-epoxy stearate (Fig. C). In this example the major ion fragment A, representing the methoxy carboxylic methyl ester, is used for quantification.

to the methoxy group gave ion 187. Typical losses of  $\text{CH}_3\text{OH}$  (32 amu), OH (17 amu), or  $\text{H}_2\text{O}$  (18 amu) were identified, giving ions 169 (201 – 32), 170 (187 – 17), 169 (187 – 18), 155 (187 – 32), 138 (170 – 32), and 137 (169 – 32). Derivatization of the vicinal hydroxy–methoxy FAME using TMAH produced a single chromatographic peak of vicinal dimethoxy FAME but, more importantly, the mass spectrum was simplified and

easily interpreted (Fig. 2C). Major fragmentation occurred between the vicinal dimethoxy groups; and the two major ion fragments formed, 201 and 157, could be used to identify and quantify the 9,10-epoxy isomer.

The precision of the method was assessed using quality control (QC) plasma, the biological material containing the least amount of lipid (1.5 mg/mL). The quantification of



U-<sup>13</sup>C-labeled 10-hydroxy methyl stearate using U-<sup>13</sup>C-labeled 9-hydroxy methyl stearate as the internal standard gave a CV of 2.7%. For 8-, 9-, 10-, 11-, 12-, and 13-hydroxy isomers, the CV of quantification was between 10 and 15% ( $n = 84$ ). It should be noted that the value of the minor isomers decreased as the mass spectrometer became dirty through sample analysis; this was reflected in the higher CV of 37 and 53% for the 15- and 16-hydroxy isomers, respectively. The 16-hydroxy isomer value decreased from 0.042 to 0.014  $\mu\text{M}$  over a 6-mon time period, but the major component values were unchanged. At this point the mass spectrometer source was cleaned. The limit of detection was 0.01  $\mu\text{M}$ . The analysis of blank samples gave values for individual hydroxy isomers of less than 0.01  $\mu\text{M}$ . It should be noted that a high 12-hydroxy was associated with certain batches of boron trifluoride. With this exception, the quantification of hydroxy isomers was the same using diazomethane or boron trifluoride (not shown). The within-batch CV of QC total plasma hydroxy was of 6.7% ( $n = 10$ ) and the between-batch CV was 10.1% ( $n = 84$ ). The 10-hydroxy and 14-hydroxy isomers derived from oxidation of the added 19:2 were constant during a 6-mon period,  $0.020 \pm 0.005 \mu\text{M}$ , and during this time no sample failed acceptable QC criteria. These values were not greater than when 19:2 was hydrogenated directly, so correction for oxidation of during-sample processing was not necessary. The 15,16-epoxy isomer was not detected in this QC plasma, and the 12,13-epoxy isomer was found at levels similar to the 15-hydroxy isomer. The within-batch CV of analysis of QC plasma epoxy was of 8.5% and the between-batch CV was 13.8%. The 9,10-epoxy isomer was found in plastic sources and should be avoided to obtain low blanks. Injection port septa also gave rise to contamination, and Teflon-coated septa or Merlin Microseal septa gave the best results. Under these conditions, blank samples gave values of around 0.03  $\mu\text{M}$  for the 9,10-epoxy isomer and less than 0.01  $\mu\text{M}$  for the 12,13-epoxy isomer.

Treatment of plasma samples with deuterium increased the mass of the hydroxy isomers proportional to the number of double bonds. This was clearly evident for the 9-hydroxy and 13-hydroxy isomers where the mass increased by 4 amu (from 171 to 175 and from 257 to 261 amu, respectively), indicating that these fragments contained two double bonds. However, little or no increase in mass was observed for the major 9,10-epoxy isomer; thus, this epoxy isomer contained no additional double bonds. Treatment of adipose tissue samples with deuterium increased the mass of the hydroxy isomers proportional to the number of double bonds. It was evident that the 12,13-epoxy isomer contained one double bond, as the mass of the fragment containing the double bond increased by 2 amu (from 243 to 245 amu). Yet there was little evidence for a similar increase in mass for the 9,10-epoxy isomer. Thus, in adipose tissue the 9,10-epoxy isomer contained no additional double bonds.

Epoxy FA and hydroxy FA were identified in the plasma of 19 men (Table 2). The 9,10-epoxy isomer was present at a higher concentration than either the 12,13-epoxy isomer or

**TABLE 2**  
**Hydroxy and Epoxy Isomers in Plasma of Man<sup>a</sup>**

Hydroxy isomer	Amount ( $\mu\text{M}$ )	Amount ( $\mu\text{M}$ )	Epoxy isomer
8-	$0.067 \pm 0.003$		
9-	$0.209 \pm 0.011$		
10-	$0.132 \pm 0.004$	$0.260 \pm 0.040$	9,10-
11-	$0.112 \pm 0.005$		
12-	$0.082 \pm 0.004$	$0.080 \pm 0.004$	12,13-
13-	$0.122 \pm 0.006$		
15-	$0.050 \pm 0.001$	$0.034 \pm 0.006$	15,16-
16-	$0.018 \pm 0.001$		
Total	$0.792 \pm 0.041$	$0.374 \pm 0.025$	Total

<sup>a</sup>Hydroxy and epoxy isomers in the plasma of 19 men were determined as described in the Methods section. Values are mean  $\pm$  SEM.

the 15,16-epoxy isomer (Table 2). The 9-, 10-, 11-, 12-, and 13-hydroxy isomers were all major products, and the pattern of hydroxy isomers was typical of oxidation of plasma unsaturated FA, in particular linoleic acid. The level of total hydroxy was related to the level of total epoxy ( $r = 0.52$ ,  $P < 0.001$ ), and this was also reflected in that the major 9,10-epoxy isomer was related to the sum of the 9-hydroxy and 10-hydroxy isomers ( $r = 0.57$ ,  $P < 0.001$ ). In these men hydroxy FA were, on average, 1.7-fold greater in concentration compared to epoxy FA. In contrast, the level of 9,10-epoxy isomer in QC plasma ( $0.752 \pm 0.023 \mu\text{M}$ ) was similar in magnitude to the level of total hydroxy isomers ( $0.720 \pm 0.031$ ).

Epoxy FA and hydroxy FA were identified in adipose tissue of the same 19 men (Table 3). Similar to that in plasma, the 9,10-epoxy isomer was present in substantially higher concentrations than either the 12,13-epoxy isomer or the 15,16-epoxy isomer (Table 3). In adipose tissue there was, on average, 4.8-fold more hydroxy than epoxy FA, with 9-, 10-, 11-, 12-, and 13-hydroxy isomers all being major products. In contrast to plasma, the 11-hydroxy isomer was the major product in adipose tissue. The levels of total hydroxy were significantly related to the levels of total epoxy ( $r = 0.65$ ,  $P < 0.005$ ), and this was reflected in the fact that the 9,10-epoxy isomer was significantly related to the sum of the 9- and 10-hydroxy isomers ( $r = 0.53$ ,  $P < 0.02$ ). It should be noted that

**TABLE 3**  
**Hydroxy and Epoxy Isomers in Adipose Tissue of Man<sup>a</sup>**

Hydroxy isomer	Amount ( $\mu\text{g/g}$ ) <sup>b</sup>	Amount ( $\mu\text{g/g}$ ) <sup>b</sup>	Epoxy isomer
8-	$4.53 \pm 0.99$		
9-	$36.47 \pm 3.88$		
10-	$16.10 \pm 1.13$	$19.24 \pm 2.98$	9,10-
11-	$40.29 \pm 4.91$		
12-	$7.32 \pm 0.44$	$2.61 \pm 0.37$	12,13-
13-	$10.79 \pm 0.69$		
15-	$2.27 \pm 0.33$	$1.46 \pm 0.10$	15,16-
16-	$1.26 \pm 0.05$		
Total	$112.9 \pm 10.4$	$23.31 \pm 3.45$	Total

<sup>a</sup>Adipose tissue from 19 men was analyzed for hydroxy and epoxy isomers as described in the Methods section.

<sup>b</sup>Values are  $\mu\text{g}$  hydroxy per g wet weight adipose tissue (mean  $\pm$  SEM).

although a weak correlation was found between plasma and adipose hydroxy isomers ( $r = 0.35$ ,  $P = 0.14$ ), there was no correlation between plasma and adipose epoxy FA ( $r = 0.12$ ,  $P = 0.60$ ). We found that the CV of adipose tissue tended to be greater than that of plasma samples from the same men. An accurate wet weight contributed to the increased error, but unlike plasma, small samples of adipose tissue were not homogeneous. Thus, adipose analyzed from a large adipose sample from a single individual gave a CV of 17% for total hydroxy ( $n = 10$ ).

## DISCUSSION

Hydroxy FA are derived directly from hydroperoxy FA and are stable end products of the body's defense mechanisms to the free radical attack (2,3). Linoleic acid is the major PUFA within the body (27). We therefore used hydroxy FA derived from linoleic acid as a surrogate measure of free radical oxidative damage (23,28). Hydroxy FA have been used as a surrogate measurement of hydroperoxy FA in biological systems in many studies (1–10). Hydrogenation is an essential step in many methods because it not only stabilizes the hydroperoxy group early in the analytical procedure (as a hydroxy group) but through elimination of double bonds also prevents further oxidation during sample workup. These methods cannot distinguish between hydroperoxy and hydroxy FA (5). The hydrogenation step described in the present paper is excellent, as demonstrated in that oxidation products derived from the added 19:2 were consistently low throughout the period of analysis and thus no autoxidation occurred during sample processing.

Methylation of FA using diazomethane, as in the original method (23), does not open up the epoxy group. Hence, FA containing monoepoxy groups were not retained on the SPE column and could not be measured. In addition to producing methyl esters, boron trifluoride in methanol opens up the epoxy group to form hydroxy-methoxy groups (14), and these compounds are retained on the SPE columns. Derivatization of hydroxy groups with TMAH improves both the chromatography and fragmentation of the hydroxy and epoxy FA esters. Two main ions are formed, and each unique ion pair defines the position of oxidation of the original carbon-carbon double bond. The method can be used to monitor and quantify all hydroxy and epoxy isomers of  $C_{18}$  FA and also measure and quantify hydroxy and epoxy isomers of  $C_{20}$  and  $C_{22}$  FA. However, in plasma and adipose tissue, the two tissues routinely sampled in human studies, the 9-, 10-, 11-, 12-, and 13-hydroxy  $C_{18}$  isomers and the 9,10-epoxy  $C_{18}$  isomer are the most abundant, and these isomers would routinely be quantified. The 9,10-epoxy isomer would, of course, be indistinguishable from the 9,10-dihydroxy isomer. However, little 9,10-dihydroxy is detected in plasma, and in samples with a high 9,10-dihydroxy concentration then measurement with and without boron trifluoride treatment would be required.

It has long been assumed that oxidized lipids are poorly absorbed (29), but it has recently been shown that hydroxy

and epoxy FA present in oils and foods are absorbed from the diet (28,30). Although consumption of oxidized fat increased the levels of hydroxy and epoxy FA during postprandial lipemia, the absorbed fat did not contribute to fasting plasma levels of oxidized lipids some 24 h later (28,30). Thus, fasting plasma hydroxy and epoxy FA may give reliable measurements of free radical damage occurring within the body. In the present study, the total fasting hydroxy FA level was  $0.792 \pm 0.041 \mu\text{mol/L}$ . It is important to note that the hydroxy FA levels are similar to the direct measurement of plasma hydroperoxy levels using other techniques (31,32). The 9- and 13-hydroxy isomers are typical of free radical oxidation of linoleic acid, and the use of deuterium confirmed that the 9- and 13-hydroxy isomers were indeed derived from linoleic acid. The 9,10-epoxy isomer was a major component in both plasma and adipose tissue and was from oleic acid. High levels of 9,10-epoxy stearate were found in blood (19), and later 9,10-epoxy octadeca-12-enoate and 12,13-epoxy octadeca-9-enoate, epoxy isomers derived from linoleic acid (20), were identified by the same researchers (20). That method, in which the epoxy group was chemically reduced to hydroxy groups, did not readily distinguish between epoxy and endogenous hydroxy FA isomers. It is possible that the high levels of 9-hydroxy and 13-hydroxy isomers in plasma were identified as epoxy isomers in those studies (20). Diffusion of epoxy FA from plastic sources into foods is now documented (33). However, there is no indication that the 9,10-epoxy stearate found in blood collected in clinical PVC bags in this and other studies (19,20) is due to a similar process. It is important to note that a plasma pool collected using glass syringes and glass tubes gave epoxy values similar to that collected using normal procedures ( $0.112 \pm 0.12$  vs.  $0.120 \pm 0.15$ ,  $n = 3$ ).

PUFA can be oxygenated by cytochrome P450 (13). This ubiquitous enzyme catalyzes the oxygenation of xenobiotics through epoxidation and hydroxylation reactions, often to detoxify these compounds, but it can also oxygenate endogenous lipids (13). Arachidonic acid, as a precursor of eicosanoids, has been studied intensively, but linoleic acid and other  $C_{18}$  FA are substrates for cytochrome P450 (11–13,34). A major hydroxylation product of cytochrome P450 is the 11-hydroxy isomer derived from linoleic acid (13). It is interesting to note that, of the two monoperoxides of linoleic acid, the rate of conversion to the 9,10-isomer is more than three times higher than the 12,13-isomer by liver (11) or soybean microsomes (34). Oleic acid is also readily oxidized to 9,10-epoxy by soybean microsomes in a mechanism consistent with hydroperoxy linoleic acid acting as an oxygen donor rather than by a free peroxy radical mechanism (34). Oxidized lipids have been detected in diseased heart tissue in pigs (22) and in humans (35), and their amounts increased with time of ischemia (22). These compounds were absent (22) or lower in concentration (35) in healthy heart tissue. Measurements were semiquantitative, but the identification of 9,10-epoxy stearate and leukotoxins (the 9,10-epoxy octadeca-12-enoate and 12,13-epoxy octadeca-9-enoate, isomers derived from

linoleic acid) led these investigators to conclude that they originated from enzymatic oxidation rather than from lipid peroxidation (35). Interestingly, in adipose tissue the 11-hydroxy isomer, a potential product of cytochrome P450 (13), was the largest component. The 9,10-epoxy isomer identified in the present study contained no additional double bonds and therefore was from the oxidation of oleic acid rather than linoleic acid. However, the present technique could not determine the stereochemistry of the isomers. Techniques to determine the stereochemistry, which might differentiate between free radical and enzymatic sources of oxygenated metabolites, have recently been reviewed (25). The origin of the 11-hydroxy and 9,10-epoxy isomer in plasma and adipose tissue requires further investigation, but it is interesting to speculate that these two products are formed enzymatically rather than from a free radical mechanism.

With the increased interest in the biological effects of epoxy FA derived from linoleic acid (11–13), there is a need for quantitative measurements. This paper describes a GC–MS technique for the quantitative analysis of hydroxy and epoxy FA derived from biological samples. The method is accurate and gives good consistency, both within batch and between batches. The method described shows good sensitivity, with 0.5 mL plasma and 20 mg adipose tissue being sufficient to measure hydroxy and epoxy isomers. Our method is a major advance over that currently available in the literature. The synthesis of hydroxy and epoxy FA from U-<sup>13</sup>C-labeled oleic acid permitted accurate quantitation. The hydrogenation step is fast and effective with no oxidation during sample preparation. Purification of hydroxy and epoxy FAME from the bulk of nonoxidized material eliminates chromatographic interference and maintains MS sensitivity for prolonged periods. Derivatization of hydroxy groups improves EI–MS readings, permitting ease of identification and simultaneous quantification of all hydroxy and epoxy isomers. Measurement of multiple isomers rather than a single ion, as in negative ion techniques, can distinguish between isomers derived from enzymatic sources and those from free radical oxidation, thus facilitating interpretation of the data.

## ACKNOWLEDGMENTS

This study was supported by a LINK Agro Food Programme grant (AFQ112). We wish to thank the Ministry of Agriculture, Food and Fisheries and the members of the Link management group—Nestlé UK Ltd., Roche Products Ltd., and Van den Bergh Foods Ltd.—for their support. R.W. was funded by EU grant (Generale Study QLRT-1999-02111). This study was also supported by an equipment grant for the purchase of the mass spectrometer from the Wellcome Foundation and the Scottish Chest, Heart and Stroke Association.

## REFERENCES

- de Zwart, L.L., Meerman, J.H., Commandeur, J.N., and Vermeulen, N.P. (1999) Biomarkers of Free Radical Damage Applications in Experimental Animals and in Humans, *Free Radic. Biol. Med.*, 26:202–226.
- Gutteridge, J.M. (1995) Lipid Peroxidation and Antioxidants as Biomarkers of Tissue Damage, *Clin. Chem.* 41:1819–1828.
- Halliwell, B. (1996) Mechanisms Involved in the Generation of Free Radicals, *Pathol. Biol.* 44:6–13.
- Offord, E., van Poppel, G., and Tyrrell, R. (2000) Markers of Oxidative Damage and Antioxidant Protection: Current Status and Relevance to Disease, *Free Radic. Res.* 33 (Suppl.), S5–S19.
- Moore, K., and Roberts, L.J. (1998) Measurement of Lipid Peroxidation, *Free Radic. Res.* 28:659–671.
- Morrow, J.D., Awad, J.A., Wu, A., Zackert, W.E., Daniel, V.C., and Roberts, L.J. (1996) Nonenzymatic Free Radical-Catalyzed Generation of Thromboxane-like Compounds (isothromboxanes) *in vivo*, *J. Biol. Chem.* 271, 23185–23190.
- Johnson, J.A., Blackburn, M.L., Bull, A.W., Welsch C.W., and Watson, J.T. (1997) Separation and Quantitation of Linoleic Acid Oxidation Products in Mammary Gland Tissue from Mice Fed Low- and High-Fat Diets, *Lipids* 32, 369–375.
- Schneider, C., Schreier, P., and Herderich, M. (1997) Analysis of Lipoyxygenase-Derived Fatty Acid Hydroperoxides by Electrospray Ionization Tandem Mass Spectrometry, *Lipids* 32, 331–336.
- Hall, L.M., and Murphy, R.C. (1998) Activation of Human Polymorphonuclear Leukocytes by Products Derived from the Peroxidation of Human Red Blood Cell Membranes, *Chem. Res. Toxicol.* 11, 1024–1031.
- Phillips, M., Greenberg, J., and Cataneo, R.N. (2000) Effect of Age on the Profile of Alkanes in Normal Human Breath, *Free Radic. Res.* 33, 57–63.
- Moghaddam, M.F., Motoba, K., Borhan, B., Pinot, F., and Hammock, B.D. (1996) Novel Metabolic Pathways for Linoleic and Arachidonic Acid Metabolism, *Biochim. Biophys. Acta* 1290, 327–339.
- Moghaddam, M.F., Grant, D.F., Cheek, J.M., Greene, J.F., Williamson, K.C., and Hammock, B.D. (1997) Bioactivation of Leukotoxins to Their Toxic Diols by Epoxide Hydrolase, *Nature Med.* 3, 562–566.
- Oliw, E.H. (1994) Oxygenation of Polyunsaturated Fatty Acids by Cytochrome P450 Monooxygenases, *Prog. Lipid Res.* 33, 329–354.
- Kleinman, R., and Spencer, G.F. (1972) Gas Chromatography–Mass Spectroscopy of Methyl Esters of Unsaturated Oxygenated Fatty Acids, *J. Am. Oil Chem. Soc.* 50, 31–38.
- Oliw, E.H. (1985) Analysis of Epoxyeicosatrienoic Acids by Gas Chromatography–Mass Spectrometry Using Chlorohydrin Adducts, *J. Chromatogr.* 339, 175–181.
- VanRollins, M., and Knapp H.R. (1995) Identification of Arachidonate Epoxides/Diols by Capillary Chromatography–Mass Spectrometry, *J. Lipid Res.* 36, 952–966.
- Fang, X., Kaduce, T.L., Weintraub, N.L., VanRollins, M., and Spector, A.A. (1996) Functional Implications of a Newly Characterized Pathway of 11,12-Epoxyeicosatrienoic Acid Metabolism in Arterial Smooth Muscle, *Circ. Res.* 79, 784–793.
- Yamane, M., Abe, A., and Yamane, S. (1994) High-Performance Liquid Chromatography–Thermospray Mass Spectrometry of Epoxy Polyunsaturated Fatty Acids and Epoxyhydroxy Polyunsaturated Fatty Acids from an Incubation Mixture of Rat Tissue Homogenate, *J. Chromatogr. B* 652, 123–136.
- Ulsaker, G.A., and Teien, G. (1983) Gas Chromatographic–Mass Spectrometric Identification of 9,10-Epoxyoctadecanoic Acid in Human Blood, *Analyst* 108, 521–524.
- Ulsaker, G.A., and Teien, G. (1986) Gas Chromatographic–Mass Spectrometric Identification of 9,10-Epoxyoctadecanoic Acid in Human Urine Using Gas Chromatography–Mass Spectrometry, *Biomed. Chromatogr.* 9, 183–187.
- Dudda, A., Spittler, G., and Kobelt, F. (1996) Lipid Oxidation

- Products in Ischemic Porcine Heart Tissue, *Chem. Phys. Lipids* 82, 39–51.
23. Wilson, R., Smith, R., Wilson, P., Shepherd, M.J., and Riemersma, R.A. (1997) Quantitative Gas Chromatography–Mass Spectrometry Isomer-Specific Measurement of Hydroxy Fatty Acids in Biological Samples and Food as a Marker of Lipid Peroxidation, *Anal. Biochem.* 248, 76–85.
  24. Christie, W.W. (1982) The Preparation of Derivatives of Lipids, in *Lipid Analysis* (Christie, W.W., ed.), pp. 51–61, Pergamon Press, Oxford.
  25. Gardner, H.W. (1997) Analysis of Plant Lipoxygenase Metabolites, in *Advances in Lipid Methodology Four* (Christie, W.W., ed.), pp. 1–44, The Oily Press, Dundee, Scotland.
  26. Christie, W.W. (1997) Structural Analysis of Fatty Acids, in *Advances in Lipid Methodology Four* (Christie, W.W., ed.), pp. 119–169, The Oily Press, Dundee, Scotland.
  27. Logan, R.L., Riemersma, R.A., Thomson M., Oliver, M.F., Olsson, A.G., Walldius, G., Rossner, S., Kaijser, L., Callmer, E., Carlson, L.A., *et al.* (1978) Risk Factors for Ischaemic Heart-Disease in Normal Men Aged 40. Edinburgh-Stockholm Study. *Lancet* 1, 949–954.
  28. Wilson, R., Lyall, K., Smyth, L., Fernie, C.E., and Riemersma R.A. (2002) Dietary Hydroxy Fatty Acids Are Absorbed in Humans—Implications for the Measurement of ‘Oxidative Stress’ *in vivo*, *Free Radic. Biol. Med.* 32, 162–168.
  29. Kubow, S. (1992) Routes of Formation and Toxic Consequences of Lipid Oxidation Products in Foods, *Free Radic. Biol. Med.* 12, 63–81.
  30. Wilson, R., Fernie, C.E., Scrimgeour, C.M., Lyall, K., Smyth, L., and Riemersma, R.A. (2002) Dietary Epoxy Fatty Acids Are Absorbed in Healthy Women, *Eur. J. Clin. Invest.* 32, 79–83.
  31. Nourooz-Zadeh, J., Tajaddini-Sarmadi, J., Ling, K.E., and Wolff, S.P. (1996) Low-Density Lipoprotein Is the Major Carrier of Lipid Hydroperoxides in Plasma. Relevance to Determination of Total Plasma Lipid Hydroperoxide Concentrations, *Biochem. J.* 313, 781–786.
  32. Zamburlini, A., Maiorino, M., Barbera, P., Roveri, A., and Ursini, F. (1995) Direct Measurement by Single Photon Counting of Lipid Hydroperoxides in Human Plasma and Lipoproteins, *Anal. Biochem.* 232, 107–113.
  33. Castle, L., Mayo, A., and Gilbert, J. (1990) Migration of Epoxidized Soya Bean Oil into Foods from Retail Packaging Materials and from Plasticised PVC Film Used in the Home, *Food Addit. Contam.* 7, 29–36.
  34. Blee, E., and Schuber, F. (1990) Efficient Epoxidation of Unsaturated Fatty Acids by a Hydroperoxide-Dependent Oxygenase, *J. Biol. Chem.* 265, 12887–12894.
  35. Carpenter, K.L., Taylor, S.E., Ballantine, J.A., Fussell, B., Halliwell, B., and Mitchinson, M.J. (1993) Lipids and Oxidized Lipids in Human Atheroma and Normal Aorta. *Biochim. Biophys. Acta* 1167, 121–130.

[Received May 16, 2002, and in revised form August 30, 2002; revision accepted September 9, 2002]



# Apolipoproteins A-I and A-II Downregulate Neutrophil Functions

Cristiane Jaciara Furlaneto<sup>a</sup>, Fernanda Pereira Ribeiro<sup>a</sup>, Elaine Hatanaka<sup>a</sup>,  
Glaucia Mendes Souza<sup>b</sup>, Marco A. Cassatella<sup>c</sup>, and Ana Campa<sup>a,\*</sup>

<sup>a</sup>Departamento de Análises Clínicas e Toxicológicas, Faculdade de Ciências Farmacêuticas, Universidade de São Paulo, CEP 05508-900 São Paulo, Brazil; <sup>b</sup>Departamento de Bioquímica, Instituto de Química, Universidade de São Paulo, CEP 05508-900, São Paulo, Brazil; and <sup>c</sup>Departamento di Patologia, Sezione di Patologia Generale, Università di Verona, CEP 37134, Verona, Italy

**ABSTRACT:** This work reports the effect of the apolipoproteins A-I and A-II (apoA-I and apoA-II) on the release of tumor necrosis factor (TNF)- $\alpha$ , interleukin (IL)-1 $\beta$ , IL-8, and IL-1 receptor antagonist (IL-1Ra) and on the oxidative burst of human neutrophils. By themselves, apoA-I and apoA-II do not affect the basal liberation of these cytokines, whereas apoA-I affects the release of IL-1 $\beta$  from lipopolysaccharide (LPS)-stimulated neutrophils and apoA-II affects IL-8 released from LPS-stimulated neutrophils. ApoA-II also decreases the production of IL-8 released by neutrophils stimulated with the acute phase apolipoprotein serum amyloid A. Both apoA-I and apoA-II exerted ~30% inhibition on the oxidative burst of neutrophils stimulated by opsonized zymosan, as revealed by the luminol-enhanced chemiluminescence assay. These findings give additional support to the idea that the role of human plasma lipoproteins and apolipoproteins goes beyond their function in lipid transport and metabolism. HDL apolipoproteins appear to be a class of mediators that can participate in the regulation of the activity of neutrophils.

Paper no. L9019 in *Lipids* 37, 925–928 (September 2002).

The biological role of human plasma lipoproteins appears to extend well beyond their function in lipid transport and metabolism. For instance, lipoproteins and their apolipoproteins can affect several immunologically relevant processes (1,2). On the other hand, significant modifications in the concentration of plasma lipids and apolipoproteins have been observed during inflammation (3). In addition, HDL suffers intense changes in composition during the acute-phase response (4), when most of the HDL<sub>3</sub> apolipoprotein A-I (apoA-I) is replaced by the acute-phase protein serum amyloid A (SAA) (4,5). The displacement of apoA-I and enrichment in SAA give rise to a new HDL particle, termed acute-phase HDL. Since HDL and its main apolipoprotein apoA-I are involved in the reverse transport of cholesterol (6) and protection against coronary artery disease (7,8), the rise of acute-phase HDL in inflammation has been considered to be a pro-atherogenic condition. In this context, HDL and apoA-I associate with neutrophils (9) and affect their cellular functions (10–12). HDL decreases the production of reactive oxygen species during the oxidative burst (10). ApoA-I was considered to have a role in the inhibition of reactive oxygen species production by HDL, since free apoA-I was shown to decrease degranulation and superoxide production by activated neutrophils (11). In neutrophils, HDL and acute-phase HDL also decrease the basal and lipopolysaccharide (LPS)-stimulated release of tumor necrosis factor- $\alpha$  (TNF- $\alpha$ ),

\*To whom correspondence should be addressed. E-mail: anacampa@usp.br  
Abbreviations: apoA-I, apolipoproteins A-I; apoA-II, apolipoproteins A-II; IL, interleukin; IL-1Ra, interleukin-1 receptor antagonist; LPS, lipopolysaccharide; RPA, RNase protection assay; SAA, serum amyloid A; TNF, tumor necrosis factor.

interleukin-1 $\beta$  (IL-1 $\beta$ ), and interleukin-8 (IL-8) (12). On the other hand, free SAA acts as a stimulus for the liberation of these proinflammatory cytokines, pointing to a role of SAA in the progression and maintenance of inflammation (12).

In this study, we focused on the effects of apoA-I and apoA-II, the two most abundant HDL proteins in serum, on the release of cytokines from LPS- and SAA-stimulated human blood neutrophils. Since apoA-II is present in the same HDL fraction with which SAA associates, i.e., HDL<sub>3</sub> (4), the effects of HDL on neutrophil functions might be the result of the combined action of these apolipoproteins.

## MATERIALS AND METHODS

Human apoA-I and apoA-II, LPS (*E. coli* 026:B6), zymosan, RPMI-1640-Hepes supplemented with L-glutamine, dextran, Histopaque®, penicillin, and streptomycin from Sigma Chemical Co. (St. Louis, MO); FBS from Gibco (Grand Island, NY); NaCl, Na<sub>2</sub>HPO<sub>4</sub>, KH<sub>2</sub>PO<sub>4</sub>, and KCl from Merck (Darmstadt, Germany); and luminol from Aldrich Chemical Co. (Milwaukee, WI) were used. Recombinant human SAA was from Peprotech Inc. (Rocky Hill, NJ). SAA is essentially endotoxin free as evaluated by the polymixin B assay as described in Morrison and Jacobs (13).

Neutrophils were obtained from blood of healthy volunteers and isolated as previously described (12) using a commercial gradient of Ficoll-Hypaque (Histopaque®). The purity of the cell preparation was higher than 98%.

**Neutrophil culture and cytokine assay.** Neutrophils (2.5  $\times$  10<sup>6</sup> cells/mL) were cultured in RPMI-1640-Hepes supplemented with 0.3 g/L L-glutamine, 2 g/L sodium bicarbonate, 100  $\mu$ g/mL streptomycin, 100 IU/mL penicillin, and 10% FBS. Neutrophils were kept in a CO<sub>2</sub> atmosphere (5%) at 37°C alone or incubated with LPS (0.5 or 5  $\mu$ g/mL), SAA (17, 40, or 100  $\mu$ g/mL), and human apoA-I or apoA-II (40 or 100  $\mu$ g/mL). After 24 h, the supernatants were collected and frozen at  $\leq$ -40°C until the determination of TNF- $\alpha$ , IL-1 $\beta$ , IL-8, and IL-1 receptor antagonist (IL-1Ra) by ELISA (Quantikine; R&D Systems, Minneapolis, MN).

**Total RNA extraction and RNase protection assay (RPA) analysis.** Purified populations of neutrophils (10<sup>7</sup> cells/mL) were cultured with 40  $\mu$ g/mL SAA in the presence or absence of apoA-I or apoA-II (40  $\mu$ g/mL) for 3 and 21 h. Total RNA was then extracted as described (14), and cytokine mRNA levels were assessed by RPA, using the Riboquant Custom Mouse Probe Set containing probes for IL-1 $\beta$ , IL-1Ra, IL-8, and actin (Pharmingen, Franklin Lakes, NJ) according to manufacturer's instructions; 5  $\mu$ g of total RNA was used per each condition.

**Chemiluminescent assay.** The effect of apoA-I or apoA-II (100  $\mu\text{g/mL}$ ) on the neutrophil oxidative burst was evaluated by the luminol chemiluminescence assay. Freshly isolated neutrophils ( $2.5 \times 10^6$  cells/mL) were stimulated with opsonized zymosan ( $1 \times 10^7$  particles/assay) in the presence of luminol (1 mM). The reaction was run at pH 7.4 in phosphate-saline buffer, containing 100 mM  $\text{CaCl}_2$ , 50 mM  $\text{MgCl}_2$ , and 1 mg/mL glucose at  $37^\circ\text{C}$  in a final volume of 0.3 mL. Chemiluminescence was followed in an EG&G Berthold LB96V Microplate Luminometer. At the concentrations used, apoA-I and apoA-II do not scavenge superoxide anion as evaluated by the absence of effect of apoA-I and apoA-II on cytochrome C reduction in the presence of the xanthine/hypoxanthine oxidase system (15).

Statistical analysis was done by two-tailed analysis with a significance level of 95%.

## RESULTS

ApoA-I and apoA-II, by themselves, do not significantly modify the small amounts of  $\text{TNF-}\alpha$ , IL-1 $\beta$ , IL-8, and IL-1Ra recovered from the supernatants of neutrophils cultured for 24 h. In contrast, apoA-I causes a significant decrease ( $\geq 47\%$ ) in IL-1 $\beta$  release, and apoA-II causes a significant decrease ( $\geq 46\%$ ) in IL-8 release from stimulated neutrophils (see Fig. 1).

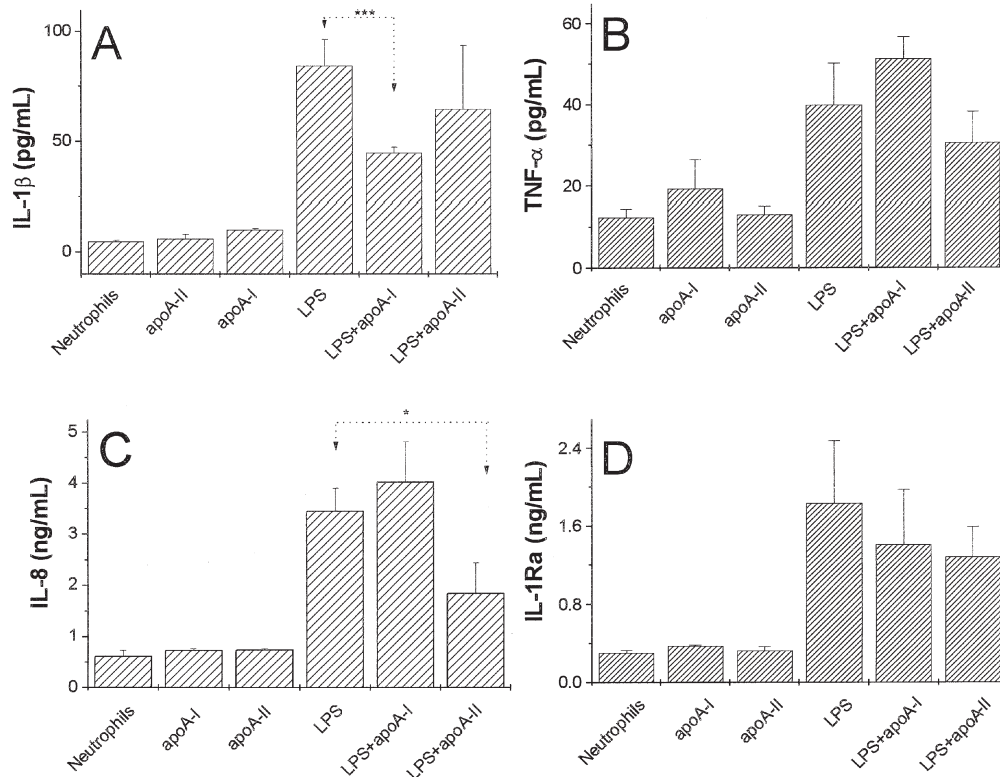
We then examined the effects of apoA-I and apoA-II on the release of IL-8 and IL-1Ra induced by SAA. SAA has previously been shown to trigger the release of neutrophil-derived

proinflammatory cytokines, particularly IL-8 (12). Figure 2 shows that only apoA-II decreases the release of SAA-induced IL-8, by approximately 44%. Neither apoA-I nor apoA-II significantly affected the release of IL-1Ra from SAA-stimulated neutrophils. ApoA-I or apoA-II neither regulate the mRNA transcripts for IL-1 $\beta$ , IL-8, and IL-1Ra nor inhibit the stimulatory effect of SAA on the related genes in 3 h-cultured neutrophils (Fig. 3). The absence of an effect of apoA-I and apoA-II on SAA regulation of mRNA transcripts of IL-1 $\beta$ , IL-1Ra, and IL-8 is also observed at longer incubation times (21 h) (data not shown).

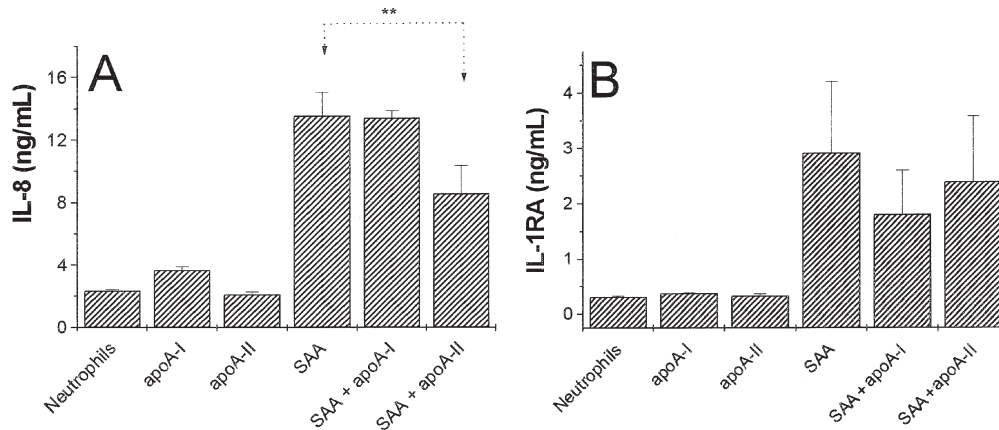
Another function that we studied was the effect of apoA-I and apoA-II on the reactive oxygen species produced by activated neutrophils. The oxidative burst was monitored by the luminol-enhanced chemiluminescence of neutrophils stimulated by opsonized zymosan (Fig. 4). The presence of either apoA-I or apoA-II does not modify the kinetic profile of light emission of opsonized zymosan-stimulated neutrophils but does decrease the integrated chemiluminescence by approximately 30%. The same magnitude of suppression was reported for apoA-I in a previous study where inhibition of superoxide anion formation was followed in neutrophils stimulated by an immunoglobulin G-coated surface (11).

## DISCUSSION

ApoA-I mediates the removal of cholesterol from peripheral tissues and carries it to the liver in a process known as reverse



**FIG. 1.** Effect of lipopolysaccharide (LPS) and the combined action of apolipoprotein A-I (apoA-I) or apolipoprotein A-II (apoA-II) plus LPS on the release of interleukin (IL)-1 $\beta$  (A), tumor necrosis factor (TNF)- $\alpha$  (B), IL-8 (C), and interleukin-1 receptor antagonist (IL-1Ra) (D) by neutrophils ( $2.5 \times 10^6$  cells/mL) after 24 h of cell culture. The concentration of apoA-I and apoA-II was 100  $\mu\text{g/mL}$  and of LPS was 5  $\mu\text{g/mL}$  for the IL-1 $\beta$  and TNF- $\alpha$  assay and 0.5  $\mu\text{g/mL}$  for the IL-8 and IL-1Ra assays. The data represent the average  $\pm$  SD of 4, 6, 5, and 2 experiments for A, B, C, and D, respectively. Significance was \* $P \leq 0.05$  and \*\*\* $P \leq 0.001$  comparing the effect of LPS alone with LPS plus apoA-I or apoA-II.



**FIG. 2.** Effect of apoA-I, apoA-II, or serum amyloid A (SAA) and the combined action of apoA-I or apoA-II plus SAA on the release of IL-8 (A) and IL-1Ra (B) by neutrophils ( $2.5 \times 10^6$  cells/mL) after 24 h of cell culture. The concentration of apoA-I and apoA-II was 100  $\mu\text{g/mL}$  and of SAA was 17  $\mu\text{g/mL}$  for the IL-8 assay and 40  $\mu\text{g/mL}$  for apoA-I, apoA-II, and SAA for the IL-1Ra assay. The data represent the average  $\pm$  SD of seven experiments for IL-8 and two experiments for IL-1Ra. Significance was  $**P \leq 0.005$  comparing the effect of SAA alone with SAA plus apoA-II. For other abbreviations see Figure 1.

cholesterol transport (6). This is considered to be a key process in the protective effect of HDL on coronary artery disease (8). Although the biological role of apoA-I is relatively well known, the functions of the second-most abundant HDL apolipoprotein, apoA-II, are still poorly understood. More recently, with the development of a mouse lineage that overexpresses apoA-II, it has been shown that, in contrast to what happens with apoA-I, HDL enriched with apoA-II lose their ability to protect against LDL oxidation and monocyte transmigration *in vitro* and promote the development of atherosclerosis *in vivo* (16). Apparently, the latter phenomenon is not a direct effect of apoA-II but rather is related to the loss of paraoxonase in the HDL particle (16).

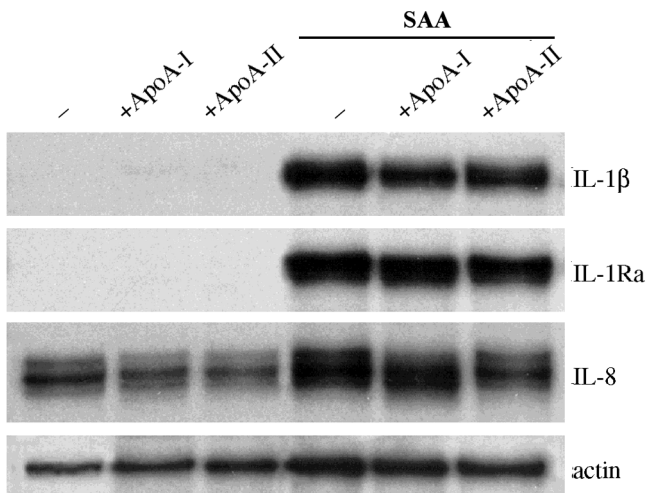
Besides the central function that apoA-I plays in lipid metabolism, apoA-I also affects neutrophil degranulation and oxidative burst (11). From the available information about the possible functions of apoA-I, it was inferred that this apolipoprotein has a general beneficial action, including an anti-inflammatory effect. In this study, we examined the par-

ticipation of both apoA-I and apoA-II in a process unrelated to lipid metabolism. Our results show that apoA-II affects the oxidative burst in a manner similar to apoA-I and that both affect the production of cytokines by neutrophils.

Cytokines are produced during the activation of innate and acquired immunity and serve to initiate the inflammatory response. The cytokine profile that predominates in a specific inflammatory process defines the magnitude and the nature of the immune response. The cytokines assayed in this study included the proinflammatory cytokines IL-1 $\beta$  and TNF- $\alpha$ , the chemokine IL-8, and the immunoregulatory cytokine IL-1Ra. At the concentration used, apoA-I and apoA-II showed inhibitory effects on IL-1 $\beta$  and IL-8 secretion, respectively, supporting the idea that they can act as anti-inflammatory compounds. Our results extend previous ones in which an inhibitory effect of apoA-I on the release of TNF- $\alpha$  and IL-1 $\beta$  from monocytes was described (17) and add an important new role for apoA-II as an inhibitor of IL-8 from neutrophils.

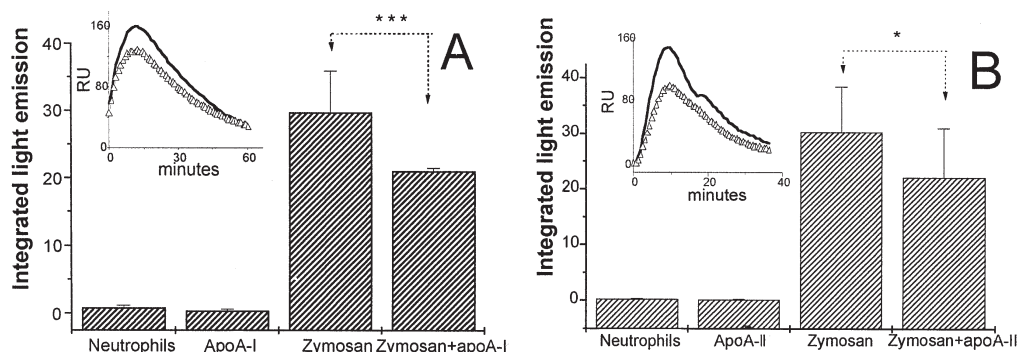
We did not observe any modulation of the various cytokine mRNA levels by either apoA-I or apoA-II in SAA-stimulated neutrophils. The regulation of the mRNA levels and the release of cytokines from neutrophils are complex and not completely understood. For instance, reduction in the mRNA levels of IL-1 $\beta$  and IL-8 in LPS-stimulated neutrophils treated with the inhibitory cytokine IL-10 was observed only at times of incubation beyond the onset of mRNA accumulation (18). Although it is possible that the reduction in the amount of cytokine released from stimulated neutrophils in the presence of apoA-I or apoA-II is due to posttranscriptional or translational effects, an effect of apoA-I and apoA-II on cytokine transcription cannot be completely discarded. This is an open question that merits further study.

Finally, the fact that apoA-I, apoA-II, and apo-SAA are found in the same HDL fraction, HDL<sub>3</sub>, indicates that an active interplay may exist between these apolipoproteins in the lipoprotein particles. Both apo-SAA (2) and apoA-II (19) can displace apoA-I from HDL particles and, although more weakly than for apoA-I, SAA also displaces apoA-II from the HDL (20). The results of the present study provide evidence that apoA-II may be one of the factors responsible for the anti-



**FIG. 3.** IL-1 $\beta$ , IL-8, and IL-1Ra mRNA expression in neutrophils incubated with apoA-I and apoA-II in the absence and presence of SAA for 3 h. The concentration of apoA-I, apoA-II, and SAA was 40  $\mu\text{g/mL}$ . The data are representative of three independent experiments. For abbreviations see Figures 1 and 2.





**FIG. 4.** Effect of apoA-I (A) and apoA-II (B) on the luminol-enhanced chemiluminescence of neutrophils ( $2.5 \times 10^6$  cells/mL) in the absence or presence of zymosan ( $1.0 \times 10^7$  particles/mL). The concentration of apoA-I and apoA-II was 100  $\mu$ g/mL. The data are the average values of the integrated light emission  $\pm$  SD of eight experiments. Significance was  $*P \leq 0.05$  and  $***P \leq 0.001$  for comparison between opsonized zymosan-stimulated neutrophils in the presence and absence of apoA-I or apoA-II. The insets show the kinetics of light emission for a representative experiment. Solid lines represent neutrophils plus zymosan; triangles represent neutrophils plus zymosan plus apoA-I (A) or apoA-II (B). RU, relative units; for other abbreviations see Figure 1.

inflammatory effect of HDL and that, during inflammation, apoA-II may be important in the control of the proinflammatory effects of SAA. Mechanisms that counterregulate neutrophil functions can prevent deleterious effects under inflammatory conditions, and apoA-I and apoA-II may be important in this process.

#### ACKNOWLEDGMENTS

The authors are indebted to the Fundação de Amparo à Pesquisa do Estado de São Paulo (FAPESP) and the Conselho Nacional de Desenvolvimento Científico e Tecnológico (CNPq) for financial support and Cristina Pinardi and Luca Crepaldi for assistance in the RPA experiments.

#### REFERENCES

- Kasiske, B.L., and Keane, W.F. (1991) Role of Lipid Peroxidation in the Inhibition of Mononuclear Cell Proliferation by Normal Lipoproteins, *J. Lipid Res.* 32, 775–781.
- Rosenfeld, S.I., Packman, C.H., and Leddy, J.P. (1983) Inhibition of the Lytic Action of Cell-Bound Terminal Complement Components by Human High Density Lipoproteins and Apoproteins, *J. Clin. Invest.* 71, 795–808.
- Alvarez, C., and Ramos, A. (1986) Lipids, Lipoproteins, and Apoproteins in Serum During Infection, *Clin. Chem.* 32, 142–145.
- Clifton, P.M., Mackinnon, A.M., and Barter, P.J. (1985) Effects of Serum Amyloid A Protein (SAA) on Composition, Size, and Density of High Density Lipoproteins in Subjects with Myocardial Infarction, *J. Lipid Res.* 26, 1389–1398.
- Coetzee, G.A., Strachan, F.A., van der Westhuyzen, D.R., Hoppe, H.C., Jeenah, M.S., and Beer, F.C. (1986) Serum Amyloid A-Containing Human High Density Lipoprotein 3. Density, Size, and Apolipoprotein Composition, *J. Biol. Chem.* 261, 9644–9651.
- Fielding, C.J., and Fielding, P.E. (1995) Molecular Physiology of Reverse Cholesterol Transport, *J. Lipid Res.* 36, 211–228.
- Tall, A.R. (1990) Plasma High Density Lipoproteins. Metabolism and Relationship to Atherogenesis, *J. Clin. Invest.* 86, 379–384.
- Karathanasis, S.K. (1992). Lipoprotein Metabolism: High Density Lipoprotein, in *Molecular Genetics of Coronary Artery Disease* (Lusis, A.J., Rotter, J.L., and Sparkes, R.S., eds.) pp. 140–171, Karger, Basel.
- Shephard, E.G., de Beer, F.C., de Beer, M.C., Jeenah, M.S., Coetzee, G.A., and van der Westhuyzen, D.R. (1987) Neutrophil Association and Degradation of Normal and Acute-Phase High-Density Lipoprotein 3, *Biochem. J.* 248, 919–926.
- Furlaneto, C.J., and Campa, A. (1997) The Effect *in vitro* of High-Density Lipoprotein from Healthy and Infected Humans on the Oxidative Metabolism of Polymorphonuclear Leukocytes, *Cell Biochem. Funct.* 15, 39–45.
- Blackburn, W.D., Jr., Dohlman, J.G., Venkatachalapathi, Y.N., Pillion, D.J., Koopmann, W.J., Segrest, J.P., and Anantharamaiah, G.M. (1991) Apolipoprotein A-I Decreases Neutrophil Degranulation and Superoxide Production, *J. Lipid Res.* 32, 1911–1918.
- Furlaneto, C.J., and Campa, A. (2000) A Novel Function of Serum Amyloid A: A Potent Stimulus for the Release of Tumor Necrosis Factor- $\alpha$ , Interleukin-1 $\beta$ , and Interleukin-8 by Human Blood Neutrophils, *Biochem. Biophys. Res. Commun.* 268, 405–408.
- Morrison, D.C., and Jacobs, D.M. (1976) Binding of Polymyxin B to the Lipid A Portion of Bacterial Lipopolysaccharides, *Immunochemistry* 13, 813–818.
- Scapini, P., Calzetti, F., and Cassatella, M.A. (1999) On the Detection of Neutrophil-Derived Vascular Endothelial Growth Factor (VEGF), *J. Immunol. Methods* 232, 121–129.
- Flohé, L., and Otting, F. (1984) Superoxide Dismutase Assays, *Methods Enzymol.* 105, 93–104.
- Castellani, L.W., Navab, M., Lenten, B.J., Hedrick, C.C., Hama, S.Y., Goto, A.M., Fogelman, A.M., and Lusis, A.J. (1997) Overexpression of Apolipoprotein AII in Transgenic Mice Converts High Density Lipoproteins to Proinflammatory Particles, *J. Clin. Invest.* 100, 464–474.
- Hyka, N., Dayer, J.M., Modoux, C., Kohno, T., Edwards, C.K., III, Roux-Lombard, P., and Burger, D., Apolipoprotein A-I Inhibits the Production of Interleukin-1 $\beta$  and Tumor Necrosis Factor- $\alpha$  by Blocking Contact-Mediated Activation of Monocytes by T Lymphocytes, *Blood* 97, 2381–2389.
- Cassatella, M.A., Meda, L., Gasperini, S., Calzetti, F., and Bonora, S. (1994) Interleukin 10 (IL-10) Upregulates IL-1 Receptor Antagonist Production from Lipopolysaccharide-Stimulated Human Polymorphonuclear Leukocytes by Delaying mRNA Degradation, *J. Exp. Med.* 179, 1695–1699.
- Lagocki, P.A., and Scanu, A.M. (1980) *In vitro* Modulation of the Apolipoprotein Composition of High Density Lipoprotein. Displacement of Apolipoprotein AI from High Density Lipoprotein by Apolipoprotein A-II, *J. Biol. Chem.* 255, 3701–3706.
- Ashby, D., Gamble, J., Vadas, M., Fidge, N., Siggins, S., Rye, K., and Barter, P.J. (2001) Lack of Effect of Serum Amyloid A (SAA) on the Ability of High-Density Lipoproteins to Inhibit Endothelial Cell Adhesion Molecule Expression, *Atherosclerosis* 154, 113–121.

[Received March 8, 2002, and in revised form June 18, 2002; revision accepted September 10, 2002]



# Supplementation with a Pine Bark Extract Rich in Polyphenols Increases Plasma Antioxidant Capacity and Alters the Plasma Lipoprotein Profile

Sridevi Devaraj<sup>a</sup>, Sonia Vega-López<sup>a</sup>, Nalini Kaul<sup>a</sup>, Frank Schönlau<sup>b</sup>, Peter Rohdewald<sup>b</sup>, and Ishwarlal Jialal<sup>a,\*</sup>

<sup>a</sup>Laboratory for Atherosclerosis and Metabolic Research, University of California, Davis, Medical Center, Sacramento, California, and <sup>b</sup>Institute of Pharmaceutical Chemistry, University of Münster, Münster, Germany

**ABSTRACT:** Pycnogenol® (PYC), an extract of French maritime pine bark (*Pinus pinaster*), is a potent antioxidant with potential health benefits. Its bioavailability has previously been shown by urinary excretion studies of constituents and metabolites of PYC. The aim of this study was to test the effect of PYC supplementation on measures of oxidative stress and the lipid profile in humans. Twenty-five healthy subjects received PYC (150 mg/d) for 6 wk. Fasting blood was collected at baseline, after 3 and 6 wk of supplementation, and again after a 4-wk washout period. After 6 wk of supplementation with PYC, a significant increase in plasma polyphenol levels was detectable, which was reversed after the 4-wk washout phase. The antioxidant effect of PYC was demonstrated by a significant increase in oxygen radical absorbance capacity (ORAC) in plasma throughout the supplementation period ( $P < 0.05$ ). The ORAC value returned to baseline after the 4-wk washout period. Moreover, in addition to its antioxidant effects, PYC significantly reduced LDL-cholesterol levels and increased HDL-cholesterol levels in plasma of two-thirds of the subjects. While the LDL changes reversed during washout, the HDL increase did not. There was no significant difference in LDL oxidizability or plasma lipid peroxides following PYC supplementation. Hence, following oral supplementation in humans, PYC significantly increases antioxidant capacity of plasma, as determined by ORAC, and exerts favorable effects on the lipid profile.

Paper no. L8982 in *Lipids* 37, 931–934 (October 2002).

Reactive oxygen species (ROS), particularly the highly reactive oxygen radicals, are produced continuously in cells as a by-product of metabolism. They can oxidize biomolecules, with the potential of causing a broad array of degenerative processes. It is now widely accepted that free radical species play an important role in the pathogenesis of various diseases. Atherosclerosis is believed to be initiated by oxidative modification of LDL (1). ROS play a decisive role in the regulation of inflammation by activating transcription factors such as NF- $\kappa$ B, which control expression of adhesion molecules and pro-inflammatory cytokines (2). ROS contribute to the

development of cancer and cardiovascular diseases (3). ROS also play a role in neurodegenerative diseases such as Alzheimer's dementia (4) and in the aging process itself (5).

Dietary micronutrients with antioxidant properties may play an important role in the prevention of atherosclerosis (6). Flavonoids are a large and diverse group of dietary micronutrients found in fruits, vegetables, tea, and wine. Epidemiological studies have shown an inverse association with flavonoid intake and coronary artery disease (CAD) risk and mortality (7,8).

Pycnogenol® (PYC), a bark extract of the French maritime pine (*Pinus pinaster*), is rich in flavonoids and was found to be among the most powerful natural antioxidants (9,10). Chemical composition of PYC has not been completely elucidated. However, it mainly consists of phenolic substances, primarily procyanidins consisting of condensed catechin and epicatechin subunits, forming oligomers up to dodecamers (9). PYC further contains monomeric catechin, taxifolin, and various phenolcarboxylic acids (9,11). PYC has been shown to recycle the ascorbic radical and to protect vitamin E against oxidation (12). In clinical studies PYC was found to counteract increased platelet aggregation in smokers (13), improve microcirculation (14), act as an anti-inflammatory agent [e.g., to inhibit UV-induced erythema (15)], increase capillary integrity in vascular disorders (16,17), and provide various other health benefits (10). These studies all demonstrate that PYC is absorbed by and exerts its action on the human body. This has been corroborated by urinary excretion studies showing that metabolites and constituents of PYC are absorbed (18,19). *In vitro* evidence exists for the potential antioxidant benefits of the flavonoid extract PYC, but dietary supplementation studies in humans are scarce. Here, we have tested the antioxidant effects of supplementation with PYC in normal healthy volunteers.

## METHODS

**Subjects.** The 25 healthy subjects in this study were included without restriction by gender, race, or socioeconomic status. The necessary criteria for participation were age  $< 50$  y, body mass index (BMI)  $< 25$  kg/m<sup>2</sup>, a diet with fewer than five servings of fruit and vegetables per day. Exclusion criteria were alcohol consumption; infection in the past 4 wk; gastrointestinal disorders (e.g., malabsorption); ingestion of vitamins, antioxidants, flavonoid supplements, hypolipidemic drugs, estrogen, thyroxin, or nonsteroidal anti-inflammatory drugs in

\*To whom correspondence should be addressed at Laboratory for Atherosclerosis and Metabolic Research, University of California, Davis, Medical Center, 4635 Second Ave., Rm. 3000, Sacramento, CA 95817. E-mail: ishwarlal.jialal@ucdmc.ucdavis.edu

Abbreviations: AAPH, 2,2'-azobis(2-amidinopropane)dihydrochloride; BMI, body mass index; CAD, coronary artery disease; CBC, complete blood count; FOX, ferrous oxide-xylene orange; ORAC, oxygen radical absorbance capacity;  $\beta$ -PE,  $\beta$ -phycoerythrin; PYC, Pycnogenol®; ROS, reactive oxygen species; TSH, thyroid-stimulating hormone.

the last month; high consumption of flavonoid-rich foods (e.g., grapes, grape products, dark chocolate, tea, red wine, berries, etc.); abnormal blood count; and abnormal renal or hepatic function. During the period of the study, subjects were advised not to change their usual diet and activity level, and they were instructed to restrict consumption of flavonoid-rich foods (grape products, fruits, fruit juices, dark chocolate, and tea). The subjects received 150 mg PYC per day for 6 wk. The protocol was approved by the Institutional Review Board at the University of Texas Southwestern Medical Center at Dallas. Written informed consent was obtained from all subjects.

**Laboratory tests.** For screening, 15 mL blood samples were collected and used to determine the complete blood count (CBC), plasma lipid and lipoprotein profile, creatinine level, liver function, blood glucose level, and level of thyroid-stimulating hormone (TSH) using standard laboratory assays. Fasting blood (50 mL) was collected in EDTA or heparin from subjects at baseline, after 3 and 6 wk of supplementation with PYC, and again after a 4-wk washout period. Plasma was separated and aliquots were stored at  $-70^{\circ}\text{C}$  for determination of polyphenols, the antioxidant potential of plasma, the lipid profile, and plasma lipid peroxides.

**Plasma total phenols.** Plasma total phenols were measured by the method of Serafini *et al.* (20). Briefly, for total phenols, 500  $\mu\text{L}$  of plasma was acidified and, following extraction of complexed phenols with alcoholic sodium hydroxide, proteins were precipitated using 0.75 M metaphosphoric acid and re-extracted with a mixture of acetone/water (1:1). Phenol content was measured by the Folin–Ciocalteu method using phenol as the standard and was expressed as mg phenol equiv/L.

**Oxygen radical absorbance capacity (ORAC) measurement.** The antioxidant potential of heparinized plasma before and after PYC supplementation was determined following deproteinization of the sample by the ORAC assay based on the procedure described by Cao and Prior (21). The method utilizes  $\beta$ -phycoerythrin ( $\beta$ -PE) as an indicator protein and 2,2'-azobis(2-amidinopropane)dihydrochloride (AAPH) as a peroxyl radical generator. Under appropriate conditions, the loss of PE fluorescence in the presence of reactive species is an index of oxidative damage of the protein. The inhibition by an antioxidant, which is reflected in the protection against the loss of PE fluorescence in the ORAC assay, is a measure of its antioxidant capacity.

**Plasma oxidation.** Plasma oxidation was measured following 4 h of oxidation with AAPH by measuring lipid peroxides using the ferrous oxide-xylene orange (FOX) assay as described previously (22).

**LDL oxidation.** LDL was isolated by sequential ultracentrifugation and the LDL (100  $\mu\text{g}/\text{mL}$ ) was oxidized using 2.5  $\mu\text{M}$  copper for 5 h. The lag phase of conjugated diene formation was assessed by absorbance at 234 nm as described previously (23).

**Plasma ascorbate.** Total ascorbic acid was measured using the ascorbate oxidase method described previously (24).

**Statistics.** Statistical analyses were carried out using Sig-mastat (SPSS Inc., Chicago, IL). Data are presented as mean  $\pm$  SD. A repeated-measures ANOVA followed by a paired *t*-test was used to analyze parametric data. A Wilcoxon signed rank test was used to assess differences relative to the baseline for nonparametric variables. The level of significance was set at  $P < 0.05$ .

## RESULTS

The participants (10 males and 15 females) had a mean age of  $30 \pm 8$  yr and a BMI of  $26 \pm 4$   $\text{kg}/\text{m}^2$ . There were no significant differences in CBC, creatinine levels, liver function tests (aspartate and alanine aminotransferases), and TSH during the study (data not shown). The lipid profile of the subjects at 0, 6, and 10 wk is shown in Table 1. Despite the lack of effect on total cholesterol and TG, PYC supplementation resulted in a significant reduction in LDL-cholesterol (7%,  $P < 0.05$ ) following 6 wk of supplementation, which returned to baseline after the 4-wk washout period. HDL-cholesterol levels were significantly elevated following supplementation and remained elevated following the 4-wk washout period (10.4%,  $P < 0.05$ ). In addition, the reduction in LDL-cholesterol and increase in HDL-cholesterol was consistent among 66% of participants.

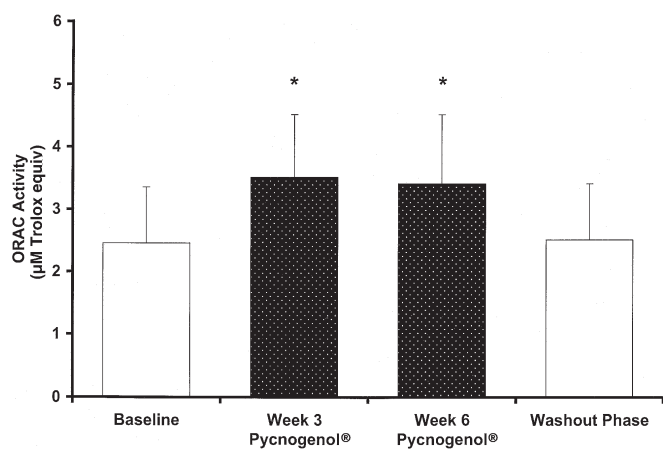
To assess compliance and determine whether the phenolic antioxidants of PYC were increased following supplementation, the total phenol level in plasma was measured at baseline and after 3 wk of supplementation. Total phenol levels increased significantly from  $4.6 \pm 1.96$  mg phenol equiv/L at baseline to  $5.67 \pm 4.1$  mg phenol equiv/L after 3 wk of PYC supplementation ( $P < 0.05$ ), demonstrating absorption of PYC in the blood. Plasma ascorbate concentrations did not change with PYC supplementation (baseline vitamin C:  $0.91 \pm 0.46$  mg/dL; 6 wk:  $0.97 \pm 0.37$  mg/dL).

The ORAC of plasma showed that PYC intake indeed significantly increased antioxidant capacity in humans (Fig. 1). Following supplementation with PYC, the ORAC values were significantly increased by about 40% over baseline ( $P < 0.005$ ). During the 4-wk washout period, the ORAC value returned back to baseline.

**TABLE 1**  
Effect of Pycnogenol® Supplementation on Lipid and Lipoprotein Profile

	Week 0	Week 6	Week 10
Total cholesterol (mg/dL)	169.30 $\pm$ 23.15	166.36 $\pm$ 21.69	167.81 $\pm$ 26.74
Total TG (mg/dL)	83.57 $\pm$ 40.08	85.65 $\pm$ 36.12	90.46 $\pm$ 36.74
LDL-cholesterol (mg/dL)	104.38 $\pm$ 17.71	97.11 $\pm$ 26.91*	104.31 $\pm$ 30.98
HDL-cholesterol (mg/dL)	48.07 $\pm$ 10.53	53.15 $\pm$ 12.63*	53.73 $\pm$ 18.01 <sup>a</sup>

<sup>a</sup> $P < 0.05$  compared to week 0.



**FIG. 1.** Oxygen radical absorbance capacity (ORAC) measured in plasma of human subjects at baseline, after daily supplementation with 150 mg Pycnogenol® for 3 and 6 wk, and following a washout period of 4 wk. Presented are mean values and SD; significant differences from baseline ( $P < 0.05$ ) are marked with an asterisk.

Supplementation with PYC did not significantly modify plasma oxidation, as determined by measuring lipid peroxides using the FOX assay (Table 2). Although this method is relatively specific for the measurement of lipid peroxides and has a CV of  $<10\%$ , it is not as sensitive as other direct methods used to determine oxidation, such as quantification of isoprostanes. Similar to plasma oxidation, the decreased susceptibility of LDL to oxidation (i.e., increase in lag phase) observed after supplementation with PYC did not reach significance (Table 2).

## DISCUSSION

PYC is known to be among the most powerful natural antioxidants (9,10). Urinary excretion studies have demonstrated that PYC is absorbed after oral consumption. Metabolites of procyanidins, taxifolin, and ferulic acid appear in the urine already after 2 h (18). Peak excretion of procyanidin metabolites was found after 8–12 h, and excretion was completed after 28–34 h. Another study showed absorption profiles of phenolic acids of PYC using ferulic acid excretion as a marker (19).

Our study demonstrates for the first time that oral consumption of PYC significantly elevates ORAC in the blood, paralleled by a significant increase in plasma concentration of phenolic compounds. During the period of PYC supplementation, the antioxidant capacity was elevated by about 40%. At the end of the 4-wk washout phase, the ORAC value returned almost to the baseline level. This finding demon-

strates that supplementation with PYC considerably improves antioxidant protection in plasma. This effect may be the basis for many of the health benefits discovered with PYC in clinical studies (11,13). A recent study has shown that consumption of PYC decreases UV-induced erythema in humans by inhibiting the redox-sensitive NF- $\kappa$ B-controlled gene expression of inflammatory mediators (15).

ESR studies have shown that PYC is able to reduce the ascorbate radical, leading to regeneration of active vitamin C (12). However, we did not detect significant differences in plasma ascorbate after PYC supplementation.

PYC was previously shown to inhibit LDL oxidation *in vitro* (25). With regard to protection of lipid components of the blood, we did not see a significant decrease in LDL-cholesterol oxidizability or in levels of lipid peroxides in subjects supplemented with PYC. However, the trend in both parameters after supplementation was reversed after the washout phase, which suggests a potentially favorable impact on these parameters. It is probable that the use of more sensitive measures of oxidative stress, such as F2-isoprostanes, may have clearly identified the antioxidant potency of PYC. Furthermore, since PYC is water soluble, it is probable that beneficial effects are not seen on LDL oxidizability, since it may not partition in the LDL particles.

Interestingly, we found that PYC supplementation reduces LDL-cholesterol levels in the blood and increases HDL-cholesterol levels and thus exerts beneficial effects on the lipid profile. Both effects of PYC, i.e., increasing HDL-cholesterol and decreasing LDL-cholesterol, will translate into a net benefit in decreasing cardiovascular events, since both are independent risk factors for CAD (26). Whether this effect is a result of the antioxidant activity of PYC is not clear. In a recent clinical trial investigating PYC to treat venous insufficiency (27), blood parameters were routinely checked. There was a significant reduction of LDL and cholesterol; HDL-cholesterol was not modified in the PYC-treated group (27). In the control group treated with horse chestnut seed extract, the cholesterol and LDL levels remained unaffected. This result points to another interesting function of PYC in influencing lipoprotein levels that is independent of its pronounced antioxidant activity.

Several clinical trials have documented beneficial modifications of the LDL/HDL ratio after intake of flavonoid- and antioxidant-containing food products. Kurowska *et al.* (28) reported that orange juice intake (750 mL/d) increased HDL-cholesterol concentrations by 21%. Fuhrman *et al.* (29) documented that supplementation with licorice root extract (0.1 g/d), which is rich in flavonoids, was associated with a 9% reduction in LDL-cholesterol concentrations in hypercholes-

**TABLE 2**  
Effect of Pycnogenol® Supplementation on Plasma and LDL Oxidizability

	Week 0	Week 3	Week 6	Week 10
Plasma lipid peroxides ( $\mu$ M)	1.8 $\pm$ 1.2	1.6 $\pm$ 1.2	1.8 $\pm$ 1.1	1.9 $\pm$ 1.4
LDL oxidizability—lag time of conjugated dienes (min)	78.5 $\pm$ 24.2	85.5 $\pm$ 36.3	83.6 $\pm$ 35.6	82.1 $\pm$ 33.3



terolemic individuals and suggested that this hypocholesterolemic effect could be secondary to an inhibitory effect on cholesterol biosynthesis. PYC could decrease LDL-cholesterol by upregulating the hepatic LDL receptor and/or enhancing sterol excretion, and it could increase HDL-cholesterol by inhibiting CETP activity. However, the specific mechanism by which PYC beneficially alters plasma lipids is beyond the scope of this study, which tested the effect of PYC on markers of oxidative stress. Future studies will be aimed at addressing these mechanisms.

This study showed that in normal healthy volunteers, PYC results in increased phenols as well as improved ORAC, and potentially also exerts an antioxidant effect. In addition, it has a favorable effect on two risk factors for CAD, i.e., decreasing LDL-cholesterol and increasing HDL-cholesterol. Future trials in larger and more diverse populations will shed light on its efficacy in cardiovascular disease prevention.

## ACKNOWLEDGMENT

This study was supported in part by a grant from the National Institutes of Health (K24 AT00596).

## REFERENCES

- Witztum, J.L., and Steinberg, D. (1991) Role of Oxidized Low Density Lipoprotein in Atherogenesis, *J. Clin. Invest.* 88, 1785–1792.
- Flohé, L., Brigelius-Flohé, R., Saliou, C., Traber, M., and Packer, L. (1997) Redox Regulation of NF- $\kappa$ B Activation, *Free Radic. Biol. Med.* 22, 1115–1126.
- Gey, K.F. (1993) Prospects for the Prevention of Free Radical Disease, Regarding Cancer and Cardiovascular Disease, *Br. Med. Bull.* 49, 679–699.
- Evans, P.H. (1993) Free Radicals in Brain Metabolism and Pathology, *Br. Med. Bull.* 49, 577–587.
- Cutler, R.G. (1991) Antioxidants and Aging, *Am. J. Clin. Nutr.* 53, 373S–379S.
- Ames, B.N., Shigenaga, M.K., and Hagen, T.M. (1993) Oxidants, Antioxidants, and the Degenerative Diseases of Aging, *Proc. Nat. Acad. Sci. USA* 90, 7915–7922.
- Katan, M.B. (1997) Flavonoids and Heart Disease, *Am. J. Clin. Nutr.* 65, 1542–1543.
- Rice-Evans, C. (1995) Plant Polyphenols: Free Radical Scavengers or Chain-Breaking Antioxidants? *Biochem. Soc. Symp.* 61, 103–116.
- Chida, M., Suzuki, K., Nakanishi-Ueda, T., Ueda, T., Yasuhara, H., Koide, R., and Armstrong, D. (1999) *In vitro* Testing of Antioxidants and Biochemical End-Points in Bovine Retinal Tissue, *Ophthalmic Res.* 31, 407–415.
- Packer, L., Rimbach, G., Virgili, F. (1999) Antioxidant Activity and Biologic Properties of a Procyanidin-Rich Extract from Pine (*Pinus maritima*) Bark, Pycnogenol®, *Free Radic. Biol. Med.* 27, 704–724.
- Rohdewald, P. (1998) Pycnogenol®, in *Flavonoids in Health and Disease* (Rice-Evans, C.A., and Packer, L., eds., pp. 405–419, Marcel Dekker, New York.
- Cossins, E., Lee, R., and Packer, L. (1998) ESR Studies of Vitamin C Regeneration, Order of Reactivity of Natural Source Phytochemical Preparations, *Biochem. Mol. Biol. Int.* 45, 583–598.
- Pütter, M., Grottemeyer, K.H.M., Würthwein, G., Arghiniknam, M., Watson, R.R., Hosseini, S., and Rohdewald, P. (1999) Inhibition of Smoking-Induced Platelet Aggregation by Aspirin and Pycnogenol, *Thromb. Res.* 95, 155–161.
- Wang, S., Tan, D., Zhao, Y., Gao, G., Gao, X., and Hu, L. (1999) The Effect of Pycnogenol® on the Microcirculation, Platelet Function and Ischemic Myocardium in Patients with Coronary Artery Diseases, *Eur. Bull. Drug Res.* 7, 19–25.
- Saliou, C., Rimbach, G., Moïni, H., McLaughlin, L., Hosseini, S., Lee, J., Watson, R.R., and Packer, L. (2001) Solar Ultraviolet-Induced Erythema in Human Skin and Nuclear Factor- $\kappa$ B-Dependent Gene Expression in Keratinocytes Are Modulated by a French Maritime Pine Bark Extract, *Free Radic. Biol. Med.* 30, 154–160.
- Spadea, L., and Balestrazzi, E. (2001) Treatment of Vascular Retinopathy with Pycnogenol®, *Phytother. Res.* 15, 219–223.
- Petrassi, C., Mastromarino, A., and Spartera, C. (2000) Pycnogenol® in Chronic Venous Insufficiency, *Phytomedicine* 7, 383–388.
- Grosse Düweler, K., and Rohdewald, P. (2000) Urinary Metabolites of French Maritime Pine Bark Extract in Humans, *Pharmazie* 55, 364–368.
- Virgili, F., Pagana, G., Bourne, L., Rimbach, G., Natella, F., Rice-Evans, C., and Packer, L. (2000) Ferulic Acid Excretion as a Marker of Consumption of a French Maritime Pine (*Pinus maritima*) Bark Extract, *Free Radic. Biol. Med.* 28, 1249–1256.
- Serafini, M., Maiani, G., and Ferro-Luzzi, A. (1998) Alcohol-Free Red Wine Enhances Plasma Antioxidant Capacity in Humans, *J. Nutr.* 128, 1003–1007.
- Cao, G., and Prior, R.L. (1999) Measurement of Oxygen Radical Absorbance Capacity in Biological Samples, *Methods Enzymol.* 299, 50–66.
- Marangon, K., Devaraj, S., Tirosh, O., Packer, L., and Jialal, I. (1999) Comparison of the Effect of  $\alpha$ -Lipoic Acid and  $\alpha$ -Tocopherol Supplementation on Measures of Oxidative Stress, *Free Radic. Biol. Med.* 27, 1114–1121.
- Jialal, I., Fuller, C.J., and Huet, B.A. (1995) The Effect of  $\alpha$ -Tocopherol Supplementation on LDL Oxidation. A Dose-Response Study, *Arterioscler. Thromb. Vasc. Biol.* 15, 190–198.
- Lee, W., Roberts, S.M., and Labbe, R.F. (1997) Ascorbic Acid Determination with an Automated Enzymatic Procedure, *Clin. Chem.* 43, 154–157.
- Nelson, A.B., Lau, B.H.S., Ide, N., and Rong, Y. (1998) Pycnogenol® Inhibits Macrophage Oxidative Burst, Lipoprotein Oxidation and Hydroxyl Radical Induced DNA Damage, *Drug Dev. Ind. Med.* 24, 1–6.
- ATPIII Panel (2001) Executive Summary of the Third Report of the National Cholesterol Education Program (NCEP) Expert Panel on Detection, Evaluation, and Treatment of High Blood Cholesterol in Adults (Adult Treatment Panel III), *J. Am. Med. Assoc.* 285, 2486–2497.
- Koch, R. (2002) Comparative Study of Venostasin and Pycnogenol in Chronic Venous Insufficiency, *Phytother. Res.* 16 (Suppl.), 2243–2250.
- Kurowska, E.M., Spence, J.D., Jordan, J., Wetmore, S., Freeman, D.J., Piche, L.A., and Serratore, P. (2000) HDL-Cholesterol-Raising Effect of Orange Juice in Subjects with Hypercholesterolemia, *Am. J. Clin. Nutr.* 72, 1095–1100.
- Fuhrman, B., Volkova, N., Kaplan, M., Presser, D., Attias, J., Hayek, T., and Aviram, M. (2002) Antiatherosclerotic Effects of Licorice Extract Supplementation on Hypercholesterolemic Patients: Increased Resistance of LDL to Atherogenic Modifications, Reduced Plasma Lipid Levels, and Decreased Systolic Blood Pressure, *Nutrition* 18, 268–273.

[Received January 10, 2002, and in revised form September 12, 2002; revision accepted September 18, 2002]



# Effects of Duodenal Seal Oil Administration in Patients with Inflammatory Bowel Disease

Gülen Arslan<sup>a,b,\*</sup>, Linn Anne Brunborg<sup>b</sup>, Livar Frøyland<sup>b</sup>, Johan G. Brun<sup>c</sup>, Merete Valen<sup>c</sup>, and Arnold Berstad<sup>a</sup>

<sup>a</sup>Division of Gastroenterology, Institute of Medicine, Haukeland University Hospital, <sup>b</sup>Institute of Nutrition, Directorate of Fisheries, and <sup>c</sup>Division of Rheumatology, Institute of Medicine, Haukeland University Hospital, Bergen, Norway

**ABSTRACT:** Long-chain n-3 PUFA in fish oil have modulating effects on inflammatory responses. The aim of this open pilot study was to investigate whether duodenal seal oil administration would benefit patients with inflammatory bowel disease (IBD). Seal oil (10 mL) was administered three times a day directly into the distal part of the duodenum *via* a nasoduodenal feeding tube for 10 d in 10 patients, 5 of whom had Crohn's disease and 5 ulcerative colitis. Nine of the 10 patients suffered from IBD-associated joint pain. Various parameters of disease activity and FA incorporation in tissues were analyzed before and after treatment. Following seal oil therapy, joint pain index, disease activity, and serum cholesterol level were significantly decreased, whereas the n-3 to n-6 ratio both in intestinal biopsies and blood was significantly increased. Measures of calprotectin concentration in gut lavage fluid, intestinal permeability, and lipid peroxidation were not significantly changed. The results suggest positive effects of seal oil in patients with IBD, especially on IBD-associated joint pain. Further controlled studies are warranted.

Paper no. L9107 in *Lipids* 37, 935–940 (October 2002).

EPA (20:5n-3) and DHA (22:6n-3) are n-3 PUFA derived from fish or marine mammals. These long-chain PUFA have been found to alter plasma membrane composition and fluidity, ion-channel flux, cell-signaling mechanisms, eicosanoid responses, cytokine release, and immune cell responses. One mechanism by which n-3 FA exert these effects might be that EPA and DHA are incorporated into membrane phospholipids by replacing arachidonic acid (AA, n-6 FA). AA is the substrate for the synthesis of eicosanoids, i.e., leukotriene B<sub>4</sub> (LTB<sub>4</sub>), thromboxane A<sub>2</sub>, and prostaglandin E<sub>2</sub> (PGE<sub>2</sub>), the latter with high inflammatory activity (1). n-3 FA have greater affinity for the cyclo- and lipoxygenase enzymes than n-6 FA. They competitively inhibit the formation of prostaglandins and leukotrienes derived from AA while serving as a substrate for prostaglandins and leukotrienes (PGE<sub>3</sub> and LTB<sub>5</sub>) with less inflammatory activity compared to the AA products (2,3). Hence, increased dietary intake of n-3 FA may shift the balance of the eicosanoid production to a less inflammatory profile.

\*To whom correspondence should be addressed at Institute of Medicine, Haukeland University Hospital, N-5021 Bergen, Norway.  
E-mail: gulen.arslan@med.uib.no

Abbreviations: AA, arachidonic acid; CD, Crohn's disease; DPA, docosapentaenoic acid; IBD, inflammatory bowel disease; LTB<sub>4</sub>, leukotriene B<sub>4</sub>; LTB<sub>5</sub>, leukotriene B<sub>5</sub>; PGE<sub>2</sub>, prostaglandin E<sub>2</sub>; UC, ulcerative colitis; VAS, visual analog scale.

In the current Western diet, n-6 FA prevail over n-3 FA, and AA is the most abundant C<sub>20</sub> PUFA converted to eicosanoids in the human body. Marine animals are good sources of n-3 FA (EPA and DHA), and the general view is that an increased intake of marine oils will improve the health of the general population.

Seal and fish oils contain approximately the same total amount of n-3 PUFA. However, seal oil contains another PUFA, namely, docosapentaenoic acid (22:5n-3, DPA), which has been shown to interfere with different pathways of eicosanoid formation (4). Seal meat is also an excellent source of minerals, particularly iron and vitamins, including vitamin B<sub>12</sub> (5).

The aims of this study were to evaluate whether administration of seal oil altered the symptoms, inflammatory activity, and FA composition of serum, buffy coat, red blood cells, and rectal mucosal biopsies in patients with inflammatory bowel disease (IBD).

## MATERIALS AND METHODS

**Patients.** Ten patients with IBD were investigated, five with Crohn's disease (CD; female/male = 4:1, age range 27–42 yr) and five with ulcerative colitis (UC; female/male = 2:3, age range 41–57 yr). Disease activity was evaluated by a simple index in CD (6) and a simple clinical colitis activity index in UC (7). Joint pain was graded by the patients on a subjective scale from 0 (no pain) to 10 (very severe pain).

An ileocecal resection had been performed earlier on two of the CD patients, and both were receiving prednisone (5 or 10 mg/d). The other patients were on the following stable medications: four on mesalazine (dose range, 2 to 3 g/d), two on sulfasalazine (3 g/d), and two on both mesalazine (3 g/d) and azathioprin (100 or 150 mg/d).

During the 10 d of the seal oil treatment, all patients lived at home, ate a normal Western diet, and continued taking their usual medications.

Five of the patients (three patients with CD, two with UC; three were receiving mesalazine, one sulfasalazine, and one prednisone) wished to try the treatment a second time. To study the repeatability of results, these five patients were investigated using the same protocol one-half to one year later, but this time with a more extensive clinical evaluation of the rheumatic disease activity, including physicians' global

assessments of joint disease activity using a 100-mm visual analog scale (VAS), duration of morning stiffness (min) and pain throughout the week (VAS), score on the Health Assessment Questionnaire (8), 28 + 2 joint counts of tender and swollen joints (9) (with ankle joints and toes added), and the number of joints with subjective pain.

This study was approved by the ethics committee at Haukeland University Hospital, and all subjects gave informed consent.

**Methods.** Blood samples were drawn from the fasting patients in two vials without anticoagulant and in one with EDTA. One serum sample was sent to the hospital's central laboratory for analysis of cholesterol and TG according to Technicon Chem method no. SA4-0305L90 and Technicon Chem method no. SA4-0324L90, respectively (Technicon Instruments, Tarrytown, NY). TBARS in serum were analyzed at the Institute of Nutrition (10). From the other sample without anticoagulant, red blood cells and buffy coat (white blood cells) were prepared, and plasma was prepared from the EDTA-containing vial.

After an overnight fast, a nasoduodenal feeding tube (Stayput®, Compat Biosystems®; Sandoz Nutrition Corporation, Boston, MA) was positioned with its tip in the distal part of the duodenum by a gastroduodenoscopy or by fluoroscopic control only. Intestinal lavage was performed using a modification of the whole-gut lavage method of Ferguson and colleagues (11,12). Two liters of an isotonic PEG solution (M.W. 3350; Laxabon®; Tika, Lund, Sweden) was administered through the tube over a period of 40 min using a peristaltic pump (505S/RL; Watson-Marlow, Falmouth, United Kingdom). The PEG solution is the same type as that used for bowel cleansing before a barium enema, colonoscopy, or colon surgery. Approximately 50  $\mu$ Ci of  $^{51}\text{Cr}$  EDTA (Amersham International, Amersham, United Kingdom) was added to the solution. Depending on intestinal permeability, trace amounts of this substance are absorbed and excreted in the urine (13). The estimated dose of radiation received during this test was  $<0.1$  mSv (effective dose equiv.), which is within the limits of natural background radiation (14). Urine was collected for 5 h, 20 min (i.e., 4 h, 40 min after finishing the infusion), and the amount of  $^{51}\text{Cr}$  EDTA excreted in the urine was quantified as percentage of the administered dose. When the PEG solution reached the distal colon, bowel movements started. The first clear fluid passed per rectum was collected for analysis of calprotectin (11).

Soon after the lavage procedure, when the patients had emptied their bowels, sigmoidoscopy was performed with a videoendoscope. Five biopsy specimens were taken from the rectum, 20–30 cm above the anus, for analysis of FA composition. These biopsies were collected on ice and stored frozen.

**Seal oil.** Seal oil was obtained from the Norwegian Institute of Fisheries and Aquaculture Inc. (Tromsø, Norway). The seal oil (mainly from harp seal, *Phagophilus groenlandicus*) was produced by A/S Rieber (Tromsø, Norway) and refined by Peter Møller A/S of Orkla A/S (Oslo, Norway). Natural tocopherols 1.5 mg/g (Covi-ox T-70; Henkel, Düsseldorf,

Germany) and DL- $\alpha$ -tocopheryl acetate (1.0 mg/g; Roche A/S, Hvidovre, Denmark) were added to the oil.

After completing the lavage and biopsy procedures, 10 mL seal oil was administered through the nasoduodenal feeding tube three times a day for 10 d. The patients thus received a total amount of 1.8 g of EPA, 1.0 g DPA, and 2.6 g of DHA per day. Seal oil was well tolerated without any noticeable side effects. The blood sample, disease activity, joint pain index, gut lavage, and biopsy procedures were repeated after the 10-d course of treatment (at day 11).

**Lavage fluid processing.** Lavage fluid was filtered through gauze, and 4.5 mL aliquots were added to tubes containing 0.5 mL of a solution with antiseptic and antiproteolytic activity. A stock solution of the latter was prepared by adding 1 mL of 10% sodium azide ( $\text{NaN}_3$ ) to 50 mL of soybean trypsin inhibitor (Sigma, Munich, Germany). The samples were stored frozen at  $-20^\circ\text{C}$  until assayed.

**Analysis of FA.** FA composition was analyzed in plasma, red blood cells, buffy coat, and biopsies. The samples were dissolved in chloroform/methanol (2:1, vol/vol) and a 19:0 FA was added as the internal standard. The samples were filtered, saponified, and methylated using 12%  $\text{BF}_3$  in methanol. FA composition of total lipids was analyzed using methods described by Lie and Lambertsen (15): The methyl esters were separated using a Carlo Erba gas chromatograph (cold on-column injection at a temperature of  $60^\circ\text{C}$ , ramped at  $25^\circ\text{C}/\text{min}$  to 160 and  $190^\circ\text{C}$ , then held at  $220^\circ\text{C}$ ) equipped with a 50-m CP-Sil 88 (Chrompack, Middelburg, The Netherlands) fused-silica capillary column (i.d. 0.32 mm). The FA were identified by retention time using standard mixtures of methyl esters (NuChek-Prep, Elysian, MN), and the FA composition (mol%) was calculated using an integrator (Turbochrom Workstation, Version 6.1.0, PerkinElmer Instruments LLC, Shelton, CT) connected to the gas-liquid chromatograph.

**Analysis of calprotectin.** The gut lavage fluid specimens were thawed and centrifuged at  $1550 \times g$  at  $4^\circ\text{C}$  before diluting the supernatant 1:50 and analyzing the calprotectin concentration by an ELISA method using the Nycotest Phical ELISA kit (Nycomed, Oslo, Norway). Microtiter plates were coated with rabbit anticalprotectin for capture, and immunoaffinity purified rabbit anticalprotectin conjugated with alkaline phosphatase was used for development (16). The ELISA read the absorbance at 405 nm for 96-well plates. The results of the test samples were calculated from the standard curves. Concentrations above 5 mg/L were not diluted further.

**Analysis of urine.** Urine was analyzed for radioactivity using a gamma counter (1282 Compugamma Counter; Wallac, Oslo, Norway). To calculate the percentage of administered dose of  $^{51}\text{Cr}$  EDTA excreted in urine, we measured the activity of a 5 mL sample of a 1/2000 dilution of the  $^{51}\text{Cr}$  EDTA solution administered and of a 5 mL sample of the pooled urine volume. The percent urinary excretion of the administered dose was calculated as in Equation 1:

$$^{51}\text{Cr EDTA}\% = \frac{(\text{urine cpm} - \text{background cpm}) \cdot \text{urine volume} \cdot 100}{(\text{standard cpm} - \text{background cpm}) \cdot \text{instilled volume}} \quad [1]$$

**Statistical analysis.** Data were analyzed using the GraphPad Prism (GraphPad Software Inc., San Diego, CA) statistical software package. All values were expressed as median with a maximum/minimum range. Differences between groups were evaluated using the Wilcoxon signed rank test.  $P$  values  $< 0.05$  were regarded as significantly different.

## RESULTS

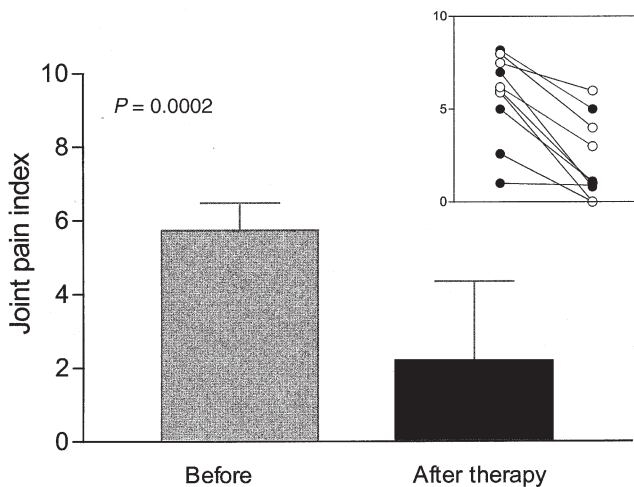
All the patients completed treatment with seal oil without relevant protocol violations. No relevant subjective side effects of the seal oil administration were detected.

Compared with pretreatment levels, the median joint pain index ( $P = 0.002$ ) (Fig. 1), disease activity ( $P = 0.01$ ) (Fig. 2), and serum cholesterol concentration ( $P = 0.002$ ) were significantly decreased after treatment with seal oil. The median serum TG concentration was also decreased but barely reached significance ( $P = 0.05$ ). The calprotectin concentration in gut lavage fluid ( $P = 0.74$ ), intestinal permeability of  $^{51}\text{Cr}$  EDTA ( $P = 0.25$ ), and serum TBARS concentration ( $P = 0.49$ ) were not significantly altered by seal oil treatment (Table 1).

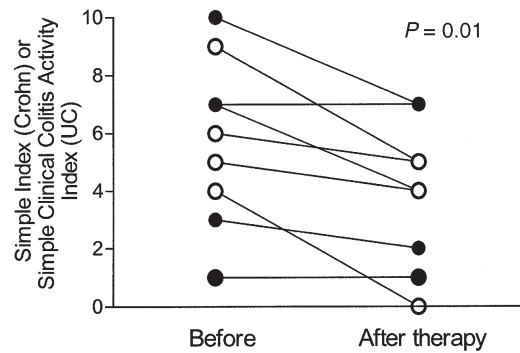
The ratio of n-3 to n-6 FA was significantly increased after treatment compared with that before treatment in serum ( $P = 0.008$ ), buffy coat ( $P = 0.006$ ), red blood cells ( $P = 0.004$ ), and colonic biopsies ( $P = 0.002$ ) (Table 1). Compositions of selected FA in serum, buffy coat, red blood cells, and biopsies from rectal mucosa are presented in Table 2. The total amount of monounsaturated FA was not changed after seal oil treatment in serum, buffy coat, and red blood cells but decreased in biopsies (Table 2).

Vitamins A and E and the FA composition of the seal oil supplied to the IBD patients were also determined (Table 3).

**Retreatment.** After the second study period, seal oil administration in five patients appeared to lower the rheumatic dis-



**FIG. 1.** Joint pain index (0 = no pain, 10 = very severe pain) in inflammatory bowel disease (IBD) patients before and after treatment with seal oil. Individual results are presented in the upper right corner ( $n = 10$ ).  $\circ$ , patients with ulcerative colitis (UC);  $\bullet$ , patients with Crohn's disease (CD).



**FIG. 2.** Individual results of disease activity index in IBD patients before and after treatment with seal oil ( $n = 10$ ).  $\circ$ , patients with UC;  $\bullet$ , patients with CD. For abbreviations see Figure 1.

ease activity but was significant only for the patients' assessment of pain ( $P = 0.04$ ) (Table 4).

## DISCUSSION

This is the first study to look at the effect of seal oil administration in patients with IBD. During the 10-d treatment period, there appeared to be a beneficial effect on joint pain, disease activity, serum cholesterol concentration, and the n-3/n-6 FA ratio in blood and tissue samples.

Fish oil has been reported to be beneficial to UC patients, but results are controversial (17–21). Three studies reported significant clinical improvement after fish oil supplementation (17–19), whereas the clinical benefit in the other two studies was limited, with no histopathological improvement compared with placebo therapy (20,21). Differences between the studies in dose, study design, composition of the supplement, and assessment of clinical improvement may explain the conflicting results (19).

Two studies examined the role of fish oil in preventing relapses in CD patients who had gone into remission with steroids (22,23). In the study by Belluzzi *et al.* (22), 78 Crohn's disease patients with a high risk of relapse were randomly assigned to receive enteric-coated fish oil capsules (total 2.7 g) or placebo (total 1.5 g, containing 60% caprylic acid and 40% capric acid). In the 1-yr follow-up, 59% of patients in the fish oil group remained in remission compared with 26% in the placebo group. In the trial of Lorenz-Meyer *et al.* (23), however, remission rates at the 1-yr follow-up were similar in the fish oil and placebo groups.

Seal oil may have important advantages over fish oil or n-3 preparations, because in seal oil EPA, DPA, or DHA are preferentially located in the *sn*-1 or *sn*-3 positions in the TAG molecule, whereas in fish oil EPA or DHA are mainly in the *sn*-2 position (24). FA in the *sn*-2 position are not easily hydrolyzed in the intestine and are therefore absorbed mainly as MG. However, FA are easily released from the *sn*-1 and *sn*-3 positions and are absorbed directly into the mucosa. Seal oil may therefore generate more FFA within the intestinal lumen than fish oil. Also, postpyloric enteral feeding, as used in the present study, may be advantageous, as higher concentrations

**TABLE 1**  
**Effects of Seal Oil Administration (10 mL three times a day) in 10 Patients with Inflammatory Bowel Disease (IBD)<sup>a</sup>**

	Before	After	P-value <sup>b</sup>
Cholesterol (mmol/L)	5.9 (3.0–9.6)	3.75 (2.6–7.6)	<b>0.002</b>
TG (mmol/L)	1.3 (0.58–3.40)	1.27 (0.52–2.22)	<b>0.05</b>
TBARS (nmol/g)	35.1 (26.1–50.7)	27.7 (20.7–45.4)	0.49
Calprotectin (mg/L)	1.2 (0.4–5.0)	1.0 (0.3–5.0)	0.74
Intestinal permeability (%)	0.09 (0.04–0.59)	0.12 (0.04–0.82)	0.25
Joint pain (score)	6.1 (1.0–8.2)	1.1 (0.0–6.0)	<b>0.002</b>
Disease activity (score)	5.5 (1.0–10.0)	4.0 (0.0–7.0)	<b>0.01</b>
n-3/n-6 serum (%)	0.2 (0.1–0.2)	0.4 (0.2–0.6)	<b>0.008</b>
n-3/n-6 buffy coat (%)	0.2 (0.1–0.4)	0.4 (0.3–0.7)	<b>0.006</b>
n-3/n-6 red cells (%)	0.4 (0.1–0.5)	0.5 (0.4–0.8)	<b>0.004</b>
n-3/n-6 biopsy (%)	0.2 (0.1–0.3)	0.5 (0.3–1.0)	<b>0.002</b>

<sup>a</sup>Median and minimum/maximum values are given. Boldfaced numbers are significant.

<sup>b</sup>Wilcoxon signed rank test.

**TABLE 2**  
**FA Composition in IBD Patients<sup>a</sup>**

FA	Before	After	P-value
<b>Serum</b>			
∑ monoenes <sup>b</sup>	23.7 ± 0.7	22.4 ± 0.6	NS
∑ n-6	38.2 ± 1.2	33 ± 1	0.0064
18:2n-6	31.1 ± 1.2	27 ± 1	0.0074
20:3n-6	1.3 ± 0.2	0.77 ± 0.06	0.0042
20:4n-6	5.8 ± 0.8	5.0 ± 0.3	NS
∑ n-3	5.7 ± 0.4	12.9 ± 0.9	0.0001
18:3n-3	0.63 ± 0.07	0.55 ± 0.05	NS
20:5n-3	1.3 ± 0.2	6.0 ± 0.6	0.0001
22:5n-3	0.7 ± 0.3	0.71 ± 0.07	NS
22:6n-3	3.3 ± 0.3	5.5 ± 0.3	0.0001
<b>Buffy coat</b>			
∑ monoenes <sup>b</sup>	22 ± 1	20 ± 2	NS
∑ n-6	31 ± 2	27 ± 2	NS
18:2n-6	20 ± 1	18 ± 2	NS
20:3n-6	1.7 ± 0.1	1.0 ± 0.1	0.0012
20:4n-6	11 ± 1	8 ± 1	0.0485
∑ n-3	7.3 ± 0.5	11 ± 1	0.0022
18:3n-3	0.38 ± 0.07	0.40 ± 0.06	NS
20:5n-3	1.2 ± 0.2	4.2 ± 0.5	0.0001
22:5n-3	1.3 ± 0.2	1.4 ± 0.2	NS
22:6n-3	4.2 ± 0.4	5.1 ± 0.7	NS
<b>Red blood cell</b>			
∑ monoenes <sup>b</sup>	17.0 ± 0.8	15.9 ± 0.6	NS
∑ n-6	24 ± 2	23 ± 2	NS
18:2n-6	13.4 ± 0.9	11.4 ± 0.02	0.0332
20:3n-6	1.5 ± 0.2	1.3 ± 0.1	NS
20:4n-6	9 ± 2	10 ± 1	NS
∑ n-3	8.8 ± 0.8	12.1 ± 0.6	0.0035
18:3n-3	0.10 ± 0.04	0.04 ± 0.04	NS
20:5n-3	1.2 ± 0.1	3.0 ± 0.3	0.0003
22:5n-3	1.7 ± 0.2	2.2 ± 0.2	NS
22:6n-3	5.6 ± 0.5	6.7 ± 0.5	NS
<b>Biopsy</b>			
∑ monoenes <sup>b</sup>	31 ± 2	24 ± 2	0.025
∑ n-6	24 ± 2	19 ± 1	0.0376
18:2n-6	16 ± 1	12.1 ± 0.6	0.0123
20:3n-6	1.5 ± 0.2	1.0 ± 0.1	NS
20:4n-6	6 ± 1	6 ± 1	NS
∑ n-3	4.1 ± 0.5	9 ± 1	0.0003
18:3n-3	0.4 ± 0.1	0.24 ± 0.08	NS
20:5n-3	0.81 ± 0.05	3.4 ± 0.4	0.0001
22:5n-3	0.6 ± 0.2	0.9 ± 0.2	NS
22:6n-3	2.2 ± 0.3	4.3 ± 0.6	0.0063

<sup>a</sup>Data are presented as percentage of total FA, mean ± SEM. The amount of FA identified ranged from 94–98%. NS, not significant. For other abbreviation see Table 1.

<sup>b</sup>∑ monoenes includes 16:1n-7, 16:1n-9, 18:1n-7, 18:1n-9, and 20:1n-9 FA.

of the active substances could reach the inflamed part of the intestine by this mode of administration compared with the oral liquid or capsules used previously (17–20).

Incorporation of FA from fish and olive oils into colonic mucosal membranes displaces AA, causing less AA to be available for cyclo- and lipoxygenase enzyme systems (25,26). In a comparison of fish and seal oil, Yoshida *et al.* (27) and Ikeda *et al.* (28) found that seal oil was more effective in reducing AA content than fish oil. In the present study administration of seal oil consistently increased the n-3 to n-6 ratio significantly in red and white blood cells as well as in biopsies from rectal mucosa.

Because PUFA are prone to oxidation, administration of PUFA to an inflamed mucosa may theoretically increase lipid peroxidation (29). Concomitant supplementation with antioxidants may counteract this potentially adverse effect of n-3

**TABLE 3**  
**Major FA and Vitamins A and E Levels in Seal Oil<sup>a</sup>**

FA	Percent	g/100 g
∑ saturated	15.3	12.7
14:0	5.3	4.4
16:0	8.5	7.1
17:0	0.3	0.3
18:0	1.0	0.8
∑ monoenes	53.2	44.2
16:1n-7	11.6	9.7
18:1n-7	4.1	3.4
18:1n-9	17.7	14.7
20:1n-9	9.8	8.1
22:1n-11	4.4	3.7
∑ n-6	2.5	2.1
18:2n-6	1.8	1.5
20:4n-6	0.4	0.4
∑ n-3	26.6	22.1
18:3n-3	0.9	0.8
20:5n-3	7.0	5.8
22:5n-3	4.0	3.3
22:6n-3	10.7	8.9
n-3/n-6	10.6	10.6
All-trans retinol		0.76 mg/100 g
All-trans dehydroretinol		0.29 mg/100 g
α-Tocopherol		5.398 mg/100 g

<sup>a</sup>Data are presented as percentage of total FA and as g/100 g oil, for vitamins A and E as mg/100 g. The amount of FA identified was 97.6%.



**TABLE 4**  
**Effects of the Second Seal Oil Administration in Five IBD Patients<sup>a</sup>**

	Before	After	P-value <sup>b</sup>
Duration of morning stiffness (min)	120 (30–180)	0 (0–30)	0.07
Number of tender joints	5 (0–7)	1 (1–4)	0.34
Number of swollen joints	0 (0–9)	1 (0–4)	0.29
Number of reported painful joints	2 (0–25)	1 (0–16)	0.20
Investigator's assessment of rheumatic disease activity (VAS)	16 (4–39)	9 (1–14)	0.14
Pain throughout the week (VAS)	57 (35–63)	12 (1–54)	<b>0.04</b>
Patient's assessment of rheumatic disease activity (VAS)	48 (45–66)	9 (2–58)	0.14
Health Assessment Score	0.875 (0.250–1.750)	0.375 (0.000–0.475)	0.08

<sup>a</sup>Median and minimum/maximum values are given. VAS, visual analog scale. For other abbreviation see Table 1. Boldface number is significant.

<sup>b</sup>Wilcoxon signed rank test.

supplementation. Most research on fish oil supplementation has failed to state the amount of concomitant antioxidants administered. In the present study we used seal oil with added antioxidants, and we found no measurable change in lipid peroxidation as measured by TBARS in blood. Calprotectin levels in stools and intestinal permeability are markers of intestinal inflammation (12,16). The lack of a beneficial effect of seal oil on these inflammatory parameters is disappointing but might be due to the short treatment period (10 d).

The total serum cholesterol concentration was significantly lower after seal oil consumption than before in the IBD patients. Findings in the literature regarding the effect of n-3 PUFA supplements on serum cholesterol are conflicting. Compared to the control group, total cholesterol, TG, and phospholipid concentrations in plasma were significantly decreased when supplements of seal or fish oil were given to patient groups (28). However, Harris observed that levels of both total and LDL cholesterol were unaffected by dietary n-3 FA (30).

For patients with rheumatoid arthritis, n-3 FA supplementation reduced neutrophil LTB<sub>4</sub>, whereas neutrophil LTB<sub>5</sub> levels increased slightly (31). The decrease in LTB<sub>4</sub> production was correlated to a decrease in the number of tender joints (32). Moreover, Volker *et al.* (33) reported that supplementation with fish oil containing 60% n-3 FA for a 15-wk period improved the clinical status of patients with rheumatoid arthritis compared to the control group (i.e., significant differences were found in early morning stiffness, the Health Assessment Questionnaire, and physicians' assessments of arthritis activity).

Peripheral "enteropathic" arthritis is seen in 15–20% of patients with IBD and is more commonly associated with CD than UC (34). In one study the prevalence of Crohn's-associated joint pain was much higher (48%) than that generally reported, possibly due to the inclusion of many patients with arthralgia or more vague rheumatic pains (35).

The weaknesses of this study are the small number of patients, choice of a nonplacebo control, and management of two distinct disease entities with different pathophysiologies and different responses to treatments. However, our 10 patients were specifically recruited because of their joint pain, which is largely independent of inflammatory disease activ-

ity. IBD patients with joint pain represent a group of patients having much suffering and few other treatment alternatives. In the present study, the effect of seal oil on joint pain was marked and appeared after only a few days of treatment. The subsequent routine follow-up indicated that the beneficial effect on the joint symptoms persisted for several months in some of the patients. These encouraging results clearly warrant further controlled studies.

#### ACKNOWLEDGMENT

The authors wish to thank Gro Maria Olderøy, Aud Sissel Hjartholm, and Agnes Nordstrand at the Gastroenterology Laboratory for help and support in conducting the clinical analysis, and Thu Thao Nguyen at the Institute of Nutrition for excellent technical assistance. This study was funded by Rieber Skinn AS, the Norwegian Fishermen Association, and the Ministry of Fisheries.

#### REFERENCES

- O'Morain, C., Tobin, A., Suzuki, Y., McColl, T., and Collins, R. (1990) Fish Oil in the Treatment of Ulcerative Colitis, *Scand. J. Gastroenterol.* 31, 267–272.
- Drevon, C. (1992) Marine Oils and Their Effects, *Nutr. Rev.* 50, 159–163.
- Nordøy, A. (1991) Is There a Rational Use for n-3 Fatty Acids (fish oils) in Clinical Medicine? *Drugs* 42, 331–342.
- Akiba, S., Murata, T., Kitatani, K., and Sato, T. (2000) Involvement of Lipooxygenase Pathway in Docosapentaenoic Acid-Induced Inhibition of Platelet Aggregation, *Biol. Pharm. Bull.* 23, 1293–1297.
- Shahidi, F., and Synowiecki, J. (1992) Seal Meat: A Unique Source of Muscle for Health and Nutrition, *Food Rev. Int.* 12, 283–302.
- Harvey, R., and Bradshaw, J. (1980) A Simple Index of Crohn's Disease Activity, *Lancet* 1, 514.
- Walmsley, R., Ayres, R., and Allan, R. (1998) A Simple Clinical Colitis Activity Index, *Gut* 43, 29–32.
- Fries, J.F., Spitz, P., Kraines, R.G., and Holman, H.R. (1980) Measurement of Patient Outcome in Arthritis, *Arthritis Rheum.* 23, 137–145.
- Fuchs, H.A., and Pincus, T. (1994) Reduced Joint Counts in Controlled Clinical Trials in Rheumatoid Arthritis, *Arthritis Rheum.* 37, 470–475.
- Schmedes, A., and Holmer, G. (1989) A New Thiobarbituric Acid (TBA) Method for Determining Free Malondialdehyde (MDA) and Hydroperoxides Selectively as a Measure of Lipid Peroxidation, *J. Am. Oil Chem. Soc.* 66, 813–817.

11. Handy, M.L., Ghosh, S., and Ferguson, A. (1995) Investigation of Neutrophil Migration into the Gut by Cytology of Whole Gut Lavage Fluid, *Eur. J. Gastroenterol. Hepatol.* 7, 53–58.
12. Acciuffi, S., Ghosh, S., and Ferguson, A. (1996) Strengths and Limitations of the Crohn's Disease Activity Index, Revealed by an Objective Gut Lavage Test of Gastrointestinal Protein Loss, *Aliment. Pharmacol. Ther.* 10, 321–326.
13. Bjarnason, I., O'Morain, C., Levi, A.J., and Peters, T.J. (1983) Absorption of <sup>51</sup>Cr EDTA in Inflammatory Bowel Disease, *Gastroenterology* 85, 18–22.
14. Bjarnason, I., Macpherson, A., and Hollander, D. (1995) Intestinal Permeability: An Overview, *Gastroenterology* 108, 1566–1581.
15. Lie, Ø., and Lambertsen, G. (1991) Fatty Acid Composition of Glycerophospholipids in Seven Tissues of Cod (*Gadus morhua*), Determined by Combined High-Performance Liquid Chromatography and Gas Chromatography, *J. Chromatogr.* 565, 119–129.
16. Berstad, A., Arslan, G., and Folvik, G. (2000) Relationship Between Intestinal Permeability and Calprotectin Concentration in Gut Lavage Fluid, *Scand. J. Gastroenterol.* 35, 64–69.
17. Lorenz, R., Weber, P.C., Szimnau, P., Heldwein, W., Strasser, T., and Loeschke, K. (1989) Supplementation with n-3 Fatty Acids from Fish Oil in Chronic Inflammatory Bowel Disease—A Randomized, Placebo-Controlled, Double-Blind Cross-Over Trial, *J. Int. Med.* 225 (Suppl. 1), 225–232.
18. McCall, T.B., O'Leary, D., Bloomfield, J., and O'Morain, C.A. (1989) Therapeutic Potential of Fish Oil in the Treatment of Ulcerative Colitis, *Aliment. Pharmacol. Ther.* 3, 415–424.
19. Stenson, W.F., Cort, D.C., Rodgers, J., Burakoff, R., DeSchryver-Kecskemeti, K., Gramlich, T.L., and Beeken, W. (1992) Dietary Supplementation with Fish Oil in Ulcerative Colitis, *Ann. Int. Med.* 116, 609–614.
20. Aslan, A., and Triadafilopoulos, G. (1992) Fish Oil Fatty Acid Supplementation in Active Ulcerative Colitis: A Double-Blind, Placebo-Controlled, Crossover Study, *Am. J. Gastroenterol.* 87, 432–437.
21. Hawthorne, A.B., Daneshmend, T.K., Hawkey, C.J., Belluzzi, A., Everitt, S.J., Holmes, G.K.T., Malkinson, C., Shaheen, M.Z., and Willars, J.E. (1992) Treatment of Ulcerative Colitis with Fish Oil Supplementation: A Prospective 12-Month Randomised Controlled Trial, *Gut* 33, 922–928.
22. Belluzzi, A., Brignola, C., Campieri, M., Pera, A., Boschi, S., and Migiolo, M. (1996) Effect of an Enteric-Coated Fish-Oil Preparation on Relapses in Crohn's Disease, *N. Engl. J. Med.* 334, 1557–1560.
23. Lorenz-Meyer, H., Nicolay, C., and Schulz, B. (1996) Omega-3 Fatty Acids and Low Carbohydrate Diet for Maintenance of Remission in Crohn's Disease: A Randomised Controlled Multi-centre Trial, *Scand. J. Gastroenterol.* 31, 778–785.
24. Ackman, R.G. (1988) Some Possible Effects on Lipid Biochemistry of Differences in the Distribution on Glycerol of Long-Chain n-3 Fatty Acids in the Fats of Marine Fish and Marine Mammals, *Atherosclerosis* 70, 171–173.
25. Hillier, K., Jewell, R., Dorrel, L., and Smith, L. (1991) Incorporation of Fatty Acids from Fish Oil and Olive Oil into Colonic Mucosal Lipids and Effects upon Eicosanoid Synthesis in Inflammatory Bowel Disease, *Gut* 32, 1151–1155.
26. Belluzzi, A., Brignola, C., Campieri, M., Camporesi, E., Gionchetti, P., and Rizzello, F. (1994) Effects of New Fish Oil Derivative and Fatty Acid Phospholipid Membrane Pattern in a Group of Crohn's Disease Patients, *Dig. Dis. Sci.* 39, 2589–2594.
27. Yoshida, H., Kummaru, J., Mawatari, M., Ikeda, I., Imaizumi, K., and Tsuji, H. (1996) Lymphatic Absorption of Seal and Fish Oils and Their Effect on Lipid Metabolism and Eicosanoid Production in Rats, *Biosci. Biotechnol. Biochem.* 60, 1293–1298.
28. Ikeda, I., Yoshida, H., Tomooka, M., Yosef, A., Imaizumi, K., and Tsuji, H. (1998) Effects of Long-Term Feeding of Marine Oils with Different Positional Distribution of Eicosapentaenoic and Docosahexaenoic Acids on Lipid Metabolism, Eicosanoid Production, and Platelet Aggregation in Hypercholesterolemic Rats, *Lipids* 33, 897–904.
29. Girelli, D., Olivieri, O., and Stanzial, A.M. (1994) Factors Affecting the Thiobarbituric Acid Test as Index of Red Blood Cell Susceptibility to Lipid Peroxidation: A Multivariate Analysis, *Clin. Chim. Acta* 227, 45–57.
30. Harris, W. (1989) Fish Oils and Plasma Lipid and Lipoprotein Metabolism in Humans: A Critical Review, *J. Lipid Res.* 30, 785–807.
31. Kremer, J.M., Jubiz, W., Michalek, A., Rynes, R., Bartholomew, L.E., and Bigouette, J. (1987) Fish Oil Fatty Acid Supplementation in Active Rheumatoid Arthritis, *Ann. Intern. Med.* 106, 497–503.
32. Kremer, J.M., Lawrence, D.A., Jubiz, W., Digiaco, R., Rynes, R., Bartholomew, L.E., and Sherman, M. (1990) Dietary Fish Oil and Olive Oil Supplementation in Patients with Rheumatoid Arthritis, *Arthritis Rheum.* 33, 810–820.
33. Volker, D., Fitzgerald, P., Major, G., and Garg, M. (2000) Efficacy of Fish Oil Concentrate in the Treatment of Rheumatoid Arthritis, *J. Rheumatol.* 27, 2343–2346.
34. Gravalles, E.M., and Kantrowitz, F.G. (1988) Arthritic Manifestations of Inflammatory Bowel Disease, *Am. J. Gastroenterol.* 83, 703–709.
35. Florin, T.H.J., Graffner, H., Nilsson, L.G., and Persson, T. (2000) Treatment of Joint Pain in Crohn's Patients with Budesonide-Controlled Ileal Release, *Clin. Exp. Pharmacol. Physiol.* 27, 295–298.

[Received September 5, 2002, and in revised form October 29, 2002; revision accepted November 14, 2002]

# EPA, but Not DHA, Decreases Mean Platelet Volume in Normal Subjects

Yongsoo Park<sup>a,b</sup> and William Harris<sup>a,b,\*</sup>

<sup>a</sup>Department of Medicine, University of Missouri–Kansas City, Missouri 64108,  
and <sup>b</sup>Lipid and Diabetes Research Center, Saint Luke's Hospital, Kansas City, Missouri 64111

**ABSTRACT:** The first indication of platelet activation is an increase in mean platelet volume (MPV). n-3 FA are known to inhibit platelet function and to reduce the risk for coronary heart disease. The purpose of this study was to determine the effects of EPA and DHA on MPV. Healthy subjects received olive oil placebo for 4 wk and then were randomly assigned to receive 4 g of ethyl esters of either safflower oil ( $n = 11$ ), EPA ( $n = 10$ ), or DHA ( $n = 12$ ) for 4 wk. At the end of placebo run-in and treatment periods, MPV (fL; mean  $\pm$  SEM) and platelet count (PLT-CT;  $10^3/\mu\text{L}$  blood) were measured in the basal state and after *ex vivo* stimulation with collagen (10  $\mu\text{g}/\text{mL}$ ), cold (4°C), and heat (37°C). Unlike DHA, EPA lowered MPV as compared with safflower oil ( $7.2 \pm 0.1$  vs.  $7.5 \pm 0.1$  fL;  $P < 0.05$ ) and raised PLT-CT ( $211 \pm 18$  vs.  $192 \pm 18$   $10^3/\mu\text{L}$ ;  $P < 0.05$ ) in the fasting state. Collagen and cold significantly increased MPV whereas heat lowered MPV regardless of treatment. All stimuli decreased PLT-CT. EPA significantly increased platelet EPA ( $0.2 \pm 0.1$  vs.  $3.3 \pm 0.4\%$ ) and docosapentaenoic acid (DPA;  $2.2 \pm 0.3$  vs.  $2.9 \pm 0.3\%$ ) concentrations, but not DHA. DHA treatment significantly increased DHA ( $1.4 \pm 0.2$  vs.  $4.1 \pm 0.5\%$ ) and DPA ( $2.0 \pm 0.4$  vs.  $3.0 \pm 0.4\%$ ) concentrations, but not EPA. In conclusion, EPA, but not DHA, reduces platelet activation, an early step in platelet aggregation.

Paper no. L9015 in *Lipids* 37, 941–946 (October 2002).

Mean platelet volume (MPV) is a marker of platelet activation (1). It has been reported that MPV is increased in patients at high risk for acute myocardial infarction (MI) (2–4). Large platelets show a higher degree of adhesion and aggregation than small ones (5). The presence of a greater number of large platelets in such patients is consistent with an elevated risk of thrombus formation. MPV is much easier to measure than agonist stimulated platelet aggregation and thus it may have clinical utility. As platelet activation increases, platelets are likely to form aggregates, leading to a decrease in single platelets in the blood. This is measured by the platelet count. A decrease in count after *ex vivo* stimulation indicates an increase in aggregates.

Interest in fish oil as an antiplatelet agent dates back 20 yr (6), and this mechanism may have played a role in the cardio-protection seen with n-3 fatty acids (FA) use in recent trials. In the GISSI-Prevention study, supplementation with n-3 FA (850 mg) reduced overall mortality in post-MI patients (already taking aspirin) by 20% and risk for sudden cardiac death by 45% (7). The Diet and Reinfarction Trial (8) and the Indian Experiment of Infarct Survival also reported that n-3 FA protected

\*To whom correspondence should be addressed at Lipid and Diabetes Research Center, Saint Luke's Hospital, 4320 Wornall Rd. MP1, Suite 128, Kansas City, MO 64111. E-mail: wharris@saint-lukes.org

Abbreviations: ACD, acid/citrate/dextrose; DPA, docosapentaenoic acid; MI, myocardial infarction; MPV, mean platelet volume; PLA<sub>2</sub>, phospholipase A<sub>2</sub>; PLT-CT, platelet count; TxA<sub>2</sub>, thromboxane A<sub>2</sub>.

against coronary artery disease. Clearly, antiplatelet drugs (e.g., aspirin) can reduce the incidence of coronary artery disease (10,11). Several studies have shown that relatively large amounts of n-3 FA can decrease platelet aggregation and prolong bleeding time (12–16); however, the effects of n-3 FA on MPV are not known.

It has been assumed that EPA is more active than DHA in altering platelet function because it is a cyclooxygenase substrate (17). However, DHA appears to decrease thromboxane A<sub>2</sub> (TxA<sub>2</sub>)/prostaglandin H<sub>2</sub> receptor affinity (18). Von Schacky and Weber (19) reported that both EPA and DHA, given for only 6 d, reduced platelet aggregation *in vitro*. Thus, both of these FA have the potential to affect platelet function. The purpose of the present study was to compare the effects of EPA and DHA separately on MPV and on MPV responses to collagen, cold, or heat during the fasting and the fed states. Like collagen, cold exposure is known to cause platelet activation (20,21) whereas heat causes platelets to contract. We tested the hypothesis that treatment with both DHA and EPA would decrease MPV, and increase platelet count (PLT-CT), as compared with safflower oil.

## MATERIALS AND METHODS

**Subjects.** Saint Luke's Hospital Institutional Review Board approved this study and informed written consent was obtained from all participants. The study consisted of three periods (4 wk each): placebo run-in, wash-out, and active treatment. Thirty-three healthy subjects, male ( $n = 17$ ) and female ( $n = 16$ ), were given olive oil capsules (4 g/d) during the placebo run-in period and then were randomized to ethyl esters of either EPA ( $n = 10$ ), DHA ( $n = 12$ ), or safflower oil ( $n = 11$ ; 4 g/d each) during the treatment period. The oils (95% pure) were provided by the Fish Oil Test Material Program of the U.S. Department of Commerce and the National Institutes of Health.

Baseline characteristics are shown in Table 1. Subjects were asked to maintain their usual lifestyle and dietary habits throughout. Intake of drugs known to affect platelet function was restricted 2 wk before blood sampling. Alcohol intake and strenuous physical exercise were also prohibited during the 48 h preceding the blood sampling. At the end of placebo run-in and treatment periods, fasting ( $\geq 12$  h overnight) blood samples were drawn from all subjects. Subjects were then asked to consume a chocolate-flavored test drink made with half-and-half (1 g fat/kg body weight), and blood samples were taken 4 h later (fed state).

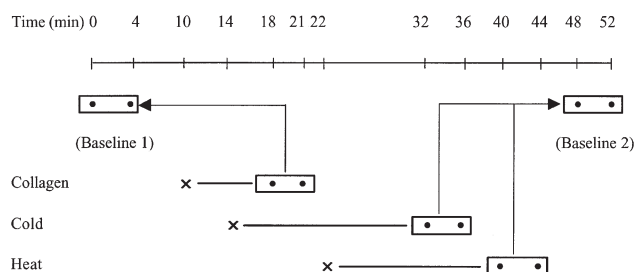
**Platelet activation.** Blood samples were drawn into acid/citrate/dextrose (ACD) tube containing 2% Na<sub>2</sub>-EDTA. This

anticoagulant cocktail reportedly prevents platelet activation for 8 h (23). Subjects were sitting during the blood draw, and an 18-gauge needle was used. The first 10 mL of blood was not used for platelet testing. MPV and PLT-CT were measured in whole blood directly from the tube using Coulter Counter MD16 (Beckman, Miami, FL) (5). The instrument was calibrated daily with commercially available controls.

MPV and PLT-CT were measured in eight separate conditions at the end of the placebo and the active treatment periods. The eight conditions were: unstimulated or stimulated with collagen, heat or cold, all in the fasting and the fed states. The effect of eating was examined because platelet activation was expected to be greater in the fed than the fasting state (24,25). Three different *ex vivo* stimuli were included in anticipation that, if EPA or DHA did not activate platelets in the basal state, they might affect platelet response to stimulation.

Within 15 min of the blood draw, a series of measurements of MPV and PLT-CT were initiated as follows (26). Three microfuge tubes were prepared: one was placed on ice, another in a 37°C water bath; to the third was added 10 µL of a 1 µg/µL collagen (type I; Chrono-log Corp., Havertown, PA), and this was kept at room temperature. ACD blood was mixed by gentle inversion seven or eight times before baseline measurements were taken. Unstimulated values were measured four times, twice before (0 and 4 min) and twice after (48 and 52 min) a series of stimulation tests (Fig. 1). Blood (1 mL each) was transferred to the collagen-containing tube, the pre-chilled tube and the pre-warmed tube at 10, 14, and 22 min, respectively, after baseline measurements were taken. MPV and PLT-CT were measured 8 and 11 min after collagen addition, and 18 and 22 min after exposure to cold and heat. Preliminary experiments showed that despite the anticoagulant cocktail, MPV gradually increased in unstimulated blood held at room temperature for 52 min by about 3% (26). Thus, control values for the platelet response to collagen (baseline 1) were defined to be the average MPV and PLT-CT at 0 and 4 min (since these samples were measured closer in time to the peak collagen response). On the other hand, the controls for the platelet responses to heat and cold (baseline 2) were defined as the mean unstimulated measurements at 48 and 52 min since the responses to temperature were assessed closer to the end of the 52 min protocol than to the beginning. All analyses were completed within 67 min from the time of the blood draw.

**Platelet FA composition.** Fasting blood was drawn in ACD tubes and centrifuged at 125 × *g* for 10 min to obtain platelet-rich plasma. Platelet-rich plasma was mixed with Brox washing buffer (63.75 mM Tris, 11.25 mM HCl, and 77 mM



**FIG. 1.** Protocol for measurement of mean platelet volume and platelet count. × indicates the time when blood was added to collagen, or when it was exposed to cold or heat; • indicates the times measurements were made; → indicates which control (baseline 1 or 2) was used for the platelet response to collagen, cold and heat.

EDTA), and the mixture was centrifuged at 500 × *g* for 15 min. After discarding the plasma, the pellet was resuspended with the buffer and centrifuged again. The platelet pellet was resuspended with 1 mL of 2% EDTA and stored at -80°C.

Diheptadecanoyl PC was added as an internal standard to the washed platelets, which were extracted with methanol/methylene chloride (1:2) for total lipids (preliminary experiments showed that >98 % of lipids were phospholipid). Glycerophospholipid FA were methylated with boron trifluoride at 100°C for 10 min (27,28) and then analyzed by GC (GC9A; Shimadzu, Corp., Columbia, MD), using a 30-m SP2330 capillary column (Supelco, Bellefonte, PA). FA were identified by comparison with known standards.

**Statistics.** Data were analyzed by ANOVA or analysis of covariance using Statistical Analysis System (Cary, NC). Differences between means were considered statistically significant at the  $P < 0.05$  level.

## RESULTS

When all data were pooled regardless of treatments (olive oil placebo, safflower oil, EPA, or DHA) or the fasting/fed status, MPV was significantly increased in response to both collagen and cold, whereas it was decreased by heat (Fig. 2). All stimuli significantly decreased PLT-CT regardless of treatments or fed/fasting status, although collagen lowered PLT-CT more than exposure to heat or cold (Fig. 2). There was no significant difference between MPV in the fasting and the fed state. EPA significantly lowered MPV and increased PLT-CT as compared to safflower oil regardless of fed/fasting state or *ex vivo* stimuli, whereas no effect was seen with DHA (Fig. 3).

Platelet responses to *ex vivo* stimuli during the olive oil placebo and the active treatment phases in both the fasting and fed states are shown in Figure 4 (MPV) and Figure 5 (PLT-CT). EPA significantly decreased MPV at baseline 1 during the fed state and at baseline 2 during the fasting state (Fig. 4). EPA significantly increased baseline 1 PLT-CT during the fasting state (Fig. 5).

The effects of treatment on the platelet FA composition (fasting state) is presented in Table 2. EPA significantly in-

**TABLE 1**  
Baseline Subject Characteristics

Subjects	Safflower oil ( <i>n</i> = 11)	EPA ( <i>n</i> = 10) <sup>a</sup>	DHA ( <i>n</i> = 12)
Age <sup>a</sup> (y)	37 ± 3	43 ± 4	41 ± 5
BMI <sup>a</sup> (kg/m <sup>2</sup> )	28 ± 1 <sup>b</sup>	25 ± 1	26 ± 1
Male/female	7/4	5/5	5/7

<sup>a</sup>Values are mean ± SEM.

<sup>b</sup>Values differ ( $P < 0.05$ ) between groups. BMI, body mass index.



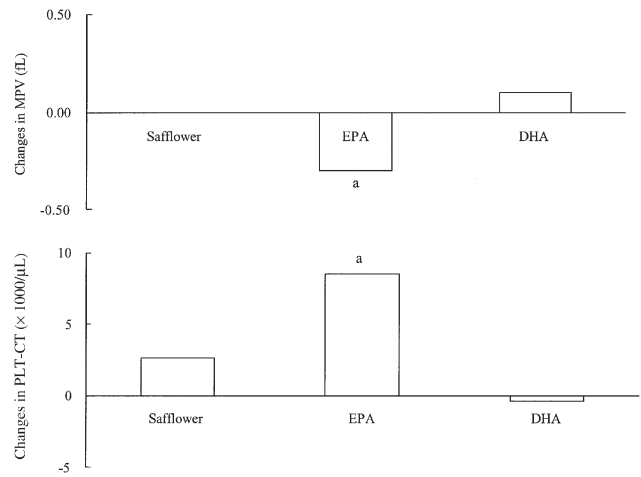
creased platelet EPA and docosapentaenoic acid (DPA) levels in an apparent exchange for stearic and arachidonic acids. DHA significantly increased DHA and DPA concentrations at the expense of palmitoleic, oleic, linoleic, and arachidonic acids. There were no significant differences in saturated, monounsaturated, and n-6 PUFA compositions between olive oil and any of the treatment groups, but total n-3 PUFA significantly increased after EPA and DHA supplementation (Table 2).

**DISCUSSION**

Changes in MPV are an early indicator of platelet activation (2,29), thus MPV may be an *in vivo* marker of the potential for platelet aggregation. Smaller platelets have less fibrinogen receptors exposed than larger ones, suggesting a reduced risk of thrombus formation (5); and larger platelets produce more TxB<sub>2</sub> when stimulated with collagen and thrombin (5).

Fish oil supplementation (including EPA and DHA) has been shown (15,16,30,31) to decrease platelet aggregation and to prolong bleeding times (12), but the separate effects of these two FA on platelet function has rarely been examined in the same setting (13–16). In this study, we found that EPA, but not DHA, decreased platelet activation as indicated by a decreased MPV and increased PLT-CT.

Hirai *et al.* (32) reported that 3.6 g of EPA for 24 d significantly inhibited collagen, ADP, and epinephrine-induced platelet aggregation, but the effect of DHA was significant only for collagen. Platelet aggregation was also significantly decreased with 2 g of EPA given for 2 and 4 wk (33,34). Von Schacky and Weber (19) reported that 6 g of EPA and DHA ethyl ester alone for 6 d caused a significant reduction in platelet aggregation with collagen, but the response to ADP was signifi-

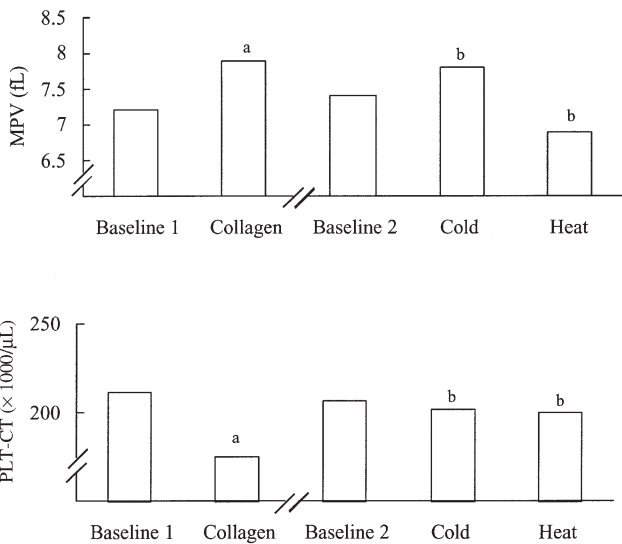


**FIG. 3.** Changes in MPV (fL; top) and PLT-CT (x 1000/μL; bottom) from olive oil to safflower oil (SAF), EPA, or DHA regardless of fed/fasting state or *ex vivo* stimuli. Mean values are presented. *n* = 33. <sup>a</sup>Values differ (*P* < 0.05) between treatments. For other abbreviations see Figure 2.

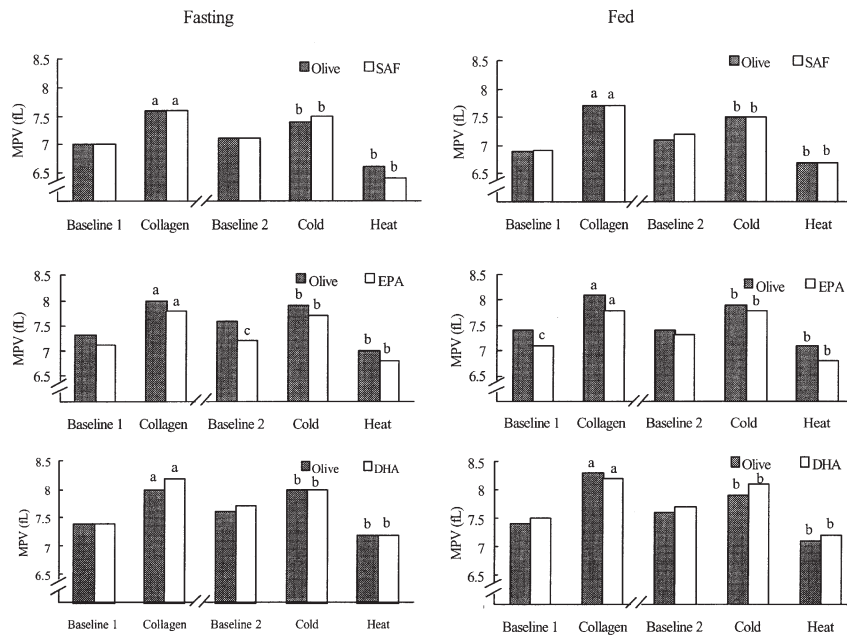
cantly lowered only by DHA. Nelson *et al.* (35) observed that adding 6 g of DHA for 90 d produced no physiological changes in blood coagulation, platelet function, or thrombotic tendencies in six healthy males. In contrast to these high dose studies, Driss *et al.* (36) reported platelet inhibitory effects with 150 mg of EPA, the lowest dose reported to alter platelet function.

Croset *et al.* (37) suggested that EPA and DHA affect platelet function in synergistic ways. EPA competes with endogenous arachidonic acid at the cyclooxygenase level to reduce the amount of TxA<sub>2</sub> formed and to generate the weakly proaggregatory TxA<sub>3</sub> (38). DHA inhibits platelet function by decreasing the affinity of TxA<sub>2</sub> for its receptor (18,39,40). In addition, Shikano *et al.* (17) reported that PE-enriched DHA is a poor substrate for phospholipase A<sub>2</sub> (PLA<sub>2</sub>), the enzyme that mobilizes eicosanoid precursors from cell membranes. What is more, EPA appears to suppress PLA<sub>2</sub> activity, resulting in reduced platelet-activating factor synthesis (41).

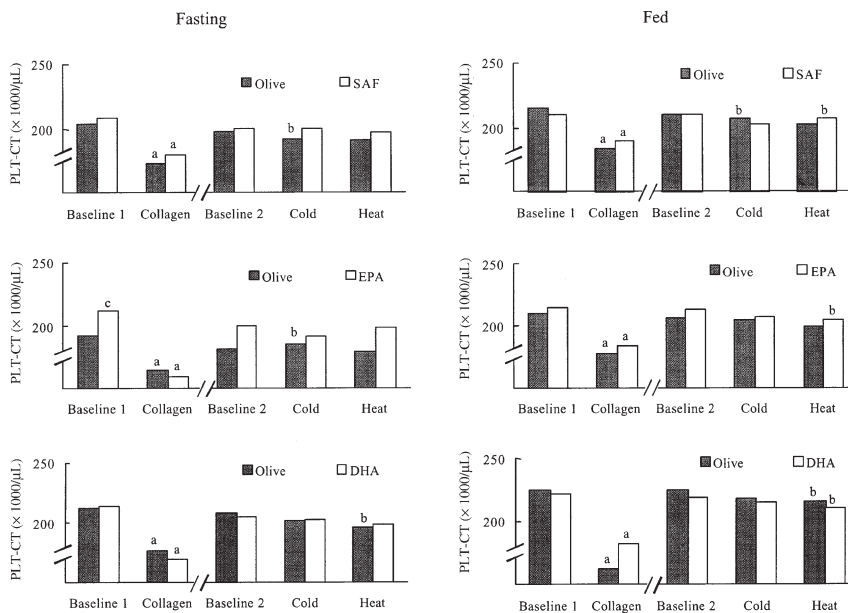
The postprandial state is considered to be more procoagulant than the fasting state. Platelet aggregation induced by ADP (24) and by collagen (25) was significantly increased in normolipemic subjects after fatty meals. Fuhrman *et al.* (24) showed that platelets maintained their hypersensitivity to aggregation 5 h after meals, at a time when plasma TG levels had returned to normal. Chylomicron remnant particles enhanced activation of platelets stimulated with ADP and collagen (42), but native chylomicrons inhibited platelet function (43). These observations imply that, although total plasma TG may not affect platelet activation, certain TG-rich lipoprotein remnants may do so. Broijerssen *et al.* (44) reported that expression of platelet selectin was increased 3 and 6 h postprandially in unstimulated and ADP-stimulated samples. However, Jakubowski *et al.* (45) found no effect of eating on platelet aggregate formation or expression of platelet-specific proaggregatory proteins. We also found that meal consumption did not significantly change MPV or PLT-CT, but PLT-CT tended to be



**FIG. 2.** Mean platelet volume (MPV; fL; top) and platelet count (PLT-CT; x 1000/μL; bottom) regardless of treatments (olive oil placebo, safflower oil, EPA or DHA) or the fasting/fed status. Mean values are presented. *n* = 33. <sup>a</sup>Values differ (*P* < 0.05) from baseline 1. <sup>b</sup>Values differ (*P* < 0.05) from baseline 2.



**FIG. 4.** Response of MPV (fL) to collagen, cold, and heat before and after supplementation with SAF (top), EPA (middle), or DHA (bottom) during the fasting (left panel) and the fed states (right panel). Mean values are presented.  $n = 33$ . <sup>a</sup>Values differ ( $P < 0.05$ ) from baseline 1 (for the same treatment). <sup>b</sup>Values differ ( $P < 0.05$ ) from baseline 2 (for the same treatment). <sup>c</sup>The change (from olive to SAF) is different ( $P < 0.05$ ) from the change (from olive to EPA). For abbreviations see Figures 2 and 3.



**FIG. 5.** Response of PLT-CT ( $\times 1000/\mu\text{L}$ ) to collagen, cold, and heat before and after supplementation with SAF (top), EPA (middle), or DHA (bottom) during the fasting (left panel) and the fed states (right panel). Mean values are presented.  $n = 33$ . <sup>a</sup>Values differ ( $P < 0.05$ ) from baseline 1 (for the same treatment). <sup>b</sup>Values differ ( $P < 0.05$ ) from baseline 2 (for the same treatment). <sup>c</sup>The change (from olive to SAF) is different ( $P < 0.05$ ) from the change (from olive to EPA). For abbreviations see Figures 2 and 3.

**TABLE 2**  
**Platelet FA Composition<sup>a</sup>**

FA	Safflower (n = 11)		EPA (n = 10)		DHA (n = 10)	
	Before	After	Before	After	Before	After
14:0	1.8 ± 0.2	1.6 ± 0.2	1.6 ± 0.1	1.5 ± 0.1	1.5 ± 0.2	1.5 ± 0.3
16:0	21.5 ± 0.6	21.5 ± 0.6	21.4 ± 0.6	20.6 ± 0.4	21.2 ± 0.6	20.6 ± 0.8
16:1	0.5 ± 0.1	0.7 ± 0.1	0.3 ± 0.1	0.4 ± 0.1	0.7 ± 0.2	0.5 ± 0.1 <sup>b</sup>
18:0	30.5 ± 1.4	28.6 ± 0.6	30.1 ± 0.8	28.2 ± 0.7	26.2 ± 1.9	27.1 ± 1.6
18:1	12.3 ± 0.3	13.6 ± 0.9	13.1 ± 1.1	13.2 ± 0.5	13.2 ± 0.8	12.3 ± 0.6 <sup>b</sup>
18:2n-6	1.9 ± 0.3	2.7 ± 0.6	1.8 ± 0.1	1.8 ± 0.1	4.2 ± 2.2	2.0 ± 0.4
18:3n-6	4.0 ± 0.7	3.4 ± 0.8	3.2 ± 0.5	3.8 ± 0.5	4.4 ± 1.3	5.7 ± 0.8
18:3n-3	1.5 ± 0.7	1.2 ± 0.8	2.4 ± 0.8	2.3 ± 1.3	0.6 ± 0.5	0.1 ± 0.1
20:1	0.6 ± 0.1	0.6 ± 0.1	0.6 ± 0.1	0.5 ± 0.1	0.7 ± 0.1	0.7 ± 0.1
20:3n-6	1.1 ± 0.1	1.1 ± 0.1	1.0 ± 0.1	1.0 ± 0.1	1.4 ± 0.2	1.4 ± 0.1
20:4n-6	20.3 ± 1.0	20.6 ± 0.9	20.2 ± 1.0	18.4 ± 0.8	21.7 ± 0.7	19.9 ± 1.6
20:5n-3	0.1 ± 0.1	0.2 ± 0.1	0.2 ± 0.1	3.3 ± 0.4 <sup>b</sup>	0.4 ± 0.1	0.4 ± 0.1
22:4n-6	0.4 ± 0.1	0.6 ± 0.2	0.4 ± 0.1	0.4 ± 0.1	0.5 ± 0.2	0.6 ± 0.1
22:5n-3	2.3 ± 0.3	2.4 ± 0.4	2.2 ± 0.3	2.9 ± 0.3 <sup>b</sup>	2.0 ± 0.4	3.0 ± 0.4 <sup>b</sup>
22:6n-3	1.3 ± 0.2	1.3 ± 0.1	1.5 ± 0.2	1.6 ± 0.3	1.4 ± 0.2	4.1 ± 0.5 <sup>b</sup>
SFA	53.8 ± 2.0	51.7 ± 1.0	53.1 ± 1.0	50.3 ± 1.1	48.9 ± 2.0	49.2 ± 2.1
MUFA	13.4 ± 0.8	14.8 ± 0.9	14.0 ± 1.0	14.2 ± 0.5	14.6 ± 0.7	13.6 ± 0.6
PUFAn-6	27.6 ± 1.4	28.5 ± 1.1	26.7 ± 1.2	25.5 ± 1.1	32.3 ± 1.9	29.5 ± 1.8
PUFAn-3	5.2 ± 0.8	5.0 ± 0.8	6.2 ± 0.8	10.0 ± 1.6 <sup>b</sup>	4.3 ± 0.9	7.6 ± 0.5 <sup>b</sup>

<sup>a</sup>Values are mean ± SEM. SFA, saturated FA; MUFA, monounsaturated FA.

<sup>b</sup>Values differ ( $P < 0.05$ ) before and after treatment.

increased in the fed state. Hansen *et al.* (46) observed that food intake increases PLT-CT, which could be due to a meal-induced release of platelets from the spleen (47).

This study suggests that EPA supplementation reduces platelet activation, an early step in platelet aggregation, whereas DHA does not. These findings constitute further evidence for an antiatherogenic potential for marine n-3 FA. Further studies are warranted to assess the effects of combined treatment with EPA and DHA on MPV, platelet membrane receptor activity, TxA<sub>2</sub> synthesis, and platelet granule constituent release.

## ACKNOWLEDGMENTS

The authors would like to thank Philip Jones for help with the statistical analysis, and Norberta Schoene for her technical advice. Grants from National Heart, Lung, and Blood Institute (HL-47468) and the Heartland Affiliate of the American Heart Association (postdoctoral fellowship for YP) supported this work.

## REFERENCES

- Willans, D.J., Mill, S.C., and Ranney, E.K. (1995) Common Thrombotic Disorders Defined by CBC Platelet Parameters, *Clin. Appl. Thrombosis Hemostasis* 1, 188–201.
- Endler, G., Klimesch, A., Sunder-Plassmann, H., Schillinger, M., Exner, M., Mannhalter, C., Jordanova, N., Christ, G., Thalhammer, R., Huber, K., and Sunder-Plassman, R. (2002) Mean Platelet Volume Is An Independent Risk Factor for Myocardial Infarction but Not for Coronary Artery Disease, *Br. J. Haematol.* 117, 399–404.
- Martin, J.F., Plumb, J., Kilbey, R.S., and Kishk, Y.T. (1983) Changes in Volume and Density of Platelets in Myocardial Infarction, *Br. Med. J.* 287, 456–459.
- Erne, P., Wardle, J., Sanders, K., Lewis, S.M., and Maseri, A. (1988) Mean Platelet Volume and Size Distribution and Their Sensitivity to Agonists in Patients with Coronary Artery Disease and Congestive Heart Failure, *Thromb. Haemost.* 59, 259–263.
- Schoene, N.W. (1997) Design Criteria: Tests Used to Assess Platelet Function, *Am. J. Clin. Nutr.* 65, 1665S–1668S.
- Knapp, H.R. (1997) Dietary Fatty Acids in Human Thrombosis and Hemostasis, *Am. J. Clin. Nutr.* 65, 1687S–1698S.
- Gissi-Prevenzione Investigators (1999) Dietary Supplementation with n-3 Polyunsaturated Fatty Acids and Vitamin E in 11,324 Patients with Myocardial Infarction: Results of the GISSI-Prevenzione Trial, *Lancet* 354, 447–455.
- Burr, M.L., Holliday, R.M., Fehily, A.M., and Whitehead, P.J. (1992) Haematological Prognostic Indices after Myocardial Infarction. Evidence from the Diet and Reinfarction Trial (DART), *Eur. Heart J.* 13, 166–170.
- Singh, R.B., Niaz, M.A., Sharma, J.P., Kumar, R., Rastogi, V., and Moshiri, M. (1997) Randomized, Double-Blind, Placebo-Controlled Trial of Fish Oil and Mustard Oil in Patients with Suspected Acute Myocardial Infarction: The Indian Experiment of Infarct Survival—4. *Cardiovasc. Drugs Ther.* 11, 485–491.
- Zucker, M.L., Trowbridge, C., Woodroof, J., Chernoff, S.B., Reynoso, L., and Dujovne, C.A. (1986) Low- vs. High-Dose Aspirin. Effects on Platelet Function in Hyperlipoproteinemic and Normal Subjects, *Arch. Intern. Med.* 146, 921–925.
- Valles, J., Santos, M.T., Aznar, J., Osa, A., Lago, A., Cosin, J., Sanchez, E., Broekman, M.J., and Marcus, A.J. (1998) Erythrocyte Promotion of Platelet Reactivity Decreases the Effectiveness of Aspirin as an Antithrombotic Therapeutic Modality: The Effect of Low-Dose Aspirin Is Less Than Optimal in Patients with Vascular Disease Due to Prothrombotic Effects of Erythrocytes on Platelet Reactivity, *Circulation* 97, 350–355.
- Brox, J., Olaussen K., Østerud, B., Elvevoll, E.O., Bjørnstad, E., Brenn, T., Brattebø, G., and Iversen, H.A. (2001) Long-Term Seal-and Cod-Liver-Oil Supplementation in Hypercholesterolemic Subjects, *Lipids* 36, 7–13.
- Mortensen, J.Z., Schmidt, E.B., Nielsen, A.H., and Dyerberg, J. (1983) The Effect of n-6 and n-3 Polyunsaturated Fatty Acids on Hemostasis, Blood Lipids and Blood Pressure, *Thromb. Haemost.* 50, 543–546.

14. Goodnight, S.H., Jr., Harris, W.S., and Connor, W.E. (1981) The Effects of Dietary Omega-3 Fatty Acids on Platelet Composition and Function in Man: A Prospective, Controlled Study, *Blood* 58, 880–885.
15. Nelson, G.J., Schmidt, P.C., and Corash, L. (1991) The Effect of a Salmon Diet on Blood Clotting, Platelet Aggregation and Fatty Acids in Normal Adult Men, *Lipids* 26, 87–96.
16. Wander, R.C., and Patton B.D. (1991) Comparison of Three Species of Fish Consumed as Part of a Western Diet: Effects on Platelet Fatty Acids and Function, Hemostasis, and Production of Thromboxane, *Am. J. Clin. Nutr.* 54, 326–333.
17. Shikano, M., Masuzawa, Y., Yazawa, K., Takayama, K., Kudo, I., and Inoue, K. (1994) Complete Discrimination of Docosahexaenoate from Arachidonate by 85 kDa Cytosolic Phospholipase A<sub>2</sub> During the Hydrolysis of Diacyl- and Alkenylacylglycerophosphoethanolamine, *Biochim. Biophys. Acta* 1212, 211–216.
18. Bayon, Y., Crosset, M., Daveloose, D., Guerbet, F., Chirouze, V., Viret, J., Kader, J.C., and Lagarde, M. (1995) Effect of Specific Phospholipid Molecular Species Incorporated in Human Platelet Membranes on Thromboxane A<sub>2</sub>/Prostaglandin H<sub>2</sub> Receptors, *J. Lipid Res.* 36, 47–56.
19. Von Schacky, C., and Weber, P.C. (1985) Metabolism and Effects on Platelet Function of the Purified Eicosapentaenoic and Docosahexaenoic Acids in Humans, *J. Clin. Invest.* 76, 2446–2450.
20. Oliver, A.E., Tablin, F., Walker N.J., and Crowe, J.H. (1999) The Internal Calcium Concentration of Human Platelets Increases During Chilling, *Biochim. Biophys. Acta* 1416, 349–360.
21. Winokur, R., and Hartwig, J.H. (1995) Mechanism of Shape Change in Chilled Human Platelets, *Blood* 85, 1796–1804.
22. Borst, C., Bos, A.N., Zwaginga, J.J., Rienks, R., de Groot, P.G., and Sixma, J.J. (1990) Loss of Blood Platelet Adhesion After Heating Native and Cultured Human Subendothelium to 100 Degrees Celsius, *Cardiovasc. Res.* 24, 665–668.
23. Thompson, C., Diaz, D., Quinn, P., Lapins, M., Kurtz, S., and Valeri, C. (1983) The Role of Anticoagulation in the Measurement of Platelet Volume, *Am. J. Clin. Nutr.* 80, 327–332.
24. Fuhrman, B., Brook, J.G., and Aviram, M. (1986) Increased Platelet Aggregation During Alimentary Hyperlipemia in Normal and Hypertriglyceridemic Subjects, *Ann. Nutr. Metab.* 30, 250–260.
25. Winterstein, G., Brook, J.G., Pillar, T., and Aviram, M. (1986) Plasma Lipoproteins and Platelet Aggregation During Alimentary Lipemia. Decreased Atherogenic Pattern in the Elderly, *J. Am. Geriatr. Soc.* 34, 569–572.
26. Park, Y., Schoene, N., and Harris, W. (2002) Mean Platelet Volume as an Indicator of Platelet Activation: Methodological Issues, *Platelets* 13:301–306.
27. Folch, J., Lees, M., and Sloane-Stanley, G.H. (1957) A Simple Method for the Isolation and Purification of Total Lipids from Animal Tissues, *J. Biol. Chem.* 226, 497–509.
28. Kojima, T., Terano, T., and Tanabe, E. (1991) Long-Term Administration of Highly Purified Eicosapentaenoic Acid Provides Improvement of Psoriasis, *Dermatologica* 182, 225–230.
29. Negrescu, E.V., De Quintana, K.L., and Siess, W. (1995) Platelet Shape Change Induced by Thrombin Receptor Activation. Rapid Stimulation of Tyrosine Phosphorylation of Novel Protein Substrates Through an Integrin- and Ca(2+)-Independent Mechanism, *J. Biol. Chem.* 270, 1057–1061.
30. Sanders, T.A.B., and Hochland, M.C. (1983) A Comparison of the Influence on Plasma Lipids and Platelet Function of Supplements of ω 3 and ω 6 Polyunsaturated Fatty Acids, *Br. J. Nutr.* 50, 521–529.
31. von Schacky, C., Fischer, S., and Weber, P.C. (1985) Long-Term Effects of Dietary Marine ω-3 Fatty Acids upon Plasma and Cellular Lipids, Platelet Function, and Eicosanoid Formation in Humans, *J. Clin. Invest.* 76, 1626–1631.
32. Hirai, A., Terano, T., Makuta, H., Kobayashi, S., Makuta, H., Ozawa, A., Fujita, T., Tamura, Y., Kitagawa, H., Kumagai, A., and Yoshida, S. (1989) Effect of Oral Administration of Highly Purified Eicosapentaenoic Acid and Docosahexaenoic Acid on Platelet Function and Serum Lipids in Hyperlipidemic Patients, *Adv. Prostaglandin Thromboxane Leukot. Res.* 19, 627–630.
33. Lillioja, S., Young, A.A., Culter, C.L., Ivy, J.L., Abbott, W.G.H., Zawadzki, J.K., Yki-Järvinen, H., Christin, L., Secomb, T.W., and Bogardus, C. (1987) Skeletal Muscle Capillary Density and Fiber Type Are Possible Determinants of *in vivo* Insulin Resistance in Man, *J. Clin. Invest.* 80, 415–424.
34. Terano, T., Hirai, A., Hamazaki, T., Kobayashi, S., Fujita, T., Tamura, Y., and Kumagai, A. (1983) Effect of Oral Administration of Highly Purified Eicosapentaenoic Acid on Platelet Function, Blood Viscosity and Red Cell Deformability in Healthy Human Subjects, *Atherosclerosis* 46, 321–331.
35. Nelson, G.J., Schmidt, P.S., Bartolini, G.L., Kelley, D.S., and Kyle, D. (1997) The Effect of Dietary Docosahexaenoic Acid on Platelet Function, Platelet Fatty Acid Composition, and Blood Coagulation in Humans, *Lipids* 32, 1129–1136.
36. Driss, F., Vericel, E., Lagarde, M., Dechavanne, M., and Darcet, P. (1984) Inhibition of Platelet Aggregation and Thromboxane Synthesis After Intake of Small Amounts of Icosapentaenoic Acid, *Thromb. Res.* 36, 389–396.
37. Crosset, M., Guichardant, M., and Lagarde, M. (1988) Different Metabolic Behavior of Long-Chain n-3 Polyunsaturated Fatty Acids in Human Platelets, *Biochim. Biophys. Acta* 961, 262–269.
38. Dyerberg, J., Bang, H.O., Stoffersen, E., Moncada, S., and Vane, J.R. (1978) Eicosapentaenoic Acid and Prevention of Thrombosis and Atherosclerosis? *Lancet* 23, 117–119.
39. Parent, C.A., Lagarde, M., Venton, D.L., and Le Breton, G.C. (1992) Selective Modulation of the Human Platelet Thromboxane A<sub>2</sub>/Prostaglandin H<sub>2</sub> Receptor by Eicosapentaenoic and Docosahexaenoic Acids in Intact Platelets and Solubilized Platelet Membranes, *J. Biol. Chem.* 267, 6541–6547.
40. VanRollins, M. (1995) Epoxygenase Metabolites of Docosahexaenoic and Eicosapentaenoic Acids Inhibit Platelet Aggregation at Concentrations Below Those Affecting Thromboxane Synthesis, *J. Pharmacol. Exp. Ther.* 274, 798–804.
41. Yeo, Y.K., Philbrick, D.J., and Holub, B.J. (1989) The Effect of Long-Term Consumption of Fish Oil on Platelet-Activating Factor Synthesis in Rat Renal Microsomes, *Biochem. Biophys. Res. Comm.* 160, 1238–1242.
42. Knofler, R., Nakano, T., Nakajima, K., and Takada, A. (1995) Remnant-Like Lipoproteins Stimulate Whole Blood Platelet Aggregation *in vitro*, *Thromb. Res.* 78, 161–171.
43. Orth, M., Luley, C., and Wieland, H. (1995) Effects of VLDL, Chylomicrons, and Chylomicron Remnants on Platelet Aggregability, *Thromb. Res.* 79, 297–305.
44. Broijersen, A., Karpe, F., Hamsten, A., Goodall, A.H., and Hjendahl, P. (1998) Alimentary Lipemia Enhances the Membrane Expression of Platelet P-Selectin Without Affecting Other Markers of Platelet Activation, *Atherosclerosis* 137, 107–113.
45. Jakubowski, J.A., Ardlie, N.G., Chesterman, C.N., McGready, J.F., and Morgan, F.J. (1985) Acute Postprandial Lipaemia Does Not Influence the *in vivo* Activity of Human Platelets, *Thromb. Res.* 39, 725–732.
46. Hansen, K., Sickelmann, F., Pietrowsky, R., Fehm, H.L., and Born, J. (1997) Systemic Immune Changes Following Meal Intake in Humans, *Am. J. Physiol.* 273, R548–R553.
47. Nossel, H.L. (1977) Bleeding, in *Principles of Internal Medicine* (Thorn, G.W., Adams, R.D., Braunwald, E., Isselbacher, K.J., Petersdorf, R.G., eds.) 8th edn., pp. 294–301, McGraw-Hill Book Company, New York.

[Received February 26, 2002, and in revised form and accepted November 12, 2002]



# Effect of Exercise on FA Profiles in n-3 FA-Supplemented and -Nonsupplemented Premenopausal Women

Julie A. Conquer\*, Heather Roelfsema, Julie Zecevic, Terry E. Graham, and Bruce J. Holub

Department of Human Biology and Nutritional Sciences, University of Guelph, Guelph, Ontario, Canada, N1G 2W1

**ABSTRACT:** The purpose of this double-blind study was to investigate the influence of exercise on the FA profile of the non-esterified FA (NEFA) and phospholipid fractions in plasma of sedentary women supplemented with n-3 FA vs. women supplemented with oil containing no n-3 FA. Twenty sedentary, premenopausal women were randomly assigned to receive 12 capsules daily of either fish oil (3.5 g EPA and 2.4 g DHA per day, each as the ethyl ester) or evening primrose oil capsules (no detectable EPA or DHA). Each subject consumed the capsules for one menstrual cycle. At the end of the supplementation period, the sedentary subjects underwent an acute exercise trial [55% maximal oxygen consumption ( $\text{VO}_2$  max), 45 min] on a cycle ergometer. Two subjects in the fish oil group were removed from all calculations owing to noncompliance for reasons not related to side effects. There were no changes in the phospholipid composition of either group of women after exercise. In both control and fish oil-supplemented women, NEFA levels in general rose after exercise. There were no changes in the percentage of any given individual NEFA in either supplementation group. However, absolute levels of certain individual NEFA (16:0, 18:0, 18:1, and 18:3n-3) increased with exercise. Women supplemented with fish oil had increased levels of n-3 NEFA [EPA, DHA, and docosapentaenoic acid (DPA)] prior to exercise. Exercise did not, however, increase the absolute levels of n-3 NEFA in the blood.

Paper no. L8979 in *Lipids* 37, 947–951 (October 2002).

Circulating nonesterified FA (NEFA) are associated with risk for cardiovascular disease (CVD), and there is evidence they play a central role in coronary heart disease development (1). The release of NEFA from intra-abdominal fat cells has been implicated in the unfavorable metabolic profile among Asian Indians (2) and others (1). The mechanism by which elevated NEFA contribute to cardiovascular pathology is not clear; however, exposure to acutely elevated levels of NEFA can be deleterious to myocardial cell activity (3–5).

Although an elevated level of NEFA is associated with CVD risk, there is some evidence to suggest that not all NEFA may

be detrimental. Particular plasma NEFA may exhibit differing effects on thrombosis and myocardial functioning (1). For example, certain saturated NEFA, such as palmitate, have been implicated in both prothrombotic and arrhythmogenic actions (1,6), whereas opposite effects (antiplatelet aggregatory and anti-arrhythmic actions) have been indicated *in vitro* for DHA in its NEFA form (7–9). Furthermore, a decreased ratio of EPA/arachidonic acid (AA) as NEFA may be a coronary risk indicator (10).

Few studies have examined the effect of n-3 supplementation on NEFA levels and composition in humans. Studies have shown that supplementation with DHA, in the absence of EPA, provides a dose-dependent rise in DHA-NEFA concentrations (11) and the maximum DHA-NEFA is formed approximately 6 h after ingestion (12). With n-3 supplementation [including EPA, DHA, and docosapentaenoic acid (DPA)], an increase in EPA, DPA, and DHA was noted in the NEFA fraction (13). Furthermore, there was a decrease in AA- and linoleic acid-NEFA and an increase in the ratio of EPA-NEFA/AA-NEFA and DHA-NEFA/AA-NEFA. n-3 supplementation does not appear to change the levels of total NEFA (11,13). n-3 FA may be incorporated into the NEFA fraction directly (12) or indirectly after release from the adipose stores where it may be stored (14,15).

Exercise has been shown to increase the potential for arrhythmia and sudden cardiac death (16). At intensities of 55% maximal oxygen consumption ( $\text{VO}_2$  max), plasma NEFA are one of the major fuels oxidized by skeletal muscle (17,18). The rate of use depends on various factors including, among other parameters, plasma availability, exercise intensity, and exercise duration. The lipolysis of NEFA from adipose tissue, for use by the skeletal muscle, increases with exercise duration and intensity to about 60%  $\text{VO}_2$  max (19). In addition, there are increases in adipose tissue and muscle blood flow with exercise and decreases in fatty acid re-esterification (20). The relative use of FA from adipose tissue is dependent on the degree of fitness (20). Although there is little evidence to suggest exercise has any effect on the types of individual NEFA released from adipose, one study has suggested that prolonged moderate exercise (60%  $\text{VO}_2$  max) increases the ratio of unsaturated/saturated NEFA in serum (21).

In our study, it was of interest to examine whether acute exercise modifies serum phospholipid (PL) and NEFA compositions in n-3 FA supplemented premenopausal women.

Present address of first author: Human Nutraceutical Research Unit, University of Guelph, Guelph, ON, Canada N1G 2W1.

\*To whom correspondence should be addressed.

E-mail: jconquer@uoguelph.ca

Abbreviations: AA, arachidonic acid; CVD, cardiovascular disease; DPA, docosapentaenoic acid; EPO, evening primrose oil; MI, myocardial infarction; NEFA, nonesterified FA; PL, phospholipid;  $\text{VO}_2$  max, maximal oxygen consumption.

## EXPERIMENTAL PROCEDURES

**Subjects and experimental design.** The subjects were 20 healthy, nonexercising, nonhormone-using, premenopausal women (average menstrual cycle 25–35 d) selected from the Guelph community. Approval for this double-blind study was granted by the Human Ethics Committee of the University of Guelph and written informed consent was obtained from each subject. The 20 subjects (aged  $34.8 \pm 1.8$  yr, mean  $\pm$  SEM) were randomly assigned (10/group) into the two supplementation groups, fish oil-supplemented and control. The encapsulated ethyl ester fish oil concentrate (product #L3020, Ocean Nutrition Canada Ltd., Bedford, Nova Scotia) contained 60% total n-3 FA, including 30% EPA and 20% DHA. The encapsulated evening primrose control oil (EPO; Bioriginal Food & Science Corp., Saskatoon, Saskatchewan) contained 0% EPA and DHA. EPO was chosen as a placebo because of the absence of EPA and DHA, as well as its slight aftertaste. This aftertaste fools many subjects into thinking they are taking fish oil. The experimental group consumed 12 fish oil capsules per day (total 3.5 g EPA/d, 2.4 g DHA/d) with their meals, and the control group consumed 12 EPO placebo capsules per day for one menstrual cycle. To minimize the variations in blood lipids associated with the different phases of the menstrual cycle, each subject began the trial during the early follicular phase (day 3–8) of her menstrual cycle and completed the trial during the same phase of her subsequent menstrual cycle. Thus, the length of the supplementation period ( $29.4 \pm 1.2$  d) varied depending on the length of a given subject's menstrual cycle ( $27.4 \pm 0.8$  d). During the supplementation period, an incremental oxygen consumption test was performed using a cycle ergometer to determine each subject's  $\text{VO}_2$  max. At the end of the supplementation period, both groups took part in an acute exercise session (cycle ergometer; 55%  $\text{VO}_2$  max; 45 min). Subjects were weighed at the beginning and the end of the trial, and height was measured at entry; there were no significant differences in these or other characteristics between the groups at entry (Table 1). Furthermore, FA profiles in the PL and NEFA fractions of subjects at entry did not differ between groups (data not shown). The weight of the subjects in either group was not affected throughout the supplementation period. All dietary records (3 d) were analyzed by the Can West Diet Analysis-Plus program, which includes comparison with the Canadian Recommended Nutrient Intakes (West Publishing Co., St. Paul, MN). The amount of fat consumed in encapsulated form (12 g/d) represented <20% of the dietary fat intake. There were no differences between daily energy intakes (average of all subjects was 8025 kJ/d; data not shown) or intakes of saturated fat, cholesterol, monounsaturated fat, or polyunsaturated fat between the two groups. Compliance was monitored by determining the FA composition of serum PL and FFA at the beginning and end of the trial and from a capsule count at the end of the study. Two subjects in the fish oil-supplemented group were dropped from all further statistics (final  $n = 8$ ) because of noncompliance as determined by blood levels of n-3 FA.

**TABLE 1**  
Subject Characteristics and Estimated Dietary Intake During Placebo or Fish Oil Supplementation<sup>a</sup>

Variable	Placebo	Fish oil
Height (m)	1.7 $\pm$ 0.0	1.6 $\pm$ 0.0
Weight (kg)	75.9 $\pm$ 3.8	67.5 $\pm$ 3.1
BMI (kg/m <sup>2</sup> )	26.7 $\pm$ 1.5	25.8 $\pm$ 1.3
Energy (kJ)	8811.5 $\pm$ 616.6	7258.5 $\pm$ 518.6
Protein (% energy)	14.3 $\pm$ 1.4	15.1 $\pm$ 1.0
Fat (% energy)	33.5 $\pm$ 2.1	31.9 $\pm$ 2.5
Carbohydrate (% energy)	51.5 $\pm$ 2.6	52.2 $\pm$ 3.2
Alcohol (% energy)	0.52 $\pm$ 0.26	0.33 $\pm$ 0.24
Menstrual cycle length (d)	26.5 $\pm$ 1.1	27.6 $\pm$ 1.0

<sup>a</sup>Values are reported as mean  $\pm$  SEM,  $n = 10$  (placebo) and  $n = 8$  (fish oil). No significant differences between the groups were found for the above variables. BMI, body mass index.

**Blood collection.** Blood was collected when the subject was fasted, in the early follicular phase of the menstrual cycle, immediately before and within 5 min of the completion of the exercise session. Blood was collected by antecubital venipuncture, by a registered technologist, into siliconized tubes containing no anticoagulant.

Blood was allowed to coagulate at room temperature (~45 min) and was then centrifuged at  $1250 \times g$  for 15 min to obtain serum. Serum was used for the measurement of total PL and NEFA compositions. Serum was stored at  $-70^\circ\text{C}$  until all samples were collected and thawed just before analyses of lipids.

**Total phospholipid and NEFA analysis.** The composition of total PL and NEFA from serum was determined as follows. Lipid extraction was performed with the addition of a known amount of heptadecaenoic acid (17:0) and PC diheptadecanoyl (17:0 PC) as described by Folch *et al.* (22). The extract was spotted on silica gel G plates and developed in heptane/isopropyl ether/acetic acid (50:50:3). The PL band and NEFA bands, respectively, were removed and methylated with 2.0 mL of boron trichloride in methanol. GLC of the FAME was performed using a Varian 3800 gas chromatograph (Palo Alto, CA) with a 60-m DB-23 capillary column (0.32 mm internal diameter).

**Statistical analysis.** All data are reported as mean  $\pm$  SEM. When observations were missing, least-squared means were calculated so that means could be compared. The general linear models procedure was used in all analyses before examination of specific differences by Fisher's protected least significant differences. Dietary intakes and subject characteristics were compared by *t*-test. Statistical analyses were done using the SAS system (SAS Institute, Inc., Cary, NC). Changes within groups as well as comparisons between groups were considered.

## RESULTS AND DISCUSSION:

Exercise has been shown to increase the potential for arrhythmia and sudden cardiac death risk (16,23). In light of the potential cardioprotective role of n-3 NEFA (6,24) and the rise in n-3 NEFA with n-3 FA supplementation (11,13), this double-blind trial examined the effects of acute exercise on changes in

PL and NEFA composition and status in sedentary premenopausal women supplemented with n-3-containing fish oil or a control oil. To our knowledge, this is the first report examining the effect of acute exercise on NEFA composition of n-3-supplemented female subjects.

The FA compositions of serum total PL (control and fish oil-supplemented) before and after exercise are given in Table 2. The levels of the various FA prior to supplementation were similar between the two groups (data not shown). EPO (control) supplementation resulted in a decrease in 18:1 (−14.7%) and an increase in 20:3n-6 (24.2%) ( $P < 0.05$ ; data not shown). Fish oil supplementation also resulted in a decrease in 18:1 (−15.0%) as well as decreases in 18:2n-6 (−24.4%), 20:3n-6 (−41.4%), AA (−10.2%), 22:4n-6 (−48.7%), and the n-6/n-3 ratio (−68.2%). Also, in the fish oil-supplemented group, increases were noted in EPA (538% overall), DHA (94% overall), and DPA (50% overall) ( $P < 0.05$ ; data not shown). Exercise appeared to have little or no effect on serum PL values.

The FA compositions of serum NEFA (control and fish oil-supplemented) before and after exercise are given in Table 3. The levels of the various FA prior to supplementation were similar between the two groups (data not shown). EPO (control) supplementation resulted in slight but nonsignificant increases in 20:3n-6, 22:4n-6, and the n-6/n-3 ratio (data not shown). Fish oil supplementation resulted in marked increases in EPA (967% overall), DHA (241% overall), and DPA (313% overall) (data not shown). Exercise had no effect on serum NEFA composition in either the fish oil- or placebo-supplemented groups.

The effects of exercise on NEFA levels ( $\mu\text{M}$ ) are given in Table 4. Total NEFA levels did not change with fish oil supplementation or with control supplementation (data not shown). Although there was no effect of supplementation with placebo on individual NEFA levels, fish oil supplementation resulted in

increased NEFA levels of EPA, DPA, and DHA [0.65 (0.20) to 14.6 (8.7)  $\mu\text{M}$ ; 0.59 (0.22) to 2.3 (0.5)  $\mu\text{M}$ ; and 2.0 (0.4) to 11.0 (2.7)  $\mu\text{M}$ , respectively]. Exercise increased levels of total NEFA in both groups. Furthermore, exercise increased absolute levels of 16:0, 18:0, 18:1, 18:2n-6, and 18:3n-3 NEFA. Absolute levels of n-3 NEFA before exercise were higher in the n-3 supplemented women compared with the women supplemented with placebo. Exercise, however, did not increase absolute levels of n-3 NEFA in either group.

Fish oil supplementation (providing 3.6 g EPA and 2.4 g DHA per day for one menstrual cycle) resulted in dramatic increases in the EPA, DHA, and DPA content of the serum NEFA and PL within approximately 28 d. This increase in n-3 NEFA is in agreement with previous studies that have shown fish oils raise the EPA, DHA, and DPA concentration of serum NEFA after supplementation with algal-source DHA (11) or seal oil (13). Exercise has been shown to increase total serum NEFA concentrations and to influence the concentrations of individual NEFA (21). That EPA is the most mobilized FA in fasted rats (25,26) and rabbits (27) has also been shown. Thus, it was hypothesized that exercise would increase the mobilization of EPA and/or DHA from adipocytes in both n-3- and non-n-3-supplemented individuals. Absolute levels of total n-3 NEFA before (41.5  $\mu\text{M}$ ) and after (45.6  $\mu\text{M}$ ) exercise, and DHA-NEFA in particular (12.9 and 12.6  $\mu\text{M}$ , before and after exercise, respectively) in the n-3-supplemented individuals, may offer cardioprotection (8,10). For example DHA-NEFA at these levels has been shown to be antiarrhythmic and antithrombotic (7–9).

The consumption of fish oil containing 3.6 g/d EPA plus 2.4 g/d DHA readily increased the percentage and absolute levels of n-3 FA in serum NEFA and the percentage of n-3 FA in serum total PL in premenopausal women. An acute exercise session (55%  $\text{VO}_2$  max; 45 min) on a cycle ergometer appeared to have little effect on the composition of serum PL. Certain individual

**TABLE 2**  
FA Composition of Total Phospholipid in Human Serum Before and After Exercise<sup>a</sup>

FA	Placebo (wt%)		Fish oil (wt%)	
	Preexercise	Postexercise	Preexercise	Postexercise
16:0	26.3 ± 0.4	26.2 ± 0.3	26.7 ± 0.3	26.5 ± 0.3
18:0	14.2 ± 0.2	14.2 ± 0.2	14.0 ± 0.2	13.9 ± 0.2
18:1	9.3 ± 0.4	9.2 ± 0.4	9.1 ± 0.3	9.4 ± 0.4
18:2n-6	20.8 ± 0.9 <sup>a</sup>	20.5 ± 0.9 <sup>a</sup>	16.8 ± 1.2 <sup>b</sup>	16.5 ± 1.2 <sup>b</sup>
18:3n-3	0.20 ± 0.03	0.18 ± 0.02	0.18 ± 0.02	0.27 ± 0.09
20:3n-6	4.1 ± 0.2 <sup>a</sup>	4.2 ± 0.2 <sup>a</sup>	1.7 ± 0.2 <sup>b</sup>	1.7 ± 0.2 <sup>b</sup>
20:4n-6 (AA)	11.8 ± 0.3 <sup>a</sup>	12.0 ± 0.3 <sup>a</sup>	8.8 ± 0.3 <sup>b</sup>	8.8 ± 0.3 <sup>b</sup>
20:5n-3 (EPA)	0.95 ± 0.1 <sup>a</sup>	0.94 ± 0.3 <sup>a</sup>	6.12 ± 0.8 <sup>b</sup>	5.96 ± 0.7 <sup>b</sup>
22:4n-6	0.33 ± 0.02 <sup>a</sup>	0.34 ± 0.02 <sup>a</sup>	0.12 ± 0.01 <sup>b</sup>	0.12 ± 0.02 <sup>b</sup>
22:5n-6	0.01 ± 0.00 <sup>a</sup>	0.02 ± 0.00 <sup>b</sup>	0.0 ± 0.0 <sup>a</sup>	0.01 ± 0.00 <sup>a</sup>
22:5n-3	0.92 ± 0.05 <sup>a</sup>	0.94 ± 0.06 <sup>a</sup>	1.41 ± 0.10 <sup>b</sup>	1.43 ± 0.11 <sup>b</sup>
22:6n-3 (DHA)	3.3 ± 0.4 <sup>a</sup>	3.4 ± 0.4 <sup>a</sup>	6.6 ± 0.4 <sup>b</sup>	6.7 ± 0.4 <sup>b</sup>
n-6/n-3	7.5 ± 0.7 <sup>a</sup>	7.6 ± 0.7 <sup>a</sup>	2.1 ± 0.3 <sup>b</sup>	2.1 ± 0.3 <sup>b</sup>
EPA/AA	0.08 ± 0.02 <sup>a</sup>	0.08 ± 0.02 <sup>a</sup>	0.68 ± 0.08 <sup>b</sup>	0.67 ± 0.08 <sup>b</sup>
DHA/AA	0.28 ± 0.03 <sup>a</sup>	0.28 ± 0.03 <sup>a</sup>	0.75 ± 0.05 <sup>b</sup>	0.76 ± 0.05 <sup>b</sup>

<sup>a</sup>Values are reported as mean ± SEM,  $n = 10$  (placebo) and  $n = 8$  (fish oil). Differing superscripts in a row indicate statistically significant differences,  $P < 0.05$ . AA, arachidonic acid.

**TABLE 2**  
**FA Composition of Nonesterified FA (NEFA) in Human Serum Before and After Exercise<sup>a</sup>**

FA	Placebo (wt%)		Fish oil (wt%)	
	Preexercise	Postexercise	Preexercise	Postexercise
16:0	24.4 ± 1.0	24.1 ± 0.8	23.3 ± 1.1	23.0 ± 0.8
18:0	10.6 ± 0.9	8.9 ± 0.5	9.7 ± 1.0	8.6 ± 0.8
18:1	37.4 ± 1.6	38.6 ± 0.9	36.9 ± 1.8	39.0 ± 1.4
18:2n-6	17.2 ± 0.8	16.9 ± 0.6	17.1 ± 2.2	17.1 ± 1.5
18:3n-3	1.2 ± 0.1	1.6 ± 0.1	1.5 ± 0.2	1.4 ± 0.1
20:3n-6	0.26 ± 0.05 <sup>a</sup>	0.25 ± 0.03 <sup>a</sup>	0.14 ± 0.03 <sup>b</sup>	0.15 ± 0.03 <sup>b</sup>
20:4n-6 (AA)	1.7 ± 0.2	1.4 ± 0.1	1.7 ± 0.4	1.5 ± 0.3
20:5n-3 (EPA)	0.17 ± 0.09 <sup>a</sup>	0.12 ± 0.03 <sup>a</sup>	1.6 ± 0.6 <sup>b</sup>	1.3 ± 0.5 <sup>b</sup>
22:4n-6	0.04 ± 0.02	0.09 ± 0.03	0.04 ± 0.02	0.05 ± 0.02
22:5n-3	0.09 ± 0.04 <sup>a</sup>	0.16 ± 0.04 <sup>a,b</sup>	0.33 ± 0.05 <sup>c</sup>	0.29 ± 0.06 <sup>b,c</sup>
22:6n-3 (DHA)	0.36 ± 0.11 <sup>a</sup>	0.53 ± 0.12 <sup>a</sup>	1.67 ± 0.23 <sup>b</sup>	1.53 ± 0.23 <sup>b</sup>
n-6/n-3	10.2 ± 0.9 <sup>a</sup>	8.8 ± 1.3 <sup>a</sup>	3.9 ± 0.4 <sup>b</sup>	4.7 ± 0.4 <sup>b</sup>
EPA/AA	0.07 ± 0.10 <sup>a</sup>	0.09 ± 0.08 <sup>a</sup>	0.78 ± 0.35 <sup>b</sup>	0.78 ± 0.26 <sup>b</sup>
DHA/AA	0.20 ± 0.04 <sup>a</sup>	0.39 ± 0.07 <sup>a</sup>	1.19 ± 0.15 <sup>b</sup>	1.17 ± 0.16 <sup>b</sup>

<sup>a</sup>Values are reported as mean ± SEM,  $n = 10$  (placebo) and  $n = 8$  (fish oil). Differing superscripts in a row indicate statistically significant differences,  $P < 0.05$ . For abbreviation see Table 2.

**TABLE 4**  
**Absolute NEFA Levels in Human Serum Before and After Exercise<sup>a</sup>**

FA	Placebo ( $\mu\text{mol/L}$ )		Fish oil ( $\mu\text{mol/L}$ )	
	Preexercise	Postexercise	Preexercise	Postexercise
16:0	154.2 ± 12.7 <sup>a</sup>	201.7 ± 10.6 <sup>b</sup>	165.4 ± 17.5 <sup>a</sup>	230.1 ± 34.8 <sup>b</sup>
18:0	58.4 ± 3.8 <sup>a</sup>	66.5 ± 3.6 <sup>b</sup>	57.5 ± 3.3 <sup>a</sup>	71.0 ± 6.6 <sup>b</sup>
18:1	224.9 ± 30.5 <sup>a</sup>	298.5 ± 23.8 <sup>b</sup>	245.9 ± 40.8 <sup>a</sup>	372.5 ± 69.7 <sup>b</sup>
18:2n-6	103.8 ± 13.9	130.9 ± 10.7	143.7 ± 48.4	187.4 ± 48.4
18:3n-3	7.7 ± 1.5 <sup>a</sup>	12.6 ± 1.9 <sup>b</sup>	10.2 ± 1.7 <sup>a</sup>	14.4 ± 2.4 <sup>b</sup>
20:3n-6	1.5 ± 0.3	1.8 ± 0.2	1.1 ± 0.4	1.6 ± 0.4
20:4n-6 (AA)	9.3 ± 1.7	8.8 ± 1.2	15.3 ± 7.2	17.4 ± 6.0
20:5n-3 (EPA)	1.0 ± 0.7 <sup>a</sup>	0.9 ± 0.3 <sup>a</sup>	16.1 ± 9.7 <sup>b</sup>	16.0 ± 8.5 <sup>b</sup>
22:4n-6	0.2 ± 0.1	0.5 ± 0.1	0.3 ± 0.2	0.5 ± 0.2
22:5n-3	0.5 ± 0.2 <sup>a</sup>	1.1 ± 0.3 <sup>a</sup>	2.2 ± 0.4 <sup>b</sup>	2.7 ± 0.8 <sup>b</sup>
22:6n-3 (DHA)	2.1 ± 0.8 <sup>a</sup>	3.6 ± 0.8 <sup>a</sup>	12.9 ± 3.4 <sup>b</sup>	12.6 ± 2.9 <sup>b</sup>
Total n-3	11.3 ± 2.7 <sup>a</sup>	18.2 ± 2.7 <sup>a</sup>	41.5 ± 13.3 <sup>b</sup>	45.6 ± 13.4 <sup>b</sup>
Total n-6	116.9 ± 16.1	145.6 ± 11.2	173.3 ± 58.4	219.4 ± 57.0
Total NEFA	580.1 ± 63.8 <sup>a</sup>	753.2 ± 49.8 <sup>b</sup>	689.3 ± 114.0 <sup>a</sup>	955.9 ± 171.4 <sup>b</sup>

<sup>a</sup>Values are reported as mean ± SEM,  $n = 10$  (placebo) and  $n = 8$  (fish oil). Differing superscripts in a row indicate statistically significant differences,  $P < 0.05$ . For abbreviations see Tables 2 and 3.

NEFA, mainly saturated and monounsaturated NEFA, increased with exercise. n-3 and n-6 NEFA, in general, however, were not mobilized to a greater extent after exercise in individuals supplemented with fish oil for a period of approximately 4 wk. Future studies could examine the effects of longer exercise durations, the effect of aerobic exercise training, and the effect of a longer duration of fish oil supplementation in order to ascertain the impact of exercise on absolute NEFA levels and composition in n-3 FA-supplemented individuals.

#### ACKNOWLEDGMENTS

We gratefully acknowledge the assistance of Dr. Diana Philbrick as well as that of Patricia Swidinsky, Cindy McLean, Dr. Farah Thong,

Premila Sathasivam, and Margaret Berry. This study was funded by a grant from the Heart and Stroke Foundation of Ontario (BJH).

#### REFERENCES

1. Frayn, K.N., Williams, C.M., and Arner, P. (1996) Are Increased Plasma Nonesterified Fatty Acid Concentrations a Risk Marker for Coronary Heart Disease and Other Diseases? *Clin. Sci.* 90, 243–253.
2. Das, U.N. (1995) Essential Fatty Acid Metabolism in Patients with Essential Hypertension, Diabetes Mellitus and Coronary Heart Disease, *Prostaglandins Leukot. Essent. Fatty Acids* 52, 387–391.
3. Corr, P.B., Gross, R.W., and Sobel, B.E. (1982) Arrhythmogenic Amphiphilic Lipids and the Myocardial Cell Membrane, *J. Mol. Cell. Cardiol.* 14, 619–626.



4. Kelly, R.A., O'Hara, D.S., Mitch, W.E., and Smith, T.W. (1986) Identification of NaK-ATPase Inhibitors in Human Plasma as Non-esterified Fatty Acids and Lysophospholipids, *J. Biol. Chem.* 261, 11704–11711.
5. Jones, R.L., Miller, J.C., Hagler, H.K., Chien, K.R., Wilerson, J.T., Buja, L.M., Bellotto, D., Buja, D., Williams, P.K., and Yang, E. (1989) Association Between Inhibition of Arachidonic Acid Release and Prevention of Loading During ATP Depletion in Cultured Rat Cardiac Myocytes, *Am. J. Pathol.* 135, 541–556.
6. Makiguchi, M., Kawaguchi, H., Tamura, M., and Yasuda, H. (1991) Effect of Palmitic Acid and Fatty Acid Binding Protein on Ventricular Fibrillation in the Perfused Rat Heart, *Cardiovasc. Drugs Ther.* 5, 753–761.
7. Gaudette, D.C., and Holub, B.J. (1991) Docosahexaenoic Acid (DHA) and Human Platelet Reactivity, *J. Nutr. Biochem.* 2, 116–121.
8. Kang, J.X., and Leaf, A. (1996) The Cardiac Anti-arrhythmic Effects of Polyunsaturated Fatty Acid, *Lipids* 31, S41–S44.
9. Krämer, H.J., Stevens, J., Grimminger, F., and Seeger, W. (1996) Fish Oil Fatty Acids and Human Platelets: Dose Dependent Decrease in Dienoic and Increase in Trienoic Thromboxane Generation, *Biochem. Pharmacol.* 52, 1211–1217.
10. Kondo, T., Ogawa K., Satake, T., Kitazawa, M., Taki, K., Sugiyama, S., and Ozawa, T. (1986) Plasma-Free Eicosapentaenoic Acid/Arachidonic Acid Ratio: A Possible New Coronary Risk Factor, *Clin. Cardiol.* 9, 413–416.
11. Conquer, J.A., and Holub, B.J., (1998) Effect of Supplementation with Different Doses of DHA on the Levels of Circulating DHA as Non-esterified Fatty Acid in Subjects of Asian Indian Background, *J. Lipid Res.* 39, 286–292.
12. Lemaitre-Delaunay, D., Pachiardi, C., Laville, M., Pousin, J., Armstrong, M., and Lagard, M. (1999) Blood Compartmental Metabolism of Docosahexaenoic Acid (DHA) in Humans After Ingestion of a Single Dose of [(13)C] DHA in Phosphatidylcholine, *J. Lipid Res.* 10, 1867–1874.
13. Conquer, J.A., Cheryk, L.A., Chan, E., Gentry, P.A., and Holub, B.J. (1999) Effect of Supplementation with Dietary Seal Oil on Selected Cardiovascular Risk Factors and Hemostatic Variables in Healthy Male Subjects, *Throm. Res.* 96, 239–250.
14. Leaf, D.A., Connor, W.E., Carstad, L., and Sexton, G. (1995) Incorporation of Dietary n-3 Fatty Acids into the Fatty Acids of Human Adipose Tissue and Plasma Lipid Classes, *Am. J. Clin. Nutr.* 62, 68–73.
15. Lin, D.S., and Connor, W.E. (1990) Are the n-3 Fatty Acids from Dietary Fish Oil Deposited in the Triglyceride Stores of Adipose Tissue? *Am. J. Clin. Nutr.* 51, 535–539.
16. Franklin, B.A., Fletcher, G.F., Gordon, N.F., Noakes, T.D., Ades, P.A., and Balady, G.J. (1997) Cardiovascular Evaluation of the Athlete. Issues Regarding Performance, Screening and Sudden Cardiac Death, *Sports Med.* 24, 97–119.
17. Coyle, E.F. (2000) Physical Activity as a Metabolic Stressor, *Am. J. Clin. Nutr.* 72, 512S–520S.
18. Romijn, J.A., Coyle, E.F., Sidossis, L.S., Rosenblatt, J., and Wolfe, R.R. (2000) Substrate Metabolism During Different Exercise Intensities in Endurance-Trained Women, *J. Appl. Physiol.* 88, 1707–1714.
19. Turcotte, L.P. (1999) Role of Fats in Exercise, *Clin. Sports Med.* 18, 485–498.
20. Horowitz, J.F., and Klein, S. (2000) Lipid Metabolism During Endurance Exercise, *Am. J. Clin. Nutr.* 72, 558S–563S.
21. Mougios, V., Kouidi, E., Kyparos, A., and Deligiannis, A. (1998) Effect of Exercise on the Proportion of Unsaturated Fatty Acids in Serum of Untrained Middle-Aged Individuals, *Br. J. Sports Med.* 32, 58–62.
22. Folch, J., Lees, M., and Sloane-Stanley, G.H. (1957) A Simple Method for the Isolation and Purification of Total Lipids from Animal Tissues, *J. Biol. Chem.* 226:497–509.
23. Siscovick, D.S. (1997) Exercise and Its Role in Sudden Cardiac Death, *Cardiol. Clin.* 15, 467–472.
24. Kanayasu-Toyoda, T., Morita, I., and Murota, S. (1996) Docosapentaenoic Acid (22:5, n-3), an Elongation Metabolite of Eicosapentaenoic Acid (20:5, n-3), Is a Potent Stimulator of Endothelial Cell Migration on Pretreatment *in vitro*, *Prostaglandins Leukot. Essent. Fatty Acids.* 54, 39–45.
25. Herzberg, G.R., Skinner, C., and Levy, R. (1996) Eicosapentaenoic Acid Is Oxidized More Rapidly than Docosahexaenoic Acid by Muscle and Liver, *Nutr. Res.* 16, 639–644.
26. Herzberg, G.R., and Farrell, B. (2000) Selective Mobilization of Fatty Acids from Skeletal Muscle Triacylglycerol, Canadian Federation of Biological Societies 43rd Annual Meeting, F097 (abstract).
27. Conner, W.E., Lin, D.S., and Colvis, C. (1996) Differential Mobilization of Fatty Acids from Adipose Tissue, *J. Lipid Res.* 37, 290–298.

[Received January 7, 2002; and in revised form October 31, 2002; accepted November 4, 2002]

# Long-Chain PUFA Supplementation Improves PUFA Profile in Infants with Cholestasis

Piotr Socha<sup>a,\*</sup>, Berthold Koletzko<sup>b</sup>, Irena Jankowska<sup>a</sup>, Joanna Pawłowska<sup>a</sup>,  
Hans Demmelmair<sup>b</sup>, Anna Stolarczyk<sup>a</sup>, Elzbieta Świątkowska<sup>a</sup>, and Jerzy Socha<sup>a</sup>

<sup>a</sup>Department of Gastroenterology, Hepatology and Nutrition, The Children's Memorial Health Institute, Warszawa, Poland, and <sup>b</sup>Department of Pediatrics, Ludwig-Maximilians-University, Muenchen, Germany

**ABSTRACT:** Long-chain PUFA (LCP) deficiency is a frequent complication in cholestatic infants. We investigated the effects of LCP-supplemented formula on EFA status in infants with cholestasis. Twenty-three infants with cholestasis (biliary atresia after surgery, 8; intrahepatic cholestasis, 15) aged 1.9 to 4.9 mon (median 3.1 mon) were randomized to receive commercial infant formulas either without LCP or with LCP from egg phospholipids for 1 mon. Liver tests, nutrient intakes, and plasma phospholipid FA (%w/w) were determined at baseline and after intervention. At baseline, patients had high serum direct bilirubin levels ( $5.9 \pm 3.0$  mg/dL; mean  $\pm$  SD), they were malnourished (body fat mass:  $40 \pm 13\%$  of normal) and presented with PUFA deficiency [plasma phospholipid PUFA: 28.43%w/w (26.56–30.53) in patients vs. 37.02%w/w (34.53–39.58) in controls; median (1st–3rd quartile)] with elevated Mead acid and palmitoleic acid. LCP-supplemented ( $n = 11$ ) and -nonsupplemented groups ( $n = 12$ ) did not differ in age, indicators of liver function, and EFA status at baseline. After the intervention, LCP-supplemented infants had higher levels of arachidonic acid [7.2 (5.9–8.8) vs. 4.2 (3.0–5.3) %w/w;  $P < 0.001$ ] and DHA [2.8 (2.2–3.2) vs. 1.6 (1.0–2.1) %w/w;  $P < 0.05$ ], accompanied by increased TBARS concentration: 1.9 (1.4–2.2) vs. 1.3 (1.1–1.6) nmol/mL;  $P < 0.05$ ]. We concluded that LCP-supplemented formulae improve LCP status of infants with severe cholestasis but may enhance lipid peroxidation.

Paper no. L9021 in *Lipids* 37, 953–957 (October 2002).

Infants and children with cholestatic liver disease often develop PUFA deficiency (1–3), which is related to both nutritional (1) and metabolic (2) factors. Since PUFA deficiency may develop early in cholestatic infants, dietary intervention may be needed to prevent functional consequences for growth (4,5) and neurodevelopment (6–8). Indeed, cholestatic children usually present with growth failure, malnutrition, and neural disturbances that have been related to deficiencies of various nutrients, including vitamin E (9). An improvement in long-chain PUFA (LCP) status by supplementation with

the precursor PUFA, linoleic acid (LA) and  $\alpha$ -linolenic acid (ALA), may not be sufficient because the conversion EFA to their long-chain derivatives seems to be impaired in cholestasis, presumably owing to hepatocyte injury (2). As an alternative approach, LCP supplementation may be considered in these patients. In this study we assessed the supplementation of infants with cholestasis with arachidonic acid (AA) and DHA in a randomized placebo-controlled trial.

## PATIENTS AND METHODS

We studied 23 infants with cholestasis (8: biliary atresia after surgery; 15: intrahepatic cholestasis, among them two with Progressive Familial Intrahepatic Cholestasis and five with cytomegalovirus infection) aged 1.9 to 4.9 mon (median 3.1 mon) treated at the Children's Memorial Health Institute. We included in the study infants who had not been breast-fed for at least 4 wk before the study started. The patients with biliary atresia were included in the study 2 wk after hepatoportocentrostomy. All children were Caucasians, only eight infants were breast-fed before entering the study (1–6 wk), eight children were born premature; the birth weight was  $2.8 \pm 0.6$  kg ( $n = 23$ ). All children studied were routinely supplemented with a lipid preparation of  $\alpha$ -tocopherol (Vitaminum E, drops; Synteza, Poznań, Poland) in a daily dose of 75 mg  $\alpha$ -tocopherol. As a reference group, we investigated 12 infants in good general health with normal weight and length, aged 1 to 11 mon (median age 5 mon) as previously described (1). The study protocol was approved by the local ethical committee, and parental written informed consent was obtained.

Cholestatic infants were randomized to receive commercial infant formulas either without LCP (Aptamil; Milupa, Friedrichsdorf, Germany) or with LCP from fractionated egg phospholipids (Aptamil with Milupan) for 1 mon. The PUFA contents of the formulas were as follows: Aptamil 1—LA 13.5%, ALA 0.55%; Aptamil with Milupan—LA 10.2–12.5%, ALA 1.2–1.5%, AA 0.3–0.4%, DHA 0.04%. Since body weight is not a reliable indicator of nutritional status in liver disease (10), we based clinical assessment of nutritional status on midarm skinfold thickness measurements with a standard caliper (Holtain Tonner/Cohirehouse caliper, A. Winter Machinery Ltd., Rapperswill, Switzerland) and arm circumference

\*To whom correspondence should be addressed at The Children's Memorial Health Institute, Department of Gastroenterology, Hepatology and Nutrition, Al. Dzieci Polskich 20, 04-736 Warszawa, Poland.  
E-mail: sochap@czd.waw.pl

Abbreviations: AA, arachidonic acid; ALA,  $\alpha$ -linolenic acid; ALAT, alanine aminotransferase; FBM, fat body mass;  $\gamma$ -GT,  $\gamma$ -glutamyl transpeptidase; LA, linoleic acid; LBM, lean body mass; LCP, long-chain PUFA; PL, phospholipids.

at baseline. Based on these parameters, we calculated lean body mass (LBM) and fat body mass (FBM) according to the following formulae (11):

$$\text{LBM (\%)} = \frac{[10 \times (\text{arm circumference}) - \pi \times (\text{skinfold thickness})]^2}{4 \times \pi} \quad [1]$$

$$\text{FBM (\%)} = \frac{[10 \times (\text{arm circumference})]^2}{4 \times \pi - (\text{LBM})} \quad [2]$$

Both LBM and FBM were expressed as a percentage of the mean normal value for age (12). At baseline and after 1 mon of treatment, we assessed nutrient intakes and liver function as well as FA composition of plasma phospholipids (PL). Intakes of energy, lipids, carbohydrates, proteins, and LA were calculated from 24-h recall protocols supplemented with a checklist of foods usually consumed at this age. The calculation was done with the Polish nutritional value database "Food 2" (Food and Nutrition Institute 1998, Warszawa, Poland). Venous blood was obtained at baseline and after a month from fasted liver patients. Serum was obtained for the measurement of total and direct bilirubin; activities of alanine aminotransferase (ALAT) and  $\gamma$ -glutamyl transpeptidase ( $\gamma$ -GT); prothrombin time; total serum bile acids, serum TG, cholesterol, and PL concentrations. Serum concentrations of retinol and  $\alpha$ -tocopherol were measured by HPLC (13).

Venous plasma was obtained with sodium EDTA (1 mg/mL) as anticoagulant and stored at  $-20^\circ\text{C}$  until analysis of the FA composition of plasma PL. Lipids were extracted from 0.5 mL plasma with chloroform/methanol, and lipid classes were separated by TLC as previously described (14). FA were transesterified with methanol and hydrochloric acid and analyzed by high-resolution capillary GLC using a Hewlett-Packard Series II 5890 gas chromatograph with split/splitless injection and FID (SGE column 60QC3/BPX70, Melbourne, Australia; column diameter 0.32 mm; column head pressure 1.5 bar; oven temperature initially  $150^\circ\text{C}$ , temperature rise by  $3^\circ\text{C}/\text{min}$  up to  $180^\circ\text{C}$ , then temperature rise by  $4^\circ\text{C}/\text{min}$  up to  $200^\circ\text{C}$ , rise by  $1^\circ\text{C}/\text{min}$  up to  $210^\circ\text{C}$ , isothermal period for 20 min). Peak identification was

verified by comparison with authentic standards (Nu-Chek-Prep. Inc., Elysian, MN; Sigma, Deisenhofen, Germany). Results are expressed as percentage (%w/w) of all FA detected having a chain length between 12 and 24 carbon atoms (15). Plasma lipid peroxides were determined with the spectrofluorometric method of Yagi (16,17) and expressed as TBARS (nmol/mL) in cholestatic patients and in 12 age-matched controls.

Results were evaluated with Statistica for Windows release 5.0 (Statsoft, Inc., Tulsa, OK). We present the data as medians with lower and upper quartiles (1st–3rd). For comparison of FA profiles, biochemical tests, and nutrient intakes in different groups, Mann-Whitney's two-sided rank test was used. The treatment effects in the same group of patients were evaluated with the Wilcoxon matched-pairs test. Differences were regarded as statistically significant at  $P < 0.05$ .

## RESULTS

At the entry to the study, the 23 patients presented with markedly elevated bilirubin levels and serum bile acids, reflecting severe cholestasis (Table 1). Severe malnutrition with an extremely low FBM was found in spite of a relatively high intake of energy, protein, and fat (Table 2). TBARS as indicators of lipid peroxidation were significantly increased relative to levels in healthy age-matched controls [1.9 (1.6–2.5) vs. 0.9 (0.7–1.0) nmol/mL]. The cholestatic patients presented with a poor PUFA status, which was mainly due to the low plasma PL levels of the precursor EFA LA (18:2n-6) and its metabolite AA (20:4n-6) (Table 3). The supplemented and placebo groups did not differ at baseline in biochemical tests (Table 1), nutritional status (Table 2), FA status (Fig. 1), and nutrient intakes except for a lower fat intake in the LCP-supplemented group (Table 2).

After the intervention, nutrient intakes of nutrients were also similar in both groups (Table 2). Bilirubin and bile acid levels decreased during the course of the study. After 1 mon, the LCP-supplemented children had significantly higher levels of LA, its metabolite AA, and DHA than the placebo

**TABLE 1**  
Clinical Chemistry in Children Supplemented with LCP and in the Placebo Group at Baseline and After 1 mon of Treatment

Parameter	At baseline		After 1 mon		Reference values
	Placebo	LCP sup.	Placebo	LCP sup.	
Total bilirubin (mg/dL)	5.7 (3.9–8.5)	6.6 (3.6–10.2)	1.4 (1.2–3.5)	1.1 (1.0–4.1)	<1
Direct bilirubin (mg/dL)	4.9 (3.0–7.3)	5.7 (3.4–8.6)	1.1 (0.5–2.9)	0.5 (0.0–4.0)	Undetectable
ALAT (IU)	86 (48–112)	108 (64–132)	62 (43–101)	81 (64–108)	8–20
$\gamma$ -GT (IU)	217 (102–519)	277 (122–539)	185 (61–291)	345 (328–774) <sup>a</sup>	9–50
Prothrombin index	1.1 (1.0–1.2)	1.1 (1.0–1.2)	1.1 (1.0–1.2)	1.0 (1.0–1.1)	0.8–1.2
Total bile acids ( $\mu\text{mol/L}$ )	145 (79–165)	130 (118–159)	30 (23–82)	40 (8–111)	<6
TG (g/L)	0.9 (0.8–1.1)	1.0 (0.9–1.4)	0.9 (0.8–1.3)	1.1 (0.7–1.6)	0.34–1.25
Cholesterol (g/L)	1.8 (1.5–2.1)	1.7 (1.3–2.2)	1.4 (1.3–1.9)	1.8 (1.6–2.4)	1.2–2.0
Phospholipids (g/L)	2.6 (2.4–2.8)	2.5 (2.1–2.8)	2.2 (1.9–3.1)	2.7 (2.4–3.1)	1.8–2.95
$\alpha$ -Tocopherol (mg/L)	2.5 (1.8–3.7)	2.0 (1.4–6.7)	1.9 (1.4–6.3)	4.3 (3.4–10.9)	3.8–16
TBARS (nmol/mL)	1.8 (1.5–2.3)	1.9 (1.7–3.1)	1.3 (1.1–1.6)	1.9 (1.4–2.2) <sup>a</sup>	

<sup>a</sup> $P < 0.05$ , LCP-supplemented group vs. placebo group (at baseline and after 1 mon of treatment). Data represent medians with lower and upper quartiles (1st–3rd). LCP, long-chain PUFA; LCP sup., LCP-supplemented; ALAT, alanine aminotransferase;  $\gamma$ -GT,  $\gamma$ -glutamyl transpeptidase.

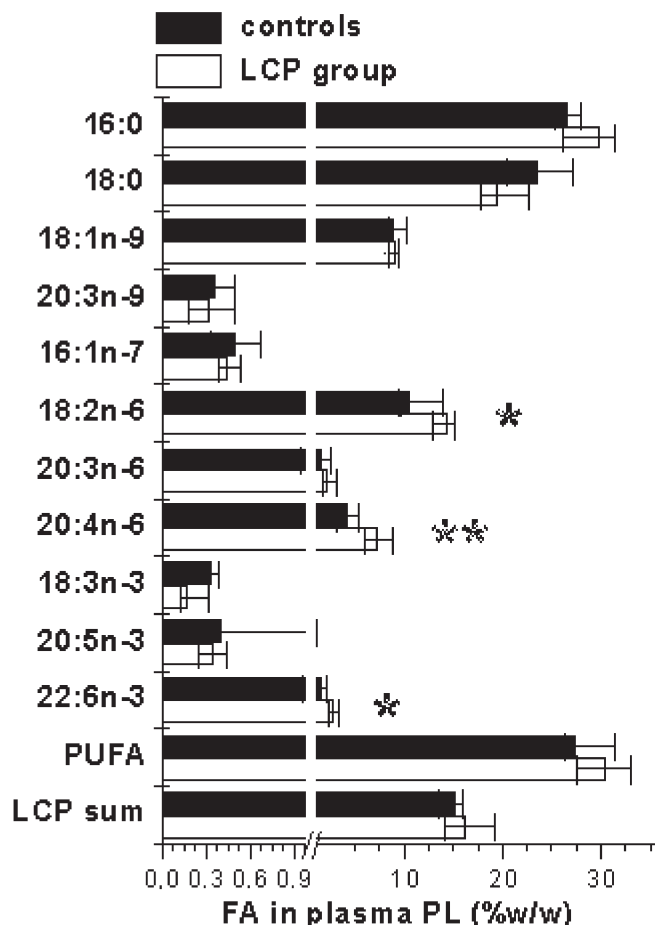
**TABLE 2**  
Nutrition and Nutritional Status in Children Supplemented with LCP and in the Placebo Group at Baseline and After 1 mon of Treatment

Parameter	At baseline		After 1 mon	
	Placebo	LCP sup.	Placebo	LCP sup.
Energy intake (kcal/kg)	127 (87–136)	110 (84–114)	119 (100–133)	114 (98–124)
Protein intake (g/kg)	3.4 (2.5–4.2)	3.2 (2.7–3.9)	2.8 (2.1–3.2)	2.5 (2.2–2.8)
Carbohydrate intake (g/kg)	14.5 (9.7–17.7)	13.6 (8.3–14.4)	13.9 (12.7–15.2)	12.3 (10.9–13.3)
Lipid intake (g/kg)	5.5 (4.8–6.5)	4.4 (3.1–5.3) <sup>a</sup>	6.3 (4.3–7.1)	6.0 (5.2–6.5)
Linoleic acid (mg/kg)	1.3 (0.9–1.4)	0.9 (0.6–1.2)	0.8 (0.7–1.0)	0.7 (0.6–0.9)
Weight (kg)	4.4 (4.0–6.1)	3.7 (3.0–4.2)		
Height (m)	0.56 (0.52–0.59)	0.52 (0.48–0.59)		
Lean body mass (% of mean normal value)	83 (77–93)	85 (75–97)		
Fat body mass (% of mean normal value)	41 (25–54)	38 (29–48)		

<sup>a</sup> $P < 0.05$ , LCP-supplemented group vs. placebo group (at baseline and after 1 mon of treatment). Data represent medians with lower and upper quartiles (1st–3rd). For abbreviation see Table 1.

group (Fig. 1). Total PUFA, AA, DHA, and total LCP increased significantly ( $P < 0.05$  for all parameters) in the LCP-supplemented group with the intervention, whereas LA and ALA remained unchanged. In contrast, there was no change of PUFA levels in the placebo group over time. After 1 mon of intervention, the LCP-supplemented group still had lower LA values than healthy controls ( $P < 0.001$ ), but AA and

DHA values had reached the levels of healthy infants. At the end of the study the placebo and LCP-supplemented groups did not differ in biochemical indicators of liver function, except for a higher  $\gamma$ -GT in LCP-supplemented infants. TBARS concentrations were higher in the LCP-supplemented group than in the placebo group (Table 1).



**FIG. 1.** Plasma phospholipid (PL) FA composition (%w/w) medians (1st–3rd quartiles) in the long-chain PUFA (LCP)-supplemented infants and in the placebo group after 1 mon of treatment. \* $P < 0.05$ ; \*\* $P < 0.001$ , LCP-supplemented group vs. controls.

**TABLE 3**  
Comparison of FA Profile in Plasma PL of Cholestatic Infants and the Reference Group [median (1st–3rd quartiles), %w/w]

FA	Cholestatic infants (n = 23)	Reference group (n = 12)
Saturated FA		
16:0	28.6 (25.8–31.5)	28.0 (27.0–28.5)
17:0	0.54 (0.44–0.78)	0.45 (0.33–0.51)
18:0	20.2 (18.1–24.3) <sup>b</sup>	14.78 (13.44–15.65)
20:0	0.68 (0.61–0.80)	0.69 (0.61–0.90)
22:0	1.26 (1.07–1.40)	1.33 (1.16–1.73)
n-9 FA		
18:1n-9	8.4 (7.5–10.7) <sup>a</sup>	11.7 (10.1–12.5)
20:1n-9	0.24 (0.16–0.39)	0.31 (0.22–0.39)
20:3n-9	0.48 (0.31–0.87) <sup>b</sup>	0.21 (0.17–0.26)
n-6 FA		
n-6 LCP	11.14 (10.11–12.75)	12.48 (11.47–14.43)
18:2n-6	13.72 (12.30–15.11) <sup>b</sup>	20.75 (18.82–22.85)
20:3n-6	2.49 (1.68–3.31)	2.16 (1.92–3.05)
20:4n-6	5.88 (4.20–6.93) <sup>b</sup>	7.87 (6.83–10.67)
n-3 FA		
n-3 LCP	2.38 (1.58–3.12) <sup>a</sup>	3.17 (2.83–3.73)
18:3n-3	0.25 (0.12–0.30)	0.17 (0.13–0.19)
20:5n-3	0.32 (0.27–0.42)	0.31 (0.24–0.53)
22:5n-3	0.35 (0.30–0.51) <sup>b</sup>	0.73 (0.56–0.98)
22:6n-3	1.48 (1.06–2.23)	2.08 (1.46–2.56)
n-7 FA		
16:1n-7	0.60 (0.03–1.00) <sup>a</sup>	0.43 (0.33–0.59)
18:1n-7	1.84 (1.27–2.43) <sup>a</sup>	1.70 (1.44–2.25)
PUFA	28.43 (26.56–30.53) <sup>b</sup>	37.02 (34.53–39.58)
LCP	13.82 (12.44–15.13)	15.66 (14.82–17.75)
LA/ALA	53.92 (39.36–112.68) <sup>a</sup>	115.18 (102.55–167.28)
LCP n-6/n-3	4.34 (3.84–6.55)	3.88 (3.45–4.42)
AA/LA	0.40 (0.29–0.49)	0.37 (0.32–0.53)
DHA/ALA	7.18 (4.15–14.00)	12.55 (7.59–16.98)

<sup>a</sup> $P < 0.05$ .

<sup>b</sup> $P < 0.001$ , patients vs. controls. PL, phospholipid; LA, linoleic acid; LCP, long-chain PUFA; ALA,  $\alpha$ -linolenic acid; AA, arachidonic acid; for other abbreviation see Table 1.



## DISCUSSION

The results presented here confirm a high risk of PUFA deficiency in young infants with cholestatic liver disease (1). Increased values of palmitoleic and Mead acids indicate the presence of PUFA deficiency in this patient population (18). The triene/tetraene ratio was not analyzed, as it is not a good indicator of PUFA deficiency in cholestasis where the decline in desaturase/elongase activity affects synthesis of both AA and Mead acid (2). The most prominent deficiencies we found were in LA and AA, whereas DHA only tended to be lower in cholestatic children. This supports the concept that both AA and DHA should be supplemented in cholestasis.

The dietary supply of PUFA, energy, and presumably of other substrates may affect PUFA status. The patients studied here showed relatively high intakes of energy and macronutrients compared to the usual consumption of healthy infants. The macronutrient intake did not change significantly over time (Table 2). However, the achieved mean caloric intake appears not to have met the high energy requirements in cholestasis of infancy, which may be well above 150 kcal/kg/d (19,20). A negative energy balance may result in enhanced oxidation of PUFA to provide energy and thus contribute to the development of PUFA deficiency. The patients presented with malnutrition, as expressed especially by low FBM, which points to short-term malnutrition. Body weight can be affected by edema, ascites, and hepatosplenomegaly. Height is more reliable, but it indicates chronic malnutrition. Skinfold thickness and arm circumference are considered to be more accurate measurements (10). A poor nutritional status may well be accompanied by a preferential utilization of nutrients as an energy source. Moreover, poor availability of antioxidants such as vitamin E may induce enhanced PUFA peroxidation and thereby also contribute to PUFA depletion (1–3). Even if the children had been treated with  $\alpha$ -tocopherol, the concentrations of vitamin E in serum tended to be low from the beginning to the end of the study. However, in a previous intervention study in another population of children with chronic cholestasis we did not find any effect of improving vitamin E status on lipid peroxidation *in vivo* and on PUFA levels (3).

At baseline, the supplemented and the placebo groups did not differ in FA status, liver parameters, nutritional status, and nutrient intakes except for a lower fat intake in the LCP-supplemented children. AA and DHA levels in the LCP-supplemented group at study's end were similar to those in healthy controls and indicated a good metabolic efficacy of the LCP-supplemented formula in the cholestatic infants. An early dietary intervention to normalize the EFA status may be very important in view of the rapid brain growth and development in early life. A number of studies performed in healthy term infants found LCP depletion with feeding of conventional infant formula without preformed LCP relative to breast-feeding or feeding LCP-supplemented formula (6–8). Some studies have related the dietary supply of preformed LCP, either with human milk or with LCP-containing formula, to im-

proved results for measures of visual acuity and neural development in healthy preterm and term infants (6–8,21–23), indicating that LCP may be conditionally essential substrates in early infancy. Cholestatic infants are at risk for neurological handicaps (9,23), which have been related in part to vitamin E deficiency (23). It is conceivable that poor availability of PUFA also could contribute to the poor growth and neurological development of cholestatic infants.

LCP are prone to lipid peroxidation owing to free radical injury. Indeed, LCP-supplemented children showed higher plasma concentrations of TBARS, indicating enhanced lipid peroxidation, than controls. The similar effect of LCP supplementation was demonstrated in healthy individuals (24), and children with cholestasis seem to be extremely vulnerable to free radical damage. Increased lipid peroxidation in children with cholestasis was shown in several studies (1–3,25), but the clinical significance of this finding remains unknown. Adequate supplementation of vitamin E and potentially other antioxidants also should be tested in children with cholestasis receiving an extra LCP supply. Moreover, the potential clinical benefits of LCP supplementation in this critical patient population need to be investigated further. We can expect that disturbances of visual function may occur in cholestatic infants although one study did not confirm this (26).

Results of the liver tests improved during the study, which reflect transient cholestasis in some subjects and improvement of bile flow in the others (e.g., biliary atresia after hepatoportoenterostomy). Still, the main factor that influenced FA status was LCP supplementation, which is indicated by higher LCP levels in the supplemented group in this randomized study. Regarding the critical period of central nervous system development in early life, LCP supplements should be considered in early infancy even if the diagnosis of cholestasis is not well established. The positive finding of our study was the relatively good absorption of LCP supplements as indicated by rising AA and DHA levels. Still, we can regard PUFA absorption in cholestatic children to be less effective than in healthy infants.

## ACKNOWLEDGMENTS

The study was supported by the Milupa company. We would like to thank Ewa Skorupa for her essential support in the laboratory work.

## REFERENCES

1. Socha, P., Koletzko, B., Świątkowska, E., Pawłowska, J., Stolarczyk, A., and Socha, J. (1998) Essential Fatty Acid Metabolism in Infants with Cholestasis, *Acta Paediatr.* 87, 278–283.
2. Socha, P., Koletzko, B., Pawłowska, P., and Socha, J. (1997) Essential Fatty Acid Status in Children with Cholestasis, in Relation to Serum Bilirubin Concentration, *J. Pediatr.* 131, 700–706.
3. Socha, P., Koletzko, B., Pawłowska, J., Prószyńska, K., and Socha, J. (1997) Treatment of Cholestatic Children with Water Soluble Vitamin E ( $\alpha$ -tocopheryl polyethylene glycol succinate): Effects on Serum Vitamin E, Lipid Peroxides and Polyunsaturated Fatty Acids, *J. Pediatr. Gastroenterol. Nutr.* 24, 189–193.
4. Koletzko, B., and Braun, M. (1991) Arachidonic Acid in Early

- Human Growth: Is There a Relation? *Ann. Nutr. Metab.* 35, S.128–S.131.
5. Carlson, S.E., Werkman, S.H., Peeples, J.M., Cooke, R.J., and Tolley, E.A. (1993) Arachidonic Acid Status Correlates with First Year Growth in Preterm Infants, *Proc. Natl. Acad. Sci. USA* 90, 1073–1077.
  6. Makrides, M., Neumann, M., Simmer, K., Pater, J., and Gibson, R. (1995) Are Long-Chain Polyunsaturated Fatty Acids Essential Nutrients in Infancy? *Lancet* 345, 1463–1468.
  7. Hoffman, D.R., Birch, E.E., Birch, D.G., Uauy, R., Castaneda, Y.S., Lapus, M.G., and Wheaton, D.H. (2000) Impact of Early Dietary Intake and Blood Composition of Long-Chain Polyunsaturated Fatty Acids on Later Visual Development, *J. Pediatr. Gastroenterol. Nutr.* 31, 540–553.
  8. Willatts, P., Forsyth, J.S., DiModugno, M.K., Varma, S., and Colvin, M. (1998) Effect of Long-Chain Polyunsaturated Fatty Acids in Infant Formula on Problem Solving at 10 Months of Age, *Lancet* 352, 688–691.
  9. Sokol, R.J., Butler-Simon, N., Conner, C., Heubi, J.E., Sinatra, F.R., Suchy, F.J., Heyman, M.B., Perrault, J., Rothbaum, R.J., and Levy, J. (1993) Multicenter Trial of *d*- $\alpha$ -Tocopheryl Polyethylene Glycol 1000 Succinate for Treatment of Vitamin E Deficiency in Children with Chronic Cholestasis, *Gastroenterology* 104, 1727–1735.
  10. Sokol, R.J., and Stall, C. (1990) Anthropometric Evaluation of Children with Chronic Liver Disease, *Am. J. Clin. Nutr.* 52, 203–208.
  11. Bhatia, S.J., Moffitt, S.D., Goldsmith, M.A., Bain, R.P., Kutner, M.H., and Rudman, D. (1981) A Method of Screening for Growth Hormone Deficiency Using Anthropometrics, *Am. J. Clin. Nutr.* 34, 281–288.
  12. Kurniewicz-Witczakowa, R. (1983) *Rozwój fizyczny dzieci i młodzieży warszawskiej (Anthropometry of Children and Adolescents in Warszawa)*, IMiD, Warszawa, 1983.
  13. De Leenheer, A.P., De Bevere, V.O.R.C., De Ruyter, M.G.M., and Claeys, A.E. (1979) Simultaneous Determination of Retinol and  $\alpha$ -Tocopherol in Human Serum by High-Performance Liquid Chromatography, *J. Chromatogr.* 162, 408–413.
  14. Koletzko, B., Schmidt, E., Bremer, H.J., Haug, M., and Harzer, G. (1989) Effects of Dietary Long-Chain Polyunsaturated Fatty Acids on the Essential Fatty Acid Status of Premature Infants, *Eur. J. Pediatr.* 148, 669–675.
  15. Decsi, T., and Koletzko, B. (1994) Fatty Acid Composition of Plasma Lipid Classes in Healthy Subject from Birth to Young Adulthood, *Eur. J. Pediatr.* 153, 520–525.
  16. Yagi, K. (1976) A Simple Fluorometric Assay for Lipoperoxide in Blood Plasma, *Biochem. Med.* 15:212–216.
  17. Yagi, K. (1982) Assay for Serum Lipid Peroxide Level and Its Clinical Significance, in *Lipid Peroxides in Biology and Medicine* (Yagi, K., ed.), Academic Press, New York, pp. 223–241.
  18. Cook, H.W. (1991) Fatty Acid Desaturation and Chain Elongation in Eucaryotes, in *Biochemistry of Lipids, Lipoproteins and Membranes* (Vance, D.E., and Vance, J., eds.), Elsevier Science Publishers, Amsterdam, pp. 141–168.
  19. Kaufman, S.S., Murray, N.D., Wood, R.P., Shaw, B.W., and Vanderhoof, J.A. (1987) Nutritional Support for the Infants with Extrahepatic Biliary Atresia, *J. Pediatr.* 10, 679–685.
  20. Robberecht, E., Koletzko, B., and Christophe, A. (1997) Several Mechanisms Contribute to the Abnormal Fatty Acid Composition of Serum Phospholipids and Cholesterol Esters in Cholestatic Children with Extrahepatic Biliary Atresia, *Prostaglandins Leukot. Essent. Fatty Acids* 56, 199–204.
  21. Carlson, S.E., and Werkman, S.H. (1996) A Randomized Trial of Visual Attention of Preterm Infants Fed Docosahexaenoic Acid Until Two Months, *Lipids* 31, 85–90.
  22. Werkman, S.H., and Carlson, S.E. (1996) A Randomized Trial of Visual Attention of Preterm Infants Fed Docosahexaenoic Acid Until Nine Months, *Lipids* 31, 91–97.
  23. SanGiovanni, J.P., Parra-Cabrera, S., Colditz, G.A., Berkey, C.S., and Dwyer, J.T. (2000) Meta-analysis of Dietary Essential Fatty Acids and Long-Chain Polyunsaturated Fatty Acids as They Relate to Visual Acuity in Healthy Preterm Infants, *Pediatrics* 105, 1292–1298.
  24. Allard, J.P., Kurian, R., Aghdassi, E., Muggli, R., and Royall, D. (1997) Lipid Peroxidation During n-3 Fatty Acid and Vitamin E Supplementation in Humans, *Lipids* 32, 535–541.
  25. Lemonnier, F., Cresteil, D., Feneant, M., Couturier, M., Bernard, O., and Alagille, D. (1987) Plasma Lipid Peroxides in Cholestatic Children, *Acta Paediatr. Scand.* 76, 928–934.
  26. Igarashi, J., Shimizu, T., Oguchim, S., Yamashiro, Y., Miyano, T., and Hayakawa, M. (2002) Retinal Neurodevelopmental Assessment with Electroretinogram in Patients with Biliary Atresia, *Pediatr. Int.* 44, 141–144.

[Received March 11, 2002, and in revised form October 8, 2002; revision accepted October 21, 2002]

# Trans Isomeric Octadecenoic Acids Are Related Inversely to Arachidonic Acid and DHA and Positively Related to Mead Acid in Umbilical Vessel Wall Lipids

Tamás Decsi<sup>a,\*</sup>, Günther Boehm<sup>b</sup>, H.M. Ria Tjoonk<sup>c</sup>, Szilárd Molnár<sup>a</sup>,  
D.A. Janneke Dijck-Brouwer<sup>d</sup>, Mijna Hadders-Algra<sup>e</sup>, Ingrid A. Martini<sup>f</sup>,  
Frits A.J. Muskiet<sup>d</sup>, and E. Rudy Boersma<sup>c</sup>

<sup>a</sup>Department of Paediatrics, University of Pécs, H-7623 Pécs, Hungary; <sup>b</sup>NUMICO Research Group, Friedrichsdorf, D-61381 Germany; <sup>c</sup>Perinatal Nutrition & Development Unit, Department of Pediatrics/Obstetrics and Gynaecology, University of Groningen, 9700 RB Groningen, The Netherlands; <sup>d</sup>Pathology and Laboratory Medicine, University Hospital Groningen, 9700 RB Groningen, The Netherlands; <sup>e</sup>Department of Neurology, University of Groningen, 9700 RB Groningen, The Netherlands; and <sup>f</sup>Laboratory Center, University Hospital Groningen, 9700 RB Groningen, The Netherlands

**ABSTRACT:** Long-chain PUFA play an important role in early human neurodevelopment. Significant inverse correlations were reported between values of *trans* isomeric and long-chain PUFA in plasma lipids of preterm infants and children aged 1–15 yr as well as in venous cord blood lipids of full-term infants. Here we report FA compositional data of cord blood vessel wall lipids in 308 healthy, full-term infants (gestational age: 39.7 ± 1.2 wk, birth weight: 3528 ± 429 g, mean ± SD). The median (interquartile range) of the sum of 18-carbon *trans* FA was 0.22 (0.13) % w/w in umbilical artery and 0.16 (0.10) % w/w in umbilical vein lipids. Nonparametric correlation analysis showed significant inverse correlations between the sum of 18-carbon *trans* FA and both arachidonic acid and DHA in artery ( $r = -0.38$ ,  $P < 0.01$ , and  $r = -0.20$ ,  $P < 0.01$ ) and vein ( $r = -0.36$ ,  $P < 0.01$ , and  $-0.17$ ,  $P < 0.01$ ) wall lipids. In addition, the sum of 18-carbon *trans* FA was significantly positively correlated to Mead acid, a general indicator of EFA deficiency, in both artery ( $r = +0.35$ ,  $P < 0.01$ ) and vein ( $r = +0.31$ ,  $P < 0.01$ ) wall lipids. The present results obtained in a large group of full-term infants suggest that maternal *trans* FA intake is inversely associated with long-chain PUFA status of the infant at birth.

Paper no. L9040 in *Lipids* 37, 959–965 (October 2002).

The long-chain PUFA, arachidonic acid (all-*cis*-5,8,11,14-arachidonic acid; 20:4n-6) and DHA (all-*cis*-4,7,10,13,16,19-DHA; 22:6n-3) play an important role in early human development (1–4). They are synthesized from the parent EFA, linoleic acid (all-*cis*-9,12-linoleic acid; 18:2n-6) and  $\alpha$ -linolenic acid (all-*cis*-9,12,15- $\alpha$ -linolenic acid; 18:3n-3), *via* a complex pathway consisting of several desaturations, chain elongations, and

peroxisomal  $\beta$ -oxidation (for biochemical details see Ref. 4), and/or consumed preformed in the diet. Oleic acid (*cis*-9-oleic acid; 18:1n-9) also may be converted *via* the same pathway into its longer-chain metabolites including Mead acid (20:3n-9). Because the affinity of 18:1n-9 for the enzymes of the pathway is considerably lower than that of 18:2n-6 and 18:3n-3, accumulation of 20:3n-9 indicates EFA deficiency.

The effect of modification of the 22:6n-3 and 20:4n-6 supply in infancy on visual and cognitive functions currently is being investigated (5–9). However, recent observations suggest that for 20:4n-6 and 22:6n-3, status at birth is one of the important determinants of postnatal changes in these FA (10). EFA status of the mother before and during pregnancy is the principal determinant of the EFA status of the infant at birth (11). Accumulating evidence indicates that factors other than maternal EFA intake may adversely affect the availability of 20:4n-6 and 22:6n-3 for the fetus.

At least four peer-reviewed publications indicated the potential interference of *trans* FA with long-chain PUFA availability in humans. First, significant inverse correlations were described between *trans*-octadecenoic acid (*t*-18:1) values and both 20:4n-6 and 22:6n-3 in plasma cholesterol esters and TAG in 29 premature infants on day 4 of life (12). Second, a significant inverse correlation was reported between *t*-18:1 and 20:4n-6 in plasma phospholipids in 53 healthy children aged 1 to 15 yr (13). Third, significant inverse correlations were seen between concentrations of *trans* FA, on the one hand and those of 22:6n-3 and 20:4n-6 on the other hand in venous cord blood plasma TAG and cholesteryl esters, respectively, in 70 healthy, full-term infants (14). Finally, significant inverse associations were described between the sum of *trans* FA and 20:4n-6 and 22:6n-3 in venous cord blood plasma phospholipids, cholesterol esters, and nonesterified FA of 42 full-term infants with an atopic trait (15).

The above-mentioned data obtained immediately or shortly after birth (12,14,15) suggest that maternal exposure to *trans* isomeric FA may be inversely related to the availability of long-chain PUFA to the fetus around birth. Shortcomings of these publications were the relatively small numbers of infants

\*To whom correspondence should be addressed at Department of Paediatrics, University of Pécs, József A. u. 7., H-7623 Pécs, Hungary.  
E-mail: tamas.decsi@aok.pte.hu

Abbreviations: *Cis* unsaturated FA: 18:1n-9, *cis*-9-oleic acid; 18:2n-6, all-*cis*-9,12-linoleic acid; 18:3n-3, all-*cis*-9,12,15- $\alpha$ -linolenic acid; 20:3n-9, all-*cis*-5,8,11-eicosatrienoic acid; 20:4n-6, all-*cis*-5,8,11,14-arachidonic acid; 22:6n-3, all-*cis*-4,7,10,13,16,19-docosahexaenoic acid. *Trans* isomeric FA: *t*-16:1, *trans*-7-hexadecenoic acid; *t*-18:1, *trans*-9/11-octadecenoic acid; *tt*-18:2, all-*trans*-9,12-octadecadienoic acid; *tc*-18:2, *trans*-9,*cis*-12-octadecadienoic acid; *ct*-18:2, *cis*-9,*trans*-12-octadecadienoic acid.



who were selected for study. Furthermore, only plasma lipids, reflecting FA status for a relatively short time, were investigated.

To avoid these shortcomings, we studied the association between five different *trans* isomeric FA and long-chain PUFA in cord blood vessel wall lipids in a large group of apparently healthy, full-term infants, all of whom were born after a normal pregnancy. In addition, a comparison was made between the FA composition of the wall of the efferent (umbilical arteries) and the afferent (umbilical vein) blood vessels of the umbilical cord.

## SUBJECTS AND METHODS

This study was part of a prospective cohort study investigating the effect of pre- and postnatal exposure to long-chain PUFA on growth and neurological development up to 18 mon of age. Apparently healthy pregnant women were informed between weeks 30 and 34 of their pregnancy about the study goal and design either by gynecologists of the University Hospital Groningen and the Martini Hospital (Groningen, The Netherlands) or by midwives in the city of Groningen. After the pregnant women gave their permission, they were called by one of the investigators who gave more detailed information. Exclusion criteria were as follows: multiple pregnancy, congenital abnormalities, and neonatal morbidity requiring intensive care. Mothers with type 1 diabetes, gestational diabetes, hypertension, and heart disease were not excluded from the study if the condition was well controlled. Written informed consent was obtained from all participants. The local medical ethical committee approved the study protocol.

We studied 308 apparently healthy, full-term infants [136 boys and 172 girls, 129 (42%) from primiparous and 179 (58%) from multiparous women]. Median maternal age was 30 yr (ranges: 18–47 yr); 24.8% of the mothers smoked during pregnancy. The mean  $\pm$  SD gestational age of the infants was  $39.7 \pm 1.2$  wk. Mean birth weight was  $3528 \pm 429$  g, and mean length at birth  $52.1 \pm 2.3$  cm.

Immediately after delivery, an approximately 7-cm sample of the umbilical cord located at the most proximal site of the placenta was removed. The sample was immediately placed in an ice-cold 0.9% NaCl solution until further processing. The two umbilical arteries and the umbilical vein were subsequently dissected from the surrounding tissue, thoroughly washed with an ice-cold 0.9% NaCl solution, and dried on paper tissue. No attempt was made to differentiate tissue layers within the blood vessel walls. Umbilical arteries and veins were weighed and subsequently transmethylated by incubating with 2 mL methanol/HCl (5:1 vol/vol; 6 mol HCl/L), which contained 5 mg BHT, at 90°C for 4 h. It was previously demonstrated in our laboratory that direct transmethylation is a suitable method in the determination of the FA composition of biological fluids and blood cells (16). All samples were stored at  $-20^\circ\text{C}$  until transported on dry ice to the Laboratory of the Department of Paediatrics, University of Pécs.

FAME were determined by high-resolution capillary GLC

with a Finnigan 9001 chromatograph (Finnigan/Tremetrics Inc., Austin, TX) with split injection (ratio: 1 to 15) and a FID. Two 30-m fused cyanopropyl columns (BPX70; SGE, Melbourne, Australia) were coupled and used for the analysis. The temperature program was as follows: an initial temperature of the injector of 80°C for 0.1 min, followed by a temperature increase of 180°C  $\text{min}^{-1}$  up to 280°C; temperature of the detector 280°C; an initial temperature of the column area of 60°C for 0.2 min, followed by a temperature increase of 20°C  $\text{min}^{-1}$  up to 160°C, followed by a 5-min isothermal period, followed by a temperature increase of 1°C  $\text{min}^{-1}$  up to 183°C, followed by a temperature increase of 5°C  $\text{min}^{-1}$  up to 200°C, followed by a 5-min isothermal period, followed by a temperature increase of 40°C  $\text{min}^{-1}$  up to 230°C, followed by a 10.65-min isothermal period. The ramped pressure program was as follows: an initial pressure of 30 psi for 0.2 min, followed by a pressure increase of 5 psi  $\text{min}^{-1}$  up to 35 psi, followed by a 9-min isobaric period, followed by a pressure increase of 5 psi  $\text{min}^{-1}$  up to 37 psi, followed by a 31.4-min isobaric period, followed by a pressure increase of 5 psi  $\text{min}^{-1}$  up to 45 psi, followed by a 9.4-min isobaric period. A typical chromatogram illustrating *trans* FA has been recently published from our laboratory (15). Identification of FA was confirmed by comparison with authentic standards (Nu-Chek-Prep, Elysian, MN). FA results were expressed as %w/w of the FA detected with a chain length between 14 and 24 carbon atoms.

We used SPSS for Windows, Release 7.5 (SPSS Inc., Chicago, IL) for the statistical analysis. The FA data are presented as median and range from the first to the third quartile values, because skewed distributions were found especially in FA present at lower concentrations. Nonparametric detection of correlation was carried out by calculating Spearman's  $\rho$  correlation coefficients. Because many ( $n = 57$ ) of the correlation analyses yielded significant results, in spite of the relatively high number of calculations ( $n = 82$ ), no attempt was made to correct for multiple testing. Results were regarded as statistically significant at  $P < 0.05$ .

## RESULTS

Percentage contributions of FA to the FA composition of umbilical cord blood vessel wall lipids are shown in Table 1. Values of *trans* FA were nearly similar in artery and vein wall lipids. In both artery and vein lipids, *trans*-7-hexadecenoic acid (*t*-16:1) was the major *trans* isomeric FA, whereas 18-carbon *trans* FA constituted about one-third of the total *trans* FA contents. Values of 20:3n-9 were about sevenfold higher in artery than in vein wall lipids.

In the wall of umbilical arteries, the sum of 18-carbon *trans* FA was positively related to 18:1n-9, 20:3n-9, and 18:3n-3, whereas it was inversely related to 20:4n-6 and 22:6n-3 (Table 2). The correlation of the sum of 18-carbon *trans* FA vs. 20:3n-9, 20:4n-6, and 22:6n-3 in umbilical artery lipids are graphically represented in Figure 1. Total *trans* FA values were positively related to 20:3n-9, 18:2n-6 and 18:3n-3, whereas they were inversely related to 20:4n-6.



**TABLE 1**  
**Fatty Acids in Umbilical Cord Blood Vessel Wall Lipids in 308 Full-Term Infants<sup>a</sup>**

FA	Umbilical artery	Umbilical vein
Saturated FA		
14:0	1.01 (0.25)	0.85 (0.21)
15:0	0.59 (0.19)	0.60 (0.21)
16:0	20.76 (1.84)	22.22 (2.22)
18:0	18.40 (1.28)	17.54 (1.21)
20:0	0.53 (0.19)	0.45 (0.18)
22:0	1.51 (0.27)	1.13 (0.22)
24:0	3.01 (0.55)	2.22 (0.42)
Sum	45.99 (2.02)	45.14 (2.46)
<i>cis</i> Monounsaturated FA		
16:1n-7	0.45 (0.18)	0.46 (0.15)
18:1n-9	11.14 (2.14)	8.57 (1.24)
18:1n-7	2.67 (0.51)	2.29 (0.46)
20:1n-9	0.52 (0.24)	0.38 (0.17)
22:1n-9	0.08 (0.08)	0.05 (0.07)
24:1n-9	4.93 (0.86)	4.60 (0.98)
Sum	20.09 (2.99)	16.60 (2.24)
<i>trans</i> FA		
<i>t</i> -16:1	0.37 (0.13)	0.44 (0.13)
<i>t</i> -18:1	0.05 (0.06)	0.06 (0.06)
<i>tt</i> -18:2	0.09 (0.07)	0.06 (0.05)
<i>tc</i> -18:2	0.02 (0.04)	0.01 (0.03)
<i>ct</i> -18:2	0.03 (0.05)	0.02 (0.03)
Sum of 18-carbon <i>trans</i>	0.22 (0.13)	0.16 (0.10)
Sum of <i>trans</i>	0.60 (0.20)	0.62 (0.19)
n-9 PUFA		
20:3n-9	2.71 (1.23)	0.37 (0.34)
n-6 PUFA		
18:2n-6	1.56 (0.49)	2.46 (0.66)
18:3n-6	0.07 (0.11)	0.04 (0.05)
20:2n-6	0.15 (0.12)	0.37 (0.18)
20:3n-6	1.58 (0.45)	2.27 (0.66)
20:4n-6	13.37 (2.38)	17.18 (1.71)
22:4n-6	3.45 (0.89)	5.88 (1.34)
22:5n-6	4.04 (1.11)	3.30 (1.09)
Sum	24.64 (3.74)	31.63 (2.42)
n-3 PUFA		
18:3n-3	0.01 (0.02)	0.01 (0.02)
20:5n-3	0.02 (0.02)	0.01 (0.03)
22:5n-3	0.35 (0.12)	0.40 (0.15)
22:6n-3	4.96 (1.22)	4.77 (1.17)
Sum	5.38 (1.24)	5.18 (1.29)

<sup>a</sup>Values are %w/w expressed as median (interquartile range).

In the wall of umbilical vein, the sum of 18-carbon *trans* FA was positively related to 18:1n-9, 20:3n-9, and 18:3n-3, whereas it was inversely related to 20:4n-6 and 22:6n-3 (Table 3). The correlation of the sum of 18-carbon *trans* FA with 20:3n-9, 20:4n-6, and 22:6n-3 in umbilical vein lipids is graphically represented in Figure 2. Total *trans* FA values were positively related to 20:3n-9, 18:2n-6, and 18:3n-3, whereas they were inversely related to 20:4n-6.

## DISCUSSION

The most notable findings of the present study are the significant inverse associations between 18-carbon *trans* isomeric FA and the most important long-chain PUFA, 20:4n-6 and 22:6n-3, in fetal tissue lipids at the end of apparently normal human pregnancies. FA compositions of fetal tissues are influenced by maternal FA supply to the fetus (11). For instance, significant positive correlations were found for almost all n-6 and n-3 FA between maternal plasma investigated during pregnancy and umbilical plasma levels (17). Parallel investigations on FA composition of the wall of umbilical cord veins and arteries allow researchers, to at least some extent, to assess maternal supply (vein) and fetal return (artery) separately.

Humans do not synthesize *trans* FA, although the human metabolism is able to elongate and desaturate ingested *trans* FA into longer-chain and more unsaturated metabolites (18). Anyhow, the *trans* FA detected in fetal tissues must have their origin in the maternal diet. In the human diet *trans* FA originate partly from the meat and milk of ruminant animals, but the major part of human *trans* FA exposure is the consequence of the production of by-products during industrial food processing, i.e., partial hydrogenation and heat-deodorization of various fats (e.g., Ref. 19). *trans* FA constitute a sizable portion of FA intake in Western-type diets. The average *trans* FA consumption was reported to be 7–12 g/d in the United States (20, 21) and 4–6 g/d in the United Kingdom (22). In pregnant and breast-feeding women, average *trans* FA intakes were estimated to be 6.4 g/d in the United States (23) and 6.9 g/d in Canada (24).

However, dietary *trans* FA intakes in The Netherlands appear to be considerably lower than those in North America. A

**TABLE 2**  
**Spearman's  $\rho$  Correlation Coefficients Between Percentage Contributions (%w/w) of *trans* FA vs. Major PUFA in Umbilical Cord Artery Wall Lipids in 308 Full-Term Infants<sup>a</sup>**

Fatty acid	<i>t</i> -16:1	<i>t</i> -18:1	<i>tt</i> -18:2	<i>tc</i> -18:2	<i>ct</i> -18:2	18-Carbon <i>trans</i>	Total <i>trans</i>
n-9 PUFA							
Oleic acid (18:1n-9)	-0.25**	+0.07	+0.09	+0.07	+0.17**	+0.16**	-0.04
Eicosatrienoic acid (20:3n-9)	-0.22**	+0.20*	+0.19**	+0.13*	+0.24**	+0.35**	+0.12*
n-6 PUFA							
Linoleic acid (18:2n-6)	+0.31**	-0.04	0.00	-0.04	-0.03	-0.04	+0.19**
Arachidonic acid (20:4n-6)	+0.17**	-0.26**	-0.17**	-0.18**	-0.29**	-0.38**	-0.19**
n-3 PUFA							
$\alpha$ -Linolenic acid (18:3n-3)	+0.27**	+0.18**	+0.07	+0.22**	+0.11*	+0.26**	+0.34**
DHA (22:6n-3)	+0.23**	-0.21**	+0.02	-0.04	-0.19**	-0.20**	+0.04

<sup>a</sup>Symbols: \* $P < 0.05$ , \*\* $P < 0.01$ . Abbreviations: *t*-16:1, *trans*-7-hexadecenoic acid; *t*-18:1, *trans*-9/11-octadecenoic acid; *tt*-18:2, all-*trans*-9,12-octadecadienoic acid; *tc*-18:2, *trans*-9-*cis*-12-octadecadienoic acid; *ct*-18:2, *cis*-9-*trans*-12-octadecadienoic acid.

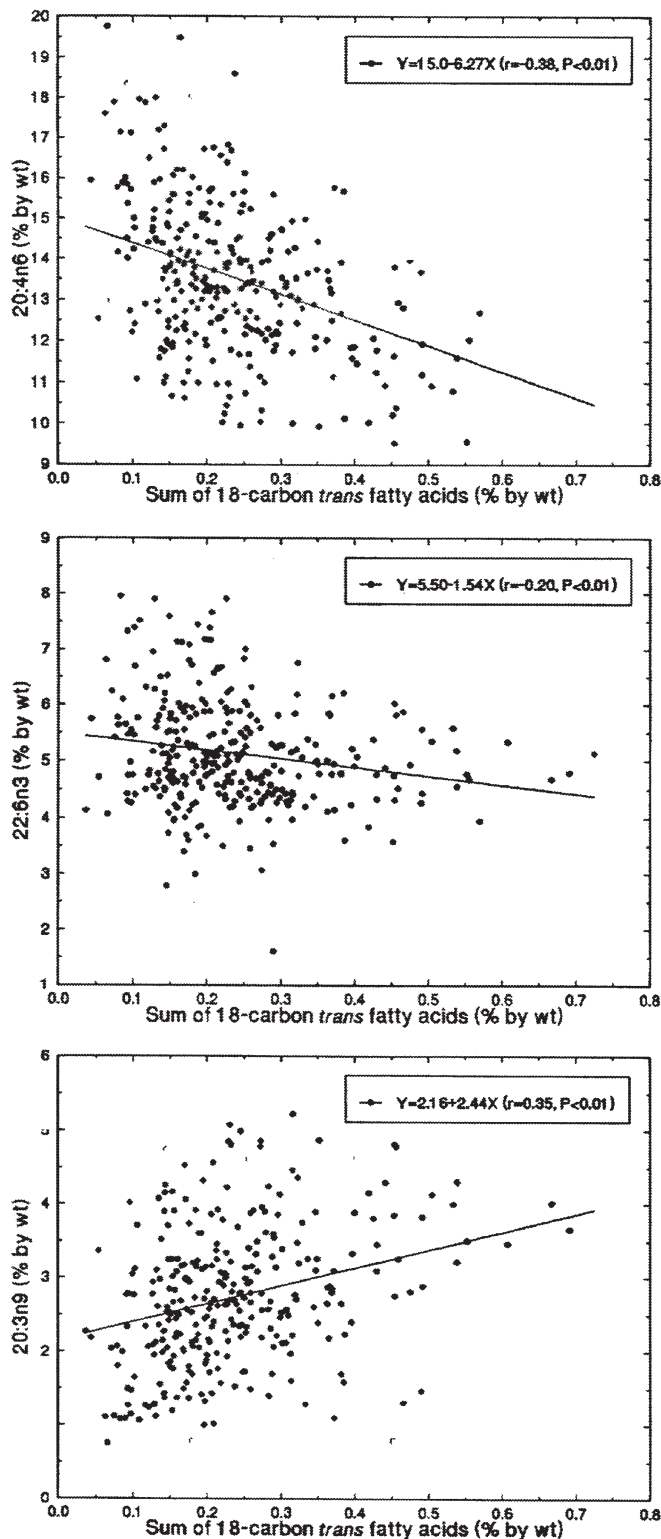


FIG. 1. Relation between the sum of 18-carbon *trans* FA (*t*-18:1 + *t*-18:2 + *tc*-18:2 + *ct*-18:2) and 20:4n-6 (top), 22:6n-3 (middle), and 20:3n-9 (bottom) in cord artery wall lipids in 305 healthy full-term infants. Because the sum of 18-carbon *trans* FA exceeded 1% by weight only in three infants (1.14, 1.43, and 2.22 % w/w), for higher graphical resolution we omitted these three data from the graph. The significance of correlation analyses (Tables 2 and 3) remained the same when calculated for the 305 infants represented in the graph. *t*-18:1, *trans*-9/11-octadecenoic acid; *t*-18:2, all-*trans*-9,12-octadecadienoic acid; *tc*-18:2, *trans*-9,*cis*-12-octadecadienoic acid; *ct*-18:2, *cis*-9,*trans*-12-octadecadienoic acid; 20:4n-6, all-*cis*-5,8,11,14-arachidonic acid; 22:6n-3, all-*cis*-4,7,10,13,16-19-DHA; 20:3n-9, all-*cis*-5,8,11-eicosatrienoic acid.

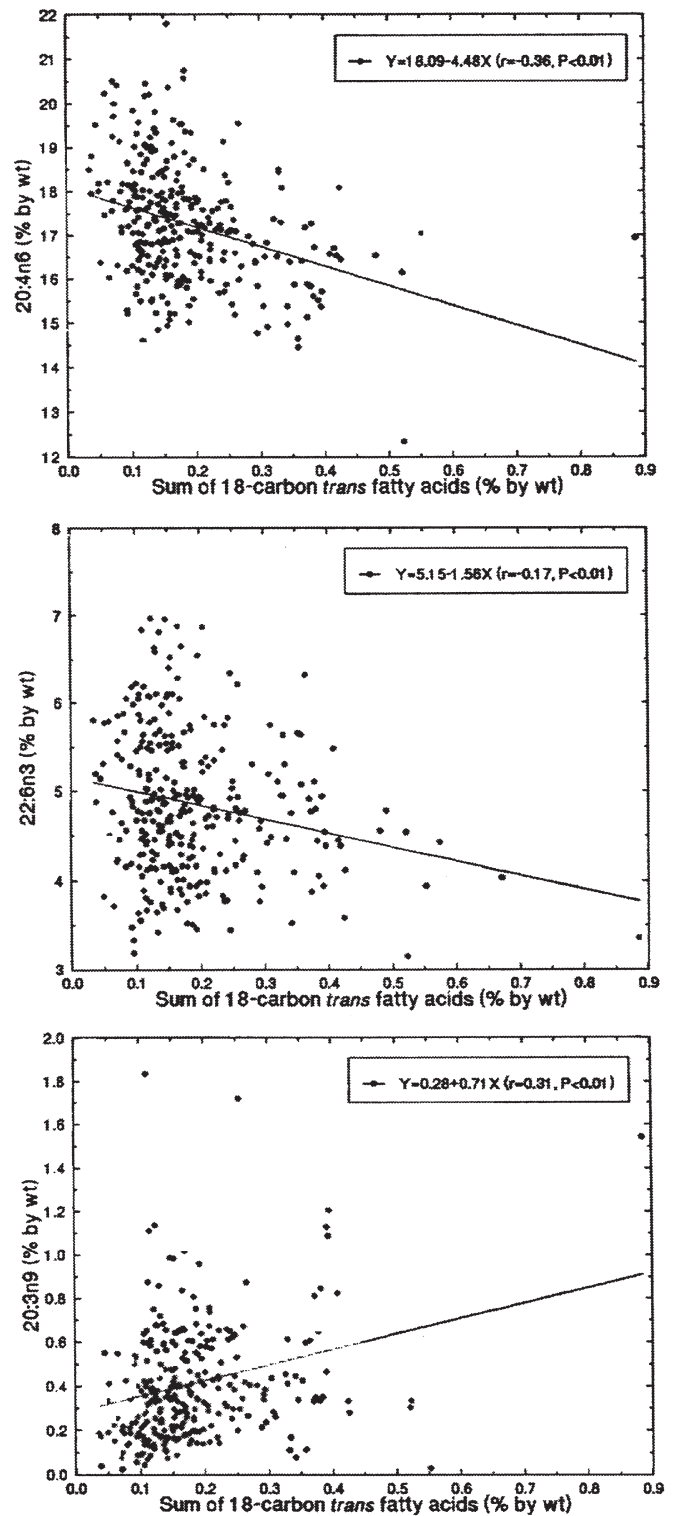


FIG. 2. Relation between the sum of 18-carbon *trans* FA (*t*-18:1 + *t*-18:2 + *tc*-18:2 + *ct*-18:2) and 20:4n-6 (top), 22:6n-3 (middle), and 20:3n-9 (bottom) in cord vein wall lipids in 305 healthy full-term infants. Because the sum of 18-carbon *trans* FA exceeded 1% by weight only in three infants (1.09, 1.21 and 1.26 % w/w), for higher graphical resolution we omitted these three data from the graph. The significance of correlation analyses (Tables 2 and 3) remained the same when calculated for the 305 infants represented in the graph. For abbreviations see Figure 1.

**TABLE 3**  
**Spearman's  $\rho$  Correlation Coefficients Between Percentage Contributions (%w/w) of *trans* Isomeric FA and Major PUFA in Umbilical Cord Vein Wall Lipids in 308 Full-Term Infants<sup>a</sup>**

Fatty acid	<i>t</i> -16:1	<i>t</i> -18:1	<i>tt</i> -18:2	<i>tc</i> -18:2	<i>ct</i> -18:2	18-Carbon <i>trans</i>	Total <i>trans</i>
n-9 PUFA							
Oleic acid (18:1n-9)	-0.05	+0.19**	+0.06	+0.18**	+0.14*	+0.14**	+0.05
Eicosatrienoic acid (20:3n-9)	-0.05	+0.23**	+0.21**	+0.11*	+0.15**	+0.31**	+0.12*
n-6 PUFA							
Linoleic acid (18:2n-6)	+0.23*	+0.13*	-0.07	+0.15**	-0.04	+0.08	+0.20**
Arachidonic acid (20:4n-6)	-0.11	-0.32**	-0.06	-0.27**	-0.23**	-0.36**	-0.33**
n-3 PUFA							
$\alpha$ -Linolenic acid (18:3n-3)	+0.27**	+0.09	-0.04	+0.11*	+0.15**	+0.13*	+0.26**
DHA (22:6n-3)	+0.15**	-0.15**	+0.05	-0.20**	-0.17*	-0.17**	+0.03

<sup>a</sup>Symbols: \* $P < 0.05$ , \*\* $P < 0.01$ . For abbreviations see Table 2.

recent report of the Dutch Health Council estimates the mean *trans* FA intake of the Dutch population to be 1.2 g/d (25). Despite this relatively low intake, it is important to note that an inverse association between *trans* isomeric and long-chain PUFA in umbilical cord blood vessel wall lipids was recorded in the present study. It may reasonably be assumed that similar or even stronger associations may be observed in populations with *trans* FA intakes exceeding the Dutch values.

The most prevalent *trans* FA in the human diet is *t*-18:1 (26,27). FA composition of blood lipids usually reflects the FA composition of the diet; for example, one of us previously investigated the contribution of *trans* FA to the FA composition of plasma lipid classes in seven age groups from birth to young adulthood and found *t*-18:1 to be the major plasma *trans* FA in all sample categories including venous cord blood (28). We are not aware of published data on the contribution of individual *trans* FA to the FA composition of cord blood vessel wall lipids.

Experimental evidence obtained in *in vitro* investigations and animal studies indicates that *trans* FA may impair the synthesis of long-chain PUFA from 18:2n-6 and 18:3n-3. Investigations both on rodent tissues (29) and on human fibroblast cultures (30) clearly demonstrated that various *trans* FA inhibit the desaturation and chain-elongation of 18:2n-6 and 18:3n-3 to their longer-chain metabolites. *In vivo* investigations in rats also showed an impairment of 18:2n-6 and 18:3n-3 metabolism with exposure to various *trans* FA (31–35). In pregnant rats, high dietary intakes of *trans* FA were associated with diminished  $\Delta 6$ -FA desaturase activity in liver microsomes and decreased contribution of longer-chain 18:3n-3 metabolites to fetal plasma lipids in the offspring (36). In an *in vitro* system of isolated human placental membranes, the presence of *t*-18:1 in the incubation medium reduced to 68–70% of binding of radio-labeled FA, whereas the inhibition of binding of 18:2n-6 and 18:3n-3 by 18:1n-9 was only around 45% (37). These data suggest that *trans* FA may effectively compete with EFA and their longer-chain metabolites for FA-binding sites in human placental membranes, thereby inhibiting the transport of these FA to the placenta (38).

In the present study it was surprising that 18-carbon *trans* FA were negatively associated with long-chain PUFA, whereas 16-carbon *trans*-FA and PUFA were positively and signifi-

cantly correlated. Industrially processed oils are usually enriched with EFA; therefore, it is reasonable to assume a positive correlation between the dietary intakes and the tissue accumulations of *trans* isomeric and EFA. However, the putative inhibitory interaction of 18-carbon *trans* FA with the metabolism of EFA may substantially influence accumulation in fetal tissues.

The significant positive correlation observed in the present study between 18-carbon *trans* FA and 20:3n-9 (Mead acid), a general indicator of EFA deficiency, may either support further the concept that high maternal intake of 18-carbon *trans* FA may impair fetal supply of long-chain PUFA, or may suggest a dietary deficiency of long-chain PUFA. Mead acid is synthesized from 18:1n-9 via  $\Delta 6$ -FA desaturation, chain elongation, and  $\Delta 5$ -FA desaturation. In classical EFA deficiency, Mead acid accumulates because of the low availability of the alternative substrates, 18:2n-6 and 18:3n-3, for  $\Delta 6$ -FA desaturation (39). However, because long-chain PUFA inhibit Mead acid synthesis, therefore, enhanced amounts of Mead acid may also indicate long-chain PUFA deficiency even if the availability of 18:2n-6 and 18:3n-3 is normal (11). The several-fold higher contribution of 20:3n-9 to cord artery than to cord vein wall lipids has been described previously by others (40) as well as by one of us (41) and is considered to represent a higher rate of substitution of 20:3n-9 for 20:4n-6 and 22:6n-3 at the efferent than at the afferent end of materno-fetal circulation.

In summary, we report a negative association between values of 18-carbon *trans* FA and that of long-chain PUFA in cord blood vessel wall lipids in a large group of apparently healthy, full-term infants. We think that the data reported here bear two immediate messages for research on PUFA. First, supply of 18-carbon *trans* isomeric FA should be taken into account as a potential independent variable in any study aimed at modifying FA supply during pregnancy. Second, individual *trans* isomeric FA rather than the parameter "sum of all *trans* fatty acids" alone should be considered as separate variable(s) in studies on the effects of *trans* FA on human health.

## REFERENCES

- Innis, S.M. (1991) Essential Fatty Acids in Growth and Development, *Prog. Lipid. Res.* 30, 39–130.

2. Decsi, T., and Koletzko, B. (1994) Polyunsaturated Fatty Acids in Infant Nutrition, *Acta Paediatr. Suppl.* 395, 31–37.
3. Carlson, S.E., and Neuringer, M. (1999) Polyunsaturated Fatty Acid Status and Neurodevelopment: A Summary and Critical Analysis of the Literature, *Lipids* 34, 171–178.
4. Decsi, T., and Koletzko, B. (2000) Role of Long-Chain Polyunsaturated Fatty Acids in Early Human Neurodevelopment, *Nutr. Neurosci.* 3, 293–306.
5. Birch, E.E., Garfield, S., Hoffman, D.R., Uauy, R., and Birch, D.G. (2000) A Randomized Controlled Trial of Early Dietary Supply of Long-Chain Polyunsaturated Fatty Acids and Mental Development in Term Infants, *Dev. Med. Child Neurol.* 42, 174–181.
6. Smit, E.N., Koopmann, M., Boersma, E.R., and Muskiet, F.A. (2000) Effect of Supplementation of Arachidonic Acid (AA) or a Combination of AA Plus Docosahexaenoic Acid on Breast-milk Fatty Acid Composition, *Prostaglandins Leukot. Essent. Fatty Acids* 62, 335–340.
7. Makrides, M., Neumann, M.A., Simmer, K., and Gibson, R.A. (2000) A Critical Appraisal of the Role of Dietary Long-Chain Polyunsaturated Fatty Acids on Neural Indices of Term Infants: A Randomized, Controlled Trial, *Pediatrics* 105, 32–38.
8. Velzing-Aarts, F.V., Klis, F.R. van der, Dijks, F.P. van der, Beusekom, C.M. van, Landman, H., Capello, J.J., and Muskiet, F.A. (2001) Effect of Three Low-Dose Fish Oil Supplements, Administered During Pregnancy, on Neonatal Long-Chain Polyunsaturated Fatty Acid Status at Birth, *Prostaglandins Leukot. Essent. Fatty Acids* 65, 51–57.
9. Auestad, N., Halter, R., Hall, R.T., Blatter, M., Bogle, M.L., Burks, W., Erickson, J.R., Fitzgerald, K.M., Dobson, V., Innis, S.M., et al. (2001) Growth and Development in Term Infants Fed Long-Chain Polyunsaturated Fatty Acids: A Double-Masked, Randomized, Parallel, Prospective, Multivariate Study, *Pediatrics* 108, 372–381.
10. Guesnet, P., Pugo-Gunsum, P., Maurage, C., Pinault, M., Graudeau, B., Alessandri, J.-M., Durand, G., Antoine, J.-M., and Couet, C. (1999) Blood Lipid Concentrations of Docosahexaenoic and Arachidonic Acids at Birth Determine Their Relative Postnatal Changes in Term Infants Fed Breast Milk or Formula, *Am. J. Clin. Nutr.* 70, 292–298.
11. Hornstra, G. (2000) Essential Fatty Acids in Mothers and Their Neonates, *Am. J. Clin. Nutr.* 71(5 Suppl.), 1262S–1269S.
12. Koletzko, B. (1992) *Trans* Fatty Acids May Impair Biosynthesis of Long-Chain Polyunsaturates and Growth in Man, *Acta Paediatr. Scand.* 81, 302–306.
13. Decsi, T., and Koletzko, B. (1995) Do *trans* Fatty Acids Impair Linoleic Acid Metabolism in Children? *Ann. Nutr. Metab.* 39, 36–41.
14. Elias, S.L., and Innis, S.M. (2001) Infant Plasma *trans*, n-6 and n-3 Fatty Acids and Conjugated Linoleic Acids Are Related to Maternal Plasma Fatty Acids, Length of Gestation, and Birth Weight and Length, *Am. J. Clin. Nutr.* 73, 807–814.
15. Decsi, T., Burus, I., Molnár, S., Minda, H., and Veitl, V. (2001) Inverse Association Between *trans* Isomeric and Long-Chain Polyunsaturated Fatty Acids in Cord Blood Lipids of Full-Term Infants, *Am. J. Clin. Nutr.* 74, 364–368.
16. Muskiet, F.A.J., Doormaal, J.J. van, Martini, I.A., Wolthers, B.G., and Slik, W. van der (1983) Capillary Gas Chromatographic Profiling of Total Long-Chain Fatty Acids and Cholesterol in Biological Materials, *J. Chromatogr. Biomed. Appl.* 278, 231–244.
17. Al, M.D., Badart-Smook, A., Houwelingen, A.C. van, Hasart, T.H., and Hornstra, G. (1996) Fat Intake of Women During Normal Pregnancy: Relationship with Maternal and Neonatal Essential Fatty Acid Status, *J. Am. Coll. Nutr.* 15, 49–55.
18. Holman, R.T., Pusch, F., Svingen, B., and Dutton, H.J. (1991) Unusual Isomeric Polyunsaturated Fatty Acids in Liver Phospholipids of Rats Fed Hydrogenated Oil, *Proc. Natl. Acad. Sci. USA* 88, 4830–4834.
19. Koletzko, B., and Decsi, T. (1997) Metabolic Aspects of *trans* Fatty Acids, *Clin. Nutr.* 16, 229–237.
20. Hunter, J.E., and Applewhite, T.H. (1991) Reassessment of *trans*-Fatty Acid Availability in the U.S. Diet, *Am. J. Clin. Nutr.* 54, 363–369.
21. Enig, M.G., Atal, S., Keeny, M., and Sampugna, J. (1990) Isomeric *trans* Fatty Acids in the U.S. Diet, *J. Am. Coll. Nutr.* 9, 471–486.
22. The British Nutrition Foundation (1995) *Unsaturated Fatty Acids. Nutritional and Physiological Significance. The Report of the British Nutrition Foundation's Task Force*, 15 pp., Chapman & Hall, London.
23. Carlson, S.E., Clandinin, M.T., Cook, H.W., Emken, E.E., and Filer, L.J. (1997) *Trans* Fatty Acids: Infant and Fetal Development, *Am. J. Clin. Nutr.* 66, 717S–736S.
24. Innis, S.M., and King, D.J. (1999) *Trans* Fatty Acids in Human Milk Are Inversely Associated with Concentrations of all-*cis* n-6 and n-3 Fatty Acids and Determine *trans*, but Not n-6 and n-3, Fatty Acids in Plasma Lipids of Breast-Fed Infants, *Am. J. Clin. Nutr.* 70, 383–390.
25. Gezondheidsraad (2001) *Voedingsnormen: energie, eiwitten, vetten en verteerbare koolhydraten*, publicatie nr. 2001/19, Gezondheidsraad, Den Haag.
26. ASCN/AIN (1996) Position Paper on *Trans* Fatty Acids. ASCN/AIN Task Force on *trans* Fatty Acids. American Society for Clinical Nutrition and American Institute of Nutrition, *Am. J. Clin. Nutr.* 63, 663–670.
27. Stender, S., Dyerberg, J., Holmer, G., Ovesen, L., and Sandström, B. (1995) The Influence of *trans* Fatty Acids on Health: A Report from The Danish Nutrition Council, *Clin. Sci.* 88, 375–392.
28. Decsi, T., and Koletzko, B. (1994) Fatty Acid Composition of Plasma Lipid Classes in Healthy Subjects from Birth to Young Adulthood, *Eur. J. Pediatr.* 53, 520–525.
29. Mahfouz, M.M., Smith, T.L., and Kummerow, F.A. (1984) Effects of Dietary Fats on Desaturase Activities and the Biosynthesis of Fatty Acids in Rat Liver Microsomes, *Lipids* 19, 214–222.
30. Rosenthal, M.D., and Doloresco, M.A. (1984) The Effects of *trans* Fatty Acids on Fatty Acyl  $\Delta 5$  Desaturation by Human Skin Fibroblasts, *Lipids* 19, 869–874.
31. Anderson, R.L., Fullmer, C.S., and Hollenbach, E.J. (1975) Effects of *trans* Isomers of Linoleic Acid on the Metabolism of Linoleic Acid in Rats, *J. Nutr.* 105, 393–400.
32. Hill, E.G., Johnson, S.B., Lawson, L.D., Mahfouz, M.M., and Holman, R.T. (1982) Perturbation of the Metabolism of Essential Fatty Acids by Dietary Partially Hydrogenated Vegetable Oils, *Proc. Natl. Acad. Sci. USA* 79, 953–957.
33. Hwang, D.H., Chanmugam, P., and Anding, R. (1982) Effects of Dietary 9-*trans*-12-*trans* Linoleate on Arachidonic Acid Metabolism in Rat Platelets, *Lipids* 17, 307–313.
34. Lawson, L.D., Hill, E.G., and Holman, R.T. (1983) Suppression of Arachidonic Acid in Lipids of Rat Tissues by Dietary Mixed Isomeric *cis* and *trans* Octadecanoates, *J. Nutr.* 113, 1827–1835.
35. Bruckner, G., Goswami, S., and Kinsella, J.E. (1984) Dietary Trilinoelaidate: Effects on Organ Fatty Acid Composition, Prostanoid Biosynthesis and Platelet Function in Rats, *J. Nutr.* 114, 58–67.
36. Larqué, E., Pérez-Llamas, F., Puerta, V., Girón, M., Suárez, M.D., Zamora, S., and Gil, A. (2000) Dietary *trans* Fatty Acids Affect Docosahexaenoic Acid Concentrations in Plasma and Liver but Not Brain of Pregnant and Fetal Rats, *Pediatr. Res.* 47, 278–283.
37. Campbell, F.M., Gordon, M.J., and Dutta-Roy, A.K. (1996)



- Preferential Uptake of Long-Chain Polyunsaturated Fatty Acids by Isolated Human Placental Membranes, *Mol. Cell. Biochem.* 155, 77–83.
38. Dutta-Roy, A.K. (1997) Transfer of Long-Chain Polyunsaturated Fatty Acids Across the Human Placenta, *Prenat. Neonat. Med.* 2, 101–107.
39. Holman, R.T., Johnson, S.B., Mercuri, O., Itarte, H.J., Rodrigo, M.A., and De Tomas, M.E. (1981) Essential Fatty Acid Deficiency in Malnourished Children, *Am. J. Clin. Nutr.* 34, 1534–1539.
40. Hornstra, G., Houwelingen, A.C. van, Simonis, M., and Gerrard, J.M. (1989) Fatty Acid Composition of Umbilical Arteries and Veins: Possible Implications for the Fetal EFA-Status, *Lipids* 24, 511–517.
41. Velzin-Aarts, F.V., Klis, F.R.M. van der, Dijs, F.P.L. van der, and Muskiet, F.A.J. (1999) Umbilical Vessels of Preeclamptic Women Have Low Contents of Both n-3 and n-6 Long-Chain Polyunsaturated Fatty Acids, *Am. J. Clin. Nutr.* 69, 293–298.

[Received April 2, 2002, and in revised form and accepted November 11, 2002]

# Lipoprotein–Apolipoprotein Changes in Renal Transplant Recipients

Maurizio Cassader<sup>a,\*</sup>, Gianluca Ruiu<sup>a</sup>, Roberto Gambino<sup>a</sup>, Natalina Alemanno<sup>a</sup>,  
Giorgio Triolo<sup>b</sup>, Fabrizio Veglia<sup>c</sup>, and Gianfranco Pagano<sup>a</sup>

<sup>a</sup>Department of Internal Medicine, University of Turin, Italy, <sup>b</sup>Nephrology and Dialysis Division, Hospital C.T.O., Turin, Italy, and <sup>c</sup>Epidemiology Unit, Institute for Scientific Interchange (ISI) Foundation, Turin, Italy

**ABSTRACT:** Recent studies have demonstrated that the incidence of cardiovascular events occurring with renal transplantation is higher than that in the general population. Renal transplantation modifies the characteristic dyslipidemia of chronic renal failure. In this study the change in lipoprotein and lipid values of 103 transplant recipients after transplantation was investigated. The aim of our work was to examine the short-term and long-term variations in lipid metabolism. The major lipoprotein fractions (VLDL, LDL, HDL) were separated by preparative ultracentrifugation, and TG and cholesterol concentrations were determined in plasma and lipoprotein fractions. Whole plasma apolipoproteins were determined by a rate immunonephelometric technique. In the pretransplant period the patients displayed the typical picture of uremics. After transplantation the most evident alterations in the lipoprotein profile occurred in our case series after 3 mon. The major finding was a 35% reduction in plasma TG. The modifications in the TG-rich lipoproteins of our transplant recipients persisted throughout the observation period. In the initial 3-mon period, total cholesterol remained steady, whereas LDL-cholesterol and total apolipoprotein B showed a significant increase. No significant changes were found in total and transported TG and cholesterol between the 3-mon and the 6-yr values. The substantial stability of cholesterol levels after transplantation and in subsequent reports, as well as a higher incidence of cardiovascular complications, may suggest that the mechanisms responsible for vessel damage must be sought mainly in the structural and physicochemical alterations of the individual lipoprotein fractions or in other risk factors.

Paper no. L9073 in *Lipids* 37, 967–974 (October 2002).

Cardiovascular complications are the main cause of death in chronic renal failure and renal transplant patients. Their incidence is much higher than in the general population (1). Atherosclerosis is the prime cause of these complications. Some of its risk factors are shared with the general population; others are typical of transplant patients (2,3). Particular attention has been directed to the effects of immunosuppressive management, the type of dialysis, and the pre- and posttransplant alterations in lipid metabolism (4–6).

\*To whom correspondence should be addressed at Dipartimento di Medicina Interna, Corso A.M. Dogliotti 14, 10126 Torino, Italy.  
E-mail: maurizio.cassader@unito.it

Abbreviations: apo, apolipoprotein; BMI, body mass index; Chol, cholesterol; CVD, cardiovascular disease; HD, hemodialysis; LPL, lipoprotein lipase; NDDG, National Diabetes Data Group; TRL, triglyceride-rich lipoproteins.

Both in the general population and in transplant recipients, lipid metabolism is of prime importance, particularly because of its presumed role in chronic organ rejection (7). The post-transplant persistence or aggravation of lipoprotein alterations has been observed for at least 20 yr and has been the subject of several studies (3,6,8,9).

At least 60% of transplant recipients display an increase in total cholesterol (Chol) and LDL-transported cholesterol (LDL-Chol), as well as an inconstant increase in plasma TG and normal HDL-Chol levels.

Various factors predisposing the patient to pretransplant dyslipidemia and its posttransplant modification have been identified: age (10), diet, posttransplant weight increases (11), pretransplant lipoprotein levels (12), renal function (7), hyperglycemia and/or hyperinsulinism (13), and immunosuppressive management (5). A genetic predisposition is also thought to play a preponderant role (14). Several studies (15,16) have shown that steroids and cyclosporine, both singly and synergistically, induce dyslipidemia, whereas cyclosporine, which has an affinity to lipoproteins, results in the direct alteration of their metabolism.

Longitudinal studies have assessed lipid profile changes following transplantation. Their evaluation over the years, however, has been confined to total Chol, HDL-Chol, and TG. This paper describes the long-term monitoring of the lipoprotein and apolipoprotein (apo) profiles of 103 nondiabetic renal transplant recipients immunosuppressed with cyclosporine plus prednisone.

## MATERIALS AND METHODS

**Patients.** Nondiabetic patients ( $n = 103$ ) were recruited at the Nephrology and Dialysis Division of San Giovanni Battista Hospital, Turin (Italy) from July 1988 to March 1992. The study was terminated in July 1998.

Thirty-eight women and 65 men (aged  $41 \pm 11.3$  yr) had been on hemodialysis (HD) for  $4.5 \pm 2.6$  yr (mean  $\pm$  SD) prior to transplantation and were not diabetic according to National Diabetes Data Group (NDDG) criteria (17). The underlying diseases leading to renal failure were chronic glomerulonephritis (52%), chronic pyelonephritis (22%), vascular nephropathy (4%), systemic lupus erythematosus (2%), blood disease (4%), toxic nephropathy (5%), cystic renal disease (5%), and interstitial nephritis (5%). Their proteinuria was  $<3.5$  g/24 h, and they

were free of thyroid and liver disease. Blood creatinine 3 mon after transplantation was  $1.6 \pm 0.4$  mg/dL.

Thirty-one hypertensive subjects were placed on loop diuretics (generally furosemide) and 14 on  $\beta$ -adrenergic blocking agents. None of the patients was in treatment with lipid-lowering agents.

All patients received cyclosporine as the immunosuppressive drug associated with prednisone. Its dose was adjusted to keep plasma levels within 150–200 ng/mL, with an average dose of  $3.75 \pm 0.15$  mg/kg/d. Acute rejection episodes were treated with 1 g i.v. methylprednisolone boluses. The mean dose of prednisone in the first year was  $4.90 \pm 1.0$  g per os and  $1.25 \pm 0.62$  g i.v., and 10 mg/d in the second. In subsequent years, it was reduced, irrespective of acute rejection episodes, to reach a mean of  $5.51 \pm 1.70$  mg/d at the end of the observation period.

The posttransplantation diet provided 25–30 kcal/kg ideal body weight/d, 35% of lipids as total calories, with a polyunsaturated/saturated ratio of 2:1 and a daily cholesterol intake less than 250 mg, about 40 g/d dietetic fibers, and elimination of simple sugar.

One hundred age-matched healthy subjects (49 male and 51 female), with a mean age of  $52 \pm 6$  yr,  $\pm 10\%$  of ideal body weight, and a negative family history of diabetes and blood lipid disorders, were randomly selected from blood donors as controls for pretransplant lipid parameters.

**Lipid and lipoprotein analysis.** All lipid and lipoprotein sample preparations and analyses were performed in a single laboratory. Blood was collected into 5% EDTA- $\text{Na}_2$  in the morning after an overnight fast, and plasma was immediately centrifuged for 30 min at  $3000 \times g$  at  $4^\circ\text{C}$  in a Beckman J6B centrifuge and separated. The blood samples were drawn at least 36 h from the last HD treatment.

Blood samples were also obtained, after an overnight fast, at 3, 6, 12, 24, 36, 48, 60, and 72 mon after transplantation.

The major lipoprotein fractions (VLDL, LDL, HDL) were separated by preparative ultracentrifugation (Beckman model L8-55M ultracentrifuge with a 50.4 Ti rotor) (18).

Concentration of TG and Chol were then determined enzymatically in plasma and lipoprotein fractions by automated methods with a Shimadzu CL-7000 enzymatic photometer (Shimadzu Instruments, Kyoto, Japan). HDL-Chol was determined after precipitation of apoB-containing lipoproteins with heparin and manganese chloride (19). HDL2-Chol was determined on whole plasma by  $\text{Mn}^{2+}$ /heparin/dextran fractionated separation (20). Whole plasma apo were determined by a rate immunonephelometric technique (Alfa-Wassermann, Milan, Italy). The coefficients of variation for apoAI, -B, -CII, and -CIII were 3.80, 4.90, 2.80, and 2.10%.

Body mass index (BMI) was calculated as weight (kg) divided by height squared ( $\text{m}^2$ ).

**Statistical analysis.** Baseline values for patients and controls were compared by unpaired *t*-tests. Short-term effects of transplantation on serum lipid values were calculated as the values measured 3 mon after transplant minus pretransplant values. Long-term effects were calculated as the mean of values measured at 3, 6, and 6+ yr after transplant minus pre-

transplant values. In order to assess the persistence of effects, we also calculated the difference between long-term (6 yr and over) and posttransplant values.

All variations were also computed as percentage differences over reference values. The significance of short- and long-term variations was assessed by paired-samples *t*-tests, and the Bonferroni correction was applied to account for the large number of tests.

Patient and graft survival and a cardiovascular disease (CVD) event rate analysis were performed by the Kaplan-Meier method, and the effect of lipid, clinical, and pharmacological variables was assessed by the log-rank test. A multivariate survival analysis was performed by the Cox proportional hazard regression method, adjusting for gender and age.

## RESULTS

**Baseline.** Baseline clinical characteristics of transplant recipients are reported in Table 1. Comparisons of the baseline lipid parameters of patients and normal subjects are reported in Table 2. A highly significant difference was observed in both men and women for total TG; VLDL-TG; LDL-TG; VLDL-Chol; HDL2-Chol; and apoAI, -AII, -CII, and -CIII. There were no differences in total Chol, LDL-Chol, and apoB levels. HDL-Chol differed significantly between male patients and controls only.

**Follow-up.** A total of 103 patients (65 male, 38 female) were enrolled and received transplants. Of this number, 93 were examined 3 mon after transplantation. By the end of the study, 25 patients had died (10 from CVD, 2 from carcinoma, 2 from liver disease, and 11 from unknown causes) and 46 had undergone explantation and were considered dropouts from the study. Forty-five patients were followed for 6 yr or longer; the median duration of follow-up was 68.4 mon (range 3–131 mon).

Clinical and lipid profiles were checked every 3 mon for the first year and annually thereafter. The statistics in Table 3 were elaborated using the findings after the first 3-mon examination, since the most significant variations from the pretransplant values occurred early. The plasma values of total TG, VLDL-TG, and apoAI in particular fell rapidly.

The average BMI was  $21.1 \pm 2.7$  before transplant, and it

**TABLE 1**  
Baseline Clinical and Anthropometric Characteristics of Transplant Patients<sup>a</sup>

Parameters	All <i>n</i> = 103		Males <i>n</i> = 65		Females <i>n</i> = 38	
	Mean	SD	Mean	SD	Mean	SD
Age (yr)	41	11.3	39.3	10.6	43.7	12
BMI ( $\text{kg}/\text{m}^2$ )	21.1	2.7	21.2	2.3	21.1	3.2
Glucose (mg/dL)	86	11	87	11	84	12
Urea (mg/dL)	142	66	123	62	154	62
Creatinine (mg/dL)	9.6	4.1	10.4	4.1	8.3	3.8
Albumin (mg/dL)	4.2	0.6	4.2	0.5	4.3	0.6

<sup>a</sup>BMI, body mass index.

**TABLE 2**  
**Baseline Lipid Parameters of Transplant Patients vs. Healthy Blood Donors**

Parameters	Males					Females				
	Cases	SD	Controls	SD	<i>P</i> -value <sup>a</sup>	Cases	SD	Controls	SD	<i>P</i> -value <sup>a</sup>
TG	202.1	78.6	118.0	45.0	<0.001	187.9	89.6	106.0	51.0	<0.001
VLDL-TG	134.1	68.0	78.0	20.0	<0.001	116.3	71.9	63.0	22.0	<0.001
LDL-TG	50.7	28.0	26.0	11.0	<0.001	53.2	25.8	30.0	22.0	<0.001
HDL-TG	17.3	11.3	14.0	4.0	NS	18.2	12.5	13.0	6.0	0.193
Chol	195.2	50.4	202.0	32.0	1.000	211.1	57.5	200.0	33.0	NS
VLDL-Chol	49.3	21.3	35.0	8.0	<0.001	43.9	24.3	29.0	9.0	0.002
LDL-Chol	109.7	38.7	118.0	33.0	NS	117.6	41.0	118.0	26.0	NS
HDL-Chol	37.7	10.1	48.0	10.0	<0.001	48.5	17.7	53.0	8.0	NS
HDL2-Chol	9.7	3.6	20.1	4.2	<0.001	13.8	8.9	25.2	5.1	<0.001
apoAI	117.1	22.7	139.0	33.0	0.001	129.8	32.5	155.0	30.0	0.006
apoAII	25.6	7.6	32.0	8.0	<0.001	27.3	10.6	46.0	6.0	<0.001
apoB	103.2	27.5	110.0	22.0	NS	109.1	30.2	102.0	17.0	NS
apoCII	4.9	2.1	3.1	2.0	<0.001	5.2	1.9	3.3	2.4	0.002
apoCIII	18.0	5.5	10.0	4.0	<0.001	19.8	8.0	8.0	3.0	<0.001
apoE	4.3	1.9	4.0	1.6	NS	5.7	3.1	4.4	2.1	NS

<sup>a</sup>Patients and controls were compared with a two-sample *t*-test and *P*-values were adjusted with a Bonferroni correction. *P*-values over 0.2 are labeled NS. Chol, cholesterol; apo, apolipoprotein.

rose to 22.1 ± 2.5 after 6 and 12 mon, respectively. Thereafter, it remained essentially stable, with a moderate increase (23.4 ± 3.2) for the 46 subjects after at least 96 mon of follow-up.

Average basal blood glucose remained fairly stable throughout the entire follow-up period, ranging from 86.3 ± 11.0 mg/dL at baseline to 92.0 ± 20 mg/dL at 36 mon.

*Lipid profile.* Table 3 shows the lipid parameter values be-

fore transplantation and at follow-up after 3 mon, 3 yr, and 6 yr. The absolute and percentage short-term (3 mon vs. pretransplant) and long-term (mean at 3 and 6 yr vs. pretransplant) differences also are included. The posttransplant pattern was determined from the differences between the 3-mon and the 6-yr values.

Column 5 illustrates a significant reduction in total plasma

**TABLE 3**  
**Baseline and Posttransplantation Lipid and Lipoprotein Values (mg/dL)<sup>a</sup>**

Parameters	Baseline <i>n</i> = 103		Posttransplant <i>n</i> = 91		Year 3 <i>n</i> = 77		Year 6 and over <i>n</i> = 45		Difference Post-baseline <i>n</i> = 91			Difference Year 3–baseline ( <i>n</i> = 77)			Difference >Year 6–baseline ( <i>n</i> = 45)			Difference >Year 6–post-baseline ( <i>n</i> = 45)		
	Mean	SD	Mean	SD	Mean	SD	Mean	SD	Mean	(%)	<i>P</i>	Mean	(%)	<i>P</i>	Mean	(%)	<i>P</i>	Mean	(%)	<i>P</i>
TG	197.0	82.6	127.8	55.5	139.0	63.4	132.8	49.8	-70.5	-35.8	<b>0.0015</b>	-57.0	-29.4	<b>0.0016</b>	-65.6	-33.3	<b>0.0015</b>	9.6	7.5	0.99
VLDL-TG	127.7	69.6	73.0	48.1	84.2	50.1	74.9	39.0	-55.6	-43.6	<b>0.0015</b>	-40.6	-34.1	<b>0.0032</b>	-53.6	-42.0	<b>0.0015</b>	6.0	8.3	1.00
LDL-TG	51.6	27.1	40.6	14.5	32.1	13.5	36.6	14.5	-11.4	-22.2	<b>0.0015</b>	-21.3	-37.7	<b>0.0016</b>	-14.5	-28.1	<b>0.003</b>	-3.1	-7.5	0.98
HDL-TG	17.6	11.7	14.6	9.1	22.7	7.6	21.9	6.6	-3.0	-16.8	0.42	4.9	28.7	<b>0.0408</b>	3.2	18.1	0.89	7.3	50.1	<b>0.0045</b>
Chol	200.9	53.3	218.4	48.2	226.4	47.9	222.6	46.0	17.0	8.5	0.13	22.4	12.7	0.07	20.0	10.0	0.34	3.6	1.7	1.00
VLDL-Chol	47.4	22.4	22.8	16.6	22.1	13.4	24.3	12.0	-24.9	-52.6	<b>0.0015</b>	-25.2	-53.4	<b>0.0016</b>	-25.0	-52.7	<b>0.0015</b>	0.6	2.7	1.00
LDL-Chol	112.6	39.5	137.3	40.6	143.9	37.9	143.0	38.8	24.5	21.8	<b>0.0015</b>	32.0	27.9	<b>0.0016</b>	33.3	29.6	<b>0.0015</b>	1.6	1.2	1.00
HDL-Chol	42.5	13.9	59.3	19.1	57.7	15.3	56.8	13.0	16.9	39.8	<b>0.0015</b>	16.1	35.6	<b>0.0016</b>	12.5	29.4	<b>0.0015</b>	-7.0	-11.7	0.15
HDL2-Chol	11.2	6.3	21.0	9.7	22.8	10.5	19.8	6.8	10.1	90.6	<b>0.0015</b>	10.1	103.9	<b>0.0016</b>	8.0	71.9	<b>0.0015</b>	-3.9	-18.6	0.21
HDL3-Chol	31.3	10.4	38.6	12.8	34.9	8.7	37.3	9.1	7.1	22.8	<b>0.0015</b>	2.7	11.3	0.81	4.7	15.1	0.21	-2.8	-7.2	0.93
apoAI	121.7	27.2	148.1	29.1	140.6	25.2	143.8	26.4	25.6	21.1	<b>0.0015</b>	15.0	15.5	<b>0.0019</b>	15.7	12.9	0.08	-14.8	-10.0	0.14
apoAII	26.2	8.8	27.0	8.4	31.6	7.8	30.2	7.4	1.1	4.1	1.00	3.7	20.5	<b>0.0056</b>	1.8	6.8	0.99	0.7	2.6	1.00
apoB	105.3	28.5	118.0	30.3	127.9	37.9	108.6	30.5	12.7	12.1	<b>0.0075</b>	20.6	21.5	<b>0.0016</b>	1.9	1.8	1.00	-9.8	-8.3	0.40
apoCII	5.0	2.1	4.4	1.6	4.8	2.2	4.4	1.4	-0.7	-13.7	<b>0.028</b>	-0.7	-4.6	0.53	-0.9	-18.0	<b>0.037</b>	-0.1	-1.9	1.00
apoCIII	18.7	6.6	16.5	5.1	14.1	6.1	12.0	4.8	-2.1	-11.0	<b>0.038</b>	-5.6	-24.5	<b>0.0016</b>	-8.2	-44.0	<b>0.0015</b>	-4.7	-28.4	<b>0.0015</b>
apoE	4.8	2.5	5.9	2.5	4.7	1.3	4.6	1.5	1.0	19.8	<b>0.025</b>	-0.7	-2.5	0.33	-0.8	-16.4	0.31	-1.4	-23.9	<b>0.0015</b>
apoB/LDL-Chol	0.990	0.2900	0.8840	0.1700	0.8910	0.1470	0.7630	0.1100	-0.099	-10.0	0.09	-0.13	-10.0	<b>0.0576</b>	-0.28	-28.3	<b>0.0015</b>	-0.10	-10.9	<b>0.074</b>
HDL2-C/HDL3-C	0.3760	0.2000	0.5720	0.2400	0.6760	0.3260	0.5470	0.2100	0.207	55.1	<b>0.0015</b>	0.27	79.8	<b>0.0016</b>	0.18	47.9	<b>0.0015</b>	-0.07	-11.9	0.96

<sup>a</sup>All differences are also reported as percentages over the reference values. The second column reports values obtained 3 mon after transplantation. The fourth column reports the means of all available values after 5 yr for subjects with at least 6 yr of follow-up. Column 5 reports the differences between values in column 2 and in column 1 for 91 subjects with at least 3 mon of follow-up. Column 7 reports the difference between column 4 and column 2 for 45 subjects with at least 6 yr of follow-up. Column 8 reports the difference between column 4 and column 1 for 45 subjects with at least 6 yr of follow-up. Within-patient differences were assessed with a paired-samples *t*-test. To account for multiple testing, according to the Bonferroni correction only *P*-values below 0.002 should be considered as significant. For abbreviations see Table 2.



**TABLE 4**  
**Baseline and Posttransplantation Lipid and Lipoprotein Values (mg/dL) According to the Occurrence of Cardiovascular Events or Rejections<sup>a</sup>**

Parameters	Baseline						Posttransplant					
	No events (no explants, <i>n</i> = 46)		CVD ( <i>n</i> = 15)		Rejections ( <i>n</i> = 46)		No events (no explants, <i>n</i> = 46)		CVD ( <i>n</i> = 15)		Rejections ( <i>n</i> = 46)	
	Mean	SD	Mean	SD	Mean	SD	Mean	SD	Mean	SD	Mean	SD
TG	194.7	75	231.5	91	188.7	86	119.7	36	158.1	79.7	128.1	64
VLDL-TG	127.8	59	150.4	79	120.3	76	67.2	34	94.2	64.8	73.4	56
LDL-TG	48.3	24	63.6	26	52	30	37.7	11	48.3	18.8	41.7	16
HDL-TG	18.5	10	17.5	16	16.5	12	14.9	7	15.5	15.8	14.1	9
Chol	205.2	53	213.9	62	194.2	52	220.8	43	233.6	65.6	211.2	48
VLDL-Chol	48.7	22	54.9	23	44	23	20.8	13	31.5	23.9	22.5	18
HDL-Chol	43.8	17	38.6	13	40	11	62.2	20	63.1	27.8	55.1	14
HDL2-Chol	12.5	8	10.9	5	9.8	4	22.2	11	22.5	11.5	19.2	8
apoAI	129.3	29	106.4	19	118	25	156.6	29	146.2	39.5	138.7	23
apoAII	28.1	10	26.4	9	23.9	8	29	9	25.5	7	25.1	7
apoB	106.5	28	120.5	30	99.8	27	118.8	29	121.3	35.9	116	31
apoCII	5.2	2	5.7	3	4.6	2	4.4	1	4.2	1.1	4.5	2
apoCIII	19.6	7	19.6	8	17.3	6	16.7	5	16.1	6.1	16.5	5
apoE	5.2	3	4.8	1.7	4.4	2	5.7	2	6.1	2.1	6	3

<sup>a</sup>None of the parameters was significantly different in the three groups after the Bonferroni correction. CVD, cardiovascular disease.

TG and all the VLDL-transported components. The protein component (especially apoCII and -CIII) was also reduced; there was thus an increase in HDL-Chol and both its fractions, especially HDL2, whose Chol load rose by 90%. The apo component of HDL increased significantly for apoAI (a 21% rise in plasma levels). In the initial 3-mon period, total Chol remained steady, whereas LDL-Chol and total apoB showed a significant increase. Column 8 shows the mean differences between the 6-yr and the 3-mon values and hence the behavior of the lipid parameters in relation to the new metabolic setting induced by the transplant. As can be seen, there were no significant changes in total and transported TG and Chol. There were slight alterations in apoAI and -B, together with a nonsignificant reduction in the apoB/LDL-Chol ratio.

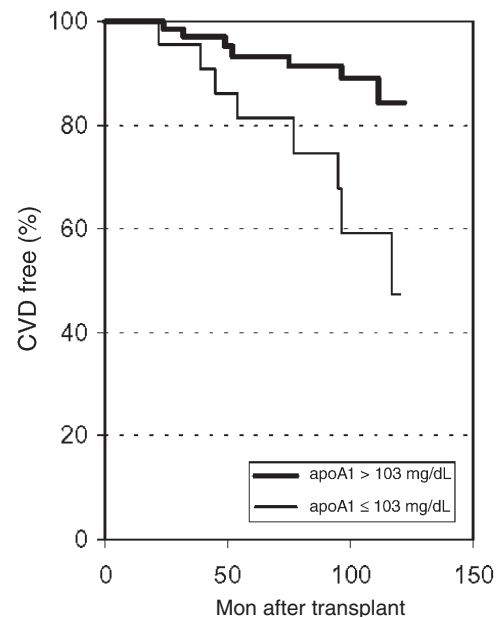
Column 7 gives the long-term variations vs. the pretransplant situation. Most of the significant changes induced after 3 mon were maintained after 6 yr. The main exceptions were the continued decrease in apoCIII and the apoB/LDL-Chol ratio.

**Mortality, rejections, and cardiovascular events.** A total of 25 deaths (25%) occurred over the follow-up period. No lipid or pharmacological parameters were significantly associated with overall mortality. Of these, 15 major cardiovascular events (fatal and nonfatal acute myocardial infarction and stroke). Baseline and posttransplant lipid levels are reported in Table 4 according to the occurrence of cardiovascular events or rejections. None of the parameters was significantly different in the three groups after the Bonferroni correction.

A Kaplan–Meier analysis of the 15 major cardiovascular events indicated that the apoAI level at the time of transplant was significantly associated with earlier events (log-rank test:

$P = 0.005$ ) (Fig. 1). A multivariate analysis with the Cox model showed that this significance was present after adjusting for age and gender ( $P = 0.006$ ). None of the other lipoprotein parameters was strongly associated with the risk of cardiovascular events, although a weak association was found for baseline LDL-Chol ( $P = 0.02$ ) and for apoB ( $P = 0.08$ ).

During follow-up, 46 rejections (estimated median organ



**FIG. 1.** Kaplan–Meier estimate of cardiovascular disease (CVD)-free survival stratified by baseline apoAI below or over the median value (103 mg/dL).

survival: 126 mon; 95% confidence interval, 87–131) occurred. Apart from the baseline apoAI ( $P = 0.048$ ), none of the biological and pharmacological parameters was associated with overall organ survival.

## DISCUSSION

Cardiovascular complications have long been regarded as one of the factors that determine the mortality of renal transplant recipients (1–3). Corroboration of this view can be found in the 1998 Annual Report of the United States Renal Data System (21), which shows that cardiac ischemia and cerebral and peripheral vasculopathies are the main cause of posttransplantation death.

Recent studies (22) also have demonstrated that the incidence of cardiovascular events in transplant recipients is higher than in the general population, with an odds ratio that rises to more than 12 in males ages 40–49.

These findings inevitably draw attention to the cardiovascular risk factors in transplant recipients—some shared with the general population, others typical of these patients—that are associated with cardiovascular events and whose correction can reduce the overall risk during the posttransplantation period (22).

All the studies directed at identifying the causes of the metabolic alterations observed in transplant recipients have illustrated the concurrence of several factors: the clinical and metabolic condition of the patient prior to transplantation, the type of dialysis, and immunosuppressive management and drug treatment (4,5,12).

A frequent finding in the literature is also the difference in the lipoprotein profile, and hence in the incidence of cardiovascular complications, of transplant recipients from different geographical areas (23–25), as in the normal population.

The pretransplant Chol and total TG values of our Caucasian subjects were similar to those described in other studies. As shown in Table 2, they displayed the typical profile of uremics prior to transplantation: elevated TG, elevated VLDL-Chol, reduced HDL-Chol in males, and a marked reduction of HDL2-Chol in both sexes with an increase in the content of TG in the LDL compared to that of a normal control population.

Our data, however, are somewhat different from those in a similar study (9), especially with regard to our higher HDL-Chol and lower LDL-Chol values. Higher HDL2-Chol levels were also observed, whereas the HDL3-Chol values were much the same in both studies. One can deduce that the profile is substantially better in our patients owing to factors that could be linked to their different characteristics, including their eating habits and possibly the dialytic management, since HDL2-Chol levels are also a reflection of the peripheral clearance of TG-rich lipoproteins (TRL) (26).

In our patients, we have taken into consideration the greatest number of lipid parameters, lipoprotein fractions, and apo levels. We hoped to characterize the profile of the patient in chronic renal failure in a precise manner as a candidate for a

renal transplant and to evaluate variations in this profile in the years following transplantation. The most evident alterations in the lipoprotein profile occur in our case series 3 mon after transplantation, a finding not always present in the literature. The first finding that emerges is the 35% reduction of plasma TG, a reduction that embraces all the lipoprotein fractions, principally the portion transported by the VLDL (–43%). The reduction in the lipid component of the VLDL involves not only the TG but also Chol (–52%). This finding indicates that the transplant has significantly modified the metabolism of the TRL. The observations of other workers (27,28) corroborate this finding in that the activity of the two enzymes involved in the clearance of these lipoproteins [hepatic TG lipase and lipoprotein lipase (LPL)] improves after transplantation. In this connection, it also becomes important to consider the circulating levels of the LPL effectors apoCII and -CIII, which in our study were measured on whole plasma and not on the isolated lipoprotein fractions. Even though this finding is indirect, their simultaneous reduction could indicate a reduction in the dimension of the particles, an expression of their better metabolism. In this connection, evaluation of the size of the VLDL before and after transplantation could provide important data.

The modifications in the TRL of our transplant recipients persisted throughout the observation period (Table 3, column 8). The substantial stability of the VLDL-transported lipid components, together with the reduction in the apoCIII levels after transplantation and during the next 6 yr, while not significant, suggest that the metabolic profile before transplantation was substantially changed. Lasting stabilization of the HDL-Chol levels after transplantation, too, can be seen as a consequence of improved TRL metabolism. The changes in the protein component of the lipoproteins follow those of the lipid component, even though the determinations were performed on whole plasma and not on the individual lipoprotein fractions. ApoCIII, an inhibitor of the enzymatic activity of LPL, fell by 10% in the 3 mon after transplantation and continued to fall throughout the 6 yr.

Chol metabolism, on the other hand, differed and is more difficult to interpret. Changes in total and transported Chol reflect both the alterations in the lipoproteins that transport the TG and quantitative changes in the LDL particles, the main plasma Chol carriers. If, in fact, an alteration in TRL metabolism (i.e., reduced clearance) changes quantitatively and qualitatively after transplantation, the result is a reduction mainly in TG, but also in the Chol transported by some lipoprotein fractions. VLDL-Chol, indeed, fell by 52% after 6 yr.

The increase in the Chol transported by the LDL and HDL, like that of the apo that characterize them (apoB and apoAI), is a very complex event. The increase in LDL-Chol can be viewed as the result of better TRL clearance, and hence better transformation into intermediate density lipoproteins and then LDL, and also as the expression of alterations in the lipoprotein structure (glycosylations, oxidations, lipoperoxidations) that significantly decrease their receptorial catabo-

lism (29,30). Moreover, the possibility cannot be ruled out that a greater flow of substrates to the liver may help to augment the circulating LDL pool.

An important role is also played by immunosuppressive management. Considerable evidence supports the pathogenic role of drugs, steroids, and cyclosporine in particular on dyslipidemia in renal transplant recipients, but the mechanism by which this is accomplished is not yet fully elucidated. *In vitro* and *in vivo* reports have shown that cyclosporine increases LDL-Chol (5,8,15,16,31) and reduces hepatic secretion of apoB and hence the production of VLDL (32). It can directly reduce the expression of the mRNA of the LDL receptor by 40% (33).

The corticosteroids, whose effect is predominantly on VLDL, are also able to reduce the expression of mRNA of the LDL receptor *in vitro* in a dose-dependent manner (34). Furthermore, data obtained *in vitro* show that the inhibitory effect on the uptake of the LDL by the two immunosuppressors is annulled with the use of the HMG-CoA reductase inhibitors (35).

On the other side, clinical reports have positively correlated the presence of dyslipidemia to the use of cyclosporine in kidney- or liver-transplant patients (15,16,36,37), whereas others found no correlation (38). The association of dyslipidemia with different immunosuppressors, such as prednisone and cyclosporine, brings an additional confusing element into its development caused by grafting. As a matter of fact, if cyclosporine or prednisone has well-characterized effects when taken alone, the combined use in patients with a preexisting altered metabolism makes interpreting their metabolic parameters much more difficult. Our work, which has followed some patients for 6 yr from transplantation with the same immunosuppressive therapy (cyclosporine and prednisone), does not clearly highlight single drug effects, nor does it allow evaluation of a direct effect of the immunosuppressive therapy on lipoprotein metabolism.

A therapeutic approach appears necessary since dyslipidemia contributes to both cardiovascular disease and mortality. It also influences the development of chronic vascular rejection in the transplant, thus having an influence on graft outcome. Drugs such as HMG-CoA reductase inhibitors (statins) are available for reducing LDL-Chol and TG efficiently (39,40). Statins also reduce the level of oxidized LDL, and they have direct effects on smooth muscle cells and the intima of the arteries (41). The statins represent the most effective Chol-lowering agents available, and side effects, myopathy in particular, are controlled with appropriate daily dosages.

Therapeutic options for treating dyslipidemia in cyclosporine-treated renal transplant recipients were limited when our study was performed. Although the use of the statins in transplant patients had begun in the early 1990s, the efficacy and tolerability of the drug were tested later in several prospective trials, as shown in a recent review (42). Hence, our patients were not given the drug since they were nearly at the end of the follow-up when statins were routinely introduced.

We should also consider the atherogenic lipid profile of our patients: We observed the simultaneous presence of improved metabolism (reduced VLDL-Chol and increased HDL-Chol) on the one hand and the occurrence of adverse events, such as the increase in LDL-Chol and structural LDL particle changes on the other. The substantial stability of Chol levels after transplantation and in subsequent reports, together with a higher incidence of cardiovascular complications, would lead one to believe that the mechanisms responsible for vessel damage must be sought mainly in the structural and physicochemical alterations of the individual lipoprotein fractions or in other risk factors. In this regard, LDL from transplant subjects undergoes not only oxidative processes but also peroxidation, glycation, and carbamoylation, making lipoprotein particles more atherogenic (43). The damage to lipid metabolism may be more consistent than it appears from the quantitative observation of the lipoprotein fractions, given that the increases in HDL-Chol and HDL2-Chol also could be related to the better exchange of lipid components between the lipoprotein classes, as mediated by the CETP following the modification of TG metabolism (44). This improvement occurred in the first 3 mon after transplantation and persisted throughout the observation period.

Last, the association between major cardiovascular events and the circulating apoAI level at the time of transplantation is a useful finding. Although the small number of events suggests that caution is necessary when interpreting this result, it is in agreement with the already known but controversial role of the apo as more sensitive markers of cardiovascular risk than such classical parameters as LDL or HDL (45).

Additional research is needed to better define the relationship between lipid abnormalities and both CVD and renal disease progression. In particular, the role of increased TG, low HDL, and associated lipoprotein compositional abnormalities in CVD should be studied. Large, multicenter trials to study the effects of lipid-lowering therapy on the rate of renal disease progression should be conducted.

## ACKNOWLEDGMENTS

This work was supported in part by grants from the Ministero dell'Università e della Ricerca Scientifica e Tecnologica (Quota 60%), Roma, Italy.

## REFERENCES

1. Levey, A.S. (1998) Controlling the Epidemic of Cardiovascular Disease in Chronic Renal Disease: Where Do We Start? *Am. J. Kidney. Dis.* 5 (Suppl. 3), S5–S13.
2. Ibels, L.S., Stewart, J.H., Mahony, J.F., and Sheil, A.G. (1974) Deaths from Occlusive Arterial Disease in Renal Allograft Recipients, *Br. Med. J.* 3, 552–554.
3. Kasiske, B.L. (1988) Risk Factors for Accelerated Atherosclerosis in Renal Transplant Recipients, *Am. J. Med.* 84, 985–992.
4. Cattran, D.C., Fenton, S.S., Wilson, D.R., and Steiner, G. (1976) Defective Triglyceride Removal in Lipemia Associated with Peritoneal Dialysis and Haemodialysis, *Ann. Intern. Med.* 85, 29–33.
5. Vathsala, A., Weinberg, R.B., Schoenberg, L., Grevel, J., Goldstein, R.A., Van Buren, C.T., Lewis, R.M., and Kahan, B.D.

- (1989) Lipid Abnormalities in Cyclosporine-Prednisone-Treated Renal Transplant Recipients, *Transplantation* 48, 37–43.
6. Lowry, R.P., Soltys, G., Peters, L., Mangel, R., and Sniderman, A.D. (1987) Type II Hyperlipoproteinemia, Hyperapobeta-lipoproteinemia, and Hyperalphalipoproteinemia Following Renal Transplantation: Implications for Atherogenic Risk, *Transplant. Proc.* 19, 3426–3430.
  7. Isoniemi, H. (1995) Hyperlipidemia After Renal Transplantation: Facts and Potential Implications, *Nephrol. Dial. Transplant.* 10, 457–459.
  8. Cassader, M., Ruiu, G., Gambino, R., Alemanno, N., Triolo, G., and Pagano, G. (1991) Lipoprotein–Apolipoprotein Changes in Renal Transplant Recipients: A 2-Year Follow-up, *Metabolism* 40, 922–925.
  9. Banyai-Falger, S., Gottsauner-Wolf, M., Stepan, E., Strobl, W., Jansen, M., Heinz, G., Horl, W.H., and Derfler, K. (1997) Lipoprotein Pattern in End-Stage Renal Disease and Following Successful Renal Transplantation, *Clin. Transplant.* 11, 545–551.
  10. Kasiske, B.L. (1998) Hyperlipidemia in Patients with Chronic Renal Disease, *Am. J. Kidney Dis.* 32 (Suppl. 3), S142–S156.
  11. Perez, R. (1993) Managing Nutrition Problems in Transplant Patients, *Nutr. Clin. Pract.* 8, 28–32.
  12. Dimeny, E., Tufveson, G., Lithell, H., Larsson, E., Siegbahn, A., and Fellstrom, B. (1993) The Influence of Pretransplant Lipoprotein Abnormalities on the Early Results of Renal Transplantation, *Eur. J. Clin. Invest.* 23, 572–579.
  13. Hughes, T.A., Gaber, A.O., Amiri, H.S., Wang, X., Elmer, D.S., Winsett, R.P., Hathaway, D.K., Hughes, S.M., and Ghawji, M. (1994) Lipoprotein Composition in Insulin-Dependent Diabetes Mellitus with Chronic Renal Failure: Effect of Kidney and Pancreas Transplantation, *Metabolism* 43, 333–347.
  14. Hricik, D.E. (1994) Post-transplant Hyperlipidemia: The Treatment Dilemma, *Am. J. Kidney Dis.* 23, 766–771.
  15. Kasiske, B.L., Tortorice, K.L., Heim-Duthoy, K.L., Awini, W.M., and Rao, K.V. (1991) The Adverse Impact of Cyclosporine on Serum Lipids in Renal Transplant Recipients, *Am. J. Kidney Dis.* 17, 700–707.
  16. Hricik, D.E., Mayes, J.T., and Schulak, J.A. (1991) Independent Effects of Cyclosporine and Prednisone on Post-transplant Hypercholesterolemia, *Am. J. Kidney Dis.* 18, 353–358.
  17. National Diabetes Data Group (1979) Classification and Diagnosis of Diabetes Mellitus and Other Categories of Glucose Intolerance, *Diabetes* 28, 1039–1057.
  18. Cassader, M., Ruiu, G., Gambino, R., Alemanno, N., Triolo, G., and Pagano, G. (1989) Apolipoprotein C and E in Diabetic Uraemic Patients, *Diabetes, Nutr. Metab.* 2, 33–38.
  19. Warnick, G.R., and Albers, J.J. (1978) A Comprehensive Evolution of the Heparin Manganese Precipitation Procedure for Estimating High Density Lipoprotein Cholesterol, *J. Lipid Res.* 29, 65–76.
  20. Gidez, L.I., Miller, G.J., Burstein, M., Slagle, S., and Eder, H.A. (1982) Separation and Quantitation of Subclasses of Human Plasma High Density Lipoproteins by a Simple Precipitation Procedure, *J. Lipid Res.* 23, 1206–1223.
  21. United States Renal Data System: USRDS 1998 Annual Data Report, National Institute of Diabetes and Digestive and Kidney Diseases, The National Institutes of Health, Bethesda, MD, 1997.
  22. Kasiske, B.L. (2000) Cardiovascular Disease After Renal Transplantation, *Seminars in Nephrology* 20, 176–187.
  23. Fassbinder, W., Brunner, F.P., Brynner, H., Ehrich, J.H., Geerlings, W., Raine, A.E., Rizzoni, G., Selwood, N.H., Tufveson, G., and Wing, A.J. (1991) Combined Report on Regular Dialysis and Transplantation in Europe, XX, 1989, *Nephrol. Dial. Transplant.* 6 (Suppl. 1), 5–35.
  24. Raine, A.E., Margreiter, R., Brunner, F.P., Ehrich, J.H., Geerlings, W., Landais, P., Loirat, C., Mallick, N.P., Selwood, N.H., and Tufveson, G. (1992) Report on Management of Renal Failure in Europe, XXII, 1991, *Nephrol. Dial. Transplant.* 7 (Suppl. 2), 7–35.
  25. Lindholm, A., Albrechtsen, D., Frodin, L., Tufveson, G., Persson, N.H., and Lundgren G. (1995) Ischemic Heart Disease—Major Cause of Death and Graft Loss After Renal Transplantation in Scandinavia, *Transplantation* 60, 451–457.
  26. Patsch, J.R., Prasad, S., Gotto, A.M., Jr., and Patsch, W. (1987) High Density Lipoprotein 2. Relationship of the Plasma Levels of This Lipoprotein Species to Its Composition, to the Magnitude of Postprandial Lipemia, and to the Activities of Lipoprotein Lipase and Hepatic Lipase, *J. Clin. Invest.* 80, 341–347.
  27. Ibels, S.L., Reardon, M.F., and Nestel, P.J. (1976) Plasma Post-heparin Lipolytic Activity and Triglyceride Clearance in Uremic and Hemodialysis Patients and Renal Allograft Recipient, *J. Lab. Clin. Med.* 87, 648–658.
  28. Crawford, G.A., Saydie, E., and Stewart, J.H. (1979) Heparin-Released Plasma Lipases in Chronic Renal Failure and After Renal Transplantation, *Clin. Sci.* 57, 155–165.
  29. Ghanem, H., van den Dorpel, M.A., Weimar, W., Man in 't Veld, A.J., El-Kannishy, M.H., and Jansen, H. (1996) Increased Low Density Lipoprotein Oxidation in Stable Kidney Transplant Recipients, *Kidney Int.* 49, 488–493.
  30. Galle, J., and Wanner, C. (1999) Modification of Lipoproteins in Uremia: Oxidation, Glycation and Carbamoylation, *Miner. Electrolyte Metab.* 25, 263–268.
  31. Quaschnig, T., Mainka, T., Nauck, M., Rump, L.C., Wanner, C., and Kramer-Guth, A. (1999) Immunosuppression Enhances Atherogenicity of Lipid Profile After Transplantation, *Kidney Int.* 71 (Suppl.), S235–S237.
  32. Kaptein, A., de Wit, E.C., and Princen, H.M. (1994) Cotranslational Inhibition of apoB-100 Synthesis by Cyclosporin A in the Human Hepatoma Cell Line HepG2, *Arterioscler. Thromb.* 14, 780–789.
  33. Rayyes, O.A., Wallmark, A., and Floren, C.H. (1996) Cyclosporine Inhibits Catabolism of Low-Density Lipoproteins in HepG2 Cells by About 25%, *Hepatology* 24, 613–619.
  34. Al Rayyes, O., Wallmark, A., and Floren, C.H. (1997) Additive Inhibitory Effect of Hydrocortisone and Cyclosporine on Low-Density Lipoprotein Receptor Activity in Cultured HepG2 Cells, *Hepatology* 26, 967–971.
  35. Al Rayyes, O., Wallmark, A., and Floren, C.H. (1997) Reversal of Cyclosporine-Inhibited Low-Density Lipoprotein Receptor Activity in HepG2 Cells by 3-Hydroxy-3-methylglutaryl Coenzyme A Reductase Inhibitors, *Hepatology* 25, 991–994.
  36. Abouljoud, M.S., Levy, M.F., Klintmalm G.B. (1995) Hyperlipidemia After Liver Transplantation: Long-Term Results of the FK506/Cyclosporine a U.S. Multicenter Trial, U.S. Multicenter Study Group, *Transplant Proc.* 27, 1121–1123.
  37. Guckelberger, O., Bechstein, W.O., Neuhaus, R., Luesebrink, R., Lemmens, H.P., Kratschmer, B., Jonas, S., and Neuhaus, P.L. (1997) Cardiovascular Risk Factors in Long-Term Follow-up After Orthotopic Liver Transplantation, *Clin Transplant.* 11, 60–65.
  38. Fernandez-Miranda, C., Guijarro, C., de la Calle, A., Loinaz, C., Gonzalez-Pinto, I., Gomez-Izquierdo, T., Larumbe, S., Moreno, E., and del Palacio, A. (1998) Lipid Abnormalities in Stable Liver Transplant Recipients—Effects of Cyclosporin, Tacrolimus, and Steroids, *Transpl. Int.* 11, 137–142.
  39. The Lipid Research Clinics Coronary Primary Prevention Trial Results I. (1984) Reduction in Incidence of Coronary Heart Disease, *JAMA* 251, 351–364.
  40. Scandinavian Simvastatin Survival Study Group (1994) Randomized Trial of Cholesterol Lowering in 4444 Patients with Coronary Heart Disease: The Scandinavian Simvastatin Survival Study (4S), *Lancet* 344, 1383–1389.



41. Kobashigawa, J.A., Katznelson, S., Laks, H., Johnson, J.A., Yeatman, L., Wang, X.M., Chia, D., Terasaki, P.I., Sabad, A., and Cogert, G.A. (1995) Effect of Pravastatin on Outcomes After Cardiac Transplantation, *N. Engl. J. Med.* 333, 621–627.
42. Kobashigawa, J.A., and Kasiske, B.L. (1997) Hyperlipidemia in Solid Organ Transplantation, *Transplantation* 63, 331–338.
43. Galle, J., and Wanner, C. (1999) Modification of Lipoproteins in Uremia: Oxidation, Glycation and Carbamoylation, *Miner. Electrolyte Metab.* 25, 263–268.
44. Yamashita, S., Hirano, K., Sakai, N., and Matsuzawa, Y. (2000) Molecular Biology and Pathophysiological Aspects of Plasma Cholesteryl Ester Transfer Protein, *Biochim. Biophys. Acta* 1529, 257–275.
45. Qureshi, A., Giles, W., Croft, J., Guterman, L., and Hopkins, N. (2002) Apolipoproteins A-1 and B and the Likelihood of Non-fatal Stroke and Myocardial Infarction—Data from The Third National Health and Nutrition Examination Survey, *Med. Sci. Monit.* 8, CR311–316.

[Received May 23, 2002, and in revised form October 17, 2002; revision accepted November 4, 2002]

# Dietary Long-Chain PUFA in the Form of TAG or Phospholipids Influence Lymph Lipoprotein Size and Composition in Piglets

Laura Amate<sup>a,b,\*</sup>, Angel Gil<sup>b</sup>, and María Ramírez<sup>a</sup>

<sup>a</sup>Research and Development Department, Abbott Laboratories, 18004 Granada, Spain, and <sup>b</sup>Department of Biochemistry and Molecular Biology, University of Granada, 18071 Granada, Spain

**ABSTRACT:** Several sources of long-chain PUFA (LCP) are currently available for infant formula supplementation. These oils differ in their FA composition, the chemical form of the FA esters [TAG or phospholipids (PL)], and presence of other lipid components. These differences may affect LCP absorption, distribution, and metabolic fate after ingestion. The purpose of this study was to evaluate the influence of different chemical forms of dietary LCP on the composition of lymph lipoproteins. Eighteen pigs (5 d old) were bottle-fed different diets for 2 wk: a control diet (C), a diet containing LCP as TAG from tuna and fungal oils (TF-TAG), or a diet containing LCP as PL from egg yolk (E-PL). We measured lipid and FA composition of lymph, main lymph fractions (TAG or PL), and the particle size of lymph lipoproteins. The average diameter of lymph lipoproteins was significantly lower in the E-PL group compared with the control and TF-TAG groups (C:  $3902 \pm 384$  Å; TF-TAG:  $3773 \pm 384$  Å; E-PL:  $2370 \pm 185$  Å). Arachidonic acid and DHA contents in lymph and lymph-TAG were significantly higher in the TF-TAG group compared to the E-PL group ( $0.50 \pm 0.03$  and  $0.24 \pm 0.03$  g/100 g vs.  $0.29 \pm 0.04$  and  $0.12 \pm 0.03$  g/100 g, respectively). The addition to the diet of LCP in the form of TAG or PL affected the size of intestinal lipoproteins and also led to a different distribution of these FA in lymph lipoproteins.

Paper no. L9004 in *Lipids* 37, 975–980 (October 2002).

The presence of DHA and arachidonic acid (AA) in human milk, together with some reports indicating that long-chain PUFA (LCP) status is improved in infants fed breast milk or LCP-containing formulas (1,2), has prompted international committees to propose the use of formulas containing balanced quantities of n-3 and n-6 LCP, similar to those found in human milk (3–6). In addition, several clinical trials have been designed to evaluate whether LCP enrichment of infant formulas has beneficial effects on the maturation of the visual system and cognitive development (7–14). These trials have shown significant functional advantages of LCP supplementation for both preterm (7–11) and term infants (12–14).

Several sources of LCP, such as fish oils, oils from unicellular organisms, or from eggs, could be used to supplement infant formulas and attain such recommendations. Fish and unicellular

oils are composed mainly of TAG, and oil fractions from commercial egg preparations are rich in phospholipids (PL). Furthermore, these lipid sources differ in the FA composition, presence of other lipid components, and the molecular structure of their TAG and PL. Because lipid digestion is a complex process involving enzymes, it is likely that these differences may affect LCP absorption, distribution, and metabolic fate.

A number of studies have focused on TAG absorption and metabolism, mainly on the importance of the *sn*-2 position (15–17). Less attention has been paid to dietary PL, but there is evidence showing TAG absorption is impaired when the supply of exogenous PL is insufficient for micelle formation during fat digestion and absorption (18–21). Moreover, clinical trials with premature infants found that DHA from egg PL was absorbed better than DHA from breast milk and DHA TAG from single-cell oils (22). Other studies have shown a positive effect of LCP-PL supplementation on fat absorption (23). PL are also essential for intestinal lipoprotein formation and for fat distribution outside the enterocytes. Data from animal studies suggest that intraduodenal infusion of triolein results in the formation of chylomicrons (CM), whereas the infusion of egg PC favors the formation of intestinal VLDL-size particles (24).

In addition, we have studied the effect of the chemical form of LCP on fasting plasma lipoprotein composition and found a different distribution of these FA in lipoprotein fractions depending on whether they were added as TAG or PL (25). In that study, the authors hypothesized that their results were due to the way LCP were packaged on lymph particles. In line with those findings, the goal of this study was to evaluate the influence of the chemical structure of the LCP added to the diet on lymph lipoprotein composition and size during active lipid absorption.

## MATERIALS AND METHODS

**Animals and diets.** Eighteen 5-d-old Yorkshire piglets at term gestation [mean body weights  $2241 \pm 67.5$  g (SD)] were obtained from Ntra. Sra. de las Mercedes Farm (La Guardia, Jaen, Spain) and were randomly assigned to one of three dietary groups. Each group of piglets was housed together and freely fed by bottle three times a day for 2 wk. Heating was provided with spot heat lamps attached above each cage. The study was approved by the Animal Care Committee at the University of Granada and conformed to the European Union Regulation of Animal Care for care and use of animals for research.

\*To whom correspondence should be addressed at Abbott Laboratories, Camino de Purchil, 68, 18004 Granada, Spain.  
E-mail: Maria.Ramirez@abbott.com

Abbreviations: AA, arachidonic acid; CM, chylomicrons; E-PL diet, diet supplemented with egg yolk phospholipid; LCP, long-chain PUFA; PL, phospholipids; TF-TAG diet, diet supplemented with tuna oil or fungal oil as a source of LCP.

Three powder formulas, identical in all ingredients except for fat composition, were designed to meet the nutrient requirement of growing piglets (26). The formulas were dissolved in warm water at a concentration of 188 g/L. The general composition of the control formula has been reported (27). Control fat was composed of a blend of olive, soy, and coconut oils and milk fat. LCP were added by supplementing with tuna oil and fungal oil (TF-TAG diet) or egg yolk-PL (E-PL diet). The final FA composition of the diets is given in Table 1. Tuna oil with a low ratio 20:5n-3/22:6n-3 was supplied by Mochida (Tokyo, Japan) and fungal oil by Suntory (Tokyo, Japan). Part of the vegetable fat blend in the control formula (2.7 g/100 g) was replaced by tuna and fungal oils to achieve an amount similar to that found in swine milk: 0.6 and 0.3 g/100 g of AA and DHA, respectively. E-PL (Ovothin 160) were supplied by Lucas Meyer (Hamburg, Germany). For this diet, 13.2 g/100 g of the fat blend in the control formula was replaced by this source of PL to reach the same concentration of AA and DHA as in the TF-TAG diet.

Because the E-PL source contained a certain amount of cholesterol, the control and the TF-TAG diets were supplemented with cholesterol to produce a final concentration of 0.33 g/100 g diet. In this fashion, dietary cholesterol effects on lipoprotein metabolism were avoided, and it was ensured that any difference found between LCP-supplemented groups was due to the particular forms of LCP in the diets.

**Experimental protocol.** One and a half hours after the intake of 120 mL of each formula, piglets were operated on under intramuscular ketamine anesthesia (15–20 mg/kg body weight). An abdominal incision was made, and the intestines were placed on the right side of the animal, keeping them at 37°C with warm saline solution. The cistern chyli was identified just distal to the right renal vein, and a small incision was made. Samples of lymph were collected with the help of a Pasteur pipet into ice-cooled tubes containing 5 µg of leupeptin to avoid protein degradation, and 40 µL of a preservative solution (25 mM EDTA, 2.5 mg/mL gentamicin sulfate,

1.25 mg/mL chloramphenicol, and 5 mg/mL sodium azide). An aliquot of lymph was separated for the electron microscopy analysis, and the rest was frozen in liquid nitrogen and stored at –80°C until analyzed (24). Since lymph was collected at 1.5 h during the digestion period, the major component of lymph was CM; therefore, sizing was performed directly on the lymph samples.

**Analytical methods.** Freshly isolated lymph samples were photographed using negative staining with electron microscopy. Samples were prepared as follows: a copper-coated grid was floated on a drop of lymph and incubated at room temperature for 4 min. Then the grid was washed twice with double-distilled water and floated on a drop of 2% uranyl acetate for 1 min. Finally, the grid was dried in a stove until it was examined. The negatively stained samples were examined with a Zeiss 10 CR electron microscope (Carl Zeiss, Thornwood, NY) at 100 kV and 50,000× magnification. To measure the particle size distribution, 300–600 particles were measured on the electron micrographs as the average length of diameters measured at 5° intervals around the centroid of each object by the image analysis software Microimage (Olympus Optical, Hamburg, Germany). The mean diameter for each group was calculated from these measurements (24).

An aliquot of lymph was extracted using hexane/isopropanol (3:2) according to Kolarovic and Fournier (28) and dried under nitrogen. The main lipid fractions from lymph extracts (TAG and PL) were separated by TLC on Silica Gel 60 plates (0.5 mm; Merck, Darmstadt, Germany) using hexane/isopropyl ether/acetic acid (75:25:1.5, by vol) according to the method previously described by Skipski and Barclay (29).

Aliquots of lymph and lymph lipid fractions were converted to FAME by transmethylation as previously described by Lepage and Roy (30). FAME were separated and quantified by GLC, using a Hewlett-Packard 5890 gas chromatograph equipped with a FID and a 60 m × 0.32 mm i.d. SP-2330 capillary column (Supelco, Bellefonte, PA) as previously described (31). A mixture of FA standards (Sigma, St. Louis, MO) was used to identify the FA peaks of the different samples.

Cholesterol and TAG in lymph were measured using commercial kits (Roche Diagnostic GmbH, Mannheim, Germany) adapted for a microplate assay. PL were measured in lipid extracts by Ziversmit's method (32). Protein content was measured by Bradford's method (33).

**Statistical analysis.** Diet group differences were investigated by one-way ANOVA using the 7D program of BMDP Statistical Software PC 90 version (Los Angeles, CA) (34). The homogeneity of variances was analyzed by Levene's test. If variances were not homogeneous, Welch's test was used to study group differences. When a significant difference was found ( $P < 0.05$ ), Bonferroni's test was used to examine individual comparisons.

## RESULTS

**Lymph lipoprotein size.** The average diameter of lymph lipoproteins was significantly lower in the E-PL group com-

**TABLE 1**  
FA Composition<sup>a</sup> of Adapted Pig Milk Formula (control) and the Same Diet Supplemented with n-6 and n-3 Long-Chain PUFA<sup>b</sup> (LCP)

FA	Control	TF-TAG	E-PL
8:0	2.3	1.9	1.7
10:0	2.8	2.5	2.2
12:0	1.6	1.7	1.8
14:0	5.6	6.2	6.2
16:0	22.3	23.4	24.9
18:0	8.6	8.4	9.9
16:1n-7	0.6	0.7	0.8
18:1n-9	36.7	35.8	35.2
18:2n-6	13.6	12.2	11.6
18:3n-3	1.2	1.1	1.2
20:4n-6	0.1	0.6	0.6
20:5n-3	—	0.14	—
22:6n-3	—	0.3	0.3

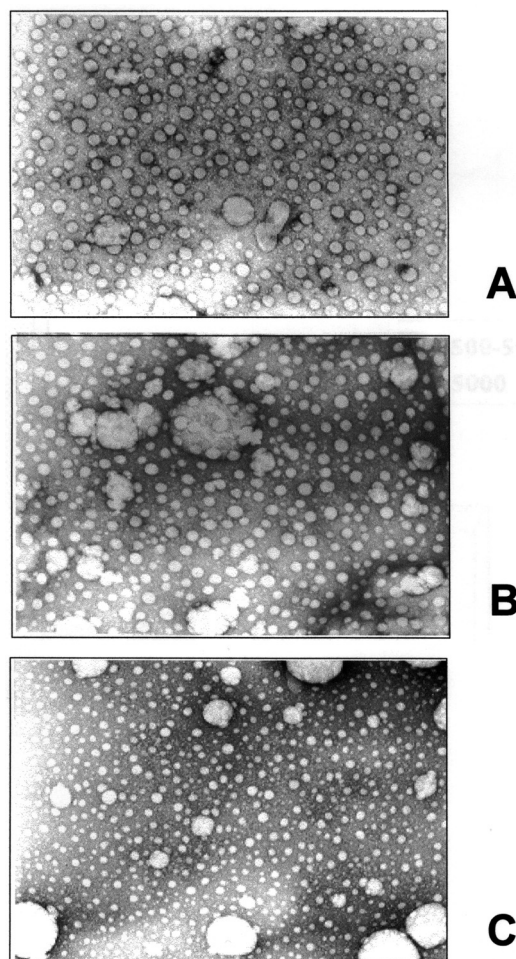
<sup>a</sup>g/100 g of total FA. —, not detected.

<sup>b</sup>Source of PUFA: fungal and tuna oils (TF-TAG) or egg yolk phospholipids (E-PL).

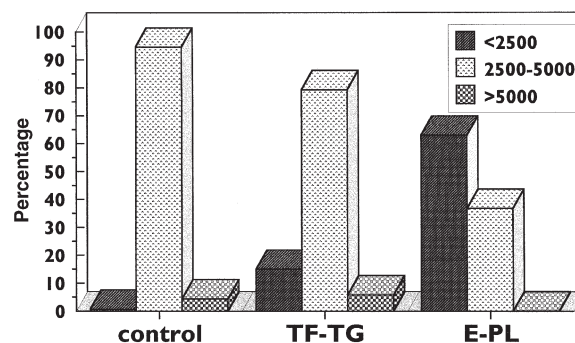
pared to the control and the TF-TAG groups (mean  $\pm$  SEM) (C:  $3902 \pm 186$  Å; TF-TAG:  $3773 \pm 384$  Å; E-PL:  $2370 \pm 185$  Å;  $P < 0.05$ ) as illustrated in Figure 1. When lymph lipoprotein size was represented in ranges, a different distribution was observed for the study groups (Fig. 2). Most of the lipoproteins in the control and TF-group were between 2500 and 5000 Å, whereas they were within the lower range (<2500 Å) in the E-PL group.

**Lipid and FA composition of lymph.** The content of lipids and proteins in lymph samples from piglets fed the study diets is shown in Table 2. There were no significant differences in the content of cholesterol, TAG, PL, and proteins of lymph among the control, the E-PL, and the TF-TAG groups.

The FA composition of total lymph and of lymph TAG and PL is shown in Table 3. The proportion of 16:0 and 16:1n-7



**FIG. 1.** Electron micrographs of intestinal lymph lipoproteins negatively stained with uranyl acetate 2% and examined with a Zeiss 10 CR electron microscope. Magnification of micrographs is 50,000 $\times$ . (A) Intestinal lymph lipoproteins from piglets fed control diet (average diameter  $\pm$  SEM:  $3902 \pm 384$  Å); (B) intestinal lymph lipoproteins from piglets fed adapted milk formula supplemented with long-chain PUFA (LCP) from fungal and tuna oils ( $3773 \pm 384$  Å); (C) intestinal lymph lipoproteins from piglets fed adapted milk formula supplemented with LCP from egg yolk phospholipids ( $2370 \pm 185$  Å).



**FIG. 2.** Distribution of sizes (Å) of lymph lipoproteins from piglets fed diets supplemented with LCP in the form of TAG or phospholipids (PL). Values are means  $\pm$  SEM,  $n = 6$ . Control: group fed adapted milk formula for piglets. TF-TAG: group fed adapted milk formula for piglets supplemented with LCP from fungal and tuna oils. E-PL: group fed adapted milk formula for piglets supplemented with LCP from egg yolk phospholipids. For abbreviation see Figure 1.

was higher and that of 18:1n-9 lower in the E-PL group than in the TF-TAG and C groups in total lymph and lymph TAG. The proportion of 18:2n-6 in lymph PL was lower in the TF-TAG group than in the E-PL and C groups. Regarding LCP, both groups of animals fed with LCP-supplemented diets had higher proportions of AA and DHA in lymph lipids. The TF-TAG group had significantly higher proportions of AA and DHA in total lymph and lymph TAG than the E-PL group. No significant differences were found in lymph PL for the FA mentioned above.

## DISCUSSION

There is some evidence that LCP added in the form of PL or TAG may not be equally digested, absorbed, or distributed. First, TAG and PL are hydrolyzed by different enzymes, yielding different products in the intestine. Pancreatic lipase cleaves the *sn*-1 and *sn*-2 position of TAG and releases 2-MAG and FFA (35). Activated pancreatic phospholipase A<sub>2</sub> releases 1-lysophospholipids and FFA from PL (24). In addition, some studies in newborn infants have indicated that dietary PL may be better absorbed than TAG. Morgan *et al.* (23) found that fat

**TABLE 2**  
**Lipid Composition<sup>a</sup> of Lymph from Infant Piglets Fed the Control Diet or Diets Supplemented with LCP in the Form of TAG or Phospholipids (PL)**

	Diet		
	Control	TF-TAG	E-PL
Protein (mg/mL)	11.97 $\pm$ 1.1	13.92 $\pm$ 3.28	10.56 $\pm$ 0.8
Cholesterol (mg/dL)	94.11 $\pm$ 19.6	70.40 $\pm$ 12.4	60.81 $\pm$ 8.1
TAG (mg/dL)	3545.6 $\pm$ 360.7	2327.7 $\pm$ 272.0	3255.0 $\pm$ 385.7
PL <sup>b</sup> (mg/dL)	33.96 $\pm$ 6.7	31.58 $\pm$ 3.37	33.13 $\pm$ 6.79

<sup>a</sup>Values are means  $\pm$  SEM,  $n = 6$ . Control: group fed adapted milk formula for piglets. TF-TAG: group fed adapted milk formula for piglets supplemented with LCP from fungal and tuna oils. E-PL: group fed adapted milk formula for piglets supplemented with LCP from egg yolk PL. For abbreviations see Table 1.

<sup>b</sup>Expressed as P<sub>i</sub>.



**TABLE 3**  
**Selected FA Composition<sup>a</sup> of Lymph and Its Fractions (g/100 g) in Infant Piglets Fed the Control Diet or Diets<sup>b</sup> Supplemented with LCP in the Form of TAG or PL**

	Total lymph			Lymph TAG			Lymph PL		
	Control	TF-TAG	E-PL	Control	TF-TAG	E-PL	Control	TF-TAG	E-PL
<b>SAT</b>									
16:0	22.02 ± 0.16 <sup>a</sup>	22.61 ± 0.40 <sup>a</sup>	23.77 ± 0.09 <sup>b</sup>	22.93 ± 0.36 <sup>a</sup>	23.80 ± 0.50 <sup>a</sup>	25.15 ± 0.10 <sup>b</sup>	22.95 ± 0.7 <sup>a</sup>	29.92 ± 0.61 <sup>b</sup>	27.01 ± 0.35 <sup>b</sup>
18:0	9.37 ± 0.27	8.44 ± 0.37	9.36 ± 0.26	8.72 ± 0.21	8.06 ± 0.37	8.74 ± 0.27	20.40 ± 0.52	21.15 ± 0.54	23.31 ± 0.16
<b>MUFA</b>									
16:1n-7	0.95 ± 0.05 <sup>a</sup>	1.08 ± 0.05 <sup>a,b</sup>	1.15 ± 0.03 <sup>b</sup>	1.11 ± 0.04 <sup>a</sup>	1.20 ± 0.05 <sup>a,b</sup>	1.37 ± 0.05 <sup>b</sup>	0.38 ± 0.03	0.39 ± 0.03	0.37 ± 0.03
18:1n-9	42.20 ± 0.26 <sup>a</sup>	40.21 ± 0.56 <sup>a</sup>	38.93 ± 0.31 <sup>b</sup>	41.90 ± 0.64 <sup>a</sup>	40.33 ± 0.63 <sup>a</sup>	38.23 ± 0.29 <sup>b</sup>	21.60 ± 0.41 <sup>a</sup>	16.73 ± 0.46 <sup>b</sup>	14.86 ± 0.13 <sup>b</sup>
<b>PUFA</b>									
<b>n-6</b>									
18:2n-6	11.81 ± 0.16	11.65 ± 0.16	11.30 ± 0.08	9.95 ± 0.22	9.69 ± 0.16	9.53 ± 0.09	20.6 ± 0.03 <sup>a</sup>	13.58 ± 0.56 <sup>b</sup>	20.02 ± 0.34 <sup>a</sup>
20:2n-6	0.18 ± 0.01	0.20 ± 0.00	0.19 ± 0.01	0.24 ± 0.02	0.25 ± 0.02	0.24 ± 0.00	0.21 ± 0.00 <sup>a</sup>	0.19 ± 0.01 <sup>a</sup>	0.18 ± 0.01 <sup>a,b</sup>
20:3n-6	0.11 ± 0.01 <sup>a</sup>	0.20 ± 0.01 <sup>b</sup>	0.13 ± 0.01 <sup>a,b</sup>	0.20 ± 0.12	0.11 ± 0.01	0.08 ± 0.00	0.39 ± 0.03	0.44 ± 0.02	0.35 ± 0.02
20:4n-6	0.55 ± 0.05 <sup>a</sup>	1.11 ± 0.06 <sup>b</sup>	0.8 ± 0.08 <sup>a</sup>	0.22 ± 0.02 <sup>a</sup>	0.50 ± 0.03 <sup>b</sup>	0.29 ± 0.04 <sup>a</sup>	2.70 ± 0.26	3.21 ± 0.25	4.14 ± 0.17
<b>n-3</b>									
22:6n-3	0.14 ± 0.02 <sup>a</sup>	0.55 ± 0.01 <sup>b</sup>	0.29 ± 0.03 <sup>c</sup>	0.05 ± 0.01 <sup>a</sup>	0.24 ± 0.03 <sup>b</sup>	0.12 ± 0.03 <sup>a</sup>	0.33 ± 0.05 <sup>a</sup>	0.71 ± 0.05 <sup>b</sup>	0.81 ± 0.04 <sup>b</sup>

<sup>a</sup>Values are means ± SEM,  $n = 6$ . Means without a common letter in a row differ,  $P < 0.05$ .

<sup>b</sup>Control: group fed adapted milk formula for piglets. TF-TAG: group fed adapted milk formula for piglets supplemented with LCP from fungal and tuna oils. E-PL: group fed adapted milk formula for piglets supplemented with LCP from egg yolk PL. For abbreviations see Table 1.

absorption was higher in term infants fed a formula containing LCP from egg yolk-PL than in those fed a standard formula without LCP. Carnielli *et al.* (36) studied a group of infants fed a formula with LCP from egg yolk-PL and a group fed a formula with LCP in the form of TAG from unicellular microorganisms. The absorption of DHA was higher in infants receiving the PL-LCP formula than in infants fed breast milk or the TAG-LCP formula. However, in the Morgan *et al.* study, no group was fed LCP in the form of TAG, and in the Carnielli *et al.* study, the quantities of LCP were not balanced in the LCP-supplemented diets; hence, the apparent absorption of DHA may simply reflect the usual greater percentage of absorption of lower intakes (37). Our own work in weanling rats supported differences in absorption between LCP sources, although these differences were related to other characteristics of the LCP source (other lipid components and FA positional distribution) rather than chemical structure (38).

On the other hand, PL are needed for intestinal lipoprotein formation and for fat distribution outside the enterocyte (18). PL may also affect the composition and metabolism of lipoproteins (24). Our result did not support differences in lipid lymph composition as inferred from the absence of significant differences in Table 2. However, this study showed evidence that dietary PL affects CM size. In fact, lymph lipoproteins from pigs fed the diet containing LCP in the form of PL were smaller than those from pigs fed the control or the LCP-TAG diet, and their size distribution was different. Another study in rats demonstrated that the intraduodenal infusion of triolein results in the formation of CM, whereas the infusion of egg PC favors the formation of intestinal VLDL-size particles (24). Unlike this previous study in which pure lipids were infused intraduodenally to rats, our study was done in piglets fed standard diets containing a mixture of vegetable oils added with LCP-PL or LCP-TAG to reach the same concentration of AA and DHA in both supplemented

diets and closer to the LCP of sow's milk. As described in the Materials and Methods section, the E-PL diet contained 13.6% of total fat as PL; this low amount (in comparison to Ref. 24) was able to produce an effect in lymph lipoproteins similar to that found using pure PL. However, in our study, lymph lipoproteins from the group fed the E-PL diet could not be considered VLDL-like particles: The majority were small CM, and a subpopulation was within the range of VLDL size (300–800 Å). The physiological implications of a different CM size in the experimental model studied may be a modification of absorption rate and/or in plasma metabolism of these lipoproteins. It has been shown that the number of particles synthesized and secreted by the small intestine remains relatively constant during fasting and active lipid absorption; and instead of increasing the number of CM, the enterocytes expand the size of the CM particles to secrete the large amounts of absorbed lipids from the intestinal mucosa (39). In considering this, the rate of absorption of dietary lipid in the E-PL group would be lower than that of the TF-TAG group, although the net absorption of both groups has not been proven to be different in our fat balance study in rats (38). Moreover, our results for lymph lipid composition (Table 2) did not support this hypothesis because there were no significant differences in PL, cholesterol, and TAG of lymph between the E-PL and TF-TAG groups and between these two groups and the control group. The amount of lymph lipids in the TF-TAG group was even lower than that of the other study groups, although not significantly different. On the other hand, it has been reported that large CM are metabolized faster than small ones (40), which means that CM from the TF-TAG would last for a shorter time in the blood stream. Therefore, LCP esterified to TF-TAG would reach target organs before LCP in the form of E-PL.

Mathews *et al.* (40) have recently reported the measurement of higher concentrations of DHA in piglets fed a diet

containing LCP-TAG from single-cell oils in comparison to piglets fed a diet containing LCP from E-PL. They also found no differences between the control group and the E-PL group in spite of the 0.3% FA as DHA in the diet. Our results showed changes in CM size and lipid fraction FA composition of lymph from piglets fed the E-PL diet. These differences may indicate, as explained above, a different absorption rate, but they do not imply a lower net absorption. In fact, in our previous experiments with fasting piglets, E-PL and the TF-TAG groups had higher plasma percentages of AA and DHA than controls, with no significant differences between both LCP-supplemented groups. In the same previous experiment, we reported an effect of LCP in the form of TAG or PL on the distribution of AA and DHA between lipoprotein fractions (22). HDL-PL contained a higher proportion of LCP when those FA were given in the diet as PL. Opposite results were found in LDL-PL, which contained a higher proportion of LCP when those FA were given in the diet as TAG. We hypothesized that this different distribution of LCP in lipoprotein PL may be explained as follows: After digestion and absorption, LCP are reesterified to the same chemical structure in which they were added to the diet (as PL or TAG) and are assembled mainly as PL on the CM surface in case of the E-PL group and mainly as TAG in the CM core in case of the TF-TAG group. Plasma CM exchange PL with HDL during intravascular catabolism (35); therefore, HDL from piglets fed an E-PL diet would contain a higher proportion of AA and DHA in HDL-PL. The results of the present study are consistent with this hypothesis: Lymph TAG from piglets fed the LCP-TAG diet contained a higher proportion of AA and DHA than lymph TAG from piglets fed the diet containing LCP in the form of PL. Opposite results were expected in lymph PL, but they were not statistically significant. However, because the data showed higher values of LCP in the lymph PL of the PL-supplemented group, the lack of significance may be due to the difficulty of analyzing the contribution of a low amount of dietary FA (less than 1% of total FA in the diet) to the PL fraction, which is the less abundant fraction of lymph lipids.

The addition to the diet of LCP in the form of TAG or PL resulted in a different distribution of these FA in lymph CM. On the other hand, LCP in the form of PL affect the packaging and secretion of intestinal lipoproteins resulting in a decrease of the lymph CM size. These results do not support an advantage of any of the LCP sources studied for infant feeding. However, the TAG source shows a lipoprotein distribution similar to the control group. Further studies would be necessary to find out whether the differences found in PL source are beneficial.

## ACKNOWLEDGMENTS

The authors thank Maria Luisa Jimenez for her help in care of animals and for her technical assistance. We also thank the Animal Nutrition Department of CSIC, especially D. José Aguilera for providing animal facilities and advice in raising piglets. This work was partly supported by a fellowship from the Spanish Ministry of Education.

## REFERENCES

1. Koletzko, B., Schmidt, E., Bremer, H.J., Haug, H., and Hazer, G. (1989) Effects of Dietary Long-Chain Polyunsaturated Fatty Acids on the Essential Fatty Acid Status of Premature Infants, *Eur. J. Pediatr.* 148, 669–675.
2. Clandinin, M.T., Parrott, A., Van Aerde, J.E., Hervada, A.R., and Lien, E. (1992) Feeding Preterm Infants a Formula Containing C20 and C22 Fatty Acids Simulated Plasma Phospholipid Fatty Acid Composition of Infants Fed Human Milk, *Early Hum. Dev.* 31, 41–51.
3. ESPGHAN Committee on Nutrition. Committee report: Aggett, P.J., Haschke, F., Heine, W., Hernell, O., Koletzko, B., Launiala, K., Rey, J., Rubino, A., Schöch, G., Senterre, J., and Tormo, R. (1991) Comment on the Content and Composition of Lipids in Infant Formulas, *Acta Paediatr. Scand.* 80, 887–896.
4. FAO/WHO Expert Committee (1994) Fats and Oils in Human Nutrition, Food and Nutrition Paper No. 57, FAO, Rome, Italy.
5. British Nutrition Foundation (1992) *Unsaturated Fatty Acids, Nutritional and Physiological Significance*, Chapman & Hall, London.
6. ISSFAL Board of Directors (1994) Recommendations for Essential Fatty Acid Requirement for Infant Formulae, *ISSFAL Newsletter* 1, 4–5.
7. Uauy, R.D., Birch, D.G., Birch, E.E., Tyson, J.E., and Hoffman, D.R. (1990) Effect of Dietary Omega-3 Fatty Acids on Retinal Function of Very-Low-Birth-Weight Neonates, *Pediatr. Res.* 28, 485–492.
8. Birch, D.G., Birch, E.E., Hoffman, D.R., and Uauy, R. (1992) Retinal Development in Very-Low-Birth-Weight Infants Fed Diets Differing in  $\omega$ -3 Fatty Acids, *Invest. Ophthalmol. Vis. Sci.* 33, 2365–2376.
9. Birch, E.E., Birch, D.G., Hoffman, D.R., and Uauy, R. (1992) Dietary Essential Fatty Acid Supply and Visual Acuity Development, *Invest. Ophthalmol. Vis. Sci.* 33, 3242–3253.
10. Carlson, S.E., Werkman, S.H., Rhodes, P.G., and Tolley, E.A. (1993) Visual-Acuity Development in Healthy Preterm Infants: Effect of Marine Oil Supplementation, *Am. J. Clin. Nutr.* 58, 35–42.
11. Carlson, S.E., and Werkman, S.H. (1996) A Randomized Trial of Visual Attention of Preterm Infants Fed Docosahexaenoic Acid Until Two Months, *Lipids* 31, 85–90.
12. Birch, E.E., Hoffman, D.R., Uauy, R., Birch, D.G., and Prestidge, C. (1998) Visual Acuity and Essentiality of Docosahexaenoic Acid and Arachidonic Acid in the Diet of Term Infants, *Pediatr. Res.* 44, 201–209.
13. Birch, E.E., Garfield, S., Hoffman, D.R., Uauy, R., and Birch, D.G. (2000) A Randomized Controlled Trial of Early Dietary Supply of Long-Chain Polyunsaturated Fatty Acids and Mental Development in Term Infants, *Dev. Med. Child Neurol.* 42, 174–181.
14. Hoffman, D.R., Birch, E.E., Birch, D.G., Uauy, R., Castaneda, Y.S., Lopus, M.G., and Wheaton, D.H. (2000) Impact of Early Dietary Intake and Blood Lipid Composition of Long-Chain Polyunsaturated Fatty Acids on Later Visual Development, *J. Pediatr. Gastroenterol. Nutr.* 31, 540–553.
15. Pufal, D.A., Quinlan, P.T., and Salter, A.M. (1995) Effect of Dietary Triacylglycerol Structure on Lipoprotein Metabolism: A Comparison of the Effects of Dioleoylpalmitoylglycerol in Which Palmitate Is Esterified to the 2- or 1(3)-Position of the Glycerol, *Biochim. Biophys. Acta* 1258, 41–48.
16. Jensen, R.G., deJong, F.A., Lambert-Davis, L.-G., and Hamosh, M. (1994) Fatty Acid and Positional Selectivities of Gastric Lipase from Premature Infants: *In vitro* Studies, *Lipids* 29, 433–435.
17. Christensen, M.S., Høy, C.E., Becker, C.C., and Redgrave, T.G. (1995) Intestinal Absorption and Lymphatic Transport of

- Eicosapentaenoic (EPA), Docosahexaenoic (DHA), and Decanoic Acids: Dependence on Intramolecular Triacylglycerol Structure, *Am. J. Clin. Nutr.* 61, 56–61.
18. O'Doherty, P.J., Kakis, G., and Kuksis, A. (1973) Role of Luminal Lecithin in Intestinal Fat Absorption, *Lipids* 8, 249–255.
  19. Tso, P., and Simmonds, W.J. (1977) Importance of Luminal Lecithin in Intestinal Absorption and Transport of Lipid in the Rat, *Aust. J. Exp. Biol. Med. Sci.* 55, 355–357.
  20. Tso, P., Balint, J.A., and Simmonds, W.J. (1977) Role of Biliary Lecithin in Lymphatic Transport of Fat, *Gastroenterology* 73, 1362–1367.
  21. Tso, P., Lam, J., and Simmonds, W.J. (1978) The Importance of the Lysophosphatidyl Choline and Choline Moiety of Bile Phosphatidylcholine in Lymphatic Transport of Fat, *Biochim. Biophys. Acta* 528, 364–372.
  22. Carnielli, V.P., Luijndijk, I.H.T., Van Goudoever, J.B., Sulkers, E.J., Boerlage, A.A., Degenhart, H.-J., and Sauer, P.J. (1995) Feeding Premature Newborn Infants Palmitic Acid in Amounts and Stereoisomeric Position Similar to That of Human Milk: Effects on Fat and Mineral Balance, *Am. J. Clin. Nutr.* 61, 1037–1042.
  23. Morgan, C., Davies, L., Corcoran, F., Stammers, J., Colley, J., Spencer, S.A., and Hull, D. (1998) Fatty Acid Balance Studies in Term Infants Fed Formula Milk Containing Long-Chain Polyunsaturated Fatty Acids, *Acta Paediatr.* 87, 136–142.
  24. Tso, P., Drake, D.S., Black, D.D., and Sabesin, S.M. (1984) Evidence for Separate Pathways of Chylomicron and Very Low-Density Lipoprotein Assembly and Transport by Rat Small Intestine, *Am. J. Physiol.* 247, G500–G600.
  25. Amate, L., Gil, A., and Ramirez, M. (2001) Feeding Infant Piglets Formula with Long-Chain Polyunsaturated Fatty Acids as Triacylglycerols or Phospholipids Influences the Distribution of These Fatty Acids in Plasma Lipoprotein Fractions, *J. Nutr.* 131, 1250–1255.
  26. Miller, E.R., and Ullrey, D.E. (1987) The Pig as Model for Human Nutrition, *Annu. Rev. Nutr.*, 361–382.
  27. Lopez-Pedrosa, J.M., Torres, M.I., Fernandez, M.I., Rios, A., and Gil, A. (1998) Severe Malnutrition Alters Lipid Composition and Fatty Acid Profile of Small Intestine in Newborn Piglets, *J. Nutr.* 128, 224–233.
  28. Kolarovic, L., and Fournier, N.C. (1986) A Comparison of Extraction Methods for the Isolation of Phospholipids from Biological Sources, *Anal. Biochem.* 156, 244–250.
  29. Skipski, V.P., and Barclay, M. (1969) Thin Layer Chromatography of Lipids, in *Methods in Enzymology* (Lowenstein, J.M., ed.), Vol. 14, pp. 530–598, Academic Press, New York.
  30. Lepage, G., and Roy, C.C. (1986) Direct Transesterification of All Classes of Lipids in a One-Step Reaction, *J. Lipid Res.* 27, 114–120.
  31. Amate, L., Ramirez, M., and Gil, A. (1999) Positional Analysis of Triglycerides and Phospholipids Rich in Long-Chain Polyunsaturated Fatty Acids, *Lipids* 34, 865–871.
  32. Ziversmit, D.B. (1950) *J. Lab. Clin. Med.* 35, 155.
  33. Bradford, M.M. (1976) A Rapid and Sensitive Method for the Quantification of Microgram Quantities of Protein Utilizing the Principle of Protein–Dye Binding, *Ann. Biochem.* 72, 248–254.
  34. Dixon, W.J., Brown, M.B., Engelman, L., and Jennrich, R.I. (1990) *BMDP Statistical Software Manual*, University of California Press, Berkeley.
  35. Mattson, F.H., and Volpenhein, R.A. (1964) The Digestion and Absorption of Triglycerides, *J. Biol. Chem.* 239, 2772–2777.
  36. Carnielli, V.P., Veriato, G., Pedrezini, F., Luijndijk, I., Boerlage, A., and Pedrotti, D. (1998) Intestinal Absorption of Long-Chain Polyunsaturated Fatty Acids in Preterm Infants Fed Breast Milk or Formula, *Am. J. Clin. Nutr.* 67, 97–103.
  37. Heird, W.C. (1999) Biological Effects and Safety Issues Related to Long-Chain Polyunsaturated Fatty Acids in Infants, *Lipids* 34, 207–214.
  38. Amate, L., Gil, A., and Ramirez, M. (2001) Dietary Long-Chain Polyunsaturated Fatty Acids from Different Sources Affect Fat and Fatty Acid Excretion in Rats, *J. Nutr.* 131, 3216–3221.
  39. Hayasi, H., Fujimoto, K., Carden, J.A., Nuting, D.F., Bergstedt, S., and Tso, P. (1990) Fat Feeding Increases Size, but Not Number, of Chylomicrons Produced by Small Intestine, *Am. J. Physiol.* 25, G709–G719.
  40. Posner, I. (1986) Metabolismo de las lipoproteínas. Dislipoproteinemias (Metabolism of Lipoproteins: Dyslipoproteinaemia), in *Bioquímica* (Herrera, E., ed.) pp. 523–541, Interamericana, Madrid.
  41. Mathews, S.A., Harrell, R.J., Oliver, W.T., Odle, J., and Diersen-Schade, D.A. (2001) Comparison of Dietary Sources of Long-Chain Polyunsaturated Fatty Acids (LC-PUFA) in the Neonatal Piglet: Assessment of Clinical Parameters, *FASEB J.* 15, A643.

[Received February 11, 2002, and in revised form and accepted November 20, 2002]

# Comparative Effect of Fenofibrate on Hepatic Desaturases in Wild-Type and Peroxisome Proliferator-Activated Receptor $\alpha$ -Deficient Mice

Hervé Guillou<sup>a</sup>, Pascal Martin<sup>b</sup>, Sophie Jan<sup>a,c</sup>, Sabine D'Andrea<sup>a</sup>, Alain Roulet<sup>b</sup>, Daniel Catheline<sup>a</sup>, Vincent Rioux<sup>a</sup>, Thierry Pineau<sup>b</sup>, and Philippe Legrand<sup>a,\*</sup>

<sup>a</sup>Laboratoire de Biochimie ENSAR-INRA, 35042 Rennes, <sup>b</sup>Laboratoire de Pharmacologie et Toxicologie INRA, 31931 Toulouse, and <sup>c</sup>Université du Maine, 72000 Le Mans, France

**ABSTRACT:** In this study is presented the effect of fenofibrate, a prototypical peroxisome proliferator of the fibrate class, on wild-type and peroxisome proliferator-activated receptor  $\alpha$  (PPAR $\alpha$ )-/- mouse liver FA profile, desaturase mRNA levels, and activities. We established that, following peroxisome proliferator exposure, the hepatic FA profile was greatly modified. These modifications in hepatic FA content required the expression of PPAR $\alpha$ , as they are suppressed in transgenic mice deficient in this nuclear receptor. Following peroxisome proliferator exposure,  $\Delta 6$ - and  $\Delta 5$ -desaturase mRNA levels and activities were increased in wild-type but not in PPAR $\alpha$ -deficient mouse liver. These results suggest the involvement of PPAR $\alpha$  in the control of hepatic  $\Delta 6$ - and  $\Delta 5$ -desaturases in mice. Their roles in minimizing long-chain PUFA depletion in the liver during peroxisome proliferator exposure are discussed.

Paper no. L9100 in *Lipids* 37, 981–989 (October 2002).

Synthetic compounds of the therapeutic class of fibrates are commonly referred to as peroxisome proliferators (PP). They have been beneficially prescribed for decades in the treatment of human hyperlipidemia and hypercholesterolemia. PP decrease circulating lipids when administered to mice, rats, and also humans (1). The molecular mode of action of these hypolipidemic drugs has been extensively studied in laboratory rodent models. The transcription of many critical genes involved in several aspects of the metabolism is altered by PP administration (2). Virtually all these effects are abolished in mice deficient in the  $\alpha$  isoform of the peroxisome proliferator-activated receptor (PPAR $\alpha$ ) (3), a member of the class 2 of the nuclear receptor family (4). PPAR $\alpha$  is a transcription factor shown to be preferentially expressed in the liver and kidney in rodent species (5). Upon ligand activation by fibrates, PUFA, or eicosanoids, it binds to the retinoid X receptor (6), and the resulting heterodimeric complex interacts with target DNA sequences to modulate gene expression levels (7). PPAR $\alpha$  target genes include a relatively homogeneous group

of genes that mainly contribute to increasing FA catabolism (3,8). Conversely, FA desaturases that catalyze the biosynthesis of unsaturated FA are thought to be increased in rodent liver following exposure to fibrates (9,10). The desaturases catalyze the introduction of double bonds at singular locations along carbon fatty acyl chains (11). In animals, three distinct desaturase enzymes introduce double bonds at the  $\Delta 9$ ,  $\Delta 6$ , and  $\Delta 5$  positions.

$\Delta 9$ -Desaturase, also called stearoyl-CoA desaturase (SCD), displays a marked substrate specificity for palmitoyl-CoA and stearoyl-CoA, which are converted by  $\Delta 9$ -desaturation to palmitoleyl-CoA and oleyl-CoA, respectively (12). The hepatic regulation of  $\Delta 9$ -desaturase activity has been extensively studied in rats and mice (12). Whereas both PUFA and fibrates are considered as PPAR $\alpha$  activators, PUFA and fibrates display opposite effects on  $\Delta 9$ -desaturase. Dietary PUFA show an inhibitory effect on  $\Delta 9$ -desaturase activity that correlates with a decreased SCD1 transcript level (13). By contrast,  $\Delta 9$ -desaturase activity is enhanced by fibrates in rodent liver (9) and in human HepG2 cells (14). In mice, this induction occurs through an increased SCD1 transcription that involves a functional peroxisome proliferator responsive element (PPRE) localized in the SCD1 promoter (15).

The  $\Delta 6$ - and  $\Delta 5$ -desaturases govern the rate-limiting steps for the biosynthesis of very long chain PUFA, which play pivotal roles in numerous biological functions. Little information is available on  $\Delta 6$ - and  $\Delta 5$ -desaturase mechanisms of regulation by PUFA and fibrates. Several groups have reported the cloning of  $\Delta 6$ - and  $\Delta 5$ -desaturases in different species (16–20). Evidence for a down-regulation of  $\Delta 6$ - and  $\Delta 5$ -desaturase gene expression by dietary PUFA (16,17) has been presented. Conversely, the hepatic expression of  $\Delta 6$ - and  $\Delta 5$ -desaturases is highly activated in transgenic mice overexpressing nuclear sterol regulatory element binding protein-1 (20), a key transcription factor in lipogenesis. Regarding the effect of fibrates, they enhance linoleic acid (18:2n-6) metabolism in rats (10) and  $\Delta 6$ - and  $\Delta 5$ -desaturase mRNA levels in mice (20). These observations suggest that, as reported for  $\Delta 9$ -desaturase (15),  $\Delta 6$ - and  $\Delta 5$ -desaturase gene expressions could be down-regulated by PUFA and stimulated by fibrate drugs.

The current study was undertaken to further investigate the

\*To whom correspondence should be addressed at Laboratoire de Biochimie INRA-ENSA Rennes, 65 Rue de Saint-Brieuc, CS 84215, France.  
E-mail: Philippe.Legrand@agrorennes.eduagri.fr

Abbreviations: AOX, peroxisomal acyl-CoA oxidase; CYP4A10, cytochrome P450 4A10; PP, peroxisome proliferator; PPAR $\alpha$ , peroxisome proliferator-activated receptor  $\alpha$ ; PPRE, peroxisome proliferator responsive element; SCD, stearoyl-CoA desaturase; TBS, Tris-buffered saline; W-T, wild-type.



*in vivo* influence of PPAR $\alpha$  on FA metabolism with particular emphasis on desaturases. This study provides evidence that PP exposure results in numerous changes of the hepatic FA profile that are dependent on the expression of PPAR $\alpha$ . We also demonstrate that fenofibrate enhances  $\Delta 6$ - and  $\Delta 5$ -desaturase mRNA levels and activities in mice. By using the PPAR $\alpha$ -null mice, we further suggest that PPAR $\alpha$  may be involved in the regulation of  $\Delta 6$ - and  $\Delta 5$ -desaturase by fenofibrate in this species. Our results strongly support the role played by hepatic  $\Delta 6$ - and  $\Delta 5$ -desaturases in counteracting exacerbated PUFA catabolism that occurs during PP exposure.

## MATERIALS AND METHODS

**Chemicals.** The Trizol solution was from Life Technologies (Paris, France). Gene Screen Plus Nylon membrane, [1-<sup>14</sup>C]-stearic acid, [1-<sup>14</sup>C] $\alpha$ -linolenic acid, and [1-<sup>14</sup>C]eicosatrienoic acid were purchased from NEN Life Science Products (Paris, France). Radiolabeled nucleotides, random priming kit (Ready Prime II), ECL Plus reagent, Phosphorcreens, Storm 840 imager, and Storm Image Analysis System were purchased from Amersham Pharmacia Biotech (Les Ulis, France). Nitrocellulose membrane was from Schleicher & Schuell (Dassel, Germany). Solvents and other chemicals were obtained from Prolabo (Paris, France) or Merck (Darmstadt, Germany), except high-purity reagents for HPLC application, which were from Fisher (Elancourt, France). Fenofibrate and standards for FA analyses were from Sigma Chemical (Saint-Quentin Fallavier, France).

**Animal housing and treatment.** Care of mice was in compliance with European Union guidelines for animal care and use. PPAR $\alpha$  homozygous-deficient mice (PPAR $\alpha$ -/-), generated initially from homologous recombinant 129Sv-ES cells (3), were interbred on a C57BL/6J genetic background (21). Age-matched wild-type (W-T) C57BL/6J male mice were obtained from Charles River (Les Oncins, France) and acclimated to local animal facility conditions for 2 wk prior to treatment. Nine-week-old mice were fed *ad libitum* on a standard chow diet (Harlan #9607, Gannat, France) with free access to water. The FA composition of the standard diet is: palmitic acid (16:0), 12.9% of total FA; stearic acid, 3.3%; oleic acid (18:1n-9), 22.8%; linoleic acid (18:2n-6), 56.1%;  $\alpha$ -linolenic acid (18:3n-3), 4.9%; total fat content (g oil/100 g diet), 4.3%. Mice were housed in groups of five in plastic cages at a temperature of 21  $\pm$  2°C with a 12 h/12 h light/dark cycle. Five W-T mice and five PPAR $\alpha$ -/- mice (9 wk old) received fenofibrate (100 mg/kg of body weight per day, suspended in a 3% aqueous sterile solution of gum arabic) by daily gavage for 14 d at 9 A.M. Five controls each of both genotypes received the vehicle alone. After 2 wk of treatment, animals were euthanized by neck dislocation. The livers were promptly removed, weighed, snap-frozen in liquid nitrogen, and stored at -80°C for later RNA extraction. About 200 mg of each fresh liver was rapidly minced for postmitochondrial supernatant preparation.

A time-course study was also performed to determine the short-term effect of fenofibrate on desaturase expression. Ten W-T mice and 10 PPAR $\alpha$ -/- mice (12 wk old) received a single dose of fenofibrate (100 mg/kg of body weight) by gavage. Two W-T and 2 PPAR $\alpha$ -/- mice were euthanized at various times after treatment (2, 4, 8, 16, and 24 h).

**Enzyme assays.** Fresh liver samples were minced in 2 mL of 50 mmol/L phosphate buffer (pH 7.4) containing 0.25 mol/L sucrose. The samples were centrifuged twice at 10,000  $\times g$  for 30 min. The resulting postmitochondrial supernatant was diluted five times and used for  $\Delta 9$ -,  $\Delta 6$ -, and  $\Delta 5$ -desaturase assays. Aliquots were stored at -20°C for subsequent protein measurements. Enzymatic activities were determined using a 1-mL assay mixture containing 100  $\mu$ L of supernatant (400 to 500  $\mu$ g protein), 150 mmol/L phosphate buffer (pH 7.16), 6 mmol/L MgCl<sub>2</sub>, 7.2 mmol/L ATP, 0.54 mmol/L CoA, and 0.8 mmol/L NADH. The reaction was started with the addition of 30 nmol of [1-<sup>14</sup>C]stearic acid (740 MBq/mmol) for  $\Delta 9$ -desaturase assay and 60 nmol of [1-<sup>14</sup>C] $\alpha$ -linolenic acid or [1-<sup>14</sup>C]eicosatrienoic acid (740 MBq/mmol) for  $\Delta 6$ - or  $\Delta 5$ -desaturase assays, respectively. The incubations were carried out in a shaking water bath at 37°C for 30 min. The reactions were stopped by adding 1 mL of 0.5 mol/L KOH in ethanol. Control assays were performed by adding KOH in ethanol before adding the substrate. FA saponification was carried out at 70°C for 30 min. After acidification, FA were extracted with diethyl ether and dried. They were converted to FA naphthacyl esters (22) and separated on HPLC (Alliance Integrated System; Waters, St. Quentin en Yvelines, France) using a Nova-Pak C18 column (4.6  $\times$  250 mm, Waters) and a guard column (Nova-Pak C18, 3.9  $\times$  20 mm). Radiolabeled substrates and products of each desaturase assay were collected and subjected to liquid scintillation counting (Packard Tri-Carb 1600 TR; Meriden, CT). Preliminary identification of FA naphthacyl esters was based on retention times obtained for naphthacyl esters prepared from radiolabeled and nonradiolabeled FA standards (23). From the amount of radioactivity found in the product compared to the radioactivity incubated, the enzyme activity could be determined and expressed as pmol substrate converted to product per min per mg of protein. The protein content in the supernatant used for enzyme assays was determined by a modified Lowry procedure (24).

**Western blotting.** The anti-rat  $\Delta 6$ -desaturase sera, named S1 and S2, were generated by immunizing two rabbits with recombinant peptides corresponding to the 108 carboxyl-terminal amino acids and the 131 amino-terminal amino acids of the  $\Delta 6$ -desaturase, respectively (25). For Western blotting analyses, 80  $\mu$ g of protein from the postmitochondrial supernatants used for the enzyme assays were diluted in Laemmli sample buffer, separated by SDS-PAGE (11% acrylamide), and blotted onto a nitrocellulose membrane. The membrane was probed with a mixture of S1 and S2 sera, both at 1:2000 dilution. The secondary antibody was a horseradish-peroxidase-conjugated sheep antirabbit immunoglobulin (IgG) (Sigma). Incubation with antibodies was carried out for 90

min in Tris-buffered saline (TBS) (20 mM Tris-HCl, 150 mM NaCl, pH 7.4) containing 0.05% Tween-20 and 10% nonfat dry milk. Washes were performed in TBS containing 0.05% Tween-20. Peroxidase activity was revealed using ECL Plus reagent according to the manufacturer's instructions and scanned with a Storm 840 Imager.

**RNA isolation and Northern blot analysis.** Hepatic mRNA levels of mouse  $\Delta 6$ -desaturase,  $\Delta 5$ -desaturase,  $\Delta 9$ -desaturase (SCD1), peroxisomal acyl-CoA oxidase (AOX), cytochrome P450 4a10 (CYP4A10), and  $\beta$ -actin were detected by Northern blotting. Total RNA was prepared from 100-mg fragments of the large lobe of the liver homogenized in 1 mL of Trizol solution using a tissue homogenizer (Ika, Jena, Germany). RNA samples were fractionated on a 1% agarose gel containing 2.2 M formaldehyde and transferred to a nylon membrane. Probes were polymerase chain reaction (PCR)-amplified from hepatic mouse or rat cDNA using the primers described in Table 1. All probes were labeled with [ $\alpha$ - $^{32}$ P]dCTP by random priming. The membranes were hybridized with each radiolabeled probe at 65°C overnight in the hybridization buffer (900 mM NaCl, 90 mM sodium citrate, pH 7.0, Denhardt's reagent, 0.5% SDS, and 20  $\mu$ g/mL salmon sperm DNA). After hybridization, the membranes were washed in 0.1  $\times$  SSC (saline-sodium citrate buffer), 0.1% SDS at 65°C. Hybridizing bands were visualized with a Storm Imager and analyzed using ImageQuant Software (Amersham Pharmacia Biosciences).

**Hepatic FA composition.** Total lipids were extracted from 100-mg liver samples homogenized in a mixture of dimethoxymethane/methanol (4:1, vol/vol) and incubated for 30 min on ice before extraction. Total hepatic lipids were

saponified for 30 min at 70°C by 1 mL of 0.5 mol/L NaOH in methanol and methylated with 1 mL BF $_3$  (14% in methanol) at 70°C for 10 min. FAME were extracted with pentane and analyzed by GC using a GIRA 1600 chromatograph (GIRA, Morlaas, France) with a split injector (1:10) at 240°C, a bonded-silica capillary column (30 m  $\times$  0.25 mm i.d., BPX 70; SGE, Villeneuve-St-Georges, France) with a stationary phase of 70% cyanopropylpolysilphenylene-siloxane (0.25  $\mu$ m film thickness). Helium was used as gas vector (1 bar). The column temperature program started at 150°C, ramping at 2°C/min to 220°C. The FID temperature was 260°C. Identification of FAME peaks was based on retention times obtained for methyl esters prepared from FA standards. The quantification of total hepatic FA was performed using heptadecanoic acid as internal standard.

**Results and statistical analysis.** All measurements were performed on samples from individual animals, and the results are expressed as mean of five animals. Statistical significance of differences was calculated by a two-tailed Student's *t*-test. A value of *P* < 0.05 was considered to be statistically significant.

## RESULTS

**Effect of a 14-d fenofibrate treatment on body and liver weight.** Fenofibrate is a prototypical PP. We investigated the effects of a 14-d fenofibrate treatment on hepatic lipids, in W-T C57Bl/6J and PPAR $\alpha$ -deficient male mice, with particular focus on FA. In W-T mice but not in PPAR $\alpha$ -deficient mice, fenofibrate administration promoted a significant liver enlargement without affecting body weight (Table 2).

**TABLE 1**  
Polymerase Chain Reaction Primer Sets for cDNA Probe Amplification

Genes	Species	Forward primer nt <sup>a</sup>	Reverse primer nt <sup>a</sup>	Accession number <sup>b</sup>
Peroxisomal acyl-CoA oxidase	Mouse	483–502	1723–1742	AB034914
CYP4A10	Mouse	181–200	1148–1168	AB018421
Skeletal $\beta$ -actin	Mouse	161–185	1146–1167	X03672
Stearoyl-CoA desaturase	Rat	103–118	1162–1180	J02585
$\Delta 6$ -Desaturase	Rat	406–425	591–610	AB021980
$\Delta 5$ -Desaturase	Rat	421–440	606–625	AF320509

<sup>a</sup>nt, nucleotide position according to accession number (from start to end of the primer).

<sup>b</sup>Accession number in Genbank<sup>TM</sup>.

**TABLE 2**  
Changes Induced by Administration of Fenofibrate in Mouse Livers

	W-T <sup>a</sup>		PPAR $\alpha$ -/-	
	-	+	-	+
Weights (g)				
Body	23.0 $\pm$ 0.91	23.5 $\pm$ 1.67	26.9 <sup>c</sup> $\pm$ 1.36	26.7 <sup>c</sup> $\pm$ 2.15
Liver	1.1 $\pm$ 0.15	1.8 <sup>b</sup> $\pm$ 0.14	1.4 $\pm$ 0.06	1.4 $\pm$ 0.22
Liver/body $\times$ 100	4.6 $\pm$ 0.53	7.6 <sup>b</sup> $\pm$ 0.35	5.0 $\pm$ 0.27	5.2 $\pm$ 0.47
Liver FA content (mg/g)	28.4 $\pm$ 3.46	43.2 <sup>b</sup> $\pm$ 4.92	71.5 <sup>c</sup> $\pm$ 18.67	57.8 <sup>c</sup> $\pm$ 9.45

<sup>a</sup>Plus or minus indicates the presence or absence of fenofibrate treatment. Results are presented as mean values  $\pm$  SD (*n* = 5 animals per group).

<sup>b</sup>Significant difference due to treatment (- vs. +; *P* < 0.05).

<sup>c</sup>Significant difference due to genotype (W-T vs. PPAR $\alpha$ -/-; *P* < 0.05). W-T, wild-type; PPAR $\alpha$ , peroxisome proliferator-activated receptor  $\alpha$ .

*Effect of a 14-d fenofibrate treatment on total lipid FA profile in the liver.* In W-T mice, PP-induced hepatomegaly was associated with an increase in hepatic FA content (Table 2). Moreover, our data emphasize a major difference in hepatic FA content between W-T and PPAR $\alpha$ -/- mice. Independently of the fenofibrate administration, the PPAR $\alpha$ -/- male mice had a higher FA content when compared to W-T mice (Table 2).

The consequences of fenofibrate treatment on liver FA composition were measured by analysis of FA from total hepatic lipids (Table 3). In our experiments, W-T mice treated with fenofibrate showed a significant increase in 16:0, 16:1n-7, 18:1n-9, and 20:3n-6, and 18:0, 18:2n-6, 20:4n-6, and 22:6n-3 contents significantly decreased (Table 3). Conversely, no significant change was detected in the total FA profile of fenofibrate-treated PPAR $\alpha$ -/- mice when compared to untreated PPAR $\alpha$ -/- mice (Table 3). Concerning monoenes, fenofibrate induced a marked increase in the 16:1n-7 and 18:1n-9 content in the W-T mice, but not in the PPAR $\alpha$ -null mice, suggesting a PPAR $\alpha$ -dependent activation of  $\Delta$ 9-desaturase. Whatever the treatment, a major difference due to genotype was observed in the relative abundance of hepatic FA: The 18:2n-6 content is much higher in the PPAR $\alpha$ -deficient mouse liver than in the W-T mouse liver (untreated  $23.68 \pm 1.21\%$ , treated  $15.77 \pm 1.51\%$ ; PPAR $\alpha$ -/-: untreated  $36.56 \pm 1.85\%$ , treated  $32.60 \pm 2.26\%$ ).

*Effect of a 14-d fenofibrate treatment on desaturase activities.* To gain further insight into the mechanisms leading to these marked changes in hepatic FA profile, we investigated the *in vivo* involvement of the  $\Delta$ 9-,  $\Delta$ 6-, and  $\Delta$ 5-desaturases in the PPAR $\alpha$ -dependent regulatory network. We first tested whether fenofibrate-induced changes in hepatic FA profile could be associated with changes in desaturase activities. On the animal livers used for FA profile analyses, desaturase activity assays were carried out.

Whatever the desaturase, the activity was significantly enhanced in W-T mice by the 14-d fenofibrate treatment:  $\Delta$ 9-,  $\Delta$ 6-, and  $\Delta$ 5-desaturase activities were induced 8-, 2-, and 2.5-fold, respectively (Fig. 1). Following 14 d of fenofibrate exposure,  $\Delta$ 6- and  $\Delta$ 5-desaturase activities were slightly increased in the liver of PPAR $\alpha$ -deficient mice; these changes were far from the range of induction observed in W-T animals (Fig. 1). Although the induction of desaturase activities after fenofibrate exposure seems to depend on PPAR $\alpha$  expression, the invalidation of PPAR $\alpha$  does not abolish desaturase activities since PPAR $\alpha$ -/- mice displayed basal desaturase activities similar to untreated W-T mice (Fig. 1).

*Effect of a 14-d fenofibrate treatment on hepatic desaturase mRNA levels.* We investigated by Northern blot whether fenofibrate could influence mouse hepatic  $\Delta$ 9- (SCD1),  $\Delta$ 6-, and  $\Delta$ 5-desaturase gene expression (Fig. 2). Since AOX and CYP4A10 are characteristic PPAR $\alpha$  target genes (3), their mRNA levels were also estimated (Fig. 2) as positive controls of transcriptional induction by fenofibrate treatment.

Following a 14-d treatment of W-T mice, fenofibrate enhanced hepatic SCD1,  $\Delta$ 6-, and  $\Delta$ 5-desaturase mRNA levels (Fig. 2). Both  $\Delta$ 9- and  $\Delta$ 6-desaturase mRNA levels were greatly increased, while the  $\Delta$ 5-desaturase mRNA level increase was weaker (Fig. 2). Conversely, fenofibrate exposure of PPAR $\alpha$ -deficient mice did not modify any desaturase mRNA levels. PPAR $\alpha$  target genes such as AOX and CYP4A10 were used as positive controls and were shown to be highly induced in W-T but not in PPAR $\alpha$ -/- mice (Fig. 2). Noticeably, all the different hepatic desaturase mRNA were detected in PPAR $\alpha$ -deficient mouse liver, suggesting that PPAR $\alpha$  is not required to sustain the constitutive level of expression of these transcripts. However, in untreated PPAR $\alpha$ -/- mice, the mRNA levels measured for SCD1 and  $\Delta$ 6-desaturase were significantly lower than in untreated W-T mice (Fig. 2).

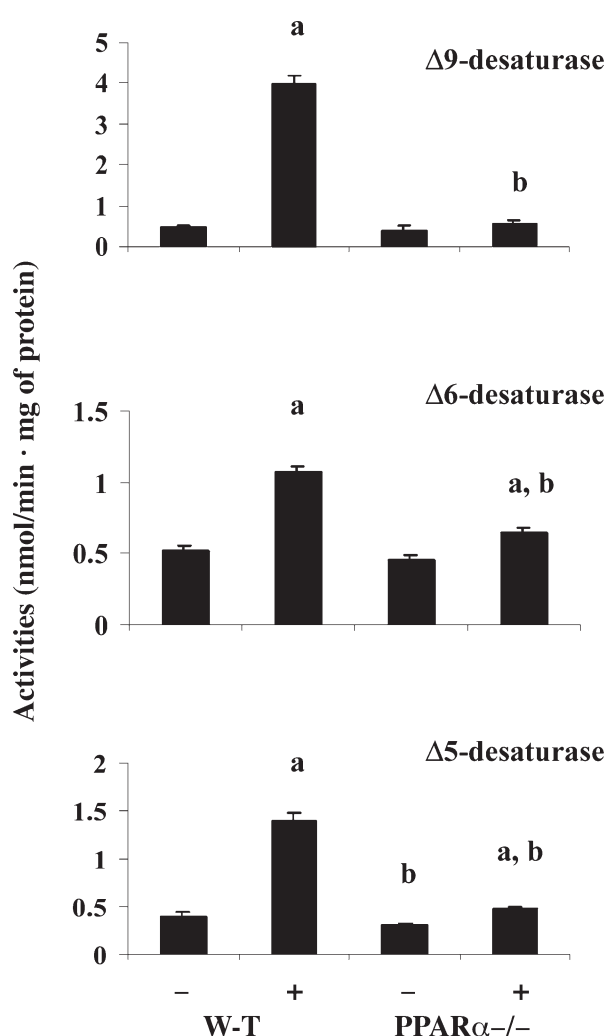
**TABLE 3**  
Effect of Fenofibrate on Total Hepatic FA Composition

FA	W-T <sup>a</sup>		PPAR $\alpha$ -/-	
	-	+	-	+
14:0	0.25 $\pm$ 0.05	0.18 $\pm$ 0.03 <sup>b</sup>	0.47 $\pm$ 0.06 <sup>c</sup>	0.3 $\pm$ 0.12 <sup>c</sup>
16:0	26.03 $\pm$ 2.08	28.59 $\pm$ 0.70 <sup>b</sup>	23.16 $\pm$ 1.12 <sup>c</sup>	23.40 $\pm$ 1.13 <sup>c</sup>
18:0	12.36 $\pm$ 0.61	8.4 $\pm$ 0.67 <sup>b</sup>	7.80 $\pm$ 1.59 <sup>c</sup>	10.61 $\pm$ 2.07
SFA	38.64 $\pm$ 2.74	37.17 $\pm$ 1.43	31.43 $\pm$ 2.77 <sup>c</sup>	34.31 $\pm$ 3.32
16:1n-9	0.27 $\pm$ 0.04	0.84 $\pm$ 0.05 <sup>b</sup>	0.29 $\pm$ 0.17	0.40 $\pm$ 0.11
18:1n-9	15.91 $\pm$ 0.83	23.95 $\pm$ 1.35 <sup>b</sup>	19.45 $\pm$ 1.99 <sup>c</sup>	19.45 $\pm$ 3.22
16:1n-7	1.63 $\pm$ 0.10	2.57 $\pm$ 0.41 <sup>b</sup>	1.91 $\pm$ 0.31	1.60 $\pm$ 0.81
18:1n-7	1.04 $\pm$ 0.86	1.74 $\pm$ 1.70	0.29 $\pm$ 0.05	0.38 $\pm$ 0.14
MFA	18.85 $\pm$ 1.83	29.1 $\pm$ 3.52 <sup>b</sup>	21.94 $\pm$ 2.52 <sup>c</sup>	21.84 $\pm$ 4.28 <sup>c</sup>
18:2n-6	23.68 $\pm$ 1.21	15.77 $\pm$ 1.51 <sup>b</sup>	36.56 $\pm$ 1.85 <sup>c</sup>	32.60 $\pm$ 2.26 <sup>c</sup>
20:3n-6	1.02 $\pm$ 0.27	3.48 $\pm$ 0.13 <sup>b</sup>	0.65 $\pm$ 0.44	0.40 $\pm$ 0.12 <sup>c</sup>
20:4n-6	11.48 $\pm$ 1.05	9.98 $\pm$ 0.61 <sup>b</sup>	5.90 $\pm$ 0.92 <sup>c</sup>	7.31 $\pm$ 1.58 <sup>c</sup>
22:5n-3	0.71 $\pm$ 0.77	0.56 $\pm$ 0.21	0.33 $\pm$ 0.09	0.33 $\pm$ 0.25
22:6n-3	5.62 $\pm$ 1.43	4.01 $\pm$ 0.75 <sup>b</sup>	3.08 $\pm$ 0.54 <sup>c</sup>	3.22 $\pm$ 1.22
PUFA	42.51 $\pm$ 4.73	33.80 $\pm$ 3.21 <sup>b</sup>	46.32 $\pm$ 3.88 <sup>c</sup>	43.86 $\pm$ 5.43 <sup>c</sup>

<sup>a</sup>Plus and minus indicate the presence or absence of a 14-d fenofibrate administration. Values are mean ratios (% weight) of each FA relative to the total FA content  $\pm$  SD ( $n = 5$ ).

<sup>b</sup>Significant difference due to treatment (- vs. +;  $P < 0.05$ ).

<sup>c</sup>Significant difference due to genotype (W-T vs. PPAR $\alpha$ -/-;  $P < 0.05$ ). SFA, saturated FA; MFA, monounsaturated FA. For other abbreviations see Table 2.



**FIG. 1.** Effect of a 14-d fenofibrate treatment on desaturase activities in wild-type (W-T) and peroxisome proliferator-activated receptor  $\alpha$  (PPAR $\alpha$ )-/- mouse liver.  $\Delta$ 9-,  $\Delta$ 6- and  $\Delta$ 5-Desaturase activities were measured on postmitochondrial liver fractions of four experimental groups: W-T mice untreated (W-T, -), W-T mice treated for 14 d with fenofibrate (W-T, +), PPAR $\alpha$ -deficient mice untreated (PPAR $\alpha$  -/-, -), and PPAR $\alpha$ -deficient mice treated for 14 d with fenofibrate (PPAR $\alpha$  -/-, +). The  $\Delta$ 9-,  $\Delta$ 6-, and  $\Delta$ 5-desaturase activities were calculated as described in the Materials and Methods section. Activities are presented as means  $\pm$  SEM of five individual assays for each group. Each assay was carried out in triplicate. <sup>a</sup>Indicates a significant difference due to fenofibrate treatment (- vs. +;  $P < 0.05$ ). <sup>b</sup>Indicates a significant difference due to genotype (W-T vs. PPAR $\alpha$  -/-;  $P < 0.05$ ).

*Effect of a 14-d fenofibrate treatment on hepatic  $\Delta$ 6-desaturase protein level.* To determine whether the fenofibrate-induced increase in  $\Delta$ 6-desaturase mRNA level was correlated with an elevated  $\Delta$ 6-desaturase protein expression, Western blot analyses were performed on hepatic postmitochondrial fractions. Rabbit sera anti-rat  $\Delta$ 6-desaturase obtained in our laboratory (25) were used (Fig. 3). Under our experimental conditions,  $\Delta$ 6-desaturase was not detected in PPAR $\alpha$ -/- mice or in untreated W-T mice (Fig. 3). Conversely, after a 14-d fenofibrate treatment, the  $\Delta$ 6-desaturase protein level strongly increased in W-T mice but not in PPAR $\alpha$ -deficient mice (Fig. 3).

*Short-term effect of fenofibrate on desaturase mRNA levels.* Desaturase mRNA levels were also analyzed 2, 4, 8, 16, and 24 h after a single intragastric administration of fenofibrate in W-T and PPAR $\alpha$ -/- mice. The results of Northern blot analyses were quantified and plotted on four separate graphics (Figs. 4A–D). A calculated model curve is represented on the figures (based on polynomial regression). We used CYP4A10, a well-documented PPAR $\alpha$  target gene, as a reference of early PPAR $\alpha$ -dependent transcriptional induction. As shown in Figure 4A, the CYP4A10 mRNA level was rapidly and strongly increased by fenofibrate in W-T animals, but it was not detected in PPAR $\alpha$ -deficient mice under the stringent washing conditions required for the W-T samples blotted on the same membrane.

As previously observed (Fig. 1), SCD1 mRNA level was markedly higher in W-T mice than in PPAR $\alpha$ -/- mice, whatever the time after treatment (Fig. 4B). A maximal difference was measured 24 h after fenofibrate exposure (Fig. 4B). We observed that  $\Delta$ 6-desaturase mRNA levels were also induced in W-T mice, but not in PPAR $\alpha$ -/- mice 16 h after treatment (Fig. 4C).  $\Delta$ 5-Desaturase mRNA level in PPAR $\alpha$ -/- mice was comparable to  $\Delta$ 5-desaturase mRNA level in W-T mice until 24 h after PP exposure (Fig. 4D). However, at 24 h after treatment, the  $\Delta$ 5-desaturase transcript level was higher in W-T animals than in PPAR $\alpha$ -/-.

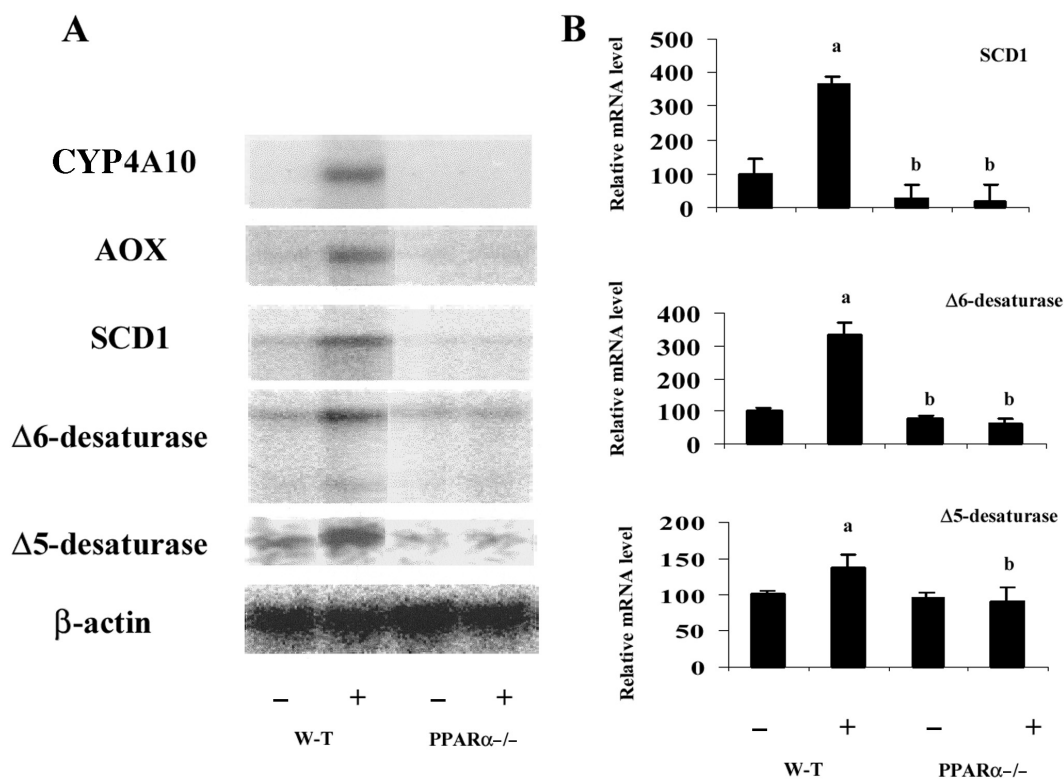
The short-term differences observed between mice from both genotypes concerning their  $\Delta$ 9-,  $\Delta$ 6-, and  $\Delta$ 5-mRNA levels are consistent with the differences reported after 2 wk of daily treatment (Fig. 1). Although SCD1 and  $\Delta$ 6-desaturase mRNA levels are rapidly and markedly increased in a PPAR $\alpha$ -dependent manner, the differential effect of PP on  $\Delta$ 5-desaturase mRNA levels between mice of both genotypes is not observed until 24 h after treatment.

## DISCUSSION

PPAR $\alpha$ -/- mice were initially investigated in pharmacological studies. This animal model led to major advances in the identification and characterization of main PPAR $\alpha$  target genes (3). Moreover, the use of PPAR $\alpha$ -deficient mice permitted a better understanding of PPAR $\alpha$  implications in metabolic adaptations (26,27) and a greater understanding of PPAR $\alpha$ -independent effects of dietary PUFA (28). The aim of our work was to document, *in vivo*, the PPAR $\alpha$ -dependent changes in hepatic FA profile and the involvement of SCD1,  $\Delta$ 6-desaturase, and  $\Delta$ 5-desaturase in the hepatic regulatory network controlled by PPAR $\alpha$  in rodents.

Our results confirm the previously mentioned PPAR $\alpha$ -deficient mice hepatic steatosis (3,21,29), for the 11-wk-old male transgenic mice had a much higher level of hepatic FA than age-matched W-T (Table 2). As has been previously reported for the liver of rats treated with PP (30), PP administration induced numerous changes in mouse hepatic FA composition (Table 3). None of the significant changes promoted in W-T mouse liver by treatment with PP occurred in the livers of PPAR $\alpha$ -deficient mice that received a similar treatment.



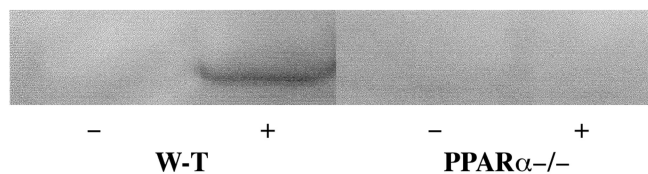


**FIG. 2.** Effect of a 14-d fenofibrate treatment on desaturase mRNA levels in W-T and PPAR $\alpha$ -/- mouse liver. (A) Total RNA was extracted from four mouse livers of the four experimental groups: W-T mice untreated (W-T, -), W-T mice treated for 14 d with fenofibrate (W-T, +), PPAR $\alpha$ -deficient mice untreated (PPAR $\alpha$ -/-, -), PPAR $\alpha$ -deficient mice treated for 14 d with fenofibrate (PPAR $\alpha$ -/-, +). Twenty micrograms of total RNA was run on a 1% formaldehyde-agarose gel, blotted onto a nylon membrane, and probed with six different random-primed  $^{32}$ P-labeled cDNA probes. cDNA probes AOX, CYP4A10, and  $\beta$ -actin were from a murine origin, whereas SCD1,  $\Delta$ 6 ( $\Delta$ 6-desaturase), and  $\Delta$ 5 ( $\Delta$ 5-desaturase) were from rat. Phosphorscreens were exposed for 24 h. (B) mRNA levels corresponding to SCD1,  $\Delta$ 6-, and  $\Delta$ 5-desaturase were analyzed for four animals of each genotype (W-T and PPAR $\alpha$ -/-) and each treatment (-: untreated, +: treated with fenofibrate) by densitometry using  $\beta$ -actin as loading control. Results are presented as means  $\pm$  SD of four individual analyses for each group. <sup>a</sup>Indicates a significant difference due to fenofibrate treatment (- vs. +;  $P < 0.05$ ). <sup>b</sup>Indicates a significant difference due to genotype (W-T vs. PPAR $\alpha$ -/-;  $P < 0.05$ ). CYP4A10, cytochrome P450; AOX, peroxisomal acyl-CoA oxidase; SCD1, stearoyl-CoA desaturase; for other abbreviations see Figure 1.

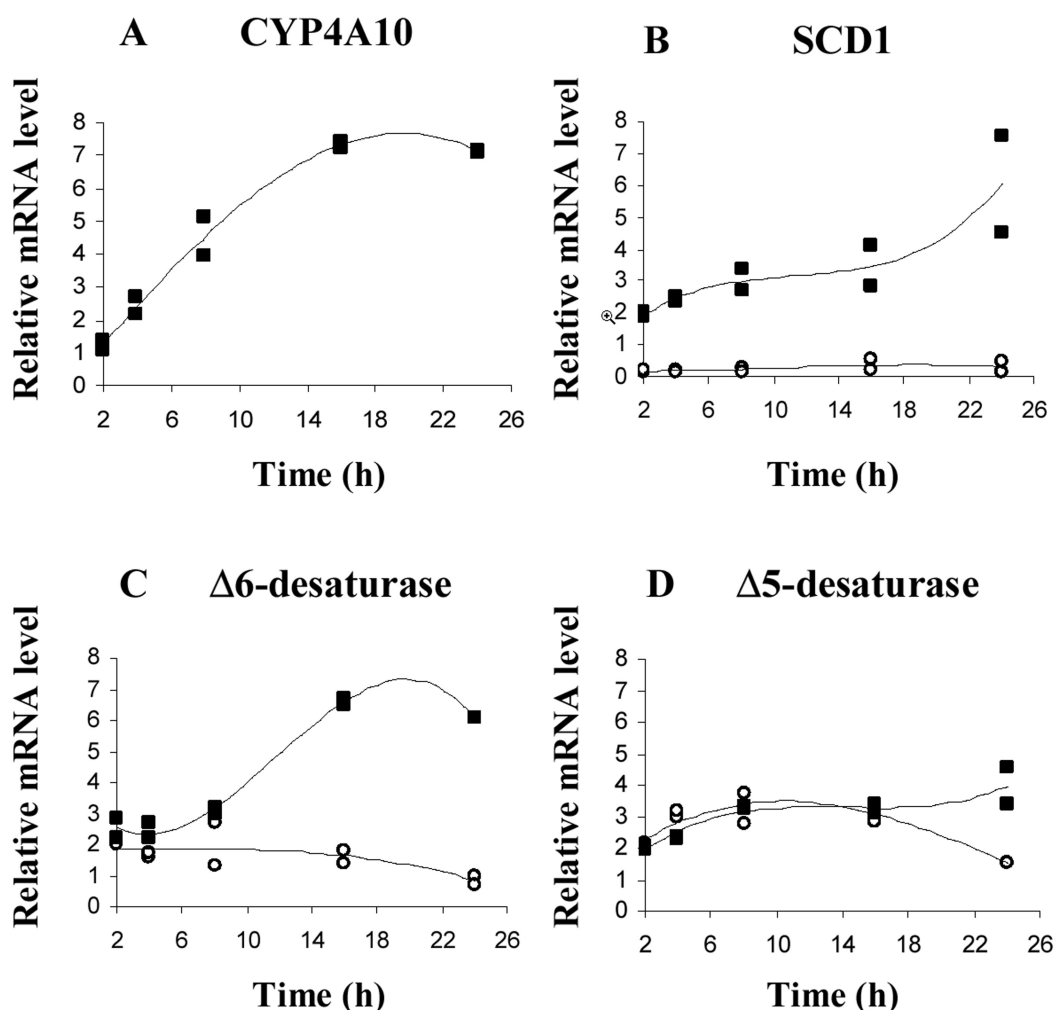
This result illustrates the major role of PPAR $\alpha$  in the regulation of FA-metabolizing enzymes.

Concerning desaturases, our data indicate that PPAR $\alpha$  is not required for their constitutive expression, as their mRNA were detected in PPAR $\alpha$ -/- mice (Fig. 2). However, SCD1 and  $\Delta$ 6-desaturase mRNA levels in untreated PPAR $\alpha$ -/- mice were significantly lower than in untreated W-T mice. Like other FA-metabolizing enzymes (31), SCD1 and  $\Delta$ 6-desaturase expression may be altered in mice lacking PPAR $\alpha$ . By contrast, the physiological consequences of PPAR $\alpha$  inactivation do not significantly alter  $\Delta$ 9- and  $\Delta$ 6-desaturase activities in 11-wk-old male mice. Therefore, the major difference in 18:2n-6 hepatic content between mice from either genotype is not correlated to a significant change in  $\Delta$ 6-desaturase activity between mice from both genotypes. We hypothesize that, as linoleic acid is by far the major FA provided by the diet, it may be less oxidized and subsequently accumulated in the liver of PPAR $\alpha$ -deficient mice.

In the liver of W-T mice treated with fenofibrate, extensive modifications in both PUFA and monoenoic FA contents were observed (Table 3). The PP-induced decrease in PUFA is consistent with the well-known induction of enzymes involved in peroxisomal  $\beta$ -oxidation, which preferentially



**FIG. 3.** Effect of a 14-d fenofibrate treatment on  $\Delta$ 6-desaturase protein level in W-T and PPAR $\alpha$ -/- mouse liver. Eighty micrograms of proteins from hepatic postmitochondrial supernatants of the four experimental groups were run on SDS-PAGE and transferred onto a nitrocellulose membrane. Rabbit polyclonal anti-rat  $\Delta$ 6-desaturase antibodies were used for the detection. For abbreviations see Figure 1.



**FIG. 4.** Short-term effect of fenofibrate treatment on desaturase mRNA levels in W-T and PPAR $\alpha$ -/- mouse liver. Total RNA was extracted from two mouse livers of the two experimental groups: W-T mice 2, 4, 8, 16, and 24 h after treatment with fenofibrate (W-T, +; ■), PPAR $\alpha$ -deficient mice 2, 4, 8, 16, and 24 h after treatment with fenofibrate (PPAR $\alpha$ -/-, +; ○). Twenty micrograms of total RNA was run on a 1% formaldehyde-agarose gel, blotted onto a nylon membrane, and probed with five different random-primed  $^{32}$ P-labeled cDNA probes. cDNA probes CYP4A10 and  $\beta$ -actin were from a murine origin, whereas SCD1,  $\Delta$ 6 ( $\Delta$ 6-desaturase), and  $\Delta$ 5 ( $\Delta$ 5-desaturase) were from rat. Phosphorscreens were exposed for 24 h CYP4A10 (A), SCD1 (B),  $\Delta$ 6-desaturase (C), and  $\Delta$ 5-desaturase (D) mRNA levels were analyzed for two animals of both genotypes at 2, 4, 8, 16, and 24 h after treatment. The results of Northern blotting were quantified and plotted on each graph as ratios relative to  $\beta$ -actin. Calculated model curves obtained by polynomial regression are represented on each graphic. For abbreviations see Figures 1 and 2.

break down PUFA (32). The increase in monoenoic FA is also consistent with a previous study that established that hepatic  $\Delta$ 9-desaturase activity was increased by a number of pharmaceutical molecules of the fibrate class (9). The mechanism underlying this phenomenon was shown to involve a transcriptional increase of SCD1 mRNA level, due to a functional PPRE in mouse SCD1 promoter (15). Consistent with these studies, we demonstrated that fenofibrate, like other PP, enhances  $\Delta$ 9-desaturase activity (Fig. 2) and SCD1 mRNA level (Fig. 3) *in vivo*. Since this induction did not occur in PPAR $\alpha$ -deficient mice, we presented evidence for a PPAR $\alpha$  requirement in this pretranslational mechanism.

Numerous studies have shown that dietary PUFA (16,17) and cholesterol (33), hormones (34,35), or lipid-lowering drugs such as fibrates (10) may regulate  $\Delta$ 6- and  $\Delta$ 5-desat-

urase activities in rodent liver. Here, we report an increase in the  $\Delta$ 6-desaturase activity (Fig. 1), mRNA level (Fig. 2), and protein level (Fig. 3) in the liver of W-T mice treated for 14 d with fenofibrate but not in PPAR $\alpha$ -/- mice. Similarly,  $\Delta$ 5-desaturase activity (Fig. 1) and mRNA level (Fig. 2) were enhanced in the liver of W-T but not PPAR $\alpha$ -/- mice after 14 d of treatment with fenofibrate. Moreover, a short-term time-course study showed that the significant effect of fenofibrate on  $\Delta$ 6- and  $\Delta$ 5-desaturase mRNA levels reported after 2 wk of daily treatment (Fig. 2) was already detectable, respectively, at 16 and 24 h after treatment (Fig. 4). Therefore, our result supports the involvement of PPAR $\alpha$  in the early control of not only  $\Delta$ 9-desaturase but also  $\Delta$ 6-desaturase and, to a lesser extent,  $\Delta$ 5-desaturase in mouse liver.

The 14-d fenofibrate treatment induced a significant

decrease in main hepatic PUFA (18:2n-6, 20:4n-6, 22:6n-3) through a PPAR $\alpha$ -mediated process (Table 3). This may have considerable physiological consequences, as PUFA perform numerous vital functions (36). Changes in the cellular availability of long-chain PUFA may indirectly contribute to delayed effects of PPAR $\alpha$  pharmacological ligands. Indeed, long-chain PUFA and certain of their derivatives, i.e., eicosanoids, are endogenous ligands for PPAR $\alpha$  itself and other nuclear receptors (37). Moreover, PUFA are known to inhibit the expression of certain lipogenic enzymes (37). Apart from these observations, it appears that changes in the activity of  $\Delta$ 6- and  $\Delta$ 5-desaturases are likely to limit the PUFA decrease in liver of mice treated by PP. Thus,  $\Delta$ 6- and  $\Delta$ 5-desaturase activities may restore secondary regulations by sustaining long-chain PUFA availability and counterbalancing their excessive degradation through peroxisomal  $\beta$ -oxidation.

Our current study shows that hepatic  $\Delta$ 6- and  $\Delta$ 5-desaturases are up-regulated by fenofibrate in W-T mice but not in PPAR $\alpha$ -/- mice after a long-term treatment. In a recent study, Cherkaoui-Malki *et al.* (38) proposed that long-term administration of PPAR $\alpha$  pharmacological ligands may result in delayed changes in gene expression occurring secondary to PPAR $\alpha$  activation and alterations in lipid metabolism. The short-term effect of fenofibrate on  $\Delta$ 6-desaturase mRNA level reported here (Fig. 4) suggests that  $\Delta$ 6-desaturase may be directly regulated by PPAR $\alpha$ . Regarding  $\Delta$ 5-desaturase, the short-term effect of fenofibrate exposure on mRNA level is less suggestive of a direct PPAR $\alpha$ -dependent control of gene expression. A molecular and functional analysis of the regulatory regions of  $\Delta$ 6- and  $\Delta$ 5-desaturase genes and the search for PPRE would further address this problem.

Dietary PUFA induce the transcription of numerous genes encoding proteins involved in FA oxidation through activation of PPAR $\alpha$ . PUFA are also known to inhibit hepatic  $\Delta$ 6- and  $\Delta$ 5-desaturase gene expression (16,17). Thus, our results document a discrepancy between fibrates and PUFA, both commonly considered as members of PPAR $\alpha$  activators, which induce opposite effects on desaturase expressions. The search for the responsive element to both PPAR $\alpha$  and other PUFA-sensitive transcription factors in the regulatory regions of  $\Delta$ 6- and  $\Delta$ 5-desaturases would contribute to elucidating this paradox.

## ACKNOWLEDGMENTS

PPAR $\alpha$ -deficient mice were a gift from Dr. Frank J. Gonzalez. We thank Dr. Christian Diot for the rat SCD1 probe and for helpful discussion. We thank Colette Bétoulière, Pablo Olivera, Anne Leborgne, and Kim L. Cung for animal care and able technical assistance. This work was supported by grants from the Région Midi Pyrénées (no. 9600469), from the Association pour la Recherche sur le Cancer (no. 1386), and from Arilait Recherches.

## REFERENCES

1. Lake, B.G. (1995) Peroxisome Proliferation: Current Mechanisms Relating to Nongenotoxic Carcinogenesis, *Toxicol. Lett.* 82–83, 673–681.
2. Reddy, J.K., and Hashimoto, T. (2001) Peroxisomal  $\beta$ -Oxidation and Peroxisome Proliferator-Activated Receptor  $\alpha$ : An Adaptive Metabolic System, *Annu. Rev. Nutr.* 21, 193–230.
3. Lee, S.S., Pineau, T., Drago, J., Lee, E.J., Owens, J.W., Kroetz, D.L., Fernandez-Salguero, P.M., Westphal, H., and Gonzalez, F.J. (1995) Targeted Disruption of the Alpha Isoform of the Peroxisome Proliferator-Activated Receptor Gene in Mice Results in Abolishment of the Pleiotropic Effects of Peroxisome Proliferators, *Mol. Cell. Biol.* 15, 3012–3022.
4. Mangelsdorf, D.J., Thummel, C., Beato, M., Herrlich, P., Schutz, G., Umesono, K., Blumberg, B., Kastner, P., Mark, M., Chambon, P., *et al.* (1995) The Nuclear Receptor Superfamily: The Second Decade, *Cell* 15, 835–839.
5. Issemann, I., and Green, S. (1990) Activation of a Member of the Steroid Hormone Receptor Superfamily by Peroxisome Proliferators, *Nature* 347, 645–650.
6. Forman, B.M., Chen, J., and Evans, R.M. (1997) Hypolipidemic Drugs, Polyunsaturated Fatty Acids, and Eicosanoids Are Ligands for Peroxisome Proliferator-Activated Receptors  $\alpha$  and  $\delta$ , *Proc. Natl. Acad. Sci. USA* 94, 4312–4317.
7. Kliewer, S.A., Umesono, K., Noonan, D.J., Heyman, R.A., and Evans, R.M. (1992) Convergence of 9-*cis* Retinoic Acid and Peroxisome Proliferator Signalling Pathways Through Heterodimer Formation of Their Receptors, *Nature* 358, 771–774.
8. Reddy, J.K., and Lalwai, N.D. (1983) Carcinogenesis by Hepatic Peroxisome Proliferators: Evaluation of the Risk of Hypolipidemic Drugs and Industrial Plasticizers to Humans, *Crit. Rev. Toxicol.* 12, 1–58.
9. Kawashima, Y., Hanioka, N., Matsumura, M., and Kozuka, H. (1983) Induction of Microsomal Stearoyl-CoA Desaturation by the Administration of Various Peroxisome Proliferators, *Biochim. Biophys. Acta* 752, 259–264.
10. Kawashima, Y., Musoh, K., and Kozuka, H. (1990) Peroxisome Proliferators Enhance Linoleic Acid Metabolism in Rat Liver. Increased Biosynthesis of Omega 6 Polyunsaturated Fatty Acids, *J. Biol. Chem.* 265, 9170–9175.
11. Tocher, D.R., Leaver, M.J., and Hodgson, P.A. (1998) Recent Advances in the Biochemistry and Molecular Biology of Fatty Acyl Desaturases, *Prog. Lipid Res.* 37, 73–117.
12. Ntambi, J.M. (1999) Regulation of Stearoyl-CoA Desaturase by Polyunsaturated Fatty Acids and Cholesterol, *J. Lipid Res.* 40, 1549–1558.
13. Landschulz, K.T., Jump, D.B., MacDougald, O.A., and Lane, M.D. (1994) Transcriptional Control of the Stearoyl-CoA Desaturase-1 Gene by Polyunsaturated Fatty Acids, *Biochem. Biophys. Res. Commun.* 200, 763–768.
14. Rodriguez, C., Cabrero A., Roglans, N., Adzet, T., Sanchez, R.M., Vazquez, M., Ciudad, C.J., and Laguna, J.C. (2001) Differential Induction of Stearoyl-CoA Desaturase and Acyl-CoA Oxidase Genes by Fibrates in HepG2 Cells, *Biochem. Pharmacol.* 61, 357–364.
15. Miller, C.W., and Ntambi, J. (1996) Peroxisome Proliferators Induce Mouse Liver Stearoyl-CoA Desaturase 1 Gene Expression, *Proc. Natl. Acad. Sci. USA* 93, 9443–9448.
16. Cho, H.P., Nakamura, M.T., and Clarke, S.D. (1999) Cloning, Expression, and Nutritional Regulation of the Mammalian  $\Delta$ 6-Desaturase, *J. Biol. Chem.* 274, 471–477.
17. Cho, H.P., Nakamura, M.T., and Clarke, S.D. (1999) Cloning, Expression, and Fatty Acid Regulation of the Human  $\Delta$ 5-Desaturase, *J. Biol. Chem.* 274, 37335–37339.
18. Aki, T., Shimada, Y., Inagaki, K., Higashimoto, H., Kawamoto, S., Shigeta, S., Ono, K., and Suzuki, O. (1999) Molecular Cloning and Functional Characterization of Rat  $\Delta$ 6 Fatty Acid Desaturase, *Biochem. Biophys. Res. Commun.* 255, 575–579.
19. Zolfaghari, R., Cifelli, C.J., Banta, M.D., and Ross, A.C. (2001) Fatty Acid  $\Delta$ (5)-Desaturase mRNA Is Regulated by Dietary Vitamin A and Exogenous Retinoic Acid in Liver of Adult Rats, *Arch. Biochem. Biophys.* 391, 8–15.

20. Matsuzaka, T., Shimano, H., Yahagi, N., Amemiya-Kudo, M., Yoshikawa, T., Hasty, A.H., Tamura, Y., Osga, J.-I., Okazaki, H., Iizuka, Y., *et al.* (2002) Dual Regulation of Mouse  $\Delta 5$ - and  $\Delta 6$ -Desaturase Gene Expression by SREBP-1 and PPAR $\alpha$ , *J. Lipid Res.* **43**, 107–114.
21. Costet, P., Legendre, C., More, J., Edgar, A., Galtier, P., and Pineau, T. (1998). Peroxisome Proliferator-Activated Receptor  $\alpha$ -Isoform Deficiency Leads to Progressive Dyslipidemia with Sexually Dimorphic Obesity and Steatosis, *J. Biol. Chem.* **273**, 29577–29585.
22. Rioux, V., Catheline, D., Bouriel, M., and Legrand, P. (1999) High-Performance Liquid Chromatography of Fatty Acids as Naphthacyl Esters, *Analisis* **27**, 186–193.
23. Rioux V., Lemarchal, P., and Legrand P. (2000) Myristic Acid, Unlike Palmitic Acid, Is Rapidly Metabolized in Cultured Rat Hepatocytes, *J. Nutr. Biochem.* **11**, 198–207.
24. Bensadoun, A., and Weinstein, D. (1976) Assay of Proteins in the Presence of Interfering Materials, *Anal. Biochem.* **70**, 241–250.
25. D'Andrea, S., Guillou, H., Jan, S., Catheline, D., Thibault, J.-N., Bouriel, M., Rioux, V., and Legrand, P. (2002) The Same Rat  $\Delta 6$ -Desaturase Not Only Acts on 18- but Also on 24-Carbon Fatty Acids in Very-Long-Chain Polyunsaturated Fatty Acid Biosynthesis, *Biochem. J.* **364**, 49–55.
26. Kroetz, D.L., Yook, P., Costet, P., Bianchi, P., and Pineau, T. (1998) Peroxisome Proliferator-Activated Receptor  $\alpha$  Controls the Hepatic CYP4A Induction Adaptive Response to Starvation and Diabetes, *J. Biol. Chem.* **273**, 31581–31589.
27. Leone, T.C., Weinheimer, C.J., and Kelly, D.P. (1999) A Critical Role for the Peroxisome Proliferator-Activated Receptor  $\alpha$  (PPAR $\alpha$ ) in the Cellular Fasting Response: The PPAR $\alpha$ -Null Mouse as a Model of Fatty Acid Oxidation Disorders, *Proc. Natl. Acad. Sci. USA* **96**, 7473–7478.
28. Ren, B., Thelen, A.P., Peters, J.M., Gonzalez, F.J., and Jump, D.B. (1997) Polyunsaturated Fatty Acid Suppression of Hepatic Fatty Acid Synthase and S14 Gene Expression Does Not Require Peroxisome Proliferator-Activated Receptor  $\alpha$ , *J. Biol. Chem.* **272**, 26827–26832.
29. Akiyama, T.E., Nicol, C.J., Fievet, C., Staels, B., Ward, J.M., Auwerx, J., Lee, S.S., Gonzalez, F.J., and Peters, J.M. (2001) Peroxisome Proliferator-Activated Receptor- $\alpha$  Regulates Lipid Homeostasis, but Is Not Associated with Obesity: Studies with Congenic Mouse Lines, *J. Biol. Chem.* **276**, 39088–39093.
30. Pennacchiotti, G.L., Maldonado, E.N., and Aveldaño, M.I. (2001) Major Clofibrate Effects on Liver and Plasma Lipids Are Independent of Changes in Polyunsaturated Fatty Acid Composition Induced by Dietary Fat, *Lipids* **36**, 121–127.
31. Aoyama, T., Peters, J.M., Iritani, N., Nakajima, T., Furihata, K., Hashimoto, T., and Gonzalez, F.J. (1998) Altered Constitutive Expression of Fatty Acid-Metabolizing Enzymes in Mice Lacking the Peroxisome Proliferator-Activated Receptor Alpha (PPARalpha), *J. Biol. Chem.* **273**, 5678–5684.
32. Reddy, J.K., and Mannaerts, G.P. (1994) Peroxisomal Lipid Metabolism, *Annu. Rev. Nutr.* **14**, 343–370.
33. Brenner, R.R., Bernasconi, A.M., Gonzales, M.S., and Rimoldi, O.J. (2002) Dietary Cholesterol Modulates  $\Delta 6$  and  $\Delta 9$  Desaturase mRNAs and Enzymatic Activity in Rats Fed a Low-EFA diet, *Lipids* **37**, 375–383.
34. Brenner, R.R. (1990) Endocrine Control of Fatty Acid Desaturation, *Biochem. Soc. Trans.* **18**, 773–775.
35. Rimoldi, O.J., Finarelli, G.S., and Brenner, R.R. (2001) Effects of Diabetes and Insulin on Hepatic  $\Delta 6$  Desaturase Gene Expression, *Biochem. Biophys. Res. Commun.* **283**, 323–326.
36. Spector, A.A. (1999) Essentiality of Fatty Acids, *Lipids* **34** (Suppl.), S1–S3.
37. Clarke, S.D. (2001) Polyunsaturated Fatty Acid Regulation of Gene Transcription: A Molecular Mechanism to Improve the Metabolic Syndrome, *J. Nutr.* **131**, 1129–1132.
38. Cherkaoui-Malki, M., Meyer, K., Cao, W.-Q., Latruffe, N., Yeldandi, A.V., Rao, M.S., Bradfield, C., and Reddy, J.K. (2001) Identification of Novel Peroxisome Proliferator-Activated Receptor  $\alpha$  (PPAR $\alpha$ ) Target Genes in Mouse Liver Using cDNA Microarray Analysis, *Gene Expr.* **9**, 291–304.

[Received June 25, 2002, and in final revised form November 5, 2002; revision accepted November 20, 2002]



# Molecular Species of PC and PE Formed During Castor Oil Biosynthesis

Jiann-Tsyh Lin\*, Jennifer M. Chen, Pei Chen, Lucy P. Liao, and Thomas A. McKeon

USDA, ARS, Western Regional Research Center, Albany, California 94710

**ABSTRACT:** As part of a program to elucidate castor oil biosynthesis, we have identified 36 molecular species of PC and 35 molecular species of PE isolated from castor microsomes after incubations with [ $^{14}\text{C}$ ]-labeled FA. The six [ $^{14}\text{C}$ ]FA studied were ricinoleate, stearate, oleate, linoleate, linolenate, and palmitate, which were the only FA identified in castor microsomal incubations. The incorporation of each of the six FA into PC was better than that into PE. The [ $^{14}\text{C}$ ]FA were incorporated almost exclusively into the *sn*-2 position of both PC and PE. The incorporation of [ $^{14}\text{C}$ ]stearate and [ $^{14}\text{C}$ ]palmitate into 2-acyl-PC was slower compared to the other four [ $^{14}\text{C}$ ]FA. The incorporation does not show any selectivity for the various *lyso*PC molecular species. The level of incorporation of [ $^{14}\text{C}$ ]FA in PC was in the order of: oleate > linolenate > palmitate > linoleate > stearate > ricinoleate, and in PE: linoleate > linolenate > oleate > palmitate > stearate > ricinoleate. In general, at the *sn*-1 position of both PC and PE, linoleate was the most abundant FA, palmitate was the next, and oleate, linolenate, stearate, and ricinoleate were minor FA. The activities of oleoyl-12-hydroxylase, oleoyl-12-desaturase seem unaffected by the FA at the *sn*-1 position of 2-oleoyl-PC. The FA in the *sn*-1 position of PC does not significantly affect the activity of phospholipase  $A_2$ , whereas ricinoleate is preferentially removed from the *sn*-2 position of PC. The results show that (i) [ $^{14}\text{C}$ ]oleate is most actively incorporated to form 2-oleoyl-PC, the immediate substrate of oleoyl-12-hydroxylase; (ii) 2-ricinoleoyl-PC is formed mostly by the hydroxylation of 2-oleoyl-PC, not from the incorporation of ricinoleate into 2-ricinoleoyl-PC; and (iii) 2-oleoyl-PE is less actively formed than 2-oleoyl-PC.

Paper no. L9031 in *Lipids* 37, 991–995 (October 2002).

Ricinoleate has many industrial uses. Its only commercial source is castor oil, in which ricinoleate constitutes 90% of the FA (1). Since castor bean contains the toxin ricin as well as potent allergens, it is hazardous to grow, harvest, and process. It would be desirable to produce ricinoleate instead in a transgenic oilseed lacking these toxic components. To develop a transgenic plant capable of producing a high level of ricinoleate in its seed oil, one must understand the biosynthesis of castor oil. The identified enzymatic steps on the path-

way regulating the production of ricinoleate-rich castor oil can be used to identify the corresponding genes to be cloned and expressed in other oilseed plants.

We have previously reported on the biosynthesis of castor oil and identified the key enzymatic steps on the pathway that drive the ricinoleate into castor oil (2,3). The main pathway is: 2-oleoyl-PC (1-acyl-2-oleoyl-*sn*-glycero-3-phosphocholine)  $\Rightarrow$  2-ricinoleoyl-PC (1-acyl-2-ricinoleoyl-*sn*-glycero-3-phosphocholine)  $\Rightarrow$  ricinoleate  $\rightarrow$  ricinoleoyl-CoA  $\rightarrow$  ricinoleoyl-*lyso*PA  $\rightarrow$  diricinoleoyl-PA  $\rightarrow$  1,2-diricinoleoyl-*sn*-glycerol  $\Rightarrow$  triricinolein. The heavy arrows ( $\Rightarrow$ ) indicate the key enzymatic steps. In castor microsomal incubation, oleoyl-CoA is rapidly incorporated into 2-oleoyl-PC by acyl-CoA:*lyso*PC acyltransferase (EC 2.3.1.23) (4,5). The 2-oleoyl-PC formed is then hydroxylated to 2-ricinoleoyl-PC by oleoyl-12-hydroxylase and desaturated to 2-linoleoyl-PC by oleoyl-12-desaturase (EC 1.3.1.35) (2). 2-Ricinoleoyl-PC is then hydrolyzed by phospholipase  $A_2$  (EC 3.1.1.4) to release ricinoleate for the biosynthesis of TAG containing ricinoleate (2). 2-Oleoyl-PE (1-acyl-2-oleoyl-*sn*-glycero-3-phosphoethanolamine) cannot be hydroxylated to 2-ricinoleoyl-PE, but can first be converted to 2-oleoyl-PC and then hydroxylated (3). The key enzyme, oleoyl-12-hydroxylase, has been characterized (5,6). We would like to extend the understanding of this pathway to the molecular species of lipid classes.

We have recently reported the molecular species of acyl-glycerols produced in microsomal incubations after incorporating six [ $^{14}\text{C}$ ] FA in castor microsomal incubations (7). The incorporations of these FA into TAG are in the order of: ricinoleate > oleate > linoleate > linolenate > stearate > palmitate. In this work, we also describe the incorporation of six [ $^{14}\text{C}$ ]FA, representing the endogenous FA, into the molecular species of PC and PE, intermediates in the biosynthesis of castor oil.

## EXPERIMENTAL PROCEDURES

**Microsomal incubation.** Microsomes from castor bean were prepared as described previously (2). To obtain suitable amounts of label incorporation for analysis, the incubation mixture was scaled up 20-fold in a total volume of 20 mL: sodium phosphate buffer (0.1 M, pH 6.3), CoA-SH (10  $\mu\text{mol}$ ), NADH (10  $\mu\text{mol}$ ), ATP (10  $\mu\text{mol}$ ),  $\text{MgCl}_2$  (10  $\mu\text{mol}$ ), catalase (20,000 units), and microsomal fraction from

\*To whom correspondence should be sent at USDA, 800 Buchanan St., Albany, CA 94710. E-mail: jtlm@pw.usda.gov

Abbreviations: 2-oleoyl-PC, 1-acyl-2-oleoyl-*sn*-glycero-3-phosphocholine; 2-oleoyl-PE, 1-acyl-2-oleoyl-*sn*-glycero-3-phosphoethanolamine; 2-ricinoleoyl-PC, 1-acyl-2-ricinoleoyl-*sn*-glycero-3-phosphocholine; RT, retention time.

endosperm of immature castor bean (300  $\mu$ L, 2.76 mg of protein). The [ $^{14}$ C]FA, ricinoleate (55 Ci/mol; American Radiolabeled Chemicals, Inc., St. Louis, MO), stearate (44 Ci/mol; NEN Life Science Products, Boston, MA), oleate (52 Ci/mol; NEN), linoleate (51 Ci/mol; NEN), linolenate (52 Ci/mol; NEN), and palmitate (56 Ci/mol; NEN) were incubated individually. The [ $^{14}$ C]FA (5.0  $\mu$ Ci) in 400  $\mu$ L ethanol was added last into a screw-capped bottle containing incubation mixture and then immediately mixed.

The mixture was then incubated in a shaking water bath for 60 min at 22°C. The incubation was stopped by suspension in 75 mL of chloroform/methanol (1:2, vol/vol). The mixture was again mixed with 12.5 mL of chloroform and 12.5 mL of water. The lower chloroform layer, containing the lipid extract, was dried and fractionated by silica HPLC to separate lipid classes as described below. For time-course studies,  $\frac{1}{2}$  of the incubation components and extraction solvents, and [ $^{14}$ C]FA (0.5  $\mu$ Ci) were used. Duplicate incubations were done at various times and the averages of incorporations were used.

**Determination of the sn-1,2 positions of [ $^{14}$ C]FA on PC and PE.** The [ $^{14}$ C]PC and [ $^{14}$ C]PE obtained from the castor microsomal incubations were hydrolyzed with 0.2 mg phospholipase A<sub>2</sub> (*Naja mossambica mossambica*, P4034; Sigma) dissolved in incubation buffer, in a total of 1 mL buffer (0.1 M Tris, pH 8.9). The PC or PE was dissolved in 20  $\mu$ L of ethanol and added to start the reaction, followed by immediate mixing. The mixture was incubated in a shaking water bath at 25°C overnight and then neutralized with HCl (0.1 M). The total lipid was extracted as described above for the castor microsomal incubation. The free FA and *lyso*PC (*lyso*PE) formed were separated by silica HPLC and counted by a flow scintillation analyzer as described below. Under these conditions, the esters at sn-2 of both PC and PE were completely hydrolyzed by phospholipase A<sub>2</sub>.

**HPLC.** HPLC was carried out on a liquid chromatograph (Waters Associates, Milford, MA), using a UV detector (Waters 2487) at 205 nm and a flow scintillation analyzer (150TR; Packard Instrument Co., Downers Grove, IL) to detect [ $^{14}$ C]-labeled compounds. Labeled lipids were separated by HPLC and where possible identified by co-chromatography with lipid standards and matching the retention times (RT) on the UV chromatogram and radiochromatogram. The PC and PE standards were purchased from Avanti Polar Lipids, Inc. (Alabaster, AL) and Sigma. The flow rate of HPLC eluents was 1 mL/min. The flow rate of liquid scintillation fluid (Ultima Flo M; Packard Instrument Co.) in the flow scintillation analyzer was 3 mL/min. The maximum scaling value of the graph from the flow scintillation analyzer was set at 10000.

(i) **Separation of lipid classes.** Lipid classes were separated according to Singleton and Stikeleather (8) on a silica column (25  $\times$  0.46 cm, 5  $\mu$ m, Luna, silica(2); Phenomenex, Torrance, CA) with a linear gradient of 2-propanol/hexane (4:3, vol/vol) to 2-propanol/hexane/water (4:3:0.75, by vol) in 20 min, then isocratically for 20 min. A prepacked silica saturator column (3  $\times$  0.46 cm, 15–25  $\mu$ m; Phenomenex) was installed between

the pump and injector to saturate the mobile phase with silica before it reached the column. To elute *lyso*PC more rapidly after phospholipase A<sub>2</sub> hydrolysis of PC, a linear gradient of 2-propanol/hexane (4:3, vol/vol) to 2-propanol/hexane/water (4:3:0.85, by vol) in 20 min, then isocratic for 30 min, was used. Eluent B is near saturation with water. In this HPLC system, RT were: 40.0 min, *lyso*PC (1-oleoyl-*lyso*PC); 30.6 min, PC (1-palmitoyl-2-oleoyl-PC); and about 3.5 min, FFA. For the separation of *lyso*PE, the former silica HPLC system (2-propanol/hexane/water, 4:3:0.75 by vol) was used, and the RT were: 22.6 min, *lyso*PE (1-oleoyl-*lyso*PE); 17.7 min, PE (1-palmitoyl-2-oleoyl-PE); and about 3.5 min, FFA.

(ii) **Separation of molecular species of PC.** Molecular species of PC were separated in 40 min as previously reported (9), using a C<sub>8</sub> column (25  $\times$  0.46 cm, 5  $\mu$ m, Luna C8; Phenomenex) with a linear gradient of 90% aqueous methanol to 100% methanol, both containing 0.1% of concentrated NH<sub>4</sub>OH. NH<sub>4</sub>OH was used as silanol-suppressing agent.

(iii) **Separation of molecular species of PE.** Molecular species of PE were separated as previously reported (10), using a C<sub>8</sub> column (Luna C8; Phenomenex) with a linear gradient of 88% aqueous methanol to 100% methanol containing 0.1% of concentrated NH<sub>4</sub>OH in 40 min.

## RESULTS AND DISCUSSION

**Separation of lipid classes.** The total lipids obtained from the incubation of each [ $^{14}$ C]FA were separated into lipid classes by silica HPLC as shown earlier (Fig. 1; Ref. 7). The lipid classes separated were AG (and FFA), PE, PC (without ricinoleoyl chain), and ricinoleoyl-PC in the order of elution. All of the six [ $^{14}$ C]FA used were incorporated into PC and PE. The levels of [ $^{14}$ C]PC were higher than those of [ $^{14}$ C]PE and [ $^{14}$ C]AG (7).

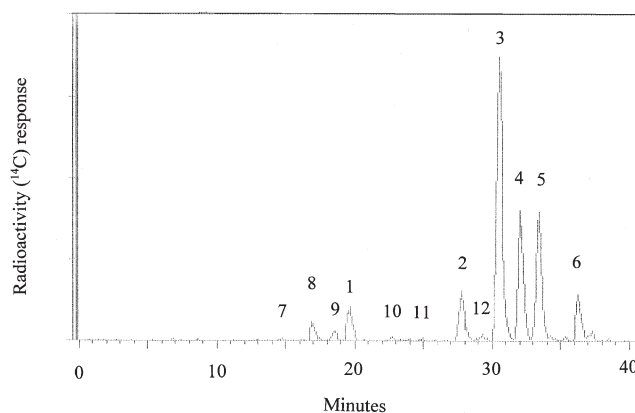
Time course studies, of up to 120 min, of microsomal incubations of the six [ $^{14}$ C]FA individually showed that in general the level incorporated by PE, PC (without ricinoleoyl chain), and ricinoleoyl-PC increased initially and then equilibrated at 45 to 60 min when the rate of incorporation from FA became equal to the rate of hydrolysis. Since ricinoleate is actively removed from the mixture of 2-acyl-PC containing different FA at sn-2 (2), the radioactivity levels at 15 min (initial rate) were used to compare the rates of incorporation. The incorporation of [ $^{14}$ C]stearate and [ $^{14}$ C]palmitate into 2-acyl-PC was slower than of the other four [ $^{14}$ C]FA. Usually these two FA are strongly excluded from the sn-2 position of phospholipids. In comparing the amount of label incorporated at the equilibrium stages, PC and PE incorporating [ $^{14}$ C]-labeled oleate, linoleate, and linolenate were at higher levels than those with ricinoleate, stearate, and palmitate. The low incorporation of label by 2-ricinoleoyl-PC at equilibrium stage may be attributed to a futile cycle of incorporation and hydrolysis. With the exception of ricinoleate, which was most actively incorporated into TAG (7), the incorporation of FA (FA preference) is similar to that observed for the incorporations of the six [ $^{14}$ C]FA into TAG. This is also consistent with

earlier studies in which [ $^{14}\text{C}$ ]oleoyl-CoA and [ $^{14}\text{C}$ ]ricinoleoyl-CoA were incorporated into [ $^{14}\text{C}$ ]PC in castor microsomal incubation (4) and when [ $^{14}\text{C}$ ]oleoyl-CoA, [ $^{14}\text{C}$ ]linoleoyl-CoA, and [ $^{14}\text{C}$ ]palmitoyl-CoA were incorporated into [ $^{14}\text{C}$ ]PC in soybean microsomal incubation (11). The incorporation of label from [ $^{14}\text{C}$ ]oleate, [ $^{14}\text{C}$ ]linoleate, and [ $^{14}\text{C}$ ]linolenate into PE was higher than that from [ $^{14}\text{C}$ ]ricinoleate, [ $^{14}\text{C}$ ]stearate, and [ $^{14}\text{C}$ ]palmitate. PE had not been previously reported in microsomal incubations of [ $^{14}\text{C}$ ]FA and [ $^{14}\text{C}$ ]acyl-CoA.

**Determination of the ratio of [ $^{14}\text{C}$ ]FA on sn-1,2 positions of [ $^{14}\text{C}$ ]PC and [ $^{14}\text{C}$ ]PE.** The [ $^{14}\text{C}$ ]PC and [ $^{14}\text{C}$ ]PE fractions collected after silica HPLC from the 60-min incubations were subjected to phospholipase A<sub>2</sub> hydrolysis to determine the ratio of [ $^{14}\text{C}$ ]FA on the sn-1 and -2 positions. The percentage of label at sn-1 in the total [ $^{14}\text{C}$ ]PC (sn-1 and -2 combined) from each [ $^{14}\text{C}$ ]FA were: 0.3% (1-[ $^{14}\text{C}$ ]ricinoleoyl-*lyso*PC, RT 47.7 min), 3.5% (1-[ $^{14}\text{C}$ ]stearoyl-*lyso*PC, 38.7 min), 2.3% (1-[ $^{14}\text{C}$ ]oleoyl-*lyso*PC, 40.0 min), 0.6% (1-[ $^{14}\text{C}$ ]linoleoyl-*lyso*PC, 40.8 min), 0.3% (1-[ $^{14}\text{C}$ ]linolenoyl-*lyso*PC, 41.2 min), and 7.3% (1-[ $^{14}\text{C}$ ]palmitoyl-*lyso*PC, 40.3 min). In earlier studies, in a soybean microsomal incubation, 95% of the [ $^{14}\text{C}$ ]PC incorporating [ $^{14}\text{C}$ ]oleoyl-CoA was labeled at the sn-2 position (11), and in a castor microsomal incubation of [ $^{14}\text{C}$ ]oleoyl-CoA, 84.4% of the [ $^{14}\text{C}$ ]PC incorporated label at the sn-2 position (4). The percentage of the label at sn-1 in the total [ $^{14}\text{C}$ ]PE (sn-1 and -2 combined) from each [ $^{14}\text{C}$ ]FA were: 2% (1-[ $^{14}\text{C}$ ]stearoyl-*lyso*PE, RT 22.3 min) and 1.8% (1-[ $^{14}\text{C}$ ]linoleoyl-*lyso*PE, 22.7 min). The levels of 1-[ $^{14}\text{C}$ ]ricinoleoyl-*lyso*PE, 1-[ $^{14}\text{C}$ ]oleoyl-*lyso*PE (22.6 min), 1-[ $^{14}\text{C}$ ]linolenoyl-*lyso*PC and 1-[ $^{14}\text{C}$ ]palmitoyl-*lyso*PC were not detectable. For both PC and PE, the [ $^{14}\text{C}$ ]FA are incorporated predominantly at the sn-2 position.

**Identification of the molecular species of [ $^{14}\text{C}$ ]PC.** The radiochromatogram separating molecular species of PC from the incubation of [ $^{14}\text{C}$ ]oleate on a C<sub>8</sub> column (9) is shown as Figure 1. Peaks #4, 5, and 6 were identified by co-chromatography with the standards 1-palmitoyl-2-oleoyl-PC, 1,2-dioleoyl-PC, and 1-stearoyl-2-oleoyl-PC. Since the standards for peaks #1, 2, and 3 were not available, they were designated as 1-ricinoleoyl-2-oleoyl-PC, 1-linolenoyl-2-oleoyl-PC, and 1-linoleoyl-2-oleoyl-PC, based on relative RT and elution characteristics of the molecular species of PC (9).

We have calculated the relative RT of the molecular species of PC from the six [ $^{14}\text{C}$ ]FA incubations based on the RT (32.15 min) of 1-palmitoyl-2-oleoyl-PC in our previous report (9) by co-chromatography with this PC standard (Lin, J.T., and McKeon, T.A., unpublished data). The calculated RT of the six 2-ricinoleoyl-PC in Figure 1 from the [ $^{14}\text{C}$ ]ricinoleate incubation are 9.4 min (1,2-ricinoleoyl-PC), 14.6 min (1-linolenoyl-2-ricinoleoyl-PC), 16.9 min (1-linoleoyl-2-ricinoleoyl-PC), 18.5 min (1-palmitoyl-2-ricinoleoyl-PC), 19.6 min (1-oleoyl-2-ricinoleoyl-PC), and 22.7 min (1-stearoyl-2-ricinoleoyl-PC). 1,2-Diricinoleoyl-PC (9.4 min) was not detected. It was probably hydrolyzed by phospholipases immediately after formation. The RT of peaks #7–10



**FIG. 1.** The C<sub>8</sub> HPLC radiochromatogram separating the molecular species of PC incorporated from [ $^{14}\text{C}$ ]oleate in castor microsomal incubation. (1) 1-Ricinoleoyl-2-oleoyl-PC; (2) 1-linolenoyl-2-oleoyl-PC; (3) 1-linoleoyl-2-oleoyl-PC; (4) 1-palmitoyl-2-oleoyl-PC; (5) 1,2-dioleoyl-PC; (6) 1-stearoyl-2-oleoyl-PC; (7) 1-linolenoyl-2-ricinoleoyl-PC; (8) 1-linoleoyl-2-ricinoleoyl-PC; (9) 1-palmitoyl-2-ricinoleoyl-PC; (10) 1-stearoyl-2-ricinoleoyl-PC; (11) 1-linolenoyl-2-linoleoyl-PC; (12) 1-palmitoyl-2-linoleoyl-PC.

are the same as the calculated RT. Labeled 1-oleoyl-2-ricinoleoyl-PC is a minor component in peak #1 (19.7 min, mostly 1-ricinoleoyl-2-oleoyl-PC), because the levels of label in 2-ricinoleoyl-PC were lower than those of 2-oleoyl-PC and the ratio of the six labeled 2-ricinoleoyl-PC to each other were similar to those of the six 2-oleoyl-PC. Similarly, the calculated RT of 2-linoleoyl-PC in Figure 1 from the incubation with [ $^{14}\text{C}$ ]linoleate were used to designate the peaks #11 (1-linolenoyl-2-linoleoyl-PC) and #12 (1-palmitoyl-2-linoleoyl-PC). The other four 2-linoleoyl-PC co-eluted with other [ $^{14}\text{C}$ ]PC as minor components. The label incorporated in 2-linoleoyl-PC was lower than in 2-ricinoleoyl-PC. The molecular species of PC incorporating the other five [ $^{14}\text{C}$ ]FA were identified and designated the same as those from [ $^{14}\text{C}$ ]oleate, except the [ $^{14}\text{C}$ ]FA were unchanged in the incubations.

The incorporations of [ $^{14}\text{C}$ ]oleoyl-CoA, [ $^{14}\text{C}$ ]oleate, and [ $^{14}\text{C}$ ]linoleate into the molecular species of PC in the microsomes prepared from soybean (11), potato tuber (12), pea leaf (13), and developing sunflower seeds (14) have been reported. The labeled PC in these systems contained two of the labeled and unlabeled oleate, linoleate, linolenate, stearate, and palmitate (no ricinoleate) at both sn-1 and sn-2 positions.

**Radioactivity levels of the molecular species of [ $^{14}\text{C}$ ]PC.** Table 1 shows the level of [ $^{14}\text{C}$ ]label in the molecular species of [ $^{14}\text{C}$ ]PC incorporating each [ $^{14}\text{C}$ ]FA during a 60-min castor microsomal incubation. The [ $^{14}\text{C}$ ]PC are primarily derived from the action of acyl-CoA:lysoPC acyltransferase with endogenous lysoPC as acyl acceptor. The lysoPC are endogenous to the microsomes and contain any of the six different FA in the sn-1 position, and the [ $^{14}\text{C}$ ]FA at sn-2 are from [ $^{14}\text{C}$ ]acyl-CoA. In general, the levels of label of [ $^{14}\text{C}$ ]PC with the FA at the sn-1 position were in the order of linoleate > palmitate > oleate > linolenate, stearate, and ricinoleate, with linoleate and palmitate as the major sn-1 component of PC.

**TABLE 1**  
**Level of Incorporation of Radiolabeled FA into Molecular Species of PC in Castor Microsomal Incubations (60 min)**

FA (nmol) <sup>a</sup>	nmol						
	RFa-PC <sup>b</sup>	LnFa-PC	LFa-PC	PFa-PC	OFa-PC	SFa-PC	Total
Ricinoleate (91)	1.3	1.4	7.6	5.3	2.2	1.6	19.4
Stearate (114)	2.0	1.5	9.1	4.9	2.1	1.2	20.8
Oleate (96)	3.0	4.8	26.8	12.7	12.7	4.0	64.0
Ricinoleate <sup>c</sup>	ND	0.2	1.5	0.9	0.9 <sup>d</sup>	0.4	3.9
Linoleate <sup>c</sup>	0.1 <sup>d</sup>	0.2	1.1 <sup>d</sup>	0.5	0.5 <sup>d</sup>	0.2 <sup>d</sup>	2.6
Linoleate (98)	1.1	2.0	17.2	6.8	3.8	2.3	33.2
Linolenate (96)	2.6	8.4	24.2	13.9	5.6	4.7	59.4
Palmitate (89)	3.6	2.4	14.6	9.5	3.5	1.8	35.4

<sup>a</sup>For each FA incubation 5.0 μCi was used. The amounts (nmol) of FA used are different because the specific radioactivities of FA are different.

<sup>b</sup>Fa is the FA shown in the FA column on the Table at the *sn*-2 position of PC.

<sup>c</sup>2-Ricinoleoyl-PC and 2-linoleoyl-PC in the incubation of [<sup>14</sup>C]-oleate.

<sup>d</sup>Estimated from the ratio of the levels of molecular species of 2-oleoyl-PC. ND, not detected; R, ricinoleate; Ln, linolenate; L, linoleate; P, palmitate; O, oleate, S, stearate.

For example, in the incorporation of [<sup>14</sup>C]ricinoleate into PC as shown in Table 1, the levels of label were 1-linoleoyl-2-ricinoleoyl-PC (7.6) > 1-palmitoyl-2-ricinoleoyl-PC (5.3) > 1-oleoyl-2-ricinoleoyl-PC (2.2). This order, reflects the relative levels of the six molecular species of *lyso*PC in castor microsomes. In previous reports of microsomal incubations of [<sup>14</sup>C]oleoyl-CoA from soybean (11), potato tuber (12), and pea leaf (13), the major PC molecular species also contained linoleate and palmitate at the *sn*-1 position. The ratios of the six PC incorporating each of the six [<sup>14</sup>C]FA were similar and thus the activity of the enzyme seems unaffected by the difference of FA at *sn*-1 position on *lyso*PC. The total [<sup>14</sup>C]-label (Table 1) from each [<sup>14</sup>C]FA was incorporated in the order: oleate > linolenate > palmitate > linoleate > stearate > ricinoleate. The acyl-CoA:*lyso*PC acyltransferase activity also may be affected by which FA more readily forms acyl-CoA, since acyl-CoA synthetase may be specific for certain FA. In soybean microsomes, acyl-CoA:*lyso*PC acyltransferase was highly specific for oleoyl-CoA and linoleoyl-CoA over palmitoyl-CoA and did not show any selectivity for the various *lyso*PC molecular species (11). In the incubation of [<sup>14</sup>C]oleate (Table 1), the proportion of label incorporated into the six 2-[<sup>14</sup>C]oleoyl-PC with different FA at *sn*-1 was similar to the proportion of the six 2-[<sup>14</sup>C]ricinoleoyl-PC and that of 2-

[<sup>14</sup>C]linoleoyl-PC from the 2-[<sup>14</sup>C]oleoyl-PC. Thus, the activities of both oleoyl-12-hydroxylase and oleoyl-12-desaturase seem not to be affected by the different FA at *sn*-1 of 2-oleoyl-PC, the immediate substrate of these two enzymes. The same conclusion was also drawn for the activity of oleoyl-12-desaturase in the microsomes of potato tuber (12) and pea leaf (13). However, the effect on oleoyl-12-hydroxylase activity has not previously been reported. Oleoyl-12-hydroxylase from *Ricinus communis* L. is an oleoyl-12-desaturase homolog (15).

*Time course for production of the molecular species of [<sup>14</sup>C]PC.* The levels of labeled molecular species of PC at various incubation times were also determined. The ratios of the levels of six molecular species of PC containing the same *sn*-2 FA from the incubations of the six [<sup>14</sup>C]FA at various times were similar to the ratio in Table 1. It seems that the activity of phospholipase A<sub>2</sub> in castor microsomes, one of the key enzymes in castor oil biosynthesis, is not significantly affected by the difference of these FA at the *sn*-1 position of PC. However, ricinoleate is preferentially removed from the *sn*-2 position of PC by phospholipase A<sub>2</sub> (2).

*Identification of the molecular species of [<sup>14</sup>C]PE.* Molecular species of PE were identified and designated as those of PC. The RT of minor [<sup>14</sup>C]PE from [<sup>14</sup>C]oleate incubation cannot be matched with our calculated RT of 2-ricinoleoyl-PE

**TABLE 2**  
**Level of Incorporation of Radiolabeled FA into Molecular Species of PE in Castor Microsomal Incubations (60 min)**

Fatty acid (nmol) <sup>a</sup>	nmol						
	RFa-PE <sup>b</sup>	LnFa-PE	LFa-PE	PFa-PE	OFa-PE	SFa-PE	Total
Ricinoleate (91)	0.01	0.01	0.28	0.22	0.02	ND	0.54
Stearate (114)	0.08	0.34	1.48	0.07	0.17	0.02	2.16
Oleate (96)	0.35	0.58	4.65	3.21	0.41	0.20	9.40
Linoleate (98)	0.32	0.46	6.26	3.94	0.56	0.43	11.97
Linolenate (96)	0.09	0.50	3.17	3.01	0.54	0.20	7.51
Palmitate (89)	0.21	0.26	2.06	0.27	0.30	0.04	3.14

<sup>a</sup>See Table 1 for description of experimental conditions.

<sup>b</sup>Fa is the FA shown in the FA column on the Table at the *sn*-2 position of PE. For abbreviations see Table 1.



and 2-linoleoyl-PE. They may be the molecular species of other lipid classes, which elute near PE on the silica HPLC including PI, PA, and PS (see Fig. 1, Ref. 2). That 2-[<sup>14</sup>C]ricinoleoyl-PE and 2-[<sup>14</sup>C]linoleoyl-PE were not detected agrees with our earlier conclusion (3) that 2-oleoyl-PE is not a substrate for oleoyl-12-hydroxylase and oleoyl-12-desaturase. Although 2-oleoyl-PE is not a substrate under these isolated conditions, we cannot yet rule it out as a substrate *in vivo*.

**Incorporation of label into molecular species of [<sup>14</sup>C]PE.** The radiolabeling of molecular species of PE incorporating the six [<sup>14</sup>C]FA in castor microsomal incubations (60 min) was lower than those of PC as shown in Table 2. Except for the PE products incorporating [<sup>14</sup>C]stearate and [<sup>14</sup>C]palmitate, PE with linoleate and palmitate at *sn*-1 position were the major PE, as for PC. Unlike PC, the levels of molecular species of PE incorporating [<sup>14</sup>C]ricinoleate were much lower than the other five [<sup>14</sup>C]FA. The labeling of PE containing only saturated FA was also very low. The total incorporation of label was in the order: linoleate > oleate > linolenate > palmitate > stearate > ricinoleate. 2-Oleoyl-PE seems less important than 2-oleoyl-PC as an intermediate in the biosynthesis of castor oil, not only because it has a lower radioactivity level but also because it cannot be hydroxylated to 2-ricinoleoyl-PE (3). Both 2-ricinoleoyl-PC and 2-ricinoleoyl-PE can be used as the substrates of phospholipid:DAG acyltransferase for the biosynthesis of triricinolein (16).

In conclusion, we have identified and quantified 36 molecular species of PC and 35 molecular species of PE in castor microsomal incubations of six [<sup>14</sup>C]FA individually. Both PC and PE are intermediates in the biosynthetic pathway of castor oil (3). The schematic overview of the plant lipid biosynthetic pathway and its compartmentation have been reported (17). The results here show that (i) 2-oleoyl-PC is actively formed as the immediate substrate of oleoyl-12-hydroxylase, comparing the six endogenous FA; (ii) 2-ricinoleoyl-PC is mostly formed by the hydroxylation of 2-oleoyl-PC, not from the incorporation of ricinoleate into 2-ricinoleoyl-PC; and (iii) 2-oleoyl-PE is not actively formed for the biosynthesis of castor oil.

## REFERENCES

- Achaya, K.T., Craig, B.M., and Youngs, C.G. (1964) The Component Fatty Acids and Glycerides of Castor Oil, *J. Am. Oil Chem. Soc.* **41**, 783–784.
- Lin, J.T., Woodruff, C.L., Lagouche, O.J., McKeon, T.A., Stafford, A.E., Goodrich-Tanrikulu, M., Singleton, J.A., and Haney, C.A. (1998) Biosynthesis of Triacylglycerols Containing Ricinoleate in Castor Microsomes Using 1-Acyl-2-oleoyl-*sn*-glycero-3-phosphocholine as the Substrate of Oleoyl-12-hydroxylase, *Lipids* **33**, 59–69.
- Lin, J.T., Lew, K.M., Chen, J.M., Iwasaki, Y., and McKeon, T.A. (2000) Metabolism of 1-Acyl-2-oleoyl-*sn*-glycero-3-phosphoethanolamine in Castor Oil Biosynthesis, *Lipids* **35**, 481–486.
- Bafor, M., Smith, M.A., Jonsson, L., Stobart, K., and Stymne, S. (1991) Ricinoleic Acid Biosynthesis and Triacylglycerol Assembly in Microsomal Preparations from Developing Castorbean (*Ricinus communis*) Endosperm, *Biochem. J.* **280**, 507–514.
- Moreau, R., and Stumpf, P.K. (1981) Recent Studies of the Enzymatic Synthesis of Ricinoleic Acid by Developing Castor Beans, *Plant Physiol.* **67**, 672–676.
- Lin, J.T., McKeon, T.A., Goodrich-Tanrikulu, M., and Stafford, A.E. (1996) Characterization of Oleoyl-12-hydroxylase in Castor Microsomes Using the Putative Substrate, 1-Acyl-2-oleoyl-*sn*-glycero-3-phosphocholine, *Lipids* **31**, 571–577.
- Lin, J.T., Chen, J.M., Liao, L.P., and McKeon, T.A. (2002) Molecular Species of Acylglycerols Incorporating Radiolabeled Fatty Acids from Castor (*Ricinus communis* L.) Microsomal Incubations, *J. Agric. Food Chem.* **50**, 5077–5081.
- Singleton, J.A., and Stikeleather, L.F. (1995) High-Performance Liquid Chromatography Analysis of Peanut Phospholipids. II. Effect of Postharvest Stress on Phospholipid Composition, *J. Am. Oil Chem. Soc.* **72**, 485–488.
- Lin, J.T., McKeon, T.A., Woodruff, C.L., and Singleton, J.A. (1998) Separation of Synthetic Phosphatidylcholine Molecular Species by High-Performance Liquid Chromatography on a C<sub>8</sub> Column, *J. Chromatogr. A* **824**, 169–174.
- Lin, J.T., Lew, K.M., Chen, J.M., and McKeon, T.A. (2000) Separation of the Molecular Species of Intact Phosphatidylethanolamines and Their *N*-Monomethyl and *N,N*-Dimethyl Derivatives by High-Performance Liquid Chromatography, *J. Chromatogr. A* **891**, 349–353.
- Demandre, C., Bahl, J., Serghini, H., Alpha, M.J., and Mazliak, P. (1994) Phosphatidylcholine Molecular Species Formed by Lysophosphatidylcholine Acyltransferase from Soya Bean Microsomes, *Phytochemistry* **35**, 1171–1175.
- Demandre, C., Tremolieres, A., Justin, A.M., and Mazliak, P. (1986) Oleate Desaturation in Six Phosphatidylcholine Molecular Species from Potato Tuber Microsomes, *Biochim. Biophys. Acta* **877**, 380–386.
- Serghini-Caid, H., Demandre, C., Justin, A.-M., and Mazliak, P. (1988) Oleoyl-phosphatidylcholine Molecular Species Desaturated in Pea Leaf Microsomes—Possible Substrates of Oleate-desaturase in Other Green Leaves, *Plant Sci.* **54**, 93–101.
- Triki, S., Demandre, C., and Mazliak, P. (1999) Biosynthesis of Triacylglycerols by Developing Sunflower Seed Microsomes, *Phytochemistry* **52**, 55–62.
- van de Loo, F.J., Broun, P., Turner, S., and Somerville, C. (1995) An Oleate 12-Hydroxylase from *Ricinus communis* L. Is a Fatty Acyl Desaturase Homolog, *Proc. Natl. Acad. Sci. USA* **92**, 6743–6747.
- Dahlqvist, A., Stahl, U., Lenman, M., Banas, A., Lee, M., Sandager, L., Ronne, H., and Stymne, S. (2000) Phospholipid:Diacylglycerol Acyltransferase: An Enzyme That Catalyzes the Acyl-CoA-Independent Formation of Triacylglycerol in Yeast and Plants, *Proc. Natl. Acad. Sci. USA* **97**, 6487–6492.
- Budziszewski, G.J., Croft, K.P.C., and Hildebrand, D.F. (1996) Uses of Biotechnology in Modifying Plant Lipids, *Lipids* **31**, 557–569.

[Received March 21, 2002, and in revised form October 22, 2002; revision accepted October 23, 2002]

# Lipase-Catalyzed Hydrolysis of TG Containing Acetylenic FA

Marcel S.F. Lie Ken Jie<sup>a,\*</sup>, Xun Fu<sup>a</sup>, Maureen M.L. Lau<sup>a</sup>, and M.L. Chye<sup>b</sup>

Departments of <sup>a</sup>Chemistry and <sup>b</sup>Botany, The University of Hong Kong, Hong Kong, SAR, P.R. China

**ABSTRACT:** Hydrolysis of symmetrical acetylenic TG of type AAA [viz., glycerol tri-(4-decynoate), glycerol tri-(6-octadecynoate), glycerol tri-(9-octadecynoate), glycerol tri-(10-undecynoate), and glycerol tri-(13-docosynoate)] in the presence of eight microbial lipases was studied. Novozyme 435 (*Candida antarctica*), an efficient enzyme for esterification, showed a significant resistance in the hydrolysis of glycerol tri-(9-octadecynoate) and glycerol tri-(13-docosynoate). Hydrolysis of acetylenic TG with Lipolase 100T (*Humicola lanuginosa*) was rapidly accomplished. Lipase PS-D (*Pseudomonas cepacia*) showed a fair resistance toward the hydrolysis of glycerol tri-(6-octadecynoate) only, which reflected its ability to recognize the  $\Delta^6$  positional isomer of 18:1. Lipase CCL (*Candida cylindracea*, syn. *C. rugosa*) and AY-30 (*C. rugosa*) were able to catalyze the release of 10-undecynoic acid and 9-octadecynoic acid from the corresponding TG, but less readily the 13-docosynoic acid in the case of glycerol tri-(13-docosynoate). The two lipases CCL and AY-30 were able to distinguish the small difference in structure of fatty acyl moieties in the TG substrate. To confirm this trend, three regioisomers of mixed acetylenic TG of type ABC (containing one each of  $\Delta^6$ ,  $\Delta^9$ , and  $\Delta^{13}$  acetylenic FA in various positions) were prepared and hydrolyzed with CCL and AY-40. The results reconfirmed the observation that AY-30 and CCL were able to distinguish the slight differences in the molecular structure (position of the acetylenic bond and chain length) of the acyl groups in the TG during the hydrolysis of such TG substrates.

Paper no. L9066 in *Lipids* 37, 997–1006 (October 2002).

Lipases are key enzymes in catalyzing the breakdown of fats and oils to FFA, DAG, MAG, and glycerol. They are important to an organism in the digestion, mobilization, and deposition of lipid molecules. By understanding the activities of various lipases as biocatalysts in the hydrolysis of TG and in the esterification of FA to glycerol, scientists have successfully utilized these properties to isolate FFA and have prepared structured TG (1–5).

For example, pancreatic lipase hydrolyzes TG to 2-MG (5,6). Lipases also show specific activities toward the hydroly-

ysis of phospholipids and PC (components of cell or neuronal membranes) (7,8).

The discovery of the nutritional importance of n-3 PUFA (viz.,  $\alpha$ -linolenic acid, EPA, and DHA) initiated an intense effort to determine the action of lipases on such PUFA (9–11).

Apart from hydrolytic activities, lipases are also efficient in reactions such as esterification, transesterification, and aminolysis. These activities have led to the development and application of various immobilized lipases for oleochemical industries (12–14).

A large amount of work has been done on the hydrolysis of saturated and polyolefinic TG (15,16), but little has been conducted on TG containing acetylenic FA, found as minor components in some seed oils (17–20).

The role of acetylenic FA is not clear, but compounds such as stearolic acid [9-octadecynoic acid; abbreviated as 18:1(9a)] act as strong DNA-binding agents (21). Acetylenic alcohols also can inactivate oxidases (22) or lipoxygenase (23,24). In view of the biological importance of acetylenic FA, this paper reports the lipase-catalyzed hydrolysis of some symmetrical structured acetylenic TG of the type AAA and unsymmetrical structured acetylenic TG of the type ABC, where the acyl groups are different positional acetylenic FA isomers or homologs. The aim of this work was to investigate the effects of the acetylenic bond located at different positions in the acyl chains on the rate of hydrolysis of acetylenic TG substrates in the presence of different lipases as biocatalysts.

## MATERIALS AND METHODS

Immobilized lipases from *Rhizomucor miehei* (Lipozyme IM 20; activity 5.8 unit/mg), *Humicola lanuginosa* (Lipolase 100T; 20.8 unit/mg), and *Candida antarctica* (Novozyme 435; 7.8 unit/mg) were gifts from Novo Nordisk A/S (Hong Kong). Lipases from *C. cylindracea*, syn. *C. rugosa* (CCL, type VII; 8.4 unit/mg) and porcine pancreatic lipase (PPL, type II; 13.4 unit/mg) were purchased from Sigma Chemical Co. (St. Louis, MO). Immobilized lipases from *Pseudomonas cepacia* (PS-D, type I; 10.5 unit/mg), *Aspergillus niger* (Lipase A-12; 2.3 unit/mg), and *C. rugosa* (Lipase AY-30; 11.4 unit/mg) were gifts from Amano Pharmaceutical Co. Ltd. (Nagoya, Japan). Lipase activity in this study was measured as the liberation of 1  $\mu$ mol of butyric acid from tributyrin per minute at 37°C. One micromole of NaOH consumed (titra-

\*To whom correspondence should be addressed at The University of Hong Kong, Pokfulam Road, Hong Kong, SAR, P.R. China.  
E-mail: hrsclkj@hkucc.hku.hk

Abbreviations: 18:1(6a), 6-octadecynoate; 18:1(9a), 9-octadecynoate; 22:1(13a), 13-docosynoate; CCL, lipase from *Candida cylindracea*, syn. *C. rugosa*; PPL, porcine pancreatic lipase; PS-D, immobilized lipase from *Pseudomonas cepacia*; triolein, glycerol tri-(9Z-octadecenoate), or [18:1(9c)]<sub>3</sub>.

tion with 0.1 M NaOH) per minute corresponds to 1 unit of lipase activity.

Glycerol tri-(9Z-octadecenoate) [triolein], 10-undecenoic acid, and glycerol (99+%) were purchased from Aldrich Chemical Co. (Milwaukee, WI). Carrot seeds and high-erucic acid rapeseed oil were obtained from local sources. Preparation of acetylenic FA from the corresponding olefinic FA or seed oils by bromination and dehydrobromination was performed by the method described elsewhere (25). 4-Decynoic acid was obtained by condensing 4-pentynoic acid with *n*-bromopentane under *n*-butyllithium as described by Gilman and Holland (26).

$^1\text{H}$  and  $^{13}\text{C}$  NMR spectra were obtained using a Bruker Avance DPX<sub>300</sub> NMR spectrometer with the sample dissolved in deuteriochloroform and with tetramethylsilane as internal reference standard. TLC analysis was done on TLC plates coated with silica gel 60 GF<sub>254</sub> (art. 7730, 70–230 mesh), and column chromatographic separation was performed on silica gel 60 (art. 9385, 230–400 mesh; Merck, Darmstadt, Germany). GC was performed on a Hewlett-Packard gas chromatograph model 5890, equipped with an FID and a Hewlett-Packard model HP3394A electronic integrator. The GC columns used were fused-silica capillary columns with Nukol<sup>TM</sup> (Supelco Inc., Bellefonte, PA) as stationary phase (15 m × 0.53 mm, 0.50 μm film thickness) and Omegawax<sup>TM</sup> (Supelco Inc.) as stationary phase (30 m × 0.32 mm, 0.25 μm film thickness), for analyzing acetylenic acid and methyl ester, respectively. The temperatures of the column oven, injection port, and detector were maintained at 200, 250, and 250°C, respectively.

*General method for the preparation of TG of type AAA by enzymatic esterification in the presence of Novozyme as exemplified by the reaction of 10-undecynoic acid with glycerol.* A mixture of glycerol (400 mg, 4.35 mmol), 10-undecynoic acid (2.40 g, 13.0 mmol), Novozyme (160 mg), molecular sieve (4 Å, 1.0 g), and *n*-hexane (24 mL) was stirred vigorously in a 50-mL round-bottomed flask at 55°C for 24 h. The mixture was centrifuged, and the supernatant liquid was loaded on a silica gel column (100 g, 3.2 mm internal diameter). The column was then eluted with a mixture of *n*-hexane/diethyl ether (9:1, vol/vol, 500 mL). The eluent was evaporated to give glycerol tri-(10-undecynoate) (1.62 g, 63%). Similar reactions were carried out for the preparation of other TG of type AAA: namely, glycerol tri-(4-decynoate) (73%), glycerol tri-(6-octadecynoate) (70%), glycerol tri-(9-octadecynoate) (62%), and glycerol tri-(13-docosynoate) (61%).

*General method for the enzymatic hydrolysis of acetylenic TG as exemplified by the hydrolysis of glycerol tri-(9-octadecynoate) in the presence of PPL.* A mixture of glycerol tri-(9-octadecynoate) (53 mg, 0.06 mmol), 0.1 M NaH<sub>2</sub>PO<sub>4</sub>–Na<sub>2</sub>HPO<sub>4</sub> buffer solution (1.2 mL, pH 7), and lipase (PPL) (22 mg) was stirred at 40°C in a glass culture tube for definite periods. The reaction mixture was then extracted with diethyl ether (3 × 2 mL) and centrifuged to remove the lipase. The ethereal layer was concentrated and loaded on a silica gel (7.0 g) column. A mixture of *n*-hexane/diethyl ether (9:1, vol/vol, 90 mL)

was used to elute unhydrolyzed TG, and a mixture of *n*-hexane/diethyl ether/acetic acid (90:10:1, by vol; 100 mL) was used to elute the free 9-octadecynoic acid. The remaining components on the column were eluted with *n*-hexane/diethyl ether (3:2, vol/vol; 100 mL) and *n*-hexane/diethyl ether (1:1, vol/vol; 100 mL) to remove DG and MG, respectively. The solvent of each fraction was evaporated under reduced pressure, and the weights of TG, FAA, DG, and MG were determined.

For the remaining hydrolysis reactions, 0.06 mmol of TG substrates was used. The amount of lipases employed for each reaction was about 300 units [Lipase A-12 (125 mg), Lipase AY-30 (25 mg), PPL (22 mg), CCL (35 mg), PS-D (28 mg), Lipolase (15 mg), Lipozyme (50 mg), and Novozyme (35 mg)].

*General method for the preparation of mixed structured TG of type ABC by enzymatic esterification as exemplified by the preparation of glycerol 1-(3)-(9-octadecynoate)/6-octadecynoate)-2-(13-docosynoate) (1).* Glycerol 1-(3)-(9-octadecynoate) was produced by esterification of glycerol (250 mg, 2.7 mmol) with 9-octadecynoic acid (1.5 g, 5.4 mmol) in *n*-hexane (10 mL) and catalyzed by Lipozyme (150 mg) at 45°C for 12 h. The yield of MG, glycerol 1-(3)-(9-octadecynoate), was 27% after column chromatographic purification. A mixture of glycerol 1-(3)-(9-octadecynoate) (780 mg, 2.2 mmol), 13-docosynoic acid (780 mg, 2.32 mmol), Novozyme (90 mg), and *n*-hexane (10 mL) was stirred at 60°C for 8 h. Glycerol 1-(3)-(9-octadecynoate)-2-(13-docosynoate) (340 mg, 23%) was isolated by column chromatography. The DG obtained (280 mg, 0.42 mmol) was further esterified with 6-octadecynoic acid (120 mg, 0.43 mmol) in *n*-hexane (3.0 mL), in the presence of Novozyme (25 mg) at 60°C for 12 h. Compound **1** (246 mg, 63.3%) was obtained after column chromatographic separation. By a similar procedure, glycerol 1-(3)-(9-octadecynoate)/13-docosynoate)-2-(6-octadecynoate) [18:1(9a)/18:1(6a)/22:1(13a)] (compound **2**) and glycerol 1-(3)-(6-octadecynoate)/13-docosynoate)-2-(9-octadecynoate) [18:1(6a)/18:1(9a)/22:1(13a)] (compound **3**) were prepared in yields of 61.0 and 61.9%, respectively, for the last esterification step.

The position ( $\alpha$  or  $\beta$ ) of the various acyl chains in compounds **1–3** was confirmed by referring to the carbon chemical shifts of the C-1, C-2, and the carbon shifts of the acetylenic carbon nuclei published by Lie Ken Jie and Lam (27). The characteristic carbon shifts were identified as follows: 173.190/172.839/172.940 (C-1 for compound **1**), 34.000/34.202/33.527 (C-2 for compound **1**), 80.020/80.320/80.194/80.223/79.245/80.800 ( $\Delta^9/\Delta^{13}/\Delta^6$  for compound **1**); 173.214/172.550/172.259 (C-1 for compound **2**), 33.993/33.694/34.040 (C-2 for compound **2**), 80.031/80.329/79.245/80.806/80.207/80.231 ( $\Delta^9/\Delta^6/\Delta^{13}$  for compound **2**); 172.945/172.798/173.246 (C-1 for compound **3**), 33.529/34.160/34.044 (C-2 for compound **3**), 79.249/80.806/80.007/80.326/80.198/80.228 ( $\Delta^6/\Delta^9/\Delta^{13}$  for compound **3**).

*General method for the hydrolysis of structured acetylenic TG catalyzed by Lipase AY-30 or CCL as exemplified by the hydrolysis of compound 1 in the presence of CCL.* A mixture



of compound **1** (500 mg, 0.54 mmol), 0.1 M  $\text{NaH}_2\text{PO}_4$ – $\text{Na}_2\text{HPO}_4$  buffer solution (10 mL, pH 7), and lipase (CCL, 200 mg) was stirred at 40°C for 5 h. [Note: In the case of compounds **2** (500 mg) and **3** (500 mg), the amount of biocatalyst used was 200 mg of CCL or 150 mg of lipase AY-30.] The reaction products were extracted with diethyl ether and fractionated by column chromatography as described above. The relative amounts of the different FFA (183 mg) were determined from the intensities of the C-1 signals in the  $^{13}\text{C}$  NMR spectrum (180.32/180.59/180.65 for  $\Delta^6/\Delta^9/\Delta^{13}$ , respectively) as 6:7:4 for 18:1(6a):18:1(9a):22:1(13a), respectively. The mixed acetylenic FA (30 mg) were esterified with 15%  $\text{BF}_3$ /methanol (5 mL) for 15 min at 70°C. GC analysis indicated that the ratio of the methyl esters of 18:1(9a) and 18:1(6a) (overlapped) to 22:1(13a) was 7:2.

The isolated mixture of DG (164 mg) was stirred with potassium hydroxide (100 mg) in 95% ethanol solution (20 mL) at 80°C for 2 h. The reaction mixture was diluted with water (50 mL), acidified with HCl (4 M, 8 mL), and extracted with diethyl ether (3 × 20 mL). The solvent was evaporated and the residue was separated by column chromatography to give a mixture of free acetylenic FA. The components and ratio of acetylenic FA positional isomers in the DG fraction were determined by  $^{13}\text{C}$ -NMR from the intensities of the C-1 signals (180.32/180.59/180.65 for  $\Delta^6/\Delta^9/\Delta^{13}$ , respectively) as 9:8:12.

The time courses of lipase-catalyzed hydrolysis of TG are graphically presented in Figures 1–4. The graphs in Figures 1A–H show the amount (based on the weight of products isolated by silica column chromatographic separation) of unhydrolyzed (recovered) acetylenic TG left at the end of the indicated hydrolysis period (maximum of 45 h). Figures 2A–H give the amount of FFA, Figures 3A–H shows the amount of DG, and Figures 4A–H gives the amount of MG isolated by silica gel column chromatography. The results are the averages of three experiments conducted for each TG under investigation with a deviation  $\leq 5\%$ .

## RESULTS AND DISCUSSION

A total of eight lipase preparations [Lipozyme (*R. miehei*), Lipolase (*H. lanuginosa*), Novozyme (*C. antarctica*), CCL (*C. cylindracea*), PPL (porcine pancreatic lipase), PS-D (*P. cepacia*), A-12 (*A. niger*), and AY-30 (*C. rugosa*)] were used as biocatalysts to study the hydrolysis of five symmetrical acetylenic TG of type AAA {viz., [10:1(4a)]<sub>3</sub>\*, [18:1(6a)]<sub>3</sub>, [18:1(9a)]<sub>3</sub>, [11:1(10a)]<sub>3</sub>, and [22:1(13a)]<sub>3</sub>} along with triolein [18:1(9c)]<sub>3</sub>. [Note: The first number denotes the chain length of the FA. The number after the colon denotes the number of unsaturation and the number within the brackets indicates the position of the unsaturation; the letter “a” stands for acetylene, “c” stands for *cis* ethylene. The number 3 outside of the square bracket means that three FA moieties are acylated to the backbone of glycerol to form a TG.]

All eight of the lipases used in our hydrolysis reactions were effective biocatalysts. Even lipases A-12 and AY-30, which were poor performers in the esterification of acetylenic

acids with *n*-butanol (28), displayed good hydrolytic activities. In most cases, less than 20% of the acetylenic TG was left unreacted after 45 h. All lipases used were able to catalyze the hydrolysis of triolein efficiently (complete hydrolysis after 45 h). Novozyme distinguished fatty acyl chains in which the triple bond was located at the 9-position {as in [18:1(9a)]<sub>3</sub>} or the 13-position {as in [22:1(13a)]<sub>3</sub>}. It was interesting to realize that Novozyme, which is a nonregiospecific but an efficient lipase for esterification, was not as efficient in the hydrolysis of these TG as many of the other lipases used here.

None of the acetylenic TG was completely resistant to hydrolysis. However, Lipase A-12 was able to show a degree of differentiation in the case of [18:1(9a)]<sub>3</sub> and [22:1(13a)]<sub>3</sub>, as the hydrolysis process appeared rather slow during the first 25 h of reaction for these substrates. Lipases CCL and AY-30 showed a significant degree of resistance to the hydrolysis of [22:1(13a)]<sub>3</sub>, and about 30% of this symmetrical TG was recovered after stirring the reaction for 25 h.

The results for FFA isolated from these experiments also showed that the release of 18:1(6a) was comparatively slow when PS-D and Lipozyme were used as biocatalysts (Fig. 2). This result could be interpreted as follows: During the hydrolysis of [18:1(6a)]<sub>3</sub> to the FFA, these two lipases were significantly affected by the acetylenic bond at the 6-position of the acyl chain at either the intermediate DG or MG stage. Hence, the release of further FFA was relatively slow.

The results of FFA in Figures 2A–H reflected quite accurately the expected amounts of FFA liberated during the hydrolysis process. Where the amount of isolated TG was high (refer to Figs. 1A–H), the amount of the corresponding FFA tended to be low. For example, in the case of AY-30 and CCL, the amount of 22:1(13a) liberated was markedly lower than those of other positional acetylenic fatty isomers or homologs. Interestingly, in the presence of AY-30 and CCL, all TG showed a quick release of FFA (>70% within the first hour of reaction) except, of course, that of [22:1(13a)]<sub>3</sub>.

The total amount of DG for each reaction was also determined, and the results are shown in Figures 3A–H. The amount of DG isolated in all cases was less than 30% yield after 45 h. Lipases CCL, Lipolase, and Novozyme showed the lowest levels of DG (<10% after 5 h of contact time with the lipases), whereas PPL showed the highest level (>15% within 25 h). The amount of DG containing 18:1(9a) was comparatively high when [18:1(9a)]<sub>3</sub> was hydrolyzed in the presence of lipases A-12 and PPL.

In the case of PS-D, the amount of DG containing 18:1(6a) was significantly high. This result could be predicted from the low amount of FFA, 18:1(6a), isolated, as discussed above (see Fig. 2E). It could therefore be concluded that PS-D had experienced difficulty in hydrolyzing the DG intermediate containing 18:1(6a) acyl groups.

Figures 4A–H shows the amounts of MG isolated from these reactions. Reactions with Lipase A-12 and PPL showed relatively high amounts of MG (1.5–7%) after 25 h of reaction time. In the case of PS-D and Lipozyme, the 18:1(6a)



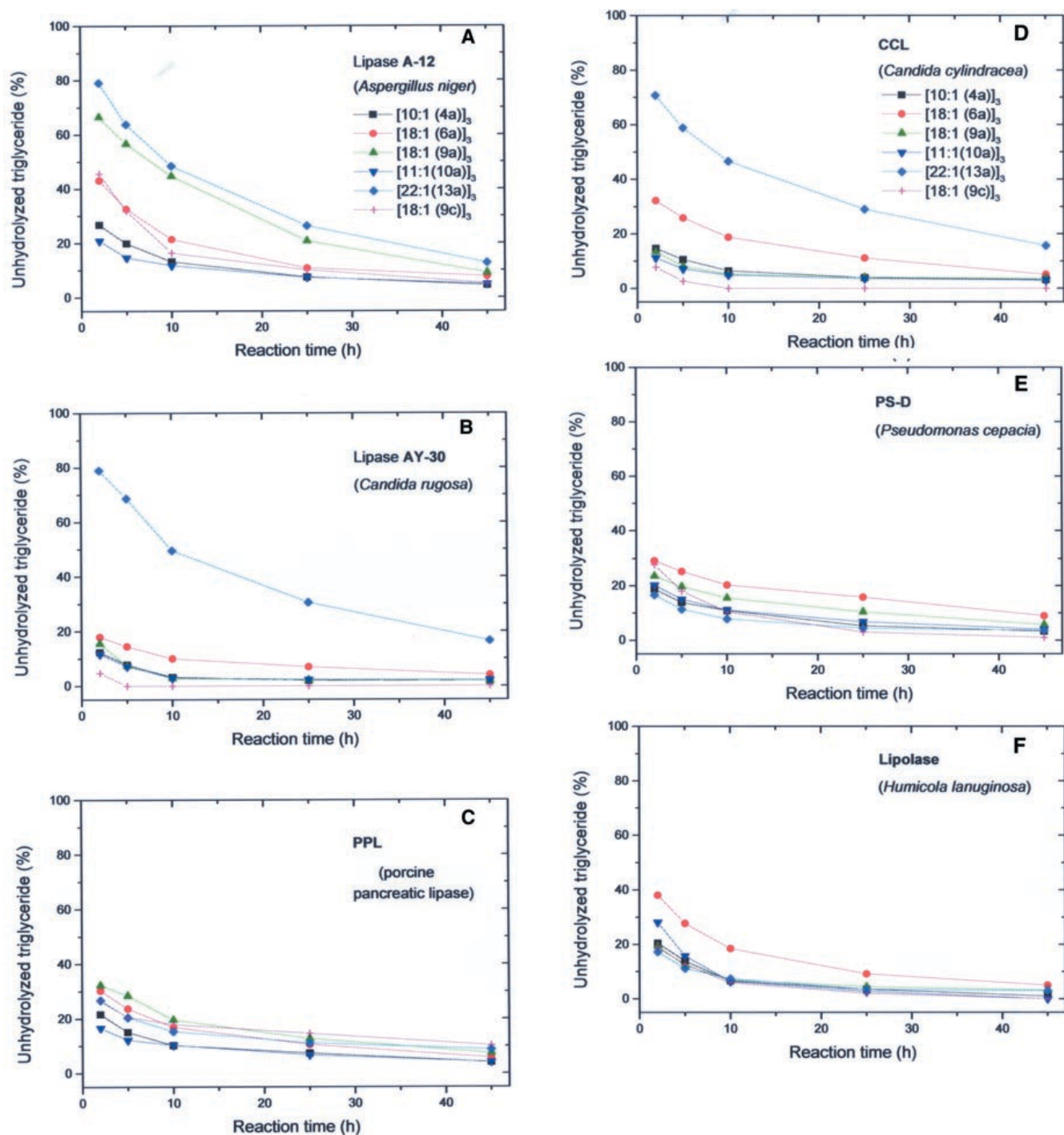


FIG. 1. Amount of unhydrolyzed TG in the hydrolysis of acetylenic TG.

MG was the highest (about 4%). The lowest amount of MG was found in the case of CCL and AY-30.

In the study of these symmetrical acetylenic TG of type AAA, lipase A-12, AY-30, and CCL were the least effective biocatalysts in the hydrolysis of  $[22:1(13a)]_3$ . Also, these three lipases exhibited different rates of hydrolysis between  $[18:1(6a)]_3$  and  $[18:1(9a)]_3$ , which are substrates containing positional isomers of  $C_{18}$  acetylenic FA. To reconfirm these observations, it was decided to prepare three regioisomeric

mixed acetylenic TG of type ABC, namely, compounds **1**, **2**, and **3**, by stepwise esterification of each acetylenic acid to glycerol. Lipase AY-30 and CCL were then used to study the hydrolysis of these three mixed acetylenic TG of type ABC.

When the mixed acetylenic TG **1**  $[18:1(9a)/22:1(13a)/18:1(6a)]$  was subjected to hydrolysis with either CCL or AY-30 for 5 h, the FFA produced from the reaction in the presence of CCL were isolated, methylated, and analyzed by GC. When CCL was used as the biocatalyst, GC analysis

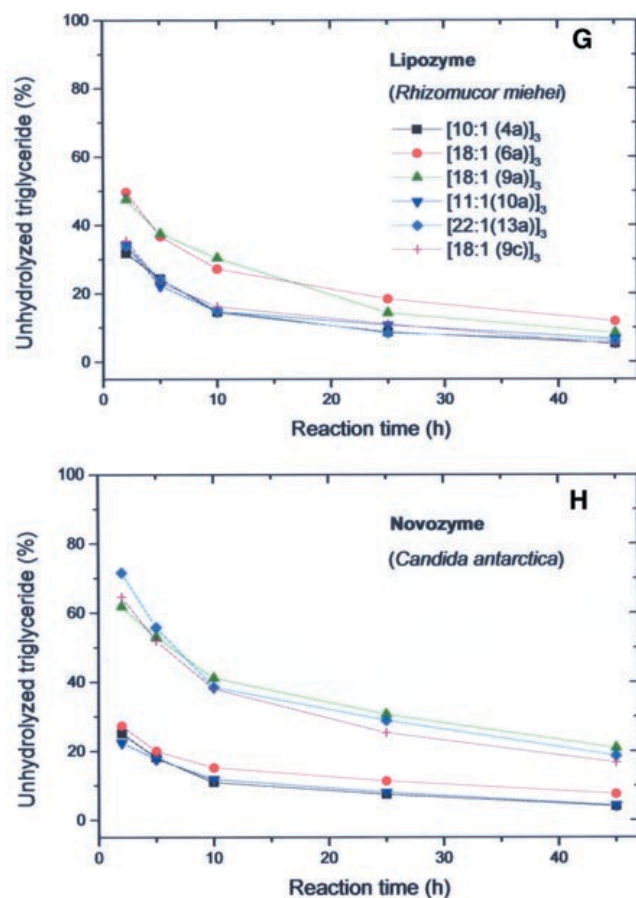


FIG. 1. Continued

showed a ratio of the combined amount of methyl esters of 18:1(9a) and 18:1(6a) (the peaks of these two component overlapped) to 22:1(13a) as 7:2. In the case where AY-30 was used as the biocatalyst, the ratio of the combined amount of methyl esters of 18:1(9a) and 18:1(6a) (GC peaks overlapped) to 22:1(13a) was 4:1. The ratios of these FFA were supported by  $^{13}\text{C}$  NMR spectroscopic analysis. The ratio of  $\Delta^6/\Delta^9/\Delta^{13}$  free acetylenic acids was 6:7:4 when CCL was used as the biocatalyst, and 3:4:2 with AY-30. This was found by comparing the intensities of C-1 signals of the corresponding acids (180.32/180.60/180.65,  $\Delta^6/\Delta^9/\Delta^{13}$ , respectively) in the  $^{13}\text{C}$  NMR spectra (27).

Thus, with the 22:1(13a) acylated to the  $\beta$ -position of the TG, the amount of free 22:1(13a) acid released was about onefold lower than either of the other two acetylenic FA. It was also found that the DG intermediates contained a comparatively larger amount (50%) of 22:1(13a) acid than that of 18:1(6a) and 18:1(9a) acid isomers combined. These results indicated that a comparatively large amount of 22:1(13a) remained unhydrolyzed on the glycerol backbone after 5 h.

When similar hydrolysis experiments were conducted on 18:1(9a)/18:1(6a)/22:1(13a) (**2**) in the presence of AY-30 and CCL, the relative ratio of FFA isolated for 18:1(6a)/18:1(9a)/22:1(13a) was 4:5:3 with CCL and 7:9:5 with AY-30. This result again showed that even though 22:1(13a) was acylated to the  $\alpha$ -position of the glycerol backbone, the amount of free

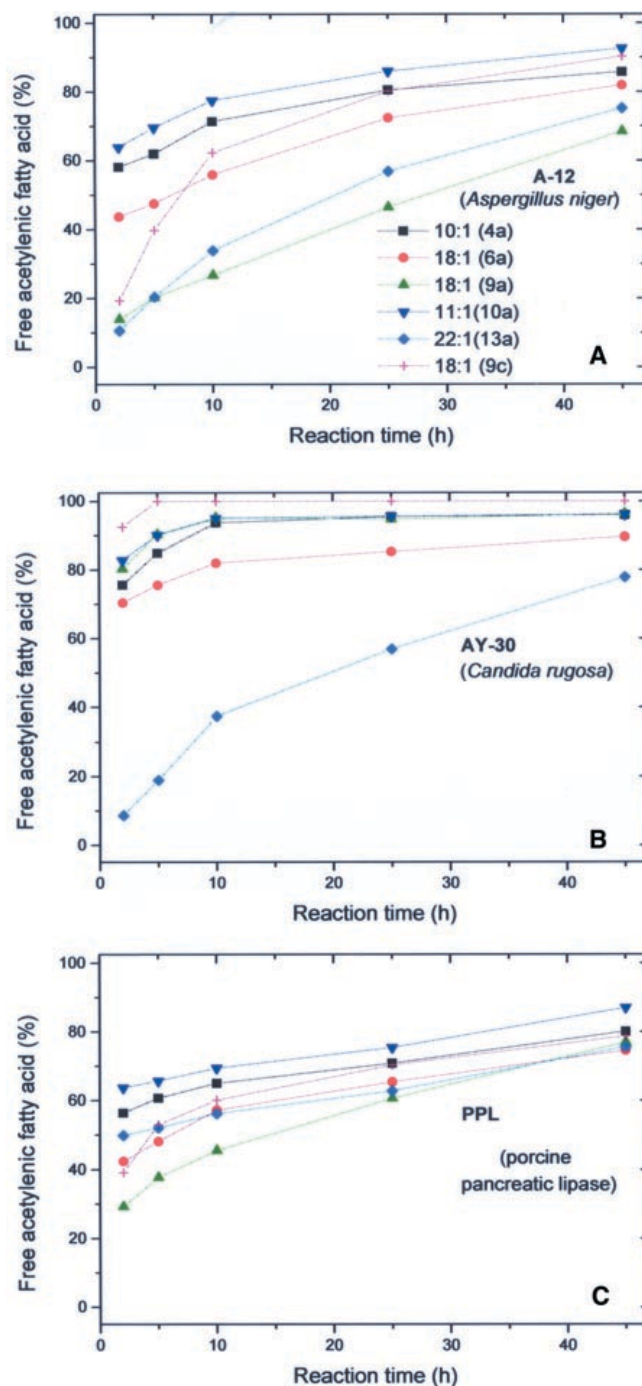


FIG. 2. Yield of released FFA in the hydrolysis of acetylenic TG.

22:1(13a) acid released was 0.3–0.8-fold lower than either one of the other two acetylenic FA [i.e., 18:1(6a) or 18:1(9a)]. The results of the hydrolysis of compound **2** [18:1(9a)/18:1(6a)/22:1(13a)] again demonstrated that lipases AY-30 and CCL were able to distinguish the 22:1(13a) acyl group. Similar observation was found in the case of the hydrolysis of 18:1(6a)/18:1(9a)/22:1(13a) (**3**). In the presence of CCL and AY-30, the relative ratio of FFA isolated from 18:1(6a)/18:1(9a)/22:1(13a) was 5:7:4 with CCL and 3:4:2 with AY-30 as the biocatalyst. Therefore, TG containing a 22:1(13a)

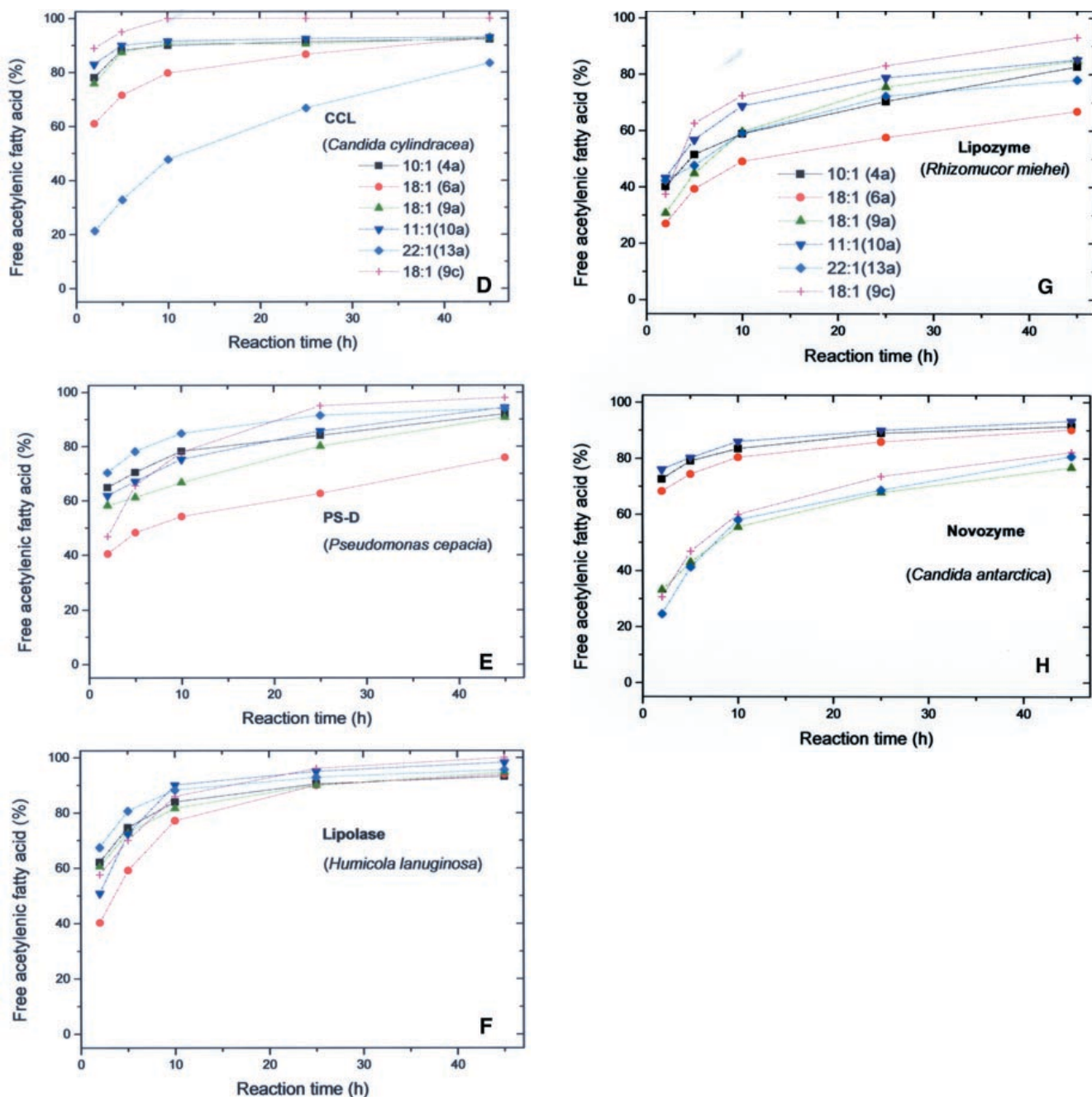


FIG. 2. Continued

acid inhibit the hydrolytic activities of CCL (*C. cylindracea*) and AY-30 (*C. rugosa*). McNeill and Sonnet (29) also reported the discrimination toward 22:1(13c) (erucic acid) in rapeseed oil by *C. rugosa* lipase (AY-30).

From these experiments it was found that some of these lipases could to some degree recognize the acyl groups of the acetylenic TG according to the position of the acetylenic bond in the acyl chains. Lipase A-12 was slow in hydrolyzing the [22:1(13a)]<sub>3</sub> and [18:1(9a)]<sub>3</sub> substrates, as compared to other symmetric TG in this study. Lipase AY-30 and CCL showed a significant resistance toward [22:1(13a)]<sub>3</sub>. The catalytic activities of PS-D and Lipozyme were also decreased in the hydrolysis of [18:1(6a)]<sub>3</sub>.

Novozyme was an efficient enzyme for esterification, but was not so efficient as many of the other lipases used in the hydrolysis of TG. Of the eight lipases studied, Lipolase appeared to be the most efficient lipase for hydrolysis. The application of this work can lead to the production of a vast range of lipid intermediates (MG, DG, and FFA) for the cosmetic, therapeutic, and nutrition industries.

#### ACKNOWLEDGMENTS

The authors thank the Lipid Research Fund, Science Faculty Collaborative Seed Grant 2001, for financial assistance, and Novo Nordisk



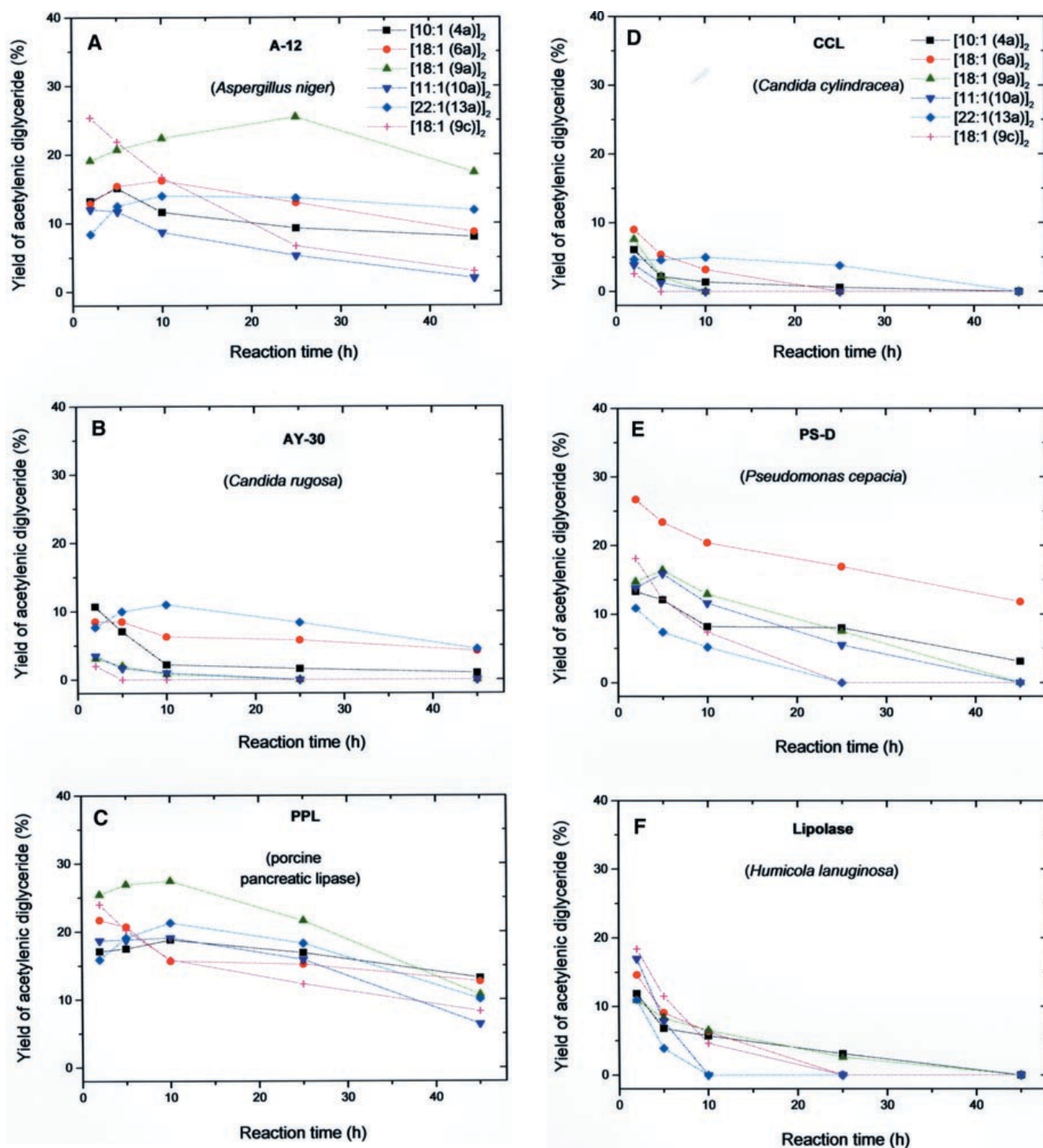


FIG. 3. Yield of DG in the hydrolysis of acetylenic TG.

A/S (Hong Kong) and Amano Pharmaceutical Co. Ltd. (Nagoya, Japan) for lipase samples.

## REFERENCES

1. Brockerhoff, H., and Jensen R.G. (1974) *Lipolytic Enzymes*, Academic Press, New York.
2. Chen, Q., Sternby, B., and Nilsson, Å. (1989) Hydrolysis of Triacylglycerol Arachidonic and Linoleic Acid Ester Bonds by Human Pancreatic Lipase and Carboxyl Ester Lipase, *Biochim. Biophys. Acta* 1004, 372–385.
3. Yang, L.-Y., Kuksis, A., and Myher, J.J. (1990) Lipolysis of Menhaden Oil Triacylglycerols and the Corresponding Fatty Acid Alkyl Esters by Pancreatic Lipase *in vitro*: A Reexamination, *J. Lipid Res.* 31, 137–148.
4. Miyashita, K., Takagi, T., and Frankel, E.N. (1990) Preferential Hydrolysis of Monohydroperoxides of Linoleoyl and Linolenoyl Triacylglycerol by Pancreatic Lipase, *Biochim. Biophys. Acta* 1045, 233–238.



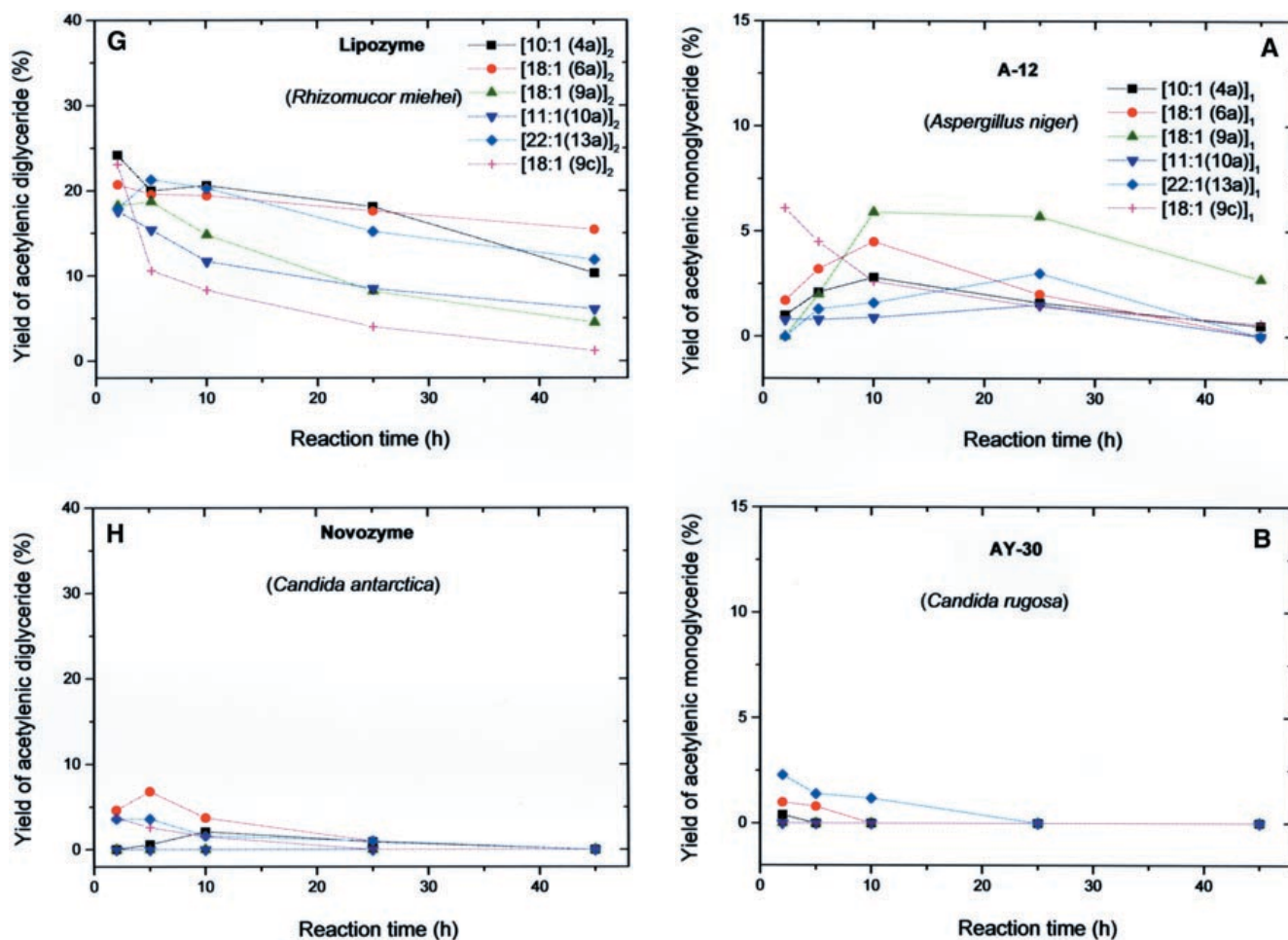


FIG. 3. Continued

5. Lee, K-T., and Akoh, C.C. (1998) Structured Lipids: Synthesis and Applications, *Food Rev. Int.* 14, 17–34.
6. Brockerhoff, H. (1965) Stereospecific Analysis of Triglycerides: An Analysis of Human Depot Fat, *Arch. Biochem. Biophys.* 110, 586–592.
7. Hara, F., Nakashima, T., and Fukuda, H. (1997) Comparative Study of Commercially Available Lipases in Hydrolysis Reaction of Phosphatidylcholine, *J. Am. Oil Chem. Soc.* 74, 1129–1132.
8. Haas, M.J., Cichowicz, D.J., Jun, W., and Scott, K. (1995) The Enzymatic Hydrolysis of Triglyceride–Phospholipid Mixtures in an Organic Solvent, *J. Am. Oil Chem. Soc.* 72, 519–525.
9. Shimada, Y., Fukushima, N., Fujita, H., Honda, Y., Sugihara, A., and Tominaga, Y. (1998) Selective Hydrolysis of Borage Oil with *Candida rugosa* Lipase: Two Factors Affecting the Reaction, *J. Am. Oil Chem. Soc.* 75, 1581–1586.
10. Wanasundara, U.N., and Shahidi, F. (1998) Lipase-Assisted Concentration of n-3 Polyunsaturated Fatty Acids in Acylglycerols from Marine Oils, *J. Am. Oil Chem. Soc.* 75, 945–951.
11. Pedersen, S.B., and Hølmer, G. (1995) Studies of the Fatty Acid Specificity of the Lipase from *Rhizomucor miehei* Toward 20:1n-9, 20:5n-3, 22:1n-9, and 22:6n-3, *J. Am. Oil Chem. Soc.* 72, 239–243.
12. Villeneuve, P., and Foglia, T.A. (1997) Lipase Specificities: Potential Application in Lipid Bioconversions, *INFORM* 8, 640–650.
13. Schmid, R.D., and Verger, R. (1998) Lipases: Interfacial En-

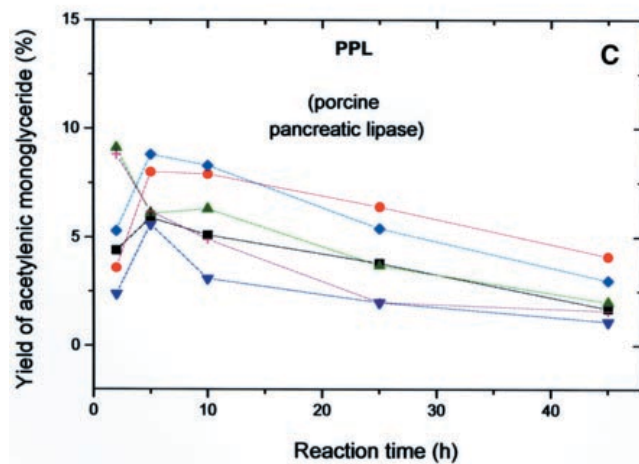


FIG. 4. Yield of MG in the hydrolysis of acetylenic TG.

- zymes with Attractive Applications, *Angew. Chem. Int. Ed.* 37, 1608–1633.
14. Villeneuve, P., Muderhwa, J.M., Graille, J., and Haas, M.J. (2000) Customizing Lipases for Biocatalysis: A Survey of Chemical, Physical, and Molecular Biological Approaches, *J. Mol. Catal. B: Biophys.* 9, 113–148.
15. Foglia, T.A., Jones, K.C., and Sonnet, P.E. (2000) Selectivity of Lipases: Isolation of Fatty Acids from Castor, Coriander, and Meadowfoam Oils, *Eur. J. Lipid Sci. Technol.* 102, 612–617.

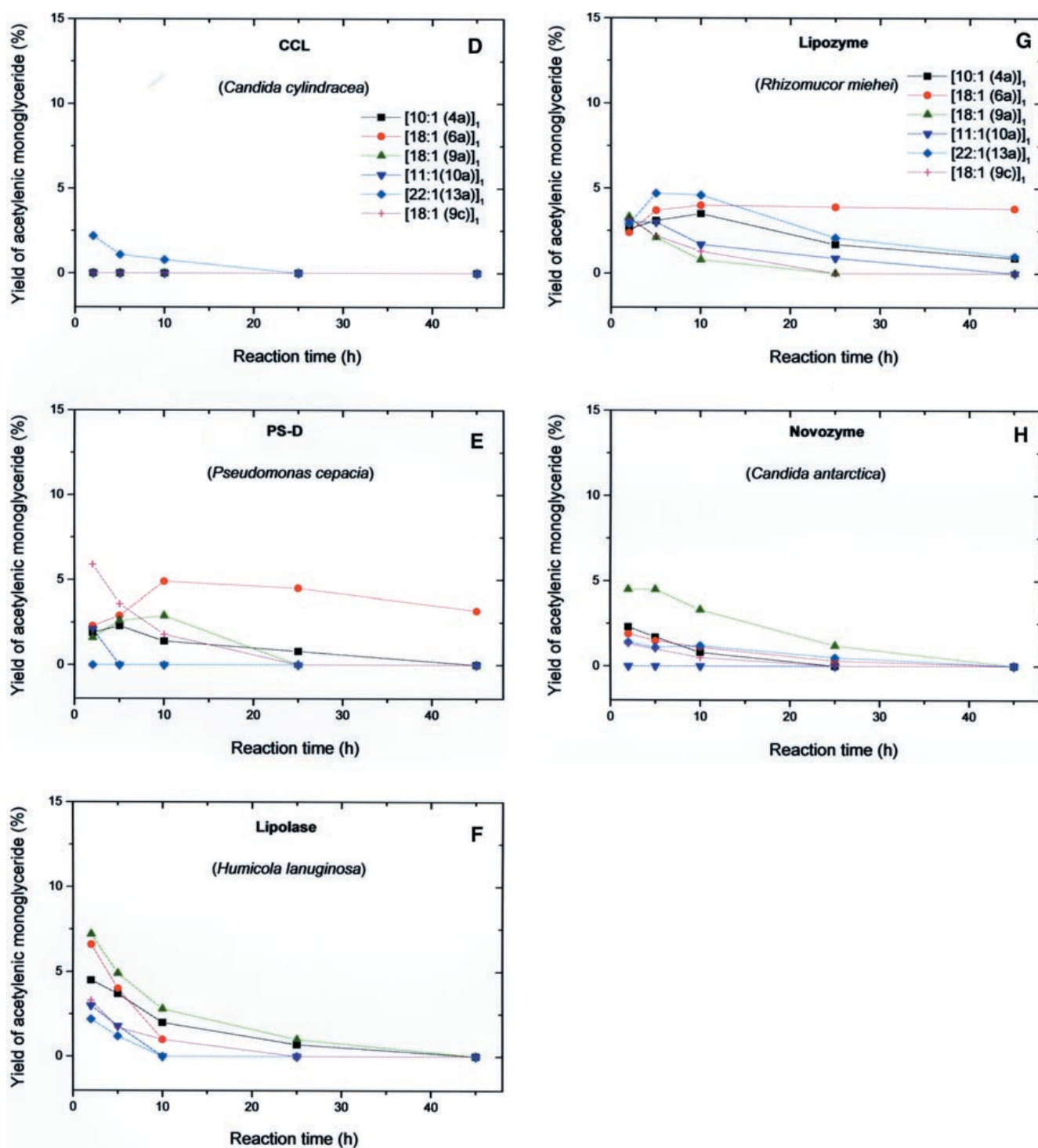


FIG. 4. Continued

16. Rice, K.E., Watkins, J., and Hill, C.G., Jr. (1999) Hydrolysis of Menhaden Oil by a *Candida cylindracea* Lipase Immobilized in a Hollow-Fiber Reactor, *Biotechnol. Bioeng.* 63, 33–45.
17. Bohlmann, F., Burkhardt, T., and Zdero, C. (1973) *Naturally Occurring Acetylenes*, Academic Press, London, pp. 326–330.
18. Spitzer, V., Tomberg, W., Hartmann, R., and Aichholz, R. (1997) Analysis of the Seed Oil of *Heisteria silvanii* (Olaaceae)—A Rich Source of a Novel C<sub>18</sub> Acetylenic Fatty Acid, *Lipids* 32, 1189–1200.
19. Fatope, M.O., Adoum, O.A., and Takeda, Y. (2000) C<sub>18</sub> Acetylenic Fatty Acids of *Ximenia americana* with Potential Pesticidal Activity, *J. Agric. Food Chem.* 48, 1872–1874.
20. Hopkins, C.Y., and Chisholm, M.J. (1964) Occurrence of Stearolic Acid in a Seed Oil, *Tetrahedron Lett.* 40, 3011–3013.
21. Berry, D.E., Chan, J.A., MacKenzie, L., and Hecht, S.M. (1991) 9-Octadecynoic Acid: A Novel DNA-Binding Agent, *Chem. Res. Toxicol.* 4, 195–198.
22. Nichols, C.S., and Cromartie, T.H. (1980) Irreversible Inactiva-

- tion of the Flavoenzyme Alcohol Oxidase with Acetylenic Alcohols, *Biochem. Biophys. Res. Comm.* 97, 216–221.
23. Schilstra, M.J., Nieuwenhuizen, W.F., Veldink, G.A., and Vliegthart, J.F.G. (1996) Mechanism of Lipoxygenase Inactivation by the Linoleic Acid Analogue Octadeca-9,12-dienoic Acid, *Biochemistry* 35, 3396–3401.
  24. Kuhn, H., Hayess, K., Holzhutter, H.G., Zabolotzski, D.A., Myagkova, G.I., and Schewe, T. (1991) Inactivation of 15-Lipoxygenases by Acetylenic Fatty Acids, *Biomed. Biochim. Acta* 50, 835–839.
  25. Lie Ken Jie, M.S.F., Syed-Rahmatullah, M.S.K., Lam, C.K., and Kalluri, P. (1994) Ultrasound in Fatty Acid Chemistry: Synthesis of a 1-Pyrroline Fatty Acid Ester Isomer from Methyl Ricinoleate, *Lipids* 29, 889–892.
  26. Gilman, N.W., and Holland, B.C. (1974) Synthesis of Some Acetylenic Acids, *Chem. Phys. Lipids* 13, 239–248.
  27. Lie Ken Jie, M.S.F., and Lam, C.C. (1995) C-13 Studies of Polyunsaturated Triacylglycerols of Type AAA and Mixed Triacylglycerols Containing Saturated, Acetylenic and Ethylenic Acyl Groups, *Chem. Phys. Lipids* 78, 1–13.
  28. Lie Ken Jie, M.S.F., and Fu, X. (1998) Studies of Lipase-Catalyzed Esterification Reactions of Some Acetylenic Fatty Acids, *Lipids* 33, 71–75.
  29. McNeill, G.P., and Sonnet, P.E. (1995) Isolation of Erucic Acid from Rapeseed Oil by Lipase-Catalyzed Hydrolysis, *J. Am. Oil Chem. Soc.* 72, 213–218.

[Received May 7, 2002; and in revised form November 8, 2002; revision accepted November 11, 2002]

# Ozonation of PC in Ethanol: Separation and Identification of a Novel Ethoxyhydroperoxide

Misako Tagiri-Endo, Kaori Ono, Kiyotaka Nakagawa,  
Mari Yotsu-Yamashita, and Teruo Miyazawa\*

Food & Biodynamic Chemistry Laboratory, Graduate School of Life Science and Agriculture, Tohoku University, Sendai, Japan

**ABSTRACT:** The product of the ozonolysis of 1-palmitoyl-2-oleoyl-*sn*-glycero-3-phosphocholine in ethanol-containing solvent was analyzed by chemiluminescence detection–HPLC with on-line electrospray MS, and characterized on the basis of NMR spectroscopy and MS in high-resolution fast atom bombardment mode. The reaction yielded a large amount of a novel ethoxyhydroperoxide compound [1-palmitoyl-2-(9-ethoxy-9-hydroperoxynonyl)-*sn*-glycero-3-phosphocholine]. In addition to a structural analysis, we speculate on the reaction pathway and discuss the possibility of ethoxyhydroperoxide as a potentially reactive ozonized lipid in food and biological materials.

Paper no. L9108 in *Lipids* 37, 1007–1012 (October 2002).

Ozone, one of the most powerful oxidants in polluted air, reacts with most organic compounds (1). Exposure of animals and humans to ozone causes lung injury, including increased epithelial macromolecular permeability and neutrophil infiltration (2,3). In addition, cell leakage and lysis are observed in bacteria such as *Escherichia coli* after ozone exposure (4). Owing to its high oxidative power, it is frequently applied to the disinfection, deodorization, and bleaching of foods, water, and air (5).

Since unsaturated lipids (i.e., phospholipid and cholesterol) are expected to be important targets of ozone in lung lining fluids, cell membranes, and foods, the reaction of ozone with lipids has been studied in detail (6–11). In the case of 1-palmitoyl-2-oleoyl-*sn*-glycero-3-phosphocholine (POPC), the ozonation of unsaturated FA (oleoyl moiety) of POPC gives an unstable 1,2,3-trioxolane (Fig. 1). The compound rapidly decomposes to give both carbonyl oxide and aldehyde (12,13). These two species (carbonyl oxide and aldehyde) recombine to give the Criegee ozonide in nonparticipating organic solvents (12). In the presence of H<sub>2</sub>O, however, the

H<sub>2</sub>O can readily react with carbonyl oxide to form an unstable hydroxyhydroperoxide. Elimination of H<sub>2</sub>O<sub>2</sub> from the hydroxyhydroperoxide yields an aldehyde-containing PC. Oxidation of the aldehyde by ozone gives a carboxylic acid-containing PC as a final product (13) (Fig. 1). Therefore, the selection of solvent might have a significant impact on the mechanism of the reaction of ozone with POPC.

According to an early study (14), Heath and Tappel studied the reaction of ozone with linoleic acid in the presence of ethanol. They found that ozone reacts with linoleic acid to give an “organic hydroperoxide” in ethanol. This compound is presumably the ethanol adduct of the carbonyl oxide; that is, the ethoxyhydroperoxide molecule [HOO–CH(OC<sub>2</sub>H<sub>5</sub>)–(CH<sub>2</sub>)<sub>7</sub>–COOH]. However, the ozonation products from POPC in the presence of alcohol have never been investigated. It seemed logical to anticipate that POPC could react with ozone in the presence of ethanol to yield the ethoxyhydroperoxide-containing PC. The compound might be a new toxic molecule arising during ozone exposure because it possesses a reactive hydroperoxide group.

Previously, we developed a chemiluminescence (CL) detection–HPLC method for sensitive and selective determination of organic hydroperoxides present in food models and biological samples (15,16). Using this method, hydroperoxidation of various kinds of molecules, such as phospholipids (15,16), TAG (17),  $\alpha$ -tocopherol (18), squalene (19), and cholesterol (20), has been demonstrated. The application of an effective CL–HPLC assay would help to understand lipid ozonation reactions in foods and biological tissues. Hence, in the present study, we investigated the structures of the ozonation products of POPC, focusing especially on ethoxyhydroperoxide-containing PC formation in the presence of ethanol using our CL–HPLC with on-line MS.

## EXPERIMENTAL PROCEDURES

**Materials.** POPC and soybean phosphatidylcholine (soyPC) were purchased from Funakoshi (Tokyo, Japan). Other reagents and solvents were of the highest grade available.

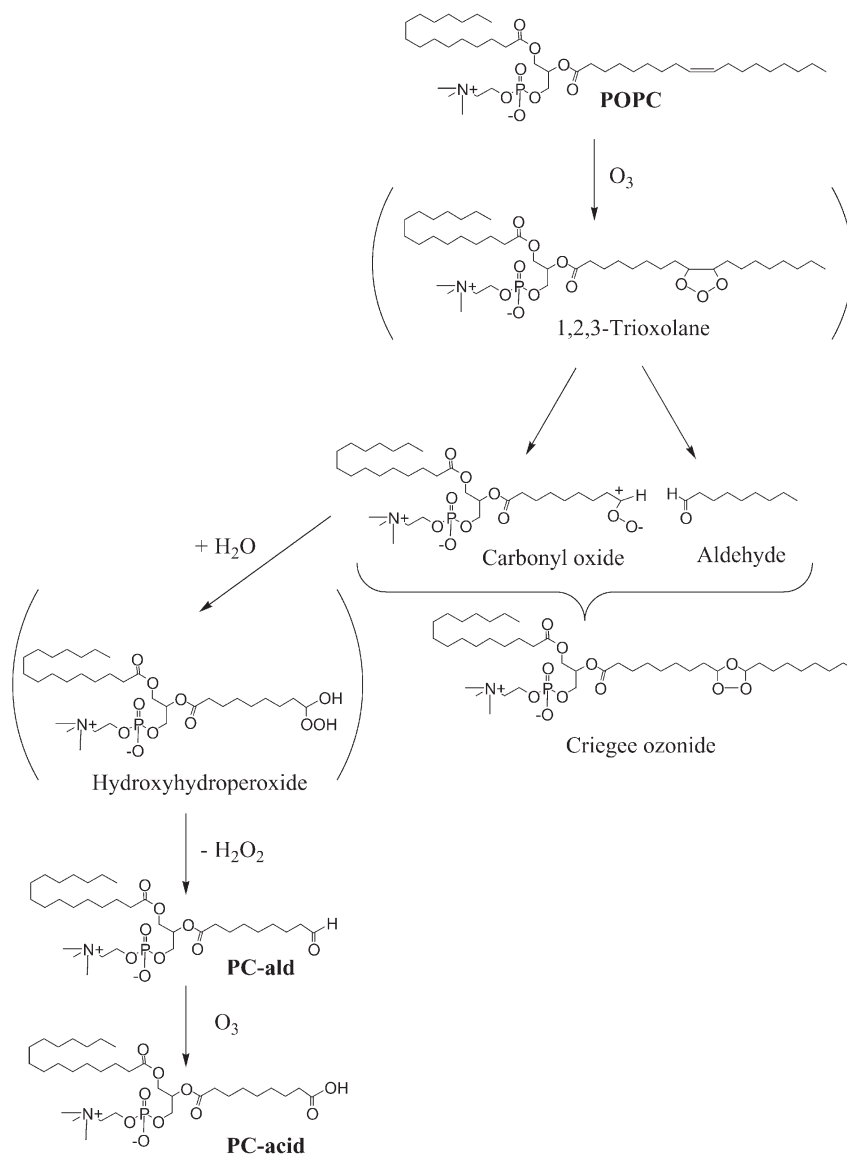
**Ozone exposure.** POPC (5  $\mu$ mol) was dissolved in 3 mL of ethanol/hexane (1:9, vol/vol). An EO-301 Okano Works ozonator was used for generating a 1.3% ozone-in-oxygen stream. POPC solution was bubbled at a flow rate of 100 mL/min for 3 min under ice-cold conditions (12,13). After ozonation, the reaction mixture was dried and redissolved in

Present address of first author: Industrial Technology Institute, Miyagi Prefectural Government, Sendai 981-3206, Japan.

\*To whom correspondence should be addressed at Food & Biodynamic Chemistry Laboratory, Graduate School of Life Science and Agriculture, Tohoku University, 1-1, Tsutsumidori Amamiyamachi, Sendai, 981-8555, Japan. E-mail: miyazawa@biochem.tohoku.ac.jp

Abbreviations: CL, chemiluminescence; HMBC, heteronuclear multiple bond correlation; HRFAB, high-resolution fast atom bombardment mode; HSQC, heteronuclear single-quantum coherence; PC-acid, 1-palmitoyl-2-(9-carboxynonyl)-*sn*-glycero-3-phosphocholine; PC-ald, 1-palmitoyl-2-(9-oxononyl)-*sn*-glycero-3-phosphocholine; PC-CE, 1-palmitoyl-2-(9-carboethoxynonyl)-*sn*-glycero-3-phosphocholine; PC-EHP, 1-palmitoyl-2-(9-ethoxy-9-hydroperoxynonyl)-*sn*-glycero-3-phosphocholine; POPC, 1-palmitoyl-2-oleoyl-*sn*-glycero-3-phosphocholine; soyPC, soybean phosphatidylcholine; TIC, total ion current.





**FIG. 1.** Chemical reaction of 1-palmitoyl-2-oleoyl-*sn*-glycero-3-phosphocholine (POPC) with ozone. PC-ald, 1-palmitoyl-2-(9-oxononanoyl)-*sn*-glycero-3-phosphocholine; PC-acid, 1-palmitoyl-2-(9-carboxynonanoyl)-*sn*-glycero-3-phosphocholine.

300  $\mu$ L of methanol. An aliquot portion (10  $\mu$ L) was subjected to CL-HPLC with on-line MS (HPLC-CL-MS). The principal ozonation products (retention times of 25 and 27 min in HPLC-CL-MS) were isolated and their chemical structures determined as described below.

In studies aimed at assigning the mechanism of product formation, the following procedure was adopted: POPC or soyPC (5  $\mu$ mol each) was dissolved in hexane containing different amounts of ethanol (0–60%, vol/vol), and treated with ozone gas for various lengths of time (0–10 min). Following the reactions, the yields of ozonized lipids were determined by HPLC-CL-MS.

**HPLC analysis.** For the HPLC-CL-MS system, an ODS column (TSKgel ODS-80Ts, 4.6  $\times$  250 mm; Tosoh, Tokyo, Japan) was used. The column was eluted using a binary gradient consisting of the following HPLC solvents: A,

methanol/water (1:1), and B, methanol. The gradient profile was as follows: 0–15 min, 70% B; 15–25 min, 70–98% B linear; 25–28 min, 98–100% B linear; 28–40 min, 100% B. The flow rate was adjusted to 1 mL/min and the column temperature was maintained at 36°C. At the column exit, the eluant was split. One of the split eluants (flow rate, 0.9 mL/min) was subsequently mixed with a hydroperoxide-specific CL cocktail (a mixture of luminol and cytochrome C in 50 mM borate buffer; pH 10) (15,16) and sent to a JASCO 825CL detector (Japan Spectroscopic Co., Tokyo, Japan). The flow rate of the CL cocktail was 1 mL/min. The other split column eluant (flow rate, 0.1 mL/min) was sent to a Mariner electrospray ionization time-of-flight mass spectrometer (PerSeptive Biosystems, Framingham, MA). MS was carried out in the positive ion measurement mode with a spray voltage of 1900 V, a nozzle potential of 150 V, and a nozzle temperature of 150°C. The flow rate

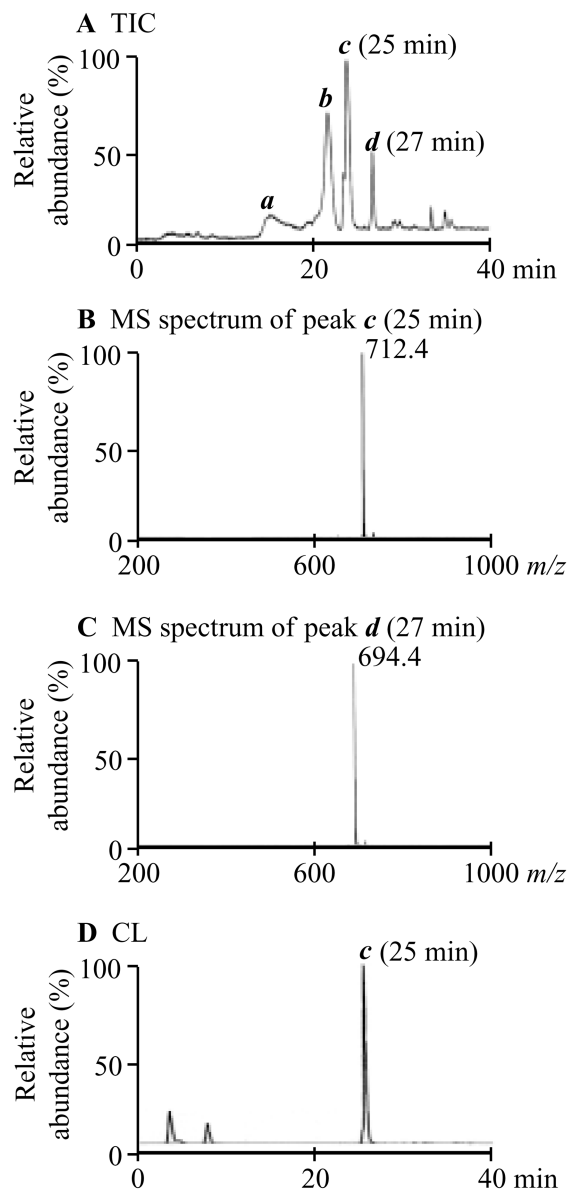
of nebulizer gas was 0.3 mL/min. Full-scan spectra were obtained by scanning masses between  $m/z$  range 200–1000.

**Identification procedures.** The accurate mass for the isolated ozonation product was determined by a JEOL-JMS-700 mass station (JEOL, Tokyo, Japan) in high-resolution fast atom bombardment mode (HRFAB). HRFAB-MS measurements were performed in the positive mode with glycerol as matrix.  $^1\text{H}$  and  $^{13}\text{C}$  NMR spectra were measured on a Varian Unity 600 spectrometer at 600 MHz for  $^1\text{H}$  NMR and at 150 MHz for  $^{13}\text{C}$  NMR, respectively, using  $\text{CDCl}_3$  as the solvent.

## RESULTS AND DISCUSSION

Figure 2A shows the typical total ion current (TIC) chromatogram when ozone gas-exposed POPC in ethanol/hexane (1:9) was subjected to HPLC-CL-MS. After only 3 min of ozonation, POPC itself was completely decomposed, and the peak components *a-d* ascribed to ozonation products appeared in the TIC chromatogram (Fig. 2A). Of these peaks, peaks *a* (retention time = 16 min) and *b* (22 min) gave molecular ions  $[\text{M} + \text{H}]^+$  at  $m/z$  666.5 and 650.5, which were identical to the well-known ozonolysis products PC-acid [1-palmitoyl-2-(9-carboxynonanoyl)-*sn*-glycero-3-phosphocholine] and PC-ald [1-palmitoyl-2-(9-oxononanoyl)-*sn*-glycero-3-phosphocholine], respectively (Fig. 1) (13). Of the other known products of ozonized POPC, the Criegee ozonide (12,21) was at trace level and the hydroxyhydroperoxide (13) could not be detected under the present experimental conditions. On the other hand, the peak components *c* (25 min) and *d* (27 min) showed molecular ions at  $m/z$  712.4 and 694.4 (Figs. 2B and C), respectively, although these components have not yet been characterized. Component *c* gave an intense CL peak (25 min) in the CL chromatogram (Fig. 2D), whereas peak *d* did not react with the CL cocktail (data not shown). The MS spectra (Figs. 2B and C) and CL properties (Fig. 2D) of peak *c* suggest that it might possess a hydroperoxy group in the molecule.

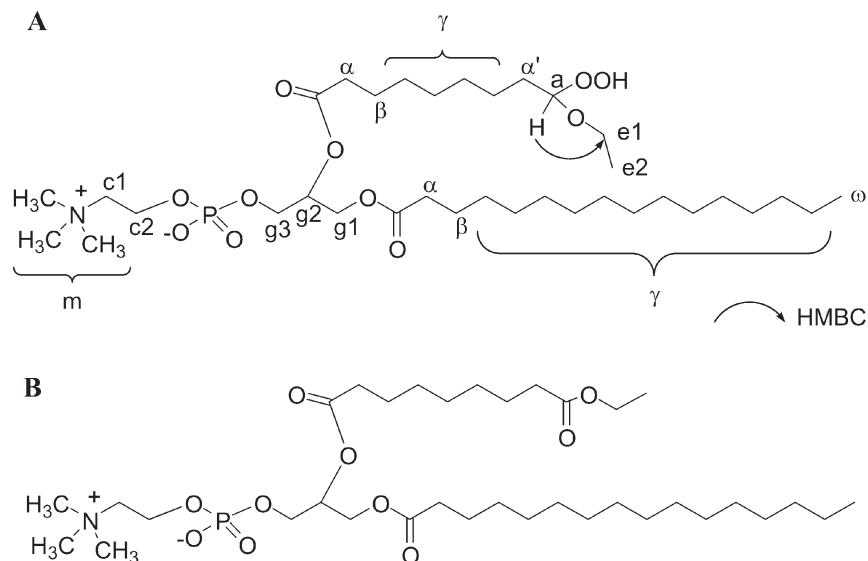
Next, to determine the chemical structures of peaks *c* and *d*, these components were isolated by HPLC (see the Experimental Procedures section), and their structures were determined by spectroscopic procedures. Peak *c*: HRFAB-MS (glycerol)  $[\text{M} + \text{H}]^+$   $m/z$  712.4767 (calcd. for  $[\text{C}_{35}\text{H}_{71}\text{N}_1\text{O}_{11}\text{P}_1]^+$   $m/z$  712.4686). Further NMR measurements, i.e., COSY, heteronuclear single-quantum coherence (HSQC) and heteronuclear multiple bond correlation (HMBC) ( $J = 8$  Hz), enabled us to identify component *c* as 1-palmitoyl-2-(9-ethoxy-9-hydroperoxynonanoyl)-*sn*-glycero-3-phosphocholine (PC-EHP, Fig. 3A). The presence of the  $\text{CH}(\text{OOH})\text{OCH}_2\text{CH}_3$  fragment in this molecule is supported by the HMBC between  $\text{H}_a$  and  $\text{C}_{e1}$ . NMR data are listed below:  $^1\text{H}$  NMR ( $\text{CDCl}_3$ ): 0.85 (*t*, 3H,  $\text{H}_w$ ), 1.18 (*t*, 3H,  $\text{H}_{e2}$ ), 1.25–1.30 (*m*, 32H,  $\text{H}_v$ ), 1.48–1.60 (*m*, 6H,  $\text{H}_\alpha$ ,  $\text{H}_\beta$ ), 2.20–2.30 (*m*, 4H,  $\text{H}_\alpha$ ), 3.35 (*s*, 9H,  $\text{H}_m$ ), 3.55 (*m*, 1H,  $\text{H}_{e1}$ ), 3.87 (*m*, 1H,  $\text{H}_{e1}$ ), 3.90 (*m*, 2H,  $\text{H}_{c1}$ ), 4.00 (*m*, 2H,  $\text{H}_{g3}$ ), 4.08 (*m*, 1H,  $\text{H}_{g1}$ ), 4.28 (*m*, 1H,  $\text{H}_{g1}$ ), 4.37 (*m*, 2H,  $\text{H}_{c2}$ ), 4.75 (*m*, 1H,  $\text{H}_a$ ), 5.18 (*m*, 1H,  $\text{H}_{g2}$ ) ppm.  $^{13}\text{C}$  NMR ( $\text{CDCl}_3$ ): 13.5 ( $\text{C}_w$ ), 14.1 ( $\text{C}_{e2}$ ), 24.3 ( $\text{C}_\alpha$ ,  $\text{C}_\beta$ ), 28.4–29.1 ( $\text{C}_v$ ), 33.5 ( $\text{C}_\alpha$ ), 54.2 ( $\text{C}_m$ ), 60.0 ( $\text{C}_{c2}$ ), 62.2 ( $\text{C}_{g1}$ ), 64.1 ( $\text{C}_{g3}$ ), 64.8 ( $\text{C}_{e1}$ ), 65.7 ( $\text{C}_{c1}$ ), 69.8 ( $\text{C}_{g2}$ ), 107.5 ( $\text{C}_a$ ) ppm.



**FIG. 2.** Ozonation products of POPC in ethanol. POPC (5  $\mu\text{mol}$ ) in ethanol/hexane (1:9) was exposed to ozone gas for 3 min and analyzed by HPLC-chemiluminescence (CL)-MS. A, total ion current (TIC) chromatogram; B, mass spectrum of the peak *c* component (25 min) in chromatogram A; C, mass spectrum of the peak *d* component (27 min) in chromatogram A; D, CL chromatogram. For other abbreviation see Figure 1.

The chemical shifts of  $^{13}\text{C}$  signals were determined by the cross-peaks in HSQC and HMBC spectra. This isolated PC-EHP was used as a reference standard in later experiments. On the other hand, peak *d* was tentatively determined as 1-palmitoyl-2-(9-carbethoxynonanoyl)-*sn*-glycero-3-phosphocholine (PC-CE, Fig. 3B) based on MS data; HRFAB-MS,  $[\text{M} + \text{H}]^+$   $m/z$  694.4662 (calcd. for  $[\text{C}_{35}\text{H}_{69}\text{N}_1\text{O}_{10}\text{P}_1]^+$   $m/z$  694.4581). NMR measurement of PC-CE could not be carried out in the present study owing to the insufficient amount of isolated PC-CE.

To help assign pathways for PC-EHP and PC-CE formation in ethanol, POPC was dissolved in hexane containing different amounts of ethanol (0–60%) and then treated with



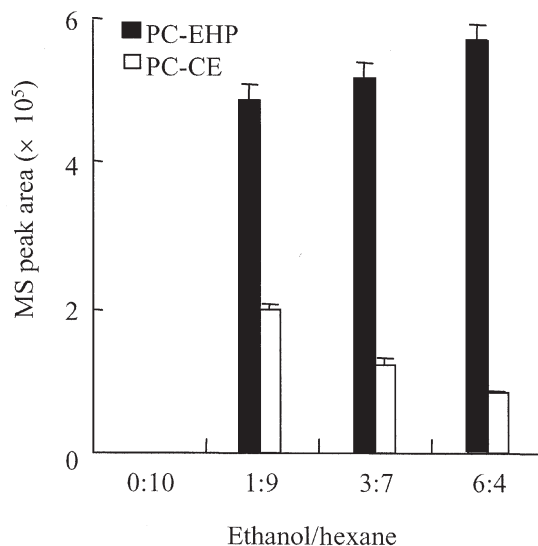
**FIG. 3.** A, Chemical structure of peak **c**: 1-palmitoyl-2-(9-ethoxy-9-hydroperoxynonyl)-*sn*-glycero-3-phosphocholine (PC-EHP). The arrow shows the heteronuclear multiple bond correlation (HMBC) between  $H_a$  and  $C_{e1}$ . The other HMBC are not shown. B, proposed structure of peak **d**: 1-palmitoyl-2-(9-carbethoxynonyl)-*sn*-glycero-3-phosphocholine (PC-CE).

ozone for 3 min. Neither PC-EHP nor PC-CE was formed in the absence of ethanol (Fig. 4). Hence, these components would appear to be principal products during ozonation in the presence of alcohol. The PC-EHP yield showed a maximum when POPC in ethanol/hexane (6:4) was treated with ozone. In contrast, the yield of PC-CE was at a maximum when exposing POPC in ethanol/hexane (1:9) to ozone gas (Fig. 4). When isolated PC-EHP was incubated in ethanol-free solvent (i.e., chloroform, hexane, and methanol), PC-EHP did not decompose (data not shown). This implied that PC-EHP is a stable compound and that PC-CE could not be formed *via* PC-EHP. Based on these findings, two possible pathways for POPC ozonation in ethanol can be envisaged (Figs. 5A and B). In the first, ethanol reacts with the carbonyl oxide to form PC-EHP (Fig. 5A). In the second, the Criegee ozonide and/or 1,2,3-trioxolane reacts with ethanol to form PC-EHP, PC-ald, the short-chain aldehyde [ $\text{CH}_3-(\text{CH}_2)_7-\text{CHO}$ ], and an ethoxyhydroperoxide molecule [ $\text{HOO}-\text{CH}(\text{OC}_2\text{H}_5)-(\text{CH}_2)_7-\text{CH}_3$ ] (Fig. 5B). PC-ald in the presence of ethanol may be in equilibrium with its ethyl hemiacetal. This compound can be transformed into PC-CE by a simple oxidation step (Fig. 5B).

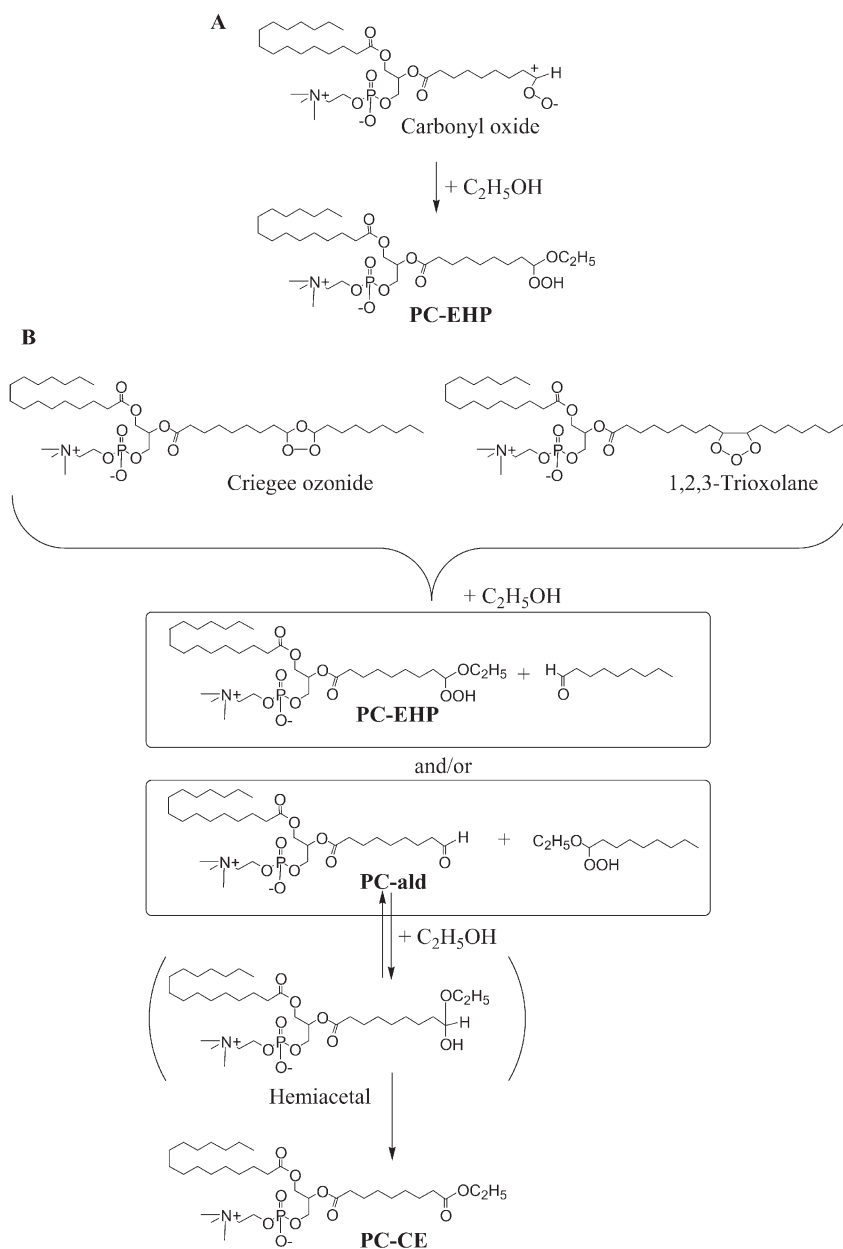
Figure 6 shows the time course of changes in the yields of ozonation products when POPC in ethanol/hexane (1:9) was exposed to ozone for 0–10 min. Interestingly, POPC itself was rapidly degraded during ozonation, but considerable amounts of PC-ald, PC-EHP, and PC-CE were formed and remained in the reaction mixture even after 10 min of ozone exposure. Hence, these products (PC-ald, PC-EHP, and PC-CE) might be useful marker molecules for ozone exposure.

For food sterilization, the use of a combination of different disinfection procedures (i.e., treatment of ozone together with alcohol or UV light) was recently recommended to enhance

the bactericidal effect (22,23). If one is applying the  $\text{O}_3$ /ethanol treatment for food disinfection, PC-EHP may be formed from food phospholipids, influencing the quality, taste, and flavor of food. To assess such a possibility, we tested the frequently used food extender soyPC. Figure 7 shows a typical CL chromatogram when soyPC (5  $\mu\text{mol}$ ) in 3 mL of ethanol/hexane (1:9) was exposed to ozone gas for 3 min. Molecular species of PC-EHP, having palmitoyl (16:0-PC-EHP) or oleoyl (18:0-PC-EHP) residues at the *sn*-1 position of the glyce-



**FIG. 4.** The yields of PC-EHP and PC-CE during ozonation of POPC in ethanol. POPC was dissolved in hexane containing different amounts of ethanol (0–60%) and then treated with ozone for 3 min. After the reaction, the samples were analyzed by HPLC–CL–MS. Values are mean  $\pm$  SD ( $n = 4$ ). For other abbreviations see Figures 2 and 3.



**FIG. 5.** Proposed pathway for the formation of PC-EHP and PC-CE during ozonation of POPC in ethanol. For abbreviations see Figures 1–3.

erol moiety, were detected in the CL chromatogram. Ethoxyhydroperoxide concentrations were determined as 0.21  $\mu\text{mol}$  for 16:0-PC-EHP and 0.11  $\mu\text{mol}$  18:0-PC-EHP/3 mL of total reaction mixture using a calibration curve generated from standard PC-EHP. This means that 6.4 mol% of soyPC is converted to the ethoxyhydroperoxide products during only 3 min of ozonation. Such high hydroperoxidation values will impair the nutritive value of soy products.

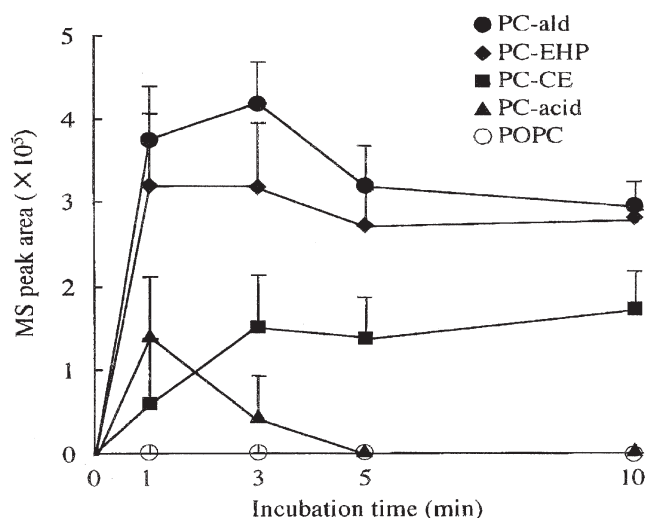
When POPC was exposed to ozone gas in the presence of ethanol, the formation of an ethoxyhydroperoxide derivative (PC-EHP) could be confirmed. The present HPLC–CL–MS system is an effective method for the structural elucidation of ozonized phospholipids. In addition, CL measurement allows

the selective and sensitive determination of PC-EHP. Applying the present method to the ozonation of soyPC in ethanol, we succeeded in detecting a large amount of PC-EHP. We anticipate that the compound may be useful as a new specific marker molecule for detecting exposure of food lipids to ozone.

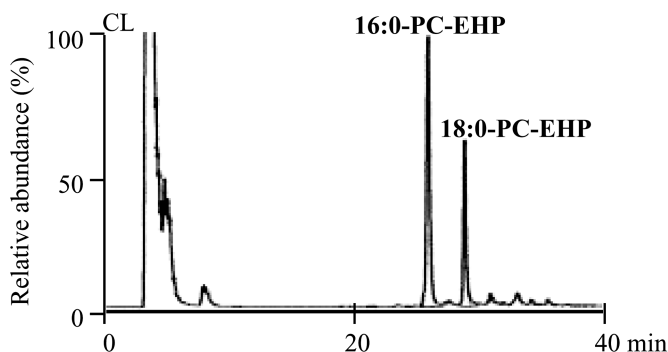
## REFERENCES

1. Mustafa, M.G. (1990) Biochemical Basis of Ozone Toxicity, *Free Radic. Biol. Med.* 9, 245–265.
2. Kehrl, H.R., Vincent, L.M., Kowalsky, R.J., Horstman, D.H., O’Neil, J.J., McCartney, W.H., and Bromberg, P.A. (1987) Ozone Exposure Increases Respiratory Epithelial Permeability in Humans, *Am. Rev. Respir. Dis.* 135, 1124–1128.





**FIG. 6.** Course of changes in the yields of ozonation products. POPC in ethanol/hexane (1:9) was exposed to ozone gas for 0–10 min. Following the reaction, the samples were analyzed by HPLC–CL–MS. Values are mean  $\pm$  SD ( $n = 4$ ). For abbreviations see Figures 1–3.



**FIG. 7.** Typical CL chromatogram of ethoxyhydroperoxide derivatives of soybean phosphatidylcholine (soyPC) during exposure to ozone. 16:0-PC-EHP, 1-palmitoyl-2-(9-ethoxy-9-hydroperoxynonanoyl)-sn-glycero-3-phosphocholine; 18:0-PC-EHP, 1-oleoyl-2-(9-ethoxy-9-hydroperoxynonanoyl)-sn-glycero-3-phosphocholine. For other abbreviation see Figure 2.

3. Seltzer, J., Bigby, B.G., Stulberg, M., Holtzman, M.J., Nadel, J.A., Ueki, I.F., Leikauf, G.D., Goetzl, E.J., and Boushey, H.A. (1986)  $O_3$ -Induced Change in Bronchial Reactivity to Methacholine and Airway Inflammation in Humans, *J. Appl. Physiol.* **60**, 1321–1326.
4. MacNair Scott, D.B., and Leshner, E.C. (1963) Effect of Ozone on Survival and Permeability of *Escherichia coli*, *J. Bacteriol.* **85**, 567–576.
5. Moore, G., Griffith, C., and Peters, A. (2000) Bactericidal Properties of Ozone and Its Potential Application as a Terminal Disinfectant, *J. Food. Prot.* **63**, 1100–1106.
6. Goldstein, B.D., Buckley, R.D., Cardenas, R., and Balchum, O.J. (1970) Ozone and Vitamin E, *Science* **169**, 605–606.
7. Chow C.K., and Tappel, A.L. (1972) An Enzymatic Protective Mechanism Against Lipid Peroxidation Damage to Lungs of Ozone-Exposed Rats, *Lipids* **7**, 518–524.

8. Pryor, W.A., Das, B., and Church, D.F. (1991) The Ozonation of Unsaturated Fatty Acids: Aldehydes and Hydrogen Peroxide as Products and Possible Mediators of Ozone Toxicity, *Chem. Res. Toxicol.* **4**, 341–348.
9. Pryor, W.A., and Wu, M. (1992) Ozonation of Methyl Oleate in Hexane, in a Thin Film, in SDS Micelles, and in Distearoylphosphatidylcholine Liposomes: Yields and Properties of the Criegee Ozonide, *Chem. Res. Toxicol.* **5**, 505–511.
10. Uppu, R.M., Cueto, R., Squadrito, G.L., and Pryor, W.A. (1995) What Does Ozone React with at the Air/Lung Interface? Model Studies Using Human Red Blood Membranes, *Arch. Biochem. Biophys.* **319**, 257–266.
11. Mudd, J.B., Dawson, P.J., and Santrock, J. (1997) Ozone Does Not React with Erythrocyte Membrane Lipids, *Arch. Biochem. Biophys.* **319**, 251–258.
12. Squadrito, G.L., Uppu, R.M., Cueto, R., Squadrito, G.L., and Pryor, W.A. (1992) Production of the Criegee Ozonide During the Ozonation of 1-Palmitoyl-2-oleoyl-sn-glycero-3-phosphocholine Liposomes, *Lipids* **27**, 955–958.
13. Santrock, J., Gorski, R.A., and O’Gara, J. (1992) Products and Mechanism of the Reaction of Ozone with Phospholipids in Unilamellar Phospholipid Vesicles, *Chem. Res. Toxicol.* **5**, 134–141.
14. Heath, R.L., and Tappel, A.L. (1976) A New Sensitive Assay for the Measurement of Hydroperoxides, *Anal. Biochem.* **76**, 184–191.
15. Miyazawa, T. (1989) Determination of Phospholipid Hydroperoxides in Human Blood Plasma by a Chemiluminescence-HPLC Assay, *Free Radic. Biol. Med.* **7**, 209–217.
16. Miyazawa, T., Suzuki, T., Fujimoto, K., and Yasuda, K. (1992) Chemiluminescent Simultaneous Determination of Phosphatidylcholine Hydroperoxide and Phosphatidylethanolamine Hydroperoxide in the Liver and Brain of the Rat, *J. Lipid Res.* **33**, 1151–1159.
17. Miyazawa, T., Kunika, H., Fujimoto, K., Endo, Y., and Kaneda, T. (1995) Chemiluminescence Detection of Mono-, Bis-, and Tris-hydroperoxy Triacylglycerols Present in Vegetable Oils, *Lipids* **30**, 1001–1006.
18. Miyazawa, T., Yamashita, T., Fujimoto, K., and Yasuda, K. (1992) Chemiluminescence Detection of 8 $\alpha$ -Hydroperoxytocopherone in Photooxidized  $\alpha$ -Tocopherol, *Lipids* **27**, 289–294.
19. Khono, T., Sakamoto, O., Nakamura, T., and Miyazawa, T. (1993) Determination of Human Skin Surface Lipid Peroxides by Chemiluminescence-HPLC, *J. Jpn. Oil Chem. Soc.* **42**, 204–209.
20. Adachi, J., Asano, M., Naito, T., Ueno, Y., and Tatsuno, Y. (1998) Chemiluminescent Determination of Cholesterol Hydroperoxides in Human Erythrocyte Membrane, *Lipids* **33**, 1235–1240.
21. Harrison, K.A., and Murphy, R.C. (1996) Direct Mass Spectrometric Analysis of Ozonide: Application to Unsaturated Glycero-phosphocholine Lipids, *Anal. Chem.* **68**, 3224–3230.
22. Naito, S. (1989) Effect of Ozone Treatment on Elongation of Hypocotyl and Microbial Counts of Bean Sprouts (Japanese), *Nippon Shokuhin Kogyo Gakkaishi* **36**, 181–188.
23. Naito, S. (1990) Effect of Ozone Treatment on the Rheological Properties of Wheat Flour (Japanese), *Nippon Shokuhin Kogyo Gakkaishi* **37**, 810–813.

[Received July 5, 2002, and in revised form September 18, 2002; revision accepted October 22, 2002]

# Synthesis of 9,9,9-Trideutero-1,4-dihydroxynonane Mercapturic Acid ( $d_3$ -DHN-MA), a Useful Internal Standard for DHN-MA Urinalysis

B. Chantegrel<sup>a,\*</sup>, C. Deshayes<sup>a</sup>, A. Doutheau<sup>a</sup>, and J.P. Steghens<sup>b</sup>

<sup>a</sup>Laboratoire de Chimie Organique INSA-Lyon, Villeurbanne, France, and <sup>b</sup>Laboratoire de Biochimie C, Hôpital Edouard Herriot, Lyon, France

**ABSTRACT:** Racemic 1,4-dihydroxynonane mercapturic acid (DHN-MA) and 9,9,9-trideutero-1,4-dihydroxynonane mercapturic acid ( $d_3$ -DHN-MA) are synthesized on a 400-mg scale (overall yield ~40%) by a two-step sequence involving Michael addition of *N*-acetyl-L-cysteine to methyl 4-hydroxynon-2(*E*)-enoate or methyl 9,9,9-trideutero-4-hydroxynon-2(*E*)-enoate, followed by reduction of the intermediate adducts with lithium borohydride. The requisite starting methyl esters are obtained, respectively, from heptanal or 7,7,7-trideuteroheptanal and methyl 4-chlorophenylsulfanylacetate *via* a sulfoxide piperidine and carbonyl reaction described in the literature. The 7,7,7-trideuteroheptanal is easily prepared by classical methods in four steps from 6-bromo-1-hexanol. <sup>13</sup>C NMR data indicate that DHN-MA as well as  $d_3$ -DHN-MA are obtained as mixtures of four diastereomers. Preliminary results show that  $d_3$ -DHN-MA could be used as an internal standard for mass spectrometric quantification of DHN-MA in human urine.

Paper no. L9123 in *Lipids* 37, 1013–1018 (October 2002).

Despite much investigation, the quantitative evaluation of oxidative stress remains a difficult task for biologists. Lipoperoxidation, one of the main consequences of oxidative stress, yields numerous cytotoxic and mutagenic aldehydes, of which malondialdehyde and 4-hydroxy-2(*E*)-nonenal (4-HNE) have been the most extensively studied (1–3). Lipoperoxidation is often estimated by the TBARS method, which is rather unspecific (4). Recently, the cell-detoxifying process of 4-HNE was discovered to result from at least three different routes. From a quantitative viewpoint, in rats and humans, its conjugation to glutathione seems the most important, and its main final product is urinary dihydroxynonane-mercapturic acid (DHN-MA) (5–8). Thus, DHN-MA may be a good candidate as a noninvasive biomarker of oxidative stress. Therefore, the preparation of a deuterium-labeled DHN-MA derivative that can be used as an internal standard for mass spectrometric quantification of DHN-MA in urine is needed. The objective of the present note is to report an improved synthesis of DHN-MA, its application to the preparation of stable 9,9,9-trideutero-1,4-dihydroxynonane mercapturic acid ( $d_3$ -DHN-MA), and preliminary re-

sults on the utilization of this trideuterated compound to quantify DHN-MA in human urine.

## EXPERIMENTAL PROCEDURES

**Materials and methods.** All reagents of analytical reagent grade were purchased from Sigma Aldrich (L'Isle d'Abeau, France) and used without further purification. Methyl 4-chlorophenylsulfanylacetate was prepared from 4-chlorothiophenol and methyl chloroacetate following a described procedure (9). THF was distilled from sodium/benzophenone ketyl and dichloromethane from phosphorus pentoxide immediately before use. Flash chromatographies were performed using Merck Silica Gel 60 (40–63  $\mu$ m), and TLC separations were carried out using Merck Kieselgel 60 F254 plates (Merck S.A., Chelles, France). IR spectra were recorded on a PerkinElmer 1310 IR spectrophotometer; the abbreviation for shoulder is sh. NMR spectra were recorded on a Bruker AC200 instrument (200/50 MHz) and for specified cases on a Bruker DRX-500 (500/125 MHz). Splitting pattern abbreviations are *s*, singlet; *d*, doublet; *t*, triplet; *p*, pentuplet; *m*, multiplet; and *app*, apparent. Multiplicity (<sup>13</sup>C NMR) was determined by distortionless enhancement by polarization transfer sequences. High-resolution negative ion fast atom bombardment MS (HR-NI-FABMS) was performed by Centre de Spectrométrie de Masse (Université Claude Bernard-Lyon 1, Villeurbanne, France).

**Synthetic procedures.** (i) *Methyl 4-hydroxynon-2(E)-enoate (2a) and methyl 9,9,9-trideutero-4-hydroxynon-2(E)-enoate (2b).* To a solution of 4 g (17.2 mmol) of methyl 4-chlorophenylsulfanylacetate (9) in 40 mL of acetonitrile was added 2.4 mL (24 mmol) of piperidine followed by dropwise addition of 2.5 g of heptanal **1a** (21.9 mmol) or 7,7,7-trideuteroheptanal **1b** (21.3 mmol). The reaction mixture was stirred overnight at room temperature and then evaporated *in vacuo*. The residue was purified by flash chromatography on silica gel (150 g; dichloromethane/diethyl ether, 90:10 vol/vol) to afford the ester **2a** or **2b** contaminated with residual methyl 4-chlorophenylsulfanylacetate. A second flash chromatography on silica gel (150 g; diethyl ether) afforded 2.16 g (67%) of pure ester **2a** or 2.32 g (71%) of pure ester **2b** as yellowish oils. **Ester 2a:** The NMR spectra were in accordance with literature data (9). **Ester 2b:** IR: (neat)  $\nu$  (cm<sup>-1</sup>): 3450 (OH); 2220, 2115, 2080 (CD); 1730, 1715 sh (CO); 1615 (C=C). <sup>1</sup>H NMR:

\*To whom correspondence should be addressed at Laboratoire de Chimie-Organique, INSA, Bâtiment Jules Verne, 17 Avenue Jean Capelle, 69621 Villeurbanne Cedex, France. E-mail: Bernard.Chantegrel@insa-lyon.fr

Abbreviations: DHN-MA, 1,4-dihydroxynonane mercapturic acid; 4-HNE, 4-hydroxy-2(*E*)-nonenal; HR, high-resolution; NI-FABMS, negative ion fast atom bombardment MS; PCC, pyridinium chlorochromate.

(CDCl<sub>3</sub>)  $\delta$ : 1.15–1.50 (6H, *m*); 1.50–1.80 (2H, *m*); 2.17 (1H, *d*,  $J = 3$  Hz); 3.73 (3H, *s*); 4.29 (1H, *m*); 6.02 (1H, *dd*,  $J = 15.7$ ,  $J = 1.6$  Hz); 6.95 (1H, *dd*,  $J = 15.7$ ,  $J = 4.9$  Hz). <sup>13</sup>C NMR: (CDCl<sub>3</sub>)  $\delta$ : 13.12 (app. *p*, C-9, <sup>1</sup> $J_{CD} = 18.8$  Hz); 22.30 (C-8); 24.95 (C-6); 31.62 (C-7); 36.64 (C-5); 51.64 (C-10); 71.06 (C-4); 119.58 (C-2); 150.92 (C-3); 167.21 (C-1).

(ii) *Michael addition of N-acetyl-L-cysteine to esters 2a,b*. To a solution of 0.85 g of ester **2a** (4.56 mmol) or ester **2b** (4.49 mmol) in methanol (20 mL) were added 665 mg (4 mmol) of *N*-acetyl-L-cysteine and 1.26 mL (9 mmol) of triethylamine. The reaction mixture was stirred under a nitrogen atmosphere at room temperature for 3 d. The solvent was evaporated *in vacuo* and the crude product was purified by flash chromatography on silica gel (170 g; chloroform/methanol/acetic acid, 10:3:0.5 by vol) to afford a mixture of diastereomeric ester **3** and diastereomeric lactone **4** as a sticky oil contaminated with residual acetic acid. A second flash chromatography on silica gel (140 g; chloroform/methanol/ether, 10:6:1 by vol) gave 1.33 g (~73%) of a **3a/4a** mixture or 1.20 g (~83%) of a **3b/4b** mixture as white solid foams. The **3a/4a** or **3b/4b** ratios were determined to be about 1:2 by <sup>1</sup>H NMR (see Results and Discussion section below). **3a/4a** mixture: IR (CHCl<sub>3</sub>)  $\nu$  (cm<sup>-1</sup>): 3600–2400 (OH, NH); 1770 (CO lactone); 1715 (CO ester and acid); 1660 (CO amide). <sup>1</sup>H NMR (500 MHz, CD<sub>3</sub>OD)  $\delta$ : 0.90 (3H, *t*); 1.10–1.90 (8H, *m*); 2.10 and 2.15 (3H, 2*s*); 2.45–2.80 (1H, *m*); 2.80–3.50 (3H, *m*); 3.60–3.90 (1H, *m* with a singlet at 3.73 ppm for the methyl ester resonance of **3a**); 4.10–5.00 (2H, *m*). **3b/4b** mixture: IR (CHCl<sub>3</sub>)  $\nu$  (cm<sup>-1</sup>): 3600–2400 (OH, NH), 2220, 2115, 2080 (CD); 1775 (CO lactone); 1720 (CO ester and acid); 1660 (CO amide). <sup>1</sup>H NMR (500 MHz, CD<sub>3</sub>OD)  $\delta$ : 1.25–1.90 (8H, *m*); 2.01 and 2.06 (3H, 2*s*); 2.45–2.75 (1H, *m*); 2.75–3.50 (3H, *m*); 3.65–3.90 (1H, *m* with a singlet at 3.73 ppm for the methyl ester resonance of **3b**); 4.25–4.75 (2H, *m*).

(iii) *DHN-MA (5a) and d<sub>3</sub>-DHN-MA (5b)*. To a stirred solution of 900 mg (~2.5 mmol) of **3a/4a** or **3b/4b** mixture in anhydrous THF (20 mL) under a nitrogen atmosphere at 0°C was added lithium borohydride (150 mg, 6.89 mmol) in one portion. After 10 min at 0°C, the cooling bath was removed and the reaction mixture was stirred for 24 h at room temperature. The reaction mixture was cooled in a water-ice bath, quenched with acetic acid (~1 mL), and concentrated *in vacuo*. The residue was purified by flash chromatography on silica gel (140 g; chloroform/methanol/acetic acid, 10:3:0.5 by vol) to afford 520 mg of **5a** or 500 mg of **5b** contaminated with residual acetic acid. A second flash chromatography on silica gel (80 g; chloroform/methanol/ether, 5:4:1 by vol) gave 432 mg (~54%) of **5a** or 418 mg (~51%) of **5b** as white solid foams that slowly decomposed at about 120°C. *DHN-MA 5a*: <sup>1</sup>H NMR (500 MHz, CD<sub>3</sub>OD)  $\delta$ : 0.92 (*t*, 3H,  $J = 6.85$  Hz); 1.25–1.40 (5H, *m*); 1.40–1.70 (4H, *m*); 1.82–1.92 (1H, *m*); 2.02 (3H, *s*; three peaks were observed by enlargement of this signal); 2.82–3.32 (3H, *m*); 3.62–3.85 (3H, *m*); 4.35–4.50 (1H, *m*). <sup>13</sup>C NMR (125 MHz, CD<sub>3</sub>OD; pertinent signals)  $\delta$ : 13.58 (C-9); 21.98 (C-5'); 49.31, 49.70, 50.63 (C-3); 55.21, 55.27 (C-2'); 59.50, 59.71 (C-1); 74.16, 74.27, 74.35, 74.50 (C-4); 172.09, 172.17 (C-4');

176.58–176.70 (C-1'). NI-FABMS:  $m/z$ : 320 (M – H)<sup>-</sup>; 191 (C<sub>9</sub>H<sub>19</sub>O<sub>2</sub>S<sup>-</sup>); 162 (C<sub>5</sub>H<sub>8</sub>NO<sub>3</sub>S<sup>-</sup>); 143 (C<sub>9</sub>H<sub>19</sub>O<sup>-</sup>). HR-NI-FABMS: (M – H)<sup>-</sup>: Calculated for C<sub>14</sub>H<sub>26</sub>NO<sub>5</sub>S, 320.1530; found, 320.1532. *d<sub>3</sub>-DHN-MA 5b*: <sup>1</sup>H NMR (500 MHz, CD<sub>3</sub>OD)  $\delta$ : 1.25–1.45 (5H, *m*); 1.45–1.70 (4H, *m*); 1.85–1.95 (1H, *m*); 2.03 (3H, *s*; three peaks were observed by enlargement of this signal); 2.82–3.35 (3H, *m*); 3.62–3.90 (3H, *m*); 4.35–4.50 (1H, *m*). <sup>13</sup>C NMR (125 MHz, CD<sub>3</sub>OD; pertinent signals)  $\delta$ : 12.59 (app. *p*, C-9, <sup>1</sup> $J_{CD} = 19.1$  Hz); 21.80 (C-5'); 49.24, 49.62, 50.58 (C-3); 55.22, 55.30 (C-2'); 59.45, 59.64 (C-1); 74.15, 74.26, 74.39, 74.52 (C-4); 172.09, 172.13, 172.22, 172.25 (C-4'); 177.10, 177.21 (C-1'). NI-FABMS:  $m/z$ : 323(M – H)<sup>-</sup>; 194 (C<sub>9</sub>H<sub>16</sub>D<sub>3</sub>O<sub>2</sub>S<sup>-</sup>); 162 (C<sub>5</sub>H<sub>8</sub>NO<sub>3</sub>S<sup>-</sup>); 146 (C<sub>9</sub>H<sub>16</sub>D<sub>3</sub>O<sup>-</sup>). HR-NI-FABMS: (M – H)<sup>-</sup>: Calculated for C<sub>14</sub>H<sub>23</sub>D<sub>3</sub>NO<sub>5</sub>S, 323.1715; found, 323.1720.

(iv) *6-Tetrahydropyran-1-bromohexane (7)*. To a stirred solution of 10 g (55 mmol) of 6-bromo-1-hexanol (**6**) in 120 mL of dichloromethane was added 6.5 mL (67 mmol) of dihydropyran in one portion, followed by 2.8 g (11 mmol) of pyridinium *p*-toluenesulfonate. After being stirred for 24 h at room temperature, the reaction mixture was washed successively with saturated aqueous sodium hydrogencarbonate (40 mL) and brine (40 mL), dried over sodium sulfate, and concentrated *in vacuo*. The residue was purified by flash chromatography on 150 g of silica gel (pentane/ethyl acetate, 95:5 vol/vol) to afford 12 g (82%) of bromide **7** as a colorless liquid (10).

(v) *7,7,7-Trideutero-1-tetrahydropyran-1-ol (8)*. To a stirred solution of 6 g (22.6 mmol) of bromide **7** in 100 mL of anhydrous THF, under a nitrogen atmosphere, was added 7 mL of a 0.1 M solution of Li<sub>2</sub>CuCl<sub>4</sub> in THF. The resulting solution was cooled in an ice-sodium chloride bath, and 25 mL of a 1 M solution of CD<sub>3</sub>MgI in diethyl ether was added dropwise. After stirring for 24 h at room temperature, the reaction mixture was quenched with saturated aqueous ammonium chloride (100 mL) and extracted with diethyl ether (3 × 40 mL). The combined extracts were washed with brine (40 mL), dried over sodium sulfate, and concentrated *in vacuo*. The residue was purified by flash chromatography on silica gel (120 g; pentane/diethyl ether, 95:5 by vol) to afford 4.1 g (89%) of **8** as a colorless liquid. IR (neat)  $\nu$  (cm<sup>-1</sup>): 2200, 2130, 2080 (CD). <sup>1</sup>H NMR (CDCl<sub>3</sub>)  $\delta$ : 1.20–1.45 (8H, *m*); 1.45–2.00 (8H, *m*); 3.30–3.60 (2H, *m*); 3.65–3.95 (2H, *m*); 4.85 (1H, *m*).

(vi) *7,7,7-Trideuteroheptan-1-ol (9)*. A solution of **8** (7 g, 34.4 mmol) and *p*-toluenesulfonic acid monohydrate (1 g, 5.26 mmol) in methanol (60 mL) was stirred for 36 h at room temperature. The solution was then neutralized by addition of solid sodium hydrogencarbonate (1.5 g). After evaporation of the solvent, 20 mL of dichloromethane was added and the solution was filtered and evaporated *in vacuo*. The residue was purified by flash chromatography on silica gel (120 g; pentane/diethyl ether, 80:20 by vol) to afford 3.55 g (86%) of trideuteroheptanol **9** as a colorless liquid. IR (neat)  $\nu$  (cm<sup>-1</sup>): 3340 (OH); 2220, 2130, 2080 (CD). <sup>1</sup>H NMR (CDCl<sub>3</sub>)  $\delta$ : 1.20–1.45 (8H, *m*); 1.45–1.65 (2H, *m*); 1.69 (1H, *s*); 3.62 (2H, *t*,  $J = 6.5$  Hz).

(vii) *7,7,7-Trideuteroheptanal (1b)*. To a stirred suspension

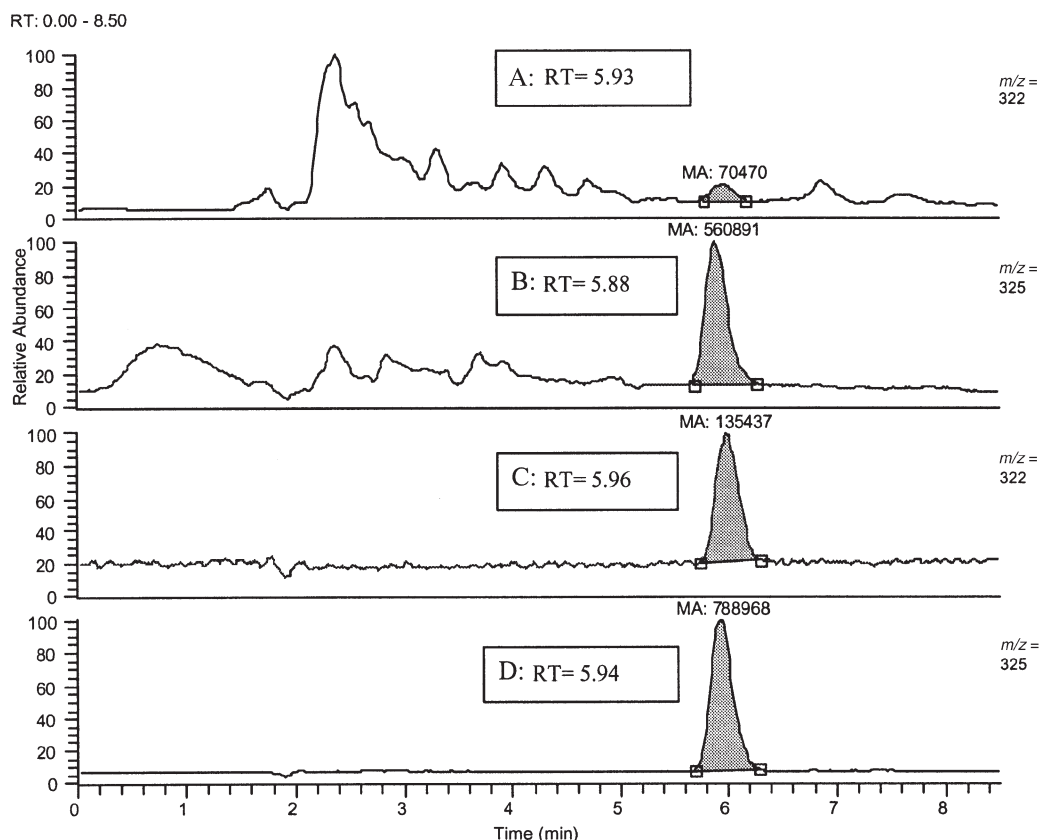


of pyridinium chlorochromate (PCC) (10 g, 46.4 mmol) and anhydrous sodium acetate (0.6 g, 7.3 mmol) in dichloromethane (50 mL) cooled in a water-ice bath was added 3.5 g (30.1 mmol) of alcohol **9** in one portion. The reaction mixture was stirred for 5 min at 0°C and then for 1 h at room temperature. After addition of 100 mL of diethyl ether, the resulting suspension was filtered through silica gel (60 g). The silica gel was washed with four 50-mL portions of diethyl ether. The combined organic eluates were concentrated *in vacuo*, and the residue was purified by flash chromatography on silica gel (50 g; dichloromethane) to afford 2.68 g (78%) of trideuteroheptanal **1b** as a colorless liquid. IR (neat)  $\nu$  ( $\text{cm}^{-1}$ ): 2220, 2130, 2080 (CD); 1725 (CO).  $^1\text{H}$  NMR ( $\text{CDCl}_3$ )  $\delta$ : 1.20–1.40 (6H, *m*); 1.55–1.75 (2H, *m*); 2.42 (2H, *td*,  $J = 7.20$ ,  $J = 1.85$  Hz); 9.77 (1H, *t*,  $J = 1.85$  Hz).

**HPLC analysis of DHN-MA 5a.** Analytical HPLC separation was performed with a Thermo Finnigan liquid chromatograph (pump P4000, injector AS 3000, and a UV/vis diode-array detector UV 6000 LP) on a  $150 \times 2$  mm Uptisphere ODB C18 cartridge (3  $\mu\text{m}$  particle size) (Interchim, Montluçon, France). The flow rate was 200  $\mu\text{L}/\text{min}$  with the cartridge kept

at 37°C and the detector set at 215 nm. The mobile phase was 10 mM ammonium acetate (final concentration) adjusted to pH 3.5 with formic acid, and 20% (vol/vol) of acetonitrile. DHN-MA (600  $\mu\text{mol}/\text{L}$ ) (10  $\mu\text{L}$  injected) was detected as a double peak at 6.6 and 6.9 min in a pattern similar to that described by Alary *et al.* (6).

**DHN-MA analysis in human urine.** Urine (100  $\mu\text{L}$ ), acidified with 10  $\mu\text{L}$  HCl (1 M) and spiked with  $d_3$ -DHN-MA, was prepared by solid-phase extraction on Oasis HLB (60 mg, Waters®) according to the manufacturer's instructions. After optimization of the washing step by using methanol/water 20:80 (vol/vol;  $2 \times 500$   $\mu\text{L}$ ), the sample was eluted with methanol, dried under vacuum, and reconstituted with 100  $\mu\text{L}$  of the mobile phase (10 mM ammonium acetate adjusted to pH 2.5 with formic acid and containing 35% vol/vol methanol). The HPLC analysis was carried out with the same device as described for HPLC analysis of DHN-MA **5a**. The sample (10  $\mu\text{L}$ ) was injected onto an Alltech (Deerfield, IL) Adsorbosphere HS C18 (150  $\times$  2 mm, 3  $\mu\text{m}$  particle size) held at 45°C, with a 200  $\mu\text{L}/\text{min}$  flow rate. Detection was with a single quadrupole mass spectrometer (Navigator Aqua, Thermo Finnigan) in electron



**FIG. 1.** Typical LC/MS chromatograms ( $[M + H]^+$ , single ion monitoring mode) of: (A, B) a human urine of a burnt patient, prepared and analyzed as described in the text, with authentic DHN-MA eluted at the retention time (RT) = 5.93 min and  $m/z = 322$  (A) and its internal  $d_3$ -DHN-MA standard recorded at RT = 5.88 min and  $m/z = 325$  (B). (C) A DHN-MA standard (140 nM) at RT = 5.96 min and  $m/z = 322$ . (D) The  $d_3$ -DHN-MA prepared like a sample and injected alone (RT = 5.94 min at  $m/z = 325$ ) to calculate the recovery for the urine sample shown in (A) and (B), i.e., around 71%. From these chromatograms it appeared that DHN-MA was present at about 102 nM in the analyzed urine sample. DHN-MA, 1,4-dihydroxynonane mercapturic acid.



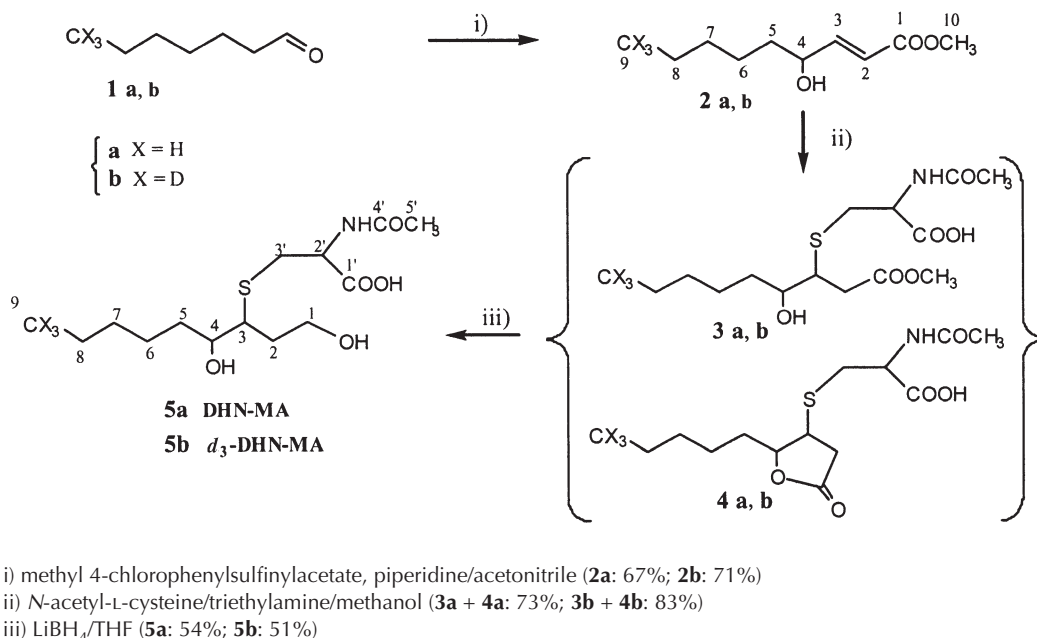
spray ionization positive mode. The probe was set at 225°C and 2.5 kV with an entrance cone voltage at 10 V. Typical chromatograms recorded in single-ion monitoring mode ( $M + H$ )<sup>+</sup> at  $m/z = 322$  and  $325$  are shown in Figure 1.

## RESULTS AND DISCUSSION

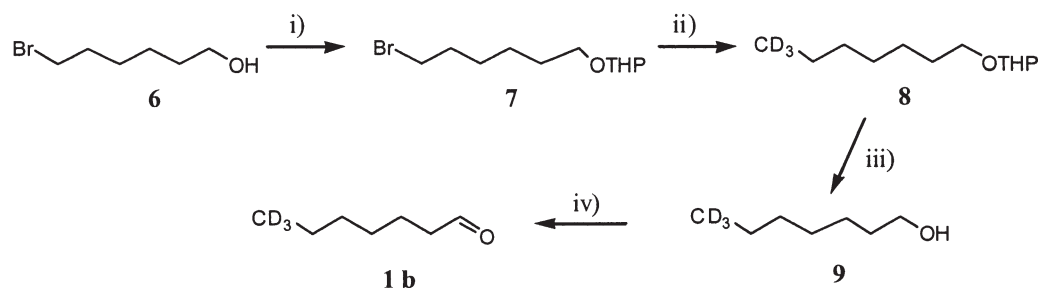
DHN-MA was first synthesized by Alary *et al.* (6) on a 5-mg scale for identification purposes. Starting from 3,3-diethoxy-1-propyne and hexanal, racemic 4-HNE diethyl acetal was prepared in two steps (11,12). Hydrolysis of 4-HNE diethyl acetal to 4-HNE was followed by Michael addition of *N*-acetyl-L-cysteine and reduction of the intermediate aldehyde to DHN-MA. Alary's synthesis could be applied to the preparation of *d*<sub>3</sub>-DHN-MA starting from 9,9,9-trideutero-4-HNE since this compound has been synthesized in five steps with a total yield of about 20% (13). However, the yield of the Michael addition–reduction steps in Alary's sequence was rather low (about 15%), presumably because the reactive intermediate saturated aldehyde, formed from 4-HNE in the Michael addition reaction, could give rise to side reactions. In an attempt to improve the yield and ease of synthesis of DHN-MA, we turned our attention to methyl 4-hydroxynon-2(*E*)-enoate as the starting material, in place of 4-HNE, for the following reasons. A facile synthesis of racemic methyl 4-hydroxynon-2(*E*)-enoate **2a**, starting from heptanal **1a** and methyl 4-chlorophenylsulfanylacetate (Scheme 1) *via* a sulfoxide piperidine and carbonyl reaction, has been described by Tanikaga *et al.* (9). The utilization of an ester should minimize the side reactions in the Michael addition step. If successful, the procedure could be easily transposed to the preparation of *d*<sub>3</sub>-DHN-MA starting from 9,9,9-trideutero-4-hydroxynon-2(*E*)-enoate **2b**.

Michael addition of *N*-acetyl-L-cysteine to racemic unsaturated ester **2a** was conducted in methanol in the presence of triethylamine for 3 d and afforded an inseparable mixture of diastereomeric ester **3a** and diastereomeric lactone **4a**. The formation of **4a** was evidenced by a deficit in the integration of the methyl ester resonance in the <sup>1</sup>H NMR together with a strong absorption at 1770 cm<sup>-1</sup> in the IR spectrum. The **3a/4a** ratio was estimated to be 1:2 by <sup>1</sup>H NMR from the integrations of the methyl ester resonances centered at 3.73 ppm for **3a** and acetamido resonances between 2.10 and 2.15 ppm for (**3a** + **4a**). The **3a/4a** ratio should presumably reflect an equilibrium between ester **3a** and lactone **4a** because the Michael addition is a slow process and **4a** can reopen to **3a** by reaction with methanol. Alary *et al.* (5) also have observed the formation of lactone **4a** in the Michael addition of *N*-acetyl-L-cysteine to 4-hydroxynon-2(*E*)-enoic acid (5). Subsequent simultaneous reduction by lithium borohydride in THF (14) of the ester and lactone functionalities in the **3a/4a** mixture gave rise to DHN-MA **5a**. This sequence allowed us to prepare DHN-MA on a 400-mg scale, with a 39% yield from ester **2a** after chromatographic purification.

The procedure was then applied to the synthesis of *d*<sub>3</sub>-DHN-MA **5b** through the key trideuterated ester **2b**, which was prepared from the 7,7,7-trideuteroheptanal **1b** (Scheme 1). This aldehyde was readily obtained from 6-bromo-1-hexanol **6** (Scheme 2) by classical methods [alcohol protection as a tetrahydropyranloxy derivative (10), reaction with trideuteroethylmagnesium iodide in the presence of lithium tetrachlorocuprate (15), deprotection, and PCC oxidation (15)] in a 49% overall yield. The spectroscopic data were in full agreement with the structure of **1b**, in particular a triplet resonance at 9.77 ppm with a <sup>3</sup>*J* coupling of 1.85 Hz, which was observed



SCHEME 1



- i) dihydropyran, pyridinium *p*-toluene sulfonate/ $\text{CH}_2\text{Cl}_2$  (82%); OTHP, tetrahydropyranyloxy  
 ii)  $\text{CD}_3\text{MgI}$ ,  $\text{Li}_2\text{CuCl}_4$ /THF (89%)  
 iii) methanol/*p*-toluene sulfonic acid (86%)  
 iv) pyridinium chlorochromate, sodium acetate/ $\text{CH}_2\text{Cl}_2$  (78%)

SCHEME 2

for the aldehydic proton in the  $^1\text{H}$  NMR spectrum, and absorption bands in the IR spectrum at  $2080\text{--}2220\text{ cm}^{-1}$  for the C–D bonds. The aldehyde **1b** was transformed into the key ester **2b** by following the procedure of Tanikaga *et al.* (9). The structure of **2b** was fully consistent with the IR,  $^1\text{H}$  NMR, and  $^{13}\text{C}$  NMR data. The presence of the hydroxyl group was confirmed by the band at  $3450\text{ cm}^{-1}$  in the IR spectrum together with the doublet at 2.17 ppm due to the  $^3J$  coupling between the OH and C4-*H* protons in the  $^1\text{H}$  NMR spectrum. The double bond was evidenced by the resonances at 6.02 ppm (C2-*H*) and 6.95 ppm (C3-*H*), occurring as doublets of doublets, in the  $^1\text{H}$  NMR spectrum and at 150.92 (C2) and 119.58 ppm (C3) in the  $^{13}\text{C}$  NMR spectrum. The presence of the  $\text{CD}_3$  group was indicated by the CD bands at  $2080\text{--}2220\text{ cm}^{-1}$  in the IR spectrum and a resonance at 13.12 ppm in the  $^{13}\text{C}$  NMR spectrum; this resonance was observed as a pentuplet, with a  $^1J_{\text{CD}}$  coupling of 18.8 Hz, in place of the expected septuplet, because the two smallest peaks were lost in the spectral noise. Michael addition of *N*-acetyl-L-cysteine to unsaturated ester **2b** afforded an inseparable mixture of diastereomeric ester **3b** and diastereomeric lactone **4b**. The **3b/4b** ratio was estimated to be 1:2 by  $^1\text{H}$  NMR in a similar manner as for the **3a/4a** mixture. Reduction of the **3b/4b** mixture, in a similar way as for the **3a/4a** mixture, afforded  $d_3$ -DHN-MA **5b**, on a 400-mg scale, with a 42% yield from **2b** after chromatographic purification.

Four diastereomers of DHN-MA **5a** and  $d_3$ -DHN-MA **5b** could be expected since three asymmetric carbons are present in these molecules. HPLC analysis of synthetic DHN-MA **5a** showed the presence of two partially resolved peaks in a pattern similar to that observed by Alary *et al.* (6) and consistent with the presence of at least two diastereomers. Examination of the complex NMR spectra of both **5a** and **5b** gave further insight into the diastereomeric composition. The  $^1\text{H}$  NMR spectrum of **5a** was in agreement with the data of Alary *et al.* (6). The  $^1\text{H}$  NMR spectra of **5a** and **5b** were impossible to analyze fully, but the presence of three diastereomers could be deduced from these spectra since three peaks were observed by enlargement of the acetyl group at about 2 ppm. A careful

examination of the  $^{13}\text{C}$  NMR spectra of **5a** and of **5b** showed that two peaks were observed for carbons C-1, C-1', or C-2', three peaks for carbon C-3, and four peaks for carbon C-4. The chemical shifts of these carbons (see Experimental Procedures section) are consistent with literature data for similar carbons, observed in 3-mercapto-2-butanol (for C-3 and C-4) and *N*-acetyl-L-cysteine (for C-1' and C-2') (16). In particular, the four C-4 resonances appeared at 74.16, 74.27, 74.35, and 74.50 ppm for **5a** and 74.15, 74.26, 74.39, and 74.52 ppm for **5b**. On this basis we concluded that DHN-MA **5a** and  $d_3$ -DHN-MA **5b** were obtained as mixtures of four diastereomers.

The structures of **5a** and **5b** were confirmed by NI-FABMS.  $(\text{M} - \text{H})^-$  base peaks appeared at  $m/z$  320 for **5a** and  $m/z$  323 for **5b**. Two other significant ions resulting from  $\text{C}_3$ -S and  $\text{C}_3$ -S bond cleavages were observed at  $m/z$  162 ( $\text{C}_5\text{H}_8\text{NO}_3\text{S}^-$ ) and 191 ( $\text{C}_9\text{H}_{19}\text{O}_2\text{S}^-$ ) for **5a** or at  $m/z$  162 ( $\text{C}_5\text{H}_8\text{NO}_3\text{S}^-$ ) and 194 ( $\text{C}_9\text{H}_{16}\text{D}_3\text{O}_2\text{S}^-$ ) for **5b**. Exact mass measurements of the  $(\text{M} - \text{H})^-$  ion by HR-NI-FABMS for both compounds were in perfect accordance with the expected values.

Preliminary analyses of human urine for DHN-MA were done on samples of burnt patients that were expected to have a high DHN-MA content. They are illustrated by the chromatograms recorded in single-ion monitoring mode  $(\text{M} + \text{H})^+$  at  $m/z = 322$  and  $325$  shown in Figure 1. Authentic urine DHN-MA is eluted at the same retention time as  $d_3$ -DHN-MA (chromatograms A, B), and this elution time is similar for synthetic DHN-MA standard (chromatogram C) or  $d_3$ -DHN-MA alone (chromatogram D). Our preliminary results allowed us to determine DHN-MA urine concentrations at a 100 nM level. Further refinements are needed to obtain an improved sensitivity for analyzing normal samples.

## REFERENCES

1. Esterbauer, H., Zollner, H., and Schaur, R.J. (1991) Chemistry and Biochemistry of 4-Hydroxynonenal, Malondialdehyde and Related Aldehydes, *Free Radic. Biol. Med.* 11, 81–128.
2. Poli, G., and Schaur, R.J. (2000) 4-Hydroxynonenal in the Pathomechanisms of Oxidative Stress, *Life* 50, 315–321.

3. Schneider, C., Tallman, K.A., Porter, N.A., and Brash, A.R. (2001) Two Distinct Pathways of Formation of 4-Hydroxynonenal. Mechanisms of Nonenzymatic Transformation of the 9- and 13-Hydroperoxides of Linoleic Acid to 4-Hydroxyalkenals, *J. Biol. Chem.* 276, 20831–20838.
4. Janero, D.R. (1990) Malondialdehyde and Thiobarbituric Acid-Reactivity as Diagnostic Indices of Lipid Peroxidation and Peroxidative Tissue Injury, *Free Radic. Biol. Med.* 9, 515–540.
5. Alary, J., Bravais, F., Cravedi, J.P., Debrauwer, L., Rao, D., and Bories, G. (1995) Mercapturic Acid Conjugates as Urinary End Metabolites of the Lipid Peroxidation Product 4-Hydroxy-2-nonenal in the Rat, *Chem. Res. Toxicol.* 8, 34–39.
6. Alary, J., Debrauwer, L., Fernandez, Y., Cravedi, J.P., Rao, D., and Bories, G. (1998) 1,4-Dihydroxynonene Mercapturic Acid, the Major End Metabolite of Exogenous 4-Hydroxy-2-nonenal, Is a Physiological Component of Rat and Human Urine, *Chem. Res. Toxicol.* 11, 130–135.
7. Laurent, A., Alary, J., Debrauwer, L., and Cravedi, J.P. (1999) Analysis in the Rat of 4-Hydroxynonenal Metabolites Excreted in Bile: Evidence of Enterohepatic Circulation of These Byproducts of Lipid Peroxidation, *Chem. Res. Toxicol.* 12, 887–894.
8. Boon, P.J.M., Marinho, H.S., Oosting, R., and Mulder, G.J. (1999) Glutathione Conjugation of 4-Hydroxy-*trans*-2,3-Nonenal in the Rat *in vivo*, the Isolated Perfused Liver and Erythrocytes, *Toxicol. Appl. Pharmacol.* 159, 214–223.
9. Tanikaga, R., Nozaki, Y., Tamura, T., and Kaji, A. (1983) Facile Synthesis of 4-Hydroxy-(*E*)-2-alkenoic Esters from Aldehydes, *Synthesis*, 134–135.
10. Clyne, D.S., and Weiler, L. (1999) The Synthesis of 14-Membered Macrocyclic Ethers, *Tetrahedron* 55, 13659–13682.
11. Esterbauer, H., and Weger, W. (1967) Action of Aldehydes on Normal and Malignant Cells. III. Synthesis of Homologous 4-Hydroxy-2-alkenals, *Monatsh. Chem.* 98, 1994–2000.
12. Bravais, F., Rao, D., Alary, J., Rao, R., Debrauwer, L., and Bories, G. (1995) Synthesis of 4-Hydroxy[4-<sup>3</sup>H]-2-(*E*)-nonen-1-yl diethyl acetal, *J. Labelled Compd. Radiopharm.* 36, 471–477.
13. Rees, M.S., Van Kuijk, F.J.G.M., Stephens, R.J., and Mundy, B.P. (1993) Synthesis of Deuterated 4-Hydroxyalkenals, *Synth. Comm.* 23, 757–763.
14. Matsuura, F., Hamada, Y., and Shioiri, T. (1992) Synthesis of a  $\gamma$ -Azetidiny- $\beta$ -hydroxy- $\alpha$ -amino Acid Derivative, a Key Intermediate for the Synthesis of Mugineic Acid, *Tetrahedron: Asymmetry* 3, 1069–1074.
15. Sabhrwal, A., Dogra, V., Sharma, S., Kalra, R., Vig, O.P., and Kad, G.L. (1990) Stereospecific Synthesis of Pipericide and 10,11-Dihydropipericide, *J. Ind. Chem. Soc.* 67, 318–320.
16. Pouchert, C.J., and Behnke, J. (1993) The Aldrich Library of <sup>13</sup>C and <sup>1</sup>H FT NMR Spectra, Edition I, Volume I, Aldrich, Milwaukee, WI, Spectra 423A (3-mercapto-2-butanol) and 1282B (*N*-acetyl-L-cysteine). Netlink: [www.sigma-aldrich.com](http://www.sigma-aldrich.com)

[Received July 18, 2002, and in revised form October 24, 2002; revision accepted November 5, 2002]

# Clinical Trial Results Support a Preference for Using CLA Preparations Enriched with Two Isomers Rather Than Four Isomers in Human Studies

Jean-Michel Gaullier\*, Grethe Berven, Henrietta Blankson, and Ola Gudmundsen

Scandinavian Clinical Research, 2027 Kjeller, Norway

**ABSTRACT:** CLA mixtures are now commercially available. They differ from each other with respect to their content of CLA isomers and their degree of purification. As a group of natural FA, CLA have been widely assumed to be safe. However, the suspected presence of both impurities and particular isomers might induce undesirable side effects. Despite this potential health risk, only a few CLA preparations have been tested under rigorous conditions for clinical efficacy and safety. Based on the limited results available, it is possible to suggest that preparations enriched in *c9,t11* and *t10,c12* isomers are preferable for human consumption compared to preparations containing four isomers, in terms both of safety and efficacy.

Paper no. L9016 in *Lipids* 37, 1019–1025 (November 2002).

The interest in CLA has developed since the 1980s when CLA was identified as a component present in fried ground beef, which exhibited anticarcinogenic properties against chemically-induced tumor formation in animal models (1). Progressively, *in vitro* and animal research have confirmed the anticarcinogenic properties of CLA in such models (2–4), and shown that CLA could be an antiatherosclerotic agent (5,6), stimulator of the immune functions (7,8), growth factor (9), and modulator of body composition in animals (10–15).

CLA refers to a mixture of linoleic acid isomers (18:2) with conjugated double bonds and not simply to a single FA. All CLA isomers are described according to the *cis* or *trans* configuration of both double bonds at any position of the carbon chain, and may be purified by silver ion-HPLC or GC with capillary columns (16). The synthesis of CLA occurs *in vivo* during the biohydrogenation of linoleic acid by rumen bacteria such as *Butyrivibrio fibrisolvens*. Incorporation of CLA into several bovine tissues renders dairy products (e.g., milk and cheese) and beef suitable as the main dietary sources of CLA for humans (17).

However, the CLA content of the human diet is far below the dose that is known to exert effects on animals. Depending on gender and diet, the average daily intake of CLA by human adults is estimated to range from 15 to 430 mg/d (18), whereas the lowest dose of CLA to obtain effects in animal

models is about 10 times higher. To provide a higher CLA intake, a number of commercial preparations containing highly purified CLA have appeared on the market. In 1997, only two companies (Natural ASA, Hovdebygda, Norway; PharmaNutrients Inc., Lake Bluff, IL) marketed CLA as a dietary supplement. Today, numerous companies are marketing CLA, claiming a variety of health benefits. The discrepancies among these preparations are huge, and all preparations may not be appropriate for human use. The marked heterogeneity and variable purity of commercial CLA preparations has already been well documented, based on state-of-the-art chemical analyses of several commercial preparations (19).

The present review will discuss the isomer content in commercial CLA products in terms of the safety and physiological effects shown in clinical studies.

*CLA preparations for humans.* Alkaline isomerization of linoleic acid (LA, *c9,c12*-18:2) is a common method used in the synthesis of mixtures of CLA isomers. The CLA concentration in the final product depends on the level of LA in the starting material. Commercial CLA preparations are usually made from sunflower oil (app. 60–70% LA) or safflower oil (70–80% LA) (20). By chemical treatment, the linoleic acid is progressively converted to CLA without affecting the saturated and monounsaturated acids present in the oil (21,22).

Whatever the chemical procedure used or the nature of the oil, the double bonds migrate to form more isomers than in the product of the initial conjugation step. As a result, the purification provides mainly four isomers: *t8,c10*; *c9,t11*; *t10,c12*; and *c11,t13* (19,23,24). The preparations are mainly in the form of gelatin capsules with CLA FFA or CLA TG.

Lately, some manufacturers have given priority to the production of CLA preparations containing a limited number of isomers, based on recent research showing that the diverse putative benefits of CLA might be due to distinct isomers.

Isomer *c9,t11*, the main isomer found in the diet, has been claimed to modulate growth (25), whereas the isomer *t10,c12* has been claimed to positively modulate body composition and diabetes in mice (11). However, the isomer *t10,c12* also has been found to increase insulin resistance in some humans with metabolic syndrome (26). Both CLA isomers could reduce the appearance or progression of some tumors in humans if their anticarcinogenic effects were similar to those found against chemically-induced tumors in rat models (27,28).

\*To whom correspondence should be addressed at Scandinavian Clinical Research AS, Gåsevikkveien 8, P.O. Box 135, 2027 Kjeller, Norway.

E-mail: j-m@scr.no

Abbreviations: *c*, *cis* configuration; LA, linoleic acid; *t*, *trans* configuration.



CLA may also have useful antiatherogenic effects on lipid metabolism in humans (29). In contrast, the isomer *c11,t13* has been shown to accumulate in the liver and in the heart muscle of pigs (30). The pigs were not shown to suffer from any growth or pathological abnormalities (15). However, incorporation and accumulation of this isomer into mitochondrial phospholipids may affect enzymes embedded in the membrane and thus lead to disorders in the long term (30). Because of this, some producers are now trying to eliminate the *c11,t13* isomer from their preparations (Table 1).

The first CLA preparations to appear on the market in 1996 were produced from sunflower oil and generally contained four isomers of CLA. In this article, such products will be referred to as "four-isomer" preparations; these contain approximately 60% CLA (Table 1). More recently, producers have purified CLA (by manipulation of temperature and time reactions) in order to obtain mainly the two apparently active isomers, *c9,t11* and *t10,c12*, and their total CLA content can reach 80%. By analogy, they will be referred to as "two-isomer" preparations (Table 1). However, one must exert caution in making assumptions about the composition of the CLA preparations since they refer to analyses by producers who might be less reliable than claimed.

Owing to the presence of catalysts as well as to trace elements and residual solvents, the conjugation of CLA may also result in the production of *cis,cis* and especially *trans,trans* isomers that can accumulate progressively with time (21). The four-isomer preparations contain between 7.3 up to 22.43% *trans,trans* and *cis,cis* isomers, whereas the two-isomer preparations contain only trace amounts of isomers other than the two main one, and less than 5% of *trans,trans* and *cis,cis* isomers.

**Clinical trials.** Based on the very promising benefits observed in animals fed CLA, 16 clinical trials were published or reported within the last five years (Table 2). Most of them can be considered early phase studies, as they include a relatively small number of subjects.

(i) **Safety.** CLA is a natural substance detected in several food products as well as in the tissues and body fluids in humans (31,32), and has generally been considered nontoxic. Nevertheless, since the recommended doses of CLA supplementation are approximately 10–200 times higher than the normal dietary intake, efforts have been made to evaluate the toxicological features and the tolerability of some of the CLA preparations whose composition is available (Table 2).

However, records and reports of side effects (based on adverse events and blood sample analyses) from clinical studies, as well as from postmarketing surveillance, have been limited. Even though adverse events have been properly reported in some CLA studies involving two-isomer preparations (33,34), adverse events have been poorly documented in the studies using four-isomer ones (35–41). The most frequent side effects reported from the studies on two-isomer preparations are gastrointestinal disturbances such as diarrhea, constipation, and flatulence; however, these adverse events have been reported as only mildly to moderately severe (33,34,42). No difference in the frequency of adverse events was found between the CLA- and placebo-treated groups (who received olive oil in the studies mentioned above). The side effects may thus be caused either by the oil ingested or by the capsule material itself. For instance, constipation can be caused by iron oxide used as a dye agent in some capsules. Nevertheless, the withdrawal rate in these studies was very low, indicating that the majority of the subjects did not experience any discomfort when taking CLA. Importantly, no acute toxic reaction has been reported in any of the clinical trials performed to date. The safety of the CLA preparations in humans can also be evaluated based on the analysis of blood parameters such as liver transferases and other serum biochemical markers. Thus far, all data obtained with the two-isomer preparations indicate that these isomers lack any observed detrimental effect on blood lipids or liver enzymes (33,34,43). Neither Berven *et al.* (33) nor Blankson *et al.* (34) reported any clinically important changes in the

**TABLE 1**  
Product Characteristics (content expressed in %) <sup>a</sup>

Product (producer) <sup>b</sup>	Number of CLA isomers	CLA <i>c9,t11</i>	CLA <i>t10,c12</i>	CLA, <i>c,c</i>	CLA, <i>C,t,t</i>	CLA <i>c11,t13</i>	CLA <i>t8,c10</i>	Other CLA (undefined)	Total CLA (form)	Other (FA and impurities)	Technique of analysis (reference)
Tonalin-FFA (Natural)	2	38.73	41	2.42	1.58	0.2	0.24	0.2	84.37 (FFA)	15.63	GC
Tonalin-TG (Natural)	2	37.49	38.02	1.88	1.95	0.6	0.39	0.44	80.77 (TG)	19.23	GC
Tonalin (PharmaNutrients)	4	11.44	14.69	6.74	6	15.34	10.79	—	65 (FFA)	35	GC
Clarinol (Loders and Croklaan)	2	39.36	38.16	0.75	0.38	0.28	Unknown	1.55	80.48 (TG)	19.52	GC
Jahreis preparation (not commercialized)	4	8.34	7.86	4.71	17.72	7.1	5.96	2.51	54.2 (TG)	45.8	GC, Ag <sup>+</sup> HPLC
CLA-capsules (Fitness Pharma)	4	21.7 (with <i>t8,c10</i> )	19.1	4.2	3.1	8.5	21.7 (with <i>t10,c12</i> )	—	56.6 (FFA)	43.4	GC

<sup>a</sup>*c*, *cis* configuration; *t*, *trans* configuration.

<sup>b</sup>Natural, Hovdebygda, Norway; PharmaNutrients Inc., Lake Bluff, IL; Loders and Croklaan, Wormerveer, The Netherlands; Fitness Pharma, Molde, Norway.

**TABLE 2**  
**Clinical Trials with CLA<sup>a</sup>**

Studies (code number and reference)	Subjects	CLA preparation	Dose g/d (duration)	Results
# 001 Atkinson (49)	80 overweight	Two isomers	2.7 (26 wk)	<i>Slight decrease:</i> BW, BFM <i>Slight increase:</i> LBM <i>Safety:</i> One patient with edema that resolved when CLA was discontinued. CLA started again without problems for the last 3 mon.
# 002 Basu <i>et al.</i> (46) Riserus <i>et al.</i> (26)	24 overweight	Two isomers	4.2 (4 wk)	<i>Decrease:</i> Sagittal abdominal diameter <i>Stable:</i> BW and BMI <i>Increase:</i> 8-iso-PGF <sub>2α</sub> and 15-oxo-dihydro-PGF <sub>2α</sub> <i>Safety:</i> No reported AE
# 003 Basu <i>et al.</i> (48) Smedman and Vessby (42)	53 healthy	Two isomers	4.2 (12 wk)	<i>Decrease:</i> BFM <i>Stable:</i> BW, BMI, and sagittal abdominal diameter <i>Increase:</i> 8-iso-PGF <sub>2α</sub> and 15-oxo-dihydro-PGF <sub>2α</sub> <i>Safety:</i> Few gastrointestinal disturbances (diarrhea)
# 004 Basu <i>et al.</i> (47)	60 healthy	Two isomers or one isomer r10,c12	3 (4 wk after 2 wk with vitamin E or COX2 inhibitor)	<i>Increase:</i> Isomer r10,c12 increases both 8-iso-PGF <sub>2α</sub> and 15-oxo-dihydro-PGF <sub>2α</sub> <i>Decrease:</i> COX2 inhibitor reduces 15-oxo-dihydro-PGF <sub>2α</sub>
# 005 Belury (53)	Diabetics type 2	Two isomers	6 (8 wk)	<i>Stable:</i> Insulin, TG, cholesterol, HDL <i>Decrease:</i> Blood glucose, leptins, BMI, and BW
# 006 Benito <i>et al.</i> (35,36) Kelley <i>et al.</i> (54,55) Medina <i>et al.</i> (37) Zambell <i>et al.</i> (39,40)	17 healthy	Four isomers	3.9 <sup>b</sup> (9 wk)	<i>Decrease:</i> Leptins <i>Increase:</i> For skinfold corrected armgirth, body mass, and leg press <i>Stable:</i> BW, BFM, and LBM; blood coagulation and platelet function; immune status (in response to influenza virus); insulin, glucose, lactate, and appetite <i>Safety:</i> No change in plasma cholesterol LDL, HDL, and TG; no reported AE; no difference in tympanic temperature or blood parameters
# 007 Berven <i>et al.</i> (33)	60 overweight	Two isomers	3.4 (12 wk)	<i>Decrease:</i> BW and BMI <i>Safety:</i> Gastrointestinal disturbances; no change in blood parameters and vital signs
# 008 Blankson <i>et al.</i> (34)	60 overweight	Two isomers	1.7, 3.4, 5.1, or 6.8 (12 wk)	<i>Decrease:</i> BFM <i>Increase:</i> LBM <i>Stable:</i> BW and BMI <i>Safety:</i> Gastrointestinal disturbances; no change in vital signs and a decrease in total cholesterol in blood
# 009 Jahreis and Loeffelholz (41)	21 bodybuilders	Four isomers	7 <sup>c</sup> (26 wk)	<i>Increase:</i> LBM <i>Decrease:</i> BFM in both groups <i>Stable:</i> Leptins <i>Safety:</i> Increase in total cholesterol and LDL in beginners but not in advanced athletes
# 10 Kreider <i>et al.</i> (56)	24 bodybuilders	Two isomers	6 (4 wk)	<i>Stable:</i> BMI, BFM, and strength <i>Safety:</i> Not recorded; no change in creatinine levels
# 11 Lowery <i>et al.</i> (43)	24 bodybuilders	Two isomers	7.2 (6 wk)	<i>Increase:</i> For skinfold corrected armgirth, body mass, and leg press <i>Stable:</i> BFM <i>Safety:</i> No difference in tympanic temperature and blood parameters (glucose, lipids, creatinine, enzymes)
# 012 Mohede <i>et al.</i> (44)	50 healthy	Two isomers	1.7 <sup>c</sup> (12 wk)	<i>Increase:</i> Seroprotection rate (in response to hepatitis B vaccination) <i>Safety:</i> Decrease of HDL; no AE recorded

Continued

**TABLE 2**  
(Cont.) Clinical Trials with CLA

Studies (code number and reference)	Subjects	CLA preparation	Dose g/d (duration)	Results
# 013 Mougios <i>et al.</i> (45)	22 healthy	Two isomers	0.7 and 1.4 (4 wk and 4 wk)	<i>Decrease:</i> Sum of skinfolds, percentage body fat, and fat mass (second period) <i>Safety:</i> No AE related to CLA supplementation; decrease in HDL
# 014 Noone <i>et al.</i> (29)	51 healthy	Two isomers (50:50 or 80:20)	3 (8 wk)	<i>Stable:</i> BW <i>Safety:</i> Decrease in TAG with the 50:50 preparation; decrease in VLDL-cholesterol with the 80:20 preparation; no effect on HDL, LDL, insulin, or glucose
# 015 Riserus <i>et al.</i> (50)	60 overweight/ obese with metabolic syndrome	Two isomers or one isomer <i>t</i> 10, <i>c</i> 1	3.4 (12 wk)	<i>Stable:</i> BW <i>No difference between groups:</i> BFW, LBM <i>Safety:</i> Decrease of HDL; <i>t</i> 10, <i>c</i> 12, increase insulin resistance and glycemia, but not the two-isomer preparation
# 016 Thom <i>et al.</i> (38)	20 healthy exercising	Four isomers	1.8 (12 wk)	<i>Decrease:</i> BFM <i>Safety:</i> One case of gastrointestinal distress

<sup>a</sup>BW, body weight; BFM, body fat mass; LBM, lean body mass; BMI, body mass index; PC<sub>F<sub>2α</sub></sub>, prostaglandin F<sub>2α</sub>; COX2, cyclooxygenase 2; AE, adverse event(s).

<sup>b</sup>According to the authors, the right dose of CLA given per day was 3.9 g (and not 3 g as mentioned in the article) out of 6 g oil in the capsules.

<sup>c</sup>CLA given as TG.

blood levels of liver enzymes during the 12-wk treatment with CLA. This is in agreement with Lowery *et al.* (43), who also found no effect of the CLA mixture on the liver enzyme transferases in novice body builders supplemented with a two-isomer preparation (3.9 g/d) for 6 wk. In Blankson *et al.* (34), the cholesterol level (total cholesterol, LDL, and HDL) was significantly reduced in all groups treated with the two-isomer preparation. A decrease in HDL was also reported after 12 wk (44) or 8 wk (45) of supplementation with a two-isomer preparation, whereas a recent study found no significant effect of both two-isomer preparations (see Table 2) on either HDL or LDL (29). The last study, however, showed a significant decrease in plasma TAG concentrations with the 50:50 blend mixture of the two-isomer preparation and a significant reduction in the VLDL-cholesterol with the 80:20 preparation enriched with the *c*9,*t*11 isomer (29). On the other hand, a four-isomer preparation containing a high percentage of *trans,trans* isomers was found to increase blood lipids (total cholesterol and LDL) (41). Interestingly, another four-isomer preparation that contained a much lower amount of *trans,trans* isomers but a substantial amount of *c*11,*t*13 (35), an isomer that is found to accumulate in cardiac lipid fractions in pigs, had no effect on blood lipid levels in humans (36).

Intriguingly, an increased level of urinary isoprostanes was observed as a possible lipid peroxidation product *in vivo* after 3 mon of supplementation with a two-isomer preparation (46–48). However, no adverse events were reported from these studies.

(ii) *Efficacy.* One of the most widely reported effects of two-isomer preparations is its influence on body composition

(26,33,34,42,43,49,50,53). Body fat mass is decreased concomitantly with an increase in or maintenance of lean body mass (also described as the fat-free mass, which includes water, bones, and musculature). However, despite 6 mon of supplementation with one two-isomer preparation, Atkinson reported only nonsignificant changes in adult humans (49). This might be due to the low dose of CLA (2.7 g/d) given to the subjects in this trial, since the only dose–response study performed to date shows that the lowest dose required to obtain changes in body composition is 3.4 g CLA/d (34).

The effect of CLA on body composition is supported by recent studies performed *in vitro* and in animals that describe the *t*10,*c*12 isomer to be responsible for the effects on body composition and diabetes (11,25,51,52). The mechanisms by which one or both isomers would exert their effects remain to be documented. One proposed mechanism implicates the hormone leptin, whose level was noted to decrease after supplementation with two-isomer preparations in diabetic (53) and healthy subjects (37).

In addition to the effects on body composition, a two-isomer preparation has been suggested to stimulate the immune response after vaccination against the hepatitis B virus (44). The results reported with four-isomer preparations have varied. Thus far, one study performed with a four-isomer preparation has shown an effect on body composition (38). Other investigations have strongly pointed out a lack of effect on several physiological parameters (35–37,39–41,54–56). For example, the four-isomer preparations have not been found to affect blood coagulation and platelet functions (35) or to increase immune stimulation in response to the influenza virus (54,55).

None of the two- and four-isomer preparations seem to alter either the glucose level (37,42,43) or the glycosylated hemoglobin level in healthy subjects (33,34). On the contrary, the two-isomer products may modulate insulin levels (26). According to a preliminary report by Belury (53), the two-isomer products could provide health benefits if the effect of reducing fasting blood glucose levels of type 2 diabetics could be confirmed. Conversely, another report found that purified *t10,c12* alone increased the insulin resistance of obese patients with metabolic syndrome, although the combination of both *c9,t11* and *t10,c12* did not (50).

## DISCUSSION

*What CLA product should be preferred in the future?* The numerous choices of commercial CLA preparations available as food supplements may be a matter of concern, since the formulations differ greatly in the content of isomers that might jeopardize health. First, *cis,cis* and *trans,trans* isomers may increase with reaction time owing to the presence of catalysts but also to other trace elements and residual solvents (21). Their presence, and especially that of *trans,trans* isomers, therefore mirrors the impurity level of the synthetic preparations. Considering that some of these impurities might be toxic, preparations with as low *trans,trans* isomer content as possible are preferable for human use. As mentioned in the previous section, this potential risk to human health is illustrated by the increase in LDL reported with a four-isomer preparation rich in *trans,trans* isomers (41). There is a consensus that a higher HDL/LDL ratio is associated with a lower risk of cardiac disease. Thus, if LDL increases due to the presence of the *trans,trans* isomers, their removal from CLA preparations would be important. In addition, even if the presence of the isomer *c11,t13* does not influence the serum lipid composition (35,36), other potential problems with this isomer in some of these formulations should not be underestimated. An accumulation of *c11,t13* in the inner membrane of the mitochondria (30) may affect energy metabolism and thus represent a danger. Consequently, preparations with a high content of *trans,trans* isomers and of *c11,t13* would best be avoided. Interestingly, the two-isomer preparations contain on average about 1/20th as much of these isomers as do some of the four-isomer preparations.

At the same time, some studies performed with two-isomer preparations have found a significant decrease in HDL that might be undesirable (44,45,50), but other studies performed with two-isomer preparations have shown no effect on HDL (29,33,34) and a significant reduction in the potentially atherogenic VLDL-cholesterol concentrations (29).

On the other hand, markers of possible lipid peroxidation *in vivo* (isoprostanes) have been found in the urine of subjects after supplementation with one two-isomer preparation (46,48).

The mechanisms behind this peroxidation are unclear (47), and we do not know whether this lipid peroxidation may be harmful to humans. Since this test has not been conducted

using the urine of subjects taking any of the four-isomer preparations, whether a four-isomer CLA preparation would lead to the same urinary findings is unknown.

Based on the limited preliminary findings on body composition, diabetes, and immune stimulation in humans, it would seem that the CLA formulations most likely to have benefits and least likely to exert adverse effects for human would be those containing high amounts of the two presumably active isomers, *c9,t11* and *t10,c12*. The notable differences in effects between the two-isomer and four-isomer preparations could be due either to a negative effect of the extra isomers (and/or contaminants) that would counterbalance the positive effects of both *c9,t11* and *t10,c12*, or to the lower dose of both *c9,t11* and *t10,c12* in the four-isomer preparations compared to those in the two-isomer ones. As Table 1 shows, the average percentage of both active isomers in the two-isomer preparation reaches 80%, whereas their average percentage in the four-isomer preparations never exceeds 30–40%. Therefore, to reach the same effective dosage as the two-isomer preparations, the four-isomer ones should be taken in higher doses, yet doing so might subsequently increase the risk of side effects.

There are indications that the *t10,c12* CLA isomer affects body composition, whereas the *c9,t11* isomer is responsible for growth modulation (11). This knowledge might lead to production of highly purified preparations containing only one of the isomers. Nevertheless, as illustrated by the study of Riserus *et al.* (50) showing that the isomer *t10,c12* might increase the insulin resistance of diabetics, it will be necessary to test (i) whether either isomer is efficacious in producing specific biological effects in humans with an acceptable safety profile, and (ii) whether there might be any advantage or disadvantage of giving both isomers together.

Taken together, the limited human safety and efficacy data available indicate that two-isomer preparations are preferable to four-isomer preparations for human supplementation studies. However, particular caution should be given to all preparations found on the market that have not been tested clinically (some soluble preparations may not contain any CLA at all; Ref. 19), and thus should not be advised for human consumption.

Finally, long-term effects (safety and efficacy) of CLA supplementation in humans need to be documented, since only supplementation periods up to 6 mon with low daily doses or up to 3 mon with higher doses have been reported thus far. Data from studies lasting one year or more should be part of the postcommercial surveillance that should be provided by the manufacturers of every CLA preparation marketed for human use.

## ACKNOWLEDGMENT

The authors' research was supported by a grant from Natural ASA.

## REFERENCES

- Ha, Y.L., Grimm, N.K., and Pariza, M.W. (1987) Anticarcinogens from Fried Ground Beef: Heat-Altered Derivatives of Linoleic Acid, *Carcinogenesis* 8, 1881–1887.
- Ip, C., Ip, M.M., Loftus, T., Shoemaker, S., and Shea-Eaton, W.



- (2000) Induction of Apoptosis by Conjugated Linoleic Acid in Cultured Mammary Tumor Cells and Premalignant Lesions of the Rat Mammary Gland, *Cancer Epidemiol. Biomarkers Prev.* 9, 689–696.
3. Kritchevsky, D. (2000) Antimutagenic and Some Other Effects of Conjugated Linoleic Acid, *Br. J. Nutr.* 83, 459–465.
  4. Pariza, M.W., Park, Y., and Cook, M.E. (2000) Mechanisms of Action of Conjugated Linoleic Acid: Evidence and Speculation, *Proc. Soc. Exp. Biol. Med.* 223, 8–13.
  5. Lee, K.N., Kritchevsky, D., and Pariza, M.W. (1994) Conjugated Linoleic Acid and Atherosclerosis in Rabbits, *Atherosclerosis* 108, 19–25.
  6. Nicolosi, R.J., Rogers, E.J., Kritchevsky, D., Scimeca, J.A., and Huth, P.J. (1997) Dietary Conjugated Linoleic Acid Reduces Plasma Lipoproteins and Early Aortic Atherosclerosis in Hypercholesterolemic Hamsters, *Artery* 22, 266–277.
  7. Cook, M.E., Miller, C.C., Park, Y., and Pariza, M. (1993) Immune Modulation by Altered Nutrient Metabolism: Nutritional Control of Immune-Induced Growth Depression, *Poult. Sci.* 72, 1301–1305.
  8. Miller, C.C., Park, Y., Pariza, M.W., and Cook, M.E. (1994) Feeding Conjugated Linoleic Acid, *Biochem. Biophys. Res. Commun.* 198, 1107–1112.
  9. Chin, S.F., Storkson, J.M., Liu, W., Albright, K.J., and Pariza, M.W. (1994) Conjugated Linoleic Acid (9,11- and 10,12-octadecadienoic acid) Is Produced in Conventional but Not Germ-Free Rats Fed Linoleic Acid, *J. Nutr.* 124, 694–701.
  10. DeLany, J.P., Blohm, F., Truett, A.A., Scimeca, J.A., and West, D.B. (1999) Conjugated Linoleic Acid Rapidly Reduces Body Fat Content in Mice Without Affecting Energy Intake, *Am. J. Physiol.* 276, R1172–R1179.
  11. Park, Y., Storkson, J.M., Albright, K.J., Liu, W., and Pariza, M.W. (1999) Evidence That the *trans*-10,*cis*-12 Isomer of Conjugated Linoleic Acid Induces Body Composition Changes in Mice, *Lipids* 34, 235–241.
  12. West, D.B., DeLany, J.P., Camet, P.M., Blohm, F., Truett, A.A., and Scimeca, J. (1998) Effects of Conjugated Linoleic Acid on Body Fat and Energy Metabolism in the Mouse, *Am. J. Physiol.* 275, R667–R672.
  13. Szymczyk, B., Pisulewski, P.M., Szczurek, W., and Hanczakowski, P. (2001) Effects of Conjugated Linoleic Acid on Growth Performance, Feed Conversion Efficiency, and Subsequent Carcass Quality in Broiler Chickens, *Br. J. Nutr.* 85, 465–473.
  14. Gavino, V.C., Gavino, G., Leblanc, M.J., and Tuchweber, B. (2000) An Isomeric Mixture of Conjugated Linoleic Acids but Not Pure *cis*-9,*trans*-11-Octadecadienoic Acid Affects Body Weight Gain and Plasma Lipids in Hamsters, *J. Nutr.* 130, 27–29.
  15. Dugan, M.E.R., Aalhus, J.L., Schaefer, A.L., and Kramer, J.K.G. (1997) The Effects of Conjugated Linoleic Acid on Fat to Lean Repartitioning and Feed Conversion in Pigs, *Can. J. Anim. Sci.* 77, 723–725.
  16. Sehat, N., Yurawecz, M.P., Roach, J.A., Mossoba, M.M., Kramer, J.K., and Ku, Y. (1998) Silver Ion High-Performance Liquid Chromatographic Separation and Identification of Conjugated Linoleic and Isomers, *Lipids* 33, 217–221.
  17. Chin, S.F., Liu, W., Storkson, J.M., Ha, Y.L., and Pariza, M.W. (1992) Dietary Sources of Conjugated Linoleic Acid, a Newly Recognized Class of Anticarcinogens, *J. Food Comp. Anal.* 5, 185–197.
  18. McGuire, M.K., McGuire, M.A., Ritzenthaler, K., and Schultz, T.D. (1999) Dietary Sources and Intakes of Conjugated Linoleic Acid in Humans, in *Advances in Conjugated Linoleic Acid Research* (Yurawecz, M.P., Mossoba, M.M., Kramer, J.K.G., Pariza, M.W., and Nelson, G.J., eds.), Vol. 1, pp. 369–377, AOCS Press, Champaign.
  19. Yurawecz, M.P., Sehat, N., Mossoba, M.M., Roach, J.A.G., Kramer, J.K.G., and Ku, Y. (1999) Variations in Isomer Distribution in Commercially Conjugated Linoleic Acid, *Fett/Lipid* 101, 277–282.
  20. Padley, F.B., Gunstone, F.D., and Harwood, J.L. (1994) Occurrence and Characteristics of Oils and Fats, in *The Lipid Handbook* (Gunstone, F.D., Harwood, J.L., and Padley, F.B., eds.), pp. 47–224, Chapman & Hall, London.
  21. Saebo, A. (2001) Commercial Production of Conjugated Linoleic Acid (CLA), *Lipid Technol. Newsl.*, 9–13.
  22. Baumgard, L.H., Corl, B.A., Dwyer, D.A., Saebo, A., and Bauman, D.E. (2000) Identification of the Conjugated Linoleic Acid Isomer That Inhibits Milk Fat Synthesis, *Am. J. Physiol. Regul. Integr. Comp. Physiol.* 278, R179–R184.
  23. Christie, W.W., Dobson, G., and Gunstone, F.D. (1997) Isomers in Commercial Samples of Conjugated Linoleic Acid, *Lipids* 32, 1231.
  24. Sébédio, J.-L., Juaneda, P., Dobson, G., Ramilison, I., Martin, J.C., Chardigny, J.M., and Christie, W.W. (1997) Metabolites of Conjugated Isomers of Linoleic Acid (CLA) in the Rat, *Biochim. Biophys. Acta* 1345, 5–10.
  25. Pariza, M.W., Park, Y., and Cook, M.E. (2001) The Biologically Active Isomers of Conjugated Linoleic Acid, *Prog. Lipid Res.* 40, 283–298.
  26. Riserus, U., Berglund, L., and Vessby, B. (2001) Conjugated Linoleic Acid (CLA) Reduced Abdominal Adipose Tissue in Obese Middle-Aged Men with Signs of the Metabolic Syndrome: A Randomized Controlled Trial, *Int. J. Obes. Relat. Metab. Disord.* 25, 1129–1135.
  27. Banni, S., Angioni, E., Casu, V., Melis, M.P., Carta, G., Corongiu, F.P., Thompson, H., and Ip, C. (1999) Decrease in Linoleic Acid Metabolites as a Potential Mechanism in Cancer Risk Reduction by Conjugated Linoleic Acid, *Carcinogenesis* 20, 1019–1024.
  28. Ip, C., Chin, S.F., Scimeca, J.A., and Pariza, M.W. (1991) Mammary Cancer Prevention by Conjugated Dienoic Derivative of Linoleic Acid, *Cancer Res.* 51, 6118–6124.
  29. Noone, E.J., Roche, H.M., Nugent, A.P., and Gibney, M.J. (2002) The Effect of Dietary Supplementation Using Isomeric Blends of Conjugated Linoleic Acid on Lipid Metabolism in Healthy Human Subjects, *Br. J. Nutr.* 88, 243–251.
  30. Kramer, J.K.G., Sehat, N., Dugan, M.E., Mossoba, M.M., Yurawecz, M.P., Roach, J.A., Eulitz, K., Aalhus, J.L., Schaefer, A.L., and Ku, Y. (1998) Distributions of Conjugated Linoleic Acid (CLA) Isomers in Tissue Lipid Classes of Pigs Fed a Commercial CLA Mixture Determined by Gas Chromatography and Silver Ion-High-Performance Liquid Chromatography, *Lipids* 33, 549–558.
  31. Parodi, P.W. (1994) Conjugated Linoleic Acid: An Anticarcinogenic Fatty Acid Present in Milk Fat, *Aust. J. Dairy Technol.* 49, 93–97.
  32. Ip, C., Scimeca, J.A., and Thompson, H.J. (1994) Conjugated Linoleic Acid. A Powerful Anticarcinogen from Animal Fat Sources, *Cancer* 74, 1050–1054.
  33. Berven, G., Bye, A., Hals, O., Blankson, H., Fagertun, H., Thom, E., Wadstein, J., and Gudmundsen, O. (2000) Safety of Conjugated Linoleic Acid (CLA) in Overweight or Obese Human Volunteers, *Eur. J. Lipid Sci. Technol.* 102, 455–462.
  34. Blankson, H., Stakkestad, J.A., Fagertun, H., Thom, E., Wadstein, J., and Gudmundsen, O. (2000) Conjugated Linoleic Acid Reduces Body Fat Mass in Overweight and Obese Humans, *J. Nutr.* 130, 2943–2948.
  35. Benito, P., Nelson, G.J., Kelley, D.S., Bartolini, G., Schmidt, P.C., and Simon, V. (2001) The Effect of Conjugated Linoleic Acid on Platelet Function, Platelet Fatty Acid Composition, and Blood Coagulation in Humans, *Lipids* 36, 221–227.
  36. Benito, P., Nelson, G.J., Kelley, D.S., Bartolini, G., Schmidt, P.C., and Simon, V. (2001) The Effect of Conjugated Linoleic Acid on Plasma Lipoproteins and Tissue Fatty Acid Composition in Humans, *Lipids* 36, 229–236.
  37. Medina, E.A., Horn, W.F., Keim, N.L., Havel, P.J., Benito, P.,

- Kelley, D.S., Nelson, G.J., and Erickson, K.L. (2000) Conjugated Linoleic Acid Supplementation in Humans: Effects on Circulating Leptin Concentrations and Appetite, *Lipids* 35, 783–788.
38. Thom, E., Wadstein, J., and Gudmundsen, O. (2001) Conjugated Linoleic Acid Reduces Body Fat in Healthy Exercising Humans, *J. Int. Med. Res.* 29, 392–396.
  39. Zambell, K.L., Keim, N.L., Van Loan, M.D., Gale, B., Benito, P., Kelley, D.S., and Nelson, G.J. (2000) Conjugated Linoleic Acid Supplementation in Humans: Effects on Body Composition and Energy Expenditure, *Lipids* 35, 777–782.
  40. Zambell, K.L., Horn, W.F., and Keim, N.L. (2001) Conjugated Linoleic Acid Supplementation in Humans: Effects on Fatty Acid and Glycerol Kinetics, *Lipids* 36, 767–772.
  41. Jahreis, G., and Loeffelholz, C.V. (2000) Influence of CLA Supplementation on Body Composition and Strength, in *CLA: What's Going On?* (Centre d'Etude sur la Recherche et l'Innovation, ed.), Vol. 4, pp. 2–3, CERIN, Paris.
  42. Smedman, A., and Vessby, B. (2001) Conjugated Linoleic Acid Supplementation in Humans—Metabolic Effects, *Lipids* 36, 773–781.
  43. Lowery, L.M., Appicelli, P., and Lemon, P.W. R. (1998) Conjugated Linoleic Acid Enhances Muscle Size and Strength Gains in Novice Bodybuilders, *Med. Sci. Sports Exerc.* 30, 182 (abstract 1038).
  44. Mohede, I., Albers R., van der Wielen, R., Brink, L., and Dorovska-Taran, V. (2001) Immunomodulation: CLA Stimulates Antigen Specific Antibody Production in Humans, 1st International Conference on Conjugated Linoleic Acid (CLA), Ålesund, Norway, p. 12 (abstract).
  45. Mougios, V., Matsakas, A., Rings, S., Petridou, A., Sagredos, A., Melissopoulou, A., and Tsigilis, N. (2001) Effects of Supplementation with Conjugated Linoleic Acid on Human Body Fat and Serum Lipids, *J. Nutr. Biochem.* 12, 585–594.
  46. Basu, S., Riserus, U., Turpeinen, A., and Vessby, B. (2000) Conjugated Linoleic Acid Induces Lipid Peroxidation in Men with Abdominal Obesity, *Clin. Sci. (London)* 99, 511–516.
  47. Basu, S., Smedman, A., and Vessby, B. (2001) Isomer Specific Effects of Conjugated Linoleic Acid (CLA) on Lipid Peroxidation and Its Regulation by COX<sub>2</sub> Inhibitor and Vitamin E in Humans, *Free Radic. Biol. Med.* 31 (Suppl. 1), 333 (abstract).
  48. Basu, S., Smedman, A., and Vessby, B. (2000) Conjugated Linoleic Acid Induces Lipid Peroxidation in Humans, *FEBS Lett.* 468, 33–36.
  49. Atkinson, R.L. (1999) Conjugated Linoleic Acid for Altering Body Composition and Treating Obesity, in *Advances in Conjugated Linoleic Acid Research* (Yurawecz, M.P., Mossoba, M.M., Kramer, J.K.G., Pariza, M.W., and Nelson, G.J., eds.), Vol. 1, pp. 348–353, AOCS Press, Champaign.
  50. Riserus, U., Arner, P., Brismar, K., and Vessby, B. (2002) Treatment with Dietary *trans*-10,*cis*-12 Conjugated Linoleic Acid Causes Isomer-Specific Insulin Resistance in Obese Men with the Metabolic Syndrome, *Diabetes Care* 25, 1516–1521.
  51. Choi, Y., Kim, Y.C., Han, Y.B., Park, Y., Pariza, M.W., and Ntambi, J.M. (2000) The *trans*-10,*cis*-12 Isomer of Conjugated Linoleic Acid Down Regulates Stearoyl-CoA Desaturase 1 Gene Expression 3T3-L1 Adipocytes, *J. Nutr.* 130, 1920–1924.
  52. Ryder, J.W., Portocarrero, C.P., Song, X.M., Cui, L., Yu, M., Combatsiaris, T., Galuska, D., Bauman, D.E., Barbano, D.M., Charron, M.J., et al. (2001) Isomer-Specific Antidiabetic Properties of Conjugated Linoleic Acid. Improved Glucose Tolerance, Skeletal Muscle Insulin Action, and UCP-2 Gene Expression, *Diabetes* 50, 1149–1157.
  53. Belury, M.A. (2002) Dietary Conjugated Linoleic Acid in Health: Physiological Effects and Mechanisms of Action, *Annu. Rev. Nutr.* 22, 505–531.
  54. Kelley, D.S., Taylor, P.C., Rudolph, I.L., Benito, P., Nelson, G.J., Mackey, B.E., and Erickson, K.L. (2000) Dietary Conjugated Linoleic Acid Did Not Alter Immune Status in Young Healthy Women, *Lipids* 35, 1065–1071.
  55. Kelley, D.S., Simon, V.A., Taylor, P.C., Rudolph, I.L., Benito, P., Nelson, G.J., Mackey, B.E., and Erickson, K.L. (2001) Dietary Supplementation with Conjugated Linoleic Acid Increased Its Concentration in Human Peripheral Blood Mononuclear Cells, but Did Not Alter Their Function, *Lipids* 36, 669–674.
  56. Kreider, R.B., Ferreira, M.P., Greenwood, M., Wilson, M., and Almada, A.L. (2002) Effects of Conjugated Linoleic Acid Supplementation During Resistance-Training on Body Composition, Bone Density, Strength, and Selected Hematological Markers, *J. Strength Cond. Res.* 3, 325–334.

[Received August 14, 2002; in final revised form and accepted November 29, 2002]

# Purification of Lipoxygenase from *Chlorella*: Production of 9- and 13-Hydroperoxide Derivatives of Linoleic Acid

Alberto Nuñez\*, Brett J. Savary, Thomas A. Foglia, and George J. Piazza

USDA, ARS, ERRC, Wyndmoor, Pennsylvania 19038

**ABSTRACT:** Oxygenation of linoleic acid by the enzyme lipoxygenase (LOX) that is present in the microalga *Chlorella pyrenoidosa* is known to produce the corresponding 9- and 13-hydroperoxide derivatives of linoleic acid (9- and 13-HPOD, respectively). Previous work with this microalga indicated that partially purified LOX, present in the 30–45 and 45–80% saturated  $(\text{NH}_4)_2\text{SO}_4$  precipitate fractions, produced both HPOD isomers but in different ratios. It was not clear, however, if the observed activity in the two isolates represented the presence of one or more isozymes. In the present work, LOX isolated from the intracellular fraction of *Chlorella* by  $(\text{NH}_4)_2\text{SO}_4$  precipitation (35–80% saturated) was purified by ion exchange and hydrophobic interaction chromatography to apparent homogeneity. Analysis of the purified protein by SDS-PAGE and subsequent native size exclusion chromatography demonstrated that LOX in *Chlorella* is a single monomeric protein with a molecular mass of approximately 47 kDa. The purified LOX produced both the 9-HPOD and 13-HPOD isomers from linoleic acid in equal amounts, and the isomer ratio was not altered over the pH range of 6 to 9. Optimal activity of LOX was at pH 7.5.

Paper no. L9022 in *Lipids* 37, 1027–1032 (November 2002).

Lipoxygenase (LOX; EC 1.13.11.12) catalyzes the addition of molecular oxygen to PUFA to form hydroperoxide derivatives. This enzyme promotes the regio- and stereoselective dioxygenation of PUFA containing one or more 1(Z),4(Z)-pentadiene bond systems to produce (Z,E)-conjugated monohydroperoxy FA (1,2). LOX is widely distributed throughout the plant and animal kingdom and can be classified according to its specificity. In higher plants, LOX is classified according to its specificity on linoleic acid (LA) or linolenic acids. The enzyme is characterized as 9-LOX when the main product formed is 9-hydroperoxy-10(E),12(Z)-octadecadienoic acid (9-HPOD) or 13-LOX when 13-hydroperoxy-9(Z),11(E)-octadecadienoic acid isomer (13-HPOD) is the product (1,3). However, other minor amounts of positional isomers also can be formed. For example, soybean LOX, which produces 13-HPOD as the main product, also produces small amounts of

9-HPOD (1). In higher plants, additional forms of the enzyme produce a mixture of HPOD isomers (1–3).

LOX activity also is found in microorganisms such as fungi (4) and microalgae (5–7). Zimmerman and Vick reported LOX activity in the single-cell microalga *Chlorella pyrenoidosa* that produced 13-HPOD as the predominant oxidation product of LA. This activity was present in the fraction from the crude intracellular extract that precipitated from 0–42% saturated  $(\text{NH}_4)_2\text{SO}_4$ . This LOX was reported to have a maximum activity at pH 7.5 (5) and an apparent M.W. of 182 kDa (8). Bisakowski and Kermasha later reported that *C. pyrenoidosa* also contained a LOX activity in the fraction precipitated from 40–80%  $(\text{NH}_4)_2\text{SO}_4$  (7). They reported that this LOX showed optimal activity at pH 4.5. Nondenaturing gel electrophoresis of this LOX-containing fraction indicated a M.W. range between 67 and 140 kDa, but product specificity was not reported. Subsequent work reported the 9-, 10-, and 13-HPOD isomers were formed from LA using a LOX fraction precipitated from 40–80%  $(\text{NH}_4)_2\text{SO}_4$  at pH 7.0 (9). These studies, however, did not establish whether the reported LOX activities were the result of one or more isozymes.

Recently we reported that in addition to its peroxidation activity, LOX present in *C. pyrenoidosa* also cleaved 13-HPOD to a  $\text{C}_5$  fragment and a  $\text{C}_{13}$  oxo-FA under anaerobic conditions (10). The LOX fraction precipitated from 40–80%  $(\text{NH}_4)_2\text{SO}_4$  was further purified by size exclusion chromatography (SEC) and hydrophobic interaction chromatography (HIC). LOX peroxidation and the anaerobic cleavage activity eluted coincidentally with these chromatographic purification techniques, as similarly reported for soybean LOX (11,12), but the LOX peroxidation products were not characterized (10).

In a following study, we reported an HPLC method with EI-MS detection (LC/EI-MS) that allowed the analysis of the methylated HPOD products formed by LOX. This method does not require derivatization of the hydroperoxy group as required by GC with mass detection (GC-MS) (13). Using the LC/EI-MS method, we analyzed the products formed by LOX present in the *C. pyrenoidosa*-derived fraction precipitated from 30–45 and 45–80%  $(\text{NH}_4)_2\text{SO}_4$ . The 30–45%  $(\text{NH}_4)_2\text{SO}_4$  fraction gave an HPOD product distribution that was dominated by the 13-HPOD isomer, consistent with the results reported by Zimmerman and Vick (5). The 45–80% fraction, however, contained primarily the 9-HPOD isomer, and the 10-HPOD isomer (10-hydroperoxy-8(E),12(Z)-octadecadienoic acid) reported by Bisakowski *et al.* (9) was

\*To whom correspondence should be addressed at USDA, ARS, ERRC, Fats, Oils and Animal Coproducts Unit, 600 East Mermaid Lane, Wyndmoor, PA 19038. E-mail: anunez@arserrc.gov

Abbreviations: HIC, hydrophobic interaction chromatography; 9-HPOD, 9-hydroperoxy-10(E),12(Z)-octadecadienoic acid; 10-HPOD, 10-hydroperoxy-8(E),12(Z)-octadecadienoic acid; 12-HPOD, 12-hydroperoxy-9(Z),13(E)-octadecadienoic acid; 13-HPOD, 13-hydroperoxy-9(Z),11(E)-octadecadienoic acid; IEC, ion exchange chromatography; LA, linoleic acid; LOX, lipoxygenase; MWCO, molecular weight cutoff; SEC, size exclusion chromatography.



not found. These results suggested the presence of two LOX isozymes.

In this study, the LOX activity present in the microalga *Chlorella* was purified to apparent electrophoretic homogeneity. The HPOD products formed from LA using this purified LOX were analyzed by LC/EI-MS to clarify previous reports that suggested the presence of LOX isozymes.

## MATERIALS AND METHODS

**Materials.** LA was purchased from Sigma Chemical (St. Louis, MO). All other reagents used were of the highest purity available. Products were methylated with diazomethane before LC/EI-MS analysis (13).

**Algae growth and protein extraction.** *Chlorella pyrenoidosa* from American Type Culture Collection (no. 11469; Manassas, VA) or its equivalent, *C. fusca*, from the Cultural Collection at UTEX (no. 251; Austin, TX) was grown, harvested, and processed for protein extraction as described previously (14). Soluble proteins from the crude extract were partially purified by  $(\text{NH}_4)_2\text{SO}_4$  precipitation at 0°C. The 0–35% fraction, containing most of the chlorophyll pigments and negligible LOX activity, was discarded and the 35–80% fraction used for further purification. Procedures for these steps as well as protein concentration assay were reported (13).

**Chromatographic protein purification.** Proteins present in the fraction precipitated from 35–80% saturated  $(\text{NH}_4)_2\text{SO}_4$  were dissolved in 5 mL of Tris buffer (10 mM, pH 8.0) and dialyzed with a 14,000 M.W. cutoff (MWCO) Spectra/Por membrane (Spectrum Laboratories, Rancho Dominguez, CA) against 4 L of buffer. Chromatography was performed on a BioCAD 700E system with Poros perfusion media (PerSeptive Biosystem, Inc., Framingham, MA). LOX activity was first separated on a Poros-HQ20 anion-exchange chromatography column (10 mm diameter  $\times$  100 mm length, column volume 7.9 mL) using Tris buffer (10 mM, pH 8.0) at 5 column vol/min with a linear gradient of 30 column vol (about 240 mL) to a final concentration 0.20 M NaCl, in the same buffer. Fractions of 0.5 column vol (ca. 4.0 mL) were collected and assayed for LOX activity. The active fractions were pooled and concentrated with a Centricon-10 membrane filter (Amicon, Beverly, MA); then  $(\text{NH}_4)_2\text{SO}_4$  was added to a final 2.0 M. The sample was then loaded onto a Poros-PE20 hydrophobic interaction chromatography column (100  $\times$  4.6 mm, column vol. 1.7 mL). The column was equilibrated with 2.0 M ammonium sulfate in Tris buffer, then developed with a linear gradient of 25 column vol (42 mL) to 0.0 M ammonium sulfate (100% 10 mM Tris buffer, pH 8.0) at a flow rate of ca. 5 mL/min. Fractions of 0.5 column vol were collected and assayed for LOX activity. The active fractions were pooled and concentrated for electrophoretic analysis and incubated with LA to determine product specificity.

Native determination of LOX M.W. involved treating the  $(\text{NH}_4)_2\text{SO}_4$ -treated *Chlorella* extract by dialysis using Spectrum CE DispoDialyzer (Spectrum Laboratories) 50,000

MWCO dialysis tubes with Tris buffer (10 mM, pH 8.0). The dialyzed fraction was passed (five times) through a DE Septra-Sorb 10-mL cartridge (Sepragen Corporation, Hayward, CA) that had previously been equilibrated with Tris buffer (10 mM, pH 8.0) containing NaCl (0.1 M). The unbound proteins containing the LOX activity (final volume of 10 mL) were concentrated and further resolved by SEC with a High Prep 26/60 Sephacryl S-200 column (Pharmacia Biototech Inc., Alameda, CA). Fractions of 5.6 mL were collected and assayed for LOX activity. The active fractions were combined, concentrated, and incubated with LA for product analysis by LC/EI-MS. Final M.W. estimation of the LOX activity eluted from the Sephacryl S-200 column was performed with a Bio-Silect SEC 125-5 column (Bio-Rad, Hercules, CA). The column was run with potassium phosphate (200 mM, pH 8.0) at 1 mL/min using a Waters Separation Module 2690 (Waters Co., Milford, MA); fractions were collected and assayed for LOX activity. The Sephacryl-S200 and the Bio-Silect SEC columns were calibrated using the following M.W. standards: glucose-oxidase (120,000), BSA (67,000), chymotrypsinogen A (25,000), and ribonuclease A (13,700).

**Electrophoresis.** Proteins were resolved by SDS-PAGE using a 12% gel in a Mini-Protein electrophoresis cell following the manufacturer's instructions (Bio-Rad). Samples were reduced using 25 mM DTT. Molecular sizes were calculated with Bio-Rad broad range M.W. marker proteins (200,000, 116,000, 97,400, 66,200, 45,000, 31,000, 21,500, 14,400, and 6,500). About 5 to 15  $\mu\text{g}$  total protein was loaded per lane, and gels were stained with Coomassie brilliant-blue R-250.

**LOX activity assay and product characterization.** Enzymatic activity was assayed by adding 5–20  $\mu\text{L}$  of the enzyme concentrate to a solution of 900  $\mu\text{L}$  LA (1 mM) in potassium phosphate (100 mM, pH 8.0) and Tween 20 (1%) to final volume of 1 mL and by monitoring the initial rate of increase in absorbance at 234 nm.

For product characterization, active LOX fractions were incubated with 50 mL of the LA solution under oxygen, and the progress of the reaction was followed spectrophotometrically at 234 nm. At the end of the reaction the products were extracted with ether, methylated, and analyzed by LC/EI-MS. LC was performed with a Waters HPLC 2690 Separation Module connected in series to a Waters 996 Photodiode Array Detector and a Waters Thermabeam Mass Detector (Integrity System). The LC portion used a Valco LiChrosorb Diol 5  $\mu\text{m}$  column (2  $\times$  250 mm) (Varian/Chrompack, Raritan, NJ) using the method reported previously (13).

## RESULTS AND DISCUSSION

**Purification of LOX activity.** Previously we reported that the fractions obtained from the protein extract of *C. pyrenoidosa* and precipitated from 45 and 80% saturated  $(\text{NH}_4)_2\text{SO}_4$  had LOX activity that produced the 9- and 13-HPOD isomers, but in different ratios (13). These results suggested the presence of two LOX isozymes, which was consistent with other reports on LOX activity in the microalga (5,9). In this study the



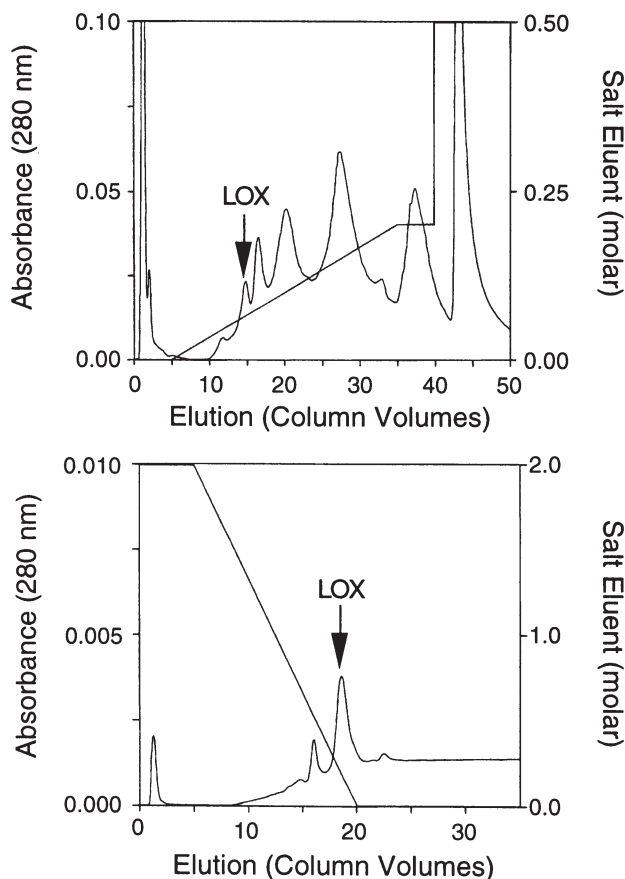
microalga *C. fusca* was used as an alternative source of *C. pyrenoidosa*, since it was found before that these two strains have the same enzymatic activity associated with LOX (10,14,15). Product characterization of LOX for both strains in the 30–45 and 45–80% fractions showed similar product distributions (see below). In addition, the *C. fusca* is offered as equivalent to *C. pyrenoidosa* by UTEX.

To determine the presence of one or more isozymes in

*Chlorella*, LOX activity expressed in the fraction precipitated from 35–80%  $(\text{NH}_4)_2\text{SO}_4$  was sequentially purified by ion exchange chromatography (IEC) and HIC. Figure 1A shows the separation of the dialyzed  $(\text{NH}_4)_2\text{SO}_4$  fraction using a Poros-HQ20 anion exchange column with protein detection at 280 nm. LOX activity eluted under the well-defined peak noted in Figure 1A, indicating the weak binding of this protein to this column in relation to the other proteins present in the 35–80% fraction. Since in a previous report the LOX activity precipitated at different percentages of  $(\text{NH}_4)_2\text{SO}_4$  seemed to determine the ratio of the HPOD isomers formed (10), the active fractions from this anion exchange column were concentrated and treated with 2 M  $(\text{NH}_4)_2\text{SO}_4$  and further resolved using HIC with a Poros-PE20 column. Figure 1B shows the HIC chromatogram with detection at 280 nm, where a single LOX activity eluted under the later peak as indicated. Table 1 summarizes the purification steps, indicating a 1.2-fold increase in the specific activity after  $(\text{NH}_4)_2\text{SO}_4$  precipitation and a 270-fold increase after IEC. Despite the removal of other proteins by HIC, however, specific activity decreased about 50% (Table 1). This significant total activity loss was associated with the concentration step of the IEC fraction after ultrafiltration at 10,000 MWCO. The reason for this loss in LOX activity is not clear and needs to be further studied. On the other hand, the elution of the LOX activity from the Poros-PE20 column was consistent with our early report of LOX activity in *C. pyrenoidosa*, in which the peroxidation and anaerobic cleavage activity eluted under the same conditions (10).

Figure 2A shows the SDS-PAGE of the purified LOX fractions after the two-mode adsorption chromatography sequence. The electrophoretic pattern indicated two major proteins in an approximate 1:1 ratio, each with an estimated M.W. of 34 and 47 kDa, respectively, but did not provide direct information on the native size of the LOX activity.

**Size exclusion purification.** SEC was used to determine the native size of LOX. The 35–80%  $(\text{NH}_4)_2\text{SO}_4$  fraction was dialyzed against a 50,000 MWCO membrane and then passed through a DEAE ion-exchange cartridge using conditions where the protein having LOX activity did not bind to the ion-exchange support (see the Materials and Methods section). The protein with LOX activity was purified further by SEC on a Sephacryl 200 column. The SEC protein fractions eluting from the column were assayed for LOX activity. The results are plotted in Figure 3A, which shows that the enzymatic



**FIG. 1.** Sequential adsorption chromatography purification of *Chlorella* fraction precipitated from 35–80%  $(\text{NH}_4)_2\text{SO}_4$ . Position of lipoxigenase (LOX) activity peaks is indicated by arrows. (A) Primary separation on Poros-HQ anion-exchange column (PerSeptive Biosystems, Inc., Framingham, MA). (B) Subsequent separation by hydrophobic interaction on Poros-HP2 column. One column-volume fractions were collected and assayed for LOX activities.

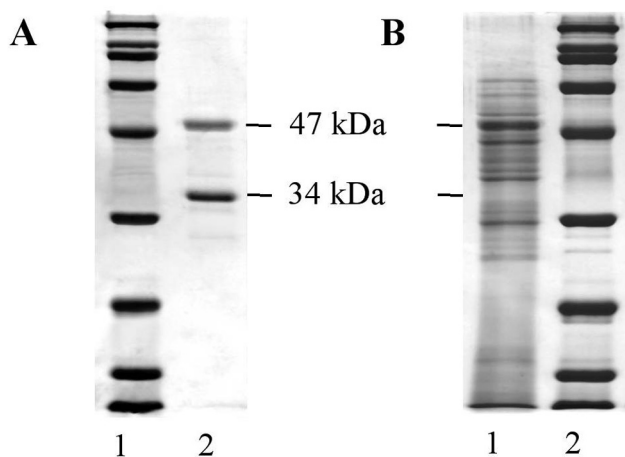
**TABLE 1**  
Purification of Lipoxigenase from *Chlorella* by Absorption Chromatography<sup>a</sup>

Stage	Total protein (mg)	Total activity ( $\mu\text{mol}/\text{min}$ )	Specific activity ( $\mu\text{mol min}^{-1} \text{mg}^{-1}$ )	Yield (%)	Purific. (fold)
Crude extract	60.1	96.3	1.6	100	1
$(\text{NH}_4)_2\text{SO}_4$	50.7	91.2	1.8	94.7	1.2
Dialysis (14 K) <sup>b</sup>	47.1	82.6	1.7	85.8	1.1
IEC	0.095	38.6	405	40.1	270
HIC	0.025	4.9	196	5.1	131

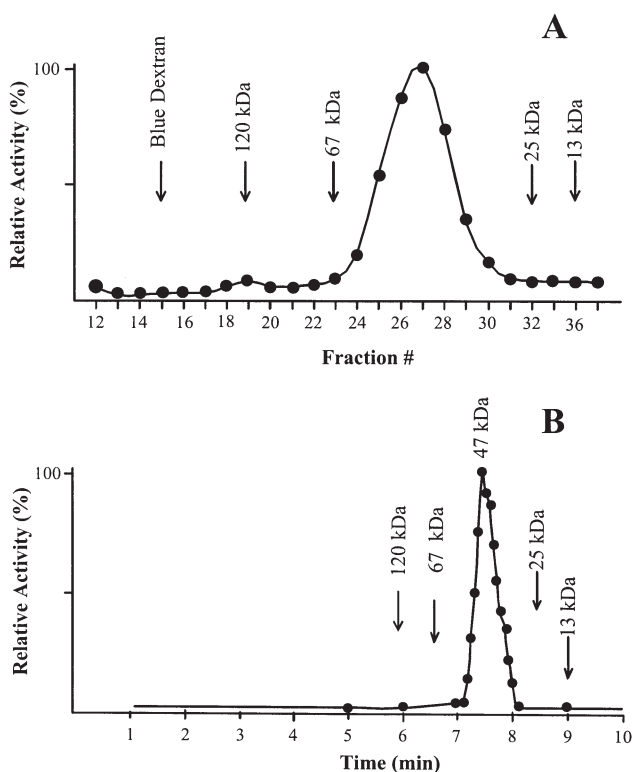
<sup>a</sup>Abbreviations: Purific., purification; IEC, ion exchange chromatography; HIC, hydrophobic interaction chromatography.

<sup>b</sup>Cutoff of 14,000 M.W.

LOX activity peaks between the 67 and 25 kDa M.W. markers. Fractions 24–30 containing the LOX activity were pooled and concentrated. SDS-PAGE analysis of the later fractions indicated the absence of the 34 kDa protein (Fig. 2A) and the



**FIG. 2.** SDS-PAGE analysis of *Chlorella* LOX. (A) LOX purified by sequential adsorption chromatography (lane 2) with M.W. markers (lane 1). (B) LOX extract resolved using size-exclusion chromatography on Sephacryl 200 (Bio-Rad, Hercules, CA) column (lane 1) with M.W. markers (lane 2). For abbreviation see Figure 1.



**FIG. 3.** LOX activity profile by native size exclusion chromatography (SEC) with molecular markers (↓). (A) Elution profile on Sephacryl S-200 column; (B) LOX activity profile (fractions 24–30, Panel A) on a Bio-Silect SEC 125-5 column (see the Materials and Methods section). For abbreviation and manufacturer, see Figures 1 and 2, respectively.

presence of an intense band at 47 kDa, as shown in Figure 2B. The active pooled fractions from the Sephacryl column were resolved using a high-resolution Bio-Silect SEC 125-5 column. Fractions from this column were collected and assayed for LOX activity, and the results are shown in Figure 3B, thus confirming that LOX activity corresponded to a protein with a M.W. of approximately 47 kDa. These results show that LOX activity in *Chlorella* is due to a monomeric enzyme of 47 kDa size, and that the smaller 34 kDa protein (Fig. 2A), which is isolated in the adsorption chromatography steps, does not have LOX activity. The native size determined for LOX, however, is not consistent with the previously reported M.W. of 182 and 120 kDa in *C. pyrenoidosa* (8,10). We have in fact observed a minor LOX activity in the  $(\text{NH}_4)_2\text{SO}_4$  fraction eluted from the Sephacryl 200 column at the previously reported size of 120 kDa, Figure 3A (10), but its activity was lost in the subsequent purification process. Analysis of the products formed by the 120 kDa LOX from the Sephacryl column were not different from the products formed by the 47 kDa LOX, suggesting the possible aggregation of LOX protein in the early purification steps.

Although most LOX enzymes reported in higher plants, animals, and fungi are in the size range of 80–120 kDa, smaller proteins with LOX activity also have been reported. In potato tubers two LOX isozymes of 35 and 85 kDa size have been reported by Reddanna *et al.* (16). The alga *Ulva lactuca* also was reported to have two LOX isozymes with the major activity corresponding to a LOX protein of 41 kDa size and a minor protein with LOX activity of 116 kDa size (17). This later report is quite consistent with the size determined for the LOX isolated from *Chlorella* in this work.

Anaerobic cleavage of the 13-HPOD by the LOX enzyme also was associated with the purified 47 kDa enzyme, as determined by GC-MS analysis of the headspace volatiles, in accordance with our previous finding of anaerobic activity associated with LOX in *Chlorella* (10).

**Characterization of purified LOX products.** Recently we reported an LC/EI-MS method that allowed for separation and identification of the methyl esters of HPOD isomers from LA (13). Characteristic ion fragments for the HPOD isomers allowed the positional assignment of the hydroperoxide group in the HPOD isomers. In general, EI-MS of HPOD isomers does not yield a molecular ion but produces characteristic ions at  $m/z$  310 [M – oxygen], 308 [M – H<sub>2</sub>O], and 293 [M – O<sub>2</sub>H]. An ion fragment at  $m/z$  185 was observed exclusively for the 9-HPOD isomer, while 13-HPOD has a characteristic ion at  $m/z$  99. Also, the 10-HPOD and 12-HPOD [12-hydroperoxy-9(Z),13(E)-octadecadienoic acid] isomers can be identified from fragment ions that are distinctive for these HPOD isomers. EI-MS analysis does not distinguish between the Z,E and E,E conjugated forms of the isomers; UV, however, provides evidence for these geometrical isomers since the Z,E and the E,E isomers have maximal absorptions at 233 and 228 nm, respectively (18).

The purified and concentrated active LOX fractions obtained by sequential adsorption chromatography were incu-

bated with LA under oxygen, and the reaction products were analyzed by LC/EI-MS after extraction and methylation. Figure 4A, the 232 nm UV chromatogram for these products, shows three peaks, which is consistent with three products having conjugated double bonds. The total ion current chromatogram (TIC) in Figure 4B shows the corresponding number of peaks. The EI spectra of the peaks gave characteristic ions for HPOD at  $m/z$  310, 308, and 293. The peaks eluting at approximately 46 and 49 min (labeled I and II in Fig. 4B) were identified as the 9(*Z*),11(*E*)- and 9(*E*),11(*E*)-13-HPOD isomers from the characteristic ion at  $m/z$  99 and UV absorptions at 232 and 228 nm, respectively (13). The peak eluting at approximately 51 min (labeled III in Fig. 4B) had an ion at  $m/z$  185 and UV absorption at 232 nm, characteristic of the 10(*E*),12(*Z*)-9-HPOD isomer. The small companion peak at 54 min (labeled IV in Fig. 4B) was identified as the 10(*E*),12(*E*)-9-HPOD. The product ratio for the 9- and 13-HPOD isomers was 49 and 51%, respectively. This product ratio also was obtained with the 35–80%  $(\text{NH}_4)_2\text{SO}_4$  fractions (see below), indicating that the LOX activity recovered after absorption chromatography retained its initial activity.

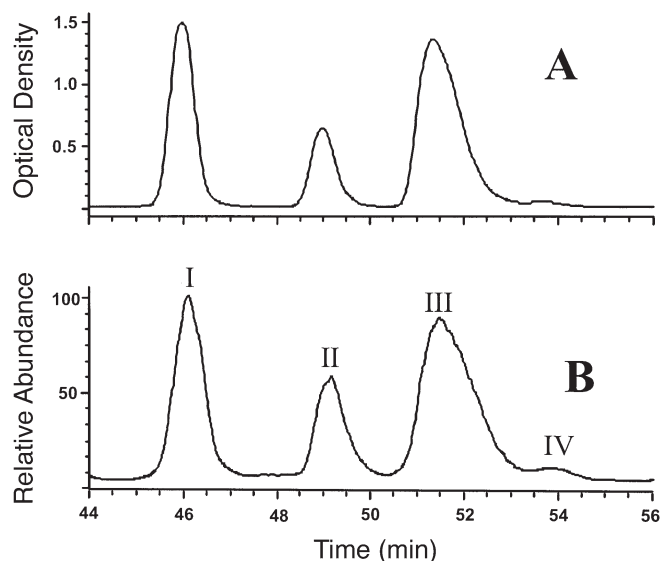
Most LOX enzymes catalyze the formation of one particular regiospecific isomer with a stereospecific configuration *S* (1,2). The stereospecificity of the *Chlorella* products has not been reported, but the product distribution found in this study is similar to the product ratio produced from LA by LOX present in the blue-green microalga *Oscillatoria* sp. (6), where the LOX products from the microalga were concluded to be 13-(*S*)-HPOD and 9-(*S*)-HPOD in a ratio of 52:48.

**pH effect on product formation.** The ratio between the 9- and 13-HPOD isomers can be affected by reaction pH. For

example, soybean LOX produces 13-HPOD almost exclusively at pH values above 8.5, whereas the 9-HPOD isomer is 25% of the total HPOD product at pH 6 (19). This pH dependency on product distribution is thought to be related to the orientation of the LA substrate at the active site. At the lowest pH, the protonated carboxylic acid group of LA can orient head-to-tail or tail-to-head at the active site, whereas at the higher pH the carboxylate anion can only be oriented one way (1,19). Since LOX from *Chlorella* produces both the 9- and 13-HPOD isomers, a pH dependency could be associated with HPOD product distribution. To investigate this aspect, the products isolated from the oxidation of LA by LOX present in the 35–80%  $(\text{NH}_4)_2\text{SO}_4$  fraction of *Chlorella* extracts at pH 6, 7, 8, and 9 were characterized by LC/EI-MS. This analysis showed that the ratio between the 9- and 13-HPOD isomers is not significantly altered, remaining in a ratio close to 50:50, indicating that pH did not alter the product ratio.

In further pH studies, activity of the purified fractions from *Chlorella* showed that the LOX activity producing the 9- and 13-HPOD isomers is maximal at pH 7.5, which is consistent with the pH for optimal activity reported by Zimmerman and Vick (5).

In this study, we purified the LOX activity in *Chlorella* producing the 9- and 13-HPOD isomers. The LOX activity was derived from a monomeric enzyme with a molecular weight of 47 kDa, as determined by SDS-PAGE after sequential adsorption chromatography and native size determination by SEC. The product distribution ratio was not dependent on pH, and the 9- and 13-HPOD isomers were formed in an equal ratio by this LOX, which has optimal activity at pH 7.5.



**FIG. 4.** LC/EI-MS analysis with a Diol column of the hydroperoxy-octadecadienoic acid products obtained by incubation of the chromatographically purified LOX activity with linoleic acid under oxygen. (A) UV chromatogram at 234 nm; (B) MS total ion chromatogram. Peak number, HPOD isomer: I, 9(*Z*),11(*E*)-13-HPOD; II, 9(*E*),11(*E*)-13-HPOD; III, 10(*E*),12(*Z*)-9-HPOD; and IV, 10(*E*),12(*E*)-9-HPOD.

## REFERENCES

- Gardner, H.W. (1991) Recent Investigation into the Lipoygenase Pathway of Plants, *Biochim. Biophys. Acta* 1084, 221–239.
- Blee, E. (1998) Phytooxypilins and Plant Defense Reaction, *Prog. Lipid Res.* 37, 33–72
- Feussner, I., and Wasternack, C. (1998) Lipoygenase-Catalyzed Oxidation of Lipids, *Fett/Lipid* 100, 146–152.
- Perraud, X., and Kermasha, S. (2000) Characterization of Lipoygenase Extracts from *Penicillium* sp., *J. Am. Oil. Chem. Soc.* 77, 335–342.
- Zimmerman, D.C., and Vick, B.A. (1973) Lipoygenase in *Chlorella pyrenoidosa*, *Lipids* 8, 264–266.
- Beneytout, J.-L., Andrianarison, R.-V., Rakotoarisoa, Z., and Tixier, M. (1989) Properties of a Lipoygenase in Green Algae (*Oscillatoria* sp.), *Plant Physiol.* 89, 367–372.
- Bisakowski, B., and Kermasha, S. (1995) Partial Purification and Characterization of Lipoygenase in *Chlorella pyrenoidosa*, *Biotechnol. Appl. Biochem.* 21, 39–48.
- Vick, B.A., and Zimmerman, D.C. (1989) Metabolism of Fatty Acid Hydroperoxides by *Chlorella pyrenoidosa*, *Plant Physiol.* 90, 125–132.
- Bisakowski, B., Perraud, X., and Kermasha, S. (1997) Characterization of Hydroperoxides and Carbonyl Compounds by Lipoygenase Extracts of Selected Microorganisms, *Biosci. Biotechnol. Biochem.* 61, 1262–1269.
- Núñez, A., Savary, B.J., Foglia, T.A., and Piazza, G.J. (2000) Anaerobic Lipoygenase Activity from *Chlorella pyrenoidosa* Responsible for the Cleavage of the 13-Hydroperoxides of

- Linoleic and Linolenic Acids, *Eur. J. Lipid Sci. Technol.* *102*, 181–188.
11. Salch, Y.P., Grove, M.J., Takamura, H., and Gardner, H.W. (1995) Characterization of a C-5,13-Cleaving Enzyme of 13(S)-Hydroperoxide of Linoleic Acid by Soybean Seed, *Plant Physiol.* *108*, 1211–1218.
  12. Garssen, G.J., Vliegthart, J.F.G., and Boldingh, J. (1971) An Anaerobic Reaction Between Lipoxygenase, Linoleic Acid and Its Hydroperoxides, *Biochem. J.* *122*, 327–332.
  13. Nuñez, A., Foglia, T.A., and Piazza, G.J. (2001) Characterization of Lipoxygenase Oxidation Products by High-Performance Liquid Chromatography with Electron Impact–Mass Spectrometric Detection, *Lipids* *36*, 851–856.
  14. Nuñez, A., Foglia, T.A., and Piazza, G.J. (1995) Improved Method for Extraction of Hydroperoxide Lyase from *Chlorella*, *Biotech. Tech.* *9*, 613–616.
  15. Nuñez, A., St. Armand, G., Foglia, T.A., and Piazza, G.J. (1997) Immobilization of Hydroperoxide Lyase from *Chlorella*, *Biotechnol. Appl. Biochem.* *25*, 75–80.
  16. Reddanna, P., Maddipati, K.R., and Channa Reddy, C. (1990) Purification of Arachidonate 5-Lipoxygenase from Potato Tubers, in *Methods in Enzymology* (Murphy, R.C., and Fitzpatrick, F.A., eds.), Vol. 187, pp. 268–276, Academic Press, New York.
  17. Kuo, J.-M., Hwang, A., and Yeh, D.-B. (1997) Purification, Substrate Specificity, and Products of a Ca<sup>2+</sup>-Stimulating Lipoxygenase from Sea Algae (*Ulva lactuca*), *J. Agric. Food Chem.* *45*, 2055–2060.
  18. Gallina Toschi, T., Stante, F., and Lercker, G. (1995) Study on Position and Geometric Configuration of Methyl Linoleate Hydroperoxides Isomers Obtained by Thermo-Oxidation: Chromatographic Analyses of Their Corresponding Hydroxy Derivatives, *J. High Resolut. Chromatogr.* *18*, 764–766.
  19. Gardner, H.W. (1989) Soybean Lipoxygenase-1 Enzymatically Forms Both (9S)- and (13S)-Hydroperoxides from Linoleic Acid by a pH-Dependent Mechanism, *Biochim. Biophys. Acta* *1001*, 274–281.

[Received March 13, 2002, and in revised form November 20, 2002; accepted November 26, 2002]



# Total Synthesis of 2-Methoxy-14-methylpentadecanoic Acid and the Novel 2-Methoxy-14-methylhexadecanoic Acid Identified in the Sponge *Agelas dispar*

Néstor M. Carballeira\*, Heidyleen Cruz, and Norma L. Ayala

Department of Chemistry, University of Puerto Rico, San Juan, Puerto Rico 00931-3346

**ABSTRACT:** The phospholipid FA composition of the Caribbean sponge *Agelas dispar* was revisited and 40 different FA were identified. Among these a novel 2-methoxylated FA, namely, the anteiso methyl-branched 2-methoxy-14-methylhexadecanoic acid, was identified together with the recently discovered iso methyl-branched 2-methoxy-14-methylpentadecanoic acid and the normal-chain 2-methoxytetradecanoic acid. The structures of the iso and anteiso methyl-branched 2-methoxylated FA were confirmed by total syntheses, which were accomplished in seven steps and in 45–48% overall yields. Other phospholipid FA identified in *A. dispar* include the unusual methyl-branched 10,13-dimethyltetradecanoic acid, 3,7,11,15-tetramethylhexadecanoic (phytanic) acid, and the 11-methyloctadecanoic acid. In addition, the  $\Delta^{5,9}$  FA (5Z,9Z)-15-methyl-5,9-hexadecadienoic acid and (5Z,9Z)-5,9-octadecadienoic acid were characterized. These findings establish alternative FA biosynthetic possibilities for these marine organisms.

Paper no. L9120 in *Lipids* 37, 1033–1037 (November 2002).

The only known 2-methoxylated FA to date have arisen from the phospholipids of sponges despite the fact that 1-*O*-(2-methoxyalkyl)glycerols have been known for some time since their initial discovery by Hallgren *et al.* in shark liver oil (1,2). These 2-methoxylated FA are of interest because the shortest member of the series, namely, the 2-methoxytetradecanoic acid, is cytotoxic against the T-cell human acute lymphocytic leukemia (CEM-SS) cell line with an average 50% toxic concentration (TC<sub>50</sub>) value of 66  $\mu$ M and against human chronic myelogenous leukemia K-562 (ATCC CCL-243) with a 50% inhibitory concentration (IC<sub>50</sub>) of 670  $\mu$ M (Carballeira, N.M., unpublished results). Therefore, the search for other types of methoxylated FA, with better antileukemic activity, is warranted. Among these 2-methoxylated FA, a series of C<sub>15</sub>–C<sub>16</sub> iso and anteiso FA were recently discovered in the phospholipids of the marine sponge *Amphimedon complanata*, most likely arising from microorganisms coexisting with the sponge (3). These unprecedented FA were characterized by GC retention times and characteristic

mass spectral fragmentations (3). However, there is a high probability that other sponges contain additional iso and anteiso 2-methoxylated FA in their phospholipids. With this hypothesis we re-examined the phospholipid FA composition of the demosponge *Agelas dispar* (family Agelasidae) and discovered a series of iso and anteiso 2-methoxylated FA including 2-methoxy-14-methylpentadecanoic acid (**1**) and the unprecedented 2-methoxy-14-methylhexadecanoic acid (**2**). In addition, we have synthesized **1** and **2** for the first time, which permitted the confirmation of the iso and anteiso methyl branching in these natural FA.

The chemical composition of *A. dispar* has been partially explored before. For example, *A. dispar* possesses an unusual phospholipid FA composition inasmuch as preliminary studies with this demosponge revealed considerable amounts of methyl-branched FA, in particular phytanic acid (3,7,11,15-tetramethylhexadecanoic acid) (4). In addition, *A. dispar* biosynthesizes a series of brominated alkaloids with diverse biological activities such as inhibitors of serotonergic receptors, noncompetitive antihistaminic agents and antifungal compounds (5,6). Moreover, immunostimulating  $\alpha$ -glycosphingolipids also have been isolated from *A. dispar* (7).

## MATERIALS AND METHODS

**Sponge collection.** *Agelas dispar* Duchassaing and Michelotti, 1860 (class Demospongiae, order Agelasida, family Agelasidae) was collected from Mona Island, Puerto Rico, during August 1992, at 20 m depth by scuba. The sponge was freeze-dried and stored at  $-20^{\circ}\text{C}$  until extraction. A voucher specimen is stored at the Chemistry Department of the University of Puerto Rico, Río Piedras campus.

**Instrumentation.** FAME were analyzed by direct ionization using a GC–MS (Hewlett-Packard 5972A MS ChemStation) at 70 eV equipped with a 30 m  $\times$  0.25 mm special performance capillary column (HP-5MS) of polymethylsiloxane cross-linked with 5% phenyl methylpolysiloxane. The temperature program was as follows: 130 $^{\circ}\text{C}$  for 1 min, then increased at a rate of 3 $^{\circ}\text{C}/\text{min}$  to 270 $^{\circ}\text{C}$  and maintained for 30 min at 270 $^{\circ}\text{C}$ . <sup>1</sup>H NMR and <sup>13</sup>C NMR were recorded on either a Bruker DPX-300 or a Bruker DRX-500 spectrometer. <sup>1</sup>H NMR chemical shifts are reported with respect to internal (CH<sub>3</sub>)<sub>4</sub>Si, and <sup>13</sup>C NMR chemical shifts are reported in parts per million relative to CDCl<sub>3</sub> (77.0 ppm).

\*To whom correspondence should be addressed at the Department of Chemistry, University of Puerto Rico, P.O. Box 23346, San Juan, Puerto Rico 00931-3346. E-mail: ncarballeira@upr.acd.upr.edu.

Abbreviations: DME, dimethoxyethane; DMDS, dimethyl disulfide; phytanic acid, 3,7,11,15-tetramethylhexadecanoic acid.

**Extraction and isolation of phospholipids.** The sponge (25 g) was carefully cleaned and cut into small pieces. Immediate extraction after collection with  $3 \times 300$  mL of  $\text{CHCl}_3/\text{MeOH}$  (1:1) yielded the total lipids (2 g). The neutral lipids (0.06 g), glycolipids (0.5 g), and phospholipids (0.6 g) were separated by column chromatography on silica gel (60–200 mesh) from the 1.5 g of total lipids that were used in the procedure of Privett *et al.* (8).

**Derivatives.** The fatty acyl components of the phospholipids were obtained as their methyl esters (0.06 g) by reaction of the phospholipids (0.50 g) with methanolic HCl followed by column chromatography. They were stored at  $-20^\circ\text{C}$  in hexane with 2,6-di-*tert*-butyl-4-methylphenol (BHT) as antioxidant and under nitrogen until analyzed in 1992. The double-bond positions in these compounds were determined by dimethyldisulfide (DMDS) derivatization following a previously described procedure (9). *N*-Acylpyrrolidide derivatives were prepared by direct treatment of the methyl esters with pyrrolidine/HOAc (10:1) in a capped vial (24 h at  $100^\circ\text{C}$ ). The methyl esters were hydrogenated in 10 mL absolute methanol in the presence of catalytic amounts of platinum oxide ( $\text{PtO}_2$ ).

**Lithium aluminum hydride reductions.** To a stirred solution of lithium aluminum hydride in dry diethyl ether (5 mL) at  $0^\circ\text{C}$  was added a solution of either 0.024 g (0.09 mmol) of the anteiso methyl ester or 0.021 g (0.09 mmol) of the iso acid dissolved in diethyl ether (5 mL). The resulting gray mixture was stirred for 2 h and then carefully quenched with a saturated aqueous ammonium chloride solution (8 mL). Diethyl ether (10 mL) was then added, and the organic layer was separated and dried over  $\text{Na}_2\text{SO}_4$ , filtered, and concentrated *in vacuo*, affording either the anteiso or iso alcohols, 0.018–0.019 g (0.08 mmol) in 99% GC yields with spectral data identical to that reported in the literature (10,11).

**Pyridinium chlorochromate oxidations.** To a stirred solution of 0.19 g (0.87 mmol) pyridinium chlorochromate in 15 mL of  $\text{CH}_2\text{Cl}_2$  was added dropwise either the anteiso or iso alcohols, 0.02–0.13 g (0.08–0.58 mmol) in 1 mL of  $\text{CH}_2\text{Cl}_2$  at room temperature. After 24 h the reaction mixture was filtered through Florisil and washed with diethyl ether (20 mL). Evaporation of the solvent afforded either the anteiso or iso aldehydes, 0.02–0.13 g (0.08–0.58 mmol) for a 99% GC yield with spectral data identical to that reported in the literature (12–14).

**Trimethylsilyl cyanide additions.** To either the iso or anteiso aldehydes, 0.04–0.13 g (0.20–0.58 mmol), in 10 mL of anhydrous  $\text{CH}_2\text{Cl}_2$ , were added dropwise 0.02–0.06 g (0.20–0.58 mmol) trimethylsilyl cyanide and catalytic amounts of  $\text{Et}_3\text{N}$  (10%) at  $0^\circ\text{C}$ . The reaction mixture was stirred for 2 h at  $0^\circ\text{C}$ . Then the solvent was removed *in vacuo*, affording 0.06–0.18 g (0.19–0.54 mmol) of either the anteiso or iso adducts for a 93% isolated yield. Spectral data for the trimethylsilyloxynitriles are presented below.

(i) *2-Trimethylsilyloxy-14-methylpentadecanonitrile.*  $^1\text{H}$  NMR ( $\text{CDCl}_3$ , 500.1 MHz)  $\delta$  4.38 (1H, *t*,  $J = 6.5$  Hz, H-2), 1.77 (2H, *m*, H-3), 1.52 (1H, *m*, H-14), 1.44 (2H, *m*, H-4), 1.29–1.25 (16H, *brs*,  $\text{CH}_2$ ), 1.14 (2H, *m*,  $\text{CH}_2$ ), 0.85 [6H, *d*,  $J = 6.6$  Hz,  $\text{CH}(\text{CH}_3)_2$ ], 0.20 [9H, *s*,  $\text{Si}(\text{CH}_3)_3$ ];  $^{13}\text{C}$  NMR

( $\text{CDCl}_3$ , 125.8 MHz)  $\delta$  120.1 (*s*, C-1), 61.5 (*d*, C-2), 39.0 (*t*, C-13), 36.2 (*t*, C-3), 29.9 (*t*), 29.7 (*t*), 29.60 (*t*), 29.56 (*t*), 29.4 (*t*), 29.3 (*t*), 28.9 (*t*), 27.9 (*d*), 27.4 (*t*), 24.5 (*t*), 22.6 [*q*,  $\text{CH}(\text{CH}_3)_2$ ],  $-0.4$  [*q*,  $\text{Si}(\text{CH}_3)_3$ ]; GC–MS *m/z* (relative intensity)  $\text{M}^+$  325 (2), 311 (24), 310 (100), 298 (26), 284 (13), 283 (56), 255 (3), 241 (2), 227 (3), 225 (3), 208 (7), 199 (4), 185 (11), 171 (23), 157 (5), 143 (12), 140 (9), 130 (6), 129 (49), 123 (5), 115 (13), 114 (14), 109 (11), 101 (19), 97 (20), 96 (13), 91 (28), 84 (21), 83 (25), 82 (20), 75 (75), 73 (74), 69 (31), 59 (10), 57 (28), 55 (35).

(ii) *2-Trimethylsilyloxy-14-methylhexadecanonitrile.*  $^1\text{H}$  NMR ( $\text{CDCl}_3$ , 500.1 MHz)  $\delta$  4.38 (1H, *t*,  $J = 6.6$  Hz, H-2), 1.68 (2H, *m*, H-3), 1.65 (1H, *m*, H-14), 1.34–1.26 (22H, *brs*,  $\text{CH}_2$ ), 0.85 (3H, *t*,  $J = 7.1$  Hz,  $-\text{CH}_2\text{CH}_3$ ), 0.83 (3H, *d*,  $J = 6.3$  Hz,  $-\text{CHCH}_3$ ), 0.20 [9H, *s*,  $\text{Si}(\text{CH}_3)_3$ ];  $^{13}\text{C}$  NMR ( $\text{CDCl}_3$ , 125.8 MHz)  $\delta$  120.1 (*s*, C-1), 61.5 (*d*, C-2), 38.7 (*t*), 36.6 (*t*), 34.4 (*d*), 30.0 (*t*), 29.7 (*t*), 29.6 (*t*), 29.5 (*t*), 29.46 (*t*), 29.43 (*t*), 29.3 (*t*), 28.9 (*t*), 27.1 (*t*), 24.5 (*t*), 19.2 (*q*, C-17), 10.9 (*q*, C-16),  $-0.4$  [*q*,  $\text{Si}(\text{CH}_3)_3$ ]; GC–MS *m/z* (relative intensity)  $\text{M}^+$  339 (2), 325 (27), 324 (100), 312 (36), 298 (15), 297 (56), 283 (12), 269 (3), 255 (2), 241 (3), 222 (9), 213 (3), 199 (4), 185 (11), 171 (21), 157 (5), 155 (3), 143 (10), 140 (10), 129 (50), 123 (7), 115 (14), 114 (13), 101 (19), 100 (12), 97 (22), 95 (24), 91 (35), 84 (24), 83 (26), 82 (22), 75 (74), 73 (81), 57 (60), 55 (44).

**Hydrolysis of the trimethylsilyloxy nitriles.** Into a 15-mL round-bottomed flask were placed the trimethylsilyloxy nitriles (0.06–0.18 g, 0.19–0.54 mmol) in 4 mL of dimethoxyethane (DME). Concentrated HCl (4 mL) was added, and the reaction mixture was heated at  $90^\circ\text{C}$  for 24 h. The reaction mixture was then cooled (ice bath) and made alkaline by the slow addition of 50% NaOH (5 mL). The reaction mixture was heated again for 2 h at  $90^\circ\text{C}$ . The mixture was then acidified with 5 mL of 6 M HCl, and the product was extracted with ether ( $2 \times 8$  mL). The organic layer was dried over  $\text{Na}_2\text{SO}_4$ , filtered, and evaporated *in vacuo*, affording 0.03–0.12 g (0.13–0.44 mmol) of either the anteiso or iso 2-hydroxy FA (68–70% isolated yields) with spectral data identical to those previously reported (15–17).

**Methylation of the 2-hydroxy FA.** Into a 15-mL round-bottomed flask provided with a magnetic stirrer and under a nitrogen atmosphere was placed 0.03–0.10 g (0.10–0.37 mmol) of the 2-hydroxy FA in 3 mL of DMSO. Two equivalents of NaH were dissolved in 2 mL of DMSO and added dropwise, after which the reaction mixture was stirred at room temperature for 10 min. An excess of  $\text{CH}_3\text{I}$  (0.18–0.74 mmol) was then added dropwise, and the reaction mixture was further stirred for 20 min, after which it was diluted with hexane/ether (1:1) and washed with  $\text{H}_2\text{O}$  ( $2 \times 8$  mL) to remove the remaining DMSO. The organic phase was dried over  $\text{MgSO}_4$ , filtered, and evaporated *in vacuo* affording 0.02–0.08 g (0.07–0.28 mmol) of the 2-methoxylated methyl esters (73–76% isolated yields). Spectral data not previously reported in the literature are presented below.

(i) *Methyl 2-methoxy-14-methylpentadecanoate.*  $^1\text{H}$  NMR ( $\text{CDCl}_3$ , 500.1 MHz)  $\delta$  3.75 (3H, *s*,  $-\text{CO}_2\text{CH}_3$ ), 3.75 (1H, X

part of ABX system, H-2), 3.37 (3H, *s*, -OCH<sub>3</sub>), 1.69 (2H, *m*, H-3), 1.50 (1H, *m*, H-14), 1.36 (2H, *m*, H-4), 1.24 (16H, *brs*, CH<sub>2</sub>), 1.13 (2H, *m*, CH<sub>2</sub>), 0.85 [6H, *d*, *J* = 6.6 Hz, CH(CH<sub>3</sub>)<sub>2</sub>]; <sup>13</sup>C NMR (CDCl<sub>3</sub>, 125.8 MHz) δ 173.3 (*s*, C-1), 80.7 (*d*, C-2), 58.1 (*q*, -OCH<sub>3</sub>), 51.7 (*q*, -CO<sub>2</sub>CH<sub>3</sub>), 39.0 (*t*, C-13), 32.8 (*t*, C-3), 29.9 (*t*), 29.7 (*t*), 29.63 (*t*), 29.60 (*t*), 29.5 (*t*), 29.4 (*t*), 29.3 (*t*), 27.9 (*d*, C-14), 27.4 (*t*), 25.1 (*t*, C-4), 22.6 [*q*, CH(CH<sub>3</sub>)<sub>2</sub>].

(ii) *Methyl 2-methoxy-14-methylhexadecanoate*. <sup>1</sup>H NMR (CDCl<sub>3</sub>, 500.1 MHz) δ 3.76 (3H, *s*, -CO<sub>2</sub>CH<sub>3</sub>), 3.76 (1H, X part of ABX system, H-2), 3.38 (3H, *s*, -OCH<sub>3</sub>), 1.70 (2H, *m*, H-3), 1.65 (1H, *m*, H-14), 1.33–1.25 (22H, *brs*, CH<sub>2</sub>), 0.85 (3H, *t*, *J* = 7.2 Hz, -CH<sub>2</sub>CH<sub>3</sub>), 0.83 (3H, *d*, *J* = 6.3 Hz, -CHCH<sub>3</sub>); <sup>13</sup>C NMR (CDCl<sub>3</sub>, 125.8 MHz) δ 173.4 (*s*, C-1), 80.7 (*d*, C-2), 58.1 (*q*, -OCH<sub>3</sub>), 51.8 (*q*, -CO<sub>2</sub>CH<sub>3</sub>), 39.0 (*t*, C-13), 38.8 (*t*), 36.7 (*t*), 34.4 (*d*, C-14), 32.8 (*t*, C-3), 30.0 (*t*), 29.71 (*t*), 29.69 (*t*), 29.6 (*t*), 29.5 (*t*), 29.4 (*t*), 27.1 (*t*), 25.1 (*t*, C-4), 19.2 (*q*, C-17), 11.4 (*q*, C-16); GC-MS *m/z* (relative intensity) M<sup>+</sup> 314 (3), 255 (100), 225 (1), 222 (1), 153 (1), 139 (2), 125 (8), 111 (25), 109 (8), 104 (8), 97 (52), 95 (17), 87 (6), 85 (20), 83 (56), 81 (18), 75 (5), 71 (64), 69 (45), 67 (18), 58 (13), 57 (57), 55 (45).

## RESULTS AND DISCUSSION

As previously reported (4), TLC showed that the main phospholipids from *A. dispar* were PE, PS, and PC. Transesterification with 1.0 M HCl/MeOH permitted the characterization of the FA as methyl esters using GC-MS. A total of 40 phospholipid FA were identified in *A. dispar*. DMDS derivatives were used to locate the double bonds in the monounsaturated methyl esters, whereas pyrrolidides were used mainly to locate methyl branching. The total phospholipid FA composition of *A. dispar* is presented in Table 1. Methyl-branched FA between C<sub>14</sub> and C<sub>20</sub> predominated in these phospholipids (59%), and in particular phytanic acid was the most abundant in this family (12.1%), but 10-methylhexadecanoic acid (9.8%) and 11-methyloctadecanoic acid (6.2%) were also abundant. The common origin of branched FA is bacterial, but phytanic acids derive from the phytol portion of chlorophyll (4). Branched-chain iso and anteiso FA accounted for 28% of the total composition, but most of these FA had chain lengths between C<sub>14</sub> and C<sub>17</sub>, which are typical chain lengths of iso and anteiso bacterial FA. The most abundant normal-chain saturated FA was palmitic acid (12.1%).

Our primary focus was the three 2-methoxylated FA that constituted 1.5% of the total phospholipid FA composition of *A. dispar*. We recently reported the presence of two of these FA, 2-methoxytetradecanoic acid and 2-methoxy-14-methylpentadecanoic acid, in two Caribbean sponges (3,18). Characterization of the remaining saturated 2-methoxylated acid (as the methyl ester) was possible using GC-MS and GC ECL values as compared to synthetic standards. For example, the mass spectrum of the novel methyl ester **2** displayed a molecular ion peak at *m/z* 314 and a strong [M<sup>+</sup>-59] peak at *m/z* 255 (100%), together with a small peak at *m/z* 104 (McLafferty

**TABLE 1**  
Identified Phospholipid FA from *Agelas dispar*

FA	Relative abundance <sup>a</sup> (wt%)
12-Methyltridecanoic (i-14:0)	0.4
Tetradecanoic (14:0)	5.4
Methyltetradecanoic (br-15:0)	0.2
13-Methyltetradecanoic (i-15:0)	6.7
12-Methyltetradecanoic (ai-15:0)	4.4
Pentadecanoic (15:0)	2.3
10,13-Dimethyltetradecanoic (16:0)	0.6
2-Methoxytetradecanoic (2-OMe-14:0)	0.5
Methylpentadecanoic (br-16:0)	0.7
14-Methylpentadecanoic (i-16:0)	2.3
(Z)-7-Hexadecenoic (16:1n-9)	0.6
(Z)-9-Hexadecenoic (16:1n-7)	2.5
(E)-9-Hexadecenoic (16:1n-7)	0.2
Hexadecanoic (16:0)	12.1
(E)-9-Methyl-10-hexadecenoic (17:1n-6)	0.7
(5Z,9Z)-15-Methyl-5,9-hexadecadienoic (i-17:2n-7)	0.3
15-Methyl-9-hexadecenoic (i-17:1n-7)	6.0
10-Methylhexadecanoic (br-17:0)	9.8
15-Methylhexadecanoic (i-17:0)	4.6
14-Methylhexadecanoic (ai-17:0)	3.3
2-Methoxy-14-methylpentadecanoic (2-OMe-i-16:0)	0.9
Heptadecanoic (17:0)	1.9
Methylheptadecanoic (br-18:0)	0.9
(5Z,9Z)-5,9-Octadecadienoic (18:2n-9)	0.2
3,7,11,15-Tetramethylhexadecanoic (br-20:0)	12.1
9-Octadecenoic (18:1n-9)	3.0
11-Octadecenoic (18:1n-7)	0.3
2-Methoxy-14-methylhexadecanoic (2-OMe-ai-17:0) <sup>b</sup>	0.1
Octadecanoic (18:0)	4.6
(E)-11-Methyl-12-octadecenoic (19:1n-6)	0.2
11-Methyloctadecanoic (br-19:0)	6.2
(Z)-12-Nonadecenoic (19:1)	3.8
5,8,11,14-Eicosatetraenoic (20:4n-6)	0.7
Eicosanoic (20:0)	0.1
Heneicosanoic (21:0)	0.4
4,7,10,13,16,19-Docosahexaenoic (22:6n-3)	0.1
7,10,13,16-Docosatetraenoic (22:4n-6)	0.4
(5Z,9Z)-5,9-Pentacosadienoic (25:2n-16)	0.2
(5Z,9Z)-5,9-Hexacosadienoic (26:2n-17)	0.3

<sup>a</sup>Relative abundance with respect to phospholipid FA.

<sup>b</sup>This FA is unprecedented in nature.

rearrangement) typical of an  $\alpha$ -methoxylated saturated methyl ester (3,18).

Despite the fact that the 2-methoxy functionality was established in these compounds by MS, the relative GC retention times of two of the 2-methoxylated methyl esters from *A. dispar* could only be explained by iso and anteiso methyl branching. For example, the methoxylated ester **1** presented an ECL value of 16.85, whereas the ester **2** had an ECL value of 17.93. Normal-chain  $\alpha$ -methoxylated FA normally have fractional chain length values of 0.17 (19). For example, the normal-chain methyl 2-methoxytetradecanoate, also identified in *A. dispar*, presented an ECL value of 15.18. These unusual ECL values of 16.85 and 17.93 could only be accommodated if **1** is an iso methyl-branched methyl ester and **2** an anteiso methyl ester (4). Therefore, we decided that it was important to confirm these structural assignments rigorously by



total synthesis since the first structures of this type were mainly confirmed by relative GC retention times. Therefore, we developed a practical synthesis for the  $\alpha$ -methoxylated methyl esters **1** and **2**.

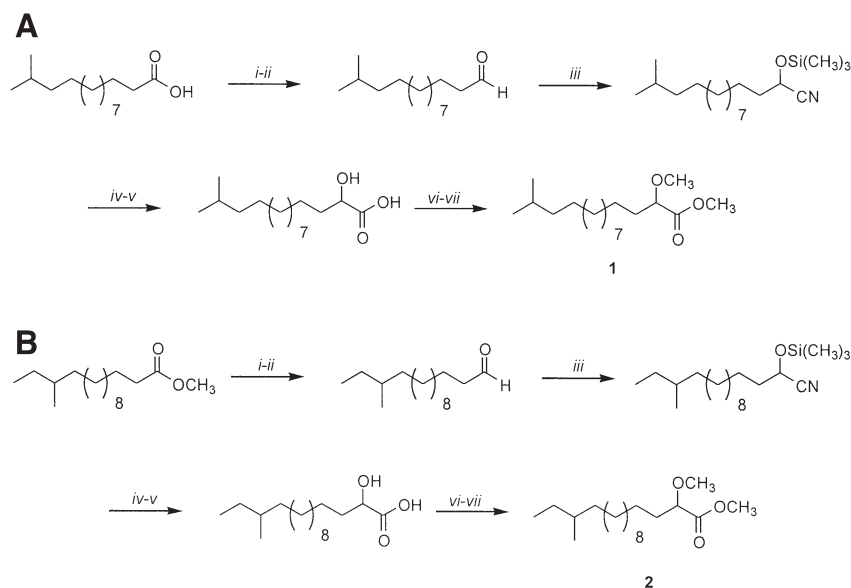
The synthesis of **1** started with commercially available (Sigma) 13-methyltetradecanoic acid, which was converted to 13-methyltetradecanal by first reducing the acid to 13-methyltetradecanol with lithium aluminum hydride in ether and then oxidizing the alcohol to the aldehyde with pyridinium chlorochromate in  $\text{CH}_2\text{Cl}_2$  in very high yield reactions (Fig. 1). The aldehyde was then reacted with trimethylsilyl cyanide and triethylamine affording the 14-methyl-2-trimethylsilyloxypentadecanonitrile in a 93% yield. The silyloxynitrile was then transformed into the known 2-hydroxy-14-methylpentadecanoic acid by first reacting the nitrile with concentrated HCl in DME followed by saponification with 50% NaOH. Final conversion into methyl 2-methoxy-14-methylpentadecanoate (**1**) was achieved by methyl esterification with 1 M HCl/MeOH and subsequent methylation of the hydroxy group with methyl iodide and sodium hydride in DMSO. The overall yield for this synthesis was 45%. The methoxylated iso ester **1** co-eluted in capillary GC with the naturally occurring methyl 2-methoxy-14-methylpentadecanoate from *A. dispar*, thus confirming the structural assignment of the iso methoxylated ester.

The synthesis of methyl 2-methoxy-14-methylhexadecanoate (**2**) was also achieved following the same synthetic scheme as described above but starting with commercially available methyl 13-methylpentadecanoate (Fig 1). The overall yield in this case was 48%. The methoxylated anteiso ester

**2** also co-eluted in capillary GC with the naturally occurring methyl 2-methoxy-14-methylhexadecanoate (**2**) from *A. dispar*, which further confirmed the structural assignment of the anteiso methoxylated ester **2**.

The noteworthy finding in this *Agelas* is that it biosynthesizes three different kinds of 2-methoxylated FA, namely, normal-chain, iso and anteiso FA. The present work is only the second report of branched  $\alpha$ -methoxylated phospholipid FA from any natural source, the first being our previous report from the sponge *Amphimedon complanata* (3). The structural similarity of these branched methoxylated FA with the known iso and anteiso 2-hydroxylated  $\text{C}_{16}$ – $\text{C}_{17}$  FA implies that these compounds could have originated, although not necessarily, from the branched 2-hydroxylated FA. For example, 2-hydroxy-14-methylpentadecanoic acid was identified in *Arthrobacter simplex* (20), and 2-hydroxy-14-methylhexadecanoic acid was found in species of the genera *Thermus* and *Meiothermus*, identified in Antarctic lake sediments, and isolated from the Actinomycetales (15–17).

The structural similarity between the iso and anteiso 2-methoxylated phospholipid FA reported here and the analogous 2-hydroxylated phospholipid FA points in the direction of a common bacterial origin for these compounds, since the 2-hydroxylated iso and anteiso  $\text{C}_{16}$ – $\text{C}_{17}$  FA are indeed bacterial (21). For example, some myxobacteria contain PE as the major phospholipid with 2-hydroxy iso-17:0 FA at the 2-position and nonhydroxy FA at the 1-position (21). Therefore, it is most likely that in *A. dispar* a novel symbiotic marine bacterium could actually contain novel PE with iso and anteiso methyl-branched 2-methoxylated FA at the 2-position (21).



**FIG. 1.** Synthesis of methoxylated ester of (A) 2-methoxy-14-methylpentadecanoic acid (**1**) and (B) 2-methoxy-14-methylhexadecanoic acid (**2**). (i)  $\text{LiAlH}_4$ -ether,  $0^\circ\text{C}$ ; (ii) PCC (1.5 eq)  $\text{CH}_2\text{Cl}_2$ ; (iii) TMS-CN,  $\text{Et}_3\text{N}$ ,  $\text{CH}_2\text{Cl}_2$ ,  $0^\circ\text{C}$ ; (iv) HCl (conc.), DME 24 h; (v) 50% NaOH, heat, 3 h; (vi) 1 N HCl-MeOH; (vii) NaH/DMSO,  $\text{CH}_3\text{I}$ . PCC, pyridinium chlorochromate; TMS-CN, trimethylsilyl cyanide; DME, dimethoxyethane.



## ACKNOWLEDGMENTS

This work was supported by a grant from the SCORE program of the National Institutes of Health (grant no. S06GM08102). Heidylen Cruz thanks the UPR-Río Piedras NIH-RISE program and Compañía de Fomento Industrial (PR) for financial assistance. Norma Ayala thanks the Howard Hughes program at UPR-Río Piedras for an undergraduate fellowship.

## REFERENCES

1. Carballeira, N.M. (2002) New Advances in the Chemistry of Methoxylated Lipids, *Prog. Lipid Res.* 41, 437–456.
2. Hallgren, B., and Stållberg, G. (1967) Methoxy-Substituted Glycerol Ethers Isolated from Greenland Shark Liver Oil, *Acta Chem. Scand.* 21, 1519–1529.
3. Carballeira, N.M., and Alicea, J. (2001) The First Naturally Occurring  $\alpha$ -Methoxylated Branched-Chain Fatty Acids from the Phospholipids of *Amphimedon complanata*, *Lipids* 36, 83–87.
4. Carballeira, N.M., Maldonado, L., and Porras, B. (1987) Isoprenoid Fatty Acids from Marine Sponges. Are Sponges Selective? *Lipids* 22, 767–769.
5. Cafieri, F., Fattorusso, E., and Tagliatalata-Scafati, O. (1998) Novel Bromopyrrole Alkaloids from the Sponge *Agelas dispar*, *J. Nat. Prod.* 61, 122–125.
6. Cafieri, F., Fattorusso, E., and Tagliatalata-Scafati, O. (1998) Novel Betaines from the Marine Sponge *Agelas dispar*, *J. Nat. Prod.* 61, 1171–1173.
7. Costantino, V., Fattorusso, E., Mangoni, A., Di Rosa, M., Ianaro, A., and Maffia, P. (1996) Glycolipids from Sponges. IV. Immunomodulating Glycosyl Ceramides from the Marine Sponge *Agelas dispar*, *Tetrahedron* 52, 1573–1578.
8. Privett, O.S., Dougherty, K.A., Erdahl, W.L., and Stolyhwo, A. (1973) Lipid Composition of Developing Soybeans, *J. Am. Oil Chem. Soc.* 50, 516–520.
9. Dunkelblum, E., Tan, S.H., and Silk, R.J. (1985) Double-Bond Location in Monounsaturated Fatty Acids by Dimethyl Disulphide Derivatization and Mass Spectrometry, *J. Chem. Ecol.* 11, 265–277.
10. Chance, D.L., Gerhardt, K.O., and Mawhinney, T.P. (1997) Gas-Liquid Chromatography–Mass Spectrometry of Primary and Secondary Fatty Alcohols and Diols as Their *tert*-Butyldimethylsilyl Derivatives, *J. Chromatogr. A* 771, 191–201.
11. Takagi, T., Itabashi, Y., and Aso, S. (1985) Fatty Acids and Fatty Alcohols of Wax Esters in the Orange Roughy: Specific Textures of Minor Polyunsaturated and Branched-Chain Components, *Lipids* 20, 675–679.
12. Shioiri, T., and Irako, N. (2000) An Efficient Synthesis of Sulfofobacin A (Flavocristamide B), Sulfofobacin B, and Flavocristamide A, *Tetrahedron* 56, 9129–9142.
13. Stein, J., and Budzikiewicz, H. (1987) Bacterial Components. XXXIII. 1-*O*-(13-Methyl-1-*Z*-tetradecenyl)-2-*O*-(13-methyl-tetradecanoyl)-glycero-3-phosphoethanolamine, a Plasmalogen from *Myxococcus stipitatus*, *Z. Naturforsch. B: Chem. Sci.* 42, 1017–1020.
14. Kishine, H., and Hayashi, A. (1997) Sphingolipids of *Euhadra hickonis*. III. Ceramides of the Viscera, *Nihon Yukagakkaishi* 46, 153–164.
15. Nobre, M.F., Carreto, L., Wait, R., Tenreiro, S., Fernandes, O., Sharp, R.J., and Da Costa, M.S. (1996) Fatty Acid Composition of the Species of the Genera *Thermus* and *Meiothermus*, *Syst. Appl. Microbiol.* 19, 303–311.
16. Matsumoto, G.I., Watanuki, K., and Torii, T. (1988) Hydroxy Acids in Antarctic Lake Sediments and Their Geochemical Significance, *Org. Geochem.* 13, 785–790.
17. Yano, I., Furukawa, Y., and Kusunose, M. (1969) Occurrence of  $\alpha$ -Hydroxy Fatty Acids in Actinomycetales, *FEBS Lett.* 4, 96–98.
18. Carballeira, N.M., and Pagán, M. (2001) New Methoxylated Fatty Acids from the Caribbean Sponge *Callyspongia fallax*, *J. Nat. Prod.* 64, 620–623.
19. Ayanoglu, E., Popov, S., Kornprobst, J.M., Aboud-Bichara, A., and Djerassi, C. (1983) Phospholipid Studies of Marine Organisms: V. New  $\alpha$ -Methoxy Acids from *Higginsia tethyoides*, *Lipids* 18, 830–836.
20. Yano, I., Furukawa, Y., and Kusunose, M. (1970) 2-Hydroxy Fatty Acid-Containing Phospholipid of *Arthrobacter simplex*, *Biochim. Biophys. Acta* 210, 105–115.
21. Yamanaka, S., Fudo, R., Kawaguchi, A., and Komagata, K. (1988) Taxonomic Significance of Hydroxy Fatty Acids in Myxobacteria with Special Reference to 2-Hydroxy Fatty Acids in Phospholipids, *J. Gen. Appl. Microbiol.* 34, 57–66.

[Received July 15, 2002, and in revised form November 29, 2002; revision accepted December 1, 2002]

# *In vitro* Desaturation and Elongation of Rumenic Acid by Rat Liver Microsomes

O. Berdeaux<sup>a,\*</sup>, S. Gnädig<sup>a</sup>, J.M. Chardigny<sup>a</sup>, O. Loreau<sup>b</sup>, J.P. Noël<sup>b</sup>, and J.-L. Sébédio<sup>a</sup>

<sup>a</sup>Institut National de la Recherche Agronomique, Unité de Nutrition Lipidique, 21065 Dijon, France, and <sup>b</sup>Commissariat à l'Énergie Atomique Saclay, Service des Molécules Marquées, 91191 Gif sur Yvette, France

**ABSTRACT:** Various nutritional studies on CLA, a mixture of isomers of linoleic acid, have reported the occurrence of conjugated long-chain PUFA after feeding experimental animals with rumenic acid, 9*c*,11*t*-18:2, the major CLA isomer, probably as a result of successive desaturation and chain elongation. In the present work, *in vitro* studies were carried out to obtain information on the conversion of rumenic acid. Experiments were first focused on the *in vitro* Δ6-desaturation of rumenic acid, the regulatory step in the biosynthesis of long-chain n-6 PUFA. The conversion of rumenic acid was compared to that of linoleic acid (9*c*,12*c*-18:2). Isolated rat liver microsomes were incubated with radiolabeled 9*c*,12*c*-18:2 and 9*c*,11*t*-18:2 under desaturation conditions. The data indicated that [1-<sup>14</sup>C]9*c*,11*t*-18:2 was a poorer substrate for Δ6-desaturase than [1-<sup>14</sup>C]-9*c*,12*c*-18:2. Next, *in vitro* elongation of 6*c*,9*c*,11*t*-18:3 and 6*c*,9*c*,12*c*-18:3 (γ-linolenic acid) was investigated in rat liver microsomes. Under elongation conditions, [1-<sup>14</sup>C]6*c*,9*c*,11*t*-18:3 was 1.5-fold better converted into [3-<sup>14</sup>C]8*c*,11*c*,13*t*-20:3 than [1-<sup>14</sup>C]6*c*,9*c*,12*c*-18:3 into [3-<sup>14</sup>C]8*c*,11*c*,14*c*-20:3. Finally, *in vitro* Δ5-desaturation of 8*c*,11*c*,13*t*-20:3 compared to 8*c*,11*c*,14*c*-20:3 was investigated. The conversion level of [1-<sup>14</sup>C]8*c*,11*c*,13*t*-20:3 into [1-<sup>14</sup>C]5*c*,8*c*,11*c*,13*t*-20:4 was 10 times lower than that of [1-<sup>14</sup>C]8*c*,11*c*,14*c*-20:3 into [1-<sup>14</sup>C]-5*c*,8*c*,11*c*,14*c*-20:4 at low substrate concentrations and 4 times lower at the saturating substrate level, suggesting that conjugated 20:3 is a poor substrate for the Δ5-desaturase.

Paper no. L8665 in *Lipids* 37, 1039–1045 (November 2002).

CLA refers to a mixture of positional and geometrical isomers of linoleic acid having two conjugated double bonds. Rumenic acid (9*c*,11*t*-18:2) is the most abundant of the CLA isomers in milk, dairy products, and meat from ruminants. It is formed as a stable intermediate in the biohydrogenation sequence of linoleic acid by anaerobic bacteria in the rumen (1,2) and also by Δ9-desaturation of vaccenic acid in the mammary gland. In addition, CLA isomers, including rumenic acid, are produced by free radical-induced isomerization of linoleic acid (4) or during commercial hydrogenation of vegetable oils (5).

\*To whom correspondence should be addressed at INRA, Unité de Nutrition Lipidique, BP 86510, 17 rue Sully, 21065 Dijon Cedex, France. E-mail: berdeaux@dijon.inra.fr

Abbreviations and acid names: Arachidonic acid, 5*c*,8*c*,11*c*,14*c*-20:4n-6; behenic acid, 23:0; dihomo-γ-linolenic acid, 8*c*,11*c*,14*c*-20:3; lignoceric acid, 24:0; linoleic acid, 9*c*,12*c*-18:2; γ-linolenic acid, 6*c*,9*c*,12*c*-18:3; rumenic acid, 9*c*,11*t*-18:2.

Research on CLA and its metabolism has been carried out in many animal experiments *in vivo* and *in vitro*. Feeding studies on animals often used synthetic mixtures of CLA, in which 9*c*,11*t*- and 10*t*,12*c*-18:2 accounted for about 90–95% of the total CLA. It has been suggested that CLA may have beneficial effects, such as anticarcinogenic and antiatherogenic effects (6–8). Moreover, it was suggested that CLA might influence body composition, as it reduced the fat-to-lean body mass ratio in various animal experiments (9,10). The mechanisms by which CLA isomers act are not yet exactly known. It has been hypothesized that CLA may modify the eicosanoid biosynthesis (11). *In vivo* feeding studies of rats by Banni *et al.* (11) and Sébédio *et al.* (12) have demonstrated the appearance of 18:3 and 20:3 conjugated metabolites from the two major CLA isomers. Recent nutritional studies on the metabolism of the 9*c*,11*t*- and 10*t*,12*c*-18:2 isomers have shown that 9*c*,11*t*-18:2 can be converted into 8*c*,11*c*,13*t*-20:3 and 10*t*,12*c*-18:3 can be converted into 6*c*,10*t*,12*c*-18:3 (11,13), probably by successive desaturation and chain elongation in the same way as 18:2n-6 into 18:3n-6 and 20:3n-6. To test the ability of CLA to act as substrate for Δ6-desaturase, a radiolabeled isomeric mixture of CLA obtained by alkaline isomerization was incubated with liver microsomes (14). It was suggested that the metabolites were the Δ6-desaturated products of CLA. But neither a differentiation in the metabolism of the individual CLA isomers nor an exact structural identification of the conversion products was carried out.

Moreover, Bretillon *et al.* (15) demonstrated the inhibitory effect of 9*c*,11*t*-18:2 on the Δ6-desaturation of linoleic acid in a dose-dependent manner, whereas 10*t*,12*c*-18:2 exhibited the same effect only at the highest concentration.

The present work describes the *in vitro* Δ6-desaturation of 9*c*,11*t*-18:2, the elongation of 6*c*,9*c*,11*t*-18:3, and the Δ5-desaturation of 8*c*,11*c*,13*t*-20:3 in comparison with their natural respective homologs using rat liver microsomes in order to obtain information on the conversion of rumenic acid into conjugated 18:3, 20:3, and 20:4 FA.

## MATERIALS AND METHODS

**Chemicals.** The FFA form of 9*c*,12*c*-18:2 was purchased from Sigma Chemicals (l'Isle d'Abeau, France). [1-<sup>14</sup>C]9*c*,12*c*-18:2 was purchased from NEN Life Science (Les Ulis, France). The 9*c*,11*t*-18:2 isomer was purchased from Natural

Lipid (Hovdebygda, Norway), and the [1-<sup>14</sup>C]9c,11t-18:2 was obtained by total synthesis as previously reported (16) with a radiochemical purity >99%. [1-<sup>14</sup>C]6c,9c,11t-18:3, [1-<sup>14</sup>C]-8c,11c,13t-20:3, and their unlabeled homologs were obtained by total synthesis (17). Coenzymes and chemicals were supplied by Sigma Chemicals.

**Animals and diets.** All animal procedures were conducted according to French regulation (authorization A21200 and 3273). Twenty-four weaning male Wistar rats (Elevage Janvier, Saint Genest, France) were fed a fat-free semisynthetic diet for 2 wk, as previously described (18). Rats (166 ± 5.9 g) were killed by decapitation.

**Microsomes preparation and incubations.** Liver microsomes were prepared at 4°C as previously reported (15). Briefly, each liver (9.4 ± 0.9 g) was homogenized in sucrose and phosphate buffer (pH 7.4). The homogenate was centrifuged at 400 × g for 5 min to pellet cellular debris. The supernatant was centrifuged at 15,000 × g for 15 min to eliminate nuclei, mitochondria, lysosomes, and peroxisomes. Finally, the supernatant was ultracentrifuged at 105,000 × g for 60 min. The pellet was resuspended in a phosphate buffer (pH 7.4)/cytosol mixture (2:1, vol/vol). Microsomal proteins were quantified according to the method of Lowry *et al.* (19).

The desaturation studies were performed at 37°C for 15 min as previously described (15). Each incubation medium contained 72 mM phosphate buffer (pH 7.4), 4.8 mM MgCl<sub>2</sub>, 0.5 mM CoA, 3.8 mM ATP, and 1.2 mM NADPH in a final volume of 2 mL. [1-<sup>14</sup>C]9c,12c-18:2, [1-<sup>14</sup>C]9c,11t-18:2, [1-<sup>14</sup>C]8c,11c,13t-20:3, and [1-<sup>14</sup>C]8c,11c,14c-20:3 were diluted in ethanol with the corresponding unlabeled molecule to a specific activity of 10 mCi/mmol. For the Δ<sup>6</sup>-desaturation studies, microsomal suspensions containing 5 mg protein were incubated in an open flask with [1-<sup>14</sup>C]9c,12c-18:2 or [1-<sup>14</sup>C]-9c,11t-18:2 at concentrations of 30, 60, 90, and 120 nmol. For the Δ<sup>5</sup>-desaturation studies, microsomal suspensions containing 5 mg protein were incubated in an open flask with [1-<sup>14</sup>C]-8c,11c,13t-20:3 or [1-<sup>14</sup>C]8c,11c,14c-20:3 at concentrations of 10, 20, 40, 60, 80, and 100 nmol.

The elongation studies were performed at 37°C for 30 min under anaerobic conditions as described by Mohrhauer *et al.* (20). Each incubation medium contained 120 mM phosphate buffer (pH 7), 3.5 mM ATP, 0.1 mM malonyl-CoA, 0.8 mM NADPH, 1.4 mM MgCl<sub>2</sub>, 0.75 mM glutathione, 0.5 mM KCN, 20 mM KF, 0.1 mM CoA, and 0.2 mM nicotinamide in a final volume of 3 mL. [1-<sup>14</sup>C]6c,9c,11t-18:3 and [1-<sup>14</sup>C]-6c,9c,12c,18:3 were diluted in ethanol with the corresponding unlabeled molecule to a specific activity of 10 mCi/mmol. Microsomal suspensions containing 5 mg protein were incubated for 30 min in a closed flask under an argon atmosphere with [1-<sup>14</sup>C]6c,9c,12c-18:3 or [1-<sup>14</sup>C]6c,9c,11t-18:3 at concentrations of 10, 20, 40, and 60 nmol.

**Analysis of the conversion product.** The incubations were stopped by the addition of KOH (12%) in ethanol. Lipids were saponified by heating at 75°C for 1 h. After extraction with hexane, the FFA were esterified into FAME using boron triflu-

oride (14%) in methanol for 15 min at room temperature. The FAME were dissolved in 600 μL of acetone and analyzed by HPLC (Waters 600; Saint Quentin en Yvelines, France) using a Nucleosil C<sub>18</sub> column (5 μm particle size, 250 × 4.6 mm i.d.; Interchim, Montluçon, France). The mobile phase was acetonitrile at a flow rate of 0.5 mL·min<sup>-1</sup>. The radioactivity was measured in the counting cell of a radiochromatographic Flo-One β detector (Series A-100; Radiomatic Instruments, Tampa, FL) after mixing the column effluent with a Uniscint BD scintillation cocktail (National Diagnostics, Atlanta, GA) in a ratio of 1:1.2 (effluent/scintillation cocktail).

Microsomal FAME were also analyzed on a Hewlett-Packard 5890 gas chromatograph (Palo Alto, CA), equipped with a splitless/split injector and a Stabilwax wide-bore column (60 m × 0.53 mm i.d.; film thickness, 0.50 μm, Restek, Evry, France) as previously described (15). The column was connected to a FID and to a radio-GC-detector (GC RAM Lablogic, Sheffield, United Kingdom). The temperatures of the injector and detector were 250 and 280°C, respectively. Helium was the carrier gas. The output flow from the column was split between the FID and the radio-GC-detector in a ratio 10:90. The data were computed using Laura software (Lablogic).

**Identification of the conversion product.** Two Hewlett-Packard HP 5890 Series II (Hewlett-Packard Ltd., Wokingham, United Kingdom) were used for GC analysis. The first was equipped with a splitless/split injector and a FID. The temperatures of the injector and detector were 250 and 280°C, respectively. Helium was the carrier gas. The analyses were performed using a BPX-70 capillary column (50 m × 0.33 mm i.d., film thickness, 0.25 μm; SGE Ltd., Melbourne, Australia). The oven temperature was programmed from 60 to 170°C at 20°C·min<sup>-1</sup>. The second one was equipped with a splitless/split injector and an FID. The temperatures of the injector and detector were 250 and 280°C, respectively. Hydrogen was the carrier gas. The analyses were performed using a CP-SIL capillary column (100 m × 0.25 mm i.d.; film thickness, 0.25 μm; Varian, Les Ulis, France). The oven temperature was programmed from 60 to 190°C at 20°C·min<sup>-1</sup>.

Data were collected using a Borwin workstation (JMBS Developments) including an acquisition interface, software, and a computer. GC-MS analyses were effected with a Hewlett-Packard 6890 gas chromatograph coupled to an HP model 5973 mass selective detector (Hewlett-Packard Ltd.). The latter was used in the EI mode at 70 eV with a source temperature of 250°C. The GC separation was performed on an HP-5-MS column (30 m × 0.25 mm i.d., film thickness 0.25 μm, Hewlett-Packard Ltd.) using helium as carrier gas. The oven temperature was programmed from 60 to 300°C at 18°C·min<sup>-1</sup>. Splitless injection was used with the injection port maintained at 250°C.

**Expression of results.** Results are expressed as means ± SD. The means were compared using an ANOVA and the Student-Newman-Keuls test using SAS software (Cary, NC). Significant differences (*P* < 0.05) are indicated by different superscript letters.

## RESULTS AND DISCUSSION

In the present work, young rats were fed a fat-free diet for 2 wk so that there would be no effect of dietary FA when, at the end of the feeding period, conversion of EFA by liver microsomes was evaluated. The FA composition of liver microsomal total lipids was determined (data not shown). Rats presented an EFA deficiency, according to the criterion accepted for EFA deficiency of Mohrhauer and Holman (21) with a 5*c*,8*c*,11*c*-20:3/5*c*,8*c*,11*c*,14*c*-20:4 ratio of 0.49. No trace of CLA or *trans* FA was present in liver microsome total lipids.

**$\Delta 6$ -Desaturation study.** In a first set of experiments, the  $\Delta 6$ -desaturation of 9*c*,11*t*-18:2 was compared to that of linoleic acid.  $\Delta 6$ -Desaturation is the rate-limiting step in the conversion of linoleic acid to arachidonic acid (20:4n-6) (22). It could be hypothesized that the conversion of CLA by  $\Delta 6$ -desaturase is essential to form further conjugated 20:4 from 9*c*,11*t*-18:2. Table 1 shows the results of the conversion of [1-<sup>14</sup>C]9*c*,12*c*-18:2 or [1-<sup>14</sup>C]9*c*,11*t*-18:2 (30–120 nmol) by liver microsomes under desaturation. Rumenic and linoleic acids were both desaturated. However, the extent of conversion of 9*c*,11*t*-18:2 was significantly lower ( $P < 0.05$ ) than that of 9*c*,12*c*-18:2 at all substrate concentrations (6.3 ± 1.0 vs. 8.7 ± 0.6 nmol at 30 nmol of substrate, and 10.2 ± 1.6 vs. 16.9 ± 1.1 nmol at 120 nmol of substrate), suggesting that rumenic acid is not as good a substrate for  $\Delta 6$ -desaturase as linoleic acid. At 120 nmol the saturating substrate concentration was reached for the conversion of linoleic acid, whereas the conversion of rumenic acid did not reach a plateau, suggesting a higher saturating substrate concentration for rumenic acid than for linoleic acid under our experimental conditions.

Under similar experimental conditions the conversion product of 9*c*,12*c*-18:2 was identified as 6*c*,9*c*,12*c*-18:3 (18,23). In contrast, the *in vitro* desaturated product of 9*c*,11*t*-18:2 had to be identified. With classical chemical methods (24) this is difficult because of the low conversion levels and low metabolite concentrations. Radio-GC, GC–MS, and GC on a high-polarity column were used to analyze the structure of the metabolites formed from 9*c*,11*t*-18:2. Radio-GC revealed two labeled compounds for FAME from liver microsomes incubated in the presence of either [1-<sup>14</sup>C]-9*c*,12*c*-18:2 (Fig. 1B) or [1-<sup>14</sup>C]9*c*,11*t*-18:2 (Fig. 1C). The retention times for rumenic acid and its desaturation product varied from

those of 9*c*,12*c*-18:2 as shown in Figures 1B and 1C because of the conjugated double bonds. GC–MS analyses showed that the desaturated compounds had molecular ions at *m/z* 292 and 294, which correspond to the M.W. of unlabeled and labeled methyl octadecatrienoate, respectively. The conjugated 18:3 metabolite formed from 9*c*,11*t*-18:2 in liver microsomes was identified as 6*c*,9*c*,11*t*-18:3 by GC on a polar column (BPX-70) by comparison with a standard obtained by total synthesis with an isomeric purity >95% (17). Moreover, 19:0 and 22:0 (behenic acid) were added to the conjugated 18:3 metabolite formed from 9*c*,11*t*-18:2 in liver microsomes and to the synthetic 6*c*,9*c*,11*t*-18:3 standard for calculation of the ECL by GC on a polar column (CP-Sil, 60–190°C). The two experimental ECL values are identical (ECL: 21.56). The formation of a metabolite by  $\Delta 6$ -desaturation of 9*c*,11*t*-18:2 is in agreement with earlier results published by Belury and Kempa-Stecko (14). They observed that a radiolabeled CLA mixture was desaturated into an 18:3 product, which was not further identified in a similar way as linoleic acid was converted into  $\gamma$ -linolenic acid.

**Elongation study.** To investigate further the hypothetical metabolic pathway of rumenic acid into conjugated PUFA, an *in vitro* elongation study was carried out using radiolabeled 6*c*,9*c*,11*t*-18:3 obtained by total stereoselective synthesis (17). The elongation of 6*c*,9*c*,11*t*-18:3 was compared to that of  $\gamma$ -linolenic acid as its nonconjugated homolog.

The chain elongation of [1-<sup>14</sup>C]6*c*,9*c*,11*t*-18:3 was carried out in the presence of malonyl-CoA and under an argon atmosphere in order to avoid desaturation (25). Table 2 shows the conversion of [1-<sup>14</sup>C]6*c*,9*c*,12*c*-18:3 into [3-<sup>14</sup>C]-8*c*,11*c*,14*c*-20:3 and [1-<sup>14</sup>C]6*c*,9*c*,11*t*-18:3 into [3-<sup>14</sup>C]-8*c*,11*c*,13*t*-20:3 at various substrate concentrations (10–60 nmol) by rat liver microsomes under elongation conditions. The [1-<sup>14</sup>C]6*c*,9*c*,11*t*-18:3 was elongated in a similar way as  $\gamma$ -linolenic acid, and its conversion rates were 1.5-fold higher ( $P < 0.05$ ) than those of [1-<sup>14</sup>C]6*c*,9*c*,12*c*-18:3 at all substrate concentrations (7.9 ± 0.3 vs. 6.3 ± 0.3 nmol with 10 nmol of substrate and 9.1 ± 1.0 vs. 5.5 ± 1.2 with 60 nmol of substrate, respectively). This suggests that 6*c*,9*c*,11*t*-18:3 is a better substrate for the chain elongation enzyme than  $\gamma$ -linolenic acid under our experimental conditions.

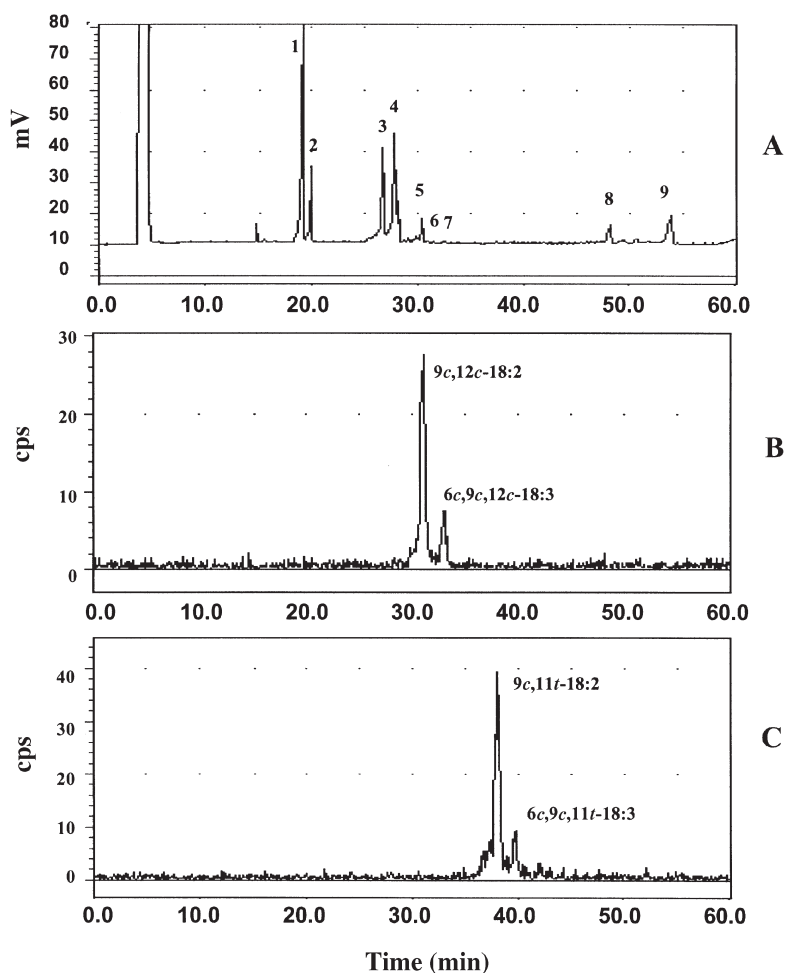
$\gamma$ -Linolenic acid and 6*c*,9*c*,11*t*-18:3 reached the saturating substrate level at 20 nmol. The slight decrease in the conversion

**TABLE 1**  
Formation of the  $\Delta 6$ -Desaturated Products (in % conversion and nmol) from Radiolabeled 9*c*,12*c*-18:2 (linoleic acid) and 9*c*,11*t*-18:2 (rumenic acid) by Rat Liver Microsomes<sup>a</sup>

<sup>14</sup> C Substrate (nmol)	9 <i>c</i> ,12 <i>c</i> -18:2		9 <i>c</i> ,11 <i>t</i> -18:2	
	Conversion (%)	nmol	Conversion (%)	nmol
30	29.1 ± 2.1	8.7 ± 0.6 <sup>a</sup>	21.0 ± 3.3	6.3 ± 1.0 <sup>b</sup>
60	20.5 ± 2.3	12.3 ± 1.4 <sup>a</sup>	12.4 ± 3.5	7.4 ± 2.1 <sup>b</sup>
90	17.4 ± 2.5	15.6 ± 2.3 <sup>a</sup>	10.3 ± 1.4	9.2 ± 1.3 <sup>b</sup>
120	14.1 ± 0.9	16.9 ± 1.1 <sup>a</sup>	8.5 ± 1.3	10.2 ± 1.6 <sup>b</sup>

<sup>a</sup>The conditions for incubations are described in the Materials and Methods section. Results are expressed as mean ± SD of four independent determinations. After ANOVA, means were compared according to the least difference and classified in decreasing order. Means in rows with different superscript letters were significantly different ( $P < 0.05$ ).





**FIG. 1.** GC analysis of the FAME obtained from liver microsomes (5 mg protein) incubated for 15 min with 60 nmol of  $[1-^{14}\text{C}]9c,12c-18:2$  (trace A: FID, trace B: radioactive signal) or with 120 nmol of  $[1-^{14}\text{C}]9c,11t-18:2$  (trace C: radioactive signal). Peak 1: 16:0; 2: 16:1; 3: 18:0; 4: 18:1; 5: 18:2n-6; 6: 18:3n-6; 7: 18:3n-3; 8: 20:3n-9; 9: 20:4n-6.

rates above this concentration could be related to an inhibitory effect of the substrate or of the metabolites. The radio-GC and GC-FID results obtained after injection on a BPX-70 column (Fig. 2B) confirmed that the  $6c,9c,11t-18:3$  was elongated into its corresponding conjugated 20:3, as evidenced by comparing the retention time with that of the  $8c,11c,13t-20:3$  standard obtained by total synthesis (17). Moreover, 23:0 and 24:0 (lignoceric acid) were added to the conjugated 20:3 metabolite formed from  $6c,9c,11t-18:3$  in liver microsomes and to  $8c,11c,13t-20:3$  standard to calculate the ECL by GC on a polar column (CP-Sil, 60–190°C) as carried out for the  $\Delta 6$ -desaturation study. The two experimental ECL values are identical (ECL: 23.55).

**$\Delta 5$ -Desaturation study.** Finally, the  $\Delta 5$ -desaturation of the  $8c,11c,13t-20:3$  was investigated in comparison to dihomo- $\gamma$ -linolenic acid ( $8c,11c,14c-20:3$ ). Table 3 presents the conversion of  $[1-^{14}\text{C}]8c,11c,13t-20:3$  and  $[1-^{14}\text{C}]8c,11c,14c-20:3$  (10–100 nmol) by liver microsomes into their corresponding  $\Delta 5$ -desaturated metabolites. Conjugated 20:3 was converted into  $5c,8c,11c,13t-20:4$ . In comparing the two incubated sub-

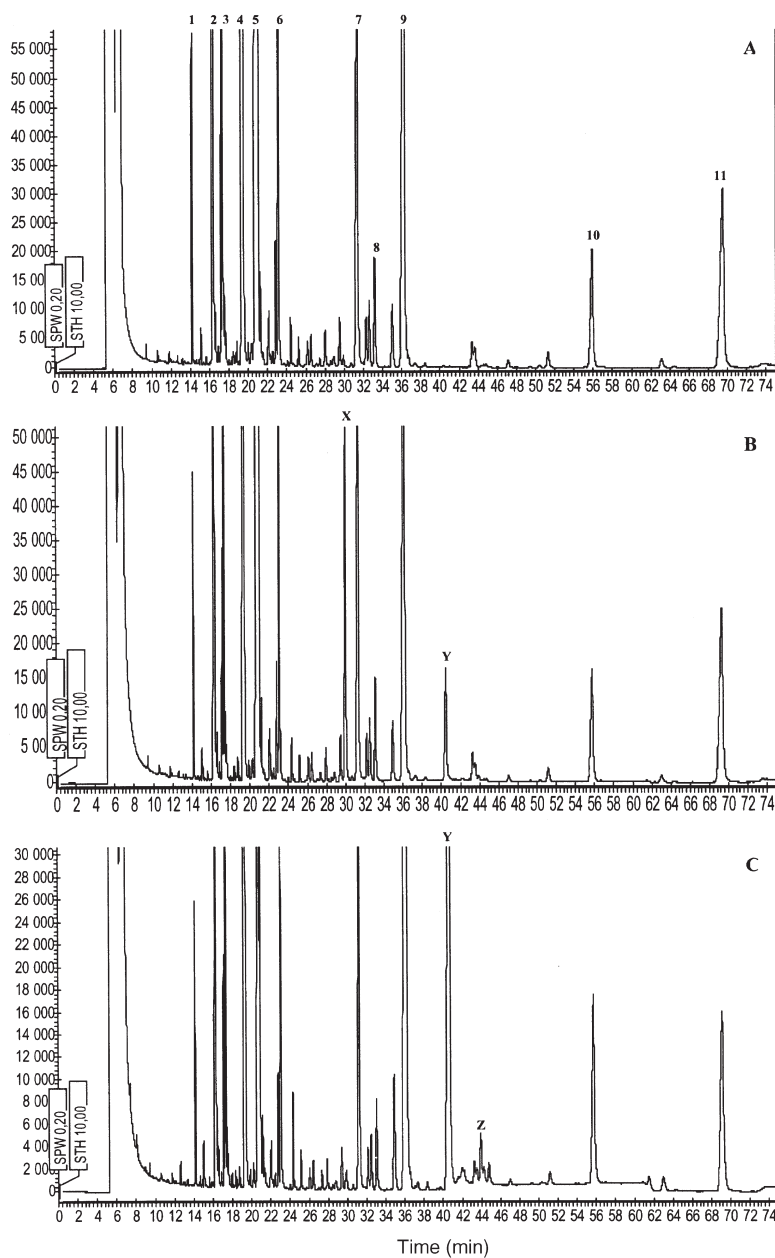
strates, the rate of conversion of  $[1-^{14}\text{C}]8c,11c,13t-20:3$  was about one-tenth that of  $8c,11c,14c-20:3$  ( $0.8 \pm 0.1$  vs.  $7.8 \pm 0.1$  nmol, respectively) at 10 nmol concentration and about one-fifth that of its natural homolog at the highest concentration ( $4.1 \pm 1.0$  vs.  $19.6 \pm 1.5$  nmol) at 100 nmol. The saturating substrate level for  $[1-^{14}\text{C}]8c,11c,14c-20:3$  was reached at 60 nmol whereas for  $[1-^{14}\text{C}]8c,11c,13t-20:3$  the plateau seemed to be reached at 100 nmol. The desaturation product of  $8c,11c,13t-20:3$  was clearly identified as  $5c,8c,11c,13t-20:4$  by GC-FID on a BPX-70 column (Fig. 2C) by comparing the retention time of the desaturation product to that of an authentic standard previously purified and characterized from adipose tissue of rats fed ruminic acid (13). Moreover, when 24:0 and 26:0 were added to the conjugated 20:4 metabolite formed from  $8c,11c,13t-20:3$  in liver microsomes and to the authentic standard containing  $5c,8c,11c,13t-20:4$  for calculation of the ECL by GC on a polar column (CP-Sil, 60–190°C), the two experimental ECL values were identical (ECL: 25.13).

The level of conversion of  $8c,11c,13t-20:3$  into  $5c,8c,11c,13t-20:4$  (arachidonic acid) was considerably lower than

**TABLE 2**  
**Formation of the Elongated Products (in % conversion and nmol) from Radiolabeled 6*c*,9*c*,12*c*-18:3 and 6*c*,9*c*,11*t*-18:3 by Rat Liver Microsomes**

<sup>14</sup> C Substrate (nmol)	6 <i>c</i> ,9 <i>c</i> ,12 <i>c</i> -18:3		6 <i>c</i> ,9 <i>c</i> ,11 <i>t</i> -18:3	
	Conversion (%)	nmol	Conversion (%)	nmol
10	63.0 ± 3.0	6.3 ± 0.3 <sup>a</sup>	79.0 ± 3.0	7.9 ± 0.3 <sup>b</sup>
20	39.5 ± 5.0	7.9 ± 1.0 <sup>a</sup>	60.0 ± 6.0	12.0 ± 1.2 <sup>b</sup>
40	16.2 ± 4.0	6.5 ± 1.6 <sup>a</sup>	25.5 ± 2.7	10.2 ± 1.1 <sup>b</sup>
60	9.2 ± 2.0	5.5 ± 1.2 <sup>a</sup>	15.2 ± 1.6	9.1 ± 1.0 <sup>b</sup>

<sup>a</sup>The conditions for incubations are described in the Materials and Methods section. Results are expressed as mean ± SD of four determinations. After ANOVA, means were compared according to the least difference and classified in decreasing order. Means in rows with different superscript letters were significantly different ( $P < 0.05$ ).



**FIG. 2.** GC analysis of the FAME obtained from liver microsomes (5 mg protein) (trace A, control) or from liver microsomes (5 mg protein) incubated for 30 min with 60 nmol of [1-<sup>14</sup>C]6*c*,9*c*,11*t*-18:3 (trace B) or from liver microsomes (5 mg protein) incubated for 15 min with 100 nmol of [1-<sup>14</sup>C]8*c*,11*c*,13*t*-20:3 (trace C) (BPX-70 column, FID). Peak 1: 14:0; 2: 16:0; 3: 16:1; 4: 18:0; 5: 18:1; 6: 18:2*n*-6; 7: 20:3*n*-9; 8: 20:3*n*-6; 9: 20:4*n*-6; 10: 22:5*n*-6; 11: 22:6*n*-3; X: 6*c*,9*c*,11*t*-18:3; Y: 8*c*,11*c*,13*t*-20:3; Z: 5*c*,8*c*,11*c*,13*t*-20:3.

**TABLE 3**  
**Formation of the  $\Delta^5$ -Desaturated Products (in % conversion and nmol) from Radiolabeled 8c,11c,14c-20:3 and 8c,11c,13t-20:3 by Rat Liver Microsomes<sup>a</sup>**

<sup>14</sup> C Substrate (nmol)	8c,11c,14c-20:3		8c,11c,13t-20:3	
	Conversion (%)	nmol	Conversion (%)	nmol
10	77.6 ± 1.3	7.8 ± 0.1 <sup>a</sup>	7.7 ± 1.0	0.8 ± 0.1 <sup>b</sup>
20	64.0 ± 1.5	12.8 ± 0.3 <sup>a</sup>	6.3 ± 0.6	1.3 ± 0.13 <sup>b</sup>
40	42.7 ± 4.7	17.1 ± 1.9 <sup>a</sup>	5.4 ± 0.8	2.1 ± 0.3 <sup>b</sup>
60	32.4 ± 2.0	19.4 ± 1.2 <sup>a</sup>	5.5 ± 0.5	3.3 ± 0.3 <sup>b</sup>
80	25.6 ± 1.4	20.5 ± 1.1 <sup>a</sup>	5.6 ± 0.1	4.5 ± 0.1 <sup>b</sup>
100	19.6 ± 1.5	19.6 ± 1.5 <sup>a</sup>	4.1 ± 1.0	4.1 ± 1.0 <sup>b</sup>

<sup>a</sup>The conditions for incubation are described in the Materials and Methods section. Results are expressed as mean ± SD of four determinations. After ANOVA, means were compared according to the least difference and classified in decreasing order. Means in rows with different superscript letters were significantly different ( $P < 0.05$ ).

for dihomog- $\gamma$ -linolenic acid, indicating that 8c,11c,13t-20:3 was a poorer substrate for the  $\Delta^5$ -desaturase.

The results obtained are in agreement with the data from the nutritional studies on rats and mice. Recently, Banni *et al.* (26) reported the occurrence of conjugated 18:3 and 20:3 FA in different lipid classes of the liver after administration of 9c,11t-18:2 to rats. The content of conjugated 20:3 FA was about fourfold higher than that of conjugated 18:3 or 20:4 FA. They measured 0.7  $\mu$ g/mg lipid of conjugated 18:3, 3.9  $\mu$ g/mg lipid of conjugated 20:3, and 1.0  $\mu$ g/mg lipid of conjugated 20:4 (26). Similar results were obtained in a feeding study on rats using pure CLA isomers (13).

Our results indicate rumenic acid (9c,11t-18:2) was mainly converted into conjugated 20:3 (8c,11c,13t-20:3), as it was only slightly converted into 6c,9c,11t-18:3 by  $\Delta^6$ -desaturation, and 6c,9c,11t-18:3 was well elongated into 8c,11c,13t-20:3. The conversion of 8c,11c,13t-20:3 to the corresponding conjugated 20:4 was very low. Rumenic acid may likely follow the same *in vivo* metabolic pathway of conversion into long-chain FA as linoleic acid. In this view, the detection of conjugated 18:3, 20:3, and 20:4 FA in tissues of CLA-fed animals would result from successive  $\Delta^6$ -desaturation, elongation, and  $\Delta^5$ -desaturation of rumenic acid.

## ACKNOWLEDGMENTS

The authors thank Bruno Pasquis and Stéphane Grégoire for technical assistance. Silke Gnädig was supported by a Marie Curie Fellowship (FAIR-CT98-5071) from the European Union.

## REFERENCES

- Kepler, C.R., and Tove, S.B. (1967) Biohydrogenation of Unsaturated Fatty Acids, *J. Biol. Chem.* 242, 5686–5692.
- Hughes, P.E., Hunter, W.J., and Tove, S.B. (1982) Biohydrogenation of Unsaturated Fatty Acids: Purification and Properties of *cis*-9,*trans*-11-Octadecadienoate Reductase, *J. Biol. Chem.* 257, 3643–3649.
- Grinari, J.M., and Bauman, D.E. (1999) Biosynthesis of Conjugated Linoleic Acid and Its Incorporation into Meat and Milk in Ruminants, in *Advances in Conjugated Linoleic Acid Research*, Vol. 1 (Yurawecz, M.P., Mossoba, M.M., Kramer, J.K.G., Pariza, M.W. and Nelson, G.J., eds.), pp. 180–200, AOCS Press, Champaign.
- Cawood, P., Wickens, D.G., Iversen, S.A., Braganza, J.M., and Dormandy, T.L. (1983) The Nature of Diene Conjugation in Human Serum, Bile and Duodenal Juice, *FEBS Lett.* 162, 239–243.
- Banni, S., Day, B.W., Evans, R.W., Corongiu, F., and Lombardi, B. (1994) Liquid Chromatographic–Mass Spectrometric Analysis of Conjugated Diene Fatty Acids in a Partially Hydrogenated Fat, *J. Am. Oil Chem. Soc.* 71, 1321–1325.
- Banni, S., and Martin, J.C. (1998) Conjugated Linoleic Acid and Metabolites, in *Trans Fatty Acids in Human Nutrition* (Sébédio, J.L., and Christie, W.W., eds.), pp. 261–302, The Oily Press, Dundee.
- Sébédio, J.L., Gnädig, S., and Chardigny, J.M. (1999) Recent Advances in Conjugated Linoleic Acid, *Curr. Opin. Clin. Nutr. Metab. Care* 2, 499–506.
- Pariza, M.W., Park, Y., and Cook, M.E. (2000) Mechanisms of Action of Conjugated Linoleic Acid: Evidence and Speculation, *Proc. Soc. Exp. Biol. Med.* 223, 8–13.
- Park, Y., Albright, K.J., Liu, W., Storkson, J.M., Cook, M.E., and Pariza, M.W. (1997) Effect of Conjugated Linoleic Acid on Body Composition in Mice, *Lipids* 32, 853–858.
- Dugan, M.E.R., Aalhus, J.L., Schaefer, A.L., and Kramer, J.K.G. (1997) The Effect of Conjugated Linoleic Acid on Fat to Lean Repartitioning and Feed Conversion in Pigs, *Can. J. Anim. Sci.* 77, 723–725.
- Banni, S., Angioni, E., Casu, V., Melis, M.P., Carta, G., Corongiu, F.P., Thompson, H., and Ip, C. (1999) Decrease in Linoleic Acid Metabolites as a Potential Mechanism in Cancer Risk Reduction by Conjugated Linoleic Acid, *Carcinogenesis* 20, 1019–1024.
- Sébédio, J.L., Juaneda, P., Dobson, G., Ramilison, I., Martin, J.C., Chardigny, J.M., and Christie, W.W. (1997) Metabolites of Conjugated Isomers of Linoleic Acid (CLA) in the Rat, *Biochim. Biophys. Acta* 1345, 5–10.
- Sébédio, J.L., Angioni, E., Chardigny, J.M., Grégoire, S., Juaneda, P., and Berdeaux, O. (2001) The Effect of Conjugated Linoleic Acid Isomers on Fatty Acid Profiles of Liver and Adipose Tissues and Their Conversion to Isomers of 16:2 and 18:3 Conjugated Fatty Acids in Rats, *Lipids* 36, 575–582.
- Belury, M.A., and Kempa-Steczko, A. (1997) Conjugated Linoleic Acid Modulates Hepatic Lipid Composition in Mice, *Lipids* 32, 199–204.
- Bretillon, L., Chardigny, J.M., Grégoire, S., Berdeaux, O., and Sébédio, J.L. (1999) Effects of Conjugated Linoleic Acid Isomers on the Hepatic Microsomal Desaturation Activities *in vitro*, *Lipids* 34, 965–969.
- Loreau, O., Maret, A., Chardigny, J.M., Sébédio, J.L. and Noël, J.P. (2001) Sequential Substitution of 1,2-Dichloro-ethene: A Convenient Stereoselective Route to (9Z,11E)-, (10E,12Z)- and (10Z,12Z)-[1-<sup>14</sup>C] Conjugated Linoleic Acid Isomers, *Chem. Phys. Lipids* 110, 57–67.
- Gnädig, S., Berdeaux, O., Loreau, O., Noël, J.P. and Sébédio,

- J.L. (2001) Synthesis of (6Z,9Z,11E)-Octadecatrienoic and (8Z,11Z,13E)-Eicosatrienoic Acids and Their [1-<sup>14</sup>C]-Radiolabeled Analogs, *Chem. Phys. Lipids* 112, 121–135.
18. Berdeaux, O., Blond, J.P., Bretillon, L., Chardigny, J.M., Mairot, T., Vatèle, J.M., Poullain, D., and Sébédio, J.L. (1998) *In vitro* Desaturation or Elongation of Monotrans Isomers of Linoleic Acid by Rat Liver Microsomes, *Mol. Cell. Biochem.* 185, 17–25.
  19. Lowry, O.H., Rosebrough, N.J., Farr, A.L., and Randall, R.J. (1951) Protein Measurement with the Folin Phenol Reagent, *J. Biol. Chem.* 193, 265–275.
  20. Mohrhauer, H., Christiansen, K., Gan, M.V., Deubic, M., and Holman, R.T. (1967) Chain Elongation of Linoleic Acid and Its Inhibition by Other Fatty Acids *in vitro*, *J. Biol. Chem.* 242, 4507–4514.
  21. Mohrhauer, H., and Holman, R. (1963) The Effect of Dose Level of Essential Fatty Acids upon Fatty Acid Composition of the Rat Liver, *J. Lipid Res.* 4, 151–159.
  22. Cook, H.W. (1991) Fatty Acid Desaturation and Chain Elongation in Eucaryotes, in *Biochemistry of Lipids, Lipoproteins and Membranes* (Vance, D.E., and Vance, J. eds.), pp. 141–169, Elsevier Science, New York.
  23. Cao, J., Blond, J.P., and Bézard, J. (1993) Inhibition of Fatty Acid  $\Delta$ 6- and  $\Delta$ 5-Desaturation by Cyclopropene Fatty Acids in Rat Liver Microsomes, *Biochim. Biophys. Acta* 1210, 27–34.
  24. Sébédio, J.L. (1994) Classical Chemical Techniques for Fatty Acid Analysis, in *New Trends in Lipids and Lipoprotein Analysis* (Sébédio, J.L., and Perkins, E.G., eds.), pp. 277–289, AOCS Press, Champaign.
  25. Brenner, R.R. (1971) The Desaturation Step in Animal Biosynthesis of Polyunsaturated Fatty Acids, *Lipids* 6, 567–571.
  26. Banni, S., Carta, G., Angioni, E., Murru, E., Scanu, P., Melis, M.P., Bauman, D.E., Fischer, S.M., and Ip, C. (2001) Distribution of Conjugated Linoleic Acid and Metabolites in Different Lipid Fractions in the Rat Liver, *J. Lipid Res.* 42, 1056–1061.

[Received October 23, 2000, and in final revised form and accepted May 22, 2002]



# Fatty Acid Mobilized by the Vascular Endothelial Growth Factor in Human Endothelial Cells

Mariarosaria Boccellino, Alfonso Giovane, Luigi Servillo,  
Ciro Balestrieri, and Lucio Quagliuolo\*

Department of Biochemistry and Biophysics, Second University of Naples, 80138 Napoli, Italy

**ABSTRACT:** Release of FFA from membrane phospholipids was observed after incubation of umbilical cord vein-derived endothelial cells (HUVEC) with vascular endothelial growth factor (VEGF). In particular, we found an increase of arachidonate, stearate, and palmitate in a time-dependent manner with a peak at 30 min. The maximum increase was reached by arachidonate (4.4-fold), followed by stearate (2.2-fold) and palmitate (1.3-fold). The arachidonate increase can be ascribed to the activation of phospholipase A<sub>2</sub> (PLA<sub>2</sub>). In fact, cells preincubated with arachidonyl trifluoromethyl ketone, a PLA<sub>2</sub> inhibitor, showed a marked reduction in arachidonate mobilization. The role of Ca<sup>2+</sup> in PLA<sub>2</sub> activation was also investigated. Cells incubated with VEGF in the presence of EGTA showed a marked decrease in arachidonate mobilization, whereas incubation with the calcium ionophore A23187 alone produced an increase in arachidonate, although to a lesser extent compared with the VEGF stimulation. Incubation with A23187 in association with PMA produced the same increase in arachidonate as the VEGF treatment. Mitogen-activated protein kinase (MAPK) activity was also found to increase as a consequence of VEGF stimulation. Taken together, these results suggest that the VEGF-mediated activation of PLA<sub>2</sub> in HUVEC is dependent on both MAPK-mediated phosphorylation and Ca<sup>2+</sup> increase. Furthermore, the increase in stearate and palmitate likely is brought about by the activation of a pathway involving phospholipase D, phosphatidate phosphohydrolase (PAP), and DAG lipase. In fact, the increase in those FFA was prevented when HUVEC were stimulated with VEGF in the presence of ethanol (which inhibits the formation of phosphatidate), propranolol (a specific inhibitor of PAP), or RHC-80267 (a specific inhibitor of DAG lipase).

Paper no. L9096 in *Lipids* 37, 1047–1052 (November 2002).

Vascular endothelial growth factor (VEGF), also known as vascular permeability factor, is a potent mitogen for vascular endothelial cells. This cytokine has been shown to play a central role in the angiogenesis associated with physiological and pathological processes (1–4). Angiogenesis, the process by which new blood vessels are formed *via* proliferation of vascular endothelial cells (5), is essential in reproduction,

development, and wound repair (6). The mechanisms involved in the initiation and progression of angioproliferative disease processes are poorly understood. Recent evidence indicates that VEGF is essential for embryonic angiogenesis (7), for angiogenesis in the female reproductive tract (8–10), and for morphogenesis of the epiphyseal growth plate and endochondral bone formation (11). Additional studies indicate that VEGF has a relevant role in pathological angiogenesis. Indeed anti-VEGF monoclonal antibodies or other VEGF inhibitors block the growth of several human tumor cell lines in nude mice (12), whereas augmented VEGF expression is correlated with increased tumor growth and vascularity (13,14).

The action of VEGF is mediated by two receptors, the human *fms*-like tyrosine kinase (Flt-1) (15) and fetal liver kinase 1 (Flk-1) (16,17), the mouse homolog of the human kinase insert domain receptor (KDR) (18). The distal signaling pathway for VEGF receptors has not been completely determined, although it is known that VEGF rapidly increases the intracellular Ca<sup>2+</sup> concentration in endothelial cells (19), causes a striking and transient increase in mitogen-activated protein kinase (MAPK) activity, and stimulates phospholipase C- $\gamma$  tyrosine phosphorylation (20). When stimulated with VEGF, human endothelial cells in culture release arachidonic acid from their phospholipid storage sites (21). Lipid metabolism plays a crucial role in cell signaling, and considerable efforts have been made to identify the pathways for arachidonate mobilization from cellular phospholipids (22). Although it is assumed that the main step involves the action of phospholipase A<sub>2</sub> (PLA<sub>2</sub>), another pathway has been suggested to play a role in arachidonate mobilization, i.e., the activation of phospholipase D (PLD), which catalyzes the hydrolysis of PC to produce choline and PA with subsequent liberation of arachidonate (23,24). However, PA itself possesses signaling properties, including the stimulation of actin stress fiber formation in porcine aortic endothelial cells (25). Furthermore, PA was found to induce the chemotactic migration of endothelial cells from established monolayers, which is an important step in angiogenesis (26).

The aim of this work was to investigate the pathways involved in the release of FFA in VEGF-stimulated human umbilical cord vein-derived endothelial cells (HUVEC). Herein we report evidence that, upon VEGF stimulation, palmitate and stearate, as well as arachidonate, are increased. This finding suggests the involvement of at least two different pathways, one taking place *via* cPLA<sub>2</sub> activation, which generates

\*To whom correspondence should be addressed at Dipartimento di Biochimica e Biofisica, Via Costantinopoli 16, 80138 Napoli, Italy.  
E-mail: lucio.quagliuolo@unina2.it

Abbreviations: AACOCF<sub>3</sub>, arachidonyl trifluoromethyl ketone; ADAM, 9-anthryldiazomethane; HUVEC, human umbilical cord vein-derived endothelial cells; KDR, kinase insert domain receptor; MAPK, mitogen-activated protein kinase; PAP, phosphatidate phosphohydrolase; PKC, protein kinase C; PLA<sub>2</sub>, phospholipase A<sub>2</sub>; PLD, phospholipase D; RHC-80267, a DAG lipase inhibitor; VEGF, vascular endothelial growth factor.

arachidonate, and the other involving PLD, phosphatidate phosphohydrolase (PAP), and DAG lipase, which brings about increases in stearate and palmitate.

## EXPERIMENTAL PROCEDURES

**Materials.** Collagenase from *Clostridium histolyticum* was from Roche S.p.A. (Monza, Italy). Human von Willebrand antiserum was from Nordic Immunology (Tilberg, The Netherlands). Anti-human histocompatibility antigens class I and class II were purchased from Becton, Dickinson, and Co. (Franklin Lakes, NJ). [ $\gamma$ - $^{32}$ P]ATP (3000 Ci/mmol) was purchased from Amersham (Arlington Heights, IL). Myelin basic protein, the calcium ionophore A23187, porcine sodium heparin, endothelial cell growth factor, PMA, BSA, and FFA standards were from Sigma (St. Louis, MO). Arachidonyl trifluoromethyl ketone (AACOCF<sub>3</sub>, a PLA<sub>2</sub> inhibitor) and 1,6-bis(cyclohexyloximino-carbonylamino) hexane (RHC-80267, a specific inhibitor of DAG lipase) were from Alexis Biochemicals (c/o Vinci-Biochem, Vinci, Italy). Fetal calf serum was from Hyclone Lab (Logan, UT). Recombinant human VEGF was from Genzyme Diagnostics (Cambridge, MA). 9-Anthryldiazomethane (ADAM) was from Molecular Probes Inc. (Eugene, OR). All other reagents were of analytical grade.

**Endothelial cell culture.** HUVEC were isolated by treatment of human umbilical cord veins with 0.2% collagenase from *C. histolyticum* (20 min, 37°C) and cultured as described previously (27) until they reached confluence. The cells were characterized by morphologic criteria and positive immunofluorescence for von Willebrand factor and class I, but not class II, histocompatibility antigens (27). Cells between passages 3 and 10 were used. Cell viability was assessed following the release of cytosolic lactate dehydrogenase activity by a cytotoxicity detection kit (Roche).

**FFA determination.** FFA were determined by HPLC using a fluorescence detector after derivatization with ADAM, a fluorescent probe that specifically reacts with free carboxyl groups. To profile the FFA released by HUVEC, cells were grown on 35 mm-diameter dishes until the cell number reached  $4.6 \times 10^5 \pm 3.2 \times 10^4$ . Cells were starved in medium without serum and growth factor for 18 h, then washed three times with PBS and incubated at 37°C in 2 mL RPMI-1640 medium with VEGF (50 ng/mL) and/or other stimuli for the appropriate time. After incubation the medium was removed, 1 nmol of eicosanoate was added as internal standard, and the incubation was stopped by adding methanol (2 mL/dish). Cells were scraped from the dish, the suspension was transferred to borosilicate tubes, and lipids were extracted according to the procedure of Bligh and Dyer (28). Total lipids were extracted into chloroform by shaking vigorously for 90 s. After centrifugation ( $1500 \times g$ , 5 min), the chloroform solution was transferred into another tube and dried under vacuum by using the Univapor Concentrator Centrifuge, model Univapo 100 H (Uni Equip, Martinsried, Germany). The dried lipids were dissolved in 450  $\mu$ L acetonitrile; 50  $\mu$ L solution containing 1 mg/mL of ADAM in acetonitrile was then

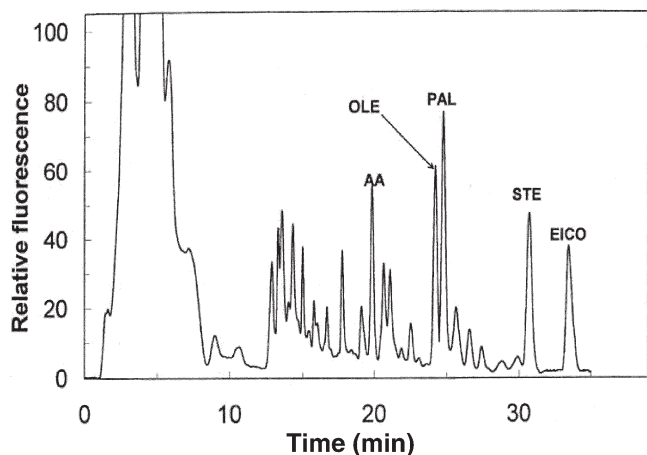
added and the mixture was incubated overnight at room temperature (29). After incubation, 100  $\mu$ L of the mixture was directly analyzed by HPLC.

The separation of ADAM-derivatized FFA was performed on a Symmetry C<sub>18</sub> reversed-phase column,  $4.6 \times 150$  mm, filled with a stationary phase of 3.5  $\mu$ m average particle size (Waters, Milford, MA), by a gradient liquid chromatograph consisting of a controller (model 600) and a pump (model 626) (Waters). The column was eluted with methanol/water (85:15, vol/vol) for 10 min, then with 100% methanol. The flow rate was 1.0 mL/min. The peaks were detected with a Shimadzu Model 160 fluorescence spectrometer equipped with a computer with the Millennium software (Waters). The excitation and emission wavelengths were 364 and 412 nm, respectively. The amount of derivatized FFA was calculated by comparing the peak area with authentic standards and, using the eicosanoate as internal standard, a recovery of  $92 \pm 5\%$  was calculated.

**MAPK assay.** Cells ( $10^5$ ) were plated on 60-mm dishes and cultured for 24 h. Confluent cells were serum-starved for 18 h and stimulated with VEGF (50 ng/mL) at different times in 1 mL of M199 medium. Incubations were terminated by aspiration of the medium and addition of 500  $\mu$ L of lysis buffer [1% Triton X-100, 20 mM Tris/HCl (pH 8), 137 mM NaCl, 10% (vol/vol) glycerol, 2 mM EDTA, 0.14 unit/mL of aprotinin, 20  $\mu$ M leupeptin, and 1 mM sodium orthovanadate] at 4°C for 20 min (30). Cells were scraped from the dish, the lysate was centrifuged at  $14,000 \times g$  for 10 min at 4°C, the supernatant was collected, and the protein concentrations were determined by the method of Bradford (31). Approximately 20  $\mu$ g of proteins were immunoprecipitated overnight at 4°C with 5  $\mu$ g/mL MAPK polyclonal antiserum (erk1-CT). Immune complexes were purified by incubation for 3 h at 4°C with 80  $\mu$ L of protein A-Sepharose slurry (40  $\mu$ L bead volume). The resin was then washed three times with Tris-buffered saline and once with kinase buffer (30 mM Tris/HCl, pH 8.0; 20 mM MgCl<sub>2</sub>; 1 mM DTT) and resuspended in 30  $\mu$ L of kinase buffer containing 7  $\mu$ g of myelin basic protein, 2  $\mu$ M ATP, and 5  $\mu$ Ci of [ $\gamma$ - $^{32}$ P]ATP (32). After incubation for 20 min at 30°C, a BSA solution was added to the suspension at final concentration of 1 mg/mL, and proteins were precipitated by adding 1 mL of 5% TCA. The samples were filtered on a glass fiber filter AP40 (Millipore, Milford, MA) and washed three times with 2 mL of 5% TCA to remove unincorporated radioactivity. The filters were transferred to scintillation vials and counted for radioactivity; counts were normalized for the amount of protein used in the immunoprecipitation step. Owing to a possible contamination of protein kinase C (PKC) in the immunoprecipitate, the substrate phosphorylation was ruled out in parallel experiments by using bisindolylmaleimide, a selective inhibitor of the PKC.

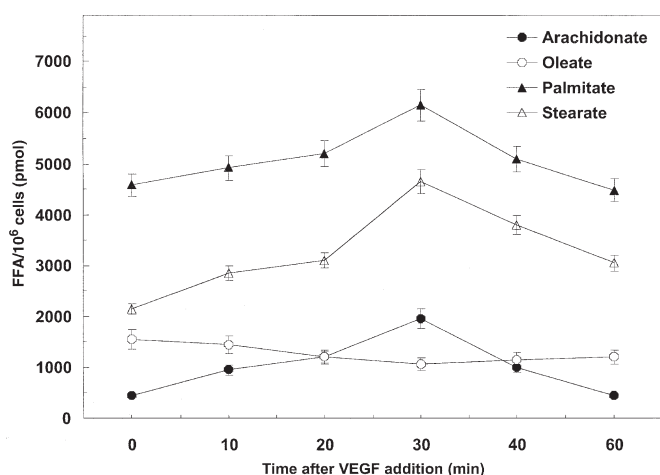
## RESULTS

**FFA release by HUVEC stimulated with VEGF.** Serum-deprived HUVEC were stimulated at various times with 50 ng/mL VEGF. After total lipids were extracted, FFA were



**FIG. 1.** Chromatogram of 9-anthryldiazomethane-derivatized FA extracted from human umbilical cord vein-derived endothelial cells (HUVEC). Cells were stimulated with vascular endothelial growth factor (VEGF) for 30 min. Eicosanoate was added as internal standard. AA, arachidonate; OLE, oleate; PAL, palmitate; STE, stearate; EICO, eicosanoate.

derivatized with ADAM and analyzed by HPLC, as described in the Experimental Procedures section. Figure 1 shows a typical chromatographic pattern of ADAM-derivatized FFA obtained from a representative experiment in which HUVEC were stimulated with VEGF for 30 min. When confluent cultures of HUVEC were treated with VEGF, a time-dependent increase in FFA occurred in the cells. As shown in Figure 2, the amount of arachidonate, palmitate, and stearate increased in the cell, with a maximum at 30 min followed by a decrease that, after 60 min, restored the initial conditions. VEGF stimulated an increase in arachidonate from 445 to 1950 pmol/ $10^6$  cells after 30 min, whereas the palmitate and stearate increases were from 4580 to 6150 pmol/ $10^6$  cells and from 2140 to 4660 pmol/ $10^6$  cells, respectively. Oleate mobiliza-

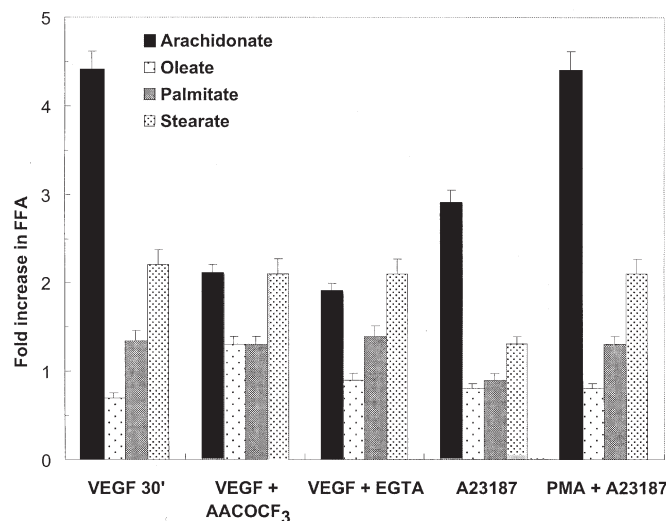


**FIG. 2.** Time course of FFA production in HUVEC stimulated with VEGF. Cells were stimulated with VEGF (50 ng/mL) for the indicated times. FFA were extracted and their amounts measured by HPLC. Data are mean  $\pm$  SD of triplicate experiments. The amount of each FFA was measured at incubation time zero and used as a control. No substantial difference was found in unstimulated cells among incubation time zero and other time points. For abbreviations see Figure 1.

tion showed a different behavior, with a limited decrease that had a minimum at 30 min (from 1550 to 1070). By expressing the data as fold of FFA increase with respect to the unstimulated cells (at the same time points), we found that the increases in arachidonate, stearate, and palmitate were 4.4-, 2.2-, and 1.3-fold, respectively, whereas oleate had a decrease of 0.7-fold.

**Role of the  $PLA_2$  in FFA release induced by VEGF.** HUVEC were preincubated for 5 min in the presence of the  $PLA_2$  inhibitor AACOCF<sub>3</sub> at a concentration of 25  $\mu$ M, followed by VEGF stimulation for an additional 30 min at 37°C. In these conditions a marked inhibition of arachidonate mobilization was observed, from 4.4- to 2.1-fold (Fig. 3), compared with VEGF alone. Instead, the  $PLA_2$  inhibitor poorly affected the production of saturated and monounsaturated FFA; however, the increase in oleate was higher than that observed with VEGF alone.

The role of calcium ions in FA mobilization was also investigated. HUVEC were incubated with either VEGF for 30 min in the presence of 2 mM EGTA, with 10  $\mu$ M calcium ionophore A23187 for 10 min, or with 1  $\mu$ M PMA for 5 min followed by A23187 (10  $\mu$ M) for 10 min. As shown in Figure 3, the chelation of divalent cations was accompanied by a reduction in arachidonate mobilization from 4.4- to 1.8-fold, indicating that the VEGF-stimulated arachidonate production is basically calcium dependent. In fact, cells incubated for 10 min with A23187 showed a consistent increase in arachidonate production, which became more pronounced when the cells were preincubated for 5 min with PMA followed by an additional 10 min in the presence of 10  $\mu$ M A23187.



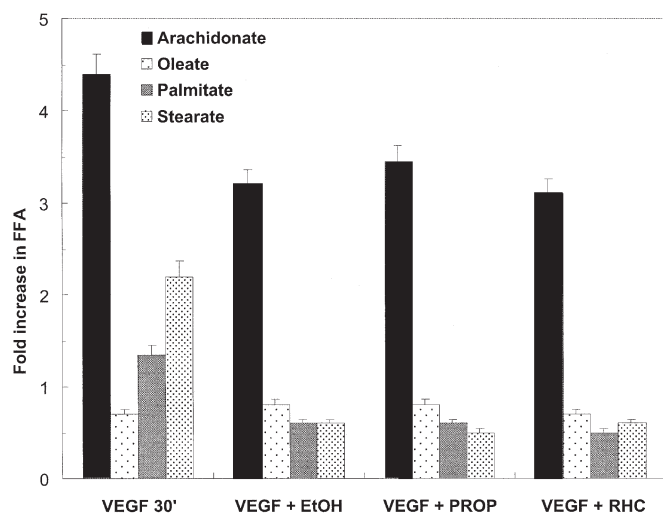
**FIG. 3.** Role of phospholipase A<sub>2</sub> ( $PLA_2$ ) on FFA production in VEGF-stimulated HUVEC. Cells were stimulated with VEGF (50 ng/mL) for 30 min, or incubated with arachidonyl trifluoromethyl ketone (AACOCF<sub>3</sub>, a  $PLA_2$  inhibitor) (25  $\mu$ M) for 5 min and then for an additional 30 min in the presence of VEGF (50 ng/mL), or with VEGF in the presence of 2 mM EGTA for 30 min. Cells were also incubated with the calcium ionophore A23187 (10  $\mu$ M) for 10 min, or with PMA (1  $\mu$ M) for 5 min and then for an additional 10 min in the presence of A23187. For other abbreviations see Figure 1.



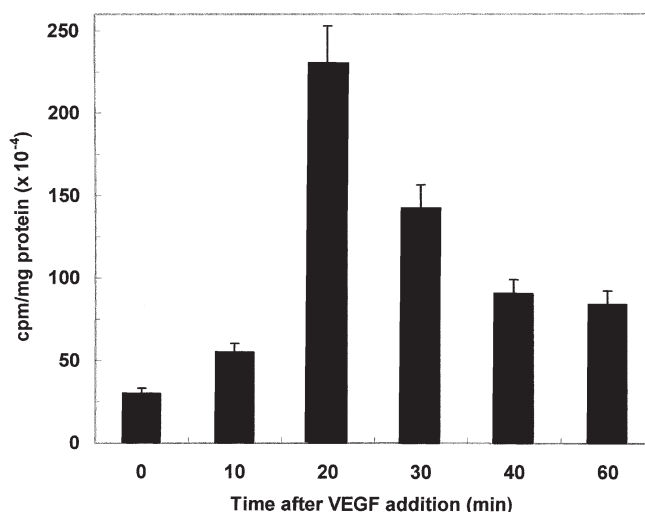
Although the A23187 incubation produced only an increase in arachidonate, the preincubation with PMA also resulted in increases in palmitate and stearate.

**Role of PLD in the FFA release induced by VEGF.** VEGF is known to induce an increase in arachidonate in HUVEC (21) due to the activation of PLA<sub>2</sub>, which specifically hydrolyzes arachidonic acid at the *sn*-2 position of phospholipids. However, the increase in saturated FFA in HUVEC stimulated with VEGF has not been reported so far. The mobilization of saturated FA could be the result of a metabolic pathway involving PLD, PAP, and DAG lipase. To verify this hypothesis, we used specific inhibitors acting at the level of each of these metabolic steps. As shown in Figure 4, cells incubated with VEGF in the presence of 2% (vol/vol) ethanol, which prevents the formation of PA by PLD, did not show any increase in stearate and palmitate, and the arachidonate production was scarcely affected. Similar results were obtained using propranolol (200 μM), which is a PAP inhibitor, and the DAG lipase inhibitor RHC-80267 (6 μM).

**Effect of VEGF on MAPK activity.** To investigate the mechanism involved in PLA<sub>2</sub> activation responsible for the arachidonate release triggered by VEGF, the role of MAPK in signal transduction was also evaluated. Indeed, the role of MAPK phosphorylation in the activation of cytosolic PLA<sub>2</sub> by phosphorylation is now recognized. As shown in Figure 5, MAPK activity, as evaluated by the incorporation of <sup>32</sup>P into the myelin basic protein (see the Experimental Procedures section), displayed a ninefold increase and reached a maximum 20 min after stimulation with VEGF. MAPK activity



**FIG. 4.** Role of phospholipase D on FFA production in VEGF-stimulated HUVEC. Cells were preincubated for 10 min with ethanol (which inhibits the formation of phosphatidate) (2%, vol/vol), for 15 min with propranolol (PROP, a specific inhibitor of phosphatidate phosphohydrolyase) (200 μM), for 5 min with RHC-80267 (a specific inhibitor of DAG lipase) (6 μM), and then stimulated with VEGF (50 ng/mL) for an additional 30 min. Following the treatment, FFA were extracted and analyzed by HPLC as described in the Experimental Procedures section. The results are expressed as the fold increase with respect to untreated cells used as a control. Data are mean ± SD of triplicate experiments. For other abbreviations see Figure 1.



**FIG. 5.** Time course of mitogen-activated protein kinase (MAPK) activity in VEGF-stimulated HUVEC. Cells were stimulated with VEGF (50 ng/mL) for the indicated times and cell lysates were immunoprecipitated with the anti-MAPK antibody. The kinase activity was determined in the immunoprecipitate by incorporation of <sup>32</sup>P into the myelin basic protein used as substrate. Results are mean ± SD of triplicate experiments. Data were corrected for radioactivity background by omitting the substrate from the incubation mixture. For other abbreviations see Figure 1.

was undetectable in unstimulated control cells. Furthermore, by using bisindolylmaleimide, a selective inhibitor of PKC, we confirmed that the phosphorylation was due only to the MAPK. In fact, since PKC is involved in the phosphorylation cascade of MAPK (33), it could be coprecipitated by the MAPK antiserum.

## DISCUSSION

The results reported herein demonstrate that in VEGF-stimulated HUVEC, at least two cell-signaling pathways, involving PLA<sub>2</sub> and PLD, are activated. It is well documented that PLA<sub>2</sub> participates in the mobilization of arachidonic acid from the *sn*-2 position of phospholipids, and recently (21,34) the activation of PLA<sub>2</sub> has been shown to take place in VEGF-mediated HUVEC stimulation in an extracellular-regulated kinase- and PKC-sensitive manner. Usually, the way to monitor the mobilization of arachidonate consists of measuring the release, following an appropriate stimulus, of radioactive arachidonate previously incorporated into the cell. This method, although very simple, does not allow the evaluation of other FFA. In this work we used a different approach based on the HPLC determination of FFA derivatized with the fluorescent agent anthryldiazomethane, which selectively reacts with the free carboxyl groups. In this way, we were able to determine different FFA at pmol levels simultaneously and to measure their relative amounts as a consequence of the cellular stimulation. In time-course experiments (Fig. 2), we observed that in VEGF-stimulated HUVEC, the amount of arachidonate increased, reaching the maximum at 30 min. The arachidonate increase was also accompanied by increases



in stearate and palmitate and by a slight decrease in oleate. The more sustained increase, however, concerned arachidonate, whose amount increased 4.4-fold, whereas the amounts of stearate and palmitate were augmented by 2.2- and 1.3-fold, respectively. The increase in arachidonate was essentially due to activation of PLA<sub>2</sub>, since we found that the inhibitor of a calcium dependent PLA<sub>2</sub>, AACOCF<sub>3</sub>, greatly reduced the VEGF-mediated release of arachidonate (Fig. 3). Furthermore, when cells were incubated with VEGF in the presence of the calcium chelator EGTA, the same result was obtained. Instead, the incubation of HUVEC with the calcium ionophore A23187 resulted in an arachidonate production that equaled that induced by VEGF when the ionophore was used in association with PMA. In fact, phorbol esters stimulate PKC, which activates PLA<sub>2</sub> via MAPK (35); therefore, calcium-dependent translocation from the cytosol to the membrane and MAPK phosphorylation act synergistically to activate PLA<sub>2</sub> (22). The involvement of MAPK was also confirmed by the increase in its activity in VEGF-stimulated HUVEC (Fig. 5). The activation of MAPK in VEGF-stimulated HUVEC was already demonstrated following the phosphorylation of PLA<sub>2</sub> (21); however, here we provide direct evidence that an increase in MAPK activity takes place.

Moreover, using the HPLC analysis, we were able to determine increases in saturated FFA, such as stearate and palmitate, that have not been reported so far in VEGF-stimulated HUVEC. Increases in saturated FFA could originate from a remodeling pathway using DAG as substrate. However, DAG can be produced directly by the action of PLC or by the combined action of PLD and PAP. The finding that in porcine aortic endothelial cells PLC activation generates essentially polyunsaturated DAG species, whereas PLD activation generates saturated/monounsaturated DAG species (36), led us to investigate the role played by PLD in VEGF-stimulated HUVEC. In fact, an increase of PLD activity in endothelial cells stimulated by VEGF was reported previously (37). Consistent with this notion, we found that HUVEC treated with VEGF in the presence of ethanol showed a strong reduction in stearate and palmitate with respect to VEGF alone (Fig. 4). In fact, PLD utilizes ethanol in a transphosphatidyl reaction, leading to the formation of phosphatidylethanol, which is a poor substrate for PAP. When propranolol, a specific inhibitor of PAP, is used in association with VEGF, we also observed a reduction in stearate and palmitate with respect to VEGF-stimulated cells. These results were further confirmed by experiments carried out using RHC-80267, a DAG lipase inhibitor. Taken together, these data clearly demonstrate that unsaturated FFA production was generated by a PLD-dependent pathway. In fact, PLD activation leads to the formation of PA, which is converted to DAG by the action of PAP (38). DAG is then involved in the phospholipid remodeling pathway through DAG lipase, which brings about the increase in saturated FFA. Unlike the mobilization of palmitate and stearate, that of oleate showed a behavior that is difficult to explain. In fact, the amount of this FFA decreased in HUVEC incubated for 30 min with VEGF.

A probable explanation for this finding is that oleate could be used in replacing the arachidonate in the lysophospholipids generated by the action of PLA<sub>2</sub>.

The results we report suggest that when HUVEC are stimulated with VEGF, at least two different pathways are activated, involving PLA<sub>2</sub> and PLD. Since PLD triggers the production of PA and DAG, which possess signaling properties (25,26), the elucidation of the PLD-dependent pathway(s) could be of great interest in understanding the molecular basis of the VEGF action in endothelial cells.

## ACKNOWLEDGMENT

This work was partly supported by a grant from the Ministero dell'Università e della Ricerca Scientifica (PRIN 2001) to L.S.

## REFERENCES

1. Ferrara, N. (1996) Vascular Endothelial Growth Factor, *Eur. J. Cancer* 32A, 2413–2422.
2. Plate, K.H., Breier, G., Weich, H.A., and Risau, W. (1992) Vascular Endothelial Growth Factor Is a Potential Tumour Angiogenesis Factor in Human Gliomas *in vivo*, *Nature* 359, 845–848.
3. Hashimoto, M., Ohsawa, M., Ohnishi, A., Naka, N., Hirota, S., Kitamura, Y., and Aozasa, K. (1995) Expression of Vascular Endothelial Growth Factor and Its Receptor mRNA in Angiosarcoma, *Lab. Invest.* 73, 859–863.
4. Benjamin, L.E., and Keshet, E. (1997) Conditional Switching of Vascular Endothelial Growth Factor (VEGF) Expression in Tumors: Induction of Endothelial Cell Shedding and Regression of Hemangioblastoma-like Vessels by VEGF Withdrawal, *Proc. Natl. Acad. Sci. USA* 94, 8761–8766.
5. Folkman, J. (1991) *Biologic Therapy of Cancer* (De Vita, V., Hellman, S., and Rosenberg, S.A., eds.), pp. 743–753, Lippincott, Philadelphia.
6. Folkman, J. (1995) Angiogenesis in Cancer, Vascular, Rheumatoid and Other Disease, *Nat. Med.* 1, 27–31.
7. Ferrara, N. (2001) Role of Vascular Endothelial Growth Factor in Regulation of Physiological Angiogenesis, *Am. J. Physiol. Cell Physiol.* 280, C1358–C1366.
8. Ravindranath, N., Little-Ihrig, L., Phillips, H.S., Ferrara, N., and Zeleznik, A.J. (1992) Vascular Endothelial Growth Factor Messenger Ribonucleic Acid Expression in the Primate Ovary, *Endocrinology* 131, 254–260.
9. Shweiki, D., Itin, A., Neufeld, G., Gitay-Goren, H., and Keshet, E. (1993) Patterns of Expression of Vascular Endothelial Growth Factor (VEGF) and VEGF Receptors in Mice Suggest a Role in Hormonally Regulated Angiogenesis, *J. Clin. Invest.* 91, 2235–2243.
10. Cullinan-Bove, K., and Koos, R.D. (1993) Vascular Endothelial Growth Factor/Vascular Permeability Factor Expression in the Rat Uterus: Rapid Stimulation by Estrogen Correlates with Estrogen-Induced Increases in Uterine Capillary Permeability and Growth, *Endocrinology* 133, 829–837.
11. Gerber, H.P., Vu, T.H., Ryan, A.M., Kowalski, J., Werb, Z., and Ferrara, N. (1999) VEGF Couples Hypertrophic Cartilage Remodeling, Ossification and Angiogenesis During Endochondral Bone Formation, *Nat. Med.* 5, 623–628.
12. Kim, K.J., Li, B., Winer, J., Armanini, M., Gillett, N., Phillips, H.S., and Ferrara, N. (1993) Inhibition of Vascular Endothelial Growth Factor-Induced Angiogenesis Suppresses Tumour Growth *in vivo*, *Nature* 362, 841–844.
13. Zhang, H.T., Craft, P., Scott, P.A., Ziche, M., Weich, H.A., Harris, A.L., and Bicknell, R. (1995) Enhancement of Tumor

- Growth and Vascular Density by Transfection of Vascular Endothelial Cell Growth Factor into MCF-7 Human Breast Carcinoma Cells, *J. Natl. Cancer Inst.* 87, 213–219.
14. Takahashi, Y., Kitadai, Y., Bucana, C.D., Cleary, K.R., and Ellis, L.M. (1995) Expression of Vascular Endothelial Growth Factor and Its Receptor, KDR, Correlates with Vascularity, Metastasis, and Proliferation of Human Colon Cancer, *Cancer Res.* 55, 3964–3968.
  15. de Vries, C., Escobedo, J.A., Ueno, H., Houck, K., Ferrara, N., and Williams, L.T. (1992) The fms-like Tyrosine Kinase, A Receptor for Vascular Endothelial Growth Factor, *Science* 255, 989–991.
  16. Millauer, B., Wизigmann-Voos, S., Schnurch, H., Martinez, R., Moller, N.P., Risau, W., and Ullrich, A. (1993) High Affinity VEGF Binding and Developmental Expression Suggest flk-1 as a Major Regulator of Vasculogenesis and Angiogenesis, *Cell* 72, 835–846.
  17. Quinn, T.P., Peters, K.G., de Vries, C., Ferrara, N., and Williams, L.T. (1993) Fetal Liver Kinase 1 Is a Receptor for Vascular Endothelial Growth Factor and Is Selectively Expressed in Vascular Endothelium, *Proc. Natl. Acad. Sci. USA* 90, 7533–7537.
  18. Terman, B.I., Dougher-Vermazen, M., Carrion, M.E., Dimitrov, D., Armellino, D.C., Gospodarowicz, D., and Bohlen, P. (1992) Identification of the KDR Tyrosine Kinase as a Receptor for Vascular Endothelial Cell Growth Factor, *Biochem. Biophys. Res. Commun.* 187, 1579–1586.
  19. Brock, T.A., Dvorak, H.F., and Senger, D.R. (1991) Tumor-Secreted Vascular Permeability Factor Increases Cytosolic Ca<sup>2+</sup> and von Willebrand Factor Release in Human Endothelial Cells, *Am. J. Pathol.* 138, 213–221.
  20. Guo, D., Jia, Q., Song, H.Y., Warren, R.S., and Donner, D.B. (1995) Vascular Endothelial Cell Growth Factor Promotes Tyrosine Phosphorylation of Mediators of Signal Transduction That Contain SH2 Domains. Association with Endothelial Cell Proliferation, *J. Biol. Chem.* 270, 6729–6733.
  21. Wheeler-Jones, C., Abu-Ghazaleh, R., Cospedal, R., Houliston, R.A., Martin, J., and Zachary, I. (1997) Vascular Endothelial Growth Factor Stimulates Prostacyclin Production and Activation of Cytosolic Phospholipase A<sub>2</sub> in Endothelial Cells via P42/P44 Mitogen-Activated Protein Kinase, *FEBS Lett.* 420, 28–32.
  22. Piomelli, D. (1996) Arachidonic Acid in Cell Signaling, *Curr. Opin. Cell Biol.* 5, 274–280.
  23. Exton, J.H. (1994) Phosphatidylcholine Breakdown and Signal Transduction, *Biochim. Biophys. Acta* 1212, 26–42.
  24. Exton, J.H. (1997) Phospholipase D: Enzymology, Mechanisms of Regulation, and Function, *Physiol. Rev.* 77, 303–320.
  25. Cross, M.J., Roberts, S., Ridley, A.J., Hodgkin, M.N., Stewart, A., Claesson-Welsh, L., and Wakelam, M.J. (1996) Stimulation of Actin Stress Fibre Formation Mediated by Activation of Phospholipase D, *Curr. Biol.* 6, 588–597.
  26. English, D., Kovala, A.T., Welch, Z., Harvey, K.A., Siddiqui, R.A., Brindley, D.N., and Garcia, J.G. (1999) Induction of Endothelial Cell Chemotaxis by Sphingosine 1-Phosphate and Stabilization of Endothelial Monolayer Barrier Function by Lysophosphatidic Acid, Potential Mediators of Hematopoietic Angiogenesis, *J. Hematother. Stem Cell Res.* 8, 627–634.
  27. Jaffe, E.A., Nachman, R.L., Becker, C.G., and Minick, C.R. (1973) Culture of Human Endothelial Cells Derived from Umbilical Veins. Identification by Morphologic and Immunologic Criteria, *J. Clin. Invest.* 52, 2745–2756.
  28. Bligh, E.G., and Dyer, W.J. (1959) A Rapid Method of Total Lipid Extraction and Purification, *Can. J. Biochem. Physiol.* 37, 911–917.
  29. Shimomura, Y., Sugiyama, S., Takamura, T., Kondo, T., and Ozawa, T. (1986) Quantitative Determination of the Fatty Acid Composition of Human Serum Lipids by High-Performance Liquid Chromatography, *J. Chromatogr.* 383, 9–17.
  30. Morrison, D.K., Kaplan, D.R., Escobedo, J.A., Rapp, U.R., Roberts, T.M., and Williams, L.T. (1989) Direct Activation of the Serine/Threonine Kinase Activity of Raf-1 Through Tyrosine Phosphorylation by the PDGF Beta-Receptor, *Cell* 58, 649–657.
  31. Bradford, M.M. (1976) A Rapid and Sensitive Method for the Quantitation of Microgram Quantities of Protein Utilizing the Principle of Protein-Dye Binding, *Anal. Biochem.* 72, 248–254.
  32. D'Angelo, G., Struman, I., Martial, J., and Weiner, R.I. (1995) Activation of Mitogen-Activated Protein Kinases by Vascular Endothelial Growth Factor and Basic Fibroblast Growth Factor in Capillary Endothelial Cells Is Inhibited by the Antiangiogenic Factor 16-kDa N-Terminal Fragment of Prolactin, *Proc. Natl. Acad. Sci. USA* 92, 6374–6378.
  33. Cobb, M.H., and Goldsmith, E.J. (1995) How MAP Kinases Are Regulated, *J. Biol. Chem.* 270, 14843–14846.
  34. Gliki, G., Abu-Ghazaleh, R., Jezequel, S., Wheeler-Jones, C., and Zachary, I. (2001) Vascular Endothelial Growth Factor-Induced Prostacyclin Production Is Mediated by a Protein Kinase C (PKC)-Dependent Activation of Extracellular Signal-Regulated Protein Kinases 1 and 2 Involving PKC- $\delta$  and by Mobilization of Intracellular Ca<sup>2+</sup>, *Biochem. J.* 353, 503–512.
  35. Lin, L.L., Wartmann, M., Lin, A.Y., Knopf, J.L., Seth, A., and Davis, R.J. (1993) cPLA<sub>2</sub> Is Phosphorylated and Activated by MAP Kinase, *Cell* 72, 269–278.
  36. Pettitt, T.R., Martin, A., Horton, T., Liou, C., Lord, J.M., and Wakelam, M.J. (1997) Diacylglycerol and Phosphatidate Generated by Phospholipases C and D, Respectively, Have Distinct Fatty Acid Compositions and Functions. Phospholipase D-Derived Diacylglycerol Does Not Activate Protein Kinase C in Porcine Aortic Endothelial Cells, *J. Biol. Chem.* 272, 17354–17359.
  37. Seymour, L.W., Shoabi, M.A., Martin, A., Ahmed, A., Elvin, P., Kerr, D.J., and Wakelam, M.J. (1996) Vascular Endothelial Growth Factor Stimulates Protein Kinase C-Dependent Phospholipase D Activity in Endothelial Cells, *Lab. Invest.* 75, 427–437.
  38. Exton, J.H. (1997) New Developments in Phospholipase D, *J. Biol. Chem.* 272, 15579–15582.

[Received June 24, 2002, and in revised form September 30, 2002; revision accepted November 8, 2002]

# Olive Oil Phenolics Protect LDL and Spare Vitamin E in the Hamster

Sheila A. Wiseman, Lilian B.M. Tijburg, and Frans H.M.M. van de Put\*

Unilever Health Institute, 3133 AT Vlaardingen, The Netherlands

**ABSTRACT:** An animal feeding trial was conducted to investigate whether olive oil phenolics can act as functional antioxidants *in vivo*. To this end, hamsters were exposed for a period of 5 wk to a dietary regime with either a phenol-rich extra virgin olive oil or extra virgin olive oil from which phenols were removed by ethanol/water-washing. The original oil used in the high olive phenol diet was also used for the preparation of the low phenol diet in order to keep the FA compositions exactly the same. In addition, the vitamin E content was kept identical in both diets. This careful preparation of the diets was undertaken in order to prevent these factors from influencing the antioxidative status in plasma and LDL. Removal of olive oil phenols was shown to reduce both the vitamin E level in plasma and the resistance of LDL to *ex vivo* oxidation. The results of this study support the idea that extra virgin olive oil phenols improve the antioxidant defense system in plasma by sparing the consumption of vitamin E under normal physiological circumstances.

Paper no. L9075 in *Lipids* 37, 1053–1057 (November 2002).

The oxidation of LDL is believed to be an important factor in the onset of the pathogenesis of atherosclerosis. Diets rich in antioxidants, such as the Mediterranean diet, are believed to provide protection against the potentially deleterious effects of oxidative stress. Epidemiological evidence supports this idea since the rate of coronary heart disease is low in Mediterranean countries (1–3).

Extra virgin olive oil (EVOV) is an important constituent of the Mediterranean diet and has a unique composition compared to refined oils, one of the main differences being that the former contains significant amounts of phenols in addition to vitamin E. Major phenolic components in EVOV are oleuropein- and ligstroside-aglycones and their respective hydrolysis products hydroxytyrosol and tyrosol. The properties of hydroxytyrosol and tyrosol have been extensively studied and have led to the conclusion that these phenols, especially hydroxytyrosol, possess powerful antioxidant properties (1).

Various studies have demonstrated that olive oil phenols strongly protect LDL against oxidation *in vitro*, possibly by retarding the consumption of vitamin E endogenously present in these particles (1,4–6). Further support has been obtained with

feeding trials in rabbits in which diets enriched with EVOV extend the resistance of LDL to oxidation compared to diets enriched with refined olive oil (7–9). Whether olive oil phenols have similar effects in humans is less clear. The bioavailability of olive oil phenols has been demonstrated by several groups (10–12). Hydroxytyrosol, tyrosol, and their metabolites are detected in urine following an oral dose of olive oil. The administration of phenol-rich olive oils also leads to a reduced urinary excretion of isoprostanes, a sensitive biomarker for lipid peroxidation (11). Whether olive oil phenols increase the antioxidant capacity in plasma and protect LDL against peroxidation in humans is, however, less clear. In men with peripheral vascular disease, EVOV increased the resistance to LDL oxidation more than refined olive oil (13). Other studies, however, failed to demonstrate a clear difference between EVOV and refined olive oil (or oleic acid-rich oils) on *ex vivo* LDL oxidizability (14–16). Not only differences in phenols but also differences in vitamin E content and lipid composition between the oils used in the same study may account for the presence or absence of these effects.

The aim of the present animal study was to investigate whether olive oil phenolics can act as functional antioxidants *in vivo*. To this end, hamsters were supplemented with a diet containing either a phenol-rich EVOV or EVOV from which phenols had been removed by ethanol/water-washing. Great care was taken in the preparation of the diets. The FA composition and the vitamin E content were identical in both diets to prevent these factors from influencing the antioxidant status. This study describes the effects of dietary supplementation of EVOV phenols on the plasma antioxidant status and on the resistance of LDL to oxidation in the hamster.

## MATERIALS AND METHODS

**Study design.** The experimental protocol was approved by the Animal Welfare Officer and the Animal Experimentation Committee of Unilever Research Vlaardingen. Twenty male F<sub>1</sub>B hybrid Syrian golden hamsters, aged 11 wk on arrival, were obtained from BioBreeders Inc. (Fitchburg, MA). The animals were individually housed in Makrolon type II cages under standard conditions (temperature 18 ± 1°C, relative humidity 65 ± 10%, and day/night cycles of 12/12 h). A layer of sawdust was provided as bedding. During the 14-d period, all animals received a semipurified diet containing refined olive oil (zero phenols) as the only fat source. At the end of the prestudy

\*To whom correspondence should be addressed at Erasmus University, Department of Health Physics, Groene Hilledijk 301, 3075 EA Rotterdam, The Netherlands. E-mail: f.h.m.m.vandeput@azr.nl

Abbreviations: EVOV, extra virgin olive oil; FRAP, ferric-reducing ability of plasma; TEAC, Trolox Equivalent Activity.



period, the animals were allocated to two groups of 10 animals each on the basis of body weight and received one of the experimental olive oil diets for a period of 5 wk. Food and drinking water were freely available throughout the prestudy and the study periods. All animals were clinically observed and weighed weekly. Food consumption was determined at 2-wk intervals. At the end of the experiment (5 wk) after fasting for 16 h, the animals were anesthetized under halothane, and retro-orbital blood samples were collected into sodium heparin-coated tubes and plasma was prepared immediately at 4°C. Plasma samples for LDL isolation were mixed with 0.6% sucrose and stored at -70°C, together with plasma samples for lipid and antioxidant activity analysis. The animals were then killed by decapitation and internal organs inspected macroscopically. Liver weights were noted, and samples of the right median lobe were fixed in 10% neutral buffered formalin. Sections of the liver were cut, stained with hematoxylin azaphloxin, and examined microscopically.

**Experimental diets.** Both semipurified olive oil diets were based on a single batch of EVOV (Van den Berg Foods, Crema, Italy) that contained 196 mg olive oil phenols per kg oil. (The method to measure the phenol concentration and composition is described below in further detail.) EVOV was washed with ethanol/water to obtain a reduction of the phenol concentration to 26 mg of olive oil phenols per kg. The washing procedure was performed by adding ethanol/water (1:1, w/w) to 10 kg of EVOV in the ratio 15:85 (vol/vol) and stirring for 15 min at 50°C. The extraction was repeated twice with an ethanol/water-olive oil ratio of 10:90 (vol/vol). This washing did not remove minor components such as chlorophyll and sterols (results not shown) but did remove about 49 mg/kg oil of  $\alpha$ -tocopherol from the resulting oil. Vitamin E was equalized to 299 mg  $\alpha$ -tocopherol per kg oil (the measured value in the original batch of EVOV) in both diets by the addition of 67% *d*- $\alpha$ -tocopherol in soybean oil (Sigma-Aldrich, Zwijndrecht, The Netherlands). The minor amount of soybean oil has a negligible influence on the composition of the treated oil (EVOV-EtOH/H<sub>2</sub>O).

All diets contained 30 energy % as olive oil, of which 4.7 energy % was saturated FA, 22.7 energy % monounsaturated FA, and 2.6 energy % PUFA. The FA composition of the original EVOV was analyzed by GC as described previously (7).

**TABLE 1**  
Characterization of the Experimental Olive Oils

Antioxidant parameter	Olive oil <sup>a</sup>	
	EVOV	EVOV-EtOH/H <sub>2</sub> O
Total phenols (ppm)	196	26
Tyrosol (ppm)	41	2
Hydroxytyrosol (ppm)	31	0
Antioxidant activity (mmol Trolox equivalents per gram oil)	1.37	0.53
$\alpha$ -Tocopherol (ppm)	270	261
$\gamma$ -Tocopherol (ppm)	< 20	< 20

<sup>a</sup>EVOV, extra virgin olive oil; EVOV-EtOH/H<sub>2</sub>O, ethanol/water-treated EVOV.

[FA distribution in percentage of the total FA in the EVOV is as follows: 14:0 (not detected), 16:0 (12.4%), 16:1 (1.0%), 18:0 (2.6%), 18:1 (74.1%), 18:2 (8.2%), 20:0 (0.8%), 20:1 (0.4%), 22:0 (0.2%), 22:1 (not detected), 24:0 (0.1%), and 24:1 (not detected)]. Various parameters were determined in the oils. The phenol and vitamin E concentrations of the olive oils were determined by HPLC as previously described (7). The total antioxidant activity in the oils was determined by accurately weighing 1 g of each oil (0.9 g/mL) into a screw-topped tube. One milliliter of heptane (0.68 g/mL) was added to give a solution of olive oil in heptane of 474 mg/mL. Aliquots of these heptane solutions were then analyzed in duplicate for the total antioxidant activity using the Trolox Equivalent Activity (TEAC) assay (17). The results of the phenol analysis and the total antioxidant activity of the experimental oils are presented in Table 1. The composition of the experimental diets is given in Table 2. Cholesterol (Merck, Darmstadt, Germany) was added to all diets at a final concentration of 0.1 g per kg.

**Plasma and LDL analyses.** (i) *Analyses of lipid and antioxidant parameters in plasma and lipoproteins.* Cholesterol and total glycerol were determined in plasma and LDL (cholesterol only) using commercial enzymatic colorimetric methods (Boehringer, Mannheim, Germany). Vitamin E was determined in plasma by HPLC as previously described (7). The plasma antioxidant activity was determined using the ferric-reducing ability of plasma assay (FRAP assay) (18).

(ii) *Isolation of LDL and determination of copper-mediated oxidizability.* LDL was isolated by means of density ultracentrifugation using a Beckman Optima tabletop centrifuge and TLA-120.2 near-vertical rotor according to the method described by Himber and coworkers (19). The protein concentration of the LDL fraction was determined with a modified Lowry protein assay (20). A sample of 20  $\mu$ g LDL protein was diluted to a total volume of 1 mL with PBS, and this solution was placed in a cuvette thermostated to a temperature of 30°C.

**TABLE 2**  
Composition of the Experimental Diets

Ingredient (g/100 g)	Group/diet	
	EVOV	EVOV-EtOH/H <sub>2</sub> O
Ca-caseinate	23.7	23.7
EVOV	13.1	0
EVOV-EtOH/H <sub>2</sub> O	0	13.1
Maize starch	55.7	55.7
Solkafloc	5.8	5.8
Mineral mix RMH88 <sup>a</sup>	1.39	1.39
Vitamin mix Vit 96 <sup>b</sup>	0.32	0.32
Cholesterol	0.01	0.01
Total	100.0	100.0

<sup>a</sup>Composition of mineral mix RMH88 (mg/MJ): KCl, 83.18; MgHPO<sub>4</sub>·3H<sub>2</sub>O, 227.21; KH<sub>2</sub>PO<sub>4</sub>, 112.89; KHCO<sub>3</sub>, 170.88; CaCO<sub>3</sub>, 70.11; C<sub>6</sub>H<sub>5</sub>O<sub>7</sub>Na<sub>3</sub>·2H<sub>2</sub>O, 168.98; MnSO<sub>4</sub>·H<sub>2</sub>O, 12.22; ferric citrate, 10.43; zinc citrate, 2.97; cupric citrate, 1.12; KIO, 0.017.

<sup>b</sup>Composition of vitamin mix Vit 96 (without vitamin E) (mg/MJ): choline chloride 50%, 119.5; myoinositol, 5.98; vitamin A 325,000 IE/g, 1.84; vitamin B<sub>1</sub>, 0.36; vitamin B<sub>2</sub>, 0.36; vitamin B<sub>6</sub>, 0.38; vitamin B<sub>12</sub> 0.1%, 3.10; vitamin D<sub>3</sub> 100,000 IE/g, 0.60; vitamin K<sub>3</sub>, 0.24; calcium panthothenate, 1.20; nicotinamide, 1.20; folic acid, 0.06; *d*-biotin, 0.012; maize starch, 43.7; calcium silicate 11.95. For abbreviations see Table 1.



The oxidation of LDL was initiated by the addition  $\text{CuCl}_2$  at a final concentration of  $1 \mu\text{M}$ . The formation of conjugated dienes was monitored spectrophotometrically at a wavelength of 234 nm at 2-min intervals using a UV-vis spectrophotometer equipped with a thermostated multicuvette holder for a period of 240 min or until oxidation was complete (Shimadzu UV 2101PC Spectrophotometer). The oxidation profile of each LDL sample was plotted against time. The lag phase before propagation of oxidation, the maximal rate of oxidation, and the maximal amounts of conjugated dienes formed were determined as described by Esterbauer *et al.* (21).

**Statistical analysis.** Data are presented as mean  $\pm$  SEM, and the Student *t*-test was used to compare the two treatments. Antioxidant parameters were tested using one-tailed comparisons. All other parameters were tested using two-tailed tests. The maximal rate of diene formation and the maximal amount of dienes formed during LDL oxidation were log-transformed before analysis. All data were evaluated using the statistical package SAS (Cary, NC).

## RESULTS

**Animals.** No differences in food consumption or body weight gain were observed in the different treatment groups. The mean weight of the hamsters was  $106.0 \pm 0.8$  g on arrival and  $120.1 \pm 1.7$  g at the end of the study. Mean food consumption was  $5.9 \pm 0.2$  g per day. All animals remained in apparent good health throughout the period of the study, and histopathological examination gave no suggestion of compromised health status.

**The antioxidant activity and the composition of the experimental olive oils.** The antioxidant activity in the oils was determined by means of the commonly used TEAC assay (17), and the results are presented in Table 1. The phenolic content of the oils is also presented in Table 1. As expected, the phenols present in the oils contributed significantly to the total antioxidant activity of the oils. Ethanol/water washing of EVOV led to a considerable loss in both phenols and antioxidant activity. The antioxidant activity in the processed oil can be explained by the presence of vitamin E, which is not removed during the ethanol/water washing of the oil. The following FA distribution was observed in the olive oil used for both diets: 74% oleic acid, 9% PUFA, 16% saturated FA, and 1% monounsaturated FA other than oleic acid. The main difference between the experimental diets was their different phenol content, and as a consequence, their antioxidant activity.

**Plasma lipids, vitamin E, antioxidant activity, and LDL lipids.** No differences were observed in the plasma and LDL cholesterol and plasma glycerol levels between the groups receiving the olive oil diets. The dietary treatments also had no effect on the total antioxidant status in plasma as measured with the FRAP assay. Plasma vitamin E concentrations were significantly reduced in the group receiving the diet containing ethanol/water-washed EVOV compared to the group receiving the original EVOV (Table 3).

**Ex vivo LDL oxidizability.** Three parameters were used to define susceptibility of LDL to copper-mediated oxidation: the

**TABLE 3**  
**Plasma Antioxidant Activity and Plasma Lipids<sup>a</sup>**

	Group/Diet	
	EVOV	EVOV-EtOH/H <sub>2</sub> O
Vitamin E ( $\mu\text{g}/\text{mL}$ )	$12.7 \pm 0.75$	$10.1 \pm 0.49^b$
Antioxidant activity (mM)	$0.51 \pm 0.01$	$0.50 \pm 0.01$
Total cholesterol (mM)	$3.90 \pm 0.18$	$3.65 \pm 0.15$
Total glycerol (mM)	$1.29 \pm 0.14$	$1.26 \pm 0.15$

<sup>a</sup>All values are the mean  $\pm$  SEM;  $n = 10$  animals for each group.

<sup>b</sup>Statistical difference compared to EVOV group, two-tailed *t*-test  $P < 0.01$ . For abbreviations see Table 1.

lag phase before initiation of oxidation, the maximal rate of LDL oxidation, and the maximal amount of conjugated dienes formed during the oxidation process (22). Similar to observations made for the plasma vitamin E content, the removal of olive oil phenols by ethanol/water-washing of EVOV diet resulted in a reduction in the lag phase compared to the diet containing the original EVOV (Table 4). The 24% reduction in the lag phase reached statistical significance ( $P = 0.05$ ). No differences were observed between the olive oil groups in terms of maximal rate of oxidation and the maximal amount of conjugated dienes formed during the copper-induced oxidation process (Table 4).

## DISCUSSION

The purpose of the present study was to investigate the effect of the phenol content in olive oil fed to hamsters as part of a semipurified diet over a period of 5 wk on the antioxidant activity in plasma and LDL. To this end, a diet containing a phenol-rich EVOV was compared with a diet containing EVOV from which virtually all phenols had been removed by ethanol/water washing. The results showed that the absence of olive oil phenols in the diet decreased the resistance of LDL to copper-mediated oxidation *ex vivo* and reduced vitamin E levels in plasma.

To rule out any effect of differences in FA composition, the FA composition in both semipurified diets was designed to be identical in the present study by using the same olive oil as the principal fat source. In addition, the  $\alpha$ -tocopherol content was equalized in both oils used in this study. It is important that these two elements not be dietary variables, as they both

**TABLE 4**  
**LDL Oxidation Resistance<sup>a</sup>**

	Group/diet	
	EVOV	EVOV-EtOH/H <sub>2</sub> O
Lag phase (min)	$62 \pm 7.2$	$47 \pm 5.4^b$
Maximal oxidation rate ( $\text{nmol dienes} \cdot \text{min}^{-1} \cdot \text{mg LDL}^{-1}$ )	$4.9 \pm 0.3$	$5.4 \pm 0.5$
Maximal amount dienes (nM)	$593 \pm 18$	$544 \pm 14$
LDL-cholesterol (mM)	$1.23 \pm 0.08$	$1.25 \pm 0.08$

<sup>a</sup>All values are the mean  $\pm$  SEM;  $n = 10$  animals for each group.

<sup>b</sup>Statistical difference compared to EVOV group, one-tailed *t*-test  $P < 0.05$ . For abbreviations see Table 1.

significantly affect the *ex vivo* oxidizability of LDL (22). In fact, several human and animal studies in which the effect of EVOV is compared with refined olive have a poor control over dietary intake of  $\alpha$ -tocopherol (8,9,13,16). This confounding element makes interpretation of the data very difficult as the difference between the oils may be explained by the differences in phenols and/or  $\alpha$ -tocopherol.

The resistance of LDL to oxidation was not the only antioxidant activity marker that was evaluated in this study. The antioxidant capacity in the plasma of the hamsters was also investigated by means of the FRAP assay following the dietary regimes. The measurements showed that the plasma antioxidant capacity did not differ between the groups. Our observations were in line with an intervention trial in humans, in which it was shown that a 3-wk supplementation of phenol-rich EVOV oil failed to increase the FRAP value of plasma prepared from fasting blood samples. Even if olive oil phenols would have increased plasma antioxidant capacity under the conditions applied in this study, it is expected that the overnight fasting reduced the circulating phenol levels to negligible levels since bioavailability studies have demonstrated that the majority of olive oil phenols are excreted in urine within 4 h following administration (5,23,24). One should, however, take into consideration that the biological relevance and the specificity of total antioxidant capacity assays are frequently questioned. One of the reasons for this is that many endogenous and exogenous antioxidants in plasma contribute in a variable manner to the measured antioxidant capacity (25).

Although dietary intake of vitamin E was the same in both groups, the plasma levels of the hamsters receiving the ethanol/water-washed EVOV were significantly lower than values observed in hamsters receiving the EVOV diets. The increased protection provided by EVOV compared to the ethanol/water-washed EVOV in the resistance of LDL to oxidation may be explained by the fact that (i) olive oil phenols have a vitamin E-sparing effect *in vivo* or, alternatively, (ii) olive oil phenols accumulate in LDL and thereby increase the resistance of LDL to oxidation. Binding of phenols to LDL is likely to occur *in vivo*, but a significant proportion is probably lost during the isolation and dilution of LDL from plasma (26,27). Their relatively poor lipophilicity compared to  $\alpha$ -tocopherol prevents the integration of phenols in the lipophilic core of the LDL particles. A consequence of this poor interaction is that the majority of phenols dissociate from LDL during isolation. This loss of phenols has been demonstrated for red wine phenolic compounds that are lost during the dialysis of LDL (27). Similar observations have been made with plasma incubated with EVOV phenols. The phenol concentration required to protect LDL after isolation is considerably higher when phenols are added directly to isolated LDL (5,6). The higher vitamin E content in plasma of the EVOV-treated group therefore explains the increased resistance of LDL to oxidation *ex vivo*. In other words, the most likely explanation for the observed protective action of the phenols present in the olive oil is that they possess a vitamin E-sparing potential *in vivo*.

This vitamin E-sparing potential of phenols and polyphenols

has been observed *in vitro* in LDL and other model membrane systems (28–30). Also, olive oil phenols retard both lipid peroxidation and vitamin E consumption in LDL subjected to an oxidative stress (4,31). The ability of phenols to interact with vitamin E has been studied in great detail with caffeic acid, a monophenolic antioxidant that structurally resembles hydroxytyrosol (32,33). Caffeic acid interacts with the surface of the LDL particle and can recycle vitamin E. During this process a radical is removed from this lipophilic environment into the surrounding aqueous medium where the radical is further stabilized. Other studies have also shown that vitamin E is only functional as a chain-breaking antioxidant provided hydrophilic co-antioxidants are present in the aqueous surroundings. This is especially relevant when radicals become trapped in LDL particles when they are exposed to a low flux of radicals (34). Indeed, vitamin C, which is even more hydrophilic than phenols and polyphenols, is efficacious in protecting lipids in LDL and plasma against peroxidation (35).

It can be reasoned that similar conditions apply in the hamster *in vivo*. Healthy hamsters experience only low levels of oxidative stress. LDL in blood plasma is, under normal physiological circumstances, protected from oxidation due to the presence of endogenous antioxidants such as ascorbate. Supplementation of olive oil phenols may further enhance this level of protection by interacting with the surface of the LDL particle. Through this interaction, olive oil phenols can either prevent oxidation of LDL by directly scavenging aqueous radicals or, in the event that radicals enter the LDL, can act as chain-breaking antioxidants by recycling vitamin E. This vitamin E-sparing potential is a continuous process that does not become apparent during a brief *in vitro* incubation of plasma with olive oil phenols (6) but appears to require a longer incubation period to become apparent. Such a condition is created during a supplementation period of 5 wk. In conclusion, the findings of this trial with hamsters are consistent with the hypothesis that olive oil phenols protect LDL *in vivo*. Phenols endogenously present in EVOV improve the antioxidant defense system in plasma by sparing the consumption of vitamin E.

## REFERENCES

1. Galli, C., and Visioli, F. (1999) Antioxidant and Other Activities of Phenolics in Olives/Olive Oil, Typical Components of the Mediterranean Diet, *Lipids* 34 (Suppl.), S23–S26.
2. Lusis, A.J. (2000) Atherosclerosis, *Nature* 407, 233–241.
3. Diaz, M.N., Frei, B., Vita, J.A., and Keaney, J.F. (1997) Mechanisms of Disease—Antioxidants and Atherosclerotic Heart Disease, *New Engl. J. Med.* 337, 408–416.
4. Visioli, F., Bellomo, G., Montedoro, G., and Galli, C. (1995) Low Density Lipoprotein Oxidation Is Inhibited *in vitro* by Olive Oil Constituents, *Atherosclerosis* 117, 25–32.
5. Fito, M., Covas, M.I., Lamuela-Raventos, R.M., Vila, J., Torrents, J., de la Torre, C., and Marrugat, J. (2000) Protective Effect of Olive Oil and Its Phenolic Compounds Against Low Density Lipoprotein Oxidation, *Lipids* 35, 633–638.
6. Leenen, R., Roodenburg, A., Vissers, M.N., Schuurbiens, J.A.E., van Putte, K.P.A.M., Wiseman, S.A., and van de Put, F.H.M.M. (2002) Supplementation of Plasma with Olive Oil Phenols and Extracts: Influence on LDL Oxidation, *J. Agric. Food Chem.* 46, 1290–1297.

7. Wiseman, S.A., Mathot, J.N., de Fouw, N.J., and Tijburg, L.B. (1996) Dietary Non-tocopherol Antioxidants Present in Extra Virgin Olive Oil Increase the Resistance of Low Density Lipoproteins to Oxidation in Rabbits, *Atherosclerosis* 120, 15–23.
8. Ochoa, J.J., Quiles, J.L., Ramirez-Tortosa, M.C., Mataix, J., and Huertas, J.R. (2002) Dietary Oils High in Oleic Acid but with Different Unsaponifiable Fraction Contents Have Different Effects in Fatty Acid Composition and Peroxidation in Rabbit LDL, *Nutrition* 18, 60–65.
9. Coni, E., Di Benedetto, R., Di Pasquale, M., Masella, R., Modesti, D., Mattei, R., and Carlini, E.A. (2000) Protective Effect of Oleuropein, an Olive Oil Biophenol, on Low Density Lipoprotein Oxidizability in Rabbits, *Lipids* 35, 45–54.
10. Visioli, F., Galli, C., Bornet, F., Mattei, A., Patelli, R., Galli, G., and Caruso, D. (2000) Olive Oil Phenolics Are Dose-Dependently Absorbed in Humans, *FEBS Lett.* 468, 159–160.
11. Visioli, F., Caruso, D., Galli, C., Viappiani, S., Galli, G., and Sala, A. (2000) Olive Oils Rich in Natural Catecholic Phenols Decrease Isoprostane Excretion in Humans, *Biochem. Biophys. Res. Commun.* 278, 797–799.
12. Miro-Casas, E., Albaladejo, M.F., Covas, M.I., Rodriguez, J.O., Colomer, E.M., Raventos, R.M.L., and de la Torre, R. (2001) Capillary Gas Chromatography–Mass Spectrometry Quantitative Determination of Hydroxytyrosol and Tyrosol in Human Urine After Olive Oil Intake, *Anal. Biochem.* 294, 63–72.
13. Ramirez-Tortosa, M.C., Urbano, G., Lopez-Jurado, M., Nestares, T., Goetz, M.C., Mir, A., Ros, E., Mataix, J., and Gil, A. (1999) Extra-Virgin Olive Oil Increases the Resistance of LDL to Oxidation More Than Refined Olive Oil in Free-Living Men with Peripheral Vascular Disease, *J. Nutr.* 129, 2177–2183.
14. Bonanome, A., Pagnan, A., Caruso, D., Toia, A., Xamin, A., Fedeli, E., Berra, B., Zamburlini, A., Ursini, F., and Galli, G. (2000) Evidence of Postprandial Absorption of Olive Oil Phenols in Humans, *Nutr. Metab. Cardiovasc. Dis.* 10, 111–120.
15. Vissers, M.N., Zock, P.L., Wiseman, S.A., Meyboom, S., and Katan, M.B. (2001) Effect of Phenol-Rich Extra Virgin Olive Oil on Markers of Oxidation in Healthy Volunteers, *Eur. J. Clin. Nutr.* 55, 334–341.
16. Nicolaiew, N., Lemort, N., Adorni, L., Berra, B., Montorfano, G., Rapelli, S., Cortesi, N., and Jacotot, B. (1998) Comparison Between Extra Virgin Olive Oil and Oleic Acid Rich Sunflower Oil: Effects on Postprandial Lipemia and LDL Susceptibility to Oxidation, *Ann. Nutr. Metab.* 42, 251–260.
17. Re, R., Pellegrini, N., Proteggente, A., Pannala, A., Yang, M., and Rice-Evans, C. (1999) Antioxidant Activity Applying an Improved ABTS Radical Cation Decolorization Assay, *Free Radic. Biol. Med.* 26, 1231–1237.
18. Benzie, I.F., and Strain, J.J. (1999) Ferric Reducing/Antioxidant Power Assay: Direct Measure of Total Antioxidant Activity of Biological Fluids and Modified Version for Simultaneous Measurement of Total Antioxidant Power and Ascorbic Acid Concentration, *Methods Enzymol.* 299, 15–27.
19. Himber, J., Buhler, E., Moll, D., and Moser, U.K. (1995) Low-Density-Lipoprotein for Oxidation and Metabolic Studies—Isolation from Small Volumes of Plasma Using a Tabletop Ultracentrifuge, *Int. J. Vitam. Nutr. Res.* 65, 137–142.
20. Markwell, M.A.K., Haas, S.M., Bieber, L.L., and Tolbert, N.E. (1978) Modification of Lowry Procedure to Simplify Protein Determination in Membrane and Lipoprotein Samples, *Anal. Biochem.* 87, 206–210.
21. Esterbauer, H., Striegl, G., Puhl, H., and Rotheneder, M. (1989) Continuous Monitoring of *in vitro* Oxidation of Human Low-Density Lipoprotein, *Free Radic. Res. Commun.* 6, 67–75.
22. Esterbauer, H., Gebicki, J., Puhl, H., and Jurgens, G. (1992) The Role of Lipid-Peroxidation and Antioxidants in Oxidative Modification of LDL, *Free Radic. Biol. Med.* 13, 341–390.
23. Tuck, K.L., Freeman, M.P., Hayball, P.J., Stretch, G.L., and Stupans, I. (2001) The *in vivo* Fate of Hydroxytyrosol and Tyrosol, Antioxidant Phenolic Constituents of Olive Oil, After Intravenous and Oral Dosing of Labeled Compounds to Rats, *J. Nutr.* 131, 1993–1996.
24. Bai, C., Yan, X.J., Takenaka, M., Sekiya, K., and Nagata, T. (1998) Determination of Synthetic Hydroxytyrosol in Rat Plasma by GC–MS, *J. Agric. Food Chem.* 46, 3998–4001.
25. Griffiths, H.R., Moller, L., Bartosz, G., Bast, A., Bertoni-Fredari, C., Collins, A., Coolen, S., Haenen, G., Hoberg, A.M., Loft, S., (2002) Biomarkers, *Mol. Aspects Med.* 23, 101–208.
26. Scheek, L.M., Wiseman, S.A., Tijburg, L.B., and van Tol, A. (1995) Dialysis of Isolated Low Density Lipoprotein Induces a Loss of Lipophilic Antioxidants and Increases the Susceptibility to Oxidation *in vitro*, *Atherosclerosis* 117, 139–144.
27. Carbonneau, M.A., Leger, C.L., Monnier, L., Bonnet, C., Michel, F., Fouret, G., Dedieu, F., and Descomps, B. (1997) Supplementation with Wine Phenolic Compounds Increases the Antioxidant Capacity of Plasma and Vitamin E of Low-Density Lipoprotein Without Changing the Lipoprotein Cu<sup>2+</sup>-Oxidizability: Possible Explanation by Phenolic Location, *Eur. J. Clin. Nutr.* 51, 682–690.
28. Witting, P.K., Westerlund, C., and Stocker, R. (1996) A Rapid and Simple Screening Test for Potential Inhibitors of Tocopherol-Mediated Peroxidation of LDL Lipids, *J. Lipid Res.* 37, 853–867.
29. Salah, N., Miller, N.J., Paganga, G., Tijburg, L., Bolwell, G.P., and Rice-Evans, C. (1995) Polyphenolic Flavonols as Scavengers of Aqueous-Phase Radicals and as Chain-Breaking Antioxidants, *Arch. Biochem. Biophys.* 322, 339–346.
30. Terao, J., Piskula, M., and Yao, Q. (1994) Protective Effect of Epicatechin, Epicatechin Gallate, and Quercetin on Lipid Peroxidation in Phospholipid Bilayers, *Arch. Biochem. Biophys.* 308, 278–284.
31. Visioli, F., and Galli, C. (1994) Oleuropein Protects Low Density Lipoprotein from Oxidation, *Life Sci.* 55, 1965–1971.
32. Laranjinha, J., and Cadenas, E. (1999) Redox Cycles of Caffeic acid,  $\alpha$ -Tocopherol, and Ascorbate: Implications for Protection of Low-Density Lipoproteins Against Oxidation, *IUBMB Life* 48, 57–65.
33. Laranjinha, J. (2001) Caffeic Acid and Related Antioxidant Compounds: Biochemical and Cellular Effects, in *Handbook of Antioxidants* (Cadenas, E., and Packer, L., eds.), pp. 279–302, Marcel Dekker, New York.
34. Thomas, S.R., Neuzil, J., Mohr, D., and Stocker, R. (1995) Co-antioxidants Make  $\alpha$ -Tocopherol an Efficient Antioxidant for Low-Density-Lipoprotein, *Am. J. Clin. Nutr.* 62, S1357–S1364.
35. Frei, B., England, L., and Ames, B.N. (1989) Ascorbate Is an Outstanding Antioxidant in Human-Blood Plasma, *Proc. Natl. Acad. of Sci. USA* 86, 6377–6381.

[Received May 24, 2002, and in revised form October 9, 2002; revision accepted December 4, 2002]



# Dietary Flax Oil Reduces Renal Injury, Oxidized LDL Content, and Tissue n-6/n-3 FA Ratio in Experimental Polycystic Kidney Disease

Malcolm R. Ogborn\*, Evan Nitschmann, Neda Bankovic-Calic, Hope A. Weiler, and Harold Aukema

University of Manitoba, Winnipeg, Manitoba, R3E 3P4 Canada

**ABSTRACT:** As whole flaxseed is beneficial in the treatment of experimental renal disease, we undertook a study to determine whether previously documented benefits of whole flaxseed could be reproduced with dietary low-lignan flax oil (FO), a rich source of  $\alpha$ -linolenic acid, in experimental polycystic kidney disease. Male offspring of Han:SPRD-*cy* heterozygous rats were fed a synthetic diet containing FO or corn oil (CO) for 8 wk from the time of weaning. Renal inflammation, fibrosis, proliferation, cystic change, and oxidized-LDL were assessed morphometrically. Hepatic and renal lipid composition was assessed using GC. FO feeding produced hepatic and renal enrichment of n-3 PUFA and an increase in C18:>C18 PUFA ratios (18-carbon PUFA compared to longer-chain PUFA), with a reduction in proportion of hepatic long-chain PUFA. The FO-based diet was associated with lower mean cystic change by 29.7% ( $P = 0.018$ ), fibrosis by 21.7% ( $P = 0.017$ ), macrophage infiltration by 31.5% ( $P < 0.0001$ ), epithelial proliferation by 18.7% ( $P = 0.0035$ ), and ox-LDL detection by 31.4% ( $P < 0.0001$ ) in Han:SPRD-*cy* heterozygotes. Serum creatinine was significantly lower in FO-fed diseased animals. A small hypocholesterolemic effect was noted in all animals fed FO. FO feeding moderates renal injury, modifies the profile of substrates available for elongation to eicosanoid precursors, and inhibits the elongation of C<sub>18</sub> PUFA in this model. The consumption of FO-based products may prove a more practical way of obtaining health benefit than attempts to increase dietary content of unrefined seed.

Paper no. L9093 in *Lipids* 37, 1059–1065 (November 2002).

Flaxseed has possible benefits in the reduction of inflammation in rheumatic disease, reduction of atherosclerosis, and modification of hormone-dependent tumor growth (1–4). A possible mechanism for health benefits of flaxseed includes increased dietary consumption of the PUFA  $\alpha$ -linolenic acid (ALA). Such enrichment has been associated with reduction in proinflammatory prostanoids or cytokines in circulating mononuclear cells (5), particularly tumor necrosis factor  $\alpha$  and interleukin-1 $\beta$  (4). Flaxseed is also the richest natural source of mammalian lignans, present in the husk of the seed as an ester secoisolaricoresinol diglycoside (SDG) that is hydro-

lyzed in the intestinal lumen to enterodiol and enterolactone (6). SDG or its hydrolyzed products may influence health or disease through estrogenic pathways, through an antioxidant effect, or through antagonism of platelet-activating factor (3). SDG is, however, lipophobic, and refined flax oil contains only negligible amounts of SDG, making it possible to separate the contribution of the oil and the lignan experimentally.

We have demonstrated that partial dietary substitution of ground flaxseed into standard rat chow to a level of 10% by weight of diet reduced renal cystic, inflammatory, and fibrotic change in the Han:SPRD-*cy* rat (7,8). This complements previous studies that showed benefits of flaxseed or flax oil (FO) in the rat-5/6 nephrectomy model (9) and murine or human lupus erythematosus (10,11). The Han:SPRD-*cy* model of polycystic kidney disease (PKD), characterized by autosomal dominant inheritance with marked sexual dimorphism in expression, is an excellent system in which to explore the modification of chronic renal injury (12). Epithelial proliferation and progressive dilatation of nephrons, marked interstitial inflammation, and fibrosis characterize the disease (13). Oxidant injury has been implicated in its pathogenesis (14). It can be ameliorated with methyl prednisolone (15), angiotensin blockade or -converting enzyme inhibition (16,17), and lovastatin (18). Amelioration occurs with dietary soy protein substitution (19,20), protein restriction (21), and citrate supplementation (22). We showed that both soy protein- and flaxseed-based diets are associated with amelioration of this disease (8,20). In both instances, this was associated with the alteration of the renal and hepatic PUFA proportion, with evidence of a reduced conversion of linoleic acid (LA) to arachidonic acid (AA) for animals on a soy diet and an increase of n-3 FA with flaxseed. A pure animal protein-based diet is associated with more rapid disease progression than that seen with mixed vegetable and animal protein-based rat chows (8,20).

To test the hypothesis that amelioration of this disease by the administration of dietary flaxseed is related to changes in PUFA composition, we undertook this study to determine the effects of FO on renal injury in Han:SPRD-*cy* rat PKD.

## MATERIALS AND METHODS

**Animals.** All animal procedures and care were examined by the University of Manitoba Committee on Animal Use and were within the guidelines of the Canadian Council on

\*To whom correspondence should be addressed at AE 208-840 Sherbrook St., Winnipeg, MB R3A 1S1, Canada. E-mail ogborn@cc.umanitoba.ca

Abbreviations: AA, arachidonic acid; ALA,  $\alpha$ -linolenic acid; CO, corn oil as dietary lipid source; FO, flax oil as dietary lipid source; GLA,  $\gamma$ -linolenic acid; LA, linoleic acid; LC-PUFA, long-chain PUFA; ox-LDL, oxidized LDL; PKD, polycystic kidney disease; SDG, secoisolaricoresinol diglycoside.



Animal Care. Male offspring of known Han:SPRD-*cy* heterozygotes from our own breeding colony were randomly assigned to treatment or control groups at weaning (3 wk of age). Males only, two-thirds of which would be heterozygous as homozygotes do not survive beyond weaning, are used owing to the more rapid progress of this disease in male animals. Animals were killed after 8 wk on the diet and kidney and liver tissue and serum collected for analysis. Diets were based on the AIN 76 formula using casein as the protein source and 5% corn oil (CO) or 5% FO (Omega Nutrition, Vancouver, Canada) as the lipid source. The diets differed mainly in LA proportion (CO, 60.5% of dietary fat; FO, 15.8%) and ALA (CO, 0.9% of dietary fat; FO, 52.3%). Cages containing one to three animals fed the CO diet were paired to cages of animals on the FO diet, with CO diet intake limited to the amount consumed by the paired FO diet cage the previous day.

**Histology and immunohistochemistry.** Tissue from the left kidney was processed using our previously described methods (8,20) for histologic and immunohistochemical analysis. These studies included hematoxylin and eosin, aniline blue staining for fibrosis, proliferating cell nuclear antigen (M 0879; Dako A/S, Glostrup, Denmark), and macrophages (MAB1435; Chemicon International Inc., Temecula, CA). Oxidized LDL (ox-LDL) staining was used as a marker of oxidant injury (23), using a polyclonal antibody (AB3230; Chemicon International Inc.). Animals were classified by one of two experienced observers (NBC, MRO) as affected on the basis of the characteristic cystic and inflammatory pathology of this disease.

**Image analysis and morphometric assessment.** Image analysis procedures were performed with a system consisting of a Cohu high-resolution black and white camera connected to a computer via a PCVisionPlus video capture board. The observer was blinded to dietary treatment, although disease status is obvious on microscopic examination. Images were captured using the Image Pro software package (Phoenix Biotechnology, Seattle, WA). Raw image analysis data was processed as previously described (8,20). Measurements of fibrosis and cellular markers were corrected to solid tissue areas of sections as we have done previously (8,20). This prevents underestimation of these parameters due to the presence of empty cystic areas on the section.

**Chemistry.** Biochemical measurements were performed by an observer (EN) blinded to disease and dietary status. Serum creatinine and cholesterol in serum were determined

by spectrophotometric methods using Sigma kits (creatinine kit #555-A, cholesterol kit #402-20; Sigma Chemical Co., St. Louis, MO) adapted to a 96-well plate reader.

**GC.** Lipids were extracted from kidney and liver and methylated for GC as previously described (8,20). GC was performed on a Varian Chrompack 3800 instrument, using a Zebron ZB Wax 30-m column (Phenomenex, Torrance, CA).

**Statistical analysis.** Morphometric data involving comparisons relevant only to cystic groups were analyzed with Student's *t*-test with the Welch correction for unequal variances. Data from both normal and PKD animals were analyzed using a general linear model ANOVA and Tukey's *post-hoc* pairwise comparisons, using the Minitab v13 software package (Minitab Inc., State College, PA).

## RESULTS

Disease was associated with significantly lower weights in both dietary groups but was not influenced by diet. Serum creatinine was elevated in Han:SPRD-*cy* heterozygotes with PKD but was significantly lower in *post-hoc* analysis in FO-fed heterozygotes compared to CO-fed heterozygotes ( $P < 0.03$ ). Both diet and disease significantly influenced serum cholesterol, with FO producing a reduction ( $P < 0.001$ ) and disease expression producing an elevation in serum cholesterol on both diets ( $P = 0.029$ ). Serum TG was not different between diet or disease groups (Table 1).

FO supplementation was associated with significant reductions in cystic change (Figs. 1A, 1B, 2), with a decrease in epithelial proliferation (Fig. 3) that was proportionate to the observed decrease in cystic change. A comparable reduction was also seen in interstitial fibrosis (Fig. 4). Macrophage infiltration (Fig. 5) and ox-LDL detection (Fig. 6) were reduced to a similar extent by FO feeding. Data from normal animals are not shown in figures, as most of these parameters are barely detectable in normal tissue.

FO-fed animals showed a higher renal proportion of ALA, EPA, and n-3 DHA. FO-fed animals with PKD also had lower renal proportions of n-6  $\gamma$ -linolenic acid (GLA) and n-6 LA, but there were no changes in FO-fed animals without PKD (Table 2). The relative amount of AA in renal lipids did not change with diet (Table 2).

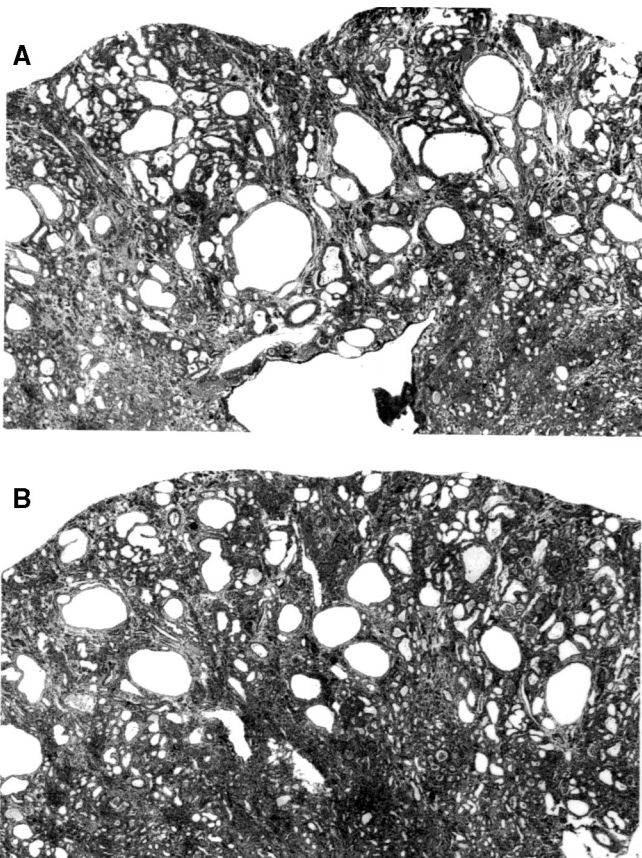
Increased relative amounts of ALA, EPA, and DHA were seen in liver tissue from all animals, with or without PKD

**TABLE 1**  
Serum Biochemistry and Weight Results<sup>a</sup>

	CO normal (n = 8)	FO normal (n = 6)	CO PKD (n = 19)	FO PKD (n = 23)	Diet effect	PKD effect
Weight (g)	370 (7.3)	373 (8.6)	320 (5.3)	315 (5.7)	NS	$P < 0.001$
Creatinine (mmol/L)	101 (15.9)	98 (18.3)	199 (10.3)	159 <sup>b</sup> (9.4)	NS	$P < 0.001$
Cholesterol (mmol/L)	2.37 (0.20)	1.51 (0.18)	2.79 (0.16)	2.04 (0.51)	$P < 0.001$	$P = 0.029$
TG (mmol/L)	0.70 (0.09)	0.60 (0.12)	0.67 (0.06)	0.52 (0.07)	NS	NS

<sup>a</sup>Results are expressed as group means with SEM in parentheses.

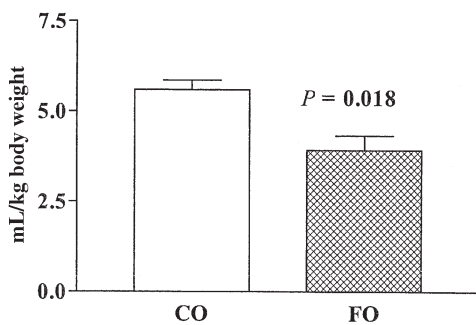
<sup>b</sup>Significantly different from polycystic kidney disease (PKD) animals fed the corn oil (CO) diet,  $P < 0.03$ . FO, flax oil; NS, not significant.



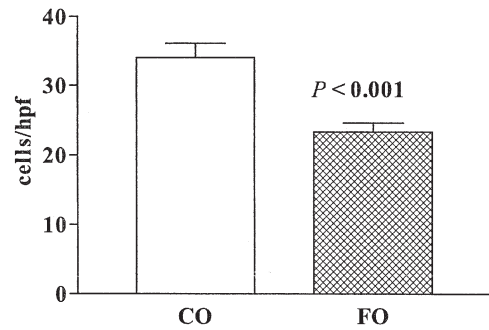
**FIG. 1.** Hematoxylin- and eosin-stained section from an 11-wk-old Han:SPRD-cy rat (A) fed corn oil (CO) diet, and (B) fed flax oil (FO) diet; 20x magnification.

(Table 2). LA, GLA, AA, and eicosatrienoic acid (20:3n-6) in liver were also significantly lower in the animals fed the FO diet.

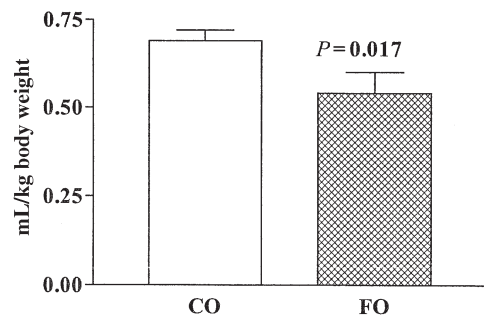
Total long-chain PUFA (LC-PUFA) was significantly decreased in the liver by FO feeding, and increased by PKD in the livers of animals on the CO diet only (Table 4). The ratio of LA/AA, although not significantly altered in kidney by diet or disease, was increased in liver by diet but was decreased in the presence of renal disease (Table 4). The ALA/(EPA + DHA) ratio was chosen as a measure of elongation of n-3 PUFA in preference to the ALA/EPA ratio owing to our inability to detect EPA in a significant number of CO samples.



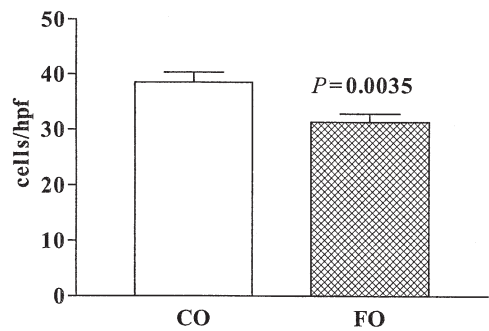
**FIG. 2.** Morphometric assessment of cystic change in animals with polycystic kidney disease (PKD). Error bars are SEM. Statistical value refers to dietary effect in animals with PKD. For abbreviations see Figure 1.



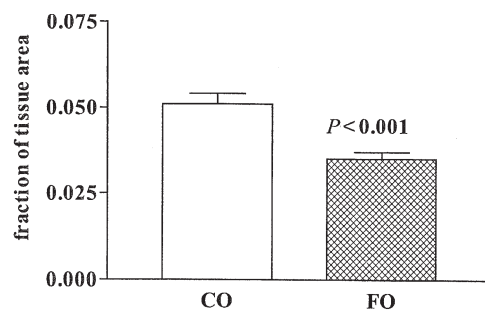
**FIG. 3.** Morphometric assessment of epithelial proliferation (proliferating cell nuclear antigen) in animals with PKD. Error bars are SEM. Statistical value refers to dietary effect in animals with PKD. hpf, high power field; for other abbreviations see Figures 1 and 2.



**FIG. 4.** Morphometric assessment of renal fibrosis in animals with PKD. Error bars are SEM. Statistical value refers to dietary effect in animals with PKD. For abbreviations see Figures 1 and 2.



**FIG. 5.** Morphometric assessment of macrophage infiltration in animals with PKD. Error bars are SEM. Statistical value refers to dietary effect in animals with PKD. For abbreviations see Figures 1, 2, and 3.



**FIG. 6.** Morphometric assessment of oxidized-LDL staining in animals with PKD. Error bars are SEM. Statistical value refers to dietary effect in animals with PKD. For abbreviations see Figures 1 and 2.

**TABLE 2**  
Renal Proportion<sup>a</sup> of Select n-6/n-3 PUFA in Han:SPRD-cy or Normal Rats Fed FO or CO Diet

	CO normal (n = 8)	FO normal (n = 6)	CO PKD (n = 19)	FO PKD (n = 23)	Diet effect P	Disease effect P
18:2n-6 (LA)	14.2 (0.9)	13.1 (1.1)	16.2 (0.6)	11.1 <sup>b</sup> (0.6)	<0.001	NS
18:3n-6 (GLA)	0.06 (0.02)	0.04 (0.02)	0.10 (0.01)	0.03 <sup>b</sup> (0.01)	<0.001	NS
18:3n-3 (ALA)	0.36 (0.90)	2.97 (1.04)	0.33 (0.62)	5.57 (0.57)	<0.001	NS
20:3n-6	0.19 (0.06)	0.24 (0.07)	0.31 (0.04)	0.20 (0.04)	NS	NS
20:3n-3	0.46 (0.10)	0.80 (0.11)	0.48 (0.07)	0.59 (0.07)	NS	NS
20:4n-6 (AA)	14.5 (2.0)	13.4 (2.3)	14.7 (1.4)	11.0 (1.3)	NS	NS
20:5n-3 (EPA)	0.02 (0.02)	0.23 (0.02)	Not detected	Not detected	NS <sup>c</sup>	NS <sup>c</sup>
22:6n-3 (DHA)	0.6 (0.1)	1.5 (0.1)	0.5 (0.1)	1.1 (0.1)	<0.001	0.021

<sup>a</sup>Results are expressed as group mean percentage of total lipids with SEM in parentheses.

<sup>b</sup>Significantly different from CO in same disease category,  $P < 0.001$  *post-hoc* testing.

<sup>c</sup>EPA was not detectable in seven samples from the CO normal group and nine samples in the CO PKD group, thus violating assumptions of normality; therefore,  $P$  values are not reported. LA, linoleic acid; GLA,  $\gamma$ -linolenic acid; ALA,  $\alpha$ -linolenic acid; AA, arachidonic acid; for other abbreviations see Table 1.

Diet produced a significant increase in this ratio in kidney and liver (Table 4). Total n-6/n-3 ratios were decreased significantly by diet in the kidney and liver (Table 4) but were significantly increased in the liver in the presence of PDK.

## DISCUSSION

Early interest in the use of FO in the treatment of renal disease was somewhat indirect, focusing on potential benefits on hypertension through modification of the renin-angiotensin system (24). Ingram *et al.* (9) demonstrated that both flaxseed and FO were protective against glomerulosclerosis in the 5/6-nephrectomy model of renal disease. FO had a greater effect on renal lipid composition and on prostanoid physiology in that model, with greater overall enrichment with n-3 PUFA and a statistically significant increase in the proportion of DHA. With mice and with humans, Hall *et al.* (10) and Clark *et al.* (11), respectively, demonstrated evidence of reduction in renal injury in lupus nephritis with use of a whole flaxseed supplement. Our earlier study in the Han:SPRD-cy rat also showed that flaxseed supplementation

was beneficial, particularly with respect to the inflammatory component of injury that is a prominent part of the Han:SPRD-cy model (8).

An important difference between this report and our earlier study is that the FO diet did result in a significant difference in the relative renal proportion of DHA (8). In our previous study, the flaxseed-supplemented diet did not increase DHA above the level seen with standard chow (control, 1.7% total lipids; flaxseed, 1.3% total lipids). This is of interest because DHA has been shown *in vitro* to inhibit macrophage response, reduce the production of pro-inflammatory cytokines, and inhibit induction of neutrophil nitric oxide synthase, a regulatory point in inflammatory events (25–28). DHA, but not EPA, *in vivo* reduces mesangial proliferation and has been proposed as a potential explanation of the apparent benefit of dietary fish oil in immunoglobulin A nephropathy (29). Expression of PKD was associated with a reduction in DHA in this study, a phenomenon also observed in the *pcy* mouse (30). In the 5/6-nephrectomy rat, Ingram *et al.* (9) demonstrated renal enrichment with ALA by both flaxseed and flax oil, and EPA only by flax oil; DHA was actually reduced by

**TABLE 3**  
Hepatic Proportion<sup>a</sup> of Select n-6/n-3 PUFA in Han:SPRD-cy or Normal Rats Fed FO or CO Diet

	CO normal (n = 8)	FO normal (n = 6)	CO PKD (n = 19)	FO PKD (n = 23)	Diet effect P	Disease effect P
18:2n-6 (LA)	20.0 (0.8)	12.1 (0.8)	20.1 (0.5)	13.9 (0.4)	<0.001	NS
18:3n-6 (GLA)	0.30 (0.03)	0.08 <sup>c</sup> (0.03)	0.52 <sup>d</sup> (0.02)	0.13 <sup>c</sup> (0.02)	<0.001 <sup>e</sup>	<0.001
18:3n-3 (ALA)	0.44 (0.26)	6.37 (0.26)	0.19 (0.15)	5.31 (0.14)	<0.001	0.003
20:3n-6	0.27 (0.02)	0.19 (0.02)	0.28 (0.01)	0.22 (0.01)	0.001	NS
20:3n-3	0.58 (0.04)	0.85 (0.04)	0.53 (0.02)	0.76 (0.02)	<0.001	0.039
20:4n-6 (AA)	14.1 (1.1)	6.4 <sup>b</sup> (1.1)	21.8 <sup>d</sup> (0.6)	9.0 (0.6)	<0.001 <sup>e</sup>	<0.001
20:5n-3 (EPA)	0.13 (0.07)	0.61 (0.07)	0.01 (0.04)	0.39 (0.04)	N/A	N/A <sup>b</sup>
22:6n-3 (DHA)	3.0 (0.4)	6.2 (0.4)	2.1 (0.2)	4.3 (0.2)	<0.001	<0.001

<sup>a</sup>Results are expressed as group mean percentage of total lipids with SEM in parentheses.

<sup>b</sup>EPA was not detectable in 4 samples from the CO normal group and 17 samples in the CO PKD group; EPA was not detectable in 7 samples from the CO normal group and 9 samples in the CO PKD group, thus violating assumptions of normality. Therefore,  $P$  values are not reported.

<sup>c</sup>Significantly different from CO in the same disease category,  $P < 0.001$  *post-hoc* testing.

<sup>d</sup>Significantly different from normal animals in the same diet category,  $P < 0.001$  *post-hoc* testing.

<sup>e</sup>Significant interaction detected between diet and PKD at  $P < 0.05$ . For abbreviations see Tables 1 and 2.



**TABLE 4**  
**Total Long-Chain PUFA (LC-PUFA) Proportions and C18:>C18 Ratios in Liver and Kidney Tissue from Animals Fed CO or FO Diets<sup>a</sup>**

	CO normal (n = 8)	FO normal (n = 6)	CO PKD (n = 19)	FO PKD (n = 23)	Diet effect P	Disease effect P
Kidney LC-PUFA <sup>b</sup>	15.8 (2.2)	16.3 (2.6)	16.0 (1.5)	13.1 (1.4)	NS	NS
Liver LC-PUFA <sup>b</sup>	19.1 (0.9)	14.2 (0.9)	24.7 (0.5)	14.3 (0.5)	<0.001 <sup>b</sup>	<0.001
Kidney n-6/n-3 ratio	21.6 (1.9)	5.3 (2.2)	25.9 (1.3)	4.0 (1.2)	<0.001	NS
Liver n-6/n-3 ratio	11.2 (1.1)	1.4 (1.1)	15.7 (0.6)	2.1 (0.6)	<0.001	0.007
Kidney LA/AA ratio	0.70 (0.52)	1.01 (0.21)	1.58 (0.52)	1.25 (0.12)	NS	NS
Liver LA/AA ratio	1.41 (0.17)	1.90 (0.12)	0.85 (0.29)	1.64 (0.06)	0.001	0.029
Kidney ALA/(EPA + DHA) ratio <sup>c</sup>	0.70 (1.11)	1.90 (1.28)	0.67 (0.77)	5.61 (0.70)	0.003	NS
Liver ALA/(EPA + DHA) ratio <sup>c</sup>	0.20 (0.08)	0.96 (0.08)	0.08 (0.04)	1.14 (0.04)	<0.001	NS

<sup>a</sup>Results are expressed as group mean percentage of total lipids; SEM is in parentheses for all results.

<sup>b</sup>Sum of proportions of 20:3n-3, 20:3n-6, AA, EPA, 22:5n-3, and DHA.

<sup>c</sup>Reported in preference to ALA/EPA ratio owing to high rate of nondetection of EPA in CO samples. C18:>C18 ratio, ratio of 18-carbon PUFA to longer-chain PUFA. For other abbreviations see Tables 1 and 2.

both flax diets (9). The reported levels of renal DHA for animals fed their standard diet were substantially higher than seen in our control animals; dietary FA analysis was not presented. In that study, AA also was increased by the flaxseed diet, causing the authors to speculate that AA metabolism to prostanoids was reduced by competition with EPA generated from increased dietary ALA. The changes in AA proportion are, however, reminiscent of those we found in Han:SPRD-cy rats fed soy protein (20), and a separate effect on FA metabolism of modification of dietary protein source, which was controlled in the study reported here, cannot be excluded as part explanation of their results.

The alterations in liver of the LA/AA ratio, ALA/(EPA + DHA) ratio, and total LC-PUFA seen in this study suggest that FO may have an inhibitory effect on  $\Delta 6$ -desaturase similar to that reported with soy protein (31). Cherian *et al.* (32) reported such inhibition in response to flaxseed supplementation in poultry. Direct modification of desaturase pathways has been proposed as a possible explanation for the anti-inflammatory and antiproliferative effects of CLA, a group of isomers of LA (33), and our results suggest a further line of inquiry to explain possible similar benefits of FO. These changes were less marked in renal tissue, with a significant difference, however, observed in ALA/(EPA + DHA). In diseased animals fed the CO diet, increased hepatic proportions of total LC-PUFA were found, and disease was also associated with lower LA/AA ratios, suggesting that the uremic state opposes diet-induced mechanisms for inhibiting elongation. The uremic state has been recognized as a proinflammatory state for many body tissues (34), but an altered content of prostanoid precursors has not yet been explored as a potential mechanism in this process.

The level of substitution of FO that we fed in these studies (approximately 2.5–3 g/kg body weight/d as ALA) would be difficult to achieve in human studies. Biologically significant effects in humans, however, are possible with dietary substitutions involving PUFA that are practical. A daily oral dose of 1800 mg of purified EPA reduces the levels of circulating remnant lipoproteins in dialysis patients, potentially stabilizing LDL and conferring some resistance to oxidation (35). Kre-

mer *et al.* (36,37) reported clinical improvements in rheumatoid arthritis patients receiving EPA-rich fish oil supplements that correlated with altered monocyte prostanoid and cytokine production. Caughey *et al.* (4) demonstrated that substitution of deodorized FO for cooking oil and in margarine-like spread caused a 74% reduction in monocyte production of tumor necrosis factor  $\alpha$  and interleukin 1 $\beta$  in healthy volunteers. Both of these cytokines have been linked to the progression of renal injury in human PKD (38). The average daily intake in that study was 13 g of FO (approximately 170 mg/kg/d assuming an average patient mass of 75 kg) (4). The study by Caughey *et al.* also represents a rare example of a direct comparison between FO and the other major dietary source of n-3 PUFA, fish oil. They found that the cytokine reduction effects correlated with the monocyte proportion of EPA (20:5), irrespective of whether FO or fish oil was the source. FO substitution in human diets has been associated with reduction in cholesterol, which may benefit renal disease progression (39) through reduced production of farnesyl phosphate and subsequent down-regulation of G-protein-mediated signaling (18). The reduction we observed in this study was very modest, however, and we failed to link hypocholesterolemic effects to disease modification in previous dietary studies (8,20).

The observation of reduced amounts of ox-LDL suggests a possible role for FO in reducing susceptibility to oxidant stress. The Han:SPRD-cy rat model of PKD involves compromised resistance to oxidant injury, both as decreased expression of antioxidant enzymes (14) and aggravation of disease by inhibition of glutathione synthesis (40). Dietary antioxidant therapy with  $\alpha$ -tocopherol, however, did not produce improvement in the prevalence of renal injury (41).

The observation that both diet and expression of renal disease were associated with significant alterations in hepatic lipids also supports previous studies in both modification of renal injury and nonrenal metabolism in early uremia (20,42). The basis for such metabolic effects in mild uremia remains as yet unexplored.

Han:SPRD-cy rat PKD is associated with a marked inflammatory component, and the infiltrating cells arise outside the kidney. As such, the profile of PUFA in these circulation-



derived cells may be important in determining the type of inflammatory lipid products released. This profile may be more dependent on hepatic regulation of FA production than the local renal lipid environment. The effect of our dietary interventions on circulating inflammatory cells in this model will be a future line of inquiry.

Boyd-Eaton *et al.* (43) pointed out that the sophistication of human society has been associated with a 10- to 20-fold increase in the ratio of n-6/n-3 FA in the human diet. Manipulations of animal diets that reproduce these trends in FA intake are associated with worsening of inflammatory and malignant disease, and, in certain models, the development of insulin resistance (24). In this anthropologic context, the intervention studied here might be viewed as a return to the dietary pattern on which our metabolic responses evolved.

Our studies confirm the importance of testing specific food ingredients in dietary intervention in renal disease, rather than broad categories such as total protein or fat content. Our results demonstrate that FO, either incorporated into common foodstuffs or given as a therapeutic supplement, may be of similar value to administration of whole flaxseed in the amelioration of renal injury.

## ACKNOWLEDGMENTS

This work was supported by an operating grant from the Strategic Development Initiative of the Manitoba Health Research Council with partnership from the Flax Council of Canada. Laboratory facilities in the John Buhler Research Centre in Winnipeg are supported by the Children's Hospital Foundation of Manitoba, Inc. Dr. Hope Weiler is the recipient of a New Investigator Award of the Canadian Institutes of Health Research.

## REFERENCES

- Tou, J.C., and Thompson, L.U. (1999) Exposure to Flaxseed or Its Lignan Component During Different Developmental Stages Influences Rat Mammary Gland Structures, *Carcinogenesis* 20, 1831–1835.
- Prasad, K. (1997) Dietary Flax Seed in Prevention of Hypercholesterolemic Atherosclerosis, *Atherosclerosis* 132, 69–76.
- Kurzer, M.S., and Xu, X. (1997) Dietary Phytoestrogens, *Annu. Rev. Nutr.* 17, 353–381.
- Caughey, G.E., Mantzioris, E., Gibson, R.A., Cleland, L.G., and James, M.J. (1996) The Effect on Human Tumor Necrosis Factor Alpha and Interleukin 1 Beta Production of Diets Enriched in n-3 Fatty Acids from Vegetable Oil or Fish Oil, *Am. J. Clin. Nutr.* 63, 116–122.
- Gibson, R.A., Neumann, M.A., James, M.J., Hawkes, J.S., Hall, C., and Cleland, L.G. (1992) Effect of n-3 and n-6 Dietary Fats on the Lipoxygenase Products from Stimulated Rat Neutrophils, *Prostaglandins Leukot. Essent. Fatty Acids* 46, 87–91.
- Borriello, S.P., Setchell, K.D., Axelson, M., and Lawson, A.M. (1985) Production and Metabolism of Lignans by the Human Faecal Flora, *J. Appl. Bacteriol.* 58, 37–43.
- Ogborn, M.R., Nitschmann, E., Bankovic-Calic, N., Buist, R., and Peeling, J. (1998) The Effect of Dietary Flaxseed Supplementation on Organic Anion and Osmolyte Content and Excretion in Rat Polycystic Kidney Disease, *Biochem. Cell Biol.* 76, 553–559.
- Ogborn, M.R., Nitschmann, E., Weiler, H., Leswick, D., and Bankovic-Calic, N. (1999) Flaxseed Ameliorates Interstitial Nephritis in Rat Polycystic Kidney Disease, *Kidney Int.* 55, 417–423.
- Ingram, A.J., Parbtani, A., Clark, W.F., Spanner, E., Huff, M.W., Philbrick, D.J., and Holub, B.J. (1995) Effects of Flaxseed and Flax Oil Diets in a Rat-5/6 Renal Ablation Model, *Am. J. Kidney Dis.* 25, 320–329.
- Hall, A.V., Parbtani, A., Clark, W.F., Spanner, E., Keeney, M., Chin Yee, I., Philbrick, D.J., and Holub, B.J. (1993) Abrogation of MRL/lpr Lupus Nephritis by Dietary Flaxseed, *Am. J. Kidney Dis.* 22, 326–332.
- Clark, W.F., Parbtani, A., Huff, M.W., Spanner, E., de Salis, H., Chin Yee, I., Philbrick, D.J., and Holub, B.J. (1995) Flaxseed: A Potential Treatment for Lupus Nephritis, *Kidney Int.* 48, 475–480.
- Cowley, B.D., Jr., Gudapaty, S., Kraybill, A.L., Barash, B.D., Harding, M.A., Calvet, J.P., and Gattone, V.H., 2nd (1993) Autosomal-Dominant Polycystic Kidney Disease in the Rat, *Kidney Int.* 43, 522–534.
- Gretz, N., Ceccherini, I., Kranzlin, B., Kloting, I., Devoto, M., Rohmeiss, P., Hoher, B., Waldherr, R., and Romeo, G. (1995) Gender-Dependent Disease Severity in Autosomal Polycystic Kidney Disease of Rats, *Kidney Int.* 48, 496–500.
- Maser, R.L., Vassmer, D., Magenheimer, B.S., and Calvet, J.P. (2002) Oxidant Stress and Reduced Antioxidant Enzyme Protection in Polycystic Kidney Disease, *J. Am. Soc. Nephrol.* 13, 991–999.
- Gattone, V.H., 2nd, Cowley, B.D., Jr., Barash, B.D., Nagao, S., Takahashi, H., Yamaguchi, T., and Grantham, J.J. (1995) Methylprednisolone Retards the Progression of Inherited Polycystic Kidney Disease in Rodents, *Am. J. Kidney Dis.* 25, 302–313.
- Keith, D.S., Torres, V.E., Johnson, C.M., and Holley, K.E. (1994) Effect of Sodium Chloride, Enalapril, and Losartan on the Development of Polycystic Kidney Disease in Han:SPRD Rats, *Am. J. Kidney Dis.* 24, 491–498.
- Ogborn, M.R., Sareen, S., and Pinette, G. (1995) Cilazapril Delays Progression of Hypertension and Uremia in Rat Polycystic Kidney Disease, *Am. J. Kidney Dis.* 26, 942–946.
- Gile, R.D., Cowley, B.D., Jr., Gattone, V.H., 2nd, O'Donnell, M.P., Swan, S.K., and Grantham, J.J. (1995) Effect of Lovastatin on the Development of Polycystic Kidney Disease in the Han:SPRD Rat, *Am. J. Kidney Dis.* 26, 501–507.
- Ogborn, M., Bankovic-Calic, N., Shoemith, C., Buist, R., and Peeling, J. (1998) Soy Protein Modification of Rat Polycystic Kidney Disease, *Am. J. Physiol.* 274 (Renal Physiol. 43), F541–F549.
- Ogborn, M.R., Nitschmann, E., Weiler, H.A., and Bankovic-Calic, N. (2000) Modification of Polycystic Kidney Disease and Fatty Acid Status by Soy Protein Diet, *Kidney Int.* 57, 159–166.
- Ogborn, M.R., and Sareen, S. (1995) Amelioration of Polycystic Kidney Disease by Modification of Dietary Protein Intake in the Rat, *J. Am. Soc. Nephrol.* 6, 1649–1654.
- Tanner, G.A. (1998) Potassium Citrate/Citric Acid Intake Improves Renal Function in Rats with Polycystic Kidney Disease, *J. Am. Soc. Nephrol.* 9, 1242–1248.
- Bosmans, J.L., Holvoet, P., Dauwe, S.E., Ysebaert, D.K., Chapelle, T., Jurgens, A., Kovacic, V., Van Marck, E.A., De Broe, M.E., and Verpooten, G.A. (2001) Oxidative Modification of Low-Density Lipoproteins and the Outcome of Renal Allografts at 1½ Years, *Kidney Int.* 59, 2346–2356.
- Simopoulos, A.P. (1989) Summary of the NATO Advanced Research Workshop on Dietary Omega 3 and Omega 6 Fatty Acids: Biological Effects and Nutritional Essentiality, *J. Nutr.* 119, 521–528.
- Khair el Din, T., Sicher, S.C., Vazquez, M.A., Chung, G.W., Stallworth, K.A., Kitamura, K., Miller, R.T., and Lu, C.Y. (1996) Transcription of the Murine iNOS Gene Is Inhibited by

- Docosahexaenoic Acid, a Major Constituent of Fetal and Neonatal Sera as Well as Fish Oils, *J. Exp. Med.* 183, 1241–1246.
26. Khair el Din, T.A., Sicher, S.C., Vazquez, M.A., Wright, W.J., and Lu, C.Y. (1995) Docosahexaenoic Acid, a Major Constituent of Fetal Serum and Fish Oil Diets, Inhibits IFN  $\gamma$ -Induced Ia-Expression by Murine Macrophages *in vitro*, *J. Immunol.* 154, 1296–1306.
  27. Dustin, L.B., Shea, C.M., Soberman, R.J., and Lu, C.Y. (1990) Docosahexaenoic Acid, a Constituent of Rodent Fetal Serum and Fish Oil Diets, Inhibits Acquisition of Macrophage Tumoricidal Function, *J. Immunol.* 144, 4888–4897.
  28. De Caterina, R., Cybulsky, M.I., Clinton, S.K., Gimbrone, M.A., Jr., and Libby, P. (1994) The Omega-3 Fatty Acid Docosahexaenoate Reduces Cytokine-Induced Expression of Proatherogenic and Proinflammatory Proteins in Human Endothelial Cells, *Arterioscler. Thromb.* 14, 1829–1836.
  29. Grande, J.P., Walker, H.J., Holub, B.J., Warner, G.M., Keller, D.M., Haugen, J.D., Donadio, J.V., Jr., and Dousa, T.P. (2000) Suppressive Effects of Fish Oil on Mesangial Cell Proliferation *in vitro* and *in vivo*, *Kidney Int.* 57, 1027–1040.
  30. Aukema, H.M., Yamaguchi, T., Takahashi, H., Celi, B., and Holub, B.J. (1992) Abnormal Lipid and Fatty Acid Compositions of Kidneys from Mice with Polycystic Kidney Disease, *Lipids* 27, 429–435.
  31. Koba, K., and Wakamatsu, K., Obata, K., and Sugano, M. (1993) Effects of Dietary Proteins on Linoleic Acid Desaturation and Membrane Fluidity in Rat Liver Microsomes, *Lipids* 28, 457–464.
  32. Cherian, G., and Sim, J. S. (2001) Maternal Dietary  $\alpha$ -Linolenic Acid (18:3n-3) Alters n-3 Polyunsaturated Fatty Acid Metabolism and Liver Enzyme Activity in Hatched Chicks, *Poult. Sci.* 80, 901–905.
  33. Smith, S.B., Hively, T.S., Cortese, G.M., Han, J.J., Chung, K.Y., Castenada, P., Gilbert, C.D., Adams, V.L., and Mersmann, H.J. (2002) Conjugated Linoleic Acid Depresses the  $\Delta 9$  Desaturase Index and Stearoyl Coenzyme A Desaturase Enzyme Activity in Porcine Subcutaneous Adipose Tissue, *J. Anim. Sci.* 80, 2110–2115.
  34. Don, B.R., and Kaysen, G.A. (2000) Assessment of Inflammation and Nutrition in Patients with End-Stage Renal Disease, *J. Nephrol.* 13, 249–259.
  35. Ando, M., Sanaka, T., and Nihei, H. (1999) Eicosapentanoic Acid Reduces Plasma Levels of Remnant Lipoproteins and Prevents *in vivo* Peroxidation of LDL in Dialysis Patients, *J. Am. Soc. Nephrol.* 10, 2177–2184.
  36. Kremer, J.M., Lawrence, D.A., Jubiz, W., DiGiacomo, R., Rynes, R., Bartholomew, L.E., and Sherman, M. (1990) Dietary Fish Oil and Olive Oil Supplementation in Patients with Rheumatoid Arthritis. Clinical and Immunologic Effects, *Arthritis Rheum.* 33, 810–820.
  37. Kremer, J.M. (2000) n-3 Fatty Acid Supplements in Rheumatoid Arthritis, *Am. J. Clin. Nutr.* 71, 349S–351S.
  38. Gardner, K.D., Jr., Burnside, J.S., Elzinga, L.W., and Locksley, R.M. (1991) Cytokines in Fluids from Polycystic Kidneys, *Kidney Int.* 39, 718–724.
  39. Harris, W.S. (1997) n-3 Fatty Acids and Serum Lipoproteins: Human Studies, *Am. J. Clin. Nutr.* 65, 1645S–1654S.
  40. Torres, V.E., Bengal, R.J., Litwiller, R.D., and Wilson, D.M. (1997) Aggravation of Polycystic Kidney Disease in Han:SPRD Rats by Buthionine Sulfoximine, *J. Am. Soc. Nephrol.* 8, 1283–1291.
  41. Torres, V.E., Bengal, R.J., Nickander, K.K., Grande, J.P., and Low, P.A. (1998) Renal Concentration of  $\alpha$ -Tocopherol: Dependence on Gender and Lack of Effect on Polycystic Kidney Disease in Han:SPRD Rats, *Am. J. Kidney Dis.* 31, 687–693.
  42. Ogborn, M.R., Nitschmann, E., Bankovic-Calic, N., Buist, R., and Peeling, J. (2000) Dietary Betaine Modifies Hepatic Metabolism but Not Renal Injury in Rat Polycystic Kidney Disease, *Am. J. Physiol. Gastrointest. Liver Physiol.* 279, G1162–G1168.
  43. Boyd-Eaton, S., Eaton, S.B., 3rd, Konner, M.J., and Shostak, M. (1996) An Evolutionary Perspective Enhances Understanding of Human Nutritional Requirements, *J. Nutr.* 126, 1732–1740.

[Received June 21, 2002, and in revised form October 30, 2002; revision accepted December 4, 2002]

# Tuna Fishmeal as a Source of DHA for n-3 PUFA Enrichment of Pork, Chicken, and Eggs

Peter R.C. Howe<sup>a,\*</sup>, Jeffrey A. Downing<sup>a,b</sup>, Brin F.S. Grenyer<sup>a</sup>,  
Elizabeth M. Grigonis-Deane<sup>a</sup>, and Wayne L. Bryden<sup>a,b</sup>

<sup>a</sup>Smart Foods Centre, University of Wollongong, NSW 2522, Australia, and <sup>b</sup>Faculty of Veterinary Science, University of Sydney, Camden, NSW 2570, Australia

**ABSTRACT:** Enriching foods with long-chain n-3 PUFA (LC n-3 PUFA) is an important approach to increasing the dietary intake of these beneficial nutrients. Enrichment of meat and eggs can be achieved by adding flaxseed, fish oil, or fishmeal to pig or poultry feeds. However, utilization of these sources, particularly fishmeal, has been limited by concerns about adverse effects on sensory qualities. In this study, we evaluated the use of PorcOmega™ (POM), a stabilized tuna fishmeal formulation, as a source of DHA for enrichment of pork and poultry products. Pigs, broilers, and laying hens were fed rations containing varying levels of POM for varying time periods, and its impact on the LC n-3 PUFA content and sensory qualities of cooked meat and eggs was examined. Pork and chicken products, including chops, sausages, and eggs, with substantially increased (up to sevenfold) levels of LC n-3 PUFA (predominantly DHA) were achieved by including up to 10% POM in rations. The increases were retained after cooking. Some sensory deficits were noted when using higher levels of POM (exceeding 15% in meat and 10% in eggs). However, at modest rates of feeding (5–10% POM), palatable meat and eggs were obtained with worthwhile levels of enrichment. The fishmeal feeding strategy used in this study offers a viable means of producing a range of alternative dietary sources of LC n-3 PUFA.

Paper no. L9070 in *Lipids* 37, 1067–1076 (November 2002).

There is increasing awareness of potential health benefits, especially cardiovascular, to be gained by increasing the consumption of long-chain n-3 PUFA (LC n-3 PUFA), *viz.*, EPA, docosapentaenoic acid (DPA), and DHA (1,2). Recommendations for dietary intakes for LC n-3 PUFA range from 200 to 1000 mg/d, the most recent being 650 mg/d as an adequate intake for adults, of which at least 200 mg/d should be DHA (3). This target is surpassed in countries with a high consumption of fish, e.g., approximately 700 mg/d in Norway and 1500 mg/d in Japan (4). However, in countries such as the United States and Australia where the relative consumption of meat is much greater, the average dietary intake of LC n-3 PUFA (150 and 190 mg/d, respectively) falls well short of recommendations (5,6). The demand in these countries for alternative dietary sources has

Present address of fifth author: School of Animal Studies, University of Queensland, Gatton, QLD 4343, Australia.

\*To whom correspondence should be addressed at Department of Physiology, University of Adelaide, SA 5005, Australia.  
E-mail: peter.howe@adelaide.edu.au

Abbreviations: ALA,  $\alpha$ -linolenic acid; DPA, docosapentaenoic acid; FQ, forequarter; FSANZ, Foods Standards Australia New Zealand; GC, gas chromatograph; LC n-3 PUFA, long-chain n-3 PUFA; POM, PorcOmega™.

prompted the food industry to add LC n-3 PUFA to a wide variety of processed foods, usually in a microencapsulated or emulsified form to protect the LC n-3 PUFA from oxidative degradation. The products of degradation may cause tainting, *i.e.*, adversely affecting the taste and flavor of the food.

Another strategy is to enrich meat and eggs naturally with LC n-3 PUFA by including appropriate sources in livestock rations. Pigs and poultry readily incorporate dietary FA in body tissues so that significant increases in the n-3 content of pork (7–9), chicken, and eggs (10–15) have been achieved by adding marine sources such as fish oil, fishmeal, or microalgae to rations. This approach is less effective in ruminants, however, unless the FA are delivered in a protective coating (16,17). As with other approaches to n-3 enrichment of foods, feeding n-3 sources to livestock may lead to tainting of the meat and egg products, thus reducing their consumer acceptability (18–23). Feeding strategies are required that aim for optimal n-3 enrichment with minimal tainting of the product.

Vegetable sources of  $\alpha$ -linolenic acid (ALA) are cheaper than marine sources of n-3 PUFA for enrichment, with possibly less likelihood of tainting (11,12,24). However, the conversion of ALA to LC n-3 PUFA is limited in animals as in humans (25). Flaxseed is therefore of limited value for increasing the LC n-3 PUFA content of pork, and it still has the capacity to cause tainting if degraded (18,24). On the other hand, flaxseed and canola have been used in poultry feeds either alone or in combination with fish oil to enrich chicken meat and eggs, the relative proportion of vegetable to fish oil influencing the cost and extent of LC n-3 PUFA enrichment (10–12).

Fishmeal offers a cheaper and more plentiful source of LC n-3 PUFA than fish oil for direct n-3 enrichment of pork and poultry (26,27). However, the potential for fishmeal to taint meat and eggs, even at relatively low rates of inclusion in rations, is widely recognized. Moreover, tainted feeds reduce feed consumption and impair livestock productivity. For this reason, it has been recommended that inclusion of fishmeal in grower and finisher pig rations be limited to 5% (28). In a previous study, however, we found that feeding a high level (20%) of stabilized tuna fishmeal (PorcOmega™, POM) to pigs resulted in substantial n-3 enrichment of pork with minimal detrimental effects (7). Tuna meal has a higher content of DHA relative to EPA than fish oil or fishmeals of many other species (other fishmeals may contain a higher content of EPA relative to DHA). As DHA is the predominant LC n-3 PUFA in animal tissues, feeding an n-3 source in which DHA

predominates is likely to be more efficient than using either an EPA- or ALA-rich source.

Following these initial promising observations, we conducted a series of studies to evaluate the use of tuna fishmeal to enrich chicken meat and eggs and pork products. Our goal was to produce foods with acceptable sensory qualities that would qualify for a new nutrition claim introduced by Foods Standards Australia New Zealand (FSANZ) in its Revised Food Standards Code, *viz.*, foods can be labeled as “a good source of omega-3” if they contain at least 60 mg of EPA and/or DHA per serving with less than 5% saturated/*trans* fat (29). The current report describes the extent of n-3 enrichment achieved and its impact on the sensory qualities of the products.

## MATERIALS AND METHODS

Production trials with pigs and poultry were conducted at the Camden Campus of The University of Sydney to compare effects of feeding experimental rations containing POM. Approval for the feeding trials was obtained from The University of Sydney’s Animal Ethics Committee. Meats and eggs obtained from the trials were used for chemical and sensory evaluation at the Smart Foods Centre, University of Wollongong. Wollongong University’s Human Research Ethics Committee approved the evaluation of products by volunteer panelists.

*Formulation of rations.* The rations were formulated to be isonitrogenous and isocaloric and to meet nutritional requirements for pigs (30) and broiler chickens and laying hens (31). POM, a tuna fishmeal formulation containing a complex antioxidant system and flavorings designed to eliminate objectionable fish odor and taint, was provided by Bartlett Grain Pty. Ltd., Sydney, Australia. POM was substituted for other ingredients typically used in a least-cost formulation, e.g., meat and bone, soy and canola meals, while maintaining an

appropriate macronutrient profile. Total fat contents of the rations averaged 4.5% of total energy for layer, 3.7% for broiler starter, 5.2% for broiler finisher, and 3.2% for pig finisher rations. Table 1 shows the FA compositions of POM and of representative finisher rations.

*Production of eggs.* Groups of 14 mature laying hens were randomized to one of seven feeding strategies as follows: (i) control diet for 42 d; (ii) 5, 10, 15, or 20% POM diet for 42 d; (iii) control diet for 14 d followed by 20% POM diet for 28 d; (iv) control diet for 28 d followed by 20% POM diet for 14 d. Eggs were collected at the end of each treatment period ( $\pm 2$  d) and were stored at 0–4°C. The logistics of conducting the sensory panels necessitated keeping eggs for up to 1 mon prior to evaluation.

*Production of chicken meat.* Groups of 54-d-old male broilers were randomized to one of nine feeding strategies as follows: (i) control diet for 42 d; (ii) 5, 10, 15, or 20% POM diet for 42 d; (iii) control diet for 18 d followed by 5, 10, 15, or 20% POM diet for 24 d. At the end of the treatment period, birds were processed to obtain skinless breast, thigh fillets, and typical aggregate meat for sausage production from each treatment group. Samples were individually wrapped and stored frozen at –15°C for subsequent chemical and sensory analysis.

*Production of pork.* Groups of three male and three female pigs were fed 15% POM for 6 wk or 20% POM for 4 wk prior to slaughter. A group of four male and four female pigs was maintained on the control ration. Samples of forequarter chops, loin chops, and leg fillets were obtained from each pig. Equal portions of suitable meat for sausages were also taken from each pig and pooled for each treatment group to produce sausages. All meat samples were individually wrapped and stored frozen at –15°C for subsequent chemical and sensory analysis.

*Chemical analysis.* Determinations of FA and cholesterol composition were made on five individual eggs from each

**TABLE 1**  
FA Composition (% of total FA) of PorcOmega™ Tuna Fishmeal<sup>a</sup> (POM)  
and of Representative Finisher Rations Fed to Broilers, Layers, and Pigs

	POM	Broiler		Layer		Pig	
		Control	10% POM	Control	10% POM	Control	15% POM
14:0	3.1	1.2	1.1	1.2	1.5	1.0	1.5
16:0	24.1	18.4	17.7	21.4	21.0	20.8	21.0
16:1	3.9	1.1	1.4	1.1	1.8	0.7	1.8
18:0	8.5	7.8	4.5	8.0	5.0	6.6	3.9
18:1n-9	19.2	35.2	29.1	30.6	23.9	21.5	17.1
18:1n-7	2.4	2.9	2.4	2.8	1.9	1.7	1.5
18:2n-6	3.5	29.9	33.1	31.2	31.5	43.1	32.5
18:3n-6	0.3	0.1	0.1	0.0	0.1		0.1
18:3n-3	1.1	2.6	3.0	2.7	0.7	3.3	3.2
20:1n-9	1.4	0.5	0.7	0.6	0.2	0.5	1.1
20:2n-6	0.3		0.1				0.2
20:4n-6	2.3		0.5		0.2		1.0
20:5n-3	4.8	0.2	1.3	0.1	2.2	0.2	2.8
22:4n-6	1.8		0.3		0.5		0.7
22:5n-3	1.1	0.2	0.2	0.2	0.4	0.2	0.5
22:6n-3	22.4	0.1	5.4	0.1	8.9	0.2	11.2

<sup>a</sup>POM, tuna fishmeal formulation containing a complex antioxidant system and flavorings designed to eliminate objectionable fish odor and taint (Bartlett Grain Pty. Ltd., Sydney, Australia).



treatment group. Eggs were broken, yolks and whites separated, and weights recorded. The yolks were gently stirred, then 100  $\mu$ L aliquots were homogenized in chloroform/methanol containing a FA internal standard (21:0; Sigma Chemical Co., St. Louis, MO) and extracted for FA analysis using a direct transesterification procedure (32). FAME were measured on a Shimadzu gas chromatograph (GC; Shimadzu Corporation, Kyoto, Japan) fitted with an FID and using a fused-silica Crossbond® polyethylene glycol capillary column (0.32 mm i.d. and 0.25  $\mu$ m film thickness, Restek Corporation, Bellefonte, PA). Samples were injected at 150°C. The oven temperature was set to increase by 20°C/min to 190°C, then by 5°C/min to 210°C, then by 1.5°C/min to 220°C, then by 2°C/min to 230°C, then by 5°C/min to a final temperature of 240°C, which was held for 3 min. The injector and detectors were maintained at 250°C and hydrogen was used as the carrier gas. Peak areas and FA percentages were quantified on an IBM-compatible workstation using Shimadzu software. A standard mixture of FAME (Sigma Chemical Co.) was used to calibrate the GC and to determine response factors. FA concentrations were estimated by reference to the recovery of the standard.

The cholesterol content of yolks was measured by an enzymatic colorimetric test on a Cobas autoanalyzer (Roche Diagnostics Corporation, Indianapolis, IN) using Roche Diagnostics test kits (Roche Diagnostics Corporation). The autoanalyzer was calibrated using a calibrator for automated systems (Roche Diagnostics Corporation).

Frozen portions of uncooked chicken breasts, thighs, and sausages were thawed and sampled for FA analyses. Three portions of each were randomly selected from each treatment group.

Portions of chicken meat that had been cooked for sensory evaluation were also used for FA analysis. Core samples weighing approximately 100 mg were obtained from lean regions of the meat using a cork borer. The total fat content of uncooked meat was also assayed in randomly selected whole untrimmed portions by Weston Analytical Laboratories (Sydney, Australia) using a Soxhlet extraction procedure (33).

Raw and cooked portions of pork loin, leg, and shoulder chops and sausages were similarly used for analyses of total fat and FA contents. One portion of each type of raw meat was randomly selected from each pig in each treatment group except for sausages, which were prepared from meat pooled from all pigs in each group.

**Sensory evaluation.** Panelists (5 men and 11 women recruited by advertisement) were specifically trained to conduct organoleptic analysis for each type of food being evaluated. Potential panelists were screened on a number of standard sensory discrimination tests assessing sweet, sour, bitter, and salt flavors. After passing these tests, they progressed to the second phase of training, which comprised 5 h of tasting regular supermarket foods over a period of 4 wk. Panelists were trained to use a common vocabulary for either meat or egg tasting and to practice discriminating the sensory attributes of flavor, texture, color, and odor. Tasting was conducted under

standard conditions. Panelists were given extensive feedback at each training session on their responses and were shown how their responses compared to the group. Panelists were thus given multiple practice and feedback sessions to improve their discrimination skills.

Tasting sessions of approximately 25 min duration were repeated on three occasions for each food tested. Eggs were served soft-boiled. All meats used for tasting were cooked in random order on a Breville Professional Grill and Sandwich Press TG-900, set to highest heat. Samples were cut into 1-cm squares and presented to the panelists on coded toothpicks. Panelists were requested to refresh their palate with water after each sample tasted. The sensory qualities tested were specific attributes related to taste, texture, aroma, mouthfeel, and hedonics. The wording of the sensory attributes and the line scale dimensions were made by the panelists in conjunction with the investigators during the training phase. This procedure ensured that all panelists were concordant with the attributes and their meaning and could agree to score quality consistently.

**Statistical analysis.** Biochemical data are presented as mean  $\pm$  SEM. Student's *t*-test was used to determine the significance of differences between means;  $P < 0.05$  was considered significant. ANOVA was applied to the sensory analysis for each variable (color, texture, odor, flavor, liking) to determine significances of differences between mean scores for these variables. *t*-Tests with Bonferroni adjustments were used to compare individual treatments.

## RESULTS

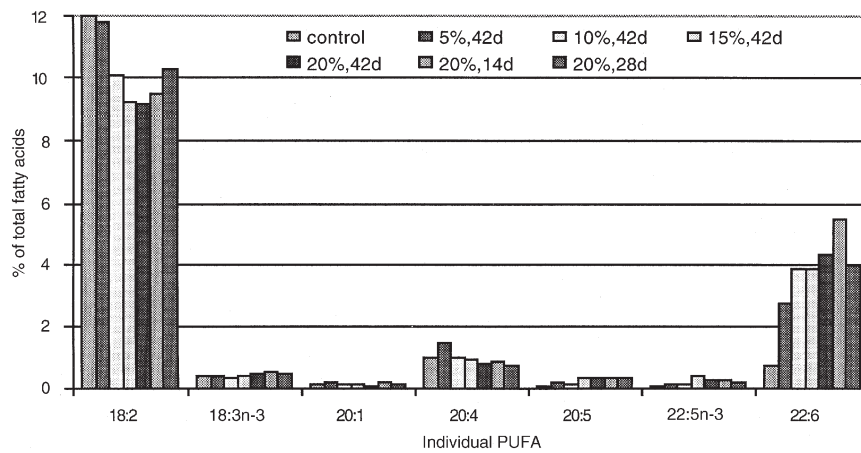
**Chemical analysis of eggs.** Table 2 shows the effect of feeding POM to laying hens on the total LC n-3 PUFA content of eggs. The concentration in yolks rose with increasing POM content of rations, reaching a maximum at 10% by weight of the feed. At the highest inclusion rate (20%), there was no apparent effect of varying the duration of feeding from 14 to 42 d. Feeding DHA-rich fishmeal resulted in a selective increase of DHA (Fig. 1). Even at the lowest POM inclusion rate (5%),

**TABLE 2**  
**Cholesterol (mg) and Total Long-Chain n-3 PUFA (LC n-3 PUFA, mg/100 g) in Eggs from Chickens Fed 5–20% of POM for 42 d, from Chickens Fed 20% of POM for 28 d, and from Chickens Fed 20% of POM for 14 d Compared with Unsupplemented Chickens<sup>a</sup> (control)**

POM treatment	Yolk weight (g)	Egg weight (g)	Cholesterol in yolk (mg)	LC n-3 PUFA in yolk (mg/100 g)	LC n-3 PUFA per egg (mg)
0%, control	18 $\pm$ 1	52 $\pm$ 3	309 $\pm$ 15	289 $\pm$ 21	51 $\pm$ 4
5%, 42 d	18 $\pm$ 1	57 $\pm$ 2	333 $\pm$ 36	969 $\pm$ 139 <sup>b</sup>	177 $\pm$ 53 <sup>b</sup>
10%, 42 d	18 $\pm$ 0	55 $\pm$ 2	328 $\pm$ 29	1806 $\pm$ 283 <sup>b</sup>	316 $\pm$ 82 <sup>b</sup>
15%, 42 d	18 $\pm$ 0	55 $\pm$ 2	411 $\pm$ 32	1390 $\pm$ 184 <sup>b</sup>	255 $\pm$ 38 <sup>b</sup>
20%, 42 d	18 $\pm$ 1	53 $\pm$ 2	314 $\pm$ 15	1502 $\pm$ 135 <sup>b</sup>	271 $\pm$ 62 <sup>b</sup>
20%, 28 d	18 $\pm$ 1	55 $\pm$ 3	413 $\pm$ 55	1372 $\pm$ 68 <sup>b</sup>	252 $\pm$ 18 <sup>b</sup>
20%, 14 d	19 $\pm$ 1	57 $\pm$ 0	388 $\pm$ 17	1603 $\pm$ 69 <sup>b</sup>	304 $\pm$ 20 <sup>b</sup>

<sup>a</sup>Data are presented as mean  $\pm$  SEM,  $n = 5$  per group.

<sup>b</sup>Significantly different from control ( $P < 0.01$ ). For abbreviation and manufacturer see Table 1.



**FIG. 1.** PUFA composition (% of total FA) of egg yolks from poultry fed different levels (5–20%) of PorcOmega™ tuna fishmeal (POM) for 28 and 42 d and unsupplemented poultry (control). POM: tuna fishmeal formulation containing a complex antioxidant system and flavorings designed to eliminate objectionable fish odor and taint (Bartlett Grain Pty. Ltd., Sydney, Australia).

there was a threefold increase in DHA content, accounting for almost all of the LC n-3 PUFA increase (from 51 mg in control eggs to 177 mg). This is equivalent to that of commercially available n-3-enriched eggs and, by yielding more than 60 mg of LC n-3 PUFA per serving, would qualify for FSANZ's "good source of omega-3" claim (29). The cholesterol content of yolks was unaffected by feeding 5 or 10% POM. However, higher rates of POM inclusion tended to raise cholesterol content. The proportions of saturated fat and PUFA in yolks remained relatively constant across treatment groups (31–34% and 15–18%, respectively).

**Sensory evaluation of eggs.** Owing to logistical limitations, eggs from only two POM treatment protocols (10% for 42 d and 20% for 14 d) were used for sensory evaluation. These treatments had resulted in the highest levels of LC n-3 PUFA enrichment (at least six times higher than control). They were compared with eggs from hens fed the control diet and with a commercial n-3-enriched egg (Body Egg™, Chanteclair Farms, Quakers Hill, NSW, Australia). The LC n-3 PUFA content of the latter was similar to that of the 5% POM eggs (approximately three times higher than controls).

Figure 2 summarizes overall assessments for the eggs, based on criteria related to each of the six sensory attributes evaluated, *viz.*, color, texture, mouthfeel, aroma, flavor, and hedonics. The experimental n-3-enriched eggs were less desirable in most characteristics than the Body Egg and, to a lesser extent, the control egg. The Body Egg was superior in color to the eggs produced in this study, probably due to the use of pigment additives. Although there were no quantitative differences in odor, more than half of the panelists detected a fishy odor in the 20% POM eggs. Overall, the 10 and 20% POM eggs were liked less than the other eggs.

**Chemical analysis of chicken.** The n-3 PUFA content of chicken meat was also increased by feeding POM-enriched diets to poultry for either 21 or 42 d. Table 3 shows the total LC n-3 PUFA concentrations in uncooked samples of chicken

breasts, thighs, and sausages from each treatment group. The group fed 15% POM for 21 d showed the greatest n-3 enrichment, with 7- to 14-fold increases in the LC n-3 PUFA content of chicken meat. Even 5% POM fed for 21 or 42 d gave three- to sixfold increases, reaching the level required for a "good source of omega-3" claim. As with the eggs, the n-3 enrichment of chicken meat was due almost entirely to increased DHA content, as exemplified by changes in the PUFA profile of chicken breasts (Fig. 3). In breasts from birds fed 10% POM for 21 d, the relative content of DHA actually exceeded that of linoleic acid (18:2n-6).

When samples of n-3 PUFA-enriched chicken breasts and thighs were cooked by grilling (Table 4), the absolute concentrations of FA, including LC n-3 PUFA, tended to be higher than in raw meat. This is probably due to loss of moisture content, as the LC n-3 PUFA content expressed as a percentage of total FA was similar. Thus, it appears that there was no selective loss of LC n-3 PUFA due to cooking.

**TABLE 3**  
Total LC n-3 PUFA (mg/100 g) in Chicken Breast, Thigh, and Sausage from Chickens Fed 5–20% of POM for 42 d and from Chickens Fed 5–20% of POM for 21 d, Compared with Unsupplemented Chickens<sup>a</sup> (control)

POM treatment	Breast	Thigh	Sausage
Control	17 ± 3	18 ± 1	23
5%, 42 d	68 ± 1 <sup>b</sup>	96 ± 1 <sup>b</sup>	68
10%, 42 d	91 ± 14 <sup>b</sup>	138 ± 30 <sup>b</sup>	90
15%, 42 d	92 ± 10 <sup>b</sup>	183 ± 56 <sup>b</sup>	153
20%, 42 d	101 ± 21 <sup>b</sup>	190 ± 41 <sup>b</sup>	184
5%, 21 d	77 ± 3 <sup>b</sup>	76 ± 3 <sup>b</sup>	131
10%, 21 d	103 ± 8 <sup>b</sup>	107 ± 9 <sup>b</sup>	110
15%, 21 d	111 ± 11 <sup>b</sup>	249 ± 53 <sup>b</sup>	199
20%, 21 d	109 ± 15 <sup>b</sup>	204 ± 56 <sup>b</sup>	146

<sup>a</sup>Data are presented as mean ± SEM for three birds per group except for sausages, where meat was batched from all birds.

<sup>b</sup>Significantly different from control ( $P < 0.01$ ). For abbreviation and manufacturer see Table 1.

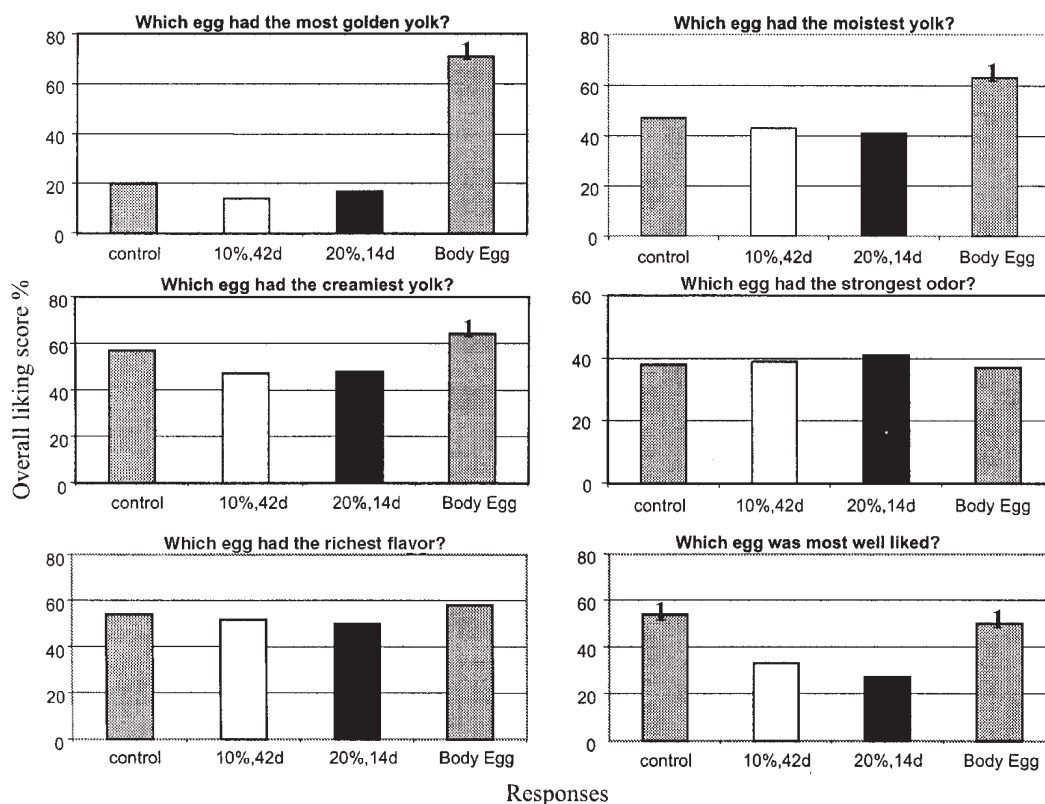


FIG. 2. Sensory evaluation (overall liking scores; %) of eggs enriched with 5 and 15% POM and unenriched (control) eggs. <sup>1</sup>Significantly different ( $P < 0.01$ ) from 10 and 20% POM treatment eggs (ANOVA). Body Egg™, commercial n-3 enriched egg (Chanteclair Farms, Quakers Hill, NSW, Australia). For abbreviation see Figure 1.

The total fat content of whole untrimmed portions of chicken was determined by the Soxhlet method (33). Average concentrations were 1.6, 6.2, and 2.3 g/100 g for breasts, thighs, and sausages, respectively. Neither the total fat content nor the proportion of saturated fat in chicken meat was significantly affected by the POM treatments. Considering that approximately one-third of total FA were saturated, it appears that the n-3 PUFA-enriched meats would qualify as

“good sources of omega-3” with respect to the disqualifying limit of 5 g/100 g for saturated/*trans* fat content (29).

*Sensory evaluation of chicken.* Samples of chicken meat from birds fed both 5 and 15% POM rations were compared with those from birds fed control rations. Breasts, thighs, and sausages were individually evaluated. Apart from having more tender texture, breasts from birds fed POM did not differ significantly from control breasts in any quantitative

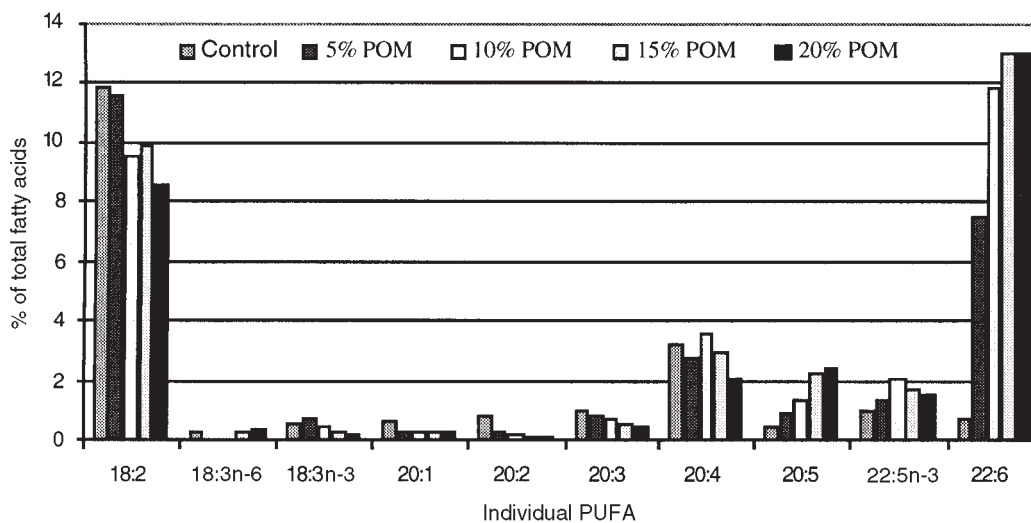


FIG. 3. PUFA composition (% of total FA) of uncooked chicken breasts from poultry fed different levels (5–20%) of POM for 42 d and of unsupplemented poultry (control). For abbreviation see Figure 1.

**TABLE 4**  
**Effect of Cooking (grilling) on Total LC n-3 PUFA in Chicken (breast, thigh, sausage)**  
**Compared with Uncooked (raw) Chicken<sup>a</sup>**

	POM treatment	Breast		Thigh		Sausage	
		Raw	Grilled	Raw	Grilled	Raw	Grilled
mg/100 g	5%, 21 d	77	105	76	149	131	121
	15%, 21 d	111	168	249	242	199	182
% of total FA	5%, 21 d	13.5	12.7	8.1	4.5	3.8	3.7
	15%, 21 d	21.9	19.1	8.5	10.8	5.6	6.4

<sup>a</sup>Data are averaged from two or three samples in each case. For abbreviation see Table 1.

assessments. There were no significant differences in any characteristics between POM-treated and control thighs and sausages, with the exception that the 15% POM-treated thighs were liked less than the controls and a mildly fishy flavor was detected in both breasts and thighs with 15% POM. Overall, there was a clear tendency for meat from birds fed 15% POM to be less well liked (Fig. 4), whereas that of birds fed 5% POM appeared to be equivalent to control chicken.

**Chemical analysis of pork.** Table 5 shows the total LC n-3 PUFA concentrations in pork chops and sausages from groups of male or female pigs fed control or POM-containing rations. Both enrichment strategies (15% POM for 42 d and 20% POM for 28 d) caused significant increases in LC n-3 PUFA levels in pork, with threefold increases in forequarter and leg chops and a 3.5-fold increase in sausages. Figure 5 shows a typical example of changes in individual FA composition of pork following n-3 enrichment. Data are averaged from samples of forequarter chops taken from control ( $n = 8$ ) and treated pigs ( $n = 12$ ). Total LC n-3 PUFA content rose from 1% of total FA in controls to 4% in forequarter chops from POM-fed pigs. As in meat from poultry fed POM, DHA increased far more than the other PUFA in pork. Cooking raised the absolute concentrations of all FA, including LC n-3 PUFA, due to loss of moisture from the meat. As with chicken, the proportionate increase of LC n-3 PUFA, especially DHA, in the pork was largely retained after cooking (Table 6).

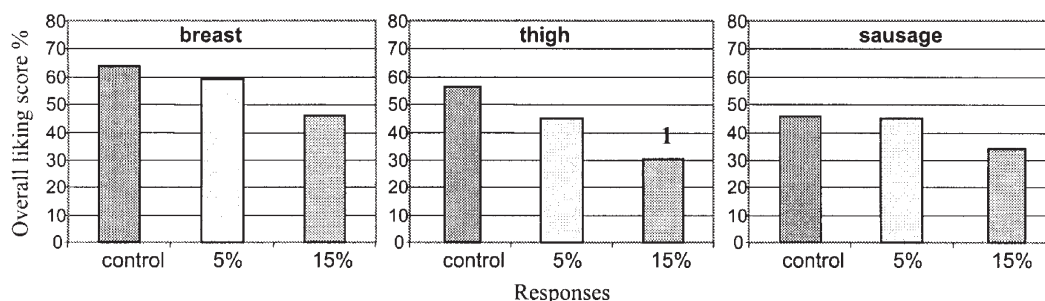
**Fat content of pork.** Soxhlet determinations of the total fat content of pork products indicated that the forequarter and loin chops (25 and 27 g/100 g, respectively) would be unlikely to qualify for the Australian n-3 nutrition claim (requiring saturated/trans fat <5 g/100 g) without significant trim-

ming of adipose tissue. However, the leg chops, with total fat content around 5 g/100 g, would qualify. Indirect assessment of total fat in the lean portions of meat used for the GC analysis of FA indicated that interstitial fat amounted to less than 2 g/100 g, of which one-third was saturated fat. Pork sausages as prepared in this study (saturated fat approximately 5.7 g/100 g) would have marginal acceptability. As with the eggs and chicken meat, the proportion of saturated fat in pork was not affected by the n-3 enrichment.

**Sensory evaluation of pork.** Loin, forequarter, and leg chops and sausages were individually evaluated for sensory qualities. Comparisons were made between each of six treatment groups, i.e., male or female pigs fed the control, 15 or 20% POM ration. There were minor but inconsistent differences in sensory qualities of enriched meat between male and female pigs, e.g., loin and forequarter chops were more tender and juicy from male (especially POM-treated) than from female pigs but female POM-treated leg chops were more tender and juicy than male leg chops. Fishy odor or flavor was detected in forequarter and loin chops from POM-treated pigs but not in leg chops. Figure 6 shows overall liking scores for pork. POM treatment caused only forequarter chops to be significantly less liked than controls. There were no significant differences in any sensory qualities of sausages between any of the treatment groups.

## DISCUSSION

Enriching foods with LC n-3 PUFA is an important approach to increase consumption of these beneficial nutrients. In this study we have demonstrated that a stabilized fishmeal product can be successfully incorporated into pig and poultry



**FIG. 4.** Sensory evaluation (overall liking scores; %) of chicken (breast, thigh, and sausage) enriched with 5 and 15% POM and unenriched (control) chicken. For abbreviation see Figure 1. <sup>1</sup>Significantly different ( $P < 0.01$ ) from control (ANOVA).



**TABLE 5**  
**Total LC n-3 PUFA (mg/100 g) in Uncooked Pork (forequarter, loin, leg chop, and sausage) from Pigs Fed 15% of POM for 42 d and from Pigs Fed 20% of POM for 28 d, Compared with Unsupplemented Pigs<sup>a</sup> (control)**

POM treatment		Forequarter	Loin	Leg	Sausage
Control	Male (4)	25 ± 3	21 ± 2	27 ± 3	87
	Female (4)	22 ± 1	17 ± 3	18 ± 2	49
15% for 42 d	Male (3)	66 ± 9 <sup>b</sup>	55 ± 11 <sup>b</sup>	48 ± 4 <sup>b</sup>	202
	Female (3)	61 ± 13 <sup>b</sup>	47 ± 5 <sup>b</sup>	43 ± 6 <sup>b</sup>	278
20% for 28 d	Male (3)	71 ± 5 <sup>b</sup>	46 ± 6 <sup>b</sup>	79 ± 18 <sup>b</sup>	208
	Female (3)	61 ± 10 <sup>b</sup>	54 ± 7 <sup>b</sup>	65 ± 5 <sup>b</sup>	218

<sup>a</sup>Values are means ± SEM (one sample from each pig) except for sausages (one pooled sample for each treatment group).

<sup>b</sup>Significantly different from control ( $P < 0.01$ ).

feeding strategies to enrich meat and eggs without tainting the foods.

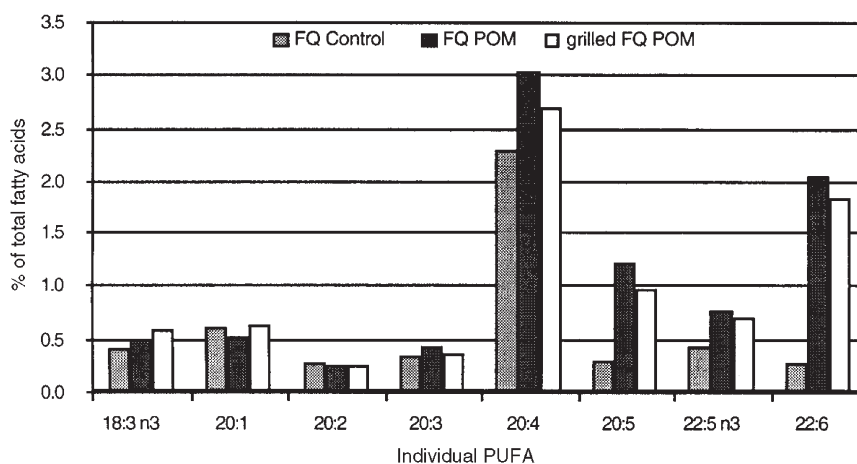
**Enrichment of pork.** This study confirms the effectiveness of fishmeal as a dietary source of LC n-3 PUFA for producing n-3-enriched pork. Moreover, by feeding DHA-rich tuna fishmeal, the enrichment was highly selective for DHA. The LC n-3 PUFA concentrations in the pork chops were lower than those achieved previously (7). In that study, however, pigs were fed 20% POM for 11 wk, whereas in the present study, an acceptable level of LC n-3 PUFA enrichment was attained after only 4 wk of feeding at that level.

LC n-3 PUFA concentrations have been measured directly in samples of lean meat (comprising muscle tissue and interstitial fat), which is likely to contain a higher relative proportion of LC n-3 PUFA than adipose tissue (15). In the previous study, the percentage of LC n-3 PUFA assayed in a lean sample of meat was multiplied by the total fat content of the whole portion of meat to estimate the LC n-3 PUFA concentration indirectly, which is likely to have been overestimated. However, the data now obtained for forequarter, loin, and leg chops by direct measurement of FA in lean samples of meat

(Table 5) is likely to underestimate the LC n-3 PUFA content of even a well-trimmed serving of pork. There is considerable latitude to increase the LC n-3 PUFA content per serving of pork by allowing more residual fat. Pork sausages give an indication of the maximal LC n-3 PUFA concentration attainable: >200 mg/100 g in sausages that had a 14% fat content (saturated fat approximately 6 g/100 g). Pork chops and sausages enriched with LC n-3 PUFA by short-term feeding of rations containing 15–20% POM could readily qualify for FSANZ's new n-3 nutrition claim (29) simply by adjusting the fat content of the products during processing.

In previous attempts to increase the LC n-3 PUFA content of pork, researchers have usually used fish oil and flaxseed oil and meal rather than fishmeal. Fishmeal is an important source of protein for pig rations, but its potential for tainting pork has led to restrictions on its use (25). Trials have been undertaken to develop recommendations for the use of fishmeal, which will minimize the retention of LC n-3 PUFA in pork and the associated risk of tainting (18,19). The same concern applies, however, if fish oil or flaxseed is used for n-3 PUFA enrichment. In fact, feeding flaxseed to pigs caused tainting of bacon without raising DHA content (24). Using a premium-quality tuna fishmeal, we sought to ascertain the highest level of LC n-3 PUFA enrichment of meat that could be attained without compromising quality.

The most important criterion for consumer acceptance of n-3 PUFA-enriched foods is sensory quality, which appears to be inversely related to the n-3 PUFA content (18–20). A compromise must therefore be reached between the extent of enrichment and deterioration of quality. The mode of enrichment will influence this relationship. Encapsulation, for example, is an important strategy for delivering n-3 PUFA in processed foods in a protected form that will minimize adverse effects on quality. Similarly, LC n-3 PUFA incorporated in muscle membrane phospholipids may be less susceptible to degradation than in adipose tissue stores (15). Presumably this accounts for the high levels of DHA retained in lean meat



**FIG. 5.** Individual LC PUFA composition (% of total FA) of control and POM pork forequarter (FQ) chops. FQ control: raw meat from untreated pigs; FQ POM: raw meat from pigs fed 15 or 20% POM; grilled FQ POM: cooked meat from pigs fed 15 and 20% POM. For abbreviation see Figure 1.

**TABLE 6**  
**Effect of Cooking (grilling) on Total LC n-3 PUFA of Pork (forequarter, loin, leg chop, and sausages) Compared with Uncooked (raw) Pork<sup>a</sup>**

	POM treatment	Forequarter		Loin		Leg		Sausage	
		Raw	Grilled	Raw	Grilled	Raw	Grilled	Raw	Grilled
mg/100 g	15%, 42 d	64	128	51	147	46	100	240	318
	20%, 28 d	66	169	50	120	72	116	213	276
% of total FA	15%, 42 d	3.5	4.5	4.4	4.0	6.4	7.2	1.8	1.3
	20%, 28 d	4.6	2.5	3.7	3.3	4.2	7.0	1.8	1.2

<sup>a</sup>Data averaged from 4 to 8 pigs/group. For abbreviation see Table 1.

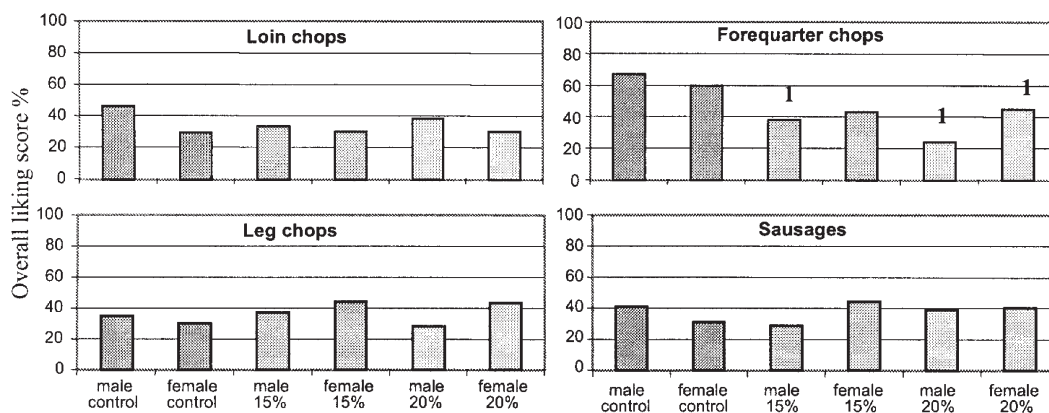
in the present study after feeding DHA-rich POM. The level of inclusion for POM was three to four times higher than the recommended upper limit for fishmeal in pig rations (25). However, the proprietary product used in this study has been fortified with antioxidants to minimize degradation of LC PUFA. Others have shown that inclusion of selected antioxidants in rations can improve the stability of n-3 PUFA in enriched meat (20–23). Livestock performance data (Downing, J., Howe, P., and Bryden, W., unpublished data) and sensory evaluation of the LC n-3 PUFA-enriched pork products justify the higher rates of inclusion of POM in rations.

It was encouraging to note that there was good retention of LC n-3 PUFA during grilling in both chops and sausages. In fact, LC n-3 PUFA concentrations actually increased, owing to loss of moisture during grilling at high temperature, but the proportionate increases in LC n-3 PUFA relative to other FA were largely unaffected. Presumably the LC n-3 PUFA in meat are also less susceptible to degradation during cooking than, for example, a LC n-3 PUFA-rich cooking oil. Except for the eggs, all foods used for sensory evaluation were frozen for at least 1 mon and thawed prior to cooking. Others have noted off-flavors and rancidity after long-term frozen storage in pork from pigs fed fishmeal (18,19). However, with the exception of forequarter chops, containing high levels of adipose tissue (25% fat), there were few consistent differences in sensory qualities between control and n-3 PUFA-enriched pork. Sausages in particular, with their high fat content and level of enrichment, were well accepted by

panelists. Sausages and other processed meat products may be preferable products for enrichment, affording greater resistance to LC n-3 PUFA degradation during storage and cooking than other cuts of meat.

*Enrichment of chicken and eggs.* Birds readily accumulate n-3 PUFA in tissues and appear more efficient than mammals at converting ALA to LC n-3 PUFA (34). There are many good examples of LC n-3 PUFA enrichment of poultry products using fish oil or microalgal sources of LC n-3 PUFA, alone or in combination with ALA sources such as flaxseed or canola (10–15). ALA accumulates in the TG fraction, whereas LC n-3 PUFA are incorporated into phospholipids, and accumulation of high levels of ALA contributes to tainting of foods (12,18,24). Direct sources of preformed LC n-3 PUFA are preferred. Fishmeal is widely used as a source of protein in poultry rations at inclusion rates of 2–5% (26). As with pigs, however, there are few reports of its use for n-3 PUFA enrichment of poultry (18,19), even though it represents a more abundant and cost-effective source than fish oil. Leskanich and Noble (10) have reviewed the use of fishmeal, fish oil, and other sources for LC n-3 PUFA enrichment in poultry and recommend using high-quality fishmeal or fish oil, together with supplemental antioxidants, and limiting inclusion rates in rations to 12 or 1%, respectively, to avoid taint.

We have now demonstrated the suitability of POM (tuna fishmeal) for n-3 PUFA enrichment of poultry. Indeed, greater relative increases in LC n-3 PUFA, particularly DHA, can be



**FIG. 6.** Sensory evaluation (overall liking scores; %) of pork (loin, leg, forequarter chop, and sausage) enriched with 15 and 20% POM and unenriched (control) pork. <sup>1</sup>Significantly different ( $P < 0.01$ ) from control (ANOVA).

achieved at lower rates of POM feeding in poultry than in pork. The increases obtained by feeding 5% POM exceeded those achieved in other studies using <12% redfish meal in broiler rations (15). This may be attributable to the substantially higher content of DHA and ratio of DHA to EPA in tuna meal compared with herring meal. When feeding 15% POM to broilers, we found that the overall liking score for chicken thighs was significantly reduced, whereas with 5% POM, there were no discernible differences in sensory characteristics from the control meat. The n-3 PUFA-enriched chicken sausages were particularly well accepted. As with pork, the LC n-3 PUFA enrichment of chicken meat appeared to be sustained during high-temperature cooking.

Numerous strategies have been used for n-3 PUFA enrichment of eggs, with DHA and total LC n-3 PUFA ranging as high as 660 and 780 mg/egg, respectively (10). High levels are obtained by including high levels of fish oil in rations. Lower levels of fish oil, with or without flaxseed oil, result in more modest levels of LC n-3 PUFA enrichment and have been used to produce a wide range of commercial eggs with acceptable sensory characteristics. Nevertheless, the high cost of the dietary oils and the special conditions for production necessitate premium prices for n-3-enriched eggs.

Fishmeal may represent a cheaper alternative source of LC n-3 PUFA for enrichment of eggs. Using tuna fishmeal, we achieved increases in the DHA and total LC n-3 PUFA content of eggs that compared favorably with results obtained using other n-3 sources in published studies and in commercial production of n-3-enriched eggs. There were insufficient eggs available in this study to assess the effect of cooking on increased n-3 content. However, experience with commercially enriched eggs indicates that there is generally satisfactory retention of LC n-3 PUFA after cooking. As fresh eggs were required for the sensory evaluation, we were unaware of their n-3 content at the time of selecting treatment groups for evaluation. Unfortunately, the levels of POM inclusion chosen for sensory evaluation proved to be unacceptably high, resulting in significant sensory deficits. In retrospect, it would have been preferable to conduct sensory evaluation on eggs from hens fed 5% POM. At this level of feeding, the LC n-3 PUFA enrichment (approximately 180 mg/egg) compared favorably with that of feeding 12% herring meal (approximately 100 mg EPA and DHA/yolk) in the only other published report on n-3 PUFA enrichment of eggs with fishmeal (14).

The present study confirms that suitably processed tuna fishmeal, a by-product of the tuna processing industry that has traditionally been used as a protein source for livestock rations, may also be used as an alternative source of LC n-3 PUFA for enrichment of meat and eggs. It demonstrates that appropriate feeding strategies can be developed to avoid sensory deficits traditionally associated with the use of fishmeal in livestock rations. Compared with the use of other LC n-3 PUFA sources, high concentrations of DHA can be achieved with a relatively low dietary inclusion rate and duration of fishmeal feeding, permitting economical production of quality n-3 enriched foods. Consumer interest in these foods will

be stimulated by new labeling options such as the nutrition claim for n-3 PUFA recently introduced in Australia and New Zealand (29), which will help to differentiate them as premium products in the market place. Although qualification for n-3 PUFA nutrition claims is based on the LC n-3 PUFA content of uncooked foods, it is essential that cooked foods deliver the n-3 benefits. We have been able to confirm that the LC n-3 PUFA in enriched chicken and pork are retained after cooking. Further studies are now being undertaken with POM to refine the livestock feeding strategies required for the n-3 PUFA enrichment of specific food products and to optimize both sensory and shelf-life characteristics.

## ACKNOWLEDGMENTS

PorcOmega™ tuna fishmeal and financial support for this study were kindly provided by Bartlett Grain Pty. Ltd. The authors are grateful to John Wingate for advice on formulation of rations, to Samantha Reis for assistance with the sensory evaluation, and Dr. Karen Murphy for assistance with revision of the manuscript. The Smart Foods Centre is a Key Centre of Teaching and Research funded by the Australian Research Council.

## REFERENCES

1. Nettleton, J.A. (1995) *Omega-3 Fatty Acids and Health*, Chapman & Hall, New York.
2. Simopoulos, A.P. (1991) Omega-3 Fatty Acids in Health and Disease and in Growth and Development, *Am. J. Clin. Nutr.* 54, 438–463.
3. Simopoulos, A.P., Leaf, A., and Salem, N., Jr. (1999) Workshop on the Essentiality of and Recommended Dietary Intakes for Omega-6 and Omega-3 Fatty Acids, *Food Australia* 51, 332–333.
4. Dolecek, T. (1992) Epidemiological Evidence of Relationships Between Dietary Polyunsaturated Fatty Acids and Mortality in the Multiple Risk Factor Intervention Trial, *Proc. Soc. Exp. Biol. Med.* 200, 177–182.
5. Kris-Etherton, P.M., Taylor, D.S., Yu-Poth, S., Huth, P., Moriarty, K., Fishell, V., Hargrove, R.L., Zhao, G., and Etherton, T.D. (2000) Polyunsaturated Fatty Acids in the Food Chain in the United States, *Am. J. Clin. Nutr.* 71, 179S–188S.
6. Ollis, T.E., Meyer, B.J., and Howe, P.R.C. (1999) Australian Food Sources and Intakes of Omega-6 and Omega-3 Polyunsaturated Fatty Acids, *Ann. Nutr. Metab.* 43, 346–355.
7. Howe, P.R.C. (1998) Omega-3 Enriched Pork, *World Rev. Nutr. Diet* 83, 132–143.
8. Leskanich, C., Matthews, K., Warkup, C., Noble, R., and Hazledine, M. (1997) The Effect of Dietary Oil Containing n-3 Fatty Acids on the Fatty Acid, Physicochemical and Organoleptic Characteristics of Pig Meat and Fat, *J. Anim. Sci.* 75, 673–683.
9. Irie, M., and Sakimoto, M. (1992) Fat Characteristics of Pigs Fed Fish Oil Containing Eicosapentaenoic and Docosahexaenoic Acids, *J. Anim. Sci.* 70, 470–477.
10. Leskanich, C.O., and Noble, R.C. (1997) Manipulation of the n-3 Polyunsaturated Fatty Acid Composition of Avian Eggs and Meat, *World's Poult. Sci. J.* 53, 155–183.
11. Farrell, D.J. (1998) Enrichment of Hen Eggs with n-3 Long-Chain Fatty Acids and Evaluation of Enriched Eggs in Humans, *Am. J. Clin. Nutr.* 68, 538–544.
12. Van Elswyk, M.E. (1997) Comparison of n-3 Fatty Acid Sources in Laying Hen Rations for Improvement of Whole Egg Nutritional Quality: A Review, *Br. J. Nutr.* 78, S61–S69.

13. Abril, R., and Barclay, W. (1998) Production of Docosa-hexaenoic Acid-Enriched Poultry Eggs and Meat Using an Algae-Based Feed Ingredient, *World Rev. Nutr. Diet* 83, 77–88.
14. Nash, D.M., Hamilton, R.M.G., and Hulan, H.W. (1995) The Effect of Dietary Herring Meal on the Omega-3 Fatty Acid Content of Plasma and Egg Yolk Lipids of Laying Hens, *Can. J. Anim. Sci.* 75, 247–253.
15. Ratnayake, W., Ackman, R., and Hulan, H. (1989) Effect of Redfish Meal-Enriched Diets on the Taste and n-3 PUFA of 42-Day-Old Broiler Chickens, *J. Sci. Food Agric.* 49, 59–74.
16. Ashes, J.R., Siebert, B.D., Gulati, S.K., Cuthbertson, A.Z., and Scott, T.W. (1992) Incorporation of n-3 Fatty Acids of Fish Oil Into Tissue and Serum Lipids of Ruminants, *Lipids* 27, 629–631.
17. Mandell, I.B., Buchanan-Smith, J.G., Holub, B.J., and Campbell, C.P. (1997) Effects of Fish Meal in Beef Cattle Diets on Growth Performance, Carcass Characteristics and Fatty Acid Composition of Longissimus Muscle, *J. Anim. Sci.* 75, 910–919.
18. Hertzman, C., Goransson, L., and Ruderus, H. (1988) Influence of Fishmeal, Rapeseed and Rapeseed Meal in Feed on the Fatty Acid Composition and Storage Stability of Porcine Body Fat, *Meat Sci.* 23, 37–53.
19. Valaja, J., Suomi, K., Alaviuhkola, T., and Immonen, I. (1992) Effect of Dietary Fishmeal on the Palatability and Fatty Acid Composition of Pork, *J. Agric. Sci.* 1, 21–26.
20. Wood, J.D., and Enser, M. (1997) Factors Influencing Fatty Acids in Meat and the Role of Antioxidants in Improving Meat Quality, *Br. J. Nutr.* 78, S49–S60.
21. Buckley, D.J., Morrissey, P.A., and Gray, J.I. (1995) Influence of Dietary Vitamin E on the Oxidative Stability and Quality of Pig Meat, *J. Anim. Sci.* 73, 3122–3130.
22. Ajuyah, A.O., Ahn, D.U., Hardin, T., and Sim, J.S. (1991) Dietary Antioxidants and Storage Affect Chemical Characteristics of  $\omega$ -3 Fatty Acid Enriched Broiler Chicken Meats, *J. Food Sci.* 61, 43–46.
23. Specht-Overholt, S.M. (1995) Commercial Manufacturing of Omega-3-Pork Products and the Effects of *d*,1- $\alpha$ -Tocopherol Acetate in Swine Diets on Lipid and Pigment Stability and Various Pork Characteristics, *Dissert. Abstr. Intl.* b 56, 587.
24. Romans, J.R., Wulf, D.M., Johnson, R.C., Libal, G.W., and Costello, W.J. (1995) Effect of Ground Flaxseed in Swine Diets on Pig Performance and on Physical and Sensory Characteristics and Omega-3 Content of Pork: II Duration of 15% Dietary Flaxseed, *J. Anim. Sci.* 73, 1987–1999.
25. Emken, E.A., Adlof, R.O., and Gulley, R.M. (1994) Dietary Linoleic Acid Influences Desaturation and Acylation of Deuterium-Labeled Linoleic and Linolenic Acids in Young Adult Males, *Biochim. Biophys. Acta* 1213, 277–288.
26. Fishmeal Information Network (2001) Fishmeal Facts and Figures (<http://www.gafta.com/fin/finfacts.html>).
27. Pike, I.H., and Barlow, S. (1999) Fish Meal and Oil to the Year 2010—Supplies for Aquaculture, World Aquaculture 99, Sydney. Proceedings available at <http://www.ifoma.com/raw.html>.
28. Van Barneveld, R. (1997) Fishmeal in Pig Diets—The Effect on Pork and Pork Product Quality, *Pig Industry News* (July), 21–23.
29. Food Standards Australia New Zealand (2000) Amendment 53 to the Food Standards Code: Part 1.2.8 Div 3: Conditions for Making Certain Nutrition Claims, 13—Claims in Relation to Omega Fatty Acid Content of Foods, *Commonwealth of Australia Gazette P30*, 68.
30. National Research Council (1998) Nutrient Requirements of Swine, 10th rev. edn., Washington, DC.
31. National Research Council (1994) Nutrient Requirements of Poultry, 9th rev. edn., Washington, DC.
32. Lepage, G., and Roy, G.C. (1986) Direct Esterification of All Classes of Lipids in a One-Step Reaction, *J. Lipid Res.* 27, 114–120.
33. Anonymous (1990) Test Methods for Evaluating Solid Waste, 3rd edn., EPA SW-846 Method 3540, U.S. Government Printing Office, Washington, DC.
34. Klashing, K.C. (1998) *Comparative Avian Nutrition*, CAB International, Wallingford, United Kingdom.

[Received May 15, 2002, and in revised form and accepted December 3, 2002]



# Effects of Dietary $\alpha$ -Linolenic Acid from Blended Oils on Biochemical Indices of Coronary Heart Disease in Indians

Ghafoorunissa\*, A. Vani, R. Laxmi, and B. Sesikeran

National Institute of Nutrition (ICMR), Hyderabad-500 007, A.P., India

**ABSTRACT:** PUFA of the n-6 and n-3 series have beneficial effects on key risk factors of coronary heart disease (CHD). Our earlier studies on the intake of FA and on the FA composition of plasma and platelet phospholipids suggested the need to improve the n-3 PUFA nutritional status in the Indian population. The present long-term study was conducted on 80 middle-aged Indian subjects (40 men and 40 women) using the subjects' own home-prepared diets to evaluate the effects of dietary n-3 PUFA on biochemical indices of CHD risk. Substitution of Blend G (equal proportions of groundnut and canola oils) for groundnut oil or substitution of Blend S (equal proportions of sunflower oil and canola oils) for sunflower oil increased  $\alpha$ -linolenic acid (ALNA) fourfold and decreased the linoleic acid (LA)/ALNA ratio from 35 to 6 and 65 to 9, respectively. Twelve subjects (six men and six women) who received Blend G were switched back to groundnut oil and were administered 0.3 g daily of long-chain (LC) n-3 PUFA from fish oil. At the end of the trial period for both blends in both sexes, plasma lipid and apolipoprotein levels had not changed, and ADP-induced aggregation had decreased. In plasma and platelet phospholipids, LA as well as LCn-3 PUFA had increased, suggesting competition between LA and ALNA for metabolism into the respective LC-PUFA. Fish oil supplementation increased LCn-3 PUFA in plasma and platelet phospholipids, decreased ADP-induced platelet aggregation, and increased plasma cholesterol. On the basis of the increased LCn-3 PUFA in plasma phospholipids, it was calculated that 0.75% energy (en%) (2.2 g) ALNA (from vegetable oils) may be required to increase LCn-3 PUFA to about the same extent as 0.1 en% (0.3 g) LCn-3 PUFA (from fish oils). Since both n-6 and n-3 PUFA play a critical role in fetal growth and development and in the programming of diet-related chronic diseases in adults, an improvement in the n-3 PUFA nutritional status in cereal-based diets through long-term use of cooking oils containing 25–40% LA and 4% ALNA may contribute to the prevention of CHD in Indians.

Paper no. L9046 in *Lipids* 37, 1077–1086 (November 2002).

PUFA comprise the parent EFA [linoleic acid (LA) and  $\alpha$ -linolenic acid (ALNA)] and their respective long-chain (LC) more unsaturated derivatives. Since the time the essentiality of PUFA was established in 1929, studies on the nutritional

effects of LA have received wide attention. However, following the Eskimo studies (1), several lines of evidence showed that the LCn-3 PUFA downregulate factors that have atherogenic potential and enhance factors that have anti-atherogenic potential (2–4). Recent studies also have focused on the effects of ALNA in preventing coronary heart disease (CHD) (5–8). Studies on FA intakes among Indians showed that LA requirements are fully met owing to their high levels in cereal, millet, and vegetable oils, but ALNA intake is low and therefore the n-6/n-3 ratio is high (9). Further, data on the FA profile of plasma and platelet phospholipids in apparently normal subjects suggested the need to improve the n-3 PUFA nutritional status in Indians (9). Metabolic studies conducted to investigate the effects of using canola oil (ALNA) or fish oil supplements (LCn-3 PUFA) compared to groundnut oil (negligible ALNA) showed that ~1.4% energy (en%) ALNA, (n-6/n-3, ~4) or 0.2 to 0.5 en% LCn-3 PUFA (n-6/n-3, ~7 to 12, respectively) may produce anti-atherogenic effects (9,10). To achieve the above levels of ALNA and an optimal n-6/n-3 ratio (5:1 to 10:1), the use of ALNA-containing oils (canola, soybean, or mustard) along with other oil(s) has been recommended (11). The present study was carried out to evaluate the long-term effects of increasing ALNA intake using combinations of ALNA-containing oil (canola) with two edible oils commonly used in south India (groundnut and sunflower) compared to the effects of fish oil supplementation on biochemical parameters of cardiovascular risk.

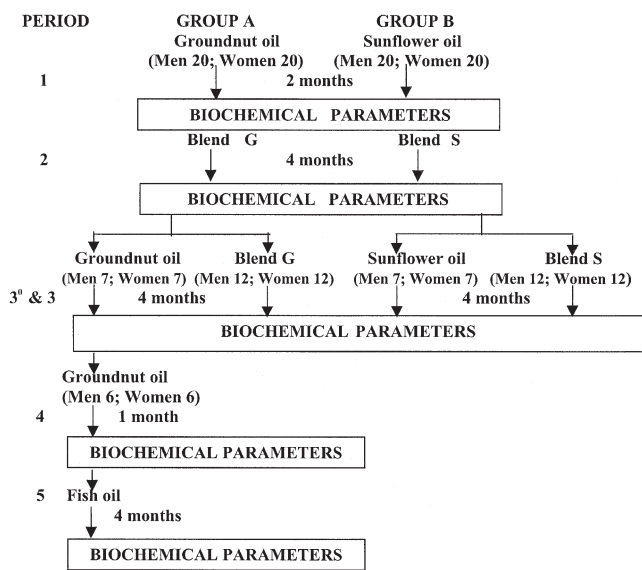
## MATERIALS AND METHODS

**Subjects.** Out of a total of 70 families to whom the study was explained, 40 were enrolled. Criteria for their selection included age between 30 and 50 years, a normal ECG, and no history of diabetes or CHD. In addition, the subjects were not in the habit of consuming frequent meals or snacks outside their homes, did not take anti-inflammatory drugs, and consumed neither tobacco nor alcohol. The subjects' diets provided >30 g/d of cooking oil. The study was approved by the Institute's ethical committee, and written consent was obtained from both husband and wife.

**Study design. (i) Period 1.** Twenty families (Scheme 1) who had used groundnut oil as the major cooking oil for more than 2 mon were provided the traditionally consumed refined groundnut oil (Postman, Ahamed Mills, Mumbai, India), and 20 families who had used sunflower oil as the major cooking oil for more than 2 mon were provided sunflower oil [Dhara,

\*To whom correspondence should be addressed at National Institute of Nutrition, Jamai Osmania P.O., Hyderabad-500 007, A.P., India.  
E-mail: ghafoorunissanin@rediffmail.com or nin@ap.ap.nic.in

Abbreviations: ALNA,  $\alpha$ -linolenic acid; CHD, coronary heart disease; DPA, docosapentaenoic acid; EMR, estimated maximal response; LA, linoleic acid; LC, long-chain; NDDB, National Dairy Development Board; PPP, platelet-poor plasma; PRP, platelet-rich plasma; WB, whole blood.



SCHEME 1

National Dairy Development Board (NDDB), Anand, Gujarat, India]. Both oils were supplied in sealed containers with instructions to use it as the only cooking fat source for a period of 2 mon.

(ii) *Period 2.* The families in Group A (Scheme 1) were switched to Blend G (equal proportions of groundnut and canola) and those in Group B were switched to Blend S (equal proportions of sunflower and canola) for a period of 4 mon. Blended oils were obtained from the NDDB. The percentage FA in Blend G and Blend S, respectively, were as follows: total saturates, 17 and 9; total monounsaturates, 52 and 44; and LA, 26 and 42. Both blends furnished ~4% ALNA compared to negligible levels in the single oils (groundnut or sunflower). The blended oils were prepared and supplied by the NDDB in 1- and 4-kg sealed containers.

(iii) *Period 3.* Twelve families each from Groups A and B continued to consume Blend G and Blend S, respectively, for the next 4 mon (Period 3), whereas seven families from each group (A and B) were switched back to the single oils (Period 3<sup>0</sup>) on which they were stabilized earlier.

(iv) *Periods 4 and 5.* Six families (six men and six women) who were switched back to groundnut oil (Period 3<sup>0</sup>) were continued for another month on groundnut oil (Period 4) and subsequently were administered one capsule of fish oil daily (MaxEPA, 180 mg; DHA, 120 mg) as well as 100 mg  $\alpha$ -tocopherol twice a week for 4 mon (Period 5).

*Diets.* During each of the study periods (1, 2, and 3), individual diet surveys were done (one on the weekend and two on weekdays) using a 24-h recall questionnaire (12), and subjects' average daily intakes of major food groups, macronutrients, and individual FA from all food items (invisible fat) were calculated using food composition tables (9,13). The intake of fat and individual FA from the total diet (invisible + visible) was calculated for each oil period. In order to monitor compliance, the subjects were requested to record the total number of meals and snacks eaten outside the home. These

records were collected at biweekly intervals throughout the study period. At the end of Period 1, body weight, height, and blood pressure were recorded; body weight was again recorded at the end of Periods 2 and 3.

*Biochemical parameters.* Fasting blood samples were collected in the morning at the end of each period after ensuring that the subjects had not taken anti-inflammatory drugs in the previous 2 wk. For platelet aggregation studies, blood was collected in a 3.8% trisodium citrate solution (9:1 vol/vol). For analysis of plasma lipids and lipoproteins, blood was collected into tubes containing EDTA (1 mg/mL).

(i) *Lipids, lipoproteins, and FA.* Blood collected in tubes with EDTA was spun at  $120 \times g$  for 10 min. The platelet-rich plasma (PRP) that was obtained was spun at  $1000 \times g$  for 15 min to get a platelet pellet and platelet-poor plasma (PPP). The platelet pellet was washed with saline and the cells were lysed. The PPP was used for analysis of lipids, apolipoproteins, and phospholipid FA composition. Total cholesterol, HDL-cholesterol, and TAG were analyzed by enzymatic methods using kits obtained from Dr. Reddy's Laboratories (Hyderabad, India). The levels of apolipoproteins B and A-1 were determined by a quantitative, immunoturbidimetric method using kits obtained from Sigma Diagnostics (St. Louis, MO). Lipids were extracted from both plasma and lysed platelets with chloroform/methanol (2:1 vol/vol) containing BHT, and the phospholipid band was separated by TLC and methylated (14). FAME were analyzed by flame ionization capillary GLC using a PC-based Perkin-Elmer autoanalyzer (Buckinghamshire, United Kingdom) as described previously (14).

(ii) *Platelet aggregation and plasma fibrinogen.* Citrated blood was diluted with saline (1:1 vol/vol), and whole blood (WB) aggregation was measured with  $2 \mu g$  collagen by the impedance method (15) using a Model 530 WB aggregometer (Chronolog Corporation, Havertown, PA); aggregation rate (slope) and lag time were calculated. PRP was obtained by spinning citrated blood as described previously (14). ADP-induced aggregation was measured in  $250 \mu L$  PRP ( $250,000$  cells/ $\mu L$ ) with varying concentrations of ADP (0.02 to  $2 \mu M$ ) as described previously (14). The threshold for ADP (dose at which no aggregation was recorded) and aggregation rate (slope) with  $2 \mu M$  ADP were determined. Plasma fibrinogen was estimated in citrated PPP by an optimized microturbidimetric assay using a two-step addition of ammonium sulfate reagent and timed turbidity measurements after 120 and 190 s at 340 nm (16).

*Statistical analysis.* The biochemical parameters were analyzed by a multi-way ANOVA to test the differences, if any, among sex, oils, and time period, and paired *t*-tests were done between single and blended oils (Period 1 vs. 2). Because the responses on the biochemical parameters were similar after 4 mon on Blend G and Blend S, the data on the two blends were pooled. A one-way ANOVA was done to determine the effects of the single oil consumed for 4 mon and the blends for 4 and 8 mon (periods 1, 2, and 3), as well as on the effects of changing back to the single oil after 4 mon of blend consumption

(Periods 1, 2, and 3<sup>0</sup>). Statistical analyses were done by using SPSS version 10 for Windows (SPSS Inc., Chicago, IL).

## RESULTS

**Compliance and dietary intake.** The clinical characteristics of subjects are given in Table 1. The average daily intakes of each of the food groups and macronutrients are presented in Table 2. The number of meals and snacks eaten outside the home were similar in Groups A and B during the 10-mon study period (70% of subjects consumed <50 and 30% of subjects consumed 51–100 meals and snacks during the entire period of the study). In 40% of the families, the average consumption of oil was higher during Periods 2 and 3 (0.9–1.8 kg/mon/family) compared to Period 1. The contribution of meals and snacks eaten outside the home and the consequent difference in the amount and type of oil was not accounted for in calculating food and nutrient intakes. The data presented in Table 3 show that the use of both Blend G and Blend S increased ALNA from ~0.2 to ~0.9 and 0.8 en%, respectively, compared to the single oils (Table 3). The intake of other FA was similar during Blend G and groundnut oil periods. The intakes of total monounsaturates were high, and LA was low during consumption of Blend S compared to sunflower oil. The ratio of LA/ALNA (n-6/n-3) was reduced from 35 during intake of groundnut oil to 6 during intake of Blend G, and from 65 during intake of sunflower oil to 9 during intake of Blend S (Table 3). During fish oil supplementation, the LA/ALNA + LCn-3 PUFA (n-6/n-3) ratio was 25.

**Effect of 4-mon intake of blended oil.** In both the groups (men and women), at the end of each oil consumption period (4 and 8 mon) body weight (data not given), plasma total cholesterol, HDL-cholesterol, TAG, and apolipoprotein A-1 and B levels were not altered (Table 4). The data on plasma phospholipid FA composition showed that during the single-oil period, ALNA and 20:5n-3 were not detectable (Table 5). At the end of trials for each blend in both sexes, ALNA could be detected only in some subjects and LA, 20:5n-3, 22:5n-3, and 22:6n-3 (LCn-3 PUFA) increased. The use of blends lowered total saturates, and only at the end of the Blend S period did monounsaturates increase. In platelet phospholipids, the use of either of the blends increased LA and 20:5n-3, and decreased 22:6n-3, dihomo- $\gamma$ -linolenic acid (20:3n-6), and docosatraenoic acid 22:4n-6 (Table 6).

**TABLE 1**  
Clinical Characteristics of the Subjects<sup>a</sup>

Parameters	Men		Women	
	Mean $\pm$ SEM	Range	Mean $\pm$ SEM	Range
Age (yr)	43 $\pm$ 0.6	34–50	37 $\pm$ 0.5	32–46
Body mass index	24 $\pm$ 0.9	18–31	25 $\pm$ 0.8	16–36
Blood pressure (mm Hg)				
Systolic	125 $\pm$ 1.6	108–146	122 $\pm$ 1.9	110–150
Diastolic	87 $\pm$ 1.1	70–100	83 $\pm$ 1.3	60–96

<sup>a</sup>n = 40 for each sex. Body mass index = weight (kg)/height<sup>2</sup> (m).

**TABLE 2**  
Average Daily Intakes of Food Groups and Macronutrients<sup>a</sup>

	Men	Women
Food groups (g/p) <sup>a</sup>		
Cereals	275 $\pm$ 11	220 $\pm$ 6
Pulses	68 $\pm$ 6	53 $\pm$ 4
Vegetables	220 $\pm$ 12	195 $\pm$ 10
Milk and milk products	390 $\pm$ 18	340 $\pm$ 21
Oil	38 $\pm$ 2	31 $\pm$ 2
Ghee	5 $\pm$ 1	5 $\pm$ 1
Nuts and oilseeds	19 $\pm$ 2	16 $\pm$ 2
Meat, eggs <sup>b</sup> , and fish	120 $\pm$ 19	95 $\pm$ 11
Sugar	25 $\pm$ 2	20 $\pm$ 2
Macronutrients		
Total energy (Kcal)	2280 $\pm$ 75	1895 $\pm$ 48
Protein (en%)	11 $\pm$ 0.3	11 $\pm$ 0.3
Carbohydrate (en%)	56 $\pm$ 0.8	55 $\pm$ 0.9
Total fat (en%)	32 $\pm$ 0.7	33 $\pm$ 0.8
Invisible fat (en%) <sup>a</sup>	16 $\pm$ 0.5	17 $\pm$ 0.5
Visible fat (en%) <sup>a</sup>	16 $\pm$ 0.7	16 $\pm$ 0.7

<sup>a</sup>Values are mean  $\pm$  SEM; n = 40 for each sex. en%, percent energy; g/p, gram/person. Visible fat, cooking oil and ghee; invisible fat, fat from all food items.

<sup>b</sup>Eighteen men and 18 women. Fish (eight men, eight women), 5 g.

In both sexes, following consumption of each blend the lag time for collagen-induced aggregation in WB was shorter and ADP-induced platelet aggregation (slope) in PRP decreased (except in men on Blend S; see Table 7). The threshold for ADP-induced aggregation and plasma fibrinogen levels was not altered (Table 7). Irrespective of the type of oil used, women had lower levels of TAG and apolipoprotein B as well as higher levels of HDL-cholesterol (Table 4), higher aggregation rates with both collagen and ADP, and lower thresholds for ADP-induced aggregation than men (Table 7).

**Effect of continued intake of blended oils or switching back to single oils.** Continued consumption of blended oils for an additional period of 4 mon (Period 3) or switching back to single oils (Period 3<sup>0</sup>) affected neither plasma lipids (TAG, cholesterol, and HDL-cholesterol) nor apolipoproteins (data not shown). In plasma phospholipids, the magnitude of increase in total LCn-3 PUFA was similar at the end of 4 and 8 mon on blends (Table 8). At the end of 4 mon after switching to the single oils (Period 3<sup>0</sup>), the total LCn-3 PUFA levels decreased; these values were higher than those of the single-oil period (Period 1). At the end of 8 mon (Period 3) of blended oil consumption, an increase in total LCn-3 PUFA in platelet phospholipids was due to 20:5n-3 and 22:5n-3.

The lag time for collagen-induced aggregation in WB decreased to the same extent at the end of 4 and 8 mon on blends compared to the single-oil period (Table 8). In subjects who were switched back to single oils (Period 3<sup>0</sup>), the lag time for collagen-induced aggregation in WB increased to the basal value. ADP-induced aggregation in PRP decreased after both 4 and 8 mon of blend consumption as well as after switching back to single oils (statistical significance was not consistent).

**Effects of blended oil vs. fish oil intake.** The data presented in Table 9 show the response of subjects to the dietary increase in ALNA from blended oils (Periods 1 and 2) compared to the increase in LCn-3 PUFA from fish oil (Periods 4 and 5) over a

**TABLE 3**  
**Average Daily Intakes of FA<sup>a</sup> (invisible fat + visible fat)**

FA (en%)	Group A		Group B	
	Period 1	Period 2	Period 1	Period 2
<b>Men</b>				
Total saturates	9.7 ± 0.6	9.1 ± 0.6	8.6 ± 0.5	8.3 ± 0.6
Total monounsaturates	11.1 ± 0.7	11.5 ± 0.5	6.3 ± 0.3	9.6 ± 0.5 <sup>b</sup>
Linoleic (18:2n-6)	5.2 ± 0.3	5.4 ± 0.3	10.4 ± 0.8	7.4 ± 0.4 <sup>b</sup>
α-Linolenic (18:3n-3)	0.2 ± 0.05	0.9 ± 0.07 <sup>b</sup>	0.2 ± 0.02	0.8 ± 0.04 <sup>b</sup>
<b>Ratios</b>				
Polyunsaturates/saturates	0.5 ± 0.04	0.7 ± 0.05 <sup>b</sup>	1.3 ± 0.09	1.0 ± 0.07 <sup>b</sup>
18:2n-6/18:3n-3	37 ± 4.7	6.1 ± 0.1 <sup>b</sup>	65 ± 6.2	9.2 ± 0.2 <sup>b</sup>
<b>Women</b>				
Total saturates	10.0 ± 0.6	9.3 ± 0.6	8.8 ± 0.5	8.5 ± 0.5
Total monounsaturates	12.3 ± 0.6	12.0 ± 0.6	6.2 ± 0.3	9.2 ± 0.4 <sup>b</sup>
Linoleic (18:2n-6)	5.5 ± 0.3	5.6 ± 0.3	10.5 ± 0.6	7.1 ± 0.3 <sup>b</sup>
α-Linolenic (18:3n-3)	0.2 ± 0.07	0.9 ± 0.05 <sup>b</sup>	0.2 ± 0.01	0.8 ± 0.03 <sup>b</sup>
<b>Ratios</b>				
Polyunsaturates/saturates	0.6 ± 0.04	0.8 ± 0.08 <sup>c</sup>	1.3 ± 0.1	0.9 ± 0.08 <sup>c</sup>
18:2n-6/18:3n-3	33 ± 3.3	6.1 ± 0.1 <sup>b</sup>	65 ± 6.1	9.2 ± 0.15 <sup>b</sup>

<sup>a</sup>Values are mean ± SEM; *n* = 20 in each period for each sex. Group A: Period 1, groundnut oil; Period 2, Blend G (equal proportions of groundnut and canola). Group B: Period 1, sunflower oil; Period 2, Blend S (equal proportions of sunflower and canola). For abbreviation see Table 2.

<sup>b</sup>*P* < 0.001.

<sup>c</sup>*P* < 0.05; statistically different from Period 1 by paired *t*-test.

period of 4 mon. In plasma phospholipids, blended oil as well as fish oil supplementation increased LA, 20:5n-3, 22:5n-3, and 22:6n-3 (total LCn-3 PUFA). In platelet phospholipids, blended oil increased LA and 20:5n-3 and decreased 20:3n-6. Fish oil supplementation increased LA, 20:5n-3, 22:5n-3, and 22:6n-3 and decreased 20:3n-6. Supplementation with fish oil decreased ADP-induced platelet aggregation in PRP (Table 9) and increased plasma total cholesterol (Fig. 1). The apolipoproteins A-1 and B and HDL-cholesterol were not altered, whereas TAG were decreased (not statistically significant). The decrease in lag time observed for WB aggregation after blended oil supplementation was not seen after fish oil supplementation (Table 9).

## DISCUSSION

**Dietary intake of FA.** The present study documents the long-term effects of increasing ALNA on various biochemical parameters associated with CHD in middle-aged Indian subjects. The use of Blend G (26% LA, 4% ALNA) increased ALNA and decreased the n-6/n-3 ratio without any change in other dietary FA. On the other hand, the use of Blend S (42% LA, 4% ALNA) increased ALNA and MUFA and decreased LA and the n-6/n-3 ratio. During the single-oil period, the daily ALNA intake was 0.6 g (0.2 en%) and LCn-3 PUFA intake was negligible compared to the ALNA + LCn-3 PUFA intake

**TABLE 4**  
**Plasma Lipids and Apolipoproteins<sup>a</sup> at the End of a 4-mon Intake of Blends**

	Group A		Group B	
	Period 1	Period 2	Period 1	Period 2
<b>Men</b>				
Lipids/apolipoproteins (mg%)				
Total cholesterol	175 ± 8.0	187 ± 9.2	172 ± 8.2	178 ± 8.4
HDL-cholesterol	32 ± 1.6	34 ± 1.8	30 ± 1.4	33 ± 1.0
TG	154 ± 18	166 ± 18	167 ± 20	168 ± 17
Apolipoprotein A-1	82 ± 4.9	83 ± 3.8	78 ± 3.5	83 ± 4.3
Apolipoprotein B	71 ± 4.2	66 ± 5.5	76 ± 4.9	68 ± 4.1
<b>Women</b>				
Lipids/apolipoproteins (mg%)				
Total cholesterol	176 ± 4.5	184 ± 4.6	152 ± 3.5	158 ± 5.8
HDL-cholesterol <sup>b</sup>	41 ± 2.2	45 ± 2.2	36 ± 1.7	39 ± 1.9
TG <sup>b</sup>	92 ± 9.2	113 ± 12.0	100 ± 8.7	111 ± 10
Apolipoprotein A-1	86 ± 2.6	86 ± 3.6	86 ± 3.6	84 ± 2.8
Apolipoprotein B <sup>b</sup>	62 ± 3.7	56 ± 2.3	57 ± 2.8	58 ± 2.8

<sup>a</sup>Values are mean ± SEM; *n* = 20 in each period for each sex. Group A: Period 1, groundnut oil; Period 2, Blend G. Group B: Period 1, sunflower oil; Period 2, Blend S. For blend components see Table 3.

<sup>b</sup>*P* < 0.05 for sex difference.



**TABLE 5**  
**FA Composition of Plasma Phospholipids<sup>a</sup> at the End of a 4-mon Intake of Blended Oils (nmol%)**

Parameters	Group A		Group B	
	Period 1	Period 2	Period 1	Period 2
<b>Men</b>				
Total saturates	56.9 ± 2.09	47.1 ± 0.84 <sup>b</sup>	56.6 ± 1.30	45.7 ± 0.58 <sup>b</sup>
Total monounsaturates	12.3 ± 1.92	13.5 ± 0.36	9.6 ± 0.46	12.5 ± 0.33 <sup>b</sup>
Linoleic (18:2n-6)	16.2 ± 0.70	18.9 ± 0.47 <sup>c</sup>	15.7 ± 0.46	19.5 ± 0.56 <sup>c</sup>
Dihomo- $\gamma$ -linolenic (20:3n-6)	3.6 ± 0.37	3.6 ± 0.3	4.3 ± 0.44	3.9 ± 0.2
Arachidonic (20:4n-6)	9.6 ± 0.72	11.7 ± 0.50	10.9 ± 0.66	11.8 ± 0.49
Docosatetraenoic (22:4n-6)	1.76 ± 0.60	2.1 ± 0.56	1.9 ± 0.25	2.2 ± 0.23
Docosapentaenoic (22:5n-6)	0.2 ± 0.01	0.2 ± 0.01	0.2 ± 0.01	0.2 ± 0.02
Total LCN-6 polyunsaturates <sup>e</sup>	15.1 ± 0.9	17.7 ± 0.7 <sup>b</sup>	17.3 ± 1.0	18.2 ± 0.5
$\alpha$ -Linolenic (18:3n-3)	ND	ND	ND	0.2 ± 0.06 (5)
Eicosapentaenoic (20:5n-3)	ND	0.3 ± 0.06 (8)	ND	0.4 ± 0.06 (12)
Docosapentaenoic (22:5n-3)	0.2 ± 0.06	1.1 ± 0.10 <sup>b</sup>	0.3 ± 0.06	1.0 ± 0.13 <sup>b</sup>
Docosahexaenoic (22:6n-3)	0.6 ± 0.11	2.4 ± 0.25 <sup>b</sup>	0.7 ± 0.16	2.2 ± 0.2 <sup>b</sup>
Total LCN-3 polyunsaturates <sup>f</sup>	0.9 ± 0.14	3.3 ± 0.27 <sup>b</sup>	1.0 ± 0.16	3.7 ± 0.39 <sup>b</sup>
<b>Women</b>				
Total saturates	55.3 ± 1.21	46.4 ± 0.76 <sup>b</sup>	56.4 ± 1.40	47.7 ± 0.95 <sup>b</sup>
Total monounsaturates	10.8 ± 0.44	11.9 ± 0.67 <sup>c</sup>	9.5 ± 0.31	11.8 ± 0.24 <sup>b</sup>
Linoleic (18:2n-6)	15.9 ± 0.75	19.3 ± 0.54 <sup>c</sup>	16.2 ± 0.47	19.7 ± 0.62 <sup>b</sup>
Dihomo- $\gamma$ -linolenic (20:3n-6)	4.4 ± 0.37	3.6 ± 0.26 <sup>d</sup>	3.9 ± 0.33	3.5 ± 0.17
Arachidonic (20:4n-6)	11.5 ± 0.64	12.0 ± 0.41	11.5 ± 0.61	11.9 ± 0.69
Docosatetraenoic (22:4n-6)	1.6 ± 0.14	2.0 ± 0.30	1.8 ± 0.39	2.3 ± 0.34
Docosapentaenoic (22:5n-6)	0.2 ± 0.01	0.2 ± 0.03	0.2 ± 0.01	0.2 ± 0.04
Total LCN-6 polyunsaturates <sup>e</sup>	17.7 ± 0.8	17.8 ± 0.5	17.4 ± 0.9	17.5 ± 0.4
$\alpha$ -Linolenic (18:3n-3)	ND	0.3 ± 0.06 (4)	ND	0.2 ± 0.05 (5)
Eicosapentaenoic (20:5n-3)	ND	0.5 ± 0.08 (13)	ND	0.6 ± 0.15 (10)
Docosapentaenoic (22:5n-3)	0.4 ± 0.07	1.0 ± 0.08 <sup>b</sup>	0.2 ± 0.06	0.9 ± 0.08 <sup>b</sup>
Docosahexaenoic (22:6n-3)	0.6 ± 0.11	2.4 ± 0.25 <sup>b</sup>	1.0 ± 0.16	2.2 ± 0.20 <sup>b</sup>
Total LCN-3 polyunsaturates <sup>f</sup>	1.0 ± 0.14	3.8 ± 0.28 <sup>b</sup>	1.2 ± 0.18	3.3 ± 0.22 <sup>b</sup>

<sup>a</sup>Values are mean ± SEM; *n* = 20 in each period for each sex except where indicated in parentheses. Group A: Period 1, groundnut oil; Period 2, Blend G. Group B: Period 1, sunflower oil; Period 2, Blend S. For blend components see Table 3. ND, not detected; LC, long-chain.

<sup>b</sup>*P* < 0.001; <sup>c</sup>*P* < 0.01; <sup>d</sup>*P* < 0.05; statistically different from Period 1 by paired *t*-test.

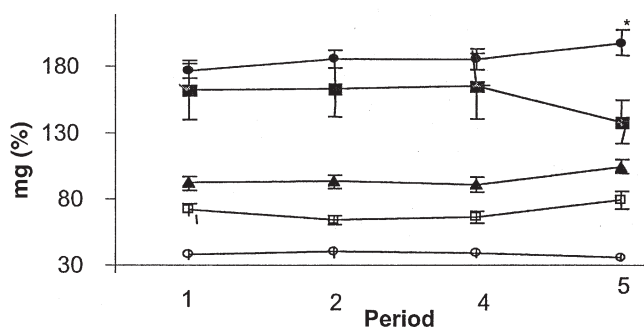
<sup>e</sup>Includes 20:3n-6, 20:4n-6, 22:4n-6, and 22:5n-6.

<sup>f</sup>Includes 20:5n-3, 22:5n-3, and 22:6n-3.

of 1–2 g common in most Western diets (17,18). In Eskimos and in populations in Japan (fishing villages) with low CHD morbidity, the daily intake of LCN-3 PUFA was about 7 and 4 g, respectively (19,20). Since subjects showed good compliance by using the oil supplied as the major cooking oil in their

homes and by eating home-prepared food, and because their body weights were similar at the end of the single-oil and blended-oil regimens, the data presented in Tables 4–8 can be attributed to differences in the type of oil consumed.

**FA composition in plasma and platelet phospholipids.** Despite having no differences in the intake of saturates, subjects' use of either of the blends decreased the total saturates in plasma phospholipids; the higher intake of oleic acid in subjects who used Blend S was reflected in plasma phospholipid values. The total LCN-3 PUFA levels in plasma and platelet phospholipids were low in the subjects studied here compared to populations consuming ALNA-rich edible oils (21,22) or fish (23–25). The observation that the magnitude of increase in total LCN-3 PUFA (20:5n-3, 22:5n-3, and 22:6n-3) in plasma phospholipids was similar at the end of 4 and 8 mon suggests that with a low dose of ALNA, the maximum improvement in n-3 PUFA status was achieved in 4 mon. At the end of 4 mon on either of the blends, 20:5n-3 increased but 22:6n-3 decreased in platelets. The reason for the decrease in 22:6n-3 is not clear. However, at the end of 8 mon, the increases in 20:5n-3 and 22:5n-3 contributed to a twofold increase in total LCN-3 PUFA. Published work on the effects of



**FIG. 1.** Effects of blended oils vs. fish oil on plasma lipids and apolipoproteins. Values are mean ± SEM (*n* = 12). \*Significantly different by ANOVA from Period 1 (*P* < 0.05). Period 1, groundnut oil; Period 2, Blend G (equal proportions of groundnut and canola) for 4 mon; Period 4, reversal to groundnut oil; Period 5, groundnut oil + 0.3 g LCN-3 PUFA. (●), Total cholesterol, (■) TG, (▲) apolipoprotein A-1, (□) apolipoprotein B, (○) HDL-cholesterol.

**TABLE 6**  
**FA Composition of Platelet Phospholipids<sup>a</sup> at the End of a 4-mon Intake of Blended Oils (nmol%)**

Parameters	Group A		Group B	
	Period 1	Period 2	Period 1	Period 2
<b>Men</b>				
Total saturates	48.8 ± 0.98	50.4 ± 2.82	48.4 ± 0.66	47.9 ± 0.76
Total monounsaturates	19.2 ± 0.74	19.4 ± 0.64	19.5 ± 0.75	18.5 ± 0.78
Linoleic (18:2n-6)	3.9 ± 0.13	4.9 ± 0.17 <sup>c</sup>	4.2 ± 0.14	5.5 ± 0.11 <sup>c</sup>
Dihomo-γ-linolenic(20:3n-6)	4.9 ± 0.52	1.3 ± 0.07 <sup>c</sup>	4.5 ± 0.50	1.4 ± 0.05 <sup>c</sup>
Arachidonic (20:4n-6)	19.9 ± 1.13	21.5 ± 0.88	20.2 ± 0.72	25.3 ± 0.64
Docosatetraenoic (22:4n-6)	2.2 ± 0.17	1.1 ± 0.18 <sup>c</sup>	2.0 ± 0.12	0.8 ± 0.20 <sup>c</sup>
Docosapentaenoic (22:5n-6)	0.2 ± 0.17	0.3 ± 0.02	0.5 ± 0.05	0.4 ± 0.01
Total LCn-6 polyunsaturates <sup>e</sup>	27.1 ± 1.0	23.8 ± 0.8 <sup>c</sup>	27.1 ± 0.9	27.8 ± 0.7
Eicosapentaenoic (20:5n-3)	ND	0.5 ± 0.06 (15)	ND	0.3 ± 0.04 (13)
Docosapentaenoic (22:5n-3)	0.4 ± 0.16	0.5 ± 0.05	0.9 ± 0.22	0.6 ± 0.03
Docosahexaenoic (22:6n-3)	1.2 ± 0.20	0.4 ± 0.04 <sup>b</sup>	0.7 ± 0.07	0.5 ± 0.05 <sup>d</sup>
Total LCn-3 polyunsaturates <sup>f</sup>	1.5 ± 0.23	1.4 ± 0.15	1.4 ± 0.13	1.5 ± 0.10
<b>Women</b>				
Total saturates	49.8 ± 1.06	51.1 ± 0.96	47.9 ± 1.35	49.8 ± 0.93
Total monounsaturates	20.5 ± 0.68	19.8 ± 0.76	18.2 ± 0.80	16.7 ± 0.37
Linoleic (18:2n-6)	4.3 ± 0.16	5.2 ± 0.11 <sup>c</sup>	4.4 ± 0.17	5.6 ± 0.15 <sup>c</sup>
Dihomo-γ-linolenic (20:3n-6)	4.7 ± 0.50	1.3 ± 0.06 <sup>c</sup>	4.7 ± 0.45	1.3 ± 0.10 <sup>c</sup>
Arachidonic (20:4n-6)	19.5 ± 0.71	21.1 ± 0.73	20.5 ± 0.97	22.5 ± 1.54
Docosatetraenoic (22:4n-6)	0.5 ± 0.04	1.3 ± 0.17 <sup>c</sup>	2.2 ± 0.16	0.9 ± 0.19 <sup>c</sup>
Docosapentaenoic (22:5n-6)	0.3 ± 0.02	0.4 ± 0.04	0.5 ± 0.05	0.3 ± 0.02
Total LCn-6 polyunsaturates <sup>e</sup>	24.8 ± 0.8	24.0 ± 0.6	27.9 ± 1.0	25.3 ± 1.1
Eicosapentaenoic (20:5n-3)	ND	0.4 ± 0.06 (16)	ND	0.3 ± 0.05 (15)
Docosapentaenoic (22:5n-3)	0.5 ± 0.13	0.7 ± 0.08	1.0 ± 0.28	0.5 ± 0.04
Docosahexaenoic (22:6n-3)	0.8 ± 0.08	0.5 ± 0.05 <sup>c</sup>	0.8 ± 0.14	0.5 ± 0.05 <sup>d</sup>
Total LCn-3 polyunsaturates <sup>f</sup>	1.3 ± 0.13	1.6 ± 0.12	1.6 ± 0.18	1.3 ± 0.10

<sup>a</sup>Values are mean ± SEM; *n* = 20 in each period for each sex except where indicated in parentheses. Group A: Period 1, groundnut oil; Period 2, Blend G. Group B: Period 1, sunflower oil; Period 2, Blend S. For blend components see Table 3. For abbreviations see Table 5.

<sup>b</sup>*P* < 0.01; <sup>c</sup>*P* < 0.001; <sup>d</sup>*P* < 0.05; statistically different from Period 1 by paired *t*-test.

<sup>e</sup>Includes 20:3n-6, 20:4n-6, 22:4n-6, and 22:5n-6.

<sup>f</sup>Includes 20:5n-3, 22:5n-3, and 22:6n-3.

**TABLE 7**  
**Platelet Aggregation and Fibrinogen at the End of a 4-mon Intake of Blended Oils<sup>a</sup>**

Parameters	Group A		Group B	
	Period 1	Period 2	Period 1	Period 2
<b>Men</b>				
WB aggregation with 2 μg collagen				
Slope (div/min)	16 ± 1.9	17 ± 2.0	18 ± 1.8	18 ± 1.7
Lag time (s)	120 ± 11.9	104 ± 7.5	130 ± 9.3	97 ± 4.6 <sup>b</sup>
PRP aggregation				
2 μM ADP (div/min)	66 ± 3.7	57 ± 1.8 <sup>c</sup>	64 ± 2.8	64 ± 3.4
Threshold (μM ADP)	0.25 ± 0.06	0.26 ± 0.04	0.26 ± 0.04	0.25 ± 0.03
Fibrinogen (mg/dL)	280 ± 34	310 ± 12	337 ± 10	316 ± 17
<b>Women</b>				
WB aggregation with 2 μg collagen				
Slope (div/min) <sup>b,d</sup>	21 ± 2.7	23 ± 2.0	22 ± 2.1	23 ± 2.2
Lag time (s)	129 ± 10.5	93 ± 6.1 <sup>b</sup>	120 ± 11	87 ± 5.7 <sup>b</sup>
PRP aggregation				
2 μM ADP (div/min) <sup>b,d</sup>	78 ± 4.5	68 ± 2.5 <sup>c</sup>	76 ± 4.4	67 ± 1.5 <sup>c</sup>
Threshold (μM ADP) <sup>b,d</sup>	0.10 ± 0.02	0.16 ± 0.02	0.17 ± 0.02	0.18 ± 0.03
Fibrinogen (mg/dL)	390 ± 26	356 ± 17	370 ± 18	337 ± 16

<sup>a</sup>Values are mean ± SEM; *n* = 20 in each period for each sex. Group A: Period 1, groundnut oil; Period 2, Blend G. Group B: Period 1, sunflower oil; Period 2, Blend S. For blend components see Table 3. WB, whole blood; PRP, platelet-rich plasma.

<sup>b</sup>*P* < 0.001; <sup>c</sup>*P* < 0.05; statistically different from Period 1 by paired *t*-test.

<sup>d</sup>Sex difference.

**TABLE 8**  
**LCn-3 PUFA in Plasma and Platelet Total Phospholipids, Platelet Aggregation, and Fibrinogen**  
**at the End of an 8-mon Intake of Blended Oils and After Changing Back to Single Oils<sup>a</sup>**

Parameters	Period 1	Period 2	Period 3	Period 1	Period 2	Period 3 <sup>0</sup>
<b>Men</b>						
Total LCn-3 polyunsaturates in phospholipids						
Plasma (nmol%)	1.0 ± 0.13	3.9 ± 0.42 <sup>b</sup>	3.4 ± 0.22 <sup>b</sup>	0.8 ± 0.22	3.6 ± 0.32 <sup>b</sup>	2.1 ± 0.22 <sup>b,c</sup>
Platelet (nmol%)	1.4 ± 0.15	1.4 ± 0.12	2.8 ± 0.22 <sup>b,c</sup>	1.1 ± 0.13	1.5 ± 0.17	2.2 ± 0.19 <sup>b,c</sup>
20:5n-3	ND	0.4 ± 0.05	0.6 ± 0.12	ND	0.4 ± 0.07	0.4 ± 0.16
22:5n-3	0.5 ± 0.18	0.6 ± 0.05	1.2 ± 0.11 <sup>b,c</sup>	0.3 ± 0.20	0.6 ± 0.05	0.9 ± 0.09 <sup>b</sup>
22:6n-3	0.9 ± 0.15	0.5 ± 0.05 <sup>b</sup>	1.1 ± 0.08 <sup>c</sup>	0.8 ± 0.08	0.5 ± 0.07 <sup>b</sup>	1.0 ± 0.15 <sup>c</sup>
Aggregation in WB						
2 $\mu$ g collagen						
Slope (div/min)	16 ± 2.1	18 ± 1.8	14 ± 1.6	15 ± 2.3	14 ± 2.0	13 ± 1.9
Lag time (s)	129 ± 6.8	98 ± 4.7 <sup>b</sup>	117 ± 9.0	140 ± 17.1	108 ± 9.1	131 ± 8.5
Aggregation in PRP						
2 $\mu$ M ADP						
Slope (div/min)	67 ± 3.6	59 ± 2.4	58 ± 3.5	60 ± 2.8	56 ± 2.2	54 ± 2.3
Threshold $\mu$ M	0.24 ± 0.04	0.28 ± 0.04	0.22 ± 0.03	0.34 ± 0.09	0.29 ± 0.04	0.26 ± 0.04
Fibrinogen (mg%)	355 ± 14.9	322 ± 18.2	282 ± 14.1 <sup>b</sup>	318 ± 19.6	288 ± 20.7	311 ± 31.6
<b>Women</b>						
Total LCn-3 polyunsaturates in phospholipids						
Plasma (nmol%)	1.2 ± 0.21	3.6 ± 0.25 <sup>b</sup>	3.6 ± 0.30 <sup>b</sup>	1.0 ± 0.16	3.4 ± 0.34 <sup>b</sup>	2.1 ± 0.21 <sup>b,c</sup>
Platelet (nmol%)	1.2 ± 0.16	1.4 ± 0.13	2.3 ± 0.17 <sup>b,c</sup>	1.4 ± 0.19	1.6 ± 0.15	2.0 ± 0.17 <sup>b</sup>
20:5n-3	ND	0.4 ± 0.08	0.4 ± 0.06	ND	0.4 ± 0.06	0.5 ± 0.10
22:5n-3	0.5 ± 0.33	0.5 ± 0.04	1.1 ± 0.09 <sup>c</sup>	0.7 ± 0.18	0.7 ± 0.10	0.8 ± 0.08
22:6n-3	0.8 ± 0.07	0.5 ± 0.06 <sup>b</sup>	0.9 ± 0.06 <sup>c</sup>	0.9 ± 0.17	0.5 ± 0.05 <sup>b</sup>	0.8 ± 0.11 <sup>c</sup>
Aggregation in WB						
2 $\mu$ g collagen						
Slope (div/min)	19 ± 2.5	23 ± 2.6	18 ± 2.7	23 ± 2.6	22 ± 1.9	16 ± 2.3 <sup>b</sup>
Lag time (s)	122 ± 13.8	98 ± 6.2	101 ± 7.7	115 ± 14.4	84 ± 7.0 <sup>b</sup>	112 ± 5.0 <sup>c</sup>
Aggregation in PRP						
2 $\mu$ M ADP						
Slope (div/min)	76 ± 6.3	68 ± 2.2	63 ± 3.1 <sup>b</sup>	75 ± 2.8	68 ± 2.5	67 ± 2.8 <sup>b</sup>
Threshold $\mu$ M	0.14 ± 0.03	0.19 ± 0.03	0.17 ± 0.02	0.12 ± 0.02	0.11 ± 0.02	0.14 ± 0.02
Fibrinogen (mg%)	385 ± 24.5	366 ± 20.9	343 ± 23.0	385 ± 25.1	347 ± 16.8	348 ± 27.0

<sup>a</sup>Values are mean  $\pm$  SEM;  $n = 24$  in each period for each sex (Periods 1, 2, and 3) and  $n = 14$  in each period for each sex (Periods 1, 2, and 3<sup>0</sup>). Statistically different by ANOVA from <sup>b</sup>Period 1 and <sup>c</sup>Period 2 ( $P < 0.05$ ). Period 1, groundnut oil or sunflower oil; Period 2, Blend G or Blend S for 4 mon; Period 3, Blend G or Blend S for 8 mon; Period 3<sup>0</sup>, groundnut oil or sunflower oil for 4 mon. For blend components see Table 3. For abbreviations see Table 7.

ALNA from flaxseed or canola oil have shown either no increase in 20:5n-3 and 22:6n-3 or only a modest increase in 20:5n-3 in plasma and platelet phospholipids. This wide variability has been attributed to differences in the dose of ALNA, duration of the experiment, LA intake, the n-6/n-3 ratio, or other nutritional and hormonal variations (21,26–29). The increase in LA in both plasma and platelet phospholipids and the decrease in 20:3n-6 in platelet phospholipids could be due to competition of ALNA with LA for the desaturases. It therefore appears that a modest increase in ALNA in cereal-based diets providing 5–7 en% LA may inhibit desaturation of LA and increase the conversion of ALNA to LCn-3 PUFA.

To determine the extent to which vegetable oils can substitute for fish oils, we studied the effects of increasing dietary ALNA compared to supplementation with LCn-3 PUFA (20:5n-3 + 22:6n-3) on plasma and platelet FA composition (Table 9). These data were obtained from the same subjects after a washout period of 5 mon so as to minimize interindividual variations. However, after the washout period LA and LCn-3 PUFA levels were higher than in the single-oil con-

sumption period, indicating that the carryover effects of blended oils may exceed 5 mon. The increase in LA in both plasma and platelet phospholipids and the decrease in 20:3n-6 in platelet phospholipids indicate that 20:5n-3 and 22:6n-3 from fish oil may inhibit the desaturation of LA (Table 9). The magnitude of increase in the LCn-3 PUFA period calculated in comparison to the respective single-oil period showed that dietary intake of  $\sim 2.2$  g (0.75 en%) ALNA or 0.3 g (0.1 en%) LCn-3 PUFA increased LCn-3 PUFA to the same extent in plasma phospholipids (efficiency of conversion was 7.5:1). However, the efficiency of conversion of ALNA to 20:5n-3 and 22:6n-3 was  $\sim 12:1$  and  $30:1$ , respectively. In our earlier short-term metabolic studies with twice the dose of ALNA or LCn-3 PUFA, the efficiency of conversion of ALNA to LCn-3 PUFA was 11:1 (10). Bioequivalence in functional responses have been achieved in some, but not all, studies by providing ALNA at levels 7–10 times that of the corresponding amounts of 22:6n-3 (29), and the efficiency of 20:5n-3 to prolong bleeding time is about twofold greater than that of ALNA (30).

**TABLE 9**  
**Effects for Blended Oils vs. Fish Oil<sup>a</sup> on Plasma and Platelet Total Phospholipid FA and Platelet Aggregation**

Parameters	Period 1	Period 2	Period 4	Period 5
Plasma phospholipids (nmol%)				
Total saturates	57.7 ± 1.8	44.2 ± 1.1 <sup>b</sup>	51.8 ± 2.2 <sup>b,c</sup>	45.8 ± 0.4 <sup>b,d</sup>
Total monounsaturates	10.1 ± 0.4	14.2 ± 0.5 <sup>b</sup>	10.5 ± 0.5 <sup>c</sup>	10.6 ± 0.2 <sup>c</sup>
Linoleic (18:2n-6)	15.6 ± 0.6	20.4 ± 0.84 <sup>b</sup>	18.7 ± 1.14 <sup>b</sup>	22.9 ± 0.6 <sup>b,c,d</sup>
Dihomo-γ-linolenic (20:3n-6)	4.1 ± 0.4	3.2 ± 0.5	4.5 ± 0.3 <sup>c</sup>	4.1 ± 0.4
Arachidonic (20:4n-6)	10.9 ± 0.9	12.2 ± 0.5	11.8 ± 0.8	10.5 ± 0.3
Docosatetraenoic (22:4n-6)	1.0 ± 0.05	1.3 ± 0.27	0.7 ± 0.1(10)	1.5 ± 0.2 (11)
Docosapentaenoic (22:5n-6)	0.2 ± 0.04	0.3 ± 0.07	0.3 ± 0.04	0.3 ± 0.03
Total LCn-6 polyunsaturates <sup>e</sup>	16 ± 1.2	17.2 ± 3.0	17.3 ± 3.3	16.3 ± 3.3 <sup>d</sup>
Eicosapentaenoic (20:5n-3)	ND	0.4 ± 0.08 (7)	0.2 ± 0.02 (5)	0.5 ± 0.06 (10)
Docosapentaenoic (22:5n-3)	0.2 ± 0.04	0.9 ± 0.14 <sup>b</sup>	<sup>b</sup> 0.4 ± 0.06 <sup>c</sup>	0.8 ± 0.07 <sup>b,d</sup>
Docosahexaenoic (22:6n-3)	0.8 ± 0.15	1.7 ± 0.30 <sup>b</sup>	1.2 ± 0.13	2.6 ± 0.21 <sup>b,c,d</sup>
Total LCn-3 polyunsaturates <sup>f</sup>	0.9 ± 0.16	3.0 ± 0.33 <sup>b</sup>	<sup>b</sup> 1.5 ± 0.18 <sup>c</sup>	3.5 ± 0.39 <sup>b,d</sup>
Platelet phospholipids (nmol%)				
Total saturates	49.8 ± 1.0	51.5 ± 0.8	47.1 ± 2 <sup>c</sup>	43.9 ± 1.2 <sup>b,c</sup>
Total monounsaturates	18.1 ± 0.8	16.5 ± 0.6	18.9 ± 0.7 <sup>c</sup>	18.9 ± 0.7 <sup>c</sup>
Linoleic (18:2n-6)	4.4 ± 0.17	5.4 ± 0.17 <sup>b</sup>	5.7 ± 0.53 <sup>b</sup>	7.3 ± 0.29 <sup>b,c,d</sup>
Dihomo-γ-linolenic (20:3n-6)	4.3 ± 0.5	1.2 ± 0.06 <sup>b</sup>	2.4 ± 0.5 <sup>b,c</sup>	1.2 ± 0.08 <sup>b,d</sup>
Arachidonic (20:4n-6)	21.5 ± 1.2	22.7 ± 0.8	23.9 ± 1.3	21 ± 1.8
Docosatetraenoic (22:4n-6)	1.5 ± 0.3	1.0 ± 0.2	1.6 ± 0.3	2.8 ± 0.8 <sup>b,c</sup>
Docosapentaenoic (22:5n-6)	0.3 ± 0.06	0.2 ± 0.07	0.4 ± 0.05	0.3 ± 0.1
Total LCn-6 polyunsaturates <sup>e</sup>	27.3 ± 4.6	25.4 ± 2.6 <sup>b,c</sup>	28.2 ± 4.9 <sup>c</sup>	25.1 ± 5.0 <sup>b,d</sup>
Eicosapentaenoic (20:5n-3)	ND	0.4 ± 0.09	ND	0.6 ± 0.14
Docosapentaenoic (22:5n-3)	0.1 ± 0.06	0.6 ± 0.06 <sup>b</sup>	0.5 ± 0.05 (7) <sup>b</sup>	1.3 ± 0.16 <sup>b,c,d</sup>
Docosahexaenoic (22:6n-3)	0.9 ± 0.07	0.4 ± 0.04 <sup>b</sup>	0.9 ± 0.16 <sup>c</sup>	1.5 ± 0.17 <sup>b,c,d</sup>
Total LCn-3 polyunsaturates <sup>f</sup>	0.9 ± 0.20	1.3 ± 0.16	1.2 ± 0.26	3.3 ± 0.29 <sup>b,c,d</sup>
WB aggregation (2 μg collagen)				
Slope (div/min)	17 ± 3.3	19 ± 2.6	15 ± 3.1	15 ± 3.1
Lag time (s)	134 ± 17	94 ± 7.2 <sup>b</sup>	127 ± 9.8 <sup>c</sup>	130 ± 11 <sup>c</sup>
PRP aggregation				
2 μM ADP (div/min)	68 ± 4.4	63 ± 2.9	65 ± 4.8	53 ± 2.5 <sup>b,d</sup>
Threshold (μM ADP)	0.2 ± 0.07	0.2 ± 0.04	0.2 ± 0.06	0.2 ± 0.05

<sup>a</sup>Values are mean ± SEM; *n* = 12 (six men, six women) in each period. Statistically different by ANOVA from <sup>b</sup>Period 1, <sup>c</sup>Period 2, and <sup>d</sup>Period 4 (*P* < 0.05). Period 1, groundnut oil; Period 2, Blend G for 4 mon; Period 4, reversal to groundnut oil; Period 5, groundnut oil + 0.3 g LCn-3 PUFA. For blend components see Table 3.

<sup>e</sup>Includes 20:3n-6, 20:4n-6, 22:4n-6, and 22:5n-6.

<sup>f</sup>Includes 20:5n-3, 22:5n-3, and 22:6n-3. For abbreviations see Tables 5 and 7.

**Platelet aggregation and fibrinogen.** The measurements of platelet aggregation *in vitro* and fibrinogen were done to assess the hemostatic effect of n-3 PUFA. ADP-induced aggregation in PRP measured by turbidometry has been widely used to assess platelet reactivity. The responsiveness to ADP-induced aggregation in PRP has been reported to be higher in a high-risk CHD group compared to a low-risk group. Further, dietary saturates (31) increase but n-3 PUFA decrease the ADP-induced platelet aggregation rate (32). Increasing dietary ALNA (Table 7) as well as supplementing with LCn-3 PUFA (Table 9) decreased ADP-induced aggregation. This decrease persisted (though statistical significance was not achieved for all values) both with the continuation of blended oils and after subjects were switched back to single oils for an additional period of 4 mon (Table 8). It is interesting that the carryover effects of ALNA in reducing ADP-induced aggregation (Table 8) parallel those observed in LCn-3 PUFA in plasma and platelet phospholipids (Table 8). However, it is not clear whether the decrease in ADP-induced aggregation rate without a corresponding change in other parameters of

coagulation (threshold for ADP and fibrinogen) will contribute to a decrease in platelet reactivity. In our earlier studies with 2–5 times higher doses of fish oil supplements, decreases in ADP-induced aggregation (33) were reported, but doubling the intake of saturates had no effect (14).

The impedance method of assessing agonist-induced WB aggregation permits measurement of platelet aggregation in its natural milieu. It reveals the formation of the first aggregates but provides scanty information about changes in platelet size (15,34). The lag time observed in collagen-induced aggregation is due to polymerization of collagen to collagen fibrils as well as stimulation and secretion of platelet contents following adhesion of platelets to collagen fibrils. Studies on collagen-induced aggregation in PRP and WB showed that n-3 PUFA decreased the aggregation rate (15,34). In Indian men, an increase in either ALNA or LCn-3 PUFA intake decreased the collagen-induced aggregation rate in WB (10). That the collagen-induced aggregation rate was not inhibited in WB, as observed in this study, could be attributed to the lower levels of either ALNA or LCn-3 PUFA. However, it is not clear whether the decrease in



lag time without a change in aggregation rate observed at the end of the blended oil period will affect the overall reactivity of platelets and would be of physiological or clinical relevance.

Platelet reactivity was higher in women as assessed by the ADP-induced aggregation rate, threshold for ADP in PRP, and collagen-induced WB aggregation rate. Johnson *et al.* (35) reported that ADP-induced aggregation increased in both sexes with age and that platelet sensitivity was greater in women. In our earlier studies, WB aggregation was measured with different levels of collagen; we found that EMR (estimated maximal response) was high in women but that the dose required for half-maximal response and lag times were similar in both sexes (14).

This study shows that a modest increase in dietary ALNA (the maximum achievable levels in cereal-based diets) leads to significant improvement in n-3 PUFA nutritional status. The observed beneficial effects are particularly important for vegetarians and for those who for various reasons do not include fish in their regular diets. We observed that although long-term use of LCn-3 PUFA from fish oils may confer benefits by having hypotriglyceridemic effects and by being about seven times more effective than ALNA in increasing total LCn-3 PUFA in plasma phospholipids, they may adversely affect cholesterol metabolism. In a recent review of epidemiological studies, Marckmann and Gronbaek (36) concluded that CHD mortality is high in people not eating fish at all, but daily consumption of 40–60 g fish is associated with reduced CHD mortality in high-risk populations. Since ALNA intake is inversely associated with risk of CHD (3,5–8), daily intake of ~2 g ALNA and an LA/ALNA ratio lower than 10:1 is recommended (6). The data presented here show that daily intake of ~2 g ALNA (vegetable oil blends) or 20:5n-3 plus 22:6n-3, which can be furnished from 20–50 g fish (2–5% fat), can improve n-3 PUFA nutritional status and reduce platelet reactivity. In India, chronic undernutrition, particularly a low intake of fat, n-3 PUFA (11), and micronutrients, may contribute to the high prevalence of low birth weights and the poor growth and development of babies (37–39). Both n-6 and n-3 PUFA play a critical role in gene regulation (40), fetal growth and development (41,42), and programming of diet-related chronic diseases in adults (43). Therefore, an improvement in the n-3 PUFA nutritional status of the Indian population throughout the life span may contribute to several health benefits, including the prevention of diet-related chronic diseases.

## ACKNOWLEDGMENTS

This project was funded (in part) by a grant-in-aid from the National Dairy Development Board (NDDB), Anand, Gujarat. The authors are grateful to Dr. Kamala Krishnaswamy, former director, NIN, and Dr. Amrita Patel, chairman, NDDB, for their keen interest and encouragement. We thank Dr. M. Vishnuvardhan Rao for help with the statistical analysis.

## REFERENCES

- Bang, H.O., and Dyerberg, J. (1972) Plasma Lipids and Lipoproteins in Greenlandic West Coast Eskimos, *Acta Med. Scand.* 192, 85–89.
- Leaf, A., and Kang, J.X. (1998)  $\omega$ -3 Fatty Acids and Cardiovascular Disease, in *The Return of  $\omega$ -3 Fatty Acids into the Food Supply* (Simopoulos, A.P., ed.), World Review of Nutrition and Dietetics, Vol. 83, pp. 24–37, S. Karger, Basel, Switzerland.
- Hu, F.B., Manson, J.E., and Willett, W.C. (2001) Types of Dietary Fat and Risk of Coronary Heart Disease: A Critical Review, *J. Am. Coll. Nutr.* 20, 5–19.
- Leaf, A. (1994) Some Effects of  $\omega$ -3 Fatty Acids on Coronary Heart Disease, in *Effects of Fatty Acids and Lipids in Health and Disease* (Galli, C., Simopoulos, A.P., and Trimoli, E., eds.), World Review of Nutrition and Dietetics, Vol. 76, pp. 1–8, S. Karger, Basel, Switzerland.
- De Lorgeril, M., Renaud, S., Mamelle, N., Salen, P., Martin, J.L., Monjaud, I., Guidollet, J., Tauboul, P., and Delaye, J. (1994) Mediterranean  $\alpha$ -Linolenic Acid-Rich Diet in Secondary Prevention of Coronary Heart Disease, *Lancet* 343, 1454–1459.
- Petithory, D.L. (2001)  $\alpha$ -Linolenic Acid and Cardiovascular Disease, *J. Nutr. Health Aging* 5, 179–183.
- Hu, F.B., Stampfer, M.J., Manson, J.E., Rimm, E.B., Wolk, A., Colditz, G.A., Hennekens, C.H., and Willett, W.C. (1999) Dietary Intake of  $\alpha$ -Linolenic Acid and Risk of Fatal Ischemic Heart Disease Among Women, *Am. J. Clin. Nutr.* 69, 890–897.
- Ascherio, A., Rimm, E.B., Giovannucci, E.L., Spiegelman, D., Stampfer, M.J., and Willett, W.C. (1996) Dietary Fat and Risk of Coronary Heart Disease in Men: Cohort Follow-Up Study in the United States, *Br. Med. J.* 313, 84–90.
- Ghafoorunissa (1996) Fats in Indian Diets and Their Nutritional and Health Implications, *Lipids* 31, S287–S291.
- Indu, M., and Ghafoorunissa (1992) n-3 Fatty Acids in Indian Diets—Comparison of the Effects of Precursor ( $\alpha$ -linolenic acid) vs. Product (long-chain n-3 polyunsaturated fatty acids), *Nutr. Res.* 12, 569–582.
- Ghafoorunissa (1998) Requirement of Dietary Fats to Meet Nutritional Needs and Prevent the Risk of Atherosclerosis—An Indian Perspective, *Ind. J. Med. Res.* 108, 191–202.
- Thimmayamma, B.V.S. (1987) *A Hand Book on Schedules and Guidelines in Socio-economic and Diet Surveys*, pp. 1–70, National Institute of Nutrition, Hyderabad, India.
- Gopalan, C., Ramasastry, B.V., and Balasubramanian, S.C. (1989) *Nutritive Value of Indian Foods* (revised and updated by Narasinga Rao, B.S., Deosthale, Y.G., and Pant, K.C.), pp. 47–91, Indian Council of Medical Research, New Delhi.
- Ghafoorunissa, Reddy, V., and Sesikeran, B. (1995) Palmolein and Groundnut Oil Have Comparable Effects on Blood Lipids and Platelet Aggregation in Healthy Indian Subjects, *Lipids* 30, 1163–1169.
- Cardinal, D.L., and Flower, R.J. (1980) The Electronic Aggregometer—A Novel Device for Assessing Platelet Behavior in Blood, *J. Pharmacol. Methods* 3, 135–158.
- Macart, M., Koffi, A., Henocque, G., Mathieu, J.F. and Guilbaud, J.C. (1989) Optimized Microturbidimetric Assay for Fibrinogen, *Clin. Chem.* 35, 211–214.
- Sanders, T.A.B. (2000) Polyunsaturated Fatty Acids in the Food Chain in Europe, *Am. J. Clin. Nutr.* 71 (Suppl.), 176S–178S.
- Kris-Etherton, P.M., Taylor, D.S., Poth, S.Y., Huth, P., Moriarty, K., Fishell, V., Hargrove, R.L., Zhao, G., and Etherton, T.D. (2000) Polyunsaturated Fatty Acids in the Food Chain in the United States, *Am. J. Clin. Nutr.* 71 (Suppl.), 179S–188S.
- Bang, H.O., Dyerberg, J., and Hjerne, N. (1976) The Composition of Food Consumed by Greenland Eskimos, *Acta Med. Scand.* 200, 69–73.
- Sugano, M., and Hirahara, F. (2000) Polyunsaturated Fatty Acids in the Food Chain in Japan, *Am. J. Clin. Nutr.* 71 (Suppl.), 189S–196S.
- Gerster, H. (1998) Can Adults Convert  $\alpha$ -Linolenic Acid (18:3n-3) to Eicosapentaenoic Acid (20:5n-3) and Docosahexaenoic Acid (22:6n-3)? *Int. J. Vitam. Nutr. Res.* 68, 159–173.

22. Sandker, G.N. (1993) Serum Cholesteryl Ester Fatty Acids and Their Relation with Serum Lipids in Elderly Men in Crete and The Netherlands, *Eur. J. Clin. Nutr.* 47, 201–208.
23. Yukio, Y., Nara, Y., Iritani, N., Workman, R.J., and Inagami, T. (1985) Comparison of Serum Phospholipid Fatty Acids Among Fishing and Farming Japanese Populations and American Inlanders, *J. Nutr. Sci. Vitaminol.* 31, 417–422.
24. Skúladóttir, G.V., Gudmundsdóttir, S., Ólafsson, G.B., Sigurdsson, S.B., Sigfússon, N., and Axelsson, J. (1995) Plasma Fatty Acids and Lipids in Two Separate but Genetically Comparable, Icelandic Populations, *Lipids* 30, 649–655.
25. Bulliyya, G., Reddy, P.C., and Reddanna, P. (1997) Traditional Fish Intake and Fatty Acid Composition in Fish-Consuming and Non-fish-Consuming Populations, *Asia Pac. J. Clin. Nutr.* 6, 230–234.
26. Thies, F., Nebe-Von-Caron, G., Powell, J.R., Yaqoob, P., Newsholme, E.A., and Calder, P.C. (2001) Dietary Supplementation with Eicosapentaenoic Acid, but Not with Other Long-Chain n-3 or n-6 Polyunsaturated Fatty Acids, Decreases Natural Killer Cell Activity in Healthy Subjects Aged Above 55 Years, *Am. J. Clin. Nutr.* 73, 539–548.
27. Sanders, T.A.B., and Roshanai, F. (1983) The Influence of Different Types of  $\omega$ -3 Polyunsaturated Fatty Acids on Blood Lipids and Platelet Function in Healthy Volunteers, *Clin. Sci.* 64, 91–99.
28. Valsta, L.M., Salminen, I., Aro, A., and Mutanen, M. (1996)  $\alpha$ -Linolenic Acid in Rapeseed Oil Partly Compensates for the Effect of Fish Restriction on Plasma Long-Chain n-3 Fatty Acids, *Eur. J. Clin. Nutr.* 50, 229–235.
29. Uauy, R., and Valenzuela, A. (2000) Marine Oils: The Health Benefits of n-3 Fatty Acids, *Nutrition* 16, 680–683.
30. Freese, R., and Mutanen, M. (1997)  $\alpha$ -Linolenic Acid and Marine Long-Chain n-3 Fatty Acids Differ Only Slightly in Their Effects of Hemostatic Factors in Healthy Subjects, *Am. J. Clin. Nutr.* 66, 591–598.
31. Renaud, S., Backer, D.E.G., Thevenon, C., Joossens, J.V., Vermeylen, J., Kornitzer, M., and Verstraetes, M. (1991) Platelet Fatty Acids and Function in Two Distinct Regions of Belgium: Relationship to Age and Dietary Habits, *J. Intern. Med.* 229, 79–88.
32. Mutanen, M., and Freese, R. (1996) Polyunsaturated Fatty Acids and Platelet Aggregation, *Curr. Opin. Lipidol.* 7, 14–19.
33. Ghafoorunissa (1999) Antiatherogenic Potential of Oils in Indian Subjects Consuming Cereal-Based Diets, *Proc. Nutr. Soc. India* 46, 33–46.
34. Schoene, N.W. (2001) Vitamin E and  $\omega$ -3 Fatty Acids: Effectors of Platelet Responsiveness, *Nutrition* 17, 793–796.
35. Johnson, M., Ramex, E., and Ramwell, P.W. (1975) Sex and Age Differences in Human Platelet Aggregation, *Nature* 253, 355–357.
36. Marckmann, P., and Gronbaek, M. (1999) Fish Consumption and Coronary Heart Disease Mortality. A Systematic Review of Prospective Cohort Studies, *Eur. J. Clin. Nutr.* 53, 585–590.
37. Gopalan, C. (1995) Micronutrient Deficiencies: Public Health Implications, *Ind. J. Pediatr.* 62, 157–167.
38. Gopalan, C. (2002) Multiple Micronutrient Supplementation in Pregnancy, *Nutr. Rev.* 60 (5), S2–S6.
39. UNICEF (1998) *The State of the World's Children*, Oxford University Press, New York.
40. Jump, D.B., and Clarke, S.D. (1999) Regulation of Gene Expression by Dietary Fat, *Annu. Rev. Nutr.* 19, 63–90.
41. Lapillonne, A., and Carlson, S.E. (2001) Polyunsaturated Fatty Acids and Infant Growth, *Lipids* 36, 901–911.
42. Innis, S.M. (1991) Essential Fatty Acids in Growth and Development, *Prog. Lipid Res.* 30, 39–103.
43. Barker, D.J.P. (1994) *Mothers, Babies and Diseases in Later Life*, pp. 80–93, BMJ Publishing, London.

[Received April 10, 2002, and in revised form September 18, 2002; revision accepted October 21, 2002]

# <sup>31</sup>P NMR Quantification and Monophasic Solvent Purification of Human and Bovine Lens Phospholipids

William C. Byrdwell<sup>a</sup>, Hidetoshi Sato<sup>b</sup>, Arne K. Schwarz<sup>b</sup>, Douglas Borchman<sup>b,\*</sup>,  
M.C. Yappert<sup>a</sup>, and Daxin Tang<sup>b</sup>

Departments of <sup>a</sup>Chemistry and <sup>b</sup>Ophthalmology and Visual Sciences, University of Louisville, Louisville, Kentucky 40202

**ABSTRACT:** Most lipid extraction procedures [Folch, J., Lees, M., and Sloane-Stanley, G.H. (1957) A Simple Method for the Isolation and Purification of Total Lipids from Animal Tissues, *J. Biol. Chem.* 226, 497–509; Bligh, E.G., and Dyer, W.J. (1959) A Rapid Method of Total Lipid Extraction and Purification, *Can. J. Biochem. Physiol.* 37, 911–917] employ biphasic solvent mixtures designed to dissolve the lipids in an organic phase and remove impurities in an aqueous phase. However, when applying these protocols to biological matrices such as that of the ocular lens, the formation of an emulsion layer between the organic and aqueous phases causes poor reproducibility in extraction yields and gives only a small amount of the lipid-containing chloroform phase. In this study, we quantified phospholipids at each step of the Folch *et al.* extraction protocol and compared the yield of human and bovine lens phospholipids obtained by the Folch-based approach and a novel monophasic methanol extraction method designed to circumvent the problems associated with biphasic extraction protocols. A monophasic methanol extraction coupled with <sup>31</sup>P NMR spectroscopy was found to be the simplest, quickest, and most effective method for quantifying the phospholipid content of the lens.

Paper no. L9008 in *Lipids* 37, 1087–1092 (November 2002).

Most lipid extraction procedures (1,2) employ biphasic solvent mixtures designed to dissolve the lipids in an organic phase and remove impurities in an aqueous phase. Upon addition of the KCl-containing aqueous buffer, however, biological matrices such as that of the ocular lens yield an emulsion layer between the organic and aqueous phases that causes low extraction yields and poor reproducibility.

These problems were circumvented in lens (3) and fungus (4) tissues by using an initial monophasic extraction with either methanol or a mixture of chloroform and methanol. The preferential solubility of phospholipids in methanol has been reported (5,6). It is reasonable, then, to expect better extraction yields using only methanol, a relatively polar solvent, rather than the less polar chloroform/methanol mixture. For this reason, we have explored the efficiency of a monophasic, methanol-based protocol for the extraction of lens phospholipids.

Present address of first author: Department of Chemistry, Florida Atlantic University, 777 Glades Rd., Box 3091, Boca Raton, FL 33401-0991.

Present address of second author: The Institute of Physical and Chemical Research (Riken), 19-1399, Koeji, Nagamachi, Aoba-Ku, Sendai, Miyagi, 980-868, Japan.

\*To whom correspondence should be addressed at Department of Ophthalmology and Visual Sciences, University of Louisville, 301 E. Muhammad Ali Blvd., Louisville, KY 40202. E-mail: borchman@louisville.edu

We have demonstrated that phospholipids obtained with a single methanolic extraction, without further purification, can be quantified by <sup>31</sup>P NMR spectroscopy. We have also determined the relative loss of phospholipids at each step of the extraction procedure and have compared the yield and composition of human and bovine lens phospholipids obtained by the Folch-based (1) approach and a monophasic methanol extraction method.

## METHODS

Through the Kentucky Lions Eye Bank and the Wisconsin Lions Eye Bank, Medical College of Wisconsin, clear human lenses were obtained within 8 h postmortem and frozen in liquid nitrogen. Bovine eyes were obtained fresh from a slaughterhouse. The lenses were removed and immediately frozen at –70°C. Spectrophotometric-grade solvents and all other chemicals were purchased from Sigma Chemicals (St. Louis, MO). All solutions and solvents were bubbled with argon gas for at least 10 min to remove oxygen. Glassware was used instead of plastic to avoid impurities present in plastics.

Buffer A was prepared as follows: 0.3 M sucrose; 10 mM *N*-2-hydroxyethylpiperazine-*N'*-2-ethane sulfonic acid, pH 7.4; and 2 mM DTT, added fresh. Buffer B was prepared as follows: 8 M urea; 0.08 M tris(hydroxymethyl)amino-methane, pH 7.4; and 2 mM DTT, added fresh.

Figure 1 shows the sequence of steps followed to compare the extraction efficiency of the most commonly used chloroform/methanol approach (Paths A1 and A2) with that of a monophasic methanol method (Path A3). The percent yields obtained with and without the use of a centrifugation step to remove water-soluble proteins prior to the Folch-based extraction are indicated (Paths A1 and A2). The loss of lipid caused by ultracentrifugation (Path A2 vs. Path A3) was also quantified.

*Paths A1, A2 (Fig. 1): Centrifugation fractionation of soluble and insoluble proteins.* We prepared three samples, S1, S2, and S3, each containing four bovine lenses. Lenses were thawed, weighed, and homogenized in 40 mL of buffer A using a mechanical tissue tearer (Biospec Products Inc., Bartlesville, OK). We dispersed the homogenate three times with 15-s bursts from a Branson Sonifier Cell disrupter 185 (Danbury, CT) at a power setting of 5, allowing 2 min between sonication periods to avoid heating the samples.

We placed samples S1 and S2 in ultracentrifuge tubes and spun them at 70,000 × *g* for 1.5 h. After centrifugation, we

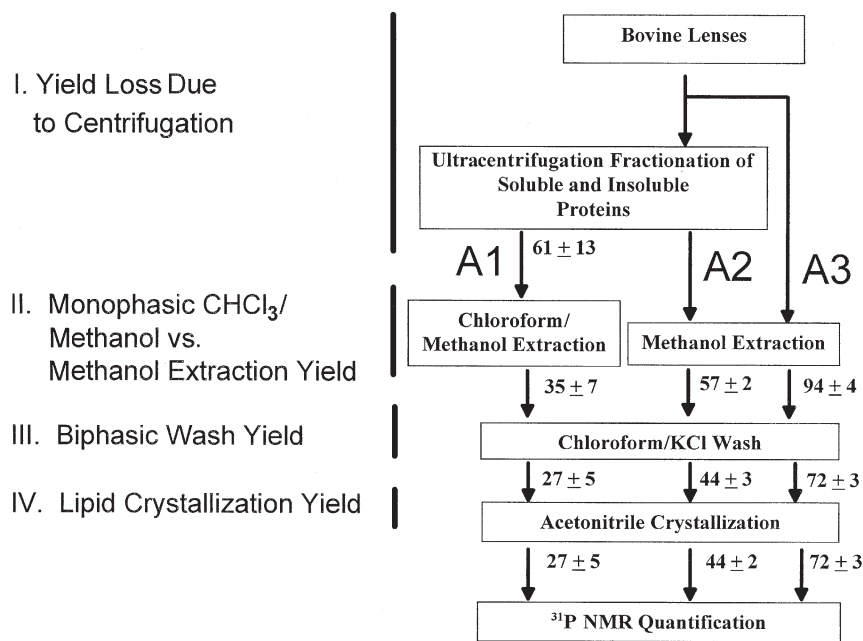


FIG. 1. Bovine lens lipid purification protocol. Data are mean (percent yields)  $\pm$  SEM ( $n = 8$ ).

decanted the supernatants and transferred the two resulting pellets to 50-mL centrifuge tubes, then added 15 mL of buffer B to each pellet. Each sample was mixed with a vortex mixer (Scientific Industries Inc., Bohemia, NY).

**Path A1 (Fig. 1): Chloroform/methanol bovine lipid extraction.** We added 30 mL of a 2:1 (vol/vol) chloroform/methanol mixture to the pellet in buffer B from sample S1. The sample was then mixed with a vortex mixer (Scientific Industries Inc.) and centrifuged at  $1,700 \times g$  for 10 min. Using a syringe with a cannula, we removed the lower (chloroform) layer and placed it in another centrifuge tube. We split the sample into two centrifuge tubes to accommodate the volume necessary for reextraction with 30 mL of chloroform/methanol. We then recombined the chloroform layers from the two tubes and evaporated the chloroform to dryness under argon. We reconstituted the resulting residue by adding 20 mL of chloroform and transferred this solution to a 50-mL centrifuge tube.

**Paths A2 and A3 (Fig. 1): Monophasic methanol bovine lipid extraction.** After centrifuging sample S2 in buffer B at  $70,000 \times g$  for 1.5 h, we decanted the supernatant and transferred the resulting pellet to a 50-mL centrifuge tube to which we added 40 mL of methanol. Samples S2 and S3 were each mixed with a vortex mixer (Scientific Industries Inc.) and spun at  $1,700 \times g$  for 10 min. We transferred the supernatants to a 100-mL rotary evaporator (Buchi Roto-Vap) flask and evaporated them to complete dryness in a water bath at  $60^\circ\text{C}$  using house vacuum. Failure to achieve complete dryness at this point resulted in cloudiness in the next step, even after centrifugation of the chloroform layer. We reconstituted the resulting residues by adding 20 mL of chloroform to each flask while swirling its contents and using a spatula to help dislodge the residue. Each solution was transferred to a 50-mL centrifuge tube.

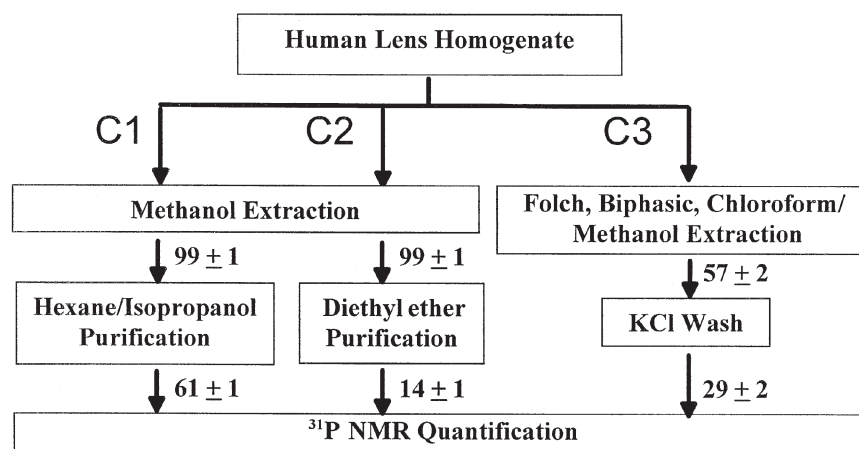
**Paths A1–A3 (Fig. 1): Chloroform/KCl wash.** We washed S1 samples from the chloroform/methanol extraction step and S2 and S3 samples from the methanol extraction step with 6 mL of 0.74% KCl solution. (NaCl was also used, with identical results.) We spun each mixture at  $1,700 \times g$  for 10 min, then aspirated off the top layer. The total volume of each sample was reduced to 1.5 mL under a stream of argon gas. Each sample was then transferred to a tared microtube.

**Paths A1–A3 (Fig. 1): Acetonitrile crystallization.** We added 20 mL of pure acetonitrile to samples S1, S2, and S3, then mixed each sample with a vortex mixer (Scientific Industries Inc.). This immediately caused precipitation of the product as a white flocculent material. We then centrifuged each tube at  $1,700 \times g$  for 10 min, and decanted and discarded the supernatant.

**Paths A1–A3 (Fig. 1): Quantification of bovine lipid.** We used eight samples for each path each time we performed the procedure in Figure 1. The percent recovery at each juncture in Figure 1 was determined by taking each sample to dryness under argon, dissolving it in 1.5 mL chloroform, and transferring it to tared microtubes. We took each sample to dryness under argon for weight determination and <sup>31</sup>P NMR analysis.

**Characterization of impurities.** Thirty-three bovine lenses that had been kept at  $-70^\circ\text{C}$  for 3 wk were thawed and weighed. We extracted lipid from these lenses as outlined in the methanol extraction protocol (Fig. 1, Path A3) except that we used a 250-mL volume of methanol. We added a 100-mL aliquot of chloroform to half the extracted and dried lipid. An insoluble white impurity was isolated by decanting the supernatant after spinning at  $1,700 \times g$  for 20 min. To the other half of the dried lipid methanol extract we added 100 mL of hexane/isopropanol (2:1, vol/vol), then followed the protocol for the hexane/isopropanol purification (Fig. 2, Path C1). The pellet from both centrifugation steps was saved for UV, IR, and <sup>31</sup>P NMR spectroscopic analysis.

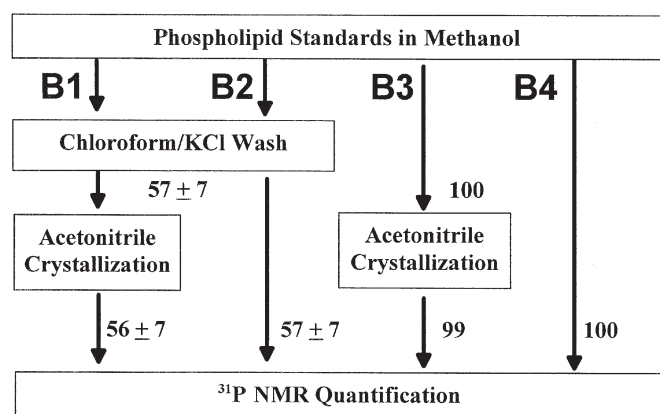




**FIG. 2.** Human lens lipid purification protocol. Data are mean (percent yields)  $\pm$  deviation ( $n = 2$ ). The amount of lipid extracted by two methanol extractions was determined to be 100% of the total lipid.

*Paths B1–B4 (Fig. 3): Purification of a synthetic mixture of phospholipids and cholesterol.* To assess the effect of the KCl wash and the acetonitrile precipitation in our method, we prepared mixtures of commercially available PS, PE, PC, and sphingomyelin, each to a concentration of 1  $\mu\text{g}/\text{mL}$ , then added cholesterol to give a final concentration of 4  $\mu\text{g}/\text{mL}$ . We analyzed an aliquot of each mixture before the extraction procedure using  $^{31}\text{P}$  NMR spectroscopy. We extracted aliquots of the standard by the method previously used to extract bovine lipids (Paths A1 and A2) with the KCl wash (Paths B1 and B2), with the acetonitrile precipitation (Paths B1 and B3), and without the KCl wash (Paths B3 and B4). PA was added as an internal standard before spectral acquisition.

*Paths C1–C3 (Fig. 2): Human lens lipid extraction and purification.* Fifteen pairs of human lenses  $44 \pm 18$  (SD) yr old were used for the extraction procedure. The lenses were weighed and homogenized in 150 mL of methanol using a mechanical tissue tearer (Biospec Products Inc.). The ho-



**FIG. 3.** Lipid standard purification protocol. PC, PS, PE, sphingomyelin, and cholesterol were used. Data are mean (percent yields)  $\pm$  SEM ( $n = 3$ ). The amount of lipid extracted by two sequential methanol extractions was determined to be 100% of the total lipid.

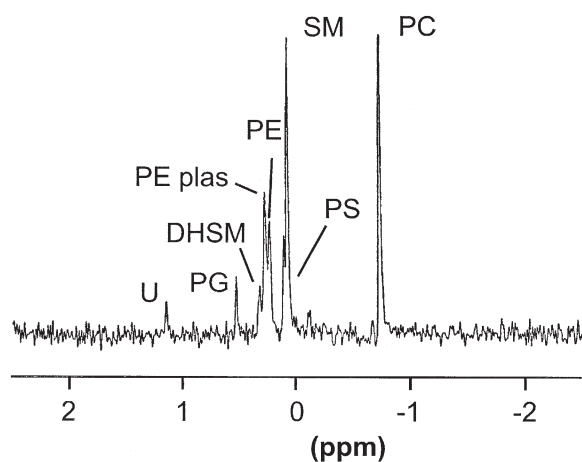
mogenate was dispersed by sonication as described above. We centrifuged samples at  $1,700 \times g$  for 10 min. We decanted and saved the supernatant, then added 150 mL of methanol to the pellet. We mixed, dispersed, and spun the pellet as described previously, then combined it with that from the first spin. Each sample was evenly divided into six tubes and weighed. The methanol in all tubes was evaporated under vacuum at  $60^\circ\text{C}$  and dried in a lyophilizer (Labconco, Kansas City, MO) for 12 h. These samples were all labeled A.

*Human lens phospholipid percent composition and quantification.* We evaluated the phospholipid composition of one of the samples labeled A by  $^{31}\text{P}$  NMR spectroscopy. To quantify the total phospholipid, we added 100  $\mu\text{L}$  of a PA solution (28 mg/mL methanol) as an internal standard. The linearity of the standard curve was demonstrated by adding known amounts of the internal standard.

*Path C1 (Fig. 2): Hexane/isopropanol purification.* We added 50 mL of hexane/isopropanol (2:1, vol/vol) to each of two samples labeled A and dispersed these samples three times with sonication as described above. We spun the mixtures at  $1,700 \times g$  for 10 min and decanted the supernatant carefully to avoid mixing the pellet. The supernatant was dried under argon. Phospholipid composition and total content were determined by  $^{31}\text{P}$  NMR spectroscopy.

*Human lens lipid diethyl ether purification (Fig. 2, Path C2).* We added 50 mL of diethyl ether to one sample labeled A and dispersed it with sonication as explained above. We spun the mixture at  $1,700 \times g$  for 10 min and decanted the supernatant. We dried the supernatant under argon and determined its phospholipid composition and total content by  $^{31}\text{P}$  NMR spectroscopy.

*Folch extraction of human lens tissue (Fig. 2, Path C3).* We added 50 mL of chloroform/methanol (2:1, vol/vol) to each of two samples labeled A and dispersed them with sonication as explained above. We added 10 mL of a 0.75% KCl aqueous solution, spun the samples at  $1,700 \times g$  for 10 min, and then removed the lower layer. We dried each lower layer under argon. Total phospholipid was determined by  $^{31}\text{P}$  NMR



**FIG. 4.** A typical  $^{31}\text{P}$  NMR spectrum of bovine lens lipid. SM, sphingomyelin; PE plas, PE plasmalogen; DHSM, dihydrosphingomyelin; PG, phosphatidylglycerol; U, unknown phospholipid.

spectroscopy. This procedure was repeated two times to assess reproducibility.

**$^{31}\text{P}$  NMR phospholipid compositional analysis and quantification.** For spectrometric compositional studies, we added 100  $\mu\text{L}$  of an internal standard solution consisting of 20 mg PA/mL of deuterated chloroform to each of the dried, extracted phospholipid samples. We then added a 400- $\mu\text{L}$  aliquot of deuterated chloroform to make a chloroform volume of 500  $\mu\text{L}$ . We vortexed this sample in the microtube and pipetted it into a 5-mm NMR tube for phospholipid quantification. We prepared a reagent consisting of 0.1 M EDTA (pH 6)/methanol (1:4, vol/vol) using KOH as the counter-cation source. At least 15 min before spectral acquisition, we added 250  $\mu\text{L}$  of the EDTA/methanol reagent (7,8) and shook the mixture. The aqueous phase was allowed to separate before analysis.

We quantified all samples using  $^{31}\text{P}$  NMR. For data acquisition, a Bruker AMX500 NMR spectrometer operating at 202.4 MHz  $^{31}\text{P}$  resonance frequency was used with the following spectral acquisition parameters: spectral width, 2032.5 Hz; resolution, 0.50 Hz; acquisition time, 1.0 s; interscan delay, 1.0 s; pulse length, 10  $\mu\text{s}$ ; dwell time, 246  $\mu\text{s}$ ; number of scans, 1,000. We treated spectral data on a personal computer using Bruker WINNMR software. All spectra were phase and baseline corrected. Deconvolution and curve fit were applied to obtain the area of each peak. A typical spectrum is shown in Figure 4. The spectral assignments are based on the chemical shifts reported previously (7,8) as well as on the spectral shifts obtained for the standard phospholipids PE, PS, sphingomyelin, and PC.

The number of moles of each phospholipid was evaluated from the ratio of the areas of the spectral bands corresponding to each phospholipid and the internal standard, for which the number of moles was known. We multiplied the number of moles thus obtained by 800 g/mol, an average phospholipid M.W., to obtain the weight of each extracted lipid. We referenced these weights to the initial amount of lens material.

## RESULTS

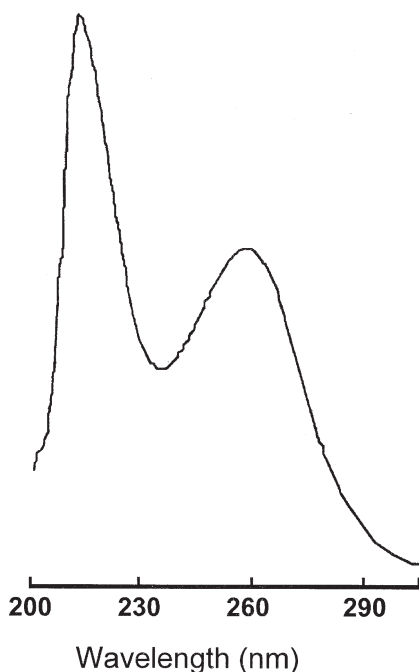
**Problems with the Folch extraction.** The advantage of using  $^{31}\text{P}$  NMR spectroscopy to quantify phospholipids is that purification is not necessary: A single-step methanolic extraction yields most, if not all, of the phospholipids at a level of purity adequate for quantification by NMR spectroscopy. However, along with the lipids, contaminants such as flavins and polysaccharides are also present. To remove these impurities, an aqueous wash is often used, as first reported by Folch *et al.* (1). This step leads to the separation of phases and results in lipid loss. Indeed, only about a third of the total phospholipid was recovered from human lenses (Fig. 2, Path C3) when using this approach.

**Comparison of extraction yields.** Centrifugation as pretreatment (Fig. 1, Paths A2 and A3) caused a twofold decrease in the yield of phospholipid as a result of lipid within the soluble-protein phase. The yield when methanol was used as the single extraction solvent was 65% higher than the yield when chloroform and methanol were used.

The effects of the KCl wash and the acetonitrile crystallization step were examined by extracting a mixture of standard phospholipids to which cholesterol had been added to emulate more closely the composition of lens membranes. As shown in Figure 3, elimination of the KCl wash produced significant increases in the amounts of phospholipid extracted. Under this condition, the average yield was 1.25 mg phospholipid/g of lens.

A monophasic extraction using methanol and no aqueous wash was advantageous as compared to the other extraction procedures. As measured by  $^{31}\text{P}$  NMR spectroscopy, 5.9 mg of phospholipid was extracted per gram of wet weight of human lens tissue. The use of a second methanol or chloroform extraction yielded undetectable levels of phospholipid, indicating that most of the total phospholipid from human lenses is recovered in a single methanol extraction. With bovine lens material, a second extraction recovered an additional 2 to 10% of phospholipid. No detectable phospholipids were recovered by a third extraction. Thus, the monophasic methanolic extraction of phospholipids coupled with  $^{31}\text{P}$  NMR is the simplest, quickest, and most precise method for quantifying phospholipid composition. In contrast, the Folch extraction and various other purification protocols decrease the yield of phospholipids.

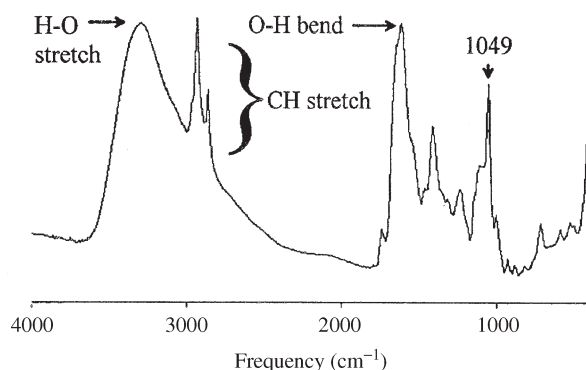
**The characteristics of impurities and phospholipid purification.** Various nonphospholipid impurities are present in the initial methanol extract of human and bovine lenses. These impurities do not interfere with the quantification of lipid using  $^{31}\text{P}$  NMR spectroscopy. The major impurity is a white hygroscopic powder that is completely soluble in water and methanol, slightly soluble in chloroform, and insoluble in hexane/isopropanol. This impurity is also composed of less than 3% protein by weight, as determined by a modified Lowry assay (9). The absorption band exhibited by the impurity at 262 nm (absorptivity = 2.2  $\text{mg}^{-1} \text{mL cm}^{-1}$ ) suggests the presence of mononucleotides or oligonucleotides (Fig. 5).



**FIG. 5.** UV absorbance spectrum of a methanol- and chloroform-soluble, hexane/isopropanol insoluble impurity in methanol as isolated from bovine lenses.

From the IR spectrum, shown in Figure 6, it appears that another component of the impurity may be a polysaccharide. Further evaluation will be necessary to confirm this assignment. Because of the high solubility of the white impurity in water, the KCl wash in the Folch (1) extraction completely removes it. Unfortunately, a considerable percentage of lipid is also lost in this step. Therefore, a purification procedure that avoids phase separation was developed.

**Purification by chloroform extraction.** Our first attempt to purify phospholipid involved evaporating the methanol from the initial phospholipid extraction and adding chloroform to the dried lipid film. The flocculent white impurity would not form a pellet even when it was centrifuged at  $200,000 \times g$  for 90 min. This indicates that the density of the impurity is similar to that of chloroform.



**FIG. 6.** IR spectrum of a methanol-soluble impurity lyophilized on a silver chloride window. The  $1049 \text{ cm}^{-1}$  band suggests that one of the impurities may be polysaccharide.

**Purification by hexane/isopropanol extraction.** The white impurity is insoluble in hexane/isopropanol, which is much less dense than chloroform. Consequently, centrifugation causes the impurity to form a pellet, leaving the purified phospholipid in the supernatant. No absorbance was detected in the supernatant at 262 nm, indicating complete removal of the impurity. When we used hexane/isopropanol purification, 60% of human phospholipid was recovered; a twofold improvement in the yield was achieved over the Folch (1) procedure (Fig. 2).

**Purification by diethyl ether extraction.** Diethyl ether is often used as an extraction solvent. However, the recovery was less than 15% of the total lipids (Fig. 2).

## DISCUSSION

We found that extraction of bovine and human lens lipids with methanol gives about 40% higher yield of phospholipids than does extraction with chloroform and methanol. Similar results have been reported using other tissues (4,5), but methanol extraction is not widely used. We also found that a 30–50% loss of phospholipids occurs at the KCl-wash step of the Folch procedure (1) even when using a mixture of phospholipid standards devoid of proteins. A centrifugation step to circumvent problems associated with insoluble protein at the aqueous–chloroform interface caused an additional 40% loss of phospholipids. The phospholipid yields at each step of the Folch extraction have never before been reported.

Because of the low yield of phospholipids obtained by the Folch protocol (1), we developed a method to extract and quantify phospholipids using a single methanol extraction. The loss of phospholipids is minimized because purification is unnecessary.  $^{31}\text{P}$  NMR spectroscopy (7,8) allows the quantification of phospholipids even when impurities are present.

When purification of phospholipids is essential, such as for biophysical characterization studies or the determination of lipid phosphate by chemical assays, we found that the addition of hexane/isopropanol to the initial dried methanol extract maintained a single phase and effectively removed the impurities. With this approach, the yield was two times higher than that obtained with the Folch (1) purification.

In conclusion, the biphasic nature of most solvent mixtures used in lipid extractions produces a lower yield of phospholipids than does the monophasic methanol extraction we have described. A single-step methanolic extraction followed by  $^{31}\text{P}$  NMR detection provides a simple, quick, and effective method for quantifying lens phospholipid. The methanol extraction followed by hexane/isopropanol purification provides the highest yield of purified phospholipids. These protocols should be advantageous for the analysis of phospholipids in all biological tissues.

## ACKNOWLEDGMENTS

Supported by Public Health Service research grants EY07975 (D.B.), EYO11657 (M.C.Y.), and the Kentucky Lions Eye Foundation (Louisville, KY), and an unrestricted grant from Research to Prevent Blindness, Inc.

## REFERENCES

1. Folch J., Lees, M., and Sloane-Stanley, G.H. (1957) A Simple Method for the Isolation and Purification of Total Lipids from Animal Tissues, *J. Biol. Chem.* 226, 497–509.
2. Bligh, E.G., and Dyer, W.J. (1959) A Rapid Method of Total Lipid Extraction and Purification, *Can. J. Biochem. Physiol.* 37, 911–917.
3. Broekhuysse, R.M. (1969) Phospholipids in Tissues of the Eye. III. Composition and Metabolism of Phospholipids in Human Lens in Relation to Age and Cataract Formation, *Biochim. Biophys. Acta* 187, 354–365.
4. Mirbod, F., Mori, S., and Nozawa, Y. (1993) Methods for Phospholipid Extraction in *Candida albicans*: An Extraction Method with High Efficiency, *J. Med. Vet. Mycol.* 31, 405–409.
5. Shuko, N., and Manami, K. (1976) Fat and Yeast Grown on Hydrocarbon Substrates II: Complete Extraction and Separation of Lipids, *Ogata Igaku Kagaku Kenkyusho Kenkyu Hokoku* 46, 91–92.
6. Ramesh, B., Adkar, S.S., Prabhudesai, A.V., and Viswanathan, C.V. (1979) Selective Extraction of Phospholipids from Egg Yolk, *J. Am. Oil Chem. Soc.* 56, 585–587.
7. Borchman, D., Byrdwell, W.C., and Yappert, M.C. (1994) Regional and Age-Dependent Differences in the Phospholipid Composition of Human Lens Membranes, *Invest. Ophthalmol. Vis. Sci.* 35, 3938–3942.
8. Merchant, T.E., Lass, J.H., Meneses, P., Greiner, J.V., and Glonek, T. (1991) Human Crystalline Lens Phospholipid Analysis with Age, *Invest. Ophthalmol. Vis. Sci.* 32, 549–555.
9. Peterson, G.L. (1977) A Simplification of the Protein Assay Method of Lowry *et al.* Which Is More Generally Applicable, *Anal. Biochem.* 83, 346–356.

[Received February 14, 2002, and in revised form and accepted December 11, 2002]



# Rapid and Improved Method for the Determination of Bile Acids in Human Feces Using MS

Shahid Perwaiz<sup>a,b,\*</sup>, Diane Mignault<sup>a,b</sup>, Beatriz Tuchweber<sup>b</sup>,  
and Ibrahim M. Yousef<sup>a,b</sup>

<sup>a</sup>Department of Pharmacology, Université de Montréal, Montréal, Canada H3C 3J7,  
and <sup>b</sup>Centre de Recherche de l'Hôpital Sainte-Justine, Montréal, Canada H3T 1C5

**ABSTRACT:** A simple method for the determination of bile acids in adult human fecal samples using GC–MS is described. Bile acids are directly extracted from feces by ethanol (95%) containing 0.1 N NaOH. Extracts are purified by passage through a reversed-phase C<sub>18</sub> silica cartridge and then analyzed by GC–MS. The present study has shown that lyophilized human feces contain mainly free bile acids, with lithocholic acid (LCA) and deoxycholic acid (DCA) as the major bile acids; however, isomers of LCA and DCA, keto-bile acids, and cholic acid are also present. Any traces of conjugated bile acids are hydrolyzed before the C<sub>18</sub> extraction by deconjugating enzymes, which are present in feces and are activated by the addition of water during the homogenization step. Thus, the analysis of fecal bile acids can be performed without the hydrolysis step in less than 4 h in comparison to traditional techniques, which usually require at least 48 h.

Paper no. L9079 in *Lipids* 37, 1093–1100 (November 2002).

Bile acids are the by-product of cholesterol and serve many important physiological functions in the maintenance of cholesterol homeostasis and the excretion and recirculation of drugs, vitamins, and lipids as well as endogenous and exogenous toxins. During their enterohepatic circulation, approximately 5% of bile acids escape into the colon, where they are modified by the intestinal flora and excreted in the feces (1–3). In recent years the analysis of fecal bile acids has been of interest because several studies have claimed a role for bile acids in colon cancer; it has been suggested that analysis of bile acid in feces may be a useful indicator of the susceptibility of individuals and populations in the development of colon cancer (4–8).

Despite the many studies reported for the analysis of fecal bile acids, data comparison is difficult principally because of the marked differences in the extraction procedures and the lack of a sensitive and accurate method. The extraction of bile acids from feces may be affected by (i) the presence of microorganisms, which hydrolyze peptide bonds of conjugated bile acids as well as dehydroxylate the 7  $\alpha$ -OH group, and (ii) binding of bile acids to particulate material (9,10). Several methods for bile acid determination in feces have been reported

\*To whom correspondence should be addressed at c/o Prof. Ibrahim M. Yousef, Département de Pharmacologie, Université de Montréal, C.P. 6128, Succ. Centre-ville, Montréal, Québec, Canada H3C 3J7.  
E-mail: pshahid@hotmail.com

Abbreviations: CA, cholic acid; DCA, deoxycholic acid; ES-MS-MS, electrospray tandem MS; LCA, lithocholic acid.

over the last three decades including GLC–MS, which is currently considered as the most reliable technique (11–14). The present study shows that bile acids present in adult human feces are mainly free bile acids, which contain lithocholic acid (LCA) and deoxycholic acid (DCA) as the major bile acids followed by isomers of LCA and DCA, keto-bile acids, cholic acid (CA), and traces of conjugated bile acids. Therefore, because bile acids are present mainly as free acids, it is possible to eliminate the hydrolysis step usually involved in fecal bile acid analysis. The present method allows the direct extraction of bile acids from feces by refluxing samples in alkaline ethanol at 80°C for 1 h followed by purification with C<sub>18</sub> columns. This procedure eliminates the time-consuming steps of homogenization and hydrolysis.

## MATERIALS AND METHODS

**Reagents.** Bile acid standards [cholic acid (CA), chenodeoxycholic acid, DCA, LCA, 5 $\beta$ -cholanic acid, and their glycine- and taurine-conjugated forms] were obtained from Calbiochem (San Diego, CA) and were at least 98% pure. Octadecyl (C<sub>18</sub>) Bakerbond™ extraction columns were obtained from J.T.Baker Inc. (Phillipsburg, NJ). All other solvents and chemicals used were either of HPLC grade or of known analytical purity and obtained from Sigma-Aldrich Chemical (St. Louis, MO).

**Preparation of standards.** Glycine and taurine conjugates of CA, chenodeoxycholic acid, DCA, and LCA as well as the internal standards (5 $\beta$ -cholanic acid) were dissolved individually in methanol at a concentration of 1 mg/mL. These solutions were kept refrigerated and were used as stock solutions.

**Homogenization of fecal samples.** Human fecal samples obtained from 14 volunteers were lyophilized and kept at –20°C until required for analysis. Cold distilled water (1 mL) was added to 200 mg of lyophilized fecal sample and homogenized for 3–5 min using a Polytron homogenizer, then incubated for 1 h at 37°C. The homogenized fecal samples were centrifuged at 1500  $\times$  g for 10 min. The supernatant (fecal water) was separated from the fecal pellet. To test the effect of incubation of lyophilized fecal samples in water on the deconjugation process, 50  $\mu$ g of taurine-conjugated LCA, DCA, and CA were added to the same fecal samples before the incubation step, and both free and conjugated bile acids were analyzed by GC–MS and electrospray tandem MS (ES-MS-MS).

**Extraction of bile acid.** Lyophilized human fecal samples (200 mg each) were directly refluxed in ethanol (5 mL)

containing 0.1 N NaOH (0.4 mL) and 100 µg of internal standard (5β-cholanic acid) at 80°C for 1 h. Samples were cooled on ice and then centrifuged at 1500 × *g* for 10 min. The supernatant was removed and dried under nitrogen, redissolved in 1 mL of HPLC water, and then subjected to a solid-phase extraction using an octadecyl (C<sub>18</sub>) Bakerbond™ cartridge. The C<sub>18</sub> cartridge was preconditioned, prior to loading the samples, with successive elutions of 2 mL of chloroform/methanol (2:1), methanol, and HPLC water solutions. After loading the samples, the column was washed with 2 mL of HPLC water and then *n*-hexane. The column was left for 10 min to drain any excess solvents. Bile acids were eluted from the cartridge with methanol (5 mL). The eluate was divided into two aliquots, which were evaporated to dryness under nitrogen. One aliquot was hydrolyzed, methylated, and acetylated; the other was methylated and acetylated but not hydrolyzed before GC–MS analysis.

**GC–MS.** The extracted samples were hydrolyzed, methylated, and acetylated as previously described (14). Identification and quantification of the bile acids were achieved by GC–MS using a Hewlett-Packard 5890 gas chromatograph equipped with a Hewlett-Packard 5971A mass selective detector employing the selected ion monitoring mode. In this method the selected ions for the different bile acids were, for CA, *m/z* 253, 368; chenodeoxycholic acid, 255, 370; DCA, 255, 370; ursodeoxycholic acid, 255, 370, keto-bile acids, 231, 446; LCA 257, 372; and 5β-cholanic acids, 217 and 374. Quantification was carried out by employing a correction factor obtained using 5β-cholanic acid as internal standard. Bile acid standards were processed and analyzed in a similar manner. The remaining half of the samples were not subjected to hydrolysis but were directly methylated and acetylated.

**Presence of deconjugating enzymes in human fecal samples.** To test for the presence of deconjugating enzymes in lyophilized human fecal samples, 100 µL of rat bile was incubated with 100 mg of lyophilized human feces homogenized in 1 mL of cold distilled water and incubated at 37°C for 1 h. Bile acids were extracted after incubation as described above and analyzed by ES-MS-MS.

**ES-MS-MS.** The ES-MS-MS methodology used for the identification of bile acids was similar to that previously described (14). The system used included a Hewlett-Packard high-performance liquid chromatograph (series 1100) equipped with an automatic sample injector that was connected to a Quattro electrospray tandem mass spectrometer (Micromass, Manchester, United Kingdom). The HPLC system was used only for injecting the samples into the mass spectrometer. Liquid nitrogen was used as nebulizer and argon as collision gas. The HPLC system was operated isocratically at a flow rate of 10 µL/min for the mobile phase (acetonitrile/water 1:1) at room temperature. Sample (10 µL) was injected into the ES-MS-MS by automatic injector. Negative ion mass spectra of the eluents were recorded using full scan mode.

**Statistical analysis.** An ANOVA test was used to evaluate the difference between the results obtained from groups analyzed with and without the hydrolysis step. A *P* value of <0.05 was considered significant.

## RESULTS

**Analysis of bile acids in human feces by GC–MS (with incubation in water).** The determination of the bile acid composition of adult human fecal samples analyzed with GC–MS was carried out in triplicate and results are presented in Tables 1 and 2. The amount of total and individual bile acids showed considerable variation between samples. The main bile acids in each fecal sample were LCA (45–50%) and DCA (30–40%), followed by isomers of LCA and DCA (10–15%), keto-bile acids (6–8%), and CA (1–2%). The concentration of total bile acid obtained by GC–MS varied between 284.72 and 678.23 µg bile acids/100 mg of feces (Tables 1 and 2). There was no significant difference between the amounts of total bile acids observed between samples that were or were not subjected to alkaline hydrolysis. To test for the presence of deconjugating enzymes, these fecal samples were spiked with 50 µg of standards of taurine-conjugated LCA, DCA, and CA and measured in a similar manner. The results obtained again showed no significant difference between the

**TABLE 1**  
Analysis<sup>a</sup> of Major Bile Acids in Human Feces Without Alkaline Hydrolysis (with incubation in water)

Samples <sup>b</sup>	LCA	DCA	CA	Keto-bile acids	Others	Total bile acid
A-1	235.91 ± 2.6	140.05 ± 4.9	5.21 ± 2.6	26.25 ± 4.9	45.11 ± 7.5	452.52 ± 8.9
A-2	159.42 ± 3.0	99.28 ± 4.6	3.12 ± 1.8	20.64 ± 5.2	33.63 ± 6.8	316.07 ± 7.5
A-3	141.75 ± 2.8	102.90 ± 3.8	4.80 ± 3.2	14.67 ± 6.5	31.80 ± 8.2	295.92 ± 8.2
A-4	194.11 ± 2.9	180.74 ± 3.6	3.63 ± 2.2	27.76 ± 5.8	43.48 ± 6.5	422.69 ± 7.8
A-5	265.56 ± 3.5	269.57 ± 4.2	1.80 ± 2.5	45.47 ± 4.2	80.26 ± 6.9	662.66 ± 8.2
S-1	280.65 ± 2.8	185.08 ± 5.2	49.51 ± 3.2	25.54 ± 3.8	42.92 ± 7.7	583.70 ± 7.9
S-2	201.20 ± 3.2	145.28 ± 4.9	43.97 ± 3.5	19.32 ± 7.2	38.52 ± 7.0	447.79 ± 8.1
S-3	185.75 ± 3.9	148.90 ± 5.3	46.54 ± 4.2	15.86 ± 8.5	29.51 ± 6.9	426.56 ± 9.2
S-4	235.08 ± 3.1	222.90 ± 4.7	44.34 ± 3.8	29.11 ± 4.9	41.63 ± 8.5	573.06 ± 8.7
S-5	308.56 ± 2.5	310.57 ± 5.9	45.50 ± 4.2	47.37 ± 5.2	82.86 ± 6.4	794.86 ± 6.9

<sup>a</sup>Values are expressed as µg bile acids/100 mg of dried feces. Each value represents the average of three determinations ± SD.

<sup>b</sup>Samples were obtained from five healthy adult subjects (A1–A5). Samples S1–S5 were the same set of samples (A1–A5) but were spiked with 50 µg of taurine conjugates of LCA (lithocholic acid), DCA (deoxycholic acid), and CA (cholic acid). Others = isomers of LCA and DCA.

**TABLE 2**  
**Analysis<sup>a</sup> of Major Bile Acids in Human Feces with Alkaline Hydrolysis (with incubation in water)**

Samples <sup>b</sup>	LCA	DCA	CA	Keto-bile acids	Others	Total bile acid
A-1	218.27 ± 2.8	140.70 ± 4.2	4.80 ± 3.1	28.12 ± 5.9	46.67 ± 7.2	438.59 ± 7.5
A-2	149.56 ± 3.2	95.31 ± 3.5	2.80 ± 2.2	18.30 ± 6.0	35.38 ± 6.8	301.28 ± 7.2
A-3	136.22 ± 2.1	96.70 ± 4.2	4.21 ± 3.5	16.30 ± 5.5	31.32 ± 8.4	284.72 ± 8.9
A-4	188.37 ± 2.8	169.32 ± 3.2	3.22 ± 1.8	26.82 ± 5.2	48.55 ± 6.9	436.22 ± 8.6
A-5	276.12 ± 2.9	273.50 ± 3.9	2.21 ± 2.9	46.66 ± 4.8	79.70 ± 5.9	678.23 ± 9.5
S-1	265.27 ± 2.7	185.51 ± 5.0	46.60 ± 2.9	25.62 ± 4.9	41.98 ± 5.7	564.99 ± 8.9
S-2	195.53 ± 4.1	142.80 ± 4.5	43.51 ± 3.2	18.40 ± 6.7	38.53 ± 5.2	438.74 ± 7.4
S-3	180.42 ± 3.5	140.50 ± 4.9	44.43 ± 3.5	17.90 ± 5.9	28.54 ± 7.4	411.79 ± 8.5
S-4	233.27 ± 2.9	215.21 ± 4.6	45.32 ± 3.5	23.82 ± 6.3	54.66 ± 7.6	572.26 ± 7.4
S-5	320.22 ± 2.2	319.33 ± 1.6	46.60 ± 5.3	52.88 ± 5.8	69.73 ± 6.8	808.79 ± 9.2

<sup>a</sup>Values are expressed as  $\mu\text{g}$  of bile acids/100 mg of dried feces. Each value represents the average of three determinations  $\pm$  SD.

<sup>b</sup>Samples were obtained from five healthy adult subjects (A1–A5). Samples S1–S5 were the same set of samples (A1–A5) but spiked with 50  $\mu\text{g}$  of taurine conjugates of LCA, DCA, and CA. Others = isomers of LCA and DCA. For abbreviations see Table 1.

groups that had or had not undergone alkaline hydrolysis (Tables 1 and 2).

*Analysis of bile acids in human feces by GC–MS (without incubation in water).* Tables 3 and 4 illustrate the bile acid profiles of five human fecal samples, not incubated in water, that were analyzed by GC–MS. The major bile acids present in all the fecal samples were LCA followed by DCA, followed by isomers of LCA and DCA (10–15%), keto-bile acids (6–8%), and CA (1–2%). The amount of total bile acids ranged from 247.0 to 415.05  $\mu\text{g}$  bile acids/100 mg of feces (Tables 3 and 4). There was no significant difference between the amount of total bile acid observed for the samples analyzed after alkaline hydrolysis and those not subjected to alkaline hydrolysis. But in the samples spiked with 50  $\mu\text{g}$  of standards of taurine-conjugated LCA, DCA, and CA, there was a significant difference in total bile acids between the groups analyzed after alkaline hydrolysis and those not exposed to alkaline hydrolysis by GC–MS. This proves that human fecal samples contain only free bile acids, and that addition of water to the lyophilized fecal sample stimulates the bacterial enzymes responsible for the deconjugation of conjugated bile acids (Tables 3 and 4).

*Fecal bile acids analyzed by ES-MS-MS.* To test the profile of bile acids as well as the presence of deconjugating enzymes in human feces, ES-MS-MS techniques were used. Figure 1 illustrates the ES-MS-MS spectrum obtained from the fecal sample, which shows the presence of only free bile acids and keto-bile acids. The ions obtained at  $m/z$  373.7, 375.7, 389.7, 391.7, and 407.8 correspond to mono-keto, mono-OH, mono-keto-mono-OH, di-OH, and trihydroxylated free bile acids, respectively (Fig. 1). There was no evidence of sulfated and glucuronidated bile acids in these samples. The other ions present in Figure 1 do not correspond to any known bile acids, and the chromatogram obtained by GC–MS (Fig. 2) confirms the presence of LCA, DCA, CA, isomers of LCA and DCA, and keto-bile acids. Figure 3 shows the full-scan spectrum of rat bile obtained by ES-MS-MS showing only taurine-conjugated di- ( $m/z$  498.7) and trihydroxylated ( $m/z$  514.7) bile acids. Figure 4 shows the spectrum obtained from ES-MS-MS after incubating 100  $\mu\text{L}$  of rat bile with fecal samples in cold distilled water. The result clearly illustrates the deconjugation of taurine-conjugated di- and trihydroxylated bile acids into their respective free forms ( $m/z$  391.7 and 407.7).

**TABLE 3**  
**Analysis<sup>a</sup> of Major Bile Acids in Human Feces Without Alkaline Hydrolysis (without incubation in water)**

Samples <sup>b</sup>	LCA	DCA	CA	Keto-bile acids	Others	Total bile acid
B-1	247.06 ± 4.6	96.48 ± 1.6	1.21 ± 3.1	24.01 ± 5.9	46.30 ± 8.6	415.05 ± 8.6
B-2	151.51 ± 4.2	104.65 ± 2.3	3.53 ± 3.8	20.49 ± 6.2	34.58 ± 8.9	314.73 ± 9.2
B-3	124.09 ± 3.8	89.57 ± 1.8	4.82 ± 4.1	15.88 ± 6.5	36.84 ± 7.8	271.18 ± 8.5
B-4	101.92 ± 5.6	83.95 ± 2.0	3.22 ± 5.1	13.57 ± 6.8	26.70 ± 8.2	257.13 ± 8.2
B-5	153.03 ± 3.9	112.95 ± 3.2	4.90 ± 3.6	25.94 ± 6.4	40.23 ± 8.1	327.05 ± 9.4
T-6	244.81 ± 4.8	108.28 ± 2.5	3.11 ± 3.9	21.32 ± 5.9	48.90 ± 7.5	426.30 ± 8.8
T-7	145.86 ± 4.9	113.51 ± 3.8	2.80 ± 4.2	20.68 ± 5.6	37.58 ± 6.8	320.43 ± 7.9
T-8	131.84 ± 6.0	107.40 ± 4.2	2.51 ± 4.5	15.63 ± 6.3	21.73 ± 7.6	279.10 ± 8.1
T-9	106.43 ± 6.2	93.65 ± 2.6	3.80 ± 3.2	12.75 ± 7.0	26.43 ± 8.0	243.06 ± 9.3
T-10	167.27 ± 5.7	115.17 ± 3.2	4.73 ± 3.1	18.63 ± 7.6	38.51 ± 7.9	344.28 ± 8.6

<sup>a</sup>Values are expressed as  $\mu\text{g}$  bile acids/100 mg of dried feces. Each value represents the average of three determinations  $\pm$  SD.

<sup>b</sup>Samples were obtained from five healthy adult subjects (B1–B5). Samples T6–T10 were the same set of samples (B1–B5) but spiked with 50  $\mu\text{g}$  of taurine conjugates of LCA, DCA, and CA. Others = isomers of LCA and DCA. For abbreviations see Table 1.

**TABLE 4**  
**Analysis<sup>a</sup> of Major Bile Acids in Human Feces with Alkaline Hydrolysis (without incubation in water)**

Samples <sup>b</sup>	LCA	DCA	CA	Keto-bile acids	Others	Total bile acid
B-1	223.80 ± 4.2	90.41 ± 1.8	3.13 ± 3.9	30.99 ± 6.2	49.41 ± 8.5	397.70 ± 7.8
B-2	124.91 ± 4.8	91.82 ± 2.5	2.80 ± 4.2	21.67 ± 6.6	47.67 ± 9.1	288.84 ± 8.9
B-3	105.53 ± 3.2	86.78 ± 2.0	2.51 ± 4.5	21.15 ± 6.8	44.61 ± 8.8	260.56 ± 8.4
B-4	92.21 ± 5.1	79.46 ± 2.2	3.81 ± 3.2	28.88 ± 5.9	42.62 ± 8.9	247.00 ± 7.8
B-5	143.60 ± 3.4	126.94 ± 3.0	4.70 ± 3.1	24.35 ± 6.2	40.59 ± 7.7	340.24 ± 9.2
T-6	319.41 ± 3.9	135.36 ± 2.8	45.73 ± 4.8	28.33 ± 5.5	45.98 ± 7.5	574.81 ± 8.1
T-7	189.18 ± 3.8	140.84 ± 3.5	44.90 ± 6.8	21.54 ± 6.1	49.11 ± 8.1	445.65 ± 7.5
T-8	165.83 ± 5.8	131.01 ± 4.9	44.12 ± 6.1	20.98 ± 5.7	47.98 ± 8.5	409.96 ± 7.6
T-9	151.21 ± 5.8	126.73 ± 2.3	46.82 ± 6.2	26.73 ± 5.9	39.42 ± 7.3	390.85 ± 9.0
T-10	209.67 ± 4.9	173.15 ± 3.0	47.30 ± 5.9	25.21 ± 6.2	40.67 ± 9.2	496.08 ± 8.2

<sup>a</sup>Values are expressed as µg bile acids/100 mg of dried feces. Each value represents the average of three determinations ± SD.

<sup>b</sup>Samples were obtained from five healthy adult subjects (B1–B5). Samples T6–T10 were the same set of sample (B1–B5) but spiked with 50 µg of taurine conjugates of LCA, DCA, and CA. Others = isomers of LCA and DCA. For abbreviations see Table 1.

## DISCUSSION

Most of the procedures currently used for the extraction and analysis (HPLC, GLC, GC–MS) of bile acids (10–15) from feces show very little advance upon the methods developed in the 1960s. The results from the present method clearly show the presence of deconjugating enzymes in the lyophilized fecal samples. Therefore, addition of water during the homogenization step causes the deconjugation of conjugated bile acids in feces into their respective free forms. Thus, fecal samples can be analyzed without the alkaline hydrolysis step.

Several studies have considered the microbial transformation of bile acid by mixed microbial cultures from human feces (8,9). In the present study, the spectrum obtained from ES-MS-MS (Fig. 1) shows that human feces contain mainly free bile acids (LCA, DCA, CA, and keto-bile acids); thus, if any conjugated bile acid is present, deconjugation occurs by the addition of water during the homogenization step as a result of the activation of deconjugating enzymes. Figure 2 further identifies the presence of the isomers of LCA and DCA. The ES-MS-MS spectra (Figs. 3 and 4) confirm the deconjugation of bile acids by deconjugating enzymes. The bile acids present in rat bile are mainly taurine-conjugated di- and tri-hydroxylated bile acids (Fig. 3), but after incubation of the same rat bile with a lyophilized human fecal sample in cold distilled water, the conjugated bile acids are significantly hydrolyzed to their respective free bile acids (Fig. 4).

For the identification and quantification of conjugated bile acids by GC–MS, alkaline hydrolysis is a necessary step to hydrolyze the peptide bond between taurine/glycine and bile acids before derivatization. Tables 1 and 2 depict the bile acid analysis by GC–MS of five adult human fecal samples following incubation in water. The results show no significant difference in the amount of total bile acid between the samples that were hydrolyzed and those that were not hydrolyzed with alkali. This proves that human feces contain only the free bile acids (Tables 1 and 4). To test the effect of water on the hydrolysis of conjugated bile acids, the same sets of fecal samples were spiked with 50 µg of standards of taurine-conjugated

LCA, DCA, and CA and analyzed in a manner similar to that for nonspiked human fecal samples. The results obtained show there was no significant difference between the groups subjected or not to alkaline hydrolysis, which further proves that hydrolysis of taurine-conjugated bile acids occurred owing to activation of bacterial enzymes when fecal samples were incubated in cold distilled water (Tables 1 and 2).

Tables 3 and 4 show the bile acid analysis by GC–MS of another five adult human fecal samples that were not incubated in water. The results obtained show no difference in the amount of total bile acids between groups analyzed with alkaline hydrolysis and without alkaline hydrolysis (Tables 3 and 4). But when the same samples were spiked with 50 µg of standards of taurine-conjugated LCA, DCA, and CA and analyzed in a manner similar to that in Tables 1 and 2, the amounts of total bile acid were significantly different between the groups analyzed with and without the alkaline hydrolysis step.

Thus, fecal bile acids can be easily extracted by refluxing the fecal samples directly in alkaline ethanol solution followed by derivatization for GC–MS analysis without the time-consuming step of the traditional alkaline hydrolysis. This method also enables fast determination (<4 h) of fecal bile acids—including extraction time, purification step, derivatization, and GC–MS analysis time—in comparison to other techniques.

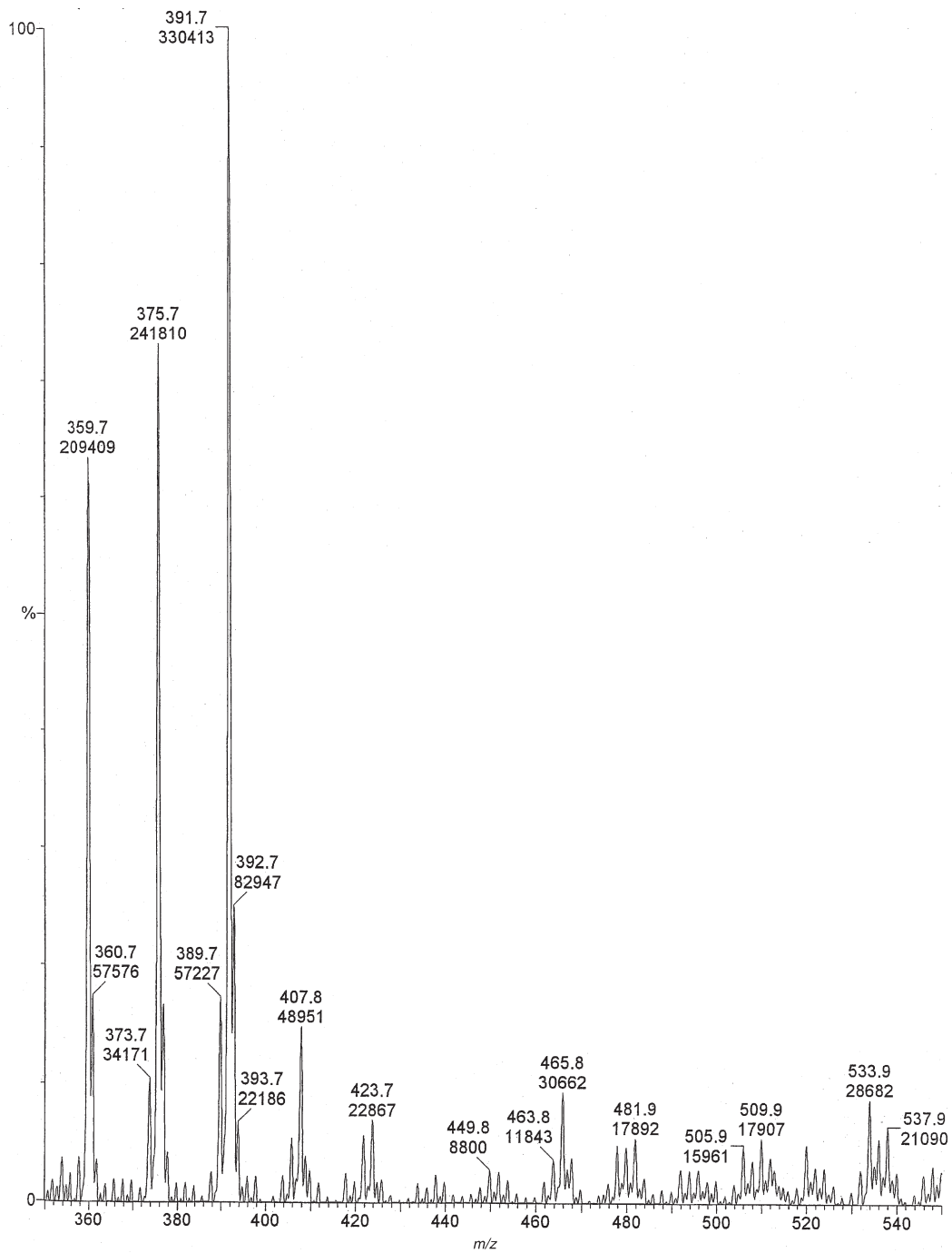
## ACKNOWLEDGMENT

This work was supported by a grant from the Canadian Liver Foundation (CLF).

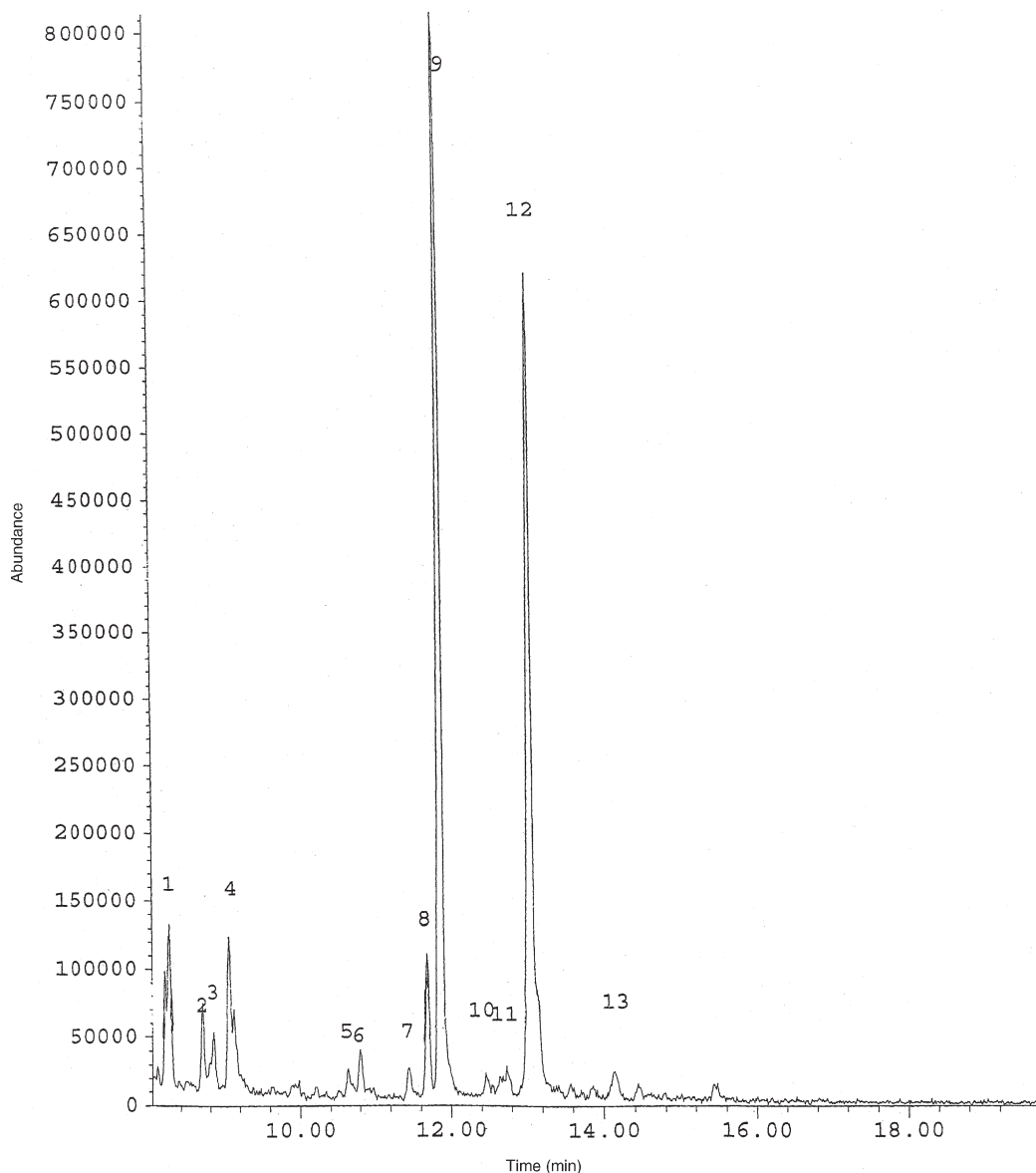
## REFERENCES

- Vlahcevic, Z.R., Pandak, W.M., and Stravitz, R.T. (1999) Regulation of Bile Acid Biosynthesis, *Gastroenterol. Clin. North Am.* 28, 1–25.
- Hoffman, A.F. (1994) Bile Acids, in *The Liver: Biology and Pathobiology* (Arias, I.M., Boyer, J., Fausto, L., Jakoby, N., and Schachter, W.B., eds.), 3rd edn., pp. 677–718, Raven Press, New York.



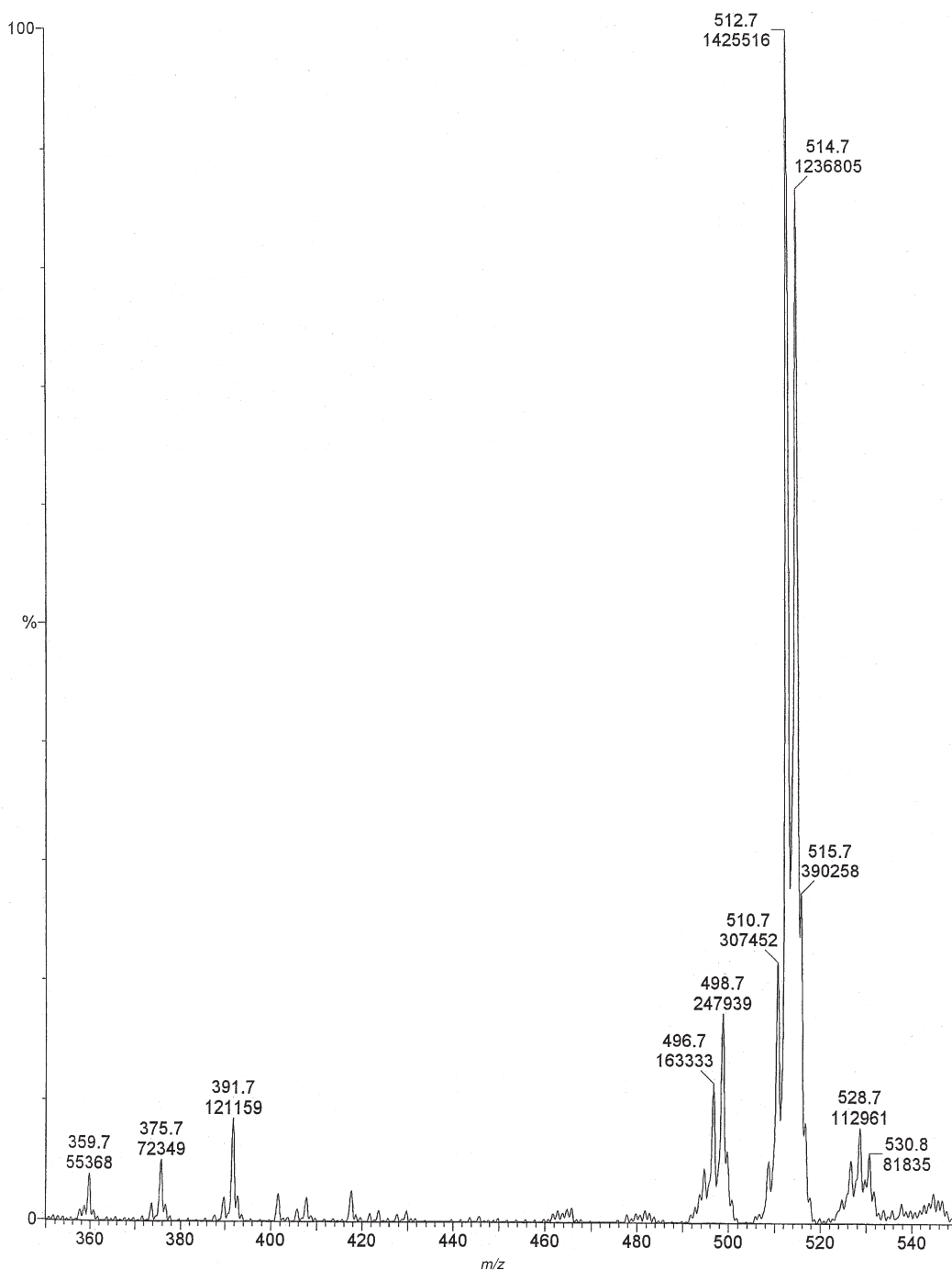


**FIG. 1.** Typical spectrum of full electrospray tandem mass spectroscopy (ES-MS-MS) scan representing a total bile acid profile in the feces obtained from an adult human. The ions obtained at  $m/z$  359.7, 373.7, 375.7, 389.7, 391.7, and 407.8 correspond to  $5\beta$ -cholic acid, mono-keto, mono-OH, mono-keto-mono-OH, di-OH, and trihydroxylated free bile acids, respectively. None of the other ions correspond to the M.W. of any known bile acids including sulfated and glucuronidated bile acids. The two numbers over each peak represent (upper) the M.W. minus 1 [ $M - H$ ] and (lower) the abundance of this ion.



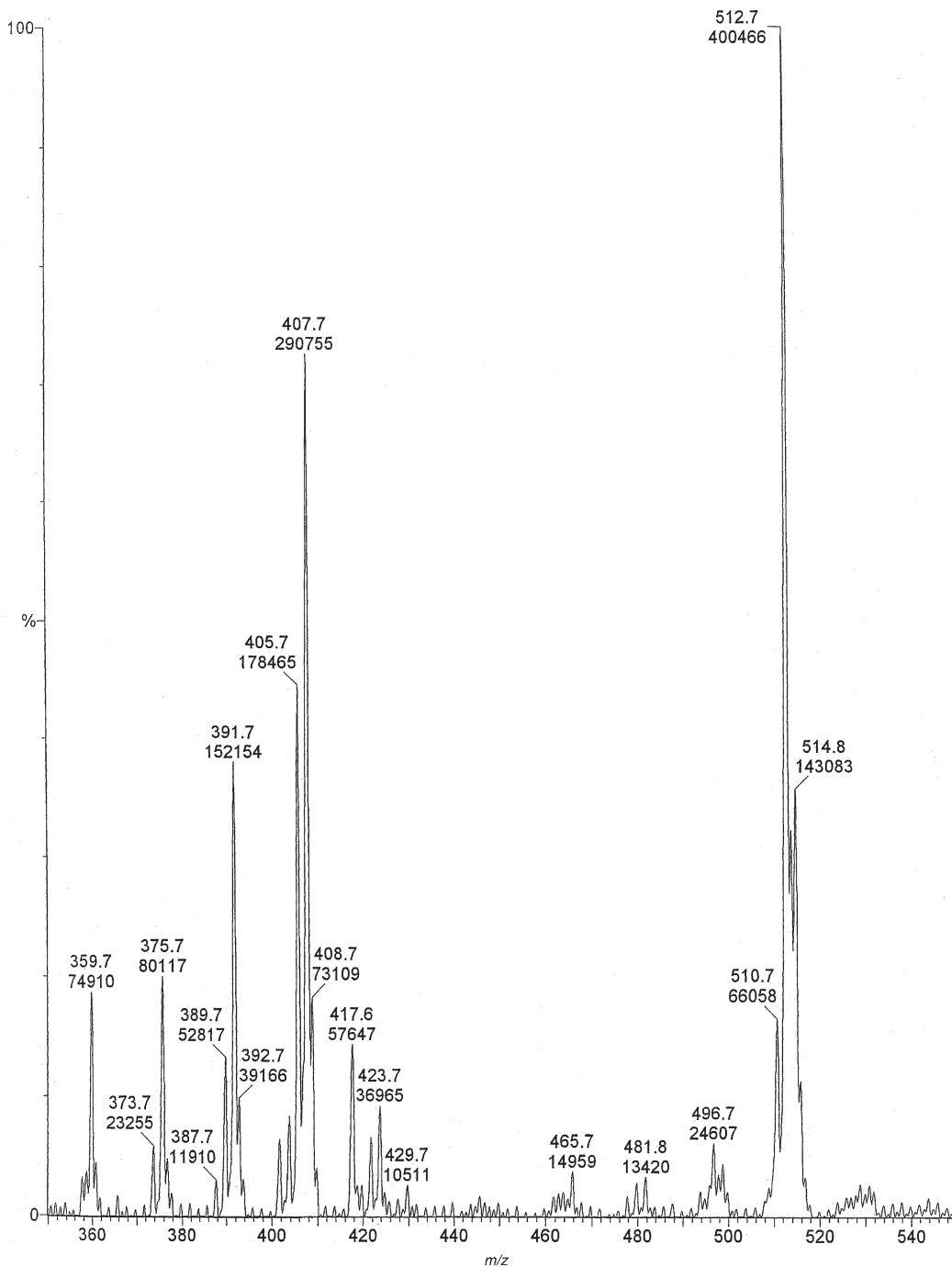
**FIG. 2.** Gas chromatogram of methyl-ester acetate derivatives of bile acids obtained from analyses of feces of a healthy adult man. The following compounds were identified: peak no. 1, 5 $\beta$ -cholanic acid; 2–6, unknown keto-bile acids; 7,8, isomers of lithocholic acid (LCA); 9, LCA; 10,11, isomers of deoxycholic acid (DCA); 12, DCA; and 13, cholic acid.

3. Carey, M.C., and Duane, W.C. (1994) Enterohepatic Circulation, in *The Liver: Biology and Pathobiology* (Arias, I.M., Boyer, J., Fausto, L., Jakoby, N., and Schachter, W.B., eds.), 3rd edn., pp. 719–768, Raven Press, New York.
4. Kasbo, J., Saleem, M., Perwaiz, S., Mignault, D., Lamireau, T., Tuchweber, B., and Yousef, I. (2002) Biliary, Fecal, and Plasma Deoxycholic Acid in Rabbit, Hamster, Guinea Pig, and Rat: Comparative Study and Implication in Colon Cancer, *Biol. Pharm. Bull.* 25, 1381–1384.
5. Bernstein, C., Bernstein, H., Garewal, H., Dinning, P., Jabi, R., Sampliner, R.E., McCuskey, M.K., Panda, M., Roe, D.J., L'Heureux, L., and Payne, C. (1999) A Bile Acid-Induced Apoptosis Assay for Colon Cancer Risk and Associated Quality Control Studies, *Cancer Res.* 59, 2353–2357.
6. Powolny, A., Xu, J., and Loo, G. (2001) Deoxycholate Induces DNA Damage and Apoptosis in Human Colon Epithelial Cells Expressing Either Mutant or Wild-Type p53, *Int. J. Biochem. Cell Biol.* 33, 193–203.
7. Reddy, B.S. (1999) Prevention of Colon Carcinogenesis by Components of Dietary Fiber, *Anticancer Res.* 19, 3681–3683.
8. Ochsenkuhn, T., Bayerdorffer, E., Meining, A., Schinkel, M., Thiede, C., Nussler, V., Sackmann, M., Hatz, R., Neubauer, A., and Paumgartner, G. (1999) Colonic Mucosal Proliferation Is Related to Serum Deoxycholic Acid Levels, *Cancer.* 85, 1664–1669.
9. Hirano, S., Masuda, N., Oda, H., and Imamura, T. (1981) Transformation of Bile Acids by Mixed Microbial Cultures from Human Feces and Bile Acid Transforming Activities of Isolated Bacterial Strains, *Microbiol. Immunol.* 25, 271–282.
10. White, B.A., Lipsky, R.L., Fricke, R.J., and Hylemon, P.B. (1980) Bile Acid Induction Specificity of 7  $\alpha$ -Dehydroxylase Activity in an Intestinal *Eubacterium* Species, *Steroids* 35, 103–109.



**FIG. 3.** Spectrum of full ES-MS-MS scan representing a total bile acid profile of rat bile. The full scan revealed the presence of prominent  $m/z$  ions at 359.7, 375.7, 391.7, 498.7, 514.7, and 528.7, which correspond to  $5\beta$ -cholanic acid (internal standard), unconjugated monohydroxy, dihydroxy, taurine-conjugated dihydroxy, trihydroxy, and glycine-conjugated dihydroxy-mono-sulfate cholanic acid, respectively. The two numbers over each peak represent (upper) the M.W. minus 1 [ $M - H$ ] and (lower) the abundance of this ion. For abbreviation see Figure 1.

11. Batta, A.K., Salen, G., Rapole, K.R., Batta, M., Batta, P., Alberts, D., and Earnest, D. (1999) Highly Simplified Method for Gas-Liquid Chromatographic Quantitation of Bile Acids and Sterols in Human Stool, *J. Lipid Res.* **40**, 1148-1154.
12. van Faassen, A., Nagengast, F.M., Hectors, M., van den Broek, W.J., Huijbregts, A.W., van der Werf, S.D., van Berge Hengouwen, G.P., and van Tongeren, J.H. (1985) Determination of Individual Human Faecal Bile Acids by Gas-Liquid Chromatography After Enzymatic Deconjugation and Simultaneous Solvolysis and Methylation Using Dimethoxypropane, *Clin. Chim. Acta* **31**, 231-239.
13. Setchell, K.D., Ives, J.A., Cashmore, G.C., and Lawson, A.M. (1987) On the Homogeneity of Stools with Respect to Bile Acid Composition and Normal Day-to-Day Variations: A Detailed Qualitative and Quantitative Study Using Capillary Column Gas Chromatography-Mass Spectrometry, *Clin. Chim. Acta* **162**, 257-275.
14. Perwaiz, S., Tuchweber, B., Mignault, D., Gilat, T., and Yousef,



**FIG. 4.** Spectrum of full ES-MS-MS scan obtained from the same rat bile sample (Fig. 3) incubated with human lyophilized fecal sample in water. The ions at  $m/z$  359.7, 375.7, 391.7, 407.7, and 514.8 correspond to  $5\beta$ -cholanic acid (internal standard), unconjugated monohydroxy, dihydroxy, trihydroxy, and taurine-conjugated trihydroxylated bile acids, respectively. Notice the presence of the ion at  $m/z$  407.7 representing the free trihydroxylated bile acid as well as increased intensity of ions at  $m/z$  391.7 and 375.7 corresponding to free dihydroxy and monohydroxylated bile acid. The two numbers over each peak represent (upper) the M.W. minus 1 [ $M - H$ ] and (lower) the abundance of this ion. For abbreviation see Figure 1.

- I. (2001) Determination of Bile Acids in Biological Fluids by Liquid Chromatography–Electrospray Tandem Mass Spectrometry, *J. Lipid Res.* 42, 114–119.
15. Ferguson, L.R., Rewcastle, G.W., Lello, J.M., Alley, P.G., and Seelye, R.N. (1984) Quantitation of Free and Conjugated Bile

Acids in Human Feces Using a High-Pressure Liquid Chromatography Counter Ion Method, *Anal. Biochem.* 143, 325–332.

[Received May 29, 2002, and in revised form October 24, 2002; revision accepted November 27, 2002]



# Simultaneous Evaluation of HMG-CoA Reductase and Cholesterol 7 $\alpha$ -Hydroxylase Activities by Electrospray Tandem MS

Marie-Yvonne Ndong-Akoume<sup>a,b</sup>, Diane Mignault<sup>a,b</sup>, Shahid Perwaiz<sup>a,b</sup>,  
Gabriel L. Plaa<sup>a</sup>, and Ibrahim M. Yousef<sup>a,b,\*</sup>

<sup>a</sup>Département de Pharmacologie, Université de Montréal, Montréal, Canada H3C 3J7,  
and <sup>b</sup>Centre de Recherche de l'Hôpital Sainte-Justine, Montréal, Canada H3T 1C5

**ABSTRACT:** Simultaneous evaluation of HMG-CoA reductase and cholesterol 7 $\alpha$ -hydroxylase activities by electrospray tandem mass spectrometry (ES-MS-MS) was performed. The assay was based on the measurement of mevalonolactone (MVL) and 7 $\alpha$ -hydroxycholesterol (7 $\alpha$ -OHC) produced by the incubation of HMG-CoA with hepatic microsomes in the presence of NADPH and glucose-6-phosphate dehydrogenase. Following extraction and purification using a cyanopropyl cartridge, MVL and 7 $\alpha$ -OHC were analyzed, without derivatization, by ES-MS-MS. The analysis was achieved in 5 min. Calibration curves were made for MVL and 7 $\alpha$ -OHC, and were linear from 0 to 100  $\mu$ g. The recovery was >97%. The procedure was validated under similar calibration and recovery experiments, by measuring the above mentioned products as dimethylethylsilyl ether derivatives using the classical technique of GC-MS. Data obtained by ES-MS-MS and GC-MS showed a good correlation, with no significant differences. ES-MS-MS is a simple and reliable method for the evaluation of HMG-CoA reductase and cholesterol 7 $\alpha$ -hydroxylase activities in liver microsomal preparations.

Paper no. L9101 in *Lipids* 37, 1101–1107 (November 2002).

Cholesterol homeostasis in the body is preserved mainly through the modulation of the activities of two enzymes located in the endoplasmic reticulum: HMG-CoA reductase, which catalyzes the formation of mevalonic acid (MVA) from HMG-CoA, considered as the rate-determining step in cholesterol synthesis (1), and cholesterol 7 $\alpha$ -hydroxylase, which catalyzes the rate-limiting step in the major pathway of degradation of cholesterol to bile acids (2).

In view of the critical role played by these enzymes in cholesterol metabolism, many efforts have been made to develop rapid and accurate methods for the simultaneous estimation of their activities. The measurement of the actual amount of mevalonolactone (MVL) and 7 $\alpha$ -hydroxycholesterol (7 $\alpha$ -OHC) enzymatically formed is considered to be a more accurate indication of the activities of HMG-CoA reductase and cholesterol 7 $\alpha$ -hydroxylase, respectively (3). For this pur-

pose, several approaches, direct and indirect, are available for measuring the mass of these products. These include double-labeling techniques (4–6), ion-exchange column chromatography (7), paper chromatography (8), HPLC (9,10), and GC-MS with selected ion monitoring (SIM) (3,11–13). GC-MS is considered to be the best method because of its superior sensitivity and accuracy, but its use entails a laborious sample preparation and a long analytical process. Although the availability of electrospray tandem mass spectrometry (ES-MS-MS) offers opportunities to overcome these disadvantages, there has been no study using this technique to evaluate HMG-CoA reductase and cholesterol 7 $\alpha$ -hydroxylase activities simultaneously. The purpose of the present work is to test this technique for this assay in rat liver microsomal preparations.

## MATERIALS AND METHODS

**Chemicals.** NADPH, EDTA, mevalonic acid lactone, HMG-CoA, glucose-6-phosphate dehydrogenase (500 U/mL), and glucose-6-phosphate were purchased from Sigma Chemical Co. (St Louis, MO). 7 $\alpha$ -OHC and 6 $\beta$ -hydroxycholestanol (6 $\beta$ -OHC) were available from Steraloids Inc. (Wilton, NH). Dimethylethylsilyl imidazole (DMESI) was obtained from Kogyo Inc. (Tokyo, Japan), and Bond Elut cyanopropyl (CN; 500 mg) from Varian (Harbor City, CA). All other reagents and solvents were of analytical grade and used without further purification.

**Preparation of internal standard for the MVL quantification.** MVL (1 mg) was acetylated in 1 mL of a mixture of 7 mL glacial acetic acid, 5 mL acetic anhydride, and 10 drops of 70% perchloric acid. Following incubation at 37°C for 60 min, 5 mL of water and 10 mL of diethyl ether were added, and tubes were mixed for 20 min. The ether layer was then transferred to other tubes and dried under nitrogen. The residue was redissolved in 1 mL methanol and stored at –20°C, then used as stock solution in the following analyses.

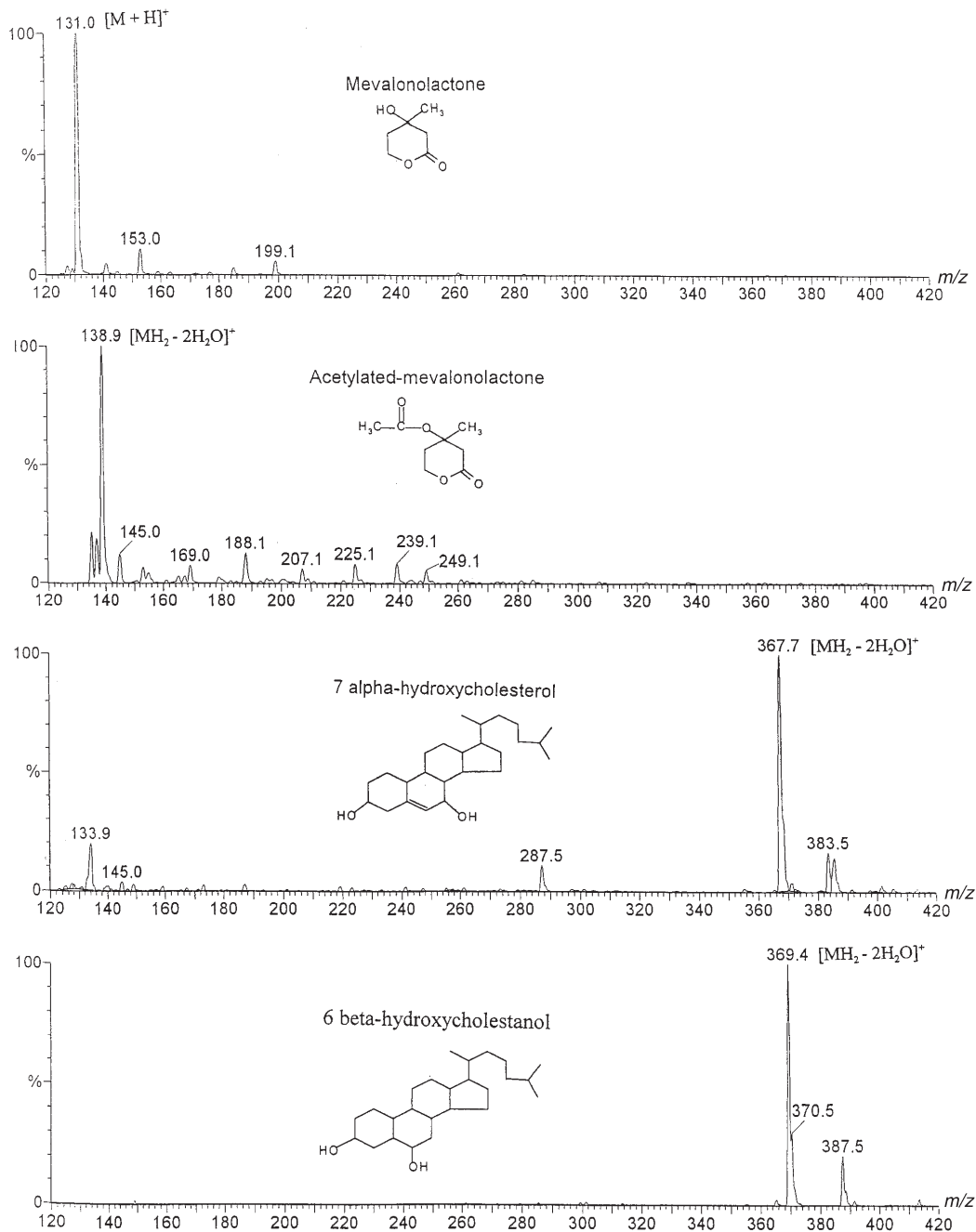
**Preparation of liver microsomes.** Liver microsomes were prepared at 4°C as described previously (11). Briefly, rat livers were excised, washed in ice-cold saline solution, weighed, and placed into 3 mL of ice-cold 50 mM Tris-HCl buffer (pH 7.4), containing 0.3 M sucrose, 10 mM DTT, 10 mM EDTA, and 50 mM sodium fluoride. The livers were minced with scissors and homogenized in a Dounce homogenizer with a loosely fitting

\*To whom correspondence should be addressed at Université de Montréal, Département de Pharmacologie, C.P. 6128, Succ. Centre-ville, Montréal, Québec, Canada H3C 3J7. E-mail: ibrahim.yousef@umontreal.ca

Abbreviations: CN, cyanopropyl; DMES, dimethylethylsilyl; DMESI, DMES imidazole; ES-MS-MS, electrospray tandem mass spectrometry; MVA, mevalonic acid; MVL, mevalonolactone; 6 $\beta$ -OHC, 6 $\beta$ -hydroxy-cholestanol; 7 $\alpha$ -OHC, 7 $\alpha$ -hydroxycholesterol; SIM, selected ion monitoring.

Teflon pestle. The homogenate (10%) was centrifuged at  $18,000 \times g$  for 20 min (SS-34 rotor, Sorval RC2-B refrigerated centrifuge), and the supernatant was centrifuged at  $100,000 \times g$  for 60 min (50.2 Ti rotor, Beckman L centrifuge). The resulting microsomal fraction was suspended in 3 mL of 0.1 M potassium phosphate buffer (pH 7.4), containing 1 mM EDTA and 5 mM DTT. Aliquots were immediately frozen in liquid nitrogen and stored at  $-80^\circ\text{C}$  to be used as the enzymatic and endogenous cholesterol sources. A small aliquot was used for protein determination according to Lowry *et al.* (14).

*Simultaneous assay of HMG-CoA reductase and 7 $\alpha$ -hydroxylase activities.* A microsomal suspension of 500  $\mu\text{L}$ , containing 5 mg protein, was preincubated for 5 min at  $37^\circ\text{C}$  with 450  $\mu\text{L}$  of 0.1 M potassium phosphate buffer, pH 7.4, containing 1 mM EDTA and 12 mM glucose-6-phosphate. The assay was initiated by adding 50  $\mu\text{L}$  of cofactor-substrate solution (0.1 mM HMG-CoA, 3 mM NADPH, and 2 U/mL glucose-6-phosphate dehydrogenase), and the incubation was performed for 30 min at  $37^\circ\text{C}$ . Care was taken to avoid exposure to light to prevent cholesterol autoxidation. The incubation



**FIG. 1.** Positive ion electrospray mass spectra of mevalonolactone, acetylated mevalonolactone, 7 $\alpha$ -hydroxycholesterol, and 6 $\beta$ -hydroxycholestanol. Electrospray tandem MS conditions are described in the Materials and Methods section.

was terminated by the addition of 50  $\mu\text{L}$  of 1 M NaOH, 10  $\mu\text{g}$  each of acetylated-MVL and 6 $\beta$ -OHC dissolved in methanol were added as internal standards. The sample was applied to the CN cartridge (preconditioned by successive elution with 2 mL each of hexane, methanol, and distilled water) and washed with 4 mL of acetonitrile/water (2:3, vol/vol) to extract MVA. After removing cholesterol with 4 mL of hexane, 7 $\alpha$ -OHC was eluted with 4 mL of methanol.

The fraction containing MVA was acidified to pH 1 with 0.6 N HCl to promote the generation of MVL. Following incubation at 37°C for 60 min, the suspension was applied to a CN cartridge (cleaned in advance with 2 mL each of hexane, methanol, and distilled water, successively), and MVL was eluted with 4 mL of acetonitrile.

Both eluate fractions were mixed and divided into two portions. One portion was used for ES-MS-MS analysis and the other for the GC-MS analysis.

**Analysis by ES-MS-MS.** The eluate mixture was evaporated under nitrogen, and the residue was analyzed by the ES-MS-MS after reconstitution in 100  $\mu\text{L}$  of methanol.

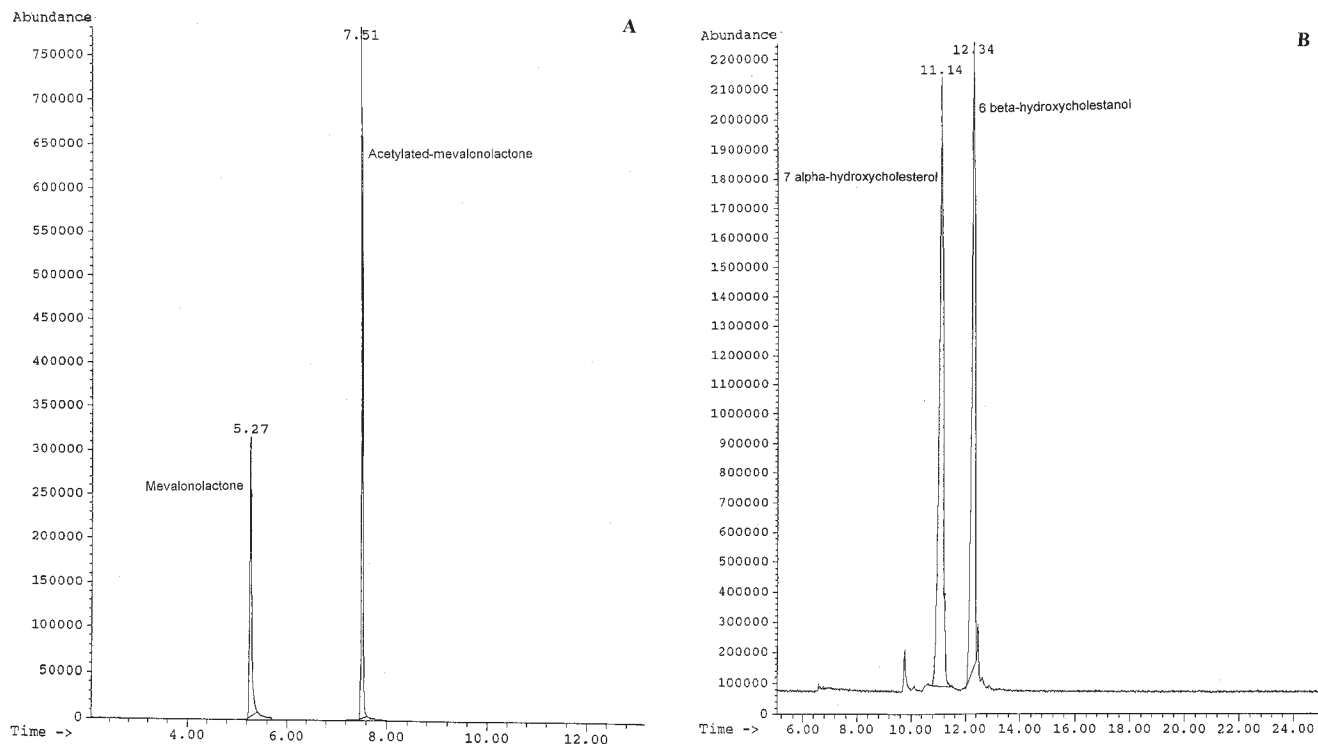
The ES-MS-MS system consisted of a Hewlett-Packard model HP1100 liquid chromatograph (HPLC) connected to a Quattro II electrospray tandem mass spectrometer (ES-MS-MS) obtained from Micromass (Manchester, United Kingdom). The HPLC system was operated isocratically without column at a 10  $\mu\text{L}/\text{min}$  flow rate for a mobile phase (acetonitrile/water; 1:1) at room temperature. Sample (10  $\mu\text{L}$ ) was injected in the ES-MS-MS by the automatic injector. Liquid ni-

trogen was used as nebulizer, and argon was used as collision gas. Cone voltage was set at 25 volts. Positive ion mass spectra of the eluents were recorded using the selective ion-recording mode. Quantification of MVL and 7 $\alpha$ -OHC was carried out using Micromass Mass Lynx 2.22 software by determining the peak area ratios of each compound with its internal standard. The enzymatic activities, expressed as pmol/min/mg of protein, were calculated by subtracting the amount present at zero time from that at the end of the incubation. Zero time was realized using microsomes previously inactivated with 1 M NaOH.

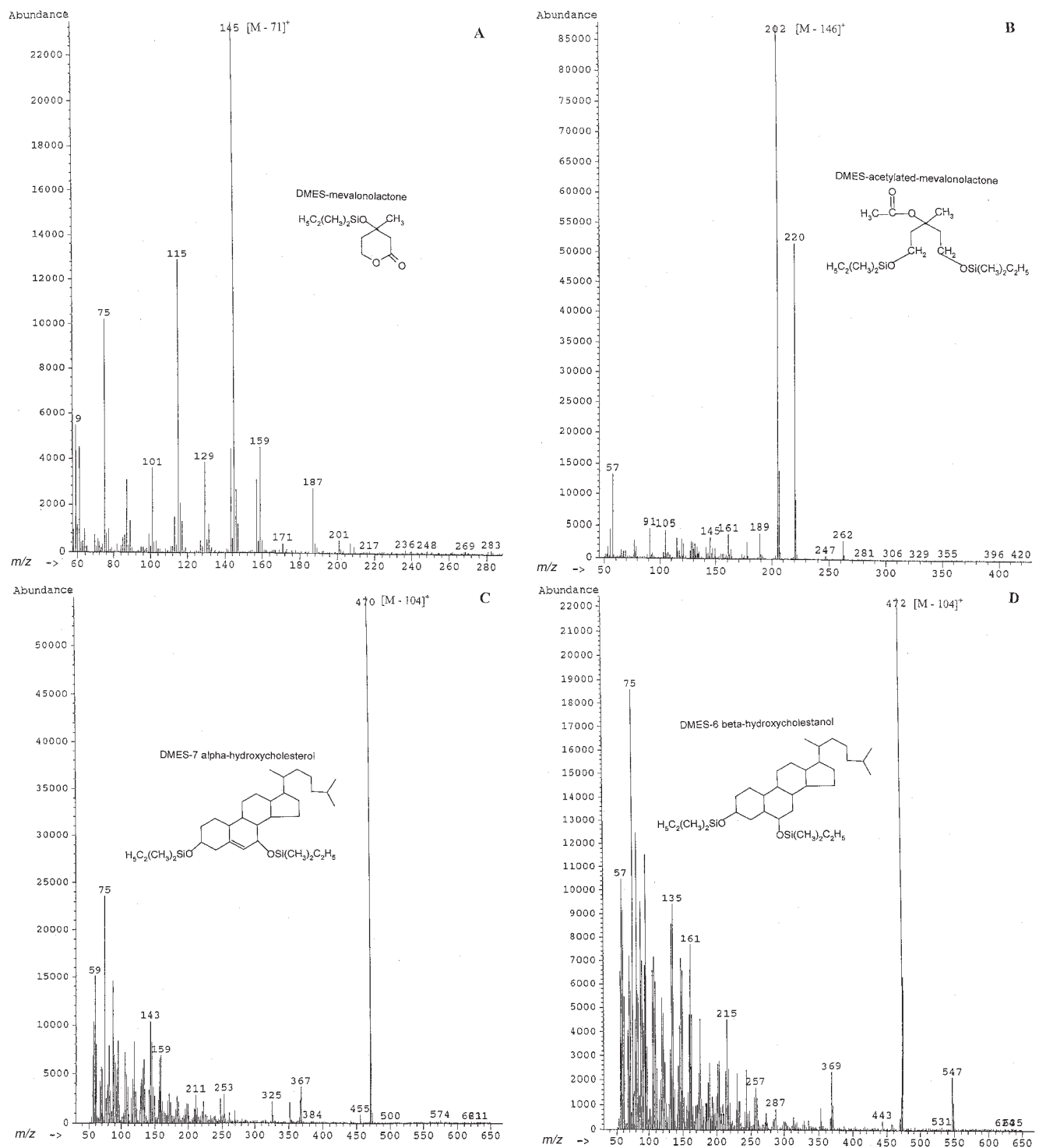
**Analysis by GC-MS.** After evaporation of the eluate mixture (MVL and 7 $\alpha$ -OHC) under nitrogen, the products were converted to dimethylethylsilyl (DMES) ether by treatment with 50  $\mu\text{L}$  pyridine-DMESI (10:2, vol/vol) at 80°C for 60 min. The derivatization solution was evaporated under nitrogen. The residue was dissolved in 100  $\mu\text{L}$  of chloroform.

GC-MS analysis was performed on an Hewlett-Packard 5890 series II gas chromatograph equipped with an HP-5 MS capillary column and connected to an HP 5971A mass spectrometer. Helium was used as the carrier gas. The column was maintained at 100°C for 2 min, then programmed from 100 to 160°C at 10°C/min and from 160 to 280°C at 20°C/min. The column temperature was kept at 280°C for 5 min. The MS transfer line was maintained at 280°C while the injection port was at 250°C. Samples (2  $\mu\text{L}$ ) were injected manually, and the SIM mode was used for quantitative determination.

**Assay validation.** The assay was validated with calibration



**FIG. 2.** Representative GC-MS chromatograms of the mixture of (A) mevalonolactone and its internal standard, acetylated-mevalonolactone, and (B) 7 $\alpha$ -hydroxycholesterol and 6 $\beta$ -hydroxycholestanol, used as internal standard. See the Materials and Methods section for derivatization and GC-MS conditions.



**FIG. 3.** Electron impact mass spectra of the dimethylethylsilyl (DMES) ether derivatives of (A) mevalonolactone, (B) acetylated mevalonolactone, (C)  $7\alpha$ -hydroxycholesterol, and (D)  $6\beta$ -hydroxycholesterol obtained by GC-MS. For conditions see the Materials and Methods section.

standards prepared by adding a constant amount (10  $\mu\text{g}$ ) of acetylated-MVL or  $6\beta$ -OHC as internal standards, to a series of tubes containing varied amounts (1–100  $\mu\text{g}$ ) of MVL or  $7\alpha$ -OHC, respectively. The content of each tube was subjected to the same procedure as microsomal preparations and analyzed by ES-MS-MS or GC-MS. A linear regression line

was fitted over the concentration range for both assays. Reproducibility of the assay was investigated in five samples, each processed in triplicate, while the recovery study was carried out by adding 15, 30, or 60  $\mu\text{g}$  of MVL and  $7\alpha$ -OHC to duplicate samples of 500  $\mu\text{L}$  of the microsomal suspension. Recoveries were calculated using the following equation:



$$\text{recovery} = \frac{(\text{amount found} - \text{basic amount})}{\text{amount added}} \times 100 \quad [1]$$

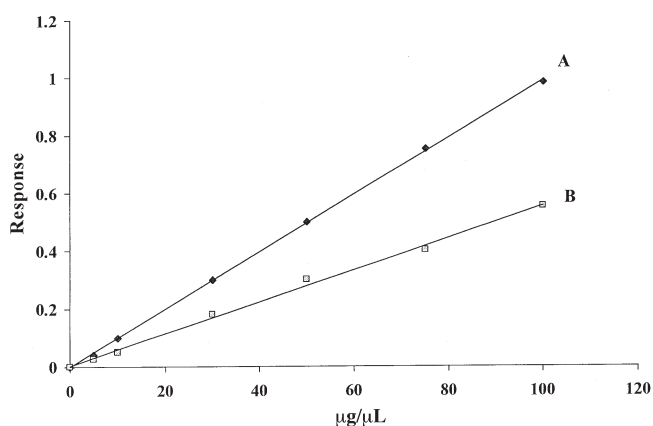
**Statistical analysis.** The statistical significance of differences between the ES-MS-MS and GC-MS methods was evaluated by one-way ANOVA, and statistical significance was accepted at the level of  $P < 0.05$ .

## RESULTS

**ES-MS-MS analysis.** Figure 1 shows the mass spectra of MVL, acetylated-MVL, 7 $\alpha$ -OHC, and 6 $\beta$ -OHC obtained in positive mode. MVL gave a high-abundance fragment ion at  $m/z$  131, which corresponded to the peak of its protonated molecule. The molecular ions of acetylated-MVL, 7 $\alpha$ -OHC, and 6 $\beta$ -OHC were not observed. However, a high-abundance fragment ion, which is formed by the loss of 2 H<sub>2</sub>O from each molecule, was detected at  $m/z$  138.9, 367, and 369 for acetylated-MVL, 7 $\alpha$ -OHC, and 6 $\beta$ -OHC, respectively.

**GC-MS analysis.** The DMES ether derivatives of MVL and its internal standard produced symmetrical peaks with elution times of 5.27 and 7.51 min, respectively (Fig. 2A). The DMES ether derivative of 7 $\alpha$ -OHC eluted from the GC column at 11.14 min, whereas the DMES ether derivative of its internal standard appeared at 12.34 min (Fig. 2B). Figure 3 shows the mass spectra of DMES ether derivatives obtained in the electron ionization mode. The fragment ions of  $[M - 71]^+$  produced at  $m/z$  145 for MVL,  $[M - 146]^+$  at  $m/z$  202 for acetylated-MVL,  $[M - 104]^+$  at  $m/z$  470 for 7 $\alpha$ -OHC, and  $[M - 104]^+$  at  $m/z$  472 for 6 $\beta$ -OHC had the highest abundances and were selected for ion monitoring analysis.

**Linearity, precision, and accuracy of the assay.** The assay was validated over the range 1–100  $\mu\text{g}$ . Representative calibration curves for MVL and 7 $\alpha$ -OHC generated by ES-MS-MS are shown in Figure 4. Table 1 lists parameters for cali-



**FIG. 4.** Calibration curves for (A) mevalonolactone and (B) 7 $\alpha$ -hydroxycholesterol obtained by linear regression analysis of the peak-area ratios of the compound to the internal standard vs. the concentrations of the compound ( $\mu\text{g}/\mu\text{L}$ ). Calibration standards were prepared as described in the Materials and Methods section.

**TABLE 1**  
Parameters for Calibration Curves Generated by Electrospray Tandem Mass Spectroscopy (ES-MS-MS) and GC-MS<sup>a</sup>

Methods	Analytes	Correlation coefficients	Calibration curve equations
ES-MS-MS	MVL	0.98	$Y = 0.190458 X$
	Acetylated-MVL	0.97	$Y = 0.008223 X$
	7 $\alpha$ -OHC 6 $\beta$ -OHC		
GC-MS	MVL	0.99	$Y = 0.085332 X$
	Acetylated-MVL	0.98	$Y = 0.008135 X$
	7 $\alpha$ -OHC 6 $\beta$ -OHC		

<sup>a</sup>Calibration curves were obtained by adding a constant amount (10  $\mu\text{g}$ ) of acetylated mevalonolactone (MVL) or 6 $\beta$ -hydroxycholesterol (6 $\beta$ -OHC), as internal standards, to a series of tubes containing varied amounts (1–100  $\mu\text{g}$ ) of MVL or 7 $\alpha$ -hydroxycholesterol (7 $\alpha$ -OHC), respectively. The contents of each tube were submitted to the same procedure as the microsomes.

**TABLE 2**  
Reproducibilities of HMG-CoA Reductase and 7 $\alpha$ -Hydroxylase Activities in the Rat Liver Microsomes<sup>a</sup>

Methods	Samples	HMG-CoA reductase		7 $\alpha$ -Hydroxylase	
		Activity (pmol/min/mg protein)	CV (%)	Activity (pmol/min/mg protein)	CV (%)
ES-MS-MS	A	141.73 $\pm$ 0.25	0.17	33.00 $\pm$ 0.08	0.24
	B	131.01 $\pm$ 0.10	0.08	27.74 $\pm$ 0.06	0.21
	C	133.90 $\pm$ 0.06	0.07	34.05 $\pm$ 0.12	0.35
	D	136.52 $\pm$ 0.27	0.19	30.00 $\pm$ 0.10	0.33
	E	142.32 $\pm$ 0.10	0.04	36.38 $\pm$ 0.15	0.41
GC-MS	A	140.43 $\pm$ 0.24	0.17	31.69 $\pm$ 0.02	0.06
	B	134.18 $\pm$ 0.09	0.06	27.24 $\pm$ 0.16	0.58
	C	134.25 $\pm$ 0.06	0.04	32.50 $\pm$ 0.11	0.33
	D	137.44 $\pm$ 0.16	0.11	31.66 $\pm$ 0.10	0.31
	E	141.57 $\pm$ 0.06	0.04	36.14 $\pm$ 0.19	0.52

<sup>a</sup>Each sample was processed in triplicate. CV is the intra-assay CV and was calculated using the following formula:  $CV = (SD/\text{mean}) \times 100$ . For abbreviation see Table 1.

bration curves obtained by ES-MS-MS and GC-MS. The correlation coefficients were  $\geq 0.97$  for all curves.

The precision and accuracy were checked by calculating the intra-assay variation for five different samples processed in triplicate. As shown in Table 2, the CV for each sample was less than 1%. The recoveries of MVL and 7 $\alpha$ -OHC determined at three different levels varied from 97 to 100% (Table 3). There were no significant differences between data obtained using both ES-MS-MS and GC-MS analytical techniques.

## DISCUSSION

The high incidence of diseases associated with increased levels of cholesterol in plasma and liver continually stimulates the interest in development of rapid and sensitive methods for the determination of the activities of HMG-CoA reductase

**TABLE 3**  
**Recovery of Mevalonolactone and 7 $\alpha$ -Hydroxycholesterol from Microsomes Analyzed by ES-MS-MS and GC-MS<sup>a</sup>**

Methods	Amount added ( $\mu$ g)	MVL		7 $\alpha$ -OHC	
		Amount found ( $\mu$ g)	Recovery (%)	Amount found ( $\mu$ g)	Recovery (%)
ES-MS-MS	0	10.72 $\pm$ 0.03		7.24 $\pm$ 0.24	
	15	25.42 $\pm$ 0.18	98.30 $\pm$ 1.17	22.06 $\pm$ 0.12	98.83 $\pm$ 0.93
	30	40.28 $\pm$ 0.36	98.43 $\pm$ 1.07	36.89 $\pm$ 0.18	98.84 $\pm$ 0.42
	60	69.86 $\pm$ 0.26	98.59 $\pm$ 0.47	65.85 $\pm$ 0.54	97.69 $\pm$ 0.84
GC-MS	0	10.72 $\pm$ 0.07		7.23 $\pm$ 0.03	
	15	25.58 $\pm$ 0.17	99.04 $\pm$ 1.04	21.97 $\pm$ 0.01	98.25 $\pm$ 0.34
	30	40.20 $\pm$ 0.33	98.25 $\pm$ 1.07	37.23 $\pm$ 0.34	100 $\pm$ 1.11
	60	70.15 $\pm$ 0.06	99.06 $\pm$ 0.47	66.19 $\pm$ 0.38	98.27 $\pm$ 0.62

<sup>a</sup>Values are mean  $\pm$  SD ( $n = 3$ ) and represent the recovery of different amounts of MVL and 7 $\alpha$ -OHC added to aliquots of 500  $\mu$ L of the microsomal suspension, containing 5 mg of protein. The assay recovery at each amount was calculated using the following equation: recovery = 100  $\times$  (amount found – basic amount)/amount added. For abbreviations see Table 1.

and cholesterol 7 $\alpha$ -hydroxylase, two key enzymes in the synthesis and degradation pathways of cholesterol (1,2). Because of the high sensitivity and accuracy of GC-MS, it is widely used in the evaluation of activities of these enzymes *in vitro*. In this method, the mass of MVL and 7 $\alpha$ -OHC formed is determined. However, this method has the drawback of being labor-intensive and slow. In the method described here, we demonstrated that the use of ES-MS-MS offers the opportunity to overcome these disadvantages. Indeed, the use of ES-MS-MS does not require preliminary derivatization procedures and takes only 5 min for analysis. Compounds are identified by their molecular mass and their characteristic fragmentations. The fragment ions at  $m/z$  131 and 367.7 were selected to identify MVL and 7 $\alpha$ -OHC, respectively. Quantitative determination of these compounds requires the addition of internal standards. Deuterated-MVL (3) and 6 $\beta$ -OHC (15) have been reported to be suitable internal standards for MVL and 7 $\alpha$ -OHC, respectively. However, since deuterated-MVL is not commercially available and is difficult to synthesize, we made an alternative internal standard, acetylated-MVL. This compound was not present in the microsomal preparation and was separated clearly from MVL by GC, suggesting that it could be a suitable internal standard. In addition, the fragment ions at  $m/z$  131 for MVL and 138.9 for acetylated-MVL, selected for the ES-MS-MS analysis, were detected with the same degree of sensitivity. The validity of this approach was achieved by comparing the results obtained by the ES-MS-MS with those obtained by the more traditional GC-MS technique, using similar conditions. No significant differences were noted. In addition, the values obtained were in agreement with the values reported by other investigators (16–23). The internal standard described is another advantage since it could be prepared easily and was found to be stable during storage and sample preparation.

We have also simplified the solid-phase extraction procedure used for the simultaneous extraction and purification of 7 $\alpha$ -OHC and MVL by reducing the number of different Bond Elut cartridges used. We used only CN cartridges to extract

and purify these two reaction products. Del Puppo *et al.* (24) found that the lactone was more readily extracted and purified than the free acid. However, the lactonization of MVA requires the use of a strong monobasic mineral acid such as hydrochloric acid, but cholesterol oxidation products are sensitive to acids (25). It was therefore necessary to separate MVA from 7 $\alpha$ -OHC prior to lactonization. For this procedure, it was necessary to demonstrate that significant quantities of MVL or 7 $\alpha$ -OHC are not lost during sample preparation, and that the preparation leads to adequate recovery of these products. These two aspects were examined by adding MVL or 7 $\alpha$ -OHC directly to a fraction of microsomal suspension. Extraction and purification were then carried out as described. An adequate separation of MVA and 7 $\alpha$ -OHC was achieved on the CN cartridges. With the purification conditions chosen, excellent recoveries of 7 $\alpha$ -OHC and the lactone form of MVA, were obtained. The use of Bond Elut CN cartridges to perform the extraction and purification simultaneously simplified the pre-analytic preparation of samples greatly and offered greater potential for automation.

The approach described here has significant advantages over other procedures used for the evaluation of HMG-CoA reductase and cholesterol 7 $\alpha$ -hydroxylase activities in liver microsomal preparations. First, the sample preparation time is dramatically reduced, and no derivatization steps are required. Second, the data acquisition time is considerably reduced when the analysis is processed by ES-MS-MS. In conclusion, we have developed a simple, rapid, and accurate method for the simultaneous evaluation of the activities of hepatic microsomal HMG-CoA reductase and cholesterol 7 $\alpha$ -hydroxylase, using the ES-MS-MS technique, a new internal standard, and a simple pre-analytic procedure.

#### ACKNOWLEDGMENTS

This work was supported by a grant from the Canada Institute of Health Research and the Canadian Liver Foundation. Marie-Yvonne Ndong-Akoume holds a Studentship from the Republic of Gabon.

## REFERENCES

1. Rodwell, V.W., Nordstrom, J.L., and Mitschelen, J.J. (1976) Regulation of HMG-CoA Reductase, *J. Lipid Res.* 14, 1–74.
2. Myant, N.B., and Mitropoulos, K.A. (1977) Cholesterol 7 $\alpha$ -Hydroxylase, *J. Lipid Res.* 18, 135–153.
3. Galli Kienle, G., Galli, G., Bosisio, E., Cighetti, G., and Paoletti, R. (1984) Evaluation of Enzyme Activities by Gas Chromatography–Mass Spectrometry: HMG-CoA Reductase and Cholesterol 7 $\alpha$ -Hydroxylase, *J. Chromatogr.* 289, 267–276.
4. Kekki, M., Miettinen, T.A., and Wahlstrom, B. (1977) Measurement of Cholesterol Synthesis in Kinetically Defined Pools Using Fecal Steroid Analysis and Double Labeling Technique in Man, *J. Lipid Res.* 18, 99–114.
5. Mitropoulos, K.A., and Balasubramaniam, S. (1972) Cholesterol 7 $\alpha$ -Hydroxylases in Rat Liver Microsomal Preparations, *Biochem. J.* 128, 1–9.
6. Einarsson, K., Angelin, B., Ewerth, S., Nilsell, K., and Bjorkhem, I. (1986) Bile Acid Synthesis in Man: Assay of Hepatic Microsomal Cholesterol 7 $\alpha$ -Hydroxylase Activity by Isotope Dilution–Mass Spectrometry, *J. Lipid Res.* 27, 82–88.
7. Ong, K.K., Khor, H.T., and Tan, D.T. (1991) Assay of 3-Hydroxy-3-Methylglutaryl CoA Reductase Activity Using Anionic Exchange Column Chromatography, *Anal. Biochem.* 196, 211–214.
8. Shapiro, D.J., Imblum, R.L., and Rodwell, V.W. (1969) Thin-Layer Chromatographic Assay for HMG-CoA Reductase and Mevalonic Acid, *Anal. Biochem.* 31, 383–390.
9. Guchhait, R.B., and Porter, J.W. (1966) A Gas–Liquid Chromatographic Method of Assay for Mevalonic Acid, *Anal. Biochem.* 15, 509–516.
10. Ogishima, T., and Okuda, K. (1986) An Improved Method for Assay of Cholesterol 7 $\alpha$ -Hydroxylase Activity, *Anal. Biochem.* 158, 228–232.
11. Honda, A., Shoda, J., Tanaka, N., Matsuzaki, Y., Osuga, T., Shigematsu, N., Tohma, M., and Miyazaki, H. (1991) Simultaneous Assay of the Activities of Two Key Enzymes in the Cholesterol Metabolism by Gas Chromatography–Mass Spectrometry, *J. Chromatogr.* 565, 53–66.
12. Bjorkhem, I., and Danielsson, H. (1974) Assay of Liver Microsomal Cholesterol 7 $\alpha$ -Hydroxylase Using Deuterated Carrier and Gas Chromatography–Mass Spectrometry, *Anal. Biochem.* 59, 508–516.
13. Sanghvi, A., Grassi, E., Bartman, C., Lester, R., Galli Kienle, M., and Galli, G. (1981) Measurement of Cholesterol 7 $\alpha$ -Hydroxylase Activity with Selected Ion Monitoring, *J. Lipid Res.* 22, 720–724.
14. Lowry, O.H., Rosebrough, N.J., Farr, A.L., and Randall, R.J. (1951) Protein Measurement with the Folin Phenol Reagent, *J. Biol. Chem.* 193, 265–275.
15. Hahn, C., Reichel, C., and Bergmann, K.V. (1995) Serum Concentration of 7 $\alpha$ -Hydroxycholesterol as an Indicator of Bile Acid Synthesis in Humans, *J. Lipid Res.* 36, 2059–2066.
16. Brown, M.S., Goldstein, J.L., and Dietschy, J.M. (1979) Active and Inactive Forms of 3-Hydroxy-3-Methylglutaryl Coenzyme A Reductase in the Liver of the Rat, *J. Biol. Chem.* 254, 5144–5149.
17. Hunter, C.F., and Rodwell, V.W. (1980) Regulation of Vertebrate Liver HMG-CoA Reductase via Reversible Modulation of Catalytic Activity, *J. Lipid Res.* 21, 399–405.
18. Makino, I., Chijiwa, K., Fukushima, K., Kameoka, N., Komura, M., Kuroki, S., Yamashita, H., and Tanaka, M. (1997) Cholesterol and Bile Acid Metabolism After Selected Portal Vein Ligation, *J. Surg. Res.* 68, 91–98.
19. Rudling, M., Parini, P., and Angelin, B. (1997) Growth Hormone and Bile Acid Synthesis: Key Role for the Activity of Hepatic Microsomal Cholesterol 7 $\alpha$ -Hydroxylase in the Rat, *J. Clin. Invest.* 99, 2239–2245.
20. Parini, P., Angelin, B., and Rudling, M. (1998) Cholesterol and Lipoprotein Metabolism in Aging Reversal of Hypercholesterolemia by Growth Hormone Treatment in Old Rats, *Arterioscler. Thromb. Vasc. Biol.* 19, 832–839.
21. Duguay, A.B., Yousef, I.M., and Plaa, G.L. (2000) Manganese-Bilirubin Effect on Cholesterol Accumulation in Rat Bile Canaliculus Membranes, *Toxicol. Sci.* 53, 150–155.
22. Post, S.M., de Wit, E.C.M., and Princen, H.M.G. (1997) Cafestol, the Cholesterol-Raising Factor in Boiled Coffee Suppresses Bile Acid Synthesis by Down Regulation of Cholesterol 7 $\alpha$ -Hydroxylase and Sterol 27-Hydroxylase in Rat Hepatocytes, *Arterioscler. Thromb. Vasc. Biol.* 17, 3064–3070.
23. Koopen, N.R., Post, S.M., Wolters, H., Havinga, R., Stellaard, F., Boverhof, R., Kuipers, F., and Princen, H.M.G. (1999) Differential Effects of 17 $\alpha$ -Ethinylestradiol on the Neutral and Acidic Pathways of Bile Salts Synthesis in the Rat, *J. Lipid Res.* 40, 100–108.
24. Del Puppo, M., Cighetti, M., Galli Kienle, G., and de Angelis, L. (1989) Measurement of Mevalonate in Human Plasma and Urine by Multiple Selected Ion Monitoring, *Biomed. Environ. Mass. Spectrom.* 18, 174–176.
25. Dzeletovis, S., Breuer, O., Lund, E., and Diczfalusy, U. (1995) Determination of Cholesterol Oxidation Products in Human Plasma by Isotope Dilution–Mass Spectrometry, *Anal. Biochem.* 225, 73–80.

[Received July 11, 2002, and in revised form and accepted November 26, 2002]

# 5,9,23-Triacontatrienoic Methyl Ester, an Elastase Inhibitor from the Marine Sponge *Chondrilla nucula*

Michèle Meyer and Michèle Guyot\*

Laboratoire de Chimie, ESA 8041 C.N.R.S., Muséum National d'Histoire Naturelle, F-75005 Paris, France

**ABSTRACT:** A polyethylenic fatty ester was isolated from the marine sponge *Chondrilla nucula*. The structure was elucidated through NMR spectral data and MS analysis as 5,9,23-triacontatrienoic methyl ester **1**. Compound **1** is an elastase inhibitor [ $ID_{50} = 10 \mu\text{g/mL}$  ( $2 \cdot 10^{-5} \text{ M}$ )].

Paper no. L8864 in *Lipids* 37, 1109–1111 (November 2002).

Marine sponges of the class Demospongiae biosynthesize long-chain FA,  $C_{24}$ – $C_{30}$ , commonly called “desmospongiac acids” (1). A number of  $C_{30}$  FA have been isolated; the most common, 5,9,23-30:3 $\Delta$ , was first isolated from *Chondrilla nucula* (2), then from *Trikenrion loeve* (along with 9,23-30:2, 23-30:1, 5,9,25-30:3, *Pseudaxinella* cf. *lunaecharta* (3), *Higginsia tethyoides* (4), and *Cinachyrella alloclada* (5). Acid 5,9-30:2 was found in *Petrosia pellasarca* (6) along with a very long chain FA, 19,22,25,28,31-34:5. Another 34:4 acid was isolated from the sponge *Amphimedon compressa* (7), and other highly unsaturated  $C_{30}$  FA, 15,18,21,24-30:4 and 15,18,21,24,27-30:5, were found in *Cliona celata* (8). All of these unsaturated acids were isolated from phospholipids. Acid 5,9,21-30:3 was isolated from *Amphimedon* sp. and described as a DNA topoisomerase I inhibitor (9).

In the course of our program devoted to the search for bioactive metabolites from marine invertebrates of the northern Mediterranean shore, the dichloromethane extract of the sponge *Chondrilla nucula* ([collected by J. Vacelet, Centre d'Océanologie de Marseille (CNRS-Université de la Méditerranée, UMR 6540 DIMAR), Station Marine d'Endoume, 13007 Marseille, France]) showed noticeable inhibition of amidolysis of Suc(Ala)<sub>3</sub>pNA by porcine pancreatic elastase (PPE) (10). Elastase inhibitors have the potential to be therapeutic agents in pulmonary emphysema (11), chronic bronchitis (12), adult respiratory distress syndrome (13), and other inflammatory disorders (14). It has been hypothesized that appropriate small-M.W. inhibitors would be therapeutically useful in the treatment of such diseases (15). Hence, we engaged

in the study of the chemistry of this sponge to isolate the active compound.

## EXPERIMENTAL PROCEDURES

<sup>1</sup>H and <sup>13</sup>C NMR spectra were recorded on a Bruker AC 300 MHz spectrometer. Chemical shifts ( $\delta$ ) are expressed in ppm from residual  $\text{CHCl}_3$  (7.25 ppm) as internal standard. Mass spectra were recorded on a Nermag 10-10 (CI,  $\text{NH}_3$ ). IR spectra were recorded on a Nicolet (impact 400D) FTIR spectrometer. TLC analyses were performed on thin-layer analytical plates 60F254 (Merck, Darmstadt, Germany).

*Chondrilla nucula* was collected near Marseille, washed with seawater, and immersed in methanol for shipping. After arrival, the methanol/water mixture was removed, and specimens were extracted with dichloromethane/methanol (1:1, vol/vol). Solvents were evaporated, and the residue was extracted with dichloromethane. The purification procedure was monitored by measuring amidolysis of *N*-succinyl-alanyl-alanyl-alanyl-*p*-nitroanilide [Suc(Ala)<sub>3</sub>pNA] (Sigma, St. Louis, MO) by PPE (Biosys, Compiègne, France) at 410 nm. Assays were performed in 0.1 M Tris buffer, pH 8, using a Ceres 900 kinetic microplate reader (Bio-Tek Instruments, Winooski, VT) in 96-well microplates. Aliquots (95  $\mu\text{L}$ ) of 40 nM PPE in 200  $\mu\text{L}$  pH 8 buffer and 25  $\mu\text{L}$  of products (25 or 2.5  $\mu\text{g}$ ) in DMSO were mixed at 25°C for 30 min prior to addition of 10  $\mu\text{L}$  of substrate solution [30  $\mu\text{mol}$  of Suc(Ala)<sub>3</sub>pNA in 1 mL of DMSO], and plates were read after 10 min. Oleic acid and methyl oleate were purchased from Sigma.

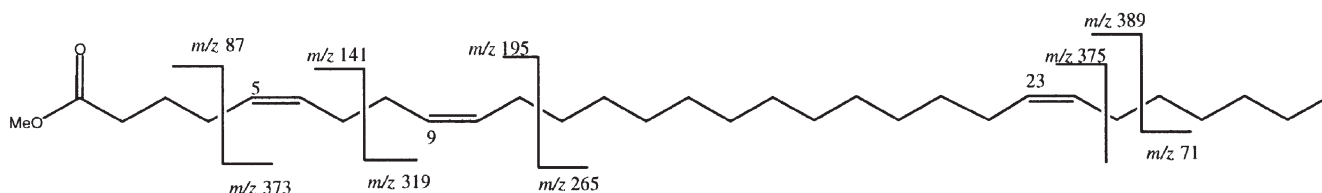
The crude dichloromethane extract was first separated by chromatography on a silica gel column using  $\text{CH}_2\text{Cl}_2$  with increasing amounts of acetone as eluent. The fraction eluted with  $\text{CH}_2\text{Cl}_2$  retained activity and was further purified on another silica gel column eluted with dichloromethane/pentane (2:8, vol/vol) to yield active compound **1**. <sup>13</sup>C NMR ( $\text{CDCl}_3$ ,  $\delta$  ppm): 174.8, 130.5, 130.4, 129.9, 129.9, 128.9, 128.8, 51.9, 39.5, 37.1, 34.1, 33.5, 32.7, 31.9, 30.6–29.1, 27.8, 27.5, 26.7, 25.3, 23.1, 14.5.

Hydrolysis of **1** was performed with  $\text{CO}_3\text{Na}_2$  in dioxane (16). After addition of water, the mixture was extracted with dichloromethane and the residue obtained after evaporation of the solvent purified through a short column of silica gel using dichloromethane as eluant to give pure **2**, MS  $m/z$  446.

\*To whom correspondence should be addressed at Laboratoire de Chimie, ESA 8041 C.N.R.S., Muséum National d'Histoire Naturelle, F-75005 Paris, France. E-mail: guyot@mnhn.fr

Abbreviations:  $ID_{50}$ , dose that is inhibitory in 50% of tests; PPE, porcine pancreatic elastase.





SCHEME 1

## RESULTS AND DISCUSSION

Active compound **1** was obtained as an oil (0.005% dry weight). It exhibits inhibition of PPE at an  $ID_{50}$  (inhibitory dose for 50% of assays) of 10  $\mu\text{g/mL}$  ( $2 \cdot 10^{-5}$  M). High-resolution MS furnished the formula  $C_{31}H_{56}O_2$  by the peak at  $m/z$  460.4275 (calculated 460.4280). The IR spectrum exhibited vibration bands corresponding to one carbonyl ( $1720\text{ cm}^{-1}$ ), ethylenic double bonds ( $1534, 1583, 1613\text{ cm}^{-1}$ ), and an ether function ( $1100\text{ cm}^{-1}$ ). There was no prominent absorption in the  $970\text{ cm}^{-1}$  region, so all double bonds were of *cis* configuration (2).

$^1\text{H}$  NMR spectrum showed signals at  $\delta$  5.35 (*m*, 6H), 3.65 (*s*, 3H,  $\text{OCH}_3$ ), 2.3 (*m*, 2H), 2.1 (*m*, 2H), 1.95 (*m*, 2H), 1.7 (*m*, 4H), 1.25 (*br s*, 32H), and 0.9 ppm (*t*, 3H,  $\text{CH}_3$ ), suggesting a triethylenic FAME. No signal at  $\delta$  2.7 ppm for a methylene-interrupted double bond was observed.

$^{13}\text{C}$  NMR spectrum of **1** showed resonances for 31 carbons: one carbonyl ester at  $\delta$  174.8 ppm, six ethylenic carbons at  $\delta$  130.5, 130.4, 129.9, 129.90, 128.9, 128.8 ppm, one methoxyl group at  $\delta$  51.9 ppm, and signals between 40 and 25 ppm, corresponding to methylene groups.  $^1\text{H}$  COSY allowed unambiguous assignment of the position of the first double bond at C-5.

In the mass spectrum (EI), the typical fragments at  $m/z$  386 and 74, the consequence of a McLafferty rearrangement of methyl esters, are observed along with the base peak at  $m/z$  81 (100%) characteristic of a  $\Delta^{5-9}$  ethylenic acid (6). Other diagnostic fragmentations are shown in Scheme 1 (above), which allowed us to propose locations of the double bonds at the 5,9,23 positions. Upon comparison of the MS spectrum of **1** with that of an authentic sample (Barnathan, G., and Kornprobst, J.M., personal communication), the two spectra were almost identical.

Previous chemical studies of *C. nucula* have led, after hydrolysis of phospholipids, to the isolation of two new 5,9 unsaturated acids. *Chondrilla nucula* collected in Florida contained 5,9,23-triacontatrienoic acid (2). Later, another sample of *C. nucula* collected in Puerto Rico furnished the unusual *cis*-5,9-hexadecadienoic acid, with 9-hexadecenoic and palmitic as the major FA (17), but it lacked 5,9,23-triacontatrienoic acid. This suggests that seasonal and (or) geographic variations may be observed in FA distribution of marine sponges.

However, previous analyses of the long-chain FA contents in *C. nucula* were carried out after acidic methanolysis of the total lipids, so if a methyl ester was present it would not have been detected. Examples of esterified FA as natural products are not rare; we can cite the isolation of the ethyl ester of a

bromopolyacetylenic acid from a sponge (18) or methyl ester of a prostaglandin from a gorgonian (19).

Little is known about biological activities of these long-chain unsaturated FA, except the DNA topoisomerase I inhibition of  $\Delta 5,9,21$ -30:3 (9). To the best of our knowledge, this is the first report of a long-chain fatty ester as an elastase inhibitor. For comparison, the free acid **2** was assayed in the same conditions but was found inactive until 100  $\mu\text{g/mL}$ , as was methyl oleate. However oleic acid gave 35% inhibition at 350  $\mu\text{M}$ , a somewhat higher concentration than that needed to inhibit human leucocyte elastase (20). We concluded that the biological activity of **1** must be accounted for by its unique structure. Synthetic studies and examination of a series of FA and their esters will be necessary to investigate this promising new antielastase agent.

## ACKNOWLEDGMENTS

We express our thanks to Arlette Longeon for the elastase assay, Maurice Baran-Marszak for recording the NMR spectra, Jean-Paul Brouard for mass spectra, and Jean-Michel Kornprobst and George Barnathan for providing the methyl ester mass spectra.

## REFERENCES

- Litchfield, C., Greenberg, A.J., Noto, G., and Morales, R.W. (1976) Unusually High Levels of  $C_{24}$ – $C_{30}$  Fatty Acids in Sponges of the Class Demospongiae (20 genera of sponges studied), *Lipids* 11, 567–570.
- Litchfield, C., Tyszkiewicz, J., and Dato, V. (1979) 5,9,23-Triacontatrienoic Acid: Principal Fatty Acid of the Marine Sponge *Chondrilla nucula*, *Lipids* 15, 200–203.
- Barnathan, G., Kornprobst, J.M., Doumenq, P., and Miralles, J. (1996) New Unsaturated Long-Chain Fatty Acids in the Phospholipids from the Axinellida Sponges *Triaktrion loeve* and *Pseudaxinella cf. lunaecharta*, *Lipids* 31, 193–200.
- Ayanoglu, E., Popov, S., Kornprobst, J.M., Aboud-Bichara, A., and Djerassi, C. (1983) Phospholipid Studies of Marine Organisms: V. New  $\alpha$ -Methoxy Acids from *Higginsia tethyoides* (a demosponge), *Lipids* 18, 830–836.
- Barnathan, G., Miralles, J., Gaydou, E.M., Boury-Esnault, N., and Kornprobst, J.M. (1992) New Phospholipid Fatty Acids from the Marine Sponge *Cinachyrella alloclada* Uliczka, *Lipids* 27, 779–784.
- Carballeira, N.M., and Reyes, E.D. (1990) Novel Very Long Chain Fatty Acids from the Sponge *Petrosia pellarca*, *J. Nat. Prod.* 53, 836–840.
- Carballeira, N.M., and Lopez, M.R. (1989) On the Isolation of 2-Hydroxydocosanoic Acid and 2-Hydroxytricosanoic Acid from the Marine Sponge *Amphimedon compressa*, *Lipids* 24, 89–91.
- Litchfield, C., Tyszkiewicz, J., Marcantonio, E.E., and Noto, G. (1979) 15,18,21,24-Triacontatetraenoic Acids: New  $C_{30}$  Fatty Acids from the Marine Sponge *Cliona celata*, *Lipids* 14, 619–622.

9. Nemoto, T., Yoshino, G., Ojika, M., and Sakagami, Y. (1997) Amphimic Acids and Related Long-Chain Fatty Acids as DNA Topoisomerase Inhibitors from an Australian Sponge, *Amphimedon* sp.: Isolation, Structure, Synthesis, and Biological Evaluation, *Tetrahedron* 53, 16699–16710.
10. La Barre, S., Longeon, A., Barthélemy, M., Guyot, M., Le Caer, J.P., and Bargibant, G. (1996) Characterization of a Novel Elastase Inhibitor from a Fan Coral, *C.R. Acad. Sci. III, Sci. Vie* 319, 365–370.
11. Janoff, A. (1985) Elastases and Emphysema. Current Assessment of the Protease–Antiprotease Hypothesis, *Am. Rev. Respir. Dis.* 13, 417–433.
12. Piccioni, P.D., Kramps, J.A., Rudolphus, A., Bulgheroni, A., and Luisetti, M. (1992) Proteinase/Proteinase Inhibitor Imbalance in Sputum Sol Phases from Patients with Chronic Obstructive Pulmonary Disease. Suggestions for a Key Role Played by Antileukoprotease, *Chest* 102, 1470–1476.
13. Merritt, T.A., Cochrane, C.G., Holcomb, K., Bohl, B., Hallman, M., Strayer, D., Edwards, D.K., 3rd, and Gluck, L. (1983) Elastase and  $\alpha$  1-Proteinase Inhibitor Activity in Tracheal Aspirates During Respiratory Distress Syndrome. Role of Inflammation in the Pathogenesis of Bronchopulmonary Dysplasia, *J. Clin. Invest.* 72, 656–666.
14. Janoff, A. (1985) Elastase in Tissue Injury, *Annu. Rev. Med.* 36, 207–216.
15. Edwards, P.D., and Bernstein, P.R. (1994) Synthetic Inhibitors of Elastase, *Med. Res. Rev.* 14, 127–194.
16. Bestmann, H.J., Kunstmann, R., and Schulz, H. (1966) Eine synthese der “Königinnensubstanz” und der *trans*-10-hydroxy-decen-(2)-säure-(1) (royal jelly acid), *Liebigs Ann. Chem.* 699, 33–39.
17. Carballeira, N.M., and Maldonado, L. (1986) Identification of 5,9-Hexadecadienoic Acid in the Marine Sponge *Chondrilla nucula*, *Lipids* 21, 470–471.
18. Bourguet, M.L., Martin, M.T., Raharimalala, M.T., and Guyot, M. (1992) Bioactive Bromopolyacetylenes from the Marine Sponge *Xestospongia testudinaria*, *Tetrahedron Lett.* 33, 225–226.
19. Weinheimer, A.J., and Spraggins, R.L. (1969) The Occurrence of Two New Prostaglandin Derivatives (15-epi-PGA<sub>2</sub> and its acetate, methyl ester) in the Gorgonian *Plexaura homomalla*. Chemistry of Coelenterates XV, *Tetrahedron Lett.* 10, 5185–5188.
20. Sklan, D., Rappaport, R., and Vered, M. (1990) Inhibition of the Activity of Human Leukocyte Elastase by Lipids Particularly Oleic Acid and Retinoic Acid, *Lung* 168, 323–332.

[Received May 25, 2001, and in final revised form and accepted November 29, 2002]

# What Is the Role of $\alpha$ -Linolenic Acid for Mammals?

Andrew J. Sinclair<sup>a,\*</sup>, Nadia M. Attar-Bashi<sup>a</sup>, and Duo Li<sup>b</sup>

<sup>a</sup>Department of Food Science, RMIT University, Melbourne, Victoria, 3001, Australia, and <sup>b</sup>Department of Food Science, Hangzhou University of Commerce, Hangzhou, China

**ABSTRACT:** This review examines the data pertaining to an important and often underrated EFA,  $\alpha$ -linolenic acid (ALA). It examines its sources, metabolism, and biological effects in various population studies, *in vitro*, animal, and human intervention studies. The main role of ALA was assumed to be as a precursor to the longer-chain n-3 PUFA, EPA and DHA, and particularly for supplying DHA for neural tissue. This paper reveals that the major metabolic route of ALA metabolism is  $\beta$ -oxidation. Furthermore, ALA accumulates in specific sites in the body of mammals (carcass, adipose, and skin), and only a small proportion of the fed ALA is converted to DHA. There is some evidence that ALA may be involved with skin and fur function. There is continuing debate regarding whether ALA has actions of its own in relation to the cardiovascular system and neural function. Cardiovascular disease and cancer are two of the major burdens of disease in the 21st century, and emerging evidence suggests that diets containing ALA are associated with reductions in total deaths and sudden cardiac death. There may be aspects of the action and, more importantly, the metabolism of ALA that need to be elucidated, and these will help us understand the biological effects of this compound better. Additionally, we must not forget that ALA is part of the whole diet and should be seen in this context, not in isolation.

Paper no. L9029 in *Lipids* 37, 1113–1123 (December 2002).

Linoleic and  $\alpha$ -linolenic acids are essential fatty acids (EFA), which means that, like vitamins, they must be obtained in the diet. The essential nature of these PUFA was established in the 1930s (1). Linoleic acid was found to be the parent or precursor for a series of PUFA, now known as the n-6 PUFA since linoleic acid itself is an n-6 PUFA; likewise,  $\alpha$ -linolenic acid (ALA) is the parent FA for the n-3 PUFA.  $\alpha$ -Linolenic acid is called ALA in order to distinguish it from  $\gamma$ -linolenic acid, an n-6 PUFA found in evening primrose oil and borage oil. All FA in the linoleic acid (n-6) PUFA family have their first double bond 6 carbons from the terminal methyl end of the molecule. Similarly, all FA in the ALA (n-3) PUFA family have their first double bond 3 carbons from the methyl end.

ALA is an EFA for mammals because they do not possess the ability to insert double bonds in 18-carbon PUFA between the methyl end and the middle of the molecule. The position of the first double bond from the methyl end of the molecule has led to describing ALA as an n-3 PUFA, since the first

double bond is 3 carbons from the methyl (omega) end of the FA. All FA with this double bond system starting 3 carbons from the methyl end are known as n-3 PUFA. ALA has three *cis* double bonds in positions 9-10, 12-13, and 15-16 counting from the carboxyl end of the FA (all-*cis*-9,12,15-octadecatrienoic acid).

ALA is found in plant chloroplast membranes where it is synthesized from linoleic acid, which in turn is derived from acetate. Cunnane *et al.* (2) argue that because human diets contain 16:2n-6 and 16:3n-3, found in green leafy vegetables, it is possible for humans to synthesize linoleic acid (18:2n-6) and ALA (18:3n-3) by chain elongation, although he concedes the amount of synthesis would be limited. Chloroplast membranes contain a very high content of ALA, which is considered to protect plants against damage during cold spells, with recent evidence showing that transgenic tobacco plants with reduced ALA, due to a silenced n-3 FA desaturase, were better able to acclimate to higher temperatures (3). Lipoxygenase products of ALA in plants include jasmonic acid and related phytohormones produced *via* the oxylipin cascade (4).

ALA is found in plants, animals, zooplankton, phytoplankton, and marine species. The most highly unsaturated FA found in terrestrial plants usually is ALA, although Simopoulos and Salem (5) have reported the presence of trace amounts of long-chain PUFA in some plants. In plants, ALA is found in leaves, mainly in glycolipids, and as TAG in certain seed oils (rapeseed, flaxseed, perilla seed, chia seed), beans (soybeans, navy beans) and nuts (walnuts) (6,7). In fresh green, leafy vegetables the ALA content ranges from 28 to 195 mg/100 g wet weight (8). In mammals, ALA is deposited in most tissues in different lipid fractions (cholesterol esters, TAG, and phospholipids) where it can subsequently be metabolized *via* a number of different metabolic routes (see below).

## FUNCTIONS OF THE n-3 FA

In mammals, linoleic acid is important for growth, reproduction, and skin function and as the precursor of arachidonic acid (9). This latter FA is the main substrate for a series of enzymes that produce the eicosanoids, such as thromboxane, prostaglandins, prostacyclins, leukotrienes and lipoxins (10). Cunnane (11) has argued that we really know little about the effects of linoleic acid deficiency, since researchers study the effect either of combined EFA deficiency (using fat-free diets) or of ALA deficiency (using diets rich in LA). He contends

\*To whom correspondence should be addressed.

E-mail: andrew.sinclair@rmit.edu.au

Abbreviations: ALA,  $\alpha$ -linolenic acid; CE, cholesterol ester; DPA, docosapentaenoic acid; PG, prostaglandin.

that the requirement for linoleic acid is lower when diets contain ALA (11).

Following the discovery of the essential nature of fat by Burr and Burr in 1930 (1), they and other authors investigated which FA were able to correct failure to grow, which FA prevented skin lesions, and which FA corrected high intake of water (presumed to be related to water loss through the skin). The initial studies of Burr and colleagues suggested that both linoleic and linolenic acids increased growth of fat-deficient rats and improved skin lesions (12). Work conducted with pure FA by Mohrhauer and Holman showed that both linoleic and linolenic acids increased the growth of fat-deficient rats; however, the final average weight of the rats fed linoleic acid was significantly greater than those fed ALA (13). This difference in weight might be regarded as significant in today's world and is supported by studies by Pan and Storlien (14), who showed that safflower oil-fed rats were heavier than rats fed diets containing a higher n-3 PUFA content.

Until the late 1970s, n-3 PUFA were regarded as being important only in marine species. Indeed, Tinoco *et al.* (15) suggested that ALA was not needed for terrestrial mammals based on a three-generation deficiency study in rats, although this was hotly contested (16). At this time, it was recognized that DHA was found in high proportions in mammalian brain and retina (17–19) and Anderson's group (20) had already reported that the maximal response of the retina to light was found in diets containing 2% (by weight) of ALA compared with diets containing 2% linoleic acid or 1% of each of the two EFA. It is now recognized that ALA, through its metabolite DHA, is essential for normal visual function based on studies in rats, monkeys, guinea pigs, and infants (21). Furthermore, a putative role for ALA as a messenger of excitation has been described in *Drosophila* photoreceptors (22).

The high levels of brain DHA across mammalian species led to early speculations that this molecule was playing a crucial role in the nervous system (18). Many studies using ALA-deficient diets in different animal species have shown reductions in the level of DHA in brain. Associated changes in brain function (auditory, olfactory, learning, memory, appetite events, neuron size, nerve growth factor levels) have been reported (23–29).

Various mechanisms have been suggested to account for these physiological changes in the brain and retina, as reviewed recently by Kurlack and Stephenson (30), Lauritzen *et al.* (31) and Salem *et al.* (32). Briefly, DHA plays a crucial role in the following: (i) membrane disorder (membrane fluidity), which can influence the function of membrane receptors such as rhodopsin (33,34); (ii) regulation of membrane-bound enzymes (Na/K-dependent ATPase) (35); (iii) dopaminergic and serotonergic neurotransmission (36); (iv) signal transduction *via* effects on inositol phosphates, DAG kinase, and protein kinase C (37); (v) regulation of the synthesis of eicosanoids derived from arachidonic acid (30); (vi) regulation of gene expression (38–40); (vii) regulation of phosphatidylserine levels (41); (viii) protection of neural cells from apoptotic death (42); (ix) stimulation of neurite outgrowth in PC12 cells

(43,44); (x) selective accumulation of DHA by synaptic growth cones during neuronal development (43,44); (xi) regulation of nerve growth factor (29); and (xii) regulation of neuron size (27,28).

There has been considerable discussion whether the true essentiality resides with the EFA themselves or with their long-chain derivatives [arachidonic acid in the case of the n-6 family, and EPA, docosapentaenoic acid (DPA), and DHA in the case of the n-3 family]. For example, dietary ALA has been shown to prevent neuronal death in an animal model of global ischemia and to protect animals treated with kainate against seizures and hippocampal lesions (45). Mixtures of linoleic acid and ALA, as FFA, have been reported to prevent elevations of blood cortisol and cholesterol levels that accompany stressful situations and to prevent rapid and repeated eye blinking in rats following chemical induction of dopamine depletion (46). Whether these effects are mediated *via* the EFA themselves, their long-chain metabolites, or eicosanoids is unknown.

Specific functions have been described for linoleic acid in skin, where there is evidence that it is required to control water permeability (47). Linoleic acid also can be metabolized to an antiproliferative compound, 13-hydroxyoctadecadienoic acid, *via* the 15-lipoxygenase pathway (48).

In plants, specific functions have been described for ALA or ALA metabolites. Plant membranes contain an abundance of ALA, which is thought to be involved in a number of important processes, including (i) being the precursor of jasmonic acid, a plant growth regulator (49); (ii) being a lipoxygenase substrate producing hydroperoxy FA, which mediate defense responses against injury or infection (50); being the substrate for phytoprostanes (dinor isoprostanes) found in high concentration during drying and storage of plants and in pollen (51); being the precursor of a stress-induced  $\alpha$ -ketol derivative of ALA, which has strong flower-inducing activity (52); and being a potent inhibitor of a wound-induced mitogen-activated protein kinase (53).

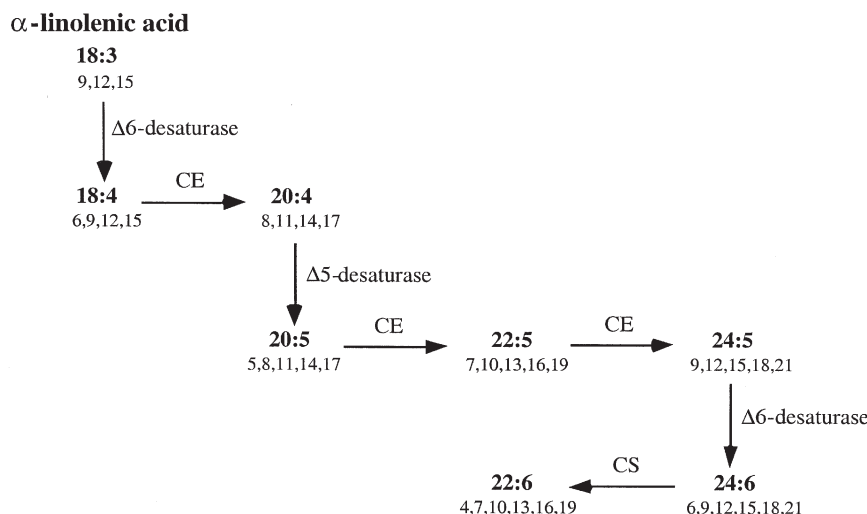
In mammals, the functions that have been described for ALA include being the precursor of the long-chain n-3 FA, being a preferred substrate for  $\beta$ -oxidation and for carbon recycling in the brain and other tissues (54), and having a putative role in skin and fur (55–57).

## $\alpha$ -LINOLENIC ACID METABOLIC PATHWAYS

**$\beta$ -Oxidation.** Studies in humans and animals reveal that a major catabolic route of metabolism of ALA is  $\beta$ -oxidation. In the rat, approximately 60% of an oral dose of labeled ALA was expired as CO<sub>2</sub> in 24 h compared with less than 20% for palmitic, stearic, and arachidonic acids (58). Pan and Storlien (14) reported that the higher the proportion of PUFA in the diet, the higher the rate of  $\beta$ -oxidation of labeled ALA in rats. In humans, between 16 and 20% of ALA was expired as CO<sub>2</sub> in 12 h (59,60); of the 18-carbon FA, ALA was the most highly oxidized while linoleic acid appeared to be somewhat conserved in humans (61).

**Carbon recycling.** Another major route of metabolism of





**FIG. 1.** Metabolic steps involved in converting  $\alpha$ -linolenic acid (18:3n-3) to docosahexaenoic acid (22:6n-3). CE = chain elongation; CS = chain-shortening reaction (peroxisomal oxidation).

ALA in rats and primates involves carbon recycling into *de novo* lipogenesis in the brain and other tissues in pregnant, lactating, fetal, and infant animals (60). When labeled ALA is fed to animals, a substantial proportion of the label ends up in brain saturated and monounsaturated FA and cholesterol (54,62,63). It is not known whether this is due to  $\beta$ -oxidation of ALA in the brain or in nonneural tissues such as liver and muscle and transport and uptake of ketones by the brain. In developing rats fed labeled ALA, the labeling of cholesterol exceeded the labeling of DHA by 4- to 16-fold (63). Edmond *et al.* (64) showed that orally fed deuterium-labeled palmitate, stearate, and oleate did not enter the brain; however, these FA were labeled in the brain owing to new synthesis (recycled deuterium). This implies that the process of  $\beta$ -oxidation in nonneural tissue is important for the supply of substrates such as ketone bodies for brain synthesis of these lipids.

**Precursor of EPA and DHA.** A third metabolic pathway for ALA, and often thought of as the main pathway, is as the precursor of longer-chain, more unsaturated FA, such as EPA, DPA (22:5n-3), and DHA (60,65). The pathway involves seven different steps, of which three are desaturases, three are chain elongations, and one is a chain-shortening reaction (Fig. 1). This pathway takes place mainly in the endoplasmic reticulum, but the final chain-shortening step involves peroxisomal oxidation of 24:6n-3 to 22:6n-3 (65,66). Patients with a peroxisomal disorder known as Zellweger syndrome cannot synthesize 22:6n-3 (67). A critical issue is whether dietary ALA can supply tissues with all the EPA and DHA needed for optimal function or whether there are some tissues that may require a dietary supply of EPA and DHA (see later).

**Skin and fur.** A putative pathway of ALA metabolism is deposition in skin (57,68,69) and secretion onto fur of small mammals (57). In a recent study in guinea pigs, more than 46% of an oral dose of  $^{14}\text{C}$ -ALA was found in the skin and fur lipids, with the highest proportion of the label being found

in the fur (57). In that study, the proportion oxidized to  $\text{CO}_2$  was estimated to be 39% of the oral dose, indicating that nearly 90% of the ALA was unavailable for other metabolic pathways. It was proposed that ALA was secreted from the skin and onto the fur by the sebaceous glands, and that its function was to protect the fur from damage by water, light, or other agents. Sebaceous gland secretion was shown to be a major route of vitamin E delivery to the skin; this mechanism was proposed to protect skin surface lipids and the upper stratum corneum from harmful oxidation (70). Preliminary data from this laboratory reveal that ALA is similarly metabolized by this route (onto the fur) in rats and mice (Sinclair, A., and Fu, Z., unpublished observations). This observation may be related to the commonly reported use of flaxseed oil (linseed oil) as a dietary supplement by dog and horse owners to provide shine to the coats of these species (71).

Several different studies have reported that ALA may play a role in skin and fur function in other species. For example, an early study in rats showed that linseed oil (rich in ALA) contained a factor that promoted fur growth compared with a fat-deficient control group, and that ALA was more effective than linoleic acid in restoring fur growth (55). A later study in capuchin monkeys reported skin lesions, fur loss, and abnormal behavior on a diet very low in ALA but rich in linoleic acid, and that there was a restoration of normal skin and fur appearance following the inclusion of linseed oil in the diet (56).

Both linoleic acid and ALA have been shown to lighten skin following UV-induced hyperpigmentation of skin in guinea pigs (72), which was believed to be due to the suppression of melanin production and enhanced desquamation of the pigment from the epidermis.

Linoleic acid prevents abnormal water loss through the skin, which occurs in EFA deficiency, with comparative studies in the rat showing ALA was not effective in reducing water loss (12,47,73). An explanation offered is that linoleic

acid is incorporated into skin acyl ceramides, whereas ALA is not (47).

**Water homeostasis studies.** In rhesus monkeys, ALA deficiency was associated with an increased water intake; however, this was balanced by increased urination rather than water loss through the skin (74). A recent report involving rats indicated that perinatal n-3 deficiency altered sodium and water homeostasis (75) and that this was associated with an increased blood pressure by the time the rats were adults (76). This suggests an important role for dietary ALA during pregnancy in rats to prevent hypertension in adults. Similar data have been obtained by Langley-Evans (77), who showed that low-protein diets containing corn oil (very low ALA levels) were associated with an elevated blood pressure, whereas low-protein diets containing soy oil were not associated with altered blood pressure.

### HOW EFFECTIVELY IS ALA METABOLIZED TO DHA?

There has been considerable discussion about the effectiveness of dietary ALA as a substrate for tissue EPA and DHA (60,78). To examine this question, several different approaches have been used, including feeding animals and humans with ALA and DHA and comparing tissue levels of DHA; using isotopically labeled ALA and determining the fractional metabolism to DHA in available tissue compartments (such as in plasma or in various tissues in the case of animal studies); and more recently measuring the amount of mRNA for the  $\Delta 6$ - and 5-desaturases in tissues.

Feeding and labeling studies indicate that DHA is a more effective source of tissue DHA than is ALA on a gram-for-gram basis. Early studies in weanling rats revealed that 0.16% of a radiolabeled oral dose of DHA was recovered in brain DHA compared with 0.008% of a radiolabeled oral dose of ALA being found in brain DHA, a 20-fold difference (62). In the guinea pig, it has been estimated that 10 times more dietary ALA than dietary DHA was required to maintain a given brain DHA level (79), whereas DHA was seven times more effective as a substrate for neural DHA than dietary ALA in baboons (80–82). When rats were fed a diet supplied with 0.45% of dietary energy as DHA, they accumulated a twofold higher amount of 22:6n-3 than rats fed a diet supplied with the same amount of ALA for 5 wk (69). In other words, in various mammalian species, dietary DHA is a more effective source of tissue DHA than dietary ALA. Woods *et al.* (82) reported that the brain DHA level was the same in artificially reared rat pups fed high intakes of ALA as in dam-reared pups (who were receiving DHA in the milk); however, retinal DHA levels in the artificially reared groups fed ALA were significantly lower than the dam-reared group.

### DIETS RICH IN ALA DO NOT NECESSARILY LEAD TO HIGH TISSUE DHA LEVELS

There is a view that most dietary ALA is either  $\beta$ -oxidized or converted to long-chain n-3 acids. We have addressed this

issue in studies using diets low or high in ALA with the same LA content (84). Guinea pigs were fed diets for 3 wk containing the same amount of LA (18% of FA) but varying in ALA content (0.3 or 17% of FA). Animals in the high-ALA diet had significantly more whole-body ALA than the low-ALA diet group (8.8 vs. 2.3 g/whole body). There was also significantly more whole-body EPA (0.06 vs. 0.01 g), but on the high-ALA diet the whole-body DPA and DHA did not increase significantly. In other words, ALA does accumulate when fed at high levels, and in the whole body even on a diet low in ALA, the major n-3 FA is ALA (>90% of total n-3 PUFA). The tissues where the most ALA accumulated were muscle, skin, and adipose tissue (approximately 90% of whole-body ALA). These data show that DHA represents a very small proportion of the whole-body n-3 content (90 mg DHA out of a total of 9140 mg). It is also revealing that brain DHA content was only approximately one-quarter of the total DHA in the body, with the carcass representing about 50% of the whole-body DHA (84).

In humans, feeding high-ALA diets (up to 15 g/d) in 4-wk studies led to small but significant increases in ALA, EPA, and 22:5n-3 in plasma TG and phospholipids and very little, if any, detectable increase in DHA in plasma, platelets, and white and red blood cells (78,85,86). Deuterium-labeling studies with ALA in humans showed that the percentage conversion of ALA to EPA and other long-chain n-3 PUFA was between 11 and 19% of the dose, and that the conversion rate was reduced by 40–54% when the diet was rich in linoleic acid (87). In a recent study, physiological compartmental analysis of ALA metabolism in adult humans was carried out. Subjects received a 1-g oral dose of an isotope tracer of ALA; only about 0.2% of the plasma ALA was destined for synthesis of EPA, approximately 63% of the plasma EPA was accessible for production of 22:5n-3, and 37% of 22:5n-3 was available for synthesis of DHA (88). The very limited conversion of ALA to EPA indicates that the biosynthesis of long-chain n-3 PUFA from ALA is limited in healthy individuals. Recently, it has been reported in studies using  $^{13}\text{C}$ -ALA that young women have a greater capacity than young men to convert ALA to DHA (89,90).

Subjects fed a liquid formula diet for 2 wk containing up to 16 energy % of ALA (approximately 35 g/d) and 4 energy% linoleic acid (9 g/d) showed marked increases in ALA in the plasma cholesterol esters (about 7% of CE FA) and also substantial increases in ALA in plasma phosphatidylcholine (PC), with significant rises in EPA in both these fractions (1 and 1.5% of PC and CE fractions, respectively) (91). The increases in ALA were accompanied by equivalent decreases in oleic acid with no significant changes in the arachidonic acid levels in either fraction. Subjects on these diets showed a 52 to 85% decrease in urinary metabolites of total prostaglandins (PG) and  $\text{PGE}_2$ , and a 74% decrease in  $\text{PGF}_{2\alpha}$  levels on the highest ALA diet. An earlier study in healthy subjects who received 30 mL linseed oil daily for 4 wk reported there was an increase in EPA by 150% and in DHA by 70% in the serum phospholipids (92). The large increase in DHA in plasma has not been reported in subsequent studies using

doses of up to 15 g ALA/d (79,86,87). Longer-term studies in adults, who increased their ALA intake by 3 g/d by substituting soy oil for perilla oil for 10 mon, demonstrated an increase in plasma DHA levels by more than 20% (93).

There could be a number of reasons for the relatively poor efficiency of the conversion of ALA to EPA and DHA. First, as noted above, a substantial proportion of the ALA is either diverted to  $\beta$ -oxidation or found distributed throughout all major tissue lipid pools (adipose, carcass, skin) as ALA; in addition, in animals ALA may be excreted onto the fur. Second, linoleic acid (the major dietary PUFA) is a competitive inhibitor of the metabolism of ALA to 18:4n-3, which is a precursor of long-chain n-3 PUFA (Fig. 1). Furthermore, diets rich in linoleic acid decrease the expression of the hepatic  $\Delta 6$ -desaturase compared with a diet rich in oleic acid, which presumably also reduces the possibility of conversion of ALA to 18:4n-3 and 24:5n-3 to 24:6n-3 (94). Based on the data that linoleic acid reduces the  $\Delta 6$ -desaturase levels (94), an obvious mechanism to promote EPA and DHA synthesis from ALA would be to reduce the dietary linoleic acid level and at the same time to increase the ALA level. This strategy has been used successfully in human dietary studies (86) and rat studies (95) to promote synthesis of EPA and DHA from ALA.

With respect to infants, there has been a substantial debate about rates of synthesis of arachidonic acid and DHA from their 18-carbon precursors, especially in preterm infants. This discussion arose when it was realized that formula-fed infants had reduced DHA levels in plasma, red blood cell, muscle, and brain compared with breast-fed infants (above) and that restoration of levels only occurred when arachidonic acid and DHA were added to the infant formula. Many commercial infant formulas contain high levels of linoleic acid and do not contain arachidonic acid and DHA, whereas breast milk contains a small proportion of arachidonic acid and DHA. There is now evidence that ALA is converted to DHA in both preterm and term infants (96,97), although there is wide variability between individual subjects. Despite the apparent ability of infants to make long-chain PUFA, Cunnane *et al.* (98) argue that this production is not sufficient to meet the accretion rate of DHA in the brain. Perhaps the period of rapid brain growth is a situation when DHA, rather than ALA alone, is required to support the accretion rate of brain DHA. It is possible that  $\Delta 6$ -desaturase is especially sensitive to linoleic acid in infants and that high levels of linoleic acid in infant formulas reduce the activity of this enzyme, thus increasing the likely requirement of arachidonic acid and DHA to maintain plasma and other tissue levels of these PUFA.

#### DO PLASMA DHA LEVELS REFLECT DHA STATUS IN OTHER TISSUES?

In studies in humans (infants and adults) with either  $^{13}\text{C}$ - or  $^2\text{H}$ -ALA, the main compartment that can be accessed is plasma. All these studies report that labeled DHA is found in plasma lipids with time, with substantial variability in stable isotope labeled-DHA formation being reported in infants

(96). It is presumed that most of the DHA found in these studies is derived from synthesis in the liver since this tissue is often considered a major site of PUFA synthesis. If other tissues have specific capacities for PUFA formation, such as the brain and testes, then examining the plasma might not reveal this capacity. For example, in the guinea pig fed 0.7% ALA in the diet (0.7 g/100 g diet), liver and heart DHA levels were less than 1% of phospholipid FA (suggesting little DHA synthesis), whereas retina and brain levels of DHA were 16 and 11%, respectively, implying DHA synthesis in these tissues (80). In other words, there are tissue-specific levels of PUFA that presumably depend on a number of factors, including the activity of the desaturases and elongases in the specific tissues, preferential transport, and decreased degradation. A possible explanation for the high brain DHA levels might be the presence of a brain FA-binding protein that supplies DHA to the developing neurons (99). In the cat, the liver apparently has the capacity to synthesize 22:5n-3 from ALA, which is then transported to the brain where DHA can be synthesized, presumably because of the presence of brain-specific enzymes (100). Recent studies on the cloning and expression of mammalian  $\Delta 6$ - and  $\Delta 5$ -desaturases provide support for the idea that tissues other than liver have high levels of desaturase activity. For example, Cho *et al.* (94,101) showed that brain had a higher  $\Delta 6$ -desaturase mRNA level than liver, lung, heart, and skeletal muscle (in mice) and that liver, brain, and heart had a higher abundance of  $\Delta 5$ -desaturase mRNA than other human tissues.

#### CAN DIETARY ALA SUPPORT ADEQUATE PHYSIOLOGICAL OUTCOMES?

In spite of the apparent differences between ALA and DHA in their efficiencies as a source of tissue DHA, it is relevant to ask "does it really matter if all that is needed is a larger dose of ALA than would be required if only DHA were supplied"?

This question can be considered in the retina and in the cardiovascular system:

(i) *The retina.* The physiological response of the retina to light is positively correlated with the supply of n-3 FA (20,21). Few studies have compared the effect of dietary ALA with that of DHA on electroretinographic amplitude responses (102–104). In the first study (in guinea pigs) there were three dietary ALA levels (low, medium, and high) and another diet containing ALA, EPA and DHA (102). The maximum electroretinographic amplitude was found in the group with the highest ALA level (2% energy). The diet containing ALA and long-chain n-3 PUFA, as well as the highest total n-3 PUFA intake (3.1% energy), gave a reduced electroretinographic signal in comparison with the ALA alone diet. In this study, it was not established whether the reduced signal might have resulted from increased peroxidation of DHA or from too much light or perhaps even an imbalance between retinal AA and DHA levels. In the second study, monkeys were fed diets with safflower oil, soybean oil (8% ALA), and a blend including tuna oil (0.6% DHA); results showed no significant

differences between the photoreceptor function in the two diet groups containing significant quantities of the n-3 PUFA (103). In the third study, infant rhesus monkeys were fed either a control diet containing ALA as the sole n-3 PUFA (2% of FA) or a supplemented diet containing 1% DHA and 1% AA from birth. The results suggested that the supplementation with DHA and AA neither harmed nor provided any substantial benefit to the development of visual acuity or retinal function in the first four postnatal months compared with the diet containing only ALA (104).

(ii) *The cardiovascular system.* A substantial role for long-chain n-3 PUFA (EPA and DHA) in the cardiovascular system has been described. The effects include regulation of eicosanoid production from arachidonic acid, plasma TAG and blood pressure-lowering effects (105,106), regulation of ion flux in cardiac cells (107), and regulation of gene expression *via* the peroxisomal proliferation system (108). There have been successful trials of secondary prevention of myocardial infarction with both ALA-rich vegetable oils (109, 110) and oils rich in EPA and DHA (111). A higher intake of ALA was inversely related to the prevalence odds ratio of coronary artery disease (113). In other studies, ALA, EPA, and DHA all prevented fatal arrhythmia in dogs following infusions of them as FFA (113).

(iii) *Platelet behavior.* Renaud and Norday (114) showed that enriching the diet of French farmers with ALA was associated with marked improvements in platelet behavior. In 1992, analysis of data from the MRFIT study of 6250 men (115) in the usual care group showed significant inverse associations between ALA and mortality from CHD ( $P < 0.04$ ), all cardiovascular disease ( $P < 0.03$ ), and all cause mortality ( $P < 0.02$ ). In 1999, Hu *et al.* (116) reported that a higher intake of ALA in the Nurses Health study of 76,283 women was protective against fatal ischemic heart disease, in a prospective cohort study. The mechanism whereby these effects are mediated has not been elucidated; however, one hypothesis involves an alteration in the balance between vasoactive PG (reducing production of vasoconstrictive thromboxane and increasing vasodilatory prostacyclin). In support of this hypothesis is a study by Ferretti and Flanagan (117), who reported that one subject fed a diet containing 5% of the energy from each of linoleic acid and ALA for 5 wk showed a significant reduction in urine excretion of 11-dehydrothromboxane B<sub>2</sub>, which returned to baseline levels following resumption of a low-ALA diet (5.9% energy of linoleic acid, 0.2% energy ALA). The PGI<sub>2</sub>-metabolite levels in urine were similarly significantly reduced during the high-ALA diet phase; however, the level of this metabolite did return to baseline, but more slowly than for that of the thromboxane metabolite. There may also be effects of n-3 rich diets *via* vasoconstrictor response to stressor hormones and reduced blood viscosity (118). ALA may also improve the elasticity of the arterial system, since it has been shown that arterial compliance is improved in obese subjects consuming 20 g of ALA from flaxseed oil for 4 wk (119).

(iv) *Coronary heart disease.* Ventricular fibrillation is a

major fatal complication of coronary heart disease. The introduction of n-3 PUFA as marine n-3 oils into the diet of rats or the acute infusion of ALA, EPA, and DHA in dogs can reverse ventricular fibrillation, strengthening the rationale for the use of these FA in preventing rhythm disorders (120,121). The presence of n-3 PUFA in the myocardial cell membranes electrically stabilizes the cells and prolongs the relative refractory period (107).

(v) *Cardiovascular disease.* The Lyon Diet Heart study of secondary prevention trial aimed to reduce the risk of CVD deaths by diet modification (110). The experimental group ( $n = 302$ ), who consumed a Mediterranean diet rich in ALA, showed a significant reduction in cardiac deaths and nonfatal myocardial infarction compared with the control group. Another prospective, randomized clinical trial using n-3 FA was reported by Singh *et al.* (109). Patients presenting with suspected myocardial infarctions ( $n = 360$ ) were randomized to placebo, marine n-3 oil (2 g of EPA + DHA per day), or mustard seed oil (containing 2.9 g of ALA per day). After one year, CHD events were significantly reduced in both n-3 FA groups.

(vi) *Coronary artery disease.* A randomized, single-blind trial in 1000 patients with angina pectoris, myocardial infarction, or surrogate risk factors for coronary artery disease showed that subjects allocated to a diet rich in whole grains, fruits, vegetables, walnuts, and almonds with soy or mustard seed oil had significantly fewer total cardiac end points, including sudden cardiac deaths and nonfatal myocardial infarctions, compared with a local diet similar to the step 1 National Cholesterol Education Program prudent diet. The intervention diet group consumed a twofold higher intake of ALA (1.8 vs. 0.8 g/d) compared with the control group (122).

## ALA AND PROSTATE CANCER

A number of prospective and case-control studies have suggested there is a positive association between diet or plasma ALA levels and the incidence of prostate cancer (123–128); however, other studies have not supported this association (129–132). The studies above estimated ALA dietary intake by using food frequency questionnaires or by measuring ALA levels in plasma or adipose tissue. The one study that measured ALA levels in prostate tissue itself from patients undergoing radical prostatectomy (133) showed that prostatic ALA levels tended to be lower in cases than in control subjects, with significantly lower levels when tumors extended to anatomical or surgical margins.

The lack of consistency in findings from these studies may be due to methodological limitations related to measurement error in estimating past dietary exposure of a nutrient like ALA from food frequency questionnaires, in measuring ALA levels in plasma that may not represent long-term dietary intake, in assuming that ALA levels in plasma are representative of ALA levels in the prostate tissue, and in choosing the sample size of the studies, which may have been too small in some studies. Measuring prostatic levels of FA, as in the study by Freeman *et al.* (133), offers advantages over self-reported



usual dietary intake since it provides an estimate of exposure at the target organ level, where the concentrations likely reflect long-term dietary intake; however, the sample size for that study was small.

At least four distinct biological mechanisms have been postulated to explain an effect of PUFA on prostate cancer growth. These include alteration in (i) the immune system response *via* eicosanoid synthesis, (ii) membrane phospholipid composition affecting permeability and receptor activity, (iii) hormone metabolism such as interference with  $5\alpha$ -reductase activity, which converts testosterone to  $5\alpha$ -dihydrotestosterone, and (iv) free radical formation from FA oxidation (134–136).

The etiology of prostate cancer remains unknown; however, it is evident that both genetic and exogenous factors are important in causing prostate cancer. The evidence of a positive association between ALA and prostate cancer is very weak and conflicting. Future research should aim at looking at the prostatic levels of ALA rather than plasma or diet in patients with prostate cancer.

## ALA AND BREAST CANCER

Several recent papers have associated a low ALA content of breast adipose tissue with an increased risk of breast cancer. The first study was a case-control study that showed an inverse association between breast adipose tissue ALA and the risk of breast cancer in 123 women with invasive, non-metastatic breast carcinoma compared with 59 women with benign breast disease (137). The second study was also a case-control study that examined breast adipose tissue from 241 patients with invasive, nonmetastatic breast carcinoma and 88 patients with benign breast disease (138). There was an inverse association between breast cancer risk and n-3 FA levels in breast adipose tissue. Furthermore, there were significant reductions of risk for women in the highest tertile of both ALA and DHA and in the highest tertile for the ratio of long-chain n-3 to n-6 PUFA. Studies in animals fed a high level of ALA suggest that rat mammary tumor growth depended on the dietary oxidative status, with vitamin E added to the ALA in the diet resulting in increased tumor growth compared with the high-ALA diet without vitamin E and prooxidants (sodium ascorbate/2-methyl-1,4-naphthoquinone) decreasing tumor growth (139).

## CASE REPORTS OF ALA DEFICIENCY IN HUMANS

Two case reports of suspected ALA deficiency in children deserve mention (137,138). In the first, a 7-yr-old child fed intravenously for 5 mon on a high-linoleic and low-ALA emulsion was reported to have experienced episodes of numbness, paresthesia, weakness, inability to walk, pain in the legs, and blurring of vision. Use of an ALA-containing emulsion was associated with a gradual and complete resolution of the paresthesias and episodes of weakness in the first 12 wk and subsequently improved nerve conduction velocities (140). The authors concluded there was a requirement for ALA of

0.54% of energy. In the second study, a 7-yr-old girl fed solely by gastric tube, with a preparation containing 16.2% energy as linoleic acid and 0.07% as ALA, from the age of 3 to the age of 7 showed little evidence of growth in this period, with weight being constant for the last 15 mon at 10.3 kg. She was supplemented with a linseed- and cod liver-oil mixture (5:1, vol/vol) for 2 mon, during which time her weight increased 0.43 kg/mon; after 5 mon, the amount of cod liver oil was increased and the weight gain increased to 0.64 kg/mon and her length increased from 117 to 122 cm in 5 mon (141). The authors concluded the n-3 requirements for this child were in the range 1.1–1.2% energy.

## RECOMMENDED DAILY INTAKES OF ALA

In 1992, the National Health and Medical research Council of Australia recommended that Australians increase their intakes of n-3 PUFA without specifying a figure for the recommended intake (142). In 1998, a European group considered the evidence for a Recommended Daily Intake for ALA and judged there was no evidence to deviate from the value of 1% energy (105). This group highlighted the need for large-scale prospective studies and randomized controlled trials focusing specifically on ALA. In 1999, a workshop sponsored by the National Institute on Alcohol Abuse and Alcoholism–NIH, the Office of Dietary Supplements–NIH, The Centre for Genetics, Nutrition & Health, and the International Society for the Study of Fatty Acids & Other Lipids suggested that the adequate intake of ALA should be 1% energy (2.22 g/d on a 2000 kcal diet) (143) with the proviso that the adequate linoleic acid intake be 2% of energy. The rationale for this suggestion was that it is only at low intakes of linoleic acid that ALA is effectively metabolized to long-chain n-3 in plasma and tissues (144,145). There is a clear need for a physiological end point related to ALA in order that requirements can be more effectively determined.

## REFERENCES

1. Burr, G.O., and Burr, M.M. (1930) On the Nature and Role of Fatty Acids Essential in Nutrition, *J. Biol. Chem.* 86, 587–621.
2. Cunnane, S.C., Ryan, M.A., Craig, K.S., Brookes, S., Koletzko, B., Demmelmair, H., Singer, J., and Kyle, D.J. (1995) Synthesis of Linoleate and  $\alpha$ -Linolenate by Chain Elongation in the Rat, *Lipids* 30, 781–783.
3. Murakami, Y., Tsuyama, M., Kobayashi, Y., Kodama, H., and Iba, K. (2000) Trienoic Fatty Acids and Plant Tolerance of High Temperature, *Science* 287, 476–479.
4. Koch, T., Krumm, T., Jung, V., Engelbert, J., and Boland, W. (1999) Differential Induction of Plant Volatile Biosynthesis in the Lima Bean by Early and Late Intermediates of the Octadecanoid-Signalling Pathway, *Plant Physiol.* 121, 153–162.
5. Simopoulos, A.P. and Salem, N., Jr. (1989) n-3 Fatty Acids in Eggs from Free-Range Greek Chickens, *N. Engl. J. Med.* 321, 1412 (letter).
6. Raper, N.R., Cronin, F.J., and Exler, J. (1992) n-3 Fatty Acid Content of the U.S. Food Supply, *J. Am. Coll. Nutr.* 11, 304–308.
7. Ayerza, R. (1995) Oil Content and Fatty Acid Composition of

- Chia (*Salvia hispanica* L.) from Five Northwestern Locations in Argentina, *J. Am. Oil Chem. Soc.* 72, 1079–1081.
8. Periera, C., Li, D., and Sinclair, A.J. (2001) The  $\alpha$ -Linolenic Acid Content of Commonly Available Green Vegetables in Australia, *Int. J. Vitam. Nutr. Res.* 71, 223–228.
  9. Holman, R.T. (1968) Biological Activities of and Requirements for Polyunsaturated Fatty Acids, *Prog. Chem. Fats Other Lipids* 9, 611–680.
  10. Yamamoto, S., and Smith, W.L. (2002) Molecular Biology of the Arachidonate Cascade (second edition), *Prostaglandins Other Lipid Mediat.* 68–69, 1 (Preface).
  11. Cunnane, S.C. (1999) The Long History of Essential Fatty Acids but Belated Knowledge About Linoleate Deficiency *per se*: A Paradox, *J. Nutr.* 129, 446.
  12. Burr, G.O. (1942) Significance of the Essential Fatty Acids, *Fed. Proc.* 1, 224–233.
  13. Mohrhauer, H., and Holman, R.T. (1963) The Effect of Dose Level of Essential Fatty Acids Upon Fatty Acid Composition of the Rat Liver, *J. Lipid Res.* 4, 151–159.
  14. Pan, D.A., and Storlien, L.H. (1993) Dietary Lipid Profile Is a Determinant of Tissue Phospholipid Fatty Acid Composition and Rate of Weight Gain in Rats, *J. Nutr.* 123, 512–519.
  15. Tinoco, J., Williams, M.A., Hincenbergs, I., and Lyman, R.L. (1971) Evidence for Non-essentiality of Linolenic Acid in the Diet of the Rat, *J. Nutr.* 101, 937–943.
  16. Crawford, M.A., and Sinclair, A.J. (1972) The Limitations of Whole Tissue Analysis to Define Linolenic Acid Deficiency, *J. Nutr.* 102, 1315–1322.
  17. O'Brien, J.S., and Sampson, E.L. (1965) Fatty Acid and Fatty Aldehyde Composition of the Major Brain Lipids in Normal Human Gray Matter, White Matter and Myelin, *J. Lipid Res.* 6, 545–551.
  18. Crawford, M.A., and Sinclair, A.J. (1972) Nutritional Influences in the Evolution of the Mammalian Brain, in *CIBA Foundation Symposium on Lipids, Malnutrition and the Developing Brain*, pp. 267–287, Associated Scientific Publishers, Amsterdam.
  19. Fleisler, S.J., and Anderson, R.E. (1983) Chemistry and Metabolism of Lipids in the Vertebrate Retina, *Prog. Lipid Res.* 22, 79–131.
  20. Wheeler, T.G., Benolken, R.M., and Anderson, R.E. (1975) Visual Membranes: Specificity of Fatty Acid Precursors for the Electrical Response to Illumination, *Science* 188, 1312–1314.
  21. Sinclair, A.J. (2000) Commentary on the Workshop Statement, Prostaglandins, *Leukot. Essent. Fatty Acids* 63, 135–137.
  22. Chyb, S., Raghu, P., and Hardie, R.C. (1999) Polyunsaturated Fatty Acids Activate the *Drosophila* Light-Sensitive Channels TRP and TRPL, *Nature* 397, 255–259.
  23. Salem, N., Jr., and Ward, G.R. (1993) Are Omega-3 Fatty Acids Essential Nutrients for Mammals? *World Rev. Nutr. Dietet.* 72, 128–147.
  24. Greiner, R.S., Moriguchi, T., Hutton, A., Slotnick, B.M., and Salem, N., Jr. (1999) Rats with Low Levels of Brain Docosahexaenoic Acid Show Impaired Performance in Olfactory-Based and Spatial Learning Tasks, *Lipids* 34, S239–S243.
  25. Bourre, J.M., Durand, G., Erre, J.P., and Aran, J.M. (1999) Changes in Auditory Brainstem Responses in  $\alpha$ -Linolenic Acid Deficiency as a Function of Age in Rats, *Audiology* 38, 13–18.
  26. Umezawa, M., Kogishi, K., Tojo, H., Yoshimura, S., Seriu, N., Ohta, A., Takeda, T., and Hosokawa, M. (1999) High-Linoleate and High  $\alpha$ -Linolenate Diets Affect Learning Ability and Natural Behavior in SAMR1 Mice, *J. Nutr.* 129, 431–437.
  27. Ahmad, A., Moriguchi, T., and Salem, N., Jr. (2002) Decrease in Neuron Size in Docosahexaenoic Acid-Deficient Brain, *Pediatr. Neurol.* 26, 210–218.
  28. Ahmad, A., Murthy, M., Greiner, R.S., Moriguchi, T., and Salem, N., Jr. (2002) A Decrease in Cell Size Accompanies a Loss of Docosahexaenoate in the Rat Hippocampus, *Nutr. Neurosci.* 5, 103–113.
  29. Ikemoto, A., Nitta, A., Furukawa, S., Ohishi, M., Nakamura, A., Fujii, Y., and Okuyama, H. (2000) Dietary n-3 Fatty Acid Deficiency Decreases Nerve Growth Factor Content in Rat Hippocampus, *Neurosci. Lett.* 285, 99–102.
  30. Kurlak, L.O., and Stephenson, T.J. (1999) Plausible Explanations for Effects of Long Chain Polyunsaturated Fatty Acids (LCPUFA) on Neonates, *Arch. Dis. Child Fetal Neonatal Ed.* 80, 148–154.
  31. Lauritzen, L., Hansen, H.S., Jorgensen, M.H., and Michaelsson, K.F. (2001) The Essentiality of Long Chain n-3 Fatty Acids in Relation to Development and Function of the Brain and Retina, *Prog. Lipid Res.* 40, 1–94.
  32. Salem, N., Jr., Litman, B., Kim, H.-Y., and Gawrisch, K. (2001) Mechanisms of Action of Docosahexaenoic Acid in the Nervous System, *Lipids* 36, 945–959.
  33. Litman, B.J., Niu, S.L., Polozova, A., and Mitchell, D.C. (2001) The Role of Docosahexaenoic Acid Containing Phospholipids in Modulating G Protein-Coupled Signaling Pathways: Visual Transduction, *J. Mol. Neurosci.* 16, 237–242.
  34. Feller, S.E., Gawrisch, K., and MacKerell, A.D. (2002) Polyunsaturated Fatty Acids in Lipid Bilayers: Intrinsic and Environmental Contributions to Their Unique Physical Properties, *J. Am. Chem. Soc.* 124, 318–326.
  35. Bowen, R.A.R., and Clandinin, M.T. (2002) Dietary Low Linolenic Acid Compared with Docosahexaenoic Acid Alter Synaptic Plasma Membrane Phospholipid Fatty Acid Composition and Sodium-Potassium ATPase Kinetics in Developing Rats, *J. Neurochem.* 83, 764–774.
  36. Zimmer, L., Delion-Vancassel, S., Durand, G., Guilloteau, D., Bodard, S., Besnard, J.C., and Farkas, T. (2000) Modification of Dopamine Neurotransmission in the Nucleus Accumbens of Rats Deficient in n-3 Polyunsaturated Fatty Acids, *J. Lipid Res.* 41, 32–40.
  37. Vaidyanathan, V.V., Rao, K.V.R., and Sastry, P.S. (1994) Regulation of Diacylglycerol Kinase in Rat Brain Membranes by Docosahexaenoic Acid, *Neurosci. Lett.* 179, 171–174.
  38. Rojas, C.V., Greiner, R.S., Martinez, J.I., Salem, N., Jr., and Uauy, R. (2002) Long-Term n-3 Fatty Acid Deficiency Modifies Peroxisome Proliferator-Activated Receptor  $\beta$  mRNA Abundance in Rat Ocular Tissues, *Lipids* 37, 367–374.
  39. Kitajka, K., Puskas, L.G., Zvara, A., Hackler, L., Jr., Barcelo-Coblijn, G., Yeo, Y.K., and Farkas, T. (2002) The Role of n-3 Polyunsaturated Fatty Acids in Brain: Modulation of Rat Brain Gene Expression by Dietary n-3 Fatty Acids, *Proc. Natl. Acad. Sci. USA* 99, 2619–2624.
  40. De Urquiza, A.M., Liu, S., Sjoberg, M., Zetterstrom, R.H., Griffiths, W., Sjoval, J., and Perlmann, T. (2000) Docosahexaenoic Acid, a Ligand for the Retinoid X Receptor in Mouse Brain, *Science* 290, 2140–2144.
  41. Garcia, M.C., Ward, G., Ma, Y.-C., Salem, N., Jr., and Kim, H.-Y. (1998) Effect of Docosahexaenoic Acid on the Synthesis of Phosphatidylserine in Rat Brain Microsomes and C6 Glioma Cells, *J. Neurochem.* 70, 24–30.
  42. Akbar, M., and Kim, H.-Y. (2002) Protective Effects of Docosahexaenoic Acid in Staurosporine-Induced Apoptosis: Involvement of Phosphatidyl-3-kinase Pathway, *J. Neurochem.* 82, 655–665.
  43. Ikemoto, A., Kobayashi, T., Watanabe, S., and Okuyama, H. (1997) Membrane Fatty Acid Modifications of PC12 Cells by Arachidonate or Docosahexaenoate Affect Neurite Outgrowth but Not Norepinephrine Release, *Neurochem. Res.* 22, 671–678.
  44. Martin, R.E. (1998) Docosahexaenoic Acid Decreases Phos-

- pholipase A<sub>2</sub> Activity in the Neurites/Nerve Growth Cones of PC12 Cells, *J. Neurosci. Res.* 54, 805–813.
45. Lauritzen, I., Blondeau, N., Heurteaux, C., Widmann, C., Romey, G., and Lazdunski, M. (2000) Polyunsaturated Fatty Acids Are Potent Neuroprotectors, *EMBO J.* 19, 1784–1793.
  46. Mostofsky, D.I., Yehuda, S., Rabinovitz, S., and Carasso, R. (2000) The Control of Blepharospasm by Essential Fatty Acids *Neuropsychobiology* 41, 154–157.
  47. Hansen, H.S., and Jensen, B. (1985) Essential Function of Linoleic Acid Esterified in Acylglucosylceramide and Acylceramide in Maintaining the Epidermal Water Permeability Barrier. Evidence from Feeding Studies with Oleate, Linoleate, Arachidonate, Columbinatate and  $\alpha$ -linolenate, *Biochim. Biophys. Acta* 834, 357–363.
  48. Ziboh, V.A., Miller, C.C., and Cho, Y. (2000) Metabolism of Polyunsaturated Fatty Acids by Skin Epidermal Enzymes: Generation of Antinflammatory and Antiproliferative Metabolites, *Am. J. Clin. Nutr.* 71, 361S–366S.
  49. Koch, T., Krumm, T., Jung, V., Engelberth, J., and Boland, W. (1999) Differential Induction of Plant Volatile Biosynthesis in the Lima Bean by Early and Late Intermediates of the Octadecanoid-Signaling Pathway, *Plant Physiol.* 121, 153–162.
  50. Martin, M., Leon, J., Dammann, C., Albar, J.P., Griffiths, G., and Sanchez-Serrano, J.J. (1999) Anti-sense Depletion of Potato Leaf Omega 3 Fatty Acid Desaturase Lowers Linolenic Acid Content and Reduces Gene Activation in Response to Wounding, *Eur. J. Biochem.* 262, 283–290.
  51. Imbusch, R., and Mueller, M.J. (2000) Formation of Isoprostane F<sub>2</sub>-like Compounds from  $\alpha$ -Linolenic Acid in Plants, *Free Radic. Biol. Med.* 28, 720–726.
  52. Yokoyama, M., Yamaguchi, S., Inomata, S., Komatsu, K., Yoshida, S., Iida, T., Yokokawa, Y., Yamaguchi, M., Kaihara, S., and Takimoto, A. (2000) Stress-Induced Factor in Flower Formation of *Lemna* Is an  $\alpha$ -Ketol Derivative of Linolenic Acid, *Plant Cell Physiol.* 41, 110–113.
  53. Baudouin, E., Meskiene, I., and Hirt, H. (1999) Unsaturated Fatty Acids Inhibit MP2C, a Protein Phosphatase 2C Involved in the Wound-Induced MAP Kinase Pathway Regulation, *Plant J.* 20, 343–348.
  54. Cunnane, S.C., Menard, C.R., Likhodii, S.S., Brenna, J.T., and Crawford, M.A. (1999) Carbon Recycling into *de novo* Lipogenesis Is a Major Pathway in Neonatal Metabolism of Linoleate and  $\alpha$ -Linolenate, *Prostaglandins Leukot. Essent. Fatty Acids* 60, 387–392.
  55. Rokkones, T. (1953) A Dietary Factor Essential for Hair Growth in Rats, *Intern. Z. Vitaminforsch.* 25, 86–98.
  56. Fiennes, R.N.T.W., Sinclair, A.J., and Crawford, M.A. (1973) Essential Fatty Acid Studies in Primates. Linolenic Acid Requirements of Capuchins, *J. Med. Prim.* 2, 155–169.
  57. Fu, Z., and Sinclair, A.J. (2000) Novel Pathway of Metabolism of  $\alpha$ -Linolenic Acid in the Guinea Pig, *Pediatr. Res.* 47, 414–417.
  58. Leyton, J., Drury, P.J., and Crawford, M.A. (1987) Differential Oxidation of Saturated and Unsaturated Fatty Acids *in vivo* in the Rat, *Br. J. Nutr.* 57, 383–393.
  59. Vermunt, S.H., Mensink, R.P., Simonis, M.M., and Hornstra, G. (2000) Effects of Dietary  $\alpha$ -Linolenic Acid on the Conversion and Oxidation of <sup>13</sup>C- $\alpha$ -Linolenic Acid, *Lipids* 35, 137–142.
  60. Brenna, J.T. (2002) Efficiency of Conversion of  $\alpha$ -Linolenic Acid to Long Chain n-3 Fatty Acids in Man, *Curr. Opin. Clin. Nutr. Metab. Care* 5, 127–132.
  61. DeLany, J.P., Windhauser, M.M., Champagne, C.M., and Bray, G.A. (2000) Differential Oxidation of Individual Dietary Fatty Acids in Humans, *Am. J. Clin. Nutr.* 79, 905–911.
  62. Sinclair, A.J. (1975) Incorporation of Radioactive Polyunsaturated Fatty Acids into Liver and Brain of the Developing Rat, *Lipids* 10, 175–184.
  63. Menard, C.R., Goodman, K.J., Corso, T.N., Brenna, J.T., and Cunnane, S.C. (1998) Recycling of Carbon into Lipids Synthesized *de novo* Is a Quantitatively Important Pathway of  $\alpha$ -[U-<sup>13</sup>C]Linolenate Utilization in the Developing Rat Brain, *J. Neurochem.* 71, 2151–2180.
  64. Edmond, J., Higa, T.A., Korsack, R.A., Bergner, E.A., and Lee, W.-N.P. (1998) Fatty Acid Transport and Utilization for the Developing Brain, *J. Neurochem.* 70, 1227–1234.
  65. Voss, A.M., Reinhart, S., Sankarappa, S., and Sprecher, H. (1991) Metabolism of 22:5n-3 to 22:6n-3 in Rat Liver Is Independent of 4-Desaturase, *J. Biol. Chem.* 266, 19995–20000.
  66. Moore, S.A., Hurt, E., Yoder, E., Sprecher, H., and Spector, A.A. (1995) Docosahexaenoic Acid Synthesis in Human Skin Fibroblasts Involves Peroxisomal Retroconversion of Tetraacosahexaenoic Acid, *J. Lipid Res.* 36, 2433–2443.
  67. Martinez, M., Vazquez, E., Garcia-Silva, M.T., Manzanares, J., Bertran, J.M., Castello, F., and Mougan, I. (2000) Therapeutic Effects of Docosahexaenoic Acid Ethyl Ester in Patients with Generalized Peroxisomal Disorders, *Am. J. Clin. Nutr.* 71, 376S–385S.
  68. Bowen, R.A., and Clandinin, M.T. (2000) High Dietary 18:3n-3 Increases the 18:3n-3 but Not the 22:6n-3 Content in the Whole Body, Brain, Skin, Epididymal Fat Pads, and Muscles of Suckling Rat Pups, *Lipids* 35, 389–394.
  69. Poumès-Ballihaut, C., Langelier, B., Houlier, F., Alessandri, J., Durand, G., Latge, C., and Guesnet, P. (2001) Comparative Bioavailability of Dietary  $\alpha$ -Linolenic Acid and Docosahexaenoic Acid in the Growing Rat, *Lipids* 36, 793–800.
  70. Thiele, J.J., Weber, S.U., and Packer, L.L. (1999) Sebaceous Gland Secretion Is a Major Physiologic Route of Vitamin E Delivery to Skin, *J. Invest. Dermatol.* 113, 1006–1010.
  71. Lloyd, D.H. (1989) Essential Fatty Acids and Skin Disease, *J. Small Anim. Prac.* 30, 207–212.
  72. Ando, H., Ryu, A., Hashimoto, A., Oka, M., and Ichihashi, M. (1998) Linoleic Acid and  $\alpha$ -Linolenic Acid Lighten Ultraviolet-Induced Hyperpigmentation of the Skin, *Arch. Dermatol. Res.* 290, 375–381.
  73. Hartop, P.J., and Prottey, C. (1976) Changes in Transepidermal Water Loss and the Composition of Epidermal Lecithin After Applications of Pure Fatty Acid Triglycerides to the Skin of Essential Fatty Acid Deficient Rats, *J. Dermatol.* 95, 255–264.
  74. Reisbick, S., Neuringer, M., and Connor, W.E. (1992) Postnatal Deficiency of Omega-3 Fatty Acids in Monkeys: Fluid Intake and Urine Concentration, *Physiol. Behav.* 51, 473–479.
  75. Armitage, J.A., Burns, P., Sinclair, A.J., Weisinger, H.S., Vingrys, A.J., and Weisinger, R.S. (2000) Perinatal Omega 3 Fatty Acid Deprivation Alters Thirst and Sodium Appetite in Adult Rats, *Appetite* 37, 258.
  76. Weisinger, H.S., Armitage, J.A., Sinclair, A.J., Vingrys, A.J., Burns, P., and Weisinger, R.S. (2001) Peri-natal Omega 3 Fatty Acid Deficiency Affects Blood Pressure, Fluid and Metabolite Homeostasis, *Nature Med.* 7, 258–259.
  77. Langley-Evans, S.C. (2000) Critical Differences Between Two Low Protein Diet Protocols in the Programming of Hypertension in the Rat, *Int. J. Food Sci. Nutr.* 51, 11–17.
  78. Gerster, H. (1998) Can Adults Adequately Convert  $\alpha$ -Linolenic Acid to Eicosapentaenoic Acid and Docosahexaenoic Acid? *Internat. J. Vit. Nutr. Res.* 68, 159–173.
  79. Abedin, L., Lien, E.L., Vingrys, A.J., and Sinclair, A.J. (1999) The Effects of Dietary  $\alpha$ -Linolenic Acid Compared with Docosahexaenoic Acid on Brain, Retina, Liver, and Heart in the Guinea Pig, *Lipids* 34, 475–482.
  80. Greiner, R.C., Winter, J., Nathanielsz, P.W., and Brenna, J.T. (1997) Brain Docosahexaenoate Accretion in Fetal Baboons: Bioequivalence of Dietary  $\alpha$ -Linolenic and Docosahexaenoic Acids, *Pediatr. Res.* 42, 826–834.



81. Su, H.M., Bernardo, L., Mirmiran, M., Ma, X.H., Nathanielsz, P.W., and Brenna, J.J. (1999) Dietary 18:3n-3 and 22:6n-3 as Sources of 22:6n-3 Accretion in Neonatal Baboon Brain and Associated Organs, *Lipids* 34, S347–S350.
82. Woods, J., Ward, G., and Salem, N., Jr. (1996) Is Docosahexaenoic Acid Necessary in Infant Formulas? Evaluation of High Linolenate Diets in the Neonatal Rat, *Pediatr. Res.* 40, 687–694.
83. Su, H.M., Huang, M.C., Saad, N.M., Nathanielsz, P.W., and Brenna, J.T. (2001) Fetal Baboons Convert 18:3n-3 to 22:6n-3 *in vivo*: A Stable Isotope Tracer Study, *J. Lipid Res.* 42, 581–586.
84. Fu, Z., and Sinclair, A.J. (2000) Increased  $\alpha$ -Linolenic Acid Intake Increases Tissue  $\alpha$ -Linolenic Acid Content and Apparent Oxidation with Little Effect on Tissue Docosahexaenoic Acid in the Guinea Pig, *Lipids* 35, 395–400.
85. Li, D., Sinclair, A., Wilson, A., Nakkote, S., Kelly, F., Abedin, L., Mann, N., and Turner, A. (1999) Effect of Dietary  $\alpha$ -Linolenic Acid on Thrombotic Risk Factors in Vegetarian Men, *Am. J. Clin. Nutr.* 69, 872–882.
86. Mantzioris, E., James, M.J., Gibson, R.A., and Cleland, L.G. (1994) Dietary Substitution with an  $\alpha$ -Linolenic Acid-rich Vegetable Oil Increases Eicosapentaenoic Acid Concentrations in Tissues, *Am. J. Clin. Nutr.* 59, 1304–1309.
87. Emken, E.A., Adlof, R.O., and Gulley, G.M. (1994) Dietary Linoleic Acid Influences the Desaturation and Acylation of Deuterium-Labelled Linoleic and  $\alpha$ -Linolenic Acid in Young Adult Males, *Biochim. Biophys. Acta* 1213, 277–288.
88. Pawlosky, R.J., Hibbeln, J.R., Novotny, J.A., and Salem, N., Jr. (2001) Physiological Compartmental Analysis of  $\alpha$ -Linolenic Acid Metabolism in Adult Humans, *J. Lipid Res.* 42, 1257–1265.
89. Burdge, G.C., and Wootton, S.A. (2002) Conversion of  $\alpha$ -Linolenic Acid to Eicosapentaenoic, Docosapentaenoic and Docosahexaenoic Acids in Young Women, *Br. J. Nutr.* 88, 411–420.
90. Burdge, G.C., Jones, A.E., and Wootton, S.A. (2002) Eicosapentaenoic and Docosapentaenoic Acids Are the Principal Products of  $\alpha$ -Linolenic Acid Metabolism in Young Men, *Br. J. Nutr.* 88, 355–363.
91. Adam, O., Wolfram, G., and Zollner, N. (1986) Effect of  $\alpha$ -Linolenic Acid in the Human Diet on Linoleic Acid Metabolism and Prostaglandin Biosynthesis, *J. Lipid Res.* 27, 421–426.
92. Mest, H.J., Beitz, J., Heinroth, I., Block, H.U., and Forster, W. (1983) The Influence of Linseed Diet on Fatty Acid Pattern in Phospholipids and Thromboxane Formation in Platelets in Man, *Klin. Wochenschr.* 61, 187–191.
93. Ezaki, O., Takahashi, M., Shigematsu, T., Shimamura, K., Kimura, J., Ezaki, H., and Gotoh, T. (1999) Long-Term Effects of Dietary  $\alpha$ -Linolenic Acid from Perilla Oil on Serum Fatty Acid Composition and on the Risk Factors of Coronary Heart Disease in Japanese Elderly Subjects, *J. Nutr. Sci. Vitaminol.* 45, 759–762.
94. Cho, H.P., Nakamura, M.T., and Clarke, S.D. (1999) Cloning, Expression, and Nutritional Regulation of the Mammalian  $\Delta$ 6-Desaturase, *J. Biol. Chem.* 274, 471–477.
95. O'Dea, K., Steel, M., Naughton, J.M., Sinclair, A.J., Hopkins, G., Angus, J., He, G.-W., Niall, M., and Martin, T.J. (1988) Butter-Enriched Diets Reduce Arterial Prostacyclin-Production in Rats, *Lipids* 23, 234–241.
96. Salem, N., Jr., Wegher, B., Mena, P., and Uauy, R. (1996) Arachidonic and Docosahexaenoic Acids Are Biosynthesized from Their 18-Carbon Precursors in Human Infants, *Proc. Natl. Acad. Sci. USA* 93, 49–54.
97. Uauy, R., Mena, P., Wegher, B., Nieto, S., and Salem, N., Jr. (2000) Long Chain Polyunsaturated Fatty Acid Formation in Neonates: Effect of Gestational Age and Intrauterine Growth, *Pediatr. Res.* 47, 127–135.
98. Cunnane, S.C., Francescutti, V., Brenna, J.T., and Crawford, M.A. (2000) Breast-fed Infants Achieve a Higher Rate of Brain and Whole Body Docosahexaenoate Accumulation Than Formula-Fed Infants Not Consuming Dietary Docosahexaenoate, *Lipids* 35, 105–111.
99. Balendiran, G.K., Schnutgen, F., Scapin, G., Borchers, T., Xhong, N., Lim, K., Godbout, R., Spener, F., and Sacchettini, J.C. (2000) Crystal Structure and Thermodynamic Analysis of Human Brain Fatty Acid-Binding Protein, *J. Biol. Chem.* 275, 27045–27054.
100. Pawlosky, R., Barnes, A., and Salem, N., Jr. (1994) Essential Fatty Acid Metabolism in the Feline: Relationship Between Liver and Brain Production of Long-Chain Polyunsaturated Fatty Acids, *J. Lipid Res.* 35, 2032–2040.
101. Cho, H.P., Nakamura, M., and Clarke, S.D. (1999) Cloning, Expression, and Fatty Acid Regulation of the Human  $\Delta$ 5-Desaturase, *J. Biol. Chem.* 274, 37335–37339.
102. Weisinger, H.S., Vingrys, A.J., and Sinclair, A.J. (1996) The Effect of Docosahexaenoic Acid on the Electroretinogram of the Guinea Pig, *Lipids* 31, 65–70.
103. Jeffrey, B.G., Mitchell, D.C., Gibson, R.A., and Neuringer, M. (2002) n-3 Fatty Acid Deficiency Alters Recovery of the Rod Photoresponse in Rhesus Monkeys, *Invest. Ophthalmol. Vis. Sci.* 43, 2806–2814.
104. Jeffrey, B.G., Mitchell, D.C., Hibbeln, J.R., Gibson, R.A., Chedester, A.L., and Salem, N., Jr. (2002) Visual Acuity and Retinal Function in Infant Monkeys Fed Long-Chain PUFA, *Lipids* 37, 839–848.
105. De Deckere, E.A.M., Korver, O., Verschuren, P.M., and Katan, M. (1998) Health Aspects of Fish and n-3 Polyunsaturated Fatty Acids from Plant and Marine Origin, *Eur. J. Clin. Nutr.* 52, 749–753.
106. Mori, T.A., Bao, D.Q., Burke, V., Puddey, I.B., and Beilin, L.J. (1999) Docosahexaenoic Acid but Not Eicosapentaenoic Acid Lowers Ambulatory Blood Pressure and Heart Rate in Humans, *Hypertension* 34, 253–260.
107. Kang, J.X., and Leaf, A. (2000) Prevention of Fatal Cardiac Arrhythmias by Polyunsaturated Fatty Acids, *Am. J. Clin. Nutr.* 71, 202S–207S.
108. Price, P.T., Nelso, C.M., and Clarke, S.D. (2000) Omega 3 Polyunsaturated Fatty Acid Regulation of Gene Expression, *Curr. Opin. Lipidol.* 11, 3–7.
109. Singh, R.B., Niaz, M.A., Sharma, J.P., Kumar, R., Rastogi, V., and Moshiri, M. (1997) Randomized, Double-Blind, Placebo-Controlled Trial of Marine Omega-3 Oil and Mustard Oil in Patients with Suspected Acute Myocardial Infarction: The Indian Experiment of Infarct Survival-4, *Cardiovasc. Drugs Therap.* 11, 485–491.
110. De Lorgeril, M., Salen, P., Martin, J.-L., Moniaud, I., Delaye, I., and Mamelle, N. (1999) Mediterranean Diet, Traditional Risk Factors and Rate of Cardiovascular Complications After Myocardial Infarction: Final Report of the Lyon Diet Heart Study, *Circulation* 99, 779–785.
111. GISSI-Prevenzione Investigators (1999) Dietary Supplementation with n-3 Polyunsaturated Fatty Acids and Vitamin E After Myocardial Infarction: Results of the GISSI-Prevenzione Trial, *The Lancet* 354, 447–455.
112. Djousse, L., Pankow, J.S., Eckfeldt, J.H., Folsom, A.R., Hopkins, P.N., Province, M.A., Hong, Y., and Ellison, R.C. (2001) Relation Between Dietary Linolenic Acid and Coronary Artery Disease in the National Heart, Lung, and Blood Institute Family Heart Study, *Am. J. Clin. Nutr.* 74, 612–619.
113. Billman, G.E., Kang, J.X., and Leaf, A. (1999) Prevention of Sudden Cardiac Death by Dietary Pure Omega-3 Polyunsaturated Fatty Acids in Dogs, *Circulation* 99, 2452–2457.



114. Renaud, S., and Nordoy, A. (1983) "Small Is Beautiful":  $\alpha$ -Linolenic Acid and Eicosapentaenoic Acid in Man, *The Lancet* (May 21), 1169.
115. Dolecek, T.A. (1992) Epidemiological Evidence of Relationships Between Dietary PUFA and Mortality in the Multiple Risk Factor Intervention Trial, *Proc. Soc. Exp. Biol. Med.* 200, 177–182.
116. Hu, F.B., Stampfer, M.J., Manson, J.E., Rimm, E.B., Wolk, A., Colditz, G.A., Hennekens, C.H., and Willett, W.C. (1999) Dietary Intake of  $\alpha$ -Linolenic Acid and Risk of Fatal Ischemic Heart Disease Among Women, *Am. J. Clin. Nutr.* 69, 890–897.
117. Ferretti, A., and Flanagan, V.P. (1996) Antithromboxane Activity of Dietary  $\alpha$ -Linolenic Acid: A Pilot Study, *Prostaglandins Leukot. Essent. Fatty Acids* 54, 451–455.
118. Appel, L.J., Miller, E.R., 3rd, Seidler, A.J., and Whelton, P.K. (1993) Does Supplementation of Diet with "Marine Omega 3 Oil" Reduce Blood Pressure? A Meta-analysis of Controlled Clinical Trials, *Arch. Intern. Med.* 153, 1429–1438.
119. Nestel, P.J., Pomeroy, S.E., Sasahara, T., Yamashita, T., Liang, Y.L., Dart, A.M., Jennings, G.L., Abbey, M., and Cameron, J.D. (1997) Arterial Compliance in Obese Subjects Is Improved with Dietary Plant n-3 Fatty Acid from Flaxseed Oil Despite Increased LDL Oxidizability, *Arterioscler. Thromb. Vasc. Biol.* 17, 1163–1170.
120. McLellan, P.L., Abewardena, M.Y., and Charnock, J.S. (1988) Dietary Marine Omega 3 Oil Prevents Ventricular Fibrillation Following Coronary Artery Occlusion and Reperfusion, *Am. Heart J.* 116, 709–717.
121. Billman, G.E., Kang, J.X., and Leaf, A. (1997) Prevention of Ischemia-Induced Cardiac Sudden Death by n-3 Polyunsaturated Fatty Acids in Dogs, *Lipids* 32, 1161–1168.
122. Singh, R.B., Dubnov, G., Niaz, M.A., Ghosh, S., Singh, R., Rastogi, S.S., Manor, O., Pella, D., and Berry, E. (2002) Effect of an Indo-Mediterranean Diet on Progression of Coronary Artery Disease in High Risk Patients (Indo-Mediterranean Diet Heart Study): A Randomized Single-Blind Trial, *Lancet* 360, 1455–1466.
123. Giovannucci, E., Rimm, E.B., Colditz, G.A., Stampfer, M., Ascherio, A., Chute, C.C., and Willett, W. (1993) A Prospective Study of Dietary Fat and Risk of Prostate Cancer, *J. Natl. Cancer Inst.* 85, 1571–1579.
124. De Stéfani, E., Deneo-Pellegrini, H., Boffetta, P., Ronco, A., and Mendilaharsu, M. (2000)  $\alpha$ -Linolenic Acid and Risk of Prostate Cancer: A Case-Control Study in Uruguay, *Cancer Epidemiol. Biomarkers Prev.* 9, 335–338.
125. Ramon, J.M., Ricard, B., Romea, S., Alkiza, M.E., Jacas, M., Ribes, J., and Oromi, J. (2000) Dietary Intake and Prostate Cancer Risk: A Case-Control Study in Spain, *Cancer Causes Control* 11, 679–685.
126. Gann, P.H., Hennekens, C.H., Sacks, F.M., Grodstein, F., Giovannucci, E.L., and Stampfer, M.J. (1994) Prospective Study of Plasma Fatty Acids and Risk of Prostate Cancer, *J. Natl. Cancer Inst.* 86, 281–286.
127. Harvei, S., Bjerve, K.S., Tretli, S., Jellum, E., Robsahm, T.E., and Vatten, L. (1997) Prediagnostic Level of Fatty Acids in Serum Phospholipids:  $\omega$ -3 and  $\omega$ -6 Fatty Acids and the Risk of Prostate Cancer, *Int. J. Cancer* 71, 545–551.
128. Newcomer, L.M., King, I.B., Wicklund, K.G., and Stanford, J.L. (2001) The Association of Fatty Acids with Prostate Cancer, *The Prostate* 47, 262–268.
129. Andersson, S.O., Wolk, A., Bergstrom, R., Giovannucci, E., Lindgren, C., Baron, J., and Adami, H.O. (1996) Energy, Nutrition Intake and Prostate Cancer Risk: A Population-Based Case-Control Study in Sweden, *Int. J. Cancer* 68, 716–722.
130. Alberg, A.J., Kafonek, S., Huang, H.Y., Hoffman, S.C., Comstock, G.W., and Helzlsouer, K.J. (1996) Fatty Acid Levels and the Subsequent Development of Prostate Cancer, *Proc. Am. Assoc. Cancer Res.* 37, 281.
131. Godley, P.A., Campbell, M.K., Gallagher, P., Martinson, F.E., Mohler, J.L., and Sandler, R.S. (1996) Biomarkers of Essential Fatty Acid Consumption and Risk of Prostatic Carcinoma, *Cancer Epidemiol. Biomarkers Prev.* 5, 889–895.
132. Schuurman, A.G., van den Brandt, P.A., Dorant, E., Brants, H.A.M., and Goldbohm, R.A. (1999) Association of Energy and Fat Intake with Prostate Carcinoma Risk: Results from the Netherlands Cohort Study, *Cancer* 86, 1019–1027.
133. Freeman, V.L., Meydani, M., Yong, S., Pyle, J., Flanagan, R.C., Waters, B., and Wojcik, E.M. (2000) Prostatic Levels of Fatty Acids and the Histopathology of Localized Prostate Cancer, *J. Urology* 164, 2168–2172.
134. Cave, W.T., Jr. (1991) Dietary n-3 ( $\omega$ -3) Polyunsaturated Fatty Acid Effects on Animal Tumorigenesis, *FASEB J.* 5, 2160–2166.
135. Liang, T., and Liao, S. (1992) Inhibition of Steroid  $5\alpha$ -Reductase by Specific Aliphatic Unsaturated Fatty Acids, *Biochem. J.* 285, 557–562.
136. Marshall, L.A., Szczesniewski, A., and Johnston, P.V. (1983) Dietary  $\alpha$ -Linolenic Acid and Prostaglandin Synthesis: A Time Course Study, *Am. J. Clin. Nutr.* 38, 895–900.
137. Klein, V., Chajes, V., Germain, E., Schulgen, G., Pinault, M., Malvy, D., Lefrancq, T., Fignon, A., Le Floch, O., Lhuillery, C., and Bougnoux, P. (2000) Low  $\alpha$ -Linolenic Acid Content of Adipose Breast Tissue Is Associated with an Increased Risk of Breast Cancer, *Eur. J. Cancer* 36, 335–340.
138. Maillard, V., Bougnoux, P., Ferrari, P., Jourdain, M.L., Pinault, M., Lavillonniere, F., Body, G., Le Floch, O., and Chajes, V. (2002) n-3 and n-6 Fatty Acids in Breast Adipose Tissue and Relative Risk of Breast Cancer in a Case-Control Study in Tours, France, *Int. J. Cancer* 98, 78–93.
139. Cognault, S., Jourdan, M.L., Germain, E., Pitavy, R., Morel, E., Durand, G., Bougnoux, P. and Lhuillery, C. (2000) Effect of an  $\alpha$ -Linolenic Acid-Rich Diet on Rat Mammary Tumor Growth Depends on the Dietary Oxidative Status, *Nutr. Cancer* 36, 33–41.
140. Holman, R.T., Johnson, S.B., and Hatch, T.F. (1982) A Case of Human Linolenic Acid Deficiency Involving Neurological Abnormalities, *Am. J. Clin. Nutr.* 35, 617–623.
141. Bjerve, K.S., Thoresen, L., and Borsting, S. (1998) Linseed and Cod Liver Oil Induce Rapid Growth in a 7-Year-Old Girl with n-3 Fatty Acid Deficiency, *JPEN J. Parenter. Enteral Nutr.* 12, 521–525.
142. NHMRC: Report of Working Party (1992) *The Role of Polyunsaturated Fatty Acids in the Australian Diet*, Australian Government Publishing Service, Canberra.
143. Simopoulos, A.P., Leaf, A., and Salem, N. (2000) Workshop Statement on the Essentiality of and Recommended Intakes for Omega 6 and Omega 3 Fatty Acids, *Prostaglandins Leukot. Essent. Fatty Acids* 63, 119–121.
144. Lands, W.E.M., Libelt, B., Morris, A., Kramer, N.C., Prewitt, T.E., Bowen, P., Schmeisser, D., and Davidson, M.H. (1992) Maintenance of Lower Proportions of (n-6) Eicosanoid Precursors in Phospholipids of Human Plasma in Response to Added Dietary (n-3) Fatty Acids, *Biochim. Biophys. Acta* 1180, 147–162.
145. Blank, C., Neumann, M.A., Makrides, M., and Gibson, R.A. (2002) Optimizing DHA Levels in Piglets by Lowering the Linoleic Acid to  $\alpha$ -Linolenic Acid Ratio, *J. Lipid Res.* 43, 1537–1543.

[Received March 18, 2002, and in revised form December 9, 2002; revision accepted December 17, 2002]

# The Effects of Vitamin E and Selenium Intake on Oxidative Stress and Plasma Lipids in Hamsters Fed Fish Oil

Johanne Poirier<sup>a</sup>, Kevin Cockell<sup>b</sup>, Nick Hidirolou<sup>b</sup>,  
Rene Madere<sup>b</sup>, Keith Trick<sup>b</sup>, and Stan Kubow<sup>a,\*</sup>

<sup>a</sup>School of Dietetics and Human Nutrition, Macdonald Campus of McGill University, Québec, H9X 3V9, Canada, and

<sup>b</sup>Nutrition Research, Food Directorate, Health Protection Branch of Health Canada, Banting Research Centre, Ottawa, Ontario, Canada K1A 0L2

**ABSTRACT:** The aim of the present work was to test the effects of large-dose supplementation of vitamin E (Vit E) and selenium (Se), either singly or in combination, on fish oil (FO)-induced tissue lipid peroxidation and hyperlipidemia. The supplementation of Se has been shown to lower blood cholesterol and increase tissue concentrations of the antioxidant glutathione (GSH); however, the effects of Se supplementation, either alone or in combination with supplemental Vit E, on FO-induced oxidative stress and hyperlipidemia have not been studied. Male Syrian hamsters received FO-based diets that contained 14.3 wt% fat and 0.46 wt% cholesterol supplemented with Vit E (129 IU D- $\alpha$ -tocopheryl acetate/kg diet) and/or Se (3.4 ppm as sodium selenate) or that contained basal requirements of both nutrients. The cardiac tissue of hamsters fed supplemental Se showed increased concentrations of lipid hydroperoxides (LPO) but decreased oxidized glutathione (GSSG) concentrations. The higher concentrations of LPO in the hearts of Se-supplemented hamsters were not lowered with concurrent Vit E supplementation. In the liver, Se supplementation was associated with higher Se-dependent glutathione peroxidase activity and an increase in the GSH/GSSG ratio, whereas a lower hepatic non-Se-dependent glutathione peroxidase activity was seen with Vit E supplementation. Supplemental intake of Se was associated with lower plasma concentrations of total cholesterol and low density lipoprotein cholesterol plus very low density lipoprotein cholesterol. In view of the pro-oxidative effects of Se supplementation on cardiac tissue, a cautionary approach needs to be taken regarding the plasma lipid-lowering properties of supplemental Se.

Paper No. L9017 in *Lipids* 37, 1125–1133 (December 2002).

Fish oil (FO) consumption generally has been associated with a beneficial lowering of plasma concentrations of triglycerides (TG) and very low density lipoprotein cholesterol (VLDL) (1). The effect of FO ingestion on plasma lipids, however, is not always beneficial, as demonstrated by increased concentrations of

plasma low density lipoprotein cholesterol (LDL) and a lowering of high density lipoprotein cholesterol (HDL) in some human and animal feeding trials (2). In addition, intake of FO without adequate antioxidant supplementation is commonly associated with increased *in vivo* lipid peroxidation and decreased tissue antioxidant content in the plasma, heart, and liver (3,4). The enhanced *in vivo* lipid peroxidation induced by FO has been attributed to an increased unsaturation of membrane phospholipids resulting from the intake of highly unsaturated n-3 PUFA, such as eicosapentaenoic acid (EPA) and docosahexaenoic acid (DHA) found in FO (3,4). Because the enzymes of cholesterol biosynthesis reside in the plasma membrane of the endoplasmic reticulum, which is rich in PUFA content, the increased lipid peroxidation associated with FO intake has been related to FO-induced hyperlipidemia (5).

Lipid peroxidation results in the formation of lipid hydroperoxides (LPO), which are substrates for cytosolic glutathione peroxidase (GSHPx). Selenium (Se) is an essential component for Se-dependent glutathione peroxidase (SeGSHPx) and has been shown to inhibit lipid peroxidation and hyperlipidemia when supplemented at doses above basal requirements (6). There is also non-selenium-dependent glutathione peroxidase (non-SeGSHPx) activity found in the cytosol that consists of the activity of some glutathione S-transferases. These glutathione S-transferases catalyze reactions of organic peroxides but not hydrogen peroxide with GSH to form oxidized glutathione (GSSG) and alcohols. The distribution of cellular SeGSHPx and glutathione S-transferases varies among tissues and species. Total GSHPx activity is measured using *t*-butylperoxide, as it detects both SeGSHPx and glutathione S-transferases.

Supplementation of Se is associated with higher hepatic concentrations of GSH (7,8), a potent intracellular inhibitor of lipid peroxidation (9). Vitamin E (Vit E), known to inhibit the chain reaction of lipid peroxidation in the membrane, has a sparing effect on the requirement of Se (10). However, the effects of a combined supplemental intake of Vit E and Se on inhibiting *in vivo* lipid peroxidation and on modulating tissue levels of GSH, SeGSHPx, and non-SeGSHPx activity have not been examined previously. Since Vit E has been shown to be only partially effective at inhibiting *in vivo* lipid peroxidation induced by FO ingestion (11), a supplemental combination of Vit E and Se could be more effective in this regard. Moreover, as supplementation of Vit E (12) and Se (6) have both been associated with decreased plasma concentrations of total cholesterol (TC) and LDL, the combined supplementation of these nutrients may

\*To whom correspondence should be addressed at School of Dietetics and Human Nutrition, Macdonald Campus of McGill University, 21,111 Lakeshore, Ste-Anne-de-Bellevue, Québec, H9X 3V9, Canada.  
E-mail: Stan.Kubow@McGill.ca

Abbreviations: DHA, docosahexaenoic acid; EPA, eicosapentaenoic acid; FO, fish oil; GSH, reduced glutathione; GSHPx, glutathione peroxidase; GSSG, oxidized glutathione; HDL, high density lipoprotein cholesterol; LDL, low density lipoprotein cholesterol; LDL + VLDL, low density lipoprotein cholesterol + very low density lipoprotein cholesterol; LPO, lipid hydroperoxides; non-SeGSHPx, non-selenium-dependent glutathione peroxidase; NRC, National Research Council; SeGSHPx, selenium-dependent glutathione peroxidase; TC, total cholesterol; TE, tocopherol equivalents; TG, triglyceride; Vit E, vitamin E; VLDL, very low density lipoprotein cholesterol.

**TABLE 1**  
**Composition of Experimental Diets (g/kg)<sup>a</sup>**

Ingredients	FO	FO + Se	FO + Vit E	FO + Vit E + Se
Casein, vitamin-free	159.1	159.1	159.1	159.1
Cornstarch	306.1	305.4	305.9	305.2
Sucrose	176.1	176.1	176.1	176.1
Dextrose	98.9	98.9	98.9	98.9
Cellulose	43	43	43	43
FO <sup>b</sup>	129	129	129	129
Safflower oil <sup>c</sup>	13.8	13.8	13.8	13.8
Cholesterol, USP <sup>d</sup>	4.2	4.2	4.2	4.2
Mineral mix <sup>e</sup>	43	43	43	43
Vitamin mix <sup>f</sup>	8.6	8.6	8.6	8.6
Choline bitartrate	11.2	11.2	11.2	11.2
Sodium selenate	0.046	0.8229	0.046	0.8229
Vit E acetate	0.052	0.052	0.256	0.256
Metabolizable energy, MJ/kg	15.4	15.4	15.4	15.4

<sup>a</sup>FO = fish oil; FO + Se = fish oil + selenium; FO + Vit E = fish oil + vitamin E; FO + Vit E + Se = fish oil + vitamin E + selenium. All diets were formulated at McGill University and prepared in pellet form by Dyets Inc. (Bethlehem, PA).

<sup>b</sup>Menhaden oil (MO) was refined and antioxidant free. FA composition of FO is as follows (% by wt): 14:0, 6.85; 15:0, 0.46; 16:0, 14.83; 16:1, 9.74; 16:2, 1.62; 16:3, 1.51; 16:4, 1.53; 17:0, 0.38; 18:0, 2.55; 18:1, 9.58; 18:2, 1.93; 18:3, 1.48; 18:4, 3.09; 19:0, 0.00; 20:0, 0.17; 20:1, 1.48; 20:2, 0.18; 20:3, 0.37; 20:4, 2.09; 20:5, 14.16; 21:5, 0.76; 22:0, 0.10; 22:1, 0.33; 22:4, 0.24; 22:5, 2.82; 22:6, 10.26; 24:0, 0.60; 24:1, 0.22. Remaining percentage is composed of the weight of unidentified FA and glycerol. MO was analyzed for pesticides and found to contain 0.07 µg/g α-BHC and 0.20 µg/g *p,p'*-DDE [method detection limit (MDL) of 0.02 µg/g]. Results of mineral analysis of MO include (µg/g): mercury <0.05, copper 0.6 (MDL of 0.3 µg/g), lead <2.5, selenium <5, arsenic <6, tin <1.8, cadmium <0.3.

<sup>c</sup>Safflower oil (SAFF) was added to prevent EFA deficiency. Vit E concentration of SAFF is 350 ppm α-tocopherol, 180 ppm other tocopherols. FA profile of SAFF included (% by wt): 14:0, trace; 16:0, 6.9; 16:1, trace; 18:0, 2.9; 18:1, 12.2; 18:2, 78.0; 18:3, trace.

<sup>d</sup>Cholesterol, USP, added to MO 4.535 g/kg. MO contains 350 mg cholesterol/100 g MO.

<sup>e</sup>The mineral mix was free of Se and was composed of (g/kg): calcium carbonate 336.4; calcium phosphate, monobasic 285.0; magnesium oxide 2.985; potassium iodate (10 mg KI/g) 0.76; potassium phosphate, dibasic 40.76; sodium chloride 11.45; cupric carbonate 0.084; cobalt chloride 0.133; sodium fluoride 0.002; ferric citrate 25.45; manganous carbonate 0.229; ammonium paramolybdate 0.008; zinc carbonate 0.53; sucrose 296.209. Sodium selenate (10 mg/g sodium selenate) was added separately to make the diets; for basal Se diets 0.046; for high Se diets 0.8229.

<sup>f</sup>The vitamin mix was free of Vit E and was composed of (g/kg): vitamin A palmitate (500 IU/g) 6.88; vitamin D<sub>3</sub> (400,000 IU/g) 0.9315; vitamin K<sub>1</sub> premix (10 mg/g) 110.0; biotin 0.03; folic acid 0.3; niacin 13.5; pantothenate (Ca) 1.5; riboflavin 2.25; thiamine HCl 3.0; pyridoxine HCl 0.9; vitamin B<sub>12</sub> (0.1%) 1.5; sucrose 866.0885. Vit E acetate (500 IU/g) was added separately to make the diets; for basal Vit E diets 0.052; for high Vit E 0.260.

exert synergistic plasma cholesterol-lowering effects in association with FO feeding.

In the present study, the effects of Vit E and Se supplementation were studied in association with FO feeding with respect to: (i) endogenously produced GSH, SeGSHPx, and non-SeGSHPx activity; (ii) *in vivo* lipid peroxidation; and (iii) plasma lipid concentrations. The plasma, heart, and liver were examined to investigate whether these tissues respond similarly to the effects of Se and Vit E supplementation on FO-induced *in vivo* lipid peroxidation.

## MATERIALS AND METHODS

**Animals and diets.** Thirty-two male Golden Syrian hamsters weighing on average 112 ± 3 g at 10 wk of age were obtained from Charles River Laboratories (St-Constant, Québec, Canada). Eight animals were randomly assigned to each one of the four dietary treatments for 3 wk after being acclimatized for 4 wk. Hamsters began consuming their respective diets in a staggered manner. The staggered procedure involved the inclusion of one hamster randomly chosen from each diet so that four hamsters began consuming their respective diets, one hamster from each diet per day. The staggered

design was necessary in order to allow for equal sampling across treatment groups at the end of the experiment when animals were killed in a staggered manner over several days. Diets were prepared in pellet form and vacuum packed by Dyets (Bethlehem, PA). Diets were kept refrigerated at 4°C. One bag was opened every week to feed the hamsters for the upcoming week. The exact composition of the diets is given in Table 1. The basal diet consisted by weight of 15.9% vitamin-free casein, 12.9% FO, 1.38% safflower oil, 0.46% cholesterol, 30.24% cornstarch, 9.9% dextrinized cornstarch, 18.64% sucrose, 4.3% cellulose, 4.3% mineral mix (without Se), 0.86% vitamin mix (without Vit E), and 1.12% choline bitartrate. Suitable vitamin and mineral mixes for hamster needs were developed following the National Research Council (NRC) requirements (13) and were given at 1.3 times the requirements to ensure an adequate intake of those nutrients. Separate additions of Se and Vit E were made for the final formulations of the diets. The basal Se diet provided 0.19 mg of Se/kg diet, whereas the supplemental Se diet provided 3.4 mg of Se/kg diet as sodium selenate (Na<sub>2</sub>SeO<sub>3</sub>). The basal Vit E diet provided 27 IU tocopherol acetate/kg diet, whereas the supplemental Vit E diet provided 129 IU of tocopherol acetate/kg diet [10 tocopherol equivalents (TE) = 10 mg D-α-



tocopherol = 15 IU]. The diets included: (i) FO; (ii) FO + Vit E; (iii) FO + Se; and (iv) FO + Vit E + Se.

Hamsters were housed in a room of controlled light (light 0700–1900 h) in plastic-bottomed cages and fed diets and tap water *ad libitum*. Fresh diets were fed to the hamsters daily and uneaten food was discarded. Food consumption was measured daily and body weights were recorded weekly. Care and handling of the hamsters conformed to the guidelines of the McGill University Animal Care Committee and Canadian Council of Animal Care (14).

**Sample preparation.** At the end of the feeding period, the hamsters were fasted 13.5 to 20 h. They were anesthetized with CO<sub>2</sub> and killed by exsanguination after cardiac puncture. Blood was drawn into vacutainer tubes containing EDTA. The plasma was immediately isolated by centrifugation at 1,500 × *g*, 4°C, for 10 min and aliquoted into microcentrifuge tubes. Liver and heart were immediately removed, rinsed in ice-cold saline, blotted, and rapidly frozen in liquid nitrogen. Both plasma and tissues were stored at –80°C until analysis.

## EXPERIMENTAL PROCEDURES

**Plasma lipids.** Automated enzymatic methodology using the Abbott VP Super System (Abbott, Irving, TX) with Abbott enzymatic reagent kits measured plasma TG (Abbott Kit 6097), TC (Abbott Kit 6095), and HDL (Abbott Kit 6039). LDL + VLDL were calculated from the difference between TC and HDL.

**Plasma TBARS.** Plasma concentrations of TBARS were measured using a modified method of Asakawa and Matsushita (15) and Wong *et al.* (16). A standard curve was constructed using a 1,1,3,3-tetramethoxypropane solution (Sigma T 9889; St. Louis, MO) (1200 μmol/L 0.01M HCl). The assay consisted of 100 μL of plasma or standard, 12.5 μL of thiobarbituric acid solution (Sigma T 5500) (110.99 mmol/L, 0.1 M NaOH), 100 μL of 85% aqueous orthophosphoric acid solution (Fisher A242-1; Fairlawn, NJ) (11.56 mmol/L), and 12.5 μL of BHT solution (Sigma B 1378) (3 mmol/L ethanol) to a final volume of 225 μL. Samples and standards were heated for 45 min at 90°C in a boiling water bath. After cooling, 250 μL of *n*-butanol (Sigma 19417) and 25 μL of saturated sodium chloride were added. Following centrifugation, the extraction of both sample and standard was accomplished with removal of 200 μL of *n*-butanol upper phase to microtiter plate wells. Plasma TBARS were expressed as μmol/mL of plasma. Absorbance was read at 540 and 590 nm using the series 750 microtiter plate reader (Cambridge Technology, Inc., Cambridge, MA).

**Total GSHPx, SeGSHPx, and non-SeGSHPx (glutathione S-transferase) activity.** Tissue supernatants were assayed for total GSHPx and SeGSHPx activity using an automated modification (17) of the coupled assay of Paglia and Valentine (18). The assay mixture was prepared fresh daily and contained 150 mM potassium phosphate buffer (pH 7.0); potassium phosphate, monobasic (Sigma P 5379); potassium phosphate, dibasic (P 5504), 5 mM EDTA, disodium salt (Sigma E 5134); 0.5 mM sodium azide (Sigma S 2002); 2 mM GSH (reduced, crystalline-free acid) (Sigma G 6654); 0.24 mM NADPH (Sigma

N 6505); and 1 U/mL of glutathione reductase (GSSGRase, EC 1.6.4.2) (Sigma G 3664). Total GSHPx activity and SeGSHPx activity were determined using 1.2 mM and 0.3 mM *t*-butylperoxide (Sigma B 2633) as substrates, respectively. The blank activity was significantly lower with 0.3 mM *t*-butylperoxide than with hydrogen peroxide, and for this reason *t*-butylperoxide was used instead. The ability to detect only SeGSHPx activity using a concentration of 0.3 mM *t*-butylperoxide was also confirmed in a study by Prohaska (19). Non-SeGSHPx activity due to glutathione S-transferases was determined from the difference between total GSHPx activity and SeGSHPx activity. Reactions were carried out using the Abbott VP Super System at 37°C with a 340/380 nm filter. The sample cuvette contained 250 μL of the assay mixture and 5 μL of sample. The reaction was initiated by the addition of substrate. One unit (U) of activity catalyzes the oxidation of 1.0 μmol of reduced NADPH per min, and was expressed as mU/mg of protein.

**Tissue GSH and GSSG.** The detection of GSH and GSSG was done using a Cayman chemical kit (GSH Assay Kit Cat# 703002; Ann Arbor, MI). The kit protocol was modified by homogenizing tissue using a homogenizing buffer made up of 5% sulfosalicylic acid (wt/vol) at pH 1.0 in order to maintain the ratio of GSH/GSSG, which is subject to radical change without the acidic pH (20). Protein content was extracted by adding metaphosphoric acid (Aldrich 23,927-5; Milwaukee, WI) and centrifuging at 3,000 × *g* for 5 min. Supernatant was then stored at –80°C for later analysis. For the final analysis, the supernatant was adjusted to pH 7.0 with the addition of triethanolamine (Aldrich T5, 830-0) and diluted so that absorbance of the sample fell within the absorbance of the standard curve values specified by the kit protocol. GSSG was measured by derivatizing GSH with 2-vinylpyridine. The ELX 8081U Ultra Microplate reader (Bio-Tek, Inc., Winooski, VT) was used along with the KC4 Kinetic software for Windows version 2.6 RevXX (Bio-TEK) using a 405 nm filter.

**Tissue LPO.** Heart and liver were analyzed for LPO using an LPO kit assay (Kamiya Biomedical, Thousand Oaks, CA) based on the method of Oshishi *et al.* (21). The lipid was extracted by the method of Folch *et al.* (22). The absorbance of the sample was determined at 620 nm using the series 750 microtiter plate reader (Cambridge Technology, Inc.).

**Tissue Vit E.** α-Tocopherol content of heart and liver tissue was measured by the HPLC method of Thompson and Hatina (23). Tissues were homogenized in water, diluted 1:1 with ethanol to de-proteinize them, and the tocopherols were extracted with heptane. Samples of 100 μL volume were injected for HPLC separation on a silica column [25 cm × 4.6 mm i.d., 5 μm particle size, Supelcosil LC-SI (Supelco Canada Ltd., Oakville, Ontario, Canada)] using a Waters 717+ autosampler (Waters Scientific Ltd., Mississauga, Ontario, Canada), Waters model 510 pump, and PerkinElmer 650 fluorescence detector. The mobile phase (1% 2-propanol in hexane) was degassed by sonication and run at a flow rate of 2 mL/min at ambient temperature. Detector settings were as follows: excitation wavelength 290 nm and slit 10 nm, emission wavelength 320 nm and slit 12 nm. A threefold higher detector



**TABLE 2**  
ANOVA of the Effects of Dietary Vit E and Se Supplementation on Body Weight Gain and Average Daily Intake of Adult Male Syrian Hamsters Fed FO Diets for 3 wk<sup>a</sup>

Variable	Dietary treatment				Significance of main and interaction effects <sup>b</sup>		
	FO	FO + Se	FO + Vit E	FO + Vit E + Se	Vit E	Se	Vit E × Se
Average daily intake (g/d)	5.90 ± 0.12 <sup>a</sup>	6.03 ± 0.12 <sup>a</sup>	5.79 ± 0.12 <sup>b</sup>	5.58 ± 0.12 <sup>b</sup>	0.05	NS	NS
Body weight gain (g)	-1.4 ± 1.9	-0.60 ± 1.9	-4.5 ± 1.9	-4.9 ± 1.9	NS	NS	NS

<sup>a</sup>Values are mean ± SEM ( $n = 8$ ). Diets and abbreviations are as indicated in Table 1. Means within rows with no common roman superscript letter differ significantly ( $P < 0.05$ ). NS = nonsignificant.

<sup>b</sup>The four interaction effects include FO = basal Vit E × basal Se; FO + Se = basal Vit E × supplemental Se; FO + Vit E = supplemental Vit E × basal Se; and FO + Vit E + Se = supplemental Vit E × supplemental Se. Main effects include the effect of basal Vit E vs. supplemental Vit E and basal Se vs. supplemental Se.

sensitivity was used for measurement of  $\alpha$ -tocopherol in heart because of the lower levels of Vit E compared to liver.

**Tissue protein.** Protein concentrations of all supernatants were determined using the biuret assay (Abbott Total Protein Kit# LN5A13-26). BSA was used as standard. Homogenates were centrifuged for 5 min at 12,000 ×  $g$  and supernatants assayed. The Abbott VP Super System was used.

**Data analysis.** Data were tested using the mixed model procedure for all analyses of SAS 6.2 (24). The aim of the study was to determine whether Vit E and Se had independent or interaction effects on the dependent variables tested. Hence, the main effects of the Vit E and Se treatments and their possible interaction effects were assessed using a fixed-effect 2 × 2 factorial design. Data were assessed for normality (univariate) and homogeneity of variance using a mixed model procedure. Blocking was an integral part of the experimental design owing to the staggered feeding that occurred in distinct blocks over time. Blocking was therefore considered

to be a source of variation and was included as a variable in the statistical model to ensure that it did not interfere with or confound the significant effect of treatment on the dependent variable. The average daily food intake and body weight gain were considered in the statistical model as co-variables; however, these co-variables were found not to affect the results significantly and so were omitted from the model. The statistical significances of the differences between least square means were determined using the Scheffé test. Differences of  $P < 0.05$  were considered significant.

## RESULTS

**Average daily food intake.** A significant main effect of Vit E ( $P < 0.05$ ) on average daily food intake was observed. Fewer grams of diet were consumed by hamsters fed the diets supplemented with Vit E than by hamsters fed the diets not supplemented with Vit E (Table 2).

**TABLE 3**  
ANOVA of the Effects of Dietary Vit E and Se Supplementation on Plasma Lipid Concentrations (TC, LDL + VLDL, HDL, TG, and LDL + VLDL/HDL Ratios) of Adult Male Syrian Hamsters Fed FO Diets for 3 wk<sup>a</sup>

Variable	Dietary treatment				Significance of main and interaction effects <sup>b</sup>		
	FO	FO + Se	FO + Vit E	FO + Vit E + Se	Vit E	Se	Vit E × Se
TC (mg/dL)	285 ± 16 <sup>a</sup>	220 ± 16 <sup>b</sup>	265 ± 15 <sup>b</sup>	233 ± 16 <sup>b</sup>	NS	0.01	NS
LDL + VLDL (mg/dL)	228 ± 16 <sup>a</sup>	171 ± 16 <sup>b</sup>	218 ± 16 <sup>a</sup>	172 ± 16 <sup>b</sup>	NS	0.005	NS
HDL (mg/dL)	57 ± 5	48 ± 5	47 ± 5	62 ± 5	NS	NS	0.05
LDL + VLDL/HDL	4 ± 2	4 ± 2	8 ± 2	3 ± 2	NS	NS	NS
TG (mg/dL)	220 ± 20	154 ± 20	181 ± 20	214 ± 20	NS	NS	0.05

<sup>a</sup>Values are mean ± SEM ( $n = 8$ ). Means within rows with no common superscript roman letter differ significantly ( $P < 0.05$ ). Diets and abbreviations are as indicated in Table 1. TC, total cholesterol; LDL + VLDL, low density lipoprotein + very low density lipoprotein cholesterol; HDL, high density lipoprotein cholesterol; LDL + VLDL/HDL, low density lipoprotein + very low density lipoprotein cholesterol/high density lipoprotein cholesterol ratio; TG, triglyceride; for other abbreviation see Table 2.

<sup>b</sup>The four interaction effects include FO = basal Vit E × basal Se; FO + Se = basal Vit E × supplemental Se; FO + Vit E = supplemental Vit E × basal Se; and FO + Vit E + Se = supplemental Vit E × supplemental Se. Main effects include the effect of basal Vit E vs. supplemental Vit E and basal Se vs. supplemental Se.

**TABLE 4**  
ANOVA of the Effects of Dietary Vit E and Se Supplementation on Heart LPO, GSH, GSSG, SeGSHPx Activity, Non-SeGSHPx Activity, and Vit E of Adult Male Syrian Hamsters Fed FO Diets for 3 wk<sup>a</sup>

Variable	Dietary treatment				Significance of main and interaction effects <sup>b</sup>		
	FO	FO + Se	FO + Vit E	FO + Vit E + Se	Vit E	Se	Vit E × Se
LPO (nmol/g protein)	834 ± 170 <sup>a</sup>	1430 ± 170 <sup>b</sup>	883 ± 170 <sup>a</sup>	1080 ± 170 <sup>b</sup>	NS	0.05	NS
GSH (μmol/g protein)	16 ± 1	16 ± 1	16 ± 1	16 ± 1	NS	NS	NS
GSSG (μmol/g protein)	11 ± 2 <sup>a</sup>	5 ± 2 <sup>b</sup>	7 ± 2 <sup>a</sup>	6 ± 2 <sup>b</sup>	NS	0.05	NS
SeGSHPx (units/mg protein)	40 ± 4	50 ± 4	45 ± 4	44 ± 4	NS	NS	NS
Non-SeGSHPx (units/mg protein)	10 ± 2	11 ± 2	9 ± 2	13 ± 2	NS	NS	NA
Vit E (μg/g protein)	10 ± 10 <sup>a</sup>	12 ± 10 <sup>a</sup>	86 ± 10 <sup>b</sup>	73 ± 10 <sup>b</sup>	0.005	NS	NS

<sup>a</sup>Values are mean ± SEM ( $n = 8$ ). Means within rows with no common superscript roman letter differ significantly ( $P < 0.05$ ). LPO, lipid hydroperoxides; GSH, glutathione; GSSG, oxidized glutathione; SeGSHPx, Se-dependent glutathione peroxidase activity; Non-SeGSHPx, non-Se-dependent glutathione peroxidase activity. Diets and abbreviations are as indicated in Tables 1 and 3.

<sup>b</sup>The four interaction effects include FO = basal Vit E × basal Se; FO + Se = basal Vit E × supplemental Se, FO + Vit E = supplemental Vit E × basal Se, and FO + Vit E + Se = supplemental Vit E × supplemental Se. Main effects include the effect of basal Vit E vs. supplemental Vit E and basal Se vs. supplemental Se.

**Body weight gain.** Neither Vit E nor Se was associated with any significant effects on body weight gain (Table 2).

**Plasma lipids.** As shown in Table 3, a significant main effect of Se on plasma TC and LDL + VLDL concentrations ( $P < 0.01$  and  $P < 0.005$ , respectively) was observed. The plasma of hamsters supplemented with Se had 18% lower TC concentrations and 23% lower LDL + VLDL than plasma of the non-Se-supplemented groups (Table 3). A significant interaction effect of Vit E × Se on plasma HDL and TG concentrations was observed ( $P < 0.05$  and  $P < 0.05$ , respectively)

(Table 3); however, no significant difference between groups was observed *via* the Scheffé multiple comparison test. Blocking was shown to affect significantly the concentrations of TC ( $P < 0.005$ ), LDL + VLDL ( $P < 0.001$ ), and TG ( $P < 0.05$ ).

**Plasma TBARS.** Neither Vit E nor Se was associated with any significant effect on plasma TBARS concentrations (data not shown).

**Tissue LPO.** A significant main effect of Se ( $P < 0.05$ ) on concentrations of LPO was observed in the heart (Table 4). The supplementation of Se to FO diets resulted in a higher

**TABLE 5**  
ANOVA of the Effects of Dietary Vit E and Se Supplementation on Liver LPO, GSH, GSSG, GSH/GSSG Ratios, SeGSHPx Activity, Non-SeGSHPx Activity, and Vit E of Adult Male Syrian Hamsters Fed FO Diets for 3 wk<sup>a</sup>

Variable	Dietary treatment				Significance of main and interaction effects <sup>b</sup>		
	FO	FO + Se	FO + Vit E	FO + Vit E + Se	Vit E	Se	Vit E × Se
LPO (nmol/g protein)	484 ± 70	494 ± 70	467 ± 70	592 ± 70	NS	NS	NS
GSH (μmol/g protein)	45 ± 4	49 ± 4	40 ± 4	40 ± 4	NS	NS	NS
GSSG (μmol/g protein)	8 ± 1	7 ± 1	8 ± 1	5 ± 1	NS	NS	NS
GSH/GSSG	6 ± 1 <sup>a</sup>	9 ± 1 <sup>b</sup>	6 ± 1 <sup>a</sup>	10 ± 1 <sup>b</sup>	NS	0.05	NS
SeGSHPx (units/mg protein)	280 ± 8 <sup>a</sup>	290 ± 8 <sup>b</sup>	257 ± 8 <sup>a</sup>	292 ± 8 <sup>b</sup>	NS	0.05	NS
Non-SeGSHPx (units/mg protein)	73 ± 6 <sup>a</sup>	66 ± 6 <sup>a</sup>	57 ± 6 <sup>b</sup>	55 ± 6 <sup>b</sup>	0.05	NS	NS
Vit E (μg/g protein)	528 ± 100 <sup>a</sup>	613 ± 100 <sup>a</sup>	1110 ± 100 <sup>b</sup>	939 ± 100 <sup>b</sup>	0.0005	NS	NS

<sup>a</sup>Values are mean ± SEM ( $n = 8$ ). Means within rows with no common superscript roman letter differ significantly ( $P < 0.05$ ). Diets and abbreviations are as indicated in Table 1. For other abbreviations see Tables 2–4.

<sup>b</sup>The four interaction effects include FO = basal Vit E × basal Se; FO + Se = basal Vit E × supplemental Se, FO + Vit E = supplemental Vit E × basal Se, and FO + Vit E + Se = supplemental Vit E × supplemental Se. Main effects include the effect of basal Vit E vs. supplemental Vit E and basal Se vs. supplemental Se.

heart concentration of LPO as compared to hamsters receiving FO alone. In the liver, neither Vit E nor Se was associated with any significant effect on LPO concentrations (Table 5). Blocking was associated with significant effects on heart and liver LPO ( $P < 0.01$ ).

**Tissue GSH.** Neither Vit E nor Se was associated with any significant effects on heart GSH concentrations (Table 4). Also in the liver, neither Vit E nor Se was associated with any significant effects on liver GSH concentrations (Table 5). Blocking was associated with significant effects on heart GSH ( $P < 0.0001$ ) and liver GSH ( $P < 0.05$ ).

**Tissue GSSG.** A significant main effect of Se ( $P < 0.05$ ) on heart GSSG concentration was observed (Table 4). The supplementation of Se was associated with significantly lower levels of GSSG in the heart as compared to the hamsters not supplemented with Se (Table 4). In the liver, neither Vit E nor Se was associated with any significant effects on GSSG concentrations (Table 5). Blocking was associated with significant differences in heart and hepatic GSSG concentrations ( $P < 0.005$ ).

**Tissue GSH/GSSG ratio.** Neither Vit E nor Se was associated with any significant effects on heart GSH/GSSG ratios (data not shown). In the liver, a significant main effect of Se ( $P < 0.05$ ) on GSH/GSSG ratios (Table 5) was seen. Hamsters fed the diets supplemented with Se had significantly higher liver GSH/GSSG ratios compared to hamsters not fed supplemental Se (Table 5). The hepatic GSH/GSSG ratio was affected significantly by blocking ( $P < 0.05$ ).

**Tissue SeGSHPx activity.** Neither Vit E nor Se was associated with any significant effects on heart SeGSHPx activity (Table 4). For liver SeGSHPx activity, a main effect of Se ( $P < 0.05$ ) was observed (Table 5). The supplementation of Se was shown to increase SeGSHPx activity in the liver. SeGSHPx activity was significantly affected by blocking in the heart ( $P < 0.05$ ) and liver ( $P < 0.0001$ ).

**Tissue non-SeGSHPx (glutathione S-transferase) activity.** Neither Vit E nor Se was associated with any significant effect on heart non-SeGSHPx activity (Table 4). In the liver, a significant main effect of Vit E ( $P < 0.05$ ) on non-SeGSHPx activity was observed (Table 5). The supplementation of Vit E was associated with a decrease in hepatic non-SeGSHPx activity. Liver non-SeGSHPx activity was affected significantly by blocking ( $P < 0.05$ ).

**Tissue Vit E.** A significant main effect of Vit E ( $P < 0.005$ ) on Vit E concentrations was observed in the heart (Table 4). The Vit E-supplemented hamsters had significantly higher concentrations of Vit E in the heart compared to the hamsters not supplemented with Vit E (Table 4). In the liver, a significant main effect of Vit E ( $P < 0.0005$ ) on Vit E concentrations was observed (Table 5). The Vit E-supplemented hamsters had significantly higher concentrations of Vit E in the liver compared to the hamsters not supplemented with Vit E (Table 5).

## DISCUSSION

The aim of the present work was to test the effects of large-dose supplementation of Vit E and Se, when provided either

singly or in combination, on FO-induced tissue lipid peroxidation and hyperlipidemia. Although Se supplementation was not associated with differences in indicators of oxidative stress in the liver and plasma, a higher cardiac LPO content was shown with Se supplementation. This observation is in marked contrast to the observations of Jamall *et al.* (25), who noted a decrease in cardiac TBARS content in myopathic Syrian Golden hamsters receiving dietary Se supplementation at a level of 1 ppm in a standard laboratory diet. In addition to differences in hamster strains, the 3.5 higher dose of Se used in the present study may have exerted a pro-oxidative action in concert with the FO-rich diet. The dose of Se (3.4 ppm) used in the present work was chosen to be comparable to, but more moderate than, the level of 5 ppm dietary Se used in the work of Vinson *et al.* (6), which showed significant plasma lipid- and plasma lipid peroxide-lowering effects in Syrian hamsters fed Se in conjunction with a low-fat diet.

The supplementation of Se also showed no detrimental effects on the histopathology of major organ systems when Syrian hamsters were fed 5 ppm Se for 25 wk in conjunction with a standard laboratory diet (26). In the present study, it is conceivable that a pro-oxidative action of Se supplementation in the heart may have been induced by the concurrent feeding of FO, as FO feeding has been shown to result in an increase in cardiac lipid peroxidation (27,28). The greater sensitivity of the heart to the pro-oxidative action of Se also may be explained by previous work showing heart tissue to be less capable than the liver of synthesizing dimethyl selenide, which is a major metabolic route for detoxifying subacute doses of Se (29). High doses of Se are processed for elimination by interacting with endogenously produced GSH, which results in the consequent methylation of Se for excretion (30). Selenotrisulfides formed inside the cell from the reaction of Se with GSH react with oxygen to produce reactive oxygen species involved in lipid peroxidation (29). In this regard, the decrease in heart GSSG content following Se supplementation could have been due to an increased formation of selenotrisulfides.

The pro-oxidant effect of Se supplementation also may have been associated with the unchanged cardiac SeGSHPx activity seen with Se supplementation. The higher LPO content in the heart tissue following Se supplementation could have inhibited the capability of Se to induce heart SeGSHPx activity, as lipid peroxidation negatively affects SeGSHPx activity (31). Alternatively, the capability of Se to induce heart SeGSHPx activity may be a species-specific effect in the hamster, as the guinea pig heart is refractory in this regard (32). It is thus possible that heart SeGSHPx activity in the hamster was not responsive to Se supplementation, although the hamster has not been studied to our knowledge in this regard. The capability of Se to induce SeGSHPx activity, however, was organ specific as SeGSHPx activity in liver tissue was increased with Se supplementation (Table 5). Previous work in the rat has shown that SeGSHPx activity in the liver is more sensitive to induction *via* Se supplementation than heart tissue (33).

The supplementation of Vit E was not associated with dif-

ferences in hepatic SeGSHPx activity, which agrees with the findings of Kaasgaard *et al.* (3), who also showed a lack of association between the Vit E supplementation and hepatic SeGSHPx activity in monkeys fed menhaden oil. On the other hand, the supplementation of Vit E was associated with a decrease in non-SeGSHPx activity in the liver (Table 5). The reasons for the lowering effect of Vit E supplementation on non-SeGSHPx activity are not clear; however, the activity of non-SeGSHPx in the hamster liver accounts for 43% of total GSHPx activity and for this reason plays an important role against oxidative stress. In the heart, both SeGSHPx and non-SeGSHPx activity were unchanged in the Vit E-supplemented hamsters, which agrees with a previous study that showed that cardiac total GSHPx activity was unaffected by Vit E in the normal Syrian hamster (34). Such differential responses of the heart and liver further illustrate that tissue-specific responses of antioxidant enzymatic defenses can occur with antioxidant supplementation.

The enhancement of lipid peroxidation with Se treatment was unaffected by the increased tocopherol content in heart tissue following Vit E supplementation (129 IU/kg diet), which provided a dietary intake approximately five times the NRC requirement for the hamster (13). Dietary supplementation of Vit E was also associated with significantly higher hepatic tocopherol concentrations. The level of Vit E supplementation used in the present work was based on the findings of Farwer *et al.* (35), which showed that 5.6 mg or 8.4 IU TE per MJ of diet were required to maintain adequate hepatic levels of Vit E in rats fed a diet high in PUFA. In both the heart and liver, however, higher tocopherol concentrations were not associated with lower tissue concentrations of LPO. Similarly, Demoz *et al.* (36) showed a lack of association between hepatic tocopherol concentrations and lipid peroxidation in the livers of EPA-fed rats. Higher dietary doses of Vit E may have been required to exert antioxidant action in hamsters fed diets containing FO-based diet; Kubow *et al.* (11) demonstrated lower hepatic lipid peroxidation concentrations in hamsters fed FO-based diets following supplementation with a 562 IU Vit E/kg diet. Supplementation of Vit E also was not associated with lower plasma concentrations of TBARS. This latter finding agrees with previous work showing an absence of effect of Vit E supplementation on decreasing plasma TBARS concentrations in humans (37) and hamsters fed FO (11).

In the present study, the supplementation of Se was associated with significantly higher hepatic GSH/GSSG ratios, which resulted in a ratio of 10:1 found in cells under normal conditions. Previous studies have shown depressed hepatic GSH concentrations in FO-fed rats (38,39); however, in the present study, hepatic GSH/GSSG ratios were within the normal range as seen in the rat fed a standard rodent diet (40,41). The effects of Se supplementation on tissue GSH concentrations have not been studied previously in association with FO-based diets. Earlier studies have shown, however, that supplementation of Se results in increased hepatic GSH concentrations in various species (7,8). In the present study, the supplementation of Se was not associated with changes in GSH/GSSG ratios in the heart and suggests tissue-specific effects in this regard.

A major decrease in plasma concentrations of LDL + VLDL and TC (Table 2) was observed with Se supplementation. Vinson *et al.* (6) reported a similar reduction in TC and LDL + VLDL in hamsters fed nonpurified diets supplemented with Se at a level of 5 mg/kg diet, comparable to the Se supplemental levels of 3.4 mg/kg diet used in the present study. The lack of significant lowering of TG concentrations shown in the present study is in contrast with previous studies that noted significant decreases in plasma TG concentrations with Se supplementation in the human (42) and the rat (43) but concurs with the findings of Vinson *et al.* (6), who observed no significant change in plasma TG concentrations in hamsters fed diets supplemented with Se.

The degree of plasma TC and LDL lowering (18 and 23%, respectively) observed with Se supplementation in the present work is similar to that observed with other potent cholesterol-lowering nutritional and pharmaceutical agents. For example, nicotinic acid is used therapeutically to lower LDL cholesterol by 15–30% and pharmaceuticals such as bile acid sequestrants and probucol lower LDL levels by 10–30% and 10–15%, respectively (44). The large magnitude of the plasma TC- and LDL-lowering effect of Se suggests that supplementation of Se could be a worthwhile avenue to explore as a treatment for diet-induced hypercholesterolemia. In this regard, a 6-wk supplementation with Se was associated with a decrease in plasma TC and LDL concentrations in a recent human study (42). Also, peroral sodium selenite therapy in hypothyroid patients was shown to be associated with lowered TC and LDL plasma concentrations (45). Thyroid hormone is one the most potent agents known to reduce serum LDL concentrations and is known to affect hepatic levels of LDL receptor by enhancing LDL receptor gene transcription when administered at physiological doses (46). As Se is needed for hepatic conversion of thyroxine ( $T_4$ ) to 3,3,5-triiodothyronine ( $T_3$ ) through Type I iodothyronine deiodinase, Se supplementation may lower plasma cholesterol concentrations indirectly *via* its key role in thyroid hormone metabolism.

Although previous work has shown the supplementation of Vit E to be associated with a reduction in plasma TC in the presence of FO feeding in the hamster (11), no significant effect of Vit E supplementation was noted in the present work. The reason for the difference between the previously mentioned studies may have been due to a 4.5-fold higher supplemental dose of Vit E provided in the earlier work. No significant effect of Se or Vit E supplementation was noted on plasma LDL/HDL ratios, which were comparable to those previously seen in hamsters fed FO diets (47). The relatively high LDL/HDL ratios may be due to the adverse lipidemic response of hamsters to FO intake; previous studies have shown that FO intake in the hamster is associated with depressed HDL concentrations (48).

Although tissue-specific effects were observed in the improvement of antioxidant indices following supplementation of Se and Vit E, antioxidant supplementation was shown to be ineffective in lowering tissue lipid peroxidation in FO-fed hamsters. Moreover, combined supplementation of Vit E and Se provided no additional benefit in terms of oxidative stress



or antioxidative indices in the presence of FO feeding. Although the supplementation of Se was associated with an increased hepatic GSH/GSSG ratio and SeGSHPx activity, no changes in liver concentrations of LPO were noted. Likewise, the higher hepatic and cardiac Vit E content following Vit E supplementation was not associated with lowered oxidative stress. In addition, the hamster heart showed a pro-oxidative response to Se supplementation in terms of lipid peroxidation despite an apparently favorable decrease in heart GSSG content. Plasma lipid peroxidation status was also refractory to both Vit E and Se supplementation. In contrast, Se supplementation showed favorable effects on plasma LDL + VLDL and TC concentrations, suggesting that antioxidative effects are unlikely to be involved in the hypolipidemic effects of Se. The mechanisms involved in the plasma lipid-lowering effects of Se supplementation and in the resistance of *in vivo* lipid peroxidation to high-dose Se and Vit E supplementation with FO feeding require additional study. In addition, the pro-oxidative effects of Se supplementation in heart tissue also need further investigation, particularly since the plasma lipid-lowering effect of Se supplementation is receiving increased research attention.

## ACKNOWLEDGMENTS

Grant support from the National Sciences and Engineering Research Council of Canada (to S. Kubow) is gratefully acknowledged. The gift of menhaden oil from Omega Protein is appreciated.

## REFERENCES

- Connor, S.L., and Connor, W.E. (1997) Are Fish Oils Beneficial in the Prevention and Treatment of Coronary Artery Disease? *Am. J. Clin. Nutr.* 66 (Suppl.), 1020S–1031S.
- Harris, W.S. (1996) n-3 Fatty Acids and Lipoproteins: Comparison of Results from Human and Animal Studies, *Lipids* 31, 243–252.
- Kaasgaard, S.G., Holmer, G., Høy, C.-E., Behrens, W.A., and Beare-Rogers, J. (1992) Effects of Dietary Linseed Oil and Marine Oil on Lipid Peroxidation in Monkey Liver *in vivo* and *in vitro*, *Lipids* 27, 740–745.
- Cho, S.H., Im, J.G., Choi, Y.S., Son, Y.S., and Chung, M.H. (1995) Lipid Peroxidation and 8-Hydroxydeoxyguanosine Formation in Rats Fed Fish Oil with Different Levels of Vitamin E, *J. Nutr. Sci. Vitaminol.* 41, 61–72.
- Kubow, S. (1998) The Role of Oxidative Stress and Antioxidant Supplementation on Lipoprotein Metabolism, *Rec. Res. Dev. Lipids Res.* 2, 81–99.
- Vinson, J.A., Stella, J.M., and Flanagan, T.J. (1998) Selenium Yeast Is an Effective *in vitro* and *in vivo* Antioxidant and Hypolipemic Agent in Normal Hamsters, *Nutr. Res.* 18, 735–742.
- Hoffman, D.J., Heinz, G.H., and Krynitsky, A.J. (1989) Hepatic Glutathione Metabolism and Lipid Peroxidation in Response to Excess Dietary Selenomethionine and Selenite in Mallard Ducklings, *J. Toxicol. Environ. Health* 27, 263–271.
- LeBoeuf, R.A., Zentner, K.L., and Hoekstra, W.G. (1985) Effects of Dietary Selenium Concentration and Duration of Selenium Feeding on Hepatic Glutathione Concentrations in Rats, *Proc. Soc. Exp. Biol. Med.* 180, 348–352.
- Comporti, M. (1987) Glutathione Depleting Agents and Lipid Peroxidation, *Chem. Phys. Lipids* 45, 143–169.
- Combs, G.F., and Scott, M.L. (1974) Antioxidant Effects of Selenium and Vitamin E Function in the Chick, *J. Nutr.* 104, 1297–1303.
- Kubow, S., Goyette, N., Kermasha, S., Stewart-Phillip, J., and Koski, K.G. (1996) Vitamin E Inhibits Fish Oil-Induced Hyperlipidemia and Tissue Lipid Peroxidation in Hamsters, *Lipids* 31, 839–847.
- Wilson, R.B., Middleton, C.C. and Sun, G.Y. (1978) Vitamin E, Antioxidants, and Lipid Peroxidation in Experimental Atherosclerosis of Rabbits, *J. Nutr.* 108, 1858–1867.
- National Research Council (1995) Nutrient Requirements of the Hamster, in *Nutrient Requirements of Laboratory Animals*, 4th rev. edn., pp.125–139, National Academy of Sciences, Washington, DC.
- Canadian Council on Animal Care (1984) *Guide to the Care and Use of Experimental Animals*, Vols. I and II, National Library of Canada, Ottawa.
- Asakawa, T., and Matsushita, S. (1980) Thiobarbituric Acid Test for Detecting Lipid Peroxides, *Lipids* 14, 401–406.
- Wong, S.H.Y., Knight, J.A., Hopfer, S.M., Zaharia, O., Leach, C.N., Jr., and Sunderman, F.W., Jr. (1987) Lipoperoxides in Plasma as Measured by Liquid-Chromatographic Separation of Malondialdehyde–Thiobarbituric Acid Adduct, *Clin. Chem.* 33, 214–220.
- L'Abbé, M.R., Fischer, P.W.F., Campbell, J.S., and Chavez, E.R. (1989) Effects of Dietary Selenium on DMBA-Induced Carcinogenesis in Rats Fed a Diet High in Mixed Fats, *J. Nutr.* 119, 757–765.
- Paglia, D.E., and Valentine, W.N. (1967) Studies on the Quantitative and Qualitative Characterization of Erythrocyte Glutathione Peroxidase, *J. Lab. Clin. Med.* 70, 158–168.
- Prohaska, J.R. (1991) Changes in Cu, Zn-Superoxide Dismutase, Cytochrome C Oxidase, Glutathione Peroxidase, and Glutathione Transferase Activities in Copper-Deficient Mice and Rats, *J. Nutr.* 121, 355–363.
- Meister, A., and Anderson, M.E. (1983) Glutathione, *Annu. Rev. Biochem.* 52, 711–760.
- Oshishi, N., Ohkawa, H., Miike, A., Tatano, T., and Yagi, Y. (1985) A New Assay Method for Lipid Peroxides Using a Methylene Blue Derivative, *Biochem. Int.* 10, 205–211.
- Folch, J., Lees, M., and Sloane-Stanley, G.H. (1957) A Simple Method for the Isolation and Purification of Total Lipids from Animal Tissues, *J. Biol. Chem.* 226, 497–503.
- Thompson, J.N., and Hatina, G. (1979) Determination of Tocopherols and Tocotrienols in Foods and Tissues by High-Performance Liquid Chromatography, *J. Liq. Chromatogr.* 2, 327–344.
- SAS USA Release 6.12, 1989–1996, by SAS Institute Inc., Cary, NC.
- Jamall, S., Haldar, D., and Wadewitz, A.G. (1987) Effects of Dietary Selenium on Lipid Peroxidation, Mitochondrial Function and Protein Profiles in the Heart of the Myopathic Syrian Golden Hamster (Bio 14.6), *Biochem. Biophys. Res. Commun.* 144, 815–820.
- Birt, D.F., Julius, A.D., and Runice, C.E. (1986) Tolerance of Low and High Dietary Selenium Throughout the Life Span of Syrian Hamsters, *Ann. Nutr. Metab.* 30, 233–240.
- L'Abbé, M.R., Trick, K.D., and Beare-Rogers, J.L. (1991) Dietary (n-3) Fatty Acids Affect Rat Heart, Liver, and Aorta Protective Enzyme Activities and Lipid Peroxidation, *J. Nutr.* 121, 1331–1340.
- Nalbone, G., Leonard, J., Termine, E., Portugal, H., Lechene, P., Pauli, A.M., and Lafont, H. (1989) Effects of Fish Oil, Corn Oil, and Lard Diets on Lipid Peroxidation Status and Glutathione Peroxidase Activities in Rat Heart, *Lipids* 24, 179–186.
- Ganther, H.E. (1966) Enzymic Synthesis of Dimethyl Selenide from Sodium Selenite in Mouse Liver Extracts, *Biochemistry* 5, 1089–1098.

30. Spallholz, J.E. (1994) On the Nature of Selenium Toxicity and Carcinostatic Activity, *Free Radic. Biol. Med.* 17, 45–64.
31. Kinter, M., and Roberts, R.J. (1996) Glutathione Consumption and Glutathione Peroxidase Inactivation in Fibroblast Cell Lines by 4-Hydroxy-2-nonenal, *Free Radic. Biol. Med.* 21, 457–462.
32. Toyoda, H., Himeno, S., and Imura, N. (1989) The Regulation of Glutathione Peroxidase Gene Expression Relevant to Species Difference and the Effects of Dietary Selenium Manipulation, *Biochim. Biophys. Acta* 1008, 301–308.
33. Bermano, G., Nicol, F., Dyer, J.A., Sunde, R.A., Beckett, G.J., Arthur, J.R., and Hesketh, J.E. (1995) Tissue-Specific Regulation of Selenoenzyme Gene Expression During Selenium Deficiency in Rats, *Biochem. J.* 311, 425–430.
34. Li, R.-K., Sole, M.J., Mickle, D.A.G., Schimmer, J., and Goldstein, D. (1998) Vitamin E and Oxidative Stress in the Heart of the Cardiomyopathic Syrian Hamster, *Free Radic. Biol. Med.* 24, 252–258.
35. Farwer, S.R., der Boer, B.C.J., Haddeman, E., Kivits, G.A.A., Wiersma, A., and Danse, B.H.J.C. (1994) The Vitamin E Nutritional Status of Rats Fed on Diets High in Fish Oil, Linseed Oil or Sunflower Seed Oil, *Br. J. Nutr.* 72, 127–145.
36. Demoz, A., Asiedu, D.K., Lie, Ø., and Berge R.K. (1994) Modulation of Plasma and Hepatic Oxidative Status and Changes in Plasma Lipid Profile by n-3 (EPA and DHA), n-6 (corn oil) and 3-Thia Fatty Acids in Rats, *Biochim. Biophys. Acta* 1199, 238–244.
37. Meydani, M., Natiello, F., Goldin, B., Free, N., Woods, M., Schaefer, E., Blumberg, J.B., and Gorbach, S.L. (1991) Effect of Long-Term Fish Oil Supplementation on Vitamin E Status and Lipid Peroxidation in Women, *J. Nutr.* 121, 484–491.
38. Atalay, M., Laaksonen, D.E., Khanna, S., Kaliste-Korhonen, E., Hänninen, O., and Sen, C.K. (1998) Vitamin E Regulates Changes in Tissue Antioxidants Induced by Fish Oil and Acute Exercise, *Med. Sci. Sports Exerc.* 32, 601–607.
39. Saito, M., and Nakatsugawa, K. (1994) Increased Susceptibility of Liver to Lipid Peroxidation After Ingestion of a High Fish Oil Diet, *Intl. J. Vitam. Nutr. Res.* 64, 144–151.
40. Tiidus, P.M., Bombardier, E., Hidioglou, N., and Madere, R. (1998) Estrogen Administration, Post Exercise Tissue Oxidative Stress and Vitamin C Status in Male Rats, *Can. J. Physiol. Pharmacol.* 76, 952–960.
41. Rauscher, F.M., Sanders, R.A., and Watkins, J.B., III, (2000) Effects of Piperine on Antioxidant Pathways in Tissues from Normal and Streptozotocin-Induced Diabetic Rats, *J. Biochem. Mol. Toxicol.* 14, 329–334.
42. Djuric, I.S., Jozanov-Stankov, O.N., Milovac, M., Jankovic, V., and Djermanovic, V. (2000) Bioavailability and Possible Benefits of Wheat Intake Naturally Enriched with Selenium and Its Products, *Biol. Trace Elem. Res.* 77, 273–285.
43. Crespo, A.M., Lanca, M.J., Vasconcelos, S., Andrade, V., Rodrigues, H., and Santos, M.C. (1995) Effect of Selenium Supplementation on Some Blood Biochemical Parameters in Male Rats, *Biol. Trace Elem. Res.* 47, 343–347.
44. Ney, D.M. (1991) The Cardiovascular System, in *Clinical Nutrition and Dietetics* (Zeman, F.J., ed.), pp. 339–397, Macmillan, New York.
45. Kauf, E., Dawczynski, H., Jahreis, G., Janitzky, E., and Winnefeld, K. (1994) Sodium Selenite Therapy and Thyroid-Hormone Status in Cystic Fibrosis Congenital Hypothyroidism, *Biol. Trace Elem. Res.* 40, 247–253.
46. Ness, G.C., and Zhao, Z. (1994) Thyroid Hormone Rapidly Induces Hepatic LDL Receptor mRNA Levels in Hypophysectomized Rats, *Arch. Biochem. Biophys.* 315, 199–202.
47. Lu, S.C., Lin, M.H., and Huang, P.C. (1996) A High Cholesterol, (n-3) Polyunsaturated Fatty Acid Diet Induces Hypercholesterolemia More Than a High Cholesterol, (n-6) Polyunsaturated Fatty Acid Diet in Hamsters, *J. Nutr.* 126, 1759–1765.
48. Hayes, K.C., Pronczuk, A., Stephen, Z.F., and Lanzkron, S. (1990) Comparative Lipemias in Hamsters and Three Monkey Species Fed Fish Oil, in *Proceedings of the AOCS Short Course on Polyunsaturated Fatty Acids and Eicosanoids* (Lands, W.E.M., ed.), pp. 334–339, American Oil Chemists' Society, Champaign.

[Received March 1, 2002, and in revised form December 15, 2002; revision accepted December 16, 2002]

# Endothelial Vasodilatory Function Is Predicted by Circulating Apolipoprotein B and HDL in Healthy Humans

Peter Steer<sup>a</sup>, Johannes Hulthe<sup>c</sup>, Jonas Millgård<sup>a</sup>, Dennis M. Sarabi<sup>a</sup>,  
Samar Basu<sup>b</sup>, Bengt Vessby<sup>b</sup>, and Lars Lind<sup>a,\*</sup>

Departments of <sup>a</sup>Medical Sciences/Internal Medicine and <sup>b</sup>Public Health and Caring Sciences/Geriatrics, University Hospital, SE-751 85 Uppsala, Sweden, and <sup>c</sup>Wallenberg Laboratory for Cardiovascular Research, Sahlgrenska University Hospital, SE-413 45 Gothenburg, Sweden

**ABSTRACT:** Endothelium-dependent vasodilation (EDV), LDL particle size, and antibodies against oxidized LDL (oxLDL<sub>ab</sub>) have been shown to be related to the development of atherosclerosis and cardiovascular disease. In this study, we investigated whether LDL particle size, oxLDL<sub>ab</sub>, apolipoproteins, and lipoproteins are related to endothelial vasodilatory function in a population sample of 58 apparently healthy subjects aged 20 to 69 yr. EDV and endothelium-independent vasodilation (EIDV) were studied in the forearm during local administration of methacholine chloride (2 and 4 µg/min) or sodium nitroprusside (5 and 10 µg/min). Forearm blood flow was determined with venous occlusion plethysmography. In multiple stepwise regression analyses, neither oxLDL<sub>ab</sub> nor small LDL particles were significantly predictive of endothelial vasodilatory function. Instead, a high level of apolipoprotein B (apoB) was an independent predictor of both attenuated EDV and EIDV ( $r = -0.43$ ,  $P < 0.01$ , and  $r = -0.34$ ,  $P < 0.05$ , respectively). HDL cholesterol, on the other hand, was the only lipid variable that was significantly related to the EDV to EIDV ratio, an index of endothelial vasodilatory function ( $r = 0.35$ ,  $P < 0.01$ ). The inverse associations between apoB and both EDV and EIDV indicate that apoB might be an early marker of structural vascular changes in healthy subjects, whereas HDL seems to be more specifically related to endothelial vasodilatory function.

Paper no. L8867 in *Lipids* 37, 1135–1140 (December 2002).

Elevated LDL cholesterol is an important predictor of cardiovascular morbidity and mortality (1). LDL particles constantly diffuse across the arterial wall and sometimes become trapped in the extracellular matrix that constitutes the subendothelial space (2). Once trapped, LDL becomes oxidized (oxLDL) (3) and takes part in the development of atheroma through a broad spectrum of mechanisms, such as inhibition of the release of nitric oxide (NO), smooth muscle cell proliferation, platelet activation, recruitment of monocytes, and uncontrolled endocytosis of oxLDL by macrophages, leading to foam cell formation (4,5). One potentially important consequence of oxLDL formation may be the elicitation of an immune response. Indeed, antibodies against oxLDL (oxLDL<sub>ab</sub>) have been detected in both human and rabbit plasma and in atherosclerotic lesions

\*To whom correspondence should be addressed at the Department of Medical Sciences/Internal Medicine, University Hospital, SE-751 85 Uppsala, Sweden. E-mail: lars.lind@medsci.uu.se

Abbreviations: apoA-1, apolipoprotein A-1; apoB, apolipoprotein B; EDV, endothelium-dependent vasodilation; EFL, endothelial function index; EIDV, endothelium-independent vasodilation; FBF, forearm blood flow; Mch, methacholine chloride; MDA, malondialdehyde; NO, nitric oxide; oxLDL, oxidized LDL; oxLDL<sub>ab</sub>, antibodies against oxLDL; SNP, sodium nitroprusside.

(6,7). However, the role of oxLDL<sub>ab</sub> in atherosclerosis is unclear, as elevated oxLDL<sub>ab</sub> titers have been reported to predict myocardial infarction (8), as well as to be inversely related to the intima-media thickness of the carotid artery in humans (9).

OxLDL also has been shown to promote atherosclerosis by impairing endothelium-dependent vasodilation (EDV) (10,11). Indeed, statin therapy, apart from lowering LDL cholesterol, also improves EDV (12). An impaired EDV is an early event in atherosclerosis (13) and is associated with several of the major cardiovascular risk factors, such as diabetes mellitus, hypertension, hypercholesterolemia, and smoking (14–17).

The inflow rate of LDL particles into the arterial wall has been suggested to increase for small LDL particles (18). Indeed, according to several cross-sectional and prospective studies, individuals with small, dense LDL particles have a higher risk of coronary artery disease (19–21).

The primary aim of this study was to investigate whether LDL particle size, oxLDL<sub>ab</sub>, or other markers of cholesterol metabolism are related to endothelial vasodilatory function in a population sample of apparently healthy subjects. In addition, we wished to investigate whether different measures of cholesterol metabolism are associated with LDL particle size and antibody titers against oxLDL.

## METHODS

**Subjects.** Subjects were randomly chosen from the population registry of Uppsala, Sweden. The study sample (Table 1) consisted of 58 healthy subjects (31 men and 27 women, 12 of whom were postmenopausal), aged 20 to 69 yr. The subjects underwent a complete history, physical examination, and a high-resolution B-mode ultrasonographic examination of the carotid arteries (Acuson 128 XP/10 with a 7.5 MHz transducer). None of the subjects had atherosclerotic plaques or an intima-media thickness in their common carotid arteries above 1.20 mm (mean value  $0.76 \pm 0.17$  mm). None of the subjects was on regular medication or had a history of any disease known to affect the cardiovascular system, or a history of any metabolic or other chronic disease. None of the women was on contraceptive or estrogen replacement therapy. Subjects with blood pressures higher than 160/95 mm Hg, fasting hyperglycemia ( $>6.0$  mmol/L), or pronounced hypercholesterolemia ( $>7.0$  mmol/L) at the investigation were not included. The study was approved by the Ethics Committee of Uppsala University and informed consent was obtained from each participant.



**TABLE 1**  
**Basic Characteristics of the Study Sample (31 men and 27 women)<sup>a</sup>**

	Means $\pm$ SD or <i>n</i>
Age (yr)	50 $\pm$ 13
Height (cm)	174 $\pm$ 9
Weight (kg)	75 $\pm$ 13
BMI (kg/m <sup>2</sup> )	24.7 $\pm$ 3.2
Systolic blood pressure (mm Hg)	121 $\pm$ 14
Diastolic blood pressure (mm Hg)	79 $\pm$ 8
S-Cholesterol (mM)	5.44 $\pm$ 1.17
S-TG (mM)	0.84 $\pm$ 0.51
S-HDL cholesterol (mM)	1.40 $\pm$ 0.36
S-LDL cholesterol (mM)	3.66 $\pm$ 1.03
S-VLDL cholesterol (mM)	0.38 $\pm$ 0.22
S-Apolipoprotein A-1 (g/L)	1.32 $\pm$ 0.19
S-Apolipoprotein B (g/L)	0.87 $\pm$ 0.23
S-Apolipoprotein A-1/S-apolipoprotein B	1.62 $\pm$ 0.50
LDL particle size (nm)	27.33 $\pm$ 0.86
S-IgG anti-MDA-LDL	0.96 $\pm$ 0.19
S-IgM anti-MDA-LDL	0.93 $\pm$ 0.27
Smokers ( <i>n</i> )	5

<sup>a</sup>BMI, body mass index; S, serum; MDA, malondialdehyde.

**Experimental procedure.** The studies began at 8 A.M. after an overnight fast and were carried out with the subjects in supine position. Room temperature was maintained at 20–22°C. An arterial catheter (1.0 mm; Ohmeda, Swindon, United Kingdom) was inserted into the brachial artery for regional infusion of methacholine chloride (Mch; Metakolinklorid, Apoteksbolaget, Umeå, Sweden), and sodium nitroprusside (SNP; Nitropress®, Abbott Labs, Chicago, IL). The arterial catheter was also used for collection of blood samples for determination of lipid metabolism.

Forearm blood flow (FBF) was measured by venous occlusion plethysmography with mercury-in-Silastic strain gauges (Elektromedicin, Kullavik, Sweden) and expressed as mL/min per 100 mL of forearm volume. Venous occlusion pressure was 40 mm Hg, and FBF was calculated as the mean value of five consecutive readings. EDV was assessed as FBF during intra-arterial infusion of Mch at doses of 2 and 4  $\mu$ g/min in the brachial artery, whereas endothelium-independent vasodilation (EIDV) was assessed as FBF during intra-arterial infusion of SNP at doses of 5 and 10  $\mu$ g/min. EDV and EIDV are expressed as the relative increase (%) in FBF during vasodilation with Mch or SNP, respectively. Registrations were performed during the fifth minute of vasodilation. EDV and EIDV were registered in random order, and washout periods of 20 min were allowed between drugs. The endothelial function index (EFI), reflecting the endothelial contribution to vasodilation, was calculated as the EDV/EIDV ratio (during administration of 4  $\mu$ g/min Mch and 10  $\mu$ g/min SNP, respectively).

The short-term (2 h) and long-term (3 wk) reproducibility of FBF during vasodilation with Mch and SNP with this method has a CV of 5–7% (22). We have recently found that the highest dose of Mch (4  $\mu$ g/min) results in a significant increase in forearm venous plasma nitrite and nitrate concentrations in healthy volunteers. The arteriovenous difference in plasma nitrite and nitrate concentrations showed more than a 10-fold increase in venous blood, indicating that Mch mediates vasodilation by an increased NO production (23).

**Biochemical studies.** LDL, VLDL, and HDL were isolated by a combination of preparative ultracentrifugation (24) and precipitation with a sodium phosphotungstate and magnesium chloride solution (25). Cholesterol concentrations were determined enzymatically in serum and in lipoprotein fractions (IL Test Cholesterol 181618-10; Instrumentation Laboratory Company, Lexington, MA), using a Monarch apparatus. The concentrations of serum apolipoprotein (apo) A-1 and B were determined by immunoturbidimetry in a Monarch apparatus (Orion Diagnostica, Espoo, Finland). LDL particle size was assessed on commercially available nondenaturing 2 to 16% polyacrylamide gradient gels as described previously (26,27). The CV (same serum run on different gels on different days) for LDL peak particle size was 0.3%, with a correlation coefficient of  $r = 0.99$ . To minimize the reading error from the gels, each lane was scanned twice. Mean values from the two readings were used in the present study.

**Antibody titers against modified lipoproteins.** Antibody titers were determined with a solid phase ELISA, as described earlier (28,29). Malondialdehyde-treated LDL (MDA-LDL) was prepared as described by Palinski *et al.* (30). As a routine procedure, modifications were checked by controlling the electrophoretic mobility in agarose gel of the modified lipoproteins. The antibody titer was defined as

$$\text{titer} = \frac{\text{absorbance (value in patient serum} - \text{that in postcoat)}}{\text{internal standard serum} - \text{that in postcoat}} \quad [1]$$

For IgG the postcoated wells gave no absorbance. Therefore, this correction was only made for IgM. We chose to determine MDA-LDL antibodies because MDA is a prominent epitope of oxLDL and seems to be more sensitive than other ligands to antibody detection (31,32).

**Statistical analysis.** A principal component factor analysis was performed to investigate the interrelationships between different measures of cholesterol metabolism. Relationships between endothelial vasodilatory function and measures of cholesterol metabolism were evaluated by linear regression analysis. A multiple stepwise regression analysis was conducted to identify independent determinants of endothelial vasodilatory function. Age and gender are related to EDV and EIDV (33) and were therefore included as confounding variables, together with the cholesterol metabolism markers in all multiple regression analyses.  $P < 0.05$  was regarded as significant, and the present sample size thereby had the power to detect a partial correlation coefficient above 0.25 as significant. Data are expressed as mean values  $\pm$  SD unless otherwise specified.

## RESULTS

Basic characteristics of the study sample are given in Table 1.

**Factor analysis.** The factor analysis, which included total cholesterol, LDL cholesterol, HDL cholesterol, LDL peak particle size, apoB, and IgM and IgG titers against oxLDL, resulted in three oblique factors (Table 2). Factor 1 was composed mainly of total cholesterol, LDL cholesterol, and apoB. Factor 2 was composed mainly of HDL cholesterol, LDL



**TABLE 2**  
Factor Analysis of the Indices of Cholesterol Metabolism Investigated<sup>a</sup>

	Factor 1	Factor 2	Factor 3
Eigenvalue	3.9	2.8	0.9
S-Total cholesterol	0.97	0.20	-0.05
S-LDL cholesterol	0.97	0.05	0.05
S-HDL cholesterol	<0.01	0.93	-0.18
S-VLDL cholesterol	0.59	-0.64	-0.18
S-LDL peak particle size	-0.31	0.87	0.05
S-Apolipoprotein A-1	0.25	0.81	-0.29
S-Apolipoprotein B	0.94	-0.28	-0.04
S-Apolipoprotein A-1/S-apolipoprotein B	-0.70	0.61	-0.09
S-IgG against MDA-LDL	0.01	-0.12	0.96
S-IgM against MDA-LDL	-0.02	0.55	<0.01

<sup>a</sup>Data are presented as correlation coefficients. For abbreviations see Table 1.

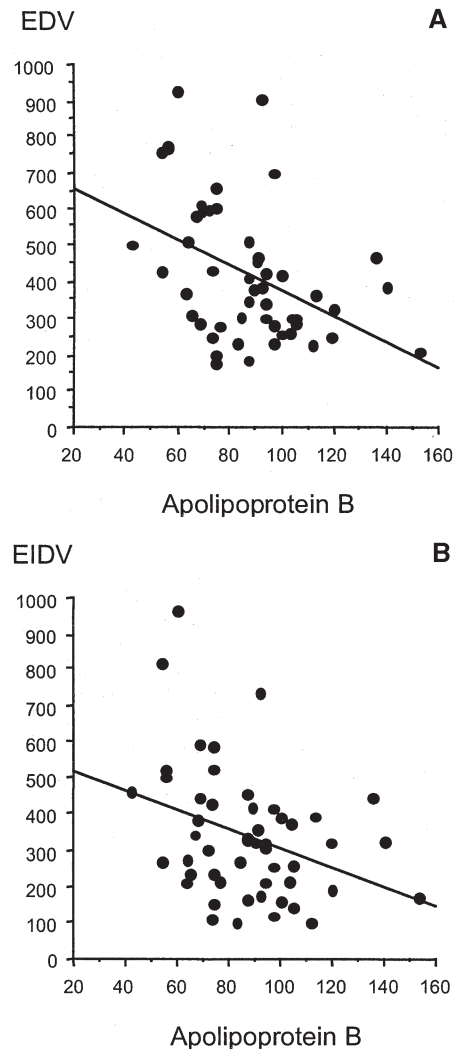
peak particle size, apoA-1, and IgM titers against oxLDL. IgG titers against oxLDL were the main constituents of Factor 3.

**Univariate regression analysis.** Univariate correlations between indices of cholesterol metabolism and endothelial vasodilatory function are presented in Table 3. EDV was significantly associated with apoB [ $r = -0.43, P < 0.01$ , during administration of 4  $\mu\text{g}/\text{min}$  Mch (Fig. 1) and  $r = -0.37, P < 0.01$  during administration of 2  $\mu\text{g}/\text{min}$  Mch], LDL cholesterol ( $r = -0.31, P < 0.05$ , during administration of 4  $\mu\text{g}/\text{min}$  Mch and  $r = -0.27, P < 0.05$ , during administration of 2  $\mu\text{g}/\text{min}$  Mch), total cholesterol ( $r = -0.29, P < 0.05$ , during administration of 4  $\mu\text{g}/\text{min}$  Mch and  $r = -0.24, P = 0.06$ , during administration of 2  $\mu\text{g}/\text{min}$  Mch), VLDL cholesterol ( $r = -0.29, P < 0.05$ , during administration of 4  $\mu\text{g}/\text{min}$  Mch and  $r = -0.25, P = 0.059$ , during administration of 2  $\mu\text{g}/\text{min}$  Mch), and the apoA-1/apoB ratio ( $r = 0.38, P < 0.01$ , during administration of 4  $\mu\text{g}/\text{min}$  Mch and  $r = 0.36, P < 0.01$ , during administration of 2  $\mu\text{g}/\text{min}$  Mch). In addition, the first factor obtained in the factor analysis was significantly associated with

**TABLE 3**  
Univariate Correlations Between Indices of Cholesterol Metabolism and Endothelial Vasodilatory Function<sup>a</sup>

	EDV	EIDV	EFI
S-Total cholesterol	-0.29*	-0.29*	0.03
S-HDL cholesterol	0.14	-0.04	0.35**
S-LDL cholesterol	-0.31*	-0.26*	-0.07
S-LDL peak particle size	0.15	0.06	0.13
S-VLDL cholesterol	-0.29*	-0.22	-0.08
S-Apolipoprotein A-1	-0.04	-0.15	0.21
S-Apolipoprotein B	-0.43**	-0.34*	-0.10
S-Apolipoprotein A-1/S-apolipoprotein B	0.38**	0.27	0.14
S-IgG against MDA-LDL	-0.02	-0.07	0.08
S-IgM against MDA-LDL	0.13	0.22	-0.11
Factor 1	-0.38**	-0.33*	-0.04
Factor 2	0.13	0.03	0.18
Factor 3	-0.07	-0.04	-0.13

<sup>a</sup>Data are presented as correlation coefficients. EDV, forearm blood flow (FBF) during administration of intra-arterial methacholine (4  $\mu\text{g}/\text{min}$ ) measuring endothelium-dependent vasodilation; EIDV, FBF during intra-arterial administration of nitroprusside (10  $\mu\text{g}/\text{min}$ ) measuring endothelium-independent vasodilation; EFI, endothelial function index calculated as FBF during intra-arterial administration of methacholine (4  $\mu\text{g}/\text{min}$ ) divided by FBF during intra-arterial administration of nitroprusside (10  $\mu\text{g}/\text{min}$ ). For other abbreviations see Table 1. \* $P < 0.05$ ; \*\* $P < 0.01$ .



**FIG. 1.** Correlations between serum apolipoprotein B and endothelium-dependent vasodilation (EDV;  $r = -0.43, P < 0.01$ ) (A) and endothelium-independent vasodilation (EIDV;  $r = -0.34, P < 0.05$ ) (B). EDV and EIDV are expressed as the relative increase (%) in forearm blood flow during administration of methacholine (4  $\mu\text{g}/\text{min}$ ) and sodium nitroprusside (10  $\mu\text{g}/\text{min}$ ), respectively.

EDV ( $r = -0.38, P < 0.01$ , during administration of 4  $\mu\text{g}/\text{min}$  Mch and  $r = -0.28, P < 0.05$ , during administration of 2  $\mu\text{g}/\text{min}$  Mch). EIDV was associated with apoB [ $r = -0.34, P < 0.05$ , during administration of 10  $\mu\text{g}/\text{min}$  SNP (Fig. 1) and  $r = -0.42, P < 0.01$ , during administration of 5  $\mu\text{g}/\text{min}$  SNP], the first factor ( $r = -0.34, P < 0.05$ , during administration of 10  $\mu\text{g}/\text{min}$  SNP and  $r = -0.27, P < 0.05$ , during administration of 5  $\mu\text{g}/\text{min}$  SNP), LDL cholesterol ( $r = -0.26, P < 0.05$ , during administration of 10  $\mu\text{g}/\text{min}$  SNP and  $r = -0.31, P < 0.05$ , during administration of 5  $\mu\text{g}/\text{min}$  SNP), and total cholesterol ( $r = -0.29, P < 0.05$ , during administration of 10  $\mu\text{g}/\text{min}$  SNP and  $r = -0.31, P < 0.05$ , during administration of 5  $\mu\text{g}/\text{min}$  SNP). The only significant predictor of the EFI was HDL cholesterol ( $r = 0.35, P < 0.01$ ).

**Multiple stepwise regression analysis.** When indices of cholesterol metabolism that were significantly associated with EDV, EIDV, or EFI in the univariate regression analysis were introduced into a multiple stepwise regression model together

with age and gender, apoB was inversely and independently related to both EDV and EIDV when evaluated at the highest dose of Mch or SNP, respectively ( $r = -0.43$ ,  $P < 0.01$ , for EDV and  $r = -0.34$ ,  $P < 0.05$ , for EIDV). HDL cholesterol was the only predictor of EFI ( $r = 0.35$ ,  $P < 0.01$ ). Neither LDL peak particle size, nor IgM and IgG titers against oxLDL, nor the factors obtained by factor analysis were independent predictors of EDV, EIDV, or EFI.

## DISCUSSION

The major finding of the present study was that neither antibody titers against oxLDL nor small LDL particles are significantly associated with endothelial vasodilatory function in apparently healthy subjects. Instead, a high level of apoB predicts attenuation in both EDV and EIDV, whereas HDL seems to be protective of endothelial vasodilatory function.

*In vitro* studies have shown that oxLDL takes part in the development of atheroma through a broad spectrum of mechanisms, including endothelial dysfunction (4,5). Hence, oxLDL, or lysolecithin from oxLDL, has been shown to impair EDV in rabbit aortic strips (10) and in perfused rabbit renal arteries under high-pressure conditions (11). Furthermore, Toikka *et al.* (34) reported an inverse relationship between EDV and plasma oxLDL levels in young men. Although immunization with oxLDL suppresses atherogenesis in rabbit models (35), the role of the immune response to oxLDL in atherosclerosis is unclear. In the present study, factor analysis revealed that IgM titers against oxLDL are associated with HDL cholesterol, apoA-1, and LDL particle size. Because high levels of HDL and apoA-1 have been shown to be associated with a lower risk of coronary artery disease and lower intima-media thickness of the carotid artery, and small LDL particles have been associated with coronary artery disease (19–21,36,37), our finding might indicate that IgM titers against oxLDL are protective against atherosclerosis. Indeed, Fukumoto *et al.* (9) recently reported that oxLDL titers are inversely associated with carotid intima-media thickness in healthy subjects. Furthermore, lower IgM titers against oxLDL have been found in patients with a history of myocardial infarction as compared to controls (28). These findings would suggest that the immune response against oxLDL might be protective under certain circumstances. On the other hand, high oxLDL titers have been reported to predict myocardial infarction and progression of carotid atherosclerosis independently in humans (8,32). Furthermore, elevated oxLDL titers have been found in insulin-dependent diabetes mellitus and hypertension (38,39), whereas other studies found no relationship between oxLDL and atherosclerotic disease (40). However, whether endothelial vasodilatory function is related to oxLDL has not been investigated previously in healthy humans. In the present study neither EDV, EIDV, nor the EFI were significantly related to oxLDL. This result is in accordance with a recent study in patients with insulin-dependent diabetes mellitus, in which no correlation was found between EDV, measured as the vasodilatory response to acetylcholine

in forearm resistance vessels, and oxLDL (38) despite elevated titers of oxLDL. Taken together, these data do not support a relationship between immune responses to oxLDL and endothelial vasodilatory function.

According to several cross-sectional and prospective studies, individuals with small, dense LDL particles have a higher risk for coronary artery disease (19–21). Although Vakkilainen *et al.* (41) found a significant relationship between small LDL particles and impaired EDV, as assessed by venous occlusion plethysmography, in healthy middle-aged men, we found no relationship between LDL particle size and endothelial vasodilatory function in the present study. This could be explained by differences in the metabolic profiles of the samples. Thus, O'Brien *et al.* (42) found a relationship between LDL particle size and EDV, as assessed by venous occlusion plethysmography, in a sample of middle-aged men with non-insulin-dependent diabetes mellitus, whereas no relationship was found between LDL particle size and EDV in healthy controls. However, in the study by Vakkilainen *et al.* (41), mean values of body mass index, serum TG and cholesterol, and LDL particle size showed a closer resemblance to the non-insulin-dependent group in the study by O'Brien *et al.* (42) than to the healthy subjects in our present study. Furthermore, in the Québec Cardiovascular Study (21) small LDL particles were significant predictors of ischemic heart disease risk only at plasma apoB levels above 1.2 g/L. The low levels of apoB in our sample might therefore contribute to the lack of correlation between LDL particle size and EDV in the present study. Only four subjects had apoB levels above 1.2 g/L, which was not high enough to stratify the sample according to normal or high levels of apoB. Thus, LDL particle size may not be closely related to endothelial vasodilatory function in healthy subjects with a favorable risk factor profile.

The EFI, reflecting the endothelial contribution to vasodilation, was associated with HDL cholesterol in the present study. Our data are corroborated by other studies, in which decreased HDL cholesterol has been shown to predict endothelial dysfunction in healthy young men as well as in men with non-insulin-dependent diabetes mellitus (34,42). HDL also has been shown to reverse the inhibitory effect of oxLDL on EDV in rabbit arterial rings (11,43) and to be inversely associated with oxLDL in healthy humans (34). In the present study, the factor analysis showed low levels of HDL cholesterol to be associated with small LDL particles and decreased levels of apoA-1 in serum. These are some of the features of the insulin resistance syndrome (44). Thus, the independent relationship between HDL cholesterol and EFI in the present study further supports a protective role for HDL cholesterol on endothelial vasodilatory function.

ApoB was independently and inversely associated with both EDV and EIDV. ApoB is present mainly in the LDL fraction under fasting conditions, and an elevated apoB/LDL cholesterol ratio is frequently observed in atherosclerotic cardiovascular disease (45). However, whether endothelial vasodilatory function is related to apoB has hitherto not been thoroughly investigated. The inverse associations of both EDV

and EIDV to apoB in the present study would suggest that apoB predicts structural vascular changes rather than endothelial dysfunction *per se*. Indeed, an elevated level of apoB has been identified as an independent predictor of increased carotid intima-media thickness and arterial stiffness in healthy subjects (37,46). In our own recent cross-sectional study, apoB was an independent predictor of both arterial stiffness, assessed as the stroke volume to pulse pressure ratio, and carotid intima-media thickness in healthy women (47). ApoB is a constituent of LDL particles, and we did indeed find a weak association between LDL cholesterol and EIDV. Creager *et al.* (15) found that EIDV, measured by venous occlusion plethysmography, was significantly lower in hypercholesterolemic subjects as compared to healthy controls, and Goode and Heagerty (48) showed that EIDV was significantly impaired in arterial rings from hypercholesterolemic humans as compared to normocholesterolemic controls.

**Limitations.** Owing to sample size, only correlation coefficients above 0.25 were significant in the present study. Thus, weak associations could not be detected. However, associations below this limit could have explained only less than 7% of the variation in the dependent variable. A number of correlations were performed, and with the chosen significance level of 5%, one correlation in 20 might be significant merely by chance. Therefore, these results must be interpreted with caution until reproduced by other investigators in larger studies. Nevertheless, the fact that similar associations were seen for both dosages of Mch and SNP minimizes the chance of type 1 errors. Relatively normal apoB levels in the sample might explain the lack of correlation between LDL particle size and EDV, as the Québec Cardiovascular Study (21) showed small LDL particles to be significant predictors of risk of ischemic heart disease only at plasma apoB levels above 1.2 g/L. Only four subjects had apoB levels above 1.2 g/L, which was not enough to stratify the sample according to normal or high levels of apoB.

In conclusion, the inverse associations between apoB and both EDV and EIDV indicate that apoB might be an early marker of structural vascular changes in healthy subjects, whereas HDL seems to be more specifically related to EDV.

**REFERENCES**

1. Jousilahti, P., Vartiainen, E., Pekkanen, J., Tuomilehto, J., Sundvall, J., and Puska, P. (1998) Serum Cholesterol Distribution and Coronary Heart Disease Risk: Observations and Predictions Among Middle-Aged Population in Eastern Finland, *Circulation* 97, 1087–1094.
2. Williams, K.J., and Tabas, I. (1995) The Response-to-Retention Hypothesis of Early Atherogenesis, *Arterioscler. Thromb. Vasc. Biol.* 15, 551–561.
3. Ylä-Herttuala, S., Palinski, W., Rosenfeld, M.E., Parthasarathy, S., Carew, T.E., Butler, S., Witztum, J.L., and Steinberg, D. (1989) Evidence for the Presence of Oxidatively Modified Low Density Lipoprotein in Atherosclerotic Lesions of Rabbit and Man, *J. Clin. Invest.* 84, 1086–1095.
4. Deckert, V., Brunet, A., Lantoine, F., Lizard, G., Millanvoveyan Brussel, E., Monier, S., Lagrost, L., David-Dufilho, M., Gambert, P., and Devynck, M.A. (1998) Inhibition by Cholesterol Oxides of NO Release from Human Vascular Endothelial Cells, *Arterioscler. Thromb. Vasc. Biol.* 18, 1054–1060.

5. Navab, M., Berliner, J.A., Watson, A.D., Hama, S.Y., Territo, M.C., Lusis, A.J., Shih, D.M., Van Lenten, B.J., Frank, J.S., Demer, L.L., *et al.* (1996) The Yin and Yang of Oxidation in the Development of the Fatty Streak. A Review Based on the 1994 George Lyman Duff Memorial Lecture, *Arterioscler. Thromb. Vasc. Biol.* 16, 831–842.
6. Ylä-Herttuala, S., Palinski, W., Butler, S.W., Picard, S., Steinberg, D., and Witztum, J.L. (1994) Rabbit and Human Atherosclerotic Lesions Contain IgG That Recognizes Epitopes of Oxidized LDL, *Arterioscler. Thromb.* 14, 32–40.
7. Palinski, W., Rosenfeld, M.E., Ylä-Herttuala, S., Gurtner, G.C., Socher, S.S., Butler, S.W., Parthasarathy, S., Carew, T.E., Steinberg, D., and Witztum, J.L. (1989) Low Density Lipoprotein Undergoes Oxidative Modification *in vivo*, *Proc. Natl. Acad. Sci. USA* 86, 1372–1376.
8. Puurunen, M., Manttari, M., Manninen, V., Tenkanen, L., Alfthan, G., Ehnholm, C., Vaarala, O., Aho, K., and Palosuo, T. (1994) Antibody Against Oxidized Low-Density Lipoprotein Predicting Myocardial Infarction, *Arch. Intern. Med.* 154, 2605–2609.
9. Fukumoto, M., Shoji, T., Emoto, M., Kawagishi, T., Okuno, Y., and Nishizawa, Y. (2000) Antibodies Against Oxidized LDL and Carotid Artery Intima-Media Thickness in a Healthy Population, *Arterioscler. Thromb. Vasc. Biol.* 20, 703–707.
10. Kugiyama, K., Kerns, S.A., Morrisett, J.D., Roberts, R., and Henry, P.D. (1990) Impairment of Endothelium-Dependent Arterial Relaxation by Lysolecithin in Modified Low-Density Lipoproteins, *Nature* 344, 160–162.
11. Galle, J., Ochslin, M., Schollmeyer, P., and Wanner, C. (1994) Oxidized Lipoproteins Inhibit Endothelium-Dependent Vasodilation. Effects of Pressure and High-Density Lipoprotein, *Hypertension* 23, 556–564.
12. Dupuis, J., Tardif, J.C., Cernacek, P., and Theroux, P. (1999) Cholesterol Reduction Rapidly Improves Endothelial Function After Acute Coronary Syndromes. The RECIFE (reduction of cholesterol in ischemia and function of the endothelium) Trial, *Circulation* 99, 3227–3233.
13. Glasser, S.P., Selwyn, A.P., and Ganz, P. (1996) Atherosclerosis: Risk Factors and the Vascular Endothelium, *Am. Heart J.* 131, 379–384.
14. Mäkimattila, S., Liu, M.L., Vakkilainen, J., Schlenzka, A., Lahdenperä, S., Syvanne, M., Mantysaari, M., Summanen, P., Bergholm, R., Taskinen, M.R., *et al.* (1999) Impaired Endothelium-Dependent Vasodilation in Type 2 Diabetes. Relation to LDL Size, Oxidized LDL, and Antioxidants, *Diabetes Care* 22, 973–981.
15. Creager, M.A., Cooke, J.P., Mendelsohn, M.E., Gallagher, S.J., Coleman, S.M., Loscalzo, J., and Dzau, V.J. (1990) Impaired Vasodilation of Forearm Resistance Vessels in Hypercholesterolemic Humans, *J. Clin. Invest.* 86, 228–234.
16. Egashira, K., Suzuki, S., Hirooka, Y., Kai, H., Sugimachi, M., Imaizumi, T., and Takeshita, A. (1995) Impaired Endothelium-Dependent Vasodilation of Large Epicardial and Resistance Coronary Arteries in Patients with Essential Hypertension. Different Responses to Acetylcholine and Substance P, *Hypertension* 25, 201–206.
17. Zeiher, A.M., Schachinger, V., and Minners, J. (1995) Long-Term Cigarette Smoking Impairs Endothelium-Dependent Coronary Arterial Vasodilator Function, *Circulation* 92, 1094–1100.
18. Björnheden, T., Babyi, A., Bondjers, G., and Wiklund, O. (1996) Accumulation of Lipoprotein Fractions and Subfractions in the Arterial Wall, Determined in an *in vitro* Perfusion System, *Atherosclerosis* 123, 43–56.
19. Austin, M.A., Breslow, J.L., Hennekens, C.H., Buring, J.E., Willett, W.C., and Krauss, R.M. (1988) Low-Density Lipoprotein Subclass Patterns and Risk of Myocardial Infarction, *JAMA* 260, 1917–1921.



20. Stampfer, M.J., Krauss, R.M., Ma, J., Blanche, P.J., Holl, L.G., Sacks, F.M., and Hennekens, C.H. (1996) A Prospective Study of Triglyceride Level, Low-Density Lipoprotein Particle Diameter, and Risk of Myocardial Infarction, *JAMA* 276, 882–888.
21. Lamarche, B., Tchernof, A., Moorjani, S., Cantin, B., Dagenais, G.R., Lupien, P.J., and Despres, J.P. (1997) Small, Dense Low-Density Lipoprotein Particles as a Predictor of the Risk of Ischemic Heart Disease in Men. Prospective Results from the Québec Cardiovascular Study, *Circulation* 95, 69–75.
22. Lind, L., Sarabi, M., and Millgård, J. (1998) Methodological Aspects of the Evaluation of Endothelium-Dependent Vasodilatation in the Human Forearm, *Clin. Physiol.* 18, 81–87.
23. Lind, L., Hall, J., Larsson, A., Annuk, M., Fellström, B., and Lithell, H. (2000) Evaluation of Endothelium-Dependent Vasodilation in the Human Peripheral Circulation, *Clin. Physiol.* 20, 440–448.
24. Havel, R.J., Eder, H.A., and Bragdon, J.H. (1955) The Distribution and Chemical Composition of Ultracentrifugally Separated Lipoproteins in Human Serum, *J. Clin. Invest.* 34, 1345–1353.
25. Seigler, L., and Wu, W.T. (1981) Separation of Serum High-Density Lipoprotein for Cholesterol Determination: Ultracentrifugation vs. Precipitation with Sodium Phosphotungstate and Magnesium Chloride, *Clin. Chem.* 27, 838–841.
26. Hulthe, J., Wiklund, O., Olsson, G., Fagerberg, B., Bokemark, L., Nivall, S., and Wikstrand, J. (1999) Computerized Measurement of LDL Particle Size in Human Serum. Reproducibility Studies and Evaluation of LDL Particle Size in Relation to Metabolic Variables and the Occurrence of Atherosclerosis, *Scand. J. Clin. Lab. Invest.* 59, 649–661.
27. Hulthe, J., Bokemark, L., Wikstrand, J., and Fagerberg, B. (2000) The Metabolic Syndrome, LDL Particle Size, and Atherosclerosis: The Atherosclerosis and Insulin Resistance (AIR) Study, *Arterioscler. Thromb. Vasc. Biol.* 20, 2140–2147.
28. Hulthe, J., Wikstrand, J., Lidell, A., Wendelhag, I., Hansson, G.K., and Wiklund, O. (1998) Antibody Titers Against Oxidized LDL Are Not Elevated in Patients with Familial Hypercholesterolemia, *Arterioscler. Thromb. Vasc. Biol.* 18, 1203–1211.
29. Hulthe, J., Bokemark, L., and Fagerberg, B. (2001) Antibodies to Oxidized LDL in Relation to Intima-Media Thickness in Carotid and Femoral Arteries in 58-Year-Old Subjectively Clinically Healthy Men, *Arterioscler. Thromb. Vasc. Biol.* 21, 101–107.
30. Palinski, W., Ylä-Herttuala, S., Rosenfeld, M.E., Butler, S.W., Socher, S.A., Parthasarathy, S., Curtiss, L.K., and Witztum, J.L. (1990) Antisera and Monoclonal Antibodies Specific for Epitopes Generated During Oxidative Modification of Low Density Lipoprotein, *Arteriosclerosis* 10, 325–335.
31. Griffin, M.E., McInerney, D., Fraser, A., Johnson, A.H., Collins, P.B., Owens, D., and Tomkin, G.H. (1997) Autoantibodies to Oxidized Low Density Lipoprotein: The Relationship to Low Density Lipoprotein Fatty Acid Composition in Diabetes, *Diabet. Med.* 14, 741–747.
32. Salonen, J.T., Ylä-Herttuala, S., Yamamoto, R., Butler, S., Korpela, H., Salonen, R., Nyyssonen, K., Palinski, W., and Witztum, J.L. (1992) Autoantibody Against Oxidized LDL and Progression of Carotid Atherosclerosis, *Lancet* 339, 883–887.
33. Sarabi, M., Millgård, J., and Lind, L. (1999) Effects of Age, Gender and Metabolic Factors on Endothelium-Dependent Vasodilation: A Population-Based Study, *J. Intern. Med.* 246, 265–274.
34. Toikka, J.O., Ahotupa, M., Viikari, J.S., Niinikoski, H., Taskinen, M., Irjala, K., Hartiala, J.J., and Raitakari, O.T. (1999) Constantly Low HDL-Cholesterol Concentration Relates to Endothelial Dysfunction and Increased *in vivo* LDL-Oxidation in Healthy Young Men, *Atherosclerosis* 147, 133–138.
35. Palinski, W., Miller, E., and Witztum, J.L. (1995) Immunization of Low Density Lipoprotein (LDL) Receptor-Deficient Rabbits with Homologous Malondialdehyde-Modified LDL Reduces Atherogenesis, *Proc. Natl. Acad. Sci. USA* 92, 821–825.
36. Castelli, W.P., Doyle, J.T., Gordon, T., Hames, C.G., Hjortland, M.C., Hulley, S.B., Kagan, A., and Zukel, W.J. (1977) HDL Cholesterol and Other Lipids in Coronary Heart Disease. The Cooperative Lipoprotein Phenotyping Study, *Circulation* 55, 767–772.
37. Sharrett, A.R., Patsch, W., Sorlie, P.D., Heiss, G., Bond, M.G., and Davis, C.E. (1994) Associations of Lipoprotein Cholesterol, Apolipoproteins A-I and B, and Triglycerides with Carotid Atherosclerosis and Coronary Heart Disease. The Atherosclerosis Risk in Communities (ARIC) Study, *Arterioscler. Thromb.* 14, 1098–1104.
38. Mäkimattila, S., Luoma, J.S., Ylä-Herttuala, S., Bergholm, R., Utriainen, T., Virkamäki, A., Mantysaari, M., Summanen, P., and Yki-Järvinen, H. (1999) Autoantibodies Against Oxidized LDL and Endothelium-Dependent Vasodilation in Insulin-Dependent Diabetes Mellitus, *Atherosclerosis* 147, 115–122.
39. Maggi, E., Marchesi, E., Ravetta, V., Martignoni, A., Finardi, G., and Bellomo, G. (1995) Presence of Autoantibodies Against Oxidatively Modified Low-Density Lipoprotein in Essential Hypertension: A Biochemical Signature of an Enhanced *in vivo* Low-Density Lipoprotein Oxidation, *J. Hypertens.* 13, 129–138.
40. van de Vijver, L.P., Steyger, R., van Poppel, G., Boer, J.M., Kruijssen, D.A., Seidell, J.C., and Princen, H.M. (1996) Autoantibodies Against MDA-LDL in Subjects with Severe and Minor Atherosclerosis and Healthy Population Controls, *Atherosclerosis* 122, 245–253.
41. Vakkilainen, J., Mäkimattila, S., Seppälä-Lindroos, A., Vehkavaara, S., Lahdenperä, S., Groop, P.H., Taskinen, M.R., and Yki-Järvinen, H. (2000) Endothelial Dysfunction in Men with Small LDL Particles, *Circulation* 102, 716–721.
42. O'Brien, S.F., Watts, G.F., Playford, D.A., Burke, V., O'Neal, D.N., and Best, J.D. (1997) Low-Density Lipoprotein Size, High-Density Lipoprotein Concentration, and Endothelial Dysfunction in Non-insulin-dependent Diabetes, *Diabet. Med.* 14, 974–978.
43. Matsuda, Y., Hirata, K., Inoue, N., Suematsu, M., Kawashima, S., Akita, H., and Yokoyama, M. (1993) High-Density Lipoprotein Reverses Inhibitory Effect of Oxidized Low Density Lipoprotein on Endothelium-Dependent Arterial Relaxation, *Circ. Res.* 72, 1103–1109.
44. Laakso, M. (1996) Insulin Resistance and Coronary Heart Disease, *Curr. Opin. Lipidol.* 7, 217–226.
45. Hattori, Y., Suzuki, M., Tsushima, M., Yoshida, M., Tokunaga, Y., Wang, Y., Zhao, D., Takeuchi, M., Hara, Y., Ryomoto, K.I., et al. (1998) Development of Approximate Formula for LDL-cholesterol, LDL-apo B and LDL-cholesterol/LDL-apo B as Indices of Hyperapobetalipoproteinemia and Small Dense LDL, *Atherosclerosis* 138, 289–299.
46. Marques, V.P., Amar, J., Cambou, J.P., and Chamontin, B. (1996) Relationships Between Blood Pressure Components, Lipids and Lipoproteins in Normotensive Men, *J. Hum. Hypertens.* 10, 239–244.
47. Steer, P., Millgård, J., Sarabi, M.D., Basu, S., Vessby, B., Kahan, T., Edner, M., and Lind, L. (2002) Cardiac and Vascular Structure and Function Are Related to Lipid Peroxidation and Metabolism, *Lipids* 37, 231–236.
48. Goode, G.K., and Heagerty, A.M. (1995) *In vitro* responses of Human Peripheral Small Arteries in Hypercholesterolemia and Effects of Therapy, *Circulation* 91, 2898–2903.

[Received July 6, 2001, and in revised form March 27, 2002; revision accepted September 30, 2002]



# The Types of Circulating Fatty Acids Influence Vascular Reactivity

Lars Lind<sup>a,c,\*</sup>, Eva Södergren<sup>b</sup>, Inga-Britt Gustafsson<sup>b</sup>, Jonas Millgård<sup>a</sup>, Mahziar Sarabi<sup>a</sup>, and Bengt Vessby<sup>b</sup>

Departments of <sup>a</sup>Internal Medicine and <sup>b</sup>Geriatrics, University Hospital, Uppsala, Sweden, and <sup>c</sup>AstraZeneca R&D, Mölndal, Sweden

**ABSTRACT:** The objective of this study was to investigate the relationship between the composition of FA in serum lipids, a marker of dietary fat intake, and vascular reactivity using a combination of cross-sectional and intervention approaches. Fifty-six middle-aged subjects were evaluated in a cross-sectional protocol regarding the relationship between the proportion of FA in serum cholesterol esters and vascular reactivity using measurements of forearm blood flow (FBF) with venous occlusion plethysmography during hyperemia. Another 19 middle-aged subjects were given a rapeseed oil-based diet rich in mono- and polyunsaturated FA or a control diet rich in saturated FA during two consecutive 4-wk periods separated by a 4-wk washout period. In the cross-sectional protocol, the FA 18:0 and 20:3 were positively related to resting FBF, whereas an inverse relationship was seen for the FA 20:5 and 22:6 ( $P < 0.05$ – $0.01$ ). Opposite relationships were seen between these four FA and the relative increase in maximal FBF during hyperemia ( $P < 0.05$ – $0.01$ ). In the intervention protocol, the saturated diet increased resting FBF, as well as the relative increase in maximal FBF during reactive hyperemia, compared to the diet rich in unsaturated FA ( $P < 0.05$ ). Both the cross-sectional and intervention data support the view that the composition of serum FA, which at least partly reflects the quality of dietary fat, plays a role in determinations of vascular reactivity. Paper no. L9043 in *Lipids* 37, 1141–1145 (December 2002).

Lipids are known to have a major impact on the development of cardiovascular diseases, and serum cholesterol levels were early identified as a major cardiovascular risk factor (1). That a high dietary intake of saturated FA is associated with an increased risk of developing coronary heart disease (CHD) is also well established (2,3). However, no consensus exists whether saturated FA should be replaced mainly by mono-unsaturated FA, PUFA, or carbohydrates. Epidemiological studies investigating the effects of mono- and polyunsaturated FA have shown divergent results (2). Intervention studies have shown beneficial lipid-lowering effects (3) but also an increased susceptibility of lipoproteins to oxidation during interventions with diets rich in PUFA (4,5).

Since the discoveries that the endothelium takes an active part in the vasodilatory process (6), and that the major substance secreted from the endothelium responsible for this vasodilatory

process is nitric oxide (NO) (7), much attention has been paid to measuring the impact of NO on cardiovascular function.

For decades, the increase in forearm blood flow (FBF) seen during the hyperemic phase following obstruction of blood flow has been used to evaluate vascular reactivity. Previously, it was claimed that vascular anatomic changes, such as vascular hypertrophy, were the major determinants of FBF during hyperemia (8). However, recent studies have shown that FBF during hyperemia also is dependent on NO production (9). By the use of a local infusion of the NO antagonist L-NMMA, both the peak in FBF that occurs immediately after release of an arterial occlusion and the following reduction in FBF were shown to be NO-dependent. Resting FBF was also largely determined by NO production (10).

The purpose of the present study was to investigate the relationship between serum FA composition and vascular reactivity using the postocclusive hyperemia forearm model, which is in part NO dependent. The study used a dual approach. First, a population of apparently healthy middle-aged subjects was studied in a cross-sectional protocol to relate the FA composition of serum cholesterol esters to vascular reactivity. In this part of the study, the FA composition of serum cholesterol esters was used as a marker of the quality of fat ingested over the weeks preceding the investigation (11,12). In the second part, another group of middle-aged subjects were given either a diet high in saturated FA or a diet rich in PUFA in a randomized cross-over fashion. Vascular reactivity was evaluated in the same way in both the cross-sectional and the intervention protocols.

## MATERIALS AND METHODS

*Cross-sectional protocol: Subjects.* The population sample, recruited from the general population in Uppsala, Sweden, consisted of 56 healthy subjects (31 men and 25 women; see Table 1) who ranged in age from 20 to 69 yr (13). None of the subjects was taking regular medication or had a history of any disease known to affect the cardiovascular system. In addition, subjects with a history of any metabolic or other serious diseases were excluded from the study. None of the women was on contraceptive pills or estrogen replacement therapy. Subjects with blood pressure  $>160/95$  mm Hg, fasting hyperglycemia ( $>6.0$  mmol/L), or pronounced hypercholesterolemia ( $>8.0$  mmol/L) at the investigation were not included. Eight of the subjects were smokers.

\*To whom correspondence should be addressed at Dept. of Internal Medicine, University Hospital, S751 85 Uppsala, Sweden.  
E-mail: lars.lind@medsci.uu.se

Abbreviations: CHD, coronary heart disease; E%, energy percent; FBF, forearm blood flow; NO, nitric oxide; RO, rapeseed oil-based diet; SAT, control diet high in saturated FA.

*Intervention protocol. (i) Subjects.* Nineteen healthy subjects (6 female/13 male) aged  $50 \pm 8$  yr with normal or moderately increased body weight and blood lipids participated in the protocol. Subjects were recruited *via* posters in nearby companies. Eligible for the study were men (age 30 to 65) and women (age 50 to 65) with serum cholesterol  $<8.0$  mmol/L, serum TG 1.3 to 5.0 mmol/L, fasting blood glucose  $<6.0$  mmol/L, diastolic blood pressure  $<95$  mm Hg, and body mass index  $<30$  kg/m<sup>2</sup>. Exclusion criteria were treatment for CHD; liver, kidney, or thyroid disease; diabetes mellitus; hypertension; estrogen replacement therapy; and regular acetyl salicylic acid medication. Two subjects were smokers. All subjects were asked to maintain their habitual lifestyles during the study.

*(ii) Study design.* The protocol was conducted using a randomized cross-over design. Two consecutive 4-wk diet periods were separated by a 4-wk washout period. The two diets tested were a rapeseed oil-based (RO) diet rich in monounsaturated FA and  $\alpha$ -linolenic acid and a control (SAT) diet with a high proportion of saturated FA. Subjects were randomly assigned to start with one of the two diets. Measurements of vascular reactivity and determinations of FA composition in phospholipids were performed at the end of the two treatment periods.

The study was approved by the Ethics Committee at Uppsala University, and each participant gave informed consent.

*(iii) Diets.* The fat quality of the two test diets (RO and SAT) was controlled by supplying fat products and food items prepared with the fats tested, in combination with dietary advice to avoid fats from other dietary sources such as fatty dairy and meat products. The subjects met a nutritionist before and during the diet periods for dietary advice and instructions on preparing their diets to ensure good adherence to the diet. Specially prepared table margarine (without rapeseed oil) for the SAT diet and ice cream (with rapeseed oil) for the RO diet were produced in pilot plants by Van den Bergh Foods AB (Helsingborg, Sweden) and Karlshamns Mejeri AB (Karlshamn, Sweden), respectively. Commercial qualities of all other cooking fats, table margarines, oils, and ice creams were purchased on the market or obtained from Karlshamns AB (Karlshamn, Sweden). Lunch meals (five per week, 10 different meals), bread (three per day), and cookies (one per day) prepared with the fats tested were supplied weekly, as well as free amounts of cooking fat, table margarine (80% fat), and oil to use for cooking, spreads, and dressings. Double portions that included the daily supply of food items and an approximate daily intake of fat products supplied were prepared on the 12 MJ energy level for each of the 10 d. The test diets were planned to contain 37 energy percent (E%) fat, 12 E% protein, and 50 E% of carbohydrates. The composition of the RO diet was aimed to represent a normal mixed-RO diet composed according to dietary recommendations, but with a fat content corresponding to the average intake of a Swedish population. The control diet contained saturated fat products instead of rapeseed oil-based fat products. Two energy levels, 9 and 12 MJ, were prepared, and the energy requirement for each subject was approximated as 146 kJ/kg body weight. The body

weight of the subjects was checked once a week to avoid weight changes, and the energy level, together with dietary advice, was adjusted when needed. Dietary intake was monitored using 3-d food records (two weekdays and one weekend day) on five occasions, one at baseline and two during each diet period. The dietary food records were analyzed by using the software program Stor MATs 4.0 (Rudans Lättdata, Västerås, Sweden) based on a Swedish-specific food database from the Swedish National Food Administration (PC-Kost 1996, SLV, Uppsala, Sweden).

*(iv) Measurement of vascular reactivity.* The vascular reactivity studies were performed after an overnight fast. The subjects were supine in an air-conditioned room at a constant temperature (20°C). FBF (measured in mL/min/100 mL tissue) was measured by venous occlusion plethysmography (Elekromedicin, Kullavik, Sweden). A mercury-in-Silastic strain gauge was placed at the upper third of the forearm, which rested comfortably slightly above the level of the heart. The strain gauge was coupled to an calibrated plethysmograph. Venous occlusion was achieved by a blood pressure cuff applied proximal to the elbow and inflated to 40 mm Hg by a rapid cuff inflator. Blood flow during reactive hyperemia was measured after occlusion of the forearm circulation by inflating a cuff in the upper part of the arm to 200 mm mercury for 5 min. After release of the cuff, FBF was measured after 5 s to obtain the maximal blood flow. Blood flow measurements were performed each 20th s thereafter in the cross-sectional study and at 80 s of hyperemia only in the intervention study. FBF at 80 s of hyperemia was considered to be a measurement of recovery after the hyperemic phase. Relative maximal FBF was defined as maximal FBF minus resting FBF divided by resting FBF. We previously showed that maximal FBF is more closely related to the muscarinic-receptor agonist-induced increase in FBF than to the increase in FBF seen during local infusion of sodium nitroprusside in the forearm (14). Recalculation of data using the relative maximal FBF instead of the absolute number for maximal FBF gave similar results.

The reproducibility of the measurement of resting FBF was previously evaluated in 10 healthy young volunteers (14), in whom the investigation was performed before and after 2 h of i.v. saline infusion, as well as after 2–3 wk. Resting FBF showed a CV of less than 10%.

Systolic and diastolic blood pressures, as well as heart rate, were measured in the supine position after 15 min of rest. A mercury sphygmomanometer was used for the measurements.

*(v) Measurements of FA composition in serum lipids.* To analyze the FA composition of the serum cholesterol esters, serum was extracted with a hexane/isopropanol solution. Cholesterol esters were separated from the extract by TLC before interesterification, and the free cholesterol liberated in the reaction was removed by an aluminum oxide column to avoid contamination of the GLC column. The percentage composition of methylated FA was determined by GC (a 25-m NB-351 silica capillary column, i.d. 0.32 mm, phase layer 0.20  $\mu$ m) with use of an FID and with helium as carrier gas. Every 25th sample was a serum control pool. The preci-

sion of the between-series analysis ( $n = 35$ ) varied from 2 (large peaks) to 10% (smaller peaks) and between successive GC runs ( $n = 17$ ) from 0.2 to 5% (CV).

(vi) *Statistical analysis.* In the cross-sectional study the relationships between continuous variables were evaluated by linear regression analysis. Interactions between several independent variables were examined with stepwise multiple regression analysis. In the intervention study differences between the diets were evaluated with Student's paired *t*-test. A test for carryover effects was used according to Jones and Kenward (15). If the carryover test was significant, only data from the first diet period were used for comparisons of the two test diets.  $P < 0.05$  was regarded as significant.

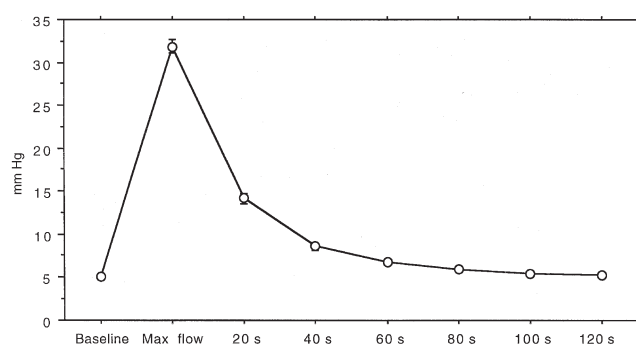
## RESULTS

*Cross-sectional protocol.* Basic characteristics of the study population are given in Table 1. FBF at different time points during reactive hyperemia are shown in Figure 1.

In comparing the composition of FA in the serum cholesterol esters (see Table 2) to the different FBF characteristics, the proportion of 18:0 was significantly related to both resting FBF ( $r = 0.31$ ,  $P < 0.05$ ) and to FBF at 80 s during hyperemia ( $r = 0.41$ ,  $P < 0.01$ ). The proportion of 20:3 was also significantly related to resting FBF ( $r = 0.32$ ,  $P < 0.05$ ). On the contrary, the proportions of both 20:5 and 22:6 were inversely related to resting FBF ( $r = -0.31$  and  $r = -0.37$ ,  $P < 0.05$  and  $< 0.01$ , respectively). Furthermore, the proportion of 22:6 was correlated to the relative maximal FBF ( $r = 0.41$ ,  $P < 0.03$ ). Although an inverse relationship was seen between the proportion of 20:3 and the relative maximal FBF ( $r = -0.35$ ,  $P < 0.05$ ), a positive relationship was seen between this vascular reactivity variable and the proportion of 20:5 ( $r = 0.29$ ,  $P < 0.05$ ). None of the other FA measured were significantly related to the measured variables evaluating vascular reactivity.

All of the significant associations reported between the proportions of different FA and indices of vascular reactivity were still significant after the influences of age and sex were taken into account in multiple regression analyses.

*Intervention protocol.* When serum lipids were measured at the end of each intervention period, serum LDL cholesterol



**FIG. 1.** Mean  $\pm$  SEM for forearm blood flow (mL/min/100 mL tissue) at different time points during reactive hyperemia following 5 min of occlusion of the forearm in the cross-sectional study. Maximal flow was measured 5 s after release of occlusion.

levels were significantly higher for the SAT diet compared to the RO diet ( $4.33 \pm 0.34$  vs.  $3.85 \pm 0.85$  mmol/L,  $P < 0.001$ ). No significant difference between the two diets was seen for serum TG levels ( $1.43 \pm 0.96$  for the SA diet vs.  $1.24 \pm 0.65$  mmol/L for the RO diet,  $P = 0.18$ ).

The relative FA composition of serum phospholipids at the end of the two diet periods is given in Table 3. In general, the proportions of saturated FA were higher for the SAT diet than for the RO diet. The reverse was generally seen for the PUFA, except that the proportion of 20:3 was significantly higher for the SAT diet.

As can be seen in Table 4, no significant differences in blood pressure were seen between the two diets. However, there was a nonsignificant tendency for the heart rate to be higher for the SAT diet than for the RO diet ( $P = 0.066$ ).

As can also be seen in Table 4, the resting FBF was significantly higher for the SAT diet than for the diet rich in PUFA. FBF at 80 s during hyperemia was also significantly increased with the SAT diet compared to the RO diet. Although the maximum FBF during hyperemia did not differ between the diets, the relative maximal FBF was attenuated with the SAT diet compared to the RO diet.

**TABLE 2**  
Proportion of FA in Serum Cholesterol Esters  
in the Cross-Sectional Protocol<sup>a</sup>

FA	Proportion
14:0	0.9 $\pm$ 0.2
15:0	0.2 $\pm$ 0.03
16:0	11.3 $\pm$ 0.6
16:1n-7	3.7 $\pm$ 1.2
18:0	0.9 $\pm$ 0.1
18:1n-9	21.7 $\pm$ 12.4
18:2n-6	50.0 $\pm$ 3.7
18:3n-6	0.8 $\pm$ 0.3
18:3n-3	0.9 $\pm$ 0.2
20:3n-6	0.7 $\pm$ 0.2
20:4n-6	6.6 $\pm$ 1.2
20:5n-3	1.9 $\pm$ 0.8
22:6n-3	1.0 $\pm$ 0.2

<sup>a</sup>Mean  $\pm$  SD given in percentages.

**TABLE 1**  
Clinical Characteristics of the Subjects in the Two Protocols<sup>a</sup>

	Cross-sectional protocol ( $n = 56$ )	Intervention protocol ( $n = 19$ )
Women/men	25/31	6/13
Age (yr)	50 $\pm$ 13	50 $\pm$ 8
BMI (kg/m <sup>2</sup> )	24.8 $\pm$ 3.2	24.5 $\pm$ 2.6
Serum cholesterol (mmol/L)	5.39 $\pm$ 0.94	6.19 $\pm$ 1.02
Serum TG (mmol/L)	0.85 $\pm$ 0.51	1.40 $\pm$ 0.61
Fasting plasma glucose (mmol/L)	4.34 $\pm$ 0.42	4.96 $\pm$ 0.29
Systolic blood pressure (mm Hg)	123 $\pm$ 11	119 $\pm$ 11
Diastolic blood pressure (mm Hg)	79 $\pm$ 14	72 $\pm$ 16

<sup>a</sup>Mean  $\pm$  SD are given. BMI, body mass index.

**TABLE 3**  
**Relative FA Composition (%) in Serum Phospholipids**  
**During the Rapeseed Oil-Based Diet (RO) and the Saturated**  
**FA Diet (SAT) in the Intervention Protocol<sup>a</sup>**

FA	RO	SAT	P value
14:0	0.42 ± 0.06	0.55 ± 0.09	<0.001
15:0	0.18 ± 0.04	0.23 ± 0.03	<0.001
16:0	29.5 ± 1.25	29.8 ± 1.24	0.12
16:1n-7	0.57 ± 0.15	0.68 ± 0.16	<0.001
17:0	0.41 ± 0.06	0.43 ± 0.06	0.11
18:0	14.0 ± 1.03	14.3 ± 0.79	0.049
18:1n-9	13.7 ± 1.23	12.8 ± 1.78	0.0016
18:2n-6	22.0 ± 1.52	22.5 ± 1.76	0.18
18:3n-3	0.57 ± 0.12	0.45 ± 0.22	<0.001
20:3n-6	2.82 ± 0.60	3.15 ± 0.51	0.004
20:4n-6	8.12 ± 1.04	8.14 ± 1.25	0.88
20:5n-3	1.79 ± 0.45	1.37 ± 0.37	<0.001
22:5n-3	1.13 ± 0.16	1.10 ± 0.18	0.37
22:6n-3	4.75 ± 0.75	4.48 ± 0.78	0.075

<sup>a</sup>Mean ± SD are given.

There were significant carryover effects (especially from the SAT diet to the second diet period) for resting FBF and FBF at 80 s during hyperemia. Therefore, for these variables only the first diet period was used for calculations.

## DISCUSSION

In both the cross-sectional and the intervention protocols of the present study, the composition of FA in serum lipids was a major determinant of both resting FBF and vascular reactivity during the hyperemic phase.

The resting FBF variable has many different determinants. It is increased in males compared to females, probably due to the higher forearm muscle mass and the need for an increased nutrient blood flow in the male forearm. Resting FBF also has been shown to be governed by NO release, as local infusion of the NO blocker L-NMMA has been shown to cause a 25–50% decrease in resting FBF (10). Other factors, such as glucose infusion, euglycemic hyperinsulinemia, or an acute elevation of FFA by means of intralipid and heparin infusion, could also increase the resting FBF (16,17). At first glance it would seem favorable to increase FBF with saturated FA, as this blood flow characteristic is in part NO dependent. How-

**TABLE 4**  
**Blood Pressure and Forearm Blood Flow (FBF, mL/min/100 mL tissue)**  
**for the RO Diet and the SAT Diet in the Intervention Protocol<sup>a</sup>**

	RO	SAT	P value
Systolic blood pressure (mm Hg)	116 ± 13	118 ± 10	0.27
Diastolic blood pressure (mm Hg)	70 ± 11	72 ± 12	0.22
Heart rate (beats/min)	56 ± 8	58 ± 10	0.066
Resting FBF <sup>b</sup>	6.4 ± 3.5	7.6 ± 3.5	0.03
Absolute maximal FBF	30.1 ± 6.4	29.4 ± 9.0	0.43
Relative maximal FBF <sup>b</sup>	4.6 ± 2.0	3.0 ± 1.3	0.02
FBF at 80 s <sup>b</sup>	4.6 ± 1.7	8.4 ± 3.4	0.002

<sup>a</sup>Mean ± SD are given. For other abbreviations see Table 3.

<sup>b</sup>Indicates a variable with a carryover effect. Data are from the first diet period only.

ever, as both the proportions of 18:0 and 20:3 were positively associated with resting FBF, it seems highly unlikely that this FA profile would be of any benefit, as this profile has been associated with the development of CHD (18).

As could be seen in the intervention part of the present study, a dietary change can induce changes in the FA profile in serum. The FA profile in serum cholesterol esters has previously been found to reflect mainly the quality of fat intake during the last weeks (11,12). That genetic and metabolic factors also influence the FA profile cannot be excluded, however, and could, at least in part, be responsible for the associations found in the cross-sectional study.

Neither in the cross-sectional study nor in the intervention was an association found between the absolute level of the maximal FBF during hyperemia, in part being NO-dependent (9,19), and FA. However, the relative maximal FBF was attenuated during the SAT diet, and positive relationships were seen in the cross-sectional study when compared to proportions of some PUFA. Although the relationships described in the intervention study were mainly because the resting FBF, and thereby also the relative maximal FBF, were altered, the relative maximal FBF also is known to be more closely related to endothelium-dependent vasodilation than to endothelium-independent vasodilation (14).

A relationship between FA composition and FBF during the decremental part of the hyperemic phase (FBF at 80 s) was shown in both the cross-sectional and the intervention protocols, suggesting that these measurements are governed by similar mechanisms.

The proportion of FA in the cholesterol esters was measured in the cross-sectional study, but in the intervention the FA in phospholipids were determined. As seen in the tables, measurements in these two compartments gave different information on the proportions of the different FA. Measuring FA in cholesterol esters is our usual approach in cross-sectional studies in which the effects of long-term dietary intake are to be evaluated. However, the proportions of long-chain FA are quite small in that compartment. Therefore, in the intervention, measurements in phospholipids were used because the proportions of long-chain FA were higher and thus the sensitivity to detect a change in these FA would be better when food intake was altered. The results would, however, be quite similar with both types of measurements. Subjects with a relative lack of long-chain FA in cholesterol esters would also have a relative shortage of these FA in the phospholipids, and vice versa.

We recently showed that different FA in serum cholesterol esters could affect the endothelium in divergent ways in apparently healthy subjects (20). In the experimental setting, divergent effects of different FA also were described. Both oleic and palmitic acids were shown to impair NO-dependent vasodilation, whereas stearic acid did not induce this effect (21,22). Furthermore, in rats given a diet rich in n-3 PUFA an improvement in NO-dependent vasodilation was seen (23). Several mechanisms might be involved in the actions of FA on vascular function. First, different FA are associated with



different degrees of lipid oxidation, a process that could both inhibit NO formation and transform NO to inactive compounds such as peroxynitrite. Second, FA affect cell membrane fluidity in different ways, altering the permeability and action of different ion pumps in the membrane. In this way, transmembrane calcium ion fluxes involved in NO formation could be altered. Third, FA are involved in the formation of both vasodilatory and vasoconstrictive prostanoid metabolites, such as prostacycline and thromboxane A<sub>2</sub>.

These studies support the view emerging from the present study that the composition of FA is a determinant of vascular reactivity and that NO, at least in part, is involved in this process.

## REFERENCES

- Castelli, W.P., Doyle, J.T., Gordon, T., Hames, C.G., Hjortland, M.C., Hulley, S.B., Kagan, A., and Zukel, W.J. (1997) HDL Cholesterol and Other Lipids in Coronary Heart Disease. The Cooperative Lipoprotein Phenotyping Study, *Circulation* 55, 767–772.
- Caggiula, A.W., and Mustad, V.A. (1997) Effects of Dietary Fat and Fatty Acids on Coronary Artery Disease Risk and Total and Lipoprotein Cholesterol Concentrations: Epidemiologic Studies, *Am. J. Clin. Nutr.* 65, 1597S–1610S.
- Mensink, R.P., and Katan, M.B. (1992) Effect of Dietary Fatty Acids on Serum Lipids and Lipoproteins. A Meta-analysis of 27 Trials, *Arterioscler. Thromb.* 12, 911–919.
- Eritsland, J. (2000) Safety Considerations of Polyunsaturated Fatty Acids, *Am. J. Clin. Nutr.* 71, 197S–201S.
- Tsimikas, S., and Reaven, P.D. (1998) The Role of Dietary Fatty Acids in Lipoprotein Oxidation and Atherosclerosis, *Curr. Opin. Lipidol.* 9, 301–307.
- Furchgott, R.F., and Zawadzki, J.V. (1980) The Obligatory Role of Endothelial Cells in the Relaxation of Arterial Smooth Muscle by Acetylcholine, *Nature* 299, 373–376.
- Palmer, R.M., Ferrige, A.G., and Moncada, S. (1987) Nitric Oxide Release Accounts for the Biological Activity of Endothelium-Derived Relaxing Factor, *Nature* 327, 524–526.
- Rosei, E.A., Rizzoni, D., Castellano, M., Porteri, E., Zulli, R., Muiesan, M.L., Bettoni, G., Salvetti, M., Muiesan, P., and Giulini, S.M. (1995) Media:Lumen Ratio in Human Small Resistance Arteries Is Related to Forearm Minimal Vascular Resistance, *J. Hypertens.* 13, 341–347.
- Tagawa, T., Imaizumi, T., Endo, T., Shiramoto, M., Harasawa, Y., and Takeshita, A. (1994) Role of Nitric Oxide in Reactive Hyperaemia in Human Forearm Vessels, *Circulation* 90, 2285–2290.
- Vallance, P., Collier, J., and Moncada, S. (1989) Effects of Endothelium-Derived Nitric Oxide on Peripheral Arterial Tone in Man, *Lancet* 2, 997–1000.
- Smedman, A.E., Gustafsson, I.B., Berglund, L.G., and Vessby, B.O. (1999) Pentadecanoic Acid in Serum as a Marker for Intake of Milk Fat: Relations Between Intake of Milk Fat and Metabolic Risk Factors, *Am. J. Clin. Nutr.* 69, 22–29.
- Zock, P.L., Mensink, R.P., Harryvan, J., deVries, J.H., and Katan, M.B. (1997) Fatty Acids in Serum Cholesteryl Esters as Quantitative Biomarkers of Dietary Intake in Humans, *Am. J. Epidemiol.* 145, 1114–1122.
- Sarabi, M., Millgård, J., and Lind, L. (1999) Effects of Age, Gender and Metabolic Factors on Endothelium-Dependent Vasodilation—A Population Based Study, *J. Intern. Med.* 246, 265–274.
- Lind, L., Sarabi, M., and Millgård, J. (1998) Methodological Aspects of the Evaluation of Endothelium-Dependent Vasodilation in the Human Forearm, *Clin. Physiol.* 18, 81–87.
- Jones, B., and Kenward, M.G. (1989) *Monographs on Statistics and Applied Probability 34: Design and Analysis of Cross-Over Trials*, Chapman & Hall, London.
- Steinberg, H.O., Tarshoby, M., Monestel, R., Hook, G., Cronin, J., Johnson, A., Bayazeed, B., and Baron, A.D. (1997) Elevated Circulating Free Fatty Acid Levels Impair Endothelium-Dependent Vasodilation, *J. Clin. Invest.* 100, 1230–1239.
- Lind, L., Fugmann, A., Vessby, B., Millgård, J., Berne, C., and Lithell, H. (2000) Impaired Endothelial Function Induced by Free Fatty Acids Is Reversed by Insulin, *Clin. Sci.* 99, 169–174.
- Öhrvall, M., Berglund, L., Salminen, I., Lithell, H., Aro, A., and Vessby, B. (1996) The Serum Cholesterol Ester Fatty Acid Composition but Not the Serum Concentration of  $\alpha$ -Tocopherol Predicts the Development of Myocardial Infarction in 50-Year-Old Men: 19 Years Follow-up, *Atherosclerosis* 127, 65–71.
- Dakak, N., Husain, S., Mulcahy, D., Andrews, N.P., Panza, J.A., Waclawiw, M., Schenke, W., and Quyyumi, A.A. (1998) Contribution of Nitric Oxide to Reactive Hyperemia: Impact of Endothelial Dysfunction, *Hypertension* 32, 9–15.
- Sarabi, M., Vessby, B., Millgård, J., and Lind, L. (2001) Endothelium-Dependent Vasodilation Is Related to Fatty Acid Composition of Serum Lipids in Healthy Subjects, *Atherosclerosis* 156, 349–355.
- Davda, R.K., Stepniakowski, K.T., Lu, G., Ullian, M.E., Goodfriend, T.T., and Egan, B.M. (1995) Oleic Acid Inhibits Endothelial Nitric Oxide Synthase by a Protein Kinase C-Independent Mechanism, *Hypertension* 26, 764–770.
- Moers, A., and Schrezenmeir, J. (1997) Palmitic Acid but Not Stearic Acid Inhibits NO Production in Endothelial Cells, *Exp. Clin. Endocrinol. Diabetes* 105 (Suppl. 2), 78–80.
- Shimokawa, H., and Vanhoutte, P.M. (1989) Dietary Omega-3 Fatty Acids and Endothelium-Dependent Relaxation in Porcine Coronary Arteries, *Am. J. Physiol.* 256, H968–H973.

[Received April 8, 2002, and in revised form November 27, 2002; revision accepted December 11, 2002]

## Are *trans* Isomers of $\alpha$ -Linolenic Acid of Nutritional Significance for Certain Populations?

Sir:

In a recent study (1), Combe and Boué established the individual daily intake and identified the origins of  $\alpha$ -linolenic (18:3n-3) acid consumed by a population of women from the southwestern region of France (Aquitaine). They showed that vegetable oils contributed only 9% to this intake, the remainder coming from animal fats (73%; mainly dairy products) and vegetable lipids (27%). The total daily intake of 18:3n-3 acid by nonpregnant women ( $n = 79$ ) was  $0.6 \pm 0.2$  g/p/d ( $0.8 \pm 0.3$  for pregnant women;  $n = 61$ ). From these data, it can be estimated that only *ca.* 60 mg of  $\alpha$ -linolenic acid is attributable to vegetable oils. In the region considered, olive oil is a significant source of  $\alpha$ -linolenic acid, contributing approximately 25 mg/p/d (1).

Olive oil (virgin) and animal fats are a source of unaltered all-*cis*-18:3n-3 acid, whereas other vegetable oils are deodorized and contain  $\alpha$ -linolenic acid geometrical isomers ( $\alpha$ -LAGI) presenting at least one *trans*-ethylenic bond (2–5). A mean proportion of 17% for the latter components (relative to total 18:3n-3 acids) could be established for different oils from different countries (5). Thus, consumption of  $\alpha$ -LAGI should not exceed, on average, 5–6 mg/p/d for the population of Aquitaine women. This quantity would include *ca.* 2 mg for each of the *trans*-9,*cis*-12,*cis*-15 and *cis*-9,*cis*-12,*trans*-15 isomers, and 1 mg of both the *cis*-9,*trans*-12,*cis*-15 and *trans*-9,*cis*-12,*trans*-15 isomers (calculated according to Ref. 5). Because these isomers are rapidly catabolized (6), only a fraction of these quantities remains for either incorporation into tissue lipids or further desaturation and elongation to longer polyunsaturated chains (7). Such trivial amounts indicate that  $\alpha$ -LAGI should not be of major nutritional significance in the adult population considered and may explain why these isomers could not be detected by gas chromatograph in the adipose tissue of the same population (8). This likely also occurs in Mediterranean countries with similar diets rich in vegetables, dairy lipids, and olive oil. However, this should not be the case in those countries where rapeseed and soybean oils are the major sources of  $\alpha$ -linolenic acid (many European countries and North America). Even in France, where the use of rapeseed or soybean oil for deep-frying is forbidden by the law, exceptions were shown to occur, either in restaurants (9)

or by individual people (10). Thus, the Aquitaine study (1) may not be representative of the whole French population, and further studies are required.

On the other hand, the metabolic fate of  $\alpha$ -LAGI may be different in lactating women, as these isomers are directly incorporated into milk lipids (10,11).  $\alpha$ -LAGI also have been shown to occur in infant formulas from France and Canada (12,13), where deodorized  $\alpha$ -linolenic acid-containing oils are added to meet the requirements for 18:3n-3 acid intake, and they may then be of nutritional importance for neonates, whether they are fed breast milk or infant formulas. Consequently, in Europe  $\alpha$ -LAGI remain of nutritional concern.

### REFERENCES

1. Combe, N.A., and Boué, C. (2001) Apports alimentaires en Acides Linoléique et alpha-Linolénique d'une Population d'Aquitaine, *Oléagineux, Corps Gras, Lipides* 8, 118–121.
2. Wolff, R.L. (1992) *Trans*-Polyunsaturated Fatty Acids in French Edible Rapeseed and Soybean Oils, *J. Am. Oil Chem. Soc.* 69, 106–110.
3. Wolff, R.L. (1993) Further Studies on Artificial Geometrical Isomers of  $\alpha$ -Linolenic Acid in Linolenic Acid-Containing Oils, *J. Am. Oil Chem. Soc.* 70, 219–224.
4. Wolff, R.L. (1993) Occurrence of Artificial *trans*-Polyunsaturated Fatty Acids in Refined (deodorized) Walnut Oils, *Sci. Aliments* 13, 155–163.
5. Wolff, R.L. (1997) *Trans* Isomers of  $\alpha$ -Linolenic Acid in Deodorized Oils, *Lipid Technol. Newslett.* 3, 36–39.
6. Bretillon, L., Chardigny, J.M., Sébédio, J.-L., Noël, J.P., Scrimgeour, C.M., Fernie, C.E., Loreau, O., Gachon, P., and Beaufrère, B. (2001) Isomerization Increases the Postprandial Oxidation of Linoleic Acid but Not  $\alpha$ -Linolenic Acid in Men, *J. Lipid Res.* 42, 995–997.
7. Brétilon, L., Chardigny, J.M., Noël, J.P., and Sébédio, J.-L. (1998) Desaturation and Chain Elongation of 1-<sup>14</sup>C Mono-*trans* Isomers of Linoleic and  $\alpha$ -Linolenic Acids in Perfused Rat Liver, *J. Lipid Res.* 39, 2228–2239.
8. Boué, C., Combe, N., Billeaud, C., Mignerot, C., Entressangles, B., Thery, G., Geoffrion, H., Brun, J.L., Dallay, D., and Leng, J.J. (2000) *Trans* Fatty Acids in Adipose Tissue of French Women in Relation to Their Dietary Sources, *Lipids* 35, 561–566.
9. Sébédio, J.-L., Grandgirard, A., Septier, C., and Prevost, J. (1987) Etat d'Altération de Quelques Huiles de Friture Prélevées en Restauration, *Rev. Fr. Corps Gras.* 34, 15–18.
10. Chardigny, J.M., Wolff, R.L., Mager, E., Sébédio, J.-L., Martine, L., and Juanéda, P. (1995) *Trans* Mono- and Polyunsaturated Fatty Acids in Human Milk, *Eur. J. Clin. Nutr.* 49, 523–531.
11. Precht, D., and Molkentin, J. (1999) C18:1, C18:2 and C18:3

Paper no. L8970 in *Lipids* 37, 1147–1148 (December 2002).

Abbreviations: g/p/d, grams per person per day; mg/p/d, milligrams per person per day.

- trans* and *cis* Fatty Acid Isomers Including Conjugated *cis*  $\Delta^9$ ,*trans*  $\Delta^{11}$  Linoleic Acid (CLA) as Well as Total Fat Composition of German Human Milk Lipids, *Nahrung* 43, 233–244.
12. Chardigny, J.M., Wolff, R.L., Mager, E., Bayard, C.C., Sébédio, J.-L., and Ratnayake, W.M.N. (1996) Fatty Acid Composition of French Infant Formulas with Emphasis on the Content and Detailed Profile of *trans* Fatty Acids, *J. Am. Oil Chem. Soc.* 73, 1595–1601.
13. Ratnayake, W.M.N., Chardigny, J.M., Wolff, R.L., Bayard, C.C., Sébédio, J.-L., and Martine, L. (1997) Essential Fatty Acids and Their *trans* Geometrical Isomers in Powdered and Liquid Infant Formulas Sold in Canada, *J. Pediatr. Gastroenterol. Nutr.* 20, 400–407.

[Received December 28, 2001; accepted December 12, 2002]

Robert L. Wolff\*  
INRA, UNL  
21065 Dijon cedex, France

\_\_\_\_\_  
\*Deceased.

# Reassessment of the Contribution of Bovine Milk Fats to the *trans*-18:1 Isomeric Acid Consumption by European Populations. Additional Data for Rumenic (*cis*-9,*trans*-11 18:2) Acid

Sir:

In 1995 (1), we published a detailed account of the contribution of ruminant fats to the daily *trans*-18:1 acid intake by European populations. New data on bovine milk consumption (2) have recently been published by the CNIEL (National Inter-Professional Center for Dairy Economics) for 15 countries of the European Union. Some slight trends could be noted between the two periods for the consumption of dairy fats in several (Mediterranean) countries; e.g., Italy, Spain, Greece, and Portugal had higher intakes, whereas other countries showed a significant decrease in their consumption (e.g., Denmark). Also, data were not available for countries such as Austria, Sweden, and Finland in our previous study.

Moreover, between our earlier study (1) and the present one, additional data were published on the accurate contents and profiles of *trans*-18:1 isomeric acids in bovine milk fats (e.g., Refs. 3 and 4). The main observation that was made was the dependence of these parameters on the manner of cattle feeding, e.g., barn vs. pasture feeding or transition times (barn to pasture feeding in spring and the reverse in late autumn). Furthermore, the negative energy balance during early lactation (*ca.* the first 10 wk of lactation) or special feeding conditions (e.g., ecological farming, supplementing the feed rations with fat additions) influence the *trans*-18:1 contents in milk fat (5). Hence, some geographical differences may exist, as cattle-raising habits in different countries may not be the same. Ireland represents an exception because cows are fed on pasture throughout the year, causing higher *trans*-18:1 contents (4).

In the present assessment, we chose a rounded average value of 3.7% for the *trans*-18:1 acid content of milk fat (4), which should take into account geographical variations as well as seasonal variations, and a mean content of 50% of vaccenic acid (6) (*trans*-11 18:1) relative to total *trans*-18:1 isomers (it itself varies with the feed). Furthermore, the daily per capita consumption of dairy fats was multiplied by 0.95 to take into account the proportion of FA in TG. Because the true values for individual countries may be slightly higher or lower, we give our data to the first decimal place only [except for rumenic (*cis*-9,*trans*-11 18:2) acid], and we do not consider at the moment the Irish conditions.

For most countries, the daily individual intake of *trans*-18:1 isomers from dairy products (Table 1) lies in the narrow range 1.0–1.6 g/p/d. Lower values are encountered in southern countries (Greece, Spain, and Portugal, 0.7), whereas higher values are observed in northern countries (Finland and Sweden: 1.6–1.8). Vaccenic acid evidently follows the same trends, from a low of 0.3 (Spain) to a high of 0.9 g/p/d (Finland). However, our data for Mediterranean countries are underestimates, as ewe and goat milk fats are nonnegligible dietary sources of *trans*-18:1 isomers in these countries (1). As an example, 5.9 million of goats are raised in Greece, but only 1.1 million in France. Corresponding data for lactating cows are 0.17 and 4.06 million (2). The respective human populations in these countries are 10.5 and 59.0 million inhabitants.

The CNIEL also provides data on the consumption of margarines and similar products, such as low-calorie spreads, but no reliable data are available for the *trans*-18:1 acid content in these foods. This is due to a switch from high- to low-*trans* partially hydrogenated vegetable oils being used for the manufacture of margarines in the years 1994–1995 in many European countries (7). On the other hand, *trans*-18:1 isomers are still present in foods containing partially hydrogenated vegetable oils, but they are so diverse and their *trans*-18:1 isomer content and profile so variable that a sound estimate can hardly be made.

Regarding the CLA rumenic acid, which has been quantified in 2,110 samples of European bovine milk (4), the daily per capita intakes are also given in Table 1 and have a mean value of 0.76% relative to total FA (4). This content nearly agrees with a newer value of 0.74% for French butters (4), but other French data from different seasons were somewhat lower (8). This may be attributable to the acid-catalyzed method employed to prepare FA derivatives in the latter study. Intakes of this CLA exactly follow the trend for total *trans*-18:1 acids as well as for *trans*-11 18:1 acid. For the 15 countries of the European Union, rumenic acid intake varies between 0.14 and 0.38 g/p/d, with higher values in the northern countries and lower values in the Mediterranean countries. Here too, ovine and caprine milks may contribute to higher rumenic acid intakes in Mediterranean countries (1). Apart from these particular cases, data in Table 1 may be increased by approximately 10% to take into account the contribution of beef and sheep meat lipids and tallow (1).

Taking mean contents of 5.9% *trans*-18:1, 3.5% vaccenic [unpublished data ( $n = 23$ )], and 1.4% rumenic acids from

Paper no. L8987 in *Lipids* 37, 1149–1150 (December 2002).

Abbreviation: g/p/d, grams per person per day.



**TABLE 1**  
**Consumption of Milk (in all its forms), Milk Fat, and Some of Its *trans* FA by the Populations from 15 Countries of the European Union**

	Germany	France	Italy	Netherlands	Belgium/ Luxemb.	United Kingdom	Ireland	Denmark	Greece	Spain	Portugal	Austria	Finland	Sweden	European Union (15)
Milk (kg/p/yr) <sup>a</sup>	384	406	300	320	328	280	285	344	207	189	199	371	496	450	326
Dairy fat (g/p/yr) <sup>b</sup>	14.2	15.0	11.1	11.8	12.1	10.4	10.5	12.7	7.7	7.0	7.4	13.7	18.4	16.7	12.1
Dairy fat (g/p/d)	38.9	41.1	30.4	32.3	33.2	28.5	28.8	34.9	21.1	19.2	20.3	37.6	50.4	45.8	33.0
Σ <i>trans</i> -18:1 g/p/d (99) <sup>c</sup>	1.4	1.4	1.1	1.1	1.2	1.0	1.6	1.2	0.7	0.7	0.7	1.3	1.8	1.6	1.2
Σ <i>trans</i> -18:1 g/p/d (94) <sup>d</sup>	1.7	1.5	1.1	1.1	1.4	1.1	1.3	1.7	0.7	0.6	0.6	— <sup>e</sup>	—	—	—
<i>trans</i> -11-18:1 g/p/d <sup>f</sup>	0.7	0.7	0.5	0.6	0.6	0.5	1.0	0.6	0.4	0.3	0.4	0.7	0.9	0.8	0.6
CLA (g/p/d) <sup>g</sup>	0.28	0.30	0.22	0.23	0.24	0.21	0.38	0.25	0.15	0.14	0.15	0.27	0.36	0.33	0.25

<sup>a</sup>Data established by the CNIEL (National Inter-Professional Center for Dairy Economics) for the year 1999. Milk quantities adjusted to a 3.7% fat content (w/w) and covering all dairy products. kg/p/yr, kilograms per person per year; g/p/d, grams per person per day.

<sup>b</sup>Value of the preceding row multiplied by 0.037. No wastage is taken into account.

<sup>c</sup>Calculated from an average total *trans*-18:1 isomeric acid content of 3.7%; value for Ireland taken as 5.9%.

<sup>d</sup>Values established in 1995 with data published in 1994 by the CNIEL.

<sup>e</sup>Not determined in 1995.

<sup>f</sup>Values based on a 50% content of vaccenic (*trans*-18:1) acid relative to total *trans*-18:1 isomers; value for Ireland of *trans*-11-18:1 taken as 3.5 wt%.

<sup>g</sup>CLA (*cis*-9,*trans*-11-18:2) calculated from an average content of 0.76%; value for Ireland calculated at 1.4%.

Ref. 4, for Ireland the daily individual intake in this country would amount to 1.6, 1.0, and 0.38 g/p/d, respectively.

Possible small differences concerning the average consumption of bovine milk fat for women and men (9) were not taken into account in this report.

## REFERENCES

- Wolff, R.L. (1995) Content and Distribution of *trans*-18:1 Acids in Ruminant Milk and Meat Fats. Their Importance in European Diets and Their Effect on Human Milk, *J. Am. Oil Chem. Soc.* 72, 259–272.
- Maurisson, E., and Tillier, S. (2001) *L'Economie Laitière en Chiffres*, p. 175, CNIEL, Paris.
- Wolff, R.L., Precht, D., and Molkentin, J. (1998) Occurrence and Distribution Profiles of *trans*-18:1 Acids in Edible Fats of Natural Origin, in *Trans Fatty Acids in Human Nutrition* (Sébédio, J.-L., and Christie, W.W., eds.), pp. 1–33, Oily Press, Dundee, Scotland.
- Precht, D., and Molkentin, J. (2000) Frequency Distributions of Conjugated Linoleic Acid and *trans* Fatty Acid Contents in European Bovine Milk Fats, *Milchwissenschaft* 55, 687–691.
- Precht, D., Voigt, J., Hagemeister, H., and Kanitz, W. (2001) The Influence of Dietary Rumen-Protected Linoleic Acid on Milk Fat Composition, Spreadability of Butter and Energy Balance in Dairy Cows, *Eur. J. Lipid Sci. Technol.* 103, 783–792.
- Precht, D., and Molkentin, J. (1997) Effect of Feeding on *trans* Positional Isomers of Octadecenoic Acid in Milk Fats, *Milchwissenschaft* 52, 564–568.
- Wolff, R.L., Combe, N.A., Destailhats, F., Boué, C., Precht, D., Molkentin, J., and Entressangles, B. (2000) Follow-Up of the Δ4 to Δ16 *trans*-18:1 Isomer Profile and Content in French Processed Foods Containing Partially Hydrogenated Vegetable Oils During the Period 1995–1999. Nutritional and Analytical Implications, *Lipids* 35, 815–825.
- Wolff, R.L., Bayard, C.C., and Fabien, R.J. (1995) Evaluation of Sequential Methods for the Determination of Butterfat Fatty Acid Composition with Emphasis on *trans*-18:1 Acids. Application to the Study of Seasonal Variations in French Butters, *J. Am. Oil Chem. Soc.* 72, 1471–1483.
- Fritsche, J., and Steinhart, H. (1997) Contents of *trans* Fatty Acids (TFA) in German Foods and Estimation of Daily Intake, *Fett/Lipid* 99, 314–318.

[Received January 22, 2002; accepted December 12, 2002]

Robert L. Wolff<sup>a,\*</sup> and Dietz Precht<sup>b,\*\*</sup>  
<sup>a</sup>INRA, UNL, 21065 Dijon cedex, France,  
and <sup>b</sup>Institute of Dairy Chemistry and Technology,  
Federal Dairy Research Centre, 24121 Kiel, Germany

\*Deceased.

\*\*To whom correspondence should be addressed at Institute of Dairy Chemistry and Technology, Federal Dairy Research Center, P.O. Box 6069, 24121 Kiel, Germany. E-mail: precht@bafm.de

## Recent Advances in Steroid Research

Presented at the 93rd AOCS Annual Meeting & Expo  
in Montréal, Canada, May 2002

**Edward J. Parish<sup>a</sup>, W. David Nes<sup>b</sup>, and John R. Williams<sup>c</sup>**

Departments of <sup>a</sup>Chemistry, Auburn University, Auburn, Alabama 36849, <sup>b</sup>Chemistry and Biochemistry, Texas Tech University, Lubbock, Texas 79409, and <sup>c</sup>Chemistry, Temple University, Philadelphia, Pennsylvania 19122

The AOCS has been a regular host to steroid symposia since 1970. The history of this symposium series has been published [Weete, J.D., Parish, E.J., and Nes, W.D. (2000) *Lipids* 35, 241]. These symposia have focused on current research in the areas of steroid structure, biosynthesis, chemistry, regulation, and function.

The 2002 Steroid Symposium, "Recent Advances in Steroid Research," was held at the AOCS Annual Meeting in Montréal, Canada. This year the symposium held special significance, for it hosted the presentation of the first G.J. Schroepfer Jr. Award for steroid research. The Award was established to honor the memory of Dr. George J. Schroepfer Jr., a prominent steroid biochemist and chemist who made major and lasting contributions to the steroid field. Much of his research dealt with the biosynthesis of cholesterol and its regulation. In addition, he maintained a strong organic synthesis program to support his biochemical studies. A biography describing many of Dr. Schroepfer's contributions can be found in this journal [Wilson, W.K. (2000) *Lipids* 35, 242]. Dr. Schroepfer was scheduled to be the keynote speaker at the last steroid symposium in Orlando, Florida in 1999, but unfortunately, he passed away on December 11, 1998. That

symposium was dedicated to Professor Schroepfer's memory and was a memorial symposium.

The first recipient of the G.J. Schroepfer Jr. Award for steroid research was Professor Geoffrey F. Gibbons of the Metabolic Research Laboratory at Oxford University. Professor Gibbons has made major contributions to the steroid field, and we were pleased with his nomination. Professor Gibbons was also our keynote speaker at the symposium and thus made a dual contribution to these proceedings.

As in past symposia, we are indebted to our corporate partners who helped make the symposium a success: AstraZeneca Pharmaceutical Co., Pharmacia Centre Source, and Steraloids, Inc. We appreciate their contribution and look forward to their continued support of our symposium series.

This symposium was sponsored by the Biotechnology Division of the AOCS. Speakers in the 2002 Sterol Symposium represented an international group of senior and junior scientists. We express here our appreciation to each of them for their cooperation during the planning process and for their participation in the symposium. By all accounts, the event was a success, and we are looking forward to the next steroid symposium.

# From Gallstones to Genes: Two Hundred Years of Sterol Research. A Tribute to George J. Schroepfer Jr.

Geoffrey F. Gibbons\*

Metabolic Research Laboratory, Nuffield Department of Clinical Medicine,  
University of Oxford, Oxford OX2 6HE, United Kingdom

**ABSTRACT:** The origins of cholesterol research can be traced to prerevolutionary France. The discovery of cholesterol as a single substance, present in human gallstones, owes much to the scientists of l'Académie Française, including Lavoisier, who contributed so much to the emergence of chemistry as a modern scientific discipline. Since that time, cholesterol probably has been the most intensively scrutinized natural product of all time, and it has been the subject of Nobel Prizes for several who have studied its structure, biosynthesis, and regulation. The pace of research into cholesterol shows no sign of diminishing, and recent discoveries have led to the recognition that the regulation of cholesterol metabolism is intimately linked with that of other metabolic pathways. Details of these interactions are only just emerging, but it is becoming apparent that under some circumstances it is difficult to reconcile, in a conventional manner, changes in regulatory gene expression with corresponding changes in pathway carbon flux. The present review includes some of our studies on the roles of the transcription factors sterol regulatory element-binding protein, liver X-receptor  $\alpha$ , and peroxisome proliferator activated receptor  $\alpha$  in the coordination of cholesterol and fatty acid synthesis and describes how some of the results obtained can best be interpreted from a Metabolic Control Analysis perspective of the regulation of pathway carbon fluxes.

Paper no. L9140 in *Lipids* 37, 1153–1162 (December 2002).

## A TRIBUTE TO GEORGE J. SCHROEPFER JR., JUNE 15, 1932–DECEMBER 11, 1998

I'd like to begin by saying how deeply honored I am to be the first recipient of the Schroepfer Medal. The award gives me particular pleasure, partly for nostalgic reasons, as it takes me back to my roots in steroid chemistry at the Medical Research Council Lipid Metabolism Unit at Hammersmith Hospital in West London. It was here, in 1973, that I first met George Schroepfer, who was passing through to visit old friends and acquaintances from the days when he worked as a young postdoc with George Popják in 1961. And it was at Hammersmith that Schroepfer made a major contribution to the momentous work of Popják and Cornforth in defining the com-

plete stereospecific enzymology of squalene biosynthesis from mevalonate, work that contributed to the award of the Nobel Prize in 1975 (1). Popják recognized Schroepfer's early contribution to this work in his memoir published in the *Journal of the American Oil Chemists' Society* in 1977 (2). George pursued his interest in the stereochemistry of enzymic catalysis during a further postdoctoral period in the laboratory of another Nobel Laureate, Konrad Bloch, at Harvard.

His work on the stereospecificity of lipid biosynthesis awakened Schroepfer's interest in the stereochemistry of steroids, which was reflected by his lifelong devotion to the study of oxygenated steroids. Many of those who read his recent monumental review in *Physiological Reviews*, which ran to 193 pages (3) and which he modestly described as only "fairly comprehensive," have wondered how long a "fully comprehensive" version would have been. But for George Schroepfer, this work was never an end in itself. As a clinician, he wanted to know the answer to the question "Why is a lot of cholesterol bad for you?" To this end, he devoted considerable effort to the development of oxygenated sterols as potential cholesterol-lowering drugs. As a chemist, George emphasized the need for unambiguous specification of steroid structure and rigorous proof of chemical and radiochemical purity before any conclusions could be made regarding biological function. He was often amazed by the slipshod methodology and unsubstantiated claims of some groups working in this area of research; the confusion caused by claims for a direct regulatory role for (im-pure) cholesterol in isolated cells comes to mind here.

Toward the end of George Schroepfer's life, it was becoming increasingly clear that oxysterols are important biological ligands for the transcription factor liver X-receptor  $\alpha$  (LXR $\alpha$ ), but the enzymology involved in the natural production of these ligands remained obscure. Together with colleagues at the Howard Hughes Institute, George showed that production of the cholesterol precursor, mevalonate, was essential for LXR $\alpha$  activation. The requirement for mevalonate could be spared by 20(*S*)-hydroxycholesterol and 22(*R*)-hydroxycholesterol, substances that he synthesized and characterized (4). It surely is a great pity that George's life was cut short and that he was unable to fully appreciate how much of his life's work is now bearing fruit.

## HISTORICAL BACKGROUND

Over a period of almost 250 years, cholesterol has been one of the most intensively studied of all natural products. It is

\*Address correspondence at Metabolic Research Laboratory, Radcliffe Infirmary, Woodstock Rd., Oxford OX2 6HE, United Kingdom.  
E-mail: geoff.gibbons@metabolic-research.oxford.ac.uk

Abbreviations: CYP7A1, cholesterol 7 $\alpha$ -hydroxylase; ER, endoplasmic reticulum; FAS, fatty acid synthase; LXR $\alpha$ , liver X-receptor  $\alpha$ ; MCA, Metabolic Control Analysis; PPAR $\alpha$ , peroxisome proliferator-activated receptor  $\alpha$ ; SCAP, SREBP cleavage-activating protein; SREBP, sterol regulatory element-binding protein.

only recently, however, that the substance has acquired a fearsome reputation, surpassed only by that of the Black Death in medieval Europe. But a lot of cholesterol is not bad for everyone. It has won the Nobel Prize for several of its more dedicated admirers, and the French chemist Michel Chevreul, to whom its discovery is normally attributed, lived to the grand old age of 103. Chevreul isolated cholesterol from human gallstones in 1815 and was the first to characterize it as a single, pure substance (5).

But the history of cholesterol predates even Chevreul. Its story goes back to the Cemetery of the Innocents in prerevolutionary Paris. In 1786 the Government commissioned the chemist Antoine Fourcroy, a member of the Academy of Sciences and a colleague of Lavoisier, to report on the condition of the Innocents' Cemetery as a potential health risk in view of its proximity to the nearby marketplace in the quartier des Halles. Fourcroy himself was an intriguing character who, following the overthrow of the *ancien régime*, subsequently became a member of the revolutionary government. Torn between his allegiance to his colleagues in the Academy and his apparatchik-like devotion to the aims of the revolution, he is often accused of betraying Lavoisier and thus being partly responsible for Lavoisier's execution in May 1794 during the Reign of Terror. But there is evidence that Fourcroy pleaded with Robespierre, the effective Head of the Revolutionary Government, to spare Lavoisier and almost ended up with his own neck on the block for his pains (6). Fourcroy's report on the condition of the Innocents' Cemetery involved an examination of the fat of putrefied corpses (7). He recognized that some of the properties of this *gras-de-cadavre* were similar to those of the substance that we now know as cholesterol, which he crystallized from human gallstones in 1789 (8) following the observation by F. Poulletier de la Salle, in 1770, that gallstone material was alcohol-soluble. It was also similar, in some respects, to spermaceti. Following Robert Boyle's maxim that if you can't prove that things are different, they must be the same, Fourcroy classified all these substances as "adipocire." Six years after Fourcroy's death in 1809, Chevreul distinguished chemically between these three substances on the basis of their saponifiability and baptized the gallstone material *cholestérine* the following year (9).

Cholesterol's story now moves eastward across the Rhine. The German chemists Heinrich Wieland and Adolf Windaus were awarded Nobel Prizes in 1927 and 1928, respectively, for their work on the structures of cholesterol and the bile acids. Windaus was the first to demonstrate the high cholesterol content of experimental atheroma (10). He also taught chemistry to several subsequent Nobel Laureates, including the young Hans Krebs, who was a medical student at Göttingen in 1919 after being discharged from the Imperial German Army at the end of World War I (11). It turned out, however, that the original proposed structure of the steroid nucleus (Fig. 1) was incorrect. In one of the first demonstrations of the enormous analytical power of X-ray crystallography, the studies of J.D. Bernal, working in the old Cavendish Laboratory in Cambridge (United Kingdom), showed clearly that the squat struc-

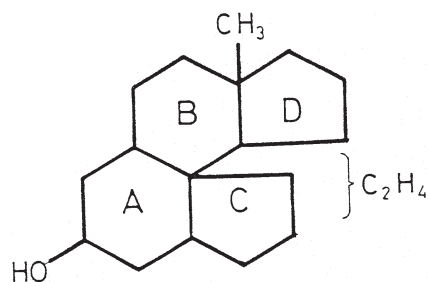


FIG. 1. Original Wieland and Windaus structure of the steroid nucleus.

ture suggested by the presence of the quaternary carbon atom was incompatible with the diffraction pattern obtained (12). Bernal never won the Nobel Prize, but he was awarded the Order of Lenin, which, given his political views, probably gave him a great deal more pleasure and satisfaction (13). The longer, more streamlined structure of the steroid nucleus that is familiar to us today was proposed independently by Wieland and Dane (14) and by Rosenheim and King in 1932 (15) and confirmed by chemical synthesis and degradation.

The discovery of the correct structure of cholesterol and the steroids now set the stage for the studies on their biosynthesis that were carried out mainly in Britain and the United States. The work of Rudolf Schoenheimer and David Rittenberg at Columbia was pivotal in this respect. Schoenheimer, who was of German origin, had worked with Adolf Windaus at Freiberg in 1926 and was one of the many Jewish intellectuals and scholars who fled Germany after the election of Hitler as Chancellor in January 1933. In 1937 Schoenheimer used deuterated water produced in Urey's laboratory at Columbia to show that cholesterol was produced in mammals as a result of the reductive polymerization of small molecules (16). In 1942, a year after Schoenheimer's untimely death, Konrad Bloch, another German emigré who had found refuge at Columbia, showed that the small monomeric building block was acetate. Bloch's later studies showed that acetate was linked biosynthetically with the cholesterol precursors squalene and lanosterol (for a review of this work, see Ref. 17). These crucial observations paved the way for the discovery, by Gordon Gould and his colleagues, that cholesterol feeding in dogs suppressed the reductive polymerization of acetate leading to cholesterol, but not to FA, in liver slices (18). This seminal work set the scene for the next 50 years' research on the regulation of cholesterol synthesis and, in more recent years, the physiological circumstances in which this regulation is integrated with that of FA synthesis (19). Another recent discovery, which emphasized the multifunctional role of cholesterol in nature, is that the proper functioning of the signaling molecule Hedgehog during vertebrate embryonic development is dependent on its covalent modification by cholesterol (20).

By 1960 it had become clear from the work of several groups, including those of Gould, Popják, Siperstein, and Lynen, that HMG-CoA reductase was an early target for the control of hepatic cholesterol synthesis, including that by dietary cholesterol. Early attempts to reproduce the *in vivo* effects of dietary cholesterol in isolated cells to which cholesterol was

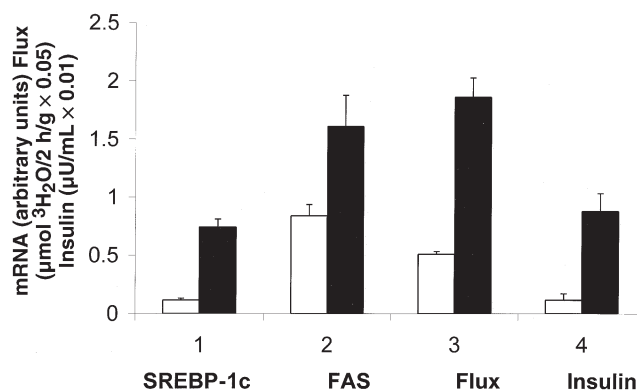


added *in vitro* were apparently successful. Real life, unfortunately, is not so simple, and this rather facile concept of direct prokaryote-like feedback inhibition was scotched by Kandutsch and Chen, who clearly showed that highly purified cholesterol added to cell cultures in a strictly defined chemical environment inhibited neither HMG-CoA reductase nor cholesterol synthesis (21). The original observations were the result of the potent inhibitory effects of small quantities of oxygenated sterol impurities present in the cholesterol added to the culture dishes. This discovery marked the beginning of a long and productive collaboration between the laboratories of Kandutsch and Schroeffer, the results of which have made a major contribution to our current understanding of the role of oxysterols in the control of transcription factor activity. The remainder of this lecture will deal with the transcriptional regulation of cholesterol and FA synthesis and will be illustrated by some of our own work at the Metabolic Research Laboratory. In particular, I would like to show how some of our results can best be understood from a Metabolic Control Analysis (MCA) perspective (22) in describing changes in overall carbon flux through these pathways.

### TRANSCRIPTIONAL REGULATION OF LIPOGENIC AND CHOLESTEROGENIC CARBON FLUX

*Interactions between sterol regulatory element-binding protein (SREBP), LXR $\alpha$ , and insulin.* Naturally occurring cholesterol precursors and oxygenated sterol metabolites of cholesterol are potent activating ligands for the transcription factor LXR $\alpha$  (4,23,24). In its ligand-bound state, LXR $\alpha$  transcriptionally activates several genes involved in the maintenance of whole-body cholesterol balance such as cholesterol 7 $\alpha$ -hydroxylase (CYP7A1) in the bile acid pathway (24) and ABC-A1 in the reverse cholesterol transport pathway (25). In mouse liver, active LXR $\alpha$  also transactivates the gene encoding SREBP-1c, another transcription factor responsible for the regulation of a portfolio of genes encoding enzymes of the lipogenic pathway (26). Feeding cholesterol in the diet of mice gives rise to an increase in the hepatic concentration of oxysterol ligands of LXR $\alpha$  (3,27) with resultant effects on target genes including SREBP-1c (28). The transcription of SREBP-1c is also regulated by insulin in a mechanism by which the insulin signal is transduced *via* insulin receptor substrate 1 (IRS-1) and PI 3-kinase (29–31). This mechanism contributes to the overall means by which insulin increases *de novo* FA synthesis (32,33).

Using mice of the SV/129 strain, we have compared the physiological consequences of changes in hepatic SREBP-1c expression caused by insulin, on the one hand, and by an LXR $\alpha$ - and oxysterol-mediated process resulting from cholesterol feeding, on the other. First, starvation for 24 h (beginning at the midpoint of the dark phase of the diurnal cycle) followed by 6 h of refeeding with a high-carbohydrate, low-fat diet (34) gave rise, as expected, to a large increase in plasma insulin ( $P < 0.001$ ) (Fig. 2). An increase in the expression of SREBP-1c mRNA ( $P < 0.001$ ) accompanied the rise in plasma insulin levels. There was also a significant increase in the

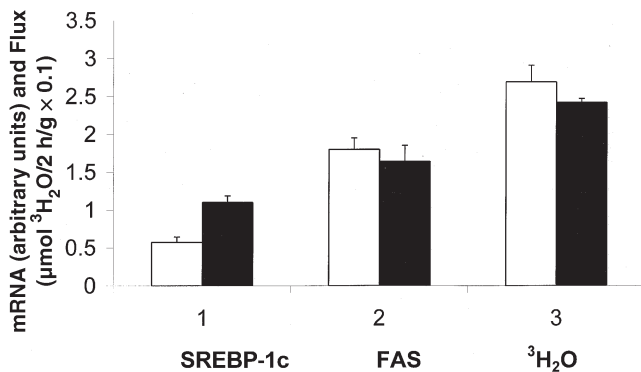


**FIG. 2.** Effects of starvation and refeeding on the lipogenic gene expression and pathway flux. Mice were starved for 24 h beginning at the midpoint of the dark phase of the diurnal cycle. They were then either killed (open bars) or fed *ad libitum* for 6 h and killed (solid bars) ( $n = 4$  in each group). In each group, at the end of the test period, some animals were injected i.p. with  $^3\text{H}_2\text{O}$  (1 mCi) 2 h before killing ( $n = 4$  in each group). Portions of the livers were used for measurement of fatty acid synthase (FAS) mRNA (columns 2) (37) and sterol regulatory element-binding protein-1c (SREBP-1c) mRNA (columns 1) (38). Measurement of the incorporation of  $^3\text{H}_2\text{O}$  into hepatic total FA (columns 3) was carried out as described previously (39). Immediately before killing, the animals were anesthetized with pentobarbital and a blood sample was taken for measurements of plasma insulin and the specific radioactivity of the plasma water. Values are presented as the mean  $\pm$  SEM for each group.

expression of an SREBP-1c target gene, fatty acid synthase (FAS) ( $P < 0.01$ ), which was itself accompanied by an increased carbon flux through the lipogenic pathway ( $P < 0.001$ ). This latter parameter was measured by injecting  $^3\text{H}_2\text{O}$  intraperitoneally *in vivo* and determining the incorporation of tritium into hepatic FA 2 h later when the animals were killed. The stoichiometry between the molar incorporation of  $^3\text{H}_2\text{O}$  and the molar incorporation of acetyl-CoA has been established (35), so this relationship can be used to determine the effects of various physiological manipulations on lipogenic carbon flux *in vivo*.

In the second experiment, mice were fed *ad libitum* for 7 d either with the standard, high-carbohydrate diet or with a similar diet supplemented with 2% (w/w) cholesterol. Cholesterol treatment, like insulin, increased the expression of SREBP-1c mRNA (Fig. 3) ( $P < 0.01$ ). However, in this case, the increase in SREBP-1c mRNA gave rise neither to an increased expression of the SREBP-1c target gene FAS nor to an increased lipogenic carbon flux. As expected, tritiated water incorporation into hepatic cholesterol *in vivo*, a measure of cholesterogenic carbon flux (36), was virtually abolished by cholesterol feeding, and there was a large decline in the expression of mRNA for HMG-CoA reductase, an enzyme with high control strength for overall pathway flux (37).

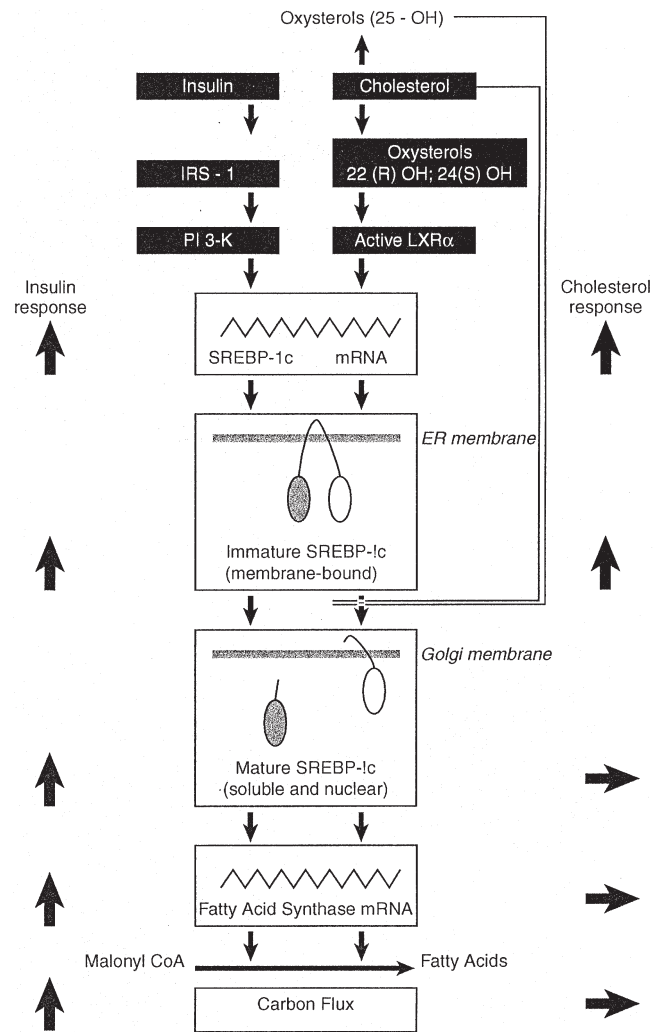
It might be argued that these results with cholesterol feeding merely confirm what has been known for many years in other mammalian species and serve to highlight the long-established fact that the effects of dietary cholesterol are specific for the hepatic cholesterogenic pathway. *De novo* lipogenic carbon flux from labeled acetate was apparently unaffected (18,40). Yet a paradox remains: What possible physiological purpose is served by an increased expression of



**FIG. 3.** Effects of dietary cholesterol on lipogenic gene expression and pathway flux. Mice were fed for 7 d with either a standard high-carbohydrate, low-fat diet (open bars) (37) or an identical diet containing 2% (w/w) cholesterol (solid bars). At the midpoint of the dark phase of the cycle, some animals from each group were killed and the livers removed for measurement of SREBP-1c mRNA (columns 1) (38) and FAS mRNA (columns 2) (37) ( $n = 4$  in each group). Other animals were injected i.p. with  $^3\text{H}_2\text{O}$  (1 mCi) and killed 2 h later ( $n = 4$  in each group) (columns 3). Values are presented as the mean  $\pm$  SEM. For abbreviations see Figure 2.

SREBP-1c mRNA when flux through a major pathway (lipogenesis) normally controlled by SREBP-1c target genes remains unchanged? The answer to this question may be found in terms of the posttranslational processing of SREBP-1c. The product of SREBP-1c mRNA translation is an immature transcription factor, which becomes active only following proteolytic cleavage (19,41). The increased expression of hepatic SREBP-1c mRNA following insulin administration either *in vivo* (30) or *in vitro* (33), which results in an increased lipogenic carbon flux (Fig. 2), was accompanied by an increase in the concentration of the mature form of SREBP (32). However, in the present work, immunoblotting of liver extracts from the cholesterol-fed mice did not show any change in the concentration of the mature form of SREBP-1c, despite the increased SREBP-1c mRNA expression (Fig. 3). This effect in mice appears to differ from the effects of cholesterol feeding in the liver of hamster, in which the mature form of SREBP-1c was reduced (42). Interestingly, the expression of SREBP-1c mRNA was not increased in the liver of the cholesterol-fed hamster (42), in contrast to that in the mouse (Fig. 3).

It has been established for some time that SREBP cleavage is sensitive to the sterol content of the intracellular membranes housing the proteolytic cleavage machinery (for reviews, see Refs. 19,41). In particular, mixtures of cholesterol and 25-hydroxycholesterol suppress the maturation of SREBP-1a in HeLa cells (43). In the absence of sterols, a specific peptide, SCAP (SREBP cleavage-activating protein) interacts with SREBP in the endoplasmic reticulum (ER) and escorts it to the Golgi, which houses the two proteases required for cleavage to give the mature form of SREBP that enters the nucleus (reviewed in Ref. 41) (Fig. 4). Sterols in some way prevent the transfer of the SCAP-SREBP complex from the ER to the Golgi, so maturation can no longer take place. It might be expected therefore that an increase in the sterol content of hepatic ER membranes following cholesterol



**FIG. 4.** Regulation and control of the SREBP-1c pathway by cholesterol and insulin in mouse liver. Insulin and cholesterol both increase SREBP-1c transcription but by different mechanisms. Cholesterol also results in a decreased cleavage of immature SREBP-1c, which imposes a constraint on the production of the mature transcription factor. The net effect of an increased transcription and translation coupled with a decreased cleavage ensures a constant production of the mature transcription factor and thus constant lipogenic carbon flux. In the absence of a constraint on cleavage, an insulin-mediated increase in transcription gives rise to an increased production of the mature transcription factor and an increased lipogenic carbon flux. IRS-1, insulin receptor substrate-1; PI 3-K, phosphatidylinositol 3-kinase; LXR $\alpha$ , liver X-receptor  $\alpha$ ; ER, endoplasmic reticulum; for other abbreviation see Figure 2.

feeding would suppress the maturation of SREBP-1c and lead to a decreased activation of its target genes. Previous experiments in the hamster have shown such a decrease in the nuclear forms of hepatic SREBP-1c and SREBP-2 following cholesterol feeding (42).

We have shown that hepatic SREBP-1c does not respond to cholesterol feeding in this manner in the mouse. In this species, in contrast to what occurs in the hamster, SREBP-1c mRNA expression increases but cleavage of the immature transcription factor remains unchanged. In the mouse, we propose that the upregulation of transcription and thus transla-

tion of SREBP-1c following cholesterol feeding compensate for an incipient sterol-mediated constraint on SREBP-1c maturation. The resulting constancy of mature SREBP-1c ensures a constant rate of target gene activation, including FAS, and thus a constant or only minimally reduced rate of lipogenic carbon flux (Figs. 3 and 4). This compensatory response in the mouse protects SREBP-1c-mediated regulation of metabolic pathways from interference by dietary cholesterol and ensures that the exogenous cholesterol response is restricted to cholesterologenic gene transcription only. In a previous study in mice, it is of interest that, although cholesterol feeding led to an almost fivefold increase in SREBP-1 mRNA expression, the expression of a target gene, FAS, was marginally decreased (44). In the liver of the hamster, however, dietary cholesterol was unable to activate hepatic LXR $\alpha$  and thus transcription of its target genes, including SREBP-1c and CYP7A1 was not increased (28). The inability of dietary cholesterol to upregulate the transcription and thus the translation of SREBP-1c in the hamster *via* a LXR $\alpha$ -mediated mechanism means that there is no opposition to the cholesterol-imposed constraint on cleavage, so the concentration of the mature form of SREBP-1c decreases. However, although there do not appear to be any reports of changes in hepatic FAS gene expression following cholesterol feeding in the hamster, rates of hepatic FA synthesis appear not to change (45).

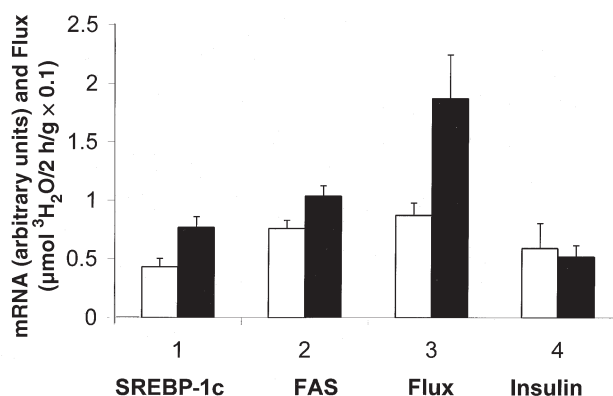
In the liver of the rat, cholesterol feeding actually upregulated total lipogenic carbon flux (46) despite the previous conclusion (40) based on the use of  $^{14}\text{C}$ -acetate only. It would be of considerable interest to determine whether the nuclear form of SREBP-1c increases under these conditions in the rat. If this is the case, then cholesterol feeding may produce sufficient LXR $\alpha$  ligands so that activation of SREBP-1c transcription outstrips the constraints on SREBP-1c peptide cleavage. Cytochrome P450 is required for the formation of LXR $\alpha$  ligands from dietary cholesterol (for a review, see Ref. 3), and it is of interest that, in the rat, administration of the P450 inhibitor ketoconazole prevented the cholesterol-mediated increase in *de novo* hepatic FA synthesis (cholesterol only:  $11.2 \pm 2.0 \mu\text{mol } ^3\text{H}_2\text{O/h/g}$ ; cholesterol plus ketoconazole:  $5.7 \pm 1.3 \mu\text{mol } ^3\text{H}_2\text{O/h/g}$ ,  $n = 6$ ,  $P < 0.05$ ) (Gibbons, G.F., and Pullinger, C.R., unpublished work).

It may turn out that, in any species, the ability to maintain equilibrium in SREBP-1c-regulated pathways following a high-cholesterol diet may depend on the magnitude of the response mounted through LXR $\alpha$ . This response may itself be determined by changes in the P450-mediated production of LXR $\alpha$ -ligands.

#### PEROXISOME PROLIFERATOR-ACTIVATED RECEPTOR $\alpha$ (PPAR $\alpha$ ) DEFICIENCY RESULTS IN ABNORMAL INSULIN REGULATION OF SREBP-1c

Another transcription factor, besides LXR $\alpha$  and the SREBP family, that contributes to hepatic lipid homeostasis, is

PPAR $\alpha$ , which targets genes involved in the regulation of FA oxidation (for reviews, see Refs. 47,48). We have previously utilized PPAR $\alpha$ -knockout mice to study the role of PPAR $\alpha$  in the regulation of SREBP-dependent metabolic pathways in the liver (37). Normal mice showed an insulin-dependent circadian periodicity of lipogenesis in the liver that was abolished under conditions of PPAR $\alpha$  deficiency. The circadian rhythm of cholesterologenesis was also abolished, although the precise role of insulin, if any, in the regulation of cholesterol synthesis is not clear. In the PPAR $\alpha$ -knockout mice, abolition of these rhythms was accompanied by a significant attenuation of the normal diurnal variations of expression of the mRNA for FAS and HMG-CoA reductase, both of which failed to increase following the increase in plasma insulin that accompanied the start of feeding at the onset of the dark phase of the cycle (37). This apparent lack of response to insulin, particularly of the lipogenic pathway, raised the possibility that SREBP-1c was abnormally regulated under conditions of PPAR $\alpha$  deficiency. To test this, we determined the expression of SREBP-1c mRNA in the livers of the normal and PPAR $\alpha$ -deficient mice at the midpoint of the dark phase of the cycle. SREBP-1c expression was compared with expression of FAS mRNA and lipogenic carbon flux (measured by  $^3\text{H}_2\text{O}$  incorporation *in vivo*) in the two genotypes. Figure 5 shows that, despite the similarity in plasma insulin concentrations and the pattern of food intake (37), the expression of SREBP-1c mRNA was significantly decreased in the liver of PPAR $\alpha$ -knockout compared to normal animals ( $P < 0.01$ ) and that this difference was accompanied by a relative decrease in the expression of FAS mRNA ( $P < 0.05$ ) and of lipogenic pathway



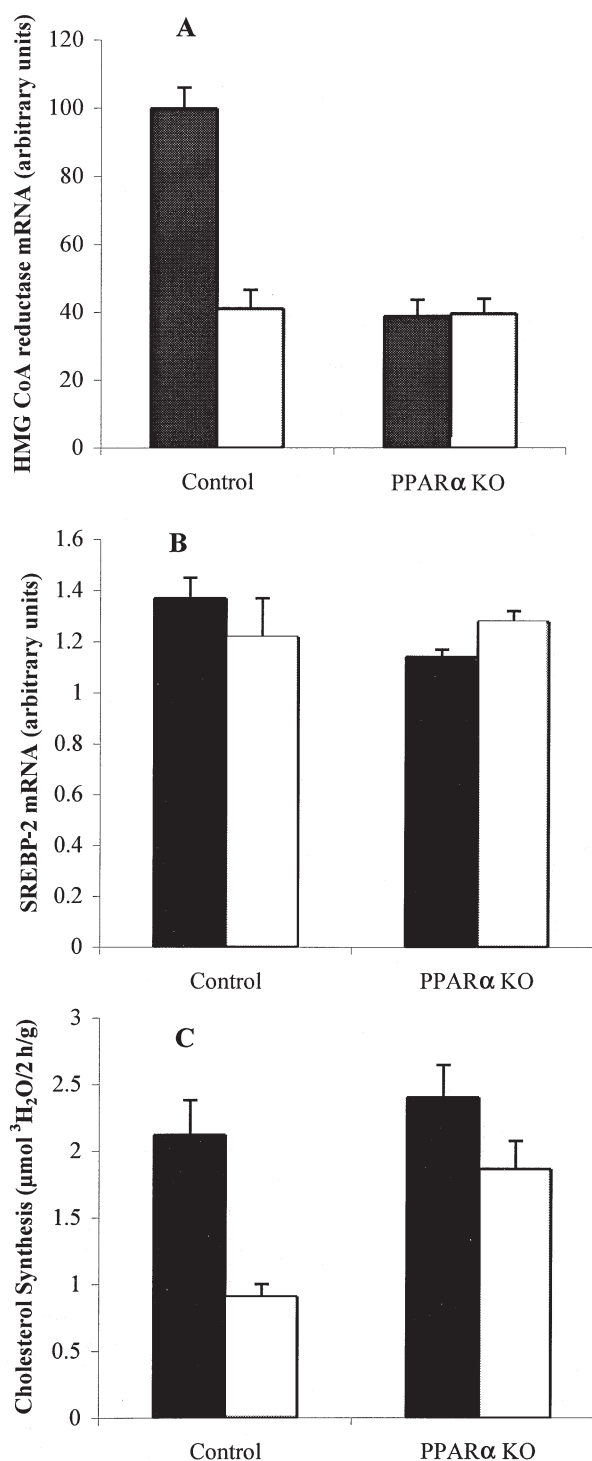
**FIG. 5.** Peroxisome proliferator-activated receptor  $\alpha$  (PPAR $\alpha$ ) deficiency results in abnormal regulation of SREBP-1c mRNA expression and lipogenic carbon flux. Groups of normal (solid bars) and PPAR $\alpha$ -knockout (open bars) mice were killed at the midpoint (sixth hour) of the dark phase of the diurnal cycle. The livers were removed and portions used to measure the concentration of the mRNA for SREBP-1c (columns 1) and FAS (columns 2) ( $n = 4$  in each group). At the same times other groups of mice were injected i.p. with  $^3\text{H}_2\text{O}$  (1 mCi) and killed 2 h later. The livers were removed for measurement of  $^3\text{H}_2\text{O}$  incorporation into FA (columns 3) (37). Immediately before killing, the animals were anesthetized with pentobarbital and blood samples taken from the descending *vena cava*. These were used for measurements of the plasma insulin concentration (columns 4) and for the specific radioactivity of plasma water. The values are presented as means  $\pm$  SEM. For abbreviations see Figure 2.

flux ( $P < 0.05$ ). Other insulin-dependent metabolic pathways in the liver also respond abnormally to starvation and refeeding in PPAR $\alpha$ -knockout mice (38), and under these conditions, the knockout mice show many of the metabolic characteristics of insulin resistance.

### PPAR $\alpha$ DEFICIENCY LEADS TO AN UNCOUPLING OF HMG-CoA REDUCTASE mRNA EXPRESSION FROM CHOLESTEROGENIC CARBON FLUX

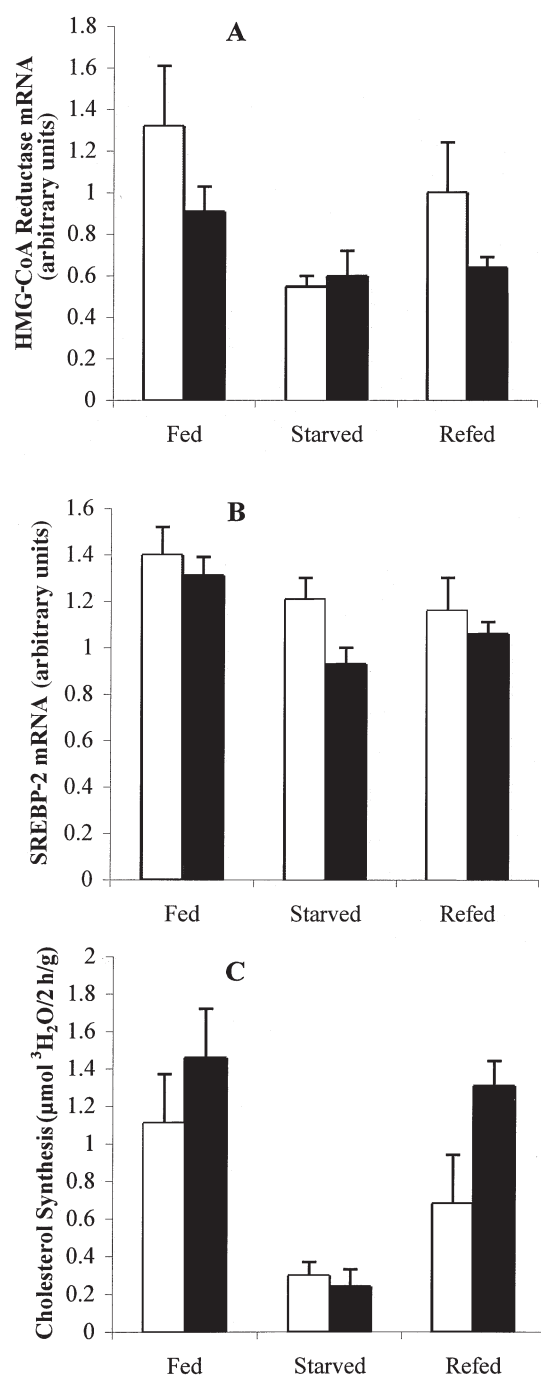
The diurnal rhythm studies showed that PPAR $\alpha$  deficiency led to an abolition of the normal variations of cholesterogenic carbon flux and HMG-CoA reductase mRNA expression. However, compared to the normal mice, carbon flux in the PPAR $\alpha$  knockout mice was maintained at a constantly high level, whereas HMG-CoA reductase mRNA remained constantly low (Fig. 6). Thus, compared to the normal mice, a higher rate of cholesterogenic carbon flux was supported by a lower expression of reductase mRNA. In other words, the functional efficiency of reductase mRNA expression for cholesterol synthesis was higher in the livers of the PPAR $\alpha$ -knockout mice than in the normal livers (34). SREBP-2 is generally considered to be a more important transcriptional activator of cholesterogenic genes, including HMG-CoA reductase, than is SREBP-1 (19). However, it is apparent from Figure 6 that there was no diurnal periodicity of SREBP-2 mRNA expression in either of the two mouse genotypes. Nor was there any difference in expression between the wild-type and the knockout mice.

It is well known that diurnal variations in cholesterogenesis and HMG-CoA reductase activity in rodents are associated with the changing pattern of food intake over the 24-h cycle (49,50), although the precise role of insulin is obscure. More extreme changes in food intake occur during starvation followed by refeeding, and these changes are again associated with parallel changes in cholesterogenic carbon flux and HMG-CoA reductase activity. We wanted to determine whether reductase expression and cholesterogenesis responded abnormally to starvation and refeeding under conditions of PPAR $\alpha$  deficiency as appeared to be the case over the diurnal cycle. To investigate this problem, mice of both genotypes were starved for 24 h (beginning at the midpoint of the dark phase of the diurnal cycle) and then either killed or refed *ad libitum* for a further 6 h. Normally fed mice of both genotypes were also tested at this point as controls (at the end of the dark phase of the cycle). Figure 7 shows that, following 24-h starvation of the normal mice, the expression of reductase mRNA decreased and then increased after refeeding. Similar changes also occurred in the rates of cholesterogenic fluxes, although the amplitudes of these changes were somewhat greater. In the liver of the PPAR $\alpha$ -knockout mice, however, although the amplitudes of the changes in cholesterogenic carbon flux were similar to or even higher than those in the normal mouse, there was very little or no change in the expression of reductase mRNA during starvation and refeeding. In particular, despite a sixfold increase in cholesterogenic



**FIG. 6.** Uncoupling of HMG-CoA reductase mRNA expression from cholesterogenic carbon flux in the livers of PPAR $\alpha$ -knockout mice. Normal (control) and PPAR $\alpha$ -knockout mice were killed at the midpoints (sixth hour) of the dark phase (solid bars) or of the light phase (open bars) of the diurnal cycle. The livers were removed, and the expression (A) of HMG-CoA reductase and (B) of SREBP-2 mRNA was determined (34) ( $n = 10$  in each group). For measurement of hepatic cholesterogenesis, other groups of mice (C) were injected with  $^3\text{H}_2\text{O}$  at the sixth hour of either the dark phase or the light phase and killed 2 h later ( $n = 12$  in each group). The values are presented as the means  $\pm$  SEM of each group. Reproduced from Reference 34 with permission. For abbreviations see Figures 2 and 5.





**FIG. 7.** Changes in cholesterogenic carbon flux are not accompanied by changes in the expression of HMG-CoA reductase mRNA during starvation and refeeding of PPAR $\alpha$ -knockout mice. Groups of normal (open bars) and PPAR $\alpha$ -deficient (solid bars) mice were starved for 24 h beginning at the midpoint of the dark phase of the diurnal cycle. Some mice in each group ( $n = 4$ ) were killed. Others were fed *ad libitum* and killed 6 h later ( $n = 4$ ). Livers were removed for measurement of SREBP-2 mRNA and HMG-CoA reductase mRNA. Identical groups of mice were used for measurement of  $^3\text{H}_2\text{O}$  incorporation into hepatic cholesterol ( $n = 4$  in each group; see legend to Fig. 2). Values are presented as the mean  $\pm$  SEM for each group. Reproduced from Reference 34 with permission. For abbreviations see Figures 2 and 5.

flux during refeeding, there was no change whatever in reductase mRNA expression.

Thus, the amounts of reductase mRNA required to support a given rate of carbon flux varied considerably in the livers of the knockout mice, whereas those in the wild-type remained relatively consistent (Table 1). Also, in the fed and refed states, the observed rates of cholesterogenesis in the livers of the knockout mice were supported by a lower level of reductase mRNA expression than those in the wild-type. In other words, the efficiency of reductase gene expression for cholesterogenic pathway flux was greater in the knockout than the wild-type animal (Table 1). Similar to the situation over the diurnal cycle, starvation and refeeding had little or no effect on the expression of SREBP-2 mRNA (Fig. 7).

To ascertain whether the abnormal responses of HMG-CoA reductase mRNA in the PPAR $\alpha$ -deficient mice described above were associated with an abnormal response to dietary cholesterol, mice of both genotypes were fed a diet enriched in cholesterol (2% w/w). In mice of both genotypes, HMG-CoA reductase mRNA expression was decreased to the same extent, as was cholesterogenic flux (34). Again, similar to the wild-type mice, cholesterol feeding increased SREBP-1c mRNA, but there was no change in the concentration of the mature form of the transcription factor.

#### MCA OF CHOLESTEROL SYNTHESIS

The above observations of uncoupling between reductase expression and cholesterogenic carbon flux in the PPAR $\alpha$ -knockout mice easily could be dismissed by assuming that, under these conditions, reductase is not “rate-limiting” for cholesterol synthesis. This is a somewhat facile explanation and begs a definition of exactly what is meant by the expression “rate-limiting step.” It is generally assumed that, within intact cells, “rate-limiting steps” are saturated with substrate and the supply of substrate for this step never becomes limiting for pathway flux. Furthermore, a quantitative relationship is considered to exist between the activity (or amount) of a rate-limiting enzyme and overall pathway flux. In other words, within a given pathway, changes in the activity (or amount) of a rate-limiting enzyme account for all of the changes in overall flux through the pathway. These assumptions have never been rigorously tested for HMG-CoA reductase, and the many instances in which experimental evidence suggests otherwise have been conveniently sidelined. On the other hand, evidence from a large number of experiments carried out in many areas of metabolic regulation suggests that overall pathway flux is determined by a number of steps, and the contribution of each step to changes in overall flux is defined by its “control strength” or “flux-control coefficient” (22). This concept, embodied in the MCA approach to the question of flux regulation, has been used successfully to explain the regulation of several pathways, including glycogen synthesis (51) and may be of universal applicability in the interpretation of functional genomic data (52) and in biotechnology and medicine (53). This approach also forces one to consider the effects, on the regulation of a particular pathway, of simultaneous changes in flux through other pathways,

**TABLE 1**  
**Efficiency<sup>a</sup> of HMG-CoA Reductase mRNA Expression for Cholesterogenic Carbon Flux<sup>b</sup>**

Fed		Starved		Refed	
Wild-type	KO	Wild-type	KO	Wild-type	KO
0.84 ± 0.21	1.64 ± 0.24	0.58 ± 0.08	0.40 ± 0.10	0.67 ± 0.19	2.08 ± 0.20

<sup>a</sup>Measured as  $\mu\text{mol } ^3\text{H}_2\text{O}$  incorporated per unit mRNA.

<sup>b</sup>During the fed/starved/refed transition in wild-type and peroxisome proliferator-activated receptor  $\alpha$ -deficient (KO) mice.

particularly those that provide and compete for common substrates.

A classic example of this situation relates to the supply and demand for the pool of acetyl-CoA in the cytosol of the cell. This pool is the common source of lipogenic and cholesterogenic carbon. One of the factors that determines supply of cytosolic acetyl-CoA is the activity of ATP:citrate lyase. This enzyme converts citrate, emerging from the mitochondrion, into cytosolic acetyl-CoA and oxaloacetate. Inhibition of ATP:citrate lyase with hydroxycitrate in cultured hepatocytes leads to a shortage of cholesterogenic precursor acetyl-CoA and a decreased cholesterogenic carbon flux. Under these conditions the  $V_{\text{max}}$  of reductase, measured under substrate-saturating conditions, increased twofold (54). This experiment suggests that reductase is not saturated with substrate in the intact cell and that enzymes affecting HMG-CoA substrate availability, such as ATP:citrate lyase, have, in terms of MCA, a high flux control coefficient for cholesterogenic pathway flux. Under these conditions, the  $V_{\text{max}}$  or capacity of reductase increases in an attempt to maintain cholesterogenic flux through the pathway. This is an analogous response to an increased LDL receptor capacity, which arises from a decreased availability of extracellular LDL cholesterol and which serves as a compensatory response to an incipient decline in cellular cholesterol influx. By the same token, an increased reductase activity does not always equate with an increased cholesterogenic pathway flux but reflects a compensatory response to a decreased substrate supply. Under these conditions of reduced substrate supply, the efficiency of reductase for maintaining cholesterol carbon flux is diminished.

Again, because lipogenesis and cholesterogenesis compete for the same common pool of acetyl-CoA, any change in lipogenic carbon flux may affect the availability of acetyl-CoA for cholesterol production. This is particularly true in organs such as the liver where the FA pathway is the "fat cat" and consumes 10 times more substrate than cholesterogenesis. In other lipogenic tissues, such as adipose tissue and lactating mammary gland, the cholesterol pathway faces even greater competition. In the latter organ, although flux into cholesterol is 10-fold lower than in the liver, HMG-CoA reductase capacity, or  $V_{\text{max}}$  (measured under substrate-saturating conditions in a cell-free preparation) is threefold higher (55). Reductase needs to operate at this high capacity simply to pump a small quantity of carbon into the cholesterol pathway in the face of a huge competitive demand for acetyl-CoA to meet the needs of FA synthesis for milk TAG production. In this

tissue therefore, the efficiency of reductase action for cholesterol synthesis is diminished. The demands of the lipogenic pathway for acetyl-CoA by the lactating mammary gland can be reduced by including fat in the diet. This manipulation also reduces *de novo* lipogenesis. Under these conditions, the rate of cholesterol synthesis does not change but remains exactly the same as that on a high-carbohydrate diet. Under these new circumstances, when a competing constraint has been partially alleviated, reductase has to work less hard to achieve a given flux, and its capacity, or  $V_{\text{max}}$ , decreases accordingly (55). The efficiency of reductase for cholesterol synthesis is now increased. Other similar compensatory effects in the cholesterol pathway for changes in flux through the lipogenic pathway have also been reported in hepatocytes (36).

To use an analogy for the effects of these changes in substrate availability, the efficiency of breathing at a Mt. Everest base camp, where atmospheric oxygen availability is limited, is obviously less than that at sea level. At high altitudes, breathing rates increase simply to maintain a constant supply of oxygen to the tissues. For an athlete competing in a track event at lower altitudes, a similar increase in breathing rate would obviously increase tissue oxygen supply in response to a greater demand by the exercising muscles. This rather mundane example serves to illustrate the fundamental principle that changes in the  $V_{\text{max}}$  of an enzyme can serve two purposes, depending on the physiological environment in which it has to operate: either to maintain flux homeostasis (regulation) or to change pathway flux (control).

The general concept of the metabolic efficiency of an enzyme is also applicable to transcription of the gene that encodes it. In this case, it is valid to refer to the functional efficiency of gene expression in terms of the amount of mRNA required to support a given flux rate through a pathway in different physiological, nutritional, or genetic environments. In the present work, when the PPAR $\alpha$  gene was deleted, a given expression of HMG-CoA reductase mRNA supported a higher rate of cholesterol pathway flux than when PPAR $\alpha$  was intact. This increased functional efficiency of reductase expression may have resulted from an increased availability of cytosolic acetyl-CoA arising from a decreased pathway flux of acetyl-CoA into FA in the PPAR $\alpha$ -knockout mouse (Fig. 5). It has also been noted recently that deletion of the LXR $\alpha$  gene was associated with an increased expression of cholesterogenic genes including HMG-CoA reductase. However, this increase was not accompanied by an increase in the rate of cholesterogenesis (44) and it is possible that, under

conditions of LXR $\alpha$  deficiency, cholesterologenic genes mount a concerted compensatory response to maintain pathway flux in the face of a constraint in substrate supply.

The general principle of MCA also can be adopted to explain the increased transcription of SREBP-1c mRNA as a compensatory response to the constraints on SREBP-1c peptide cleavage imposed by cholesterol feeding in the mouse. The unchanged concentration of mature SREBP-1c is the result of these two opposing effects and ensures that lipogenic flux in mouse liver remains unchanged or only minimally decreased (Fig. 3). Responses such as this may reflect the biological equivalent of the physicochemical principle of Le Chatelier: "When a constraint is placed upon a system, the system reacts in a manner which tends to remove the constraint." In any event, it is becoming clear that changes at every level of regulation and control from that of the gene to that of the activity of its ultimate product may serve to maintain metabolic equilibrium rather than to change metabolic flux when physiological, nutritional, or genetic constraints are imposed on an organism.

## ACKNOWLEDGMENTS

I would like to thank all my former colleagues, particularly Dr. John Goad (University of Liverpool, United Kingdom), the late Professor William R. Nes (Drexel University, Philadelphia, PA), Dr. Nick B. Myant [Medical Research Council (MRC) Lipid Metabolism Unit, Hammersmith, United Kingdom], Dr. Andrew A. Kandutsch (Jackson Laboratory, Bar Harbor, ME) and the late Dr. Derek H. Williamson (University of Oxford, United Kingdom) for their help, advice, and encouragement. Thanks are also due to my colleagues in the Metabolic Research Laboratory, Oxford, particularly David Wiggins, Abdel Hebbachi, and Anna-Marie Brown. I am also indebted to my colleagues at the Imperial College School of Medicine, Hammersmith Hospital (London, United Kingdom), Drs. Brian Knight and Dilip Patel, who made important contributions to the experimental work described in this review. I am grateful to Drs. Jeffrey Peters and Frank Gonzalez (National Institutes of Health, Bethesda, MD) for providing the mating pairs of PPAR $\alpha$ -knockout mice. The experimental work described in this paper was funded by the MRC of the United Kingdom and the British Heart Foundation (BHF) (United Kingdom). I thank the MRC and BHF for their support.

## REFERENCES

- Cornforth, J.W. (1976) Asymmetry and Enzyme Action, in *Les Prix Nobel en 1975*, pp. 119–132, Nobel Foundation, Stockholm.
- Popják, G. (1977) "As I Remember It." Research on Biosynthesis of Fatty Acids, Triglycerides, Squalene and Cholesterol, *J. Am. Oil Chem. Soc.* 54, 647A–659A.
- Schroepfer, G.F., Jr. (2000) Oxysterols: Modulators of Cholesterol Metabolism and Other Processes, *Physiol. Rev.* 80, 361–554.
- Forman, B.M., Ruan, B., Chen, J., Schroepfer, G.J., Jr., and Evans, R.M. (1997) The Orphan Nuclear Receptor LXR $\alpha$  Is Positively and Negatively Regulated by Distinct Products of Mevalonate Metabolism, *Proc. Natl. Acad. Sci. USA* 94, 10588–10593.
- Chevreur, M.E. (1815) *Ann. Chim. Phys.* 95, 5.
- Smeaton, W.A. (1962) *Fourcroy: Chemist and Revolutionary 1755–1809*, pp. 53–59, Heffer, London.
- Fourcroy, A. (1790) Memoire sur les differens états de cadavres trouves dans les fouilles du cimetiére des Innocens en 1786 et 1787, *Ann. Chim.* 5, 154–185.
- Fourcroy, A. (1789) Examen chimique de la substance feuilletée et cristalline continue dans les calculs biliaires; et de la nature des concrections cystiques cristallisées, *Ann. Chim.* 3, 242–252.
- Chevreur, M.E. (1816) Examen des graisses d'homme, de mouton, de boeuf, de jaguar et d'oie, *Ann. Chim. Phys.* 2, 339–372.
- Windaus, A. (1910) Über den Gehalt normaler und athermatöser Aorten an Cholesterin und Cholesterinester, *Z. Physiol. Chem.* 67, 174–184.
- Krebs, H.A. (1981) *Reminiscences and Reflections*, Oxford University Press, Oxford, United Kingdom.
- Bernal, J.D. (1932) Carbon Skeleton of the Sterols, *Chem. Ind.* 51, 466.
- Perutz, M. (2001) The Great Sage, *Chem. Br.* 37, 56–57.
- Wieland, H., and Dane, E. (1932) Untersuchungen über die Konstitution der Gallensäuren. 39. Mitteilung. Zur Kenntnis der 12-oxy-cholansäure, *Zt. Physiol. Chem.* 210, 268–281.
- Rosenheim, O., and King, H. (1932) The Ring System of Sterols and Bile Acids, *Nature* 130, 315.
- Florkin, M., and Stotz, E.H. (1979) History of Biochemistry, *Comp. Biochem.* 33A, 1–26.
- Cornforth, J.W. (2002) Sterol Biosynthesis: The Early Days, *Biochem. Biophys. Res. Commun.* 292, 1129–1138.
- Gould, R.G., Taylor, C.B., Hagerman, J.S., Warner, I., and Campbell, D.J. (1953) Cholesterol Metabolism. I. Effect of Dietary Cholesterol on the Synthesis of Cholesterol in Dog Tissues *in vitro*, *J. Biol. Chem.* 201, 519–528.
- Horton, J.D., Goldstein, J.L., and Brown, M.S. (2002) SREBPs: Activators of the Complete Program of Cholesterol and Fatty Acid Synthesis in the Liver, *J. Clin. Invest.* 109, 1125–1131.
- Ingham, P.W. (2001) Hedgehog Signaling: A Tale of Two Lipids, *Science* 294, 1879–1881.
- Kandutsch, A.A., and Chen, H.W. (1973) Inhibition of Sterol Synthesis in Cultured Mouse Cells by 7 $\alpha$ -Hydroxycholesterol, 7 $\beta$ -Hydroxycholesterol and 7-Ketocholesterol, *J. Biol. Chem.* 248, 8408–8417.
- Fell, D., ed. (1997) *Understanding the Control of Metabolism, Frontiers in Metabolism Series 2* (Snell, K., series ed.), 300 pp., Portland Press, London.
- Janowski, B.A., Willy, P.J., Devi, T.R., Falck, J.R., and Mangelsdorf, D.J. (1996) An Oxysterol Signalling Pathway Mediated by the Nuclear Receptor LXR $\alpha$ , *Nature* 383, 728–731.
- Lehmann, J.M., Kliewer, S.A., Moore, L.B., Smith-Oliver, T.A., Oliver, B.B., Su, J.L., Sundseth, S.S., Winegar, D.A., Blanchard, D.E., Spencer, T.A., and Willson, T.M. (1997) Activation of the Nuclear Receptor LXR by Oxysterols Defines a New Hormone Response Pathway, *J. Biol. Chem.* 272, 3137–3140.
- Repa, J.J., Turley, S.D., Lobaccaro, J.A., Medina, J., Li, L., Lustig, K., Shan, B., Heyman, R.A., Dietschy, J.M., and Mangelsdorf, D.J. (2000) Regulation of Absorption and ABC1-Mediated Efflux of Cholesterol by RXR Heterodimers, *Science* 289, 1524–1529.
- Schultz, J.R., Tu, H., Luk, A., Repa, J.J., Medina, J.C., Li, L., Schwendner, S., Wang, S., Thoolen, M., Mangelsdorf, D.J., Lustig, K.D., and Shan, B. (2000) Role of LXRs in Control of Lipogenesis, *Genes Dev.* 14, 2831–2838.
- Saucier, S.E., Kandutsch, A.A., Gayen, A.K., Swahn, D.K., and Spencer, T.A. (1989) Oxysterol Regulators of 3-Hydroxy-3-methylglutaryl-CoA Reductase in Liver. Effect of Dietary Cholesterol, *J. Biol. Chem.* 264, 6863–6869.
- Repa, J.J., Liang, G., Ou, J., Bashmakov, Y., Lobaccaro, J.M., Shimomura, I., Shan, B., Brown, M.S., Goldstein, J.L., and Mangelsdorf, D.J. (2000) Regulation of Mouse Sterol Regulatory Element-Binding Protein-1c Gene (SREBP-1c) by Oxysterol Receptors, LXR $\alpha$  and LXR $\beta$ , *Genes Dev.* 14, 2819–2830.
- Matsumoto, M., Ogawa, W., Teshigawara, K., Inoue, H.,

- Miyake, K., Sakaue, H., and Kasuga, M., (2002) Role of the Insulin Receptor Substrate 1 and Phosphatidylinositol 3-Kinase Signaling Pathway in Insulin-Induced Expression of Sterol Regulatory Element Binding Protein 1c and Glucokinase Genes in Rat Hepatocytes, *Diabetes* 51, 1672–1680.
30. Shimomura, I., Matsuda, M., Hammer, R.E., Bashmakov, Y., Brown, M.S., and Goldstein, J.L. (2000) Decreased IRS-2 and Increased SREBP-1c Lead to Mixed Insulin Resistance and Sensitivity in Livers of Lipodystrophic and ob/ob Mice, *Mol. Cell* 6, 77–86.
  31. Fleischmann, M., and Iynedjian, P.B. (2000) Regulation of Sterol Regulatory-Element Binding Protein 1 Gene Expression in Liver: Role of Insulin and Protein Kinase B/cAkt, *Biochem. J.* 349, 13–17.
  32. Shimomura, I., Bashmakov, Y., Ikemoto, S., Horton, J.D., Brown, M.S., and Goldstein, J.L. (1999) Insulin Selectively Increases SREBP-1c mRNA in the Livers of Rats with Streptozotocin-Induced Diabetes, *Proc. Natl. Acad. Sci. USA* 96, 13656–13661.
  33. Foretz, M., Pacot, C., Dugail, I., Lemarchand, P., Guichard, C., Le-Liepvre, X., Berthelie-Lubrano, C., Spiegelman, B., Kim, J.B., Ferré, P., and Foufelle, F. (1999) ADD1/SREBP-1c Is Required in the Activation of Hepatic Lipogenic Gene Expression by Glucose, *Mol. Cell Biol.* 19, 3760–3768.
  34. Gibbons, G.F., Patel, D.D., Wiggins, D., and Knight, B.L. (2002) The Functional Efficiency of Lipogenic and Cholesterogenic Gene Expression in Normal Mice and in Mice Lacking the Peroxisomal Proliferator-Activated Receptor  $\alpha$  (PPAR- $\alpha$ ), *Adv. Enzyme Regul.* 42, 227–247.
  35. Jungas, R.L. (1968) Fatty Acid Synthesis in Adipose Tissue Incubated in Tritiated Water, *Biochemistry* 7, 3708–3717.
  36. Gibbons, G.F., Björnsson, O.G., and Pullinger, C.R. (1984) Evidence That Changes in Hepatic 3-Hydroxy-3-methylglutaryl Coenzyme A Reductase Activity Are Required Partly to Maintain a Constant Rate of Sterol Synthesis, *J. Biol. Chem.* 259, 14399–14405.
  37. Patel, D.D., Knight, B.L., Wiggins, D., Humphreys, S.M., and Gibbons, G.F. (2001) Disturbances in the Normal Regulation of SREBP-Sensitive Genes in PPAR- $\alpha$ -Deficient Mice, *J. Lipid Res.* 42, 328–333.
  38. Sugden, M.C., Bulmer, K., Gibbons, G.F., Knight, B.L., and Holness, M.J. (2002) Peroxisome-Proliferator-Activated Receptor- $\alpha$  (PPAR- $\alpha$ ) Deficiency Leads to Dysregulation of Hepatic Lipid and Carbohydrate Metabolism by Fatty Acids and Insulin, *Biochem. J.* 364, 361–368.
  39. de Vasconcelos, P.R.L., Kettlewell, M.G.W., Gibbons, G.F., and Williamson, D.H. (1989) Increased Rates of Hepatic Cholesterogenesis and Lipogenesis in Septic Rats *in vivo*. Evidence for the Possible Involvement of Insulin, *Clin. Sci.* 76, 205–211.
  40. Siperstein, M.D., and Guest, M.J. (1960) Studies on the Site of the Feedback Control of Cholesterol Synthesis, *J. Clin. Invest.* 39, 642–652.
  41. Shimano, H. (2001) Sterol Regulatory Element-Binding Proteins (SREBPs): Transcriptional Regulators of Lipid Synthetic Genes, *Prog. Lipid Res.* 40, 439–452.
  42. Shimomura, I., Bashmakov, Y., Shimano, H., Horton, J.D., Goldstein, J.L., and Brown, M.S. (1997) Cholesterol Feeding Reduces Nuclear Forms of Sterol Regulatory Element Binding Proteins in Hamster Liver, *Proc. Natl. Acad. Sci. USA* 94, 12354–12359.
  43. Wang, X., Sato, R., Brown, M.S., Hua, X., and Goldstein, J.L. (1994) SREBP-1, a Membrane-Bound Transcription Factor Released by Sterol-Regulated Proteolysis, *Cell* 77, 53–62.
  44. Peet, D.J., Turley, S.D., Ma, W., Janowski, B.A., Lobaccaro, J.M., Hammer, R.E., and Mangelsdorf, D.J. (1998) Cholesterol and Bile Acid Metabolism Are Impaired in Mice Lacking the Nuclear Oxysterol Receptor LXR $\alpha$ , *Cell* 93, 693–704.
  45. Fungwe, T.V., Cagen, L.M., Wilcox, H.G., and Heimberg, M. (1994) Effects of Dietary Cholesterol on Hepatic Metabolism of Free Fatty Acid and Secretion of VLDL in the Hamster, *Biochem. Biophys. Res. Commun.* 200, 1505–1511.
  46. Fungwe, T.V., Fox, J.E., Cagen, L.M., Wilcox, H.-G., and Heimberg, M. (1994) Stimulation of Fatty Acid Biosynthesis by Dietary Cholesterol and of Cholesterol Synthesis by Dietary Fatty Acid, *J. Lipid Res.* 35, 311–318.
  47. Reddy, J.K., and Hashimoto, T. (2001) Peroxisomal  $\beta$ -Oxidation and Peroxisome Proliferator-Activated Receptor  $\alpha$ : An Adaptive Metabolic System, *Annu. Rev. Nutr.* 21, 193–230.
  48. Fruchart, J.C., Duriez, P., and Staels, B. (1999) Peroxisome Proliferator-Activated Receptor- $\alpha$  Activators Regulate Genes Governing Lipoprotein Metabolism, Vascular Inflammation and Atherosclerosis, *Curr. Opin. Lipidol.* 10, 245–257.
  49. Brown, M.S., Goldstein, J.L., and Dietschy, J.M. (1979) Active and Inactive Forms of 3-Hydroxy-3-methylglutaryl Coenzyme A Reductase in the Liver of the Rat. Comparison with the Rate of Cholesterol Synthesis in Different Physiological States, *J. Biol. Chem.* 254, 5144–5149.
  50. Edwards, P.A., Fogelman, A.M., and Tanaka, R.D. (1983) Physiological Control of HMG-CoA Reductase, in *3-Hydroxy-3-Methylglutaryl Coenzyme A Reductase* (Sabine, J.R., ed.), pp. 93–105, CRC Press, Boca Raton.
  51. Shulman, R.G., and Rothman, D.L. (2001)  $^{13}\text{C}$  NMR of Intermediary Metabolism: Implications for Systemic Physiology, *Annu. Rev. Physiol.* 63, 15–48.
  52. Wildermuth, M.C. (2000) Metabolic Control Analysis: Biological Applications and Insights, *Genome Biol.* 1, 1031.
  53. Bowden, A.C. (1999) Metabolic Control Analysis in Biotechnology and Medicine, *Nat. Biotechnol.* 17, 641–643.
  54. Pullinger, C.R., and Gibbons, G.F. (1983) The Role of Substrate Supply in the Regulation of Cholesterol Biosynthesis in Rat Hepatocytes, *Biochem. J.* 210, 625–632.
  55. Gibbons, G.F., Pullinger, C.R., Munday, M.R., and Williamson, D.H. (1983) Regulation of Cholesterol Synthesis in the Liver and Mammary Gland of the Lactating Rat, *Biochem. J.* 212, 843–848.

[Received August 26, 2002, and in final form and accepted December 4, 2002]



# The Role of Cytochrome P450 in the Regulation of Cholesterol Biosynthesis

Geoffrey F. Gibbons\*

Metabolic Research Laboratory, Nuffield Department of Clinical Medicine,  
University of Oxford, Oxford OX2 6HE, United Kingdom

**ABSTRACT:** A ubiquitously expressed member of the cytochrome P450 superfamily, CYP51, encodes lanosterol 14 $\alpha$ -demethylase, the first step in the conversion of lanosterol into cholesterol in mammals. The biosynthetic intermediates of lanosterol 14 $\alpha$ -demethylation are oxysterols, which inhibit HMG-CoA reductase and sterol synthesis in mammalian cells *in vitro*. These oxysterols (5 $\alpha$ -lanost-8-en-3 $\beta$ ,32-diol and 3 $\beta$ -hydroxy-5 $\alpha$ -lanost-8-en-32-al) are efficiently converted into cholesterol *in vitro* and are generally considered to be natural cholesterol precursors. When added to hepatocytes in high concentrations, besides their conversion into cholesterol, they are also rapidly metabolized into more polar sterols and into steryl esters. The 15 $\alpha$ - and 15 $\beta$ -hydroxy epimers of 5 $\alpha$ -lanost-8-en-3 $\beta$ -ol are also rapidly metabolized into more polar sterols and steryl esters but are not converted efficiently into cholesterol. Polar sterol formation from all these oxysterols is dependent on an active form of cytochrome P450. Oxysterols are potent regulators of the activities of transcription factors of the sterol regulatory element-binding protein family and of liver X-receptor  $\alpha$ . It is proposed that the rapid, cytochrome P450-dependent metabolism of naturally occurring regulatory oxysterols provides a route for their deactivation so that they become incapable of affecting gene transcription. Inhibition of cytochrome P450 by the drug ketoconazole prevents the inactivation of such oxysterols, leading to a prolonged suppression of hepatic HMG-CoA reductase *in vivo* and *in vitro*.

Paper no. L9141 in *Lipids* 37, 1163–1170 (December 2002).

Early experiments designed to determine the stereochemistry of cholesterol biosynthesis from mevalonic acid showed that the 15 $\alpha$ -hydrogen of lanosterol (Scheme 1) was stereospecifically removed (1), resulting in the formation of 5 $\alpha$ -lanosta-8,14,24-trien-3 $\beta$ -ol (IV, Scheme 1) (for reviews, see Refs. 2,3). The conjugated 8,14-diene is the immediate steroidal product of lanosterol 14 $\alpha$ -demethylation, a process that in both mammalian liver and yeast was shown to require an active form of cytochrome P450 (4,5). Subsequent work showed that of the more than 1,000 known members of the cytochrome P450 superfamily, only this particular type is ubiquitously expressed throughout the animal and plant kingdoms (6,7) and is now known as CYP51 (8). The C-32 oxy-

gen-functionalized lanosterol derivatives 5 $\alpha$ -lanost-8-en-3 $\beta$ ,32-diol (II) and 3 $\beta$ -hydroxy-5 $\alpha$ -lanost-8-en-32-al (III, Scheme 1) are obligatory intermediates in the cytochrome P450-dependent removal of the 14 $\alpha$ -methyl group (9,10), and these oxysterols are now generally considered to be natural cholesterol precursors (11). On the other hand, the 15 $\alpha$ - and 15 $\beta$ -hydroxy epimers of lanost-8-en-3 $\beta$ -ol (V and VI, Scheme 1) are poor precursors of cholesterol and are probably not natural intermediates (9).

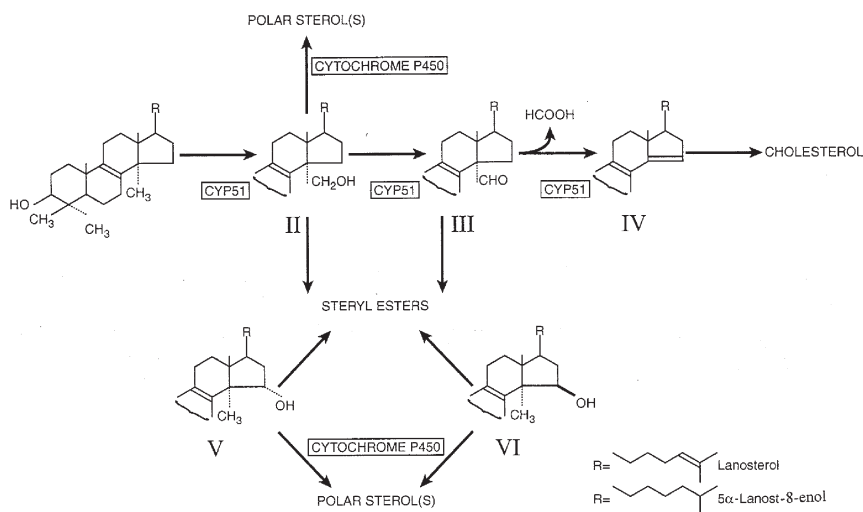
The seminal work of Kandutsch and colleagues showed convincingly that certain types of oxygenated sterol derivatives, rather than cholesterol itself, were potent inhibitory regulators of *de novo* sterol biosynthesis *in vitro* (12,13) and that an important target enzyme was HMG-CoA reductase. Subsequent work, summarized in the review by Schroepfer (14), related oxysterol structure to inhibitory potency. More recently, the discovery of the sterol regulatory element-binding protein (SREBP) family of transcription factors by Brown, Goldstein, and their colleagues (reviewed in Refs. 15,16) provided an explanation for the inhibitory action of oxysterols, particularly 25-hydroxycholesterol, on several cholesterologenic enzymes, including HMG-CoA reductase. Thus, interference with the proteolytic maturation of SREBP by oxysterols prevented the formation of the transcriptionally active N-terminal peptide of SREBP so that target genes were not activated. Later work demonstrated that other oxysterols regulated gene transcription by virtue of their role as activating ligands for the transcription factor liver X-receptor  $\alpha$  (LXR $\alpha$ ) (17–20). Target genes for activated LXR $\alpha$  include those involved in the regulation of whole-body cholesterol balance such as SREBP (21), cholesterol 7 $\alpha$ -hydroxylase (CYP7A1) (19), and the cholesterol transporter ABCA1 (22).

Despite the potency with which oxysterols regulate gene transcription by the SREBP and LXR $\alpha$  pathways, there remains uncertainty concerning the structure(s) of the naturally occurring regulatory oxysterols and the enzymology involved in their biosynthesis and metabolism. This paper revisits some of our previous work in this area (23–26), which suggests that the oxygenated, naturally occurring cholesterol precursors II and III (Scheme 1) may have a regulatory role, either as inhibitors of SREBP maturation or as activating ligands for LXR $\alpha$ . This paper will also reassess the results of some of our original studies on the regulation of cholesterol biosynthesis (27,28) in terms of factors that affect the steady-state concentration and turnover of natural regulatory oxysterols.

\*Address correspondence at Metabolic Research Laboratory, Radcliffe Infirmary, Woodstock Rd., Oxford OX2 6HE, United Kingdom.

E-mail: geoff.gibbons@metabolic-research.oxford.ac.uk

Abbreviations: lanosterol, 5 $\alpha$ -lanosta-8,14-dien-3 $\beta$ -ol; LXR $\alpha$ , liver X-receptor  $\alpha$ ; SREBP, sterol regulatory element-binding protein.



SCHEME 1

## MATERIALS AND METHODS

Preparation of the tritium-labeled sterols functionalized at C-32 was carried out by acetolysis of 3 $\beta$ -acetoxy-5 $\alpha$ -lanostan-7 $\alpha$ ,32-oxide (23). Sterols functionalized at C-15 were prepared from 3 $\beta$ -hydroxy-5 $\alpha$ -lanost-7-en-15-one (29) and were labeled with tritium at C-16 (30).

The formation of polar and nonpolar sterol products of the functionalized lanostenols by cells cultured *in vitro* was determined by solvent extraction of the total lipids followed by TLC (23). The metabolism of the labeled 15-hydroxy epimers of lanost-8-en-ol by subcellular fractions of rat liver was determined as described in Reference 25. Characterization of the polar sterols was carried out by GC-MS.

Measurement of HMG-CoA reductase activity in cell cultures was carried out using the method described by Gibbons *et al.* (23). Isolation of the microsomal fraction from rat liver was carried out as described by Marco de la Calle *et al.* (27). Measurement of HMG-CoA reductase activity in rat liver microsomes was carried out using the method of Brown *et al.* (31).

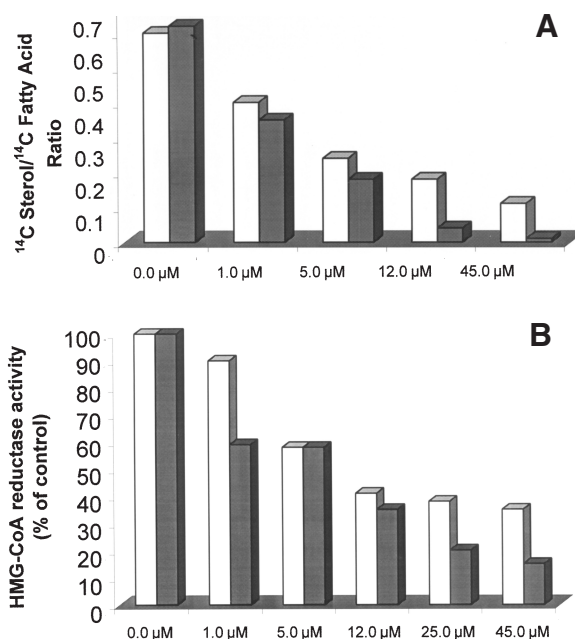
Rats (250–300 g) treated with ketoconazole received the drug intragastrically in 0.1 M HCl (1.5 mL of a 4.0 mg/mL solution). The drug was administered at different times (1, 6, 12, 17, and 24 h) before injection (i.p.) of  $^3\text{H}_2\text{O}$  (0.2 mL, 4.0 mCi), and the animals were killed 1 h later. The livers were removed and a portion was used for determination of tritium incorporation into sterols (27). The remainder was used for preparation of microsomes (see above).

Experiments using live animals were carried out in accordance with British Government Home Office-approved procedures under the authority of project licence number PPL 3001446.

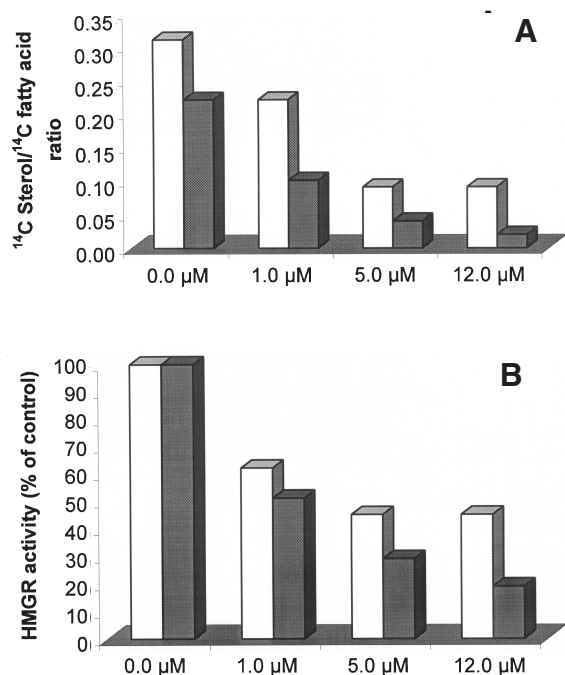
## RESULTS

*Oxysterol precursors of cholesterol inhibit HMG-CoA reductase.* The cholesterol precursors **II** and **III** (Scheme 1) were

added to primary cultures of mouse fetal liver cells at concentrations ranging from 0 to 45  $\mu\text{M}$  for 12 h. Cells from some of the flasks were harvested at this time, and HMG-CoA reductase activity was determined. To the remaining flasks was added [ $^{14}\text{C}$ ]acetate for a further 2 h, and the cells were harvested for measurement of sterol and fatty acid (FA)



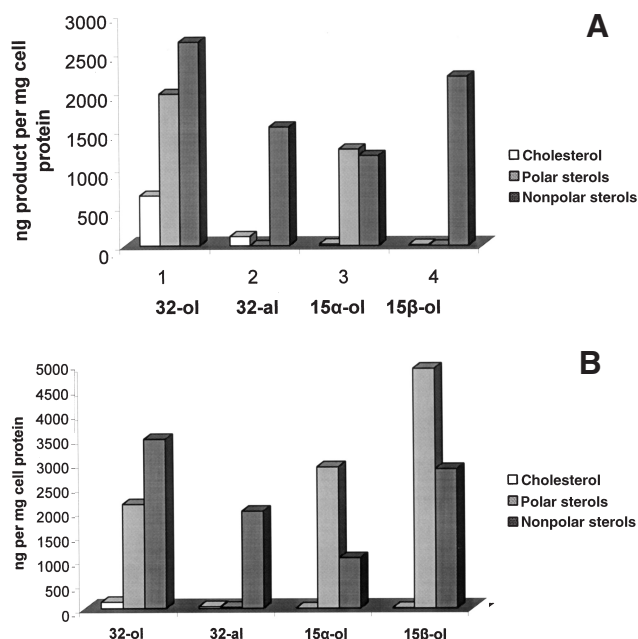
**FIG. 1.** Inhibition of (A) sterol synthesis and (B) HMG-CoA reductase by 32-functionalized lanost-8-en-ols in fetal liver. 5 $\alpha$ -Lanost-8-en-3 $\beta$ ,32-diol (open bars) and 3 $\beta$ -hydroxy-5 $\alpha$ -lanost-8-en-32-al (solid bars) were added to cultures of mouse fetal liver at concentrations ranging from 0–45  $\mu\text{M}$  (23) for 12 h. The cultures were then either harvested and used for measurement of HMG-CoA reductase activity (B) or cultured for a further 2 h in the presence of [ $^{14}\text{C}$ ]acetate (A). Measurements of HMG-CoA reductase and acetate incorporation into sterols and FA were carried out as described in Reference 23.



**FIG. 2.** Inhibition by 32-functionalized 5 $\alpha$ -lanost-8-enols of (A) sterol synthesis and (B) HMG-CoA reductase activity in Chinese hamster lung cells. Sterols as described in the caption of Figure 1 were incubated with Chinese hamster lung cells for 6 h. The cells were subsequently treated as described in the caption to Figure 1.

synthesis (23). Figure 1 shows that HMG-CoA reductase activity was inhibited by low concentrations of both **II** and **III**. Concentrations required for 50% inhibition of reductase were 6.7 and 4.9  $\mu$ M, respectively. The overall rates of sterol synthesis from [<sup>14</sup>C]acetate were somewhat more sensitive to inhibition by the 32-oxygenated lanostenols than were HMG-CoA reductase activities, particularly at the higher end of the concentration range (Fig. 1).

The experiment described above was repeated using a line of Chinese hamster lung (Dede) cells in which case the cells were cultured for 6 h in the presence of the sterols (0–12  $\mu$ M) before assay of HMG-CoA reductase. As with the fetal liver cells, [<sup>14</sup>C]acetate was added to some flasks for a further 2 h to measure rates of FA and sterol synthesis (23). The inhibitory effects of the sterols are shown in Figure 2. The rates of sterol synthesis and HMG-CoA reductase activities were somewhat more sensitive to inhibition by the 32-oxygenated



**FIG. 3.** Cholesterogenic and noncholesterogenic metabolism of oxygenated lanost-8-enols (A) and lanost-7-enols (B). The  $\Delta^7$  and  $\Delta^8$  isomers of labeled 5 $\alpha$ -lanosten-3 $\beta$ ,32-diol (32-ol), 3 $\beta$ -hydroxy-5 $\alpha$ -lanosten-3 $\beta$ ,15 $\alpha$ -diol (15 $\alpha$ -ol) and 5 $\alpha$ -lanosten-3 $\beta$ ,15 $\beta$ -diol (15 $\beta$ -ol) were incubated with fetal mouse liver cultures for 12 h. Metabolic products were separated and quantified as described in Reference 23.

sterols in the Dede cells than in the primary liver cell cultures. In this case, concentrations required for 50% inhibition of reductase were 2.8 and 1.4  $\mu$ M for **II** and **III** (Scheme 1), respectively. Again, in the Dede cells, the overall rates of sterol synthesis were more susceptible to inhibition than HMG-CoA reductase. A mutant strain of Dede cells (A2-1) selected for resistance to the metabolic effects of 25-hydroxycholesterol was also resistant to the inhibitory effect of the 32-oxygenated lanostenol derivatives on HMG-CoA reductase activity (23,24). Similar inhibitory effects of the lanostenol derivatives on rates of sterol synthesis and HMG-CoA reductase activities were also observed in L-cells, a subline of mouse fibroblasts (23). Like the Dede cells, HMG-CoA reductase activity was more sensitive to inhibition in the L-cell line than in the primary liver cell culture (concentrations required for 50% inhibitions were 2.5 and 2.8  $\mu$ M for **II** and **III**, respectively).

**TABLE 1**  
Metabolism of <sup>3</sup>H-Labeled C-32-Oxygenated Lanostenols<sup>a</sup> by L-Cells and Primary Cultures of Fetal Liver

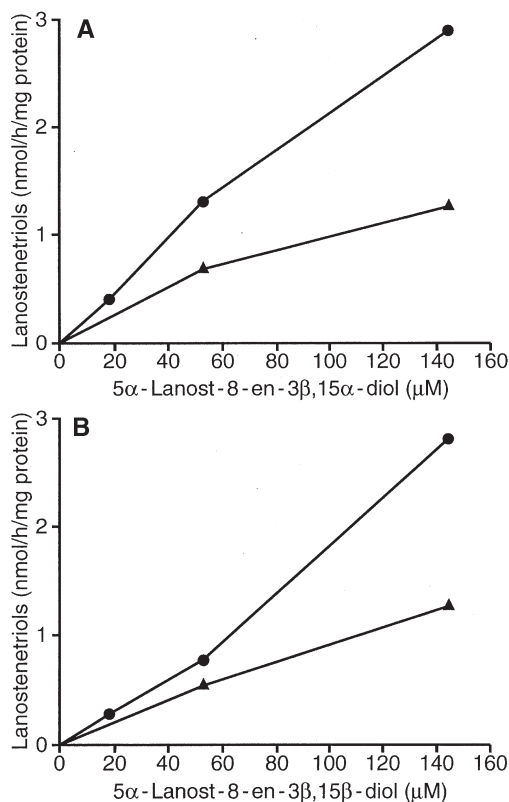
	Cholesterol		Polar sterols		Nonpolar sterols	
	L-cells	Liver	L-cells	Liver	L-cells	Liver
Precursor sterol			(ng/mg protein)			
5 $\alpha$ -Lanost-8-ene 3 $\beta$ ,32-diol	182	643	ND	1960	368	2630
3 $\beta$ -Hydroxy-5 $\alpha$ -lanost-8-en-32-al	109	116	ND	ND	352	1532
5 $\alpha$ -Lanost-7-ene 3 $\beta$ ,32-diol	127	131	33	2153	729	3509
3 $\beta$ -Hydroxy-5 $\alpha$ -lanost-7-en-32-al	27	38	63	22	305	2005

<sup>a</sup>The values are adapted from those shown in Table IV of Reference 23. The labeled sterols were incubated for 5 h, and the labeled metabolites were separated by TLC. ND = not detected.

Oxygenated lanosterol derivatives are rapidly metabolized by noncholesterogenic pathways. The C-32 functionalized lanosterol derivatives **II** and **III** (Scheme 1) were labeled with tritium (9) and added to cultures of mouse fetal liver cells for 12 h (23). Their metabolism to cholesterol and to noncholesterol products was determined at the end of this period. Similar experiments were carried out with the  $\Delta^7$  isomers of these derivatives. Figure 3 shows that, although these substances were converted, as expected, into cholesterol, they were converted much more efficiently into nonpolar substances with the chromatographic properties of steryl esters. Alkaline hydrolysis of these substances yielded labeled materials with the same properties as the substrates, adding further support for their esterified nature (results not shown). The labeled C-32 alcohols were also extensively converted into more polar substances with the chromatographic properties of lanostenetriols. To determine whether these metabolic patterns were characteristic of noncholesterogenic as well as cholesterogenic oxygenated lanosterol derivatives, we utilized the labeled 15 $\alpha$ - and 15 $\beta$ -hydroxyl epimers of 5 $\alpha$ -lanost-8-en-3 $\beta$ -ol and 5 $\alpha$ -lanost-7-en-3 $\beta$ -ol, which we had previously shown to be much poorer cholesterol precursors than the naturally occurring 32-functionalized derivatives (9). Again, all these labeled compounds were extensively esterified to nonpolar derivatives, and three of them were converted even more efficiently into more polar sterols, which suggested the introduction of a further oxygen function (Fig. 3).

Similar experiments using mouse fibroblasts (L-cells) instead of fetal liver cells showed that, in this case, cholesterol was relatively a much more important metabolite of the C-32-functionalized lanost-8-enols (Table 1). The capacity of L-cells to esterify these labeled substances was decreased compared to that of the primary liver cells, and the capacity for polar sterol formation was almost abolished.

*Oxidative metabolism of oxygenated lanostenols is dependent on cytochrome P450.* Although L-cells and fetal liver cells were broadly similar in their ability to convert the  $\Delta^7$  and  $\Delta^8$  C-32 alcohols into cholesterol, in most cases polar sterol formation from these substances in the former cells was virtually abolished. Since many types of cytochrome P450 are more highly expressed in the liver than in nonhepatic tissues, we considered the possibility that the formation of polar sterols in the liver was a cytochrome P450-dependent process. To test this idea, we examined the effects of gas mixtures containing carbon monoxide (CO), a broad-range P450 inhibitor, on polar sterol formation from the labeled 15 $\alpha$ -hydroxy and 15 $\beta$ -hydroxy epimers of 5 $\alpha$ -lanost-8-en-3 $\beta$ -ol in subcellular fractions of rat liver (25). Our previous studies with this system used GC-MS to investigate the nature of the polar materials. The fragmentation patterns suggested that the polar structures consisted of 5 $\alpha$ -lanostenetriols in which the third hydroxyl group was situated at C-7 (results not shown). Figure 4 shows that replacement of N<sub>2</sub> with CO in gas mixtures containing oxygen resulted in a 50–60% decrease in the rate of oxidative metabolism of both the 3 $\beta$ ,15 $\alpha$  and 3 $\beta$ ,15 $\beta$  lanostenediols, suggesting the involvement of cytochrome

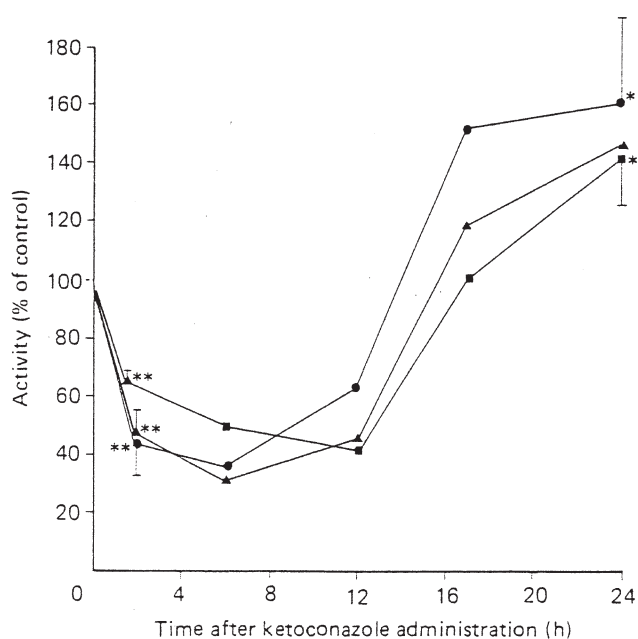


**FIG. 4.** Carbon monoxide inhibits the oxidative metabolism of the labeled (A) 15 $\alpha$ - and (B) 15 $\beta$ -hydroxy epimers of 5 $\alpha$ -lanost-8-enol. Tritium-labeled 5 $\alpha$ -lanost-8-en-3 $\beta$ ,15 $\alpha$ -diol (A) and 5 $\alpha$ -lanost-8-en-3 $\beta$ ,15 $\beta$ -diol (B) were incubated with subcellular fractions of rat liver for 45 min in the presence of gas mixtures consisting of nitrogen plus oxygen (9:1 vol/vol, ●) or carbon monoxide plus oxygen (9:1 vol/vol, ▲). The oxidative products (lanostenetriols) were separated and quantified by TLC as described in Reference 25.

P450. Another cytochrome P450 inhibitor, ketoconazole, also inhibited the metabolism of the C-32-functionalized lanost-8-enols into more polar sterols by cholesterogenically competent subcellular fractions of rat liver (32). Under similar conditions, when [<sup>14</sup>C]mevalonate was the sterol precursor, ketoconazole caused the accumulation of labeled sterols more polar than cholesterol, including the cholesterol precursor 3 $\beta$ -hydroxy-5 $\alpha$ -en-32-al (**II**, Scheme 1) (28).

*Inhibition of cytochrome P450 in vivo and in vitro suppresses hepatic HMG-CoA reductase activity and sterologenic carbon flux.* In view of the above inhibitory effects of CO, suggestive of the participation of cytochrome P450 in the oxidative metabolism of oxysterol regulators of HMG-CoA reductase, we determined the effects of administering the potent cytochrome P450 inhibitor ketoconazole on hepatic HMG-CoA reductase activity and carbon flux through the sterol pathway in intact animals (27) and in hepatocyte culture (28). In the experiments with intact animals, a solution of ketoconazole was administered intragastrically to groups of animals, and the animals were killed at various times thereafter. At each time point, 1 h before killing, <sup>3</sup>H<sub>2</sub>O was injected intraperitoneally. The livers were removed from the animals and





**FIG. 5.** Time course of the effects of ketoconazole on hepatic HMG-CoA reductase activity and sterologenes. Rats were treated intragastrically with a solution of ketoconazole and killed at various times later. One hour before killing, the rats were injected intraperitoneally with  $^3\text{H}_2\text{O}$  (4 mCi). Parts of each liver were used to prepare microsomes to measure the expressed (i.e., dephosphorylated) and total (phosphorylated plus dephosphorylated) forms of HMG-CoA reductase (31). The remaining liver was used to measure  $^3\text{H}_2\text{O}$  incorporation into nonsaponifiable lipids (sterologenes). (●) Expressed activity of HMG-CoA reductase; (▲) total activity of HMG-CoA reductase; (■)  $^3\text{H}_2\text{O}$  incorporation into nonsaponifiable lipids. Values marked \* and \*\* are significantly different ( $P < 0.05$  and  $P < 0.01$ ) from the corresponding zero time control value.

a portion was used for preparation of microsomes for the assay of the expressed (i.e., dephosphorylated) and total (phosphorylated plus dephosphorylated) forms of HMG-CoA reductase (31). The remainder was used for isolation of the  $^3\text{H}$ -labeled nonsaponifiable lipid and cholesterol-containing fractions (27). The  $^3\text{H}$  content of these fractions was determined, and the values were used as a measure of carbon flux through the sterol pathway (33). Figure 5 shows that at as little as 2 h after ketoconazole administration, both HMG-CoA reductase activity and sterologenic carbon flux were decreased. These activities remained suppressed for a further 10 h after which time suppression was abolished. At 24 h following ketoconazole treatment, there was an "overshoot" of HMG-CoA reductase activities and sterol carbon flux such that these values were significantly greater than those immediately before treatment. Addition of ketoconazole (0–2  $\mu\text{M}$ ) directly to primary cultures of rat hepatocytes also gave rise to a suppression of HMG-CoA reductase activity (28), showing that the hepatic effects observed *in vivo* were not an indirect result of ketoconazole action.

*Chronic exposure of the liver to ketoconazole induces CYP51 activity.* In the experiments with intact rats described above, samples of the hepatic microsomes were used to assay lanosterol 14 $\alpha$ -demethylase activity as measured by the amounts

of labeled cholesterol produced from [ $^{14}\text{C}$ ]lanosterol. At 24 h following ketoconazole treatment, when HMG-CoA reductase activity was significantly increased, cholesterol formation from [ $^{14}\text{C}$ ]lanosterol was also increased, suggesting an induction of 14 $\alpha$ -demethylase (CYP51) activity (27). Also, in subcellular fractions of rat liver capable of cholesterol synthesis from [ $^{14}\text{C}$ ]mevalonic acid, there is usually some accumulation of label in lanosterol. The proportion of such label was significantly decreased in liver fractions from rats that had consumed ketoconazole in the diet for the previous 24 h. Finally, in the livers of rats that had been continually pretreated with the drug (2 doses) over the previous 48 h, an acute dose of ketoconazole (2 h) was not so effective as suppressing sterol synthesis and lanosterol 14- $\alpha$  demethylation compared with that in nonpretreated animals (27).

## DISCUSSION

The functional role of a species of cytochrome P450 during lanosterol 14 $\alpha$ -demethylation was first described in mammalian liver in 1973 (4) and in yeast the following year (5). Since that time the enzyme involved, lanosterol 14 $\alpha$ -demethylase (P45014DM), has been the subject of increasing scrutiny, particularly in view of its role as a target enzyme for the azole group of antibiotics (34,35). The enzyme is encoded by CYP51 (8), the only member of the cytochrome P450 superfamily that is ubiquitously expressed in all the biological phyla (6). The importance of CYP51 is further emphasized by the finding that in mammals, the C-32-oxygenated intermediates of lanosterol 14 $\alpha$ -methylase (**II** and **III**, Scheme 1), which are natural cholesterol precursors (2,9,10), are potent inhibitors of sterol synthesis and HMG-CoA reductase activity in mammalian cells (23; reviewed in Ref. 11). The immediate steroidal product of lanosterol 14 $\alpha$ -demethylase is 5 $\alpha$ -lanosta-8,14,24-trien-3 $\beta$ -ol (2,3). Steroids containing the conjugated  $\Delta^{8,14}$  diene grouping are potently active stimulators of meiosis in oocytes (36,37) and also play a role as activating ligands for the transcription factor LXR $\alpha$  (17). Oxysterols suppress cholesterol synthesis by interfering with the proteolytic cleavage of the immature transcription factor SREBP-2 (16) to give a mature form that normally enters the nucleus and transactivates a large portfolio of cholesterol genes, including HMG-CoA reductase (15,38). It is likely that interference with SREBP-2 maturation is the means by which the oxygenated cholesterol precursors **II** and **III** suppress HMG-CoA reductase *in vitro*. However, in some cases, the rapidity with which effects are observed (e.g., Fig. 5) might suggest a mechanism in addition to that which involves changes in gene expression. In this respect, a recent report (39) has suggested that oxysterols in some way shift the balance of cellular cholesterol from the cell membrane to the endoplasmic reticulum. This may result in increased degradation of HMG-CoA reductase. Whether substances **II** and **III** (Scheme 1) play a natural regulatory role *in vivo* is more controversial, although **III** accumulates in cells during conditions in which HMG-CoA reductase becomes suppressed (11,40,41). If, as seems

likely, they do play a natural regulatory role, then the activity of CYP51 may be crucial in determining their steady-state concentration. In this respect, an accumulation of the C-32 aldehyde **III** (Scheme 1) decreases the catalytic activity of CYP51, leading to an accumulation of its substrate lanosterol (23,42). CYP51 is also regulated transcriptionally by SREBP-2, and this process is inhibited by oxysterols such as 25-hydroxycholesterol (6). Oxysterols of diverse structure are also activating ligands for the transcription factor LXR $\alpha$  (17,40). Although the C-32-oxygenated cholesterol precursors have not yet been tested for biological potency in this respect, such a role would provide a link between the regulation of cholesterol synthesis and regulation of bile acid production *via* CYP7A1, an LXR $\alpha$  target gene.

The availability of systems for the rapid inactivation of regulatory molecules is an obvious prerequisite for control of their effective concentration within the cell. Such mechanisms must exist for all natural oxysterol regulators of SREBP cleavage and LXR $\alpha$  activation. The present review shows that the liver has an extraordinarily high capacity for converting sterols such as this to more polar sterols *via* a mechanism that involves cytochrome P450 (Fig. 4, Scheme 1). The structure(s) of these more polar sterols remains a matter for conjecture. Nevertheless, it has been reported that introduction of a third hydroxyl group into certain active oxysterol inhibitors of HMG-CoA reductase decreases their inhibitory potency (44,45), an effect that is also shown following 7 $\alpha$ -hydroxylation of 27-hydroxycholesterol by CYP7B (46). Multiple hydroxylation of the cholesterol side chain also decreases the potency of the resultant triols as activating ligands for LXR $\alpha$  (43).

It is likely that hepatic cholesterol balance is normally maintained, at least in part, by the steady-state concentration of natural oxysterol regulators operating *via* SREBP-2 maturation or by activation of LXR $\alpha$ . These oxysterols originate during both *de novo* cholesterol synthesis and cholesterol metabolism (14), and their effective concentration would be determined by the balance of their production and degradation. The present review provides evidence that cytochrome P450 is required for the oxidative degradation of oxysterols. Interference with this natural regulatory process in the liver by inhibition of cytochrome P450 might be expected to lead to abnormalities of *de novo* cholesterol synthesis. Thus, inhibition of hepatic cytochrome P450 action *in vivo* by ketoconazole led acutely to a downregulation of HMG-CoA reductase and sterologenic carbon flux (Fig. 5), possibly by preventing the inactivation of natural endogenous oxysterol regulators. Similar conditions in hepatocytes give rise to an accumulation of 3 $\beta$ -hydroxylanost-8-en-32-al (28) and, probably, to other natural oxysterols. Chronic administration of ketoconazole induces P45014DM, as evidenced by the increased lanosterol 14 $\alpha$ -demethylase activity (27), and it is likely that other members of the cytochrome P450 family such as CYP7A are similarly induced under these conditions (47). Such an effect would explain the enhanced hepatic HMG-CoA reductase ac-

tivity and sterologenic carbon flux observed 24 h following ketoconazole treatment that would result from an increased P450-mediated oxidative degradation of endogenously produced oxysterols. It is also of interest that chronic treatment of HepG2 cells with ketoconazole also gave rise to an increased HMG-CoA reductase activity, possibly *via* a similar mechanism (48).

## ACKNOWLEDGMENTS

This work was carried out over a number of years, and I am indebted to several colleagues who have made important contributions at different times. These include Clive Pullinger, Kostas Mitropoulos, Andrew Kandutsch, Webster Cavenee, Ken Alexander, Carmen Marco, and José Iglesias. I would also like to thank Nick Myant and the late Derek Williamson for their constant encouragement and support. The work described in this paper was funded by the Medical Research Council (United Kingdom), and I thank the Council for its support.

## REFERENCES

- Gibbons, G.F., Goad, L.J. and Goodwin, T.W. (1968) The Stereochemistry of Hydrogen Elimination from C-15 During Cholesterol Biosynthesis, *J. Chem. Soc. Chem. Commun.*, 1458–1460.
- Akhtar, M., Freeman, C.W., Wilton, D.C., Boar, R.B., and Copey, D.B. (1977) Oxidative Metabolism of Lanosterol in the Biosynthesis of Cholesterol, *Bioorg. Chem.* 6, 473–481.
- Gibbons, G.F., Mitropoulos, K.A., and Myant, N.B. (1982), *Biochemistry of Cholesterol*, pp. 131–188, Elsevier Biomedical Press, Amsterdam.
- Gibbons, G.F., and Mitropoulos, K.A. (1973) The Role of Cytochrome P-450 in Cholesterol Biosynthesis, *Eur. J. Biochem.* 40, 267–273.
- Alexander, K.T.W., Mitropoulos, K.A., and Gibbons, G.F. (1974) A Possible Role for Cytochrome P450 During the Biosynthesis of Zymosterol from Lanosterol by *Saccharomyces cerevisiae*, *Biochem. Biophys. Res. Commun.* 60, 460–467.
- Stromstedt, M., Rozman, D., and Waterman, M.R. (1996) The Ubiquitously Expressed Human CYP51 Encodes Lanosterol 14 $\alpha$ -Demethylase, a Cytochrome P450 Whose Expression Is Regulated by Oxysterols, *Arch. Biochem. Biophys.* 329, 73–81.
- Debeljak, N., Horvat, S., Vouk, K., Lee, M., and Rozman, D. (2000) Characterization of the Mouse Lanosterol 14 $\alpha$ -Demethylase (CYP51), a New Member of the Evolutionarily Most Conserved Cytochrome P450 Family, *Arch. Biochem. Biophys.* 379, 37–45.
- Nelson, D.R., Kamataki, T., Waxman, D.J., Guengerich, F.P., Estabrook, R.W., Feyereisen, R., Gonzalez, F.J., Coon, M.J., Gunsalus, I.C., Gotoh, O., *et al.* (1993) The P450 Superfamily: Update on New Sequences, Gene Mapping, Accession Numbers, Early Trivial Names of Enzymes, and Nomenclature, *DNA Cell Biol.* 12, 1–51.
- Gibbons, G.F., Mitropoulos, K.A., and Pullinger, C.R. (1976) Lanosterol 14 $\alpha$ -Demethylase. The Metabolism of Some Potential Intermediates by Cell-free Systems from Rat Liver, *Biochem. Biophys. Res. Commun.* 69, 781–789.
- Akhtar, M., Alexander, K., Boar, R.B., McGhie, J.F., and Barton, D.H. (1978) Chemical and Zymic Studies on the Characterization of Intermediates During the Removal of the 14 $\alpha$ -Methyl Group in Cholesterol Biosynthesis. The Use of 32-Functionalized Lanostane Derivatives, *Biochem. J.* 169, 449–463.

11. Trzaskos, J.M. (1995) Oxysterols as Modifiers of Cholesterol Biosynthesis, *Prog. Lipid Res.* 34, 99–116.
12. Kandutsch, A.A., and Chen, H.W. (1973) Inhibition of Sterol Synthesis in Cultured Mouse Cells by 7 $\alpha$ -Hydroxycholesterol, 7 $\beta$ -Hydroxycholesterol and 7-Ketocholesterol, *J. Biol. Chem.* 248, 8408–8417.
13. Kandutsch, A.A., Chen, H.W., and Heiniger, H.J. (1978) Biological Activity of Some Oxygenated Sterols, *Science* 201, 498–501.
14. Schroeffer, G.J., Jr. (2000) Oxysterols: Modulators of Cholesterol Metabolism and Other Processes, *Physiol. Rev.* 80, 361–554.
15. Horton, J.D., Goldstein, J.L., and Brown, M.S. (2002) SREBPs: Activators of the Complete Program of Cholesterol and Fatty Acid Synthesis in the Liver, *J. Clin. Invest.* 109, 1125–1131.
16. Brown, M.S., and Goldstein, J.L. (1999) A Proteolytic Pathway That Controls the Cholesterol Content of Membranes, Cells, and Blood, *Proc. Natl. Acad. Sci. USA* 96, 11041–11048.
17. Janowski, B.A., Willy, P.J., Devi, T.R., Falck, J.R., and Mangelsdorf, D.J. (1996) An Oxysterol Signalling Pathway Mediated by the Nuclear Receptor LXR $\alpha$ , *Nature* 383, 728–731.
18. Peet, D.J., Turley, S.D., Ma, W., Janowski, B.A., Lobaccaro, J.M., Hammer, R.E., and Mangelsdorf, D.J. (1998) Cholesterol and Bile Acid Metabolism Are Impaired in Mice Lacking the Nuclear Oxysterol Receptor LXR $\alpha$ , *Cell* 93, 693–704.
19. Lehmann, J.M., Kliewer, S.A., Moore, L.B., Smith-Oliver, T.A., Oliver, B.B., Su, J.L., Sundseth, S.S., Winegar, D.A., Blanchard, D.E., Spencer, T.A., and Willson, T.M. (1997) Activation of the Nuclear Receptor LXR by Oxysterols Defines a New Hormone Response Pathway, *J. Biol. Chem.* 272, 3137–3140.
20. Forman, B.M., Ruan, B., Chen, J., Schroeffer, G.J., Jr., and Evans, R.M. (1997) The Orphan Nuclear Receptor LXR $\alpha$  is Positively and Negatively Regulated by Distinct Products of Mevalonate Metabolism, *Proc. Natl. Acad. Sci. USA* 94, 10588–10593.
21. Schultz, J.R., Tu, H., Luk, A., Repa, J.J., Medina, J.C., Li, L., Schwendner, S., Wang, S., Thoolen, M., Mangelsdorf, D.J., *et al.* (2000) Role of LXRs in Control of Lipogenesis, *Genes Dev.* 14, 2831–2838.
22. Repa, J.J., Turley, S.D., Lobaccaro, J.A., Medina, J., Li, L., Lustig, K., Shan, B., Heyman, R.A., Dietschy, J.M., and Mangelsdorf, D.J. (2000) Regulation of Absorption and ABC1-Mediated Efflux of Cholesterol by RXR Heterodimers, *Science* 289, 1524–1529.
23. Gibbons, G.F., Pullinger, C.R., Chen, H.W., Cavenee, W.K., and Kandutsch, A.A. (1980) Regulation of Cholesterol Synthesis in Cultured Cells by Probable Natural Precursor Sterols. *J. Biol. Chem.* 255, 375–400.
24. Cavenee, W.K., Gibbons, G.F., Chen, H.W., and Kandutsch, A.A. (1979) Effects of Various Oxygenated Sterols on Cellular Sterol Biosynthesis in Chinese Hamster Lung Cells Resistant to 25-Hydroxycholesterol, *Biochim. Biophys. Acta* 575, 255–265.
25. Gibbons, G.F., Pullinger, C.R., Baillie, T.A., and Clare, R.A. (1980) Metabolism of Hydroxysterols by Rat Liver, *Biochim. Biophys. Acta* 619, 98–106.
26. Gibbons, G.F. (1983) The Role of Oxysterols in the Regulation of HMG-CoA Reductase, *Biochem. Soc. Trans.* 11, 649–651.
27. Marco de la Calle, C., Hwang, W., Pullinger, C.R., and Gibbons, G.F. (1988) A Relationship Between the Activities of Hepatic Lanosterol 14 $\alpha$ -Demethylase and 3-Hydroxy-3-methylglutaryl CoA Reductase, *Biochem. J.* 250, 33–39.
28. Iglesias, J., and Gibbons, G.F. (1989) Regulation of Hepatic Cholesterol Biosynthesis. Effects of a Cytochrome P-450 Inhibitor on the Formation and Metabolism of Oxygenated Products of Lanosterol, *Biochem. J.* 264, 495–502.
29. Gibbons, G.F., and Ramananda, K. (1975) Synthesis and Con-  
figuration at C-15 of the Epimeric 5 $\alpha$ -Lanost-8-en-3 $\beta$ ,15-diols, *J. Chem. Soc. Chem. Commun.*, 213.
30. Gibbons, G.F., Mitropoulos, K.A., and Pullinger, C.R. (1976) Lanosterol 14 $\alpha$ -Demethylase. The Metabolism of Some Potential Intermediates by Cell-free Systems from Rat Liver, *Biochem. Biophys. Res. Commun.* 69, 781.
31. Brown, M.S., Goldstein, J.L., and Dietschy, J.M. (1979) Active and Inactive Forms of 3-Hydroxy-3-methylglutaryl Coenzyme A Reductase in the Liver of the Rat. Comparison with the Rate of Cholesterol Synthesis in Different Physiological States, *J. Biol. Chem.* 254, 5144–5149.
32. Iglesias, J. and Gibbons, G.F. (1989) Oxidative Metabolism of Cholesterol Precursors. Sensitivity to Ketoconazole, an Inhibitor of Cytochrome P-450, *Steroids* 53, 311–328.
33. Pullinger, C.R., and Gibbons, G.F. (1983) The Relationship Between the Rate of Hepatic Sterol Synthesis and the Incorporation of [<sup>3</sup>H] Water, *J. Lipid Res.* 24, 1321–1328.
34. Bellamine, A., Mangla, A.T., Nes, W.D., and Waterman, M.R. (1999) Characterization and Catalytic Properties of the Sterol 14 $\alpha$ -Demethylase from *Mycobacterium tuberculosis*, *Proc. Natl. Acad. Sci. USA* 96, 8937–8942.
35. Podust, L.M., Poulos, T.L. and Waterman, M.R. (2001) Crystal Structure of Cytochrome P450 14 $\alpha$ -Sterol Demethylase (CYP51) from *Mycobacterium tuberculosis* in Complex with Azole Inhibitors, *Proc. Natl. Acad. Sci. USA* 98, 3068–3073.
36. Byskov, A.G., Andersen, C.Y., Nordholm, L., Thogersen, H., Xia, G., Wassmann, O., Andersen, J.V., Guddal, E., and Roed, T. (1995) Chemical Structure of Sterols That Activate Oocyte Meiosis, *Nature* 374, 559–562.
37. Rozman, D., and Waterman, M.R. (1998) Lanosterol 14 $\alpha$ -Demethylase (CYP51) and Spermatogenesis, *Drug Metab. Dispos.* 26, 1199–1201.
38. Shimano, H. (2001) Sterol Regulatory Element-Binding Proteins (SREBPs): Transcriptional Regulators of Lipid Synthetic Genes, *Prog. Lipid Res.* 40:439–452.
39. Brown, A.J., Sun, L., Feramisco, J.D., Brown, M.S., and Goldstein, J.L. (2002) Cholesterol Addition to ER Membranes Alters Conformation of SCAP, the SREBP Escort Protein That Regulates Cholesterol Metabolism, *Mol. Cell.* 10, 237–245.
40. Saucier, S.E., Kandutsch, A.A., Phirwa, S., and Spencer, T.A. (1987) Accumulation of Regulatory Oxysterols, 32-Oxolanosterol and 32-Hydroxylanosterol in Mevalonate-Treated Cell Cultures. *J. Biol. Chem.* 262, 14056–14062.
41. Tabacik, C., Aliau, S., Astruc, M., and Crastes de Paulet, A. (1981) Post-HMG-CoA Reductase Regulation of Cholesterol Biosynthesis in Normal Human Lymphocytes and Lanosten-3 $\beta$ -ol-32-al, a Natural Inhibitor, *Biochem. Biophys. Res. Commun.* 101, 1087–1095.
42. Gibbons, G.F., Pullinger, C.R., and Mitropoulos, K.A. (1979) Studies on the Mechanism of Lanosterol 14 $\alpha$ -Demethylase. A Requirement for Two Distinct Types of Mixed Function Oxidase, *Biochem. J.* 183, 309–315.
43. Janowski, B.A., Grogan, M.J., Jones, S.A., Wisely, G.B., Kliewer, S.A., Corey, E.J., and Mangelsdorf, D.J. (1999) Structural Requirements of Ligands for the Oxysterol Liver X Receptors LXR $\alpha$  and LXR $\beta$ , *Proc. Natl. Acad. Sci. U.S.A.* 96, 266–271.
44. Kandutsch, A.A., and Chen, H.W. (1974) Inhibition of Sterol Synthesis in Cultured Mouse Cells by Cholesterol Derivatives Oxygenated in the Side Chain, *J. Biol. Chem.* 249, 6057–6061.
45. Kandutsch, A.A., and Chen, H.W. (1978) Inhibition of Cholesterol Synthesis by Oxygenated Sterols, *Lipids* 13, 704–707.
46. Martin, K.O., Reiss, A.B., Lathe, R., and Javitt, N.B. (1997) 7 $\alpha$ -Hydroxylation of 27-Hydroxycholesterol: Biologic Role in the Regulation of Cholesterol Synthesis, *J. Lipid Res.* 38, 1053–1058.

47. Kuipers, F., Havinga, R., Huijsmans, C.M., Vonk, R.J., and Princen, H.M. (1989) Inhibition and Induction of Bile Acid Synthesis by Ketoconazole. Effects on Bile Formation in the Rat, *Lipids* 24, 759–764.
48. Kempen, H.J., van Son, K., Cohen, L.H., Griffioen, M., Verboom, H., and Havekes, L. (1987) Effect of Ketoconazole on Cholesterol Synthesis and on HMG-CoA Reductase and LDL-Receptor Activities in Hep G2 cells, *Biochem. Pharmacol.* 36, 1245–1249.
- [Received August 26, 2002, and in revised form and accepted December 11, 2002]



# Subcellular Localization of Oxidosqualene Cyclases from *Arabidopsis thaliana*, *Trypanosoma cruzi*, and *Pneumocystis carinii* Expressed in Yeast

P. Milla<sup>a</sup>, F. Viola<sup>a</sup>, S. Oliaro Bosso<sup>a</sup>, F. Rocco<sup>a</sup>, L. Cattel<sup>a</sup>, B.M. Joubert<sup>b</sup>,  
R.J. LeClair<sup>b</sup>, S.P.T. Matsuda<sup>b</sup>, and G. Balliano<sup>a,\*</sup>

<sup>a</sup>Università degli Studi di Torino, Dipartimento di Scienza e Tecnologia del Farmaco, I-10125 Torino, Italy, and <sup>b</sup>Departments of Chemistry and of Biochemistry and Cell Biology, Rice University, Houston, Texas 77005

**ABSTRACT:** Cycloartenol synthase from *Arabidopsis thaliana* and lanosterol synthase from *Trypanosoma cruzi* and *Pneumocystis carinii* were expressed in yeast, and their subcellular distribution in the expressing cells was compared. Determination of enzymatic (oxidosqualene cyclase, OSC) activity and SDS-PAGE analysis of subcellular fractions proved that enzymes from *T. cruzi* and *A. thaliana* have high affinity for lipid particles, a subcellular compartment rich in triacylglycerols, and steryl esters, harboring several enzymes of lipid metabolism. In lipid particles of strains expressing the *P. carinii* enzyme, neither OSC activity nor the electrophoretic band at the appropriate M.W. were detected. Microsomes from the three expressing strains retained some OSC activity. Affinity of enzymes from *A. thaliana* and *T. cruzi* for lipid particles is similar to that of OSC of *Saccharomyces cerevisiae*, which is mainly located in this compartment. A different distribution of OSC in yeast cells suggests that they differ in some structural features critical for the interaction with the surface of lipid particles. Computer analysis supports the hypothesis of the structural difference since OSC from *S. cerevisiae*, *A. thaliana*, and *T. cruzi* lack or contain only one transmembrane spanning domain (a structural feature that makes a protein poorly inclined to associate with lipid particles), whereas OSC from *P. carinii* possesses six transmembrane domains. In the strain expressing cycloartenol synthase from *A. thaliana*, the accumulation of lipid particles largely exceeded that of the other strains.

Paper no. L9150 in *Lipids* 37, 1171–1176 (December 2002).

Oxidosqualene cyclases (OSC) are crucial enzymes of sterol biosynthesis in eukaryotes as they transform 2,3-oxidosqualene, the last acyclic precursor of the metabolic path, into a variety of cyclized products (1,2). These enzymes contribute to maintaining the physiological balance between precursors and end products of sterol biosynthesis by effectively channeling oxidosqualene into the metabolic path, thus preventing accumulation of acyclic precursors within the cell. In the last few years a great effort has been made to unravel questions of homeostasis and intracellular trafficking of sterols and sterol precursors and of the complex metabolic interactions among the different steps of sterol biosynthesis. An essential result of this effort was the determination of subcellular

localization of enzymes involved in the late steps of biosynthesis and of those responsible for steryl ester formation. In yeast (*Saccharomyces cerevisiae*), the picture of the subcellular distribution is almost complete, as localization of many enzymes has been identified, including squalene epoxidase (Erg1p) (3), sterol- $\Delta^{24}$ -methyltransferase (Erg6p) (4), OSC (Erg7p) (5), sterol C-24(28) reductase (Erg4p) (6), and steryl ester synthases Are1p and Are2p (7). Three of these enzymes, namely, Erg1p, Erg6p, and Erg7p, are located (Erg1p and Erg7p almost exclusively) in the so-called lipid particles, a compartment containing high levels of triacylglycerols and steryl esters and harboring several enzymes of lipid metabolism (8,9). Taking advantage of these studies, we considered using yeast mutants expressing OSC of other eukaryotes as models for studying the subcellular distribution of these enzymes. In the present work we compared the subcellular distribution of three OSC expressed in yeast: cycloartenol synthase from *Arabidopsis thaliana*, lanosterol synthase from *Trypanosoma cruzi*, and lanosterol synthase from *Pneumocystis carinii*. The first two enzymes already have been characterized, cloned, and expressed in yeast (10,11); the cloning and the expression of lanosterol synthase from *P. carinii* in yeast are reported here for the first time. The work also aimed to (i) evaluate whether the high affinity of yeast lanosterol synthase for lipid particles (5) is common to other oxidosqualene cyclases, (ii) recognize any structural features responsible for the addressing of OSC to subcellular compartments, and (iii) evaluate whether the possible propensity of other OSC expressed in yeast to accumulate into lipid particles could be used for their purification and characterization.

## EXPERIMENTAL PROCEDURES

**Strains and culture conditions.** The strains *S. cerevisiae* SMY8[pSM60.21] (MATa erg7::HIS3 hem1::TRP1 ura3-52 trp1- $\Delta$ 63 LEU2::CAS1 his3- $\Delta$ 200 ade2 Gal+), SMY8[pBJ1.21] (MATa erg7::HIS3 hem1::TRP1 ura3-52 trp1- $\Delta$ 63 LEU2::OSC *T. cruzi* his3- $\Delta$ 200 ade2 Gal+), and SMY8[pBJ4.21] (MATa erg7::HIS3 hem1::TRP1 ura3-52 trp1- $\Delta$ 63 LEU2::OSC *P. carinii* his3- $\Delta$ 200 ade2 Gal+) were used throughout this study. Cells were grown aerobically to the early stationary phase at 30°C in YPD medium containing 1% yeast extract (Oxoid, Basingstoke, England), 2% peptone (Oxoid), 2% glucose

\*To whom correspondence should be addressed at Dipartimento di Scienza e Tecnologia del Farmaco, Via P. Giuria 9, I-10125 Torino, Italy.  
E-mail: gianni.balliano@unito.it

Abbreviations: MES, morpholine ethanesulfonic acid; OSC, oxidosqualene cyclase; TM, transmembrane.

(Merck, Darmstadt, Germany), and supplemented with heme (13  $\mu\text{g}/\text{mL}$ , added from a stock solution of 1.3  $\text{mg}/\text{mL}$  heme in 1:1 ethanol/10  $\text{mM}$  NaOH) and ergosterol (20  $\mu\text{g}/\text{mL}$ , added from a stock solution of 2  $\text{mg}/\text{mL}$  ergosterol in 1:1 ethanol/Tween 80). Precultures were grown aerobically for 48 h. For the expression, cells (1 mL of inocula per 100 mL of expression medium) were grown for 48–72 h in 1% yeast extract, 2% peptone, 2% galactose, and 13  $\mu\text{g}/\text{mL}$  heme.

**Cloning and characterization of a *P. carinii* lanosterol synthase.** A BLAST search (<http://biology.uky.edu/Pc/>) for putative OSC sequences uncovered the partially sequenced *P. carinii* cDNA S18F10. Dr. Charles Staben kindly provided the clone, which was completely sequenced on both strands using vector-derived primers and synthetic oligonucleotides corresponding to the cDNA sequence. To facilitate yeast expression, restriction sites for subcloning into expression vectors were introduced by PCR (40 cycles of 95°C for 30 s, 56°C for 30 s, 72°C for 4 min). The S18F10 plasmid was used as a template with the oligonucleotides Pca7.3 (gggtcgacaaaatgattatgggtatcc) and Pca7.4 (cgcggcgcgtaaggtcttaaatattacc) and *Pfu* high-fidelity polymerase (Stratagene, La Jolla, CA) in the reaction. The resulting 2.2 kbp fragment was subcloned into the integrative, galactose-inducible yeast expression vector pRS305GAL (12) and the high-copy, galactose-inducible yeast expression vector pRS426GAL (13) to generate pBJ4.21 and pBJ4.22, respectively. These constructs and a positive control plasmid expressing *S. cerevisiae* lanosterol synthase (12) from pRS305GAL were transformed into the *S. cerevisiae* lanosterol synthase mutant SMY8 (12) to test for genetic complementation and into the *S. cerevisiae* squalene synthase/lanosterol synthase double mutant LHY4 (13) to accurately quantify triterpene alcohol production. Complementation was tested on 1% yeast extract, 2% peptone, and 2% galactose supplemented with 13  $\text{mg}/\text{L}$  hemin chloride. A preparative-scale (1-L culture) incubation with substrate was conducted essentially as described previously (13). A 40% slurry of LHY4[pBJ4.22] yeast cells in 100  $\text{mM}$  potassium phosphate (pH 6.2) buffer was lysed using a French press, and then the slurry was diluted to 20% with the same buffer and incubated with 50  $\text{mg}$  of racemic oxidosqualene (14) (final concentration: 1  $\text{mg}/\text{mL}$  oxidosqualene, 1% Triton X-100) for 24 h at 25°C. Triterpene alcohols were isolated as described (13). The crude triterpene alcohol product was chromatographed (5:1 hexane/methylene chloride) on silica gel to provide 11  $\text{mg}$  (44% yield) of pure triterpene alcohol.

**Isolation of yeast subcellular fractions.** Lipid particles were obtained at high purity by the method of Leber *et al.* (4). Briefly, yeast cells were grown in expression medium to the late exponential phase and converted to spheroplasts (15). Spheroplasts were washed twice with 20  $\text{mM}$  potassium phosphate buffer (pH 7.4) containing 1.2  $\text{M}$  sorbitol and then homogenized in breaking buffer containing 10  $\text{mM}$  morpholine ethanesulfonic acid (MES)/Tris (pH 6.9)/12% Ficoll 400/0.2  $\text{mM}$  EDTA/1  $\text{mM}$  phenylmethylsulfonyl fluoride (PMSF) at a final concentration of 0.5 g of cell wet weight per mL. The homogenate was centrifuged at 5,000  $\times g$  for 5 min, and the resulting supernatant was overlaid with breaking buffer and

centrifuged for 1 h at 28,000 rpm (100,000  $\times g$ ) in a Beckman SW-28 swing-out rotor. The floating layer was collected from the top of the gradient and subjected to two additional sequential flotation steps in (i) 10  $\text{mM}$  MES/Tris (pH 6.9)/8% Ficoll 400/0.2  $\text{mM}$  EDTA, and (ii) 10  $\text{mM}$  MES/Tris (pH 6.9)/0.25  $\text{M}$  sorbitol/0.2  $\text{mM}$  EDTA at 28,000  $\times g$  for 30 min each. The floating layer from the top of the last gradient contained lipid particles at high purity.

For the preparation of microsomes, yeast cells were grown in expression medium and converted to spheroplasts (15). Spheroplasts were homogenized in 10  $\text{mM}$  Tris/HCl (pH 7.4)/0.6  $\text{M}$  mannitol, and the homogenate was centrifuged for 30 min at 20,000  $\times g$ . The resulting supernatant was centrifuged at 30,000  $\times g$  for 30 min. To obtain highly purified 30,000  $\times g$  microsomes, the respective pellet was subjected to two additional washing steps by suspension in 10  $\text{mM}$  Tris/HCl (pH 7.5) and centrifugation at 30,000  $\times g$ .

**Characterization of subcellular fractions.** Protein was quantified by the method of Lowry *et al.* (16) using BSA as a standard. Proteins of microsomal and cytosolic fractions were precipitated from the aqueous phase with TCA (10% final concentration) and solubilized in 0.1% SDS/0.1% NaOH. Prior to protein analysis of the lipid particle fraction, samples were delipidated: Nonpolar lipids were extracted with 2 vol of diethyl ether, the organic phase was withdrawn, residual diethyl ether was removed under a stream of nitrogen, and proteins were precipitated from the extracted aqueous phase as described above.

SDS-PAGE was carried out by the method of Laemmli (17) on 10% SDS-polyacrylamide gel. Protein was precipitated with 10% TCA, washed twice with ethanol/diethyl ether (1:1, vol/vol), and dissolved in dissociation buffer. Prior to precipitation of protein in the lipid particle fraction, samples were delipidated as described. Protein bands on the gel were stained with Coomassie Brilliant Blue B.

**Incorporation of [ $^{14}\text{C}$ ]acetate into sterols.** Sterol biosynthesis in whole yeast cells was followed by incorporation of [ $^{14}\text{C}$ ]acetate into nonsaponifiable lipids as described (18). Briefly, washed cells (10–20  $\times 10^6$  cells) were suspended in 5 mL of 25  $\text{mM}$   $\text{KH}_2\text{PO}_4/\text{NaOH}$  buffer (pH 6.5) containing 1% galactose and 0.1  $\text{mg}/\text{mL}$  Tween 80, incubated with 2  $\mu\text{Ci}$  [ $^{14}\text{C}$ ]acetate (50  $\text{mCi}/\text{mM}$ ), and shaken for 3 h at 30°C. Cells were then harvested by centrifugation and saponified in 50% ethanol containing 15% KOH for 2 h at 80°C. Nonsaponifiable lipids were extracted twice with 1 mL light petroleum and separated on silica gel plates (Merck) using *n*-hexane/ethyl acetate (85:15, vol/vol) as developing solvent and authentic standards of ergosterol, lanosterol, dioxidosqualene, oxidosqualene, and squalene. Radioactivity in separated bands was measured using a System 2000 Imaging Scanner (Packard, Downers Grove, IL).

**OSC assay.** [ $^{14}\text{C}$ ]3S-2,3-Oxidosqualene was prepared as described in Reference 5. OSC activity in total yeast homogenate (6  $\text{mg}$  protein/mL), lipid particles (0.03  $\text{mg}$  protein/mL), and microsomes (0.5  $\text{mg}$  protein/mL) was determined as described elsewhere (18). Briefly, 0.5 mL of the different subcellular fractions was incubated with [ $^{14}\text{C}$ ]3S-2,3-oxidosqualene (2000 cpm, 25  $\mu\text{M}$ ) in the presence of Tween 80 (0.2  $\text{mg}/\text{mL}$ ) and Triton X-100 (1  $\text{mg}/\text{mL}$ ) in 10

mM MES/Tris (pH 6.9) and 0.2 mM EDTA for 30 min at 35°C under vigorous shaking. The reaction was stopped by adding 1 mL of 15% KOH in methanol, and lipids were saponified at 80°C for 30 min. The nonsaponifiable lipids were extracted twice with 1 mL of light petroleum and separated on silica gel plates using dichloromethane as developing solvent. Radioactivity in 2,3-oxidosqualene and lanosterol (or cycloartenol) was counted using a System 2000 Imaging Scanner (Packard). The amount of product formed was used to calculate the enzyme activity.

*In silico sequence analysis.* Determination of hypothetical transmembrane spanning domains was performed with HMMTOP 2.0 on-line software (<http://www.enzim.hu/hmmtop/server>) (19,20). Hydrophobicity analysis was performed according to Kyte and Doolittle (21) with a window size of 15 amino acids.

## RESULTS

*Characterization of a P. carinii OSC cDNA and development of a yeast expression strain.* The 2.3-kbp S18F10 cDNA clone (GenBank accession number AF285825) encodes a predicted 720-residue protein that is 57–62% identical to known lanosterol synthases and 50–57% identical to known cycloartenol synthases. This clone genetically complemented the sterol auxotrophy in the lanosterol synthase mutant SMY8 when expressed from the GAL1 promoter, consistent with the cDNA encoding a functional lanosterol synthase. Triterpene alcohol isolated from an *in vitro* reaction was shown to be lanosterol by NMR. Key <sup>1</sup>H NMR (400 MHz) signals were within 0.007 ppm of literature values (22) for lanosterol:  $\delta$  0.687 (C-18, 3H, s), 0.808 (C-29, 3H, s), 0.873 (C-30, 3H, s), 0.909 (C-21, 3H, d, *J* = 6.4 Hz), 0.980 (C-19, 3H, s), 0.998 (C-28, 3H, s), 1.599 (C-27, 3H, s), 1.681 (C-26, 3H, s), 3.23 (C-3, 1H, m), 5.10 (C-24, 1H, m). The alcohol product was acetylated and analyzed by GC as previously described (13). Lanosteryl acetate was the sole triterpenyl acetate observed; neither parkeyl acetate nor cycloartenyl acetate was present at detectable levels (<1% of lanosteryl acetate if any). No unidentified signals suggesting other triterpene products were observed. These ex-

periments establish that *P. carinii* clone S18F10 encodes a lanosterol synthase.

*Expression of active OSC in cell culture.* The level of expression of cycloartenol and lanosterol synthases in different strains were evaluated by incorporation of [<sup>14</sup>C]acetate into nonsaponifiable lipids extracted from cells grown under aerobic conditions. In strains expressing lanosterol synthases from *T. cruzi* and *P. carinii*, the bulk of radioactivity accumulated into ergosterol, indicating that the expressed enzymes perfectly complemented the yeast lanosterol synthase activity. In strains expressing cycloartenol synthase, a major fraction of radioactivity was entrapped by cycloartenol and compounds co-chromatographing with 4-monomethyl sterols such as cycloeucaenol and obtusifoliol (Table 1, Fig. 1), while a minor fraction of radioactivity accumulated into a compound co-chromatographing with ergosterol. The negligible level of radioactive oxidosqualene in all three expressing strains indicated that the ability of the expressed enzymes to channel their substrate into the metabolic path is comparable with that of the wild-type strain.

*Subcellular distribution of OSC expressed in yeast.* Subcellular distribution of activity of the different OSC expressed in yeast was compared with that of a wild-type strain (Table 2). In strains expressing enzymes from *A. thaliana* and *T. cruzi*, distribution was comparable with that of the wild-type: The enrichment relative to the homogenate indicates a clear preference of the expressed OSC for the lipid particles compartment, even though some activity was retained in microsomes to a higher extent than in the wild-type. No activity was detected in lipid particles of the strain expressing lanosterol synthase from *P. carinii*. The homogenate was as active as that of the other expressing strains, and the enrichment of the activity in microsomes was comparable and not so high as to support the hypothesis of the preference for the endoplasmic reticulum. The enzyme might then not be properly shaped for insertion in lipid particles as suggested by computer analysis (Table 3).

In the strain expressing cycloartenol synthase, production of lipid particles largely exceeded the production of the other strains, as judged by (i) the total amount of proteins recovered in lipid particles (Table 2) and (ii) the thickness of the

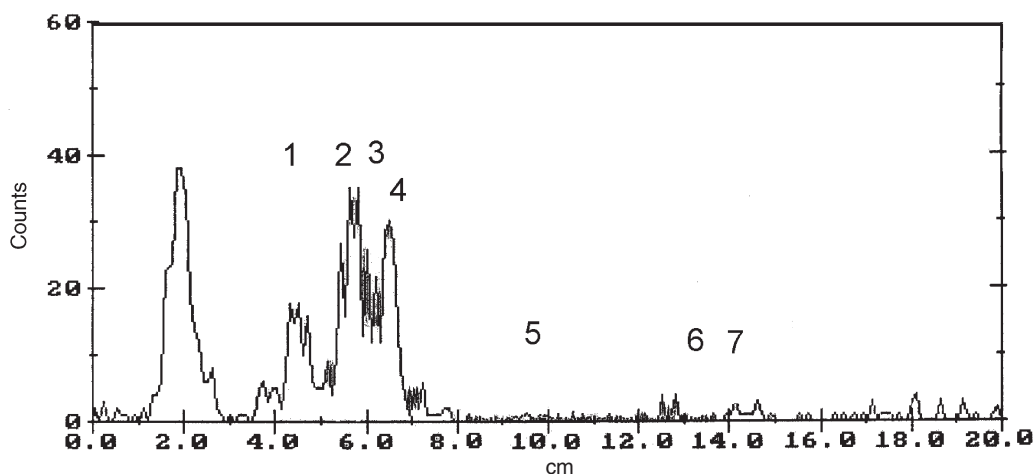
**TABLE 1**  
Incorporation of [<sup>14</sup>C]Acetate into Nonsaponifiable Lipids of Different Strains<sup>a</sup>

Strain	Squalene	Oxidosqualene	4,4-Dimethyl sterols <sup>b</sup>	4-Monomethyl sterols <sup>b</sup>	4,4-Desmethyl sterols <sup>b</sup>
FL100 <sup>c</sup> (wild-type)	2.0	ND	13.6	—	84.4
Expressor <i>A. thaliana</i>	ND	ND	22.5	61.1	16.4
Expressor <i>T. cruzi</i>	8.1	2.1	12.3	—	77.9
Expressor <i>P. carinii</i>	10.4	1.5	4.7	—	83.5

<sup>a</sup>Results are the mean values of two separate experiments with duplicate incubations each. The maximum deviation from the mean was less than 10%. ND, not detectable; *A. thaliana*, *Arabidopsis thaliana*; *T. cruzi*, *Trypanosoma cruzi*; *P. carinii*, *Pneumocystis carinii*.

<sup>b</sup>Nonsaponifiable extract contains free sterols and sterols from steryl esters.

<sup>c</sup>Data from Reference 5.



**FIG. 1.** Incorporation of [ $^{14}\text{C}$ ]acetate into nonsaponifiable lipids of the strain expressing cycloartenol synthase from *Arabidopsis thaliana*. Cells were cultured aerobically as described in the Experimental Procedures section. Nonsaponifiable lipids were then chromatographed on silica gel plates (see Experimental Procedures section) with authentic references of ergosterol (1), obtusifoliol (2), cycloeucaenol (3), cycloartenol (4), dioxidosqualene (5), oxidosqualene (6), and squalene (7).

lipid floating layer recovered at the end of gradient centrifugation passages (see the Experimental Procedures section).

**Protein pattern of subcellular fractions isolated from expressing strains.** The protein content of lipid particles and microsomes isolated from the three expressing strains was analyzed by SDS-PAGE. Results confirmed the high preference of cycloartenol synthase from *A. thaliana* and lanosterol synthase from *T. cruzi* for yeast lipid particles, as indicated by the intense protein bands at 86 and 101 kDa, respectively (Fig. 2). In lipid particles of the strain expressing cycloartenol synthase, the enzyme represents the large majority of proteins. No band at 83 kDa, the predicted M.W. of lanosterol synthase of *P. carinii*, was visible among the proteins from the lipid particles of the strain expressing enzyme of *P. carinii* (Fig. 2). In microsomal preparations, protein bands corresponding to OSC were barely detectable.

**In silico sequence analysis.** Computer analysis revealed that OSC from *A. thaliana* and *S. cerevisiae* (8) lack transmembrane (TM) spanning domains, and OSC from *T. cruzi* contains only one hypothetical TM domain (Table 3). Inter-

estingly, six TM domains were present in the OSC from *P. carinii*. Structure prediction seems to agree with the observation that proteins lacking TM domains are highly inclined to associate with the phospholipid monolayer of lipid particles, whereas proteins containing multiple TM domains may hardly interact with the organelle surface (8).

## DISCUSSION

The phylogenetic position of *P. carinii* has been controversial, and the presence of lanosterol synthase in *P. carinii* supports the view that this pathogen is a fungus rather than an amoeba. Fungi, animals, and kinetoplastid protists share a sterol biosynthetic route through lanosterol, whereas plants and numerous other protists (e.g., *Naegleria*, *Dictyostelium*, and *Euglena*) make sterols from cycloartenol. The yeast strain expressing the *P. carinii* OSC, described here for the first time, will allow convenient screening for derivatives of known OSC inhibitors active on the *P. carinii* lanosterol synthase without cultivation of the pathogen. The heterologous

**TABLE 2**  
**Enzymatic Activity of Oxidosqualene Cyclase (OSC) in Homogenate and Subcellular Fractions of Different Strains<sup>a</sup>**

Strain	Production of lipid particles ( $\mu\text{g}$ protein/g wet weight cells)	Specific OSC activity <sup>a</sup> (nmol/h/mg protein)		
		Homogenate	Lipid particles	Microsomes 30,000 $\times$ g
FL100 (wild-type)	2.97	2.96 <sup>b</sup>	686 (232) <sup>b</sup>	5.11 (1.7) <sup>b</sup>
Expressor <i>A. thaliana</i>	58.7	5.38	808.9 (150)	25.1 (4.66)
Expressor <i>T. cruzi</i>	15.6	2.19	267.8 (122)	13.9 (6.35)
Expressor <i>P. carinii</i>	12.8	4.21	No activity	22.0 (5.22)

<sup>a</sup>OSC activity was measured in the presence of 1 mg/mL Triton X-100. Results are the means of two separate experiments with duplicate incubations each. The maximum deviation from the mean was 10%. Numbers in parentheses are enrichment over the homogenate. For other abbreviations see Table 1.

<sup>b</sup>Data from Reference 5.



**TABLE 3**  
**Characterization of Different OSC**

Protein	Transmembrane spanning domains <sup>a</sup>	Hydrophobicity domain $\geq 2$ <sup>b</sup>	Occurrence in lipid particles
OSC <i>S. cerevisiae</i>	0 <sup>c</sup>	1 (C terminal) <sup>c</sup>	Present
OSC <i>A. thaliana</i>	0	0	Present
OSC <i>T. cruzi</i>	1	1 (N terminal)	Present
OSC <i>P. carinii</i>	6	1 (N terminal)	Absent

<sup>a</sup>Transmembrane spanning domains predicted by HMMTOP 2.0 (19,20).

<sup>b</sup>Hydrophobicity index from Kyte and Doolittle plots (21), window size 15 amino acids.

<sup>c</sup>Data from Reference 8. *S. cerevisiae*, *Saccharomyces cerevisiae*; for other abbreviations see Tables 1 and 2.

expression system will also be useful for high-throughput screening of unbiased chemical libraries for potential chemotherapeutic agents.

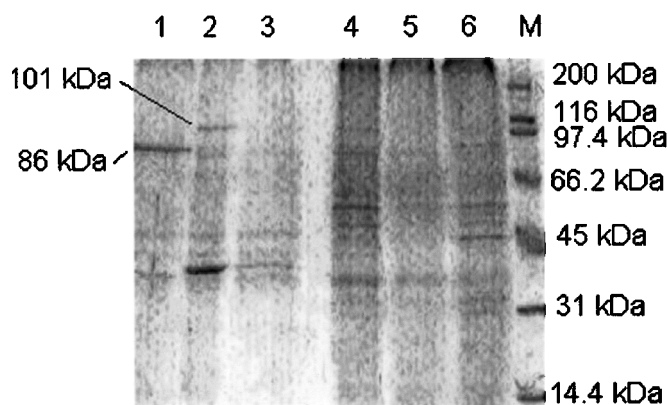
The *P. carinii* lanosterol synthase conserves residues known to be catalytically essential in *S. cerevisiae* lanosterol synthase [Asp456 (23), His146 (23), His234 (23), Tyr410 (24), and Val454 (25)]. These similarities between the *P. carinii* and *S. cerevisiae* lanosterol synthases probably underlie the observation that several established lanosterol synthase inhibitors also inhibit *P. carinii* growth (26), consistent with the two enzymes employing similar catalytic motifs.

Cycloartenol synthase from *A. thaliana* and lanosterol synthase from *T. cruzi* expressed in yeast *S. cerevisiae* showed a high propensity to associate with yeast lipid particles, as demonstrated by the high specific OSC activity of lipid particles prepared from the expressing strains and by the results of SDS-PAGE analysis of subcellular fractions. The affinity of the expressed enzymes for yeast lipid particles is similar to that of the endogenous yeast lanosterol synthase, which has recently been recognized as a peculiar protein of this subcellular compartment (5). It was suggested (8) that the preferential occurrence of a protein in the surface monolayer surrounding lipid particles depends on the lack or paucity of transmembrane spanning domains, a structural feature that seems shared by OSC of

*Arabidopsis* and *Trypanosoma*. Distribution of OSC from *S. cerevisiae*, *A. thaliana*, and *T. cruzi* in yeast cells provides indirect evidence of the structural similarity of the different eukaryotic cyclases, suggesting that they are properly shaped for the insertion in oil body-like organelles. The high sequence homology between the above-mentioned OSC and squalene hopene cyclase of *Alicyclobacillus acidocaldarius*, the structure of which was solved a few years ago (27,28), reinforces the view of the OSC as proteins shaped for association with lipid particles. The bacterial membrane protein, in fact, belongs to the so-called monotopic proteins, membrane proteins that are shaped so as to submerge from one side of the membrane into the non-polar part of the phospholipid bilayer without protruding through it (28). If the OSC are similarly shaped, their preferential association with lipid particles might be easily described by the "budding model," recently proposed for the formation of lipid particles from endoplasmic reticulum in yeast (8). According to this model, lipid particles arise from droplets of neutral lipids formed between the two leaflets of the endoplasmic reticulum membrane bilayer. After reaching a certain size, droplets, wrapped with the outer phospholipid leaflet of the endoplasmic reticulum, bud off, carrying proteins associated with the outer leaflet. Undoubtedly, the monotopic-shaped proteins have a high probability of remaining associated with the phospholipid monolayer during such a budding process.

The absence of OSC activity in lipid particles of the strain expressing the enzyme of *P. carinii* suggests that the enzyme is not properly shaped for association with lipid particles. Computer analysis seems to support the structural hypothesis, since OSC from *S. cerevisiae*, *A. thaliana*, and *T. cruzi* have no or few transmembrane domains, whereas lanosterol synthase from *P. carinii* possesses six transmembrane domains (Table 3), a structural feature that makes a protein poorly inclined to associate with lipid particles (8).

In the strain expressing cycloartenol synthase, the production of lipid particles largely exceeded that of the other strains. This result, together with the comparison of protein patterns of subcellular fractions prepared from different strains, might shed new light on the question of the driving force leading to the production of lipid particles in yeast. In the strain expressing cycloartenol synthase, in fact, the large majority of lipid particle proteins is represented by cycloartenol synthase; the enrichment over the homogenate is so high that the electrophoretic protein pattern of lipid particles looks like that of the final steps of a purification process. Our hypothesis is that the overexpression of a protein highly inclined to associate with lipid particles, such as cycloartenol synthase, forces the cell to accumulate the compartment material associated with the protein. An additional driving force could result, in the strain expressing cycloartenol synthase, from the formation of cycloartenol instead of lanosterol. The experiments with labeled acetate indicate that the channeling of cycloartenol into ergosterol biosynthesis is difficult in this strain, resulting in an accumulation of cycloartenol and possibly other intermediates of sterol biosynthesis. These precursors, bearing "extra" methyl groups compared to ergosterol, the final product, are considered less effective than the final product as membrane



**FIG. 2.** SDS-PAGE analysis of proteins of lipid particles and microsomes isolated from yeast strain expressing cycloartenol synthase from *A. thaliana* (*At*) and lanosterol synthase from *Trypanosoma cruzi* (*Tc*) and *Pneumocystis carinii* (*Pc*). Lanes 1, 2, and 3, 10 µg of lipid particles from expressors *At*, *Tc*, and *Pc*, respectively; lanes 4, 5, and 6, 30 µg of 30,000 × g microsomes from expressors *At*, *Tc*, and *Pc*, respectively.

reinforcers, as inferred from a study on comparative properties of cholesterol and its precursors as growth factors for sterol auxotrophs (29). A strain accumulating these intermediates may be induced to accumulate the lipid particle compartment for storing, as ester derivatives, possible membrane-weakening compounds. The above observations are in agreement with the cited "budding hypothesis" suggested by Daum for the formation of lipid particles in yeast (8).

The overexpression of three OSC in yeast was a useful tool for comparing their structural/functional properties and shed new light on the process of lipid particle formation in yeast. Results of the work suggested also that lipid particles may be regarded as a natural enrichment device for purifying eukaryotic OSC through their expression in yeast.

## ACKNOWLEDGMENTS

This work was supported by the Ministero dell'Università e della Ricerca Scientifica e Tecnologica (MURST), Italy (ex 60%), the National Institutes of Health (AI41598) and the Robert A. Welch Foundation (C-1323). We are grateful to Dr. Charles Staben for cDNA clone S18F10, which was generated as part of the Pneumocystis Genome Project funded by the National Institutes of Health (1R01AI44651-01).

## REFERENCES

- Nes, W.D. (1989) Control of Sterol Biosynthesis and Its Importance to Developmental Regulation and Evolution, *Recent Adv. Phytochem.* 24, 283–327.
- Abe, I., Rohmer, M., and Prestwich, G.D. (1993) Enzymatic Cyclization of Squalene and Oxidosqualene to Sterols and Triterpenes, *Chem. Rev.* 93, 2189–2206.
- Leber, R., Landl, K., Zinser, E., Ahorn, H., Spök, A., Kohlwein, S.D., Turnowsky, F., and Daum, G. (1998) Dual Localization of Squalene Epoxidase, Erg1p, in Yeast Reflects a Relationship Between the Endoplasmic Reticulum and Lipid Particles, *Mol. Biol. Cell.* 9, 375–386.
- Leber, R., Zinser, E., Zellnig, G., Paltauf, F., and Daum, G. (1994) Characterization of Lipid Particles of the Yeast, *Saccharomyces cerevisiae*, *Yeast* 10, 1421–1428.
- Milla, P., Athenstaedt, K., Viola, F., Oliaro Bosso, S., Kohlwein, S.D., Daum, G., and Balliano, G. (2002) Yeast Oxidosqualene Cyclase (Erg7p) Is a Major Component of Lipid Particles, *J. Biol. Chem.* 277, 2406–2412.
- Zweytick, D., Hrastnik, C., Kohlwein, S.D., and Daum, G. (2000) Biochemical Characterization and Subcellular Localization of the Sterol C-24(28) Reductase, Erg4p, from the Yeast *Saccharomyces cerevisiae*, *FEBS Lett.* 470, 83–87.
- Zweytick, D., Leitner, E., Kohlwein, S.D., Yu, C., Rothblatt, R., and Daum, G. (2000) Contribution of Are1 and Are2 to Steryl Ester Synthesis in the Yeast *Saccharomyces cerevisiae*, *J. Biochem.* 267, 1075–1082.
- Athenstaedt, K., Zweytick, D., Jandrositz, A., Kohlwein, S.D., and Daum, G. (1999) Identification and Characterization of Major Lipid Particle Proteins of the Yeast *Saccharomyces cerevisiae*, *J. Bacteriol.* 181, 6441–6448.
- Zweytick, D., Athenstaedt, K., and Daum, G. (2000) Intracellular Lipid Particles of Eukaryotic Cells, *Biochim. Biophys. Acta* 1469, 101–120.
- Corey, E.J., Matsuda, S.P.T., and Bartel, B. (1993) Isolation of an *Arabidopsis thaliana* Gene Encoding Cycloartenol Synthase by Functional Expression in a Yeast Mutant Lacking Lanosterol Synthase by the Use of a Chromatographic Screen, *Proc. Natl. Acad. Sci. USA* 90, 11628–11632.
- Joubert, B.M., Buckner, F.S., and Matsuda, S.P.T. (2001) Trypanosome and Animal Lanosterol Synthase Use Different Catalytic Motifs, *Org. Lett.* 3, 1957–1960.
- Corey, E.J., Matsuda, S.P.T., Baker, C.H., Ting, A.Y., and Cheng, H. (1996) Molecular Cloning of a *Schizosaccharomyces pombe* cDNA Encoding Lanosterol Synthase and Investigation of Conserved Tryptophan Residues, *Biochem. Biophys. Res. Commun.* 219, 327–331.
- Hart, E.A., Hua, L., Darr, L.B., Wilson, W.K., Pang, J., and Matsuda, S.P.T. (1999) Directed Evolution to Investigate Steric Control of Enzymatic Oxidosqualene Cyclization. An Isoleucine to Valine Mutation in Cycloartenol Synthase Allows Lanosterol and Parkeol Biosynthesis, *J. Am. Chem. Soc.* 121, 9887–9888.
- Nadeau, R.G., and Hanzlik, R.P. (1968) Synthesis of Labeled Squalene and Squalene 2,3-oxide, *Methods Enzymol.* 15, 346–351.
- Daum, G., Böhni, P.C., and Schatz, G. (1982) Import of Proteins into Mitochondria, *J. Biol. Chem.* 257, 13028–13033.
- Lowry, O.H., Rosebrough, N.J., Farr, A.L., and Randall, R.J. (1951) Protein Measurement with the Folin Phenol Reagent, *J. Biol. Chem.* 193, 265–275.
- Laemmli, U.K. (1970) Cleavage of Structural Protein During the Assembly of the Head of the Bacteriophage T4, *Nature* 227, 680–685.
- Balliano, G., Viola, F., Ceruti, M., and Cattel, L. (1988) Inhibition of Sterol Biosynthesis in *Saccharomyces cerevisiae* by *N,N*-Diethylazasqualene and Derivatives, *Biochim. Biophys. Acta* 959, 9–19.
- Tusnády, G.E., and Simon, I. (1998) Principles Governing Amino Acid Composition of Integral Membrane Proteins: Applications to Topology Prediction, *J. Mol. Biol.* 283, 489–506.
- Tusnády, G.E. and Simon, I. (2001) The HMMTOP Transmembrane Topology Prediction Server, *Bioinformatics* 17, 849–850.
- Kyte, J., and Doolittle, R.F. (1982) A Simple Method for Displaying the Hydrophobic Character of a Protein, *J. Mol. Biol.* 157, 105–132.
- Emmons, G.T., Wilson, W.K., and Schroepfer, G.J., Jr. (1989) <sup>1</sup>H and <sup>13</sup>C NMR Assignments for Lanostan-3 $\beta$ -ol Derivatives: Revised Assignments for Lanosterol, *Magn. Res. Chem.* 27, 1012–1024.
- Corey, E.J., Cheng, H., Baker, C.H., Matsuda, S.P.T., Li, D., and Song, X. (1997) Studies on the Substrate Binding Segments and Catalytic Action of Lanosterol Synthase. Affinity Labeling with Carbocations Derived from Mechanism-Based Analogs of 2,3-Oxidosqualene and Site-Directed Mutagenesis Probes, *J. Am. Chem. Soc.* 119, 1289–1296.
- Meyer, M.M., Segura, M.J.R., Wilson, W.K., and Matsuda, S.P.T. (2000) Oxidosqualene Cyclase Residues That Promote Formation of Cycloartenol, Lanosterol, and Parkeol, *Angew. Chem.* 112, 4256–4258.
- Joubert, B.M., Hua, L., and Matsuda, S.P.T. (2000) Steric Bulk at Position 454 in *Saccharomyces cerevisiae* Lanosterol Synthase Influences B-ring Formation but Not Deprotonation, *Org. Lett.* 2, 339–341.
- Kaneshiro, E.S., Collins, M.S., and Cushion, M.T. (2000) Inhibitors of Sterol Biosynthesis and Amphotericin B Reduce the Viability of *Pneumocystis carinii* f. sp. *carinii*, *Antimicrob. Agents Chemother.* 44, 1630–1638.
- Wendt, K.U., Poralla, K., and Schulz, G.E. (1997) Structure and Function of Squalene Cyclase, *Science* 277, 1811–1815.
- Wendt, K.U., Lenhart, A., and Schulz, G.E. (1999) The Structure of Membrane Protein Squalene-Hopene Cyclase at 2 Å Resolution, *J. Mol. Biol.* 286, 175–187.
- Bloch, K. (1994) Evolutionary Perfection of a Small Molecule, in *Blondes in Venetian Paintings, the Nine-Banded Armadillo, and Other Essays in Biochemistry*, pp.14–36, Yale University Press, New Haven.

[Received September 11, 2002; accepted December 2, 2002]

# Evidence for Multiple Sterol Methyl Transferase Pathways in *Pneumocystis carinii*

Wenxu Zhou<sup>a</sup>, Thi Thuy Minh Nguyen<sup>a</sup>, Margaret S. Collins<sup>a</sup>,  
Melanie T. Cushion<sup>b,c</sup>, and W. David Nes<sup>a,\*</sup>

<sup>a</sup>Department of Chemistry and Biochemistry, Texas Tech University, Lubbock, Texas 79409-1061, <sup>b</sup>Department of Internal Medicine, University of Cincinnati College of Medicine, Cincinnati, Ohio 45267, and <sup>c</sup>Veterans Administration Medical Center, Cincinnati, Ohio

**ABSTRACT:** The sterol composition of *Pneumocystis carinii*, an opportunistic pathogen responsible for life-threatening pneumonia in immunocompromised patients, was determined. Our purpose was to identify pathway-specific enzymes to impair using sterol biosynthesis inhibitors. Prior to this study, cholesterol **15** (ca. 80% of total sterols), lanosterol **1**, and several phytosterols common to plants (sitosterol **31**, 24 $\alpha$ -ethyl and campesterol, 24 $\alpha$ -methyl **30**) were demonstrated in the fungus. In this investigation, we isolated all the previous sterols and many new compounds from *P. carinii* by culturing the microorganism in steroid-immunosuppressed rats. Thirty-one sterols were identified from the fungus (total sterol = 100 fg/cell), and seven sterols were identified from rat chow. Unusual sterols in the fungus not present in the diet included, 24(28)-methyl-enlanosterol **2**; 24(28)*E*-ethylidene lanosterol **3**; 24(28)*Z*-ethylidene lanosterol **4**; 24 $\beta$ -ethyl lanosta-25(27)-dienol **5**; 24 $\beta$ -ethylcholest-7-enol **6**; 24 $\beta$ -ethylcholesterol **7**; 24 $\beta$ -ethylcholesta-5,25(27)-dienol **8**; 24-methyl lanosta-7-enol **9**; 24-methyl-desmosterol **10**; 24(28)-methylenecholest-7-enol **11**; 24 $\beta$ -methylcholest-7-enol **12**; and 24 $\beta$ -methylcholesterol **13**. The structural relationships of the 24-alkyl groups in the sterol side chain were demonstrated chromatographically relative to authentic specimens, by MS and high-resolution <sup>1</sup>H NMR. The hypothetical order of these compounds poses multiple phytosterol pathways that diverge from a common intermediate to generate 24 $\beta$ -methyl sterols: route 1, **1** → **2** → **11** → **12** → **13**; route 2, **1** → **2** → **9** → **10** → **13**; or 24 $\beta$ -ethyl sterols: route 3, **1** → **2** → **4** → **6** → **7**; route 4, **1** → **2** → **5** → **8** → **7**. Formation of **3** is considered to form an interrupted sterol pathway. Taken together, operation of distinct sterol methyl transferase (SMT) pathways that generate 24 $\beta$ -alkyl sterols in *P. carinii* with no counterpart in human biochemistry suggests a close taxonomic affinity with fungi and provides a basis for mechanism-based inactivation of SMT enzyme to treat *Pneumocystis pneumonia*.

Paper no. L9139 in *Lipids* 37, 1177–1186 (December 2002).

The sterols of *Pneumocystis carinii*, an opportunistic pathogen responsible for life-threatening pneumonia in immunocompromised patients, have been studied extensively and found to be unusual structurally (1–4). An important pe-

culiarity of this fungus is the presence of several phytosterols as well as a high level of cholesterol. Lanosterol, the central intermediate in the biosynthesis of phytosterols and cholesterol, was detected in *P. carinii* (3). A lanosterol-based pathway is consistent with this organism being a fungus (5). Several distinct pathways of sterol biosynthesis can occur that involve transformation of the lanosterol side chain. The evolutionary history of these pathways and the response of enzymes along the pathway to sterol biosynthesis inhibitors (SBI) is of considerable interest since *P. carinii* recently was proposed to have a close phylogenetic affinity to advanced fungal forms, particularly the Ascomycetes (6,7), and to be resistant to common antifungal SBI that target 14 $\alpha$ -demethylase activity (8). Another peculiarity is that 24-ethyl sterols, a characteristic of plant biochemistry (5), were found in *P. carinii* (Table 1). In fungi, as in plants (9), 24-ethyl sterols can function as membrane inserts (10,11) or act as intermediates to steroid hormones that control sexual reproduction (12). The configuration of the 24-ethyl group of *P. carinii* sterols has not been determined to date but is tacitly assumed to be  $\beta$ -oriented (1).

Sterol evolution in fungi proceeded down a different path

**TABLE 1**  
Sterol Composition of *Pneumocystis carinii* as Reported in the Literature

Sterol (trivial name)	References
Cholest-5-enol (cholesterol)	1 2 4
24 $\alpha$ -Methylcholest-5-enol (campesterol)	1 2 4
24 $\beta$ -Methylcholest-7-enol (fungisterol)	1 4
24 $\alpha$ -Ethylcholest-5-enol (sitosterol)	1 2 4
24-Ethylcholest-7-enol	1 2 4
24(28) <i>Z</i> -Ethylidenecholest-7-enol	1 4
24(28)-Methylenelanost-8-enol (eburicol)	3
24(28) <i>Z</i> -Ethylidenelanosterol (pneumocysterol)	3
24-Methylcholesta-5,24-dienol (24-methyl-desmosterol)	4
24(28)-Methylenecholest-7-enol	4
24-Ethylcholesta-5,24-dienol	4
Cholesta-8,14,24-trienol	4
Cholesta-8,24-dienol (zymosterol)	4
Cholesta-5,24-dienol (desmosterol)	1
24-Methylcholesta-5,7,22-trienol (ergosterol)	1
24-Ethylcholesta-5,22-dienol (stigmasterol)	1 2
24-Methylcholesta-5,22-dienol (brassicasterol)	1
4,4,14-Trimethylcholesta-8,24-dienol (lanosterol)	2 3

\*To whom correspondence should be addressed.  
E-mail: w david.nes@ttu.edu

Abbreviations: NSF, nonsaponifiable lipid fraction; RRT<sub>c</sub>, relative retention time of cholesterol; SBI, sterol biosynthesis inhibitor; SMT, sterol methyl transferase.



from plants. For fungi, two extreme categories of sterol structure modification exist. In category I, represented by the primitive fungi consisting of the Chytridomycetes and Oomycetes, cholesterol and 24-ethylidene sterol are the major sterols, whereas in category II, consisting of the most advanced fungi and represented by the Ascomycetes and Basidiomycetes, 24 $\beta$ -methyl sterols are the major sterols (13–15). 24(28)-Ethylidene sterols occur variably in fungi, with the E-geometry synthesized by primitive forms (12,16) and the Z-geometry synthesized by advanced forms (17). When a sterol auxotroph, *Saccharomyces cerevisiae* strain GL7, was fed fucosterol [24(28)E-ethylidene] and isofucosterol [24(28)Z-ethylidene], the cells reduced stereoselectively only the 24(28)Z-ethylidene side chain to produce a 24 $\beta$ -ethyl sterol (18), suggesting that 24 $\beta$ -ethyl sterols can also be a characteristic of the fungal sterol mixture. For plants, two extreme categories of sterol side chain structure exist. In category I, represented by less-advanced plants, including the algae, the major sterols contain a 24 $\beta$ -methyl group. In category II, the major sterols of advanced plants, represented by vascular plants, contain a 24 $\alpha$ -ethyl group (4,19). Cholesterol with a 24-hydrogen atom is usually a minor sterol in plants. The differences in sterol C-methylation patterns in fungi and plants suggest that the evolutionary history of the sterol methyl transferase (SMT) enzyme contributed to the evolution of *P. carinii* and can provide a basis for rational drug design.

In this investigation we analyzed the sterol composition of a mixed population of *P. carinii* trophic and cyst forms isolated from rat-infected lung, determined the sterol composition of the rat chow, and deduced the evolution of an SMT that constitutes the phytosterol pathway from less-advanced to more-advanced fungi. Our findings of a unique sterol profile for *P. carinii* compared to the sterol profiles described for related fungi raised certain important questions. What is the endogenous sterol pathway in this organism? Can the sterol composition of the species reveal something about its evolutionary history? At what stage of development are these sterols actually synthesized, and how do they function during membrane assembly and in sexual reproduction? What role does oxygen from the lungs play in controlling sterol biosynthesis and sterol absorption during infection? What group of SBI or complexing agents can be used to treat the disease? In the present investigation, we have explored the answers to the first two questions. A second paper is forthcoming that will address the latter questions.

## MATERIALS AND METHODS

**Fungal cultures.** Mixed life-cycle preparations of *P. carinii* f. sp. *carinii*, consisting of approximately 80% trophic forms and 20% cystic forms, were isolated from lungs of corticosteroid-immunosuppressed rats and purified from host contaminants by a series of gravity sedimentation steps and by microfiltration as described previously (20,21). The animals were fed balanced rat chow (Teklad type LM-485 sterilizable rat chow; Harlan, Madison, WI) and hyperchlorinated water.

*Pneumocystis* was isolated from infected lungs ca. 8 to 10 wk postinoculation when the animals were moribund with the disease. Approximately 900  $\mu$ g of fresh fungal culture representing  $1.2 \times 10^{10}$  cells was used to establish the sterol composition.

**Sterol analysis.** Total sterols were extracted and separated from the neutral lipids after saponification and analyzed initially by GLC (3% SE-30 packed column operated isothermally at 245°C) and reversed-phase HPLC [Phenomenex 25-cm semipreparative (10- $\mu$ m) column eluted with methanol at ambient temperature]. The chromatographs were attached to a multiple-wavelength diode array detector (Agilent 1100 series) to monitor each of the fractions by the peak purity method (22). The 4,4-dimethyl, 4-monomethyl, and 4,4-desmethyl sterols in the nonsaponifiable lipid fraction (NSF) were separated by analytical TLC (Alltech silica gel plates, 250  $\mu$ m) and  $R_f$  values for individual compounds were determined using two developments with benzene/diethyl ether (85:15, vol/vol). Sterol mixtures eluted from the TLC plate were injected into the high-performance liquid chromatograph to resolve compounds for GC-MS and  $^1\text{H}$  NMR analysis (22). Data from the GLC, HPLC, and  $^1\text{H}$  NMR analyses were used for quantification of the individual components. Authentic specimens used as reference samples were part of our steroid collection (18,19,22–26). Retention times of sterols in GLC are relative to the retention time of cholesterol (RRT<sub>c</sub>).

The instrumentation and techniques for the GLC (Hewlett-Packard 5890 series II) and HPLC (Agilent 1100 series) have been described earlier (22–24). Mass spectra were obtained by GC-MS using a Hewlett-Packard 6890 gas chromatograph coupled to a 5973 mass selective detector.  $^1\text{H}$  NMR spectroscopy was performed at 500 MHz at ambient temperature on a Varian Unity Inova 500, in  $\text{CDCl}_3$ , with tetramethylsilane as internal standard.

## RESULTS

Previous investigations of the sterol content of *P. carinii* revealed the presence of 18 sterols in the organism tentatively identified by GC-MS and HPLC (Table 1) (1–4). In one report, the published gas-liquid chromatogram of the total sterol fraction showed at least 23 peaks that corresponded to sterols (2), suggesting that several additional sterols could be present in the sterol mixture. In none of the earlier studies was the configuration at C-24 of the 24-alkyl group in the sterol side chain determined. Several  $\Delta^7$ -sterols not present in rat lung controls were common to all the investigations (24-methylcholest-7-enol, 24(28)-ethylcholest-7-enol, and 24-ethylidenecholest-7-enol), suggesting that these sterols are formed endogenously (1–3). Alternatively, the  $\Delta^5$ -sterols campesterol and sitosterol, identified in rat lungs not infected with *P. carinii*, are assumed to be of dietary origin (2).

We found, as others reported (1–3), that the cells of *P. carinii* contained predominantly cholesterol (ca. 80% of the total sterol). In addition, a substantial amount (ca. 20%) of



**TABLE 2**  
**Analysis of *P. carinii* Total Sterols**

Sterol (trivial name)	Structure <sup>a</sup>	RRT <sub>c</sub>	R <sub>f</sub>	M <sup>+</sup>	Amount (µg/mg of cells)	Percentage of total sterol without cholesterol
4,4,14-Trimethylcholesta-8,24-dienol (lanosterol)	<b>1</b>	1.29	0.50	426	0.017	6
24(28)-Methylenelanost-8-enol (eburicol)	<b>2</b>	1.42	0.50	440	0.003	1
24(28) <i>E</i> -Ethylidenelanosterol	<b>3</b>	1.64	0.50	454	0.006	2
24(28) <i>Z</i> -Ethylidenelanosterol (pneumcysterol)	<b>4</b>	1.60	0.50	454	Trace <sup>b</sup>	Trace
24β-Ethyl-25(27)-dehydrolanosterol	<b>5</b>	1.56	0.50	454	Trace	Trace
24β-Ethylcholest-7-enol (schottenol)	<b>6</b>	1.36	0.30	414	0.031	11
24β-Ethylcholest-5-enol (clionasterol)	<b>7</b>	1.26	0.30	414	0.008	3 <sup>c</sup>
24β-Ethylcholesta-5,25(27)-dienol	<b>8</b>	1.23	0.30	412	0.003	1
24-Methyllanosta-7,24-dienol	<b>9</b>	1.69	0.50	440	0.003	1
24-Methylcholesta-5,24-dienol (24-methyl-desmosterol)	<b>10</b>	1.23	0.30	398	Trace	Trace
24(28)-Methylenecholest-7-enol	<b>11</b>	1.18	0.30	398	0.003	1
24β-Methylcholest-7-enol (fungisterol)	<b>12</b>	1.21	0.30	400	0.048	17
24β-Methylcholest-5-enol (epicampesterol)	<b>13</b>	1.12	0.30	400	0.022	82
24,25-Dihydrolanosterol	<b>14</b>	1.22	0.50	428	Trace	Trace
Cholest-5-enol (cholesterol)	<b>15</b>	1.00	0.30	386	1.120	NC <sup>d</sup>
14-Norlanosterol	<b>16</b>	1.29	0.50	412	Trace	Trace
4α-Methylcholesta-8,24-dienol	<b>17</b>	1.17	0.46	398	Trace	Trace
Cholesta-8,24-dienol (zymosterol)	<b>18</b>	1.05	0.30	384	Trace	Trace
Cholest-8-enol	<b>19</b>	1.06	0.30	386	0.003	1
Cholesta-7,24-dienol	<b>20</b>	1.10	0.30	384	0.003	1
Cholesta-5,7,24-trienol	<b>21</b>	1.07	0.30	382	Trace	Trace
Cholesta-5,24-dienol (desmosterol)	<b>22</b>	1.04	0.30	384	Trace	Trace
24(28)-Methylenelanosta-8,14-dienol	<b>23</b>	1.42	0.50	424	Trace	Trace
14-Nor-24(28)-methylenelanost-8-enol	<b>24</b>	1.43	0.50	426	0.006	2
4α-Methyl-24(28)-methylenecholest-8-enol	<b>25</b>	1.31	0.46	412	0.003	1
24(28)-Methylenecholest-8-enol (fecosterol)	<b>26</b>	1.14	0.30	398	0.003	1
4α-Methyl-24(28) <i>Z</i> -ethylidenecholest-8-enol	<b>27</b>	1.45	0.46	426	0.003	1
24(28) <i>Z</i> -Ethylidenecholest-8-enol	<b>28</b>	1.32	0.30	412	0.006	2
24(28) <i>Z</i> -Ethylidenecholest-7-enol	<b>29</b>	1.41	0.30	412	0.056	20
24α-Methylcholest-5-enol (campesterol)	<b>30</b>	1.12	0.30	400	0.022	8 <sup>c</sup>
24α-Ethylcholest-5-enol (sitosterol)	<b>31</b>	1.23	0.30	414	0.034	12 <sup>c</sup>

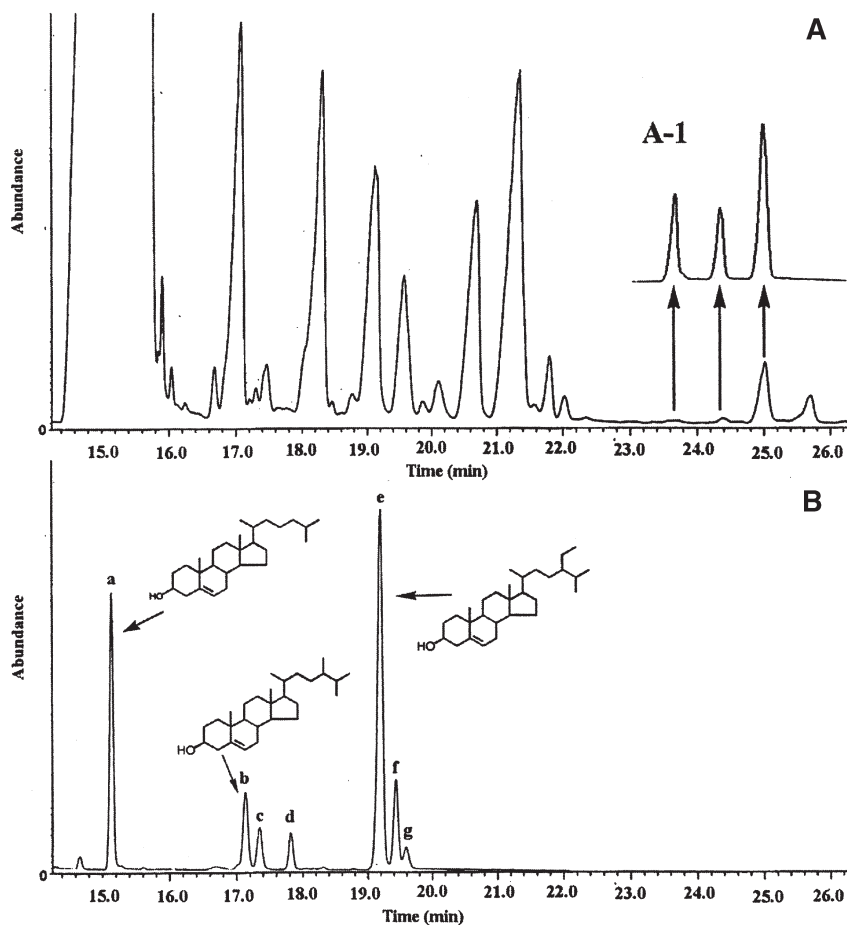
<sup>a</sup>Structure of sterols is shown in Figure 2.<sup>b</sup>Trace, less than 1% of the total sterol.<sup>c</sup>The ratio of epimers was determined by HPLC or <sup>1</sup>H NMR.<sup>d</sup>NC, not considered. As shown in Figure 1, cholesterol constitutes ca. 80% of total sterol.

phytosterol was detected in the organism (Table 2). All the sterols reported by earlier investigators, except for stigmasterol and brassicasterol, were detected, as well as 13 additional sterols that eluted in GLC (Fig. 1A and Table 2). Some 24-alkyl sterols coeluted in GLC, particularly sterols that occurred as C-24 epimers. The 29 sterols detected in GLC could be grouped into two series based on the metabolism of the Δ<sup>24</sup>-bond: as a 24-desalkyl series (24-hydrogen) and as a 24-alkyl (24-methyl or 24-ethyl). The two series of compounds gave rise to paths **a** and **b**, respectively, as shown in Figure 2. By using TLC fractionation of the NSF to separate sterols based on the degree of C-4 substitution (22), a total of ten 4,4-dimethyl, three 4-monomethyl, and sixteen 4-desmethyl sterols were detected. Of the ten 4,4-dimethyl sterols, only three (**1**, **2**, and **4**) were reported previously (2,3). Of the 4-desmethyl sterols, two pairs of 24-alkyl sterols were found to be an epimeric mixture: 24-methylcholesterol and 24-ethylcholesterol. The absolute amounts and the percent compositions of each of these sterols are given in Table 2. On a per cell basis, the amount of total sterol was calculated to be 108 fg/cell. The minor sterols in the sterol mixture were also estimated from the gas-liquid chro-

matogram (Fig. 1), based on the absence of cholesterol, to highlight their contribution to sterol synthesis in *P. carinii*.

Cholesta-5,7,24-trienol **21**, a 4-desmethyl sterol, was identified for the first time in the organism. Its structure was supported by a comparison of its elution time and mass spectrum to the elution time and mass spectrum of an authentic specimen (23). A maximum absorption at λ<sub>max</sub> 282 nm in the UV spectrum of the sample is characteristic of a Δ<sup>5,7</sup>-steroid (22). All the other sterols eluting in HPLC exhibited end-absorption UV spectra, except for compound **23**. Its spectrum contained a fingerprint at 248 nm characteristic of a Δ<sup>8,14</sup>-diene steroid (22), consistent with the assigned structures reported in Table 2. The presence of common 24-methyl sterols found in yeast (26) and of unusual 24-alkylated Δ<sup>24(25)</sup>-sterols, such as 24-methyl desmosterol and 24-ethylidenelanosterol, found in the fungus *Gibberella fujikuroi* (25), were detected in varying amounts in the sterol mixture (Table 2).

Three 24-alkyl sterols in the 4-desmethyl fraction were isolated from the initial HPLC separation to assess the configurational purity at C-24: 24-methylcholesterol, 24-ethylcholesterol, and 24-ethylcholest-7-enol. The two 24-ethyl



**FIG. 1.** GC analysis (a total ion current chromatogram) of the nonsaponifiable lipids extracted from *Pneumocystis carinii* (A) or rat chow (B). Inset A-1 shows the GC trace corresponding to the hexane-extractable product of lanosterol used by the recombinant soybean sterol methyl transferase (SMT) (see text for details of the experiment). The sterols in the GC trace in Panel B labeled **a** to **g** are discussed in the Results section of the text.

sterols possessed similar M.W. ( $M^+$  414), suggesting one double bond in the molecule. They were isolated from HPLC in sufficient amounts for  $^1\text{H}$  NMR analysis. In the case of the 24-ethyl sterol, with a chromatographic behavior and fragmentation pattern of 24-ethylcholest-7-enol, the  $^1\text{H}$  NMR spectrum [H18 (0.531, *s*), H19 (0.791, *s*), H21 (0.926, *d*, 6.4), H26 (0.828, *d*, 6.9), H27 (0.807, *d*, 6.9), H29 (0.851, *t*, 7.4)] supported the structure with a 24 $\beta$ -ethyl group. Based on the signals for C-29 and C-21 in the  $^1\text{H}$  NMR, the 24-ethylcholest-7-enol was epimerically pure at C-24. In contrast to the configuration of the 24-ethyl group of 24-ethylcholest-7-enol, the sample with chromatographic behavior and a fragmentation pattern consistent with the structure 24-ethylcholest-5-enol was found by  $^1\text{H}$  NMR to be a mixture of 24 $\alpha/\beta$ -ethylcholesterol in a 4:1 ratio of 24 $\alpha/\beta$ -ethyl. Peaks in the  $^1\text{H}$  NMR detected for the mixture of sterols were as follows: H18 (0.679/0.679, *s*), H19 (1.009/1.009, *s*), H21 (0.921, *d*, 6.4/0.914, *d*, 6.6), H26 (0.834, *d*, 6.9/0.830, *d*, 6.9), H27 (0.812, *d*, 6.9/0.810, *d*, 6.9), H29 (0.845, *t*, 7.4/0.853, *t*, 7.4). The doublet for H21 and the triplet for H29 of the pair of 24-ethyl epimers sitosterol/

clionasterol is characteristic of an  $\alpha/\beta$ -ethyl group configuration (22,26). The 24-methyl sterol isolated from the initial HPLC (Phenomenex reversed-phase  $\text{C}_{18}$  column eluted with methanol at ambient temperature) as a single component was insufficient for  $^1\text{H}$  NMR; therefore, it was chromatographed further using a reversed-phase TSK gel  $\text{C}_{18}$  column (eluted with acetonitrile/isopropanol at 4°C) to separate the pair of 24 $\alpha/\beta$ -methyl sterols (23). The chromatographic mobility of the 24-methyl sterols relative to the elution of campesterol and 24-epicampesterol standards indicated an epimeric mixture of 24-methylcholesterols in a 1:1 ratio of 24 $\alpha/24\beta$ -methyl.

Four 4,4-dimethyl sterols eluting late in GLC, between 23 and 26 min (Fig. 1), possessed M.W. and fragmentation patterns suggesting a series of 24-ethylstanoid isomers ( $M^+$  454) and a 24-methylstanoid ( $M^+$  440) (Fig. 3). Standards of the three 24-ethyl sterol isomers were prepared by incubating the soybean SMT with 24(28)-methylene lanosterol (27), whereas standards of 24-methylstanoids were prepared in our study of ergosterol biosynthesis in *G. fujikuroi* (25). The plant SMT converted 24(28)-methylene lanosterol to a mixture

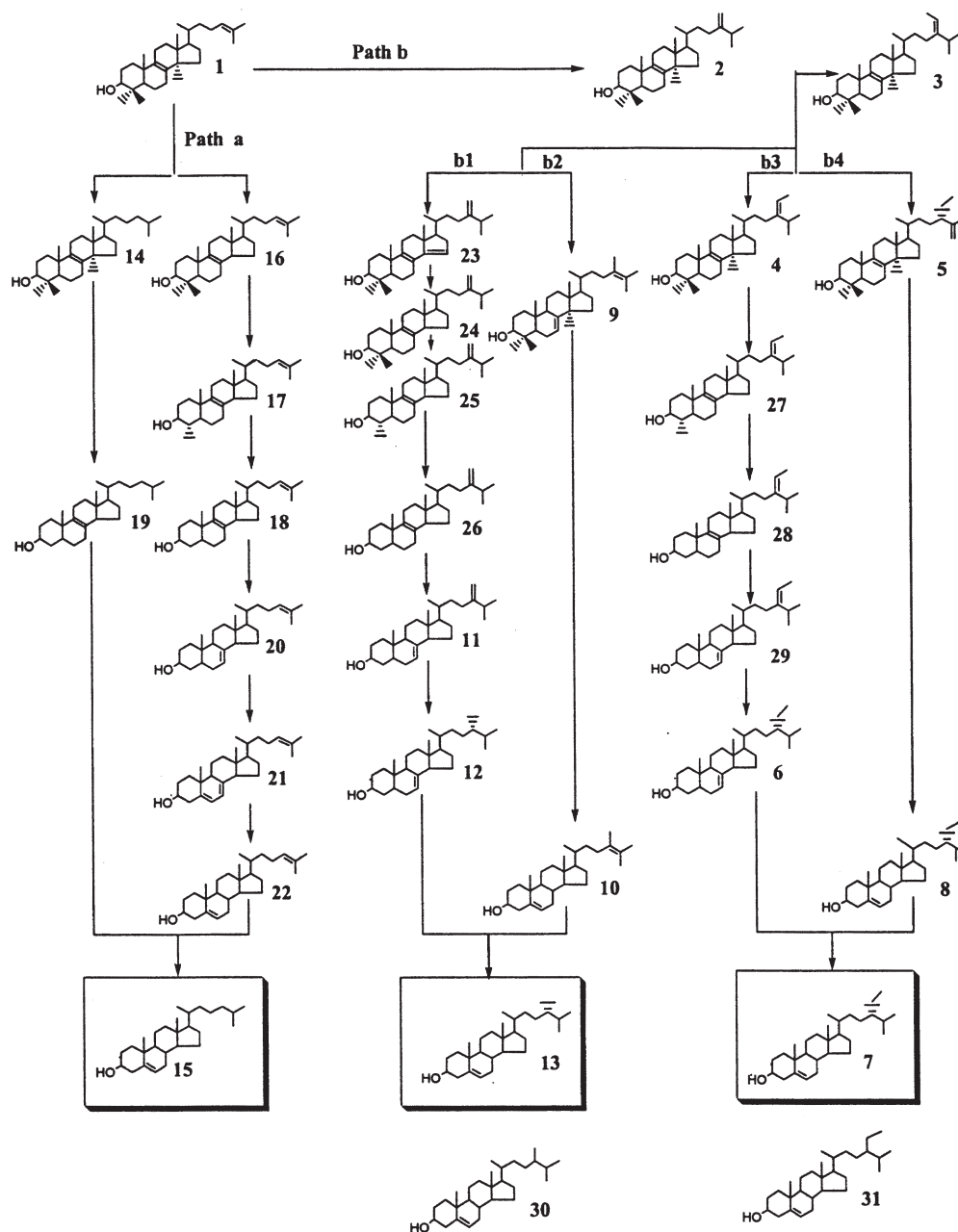


FIG. 2. Hypothetical sterol pathway for *P. carinii*.

of three 24-ethyl sterol isomers as shown in Figure 1, inset A-1. In a related study, 24(28)-methylene cycloartenol was converted to the same set of 24-ethyl sterol isomers. The individual enzyme-generated products were purified by HPLC, and the olefins were characterized by GC-MS and  $^1\text{H}$  NMR (23,27).

The sterol composition of rat chow is a mixture of cholesterol and phytosterols, including 24-methylcholesterol and 24-ethylcholesterol. Major compounds eluting in GLC, as shown in Figure 1B, and their mass spectra (M.W.,  $M^+$ ) are as follows: **a**, cholesterol ( $M^+$  386); **b**, campesterol ( $M^+$  400); **c**, campestanol ( $M^+$  402); **d**, stigmasterol ( $M^+$  412); **e**, sitosterol ( $M^+$  414); **f**, sitostanol ( $M^+$  416); and **g**, isofucosterol

( $M^+$  412). The ingredients listed for rat chow include soybean meal, wheat, cane, oats, alfalfa, fish, beets, wheat germ, corn, menadione dimethylpyrimidinol sulfite, and brewer's yeast, among other things. The source of phytosterols in the rat chow is plant material, and the source of cholesterol is likely fish. The amount of sterol in the rat chow was estimated at 0.43 mg sterol/g chow. The 24-methylcholesterol and 24-ethylcholesterol components of the rat chow were isolated from the sterol mixture by HPLC, and the configuration at C-24 was determined by  $^1\text{H}$  NMR and HPLC using a TSK gel  $C_{18}$  column. The 24-ethyl group in sitosterol was found to be pure 24 $\alpha$ -ethyl, whereas the "campesterol" sample, considered to be

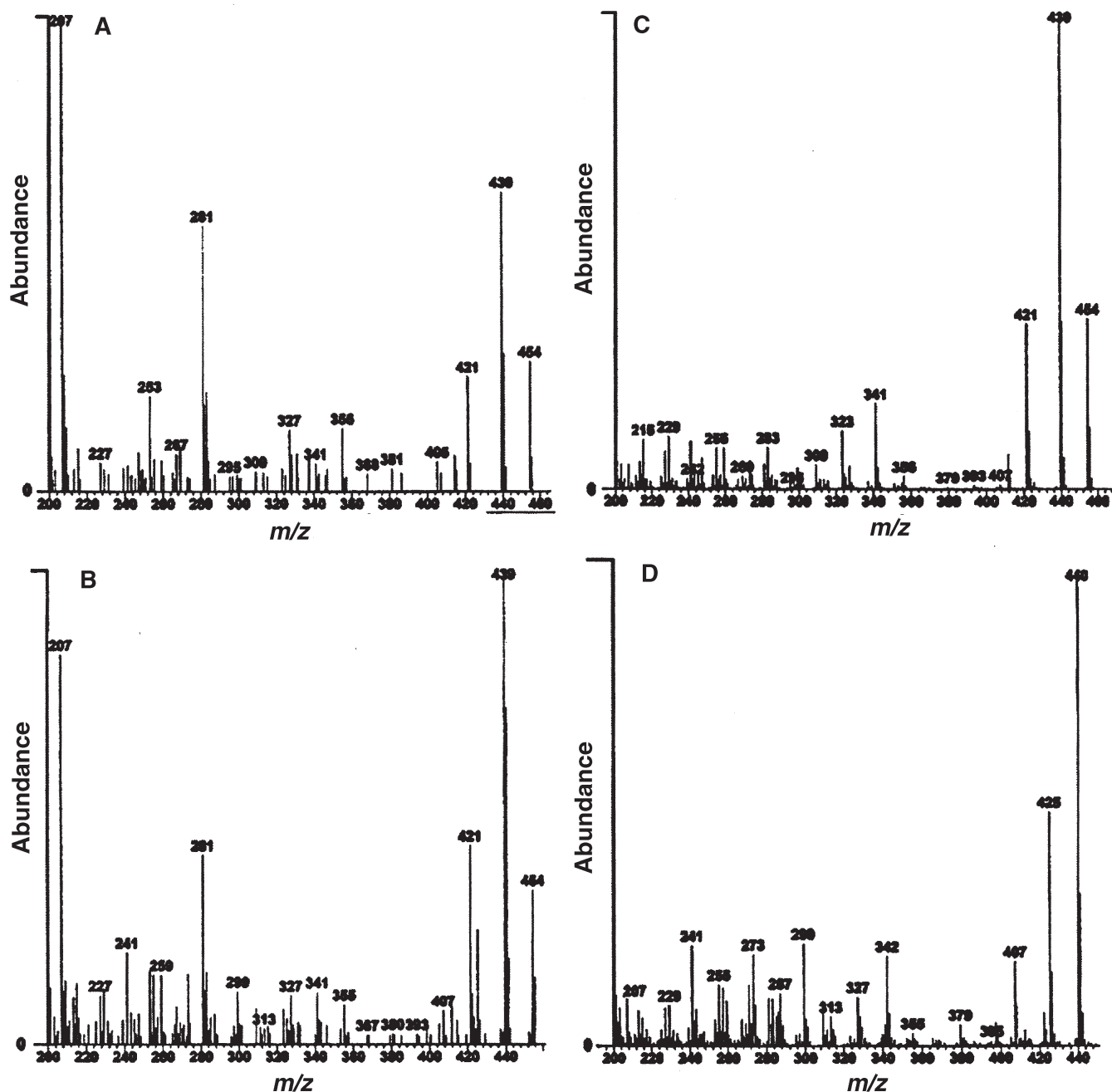


FIG. 3. Mass spectra of sterols detected in *P. carinii* by GC-MS. The mass spectrum reported in Panel A is for the GC peak at 23.7 min [relative retention time of cholesterol ( $RRT_c$ ) = 1.56], Panel B is for the GC peak at 24.4 min ( $RRT_c$  = 1.60), Panel C is for the GC peak at 25.0 min ( $RRT_c$  = 1.64), and Panel D is for the GC peak at 25.7 min ( $RRT_c$  = 1.69).

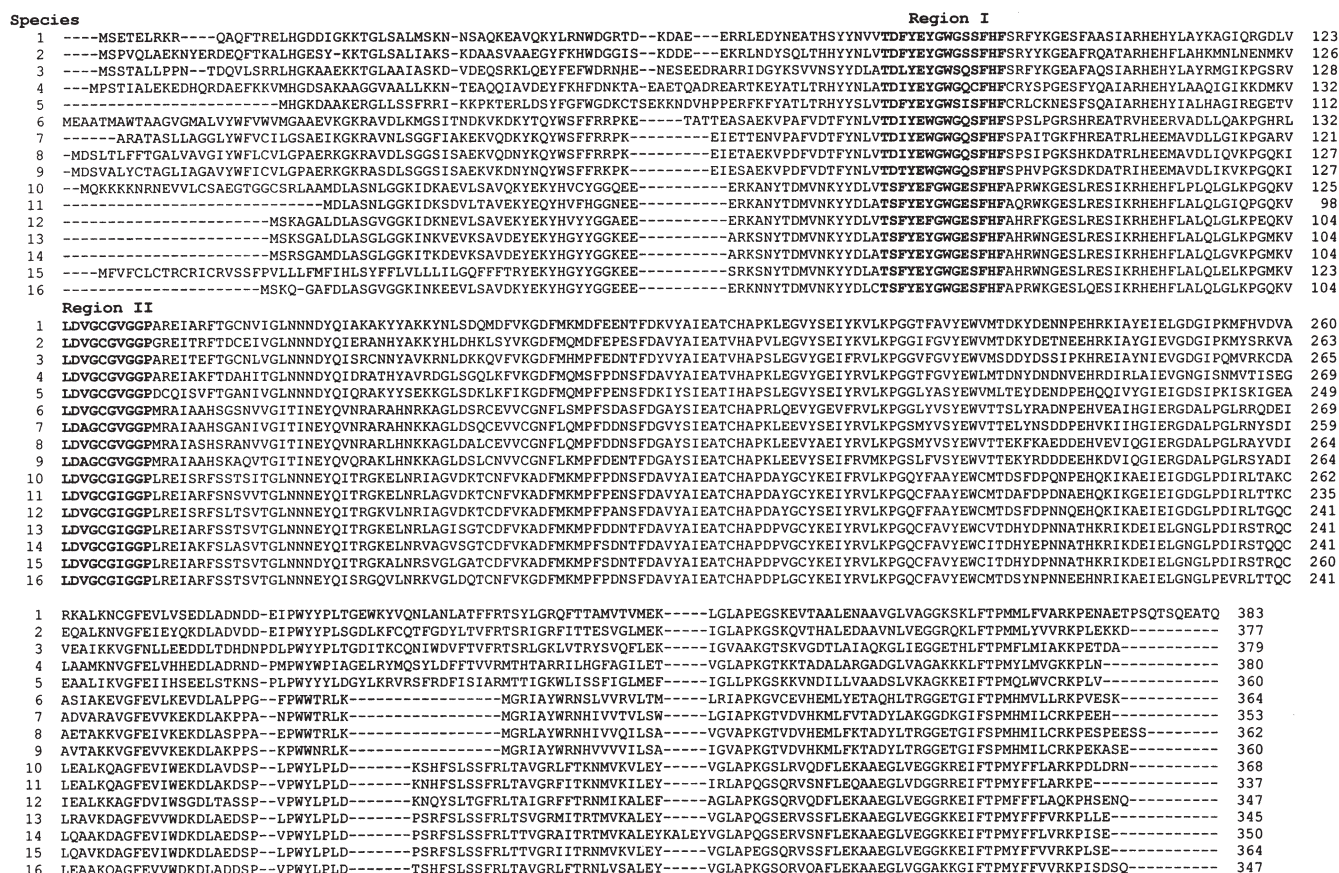
epimerically pure 24 $\alpha$ -methyl (2), was found to be a mixture of campesterol (24 $\alpha$ -methyl) and 24-epicampesterol (24 $\beta$ -methyl) in a *ca.* 2:1 mixture, consistent with the reported purity of 24-ethyl and 24-methyl sterols from vascular plants (28).

## DISCUSSION

The aim of these studies was to identify as many sterols as possible from *P. carinii* in order to establish a reasonable

sterol biosynthetic pathway for the organism after which its evolution could be considered and enzymes could be identified and targeted for rational drug design. Investigation of the sterol composition of *P. carinii* revealed interesting and noteworthy differences in comparison to related yeasts such as *Saccharomyces cerevisiae* (12). In contrast to *S. cerevisiae* and other yeasts, which usually contain predominantly ergosterol, *P. carinii* was found to contain cholesterol to about 80% of the total sterols. The enzymatic systems responsible for



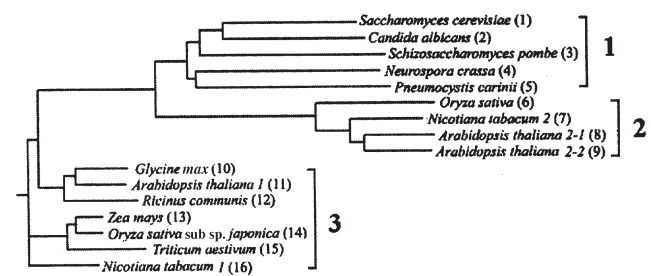


**FIG. 4.** Alignment of plant and fungal SMT. Sequences were aligned with the AlignX program (Vector NTI suite; Informax, Bethesda, MD). Region I, corresponding to the sterol binding domain, and Region II, corresponding to the AdoMet binding domain, are boldface. Complete amino acid sequences for each species of SMT are available in the GenBank corresponding to the following accession numbers: 1, CAA52308; 2, AAC26626; 3, CAB16897; 4, CAB97289; 5, AAK54439; 6, AAC34988; 7, AAC34989; 8, AAC34951; 9, T03848; 10, AAG28462; 11, CAA61966; 12, AAB62809; 13, AAB04057; 14, AAB62812; 15, AAC04265; 16, AAB37769. For abbreviation see Figure 1.

conversion of lanosterol to cholesterol accept a variety of closely related substrates, which have allowed many phytosterols structurally similar to cholesterol and to its intermediates to be detected in the organism. Eight intermediates that lie in the pathway between lanosterol and cholesterol were detected in the organism, suggesting an endogenous pathway to chole-

sterol: path **a** in Figure 2. The ability of an advanced fungus to synthesize and accumulate high levels of cholesterol was unexpected. However, cholesterol can accumulate in yeast cells. For instance, *S. cerevisiae* cultured anaerobically will absorb cholesterol from the medium and use the 24-desalkyl sterol as a bulk membrane insert replacing ergosterol (29). Anaerobic conditions are known to downregulate the postsqualene pathway in yeast, thereby upregulating sterol auxotrophy and permitting uptake of sterol from the medium (30). When deprived of oxygen, *P. carinii* growing as a parasite in the rat lung can mimic *S. cerevisiae* cultured anaerobically and absorb a significant amount of cholesterol synthesized by the host and phytosterol derived from the rat chow in a nondiscriminate manner. When the fungus is provided adequate oxygen, the organism can synthesize a portion of its cellular sterol by an acetate-mevalonate pathway (1,31). The degree to which cholesterol enters the organism may reflect a downregulation of phytosterol synthesis. This condition can affect whether the organism will resist treatment with a sterol biosynthesis inhibitor.

The *P. carinii* SMT catalyzing lanosterol **1** and 24(28)-methylenlanosterol **2** to phytosterols (32) is considered to be



**FIG. 5.** Dendrogram constructed for fungal and plant SMT. Boldface numbers refer to the grouping of SMT based on sequence homology. Sequence alignments of these enzymes are given in Figure 4. For abbreviation see Figure 1.

a key enzyme in fungi since it is not synthesized by animal systems. The enzyme also has attracted attention because of its regulatory role in phytosterol synthesis, thereby serving as a target for drug therapy (33). Indeed, as we will report elsewhere (Cushion, M.T., and Nes, W.D., unpublished report), the inhibitors of SMT action 24-aminolanosterol and 25-azalanosterol tested with *P. carinii* (33) were potent inhibitors in a cytotoxicity assay based on an ATP-driven bioluminescent reaction (6). Moreover, 24(*R,S*),25-epiminolanosterol, a potent inhibitor of SMT catalysis (33), was found to impair SMT action in whole cells of *P. carinii* (4).

Phytosterols of fungi are assumed to be of the 24 $\beta$ -alkyl series; therefore, the presence of 24 $\alpha$ -alkylsterols in *P. carinii* must be of dietary origin. Ten phytosterols with a 24-ethyl group were identified in the cells. Of these phytosterols, the  $\Delta^{25(27)}$ -olefins such as clerosterol **8** are unique to plants (5). Both  $\Delta^{24(28)}$ -*Z*-ethylidene and  $\Delta^{24(28)}$ -*E*-ethylidene sterols have been detected in fungi, but their co-occurrence with the  $\Delta^{25(27)}$ -olefin is unique to *P. carinii*. The C-24 configuration of 24-ethyl sterols from *P. carinii* showed a pattern similar to fungi (15), in which the 24 $\beta$ -ethyl stereochemistry is associated with a pathway routed through either a  $\Delta^{24(28)}$ -*Z*-ethylidene or a  $\Delta^{25(27)}$ -olefin to a  $\Delta^{24(28)}$ - or  $\Delta^{25(27)}$ -reductase-type enzyme (Fig. 2, paths **b3** and **b4**), whereas sterols lacking these specific pathways have a 24 $\alpha$ -ethyl stereochemistry. Unlike plants that can isomerize the  $\Delta^{24(28)}$ -bond to the  $\Delta^{24(25)}$ -position and in turn reduce the  $\Delta^{24(25)}$ -bond of a 24-methylsterol to either the 24 $\alpha$ - or 24 $\beta$ -configuration, fungi are known to reduce only the  $\Delta^{24(25)}$ -bond or the  $\Delta^{24(28)}$ -bond in the 24-methyl and 24-ethyl series to the 24 $\beta$ -methyl configuration. The presence of two distinct double bond series,  $\Delta^{24(28)}$ - and  $\Delta^{24(25)}$ - attached initially to a 24-methylstanostane skeleton implies the existence of two separate biosynthetic pathways to 24 $\beta$ -methylcholesterol (Fig. 2, paths **b1** and **b2**). Although the immediate precursor of 24 $\beta$ -methyl cholesterol in the **b1** pathway was not detected, the isolation of the corresponding  $\Delta^{5,7}$ -sterol in the cholesterol series suggests that the 24-alkyl compound is actually synthesized under physiological conditions.

Phylogenetic analyses based on sequence data for enzymes that constitute the sterol pathway of *P. carinii* are limited. From a comparison of the deduced amino acid sequence with that currently available, it appears that the SMT from *P. carinii* encodes an array similar to SMT enzymes from fungi and plants and belongs to the AdoMet-dependent methyl transferase superfamily (Fig. 4). As shown in the dendrogram in Figure 5, the SMT have a close evolutionary relationship to one another, with three classes based on sequence identity: In Group 1, the *P. carinii* gene shares at least 49 to 52% identity with other fungal *ERG6* genes, in Group 2, the *P. carinii* gene shares 37 to 40% identity with the plant SMT genes considered to catalyze "SMT2" activity (catalyze the second C<sub>1</sub>-transfer), and in Group 3, the *P. carinii* gene shares 32 to 38% identity with plant homologs that catalyze "SMT1" activity (catalyze the first C<sub>1</sub>-transfer). Pairwise sequence comparisons of the *ERG6* gene from *S. cerevisiae* or *P. carinii* with

related genes revealed a highly conserved hydrophobic region rich in aromatic amino acids, referred to as Region I, (Fig. 4) containing a signature motif Y81EYGWX86 not present in other AdoMet-dependent methyl transferases. As each of these enzymes uses zymosterol (cholest-8,24-dienol) as the sterol acceptor molecule, the aromatic-rich domain of Region I, spanning amino acids 78 to 91, has been proposed to be involved in substrate binding and possibly product formation by stabilizing intermediate carbenium ions generated during sterol C-methylation (34). Recent work from this laboratory has confirmed the role of Region I as part of the sterol binding site by chemical affinity labeling and site-directed mutagenesis experiments (34–36). A second highly conserved domain recently shown to be a part of the AdoMet binding site by photoaffinity labeling and site-directed mutagenesis experiments using the *S. cerevisiae* SMT spans amino acids 127 to 137 (Marshall, J.A., and Nes, W.D., unpublished report). We refer to this domain as Region II. Sequence homology analyses (37) and the structure of several AdoMet-dependent methyl transferase enzymes have been reported (38), supporting Region II as a wall of the AdoMet-binding site for the SMT. In a 3-D perspective of the crystal structures of AdoMet-dependent methyl transferases, a similar folding pattern with the central parallel  $\beta$ -sheet surrounded by  $\alpha$ -helices is observed. Although no information is available to date on the crystal structure of an SMT, all share with at least one other family member a minimum of 32 to 91% sequence identity over the entire length of the protein, ranging from 336 to 383 amino acids, and strongly indicate that SMT maintain similar 3-D conformations (39). One key feature of many AdoMet-dependent methyl transferase enzymes is the structural arrangement of their catalytic domain. This domain is built around a Rossmann fold, and it appears from the sequence alignment that SMT contain this domain at or near Region II. Regions I and II identified in the *ERG6p* gene are always found in the same order on the polypeptide chain and are separated by comparable intervals in SMT sequences. Evidence for a common fold and similar secondary structure in SMT is provided by the degree of shared amino acid identity and the fact that all family members align without large gaps connecting secondary structure elements (Bujnicki, J.M., and Nes, W.D., unpublished report). The sequence alignment data for the catalytic motifs of SMT, independent of the apparent substrate specificity, are consistent with *P. carinii* having a close phylogenetic association with yeast forms of the ascomycetous fungi.

The two sequence-related classes of plant SMT proteins catalyzing the first (SMT1) and second (SMT2) C<sub>1</sub>-transfer reactions and their strict specificity for cycloartenol and 24(28)-methylene lophenol, respectively, suggest their roles in distinct enzymatic steps in the pathway (40). A similar distinction for operation of the successive two-stage C-methylation activity in the SMT pathway of fungi is not observed, suggesting that a SMT1 and SMT2 are not required in the pathway of 24-ethyl sterols synthesized by fungi. The SMT from the yeast *S. cerevisiae* prefers zymosterol as substrate,



whereas *P. carinii* prefers lanosterol as substrate to catalyze the first C<sub>1</sub>-transfer reaction (32,33). The substrate specificity of the SMT for zymosterol or lanosterol has influenced the order of intermediates in the pathway, which can affect fungal sensitivity to C-methylation inhibitors (33). To explain the evolution in substrate specificity and the C-methylation activities that gave rise to more efficient SMT, we propose that a few amino acid substitutions in the topology of the active site occurred that affected catalytic competency and substrate channeling, as recently evidenced in site-directed mutagenesis experiments related to directed evolution of the SMT (35,36).

## ACKNOWLEDGMENTS

This study was funded in part by the Welch Foundation (D-1276) and the National Institutes of Health (NIH) (GM63477) to W.D.N. and the NIH (AI75319) to M.T.C. It represents partial fulfillment of the doctoral degree in chemistry at Texas Tech University for W.Z. A portion of this work was presented at the meeting of the American Oil Chemists' Society Steroid Symposium in May 2002 in Montréal, Canada.

## REFERENCES

- Furlong, S.T., Samia, J.A., Rose, R.M., and Fishman, J.A. (1994) Phytosterols Are Present in *Pneumocystis carinii*, *Antimicrob. Agents Chemother.* 38, 2534–2540.
- Kaneshiro, E.S., Ellis, J.E., Jayasimhulu, K., and Beach, D.H. (1994) Evidence for the Presence of "Metabolic Sterols" in *Pneumocystis*: Identification and Initial Characterization of *Pneumocystis carinii* Sterols, *J. Eukaryot. Microbiol.* 4, 78–85.
- Kaneshiro, E.S., Amit, Z., Swonger, M.M., Kreishman, G.P., Brooks, E.E., Kreishman, M., Jayasimhulu, K., Parish, E.J., Sun, H., Kizito, S.A., et al. (1999) Pneumocysterol [(24Z)-ethylidenelanost-8-en-3 $\beta$ -ol], a Rare Sterol Detected in the Opportunistic Pathogen *Pneumocystis carinii hominis*: Structural Identity and Chemical Synthesis, *Proc. Natl. Acad. Sci. USA* 96, 97–102.
- Urbina, J.A., Visbal, G., Contreras, L.M., McLaughlin, G., and Docampo, R. (1997) Inhibitors of  $\Delta^{24(25)}$ -Sterol Methyl Transferase Block Sterol Synthesis and Cell Proliferation in *Pneumocystis carinii*, *Antimicrob. Agents Chemother.* 41, 1428–1432.
- Nes, W.R., and Nes, W.D. (1980) *Lipids in Evolution*, Plenum Press, New York, 244 pp.
- Gargas, A., DePriest, P.T., Grube, M., and Tehler, A. (1995) Multiple Origins of Lichen Symbioses in Fungi Suggested by SSU rDNA Phylogeny, *Science* 268, 1492–1495.
- Cushion, M.T. (1998) Taxonomy, Genetic Organization, and Life Cycle of *Pneumocystis carinii*, *Semin. Respir. Infect.* 13, 304–312.
- Bartlett, M.S., Queener, S.F., Shaw, M.M., Richardson, J.D., and Smith, J.W. (1994) *Pneumocystis carinii* Is Resistant to Imidazole Antifungal Agents, *Antimicrob. Agents Chemother.* 38, 1859–1861.
- Hartman, M. (1998) Plant Sterols and the Membrane Environment, *Trends Plant Sci.* 3, 170–174.
- Nes, W.D. (1987) Biosynthesis and Requirement for Sterols in the Growth and Reproduction of Oomycetes, *Am. Chem. Soc. Symp. Ser.* 325, 304–328.
- Nes, W.D., Janssen, G.G., Crumley, F.G., Kalinowska, M., and Akihisa, T. (1993) The Structural Requirements of Sterol for Membrane Function in *Saccharomyces cerevisiae*, *Arch. Biochem. Biophys.* 300, 724–733.
- White, R.H., and McMorris, T.C. (1978) Biosynthetic Intermediates in the Conversion of Fucosterol and Oogoniol, *Phytochemistry* 17, 1800–1802.
- Weete, J.D., Fuller, M.S., Huang, H.Q., and Gandhi, S. (1989) Fatty and Sterols of Selected Hypochytriomycetes and Chytridomycetes, *Exp. Mycol.* 13, 183–195.
- Weete, J.D., and Gandhi, S.R. (1997) Sterols of the Phylum Zygomycota: Phylogenetic Implications, *Lipids* 32, 1309–1316.
- Patterson, G.W. (1994) Phylogenetic Distribution of Sterols, *Am. Chem. Soc. Symp. Ser.* 562, 90–108.
- Herber, R., Villoutreix, J., Granger, P., and Chapelle, S. (1983) Influence of l'Anaerobiose sur la Composition en Sterols de *Mucor hiemalis*, *Can. J. Microbiol.* 29, 606–611.
- Abreu, P.M., Lobo, M., and Prabhakar, S. (1991) Revision of C-22, C-23 Configurations of Two Triterpenoids of the Fungus *Pisolithus tinctorius*, *Phytochemistry* 30, 3818–3819.
- Li, S. (1996) Stereochemical Studies on the Metabolism of Sterols by *Saccharomyces cerevisiae* Strain GL7, Master's Thesis, Texas Tech University, Lubbock, pp. 1–123.
- Nes, W.D., Norton, R.A., Crumley, F.G., Madigan, S.J., and Katz, E.R. (1990) Sterol Phylogenesis and Algal Evolution, *Proc. Natl. Acad. Sci. USA* 87, 7565–7569.
- Chen, F., and Cushion, M.T. (1994) Use of an ATP Bioluminescent Assay to Evaluate Viability of *Pneumocystis carinii* from Rats, *J. Clin. Microbiol.* 32, 2791–2800.
- Cushion, M.T., Chen, F., and Kloepfer, N. (1997) A Cytotoxicity Assay for Evaluation of Candidate Anti-*Pneumocystis* Agents, *Antimicrob. Agents Chemother.* 41, 379–384.
- Norton, R.A., and Nes, W.D. (1991) Identification of Ergosta-6(7),8(14),25(27)-trien-3 $\beta$ -ol and Ergosta-5(6),7(8),25(27)-trien-3 $\beta$ -ol, Two New Steroidal Trienes Synthesized by *Prototheca wickerhamii*, *Lipids* 26, 247–249.
- Guo, D., Venkatramesh, M., and Nes, W.D. (1995) Developmental Regulation of Sterol Biosynthesis in *Zea mays*, *Lipids* 30, 203–219.
- Venkatramesh, M., Guo, D., Jia, Z., and Nes, W.D. (1996) Mechanism and Structural Requirements for Transformation of Substrates by the (S)-Adenosyl-L-methionine: $\Delta^{24(25)}$ -Sterol Methyl Transferase from *Saccharomyces cerevisiae*, *Biochim. Biophys. Acta* 1299, 313–324.
- Nes, W.D., and Le, P.H. (1990) Evidence for Separate Intermediates in the Biosynthesis of 24 $\beta$ -Methyl Sterols End Products by *Gibberella fujikuroi*, *Biochim. Biophys. Acta* 1042, 119–125.
- Nes, W.D., Xu, S., and Haddon, W.F. (1988) Evidence for Similarities and Differences in the Biosynthesis of Fungal Sterols, *Steroids* 53, 533–558.
- Dennis, A.L., and Nes, W.D. (2002) Sterol Methyl Transferase. Evidence for Successive C-Methyl Transfer Reactions Generating  $\Delta^{24(28)}$ - and  $\Delta^{25(27)}$ -Olefins by a Single Plant Enzyme, *Tetrahedron Lett.* 43, 7017–7021.
- Nes, W.R., Krevitz, K., and Behzadan, S. (1976) Configuration at C-24 of 24-Methyl and 24-Ethylcholesterol, *Lipids* 11, 118–126.
- Nes, W.R., Dhanuka, I.C., and Pinto, W.J. (1986) Evidence for Facilitated Transport in the Absorption of Sterols by *Saccharomyces cerevisiae*, *Lipids* 21, 102–106.
- Pinto, W.J., and Nes, W.R. (1983) Stereochemical Specificity for Sterols in *Saccharomyces cerevisiae*, *J. Biol. Chem.* 258, 4472–4476.
- Florin-Christensen, M., Florin-Christensen, J., Wu, Y.P., Zhou, L., Gupta, A., Rudney, H., and Kaneshiro, E.S. (1994) Occurrence of Specific Sterols in *Pneumocystis carinii*, *Biochem. Biophys. Res. Commun.* 14, 236–242.
- Kaneshiro, E.S., Rosenfeld, J.A., Basselin-Eiweida, M., Stringer, J.R., Keely, S.P., Smulian, A.G., and Giner, J.-L. (2002) The *Pneumocystis carinii* Drug Target S-Adenosyl-L-

- methionine: Sterol C-24 Methyl Transferase Has a Unique Substrate Preference, *Mol. Microbiol.* *44*, 989–999.
33. Nes, W.D. (2000) Sterol Methyl Transferase: Enzymology and Inhibition, *Biochim. Biophys. Acta* *1529*, 63–88.
34. Nes, W.D., McCourt, B.S., Zhou, W., Ma, J., Marshall, J.A., Peek, L.-A., and Brennan, M. (1998) Overexpression, Purification, and Stereochemical Studies of the Recombinant (*S*)-Adenosyl-L-methionine:  $\Delta^{24(25)}$ - to  $\Delta^{24(28)}$ -Sterol Methyl Transferase from *Saccharomyces cerevisiae*, *Arch. Biochem. Biophys.* *353*, 297–311.
35. Nes, W.D., McCourt, B.S., Marshall, J.A., Ma, J., Dennis, A.L., Lopez, M., and Le, H. (1999) Site-Directed Mutagenesis of the Sterol Methyl Transferase Active Site from *Saccharomyces cerevisiae* Results in Formation of Novel 24-Ethyl Sterols, *J. Org. Chem.* *64*, 1535–1542.
36. Nes, W.D., Marshall, J.A., Jia, Z., Jaradat, T.T., Song, Z., and Jayasimha, P. (2002) Active Site Mapping and Substrate Channeling in the Sterol Methyl Transferase Pathway, *J. Biol. Chem.* *277*, 42549–42556.
37. Kagan, R.M., and Clarke, S. (1994) Widespread Occurrence of Three Sequence Motifs in Diverse S-Adenosylmethionine-Dependent Methyl Transferases Suggests a Common Structure for These Enzymes, *Arch. Biochem. Biophys.* *310*, 41–427.
38. Niewmierzycka, A., and Clarke, S. (1999) S-Adenosylmethionine-Dependent Methylation in *Saccharomyces cerevisiae*, *J. Biol. Chem.* *274*, 814–824.
39. Hrmova, M., and Fincher, G.B. (2001) Plant Enzyme Structure. Explaining Substrate Specificity and the Evolution of Function, *Plant Physiol.* *125*, 54–57.
40. Bouvier-Nave, P., Husselstein, T., and Benveniste, P. (1998) Two Families of Sterol Methyl Transferase Are Involved in the First and the Second Methylation Steps of Plant Sterol Biosynthesis, *Eur. J. Biochem.* *256*, 88–96.

[Received August 26, 2002; accepted November 29, 2002]



# Transformations of DHEA and Its Metabolites by Rat Liver

Henry Lardy\*, Ashok Marwah, and Padma Marwah

Department of Biochemistry and Institute for Enzyme Research, University of Wisconsin–Madison, Madison, Wisconsin 53705

**ABSTRACT:** Because dehydroepiandrosterone (DHEA) has a wide variety of weak beneficial effects in experimental animals and humans, we searched for metabolites of this steroid in the hope of finding more active compounds that might qualify for the title “steroid hormone.” Incubation of DHEA with rat liver homogenate fortified with energy-yielding substrates resulted in rapid hydroxylation at the 7 $\alpha$ -position of the molecule and subsequent conversion to other 7-oxygenated steroids in the sequence DHEA  $\rightarrow$  7 $\alpha$ -hydroxyDHEA  $\rightarrow$  7-oxoDHEA  $\rightarrow$  7 $\beta$ -hydroxyDHEA, with branching to diols, triols, and sulfate esters. The ability of these metabolites to induce the formation of liver thermogenic enzyme activity increased from left to right in that sequence. A total of 25 different steroids were characterized, and at least six additional structures that are currently under study were produced from DHEA. 7-OxoDHEA is more effective than DHEA in enhancing memory performance in old mice and in reversing the amnesic effects of scopolamine.

Paper no. L9137 in *Lipids* 37, 1187–1191 (December 2002).

The study of naturally occurring steroids has been so extensive and has been conducted by such intellectually and experimentally gifted investigators that one might assume that there are no more interesting steroids to be found. However, as was the case when John Horgan (1) erroneously decreed in 1996 that we had reached the “twilight of the Scientific Age,” many interesting structures are still to be found among the steroids.

This essay deals with steroids derived metabolically from dehydroepiandrosterone (DHEA) (1, see Scheme 1), which is produced in the adrenals, testes, ovaries, and brain (2,3) and serves as an intermediate in the biosynthesis of testosterone and estrogens from cholesterol. In humans the adrenal glands are the main source of DHEA and of its sulfate ester (DHEAS), which is the main circulating form of this steroid. The prenatal adrenals are very active in synthesizing this steroid, but the fetal zone of the gland atrophies after birth and the synthesis is renewed in the zona reticularis at about 7 yr of age (adrenarch). The blood plasma concentration of DHEAS peaks at about 20 to 30 yr of age, when it reaches 200 to 500  $\mu\text{g}/100\text{ mL}$ —10 times the concentration of glucocorticoids (2). The concentration in blood plasma of women is somewhat lower. As humans age, blood DHEAS concen-

trations decrease so that at ages 70–80 the amount is only about 10% that in the prime years.

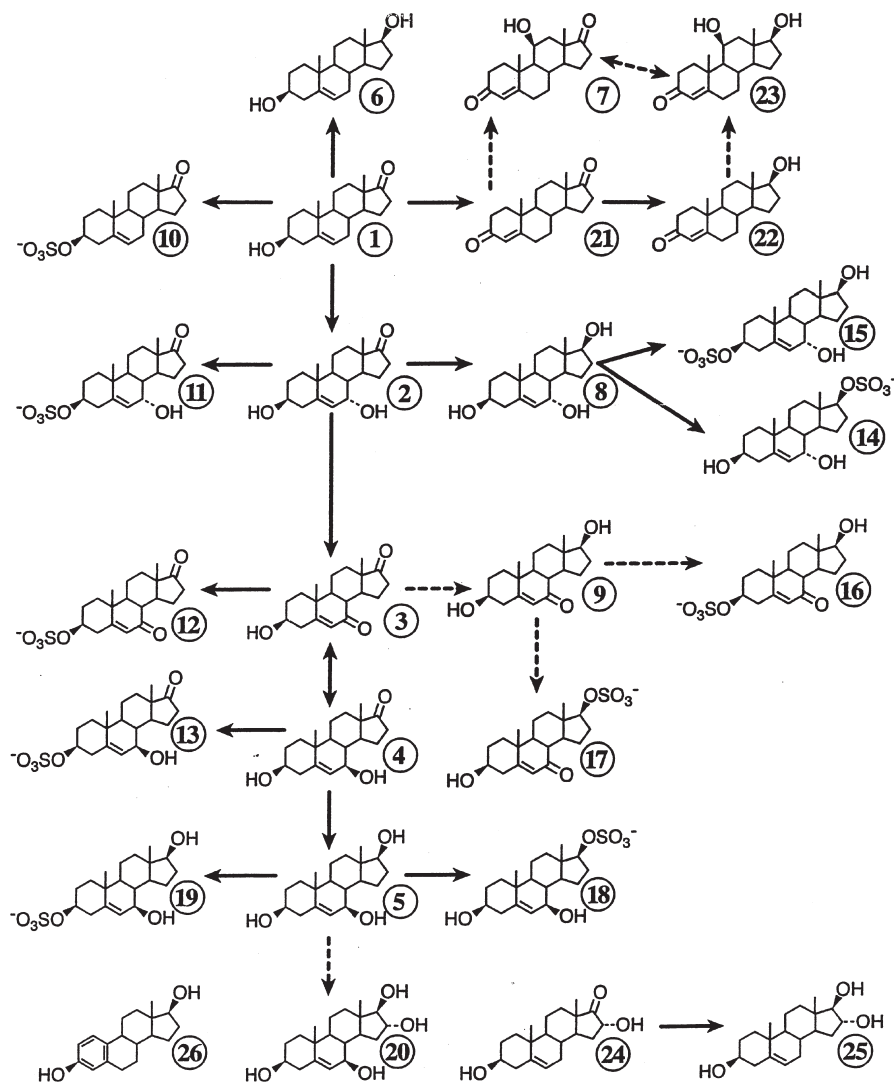
Orally administered DHEA exerts several beneficial effects in animals apart from its role in the formation of androgens and estrogens. It decreases obesity (4–8), decreases blood cholesterol (8–10), decreases blood sugar in diabetic animals (11), enhances the activity of the immune system (12,13), inhibits tumor development (14,15), and improves memory (16,17). DHEA has been found to have some limited beneficial effects in human subjects (18–27).

The suitability of DHEA as a therapeutic agent in humans is limited because of the large doses required and because it increases blood testosterone when given to women. The large amounts (*ca.* 0.5% of the diet) needed to obtain effects in animals and the fact that no receptor for DHEA has been isolated indicate that, in the systems that respond, DHEA may be acting as a precursor of a more active steroid just as it is a precursor of androgens and estrogens. We therefore initiated a search for possible metabolites of DHEA in the hope of finding more active steroids that would be more selective in their metabolic effects. That such a search requires a suitable assay system was clearly stated by Allen and Doisy in 1923 when they sought the substance responsible for their newly discovered estrogen activity: “Without a practicable test, the search for any hormone is obviously a very haphazard and uncertain task” (28). Such a “practicable test” for the DHEA problem was developed in our laboratory.

The suggestion, in 1958, from two different research groups (29,30) that mitochondrial glycerophosphate dehydrogenase (GPDH) could oxidize NADH generated by glycolysis using a pathway that skipped the mitochondrial phosphorylation site between NADH and ubiquinone at once indicated that this system (glycerophosphate shuttle) would be thermogenic. The best-known thermogenic agent in homeotherms is the thyroid hormone (31,32), which *ipso facto* increases the metabolic cost of work (33,34). We found that feeding desiccated thyroid substance increased liver mitochondrial GPDH 20-fold above that in normal animals and that thyroidectomy greatly decreased the enzyme (35,36). When DHEA was demonstrated to decrease metabolic efficiency (4) and to be thermogenic (37), we found that it too induced the formation of increased amounts of liver GPDH (38,39). Elsewhere (38,40) we have pointed out that sending electrons from glycolytically generated cytosolic NADH directly to ubiquinone could decrease metabolic efficiency only about 5%, whereas efficiency is decreased

\*To whom correspondence should be addressed.  
E-mail: haldary@facstaff.wisc.edu

Abbreviations: DHEA, dehydroepiandrosterone; DHEAS, the sulfate ester of dehydroepiandrosterone; GPDH, glycerophosphate dehydrogenase.



SCHEME 1

about 35% in hyperthyroid subjects (33,34). We have described a system involving GPDH and malic enzyme in liver that can shunt electrons from the tricarboxylic acid cycle, bypassing the first phosphorylation site, and thus decrease metabolic efficiency by one-third. We had demonstrated earlier (41) that reducing equivalents generated in the tricarboxylic acid cycle directly reduce oxalacetate to form malate, which is transported from the mitochondria to the cytosol. In liver, malic enzyme converts malate to pyruvate, which can recirculate to the mitochondria. The NADPH generated is used to reduce dihydroxyacetone phosphate to glycerophosphate (42), the substrate for the dehydrogenase located on the mitochondrial membrane.

Muscle has high GPDH activity, and if a system exists to transfer reducing equivalents from mitochondria to the cytosol in that tissue, it could account for the increased energy cost of work by hyperthyroid subjects (34). We are currently searching for such a possible transport mechanism.

We have used the induction of these two enzymes as an assay for DHEA-like activity of a large number of new steroids

we have synthesized (38,39,43-47). In a parallel study we have examined the metabolic conversion of DHEA to related steroid structures (48). By following the conversion at short and frequent time intervals, it is possible to deduce the sequence by which DHEA moves on to become more active molecules.

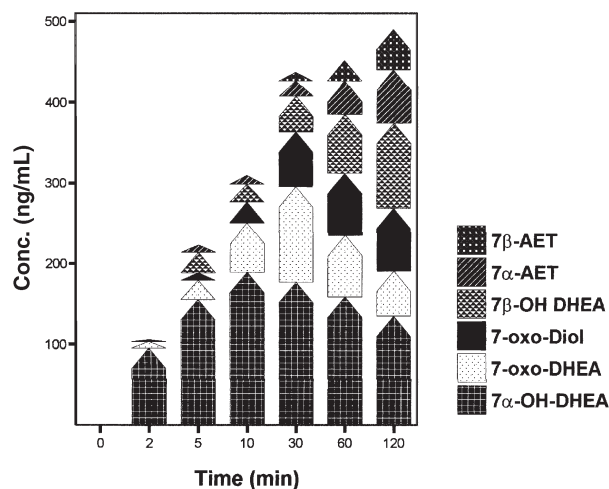
*Metabolic conversions of DHEA.* Many investigators have studied the conversion of DHEA to a variety of metabolites. Usually a specific tissue fraction was used as the enzyme source, and only a few products were identified. We examined the conversion of DHEA to neutral free steroids as well as to acidic and neutral conjugated molecules in whole-liver homogenates so that the different types of relevant enzymes in different organelles or cell compartments could have access to all metabolites as they were formed, as might be the case in the intact liver. The product of one organelle can be the substrate for another.

The first experiments were conducted with 1  $\mu$ g of DHEA (Humanetics Corp., Chanhassen, MN) per 40 mg of liver homogenized in isotonic medium to retain mitochondrial structure (48). The incubation mixture contained NADPH and malic

**TABLE 1**  
Steroids Formed from Dehydroepiandrosterone by Rat Liver Homogenate

Number	Steroid
1	3 $\beta$ -Hydroxyandrost-5-en-17-one (DHEA, starting steroid)
2	3 $\beta$ , $\alpha$ -Dihydroxyandrost-5-en-17-one
3	3 $\beta$ -Hydroxyandrost-5-ene-7,17-dione
4	3 $\beta$ ,7 $\beta$ -Dihydroxyandrost-5-en-17-one
5	Androst-5-ene-3 $\beta$ ,7 $\beta$ ,17 $\beta$ -triol
6	Androst-5-ene-3 $\beta$ ,17 $\beta$ -diol
7	11 $\beta$ -Hydroxyandrost-4-ene-3,17-dione
8	Androst-5-ene-3 $\beta$ ,7 $\alpha$ ,17 $\beta$ -triol
9	3 $\beta$ ,17 $\beta$ -Dihydroxyandrost-5-en-7-one
10	3 $\beta$ -Sulfooxyandrost-5-en-17-one
11	3 $\beta$ -Sulfooxy-7 $\alpha$ -hydroxyandrost-5-en-17-one
12	3 $\beta$ -Sulfooxyandrost-5-ene-7,17-dione
13	3 $\beta$ -Sulfooxy,7 $\beta$ -hydroxyandrost-5-en-17-one
14	3 $\beta$ ,7 $\alpha$ -Dihydroxyandrost-5-ene-17 $\beta$ -sulfate
15	3 $\beta$ -Sulfooxyandrost-5-ene-7 $\alpha$ ,17 $\beta$ -diol
16	3 $\beta$ -Sulfooxy-17 $\beta$ -hydroxyandrost-5-en-17-one
17	3 $\beta$ -Hydroxy-17 $\beta$ -sulfooxyandrost-5-en-7-one
18	3 $\beta$ ,7 $\beta$ -Dihydroxyandrost-5-ene-17 $\beta$ -sulfate
19	3 $\beta$ -Sulfooxyandrost-5-ene-7 $\beta$ ,17 $\beta$ -diol
20	Androst-5-ene-3 $\beta$ ,7 $\beta$ ,16 $\alpha$ ,17 $\beta$ -tetrol
21	Androst-4-ene-3,17-dione
22	17 $\beta$ -Hydroxyandrost-4-en-3-one (testosterone)
23	11 $\beta$ ,17 $\beta$ -Dihydroxyandrost-4-en-3-one
24	3 $\beta$ ,16 $\alpha$ -Dihydroxyandrost-5-en-17-one
25	Androst-5-ene-3 $\beta$ ,16 $\alpha$ ,17 $\beta$ -triol
26	1,3,5(10)Estratriene-3,17 $\beta$ -diol (estradiol)

acid to provide reducing power for the P450 oxidoreductase. After various incubation times, samples were removed, extracted with 50% acetonitrile, then with acetonitrile with methanol, and the solvents were evaporated. Detailed descriptions of the extraction, fractionation, and analytical procedures are presented elsewhere (48,49).



**FIG. 1.** Yield of metabolites from 1  $\mu$ g of dehydroepiandrosterone (DHEA) and homogenate from 40 mg of rat liver in 1 mL final volume. The isotonic medium was fortified with 2 mM malic acid,  $\text{MgSO}_4$ , and glucose 6-phosphate each at 1 mM, and ATP and NADPH each at 25  $\mu$ M, incubated at 37°C and sampled at the times indicated. AET, androstene triol.

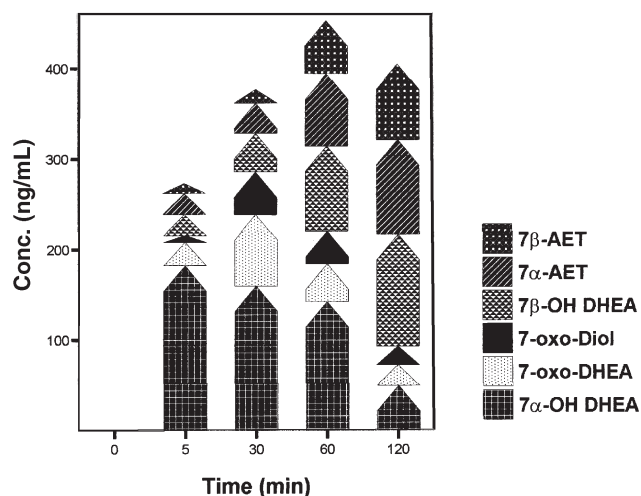
All analyses by HPLC–MS were conducted after selecting columns and solvents that permitted separation of individual compounds in each of the fractions (48,49). External and internal standards of known, synthesized steroids defined retention times, recoveries, and fragmentation patterns.

Table 1 lists 25 compounds produced from DHEA that were isolated from the incubation mixtures and identified; their structures are depicted in Scheme 1. Steroids 1 to 4 readily form 3 $\beta$ -sulfate esters. The diol and triols formed are susceptible to sulfation at either the 3 $\beta$ - or 17 $\beta$ -positions.

We were astonished that nearly all the DHEA-related structures that have been found in nature were produced in these incubations. It is clear from Figure 1 that 7 $\alpha$ -hydroxyDHEA was the first product formed from DHEA. Nearly 10% of the added DHEA accumulated as the 7 $\alpha$  derivative in the first 2 min; very small amounts of 7-oxoDHEA, but no 7 $\beta$  derivative, were formed in that interval. 7 $\alpha$ -HydroxyDHEA reached a peak at 10 min and then declined as it was converted to 7-oxoDHEA and other metabolites. After 5 min of incubation, 7 $\beta$ -hydroxyDHEA was as abundant as the 7-oxo steroid, and small amounts of 7-oxodiols and 3 $\beta$ ,7 $\alpha$ ,17 $\beta$ -triol were present. The addition of pyruvate to keep cytosolic NAD<sup>+</sup> in the oxidized state retarded the hydroxylation and the formation of other metabolites.

In liver homogenate supplemented with lactate and NADH, 7 $\alpha$ -hydroxyDHEA was again the early product (Fig. 2). Despite the presumed continued production, the total amount declined as it was converted first to 7-oxoDHEA, then to 7 $\beta$ -hydroxyDHEA and the two triols. In incubations with DHEA as substrate, small amounts of sulfate esters were formed; much larger amounts were formed when the starting steroid was 7-oxoDHEA, 7 $\beta$ -hydroxyDHEA, or 7 $\beta$ -triol. Among the metabolites still to be characterized, there is evidence for glucuronides and possibly acyl esters.

The specific ability to induce the liver thermogenic enzymes, mitochondrial *sn*-glycerol-3-phosphate dehydrogenase



**FIG. 2.** Metabolites produced from liver homogenate. Conditions are as in Figure 1, except that 2 mM lactate replaced malate and NADH replaced NADPH. For abbreviations see Figure 1.

and cytosolic malic enzyme, increases in the order DHEA  $\rightarrow$  7 $\alpha$ -hydroxyDHEA  $\rightarrow$  7-oxoDHEA  $\rightarrow$  7 $\beta$ -hydroxyDHEA. At low steroid concentrations in the diet, 7-oxoDHEA induces levels of enzyme activity equivalent to those produced by three to four times as much DHEA (44). The activity of 7 $\alpha$ -hydroxyDHEA falls between these two, whereas 7 $\beta$ -hydroxyDHEA is considerably more active than 7-oxoDHEA. Androst-5-ene-3 $\beta$ ,7 $\beta$ ,17 $\beta$ -triol and 3 $\beta$ ,7 $\beta$ ,16 $\alpha$ -trihydroxyandrost-5-en-17-one are about as active as 7 $\beta$ -hydroxyDHEA. The comparisons must be made within a given experiment because the responses vary between different batches of rats.

7-OxoDHEA is also more active than DHEA as an enhancer of memory performance and in its ability to abolish the amnesic effect of scopolamine (50).

## REFERENCES

- Horgan, J. (1997). *End of Science: Facing the Limits of Knowledge in the Twilight of the Scientific Age*, Addison-Wesley, Reading, MA.
- Parker, L. (1989) *Adrenal Androgens in Clinical Medicine*, Academic Press, San Diego.
- Le Goascogne, C., Robel, P., Guezou, M., Sananes, N., Baulieu, E.E., and Waterman, M. (1987) Neurosteroids: Cytochrome P450ssc in Rat Brain, *Science* 237, 1212–1215.
- Yen, T.T., Allan, J.A., Pearson, D.V., Acton, J.M., and Greenberg, M.M. (1977) Prevention of Obesity in Avy/a Mice by Dehydroepiandrosterone, *Lipids* 12, 409–413.
- Cleary, M.P. (1989) Antiobesity Effect of Dehydroepiandrosterone in the Zucker Rat, in *Hormones, Thermogenesis, and Obesity* (Lardy, H., and Stratman, F., eds.), pp. 365–376, Elsevier, New York.
- Kurzman, I.D., MacEwen, E.G., and Haffa, L.M. (1990) Reduction in Body Weight and Cholesterol in Spontaneously Obese Dogs by Dehydroepiandrosterone, *Int. J. Obes.* 14, 95–104.
- Lee-Currie, Y.R., Wen, P., and McIntosh, M.K. (1997) Dehydroepiandrosterone-Sulfate (DHEAS) Reduces Adipocyte Hyperplasia Associated with Feeding Rats a High-Fat Diet, *Int. J. Obes.* 21, 1058–1064.
- Kurzman, I.D., Panciera, D., Miller, J.B., and MacEwen, E.G. (1998) The Effect of Dehydroepiandrosterone Combined with a Low-Fat Diet in Spontaneously Obese Dogs: A Clinical Trial, *Obes. Res.* 6, 20–28.
- Kritchevsky, D., Tepper, S., Klurfeld, D., and Schwartz, A.S. (1983) Influence of Dehydroepiandrosterone (DHEA) on Cholesterol Metabolism in Rats, *Pharmacol. Res. Commun.* 15, 797–803.
- Ben-David, M., Dikstein, S., Bismuth, G., and Sulman, F.G. (1967) Antihypercholesterolemic Effect of Dehydroepiandrosterone in Rats, *Proc. Soc. Exp. Biol. Med.* 125, 1136–1140.
- Coleman, D.L., Schwizer, R.L., and Leiter, E.H. (1984) Effect of Genetic Background on the Therapeutic Effects of Dehydroepiandrosterone (DHEA) in Diabetes–Obesity Mutants and in Aged Normal Mice, *Diabetes* 33, 26–32.
- Loria, R., Inge, T.H., Cook, S.S., Szokol, A., and Regelson, W. (1988) Protection Against Acute Lethal Viral Infections with the Native Steroid Dehydroepiandrosterone (DHEA), *Med. Virol.* 26, 301–314.
- Ben-Nathan, D., Lustig, S., Kobilar, D., Danenberg, H.D., Lupu, E., and Feuerstein, G. (1992) Dehydroepiandrosterone Protects Mice Inoculated with West Nile Virus and Exposed to Cold Stress, *J. Med. Virol.* 38, 159–166.
- Schwartz, A.G. (1979) Inhibition of Spontaneous Breast Cancer Formation in Female C3H(Avy/a) Mice by Long-Term Treatment with Dehydroepiandrosterone, *Cancer Res.* 39, 1129–1132.
- Nyce, J.W., Magee, P.N., Hard, G.C., and Schwartz, A.G. (1984) Inhibition of 1,2-Dimethylhydrazine-Induced Colon Tumorigenesis in Balb/c Mice by Dehydroepiandrosterone, *Carcinogenesis* 5, 57–62.
- Flood, J.F., Smith, G.E., and Roberts, E. (1988) Dehydroepiandrosterone and Its Sulfate Enhance Memory Retention in Mice, *Brain Res.* 447, 269–278.
- Flood, J.F., and Roberts, E. (1988) Dehydroepiandrosterone Sulfate Improves Memory in Aging Mice, *Brain Res.* 448, 178–181.
- Kalimi, M., and Regelson, W. (eds.) (1990) *The Biological Role of Dehydroepiandrosterone (DHEA)*, DeGruyter, Berlin.
- Mortola, J.F., and Yen, S.S. (1990) The Effects of Oral Dehydroepiandrosterone on Endocrine-Metabolic Parameters in Postmenopausal Women, *J. Clin. Endocrinol. Metab.* 71, 696–704.
- Morales, A.J., Nolan, J.J., Nelson, J.C., and Yen, S.S. (1994) Effects of Replacement Doses of Dehydroepiandrosterone in Men and Women of Advancing Age, *J. Clin. Endocrinol. Metab.* 78, 1360–1367.
- Labrie, F., Diamond, P., Cusan, L., Gomez, J.-L., Belanger, A., and Candas, B. (1997) Effect of 12-Month Dehydroepiandrosterone Replacement Therapy on Bone, Vagina, and Endometrium in Postmenopausal Women, *J. Clin. Endocrinol. Metab.* 82, 3498–3505.
- Morales, A.J., Haubrich, R.H., Hwang, J.Y., Asakura, H., and Yen, S.S. (1998) The Effect of Six Months Treatment with a 100 mg Daily Dose of Dehydroepiandrosterone (DHEA) on Circulating Sex Steroids, Body Composition and Muscle Strength in Age-Advanced Men and Women, *Clin. Endocrinol.* 49, 421–432.
- Labrie, F. (1998) DHEA as a Physiological Replacement Therapy at Menopause, *J. Endocrinol. Invest.* 21, 399–401.
- Barry, N.N., McGuire, J.L., and van Vollenhoven, R. (1998) Dehydroepiandrosterone in Systemic Lupus Erythematosus: Relationship Between Dosage, Serum Levels, and Clinical Response, *J. Rheumatol.* 27, 2352–2356.
- Bloch, M., Schmidt, P.J., Danaceau, M., Adams, L.F., and Rubinow, D.R. (1999) Dehydroepiandrosterone Treatment of Midlife Dysthymia, *Biol. Psychiatry* 45, 1533–1541.
- van Vollenhoven, R.F. (2000) Dehydroepiandrosterone in Systemic Lupus Erythematosus, *Rheum. Dis. Clin. North Am.* 26, 349–362.
- Arlt, W., Callies, F., and Allolio, B. (2000) DHEA, Replacement in Women with Adrenal Insufficiency: Pharmacokinetics, Bioconversion, and Clinical Effects on Well-Being, Sexuality, and Cognition, *Endocr. Res.* 26, 505–511.
- Allen, E., and Doisy, E.A. (1923) An Ovarian Hormone. Preliminary Report on Its Location, Extraction and Partial Purification, and Action in Test Animals, *J. Am. Med. Assoc.* 81, 819–821.
- Bucher, T., and Klingenberg, M. (1958) Weg des Wasserstoffs in der lebendigen Organization, *Angew. Chem.* 70, 552–570.
- Estabrook, R.W., and Sacktor, B. (1958)  $\alpha$ -Glycerophosphate Oxidase of Flight Muscle Mitochondria, *J. Biol. Chem.* 233, 1014–1019.
- Harington, C.R. (1933) *The Thyroid Gland, Its Chemistry and Physiology*, Oxford University Press, London.
- Cori, G.T. (1921) Experimentelle untersuchungen an einem kongenitalen Myxodem, *Z. Ges. Exper. Med.* 25, 150–169.
- Plummer, H.S., and Boothby, W.M. (1923) The Cost of Work in Exophthalmic Goiter, *Am. J. Physiol.* 63, 406–407.
- Briard, S.P., McClintock, J.T., and Baldrige, C.W. (1935) Cost of Work in Patients with Hypermetabolism Due to Leukemia and to Exophthalmic Goiter, *Arch. Int. Med.* 56, 30–37.
- Lee, Y.-P., Takemori, A., and Lardy, H. (1959) Enhanced Oxidation of  $\alpha$ -Glycerophosphate by Mitochondria of Thyroid-Fed Rats, *J. Biol. Chem.* 234, 3051–3054.
- Lee, Y.-P., and Lardy, H.A. (1965) Influence of Thyroid Hormones on L- $\alpha$ -Glycerophosphate Dehydrogenase and Other



- Dehydrogenases in Various Organs of the Rat, *J. Biol. Chem.* 240, 1427–1436.
37. Tagliaferro, A., Davis, J.R., Truchon, S., and Van Hamont, N. (1986) Effects of Dehydroepiandrosterone Acetate on Metabolism, Body Weight, and Composition of Male and Female Rats, *J. Nutr.* 116, 1977–1983.
  38. Lardy, H., Su, C.-Y., Kneer, N., and Wielgus, S. (1989) Dehydroepiandrosterone Induces Enzymes That Permit Thermogenesis and Decrease Metabolic Efficiency, in *Hormones, Thermogenesis, and Obesity* (Lardy, H., and Stratman, F., eds.), pp. 415–426, Elsevier, New York.
  39. Su, C.-Y., and Lardy, H.A. (1991) Induction of Hepatic Glycero-phosphate Dehydrogenase in Rats by Dehydroepiandrosterone, *J. Biochem. (Tokyo)* 110, 207–213.
  40. Lardy, H. (1999) Dehydroepiandrosterone and Ergosteroids Affect Energy Expenditure, in *Health Promotion and Aging: The Role of Dehydroepiandrosterone (DHEA)* (Watson, R.R., ed.), p. 33–42, Harwood, Amsterdam.
  41. Lardy, H., Paetkau, V., and Walter, P. (1965) Paths of Carbon in Gluconeogenesis and Lipogenesis: The Role of Mitochondria in Supplying Precursors of Phosphoenolpyruvate, *Proc. Natl. Acad. Sci. USA* 53, 1410–1415.
  42. Bobyleva, V., Kneer, N., Bellei, M., Battelli, D., and Lardy, H. (1993) Concerning the Mechanism of Increased Thermogenesis in Rats Treated with Dehydroepiandrosterone, *J. Bioenerg. Biomembr.* 25, 313–321.
  43. Lardy, H., Partridge, B., Kneer, N., and Wei, Y. (1995) Ergosteroids: Induction of Thermogenic Enzymes in Liver of Rats Treated with Steroids Derived from Dehydroepiandrosterone, *Proc. Natl. Acad. Sci. USA* 92, 6617–6619.
  44. Lardy, H., Kneer, N., Wei, Y., Partridge, B., and Marwah, P. (1998) Ergosteroids II: Biologically Active Metabolites and Synthetic Derivatives of Dehydroepiandrosterone, *Steroids* 63, 158–165.
  45. Reich, I.L., Lardy, H., Wei, Y., Marwah, P., Kneer, N., Powell, D.R., and Reich, H.J. (1998) Ergosteroids III: Syntheses and Biological Activity in Secosteroids Related to Dehydroepiandrosterone, *Steroids* 63, 542–553.
  46. Marwah, P., Marwah, A., Kneer, N., and Lardy, H. (2001) Ergosteroids IV: Synthesis and Biological Activity of Steroid Glucuronides, Ethers, and Alkylcarbonates, *Steroids* 66, 581–595.
  47. Reich, I.L., Reich, H.J., Kneer, N., and Lardy, H. (2002) Ergosteroids V: Preparation and Biological Activity of Various D-Ring Derivatives in the 7-Oxo-dehydroepiandrosterone Series, *Steroids* 67, 221–233.
  48. Marwah, A., Marwah, P., and Lardy, H. (2002) Ergosteroids VI: Metabolism of Dehydroepiandrosterone *in vitro*: A Liquid Chromatographic–Mass Spectrometric Study, *J. Chromatogr. B* 767, 285–299.
  49. Marwah, A., Marwah, P., and Lardy, H. (2001) High-Performance Liquid Chromatographic Analysis of Dehydroepiandrosterone, *J. Chromatogr. A* 935, 279–296.
  50. Shi, J., Schulze, S., and Lardy, H. (2000) The Effect of 7-Oxo-DHEA Acetate on Memory in Young and Old C57BL/6 Mice, *Steroids* 65, 124–129.

[Received August 16, 2002; accepted December 2, 2002]

# Studies Toward the Synthesis of the Shark Repellent Pavoninin-5

John R. Williams\*, Deping Chai, Hua Gong, Wei Zhao, and Dominic Wright

Department of Chemistry, Temple University, Philadelphia, Pennsylvania 19122-2585

**ABSTRACT:** Sharks are the most dangerous predators of people in the sea, resulting in people being mauled and killed each year. A shark repellent could help to diminish this danger. The aglycone of the shark repellent pavoninin-5, (25*R*)-cholest-5-en-3 $\beta$ ,15 $\alpha$ ,26-triol (**5a**), was synthesized from diosgenin (**9**). Removing mercury from the Clemmensen reduction of **9** gave a higher yield of (25*R*)-cholest-5-en-3 $\beta$ ,16 $\beta$ ,26-triol, **10a**, and was also more environmentally friendly. Attempted methods for the transposition of the C-16 $\beta$  hydroxyl to the 15 $\alpha$  position are described. A successful method for this transposition *via* the 15 $\alpha$ -hydroxy-16-ketone, **8a**, using the Barton deoxygenation reaction on the 16-alcohol **14b**, is reported.

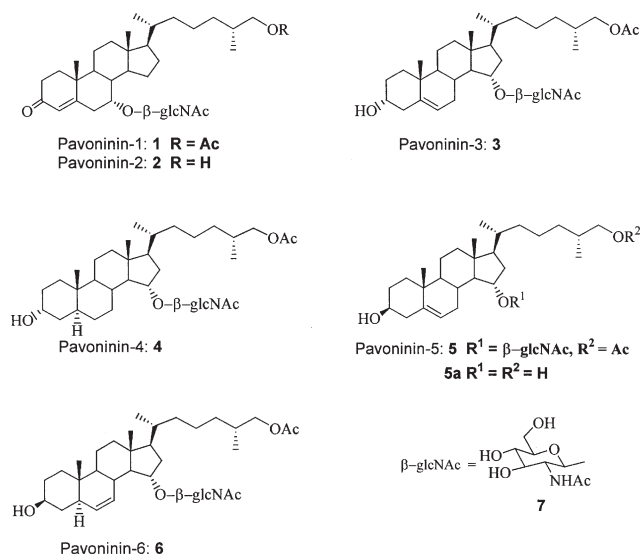
Paper no. L9136 in *Lipids* 37, 1193–1195 (December 2002).

Surveys by the National Geographic Society have shown that “shark” is the most feared word in the English language, probably as a result of the movie *Jaws*. This fear is well founded since sharks as a group are the most dangerous predators to humans in the sea.

Certain species of fish are known to kill other fish in the same tank without any traumatic device. These fish have special secretory cells that emit ichthyotoxic substances, and thus they are called ichthyocrinotoxic fish (1–3). *Paradachirus pavoninus*, a sole that lives in the tropical region of the western Pacific and eastern Indian Ocean, is an ichthyotoxic fish. The secretion from *P. pavoninus* has been isolated, separated, and characterized as pavoninins 1–6 (Scheme 1) (4). These shark-repelling pavoninins are ichthyotoxic steroids, *N*-acetylglucosaminides. It is believed that pavoninins are potent cell disrupters that should have important pharmacological properties. The toxicity of these steroid glycosides is believed to relate to their surfactant properties. The steroid backbone is considered to be the hydrophobic region, whereas the *N*-acetyl-D-glucosamide sugar is hydrophilic. The synthesis of pavoninin-1 (**1**) (5) and the aglycones of pavoninin-1 (**1a**) and -2 (**2a**) have been reported (6). In this article, we report our efforts to synthesize the aglycone of pavoninin-5 (**5a**).

Figure 1 outlines a retrosynthetic analysis of pavoninin-5 (**5**). The *N*-acetyl glucosamine (**7**) may be added to the aglycone **5a** to yield pavoninin-5. The aglycone **5a** can be prepared from the intermediate 15 $\alpha$ -hydroxy-16-ketone (**8**). This

\*To whom correspondence should be addressed at Department of Chemistry, Temple University, 13 & Norris Sts., Philadelphia, PA 19122-2585.  
E-mail: john.r.williams@temple.edu  
Abbreviations: MEM, methoxyethoxymethyl; TBDMS, tert-butyldimethylsilyl.



SCHEME 1

can be prepared from the commercially available diosgenin (**9**).

## RESULTS AND DISCUSSION

The structure of pavoninin-5 aglycone (**5a**) may be described as cholesterol with two additional hydroxyl groups at C-15 $\alpha$  and C-26. A logical starting material for the synthesis of **5a** is the commercially available **9**, which has functionality in positions suitable for conversion to **5a**. Zinc and hydrochloric acid reduction of **9** afforded the 3 $\beta$ ,16 $\beta$ ,26-triol, **10a**, in 85% yield. This is a significant improvement over the original

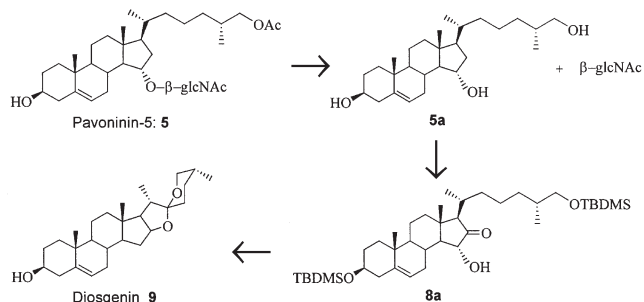
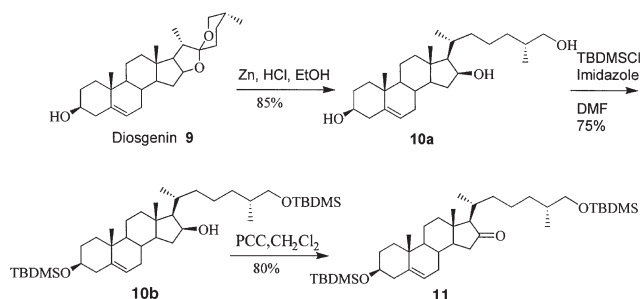


FIG. 1. Retrosynthesis of pavoninin-5 (**5**). TBDMS, *tert*-butyldimethylsilyl.



**FIG. 2.** Synthesis of C-16 ketone (**11**). PCC, pyridinium chlorochromate; DMF, dimethylformamide; for other abbreviation see Figure 1.

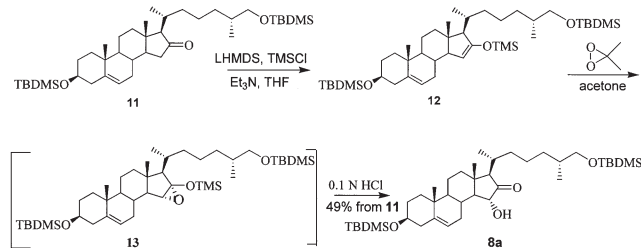
Clemmensen reduction since the yield of **10a** is higher, 85 vs. ~60% previously (7). That mercury is not used in the reduction renders the reaction more environmentally friendly (8).

The 3 $\beta$ ,16 $\beta$ ,26-triol **10a** was selectively protected as the 3 $\beta$ ,26-bissilyloxy ether **10b** (9). Oxidation of the unprotected alcohol in **10b** with pyridinium chlorochromate afforded the 16-ketone **11** (Fig. 2).

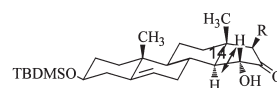
A number of methods were used in attempts to  $\alpha$ -hydroxylate **11** into **8a** in one step. The first method utilizing the Davis reagent (10,11), was unsuccessful, probably owing to the large size of the Davis reagent, which prevented it from approaching the substrate. To reduce the steric congestion in this hydroxylation reaction, the second method used a small reagent, dimethyldioxirane (12). Again the reaction was unsuccessful.

Because of the difficulty of direct hydroxylation of **11**, we proposed another route to synthesize **12**, through silyl enol ether (13) (Fig. 4). Treatment of **11** with lithium diisopropylamide (LDA) yielded the thermodynamic enolate. After many attempts, the silyl enol ether **12** was finally synthesized by using the method of Corey and Gross (14). Adding lithium hexamethyldisilazane to the solution of **11** and trimethylsilyl chloride at  $-78^{\circ}\text{C}$ , followed by addition of redistilled triethylamine, then quenching the reaction with saturated  $\text{NaHCO}_3$ , afforded the enol ether **12**. The structure of **12** was confirmed by  $^1\text{H}$  NMR, which showed the chemical shift of 15-H at 4.6.

Enol ether **12** was not purified because it is sensitive to silica gel. Oxidation of **12** with dimethyldioxirane at  $-78^{\circ}\text{C}$  probably forms the labile  $\alpha$ -epoxysilyl ether **13**, which



**FIG. 3.** Formation of  $\alpha$ -hydroxy ketone (**8a**). LHMDS, lithium hexamethyldisilazane; TMSCl, trimethylsilyl chloride; TMS, trimethylsilyl; for other abbreviations see Figure 1.



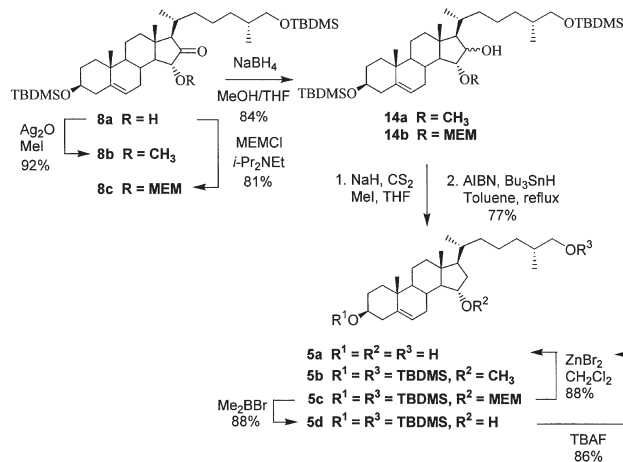
**FIG. 4.** Coupling constant between 14 $\alpha$ -H and 15 $\beta$ -H in **8a** is 10–12 Hz.

decomposes in the presence of acid to afford the  $\alpha$ -hydroxy ketone **8a** (Fig. 3). The  $^1\text{H}$  NMR spectrum of **8a** showed a coupling constant between 15-H and 14-H of 12 Hz, which indicates the 15-H should be in the  $\beta$  position (Fig. 4). The formation of this structure may be explained by steric reasons. The large groups at the C-13 $\beta$  and C-17 $\beta$  positions shielded the  $\beta$  face, causing the oxidant to attack the  $\alpha$  face and resulting in the 15 $\alpha$ -hydroxy-16-ketone **8a**.

The next step was the deoxygenation of the C-16 ketone. Attempts to prepare the thioketal of **8a** were unsuccessful. One can rationalize the failure to form a thioketal as being due to steric congestion. Efforts to carry out a Wolff–Kishner reduction also were unsuccessful. A survey of the literature revealed an absence of a description of the deoxygenation of  $\alpha$ -hydroxy ketones.

Owing to the failure of direct deoxygenation of **8a**, we planned to reduce the 16-position carbonyl group to a hydroxyl group, then deoxygenate the alcohol using the Barton reaction (15). We proposed this scheme because the hydroxyl group in the Barton reaction functions as a nucleophile to attack carbon disulfide, which can avoid the steric congestion of the C-16 position. First we had to protect the hydroxyl group in the 15 $\alpha$ -position. Our initial choice was the methyl group as the protecting group because it had the smallest steric size, and we did not want the protecting group at the 15-position to block the Barton reaction in the later step.

Because of the sensitivity of the 15 $\beta$  hydrogen in **8a**, we used  $\text{CH}_3\text{I}$  and silver oxide under neutral, mild methylating conditions to protect the hydroxyl group. The C-16 ketone of the methyl ether **8b** was reduced to a mixture of 16 $\alpha$  and - $\beta$



**FIG. 5.** Synthesis of pavoninin-5 aglycone (**5a**). MEM, methoxyethoxymethyl; AIBN, 2,2'-azobisisobutyronitrile; TBAF, tetrabutylammonium fluoride; for other abbreviation see Figure 1.

alcohols (**14a**) by sodium borohydride. The Barton reaction on **14a** first afford a thioester, which on radical reduction gave the desoxy methyl ether **5b** (see Scheme 4). Unfortunately, the methyl ether could not be cleaved without the concomitant cleavage of the TBDMS groups (16). The methoxyethoxymethyl (MEM) group was chosen as a protecting group (17) because it is easier to cleave MEM ether than methyl ether. The hydroxy group in **8a** was first protected using MEM chloride to afford the MEM ether, **8c**. Then, as for the methyl ether, the ketone was reduced with sodium borohydride and the resulting alcohols were deoxygenated by the Barton reaction to give the MEM ether, **5c**. The general method for cleavage of a MEM group is to use anhydrous zinc bromide in dry methylene chloride (17), but in this reaction, ZnBr<sub>2</sub> again cleaved the TBDMS group as well. This now constitutes a successful route for the synthesis of pavoninin-5 aglycone, **5a**, in 10 steps with 12% overall yield.

To selectively cleave the MEM group in **5c** without affecting the TBDMS (Fig. 4), bromodimethylborane (18) was used and yielded the 3 $\beta$ ,26-bissilyloxy protected ether **5d**. The protected ether **5d** is a suitable substrate for the attachment of N-acetylglucosamine at C-15 $\alpha$ , and removal of the protecting groups should afford the shark-repelling 26-desacetyl-pavoninin-5 (4).

We report the first synthesis of pavoninin-5 aglycone, **5a**, in 10 steps in 12% overall yield. An improved method for the reductive cleavage of diosgenin, **9**, was exploited.  $\alpha$ -Hydroxy ketones were found to be resistant to the usual ketone deoxygenation methods. A way around this problem using Barton's method of deoxygenation of alcohols was developed. A regioselective method for the 1,2 transposition of an alcohol in a five-membered ring was devised.

## ACKNOWLEDGMENTS

Financial support for this research was provided by a grant from the Temple University Research Incentive Fund and a GlaxoSmithKline Fellowship (D.C.). Also, D.W. was supported in part by a Howard Hughes Medical Institute grant to the Undergraduate Biological Sciences Education Program at Temple University. Financial support was also provided by Wyeth-Ayerst, Bristol-Myers Squibb, and Merck. We thank Dr. Stephen Wilson of the Chemistry Department at New York University for suggesting the modified Clemmensen reduction conditions.

## REFERENCES

1. Yasumoto, T., and Murata, M. (1993) Marine Toxins, *Chem. Rev.* **93**, 1897–1909.
2. Pawlik, J.R. (1993) Marine Invertebrate Chemical Defenses, *Chem. Rev.* **93**, 1911–1922.
3. Oren, Z., and Shai, Y. (1996) A Class of Highly Potent Antibacterial Peptides Derived from Pardaxin, a Pore-forming Peptide Isolated from Moses Sole Fish *Pardachirus marmoratus*, *Eur. J. Biochem.* **66**, 6389–6393.
4. Tachibana, K., Sakaitani, M., and Nakanishi, K. (1985) Pavoninins, Shark-Repelling and Ichthyotoxic Steroid N-Acetylglucosamides from the Defense Secretion of the Sole *Pardachirus pavoninus* (Soleidae), *Tetrahedron* **41**, 1027–1037.
5. Ohnishi, Y., and Tachibana, K. (1997) Synthesis of Pavoninin-1, a Shark Repellent Substance, and Its Structural Analogues Toward Mechanistic Studies on Their Membrane Perturbation, *Bioorg. Med. Chem.* **5**, 2251–2265.
6. Kim, H.S., Kim, I.C., and Lee, S.O. (1997) Synthesis of Two Marine Natural Products: The Aglycones of Pavoninin-1 and 2, *Tetrahedron* **53**, 8129–8136.
7. Marker, R.E., and Turner, D.L. (1941) Sterols CXV. Sapogenins XLIV. The Relation Between Diosgenin and Cholesterol, *J. Am. Chem. Soc.* **63**, 767–771.
8. Williams, J.R., Chai, D., and Wright, D. (2002) Synthesis of (25R)-26-Hydroxycholesterol, *Steroids* **67**, 1041–1044.
9. Kim, H.S., Wilson, W.K., Needleman, D.H., Pinkerton, F.D., Wilson, D.K., Quiocho, F.A., and Schroepfer, G.J., Jr. (1989) Inhibitors of Sterol Synthesis. Chemical Synthesis, Structure, and Biological Activities of (25R)-3 $\beta$ ,26-Dihydroxy-5 $\alpha$ -cholest-8(14)-en-15-one, a Metabolite of 3 $\beta$ -Hydroxy-5 $\alpha$ -cholest-8(14)-en-15-one, *J. Lipid Res.* **30**, 247–261.
10. Davis, F.A., Billmers, J.M., Gosciniak, D.J., Towson, J.C., and Bach, R.D. (1986) Chemistry of Oxaziridines. 7. Kinetics and Mechanism of the Oxidation of Sulfoxides and Alkenes by 2-Sulfonyloxaziridines. Relationship to the Oxygen-Transfer Reactions of Metal Peroxides, *J. Org. Chem.* **51**, 4240–4245.
11. Davis, F.A., Towson, J.C., Weismiller, M.C., Lal, S., and Carroll, P.J. (1988) Chemistry of Oxaziridines. 11. (Camphorylsulfonyl)oxaziridine: Synthesis and Properties, *J. Am. Chem. Soc.* **110**, 8477–8482.
12. Adam, W., Chan, Y.Y., Cremer, D., Gauss, J., Scheutzwow, D., and Schindler, M. (1987) Spectral and Chemical Properties of Dimethyldioxirane as Determined by Experiment and *ab initio* Calculations, *J. Org. Chem.* **52**, 2800–2803.
13. Guertin, K.R., and Chan, T.-H. (1991) Facile Synthesis of  $\alpha$ -Hydroxy Carbonyl Compounds by Enolate Oxidation with Dimethyldioxirane, *Tetrahedron Lett.* **32**, 715–718.
14. Corey, E.J., and Gross, A.W. (1984) Highly Selective, Kinetically Controlled Enolate Formation Using Lithium Dialkylamides in the Presence of Trimethylchlorosilane, *Tetrahedron Lett.* **25**, 495–498.
15. Barton, D.H.R., and McCombie, S.W. (1975) New Method for the Deoxygenation of Secondary Alcohols, *J. Chem. Soc., Perkin Trans. 1*, **16**, 1574–1585.
16. Niwa, H., Hida, T., and Yamada, K. (1981) A New Method for Cleavage of Aliphatic Methyl Ethers, *Tetrahedron Lett.* **22**, 4239–4240.
17. Corey, E.J., Gras, J.L., and Ulrich, P. (1976) A New General Method for Protection of the Hydroxyl Function, *Tetrahedron Lett.* **11**, 809–812.
18. Guindon, Y., Yoakim, C., and Morton, H.E. (1984) Dimethylboron Bromide and Diphenylboron Bromide: Cleavage of Acetals and Ketals, *J. Org. Chem.* **49**, 3912–3920.

[Received August 16, 2002; accepted 2002]



# New Chemical Syntheses of Cholest-4,6-dien-3-one

Edward J. Parish\*, Hang Sun, Ding Lu, Stephen A. Kizito, and Zhihai Qiu

Department of Chemistry, Auburn University, Alabama 36849-5312

**ABSTRACT:** Steroidal dienones represent a significant class of compounds that are useful intermediates in the further functionalization of the steroid nucleus. Their chemical synthesis can be problematic owing to the lack of a simplified method of preparation and the occurrence of impurities that can be difficult to remove. We have endeavored to develop new methods of chemical synthesis of cholest-4,6-dien-3-one that would yield a product of high purity.

Paper no. L9153 in *Lipids* 37, 1197–1200 (December 2002).

Steroidal 4,6-dien-3-ones are an important class of steroids that have been useful as intermediates in the synthesis of a variety of ring A and B modified steroids (1–10). During our studies on the synthesis of steroidal inhibitors of estrogen synthase (aromatase), we required a quantity of cholest-4,6-dien-3-one (**1**) for use as a model compound in our synthesis work. Typical literature syntheses of this compound required a multistep reaction sequence for the preparation of a purified sample. Other shortened procedures provided mixtures of products that would require extensive chromatographic purification or produce only poor yields of product. In the present work, we endeavored to develop new synthetic approaches to this compound that would make this product more readily available for experimental use.

## METHODS OF ORGANIC SYNTHESIS

The synthesis of cholesta-4,6-dien-3-one (**1**) has been reported by many research groups (2,11–13). Tachibana (2) treated cholesta-4,6-dien-3 $\beta$ -ol with various oxidizing agents [e.g., 2,3-dichloro-5,6-dicyano-1,4-benzoquinone, and pyridinium chlorochromate (PCC)] to give 50–85% yields (Scheme 1). Unfortunately, the starting material cholesta-4,6-dien-3 $\beta$ -ol is not easy to obtain; it requires many steps to be synthesized from commercially available steroids. Sondheimer *et al.* (11) found that cholesterol could be oxidized to **1** directly by means of manganese dioxide (MnO<sub>2</sub>). This method is interesting and facile but gives only a 27% yield. Wettstein (12) and Djerassi (13) also reported that cholesterol could be oxidized under the Oppenauer conditions with *p*-quinone as the hydrogen acceptor to afford **1** in one step. This reaction also gives poor yields (<50%). The reaction of steroidal-4-en-3-ones with chloranil (tetrachlorobenzo-

quinone) also gives steroidal-4,6-dien-3-ones in good yields (4). However, steroidal-4-en-3-ones may require an additional synthesis.

In the present work we developed new procedures to yield **1** in high purity. In our first attempt, using commercially available cholesterol as a starting material, we designed the chemical synthesis shown in Scheme 2 (where DMF = dimethylformamide and NBS = *N*-bromosuccinimide). In the last step, treatment of the bromide with base (2,4,6-trimethylpyridine, collidine; 1,5-diazabicyclo[4.3.0]non-5-ene, DBN; or 1,8-diazabicyclo[5.4.0]undec-7-ene, DBU) resulted in elimination of HBr to produce the products **1** and cholest-4-en-3-one (**2**) as a mixture. The enone **2** is difficult to remove and would require chromatographic separation.

We then turned our attention to the approach shown in Scheme 3. Again using cholesterol as a starting material, we treated the final dibromide (in the last reaction) with base (collidine, DBN, or DBU) and again observed a mixture of reaction products (**1** and **2**).

Using methods modified from the literature (14,15), we completed the synthesis shown in Scheme 4. This procedure resulted in the formation of **1** as the only product in high yield (90%). However, a synthesis of several steps was required.

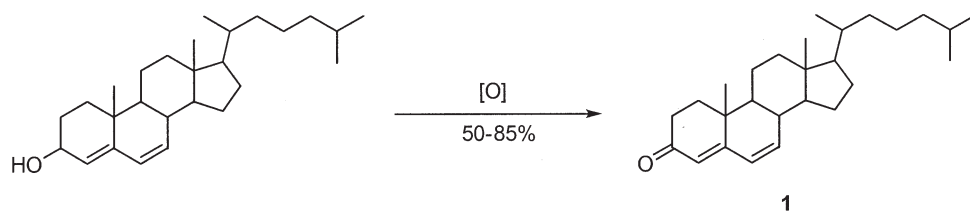
To reduce the number of steps during the preparation of **1**, we focused our efforts on the use of manganese dioxide to yield **1** directly from cholesterol (Scheme 5). This type of reaction had been described previously for the direct conversion of steroidal 5-en-3 $\beta$ -ols to 4,6-dienones (11). Using cholesterol as a starting material, we were able to produce **1** in modest yields ranging from 11 to 21%.

The results obtained using manganese dioxide were encouraging. We then explored the use of similar reagents to improve the yield of **1**. One reagent, chromium dioxide (Magtrieve™, product brochure; Aldrich Chemical Co., Milwaukee, WI) was described as a more effective reagent than manganese dioxide in many organic reactions (16). When cholesterol was treated with Magtrieve, **1** was produced in good yields (Scheme 6). Using acetonitrile as a solvent resulted in the formation of **1** in 74% yield. In addition to the major product **1**, a small quantity of 7-hydroxycholest-4-en-3-one was produced. This polar product was easily removed by silica gel column chromatography to yield purified **1**. We feel this procedure is the most efficient preparation of **1** currently available.

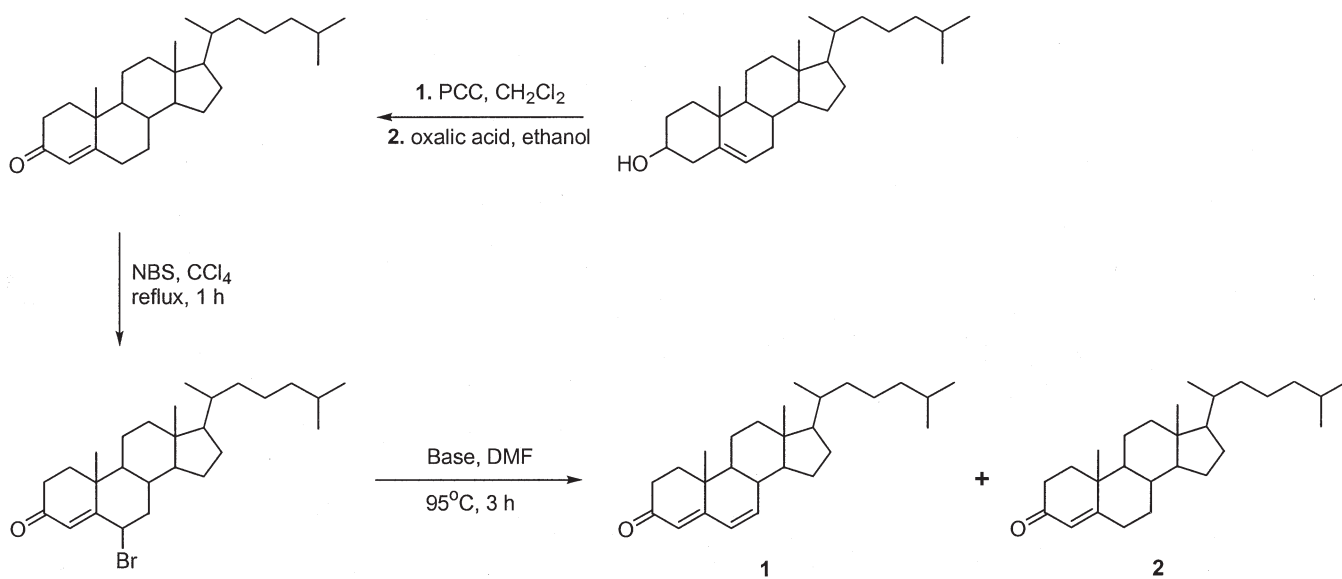
In conclusion, we feel the results presented herein provide useful information concerning the chemical synthesis of cholest-4,6-dien-3-one (**1**). In addition, we have attempted to develop novel and efficient approaches to the synthesis of **1** that will be efficient and give **1** in good yields.

\*To whom correspondence should be addressed.  
E-mail: parisej@auburn.edu

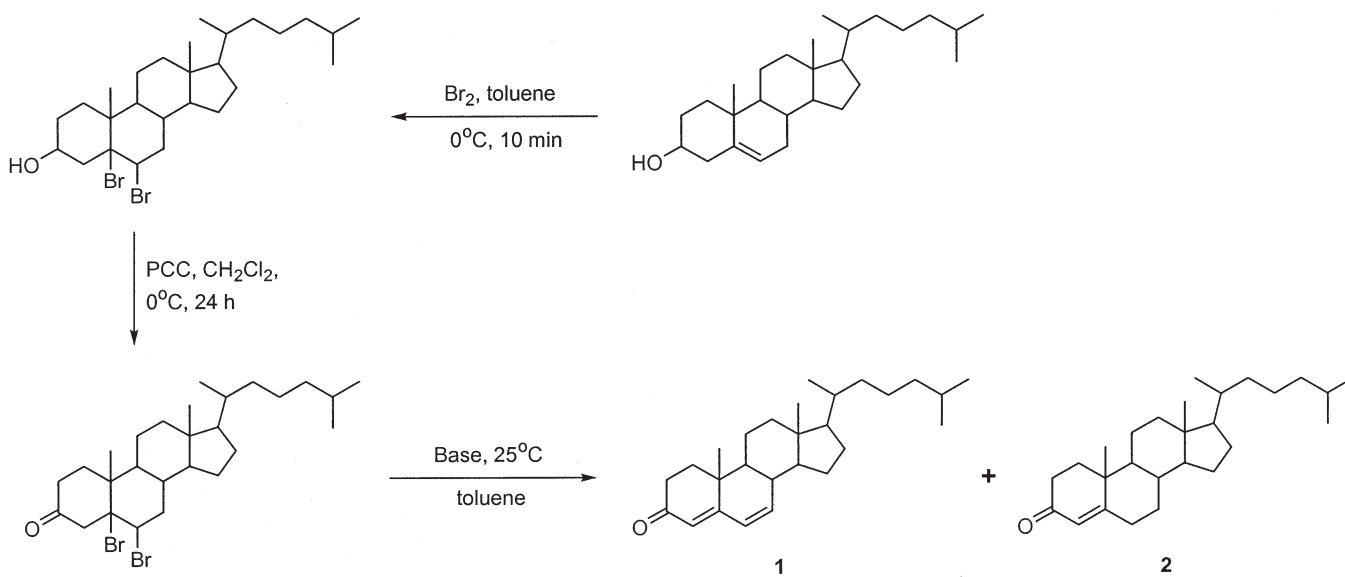
Abbreviations: Collidine, 2,4,6-trimethylpyridine; DBN, 1,5-diazabicyclo[4.3.0]non-5-ene; DBU, 1,8-diazabicyclo[5.4.0]undec-7-ene; DDQ, 2,3-dichloro-5,6-dicyano-1,4-benzoquinone; DMF, dimethylformamide; NBS, *N*-bromosuccinimide; PCC, pyridinium chlorochromate.



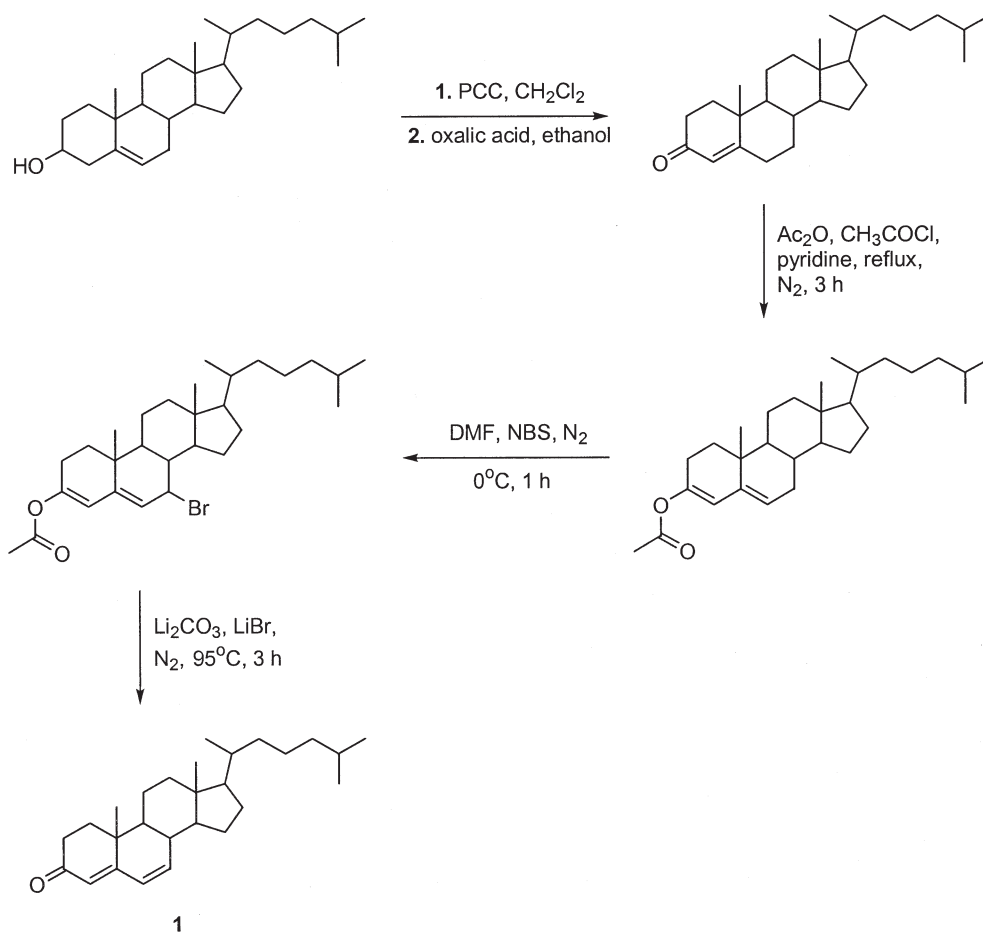
SCHEME 1



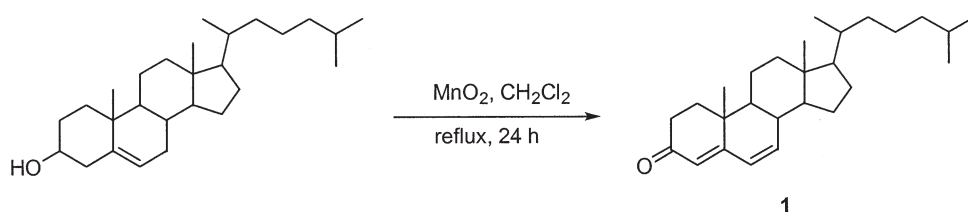
SCHEME 2



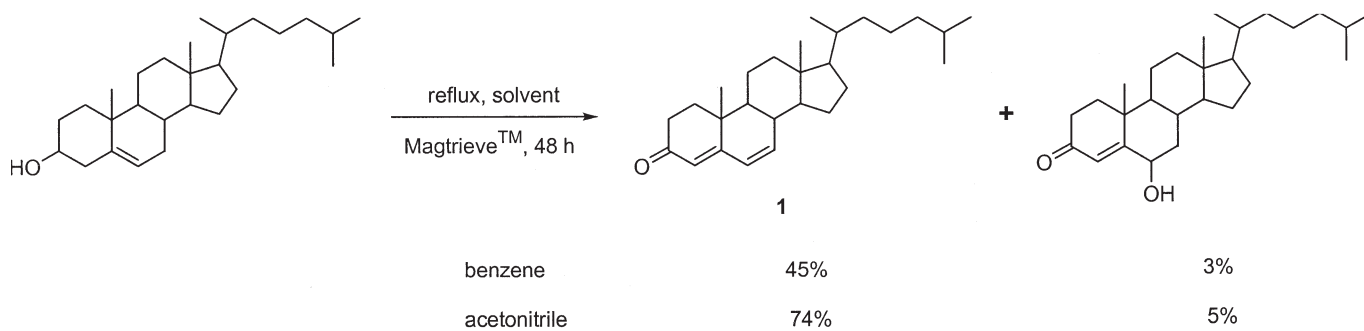
SCHEME 3



SCHEME 4



SCHEME 5



SCHEME 6

## REFERENCES

1. Cook, R.P. (1958) *Cholesterol, Chemistry, Biochemistry, and Pathology*, pp. 46–47, Academic Press, New York.
2. Tachibana, Y. (1986) A Convenient Synthesis of Cholesta-1,5,7-trien-3 $\beta$ -ol, *Bull. Chem. Soc. Jpn.* 59, 3702–3710.
3. Grunwell, J.F., Benson, H.D., Johnson, J.O., and Petrow, V. (1976) Antiprogestational Agents: The Synthesis of 7-Alkyl Steroidal Ketones with Anti-implantational and Antidecidual Activity, *Steroids* 27, 759–771.
4. Brueggemeier, R.W., Floyed, E.E., and Counsell, R.E. (1978) Synthesis and Biochemical Evaluation of Inhibitors of Estrogen Biosynthesis, *J. Med. Chem.* 21, 1007–1011.
5. Solo, A.J., Caroli, C., Darby, M.V., McKay, T., Slaunwhite, W.D., and Hebborn, P. (1982) 7 $\alpha$ -Alkyltestosterone Derivatives: Synthesis and Activity as Androgens and as Aromatase Inhibitors, *Steroids* 40, 603–614.
6. Campbell, J.A., and Babcock, J.C. (1959) The Synthesis of Some 7 $\alpha$ - and 7 $\beta$ -Methyl Steroid Hormones, *J. Am. Chem. Soc.* 81, 4069–4074.
7. Nickisch, K., and Laurent, H. (1988) Stereoselective Synthesis of 7 $\alpha$ -Allyl- and 7 $\alpha$ -Propylsteroids, *Tetrahedron Lett.* 29, 1533–1536.
8. Modi, S.P., Gardner, J.O., Milowsky, A., Wierzba, M., Forgiione, L., Mazur, P., Solo, A.J., Duax, W.L., Galdecki, Z., Grochulski, P., and Wawrzak, Z. (1989) Conjugate Addition of Grignard Reagents to Enones and Dienones, *J. Org. Chem.* 54, 2317–2321.
9. Bowler, J., Lilley, T.J., Pittam, J.D., and Wakeling, A.E. (1989) Novel Steroidal Pure Antiestrogens, *Steroids* 54, 71–99.
10. French, A.N., Wilson, S.R., Welch, M.J., and Katzenellenbogen, J.A. (1993) A Synthesis of 7 $\alpha$ -Substituted Estradiols: Synthesis and Biological Evaluation of a 7 $\alpha$ -Pentyl-Substituted BODIPY Fluorescent Conjugate and a Fluorine-18-Labeled 7 $\alpha$ -Pentylestradiol Analog, *Steroids* 58, 157–169.
11. Sondheimer, F., Amendolla, C., and Rosenkranz G. (1953) Steroids, LI.  $\Delta^{4,6}$ -Dien-3-ones, *J. Am. Chem. Soc.* 75, 5932–5935.
12. Wettstein, A. (1940) Steroids XXIV: The  $\Delta^{4,6}$ -3-Ketones of the Androstane and Pregnane Series, *Helv. Chim. Acta* 23, 388–399.
13. Djerassi, C. (1949) The Scope and Mechanism of the Reaction of Dinitrophenylhydrazine with Steroidal Bromo Ketones, *J. Am. Chem. Soc.* 71, 1003–1010.
14. Velluz, L., Goffinet, B., and Amiard, G. (1958) Photochemical Behavior of the 19-Nor- $\Delta^{5,7}$ -Steroids, *Tetrahedron* 4, 241–245.
15. Bohme, R.M., and Kempfle, M.A. (1994) Synthesis of Fluorescent 4,6,8(14)-Trien-3-one Steroids via 3,5,7-Trien-3-ol Ethers. Important Probes for Steroid-Protein Interactions, *Steroids* 59, 265–269.
16. Lee, R.A., and Donald, D.S. (1997) Magtrieve™, an Efficient, Magnetically Retrievable and Recyclable Oxidant, *Tetrahedron Lett.* 38, 3857–3860.

[Received September 17, 2002; accepted December 3, 2002]



# Temperature-Enhanced Alumina HPLC Method for the Analysis of Wax Esters, Sterol Esters, and Methyl Esters

Robert A. Moreau<sup>a,\*</sup>, Karen Kohout<sup>a</sup>, and Vijay Singh<sup>b</sup>

<sup>a</sup>ERRC, ARS, USDA, Wyndmoor, Pennsylvania, and <sup>b</sup>Department of Agricultural Engineering, University of Illinois, Urbana, Illinois 61801

**ABSTRACT:** Previous attempts at separating nonpolar lipid esters (including wax esters, sterol esters, and methyl esters) have achieved only limited success. Among the several normal-phase methods tested, a single recent report of a method employing an alumina column at 30°C with a binary gradient system was the most promising. In the current study, modification of the alumina method by increasing the column temperature to 75°C improved the separation of standards of wax esters and sterol esters. Elevated column temperature also enhanced the separation of FAME with differing degrees of unsaturation. Evidence was also presented to indicate that the method similarly separated phytosterol esters, based on their levels of unsaturation. With the increased interest in phytosterol- and phytostanol ester-enriched functional foods, this method should provide a technique to characterize and compare these products.

Paper no. L9154 in *Lipids* 37, 1201–1204 (December 2002).

Numerous HPLC methods have been reported for the separation of polar and nonpolar lipids (1,2). Approaches to the separation of nonpolar lipid classes have included the use of Diol (3,4), cyanopropyl (CN) (5,6), and alumina (7) columns. Among the nonpolar lipid classes, wax esters (a wax ester is defined as a FA esterified to a fatty alcohol) and sterol esters (including phytosterol fatty acyl esters) have proven to be the most difficult to separate, and the evidence reported in the latter alumina method (with a column temperature of 30°C) indicates that it is the most promising one (7). While employing the alumina method to separate grain seed extracts that were high in both wax esters and phytosterol esters, we noted that when the temperature of the alumina column was increased (up to 75°C) the separation between wax esters and sterol esters was enhanced. In addition, the phytosterol esters were subfractionated into several distinct peaks that appeared to be related to the degree of unsaturation. With the increased interest in phytosterol- and phytostanol-ester enriched functional foods, this method should provide a way to characterize and compare the types of sterol esters in these products.

## MATERIALS AND METHODS

Lipid standards and jojoba oil were purchased from Sigma Chemical Co. (St. Louis, MO). Benecol and Take Control

\*To whom correspondence should be addressed at Eastern Regional Research Center, ARS, USDA, 600 E. Mermaid Lane, Wyndmoor, PA 19038. E-mail: rmoreau@arserrc.gov

margarines were purchased from local grocers and were extracted with hexane (150 mg sample per 30 mL hexane), rinsed in a separatory funnel with an equal volume of water, dried under N<sub>2</sub>, and redissolved in hexane (with 0.01% BHT) for HPLC injection. CookSmart, a phytosterol ester-enriched cooking oil, was purchased on-line from Procter & Gamble (Cincinnati, OH) during a limited test-market period. Corn fiber oil (unrefined) was extracted as previously described (3).

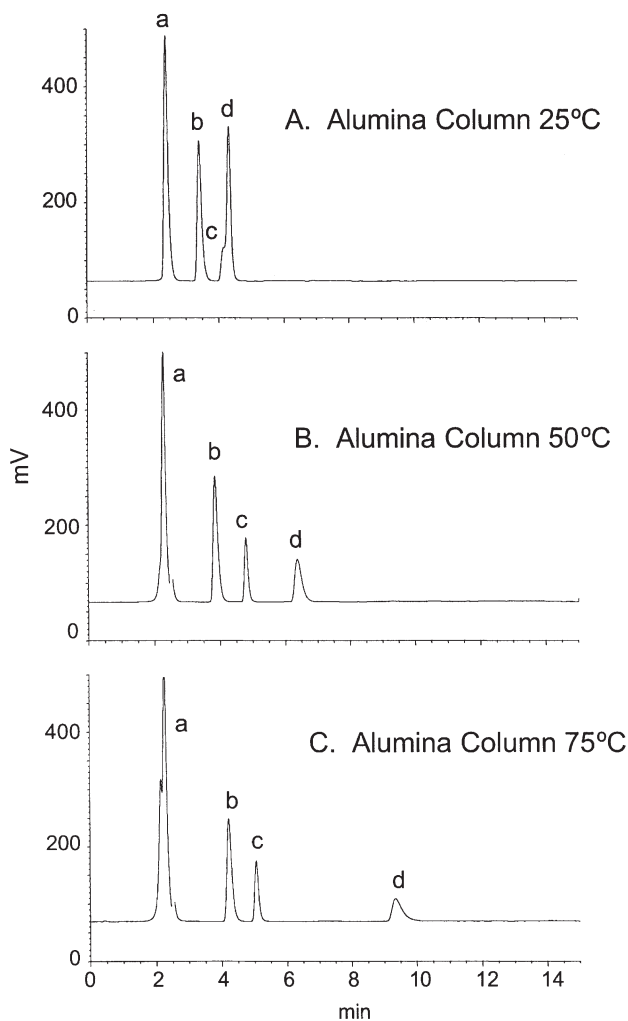
**Alumina HPLC method.** All HPLC analyses were performed with a Hewlett-Packard Model 1100 HPLC with autosampler, column heater, and detection by both an HP Model 1100 diode-array UV-vis detector (Agilent Technologies, Collegeville, PA) and a Sedex Model 55 Evaporative Light Scattering Detector (Richard Scientific, Modesto, CA) operated at 30°C and a nitrogen gas pressure of 2 bar. For alumina column separations, the column was an Aluspher Al 100, 5 μm column (125 × 4 mm), packed in a LiChroCART cartridge (Merck KGaA, Darmstadt, Germany). The binary gradient had a constant flow rate of 0.6 mL/min with Solvent A = hexane/THF, 1000:1, and Solvent B = isopropanol. The gradient timetable was as follows: at 0 min, 100% A/0% B; at 10 min, 100% A/0% B; at 20 min, 95% A/5% B; at 21 min, 100% A/0% B; and at 60 min, 100% A/0% B.

**Other HPLC methods.** A LiChrosorb 7 μm Diol column, a LiChrosorb Si 60 column, and a LiChrosorb CN column (all packed in ChromSep 3 × 100 mm cartridge columns by Chrompack, Raritan, NJ) were compared using the same gradient method except that the flow rate was decreased to 0.4 mL/min to compensate for the smaller column diameter.

## RESULTS AND DISCUSSION

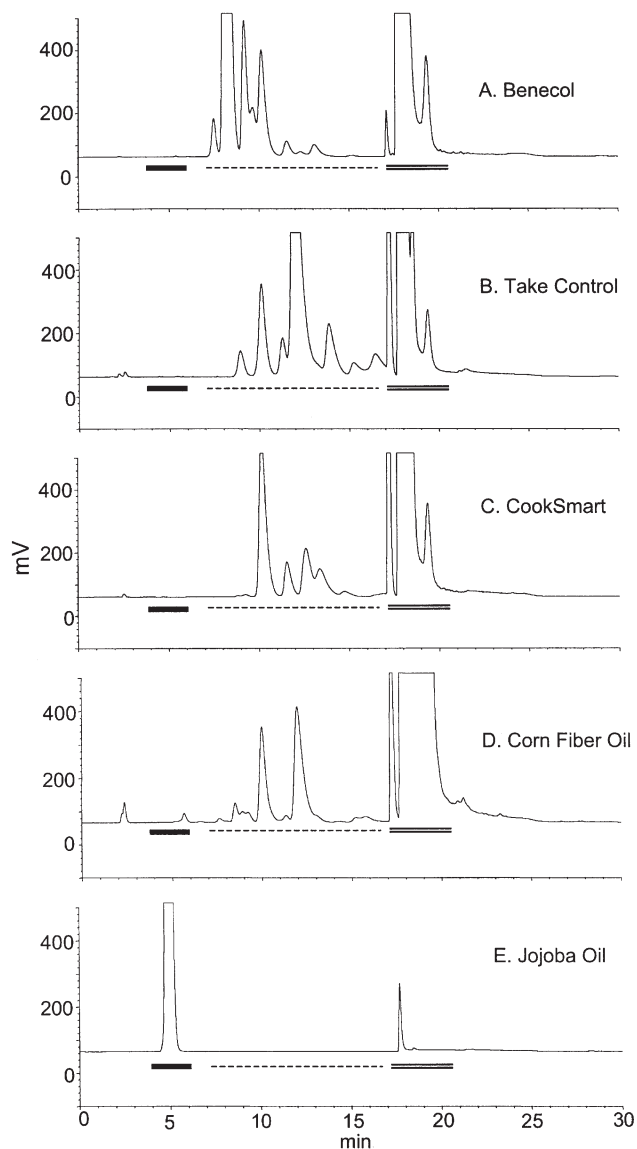
Standards of hydrocarbon (squalene), wax ester (stearyl stearate), and sterol ester (cholesterol stearate) were separated at a column temperature of 25°C (Fig. 1) using an Aluspher column and a gradient method very similar to that reported by Nordbäck and Lundburg (7). A fourth standard, methyl stearate, was also included in this mixture, and it appeared as a shoulder that preceded the peak of sterol ester. Increasing the column temperature to 50°C enhanced the separation of all four components, and further increasing it to 75°C had little effect on the first three peaks but increased the retention time of cholesterol stearate from about 6 to about 9 min.

Samples of four phytosterol ester-rich food products were injected into the HPLC system using this alumina method at



**FIG. 1.** Effect of column temperature on the separation of nonpolar lipid standards, separated on an alumina column (Aluspher Al 100, 5  $\mu$ m, 4  $\times$  125 mm, 0.6 mL/min solvent flow rate) with a binary gradient mobile phase. Abbreviations: a = squalene, b = stearyl stearate, c = methyl stearate, and d = cholesterol stearate, each at 0.5  $\mu$ g per injection.

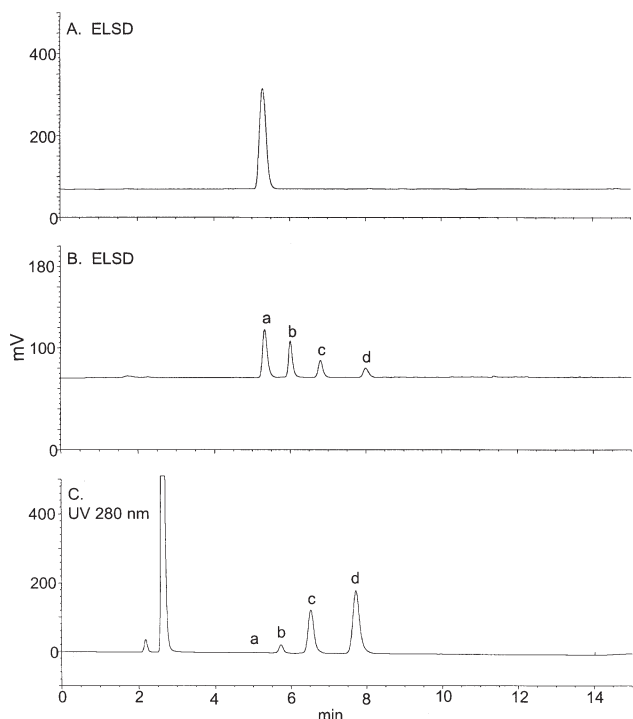
75°C (Fig. 2), and the major components in each were TAG, eluting as a broad peak at 17 to 20 min. The chromatograms obtained for all four samples also contained multiple peaks in the retention time region of 7 to 16 min, and these peaks appeared to be subfractions of phytosterol esters. Benecol, a spread containing phytosterol (completely saturated phytosterols obtained by hydrogenating phytosterols) esters, had a major peak at 8 min, and TakeControl, another spread containing phytosterol esters, had a major peak at about 12 min. CookSmart (a phytosterol ester containing cooking oil that was test-marketed for a short time by Procter & Gamble) had a major peak at about 10 min. Corn fiber oil (3), which contains both phytosterol and phytosterol esters, had major peaks at 10 and 12 min. The Benecol and TakeControl chromatograms indicate that multiple peaks of phytosterol esters may be separated based on the degree of unsaturation, partially eluting in order of increasing number of carbon-carbon double bonds in the esters.



**FIG. 2.** Separation of nonpolar ester-rich samples with the alumina column method at 75°C. (A) Benecol (65  $\mu$ g lipid injected), (B) Take Control (40  $\mu$ g lipid), (C) CookSmart (69  $\mu$ g lipid), (D) corn fiber oil (165  $\mu$ g lipid), and (E) jojoba oil (7  $\mu$ g lipid). The solid line indicates the retention time range for wax esters, the dashed line indicates the retention time range for sterol esters, and the double solid line indicates the retention time region for TAG elution.

Jojoba oil is an unusual seed oil that contains no TAG, and the storage form of lipid in the oil is entirely wax esters (20- and 22-carbon FA esterified to 20- and 22-carbon fatty alcohols) (8). The chromatogram of jojoba oil contained a major broad peak at 5 min (Fig. 2), similar to that of the wax ester standard in Figure 1.

Various FAME were then injected in the 75°C alumina method (Fig. 3). A mixture of methyl esters of four saturated FA (myristate, palmitate, stearate, and arachidate) eluted as a single peak at about 5 min. A second mixture of 18-carbon methyl esters of stearate, oleate, linoleate, and linolenate

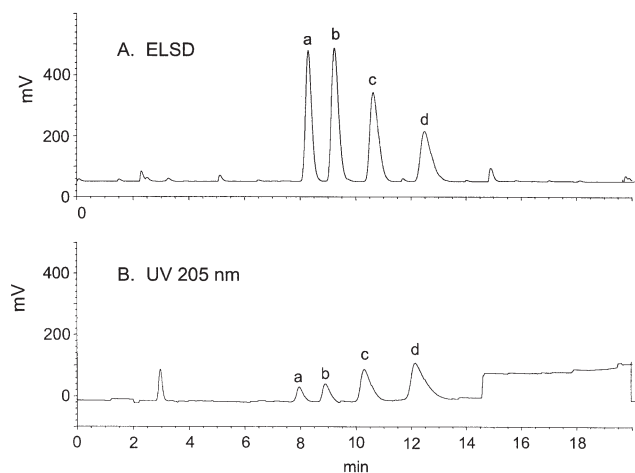


**FIG. 3.** Separation of FAME with the alumina column method at 75°C. (A) injection of saturated FAME. The injected mixture contained methyl myristate, methyl palmitate, methyl stearate, and methyl arachidate, with 0.5 µg of each component per injection. (B) Injection of C-18 saturated and unsaturated FAME. The injected mixture contained methyl myristate (a), methyl oleate (b), methyl linoleate (c), and methyl linolenate (d), with 0.5 µg of each component per injection. Detection *via* ELSD. (C) Same components as B with detection *via* UV at 205 nm.

exhibited peaks for each at 5, 6, 7, and 8 min, respectively, as detected with both the ELSD and the UV at 205 nm. The UV chromatogram verifies the increased signal of these four 18-carbon FAME, with increasing number of carbon-carbon double bonds. As conjectured for phytosterol esters in Figure 2, these FAME data (Fig. 3) similarly appear to demonstrate a separation based on the number of carbon-carbon double bonds (degree of unsaturation) of these esters.

Various cholesteryl fatty acyl esters were then injected to investigate their separation with this same elevated temperature alumina method (Fig. 4). A mixture of cholesteryl esters of stearate, oleate, linoleate, and linolenate exhibited peaks at about 8, 9, 10, and 12 min, respectively, as detected by both the ELSD (Fig. 4A) and UV205 nm detection (Fig. 4B). Cholesteryl palmitate eluted at a retention time nearly identical to cholesteryl stearates; as with the FAME (Fig. 3), the separation of cholesteryl esters correlated with the degree of unsaturation.

Because of the temperature-enhanced separation of nonpolar lipid classes displayed with the alumina column (Fig. 1), we then investigated the hypothesis that a similar temperature-enhanced separation of these same standards could be achieved with three other popular “normal-phase” columns. Increasing the temperature of the silica column caused two



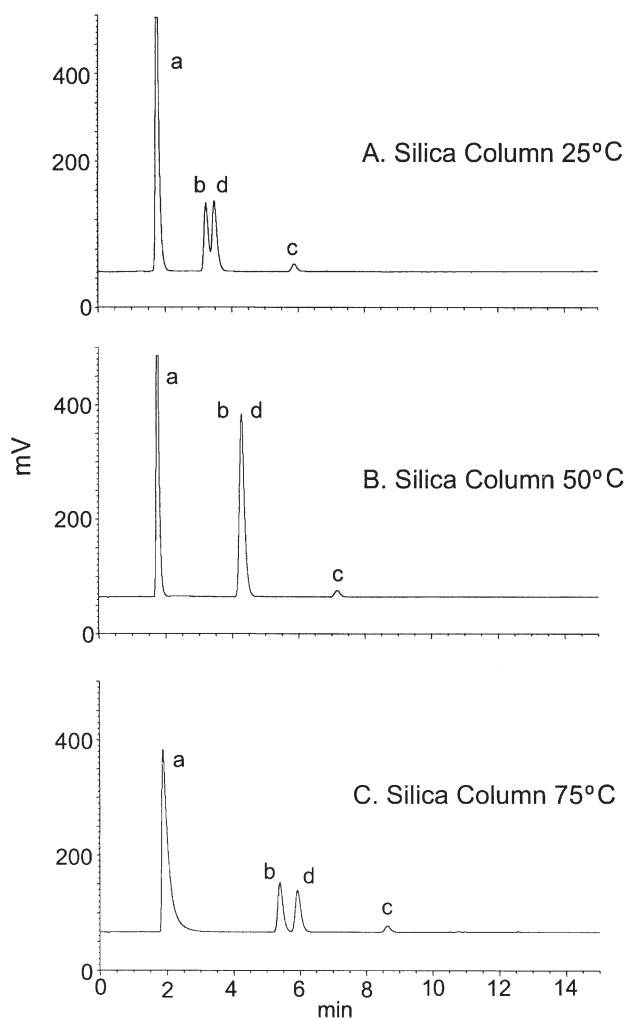
**FIG. 4.** Separation of cholesteryl esters with the alumina column method at 75°C. (A) Injection of standards, 0.5 µg each, of cholesteryl stearate (a), cholesteryl oleate (b), cholesteryl linoleate (c), and cholesteryl linolenate (d) with detection *via* ELSD. (B) Same components as A with detection *via* UV at 205 nm.

effects: (i) It progressively increased the retention time of the FAME, and (ii) it worsened the separation of the wax ester and sterol ester at 50°C and slightly improved their separation at 75°C. Of these three types of esters, wax esters and sterol esters occur naturally in many types of plant and animal material. Elevated temperatures with the silica column did not significantly improve the separation of these natural esters (Fig. 5). FAME are rarely found in natural samples and are most often obtained by chemically methylating FFA. The temperature-enhanced separation of FAME on the silica column warrants further investigation.

Two other popular normal-phase columns, CN and Diol columns, were then evaluated to determine whether elevated temperature could increase the separation of nonpolar esters, as observed with the alumina (Fig. 1–4) and Si (Fig. 5) columns. With the CN or Diol columns, standards of wax ester, sterol ester, and FAME had nearly identical retention times, and increasing the column temperature had very little effect on the retention time of these three ester classes with both columns was about 2 min; data not shown).

Besides Nordbäck and Lundburg (7), the only previous report of the HPLC of lipids *via* an alumina column was a method for the separation of cholesterol oxides with a column consisting of 16% alumina/84% silica (9).

This alumina method at 75°C appears to separate nonpolar esters *via* typical normal-phase separation in order of increasing polarity, and it also appears to separate compounds of nearly identical polarity based on the degree of unsaturation (retention time is longer for each additional carbon-carbon double bond). Although the ability of the alumina method to separate nonpolar lipid esters based on degree of unsaturation appears to have similarities to the type of separation of unsaturated compounds that is achieved by silver ion chromatog-



**FIG. 5.** Effect of column temperature on the separation of nonpolar lipid standards, separated on a silica column (LiChrosorb Si 60-5, 5  $\mu\text{m}$ , 3  $\times$  100 mm, 0.4 mL/min solvent flow rate) with a binary gradient mobile phase. For abbreviations see Figure 1.

raphy (10), separation of free and derivatized FA, based solely on degree of unsaturation, was also previously described using normal-phase silica HPLC (11).

With the current high level of interest in the cholesterol-lowering properties of phytosterol and phytostanol esters (12), this new method provides a technique to compare intact esters in various natural and semisynthetic products.

Although it should be possible to separate molecular species of phytosterol and phytostanol esters *via* reversed-phase HPLC, as has been successfully achieved with TAG (1), we are not aware of any similar reverse-phase methods that have been published to separate phytosterol ester molecular species.

## REFERENCES

1. Moreau, R.A., and Christie, W.W. (1999) The Impact of the Evaporative Light Scattering Detector on Lipid Research, *INFORM 10*, 471–478.
2. Moreau, R.A., and Gerard, H.C. (1993) High-Performance Liquid Chromatography as a Tool for the Lipid Chemist and Biochemist, in *CRC Handbook of Chromatography: Analysis of Lipids* (Mukherjee, K.D., and Weber, N., eds.), pp. 41–55, Chemical Rubber Co., Boca Raton.
3. Moreau, R.A., Powell, M.J., and Hicks, K.B. (1996). Extraction and Quantitative Analysis of Oil from Commercial Corn Fiber, *J. Agric. Food Chem.* **44**, 2149–2154.
4. Inger-Elfman-Börjesson, I., and Härröd, M. (1997) Analysis of Nonpolar Lipids by HPLC on a Diol Column, *J. High Resolut. Chromatogr.* **20**, 516–518.
5. El-Hamdy, A.H., and Christie, W.W. (1993) Separation of Nonpolar Lipids by High-Performance Liquid Chromatography on a Cyanopropyl Column, *J. High Resolut. Chromatogr.*, **16**, 55–57.
6. Foglia, T.S., and Jones, K.C. (1997) Quantitation of Neutral Lipid Mixtures Using High-Performance Liquid Chromatography with Light Scattering Detection, *J. Liq. Chromatogr. Rel. Technol.* **20**, 1829–1838
7. Nordbäck, J., and Lundburg, E. (1999) High-Resolution Separation of Nonpolar Lipid Classes by HPLC–ELSD Using Alumina as Stationary Phase, *J. High Resolut. Chromatogr.* **22**, 483–486.
8. Wisniak, J., (1987) *The Chemistry and Technology of Jojoba Oil*, American Oil Chemists' Society, Champaign.
9. Lakratz, L., and Jones, K.C. (1997) Separation and Quantitation of Cholesterol Oxides by HPLC with an Evaporative Light Scattering Detector in a Model System, *J. Am. Oil Chem. Soc.* **74**, 943–946.
10. Dobson, G., Christie, W.W., and Nikolova-Damyanova, B. (1995) Silver Ion Chromatography of Lipids and Fatty Acids, *J. Chromatogr. B.* **671**, 197–222.
11. Christie, W.W. (1987) *High-Performance Liquid Chromatography and Lipids: A Practical Guide*, 156 pp., Pergamon Press, Oxford.
12. Hicks, K.B., and Moreau, R.A. (2001) Phytosterols and Phytostanols: Functional Food Cholesterol Busters, *Food Technol.* **55**, 63–67.

[Received September 17, 2002; accepted December 10, 2002]